Scientific and Technical Aerospace Reports

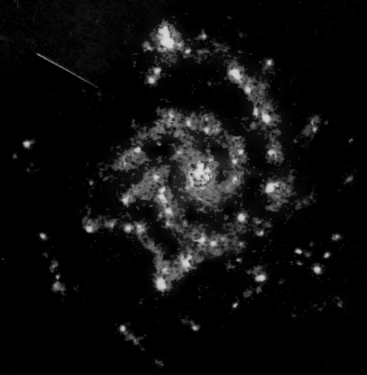

An Abstract Journal

Volume 33, Number 4
April 1995
N95-15919 to N95-17933

The NASA STI Office ... in Profile

Since its founding, NASA has been dedicated to the advancement of aeronautics and space science. The NASA Scientific and Technical Information (STI) Office plays a key part in helping NASA maintain this important role.

The NASA STI Office provides access to the NASA STI Database, the largest collection of aeronautical and space science STI in the world. The Office is also NASA's institutional mechanism for disseminating the results of its research and development activities.

Specialized services that help round out the Office's diverse offerings include creating custom thesauri, translating material to or from 34 foreign languages, building customized databases, organizing and publishing research results ... even providing videos.

For more information about the NASA STI Office, you can:

- **Phone** the NASA Access Help Desk at (301) 621-0390
- **Fax** your question to the NASA Access Help Desk at (301) 621-0134
- **E-mail** your question via the **Internet** to help@sti.nasa.gov
- **Write** to:

NASA Access Help Desk
NASA Center for AeroSpace Information
800 Elkridge Landing Road
Linthicum Heights, MD 21090-2934

Scientific and Technical Aerospace Reports

Scientific and Technical Aerospace Reports (STAR), is published each month as a major product of the NASA Scientific and Technical Information (STI) Office.

Inside this issue you will find:

- **Front Matter** containing a typical citation and abstract sample explaining the standard format, including codes for ordering reports
- **An Abstract Section** containing citations and abstracts of reports and publications that provide comprehensive coverage of worldwide aerospace-related topics including aeronautics and space science technology. *STAR* lists published and publicly available reports entered into the NASA STI Database during the four weeks preceding publication of this issue. These citations and abstracts are listed by subject categories.
- **An Index Section**
  - Subject
  - Personal author
  - Corporate source
  - Contract number
  - Report number
- **An Appendix** containing a guide for ordering cited reports, registering with the NASA STI Office, and using the available products and services. Additionally, price schedules, phone numbers, and addresses are included in this information packed section.

NASA also sponsors the companion journal, *NASA Open Volumes on Aerospace (NOVA)*, which lists abstracts of the open literature on aerospace subjects available worldwide. *NOVA* is for internal NASA use only, available from the NASA Center for AeroSpace Information (CASI).

Entries found in *STAR* are available through the NASA online retrieval service, RECON, and through DIALOG as the Aerospace Database.

The NASA STI Office gathers information through national and international agreements and exchanges and makes this information available to the NASA community and to the public in many forms through various outlets.

For additional information on the NASA STI Office, call the NASA Access Help Desk at (301) 621-0390, or write to:

NASA Center for AeroSpace Information
800 Elkridge Landing Road
Linthicum Heights, Maryland 21090-2934

US ISSN 0036-8741

This publication was prepared by the NASA Center for AeroSpace Information,
800 Elkridge Landing Road, Linthicum Heights, MD 21090-2934, (301) 621-0390.

Volume 33 Number 4 / April 1995

TABLE OF CONTENTS

AERONAUTICS For related information see also *Astronautics.*

01 AERONAUTICS (GENERAL) **649**

02 AERODYNAMICS **654**
Includes aerodynamics of bodies, combinations, wings, rotors, and control surfaces; and internal flow in ducts and turbomachinery. For related information see also *34 Fluid Mechanics and Heat Transfer.*

03 AIR TRANSPORTATION AND SAFETY **664**
Includes passenger and cargo air transport operations; and aircraft accidents. For related information see also *16 Space Transportation* and *85 Urban Technology and Transportation.*

04 AIRCRAFT COMMUNICATIONS AND NAVIGATION **665**
Includes digital and voice communication with aircraft; air navigation systems (satellite and ground based); and air traffic control. For related information see also *17 Space Communications, Spacecraft Communications, Command and Tracking* and *32 Communications and Radar.*

05 AIRCRAFT DESIGN, TESTING AND PERFORMANCE **666**
Includes aircraft simulation technology. For related information see also *18 Spacecraft Design, Testing and Performance* and *39 Structural Mechanics.* For land transportation vehicles see *85 Urban Technology and Transportation.*

06 AIRCRAFT INSTRUMENTATION **669**
Includes cockpit and cabin display devices; and flight instruments. For related information see also *19 Spacecraft Instrumentation* and *35 Instrumentation and Photography.*

07 AIRCRAFT PROPULSION AND POWER **670**
Includes prime propulsion systems and systems components, e.g., gas turbine engines and compressors; and onboard auxiliary power plants for aircraft. For related information see also *20 Spacecraft Propulsion and Power, 28 Propellants and Fuels,* and *44 Energy Production and Conversion.*

08 AIRCRAFT STABILITY AND CONTROL **670**
Includes aircraft handling qualities; piloting; flight controls; and autopilots. For related information see also *05 Aircraft Design, Testing and Performance.*

09 RESEARCH AND SUPPORT FACILITIES (AIR) **671**
Includes airports, hangars and runways; aircraft repair and overhaul facilities; wind tunnels; shock tubes; and aircraft engine test stands. For related information see also *14 Ground Support Systems and Facilities (Space).*

ASTRONAUTICS For related information see also *Aeronautics.*

12 ASTRONAUTICS (GENERAL) **672**
For extraterrestrial exploration see *91 Lunar and Planetary Exploration.*

13 ASTRODYNAMICS **673**
Includes powered and free-flight trajectories; and orbital and launching dynamics.

14 GROUND SUPPORT SYSTEMS AND FACILITIES (SPACE) ..... **N.A.**
Includes launch complexes, research and production facilities; ground support equipment, e.g., mobile transporters; and simulators. For related information see also *09 Research and Support Facilities (Air).*

15 LAUNCH VEHICLES AND SPACE VEHICLES **675**
Includes boosters; operating problems of launch/space vehicle systems; and reusable vehicles. For related information see also *20 Spacecraft Propulsion and Power.*

16 SPACE TRANSPORTATION **676**
Includes passenger and cargo space transportation, e.g., shuttle operations; and space rescue techniques. For related information see also *03 Air Transportation and Safety* and *18 Spacecraft Design, Testing and Performance.* For space suits see *54 Man/System Technology and Life Support.*

17 SPACE COMMUNICATIONS, SPACECRAFT COMMUNICATIONS, COMMAND AND TRACKING **676**
Includes telemetry; space communications networks; astronavigation and guidance; and radio blackout. For related information see also *04 Aircraft Communications and Navigation* and *32 Communications and Radar.*

N.A.—No abstracts were assigned to this category for this issue.

18 SPACECRAFT DESIGN, TESTING AND PERFORMANCE **708**
Includes satellites; space platforms; space stations; spacecraft systems and components such as thermal and environmental controls; and attitude controls. For life support systems see *54 Man/System Technology and Life Support.* For related information see also *05 Aircraft Design, Testing and Performance*, *39 Structural Mechanics*, and *16 Space Transportation.*

19 SPACECRAFT INSTRUMENTATION ..... **N.A.**
For related information see also *06 Aircraft Instrumentation* and *35 Instrumentation and Photography.*

20 SPACECRAFT PROPULSION AND POWER **711**
Includes main propulsion systems and components, e.g., rocket engines; and spacecraft auxiliary power sources. For related information see also *07 Aircraft Propulsion and Power*, *28 Propellants and Fuels*, *44 Energy Production and Conversion*, and *15 Launch Vehicles and Space Vehicles.*

CHEMISTRY AND MATERIALS

23 CHEMISTRY AND MATERIALS (GENERAL) **721**

24 COMPOSITE MATERIALS **723**
Includes physical, chemical, and mechanical properties of laminates and other composite materials. For ceramic materials see *27 Nonmetallic Materials.*

25 INORGANIC AND PHYSICAL CHEMISTRY **726**
Includes chemical analysis, e.g., chromatography; combustion theory; electrochemistry; and photochemistry. For related information see also *77 Thermodynamics and Statistical Physics.*

26 METALLIC MATERIALS **733**
Includes physical, chemical, and mechanical properties of metals, e.g., corrosion; and metallurgy.

27 NONMETALLIC MATERIALS **739**
Includes physical, chemical, and mechanical properties of plastics, elastomers, lubricants, polymers, textiles, adhesives, and ceramic materials. For composite materials see *24 Composite Materials.*

28 PROPELLANTS AND FUELS **748**
Includes rocket propellants, igniters and oxidizers; their storage and handling procedures; and aircraft fuels. For related information see also *07 Aircraft Propulsion and Power*, *20 Spacecraft Propulsion and Power*, and *44 Energy Production and Conversion.*

29 MATERIALS PROCESSING **750**
Includes space-based development of products and processes for commercial application. For biological materials see *55 Space Biology:*

ENGINEERING For related information see also *Physics.*

31 ENGINEERING (GENERAL) **750**
Includes vacuum technology; control engineering; display engineering; cryogenics; and fire prevention.

32 COMMUNICATIONS AND RADAR **751**
Includes radar; land and global communications; communications theory; and optical communications. For related information see also *04 Aircraft Communications and Navigation* and *17 Space Communications, Spacecraft Communications, Command and Tracking.* For search and rescue see *03 Air Transportation and Safety*, and *16 Space Transportation.*

33 ELECTRONICS AND ELECTRICAL ENGINEERING **762**
Includes test equipment and maintainability; components, e.g., tunnel diodes and transistors; microminiaturization; and integrated circuitry. For related information see also *60 Computer Operations and Hardware* and *76 Solid-State Physics.*

34 FLUID MECHANICS AND HEAT TRANSFER **769**
Includes boundary layers; hydrodynamics; fluidics; mass transfer and ablation cooling. For related information see also *02 Aerodynamics* and *77 Thermodynamics and Statistical Physics.*

35 INSTRUMENTATION AND PHOTOGRAPHY **774**
Includes remote sensors; measuring instruments and gauges; detectors; cameras and photographic supplies; and holography. For aerial photography see *43 Earth Resources and Remote Sensing.* For related information see also *06 Aircraft Instrumentation* and *19 Spacecraft Instrumentation.*

36 LASERS AND MASERS **776**
Includes parametric amplifiers. For related information see also *76 Solid-State Physics.*

37 MECHANICAL ENGINEERING **780**
Includes auxiliary systems (nonpower); machine elements and processes; and mechanical equipment.

38 QUALITY ASSURANCE AND RELIABILITY **783**
Includes product sampling procedures and techniques; and quality control.

39 STRUCTURAL MECHANICS **784**
Includes structural element design and weight analysis; fatigue; and thermal stress. For applications see *05 Aircraft Design, Testing and Performance* and *18 Spacecraft Design, Testing and Performance.*

GEOSCIENCES For related information see also *Space Sciences.*

42 GEOSCIENCES (GENERAL) ..... **N.A.**

43 EARTH RESOURCES AND REMOTE SENSING **790**
Includes remote sensing of earth resources by aircraft and spacecraft; photogrammetry; and aerial photography. For instrumentation see *35 Instrumentation and Photography.*

44 ENERGY PRODUCTION AND CONVERSION **791**
Includes specific energy conversion systems, e.g., fuel cells; global sources of energy; geophysical conversion; and windpower. For related information see also *07 Aircraft Propulsion and Power, 20 Spacecraft Propulsion and Power,* and *28 Propellants and Fuels.*

45 ENVIRONMENT POLLUTION **794**
Includes atmospheric, noise, thermal, and water pollution.

46 GEOPHYSICS **798**
Includes aeronomy; upper and lower atmosphere studies; ionospheric and magnetospheric physics; and geomagnetism. For space radiation see *93 Space Radiation.*

47 METEOROLOGY AND CLIMATOLOGY **800**
Includes weather forecasting and modification.

48 OCEANOGRAPHY **803**
Includes biological, dynamic, and physical oceanography; and marine resources. For related information see also *43 Earth Resources and Remote Sensing.*

LIFE SCIENCES

51 LIFE SCIENCES (GENERAL) **807**

52 AEROSPACE MEDICINE **818**
Includes physiological factors; biological effects of radiation; and effects of weightlessness on man and animals.

53 BEHAVIORAL SCIENCES **825**
Includes psychological factors; individual and group behavior; crew training and evaluation; and psychiatric research.

54 MAN/SYSTEM TECHNOLOGY AND LIFE SUPPORT **829**
Includes human engineering; biotechnology; and space suits and protective clothing. For related information see also *16 Space Transportation.*

55 SPACE BIOLOGY ..... **N.A.**
Includes exobiology; planetary biology; and extraterrestrial life.

MATHEMATICAL AND COMPUTER SCIENCES

59 MATHEMATICAL AND COMPUTER SCIENCES (GENERAL) **832**

60 COMPUTER OPERATIONS AND HARDWARE **832**
Includes hardware for computer graphics, firmware, and data processing. For components see *33 Electronics and Electrical Engineering.*

61 COMPUTER PROGRAMMING AND SOFTWARE **833**
Includes computer programs, routines, algorithms, and specific applications, e.g., CAD/CAM.

62 COMPUTER SYSTEMS **844**
Includes computer networks and special application computer systems.

63 CYBERNETICS **851**
Includes feedback and control theory, artificial intelligence, robotics and expert systems. For related information see also *54 Man/System Technology and Life Support.*

64 NUMERICAL ANALYSIS **859**
Includes iteration, difference equations, and numerical approximation.

65 STATISTICS AND PROBABILITY **864**
Includes data sampling and smoothing; Monte Carlo method; and stochastic processes.

66 SYSTEMS ANALYSIS ..... **N.A.**
Includes mathematical modeling; network analysis; and operations research.

67 THEORETICAL MATHEMATICS ..... **N.A.**
Includes topology and number theory.

PHYSICS For related information see also *Engineering.*

70 PHYSICS (GENERAL) **868**
For precision time and time interval (PTTI) see *35 Instrumentation and Photography*; for geophysics, astrophysics or solar physics see *46 Geophysics, 90 Astrophysics*, or *92 Solar Physics.*

71 ACOUSTICS **869**
Includes sound generation, transmission, and attenuation. For noise pollution see *45 Environment Pollution.*

72 ATOMIC AND MOLECULAR PHYSICS **871**
Includes atomic structure, electron properties, and molecular spectra.

73 NUCLEAR AND HIGH-ENERGY PHYSICS **879**
Includes elementary and nuclear particles; and reactor theory. For space radiation see *93 Space Radiation.*

74 OPTICS **883**
Includes light phenomena and optical devices. For lasers see *36 Lasers and Masers.*

75 PLASMA PHYSICS **888**
Includes magnetohydrodynamics and plasma fusion. For ionospheric plasmas see *46 Geophysics.* For space plasmas see *90 Astrophysics.*

76 SOLID-STATE PHYSICS **894**
Includes superconductivity. For related information see also *33 Electronics and Electrical Engineering* and *36 Lasers and Masers.*

77 THERMODYNAMICS AND STATISTICAL PHYSICS **902**
Includes quantum mechanics; theoretical physics; and Bose and Fermi statistics. For related information see also *25 Inorganic and Physical Chemistry* and *34 Fluid Mechanics and Heat Transfer.*

SOCIAL SCIENCES

80 SOCIAL SCIENCES (GENERAL) **904**
Includes educational matters.

81 ADMINISTRATION AND MANAGEMENT **904**
Includes management planning and research.

82 DOCUMENTATION AND INFORMATION SCIENCE **905**
Includes information management; information storage and retrieval technology; technical writing; graphic arts; and micrography. For computer documentation see *61 Computer Programming and Software.*

83 ECONOMICS AND COST ANALYSIS **914**
Includes cost effectiveness studies.

84 LAW, POLITICAL SCIENCE AND SPACE POLICY ..... **N.A.**
Includes NASA appropriation hearings; aviation law; space law and policy; international law; international cooperation; and patent policy.

85 URBAN TECHNOLOGY AND TRANSPORTATION ..... **N.A.**
Includes applications of space technology to urban problems; technology transfer; technology assessment; and surface and mass transportation. For related information see *03 Air Transportation and Safety, 16 Space Transportation,* and *44 Energy Production and Conversion.*

SPACE SCIENCES For related information see also *Geosciences.*

88 SPACE SCIENCES (GENERAL) ..... **N.A.**

89 ASTRONOMY **914**
Includes radio, gamma-ray, and infrared astronomy; and astrometry.

90 ASTROPHYSICS **916**
Includes cosmology; celestial mechanics; space plasmas; and interstellar and interplanetary gases and dust. For related information see also *75 Plasma Physics.*

91 LUNAR AND PLANETARY EXPLORATION **917**
Includes planetology; and manned and unmanned flights. For spacecraft design or space stations see *18 Spacecraft Design, Testing and Performance.*

92 SOLAR PHYSICS **923**
Includes solar activity, solar flares, solar radiation and sunspots. For related information see also *93 Space Radiation.*

93 SPACE RADIATION **924**
Includes cosmic radiation; and inner and outer earth's radiation belts. For biological effects of radiation see *52 Aerospace Medicine.* For theory see *73 Nuclear and High-Energy Physics.*

GENERAL

Includes aeronautical, astronautical, and space science related histories, biographies, and pertinent reports too broad for categorization; histories or broad overviews of NASA programs.

99 GENERAL **924**

SUBJECT INDEX **I-1**

PERSONAL AUTHOR INDEX **I-117**

CORPORATE SOURCE INDEX **I-131**

CONTRACT NUMBER INDEX **I-151**

REPORT NUMBER INDEX **I-155**

APPENDIX **A-1**

TYPICAL CITATION AND ABSTRACT

NASA SPONSORED — ON MICROFICHE

ACCESSION NUMBER → **N95-10148*#** National Aeronautics and Space Administration. Lewis Research Center, Cleveland, OH. ← CORPORATE SOURCE

TITLE → **EFFECTS OF A FORWARD-SWEPT FRONT ROTOR ON THE FLOWFIELD OF A COUNTERROTATION PROPELLER**

AUTHORS → M. Nallasamy (NYMA, Inc., Brook Park, OH.) and Gary G. Podboy Aug. 1994 19 p Presented at the 30th Joint Propulsion Conference, Indianapolis, IN, 27-29 Jun. 1994; sponsored by AIAA, ASME, SAE, and ASEE ← PUBLICATION DATE

CONTRACT OR GRANT → (Contract NAS3-27186; RTOP 538-03-11)

REPORT NUMBERS → (NASA-TM-106671; E-8994; NAS 1.15:106671; AIAA Paper 94-2694) Avail: CASI HC A03/MF A01; 6 functional color pages ← AVAILABILITY SOURCE AND PRICE CODE

The effects of a forward-swept front rotor on the flowfield of a counterrotation model propeller at takeoff conditions at zero degree angle of attack are studied by solving the unsteady three-dimensional Euler equations. The configuration considered is an uneven blade count counterrotation model with twelve forward-swept blades on the fore rotor and ten aft-swept blades on the aft rotor. The flowfield is compared with that of a reference aft-swept counterrotation geometry and Laser Doppler Velocimeter (LDV) measurements. At the operating conditions considered, the forward-swept blade experiences a higher tip loading and produces a stronger tip vortex compared to the aft-swept blade, consistent with the LDV and acoustic measurements. Neither the solution nor the LDV data indicated the formation of a leading edge vortex. The predicted radial distribution of the circumferentially averaged axial velocity at the measurement station agreed very closely with LDV data, while crossflow velocities showed poor agreement. The discrepancy between prediction and LDV data of tangential and radial velocities is due in part to the insufficient mesh resolution in the region between the rotors and in the tip region to track the tip vortex. The vortex is diffused by the time it arrives at the measurement station. The uneven blade count configuration requires the solution to be carried out for six blade passages of the fore rotor and five passages of the aft rotor, thus making grid refinement prohibitive.

Author

VOLUME 33 NUMBER 4 / April 1995

Scientific and Technical Aerospace Reports

A Monthly Publication of the National Aeronautics and Space Administration

01 AERONAUTICS (GENERAL)

N95-16249# Nanjing Univ. of Aeronautics and Astronautics, Nanjing, Jiangsu (China).
JOINT PROCEEDINGS ON AERONAUTICS AND ASTRONAUTICS (JPAA)
Jianying Zhu, ed. and G. L. Degtyarev, ed. May 1993 271 p Prepared in cooperation with Kazan Inst. of Aviation, USSR
(ISBN-7-80-046602-7) Avail: CASI HC A12/MF A03

These proceedings contain the papers presented at a joint Chinese - Russian symposium dealing with: aerodynamic characteristics of airfoils, aircraft design, liquid fuels for aircraft, wind tunnel equipment and testing, mathematical modeling of dynamic systems, signal processing, aircraft engine testing and maintainability, radar imaging, radioelectronic equipment design, aircraft landing systems, computational mathematics, computer aided design and manufacturing, and robotics. For individual titles, see N95-16250 through N95-16281.

N95-16250# Nanjing Univ. of Aeronautics and Astronautics, Nanjing, Jiangsu (China). Research Inst. of Helicopter Technique.
INVESTIGATION OF DYNAMIC INFLOW'S INFLUENCE ON ROTOR CONTROL DERIVATIVES **c34**
Xiaogu Zhang and Jinsong Bao *In its* Joint Proceedings on Aeronautics and Astronautics (JPAA) May 1993 p 1-10 Sponsored by the Aeronautical Science Foundation of China (For primary document see N95-16249 04-01)
Avail: CASI HC A02/MF A03

A method including dynamic inflow model is developed to analyze rotor force and moments. Rotor model tests are performed to measure rotor control derivatives. The dynamic inflow model is verified through the comparative study between analytical results and test data. The influence of dynamic inflow on different conditions is investigated. A simplified analytical model is used to investigate the influence of dynamic inflow on the different rotor configurations. The correlation between theoretical predictions with dynamic inflow and test results is excellent. Author

N95-16251# Nanjing Univ. of Aeronautics and Astronautics, Nanjing, Jiangsu (China). Research Inst. of Pilotless Aircraft.
AN APPROACH TO AERODYNAMIC CHARACTERISTICS OF LOW RADAR CROSS-SECTION FUSELAGES **c02**
Jiazheng Pan, Yifei Wang, and Caiwen Zhang *In its* Joint Proceedings on Aeronautics and Astronautics (JPAA) May 1993 p 11-18 (For primary document see N95-16249 04-01)
Avail: CASI HC A02/MF A03

This paper proves that polygonal section fuselages are better than circular section fuselage not only in stealthy characteristics (low radar cross section (RCS)), but also in aerodynamic characteristics, especially in lift force and maximum lift-drag ratio, by investigating low speed aerodynamic characteristics for three 'panel' polygonal section fuselage models with low RCS and one regular circular section fuselage model, through low speed tunnel testing of measuring forces, water tunnel field visualization and comparison between the results of the engineering evaluation and experiments at an angle of attack up to 50 degrees. Moreover, they can produce steady side forces larger than those of the circular section fuselage at high angles of attack and zero sideslip, and the produced angle of attack is lower than that of a circular one. The calculation method of polygonal section fuselages has not yet been perfected. In this paper a correction evaluation method is proposed that is given according to the contour characteristics of the corresponding section on the basis of the calculation method of a low aspect ratio wing and the calculated results are in good agreement with those of the experiments. Author (revised)

N95-16252# Nanjing Univ. of Aeronautics and Astronautics, Nanjing, Jiangsu (China). Research Inst. of Pilotless Aircraft.
AN IMPROVED METHOD OF AIRFOIL DESIGN **c02**
Caiwen Zhang *In its* Joint Proceedings on Aeronautics and Astronautics (JPAA) May 1993 p 19-22 See also A91-44768 (For primary document see N95-16249 04-01)
Avail: CASI HC A01/MF A03

An improved method of airfoil design is proposed in this paper, which transforms the design problem into the solution of a minimization problem of a multivariable function. It can be applied to the subcritical airfoil design, taking viscosity into consideration. Author

N95-16253# Nanjing Univ. of Aeronautics and Astronautics, Nanjing, Jiangsu (China). Dept. of Power Engineering.
EXPERIMENTAL INVESTIGATION OF TURBULENT SEPARATED-REATTACHMENT FLOW BY USING LDV **c34**
Junfei Yin and Shaozhi Yu *In its* Joint Proceedings on Aeronautics and Astronautics (JPAA) May 1993 p 23-32 (For primary document see N95-16249 04-01)
Avail: CASI HC A02/MF A03

A turbulent separation-reattachment flow in a two-dimensional asymmetrical curved-wall diffuser was surveyed with a two-dimensional laser doppler velocimeter. The turbulent boundary layer was separated on the lower curved wall under strong pressure gradient and then reattached subsequently on a parallel channel. At the inlet of the diffuser, the Reynolds number based on the diffuser height is 1.2 x 10(exp 5) and the velocity is 25.2 m/s. The results of the experiments in newly defined streamline-aligned coordinates are presented and analyzed. The experiment showed that after Transitory Detachment there was a second extremum of normal Reynolds stress and shear stress appeared as a minus in the near-wall backflow region. A scale was formed using the maximum Reynolds shear stress. It was found that Reynolds shear stress similarity exists from separation to reattachment and the Schofield-Perry velocity law exists in the forward shear flow. Both profiles were used in the experimental work that led to the design of a new eddy-viscosity model. The length scale came from that developed by Schofield and Perry. the composite velocity scale was formed by the maximum Reynolds shear stress and Schofield-Perry velocity scale as well as the edge velocity of the boundary layer. The results of these experiments are presented in this paper. Author

N95-16254# Nanjing Univ. of Aeronautics and Astronautics, Nanjing, Jiangsu (China). Dept. of Power Engineering.
IMPROVED METHOD FOR ESTIMATION OF THE MAXIMUM INSTANTANEOUS DISTORTION VALUES **c34**
Dewang Liang and Shiying Zhang *In its* Joint Proceedings on Aeronautics and Astronautics (JPAA) May 1993 p 33-42 See also A92-49076 (For primary document see N95-16249 04-01)
Avail: CASI HC A02/MF A03

In this paper, the statistical method for estimating the maximum instantaneous distortion is developed further to estimate the maximum values of the instantaneous distortions which the operation of peak values of dynamic pressures and correlations between fluctuations pressures are involved. The effects of the correlations on the estimation are discussed.

Comparison between the estimated values and the experimental results shows that the newly developed method can quite accurately estimate the maximum value of the instantaneous distortion with operation of peak values of dynamic pressures involved, such as the distortion of DC(sub theta). The accuracy of the estimation of maximum instantaneous distortion can be improved by considering the correlation between fluctuation pressures, yet when the mean correlation coefficient is less than 0.1, the estimation can be effected by dispensing with correlation. Author

N95-16255# Kazan Aviation Inst. (USSR).
SURFACE HEAT TRANSFER IN A CHANNEL WITH POROUS INSERT **c34**

Yu. F. Gortyshov *In* Nanjing Univ. of Aeronautics and Astronautics, Joint Proceedings on Aeronautics and Astronautics (JPAA) May 1993 p 43-47 (For primary document see N95-16249 04-01)
Avail: CASI HC A01/MF A03

One of the possible ways of the effective intensification is the realization of heat carrier flows in porous structures. For this purpose inserts are placed in moving heat carrier channels. Despite a large number of publications, net-like, fibrous, brush, caked and powder structures of low and mean porosity (epsilon less than or equal to 0.6) are studied. Application of high-porous permeable honeycomb materials (HPHM) shows, that among the the well-known porous materials possessing maximal permeability (penetrability factors are 10(exp -8) ...10(exp -9) sq m). HPHM's have a characteristic three-dimensional net-like honeycomb structure with high repeatability of cells. All the frame substance is concentrated in stripping ribs, which bound each separate cell. In coolant flowing in the channel with porous insert the transfer of energy from the heated wall into the channel interior originates at the expense of the frame material heat conduction and lateral conduction and lateral convective mixing of flow. In this paper we present the results of analytical and experimental heat transfer investigation at forced heat carrier, flowing in the channel that is filled-in by porous HPHM medium. Author

N95-16256# Kazan Aviation Inst. (USSR).
SERVICE AND PHYSICAL PROPERTIES OF LIQUID-JET FUELS **c25**

V. I. Skomorokhov and A. F. Dregalin *In* Nanjing Univ. of Aeronautics and Astronautics, Joint Proceedings on Aeronautics and Astronautics (JPAA) May 1993 p 48-52 (For primary document see N95-16249 04-01)
Avail: CASI HC A01/MF A03

In the present paper we discuss a relation between the service physical properties of liquid composite aircraft and rocket fuels. We give also calculation methods of physical fuel mixture properties, on the net-component basis. Author

N95-16257# Nanjing Univ. of Aeronautics and Astronautics, Nanjing, Jiangsu (China). Dept. of Aerodynamics.
WALL-SIGNATURE METHODS FOR HIGH SPEED WIND TUNNEL WALL INTERFERENCE CORRECTIONS **c02**

Qiwei Zhang *In its* Joint Proceedings on Aeronautics and Astronautics (JPAA) May 1993 p 53-62 See also A93-20803 (For primary document see N95-16249 04-01)
Avail: CASI HC A02/MF A03

Wall-signature methods for wall interference correction in NH-1 high speed wind tunnel model tests are presented. The methods correct tunnel wall interference effects using the measured pressure distribution near tunnel walls and the model force data. They do not require the knowledge of wall cross-flow properties, so can be used for various ventilated wall or solid wall wind tunnels. Hundreds of test cases of several models in various tunnels including solid wall, adaptive wall, perforated wall, slotted wall test sections are corrected by these methods. The test Mach number range is 0.5 to 0.9. The test Reynolds number range is 2x10(exp 6) to 1x10(exp 7). The corrected results are compared with other correcting methods and Navier-Stokes free-air solutions. The correctness and practicality of these methods are proved. Author

N95-16258# Nanjing Univ. of Aeronautics and Astronautics, Nanjing, Jiangsu (China). Dept. of Aerodynamics.
AN INVESTIGATION OF POLYNOMIAL CALIBRATIONS METHODS FOR WIND TUNNEL BALANCES **c09**

Buzhang Han and Ingmar Johnson (Aeronautical Research Inst. of Sweden, Bromma.) *In its* Joint Proceedings on Aeronautics and Astronautics (JPAA) May 1993 p 63-66 (For primary document see N95-16249 04-01)
Avail: CASI HC A01/MF A03

For wind tunnel balance calibration the factorial method is used in Sweden, whereas the orthogonal method is used in China. This report is a comparison between calibration results of these two methods, by using a certain six component wind tunnel balance in the MK6 calibrating rig at FFA Sweden. Author

N95-16259# Nanjing Univ. of Aeronautics and Astronautics, Nanjing, Jiangsu (China). Dept. of Aircraft Engineering.
A CONSISTENT LARGE DEFLECTION THEORY OF COMPOSITE SANDWICH SHELLS **c39**

Jinfu Zhu *In its* Joint Proceedings on Aeronautics and Astronautics (JPAA) May 1993 p 67-73 See also A93-20816 (For primary document see N95-16249 04-01)
Avail: CASI HC A02/MF A03

Composite sandwich shells are important structures in aeronautical and astronautical industry. The theory, especially nonlinear theory, of them is still required to be advanced so as to meet the demand of engineering application. With Lagrangian description, the consistent Green strain tensor, the compatibility equations and the second Piola-Kirchhoff stress tensor of the composite sandwich shells are obtained. Based on these results and several assumptions, the constitutive equations relating the stress resultants to the strains, the strain energy density and the potential energy functional are further developed. In terms of minimum potential energy principle, the equilibrium equations and associated boundary conditions are obtained, which are consistent with the first order approximation under the conditions of small strain accompanied with moderate/small rotation. In terms of the structural features of the shallow composite sandwich shells, the equations obtained are further processed approximately and Donnel-type equations for the shallow composite sandwich shells are obtained. Author

N95-16260# Nanjing Univ. of Aeronautics and Astronautics, Nanjing, Jiangsu (China). Research Inst. of Vibration Engineering.
A SUPER-ELEMENT SIMPLIFIED ANALYSIS FOR VIBRATION SYSTEMS OF COMPLEX STRUCTURES **c39**

Guoping Chen and Demao Zhu *In its* Joint Proceedings on Aeronautics and Astronautics (JPAA) 74-80 (SEE N95-16249 04-01) May 1993 See also A92-27903 (For primary document see N95-16249 04-01)
Avail: CASI HC A02/MF A03

In this paper, a super-element analysis method based on the common finite element model is developed to reduce the degrees of freedom (DOF) for the vibration systems of large complex structures. A simplified dynamic reduction is used in the internal domains of the super-elements, and a local displacement field re-assumption is introduced on the boundary areas. This method greatly reduces the order of DOF, expands the ability of solution, and is simple to program and convenient to calculate. A reduction criterion of internal DOF is suggested through the perturbation analysis. Some numerical examples verify that the method is very effective and has high calculation precision. Author

N95-16261# Nanjing Univ. of Aeronautics and Astronautics, Nanjing, Jiangsu (China). Research Inst. of Vibration Engineering.
NUMERICAL ANALYSIS ON PERIODIC RESPONSE OF NONSMOOTH DYNAMIC SYSTEMS **c39**

Haiyan Hu *In its* Joint Proceedings on Aeronautics and Astronautics (JPAA) May 1993 p 81-88 Sponsored by the Aeronautical Science Foundation of China (For primary document see N95-16249 04-01)
Avail: CASI HC A02/MF A03

The periodic response analysis of a nonlinear dynamic system, which is of great significant in engineering, is usually carried out by using numerical methods because of high dimension and complicated characters of the system. The current well-known numerical schemes like shooting and incremental harmonic balancing, however, cannot cope with the engineering systems with nonsmooth physical factors, such as elastoplasticity, clearance and dry friction, and also fail to get the strong nonlinear periodic response of smooth dynamic systems sometimes. In the paper the author analyzes the above shortcomings and points out that they result from the explicit or implicit Newton iteration in the schemes. The paper presents eight new schemes based on quasi-Newton iteration or unconstrained function

minimization to improve the shooting and the incremental harmonic balancing. The convergence, accuracy and computation efficiency of these new schemes are examined and four of them are suggested for engineering use. Author

N95-16262# Nanjing Univ. of Aeronautics and Astronautics, Nanjing, Jiangsu (China). Research Inst. of Vibration Engineering.

A NEW REGULARIZATION APPROACH IN STRUCTURAL SYSTEM IDENTIFICATION **c39**

Lingmi Zhang and Baiqing He *In its* Joint Proceedings on Aeronautics and Astronautics (JPAA) May 1993 p 89-93 (For primary document see N95-16249 04-01)

Avail: CASI HC A01/MF A03

Singular-value decomposition (SVD) technique has been utilized for regularization to solve ill-conditioned linear equations arising in modal analysis and structural system identification in the past decade. A new approach named Epsilon decomposition is developed, as an alternative to SVD, which is more efficient for large matrix with small rank deficiency. An Improved Epsilon-decomposition (IED) approach is proposed in this paper, which needs only to solve ordinary linear equations instead of eigenvalue problem in ED and hence the computation effort to solve ill-conditioned equations is dramatically reduced. It is proved in the paper that ED is a first order approximation of SVD, and ED is a second order approximation. A numerical example is given to show the feasibility and efficiency of IED. Author

N95-16263# Nanjing Univ. of Aeronautics and Astronautics, Nanjing, Jiangsu (China). Dept. of Aircraft Engineering.

THERMOELASTICITY ANALYSIS OF LAMINATED PLATES AND SHELLS USING HYBRID-STRESS ELEMENTS **c39**

Shu Li and Liangxin Sun *In its* Joint Proceedings on Aeronautics and Astronautics (JPAA) May 1993 p 94-102 See also N91-43506 Sponsored by the Aeronautical Science Foundation of China (For primary document see N95-16249 04-01)

Avail: CASI HC A02/MF A03

Based on Hellinger-Reissner variational principle, a hybrid-stress model for the thermoelasticity analysis of laminated plates and shells is derived in this paper. The elements contain a few number of stress parameters which are invariant. Besides, in order to include the effect of the transverse shear deformation and based upon the Reissner-Mindlin type, the hypothesis of a sectionized straight line is suggested that divides the straight line along the thickness direction into broken lines. Each broken line contains a certain number of layers. The numerical results show that the element and the hypothesis are precise, economic and practical. Author

N95-16264# Kazan Aviation Inst. (USSR). Scientific School of Aircraft Strength.

DEVELOPMENT OF STRENGTH ANALYSIS METHODS AND DESIGN MODEL FOR AIRCRAFT CONSTRUCTIONS IN KAZAN AVIATION INSTITUTE **c05**

M. V. Vakhitov *In* Nanjing Univ. of Aeronautics and Astronautics, Joint Proceedings on Aeronautics and Astronautics (JPAA) May 1993 p 103-106 (For primary document see N95-16249 04-01)

Avail: CASI HC A01/MF A03

Research on problems of aircraft structural strength have been carried out at Kazan Aviation Institute since the day of foundation of the chair 'Aircraft strength analysis' in 1938. The well known school of aircraft strength was developed under Yu G. Odinokov's supervision. Eight doctoral dissertations and more than 70 master's theses give witness to its fruitfullness and success. Its followers work as the leading engineers in the field of strength analysis in two large national centers - Central Aerohydrodynamic Institute and the Siberian Aircraft Research Institute and at a number of higher education institutions. Author (revised)

N95-16265# Kazan Aviation Inst. (USSR).

THEORETICAL FUNDAMENTALS OF THE AIRCRAFT GTE TESTS **c07**

Yu. V. Kozhevnikov *In* Nanjing Univ. of Aeronautics and Astronautics, Joint Proceedings on Aeronautics and Astronautics (JPAA) May 1993 p 107-111 (For primary document see N95-16249 04-01)

Avail: CASI HC A01/MF A03

We discuss the methodology of a new scientific theory taking as an example the aircraft gas turbine engine (GTE) tests. We formulate a theory of construction principles and practical approaches to the problem. Author (revised)

N95-16266# Kazan Aviation Inst. (USSR).

DEVELOPMENT OF THE VIBRATION TEST EQUIPMENT FOR TESTING THE PRODUCTS OF AIRCRAFT AND SPACE TECHNOLOGY WITH SIMULATION OF OPERATING CONDITIONS **c14**

Ya. S. Uretskii *In* Nanjing Univ. of Aeronautics and Astronautics, Joint Proceedings on Aeronautics and Astronautics (JPAA) May 1993 p 112-117 (For primary document see N95-16249 04-01)

Avail: CASI HC A02/MF A03

The final results of vibration tests depend to a considerable degree on completeness of the operating conditions simulation, which is hard to obtain due to imperfections in the vibration measuring and test facilities. Nowadays, vibration tests are based on a system of model vibration effects which are approximated as closely as possible to the operating conditions. This paper presents the following operating models (with regard for modern and long-range possibilities for vibration measurement and test methods): (1) a multi-point scalar vibration, represented as a vector of the vibration spectra of vibrations at check points of the object, and (2) the single-point scalar vibration, the spectral characteristic of which is either the vibration spectra or the vector of the spectral power densities. The following methods are briefly discussed: (1) excitation of mechanical vibration; (2) formation of exciting signal; (3) control of vibration spectra; and (4) design and optimization of vibrational spectrum formation systems, as well as means of forming the exciting signal, controlling the random vibration spectrum and forming the vibrational spectrum. Author (revised)

N95-16267# Nanjing Univ. of Aeronautics and Astronautics, Nanjing, Jiangsu (China). Research Inst. of Vibration Engineering.

RESEARCHES ON GEAR FAULT DIAGNOSIS TECHNIQUES **c37**

Ming Bao and Chunsheng Zhao *In its* Joint Proceedings on Aeronautics and Astronautics (JPAA) May 1993 p 118-123 See also A93-20811 (For primary document see N95-16249 04-01)

Avail: CASI HC A02/MF A03

Seeking effective methods is one of the most important goals in machinery fault diagnosis. The effective methods for gear fault diagnosis have been successively developed in our Institute. This paper is a comprehensive treatise based on our research work of recent years. A mathematical model of vibration signals for defective gears is physically described. Five effective new methods for gear fault diagnosis, such as zoom complex envelope analysis, wideband demodulation technique, bispectrum analysis, correlative spectrum analysis, and maximum entropy spectrum analysis for phase modulated signals, are summarily presented. The listed illustrations prove sufficiently the validation of these methods. Author

N95-16268# Nanjing Univ. of Aeronautics and Astronautics, Nanjing, Jiangsu (China). Dept. of Electronic Engineering.

LINEAR PREDICTION DATA EXTRAPOLATION SUPERRESOLUTION RADAR IMAGING **c32**

Zhaoda Zhu, Zhenru Ye, and Xiaoqing Wu *In its* Joint Proceedings on Aeronautics and Astronautics (JPAA) 125-130 (SEE N95-16249 04-01) May 1993 Sponsored by the Aeronautical Science Foundation of China (For primary document see N95-16249 04-01)

Avail: CASI HC A02/MF A03

Range resolution and cross-range resolution of range-doppler imaging radars are related to the effective bandwidth of transmitted signal and the angle through which the object rotates relatively to the radar line of sight (RLOS) during the coherent processing time, respectively. In this paper, linear prediction data extrapolation discrete Fourier transform (LPDEDFT) superresolution imaging method is investigated for the purpose of surpassing the limitation imposed by the conventional FFT range-doppler processing and improving the resolution capability of range-doppler imaging radar. The LPDEDFT superresolution imaging method, which is conceptually simple, consists of extrapolating observed data beyond the observation windows by means of linear prediction, and then performing the conventional IDFT of the extrapolated data. The live data of a metalized scale model B-52 aircraft mounted on a rotating platform in a microwave anechoic chamber and a flying Boeing-727 aircraft were processed. It is concluded that, compared to the conventional Fourier method, either higher resolution for

the same effective bandwidth of transmitted signals and total rotation angle of the object or equal-quality images from smaller bandwidth and total angle may be obtained by LPDEDFT. Author

N95-16269# Nanjing Univ. of Aeronautics and Astronautics, Nanjing, Jiangsu (China). Dept. of Electronic Engineering.
DETECTING THE NUMBER OF TARGETS IN SPATIALLY COLORED NOISE USING SAMPLED APERTURE RADARS **c32**
Zhaoda Zhu and Zhishun She *In its* Joint Proceedings on Aeronautics and Astronautics (JPAA) May 1993 p 131-136 See also A91-30858 Sponsored by the Aeronautical Science Foundation of China (For primary document see N95-16249 04-01)
Avail: CASI HC A02/MF A03

In this paper the detection of multiple targets of an unknown number with unknown directions using array processing is investigated. A noncoherent pulsed radar with an array antenna is assumed. Two criteria for estimating the number of targets, based on information theoretic and eigen decomposition based ideas that assume a known noise covariance, are described briefly. A fast convergent and numerically robust algorithm of signal eigen-analysis is presented. Simulation results are included, showing the performance of the criteria in combination with an estimate of the noise covariance obtained from reference noise samples when applied in an environment of spatially colored noise background. Author

N95-16270# Nanjing Univ. of Aeronautics and Astronautics, Nanjing, Jiangsu (China). Dept. of Electronic Engineering.
FAST ACQUISITION OF BURST DIRECT SEQUENCE SPREAD SPECTRUM SIGNALS THROUGH SATELLITE CHANNELS **c32**
Shuyao Yang *In its* Joint Proceedings on Aeronautics and Astronautics (JPAA) May 1993 p 137-146 See also A93-20859 (For primary document see N95-16249 04-01)
Avail: CASI HC A02/MF A03

The paper discusses the fast acquisition of direct sequence (DS) spread spectrum signals through satellite channels using intermediate-frequency recirculation (IFREC). Fundamental principles of IFREC loop and some problems in the design are described. Finally, the experimental results are shown for signals passing the satellite channel. Author

N95-16271# Kazan Aviation Inst. (USSR).
METHOD OF CALCULATING THE OPTIMAL RADIOELECTRONIC EQUIPMENT DESIGN **c33**
Yu. P. Ermolaev *In* Nanjing Univ. of Aeronautics and Astronautics, Joint Proceedings on Aeronautics and Astronautics (JPAA) May 1993 p 147-151 (For primary document see N95-16249 04-01)
Avail: CASI HC A01/MF A03

In designing the competitive radio-electronic equipment there inevitably arises the justified optimal constructional decision problem that accounts for many quality indexes. A totality of these quality indexes can be conveniently represented by the vector in a multi-dimensional space, on the coordinate axes of which the specific quantities of all the accountable indexes of quality are laid off. Inevitability of accounting for a variety of quality indexes, when choosing optimal decision, raises a problem of vector (multi-objective) optimization of the object developed. Author

N95-16272# Kazan Aviation Inst. (USSR).
GENERALIZED METHOD OF SOLVING TOPOLOGICAL OPTIMIZATION PROBLEMS FOR ELECTRICAL AIRPLANE EQUIPMENT SYSTEMS IN COMPUTER-AIDED DESIGN **c61**
V. S. Tereshchuk *In* Nanjing Univ. of Aeronautics and Astronautics, Joint Proceedings on Aeronautics and Astronautics (JPAA) May 1993 p 152-156 (For primary document see N95-16249 04-01)
Avail: CASI HC A01/MF A03

In developing a computer-aided design system for electric airborne equipment used by an aircraft design bureau, a number of optimization topological and parametric problems must be solved. We represent a set of all the components of the electric equipment systems arranged on board in accordance with their functional features or special requirements. The set of components can either be united into electrical structures or subject to the arrangement only. A system model of a multi-level structure of airborne equipment in the process of its disintergration is proposed and an algorithm of the electric equipment synthesis that makes it possible to find a solution for a number of separately unsolvable problems is given. Author (revised)

N95-16273# Kazan Aviation Inst. (USSR).
THEORY OF ONE-DIMENSIONAL AND TWO-DIMENSIONAL DISTRIBUTED SENSORS FOR MEASURING THE SPATIAL CHARACTERISTICS OF THERMOPHYSICAL AND HYDRODYNAMIC FIELDS **c35**
Yu. K. Evdokimov and M. P. Vyaselev *In* Nanjing Univ. of Aeronautics and Astronautics, Joint Proceedings on Aeronautics and Astronautics (JPAA) 157-160 (SEE N95-16249 04-01) May 1993 (For primary document see N95-16249 04-01)
Avail: CASI HC A01/MF A03

A conventional approach to measuring of the physical field parameters (temperature, concentration, velocity, etc.) lies in using point distributed sensors, located in the examined field points. Another approach that is discussed in the present paper is based on measurement implementation by means of the distributed sensors, which ensure continuous spatially-distributed measurement. For further use we shall introduce the term 'distributed sensor' (DS) and its quantitative characteristic. We define it using the notion of dimensional representation, that is, DS is the sensor having the topological sensitive element dimension D within the limits 0 less than D less than or equal to 3. In what follows we turn our attention to a description of constructional methods and theory of the one-dimensional (D=1) distributed sensors. The measurements made using similar distributed sensors are tantamount to the measurements made with the aid of a set of the discrete sensors. Author

N95-16274# Kazan Aviation Inst. (USSR).
METHODS OF WAVE-FRONT IDENTIFICATION BY CONTROL IMAGES **c64**
G. L. Degtyarev, A. V. Makhanko, and S. M. Chernyavskii *In* Nanjing Univ. of Aeronautics and Astronautics, Joint Proceedings on Aeronautics and Astronautics (JPAA) May 1993 p 161-168 (For primary document see N95-16249 04-01)
Avail: CASI HC A02/MF A03

The distortions of the wave front (WF) formed by an optical system result in lowering the indexes of the system quality. In designing the adaptive optical systems, which must perform a real-time WF correction with the aid of the controllable devices, e.q. mirrors, the measurements of these distortions, that is WF identification, is a necessary condition. In the present paper we examine two supplementary methods. In the first method, the aperture is divided into five sub-apertures that are covered in succession, obeying the specified cyclic law. The images obtained contain complete WF information. The second method is iterative and can be used for self-aligning the controllable mosaic mirror segments. On the basis of the source image that corresponds to the running angular position of segments we can define roughly their deflections from the position aligned. These deviations are corrected by the angular position control system and the cycle of measurements is repeated. The numeric simulation shows that 3-4 iterative cycle results in high-precision system alignment. Author

N95-16275# Nanjing Univ. of Aeronautics and Astronautics, Nanjing, Jiangsu (China). Dept. of Test and Measurement Engineering.
THE COMBINATION PROBE OF OPTICAL FIBERS AND ITS APPLICATIONS **c74**
Baoqi Tao and Weixuan Li *In its* Joint Proceedings on Aeronautics and Astronautics (JPAA) May 1993 p 169-178 (For primary document see N95-16249 04-01)
Avail: CASI HC A02/MF A03

This article introduces a kind of fiber optic combining probe which is composed of sending and receiving fibers, light emitting elements, sensitive and compensating photosensors, all of which are made into a whole body. The probe can be used to transform the change of displacement into that of light intensity and gives out electrical signal. It is an ideal tool of noncontact measurements. This article discusses the influence of the structure of probes and the shape of the reflective mirror. The probe is small in size and wide in use. We also introduce: (1) the static displacement transducers which consist of the fiber optic combining probe and its measuring circuits; (2) optical fiber extensometer used to measure the mechanical properties of materials; (3) optical fiber dynamic displacement

transducer; and (4) optical fiber angle and torque transducer and the principle and configuration of optical fiber torque transducer equipped with a single chip computer. Author

N95-16276# Kazan Aviation Inst. (USSR).
PROBLEM OF CONSTRUCTING THE LYAPUNOV'S FUNCTIONS IN LUMPED PARAMETER SYSTEMS c64
T. K. Sirazetdinov *In* Nanjing Univ. of Aeronautics and Astronautics, Joint Proceedings on Aeronautics and Astronautics (JPAA) May 1993 p 179-183 (For primary document see N95-16249 04-01)
Avail: CASI HC A01/MF A03

We consider the problem of constructing the Lyapunov's functions in studying a stability of linear and some non-linear partial differential equation systems solution. Author

N95-16277# Nanjing Univ. of Aeronautics and Astronautics, Nanjing, Jiangsu (China). Dept. of Automatic Control.
APPLICATION OF GPS/SINS/RA INTEGRATED SYSTEM TO AIRCRAFT APPROACH LANDING c04
Xin Yuan, Jianye Liu, and Yongxi Ni *In its* Joint Proceedings on Aeronautics and Astronautics (JPAA) May 1993 p 184-190 See also A92-21466 (For primary document see N95-16249 04-01)
Avail: CASI HC A02/MF A03

A design scheme for integrating a global positioning system (GPS), strap down inertial navigation system (SINS) and a radio altimeter (RA) for precise aircraft landing is presented and the dynamic model is established with the application of a Kalman filter technique. The simulation for the GPS/SINS/RA performance is carried out, using a SPS simulator, considering a glide slope inclination of 3 degrees for aircraft landings. Simulation results indicate that the integrated system, on condition that the GPS receiver uses either P code, or C/A code with the aid of pseudolite technology, and works in the differential mode, is able to meet the ICAO positioning requirements for aircraft precision landing. Author (revised)

N95-16278# Nanjing Univ. of Aeronautics and Astronautics, Nanjing, Jiangsu (China). Dept. of Automatic Control.
THE COMPUTER ANALYSIS OF THE PREDICTION OF AIRCRAFT ELECTRICAL POWER SUPPLY SYSTEM RELIABILITY c33
Xinhua Mu, Yangguang Yan, and Jibing Pen *In its* Joint Proceedings on Aeronautics and Astronautics (JPAA) May 1993 p 191-197 See also A92-37958 (For primary document see N95-16249 04-01)
Avail: CASI HC A02/MF A03

With the fast development of aviation technique, the requirements of the aircraft electrical power supply system reliability become much higher. In view of this, the reliability prediction method of simple systems can not meet the need of the research on modern aircraft electrical power supply systems. Therefore, the reliability prediction of complex systems by computers is significant. In this paper a network model of aircraft electrical power supply system is analyzed according to the reliability theory. The minimal path non-coherent technique and the computer realization process are discussed. The program flow-chart is given in detail. The reliability of an example aircraft DC electrical power supply system is calculated. Curves of system reliability are obtained by which the basis for the system reliability design is provided. Author

N95-16279# Nanjing Univ. of Aeronautics and Astronautics, Nanjing, Jiangsu (China). Dept. of Mechanical Engineering.
APPROACH TO IN-PROCESS TOOL WEAR MONITORING IN DRILLING: APPLICATION OF KALMAN FILTER THEORY c31
Ning He, Youzhen Zhang, and Liangxian Pan *In its* Joint Proceedings on Aeronautics and Astronautics (JPAA) May 1993 p 199-208 (For primary document see N95-16249 04-01)
Avail: CASI HC A02/MF A03

The two parameters often used in adaptive control, tool wear and wear rate, are the important factors affecting machinability. In this paper, it is attempted to use the modern cybernetics to solve the in-process tool wear monitoring problem by applying the Kalman filter theory to monitor drill wear quantitatively. Based on the experimental results, a dynamic model, a measuring model and a measurement conversion model suitable for Kalman filter are established. It is proved that the monitoring system possesses complete observability but does not possess complete controllability. A discriminant for selecting the characteristic parameters is put forward. The thrust force Fz is selected as the characteristic parameter in monitoring the tool wear by this discriminant. The in-process Kalman filter drill wear monitoring system composed of force sensor microphotography and microcomputer is well established. The results obtained by the Kalman filter, the common indirect measuring method and the real drill wear measured by the aid of microphotography are compared. The result shows that the Kalman filter has high precision of measurement and the real time requirement can be satisfied. Author

N95-16280# Nanjing Univ. of Aeronautics and Astronautics, Nanjing, Jiangsu (China). Dept. of Mechanical Engineering.
AN IMPROVED POSITION/FORCE CONTROL OF MANIPULATORS c37
Xiaoxi Huang, Sicong Li, and Jianying Zhu *In its* Joint Proceedings on Aeronautics and Astronautics (JPAA) May 1993 p 209-213 (For primary document see N95-16249 04-01)
Avail: CASI HC A01/MF A03

Robotic active force control is discussed in the paper. A velocity based force and motion control structure is proposed, some experimental researches about free drawing, surface following and peg-in-hole insertion are implemented in an Adept Three robotic manipulator. It is proved that the control strategies are feasible and effective. Author

N95-16281# Kazan Aviation Inst. (USSR).
DEVELOPMENT OF PROCESSES, MEANS, AND THEORETICAL PRINCIPLES OF THIN-WALLED DETAIL PLASTIC FORMING AT KAZAN AVIATION INSTITUTE c31
I. M. Zakirov *In* Nanjing Univ. of Aeronautics and Astronautics, Joint Proceedings on Aeronautics and Astronautics (JPAA) May 1993 p 214-216 (For primary document see N95-16249 04-01)
Avail: CASI HC A01/MF A03

The scientific school of thin-walled detail plastic forming was established at Kazan Aviation Institute in the transition period from wood to metal aircraft construction. High precision requirements to thin walled detail plastic forming drove the development of new processes to secure high productivity and a work culture under conditions of low volume production. Author (revised)

N95-16560*# National Aeronautics and Space Administration. Langley Research Center, Hampton, VA.
MEASUREMENTS OF UNSTEADY PRESSURE AND STRUCTURAL RESPONSE FOR AN ELASTIC SUPERCRITICAL WING
Clinton V. Eckstrom, David A. Seidel, and Maynard C. Sandford Nov. 1994 140 p
(RTOP 505-63-50-13)
(NASA-TP-3443; L-17073; NAS 1.60:3443) Avail: CASI HC A07/MF A02

Results are presented which define unsteady flow conditions associated with the high-dynamic structural response of a high-aspect-ratio, elastic, supercritical wing at transonic speeds. The wing was tested in the Langley Transonic Dynamics Tunnel with a heavy gas test medium. The supercritical wing, designed for a cruise lift coefficient of 0.53 at a Mach number of 0.80, experienced the high-dynamic structural response from Mach 0.90 to 0.94 with the maximum response occurring at about Mach 0.92. At the maximum response conditions of the wing, the forcing function appears to be the oscillatory chordwise movement of strong shocks located on the upper and lower surfaces of the wing in conjunction with the flow separation on the lower surface of the wing in the trailing-edge cove region. Author

N95-17451 National Defence Research Establishment, Stockholm (Sweden). Huvudavdelning foer Foersvarsanalys.
MILITARY AVIATION MAINTENANCE INDUSTRY IN WESTERN EUROPE: CONCENTRATION AND INTERNATIONALIZATION [MILITAERA FLYGUNDERHALLSINDUSTRIN I VAESTEUROPA: DESS KONCENTRATION OCH INTERNATIONALISERING]
K. Baecklund and K. Nyblom Jan. 1994 129 p In SWEDISH
(PB94-189180; FOA-C-10358-1.3) Avail: Issuing Activity (National Technical Information Service (NTIS))

The study presents the market structure and its development in the military aviation maintenance industry in Western Europe. Chapter 1-3 gives the purpose, method, and theoretical frame of the report as well as some definitions. The situations and the companies on the military aviation maintenance market in Germany, Great Britain, France, Belgium, the

Netherlands, Spain, Portugal, and Italy are described in chapter 4. The most important maintenance companies are compared according to the variables the authors pointed out as the most important ones. They close the discussion in chapter 6 with conclusions and reflections. The result of the study shows that although the market for the military aviation maintenance is overestablished it is rare that companies totally withdraw from the market. However, there is a clear tendency among the companies to diversify away from the military sector. NTIS

N95-17466 Battelle Columbus Labs., OH.
BICARBONATE OF SODA BLASTING TECHNOLOGY FOR AIRCRAFT WHEEL DEPAINTING Report, Jun. 1991 - May 1992
A. S. C. Chen, L. A. Smith, and R. F. Olfenbuttel Jul. 1994 82 p Prepared for Environmental Protection Agency, Cincannati, OH Limited Reproducibility: More than 20% of this document may be affected by microfiche quality
(Contract EPA-68-C0-0003)
(PB94-193323; EPA/600/R-94/127) Avail: CASI HC A05

This evaluation addressed product quality, waste reduction/pollution prevention and economics in replacing chemical solvent strippers with a bicarbonate of soda blasting technology for removal of paint from aircraft wheels. Because the paint being removed contained hazardous metal constituents, the liquid and solid wastes as well as the cloud of spray generated were evaluated for metal concentrations present and their leachability. Analyses for Cd, Cr, Cu, Pb, Mn, Ni, and Zn were made as well as total metals concentrations, pH, total suspended solids, and oil and grease. The blasting technology is effective for removing paint from aircraft wheels without significant damage to the anodized surface under the paint. In comparison to solvent depainting this technology reduced the amount of hazardous waste generated as well as cost savings due to operating and disposal costs, resulting in a 15% return on investment in about 4 years. NTIS

N95-17512# Federal Aviation Administration, Washington, DC.
FEDERAL AVIATION ADMINISTRATION AVIATION SYSTEM CAPITAL INVESTMENT PLAN, 1993
Dec. 1993 310 p See also PB92-187642
(PB94-171956) Avail: CASI HC A14/MF A03

The 1993 CIP Capital Investment Plan reflects two new policy directions for the National Airspace System (NAS) that merit added emphasis: first, an accelerated commitment to a satellite-based navigation system that uses the global positioning system (GPS) as its foundation; and second, a commitment to limited terminal radar approach control (TRACON) consolidation. The FAA will establish metroplex control facilities in a limited number of very large metropolitan areas instead of consolidating all TRACON operations into Area Control Facilities. Approximately 170 TRACON's will be modernized but will remain as stand-alone facilities. This will enable the FAA to create a simpler, more efficient local airspace management structure. NTIS

N95-17657*# National Aeronautics and Space Administration. Lewis Research Center, Cleveland, OH.
MICROGRAVITY ISOLATION SYSTEM DESIGN: A CASE STUDY
R. D. Hampton (McNeese State Univ., Lake Charles, LA.), C. R. Knospe (Virginia Univ., Charlottesville, VA.), P. E. Allaire (Virginia Univ., Charlottesville, VA.), and C. M. Grodsinsky Dec. 1994 21 p Sponsored by Commonwealth of Virginia's Center for Innovative Technology
(Contract NCC3-365; RTOP 963-70-OH)
(NASA-TM-106804; E-9282; NAS 1.15:106804) Avail: CASI HC A03/MF A01

Many acceleration-sensitive, microgravity science experiments will require active vibration isolation from manned orbiters on which they will be mounted. The isolation problem, especially in the case of a tethered payload, is a complex three-dimensional one that is best suited to modern-control design methods. In this paper, extended H(sub 2) synthesis is used to design an active isolator (i.e., controller) for a realistic single-input-multiple-output (SIMO) microgravity vibration isolation problem. Complex mu-analysis methods are used to analyze the isolation system with respect to sensor, actuator, and umbilical uncertainties. The paper fully discusses the design process employed and the insights gained. This design case study provides a practical approach for isolation problems of greater complexity. Issues addressed include a physically intuitive state-space description of the system, disturbance and noise filters, filters for frequency weighting, and uncertainty models. The controlled system satisfies all the performance specifications and is robust with respect to model uncertainties. Author

N95-17702* National Aeronautics and Space Administration, Washington, DC.
AERONAUTICAL ENGINNERING: A CUMULATIVE INDEX TO A CONTINUING BIBLIOGRAPHY (SUPPLEMENT 312)
Dec. 1994 382 p
(NASA-SP-7037(312); NAS 1.21:7037(312)) Avail: CASI HC A17

This is a cumulative index to the abstracts contained in NASA SP-7037 (301) through NASA SP-7073 (311) of Aeronautical Engineering: A Continuing Bibliography. NASA SP-7037 and its supplements have been compiled by the Center for AeroSpace Information of the National Aeronautics and Space Administration (NASA). This cumulative index includes subject, personal author, corporate source, foreign technology, contract number, report number, and accession number indexes. Author

N95-17704* National Aeronautics and Space Administration, Washington, DC.
AERONAUTICAL ENGINEERING: A CONTINUING BIBLIOGRAPHY WITH INDEXES (SUPPLEMENT 311)
Dec. 1994 22 p
(NASA-SP-7037(311); NAS 1.21:7037(311)) Avail: CASI HC A03

This report lists 4 reports, articles and other documents recently announced in the NASA STI Database. Author

02 AERODYNAMICS

Includes aerodynamics of bodies, combinations, wings, rotors, and control surfaces; and internal flow in ducts and turbomachinery.

For related information see also *34 Fluid Mechanics and Heat Transfer.*

N95-15994# Naval Postgraduate School, Monterey, CA.
AN INVESTIGATION OF THE TRANSONIC PRESSURE DRAG COEFFICIENT FOR AXI-SYMMETRIC BODIES M.S. Thesis
Eddy Priyono Mar. 1994 94 p
(AD-A280990) Avail: CASI HC A05/MF A01

This thesis investigates the pressure drag coefficient in the transonic regime over an axi-symmetric body, with a set of unique contour surfaces developed in a previous thesis. The contour surfaces were obtained by an exact solution of the small perturbation transonic equation, using the guidelines and tools developed at NPS. In this work, computational fluid dynamics (CFD) was not only used to compute the afterbody contour surface, but also to investigate a conical afterbody and complete bodies, which are composed of an arbitrary forebody (ellipsoid) and a variable afterbody (contour and conical). Euler as well as Navier-Stokes flow-solvers were applied to the geometries of interest, giving Mach-number contours for viscous and inviscid flow, pressure drag coefficient magnitude, and depicting shock wave location. On the basis of these results, it can be verified that our contour surface afterbodies will decrease by 15 percent the peak of the pressure drag coefficient (C sub d) versus Mach number curves in the transonic regime. These results can be used to design low pressure drag surfaces for missiles, projectiles, and aircraft engine nacelles. DTIC

N95-16038*# National Aeronautics and Space Administration. Lewis Research Center, Cleveland, OH.
NUMERICAL SIMULATION OF SUPERSONIC COMPRESSION CORNERS AND HYPERSONIC INLET FLOWS USING THE RPLUS2D CODE
Kamlesh Kapoor, Bernhard H. Anderson, and Robert J. Shaw Nov. 1994 14 p Original contains color illustrations
(RTOP 537-02-23)
(NASA-TM-106580; E-8840; NAS 1.15:106580) Avail: CASI HC A03/MF A01; 1 functional color page

A two-dimensional computational code, PRLUS2D, which was developed for the reactive propulsive flows of ramjets and scramjets, was validated for two-dimensional shock-wave/turbulent-boundary-layer interactions. The problem of compression corners at supersonic speeds was solved using the RPLUS2D code. To validate the RPLUS2D code for hypersonic speeds,

it was applied to a realistic hypersonic inlet geometry. Both the Baldwin-Lomax and the Chien two-equation turbulence models were used. Computational results showed that the RPLUS2D code compared very well with experimentally obtained data for supersonic compression corner flows, except in the case of large separated flows resulting from the interactions between the shock wave and turbulent boundary layer. The computational results compared well with the experiment results in a hypersonic NASA P8 inlet case, with the Chien two-equation turbulence model performing better than the Baldwin-Lomax model. Author

N95-16069*# National Aeronautics and Space Administration. Langley Research Center, Hampton, VA.
EXPERIMENTAL STUDY AT LOW SUPERSONIC SPEEDS OF A MISSILE CONCEPT HAVING OPPOSING WRAPAROUND TAILS
Jerry M. Allen and Carolyn B. Watson Nov. 1994 57 p
(RTOP 505-59-30-01)
(NASA-TM-4582; L-17337; NAS 1.15:4582) Avail: CASI HC A04/MF A01

A wind-tunnel investigation has been performed at low supersonic speeds (at Mach numbers of 1.60, and 2.16) to evaluate the aerodynamic characteristics of a missile concept capable of being tube launched and controlled with a simple one-axis canard controller. This concept, which features an axisymmetric body with two planar canards and four wraparound tail fins arranged in opposing pairs, must be in rolling motion to be controllable in any radial plane with the planar canards. Thus, producing a constant rolling moment that is invariant with speed and attitude to provide the motion is desirable. Two tail-fin shaping designs, one shaved and one beveled, were evaluated for their efficiency in producing the needed rolling moments, and the results showed that the shaved fins were much more desirable for this task than the beveled fins. Author

N95-16076 Physical Sciences, Inc., Andover, MA.
ULTRAVIOLET EMISSIONS OCCURRING ABOUT HYPERSONIC VEHICLES IN RAREFIED FLOWS Final Report, 4 Jun. 1993 - 4 Feb. 1994
George E. Caledonia and Robert H. Krech Apr. 1994 60 p Limited Reproducibility: More than 20% of this document may be affected by microfiche quality
(Contract DAAH04-93-C-0015)
(AD-A281452; PSI-1177/TR-1305; ARO-31210.2-EG-SDI) Avail: CASI HC A04

This report includes: (1) an investigation of the kinetic mechanisms for the visible shuttle glow; (2) an overview of flight and laboratory investigations of VUV to IR surface glows observed at hypersonic velocities in low earth orbit conditions; (3) a summary of the flight-measured absolute intensities observed for rarefied ram flow at VUV, UV and visible wavelengths as a function of altitude; and (4) a brief look at seeker sensor survivability/viability issues associated with a High Velocity Missile (HVM) intended for boost phase interception. DTIC

N95-16099 Ohio State Univ., Columbus.
WING-BODY JUNCTURE FLOWS Final Report
Richard J. Bodonyl Jan. 1994 44 p Limited Reproducibility: More than 20% of this document may be affected by microfiche quality
(Contract DAAL03-90-G-0186)
(AD-A281526; ARO-28249.2-EG) Avail: Issuing Activity (Defense Technical Information Center (DTIC))

Researchers have considered the flow structure near a small-scale wing-body combination within the framework of triple-deck theory. Thin airfoil theory was used to obtain the pressure distribution around a wing which in turn triggers a viscous-inviscid interaction near the wing-body juncture. As part of the formulation of the problem they have followed the lead of Smith and Gajjar, utilizing the concept of an 'effective hump shape' in the formulation of the nonlinear problem. This technique not only simplifies the pressure expression but also enhances the convergence of the numerical scheme even though the concept itself is just a transformation to convert the wing-body problem into a more conventional problem for computational efficiency. DTIC

N95-16160# Stanford Univ., CA. Dept. of Aeronautics and Astronautics.
HIGH ALTITUDE HYPERSONIC FLOWFIELD RADIATION Final Report, 1 Jan. 1990 - 31 Mar. 1994
Robert W. MacCormack and Dean R. Chapman Apr. 1994 9 p
(Contract DAAL03-90-G-0031)
(AD-A281386; ARO-27480.6-EG-SDI) Avail: CASI HC A02/MF A01

Methods for computing radiation spectra and intensity are compared with available experimental data from three flight tests and five laboratory experiments. These involve both nonequilibrium and equilibrium flow. The comparison was facilitated by development of an improved radiation code, termed NEQAIR 2, incorporating vectorized programming to enable fine-structure spectra to be computed in a practical amount of time. The main sources of computational inaccuracy are found to stem from imperfect understanding of (1) what temperature or combination thereof in a multitemperature flowfield governs electronic excitation; (2) the physics of rotational relaxation at very high temperatures; and (3) the reaction rates for NO production at very high temperatures. Computed radiation is most accurate at low altitudes and hypersonic velocities, and least accurate at high altitudes and velocities. DTIC

N95-16589*# California Univ., Davis, CA. Dept. of Mechanical and Aeronautical Engineering.
NUMERICAL SIMULATION OF HELICOPTER ENGINE PLUME IN FORWARD FLIGHT Final Report
Arsenio C. B. Dimanlig, Cornelis P. vanDam, and Earl P. N. Duque (Army Aviation Systems Command, Moffett Field, CA.) 1994 12 p Original contains color illustrations
(Contract NCC2-5061)
(NASA-CR-197488; NAS 1.26:197488) Avail: CASI HC A03/MF A01; 5 functional color pages

Flowfields around helicopters contain complex flow features such as large separated flow regions, vortices, shear layers, blown and suction surfaces and an inherently unsteady flow imposed by the rotor system. Another complicated feature of helicopters is their infrared signature. Typically, the aircraft's exhaust plume interacts with the rotor downwash, the fuselage's complicated flowfield, and the fuselage itself giving each aircraft a unique IR signature at given flight conditions. The goal of this project was to compute the flow about a realistic helicopter fuselage including the interaction of the engine air intakes and exhaust plume. The computations solve the Think-Layer Navier Stokes equations using overset type grids and in particular use the OVERFLOW code by Buning of NASA Ames. During this three month effort, an existing grid system of the Comanche Helicopter was to be modified to include the engine inlet and the hot engine exhaust. The engine exhaust was to be modeled as hot air exhaust. However, considerable changes in the fuselage geometry required a complete regriding of the surface and volume grids. The engine plume computations have been delayed to future efforts. The results of the current work consists of a complete regeneration of the surface and volume grids of the most recent Comanche fuselage along with a flowfield computation. Author

N95-16808# Wright Lab., Wright-Patterson AFB, OH.
NUMERICAL SIMULATION OF TRANSIENT VORTEX BREAKDOWN ABOVE A PITCHING DELTA WING Final Report, 1 Jan. - 31 Dec. 1992
Miguel R. Visbal 4 May 1994 43 p
(AF Proj. 2307)
(AD-A281075; WL-TR-93-3048) Avail: CASI HC A03/MF A01

Computational results are presented for transient vortex breakdown above a delta wing subject to a pitch-and-hold maneuver to high angle of attack. The flows are simulated by solving the full three-dimensional Navier-Stokes equations on a moving grid using the implicit Beam-Warming algorithm. An assessment of the effects of numerical resolution and favorable comparison with experimental data suggest the computational approach captures the basic dynamics of this transient breakdown. The pressure gradient along the vortex axis is found to play a dominant role in the initiation of breakdown. A description of the three-dimensional instantaneous structure of the flow field is provided using critical-point theory. The reversed-flow region in the vortex core is associated with pairs of opposite spiral/saddle critical points. At its onset, the vortex breakdown is fairly axisymmetric; however, as it proceeds upstream and a stronger transition takes place along the axis, asymmetric effects become important and result in the formation of a bubble-type breakdown. This bubble structure is open and contains within itself a pair of stagnation points which are diametrically opposed and which rotate in the same sense as the base flow. DTIC

N95-16824# Naval Postgraduate School, Monterey, CA.
MACH NUMBER, FLOW ANGLE, AND LOSS MEASUREMENTS DOWNSTREAM OF A TRANSONIC FAN-BLADE CASCADE M.S. Thesis
Jeffrey G. Austin Mar. 1994 85 p
(AD-A280907) Avail: CASI HC A05/MF A01

Two dimensional flow measurements of Mach number and flow angle were conducted downstream of a transonic fan-blade cascade at a Mach number of 1.4 to provide baseline data for assessing the effect of vortex generating devices on the suction surface shock-boundary layer interaction. The experimental program consisted of the design and calibration of a traversing three-port pneumatic probe to measure Mach number and flow angle and initial cascade measurements to provide baseline data for the fully-mixed-out total pressure loss coefficient and flow turning angle. Similar tests are planned with the vortex generating devices installed. Comparisons with and without the vortex generating devices are needed to quantify the overall effect on the shock-boundary interaction in a transonic fan-blade passage, and to assess the potential for using vortex generating devices in military engine fans. DTIC

N95-16858*# National Aeronautics and Space Administration. Hugh L. Dryden Flight Research Center, Edwards, CA.
DEVELOPMENT OF A LOW-ASPECT RATIO FIN FOR FLIGHT RESEARCH EXPERIMENTS
David M. Richwine (Planning Research Corp., Edwards, CA.) and John H. DelFrate Washington Aug. 1994 16 p Presented at the 6th Biennial Flight Test Conference, Colorado Springs, CO, 20-23 Jun. 1993 Original contains color illustrations
(RTOP 505-68-00)
(NASA-TM-4596; H-1993; NAS 1.15:4596; AIAA Paper 94-2133) Avail: CASI HC A03/MF A01; 3 functional color pages

A second-generation flight test fixture, developed at NASA Dryden Flight Research Center, offers a generic testbed for aerodynamic and fluid mechanics research. The new fixture, a low-aspect ratio vertical fin shape mounted on the centerline of an F-15B aircraft lower fuselage, is designed for flight research at Mach numbers up to 2.0. The new fixture is a composite structure with a modular configuration and removable components for functional flexibility. This report describes the multidisciplinary design and analysis approach used to develop the fixture. The approach integrates conservative assumptions with simple analysis techniques to minimize the time and cost associated with its development. Presented are the principal disciplines required for this effort, which include aerodynamics, structures, stability, and operational considerations. In addition, preliminary results from the first phase of flight testing are presented. Acceptable directional stability and flow quality are documented and show agreement with predictions. Future envelope expansion activities will minimize current limitations so that the fixture can be used for a wide variety of high-speed aerodynamic and fluid mechanics research experiments. Author

N95-16887*# Sverdrup Technology, Inc., Brook Park, OH.
AN ANALYSIS CODE FOR THE RAPID ENGINEERING ESTIMATION OF MOMENTUM AND ENERGY LOSSES (REMEL) Final Report
Lawrence J. DeChant Cleveland, OH NASA Nov. 1994 86 p
(Contract NAS3-25266; RTOP 505-69-50)
(NASA-CR-191178; E-8079; NAS 1.26:191178) Avail: CASI HC A05/MF A01

Nonideal behavior has traditionally been modeled by defining efficiency (a comparison between actual and isentropic processes), and subsequent specification by empirical or heuristic methods. With the increasing complexity of aeropropulsion system designs, the reliability of these more traditional methods is uncertain. Computational fluid dynamics (CFD) and experimental methods can provide this information but are expensive in terms of human resources, cost, and time. This report discusses an alternative to empirical and CFD methods by applying classical analytical techniques and a simplified flow model to provide rapid engineering estimates of these losses based on steady, quasi-one-dimensional governing equations including viscous and heat transfer terms (estimated by Reynold's analogy). A preliminary verification of REMEL has been compared with full Navier-Stokes (FNS) and CFD boundary layer computations for several high-speed inlet and forebody designs. Current methods compare quite well with more complex method results and solutions compare very well with simple degenerate and asymptotic results such as Fanno flow, isentropic variable area flow, and a newly developed, combined variable area duct with friction flow solution. These solution comparisons may offer an alternative to transitional and CFD-intense methods for the rapid estimation of viscous and heat transfer losses in aeropropulsion systems. Author

N95-16908*# National Aeronautics and Space Administration. Langley Research Center, Hampton, VA.
COMPARISON OF COMPUTATIONAL AND EXPERIMENTAL RESULTS FOR A SUPERCRITICAL AIRFOIL
Melissa B. Rivers and Richard A. Wahls Nov. 1994 30 p
(RTOP 505-59-10-31)
(NASA-TM-4601; L-17330; NAS 1.15:4601) Avail: CASI HC A03/MF A01

A computational investigation was performed to study the flow over a supercritical airfoil model. Solutions were obtained for steady-state transonic flow conditions using a thin-layer Navier-Stokes flow solver. The results from this computational study were compared with time-averaged experimental data obtained over a wide Reynolds number range at transonic speeds in the Langley 0.3-Meter Transonic Cryogenic Tunnel. Comparisons were made at a nominal Mach number of 0.72 and at Reynolds numbers ranging from 6 x 10(exp 6) to 35 x 10(exp 6). Author

N95-17178# Defence Science and Technology Organization, Melbourne (Australia).
DATA ACQUISITION AND PROCESSING SOFTWARE FOR THE LOW SPEED WIND TUNNEL TESTS OF THE JINDIVIK AUXILIARY AIR INTAKE
S. S. Lam Aug. 1994 46 p
(AD-A285455; DSTO-TR-0043; DODA-AR-007-100) Avail: CASI HC A03/MF A01

Data acquisition software has been developed for the wind tunnel tests of the auxiliary air intake of the Jindivik pilotless target aircraft in the AMRL Low Speed Wind Tunnel (LSWT) using the new Pressure Systems Incorporated (PSI) 8400 Measurement System under the control of an IBM PS/2 computer. The recent upgrade of the data acquisition system for the LSWT and the replacement of the mechanical Scanivalve pressure measuring system with PSI electronic pressure scanners has required major modifications to be made to existing software. To minimize the changes needed and to provide compatibility with data processing for previous tests, the data acquired by the PSI electronic pressure equipment are transferred to the dedicated LSWT DEC PDP-11/44 mini-computer for storage and processing. This report describes the development and operation of new software for the LSWT tests of the Jindivik auxiliary air intake. DTIC

N95-17273*# Vigyan Research Associates, Inc., Hampton, VA.
TRANSONIC NAVIER-STOKES CALCULATIONS ABOUT A 65 DEG DELTA WING Final Report
W. Kelly Londenberg NASA Nov. 1994 71 p
(Contract NAS1-18585; RTOP 505-59-54-01)
(NASA-CR-4635; NAS 1.26:4635) Avail: CASI HC A04/MF A01

A computational study has been conducted in which the CFL3D Navier-Stokes solver coupled with an algebraic and a one-equation nonequilibrium turbulence model has been used to predict the flow over a 65 degree delta wing at transonic conditions for Reynolds numbers ranging from 6 x 10(exp 6) to 120 x 10(exp 6) based on mean aerodynamic chord. Solutions obtained indicated that the computational method when used with the one-equation turbulence model predicts results that compare well with experiment for attached flow conditions. Comparisons with experimental pressure at separated conditions show that the computational method, even though primary flow-field features are predicted well, does not predict secondary flow features. Author

N95-17435 Naval Postgraduate School, Monterey, CA.
NUMERICAL OPTIMIZATION OF SYNERGETIC MANEUVERS M.S. Thesis
John C. Nicholson Jun. 1994 181 p Limited Reproducibility: More than 20% of this document may be affected by microfiche quality
(AD-A283398) Avail: Issuing Activity (Defense Technical Information Center (DTIC))

The use of atmospheric forces to produce an orbital plane change requires less energy than a pure exoatmospheric propulsion maneuver. The combination of aerodynamic and propulsive forces to cause a change

in orbital inclination is termed a synergetic maneuver. Several methods have been proposed to control the critical heating rate while performing the procedure. This thesis examines these control methods by numerically optimizing the trajectory for several fuel weights and heat rate constraints. The Program to Optimize Simulated Trajectories (POST) is used to simulate the maneuvers and control schemes and to perform the optimization. For no active heat constraints, it is shown that a gliding atmospheric entry followed by a maximum throttle bang produces significantly more inclination change than other proposed maneuvers. If the heat constraints are active, the recently proposed aerobang maneuvers produces a substantial inclination change while providing significant heating rate control and shows definite advantages over the long-studied aerocruise maneuver. DTIC

N95-17846# Advisory Group for Aerospace Research and Development, Neuilly-Sur-Seine (France). Fluid Dynamics Panel.

A SELECTION OF EXPERIMENTAL TEST CASES FOR THE VALIDATION OF CFD CODES, VOLUME 2 [RECUEIL DE CAS D'ESSAI EXPERIMENTAUX POUR LA VALIDATION DES CODES DE L'AERODYNAMIQUE, VOLUME 2]

Aug. 1994 577 p

(AGARD-AR-303-Vol-2; ISBN-92-836-1003-2) Copyright Avail: CASI HC A25/MF A06

This report presents the results of a study by Working Group 14 of the AGARD Fluid Dynamics Panel. The thirty nine test cases that are documented cover the subsonic, transonic, and supersonic flow regimes and five classes of geometries. Included in the five classes of geometries are: Two Dimensional Airfoils; Three Dimensional Wings, designed for predominantly attached flow conditions; Slender Bodies, typical of missile type configurations; Delta Wings, characterized by a conical type of vortex flow; and Complex Configurations, either in a geometrical sense or because of complicated flow interactions. The report is presented in two volumes. Volume 1 provides a review of the theoretical and experimental requirements, a general introduction, summary of the test cases and recommendations for the future. Volume 2 contains detailed information on the test cases. Relevant data has been compiled on floppy disks. For individual titles, see N95-17847 through N95-17885.

N95-17847# Deutsche Forschungsanstalt fuer Luft- und Raumfahrt, Brunswick (Germany). Inst. fuer Entwurfsaerodynamik.

2-D AIRFOIL TESTS INCLUDING SIDE WALL BOUNDARY LAYER MEASUREMENTS **c34**

W. Bartelheimer, K. H. Horstmann, and W. Puffert-Meissner *In* AGARD, A Selection of Experimental Test Cases for the Validation of CFD Codes, Volume 2 Aug. 1994 11 p (For primary document see N95-17846 04-02)

Copyright Avail: CASI HC A03/MF A06

The data presented in this contribution were obtained in the DLR Transonic Wind Tunnel Braunschweig. The intent of the experiment was to provide data giving information on the development of the TWB-side wall boundary layer in the presence of a typical transonic airfoil model for further investigation of the influence of the side wall boundary layer on 2-D airfoil measurements. For this purpose boundary layer pitot pressure were measured in 13 different side wall positions around the airfoil. Airfoil pressure distributions were obtained in several spanwise positions by sliding the airfoil model in a spanwise direction. The test cases investigated correspond to the design conditions of the airfoil (Ma = 0.73, alpha = 1.5 deg) and to a slow (alpha = 0 deg) and a high (alpha = 3.0 deg) lift value at the same Mach number. For these cases wall pressure distributions were measured on the center slat of the top and bottom walls. Additionally to the pressure measurements some oil flow pictures were made on the upper airfoil surface and the adjacent wind tunnel side wall to get more insight in the structure of the flow. In order to have well defined wind tunnel boundary conditions for the evaluation by computational methods, the slotted top and bottom walls of the test section were closed for these specific tests. This means, of course, that the presented airfoil pressure distributions do not correspond to free flight conditions and are not comparable to wind tunnel results obtained in slotted or perforated transonic test sections. Author

N95-17848# Defence Research Agency, Farnborough, Hampshire (England).

MEASUREMENTS ON A TWO-DIMENSIONAL AEROFOIL WITH HIGH-LIFT DEVICES

I. R. M. Moir *In* AGARD, A Selection of Experimental Test Cases for the Validation of CFD Codes, Volume 2 Aug. 1994 12 p (For primary document see N95-17846 04-02)

Copyright Avail: CASI HC A03/MF A06

The tests detailed in this submission were carried out by the former British Aircraft Corporation in support of the National High Lift Programme. This Programme was a collaborative project between the Royal Aerospace Establishment Farnborough (now part of the the DRA) and the aircraft industry with the aim of increasing the understanding and knowledge of all aspects of high-lift systems, and to provide a fund of data which would benefit the design of future transport aircraft. Wind-Tunnel tests were carried out on four models: (1) A 3-D half model (RAE); (2) a swept panel wing (HSA Hatfield); (3) a quasi-2D (end-plate) model (BAC Weybridge); and (4) a 2D model (BAC Weybridge). BAC Warton also carried out structural analyses on various leading-edge and trailing-edge devices. The present cases are results from the 2D tests which covered investigations into two leading-edge and two trailing-edge devices. The model had a supercritical aerofoil section, a chord of 0.7635m, and was mounted between turnables in the floor and roof of the BAC 3.96m x 2.74m low-speed wind-tunnel. Two-dimensional conditions were maintained by local suction around the wing/wall junctions. Surface pressures were measured on all the components of the wing, at two spanwise stations, one near the tunnel centerline, and one near the roof. These pressures were integrated to give overall lift, drag and pitching moment coefficients. A pilot/static transverse through the wake provided the total momentum deficit. Traverses perpendicular to the wing surface at various chordwise locations provided information on wake and boundary layer development and interaction. Flow visualization was provided by tufting of the wing surfaces. Author

N95-17849# Defence Research Agency, Bedford (England).

INVESTIGATION OF THE FLOW OVER A SERIES OF 14 PERCENT-THICK SUPERCRITICAL AEROFOILS WITH SIGNIFICANT REAR CAMBER

P. R. Ashill *In* AGARD, A Selection of Experimental Test Cases for the Validation of CFD Codes, Volume 2 Aug. 1994 13 p (For primary document see N95-17846 04-02)

Copyright Avail: CASI HC A03/MF A06

The experiments described in this submission were performed on various airfoil sections, all of 14 percent thickness/chord ratio and with significant rear camber. The main aim was to obtain an improved understanding of viscous effects on flows over airfoils with severe adverse pressure gradients. Such gradients can be found at the rear airfoils with significant rear camber and at the foot of shock waves. The tests were performed in the 8ft x 8ft Pressurized, Subsonic/Supersonic Wind Tunnel at the Defense Research Agency (DRA, formerly the Royal Aerospace Establishment) Bedford between November 1976 and February 1982. This wind tunnel has solid walls and, since the airfoil chord to tunnel height is relatively large (0.26), the data are strictly not correctable. This was recognized from the outset, the main concern of the investigation being studying flows rather than performing tests on a prescribed shape. However, the wall boundary conditions are well defined and so the data may be useful for validating CFD codes which include allowance for the wind-tunnel walls. In addition, measurements were made of the static pressures on the roof and floor of the working section, providing an independent check on the accuracy of the representation of the walls in any CFD method. Despite the caveat above about correctability, it is believed that the cases presented having weak shock waves may be used to assess free-air calculation methods provided that allowance is made in the calculation for wall-induced camber. Cases suitable for such work are highlighted in Section 6.2 where details are also given of the camber correction. Author

N95-17850# National Research Council of Canada, Ottawa (Ontario). Inst. for Aerospace Research.

SURFACE PRESSURE AND WAKE DRAG MEASUREMENTS ON THE BOEING A4 AIRFOIL IN THE IAR 1.5X1.5m WIND TUNNEL FACILITY

D. J. Jones and Y. Nishimura *In* AGARD, A Selection of Experimental Test Cases for the Validation of CFD Codes, Volume 2 Aug. 1994

10 p (For primary document see N95-17846 04-02)
Copyright Avail: CASI HC A02/MF A06

This 10.2 percent maximum thickness to chord airfoil has become a standard airfoil for Boeing wind tunnel tests in the IAR 1.5 X 1.5m facility. In order to study wall constraint effects, several different chord lengths have been used in the narrow span (38.1 cm) IAR facility and a 30.5 cm chord model was tested in the 1.5 wide facility. The latter data from the wide span facility are presented here. This data has a small sidewall correction while the upper and lower walls are accounted for using Mokry's wall correction procedures. Transition was fixed at 10 percent and all runs were made at a chord Reynolds number of 14 million. The tests were carried out in June-July, 1991. Author

N95-17851# McDonnell-Douglas Corp., Long Beach, CA.
2-D AILERON EFFECTIVENESS STUDY
V. D. Chin, C. J. Dominik, F. T. Lynch, and D. L. Rodriguez *In* AGARD, A Selection of Experimental Test Cases for the Validation of CFD Codes, Volume 2 Aug. 1994 20 p (For primary document see N95-17846 04-02)
Copyright Avail: CASI HC A03/MF A06

The experimental data described in this contribution were obtained in the IAR High Reynolds Number 60 x 15 (1.5m x 0.38m) Two-Dimensional Test Facility. The purpose of the experiment was to investigate the effects of Reynolds number and Mach number on aileron effectiveness and to evaluate effectiveness of viscous scaling techniques that attempt to simulate flow at higher Reynolds numbers. The advent of the modern transport wing has prompted a renewed interest in the transonic characteristics of ailerons. In addition to their traditional role of lateral (roll) control, aileron are used for wing load alleviation and to improve cruise performance through the 'drooped aileron' concept. An understanding of the prevailing flow physics which limit the transonic performance of ailerons is necessary for the successful design of a control system that satisfies the multi-role requirements of the aileron. Results showed a linear variation of lift for upward trailing edge deflections but a highly nonlinear variation for downward deflections. This nonlinear behavior, equivalent to a loss in aileron effectiveness, became worse at higher angles of attack and higher Mach numbers. In addition, the viscous scaling technique that was used at lower Reynolds numbers was found to be inadequate for modeling flow at higher Reynolds numbers. The data acquired from this test were for a series of aileron deflections varying from -5 to +5 deg at Mach numbers of 0.717 and 0.746 and chord Reynolds numbers of 5, 15, and 25 million. The following types of data were obtained: airfoil surface pressure distributions; wake drag, which was determined by wake transversing probes; lift and drag forces and pitching moment, which were determined by force balance readings and surface pressure integrations; and floor and ceiling pressure distributions, which were used to compute wall interference effects. One of the difficulties in wind tunnel testing is accounting for the effects of wall interference to reinterpret the data for 'free air' conditions. Corrections for interference effects of the floor and ceiling and for the wall sidewall boundary layer effects were applied to the data. The data are available corrected for floor and ceiling effects, and corrected for both floor and ceiling interference and sidewall boundary layer effects. Author

N95-17852# Technische Hochschule, Aachen (Germany). Aerodynamisches Inst.
INVESTIGATION OF AN NLF(1)-0416 AIRFOIL IN COMPRESSIBLE SUBSONIC FLOW
P. Guntermann and G. Dietz *In* AGARD, A Selection of Experimental Test Cases for the Validation of CFD Codes, Volume 2 Aug. 1994 10 p (For primary document see N95-17846 04-02)
Copyright Avail: CASI HC A02/MF A06

The data presented in this contribution were obtained in the 40 x 40 sq cm Transonic Wind Tunnel at the Aerodynamisches Institut of the RWTH Aachen within the research program 'Entwicklung von Berechnungsverfahren fur Probleme der Stromungsmechanik' sponsored by the Stiftung Volkswagenwerk. The aim of the experimental part of the research program was to investigate the influence of compressibility on the location of transition. For this purpose a natural-laminar-flow airfoil NLF (1)-0416, designed for incompressible flow, was investigated. Starting with incompressible free stream conditions the Mach number was increased until transonic flow was obtained. The experiments on the NLF(1)-0416 should provide aerodynamical forces such as lift and drag and data concerning the location and the underlying physical mechanism of transition. Therefore different measuring techniques, e.g. liquid crystal coating and multi-sensor hot-film technique, were tested. To verify the existence of a laminar separation bubble the topology of the boundary layer was visualized. Regarding the different turbulence levels there is a good agreement of the experimental results with those obtained at NASA-Langley, which are available up to Mach numbers of 0.4. Numerical results correspond to the experiments at higher Mach numbers too. Experiments were carried out to get information about the influence of small disturbances of the profile surface on the pressure distribution, the drag, and the location of transition. In continuation of this research a wind tunnel model with adjustable geometry of its upper surface was developed and manufactured. The influence of small surface variations on the location of transition or separation will be investigated experimentally, but these tests are not part of the presented data set. Author

N95-17853# Technische Hogeschool, Delft (Netherlands). Low Speed Aerodynamics Lab.
EXPERIMENTS IN THE TRAILING EDGE FLOW OF AN NLR 7702 AIRFOIL
L. H. J. Absil and D. M. Passchier *In* AGARD, A Selection of Experimental Test Cases for the Validation of CFD Codes, Volume 2 Aug. 1994 16 p (For primary document see N95-17846 04-02)
Copyright Avail: CASI HC A03/MF A06

Detailed mean flow and turbulence properties are presented of the flow in the vicinity of an airfoil trailing edge, to provide data for the development of turbulence models and the validation of computational methods. Author

N95-17854# National Aerospace Lab., Amsterdam (Netherlands).
TWO-DIMENSIONAL 16.5 PERCENT THICK SUPERCRITICAL AIRFOIL NLR 7301
S. O. T. H. Han *In* AGARD, A Selection of Experimental Test Cases for the Validation of CFD Codes, Volume 2 Aug. 1994 11 p (For primary document see N95-17846 04-02)
Copyright Avail: CASI HC A03/MF A06

This thick supercritical airfoil designed for a lift-coefficient of 0.595 at a Mach number of 0.721 (potential flow conditions) was an early NLR design of a supercritical airfoil made in 1973. The airfoil was designed with the hodograph method and has a rather blunt nose with a roof-top type pressure distribution. A typical other feature of this airfoil is that it is highly rear loaded, both on the upper surface and on the lower surface. Because of this rear loading, the airfoil is close to trailing edge separation on the upper surface and separation in the cove region around 70% chord at the lower surface. Tests have been made originally in the NLR (Transonic) Pilot Tunnel at a Reynolds number of 2.2 million (the design condition). The results of these tests have been included in AGARDograph AR-138. At about the same time test were made in the Compressible Flow Facility CFD) of Lockheed (Georgia, USA) for the Reynolds number of 10, 20 and 30 million. In the eighties, when more advanced computer codes became available that could cope with airfoils that experienced a limited extent of separation, there was an urgent need for reliable data to validate the computer codes for these conditions. Also, the problem of scaling (low Reynolds number) wind tunnel tests to (the much higher) flight Reynolds numbers raised (again) considerably interest. For both reasons it was decided to repeat the original NLR 7301 experiments on a larger two-dimensional model in the large transonic wind tunnel HST of NLR. The tests covered the low speed and transonic speed regimes whereas part of the measurements was performed at constant lift for range of Reynolds numbers of study the indirect Reynolds number effects in more detail. Author

N95-17855# National Aerospace Lab., Amsterdam (Netherlands).
LOW-SPEED SURFACE PRESSURE AND BOUNDARY LAYER MEASUREMENT DATA FOR THE NLR 7301 AIRFOIL SECTION WITH TRAILING EDGE FLAP
B. vandenBerg and J. H. M. Gooden *In* AGARD, A Selection of Experimental Test Cases for the Validation of CFD Codes, Volume 2 Aug. 1994 12 p (For primary document see N95-17846 04-02)
Copyright Avail: CASI HC A03/MF A06

Test data are given for a two-dimensional wing flap configuration, which has been so designed that nowhere flow separations occur, apart from a

small laminar separation bubble on the wing nose. The 32% chord trailing edge flap is deflected 20 deg. Two widths of the gap between wing and flap have been applied, with mixing of the wing wake and flap boundary layer occurring with the smaller gap. The experiment has been carried out at a Reynolds number Re, c = 2.51 * E6 and a Mach number of about Ma = 0.185. The measurements comprise surface pressure data, from which lift and pitching moment coefficients were calculated, at various angles of attack from zero up to beyond stall. At three angles of attack the drag has been determined from wake traverses. At these angles mean flow measurements in the boundary layer and wake have been executed at 16 stations. In addition turbulence data were obtained at 5 stations in the wing wake above the flap. Surface flow visualization data are also available. Author

N95-17856# Office National d'Etudes et de Recherches Aerospatiales, Toulouse (France).

DATA FROM THE GARTEur (AD) ACTION GROUP 02 AIRFOIL CAST 7/DOA1 EXPERIMENTS

A. Mignosi, J. P. Archambaud, and E. Stanewsky (Deutsche Forschungs- und Versuchsanstalt fuer Luft- und Raumfahrt, Goettingen, Germany.) *In* AGARD, A Selection of Experimental Test Cases for the Validation of CFD Codes, Volume 2 Aug. 1994 12 p (For primary document see N95-17846 04-02)

Copyright Avail: CASI HC A03/MF A06

In order to gain a better understanding of the various forms and the magnitude of wind tunnel interferences that may arise in two-dimensional testing and to find improved methods of correction, a GARTEur Action Group was formed in 1979 with the primary objectives of (1) comparing test results obtained with one airfoil (CAST 7) in a number of facilities in order to assess wall interference in the individual tunnels and to assess the accuracy of correction methods currently used and (2) evaluating three-dimensional interference effects associated with the side wall boundary layer. The wind tunnels considered consisted of five conventional tunnels with either slotted or perforated test section walls and two adaptive wall wind tunnels. Based on a comparison of the results from these tunnels, it was concluded that for these two-dimensional airfoil tests the freestream conditions, Mach number and angle of attack, were generally predicted with an accuracy of delta M infinity = plus or minus 0.002 and delta alpha = plus or minus 0.1 deg to plus or minus 0.05 deg, respectively, and the lift and drag coefficients with an accuracy of delta C(sub L) = plus or minus 0.015 and delta C(sub D) = plus or minus 0.0003 deg, respectively. For the adaptive wall wind tunnel T2 of ONERA/CERT the accuracy in freestream conditions was determined to be delta M infinity = plus or minus 0.001 and delta alpha = plus or minus 0.03 deg. Due to their relatively high accuracy, only the ONERA T2 adaptive wall tests are considered hereafter. The data, obtained with well defined boundary conditions, are believed to be the most suitable for CFD - assessment. Author

N95-17857# Office National d'Etudes et de Recherches Aerospatiales, Toulouse (France).

OAT15A AIRFOIL DATA

A. M. Rodde and J. P. Archambaud *In* AGARD, A Selection of Experimental Test Cases for the Validation of CFD Codes, Volume 2 Aug. 1994 13 p (For primary document see N95-17846 04-02)

Copyright Avail: CASI HC A03/MF A06

The OAT15A airfoil is a supercritical airfoil for transport aircraft designed a few years ago within the framework of an ONERA/Aerospatiale joint programme devoted to the study of various designs. The design point is M = 0.73, C(sub L) = 0.65 and the thickness to chord ratio of the airfoil is 12.3 percent. The tests which were performed in the ONERA/CERT T2 wind tunnel were devoted to the Reynolds number effects on the airfoil performance. These effects were investigated within the range 3-20 10(exp 6) taking advantage of the cryogenic capability of the tunnel. The adaptive top and bottom walls of the tunnel give quasi free air conditions. However some sidewall effects are present and are taken into account in the correction procedure. Tests performed on another model in the S3MA wind tunnel with perforated top and bottom walls show good agreement with the T2 tests which give more confidence concerning the quality of the data. The proposed test cases concern mainly pressure distributions for various Reynolds numbers with fixed transition. However for a selected number of test cases boundary layer measurements with an external probe and LDV flow field data are also given. The set of data can be used for different purposes: (1) computer code capability for the prediction of Reynolds number effect; and (2) detailed 2D computer code assessment. Author (revised)

N95-17858*# National Aeronautics and Space Administration. Ames Research Center, Moffett Field, CA.

A SUPERCRITICAL AIRFOIL EXPERIMENT

George G. Mateer, H. Lee Seegmiller, Lawrence A. Hand, and Joachim Szodruch (Messerschmitt-Boelkow-Blohm G.m.b.H., Bremen, Germany.) *In* AGARD, A Selection of Experimental Test Cases for the Validation of CFD Codes, Volume 2 Aug. 1994 12 p (For primary document see N95-17846 04-02)

Copyright Avail: CASI HC A03/MF A06

The purpose of this investigation is to provide a comprehensive data base for the validation of numerical simulations. The initial results of the study (single angle of attack) were presented in ref. 1, where the effects of various parameters and the adequacies of selected turbulence models were discussed. The objective of the present paper is to provide a tabulation of the experimental data. The data were obtained in the two-dimensional, transonic flowfield surrounding a supercritical airfoil. A variety of flows were studied in which the boundary layer at the trailing edge of the model was either attached or separated. Unsteady flows were avoided by controlling the Mach number and angle of attack. Surface pressures were measured on both the model and wind tunnel walls, and the flowfield surrounding the model was documented using a laser Doppler velocimeter (LDV). Although wall interference could not be completely eliminated, its effect was minimized by employing the following techniques. Sidewall boundary layers were reduced by aspiration, and upper and lower walls were contoured to accommodate the flow around the model and the boundary-layer growth on the tunnel walls. A data base with minimal interference from a tunnel with solid walls provides an ideal basis for evaluating the development of codes for the transonic speed range because the codes can include the wall boundary conditions more precisely than interference corrections can be made to the data sets. Author

N95-17859# Boeing Commercial Airplane Co., Seattle, WA.

TWO-DIMENSIONAL HIGH-LIFT AIRFOIL DATA FOR CFD CODE VALIDATION

G. W. Brune *In* AGARD, A Selection of Experimental Test Cases for the Validation of CFD Codes, Volume 2 Aug. 1994 13 p (For primary document see N95-17846 04-02)

Copyright Avail: CASI HC A03/MF A06

The purpose of the experimental investigation summarized below was to provide a complete data set for the validation of two-dimensional multi-element airfoil computer codes. The airfoil model used for this investigation features four elements including a double slotted trailing edge flap and a slotted leading edge device representing a section of a transport wing in high-lift configuration with take-off flap setting. The leading edge flap was tested in a nonoptimum setting in order to produce a thick confluent boundary layer on the upper airfoil surface. In this wind tunnel experiment, all data were measured on a single high-lift airfoil configuration with a fixed flap setting at one tunnel freestream condition. Emphasis was placed on the acquisition of a few high quality airfoil data with many repeat runs and redundant measurements. Measured data comprise airfoil lift, drag, pitching moment, surface pressures, mean velocity profiles and Reynolds stresses of the confluent boundary layer. The data was obtained in the Boeing Research Wind Tunnel located in Seattle at 0.11 Mach number and 1.55 million Reynolds number based on tunnel freestream velocity and a flaps-up airfoil chord of 0.6096 m (2 ft). Care was taken to achieve a close approximation to two-dimensional flow by means of turntable and tunnel side wall blowing. Two-dimensional flow was verified by comparing boundary layer mean velocity and turbulence profiles at several spanwise stations, and by various surface flow visualizations methods. In addition, lift curves from balance measurements and an integration of surface pressures were compared. Confluent boundary layer measurements were conducted employing a Pitot probe and hot wires. Probes were mounted on a mechanical traverser designed to minimize disturbances of overall airfoil circulation and of the local flow at the measuring station. Author

N95-17860# Defence Research Agency, Farnborough, Hampshire (England). Aerodynamics and Propulsion Dept.

MEASUREMENTS OF THE FLOW OVER A LOW ASPECT-RATIO WING IN THE MACH NUMBER RANGE 0.6 TO 0.87 FOR THE PURPOSE OF VALIDATION OF COMPUTATIONAL METHODS. PART 1: WING DESIGN, MODEL CONSTRUCTION, SURFACE FLOW. PART 2: MEAN FLOW IN THE BOUNDARY LAYER AND WAKE, 4 TEST CASES

M. C. P. Firmin and M. A. McDonald *In* AGARD, A Selection of Experimental Test Cases for the Validation of CFD Codes, Volume 2 Aug. 1994 18 p (For primary document see N95-17846 04-02)

Copyright Avail: CASI HC A03/MF A06

The experiments presented should improve the understanding of the flow over a wing as the speed is increased towards the buffet and separation boundaries. These boundaries limit the flight envelopes of both military and civil aircraft, and the measurements reported will allow Computational Fluid Dynamic (CFD) methods for viscous flow to be validated. The measurements are reported in two documents (Parts 1 & 2) giving detailed measurements of the subsonic free stream flow over a low aspect-ratio wing (RAE Model 2155) at conditions where the boundary layers are subjected to severe adverse pressure gradients. Part 1 provides measurements of pressure distributions on both the wing and on the tunnel walls for a wide range of Mach numbers and lift coefficients, as well as of wing surface skin friction and surface flow direction measurements for four test cases, while Part 2 contains detailed mean flow measurements within the shear layers. For this detailed study, the same four test cases have been used, as presented in Part 1. They were chosen to provide examples of flows with severe adverse pressure gradients, including those with shock waves, and leading in some cases to separation. Author

N95-17861# Defence Research Agency, Bedford (England).

DETAILED STUDY AT SUPERSONIC SPEEDS OF THE FLOW AROUND DELTA WINGS

M. J. Simmons *In* AGARD, A Selection of Experimental Test Cases for the Validation of CFD Codes, Volume 2 Aug. 1994 17 p (For primary document see N95-17846 04-02)

Copyright Avail: CASI HC A03/MF A06

The tests described in this submission were made on two half-models of delta-wing/body configuration suitable for supersonic combat aircraft. The aim of the program of work was to improve the understanding of supersonic flows over wing with rounded leading edges. The reason for choosing the large half-model design were: (1) the attainment of high chordal Reynolds numbers; (2) the facility to make detailed flow measurements; and (3) the ability to manufacture the large wing to the desired model accuracy with conventional machine tolerances. The last requirement is particularly important in the highly-curved region of the leading edge which controls the development of transonic flows on the upper surface. Both wings are of the same quasi-delta planform of 60 leading edge sweep and thickness form of 4% thickness/chord ratio but with differing camber distributions. Wing A has a complex camber surface with camber in both spanwise and streamwise planes. Wing C has an umcambered symmetrical section and was used as a datum case for the study. The only design constraint on model size was the need to ensure that the flow over the wing was not disturbed by shock-wave reflections from the solid walls of the tunnel. The tests were performed in the 8ft x 8ft Pressurized, Subsonic/Supersonic Wind Tunnel at the Defense Research Agency (DRA Aerospace Division, formerly the Royal Aerospace Establishment) Bedford in July 1985. Author (revised)

N95-17862# Defence Research Agency, Bedford (England).

PRESSURE DISTRIBUTIONS ON RESEARCH WING W4 MOUNTED ON AN AXISYMMETRIC BODY

J. L. Fulker *In* AGARD, A Selection of Experimental Test Cases for the Validation of CFD Codes, Volume 2 Aug. 1994 12 p (For primary document see N95-17846 04-02)

Copyright Avail: CASI HC A03/MF A06

The experiments described in this submission were performed on a wing-body configuration suitable for a civil transport aircraft. When the wing was designed (1972) it was recognized that, in order to achieve an advance in technology, a significant increase in rear loading would be required compared to that of earlier designs. As a consequence, the boundary layer conditions close to the trailing edge on the upper surface were expected to be more adverse than in previous designs. This requirement led to the need for a high test Reynolds number, which was achieved by testing a large half model in the Defense Research Agency (DRA) 8ft x 8ft Wind Tunnel at Reynolds numbers, based on geometric mean chord, of up to 15 x 10(exp 6). Complementary tests were also performed on a smaller complete model in order to provide an accurate assessment of the drag characteristics of the wing. The wing was designed to have a weak shock wave near mid chord on the upper surface at the cruise condition (C(sub L) = 0.32, M = 0.78). The overall aims of the investigation were to obtain an improved understanding of the behavior of the flow over wings of this type over a wide range of subsonic Mach numbers and Reynolds numbers. The tests were performed during 1977 on the complete model and 1978 on the half model. The wind tunnel has solid walls, and since the models are relatively large, the data are strictly not correctable. However, the wall boundary conditions are well defined and so the data may be useful for validating CFD codes which include allowance for the wind-tunnel walls. In addition measurements were made on the static pressures on the roof and floor of the working section, providing an independent check on the accuracy of the representation of the walls in any CFD method. Derived from text

N95-17863# Deutsche Forschungsanstalt fuer Luft- und Raumfahrt, Brunswick (Germany). Inst. fuer Entwurfsaerodynamik.

DLR-F4 WING BODY CONFIGURATION **c05**

G. Redeker *In* AGARD, A Selection of Experimental Test Cases for the Validation of CFD Codes, Volume 2 Aug. 1994 21 p (For primary document see N95-17846 04-02)

Copyright Avail: CASI HC A03/MF A06

These tests have been carried out under the auspices of GARTEUR in order to provide an experimental data base for a modern commercial transport type aircraft against which results of various computational methods may be checked. The tests were carried out in three major European wind tunnels (NLR-HST, ONERA-S2MA, and DRA-8ft x 8ft DRA Bedford) in order to compare the results of the same model in different wind tunnels. For the purpose of these tests the available geometry of the DLR-F4 model of a wing body configuration, which was developed as a research configuration of a modern transport type aircraft, was selected by the GARTEUR Action Group AD (AG01) 'Wing body aerodynamics at transonic speeds.' Derived from text

N95-17864# Deutsche Forschungsanstalt fuer Luft- und Raumfahrt, Goettingen (Germany).

DLR-F5: TEST WING FOR CFD AND APPLIED AERODYNAMICS

H. Sobieczky *In* AGARD, A Selection of Experimental Test Cases for the Validation of CFD Codes, Volume 2 Aug. 1994 11 p (For primary document see N95-17846 04-02)

Copyright Avail: CASI HC A03/MF A06

A swept wing with symmetrical sections was originally created to serve two purposes. First, the surface generator used for data definition was under development for aerodynamic design and optimization. The wing created was intended therefore to be a selected case of a whole family of configurations obtained by variation of the input parameters. Aerodynamic design and optimization strategies call for such variations. Second, CFD code development needs both accurate test case geometries as well as experimental results from wind tunnels. The latter usually suffer from corrections which still might suit practical purposes of measuring aerodynamic coefficients but fall short of the requirement to define the flow conditions to the same accuracy as geometrical boundaries are known. Using the generator software, a compromise was chosen by including the closed wind tunnel wall geometry as a channel boundary surrounding an aerodynamic component. In order to also avoid model support problems, a wing half model mounted on and including a splitter plate was used as 'configuration.' Geometry of the flow boundaries was completely defined through the simple rectangular channel geometry completed by chosen inlet and exit planes. Flow data were required at these planes to formulate a boundary value problem for CFD. In a workshop to compare CFD results with the first test case experiment (1986), partners had obtained and used a computer code to generate the wing and the wind tunnel boundary conditions, along with the absolutely necessary parameters to formulate fluid dynamic boundary conditions for the Navier-Stokes equations. This software is a simplified version of the geometry generator for aerospace configurations and CFD grid generation which has since been further developed as an industrial tool for design aerodynamics. The experiment

and the refined half-model technique was published and the results of the workshop, comparing numerical results, have been summarized. Based on these results we may conclude that for CFD this test case turns out to be a complicated one basically because of the observed viscous flow phenomena on the wing. On the other hand, the definition of the complete boundary value problem makes the case rather unique and, with the help of generator software and experimental data, easy to implement for CFD validation. The workshop software and experimental results for surface pressure distributions is made available in one package.

Derived from text

N95-17865*# National Aeronautics and Space Administration. Ames Research Center, Moffett Field, CA.

LOW ASPECT RATIO WING EXPERIMENT

Mike Olsen and H. Lee Seegmiller *In* AGARD, A Selection of Experimental Test Cases for the Validation of CFD Codes, Volume 2 Aug. 1994 11 p (For primary document see N95-17846 04-02)

Copyright Avail: CASI HC A03/MF A06

This test was initiated to provide validation data on low aspect ratio wings at transonic speeds. The test was conducted so that the data obtained would be useful in the validation of codes, and all boundary condition data required would be measured as part of the test. During the conduct of the test, the measured quantities were checked for repeatability, and when the data would not repeat, the cause was tracked down and either eliminated or included in the measurement uncertainty. The accuracy of the data was in the end limited by wall imperfections of the wind tunnel in which the test was run. Derived from text

N95-17866# Deutsche Forschungsanstalt fuer Luft- und Raumfahrt, Cologne (Germany). Hauptabeilung Windkanaele.

WIND TUNNEL INVESTIGATIONS OF THE APPEARANCE OF SHOCKS IN THE WINDWARD REGION OF BODIES WITH CIRCULAR CROSS SECTION AT ANGLE OF ATTACK

H. Esch *In* AGARD, A Selection of Experimental Test Cases for the Validation of CFD Codes, Volume 2 Aug. 1994 16 p (For primary document see N95-17846 04-02)

Copyright Avail: CASI HC A03/MF A06

Originally the model was designed to investigate differences in the interference of fuselage and control surfaces attached to bodies of circular and rectangular cross sections. During the test it was found difficult to define the interference since the reference configuration, the isolated body without controls, showed some disturbances in the pressure distribution at certain combinations of Mach number and angle of attack. These disturbances are connected with the appearance of shock waves on the windward side of isolated circular bodies. By checking schlieren pictures made during earlier test series of missiles the range could be defined in which this type of shock occurs. Pressure distribution measurements were made in order to find an explanation for the formation of the shocks and their bending into the windward region. It is believed that three conditions must be fulfilled: (1) Crossflow Mach number must be high enough that a shock forms in front of the wedge-like primary separation. (2) The primary separation line must move towards the windward side of the body. As a result the local Mach number normal to the separation line decreases, and eventually the shock detaches - if the crossflow Mach number is not too high. (3) When the local surface Mach number normal to the body axis is less than one, the disturbances propagates towards the windward region of the body. In some cases this type of disturbance may lead to confusion especially when there are not enough pressure taps: in the pressure distribution one finds only one or two peaks and from this, one cannot identify the shock trace. The model is extremely simple and thus the generation of a grid should not be too expensive. The data are considered valuable for CFD validation but on the other hand CFD should be useful to get more information of the outer flow field and further insight into this more fundamental flow phenomenon. Derived from text

N95-17867# Deutsche Forschungsanstalt fuer Luft- und Raumfahrt, Goettingen (Germany). Inst. fuer Stroemungsmechanik.

THREE-DIMENSIONAL BOUNDARY LAYER AND FLOW FIELD DATA OF AN INCLINED PROLATE SPHEROID **c34**

H.-P. Kreplin *In* AGARD, A Selection of Experimental Test Cases for the Validation of CFD Codes, Volume 2 Aug. 1994 12 p (For primary document see N95-17846 04-02)

Copyright Avail: CASI HC A03/MF A06

A research project on the investigation of three-dimensional boundary layers on inclined bodies of revolution has been carried out. Experimental data for such flows were provided which can be used for the validation of calculation methods and the testing and development of turbulence models for three-dimensional flows. Problems of laminar-turbulent boundary layer separation have been studied for a range of angles of incidence and Reynolds number. Derived from text

N95-17868# Deutsche Forschungsanstalt fuer Luft- und Raumfahrt, Goettingen (Germany).

FORCE AND PRESSURE DATA OF AN OGIVE-NOSED SLENDER BODY AT HIGH ANGLES OF ATTACK AND DIFFERENT REYNOLDS NUMBERS

K. Hartmann *In* AGARD, A Selection of Experimental Test Cases for the Validation of CFD Codes, Volume 2 Aug. 1994 13 p (For primary document see N95-17846 04-02)

Copyright Avail: CASI HC A03/MF A06

Force, moment, flow field, and pressure measurements (steady and unsteady) were carried out on an ogive-nosed circular cylinder body with a smooth surface. The tests were performed in the two open jet low speed wind tunnels of the DLR in Gottingen (NWG, test section size 3 m x 3 m) and in Braunschweig (NWB, test section size 2.8 m x 3.25 m). A body diameter of D = 200 mm was chosen to achieve Reynolds numbers as high as possible at the maximum speed in these tunnels. The tests comprise angles of attack from 0 to 90 deg and Reynolds numbers of 2.5 x 10(exp 5), 3.7 x 10(exp 5), and 7.7 x 10(exp 5) (based on body diameter and freestream conditions). For six angles of attack between 20 and 70 deg the dependence on different roll positions of the body was systematically investigated with a complete coverage of 360 deg. In some cases the turbulence level of the freestream was varied. The body vortices were visualized in a water towing tank using hydrogen bubbles and in the wind tunnel with the aid of smoke and a laser light sheet. Derived from text

N95-17869# Office National d'Etudes et de Recherches Aerospatiales, Paris (France).

ELLIPSOID-CYLINDER MODEL **c34**

D. Barberis *In* AGARD, A Selection of Experimental Test Cases for the Validation of CFD Codes, Volume 2 Aug. 1994 11 p (For primary document see N95-17846 04-02)

Copyright Avail: CASI HC A03/MF A06

The data presented in this contribution were obtained in the F2 subsonic wind tunnel of the ONERA Fauga-Mauzac Center. The objective of this work was to obtain detailed experimental data on a separated vortex flow. The model shape has been chosen to be as simple as possible in order to facilitate the mathematical modeling. This model has been defined after preliminary studies in a water tunnel. The present document reports the results obtained with an axisymmetric model at incidence. Attention has been focused on the boundary layer evolution in the zone of separation and on the mechanism leading to the formation of a well detached primary vortex. The flow has been investigated in great detail by using several experimental techniques: surface flow visualizations, surface pressure measurements, field explorations by multihole pressure probes, and an LDV system. Derived from text

N95-17870# Office National d'Etudes et de Recherches Aerospatiales, Paris (France).

SUPERSONIC VORTEX FLOW AROUND A MISSILE BODY

D. Barberis *In* AGARD, A Selection of Experimental Test Cases for the Validation of CFD Codes, Volume 2 Aug. 1994 11 p (For primary document see N95-17846 04-02)

Copyright Avail: CASI HC A03/MF A06

Boundary-layer separation occurring on a missile body at moderate or high angle of incidence leads to the formation of well organized vortical structures, especially at supersonic flight Mach numbers. Even though a certain number of experimental results are available for this type of flow, none of the published data provide complete information for a supersonic flow. A experimental study of the flowfield around a 3 caliber tangent ogive-cylinder body in a supersonic flow has been carried out to provide a consistent description of the flow. This experiment includes oil flow visualizations, primary separation line determination, surface pressure

measurements and five hole pressure probe surveys for a Mach number of 2 and an angle of incidence varying from 0 to 20 deg. Results are obtained for a natural and fixed transition. Author

N95-17871# Office National d'Etudes et de Recherches Aerospatiales, Paris (France).

TEST DATA ON A NON-CIRCULAR BODY FOR SUBSONIC, TRANSONIC AND SUPERSONIC MACH NUMBERS **c34**

P. Champigny *In* AGARD, A Selection of Experimental Test Cases for the Validation of CFD Codes, Volume 2 Aug. 1994 11 p (For primary document see N95-17846 04-02)

Copyright Avail: CASI HC A03/MF A06

Measurements on a non-circular body were made in ONERA wind tunnels. This body, representative of non-conventional missile shapes, was studied for Mach numbers from 0.4 to 3.0 (S2MA wind-tunnel) and 4.5 (S3MA wind-tunnel), angles of attach up to 20 deg and sideslip angles up to 10 deg, with a free transition. The data base consists of static pressure measurements. The intent of the experiment was to provide data for evaluation of three-dimensional flow computation methods, as part of a research program sponsored by the 'Direction des Recherches, Etudes et Techniques' of the French Ministry of Defense. The flow exhibits large separation regions and strong vortices, even at low angles of attack, due to the particular shape of the body (lenticular cross-section). Author

N95-17872# National Aerospace Lab., Amsterdam (Netherlands).

WIND TUNNEL TEST ON A 65 DEG DELTA WING WITH A SHARP OR ROUNDED LEADING EDGE: THE INTERNATIONAL VORTEX FLOW EXPERIMENT

A. Elsenaar *In* AGARD, A Selection of Experimental Test Cases for the Validation of CFD Codes, Volume 2 Aug. 1994 18 p (For primary document see N95-17846 04-02)

Copyright Avail: CASI HC A03/MF A06

The windtunnel tests carried out on this model resulted from an international co-operation that involved the aeronautical laboratories AFWAL (US), DLR (Germany), FFA (Sweden), NLR (The Netherlands) and the Universities of Braunschweig (Germany) and Delft (The Netherlands). It was the basic aim of these measurements to provide detailed pressure and flow field data on a 65 deg delta wing configuration of a generic shape for the validation of CFD methods, notably Euler methods. For this reason one of the basic configurations had a sharp leading edge. However, there was also considerable interest for configurations with more realistic features and therefore other configurations were added. These featured a wing with a smaller sweep angle (55 instead of 65 deg), a rounded instead of a sharp leading edge shape, a drooped leading edge and the addition of a canard wing. The windtunnel tests were made in different wind tunnels with different models. They covered a large range of flow conditions and measuring techniques (including force, pressure and flow field measurements). The test case to be described here covers only the force and pressure measurements as carried out at NLR in the transonic windtunnel HST and the supersonic windtunnel SST. The measurements executed at DLR, including flow field measurements, can be found in case D-4. Author

N95-17873# Office National d'Etudes et de Recherches Aerospatiales, Paris (France).

DELTA-WING MODEL

D. Barberis *In* AGARD, A Selection of Experimental Test Cases for the Validation of CFD Codes, Volume 2 Aug. 1994 11 p (For primary document see N95-17846 04-02)

Copyright Avail: CASI HC A03/MF A06

A detailed study has been made on the flow around a 75 sweep angle delta wing to provide reference material or numerical codes. Experiments were carried out in the F2 wind tunnel of the ONERA Le Fauga - Mauzac Centre. Firstly an examination of the surface flow properties was carried out using surface pressure measurements an surface flow visualizations with a viscous coating. The angle of incidence was varied between 5 and 30 deg and the upstream velocity between 10 and 75 m/s. Secondly,the aerodynamic field was characterized by means of laser tomography visualizations and surveys with a two component laser Doppler velocimeter system. Mean and fluctuating velocity fields were determined in several vertical planes normal to the wind tunnel longitudinal axis. These measurements were carried out for an angle of incidence of 20 deg and for two values of the upstream velocity (24 m/s and 40 m/s). Author

N95-17874# Technische Hogeschool, Delft (Netherlands). Faculty of Aerospace Engineering.

EXPERIMENTAL INVESTIGATION OF THE VORTEX FLOW OVER A 76/60-DEG DOUBLE DELTA WING

N. G. Verhaagen and J. E. J. Maseland *In* AGARD, A Selection of Experimental Test Cases for the Validation of CFD Codes, Volume 2 Aug. 1994 15 p (For primary document see N95-17846 04-02)

Copyright Avail: CASI HC A03/MF A06

Data was obtained from a low-speed wind-tunnel experiment carried out on a sharp-edged 76/60-deg double-delta wing. The objective of the investigation was to generate data on the vortex interaction downstream of the strake-wing leading-edge kink of a double-delta wing. An oil-flow and laserlight-sheet technique was used to visualize the flow on and off the surface of the wing. Balance measurements were performed to determine the forces and moments acting on the wing. In addition, the pressure on the upper surface of the wing was measured at several wing chordwise stations. Using a thin five-hole probe, the flowfield over the wing panel was surveyed in detail for an incidence of 20 deg. The data provide information on the interaction process of the wing and strake vortex as well as the development of the secondary separation downstream of the leading-edge kink. Author

N95-17875# Deutsche Forschungsanstalt fuer Luft- und Raumfahrt, Goettingen (Germany).

WIND TUNNEL TEST ON A 65 DEG DELTA WING WITH ROUNDED LEADING EDGES: THE INTERNATIONAL VORTEX FLOW EXPERIMENT

K. Hartmann, K. A. Buetefisch, and H. Pszolla *In* AGARD, A Selection of Experimental Test Cases for the Validation of CFD Codes, Volume 2 Aug. 1994 12 p (For primary document see N95-17846 04-02)

Copyright Avail: CASI HC A03/MF A06

The wind tunnel tests carried out on this model resulted from an international cooperation that involved the aeronautical laboratories AFWAL (US), DLR (Germany), FFA (Sweden), NLR (The Netherlands) and the Universities of Braunschweig (Germany) and Delft (The Netherlands). It was the basic aim of these measurements to provide detailed pressure and flow field data on a 65 deg delta wing configuration of a generic shape for the validation of CFD methods, notably Euler methods. For this reason one of the basic configurations had a sharp leading edge. However, there was also considerable interest for configurations with more realistic features and therefore other configurations were added. These featured a wing with a smaller sweep angle (55 instead of 65 deg), a rounded instead of a sharp leading edge shape, a drooped leading edge and the addition of a canard wing. The wind tunnel tests were made in different wind tunnels with different models. They covered a large range of flow conditions and measuring techniques including force, pressure and flow field measurements. The test case to be described here covers the force, pressure and flow field measurements and flow visualization as carried out at DLR in the transonic wind tunnel TWG on the smaller scale model with round leading edges. This configuration was designed and manufactured by the MBB company in Germany. Author

N95-17876# Aircraft Research Association Ltd., Bedford (England).

INVESTIGATION OF THE FLOW DEVELOPMENT ON A HIGHLY SWEPT CANARD/WING RESEARCH MODEL WITH SEGMENTED LEADING- AND TRAILING-EDGE FLAPS

D. Stanniland *In* AGARD, A Selection of Experimental Test Cases for the Validation of CFD Codes, Volume 2 Aug. 1994 18 p (For primary document see N95-17846 04-02)

Copyright Avail: CASI HC A03/MF A06

The results included in this submission are drawn from the extensive testing which has been carried out on a simple canard/wing research model with a low aspect ratio (2.3), highly swept (58 deg) wing with leading- and trailing-edge flaps. The purpose of these tests was to improve the understanding of the flow development of this class of configuration, to validate the CFD method and philosophy used for the wing design and to provide and extensive data base of pressure data on a precisely specified model geometry for the validation of CFD methods which are capable of handling more complex geometries. The wing was designed using an FP wing/body code, aiming for attached flow at a high subsonic maneuver

design point. This results in a highly cambered and twisted wing with a complex flow breakdown on the upper surface. The use of a segmented leading-edge flap means that the vortical flow develops as a series of part-span vortices, even at a constant flap setting with the gaps between the flap segments sealed. The model has been tested in the ARA 9ft by 8ft Transonic Wind Tunnel over the period 1985 - 1992 to investigate: (1) the effect of a canard, including variation in its position and setting angle; (2) the effect of alternative leading- and trailing-edge flap angles, including both positive and negative settings, although the model is capable of being tested with graded settings across the span (this option has not been investigated to date); (3) a three surface configuration (canard/wing/tailplane); and (4) a blended wing/body derivative of the model, using the existing outer wing and canard designs. Obviously these tests provide an extensive data base and the results included here comprise the datum wing without flap deflection, both with and without a canard.
Author

N95-17877# Deutsche Forschungsanstalt fuer Luft- und Raumfahrt, Brunswick (Germany). Inst. fuer Entwurfsaerodynamik.
SUBSONIC FLOW AROUND US-ORBITER MODEL FALKE IN THE DNW
R. Radespiel and A. Quast *In* AGARD, A selection of Experimental Test Cases for the Validation of CFD Codes, Volume 2 Aug. 1994 13 p (For primary document see N95-17846 04-02)
Copyright Avail: CASI HC A03/MF A06

The contribution describes wind tunnel measurements of aerodynamic forces, pressure distributions and surface visualization for the FALKE model. FALKE is a model of the US-Orbiter in the scale 1:5.427. The test results taken in the subsonic wind tunnel DNW enable validation of computational methods for reentry vehicles in landing conditions at high Reynolds numbers, where strong vortical flow occurs on the upper side of the configuration.
Author

N95-17878# Deutsche Forschungsanstalt fuer Luft- und Raumfahrt, Brunswick (Germany). Inst. fuer Entwurfsaerodynamik.
PRESSURE DISTRIBUTION MEASUREMENTS ON AN ISOLATED TPS 441 NACELLE
R. Kiock and W. Baumert (Deutsche Forschungsanstalt fuer Luft- und Raumfahrt, Goettingen, Germany.) *In* AGARD, A Selection of Experimental Test Cases for the Validation of CFD Codes, Volume 2 Aug. 1994 9 p (For primary document see N95-17846 04-02)
Copyright Avail: CASI HC A02/MF A06

The demand for even more economic jet engines requires extensive experimental investigations of the complete flow field around wing-body-engine-pylon (WBEP) configurations. The engine can be simulated best by pressure-driven devices, so-called Turbine-Powered Simulators (TPS). Though they have been applied for about 20 years, very few nacelle surface pressure measurements were carried out up to now. The reason is seen in the small size of the engine and in the poor theoretical capabilities in the past. Nowadays, WBEP configurations are handled by the Euler code, but experimental validation is required. One pre-step is the experimental investigation of the isolated nacelle which is presented here.
Author

N95-17879*# National Aeronautics and Space Administration. Langley Research Center, Hampton, VA.
SINGLE-ENGINE TAIL INTERFERENCE MODEL
Bobby L. Berrier *In* AGARD, A Selection of Experimental Test Cases for the Validation of CFD Codes, Volume 2 Aug. 1994 23 p (For primary document see N95-17846 04-02)
Copyright Avail: CASI HC A03/MF A06

The data presented in this contribution were obtained in the NASA Langley 16-Foot Transonic Tunnel. Multiple test entries were completed and the results have been completely reported in five NASA reports. The objective of the initial investigation was to determine the effect of empennage (tail) interference on the drag characteristics of an axisymmetric model with a single engine fighter aft-end with convergent divergent nozzles. Two nozzle power settings, dry and maximum afterburning, were investigated. Several empennage arrangements and afterbody modifications were investigated during the initial investigation. Subsequent investigations were used to determine the effects of other model variables including tail incidence, tail span, and nozzle shape. For the final investigation, extensive surface pressure instrumentation was added to the model in order to develop and understanding of the flow interactions associated with afterbody/empennage integration and also to provide data for code validation. Extensive computational analysis has been conducted on the staggered empennage configuration at a Mach number of 0.6 utilizing a three-dimensional Navier Stokes code. Most of the investigations were conducted at Mach numbers from 0.60 to 1.20 and at ratios of jet total pressure to free stream static pressure (nozzle pressure ratio) from 0.1 (jet off) to 8.0. Some angle of attack variation was obtained at jet off conditions.
Author

N95-17880*# National Aeronautics and Space Administration. Langley Research Center, Hampton, VA.
TWIN ENGINE AFTERBODY MODEL
David J. Wing *In* AGARD, A Selection of Experimental Test Cases for the Validation of CFD Codes, Volume 2 Aug. 1994 17 p (For primary document see N95-17846 04-02)
Copyright Avail: CASI HC A03/MF A06

This test was originally conducted to determine the effects of several empennage and afterbody parameters on the aft-end aerodynamic characteristics of a twin-engine fighter-type configuration. Model variables were as follows: horizontal tail axial location and incidence, vertical tail axial location and configuration (twin-vs single-tail arrangements), tail booms, and nozzle power setting. Jet propulsion was simulated by exhausting high-pressure, cold-flow air from the nozzles. Following a successful test conducted on a single engine nacelle model to validate a CFD code, this model was chosen to be instrumented with pressure taps on the afterbody and nozzles and used as a follow-on test, providing a more complex geometry for the CFD code validation. A more limited test matrix was run to collect the pressure data, employing only the twin-tail configuration and varying only the horizontal and vertical tail locations. Mach number was varied from 0.6 to 1.2. Nozzle pressure ratio was varied from jet-off to 8. Angle-of-attack varied from 0 to 8 deg.
Author

N95-17881*# National Aeronautics and Space Administration. Ames Research Center, Moffett Field, CA.
STOVL CFD MODEL TEST CASE
Karlin R. Roth *In* AGARD, A Selection of Experimental Test Cases for the Validation of CFD Codes, Volume 2 Aug. 1994 16 p (For primary document see N95-17846 04-02)
Copyright Avail: CASI HC A03/MF A06

The transitional flight characteristics of a geometrically simplified Short Take-Off Vertical Landing (STOVL) aircraft configuration have been measured in the NASA Ames 7- by 10-Foot Wind Tunnel. The experiment is the first in a sequence of tests designed to provide detailed data for evaluating the capability of computational fluid dynamics methods to predict the important flow parameters for powered lift. The model consists of a 60 deg cropped delta wing platform, blended fuselage and two circular in-line jets that exit perpendicularly from the flat lower surface. The measured flows have a maximum freestream Mach number of 0.2. Model angle of attack is varied between -10 and +20 deg. The flow is ambient temperature in both jet exits and the nozzle pressure ratios are varied between 1 and 3. The data presented includes forces and moments, pressures measured at 281 surface pressure ports and the pressures of the jets. Measurements of the flow are also made in the tunnel test section upstream and downstream of the model and at the jet exits to guide boundary condition selection for the planned computations. Flow visualization and total pressure measurements in the jet plumes provide a description of the three-dimensional jet efflux flowfield.
Author

N95-17882# Aeronautical Research Inst. of Sweden, Bromma. Flygtekniska Foersoeksanstalten.
LOW SPEED PROPELLER SLIPSTREAM AERODYNAMIC EFFECTS
I. Samuelsson *In* AGARD, A Selection of Experimental Test Cases for the Validation of CFD Codes, Volume 2 Aug. 1994 21 p (For primary document see N95-17846 04-02)
Copyright Avail: CASI HC A03/MF A06

The data presented in this contribution to AGARD WG-14: 'EXPERIMENTAL TEST CASES FOR CFD VALIDATION' were obtained at tests in the FFA Low Speed Wind Tunnel LT1 (diameter 3.6 m) as part of an aeronautical research programme sponsored by the Swedish Board for Technical Development (STU). The intent of the experiment was two-fold: (1) to gain some physical insight to the complex aerodynamic interference

phenomena occurring when the slip-stream from a highly loaded propeller washes downstream located surfaces (nacelle and wing); (2) to provide surface pressures and flow field data for evaluation of three-dimensional flow computation methods. The performed wind tunnel tests show that in high power conditions at low speeds large asymmetrical loads can develop on the nacelle and on the wing. For e.g. an aircraft with two propellers having the same sense of rotation these loads do not cancel out but combine to a net increase in asymmetrical loads (in particular side force and yawing moment). These effects, if not known or accounted for in advance, could lead to a resizing of the aircraft control surfaces and/or necessary trim changes with subsequent increased trim drag. Author

N95-17883# Maryland Univ., College Park, MD. Center for Rotorcraft Education and Research.
EXPERIMENTAL DATA ON THE AERODYNAMIC INTERACTIONS BETWEEN A HELICOPTER ROTOR AND AN AIRFRAME
J. G. Leishman and Nai-Pei Bi *In* AGARD, A Selection of Experimental Test Cases for the Validation of CFD Codes, Volume 2 Aug. 1994 17 p (For primary document see N95-17846 04-02)
Copyright Avail: CASI HC A03/MF A06

The data presented in this contribution were obtained at the Center for Rotorcraft Education and Research at the University of Maryland under part of a research program sponsored by the United States Army Research Office. The experiments were performed in several wind-tunnel entries during the period from June 1988 through June 1990. The purpose of the experiments was to provide a better understanding into the origin of rotor/airframe interactional aerodynamic effects that are present on helicopters and other rotary wing aircraft. The measured results provide several unique and challenging engineering test cases for computational fluid dynamic methods used to model helicopter rotor wakes and rotor/airframe interaction phenomena. Author

N95-17884# Aircraft Research Association Ltd., Bedford (England).
INVESTIGATION INTO THE AERODYNAMIC CHARACTERISTICS OF A COMBAT AIRCRAFT RESEARCH MODEL FITTED WITH A FORWARD SWEPT WING
D. Stanniland *In* AGARD, A Selection of Experimental Test Cases for the Validation of CFD Codes, Volume 2 Aug. 1994 26 p (For primary document see N95-17846 04-02)
Copyright Avail: CASI HC A03/MF A06

The submission covers a series of tests on a combat aircraft research model fitted with a forward swept wing. The purpose of the tests was to investigate the flow development of the upper surface of the wing and to establish a level of confidence in the CFD methods used for the wing design. The fuselage was specified algebraically in order to permit a precise definition of the geometry both for CFD calculations and model manufacture, and the model was fitted with pressure tappings on the wing, fuselage and canard. The tests were performed in the ARA 9ft x 8ft Transonic Wind Tunnel in February 1985. Author

N95-17885# Aircraft Research Association Ltd., Bedford (England).
INVESTIGATION OF THE INFLUENCE OF PYLONS AND STORES ON THE WING LOWER SURFACE FLOW
D. Stanniland *In* AGARD, A Selection of Experimental Test Cases for the Validation of CFD Codes, Volume 2 Aug. 1994 16 p (For primary document see N95-17846 04-02)
Copyright Avail: CASI HC A03/MF A06

The submission describes a series of tests on a large half model with a constant chord, untwisted, constant section wing with 25 sweep. The aim of these tests was to investigate the influence of pylons and stores on the wing surface flow, particularly the development of shocks and separations around the pylons with an associated increase in drag. To this end a large number of surface pressure tappings were provided on the wing lower surface (17 stations), on the inboard and outboard sides of each of the pylons and around the mid-pylon store. Since these data were to be used primarily for the validation of CFD codes, for this class of configuration, the fuselage and store are precisely defined bodies of revolution which can be modelled easily by the CFD geometry packages. The tests were performed in the ARA 9ft x 8 ft Transonic Wind Tunnel in February 1986. Author

N95-16251# Nanjing Univ. of Aeronautics and Astronautics, Nanjing, Jiangsu (China). Research Inst. of Pilotless Aircraft.
AN APPROACH TO AERODYNAMIC CHARACTERISTICS OF LOW RADAR CROSS-SECTION FUSELAGES
Jiazheng Pan, Yifei Wang, and Caiwen Zhang *In its* Joint Proceedings on Aeronautics and Astronautics (JPAA) May 1993 p 11-18 (For primary document see N95-16249 04-01)
Avail: CASI HC A02/MF A03

N95-16252# Nanjing Univ. of Aeronautics and Astronautics, Nanjing, Jiangsu (China). Research Inst. of Pilotless Aircraft.
AN IMPROVED METHOD OF AIRFOIL DESIGN
Caiwen Zhang *In its* Joint Proceedings on Aeronautics and Astronautics (JPAA) May 1993 p 19-22 See also A91-44768 (For primary document see N95-16249 04-01)
Avail: CASI HC A01/MF A03

N95-16257# Nanjing Univ. of Aeronautics and Astronautics, Nanjing, Jiangsu (China). Dept. of Aerodynamics.
WALL-SIGNATURE METHODS FOR HIGH SPEED WIND TUNNEL WALL INTERFERENCE CORRECTIONS
Qiwei Zhang *In its* Joint Proceedings on Aeronautics and Astronautics (JPAA) May 1993 p 53-62 See also A93-20803 (For primary document see N95-16249 04-01)
Avail: CASI HC A02/MF A03

N95-16563# National Technical Univ., Athens (Greece). Lab. of Thermal Turbomachines.
SINGLE-PASS METHOD FOR THE SOLUTION OF INVERSE POTENTIAL AND ROTATIONAL PROBLEMS. PART 1: 2-D AND QUASI 3-D THEORY AND APPLICATION
P. Chaviaropoulos, V. Dedoussis (Piraeus Univ., Piraeus, Greece.), and K. D. Papailiou *In* AGARD, Optimum Design Methods for Aerodynamics Nov. 1994 19 p (For primary document see N95-16562 04-05)
Copyright Avail: CASI HC A03/MF A03

N95-16564# National Technical Univ., Athens (Greece). Lab. of Thermal Turbomachines.
SINGLE-PASS METHOD FOR THE SOLUTION OF INVERSE POTENTIAL AND ROTATIONAL PROBLEMS. PART 2: FULLY 3-D POTENTIAL THEORY AND APPLICATIONS
P. Chaviaropoulos, V. Dedoussis (Piraeus Univ., Piraeus, Greece.), and K. D. Papailiou *In* AGARD, Optimum Design Methods for Aerodynamics Nov. 1994 14 p (For primary document see N95-16562 04-05)
Copyright Avail: CASI HC A03/MF A03

N95-17291*# Jet Propulsion Lab., California Inst. of Tech., Pasadena, CA.
FIELD VERIFICATION OF THE WIND TUNNEL COEFFICIENTS
W. K. Gawronski and J. A. Mellstrom *In its* The Telecommunications and Data Acquisition Report 15 Nov. 1994 p 210-220 (For primary document see N95-17279 04-32)
(RTOP 314-40-52-01-02)
Avail: CASI HC A03/MF A03

03 AIR TRANSPORTATION AND SAFETY

Includes passenger and cargo air transport operations; and aircraft accidents.

For related information see also *16 Space Transportation* and *85 Urban Technology and Transportation.*

N95-16404# Army Aeromedical Research Lab., Fort Rucker, AL.
A CORRELATIVE INVESTIGATION OF SIMULATED OCCUPANT MOTION AND ACCIDENT REPORT IN A HELICOPTER CRASH
David G. Beale, Nabih M. Alem, and Barclay P. Butler Aug. 1994 31 p (AD-A285190; USAARL-94-42) Avail: CASI HC A03/MF A01

In 1987, an Army Apache helicopter crashed during a training mission at Fort Rucker, Alabama, resulting in fatal injuries to the rear seat pilot and survivable injuries to the front seat copilot. U.S. Army Safety Center (USASC) investigators at Fort Rucker, Alabama, reported the aircraft damage

assessment and aircrew member injuries. U.S. Army Aeromedical Research Laboratory (USAARL) researchers at Fort Rucker, Alabama, concurrently examined the helmets, restraint systems, and crashworthy seats. Crash kinematics were derived from the investigation; including estimates of the motion of the harnessed occupants during the crash. DTIC

N95-16964# Argonne National Lab., IL.
STATISTICAL PROPERTIES OF AN ALGORITHM USED FOR ILLICIT SUBSTANCE DETECTION BY FAST-NEUTRON TRANSMISSION
D. L. Smith, L. Sagalovsky, B. J. Micklich, M. K. Harper, and A. H. Novick 1994 7 p Presented at the 4th International Conference on Applications of Nuclear Techniques: Neutrons and their Applications, Crete, Greece, 12-18 Jun. 1994
(Contract W-31-109-eng-38)
(DE94-013868; ANL/TD/CP-83205; CONF-9406176-2) Avail: CASI HC A02/MF A01

A least-squares algorithm developed for analysis of fast-neutron transmission data resulting from non-destructive interrogation of sealed luggage and containers is subjected to a probabilistic interpretation. The approach is to convert knowledge of uncertainties in the derived areal elemental densities, as provided by this algorithm, into probability information that can be used to judge whether an interrogated object is either benign or potentially contains an illicit substance that should be investigated further. Two approaches are considered in this paper. One involves integration of a normalized probability density function associated with the least-squares solution. The other tests this solution against a hypothesis that the interrogated object indeed contains illicit material. This is accomplished by an application of the F-distribution from statistics. These two methods of data interpretation are applied to specific sets of neutron transmission results produced by Monte Carlo simulation. DOE

N95-17476# Federal Aviation Administration, Washington, DC.
FEDERAL AVIATION REGULATIONS, PART 91. GENERAL OPERATING AND FLIGHT RULES. CHANGE 5
15 May 1994 24 p See also PB94-159944
(PB94-194883) Avail: CASI HC A03/MF A01

This change incorporates three amendments on Special Visual Flight Rules (SVFR)--Amendments 91-236, 91-237, and 91-128--which affect Appendix D. This change also incorporates Amendment 91-239, Airspace Reclassification, issued March 7, which affects Sections 91.126, 91.127, and 91-130. NTIS

N95-17646# National Transportation Safety Board, Washington, DC.
AIRCRAFT ACCIDENT REPORT: STALL AND LOSS OF CONTROL ON FINAL APPROACH, ATLANTIC COAST AIRLINES, INC./UNITED EXPRESS FLIGHT 6291 JETSTREAM 4101, N304UE COLUMBUS, OH, 7 JANUARY 1994
6 Oct. 1994 124 p
(PB94-910409; NTSB/AAR-94/07) Avail: CASI HC A06/MF A02

This report explains the crash of United Express flight 6291, a Jetstream 4101 airplane, while on approach to runway 28L at Port Columbus International Airport, Columbus, Ohio, on January 7, 1994. The safety issues in the report focused on aircraft safety belts and training programs for Part 135 pilots that emphasize stall warning recognition and recovery techniques, and that lead to proficiency in both high speed and coupled approaches. Safety recommendations concerning these issues were made to the Federal Aviation Administration. Author

N95-17748# National Transportation Safety Board, Washington, DC.
ANNUAL REVIEW OF AIRCRAFT ACCIDENT DATA: US AIR CARRIER OPERATIONS, CALENDAR YEAR 1992
15 Sep. 1994 73 p
(PB95-100319; NTSB/ARC-94/02) Avail: CASI HC A04/MF A01

This publication presents the record of aviation accidents involving revenue operations of U.S. Air Carriers including Commuter Air Carriers and On Demand Air Taxis for calendar year 1992. The report is divided into three major sections according to the federal regulations under which the flight was conducted - 14 CFR 121, Scheduled 14 CFR 135, or Nonscheduled 14 CFR 135. In each section of the report tables are presented to describe the losses and characteristics of 1992 accidents to enable comparison with prior years. NTIS

04 AIRCRAFT COMMUNICATIONS AND NAVIGATION

Includes digital and voice communication with aircraft; air navigation systems (satellite and ground based); and air traffic control.

For related information see also *17 Space Communications, Spacecraft Communications, Command and Tracking* and *Communications and Radar.*

N95-16375 Computer Technology Associates, Inc., McKee City, NJ.
APPLICATION OF RESEARCH TECHNIQUES FOR DOCUMENTING COGNITIVE PROCESSES IN AIR TRAFFIC CONTROL: SECTOR COMPLEXITY AND DECISION MAKING Technical Note, Jul. 1991 - Mar. 1992
R. H. Mogford, E. E. Murphy, R. J. Roske-Hofstrand, G. Yastrop, and J. A. Guttman Jun. 1994 115 p Sponsored by FAA Limited Reproducibility: More than 20% of this document may be affected by microfiche quality
(AD-A282336; DOT/FAA/CT-TN94/3) Avail: Issuing Activity (Defense Technical Information Center (DTIC))

Air traffic controller decision making is a key contributor to safety in the National Airspace System (NAS). Little systematic attention has been paid, however, to investigating the parameters of controller decision making or the factors that affect decision making in the air traffic control (ATC) environment. Because controller decision making takes place within the context of controlled airspace, it is necessary to understand the elements of that context as potential influences on decision-making outcomes. Previous research was conducted on sector complexity in the Great Lakes Region. The research documented in this report was designed to further investigate the elements of en route sector complexity in the Southeast Region and to examine the effects of those elements on controller decision making. Nineteen candidate factors were generated through the use of direct and indirect methods. Of these 19 factors, 11 had significant product-moment correlations, with overall ratings of sector complexity. The results suggested that the use of indirect approaches for knowledge elicitation did not prove to have any distinct advantage in terms of information yield over directly asking controllers for candidate complexity factors. DTIC

N95-17373 CCG Associates, Inc., Silver Spring, MD.
IDENTIFICATION OF ARTIFICIAL INTELLIGENCE (AI) APPLICATIONS FOR MAINTENANCE, MONITORING, AND CONTROL OF AIRWAY FACILITIES Final Report, Jul. 1991 - Mar. 1992
Lori Adkisson, Kamal Karna, Donald Katz, Anita Karna, and Kejitan Dontas May 1994 172 p Limited Reproducibility: More than 20% of this document may be affected by microfiche quality
(AD-A282479; DOT/FAA/CT-TN92/41-I) Avail: Issuing Activity (Defense Technical Information Center (DTIC))

This document provides information acquired from a study conducted on artificial intelligence (AI). The study had four goals, as follows: (1) to identify airway facilities (AF) maintenance, monitoring, and control of activities suitable for AI application development; (2) to determine the AI technologies, tools, architectures, and algorithms that would be most suitable for the identified applications; (3) to develop a set of criteria for AI applications development, and evaluate each of the identified applications in terms of this criteria; and (4) to make short- and long-term recommendations for AI applications development within AF. DTIC

N95-17384*# National Aeronautics and Space Administration. Langley Research Center, Hampton, VA.
MODELING OF INSTRUMENT LANDING SYSTEM (ILS) LOCALIZER SIGNAL ON RUNWAY 25L AT LOS ANGELES INTERNATIONAL AIRPORT
Richard M. Hueschen and Charles E. Knox Nov. 1994 30 p
(RTOP 505-64-13-04)
(NASA-TM-4588; L-17334; NAS 1.15:4588) Avail: CASI HC A03/MF A01

A joint NASA/FAA flight test has been made to record instrument landing system (ILS) localizer receiver signals for use in mathematically modeling the ILS localizer for future simulation studies and airplane flight tracking tasks. The flight test was conducted on a portion of the ILS localizer installed on runway 25L at the Los Angeles International Airport. The tests covered the range from 10 to 32 n.mi. from the localizer antenna.

Precision radar tracking information was compared with the recorded localizer deviation data. Data analysis showed that the ILS signal centerline was offset to the left of runway centerline by 0.071 degrees and that no significant bends existed on the localizer beam. Suggested simulation models for the ILS localizer are formed from a statistical analysis. Author

N95-17508 Army Topographic Engineering Center, Fort Belvoir, VA.
GPS TIDES AND DATUMS
Stephen R. DeLoach Jul. 1994 10 p Limited Reproducibility: More than 20% of this document may be affected by microfiche quality
(AD-A282422; USATEC-R-229) Avail: CASI HC A02

The recent development of On-The-Fly (OTF) ambiguity resolution techniques with Global Positioning System observations has created a powerful tool for the study of dynamic time series, such as tidal analysis or the study of water level heights. Using OTF technology it should be possible to obtain a time series of water surface heights to an accuracy of 1 to 2 centimeters, at a 1 second sampling rate, many kilometers from the nearest land. Subsequent time series analysis will yield a water surface datum at the receiver location. DTIC

N95-17706 Carnegie-Mellon Univ., Pittsburgh, PA. Robotics Inst.
A FEEDFORWARD CONTROL APPROACH TO THE LOCAL NAVIGATION PROBLEM FOR AUTONOMOUS VEHICLES
Alonzo Kelly 2 May 1994 71 p Limited Reproducibility: More than 20% of this document may be affected by microfiche quality
(Contracts DACA76-89-C-0014; DAAE07-90-C-R059)
(AD-A282787; CMU-RI-TR-94-17) Avail: CASI HC A04

RANGER is an acronym for Real-time Autonomous Navigator with a Geometric Engine. This report describes the 'geometric engine' part of RANGER - the state space model and the associated control algorithms. A new approach to the high speed autonomy problem is presented which is based fundamentally on the state space representation of a multi-input multi-output linear system. The system closes the overall perceive-think-act loop for a robot vehicle at relatively high update bandwidth and incorporates both somatic and environmental feedback. A high fidelity feedforward actuator dynamics and terrain following model is introduced which formulates the local navigation problem as an optimal control problem. The system is concerned with the high level coordinated control problem. It is a state space controller because it explicitly forms an expression of the vehicle dynamic state vector in order to predict the hazard signals upon which decisions are based. Derived from text

N95-16277# Nanjing Univ. of Aeronautics and Astronautics, Nanjing, Jiangsu (China). Dept. of Automatic Control.
APPLICATION OF GPS/SINS/RA INTEGRATED SYSTEM TO AIRCRAFT APPROACH LANDING
Xin Yuan, Jianye Liu, and Yongxi Ni *In its* Joint Proceedings on Aeronautics and Astronautics (JPAA) May 1993 p 184-190 See also A92-21466 (For primary document see N95-16249 04-01)
Avail: CASI HC A02/MF A03

N95-17196*# Centre National d'Etudes Spatiales, Toulouse (France).
A PROCESSING CENTRE FOR THE CNES CE-GPS EXPERIMENTATION
Norbert Suard and Jean-Claude Durand *In* NASA. Goddard Space Flight Center, Third International Symposium on Space Mission Operations and Ground Data Systems, Part 1 Nov. 1994 p 149-154 (For primary document see N95-17179 04-17)
Avail: CASI HC A02/MF A06

05 AIRCRAFT DESIGN, TESTING AND PERFORMANCE

Includes aircraft simulation technology.

For related information see also *18 Spacecraft Design, Testing and Performance* and *39 Structural Mechanics*.For land transportation vehicles see *85 Urban Technology and Transportation.*

N95-15971*# Rockwell International Corp., Downey, CA. Space Systems Div.
PROGRAM TEST OBJECTIVES MILESTONE 3
T. L. Gaynor 15 Nov. 1994 78 p
(Contract NCC8-47)
(NASA-CR-197030; NAS 1.26:197030; SSD94D0335) Avail: CASI HC A05/MF A01

The following conclusions have been developed relative to propulsion system technology adequacy for efficient development and operation of recoverable and expendable launch vehicles (RLV and ELV) and the benefits which the integrated propulsion technology demonstrator will provide for enhancing technology: (1) Technology improvements relative to propulsion system design and operation can reduce program cost. Many features or improvement needs to enhance operability, reduce cost, and improve payload are identified. (2) The Integrated Propulsion Technology Demonstrator (IPTD) Program provides a means of resolving the majority of issues associated with improvement needs. (3) The IPTD will evaluate complex integration of vehicle and facility functions in fluid management and propulsion control systems, and provides an environment for validating improved mechanical and electrical components. (4) The IPTD provides a mechanism for investigating operational issues focusing on reducing manpower and time to perform various functions at the launch site. These efforts include model development, collection of data to validate subject models, and ultimate development of complex time line models. (5) The IPTD provides an engine test bed for tri/bi-propellant engine development firings which is representative of the actual vehicle environment. (6) The IPTD provides for only a limited multiengine configuration integration environment for RLV. Multiengine efforts may be simulated for a number of subsystems and a number of subsystems are relatively independent of the multiengine influences. Derived from text

N95-16171# Loral Systems, Inc., Orlando, FL. Adst Program Office.
ADST SYSTEM TEST REPORT FOR THE ROTARY WING AIRCRAFT AIRNET AEROMODEL AND WEAPON MODEL MERGE WITH THE ATAC 2 BASELINE
Joe Almanza, Lynn Thompson, and Mary Kruck 20 Jan. 1994 290 p
(Contract N61339-91-D-0001)
(AD-A281580; ADST/WDL/TR-93-003274) Avail: CASI HC A13/MF A03

The results and corrective actions of the AIRNET/ATAC 2 test activities which were conducted at the Ft Rucker, AL, Aviation Training Facility during the periods of 8-12 February 1993 and 9-18 August 1993 are documented. DTIC

N95-16356# Naval Postgraduate School, Monterey, CA.
LOW RATE INITIAL PRODUCTION IN ARMY AVIATION SYSTEMS DEVELOPMENT M.S. Thesis
Lawrence P. Medler Mar. 1994 123 p
(AD-A281871) Avail: CASI HC A06/MF A02

The purpose of this thesis is to analyze DOD's use of Low Rate Initial Production (LRIP) on selected Army Aviation programs within the acquisitior. life cycle of weapon systems development. A comparative analysis is conducted on the selected programs concentrating on significant issues which affect the use of LRIP. The thesis focuses on the preproduction phases of the acquisition process, the organizations that influence LRIP policies and future trends in procurement policy. The research includes an examination of the AH-64 Longbow Apache, the OH-58D Kiowa Warrior, the MH-47 and the EH-60 Special Operations Aircraft and the RAH-66 Comanche. This thesis concludes that premature entry into LRIP is a systemic deficiency in acquisition oversight which leads to a proliferation in the required number of LRIP systems. A recommendation to overcome this deficiency and obtain a more accurate number is to identify the three LRIP quantity determination elements separately. This would provide the Milestone II Decision Authority more accurate data with which to render a decision. DTIC

N95-16562# Advisory Group for Aerospace Research and Development, Neuilly-Sur-Seine (France). Fluid Dynamics Panel.
OPTIMUM DESIGN METHODS FOR AERODYNAMICS [LES METHODES DE CONCEPTION OPTIMALE POUR L'AERODYNAMIQUE]
Nov. 1994 270 p Special course held in Rhode-Saint-Genese, Belgium, 25-29 Apr. 1994; sponsored by AGARD and VKI
(AGARD-R-803; ISBN-92-836-1007-5) Copyright Avail: CASI HC A12/MF A03

The course addresses the ingredients of new algorithms for accurate

and cost effective numerical solutions of design problems. A special emphasis is given to the following topics: fundamental mathematical properties of methodologies for solving optimization problems using control theory and variational formulations; numerical aspects of fast algorithms coupling constrained optimizers and flow analysis solvers and their implementation; geometric representations and choice of design variables; and real life 3-D applications encountered in Aerospace Engineering in order to demonstrate the usefulness of these design methodologies to practical design problems. For individual titles, see N95-16563 through N95-16573.

N95-16563# National Technical Univ., Athens (Greece). Lab. of Thermal Turbomachines.

SINGLE-PASS METHOD FOR THE SOLUTION OF INVERSE POTENTIAL AND ROTATIONAL PROBLEMS. PART 1: 2-D AND QUASI 3-D THEORY AND APPLICATION **c02**

P. Chaviaropoulos, V. Dedoussis (Piraeus Univ., Piraeus, Greece.), and K. D. Papailiou *In* AGARD, Optimum Design Methods for Aerodynamics Nov. 1994 19 p (For primary document see N95-16562 04-05)

Copyright Avail: CASI HC A03/MF A03

A methodology for the solution of the 2-D and 3-D inverse inviscid subsonic flow problem is introduced. The proposed methodology handles the 2-D and axisymmetric rotational and the 3-D potential target pressure problem in a single-pass manner. The method is based on a potential function/stream function formulation where the physical space is mapped onto a natural one using the potential and stream function(s) as body-fitted coordinates. A novel procedure based on differential geometry and generalized tensor analysis arguments is employed to formulate the method in a modular way. The governing equations for the inverse problem are derived through the metrics compatibility condition on the natural space. Geometry is determined by integrating generalized Frenet equations along the natural coordinate lines. Rotationality, when present, is due to incoming (stagnation) thermodynamic quantities and/or preswirl gradients. The Clebsch formulation is, then, adopted to decompose the velocity field into a potential and a rotational part. To validate the method inverse calculation results are compared to results of direct 'reproduction' calculations. The design procedure of some optimized shapes is also presented. Part 1 of this lecture focuses on 2-D and axisymmetric inverse potential or rotational flow problems, while the fully 3-D inverse potential problem is considered in Part 2. Author

N95-16564# National Technical Univ., Athens (Greece). Lab. of Thermal Turbomachines.

SINGLE-PASS METHOD FOR THE SOLUTION OF INVERSE POTENTIAL AND ROTATIONAL PROBLEMS. PART 2: FULLY 3-D POTENTIAL THEORY AND APPLICATIONS **c02**

P. Chaviaropoulos, V. Dedoussis (Piraeus Univ., Piraeus, Greece.), and K. D. Papailiou *In* AGARD, Optimum Design Methods for Aerodynamics Nov. 1994 14 p (For primary document see N95-16562 04-05)

Copyright Avail: CASI HC A03/MF A03

A potential function/stream function formulation is introduced for the solution of the fully 3-D inverse potential 'target pressure' problem. Potential function and two stream vectors are used as the independent natural coordinates, whilst the velocity magnitude, as well as, the aspect ratio and the cross-section angle of the elementary stream tubes are assumed to be the dependent ones. A novel procedure based on differential geometry is employed to formulate the method. The governing differential equations are derived by requiring the curvature tensor of the flat 3-D physical Euclidean space, expressed in terms of the curvilinear natural coordinates, to be zero. The resulting equations are discussed and investigated with particular emphasis to the existence and uniqueness of their solution. It is shown that the general 3-D inverse potential problem with target pressure boundary conditions only, is ill-posed accepting multiple solutions. This multiplicity is alleviated by considering elementary stream tubes with orthogonal cross-sections. The assumption of orthogonal stream surfaces reduces the number of dependent variables by one, simplifying the governing equations to an elliptic PDE, for the the velocity magnitude and to a second order ODE for the stream tube aspect ratio. The solution of these two equations provides the flow field. Geometry is determined independently by integrating Frenet equations along the natural coordinate lines, after the flow field has been calculated. The numerical implementation as well as validation test cases for the proposed inverse methodology are presented in the last part of the lecture. Author

N95-16565# Princeton Univ., NJ. Dept. of Mechanical and Aerospace Engineering.

OPTIMUM AERODYNAMIC DESIGN VIA BOUNDARY CONTROL

Antony Jameson *In* AGARD, Optimum Design Methods for Aerodynamics Nov. 1994 33 p Sponsored in cooperation with USRA (For primary document see N95-16562 04-05)

(Contract AF-AFOSR-0391-91; N00014-92-J-1976)

Copyright Avail: CASI HC A03/MF A03

These lectures describe the implementation of optimization techniques based on control theory for airfoil and wing design. In previous studies it was shown that control theory could be used to devise an effective optimization procedure for two-dimensional profiles in which the shape is determined by a conformal transformation from a unit circle, and the control is the mapping function. Recently the method has been implemented in an alternative formulation which does not depend on conformal mapping, so that it can more easily be extended to treat general configurations. The method has also been extended to treat the Euler equations, and results are presented for both two and three dimensional cases, including the optimization of a swept wing. Author

N95-16566# National Aerospace Lab., Amsterdam (Netherlands). Theoretical Aerodynamics Dept.

RESIDUAL-CORRECTION TYPE AND RELATED COMPUTATIONAL METHODS FOR AERODYNAMIC DESIGN. PART 1: AIRFOIL AND WING DESIGN

Th. E. Labrujere *In* AGARD, Optimum Design Methods for Aerodynamics Nov. 1994 24 p (For primary document see N95-16562 04-05)

Copyright Avail: CASI HC A03/MF A03

The present paper discusses the problem of inverse shape design, where the geometry of a wing should be determined such that it will have a prescribed surface pressure distribution at the design condition considered. A survey is given of so-called decoupled-solution methods or this problem. With this type of methods the flow field around a current estimate of the wing and a subsequent new estimate of the wing are determined by two separate computational steps in an iterative process. A global description is given of the main features of the underlying theories and some examples of application are given. A detailed description is given of the NLR method for inverse shape design based on the residual-correction approach. Author

N95-16567# National Aerospace Lab., Amsterdam (Netherlands). Theoretical Aerodynamics Dept.

RESIDUAL-CORRECTION TYPE AND RELATED COMPUTATIONAL METHODS FOR AERODYNAMIC DESIGN. PART 2: MULTI-POINT AIRFOIL DESIGN

Th. E. Labrujere *In* AGARD, Optimum Design Methods for Aerodynamics Nov. 1994 31 p (For primary document see N95-16562 04-05)

Copyright Avail: CASI HC A03/MF A03

The present paper considers the problem of multi-point airfoil design, where the geometry of an airfoil is to be determined such that it will approximate simultaneously, at different design points, a priori specified aerodynamic requirements. Some attention is paid to approaches published in the open literature. The main part of the paper concerns work in progress at NLR. Some preliminary results are shown. Author

N95-16568# Paris VI Univ. (France). Lab. Analyse Numerique.

OPTIMAL SHAPE DESIGN FOR AERODYNAMICS

O. Pironneau *In* AGARD, Optimum Design Methods for Aerodynamics Nov. 1994 38 p (For primary document see N95-16562 04-05)

Copyright Avail: CASI HC A03/MF A03

After a brief recall on the history of the field of optimal shape design, we shall present a few applications to aerodynamics, then recall the variational approach, the numerical methods and the recent developments both in applied mathematics and in computer sciences. Author

N95-16569*# National Aeronautics and Space Administration. Lewis Research Center, Cleveland, OH.

AIRFOIL OPTIMIZATION BY THE ONE-SHOT METHOD

G. Kuruvila (Vigyan Research Associates, Inc., Hampton, VA.), Shlomo

Taasan (Institute for Computer Applications in Science and Engineering, Hampton, VA.), and M. D. Salas *In* AGARD, Optimum Design Methods for Aerodynamics Nov. 1994 21 p (For primary document see N95-16562 04-05)
Copyright Avail: CASI HC A03/MF A03

An efficient numerical approach for the design of optimal aerodynamic shapes is presented in this paper. The objective of any optimization problem is to find the optimum of a cost function subject to a certain state equation (Governing equation of the flow field) and certain side constraints. As in classical optimal control methods, the present approach introduces a costate variable (Language multiplier) to evaluate the gradient of the cost function. High efficiency in reaching the optimum solution is achieved by using a multigrid technique and updating the shape in a hierarchical manner such that smooth (low-frequency) changes are done separately from high-frequency changes. Thus, the design variables are changed on a grid where their changes produce nonsmooth (high-frequency) perturbations that can be damped efficiently by the multigrid. The cost of solving the optimization problem is approximately two to three times the cost of the equivalent analysis problem. Author

N95-16570# Deutsche Airbus G.m.b.H., Bremen (Germany). Aerodynamic Design Section.
TOOLS FOR APPLIED ENGINEERING OPTIMIZATION
A. VanderVelden *In* AGARD, Optimum Design Methods for Aerodynamics Nov. 1994 10 p (For primary document see N95-16562 04-05)
Copyright Avail: CASI HC A02/MF A03

This paper is an introduction to applied optimization of engineering problems, with an emphasis on aircraft design. First, the optimization problem is described-namely, the objective function and the problems often involved in its optimization, the variables or parameters over which the objective function is optimized, and the constraints upon the objective function. Formulation of the optimization problem to ensure rapid and accurate convergence is discussed and illustrated with specific examples. Three classes of optimization methods: evolution, downhill simplex and gradient optimization, are discussed. The robustness and spéed of these optimization methods are evaluated and compared. Finally, a number of practical implementation issues related to optimization are highlighted. Author

N95-16571# Deutsche Airbus G.m.b.H., Bremen (Germany). Aerodynamic Design Section.
THE GLOBAL AIRCRAFT SHAPE
A. VanderVelden *In* AGARD, Optimum Design Methods for Aerodynamics Nov. 1994 11 p (For primary document see N95-16562 04-05)
Copyright Avail: CASI HC A03/MF A03

This work describes the methodology used to compare supersonic design concepts and its use in industry. The design concepts are analyzed with a modular synthesis model and compared on the basis of operating economy with specified performance and environmental impact. The analysis routines of the synthesis model are mainly configuration independent and represent fixed levels of structural, aerodynamic and propulsion technology. The specialist departments are responsible for the content of the routines, and later verify the design with more refined methods. At present more than two hundred variables describe the aircraft geometry, engine characteristics and mission. More than twenty of those variables representing the aircraft and its flight-profile are optimized simultaneously as a function of Mach number, payload and range. Because the various designs are analyzed with the same routines and optimization procedures they can be easily compared. This aircraft pre-optimization results in a significant reduction of the number of follow-on detail-design cycles, especially for non-conventional designs. Author

N95-16572# Deutsche Airbus G.m.b.H., Bremen (Germany). Aerodynamic Design Section.
AERODYNAMIC SHAPE OPTIMIZATION
A. VanderVelden *In* AGARD, Optimum Design Methods for Aerodynamics Nov. 1994 13 p (For primary document see N95-16562 04-05)
Copyright Avail: CASI HC A03/MF A03

This paper will discuss examples of aerodynamic shape optimization at Deutsche Airbus in Bremen. First, we will introduce a general approach to aerodynamic shape design based on minimization of aircraft life energy costs. Realistic constraints are introduced on lift, pitching moments and thickness. This method is applied to the quasi-3D design of multipoint transonic wings which are analyzed by a full potential code with a coupled boundary layer calculation. Finally, this method is applied to the wing-body design of a Supersonic Civil Transport that is analyzed with a linear potential code with real flow corrections and a decoupled boundary layer calculations. Author

N95-16573# Avions Marcel Dassault-Breguet Aviation, Saint-Cloud (France).
REVIEW OF THE EUROPT PROJECT AERO-0026
B. Mantel, J. Periaux, and B. Stoufflet *In* AGARD, Optimum Design Methods for Aerodynamics Nov. 1994 43 p (For primary document see N95-16562 04-05)
(Grant Brite-Euram-AERO-0026)
Copyright Avail: CASI HC A03/MF A03

Despite progress toward automated shape design in Industry has been penalized until now by excessive computing costs, useful innovative design methodologies have been recently proposed for computing different academic and industrial designs of nozzles, airfoils and wing-body combinations operating in inviscid flows modelled by the potential and Euler equations. Since the designer has a precise idea of the pressure distribution that will produce the desired performance, not only optimization problems but also inverse problems have to be considered in current design. The goal of this lecture is to describe the major ingredients of new algorithms developed by european partners of the AERO 89-0026 project, which allow accurate and cost effective numerical solutions of optimization problems and also to illustrate the capabilities of design software on test cases proposed in a Workshop for validation purpose. Industrial applications illustrating these methodologies are also presented. Finally a new emergent search method for non linear optimization problems provided by simple Genetic Algorithms (GA's) is briefly described and illustrated by a few examples related to inverse problems and applied to reduction of viscous drag. Author

N95-16899*# Old Dominion Univ., Norfolk, VA. Dept. of Mathematics and Statistics.
AUTOMATION OF REVERSE ENGINEERING PROCESS IN AIRCRAFT MODELING AND RELATED OPTIMIZATION PROBLEMS Progress Report, period ending Dec. 1994
W. Li and J. Swetits Nov. 1994 87 p
(Contract NCC1-68)
(NASA-CR-197109; NAS 1.26:197109; ODURF-124303) Avail: CASI HC A05/MF A01

During the year of 1994, the engineering problems in aircraft modeling were studied. The initial concern was to obtain a surface model with desirable geometric characteristics. Much of the effort during the first half of the year was to find an efficient way of solving a computationally difficult optimization model. Since the smoothing technique in the proposal 'Surface Modeling and Optimization Studies of Aerodynamic Configurations' requires solutions of a sequence of large-scale quadratic programming problems, it is important to design algorithms that can solve each quadratic program in a few interactions. This research led to three papers by Dr. W. Li, which were submitted to SIAM Journal on Optimization and Mathematical Programming. Two of these papers have been accepted for publication. Even though significant progress has been made during this phase of research and computation times was reduced from 30 min. to 2 min. for a sample problem, it was not good enough for on-line processing of digitized data points. After discussion with Dr. Robert E. Smith Jr., it was decided not to enforce shape constraints in order in order to simplify the model. As a consequence, P. Dierckx's nonparametric spline fitting approach was adopted, where one has only one control parameter for the fitting process - the error tolerance. At the same time the surface modeling software developed by Imageware was tested. Research indicated a substantially improved fitting of digitalized data points can be achieved if a proper parameterization of the spline surface is chosen. A winning strategy is to incorporate Dierckx's surface fitting with a natural parameterization for aircraft parts. The report consists of 4 chapters. Chapter 1 provides an overview of reverse engineering related to aircraft modeling and some preliminary findings of the effort in the second half of the year. Chapters 2-4 are the research results by Dr. W. Li on penalty functions and conjugate gradient methods for quadratic programming problems. Author (revised)

N95-16969# Electronics Research Lab., Salisbury (Australia).
A PC-BASED INTERACTIVE SIMULATION OF THE F-111C PAVE TACK SYSTEM AND RELATED SENSOR, AVIONICS AND AIRCRAFT ASPECTS
David A. Fogg, Mike Davies, Fred D. Bowden, and Ray Janus Mar. 1994 217 p
(AD-A285500; ERL-0656-RR; DODA-AR-007-005) Avail: CASI HC A10/MF A03

Pave Tack is an all weather, day and night, navigation and weapon delivery system fitted to the F-111C aircraft. A PC-based, interactive digital computer simulation has been written which can be used to assess the performance of the Pave Tack system and also as a computer-aided training device. In forming the simulation, it was necessary to model a number of avionics and sensor aspects and an F-111C flight path generator was used to produce accurate data off-line. This report details the history, structure and general capabilities of the F-111C Pave Tack Simulation (FPTS). DTIC

N95-16982* National Aeronautics and Space Administration, Washington, DC.
REVITALIZING GENERAL AVIATION (Videotape)
20 Jul. 1994 Videotape: 6 min. 30 sec. playing time, in color, with sound
(NASA-TM-110113; NASA-ASR-268; NONP-NASA-VT-95-35013) Avail: CASI VHS A02/BETA A22

This video contains a short feature of NASA and the FAA joint effort to incorporate new technology into the design of general aviation aircraft. CASI

N95-17397*# National Aeronautics and Space Administration. Langley Research Center, Hampton, VA.
ACTIVE LOAD CONTROL DURING ROLLING MANEUVERS
Jessica A. Woods-Vedeler, Anthony S. Pototzky (Lockheed Engineering and Sciences Co., Hampton, VA.), and Sherwood T. Hoadley Oct. 1994 61 p
(RTOP 505-63-36-01)
(NASA-TP-3455; L-17053; NAS 1.60:3455) Avail: CASI HC A04/MF A01

A rolling maneuver load alleviation (RMLA) system has been demonstrated on the active flexible wing (AFW) wind tunnel model in the Langley Transonic Dynamics Tunnel (TDT). The objective was to develop a systematic approach for designing active control laws to alleviate wing loads during rolling maneuvers. Two RMLA control laws were developed that utilized outboard control-surface pairs (leading and trailing edge) to counteract the loads and that used inboard trailing-edge control-surface pairs to maintain roll performance. Rolling maneuver load tests were performed in the TDT at several dynamic pressures that included two below and one 11 percent above open-loop flutter dynamic pressure. The RMLA system was operated simultaneously with an active flutter suppression system above open-loop flutter dynamic pressure. At all dynamic pressures for which baseline results were obtained, torsion-moment loads were reduced for both RMLA control laws. Results for bending-moment load reductions were mixed; however, design equations developed in this study provided conservative estimates of load reduction in all cases. Author

N95-17631# Naval Air Warfare Center, Warminster, PA. Air Vehicle and Crew Systems Technology Dept.
EVALUATION OF ALTERNATE F-14 WING LUG COATING Final Report, 1 Jan. 1991 - 30 Sep. 1993
Janet L. McGovern and Alan E. Ankeny 1 Dec. 1993 28 p
(AD-A283207; NAWCADWAR-93082-60) Avail: CASI HC A03/MF A01

The F-14 wing lug is coated with specific formulation polyurethane coating which prevents scoring of the wing lug by providing a wear surface for the outside diameter of the wing pivot bearing. The manufacture of this coating material was discontinued in 1991 because the original formulation used talcs which contained asbestos as impurities. The new formulation, containing asbestos free talcs, was inadequate in providing the abrasion resistance required to protect the F-14 wing lug. A new coating or coating process was required. A centrifugation processing procedure for the new formulation was developed which appeared to provide a coating that exhibited similar wear characteristics as the original coating. Oscillation wear tests were required to determine bearing wear performance of the alternate coating under normal and high stress in both the dry and fluid contaminated states. DTIC

N95-17661# Veda, Inc., Dayton, Ohio,
INDUSTRY REVIEW OF A CREW-CENTERED COCKPIT DESIGN PROCESS AND TOOLSET Interim Report, Aug. - Sep. 1993
Edward Lehman, Michael Rountree, Katherine Jackson, Brett Storey, and Philip Kulwicki Apr. 1994 81 p
(Contract F33615-92-C-5936)
(AD-A282966; Rept-63193-94U/P60099; AL/CF-TR-1994-0063) Avail: CASI HC A05/MF A01

This report contains the results of an industry review done for the Crew-Centered Cockpit Design (CCCD) Field Demonstration Program, USAF Contract F33615-92-C-5936. The objectives of the program are to upgrade and validate a new system for cockpit design. The system consists of a crew-centered system design process (CSDP) and a cockpit design system (CDS). The CSDP is intended to improve design practice, allowing designers to base decisions on mission requirements and crew capabilities while meeting installation constraints. The CDS offers improved design efficiency and includes traceability functions that preserve the rationale for design decisions. The CCCD Program Office recognizes that the acceptance and long-term utility of the CCCD products depend on the interest and support of the cockpit development community, which includes aircraft prime contractors and government aircraft acquisition organizations. For this reason, a survey of four aircraft prime contracts was made during August and September of 1993. The objective of the survey was to elicit end-user requirements for CCCD products. Information was obtained from engineers, scientists, and managers who are involved in different crew station activities including pilot-vehicle interface (PVI) design, crew station design, human factors analysis, systems engineering, and operational analysis. The report documents the results of the survey. DTIC

N95-16264# Kazan Aviation Inst. (USSR). Scientific School of Aircraft Strength.
DEVELOPMENT OF STRENGTH ANALYSIS METHODS AND DESIGN MODEL FOR AIRCRAFT CONSTRUCTIONS IN KAZAN AVIATION INSTITUTE
M. V. Vakhitov *In* Nanjing Univ. of Aeronautics and Astronautics, Joint Proceedings on Aeronautics and Astronautics (JPAA) May 1993 p 103-106 (For primary document see N95-16249 04-01)
Avail: CASI HC A01/MF A03

N95-17863# Deutsche Forschungsanstalt fuer Luft- und Raumfahrt, Brunswick (Germany). Inst. fuer Entwurfsaerodynamik.
DLR-F4 WING BODY CONFIGURATION
G. Redeker *In* AGARD, A Selection of Experimental Test Cases for the Validation of CFD Codes, Volume 2 Aug. 1994 21 p (For primary document see N95-17846 04-02)
Copyright Avail: CASI HC A03/MF A06

06 AIRCRAFT INSTRUMENTATION

Includes cockpit and cabin display devices; and flight instruments.

For related information see also *19 Spacecraft Instrumentation* and *35 Instrumentation and Photography.*

N95-15970*# National Aeronautics and Space Administration. Lewis Research Center, Cleveland, OH.
SENSOR FAULT DETECTION AND DIAGNOSIS SIMULATION OF A HELICOPTER ENGINE IN AN INTELLIGENT CONTROL FRAMEWORK
Jonathan Litt (Army Research Lab., Cleveland, OH.), Mehmet Kurtkaya (Florida Atlantic Univ., Boca Raton, FL.), and Ahmet Duyar (Florida Atlantic Univ., Boca Raton, FL.) Nov. 1994 15 p Presented at the 1994 Conference of Military, Government and Aerospace Simulation, San Diego, CA, 11-13 Apr. 1994; sponsored by Society for Computer Simulation Prepared in cooperation with Army Research Lab., Cleveland, OH
(Grant NAG3-1198; RTOP 505-62-0X; DA Proj. 1L1-61102-AH-45)
(NASA-TM-106784; E-9237; NAS 1.15:106784; ARL-TR-637) Avail: CASI HC A03/MF A01

This paper presents an application of a fault detection and diagnosis

scheme for the sensor faults of a helicopter engine. The scheme utilizes a model-based approach with real time identification and hypothesis testing which can provide early detection, isolation, and diagnosis of failures. It is an integral part of a proposed intelligent control system with health monitoring capabilities. The intelligent control system will allow for accommodation of faults, reduce maintenance cost, and increase system availability. The scheme compares the measured outputs of the engine with the expected outputs of an engine whose sensor suite is functioning normally. If the differences between the real and expected outputs exceed threshold values, a fault is detected. The isolation of sensor failures is accomplished through a fault parameter isolation technique where parameters which model the faulty process are calculated on-line with a real-time multivariable parameter estimation algorithm. The fault parameters and their patterns can then be analyzed for diagnostic and accommodation purposes. The scheme is applied to the detection and diagnosis of sensor faults of a T700 turboshaft engine. Sensor failures are induced in a T700 nonlinear performance simulation and data obtained are used with the scheme to detect, isolate, and estimate the magnitude of the faults. Author

N95-16456*# National Aeronautics and Space Administration. Langley Research Center, Hampton, VA.
A STUDY OF SOFTWARE STANDARDS USED IN THE AVIONICS INDUSTRY
Kelly J. Hayhurst *In its* The Role of Computers in Research and Development at Langley Research Center Oct. 1994 p 85-105 (For primary document see N95-16453 04-62)
Avail: CASI HC A03/MF A06

07 AIRCRAFT PROPULSION AND POWER

Includes prime propulsion systems and systems components, e.g., gas turbine engines and compressors; and onboard auxilliary power plants for aircraft.

For related information see also *20 Spacecraft Propulsion and Power, 28 Propellants and Fuels,* and *44 Energy Production and Conversion.*

N95-17371# Pacific Northwest Lab., Richland, WA.
AN ARTIFICIAL NEURAL NETWORK SYSTEM FOR DIAGNOSING GAS TURBINE ENGINE FUEL FAULTS
O. J. Illi, Jr. (Army Ordnance Center and School, Aberdeen Proving Ground, MD.), F. L. Greitzer, L. J. Kangas, and T. Reeve (Expert Solutions, Stratford, CT.) Apr. 1994 10 p Presented at the Mechanical Failures Prevention Group Conference, Wakefield, MA, 19-21 Apr. 1994
(Contract DE-AC06-76RL-01830)
(DE94-013960; PNL-SA-22914; CONF-9404179-1) Avail: CASI HC A02/MF A01

The US Army Ordnance Center and School and Pacific Northwest Laboratories are developing a turbine engine diagnostic system for the M1A1 Abrams tank. This system employs artificial neural network (ANN) technology to perform diagnosis and prognosis of the tank's AGT-1500 gas turbine engine. This paper describes the design and prototype development of the ANN component of the diagnostic system, which we refer to as 'TEDANN' for turbine engine diagnostic artificial neural networks. DOE

N95-17402*# Case Western Reserve Univ., Cleveland, OH. Dept. of Mechanical and Aerospace Engineering.
THREE DIMENSIONAL COMPRESSIBLE TURBULENT FLOW COMPUTATIONS FOR A DIFFUSING S-DUCT WITH/WITHOUT VORTEX GENERATORS Final Report
Soo-Yong Cho and Isaac Greber NASA Dec. 1994 216 p
(Contract NCC3-181; RTOP 505-62-52)
(NASA-CR-195390; E-9160; NAS 1.26:195390) Avail: CASI HC A10/MF A03

Numerical investigations on a diffusing S-duct with/without vortex generators and a straight duct with vortex generators are presented. The investigation consists of solving the full three-dimensional unsteady compressible mass averaged Navier-Stokes equations. An implicit finite volume lower-upper time marching code (RPLUS3D) has been employed and modified. A three-dimensional Baldwin-Lomax turbulence model has been modified in conjunction with the flow physics. A model for the analysis of vortex generators in a fully viscous subsonic internal flow is evaluated. A vortical structure for modeling the shed vortex is used as a source term in the computation domain. The injected vortex paths in the straight duct are compared with the analysis by two kinds of prediction models. The flow structure by the vortex generators are investigated along the duct. Computed results of the flow in a circular diffusing S-duct provide an understanding of the flow structure within a typical engine inlet system. These are compared with the experimental wall static-pressure, static- and total-pressure field, and secondary velocity profiles. Additionally, boundary layer thickness, skin friction values, and velocity profiles in wall coordinates are presented. In order to investigate the effect of vortex generators, various vortex strengths are examined in this study. The total-pressure recovery and distortion coefficients are obtained at the exit of the S-duct. The numerical results clearly depict the interaction between the low velocity flow by the flow separation and the injected vortices. Author

N95-17749 Jiaotong Univ., Shanghai (China).
SIMULATION INVESTIGATION ON SYSTEM IDENTIFICATION OF GAS TURBINE
M. Su 1993 8 p Sponsored by Institute of Scientific and Technical Information of China, Beijing
(PB95-104238; ISTIC-TR-93123) Avail: Issuing Activity (National Technical Information Service (NTIS))

To this paper the hybrid simulation system for identification is introduced. The analysis and the comparison between the results in open loop and closed loop are made. Three different speed regulators are tested in closed loop identification simulation experiments. The effect of external input signal on identification results is examined. A piecewise linear model of a marine gas turbine is developed. NTIS

N95-16265# Kazan Aviation Inst. (USSR).
THEORETICAL FUNDAMENTALS OF THE AIRCRAFT GTE TESTS
Yu. V. Kozhevnikov *In* Nanjing Univ. of Aeronautics and Astronautics, Joint Proceedings on Aeronautics and Astronautics (JPAA) May 1993 p 107-111 (For primary document see N95-16249 04-01)
Avail: CASI HC A01/MF A03

N95-16317# General Electric Co., Cincinnati, OH. Aircraft Engine Div.
SCRAMJET TESTING GUIDELINES Status Report
P. Kutschenreuter *In* JHU, The 1993 JANNAF Propulsion Meeting, Volume 1 Nov. 1993 p 247-259 (For primary document see N95-16312 04-20)
Avail: CPIA, 10630 Little Patuxent Pkwy., Suite 202, Columbia, MD 21044-3200 HC

N95-16323# Sundstrand Power Systems, San Diego, CA.
SMALL TURBOJETS: DESIGNS AND INSTALLATIONS
C. Rodgers *In* JHU, The 1993 JANNAF Propulsion Meeting, Volume 1 Nov. 1993 p 335-352 (For primary document see N95-16312 04-20)
Avail: CPIA, 10630 Little Patuxent Pkwy., Suite 202, Columbia, MD 21044-3200 HC

08 AIRCRAFT STABILITY AND CONTROL

Includes aircraft handling qualities; piloting; flight controls; and autopilots.

For related information see also *05 Aircraft Design, Testing and Performance.*

N95-16109 Naval Postgraduate School, Monterey, CA.
A COMPUTATIONAL INVESTIGATION OF WAKE-INDUCED AIRFOIL FLUTTER IN INCOMPRESSIBLE FLOW AND ACTIVE FLUTTER CONTROL M.S. Thesis
Mark A. Turner Mar. 1994 108 p Limited Reproducibility: More than 20% of this document may be affected by microfiche quality
(AD-A281534) Avail: Issuing Activity (Defense Technical Information Center (DTIC))

Several incompressible oscillatory flow and flutter problems were investigated. A previously developed unsteady panel code for single airfoil bending torsion flutter analysis was compared to Theodorsen's classical

theory. The panel code agrees with Theodorsen's bending-torsion flutter analysis for natural frequency ratios (omega sub h/omega sub alpha) less than 1.2. Also, a two airfoil unsteady panel code was modified for one degree of freedom flutter analysis. Code verification was completed by first comparing flat plate theory to the unsteady aerodynamic force and moment coefficients and then using the equation of motion to determine regions of instability. The possibility of active flutter control was investigated by positioning a small control airfoil in front of a neutrally stable reference airfoil. Results show that the flutter boundary may be changed through the placement, oscillation, or scaling of a second airfoil upstream. A comparison with pitch damping curves published by Loewy confirms that the code is capable of predicting wake-induced airfoil flutter. DTIC

N95-16381 Wright Lab., Eglin AFB, FL. Armament Directorate.
AUTONOMOUS WEAPON GUIDANCE Final Report, Jan. - Sep. 1993
John L. Dargan 3 May 1994 66 p Limited Reproducibility: More than 20% of this document may be affected by microfiche quality
(AF Proj. 670B)
(AD-A282715; WL-TR-94-7033) Avail: CASI HC A04

Precision guided weapons are becoming more and more sophisticated. Terminology such as global positioning system, differential global positioning system, laser radar, synthetic aperture radar, inertial navigation system, and Kalman filtering have become prevalent as weapons are made smarter and more precise. This study comprised an examination of the midcourse and terminal navigation and guidance schemes implemented in the Armament Directorate's advanced development guidance programs. The implementation of these navigation and guidance schemes allows the weapon to be more precise. This report describes these implementations and provides a background for the engineer or manager on the elements that comprise an autonomously guided weapon. DTIC

N95-16392# National Aeronautical Lab., Bangalore (India). Civil Aviation Unit.
EVALUATION OF THE DYNAMIC STABILITY CHARACTERISTICS OF THE NAL LIGHT TRANSPORT AIRCRAFT
S. M. Kannan Dec. 1992 33 p
(NAL Proj. ID-8-117L)
(NAL-PD-CA-9217) Avail: CASI HC A03/MF A01

A study of the dynamic stability characteristics of the NAL Light Transport Aircraft, LTA-7 is made in this report. The dynamic stability derivatives of the aircraft are evaluated at low angles of attack (unseparated flows) and incompressible flows. A comparison is made of the estimated derivatives with the range of experimental values available in the open literature for light aircraft for validation of the computer code used. The characteristic equations of the linear small disturbance equations of motion for both the longitudinal and the lateral dynamics are solved and the stability characteristics evaluated. A discussion of the flying qualities vis-a-vis the FAR regulations is also made. Author

N95-17404*# Maryland Univ., College Park, MD. Dept. of Aerospace Engineering.
COOPERATIVE CONTROL THEORY AND INTEGRATED FLIGHT AND PROPULSION CONTROL Final Report, 1990-1993
David K. Schmidt and John D. Schierman Nov. 1994 104 p
(Grant NAG3-998)
(NASA-CR-197493; NAS 1.26:197493) Avail: CASI HC A06/MF A02

This report documents the activities and research results obtained under a grant (NAG3-998) from the NASA Lewis Research Center. The focus of the research was the investigation of dynamic interactions between airframe and engines for advanced ASTOVL aircraft configurations, and the analysis of the implications of these interactions on the stability and performance of the airframe and engine control systems. In addition, the need for integrated flight and propulsion control for such aircraft was addressed. The major contribution of this research was the exposition of the fact that airframe and engine interactions could be present, and their effects could include loss of stability and performance of the control systems. Also, the significance of two directional, as opposed to one-directional, coupling was identified and explained. A multi variable stability and performance analysis methodology was developed, and applied to several candidate aircraft configurations. Also exposed was the fact that with interactions present along with some integrated control approaches, the engine command/limiting logic (which represents an important non-linear component of the engine control system) can impact closed-loop airframe/engine system stability. Finally, a brief investigation of control-law synthesis techniques appropriate for the class of systems was pursued, and it was determined that multi variable techniques, included model-following formulations of LQG and/or H (infinity) methods showed promise. However, for practical reasons, decentralized control architectures are preferred, which is an architecture incompatible with these synthesis methods.
Author (revised)

N95-17454 National Defence Research Establishment, Stockholm (Sweden). Dept. of Weapon Systems, Effects and Protection.
EVALUATION OF AN AUTOPILOT BASED MULTIMODELLING [UTVAERDERING AV STYRAUTOMAT FOER MISSILER, BASERAD PA MULTIMODELLERING]
S. L. Wirkander Jan. 1994 49 p In SWAHILI
(PB94-190725; FOA-C-20957-2.1) Avail: Issuing Activity (National Technical Information Service (NTIS))

The report describes an investigation and development of the autopilot, which was described in an earlier report. This autopilot law was based on a library, consisting of missile models corresponding to different speeds and altitudes, which makes it possible to give the missile the same guidance properties independently of speed and altitude. In the present report an autopilot of a conventional type is constructed, with the intention to constitute an object of comparison for the multimodel autopilot. The report presents such a comparison, in which it is demonstrated that the multimodel autopilot works satisfactorily for all speeds and altitudes for which it has models, whereas the conventional one works only in the neighborhood of one special (nominal) speed-altitude combination. It is also shown that the multimodel autopilot can be improved by means of interpolation between the models in the library. This version of multimodel autopilot is always preferable, because of its superior controlling qualities. In this investigation the same library has been used as in the earlier report. NTIS

09 RESEARCH AND SUPPORT FACILITIES (AIR)

Includes airports, hangars and runways; aircraft repair and overhaul facilities; wind tunnels; shock tubes; and aircraft engine test stands.

For related information see also *14 Ground Support Systems and Facilities (Space).*

N95-16509# Sandia National Labs., Albuquerque, NM.
ERROR PROPAGATION EQUATIONS FOR ESTIMATING THE UNCERTAINTY IN HIGH-SPEED WIND TUNNEL TEST RESULTS
E. L. Clark 1994 22 p Presented at the 18th American Institute of Aeronautics and Astronautics (AIAA) Aerospace Ground Test Conference, Colorado Springs, CO, 20-23 Jun. 1994
(Contract DE-AC04-94AL-85000)
(DE94-014136; SAND-93-0208C; CONF-9406188-1) Avail: CASI HC A03/MF A01

Error propagation equations, based on the Taylor series model, are derived for the nondimensional ratios and coefficients most often encountered in high-speed wind tunnel testing. These include pressure ratio and coefficient, static force and moment coefficients, dynamic stability coefficients, and calibration Mach number. The error equations contain partial derivatives, denoted as sensitivity coefficients, which define the influence of free-steam Mach number, M sub infinity, on various aerodynamic ratios. To facilitate use of the error equations, sensitivity coefficients are derived and evaluated for five fundamental aerodynamic ratios which relate free-steam test conditions to a reference condition. DOE

N95-17388# Advisory Group for Aerospace Research and Development, Neuilly-Sur-Seine (France). Flight Mechanics Panel.
AIRCRAFT AND SUB-SYSTEM CERTIFICATION BY PILOTED SIMULATION [HOMOLOGATION DES AERONEFS ET DE LEURS SOUS-SYSTEMES PAR LA SIMULATION PILOTEE]
Sep. 1994 53 p
(AGARD-AR-278; ISBN-92-835-0757-6) Copyright Avail: CASI HC A04/MF A01

There is a steadily increasing tendency to use piloted flight simulators for official clearance of selected areas of flight envelopes and of system behavior or malfunctions. This is a natural and desirable evolution from

the wide use of simulation during the development of new aircraft. However, there is a lack of guidance for certification authorities and aircraft manufacturers on simulation standards, validation procedures and general information on the advantages and disadvantages of using simulation as part of a clearance program. This could lead to either inappropriate use of simulators, or unnecessary (and costly) reluctance to use simulation when it is appropriate. In particular, there is concern by many involved with research and engineering development simulators that subjective pilot opinion is often the primary criterion for acceptance of simulators for certification activities. However, clearance demonstrations on a simulator will not usually be experienced in flight until an operational pilot encounters the conditions or configurations of the clearance. Thus validation of the simulator for clearance tasks must involve rigorous model and simulation system validation as well as pilot subjective tests. Subjective adjustments are unacceptable. Working Group 16 was formed by the Flight Mechanics Panel of AGARD to produce an Advisory Report on this subject. The aim was to provide advice and guidance to Certification and Acceptance Authorities, and Aircraft Manufacturers on the appropriate use of piloted simulation as the sole demonstration for aircraft and system flight clearances. The Group included members from Canada, Germany, Italy, Netherlands, United Kingdom and the United States. Government R&D Establishments, Armed Service R&D Establishments, and aircraft and simulator manufacturers were all represented. Author

N95-17444 Air Force Inst. of Tech., Wright-Patterson AFB, OH. School of Engineering.
DEVELOPMENT OF AN AUTOMATED AIRFIELD DYNAMIC CONE PENETROMETER (AADCP) PROTOTYPE AND THE EVALUATION OF UNSURFACED AIRFIELD SEISMIC SURVEYING USING SPECTRAL ANALYSIS OF SURFACE WAVES (SASW) TECHNOLOGY M.S. Thesis
David Weintraub Dec. 1993 327 p Limited Reproducibility: More than 20% of this document may be affected by microfiche quality
(AD-A281985; AFIT/CI/CIA-94-013D) Avail: Issuing Activity (Defense Technical Information Center (DTIC))

The mission of U.S. Air Force Combat Controllers is to infiltrate unused airfields. A specially trained evaluation team, carrying limited portable testing equipment, evaluates the unsurfaced airfield for use as a landing zone. The equipment used to evaluate the bearing capacity of the airfield is the Dynamic Cone Penetrator (DCP). Empirically based relationships are used to predict the type and number of aircraft passes on the unsurfaced airfield based on inputs from the DCP. It was the goal of this research to improve on the field testing equipment used in the unsurfaced airfield evaluation process. DTIC

N95-16258# Nanjing Univ. of Aeronautics and Astronautics, Nanjing, Jiangsu (China). Dept. of Aerodynamics.
AN INVESTIGATION OF POLYNOMIAL CALIBRATIONS METHODS FOR WIND TUNNEL BALANCES
Buzhang Han and Ingmar Johnson (Aeronautical Research Inst. of Sweden, Bromma.) *In its* Joint Proceedings on Aeronautics and Astronautics (JPAA) May 1993 p 63-66 (For primary document see N95-16249 04-01)
Avail: CASI HC A01/MF A03

N95-16318# Arnold Engineering Development Center, Arnold AFS, TN.
A MODEL FOR PRELIMINARY FACILITY DESIGN INCLUDING SIMULATION ISSUES
E. S. Powell *In* JHU, The 1993 JANNAF Propulsion Meeting, Volume 1 Nov. 1993 p 261-274 (For primary document see N95-16312 04-20)
Avail: CPIA, 10630 Little Patuxent Pkwy., Suite 202, Columbia, MD 21044-3200 HC

N95-16319# Arnold Engineering Development Center, Arnold AFS, TN.
HYPERSONIC AIR-BREATHING AEROPROPULSION FACILITY TEST SUPPORT REQUIREMENTS
Brian Wettlaufer *In* JHU, The 1993 JANNAF Propulsion Meeting, Volume 1 Nov. 1993 p 275-292 (For primary document see N95-16312 04-20)
Avail: CPIA, 10630 Little Patuxent Pkwy., Suite 202, Columbia, MD 21044-3200 HC

N95-16320*# General Applied Science Labs., Inc., Ronkonkoma, NY.
FREE-JET TESTING AT MACH 3.44 IN GASL'S AERO/THERMO TEST FACILITY
D. Cresci, S. Koontz, and C. Y. Tsai *In* JHU, The 1993 JANNAF Propulsion Meeting, Volume 1 Nov. 1993 p 293-307 (For primary document see N95-16312 04-20)
(Contract NAS1-18450)
Avail: CPIA, 10630 Little Patuxent Pkwy., Suite 202, Columbia, MD 21044-3200 HC

12 ASTRONAUTICS (GENERAL)

For extraterrestrial exploration see *91 Lunar and Planetary Exploration.*

N95-16033*# National Academy of Sciences - National Research Council, Washington, DC.
[ACTIVITIES OF THE SPACE STUDIES BOARD] Annual Report, 1993
1994 51 p
(Contracts NASw-4627; NOAA-50-DGNE-1-00138; N00173-93-P-6207)
(NASA-CR-197105; NAS 1.26:197105) Avail: CASI HC A04/MF A01

This 1993 annual report of the Space Studies Board of the National research Council (NRC) describes the activities of the Board during a year filled with questions and change in the nation's civil space program. The accounts contained in this report briefly describe the activities of the Board and its committees and sketch out major space research issues. Two major reports are summarized, and the full text of three letter reports is included. Items considered include: (1) robotic missions to explore the Earth, the solar system, and the far reaches of the universe; (2) instability in the human flight program; (3) the redesign of the International Space Station; and (4) federal funding of research in all fields, especially basic research. Author (revised)

N95-16530# Massachusetts Inst. of Tech., Cambridge. Lincoln Lab.
PROCEEDINGS OF THE 12TH ANNUAL SPACE SURVEILLANCE WORKSHOP, VOLUME 1
K. P. Schwan 7 Apr. 1994 253 p Workshop held in Lexington, MA, 5-7 Apr. 1994
(Contract F19628-90-C-0002)
(AD-A285265; STK-221-Vol-1; ESC-TR-94-083-Vol-1) Avail: CASI HC A12/MF A03

The twelfth Annual Space Surveillance Workshop hosted by MIT Lincoln Laboratory was held 5-7 April 1994. The purpose of this series of workshops is to provide a forum for the presentation and discussion of space surveillance issues. This Proceedings documents most of the presentations from this workshop. The papers contained were reproduced directly from copies supplied by their authors (with minor mechanical changes where necessary). It is hoped that this publication will enhance the utility of the workshop. DTIC

N95-16842 Massachusetts Inst. of Tech., Lexington. Lincoln Lab.
PROCEEDINGS OF THE 12TH SPACE SURVEILLANCE WORKSHOP, VOLUME 2
K. P. Schwan 7 Apr. 1994 67 p Workshop held in Lexington, MA, 5-7 Apr. 1994 Limited Reproducibility: More than 20% of this document may be affected by microfiche quality
(Contract F19628-90-C-0002)
(AD-A285115; STK-221-Vol-2; ESC-TR-94-091-Vol-2) Avail: CASI HC A04

The twelfth Annual Space Surveillance Workshop hosted by MIT Lincoln Laboratory was held 5-7 April 1994. The purpose of this series of workshops is to provide a forum for the presentation and discussion of space surveillance issues. This Proceedings documents most of the presentations from this workshop that did not appear in Vol. 1. The papers contained were reproduced directly from copies supplied by their authors (with minor mechanical changes where necessary). It is hoped that this publication will enhance the utility of the workshop. DTIC

N95-17427 RAND Corp., Santa Monica, CA.
EMERGING NATIONAL SPACE LAUNCH PROGRAMS: ECONOMICS AND SAFEGUARDS

Brian G. Chow 1993 85 p Limited Reproducibility: More than 20% of this document may be affected by microfiche quality
(Contract MDA903-90-C-0004)
(AD-A282107; RAND/R-4179-USDP) Avail: Issuing Activity (Defense Technical Information Center (DTIC))

Most ballistic missile nonproliferation studies have focused on trends in the numbers and performance of missiles and the resulting security threats. This report concentrates on the economic viability of emerging national space launch programs and the prospects for imposing effective safeguards against the use of space launch technology for military missiles. For the convenience of discussion in this report, a reference to ballistic missiles hereafter means surface-to-surface guided ballistic missiles only. Space launch vehicles (SLV's) are surface-to-space ballistic missiles, and they will be referred to explicitly as 'space launch vehicles' or 'space launchers'. Surface-to-surface unguided ballistic missiles will be referred to as 'rockets.' DTIC

N95-15978*# Jet Propulsion Lab., California Inst. of Tech., Wrightwood, CA.
USING VIRTUAL REALITY FOR SCIENCE MISSION PLANNING: A MARS PATHFINDER CASE
Jacqueline H. Kim, Richard J. Weidner, and Allan L. Sacks *In* NASA. Johnson Space Center, ISMCR 1994: Topical Workshop on Virtual Reality. Proceedings of the Fourth International Symposium on Measurement and Control in Robotics Nov. 1994 p 37-46 (For primary document see N95-15972 04-63)
Avail: CASI HC A02/MF A02

N95-17212*# Massachusetts Inst. of Tech., Cambridge. Lincoln Lab.
MISSION PLANNING FOR SPACE BASED SATELLITE SURVEILLANCE EXPERIMENTS WITH THE MSX
R. Sridharan, T. Fishman, E. Robinson, H. Viggh, and A. Wiseman *In* NASA. Goddard Space Flight Center, Third International Symposium on Space Mission Operations and Ground Data Systems, Part 1 Nov. 1994 p 295-303 (For primary document see N95-17179 04-17)
Avail: CASI HC A02/MF A06

N95-17213*# European Space Agency. European Space Operations Center, Darmstadt (Germany).
ENGINEERING ULYSSES EXTENDED MISSION
Shaun Standley *In* NASA. Goddard Space Flight Center, Third International Symposium on Space Mission Operations and Ground Data Systems, Part 1 Nov. 1994 p 305-309 (For primary document see N95-17179 04-17)
Avail: CASI HC A01/MF A06

N95-17215*# Massachusetts Inst. of Tech., Cambridge. Lincoln Lab.
JOINT OPERATIONS PLANNING FOR SPACE SURVEILLANCE MISSIONS ON THE MSX SATELLITE
Grant Stokes and Andrew Good (Johns Hopkins Univ., Laurel, MD.) *In* NASA. Goddard Space Flight Center, Third International Symposium on Space Mission Operations and Ground Data Systems, Part 1 Nov. 1994 p 319-326 (For primary document see N95-17179 04-17)
Avail: CASI HC A02/MF A06

N95-17216*# Jet Propulsion Lab., California Inst. of Tech., Pasadena, CA.
INTERNATIONAL MISSION PLANNING FOR SPACE VERY LONG BASELINE INTERFEROMETRY
James S. Ulvestad *In* NASA. Goddard Space Flight Center, Third International Symposium on Space Mission Operations and Ground Data Systems, Part 1 Nov. 1994 p 329-336 (For primary document see N95-17179 04-17)
Avail: CASI HC A02/MF A06

13 ASTRODYNAMICS

Includes powered and free-flight trajectories; and orbital and launching dynamics.

N95-17648# Instituto de Pesquisas Espaciais, Sao Paulo (Brazil).
OPTIMAL TRANSFER AND SWING-ORBITS IN THE TWO- AND THREE-BODY PROBLEMS Ph.D. Thesis - Texas Univ.
Antonio Fernando BertachinideAlmeidaPrado 1993 256 p
(INPE-5572-TAE/022) Avail: CASI HC A12/MF A03

This dissertation deals with the general topic of transfer orbits in the two- and three-body problems. Several problems are considered. Those problems are related to each other in the sense that they all have similar goals (to find transfer orbits suitable for a defined task) and that they use similar models for the dynamics (two-body Keplerian orbits or restricted three-body problem). In that way, every chapter can be studied separately and all the background information required from previous chapters is mentioned briefly. An effort is made to keep the duplication of information in the whole dissertation to a minimum level, just enough for the clarity of the ideas presented. The nomenclature used is the standard in the literature for each problem. Every symbol is defined the first time that it is used. In a few cases the same symbol is used for two different chapters with different meanings. An effort is made to keep this repetition of symbols to a minimum, to avoid confusion. The total elimination of this repetition would introduce too many symbols completely different from the standard ones used in the literature. Every time this duplication occurs, it is identified and the new meaning of the symbol is redefined. There is no such repetition in a single chapter. The goals and motivation of this dissertation and the definition of each particular problem treated are made in every chapter, since they vary from chapter to chapter. The conclusions are also presented in each chapter, instead of in an exclusive chapter, for the same reason. Derived from text

N95-17544*# Storm Integration, Inc., San Jose, CA.
IMPLEMENTATION OF A LOW-COST, COMMERCIAL ORBIT DETERMINATION SYSTEM
Jim Corrigan *In* NASA. Goddard Space Flight Center, Third International Symposium on Space Mission Operations and Ground Data Systems, Part 2 Nov. 1994 p 773-783 (For primary document see N95-17531 04-17)
Avail: CASI HC A03/MF A06

N95-17547*# Mitre Corp., Bedford, MA.
TDRS ORBIT DETERMINATION BY RADIO INTERFEROMETRY
Michael S. Pavloff *In* NASA. Goddard Space Flight Center, Third International Symposium on Space Mission Operations and Ground Data Systems, Part 2 Nov. 1994 p 799-806 (For primary document see N95-17531 04-17)
Avail: CASI HC A02/MF A06

14 GROUND SUPPORT SYSTEMS AND FACILITIES (SPACE)

Includes launch complexes, research and production facilities; ground support equipment, e.g., mobile transporters; and simulators.

For related information see also *09 Research and Support Facilities (Air).*

N95-16266# Kazan Aviation Inst. (USSR).
DEVELOPMENT OF THE VIBRATION TEST EQUIPMENT FOR TESTING THE PRODUCTS OF AIRCRAFT AND SPACE TECHNOLOGY WITH SIMULATION OF OPERATING CONDITIONS
Ya. S. Uretskii *In* Nanjing Univ. of Aeronautics and Astronautics, Joint Proceedings on Aeronautics and Astronautics (JPAA) May 1993 p 112-117 (For primary document see N95-16249 04-01)
Avail: CASI HC A02/MF A03

N95-17223*# Centre National d'Etudes Spatiales, Toulouse (France).
SPOT4 MANAGEMENT CENTRE
Yves Labrune, X. Labbe (Compagnie Internationale de Service en

Informatique, Toulouse, France.), A. Roussel (Compagnie Internationale de Service en Informatique, Toulouse, France.), and P. Vielcanet (Compagnie Internationale de Service en Informatique, Toulouse, France.) *In* NASA. Goddard Space Flight Center, Third International Symposium on Space Mission Operations and Ground Data Systems, Part 1 Nov. 1994 p 389-396 (For primary document see N95-17179 04-17)
Avail: CASI HC A02/MF A06

N95-17250*# Centre National d'Etudes Spatiales, Toulouse (France).
TOWARDS CHEAPER CONTROL CENTERS
Lionel Baize *In* NASA. Goddard Space Flight Center, Third International Symposium on Space Mission Operations and Ground Data Systems, Part 1 Nov. 1994 p 617-624 (For primary document see N95-17179 04-17)
Avail: CASI HC A02/MF A06

N95-17251*# European Space Agency, Redu (Belgium).
THE SILEX EXPERIMENT SYSTEM OPERATIONS
B. Demelenne *In* NASA. Goddard Space Flight Center, Third International Symposium on Space Mission Operations and Ground Data Systems, Part 1 Nov. 1994 p 625-631 (For primary document see N95-17179 04-17)
Avail: CASI HC A02/MF A06

N95-17253*# European Space Agency. European Space Operations Center, Darmstadt (Germany). Flight Control Systems Dept.
SCOS 2: ESA'S NEW GENERATION OF MISSION CONTROL SYSTEM
M. Jones, N. C. Head, K. Keyte (Vitrociset S.p.A., Rome, Italy.), P. Howard (Science Systems Ltd., Bristol, England.), and S. Lynenskjold (Computer Resources International A/S, Denmark.) *In* NASA. Goddard Space Flight Center, Third International Symposium on Space Mission Operations and Ground Data Systems, Part 1 Nov. 1994 p 641-654 (For primary document see N95-17179 04-17)
Avail: CASI HC A02/MF A06

N95-17254*# Compagnie Internationale de Service en Informatique, Toulouse (France). Aerospace Branch.
CCS-MIP: LOW COST CUSTOMIZABLE CONTROL CENTRE
Christian Labezin and Pierre Vielcanet *In* NASA. Goddard Space Flight Center, Third International Symposium on Space Mission Operations and Ground Data Systems, Part 1 Nov. 1994 p 649-654 (For primary document see N95-17179 04-17)
Avail: CASI HC A02/MF A06

N95-17255*# Computer Sciences Corp., Lanham, MD. Astronomy Programs.
THE IUE SCIENCE OPERATIONS GROUND SYSTEM
Ronald E. Pitts and Richard Arquilla *In* NASA. Goddard Space Flight Center, Third International Symposium on Space Mission Operations and Ground Data Systems, Part 1 Nov. 1994 p 655-662 (For primary document see N95-17179 04-17)
Avail: CASI HC A02/MF A06

N95-17256*# Loral AeroSys, Seabrook, MD.
EFFICIENT MISSION CONTROL FOR THE 48-SATELLITE GLOBALSTAR CONSTELLATION
Dan Smith *In* NASA. Goddard Space Flight Center, Third International Symposium on Space Mission Operations and Ground Data Systems, Part 1 Nov. 1994 p 663-670 (For primary document see N95-17179 04-17)
Avail: CASI HC A02/MF A06

N95-17257*# Centre National d'Etudes Spatiales, Toulouse (France).
MINI ALL-PURPOSE SATELLITE CONTROL CENTER (MASCC)
Gerard Zaouche *In* NASA. Goddard Space Flight Center, Third International Symposium on Space Mission Operations and Ground Data Systems, Part 1 Nov. 1994 p 671-678 (For primary document see N95-17179 04-17)
Avail: CASI HC A02/MF A06

N95-17532*# MATRA Marconi Space, Toulouse (France).
DELIVERING SPACECRAFT CONTROL CENTERS WITH EMBEDDED KNOWLEDGE-BASED SYSTEMS: THE METHODOLOGY ISSUE
S. Ayache, M. Haziza, and D. Cayrac *In* NASA. Goddard Space Flight Center, Third International Symposium on Space Mission Operations and Ground Data Systems, Part 2 Nov. 1994 p 681-688 Sponsored by Cap Gemini Innovation; Westfield College; Sintef Delab; Eritel; and ITMI (For primary document see N95-17531 04-17)
(ESPRIT Proj. 6083)
Avail: CASI HC A02/MF A06

N95-17535*# National Aeronautics and Space Administration. Goddard Space Flight Center, Greenbelt, MD.
USING GRAPHICS AND EXPERT SYSTEM TECHNOLOGIES TO SUPPORT SATELLITE MONITORING AT THE NASA GODDARD SPACE FLIGHT CENTER
Peter M. Hughes, Gregory W. Shirah, and Edward C. Luczak (Computer Sciences Corp., Lanham, MD.) *In its* Third International Symposium on Space Mission Operations and Ground Data Systems, Part 2 Nov. 1994 p 707-712 (For primary document see N95-17531 04-17)
Avail: CASI HC A02/MF A06

N95-17537*# European Space Agency. European Space Operations Center, Darmstadt (Germany). Mission Operations Dept.
SCOSII: ESA'S NEW GENERATION OF MISSION CONTROL SYSTEMS: THE USER'S PERSPECTIVE
P. Kaufeler, M. Pecchioli, and I. Shurmer (VEGA Space Systems Engineering Ltd., Harpenden, England.) *In* NASA. Goddard Space Flight Center, Third International Symposium on Space Mission Operations and Ground Data Systems, Part 2 Nov. 1994 p 719-725 (For primary document see N95-17531 04-17)
Avail: CASI HC A02/MF A06

N95-17550*# MATRA Marconi Space, Toulouse (France).
DESIGN OF GROUND SEGMENTS FOR SMALL SATELLITES
Guy Mace *In* NASA. Goddard Space Flight Center, Third International Symposium on Space Mission Operations and Ground Data Systems, Part 2 Nov. 1994 p 825-835 (For primary document see N95-17531 04-17)
Avail: CASI HC A03/MF A06

N95-17553*# National Aeronautics and Space Administration. Goddard Space Flight Center, Greenbelt, MD.
EMBEDDED PARALLEL PROCESSING BASED GROUND CONTROL SYSTEMS FOR SMALL SATELLITE TELEMETRY
Michael L. Forman, Tushar K. Hazra (Martin Marietta Services, Inc., Greenbelt, MD.), Gregory M. Troendly (Martin Marietta Services, Inc., Greenbelt, MD.), and William G. Nickum (Martin Marietta Services, Inc., Greenbelt, MD.) *In its* Third International Symposium on Space Mission Operations and Ground Data Systems, Part 2 Nov. 1994 p 857-864 (For primary document see N95-17531 04-17)
(Contract NAS5-31739)
Avail: CASI HC A02/MF A06

N95-17554*# Jet Propulsion Lab., California Inst. of Tech., Pasadena, CA.
OPEN SOLUTIONS TO DISTRIBUTED CONTROL IN GROUND TRACKING STATIONS
William Randy Heuser *In* NASA. Goddard Space Flight Center, Third International Symposium on Space Mission Operations and Ground Data Systems, Part 2 Nov. 1994 p 865-877 (For primary document see N95-17531 04-17)
Avail: CASI HC A03/MF A06

N95-17556*# National Aeronautics and Space Administration. Goddard Space Flight Center, Greenbelt, MD.
ADVANCED GROUND STATION ARCHITECTURE
David Zillig and Ted Benjamin (Stanford Telecommunications, Inc., Reston, VA.) *In its* Third International Symposium on Space Mission Operations and Ground Data Systems, Part 2 Nov. 1994 p 889-896 (For primary document see N95-17531 04-17)
Avail: CASI HC A02/MF A06

N95-17565*# Hughes STX, Inc., Greenbelt, MD. Technology Applications Group.
OOD/OOP EXPERIENCE IN THE SCIENCE OPERATIONS CENTER PART OF THE GROUND SYSTEM FOR X RAY TIMING EXPLORER MISSION
Abdur Rahim Choudhary *In* NASA. Goddard Space Flight Center, Third International Symposium on Space Mission Operations and Ground Data Systems, Part 2 Nov. 1994 p 963-970 (For primary document see N95-17531 04-17)
Avail: CASI HC A02/MF A06

N95-17568*# Computer Sciences Corp., Lanham, MD.
INTEGRATION OF A SATELLITE GROUND SUPPORT SYSTEM BASED ON ANALYSIS OF THE SATELLITE GROUND SUPPORT DOMAIN
R. D. Pendley, E. J. Scheidker, D. S. Levitt, C. R. Myers, and R. D. Werking *In* NASA. Goddard Space Flight Center, Third International Symposium on Space Mission Operations and Ground Data Systems, Part 2 Nov. 1994 p 993-1000 (For primary document see N95-17531 04-17)
Avail: CASI HC A02/MF A06

N95-17573*# National Aeronautics and Space Administration. Goddard Space Flight Center, Greenbelt, MD.
SOLAR AND HELIOSPHERIC OBSERVATORY (SOHO) EXPERIMENTERS' OPERATIONS FACILITY (EOF)
Eliane Larduinat (Allied-Signal Technical Services Corp., Alexandria, VA.) and William Potter *In its* Third International Symposium on Space Mission Operations and Ground Data Systems, Part 2 Nov. 1994 p 1031-1038 (For primary document see N95-17531 04-17)
(Contract NAS5-27772)
Avail: CASI HC A02/MF A06

N95-17576*# National Aeronautics and Space Administration. Goddard Space Flight Center, Greenbelt, MD.
NCCDS PERFORMANCE MODEL
Eric Richmond and Antonio Vallone (Computer Sciences Corp., Lanham, MD.) *In its* Third International Symposium on Space Mission Operations and Ground Data Systems, Part 2 Nov. 1994 p 1055-1062 (For primary document see N95-17531 04-17)
Avail: CASI HC A02/MF A06

N95-17581*# National Aeronautics and Space Administration. Goddard Space Flight Center, Greenbelt, MD.
TEST/SCORE/REPORT: SIMULATION TECHNIQUES FOR AUTOMATING THE TEST PROCESS
Barbara H. Hageman (Integral Systems, Inc., Lanham, MD.), Clayton B. Sigman, and John T. Koslosky *In its* Third International Symposium on Space Mission Operations and Ground Data Systems, Part 2 Nov. 1994 p 1103-1109 (For primary document see N95-17531 04-17)
Avail: CASI HC A02/MF A06

N95-17582*# National Aeronautics and Space Administration. Goddard Space Flight Center, Greenbelt, MD.
SPACECRAFT DATA SIMULATOR FOR THE TEST OF LEVEL ZERO PROCESSING SYSTEMS
Jeff Shi (RMS Technologies, Inc., Landover, MD.), Julie Gordon (RMS Technologies, Inc., Landover, MD.), Chandru Mirchandani (Loral AeroSys, Seabrook, MD.), and Diem Nguyen (Loral AeroSys, Seabrook, MD.) *In its* Third International Symposium on Space Mission Operations and Ground Data Systems, Part 2 Nov. 1994 p 1111-1120 (For primary document see N95-17531 04-17)
Avail: CASI HC A02/MF A06

N95-17589*# McDonnell-Douglas Corp., Cape Canaveral, FL. Space and Defense Systems.
CONFIGURABLE TECHNOLOGY DEVELOPMENT FOR REUSABLE CONTROL AND MONITOR GROUND SYSTEMS
David R. Uhrlaub *In* NASA. Goddard Space Flight Center, Third International Symposium on Space Mission Operations and Ground Data Systems, Part 2 Nov. 1994 p 1177-1184 (For primary document see N95-17531 04-17)
Avail: CASI HC A02/MF A06

N95-17601*# National Aeronautics and Space Administration. Goddard Space Flight Center, Greenbelt, MD.
MISSION OPERATIONS CENTERS (MOCs): INTEGRATING KEY SPACECRAFT GROUND DATA SYSTEM COMPONENTS
Randy Harbaugh and Donna Szakal (Computer Sciences Corp., Laurel, MD.) *In its* Third International Symposium on Space Mission Operations and Ground Data Systems, Part 2 Nov. 1994 p 1281-1288 (For primary document see N95-17531 04-17)
Avail: CASI HC A02/MF A06

15 LAUNCH VEHICLES AND SPACE VEHICLES

Includes boosters; operating problems of launch/space vehicle systems; and reusable vehicles.

For related information see also *20 Spacecraft Propulsion and Power.*

N95-16005# Utah State Univ., Logan, UT.
DEVELOPMENT OF A MEDIUM ENERGY MODULATED ELECTRON GUN FOR ORBITAL EXPERIMENTS Final Technical Report, Aug. 1991 - Sep. 1992
W. J. Raitt May 1994 20 p
(Contract F19628-91-K-0037)
(AD-A281021; RL-TR-94-50) Avail: CASI HC A03/MF A01

Rome Laboratory has provided funding support for the development of a medium powered modulated electron gun to be flight tested on a NASA sounding rocket designated CHARGE-2B. The objective of the flight test was to study both the generation and the propagation of VLF electromagnetic waves in the near and far fields of the waves. DTIC

N95-17419*# National Aeronautics and Space Administration. Lewis Research Center, Cleveland, OH.
CONCEPTUAL DESIGN OF THE SPACE STATION COMBUSTION MODULE
Daniel P. Morilak, Dennis W. Rohn, and Jennifer L. Rhatigan Nov. 1994 13 p Presented at the 33rd Aerospace Sciences Meeting and Exhibit, Reno, NV, 9-12 Jan. 1995; sponsored by AIAA
(NASA-TM-106788; E-9244; NAS 1.15:106788; AIAA Paper 95-0692)
Copyright Avail: CASI HC A03/MF A01

The purpose of this paper is to describe the conceptual design of the Combustion Module for the International Space Station Alpha (ISSA). This module is part of the Space Station Fluids/Combustion Facility (SS FCF) under development at the NASA Lewis Research Center. The Fluids/Combustion Facility is one of several science facilities which are being developed to support microgravity science investigations in the US Laboratory Module of the ISSA. The SS FCF will support a multitude of fluids and combustion science investigations over the lifetime of the ISSA and return state-of-the-art science data in a timely and efficient manner to the scientific communities. This will be accomplished through modularization of hardware, with planned, periodic upgrades; modularization of like scientific investigations that make use of common facility functions; and through the use of orbital replacement units (ORU's) for incorporation of new technology and new functionality. The SS FCF is scheduled to become operational on-orbit in 1999. The Combustion Module is presently scheduled for launch to orbit and integration with the Fluids/Combustion Facility in 1999. The objectives of this paper are to describe the history of the Combustion Module concept, the types of combustion science investigations which will be accommodated by the module, the hardware design heritage, the hardware concept, and the hardware breadboarding efforts currently underway. Author

N95-17493*# California Univ., Los Angeles, CA. Dept. of Mechanical, Aerospace and Nuclear Engineering.
DEMONSTRATION OF THE DYNAMIC FLOWGRAPH METHODOLOGY USING THE TITAN 2 SPACE LAUNCH VEHICLE DIGITAL FLIGHT CONTROL SYSTEM
M. Yau, S. Guarro, and G. Apostolakis Jun. 1993 102 p
(Contract NCC2-374; NAG5-1440)
(NASA-CR-197517; NAS 1.26:197517; UCLA ENG-93-43) Avail: CASI HC A06/MF A02

Dynamic Flowgraph Methodology (DFM) is a new approach developed

to integrate the modeling and analysis of the hardware and software components of an embedded system. The objective is to complement the traditional approaches which generally follow the philosophy of separating out the hardware and software portions of the assurance analysis. In this paper, the DFM approach is demonstrated using the Titan 2 Space Launch Vehicle Digital Flight Control System. The hardware and software portions of this embedded system are modeled in an integrated framework. In addition, the time dependent behavior and the switching logic can be captured by this DFM model. In the modeling process, it is found that constructing decision tables for software subroutines is very time consuming. A possible solution is suggested. This approach makes use of a well-known numerical method, the Newton-Raphson method, to solve the equations implemented in the subroutines in reverse. Convergence can be achieved in a few steps. Author

N95-17509 Naval Postgraduate School, Monterey, CA.
A SURVEY OF COMMERCIALLY AVAILABLE EXPENDABLE HEAVY LIFT LAUNCH VEHICLES M.S. Thesis
Joseph J. Mihal, Jr. Jun. 1994 115 p Limited Reproducibility: More than 20% of this document may be affected by microfiche quality
(AD-A282429) Avail: CASI HC A06

This thesis examines the launch vehicle options available to place a heavy payload, 10 tons, into a low-earth-orbit. The study provides the current status of the space launch vehicle market for heavy lift launchers. The following launchers are looked at in detail: Titan 3, Proton, Energia, Long March 3, Ariane 5, and the H-2. Vehicle design history and launch record are examined. Each launcher is then examined and broken down by stages, including the payload sections. A typical launch sequence is included for each vehicle. Finally, the cost of the various launchers is examined. Conclusions regarding the future need of heavy lift launch vehicles and a look at the current political environment is made. DTIC

16 SPACE TRANSPORTATION

Includes passenger and cargo space transportation, e.g., shuttle operations; and space rescue techniques.

For related information see also *03 Air Transportation and Safety* and *18 Spacecraft Design, Testing and Performance*. For space suits see *54 Man/System Technology and Life Support*.

N95-17262*# National Aeronautics and Space Administration. John F. Kennedy Space Center, Cocoa Beach, FL.
DEBRIS/ICE/TPS ASSESSMENT AND INTEGRATED PHOTOGRAPHIC ANALYSIS OF SHUTTLE MISSION STS-64 ON 9 AUGUST 1994 Final Report, 8-22 Sep. 1994
J. Bradley Davis, Barry C. Bowen, Jorge E. Rivera, Robert F. Speece, and Gregory N. Katnik Oct. 1994 91 p Original contains color illustrations
(NASA-TM-109206; NAS 1.15:109206) Avail: CASI HC A05/MF A01; 28 functional color pages

A debris/ice/thermal protection system assessment and integrated photographic analysis was conducted for Shuttle mission STS-64. Debris inspections of the flight elements and launch pad were performed before and after launch. Icing conditions on the External Tank were assessed by the use of computer programs, nomographs, and infrared scanner data during cryogenic loading of the vehicle followed by on-pad visual inspection. High speed photography of the launch was analyzed to identify ice/debris sources and evaluate potential vehicle damage and/or in-flight anomalies. This report documents the ice/debris/thermal protection system conditions and integrated photographic analysis of Shuttle mission STS-64, and the resulting effect on the Space Shuttle Program. Author

N95-16769*# National Aeronautics and Space Administration, Washington, DC.
SLS-1: THE FIRST DEDICATED LIFE SCIENCES SHUTTLE FLIGHT Abstract Only
Robert W. Phillips *In* Aerospace Medical Association, Aerospace Medical Association 63rd Annual Scientific Meeting Program 14 May 1992 1 p (For primary document see N95-16737 04-51)
Avail: CASI HC A01/MF A02

17 SPACE COMM., SPACECRAFT COMM., COMMAND & TRACKING

Includes telemetry; space communications networks; astronavigation and guidance; and radio blackout.

For related information see also *04 Aircraft Communications and Navigation* and *32 Communications and Radar*.

N95-17179*# National Aeronautics and Space Administration. Goddard Space Flight Center, Greenbelt, MD.
THIRD INTERNATIONAL SYMPOSIUM ON SPACE MISSION OPERATIONS AND GROUND DATA SYSTEMS, PART 1
James L. Rash, ed. Nov. 1994 666 p Symposium held in Greenbelt, MD, 15-18 Nov. 1994
(RTOP 500-00-00)
(NASA-CP-3281-Pt-1; Rept-94B00135-Pt-1; NAS 1.55:3281-Pt-1) Avail: CASI HC A99/MF A06

Under the theme of 'Opportunities in Ground Data Systems for High Efficiency Operations of Space Missions,' the SpaceOps '94 symposium included presentations of more than 150 technical papers spanning five topic areas: Mission Management, Operations, Data Management, System Development, and Systems Engineering. The papers focus on improvements in the efficiency, effectiveness, productivity, and quality of data acquisition, ground systems, and mission operations. New technology, techniques, methods, and human systems are discussed. Accomplishments are also reported in the application of information systems to improve data retrieval, reporting, and archiving; the management of human factors; the use of telescience and teleoperations; and the design and implementation of logistics support for mission operations. For individual titles, see N95-17180 through N95-17257.

N95-17180*# Jet Propulsion Lab., California Inst. of Tech., Pasadena, CA.
TELECOMMUNICATIONS END-TO-END SYSTEMS MONITORING ON TOPEX/POSEIDON: TOOLS AND TECHNIQUES
Bruno J. Calanche *In* NASA. Goddard Space Flight Center, Third International Symposium on Space Mission Operations and Ground Data Systems, Part 1 Nov. 1994 p 3-9 (For primary document see N95-17179 04-17)
Avail: CASI HC A02/MF A06

The TOPEX/Poseidon Project Satellite Performance Analysis Team's (SPAT) roles and responsibilities have grown to include functions that are typically performed by other teams on JPL Flight Projects. In particular, SPAT Telecommunication's role has expanded beyond the nominal function of monitoring, assessing, characterizing, and trending the spacecraft (S/C) RF/Telecom subsystem to one of End-to-End Information Systems (EEIS) monitoring. This has been accomplished by taking advantage of the spacecraft and ground data system structures and protocols. By processing both the received spacecraft telemetry minor frame ground generated CRC flags and NASCOM block poly error flags, bit error rates (BER) for each link segment can be determined. This provides the capability to characterize the separate link segments, determine science data recovery, and perform fault/anomaly detection and isolation. By monitoring and managing the links, TOPEX has successfully recovered approximately 99.9 percent of the science data with an integrity (BER) of better than 1 x 10(exp 8). This paper presents the algorithms used to process the above flags and the techniques used for EEIS monitoring. Author

N95-17181*# European Space Agency. European Space Operations Center, Darmstadt (Germany).
COMMUNICATION NETWORK FOR DECENTRALIZED REMOTE TELE-SCIENCE DURING THE SPACELAB MISSION IML-2
Uwe Christ, Klaus-Juergen Schulz, and Marco Incollingo *In* NASA. Goddard Space Flight Center, Third International Symposium on Space Mission Operations and Ground Data Systems, Part 1 Nov. 1994 p 11-20 (For primary document see N95-17179 04-17)
Avail: CASI HC A02/MF A06

The ESA communication network for decentralized remote telescience during the Spacelab mission IML-2, called Interconnection Ground Subnetwork (IGS), provided data, voice conferencing, video distribution/conferencing and high rate data services to 5 remote user

centers in Europe. The combination of services allowed the experimenters to interact with their experiments as they would normally do from the Payload Operations Control Center (POCC) at MSFC. In addition, to enhance their science results, they were able to make use of reference facilities and computing resources in their home laboratory, which typically are not available in the POCC. Characteristics of the IML-2 communications implementation were the adaptation to the different user needs based on modular service capabilities of IGS and the cost optimization for the connectivity. This was achieved by using a combination of traditional leased lines, satellite based VSAT connectivity and N-ISDN according to the simulation and mission schedule for each remote site. The central management system of IGS allows minimization of staffing and the involvement of communications personnel at the remote sites. The successful operation of IGS for IML-2 as a precursor network for the Columbus Orbital Facility (COF) has proven the concept for communications to support the operation of the COF decentralized scenario. Author

N95-17182*# National Aeronautics and Space Administration. Goddard Space Flight Center, Greenbelt, MD.

EARTH OBSERVING SYSTEM (EOS) COMMUNICATION (Ecom) MODELING, ANALYSIS, AND TESTBED (EMAT) ACTIVIY

Vishal Desai *In its* Third International Symposium on Space Mission Operations and Ground Data Systems, Part 1 Nov. 1994 p 21-28 (For primary document see N95-17179 04-17)

Avail: CASI HC A02/MF A06

This paper describes the Earth Observing System (EOS) Communication (Ecom) Modeling, Analysis, and Testbed (EMAT) activity performed by Code 540 in support of the Ecom project. Ecom is the ground-to-ground data transport system for operational EOS traffic. The National Aeronautic and Space Administration (NASA) Communications (Nascom) Division, Code 540, is responsible for implementing Ecom. Ecom interfaces with various systems to transport EOS forward link commands, return link telemetry, and science payload data. To understand the complexities surrounding the design and implementation of Ecom, it is necessary that sufficient testbedding, modeling, and analysis be conducted prior to the design phase. These activities, when grouped, are referred to as the EMAT activity. This paper describes work accomplished to date in each of the three major EMAT activities: modeling, analysis, and testbedding. Author

N95-17183*# Stanford Telecommunications, Inc., Seabrook, MD.

S-BAND AND Ku-BAND RETURN SERVICE INTERFERENCE BETWEEN TDRSS USERS

Linda Harrell *In* NASA. Goddard Space Flight Center, Third International Symposium on Space Mission Operations and Ground Data Systems, Part 1 Nov. 1994 p 29-40 (For primary document see N95-17179 04-17)

Avail: CASI HC A03/MF A06

The Tracking Data Relay Satellite System (TDRSS) return service performance can be degraded by interference from another user when two or more spacecraft communicate with the same Tracking Data Relay Satellite (TDRS) at the same time. This paper describes the S-band and Ku-band return service self interference environment expected in the 1996 - 2010 timeframe and shows the self-interference expected for selected TDRSS users based on Communications Link Analysis and Simulation System (CLASS) Automated Conflict Resolution System (ACRS) and Interference Monitor (IM) tools. The results show: which user links are susceptible to interference from other users, the interference statistics, and whether or not interference can be avoided with appropriate interference mitigation techniques such as scheduling, cross-polarization, or Pseudo random Noise (PN) spreading. The analysis results enable Space Network (SN) managers to determine the impacts of self-interference on the TDRSS service availability. They also enable project offices to determine whether they should select return service communications parameters, such as polarization and PN spreading, to minimize the probability of being impacted by self-interference; try to schedule TDRSS support around other user spacecraft communications schedules; or accept communication outages due to self-interference. Author

N95-17184*# National Space Development Agency, Tsukuba (Japan).

ATTEMPT OF AUTOMATED SPACE NETWORK OPERATIONS AT ETS-VI EXPERIMENTAL DATA RELAY SYSTEM

Kiyoomi Ishihara and Masayuki Sugawara *In* NASA. Goddard Space Flight Center, Third International Symposium on Space Mission Operations and Ground Data Systems, Part 1 Nov. 1994 p 41-47 (For primary document see N95-17179 04-17)

Avail: CASI HC A02/MF A06

National Space Development Agency of Japan (NASDA) is to perform experimental operations to acquire necessary technology for the future inter-satellite communications configured with a data relay satellite. This paper intends to overview functions of the experimental ground system which NASDA has developed for the Engineering Test Satellite VI (ETS-VI) Data Relay and Tracking Experiment, and to introduce Space Network System Operations Procedure (SNSOP) method with an example of Ka-band Single Access (KSA) acquisition sequence. To reduce operational load, SNSOP is developed with the concept of automated control and monitor of both ground terminal and data relay satellite. To perform acquisition and tracking operations fluently, the information exchange with user spacecraft controllers is automated by SNSOP functions. Author

N95-17185*# Telos Information Systems, Pasadena, CA.

TABLE-DRIVEN CONFIGURATION AND FORMATTING OF TELEMETRY DATA IN THE DEEP SPACE NETWORK

Evan Manning *In* NASA. Goddard Space Flight Center, Third International Symposium on Space Mission Operations and Ground Data Systems, Part 1 Nov. 1994 p 49-56 Sponsored by JPL (For primary document see N95-17179 04-17)

Avail: CASI HC A02/MF A06

With a restructured software architecture for telemetry system control and data processing, the NASA/Deep Space Network (DSN) has substantially improved its ability to accommodate a wide variety of spacecraft in an era of 'better, faster, cheaper'. In the new architecture, the permanent software implements all capabilities needed by any system user, and text tables specify how these capabilities are to be used for each spacecraft. Most changes can now be made rapidly, outside of the traditional software development cycle. The system can be updated to support a new spacecraft through table changes rather than software changes, reducing the implementation, test, and delivery cycle for such a change from three months to three weeks. The mechanical separation of the text table files from the program software, with tables only loaded into memory when that mission is being supported, dramatically reduces the level of regression testing required. The format of each table is a different compromise between ease of human interpretation, efficiency of computer interpretation, and flexibility. Author

N95-17186*# National Aeronautics and Space Administration. Goddard Space Flight Center, Greenbelt, MD.

END-TO-END COMMUNICATION TEST ON VARIABLE LENGTH PACKET STRUCTURES UTILIZING AOS TESTBED

Warner H. Miller, V. Sank (Herold, Fredrick and Associates, Inc., Greenbelt, MD.), Wai Fong, J. Miko, M. Powers, John Folk (Advanced Technology and Research, Inc., Laurel, MD.), B. Conaway (Herold, Fredrick and Associates, Inc., Greenbelt, MD.), K. Michael, and Pen-Shu Yeh *In its* Third International Symposium on Space Mission Operations and Ground Data Systems, Part 1 Nov. 1994 p 57-64 (For primary document see N95-17179 04-17)

Avail: CASI HC A02/MF A06

This paper describes a communication test, which successfully demonstrated the transfer of losslessly compressed images in an end-to-end system. These compressed images were first formatted into variable length Consultative Committee for Space Data Systems (CCSDS) packets in the Advanced Orbiting System Testbed (AOST). The CCSDS data Structures were transferred from the AOST to the Radio Frequency Simulations Operations Center (RFSOC), via a fiber optic link, where data was then transmitted through the Tracking and Data Relay Satellite System (TDRSS). The received data acquired at the White Sands Complex (WSC) was transferred back to the AOST where the data was captured and decompressed back to the original images. This paper describes the compression algorithm, the AOST configuration, key flight components, data formats, and the communication link characteristics and test results. Author

N95-17187*# National Aeronautics and Space Administration. Goddard Space Flight Center, Greenbelt, MD.

DEMAND ACCESS COMMUNICATIONS FOR TDRSS USERS

David Zillig, Aaron Weinberg (Stanford Telecommunications, Inc., Reston,

VA.), and Robert McOmber (Stanford Telecommunications, Inc., Reston, VA.) *In its* Third International Symposium on Space Mission Operations and Ground Data Systems, Part 1 Nov. 1994 p 65-74 (For primary document see N95-17179 04-17)
Avail: CASI HC A02/MF A06

The Tracking and Data Relay Satellite System (TDRSS) has long been used to provide reliable low and high-data rate relay services between user spacecraft in Earth orbit and the ground. To date, these TDRSS services have been implemented via prior scheduling based upon estimates of user needs and mission event timelines. While this approach may be necessary for large users that require greater amounts of TDRSS resources, TDRSS can potentially offer the planned community of smaller science missions (e.g., the small explorer missions), and other emerging users, the unique opportunity for services on demand. In particular, innovative application of the existing TDRSS Multiple Access (MA) subsystem, with its phased array antenna, could be used to implement true demand access services without modification to either the TDRSS satellites or the user transponder, thereby introducing operational and performance benefits to both the user community and the Space Network. In this paper, candidate implementations of demand access service via the TDRSS MA subsystem are examined in detail. Both forward and return link services are addressed and a combination of qualitative and quantitative assessments are provided. The paper also identifies further areas for investigation in this ongoing activity that is being conducted by GSFC/Code 531 under the NASA Code O Advanced Systems Program. Author

N95-17188*# National Aeronautics and Space Administration. Goddard Space Flight Center, Greenbelt, MD.
THE GRO REMOTE TERMINAL SYSTEM
David J. Zillig and Joe Valvano (Allied-Signal Technical Services Corp., Columbia, MD.) *In its* Third International Symposium on Space Mission Operations and Ground Data Systems, Part 1 Nov. 1994 p 75-82 (For primary document see N95-17179 04-17)
Avail: CASI HC A02/MF A06

In March 1992, NASA HQ challenged GSFC/Code 531 to propose a fast, low-cost approach to close the Tracking Data Relay Satellite System (TDRSS) Zone-of-Exclusion (ZOE) over the Indian Ocean in order to provide global communications coverage for the Compton Gamma Ray Observatory (GRO) spacecraft. GRO had lost its tape recording capability which limited its valuable science data return to real-time contacts with the TDRS-E and TDRS-W synchronous data relay satellites, yielding only approximately 62 percent of the possible data obtainable. To achieve global coverage, a TDRS spacecraft would have to be moved over the Indian Ocean out of line-of-sight control of White Sands Ground Terminal (WSGT). To minimize operations life cycle costs, Headquarters also set a goal for remote control, from the WSGT, of the overseas ground station which was required for direct communications with TDRS-1. On August 27, 1992, Code 531 was given the go ahead to implement the proposed GRO Relay Terminal System (GRTS). This paper describes the Remote Ground Relay Terminal (RGRT) which went operational at the Canberra Deep Space Communications Complex (CDSCC) in Canberra, Australia in December 1993 and is currently augmenting the TDRSS constellation in returning between 80-100 percent of GRO science data under the control of a single operator at WSGT.
Author

N95-17189*# European Space Agency. European Space Operations Center, Darmstadt (Germany). METEOSAT Exploitation Project.
OVERVIEW ON METEOSAT GEOMETRICAL IMAGE DATA PROCESSING
Frank J. Diekmann *In* NASA. Goddard Space Flight Center, Third International Symposium on Space Mission Operations and Ground Data Systems, Part 1 Nov. 1994 p 85-93 (For primary document see N95-17179 04-17)
Avail: CASI HC A02/MF A06

Digital Images acquired from the geostationary METEOSAT satellites are processed and disseminated at ESA's European Space Operations Centre in Darmstadt, Germany. Their scientific value is mainly dependent on their radiometric quality and geometric stability. This paper will give an overview on the image processing activities performed at ESOC, concentrating on the geometrical restoration and quality evaluation. The performance of the rectification process for the various satellites over the past years will be presented and the impacts of external events as for instance the Pinatubo eruption in 1991 will be explained. Special developments both in hard and software, necessary to cope with demanding tasks as new image resampling or to correct for spacecraft anomalies, are presented as well. The rotating lens of MET-5 causing severe geometrical image distortions is an example for the latter. Author

N95-17190*# Jet Propulsion Lab., California Inst. of Tech., Pasadena, CA.
USE OF A MULTIMISSION SYSTEM FOR COST EFFECTIVE SUPPORT OF PLANETARY SCIENCE DATA PROCESSING
William B. Green *In* NASA. Goddard Space Flight Center, Third International Symposium on Space Mission Operations and Ground Data Systems, Part 1 Nov. 1994 p 97-103 (For primary document see N95-17179 04-17)
Avail: CASI HC A02/MF A06

JPL's Multimission Operations Systems Office (MOSO) provides a multimission facility at JPL for processing science instrument data from NASA's planetary missions. This facility, the Multimission Image Processing System (MIPS), is developed and maintained by MOSO to meet requirements that span the NASA family of planetary missions. Although the word 'image' appears in the title, MIPS is used to process instrument data from a variety of science instruments. This paper describes the design of a new system architecture now being implemented within the MIPS to support future planetary mission activities at significantly reduced operations and maintenance cost. Author

N95-17191*# National Aeronautics and Space Administration. Goddard Space Flight Center, Greenbelt, MD.
A SECOND GENERATION 50 Mbps VLSI LEVEL ZERO PROCESSING SYSTEM PROTOTYPE
Jonathan C. Harris (RMS Technologies, Inc., Landover, MD.), Jeff Shi (RMS Technologies, Inc., Landover, MD.), Nick Speciale, and Toby Bennett *In its* Third International Symposium on Space Mission Operations and Ground Data Systems, Part 1 Nov. 1994 p 105-115 (For primary document see N95-17179 04-17)
Avail: CASI HC A03/MF A06

Level Zero Processing (LZP) generally refers to telemetry data processing functions performed at ground facilities to remove all communication artifacts from instrument data. These functions typically include frame synchronization, error detection and correction, packet reassembly and sorting, playback reversal, merging, time-ordering, overlap deletion, and production of annotated data sets. The Data Systems Technologies Division (DSTD) at Goddard Space Flight Center (GSFC) has been developing high-performance Very Large Scale Integration Level Zero Processing Systems (VLSI LZPS) since 1989. The first VLSI LZPS prototype demonstrated 20 Megabits per second (Mbp's) capability in 1992. With a new generation of high-density Application-specific Integrated Circuits (ASIC) and a Mass Storage System (MSS) based on the High-performance Parallel Peripheral Interface (HiPPI), a second prototype has been built that achieves full 50 Mbp's performance. This paper describes the second generation LZPS prototype based upon VLSI technologies. Author

N95-17192*# Institute of Space Research, Moscow (USSR).
FAST COMPUTATIONAL SCHEME OF IMAGE COMPRESSION FOR 32-BIT MICROPROCESSORS **c61**
Leonid Kasperovich *In* NASA. Goddard Space Flight Center, Third International Symposium on Space Mission Operations and Ground Data Systems, Part 1 Nov. 1994 p 119-123 (For primary document see N95-17179 04-17)
Avail: CASI HC A01/MF A06

This paper presents a new computational scheme of image compression based on the discrete cosine transform (DCT), underlying JPEG and MPEG International Standards. The algorithm for the 2-d DCT computation uses integer operations (register shifts and additions / subtractions only); its computational complexity is about 8 additions per image pixel. As a meaningful example of an on-board image compression application we consider the software implementation of the algorithm for the Mars Rover (Marsokhod, in Russian) imaging system being developed as a part of Mars-96 International Space Project. It's shown that fast software solution for 32-bit microprocessors may compete with the DCT-based image compression hardware. Author

N95-17193*# National Aeronautics and Space Administration. Goddard Space Flight Center, Greenbelt, MD.

THE DEVELOPMENT AND OPERATION OF THE INTERNATIONAL SOLAR-TERRESTRIAL PHYSICS CENTRAL DATA HANDLING FACILITY **c82**

Kenneth Lehtonen *In its* Third International Symposium on Space Mission Operations and Ground Data Systems, Part 1 Nov. 1994 p 125-132 (For primary document see N95-17179 04-17)

Avail: CASI HC A02/MF A06

The National Aeronautics and Space Administration (NASA) Goddard Space Flight Center (GSFC) International Solar-Terrestrial Physics (ISTP) Program is committed to the development of a comprehensive, multi-mission ground data system which will support a variety of national and international scientific missions in an effort to study the flow of energy from the sun through the Earth-space environment, known as the geospace. A major component of the ISTP ground data system is an ISTP-dedicated Central Data Handling Facility (CDHF). Acquisition, development, and operation of the ISTP CDHF were delegated by the ISTP Project Office within the Flight Projects Directorate to the Information Processing Division (IPD) within the Mission Operations and Data Systems Directorate (MO&DSD). The ISTP CDHF supports the receipt, storage, and electronic access of the full complement of ISTP Level-zero science data; serves as the linchpin for the centralized processing and long-term storage of all key parameters generated either by the ISTP CDHF itself or received from external, ISTP Program approved sources; and provides the required networking and 'science-friendly' interfaces for the ISTP investigators. Once connected to the ISTP CDHF, the online catalog of key parameters can be browsed from their remote processing facilities for the immediate electronic receipt of selected key parameters using the NASA Science Internet (NSI), managed by NASA's Ames Research Center. The purpose of this paper is twofold: (1) to describe how the ISTP CDHF was successfully implemented and operated to support initially the Japanese Geomagnetic Tail (GEOTAIL) mission and correlative science investigations, and (2) to describe how the ISTP CDHF has been enhanced to support ongoing as well as future ISTP missions. Emphasis will be placed on how various project management approaches were undertaken that proved to be highly effective in delivering an operational ISTP CDHF to the Project on schedule and within budget. Examples to be discussed include: the development of superior teams; the use of Defect Causal Analysis (DCA) concepts to improve the software development process in a pilot Total Quality Management (TQM) initiative; and the implementation of a robust architecture that will be able to support the anticipated growth in the ISTP Program science requirements with only incremental upgrades to the baseline system. Further examples include the use of automated data management software and the implementation of Government and/or industry standards, whenever possible, into the hardware and software development life-cycle. Finally, the paper will also report on several new technologies (for example, the installation of a Fiber Data Distribution Interface network) that were successfully employed.

Author

N95-17194*# Jet Propulsion Lab., California Inst. of Tech., Pasadena, CA.

ECONOMICAL GROUND DATA DELIVERY **c82**

Richard W. Markley, Russell H. Byrne, and Daniel E. Bromberg *In* NASA. Goddard Space Flight Center, Third International Symposium on Space Mission Operations and Ground Data Systems, Part 1 Nov. 1994 p 133-138 (For primary document see N95-17179 04-17)

Avail: CASI HC A02/MF A06

Data delivery in the Deep Space Network (DSN) involves transmission of a small amount of constant, high-priority traffic and a large amount of bursty, low priority data. The bursty traffic may be initially buffered and then metered back slowly as bandwidth becomes available. Today both types of data are transmitted over dedicated leased circuits. The authors investigated the potential of saving money by designing a hybrid communications architecture that uses leased circuits for high-priority network communications and dial-up circuits for low-priority traffic. Such an architecture may significantly reduce costs and provide an emergency backup. The architecture presented here may also be applied to any ground station-to-customer network within the range of a common carrier. The authors compare estimated costs for various scenarios and suggest security safeguards that should be considered.

Author

N95-17195*# National Aeronautics and Space Administration. Lyndon B. Johnson Space Center, Houston, TX.

NASA JOHNSON SPACE CENTER LIFE SCIENCES DATA SYSTEM **c82**

Hasan Rahman (Martin Marietta Corp., Houston, TX.) and Jeffery Cardenas *In* NASA. Goddard Space Flight Center, Third International Symposium on Space Mission Operations and Ground Data Systems, Part 1 Nov. 1994 p 139-147 (For primary document see N95-17179 04-17)

Avail: CASI HC A02/MF A06

The Life Sciences Project Division (LSPD) at JSC, which manages human life sciences flight experiments for the NASA Life Sciences Division, augmented its Life Sciences Data System (LSDS) in support of the Spacelab Life Sciences-2 (SLS-2) mission, October 1993. The LSDS is a portable ground system supporting Shuttle, Spacelab, and Mir based life sciences experiments. The LSDS supports acquisition, processing, display, and storage of real-time experiment telemetry in a workstation environment. The system may acquire digital or analog data, storing the data in experiment packet format. Data packets from any acquisition source are archived and meta-parameters are derived through the application of mathematical and logical operators. Parameters may be displayed in text and/or graphical form, or output to analog devices. Experiment data packets may be retransmitted through the network interface and database applications may be developed to support virtually any data packet format. The user interface provides menu- and icon-driven program control and the LSDS system can be integrated with other workstations to perform a variety of functions. The generic capabilities, adaptability, and ease of use make the LSDS a cost-effective solution to many experiment data processing requirements. The same system is used for experiment systems functional and integration tests, flight crew training sessions and mission simulations. In addition, the system has provided the infrastructure for the development of the JSC Life Sciences Data Archive System scheduled for completion in December 1994.

Author

N95-17196*# Centre National d'Etudes Spatiales, Toulouse (France).

A PROCESSING CENTRE FOR THE CNES CE-GPS EXPERIMENTATION **c04**

Norbert Suard and Jean-Claude Durand *In* NASA. Goddard Space Flight Center, Third International Symposium on Space Mission Operations and Ground Data Systems, Part 1 Nov. 1994 p 149-154 (For primary document see N95-17179 04-17)

Avail: CASI HC A02/MF A06

CNES is involved in a GPS (Global Positioning System) geostationary overlay experimentation. The purpose of this experimentation is to test various new techniques in order to select the optimal station synchronization method, as well as the geostationary spacecraft orbitography method. These new techniques are needed to develop the Ranging GPS Integrity Channel services. The CNES experimentation includes three transmitting/receiving ground stations (manufactured by IN-SNEC), one INMARSAT 2 C/L band transponder and a processing center named STE (Station de Traitements de l'Experimentation). Not all the techniques to be tested are implemented, but the experimental system has to include several functions; part of the future system simulation functions, such as a servo-loop function, and in particular a data collection function providing for rapid monitoring of system operation, analysis of existing ground station processes, and several weeks of data coverage for other scientific studies. This paper discusses system architecture and some criteria used in its design, as well as the monitoring function, the approach used to develop a low-cost and short-life processing center in collaboration with a CNES sub-contractor (ATTDATAID), and some results.

Author (revised)

N95-17197*# McDonnell-Douglas Space Systems Co., Cocoa Beach, FL.

SINGLE STAGE ROCKET TECHNOLOGY'S REAL TIME DATA SYSTEM **c82**

Steven D. Voglewede *In* NASA. Goddard Space Flight Center, Third International Symposium on Space Mission Operations and Ground Data Systems, Part 1 Nov. 1994 p 155-168 (For primary document see N95-17179 04-17)

Avail: CASI HC A03/MF A06

The Single Stage Rocket Technology (SSRT) Delta Clipper Experimental (DC-X) Program is a United States Air Force Ballistic Missile Defense Organization (BMDO) rapid prototyping initiative that is currently

demonstrating technology readiness for reusable suborbital rockets. The McDonnell Douglas DC-X rocket performed technology demonstrations at the U.S. Army White Sands Missile Range in New Mexico from April-October in 1993. The DC-X Flight Operations Control Center (FOCC) contains the ground control system that is used to monitor and control the DC-X vehicle and its Ground Support Systems (GSS). The FOCC is operated by a flight crew of three operators. Two operators manage the DC-X Flight Systems and one operator is the Ground Systems Manager. A group from McDonnell Douglas Aerospace at KSC developed the DC-X ground control system for the FOCC. This system is known as the Real Time Data System (RTDS). The RTDS is a distributed real time control and monitoring system that utilizes the latest available commercial off-the-shelf computer technology. The RTDS contains front end interfaces for the DC-X RF uplink/downlink and fiber optic interfaces to the GSS equipment. This paper describes the RTDS architecture and FOCC layout. The DC-X applications and ground operations are covered. Author (revised)

N95-17198*# Jet Propulsion Lab., California Inst. of Tech., Pasadena, CA.

INTERNATIONAL DATA TRANSFER FOR SPACE VERY LONG BASELINE INTERFEROMETRY **c32**

Alexandria B. Wiercigroch *In* NASA. Goddard Space Flight Center, Third International Symposium on Space Mission Operations and Ground Data Systems, Part 1 Nov. 1994 p 169-175 (For primary document see N95-17179 04-17)

Avail: CASI HC A02/MF A06

Space very long baseline interferometry (SVLBI) experiments using a TDRSS satellite have successfully demonstrated the capability of using spacecraft to extend the effective baseline length of VLBI observations beyond the diameter of the Earth, thereby improving the resolution for imaging of active galactic nuclei at centimeter wavelengths. As a result, two spacecraft dedicated to SVLBI, VSOP (Japan) and RadioAstron (Russia), are scheduled to be launched into high Earth orbit in 1996 and 1997. The success of these missions depends on the cooperation of the international community in providing support from ground tracking stations, ground radio telescopes, and correlation facilities. The timely exchange and monitoring of data among the participants requires a well-designed and automated international data transfer system. In this paper, we will discuss the design requirements, data types and flows, and the operational responsibilities associated with the SVLBI data transfer system. Author

N95-17199*# Jet Propulsion Lab., California Inst. of Tech., Pasadena, CA.

ARACHNID: A PROTOTYPE OBJECT-ORIENTED DATABASE TOOL FOR DISTRIBUTED SYSTEMS **c82**

Herbert Younger, John OReilly (MIMD Systems, Inc., Palo Alto, CA.), and Bjorn Frogner (MIMD Systems, Inc., Palo Alto, CA.) *In* NASA. Goddard Space Flight Center, Third International Symposium on Space Mission Operations and Ground Data Systems, Part 1 Nov. 1994 p 177-183 (For primary document see N95-17179 04-17)

(Contract NAS7-1156)

Avail: CASI HC A02/MF A06

This paper discusses the results of a Phase 2 SBIR project sponsored by NASA and performed by MIMD Systems, Inc. A major objective of this project was to develop specific concepts for improved performance in accessing large databases. An object-oriented and distributed approach was used for the general design, while a geographical decomposition was used as a specific solution. The resulting software framework is called ARACHNID. The Faint Source Catalog developed by NASA was the initial database testbed. This is a database of many giga-bytes, where an order of magnitude improvement in query speed is being sought. This database contains faint infrared point sources obtained from telescope measurements of the sky. A geographical decomposition of this database is an attractive approach to dividing it into pieces. Each piece can then be searched on individual processors with only a weak data linkage between the processors being required. As a further demonstration of the concepts implemented in ARACHNID, a tourist information system is discussed. This version of ARACHNID is the commercial result of the project. It is a distributed, networked, database application where speed, maintenance, and reliability are important considerations. This paper focuses on the design concepts and technologies that form the basis for ARACHNID. Author

N95-17200*# National Aeronautics and Space Administration. Goddard Space Flight Center, Greenbelt, MD.

A LOW-COST TRANSPORTABLE GROUND STATION FOR CAPTURE AND PROCESSING OF DIRECT BROADCAST EOS SATELLITE DATA

Don Davis, Toby Bennett, and Nicholas M. Short, Jr. *In its* Third International Symposium on Space Mission Operations and Ground Data Systems, Part 1 Nov. 1994 p 187-195 (For primary document see N95-17179 04-17)

Avail: CASI HC A02/MF A06

The Earth Observing System (EOS), part of a cohesive national effort to study global change, will deploy a constellation of remote sensing spacecraft over a 15 year period. Science data from the EOS spacecraft will be processed and made available to a large community of earth scientists via NASA institutional facilities. A number of these spacecraft are also providing an additional interface to broadcast data directly to users. Direct broadcast of real-time science data from overhead spacecraft has valuable applications including validation of field measurements, planning science campaigns, and science and engineering education. The success and usefulness of EOS direct broadcast depends largely on the end-user cost of receiving the data. To extend this capability to the largest possible user base, the cost of receiving ground stations must be as low as possible. To achieve this goal, NASA Goddard Space Flight Center is developing a prototype low-cost transportable ground station for EOS direct broadcast data based on Very Large Scale Integration (VLSI) components and pipelined, multiprocessing architectures. The targeted reproduction cost of this system is less than $200K. This paper describes a prototype ground station and its constituent components. Author (revised)

N95-17201*# National Aeronautics and Space Administration. Goddard Space Flight Center, Greenbelt, MD.

APPLICATIONS OF MASSIVELY PARALLEL COMPUTERS IN TELEMETRY PROCESSING

Tarek A. El-Ghazawi (George Washington Univ., Washington, DC.), Jim Pritchard, and Gordon Knoble *In its* Third International Symposium on Space Mission Operations and Ground Data Systems, Part 1 Nov. 1994 p 197-204 (For primary document see N95-17179 04-17)

Avail: CASI HC A02/MF A06

Telemetry processing refers to the reconstruction of full resolution raw instrumentation data with artifacts, of space and ground recording and transmission, removed. Being the first processing phase of satellite data, this process is also referred to as level-zero processing. This study is aimed at investigating the use of massively parallel computing technology in providing level-zero processing to spaceflights that adhere to the recommendations of the Consultative Committee on Space Data Systems (CCSDS). The workload characteristics, of level-zero processing, are used to identify processing requirements in high-performance computing systems. An example of level-zero functions on a SIMD MPP, such as the MasPar, is discussed. The requirements in this paper are based in part on the Earth Observing System (EOS) Data and Operation System (EDOS).

Author

N95-17202*# Jet Propulsion Lab., California Inst. of Tech., Pasadena, CA.

TEST TELEMETRY AND COMMAND SYSTEM (TTACS)

Alvin J. Fogel *In* NASA. Goddard Space Flight Center, Third International Symposium on Space Mission Operations and Ground Data Systems, Part 1 Nov. 1994 p 205-212 (For primary document see N95-17179 04-17)

Avail: CASI HC A02/MF A06

The Jet Propulsion Laboratory has developed a multimission Test Telemetry and Command System (TTACS) which provides a multimission telemetry and command data system in a spacecraft test environment. TTACS reuses, in the spacecraft test environment, components of the same data system used for flight operations; no new software is developed for the spacecraft test environment. Additionally, the TTACS is transportable to any spacecraft test site, including the launch site. The TTACS is currently operational in the Galileo spacecraft testbed; it is also being provided to support the Cassini and Mars Surveyor Program projects. Minimal personnel data system training is required in the transition from pre-launch spacecraft test to post-launch flight operations since test personnel are already familiar with the data system's operation. Additionally, data system components, e.g. data display, can be reused to support spacecraft software development;

and the same data system components will again be reused during the spacecraft integration and system test phases. TTACS usage also results in early availability of spacecraft data to data system development and, as a result, early data system development feedback to spacecraft system developers. The TTACS consists of a multimission spacecraft support equipment interface and components of the multimission telemetry and command software adapted for a specific project. The TTACS interfaces to the spacecraft, e.g., Command Data System (CDS), support equipment. The TTACS telemetry interface to the CDS support equipment performs serial (RS-422)-to-ethernet conversion at rates between 1 bps and 1 mbps, telemetry data blocking and header generation, guaranteed data transmission to the telemetry data system, and graphical downlink routing summary and control. The TTACS command interface to the CDS support equipment is nominally a command file transferred in non-real-time via ethernet. The CDS support equipment is responsible for metering the commands to the CDS; additionally for Galileo, TTACS includes a real-time-interface to the CDS support equipment. The TTACS provides the basic functionality of the multimission telemetry and command data system used during flight operations. TTACS telemetry capabilities include frame synchronization, Reed-Solomon decoding, packet extraction and channelization, and data storage/query. Multimission data display capabilities are also available. TTACS command capabilities include command generation verification, and storage. Author (revised)

N95-17203*# European Space Agency. European Space Operations Center, Darmstadt (Germany). Technology Development Div.

GROUND EQUIPMENT FOR THE SUPPORT OF PACKET TELEMETRY AND TELECOMMAND

Wolfgang Hell *In* NASA. Goddard Space Flight Center, Third International Symposium on Space Mission Operations and Ground Data Systems, Part 1 Nov. 1994 p 213-224 (For primary document see N95-17179 04-17)

Avail: CASI HC A03/MF A06

This paper describes ground equipment for packet telemetry and telecommand which has been recently developed by industry for the European Space Agency. The architectural concept for this type of equipment is outlined and the actual implementation is presented. Focus is put on issues related to cross support and telescience as far as they affect the design of the interfaces to the users of the services provided by the equipment and to the management entities in charge of equipment control and monitoring. Author

N95-17204*# Jet Propulsion Lab., California Inst. of Tech., Pasadena, CA.

PROCESS AND METHODOLOGY OF DEVELOPING CASSINI G AND C TELEMETRY DICTIONARY

Edwin P. Kan *In* NASA. Goddard Space Flight Center, Third International Symposium on Space Mission Operations and Ground Data Systems, Part 1 Nov. 1994 p 225-232 (For primary document see N95-17179 04-17)

Avail: CASI HC A02/MF A06

While the Cassini spacecraft telemetry design had taken on the new approach of 'packetized telemetry', the AACS (Attitude and Articulation Subsystem) had further extended into the design of 'mini-packets' in its telemetry system. Such telemetry packet and mini-packet design produced the AACS Telemetry Dictionary; iterations of the latter in turn provided changes to the former. The ultimate goals were to achieve maximum telemetry packing density, optimize the 'freshness' of more time-critical data, and to effect flexibility, i.e., multiple AACS data collection schemes, without needing to change the overall spacecraft telemetry mode. This paper describes such a systematic process and methodology, evidenced by various design products related to, or as part of, the AACS Telemetry Dictionary. Author

N95-17205*# Jet Propulsion Lab., California Inst. of Tech., Pasadena, CA.

MULTIMISSION TELEMETRY VISUALIZATION (MTV) SYSTEM: A MISSION APPLICATIONS PROJECT FROM JPL'S MULTIMEDIA COMMUNICATIONS LABORATORY

Ernest Koeberlein, III and Shaw Exum Pender *In* NASA. Goddard Space Flight Center, Third International Symposium on Space Mission Operations and Ground Data Systems, Part 1 Nov. 1994 p 233-240 (For primary document see N95-17179 04-17)

Avail: CASI HC A02/MF A06

This paper describes the Multimission Telemetry Visualization (MTV) data acquisition/distribution system. MTV was developed by JPL's Multimedia Communications Laboratory (MCL) and designed to process and display digital, real-time, science and engineering data from JPL's Mission Control Center. The MTV system can be accessed using UNIX workstations and PC's over common datacom and telecom networks from worldwide locations. It is designed to lower data distribution costs while increasing data analysis functionality by integrating low-cost, off-the-shelf desktop hardware and software. MTV is expected to significantly lower the cost of real-time data display, processing, distribution, and allow for greater spacecraft safety and mission data access. Author

N95-17206*# National Aeronautics and Space Administration. Goddard Space Flight Center, Greenbelt, MD.

VLSI TECHNOLOGY FOR SMALLER, CHEAPER, FASTER RETURN LINK SYSTEMS

Kathy Nanzetta, Parminder Ghuman, Toby Bennett, Jeff Solomon (RMS Technologies, Inc., Landover, MD.), Jason Dowling (Loral AeroSys, Seabrook, MD.), and John Welling (Loral AeroSys, Seabrook, MD.) *In its* Third International Symposium on Space Mission Operations and Ground Data Systems, Part 1 Nov. 1994 p 241-248 (For primary document see N95-17179 04-17)

Avail: CASI HC A02/MF A06

Very Large Scale Integration (VLSI) Application-specific Integrated Circuit (ASIC) technology has enabled substantially smaller, cheaper, and more capable telemetry data systems. However, the rapid growth in available ASIC fabrication densities has far outpaced the application of this technology to telemetry systems. Available densities have grown by well over an order magnitude since NASA's Goddard Space Flight Center (GSFC) first began developing ASIC's for ground telemetry systems in 1985. To take advantage of these higher integration levels, a new generation of ASIC's for return link telemetry processing is under development. These new submicron devices are designed to further reduce the cost and size of NASA return link processing systems while improving performance. This paper describes these highly integrated processing components. Author

N95-17207*# Satellite Operational Services G.m.b.H., Gilching (Germany).

TELEMETRY DISTRIBUTION AND PROCESSING FOR THE SECOND GERMAN SPACELAB MISSION D-2

E. Rabenau and W. Kruse (Deutsche Forschungs- und Versuchsanstalt fuer Luft- und Raumfahrt, Oberpfaffenhofen, Germany.) *In* NASA. Goddard Space Flight Center, Third International Symposium on Space Mission Operations and Ground Data Systems, Part 1 Nov. 1994 p 249-256 (For primary document see N95-17179 04-17)

Avail: CASI HC A02/MF A06

For the second German Spacelab Mission D-2 all activities related to operating, monitoring and controlling the experiments on board the Spacelab were conducted from the German Space Operations Control Center (GSOC) operated by the Deutsche Forschungsanstalt fur Luft- und Raumfahrt (DLR) in Oberpfaffenhofen, Germany. The operational requirements imposed new concepts on the transfer of data between Germany and the NASA centers and the processing of data at the GSOC itself. Highlights were the upgrade of the Spacelab Data Processing Facility (SLDPF) to real time data processing, the introduction of packet telemetry and the development of the high-rate data handling front end, data processing and display systems at GSOC. For the first time, a robot on board the Spacelab was to be controlled from the ground in a closed loop environment. A dedicated forward channel was implemented to transfer the robot manipulation commands originating from the robotics experiment ground station to the Spacelab via the Orbiter's text and graphics system interface. The capability to perform telescience from an external user center was implemented. All interfaces proved successful during the course of the D-2 mission and are described in detail in this paper. Author

N95-17208*# National Aeronautics and Space Administration. Goddard Space Flight Center, Greenbelt, MD.

LESSONS LEARNED SUPPORTING ONBOARD SOLID-STATE RECORDERS c35

Jeff Shi (RMS Technologies, Inc., Landover, MD.), Tony Mao (RMS Technologies, Inc., Landover, MD.), Tim Clotworthy (RMS Technologies, Inc., Landover, MD.), and Gerald Grebowsky *In its* Third International Symposium on Space Mission Operations and Ground Data Systems, Part 1 Nov. 1994 p 257-264 (For primary document see N95-17179 04-17)
Avail: CASI HC A02/MF A06

With the advance of semiconductor technology, Solid-State Recorders (SSR) have matured and been accepted as primary onboard data storage devices. Their high reliability, simpler interface and control, and high flexibility have made the SSR's a superb choice in today's spacecraft design. While there are many benefits, the use of SSR's may also add significant complexity to ground data systems. For instance, real-time and playback data may be interleaved into the same data stream, making data sequencing and time ordering difficult. Stored data may be played back out of time order, increasing processing load significantly. Data may also be played back after being sorted by Virtual Channels in the SSR, potentially creating bursts in packet rates that exceed the real-time processing capabilities of the ground systems. This paper presents a summary of lessons learned through the efforts in supporting a number of NASA's missions that employ SSR's. It describes various problems encountered through the design process, and their potential impact on ground system performance, resources, and cost. Recommended approaches to minimizing the impact are demonstrated by examples. The discussion leads to the conclusion that the use of SSR's demands an even higher level of cooperation between spacecraft and ground system designers in order to build the most cost effective end-to-end system. Author

N95-17209*# European Space Agency. European Space Operations Center, Darmstadt (Germany).
EXPERIENCE WITH THE EURECA PACKET TELEMETRY AND PACKET TELECOMMAND SYSTEM
Erik Mose Sorensen and Paolo Ferri *In* NASA. Goddard Space Flight Center, Third International Symposium on Space Mission Operations and Ground Data Systems, Part 1 Nov. 1994 p 265-272 (For primary document see N95-17179 04-17)
Avail: CASI HC A02/MF A06

The European Retrieval Carrier (EURECA) was launched on its first flight on the 31st of July 1992 and retrieved on the 29th of June 1993. EURECA is characterized by several new on-board features, most notably Packet telemetry, and a partial implementation of packet telecommanding, the first ESA packetised spacecraft. Today more than one year after the retrieval the data from the EURECA mission has to a large extent been analysed and we can present some of the interesting results. This paper concentrates on the implementation and operational experience with the EURECA Packet Telemetry and Packet Telecommanding. We already discovered during the design of the ground system that the use of packet telemetry has major impact on the overall design and that processing of packet telemetry may have significant effect on the computer loading and sizing. During the mission a number of problems were identified with the on-board implementation resulting in very strange anomalous behaviors. Many of these problems directly violated basic assumptions for the design of the ground segment adding to the strange behavior. The paper shows that the design of a telemetry packet system should be flexible enough to allow a rapid configuration of the telemetry processing in order to adapt it to the new situation in case of an on-board failure. The experience gained with the EURECA mission control should be used to improve ground systems for future missions. Author

N95-17210*# Jet Propulsion Lab., California Inst. of Tech., Pasadena, CA.
GALILEO MISSION PLANNING FOR LOW GAIN ANTENNA BASED OPERATIONS **c32**
R. Gershman, K. L. Buxbaum, J. M. Ludwinski, and B. G. Paczkowski *In* NASA. Goddard Space Flight Center, Third International Symposium on Space Mission Operations and Ground Data Systems, Part 1 Nov. 1994 p 279-286 (For primary document see N95-17179 04-17)
Avail: CASI HC A02/MF A06

The Galileo mission operations concept is undergoing substantial redesign, necessitated by the deployment failure of the High Gain Antenna, while the spacecraft is on its way to Jupiter. The new design applies state-of-the-art technology and processes to increase the telemetry rate available through the Low Gain Antenna and to increase the information density of the telemetry. This paper describes the mission planning process being developed as part of this redesign. Principal topics include a brief description of the new mission concept and anticipated science return (these have been covered more extensively in earlier papers), identification of key drivers on the mission planning process, a description of the process and its implementation schedule, a discussion of the application of automated mission planning tool to the process, and a status report on mission planning work to date. Galileo enhancements include extensive reprogramming of on-board computers and substantial hard ware and software upgrades for the Deep Space Network (DSN). The principal mode of operation will be onboard recording of science data followed by extended playback periods. A variety of techniques will be used to compress and edit the data both before recording and during playback. A highly-compressed real-time science data stream will also be important. The telemetry rate will be increased using advanced coding techniques and advanced receivers. Galileo mission planning for orbital operations now involves partitioning of several scarce resources. Particularly difficult are division of the telemetry among the many users (eleven instruments, radio science, engineering monitoring, and navigation) and allocation of space on the tape recorder at each of the ten satellite encounters. The planning process is complicated by uncertainty in forecast performance of the DSN modifications and the non-deterministic nature of the new data compression schemes. Key mission planning steps include quantifying resource or capabilities to be allocated, prioritizing science observations and estimating resource needs for each, working inter-and intra-orbit trades of these resources among the Project elements, and planning real-time science activity. The first major mission planning activity, a high level, orbit-by-orbit allocation of resources among science objectives, has already been completed; and results are illustrated in the paper. To make efficient use of limited resources, Galileo mission planning will rely on automated mission planning tools capable of dealing with interactions among time-varying downlink capability, real-time science and engineering data transmission, and playback of recorded data. A new generic mission planning tool is being adapted for this purpose. Author

N95-17211*# National Aeronautics and Space Administration. Marshall Space Flight Center, Huntsville, AL.
A DISTRIBUTED PLANNING CONCEPT FOR SPACE STATION PAYLOAD OPERATIONS **c66**
Jeff Hagopian, Theresa Maxwell, and Tracey Reed *In* NASA. Goddard Space Flight Center, Third International Symposium on Space Mission Operations and Ground Data Systems, Part 1 Nov. 1994 p 287-294 (For primary document see N95-17179 04-17)
Avail: CASI HC A02/MF A06

The complex and diverse nature of the payload operations to be performed on the Space Station requires a robust and flexible planning approach. The planning approach for Space Station payload operations must support the phased development of the Space Station, as well as the geographically distributed users of the Space Station. To date, the planning approach for manned operations in space has been one of centralized planning to the n-th degree of detail. This approach, while valid for short duration flights, incurs high operations costs and is not conducive to long duration Space Station operations. The Space Station payload operations planning concept must reduce operations costs, accommodate phased station development, support distributed users, and provide flexibility. One way to meet these objectives is to distribute the planning functions across a hierarchy of payload planning organizations based on their particular needs and expertise. This paper presents a planning concept which satisfies all phases of the development of the Space Station (manned Shuttle flights, unmanned Station operations, and permanent manned operations), and the migration from centralized to distributed planning functions. Identified in this paper are the payload planning functions which can be distributed and the process by which these functions are performed. Author

N95-17212*# Massachusetts Inst. of Tech., Cambridge. Lincoln Lab.
MISSION PLANNING FOR SPACE BASED SATELLITE SURVEILLANCE EXPERIMENTS WITH THE MSX **c12**
R. Sridharan, T. Fishman, E. Robinson, H. Viggh, and A. Wiseman *In* NASA. Goddard Space Flight Center, Third International Symposium on Space Mission Operations and Ground Data Systems, Part 1 Nov. 1994 p 295-303 (For primary document see N95-17179 04-17)
Avail: CASI HC A02/MF A06

The Midcourse Space Experiment is a BMDO-sponsored scientific satellite set for launch within the year. The satellite will collect phenomenology data on missile targets, plumes, earth limb backgrounds and deep space backgrounds in the LWIR, visible and ultra-violet spectral bands. It will also conduct functional demonstrations for space-based space surveillance. The Space-Based Visible sensor, built by Lincoln Laboratory, Massachusetts Institute of Technology, is the primary sensor on board the MSX for demonstration of space surveillance. The SBV Processing, Operations and Control Center (SPOCC) is the mission planning and commanding center for all space surveillance experiments using the SBV and other MSX instruments. The guiding principle in the SPOCC Mission Planning System was that all routine functions be automated. Manual analyst input should be minimal. Major concepts are: (I) A high level language, called SLED, for user interface to the system; (2) A group of independent software processes which would generally be run in a pipe-line mode for experiment commanding but can be run independently for analyst assessment; (3) An integrated experiment cost computation function that permits assessment of the feasibility of the experiment. This paper will report on the design, implementation and testing of the Mission Planning System. Author

N95-17213*# European Space Agency. European Space Operations Center, Darmstadt (Germany).

ENGINEERING ULYSSES EXTENDED MISSION **c12**

Shaun Standley *In* NASA. Goddard Space Flight Center, Third International Symposium on Space Mission Operations and Ground Data Systems, Part 1 Nov. 1994 p 305-309 (For primary document see N95-17179 04-17)

Avail: CASI HC A01/MF A06

The Ulysses Mission is a collaboration between the European Space Agency (ESA) and the National Aeronautics and Space Administration (NASA). The mission is unique, enabling exploration of the heliosphere within a few astronomical units of the Sun over a full range of heliographic latitudes adding a third dimension to our understanding of the Solar System. The advanced scientific instrumentation on Ulysses continually measures the properties of the heliospheric magnetic field, the solar wind, solar radio bursts and plasma waves, galactic cosmic rays, energetic particles, solar X-rays, and interstellar neutral gas. By the end of 1995, the spacecraft will have completed measurements at heliographic latitudes up to 80 degrees over a single orbit of the Sun. The properties of the heliosphere are solar cycle dependent, and Ulysses' first orbit of the Sun will have taken place around a solar minimum. In order to characterize the heliosphere over a full (11 year) solar cycle, it is desirable to continue measurements over a second orbit of the Sun, a new Odyssey that will extend through 2001. Since the spacecraft was only designed for a five-year mission, a number of technical challenges have been surmounted in order to demonstrate the engineering feasibility of this unparalleled scientific opportunity. This paper describes the changes that were necessary to the Ulysses mission engineering and mission operations in order to ensure continual, effective payload operation throughout 1996-2001. Author

N95-17214*# National Aeronautics and Space Administration, Washington, DC.

ACCURACY ANALYSIS OF TDRSS DEMAND FORECASTS **c32**

Daniel C. Stern, Allen J. Levine (National Aeronautics and Space Administration. Goddard Space Flight Center, Greenbelt, MD.), and Karl J. Pitt (Mitre Corp., Greenbelt, MD.) *In* NASA. Goddard Space Flight Center, Third International Symposium on Space Mission Operations and Ground Data Systems, Part 1 Nov. 1994 p 311-318 (For primary document see N95-17179 04-17)

Avail: CASI HC A02/MF A06

This paper reviews Space Network (SN) demand forecasting experience over the past 16 years and describes methods used in the forecasts. The paper focuses on the Single Access (SA) service, the most sought-after resource in the Space Network. Of the ten years of actual demand data available, only the last five years (1989 to 1993) were considered predictive due to the extensive impact of the Challenger accident of 1986. NASA's Space Network provides tracking and communications services to user spacecraft such as the Shuttle and the Hubble Space Telescope. Forecasting the customer requirements is essential to planning network resources and to establishing service commitments to future customers. The lead time to procure Tracking and Data Relay Satellites (TDRS's) requires demand forecasts ten years in the future a planning horizon beyond the funding commitments for missions to be supported. The long range forecasts are shown to have had a bias toward underestimation in the 1991 -1992 period. The trend of underestimation can be expected to be replaced by overestimation for a number of years starting with 1998. At that time demand from new missions slated for launch will be larger than the demand from ongoing missions, making the potential for delay the dominant factor. If the new missions appear as scheduled, the forecasts are likely to be moderately underestimated. The SN commitment to meet the negotiated customer's requirements calls for conservatism in the forecasting. Modification of the forecasting procedure to account for a delay bias is, therefore, not advised. Fine tuning the mission model to more accurately reflect the current actual demand is recommended as it may marginally improve the first year forecasting. Author

N95-17215*# Massachusetts Inst. of Tech., Cambridge. Lincoln Lab.

JOINT OPERATIONS PLANNING FOR SPACE SURVEILLANCE MISSIONS ON THE MSX SATELLITE **c12**

Grant Stokes and Andrew Good (Johns Hopkins Univ., Laurel, MD.) *In* NASA. Goddard Space Flight Center, Third International Symposium on Space Mission Operations and Ground Data Systems, Part 1 Nov. 1994 p 319-326 (For primary document see N95-17179 04-17)

Avail: CASI HC A02/MF A06

The Midcourse Space Experiment (MSX) satellite, sponsored by BMDO, is intended to gather broad-band phenomenology data on missiles, plumes, naturally occurring earthlimb backgrounds and deep space backgrounds. In addition the MSX will be used to conduct functional demonstrations of space-based space surveillance. The JHU/Applied Physics Laboratory (APL), located in Laurel, MD, is the integrator and operator of the MSX satellite. APL will conduct all operations related to the MSX and is charged with the detailed operations planning required to implement all of the experiments run on the MSX except the space surveillance experiments. The non-surveillance operations are generally amenable to being defined months ahead of time and being scheduled on a monthly basis. Lincoln Laboratory, Massachusetts Institute of Technology (LL), located in Lexington, MA, is the provider of one of the principle MSX instruments, the Space-Based Visible (SBV) sensor, and the agency charged with implementing the space surveillance demonstrations on the MSX. The planning timelines for the space surveillance demonstrations are fundamentally different from those for the other experiments. They are generally amenable to being scheduled on a monthly basis, but the specific experiment sequence and pointing must be refined shortly before execution. This allocation of responsibilities to different organizations implies the need for a joint mission planning system for conducting space surveillance demonstrations. This paper details the iterative, joint planning system, based on passing responsibility for generating MSX commands for surveillance operations from APL to LL for specific scheduled operations. The joint planning system, including the generation of a budget for spacecraft resources to be used for surveillance events, has been successfully demonstrated during ground testing of the MSX and is being validated for MSX launch within the year. The planning system developed for the MSX forms a model possibly applicable to developing distributed mission planning systems for other multi-use satellites. Author

N95-17216*# Jet Propulsion Lab., California Inst. of Tech., Pasadena, CA.

INTERNATIONAL MISSION PLANNING FOR SPACE VERY LONG BASELINE INTERFEROMETRY **c12**

James S. Ulvestad *In* NASA. Goddard Space Flight Center, Third International Symposium on Space Mission Operations and Ground Data Systems, Part 1 Nov. 1994 p 329-336 (For primary document see N95-17179 04-17)

Avail: CASI HC A02/MF A06

Two spacecraft dedicated to Very Long Baseline Interferometry (VLBI) will be launched in 1996 and 1997 to make observations using baselines between the space telescopes and many of the world's ground radio telescopes. The Japanese Institute of Space and Astronautical Science (ISAS) will launch VSOP (VLBI Space Observatory Program) in September 1996, while the Russian Astro Space Center (ASC) is scheduled to launch RadioAstron in 1997. Both spacecraft will observe radio sources at frequencies near 1.7, 4.8, and 22 GHz; RadioAstron will also observe at 0.33 GHz. The baselines between space and ground telescopes will provide

3-10 times the resolution available for ground VLBI at the same observing frequencies. Ground tracking stations on four continents will supply the required precise frequency reference to each spacecraft measure the two-way residual phase and Doppler on the ground-space link, and record 128 Megabit/s of VLBI data downlinked from the spacecraft. The spacecraft data are meaningless without cross-correlation against the data from Earth-bound telescopes, which must take place at special-purpose VLBI correlation facilities. Therefore, participation by most of the world's radio observatories is needed to achieve substantial science return from VSOP and RadioAstron. The collaboration of several major space agencies and the ground observatories, which generally follow very different models for allocation of observing time and for routine operations, leads to great complexity in mission planning and in day-to-day operations. This paper describes some of those complications and the strategies being developed to assure productive scientific missions. Author

N95-17217*# Deutsche Forschungs- und Versuchsanstalt fuer Luft- und Raumfahrt, Oberpfaffenhofen (Germany).
GEOSTATIONARY SATELLITE POSITIONING BY DLR/GSOC OPERATIONS AND MANAGEMENT METHODS **c66**
Peter Brittinger *In* NASA. Goddard Space Flight Center, Third International Symposium on Space Mission Operations and Ground Data Systems, Part 1 Nov. 1994 p 339-346 (For primary document see N95-17179 04-17)
Avail: CASI HC A02/MF A06

Starting with a short description of the GSOC (German Space Operations Center) and its role within the wider framework of the research institute DLR, this paper provides a review of the geostationary telecommunications satellites positioned by the GSOC. The paper then proceeds to describe the evolution of the operations and management structures and methods which have been effectively used to accomplish these missions. Author

N95-17218*# Martin Marietta Corp., Denver, CO.
MAGELLAN PROJECT: EVOLVING ENHANCED OPERATIONS EFFICIENCY TO MAXIMIZE SCIENCE VALUE **c66**
Allan R. Cheuvront, James C. Neuman, and J. Franklin McKinney *In* NASA. Goddard Space Flight Center, Third International Symposium on Space Mission Operations and Ground Data Systems, Part 1 Nov. 1994 p 347-354 Sponsored by JPL (For primary document see N95-17179 04-17)
Avail: CASI HC A02/MF A06

Magellan has been one of NASA's most successful spacecraft, returning more science data than all planetary spacecraft combined. The Magellan Spacecraft Team (SCT) has maximized the science return with innovative operational techniques to overcome anomalies and to perform activities for which the spacecraft was not designed. Commanding the spacecraft was originally time consuming because the standard development process was envisioned as manual tasks. The Program understood that reducing mission operations costs were essential for an extended mission. Management created an environment which encouraged automation of routine tasks, allowing staff reduction while maximizing the science data returned. Data analysis and trending, command preparation, and command reviews are some of the tasks that were automated. The SCT has accommodated personnel reductions by improving operations efficiency while returning the maximum science data possible. Author

N95-17219*# European Space Agency. Ulysses Office, Pasadena, CA.
GRAND MISSION VERSUS SMALL OPS TEAM: CAN WE HAVE BOTH? **c66**
Raul Garcia-Perez *In* NASA. Goddard Space Flight Center, Third International Symposium on Space Mission Operations and Ground Data Systems, Part 1 Nov. 1994 p 355-360 (For primary document see N95-17179 04-17)
Avail: CASI HC A02/MF A06

Space Missions are growing more ambitious, but resources are getting smaller. Is this is a contradiction in terms, or is it a healthy challenge? This paper offers the author's point of view as a member of a small Mission Operations Team that carries out an ambitious international mission (Ulysses ESA/NASA). Author

N95-17220*# Johns Hopkins Univ., Laurel, MD. Applied Physics Lab.
THE ROLE OF MISSION OPERATIONS IN SPACECRAFT INTEGRATION AND TEST **c66**
Raymond J. Harvey *In* NASA. Goddard Space Flight Center, Third International Symposium on Space Mission Operations and Ground Data Systems, Part 1 Nov. 1994 p 361-369 (For primary document see N95-17179 04-17)
Avail: CASI HC A02/MF A06

The participation of mission operations personnel in the spacecraft integration and test process offers significant benefits to spacecraft programs in terms of test efficiency, staffing and training efficiency, test completeness, and subsequent cost containment. Operations personnel who have had real-time contact experience and have been responsible for the assessment of on orbit spacecraft operations bring a unique view of spacecraft operations to pre-launch spacecraft test activities. Because of the unique view of the spacecraft/ground interface that experienced operations personnel have, they can propose optimum test approaches and optimum test data analysis techniques. Additionally, the testing that is typically required to validate operations methodologies can be integrated into spacecraft performance testing scenarios. Author

N95-17221*# European Space Agency. European Space Research and Technology Center, ESTEC, Noordwijk (Netherlands).
PAYLOAD OPERATIONS MANAGEMENT OF A PLANNED EUROPEAN SL-MISSION EMPLOYING ESTABLISHMENTS OF ESA AND NATIONAL AGENCIES **c66**
Rolf Joensson and Karl L. Mueller (Deutsche Forschungsanstalt fuer Luft- und Raumfahrt, Cologne, Germany.) *In* NASA. Goddard Space Flight Center, Third International Symposium on Space Mission Operations and Ground Data Systems, Part 1 Nov. 1994 p 371-376 (For primary document see N95-17179 04-17)
Avail: CASI HC A02/MF A06

Spacelab (SL)-missions with Payload Operations (P/L OPS) from Europe involve numerous space agencies, various ground infrastructure systems and national user organizations. An effective management structure must bring together different entities, facilities and people, but at the same time keep interfaces, costs and schedule under strict control. This paper outlines the management concept for P/L OPS of a planned European SL-mission. The proposal draws on the relevant experience in Europe, which was acquired via the ESA/NASA mission SL-1, by the execution of two German SL-missions and by the involvement in, or the support of, several NASA-missions. Author

N95-17222*# Stanford Telecommunications, Inc., Reston, VA.
EVALUATING SPACE NETWORK (SN) SCHEDULING OPERATIONS CONCEPTS THROUGH STATISTICAL ANALYSIS **c66**
Carl Kwadrat and Nadine Happell *In* NASA. Goddard Space Flight Center, Third International Symposium on Space Mission Operations and Ground Data Systems, Part 1 Nov. 1994 p 377-388 (For primary document see N95-17179 04-17)
Avail: CASI HC A03/MF A06

The Network Control Center (NCC) currently uses the NCC Data System (NCCDS) to schedule customer spacecraft communication requests for the Space Network (SN). The NCC/Request Oriented Scheduling Engine (NCC/ROSE), which implements an operational concept called flexible scheduling, is being tested as a potential replacement for the NCCDS scheduler in an effort to increase the efficiency of the NCC scheduling operations. This paper describes the high fidelity benchmark tests being conducted on NCC/ROSE, the evaluation techniques used to compare schedules, and the results of the tests. This testing will verify the increases in efficiency and productivity that can help the NCC meet the anticipated scheduling loads well into the next century. Author

N95-17223*# Centre National d'Etudes Spatiales, Toulouse (France).
SPOT4 MANAGEMENT CENTRE **c14**
Yves Labrune, X. Labbe (Compagnie Internationale de Service en Informatique, Toulouse, France.), A. Roussel (Compagnie Internationale de Service en Informatique, Toulouse, France.), and P. Vielcanet (Compagnie Internationale de Service en Informatique, Toulouse, France.) *In* NASA. Goddard Space Flight Center, Third International Symposium on Space Mission Operations and Ground Data Systems, Part 1 Nov. 1994

p 389-396 (For primary document see N95-17179 04-17)
Avail: CASI HC A02/MF A06

In the context of the CNES SPOT4 program CISI is particularly responsible for the development of the SPOT4 Management Centre, part of the SPOT4 ground control system located at CNES Toulouse (France) designed to provide simultaneous control over two satellites. The main operational activities are timed to synchronize with satellite visibilities (ten usable passes per day). The automatic capability of this system is achieved through agenda services (sequence of operations as defined and planned by operator). Therefore, the SPOT4 Management Centre offers limited, efficient and secure human interventions for supervision and decision making. This paper emphasizes the main system characteristics as degree of automation, level of dependability and system parameterization. Author

N95-17224*# National Aeronautics and Space Administration. Goddard Space Flight Center, Greenbelt, MD.
NICKEL CADMIUM BATTERY OPERATIONS AND PERFORMANCE c33
Gopalakrishna Rao, Jill Prettyman-Lukoschek (Loral AeroSys, Seabrook, MD.), Richard Calvin (Martin Marietta Services, Inc., Greenbelt, MD.), Thomas Berry (Allied-Signal Technical Services Corp., Columbia, MD.), Robert Bote (Allied-Signal Technical Services Corp., Columbia, MD.), and Mark Toft (Jackson and Tull, Inc., Seabrook, MD.) *In its* Third International Symposium on Space Mission Operations and Ground Data Systems, Part 1 Nov. 1994 p 399-408 (For primary document see N95-17179 04-17)
Avail: CASI HC A02/MF A06

The Earth Radiation Budget Satellite (ERBS), Compton Gamma Ray Observatory (CGRO), Upper Atmosphere Research Satellite (UARS), and Extreme Ultraviolet Explorer (EUVE) spacecraft are operated from NASA's Goddard Space Flight Center (GSFC) in Greenbelt, Maryland. On-board power subsystems for each satellite employ NASA Standard 50 Ampere-hour (Ah) nickel-cadmium batteries in a parallel configuration. To date, these batteries have exhibited degradation over periods from several months (anomalous behavior, UARS and CGRO (MPS-1); to little if any, EUVE) to several years (old age, normal behavior, ERBS). Since the onset of degraded performance, each mission's Flight Operations Team (FOT), under the direction of their cognizant GSFC Project Personnel and Space Power Application Branch's Engineers has closely monitored the battery performance and implemented several charge control schemes in an effort to extend battery life. Various software and hardware solutions have been developed to minimize battery overcharge. Each of the four sections of this paper covers a brief overview of each mission's operational battery management and its associated spacecraft battery performance. Also included are new operational procedures developed on-orbit that may be of special interest to future mission definition and development. Author

N95-17225*# Loral AeroSys, Seabrook, MD.
MISSION OPERATIONS MANAGEMENT c66
David A. Rocco *In* NASA. Goddard Space Flight Center, Third International Symposium on Space Mission Operations and Ground Data Systems, Part 1 Nov. 1994 p 409-416 (For primary document see N95-17179 04-17)
Avail: CASI HC A02/MF A06

Redefining the approach and philosophy that operations management uses to define, develop, and implement space missions will be a central element in achieving high efficiency mission operations for the future. The goal of a cost effective space operations program cannot be realized if the attitudes and methodologies we currently employ to plan, develop, and manage space missions do not change. A management philosophy that is in synch with the environment in terms of budget, technology, and science objectives must be developed. Changing our basic perception of mission operations will require a shift in the way we view the mission. This requires a transition from current practices of viewing the mission as a unique end product, to a 'mission development concept' built on the visualization of the end-to-end mission. To achieve this change we must define realistic mission success criteria and develop pragmatic approaches to achieve our goals. Custom mission development for all but the largest and most unique programs is not practical in the current budget environment, and we simply do not have the resources to implement all of our planned science programs. We need to shift our management focus to allow us the opportunity make use of methodologies and approaches which are based on common building blocks that can be utilized in the space, ground, and mission unique segments of all missions. Author

N95-17226*# Allied-Signal Technical Services Corp., Columbia, MD.
GRTS OPERATIONS MONITOR/CONTROL SYSTEM c66
Richard A. Rohrer *In* NASA. Goddard Space Flight Center, Third International Symposium on Space Mission Operations and Ground Data Systems, Part 1 Nov. 1994 p 417-423 (For primary document see N95-17179 04-17)
Avail: CASI HC A02/MF A06

An Operations Monitor/Control System (OMCS) was developed to support remote ground station equipment. The ground station controls a Tracking Data Relay Satellite (TDRS) relocated to provide coverage in the tracking system's zone of exclusion. The relocated satellite significantly improved data recovery for the Gamma Ray Observatory mission. The OMCS implementation, performed in less than 11 months, was mission critical to TDRS drift operations. Extensive use of Commercial Off The Shelf (COTS) hardware and software products contributed to implementation success. The OMCS has been operational for over 9 months with no significant problems. This paper will share our experiences in OMCS development and integration. Author

N95-17227*# National Aeronautics and Space Administration. Marshall Space Flight Center, Huntsville, AL.
INTERNATIONAL SPACE STATION ALPHA USER PAYLOAD OPERATIONS CONCEPT c66
Ronald A. Schlagheck, William B. Crysel (Boeing Defense and Space Group, Huntsville, AL.), Elaine F. Duncan, and James W. Rider (Teledyne Brown Engineering, Huntsville, AL.) *In* NASA. Goddard Space Flight Center, Third International Symposium on Space Mission Operations and Ground Data Systems, Part 1 Nov. 1994 p 425-433 (For primary document see N95-17179 04-17)
Avail: CASI HC A02/MF A06

International Space Station Alpha (ISSA) will accommodate a variety of user payloads investigating diverse scientific and technology disciplines on behalf of five international partners: Canada, Europe, Japan, Russia, and the United States. A combination of crew, automated systems, and ground operations teams will control payload operations that require complementary on-board and ground systems. This paper presents the current planning for the ISSA U.S. user payload operations concept and the functional architecture supporting the concept. It describes various NASA payload operations facilities, their interfaces, user facility flight support, the payload planning system, the onboard and ground data management system, and payload operations crew and ground personnel training. This paper summarizes the payload operations infrastructure and architecture developed at the Marshall Space Flight Center (MSFC) to prepare and conduct ISSA on-orbit payload operations from the Payload Operations Integration Center (POIC), and from various user operations locations. The authors pay particular attention to user data management, which includes interfaces with both the onboard data management system and the ground data system. Discussion covers the functional disciplines that define and support POIC payload operations: Planning, Operations Control, Data Management, and Training. The paper describes potential interfaces between users and the POIC disciplines, from the U.S. user perspective. Author

N95-17228*# Jet Propulsion Lab., California Inst. of Tech., Pasadena, CA.
SHARED MISSION OPERATIONS CONCEPT c66
Gary L. Spradlin, Richard P. Rudd, and Susan H. Linick *In* NASA. Goddard Space Flight Center, Third International Symposium on Space Mission Operations and Ground Data Systems, Part 1 Nov. 1994 p 435-442 (For primary document see N95-17179 04-17)
Avail: CASI HC A02/MF A06

Historically, new JPL flight projects have developed a Mission Operations System (MOS) as unique as their spacecraft, and have utilized a mission-dedicated staff to monitor and control the spacecraft through the MOS. NASA budgetary pressures to reduce mission operations costs have led to the development and reliance on multimission ground system capabilities. The use of these multimission capabilities has not eliminated an ongoing requirement for a nucleus of personnel familiar with a given spacecraft and its mission to perform mission-dedicated operations. The high cost of skilled personnel required to support projects with diverse mission objectives has the potential for significant reduction through shared mission operations among mission-compatible projects. Shared mission operations are feasible if: (1) the missions do not conflict with one another

in terms of peak activity periods, (2) a unique MOS is not required, and (3) there is sufficient similarity in the mission profiles so that greatly different skills would not be required to support each mission. This paper will further develop this shared mission operations concept. We will illustrate how a Discovery-class mission would enter a 'partner' relationship with the Voyager Project, and can minimize MOS development and operations costs by early and careful consideration of mission operations requirements.
Author

N95-17229*# Jet Propulsion Lab., California Inst. of Tech., Pasadena, CA.
MARS PATHFINDER MISSION OPERATIONS CONCEPTS **c66**
Francis M. Sturms, Jr., William C. Dias, Albert Y. Nakata, and Wallace S. Tai *In* NASA. Goddard Space Flight Center, Third International Symposium on Space Mission Operations and Ground Data Systems, Part 1 Nov. 1994 p 443-450 (For primary document see N95-17179 04-17)
Avail: CASI HC A02/MF A06

The Mars Pathfinder Project plans a December 1996 launch of a single spacecraft. After jettisoning a cruise stage, an entry body containing a lander and microrover will directly enter the Mars atmosphere and parachute to a hard landing near the sub-solar latitude of 15 degrees North in July 1997. Primary surface operations last for 30 days. Cost estimates for Pathfinder ground systems development and operations are not only lower in absolute dollars, but also are a lower percentage of total project costs than in past planetary missions. Operations teams will be smaller and fewer than typical flight projects. Operations scenarios have been developed early in the project and are being used to guide operations implementation and flight system design. Recovery of key engineering data from entry, descent, and landing is a top mission priority. These data will be recorded for playback after landing. Real-time tracking of a modified carrier signal through this phase can provide important insight into the spacecraft performance during entry, descent, and landing in the event recorded data is never recovered. Surface scenarios are dominated by microrover activity and lander imaging during 7 hours of the Mars day from 0700 to 1400 local solar time. Efficient uplink and downlink processes have been designed to command the lander and microrover each Mars day.
Author

N95-17230*# MATRA Marconi Space, Toulouse (France).
TOWARDS A NEW GENERATION OF MISSION PLANNING SYSTEMS: FLEXIBILITY AND PERFORMANCE **c66**
A. Gasquet, Y. Parrod, and A. DeSaintVincent *In* NASA. Goddard Space Flight Center, Third International Symposium on Space Mission Operations and Ground Data Systems, Part 1 Nov. 1994 p 453-460 (For primary document see N95-17179 04-17)
Avail: CASI HC A02/MF A06

This paper presents some new approaches which are required for a better adequacy of Mission Planning Systems. In particular, the performance flexibility and genericity issues are discussed based on experience acquired through various Mission Planning systems developed by Matra Marconi Space.
Author

N95-17231*# National Aeronautics and Space Administration. Marshall Space Flight Center, Huntsville, AL.
GENERIC MISSION PLANNING AND SCHEDULING: THE AXAF SOLUTION **c81**
O. T. Guffin and M. Newhouse (Computer Sciences Corp., Huntsville, AL.) *In* NASA. Goddard Space Flight Center, Third International Symposium on Space Mission Operations and Ground Data Systems, Part 1 Nov. 1994 p 461-466 (For primary document see N95-17179 04-17)
Avail: CASI HC A02/MF A06

During SpaceOps 92 the idea of generic mission planning concepts for space astronomy missions, that could be applied to future missions in order to simplify software development, was introduced. It was proposed that mission planning systems could be decomposed into functional elements that could be standardized and then organized into optimal functional flows for each individual mission. In addition, it was further suggested that these flows themselves could be reduced to a small set of possibilities by describing them in terms of generic mission type, such as manned, unmanned, high orbit, low orbit, etc. The Advanced X-ray Astrophysics Facility (AXAF), planned for launch in the latter part of '98, represents the first application of this idea on an unmanned mission. This paper examines the AXAF Mission Planning and Scheduling concept in light of the generic system theory. Each functional element is evaluated according to AXAF characteristics and requirements and then compared to its generic counterpart. Functional flow considerations are then derived from the overall AXAF mission planning concept to determine the viability and sensitivity of the generic flow to actual requirements. The results of this analysis are then used to update the generic system concept and to define the level of commonality and core system components that are practical to achieve across multiple missions.
Author

N95-17232*# Centre National d'Etudes Spatiales, Toulouse (France).
A PC BASED TOOL FOR MISSION PLAN PRODUCTION **c66**
Jean-Pierre Joli and Clet Yven *In* NASA. Goddard Space Flight Center, Third International Symposium on Space Mission Operations and Ground Data Systems, Part 1 Nov. 1994 p 467-471 (For primary document see N95-17179 04-17)
Avail: CASI HC A01/MF A06

Satellite positioning is managed according to a mission plan (MP) which provides, on a minute accuracy basis, a chronological list of events and associated actions to be performed. This tool, called MM2, is designed under the Windows environment. Excel is used to provide the MP itself. A Visual Basic process then translates it into a graphic symbolic representation called flight plan (FP). During operations, MM2 is also used to log the actual event dates and/or dated OPS Manager live comments.
Author (revised)

N95-17233*# European Space Agency. European Space Operations Center, Darmstadt (Germany).
TOWARDS A CLASS LIBRARY FOR MISSION PLANNING **c66**
Oliver Pujo, Simon T. Smith (Cray Systems, Bristol, England.), Paul Starkey (Cray Systems, Bristol, England.), and Thilo Wolff *In* NASA. Goddard Space Flight Center, Third International Symposium on Space Mission Operations and Ground Data Systems, Part 1 Nov. 1994 p 473-480 (For primary document see N95-17179 04-17)
Avail: CASI HC A02/MF A06

The PASTEL Mission Planning System (MPS) has been developed in C++ using an object-oriented (OO) methodology. While the scope and complexity of this system cannot compare to that of an MPS for a complex mission one of the main considerations of the development was to ensure that we could reuse some of the classes in future MPS. We present here PASTEL MPS classes which could be used in the foundations of a class library for MPS.
Author

N95-17234*# National Aeronautics and Space Administration. Goddard Space Flight Center, Greenbelt, MD.
AUTONOMOUS MISSION PLANNING AND SCHEDULING: INNOVATIVE, INTEGRATED, RESPONSIVE **c66**
Charisse Sary (Computer Sciences Corp., Beltsville, MD.), Simon Liu (Computer Sciences Corp., Beltsville, MD.), Larry Hull, and Randy Davis (Colorado Univ., Boulder, CO.) *In its* Third International Symposium on Space Mission Operations and Ground Data Systems, Part 1 Nov. 1994 p 481-488 (For primary document see N95-17179 04-17)
Avail: CASI HC A02/MF A06

Autonomous mission scheduling, a new concept for NASA ground data systems, is a decentralized and distributed approach to scientific spacecraft planning, scheduling, and command management. Systems and services are provided that enable investigators to operate their own instruments. In autonomous mission scheduling, separate nodes exist for each instrument and one or more operations nodes exist for the spacecraft. Each node is responsible for its own operations which include planning, scheduling, and commanding; and for resolving conflicts with other nodes. One or more database servers accessible to all nodes enable each to share mission and science planning, scheduling, and commanding information. The architecture for autonomous mission scheduling is based upon a realistic mix of state-of-the-art and emerging technology and services, e.g., high performance individual workstations, high speed communications, client-server computing, and relational databases. The concept is particularly suited to the smaller, less complex missions of the future.
Author

N95-17235*# Deutsche Forschungsanstalt fuer Luft- und Raumfahrt, Wessling (Germany).

A MISSION PLANNING CONCEPT AND MISSION PLANNING SYSTEM FOR FUTURE MANNED SPACE MISSIONS **c66**

Martin Wickler *In* NASA. Goddard Space Flight Center, Third International Symposium on Space Mission Operations and Ground Data Systems, Part 1 Nov. 1994 p 489-497 (For primary document see N95-17179 04-17)

Avail: CASI HC A02/MF A06

The international character of future manned space missions will compel the involvement of several international space agencies in mission planning tasks. Additionally, the community of users requires a higher degree of freedom for experiment planning. Both of these problems can be solved by a decentralized mission planning concept using the so-called 'envelope method,' by which resources are allocated to users by distributing resource profiles ('envelopes') which define resource availabilities at specified times. The users are essentially free to plan their activities independently of each other, provided that they stay within their envelopes. The new developments were aimed at refining the existing vague envelope concept into a practical method for decentralized planning. Selected critical functions were exercised by planning an example, founded on experience acquired by the MSCC during the Spacelab missions D-1 and D-2. The main activity regarding future mission planning tasks was to improve the existing MSCC mission planning system, using new techniques. An electronic interface was developed to collect all formalized user inputs more effectively, along with an 'envelope generator' for generation and manipulation of the resource envelopes. The existing scheduler and its data base were successfully replaced by an artificial intelligence scheduler. This scheduler is not only capable of handling resource envelopes, but also uses a new technology based on neuronal networks. Therefore, it is very well suited to solve the future scheduling problems more efficiently. This prototype mission planning system was used to gain new practical experience with decentralized mission planning, using the envelope method. In future steps, software tools will be optimized, and all data management planning activities will be embedded into the scheduler. Author

N95-17236*# OAO Corp., Altadena, CA.

OPERATIONS AUTOMATION **c66**

Charles Thomas Boreham *In* NASA. Goddard Space Flight Center, Third International Symposium on Space Mission Operations and Ground Data Systems, Part 1 Nov. 1994 p 501-505 (For primary document see N95-17179 04-17)

Avail: CASI HC A01/MF A06

This is truly the era of 'faster-better-cheaper' at the National Aeronautics and Space Administration/Jet Propulsion Laboratory (NASA/JPL). To continue JPL's primary mission of building and operating interplanetary spacecraft, all possible avenues are being explored in the search for better value for each dollar spent. A significant cost factor in any mission is the amount of manpower required to receive, decode, decommutate, and distribute spacecraft engineering and experiment data. The replacement of the many mission-unique data systems with the single Advanced Multimission Operations System (AMMOS) has already allowed for some manpower reduction. Now, we find that further economies are made possible by drastically reducing the number of human interventions required to perform the setup, data saving, station handover, processed data loading, and tear down activities that are associated with each spacecraft tracking pass. We have recently adapted three public domain tools to the AMMOS system which allow common elements to be scheduled and initialized without the normal human intervention. This is accomplished with a stored weekly event schedule. The manual entries and specialized scripts which had to be provided just prior to and during a pass are now triggered by the schedule to perform the functions unique to the upcoming pass. This combination of public domain software and the AMMOS system has been run in parallel with the flight operation in an online testing phase for six months. With this methodology, a savings of 11 man-years per year is projected with no increase in data loss or project risk. There are even greater savings to be gained as we learn other uses for this configuration. Author

N95-17237*# National Aeronautics and Space Administration. Goddard Space Flight Center, Greenbelt, MD.

PRODUCTION AND QUALITY ASSURANCE AUTOMATION IN THE GODDARD SPACE FLIGHT CENTER FLIGHT DYNAMICS FACILITY **c38**

K. B. Chapman (Computer Sciences Corp., Lanham, MD.), C. M. Cox (Computer Sciences Corp., Lanham, MD.), C. W. Thomas (Computer Sciences Corp., Lanham, MD.), O. O. Cuevas, and R. M. Beckman *In its* Third International Symposium on Space Mission Operations and Ground Data Systems, Part 1 Nov. 1994 p 509-516 (For primary document see N95-17179 04-17)

(Contract NAS5-31500)

Avail: CASI HC A02/MF A06

The Flight Dynamics Facility (FDF) at the NASA Goddard Space Flight Center (GSFC) generates numerous products for NASA-supported spacecraft, including the Tracking and Data Relay Satellites (TDRS's), the Hubble Space Telescope (HST), the Extreme Ultraviolet Explorer (EUVE), and the space shuttle. These products include orbit determination data, acquisition data, event scheduling data, and attitude data. In most cases, product generation involves repetitive execution of many programs. The increasing number of missions supported by the FDF has necessitated the use of automated systems to schedule, execute, and quality assure these products. This automation allows the delivery of accurate products in a timely and cost-efficient manner. To be effective, these systems must automate as many repetitive operations as possible and must be flexible enough to meet changing support requirements. The FDF Orbit Determination Task (ODT) has implemented several systems that automate product generation and quality assurance (QA). These systems include the Orbit Production Automation System (OPAS), the New Enhanced Operations Log (NEOLOG), and the Quality Assurance Automation Software (QA Tool). Implementation of these systems has resulted in a significant reduction in required manpower, elimination of shift work and most weekend support, and improved support quality, while incurring minimal development cost. This paper will present an overview of the concepts used and experiences gained from the implementation of these automation systems.

Author (revised)

N95-17238*# Centre National d'Etudes Spatiales, Toulouse (France).

GRAPHIC SERVER: A REAL TIME SYSTEM FOR DISPLAYING AND MONITORING TELEMETRY DATA OF SEVERAL SATELLITES

Stephane Douard *In* NASA. Goddard Space Flight Center, Third International Symposium on Space Mission Operations and Ground Data Systems, Part 1 Nov. 1994 p 517-523 (For primary document see N95-17179 04-17)

Avail: CASI HC A02/MF A06

Known as a Graphic Server, the system presented was designed for the control ground segment of the Telecom 2 satellites. It is a tool used to dynamically display telemetry data within graphic pages, also known as views. The views are created off-line through various utilities and then, on the operator's request, displayed and animated in real time as data is received. The system was designed as an independent component, and is installed in different Telecom 2 operational control centers. It enables operators to monitor changes in the platform and satellite payloads in real time. It has been in operation since December 1991. Author (revised)

N95-17239*# Allied-Signal Aerospace Co., Seabrook, MD.

ADVANCED TECHNOLOGIES IN THE ASI MLRO TOWARDS A NEW GENERATION LASER RANGING SYSTEM **c36**

Thomas Varghese and Giuseppe Bianco (Italian Space Agency, Matera.) *In* NASA. Goddard Space Flight Center, Third International Symposium on Space Mission Operations and Ground Data Systems, Part 1 Nov. 1994 p 525-530 (For primary document see N95-17179 04-17)

Avail: CASI HC A02/MF A06

Matera Laser Ranging Observatory (MLRO) is a high performance, highly automated optical and astronomical observatory currently under design and development by AlliedSignal for the Italian Space Agency (ASI). It is projected to become operational at the Centro Geodesia Spaziale in Matera, Italy, in 1997. MLRO, based on a 1.5-meter astronomical quality telescope, will perform ranging to spacecraft in earthbound orbits, lunar reflectors, and specially equipped deep space missions. The primary emphasis during design is to incorporate state-of-the-art technologies to produce an intelligent, automated, high accuracy ranging system that will mimic the characteristic

features of a fifth generation laser ranging system. The telescope has multiple ports and foci to support future experiments in the areas of laser communications, lidar, astrometry, etc. The key features providing state-of-the-art ranging performance include: a diode-pumped picosecond (50 ps) laser, high speed (3-5 GHz) optoelectronic detection and signal processing, and a high accuracy (6 ps) high resolution (less than 2 ps) time measurement capability. The above combination of technologies is expected to yield millimeter laser ranging precision and accuracy on targets up to 300,000 km, surpassing the best operational instrument performance to date by a factor of five or more. Distributed processing and control using a state-of-the-art computing environment provides the framework for efficient operation, system optimization, and diagnostics. A computationally intelligent environment permits optimal planning, scheduling, tracking, and data processing. It also supports remote access, monitor, and control for joint experiments with other observatories. Author

N95-17240*# Deutsche Forschungsanstalt fuer Luft- und Raumfahrt, Oberpfaffenhofen (Germany).

THE SEQUENCE OF EVENTS GENERATOR: A POWERFUL TOOL FOR MISSION OPERATIONS c66

Hubertus Wobbe and Armin Braun *In* NASA. Goddard Space Flight Center, Third International Symposium on Space Mission Operations and Ground Data Systems, Part 1 Nov. 1994 p 531-537 (For primary document see N95-17179 04-17)

Avail: CASI HC A02/MF A06

The functions and features of the sequence of events (SOE) and flight operations procedures (FOP) generator developed and used at DLR/GSOC for the positioning of EUTELSAT 2 satellites are presented. The SOE and FOP are the main operational documents that are prepared for nominal as well as for non-nominal mission execution. Their structure and application are described. Both of these documents are generated, validated, and maintained by a common software tool. Its main features and advantages are demonstrated. The tool has been improved continuously over the last 5 years. Due to its flexibility it can easily be applied to other projects and new features may be added. Author

N95-17241*# California Univ., Berkeley, CA. Center for EUV Astrophysics.

DESIGNING AN AUTONOMOUS ENVIRONMENT FOR MISSION CRITICAL OPERATION OF THE EUVE SATELLITE c66

Annadiana Abedini and Roger F. Malina *In* NASA. Goddard Space Flight Center, Third International Symposium on Space Mission Operations and Ground Data Systems, Part 1 Nov. 1994 p 541-546 (For primary document see N95-17179 04-17)

(Contracts NAS5-29298; NCC2-838)

Avail: CASI HC A02/MF A06

Since the launch of NASA's Extreme Ultraviolet Explorer (EUVE) satellite in 1992, there has only been a handful of occurrences that have warranted manual intervention in the EUVE Science Operations Center (ESOC). So, in an effort to reduce costs, the current environment is being redesigned to utilize a combination of off-the-shelf packages and recently developed artificial intelligence (AI) software to automate the monitoring of the science payload and ground systems. The successful implementation of systemic automation would allow the ESOC to evolve from a seven day/week, three shift operation, to a seven day/week one shift operation. First, it was necessary to identify all areas considered mission critical. These were defined as follows: (1) The telemetry stream must be monitored autonomously and anomalies identified. (2) Duty personnel must be automatically paged and informed of the occurrence of an anomaly. (3) The 'basic' state of the ground system must be assessed. (4) Monitors should check that the systems and processes needed to continue in a 'healthy' operational mode are working at all times. (5) Network loads should be monitored to ensure that they stay within established limits. (6) Connectivity to Goddard Space Flight Center (GSFC) systems should be monitored as well, not just for connectivity of the network itself but also for the ability to transfer files. (7) All necessary peripheral devices should be monitored. This would include the disks, routers, tape drives, printers, tape carousel, and power supplies. (8) System daemons such as the archival daemon, the Sybase server, the payload monitoring software, and any other necessary processes should be monitored to ensure that they are operational. (9) The monitoring system needs to be redundant so that the failure of a single machine will not paralyze the monitors. (10) Notification should be done by means of looking though a table of the pager numbers for current 'on call' personnel. The software should be capable of dialing out to notify, sending email, and producing error logs. (11) The system should have knowledge of when real-time passes and tape recorder dumps will occur and should know that these passes and data transmissions are successful. Once the design criteria were established, the design team split into two groups: one that addressed the tracking, commanding, and health and safety of the science payload and another group that addressed the ground systems and communications aspects of the overall system. Author

N95-17242*# Jet Propulsion Lab., California Inst. of Tech., Pasadena, CA.

INCREASES IN EFFICIENCY AND ENHANCEMENTS TO THE MARS OBSERVER NON-STORED COMMANDING PROCESS c66

Robert N. Brooks, Jr. and J. Leigh Torgerson *In* NASA. Goddard Space Flight Center, Third International Symposium on Space Mission Operations and Ground Data Systems, Part 1 Nov. 1994 p 547-558 (For primary document see N95-17179 04-17)

Avail: CASI HC A03/MF A06

The Mars Observer team was, until the untimely loss of the spacecraft on August 21, 1993, performing flight operations with greater efficiency and speed than any previous JPL mission of its size. This level of through-put was made possible by a mission operations system which was composed of skilled personnel using sophisticated sequencing and commanding tools. During cruise flight operations, however, it was realized by the project that this commanding level was not going to be sufficient to support the activities planned for mapping operations. The project had committed to providing the science instrument principle investigators with a much higher level of commanding during mapping. Thus, the project began taking steps to enhance the capabilities of the flight team. One mechanism used by project management was a tool available from total quality management (TQM). This tool is known as a process action team (PAT). The Mars Observer PAT was tasked to increase the capacity of the flight team's nonstored commanding process by fifty percent with no increase in staffing and a minimal increase in risk. The outcome of this effort was, in fact, to increase the capacity by a factor of 2.5 rather than the desired fifty percent and actually reduce risk. The majority of these improvements came from the automation of the existing command process. These results required very few changes to the existing mission operations system. Rather, the PAT was able to take advantage of automation capabilities inherent in the existing system and make changes to the existing flight team procedures. Author

N95-17243*# Interface and Control Systems, West Melbourne, FL.

SCL: AN OFF-THE-SHELF SYSTEM FOR SPACECRAFT CONTROL c18

Brian Buckley and James VanGaasbeck *In* NASA. Goddard Space Flight Center, Third International Symposium on Space Mission Operations and Ground Data Systems, Part 1 Nov. 1994 p 559-568 (For primary document see N95-17179 04-17)

Avail: CASI HC A02/MF A06

In this age of shrinking military, civil, and commercial space budgets, an off-the-shelf solution is needed to provide a multimission approach to spacecraft control. A standard operational interface which can be applied to multiple spacecraft allows a common approach to ground and space operations. A trend for many space programs has been to reduce operational staff by applying autonomy to the spacecraft and to the ground stations. The Spacecraft Command Language (SCL) system developed by Interface and Control Systems, Inc. (ICS) provides an off-the-shelf solution for spacecraft operations. The SCL system is designed to provide a hyper-scripting interface which remains standard from program to program. The spacecraft and ground station hardware specifics are isolated to provide the maximum amount of portability from system to system. Uplink and downlink interfaces are also isolated to allow the system to perform independent of the communications protocols chosen. The SCL system can be used for both the ground stations and the spacecraft, or as a value added package for existing ground station environments. The SCL system provides an expanded stored commanding capability as well as a rule-based expert system on-board. The expert system allows reactive control on-board the spacecraft for functions such as electrical power systems (EPS), thermal control, etc. which have traditionally been performed on the ground. The SCL rule and scripting capability share a common syntax

allowing control of scripts from rules and rules from scripts. Rather than telemeter over sampled data to the ground, the SCL system maintains a database on-board which is available for interrogation by the scripts and rules. The SCL knowledge base is constructed on the ground and uploaded to the spacecraft. The SCL system follows an open-systems approach allowing other tasks to communicate with SCL on the ground and in space. The SCL system was used on the Clementine program (launched January 25, 1994) and is required to have bidirectional communications with the guidance, navigation, and control (GNC) algorithms which were written as another task. Sequencing of the spacecraft maneuvers are handled by SCL, but the low-level thruster pulse commands are handled by the GNC software. Attitude information is reported back as telemetry, allowing the SCL expert system to inference on the changing data. The Clementine SCL flight software was largely reused from another Naval Center for Space Technology (NCST) satellite program. This paper details the SCL architecture and how an off-the-shelf solution makes sense for multimission spacecraft programs. The Clementine mission will be used as a case study in the application of the SCL to a 'fast track' program. The benefits of such a system in a 'better, cheaper, faster' climate will be discussed. Author

N95-17244*# Jet Propulsion Lab., California Inst. of Tech., Pasadena, CA.

MISSION OPERATIONS DATA ANALYSIS TOOLS FOR MARS OBSERVER GUIDANCE AND CONTROL **c66**

Edwin P. Kan *In* NASA. Goddard Space Flight Center, Third International Symposium on Space Mission Operations and Ground Data Systems, Part 1 Nov. 1994 p 569-576 (For primary document see N95-17179 04-17)

Avail: CASI HC A02/MF A06

Mission operations for the Mars Observer (MO) Project at the Jet Propulsion Laboratory were supported by a variety of ground data processing software and analysis tools. Some of these tools were generic to multimission spacecraft mission operations, some were specific to the MO spacecraft, and others were custom tailored to the operation and control of the Attitude and Articulation Control Subsystem (AACS). The focus of this paper is on the data analysis tools for the AACS. Four different categories of analysis tools are presented; with details offered for specific tools. Valuable experience was gained from the use of these tools and through their development. These tools formed the backbone and enhanced the efficiency of the AACS Unit in the Mission Operations Spacecraft Team. These same tools, and extensions thereof, have been adopted by the Galileo mission operations, and are being designed into Cassini and other future spacecraft mission operations. Author

N95-17245*# National Aeronautics and Space Administration. Goddard Space Flight Center, Greenbelt, MD.

GENERIC TRENDING AND ANALYSIS SYSTEM **c82**

Lori Keehan and Jay Reese (Loral AeroSys, Seabrook, MD.) *In its* Third International Symposium on Space Mission Operations and Ground Data Systems, Part 1 Nov. 1994 p 577-582 (For primary document see N95-17179 04-17)

Avail: CASI HC A02/MF A06

The Generic Trending and Analysis System (GTAS) is a generic spacecraft performance monitoring tool developed by NASA Code 511 and Loral Aerosys. It is designed to facilitate quick anomaly resolution and trend analysis. Traditionally, the job of off-line analysis has been performed using hardware and software systems developed for real-time spacecraft contacts; then, the systems were supplemented with a collection of tools developed by Flight Operations Team (FOT) members. Since the number of upcoming missions is increasing, NASA can no longer afford to operate in this manner. GTAS improves control center productivity and effectiveness because it provides a generic solution across multiple missions. Thus, GTAS eliminates the need for each individual mission to develop duplicate capabilities. It also allows for more sophisticated tools to be developed because it draws resources from several projects. In addition, the GTAS software system incorporates commercial off-the-shelf tools software (COTS) packages and reuses components of other NASA-developed systems wherever possible. GTAS has incorporated lessons learned from previous missions by involving the users early in the development process. GTAS users took a proactive role in requirements analysis, design, development, and testing. Because of user involvement, several special tools were designed and are now being developed. GTAS users expressed considerable interest in facilitating data collection for long term trending and analysis. As a result, GTAS provides easy access to large volumes of processed telemetry data directly in the control center. The GTAS archival and retrieval capabilities are supported by the integration of optical disk technology and a COTS relational database management system. Author

N95-17246*# Centre National d'Etudes Spatiales, Toulouse (France).

A GRAPHIC SYSTEM FOR TELEMETRY MONITORING AND PROCEDURE PERFORMING AT THE TELECOM SCC

Jean Philippe Loubeyre *In* NASA. Goddard Space Flight Center, Third International Symposium on Space Mission Operations and Ground Data Systems, Part 1 Nov. 1994 p 583-590 (For primary document see N95-17179 04-17)

Avail: CASI HC A02/MF A06

The increasing amount of telemetry parameters and the increasing complexity of procedures used for the in-orbit satellite follow-up has led to the development of new tools for telemetry monitoring and procedures performing. The name of the system presented here is Graphic Server. It provides an advanced graphic representation of the satellite subsystems, including real-time telemetry and alarm displaying, and a powerful help for decision making with on line contingency procedures. Used for 2.5 years at the TELECOM S.C.C. for procedure performing, it has become an essential part of the S.C.C. Author

N95-17247*# Jet Propulsion Lab., California Inst. of Tech., Pasadena, CA.

SMALL SCALE SEQUENCE AUTOMATION PAYS BIG DIVIDENDS **c18**

Bill Nelson *In* NASA. Goddard Space Flight Center, Third International Symposium on Space Mission Operations and Ground Data Systems, Part 1 Nov. 1994 p 591-597 (For primary document see N95-17179 04-17)

Avail: CASI HC A02/MF A06

Galileo sequence design and integration are supported by a suite of formal software tools. Sequence review, however, is largely a manual process with reviewers scanning hundreds of pages of cryptic computer printouts to verify sequence correctness. Beginning in 1990, a series of small, PC based sequence review tools evolved. Each tool performs a specific task but all have a common 'look and feel'. The narrow focus of each tool means simpler operation, and easier creation, testing, and maintenance. Benefits from these tools are (1) decreased review time by factors of 5 to 20 or more with a concomitant reduction in staffing, (2) increased review accuracy, and (3) excellent returns on time invested. Author

N95-17248*# European Space Agency. European Space Operations Center, Darmstadt (Germany).

SAFETY ASPECTS OF SPACECRAFT COMMANDING

N. Peccia *In* NASA. Goddard Space Flight Center, Third International Symposium on Space Mission Operations and Ground Data Systems, Part 1 Nov. 1994 p 599-605 (For primary document see N95-17179 04-17)

Avail: CASI HC A02/MF A06

The commanding of spacecraft is a potentially hazardous activity for the safety of the spacecraft. Present day control systems contain safety features in their commanding subsystem and in addition, strict procedures are also followed by operations staff. However, problems have occurred on a number of missions as a result of erroneous commanding leading in some cases to spacecraft contingencies and even to near loss of the spacecraft. The problems of checking commands in advance are increased by the tendency in modern spacecraft to use blocked/time-tagged commands and the increased usage of on-board computers, for which commands changing on-board software tables can radically change spacecraft or subsystem behavior. This paper reports on an on-going study. The study aims to improve the approach to safety of spacecraft commanding. It will show how ensuring 'safe' commanding can be carried out more efficiently, and with greater reliability, with the help of knowledge based systems and/or fast simulators. The whole concept will be developed based on the Object-Oriented approach. Author

N95-17249*# National Aeronautics and Space Administration. Goddard Space Flight Center, Greenbelt, MD.

THE DEVELOPMENT AND VALIDATION OF COMMAND SCHEDULES FOR SeaWiFS

Robert H. Woodward (General Sciences Corp., Laurel, MD.), Watson W. Gregg, and Frederick S. Patt (General Sciences Corp., Laurel, MD.) *In its* Third International Symposium on Space Mission Operations and Ground Data Systems, Part 1 Nov. 1994 p 607-614 (For primary document see N95-17179 04-17)

Avail: CASI HC A02/MF A06

An automated method for developing and assessing spacecraft and instrument command schedules is presented for the Sea-viewing Wide Field-of-view Sensor (SeaWiFS) project. SeaWiFS is to be carried on the polar-orbiting SeaStar satellite in 1995. The primary goal of the SeaWiFS mission is to provide global ocean chlorophyll concentrations every four days by employing onboard recorders and a twice-a-day data downlink schedule. Global Area Coverage (GAC) data with about 4.5 km resolution will be used to produce the global coverage. Higher resolution (1.1 km resolution) Local Area Coverage (LAC) data will also be recorded to calibrate the sensor. In addition, LAC will be continuously transmitted from the satellite and received by High Resolution Picture Transmission (HRPT) stations. The methods used to generate commands for SeaWiFS employ numerous hierarchical checks as a means of maximizing coverage of the Earth's surface and fulfilling the LAC data requirements. The software code is modularized and written in Fortran with constructs to mirror the pre-defined mission rules. The overall method is specifically developed for low orbit Earth-observing satellites with finite onboard recording capabilities and regularly scheduled data downlinks. Two software packages using the Interactive Data Language (IDL) for graphically displaying and verifying the resultant command decisions are presented. Displays can be generated which show portions of the Earth viewed by the sensor and spacecraft sub-orbital locations during onboard calibration activities. An IDL-based interactive method of selecting and testing LAC targets and calibration activities for command generation is also discussed. Author

N95-17250*# Centre National d'Etudes Spatiales, Toulouse (France).

TOWARDS CHEAPER CONTROL CENTERS c14

Lionel Baize *In* NASA. Goddard Space Flight Center, Third International Symposium on Space Mission Operations and Ground Data Systems, Part 1 Nov. 1994 p 617-624 (For primary document see N95-17179 04-17)

Avail: CASI HC A02/MF A06

Today, any approach to the design of new space systems must take into consideration an important constraint, namely costs. This approach is our guideline for new missions and also applies to the ground segment, and particularly to the control center. CNES has carried out a study on a recent control center for application satellites in order to take advantage of the experience gained. This analysis, the purpose of which is to determine, a posteriori, the costs of architecture needs and choices, takes hardware and software costs into account and makes a number of recommendations. Author

N95-17251*# European Space Agency, Redu (Belgium).

THE SILEX EXPERIMENT SYSTEM OPERATIONS c14

B. Demelenne *In* NASA. Goddard Space Flight Center, Third International Symposium on Space Mission Operations and Ground Data Systems, Part 1 Nov. 1994 p 625-631 (For primary document see N95-17179 04-17)

Avail: CASI HC A02/MF A06

The European Space Agency is going to conduct an inter orbit link experiment which will connect a low Earth orbiting satellite and a Geostationary satellite via optical terminals. This experiment has been called SILEX (Semiconductor Inter satellite Link EXperiment). Two payloads will be built. One called PASTEL (PASsager de TELecommunication) will be embarked on the French Earth observation satellite SPOT4. The future European experimental data relay satellite ARTEMIS (Advanced Relay and TEchnology MISsion) will carry the OPALE terminal (Optical PAyload Experiment). The principal characteristic of the mission is a 50 Megabits flow of data transmitted via the optical satellite link. The relay satellite will route the data via its feeder link thus permitting a real time reception in the European region of images taken by the observation satellite. The PASTEL terminal has been designed to cover up to 9 communication sessions per day with an average of 5. The number of daily contact opportunities with the low earth orbiting satellite will be increased and the duration will be much longer than the traditional passes over a ground station. The terminals have an autonomy of 24 hours with respect to ground control. Each terminal will contain its own orbit model and that of its counter terminal for orbit prediction and for precise computation of pointing direction. Due to the very narrow field of view of the communication laser beam, the orbit propagation calculation needs to be done with a very high accuracy. The European Space Agency is responsible for the operation of both terminals. A PASTEL Mission Control System (PMCS) is being developed to control the PASTEL terminal on board SPOT4. The PMCS will interface with the SPOT4 Control Centre for the execution of the PASTEL operations. The PMCS will also interface with the ARTEMIS Mission Control System for the planning and the coordination of the operation. It is the first time that laser technology will be used to support inter-satellite links in Europe. Due to the complexity and experimental character of this new optical technology, the SILEX experiment control facilities will be designed to allow as much operational flexibility as possible. Author

N95-17252*# European Space Agency. European Space Operations Center, Darmstadt (Germany).

EURECA MISSION CONTROL EXPERIENCE AND MESSAGES FOR THE FUTURE

H. Huebner, P. Ferri, and W. Wimmer *In* NASA. Goddard Space Flight Center, Third International Symposium on Space Mission Operations and Ground Data Systems, Part 1 Nov. 1994 p 633-640 (For primary document see N95-17179 04-17)

Avail: CASI HC A02/MF A06

EURECA is a retrievable space platform which can perform multi-disciplinary scientific and technological experiments in a Low Earth Orbit for a typical mission duration of six to twelve months. It is deployed and retrieved by the NASA Space Shuttle and is designed to support up to five flights. The first mission started at the end of July 1992 and was successfully completed with the retrieval in June 1993. The operations concept and the ground segment for the first EURECA mission are briefly introduced. The experiences in the preparation and the conduction of the mission from the flight control team point of view are described. Author

N95-17253*# European Space Agency. European Space Operations Center, Darmstadt (Germany). Flight Control Systems Dept.

SCOS 2: ESA'S NEW GENERATION OF MISSION CONTROL SYSTEM c14

M. Jones, N. C. Head, K. Keyte (Vitrociset S.p.A., Rome, Italy.), P. Howard (Science Systems Ltd., Bristol, England.), and S. Lynenskjold (Computer Resources International A/S, Denmark.) *In* NASA. Goddard Space Flight Center, Third International Symposium on Space Mission Operations and Ground Data Systems, Part 1 Nov. 1994 p 641-654 (For primary document see N95-17179 04-17)

Avail: CASI HC A02/MF A06

New mission-control infrastructure is currently being developed by ESOC, which will constitute the second generation of the Spacecraft Control Operations system (SCOS 2). The financial, functional and strategic requirements lying behind the new development are explained. The SCOS 2 approach is described. The technological implications of these approaches is described: in particular it is explained how this leads to the use of object oriented techniques to provide the required 'building block' approach. The paper summarizes the way in which the financial, functional and strategic requirements have been met through this combination of solutions. Finally, the paper outlines the development process to date, noting how risk reduction was achieved in the approach to new technologies and summarizes the current status future plans. Author

N95-17254*# Compagnie Internationale de Service en Informatique, Toulouse (France). Aerospace Branch.

CCS-MIP: LOW COST CUSTOMIZABLE CONTROL CENTRE c14

Christian Labezin and Pierre Vielcanet *In* NASA. Goddard Space Flight Center, Third International Symposium on Space Mission Operations and Ground Data Systems, Part 1 Nov. 1994 p 649-654 (For primary document see N95-17179 04-17)

Avail: CASI HC A02/MF A06

The positioning and station keeping of French national satellites are among the main missions of CNES French Space Agency CNES. The

related experience and skills of the Toulouse Space Centre are reknown and often required at international level for a wide range of missions. CISI, a software engineering company, has been contributing during the last 20 years to the development of the French space programs, particularly in the field of space missions ground control segments. The CCS-MIP system, presented here, is a satellite positioning and station-keeping system designed to answer the CNES multi-mission needs, easily adaptable for a wide range of applications. Author

N95-17255*# Computer Sciences Corp., Lanham, MD. Astronomy Programs.
THE IUE SCIENCE OPERATIONS GROUND SYSTEM **c14**
Ronald E. Pitts and Richard Arquilla *In* NASA. Goddard Space Flight Center, Third International Symposium on Space Mission Operations and Ground Data Systems, Part 1 Nov. 1994 p 655-662 (For primary document see N95-17179 04-17)
Avail: CASI HC A02/MF A06

The International Ultraviolet Explorer (IUE) Science Operations System provides full realtime operations capabilities and support to the operations staff and astronomer users. The components of this very diverse and extremely flexible hardware and software system have played a major role in maintaining the scientific efficiency and productivity of the IUE. The software provides the staff and user with all the tools necessary for pre-visit and real-time planning and operations analysis for any day of the year. Examples of such tools include the effects of spacecraft constraints on target availability, maneuver times between targets, availability of guide stars, target identification, coordinate transforms, e-mail transfer of Observatory forms and messages, and quick-look analysis of image data. Most of this extensive software package can also be accessed remotely by individual users for information, scheduling of shifts, pre-visit planning, and actual observing program execution. Astronomers, with a modest investment in hardware and software, may establish remote observing sites. We currently have over 20 such sites in our remote observers' network. Author

N95-17256*# Loral AeroSys, Seabrook, MD.
EFFICIENT MISSION CONTROL FOR THE 48-SATELLITE GLOBALSTAR CONSTELLATION **c14**
Dan Smith *In* NASA. Goddard Space Flight Center, Third International Symposium on Space Mission Operations and Ground Data Systems, Part 1 Nov. 1994 p 663-670 (For primary document see N95-17179 04-17)
Avail: CASI HC A02/MF A06

The Globalstar system is being developed by Globalstar, Limited Partnership and will utilize 48 satellites in low earth orbit (See Figure 1) to create a world-wide mobile communications system consistent with Vice President Gore's vision of a Global Information Infrastructure. As a large long term commercial system developed by a newly formed organization, Globalstar provides an excellent opportunity to explore innovative solutions for highly efficient satellite command and control. Design and operational concepts being developed are unencumbered by existing physical and organizational infrastructures. This program really is 'starting with a clean sheet of paper'. Globalstar operations challenges can appear enormous. Clearly, assigning even a single person around the clock to monitor and control each satellite is excessive for Globalstar (it would require a staff of 200! . Even with only a single contact per orbit per satellite, data acquisitions will start or stop every 45 seconds! Although essentially identical, over time the satellites will develop their own 'personalities'and will re quire different data calibrations and levels of support. This paper discusses the Globalstar system and challenges and presents engineering concepts, system design decisions, and operations concepts which address the combined needs and concerns of satellite, ground system, and operations teams. Lessons from past missions have been applied, organizational barriers broken, partnerships formed across the mission segments, and new operations concepts developed for satellite constellation management. Control center requirements were then developed from the operations concepts. Author

N95-17257*# Centre National d'Etudes Spatiales, Toulouse (France).
MINI ALL-PURPOSE SATELLITE CONTROL CENTER (MASCC) **c14**
Gerard Zaouche *In* NASA. Goddard Space Flight Center, Third International Symposium on Space Mission Operations and Ground Data Systems, Part 1 Nov. 1994 p 671-678 (For primary document see N95-17179 04-17)
Avail: CASI HC A02/MF A06

A new generation of Mini All-purpose Satellite Control Centers (MASCC) has been developed by CNES (F). They turn out to be easily adaptable to different kinds of satellites, both Low Earth Orbital or Geostationary. The features of MASCC allow both standard satellite control activities, and checking of passengers experiments hosted on a space platform. In the different environments in which it may be used, MASCC provides standard broadcasting of telemetry parameters on animated synoptics (curves, bar graphs, alphanumeric displays, ...), which turns out to be a very useful and ergonomic medium for operational teams or satellite specialists. Special care has been taken during the MASCC development about two points: - automation of all routine tasks, allowing automated operation, and limiting human commitment to system supervision and decision making, - software adaptability. To reach these two main objectives, the MASCC design provides:(1) a simple, robust and flexible hardware architecture, based on powerful distributed workstations; and (2) a table-driven software architecture, easily adapted to various operational needs. Satellite characteristics are described in a central Data Base. Hence, the processing of telemetry and commands is largely independent from the satellite itself. In order to validate these capabilities, the MASCC has been customized to several types of satellites and orbital platforms: (1) SPOT4, the French new generation of remote sensing satellites; (2) TELECOM2, the French geostationary TV and telecommunication satellite; and (3) MIR, the Russian orbital platform. MASCC development has been completed by the third quarter of 1993. This paper will provide first a description of the MASCC basic functions, of its hardware and software design. It will then detail the increased automation capability, along with the easy adaptation of the MASCC to new satellites with minimal software modifications. Author

N95-17531*# National Aeronautics and Space Administration. Goddard Space Flight Center, Greenbelt, MD.
THIRD INTERNATIONAL SYMPOSIUM ON SPACE MISSION OPERATIONS AND GROUND DATA SYSTEMS, PART 2
James L. Rash, ed. Washington Nov. 1994 700 p Symposium held in Greenbelt, MD, 15-18 Nov. 1994
(RTOP 500-00-00)
(NASA-CP-3281-Pt-2; Rept-94B00135-Pt-2; NAS 1.55:3281-Pt-2) Avail: CASI HC A99/MF A06

Under the theme of 'Opportunities in Ground Data Systems for High Efficiency Operations of Space Missions,' the SpaceOps '94 symposium included presentations of more than 150 technical papers spanning five topic areas: Mission Management, Operations, Data Management, System Development, and Systems Engineering. The symposium papers focus on improvements in the efficiency, effectiveness, and quality of data acquisition, ground systems, and mission operations. New technology, methods, and human systems are discussed. Accomplishments are also reported in the application of information systems to improve data retrieval, reporting, and archiving; the management of human factors; the use of telescience and teleoperations; and the design and implementation of logistics support for mission operations. This volume covers expert systems, systems development tools and approaches, and systems engineering issues. For individual titles, see N95-17532 through N95-17614.

N95-17532*# MATRA Marconi Space, Toulouse (France).
DELIVERING SPACECRAFT CONTROL CENTERS WITH EMBEDDED KNOWLEDGE-BASED SYSTEMS: THE METHODOLOGY ISSUE **c14**
S. Ayache, M. Haziza, and D. Cayrac *In* NASA. Goddard Space Flight Center, Third International Symposium on Space Mission Operations and Ground Data Systems, Part 2 Nov. 1994 p 681-688 Sponsored by Cap Gemini Innovation; Westfield College; Sintef Delab; Eritel; and ITMI (For primary document see N95-17531 04-17)
(ESPRIT Proj. 6083)
Avail: CASI HC A02/MF A06

Matra Marconi Space (MMS) occupies a leading place in Europe in the domain of satellite and space data processing systems. The maturity of the knowledge-based systems (KBS) technology, the theoretical and practical experience acquired in the development of prototype, pre-operational and operational applications, make it possible today to consider the wide operational deployment of KBS's in space applications. In this perspective, MMS has to prepare the introduction of the new methods and support

tools that will form the basis of the development of such systems. This paper introduces elements of the MMS methodology initiatives in the domain and the main rationale that motivated the approach. These initiatives develop along two main axes: knowledge engineering methods and tools, and a hybrid method approach for coexisting knowledge-based and conventional developments. Author

N95-17533*# European Space Agency. European Space Operations Center, Darmstadt (Germany). Flight Control Systems Dept.

SCOSII OL: A DEDICATED LANGUAGE FOR MISSION OPERATIONS **c61**

Andrea Baldi, Dennis Elgaard (Computer Resources International A/S, Denmark.), Steen Lynenskjold (Computer Resources International A/S, Denmark.), and Mauro Pecchioli *In* NASA. Goddard Space Flight Center, Third International Symposium on Space Mission Operations and Ground Data Systems, Part 2 Nov. 1994 p 689-696 (For primary document see N95-17531 04-17)

Avail: CASI HC A02/MF A06

The Spacecraft Control and Operations System 2 (SCOSII) is the new generation of Mission Control Systems (MCS) to be used at ESOC. The system is generic because it offers a collection of standard functions configured through a database upon which a dedicated MCS is established for a given mission. An integral component of SCOSII is the support of a dedicated Operations Language (OL). The spacecraft operation engineers edit, test, validate, and install OL scripts as part of the configuration of the system with, e.g., expressions for computing derived parameters and procedures for performing flight operations, all without involvement of software support engineers. A layered approach has been adopted for the implementation centered around the explicit representation of a data model. The data model is object-oriented defining the structure of the objects in terms of attributes (data) and services (functions) which can be accessed by the OL. SCOSII supports the creation of a mission model. System elements as, e.g., a gyro are explicit, as are the attributes which described them and the services they provide. The data model driven approach makes it possible to take immediate advantage of this higher-level of abstraction, without requiring expansion of the language. This article describes the background and context leading to the OL, concepts, language facilities, implementation, status and conclusions found so far. Author

N95-17534*# MATRA Marconi Space, Toulouse (France).

DIAMS REVISITED: TAMING THE VARIETY OF KNOWLEDGE IN FAULT DIAGNOSIS EXPERT SYSTEMS **c63**

M. Haziza, S. Ayache, J.-M. Brenot, D. Cayrac, and D.-P. Vo *In* NASA. Goddard Space Flight Center, Third International Symposium on Space Mission Operations and Ground Data Systems, Part 2 Nov. 1994 p 697-706 Sponsored by Cap Gemini Innovation; Westfield College; Sintef Delab; Eritel; and ITMI (For primary document see N95-17531 04-17) (ESPRIT Proj. 6083)

Avail: CASI HC A02/MF A06

The DIAMS program, initiated in 1986, led to the development of a prototype expert system, DIAMS-1 dedicated to the Telecom 1 Attitude and Orbit Control System, and to a near-operational system, DIAMS-2, covering a whole satellite (the Telecom 2 platform and its interfaces with the payload), which was installed in the Satellite Control Center in 1993. The refinement of the knowledge representation and reasoning is now being studied, focusing on the introduction of appropriate handling of incompleteness, uncertainty and time, and keeping in mind operational constraints. For the latest generation of the tool, DIAMS-3, a new architecture has been proposed, that enables the cooperative exploitation of various models and knowledge representations. On the same baseline, new solutions enabling higher integration of diagnostic systems in the operational environment and cooperation with other knowledge intensive systems such as data analysis, planning or procedure management tools have been introduced. Author

N95-17535*# National Aeronautics and Space Administration. Goddard Space Flight Center, Greenbelt, MD.

USING GRAPHICS AND EXPERT SYSTEM TECHNOLOGIES TO SUPPORT SATELLITE MONITORING AT THE NASA GODDARD SPACE FLIGHT CENTER **c14**

Peter M. Hughes, Gregory W. Shirah, and Edward C. Luczak (Computer Sciences Corp., Lanham, MD.) *In its* Third International Symposium on Space Mission Operations and Ground Data Systems, Part 2 Nov. 1994 p 707-712 (For primary document see N95-17531 04-17)

Avail: CASI HC A02/MF A06

At NASA's Goddard Space Flight Center, fault-isolation expert systems have been developed to support data monitoring and fault detection tasks in satellite control centers. Based on the lessons learned during these efforts in expert system automation, a new domain-specific expert system development tool named the Generic Spacecraft Analysts Assistant (GenSAA), was developed to facilitate the rapid development and reuse of real-time expert systems to serve as fault-isolation assistants for spacecraft analysts. This paper describes GenSAA's capabilities and how it is supporting monitoring functions of current and future NASA missions for a variety of satellite monitoring applications ranging from subsystem health and safety to spacecraft attitude. Finally, this paper addresses efforts to generalize GenSAA's data interface for more widespread usage throughout the space and commercial industry. Author

N95-17536*# Deutsche Forschungsanstalt fuer Luft- und Raumfahrt, Cologne (Germany).

DEVELOPMENT OF USE OF AN OPERATIONAL PROCEDURE INFORMATION SYSTEM (OPIS) FOR FUTURE SPACE MISSIONS **c82**

N. Illmer, L. Mies, A. Schoen, and A. Jain (WIB G.m.b.H., Berlin, Germany.) *In* NASA. Goddard Space Flight Center, Third International Symposium on Space Mission Operations and Ground Data Systems, Part 2 Nov. 1994 p 713-717 (For primary document see N95-17531 04-17)

Avail: CASI HC A01/MF A06

A MS-Windows based electronic procedure system, called OPIS (Operational Procedure Information System), was developed. The system consists of two parts, the editor, for 'writing' the procedure and the notepad application, for the usage of the procedures by the crew during training and flight. The system is based on standardized, structured procedure format and language. It allows the embedding of sketches, photos, animated graphics and video sequences and the access to off-nominal procedures by linkage to an appropriate database. The system facilitates the work with procedures of different degrees of detail, depending on the training status of the crew. The development of a 'language module' for the automatic translation of the procedures, for example into Russian, is planned. Author

N95-17537*# European Space Agency. European Space Operations Center, Darmstadt (Germany). Mission Operations Dept.

SCOSII: ESA'S NEW GENERATION OF MISSION CONTROL SYSTEMS: THE USER'S PERSPECTIVE **c14**

P. Kaufeler, M. Pecchioli, and I. Shurmer (VEGA Space Systems Engineering Ltd., Harpenden, England.) *In* NASA. Goddard Space Flight Center, Third International Symposium on Space Mission Operations and Ground Data Systems, Part 2 Nov. 1994 p 719-725 (For primary document see N95-17531 04-17)

Avail: CASI HC A02/MF A06

In 1974 ESOC decided to develop a reusable Mission Control System infrastructure for ESA's missions operated under its responsibility. This triggered a long and successful product development line, which started with the Multi Mission Support System (MSSS) which entered in service in 1977 and is still being used today by the MARECS and ECS missions; it was followed in 1989 by a second generation of systems known as SCOS-I, which was/is used by the Hipparcos, ERS-1 and EURECA missions and will continue to support all future ESCO controlled missions until approximately 1995. In the meantime the increasing complexity of future missions together with the emergence of new hardware and software technologies have led ESOC to go for the development of a third generation of control systems, SCOSII, which will support their future missions up to at least the middle of the next decade. The objective of the paper is to present the characteristics of the SCOSII system from the perspective of the mission control team; i.e. it will concentrate on the improvements and advances in the performance, functionality and work efficiency of the system. Author

N95-17538*# Jet Propulsion Lab., California Inst. of Tech., Pasadena, CA.

A SOFTWARE ARCHITECTURE FOR AUTOMATING OPERATIONS PROCESSES **c61**

Kevin J. Miller *In* NASA. Goddard Space Flight Center, Third International Symposium on Space Mission Operations and Ground Data Systems, Part 2 Nov. 1994 p 729-734 (For primary document see N95-17531 04-17)
Avail: CASI HC A02/MF A06

The Operations Engineering Lab (OEL) at JPL has developed a software architecture based on an integrated toolkit approach for simplifying and automating mission operations tasks. The toolkit approach is based on building adaptable, reusable graphical tools that are integrated through a combination of libraries, scripts, and system-level user interface shells. The graphical interface shells are designed to integrate and visually guide a user through the complex steps in an operations process. They provide a user with an integrated system-level picture of an overall process, defining the required inputs and possible output through interactive on-screen graphics. The OEL has developed the software for building these process-oriented graphical user interface (GUI) shells. The OEL Shell development system (OEL Shell) is an extension of JPL's Widget Creation Library (WCL). The OEL Shell system can be used to easily build user interfaces for running complex processes, applications with extensive command-line interfaces, and tool-integration tasks. The interface shells display a logical process flow using arrows and box graphics. They also allow a user to select which output products are desired and which input sources are needed, eliminating the need to know which program and its associated command-line parameters must be executed in each case. The shells have also proved valuable for use as operations training tools because of the OEL Shell hypertext help environment. The OEL toolkit approach is guided by several principles, including the use of ASCII text file interfaces with a multimission format, Perl scripts for mission-specific adaptation code, and programs that include a simple command-line interface for batch mode processing. Projects can adapt the interface shells by simple changes to the resources configuration file. This approach has allowed the development of sophisticated, automated software systems that are easy, cheap, and fast to build. This paper will discuss our toolkit approach and the OEL Shell interface builder in the context of a real operations process example. The paper will discuss the design and implementation of a Ulysses toolkit for generating the mission sequence of events. The Sequence of Events Generation (SEG) system provides an adaptable multimission toolkit for producing a time-ordered listing and timeline display of spacecraft commands, state changes, and required ground activities. Author

N95-17539*# Storm Integration, Inc., Herndon, VA.
SPACECRAFT COMMAND AND CONTROL USING EXPERT SYSTEMS
Scott Norcross and William H. Grieser *In* NASA. Goddard Space Flight Center, Third International Symposium on Space Mission Operations and Ground Data Systems, Part 2 Nov. 1994 p 735-740 (For primary document see N95-17531 04-17)
Avail: CASI HC A02/MF A06

This paper describes a product called the Intelligent Mission Toolkit (IMT), which was created to meet the changing demands of the spacecraft command and control market. IMT is a command and control system built upon an expert system. Its primary functions are to send commands to the spacecraft and process telemetry data received from the spacecraft. It also controls the ground equipment used to support the system, such as encryption gear, and telemetry front-end equipment. Add-on modules allow IMT to control antennas and antenna interface equipment. The design philosophy for IMT is to utilize available commercial products wherever possible. IMT utilizes Gensym's G2 Real-time Expert System as the core of the system. G2 is responsible for overall system control, spacecraft commanding control, and spacecraft telemetry analysis and display. Other commercial products incorporated into IMT include the SYBASE relational database management system and Loral Test and Integration Systems' System 500 for telemetry front-end processing. Author

N95-17540*# Jet Propulsion Lab., California Inst. of Tech., Pasadena, CA.
SEQ-GEN: A COMPREHENSIVE MULTIMISSION SEQUENCING SYSTEM c61
Jose Salcedo and Thomas J. Starbird *In* NASA. Goddard Space Flight Center, Third International Symposium on Space Mission Operations and Ground Data Systems, Part 2 Nov. 1994 p 741-748 (For primary document see N95-17531 04-17)
Avail: CASI HC A02/MF A06

SEQ-GEN is a user-interactive computer program used to plan and generate a sequence of commands for spacecraft. Desired activities are specified by the user of SEQ-GEN; SEQ-GEN in turn expands these activities, deriving the spacecraft commands necessary to accomplish the desired activities. SEQ-GEN models the effects on the spacecraft of the commands, predicting the state as a function of time, flagging any conflicts and rule violations. These states, conflicts, and violations are viewable both graphically and textually at the user's request. SEQ-GEN also displays the entire sequence graphically, showing each requested activity as a bar on its graphical timeline. SEQ-GEN immediately revalidates the sequence, updating its models and calculations along with its displays based on these changes. Because it has the ability to recalculate spacecraft states immediately, the user is able to perform 'what-if' sessions easily. SEQ-GEN, a multimission tool, is adaptable to any flight project. A flight project writes its adaptation files containing project unique information including in its simplest form, only spacecraft commands. For more involved projects the adaptation files may also contain flight and mission rules, description of the spacecraft and ground models, and the definition of activities. SEQ-GEN operates at whatever level of detail the adaptation files imply. Simple adaptations are straight forward to do. There is, however, no limit to the complexity of activity definitions or of spacecraft models: both may involve unlimited logical decision points. Commands and activities may involve any number of parameters of a wide variety of data types, including integer, float, time, boolean, and character strings. SEQ-GEN will be used by the Mars Pathfinder, Cassini, and VIM (Voyager Interstellar Mission) project in an effort to speed up adaptation time and to keep sequence generation costs down. SEQ-GEN is hosted on UNIX workstations. It uses MOTIF and X for windowing, and was designed and coded in an object-oriented style in the language C++. Author

N95-17541*# Computer Sciences Corp., Lanham, MD.
THE PACOR 2 EXPERT SYSTEM: A CASE-BASED REASONING APPROACH TO TROUBLESHOOTING
Charisse Sary *In* NASA. Goddard Space Flight Center, Third International Symposium on Space Mission Operations and Ground Data Systems, Part 2 Nov. 1994 p 749-756 (For primary document see N95-17531 04-17)
Avail: CASI HC A02/MF A06

The Packet Processor 2 (Pacor 2) Data Capture Facility (DCF) acquires, captures, and performs level-zero processing of packet telemetry for spaceflight missions that adhere to communication services recommendations established by the Consultative Committee for Space Data Systems (CCSDS). A major goal of this project is to reduce life-cycle costs. One way to achieve this goal is to increase automation. Through automation, using expert systems, and other technologies, staffing requirements will remain static, which will enable the same number of analysts to support more missions. Analysts provide packet telemetry data evaluation and analysis services for all data received. Data that passes this evaluation is forwarded to the Data Distribution Facility (DDF) and released to scientists. Through troubleshooting, data that fails this evaluation is dumped and analyzed to determine if its quality can be improved before it is released. This paper describes a proof-of-concept prototype that troubleshoots data quality problems. The Pacor 2 expert system prototype uses the case-based reasoning (CBR) approach to development, an alternative to a rule-based approach. Because Pacor 2 is not operational, the prototype has been developed using cases that describe existing troubleshooting experience from currently operating missions. Through CBR, this experience will be available to analysts when Pacor 2 becomes operational. As Pacor 2 unique experience is gained, analysts will update the case base. In essence, analysts are training the system as they learn. Once the system has learned the cases most likely to recur, it can serve as an aide to inexperienced analysts, a refresher to experienced analysts for infrequently occurring problems, or a training tool for new analysts. The Expert System Development Methodology (ESDM) is being used to guide development. Author

N95-17542*# National Aeronautics and Space Administration. Goddard Space Flight Center, Greenbelt, MD.
AN INTELLIGENT AUTOMATED COMMAND AND CONTROL SYSTEM FOR SPACECRAFT MISSION OPERATIONS
A. William Stoffel *In its* Third International Symposium on Space Mission

Operations and Ground Data Systems, Part 2 Nov. 1994 p 757-763 (For primary document see N95-17531 04-17)
Avail: CASI HC A02/MF A06

The Intelligent Command and Control (ICC) System research project is intended to provide the technology base necessary for producing an intelligent automated command and control (C&C) system capable of performing all the ground control C&C functions currently performed by Mission Operations Center (MOC) project Flight Operations Team (FOT). The ICC research accomplishments to date, details of the ICC, and the planned outcome of the ICC research, mentioned above, are discussed in detail. Author

N95-17543*# Jet Propulsion Lab., California Inst. of Tech., Pasadena, CA.
DSN CO-OBSERVING OPERATIONS TO SUPPORT SPACE VLBI MISSIONS
Valery I. Altunin, Thomas B. Kuiper, and Pamela R. Wolken (Allied-Signal Technical Services Corp., Alexandria, VA.) *In* NASA. Goddard Space Flight Center, Third International Symposium on Space Mission Operations and Ground Data Systems, Part 2 Nov. 1994 p 767-772 (For primary document see N95-17531 04-17)
Avail: CASI HC A02/MF A06

Reliable radio astronomy support of space very long baseline interferometry (VLBI) missions by ground radio telescopes is mandatory in order to achieve a high scientific return from the missions. The 70 m DSN antennas along with other ground radio telescopes will perform as the ground segment of the earth-space interferometer. Improvements of radio astronomy VLBI operations at the DSN to achieve higher reliability, efficiency, flexibility, and lower operations costs is a major goal in preparing for radio astronomy support of SVLBI. To help realize this goal, a remote control and monitoring mode for radio astronomy operations at the DSN has been developed. Author

N95-17544*# Storm Integration, Inc., San Jose, CA.
IMPLEMENTATION OF A LOW-COST, COMMERCIAL ORBIT DETERMINATION SYSTEM **c13**
Jim Corrigan *In* NASA. Goddard Space Flight Center, Third International Symposium on Space Mission Operations and Ground Data Systems, Part 2 Nov. 1994 p 773-783 (For primary document see N95-17531 04-17)
Avail: CASI HC A03/MF A06

Traditional satellite and launch control systems have consisted of custom solutions requiring significant development and maintenance costs. These systems have typically been designed to support specific program requirements and are expensive to modify and augment after delivery. The expanding role of space in today's marketplace combined with the increased sophistication and capabilities of modern satellites has created a need for more efficient, lower cost solutions to complete command and control systems. Recent technical advances have resulted in commercial-off-the-shelf products which greatly reduce the complete life-cycle costs associated with satellite launch and control system procurements. System integrators and spacecraft operators have, however, been slow to integrate these commercial based solutions into a comprehensive command and control system. This is due, in part, to a resistance to change and the fact that many available products are unable to effectively communicate with other commercial products. The United States Air Force, responsible for the health and safety of over 84 satellites via its Air Force Satellite Control Network (AFSCN), has embarked on an initiative to prove that commercial products can be used effectively to form a comprehensive command and control system. The initial version of this system is being installed at the Air Force's Center for Research Support (CERES) located at the National Test Facility in Colorado Springs, Colorado. The first stage of this initiative involved the identification of commercial products capable of satisfying each functional element of a command and control system. A significant requirement in this product selection criteria was flexibility and ability to integrate with other available commercial products. This paper discusses the functions and capabilities of the product selected to provide orbit determination functions for this comprehensive command and control system. Author

N95-17545*# Jet Propulsion Lab., California Inst. of Tech., Pasadena, CA.
DEVELOPMENT OF A PROTOTYPE REAL-TIME AUTOMATED FILTER FOR OPERATIONAL DEEP SPACE NAVIGATION
W. C. Masters and V. M. Pollmeier *In* NASA. Goddard Space Flight Center, Third International Symposium on Space Mission Operations and Ground Data Systems, Part 2 Nov. 1994 p 785-789 (For primary document see N95-17531 04-17)
Avail: CASI HC A01/MF A06

Operational deep space navigation has been in the past, and is currently, performed using systems whose architecture requires constant human supervision and intervention. A prototype for a system which allows relatively automated processing of radio metric data received in near real-time from NASA's Deep Space Network (DSN) without any redesign of the existing operational data flow has been developed. This system can allow for more rapid response as well as much reduced staffing to support mission navigation operations. Author

N95-17546*# National Aeronautics and Space Administration. Goddard Space Flight Center, Greenbelt, MD.
MAGNETOMETER-ONLY ATTITUDE AND RATE DETERMINATION FOR A GYRO-LESS SPACECRAFT
G. A. Natanson (Computer Sciences Corp., Lanham, MD.), M. S. Challa (Computer Sciences Corp., Lanham, MD.), J. Deutschmann, and D. F. Baker *In its* Third International Symposium on Space Mission Operations and Ground Data Systems, Part 2 Nov. 1994 p 791-798 (For primary document see N95-17531 04-17)
(Contract NAS5-31500)
Avail: CASI HC A02/MF A06

Attitude determination algorithms that requires only the earth's magnetic field will be useful for contingency conditions. One way to determine attitude is to use the time derivative of the magnetic field as the second vector in the attitude determination process. When no gyros are available, however, attitude determination becomes difficult because the rates must be propagated via integration of Euler's equation, which in turn requires knowledge of the initial rates. The spacecraft state to be determined must then include not only the attitude but also rates. This paper describes a magnetometer-only attitude determination scheme with no a priori knowledge of the spacecraft state, which uses a deterministic algorithm to initialize an extended Kalman filter. The deterministic algorithm uses Euler's equation to relate the time derivatives of the magnetic field in the reference and body frames and solves the resultant transcendental equations for the coarse attitude and rates. An important feature of the filter is that its state vector also includes corrections to the propagated rates, thus enabling it to generate highly accurate solutions. The method was tested using in-flight data from the Solar, Anomalous, and Magnetospheric Particles Explorer (SAMPEX), a Small Explorer spacecraft. SAMPEX data using several eclipse periods were used to simulate conditions that may exist during the failure of the on-board digital sun sensor. The combined algorithm has been found effective, yielding accuracies of 1.5 deg in attitude (within even nominal mission requirements) and 0.01 degree per second (deg/sec) in the rates. Author

N95-17547*# Mitre Corp., Bedford, MA.
TDRS ORBIT DETERMINATION BY RADIO INTERFEROMETRY **c13**
Michael S. Pavloff *In* NASA. Goddard Space Flight Center, Third International Symposium on Space Mission Operations and Ground Data Systems, Part 2 Nov. 1994 p 799-806 (For primary document see N95-17531 04-17)
Avail: CASI HC A02/MF A06

In support of a NASA study on the application of radio interferometry to satellite orbit determination, MITRE developed a simulation tool for assessing interferometry tracking accuracy. The Orbit Determination Accuracy Estimator (ODAE) models the general batch maximum likelihood orbit determination algorithms of the Goddard Trajectory Determination System (GTDS) with the group and phase delay measurements from radio interferometry. ODAE models the statistical properties of tracking error sources, including inherent observable imprecision, atmospheric delays, clock offsets, station location uncertainty, and measurement biases, and through Monte Carlo simulation, ODAE calculates the statistical properties of errors in the predicted satellites state vector. This paper presents results from ODAE application to orbit determination of the Tracking and Data Relay

Satellite (TDRS) by radio interferometry. Conclusions about optimal ground station locations for interferometric tracking of TDRS are presented, along with a discussion of operational advantages of radio interferometry.

Author

N95-17548*# Johns Hopkins Univ., Laurel, MD. Applied Physics Lab.

COST EFFICIENT OPERATIONS FOR DISCOVERY CLASS MISSIONS **c66**

G. E. Cameron, J. A. Landshof, and G. W. Whitworth *In* NASA. Goddard Space Flight Center, Third International Symposium on Space Mission Operations and Ground Data Systems, Part 2 Nov. 1994 p 809-816 (For primary document see N95-17531 04-17)

Avail: CASI HC A02/MF A06

The Near Earth Asteroid Rendezvous (NEAR) program at The Johns Hopkins University Applied Physics Laboratory is scheduled to launch the first spacecraft in NASA's Discovery program. The Discovery program is to promote low cost spacecraft design, development, and mission operations for planetary space missions. The authors describe the NEAR mission and discuss the design and development of the NEAR Mission Operations System and the NEAR Ground System with an emphasis on those aspects of the design that are conducive to low-cost operations. Author

N95-17549*# Rutherford Appleton Lab., Chilton (England).

GROUND STATION SUPPORT FOR SMALL SCIENTIFIC SATELLITES **c66**

R. Holdaway, E. Dunford, and P. H. McPherson *In* NASA. Goddard Space Flight Center, Third International Symposium on Space Mission Operations and Ground Data Systems, Part 2 Nov. 1994 p 817-824 (For primary document see N95-17531 04-17)

Avail: CASI HC A02/MF A06

In order to keep the cost of a complete small satellite program low, it is necessary to minimize the cost of the ground station operations and support. This is required not only for the operations and support per se, but also in the development of ground station hardware and the mission associated software. Recent experiences at the Rutherford Appleton Laboratory (RAL) on two international projects, IRAS and AMPTE, have shown that the low cost objectives of operations using smaller national facilities can be achieved. This paper describes the facilities at RAL, and the methods by which low cost support are provided by considering the differing implications of hardware/software system modularity, reliability, and small numbers of dedicated and highly skilled operations staff. Author

N95-17550*# MATRA Marconi Space, Toulouse (France).

DESIGN OF GROUND SEGMENTS FOR SMALL SATELLITES **c14**

Guy Mace *In* NASA. Goddard Space Flight Center, Third International Symposium on Space Mission Operations and Ground Data Systems, Part 2 Nov. 1994 p 825-835 (For primary document see N95-17531 04-17)

Avail: CASI HC A03/MF A06

New concepts must be implemented when designing a Ground Segment (GS) for small satellites to conform to their specific mission characteristics: low cost, one main instrument, spacecraft autonomy, optimized mission return, etc. This paper presents the key cost drivers of such ground segments, the main design features, and the comparison of various design options that can meet the user requirements. Author

N95-17551*# Alenia Spazio S.p.A., Turin (Italy).

THE SAX ITALIAN SCIENTIFIC SATELLITE. THE ON-BOARD IMPLEMENTED AUTOMATION AS A SUPPORT TO THE GROUND CONTROL CAPABILITY **c18**

Andrea Martelli *In* NASA. Goddard Space Flight Center, Third International Symposium on Space Mission Operations and Ground Data Systems, Part 2 Nov. 1994 p 837-846 (For primary document see N95-17531 04-17)

Avail: CASI HC A02/MF A06

This paper presents the capabilities implemented in the SAX system for an efficient operations management during its in-flight mission. SAX is an Italian scientific satellite for x-ray astronomy whose major mission objectives impose quite tight constraints on the implementation of both the space and ground segment. The most relevant mission characteristics require an operative lifetime of two years, performing scientific observations both in contact and in noncontact periods, with a low equatorial orbit supported by one ground station, so that only a few minutes of communications are available each orbit. This operational scenario determines the need to have a satellite capable of performing the scheduled mission automatically and reacting autonomously to contingency situations. The implementation approach of the on-board operations management, through which the necessary automation and autonomy are achieved, follows a hierarchical structure. This has been achieved adopting a distributed avionic architecture. Nine different on-board computers, in fact, constitute the on-board data management system. Each of them performs the local control and monitors its own functions while the system level control is performed at a higher level by the data handling applications software. The SAX on-board architecture provides the ground operators with different options of intervention by three classes of telecommands. The management of the scientific operations will be scheduled by the operation control center via dedicated operating plans. The SAX satellite flight mode is presently being integrated at Alenia Spazio premises in Turin for a launch scheduled for the end of 1995. Once in orbit, the SAX satellite will be subject to intensive check-out activities in order to verify the required mission performances. An overview of the envisaged procedure and of the necessary on-ground activities is therefore depicted as well. Author

N95-17552*# Computer Technology Associates, Inc., McLean, VA. Space Systems.

SMALL SATELLITE SPACE OPERATIONS **c66**

Keith Reiss *In* NASA. Goddard Space Flight Center, Third International Symposium on Space Mission Operations and Ground Data Systems, Part 2 Nov. 1994 p 847-853 (For primary document see N95-17531 04-17)

Avail: CASI HC A02/MF A06

CTA Space Systems has played a premier role in the development of the 'lightsat' programs of the 80's and 90's. The high costs and development times associated with conventional LEO satellite design, fabrication, launch, and operations continue to motivate the development of new methodologies, techniques, and generally low cost and less stringently regulated satellites. These spacecraft employ low power 'lightsat' communications (versus TDRSS for NASA's LEO's) and typically fly missions with payload/experiment suites that can succeed, for example, without heavily redundant backup systems and large infrastructures of personnel and ground support systems. Such small yet adaptable satellites are also typified by their very short contract-to-launch times (often one to two years). This paper reflects several of the methodologies and perspectives of our successful involvement in these innovative programs and suggests how they might relieve NASA's mounting pressures to reduce the cost of both the spacecraft and their companion mission operations. It focuses on the use of adaptable, sufficiently powerful yet inexpensive PC-based ground systems for wide ranging user terminal (UT) applications and master control facilities for mission operations. These systems proved themselves in successfully controlling more than two dozen USAF, USN, and ARPA satellites at CTA/SS. UT versions have linked with both GEO and LEO satellites and functioned autonomously in relay roles often in remote parts of the world. LEO applications particularly illustrate the efficacy of these concepts since a user can easily mount a lightweight antenna, usually an omni or helix with light duty rotors and PC-based drivers. A few feet of coax connected to a small transceiver module (the size of a small PC) and a serial line to an associated PC establishes a communications link and together with the PC constitute a viable ground station. Applications included geomagnetic mapping; spaceborne solid state recorder validation; global store-and-forward data communications for both scientific and military purposes such as Desert Storm; UHF transponder services for both digital data and voice using a constellation; remote sensor monitoring of weather and oceanographic conditions; classified payloads; and UHF spectrum surveillance. Ground processing has been accomplished by automatic unattended or manual operation. Management of multiple assets highlights the relative ease with which two constellations totaling nine satellites were controlled from one system including constellation station keeping. Our experience in small end-to-end systems including concurrent design, development, and testing of the flight and operational ground systems offers low cost approaches to NASA scientific satellite operations of the 1990's. Author

N95-17553*# National Aeronautics and Space Administration. Goddard Space Flight Center, Greenbelt, MD.

EMBEDDED PARALLEL PROCESSING BASED GROUND CONTROL SYSTEMS FOR SMALL SATELLITE TELEMETRY **c14**

Michael L. Forman, Tushar K. Hazra (Martin Marietta Services, Inc., Greenbelt, MD.), Gregory M. Troendly (Martin Marietta Services, Inc., Greenbelt, MD.), and William G. Nickum (Martin Marietta Services, Inc., Greenbelt, MD.) *In its* Third International Symposium on Space Mission Operations and Ground Data Systems, Part 2 Nov. 1994 p 857-864 (For primary document see N95-17531 04-17)

(Contract NAS5-31739)

Avail: CASI HC A02/MF A06

The use of networked terminals which utilize embedded processing techniques results in totally integrated, flexible, high speed, reliable, and scalable systems suitable for telemetry and data processing applications such as mission operations centers (MOC). Synergies of these terminals, coupled with the capability of terminal to receive incoming data, allow the viewing of any defined display by any terminal from the start of data acquisition. There is no single point of failure (other than with network input) such as exists with configurations where all input data goes through a single front end processor and then to a serial string of workstations. Missions dedicated to NASA's ozone measurements program utilize the methodologies which are discussed, and result in a multimission configuration of low cost, scalable hardware and software which can be run by one flight operations team with low risk. Author

N95-17554*# Jet Propulsion Lab., California Inst. of Tech., Pasadena, CA.

OPEN SOLUTIONS TO DISTRIBUTED CONTROL IN GROUND TRACKING STATIONS **c14**

William Randy Heuser *In* NASA. Goddard Space Flight Center, Third International Symposium on Space Mission Operations and Ground Data Systems, Part 2 Nov. 1994 p 865-877 (For primary document see N95-17531 04-17)

Avail: CASI HC A03/MF A06

The advent of high speed local area networks has made it possible to interconnect small, powerful computers to function together as a single large computer. Today, distributed computer systems are the new paradigm for large scale computing systems. However, the communications provided by the local area network is only one part of the solution. The services and protocols used by the application programs to communicate across the network are as indispensable as the local area network. And the selection of services and protocols that do not match the system requirements will limit the capabilities, performance, and expansion of the system. Proprietary solutions are available but are usually limited to a select set of equipment. However, there are two solutions based on 'open' standards. The question that must be answered is 'which one is the best one for my job?' This paper examines a model for tracking stations and their requirements for interprocessor communications in the next century. The model and requirements are matched with the model and services provided by the five different software architectures and supporting protocol solutions. Several key services are examined in detail to determine which services and protocols most closely match the requirements for the tracking station environment. The study reveals that the protocols are tailored to the problem domains for which they were originally designed. Further, the study reveals that the process control model is the closest match to the tracking station model. Author

N95-17555*# National Aeronautics and Space Administration. Goddard Space Flight Center, Greenbelt, MD.

AN AGENT-ORIENTED APPROACH TO AUTOMATED MISSION OPERATIONS **c66**

Walt Truszkowski and Jide Odubiyi (Loral AeroSys, Seabrook, MD.) *In its* Third International Symposium on Space Mission Operations and Ground Data Systems, Part 2 Nov. 1994 p 879-887 Sponsored by NASA, Washington (For primary document see N95-17531 04-17)

Avail: CASI HC A02/MF A06

As we plan for the next generation of Mission Operations Control Center (MOCC) systems, there are many opportunities for the increased utilization of innovative knowledge-based technologies. The innovative technology discussed is an advanced use of agent-oriented approaches to the automation of mission operations. The paper presents an overview of this technology and discusses applied operational scenarios currently being investigated and prototyped. A major focus of the current work is the development of a simple user mechanism that would empower operations staff members to create, in real time, software agents to assist them in common, labor intensive operations tasks. These operational tasks would include: handling routine data and information management functions; amplifying the capabilities of a spacecraft analyst/operator to rapidly identify, analyze, and correct spacecraft anomalies by correlating complex data/information sets and filtering error messages; improving routine monitoring and trend analysis by detecting common failure signatures; and serving as a sentinel for spacecraft changes during critical maneuvers enhancing the system's capabilities to support nonroutine operational conditions with minimum additional staff. An agent-based testbed is under development. This testbed will allow us to: (1) more clearly understand the intricacies of applying agent-based technology in support of the advanced automation of mission operations and (2) access the full set of benefits that can be realized by the proper application of agent-oriented technology in a mission operations environment. The testbed under development addresses some of the data management and report generation functions for the Explorer Platform (EP)/Extreme UltraViolet Explorer (EUVE) Flight Operations Team (FOT). We present an overview of agent-oriented technology and a detailed report on the operation's concept for the testbed. Author

N95-17556*# National Aeronautics and Space Administration. Goddard Space Flight Center, Greenbelt, MD.

ADVANCED GROUND STATION ARCHITECTURE **c14**

David Zillig and Ted Benjamin (Stanford Telecommunications, Inc., Reston, VA.) *In its* Third International Symposium on Space Mission Operations and Ground Data Systems, Part 2 Nov. 1994 p 889-896 (For primary document see N95-17531 04-17)

Avail: CASI HC A02/MF A06

This paper describes a new station architecture for NASA's Ground Network (GN). The architecture makes efficient use of emerging technologies to provide dramatic reductions in size, operational complexity, and operational and maintenance costs. The architecture, which is based on recent receiver work sponsored by the Office of Space Communications Advanced Systems Program, allows integration of both GN and Space Network (SN) modes of operation in the same electronics system. It is highly configurable through software and the use of charged coupled device (CCD) technology to provide a wide range of operating modes. Moreover, it affords modularity of features which are optional depending on the application. The resulting system incorporates advanced RF, digital, and remote control technology capable of introducing significant operational, performance, and cost benefits to a variety of NASA communications and tracking applications. Author

N95-17557*# Jet Propulsion Lab., California Inst. of Tech., Pasadena, CA.

AUTOMATING TESTBED DOCUMENTATION AND DATABASE ACCESS USING WORLD WIDE WEB (WWW) TOOLS **c82**

Charles Ames, Brent Auernheimer (California State Univ., Fresno, CA.), and Young H. Lee *In* NASA. Goddard Space Flight Center, Third International Symposium on Space Mission Operations and Ground Data Systems, Part 2 Nov. 1994 p 899-904 (For primary document see N95-17531 04-17)

Avail: CASI HC A02/MF A06

A method for providing uniform transparent access to disparate distributed information systems was demonstrated. A prototype testing interface was developed to access documentation and information using publicly available hypermedia tools. The prototype gives testers a uniform, platform-independent user interface to on-line documentation, user manuals, and mission-specific test and operations data. Mosaic was the common user interface, and HTML (Hypertext Markup Language) provided hypertext capability. Author

N95-17558*# Vitrociset S.p.A., Rome (Italy).

TOWARDS AN INTEGRAL COMPUTER ENVIRONMENT SUPPORTING SYSTEM OPERATIONS ANALYSIS AND CONCEPTUAL DESIGN **c60**

E. Barro, A. DelBufalo, and F. Rossi *In* NASA. Goddard Space Flight Center, Third International Symposium on Space Mission Operations and Ground Data Systems, Part 2 Nov. 1994 p 905-913 (For primary

document see N95-17531 04-17)
Avail: CASI HC A02/MF A06

VITROCISET has in house developed a prototype tool named System Dynamic Analysis Environment (SDAE) to support system engineering activities in the initial definition phase of a complex space system. The SDAE goal is to provide powerful means for the definition, analysis, and trade-off of operations and design concepts for the space and ground elements involved in a mission. For this purpose SDAE implements a dedicated modeling methodology based on the integration of different modern (static and dynamic) analysis and simulation techniques. The resulting 'system model' is capable of representing all the operational, functional, and behavioral aspects of the system elements which are part of a mission. The execution of customized model simulations enables: the validation of selected concepts with respect to mission requirements; the in-depth investigation of mission specific operational and/or architectural aspects; and the early assessment of performances required by the system elements to cope with mission constraints and objectives. Due to its characteristics, SDAE is particularly tailored for nonconventional or highly complex systems, which require a great analysis effort in their early definition stages. SDAE runs under PC-Windows and is currently used by VITROCISET system engineering group. This paper describes the SDAE main features, showing some tool output examples. Author

N95-17559*# Jet Propulsion Lab., California Inst. of Tech., Pasadena, CA.
SEQ-POINTER: NEXT GENERATION, PLANETARY SPACECRAFT REMOTE SENSING SCIENCE OBSERVATION DESIGN TOOL
Jeffrey S. Boyer *In* NASA. Goddard Space Flight Center, Third International Symposium on Space Mission Operations and Ground Data Systems, Part 2 Nov. 1994 p 915-922 (For primary document see N95-17531 04-17)
Avail: CASI HC A02/MF A06

Since Mariner, NASA-JPL planetary missions have been supported by ground software to plan and design remote sensing science observations. The software used by the science and sequence designers to plan and design observations has evolved with mission and technological advances. The original program, PEGASIS (Mariners 4, 6, and 7), was re-engineered as POGASIS (Mariner 9, Viking, and Mariner 10), and again later as POINTER (Voyager and Galileo). Each of these programs were developed under technological, political, and fiscal constraints which limited their adaptability to other missions and spacecraft designs. Implementation of a multi-mission tool, SEQ POINTER, under the auspices of the JPL Multimission Operations Systems Office (MOSO) is in progress. This version has been designed to address the limitations experienced on previous versions as they were being adapted to a new mission and spacecraft. The tool has been modularly designed with subroutine interface structures to support interchangeable celestial body and spacecraft definition models. The computational and graphics modules have also been designed to interface with data collected from previous spacecraft, or on-going observations, which describe the surface of each target body. These enhancements make SEQ POINTER a candidate for low-cost mission usage, when a remote sensing science observation design capability is required. The current and planned capabilities of the tool will be discussed. The presentation will also include a 5-10 minute video presentation demonstrating the capabilities of a proto-Cassini Project version that was adapted to test the tool. The work described in this abstract was performed by the Jet Propulsion Laboratory, California Institute of Technology, under contract to the National Aeronautics and Space Administration. Author

N95-17560*# National Aeronautics and Space Administration. Goddard Space Flight Center, Greenbelt, MD.
KNOWLEDGE-BASED CRITIQUING OF GRAPHICAL USER INTERFACES WITH CHIMES **c61**
Jianping Jiang (Computer Technology Associates, Inc., Rockville, MD.), Elizabeth D. Murphy (Computer Technology Associates, Inc., Rockville, MD.), Leslie E. Carter (Computer Technology Associates, Inc., Rockville, MD.), and Walter F. Truszkowski *In its* Third International Symposium on Space Mission Operations and Ground Data Systems, Part 2 Nov. 1994 p 923-928 (For primary document see N95-17531 04-17)
Avail: CASI HC A02/MF A06

CHIMES is a critiquing tool that automates the process of checking graphical user interface (GUI) designs for compliance with human factors design guidelines and toolkit style guides. The current prototype identifies instances of non-compliance and presents problem statements, advice, and tips to the GUI designer. Changes requested by the designer are made automatically, and the revised GUI is re-evaluated. A case study conducted at NASA-Goddard showed that CHIMES has the potential for dramatically reducing the time formerly spent in hands-on consistency checking. Capabilities recently added to CHIMES include exception handling and rule building. CHIMES is intended for use prior to usability testing as a means, for example, of catching and correcting syntactic inconsistencies in a larger user interface. Author

N95-17561*# Jet Propulsion Lab., California Inst. of Tech., Pasadena, CA.
SEQ-REVIEW: A TOOL FOR REVIEWING AND CHECKING SPACECRAFT SEQUENCES
Pierre F. Maldague, Mekki El-Boushi, Thomas J. Starbird, and Steven J. Zawacki *In* NASA. Goddard Space Flight Center, Third International Symposium on Space Mission Operations and Ground Data Systems, Part 2 Nov. 1994 p 929-936 (For primary document see N95-17531 04-17)
Avail: CASI HC A02/MF A06

A key component of JPL's strategy to make space missions faster, better and cheaper is the Advanced Multi-Mission Operations System (AMMOS), a ground software intensive system currently in use and in further development. AMMOS intends to eliminate the cost of re-engineering a ground system for each new JPL mission. This paper discusses SEQ-REVIEW, a component of AMMOS that was designed to facilitate and automate the task of reviewing and checking spacecraft sequences. SEQ-REVIEW is a smart browser for inspecting files created by other sequence generation tools in the AMMOS system. It can parse sequence-related files according to a computer-readable version of a 'Software Interface Specification' (SIS), which is a standard document for defining file formats. It lets users display one or several linked files and check simple constraints using a Basic-like 'Little Language'. SEQ-REVIEW represents the first application of the Quality Function Development (QFD) method to sequence software development at JPL. The paper will show how the requirements for SEQ-REVIEW were defined and converted into a design based on object-oriented principles. The process starts with interviews of potential users, a small but diverse group that spans multiple disciplines and 'cultures'. It continues with the development of QFD matrices that related product functions and characteristics to user-demanded qualities. These matrices are then turned into a formal Software Requirements Document (SRD). The process concludes with the design phase, in which the CRC (Class, Responsibility, Collaboration) approach was used to convert requirements into a blueprint for the final product. Author

N95-17562*# Jet Propulsion Lab., California Inst. of Tech., Pasadena, CA.
SIMPLIFYING OPERATIONS WITH AN UPLINK/DOWNLINK INTEGRATION TOOLKIT
Susan C. Murphy, Kevin J. Miller, Ana Maria Guerrero, Chester Joe, John J. Louie, and Christine Aguilera *In* NASA. Goddard Space Flight Center, Third International Symposium on Space Mission Operations and Ground Data Systems, Part 2 Nov. 1994 p 937-943 (For primary document see N95-17531 04-17)
Avail: CASI HC A02/MF A06

The Operations Engineering Lab (OEL) at JPL has developed a simple, generic toolkit to integrate the uplink/downlink processes, (often called closing the loop), in JPL's Multimission Ground Data System. This toolkit provides capabilities for integrating telemetry verification points with predicted spacecraft commands and ground events in the Mission Sequence Of Events (SOE) document. In the JPL ground data system, the uplink processing functions and the downlink processing functions are separate subsystems that are not well integrated because of the nature of planetary missions with large one-way light times for spacecraft-to-ground communication. Our new closed-loop monitoring tool allows an analyst or mission controller to view and save uplink commands and ground events with their corresponding downlinked telemetry values regardless of the delay in downlink telemetry and without requiring real-time intervention by the user. An SOE document is a time-ordered list of all the planned ground and spacecraft events, including all commands, sequence loads, ground events, significant mission activities, spacecraft status, and resource

allocations. The SOE document is generated by expansion and integration of spacecraft sequence files, ground station allocations, navigation files, and other ground event files. This SOE generation process has been automated within the OEL and includes a graphical, object-oriented SOE editor and real-time viewing tool running under X/Motif. The SOE toolkit was used as the framework for the integrated implementation. The SOE is used by flight engineers to coordinate their operations tasks, serving as a predict data set in ground operations and mission control. The closed-loop SOE toolkit allows simple, automated integration of predicted uplink events with correlated telemetry points in a single SOE document for on-screen viewing and archiving. It automatically interfaces with existing real-time or non real-time sources of information, to display actual values from the telemetry data stream. This toolkit was designed to greatly simplify the user's ability to access and view telemetry data, and also provide a means to view this data in the context of the commands and ground events that are used to interpret it. A closed-loop system can prove especially useful in small missions with limited resources requiring automated monitoring tools. This paper will discuss the toolkit implementation, including design trade-offs and future plans for enhancing the automated capabilities.

Author

N95-17563*# Centre National d'Etudes Spatiales, Toulouse (France).

ELISA, A DEMONSTRATOR ENVIRONMENT FOR INFORMATION SYSTEMS ARCHITECTURE DESIGN **c82**

Chantal Panem *In* NASA. Goddard Space Flight Center, Third International Symposium on Space Mission Operations and Ground Data Systems, Part 2 Nov. 1994 p 945-952 (For primary document see N95-17531 04-17)

Avail: CASI HC A02/MF A06

This paper describes an approach of reusability of software engineering technology in the area of ground space system design. System engineers have lots of needs similar to software developers: sharing of a common data base, capitalization of knowledge, definition of a common design process, communication between different technical domains. Moreover system designers need to simulate dynamically their system as early as possible. Software development environments, methods and tools now become operational and widely used. Their architecture is based on a unique object base, a set of common management services and they host a family of tools for each life cycle activity. In late '92, CNES decided to develop a demonstrative software environment supporting some system activities. The design of ground space data processing systems was chosen as the application domain. ELISA (Integrated Software Environment for Architectures Specification) was specified as a 'demonstrator', i.e. a sufficient basis for demonstrations, evaluation and future operational enhancements. A process with three phases was implemented: system requirements definition, design of system architectures models, and selection of physical architectures. Each phase is composed of several activities that can be performed in parallel, with the provision of Commercial Off the Shelves Tools. ELISA has been delivered to CNES in January 94, currently used for demonstrations and evaluations on real projects (e.g. SPOT4 Satellite Control Center). It is on the way of new evolutions. Author

N95-17564*# Telos Corp., Pasadena, CA.

SOFTWARE INTERFACE VERIFIER **c61**

Tomas J. Soderstrom, Laura A. Krall, Sharon A. Hope, and Brian S. Zupke *In* NASA. Goddard Space Flight Center, Third International Symposium on Space Mission Operations and Ground Data Systems, Part 2 Nov. 1994 p 953-960 (For primary document see N95-17531 04-17)

Avail: CASI HC A02/MF A06

A Telos study of 40 recent subsystem deliveries into the DSN at JPL found software interface testing to be the single most expensive and error-prone activity, and the study team suggested creating an automated software interface test tool. The resulting Software Interface Verifier (SIV), which was funded by NASA/JPL and created by Telos, employed 92 percent software reuse to quickly create an initial version which incorporated early user feedback. SIV is now successfully used by developers for interface prototyping and unit testing, by test engineers for formal testing, and by end users for non-intrusive data flow tests in the operational environment. Metrics, including cost, are included. Lessons learned include the need for early user training. SIV is ported to many platforms and can be successfully used or tailored by other NASA groups. Author

N95-17565*# Hughes STX, Inc., Greenbelt, MD. Technology Applications Group.

OOD/OOP EXPERIENCE IN THE SCIENCE OPERATIONS CENTER PART OF THE GROUND SYSTEM FOR X RAY TIMING EXPLORER MISSION **c14**

Abdur Rahim Choudhary *In* NASA. Goddard Space Flight Center, Third International Symposium on Space Mission Operations and Ground Data Systems, Part 2 Nov. 1994 p 963-970 (For primary document see N95-17531 04-17)

Avail: CASI HC A02/MF A06

The Science Operations Center (SOC) for the X-ray Timing Explorer (XTE) mission is an important component of the XTE ground system. Its mandate includes: (1) command and telemetry for the three XTE instruments, using CCSDS standards; (2) monitoring of the real-time science operations, reconfiguration of the experiment and the instruments, and real-time commanding to address the targets of opportunity (TOO) and alternate observations; and (3) analysis, processing, and archival of the XTE telemetry, and the timely delivery of the data products to the principal investigator (PI) teams and the guest observers (GO). The SOC has two major components: the science operations facility (SOF) that addresses the first two objectives stated above and the guest observer facility (GOF) that addresses the third. The SOF has subscribed to the object oriented design and implementation; while the GOF uses the traditional approach in order to take advantage of the existing software developed in support of previous missions. This paper details the SOF development using the object oriented design (OOD), and its implementation using the object oriented programming (OOP) in C++ under Unix environment on client-server architecture using Sun workstations. It also illustrates how the object oriented (OO) and the traditional approaches coexist in SOF and GOF, the lessons learned, and how the OOD facilitated the distributed software development collaboratively by four different teams. Details are presented for the SOF system, its major subsystems, its interfaces with the rest of the XTE ground data system, and its design and implementation approaches. Author

N95-17566*# National Aeronautics and Space Administration. Goddard Space Flight Center, Greenbelt, MD.

A PROVEN APPROACH FOR MORE EFFECTIVE SOFTWARE DEVELOPMENT AND MAINTENANCE **c61**

Rose Pajerski, Dana Hall (Science Applications International Corp., McLean, VA.), and Craig Sinclair (Science Applications International Corp., McLean, VA.) *In its* Third International Symposium on Space Mission Operations and Ground Data Systems, Part 2 Nov. 1994 p 975-983 (For primary document see N95-17531 04-17)

Avail: CASI HC A02/MF A06

Modern space flight mission operations and associated ground data systems are increasingly dependent upon reliable, quality software. Critical functions such as command load preparation, health and status monitoring, communications link scheduling and conflict resolution, and transparent gateway protocol conversion are routinely performed by software. Given budget constraints and the ever increasing capabilities of processor technology, the next generation of control centers and data systems will be even more dependent upon software across all aspects of performance. A key challenge now is to implement improved engineering, management, and assurance processes for the development and maintenance of that software; processes that cost less, yield higher quality products, and that self-correct for continual improvement evolution. The NASA Goddard Space Flight Center has a unique experience base that can be readily tapped to help solve the software challenge. Over the past eighteen years, the Software Engineering Laboratory within the code 500 Flight Dynamics Division has evolved a software development and maintenance methodology that accommodates the unique characteristics of an organization while optimizing and continually improving the organization's software capabilities. This methodology relies upon measurement, analysis, and feedback much analogous to that of control loop systems. It is an approach with a time-tested track record proven through repeated applications across a broad range of operational software development and maintenance projects. This paper describes the software improvement methodology employed by the Software Engineering Laboratory, and how it has been exploited within the Flight Dynamics Division with GSFC Code 500. Examples of specific improvement in the software itself and its processes are presented to illustrate the

effectiveness of the methodology. Finally, the initial findings are given when this methodology was applied across the mission operations and ground data systems software domains throughout Code 500. Author

N95-17567*# European Space Agency. European Space Operations Center, Darmstadt (Germany).

XMM INSTRUMENT ON-BOARD SOFTWARE MAINTENANCE CONCEPT c61

N. Peccia and F. Giannini (European Space Agency. European Space Research and Technology Center, ESTEC, Noordwijk, Netherlands.) *In* NASA. Goddard Space Flight Center, Third International Symposium on Space Mission Operations and Ground Data Systems, Part 2 Nov. 1994 p 985-992 (For primary document see N95-17531 04-17)

Avail: CASI HC A02/MF A06

While the pre-launch responsibility for the production, validation and maintenance of instrument on-board software traditionally lies with the experimenter, the post-launch maintenance has been the subject of ad hoc arrangements with the responsibility shared to different extent between the experimenter, ESTEC and ESOC. This paper summarizes the overall design and development of the instruments on-board software for the XMM satellite, and describes the concept adopted for the maintenance of such software post-launch. The paper will also outline the on-board software maintenance and validation facilities and the expected advantages to be gained by the proposed strategy. Conclusions with respect to adequacy of this approach will be presented as well as recommendations for future instrument on-board software developments. Author

N95-17568*# Computer Sciences Corp., Lanham, MD.

INTEGRATION OF A SATELLITE GROUND SUPPORT SYSTEM BASED ON ANALYSIS OF THE SATELLITE GROUND SUPPORT DOMAIN c14

R. D. Pendley, E. J. Scheidker, D. S. Levitt, C. R. Myers, and R. D. Werking *In* NASA. Goddard Space Flight Center, Third International Symposium on Space Mission Operations and Ground Data Systems, Part 2 Nov. 1994 p 993-1000 (For primary document see N95-17531 04-17)

Avail: CASI HC A02/MF A06

This analysis defines a complete set of ground support functions based on those practiced in real space flight operations during the on-orbit phase of a mission. These functions are mapped against ground support functions currently in use by NASA and DOD. Software components to provide these functions can be hosted on RISC-based work stations and integrated to provide a modular, integrated ground support system. Such modular systems can be configured to provide as much ground support functionality as desired. This approach to ground systems has been widely proposed and prototyped both by government institutions and commercial vendors. The combined set of ground support functions we describe can be used as a standard to evaluate candidate ground systems. This approach has also been used to develop a prototype of a modular, loosely-integrated ground support system, which is discussed briefly. A crucial benefit to a potential user is that all the components are flight-qualified, thus giving high confidence in their accuracy and reliability. Author

N95-17569*# National Aeronautics and Space Administration. Goddard Space Flight Center, Greenbelt, MD.

SOFTWARE PROCESS ASSESSMENT (SPA) c61

Linda H. Rosenberg (Unisys Corp., Lanham, MD.), Sylvia B. Sheppard, and Scott A. Butler (Maryland Univ., College Park, MD.) *In its* Third International Symposium on Space Mission Operations and Ground Data Systems, Part 2 Nov. 1994 p 1001-1008 (For primary document see N95-17531 04-17)

Avail: CASI HC A02/MF A06

NASA's environment mirrors the changes taking place in the nation at large, i.e. workers are being asked to do more work with fewer resources. For software developers at NASA's Goddard Space Flight Center (GSFC), the effects of this change are that we must continue to produce quality code that is maintainable and reusable, but we must learn to produce it more efficiently and less expensively. To accomplish this goal, the Data Systems Technology Division (DSTD) at GSFC is trying a variety of both proven and state-of-the-art techniques for software development (e.g., object-oriented design, prototyping, designing for reuse, etc.). In order to evaluate the effectiveness of these techniques, the Software Process Assessment (SPA) program was initiated. SPA was begun under the assumption that the effects of different software development processes, techniques, and tools, on the resulting product must be evaluated in an objective manner in order to assess any benefits that may have accrued. SPA involves the collection and analysis of software product and process data. These data include metrics such as effort, code changes, size, complexity, and code readability. This paper describes the SPA data collection and analysis methodology and presents examples of benefits realized thus far by DSTD's software developers and managers. Author

N95-17570*# National Aeronautics and Space Administration. Goddard Space Flight Center, Greenbelt, MD.

TAKING ADVANTAGE OF GROUND DATA SYSTEMS ATTRIBUTES TO ACHIEVE QUALITY RESULTS IN TESTING SOFTWARE c82

Clayton B. Sigman, John T. Koslosky, and Barbara H. Hageman (Integral Systems, Inc., Lanham, MD.) *In its* Third International Symposium on Space Mission Operations and Ground Data Systems, Part 2 Nov. 1994 p 1009-1014 (For primary document see N95-17531 04-17)

Avail: CASI HC A02/MF A06

During the software development life cycle process, basic testing starts with the development team. At the end of the development process, an acceptance test is performed for the user to ensure that the deliverable is acceptable. Ideally, the delivery is an operational product with zero defects. However, the goal of zero defects is normally not achieved but is successful to various degrees. With the emphasis on building low cost ground support systems while maintaining a quality product, a key element in the test process is simulator capability. This paper reviews the Transportable Payload Operations Control Center (TPOCC) Advanced Spacecraft Simulator (TASS) test tool that is used in the acceptance test process for unmanned satellite operations control centers. The TASS is designed to support the development, test and operational environments of the Goddard Space Flight Center (GSFC) operations control centers. The TASS uses the same basic architecture as the operations control center. This architecture is characterized by its use of distributed processing, industry standards, commercial off-the-shelf (COTS) hardware and software components, and reusable software. The TASS uses much of the same TPOCC architecture and reusable software that the operations control center developer uses. The TASS also makes use of reusable simulator software in the mission specific versions of the TASS. Very little new software needs to be developed, mainly mission specific telemetry communication and command processing software. By taking advantage of the ground data system attributes, successful software reuse for operational systems provides the opportunity to extend the reuse concept into the test area. Consistency in test approach is a major step in achieving quality results. Author

N95-17571*# Computer Resources International A/S (Denmark).

SCOS 2: AN OBJECT ORIENTED SOFTWARE DEVELOPMENT APPROACH c61

Martin Symonds, Steen Lynenskjold, and Christian Mueller *In* NASA. Goddard Space Flight Center, Third International Symposium on Space Mission Operations and Ground Data Systems, Part 2 Nov. 1994 p 1015-1022 (For primary document see N95-17531 04-17)

Avail: CASI HC A02/MF A06

The Spacecraft Control and Operations System 2 (SCOS 2), is intended to provide the generic mission control system infrastructure for future ESA missions. It represents a bold step forward in order to take advantage of state-of-the-art technology and current practices in the area of software engineering. Key features include: (1) use of object oriented analysis and design techniques; (2) use of UNIX, C++ and a distributed architecture as the enabling implementation technology; (3) goal of re-use for development, maintenance and mission specific software implementation; and (4) introduction of the concept of a spacecraft control model. This paper touches upon some of the traditional beliefs surrounding Object Oriented development and describes their relevance to SCOS 2. It gives rationale for why particular approaches were adopted and others not, and describes the impact of these decisions. The development approach followed is discussed, highlighting the evolutionary nature of the overall process and the iterative nature of the various tasks carried out. The emphasis of this paper is on the process of the development with the following being covered: (1) the three phases of the SCOS 2 project - prototyping & analysis, design & implementation and configuration / delivery of mission specific systems; (2) the close cooperation and continual interaction with the users during the development; (3) the management approach - the

split between client staff, industry and some of the required project management activities; (4) the lifecycle adopted being an enhancement of the ESA PSS-05 standard with SCOS 2 specific activities and approaches defined; and (5) an examination of some of the difficulties encountered and the solutions adopted. Finally, the lessons learned from the SCOS 2 experience are highlighted, identifying those issues to be used as feedback into future developments of this nature. This paper does not intend to describe the finished product and its operation, but focusing on the journey to arrive there, concentrating therefore on the process and not the products of the SCOS 2 software development. Author

N95-17572*# National Aeronautics and Space Administration. Goddard Space Flight Center, Greenbelt, MD.

EVALUATING MODELING TOOLS FOR THE EDOS **c66**

Gordon Knoble, Frederick McCaleb, Tanweer Aslam (Computer Sciences Corp., Lanham, MD.), and Paul Nester (Computer Sciences Corp., Lanham, MD.) *In its* Third International Symposium on Space Mission Operations and Ground Data Systems, Part 2 Nov. 1994 p 1025-1030 (For primary document see N95-17531 04-17)

Avail: CASI HC A02/MF A06

The Earth Observing System (EOS) Data and Operations System (EDOS) Project is developing a functional, system performance model to support the system implementation phase of the EDOS which is being designed and built by the Goddard Space Flight Center (GSFC). The EDOS Project will use modeling to meet two key objectives: (1) manage system design impacts introduced by unplanned changed in mission requirements; and (2) evaluate evolutionary technology insertions throughout the development of the EDOS. To select a suitable modeling tool, the EDOS modeling team developed an approach for evaluating modeling tools and languages by deriving evaluation criteria from both the EDOS modeling requirements and the development plan. Essential and optional features for an appropriate modeling tool were identified and compared with known capabilities of several modeling tools. Vendors were also provided the opportunity to model a representative EDOS processing function to demonstrate the applicability of their modeling tool to the EDOS modeling requirements. This paper emphasizes the importance of using a well defined approach for evaluating tools to model complex systems like the EDOS. The results of this evaluation study do not in any way signify the superiority of any one modeling tool since the results will vary with the specific modeling requirements of each project. Author

N95-17573*# National Aeronautics and Space Administration. Goddard Space Flight Center, Greenbelt, MD.

SOLAR AND HELIOSPHERIC OBSERVATORY (SOHO) EXPERIMENTERS' OPERATIONS FACILITY (EOF) **c14**

Eliane Larduinat (Allied-Signal Technical Services Corp., Alexandria, VA.) and William Potter *In its* Third International Symposium on Space Mission Operations and Ground Data Systems, Part 2 Nov. 1994 p 1031-1038 (For primary document see N95-17531 04-17)

(Contract NAS5-27772)

Avail: CASI HC A02/MF A06

This paper describes the SOHO Instrumenters' Operations Facility (EOF) project. The EOF is the element of the SOHO ground system at the Goddard Space Flight Center that provides the interface between the SOHO scientists and the other ground system elements. This paper first describes the development context of the SOHO EOF. It provides an overview of the SOHO mission within the International Solar-Terrestrial Physics (ISTP) project, and discusses the SOHO scientific objectives. The second part of this paper presents the implementation of the SOHO EOF, its innovative features, its possible applications to other missions, and its potential for use as part of a fully integrated ground control system. Author

N95-17574*# Jet Propulsion Lab., California Inst. of Tech., Pasadena, CA.

GALILEO SPACECRAFT MODELING FOR ORBITAL OPERATIONS **c18**

Bruce A. McLaughlin and Erik N. Nilsen *In* NASA. Goddard Space Flight Center, Third International Symposium on Space Mission Operations and Ground Data Systems, Part 2 Nov. 1994 p 1039-1044 (For primary document see N95-17531 04-17)

Avail: CASI HC A02/MF A06

The Galileo Jupiter orbital mission using the Low Gain Antenna (LGA) requires a higher degree of spacecraft state knowledge than was originally anticipated. Key elements of the revised design include onboard buffering of science and engineering data and extensive processing of data prior to downlink. In order to prevent loss of data resulting from overflow of the buffers and to allow efficient use of the spacecraft resources, ground based models of the spacecraft processes will be implemented. These models will be integral tools in the development of satellite encounter sequences and the cruise/playback sequences where recorded data is retrieved. Author

N95-17575*# Computer Technology Associates, Inc., Rockville, MD.

THE ADVANCED ORBITING SYSTEMS TESTBED PROGRAM: RESULTS TO DATE **c82**

John F. Otranto and Penny A. Newsome *In* NASA. Goddard Space Flight Center, Third International Symposium on Space Mission Operations and Ground Data Systems, Part 2 Nov. 1994 p 1045-1054 Sponsored by NASA, Washington (For primary document see N95-17531 04-17)

Avail: CASI HC A02/MF A06

The Consultative Committee for Space Data Systems (CCSDS) Recommendations for Packet Telemetry (PT) and Advanced Orbiting Systems (AOS) propose standard solutions to data handling problems common to many types of space missions. The Recommendations address only space/ground and space/space data handling systems. Goddard Space Flight Center's (GSFC's) AOS Testbed (AOST) Program was initiated to better understand the Recommendations and their impact on real-world systems, and to examine the extended domain of ground/ground data handling systems. The results and products of the Program will reduce the uncertainties associated with the development of operational space and ground systems that implement the Recommendations. Author

N95-17576*# National Aeronautics and Space Administration. Goddard Space Flight Center, Greenbelt, MD.

NCCDS PERFORMANCE MODEL **c14**

Eric Richmond and Antonio Vallone (Computer Sciences Corp., Lanham, MD.) *In its* Third International Symposium on Space Mission Operations and Ground Data Systems, Part 2 Nov. 1994 p 1055-1062 (For primary document see N95-17531 04-17)

Avail: CASI HC A02/MF A06

The NASA/GSFC Network Control Center (NCC) provides communication services between ground facilities and spacecraft missions in near-earth orbit that use the Space Network. The NCC Data System (NCCDS) provides computational support and is expected to be highly utilized by the service requests needed in the future years. A performance model of the NCCDS has been developed to assess the future workload and possible enhancements. The model computes message volumes from mission request profiles and SN resource levels and generates the loads for NCCDS configurations as a function of operational scenarios and processing activities. The model has been calibrated using the results of benchmarks performed on the operational NCCDS facility and used to assess some future SN service request scenarios. Author

N95-17577*# National Aeronautics and Space Administration. Goddard Space Flight Center, Greenbelt, MD.

EVALUATION OF NASA'S END-TO-END DATA SYSTEMS USING DSDS+ **c82**

Christopher Rouff, William Davenport, and Philip Message (Stanford Telecommunications, Inc., Seabrook, MD.) *In its* Third International Symposium on Space Mission Operations and Ground Data Systems, Part 2 Nov. 1994 p 1063-1069 (For primary document see N95-17531 04-17)

Avail: CASI HC A02/MF A06

The Data Systems Dynamic Simulator (DSDS+) is a software tool being developed by the authors to evaluate candidate architectures for NASA's end-to-end data systems. Via modeling and simulation, we are able to quickly predict the performance characteristics of each architecture, to evaluate 'what-if' scenarios, and to perform sensitivity analyses. As such, we are using modeling and simulation to help NASA select the optimal system configuration, and to quantify the performance characteristics of this system prior to its delivery. This paper is divided into the following six sections: (1) The role of modeling and simulation in the systems engineering process. In this section, we briefly describe the different types of results obtained by modeling each phase of the systems engineering life cycle, from concept definition through operations and maintenance; (2)

Recent applications of DSDS+. In this section, we describe ongoing applications of DSDS+ in support of the Earth Observing System (EOS), and we present some of the simulation results generated of candidate system designs. So far, we have modeled individual EOS subsystems (e.g. the Solid State Recorders used onboard the spacecraft), and we have also developed an integrated model of the EOS end-to-end data processing and data communications systems (from the payloads onboard to the principle investigator facilities on the ground); (3) Overview of DSDS+. In this section we define what a discrete-event model is, and how it works. The discussion is presented relative to the DSDS+ simulation tool that we have developed, including it's run-time optimization algorithms that enables DSDS+ to execute substantially faster than comparable discrete-event simulation tools; (4) Summary. In this section, we summarize our findings and 'lessons learned' during the development and application of DSDS+ to model NASA's data systems; (5) Further Information; and (6) Acknowledgements. Author

N95-17578*# National Aeronautics and Space Administration. Goddard Space Flight Center, Greenbelt, MD.

ANALYSIS OF SPACE NETWORK LOADING

Mark Simons and Gus Larrson (Allied-Signal Technical Services Corp., Columbia, MD.) *In its* Third International Symposium on Space Mission Operations and Ground Data Systems, Part 2 Nov. 1994 p 1071-1077 (For primary document see N95-17531 04-17)

Avail: CASI HC A02/MF A06

The NASA Space Network (SN) consists of several geosynchronous communications satellites, in addition to ground support facilities. Space Network management must predict years in advance what network resources are necessary to adequately satisfy all SN users. Similarly, users of the Space Network must know throughout all stages of mission planning and operations to what extent their communication support requirements can be met. NASA, at the Goddard Space Flight Center, performs Space Network and Mission Modeling using The Network Planning and Analysis System (NPAS), to determine the answers to these questions. Author

N95-17579*# European Space Agency. European Space Operations Center, Darmstadt (Germany). Stations and Communications Engineering Dept.

MODELING ESA'S TT/C SYSTEMS

Enrico Vassallo *In* NASA. Goddard Space Flight Center, Third International Symposium on Space Mission Operations and Ground Data Systems, Part 2 Nov. 1994 p 1079-1090 (For primary document see N95-17531 04-17)

Avail: CASI HC A03/MF A06

After a brief introduction on the need for simulation packages for the analysis and design of satellite communications systems, the software tool developed for the European Space Agency (ESA), its main objectives and the design choices made during the development are presented. A very concise description of the available communications and measurement block follows. The ESA standard Telemetry, Tracking and Command (TT&C) system simulator is then introduced along with a description of the ESA standard modulation and coding schemes. As an example, the simulation of the ranging system which is a non-standard communications block, is described in details. Several examples of TT&C simulations outputs are given and compared with measurement results or theoretical approximations, when available. Finally, future developments like the support of advanced modulation schemes and the dynamic satellite link simulation are presented. Author

N95-17580*# National Aeronautics and Space Administration. Goddard Space Flight Center, Greenbelt, MD.

A GENERAL MISSION INDEPENDENT SIMULATOR (GMIS) AND SIMULATOR CONTROL PROGRAM (SCP) **c61**

Paul L. Baker (Global Science and Technology, Inc., Greenbelt, MD.), J. Michael Moore, and John Rosenberger (Computer Technology Associates, Inc., Rockville, MD.) *In its* Third International Symposium on Space Mission Operations and Ground Data Systems, Part 2 Nov. 1994 p 1093-1100 (For primary document see N95-17531 04-17)

Avail: CASI HC A02/MF A06

GMIS is a general-purpose simulator for testing ground system software. GMIS can be adapted to any mission to simulate changes in the data state maintained by the mission's computers. GMIS was developed in Code 522 NASA Goddard Space Flight Center. The acronym GMIS stands for GOTT Mission Independent Simulator, where GOTT is the Ground Operations Technology Testbed. Within GOTT, GMIS is used to provide simulated data to an installation of TPOCC - the Transportable Payload Operations Control Center. TPOCC was developed by Code 510 as a reusable control center. GOTT uses GMIS and TPOCC to test new technology and new operator procedures. Author

N95-17581*# National Aeronautics and Space Administration. Goddard Space Flight Center, Greenbelt, MD.

TEST/SCORE/REPORT: SIMULATION TECHNIQUES FOR AUTOMATING THE TEST PROCESS **c14**

Barbara H. Hageman (Integral Systems, Inc., Lanham, MD.), Clayton B. Sigman, and John T. Koslosky *In its* Third International Symposium on Space Mission Operations and Ground Data Systems, Part 2 Nov. 1994 p 1103-1109 (For primary document see N95-17531 04-17)

Avail: CASI HC A02/MF A06

A Test/Score/Report capability is currently being developed for the Transportable Payload Operations Control Center (TPOCC) Advanced Spacecraft Simulator (TASS) system which will automate testing of the Goddard Space Flight Center (GSFC) Payload Operations Control Center (POCC) and Mission Operations Center (MOC) software in three areas: telemetry decommutation, spacecraft command processing, and spacecraft memory load and dump processing. Automated computer control of the acceptance test process is one of the primary goals of a test team. With the proper simulation tools and user interface, the task of acceptance testing, regression testing, and repeatability of specific test procedures of a ground data system can be a simpler task. Ideally, the goal for complete automation would be to plug the operational deliverable into the simulator, press the start button, execute the test procedure, accumulate and analyze the data, score the results, and report the results to the test team along with a go/no recommendation to the test team. In practice, this may not be possible because of inadequate test tools, pressures of schedules, limited resources, etc. Most tests are accomplished using a certain degree of automation and test procedures that are labor intensive. This paper discusses some simulation techniques that can improve the automation of the test process. The TASS system tests the POCC/MOC software and provides a score based on the test results. The TASS system displays statistics on the success of the POCC/MOC system processing in each of the three areas as well as event messages pertaining to the Test/Score/Report processing. The TASS system also provides formatted reports documenting each step performed during the tests and the results of each step. A prototype of the Test/Score/Report capability is available and currently being used to test some POCC/MOC software deliveries. When this capability is fully operational it should greatly reduce the time necessary to test a POCC/MOC software delivery, as well as improve the quality of the test process. Author

N95-17582*# National Aeronautics and Space Administration. Goddard Space Flight Center, Greenbelt, MD.

SPACECRAFT DATA SIMULATOR FOR THE TEST OF LEVEL ZERO PROCESSING SYSTEMS **c14**

Jeff Shi (RMS Technologies, Inc., Landover, MD.), Julie Gordon (RMS Technologies, Inc., Landover, MD.), Chandru Mirchandani (Loral AeroSys, Seabrook, MD.), and Diem Nguyen (Loral AeroSys, Seabrook, MD.) *In its* Third International Symposium on Space Mission Operations and Ground Data Systems, Part 2 Nov. 1994 p 1111-1120 (For primary document see N95-17531 04-17)

Avail: CASI HC A02/MF A06

The Microelectronic Systems Branch (MSB) at Goddard Space Flight Center (GSFC) has developed a Spacecraft Data Simulator (SDS) to support the development, test, and verification of prototype and production Level Zero Processing (LZP) systems. Based on a disk array system, the SDS is capable of generating large test data sets up to 5 Gigabytes and outputting serial test data at rates up to 80 Mbps. The SDS supports data formats including NASA Communication (Nascom) blocks, Consultative Committee for Space Data System (CCSDS) Version 1 & 2 frames and packets, and all the Advanced Orbiting Systems (AOS) services. The capability to simulate both sequential and non-sequential time-ordered downlink data streams with errors and gaps is crucial to test LZP systems. This paper describes the system architecture, hardware and software designs, and test data

designs. Examples of test data designs are included to illustrate the application of the SDS. Author

N95-17583*# Jet Propulsion Lab., California Inst. of Tech., Pasadena, CA.

RE-ENGINEERING THE MULTIMISSION COMMAND SYSTEM AT THE JET PROPULSION LABORATORY

Scott Alexander, Jeff Biesiadecki, Nagin Cox, Susan C. Murphy, and Tim Reeve *In* NASA. Goddard Space Flight Center, Third International Symposium on Space Mission Operations and Ground Data Systems, Part 2 Nov. 1994 p 1123-1131 (For primary document see N95-17531 04-17)

Avail: CASI HC A02/MF A06

The Operations Engineering Lab (OEL) at JPL has developed the multimission command system as part of JPL's Advanced Multimission Operations System. The command system provides an advanced multimission environment for secure, concurrent commanding of multiple spacecraft. The command functions include real-time command generation, command translation and radiation, status reporting, some remote control of Deep Space Network antenna functions, and command file management. The mission-independent architecture has allowed easy adaptation to new flight projects and the system currently supports all JPL planetary missions (Voyager, Galileo, Magellan, Ulysses, Mars Pathfinder, and CASSINI). This paper will discuss the design and implementation of the command software, especially trade-offs and lessons learned from practical operational use. The lessons learned have resulted in a re-engineering of the command system, especially in its user interface and new automation capabilities. The redesign has allowed streamlining of command operations with significant improvements in productivity and ease of use. In addition, the new system has provided a command capability that works equally well for real-time operations and within a spacecraft testbed. This paper will also discuss new development work including a multimission command database toolkit, a universal command translator for sequencing and real-time commands, and incorporation of telecommand capabilities for new missions. Author

N95-17584*# National Aeronautics and Space Administration. Goddard Space Flight Center, Greenbelt, MD.

RE-ENGINEERING NASCOM'S NETWORK MANAGEMENT ARCHITECTURE **c32**

Brian C. Drake and David Messent (Computer Sciences Corp., Lanham, MD.) *In its* Third International Symposium on Space Mission Operations and Ground Data Systems, Part 2 Nov. 1994 p 1133-1141 (For primary document see N95-17531 04-17)

Avail: CASI HC A02/MF A06

The development of Nascom systems for ground communications began in 1958 with Project Vanguard. The low-speed systems (rates less than 9.6 Kbs) were developed following existing standards; but, there were no comparable standards for high-speed systems. As a result, these systems were developed using custom protocols and custom hardware. Technology has made enormous strides since the ground support systems were implemented. Standards for computer equipment, software, and high-speed communications exist and the performance of current workstations exceeds that of the mainframes used in the development of the ground systems. Nascom is in the process of upgrading its ground support systems and providing additional services. The Message Switching System (MSS), Communications Address Processor (CAP), and Multiplexer/Demultiplexer (MDM) Automated Control System (MACS) are all examples of Nascom systems developed using standards such as, X-windows, Motif, and Simple Network Management Protocol (SNMP). Also, the Earth Observing System (EOS) Communications (Ecom) project is stressing standards as an integral part of its network. The move towards standards has produced a reduction in development, maintenance, and interoperability costs, while providing operational quality improvement. The Facility and Resource Manager (FARM) project has been established to integrate the Nascom networks and systems into a common network management architecture. The maximization of standards and implementation of computer automation in the architecture will lead to continued cost reductions and increased operational efficiency. The first step has been to derive overall Nascom requirements and identify the functionality common to all the current management systems. The identification of these common functions will enable the reuse of processes in the management architecture and promote increased use of automation throughout the Nascom network. The MSS, CAP, MACS, and Ecom projects have indicated the potential value of commercial-off-the-shelf (COTS) and standards through reduced cost and high quality. The FARM will allow the application of the lessons learned from these projects to all future Nascom systems. Author

N95-17585*# National Aeronautics and Space Administration, Washington, DC.

RE-ENGINEERING NASA'S SPACE COMMUNICATIONS TO REMAIN VIABLE IN A CONSTRAINED FISCAL ENVIRONMENT **c32**

Rhoda Shaller Hornstein, Donald J. Hei, Jr. (National Aeronautics and Space Administration. Goddard Space Flight Center, Greenbelt, MD.), Angelita C. Kelly (National Aeronautics and Space Administration. Goddard Space Flight Center, Greenbelt, MD.), Patricia C. Lightfoot (National Aeronautics and Space Administration. Goddard Space Flight Center, Greenbelt, MD.), Holland T. Bell (National Aeronautics and Space Administration. Wallops Flight Facility, Wallops Island, VA.), Izeller E. Cureton-Snead (Jet Propulsion Lab., California Inst. of Tech., Pasadena, CA.), William J. Hurd (Jet Propulsion Lab., California Inst. of Tech., Pasadena, CA.), and Charles H. Scales (National Aeronautics and Space Administration. Marshall Space Flight Center, Huntsville, AL.) *In* NASA. Goddard Space Flight Center, Third International Symposium on Space Mission Operations and Ground Data Systems, Part 2 Nov. 1994 p 1143-1150 (For primary document see N95-17531 04-17)

Avail: CASI HC A02/MF A06

Along with the Red and Blue Teams commissioned by the NASA Administrator in 1992, NASA's Associate Administrator for Space Communications commissioned a Blue Team to review the Office of Space Communications (Code O) Core Program and determine how the program could be conducted faster, better, and cheaper. Since there was no corresponding Red Team for the Code O Blue Team, the Blue Team assumed a Red Team independent attitude and challenged the status quo, including current work processes, functional distinctions, interfaces, and information flow, as well as traditional management and system development practices. The Blue Team's unconstrained, non-parochial, and imaginative look at NASA's space communications program produced a simplified representation of the space communications infrastructure that transcends organizational and functional boundaries, in addition to existing systems and facilities. Further, the Blue Team adapted the 'faster, better, cheaper' charter to be relevant to the multi-mission, continuous nature of the space communications program and to serve as a gauge for improving customer services concurrent with achieving more efficient operations and infrastructure life cycle economies. This simplified representation, together with the adapted metrics, offers a future view and process model for reengineering NASA's space communications to remain viable in a constrained fiscal environment. Code O remains firm in its commitment to improve productivity, effectiveness, and efficiency. In October 1992, the Associate Administrator reconstituted the Blue Team as the Code O Success Team (COST) to serve as a catalyst for change. In this paper, the COST presents the chronicle and significance of the simplified representation and adapted metrics, and their application during the FY 1993-1994 activities. Author

N95-17586*# National Space Development Agency, Tokyo (Japan). Tracking and Data Acquisition Dept.

A SYSTEM STUDY FOR SATELLITE OPERATION AND CONTROL IN NEXT GENERATION **c66**

K. Nakayama, T. Shigeta, T. Gotanda (LTCB Systems Co. Ltd., Japan.), K. Yamamoto (LTCB Systems Co. Ltd., Japan.), and Y. Yokokawa (LTCB Systems Co. Ltd., Japan.) *In* NASA. Goddard Space Flight Center, Third International Symposium on Space Mission Operations and Ground Data Systems, Part 2 Nov. 1994 p 1151-1157 (For primary document see N95-17531 04-17)

Avail: CASI HC A02/MF A06

Ever since the first satellite, ETS-1, in 1975, 28 NASDA satellites in total have been launched. With regards to satellite operations, NASDA has developed realtime TLM/CMD processing systems which could be commonly used for different types of satellite. Presently the third generation system is operational. Meanwhile, the recent trend of satellite operations is becoming more complicated, for example, CCSDS-adapted Satellites are emerging and computer technology is developing quite rapidly. Moreover, NASDA's role in satellite operations is changing from mainly Satellite Bus operations

to experimental/whole satellite missions operations. Considering these circumstances, NASDA has initiated a study for the next generation system which is suitable for operations of future satellites keeping in mind the following viewpoints: (1) demands from mission support; (2) trend of satellite design; and (3) progress of computer environment. This is an interim report of the study. Author

N95-17587*# National Aeronautics and Space Administration. Goddard Space Flight Center, Greenbelt, MD.

TRANSPORTABLE PAYLOAD OPERATIONS CONTROL CENTER REUSABLE SOFTWARE: BUILDING BLOCKS FOR QUALITY GROUND DATA SYSTEMS c61

Ron Mahmot, John T. Koslosky, Edward Beach (Computer Sciences Corp., Lanham, MD.), and Barbara Schwarz (Integral Systems, Inc., Lanham, MD.) *In its* Third International Symposium on Space Mission Operations and Ground Data Systems, Part 2 Nov. 1994 p 1161-1169 (For primary document see N95-17531 04-17)

Avail: CASI HC A02/MF A06

The Mission Operations Division (MOD) at Goddard Space Flight Center builds Mission Operations Centers which are used by Flight Operations Teams to monitor and control satellites. Reducing system life cycle costs through software reuse has always been a priority of the MOD. The MOD's Transportable Payload Operations Control Center development team established an extensive library of 14 subsystems with over 100,000 delivered source instructions of reusable, generic software components. Nine TPOCC-based control centers to date support 11 satellites and achieved an average software reuse level of more than 75 percent. This paper shares experiences of how the TPOCC building blocks were developed and how building block developer's, mission development teams, and users are all part of the process. Author

N95-17588*# Jet Propulsion Lab., California Inst. of Tech., Pasadena, CA.

CUSTOMIZING THE JPL MULTIMISSION GROUND DATA SYSTEM: LESSONS LEARNED c82

Susan C. Murphy, John J. Louie, Ana Maria Guerrero, Daniel Hurley, and Dana Flora-Adams *In* NASA. Goddard Space Flight Center, Third International Symposium on Space Mission Operations and Ground Data Systems, Part 2 Nov. 1994 p 1171-1175 (For primary document see N95-17531 04-17)

Avail: CASI HC A01/MF A06

The Multimission Ground Data System (MGDS) at NASA's Jet Propulsion Laboratory has brought improvements and new technologies to mission operations. It was designed as a generic data system to meet the needs of multiple missions and avoid re-inventing capabilities for each new mission and thus reduce costs. It is based on adaptable tools that can be customized to support different missions and operations scenarios. The MGDS is based on a distributed client/server architecture, with powerful Unix workstations, incorporating standards and open system architectures. The distributed architecture allows remote operations and user science data exchange, while also providing capabilities for centralized ground system monitor and control. The MGDS has proved its capabilities in supporting multiple large-class missions simultaneously, including the Voyager, Galileo, Magellan, Ulysses, and Mars Observer missions. The Operations Engineering Lab (OEL) at JPL has been leading Customer Adaptation Training (CAT) teams for adapting and customizing MGDS for the various operations and engineering teams. These CAT teams have typically consisted of only a few engineers who are familiar with operations and with the MGDS software and architecture. Our experience has provided a unique opportunity to work directly with the spacecraft and instrument operations teams and understand their requirements and how the MGDS can be adapted and customized to minimize their operations costs. As part of this work, we have developed workstation configurations, automation tools, and integrated user interfaces at minimal cost that have significantly improved productivity. We have also proved that these customized data systems are most successful if they are focused on the people and the tasks they perform and if they are based upon user confidence in the development team resulting from daily interactions. This paper will describe lessons learned in adapting JPL's MGDS to fly the Voyager, Galileo, and Mars Observer missions. We will explain how powerful, existing ground data systems can be adapted and packaged in a cost effective way for operations of small and large planetary missions. We will also describe how the MGDS was adapted to support operations within the Galileo Spacecraft Testbed. The Galileo testbed provided a unique opportunity to adapt MGDS to support command and control operations for a small autonomous operations team of a handful of engineers flying the Galileo Spacecraft flight system model. Author

N95-17589*# McDonnell-Douglas Corp., Cape Canaveral, FL. Space and Defense Systems.

CONFIGURABLE TECHNOLOGY DEVELOPMENT FOR REUSABLE CONTROL AND MONITOR GROUND SYSTEMS c14

David R. Uhrlaub *In* NASA. Goddard Space Flight Center, Third International Symposium on Space Mission Operations and Ground Data Systems, Part 2 Nov. 1994 p 1177-1184 (For primary document see N95-17531 04-17)

Avail: CASI HC A02/MF A06

The control monitor unit (CMU) uses configurable software technology for real-time mission command and control, telemetry processing, simulation, data acquisition, data archiving, and ground operations automation. The base technology is currently planned for the following control and monitor systems: portable Space Station checkout systems; ecological life support systems; Space Station logistics carrier system; and the ground system of the Delta Clipper (SX-2) in the Single-Stage Rocket Technology program. The CMU makes extensive use of commercial technology to increase capability and reduce development and life-cycle costs. The concepts and technology are being developed by McDonnell Douglas Space and Defense Systems for the Real-Time Systems Laboratory at NASA's Kennedy Space Center under the Payload Ground Operations Contract. A second function of the Real-Time Systems Laboratory is development and utilization of advanced software development practices. Author

N95-17590*# European Space Agency. European Space Operations Center, Darmstadt (Germany).

A NEW COMMUNICATION PROTOCOL FAMILY FOR A DISTRIBUTED SPACECRAFT CONTROL SYSTEM

Andrea Baldi and Marco Pace (Vitrociset S.p.A., Rome, Italy.) *In* NASA. Goddard Space Flight Center, Third International Symposium on Space Mission Operations and Ground Data Systems, Part 2 Nov. 1994 p 1187-1195 (For primary document see N95-17531 04-17)

Avail: CASI HC A02/MF A06

In this paper we describe the concepts behind and architecture of a communication protocol family, which was designed to fulfill the communication requirements of ESOC's new distributed spacecraft control system SCOS 2. A distributed spacecraft control system needs a data delivery subsystem to be used for telemetry (TLM) distribution, telecommand (TLC) dispatch and inter-application communication, characterized by the following properties: reliability, so that any operational workstation is guaranteed to receive the data it needs to accomplish its role; efficiency, so that the telemetry distribution, even for missions with high telemetry rates, does not cause a degradation of the overall control system performance; scalability, so that the network is not the bottleneck both in terms of bandwidth and reconfiguration; flexibility, so that it can be efficiently used in many different situations. The new protocol family which satisfies the above requirements is built on top of widely used communication protocols (UDP and TCP), provides reliable point-to-point and broadcast communication (UDP+) and is implemented in C++. Reliability is achieved using a retransmission mechanism based on a sequence numbering scheme. Such a scheme allows to have cost-effective performances compared to the traditional protocols, because retransmission is only triggered by applications which explicitly need reliability. This flexibility enables applications with different profiles to take advantage of the available protocols, so that the best rate between sped and reliability can be achieved case by case. Author

N95-17591*# McDonnell-Douglas Aerospace, Huntington Beach, CA. Space Station Div.

STANDARDIZING THE INFORMATION ARCHITECTURE FOR SPACECRAFT OPERATIONS c82

C. R. Easton *In* NASA. Goddard Space Flight Center, Third International Symposium on Space Mission Operations and Ground Data Systems, Part 2 Nov. 1994 p 1197-1204 (For primary document see N95-17531 04-17)

Avail: CASI HC A02/MF A06

This paper presents an information architecture developed for the Space Station Freedom as a model from which to derive an information architecture standard for advanced spacecraft. The information architecture provides a way of making information available across a program, and among programs, assuming that the information will be in a variety of local formats, structures and representations. It provides a format that can be expanded to define all of the physical and logical elements that make up a program, add definitions as required, and import definitions from prior programs to a new program. It allows a spacecraft and its control center to work in different representations and formats, with the potential for supporting existing spacecraft from new control centers. It supports a common view of data and control of all spacecraft, regardless of their own internal view of their data and control characteristics, and of their communications standards, protocols and formats. This information architecture is central to standardizing spacecraft operations, in that it provides a basis for information transfer and translation, such that diverse spacecraft can be monitored and controlled in a common way. Author

N95-17592*# Loral Space and Range Systems, Sunnyvale, CA.
A STANDARD SATELLITE CONTROL REFERENCE MODEL
Constance Golden *In* NASA. Goddard Space Flight Center, Third International Symposium on Space Mission Operations and Ground Data Systems, Part 2 Nov. 1994 p 1205-1212 Sponsored by AF (For primary document see N95-17531 04-17)
Avail: CASI HC A02/MF A06

This paper describes a Satellite Control Reference Model that provides the basis for an approach to identify where standards would be beneficial in supporting space operations functions. The background and context for the development of the model and the approach are described. A process for using this reference model to trace top level interoperability directives to specific sets of engineering interface standards that must be implemented to meet these directives is discussed. Issues in developing a 'universal' reference model are also identified. Author

N95-17593*# Jet Propulsion Lab., California Inst. of Tech., Pasadena, CA.
STANDARD PROTOCOL STACK FOR MISSION CONTROL c66
Adrian J. Hooke *In* NASA. Goddard Space Flight Center, Third International Symposium on Space Mission Operations and Ground Data Systems, Part 2 Nov. 1994 p 1213-1220 (For primary document see N95-17531 04-17)
Avail: CASI HC A02/MF A06

It is proposed to create a fully 'open' architectural specification for standardized space mission command and control. By being open, i.e., independent for any particular implementation, diversity and competition will be encouraged among future commercial suppliers of space equipment and systems. Customers of the new standard capability are expected to include: (1) the civil space community (e.g., NASA, NOAA, international Agencies); (2) the military space community (e.g., Air Force, Navy, intelligence); and (3) the emerging commercial space community (e.g., mobile satellite service providers). Author

N95-17594*# Science Applications International Corp., McLean, VA.
THE SPACE COMMUNICATIONS PROTOCOL STANDARDS PROGRAM
Alan Jeffries and Adrian J. Hooke (Jet Propulsion Lab., California Inst. of Tech., Pasadena, CA.) *In* NASA. Goddard Space Flight Center, Third International Symposium on Space Mission Operations and Ground Data Systems, Part 2 Nov. 1994 p 1221-1228 (For primary document see N95-17531 04-17)
Avail: CASI HC A02/MF A06

In the fall of 1992 NASA and the Department of Defense chartered a technical team to explore the possibility of developing a common set of space data communications standards for potential dual-use across the U.S. national space mission support infrastructure. The team focused on the data communications needs of those activities associated with on-lined control of civil and military aircraft. A two-pronged approach was adopted: a top-down survey of representative civil and military space data communications requirements was conducted; and a bottom-up analysis of available standard data communications protocols was performed. A striking intersection of civil and military space mission requirements emerged, and an equally striking consensus on the approach towards joint civil and military space protocol development was reached. The team concluded that wide segments of the U.S. civil and military space communities have common needs for: (1) an efficient file transfer protocol; (2) various flavors of underlying data transport service; (3) an optional data protection mechanism to assure end-to-end security of message exchange; and (4) an efficient internetworking protocol. These recommendations led to initiating a program to develop a suite of protocols based on these findings. This paper describes the current status of this program. Author

N95-17595*# European Space Agency. European Space Operations Center, Darmstadt (Germany).
THE ESA STANDARD FOR TELEMETRY AND TELECOMMAND PACKET UTILISATION: PUS
Jean-Francois Kaufeler *In* NASA. Goddard Space Flight Center, Third International Symposium on Space Mission Operations and Ground Data Systems, Part 2 Nov. 1994 p 1229-1234 (For primary document see N95-17531 04-17)
Avail: CASI HC A02/MF A06

ESA has developed standards for packet telemetry and telecommand, which are derived from the recommendations of the Inter-Agency Consultative Committee for Space Data Systems (CCSDS). These standards are now mandatory for future ESA programs as well as for many programs currently under development. However, while these packet standards address the end-to-end transfer of telemetry and telecommand data between applications on the ground and Application Processes on-board, they leave open the internal structure or content of the packets. This paper presents the ESA Packet Utilization Standard (PUS) which addresses this very subject and, as such, serves to extend and complement the ESA packet standards. The goal of the PUS is to be applicable to future ESA missions in all application areas (Telecommunications, Science, Earth Resources, microgravity, etc.). The production of the PUS falls under the responsibility of the ESA Committee for Operations and EGSE Standards (COES). Author

N95-17596*# European Space Agency. European Space Operations Center, Darmstadt (Germany).
PACKET UTILISATION DEFINITIONS FOR THE ESA XMM MISSION
H. R. Nye *In* NASA. Goddard Space Flight Center, Third International Symposium on Space Mission Operations and Ground Data Systems, Part 2 Nov. 1994 p 1235-1242 (For primary document see N95-17531 04-17)
Avail: CASI HC A02/MF A06

XMM, ESA's X-Ray Multi-Mirror satellite, due for launch at the end of 1999 will be the first ESA scientific spacecraft to implement the ESA packet telecommand and telemetry standards and will be the first ESOC-controlled science mission to take advantage of the new flight control system infrastructure development (based on object-oriented design and distributed-system architecture) due for deployment in 1995. The implementation of the packet standards is well defined at packet transport level. However, the standard relevant to the application level (the ESA Packet Utilization Standard) covers a wide range of on-board 'services' applicable in varying degrees to the needs of XMM. In defining which parts of the ESA PUS to implement, the XMM project first considered the mission objectives and the derived operations concept and went on to identify a minimum set of packet definitions compatible with these aspects. This paper sets the scene as above and then describes the services needed for XMM and the telecommand and telemetry packet types necessary to support each service. Author

N95-17597*# European Space Agency. European Space Operations Center, Darmstadt (Germany).
USE OF DATA DESCRIPTION LANGUAGES IN THE INTERCHANGE OF DATA c61
M. Pignede, B. Real-Planells, and S. R. Smith (Logica Ltd., London, England.) *In* NASA. Goddard Space Flight Center, Third International Symposium on Space Mission Operations and Ground Data Systems, Part 2 Nov. 1994 p 1243-1251 (For primary document see N95-17531 04-17)
Avail: CASI HC A02/MF A06

The Consultative Committee for Space Data Systems (CCSDS) is developing Standards for the interchange of information between systems, including those operating under different environments. The objective is to perform the interchange automatically, i.e. in a computer interpretable

manner. One aspect of the concept developed by CCSDS is the use of a separate data description to specify the data being transferred. Using the description, data can then be automatically parsed by the receiving computer. With a suitably expressive Data Description Language (DDL), data formats of arbitrary complexity can be handled. The advantages of this approach are: (1) that the description need only be written and distributed once to all users, and (2) new software does not need to be written for each new format, provided generic tools are available to support writing and interpretation of descriptions and the associated data instances. Consequently, the effort of 'hard coding' each new format is avoided and problems of integrating multiple implementations of a given format by different users are avoided. The approach is applicable in any context where computer parsable description of data could enhance efficiency (e.g. within a spacecraft control system, a data delivery system or an archive). The CCSDS have identified several candidate DDL's: EAST (Extended Ada Subset), TSDN (Transfer Syntax Data Notation) and MADEL (Modified ASN.1 as a Data Description Language -- a DDL based on the Abstract Syntax Notation One - ASN.1 - specified in the ISO/IEC 8824). This paper concentrates on ESA's development of MADEL. ESA have also developed a 'proof of concept' prototype of the required support tools, implemented on a PC under MS-DOS, which has successfully demonstrated the feasibility of the approach, including the capability within an application of retrieving and displaying particular data elements, given its MADEL description (i.e. a data description written in MADEL). This paper outlines the work done to date and assesses the applicability of this modified ASN.1 as a DDL. The feasibility of the approach is illustrated with several examples. Author

N95-17598*# National Aeronautics and Space Administration. Goddard Space Flight Center, Greenbelt, MD.

CROSS SUPPORT OVERVIEW AND OPERATIONS CONCEPT FOR FUTURE SPACE MISSIONS **c66**

William Stallings and Jean-Francois Kaufeler (European Space Agency. European Space Operations Center, Darmstadt, Germany.) *In its* Third International Symposium on Space Mission Operations and Ground Data Systems, Part 2 Nov. 1994 p 1253-1260 (For primary document see N95-17531 04-17)

Avail: CASI HC A02/MF A06

Ground networks must respond to the requirements of future missions, which include smaller sizes, tighter budgets, increased numbers, and shorter development schedules. The Consultative Committee for Space Data Systems (CCSDS) is meeting these challenges by developing a general cross support concept, reference model, and service specifications for Space Link Extension services for space missions involving cross support among Space Agencies. This paper identifies and bounds the problem, describes the need to extend Space Link services, gives an overview of the operations concept, and introduces complimentary CCSDS work on standardizing Space Link Extension services. Author

N95-17599*# European Space Agency. European Space Operations Center, Darmstadt (Germany).

THE CCSDS RETURN ALL FRAMES SPACE LINK EXTENSION SERVICE

Hans Uhrig, John Pietras (Mitre Corp., Greenbelt, MD.), and Michael Stoloff (Jet Propulsion Lab., California Inst. of Tech., Pasadena, CA.) *In* NASA. Goddard Space Flight Center, Third International Symposium on Space Mission Operations and Ground Data Systems, Part 2 Nov. 1994 p 1261-1269 (For primary document see N95-17531 04-17)

Avail: CASI HC A02/MF A06

Existing Consultative Committee for Space Data Systems (CCSDS) Recommendations for Telemetry Channel Coding, Packet Telemetry, Advanced Orbiting Systems, and Telecommand have facilitated cross-support between Agencies by standardizing the link between spacecraft and ground terminal. CCSDS is currently defining a set of Space Link Extension (SLE) services that will enable remote science and mission operations facilities to access the ground termination of the Space Link services in a standard manner. The first SLE service to be defined is the Return All Frames (RAF) service. The RAF service delivers all CCSDS link-layer frames received on a single space link physical channel. The service provides both on-line and off-line data transfer modes to accommodate the variety of access methods typical of space mission operations. This paper describes the RAF service as of the Summer of 1994. It characterizes the behavior of the service as seen across the interface between the user and the service and gives an overview of the interactions involved in setting up and operating the service in a cross-support environment. Author

N95-17600*# Allied-Signal Technical Services Corp., Lanham, MD. Flight Operations Dept.

PROPOSAL FOR IMPLEMENTATION OF CCSDS STANDARDS FOR USE WITH SPACECRAFT ENGINEERING/HOUSEKEEPING DATA

Dave Welch *In* NASA. Goddard Space Flight Center, Third International Symposium on Space Mission Operations and Ground Data Systems, Part 2 Nov. 1994 p 1271-1276 (For primary document see N95-17531 04-17)

Avail: CASI HC A02/MF A06

Many of today's low earth orbiting spacecraft are using the Consultative Committee for Space Data Systems (CCSDS) protocol for better optimization of down link RF bandwidth and onboard storage space. However, most of the associated housekeeping data has continued to be generated and down linked in a synchronous, Time Division Multiplexed (TDM) fashion. There are many economies that the CCSDS protocol will allow to better utilize the available bandwidth and storage space in order to optimize the housekeeping data for use in operational trending and analysis work. By only outputting what is currently important or of interest, finer resolution of critical items can be obtained. This can be accomplished by better utilizing the normally allocated housekeeping data down link and storage areas rather than taking space reserved for science. Author

N95-17601*# National Aeronautics and Space Administration. Goddard Space Flight Center, Greenbelt, MD.

MISSION OPERATIONS CENTERS (MOCs): INTEGRATING KEY SPACECRAFT GROUND DATA SYSTEM COMPONENTS **c14**

Randy Harbaugh and Donna Szakal (Computer Sciences Corp., Laurel, MD.) *In its* Third International Symposium on Space Mission Operations and Ground Data Systems, Part 2 Nov. 1994 p 1281-1288 (For primary document see N95-17531 04-17)

Avail: CASI HC A02/MF A06

In an environment characterized by decreasing budgets, limited system development time, and user needs for increased capabilities, the Mission Operations Division (MOD) at the National Aeronautics and Space Administration Goddard Space Flight Center initiated a new, cost-effective concept in developing its spacecraft ground data systems: the Mission Operations Center (MOC). In the MOC approach, key components are integrated into a comprehensive and cohesive spacecraft planning, monitoring, command, and control system with a single, state-of-the-art graphical user interface. The MOD is currently implementing MOC's, which feature a common, reusable, and extendable system architecture, to support the X-Ray Timing Explorer (XTE), Tropical Rainfall Measuring Mission (TRMM), and Advanced Composition Explorer (ACE) missions. As a result of the MOC approach, mission operations are integrated, and users can, with a single system, perform real-time health and safety monitoring, real-time command and control, real-time attitude processing, real-time and predictive graphical spacecraft monitoring, trend analysis, mission planning and scheduling, command generation and management, network scheduling, guide star selection, and (using an expert system) spacecraft monitoring and fault isolation. The MOD is also implementing its test and training simulators under the new MOC management structure. This paper describes the MOC concept, the management approaches used in developing MOC systems, the technologies employed and the development process improvement initiatives applied in implementing MOC systems, and the expected benefits to both the user and the mission project in using the MOC approach. Author

N95-17602*# European Space Agency. European Space Operations Center, Darmstadt (Germany).

ATOS: INTEGRATION OF ADVANCED TECHNOLOGY SOFTWARE WITHIN DISTRIBUTED SPACECRAFT MISSION OPERATIONS SYSTEMS **c61**

M. Jones, J. Wheadon, W. OMullane, D. Whitgift (Logica Ltd., London, England.), K. Poulter (Logica Ltd., London, England.), M. Niezette (Space Applications Services, Brussels, Belgium.), R. Timmermans (Space Applications Services, Brussels, Belgium.), Ivan Rodriguez (Universidad Politecnica de Madrid, Spain.), and R. Romero (Universidad Politecnica de Madrid, Spain.) *In* NASA. Goddard Space Flight Center, Third International

Symposium on Space Mission Operations and Ground Data Systems, Part 2 Nov. 1994 p 1289-1296 (For primary document see N95-17531 04-17)
Avail: CASI HC A02/MF A06

The Advanced Technology Operations System (ATOS) is a program of studies into the integration of advanced applications (including knowledge based systems (KBS)) with ground systems for the support of spacecraft mission operations. Author

N95-17603*# National Aeronautics and Space Administration. Goddard Space Flight Center, Greenbelt, MD.
THE NASA MISSION OPERATIONS AND CONTROL ARCHITECTURE PROGRAM **c66**
Paul J. Ondrus, Richard D. Carper (Science Applications International Corp., McLean, VA.), and Alan J. Jeffries (Science Applications International Corp., McLean, VA.) *In its* Third International Symposium on Space Mission Operations and Ground Data Systems, Part 2 Nov. 1994 p 1297-1303 (For primary document see N95-17531 04-17)
Avail: CASI HC A02/MF A06

The conflict between increases in space mission complexity and rapidly declining space mission budgets has created strong pressures to radically reduce the costs of designing and operating spacecraft. A key approach to achieving such reductions is through reducing the development and operations costs of the supporting mission operations systems. One of the efforts which the Communications and Data Systems Division at NASA Headquarters is using to meet this challenge is the Mission Operations Control Architecture (MOCA) project. Technical direction of this effort has been delegated to the Mission Operations Division (MOD) of the Goddard Space Flight Center (GSFC). MOCA is to develop a mission control and data acquisition architecture, and supporting standards, to guide the development of future spacecraft and mission control facilities at GSFC. The architecture will reduce the need for around-the-clock operations staffing, obtain a high level of reuse of flight and ground software elements from mission to mission, and increase overall system flexibility by enabling the migration of appropriate functions from the ground to the spacecraft. The end results are to be an established way of designing the spacecraft-ground system interface for GSFC's in-house developed spacecraft, and a specification of the end to end spacecraft control process, including data structures, interfaces, and protocols, suitable for inclusion in solicitation documents for future flight spacecraft. A flight software kernel may be developed and maintained in a condition that it can be offered as Government Furnished Equipment in solicitations. This paper describes the MOCA project, its current status, and the results to date. Author

N95-17604*# National Aeronautics and Space Administration. Goddard Space Flight Center, Greenbelt, MD.
RENAISSANCE ARCHITECTURE FOR GROUND DATA SYSTEMS **c82**
Dorothy C. Perkins and Lawrence B. Zeigenfuss *In its* Third International Symposium on Space Mission Operations and Ground Data Systems, Part 2 Nov. 1994 p 1305-1316 (For primary document see N95-17531 04-17)
Avail: CASI HC A03/MF A06

The Mission Operations and Data Systems Directorate (MO&DSD) has embarked on a new approach for developing and operating Ground Data Systems (GDS) for flight mission support. This approach is driven by the goals of minimizing cost and maximizing customer satisfaction. Achievement of these goals is realized through the use of a standard set of capabilities which can be modified to meet specific user needs. This approach, which is called the Renaissance architecture, stresses the engineering of integrated systems, based upon workstation/local area network (LAN)/fileserver technology and reusable hardware and software components called 'building blocks.' These building blocks are integrated with mission specific capabilities to build the GDS for each individual mission. The building block approach is key to the reduction of development costs and schedules. Also, the Renaissance approach allows the integration of GDS functions that were previously provided via separate multi-mission facilities. With the Renaissance architecture, the GDS can be developed by the MO&DSD or all, or part, of the GDS can be operated by the user at their facility. Flexibility in operation configuration allows both selection of a cost-effective operations approach and the capability for customizing operations to user needs. Thus the focus of the MO&DSD is shifted from operating systems that we have built to building systems and, optionally, operations as separate services. Renaissance is actually a continuous process. Both the building blocks and the system architecture will evolve as user needs and technology change. Providing GDS on a per user basis enables this continuous refinement of the development process and product and allows the MO&DSD to remain a customer-focused organization. This paper will present the activities and results of the MO&DSD initial efforts toward the establishment of the Renaissance approach for the development of GDS, with a particular focus on both the technical and process implications posed by Renaissance to the MO&DSD. Author

N95-17605*# Tokyo Univ., Sagamihara (Japan). Inst. of Space and Astronautical Science.
ARCHITECTURE OF A DISTRIBUTED MULTIMISSION OPERATIONS SYSTEM **c66**
Takahiro Yamada *In* NASA. Goddard Space Flight Center, Third International Symposium on Space Mission Operations and Ground Data Systems, Part 2 Nov. 1994 p 1317-1324 (For primary document see N95-17531 04-17)
Avail: CASI HC A02/MF A06

This paper presents an architecture to develop a multimission operations systems, which we call DIOSA. In this architecture, a component used as a building block is called a functional block. Each functional block has a standard structure, and the interface between functional blocks are defined with a set of standard protocols. This paper shows the structure of the database used by functional blocks, the structure of interfaces between functional blocks, and the structure of system management. Finally, examples of typical functional blocks and an example of a system constructed with this architecture is shown. Author

N95-17606*# National Aeronautics and Space Administration. Goddard Space Flight Center, Greenbelt, MD.
RE-ENGINEERING THE MISSION LIFE CYCLE WITH ABC AND IDEF **c66**
Daniel Mandl, Michael Rackley, and Jay Karlin (Viable Systems, Inc., Germantown, MD.) *In its* Third International Symposium on Space Mission Operations and Ground Data Systems, Part 2 Nov. 1994 p 1327-1334 (For primary document see N95-17531 04-17)
Avail: CASI HC A02/MF A06

The theory behind re-engineering a business process is to remove the non-value added activities thereby lowering the process cost. In order to achieve this, one must be able to identify where the non-value added elements are located which is not a trivial task. This is because the non-value added elements are often hidden in the form of overhead and/or pooled resources. In order to be able to isolate these non-value added processes from among the other processes, one must first decompose the overall top level process into lower layers of sub-processes. In addition, costing data must be assigned to each sub-process along with the value the sub-process adds towards the final product. IDEF0 is a Federal Information Processing Standard (FIPS) process-modeling tool that allows for this functional decomposition through structured analysis. In addition, it illustrates the relationship of the process and the value added to the product or service. The value added portion is further defined in IDEF1X which is an entity relationship diagramming tool. The entity relationship model is the blueprint of the product as it moves along the 'assembly line' and therefore relates all of the parts to each other and the final product. It also relates the parts to the tools that produce the product and all of the paper work that is used in their acquisition. The use of IDEF therefore facilitates the use of Activity Based Costing (ABC). ABC is an essential method in a high variety, product-customizing environment, to facilitate rapid response to externally caused change. This paper describes the work being done in the Mission Operations Division to re-engineer the development and operation life cycle of Mission Operations Centers using these tools. Author

N95-17607*# Loral AeroSys, Seabrook, MD.
MO/DSD ONLINE INFORMATION SERVER AND GLOBAL INFORMATION REPOSITORY ACCESS **c82**
Diem Nguyen, Kam Ghaffarian, Keith Hogie (Computer Sciences Corp., Lanham, MD.), and William Mackey (Computer Sciences Corp., Lanham, MD.) *In* NASA. Goddard Space Flight Center, Third International Symposium on Space Mission Operations and Ground Data Systems, Part

2 Nov. 1994 p 1335-1342 (For primary document see N95-17531 04-17)
Avail: CASI HC A02/MF A06

Often in the past, standards and new technology information have been available only in hardcopy form, with reproduction and mailing costs proving rather significant. In light of NASA's current budget constraints and in the interest of efficient communications, the Mission Operations and Data Systems Directorate (MO&DSD) New Technology and Data Standards Office recognizes the need for an online information server (OLIS). This server would allow: (1) dissemination of standards and new technology information throughout the Directorate more quickly and economically; (2) online browsing and retrieval of documents that have been published for and by MO&DSD; and (3) searching for current and past study activities on related topics within NASA before issuing a task. This paper explores a variety of available information servers and searching tools, their current capabilities and limitations, and the application of these tools to MO&DSD. Most importantly, the discussion focuses on the way this concept could be easily applied toward improving dissemination of standards and new technologies and improving documentation processes. Author

N95-17608*# National Aeronautics and Space Administration. Goddard Space Flight Center, Greenbelt, MD.
THE REQUIREMENTS GENERATION SYSTEM: A TOOL FOR MANAGING MISSION REQUIREMENTS **c66**
Sylvia B. Sheppard *In its* Third International Symposium on Space Mission Operations and Ground Data Systems, Part 2 Nov. 1994 p 1345-1351 (For primary document see N95-17531 04-17)
Avail: CASI HC A02/MF A06

Historically, NASA's cost for developing mission requirements has been a significant part of a mission's budget. Large amounts of time have been allocated in mission schedules for the development and review of requirements by the many groups who are associated with a mission. Additionally, tracing requirements from a current document to a parent document has been time-consuming and costly. The Requirements Generation System (RGS) is a computer-supported cooperative-work tool that assists mission developers in the online creation, review, editing, tracing, and approval of mission requirements as well as in the production of requirements documents. This paper describes the RGS and discusses some lessons learned during its development. Author

N95-17609*# Massachusetts Inst. of Tech., Lexington. Lincoln Lab.
AN OPPORTUNITY ANALYSIS SYSTEM FOR SPACE SURVEILLANCE EXPERIMENTS WITH THE MSX **c66**
Ramaswamy Sridharan, Gary Duff, Tony Hayes, and Andy Wiseman *In* NASA. Goddard Space Flight Center, Third International Symposium on Space Mission Operations and Ground Data Systems, Part 2 Nov. 1994 p 1353-1360 (For primary document see N95-17531 04-17)
Avail: CASI HC A02/MF A06

The Mid-Course Space Experiment consists of a set of payloads on a satellite being designed and built under the sponsorship of Ballistic Missile Defense Office. The MSX satellite will conduct a series of measurements of phenomenology of backgrounds, missile targets, plumes and resident space objects (RSO's); and will engage in functional demonstrations in support of detection, acquisition and tracking for ballistic missile defense and space-based space surveillance missions. A complex satellite like the MSX has several constraints imposed on its operation by the sensors, the supporting instrumentation, power resources, data recording capability, communications and the environment in which all these operate. This paper describes the implementation of an opportunity and feasibility analysis system, developed at Lincoln Laboratory, Massachusetts Institute of Technology, specifically to support the experiments of the Principal Investigator for space-based surveillance. Author

N95-17610*# Jet Propulsion Lab., California Inst. of Tech., Pasadena, CA.
MATRIX EVALUATION OF SCIENCE OBJECTIVES **c66**
Randii R. Wessen *In* NASA. Goddard Space Flight Center, Third International Symposium on Space Mission Operations and Ground Data Systems, Part 2 Nov. 1994 p 1361-1368 (For primary document see N95-17531 04-17)
Avail: CASI HC A02/MF A06

The most fundamental objective of all robotic planetary spacecraft is to return science data. To accomplish this, a spacecraft is fabricated and built, software is planned and coded, and a ground system is designed and implemented. However, the quantitative analysis required to determine how the collection of science data drives ground system capabilities has received very little attention. This paper defines a process by which science objectives can be quantitatively evaluated. By applying it to the Cassini Mission to Saturn, this paper further illustrates the power of this technique. The results show which science objectives drive specific ground system capabilities. In addition, this process can assist system engineers and scientists in the selection of the science payload during pre-project mission planning; ground system designers during ground system development and implementation; and operations personnel during mission operations. Author

N95-17611*# National Aeronautics and Space Administration. Goddard Space Flight Center, Greenbelt, MD.
A NEW SYSTEMS ENGINEERING APPROACH TO STREAMLINED SCIENCE AND MISSION OPERATIONS FOR THE FAR ULTRAVIOLET SPECTROSCOPIC EXPLORER (FUSE) **c66**
Madeline J. Butler, George Sonneborn, and Dorothy C. Perkins *In its* Third International Symposium on Space Mission Operations and Ground Data Systems, Part 2 Nov. 1994 p 1371-1376 (For primary document see N95-17531 04-17)
Avail: CASI HC A02/MF A06

The Mission Operations and Data Systems Directorate (MO&DSD, Code 500), the Space Sciences Directorate (Code 600), and the Flight Projects Directorate (Code 400) have developed a new approach to combine the science and mission operations for the FUSE mission. FUSE, the last of the Delta-class Explorer missions, will obtain high resolution far ultraviolet spectra (910 - 1220 A) of stellar and extragalactic sources to study the evolution of galaxies and conditions in the early universe. FUSE will be launched in 2000 into a 24-hour highly eccentric orbit. Science operations will be conducted in real time for 16-18 hours per day, in a manner similar to the operations performed today for the International Ultraviolet Explorer. In a radical departure from previous missions, the operations concept combines spacecraft and science operations and data processing functions in a single facility to be housed in the Laboratory for Astronomy and Solar Physics (Code 680). A small missions operations team will provide the spacecraft control, telescope operations and data handling functions in a facility designated as the Science and Mission Operations Center (SMOC). This approach will utilize the Transportable Payload Operations Control Center (TPOCC) architecture for both spacecraft and instrument commanding. Other concepts of integrated operations being developed by the Code 500 Renaissance Project will also be employed for the FUSE SMOC. The primary objective of this approach is to reduce development and mission operations costs. The operations concept, integration of mission and science operations, and extensive use of existing hardware and software tools will decrease both development and operations costs extensively. This paper describes the FUSE operations concept, discusses the systems engineering approach used for its development, and the software, hardware and management tools that will make its implementation feasible. Author

N95-17612*# Loral AeroSys, Landover, MD.
RISK REDUCTION METHODOLOGIES AND TECHNOLOGIES FOR THE EARTH OBSERVING SYSTEM (EOS) OPERATIONS CENTER (EOC) **c66**
Richard K. Hudson and Nelson V. Pingitore *In* NASA. Goddard Space Flight Center, Third International Symposium on Space Mission Operations and Ground Data Systems, Part 2 Nov. 1994 p 1377-1381 (For primary document see N95-17531 04-17)
Avail: CASI HC A01/MF A06

This paper will discuss proposed Flight Operations methodologies and technologies for the Earth Observing System (EOS) Operations Center (EOC), to reduce risks associated with the operation of complex multi-instrument spacecraft in a multi-spacecraft environment. The EOC goals are to obtain 100 percent science data capture and maintain 100 percent spacecraft health, for each EOS spacecraft. Operations risks to the spacecraft and data loss due to operator command error, mission degradation due to mis-identification of an anomalous trend in component performance or mis-management of resources, and total mission loss due to improper subsystem configuration or mis-identification of an anomalous condition. This paper discusses automation of routine Flight Operations

Team (FOT) responsibilities, Expert systems for real-time non-nominal condition decision support, and Telemetry analysis systems for in-depth playback data analysis and trending. Author

N95-17613*# National Aeronautics and Space Administration. Goddard Space Flight Center, Greenbelt, MD.
EDOS OPERATIONS CONCEPT AND DEVELOPMENT APPROACH c66
G. Knoble, C. Garman, G. Alcott, C. Ramchandani (Computer Sciences Corp., Lanham, MD.), and J. Silvers (Computer Sciences Corp., Lanham, MD.) *In its* Third International Symposium on Space Mission Operations and Ground Data Systems, Part 2 Nov. 1994 p 1383-1390 (For primary document see N95-17531 04-17)
Avail: CASI HC A02/MF A06

The Earth Observing System (EOS) Data and Operations System (EDOS) is being developed by the National Aeronautics and Space Administration (NASA) Goddard Space Flight Center (GSFC) for the capture, level zero processing, distribution, and backup archiving of high speed telemetry data received from EOS spacecraft. All data received will conform to the Consultative Committee for Space Data Standards (CCSDS) recommendations. The major EDOS goals are to: (1) minimize EOS program costs to implement and operate EDOS; (2) respond effectively to EOS growth requirements; and (3) maintain compatibility with existing and enhanced versions of NASA institutional systems required to support EOS spacecraft. In order to meet these goals, the following objectives have been defined for EDOS: (1) standardize EDOS interfaces to maximize utility for future requirements; (2) emphasize life-cycle cost (LCC) considerations (rather than procurement costs) in making design decisions and meeting reliability, maintainability, availability (RMA) and upgradability requirements; (3) implement data-driven operations to the maximum extent possible to minimize staffing requirements and to maximize system responsiveness; (4) provide a system capable of simultaneously supporting multiple spacecraft, each in different phases of their life-cycles; (5) provide for technology insertion features to accommodate growth and future LCC reductions during the operations phase; and (6) provide a system that is sufficiently robust to accommodate incremental performance upgrades while supporting operations. Operations concept working group meetings were facilitated to help develop the EDOS operations concept. This provided a cohesive concept that met with approval of responsible personnel from the start. This approach not only speeded up the development process by reducing review cycles, it also provided a medium for generating good ideas that were immediately molded into feasible concepts. The operations concept was then used as a basis for the EDOS specification. When it was felt that concept elements did not support detailed requirements, the facilitator process was used to resolve discrepancies or to add new concept elements to support the specification. This method provided an ongoing revisal of the operations concept and prevented large revisions at the end of the requirement analysis phase of system development. Author

N95-17614*# Johns Hopkins Univ., Laurel, MD. Applied Physics Lab.
CONCURRENT ENGINEERING: SPACECRAFT AND MISSION OPERATIONS SYSTEM DESIGN c66
J. A. Landshof, R. J. Harvey, and M. H. Marshall *In* NASA. Goddard Space Flight Center, Third International Symposium on Space Mission Operations and Ground Data Systems, Part 2 Nov. 1994 p 1391-1397 (For primary document see N95-17531 04-17)
Avail: CASI HC A02/MF A06

Despite our awareness of the mission design process, spacecraft historically have been designed and developed by one team and then turned over as a system to the Mission Operations organization to operate on-orbit. By applying concurrent engineering techniques and envisioning operability as an essential characteristic of spacecraft design, tradeoffs can be made in the overall mission design to minimize mission lifetime cost. Lessons learned from previous spacecraft missions will be described, as well as the implementation of concurrent mission operations and spacecraft engineering for the Near Earth Asteroid Rendezvous (NEAR) program. Author

N95-17292*# Jet Propulsion Lab., California Inst. of Tech., Pasadena, CA.
TRACKING THE GALILEO SPACECRAFT WITH THE DSCC GALILEO TELEMETRY PROTOTYPE
T. T. Pham, S. Shambayati, D. E. Hardi, and S. G. Finley *In its* The Telecommunications and Data Acquisition Report 15 Nov. 1994 p 221-235 (For primary document see N95-17279 04-32)
(RTOP 314-30-61-02-10)
Avail: CASI HC A03/MF A03

18 SPACECRAFT DESIGN, TESTING AND PERFORMANCE

Includes satellites; space platforms; space stations; spacecraft systems and components such as thermal and environmental controls; and attitude controls.

For life support systems see *54 Man/System Technology and Life Support*. For related information see also *05 Aircraft Design, Testing and Performance, 39 Structural Mechanics*, and *16 Space Transportation*.

N95-16131# Naval Postgraduate School, Monterey, CA.
SURVEY OF UNITED STATES COMMERCIAL SATELLITES IN GEOSYNCHRONOUS EARTH ORBIT M.S. Thesis
Lawerence D. Hunt and Jeffrey L. Miller Sep. 1994 329 p
(AD-A284969) Avail: CASI HC A15/MF A03

This thesis examines the domestic commercial satellite options available for telecommunication and remote sensing services. The study provides a single source, comprehensive examination of the available commercial U.S. geosynchronous telecommunications satellites as well as the remote sensing spacecraft which may be utilized for commercial purposes. A general satellite communications technology overview is provided as background material for the more detailed satellite compendium. The following telecommunications operators are included with their respective domestic communications satellites: Alascom, Alpha Lyracom Pan American, AT&T, Comsat, GE Americom, GTE Spacenet, Hughes and Intelsat. Satellite evolution, overview, key design features, and performance parameters are catalogued. Additionally, each satellite's communications payload is examined in detail. Emerging technologies in the remote sensing field are presented. The current GOES and NOAA satellite systems are surveyed with an emphasis on each satellite's capabilities and operational status. DTIC

N95-16304 Pennsylvania State Univ., University Park, PA. Dept. of Engineering Science and Mechanics.
INTEGRATED PASSIVE AND ACTIVE CONTROL OF STRUCTURES Final Report, May 1990 - May 1993
Vernon H. Neubert Dec. 1993 100 p Limited Reproducibility: More than 20% of this document may be affected by microfiche quality
(Contract F33615-90-C-3205)
(AD-A282684; WL-TR-93-3112) Avail: CASI HC A05

A combination of passive damping and active control is needed on practical structures where sufficient modal damping is not achievable with passive damping alone. The modal theories for structural equations in state space are reviewed and some eigenvector relationship are presented which are not available elsewhere, for use later in the report. Methods for determining sensitivities of eigenvalues and eigenvectors to plant matrix and control inputs are summarized and numerical examples are presented. Procedures are developed for optimizing passive damping through use of the sensitivities of the eigenproperties, for free vibration and forced, random vibrations. Frequency-dependent behavior of viscoelastic damping material by curve-fitting is discussed, which is then used in an overdamped mini-oscillator technique for analysis of an example ten-bar truss. Two approaches are presented for designing the combination of passive viscous damping and full state feedback control. The first is iterative and makes use of eigenvalue sensitivities. The second is based on a perturbation formulation, where the desired changes in eigenvalues and eigenvectors are specified and the corresponding changes in the closed loop characteristic matrix in state space are predicted. Restrictions on the choice of eigenvalues and eigenvectors are discussed in light of related literature on eigenstructure assignment. Fortran computer programs, one coupled with the constrained function minimization program CONMIN, have been written for each type of problem. DTIC

N95-16352# National Academy of Sciences - National Research Council, Washington, DC. Commission on Engineering and Technical Systems.
[ASSESSMENT OF THE SPACE STATION PROGRAM]
Jack L. Kerrebrock (Massachusetts Inst. of Tech., Cambridge.) 27 Jun. 1994 6 p
Avail: CASI HC A02/MF A01

This letter report by the National Research Council's (NRC's) Aeronautics and Space Engineering Board addresses comments on NASA's response to the Board's 1993 letter report, NASA's response to technical and management recommendations from previous NRC technical reports on the Space Station, and an assessment of the current International Space Station Alpha (ISSA) program. CASI

N95-16559*# National Aeronautics and Space Administration. Langley Research Center, Hampton, VA.
NATURAL FREQUENCY OF UNIFORM AND OPTIMIZED TETRAHEDRAL TRUSS PLATFORMS
K. Chauncey Wu and Mark S. Lake Nov. 1994 34 p
(RTOP 506-43-41-02)
(NASA-TP-3461; L-17307; NAS 1.60:3461) Avail: CASI HC A03/MF A01

Qualitative and quantitative estimates for the fundamental frequency of uniform and optimized tetrahedral truss platforms are determined. A semiempirical equation is developed for the frequency of free-free uniform trusses as a function of member material properties, truss dimensions, and parasitic (nonstructural) mass fraction Mp/Mt. Optimized trusses with frequencies approximately two times those of uniform trusses are determined by varying the cross-sectional areas of member groups. Trusses with 3 to 8 rings, no parasitic mass, and member areas up to 25 times the minimum area are optimized. Frequencies computed for ranges of both Mp/Mt and the ratio of maximum area to minimum area are normalized to the frequency of a uniform truss with no parasitic mass. The normalized frequency increases with the number of rings, and both frequency and the ratio of maximum area to minimum area decrease with increasing Mp/Mt. Frequency improvements that are achievable with a limited number of member areas are estimated for a 3-ring truss by using Taguchi methods. Joint stiffness knockdown effects are also considered. Comparison of optimized and baseline uniform truss frequencies indicates that tailoring can significantly increase structural frequency; maximum gains occur for trusses with low values of Mp/Mt. This study examines frequency trends for ranges of structural parameters and may be used as a preliminary design guide. Author

N95-16857*# National Aeronautics and Space Administration. Langley Research Center, Hampton, VA.
EXPERIMENTAL VALIDATION OF AN INTEGRATED CONTROLS-STRUCTURES DESIGN METHODOLOGY FOR A CLASS OF FLEXIBLE SPACE STRUCTURES
Peiman G. Maghami, Sandeep Gupta (Vigyan Research Associates, Inc., Hampton, VA.), Kenny B. Elliott, Suresh M. Joshi, and Joseph E. Walz Nov. 1994 46 p
(RTOP 233-01-01-05)
(NASA-TP-3462; L-17358; NAS 1.60:3462) Avail: CASI HC A03/MF A01

This paper describes the first experimental validation of an optimization-based integrated controls-structures design methodology for a class of flexible space structures. The Controls-Structures-Interaction (CSI) Evolutionary Model, a laboratory test bed at Langley, is redesigned based on the integrated design methodology with two different dissipative control strategies. The redesigned structure is fabricated, assembled in the laboratory, and experimentally compared with the original test structure. Design guides are proposed and used in the integrated design process to ensure that the resulting structure can be fabricated. Experimental results indicate that the integrated design requires greater than 60 percent less average control power (by thruster actuators) than the conventional control-optimized design while maintaining the required line-of-sight performance, thereby confirming the analytical findings about the superiority of the integrated design methodology. Amenability of the integrated design structure to other control strategies is considered and evaluated analytically and experimentally. This work also demonstrates the capabilities of the Langley-developed design tool CSI DESIGN which provides a unified environment for structural and control design. Author

N95-16862*# National Aeronautics and Space Administration. Lewis Research Center, Cleveland, OH.
AURORAL INTERACTIONS WITH ISSA
Carolyn K. Purvis, David B. Snyder, and Gary A. Jongeward (Maxwell Labs., Inc., La Jolla, CA.) Dec. 1994 20 p
(RTOP 233-01-0E)
(NASA-TM-106794; E-9258; NAS 1.15:106794) Avail: CASI HC A03/MF A01

Due to its high inclination orbit, International Space Station Alpha (ISSA) will occasionally experience surface charging by the high energy electrons of the auroral environment. This study looks at the frequency of these occurrences and recapitulates a charging model. ISSA should expect about 80 auoral encounters annually. If the plasma contactor is not run continuously, the vehicle may charge several hundred volts. Charge storage on standard space station coatings should not be a problem, but care must be taken that materials are not introduced inadvertently that cannot bleed off accumulated charge in a reasonable time. A conductivity requirement may be used to ensure surface materials do not charge to high voltages, or store charge for long periods of time. Author

N95-16902*# National Aeronautics and Space Administration. Langley Research Center, Hampton, VA.
CONSTRAINED MINIMIZATION OF SMOOTH FUNCTIONS USING A GENETIC ALGORITHM
Daniel D. Moerder and Bandu N. Pamadi (Vigyan Research Associates, Inc., Hampton, VA.) Nov. 1994 31 p
(RTOP 506-59-61-01)
(NASA-TP-3329; L-17221; NAS 1.60-3329) Avail: CASI HC A03/MF A01

The use of genetic algorithms for minimization of differentiable functions that are subject to differentiable constraints is considered. A technique is demonstrated for converting the solution of the necessary conditions for a constrained minimum into an unconstrained function minimization. This technique is extended as a global constrained optimization algorithm. The theory is applied to calculating minimum-fuel ascent control settings for an energy state model of an aerospace plane. Author

N95-16941* National Aeronautics and Space Administration. Lyndon B. Johnson Space Center, Houston, TX.
HOUSTON, I THINK WE'VE GOT A SATELLITE (Videotape)
1992 Videotape: 30 min. playing time, in color, with sound
(NASA-TM-109987; NONP-NASA-VT-95-34902) Avail: CASI VHS A02/BETA A22

This video highlights the record breaking mission of STS-49, the maiden voyage of the Space Shuttle Endeavor. It includes the dramatic capture, repair, and reboost of the INTELSAT VI Satellite, as well as the ASEM experiment. The effectiveness of certain EVA techniques for the future construction of a space station is demonstrated. JSC

N95-17275*# National Aeronautics and Space Administration. Lewis Research Center, Cleveland, OH.
REACTION AND PROTECTION OF ELECTRICAL WIRE INSULATORS IN ATOMIC-OXYGEN ENVIRONMENTS
Ching-cheh Hung and Gidget Cantrell (Cleveland State Univ., OH.) Nov. 1994 24 p Presented at the AE-8D Wire and Cable Subcommittee Meeting, Albuquerque, NM, 12-14 Apr. 1994; sponsored by the Society of Automotive Engineers
(RTOP 506-41-41)
(NASA-TM-106767; E-9210; NAS 1.15:106767) Avail: CASI HC A03/MF A01

Atomic-oxygen erosion on spacecraft in low Earth orbit is an issue which is becoming increasingly important because of the growing number of spacecraft that will fly in the orbits which have high concentrations of atomic oxygen. In this investigation, the atomic-oxygen durability of three types of electrical wire insulation (carbon-based, fluoropolymer, and polysiloxane elastomer) were evaluated. These insulation materials were exposed to thermal-energy atomic oxygen, which was obtained by RF excitation of air at a pressure of 11-20 Pa. The effects of atomic-oxygen exposure on insulation materials indicate that all carbon-based materials erode at about the same rate as polyamide Kapton and, therefore, are not atomic-oxygen durable. However, the durability of fluoropolymers needs to be evaluated on a case by case basis because the erosion rates of

fluoropolymers vary widely. For example, experimental data suggest the formation of atomic fluorine during atomic-oxygen amorphous-fluorocarbon reactions. Dimethyl polysiloxanes (silicone) do not lose mass during atomic-oxygen exposure, but develop silica surfaces which are under tension and frequently crack as a result of loss of methyl groups. However, if the silicone sample surfaces were properly pretreated to provide a certain roughness, atomic oxygen exposure resulted in a sturdy, non-cracked atomic-oxygen durable SiO2 layer. Since the surface does not crack during such silicone-atomic oxygen reaction, the crack-induced contamination by silicone can be reduced or completely stopped. Therefore, with proper pretreatment, silicone can be either a wire insulation material or a coating on wire insulation materials to provide atomic-oxygen durability. Author

N95-17331*# Booz-Allen and Hamilton, Inc., Houston, TX.
INTERNATIONAL SPACE STATION ALPHA (ISSA) INTEGRATED TRAFFIC MODEL
Robert E. Gates 24 Oct. 1994 8 p
(Contract NAS15-10000)
(NASA-CR-197566; NAS 1.26:197566) Copyright Avail: CASI HC A02/MF A01

The paper discusses the development process of the International Space Station Alpha (ISSA) Integrated Traffic Model which is a subsystem analyses tool utilized in the ISSA design analysis cycles. Fast-track prototyping of the detailed relationships between daily crew and station consumables, propellant needs, maintenance requirements, and crew rotation via spread sheets provides adequate bench marks to assess cargo vehicle design and performance characteristics. Author

N95-17359# Lawrence Livermore National Lab., Livermore, CA.
ENERGY AND TECHNOLOGY REVIEW
Jul. 1994 18 p
(Contract W-7405-eng-48)
(DE95-000321; UCRL-52000-94-7) Avail: CASI HC A03/MF A01

Satellites have shrunk the world to the size of the proverbial global village. They track weather and the traffic patterns of ships and aircraft, and monitor our environment. Defense satellites provide high-resolution images of objects on the ground to protect our troops and allies. Telecommunication satellites have interwoven business sectors, corporations, and markets into global networks. Nevertheless, orbiting satellites may not be the best choice for all applications requiring a high vantage point. satellites and their payloads are expensive, and launching them by rocket is expensive and risky. They must operate in the extreme conditions of space, bombarded by radiation and with no airflow to cool their electronics. Only valuable, long-term missions would seem to justify the expense and risk of a satellite. Even then, satellites are not always the best choice. They typically cannot hop to a new orbit, and some uses, such as local and global communications, require a large number of satellites to ensure adequate coverage. There is clearly a large potential role for high-altitude, atmospheric vehicles that can stay aloft for very long periods (weeks or months) and can roam virtually anywhere. DOE

N95-17622# Naval Postgraduate School, Monterey, CA.
A COMPARISON OF DIFFERENT CONTROL METHODS FOR VIBRATION SUPPRESSION OF FLEXIBLE STRUCTURES USING PIEZOELECTRIC ACTUATORS M.S. Thesis
Mark G. Feuerstein Jun. 1994 55 p
(AD-A282958) Avail: CASI HC A04/MF A01

This paper compares the use of phase lead control and integral control methods to the positive position feedback (PPF) method of suppressing the primary and secondary modes of vibration of a flexible structure. The basic characteristics of piezoelectric sensors and actuators are reviewed. Integral, phase lead, and PPF control methods of interest are also reviewed. The integral and phase lead control methods prove to be comparable to that of PPF while offering a simpler implementation. DTIC

N95-16344# Thiokol Corp., Brigham City, UT.
FOAM INFLATED RIGIDIZED STRUCTURES FOR SPACE APPLICATIONS
D. M. Lester, M. J. Warner, and M. Blair *In* JHU, The 1993 JANNAF Propulsion Meeting, Volume 2 Nov. 1993 p 243-251 (For primary document see N95-16324 04-20)
Avail: CASI HC A02/MF A04

N95-16772*# National Aeronautics and Space Administration. Lyndon B. Johnson Space Center, Houston, TX.
MEDICAL CARE CAPABILITIES FOR SPACE STATION FREEDOM: A PHASE APPROACH Abstract Only
C. R. Doarn (Krug Life Sciences, Inc., Houston, TX.) and C. W. Lloyd *In* Aerospace Medical Association, Aerospace Medical Association 63rd Annual Scientific Meeting Program 14 May 1992 1 p (For primary document see N95-16737 04-51)
Avail: CASI HC A01/MF A02

N95-16776*# Krug Life Sciences, Inc., Houston, TX.
A SURGICAL SUPPORT SYSTEM FOR SPACE STATION FREEDOM Abstract Only
M. R. Campbell, R. D. Billica, and S. L. Johnston *In* Aerospace Medical Association, Aerospace Medical Association 63rd Annual Scientific Meeting Program 14 May 1992 1 p Sponsored by NASA. Lyndon B. Johnson Space Center, Houston, TX (For primary document see N95-16737 04-51)
Avail: CASI HC A01/MF A02

N95-17243*# Interface and Control Systems, West Melbourne, FL.
SCL: AN OFF-THE-SHELF SYSTEM FOR SPACECRAFT CONTROL
Brian Buckley and James VanGaasbeck *In* NASA. Goddard Space Flight Center, Third International Symposium on Space Mission Operations and Ground Data Systems, Part 1 Nov. 1994 p 559-568 (For primary document see N95-17179 04-17)
Avail: CASI HC A02/MF A06

N95-17247*# Jet Propulsion Lab., California Inst. of Tech., Pasadena, CA.
SMALL SCALE SEQUENCE AUTOMATION PAYS BIG DIVIDENDS
Bill Nelson *In* NASA. Goddard Space Flight Center, Third International Symposium on Space Mission Operations and Ground Data Systems, Part 1 Nov. 1994 p 591-597 (For primary document see N95-17179 04-17)
Avail: CASI HC A02/MF A06

N95-17551*# Alenia Spazio S.p.A., Turin (Italy).
THE SAX ITALIAN SCIENTIFIC SATELLITE. THE ON-BOARD IMPLEMENTED AUTOMATION AS A SUPPORT TO THE GROUND CONTROL CAPABILITY
Andrea Martelli *In* NASA. Goddard Space Flight Center, Third International Symposium on Space Mission Operations and Ground Data Systems, Part 2 Nov. 1994 p 837-846 (For primary document see N95-17531 04-17)
Avail: CASI HC A02/MF A06

N95-17574*# Jet Propulsion Lab., California Inst. of Tech., Pasadena, CA.
GALILEO SPACECRAFT MODELING FOR ORBITAL OPERATIONS
Bruce A. McLaughlin and Erik N. Nilsen *In* NASA. Goddard Space Flight Center, Third International Symposium on Space Mission Operations and Ground Data Systems, Part 2 Nov. 1994 p 1039-1044 (For primary document see N95-17531 04-17)
Avail: CASI HC A02/MF A06

19 SPACECRAFT INSTRUMENTATION

For related information see also *06 Aircraft Instrumentation* and *35 Instrumentation and Photography.*

N95-16201*# Max-Planck-Inst. fuer Chemie, Mainz (Germany).
ALPHA PROTON X RAY SPECTROMETER Abstract Only
Rudi Rieder, H. Waeke, and T. Economou (Chicago Univ., Chicago, IL.) *In* Lunar and Planetary Inst., Mars Pathfinder Landing Site Workshop 1994 p 36-37 (For primary document see N95-16176 04-91)
Avail: CASI HC A01/MF A01

N95-16202*# National Aeronautics and Space Administration. Ames Research Center, Moffett Field, CA.
ATMOSPHERE STRUCTURE AND METEOROLOGY INSTRUMENT FOR MARS PATHFINDER Abstract Only
Alvin Seiff (San Francisco State Univ., CA.) *In* Lunar and Planetary Inst., Mars Pathfinder Landing Site Workshop 1994 p 37 (For primary document see N95-16176 04-91)
Avail: CASI HC A01/MF A01

N95-16206*# Arizona Univ., Tucson, AZ. Lunar and Planetary Lab.
IMAGER FOR MARS PATHFINDER (IMF) Abstract Only
Peter H. Smith *In* Lunar and Planetary Inst., Mars Pathfinder Landing Site Workshop 1994 p 40-41 (For primary document see N95-16176 04-91)
Avail: CASI HC A01/MF A01

20 SPACECRAFT PROPULSION AND POWER

Includes main propulsion systems and components, e.g., rocket engines; and spacecraft auxilliary power sources.

For related information see also *07 Aircraft Propulsion and Power, 28 Propellants and Fuels, 44 Energy Production and Conversion,* and *15 Launch Vehicles and Space Vehicles.*

N95-15968*# NYMA, Inc., Brook Park, OH. Engineering Services Div.
CONTINUING LIFE TEST OF A XENON HOLLOW CATHODE FOR A SPACE PLASMA CONTACTOR Final Report
Timothy R. Sarver-Verhey Nov. 1994 18 p Presented at the 30th Joint Propulsion Conference, Indianapolis, IN, 27-29 Jun. 1994; sponsored by AIAA, ASME, SAE, and ASEE
(Contract NAS3-27186; RTOP 478-43-00)
(NASA-CR-195401; E-9245; NAS 1.26:195401) Avail: CASI HC A03/MF A01

Implementation of a hollow cathode plasma contactor for charge control on the Space Station has required validation of long-life hollow cathodes. A test series of hollow cathodes and hollow cathode plasma contactors was initiated as part of the plasma contactor development program. An on-going wear-test of a hollow cathode has demonstrated cathode operation in excess of 10,000 hours with small changes in operating parameters. The discharge has experienced 10 shutdowns during the test, all of which were due to test facility failures or expellant replenishment. In all cases, the cathode was re-ignited at approximately 42 volts and resumed typical operation. This test represents the longest demonstrated stable operation of a high current (greater than 1 A) xenon hollow cathode reported to date. Author

N95-16044*# National Aeronautics and Space Administration. Lewis Research Center, Cleveland, OH.
FIRST NASA WORKSHOP ON WIRING FOR SPACE APPLICATIONS
Ahmad Hammond, comp. (NYMA, Inc., Brook Park, OH.) and Mark W. Stavnes, comp. (NYMA, Inc., Brook Park, OH.) Sep. 1994 181 p Workshop held in Cleveland, OH, 23-24 Jul. 1991; sponsored by NASA, Washington
(Contract NAS3-27186; RTOP 323-15-03)
(NASA-CP-10145; E-9021; NAS 1.55:10145) Avail: CASI HC A09/MF A02

This document contains the proceedings of the First NASA Workshop on Wiring for Space Applications held at NASA Lewis Research Center in Cleveland, OH, July 23-24, 1991. The workshop was sponsored by NASA Headquarters Code QE Office of Safety and Mission Quality, Technical Standards Division and hosted by the NASA Lewis Research Center, Power Technology Division, Electrical Components and Systems Branch. The workshop addressed key technology issues in the field of electrical power wiring for space applications. Speakers from government, industry and academia presented and discussed topics on arc tracking phenomena, wiring applications and requirements, and new candidate insulation materials and constructions. Presentation materials provided by the various speakers are included in this document. For individual titles, see N95-16045 through N95-16057.

N95-16045*# National Aeronautics and Space Administration. Lyndon B. Johnson Space Center, Houston, TX.
KAPTON WIRE CONCERNS FOR AEROSPACE VEHICLES **c33**
J. VanLaak *In* NASA. Lewis Research Center, First NASA Workshop on Wiring for Space Applications Sep. 1994 p 11-17 (For primary document see N95-16044 04-20)
Avail: CASI HC A02/MF A02

This presentation outlines the background to the concern of using Kapton wire for aerospace vehicles and proposes it should not be utilized in new builds for spacecraft power applications. A NASA HQ investigation concluded that the risk of Kapton arc-tracking/flashover is a credible threat to the shuttle orbiter, but rationale is presented for continued flight for the time being. Recommendations for the protection of the shuttle and the build of the space station are given. CASI

N95-16046*# Rockwell International Corp., Downey, CA.
ORBITER KAPTON WIRE OPERATIONAL REQUIREMENTS AND EXPERIENCE **c33**
R. V. Peterson *In* NASA. Lewis Research Center, First NASA Workshop on Wiring for Space Applications Sep. 1994 p 19-41 (For primary document see N95-16044 04-20)
Avail: CASI HC A03/MF A02

The agenda of this presentation includes the Orbiter wire selection requirements, the Orbiter wire usage, fabrication and test requirements, typical wiring installations, Kapton wire experience, NASA Kapton wire testing, summary, and backup data. CASI

N95-16047*# National Aeronautics and Space Administration. White Sands Test Facility, NM.
WSTF ELECTRICAL ARC PROJECTS **c33**
Larry Linley *In* NASA. Lewis Research Center, First NASA Workshop on Wiring for Space Applications Sep. 1994 p 43-60 (For primary document see N95-16044 04-20)
Avail: CASI HC A03/MF A02

The objectives of these projects include the following: validate method used to screen wire insulation with arc tracking characteristics; determine damage resistance to arc as a function of source voltage and insulation thickness; investigate propagation characteristics of Kapton at low voltages; and investigate pyrolytic properties of polyimide insulated (Kapton) wire for low voltage (less than 35 VDC) applications. Supporting diagrams and tables are presented. Derived from text

N95-16048*# Naval Research Lab., Washington, DC.
PROBLEMS WITH AGING WIRING IN NAVAL AIRCRAFT **c33**
Frank J. Campbell *In* NASA. Lewis Research Center, First NASA Workshop on Wiring for Space Applications Sep. 1994 p 61-71 (For primary document see N95-16044 04-20)
Avail: CASI HC A03/MF A02

The Navy is experiencing a severe aircraft electrical wiring maintenance problem as a result of the extensive use of an aromatic polyimide insulation that is deteriorating at a rate that was unexpected when this wire was initially selected. This problem has significantly affected readiness, reliability, and safety and has greatly increased the cost of ownership of Naval aircraft. Failures in wire harnesses have exhibited arcing and burning that will propagate drastically, to the interruption of many electrical circuits from a fault initiated by the failure of deteriorating wires. There is an urgent need for a capability to schedule aircraft rewiring in an orderly manner with a logically derived determination of which aircraft have aged to the point of absolute necessity. Excessive maintenance was demonstrated to result from the accelerated aging due to the parameters of moisture, temperature, and strain that exist in the Naval Aircraft environment. Laboratory studies have demonstrated that MIL-W-81381 wire insulation when aged at high humidities followed the classical Arrhenius thermal aging relationship. In an extension of the project a multifactor formula was developed that is now capable of predicting life under varying conditions of these service parameters. An automated test system has also been developed to analyze the degree of deterioration that has occurred in wires taken from an aircraft in order to obtain an assessment of remaining life. Since it is both physically and financially impossible to replace the wiring in all the Navy's aircraft at once, this system will permit expedient scheduling so that those aircraft that are most probable to have wiring failure problems can be overhauled first. Author

N95-16049*# Sverdrup Technology, Inc., Cleveland, OH.
KAPTON PYROLYSIS ON SPACE STATION FREEDOM'S SOLAR ARRAY FLEXIBLE CURRENT CARRIER **c33**
Thomas J. Stueber *In* NASA. Lewis Research Center, First NASA Workshop on Wiring for Space Applications Sep. 1994 p 73-80 (For primary document see N95-16044 04-20)
Avail: CASI HC A02/MF A02

The objectives of this research were to investigate possible events that could cause the Kapton to pyrolyze, and to investigate the degree of damage when the Kapton pyrolyzes. Supporting diagrams and tables are presented. Derived from text

N95-16050*# National Aeronautics and Space Administration. Lewis Research Center, Cleveland, OH.
COMBUSTION AND FIRES IN LOW GRAVITY **c25**
Robert Friedman *In its* First NASA Workshop on Wiring for Space Applications Sep. 1994 p 81-90 (For primary document see N95-16044 04-20)
Avail: CASI HC A02/MF A02

Fire safety always receives priority attention in NASA mission designs and operations, with emphasis on fire prevention and material acceptance standards. Recently, interest in spacecraft fire-safety research and development has increased because improved understanding of the significant differences between low-gravity and normal-gravity combustion suggests that present fire-safety techniques may be inadequate or, at best, non-optimal; and the complex and permanent orbital operations in Space Station Freedom demand a higher level of safety standards and practices. This presentation outlines current practices and problems in fire prevention and detection for spacecraft, specifically the Space Station Freedom's fire protection. Also addressed are current practices and problems in fire extinguishment for spacecraft. Derived from text

N95-16051*# National Aeronautics and Space Administration. Lewis Research Center, Cleveland, OH.
SPACE STATION FREEDOM PRIMARY POWER WIRING REQUIREMENTS
Thomas J. Hill *In its* First NASA Workshop on Wiring for Space Applications Sep. 1994 p 95-98 (For primary document see N95-16044 04-20)
Avail: CASI HC A01/MF A02

The Space Station Freedom (SSF) Program requirements are a 30 year reliable service life in low Earth orbit in hard vacuum or pressurized module service without detrimental degradation. Specific requirements are outlined in this presentation for SSF primary power and cable insulation. The primary power cable status and the WP-4 planned cable test program are also reviewed along with Rocketdyne-WP04 prime insulation candidates. CASI

N95-16052*# Boeing Aerospace and Electronics Co., Huntsville, AL. Interconnecting Cabling Space Station Program.
SPACE STATION FREEDOM SECONDARY POWER WIRING REQUIREMENTS
C. R. Sawyer *In* NASA. Lewis Research Center, First NASA Workshop on Wiring for Space Applications Sep. 1994 p 99-110 Sponsored by NASA. Marshall Space Flight Center (For primary document see N95-16044 04-20)
Avail: CASI HC A03/MF A02

Secondary power is produced by DDCU's (direct current to direct current converter units) and routed to and through secondary power distribution assemblies (SPDA's) to loads or tertiary distribution assemblies. This presentation outlines requirements of Space Station Freedom (SSF) EEE (electrical, electronic, and electromechanical) parts wire and the approved electrical wire and cable. The SSF PDRD (Program Definition and Requirements Document) language problems and resolution are reviewed. The cable routing to and from the SPDA's is presented as diagrams and the wire recommendations and characteristics are given. CASI

N95-16053*# Auburn Univ., AL. Space Power Inst.
A STUDY OF ELECTRIC TRANSMISSION LINES FOR USE ON THE LUNAR SURFACE **c33**
Krista L. Gaustad, Lloyd B. Gordon, and Jennifer R. Weber *In* NASA. Lewis Research Center, First NASA Workshop on Wiring for Space Applications Sep. 1994 p 115-124 (For primary document see N95-16044 04-20)
Avail: CASI HC A02/MF A02

The sources for electrical power on a lunar base are said to include solar/chemical, nuclear (static conversion), and nuclear (dynamic conversion). The transmission of power via transmission lines is more practical than power beaming or superconducting because of its low cost and reliable, proven technology. Transmission lines must have minimum mass, maximum efficiency, and the ability to operate reliably in the lunar environment. The transmission line design includes conductor material, insulator material, conductor geometry, conductor configuration, line location, waveform, phase selection, and frequency. This presentation oulines the design. Liquid and gaseous dielectrics are undesirable for long term use in the lunar vacuum due to a high probability of loss. Thus, insulation for high voltage transmission line will most likely be solid dielectric or vacuum insulation. CASI

N95-16054*# National Aeronautics and Space Administration. Lewis Research Center, Cleveland, OH.
KAPTON PYROLYSIS, THE SPACE ENVIRONMENT AND WIRING REQUIREMENTS **c33**
Dale C. Ferguson *In its* First NASA Workshop on Wiring for Space Applications Sep. 1994 p 125-131 (For primary document see N95-16044 04-20)
Avail: CASI HC A02/MF A02

New Low Earth Orbit (LEO) requirements of space environment wiring are compared with traditional requirements. The pyrolysis of Kapton is reviewed for the LeRc vacuum chamber and the 1989 SSF. SEEB modeling of Kapton pyrolysis is also presented. CASI

N95-16055*# Wright Lab., Wright-Patterson AFB, OH. Aero Propulsion and Power Directorate.
HIGH TEMPERATURE POLYMER DIELECTRIC FILM-WIRE INSULATION **c27**
John G. Nairus *In* NASA. Lewis Research Center, First NASA Workshop on Wiring for Space Applications Sep. 1994 p 137-142 (For primary document see N95-16044 04-20)
Avail: CASI HC A02/MF A02

The highlights of the program are outlined including two major accomplishments. TRW identified and demonstrated the potential of two aromatic/heterocyclic polymers to have an outstanding and superior combination of electrical, thermal, and chemical resistance properties versus state-of-the-art Kapton for spacecraft and/or aircraft dielectric insulation applications. (Supporting data is provided in tables.) Feasibility was demonstrated for supporting/enabling technologies such as ceramic coatings, continuous film casting, and conductor wire wrapping, which are designed to accelerate qualification and deployment of the new wire insulation materials for USAF systems applications during the mid- to late-1990's. Derived from text

N95-16056*# Wright Lab., Wright-Patterson AFB, OH.
NEW INSULATION CONSTRUCTIONS FOR AEROSPACE WIRING APPLICATIONS **c33**
George Slenski *In* NASA. Lewis Research Center, First NASA Workshop on Wiring for Space Applications Sep. 1994 p 143-162 (For primary document see N95-16044 04-20)
Avail: CASI HC A03/MF A02

Outlined in this presentation is the background to insulation constructions for aerospace wiring applications, the Air Force wiring policy, the purpose and contract requirements of new insulation constructions, the test plan, and the test results. CASI

N95-16057*# Foster-Miller Associates, Inc., Waltham, MA.
HIGH PERFORMANCE DIELECTRIC MATERIALS DEVELOPMENT **c33**
Joe Piche, Ted Kirchner, and K. Jayaraj *In* NASA. Lewis Research Center, First NASA Workshop on Wiring for Space Applications Sep. 1994 p 173-180 (For primary document see N95-16044 04-20)
Avail: CASI HC A02/MF A02

The mission of polymer composites materials technology is to develop materials and processing technology to meet DoD and commercial needs. The following are outlined in this presentation: high performance capacitors, high temperature aerospace insulation, rationale for choosing Foster-Miller

(the reporting industry), the approach to the development and evaluation of high temperature insulation materials, and the requirements/evaluation parameters. Supporting tables and diagrams are included. CASI

N95-16066*# National Aeronautics and Space Administration. Lewis Research Center, Cleveland, OH.

COMPUTATIONAL FLUID DYNAMICS STUDIES OF NUCLEAR ROCKET PERFORMANCE

Robert M. Stubbs, Suk C. Kim, and Thomas J. Benson Jun. 1994 13 p Presented at Advanced Exploration Initiative Technologies Conference, Cleveland, OH, 4-6 Sep. 1991; cosponsored by AIAA, and OAI Original contains color illustrations

(Contract NAS3-252662-52; RTOP 505-62-52)

(NASA-TM-105436; E-6858; NAS 1.15:105436; AIAA Paper 91-3577)

Avail: CASI HC A03/MF A01; 2 functional color pages

A CFD analysis of a low pressure nuclear rocket concept is presented with the use of an advanced chemical kinetics, Navier-Stokes code. The computations describe the flow field in detail, including gas dynamic, thermodynamic and chemical properties, as well as global performance quantities such as specific impulse. Computational studies of several rocket nozzle shapes are conducted in an attempt to maximize hydrogen recombination. These Navier-Stokes calculations, which include real gas and viscous effects, predict lower performance values than have been reported heretofore. Author

N95-16302 Aerospace Corp., El Segundo, CA. Technology Operations.

ELECTRIC PROBE MEASUREMENTS IN THE PLUME OF THE UK-10 ION THRUSTER

P. C. DeBoer 1 Mar. 1994 33 p Limited Reproducibility: More than 20% of this document may be affected by microfiche quality

(Contract F04701-88-C-0089)

(AD-A282460; TR-93(3507)-1; SMC-TR-94-28) Avail: Issuing Activity (Defense Technical Information Center (DTIC))

Results are presented of measurements with double and single electric probes in the beam of the UK-10 ion thruster, using xenon as the propellant gas. The probe material consisted of tungsten, and secondary emission was of negligible importance. As a consequence of the large directed velocity of the ions, the ion current to a probe was essentially independent of probe voltage. Since the Debye length was small compared with the probe radius, no ions or electrons were collected on the downstream part of a probe. Detailed results are given for ion flux profiles and ion density in the beam, as well as for floating potential profiles. Attention is given to the determination of characteristic electron energies. Evidence is obtained that the electron gas has a non-Maxwellian speed distribution function. Estimates are derived for the degree of non-neutralization in the beam. The neutralization process is discussed in some detail, as is the charge-exchange plasma that exists outside the main beam near the outlet of the thruster. DTIC

N95-16312# Johns Hopkins Univ., Columbia, MD. Chemical Propulsion Information Agency.

THE 1993 JANNAF PROPULSION MEETING, VOLUME 1

Debra S. Eggleston, ed. Nov. 1993 464 p Meeting held in Monterey, CA, 15-19 Nov. 1993; sponsored by the Joint NASA, Army, Navy, Air Force Interagency Committee

(Contract N00014-91-C-0001)

(CPIA-Publ-602-Vol-1) Avail: CPIA, 10630 Little Patuxent Pkwy., Suite 202, Columbia, MD 21044-3200 HC

This volume, the first of six volumes, is a collection of 34 unclassified/unlimited distribution papers which were presented at the 1993 Joint Army-Navy-NASA-Air Force (JANNAF) Propulsion Meeting, held 15-19 November 1993 at the Hyatt Regency Hotel and Conference Center and the Naval Postgraduate School in Monterey, California. Specific subjects discussed include the following: (1) propellant liners; (2) bondlines; (3) booster motors; (4) motor case manufacturing; (5) hazard and sensitivity assessment; (6) divert propulsion; (7) insensitive munitions; (8) scramjets; (9) tubojets; (10) free-jet testing; (11) large caliber guns; and (12) LOVA propellants. For individual titles, see N95-16313 through N95-16323.

N95-16313# TRW, Inc., Redondo Beach, CA. Space and Electronics Group.

DESIGN MARGIN TESTING OF PEACEKEEPER SOLID ROCKET BOOSTERS

A. E. Samsonov and V. R. Betzen (TRW, Inc., San Bernardino, CA.) *In* JHU, The 1993 JANNAF Propulsion Meeting, Volume 1 Nov. 1993 p 39-50 (For primary document see N95-16312 04-20)

(Contract F04704-92-C-0005)

Avail: CPIA, 10630 Little Patuxent Pkwy., Suite 202, Columbia, MD 21044-3200 HC

This paper presents the Design Margin Test program performed on the three solid propulsion stages of the Peacekeeper ICBM. The objective of the Design Margin Tests was to validate structural models used to establish the margins of safety for two of the most critical environments in the life of a solid booster: long term storage and motor ignition. The critical failure modes evaluated by these tests were inner bore cracking and propellant/insulation debonding. Full scale motors with special imbedded instrumentation were exposed to two separate environments: (1) slow rate cool-down to validate the thermal structural models and to assess margins of safety under long term storage conditions; and (2) high rate pressurization using an inert medium to validate ignition structural models and to assess margins of safety under motor ignition conditions. These models were subsequently adjusted and validated by comparing actual test measurements to predictions and utilizing the actual material properties extracted from the test articles by means of dissection of plugging techniques. The results of the program revealed a number of corrections required to the initial margin of safety analysis in the area of induced strains and stresses as well as actual propellant and bond properties in full scale motors. Author

N95-16314# Aerojet-General Corp., Sacramento, CA. Propulsion Div.

HYDROMINING A FULL-SCALE CLASS 1.1 SOLID ROCKET MOTOR

M. F. Young, O. W. Chleborad, P. J. Cova, D. B. Eccli, T. J. Glad, and D. M. Kunkle *In* JHU, The 1993 JANNAF Propulsion Meeting, Volume 1 Nov. 1993 p 61-65 (For primary document see N95-16312 04-20)

Avail: CPIA, 10630 Little Patuxent Pkwy., Suite 202, Columbia, MD 21044-3200 HC

A class 1.1 full-scale Stage 2 Small Intercontinental Ballistic Missile (SICBM) was successfully deloaded using high pressure water jets at approximately 689 N (10,000 psia). The SICBM Stage 2 rocket motor contains approximately 2948 kg (6500 lb) of Class 1.1 propellant (nitrato ester polyester based propellant). A vertical hydromining facility was constructed to simulate a production operational mode in which the system water was continuously recycled to the high pressure water jet nozzles. A series of four in-line carbon absorption filter pairs were used to reduce nitrato ester concentrations to acceptable safety levels (e.g., less than 1 ppm of nitroglycerin). This paper will summarize the operating conditions used and the results of the successful study. Author

N95-16315# Rocket Research Corp., Redmond, WA.

UPDATED TEST RESULTS OF A PUMPED MONOPROPELLANT PROPULSION SYSTEM

Jeffrey C. Maybee, Don G. Swink, and John C. Whitehead (Lawrence Livermore National Lab., Livermore, CA.) *In* JHU, The 1993 JANNAF Propulsion Meeting, Volume 1 Nov. 1993 p 131-144 Sponsored by Ballistic Missile Defense Organization (For primary document see N95-16312 04-20)

Avail: CPIA, 10630 Little Patuxent Pkwy., Suite 202, Columbia, MD 21044-3200 HC

Significant progress was made in 1992 and 1993 towards demonstration at the system level of a high-performance pumped monopropellant propulsion system. Two separate breadboard systems were designed, fabricated and tested with hydrazine at vacuum and sea level conditions. Both designs utilized improved warm-gas-driven reciprocating pumps to transfer fuel from a low-pressure hydrazine tank (70 psig) directly to a pair of 56-lbf thrusters operating at 580 psia chamber pressure. The system most recently tested included direct warm gas pressurization of the hydrazine tank. This novel propulsion system design has been presented and discussed in various configurations in previous papers. This paper will provide an update to test results presented in 1991. This recent testing of these latest system designs included a continuous 60-second burn of a 42-lbf thruster operating at sea level, in addition bootstrap and pulse-mode firings. These results have demonstrated that improvements to the 3-way valve design of the pump

were successful, and have verified performance predictions obtained from a mathematical model of the system. Further testing of a more advanced breadboard system is planned for late 1993. Author

N95-16316# Delavan, Inc., West Des Moines, IA.
THERMAL CHEMICAL ENERGY OF ABLATING SILICA SURFACES IN AIR BREATHING SOLID ROCKET ENGINES M.S. Thesis - George Washington Univ.
Michael D. Cornwell *In* JHU, The 1993 JANNAF Propulsion Meeting, Volume 1 Nov. 1993 p 237-245 (For primary document see N95-16312 04-20)
Avail: CPIA, 10630 Little Patuxent Pkwy., Suite 202, Columbia, MD 21044-3200 HC

This paper provides theoretical adaptation and extension of current industry methodologies for analytical predictions of insulation ablation in solid fuel ramjets. Solid fuel ramjets predominantly operate in a fuel-lean state and require thermal protection systems that are highly oxidation resistant, such as insulation materials that form silica-based char. However, local regions of fuel rich gases exist in ramjets where mixing and combustion of fuel and air is incomplete. Modeling corrosion of silica based char in fuel rich regions of the combustor requires new methods. Accurate ablation prediction of these fuel rich regions are in the design of ramjets. Current analytical methods used to model the ablation of insulation are most suitable for oxidative corrosion of carbonaceous insulation char. Silica-based insulation will ablate corrosively by reduction reactions with carbon and carbon based fuels. Silica ablation by carbon reduction reactions with silica is not correctly modeled by the current industry code, ACE. This paper describes the causes of the current limitations and provides extensions to the ACE methodology to allow for the modeling of silica ablation. Author

N95-16317# General Electric Co., Cincinnati, OH. Aircraft Engine Div.
SCRAMJET TESTING GUIDELINES Status Report **c07**
P. Kutschenreuter *In* JHU, The 1993 JANNAF Propulsion Meeting, Volume 1 Nov. 1993 p 247-259 (For primary document see N95-16312 04-20)
Avail: CPIA, 10630 Little Patuxent Pkwy., Suite 202, Columbia, MD 21044-3200 HC

This is the first status report on the JANNAF Airbreathing Engine Testing Panel's project of developing scramjet testing guidelines. The motivation for such an effort is driven by the perceived need to get more meaningful results from the shrinking U.S. resources available for high Mach number airbreathing propulsion development considering recent significant changes in the political and economic environment. It is the panel's vision that formulation and use of these guidelines would make such a contribution. A quick, first rough cut at their preparation was completed in less than 12 months, including an evaluation designed to identify required areas of refinement. These interim results are the subject of this paper. Author

N95-16318# Arnold Engineering Development Center, Arnold AFS, TN.
A MODEL FOR PRELIMINARY FACILITY DESIGN INCLUDING SIMULATION ISSUES **c09**
E. S. Powell *In* JHU, The 1993 JANNAF Propulsion Meeting, Volume 1 Nov. 1993 p 261-274 (For primary document see N95-16312 04-20)
Avail: CPIA, 10630 Little Patuxent Pkwy., Suite 202, Columbia, MD 21044-3200 HC

A new procedure has been developed to aid in the preliminary design of aerodynamic simulation facilities using instream combustion as an energy source. The aerothermodynamic parameters necessary to address the issue of simulation are calculated for each simulation point considered. The new procedure uses the desired simulation conditions as input. Those conditions and the equations for the conservation of mass, momentum, energy, entropy, and the thermally perfect equation of state are used to determine facility flow rates, pressures, and nozzle expansion ratio. Accepted procedures are used to calculate the test medium thermodynamic and transport properties. Simplifying assumptions and engineering approximations have been made where they do not adversely affect accuracy of the predictions. The new procedure is easy to use and is accurate when compared to an accepted equilibrium expansion code. The new procedure requires minimal computational resources. A facility to test a hypersonic propulsion system will be used as an example. Author

N95-16319# Arnold Engineering Development Center, Arnold AFS, TN.
HYPERSONIC AIR-BREATHING AEROPROPULSION FACILITY TEST SUPPORT REQUIREMENTS **c09**
Brian Wettlaufer *In* JHU, The 1993 JANNAF Propulsion Meeting, Volume 1 Nov. 1993 p 275-292 (For primary document see N95-16312 04-20)
Avail: CPIA, 10630 Little Patuxent Pkwy., Suite 202, Columbia, MD 21044-3200 HC

The ground testing of hypersonic propulsion systems presents some interesting issues and challenges for today's facilities. The current concepts of hypersonic propulsion systems for vehicles indicate that they will be highly integrated with the airframe and use vehicle forebody and afterbody surfaces for compression and expansion surfaces. The trade studies indicate that these propulsion systems will be large devices and will probably use cryogenic fuels for engine and airframe active cooling. This makes the operational characteristics and performance of the engine highly dependent on the thermal loads on the engine and the vehicle. Test articles used for development testing in a ground test facility will also be very large because they must include or simulate the complete thermal cycle of the propulsion device, and the kinetics of the combustion process are not scalable. The ground test facilities to support development testing on hypersonic propulsion systems must be capable of providing the proper test conditions, be of adequate size, and provide ample testing durations to accommodate thermal stabilization of large test articles. Current propulsion ground test facilities with near-term enhancements are capable of supporting full-size propulsion test articles to Mach 3.8 and small propulsion test articles or component test rigs to about Mach 7 true temperature and pressure conditions. This paper will review the hypersonic ground test requirements for the development of hypersonic air-breathing propulsion systems. It will review the direct-connect and freejet testing approach using reference planes, the facility configurations, as well as their capabilities and shortfalls. Facility adequacy will be evaluated and future needs will be assessed. Author

N95-16320*# General Applied Science Labs., Inc., Ronkonkoma, NY.
FREE-JET TESTING AT MACH 3.44 IN GASL'S AERO/THERMO TEST FACILITY **c09**
D. Cresci, S. Koontz, and C. Y. Tsai *In* JHU, The 1993 JANNAF Propulsion Meeting, Volume 1 Nov. 1993 p 293-307 (For primary document see N95-16312 04-20)
(Contract NAS1-18450)
Avail: CPIA, 10630 Little Patuxent Pkwy., Suite 202, Columbia, MD 21044-3200 HC

A supersonic blow-down tunnel has been used to conduct tests of a hydrogen burning ramjet engine at simulated Mach 3.44 conditions. A pebble-bed type storage heater, a free standing test cabin, and a 48 foot diameter vacuum sphere are used to simulate the flight conditions at nearly matched enthalpy and dynamic pressure. A two dimensional nozzle with a nominal 13.26 inch square exit provides a free-jet test environment. The facility used for these tests is described as are the results of a flow calibration performed on the M = 3.44 nozzle. Some facility/model interactions are discussed as are the eventual hardware modifications and operational procedures required to alleviate the interactions. Some engine test results are discussed briefly to document the success of the test program. Author

N95-16321# Applied Thermal Sciences, Orono, ME.
COMBUSTOR KINETIC ENERGY EFFICIENCY ANALYSIS OF THE HYPERSONIC RESEARCH ENGINE DATA
K. V. Hoose *In* JHU, The 1993 JANNAF Propulsion Meeting, Volume 1 Nov. 1993 p 309-317 (For primary document see N95-16312 04-20)
Avail: CPIA, 10630 Little Patuxent Pkwy., Suite 202, Columbia, MD 21044-3200 HC

A one-dimensional method for measuring combustor performance is needed to facilitate design and development scramjet engines. A one-dimensional kinetic energy efficiency method is used for measuring inlet and nozzle performance. The objective of this investigation was to assess the use of kinetic energy efficiency as an indicator for scramjet combustor performance. A combustor kinetic energy efficiency analysis was performed on the Hypersonic Research Engine (HRE) data. The HRE data was chosen for this analysis due to its thorough documentation and availability. The combustor, inlet, and nozzle kinetic energy efficiency values were utilized to determine an overall engine kinetic energy efficiency. Finally,

a kinetic energy effectiveness method was developed to eliminate thermochemical losses from the combustion of fuel and air. All calculated values exhibit consistency over the flight speed range. Effects from fuel injection, altitude, angle of attack, subsonic-supersonic combustion transition, and inlet spike position are shown and discussed. The results of analyzing the HRE data indicate that the kinetic energy efficiency method is effective as a measure of scramjet combustor performance. Author

N95-16322# Wright Lab., Wright-Patterson AFB, OH.
AN ENGINEERING CODE TO ANALYZE HYPERSONIC THERMAL MANAGEMENT SYSTEMS **c34**
Valerie J. VanGriethuysen and Clark E. Wallace (Science Applications International Corp., Torrance, CA.) *In* JHU The 1993 JANNAF Propulsion Meeting, Volume 1 Nov. 1993 p 319-333 (For primary document see N95-16312 04-20)
(Contract F33615-91-C-2169)
Avail: CPIA, 10630 Little Patuxent Pkwy., Suite 202, Columbia, MD 21044-3200 HC

This paper will describe an effort that is underway within the Advanced Propulsion Division of the Aero Propulsion and Power Directorate at Wright Patterson AFB to develop an engineering computer code to aid in the development of hypersonic thermal management systems. The goal of the Vehicle Integrated Thermal Management Code (VITMAC), is to thermally model the entire thermal management system on an integrated basis for an entire vehicle. A further goal is for it to be a stand-alone code. In other words, to predict the aerodynamic heating on the vehicle surface during the trajectory, to the heat loads from the propulsion system, subsystems and avionics, and to the heat transfer through the structure and insulation. In addition, VITMAC will be able to model the flow of the coolant through the network. All this is to determine if the vehicle is thermally balanced and if there are any areas in risk of melting or thermal degradation. The code also has the option to accept user data for aerodynamic heating, heat loads and user-specific components. To aid the user while inputting the vehicle configuration, geometry, components, and 'plumbing' data, a graphical user interface is being incorporated within te code. This will enable the user, even those with little experience in the area, with the aid of a mouse, to literally see the network on the screen as it is being inputted. This capability will speed up the input process, particularly for complex systems, as well as aid in error detection. This paper will further discuss the architecture of VITMAC. Also discussed will be its developmental status and capabilities, computer system that supports the code, its relevancy to other types of vehicles and applications, expansion capability and future plans. Author

N95-16323# Sundstrand Power Systems, San Diego, CA.
SMALL TURBOJETS: DESIGNS AND INSTALLATIONS **c07**
C. Rodgers *In* JHU, The 1993 JANNAF Propulsion Meeting, Volume 1 Nov. 1993 p 335-352 (For primary document see N95-16312 04-20)
Avail: CPIA, 10630 Little Patuxent Pkwy., Suite 202, Columbia, MD 21044-3200 HC

Smaller, smarter airbreathing propelled tactical missiles are being proposed and developed. They will function for various operational duties currently performed by larger, limited range missiles or manned interdiction aircraft. The extreme compactness of these advanced missiles require relatively high power density small turbojets. Several design configuration options are possible for these turbojets, including centrifugal and axial turbomachinery compressor and turbines, straight annular and reverse flow annular combustors, and various types of fuel injection systems. The attributes of candidate configurations are discussed with respect to maximum thrust per frontal area, range, and endurance optimization, and low manufacturing costs. Installation constraints upon engine design, in particular, the inlet and exhaust nozzle and start system are reviewed. Early recognition of these constraints is paramount in minimizing overall propulsion system cost, and volume; thereby producing maximum weapon system effectiveness. Author

N95-16324# Johns Hopkins Univ., Columbia, MD. Chemical Propulsion Information Agency.
THE 1993 JANNAF PROPULSION MEETING, VOLUME 2
Debra S. Eggleston, ed. Nov. 1993 392 p Meeting held in Monterey, CA, 15-19 Nov. 1993; sponsored by the Joint NASA, Army, Navy, Air Force Interagency Committee
(Contract N00014-91-C-0001)
(CPIA-Publ-602-Vol-2) Avail: CASI HC A17/MF A04

This second of six volumes is a collection of 30 papers presented at the 1993 Joint Army-Navy-NASA-Air Force (JANNAF) Propulsion Meeting. Specific subjects discussed include grain integrity, hybrid motors, liquid engines, turbopumps, reaction control systems, composite motor cases, continuous propellant mixing, nondestructive testing, solar propulsion, combustion chambers, and foreign propulsion technology. For individual titles, see N95-16325 through N95-16351.

N95-16325# Virginia Polytechnic Inst. and State Univ., Blacksburg, VA. Dept. of Engineering Science and Mechanics.
GLOBAL AND NEAR TIP RESPONSE OF CRACKED SOLID PROPELLANT
C. W. Smith and C. T. Liu (Phillips Lab., Edwards AFB, CA.) *In* JHU, The 1993 JANNAF Propulsion Meeting, Volume 2 Nov. 1993 p 1-10 (For primary document see N95-16324 04-20)
(Contract F04611-92-C-0012)
Avail: CASI HC A02/MF A04

A series of tensile tests were conducted at two head rates (2.54 and 12.7 mm/min) and three temperatures (-65 F, 72 F, and 165 F) on edge cracked biaxial solid propellant specimens of two thicknesses (2.54 and 12.7 mm) to simulate typical curing, transport, and storage conditions. A grating of negligible stiffness was inscribed on the specimen surfaces near the crack tip and photographs of the grating were taken at various time intervals from which near tip displacement and strain fields, and the dominant eigenvalues, were extracted. A companion test program on uncracked biaxial specimens was conducted to obtain global stress-strain and stress relaxation data. Results of the cracked specimen tests suggested a blunt-growth-blunt-growth mechanism of extension which was highly nonlinear with the blunting preceded by extensive local voiding ahead of the crack tip except in the thick models at -65 F, where a classic brittle fracture resulted with negligible voiding. Reasonable estimates of the dominant eigenvalues were obtained for all cases. The head rate effect was considered small relative to that of temperature and the relaxation modulus followed generally the WLF predictions. Explanations are suggested for the development of brittle fractures. Author

N95-16326*# National Aeronautics and Space Administration. Marshall Space Flight Center, Huntsville, AL.
PRECISION AQUEOUS CLEANER FOR RSRM **c25**
D. E. Hutchens (Thiokol Chemical Corp., Huntsville, AL.), J. M. Keen (Thiokol Chemical Corp., Huntsville, AL.), P. A. Doan (Thiokol Chemical Corp., Huntsville, AL.), C. D. DeWeese, H. D. Burns, Jr., and J. H. Vickers *In* JHU, The 1993 JANNAF Propulsion Meeting, Volume 2 Nov. 1993 p 21-36 (For primary document see N95-16324 04-20)
(Contract NAS8-38100)
Avail: CASI HC A03/MF A04

Chlorinated solvents such as freon and 1,1,1 trichloroethane (TCA) are both environmental and physiological hazards which deplete stratospheric ozone. These chemicals are the primary degreasing solvents (vapor, vat, and hand operations) in redesigned solid rocket motor (RSRM) manufacturing. Due to the mandates of the Clean Air Act, substitutes must be identified for RSRM cleaning processes. The initial phase of laboratory testing identified candidate cleaners to replace 1,1,1 trichloroethane for cleaning, potentially reducing annual TCA consumption by 800,000 lbs. This paper describes RSRM testing which elucidated the effects of several interdependent variable including: definition of surface cleanliness criteria, validation of cleaning power of new candidates, the effect of immersion cleaning versus spray cleaning on cleaning, any effect of the cleaner and/or inhibitor upon bondline aging, and compatibility of the cleaners with nonmetallic tooling and processing materials. Author (revised)

N95-16327# American Rocket Co., Ventura, CA.
LARGE-SCALE HYBRID MOTOR PERFORMANCE AND DESIGNS FOR USE IN LAUNCH VEHICLE APPLICATIONS
K. J. Flittie and P. Estey *In* JHU, The 1993 JANNAF Propulsion Meeting, Volume 2 Nov. 1993 p 37-50 (For primary document see N95-16324 04-20)
Avail: CASI HC A03/MF A04

The American Rocket Company has developed two large-scale liquid

oxygen/polybutadiene hybrid rocket motors at 334,000 N (75,000 lbf) and 1,112,000 N (250,000 lbf) thrust. These hybrid rocket motors or derivatives of these motors can be used as strap-on boosters to replace or upgrade the existing strap-on boosters for the fleet of U.S. launch vehicles and for the planned next generation launch vehicle. Hybrid rocket boosters offer a new solution for boost propulsion since hybrids solve many of the safety and environmental concerns facing solid rocket motor manufacture and operation, yet deliver performance comparable to liquid rocket engines with much less hardware and operational complexity. This paper presents motor performance data from AMROC's 334,000 N and 1,112,000 N thrust hybrid rocket motors. A description of these hybrid motors, their performance specifications, and the key enabling technologies that have been developed at AMROC is presented. The design and development approach for an 850K thrust hybrid motor is described. Author

N95-16328*# National Aeronautics and Space Administration. Lewis Research Center, Cleveland, OH.

TEST RESULTS FROM A SIMPLE, LOW-COST, PRESSURE-FED LIQUID HYDROGEN/LIQUID OXYGEN ROCKET COMBUSTOR

G. A. Dressler (TRW, Inc., Redondo Beach, CA.), F. J. Stoddard (TRW, Inc., Redondo Beach, CA.), K. R. Gavitt (TRW, Inc., Redondo Beach, CA.), and M. D. Klem *In* JHU, The 1993 JANNAF Propulsion Meeting, Volume 2 Nov. 1993 p 51-67 (For primary document see N95-16324 04-20)

Avail: CASI HC A03/MF A04

A simple, low-cost rocket engine was designed, fabricated, and successfully hot fire tested over a wide range of interface conditions and operating parameters. The engine used low enthalpy hydrogen (45 to 70 R, 200 to 390 psia) and oxygen (139 to 163 R, 210 to 480 psia) propellants pressure-fed directly from facility cryogenic tanks. The engine demonstrated excellent performance, with 97% average combustion efficiency, and absence of combustion instabilities. Engine design chamber pressure was 300 psia, yielding about 16,500 pounds thrust at sea level with a 3:1 expansion ration test nozzle. The engine used a fixed-element injector based on TRW's unique coaxial pintle design, but was operated at 60%, 80%, and 100% thrust levels by throttling facility propellant valves. The engine was tested at propellant mixture ratios (O/F) from 5.8 to 8.4; design O/F was 6.6. To document combustion stability, in five tests RDX explosive pulse guns were detonated in radial and tangential directions across the combustion chamber during steady-state operation. The largest disturbance consisted of simultaneous detonation of a 20-grain radial gun and a 40-grain tangential gun. In no case was an instability, either feed system mode or chamber acoustic mode, excited. High-frequency piezoelectric pressure transducers documented stable recovery from disturbance overpressures within 40 milliseconds of peak pressure. A total of 67 firing tests, accumulating 149 seconds of firing time above 10% P(sub c), were performed. Since parametric testing required run durations of only 2 to 3 seconds, a heat sink combustion chamber was employed for most runs. To evaluate the feasibility of a low-cost ablative system for a flight engine design, one 20-second continuous firing was conducted with a silicone rubber chamber/throat/nozzle liner cast in one piece directly into the engine. The ablative engine operated at the equivalent of 309 seconds sea level specific impulse, when adjusted to a 98% efficient 6:1 expansion ration nozzle, and 430 seconds vacuum specific impulse, when adjusted to a 98% efficient 50:1 expansion ratio nozzle. This engine and test series represent an initial subscale demonstration of a new booster-class engine that eliminates the cost and complexity associated with regenerative cooling and typical engine cycles. This paper presents a description of the engine design and discussion and summary data plots of the performance measured during the parametric testing. Author

N95-16329*# National Aeronautics and Space Administration. Marshall Space Flight Center, Huntsville, AL.

NUMERICAL STUDY OF BASE PRESSURE CHARACTERISTIC CURVE FOR A FOUR-ENGINE CLUSTERED NOZZLE CONFIGURATION

Ten-See Wang *In* JHU, The 1993 JANNAF Propulsion Meeting, Volume 2 Nov. 1993 p 69-77 (For primary document see N95-16324 04-20)

Avail: CASI HC A02/MF A04

The objective of this study is to benchmark a four-engine clustered nozzle base flowfield with a computational fluid dynamics (CFD) model. The CFD model is a three-dimensional pressure-based, viscous flow formulation. An adaptive upwind scheme is employed for the spatial discretization. The upwind scheme is based on second and fourth order central differencing with adaptive artificial dissipation. Qualitative base flow features such as the reverse jet, wall jet, recompression shock, and plume-plume impingement have been captured. The computed quantitative flow properties such as the radial base pressure distribution, model centerline Mach number and static pressure variation, and base pressure characteristic curve agreed reasonably well with those of the measurement. Parametric study on the effect of grid resolution, turbulence model, inlet boundary condition and difference scheme on convective terms has been performed. The results showed that grid resolution had a strong influence on the accuracy of the base flowfield prediction. Author

N95-16330*# National Aeronautics and Space Administration. Marshall Space Flight Center, Huntsville, AL.

SPACE SHUTTLE MAIN ENGINE OPAD: THE SEARCH FOR A HARDWARE ENHANCED PLUME

W. T. Powers, A. E. Cooper, Tim L. Wallace (Sverdrup Technology, Inc., Arnold AFS, TN.), W. L. Buntine (Research Inst. for Advanced Computer Science, Moffett Field, CA.), and K. W. Whitaker (Alabama Univ., Tuscaloosa, AL.) *In* JHU, The 1993 JANNAF Propulsion Meeting, Volume 2 Nov. 1993 p 79-92 (For primary document see N95-16324 04-20)

Avail: CASI HC A03/MF A04

The process of applying spectroscopy to the Space Shuttle Main Engine (SSME) for plume diagnostics, as it exists today, originated at Marshall Space Flight Center in Huntsville, Alabama, and its implementation was assured largely through the efforts of Sverdrup AEDC, in Tullahoma, Tennessee. This team continues to lead and guide efforts in the plume diagnostics arena. The process, Optical Plume Anomaly Detection (OPAD), formed the basis for various activities in the development of ground-based systems as well as the development of in-flight plume spectroscopy. OPAD currently provides and will continue to provide valuable information relative to future systems definitions, instrumentation development, code validation, and data diagnostic processing. OPAD is based on the detection of anomalous atomic and molecular species in the SSME plume using two complete, stand-alone optical spectrometers. To-date OPAD has acquired data on 44 test firings of the SSME at the Technology Test Bed (TTB) at MSFC. The purpose of this paper will be to provide an introduction to the OPAD system by discussing the process of obtaining data as well as the methods of examining and interpreting the data. It will encompass such issues as selection of instrumentation correlation of data to nominal engine operation, investigation of SSME component erosion via OPAD spectral data, necessity and benefits of plume seeding, application of artificial intelligence (AI) techniques to data analysis, and the present status of efforts to quantify speçie erosion utilizing standard plume and chemistry codes as well as radiative models currently under development. Author

N95-16331*# Allied-Signal Aerospace Co., Torrance, CA. Systems and Equipment Div.

CRYOGENIC FOIL BEARING TURBOPUMPS

Alston L. Gu *In* JHU, The 1993 JANNAF Propulsion Meeting, Volume 2 Nov. 1993 p 93-102 Sponsored by NASA. Lewis Research Center, NASA. Marshall Space Flight Center, NASA. Stennis Space Center, NASA. White Sands Test Facility, AF Phillips Lab., and NRL (For primary document see N95-16324 04-20)

Avail: CASI HC A02/MF A04

Cryogenic foil bearing turbopumps offer high reliability and low cost. The fundamental cryogenic foil bearing technology has been validated in both liquid hydrogen and liquid oxygen. High load capacity, excellent rotor dynamics, and negligible bearing wear after over 100 starts and stops, and over many hours of testing, were observed in both fluids. An experimental liquid hydrogen foil bearing turbopump was also successfully demonstrated. The results indicate excellent stability, high reliability, wide throttle-ability, low bearing cooling flow, and two-phase bearing operability. A liquid oxygen foil bearing turbopump has been built and is being tested at NASA MSFC. Author

N95-16332*# National Aeronautics and Space Administration. White Sands Test Facility, NM.

SPACE SHUTTLE REACTION CONTROL SYSTEM THRUSTER METAL NITRATE REMOVAL AND CHARACTERIZATION

R. L. Saulsberry and P. A. McCartney *In* JHU, The 1993 JANNAF

Propulsion Meeting, Volume 2 Nov. 1993 p 103-113 (For primary document see N95-16324 04-20)
Avail: CASI HC A03/MF A04

The Space Shuttle hypergolic primary reaction control system (PRCS) thrusters continue to fail-leak or fail-off at a rate of approximately 1.5 per flight, attributed primarily to metal nitrate formation in the nitrogen tetroxide (N2O4) pilot operated valves (POV's). The failures have continued despite ground support equipment (GSE) and subsystem operational improvements. As a result, the Johnson Space Center (JSC) White Sands Test Facility (WSTF) performed a study to characterize the contamination in the N204 valves. This study prompted the development and implementation of a highly successful flushing technique using deionized (DI) water and gaseous nitrogen (GN2) to remove the contamination while minimizing Teflon seat damage. Following flushing a comprehensive acceptance test is performed before the thruster is deemed recovered. Between the time WSTF was certified to process flight thrusters (March 1992) and September 1993, a 68 percent thruster recovery rate was achieved. The contamination flushed from these thrusters was analyzed and has provided insight into the corrosion process, which is reported in this publication. Additionally, the long-term performance of 24 flushed thrusters installed in the WSTF Fleet Leader Shuttle reaction control subsystem (RCS) test articles is being assessed. WSTF continues to flush flight and test article thrusters and compile data to investigate metal nitrate formation characteristics in leaking and nonleaking valves. Author

N95-16333# Hercules Aerospace Co., Magna, UT. Bacchus Works.
RECENT ADVANCES IN GRAPHITE/EPOXY MOTOR CASES
William G. Wilson, Paul E. Christensen, and James L. York *In* JHU, The 1993 JANNAF Propulsion Meeting, Volume 2 Nov. 1993 p 115-123 (For primary document see N95-16324 04-20)
Avail: CASI HC A02/MF A04

Much has been published concerning improvements and enhancements in materials and technology used in the design and construction of solid rocket motors. However, there are important aspects of the improvement process that are seldom discussed, particularly process control and continuous improvement. This has been applied successfully to the resolution of challenges, which remained at the termination of the Filament Wound Case (FWC) Program. The FWC Program for the Space Shuttle boosters was terminated in 1986. At that time, although the FWC met all requirements, there were issues with composites that needed improvement. This paper discusses the success in resolving those challenges and describes how the continuous improvement methodologies were implemented at Hercules for design and fabrication of graphite/epoxy motor cases. Advancements in materials and engineering data are first evaluated. The implementation of an approach that includes concurrent engineering, process controls, statistical process controls, continuous improvement, and product acceptance are then discussed. The successes in recent years have been realized from application of these principles. Discrepancies have been reduced by an order of magnitude. Delaminations have been virtually eliminated. Voids have been reduced to 'hardly detectable.' Enhancements in manufacturing technology and cost reductions have also been realized. The application of process control and continuous improvement principles has resulted in 100 percent flight performance success while simultaneously achieving improved vehicle performance. Author

N95-16334*# Aerojet-General Corp., Sacramento, CA. Propulsion Div.
THE USE OF DESIGNED EXPERIMENTS IN THE PROCESS DEVELOPMENT OF CONTINUOUS PROPELLANT MIXING **c28**
J. A. Campbell, K. T. Clemons, and M. K. Wong *In* JHU, The 1993 JANNAF Propulsion Meeting, Volume 2 Nov. 1993 p 125-133 (For primary document see N95-16324 04-20)
(Contract NAS8-37800)
Avail: CASI HC A02/MF A04

A continuous mix pilot plant was constructed at Aerojet Propulsion Division in Sacramento, California to develop a robust propellant mixing process for the full scale plant that was to be built at the NASA Advanced Solid Rocket Motor facility Yellow Creek, Mississippi. The plant was used to conduct dozens of subsystem and full system mixing tests for evaluation of equipment, processing methods, and control schemes for later use at the production plant. As a culmination to this work, a series of designed experiments were conducted using an eight run Taguchi analysis with four factors at two levels each to determine the primary effect of processing parameters on propellant ballistic and mechanical properties. The factors examined in these runs included the propellant production rate (454 (1000) and 622 kg/hr (1371 lb/hr)), the product temperature out of the mixer (49 (120) and 63 deg C (145 deg F)), mixer screw speed (75 and 90 rpm), and the deaerator excess capacity (20 and 80 percent). Measured response variables included the uncured and cured density, Crawford Bomb liquid strand burning rates, and selected mechanical properties. The experiment revealed that several of the response variables displayed significant changes from run-to-run with the product temperature being the single most important factor. After concluding this experiment, a twenty-six hour confirmation run was conducted to verify the conclusions reached in the designed experiment. The extended run produced over 12,250 kgs (27,000 lbs) of propellant meeting all of the pre-run targeted properties including density (1.803 g/cc (0.065 lb/in(exp 3)) with a 0.12 percent coefficient of variation (CV) at 25 deg C (77 deg F)), liquid strand burn rate (0.889 cm/s (0.350 in/s) with a 0.69 percent CV at 4210 KPa (610 psig), 15.6 deg C (60 deg F)), nominal maximum stress (828 KPa (120 psig) with a 2.84 percent CV, S&E at 25 deg C (77 deg F), 5.08 cm/min (2 in/min)), strain at nominal maximum (47.4 percent with a 3.96 percent CV), and initial tangent modulus (5349 KPa (775 psig) with a 7.26 percent CV). Author

N95-16335*# Thiokol Corp., Brigham City, UT.
IGNITION PROPAGATION AND HEAT EFFECTS OF PROPELLANT CHIPS EMBEDDED IN CASTABLE INHIBITOR USING A LASER FLUX TEST BOMB **c28**
Douglas E. Bolton, Jr. *In* JHU, The 1993 JANNAF Propulsion Meeting, Volume 2 Nov. 1993 p 135-145 (For primary document see N95-16324 04-20)
(Contract NAS8-38100)
Avail: CASI HC A03/MF A04

A castable inhibitor is applied to the aft face of the Space Shuttle Redesigned Solid Rocket Motor (RSRM) forward segment propellant grain to control propellant surface burn area. During fabrication, the propellant surface is trimmed prior to the inhibitor application. This produces a potential for small propellant chips to remain undetected on the propellant surface and contaminate the inhibitor during application. The concern was that undetected propellant chips in the inhibitor might provide a fuse path for premature propellant ignition underneath the inhibitor. To evaluate the fuse path potential, testing was performed on inhibitor samples with embedded propellant. The internal motor environment was simulated with a calibrated CO2 laser beam directed onto a sample which was placed in a 4100 kPa (600 psi) nitrogen pressurized bomb (laser bomb). The testing showed definitive results pertaining to fuse path formation. Embedded propellant chips did not autoignite until the receding heat affected inhibitor surface reached, or passed, the propellant chip. Samples with embedded propellant chips in alignment did not propagate ignition from one chip to another with separation distances as small as 0.010 cm(0.004 inc) and some as little as 0.0051 cm (0.002 in). Propellant chips with volumes approximately less than 0.025 cu cm (0.0015 cu in) (which did not propagate ignition) did not increase the inhibitor material decomposition depth more than the resulting void cavity of the burned out propellant chip. In addition, the depth of this void cavity did not increase until it was overtaken by the surrounding material decomposition depth. This was due, in part, to the retention of the protective inhibitor char layer. Samples with embedded propellant strings, whose thicknesses were below 0.023 cm (0.009 in), did not propagate ignition. Propellant string thicknesses above 0.038 cm (0.015 in) did propagate ignition. Test sample char and heat affected layer measurements and observations compared well with those from the Space Shuttle Solid Rocket Motor (SRM) Technical Evaluation Motor no. 9(TEM-9). Author

N95-16336# Rockwell International Corp., Canoga Park, CA. Rocketdyne Div.
INTEGRATED MODULAR ENGINE CONFIGURATION OPTIONS
T. J. Harmon and G. L. Briley *In* JHU, The 1993 JANNAF Propulsion Meeting, Volume 2 Nov. 1993 p 147-154 (For primary document see N95-16324 04-20)
(Contract F04701-91-C-0076)
Avail: CASI HC A02/MF A04

Engine concepts characterized by modular architecture, advanced technologies, and enhanced operability applicability to a wide range of missions (i.e., upper stage, space-based, transfer, lunar lander, ascent, and Mars lander propulsion systems). Two widely different propulsion system

applications, a launch vehicle upper stage and a lunar lander vehicle, were developed around a common propulsion system architecture. These Integrated Modular Engine (IME) systems include propellant tanks, propellant distribution, and the rocket engines. This approach focused on automating and minimizing operations required for preparing and placing a propulsion system into operation. The versatility of the IME system architecture is described along with options to further integrate stage or vehicle functions. Author

N95-16337*# National Aeronautics and Space Administration. Lewis Research Center, Cleveland, OH.

STRUCTURALLY-COMPLIANT ROCKET ENGINE COMBUSTION CHAMBER: EXPERIMENTAL/ANALYTICAL VALIDATION

R. S. Jankovsky, J. M. Kazaroff, G. R. Galford, and V. K. Arya (Toledo Univ., OH.) *In* JHU, The 1993 JANNAF Propulsion Meeting, Volume 2 Nov. 1993 p 155-168 (For primary document see N95-16324 04-20)
Avail: CASI HC A03/MF A04

A new, structurally-compliant rocket engine combustion chamber design has been validated through analysis and experiment. Subscale, tubular channel chambers have been cyclically tested, and analytically evaluated. Cyclic lives were determined to have a potential for 1000 percent increase in life over that of rectangular channel designs, the current state-of-the-art. Greater structural compliance in the circumferential direction gives rise to lower thermal strains during hot firing, resulting in lower thermal strain ratcheting and longer predicted fatigue lives. Thermal/durability analyses of the combustion chamber design, involving cyclic temperatures, strains, and low-cycle fatigue lives have corroborated the experimental observations. Author

N95-16338*# National Aeronautics and Space Administration. Goddard Space Flight Center, Greenbelt, MD.

NONDESTRUCTIVE EXAMINATION OF THE TRMM RCS PROPELLANT TANKS **c38**

James M. Free *In* JHU, The 1993 JANNAF Propulsion Meeting, Volume 2 Nov. 1993 p 169-179 (For primary document see N95-16324 04-20)
Avail: CASI HC A03/MF A04

This paper assesses the feasibility of using eddy current nondestructive examination of determine flaw sizes in completely assembled hydrazine propellant tanks. The study was performed by the NASA Goddard Space Flight Center for the Tropical Rainfall Measuring Mission (TRMM) project to help determine whether existing propellant tanks could meet the fracture analysis requirements of the current pressure vessel specification, MIL-STD-1522A and, therefore be used on the TRMM spacecraft. After evaluating several nondestructive test methods, eddy current testing was selected as the most promising method for determining flaw sizes on external and internal surfaces of completely assembled tanks. Tests were conducted to confirm the detection capability of the eddy current NDE, procedures were developed to inspect two candidate tanks, and the test support equipment was designed. The non-spherical tank eddy current NDE test program was terminated when the decision was made to procure new tanks for the TRMM propulsion subsystem. The information on the development phase of this test program is presented in this paper as a reference for future investigation on the subject. Author

N95-16339*# National Aeronautics and Space Administration. Lewis Research Center, Cleveland, OH.

THE PREDICTION OF NOZZLE PERFORMANCE AND HEAT TRANSFER IN HYDROGEN/OXYGEN ROCKET ENGINES WITH TRANSPIRATION COOLING, FILM COOLING, AND HIGH AREA RATIOS

Kenneth J. Kacynski and Joe D. Hoffman (Purdue Univ., West Lafayette, IN.) *In* JHU, The 1993 JANNAF Propulsion Meeting, Volume 2 Nov. 1993 p 181-202 (For primary document see N95-16324 04-20)
Avail: CASI HC A03/MF A04

An advanced engineering computational model has been developed to aid in the analysis and design of hydrogen/oxygen chemical rocket engines. The complete multi-species, chemically reacting and diffusing Navier-Stokes equations are modelled, finite difference approach that is tailored to be conservative in an axisymmetric coordinate system for both the inviscid and viscous terms. Demonstration cases are presented for a 1030:1 area ratio nozzle, a 25 lbf film cooled nozzle, and transpiration cooled plug-and-spool rocket engine. The results indicate that the thrust coefficient predictions of the 1030:1 nozzle and the film cooled nozzle are within 0.2 to 0.5 percent, respectively, of experimental measurements when all of the chemical reaction and diffusion terms are considered. Further, the model's predictions agree very well with the heat transfer measurements made in all of the nozzle test cases. The Soret thermal diffusion term is demonstrated to have a significant effect on the predicted mass fraction of hydrogen along the wall of the nozzle in both the laminar flow 1030:1 nozzle and the turbulent plug-and-spool rocket engine analysis cases performed. Further, the Soret term was shown to represent a significant fraction of the diffusion fluxes occurring in the transpiration cooled rocket engine. Author

N95-16340# Ultramet Co., Pacoima, CA.

MATERIALS CHARACTERIZATION AND DESIGN FOR SOLAR-THERMAL PROPULSION

M. J. DelaRosa and R. H. Tuffias *In* JHU, The 1993 JANNAF Propulsion Meeting, Volume 2 Nov. 1993 p 203-211 (For primary document see N95-16324 04-20)
(Contract F29601-92-C-0119)
Avail: CASI HC A02/MF A04

Solar-thermal propulsion relies on the convection of concentrated solar energy into kinetic energy (in the exhaust gases) in order to provide thrust. Solar radiation is focused into a blackbody cavity in which the heat is absorbed and transferred to the hydrogen fuel through a thermal absorber/heat exchanger. Performance increases are obtained by increasing the efficiency of the absorber, thereby increasing the heat transfer to the hydrogen fuel. The absorber/exchanger itself provides structural properties, which involves the severe structural constraint of needing to withstand the high internal hydrogen pressure. Thus, the absorber/exchanger becomes the critical component in the thruster, and the enabling technology for the development of a successful solar-heated hydrogen propulsion system is a combination of materials and processing. The maximum operating temperature of a solar-thermal propulsion devices is governed primarily by the strength and resistance of hydrogen degradation of the constituent materials at the operating temperature of 3000 K and above. Six candidate refractory materials were selected for investigation with regard to their potential for use in solar-thermal propulsion, with the aim of developing a properties and processing database in advance of designing, fabricating, and testing a solar-powered rocket engine (SPRE). Author

N95-16341# Hercules Aerospace Co., Magna, UT.

SOLAR-POWERED ROCKET ENGINE OPTIMIZATION FOR HIGH SPECIFIC IMPULSE

J. Bradley Pande *In* JHU, The 1993 JANNAF Propulsion Meeting, Volume 2 Nov. 1993 p 213-218 (For primary document see N95-16324 04-20)
Avail: CASI HC A02/MF A04

Hercules Aerospace is currently developing a solar-powered rocket engine (SPRE) design optimized for high specific impulse (Isp). The SPRE features a low loss geometry in its light-gathering cavity, which includes an integral secondary concentrator. The simple one-piece heat exchanger is made from refractory metal and/or ceramic open-celled foam. The foam's high surface-area-to-volume ratio will efficiently transfer the thermal energy to the hydrogen propellant. The single-pass flow of propellant through the heat exchanger further boosts thermal efficiency by regeneratively cooling surfaces near the entrance of the optical cavity. These surfaces would otherwise reradiate a significant portion of the captured solar energy back out of the solar entrance. Such design elements promote a high overall thermal efficiency and hence, a high operating Isp Author

N95-16342# California State Univ., Los Angeles, CA.

CONCEPTUAL DESIGN STUDY OF A SOLAR CONCENTRATOR/SUPPORT STRUCTURE: A THREE DIMENSIONAL FINITE ELEMENT MODEL

R. Purasinghe and K. K. Lau (Phillips Lab., Edwards AFB, CA.) *In* JHU, The 1993 JANNAF Propulsion Meeting, Volume 2 Nov. 1993 p 219-231 Sponsored by AFOSR (For primary document see N95-16324 04-20)
Avail: CASI HC A03/MF A04

Under the space environment the paraboloid solar concentrators and support structures can deform and hence the focal point of the concentrators can diffuse. If this diffusion is large, energy will not concentrate on the thruster as desired. This paper addresses this aspect of pointing and

accuracy analysis of solar concentrators, due to equivalent thrust loads. The previous studies were limited to the concentrator system being modeled with a simplified finite element model that includes only the support struts and torus. The torus model was made up of several equal length beams. The simple model did not contain the paraboloid reflector, and assumes the reflector does not effect the deformation of the torus. In the present study the inflated parabolic reflector is included in the model. The results demonstrate the nonuniform displacements on the reflector that confirms the reflector's potato chipping effect. Author

N95-16343# Spectra Research Systems, Inc., Huntsville, AL.
PREDICTION OF THE RESPONSE OF A POLYIMIDE CONCENTRATOR FOR SOLAR THERMAL PROPULSION
Paul Armin Gierow and James D. Moore *In* JHU, The 1993 JANNAF Propulsion Meeting, Volume 2 Nov. 1993 p 233-242 (For primary document see N95-16324 04-20)
(Contract F29601-92-C-0076)
Avail: CASI HC A02/MF A04

Solar Thermal propulsion requires the use of large solar collectors to focus solar energy into an absorber which heats a propellant gas that is expanded through a nozzle creating thrust. The solar thermal rocket offers specific heat impulse (Isp) on the order of 900-1000 seconds at moderate thrust levels for orbiter transfer vehicles. These Isp and thrust levels are contingent on proper design, fabrication and operation of large solar collectors. Thin film polyimide materials developed by NASA Langley Research Center (LaRC) have been used to construct large inflatable concentrators for space deployable collectors. Concentrators of sizes up to five meters in diameter have been cast and cured in the laboratory with a 0.0254mm (0.001 in) film thickness. The films are cast on double curvature mandrels in solution form and cured, resulting in a large one piece parabolic concentrator without seams. The polyimide films do not exhibit orthotropic material properties when fabricated using these processes. An analytical model of a uniformly loaded parabolic membrane was developed to predict the deflection of the membrane under prescribed loading conditions and varying material properties. A symmetrical parabolic and off-axis geometry concentrator have been modeled. The analytical model uses finite element analysis of a membrane material under a variety of stress conditions. Prediction of the deformations of the membrane as a result of material properties and loading conditions is required to select and develop appropriate polyimide materials. The predicted membrane deflections are also integrated into an optical ray trace program to estimate the solar flux distribution at the focal point of the primary collector. The edge effects of inflatable concentrators can greatly affect the flux distribution at the focal plane of the concentrator. The overall concentration ratio of a primary collector directly relates to the achievable working fluid temperatures. This paper will present the analytical results of the finite element and ray trace analyses performed to support the fabrication of operational thin film polyimide concentrators. Author

N95-16344# Thiokol Corp., Brigham City, UT.
FOAM INFLATED RIGIDIZED STRUCTURES FOR SPACE APPLICATIONS **c18**
D. M. Lester, M. J. Warner, and M. Blair *In* JHU, The 1993 JANNAF Propulsion Meeting, Volume 2 Nov. 1993 p 243-251 (For primary document see N95-16324 04-20)
Avail: CASI HC A02/MF A04

Large lightweight stowable structures that can be deployed in space without astronaut extra vehicular activity are vital to expanding space exploration and utilization. To meet this challenge Foam Inflated Rigidized (FIR) structures have been developed by Thiokol Corporation on the Air Forces's Gossamer Baggie Torus program. In this paper the development, proof of concept demonstration of an eight foot diameter octagonal torus, and design application of this technology for structural elements to stabilize the solar collector of a solar thermal rocket are discussed. A FIR structure uses foam to inflate and pre-stress a resin impregnated fabric skin. The predeployed foam used was a solvent swelled polymer that foams immediately when exposed to vacuum due to rapid solvent loss. This property allows a very simple deployment mechanism to be used in erecting these structures. Once inflated, the skin resin is cured using the available ultraviolet radiation. By using high strength and stiffness fiber materials a stiff, strong lightweight structure was produced. Author

N95-16345*# National Aeronautics and Space Administration. John F. Kennedy Space Center, Cocoa Beach, FL.
GENERIC PROPELLANT TRANSFER UNIT: A PROJECT UPDATE **c28**
C. L. Davis *In* JHU, The 1993 JANNAF Propulsion Meeting, Volume 2 Nov. 1993 p 253-268 (For primary document see N95-16324 04-20)
Avail: CASI HC A03/MF A04

Currently, most satellite programs use dedicated hypergolic propellant ground servicing equipment. These 'carts' are typically program specific (non-interchangeable), costly, and non-Department of Transportation (DOT) compliant. They require safety waivers when used on government property and must be emptied before off-site transport. The emptying process usually generates large amounts of Hazardous Wastes. Fuel carts are usually loaded from multiple 208-liter (55 gallon) drums and oxidizer carts from 909-kg (2000 lb) cylinders. This further increases operating costs due to additional container samples and cart-filling transfers. NASA, Kennedy Space Center has developed reusable, generic, DOT compliant propellant delivery containers as possible replacements for the propellant-tank portion of servicing carts. Our ultimate goal is to reduce operating expenses by minimizing propellant transfers, samples, and waste generation through use of bulk propellant operations, minimizing drum or cylinder operations. This has the added benefit of increasing operating safety by decreasing overall propellant operations. Author

N95-16346*# National Aeronautics and Space Administration. Lewis Research Center, Cleveland, OH.
TESTING AND EVALUATION OF OXIDE-COATED IRIDIUM/RHENIUM CHAMBERS
Brian D. Reed *In* JHU, The 1993 JANNAF Propulsion Meeting, Volume 2 Nov. 1993 p 269-278 (For primary document see N95-16324 04-20)
Avail: CASI HC A02/MF A04

Iridium-coated rhenium provides long life operation of radiation-cooled rockets at temperatures up to 2200 C. Ceramic oxide coatings could be used to increase iridium/rhenium rocket lifetimes and allow operation in highly oxidizing environments. Ceramic oxide coatings promise to serve as both thermal and diffusion barriers for the iridium layer. Seven ceramic oxide-coated iridium/rhenium, 22 N rocket chambers were tested on gaseous hydrogen/gaseous oxygen propellants. Five chambers had thick (over 10 mils), monolithic coatings of either hafnia or zirconia. Two chambers had coatings with thicknesses less than 5 mils. One of these chambers had a thin-walled coating of zirconia infiltrated with sol gel hafnia. The other chamber had a coating composed of an iridium/oxide composite. The purpose of this test program was to assess the ability of the oxide coatings to withstand the thermal shock of combustion initiation, adhere under repeated thermal cycling, and operate in aggressively oxidizing environments. All of the coatings survived the thermal shock of combustion and demonstrated operation at mixture ratios up to 11. The iridium/oxide composite coated chamber included testing for over 29 minutes at mixture ratio 16. The thicker-walled coatings provided the larger temperature drops across the oxide layer (up to 570 C), but were susceptible to macrocracking and eventual chipping at a stress concentrator. The cracks apparently resealed during firing, under compression of the oxide layer. The thinner-walled coatings did not experience the macrocracking and chipping of the chambers seen with the thick, monolithic coatings. However, burnthroughs in the throat region did occur in both of the thin-walled chambers at mixture ratios well above stochiometric. The burn-throughs were probably the result of oxygen-diffusion through the oxide coating that allowed the underlying iridium and rhenium layers to be oxidized. The results of this test program indicated that the thin-walled oxide coatings are better suited for repeated thermal cycling than the thick-walled coating, while thicker coatings may be required for operation in aggressively oxidizing environments. Author

N95-16347*# Ultramet Co., Pacoima, CA.
DESIGN, ANALYSIS, AND FABRICATION OF OXIDE-COATED IRIDIUM/RHENIUM COMBUSTION CHAMBERS
Q. Jang, R. H. Tuffias, R. LaFerla, and N. M. Ghoniem (California Univ., Los Angeles, CA.) *In* JHU, The 1993 JANNAF Propulsion Meeting, Volume 2 Nov. 1993 p 279-288 (For primary document see N95-16324 04-20)
(Contract NAS3-26253)
Avail: CASI HC A02/MF A04

Iridium-coated rhenium (Ir/Re) combustion chambers provide high temperature, oxidation-resistant operation for radiation-cooled liquid-fueled rocket engines. A 22-N (5-lb(sub f)) chamber has been operated for 15 hours at 2200 C (4000 F) using nitrogen tetroxide/monomethyl hydrazine (NTO/MMH) propellant, with negligible internal erosion. The oxidation resistance of these chambers could be further increased by the addition of refractory oxide coatings, providing longer life and/or operation in more oxidizing and higher temperature environments. The oxide coatings would serve as a thermal and diffusion barrier for the iridium coating, lowering the temperature of the iridium layer while also preventing the ingress of oxygen and egress of iridium oxides. This would serve to slow the failure mechanisms of Ir/Re chambers, namely the diffusion of rhenium to the inner surface and the oxidation of iridium. Such protection could extend chamber lifetimes by tens or perhaps hundreds of hours, and allow chamber operation on stoichiometric or higher mixture ratio oxygen/hydrogen (O2/H2) propellant. Extensive thermomechanical, thermochemical, and mass transport modeling was performed as a key material/structure design tool. Based on the results of these analyses, several 22-N oxide-coated Ir/Re chambers were fabricated and delivered to NASA Lewis Research Center for hot-fire testing. Author

N95-16348# Sverdrup Technology, Inc., Arnold AFS, TN.
STRUCTURAL ANALYSIS OF SOLID-PROPELLANT ROCKET MOTORS WITH AND WITHOUT FLAWS
L. R. Deken *In* JHU, The 1993 JANNAF Propulsion Meeting, Volume 2 Nov. 1993 p 289-295 (For primary document see N95-16324 04-20)
Avail: CASI HC A02/MF A04

The results of a study to define a procedure for the structural analysis of Solid Rocket Motors (SRM) are presented. Flaws have been shown to have a significant impact on the structural integrity of a SRM during a firing and therefore, must be included in the analysis procedure. Since costs associated with the failure of a SRM can be extensive, an intelligent decision on the success of a firing can only be made if an analysis of its structural integrity is made. For a complete structural integrity analysis, the structural analysis must ce coupled with a SRM propellant grain recession, crack combustion, and a fracture, crack, or debond analysis. This study concentrates on the structural analysis and includes the evaluation of element types, model types, material property requirements and availability, and flaw analysis capabilities. Author

N95-16349# Marotta Scientific Controls, Inc., Montville, NJ.
A LIFTING BALL VALVE FOR CRYOGENIC FLUID APPLICATIONS **c37**
Joseph M. Cardin, Robert H. Reinicke, and Stephen D. Bruneau *In* JHU, The 1993 JANNAF Propulsion Meeting, Volume 2 Nov. 1993 p 297-312 (For primary document see N95-16324 04-20)
Avail: CASI HC A03/MF A04

Marotta Scientific Controls, Inc. has designed a Lifting Ball Valve (LBV) capable of both flow modulation and tight shutoff for cryogenic and other applications. The LBV features a thin-walled visor valving element that lifts off the seal with near axial motion before rotating completely out of the flow path. This is accomplished with a simple, robust mechanism that minimizes cost and weight. Conventional spherical rotating seats ar plagued by leakage due to 'scuffing' as the seal and seat slide against one another while opening. Cryogenic valves, which typically utilize plastic seals, are particularly susceptible to this type of damage. The seat in the LBV lifts off the seal without 'scuffing' making it immune to this failure mode. In addition, the LBV lifting mechanism is capable of applying the very high seating loads required to seal at cryogenic temperatures. These features make the LBV ideally suited for cryogenic valve applications. Another major feature of the LBV is the fact that the visor rotates completely out of the flow path. This allows for a smaller, lighter valve for a given flow capacity, especially for line sizes above one inch. The LBV is operated by a highly integrated 'wetted' DC brushless motor. The motor rotor is 'wetted' ion that it is immersed in the fluid. To ensure compatibility, the motor rotor is encased in a thin-walled CRES weldment. The motor stator is outside the fluid containment weldment and therefore is not in direct contact with the fluid. To preclude the potential for external leakage there are no static or dynamic seals or bellows across the pressure boundary. The power required to do the work of operating the valving mechanism is transmitted across the pressure boundary by electromagnetic interaction between the motor rotor and the stator. Commutation of the motor is accomplished using the output of a special 'wetted' resolver. This paper describes the design, operation, and element testing of the LBV. Author

N95-16350# Atlantic Research Corp., Gainesville, VA.
FILAMENT OVERWRAPPED MOTOR CASE TECHNOLOGY
Joel P. Compton *In* JHU, The 1993 JANNAF Propulsion Meeting, Volume 2 Nov. 1993 p 321-330 (For primary document see N95-16324 04-20)
(Contract N00060-86-C-4971)
Avail: CASI HC A02/MF A04

Atlantic Research Corporation (ARC) joined with the French Societe Europeenne de Propulsion (SEP) to develop and deliver to the U.S. Navy a small quantity of composite filament wound rocket motors to demonstrate a manufacturing technique that was being applied at the two companies. It was perceived that the manufacturing technique could produce motors that would be light in weight, inexpensive to produce, and that had a good chance of meeting insensitive munitions (IM) requirements that were being formulated by the Navy in the early 1980s. Under subcontract to ARC, SEP designed, tested, and delivered 2.75-inch rocket motors to the U.S. Navy for IM tests that were conducted in 1989 at China Lake, California. The program was one of the first to be founded by Nunn Amendment money. The Government-to-Government program was sponsored by the Naval Air Systems Command and was monitored by the Naval Surface Warfare Center, Indian Head (NSWC-IH), Maryland. The motor propellant that was employed was a new, extruded composite formulation that was under development at the Naval Surface Warfare Center. The following paper describes the highlights of the program and gives the results of structural and ballistic static tests and insensitive munitions tests that were conducted on demonstration motors. Author

N95-16351# Naval Air Warfare Center, China Lake, CA. Weapons Div.
OVERVIEW OF TTCP AND AGARD PROPULSION ACTIVITIES **c82**
R. L. Derr and C. F. Markarian *In* JHU, The 1993 JANNAF Propulsion Meeting, Volume 2 Nov. 1993 p 331-343 (For primary document see N95-16324 04-20)
Avail: CASI HC A03/MF A04

This paper reviews two important international programs that serve as multinational exchanges for propulsion technology. The purpose of the paper is to provide information for members of the JANNAF Interagency propulsion committee propulsion community to understand how these programs operate and how to obtain information from propulsion activities associated with these programs. Author

N95-17265*# Sverdrup Technology, Inc., Brook Park, OH.
EXTENDED TEST OF A XENON HOLLOW CATHODE FOR A SPACE PLASMA CONTACTOR Final Report
Timothy R. Sarver-Verhey Nov. 1994 21 p Presented at the International Electric Propulsion Conference, Seattle, WA, 13-17 Sep. 1993; sponsored by AIAA, AIDAA, DGLR, and JSASS
(Contract NAS3-25266; RTOP 506-42-31)
(NASA-CR-195402; E-9246; NAS 1.26:195402) Avail: CASI HC A03/MF A01

Implementation of a hollow cathode plasma contactor for charge control on the Space Station has required validation of long-life hollow cathodes. A test series of hollow cathodes and hollow cathode plasma contactors was initiated as part of the plasma contactor development program. An on-going wear-test of a hollow cathode has demonstrated cathode operation in excess of 4700 hours with small changes in operating parameters. The discharge experienced 4 shutdowns during the test, all of which were due to test facility failures or expellant replenishment. In all cases, the cathode was reignited at approximately 42 volts and resumed typical operation. This test represents the longest demonstrated stable operation of a high current (greater than 1A) xenon hollow cathode reported to date. Author

N95-17269*# National Aeronautics and Space Administration. Lewis Research Center, Cleveland, OH.
MULTI-OBJECTIVE DECISION-MAKING UNDER UNCERTAINTY: FUZZY LOGIC METHODS
Terry L. Hardy Dec. 1994 16 p Presented at the Computing in Aerospace 10 Meeting, San Antonio, TX, 28-30 Mar. 1995; sponsored by AIAA

(RTOP 323-41-22)
(NASA-TM-106796; E-9263; NAS 1.15:106796) Avail: CASI HC A03/MF A01

Selecting the best option among alternatives is often a difficult process. This process becomes even more difficult when the evaluation criteria are vague or qualitative, and when the objectives vary in importance and scope. Fuzzy logic allows for quantitative representation of vague or fuzzy objectives, and therefore is well-suited for multi-objective decision-making. This paper presents methods employing fuzzy logic concepts to assist in the decision-making process. In addition, this paper describes software developed at NASA Lewis Research Center for assisting in the decision-making process. Two diverse examples are used to illustrate the use of fuzzy logic in choosing an alternative among many options and objectives. One example is the selection of a lunar lander ascent propulsion system, and the other example is the selection of an aeration system for improving the water quality of the Cuyahoga River in Cleveland, Ohio. The fuzzy logic techniques provided here are powerful tools which complement existing approaches, and therefore should be considered in future decision-making activities. Author

N95-17274*# National Aeronautics and Space Administration. Lewis Research Center, Cleveland, OH.
AN OBJECT-ORIENTED GRAPHICAL USER INTERFACE FOR A REUSABLE ROCKET ENGINE INTELLIGENT CONTROL SYSTEM
Jonathan S. Litt (Army Research Lab., Cleveland, OH.), Jeffrey L. Musgrave, Ten-Huei Guo, Daniel E. Paxson, Edmond Wong, Joseph R. Saus, and Walter C. Merrill Oct. 1994 24 p Original contains color illustrations
(RTOP 468-01-11; DA Proj. 1L1-61102-AH-45)
(NASA-TM-106750; E-9166; NAS 1.15:106750; ARL-TR-598) Avail: CASI HC A03/MF A01; 8 functional color pages

An intelligent control system for reusable rocket engines under development at NASA Lewis Research Center requires a graphical user interface to allow observation of the closed-loop system in operation. The simulation testbed consists of a real-time engine simulation computer, a controls computer, and several auxiliary computers for diagnostics and coordination. The system is set up so that the simulation computer could be replaced by the real engine and the change would be transparent to the control system. Because of the hard real-time requirement of the control computer, putting a graphical user interface on it was not an option. Thus, a separate computer used strictly for the graphical user interface was warranted. An object-oriented LISP-based graphical user interface has been developed on a Texas Instruments Explorer 2+ to indicate the condition of the engine to the observer through plots, animation, interactive graphics, and text. Author

N95-17276*# National Aeronautics and Space Administration. Lewis Research Center, Cleveland, OH.
A MODULAR ELECTRIC POWER SYSTEM TEST BED FOR SMALL SPACECRAFT
Robert M. Button and Anastacio N. Baez Dec. 1994 11 p Presented at the 33rd Aerospace Sciences Meeting and Exhibit, Reno, NV, 9-12 Jan. 1995; sponsored by AIAA
(RTOP 233-01-OC)
(NASA-TM-106812; E-9335; NAS 1.15:106812; AIAA Paper 95-0030)
Avail: CASI HC A03/MF A01

In the new climate of smaller, faster, and cheaper space science satellites, a new power system topology has been developed at the NASA Lewis Research Center. This new topology is based on a series connected boost converter (SCBC) and can greatly affect the size, weight, fault tolerance, and cost of any small spacecraft using photovoltaic solar arrays. The paper presents electric power system design factors and requirements as background information. The series connected boost converter topology is discussed and several advantages over existing technologies are illustrated. Besides being small, lightweight, and efficient, this topology has the added benefit of inherent fault tolerance. A positive ground power system test bed has been developed for the TROPIX spacecraft program. Performance of the SCBC in the test bed is described in detail. SCBC efficiencies of 95 percent to 98 percent have been measured. Finally, a modular, photovoltaic regulator 'kit' concept is presented. Two SCBC's are used to regulate solar array charging of batteries and to provide 'utilitytype' power to the user loads. The kit's modularity will allow a spacecraft electric power system to be built from off-the-shelf hardware; resulting in smaller, faster, and cheaper spacecraft. Author

N95-17278# Advisory Group for Aerospace Research and Development, Neuilly-Sur-Seine (France). Propulsion and Energetics Panel.
EXPERIMENTAL AND ANALYTICAL METHODS FOR THE DETERMINATION OF CONNECTED-PIPE RAMJET AND DUCTED ROCKET INTERNAL PERFORMANCE [METHODES EXPERIMENTALES ET ANALYTIQUES POUR LA DETERMINATION EN CONDUITE FORCEE DES PERFORMANCES DES STATOREACTEURS ET DES STATOFUSEES]
Jul. 1994 103 p
(AGARD-AR-323; ISBN-92-835-0755-X) Copyright Avail: CASI HC A06/MF A02

Connected-pipe, subsonic combustion ramjet and ducted rocket performance determination procedures used by the NATO countries have been reviewed and evaluated. A working document has been produced which provides recommended methods for reporting test results and delineates the parameters that are required to be measured. Explanations and detailed numerical examples are presented covering the determination of both theoretical and experimental performances, the use of air heaters and uncertainty and error analysis. Author

N95-17448 Naval Postgraduate School, Monterey, CA.
EROSION EFFECTS ON TVC VANE HEAT TRANSFER CHARACTERISTICS M.S. Thesis
Steven R. Gardner Mar. 1994 115 p Limited Reproducibility: More than 20% of this document may be affected by microfiche quality
(AD-A282006) Avail: Issuing Activity (Defense Technical Information Center (DTIC))

This work describes the effects of erosion on the heat transfer characteristics on thrust vector control vanes exposed to aluminized propellant exhaust flows. This was accomplished using an inverse heat transfer parameter identification of quarter scale models. The model is based on a four node lumped parameter system with two heat energy inputs. The erosion is modeled as decreasing the geometric dimensions linearly as function of time and percentage of aluminum in the propellant. Excellent agreement was found between experimental and model temperature profiles. The heat transfer coefficients of the vanes were found to decrease with increasing erosion rates. DTIC

N95-17626 Naval Postgraduate School, Monterey, CA.
AN ANALYSIS OF A SINGLE-BURN ALGORITHM FOR LOW-EARTH ORBIT MAINTENANCE M.S. Thesis
Paul A. Gardner Jun. 1994 88 p Limited Reproducibility: More than 20% of this document may be affected by microfiche quality
(AD-A283418) Avail: CASI HC A05

With the requirement for a spacecraft to maintain an orbital altitude band, a simple energy balance algorithm has been developed using a combination of radial distance and spacecraft specific energy for fixed-vector thruster control. While each trajectory produces a unique band, initial attempts at producing a prespecified band have been unsuccessful. It is theorized that a certain radial bandwidth would correspond to a specific set of control parameters, and that by creating maps of the relationship between the two for various spacecraft configurations a method of maintaining the prespecified band could be found. This thesis studies variations in spacecraft configurations and finds dependence of orbital bandwidth on thrust-to-drag ratio and ballistic coefficient. Also, within certain ranges of control parameters, multiple trajectories produce equivalent radial bands. Analysis shows that all single-burn trajectories are characterized by similar efficiencies, and are less efficient than a forced Keplerian trajectory (FKT). DTIC

23 CHEMISTRY AND MATERIALS (GENERAL)

N95-16035*# Colorado Univ., Boulder, CO. Dept. of Chemical Engineering.
PHASE SEGREGATION DUE TO SIMULTANEOUS MIGRATION AND COALESCENCE Progress Report, Jan. - Nov. 1994

Robert H. Davis 1994 7 p
(Grant NAG3-1389)
(NASA-CR-196819; NAS 1.26:196819) Avail: CASI HC A02/MF A01

The primary objective of the research is to perform ground-based analysis and experiments on the interaction and coalescence of drops (or bubbles) leading to macroscopic phase separation. Migration of the drops occurs as a result of the individual and collective action of gravity and thermocapillary effects. Larger drops migrate faster than smaller ones, leading to the possibility of collisions and coalescence. Coalescence increases the rate of macroscopic phase separation, since the result is larger drops with higher migration rates. It is hoped that the understanding gained will lead to the design of microgravity experiments to further elucidate the mechanisms governing coalescence and phase separation. Derived from text

N95-16058# Ames Lab., IA.
THE MECHANISM OF THE OLIGOMERIZATION OF THIOPHENE-BASED PARA-QUINODIMETHANES Ph.D. Thesis
Yili Wang 24 Apr. 1994 97 p
(Contract W-7405-eng-82)
(DE94-014232; IS-T-1685) Avail: CASI HC A05/MF A02

For the last decade, the Trahanovsky research group has focused on the study of various reactive molecules such as o-quinodimethanes (o-QDM's) and p-quinodimethanes (p-QDM's) derived from benzene, furan, and thiophene. These types of molecules are reactive and dimerize or polymerize at room temperature. One of the group's interests is to understand the dimerization mechanism of these molecules. Paper 1 describes the preparation and dimerization product analyses of 2-ethylidene-5-methylene-2,5-dihydrothiophene. Insights provided by these results into the mechanism of the dimerization of 2,5-dimethylene-2,5-dihydrothiophene are discussed. In paper 2, a convenient synthesis of cyclooctadecane is presented. DOE

N95-16087 University of Western Michigan, Kalamazoo, MI. Dept. of Chemistry.
THE REMOVAL OF HETEROATOMS FROM ORGANIC COMPOUNDS BY SUPERCRITICAL WATER Final Report, 15 Mar. 1990 - 14 Dec. 1993
Thomas Houser 14 Mar. 1994 11 p Limited Reproducibility: More than 20% of this document may be affected by microfiche quality
(Contract DAAL03-90-G-0028)
(AD-A281532; ARO-27505.5-CH) Avail: Issuing Activity (Defense Technical Information Center (DTIC))

This study was initiated to determine if and under what conditions supercritical water (SW) would facilitate the removal of heteroatoms (specifically N, Cl and S) from organic compounds. These atoms are representative of those which are present in many hazardous materials which may require efficient methods of disposal. The compounds investigated were: trihexylamine, quinuclidine, benzylidene benzylamine, quinoline, phenylpiperidine, phenylpyridine, nitrotoluene, dinitrotoluene, ethyl benzilate, cyclohexyl acetate, benzaldehyde, benzyl alcohol, benzyl benzoate, benzoic acid, 1-chlorohexane, 1-chlorododecane, 1-phenyl-3-chloropropane, 2-chlorotoluene, benzyl sulfide and thianaphthene. It was found that some compounds could be converted in good yields to useful materials in SW, particularly with the aid of catalytic additives. This may be a useful alternative to using methods such as oxidation/combustion for their complete destruction. The presence of SW was effective, without the aid of a catalyst, in facilitating the removal of aromatic Cl atoms, which were fairly unreactive under pyrolytic conditions. Finally, the HCl formed from chloro compounds quantitatively reacted with the reactors' metal walls producing hydrogen and metal chlorides. DTIC

N95-16100# Texas Univ., Austin, TX. Dept. of Chemistry and Biochemistry.
AUGMENTATION FOR RESEARCH TRAINING: SURFACE-MEDIATED PHOTOCATALYSIS Final Report, 5 Jan. 1992 - 30 Apr. 1994
Marye A. Fox Jun. 1994 4 p
(Contract DAAL03-92-G-0089)
(AD-A281591; ARO-29548.8-CH-AAS) Avail: CASI HC A01/MF A01

Three areas have been investigated: application of esr spectroscopy and time-resolved reflectance absorption and emission spectroscopy to establish mechanisms in photocatalytic oxidative degradations of organic molecules; exploration of controlled oxidation chemistry for new heteroatom-containing organic molecules; and synthesis and characterization of new quantized semiconductor-support systems. We have successfully demonstrated that photocatalytic oxidation on irradiated semiconductor surfaces is a useful route for degradation of various organic materials under constrained, highly controlled conditions. DTIC

N95-16513# North Dakota State Univ., Fargo, ND.
NEW APPROACHES TO NOVEL ORGANOSILANES Final Technical Report, 1 Apr. 1993 - 31 Mar. 1994
Philip Boudjouk 30 Apr. 1994 21 p Sponsored by AFOSR
(AD-A285253; AFOSR-94-0599TR) Avail: CASI HC A03/MF A01

This report summarizes the results of research in the following areas: (1) the completion of a project on di-t-butylsilylene; (2) a novel route tobinary semiconducting materials composed from the elements tin, germanium, lead, sulfur, selenium, and tellurium; (3) a new method of making ternary composites using the elements mentioned in 2; (4) the development of convenient procedures for making gallium arsenide, gallium phosphide and indium phosphide; (5) expansion of the chemistry ofsiliranes; (6) the synthesis of three stable aromatic species containing silicon; (7) the synthesis of the first stable adduct of dichlorosilane; (8) the initial studies on the synthesis of silicon-based dendrimers; (9) the initial studies on the synthesis of doped silicon carbides; (10) the development of a new procedure for preparing very high molecular weight polysilanes. Silylenes DTIC

N95-16734# Prins Maurits Lab. TNO, Rijswijk (Netherlands).
MASS SPECTRAL DATA OF ALKYL AND CYCLOALKYL METHYLPHOSPHONOFLUORIDATES
E. R. J. Wils and A. L. deJong Jul. 1994 35 p
(AD-A285312; PML-1994-A24; TDCK-94-0028) Avail: CASI HC A03/MF A01

Electron impact (EI) mass spectra of over 60 alkyl and cycloalkyl methylphosphonofluoridates (alkyl/cycloalkyl greater or equal C10) were recorded and taken up in databases. Each compound was prepared in situ by mixing an alcohol with methylphosphonodifluoride followed by gas chromatographic-mass spectrometric analysis (GC-MS) of the reaction mixture. The choice of the alcohols was restricted to relatively inexpensive, primary and secondary alcohols. The EI mass spectra and a short description of the fragmentation patterns of the methylphosphonofluoridates are presented. DTIC

N95-16905*# National Aeronautics and Space Administration. Lewis Research Center, Cleveland, OH.
STATIC AND DYNAMIC FRICTION BEHAVIOR OF CANDIDATE HIGH TEMPERATURE AIRFRAME SEAL MATERIALS
C. DellaCorte, V. Lukaszewicz (Calspan Corp., Fairview Park, OH.), D. E. Morris (Rockwell International Corp., Canoga Park, CA.), and B. M. Steinetz Dec. 1994 20 p
(Contract NAS3-25685; RTOP 505-63-1A)
(NASA-TM-106571; E-8774; NAS 1.15:106571) Avail: CASI HC A03/MF A01

The following report describes a series of research tests to evaluate candidate high temperature materials for static to moderately dynamic hypersonic airframe seals. Pin-on-disk reciprocating sliding tests were conducted from 25 to 843 C in air and hydrogen containing inert atmospheres. Friction, both dynamic and static, was monitored and serves as the primary test measurement. In general, soft coatings lead to excessive static friction and temperature affected friction in air environments only. Author

N95-17745# Lawrence Livermore National Lab., Livermore, CA.
COMPUTER MODELING OF ORGANIC AEROGELS, 93-SR-062 Final Report
E. A. Chandler, D. Calef, and A. J. C. Ladd 10 Jun. 1994 5 p
(Contract W-7405-eng-48)
(DE94-016485; UCRL-ID-117435) Avail: CASI HC A01/MF A01

Goal of the work was to develop computer models of organic aerogel structures, and to study transport process within these materials. During the course of the research understanding of the structure of all aerogels including acid and neutral-catalyzed silica aerogel was developed. The modeling of transport focused on fluid flow in aerogels. We successfully modified a novel state-of-the-art lattice Boltzmann code to simulate flow at low Knudsen number, and developed a simple molecular dynamics code

for gas flow at extremely high Knudsen number (low density). These flow-modeling techniques can be used to study aerogel applications for technology transfer; in addition, these techniques can be used to study flow through other porous materials. DOE

24 COMPOSITE MATERIALS

Includes physical, chemical, and mechanical properties of laminates and other composite materials.

For ceramic materials see *27 Nonmetallic Materials.*

N95-16016# Cornell Univ., Ithaca, NY. Dept. of Materials Science and Engineering.

CORNELL PROGRAM FOR THE DESIGN AND SYNTHESIS OF ADVANCED MATERIALS Annual Report No. 1 May 1993 - 30 Apr. 1994

Stephen L. Sass May 1994 48 p

(Contract F49620-93-1-0235)

(AD-A281352; TR-5; AFOSR-94-0412TR) Avail: CASI HC A03/MF A01

The fracture toughness of brittle ceramic materials can be increased by the addition of a dispersed second phase such as a ductile metal. Metal-ceramic and ceramic-ceramic microstructures are produced by a variety of in situ processing techniques. The mechanical properties are evaluated for correlation with the microstructures as a means of searching for optimum properties. Mechanics modeling is performed to calculate the mechanical properties associated with the microstructures. After checking the validity of the predictions of the mechanics calculation by comparison with the experimental measurements of the mechanical properties, the theoretical models are used to predict microstructures, e.g. size, morphology, and distribution of metallic and ceramic phases, that give optimum mechanical properties. Derived from text

N95-16019# University of Southern Mississippi, Hattiesburg, MS.

PROPERTY CONTROL OF (PERFLUORINATED IONOMER)/(INORGANIC OXIDE) COMPOSITES BY TAILORING THE NANOSCALE MORPHOLOGY Annual Report No. 1, Apr. 1993 - 31 Mar. 1994

Kenneth A. Mauritz and Robert B. Moore 10 Jun. 1994 158 p

(Contract F49620-93-1-0189)

(AD-A281370; AFOSR-94-0417TR) Avail: CASI HC A08/MF A02

Unique perfluoro-organic/inorganic oxide hybrid materials have been formulated by merging processes recently developed by us for the solution and melting processing of perfluorosulfonate ionomers (PFSI's) and the production of nanocomposites by the in situ sol-gel reaction for silicon and metal alkoxides within the polar clusters of PFSI's. Our working hypothesis is that the resultant morphology of the inorganic phase is ordered by the nanophase-separated morphology of the PFSI matrix. The three-dimensional morphological template presented by the PFSI is tailored by manipulating the primary polymer structure, polymer solution conditions, film casting procedure, and post-processing (e.g. drying, annealing, melt-quenching, and mechanical orientation). The nanocomposites are then characterized for microstructure broadly ranging from light microscopic resolution down to the level of Angstroms using various microscopic, scattering, diffraction, and spectroscopic methods. DTIC

N95-16041# Colorado State Univ., Fort Collins, CO. Dept. of Chemistry.

ANIONICALLY-CONDUCTIVE ULTRATHIN FILM COMPOSITE MEMBRANES Annual Technical Report, 1 Jun. 1993 - 31 May 1994

Charles R. Martin 19 Aug. 1994 8 p

(Contract F49620-83-1-0343)

(AD-A284944; Rept-53-2452; AFOSR-94-0550TR) Avail: CASI HC A02/MF A01

As noted in the previous technical report, we are interested in using interfacial polymerization to synthesize ultrathin film composite membranes based on electronically conductive polymers. During the previous year of AASERT funding we have expanded on this idea in a number of ways. We have done such interfacial polymerizations to make new composites for membrane-based separations, and to make novel coated-hollow fiber membranes. DTIC

N95-16126# Georgia Tech Research Inst., Atlanta, GA.

STUDY OF THE COMPRESSION BEHAVIOR OF HIGH PERFORMANCE FIBERS Annual Report, 1 Apr. 1993 - 30 Jun. 1994

Satish Kumar 25 Aug. 1994 115 p

(Grant AF-AFOSR-0194-91)

(AD-A284959; AFOSR-94-0560TR) Avail: CASI HC A06/MF A02

Kink band analysis has been carried out in PBZT, methyl PBZT, and Kevlar samples. Methyl PBZT and methyl PBO samples heat treated to various times and temperatures have been studied using swelling behavior in 85% and 100% methane sulfonic acid. Raman spectroscopic studies have been carried out on PAN precursor fiber, and the fiber stabilized and carbonized at different temperature (270, 400, 800, 1800, 2800 deg C). A study on the compression behavior of polymeric resins has been conducted. A review has been written on the compression behavior of polymeric materials. PBO/sulfuric acid interaction has been studied using thermogravimetric analysis, wide angle x-ray diffraction, and using 13C solid state NMR. DTIC

N95-16225# Oak Ridge National Lab., TN.

CHEMICAL VAPOR INFILTRATION OF NON-OXIDE CERAMIC MATRIX COMPOSITES

T. M. Besmann, D. P. Stinton, and R. A. Lowden 1993 9 p Presented at the Fall Meeting of the Materials Research Society (MRS), Boston, MA, 29 Nov. - 3 Dec. 1993

(Contract DE-AC05-84OR-21400)

(DE94-017770; CONF-931108-105) Avail: CASI HC A02/MF A01

Continuous fiber ceramic composites are enabling new, high temperature structural applications. Chemical vapor infiltration methods for producing these composites are being investigated, with the complexity of filament weaves and deposition chemistry merged with standard heat and mass transport relationships. Silicon carbide- based materials are, by far, the most mature, and are already being used in aerospace applications. This paper addresses the state-of-the-art of the technology and outlines current issues. DOE

N95-16397 Academy of Sciences (USSR), Moscow (USSR). Inst. of Applied Mechanics.

US-RUSSIAN WORKSHOP ON COMPUTER SYNTHESIS OF STRUCTURE AND PROPERTIES OF ADVANCED COMPOSITES Final Report

Yuri G. Yanovsky 13 May 1994 86 p Limited Reproducibility: More than 20% of this document may be affected by microfiche quality

(Contract DAAH04-94-G-0090)

(AD-A281647; ARO-33007.1-MS-CF) Avail: CASI HC A05

The objective of this workshop is to discuss the results of recent studies and experience accumulated by Russian and American scientists in the development of fundamental theoretical concepts, computer programs, methodology, and techniques for numerical and experimental modeling of structure and mechanical properties of advanced composite materials, in particular with polymer matrices. DTIC

N95-16415 California Univ., Santa Barbara, CA. Dept. of Materials.

EXPERIMENTAL STUDIES OF STRESS MEASUREMENT BY OPTICAL FLUORESCENCE Final Report, Jan. 1991 - Dec. 1993

David R. Clarke Dec. 1993 137 p Limited Reproducibility: More than 20% of this document may be affected by microfiche quality

(Contract N00014-91-J-1875)

(AD-A282337) Avail: CASI HC A07

A new method for the noncontact measurement of stresses in ceramics has been developed and applied to measuring the stress distribution in a wide variety of composites and polycrystalline ceramics. The basis of the technique is that stresses in a material alter the energy of the luminescence spectra from substitutional dopants. The technique of optical fluorescence was used to directly measure stress distribution and resolve a number of outstanding issues concerning residual stresses in composites. The residual stress distribution along sapphire fibers due to thermal expansion mismatch with the surrounding matrix were determined and used to test elasticity models for residual stress distribution. The report also introduced a method of obtaining the depth distribution along fibers by exploiting the finite depth of field of a microscope lens. The stress distribution in fibers was measured in-situ during the push-out of a fiber. By combining the measurements with finite element simulations, the residual stress distribution, the debond length

as a function of applied load, the debond energy, and the sliding stress were all determined for sapphire fibers having a variety of coatings in a TiAl matrix. Another method of obtaining the stress distribution, appropriate to long continuous fibers, is described. DTIC

N95-16492# Colorado State Univ., Fort Collins, CO. Dept. of Chemistry.
ELECTROCHEMICAL SYNTHESIS OF ULTRATHIN FILM COMPOSITE MEMBRANES Final Technical Report, 1 Apr. 1993 - 31 Mar. 1994
Charles R. Martin 19 Aug. 1994 8 p
(Contract F49620-93-1-0234)
(AD-A285075; AFOSR-94-0566TR) Avail: CASI HC A02/MF A01

During the duration of this contract we have explored a variety of aspects of a general theme. The general theme is that of 'ultrathin film composite membranes.' Such membranes resulted from the need to make membranes-based separations that show high chemical selectivity yet also show high permeant flux. We have shown in the AFOSR work that these two goals (usually mutually exclusive) can be achieved and are quite useful in a variety of areas including chemical sensors and electrochemistry. Author (DTIC)

N95-16597*# Texas A&M Univ., College Station, TX. Dept. of Aerospace Engineering.
FAILURE ANALYSIS OF 2D AND 3D WOVEN COMPOSITES (Diskette Supplement) Final Report, 1 Sep. 1991 - 31 Dec. 1994
John D. Whitcomb 31 Dec. 1994 166 p Diskette supplement: two 3.5-inch DSHD
(Grant NAG1-1324)
(NASA-CR-197247; NAS 1.26:197247; NONP-NASA-Suppl-DK-94-31824)
Avail: CASI SET A11 (HC,DK)

Part 1 of this report includes copies of publications resulting from NASA Grant NAG1-1324. In order to give a better overall view of the project, Part 1 begins with a summary of the primary conclusions and accomplishments. Specialized analysis software was developed as part of this project. Part 2 documents the use of this software. Part 2 includes user's manuals and a description of the files on the media provided with this report. The objective of this project was to develop an analysis for predicting the failure of woven composites and to use the analysis to enhance understanding of their mechanical behavior, especially the failure process. Woven components present a formidable analytical challenge. The complex architecture makes routine application of finite element analysis impractical. Accordingly, a considerable part of this effort concentrated on developing novel analytical methods. In particular, special finite elements were developed which account for microstructure within a single element and global/local analysis methods were developed and evaluated. Use of these analyses indicated that the behavior of woven composites is complex, but that much can be learned using these numerical tools on even moderate size workstations. Author

N95-16833# Agency of Industrial Science and Technology, Osaka (Japan).
STUDIES ON IMPROVEMENT OF OXIDATION RESISTIVITY OF CARBON MATERIALS BY GLASS IMPREGNATION AND SiC FORMATION
Shigeru Ikeda, Hiroshi Shioyama, Osamu Nakamura, Shouji Hori, Shinichi Otsuki, Masakazu Adachi, Kiyohisa Eguchi, Rokuro Fujii, Kanji Matsuo, and Toshiaki Sogabe et al 28 Mar. 1994 128 p
(DE94-796529; ETDE/JP-mf-94796529) Avail: CASI HC A07/MF A02

The paper describes a study of the production method for high-performance carbon materials by glass impregnation, development of borosilicate glass impregnated carbon materials which are high in oxidation resistivity, wear resistance and mechanical strength. In the glass impregnation experiment on carbon materials having pore structures, it was found that as the temperature/pressure increase and the retention time lengthens, glass is impregnated deeply from the surface and that the degree of impregnation depends on the pore structure of carbon materials. Physical properties obtained in case of impregnating borosilicate glass are as follows: the oxidation rate markedly decreases in the vicinity of the softening point of impregnated glass; flexural strength, compressive strength and elastic modulus increase to 1.5 - 3 times, 1.5 - 2 times and 1.7 - 2 times, respectively; gas permeability is under 10(exp 7)cm(exp 2)/s. Wear properties are also good, showing a fixed friction coefficient under pressure over 0.5 MPa. In 80-day impregnation examinations on sodium hydroxide, aqueous ammonia, nitric acid, hydrochloric acid, methyl alcohol and benzene, etc., resistivity to chemicals is good. DOE

N95-16859*# Analytical Services and Materials, Inc., Hampton, VA.
COMPOSITE CHRONICLES: A STUDY OF THE LESSONS LEARNED IN THE DEVELOPMENT, PRODUCTION, AND SERVICE OF COMPOSITE STRUCTURES Final Report
Louis F. Vosteen and Richard N. Hadcock (RNH Associates, Huntington, NY.) NASA Nov. 1994 59 p
(Contract NAS1-19317; RTOP 510-02-13-01)
(NASA-CR-4620; NAS 1.26:4620) Avail: CASI HC A04/MF A01

A study of past composite aircraft structures programs was conducted to determine the lessons learned during the programs. The study focused on finding major underlying principles and practices that experience showed have significant effects on the development process and should be recognized and understood by those responsible for using of composites. Published information on programs was reviewed and interviews were conducted with personnel associated with current and past major development programs. In all, interviews were conducted with about 56 people representing 32 organizations. Most of the people interviewed have been involved in the engineering and manufacturing development of composites for the past 20 to 25 years. Although composites technology has made great advances over the past 30 years, the effective application of composites to aircraft is still a complex problem that requires experienced personnel with special knowledge. All disciplines involved in the development process must work together in real time to minimize risk and assure total product quality and performance at acceptable costs. The most successful programs have made effective use of integrated, collocated, concurrent engineering teams, and most often used well-planned, systematic development efforts wherein the design and manufacturing processes are validated in a step-by-step or 'building block' approach. Such approaches reduce program risk and are cost effective. Author

N95-16926# Oak Ridge National Lab., TN.
MODELING OF CHEMICAL VAPOR INFILTRATION FOR COMPOSITE FABRICATION
T. L. Starr (Georgia Inst. of Tech., Atlanta, GA.) and T. M. Besmann 1993 9 p Presented at the International Conference on High Temperature Ceramic Matrix Composites, Bordeaux, France, 20-25 Sep. 1993
(Contract DE-AC05-84OR-21400)
(DE93-001715; CONF-930961-1) Avail: CASI HC A02/MF A01

We describe our ongoing efforts to develop a general, validated, 3-D, finite-volume model for the chemical vapor infiltration (CVI) process. The model simulates preform densification for both isothermal (ICVI) and forced flow-thermal gradient (FCVI) variations of the process, but is most useful for FCVI where specification and control of flow rates and temperature profiles are critical to rapid, uniform densification. The model has been validated experimentally for both ICVI and FCVI fabrication of SiC/SiC composites. DOE

N95-16930 Rockwell International Corp., Thousand Oaks, CA. Science Center.
LIFE PREDICTION FOR BRIDGED FATIGUE CRACKS
B. N. Cox 1994 42 p Presented at the Life Prediction Methodology for Titanium Matrix Composites Symposium, Hilton Head, SC, 22-24 Mar. 1994 Limited Reproducibility: More than 20% of this document may be affected by microfiche quality
(Contract DE-FG03-89ER-45400)
(DE94-016000; CONF-940399-1) Avail: CASI HC A03

One of the more promising classes of composites touted for high temperature applications, and certainly the most available, is that of relatively brittle matrices, either ceramic or intermetallic, reinforced by strong, aligned, continuous fibers. Under cyclic loading in the fiber direction, these materials develop matrix cracks that often run perpendicular to the fibers, while the fibers remain intact in the crack wake, supplying bridging tractions across the fracture surfaces. The bridging tractions shield the crack tip from the applied load, dramatically reducing the crack velocity from that expected in an unreinforced material subjected to the same value, (Delta)K(sub a), of the cyclic applied stress intensity factor. An important issue in reliability is the prediction of the growth rates of the bridged cracks. The growth rates of matrix fatigue cracks bridged by sliding fibers are now commonly predicted

by models based on the micromechanics of frictional interfaces. However, there exist many reasons, both theoretical and experimental, for suspecting that the most popular micromechanical models are probably wrong in detail in the context of fatigue cracks. Furthermore, a review of crack growth data reveals that the validity of the micromechanics-based predictive model has never been tested and may never be tested. In this paper, two alternative approaches are suggested to the engineering problem of predicting the growth rates of bridged cracks without explicit recourse to micromechanics. Instead, it is shown that the material properties required to analyze bridging effects can be deduced directly from crack growth data. Some experiments are proposed to test the validity of the proposals. DOE

N95-16970# Institute for Defense Analyses, Alexandria, VA.
GRAPHITE-REINFORCED POLYCYANATE COMPOSITES FOR SPACE AND MISSILE APPLICATIONS Final Report, Jun. - Dec. 1993
Janet M. Sater and Michael Rigdon Nov. 1993 481 p
(Contract MDA903-89-C-0003)
(AD-A285509; IDA-D-1454; IDA/HQ-93-44719; AD-E501839) Avail: CASI HC A21/MF A04

Lt. Col. Michael Obal of the BMDO Materials and Structures Office sponsored this workshop to promote communications among the participating groups and to identify technical issues and limitations associated with graphite-reinforced polycyanate composites. Some of the identified issues include a lack of standard materials and associated process specifications due to continuing changes in resin and prepeg formulations. Perhaps the most discussed issue was the lack of a statistical database, due, in part, to the changing formulations just mentioned. Development of a handbook via government coordination of existing information may be one way to provide data to designers and increase material acceptance. In addition, high resin contents in prepeg tapes; a lack of appropriate protective coatings; a need for structural bonding processes; a need for additional, environment-related data, particularly effects on mechanical/physical properties; a need for joint tests and subsystem level tests of structural components; and limited design tools and standards for using composites were discussed. DTIC

N95-16974 Materials Systems, Inc., Concord, MA.
COST-EFFECTIVE METHOD FOR SYNTHESIZING INNOVATIVE TRANSDUCER MATERIALS FOR SENSORS AND ACTUATORS Final Report
22 Jun. 1994 27 p Limited Reproducibility: More than 20% of this document may be affected by microfiche quality
(Contract N00014-94-C-0019)
(AD-A282339) Avail: Issuing Activity (Defense Technical Information Center (DTIC))

The overall objective is to design, demonstrate, and implement a cost-effective tooling technology for manufacturing piezoelectric composite materials by injection molding. This requires a new tooling approach which complements the existing MSI low cost PZT ceramics injection molding technology, currently used in 1-3 piezocomposite research and manufacturing. DTIC

N95-17368 Oak Ridge National Lab., TN.
ABSTRACTS: EIGHTH ANNUAL CONFERENCE ON FOSSIL ENERGY MATERIALS Abstracts Only
1994 45 p Conference held in Oak Ridge, TN, 10-12 May 1994 Limited Reproducibility: More than 20% of this document may be affected by microfiche quality
(Contract DE-AC05-84OR-21400)
(DE94-014053; ORNL/M-3677; CONF-9405143-Absts) Avail: CASI HC A03

Abstracts are presented for 39 papers. The Fossil Energy Advanced Research and Technology Development Materials program is an integrated materials research activity of the Fossil Energy Coal Program, whose objective is to conduct research and development for all advanced coal conversion and utilization technologies. The program is aimed at understanding materials behavior in coal system environments and the development of new materials for improving plant operations and reliability. A generic approach is used for addressing multiple coal technologies; for example, the hot-gas particulate filter development is applicable to pressurized fluidized bed combustion, integrated coal gasification combined-cycle, coal combustion, and indirectly fired combined-cycle systems. DOE

N95-17457 Minnesota Univ., Minneapolis, MN.
MICROMECHANICS OF INTERFACES IN METAL MATRIX COMPOSITES Final Technical Report
William W. Gerberich and David L. Kohlstedt 12 Jul. 1994 67 p Limited Reproducibility: More than 20% of this document may be affected by microfiche quality
(Contract N00014-92-J-1962)
(AD-A282404) Avail: CASI HC A04

The mechanical properties of the interfaces in an Al2O3 fiber reinforced beta-2lS titanium have been evaluated by using fiber pushout tests. The Al2O3 fibers were coated with a refractory metal and Y2O3 which served as a diffusion barrier during the HIPing used to produce the metal matrix composites. By doing fiber pushout tests the interfacial fracture was found to occur at the interface between the refractory metal and the Y2O3. The interfacial shear strength and interfacial frictional stress were measured to be 323 and 312 + or - 2 MPa, respectively. The interfacial frictional stress, which is due to asperity interlocking during the fiber sliding, was correlated to the surface roughness of the coated Al2O3 fiber obtained with the aid of an atomic force microscope. The measured surface roughness of 18.8 + or - 2.2 nm was related to the frictional stress through Hutchinson's model. The frictional coefficient between the Al2O3 fiber and the Ti matrix calculated to be 0.32 + or - 0.02. DTIC

N95-17659*# National Aeronautics and Space Administration. Lewis Research Center, Cleveland, OH.
MODELING OF STRESS/STRAIN BEHAVIOR OF FIBER-REINFORCED CERAMIC MATRIX COMPOSITES INCLUDING STRESS REDISTRIBUTION
Subodh K. Mital (Toledo Univ., OH.), Pappu L. N. Murthy, and Christos C. Chamis Dec. 1994 11 p
(RTOP 505-63-12)
(NASA-TM-106789; E-9249; NAS 1.15:106789) Avail: CASI HC A03/MF A01

A computational simulation procedure is presented for nonlinear analyses which incorporates microstress redistribution due to progressive fracture in ceramic matrix composites. This procedure facilitates an accurate simulation of the stress-strain behavior of ceramic matrix composites up to failure. The nonlinearity in the material behavior is accounted for at the constituent (fiber/matrix/interphase) level. This computational procedure is a part of recent upgrades to CEMCAN (Ceramic Matrix Composite Analyzer) computer code. The fiber substructuring technique in CEMCAN is used to monitor the damage initiation and progression as the load increases. The room-temperature tensile stress-strain curves for SiC fiber reinforced reaction-bonded silicon nitride (RBSN) matrix unidirectional and angle-ply laminates are simulated and compared with experimentally observed stress-strain behavior. Comparison between the predicted stress/strain behavior and experimental stress/strain curves is good. Collectively the results demonstrate that CEMCAN computer code provides the user with an effective computational tool to simulate the behavior of ceramic matrix composites. Author

N95-17905# Dow Corning Corp., Midland, MI.
RESEARCH AND DEVELOPMENT OF MATERIAL/PROCESSING METHODS FOR THE CONTINUOUS FIBER CERAMIC COMPOSITES PROGRAM
A. Szweda 1994 13 p
(Contract DE-FC02-92CE-40993)
(DE94-018569; DOE/CE-40993/T1) Avail: CASI HC A03/MF A01

Higher levels of matrix filler in the CFCC has been found to increase the fatigue life of CFCC's at both 982 and 1204 C. DOE

25 INORGANIC AND PHYSICAL CHEMISTRY

Includes chemical analysis, e.g., chromatography; combustion theory; electrochemistry; and photochemistry.

For related information see also *77 Thermodynamics and Statistical Physics.*.

N95-15967*# Old Dominion Univ., Norfolk, VA. Inst. for Computational and Applied Mechanics.

PARAMETRIC STUDY OF SHOCK-INDUCED COMBUSTION IN A HYDROGEN AIR SYSTEM Progress Report, Jun. - Dec. 1993

J. K. Ahuja and Surendra N. Tiwari Jun. 1994 62 p Presented at the 32nd Aerospace Sciences Meeting, Reno, NV, 10-13 Jan. 1994

(Grant NAG1-363)

(NASA-CR-197134; NAS 1.26:197134; ODU/ICAM-94-101; AIAA Paper 94-0674) Avail: CASI HC A04/MF A01

A numerical parametric study is conducted to simulate shock-induced combustion under various free-stream conditions and varying blunt body diameter. A steady combustion front is established if the free-stream Mach number is above the Chapman-Jouguet speed of the mixture, whereas an unsteady reaction front is established if the free-stream Mach number is below or at the Chapman-Jouguet speed of the mixture. The above two cases have been simulated for Mach 5.11 and Mach 6.46 with a projectile diameter of 15 mm. Mach 5.11, which is an underdriven case, shows an unsteady reaction front, whereas Mach 6.46, which is an overdriven case, shows a steady reaction front. Next for Mach 5. 11 reducing the diameter to 2.5 mm causes the instabilities to disappear, whereas, for Mach 6.46 increasing the diameter of the projectile to 225 mm causes the instabilities to reappear, indicating that Chapman-Jouguet speed is not the only deciding factor for these instabilities to trigger. The other key parameters are the projectile diameter, induction time, activation energy and the heat release. The appearance and disappearance of the instabilities have been explained by the one-dimensional wave interaction model. Author

N95-16001# Johns Hopkins Univ., Baltimore, MD. School of Medicine.

LIGAND FIELD STABILIZATION CONTROL OF METAL ION BINDING Final Report, 15 Mar. 1990 - 14 Mar. 1993

Jeremy M. Berg 30 Apr. 1994 4 p

(Contract N00014-90-J-1700)

(AD-A281011) Avail: CASI HC A01/MF A01

Specific metal ions bind to particular sites within proteins. The factors that might influence the thermodynamics of metal ion binding to proteins include metal ion radius, hard-soft acid-base effects, and ligand field stabilization energy changes. We have probed the contributions of these effects through the use of a series of peptides based on naturally occuring 'zinc finger' domains. The metal ion binding sites studied include Cys2His2, Cys3His, Cys4, and Cys2His(X) where X = OH2, Cl(-), N(-) methylimidazole, and (-)SCH2CH2OH. Metal ions tested included Zn(II), Co(II), Cd(II), Fe(II), Ni(II), and Mn(II). We found that ligand field stabilization energy changes quantitatively account for preferences for Zn(II) over Co(II). For Cd(II), hard-soft acid-base effects are dominant with a greater than 100-fold increase in affinity for Cd(II) over Zn(II) for each Cys for 'His' replacement. For other metal ions, multiple factors clearly contribute. These studies provide components for a rational basis for the design of specific metal binding sites for biosensors and other applications. DTIC

N95-16008 Virginia Polytechnic Inst. and State Univ., Blacksburg, VA.

ENERGY DECAY AND CONTROL FOR ELASTIC AND VISCOELASTIC DISTRIBUTED PARAMETER SYSTEMS Final Report, 15 Nov. 1990 - 14 Apr. 1994

Kenneth B. Hannsgen and Robert L. Wheeler 8 Jun. 1994 13 p Limited Reproducibility: More than 20% of this document may be affected by microfiche quality

(Contract AF-AFOSR-0083-91)

(AD-A281312; AFOSR-94-0391TR) Avail: Issuing Activity (Defense Technical Information Center (DTIC))

Research is reported on the dynamic behavior of viscoelastic structures, with emphasis on the interaction between passive damping and active feedback control mechanisms. A main focus is the approximation of optimal compensators for simple mechanical systems involving viscoelastic elements by realizable compensators. In the frequency domain, this corresponds to the mathematical problem of approximating a transcendental function by a rational one, under suitable stability constraints and performance criteria. The work involves the analytic study of partial product approximations to transfer functions for rods and beams, as well as a mainly numerical study concerned with replacing the complex modulus for the viscoelastic material by a rational function that reflects the most significant properties of the material. A second focus of the research is a new formula that makes clear the relation between initial data and the smoothness and decay rates of solutions of the equations for a viscoelastic system with stabilizing boundary feedback. DTIC

N95-16017 Cornell Univ., Ithaca, NY.

CARBON CLUSTERS STUDIED BY NEUTRALIZATION-REIONIZATION MASS SPECTROMETRY Final Report, 1991-1994

Fred W. McLafferty 25 Jun. 1994 4 p Limited Reproducibility: More than 20% of this document may be affected by microfiche quality

(Contract N00014-90-J-1948)

(AD-A281367) Avail: CASI HC A01

The chemistry of C(n) molecules and ions in plasmas (carbon arcs, laser ablation) and in the formation of polynuclear aromatics, diamond films, and soot has been the subject of extensive theoretical and experimental research. In these studies, ab initio calculations of isomeric carbon clusters C(n)(sup 0) and C(n)(+), n = 2-4, yield structures and energies similar to previous reports, although five (not two) C4(+) structures have local energy minima. Dissociative ionization of structurally varied precursors was used to prepare C3 and C4 ionic and neutral isomers; however, their mass spectra from collisionally activated dissociation (CAD) and neutralization-reionization (NR) under a wide variety of conditions are indistinguishable, indicating only one isomer or the same mixture of isomers. DTIC

N95-16042# University of Southern California, Los Angeles, CA. Dept. of Chemistry.

GAS-SURFACE INTERACTIONS NEAR DISSOCIATION THRESHOLD Annual Report, 1 May 1993 - 30 Apr. 1994

Hanna Reisler and Curt Wittig Jul. 1994 3 p

(Contract F49620-92-J-0230)

(AD-A284945; AFOSR-94-0569TR) Avail: CASI HC A01/MF A01

Our earlier studies of molecule-surface CID were extended to the case of NO2, which has been implicated as the emitting species in shuttle glow phenomena. The glow is believed to derive from the recombination of NO and atomic oxygen, yielding internally excited NO2. Because the NO2 zeroth order 2B2 excited state is strongly coupled to the 2A1 ground state, levels formed in recombination reactions emit throughout the visible. In our experiments, the reverse process was examined. Namely, NO2 entrained in a molecular beam was directed at a crystal surface and was photoexcited 2 cm (10 ms) before reaching the surface. The incident molecules had enough internal plus translational energy to undergo CID, which was observed for a range of NO2 internal excitations. Unexcited NO2 yielded no signal. Additionally, NO was detected with state and angular resolution and it was shown that products were scattered preferentially in the specular direction, ruling out a long residence time on the surface. It is most likely that NO2 decomposes rapidly following impact with the surface, in accord with k(E) measurements that indicate subpicosecond lifetimes for excess energies - 500 cm. This was the first demonstration of such an effect and supports the thesis that NO2 is responsible for the shuttle glow. DTIC

N95-16142# Clemson Univ., SC. Dept. of Chemical Engineering.

SUPERCRITICAL FLUID EXTRACTION: PREPARING A SUPERIOR MESOPHASE PRECURSOR FOR CARBON FIBERS Final Report

Mark C. Thies 1 Aug. 1994 12 p

(Contract DAAL03-92-G-0194)

(AD-A284933) Avail: CASI HC A03/MF A01

Supercritical fluid (SCF) extraction is being investigated for the production of mesophase pitch, the liquid-crystalline precursor for the manufacture of high-performance carbon fibers. The mesophase pitch is produced by fractionation of an isotropic petroleum pitch with supercritical toluene in a region of liquid-liquid equilibrium that exists at pressures above 40 bar. Dramatic improvements in the reliability of our apparatus have recently been made, and mesophase pitch can now be produced on a routine basis. An experimental program was conducted to explore the effects of temperature, solvent-to-pitch (S/P) ratio, and solvent solubility parameter

on the properties of the mesophase pitch produced. Temperatures of 320 and 360 deg C, solubility parameters of 3.7 and 5.0 (cal/cc)exp(1/2), and S/P ratios of 2.5 and 3.5 were chosen to conform to a two-level, augmented factorial experiment. A linear model correlated the data to a high degree of certainty. Results indicate that we can adjust SCF operating conditions and tailor-make a mesophase pitch for a given end use. We have discovered a semitheoretical method for predicting a priori the softening point and yield of mesophase pitch for a given set of SCF operating conditions. The SCF extraction process can be represented on a pseudoternary phase diagram, and good estimates of product yields and softening points can be made from a limited experimental data measured at other conditions. DTIC

N95-16144# California Univ., Los Angeles, CA. Dept. of Chemistry and Biochemistry.

NEW METHODS FOR TREATMENT OF ELECTRON CORRELATION AND SURFACE DYNAMICS (FY91 AASERT) Annual Report, 1 Jun. 1993 - 30 May 1994

Emily A. Carter 30 May 1994 4 p

(Contract F49620-92-J-0244)

(AD-A285177; AFOSR-94-0586TR) Avail: CASI HC A01/MF A01

The SiGe results were discussed in detail in the last AASERT report, so we eschew them here. The F2 reactive scattering on Si(100) was the first study in a series to ascertain the kinetics of surface processes, including etching of silicon. We calculated reaction probabilities for F2 impinging on silicon, as a function of translational and vibrational energy in the F2 molecules. We find that translational excitation is slightly more effective than vibrational excitation at increasing the reactivity of F2, but that vibrational excitation is most effective for producing precursors leading to etching (SiF2). We find that F-atom abstraction, where one Si-F bond is formed while the other F atom in the F2 molecule leaves the surface, is a very probable reaction due to the enormous exothermicity of the reaction (-100 kcal/mol exothermic do deposit only one F on the silicon surface and -200 kcal/mol to deposit both F atoms). These scattered F atoms do not have time to equilibrate with the surface, as is illustrated by the fact that they are translationally hot and do not come off in a cosine distribution. We have also recently studied the reaction of F2 molecules with stepped and defective Si(100) surfaces. DTIC

N95-16150# Ohio State Univ., Columbus.

IN SITU LASER ACTIVATION OF ELECTROCHEMICAL KINETICS AT CARBON ELECTRODES Final Report, 1 Mar. 1991 - 28 Feb. 1994

Richard L. McCreery 31 May 1994 108 p

(Grant AF-AFOSR-0213-91)

(AD-A280892; OSURF-768992/724639; AFOSR-94-0389TR) Avail: CASI HC A06/MF A02

The overall objective of the project is to identify the structural factors which control electrochemical reactivity at carbon electrode surfaces. The approach combines structural probes such as Raman spectroscopy, XPS, and scanning tunneling microscopy (STM) with measures of reactivity, including electron transfer rate constant and adsorption. Laser activation by short but intense laser pulses was used to modify electrode surfaces and enhance reactivity. Work to date has revealed two important conclusions. First, the electronic properties of carbon can differ substantially from that of metals, with major effects on both kinetics and absorption. Second, the importance of carbon structure to kinetics depends strongly on the redox system in question. DTIC

N95-16362# Sandia National Labs., Albuquerque, NM.

THE RESPONSE OF THE SANDIA ROBUST WIDE RANGE HYDROGEN SENSOR TO H2-O2 MIXTURES

R. C. Hughes, D. J. Moreno, M. W. Jenkins, and J. L. Rodriguez 1994 4 p Presented at the 1994 Solid-State Sensor and Actuator Workshop, Hilton Head, SC, 13-16 Jun. 1994

(Contract DE-AC04-94AL-85000)

(DE94-013763; SAND-94-0047C; CONF-9406166-4) Avail: CASI HC A01/MF A01

The Sandia Robust Hydrogen (SRH) sensor can detect partial pressures of H2 over a wide range (approximately 1 ppm to pure H2) because it employs two different kinds of catalytic metal sensors. A Field Effect Transistor (FET) with a catalytic gate detects low H2 concentrations and a resistor of the same metal is accurate for the higher concentrations. The use of Pd alloys with Ni preserves sensor reversibility by preventing the hydride phase transition under normal operating conditions. Mixing O2 with H2 does change the sensor signal under some conditions and comparisons of the behavior of a pure Pd device with a Pd/Ni device is given. The H2 concentration in flammable mixtures can be obtained, but an additional sensor is needed to measure the concentration of oxidant. DOE

N95-16363# Argonne National Lab., IL.

REDUCTION AND AGGREGATION OF SILVER IN AQUEOUS GELATIN AND SILICA SUSPENSIONS

S. Kapoor, D. Lawless, P. Kennepohl, D. Meisel, and N. Serpone (Concordia Univ., Montreal, Quebec.) 1994 5 p Presented at the Physics and Chemistry of Imaging Systems Conference, Rochester, NY, 15-20 May 1994

(Contract W-31-109-eng-38)

(DE94-013998; ANL/CHM/CP-81481; CONF-9405179-1) Avail: CASI HC A01/MF A01

The investigation of silver reduction and aggregation processes are of specific interest to the photographic industry, which relies heavily on photochemical equivalents of these reactions. Mechanistic insights into the formation of small silver clusters in aqueous solution have been obtained from both pulse and gamma-radiolytic studies. This paper examines the reduction of silver ions and the subsequent formation of silver clusters in aqueous gelatin solutions and on colloidal silica particles using the pulse radiolysis technique. The aggregation processes are compared with the parallel reactions in aqueous solutions. DOE

N95-16373# Northeastern Univ., Boston, MA.

METHODS DEVELOPMENT TOWARD THE MEASUREMENT OF POLYAROMATIC HYDROCARBON-DNA ADDUCTS BY MASS SPECTROMETRY

R. W. Giese and P. Vouros Oct. 1993 46 p

(Contract RFA-85-2)

(PB94-182722; HEI/RR-61/93) Copyright Avail: CASI HC A03/MF A01

Advances in sensitivity have been achieved for two modes of mass spectrometry applied to standards related to DNA adducts: gas chromatography with electron-capture negative ion mass spectrometry and fast-atom-bombardment mass spectrometry. These advances involve both sample preparation and instrument conditions. For sample preparation, three new chemical techniques, each targeted toward a class of PAH-DNA adducts, show promise for measuring DNA adducts with increased sensitivity or scope by mass spectrometry: superoxide oxidation, hydrazinolysis, and hydrogenation. Most attention was given to the superoxide oxidation technique, which was brought to the femtomole level for the measurement of a standard of benzo(a)pyrene- r-7, t-8, c-10- tetrahydrotetrol as a model analyte. Improved instrument conditions increased the sensitivity for measuring polyaromatic hydrocarbon-DNA adducts by fast-atom-bombardment mass spectrometry. Author (revised)

N95-16384 Defence Research Establishment Ottawa, Ottawa (Ontario).

AN X-RAY PHOTOELECTRON SPECTROSCOPY (XPS) STUDY OF ACTIVATED CARBONS IMPREGNATED WITH SOME ORGANOCOPPER COMPLEXES

S. H. Liang Oct. 1993 58 p Limited Reproducibility: More than 20% of this document may be affected by microfiche quality

(AD-A282721; DREO-1196) Avail: Issuing Activity (Defense Technical Information Center (DTIC))

Five organocopper complexes were impregnated on an activated carbon surface, and the surface composition of the resulting impregnated carbon investigated by x-ray photoelectron spectroscopy (XPS). From surface composition, and the high-resolution C(1s) and Cu(2p(3/2)) XPS spectra, the ratios of O/Cu, N/Cu, F/Cu, and C/Cu could be calculated. It was found that three of the complexes were either unstable or decomposed on the carbon surface. This evidence could only be obtained by XPS technique, and the analytical method employed in this report. DTIC

N95-16387# Consultec Scientific, Inc., Knoxville, TN.

ASSESSMENT OF RESEARCH NEEDS FOR ADVANCED HETEROGENEOUS CATALYSTS FOR ENERGY APPLICATIONS, VOLUME 2

G. A. Mills Apr. 1994 224 p
(Contract DE-FG02-92ER-30201)
(DE94-015890; DOE/ER-30201-H1-Vol-2) Avail: CASI HC A10/MF A03

This report assesses the direction, technical content, and priority of research needs judged to provide the best chance of yielding new and improved heterogeneous catalysts for energy-related applications over the period of 5-20 years. It addresses issues of energy conservation, alternate fuels and feedstocks, and the economics and applications that could alleviate pollution from energy processes. Recommended goals are defined in 3 research thrusts: catalytic science, environmental protection by catalysis, and industrial catalytic applications. This study was conducted by an 11-member panel of experts from industry and academia, including one each from Japan and Europe. This volume first presents an in-depth overview of the role of catalysis in future energy technology in chapter 1; then current catalytic research is critically reviewed and research recommended in 8 topic chapters: catalyst preparation (design and synthesis), catalyst characterization (structure/function), catalyst performance testing, reaction kinetics/reactor design, catalysis for industrial chemicals, catalysis for electrical applications (clean fuels, pollution remediation), catalysis for control of exhaust emissions, and catalysts for liquid transportation fuels from petroleum, coal, residual oil, and biomass. DOE

N95-16406# Pittsburgh Univ., Pittsburgh, PA. Dept. of Chemistry.
REACTION OF METHANOL WITH POROUS SILICON
J. A. Glass, Jr., E. A. Wovchko, and J. T. Yates, Jr. 6 Oct. 1994 36 p
(Contract N00014-91-J-1641)
(AD-A285518; TR-62) Avail: CASI HC A03/MF A01

The reaction of both porous silicon and hydrogen covered (passivated) porous silicon with methanol was investigated. Adsorption of methanol onto porous silicon at 300 K resulted in cleavage of the 0-H bond and formation of Si-OCH3 and Si-H surface species. Heating of these surface species to approx. 500 K caused breakage of both the C-0 and C-H bonds. This resulted in the formation of Si-H surface species and the incorporation of oxygen and carbon into the porous silicon layer. Attempts to adsorb methanol onto passivated porous silicon proved unsuccessful until removal of the Si-H surface species commenced at 600 K. In addition to oxygen and carbon incorporation, Si-OCH3, Si-CH3, and Si-H surface species were observed when excess CH30H (g) was used to drive the decomposition reaction. The stability of the Si-CH3 species when excess CH30H (g) was present is likely due to oxygen and/or carbon passivation of the silicon surface. DTIC

N95-16419# Oak Ridge National Lab., TN.
ATOMIC SCALE STRUCTURE AND CHEMISTRY OF INTERFACES BY Z-CONTRAST IMAGING AND ELECTRON ENERGY LOSS SPECTROSCOPY IN THE STEM
M. M. McGibbon, N. D. Browning, M. F. Chisholm, A. J. McGibbon, S. J. Pennycook, V. Ravikumar (Northwestern Univ., Evanston, IL.), and V. P. Dravid (Northwestern Univ., Evanston, IL.) May 1994 7 p Presented at the Spring Meeting of the Materials Research Society, San Francisco, CA, 4-8 Apr. 1994
(Contracts DE-AC05-84OR-21400; DE-FG02-92ER-45475)
(DE94-013632; CONF-940411-26) Avail: CASI HC A02/MF A01

The macroscopic properties of many materials are controlled by the structure and chemistry at grain boundaries. A basic understanding of the structure-property relationship requires a technique which probes both composition and chemical bonding on an atomic scale. High-resolution Z-contrast imaging in the scanning transmission electron microscope (STEM) forms an incoherent image in which changes in atomic structure and composition across an interface can be interpreted directly without the need for preconceived atomic structure models. Since the Z-contrast image is formed by electrons scattered through high angles, parallel detection electron energy loss spectroscopy (PEELS) can be used simultaneously to provide complementary chemical information on an atomic scale. The fine structure in the PEEL spectra can be used to investigate the local electronic structure and the nature of the bonding across the interface. In this paper we use the complimentary techniques of high resolution Z-contrast imaging and PEELS to investigate the atomic structure and chemistry of a 25 degree symmetric tilt boundary in a bicrystal of the electroceramic SrTiO3. DOE

N95-16426# Argonne National Lab., IL. Analytical Chemistry Lab.
THE STABILITY OF CALIBRATION STANDARDS FOR ICP/AES ANALYSIS: A TWO-YEAR STUDY
D. R. Huff and E. A. Huff 1994 15 p Presented at the 10th Annual Waste Testing and Quality Assurance Symposium, Arlington, VA, 11-15 Jul. 1994
(Contract W-31-109-eng-38)
(DE94-013398; ANL/CMT-ACL/CP-82364; CONF-940790-1) Avail: CASI HC A03/MF A01

The stability of instrument calibration standards for Inductively Coupled Plasma/Atomic Emission Spectrometric analysis was studied over a two-year period. Data were obtained as functions of analyte concentration, acid type, and acidity. The impact of acid concentration on signal-to-background ratios was also assessed. The results show that, with the appropriate choice of inorganic acid preservatives, most analytes maintain their integrity over extended periods; thus frequent standard preparations are not necessary to obtain valid analytical data. This conclusion allows for more efficient use of commercially purchased reference materials, which should reduce procurement costs and minimize chemical waste. DOE

N95-16485# Argonne National Lab., IL.
RADICAL CATIONS OF QUADRICYCLANE AND NORBORNADIENE IN POLAR ZSM-5 MATRICES: RADICAL CATION PHOTOCHEMICAL TRANSFORMATIONS WITHOUT PHOTONS
M. V. Barnabas and A. D. Trifunac 1994 7 p
(Contract W-31-109-eng-38)
(DE94-014007; ANL/CHM/PP-77639) Avail: CASI HC A02/MF A01

Radical cations of quadricyclane (Q) and norbornadiene (NBD) are produced by gamma radiolysis in zeolites. In polar ZSM-5, only one radical cation is initially observed below 100 K. Increasing the temperature above 200 K gives rise to the cyclopentadiene radical cation. Higher temperatures (greater than 360 K) give rise to the cyclopenten-4-yl radical. The observation of cyclopentadiene radical cation implies the occurrence of the reverse Diels-Alder reaction. This is a thermally forbidden, photochemically allowed process, which is made possible by the interaction of the polar zeolite matrix sites with parent NBD and Q radical cations. DOE

N95-16497# Rockwell International Science Center, Thousand Oaks, CA.
THERMAL DISSOCIATION OF HALOGEN AZIDES Final Technical Report, 15 Apr. 1990 - 30 Jun. 1994
D. J. Benard Sep. 1994 160 p
(Contract F49620-94-C-0025)
(AD-A285088; SC71024.FR; AFOSR-94-0512TR) Avail: CASI HC A08/MF A02

Both FN3 and ClN3 were dissociated in the presence of a variety of donor molecules, either by pulsed CO2 laser excitation (using SF6 as a sensitizer) or by thermal excitation in a chemically driven shock tube. The donors were selected to support energy transfer from the metastable NF(a) and NCl(a) products of the azide dissociation reactions, and optical diagnostics were employed to study energy transfer rates, optical gain and lasing visible wavelengths. Product of NCl(a) was shown to be inefficient, however, both gain and lasing were achieved in two systems driven by NF(a). Lasting at 471 nm on the BiF9(A-X) transition was obtained by transient heating of FN3/Bi(CH3)3 gas mixtures, however, power extraction was highly inefficient due to the low gain provided by the emitter and the short duration of the shock tube experiment. Much higher gain coefficients were obtained by CO2 laser heating of FN3/B2H6/SF6 gas mixtures, which produced intense BH(A-x) chemiluminescence and lasing at 433 nm in a low volume cavity with a threshold gain of 2.5 percent/cm. An improved BH donor was synthesized by reacting B2H6 with NH3 in a heated capillary oven and optical absorption diagnostics were developed for the dark BH(X) and BH(a) states. Author (DTIC)

N95-16608 Wien Univ. (Austria).
INTERNATIONAL WINTERSCHOOL ON ELECTRONIC PROPERTIES OF NOVEL MATERIALS: PROGRESS IN FULLERENE RESEARCH
12 Mar. 1994 94 p Winterschool held in Tyrol, Austria, 3-12 Mar. 1993
Limited Reproducibility: More than 20% of this document may be affected by microfiche quality
(Contract N68171-94-M-5319)
(AD-A282128; R/D-7294-CH-03) Avail: Issuing Activity (Defense Technical Information Center (DTIC))

The winterschool will be focused on new developments in research and application of fullerene and fullerene derived materials. Particular attention will be paid to structural properties, doping, endohedral compounds, higher fullerenes, nanotubes, photo-physics and photochemistry of fullerenes and chemically modified fullerenes. The relevance of these materials to conductivity, photo- and superconducting, magnetic and optical properties including IR, magnetic response, Raman scattering, neutron scattering and high energy spectroscopy will be discussed. DTIC

N95-16622# Stanford Univ., CA. Center for Integrated Systems.
LOW VOLTAGE ELECTRON BEAM LITHOGRAPHY Monthly Report, Apr. 1994
R. Browning and R. F. Pease Apr. 1994 2 p
(Contract N00014-92-J-1996)
(AD-A281046) Avail: CASI HC A01/MF A01

The contract has three parts covering aspects of high precision electron beam lithography: (1) comprehensive computer modeling of the electron beam tool; (2) experimental determination of the properties of sources, columns, and targets; and (3) the use of silicon single crystals as straightness and orthogonality standards using orientation dependent etching techniques. DTIC

N95-16627# Rensselaer Polytechnic Inst., Troy, NY. Dept. of Physics.
IN-SITU X-RAY CHARACTERIZATION OF THE ELECTROLYTE-SOLID INTERFACE Final Report, 1 Dec. 1989 - 31 May 1994
T. M. Hayes 31 May 1994 17 p
(Contract N00014-90-J-1332)
(AD-A281165) Avail: CASI HC A03/MF A01

Electrochemically controlled surfaces are expected to be very different from those in vacuum due to high electric fields at the electrolyte-metal interface. Microscopic knowledge of that interface is essential in understanding technologically important processes like corrosion and electroplating. Underpotentially-deposited (UPD) layers of one metal on another are relatively stable, prototypical systems for such research. The Cu atomic-scale environment in a layer of Cu deposited electrochemically on a large polycrystalline Pt electrode has been studied in situ using both fluorescence detection x-ray absorption spectroscopy (XAS) and measurements of x-ray reflectivity. Measurements were made on the same layer with the x-ray electric field vector both parallel and perpendicular to the surface normal vector, essential for the determination of the number of neighboring atoms. After a substantial effort in XAS experimental design and technique development, we have obtained significantly higher quality data than others. Moreover, we have achieved a consistent interpretation for these spectra, involving O, Cu, and Pt atoms as near neighbors. Their distances from Cu are identical in the two polarizations, but their amplitudes are different. These differences provide geometrical constraints on models proposed for the structure of the interface. DTIC

N95-16635# University of Northern Illinois, De Kalb, IL. Dept. of Chemistry.
CHARGE TRANSFER PROCESSES ON LIQUID/LIQUID INTERFACES: THE STATUS IN 1994
Petr Vanysek 21 Sep. 1994 24 p
(Contract N00014-91-J-1058)
(AD-A285067; TR-057) Avail: CASI HC A03/MF A01

Electrochemistry dealing with interfaces between two immiscible and ionic conductive solutions (ITIES) has been documented in literature for over a hundred years. The thermodynamically grounded interest in electric interfaces is now just over a century old and it closely follows the establishment of physical chemistry as an individual scientific discipline. Its first specialized journal, the Zeitschrift fur physikalische Chemie, was in its early years devoted mainly to electrochemical research. There, in 1988 the derivation of the Nernst equation appears, which can be applied not only to metal/solution interfaces, but to liquid/liquid interfaces as well. Systematic study of charge transport across immiscible interfaces and its implications to electrochemistry and electro-analysis as a separate discipline is relatively young. Its beginning can be placed in the middle 1970's. DTIC

N95-16790 California Univ., San Diego, La Jolla, CA. Dept. of Chemistry.
CHEMISORPTION ENERGETICS OF SUPERACTIVE CHLORINE CONTAINING SPECIES ON GALLIUM ARSENIDE SURFACES Final Report, 15 Mar. - 14 Dec. 1993
Andrew C. Kummel Dec. 1993 5 p Limited Reproducibility: More than 20% of this document may be affected by microfiche quality
(Contract F49620-93-1-0176)
(AD-A281311; AFOSR-94-0396TR) Avail: CASI HC A01

The chemisorption mechanisms of Cl2, Br2, and I2 on Si(100) 2x1 are quite similar while those of F2 and O2 are quite distinct. For the heavy diatomic halogens (Cl2, Br2, and Cl2), the sticking probability increases with incident translation energies above 0.1 eV, and the largest initial sticking probabilities are obtained at the highest incident energies, with SO equal to 95 - 100% for I2 and Br2, at low incident energies the initial sticking probability, SO, decreases with increasing surface temperature while at high incident energies the sticking probability is independent of surface temperature. In addition, for Cl2 very low energy molecular beams can be prepared, and the sticking probability is observed to decrease with increasing incident energies between 0.02 eV and 0.06 eV. Therefore, all these heavy diatomic halogens can adsorb via precursor - mediated chemisorption at low incident translation energy and via direct - activated chemisorption activated chemisorption at high incident translational energy. For all incident kinetic energies, the chemisorption probability decreases linearly with coverage (S=SO(1-Theta)) for the three diatomic halogen gases. This suggests that a single site is required to initiate the direct chemisorption process and the precursor is intrinsic. DTIC

N95-16791 Kansas State Univ., Manhattan, KS. Dept. of Chemistry.
NANO-SCALE METAL OXIDE PARTICLES AS MATERIALS FOR AIR PURIFICATION Final Report, 15 May 1990 - 31 Dec. 1993
Kenneth J. Klabunde 22 Feb. 1994 14 p Limited Reproducibility: More than 20% of this document may be affected by microfiche quality
(Contract DAAL03-90-G-0121)
(AD-A281394; ARO-27775.15-CH) Avail: Issuing Activity (Defense Technical Information Center (DTIC))

A final report on the study of ultrafine metal oxide particles as destructive adsorbents for toxic substances is presented. Successful treatment of organophosphorous compounds and chlorocarbons, where heteroatoms are extracted forming nontoxic metal phosphates and chlorides, has been carried out. Methods for preparing the nanoscale particles, including core/shell overlayer particles, have been worked out. Surface characterization, surface chemistry, heats of adsorption, surface catalyzed CH/D2 yields CD/H exchange, effect of surface --OH groups, electron transfer processes, (16)O/(18)O exchange, and studies of molecular metal oxides have been reported. A patentable invention dealing with Fe2O3/MgO core/shell structures is also described. DTIC

N95-16846# California Univ., Berkeley, CA. Sponsored Projects Office.
SPECTROSCOPY OF THE TRANSITION STATE REGION IN HYDROGEN TRANSFER REACTIONS Final Report, 1 Nov. 1990 - 30 Apr. 1994
Daniel M. Neumark 9 Aug. 1994 6 p
(Grant AF-AFOSR-0084-91)
(AD-A285151; AFOSR-94-0553TR) Avail: CASI HC A02/MF A01

The research supported by this grant is centered on probing the spectroscopy and dynamics of a variety of transient species using two anion photodetachment techniques: photoelectron spectroscopy and zero electron kinetic energy spectroscopy. Most of the research effort was devoted to the transition state spectroscopy of reactions involving H atom abstraction by fluorine atoms. We have also measured electron affinities of several radicals, and have characterized several of the excited electronic states O3 for the first time. Finally, we have begun studying weakly bound clusters in which a halide ion is solvated by known number of CO2 molecules. Author (DTIC)

N95-16866# Case Western Reserve Univ., Cleveland, OH. Dept. of Macromolecular Science.

THE INFLUENCE OF THE COMPLEXATION OF SODIUM AND LITHIUM TRIFLATE ON THE SELF-ASSEMBLY OF TUBULAR-SUPRAMOLECULAR ARCHITECTURES DISPLAYING A COLUMNAR MESOPHASE BASED ON TAPER-SHAPED MONOESTERS OF OLIGOETHYLENEOXIDE WITH 3,4,5-TRIS(P-(N-DODECAN-L-YLOXY)BENZYLOXY)BENZOIC ACID AND OF THEIR POLYMETHACRYLATES

Virgil Percec, James Heck, Dimitris Tomazos, and Goran Ungar 30 Jun. 1994 33 p

(Contract N00014-89-J-1828)

(AD-A281403) Avail: CASI HC A03/MF A01

The monoesters of mono-(la), di(lb), tri(1c) and tetra(ld) ethylene glycol with 3,4,5-tris (p-(n-dodecan-1-yloxy) benzyloxy)benzoic acid (1), the polymethacrylates derived from them (2) and the complexes of both 1 and 2 with LiCF3SO3 and NaCF3SO3 self-assemble into cylindrical supramolecular architectures which exhibit a hexagonal columnar (Phi(sub h)) mesophase. The generation of the Phi(sub h) mesophase depends on the stabilization of this assembly by endo-recognition in the core of the cylinder (H-bonding and ionic interactions) and exo-recognition that occurs between the tapered groups and also between the cylinders (i.e., the hexagonal arrangement of the columns). The low molecular weight compounds 1 are able to complex more salt in the Phi(sub h) mesophase and have larger increases in (Phi(sub h)-isotropic transition temperature (T Phi(sub h-i)) per increase in salt concentration than the corresponding polymethacrylates 2 derived from them. Molecular modeling appears to indicated that positional and conformational restrictions imposed by both the tapered side groups and the polymer backbone are responsible for these results. Both the polymers and the low molar mass compounds have their T Phi(sub h-i) shifted to lower temperatures and allow more LiCF3SO3 to be complexed with the increase in the number of oxyethylene segments present in the flexible spacer. A comparison of the difference in the effectiveness Of the Li cation versus the Na cation in providing an increased stabilization of the Phi sub h mesophase does not show any significant differences between the two cations. DTIC

N95-16882 Pennsylvania State Univ., University Park, PA.

COMBUSTION INSTABILITY PHENOMENA OF IMPORTANCE TO LIQUID PROPELLANT ENGINES Final Report, 1 Jul. 1991 - 30 Jun. 1994

Robert J. Santoro and William E. Anderson 31 Aug. 1994 80 p Limited Reproducibility: More than 20% of this document may be affected by microfiche quality

(Grant AF-AFOSR-0336-91; AF Proj. 2308)

(AD-A284780; AFOSR-94-0578TR) Avail: CASI HC A05

A systematic study of the atomization of impinging liquid jets was performed. Effects of jet flow condition, orifice diameter, impingement angle, preimpingement length, fabrication procedure, and jet velocity at steady and oscillating, atmospheric- and high-pressure ambient conditions were investigated. Measurements of sheet breakup length, drop size and velocity distribution, and the length between sheet structures and detached ligaments were made. Results of the experiments were compared to theoretical predictions. It appears that primary breakup of the sheets formed by turbulent impinging jets is controlled by pressure and momentum fluctuations in the liquid that are accentuated near the impingement point and that have their origin in the jet prior to impingement. Based on these results, approaches to modeling impinging jet atomization should focus on preimpingement jet conditions and the physics near the jet impingement point. Experimental results were also studied in the context of an empirical correlation used in industry for the prediction of combustion stability. The frequency with which the periodic disturbances that control primary breakup are formed has a marked similarity to the combustion instability frequency predicted by the stability correlation. Furthermore, an increase in predicted stability coincides with an increase in measured mean drop size and an increase in the polydispersity of the drop size distribution. DTIC

N95-16955# Illinois Univ., Urbana-Champaign, IL. Dept. of Mechanical and Industrial Engineering.

SHOCK INITIATION OF CRYSTALLINE BORON IN OXYGEN AND FLUORINE COMPOUNDS Annual Technical Report

Herman Krier, Rodney L. Burton, and S. R. Pirman Aug. 1994 135 p

(Contract N00014-93-1-0654)

(AD-A284266; UILU-ENG-94-4010) Avail: CASI HC A07/MF A02

The ignition delay and combustion of amorphous and crystalline boron particles is investigated at elevated temperatures and pressures for wet, dry, and fluorine-containing atmospheres. Particles ranging from submicron to 32 microns in diameter are ignited in the ambient conditions produced by a reflected shock wave in a shock tube. The ignition delay and combustion times are examined as a function of temperature for pressures of 8.5, 17, and 34 atm and for oxidizer mixtures of 100% oxygen, 30% water vapor, 1-3% sulfur hexafluoride, and 6-12% hydrogen fluoride. Results indicate that pressure in the range studied does not affect the ignition delay or burn time. The additives, water vapor and sulfur hexafluoride, reduce the ignition delay time for amorphous and sub-micron crystalline boron when compared to oxygen. For 20 microns particles, H2O and SF6 reduce the ignition temperature limit from 2500 K in pure oxygen to 2200 K and 1900 K, respectively. Burn time is unaffected by the additives. Hydrogen fluoride did not show any change in ignition delay or burn time compared to pure oxygen. At the range of temperatures tested, very little (less than 2%) of HF is dissociated into H and F atoms. The report also presents reviews of previous chemical and physical models that have attempted to explain why boron powder is relatively difficult to ignite. DTIC

N95-16973 Hawaii Univ., Manoa, HI.

CHARGING HYDROGEN INTO Ni IN HYDRIDE-CONTAINING MOLTEN SALTS Interim Report

Bor Y. Liaw and Yi Ding Jan. 1994 12 p Limited Reproducibility: More than 20% of this document may be affected by microfiche quality

(Contract N00014-92-J-1673)

(AD-A282335; TR-4) Avail: Issuing Activity (Defense Technical Information Center (DTIC))

Elevated-temperature calorimetric measurements were performed using a cell: Al 6061 alloy I LiH(saturated), LiCl-KCl eutectic I Ni with a charging current of about 600 mA. An anomalous positive temperature excursion was observed, which was difficult to explain based on our understanding of the electrochemical reactions occurring in the cell and the associated enthalpies. The potential between the working and counter electrodes fell in two peculiar ranges: in the initial stage, 0.7-1.2V, and the later stage, 2.3-2.6V -- a range of great interest -- due to its similarity to the condition of an excess heat event that we reported in the Pd-D system in which significant excess heat was measured. DTIC

N95-17140 University of Southern California, Downey, CA.

GAS-SURFACE INTERACTIONS NEAR DISSOCIATION THRESHOLD Annual Report, 1 Mar. 1993 - 30 Jun. 1994

Hanna Reisler and Curt Wittig 30 Jun. 1994 6 p Limited Reproducibility: More than 20% of this document may be affected by microfiche quality

(Contract F49620-92-J-0168)

(AD-A282726; AFOSR-94-0458TR) Avail: CASI HC A02

The 365 nm photodissociation of nitrosyl chloride adsorbed on smooth MgO(100) surfaces at 90 K has been studied with mass spectrometric product detection, as well as state-selective ionization detection of NO. Results of photofragment time-of-flight (TOF) spectra of Cl and NO, state-selective detection of the NO photofragment and temperature programmed desorptions can be rationalized by a mechanism in which ClNO grows on the surface in islands with MgO defects serving as nucleation centers. No significant differences are observed between the rough and smooth surfaces, although the number of defect sites, especially oxygen vacancies, on the latter is substantially reduced. An attempt was made to determine the geometry of the adsorbates on the surface using FTIR. The results did not show any particular order, reinforcing the conclusions of clustering and lack or orientation. Preliminary attempts to dissociate ClNO by impact of hyperthermal Xe atoms led to deposition of Xe on the surface without evidence of dissociation. Collision induced dissociation (CID) of highly excited NO2 has been observed for well characterized MgO(100) surfaces with parent and product angular resolution at various internal and incident translational energies. DTIC

N95-17141 Drexel Univ., Philadelphia, PA. Dept. of Chemistry.

CHEMICAL PROPERTIES OF THE FULLERENES Final Report, Jun. - Dec. 1992

Allan L. Smith Nov. 1993 46 p Limited Reproducibility: More than

20% of this document may be affected by microfiche quality
(Contract DAAL03-91-C-0034)
(AD-A282730; ERDEC-CR-086) Avail: CASI HC A03

The UV-visible absorption spectra of pure C60, C70, and C60O dissolved in toluene were used to perform multicomponent analysis of graphitic soot extracts and to assess the purity of fullerene samples. Diffuse-reflectance FTIR spectroscopy of 1-2 mg solid C60 and C70 samples was used to determine the fraction of hydrocarbon impurities at the level of 0.01 atom fraction H. Vacuum sublimation is the only way to produce C60 and C70 samples free of hydrocarbon impurities. The solubility of C60 and C70 in toluene was measured as a function of temperature for 25 deg C less than T less than 80 deg C, and for C60 in CS2 for 25 less than T less than 45 deg C. At 30 deg C, C60 is three times as soluble as C70, but both solubilities decrease with increasing temperature. This unusual temperaiure dependence, exhibited by virtually no other organic solids in organic solvents, is attributed to the formation of solvated fullerene solids. The heat of combustion of C60(cr) was determined with the NIST adiabatic bomb calorimeter, and used to determine the enthalpy of formation of C60, 2193 +/- 9.6 kJ/mol. The average strength of the carbon-carbon bonds in C60 is 453 kJ/mole. The absorption spectrum of C60 gas in equilibrium with the solid was recorded between 500 and 680 deg C. From the slope of the ln(P (sub vap)) vs 1/T plot, an enthalpy of sublimation for C60 of 159 kJ/mol was determined. DTIC

N95-17142 Idaho Univ., Moscow, ID.
RESEARCH ON ORGANOFLUORINE CHEMISTRY FOR 700 F THERMOOXIDATIVE STABILITY Final Technical Report
Jeanne M. Shreeve and Robert L. Kirchmeier 29 Jun. 1994 22 p Limited Reproducibility: More than 20% of this document may be affected by microfiche quality
(Grant AF-AFOSR-0189-91)
(AD-A282767; AFOSR-94-0455TR) Avail: Issuing Activity (Defense Technical Information Center (DTIC))

Much exciting chemistry has been completed over the three year course of this grant. The 32-membered fluorinated multifunctional heterocycle (C(O)N(CH3) SO2(CF2)2O(CF2) 4O(CF2)2(SO2) (CH3)NC(O))2 was prepared and a crystal structure was obtained. New, efficient routes for the preparation of fluorinated amines and azaalkenes have been developed, and several members of a nearly unknown class of compounds, i.e., fluoroalkyl (aryl) tetraazanes were prepared and characterized. Methods were also developed for the synthesis of perfluoropropylidene containing aromatic and alkyl ethers. R, transfer reagents, e.g., CF3Si(CH3)3 and C6F5Si(CH3)3 as well as R(sub f)OSi(CH3)3 were prepared and applied to the preparation of novel ethers, and substituted aromatic compounds. Several fluorinated macroheterocycles were synthesized using multifunctional silanes and siloxanes. The chemistry of perfluorovinylamines has been explored in some detail. DTIC

N95-17157# Los Alamos National Lab., NM.
USE OF MAGNESIUM FOR RECOVERING HYDROGEN ISOTOPES FROM TRITIATED WATER
R. S. Willms, Satoshi Konishi (Japan Atomic Energy Research Inst., Naka, Japan.), and Kenji Okuno (Japan Atomic Energy Research Inst., Naka, Japan.) 1994 6 p Presented at the 11th Topical Meeting on the Technology of Fusion Energy, New Orleans, LA, 19-24 Jun. 1994
(Contract W-7405-eng-36)
(DE94-014471; LA-UR-94-2063; CONF-940630-14) Avail: CASI HC A02/MF A01

Reacting tritiated water with hot metal to recover the tritium from tritiated water has been practiced for considerable time. A metal frequently used for this purpose has been uranium. Recent work at the Tritium Systems Test Assembly at Los Alamos National Laboratory has focused on using magnesium for this purpose. This work was done as part of the Annex 4 collaboration between the US Department of Energy/TSTA and the Japan Atomic Energy Research Institute/Tritium Processing Laboratory. Magnesium appears to have reactive properties that are as good as uranium and possibly better, and, of course, magnesium is easier to handle and less strictly controlled. Both bench-scale and practical-scale experiments were conducted with magnesium, including tests with tritiated water. Mg bed construction techniques and operating parameters were determined. Testing showed that the Mg packed bed was very effective for recovering hydrogen isotopes from water. However, when used for this purpose either Mg or U is irreversibly consumed and must be disposed of as tritiated waste. It follows that this processing technique would be inappropriate for a large tritiated water processing operation. However, this technique may find utility for small-scale systems. DOE

N95-17161# Oregon Graduate Inst. of Science and Technology, Beaverton, OR.
FUNDAMENTAL STUDIES IN OXIDATION-REDUCTION IN RELATION TO WATER PHOTOLYSIS
J. K. Hurst 1994 18 p
(Contract DE-FG06-87ER-13664)
(DE94-014598; DOE/ER-13664/7) Avail: CASI HC A03/MF A01

Broad objectives are to improve the conceptual view of ways in which membranes and interfaces can be used to control chemical reactivity. Focus was on three elementary processes central to developing membrane-based integrated chemical systems for water photolysis or related photoconversion/photostorage processes. It was sought to identify the influence of interfaces on charge separation/recombination reactions, pathways for transmembrane charge separation across hydrocarbon bilayer membranes, and mechanisms of water oxidation catalyzed by transition metal coordination complexes. The supramolecular assemblies studied comprise primarily small unilamellar vesicles doped with amphiphilic viologens (N,N'dialkyl-4,4'-bipyridinium ions) which can function as transmembrane charge relays. DOE

N95-17163# New Orleans Univ., LA. Dept. of Chemistry.
IDENTIFICATION AND TEMPORAL BEHAVIOR OF RADICAL INTERMEDIATES FORMED DURING THE COMBUSTION AND PYROLYSIS OF GASEOUS FUELS: KINETIC PATHWAYS TO SOOT FORMATION
R. D. Kern and H. Chen Jan. 1994 29 p
(Contract DE-FG05-85ER-13400)
(DE94-014681; DOE/ER-13400/13) Avail: CASI HC A03/MF A01

Four of the five major areas of research have been completed: C2H2 and C4H4, chlorobenzene, toluene, and propargyl chloride. The remaining area (cyclopentadiene decomposition) will be addressed. Testing of the data acquisition for the shock tube/time-of-flight mass spectrometer is described. DOE

N95-17387*# National Aeronautics and Space Administration. Lewis Research Center, Cleveland, OH.
STRUCTURE OF 4-METHYLPYRIDINIUM HYDROGEN SULFIDE
Maria T. Andras, Aloysius F. Hepp, Phillip E. Fanwick (Purdue Univ., West Lafayette, IN.), Robert A. Martuch (Cleveland State Univ., OH.), Stan A. Duraj (Cleveland State Univ., OH.), and Edward M. Gordon (Wilberforce Univ., OH.) Nov. 1994 6 p
(RTOP 233-01-0A)
(NASA-TM-106778; E-9231; NAS 1.15:106778) Avail: CASI HC A02/MF A01

4-Methylpyridinium hydrogen sulfide, (C6H7NH)HS, M(sub r) = 127.21, consists of C6H7NH(+) cations and HS(-) anions. Z = 2 for the crystal with monoclinic space group Cm (#8), dimensions of a = 8.679(2) A, b = 7.964(1) A, and c = 4.860(2) A, an angle beta of 101.10(2) degrees, and a volume of V = 329.6(3) A(exp 3). R = 0.039 and R(sub w) = 0.048 for 385 reflections with F(sub o)(exp 2) greater than 3 sigma(F(sub o)(exp 2)) and 59 variables. Both the C6H7NH(+) cation and the HS(-) anion lie on crystallographic mirror planes with the N,S, two carbon atoms, and two hydrogen atoms positioned in the planes. The hydrogen atom of the HS(-) anion was not located. Author

N95-17425 Brandeis Univ., Waltham, MA. Dept. of Chemistry.
KINETICS AND MECHANISM OF CHEMICAL MARKER FORMATION AND WATER-ACTIVATED HEAT GENERATION Final Report, 1 Jan. 1991 - 31 Dec. 1993
Kenneth Kustin 1 May 1994 16 p Limited Reproducibility: More than 20% of this document may be affected by microfiche quality
(Contract DAAL03-91-G-0005)
(AD-A281407; ARO-28691.2-LS) Avail: CASI HC A03

Research has been conducted on two projects: (1) intrinsic chemical markers; and (2) water-activated chemical heaters. It has recently been discovered at the Army's Natick, Massachusetts Research Development & Engineering Center that certain chemical substances produced as a result

of the thermal treatment of food can serve as chemical indicators of sterility. The relationship between marker formation and bacteria destruction has been established through mathematical models an verified experimentally and by computer simulation of different thermoprocessing profiles. It has also been shown at Natick that packaged foods can be readily heated using a flameless chemical heater Kinetics and calorimetric studies have been carried out to determine which physical and chemical factors are most responsible for the energy released when water reacts with a magnesium-iron mixture in the presence of electrolyte in the heater. A mechanism for reaction and heat generation has bee developed which can serve as the basis for a dynamical model of the heater. On the basis of this mechanism, a strategy has been developed for suppression of the concomitantly generated H2 gas. DTIC

N95-17437 California Univ., Berkeley. Lawrence Berkeley Lab, CA.
EXPERIMENTAL STUDY OF PREMIXED FLAMES IN INTENSE ISOTROPIC TURBULENCE
B. Bedat and R. K. Cheng Apr. 1994 22 p Presented at the 25th International Symposium on Combustion, Irvine, CA, 31 Jul. - 5 Aug. 1994 Limited Reproducibility: More than 20% of this document may be affected by microfiche quality
(Contract DE-AC03-76SF-00098)
(DE94-016868; LBL-35559; CONF-940711-17) Avail: CASI HC A03

A methodology for investigating premixed turbulent flames propagating in intense isotropic turbulence has been developed. The burner uses a turbulence generator developed by Videto and Santavicca and the flame is stabilized by weak-swirl generated by air injectors. This set-up produces stable premixed turbulent flames under a wide range of mixture conditions and turbulence intensities. The experiments are designed to investigate systematically the changes in flame structures for conditions which can be classified as wrinkled laminar flames, corrugated flames, and flames with distributed reaction zones. Laser Doppler anemometry and Rayleigh scattering techniques are used to determine the turbulence and scalar statistics. In the intense turbulence, the flames are found to produce very little changes in the mean and rms velocities. Their flame speeds increase linearly with turbulence intensity as for wrinkled laminar flames. The Rayleigh scattering pdfs for flames within the distributed reaction zone regime are distinctly bimodal. The probabilities of the reacting states (i.e. contributions from within the reaction zone) is not higher than those of wrinkled laminar flame. These results show that there is no drastic changes in flame structures at Karlovitz number close to unity. This suggests that the Klimov-Williams criterion underpredicts the resilience of wrinkled flamelets to intense turbulence. DOE

N95-17479 Department of the Navy, Washington, DC.
VOLATILE CVD PRECURSORS BASED ON COPPER ALKOXIDES AND MIXED GROUP IIA-COPPER ALKOXIDES Patent
Andrew Purdy, inventor (to Navy) 26 Apr. 1994 4 p Filed 10 Mar. 1993
(AD-D016380; US-Patent-5,306,836; US-Patent-Appl-SN-034802; US-Patent-Class-556-112) Avail: 'JS Patent and Trademark Office

This invention relates to novel chemical compositions for use in chemical vapor deposition. More specifically, it relates to fluorinated copper alkoxides and fluorinated calcium-copper, strontium-copper, and barium-copper alkoxides having superior physical properties for application in chemical vapor deposition to form thin films. The compounds should also be useful for the preparation of calcium, strontium, and barium-copper oxides by sol-gel processes. DTIC

N95-17524# Oak Ridge National Lab., TN.
ELECTRO-SEPARATIONS: EFFICIENT PROCESSING FOR THE TWENTY-FIRST CENTURY
C. H. Byers and A. Amarnath (Electric Power Research Inst., Chattanooga, TN.) 18 Apr. 1994 29 p Presented at the Spring Meeting of the American Institute of Chemical Engineers, Atlanta, GA, 17-21 Apr. 1994
(Contract DE-AC05-84OR-21400)
(DE94-012656; CONF-940433-5) Avail: CASI HC A03/MF A01

Electro-separations, the separation of mixtures driven by electricity, either directly or indirectly are shown to have significant application to the process industries. Categories discussed include, electric current phenomena, field-driving processes, convective transport enhancement, and flow stabilization. In each case, the status of a currently significant separation technique is reviewed. A general discussion of developing techniques and research and development needs and opportunities concludes the discussion. DOE

N95-17639 Lawrence Livermore National Lab., Livermore, CA.
HYDROGEN PRODUCTION BY GASIFICATION OF MUNICIPAL SOLID WASTE
R. Rogers, III 20 May 1994 15 p Limited Reproducibility: More than 20% of this document may be affected by microfiche quality
(Contract W-7405-eng-48)
(DE94-016483; UCRL-ID-117603) Avail: CASI HC A03

As fossil fuel reserves run lower and lower, and as their continued widespread use leads toward numerous environmental problems, the need for clean and sustainable energy alternatives becomes ever clearer. Hydrogen fuel holds promise as such as energy source, as it burns cleanly and can be extracted from a number of renewable materials such as municipal solid waste (MSW), which can be considered largely renewable because of its high content of paper and biomass-derived products. A computer model is being developed using ASPEN Plus flow sheeting software to simulate a process which produces hydrogen gas from MSW; the model will later be used in studying the economics of this process and is based on an actual Texaco coal gasification plant design. This paper gives an overview of the complete MSW gasification process, and describes in detail the way in which MSW is modeled by the computer as a process material. In addition, details of the gasifier unit model are described; in this unit modified MSW reacts under pressure with oxygen and steam to form a mixture of gases which include hydrogen. DOE

N95-17642 Southwest Research Inst., San Antonio, TX.
MICRO-ULTRAVIOLET SPECTROGRAPH (MICRO-UVS)
S. A. Stern and D. C. Slater 30 Apr. 1994 33 p Prepared for Lawrence Livermore National Lab., Livermore, CA Limited Reproducibility: More than 20% of this document may be affected by microfiche quality
(Contract W-7405-eng-48)
(DE94-016704; UCRL-CR-118201) Avail: CASI HC A03

In this report, the authors present a low-mass (less than 2 kg), low-power (approximately 2 W), and low-cost (less than $0.5M) Far UV spectrometer design, capable of performing high-resolution ((lambda)/(delta)(lambda) approximately equal to 100-200) spectroscopy of planetary atmospheres in the extreme ultraviolet wavelength regime (700 (angstrom) less than (lambda) less than 1500 (angstrom)). This spectrograph, referred to in this report as the MicroUVS, is in part based on the integrated UV/VIS/IR Pluto Fast Flyby (PFF) design being developed for NASA, but is tailored to be a stand-alone instrument suitable for future BMDO/LLNL missions. Design objectives and performance of the spectrometer are discussed in detail. DOE

N95-17700 Technische Univ., Delft (Netherlands).
DEVELOPMENT OF HETEROGENEOUS WACKER OXIDATION CATALYSTS: THE ROLE OF THE SUPPORT AND THE REDOX COMPONENT Ph.D. Thesis
A. W. Stobbe-Kreemers 7 Dec. 1993 182 p See also PB92-127299
(PB94-201431; ISBN-90-6275-925-4) Copyright Avail: Issuing Activity

The Wacker process is a liquid phase catalytic process for the direct oxidation of ethene to acetaldehyde. The homogeneous catalyst consists of an aqueous solution of palladium(II) chloride and copper(II) chloride, with copper(II) chloride acting as a co-catalyst for the in situ reoxidation of palladium. The most important drawbacks are the lower reaction rate of higher alkenes and the increased production of (undesired) chlorinated side products. To overcome these disadvantages several attempts have been made to develop a heterogeneous version of the process in which alkenes are oxidized in the gas phase. One of the objectives of the research described in this thesis was to further investigate and explain the influence of the support and of the redox component activity of the catalyst. The work described in this thesis shows that it is possible to oxidize 1-butene in the gas phase over a heterogeneous catalyst with high selectivity and a good activity. The Heteropolyanion (HPA) and Palladium salts of heteropolyanions (PdHPA) catalysts appear to be the most promising heterogeneous catalysts. Their initial activity is of the same order of magnitude as the activity of the homogeneous Wacker catalyst. NTIS

N95-17744# Sandia National Labs., Albuquerque, NM.
SURFTHERM: A PROGRAM TO ANALYZE THERMOCHEMICAL AND KINETIC DATA IN GAS-PHASE AND SURFACE CHEMICAL REACTION MECHANISMS
M. E. Coltrin and H. K. Moffat Jun. 1994 46 p
(Contract DE-AC04-94AL-85000)
(DE94-016145; SAND-94-0219) Avail: CASI HC A03/MF A01

This report documents the Surftherm program that analyzes transport coefficient, thermochemical- and kinetic rate information in complex gas-phase and surface chemical reaction mechanisms. The program is designed for use with the Chemkin (gas-phase chemistry) and Surface Chemkin (heterogeneous chemistry) programs. It was developed as a 'chemist's companion' in using the Chemkin packages with complex chemical reaction mechanisms. It presents in tabular form detailed information about the temperature and pressure dependence of chemical reaction rate constants and their reverse rate constants, reaction equilibrium constants, reaction thermochemistry, chemical species thermochemistry and transport properties. This report serves as a user's manual for use of the program, explaining the required input and the output. DOE

N95-17911# Oak Ridge National Lab., TN.
RAMAN SPECTROSCOPY OF C-IRRADIATED GRAPHITE
D. M. Hembree, Jr., D. F. Pedraza, G. R. Romanoski, S. P. Withrow, and B. K. Annis 1994 8 p Presented at the 16th Materials Research Society (MRS) Fall Meeting, Boston, MA, 30 Nov. - 5 Dec. 1992
(Contract DE-AC05-84OR-21400)
(DE94-018705; CONF-921101-143) Avail: CASI HC A02/MF A01

Highly oriented pyrolytic graphite samples were irradiated with C(+) ions at 35 keV in a direction normal to the basal plane and subsequently annealed up to 1373 K. Substantial surface topography changes were observed at fluences of 5 x 10(exp 18) ions/sq m and higher using scanning electron and atomic force microscopies. Intricate networks of surface cracks and ridges developed after high dose implantation. A systematic study of the irradiation effects was conducted using Raman spectroscopy. Microstructural changes in irradiated regions were first detected at a dose of 1 x 10(exp 17) ions/sq m through the appearance of the Raman D-line at approximately 1360 cm(exp -1). The intensity of this line increases while that of the Raman G-line at 1580 cm(exp -1) decreases as the irradiation dose is increased or the irradiation temperature is decreased. After irradiation at 280 K to a fluence of 5 x 10(exp 19) ions/sq m or higher the first order spectrum exhibits one single line at a wavelength intermediate between the D- and G-lines. Damage recovery upon thermal annealing depends not only on the initial damage state but also on the annealing temperature sequence. Samples irradiated to a damage level where two distinct Raman peaks are no longer resolvable exhibited upon direct annealing at a high temperature two distinct Raman lines. By contrast, pre-annealing these highly irradiated specimens at lower temperatures produced less pronounced changes in the Raman spectra. Pre-annealing appears to stabilize damage structures that are more resistant to high-temperature annealing than those induced by irradiation. DOE

N95-17912# Pacific Northwest Lab., Richland, WA.
AN XAFS STUDY OF THE OXIDATION OF STRUCTURAL IRON IN BIOTITE MICA BY SOLUTIONS CONTAINING Br2 OR H2O2
S. M. Heald, J. E. Amonette, G. D. Turner, and A. D. Scott (Iowa State Univ. of Science and Technology, Ames, IA.) Aug. 1994 8 p Presented at the 8th International Conference on X-ray Absorption Fine Structure, Berlin, Germany, 28 Aug. - 2 Sep. 1994
(Contract DE-AC06-76RL-01830)
(DE94-018721; PNL-SA-24814; CONF-9408131-3) Avail: CASI HC A02/MF A01

X ray absorption fine structure (XAFS) measurements were made on the Fe edge for a series of biotite micas oxidized to different extents by solutions containing either Br2 or H2O2. The Fe in the Br2-treated sample was nearly completely oxidized to Fe3, while the H2O2-treated samples showed an intermediate degree of oxidation. Both the near-edge and XAFS for the H2O2 samples could have been fit well by a linear combination of the untreated and Br2-treated samples. This indicates that the partially oxidized samples had the two forms of Fe in distinct sites. Detailed analysis for the oxidized site gave a coordination of 5.7 +/- 0.5 with a Fe-O distance of 1.99 (angstrom). DOE

N95-16050*# National Aeronautics and Space Administration. Lewis Research Center, Cleveland, OH.
COMBUSTION AND FIRES IN LOW GRAVITY
Robert Friedman *In its* First NASA Workshop on Wiring for Space Applications Sep. 1994 p 81-90 (For primary document see N95-16044 04-20)
Avail: CASI HC A02/MF A02

N95-16256# Kazan Aviation Inst. (USSR).
SERVICE AND PHYSICAL PROPERTIES OF LIQUID-JET FUELS
V. I. Skomorokhov and A. F. Dregalin *In* Nanjing Univ. of Aeronautics and Astronautics, Joint Proceedings on Aeronautics and Astronautics (JPAA) May 1993 p 48-52 (For primary document see N95-16249 04-01)
Avail: CASI HC A01/MF A03

N95-16326*# National Aeronautics and Space Administration. Marshall Space Flight Center, Huntsville, AL.
PRECISION AQUEOUS CLEANER FOR RSRM
D. E. Hutchens (Thiokol Chemical Corp., Huntsville, AL.), J. M. Keen (Thiokol Chemical Corp., Huntsville, AL.), P. A. Doan (Thiokol Chemical Corp., Huntsville, AL.), C. D. DeWeese, H. D. Burns, Jr., and J. H. Vickers *In* JHU, The 1993 JANNAF Propulsion Meeting, Volume 2 Nov. 1993 p 21-36 (For primary document see N95-16324 04-20)
(Contract NAS8-38100)
Avail: CASI HC A03/MF A04

26 METALLIC MATERIALS

Includes physical, chemical, and mechanical properties of metals, e.g., corrosion; and metallurgy.

N95-16091# Naval Surface Warfare Center, Silver Spring, MD.
ATOMIC STRUCTURE AND VALENCY OF NICKEL IN SOME OF ITS OXYCOMPOUNDS Technical Report No. 2
A. N. Mansour, C. A. Melendres, M. Pankuch, and R. A. Brizzolare 28 Jun. 1994 11 p
(Contract N00014-93-WX-24290)
(AD-A281109) Avail: CASI HC A03/MF A01

The structure of the higher oxide forms of nickel (where Ni has a valency greater than +2) is of great interest from the standpoint of developing advanced nickel batteries for consumer applications and for electric vehicle propulsion. In spite of the considerable research work that has been published, there is still much uncertainty and confusion as to the stoichiometry and structure of the various oxides (hydroxides) that are formed during the charging (and discharging) of the nickel electrode. The difficulty stems in part from the highly disordered or amorphous nature of the phases formed which makes structural determination by x-ray diffraction difficult. X-ray absorption spectroscopy (XAS) consisting of the x-ray absorption near edge structure (XANES) and the extended x-ray absorption fine structure (EXAFS) is an excellent technique for the characterization of such materials which have no long range order. Preliminary to using the technique for in-situ structural determinations in an electrochemical cell, we have used XAS to study a number of standard samples for subsequent use as reference. We report initial XANES and EXAFS results that give the valency and structure of nickel in some compounds of interest in battery work. DTIC

N95-16104# Pennsylvania State Univ., University Park, PA. Dept. of Materials Science and Engineering.
DUCTILE FRACTURE AND FAILURE CRITERIA OF STRUCTURAL STEELS Progress Report, 1 Mar. 1993 - 31 May 1994
D. A. Koss 20 Jun. 1994 13 p
(Contract N00014-91-J-1414)
(AD-A280754; TR-9-ONR) Avail: CASI HC A03/MF A01

Progress is reviewed for a program which examines aspects of ductile fracture of structural steels. The research seeks to establish multiaxial failure criteria which have sufficient microstructural sensitivity to account for variations in microstructure such that fracture initiation can be predicted. The research involves both experimental and computational analysis. Progress for the period March 1 to May 31, 1994 is reviewed for (1) the

initiation of a study of failure criteria of structural steels and (2) the conclusions of a two-dimensional modeling study of void linking during ductile, microvoid fracture. DTIC

N95-16229# Naval Postgraduate School, Monterey, CA.
A PRELIMINARY ATTEMPT AT SINTERING AN ULTRAFINE ALUMINA POWDER USING MICROWAVES M.S. Thesis
Edgar M. Alhambra 22 Sep. 1994 102 p
(AD-A284978) Avail: CASI HC A06/MF A02

A commercially available microwave oven was used to sinter ultrafine alumina powders (0.02-0.05 micrometers particle size) with and without CaO sintering aid. The oven was modified by inserting a thermocouple probe through the bottom housing, and thoroughly insulating the interior with insulating material. The oven was placed in a glove box and filled with argon to prevent degradation of the thermocouple, and oxidation of the powdered graphite susceptor. Heating rates of 50-75 deg C/sec with a maximum temperature of 1575 deg C were obtained. Limited success in sintering of the the powder compacts was achieved in this preliminary effort. The microstructures of the sintered products were examined by scanning electron microscopy. It was concluded that further work is necessary to develop this technique into one which can be used for the routine sintering of fine powdered ceramic material. A review of the literature on microwave sintering of ceramic powders is also reported. DTIC

N95-16364# Argonne National Lab., IL.
THE CHEMISTRY AND PHYSICS OF TRANSITION METAL CLUSTERS
E. K. Parks, J. Jellinek, M. B. Knickelbein, and S. J. Riley 1994 5 p Presented at the 9th DOE/BES Heterogeneous Catalysis Surface Chemistry Meeting, Oconomowoc, WI, 24-27 May 1994
(Contract W-31-109-eng-38)
(DE94-014012; ANL/CHM/CP-83188; CONF-9405181-1) Avail: CASI HC A01/MF A01

In this program the authors study the fundamental properties of isolated clusters of transition metal atoms. Experimental studies of cluster chemistry include determination of cluster structure, reactivity, and the nature of cluster-adsorbate interactions. Studies of physical properties include measurements of cluster ionization potentials and photoabsorption cross sections. Theoretical studies focus on the structure and dynamics of clusters, including isomers, phases and phase changes, interactions with molecules, and fragmentation process. DOE

N95-16370# DACCO SCI, Inc., Columbia, MD.
THE USE OF ELECTROCHEMISTRY AND ELLIPSOMETRY FOR IDENTIFYING AND EVALUATING CORROSION ON AIRCRAFT Annual Report, 15 Jul. - 14 Aug. 1994
Chester M. Dacres 14 Aug. 1994 2 p
(Contract F49620-94-C-0042)
(AD-A285276; AFOSR-94-0607TR) Avail: CASI HC A01/MF A01

Aluminum 2024-T3 samples have been purchased, machined and coated. Electrochemical corrosion testing is in the process of being performed on these samples, using AC impedance measurement, ellipsometry and X-Ray Photoelectron Spectroscopy (XPS). Electrochemical impedance measurements are being used to acquire a precise impedance signature which will be used to develop a sensor for detecting corrosion processes on aircraft. The objective of this Phase 1 project is to show that a distinct signature obtained from a corroding aircraft surface can be used to develop a sensor. Data have been collected using AC impedance testing and X-Ray Photoelectron Spectroscopy. DTIC

N95-16371# DACCO SCI, Inc., Columbia, MD.
THE USE OF ELECTROCHEMISTRY AND ELLIPSOMETRY FOR IDENTIFYING AND EVALUATING CORROSION ON AIRCRAFT Annual Report
Chester M. Dacres 14 Sep. 1994 2 p
(Contract F49620-94-C-0042)
(AD-A285323; AFOSR-94-0640TR) Avail: CASI HC A01/MF A01

Electrochemical corrosion testing using AC Impedance measurements, ellipsometry and X-Ray Photoelectron Spectroscopy (XPS) is progressing according to the Plan of Action and Milestones (POAM) submitted in July, 1994. The development of the corrosion sensor is on schedule and the feasibility study shows that the proposal to build the sensor is technically sound. A detailed report dated August 15, 1994 was presented to the Program Manager explaining the theory of the AC Impedance, ellipsometry and XPS. The report also explained what the physical concept of the corrosion monitor is, and how it will respond to the various stages of corrosion. The preliminary data presented in the report showed the 'signature' of the initial stages of corroding aircraft structures. DTIC

N95-16380 Army Armament Research, Development and Engineering Center, Watervliet, NY.
EXPERIMENTAL HEAT TREATMENT OF BERYLLIUM COPPER ALLOY Final Report
Kathryn E. Noll May 1994 20 p Limited Reproducibility: More than 20% of this document may be affected by microfiche quality
(AD-A282714; ARCCB-TR-94018) Avail: CASI HC A03

A cold-rolled beryllium copper alloy, in bar form, was experiencing deformation (bowing) during machining. Several experimental heat treatments were performed in order to develop a procedure that would alleviate this condition. These treatments consisted of (1) an age-hardening (overaging) and (2) a solution treatment and age-hardening. The minimum desired ultimate tensile strength (UTS) value was achieved in both heat-treating experiments conducted. For the age-hardening experiment, any aging time between one-half hour and two hours would obtain the desired UTS. For the solution treatment and age-hardening experiment, aging for one-half hour or greater at 500 F would fulfill the UTS requirement. Our recommendation for the remaining beryllium copper bars was a one hour age-hardening at 900 F. DTIC.

N95-16420 National Defence Research Establishment, Stockholm (Sweden). Dept. of Weapon Systems, Effects and Protection.
MATERIAL AND BALLISTIC INVESTIGATION OF A TUNGSTEN-26 PERCENT RHENIUM ALLOY [STUDIUM AV EN VOLFRAM-RHENIUMLEGERING FOER ANVAENDNING SOM PROJEKTILMATERIAL]
H. Oskarsson Feb. 1994 26 p In SWEDISH
(PB94-189156; FOA-C-20962-2.3) Avail: Issuing Activity (National Technical Information Service (NTIS))

Tungsten-rhenium alloys (W-Re) exhibit a combination of ductility, strength and density that makes them a candidate material for armor piercing projectiles. The present investigation contains a literature review on the mechanical properties of tungsten-rhenium alloys and a study of metallography, static and dynamic mechanical properties and terminal ballistics of W-26 percent Re. The literature review deals with different aspects of the ductilizing effect of rhenium in tungsten and on the different deformation mechanisms present. The experimental study revealed a completely dense, textured material of Hv 550. The mechanical properties were investigated at three strain rates, 0.01, 10 and 400 /s. Yield stress and ultimate stress varied with the strain rate with maximum values of 2024 and 2300 MPa respectively, the ultimate elongation varied between 12.6 and 18 percent without correlation to the strain rate and the modulus of elasticity was 300 GPa. The terminal ballistics testing indicated that W-26 percent Re has improved penetration behavior compared with conventional tungsten-iron-nickel penetrator. NTIS

N95-16505 Minnesota Univ., Minneapolis, MN. Dept. of Chemical Engineering and Materials Science.
SELF-ASSEMBLY OF LOW-DIMENSIONAL CONDUCTORS ON Au(111) SURFACES Technical Report No. 3, 1 May 1993 - 30 Jun. 1994
J. H. Schott and M. D. Ward 23 Jun. 1994 32 p Limited Reproducibility: More than 20% of this document may be affected by microfiche quality
(Contract N00014-93-1-0563)
(AD-A280936; TR-3-ONR) Avail: CASI HC A03

Two-dimensional nanoclusters of (TTF) (TCNQ) (TTF = tetrathiafulvalene, TCNQ = tetracyano quinodmethane) and Li+ TCNQ-, formed on Au (111) surfaces by vapor phase sublimation under ambient conditions prior to growth of bulk crystals of these low-dimensional organic conductors, have been observed with scanning tunneling microscopy (STM) and scanning electron microscopy (SEM). The molecular planes of the constituents in individual nanoclusters are oriented perpendicular to the Au (111) substrate, while the clusters exhibit azimuthal orientations conforming to the threefold Au (110) directions. The nanocluster morphology and structure suggest that self-assembly of nanoclusters is governed by specific interactions between the molecular species and the substrate and molecular diffusion along (110) troughs on the Au (111) substrate surface. In the

case of the (TTF) (TCNQ) nanoclusters, TTF and TCNQ molecules assemble into molecular rows normal to the stacking direction, with intermolecular distances along the stacking direction which are nearly identical to those observed in bulk (TTF) (TCNQ). DTIC

N95-16514# Rockwell International Science Center, Thousand Oaks, CA.
PROCESSING - PROPERTY RELATIONSHIP IN ADVANCED INTERMETALLICS Final Report, 4 Mar. 1991 - 3 Mar. 1994
D. A. Hardwick and P. L. Martin Jul. 1994 66 p
(Contract F49620-91-C-0027)
(AD-A285262; SC71047.FR; AFOSR-94-0567TR) Avail: CASI HC A04/MF A01

The feasibility of using the exothermic reaction between Mo and Si for the synthesis of MoSi2 has been demonstrated. The reaction-HIP process begins with high purity elemental powder and produces a low oxygen, fully-dense MoSi2 with a grain size of approx. 40 micrometers. All of the powder handling steps were done in a low oxygen, inert gas environment to explore the limits of the precautions that are necessary to eliminate SiO2 contamination. Compression testing of reactively HIP processed material showed that this material enjoys a strength advantage over material processed by HIP from commercial powder. The compression testing was done as a function of temperature, in the range 1200-1450 deg C, and of strain rate, in the range 10(exp -3) to 10(exp -5) per second. The deformation mechanism was determined to be a combination of microcracking and dislocation glide+climb. Large strain deformation resulted in dynamic of the recrystallization MoSi2. Backscatter SEM and EM were used to characterize the deformed microstructures. DTIC

N95-16519# Fairfax Materials Research, Inc., Alexandria, VA.
COMPUTER MODELLING OF CYCLIC DEFORMATION OF HIGH-TEMPERATURE MATERIALS Technical Progress Report, 1 Jun. - 30 Aug. 1994
M. S. Duesbery and N. P. Louat 30 Aug. 1994 11 p
(AD-A285212) Avail: CASI HC A03/MF A01

This program aims at improving current methods of lifetime assessment by building in the characteristics of the micro-mechanisms known to be responsible for damage and failure. The broad approach entails the integration and, where necessary, augmentation of the micro-scale research results currently available in the literature into a macro-scale model with predictive capability. DTIC

N95-16531# Naval Surface Warfare Center, Bethesda, MD.
EXPERIMENTAL APPLICATION OF METHODOLOGIES TO QUANTIFY THE EFFECT OF CONSTRAINT ON JC FOR A 3-D FLAW GEOMETRY
W. C. Porr, Jr., R. E. Link, J. P. Waskey, and R. H. Dodds, Jr. Aug. 1994 26 p
(AD-A285309; CARDIVNSWC/TR-61-94/25) Avail: CASI HC A03/MF A01

In an effort to validate methodologies to quantify the effect of crack tip constraint on cleavage fracture toughness, a series of experiments were conducted to measure the cleavage fracture toughness, J(sub c), of an ASTM A515 Grade 70 steel utilizing large plate bend specimens containing semi-elliptical surface cracks, SC(B), (3-D flaw geometry). Jc was estimated with modified EPRI and Turner design curve schemes from load and remote strains measured at initiation. The cleavage toughness of the A515 steel used for this testing was previously characterized using a series of through-cracked single edge notch bend specimens, SE(B), (2-D flaw geometry) with various initial crack-length to specimen-width ratios, a/W. The toughness values measured for the surface cracked plate specimens were consistent with the toughness ranges predicted from the SE(B) results using the toughness scaling and two parameter fracture mechanics (J-Q) methodologies to account for differences in crack tip constraint. This result verifies the applicability of small specimen, constraint adjusted, results to engineering structural integrity prediction for the case of cleavage fracture. DTIC

N95-16540# Ames Lab., IA.
THE ANALYSIS AND MINIMIZATION OF OXYGEN CONTAMINATION IN THE POWDER PROCESSING OF MOLYBDENUM DISILICIDE Ph.D. Thesis
K. Shannon 24 Apr. 1994 105 p
(Contract W-7405-eng-82)
(DE94-014234; IS-T-1663) Avail: CASI HC A06/MF A02

Problems with MoSi2 include low-temperature fracture toughness, high-temperature creep resistance, and 'pest' phenomena. Oxygen introduced by powder processing may be the cause of some of these problems. This study led to the following conclusions: Supplied powders have significant oxygen present prior to processing (up to 2.5%), in the form of silica on the surface. This oxygen contamination did not increase by exposure to air at room temperature. An improved powder processing method was developed that uses glass encapsulation. Analysis of microstructures created from powders that contained 4900 to 24,100 ppM oxygen showed that the silica was transferred to the fully dense MoSi2 as SiO2 inclusions. A method of producing MoSi2 with less oxygen was attempted. DOE

N95-16606# Naval Surface Weapons Center, Silver Spring, MD.
XAFS SPECTRA AND THE OXIDATION STATE OF NICKEL IN SOME OF ITS OXYCOMPOUNDS
A. N. Mansour, C. A. Melendres, M. Pankuch, and R. A. Brizzolara 28 Jun. 1994 15 p
(AD-A281137; TR-1) Avail: CASI HC A03/MF A01

X-ray absorption near edge structure (XANES) spectra of nickel K-edge and x-ray diffraction patterns of several nickel oxycompounds were measured. The shift in energy of the Ni K-absorption edge towards higher values correlates well with the increase in the oxidation state of nickel from +2 to +4 in the compounds studied. The inflection point energy of the Ni pre-edge structure shifts approximately 1 eV per unit change in valency. Our results provide evidence which supports the assignment that the valency of Ni in Beta-NiOOH is +3; Ni3O2(OH)4 and commercial 'nickel peroxide' (NiO2) likewise contain trivalent nickel. The edge shift for quadrivalent nickel in KNiIO6 is reported for the first time. DTIC

N95-16786# Berkeley Applied Science and Engineering, Inc., San Francisco, CA.
STRUCTURAL INTEGRITY OF INTELLIGENT MATERIALS AND STRUCTURES. CONSTITUTIVE MODELING OF SHAPE MEMORY ALLOYS Final Technical Report, 1 Aug. 1993 - 31 Mar. 1994
M. Panahandeh, A. Masud, and F. Auricchio May 1994 108 p
(Contract F49620-93-C-0028)
(AD-A281301; Rept-83-148; AFOSR-94-0411TR) Avail: CASI HC A06/MF A02

A full-scale application of shape memory alloys in intelligent structures requires that the complex interaction between active elements (sensors, actuators, processors) and the host material be investigated and a modeling tool to simulate the behavior of these structures be developed. This research is an effort toward this direction with the following objectives: (1) Development of a constitutive theory for pseudoelastic behavior of shape memory alloys based on phase transformation in these alloys; (2) Extension of the theory to finite kinematics and developments of numerical algorithms for solution of the nonlinear pseudoelastic system; (3) Formulation of a multi-director shell theory for finite element modeling of composite laminates; (4) Numerical implementation of the theory in a suitable finite element program with nonlinear capabilities; and (5) Simulation of cyclic loading and partial loading/unloading in shape memory alloys. DTIC

N95-16788# Naval Surface Warfare Center, Silver Spring, MD.
X-RAY ABSORPTION SPECTRA AND STRUCTURE OF SOME NICKEL OXIDES (HYDROXIDES)
A. N. Mansour and C. A. Melendres 28 Jun. 1994 10 p
(Contract N00014-93-WX-24290)
(AD-A281305; TR-3-ONR) Avail: CASI HC A02/MF A01

The structure of the higher oxide forms of nickel (where Ni has a valency greater than +2) is of great interest from the standpoint of developing advanced nickel batteries for consumer applications and for electric vehicle propulsion. In spite of various research efforts, much uncertainty and confusion still exists with regard to the stoichiometry and structure of the various oxides (hydroxides) that are formed during the charging (and discharging) of the nickel electrode. The difficulty stems in part from the highly disordered or amorphous nature of the phases formed which makes structural determination by X-ray diffraction difficult. X-ray absorption fine structure (XAFS) spectroscopy is an excellent technique for

the characterization of such materials which have no longer range order and can be used for in situ measurements. DTIC

N95-16793# State Univ. of New York, Stony Brook, NY. Dept. of Materials Science and Engineering.
INVESTIGATION INTO THE SUSCEPTIBILITY OF CORROSION RESISTANT ALLOYS TO BIOCORROSION Technical Report No. 2, Jun. 1993 - Jun. 1994
Clive R. Clayton 30 Jun. 1994 16 p
(Contract N00014-92-J-4089)
(AD-A281066) Avail: CASI HC A03/MF A01

It has long been recognized that sulfate reducing bacteria (SRB) found in natural and industrial waste waters promote microbiologically influenced corrosion (MIC) of certain metals and alloys. Corrosion may be enhanced biologically, through direct enzymatic action of the bacteria, or abiotically, as a result of reaction with metabolic byproducts or change in local conditions (for example, pH) brought about by bacterial activity. In this study, x-ray photoelectron spectroscopy (XPS) is utilized in conjunction with conventional microbiological and quantitative chemical analytical techniques to analyze the effects of localized environmental conditions similar to those found near the surface of a passive stainless steel on the behavior of SRB, and to determine the ability of these bacteria to alter local environmental conditions in such a way as to create conditions that accelerate corrosion. Specifically, the interactions of Fe, Cr, Ni, and Mo ions with Desulfovibrio sp. under anoxic conditions were studied in order to determine the influence of passive dissociation products on the extent of sulfate reduction and to determine the resulting speciation of the metal ions and sulfur.
Author (DTIC)

N95-16807# Oak Ridge National Lab., TN.
EFFECTS OF SUBSTRATE TEMPERATURE ON METAL COLLOID FORMATION AND ON OPTICAL RESPONSE IN METAL ION IMPLANTED SILICA
R. H. Magruder, III (Vanderbilt Univ., Nashville, TN.), R. A. Weeks (Vanderbilt Univ., Nashville, TN.), T. S. Anderson (Vanderbilt Univ., Nashville, TN.), D. H. Osborne, Jr. (Vanderbilt Univ., Nashville, TN.), R. A. Zuhr, and C. W. White Apr. 1994 9 p Presented at the 8th World Ceramic Congress, Florence, Italy, 29 Jun. - 4 Jul. 1994
(Contract DE-AC05-84OR-21400)
(DE94-013633; CONF-940641-1) Avail: CASI HC A02/MF A01

The effects of substrate temperature during implantation of Au and Cu in high purity silica on particle sizes and optical properties are examined. The implantations result in the formation of nanometer dimension Au and Cu metal particles in the silica substrates. Increasing substrate temperature during implantation results in increasing particle size in both systems. The linear absorption increases and the intensity dependent part of the refraction index, n(sub 2), increases with increasing particle size. DOE

N95-16860*# Analytical Services and Materials, Inc., Hampton, VA.
MULTI-LAB COMPARISON ON R-CURVE METHODOLOGIES: ALLOY 2024-T3 Final Report
Anthony P. Reynolds Oct. 1994 41 p
(Contract NAS1-19708; RTOP 537-06-20-06)
(NASA-CR-195004; NAS 1.26:195004) Avail: CASI HC A03/MF A01

In an effort to determine an optimum method for ranking the fracture toughness of developmental aluminum alloys for High Speed Civil Transport applications, five labs performed K and/or J based fracture tests on aluminum alloy 2024-T3. Two material thicknesses were examined: 0.063 in. and 0.125 in. Middle crack tension and compact tension specimens were excised from 60 in. wide middle crack tension panels which had been previously tested at Boeing. The crack resistance curves generated were compared to the R-curves from 60 in. wide specimens. The experimental program indicated that effective stress intensity from secant compliance based crack length and stress intensity calculated from J-integral testing were equivalent. In addition, comparison of different specimen sizes and configurations indicated that standard validity requirements for compact tension specimens may be overly restrictive. Author

N95-16878# Texas Instruments, Inc., Dallas. Defense Systems and Electronics Group.
LIQUEFIED METAL JET PROGRAM AUTOMATION AND ROBOTICS RESEARCH INSTITUTE (ARRI) Research and Development Quarterly Status Report, 15 Jul. - 15 Oct. 1994
Nick Dringenburg, Charles Smith, Patrick DuBois, Elwin Whetsel, and John Priest 12 Oct. 1994 11 p
(Contract MDA972-93-C-0035; ARPA Order 9328)
(AD-A285470) Avail: CASI HC A03/MF A01

No lead system integration began with the testing of ball deflection. Problems with ball mass, distance to apply deflection forces, and field strength dictated a decreased ball size and increased deflection length.
DTIC

N95-17159# Pacific Northwest Lab., Richland, WA.
MIXED-MODE I/III FRACTURE TOUGHNESS OF A FERRITIC/MARTENSITIC STAINLESS STEEL
Hua-Xin Li (Associated Western Universities, Inc., Salt Lake City, UT.), R. H. Jones, D. S. Gelles, and J. P. Hirth (Washington State Univ., Pullman, WA.) Oct. 1993 17 p Presented at the Fall Meeting of the Minerals, Metals and Materials Society: Physical Metallurgy and Materials, Pittsburgh, PA, 17-21 Oct. 1993
(Contract DE-AC06-76RL-01830)
(DE94-014492; PNL-SA-22493; CONF-931009-27) Avail: CASI HC A03/MF A01

The critical J-integrals of mode I (J(sub IC)), mixed-mode I/III (J(sub MC)), and mode III (J(sub IIIC)) were examined for a ferritic stainless steel (F-82H) at ambient temperature. A determination of J(sub MC) was made using modified compact-tension specimens. Different ratios of tension/shear stress were achieved by varying the principal axis of the crack plane between 0 and 55 degrees from the load line. Results showed that J(sub MC) and tearing modulus (T(sub M)) values varied with the crack angles and were lower than their mode I and mode III counterparts. Both the minimum J(sub MC) and T(sub M) values occurred at a crack angle between 40 and 50 degrees, where the load ratio of sigma(sub i)/sigma(sub iii) was 1.2 to 0.84. The J(sub min) was 240 kJ/m(exp 2), and ratios of J(sub IC)/J(sub min) and J(sub IIIC)/J(sub min) were 2.1 and 1.9, respectively. The morphology of fracture surfaces was consistent with the change of J(sub MC) and T(sub M) values. While the upper shelf-fracture toughness of F-82H depends on loading mode, the J(sub min) remains very high. Other important considerations include the effect of mixed-mode loading on the DBT temperature, and effects of hydrogen and irradiation on J(sub min). DOE

N95-17378# Lawrence Livermore National Lab., Livermore, CA.
THE INFLUENCE OF TUNGSTEN ALLOYING ON THE MECHANICAL PROPERTIES OF TANTALUM
W. H. Gourdin, D. H. Lassila, M. M. LeBlanc, and A. L. Shields 3 Feb. 1994 6 p Presented at the EURODYMAT 1994: 1st International Conference on Mechanical and Physical Behavior of Materials Under Dynamic Loading, Oxford, England, 26-30 Sep. 1994
(Contract W-7405-eng-48)
(DE94-010071; UCRL-JC-114732; CONF-940956-8) Avail: CASI HC A02/MF A01

In mechanical tests of tantalum-tungsten alloys with nominal tungsten contents between 0 and 10 wt % for strain rates between 0.000016 and 6800s(sup (minus)1) and temperatures between 77 and 400 K, the addition of tungsten noticeably reduces the strain-rate dependence of the flow stress of tantalum near yield. It also subtly alters the strain-rate behavior of the work hardening, making it more like that of copper, an fcc metal. These effects are reflected in the limiting strains for uniform plastic deformation calculated from our flow curves. For unalloyed tantalum, the instability strain appears to drop dramatically for strain rates in excess of approximately 0.005s(sup (minus)1), whereas for tungsten bearing alloys, it remains unchanged or increases slightly. Tungsten alloys may therefore be preferable to unalloyed tantalum in applications that demand substantial ductility at high rates of strain. We briefly discuss possible mechanisms for plastic flow in tantalum and how they might be affected by tungsten additions to produce the effects we observe. DOE

N95-17398 Wright Lab., Wright-Patterson AFB, OH. Materials Directorate.
THE MECHANICAL PROPERTY DATA BASE FROM AN AIR FORCE/INDUSTRY COOPERATIVE TEST PROGRAM ON HIGH TEMPERATURE ALUMINUM ALLOYS Final Report, Nov. 1989 - Jan. 1994
Mary A. Phillips and Steven R. Thompson Feb. 1994 227 p Limited Reproducibility: More than 20% of this document may be affected by microfiche quality
(AD-A282911; WL-TR-94-4027) Avail: CASI HC A11

A mechanical property data base on high temperature aluminum alloys produced by Allied Signal (8009 sheet and extrusion) and Alcoa (CZ42 sheet and extrusion, 8019 extrusion) was generated. Mechanical property data consisted of tension, compression, shear, bearing, and fracture toughness values, fatigue, fatigue crack growth rate, and spectrum fatigue crack growth rate data were generated. DTIC

N95-17486 Army Research Lab., Watertown, MA. Materials Directorate.
METALLURGICAL EXAMINATION OF FAILED T-158 CAST AUSTEMPERED DUCTILE IRON (CADI) TRACK SHOES Final Report
V. Champagne, M. Pepi, B. Pothier, D. J. Snoha, and G. Wechsler Jun. 1994 47 p Limited Reproducibility: More than 20% of this document may be affected by microfiche quality
(AD-A282433; ARL-TR-451) Avail: Issuing Activity (Defense Technical Information Center (DTIC))

The U.S. Army Research Laboratory (ARL), Materials Directorate (MD) conducted a metallurgical examination of prototype cast austempered ductile iron (CADI) tank track shoe bodies at the request of the U.S. Army Tank-Automotive Command (TACOM). The T-158 track bodies had failed during field testing on an MI/Al battle tank. Each of the failed parts had been previously fitted with an ice cleat in service which most likely caused an undue stress concentration. The test results indicated that the failure was the result of poor part design and process control. The CADI track shoes had been fabricated according to the dimensional requirements of a forged component, instead of a separate cast design. The CADI material exhibited a variation in mechanical properties. Retained austenite measurements by X-ray diffraction correlated with the differences observed in mechanical properties. Chemical analysis revealed a high level of silicon which adversely affected the fracture toughness of the material. The CADI contained a low (but acceptable) nodule count and some of the nodules were flaked which decreased fatigue and impact resistance. Recommendations were made by ARL to redesign the track shoe utilizing casting technology criteria and to control the chemistry and microstructure. DTIC

N95-17513# Oak Ridge National Lab., TN.
EFFECT OF EXTRUSION PARAMETERS ON CONSOLIDATION OF TUNGSTEN-HAFNIUM AND TUNGSTEN-STEEL POWDERS
E. K. Ohriner, V. K. Sikka, and D. Kapoor (Army Armament Research, Development and Engineering Center, Picatinny Arsenal, NJ.) 1994 24 p Presented at the International Mining Trade Show and 96th Annual Meeting of the Canadian Institute of Mining, Metallurgy and Petroleum, Toronto, Ontario, 1-4 May 1994
(Contract DE-AC05-84OR-21400)
(DE94-013270; CONF-940521-1) Avail: CASI HC A03/MF A01

The purpose of this study was to evaluate the fabrication of tungsten-steel and tungsten-hafnium composite materials by hot extrusion of canned powders. The W-28 wt percent Hf composite was consolidated by extrusion of blended powders with preheat temperatures over the temperature range of 1100 to 1400 C. Materials were fully dense and exhibited substantial elongation of the tungsten phase within the hafnium matrix, which was further elongated by re-extrusion. The flow stress, as characterized by the extrusion constant, decreased with increasing temperature up to 1300 C and increased substantially at 1400 C as significant quantities of intermetallic phase were formed during preheating. A mixture of tungsten powder with 10 wt percent steel powder was consolidated to full density by hot extrusion at a 1600 C preheat temperature and a reduction ratio of 4.2. Microstructures were found to be essentially fully recrystallized at 1300 C preheat and to be partially recrystallized at lower preheat temperatures. DOE

N95-17616# National Inst. of Standards and Technology, Gaithersburg, MD. Corrosion Group.
CHARACTERIZATION OF THE HYDROGEN INDUCED COLD CRACKING SUSCEPTIBILITY AT SIMULATED WELD ZONES IN HSLA-100 STEEL
M. R. Stoudt and R. E. Ricker 1994 71 p See also AD-A224341
(Contract N00014-89-F-0101)
(PB94-174505; AD-A279759; NISTIR-5408) Avail: CASI HC A04/MF A01

The relative susceptibilities to hydrogen induced cold cracking were evaluated for HY-100, a steel presently in service in naval applications, and for HSLA-100. The martensitic microstructure of the HY-100 undergoes wide variations in the heat affected zone during welding which strongly influence the resistance of that alloy to cold cracking. The HSLA-100, a low carbon, precipitation hardened steel with similar strength and toughness to that of the HY-100, possesses a significantly lower degree of hardenability which results in minimal microstructural variations in the heat affected zone under the same simulated welding conditions. The mechanical properties of the base metal and the heat affected zone created during a simulated, single welding pass were characterized by the slow strain rate technique for both steels in an inert environment and in artificial seawater under free corrosion and controlled hydrogen fugacities. The electrochemical behaviors of both steels were also evaluated in artificial seawater. NTIS

N95-17637 Westinghouse Hanford Co., Richland, WA.
CHARACTERIZATION OF THE CORROSION BEHAVIOR OF THE CARBON STEEL LINER IN HANFORD SITE SINGLE-SHELL TANKS
R. P. Anantatmula, E. B. Schwenk, and M. J. Danielson (Pacific Northwest Lab., Richland, WA.) Jun. 1994 74 p Limited Reproducibility: More than 20% of this document may be affected by microfiche quality
(Contract DE-AC06-87RL-10930)
(DE94-016475; WHC-EP-0772) Avail: Issuing Activity (Department of Energy (DOE))

Six safety initiatives have been identified for accelerating the resolution of waste tank safety issues and closure of unreviewed safety questions. Safety Initiative 5 is to reduce safety and environmental risk from tank leaks. Item d of Safety Initiative 5 is to complete corrosion studies of single-shell tanks to determine failure mechanisms and corrosion control options to minimize further degradation by June 1994. This report has been prepared to fulfill Safety Initiative 5, Item d. The corrosion mechanisms that apply to Hanford Site single-shell tanks are stress corrosion cracking, pitting/crevice corrosion, uniform corrosion, hydrogen embrittlement, and microbiologically influenced corrosion. The corrosion data relevant to the single-shell tanks dates back three decades, when results were obtained from in-situ corrosion coupons in a few single-shell tanks. Since that time there have been intertank transfers, evaporation, and chemical alterations of the waste. These activities have changed the character and the present composition of the waste is not well characterized. All conclusions and recommendations are made in the absence of relevant laboratory experimental data and tank inspection data. The report attempts to identify the failure mechanisms by a literature survey of carbon steel data in environments similar to the single-shell tank wastes, and by a review of the work performed at the Savannah River Site where similar wastes are stored in similar carbon steel tanks. Based on these surveys, and in the absence of data specific to Hanford single-shell tanks, it may be concluded that the single-shell tanks identified as leakers failed primarily by stress corrosion cracking due to the presence of high nitrate/low hydroxide wastes and residual stresses. In addition, some failures may be attributed to pitting under crevices in low hydroxide locations. DOE

N95-17641 Los Alamos National Lab., NM.
RIETVELD REFINEMENT OF MAGNETIC STRUCTURES FROM PULSED-NEUTRON-SOURCE POWDER-DIFFRACTION DATA
R. A. Robinson, A. C. Lawson, A. C. Larson, R. B. VonDreele, and J. A. Goldstone 1994 14 p Presented at the Neutron Scattering, Sendai, Japan, 11-14 Oct. 1994 Limited Reproducibility: More than 20% of this document may be affected by microfiche quality
(Contract W-7405-eng-36)
(DE94-016599; LA-UR-94-2574; CONF-9410165-2) Avail: CASI HC A03

The General Structure Analysis System, GSAS, has recently been modified to include magnetic neutron-scattering cross-sections. Low-temperature diffraction data have been taken on the hexagonal

noncollinear antiferromagnet UPdSn on both the HIPD and the NPD powder diffractometers at LANSCE. The low-resolution data reveal that the magnetic structure has orthorhombic symmetry (magnetic space group P(sub c)m(prime)c2(sub 1)) between 25K and 40K, and monoclinic symmetry (magnetic space group PC(sub 112)(sub 1)) below 25K. The high-resolution data reveal that there are structural distortions with corresponding symmetry changes in each of these phases, to give chemical space groups Cmc2(sub 1) and P2(sub 1), respectively, while the paramagnetic phase above 40K has space group P6(sub 3)mc. Using GSAS, we have refined data sets from both diffractometers simultaneously, including both magnetic and structural cross-sections. Magnetoelastic coefficients for the distortions have been extracted and we have determined the sign of the coupling between the structural monoclinicity and the magnetic monoclinicity. The magnetic results from Rietveld refinement are in good agreement with model fitting to the integrated intensities of seven independent magnetic reflections and these, in turn, agree with measurements made on the same sample using the constant-wavelength reactor technique. Our results therefore validate, to some level, both the technique of using spallation sources for complicated magnetic structures and the specifics of the GSAS Rietveld code. DOE

N95-17663# California Univ., Los Angeles, CA. Dept. of Materials Science and Engineering.

ANALYSIS OF THE THROUGH-THICKNESS MICROPORE AND CONSTITUENT PARTICLE POPULATION GRADIENTS IN THE 7050-T7451 PLATE ALUMINUM ALLOYS

Marek A. Przystupa, Jimin Zhang, and Annetta J. Luevano Mar. 1994 56 p

(Contract N00014-91-J-1299)

(AD-A282970) Avail: CASI HC A04/MF A01

This report contains final results of the quantitative characterizations of the pore and constituent particle morphologies in two different variants of the 7050-T7451 six-inch-thick plate alloys. The purpose of those characterizations was to find volume fraction, size, shape, and spatial distributions of both phases and their through-thickness gradients. This characterization provides data necessary for the prediction of the size distributions of the fatigue crack initiating flaws, and for the development and test of all microstructure based fatigue life prediction and durability models. The sizes, shapes, and orientations of both phases were analyzed using the linear intercept method. Their spatial distributions were quantified using the nearest neighbor spacings obtained via Voronoi (Dirichlet) tessellation techniques. Two types of intercept lengths, global and average, have been used to represent sizes of both phases on differently oriented test planes and at different locations within the plates. The distributions of those size measures for both features were lognormal. Author (DTIC)

N95-17664# Virginia Univ., Charlottesville, VA. Dept. of Materials Science and Engineering.

FUNDAMENTAL CONCEPTS RELATING LOCAL ATOMIC ARRANGEMENTS, DEFORMATION, AND FRACTURE OF INTERMETALLIC ALLOYS Final Report, Apr. 1993 - 31 Mar. 1994

J. A. Wert Apr. 1994 119 p

(Contract F49620-93-1-0245)

(AD-A282971; UVA/525771/MSE94/101; AFOSR-94-0472TR) Avail: CASI HC A06/MF A02

The creep resistance of a TiAl/Ti3Al alloy with a lamellar microstructure has been previously found to be superior to the creep resistance of single-phase TiAl and Ti3Al alloys with compositions close to the compositions of the individual phases in the lamellar alloy. The objectives of the present research project were to identify the origin of the enhanced creep resistance of the TiAl/Ti3Al lamellar alloy, to formulate a model capable of predicting the creep strength of the TiAl/Ti3Al lamellar alloy, and to evaluate the effect of thermal exposure on the creep strength of the TiAl/Ti3Al lamellar alloy. The results, analyses, and interpretations show that the enhanced creep resistance of the TiAl/Ti3Al lamellar alloy arises from the lamellar morphology of the TiAl and Ti3Al phases. The lamellar morphology provides a large interphase interfacial area per unit volume, which is proposed to introduce a high density of dislocation sources. The high density of dislocation sources is thought to increase the work hardening rate of the lamellar alloy relative to the individual single phase alloys, an effect which contributes to the small primary creep strain and low secondary creep rate exhibited by the lamellar alloy. When the increased work hardening rate is accounted for in the constitutive equations for creep of the individual TiAl and Ti3Al phases, an analytical model formulated for creep of discontinuous, lamellar-reinforced composites can be used to predict the creep strength of the TiAl/Ti3Al lamellar alloy from the creep properties of the single phase alloys. DTIC

N95-17679# Oak Ridge National Lab., TN.

EFFECT OF HEAT TREATMENT TEMPERATURE ON CREEP-RUPTURE PROPERTIES OF Fe3Al-BASED ALLOYS

C. G. McKamey and P. J. Maziasz 1994 15 p Presented at the 8th Annual Conference on Fossil Energy Materials, Oak Ridge, TN, 10-12 May 1994

(Contract DE-AC05-84OR-21400)

(DE94-018054; CONF-9405143-5) Avail: CASI HC A03/MF A01

The effects of heat treatment at 1100 to 1250 C on the creep-rupture properties of an Fe3Al-based alloy were studied. Tests were conducted at 593 C (1100 F) and 207 MPa (30 ksi) in air. The modes of fracture were identified using optical metallography and scanning electron microscopy. Analytical electron microscopy was also used to study characteristics of the microstructure, including dislocations, ordered domains, and precipitates. The creep results showed maximum creep-rupture resistance with a heat treatment at approximately 1150 C, with significant decreases in rupture life after heat treatments at both lower and higher temperatures. The peak in creep life was associated with fine precipitates that were observed after the 1150 C heat treatment and persisted during prolonged creep at 593 C. Heat treatment at 1150 C appeared to cause dissolution of coarser precipitates which then reprecipitated as new fine particles upon cooling or during creep. These fine precipitates then pinned dislocations and grain boundaries to produce strength during creep. DOE

N95-17681 Massachusetts Inst. of Tech., Cambridge. Research Lab. of Electronics.

THEORETICAL STUDIES OF THE STRENGTHS OF MATRIX SECOND PHASE PARTICLE INTERFACES Annual Report, 1 Mar. 1993 - 28 Feb. 1994

J. D. Joannopoulos 14 Jun. 1994 7 p Limited Reproducibility: More than 20% of this document may be affected by microfiche quality

(Contract N00014-92-J-1752)

(AD-A280703) Avail: CASI HC A02

Work is summarized for the progress toward the goal to theoretically model accurately and understand the properties of interfaces between grains of particles in general and matrix/second-phase particles in particular. Accomplishments have been along the following four directions: (1) the development of a new theoretical method for performing all-electron calculations; (2) the extension and generalization of the chemical concept of electron softness to investigate the effects of impurity segregation at grain boundaries; (3) the development of the first ab-initio theory of dislocation interactions; and (4) an ab-initio calculation of atomic image Scanning Tunneling Microscopy signatures for Cu, Si, and O atoms.

Derived from text

N95-17699 Department of the Navy, Washington, DC.

CORROSION INHIBITION IN HIGH TEMPERATURE ENVIRONMENT Patent

Robert L. Jones, inventor (to Navy) 17 May 1994 5 p Filed 28 Jun. 1993

(AD-D016372; US-Patent-5,312,585; US-Patent-Appl-SN-082640; US-Patent-Class-422-7) Avail: US Patent and Trademark Office

This invention pertains to the use of tin oxide as a corrosion resistant material for preventing or inhibiting high temperature corrosion by molten sulfate-vanadate deposits and gaseous sulfur trioxide formed in engines or other high temperature apparatus which burn materials containing sodium, sulfur, and vanadium. DTIC

N95-17726# Oak Ridge National Lab., TN.

SELECTED PROPERTIES OF IRON ALUMINIDES

J. H. Schneibel 1994 14 p Presented at the Metallurgical Society Annual Meeting, San Francisco, CA, 27 Feb. - 3 Mar. 1994

(Contract DE-AC05-84OR-21400)

(DE94-018057; CONF-940286-5) Avail: CASI HC A03/MF A01

Important properties of iron aluminides have been compiled in order to help engineers and scientists to be able to quickly assess this materials system. This compilation is by no means exhaustive, but it represents a

reasonable first effort to summarize the properties of iron aluminides. Considerable care has been used in assembling the data into tables. However, no guarantee can be made that all the values compiled here are correct; and in case of doubt, or in order to obtain more detailed information, the original sources should always be consulted. DOE

N95-17728# Oak Ridge National Lab., TN.
FORGING OF FeAl INTERMETALLIC COMPOUNDS
O. Flores (Universidad Nacional Autonoma de Mexico, Cuernavaca.), J. Juarez (Universidad Nacional Autonoma de Mexico, Cuernavaca.), B. Campillo (Universidad Nacional Autonoma de Mexico, Cuernavaca.), L. Martinez (Universidad Nacional Autonoma de Mexico, Cuernavaca.), and J. H. Schneibel 1994 8 p Presented at the Metallurgical Society Annual Meeting, San Francisco, CA, 27 Feb. - 3 Mar. 1994
(Contract DE-AC05-84OR-21400)
(DE94-018124; CONF-940286-6) Avail: CASI HC A02/MF A01

Much activity has been concentrated on the development of intermetallic compounds with the aim of improving tensile ductility, fracture toughness and high notch sensitivity in order to develop an attractive combination of properties for high and low temperature applications. This paper reports experience in processing and forging of FeAl intermetallic of B2 type. During the experiments two different temperatures were employed, and the specimens were forged after annealing in air, 10(exp -2) torr vacuum and argon. From the results it was learned that annealing FeAl in argon atmosphere prior to forging resulted in better deformation behavior than for the other two environments. For the higher forging temperature used in the experiments (700 C), the as-cast microstructure becomes partially recrystallized. DOE

N95-17747# Oak Ridge National Lab., TN.
ENVIRONMENTAL EFFECTS ON IRON ALUMINIDE
J. H. DeVan, P. F. Tortorelli, and M. J. Bennett (Bennett, M. J., South Moreton, England.) 1994 13 p Presented at the 8th Annual Conference on Fossil Energy Materials, Oak Ridge, TN, 10-12 May 1994
(Contract DE-AC05-84OR-21400)
(DE94-017900; CONF-9405143-4) Avail: CASI HC A03/MF A01

Air oxidation tests of iron-aluminum alloys containing 16 and 28 atom % Al, respectively, were conducted at 1300C to determine the effect of alloy composition and section thickness on time to breakdown of oxidation resistance. Oxidation rates of 16% Al were significantly higher than for 28% Al (Fe3Al). The times over which the oxide scales remained protective correlated with extent of aluminum depletion of the alloy matrix and were therefore a direct function of the initial aluminum content of the alloy, the section thickness, and oxidation rate. The oxidation rate of the Fe3Al alloys was significantly reduced by addition of 0.1% Zr, which improved the adherence of the scale during thermal cycling to room temperature. However, the oxidation rates of the Fe3Al alloys were higher at 1300C than those reported for oxide-dispersion-strengthened (ODS) Fe-18%Cr-10%Al alloys containing Y2O3. Times to the onset of breakaway oxidation were similar for zirconium-containing Fe3Al and the ODS alloys, the lower oxidation rate of the latter offsetting the higher initial aluminum of the former. Studies of the effects of chlorine (HCl) on the oxidation/sulfidation resistance of Fe3Al-based alloys were conducted using test facilities at the National Physical Laboratory (NPL) in the United Kingdom. Alloys were exposed to a test gas composed of CO2, H2, H2O, and H2S plus 1000 to 5000 ppm HCl at 450 and 550C for 1000 h. Weight gains were relatively low and were generally less than companion specimens of Fe-Cr-Al alloys. DOE

27 NONMETALLIC MATERIALS

Includes physical, chemical, and mechanical properties of plastics, elastomers, lubricants, polymers, textiles, adhesives, and ceramic materials.

For composite materials see *24 Composite Materials.*

N95-15943# Department of Energy, Washington, DC. Assistant Secretary for Environmental Management.
HIGH-LEVEL WASTE BOROSILICATE GLASS: A COMPENDIUM OF CORROSION CHARACTERISTICS
J. C. Cunnane, comp. (Argonne National Lab., IL.), J. K. Bates (Argonne National Lab., IL.), and C. R. Bradley (Argonne National Lab., IL.) Mar. 1994 149 p
(DE94-016636; DOE/EM-0177-Vol-1) Avail: CASI HC A07/MF A02

Current plans call for the United States Department of Energy (DOE) to start up facilities for vitrification of high-level radioactive waste (HLW) stored in tanks at the Savannah River Site, Aiken, South Carolina, in 1995; West Valley Demonstration Project, West Valley, New York, in 1996; and at the Hanford Site, Richland, Washington, after the year 2000. The product from these facilities will be canistered HLW borosilicate glass, which will be stored, transported, and eventually disposed of in a geologic repository. The behavior of this glass waste product, under the range of likely service conditions, is the subject of considerable scientific and public interest. Over the past few decades, a large body of scientific information on borosilicate waste glass has been generated worldwide. The intent of this document is to consolidate information pertaining to our current understanding of waste glass corrosion behavior and radionuclide release. The objective, scope, and organization of the document are discussed in Section 1.1, and an overview of borosilicate glass corrosion is provided in Section 1.2. The history of glass as a waste form and the international experience with waste glass are summarized in Sections 1.3 and 1.4, respectively. DOE

N95-15996# Carnegie-Mellon Univ., Pittsburgh, PA. Dept. of Chemistry.
SONOCHEMICAL SYNTHESIS OF POLYSILYLENES BY REDUCTIVE COUPLING OF DISUBSTITUTED DICHLOROSILANES WITH ALKALI METALS
Krzysztof Matyjaszewski, D. Greszta, J. Hrkach, and H. K. Kim 30 Jun. 1994 66 p
(Contract N00014-94-1-0101)
(AD-A280994; TR-11) Avail: CASI HC A04/MF A01

Monomodal polysilylenes with relatively narrow molecular weight distributions (M sub w/M sub n less than 1.5) have been prepared by the reductive coupling of methylphenyldichlorosilane and di-n-hexyldichlorosilane with alkali metals in toluene in the presence of ultrasound. The optimum conditions for the sonochemical synthesis of well-defined polysilylenes in the presence of an immersion-type probe were studied. Sonochemical synthesis is accompanied by selective degradation which decreases the molecular weight to the limitng value of M sub n approximately 50,000 and polydispersities (M sub w/M sub n less than 1.2). Polymerization depends strongly on the substituents on silicon atoms, solvents, alkali metals, and temperature. For example, the polymerization of methylphenyldichlorosilane in toluene with potassium, in contrast to that with sodium, does not produce a polysilylene because the reactivity of potassium is too high leading to side reaction. DTIC

N95-16000# Vermont Univ., Burlington, VT. Dept. of Chemistry.
POLYMERIC PRECURSORS TO BINARY INORGANIC MATERIALS Final Report
Christopher W. Allen 29 Jun. 1994 7 p
(Contract N00014-89-J-1041)
(AD-A281010) Avail: CASI HC A02/MF A01

The research supported in this contract, and a previous ORN contract ('Organofunctional Phosphazenes and Organofunctional Phosphazene Polymers') has led to the establishment of an entire new class of hybrid inorganic/organic materials. The work supported by this contract was concerned with the preparation and polymerization of functionalized inorganic ring systems followed by thermal decomposition reactions to provide interesting and useful materials such as boron nitride ceramics. The general approach involved a three step process which started with the affixing of a vinyl group to an inorganic ring system (with the emphasis being on cyclophosphazenes and cycloborazines). DTIC

N95-16013# Northwestern Univ., Evanston, IL. Dept. of Chemistry.
FUNDAMENTAL STUDIES OF POLYPHOSPHAZENE AND POLYSILOXANE POLYELECTROLYTES FOR ELECTROCHEMICAL DEVICES Final Report, 12 Feb. 1990 - 11 Feb. 1994
D. F. Shriver and M. A. Ratner 1 Apr. 1994 9 p
(Contract DAAL03-90-G-0044)
(AD-A281339; ARO-27054.14-CH) Avail: CASI HC A02/MF A01

New polymeric ionic conductors were synthesized and characterized both chemically and through complex dielectric measurements, which provided information on ionic conductivity. Parallel with this experimental

program, a series of theoretical studies were performed to elucidate the mechanisms of ion transport in polymers. Some major accomplishments were the demonstration that cryptands enhance ionic conductivity in phosphazene polyelectrolytes, the theoretical indication of ion clustering, and the role of such clusters in ion transport. Considerable insight into the conduction processes in these materials was also gained from conductivity and dielectric constant measurements from DC to 6 GHz, which suggest that the attempt frequency for ion motion is above 6 GHz. The research on polyphosphazenes inspired new research on polyaluminosilicates which have excellent conductivity. DTIC

N95-16073# Japan Atomic Energy Research Inst., Tokyo (Japan).
MICROCHANNEL FORMATION IN POLYIMIDE BY HEAVY ION IRRADIATION

Yasuyo Matsumoto (Sumitomo Electric Industries Ltd., Osaka, Japan.), Yuki Matsuura (Sumitomo Electric Industries Ltd., Osaka, Japan.), Yutaka Hibino (Sumitomo Electric Industries Ltd., Osaka, Japan.), Koichi Kawakami (Sumitomo Electric Industries Ltd., Osaka, Japan.), Yoshihide Komaki, Niro Ishikawa, Tsutomu Sakurai, and Enzo Tachikawa Oct. 1993 47 p
(DE94-753315; JAERI-M-93-196) Avail: CASI HC A03/MF A01

The relations between the formation of microchannels and the conditions of heavy ion irradiation and the etching have been examined for 35 mu m thick polyimide mounted on copper plate, which was irradiated over a mask by the heavy ions. A NaClO aqueous solution was suitable for etching the irradiated polyimide without any attack for copper and the adhesion. The sharp etched pattern of micro-channels in polyimide was obtained by irradiation of heavier ions (10(exp 10)-10(exp 12)/cm(exp 2)). The sharp pattern was also obtained by the subsequent exposure of the irradiated polyimide to gamma-ray (more than 1 MGy) prior to etching. The short-wave ultraviolet light was less effective than gamma-rays. The residual ions in etched polyimide was confirmed by activation analysis. Dissolution of the polyimide up to the calculated range of ion was found to leave, yet the residual ions therein and the excess dissolution of 10% over the calculated range to decrease the residual ions in the etched polyimide below the detection limit. Injected ions increase their ranges during the time of irradiation, because the characteristics of polymer change in irradiation. For the period calculated from the track etching rate, about several % of injected ions were estimated to remain in etched polyimide. Irradiation by heavy ions leads to degradation of imide group and increase in groups of C double bond O, CO, and CN in polyimide, which results in easy etchability. DOE

N95-16085 Texas Univ., El Paso, TX.
ELECTROMAGNETIC PROCESSING OF REFRACTORY METAL SILICIDE/OXIDE COMPOSITES Final Report, 1 Aug. 1990 - 31 Jan. 1994

Arturo Bronson and Joseph Pierluissi 28 Mar. 1994 22 p Limited Reproducibility: More than 20% of this document may be affected by microfiche quality
(Contract DAAL03-90-G-0194)
(AD-A281470; ARO-28198.1-MS-SAH) Avail: CASI HC A03

The electromagnetic processing of refractory metal ceramic materials within the hot zone of an induction furnace was investigated by modeling the electromagnetic field at high temperatures (i.e., 1800 deg C) and by characterizing the microstructure after annealing zirconium disilicide powder which sustained the field. The finite element analysis (FEA) of the electromagnetic field within the furnace determined that the magnetic vector potential was significant just outside the center axis. The analysis also determined that the magnetic vector potential can substantially generate a temperature rise within the zirconium disilicide phase because of its conductivity at 1800 deg C. With ceramic powders averaging in size of 3-l0 microns, a reaction couple of ZrSi/SiO2 was prepared in-situ and annealed at temperatures greater than 1900 deg C. The reaction couple developed an interdiffusion zone near the SiO2/air interface and an inner core. Within the interdiffusion zone, reaction products consisting ZrO2 and SiO2 precipitates resulted from the diffusion of oxygen through a silica layer. During the annealing process, the couple's inner core consisted of ZrSi and liquid silicide, which upon solidification resulted in ZrSi, ZrSi2 and a Si/ZrSi2 eutectic structure. DTIC

N95-16092# Missouri Univ., Rolla, MO. Dept. of Chemistry.
LOG-(CHI(EXP 2)) DISTRIBUTION OF CORRELATION TIMES REVISITED

Robert D. OConnor and Frank D. Blum 28 Jun. 1994 15 p Submitted for publication
(Contract N00014-91-J-1274)
(AD-A281123; UMR-FDB-39) Avail: CASI HC A03/MF A01

The log-(Chi(exp 2)) distribution of correlation times and its application to polymer systems are examined. It is found that the original mean correlation-time parameter, tau sub o, does not represent the true mean of the distribution. A properly parameterized log-(Chi(exp 2)) distribution and function relating the original tau sub o and width parameters, p and b, to the true mean are derived. Fitting of both the original log-(Chi(exp 2)), corrected log-(Chi(exp 2)), and log-normal distribution to experimental data is discussed and the log-normal distribution is proposed as an alternative. Interpretations of NMR data from polymer/solvent systems can be different for the log-(Chi(exp 2)) and log-normal distributions. Due to its better defined moments, the log-normal's results are believed to be more physically realistic when large widths are required. DTIC

N95-16096 Virginia Polytechnic Inst. and State Univ., Blacksburg, VA.
THERMOPLASTIC AND THERMOSETTING HIGH GLASS TRANSITION TEMPERATURE MATRIX RESINS Final Report, 1 May 1991 - 30 Jun. 1993

James E. McGrath 1 May 1994 4 p Limited Reproducibility: More than 20% of this document may be affected by microfiche quality
(Contract DAAL03-91-G-0140)
(AD-A281508) Avail: Issuing Activity (Defense Technical Information Center (DTIC))

High performance polymers based upon 3-F containing diamines and bisaminophenols were prepared via careful molecular design. Extremely high glass transition temperatures of more than 430 C could be produced while still maintaining solubility in organic solvents. Alternatively, phenyl ethynyl endcaps were synthesized, which permitted solvent resistant cured composite matrix resins and adhesives to be prepared. With proper design, crystallizable semicrystalline materials, which melted over 400 C, were also prepared. Selected copolyimides were prepared that appear to be melt-processable and still show melting characteristics greater than 400 C. Knowledge transfer of these findings was successfully achieved in cooperation with the Lockheed Company and, as a result, void-free panels were prepared showing cured glass transition temperatures of 700 F or higher. DTIC

N95-16101# Stanford Univ., CA. Dept. of Chemistry.
SYNTHESIS OF TUNGSTEN NITRENE COMPLEXES AS PRECURSORS FOR TUNGSTEN NITRIDE Final Report

Lisa McElwee-White 16 Jun. 1994 4 p
(Contract DAAL03-91-G-0130)
(AD-A281592; ARO-28353.7-CH) Avail: CASI HC A01/MF A01

Chemical vapor deposition using organometallic precursors (MOCVD) provides a method for the preparation of thin films. Low valent tungsten nitrene complexes were synthesized as potential precursors to tungsten nitride (WN(x)), a material used in diffusion barriers for Si or GaAs semiconductor devices. The original target precursors for MOCVD of WN(x) were the carbonyl-containing complexes (CO)(5-n)(PR3)(n)W=NR, where R is an alkyl or aryl group. Later synthetic work involved the tungsten (IV) imido (or nitrene) complexes (CO)2I2LW triple bonds NPh, which were prepared by oxidation of the zwitterionic species (CO)5WNPhNPhC(OMe)Ph with one equivalent of I2 followed by addition of the coordinating species L (L=THF, pyridine, PMe3, P(OMe)3). DTIC

N95-16165 Carnegie-Mellon Univ., Pittsburgh, PA. Dept. of Chemistry.
WELL-DEFINED POLYPHOSPHAZENES BY ANIONIC POLYMERIZATION OF PHOSPHORANIMINES Final Report, 1 Jun. 1991 - 31 May 1994

Krzysztof Matyjaszewski 20 Jun. 1994 5 p Limited Reproducibility: More than 20% of this document may be affected by microfiche quality
(Contract DAAL03-91-G-0126)
(AD-A281414; ARO-28631.24-CH) Avail: CASI HC A01

Polyphosphazenes form an important class of polymers with unique properties which include a combination of high temperature stability, low temperature flexibility, low surface energy, biofriendliness, inflammability, etc. The classic synthetic approach provides very high molecular weight

polymers with broad polydispersities and with no control of end groups in low yields and under extreme conditions (a few days at temperatures above 200 C in a highly corrosive medium). The purpose of the project investigated in our laboratories was to develop alternative routes to polyphosphazenes. New synthesis should provide well defined polymers in higher yields and under milder conditions. Especially important is the control of structural features of polyphosphazenes including control of molecular weights, polydispersities, tacticities, and terminal functionalities. We focused our research on catalyzed polymerization of phosphoranimines and synthesis of poly(diarylphosphazenes) via silyl azide intermediates. DTIC

N95-16230# University of Southern California, Los Angeles, CA. Dept. of Chemistry.
DESIGN OF NEW MULTI-FUNCTIONAL ELECTROACTIVE POLYMERS WITH EMPHASIS ON OPTICAL NONLINEARITY Final Technical Report, 1 Jun. 1991 - 31 Mar. 1994
Larry R. Dalton 16 Aug. 1994 59 p
(Contract F49620-91-C-0054)
(AD-A284983; AFOSR-94-0549TR) Avail: CASI HC A04/MF A01

Synthesis and processing of organic second-order nonlinear optical materials for fabrication of electro-optic modulators are discussed. Topics dealt with in order include (1) synthesis of chromophores characterized by large hyperpolarizability and good thermal stability, (2) covalent coupling of nonlinear optical chromophores to polymer lattices, (3) lattice hardening reactions which permit locking-in of electric field poling-induced macroscopic noncentrosymmetric order, (4) fabrication of buried channel nonlinear optical waveguides by photochemical and reactive ion etching techniques, (5) coupling of nonlinear optical waveguides to fiber optic transmission lines and drive electronics, and (6) prototype device fabrication and evaluation. Various device configurations are reviewed and recent advances in applications are discussed. Comparison is made between the performance of organic and inorganic materials for electro-optic modulation applications. Author (DTIC)

N95-16354# Cornell Univ., Ithaca, NY. Dept. of Chemistry.
RESIST MATERIALS DESIGN: BASE-CATALYZED CHEMICAL AMPLIFICATION
C. G. Willson, J. F. Cameron, S. A. MacDonald, C. P. Niesert, and J. M. Frechet 30 Jun. 1994 14 p
(Contract N00014-91-J-1338)
(AD-A281805) Avail: CASI HC A03/MF A01

Many chemically amplified resists that function on the basis of acid catalysis of thermolytic actions have been described as well as systems that function on the basis of free radical chain reactions. But there have been very few reports on the use of base catalysis, of chemical transformations in resist materials. We describe here our initial results on base catalyzed chemically amplified deep-UV photoresists. Photogenerated amines were used as catalysts for the decarboxylation of carboxylic acids. Two approaches to building resists around this chemistry were investigated. (1) Decarboxylation of a low molecular weight carboxylic acid led to base induced dissolution inhibition of a phenolic polymer giving negative tone images. (2) A carboxylic acid polymer was synthesized which also is susceptible towards base catalyzed decarboxylation. Wet development of this resist material gives negative tone images. Site specific gas-phase silylation of the carboxylic acid allows the use of this material in a positive tone dry develop process. A 0.5 micrometers line-space pattern obtained by this dry develop process illustrates the potential of base-catalyzed chemical amplification. DTIC

N95-16355# Georgia Inst. of Tech., Atlanta, GA. School of Mechanical Engineering.
DEFORMATION BEHAVIOR OF THIN LUBRICANT FILMS AT ELEVATED PRESSURE Annual Report, 1 Feb. 1993 - 1 Jan. 1994
Scott Bair 1 Jan. 1994 5 p
(AD-A281848) Avail: CASI HC A01/MF A01

Significant progress has been made over the past year toward understanding the mechanisms which control friction in concentrated contact. The coefficient of friction in concentrated contact is still often dealt with as a disposable parameter in numerical analyses. Boundary and elastohydrodynamic (EHD) lubrication have been recognized as separate regimes of concentrated contact lubrication since the EHD solution of Ertel-Grubin. However, the delineation of these regimes is nearly always in practice based on the magnitude of the film thickness relative to surface roughness rather than a transition in friction. It has been observed in boundary lubrication and in some aspects of elastohydrodynamic lubrication that friction is nearly Coulombic in nature - the friction coefficient is only weakly dependent upon load and sliding velocity. In some instances the friction coefficient may be so similar in the boundary and EHD regimes that friction alone does not clearly discriminate the transition from one to the other. These attributes of liquid lubrication would seem enigmatic. DTIC

N95-16369 David Sarnoff Research Center, Princeton, NJ.
CERAMIC/METAL COMPOSITE CIRCUIT-BOARD-LEVEL TECHNOLOGY FOR APPLICATION SPECIFIC ELECTRONIC MODULES (ASEMs) Technical Report, 24 Jun. - 21 Sep. 1994
Barry J. Thaler 21 Sep. 1994 28 p Limited Reproducibility: More than 20% of this document may be affected by microfiche quality
(Contract DAAB07-94-C-C009; ARPA Order A840)
(AD-A285066) Avail: CASI HC A03

Most of the major elements of the LTCC-M technology have been developed, and all have been shown to be compatible. The development of the green tape ceramic has been completed. The materials and processing have been developed to fire this green tape to a Cu/Mo/Cu metal core such that a very dense ceramic is formed with zero lateral (x-y plane) shrinkage. Thick film conductors have been developed for use with this tape. The process for mass fabrication of electrical feedthroughs in the Cu/Mo/Cu core has been successfully extended to laser drilled holes as small as 7 mils in diameter. Additionally, thin film overlays with a photosensitive BCB (from Dow Chemical) dielectric have been deposited on top of the fired ceramic. DTIC

N95-16393 Vanderbilt Univ., Nashville, TN. Dept. of Chemistry.
ENCAPSULATED ALKALINE-EARTH ORGANOMETALLICS AS CONTROLLED SOURCES OF CALCIUM, STRONTIUM, AND BARIUM IONS Final Report, 1 Jan. 1991 - 30 Apr. 1994
Timothy P. Hanusa 28 Jun. 1994 27 p Limited Reproducibility: More than 20% of this document may be affected by microfiche quality
(Contract DAAL03-91-G-0008)
(AD-A281547; ARO-28402.6-CH) Avail: CASI HC A03

Cyclopentadienyl rings with substituents that interlock with those of a second ring form 'encapsulated' metallocenes ((C5R5)2M) with the alkaline-earth metals (Ca, Sr, Ba). These metallocenes are conveniently manipulated, volatile, hydrocarbon-soluble sources of the metal cations, which make the compounds attractive as precursors to metal oxides and ceramics. The physical properties of the metallocenes are highly sensitive to the degree of encapsulation and to the geometry of the encapsulating ligands; more flexible rings reduce the ability of complexes to pack into lattices, and oils and waxes will be formed. Other main-group metals (Sn, Pb) and lanthanide elements (Sm) can be encapsulated with the same ligands used for the alkaline-earths. Under the proper conditions, a ring can be displaced from an encapsulated metallocene, exposing the metal center and activating the complex. Disproportionation of the resulting mono(ring) complexes (C5R5)M(E) into symmetrical (C5R5)2M and M(E)2 species can be blocked. 'Ligand synergism' in mono(ring) complexes can enhance their chemical and thermal stabilities relative to those of the parent symmetrical species. DTIC

N95-16409 Texas A&M Univ., College Station, TX. Dept. of Chemistry.
DETECTION OF CROSSLINK FORMATION BY 2 + 2 PHOTOCYCLOADDITION IN POLY (VINYL CINNAMATE) BY C-13 SOLID-STATE NMR Technical Report, 1 Jun. 1993 - 31 May 1994
Timothy W. Skloss and James F. Haw 13 Jul. 1994 11 p Limited Reproducibility: More than 20% of this document may be affected by microfiche quality
(Contract N00014-91-J-1475)
(AD-A281955; TR-7) Avail: Issuing Activity (Defense Technical Information Center (DTIC))

Poly (vinyl cinnamate), PVCN, is one of the more important polymers used in NLO research. It is frequently used as a host polymer into which suitable dyes are introduced, especially those with limited solubilities in other polymers. During the poling process, the polymer may be irradiated with UV light to yield a material with superior second harmonic generation (SHG) retention and reduced solubility. This is frequently assumed to be

due to photocrosslinking reactions between cinnamoyl groups in different chains or alternatively between cinnamoyl groups and NLO dye molecules with suitable structures. The mechanism of this crosslinking is proposed to be 2 + 2 cycloaddition of the olefinic groups to yield four-membered-ring crosslink sites. Although this mechanism is appealing in that it is consistent with well characterized reactions in solution, experimental evidence for this important reaction in NLO polymers has been lacking, and its acceptance has not been universal. DTIC

N95-16427 Massachusetts Univ., Lowell, MA. Dept. of Chemistry.
SELF ASSEMBLED SPIN COATED AND BULK FILMS OF A NOVEL POLYDIACETYLENE AS SECOND ORDER NLO POLYMERS Technical Report, 1 Jun. 1993 - 31 May 1994
W. H. Kim, B. Bihari, R. Moody, N. B. Kodali, and J. Kumar 31 May 1994 32 p Limited Reproducibility: More than 20% of this document may be affected by microfiche quality
(Contract N00014-90-J-1148)
(AD-A282271; TR-94-12) Avail: CASI HC A03

The polymer chains of a novel asymmetric polydiacetylene, namely poly(((8-butoxy carbonyl) methyl urethanyl) 1-(5-pyrimidyl)-octa-1,3-diyne) (BPOD), in the absence of nonlinear optically active chromophores and without recourse to poling assemble in an acentric stable polar organization upon spin coating or solution casting. Asymmetry of the side groups and the- spontaneous alignment of the urethane side groups by means of hydrogen bonds appear to be responsible for this organization. An abrupt decrease of SH intensity at around 130 C is found to be closely related to the breaking of noncentrosymmetry in the films in conjunction with the disruption of intramolecular hydrogen bonds. The changes observed were reversible below 130 C but becomes irreversible above this temperature. Comparison of absorption spectra of the poly(BPOD) films before and after thermal treatment indicate that only a slight change occurred in the absorption characteristics of the polymer backbone. FT-IR and dielectric spectroscopy confirm the relaxation of the stable hydrogen bonded polar organization at higher temperatures. Activation energies involved in this process were found to be a little higher than hydrogen bonding dissociation energies calculated from polyamide and polyurethane. The larger activation energies observed here indicate the combined effect of the hydrogen bonds followed by relaxation. DTIC

N95-16434# North Carolina Univ., Chapel Hill, NC. Chemistry Lab.
ELECTROCHEMICAL PROPERTIES OF LITHIUM ION CONDUCTING SOLID POLYMER ELECTROLYTES
M. Watanabe, C. S. Velazquez, Zeev Porat, Otto Haas, and T. T. Wooster 19 Jul. 1994 19 p Sponsored by NSF; DOE; and ONR
(AD-A281875) Avail: CASI HC A03/MF A01

In 1985 our laboratory initiated an investigation of the electrochemical reactions of molecular electron donor/acceptor species dissolved in solid and semi-solid solvents. Poly-ether polymer electrolytes were selected as the model solid and semi-solid solvents, and the redox species have included ferrocenes, metal bipyridine complexes, tetracyano quinodimethane (TCNQ), and derivatives in which poly-ether chains have been attached to such species. The thrust of this investigation was firstly, to develop methodology for obtaining quantitatively interpretable electron transfer and mass transport rates of such molecular solutes in solid or semi-solid solvents, and secondly, to explore ways in which their solid state behavior differs form that familiar in fluid electrolyte solutions. This paper will draw together the essential aspects of the microelectrode-based solid state voltammetry methodology developed, and describe some of the special aspects of electron transfer and mass transport dynamics observed during this still ongoing investigation. DTIC

N95-16449# Carnegie-Mellon Univ., Pittsburgh, PA. Dept. of Chemistry.
CONTROL OF MOLECULAR WEIGHTS AND POLYDISPERSITIES IN RADICAL POLYMERIZATION OF STYRENE IN THE PRESENCE OF STABLE RADICALS
Daniela Mardare, Krzysztof Matyjaszewski, and Takeo Shigemoto 30 Jun. 1994 5 p
(Contract N00014-94-1-0101)
(AD-A281040; TR-8) Avail: CASI HC A01/MF A01

Radical polymerization of styrene was investigated by initiation with benzoyl peroxide and 2,2'-azobis(2-methylpropionitrile) (AIBN), in the presence of nitroxy-based stable radical scavengers. The effects of the nature and concentration of nitroxy radicals and the nature and concentration of the radical initiators on the kinetics, evolution of molecular weights, and polydispersities of polystyrenes prepared at various temperatures are also discussed. DTIC

N95-16450# Carnegie-Mellon Univ., Pittsburgh, PA. Dept. of Chemistry.
REGIOCHEMISTRY OF POLYSILANES PREPARED BY RING OPENING POLYMERIZATION
Eric Fossum and Krzysztof Matyjaszewski 30 Jun. 1994 4 p
(Contract N00014-94-1-0101)
(AD-A281041; TR-19) Avail: CASI HC A01/MF A01

A series of cyclotetrasilanes bearing varying numbers of methyl and phenyl substituents, Me(n)Ph(8-n)Si4, have been prepared and characterized using H-1, C-13, and Si-29 NMR spectroscopy. The cyclotetrasilanes were polymerized employing silyl cuprates as initiators resulting in monomodal polysilanes with interesting regiochemistries. The regiochemistry of the polymerizations was studied by Si-29 NMR spectra of the polymers. The polymers resulting from ring opening polymerization of Me3Ph5Si4, Me5Ph3Si4, and Me6Ph2Si4 showed absorbance maxima lambda sub max = 343, 332, and 328 nm, respectively. DTIC

N95-16451# Carnegie-Mellon Univ., Pittsburgh, PA. Dept. of Chemistry.
LIVING RADICAL POLYMERIZATION. 1: POSSIBILITIES AND LIMITATIONS
Krzysztof Matyjaszewski, Dorota Greszta, and Daniela Mardare 30 Jun. 1994 27 p
(Contract N00014-94-1-0101)
(AD-A281042; TR-16-1) Avail: CASI HC A03/MF A01

Possibility of the synthesis of well-defined polymers by radical polymerization is discussed. Kinetic analysis demonstrates that the preparation of polymers with controlled macromolecular structure in a 'living' radical process requires low stationary concentration of growing radicals which are in a dynamic equilibrium with dormant species. Three approaches are described: first, when growing radicals react reversibly with scavenging radicals to form covalent species, second when growing radicals react reversibly with covalent species to produce persistent radicals, and the third in which growing radicals participate in the degenerative transfer reaction which regenerates the same type of radicals. Some of the reported 'living' radical systems are critically evaluated. DTIC

N95-16483# Purdue Univ., West Lafayette, IN.
NONLINEAR OPTICAL AND CHARGE DISTRIBUTION STUDIES PROBING ELECTRIC FIELD EFFECTS IN POLYMER THIN FILMS FOR SECOND ORDER NONLINEAR OPTICS End-of-year Technical Report, 1 May 1993 - 30 Apr. 1994
Hilary S. Lackritz 3 May 1994 24 p
(Contract F49620-93-1-0158)
(AD-A280980; AFOSR-94-0387TR) Avail: CASI HC A03/MF A01

The effect of large magnitude electric fields on polymer thin films is investigated in order to improve poling efficiencies in polymer films for second order nonlinear optical applications. This research determines the charge distribution, symmetry, and magnitude across doped and undoped glassy polymer thin films as a function of temperature, time, and poling (processing). Electrochromism, second order nonlinear optics, dielectric relaxation, isothermal current and surface voltage decay measurements will be used to determine the material properties. Trapping levels and sites will also be examined. By using dielectric relaxation and optical techniques we will explore how applied electric fields affect rotational mobility of small chromophores in polymer hosts. We expect to be able to improve poling efficiency and thus device performance both by achieving the greatest possible fields with the best magnitude and symmetry characteristics, and enhancing the temporal and thermal properties of the films by manipulating their charge storage and transport properties. This understanding will allow the most efficient development and design for nonlinear optical materials. DTIC

N95-16488# North Carolina State Univ., Raleigh, NC. Dept. of Materials Science and Engineering.
THE DEPOSITION OF ELECTRO-OPTIC FILMS ON SEMICONDUCTORS Final Report, 1 May 1993 - 30 Apr. 1994
Angus I. Kingon, Orlando H. Auciello, and Klaus J. Bachmann 30 Apr.

1994 51 p
(Contract N00014-91-J-1307)
(AD-A285068) Avail: CASI HC A04/MF A01

Highly epitaxial, dense potassium niobate thin films can be reproducibly grown on various substrates including magnesium oxide, magnesium spinel, and potassium tantalate by ion-beam sputter deposition. A strong correlation between lattice mismatch and epitaxial film quality can be made as films on potassium tantalate, which possess the lowest lattice mismatch, displayed the smallest amount of grain tilt. Lower optical losses were measured for thinner potassium niobate films as streak lengths of greater than 8 mm were observed. The dominant loss mechanism in these films can be attributed to volume scattering, possibly originating from twin domains or low angle grain boundaries. Second harmonic generation of green light has been demonstrated for these potassium niobate thin film planar waveguides both in the bulk and waveguide configurations. Author (DTIC)

N95-16500# Carnegie-Mellon Univ., Pittsburgh, PA. Dept. of Chemistry.
LIVING RADICAL POLYMERIZATION OF VINYL ACETATE
D. Mardare and K. Matyjaszewski 30 Jun. 1994 29 p
(Contract N00014-94-I-0101)
(AD-A280901; TR-17) Avail: CASI HC A03/MF A01

Synthesis of well-defined poly(vinyl acetate) in 'living' radical polymerization is reported. Straight lines in semilogarithmic plots up to greater than 90% conversion indicate internal first order in monomer and a constant concentration of growing species. Molecular weights increase linearly with conversion. The initiating system might involve persistent radicals formed by the ternary complexes of organoaluminum compounds with Lewis bases and stable radicals. This article focuses on Al(iBu)3:DPy:TEMPO system. The effect of the composition of the initiating system and its aging is described. DTIC

N95-16501# Carnegie-Mellon Univ., Pittsburgh, PA. Dept. of Chemistry.
FROM LIVING CARBOCATIONIC TO LIVING RADICAL POLYMERIZATION
Krzysztof Matyjaszewski 30 Jun. 1994 14 p
(Contract N00014-94-I-0101)
(AD-A280902; TR-18) Avail: CASI HC A03/MF A01

'Living' carbocationic polymerization is compared to 'living' radical process. Similarities and differences are discussed. 'Living' radical polymerization of vinyl acetate and methyl methacrylate to provide polymers with controlled molecular weights and narrow molecular weight distribution (M(sub w)/M(sub n) less than 1.2) are presented. DTIC

N95-16507# Connecticut Univ., Storrs, CT. Inst. of Materials Science.
THE EFFECT OF BRUSH POLYDISPERSITY ON THE INTERPHASE BETWEEN END-GRAFTED BRUSHED AND POLYMERIC MATRICES
Charles F. Laub and Jeffery T. Koberstein 20 Jun. 1994 40 p
(Contract N00014-91-J-1786)
(AD-A280975) Avail: CASI HC A03/MF A01

A self-consistent computer simulation has been used to calculate the concentration profile of an end-tethered polymer chain in a polymer matrix in order to investigate the influence of brush polydispersity on the width of the interphase. It was found that increasing the brush polydispersity increased the width of the interphase between the brush and the matrix. The results suggest that highly polydisperse brushes will result in increased adhesion when compared with an analogous brush of narrow molecular weight distribution. DTIC

N95-16625# North Carolina State Univ., Raleigh, NC. Dept. of Materials Science and Engineering.
LOW TEMPERATURE DEPOSITION AND CHARACTERIZATION OF N- AND P-TYPE SILICON CARBIDE THIN FILMS AND ASSOCIATED OHMIC AND SCHOTTKY CONTACTS Semiannual Technical Report, 1 Jan. - 30 Jun. 1994
Robert F. Davis and Robert J. Nemanich Jun. 1994 46 p
(Contract N00014-92-J-1500)
(AD-A281060) Avail: CASI HC A03/MF A01

Monocrystalline silicon carbide (SiC) films have been grown on vicinal 6H-SiC (0001) substrates via gas source molecular beam epitaxy at 1050-1250 C. Using transmission electron microscopy, step bunching was observed at the outset of the initial stage of growth using C3H4/Si2H6 ratios of 1, 2, or 10. Subsequent growth occurred via island formation (C2H4-rich) or step-flow (1:1 ratio). Occurrence of the different growth modes may be controlled by changes in the surface diffusion length caused by surface reconstruction as a result of changing the C/Si ratio. Cubic beta-SiC and hexagonal 6H-SiC deposit using high and 1:1 C/Si ratios, respectively. Unintentionally doped films are n-type with n = (0.2-1.0) x 10(exp 17)/cu cm. Similar atomic and hole concentration of 5 x 10(exp 18) and 1.2 x 10(exp 18), respectively, were measured in Al-doped p-type films. AlN deposited on 6H-SiC (0001) substrates possess a negative electron affinity. The surface Fermi level of the AlN is approxately 3.5 eV above the valence band maximum. Thin film electrical contacts of Co exhibited rectifying behavior with n less than 1.06 and a leakage current of 2.0 x 10(exp -8) at -10 V. After annealing at 1000 C for 2 min, ohmic-like behavior was observed as a result of significant interface reaction. DTIC

N95-16628# South Carolina Univ., Columbia, SC.
SYNTHESIS OF LOW BAND GAP ZWITTERIONIC AND PLANAR CONJUGATED PYRROLE-DERIVED POLYMERS. REVERSIBLE OPTICAL ABSORBANCES FROM THE UV TO THE NEAR-IR
Thorsten W. Brockmann and James M. Tour 28 Jun. 1994 15 p
(Contract N00014-89-J-3062)
(AD-A281174; TR-28) Avail: CASI HC A03/MF A01

Described is the synthesis of a zwitterionic pyrrole-derived polymer. The monomer is formally an azomethine ylide and it was synthesized in three steps from pyrrole. The monomer was polymerized using copper-bronze in DME. The polymer had a strong optical absorbance at 512 nm in THF and an interunit ionic interaction is proposed to explain this large red-shifted band. If aqueous NaOH is added to the THF solution, or a Lewis basic solvent used instead of THF/NaOH, then a tremendous bathochromic shift occurs to 881 or 901 nm, respectively. The large shifts are attributed to a dramatic structural change in the polymer induced by hydroxide or Lewis base attack on the iminium unit. This causes a cascade of electron shifts to form a fully conjugated polymer that is fixed into a planar conformation. The planarization process is reversible so that addition of acid or shifting to a weaker Lewis basic solvent causes the polymer to recover its zwitterionic form and its original optical absorption characteristics. Moreover, upon mild reduction of the zwitterionic polymer with Pd/C and H2 (1 atm), some of the extended conjugation is lost but a polymer forms that has an enormous optical absorption maximum range from the near-UV to the near-IR (Lambda sub max = 886 nm) depending on the solvent or hydroxide concentration. Further, a sample of the reduced polymer can be dispersed in plasticized poly(vinyl chloride). The flexible polymer composite reversibly changed from dark blue-brown in aqueous hydroxide to bright yellow-orange in aqueous HCl. DTIC

N95-16630# South Carolina Univ., Columbia, SC.
SYNTHESIS OF PLANAR POLY(P-PHENYLENE) DERIVATIVES FOR MAXIMIZATION OF EXTENDED PI-CONJUGATION
James M. Tour and Jaydeep S. Lamba 28 Jun. 1994 9 p
(Contract N00014-89-J-3062)
(AD-A281179; TR-36) Avail: CASI HC A02/MF A01

Described is the synthesis of ladder polymers with a poly(p-phenylene) (PPP) backbone. The main PPP backbone was synthesized via palladium-catalyzed coupling of an arylbis(boronic ester) with an aryl dibromide. Imine bridges, formed by exposure of the polymer to trifluoroacetic acid, are used to force the consecutive units into planarity. The bridging units are sp2 hybridized thus allowing for greater pi-electron flow between the consecutive phenyl units by lowering the band gap between the hydroquinoidal and the quinoidal forms of the phenylene backbone. Upon planarization, bathochromic shifts of 210-240 nm occur for the n-dodecyl substituted polymer. The optical spectra of the planar systems are compared to that of the parent nonplanarized polymers, oligo(p-phenylenes), PPP, and other near-planar PPP derivatives. When the bridges are n-dodecyl substituted, the fully planar structures can be made into flexible free standing films. DTIC

N95-16783# South Carolina Univ., Columbia, SC. Dept. of Chemistry.
SYNTHESIS OF POLYPHENYLENES AND POLYNAPHTHALENES BY THERMOLYSIS OF ENEDIYNESS AND DIALKYNYLBENZENES
James M. Tour and Jens A. John 28 Jun. 1994 10 p
(Contract N00014-89-J-3062)
(AD-A281294; TR-30-ONR) Avail: CASI HC A02/MF A01

Described are the syntheses of substituted enediynes and

dialkynylbenzenes using Pd- or Pd/Cu-catalyzed cross coupling procedures. The products were then thermalized, generally in benzene, to afford the corresponding poly(p-phenylene)s and poly(1,4-naphthalene)s. Thirteen examples are provided that show the scope of the polymerization process based upon substituent patterns and cyclization moieties. The superb thermal resiliency of the newly derived polymers is demonstrated using thermogravimetric analysis. The polymer structure was generally confirmed using IR data correlations to small molecules that resembled the polymer's repeat unit structure. Radical trapping of dimeric intermediates, that were analyzed by GCMS, further substantiated the proposed mechanistic route. The step-growth polymerization pattern was determined by monitoring the degree of monomer consumption versus the polymer molecular weight.
DTIC

N95-16792 Texas Univ., Austin, TX. Dept. of Chemistry and Biochemistry.
SOLUBILIZATION OF HYDROPHOBIC SUBSTANCES INTO BLOCK COPOLYMER MICELLES IN AQUEOUS MEDIA AND THEIR RELEASE
Final Report, 25 Jul. 1993 - 24 Jan. 1994
P. Munk and S. E. Webber 20 Feb. 1994 9 p Limited Reproducibility: More than 20% of this document may be affected by microfiche quality
(Contract DAAH04-93-G-0405)
(AD-A281395; ARO-32305.3-CH) Avail: Issuing Activity (Defense Technical Information Center (DTIC))

The objective of this research project was the study of properties of polymer micelles that control the uptake or release of hydrophobic species from aqueous solution. Fluorescence techniques were used to monitor the rate of equilibration of small molecule fluorophores with respect to the micelle interior. An additional goal was to characterize how the properties of the polymer influence the final micelle properties (e.g. aggregation number, hydrodynamic diameter, radius of gyration, eta.). The conditions that permit exchange of individual polymers between micelles have also been determined. Most of our work has involved polymer micelles with polystyrene cores and poly(methylmethacrylate) or poly(t-butylmethacrylate) coronas in organic solvents and poly(methacrylic acid) coronas in aqueous solution.
DTIC

N95-16829 Sandia National Labs., Albuquerque, NM.
RELATIONSHIPS BETWEEN FERROELECTRIC 90 DEG DOMAIN FORMATION AND ELECTRICAL PROPERTIES OF CHEMICALLY PREPARED Pb(Zr,Ti)O3 THIN FILMS
B. A. Tuttle, T. J. Garino, J. A. Voigt, T. J. Headley, D. Dimos, and M. O. Eatough 1994 20 p Presented at the NATO Advanced Research Workshop on Electroceramic Films, Villa Del Mar (Italy), 20 Jun. 1994 Limited Reproducibility: More than 20% of this document may be affected by microfiche quality
(Contract DE-AC04-94AL-85000)
(DE94-015274; SAND-94-1629C; CONF-9406220-1) Avail: CASI HC A03

For PZT films deposited on Pt coated substrates, remanent polarization is a monotonic function of thermal expansion of the substrate, a result of 90(degree) domain formation occurring as the film is cooled through the transformation temperature. PZT film stress in the vicinity of the Curie point controls 90 deg domain assemblages within the film. PZT films under tension at the transformation temperature area-domain oriented; whereas, films under compression at the transformation temperature are c-domain oriented. From XRD electrical switching of 90 deg domains is severely limited. Thus, formation of these 90 deg domains in vicinity of the Curie point is dominant in determination of PZT film dielectric properties. Chemically prepared PZT thin films with random crystallite orientation, but preferential a-domain orientation, have low remanent polarization (24 (mu)C/sq cm) and high dielectric constant (1000). Conversely, PZT films of similar crystalline orientation, but of preferential c-domain orientation, have large remanent polarizations (37 (mu)C/sq cm) and low dielectric constants (700). This is consistent with single-crystal properties of tetragonally distorted, simple perovksite ferroelectrics. Further, for our films that grain size - 90 deg domain relationships appear similar to those in the bulk. The effect of grain size on 90 deg domain formation and electrical properties are discussed.
DOE

N95-16844# Boeing Defense and Space Group, Seattle, WA.
PROCESSING, FABRICATION, CHARACTERIZATION AND DEVICE DEMONSTRATION OF HIGH TEMPERATURE SUPERCONDUCTING CERAMICS Quarterly Technical Report No. 3, 30 Apr. - 30 Jul. 1994
Thomas S. Luhman and Ilhan A. Aksay 30 Jul. 1994 27 p
(Contract F49620-90-C-0079)
(AD-A285145; AFOSR-94-0602TR) Avail: CASI HC A03/MF A01

A detailed small-angle neutron scattering study of the vortex lattice in a single crystal of YBa2Cu3O(7-x) was made for a field of 0.5 tesla inclined at angles between 0 and 80 degrees to the crystalline c axis. The vortex lattice is triangular for all angles. For angles less than or equal to 70 degrees its orientation adjusts itself to maximize the pinning energy to densely and highly regularly spaced twin planes. These observations have important implications for the microscopic flux-pinning mechanism, and hence for the critical current achievable in YBa2Cu3O(7-x). For large angles (about 80 degrees) the vortex lattice consists of independent chains in the orientation predicted by anisotropic London theory.
Author (DTIC)

N95-16863 Spire Corp., Bedford, MA.
EPITAXIAL MOCVD OF THIN FILM CERAMICS FOR PYROELECTRIC DETECTORS Final Report, 1 Jun. - 1 Dec. 1993
1 Dec. 1993 20 p Limited Reproducibility: More than 20% of this document may be affected by microfiche quality
(Contract DAAB07-93-C-U009)
(AD-A281397; FR-60288) Avail: CASI HC A03

The objective of this research is to increase the sensitivity of pyroelectric detectors by growing a thin-film single crystal of lead-titanate (PTO) on cobalt-silicide (CoSi2) on silicon using metalorganic chemical vapor deposition (MOCVD). A thermal isolated, aligned film should increase detectivity. In Phase 1 of this research Spire demonstrated MOCVD of PTO on CoSi2 on silicon by MOCVD using a diffusion barrier between the films. Small capacitors were fabricated and the dielectric constant was formed to vary with temperature as expected. Multiple films were required to preserve the heteroepitaxial crystal structure while preventing chemical interactions and interdiffusion. Formation of silicon-dioxide prevents direct deposition of epitaxial oxide films on silicon, so that CoSi2 was deposited first. This was followed by laser ablation deposition of the conducting film yttrium-barium copper-oxide to prevent inter-diffusion of lead. The PTO film was then put down by MOCVD, and the structure was verified' by X-ray diffraction.
DTIC

N95-16865# Case Western Reserve Univ., Cleveland, OH. Dept. of Macromolecular Science.
SYNTHESIS AND MESOMORPHIC BEHAVIOR OF POLY((2S, 3S)-(+)-2-CHLORO-3-METHYLPENTYL 4'-(OMEGA-VINYLOXYALKYLOXY)BIPHENYL-4-CARBOXYLATE S WITH ETHYL AND PROPYL ALKYL GROUPS
V. Percec and Q. Zheng 30 Jun. 1994 11 p
(Contract N00014-89-J-1828)
(AD-A281402; TR-9) Avail: CASI HC A03/MF A01

The synthesis and cationic polymerization of (2S, 3S)-(+)-2 chloro 3-methylpentyl 4'-(2-vinyloxyethyloxy) biphenyl 4-carboxylate (15-2) and (2S, 3S)-(+)-2-chloro 3-methylpentyl 4'-(3-vinyloxyethyloxy) biphenyl 4-carboylate (15-3) are described. The mesogenic behavior of the resulting polymers is discussed as a function of the molecular weight and spacer length. Based on the second and subsequent heating and cooling scans, poly(15-2)s exhibit an enantiotropic S(x) (unidentified smectic) phase. Poly (15-3)s show an enantiotropic cholesteric phase and an inverse monotropic S(x) phase.
DTIC

N95-16934 Sandia National Labs., Albuquerque, NM. Ceramic Synthesis and Inorganic Chemistry Dept.
STRUCTURE-PROPERTY RELATIONSHIPS IN SOL-GEL-DERIVED THIN FILMS
C. J. Brinker, N. K. Raman (New Mexico Univ., Albuquerque, NM.), R. Sehgal (New Mexico Univ., Albuquerque, NM.), and D. Hua (New Mexico Univ., Albuquerque, NM.) 1994 22 p Presented at the 205th American Chemical Society National Meeting, Denver, CO, 28 Mar. - 2 Apr. 1993 Limited Reproducibility: More than 20% of this document may be affected by microfiche quality
(Contract DE-AC04-94AL-85000)
(DE94-016149; SAND-94-1669C; CONF-930304-33) Avail: CASI HC A03

The molecular-scale species distributions and intermediate-scale structure of silicate sols influence the microstructures of the corresponding thin films prepared by dip-coating. Using multi-step hydrolysis procedures, the authors find that, depending on the sequence and timing of the successive steps, the species distributions (determined by (29)Si NMR) and intermediate scale structure (determined by SAXS) can change remarkably for sols prepared with the same nominal composition. During film formation, these kinetic effects cause differences in the efficiency of packing of the silicate species, leading to thin film structures with different porosities. DOE

N95-16935 Lawrence Livermore National Lab., Livermore, CA.
SUPERPLASTICITY AND SUPERPLASTIC FORMING OF CERAMICS
T. G. Nieh and J. Wadsworth May 1994 12 p Limited Reproducibility: More than 20% of this document may be affected by microfiche quality
(Contract W-7405-eng-48)
(DE94-016172; UCRL-CR-117234) Avail: CASI HC A03

Recent advances in the basic understanding of superplasticity and superplastic forming of ceramics are reviewed. Deformation mechanisms as well as microstructural requirements for superplastic ceramics are discussed. Microstructural effects, such as grain size, dynamic grain growth, and the presence of grain-boundary liquid phases, on the superplastic properties and deformation behavior of ceramics are addressed. Superplastic forming, and particularly biaxial gas-pressure forming, of several ceramics, including YTZP and Al2O3/YTZP, is also presented. The forming behavior of these ceramics is correlated with that obtained from conventional uniaxial tests. Examples of concurrent superplastic forming and diffusion bonding (SPF/DB) of metal-ceramic hybrids are given. DOE

N95-16938 Los Alamos National Lab., NM.
INTENSE ION BEAM CHARACTERIZATION AND THERMAL MODELING FOR BEAM MATERIALS PROCESSING
H. A. Davis, D. J. Rej, W. J. Waganaar, G. P. Johnston (New Mexico Univ., Albuquerque, NM.), C. L. Ruiz (Sandia National Labs., Albuquerque, NM.), and F. A. Schmidllap (Sandia National Labs., Albuquerque, NM.) 1994 9 p Presented at the 10th International Conference on High Power Particle Beams, San Diego, CA, 20-24 Jun. 1994 Limited Reproducibility: More than 20% of this document may be affected by microfiche quality
(Contract W-7405-eng-36)
(DE94-016281; LA-UR-94-2437; CONF-940634-14) Avail: CASI HC A02

The authors have developed an intense ion beam to investigate materials processing applications. Initial experiments have focused on thin film formation by depositing beam-ablated target material on substrates. Measurements of beam properties governing target ablation are presented here. Techniques include Thomson parabola particle spectroscopy to measure the ion beam atomic composition and the energy spectrum of each beam component, and thermal imaging to measure the beam incident energy density. Measurements are used as input to a computer model of the beam-target interaction. Comparison of computational results with target ablation and target energy absorption are found to be in good agreement. DOE

N95-17160# Argonne National Lab., IL.
TRIBOLOGICAL PROPERTIES OF REACTIVELY SPUTTERED NITRIDES AND CARBIDES OF TITANIUM, ZIRCONIUM AND HAFNIUM
M. E. Graham, P. Chang, and W. D. Sproul Jun. 1994 42 p Prepared in cooperation with Northwestern Univ., Evanston, IL
(Contract W-31-109-eng-38)
(DE94-014583; ANL/OTM/CR-8) Avail: CASI HC A03/MF A01

Objective was to determine the tribological properties of hard, wear-resistant coatings on steel substrates in order to expedite their use on coated roller bearings, transmission gears, cams, etc. Specific coatings investigated were TiN, TiC, ZrN, ZrC, HfN, and HfC; they were deposited by high-rate-reactive magnetron sputtering. Both nitrides and carbides improved the wear performance of steel, often by orders of magnitude. These coatings have proven to be beneficial for dry sliding, lubricated sliding, rolling, and mixed rolling/sliding wear. The rolling contact fatigue studies showed remarkable improvements of lifetime that could be achieved with very thin coatings (less than one micron); thicker coatings were not useful. Coating and substrate properties (hardness) should be matched for best performance. Properties and performance of the hard coatings are controlled by process parameter settings; these parameters can be controlled in magnetron sputtering to achieve excellent results. DOE

N95-17299 Centre National de la Recherche Scientifique, Paris (France). Theoretical Physical Chemistry Lab.
MORPHOLOGY AND DYNAMICS OF MEMBRANE SYSTEMS [MORPHOLOGIES ET DYNAMIQUE DES SYSTEMES MEMBRANAIRES]
6 Aug. 1993 22 p In FRENCH Sponsored by Direction des Recherches, Etudes et Techniques, Paris (France)
(PB94-184660) Avail: Issuing Activity

To understand the physical behavior of membranes, the authors performed numerical simulations to construct simplified models of essential elements and to test the validity of those models. The team opted for the molecular dynamics method, in which the surface is defined by a collection of interacting molecules. Though difficult to implement, it allows for the modeling of 'liquid' membranes, that is, membranes in which neighboring molecules can move until they are no longer next to one another. This report describes how the team added the effect of pressure forces and volume constraints into a previously developed simulation program. The algorithm they developed is not far removed from recent, independent developments in computer graphics. The report also discusses research into the mechanical properties of the semiflexible polymer, actine. The team developed a detailed theory to demonstrate that apparent contradictions found in earlier experiments were not real. NTIS

N95-17305 Ecole Nationale Superieure d'Arts et Metiers, Bordeaux (France).
IMPACT VULNERABILITY OF THERMOPLASTIC-MATRIX COMPOSITES [VULNERABILITE A L'IMPACT DE COMPOSITES A MATRICE THERMOPLASTIQUE]
V. Martin 1994 26 p In FRENCH Sponsored by Direction des Recherches, Etudes et Techniques and Centre de Documentation de l'Armement
(PB94-201274) Avail: Issuing Activity (National Technical Information Service (NTIS))

The accidental nature of low energy impacts (birds, hail, falling objects) on composite structures makes it impossible to observe stresses directly. This study implements a system that allows good control of experimental conditions and reliable, exact measurement of behavior under dynamic stress. Results show explicitly that the initiation and development of damage mechanisms in equally stiff composite plates have little or no influence on their overall response. But the damage induced here was highly localized and limited, which may account for the insignificant change in the structure's overall response. Initial results show that matrix cracking is the first type of damage, followed by delamination. Damage initiation and growth are affected by the manufacturing method, and thus by the quality of interfaces between plies running in different directions, and by the plates' mesostructure. Resin type affects the plates' response to localized impact, with thermoplastic resins tending to produce punctures, i.e. matrix cracking without delamination. NTIS

N95-17379# Lawrence Livermore National Lab., Livermore, CA.
COMPUTER STUDIES OF THE DYNAMIC STRENGTH OF CERAMICS
D. J. Steinberg 14 Mar. 1994 6 p Presented at the EURODYMAT 1994: 1st International Conference on Mechanical and Physical Behavior of Materials Under Dynamic Loading, Oxford, England, 26-30 Sep. 1994
(Contract W-7405-eng-48)
(DE94-010890; UCRL-JC-116952; CONF-940956-9) Avail: CASI HC A02/MF A01

Our previous constitutive model for fully dense ceramics has been extended to include Al2O3 (AD999) and Si3N4; there are now parameters for seven materials. New experimental data, such as spall and double-shock wave-profiles for SiC and B4C, have been successfully simulated. Additional experiments are proposed which should help elucidate the remaining problems. DOE

N95-17434 State Univ. of New York, Buffalo, NY. Dept. of Chemistry.
SURFACE COMPOSITION OF A SERIES OF DIMETHYLSILOXANE UREA, URETHANE SEGMENTED COPOLYMERS STUDIED BY ELECTRON SPECTROSCOPY FOR CHEMICAL ANALYSIS
Xin Chen, Joseph A. Gardella, Jr., and Tai Ho (George Mason Univ., Fairfax, VA.) Mar. 1994 63 p Limited Reproducibility: More than 20%

of this document may be affected by microfiche quality
(Contract N00014-93-1-0058)
(AD-A282872; TR-94-01) Avail: CASI HC A04

Surface composition of a series of segmented poly(siloxane urea urethane)'s have been determined by angle- and energy-dependent electron spectroscopy for chemical analysis (ESCA). The polymers are based on aminopropyl end-capped dimethylsiloxane oligomers, isophorone diisocyanate, and 1,4-benzene dimethanol. Effects of segmental length and annealing on the surface composition were investigated. It was found that when the average molecular weight of the siloxane segments reaches 27K, the topmost surface region (within 18 A of the free surface) of a film cast from tetrahydrofuran solution is nearly siloxane phase. To achieve a comparable degree of surface phase enrichment in films of copolymers with siloxane segmental molecular weight of 10K, annealing at 120 C for 15 minutes was required. Depth profiles based on these data showed that in as-cast films a siloxane deficient phase several nanometers thick occurs beneath the siloxane surface layer. Annealing increases the thickness of both surface phases. DTIC

N95-17438 Lehigh Univ., Bethlehem, PA. Materials Research Center.
MULTIPHASE CERAMICS FOR MECHANICAL AND STRUCTURAL RELIABILITY AT LOW AND ELEVATED TEMPERATURES Final Report, 15 Dec. 1990 - 30 Jun. 1994
M. P. Harmer, H. M. Chan, G. A. Miller, A. M. Thompson, and J. Zhao 30 Jun. 1994 206 p Limited Reproducibility: More than 20% of this document may be affected by microfiche quality
(Grant AF-AFOSR-0126-91)
(AD-A285497; AFOSR-94-0623TR) Avail: CASI HC A10

AFOSR project 91-0126 was undertaken to develop a design approach for improving the high-temperature structural reliability (e.g., resistance to creep, fracture and grain growth) and room temperature mechanical reliability (e.g., flaw tolerance) of structural ceramics. Some of the major accomplishments of this work are highlighted below: (1) Engineering of the grain boundary chemistry in alumina resulted in a lowering of the creep rate by over two orders of magnitude by the addition of l000 ppm of Y2O3. It is conjectured that the presence of a highly segregated oversized (similarly charged) ion at the grain boundaries is responsible for inhibiting grain boundary diffusion and lowering the creep rate. (2) Duplex microstructures of Al2O3:YAG and Al2O3:ZrO2 exhibited lower creep rates and higher fracture toughness values than their single phase constituents. The creep data was well described by a composite creep equation developed for isostrain behavior (i.e. the strain rates are the same for each phase). The higher fracture toughness was attributed to the contribution of low energy interphase boundaries to the overall composite toughness. DTIC

N95-17456# National Inst. of Standards and Technology, Gaithersburg, MD. Ceramics Div.
LOW-TEMPERATURE FABRICATION OF TRANSPARENT SILICON NITRIDE
Wei Chen, S. G. Malghan, S. C. Danforth (Rutgers Univ., Piscataway, NJ.), and A. Pechenik (Air Force Office of Scientific Research, Bolling AFB, Washington, DC.) 31 May 1994 20 p Prepared for Oak Ridge National Lab., TN
(Contract DE-AC05-84OR-21400)
(DE94-014902; ORNL/Sub-92-22041/01) Avail: CASI HC A03/MF A01

Feasibility of producing nano-phase Si3N4 with improved properties, and ultrafine-grained nano-phase transparent Si3N4 by working with amorphous nano-size powders without the use of sintering aids was investigated. The approach uses cryogenic compaction of nano-size particles under liquid nitrogen followed by pressureless sintering. DOE

N95-17462 Department of the Navy, Washington, DC.
FIRE PROTECTIVE COATING AND METHOD FOR APPLYING SAME TO A STRUCTURE Patent
Usman A. Sorathia, inventor (to Navy) and Timothy L. Dapp, inventor (to Navy) 14 Jun. 1994 4 p Filed 28 Aug. 1991
(AD-D016405; US-Patent-5,320,870; US-Patent-Appl-SN-752249) Avail: US Patent and Trademark Office

A fire protective coating and method for applying same to a composite structure are provided. The coating is a composition of matter comprising a phenolic resin and strength reinforcing fibers embedded within the phenolic resin. The method of coating the structure with the composition of matter uses a phenolic resin in the liquid state. In this way, a mixture of the phenolic resin and strength reinforcing fibers can be applied to the structure's surface by conventional spraying techniques. As the mixture on the surface cures, a fire protective coating is formed on the structure's surface. DTIC

N95-17485 University of Southern Mississippi, Hattiesburg, MS. Dept. of Polymer Science.
SYNTHESIS AND CHARACTERIZATION OF A NEW CLASS OF THERMOSETTING RESINS: ALLYL AND PROPARGYL SUBSTITUTED CYCLOPENTADIENE DERIVATIVES Technical Report, 1 Jun. 1993 - 31 May 1994
L. J. Mathias and J. Muthiah 15 Jul. 1994 34 p Limited Reproducibility: More than 20% of this document may be affected by microfiche quality
(Contract N00014-89-J-1225)
(AD-A281976; TR-74) Avail: Issuing Activity (Defense Technical Information Center (DTIC))

A series of all-hydrocarbon resins were synthesized by reacting cyclopentadiene with allyl chloride, propargyl chloride, or a mixture of allyl chloride and propargyl chloride, under phase transfer conditions. Phase transfer reactions with and without added solvents, and with either quaternary ammonium or crown ether type catalysts, yielded similar products consisting of a mixture oa 1,1-disubstituted cyclopentadiene (minor amount) and 2-3 isomers each of tri-, penta-, and hexa-substituted derivatives. No further reaction of each of these components was possible. The overall substitution pattern varied little with changes in reaction conditions although limiting the allyl chloride content led to still reactive, partially substituted products. Incorporation of all-propargyl and high propargyl-to-allyl mixed functionalities on cyclopentadiene yielded products whose stability was very low, hindering their thorough characterization. Preliminary evaluation was therefore carried out for mixed resins with lower propargyl functionality. The allyl substituted resin (allylated cyclopentadiene, ACP) underwent thermal cure (without initiator) at around 200 C while allyl/propargyl substituted resin (7:1 ratio, APCP) showed a faster, lower temperature cure at around 120 C. Cationic cure of ACP was also initiated by a novel sulfonium salt at around 100 C. DTIC

N95-17654*# Cleveland State Univ., OH. Dept. of Physics.
CHARACTERIZATION ON DEFECT SOLIDS Final Report, Jan. 1992 - Dec. 1994
Herbert Schlosser Dec. 1994 7 p
(Grant NAG3-1313)
(NASA-CR-197540; NAS 1.26:197540) Avail: CASI HC A02/MF A01

The purpose of this research has been to develop new semi-empirical techniques to describe ceramics, alloys, and metal/ceramic interfaces with applications in mind that support the materials aspects of the high speed civil transport program (HSCT). HSCT requires methods that aid in the design of alloys and ceramics for new high strength, high temperature applications. Current theoretical methods are not capable of carrying out this mission. Hence, new accurate and more efficient theoretical techniques are needed to facilitate the design of new materials and the examination of their properties. This program concentrated on modeling ceramics, but also dealt with alloy properties to a lesser degree. The primary accomplishment of this research was the development of a new equation of state (EOS) that models the energy/bond length relationship and includes terms that represent charge transfer between cations and anions. The new EOS has been used by researchers at the Naval Research Laboratory to develop a new semi-empirical method for calculating properties of ceramics and metal ceramic interfaces based on the embedded atom method. The results of the director's discretionary fund (DDF) research describing the binding energy relation was the enabling theoretical basis. Also the workers at Cleveland State and NASA Lewis have detailed an approach based on equivalent crystal theory as part of the DDF which is currently under development. In addition, initial results for using the Harris functional method have been developed. Finally, the techniques developed by us have proved useful for the study of high pressure properties of solids and have been used extensively by researchers in this field.
Author

N95-17662# Illinois Univ., Urbana, IL.
MATERIALS DEGRADATION AND FATIGUE UNDER EXTREME CONDITIONS Annual Report, 1 Apr. 1993 - 31 Mar. 1994

Jiri Jonas Mar. 1994 10 p
(Contract F49620-93-1-0241)
(AD-A282969; AFOSR-94-0446TR) Avail: CASI HC A02/MF A01

As outlined in the original proposal our work deals with NMR and laser Raman scattering experiments on highly viscous liquids, including lubricants, both in bulk and confined geometries, over a wide range of pressures and temperatures. In a general sense we focus on the relationship between molecular level properties as obtained from our experiments and the macroscopic properties of the fluid studied, including fluids at the fluid-solid interface. As continuation of our systematic efforts to improve the understanding of the dynamic behavior of confined fluids we carried out NMR relaxation experiments on a number of molecular fluids including model lubricants. Of particular interest are the unique experiments dealing with pressure effects on confined liquids. As far as the development of new instrumentation is concerned we designed and fabricated NMR probes and pressure generating systems which allow measurements up to 10 kbar pressures. DTIC

N95-17682 Northwestern Univ., Evanston, IL. Dept. of Chemistry.
ION MODULATED ELECTROACTIVITY IN THIN-FILM POLYMERS DERIVED FROM BIPYRIDYL AND PHENANTHROLINE COMPLEXES OF IRON
L. A. Lyon, Mark A. Ratner, and Joseph T. Hupp 10 Jun. 1994 17 p
Limited Reproducibility: More than 20% of this document may be affected by microfiche quality
(Contract N00014-91-J-1035)
(AD-A280704; TR-20-ONR) Avail: CASI HC A03

Profound changes in the metal-centered electroactivity of thin-film redox polymer/electrolyte systems accompany the replacement of a conventional electrolyte solution (aqueous tetraethylammonium perchlorate) by any of several aq. CH3(CH2)SO3-Na(+) solutions. For example for a poly-Fe(4-methyl 4'-vinyl 2,2'-bipyridine) 3m+ film in contact with an aq. sodium decanesulfonate solution: (1) the overall redox capacity decreases by roughly half an order of magnitude, (2) the rate of hopping-based electron transport during charging decreases by 20-fold, and (3) the thermodynamic potential for metallopolymer oxidation moves to a significantly less positive value, in comparison to films equilibrated with conventional solutions. Further experiments show that the modulation behavior is associated with the uptake and release of charge-compensating anions during film oxidation and reduction (i.e. cations are excluded), that the degree of modulation increases with increasing counter anion size, and that the modulation phenomenon is chemically reversible. These unusual effects are tentatively attributed to polymer-based steric constraints on large alkanesulfonate ion incorporation, together with hydrophobic partitioning effects. These factors apparently conspire to couple film-based electron motion strongly to counter-anion motion. Finally, spectroelectrochemical measurements show that CH3(CH2)9SO3-containing films are reversibly confined to a predominantly mixed-valent form (Fe(II)+Fe(III)), even at electrochemical potentials for removed from the formal potential for redox processes in the film. DTIC

N95-17685# Connecticut Univ., Storrs, CT. Inst. of Materials Science.
MOBILITY MEASUREMENT AND COMPUTER SIMULATION AT SPECIFIC SITES IN POLYSTYRENE SOLUTIONS AND GELS Technical Report, Jun. 1993 - May 1994
Y. S. Kim, Chong S. Sung, Y. H. Kim, and A. Glynn 1 Jun. 1994 4 p
(Contract N00014-89-J-1145)
(AD-A281214; TR-40-ONR) Avail: CASI HC A01/MF A01

Trans - cis photoisomerization of azobenzene chromophore labeled at the chain center, the chain end, or as a side chain of polystyrene as well as free probe was studied to investigate the mobility at specific chain sites in polymer solutions and gels. The site dependency of the chain mobility indicated that the chain center was least affected by increasing concentration, followed by the chain end and the side chain. Computer simulation to predict segmental density near the chromophore supports the experimental trends. Also photoisomerization of 50% atactic polystyrene (aPS) solutions in toluene and tetrahydrofuran was studied as a function of temperature from 25 deg C to -60 deg C. In aPS / toluene gel, the chain mobilities of the chain center and the chain end showed significant changes near the T sub gel, while side chain and free probe exhibited little change. Effects of concentration and temperature were characterized by bulk viscosity measurement to see how chain mobility is influenced at specific sites. DTIC

N95-17690# Allied-Signal Aerospace Co., Kansas City, MO.
ANTENNA DIELECTRIC SEALING PROCESS CHARACTERIZATION
M. L. Busby and S. S. Yerganian Apr. 1994 79 p
(Contract DE-AC04-76DP-00613)
(DE94-015864; KCP-613-5318) Avail: CASI HC A05/MF A01

An antenna assembly experienced leak test failures during TMS testing. The leaks were occurring between the dielectric and housing. The antenna assembly dielectric is sealed into a nickel-plated aluminum housing using a tin catalyzed condensation cure silicone (RTV). In preparation for sealing, the dielectric and housing are chemically cleaned and then plasma cleaned. The surfaces to be sealed are primed, RTV is applied, and the RTV is cured in a humidity chamber. This report is an evaluation of the production process and includes FEM analysis and process characterization and control (PC&C) data. DOE

N95-17693 Department of the Navy, Washington, DC.
SELECTIVE AREA PLATINUM FILM DEPOSITION Patent
David S. Hsu, inventor (to Navy) 14 Jun. 1994 8 p Filed 30 Jul. 1993
(AD-D016355; US-Patent-5,320,978; US-Patent-Appl-SN-099510) Avail: US Patent and Trademark Office

A process for selectively depositing platinum on a conductive or semiconductive substrate has the steps of: patterning a polyimide layer on the substrate to have exposed areas and unexposed areas; and, at an operating temperature and an operating pressure, flowing a platinum precursor gas over the substrate. DTIC

N95-17694# Department of the Navy, Washington, DC.
ADHESION OF SILICON OXIDE TO DIAMOND Patent Application
Michael J. Marchywka, inventor (to Navy) 22 Oct. 1993 16 p
(AD-D016356; US-Patent-Appl-SN-140388) Avail: CASI HC A03/MF A01

An electronic semiconductor device has a capability for storing a charge, is non-responsive to visible light and has a low leakage. The device includes a diamond substrate which is securely adhered to a robust layer of silica layer that cannot be scratched by a tungsten probe or delaminated from the diamond substrate by pulling on a gold wire secured to the silica layer. This electronic device can be made by electrochemically cleaning the diamond substrate to remove non-diamond carbon adhering thereto, depositing a fragile layer of silica which weakly bonds to the cleaned diamond, and annealing the fragile silica layer to convert it into a strongly bonded and robust silicon dioxide layer. DTIC

N95-17719# Rockwell International Corp., Thousand Oaks, CA. Science Center.
MECHANISMS OF MECHANICAL FATIGUE IN CERAMICS
B. Cox Jul. 1994 7 p
(Contract DE-FG03-89ER-45400)
(DE94-016040; DOE/ER-45400/T6) Avail: CASI HC A02/MF A01

This report covers work done in the second year of the three-year follow-on contract. The theme of our work in this period continued to be the theory and measurement of rate-dependent bridging phenomena in fracture and fatigue. This covers both room temperature phenomena such as cycle-dependent attrition of crack bridging ligaments and high temperature phenomena such as viscosity and creep in bridging or cohesive zones. Our theoretical work focused on analytical solutions to rate dependent bridging problems. Our experimental work focused on developing high temperature in situ imaging methods. We obtained our first crack opening displacement measurements at elevated temperature in a graphite/SiC composite. DOE

N95-17722 National Inst. of Standards and Technology, Gaithersburg, MD. Ceramics Div.
WORKSHOP ON CHARACTERIZING DIAMOND FILMS, 3
A. Feldman, S. Holly (Rockwell International Corp., Canoga Park, CA.), C. A. Klein (CAK Analytics, Lexington, MA.), and G. Lu (Norton Diamond Film, Northboro, MA.) Apr. 1994 56 p Workshop held in Gaithersburg, MD, 23-24 Feb. 1994 See also PB92-205426 and PB93-207157 Limited

Reproducibility: More than 20% of this document may be affected by microfiche quality
(PB94-187663; NISTIR-5418) Avail: CASI HC A04

The third in a series of workshops was held at NIST on February 23rd and 24th, 1994 to discuss the characterization of diamond films and the need for standards in diamond technology. The audience targeted for this workshop were producers and potential users of chemical vapor deposition (CVD) diamond technology in the United States. Three technical topics that have relevance to applications of CVD diamond films were discussed: characterizing brazing and polishing, standardization of thermal conductivity measurement, and characterizing stress, strain, and fracture. NTIS

N95-17724# Nebraska Univ., Lincoln, NE. Dept. of Chemistry.
POLING DYNAMICS AND RELAXATION OF POLAR ORDER IN GUEST/HOST POLYMERS BY SECOND HARMONIC GENERATION
H. W. Guan, C. H. Wang, and S. H. Gu 15 Jun. 1994 24 p
(AD-A283291; Rept-26) Avail: CASI HC A03/MF A01

A detailed study of the decay of the second-harmonic generation (SHG) signals of several guest/host nonlinear optical polymer systems has been carried out. The decay of the SHG signal is found to be affected by surface and trapped space charges. A fast component is observed at a low poling field and is found to be mainly due to surface charges which orient the chromophores near the surface. A second component, associated with macroscopic polarization, is induced at high field. The intensity of the second component, which decays considerably slower than the fast component, rapidly increases when the poling field is greater than a threshold voltage. Above the temperature of glass transition, T sub g, a single exponential function gives a good fit to the shape of the second component of the SHG intensity decay curve. The time constant of the slow component is found to increase with successive poling-decay cycles and reaches a steady state value after several cycles have been performed. This lengthening effect is found both above and below T sub g. Furthermore, the relaxation time of the slow component is found also to depend on the poling field strength. The temperature dependence of the steady state relaxation time is not Arrhenius; the Vogel-Fulcher-Tammann equation gives a satisfactory fit to the temperature dependence data. DTIC

N95-17892# Los Alamos National Lab., NM.
CONDUCTING POLYMERS AS CORROSION RESISTANT COATINGS
D. A. Wrobleski and B. C. Benicewicz 1994 4 p Presented at the Workshop on Chromate Replacements in Light Metal Finishing, Albuquerque, NM, 18-19 Aug. 1994
(Contract W-7405-eng-36)
(DE94-018265; LA-UR-94-2734; CONF-9408156-1) Avail: CASI HC A01/MF A01

Although the majority of top coatings used for corrosion protection are electrically insulating, previous workers have proposed using an electrically active barrier for corrosion control. The most effective corrosion resistant undercoatings in use today are based on chromium compounds. Coatings based on other materials will need to replace these coatings by the turn of the century because of environmental and health concerns. For this reason the authors have begun an investigation of the use of conducting polymers as corrosion resistant coatings as an alternative to metal-based coatings. Conducting polymers have long been considered to be unsuitable for commercial processing, hindering their use for practical applications. Research in the field of electrically conducting polymers has recently produced a number of polymers such as polyaniline and its derivatives which are readily soluble in common organic solvents. The authors coating system, consisting of a conducting polyaniline primer layer, topcoated with epoxy or polyurethane, has been evaluated for corrosion resistance on mild steel substrates. In this paper, the authors report the results of laboratory testing under acidic and saline conditions and the results of testing in the severe launch environment at the Beach Testing Facility at Kennedy Space Center. The launch environment consists of exposure to corrosive HCl exhaust fumes and the salt spray from the Atlantic Ocean. DOE

N95-17913# Pacific Northwest Lab., Richland, WA.
VACUUM DEPOSITED POLYMER/SILVER REFLECTOR MATERIAL
J. Affinito, P. Martin, M. Gross, and W. Bennett Jul. 1994 9 p Presented at the Annual Meeting of the Society of Photo-Optical Instrumentation Engineers, San Diego, CA, 24-29 Jul. 1994
(Contract DE-AC06-76RL-01830)
(DE94-018729; PNL-SA-24678; CONF-940723-27) Avail: CASI HC A02/MF A01

Weatherable, low cost, front surface, solar reflectors on flexible substrates would be highly desirable for lamination to solar concentrator panels. The method to be described in this paper may permit such reflector material to be fabricated for less than 50 cents per square foot. Vacuum deposited Polymer/Silver/Polymer reflectors and Fabry-Perot interference filters were fabricated in a vacuum web coating operation on polyester substrates. Reflectivities were measured in the wavelength range from .4 (mu)m to .8 (mu)m. It is hoped that a low cost substrate can be used with the substrate laminated to the concentrator and the weatherable acrylic polymer coating facing the sun. This technique should be capable of deposition line speeds approaching 1500 linear feet/minute. Central to this technique is a new vacuum deposition process for the high rate deposition of polymer films. This polymer process involves the flash evaporation of an acrylic monomer onto a moving substrate. The monomer is subsequently cured by an electron beam or ultraviolet light. This high speed polymer film deposition process has been named the PML process - for Polymer Multi-Layer. DOE

N95-16055*# Wright Lab., Wright-Patterson AFB, OH. Aero Propulsion and Power Directorate.
HIGH TEMPERATURE POLYMER DIELECTRIC FILM-WIRE INSULATION
John G. Nairus *In* NASA. Lewis Research Center, First NASA Workshop on Wiring for Space Applications Sep. 1994 p 137-142 (For primary document see N95-16044 04-20)
Avail: CASI HC A02/MF A02

28 PROPELLANTS AND FUELS

Includes rocket propellants, igniters, and oxidizers; their storage and handling procedures; and aircraft fuels.

For related information see also *07 Aircraft Propulsion and Power, 20 Spacecraft Propulsion and Power,* and *44 Energy Production and Conversion.*

N95-16029*# Tennessee Univ., Tullahoma, TN. Center for Space Transportation and Applied Research.
SSME PROPELLANT PATH LEAK DETECTION REAL-TIME Final Report, 20 Nov. 1989 - 31 Jul. 1994
R. A. Crawford and L. M. Smith 1994 54 p
(Grant NAG8-140)
(NASA-CR-197032; NAS 1.26:197032) Avail: CASI HC A04/MF A01

Included are four documents that outline the technical aspects of the research performed on NASA Grant NAG8-140: 'A System for Sequential Step Detection with Application to Video Image Processing'; 'Leak Detection from the SSME Using Sequential Image Processing'; 'Digital Image Processor Specifications for Real-Time SSME Leak Detection'; and 'A Color Change Detection System for Video Signals with Applications to Spectral Analysis of Rocket Engine Plumes'. CASI

N95-16214# Sandia National Labs., Albuquerque, NM.
MECHANICAL EFFECTS IN COOKOFF MODELING
R. J. Gross, M. R. Baer, and M. L. Hobbs 1994 12 p Presented at the 20th International Pyrotechnics Seminar, Colorado Springs, CO, 25-29 Jul. 1994
(Contract DE-AC04-94AL-85000)
(DE94-014174; SAND-94-1577C; CONF-940776-5) Avail: CASI HC A03/MF A01

Complete cookoff modeling of energetic material in confined geometries must couple thermal, chemical and mechanical effects. In the past, modeling has focused on the prediction of the onset of combustion behavior based only on thermal-chemistry effects with little or no regard to the mechanical behavior of the energetic material. In this paper, an analysis tool is outlined which couples thermal, chemical, and mechanical behavior for one-dimensional geometries comprised of multi-materials. A reactive heat flow code, XCHEM, and a quasistatic mechanics code, SANTOS, have been completely coupled using a reactive, elastic-plastic constitutive model describing pressurization of the energetic material. This new Thermally Reactive Elastic-plastic explosive code, TREX, was developed to assess

the coupling of mechanics with thermal chemistry making multidimensional cookoff analysis possible. In this study, TREX is applied to confined and unconfined systems. The confined systems simulate One-Dimensional Time to explosion (ODTX) experiments in both spherical and cylindrical configurations. The spherical ODTX system is a 1.27 cm diameter sphere of TATB confined by aluminum exposed to a constant external temperature. The cylindrical ODTX system is an aluminum tube filled with HMX, NC, and inert exposed to a constant temperature bath. Finally, an unconfined system consisting of a hollow steel cylinder filled with a propellant composed of Al, RMX, and NC, representative of a rocket motor, is considered. This model system is subjected to transient internal and external radiative/convective boundary conditions representative of 5 minutes exposure to a fire. The confined systems show significant pressure prior to ignition, and the unconfined system shows extrusion of the propellent suggesting that the energetic material becomes more shock sensitive. DOE

N95-16499# Vanderbilt Univ., Nashville, TN. Combustion and Propulsion Group.

SHOTGUN/DROP-WEIGHT INITIATION OF ENERGETIC MATERIALS Final Report

K. P. Duffy, J. E. Miller, and A. M. Mellor 30 Jun. 1994 114 p

(Contract DAAL03-89-K-0061)

(AD-A285090) Avail: CASI HC A06/MF A02

Shotgun impact tests were performed by firing plexiglas projectiles at 6 mm long by 12 mm diameter propellant samples at 150 and 200 m/s impact velocities. Three different HTPB/AP propellants were tested: an Army fielded munition and two research propellants. The feasibility of a new technique, laser obscuration, was evaluated for measuring the pre- and post-impact projectile velocity history. Using less than ideal optical components, the present system is able to measure the pre-impact velocity but does not provide adequate resolution of the crucial post-impact velocity. The limits of even state-of-the-art optical components coupled with the small length of the sample (6 mm) precludes using this type of laser system for future testing. A light detection system provided severity of and time to reaction information for the three propellants tested. The performance of PVDF stress gauges for determining critical energy was marginal with calculated values that qualitatively support lower velocity drop-weight results. For two of the three propellants, critical energy density decreased at the higher shotgun impact velocities as expected. Attempts were made to correlate the go/no go and severity of reaction response to several stress gauge output parameters, but due to the limited data obtained in this one-year program, no strong correlations were obtained. DTIC

N95-16512# Massachusetts Inst. of Tech., Cambridge. Dept. of Mechanical Engineering.

PHASE TRANSFORMATIONS, ULTRASTRUCTURE AND PROPERTIES OF RIGID-ROD FIBERS Final Report

Edwin L. Thomas 31 Mar. 1994 9 p

(Grant AF-AFOSR-0078-91)

(AD-A285249; AFOSR-94-0609TR) Avail: CASI HC A02/MF A01

The proposal was directed towards the fundamental understanding of two areas of polymer materials: (1) Phase Transformations and Microstructure, (2) Ultrastructure and Mechanical Properties. Years 1 and 2 were primarily concerned with rigid rod PBX-type materials. During Year 2 and especially in Year 3 emphasis was redirected toward technique development (AFM and LVHRSEM) for materials characterization, and materials processing (roll casting of block copolymers and magnetic field alignment of liquid crystalline polymers). As well, efforts shifted to block copolymer materials during the second half of the grant. DTIC

N95-16542# Lawrence Livermore National Lab., Livermore, CA.

SYNTHESIS OF PURE RDX

P. F. Pagoria 25 Mar. 1994 3 p

(Contract W-7405-eng-48)

(DE94-014356; UCRL-ID-117229) Avail: CASI HC A01/MF A01

For the bioremediation of explosives, there is the need for RDX uncontaminated by HMX. In the Bachmann process, RDX always has residual HMX. There are two methods for synthesizing pure RDX: one involving oxidation of R-salt, the other nitration of hexamine. Absence of HMX in the RDX samples was confirmed by NMR and melting points. DOE

N95-17919# Lawrence Livermore National Lab., Livermore, CA.

CHEETAH 1.0 USER'S MANUAL

L. E. Fried 24 Jun. 1994 142 p

(Contract W-7405-eng-48)

(DE94-014727; UCRL-MA-117541) Avail: CASI HC A07/MF A02

CHEETAH is an effort to bring the TIGER thermochemical code into the 1990s. A wide variety of improvements have been made in Version 1.0, and a host of others will be implemented in the future. In CHEETAH 1.0 I have improved the robustness and ease of use of TIGER. All of TIGER's solvers have been replaced by new algorithms. I find that CHEETAH solves a wider variety of problems with no user intervention (e.g. no guesses for the C-J state) than TIGER did. CHEETAH has been made simpler to use than TIGER; typical use of the code occurs with the new standard run command. I hope that CHEETAH makes the use of thermochemical codes more attractive to practical explosive formulators. In the future I plan to improve the underlying science in CHEETAH. More accurate equations of state will be used in the gas and the condensed phase. A kinetics capability will be added to the code that will predict reaction zone thickness. CHEETAH is currently a numerical implementation of C-J theory. It will become an implementation of ZND theory. Further ease of use features will eventually be added; an automatic formulator that adjusts concentrations to match desired properties is planned. DOE

N95-17923# Energy Information Administration, Washington, DC. Office of Coal, Nuclear, Electric and Alternate Fuels.

ALTERNATIVES TO TRADITIONAL TRANSPORTATION FUELS: AN OVERVIEW

Jun. 1994 148 p

(DE94-014979; DOE/EIA-0585-O) Avail: CASI HC A07/MF A02

This report presents the first compilation by the Energy Information Administration (EIA) of information on alternatives to gasoline and diesel fuel. The purpose of the report is: (1) to provide background information on alternative transportation fuels and replacement fuels compared with gasoline and diesel fuel; and (2) to furnish preliminary estimates of alternative transportation fuels and alternative fueled vehicles as required by the Energy Policy Act of 1992 (EPACT), Title 5, Section 503, 'Replacement Fuel Demand Estimates and Supply Information.' Specifically, Section 503 requires the EIA to report annually on: (1) the number and type of alternative fueled vehicles in existence the previous year and expected to be in use the following year; (2) the geographic distribution of these vehicles; (3) the amounts and types of replacement fuels consumed; and (4) the greenhouse gas emissions likely to result from replacement fuel use. Alternative fueled vehicles are defined in this report as motorized vehicles licensed for on-road use, which may consume alternative transportation fuels. (Alternative fueled vehicles may use either an alternative transportation fuel or a replacement fuel.) The intended audience for the first section of this report includes the Secretary of Energy, the Congress, Federal and State agencies, the automobile manufacturing industry, the transportation fuel manufacturing and distribution industries, and the general public. The second section is designed primarily for persons desiring a more technical explanation of and background for the issues surrounding alternative transportation fuels. DOE

N95-16334*# Aerojet-General Corp., Sacramento, CA. Propulsion Div.

THE USE OF DESIGNED EXPERIMENTS IN THE PROCESS DEVELOPMENT OF CONTINUOUS PROPELLANT MIXING

J. A. Campbell, K. T. Clemons, and M. K. Wong *In* JHU, The 1993 JANNAF Propulsion Meeting, Volume 2 Nov. 1993 p 125-133 (For primary document see N95-16324 04-20)

(Contract NAS8-37800)

Avail: CASI HC A02/MF A04

N95-16335*# Thiokol Corp., Brigham City, UT.

IGNITION PROPAGATION AND HEAT EFFECTS OF PROPELLANT CHIPS EMBEDDED IN CASTABLE INHIBITOR USING A LASER FLUX TEST BOMB

Douglas E. Bolton, Jr. *In* JHU, The 1993 JANNAF Propulsion Meeting, Volume 2 Nov. 1993 p 135-145 (For primary document see N95-16324 04-20)

(Contract NAS8-38100)

Avail: CASI HC A03/MF A04

N95-16345*# National Aeronautics and Space Administration. John F. Kennedy Space Center, Cocoa Beach, FL.
GENERIC PROPELLANT TRANSFER UNIT: A PROJECT UPDATE
C. L. Davis *In* JHU, The 1993 JANNAF Propulsion Meeting, Volume 2 Nov. 1993 p 253-268 (For primary document see N95-16324 04-20)
Avail: CASI HC A03/MF A04

29 MATERIALS PROCESSING

Includes space-based development of products and processes for commercial applications.

For biological materials see *55 Space Biology.*

N95-16065*# Alabama Univ., Huntsville, AL. Dept. of Chemistry and Materials Science Program.
CHARACTERIZATION OF SURFACES Final Report
James M. VanAlstine 15 Sep. 1992 8 p
(Grant NAG8-955)
(NASA-CR-196995; NAS 1.26:196995) Avail: CASI HC A02/MF A01

Low gravity biotechnology experiments indicate a need to better understand and control a host of liquid-solid interfacial phenomena which reduce the efficiency of bioseparations methods on earth as well as in space. We have improved and utilized polymeric and silane derivatives, developed in association with MSFC, in order to control such phenomena. The objectives of the proposed research have been obtained. They were to improve NASA-patented coatings capable of controlling macromolecular adsorption, electroosmosis, and particle electrophoresis over a wide range of pH, and to further characterize the ability of polymeric coatings to control wall wetting interactions. To date this research has resulted in six publications and four abstracts. It has also aided researchers at MSFC with studies on the electrophoresis of large DNA molecules in free solution. It will continue to enhance NASA's efforts to exploit the space environment to enhance knowledge of phenomena relevant to biotechnology, and obtain bioseparations currently unobtainable on Earth. Abstracts from the 1994 ACS Meeting in Birmingham are attached. Author

N95-16880*# Wisconsin Univ., Milwaukee, WI. Dept. of Physics.
CHEMICAL VAPOR DEPOSITION OF HIGH T(SUB c) SUPERCONDUCTING FILMS IN A MICROGRAVITY ENVIRONMENT Final Technical Report, 1 Jun. 1991 - 14 Jun. 1994
Moises Levy and Bimal K. Sarma 14 Jun. 1994 25 p
(Grant NAG3-1274)
(NASA-CR-197527; NAS 1.26:197527) Avail: CASI HC A03/MF A01

Since the discovery of the YBaCuO bulk materials in 1987, Metalorganic Chemical Vapor Deposition (MOCVD) has been proposed for preparing HTSC high T(sub c) films. This technique is now capable of producing high-T(sub c) superconducting thin films comparable in quality to those prepared by any other methods. The MOCVD technique has demonstrated its superior advantage in making large area high quality HTSC thin films and will play a major role in the advance of device applications of HTSC thin films. The organometallic precursors used in the MOCVD preparation of HTSC oxide thin films are most frequently metal beta-diketonates. High T(sub c) superconductors are multi-component oxides which require more than one component source, with each source, containing one kind of precursor. Because the volatility and stability of the precursors are strongly dependent on temperature, system pressure, and carrier gas flow rate, it has been difficult to control the gas phase composition, and hence film stoichiometry. In order circumvent these problems we have built and tested a single source MOCVD reactor in which a specially designed vaporizer was employed. This vaporizer can be used to volatilize a stoichiometric mixture of diketonates of yttrium, barium and copper to produce a mixed vapor in a 1:2:3 ratio respectively of the organometellics. This is accomplished even though the three compounds have significantly different volatilities. We have developed a model which provides insight into the process of vaporizing mixed precursors to produce high quality thin films of Y1Ba2Cu3O7. It shows that under steady state conditions the mixed organometallic vapor must have a stoichiometric ratio of the individual organometallics identical to that in the solid mixture. Author

N95-17730 Academia Sinica, Beijing (China).
STUDY OF SIMULATION IN MICROGRAVITY ENVIRONMENT
X. Jiang and Y. Lou 1993 8 p Sponsored by Institute of Scientific and Technical Information of China, Beijing
(PB95-104261; ISTIC-TR-93128) Avail: Issuing Activity (National Technical Information Service (NTIS))

This paper discusses the mathematical model of dropcapsule in the field of microgravity research and analyses the affection of attitude deviation to microgravity level and presents the expression of the microgravity acceleration induced by attitude deviation at arbitrary point in dropcapsule. The attitude control system is presented and the controller is designed. Simulation in the microgravity environment is carried out. The simulation results show that the micro-g level of the microgravity dropcapsule with an attitude control system rises. All of these will provide valuable information and experience for doing research work in the field of microgravity study. NTIS

N95-17893*# National Aeronautics and Space Administration. Lewis Research Center, Cleveland, OH.
SUMMARY REPORT OF MISSION ACCELERATION MEASUREMENTS FOR STS-62, LAUNCHED 4 MARCH 1994
Melissa J. B. Rogers (Tal-Cut Co., Beachwood, OH.) and Richard DeLombard Nov. 1994 241 p Original contains color illustrations
(RTOP 963-60-OD)
(NASA-TM-106773; E-9222; NAS 1.15:106773) Avail: CASI HC A11/MF A03; 60 functional color pages

The second mission of the United States Microgravity Payload on-board the STS-62 mission was supported with three accelerometer instruments: the Orbital Acceleration Research Experiment (OARE) and two units of the Space Acceleration Measurements System (SAMS). The March 4, 1994 launch was the fourth successful mission for OARE and the ninth successful mission for SAMS. The OARE instrument utilizes a sensor for very low frequency measurements below one Hertz. The accelerations in this frequency range are typically referred to as quasisteady accelerations. One of the SAMS units had two remote triaxial sensor heads mounted on the forward MPESS structure between two furnance experiments, MEPHISTO and AADSF. These triaxial heads had low-pass filter cut-off frequencies at 10 and 25 Hz. The other SAMS unit utilized three remote triaxial sensor heads. Two of the sensor heads were mounted on the aft MPESS structure between the two experiments IDGE and ZENO. These triaxial heads had low-pass filter cut-off frequencies at 10 and 25 Hz. The third sensor head was mounted on the thermostat housing inside the IDGE experiment container. This triaxial head had a low-pass filter cut-off frequency at 5 Hz. This report is prepared to furnish interested experiment investigators with a guide to evaluating the acceleration environment during STS-62 and as a means of identifying areas which require further study. To achieve this purpose, various pieces of information are included, such as an overview of the STS-62 mission, a description of the accelerometer system flown on STS-62, some specific analysis of the accelerometer data in relation to the various mission activities, and an overview of the low-gravity environment during the entire mission. An evaluation form is included at the end of the report to solicit users' comments about the usefulness of this series of reports. Author

31 ENGINEERING (GENERAL)

Includes vacuum technology; control engineering; display engineering; cryogenics; and fire prevention.

N95-16853# Air Force Civil Engineering Center, Tyndall AFB, FL.
FIRE PROTECTION ENGINEERING CRITERIA: ELECTRONIC EQUIPMENT INSTALLATIONS Engineering Technical Letter Report
22 Dec. 1993 9 p Supersedes ETL-89-3
(AD-A285174; AFCESA/ETL-93-5; AFCESA/ETL-89-3) Avail: CASI HC A02/MF A01

Electronic equipment requires protection from smoke and fire. Threats to this electronic equipment may originate from both inside and outside the electronic equipment space. The most significant fire and smoke threat originates outside the electronic equipment space and not within the electronic equipment space itself. The Secretary of the Air Force has provided guidance on the use of halongenated fire extinguished agents (halon systems) for the protection of the earth's atmospheric ozone. These

requirements call for the reduction and eventual elimination of the agents. DTIC

N95-17632# Naval Research Lab., Washington, DC.
USE OF COPPER POWDER EXTINGUISHERS ON LITHIUM FIRES
Joseph T. Leonard, R. Burns, J. Beither, R. Ouelette, and R. Darwin 8 Jul. 1994 26 p
(AD-A283213; NRL/MR/6180-94-7490) Avail: CASI HC A03/MF A01

The suitability of using copper powder extinguishers for controlling lithium fires resulting from a damaged Mark 50 Torpedo boiler assembly was evaluated. The results indicated that under ideal conditions, i.e., unobstructed access to the fire, copper powder will extinguish burning lithium when applied at the recommended rate of 4.5 kg (10 lb) of copper per 0.45 kg (1 lb) of lithium. However, the presence of obstructions or of high spots on the surface of the burning lithium increases the quantity of copper powder required for extinguishment. DTIC

N95-17738# Lawrence Livermore National Lab., Livermore, CA.
PRECISION MACHINING AND POLISHING OF SCINTILLATING CRYSTALS FOR LARGE CALORIMETERS AND HODOSCOPES
C. R. Wuest, B. A. Fuchs, F. R. Holdener, and J. L. Heck, Jr. (Oak Ridge National Lab., TN.) Apr. 1994 8 p Presented at the Spring Meeting of the Materials Research Society, San Francisco, CA, 4-8 Apr. 1994 Revised
(Contract W-7405-eng-48)
(DE94-012060; UCRL-JC-114014-Rev-1; CONF-940411-19-Rev-1) Avail: CASI HC A02/MF A01

New machining and polishing techniques have been developed for large scintillating crystal arrays such as the Barium Fluoride Electromagnetic Calorimeter for the GEM Detector at SSCL, the Crystal Clear Collaboration's cerium fluoride or lead tungstenate calorimeter at the proposed LHC and CERN, the PHENIX Detector at RHIC (barium fluoride), and the cesium iodide Calorimeter for the BaBar Detector at PEP-2 B Factory at SLAC. The machining and polishing methods to be presented in this paper provide crystalline surfaces without sub-surface damage or deformation as verified by Rutherford Back-scattering (RBS) analysis. Surface roughness of about 10-20 A and sub-micron mechanical tolerances have been demonstrated on large barium fluoride crystal samples. Mass production techniques have also been developed for machining the proper angled surfaces and polishing up to five 50 cm long crystals at one time. These techniques utilize kinematic mount technology developed at LLNL to allow precision machining and polishing of complex surfaces. They will present this technology along with detailed surface studies of barium fluoride and cerium fluoride crystals polished with this technique. DOE

N95-17909# Oak Ridge National Lab., TN.
TEST RESULTS OF SUPERCONDUCTING AC MAGNETS FOR MAGNETIC REFRIGERATION EXPERIMENT
J. W. Lue, J. N. Luton, S. W. Schwenterly, and C. T. Wilson 1994 4 p Presented at the 13th International Conference on Magnet Technology, Victoria, British Columbia, 20-24 Sep. 1993
(Contract DE-AC05-84OR-21400)
(DE94-018695; CONF-930926-40) Avail: CASI HC A01/MF A01

Magnetic refrigeration can be achieved by cycling the magnetic field while leaving the magnetic material and the magnet stationary to avoid the large electromagnetic force problem. Two superconducting magnets were used to test this approach. First, we reconfigured a force-cooled cable-in-conduit magnet to operate with liquid rather than supercritical helium. Limited by the available power supply voltage, the fastest charging rate achieved was 10 s to 5 T. A second low loss magnet was acquired for operation to 7 T with a 6-s duty cycle. This is a bath-cooled magnet with potted sub-coils. The conductor is a 20-strand Rutherford-type cable with Ebanol insulation on each strand. This magnet quenched prematurely at 6.4 T. It was charge rate sensitive and the fastest charging rate achieved was 10 s to 5.8 T. DOE

N95-16279# Nanjing Univ. of Aeronautics and Astronautics, Nanjing, Jiangsu (China). Dept. of Mechanical Engineering.
APPROACH TO IN-PROCESS TOOL WEAR MONITORING IN DRILLING: APPLICATION OF KALMAN FILTER THEORY
Ning He, Youzhen Zhang, and Liangxian Pan *In its* Joint Proceedings on Aeronautics and Astronautics (JPAA) May 1993 p 199-208 (For primary document see N95-16249 04-01)
Avail: CASI HC A02/MF A03

N95-16281# Kazan Aviation Inst. (USSR).
DEVELOPMENT OF PROCESSES, MEANS, AND THEORETICAL PRINCIPLES OF THIN-WALLED DETAIL PLASTIC FORMING AT KAZAN AVIATION INSTITUTE
I. M. Zakirov *In* Nanjing Univ. of Aeronautics and Astronautics, Joint Proceedings on Aeronautics and Astronautics (JPAA) May 1993 p 214-216 (For primary document see N95-16249 04-01)
Avail: CASI HC A01/MF A03

32 COMMUNICATIONS AND RADAR

Includes radar; land and global communications; communications theory; and optical communications.

For related information see also *04 Aircraft Communications and Navigation* and *17 Space Communications, Spacecraft Communications, Command and Tracking.* For search and rescue see *03 Air Transportation and Safety,* and *16 Space Transportation.*

N95-15993# Naval Postgraduate School, Monterey, CA.
HIGH SPEED TRANSPORT PROTOCOLS: AN ATTEMPT TO FIND THE BEST SOLUTION M.S. Thesis
Konstantinos A. Lazaris Mar. 1994 94 p
(AD-A280989) Avail: CASI HC A05/MF A01

The development and advances in fiber optic technology are leading to major changes in modern telecommunications systems. In short, the transmission of data through optical fiber has become so fast that the computers which the fibers connect have become a bottleneck. The transport layer protocol, which is the software interface between the network and the computer, is one of the most important sources of this bottleneck. The purpose of this thesis is to investigate several 'high-speed' transport protocols, evaluate them, and attempt to determine which transport protocol or combination of transport protocols is optimal for high speed networks of the future. The approach is to first study the requirements of transport protocols for high speed networks. Then the properties of several specific transport protocols are studied with these requirements in mind. A detailed analysis of the strengths and shortcomings of Transmission Control Protocol/Internet Protocol (TCP/IP), Xpress Transfer Protocol (XTP), and SNR are presented. TCP/IP, which is in wide use today, was designed when transmission rates were much slower and error rates were much higher than today. XTP and SNR are two new experimental transport layer protocols which have been recently designed with high speed networks in mind. The primary contribution of this thesis is an evaluation of the requirements of future transport protocols. In short, TCP/IP in its present form is simply not adequate; it must change and adapt, or be replaced by a new transport protocol like XTP or SNR. DTIC

N95-16002# Naval Research Lab., Washington, DC.
USING LIDAR TOMOGRAPHY TO CHARACTERIZE SCATTERING IN A TURBULENT MEDIA
William P. Hooper 28 Mar. 1994 14 p
(NR Proj. RR0-3103)
(AD-A281014; NRL/MR/7220-94-7478) Avail: CASI HC A03/MF A01

A tomographic method for objectively determining extinction and backscatter using a single, scanning wavelength lidar is outlined. In the theoretical analysis, the scattering media is observed from different directions by a lidar which is either moved or observes the structures as they drift past the lidar. A matrix equation is developed and tested by randomly selecting extinction and backscatter values on a five by five grid. Measurement and turbulence induced errors are modeled and the measurement accuracies are assessed. Results for the theoretical calculations suggest that the method would provide accurate results for a scanning airborne lidar, but not from a scanning system that does not move. DTIC

N95-16094# Advanced Technology and Research, Inc., Laurel, MD.
SIGNAL WAVE GENERATOR SIGNALS RECORDED BY THE FEDERAL OUTDOOR IMPACT LABORATORY'S ON-BOARD DATA ACQUISITION SYSTEM Final Report
C. Brown and B. Liu Jul. 1994 47 p
(Contract DTFH61-91-Z-00002)
(PB94-186525; FHWA/RD-93/038) Avail: CASI HC A03/MF A01

The document contains signal wave generator signals recorded by the data acquisition system (DAS) used by the Federal Highway Administration's Federal Outdoor Impact Laboratory (FOIL) located at the Turner-Fairbank Highway Research Center (TFHRC) in McLean, Virginia. The FOIL Test Director and Junior Engineer performed the evaluation testing on September 29, 1993. The Contracting Officer's Technical Representative (COTR) supervised the project. The document is accompanied by one 3.5-in (88.9-mm) floppy disk. The disk contains the data that was collected during the testing. In addition to the curve files, header files are also included on the disk. The tests were performed by injecting standard signals from a signal wave generator, serial number 7 (SWG), provided by the National Highway Traffic Safety Administration (NHTSA) into each channel of the FOIL's data acquisition system. Author

N95-16097 Massachusetts Inst. of Tech., Lexington.
SOLID STATE RADAR DEMONSTRATION TEST RESULTS AT THE FAA TECHNICAL CENTER
Richard L. Ferranti 17 Jun. 1994 39 p Limited Reproducibility: More than 20% of this document may be affected by microfiche quality
(Contract DTFA01-93-Z-02012)
(AD-A281520; ATC-221) Avail: Issuing Activity (Defense Technical Information Center (DTIC))

In 1992 and 1993 ITT Gilfillan teamed with Thomson CSF to develop a solid state transmitter system for airport surveillance radar applications. Because of the low peak power limitations of the solid state transmitter, the radar uses pulse compression techniques to obtain 55 nmi detection performance. In the fall of 1992 ITT/Thompson executed a Cooperative Research and Development Agreement with the FAA's Terminal Area Surveillance System (TASS) program office to demonstrate the transmitter at the FAA Technical Center using the FAATC's ASR-9. The laboratory participated in these tests, which were completed in April 1993. The laboratory test plan included an assessment of the solid state radar's time sidelobe levels, stability, susceptibility to short pulse interference, and target detection performance. Although the tests were limited in scope and the data required several post-collection processing corrections, the radar exhibited very low time sidelobe levels, had excellent stability, and showed adequate detection performance. The pulse compression receiver was vulnerable to short pulse interference and will require specialized processing techniques to minimize its effects. It was not possible to take weather data, and the FAA Technical Center radar environment has no stressing clutter. Recommendations are made for the follow-on effort at a mountainous site to more completely characterize the solid state ATC radar. DTIC

N95-16117# Naval Postgraduate School, Monterey, CA.
ELIMINATION OF ELECTROMAGNETIC INTERFERENCE TO RECEIVERS AND SENSITIVE EQUIPMENT GENERATED BY SWITCHING SYSTEMS M.S. Thesis
Emmanuel Stelioudakis Mar. 1994 78 p
(AD-A281643) Avail: CASI HC A05/MF A01

Recently installed equipment in naval receiving sites such as digital telephone switching systems, uninterruptible power supplies, laser printers, etc., induce electromagnetic interference (EMI) into receiver systems, thus limiting the performance of the receiving site. EMI is injected into receiver systems by conductive, inductive, and capacitive paths associated with poor compartment shielding, grounds, or cable shielding. The MITEL SX-20 automatic digital telephone switching system is studied as an EMI source. Temporal and spectral properties of EMI generated by the MITEL SX-20 system are examined over a frequency range of 0 to 100 MHz. The effectiveness of a barrier, filter, and ground architecture in containing/eliminating the generated EMI is tested under various operating conditions. Possible solutions are proposed for similar EMI sources. DTIC

N95-16123# Electronics Research Lab., Salisbury (Australia).
AN INTRODUCTION TO INTELLIGENT NETWORKS
Wolf Getto Feb. 1994 36 p
(AD-A284284; ERL-0825-RE; DODA-AR-008-866) Avail: CASI HC A03/MF A01

Intelligent networking is a new and developing technology that is already having significant impact on telecommunications architectures. This paper offers a summary of this technology, concluding with a brief discussion of how it is likely to affect the military communications of the Australian Defence Force (ADF). DTIC

N95-16129# Massachusetts Inst. of Tech., Lexington. Lincoln Lab.
A COMPARISON OF SIGNAL-PROCESSING FRONT ENDS FOR AUTOMATIC SPEECH RECOGNITION
C. R. Jankowski, Jr., H.-D. H. Vo, and R. P. Lippmann 18 Jul. 1994 33 p
(Contract F19628-90-C-0002)
(AD-A284962; TR-1002; ESC-TR-94-081) Avail: CASI HC A03/MF A01

The first stage of any system for automatic speech recognition (ASR) is a signal-processing front end that converts a sampled speech waveform into a more suitable representation for later processing. Several front ends are compared, three of which are based on knowledge about the human auditory system. The performance of an ASR system with these front ends was compared to a control mel filter bank (MFB)-based cepstral representation in clean speech and with speech degraded by noise and spectral variability. Using the TI-105 isolated word data base, it was found that auditory front ends performed comparably to MFB cepstra, sometimes slightly better in noise. With MFB cepstral recognition error rates ranging from 0.5% to 26.9%, depending on signal-to-noise ratio (SNR), auditory models could perform as high as four percentage points better. With speech degraded by linear filtering, where MFB cepstra showed error rates ranging from 0.5% to 3.1%, auditory outputs could improve performance by as much as 0.4% for conditions with high baseline error rates. This performance gain comes at a significant computational expense-approximately one-third real time for MFB cepstra as opposed to as much as over 100 times real time for auditory models. These results disagree with previous studies that suggest considerably more improvement with auditory models. However, these earlier studies used a linear predictive coding (LPC)-based control front end, which is shown to perform significantly worse than MFB cepstra under noisy conditions (e.g., 2.7% error rate with mel-cepstra vs. 25.3% with LPC at 18-dB SNR). Data-reduction techniques such as principal component analysis (PCA) and linear discriminant analysis (LDA) were also evaluated. PCA provided no gain in noise and slight gain with spectral variability. DTIC

N95-16143# Aerospace Corp., El Segundo, CA. Technology Operations.
OPTIMUM TRUNCATION OF A GAUSSIAN BEAM IN THE PRESENCE OF RANDOM JITTER
H. T. Yura 15 Sep. 1994 18 p
(Contract F04701-93-C-0094)
(AD-A284951; TR-94(4925)-4; SMC-TR-94-35) Avail: CASI HC A03/MF A01

We consider the far-field (or focal-plane) irradiance distribution of a Gaussian beam truncated by a circular aperture in the presence of random angular jitter. First, in the absence of jitter, we derive an accurate analytical approximation for the irradiance distribution within the main lobe of the beam for the case where the beam diameter is less than the aperture diameter. We then obtain the corresponding mean irradiance distribution in the presence of circularly symmetric, normally distributed jitter. By maximizing the on-axis intensity, we obtain the optimum ratio of the beam diameter to the aperture diameter in the presence of jitter and present results for the corresponding maximum on-axis intensity and encircled power as a function of the jitter statistics. DTIC

N95-16146# Physics and Electronics Lab. TNO, The Hague (Netherlands).
EVALUATION OF FEL IMAGE PROCESSING ALGORITHM FOR 12-BIT CCD-IMAGES AS FUNCTION OF VARIOUS ATMOSPHERIC CONDITIONS [EVALUATIE VAN HET TNO-FEL ALGORITME VOOR BEELDVERBETERING MET 12-BITS CCD CAMERABEELDEN ALS FUNCTIE VAN DIVERSE ATMOPSFERISCHE OMSTANDIGHEDEN]
J. A. Boden Feb. 1994 54 p
(AD-A285187; FEL-93-A323; TDCK-93-3418) Avail: CASI HC A04/MF A01

A survey is given of processing results of 12-bit pictures with the FEL image processing algorithm. The results are illustrated with examples. The pictures have been taken with the first FEL 12-bit CCD camera system under various atmospheric conditions. Some relations between processing parameters and atmospheric conditions are analysed. An indication of a quantitative visibility range improvements is given. DTIC

N95-16148# Naval Command, Control and Ocean Surveillance Center, San Diego, CA.
ROUGH SURFACE MODELS IMPLEMENTED WITHIN THE SPLIT-STEP PARABOLIC EQUATION ALGORITHM Final Report, 1 May - 31 Oct. 1993
Amalia E. Barrios and Kenneth H. Craig Apr. 1994 48 p
(AD-A280843; NRAD-TD-2630) Avail: CASI HC A03/MF A01

Three split-step parabolic equation (PE) rough surface models - mixed transform (MT), surface loss function (SLF), and approximate solution (AS) - were investigated and compared with a reference waveguide model called MLAYER. The MT and SLF models are shown to agree well with MLAYER; the AS model, however, generally showed poor agreement. The MT model, though the most accurate, is the most time-consuming of the three. The AS model, the most numerically efficient, shows the poorest match to MLAYER. In using one of these rough surface models, whether it be to model rough surface effects over ocean or variable terrain, a satisfactory compromise may be to use some form of the SLF model since it is shown to agree fairly well with MLAYER and is still fairly efficient. DTIC

N95-16227# Naval Undersea Warfare Center, Newport, RI.
OBSERVATIONS OF ELF PROPAGATION AT HIGH LATITUDES DURING THE SPORADIC-E CONDITIONS OF NOVEMBER 1986 Final Report
J. R. Katan and D. J. Saleem 11 Aug. 1994 74 p
(NR Proj. M51-007)
(AD-A284973; NUWC-NPT-TR-10687) Avail: CASI HC A04/MF A01

Researchers in extremely low frequency (ELF) radio propagation have speculated on the effects of disturbed ionospheric conditions. Over the years, it has been observed that, although the propagation of ELF signals is remarkable for its relative stability, these signals are nevertheless influenced by many of the same types of disturbances that afflict higher frequency bands. Some of the early measurements revealed not only ELF's stable, predictive features (e.g., the smooth transitions through daytime and nighttime periods), but also its unexplainable, sudden decreases in nighttime signal strength. One of the most dramatic natural events for the radio propagationist to study is the solar proton event (SPE). During polar-cap absorption (PCA) events, an earthly response to an SPE, energetic protons from the sun penetrate the polar ionosphere. In the process, interactions with a variety of atmospheric constituents result in an increase in the ionization density to altitudes of 30 km or less. DTIC

N95-16231# Naval Postgraduate School, Monterey, CA.
MODIFICATION OF THE NAVAL POSTGRADUATE SCHOOL LIDAR SYSTEM M.S. Thesis
Gary Mallo Sep. 1994 53 p
(AD-A284987) Avail: CASI HC A04/MF A01

The Naval Postgraduate School (NPS) Lidar System was modified to allow comparison of lidar profiles with radiosonde profiles preparatory to evaluation of the lidar as a monitor for changes in the boundary layer. The detector package was modified to permit day and night operation and to reduce the overlap-limited minimum measurement range. Redesign of the transmitter beam expansion optics raised the power threshold for internal optics damage while improving the filling of the 18 output mirror and maintaining eye safe operation. Tests of the system on completion of modification demonstrated clear-air returns to ranges of 1 to 1.5 kilometers. Direct comparison of clear-air lidar returns with radiosonde balloon launches can now be undertaken to evaluate correlation of changes. DTIC

N95-16232# Naval Postgraduate School, Monterey, CA.
PERFORMANCE OF A FAST FREQUENCY-HOPPED NONCOHERENT MFSK RECEIVER WITH NON-IDEAL NOISE NORMALIZATION COMBINING OVER RICEAN FADING CHANNELS WITH PARTIAL-BAND INTERFERENCE M.S. Thesis
Hidetoshi Iwasaki Sep. 1994 85 p
(AD-A284989) Avail: CASI HC A05/MF A01

An error probability analysis is performed for a noncoherent M-ary orthogonal frequency-shift keying (MFSK) communication system employing fast frequency-hopped (FFH) spread spectrum. The signal is assumed to be transmitted through a frequency-nonselective, slowly fading channel with partial-band interference. The partial-band interference is modeled as a Gaussian process. The noise normalized receiver is employed to minimize partial-band interference effects, and the effect of inaccurate noise measurement on the ability of the noise-normalized receiver to reject partial-band interference is examined. Each diversity reception is assumed to fade independently according to a Ricean process. Thermal noise is also included in the analysis. It is found that diversity dramatically reduces the degradation due to partial-band interference, and noise measurement error does not significantly degrade receiver performance. The robustness of the receiver with regard to noise measurement error is independent of the strength of channel fading. DTIC

N95-16233# Naval Air Warfare Center, China Lake, CA. Weapons Div.
SUPERSPHEROID GEOMETRIES FOR RADOME ANALYSIS Final Report, Jan. - Aug. 1994
P. L. Overfelt Sep. 1994 34 p
(AD-A285405; NAWC-WPNS-TP-8216) Avail: CASI HC A03/MF A01

In the following, we use the arc described by the two-dimensional super quadratic equation (taking its exponent v, to be any positive real number) in the first quadrant only and revolve it about its major axis to obtain a body of revolution family of geometric shapes called super spheroids. For certain values of length and radius, and assuming that 1 less than v less than 2, we have determined new shapes that are appropriate for high speed missile radomes. We have found that the super spheroid with optimized exponent value v = 1.381 can almost exactly reproduce the traditional Von Karman radome geometry. Incidence angle maps and geometric properties have been determined for this super spheroidal family. We have used a ray tracing analysis to obtain boresight error induced by this family of shapes as a function of gimbal angle. The super spheroids are mathematically simple, can approximate most of the traditional radome geometries quite well, and are exceptionally easy to either program or use analytically. DTIC

N95-16240 Rome Lab., Hanscom AFB, MA.
CLUTTER SIGNAL POLARIZATION IN BISTATIC RADAR: EFFECT OF ANTENNA SIDELOBE CLUTTER Report, Nov. 1993 - May 1994
Daniel S. Fallon and J. L. Poirier May 1994 34 p Limited Reproducibility: More than 20% of this document may be affected by microfiche quality
(AF Proj. 4600)
(AD-A282300; RL-TR-94-106) Avail: CASI HC A03

Sidelobe contributions to a radar signal's polarization may distort the polarization of clutter originating in the mainbeam. To assure that radar clutter polarization measurements are accurate and that polarization nulling algorithms under consideration would work properly, it is necessary to analyze the contributions of antenna sidelobe clutter to signal polarization. This report considers two bistatic radar configurations over homogeneous terrain. The terrain is represented by the two-scale-of-roughness bistatic scattering model. Two antenna models are used, one a square aperture and the other a simple approximation to a circular aperture with adjustable sidelobe levels. The results for the square aperture show a small change in the signal polarization from the mainbeam-only value when the sidelobes are added in. For the adjustable sidelobe level antenna the sidelobe corruption is small until the uniform sidelobe level reaches -20 dB. DTIC

N95-16300# Air Force Inst. of Tech., Wright-Patterson AFB, OH.
DETECTABILITY MODELS AND WAVEFORM DESIGN FOR MULTIPLE ACCESS LOW-PROBABILITY-OF-INTERCEPT NETWORKS Ph.D. Thesis
Robert F. Mills 5 Apr. 1994 123 p
(AD-A281864; AFIT/CI/CIA-94-016) Avail: CASI HC A06/MF A02

Increased connectivity demands in the tactical battlefield have led to the development of multiple access low probability-of-intercept (LPI) communication networks. Most detectability studies of LPI networks have focused on the individual network links, in which detectability calculations are carried out for a single network emitter. This report, however, presents a different approach to network detectability analysis: it is assumed that the interceptor does not attempt to distinguish one emitter from another, but rather decides only if a network is operating or not. What distinguishes this approach from conventional link intercept analysis is that detection

decisions are based on energy received from multiple sources. The following multiple access schemes are considered: frequency division, time division, direct sequence code division, and frequency hop code division. The wideband radiometer and its hybrids, such as the channelized radiometer, are used as potential network intercept receivers. DTIC

N95-16448# Naval Postgraduate School, Monterey, CA.
SPREAD SPECTRUM APPLICATIONS IN UNMANNED AERIAL VEHICLES M.S. Thesis
Philip K. Bess Jun. 1994 99 p
(AD-A281035) Avail: CASI HC A05/MF A02

This thesis is part of an ongoing Naval Postgraduate School research project to develop unmanned aerial vehicles (UAV's) using current off the shelf (COTS) technology. This thesis specifically evaluated a spread spectrum UHF data link between a UAV and ground terminal. The command and control (C2) process and its role as the fundamental premise of the warfare commander were discussed. A review of the Pioneer remotely piloted vehicle (RPV), which gained such wide recognition during Operations Desert Storm and Desert Shield, was provided to the reader for familiarization with the workings of a generic UAV. An investigation of two common spread spectrum techniques and their associated benefits was made. A link budget calculation was made. The choice of a spread spectrum radio transceiver was reviewed. The requirements and design of the UAV and ground terminal antenna were discussed. A link budget analysis was performed. An atmospheric path propagation prediction was performed. The details of an actual flight test and the data gathered were examined. Future changes to enhance the data link performance and increase its capabilities were introduced. The COTS spread spectrum data link will enhance the role of the UAV in its command and control mission for the warfare commander. DTIC

N95-16495# Massachusetts Inst. of Tech., Lexington. Lincoln Lab.
A SIMPLE EHF HEMISPHERIC COVERAGE ANTENNA
J. C. Lee 8 Aug. 1994 52 p
(Contract F19628-90-C-0002)
(AD-A285078; TR-1001; ESC-TR-93-364) Avail: CASI HC A04/MF A01

A circulary polarized, axially symmetric, wide-beam radiator is required in many applications, including TT&C for UAV's and satellites. This report discusses some existing wide-beam antenna designs including divergent lenses and reflectors and introduces a new antenna design. Using a simple dielectric ring in conjunction with a dielectric loaded circular waveguide opening, a near ideal, axially symmetric, hemispheric coverage antenna with circular polarization of good axial ratio and wide-band impedance match is realized. Mechanically, the antenna is small, lightweight, and low cost. The dielectric used is the common Rexolite. Since no lossy materials or resonant scatterers are used, the antenna performance is inherently broadband and low loss. A K sub a-band prototype as well as compact designs for both Q- and K-bands are described. DTIC

N95-16549# Department of the Navy, Washington, DC.
AN AUTOMATIC REPEATER STATION FOR SIGNAL TRANSMISSIONS Patent Application
Douglas Bancroft, inventor (to Navy), Yoram Levy, inventor (to Navy), and Elliot L. Ressler, inventor (to Navy) 16 Aug. 1994 32 p
(AD-D016454; US-Patent-Appl-SN-106746) Avail: CASI HC A03/MF A01

An automatic repeater station, sometimes called a relay system, is disclosed. The relay system receives signals, preferably at one band of frequencies, then filters and restores their inherent information, and finally transmits the restored information, preferably at another band of frequencies. Unlike the prior art systems utilizing transceivers and electronically tunable filters, the present invention uses separate receivers and transmitters and is devoid of electronically tunable filters. DTIC

N95-16612# Helsinki Univ. of Technology, Espoo (Finland). Electronics Lab.
DUALITY TRANSFORMATIONS, GREEN DYADICS AND PLANE-WAVE SOLUTIONS FOR A CLASS OF BIANISOTROPIC MEDIA
I. V. Lindell and F. Olyslager Feb. 1994 17 p
(PB94-197670; ISBN-951-22-2002-4) Avail: CASI HC A03/MF A01

Duality transformations, defined as linear transformations between pairs of vector fields and sources, are seen to leave a class of bianisotropic media invariant with the permittivity, permeability and Tellegen parameters multiples of the same dyadic and the chirality parameter an arbitrary dyadic. This kind of media is called self dual in the duality transformations in question. Any sources and fields in such a medium can be decomposed in two self-dual components which do not couple and actually see the bianisotropic medium as two equivalent anisotropic media of affine-isotropic type. The Green dyadics in these two media are solved through affine transformations and the Green dyadics of the original bianisotropic medium is written as a combination of them in explicit analytic form. Finally, the plane-wave dispersion equation is solved through the self-dual decomposition of fields. NTIS

N95-16613# Helsinki Univ. of Technology, Espoo (Finland). Electromagnetics Lab.
ELECTROMAGNETOSTATICS IN UNIAXIAL BIANISOTROPIC MEDIA
I. V. Lindell and A. H. Sihvola Mar. 1994 13 p
(PB94-197688; ISBN-951-22-1610-8) Avail: CASI HC A03/MF A01

The problem of electric and magnetic fields arising from static charge and current sources in the general bianisotropic medium is expressed in differential equation form. The fields are seen to be expressable in integral form in terms of a dyadic Green function satisfying a differential equation of the fourth order. It is shown that for the most general uniaxial bianisotropic medium with eight medium parameters and a given axial direction, the problem can be reduced to finding two scalar Green functions from equations of the second order which can be solved. The static solution obtained is applicable to quasi-static analyses of electromagnetic problems involving uniaxial media. NTIS

N95-16621# Rome Lab., Griffiss AFB, NY.
A VHF/UHF ANTENNA FOR THE PRECISION ANTENNA MEASUREMENT SYSTEM (PAMS)
Daniel E. Warren Jul. 1994 33 p
(AF Proj. 3321)
(AD-A285673; RL-TR-94-85) Avail: CASI HC A03/MF A01

This report describes the development of an antenna concept that is to be used to extend the lower frequency limit of the Precision Antenna Measurement System (PAMS) down to 30 MHz. It includes a discussion of the concepts of reflection ranges, log periodic antennas, half space antennas, non-steerable antennas, and numerical definition of antenna patterns in two dimensions. PAMS is located at the Verona Research Facility, and is a system for measuring the radiation patterns of antennas on aircraft while they are in flight. DTIC

N95-16624# Rome Lab., Hanscom AFB, MA.
FORMULATION OF PROBE-CORRECTED TIME-DOMAIN PLANAR NEAR-FIELD MEASUREMENTS Report, Sep. 1992 - Aug. 1993
Thorkild B. Hansen and Arthur D. Yaghjian Apr. 1994 44 p
(AD-A281053; RL-TR-94-74) Avail: CASI HC A03/MF A01

Probe-corrected planar near-field formulas in the time domain are derived for both acoustic and electromagnetic fields, so that a single set of near-field measurements in the time domain yields the fields of the test antenna directly in the time domain. The time-domain probe-corrected formulas are first derived by taking the inverse Fourier transform of the corresponding frequency-domain formulas, and then by using a time-domain expansion for the fields of the test antenna and a time-domain receiving characteristic of the probe. Because these general formulas, which involve a double integral over the scan plane and an infinite time-convolution integral, are rather complicated, we consider a special probe whose output due to an incoming time-domain plane wave is proportional to the time derivative of the field of that plane wave. For this special D-dot probe, the probe-corrected formulas simplify to give the time-domain far-field pattern as a double spatial integral of the time-domain output of the probe over the scan plane multiplied by the angular dependence of the receiving characteristic of the probe. Time-domain reciprocity relations are derived for reciprocal probes, and their time-domain receiving characteristics are related to their far fields. A time-domain sampling theorem is derived and a numerical example illustrates the use of the time-domain probe-corrected formulas. DTIC

N95-16794# Naval Research Lab., Washington, DC.
IMPLEMENTATION OF A REAL-TIME DATA PROCESSING SYSTEM

FOR RADAR BANDWIDTH EXTRAPOLATION AND STRETCH
Athena R. Caul-Toskin 10 Jun. 1994 25 p
(AD-A281195; NRL/MR/5320-94-7456) Avail: CASI HC A03/MF A01

An existing system using NRL's Senrad radar is being used to demonstrate the utility of wideband waveforms in radar surveillance. This system processes data using a stretch technique to yield high resolution range profiles of the target. To provide some of the benefits of greater bandwidth without implementing the wideband waveforms, it was suggested to add bandwidth extrapolation processing. The addition of this processing necessitated changes to the existing system for real-time processing. The changes included modifying the Volume Surveillance system hardware, constructing an interface between the existing system and the Volume Surveillance processor and modifying the stretch and bandwidth extrapolation software for a new processor. The changes were implemented and the modified hardware operated correctly. The software modifications were tested successfully with recorded and real-time data. The processing times met the time specifications necessary for real-time operation. DTIC

N95-16800 Army Test and Evaluation Command, Aberdeen Proving Ground, MD.
ELECTROMAGNETIC INTERFERENCE TESTS Final Report
31 May 1994 26 p Supersedes TOP-6-2-542 (AD-775446) Limited Reproducibility: More than 20% of this document may be affected by microfiche quality
(AD-A281396; TOP-6-2-542) Avail: Issuing Activity (Defense Technical Information Center (DTIC))

This TOP is a general guideline for electromagnetic interference testing of electronic, electrical, and electromechanical equipment, subsystems, and systems. This TOP is applicable to the measurement of emissions and the identification of susceptibilities for all systems and in all test categories. DTIC

N95-16816# Organisatie voor Toegepast Natuurwetenschappelijk Onderzoek, The Hague (Netherlands). Fysisch en Elektronisch Lab.
FIELDS AND WAVES IN ELLIPTIC WAVEGUIDES
H. J. Visser Feb. 1994 14 p
(AD-A285337; FEL-93-B227; TDCK-93-2434) Avail: CASI HC A03/MF A01

In order to calculate cut-off wavelengths of elliptic waveguides without trying to solve the roots of Mathieu functions, a first order approximation is derived. The elliptic waveguide is decomposed in two circular waveguides for even and odd mode propagation. The cut-off wavelengths of these waveguides are calculated and used as approximate cut-off wavelengths of the elliptic waveguide. Cut-off wavelengths for the dominant TE11-mode can be approximated with a maximum error of 5 percent for all eccentricities. The approximation is also valid for the other modes for small eccentricities. DTIC

N95-16825# Mitre Corp., Bedford, MA.
MITRE ADAPTIVE PROCESSING CAPABILITY
Jun. 1994 61 p
(AD-A281078; Mitre-MP-94B0000074) Avail: CASI HC A04/MF A01

Adaptive processing provides a means for removing jamming and clutter interference from radar and communications systems. The interference could come from hostile or friendly forces. Adaptive processing will become an increasingly important element in radar, command and control, and communications systems in both peace and wartime environments. DTIC

N95-16841# Air Force Inst. of Tech., Wright-Patterson AFB, OH. School of Engineering.
WAVELETS, SIGNAL PROCESSING AND MATRIX COMPUTATIONS Final Report, Oct. 1993 - Sep. 1994
Bruce W. Suter Sep. 1994 16 p
(AD-A283832; AFIT/EN-TR-94-04) Avail: CASI HC A03/MF A01

Key scientific results were found in the following four areas: (1) multidimensional Malvar wavelets; (2) time/spatial varying filter banks; (3) vector filter banks and vector-valued wavelets; and (4) multirate time-frequency. These results have opened the following new areas of research: nonseparable multidimensional Malvar wavelets, vector-valued wavelets and vector filter banks, and multirate time-frequency analysis. These results also provide fundamental tools in many Air Force and industrial applications, such as modeling of turbulence, compression of images/video images, etc. Author (revised)

N95-16886*# Analex Corp., Brook Park, OH.
SLOW WAVE VANE STRUCTURE WITH ELLIPTICAL CROSS-SECTION SLOTS, AN ANALYSIS Final Report
Henry G. Kosmahl Cleveland, OH NASA Nov. 1994 32 p
(Contract NAS3-25776; RTOP 235-01-0A)
(NASA-CR-195352; E-8888; NAS 1.26:195352) Avail: CASI HC A03/MF A01

Mathematical analysis of the wave equation in cylinders with elliptical cross-section slots was performed. Compared to slow wave structures with rectangular slots higher impedance and lower power dissipation losses are evident. These features could lead to improved designs of traveling wave magnetrons and gigahertz backward-wave oscillators as well as linear traveling wave tubes with relatively shallow slots. Author

N95-16956# Electronics Research Lab., Salisbury (Australia).
IN-FIBRE BRAGG GRATINGS FOR MILLIMETRE-WAVE EW SYSTEMS
Anthony C. Lindsay Mar. 1994 24 p
(AD-A284283; ERL-0827-RR; DODA-AR-008-868) Avail: CASI HC A03/MF A01

Fibre-optic microwave and millimetre wave systems technology has matured rapidly over the last few years. The report examines some possibilities for very wide bandwidth signal distribution and analysis based on in-fibre Bragg gratings. The gratings are fabricated within the fibre core and become integral property of the optical fibre material. DTIC

N95-16968# Tennessee Univ., Knoxville, TN. Plasma Science Lab.
INTERACTION OF ELECTROMAGNETIC FIELDS WITH MAGNETIZED PLASMAS Final Report, 1 Apr. 1989 - 31 Mar. 1994
J. R. Roth 31 Mar. 1994 328 p
(Grant AF-AFOSR-0319-89)
(AD-A285496; UTK-PSL-94-3; AFOSR-94-0594TR) Avail: CASI HC A15/MF A03

This Final Scientific Report describes research at the UTK Plasma Science Laboratory which was supported by the Air Force Office of Scientific Research, contract AFOSR 89-0319, with Dr. Robert J. Barker, Program Manager. Eight archival scientific papers were published, 19 oral or poster conference papers were presented at the annual APS and IEEE plasma meetings and one patent was obtained and two additional patents were filed for. This contract also supported three graduate theses, including partial support for one Ph.D. dissertation, and two Master of Science in Electrical Engineering theses. This contract additionally supported approximately eight person-years of half time GRA research and training, and the preparation of nine routine reports to the Air Force. This contract also supported Professor Shenggang Liu, UTK's first Visiting Distinguished Professor, for a period of one year. DTIC

N95-17173 Naval Postgraduate School, Monterey, CA.
DATA LINK LEVEL INTERCONNECTION OF REMOTE FIBER DISTRIBUTED DATA INTERFACE LOCAL AREA NETWORKS (FDDI LANs) THROUGH THE CRITICAL DATA LINK (CDL) M.S. Thesis
Selcuk Karayakaylar Jun. 1994 180 p Limited Reproducibility: More than 20% of this document may be affected by microfiche quality
(AD-A284307) Avail: CASI HC A09

This thesis deals with the features and performance of a network interface device to interconnect two remote Fiber Distributed Data Interface (FDDI) Local Area Networks (LAN's) through the Critical Data Link (CDL) which is a full-duplex, jam-resistant, point-to-point microwave communications system for use in imagery and signals intelligence collection systems. In particular, OPNET, a commercially available network engineering tool is used to model a medium access level remote bridge interface connecting two LAN's. The effectiveness of two different load balancing techniques used to distribute traffic over the multiple channels of the CDL has been studied. Also, the effect of different jamming patterns on the bit error rate seen by the users has been studied. DTIC

N95-17279*# Jet Propulsion Lab., California Inst. of Tech., Pasadena, CA.
THE TELECOMMUNICATIONS AND DATA ACQUISITION REPORT Progress Report, Jul. - Sep. 1994

Joseph H. Yuen, ed. 15 Nov. 1994 300 p
(NASA-CR-197249; JPL-TDA-PR-42-119; NAS 1.26:197249) Avail: CASI HC A13/MF A03

This quarterly publication provides archival reports on developments in programs in space communications, radio navigation, radio science, and ground-based radio and radar astronomy. It reports on activities of the Deep Space Network (DSN) in planning, supporting research and technology, implementation, and operations. Also included are standardization activities at the Jet Propulsion Laboratory for space data and information systems. For individual titles, see N95-17280 through N95-17297.

N95-17280*# Jet Propulsion Lab., California Inst. of Tech., Pasadena, CA.

EVALUATION OF CURRENT TROPOSPHERIC MAPPING FUNCTIONS BY DEEP SPACE NETWORK VERY LONG BASELINE INTERFEROMETRY

O. J. Sovers and G. E. Lanyi *In its* The Telecommunications and Data Acquisition Report 15 Nov. 1994 p 1-11 (For primary document see N95-17279 04-32)
(RTOP 314-30-56-28-50)
Avail: CASI HC A03/MF A03

To compare the validity of current algorithms that map zenith tropospheric delay to arbitrary elevation angles, 10 different tropospheric mapping functions are used to analyze the current data base of Deep Space Network Mark 3 intercontinental very long baseline interferometric (VLBI) data. This analysis serves as a stringent test because of the high proportion of low-elevation observations necessitated by the extremely long baselines. Postfit delay and delay-rate residuals are examined, as well as the scatter of baseline lengths about the time-linear model that characterizes tectonic motion. Among the functions that utilize surface meteorological data as input parameters, the Lanyi 1984 mapping shows the best performance both for residuals and baselines, through the 1985 Davis function is statistically nearly identical. The next best performance is shown by the recent function of Niell, which is based on an examination of global atmospheric characteristics as a function of season and uses no weather data at the time of the measurements. The Niell function shows a slight improvement in residuals relative to Lanyi, but also an increase in baseline scatter that is significant for the California-Spain baseline. Two variants of the Chao mapping function, as well as the Chao tables used with the interpolation algorithm employed in the Orbit Determination Program software, show substandard behavior for both VLBI residuals and baseline scatter. The length of the California-Australia baseline (10,600 km) in the VLBI solution can vary by as much as 5 to 10 cm for the 10 mapping functions. Author

N95-17281*# Jet Propulsion Lab., California Inst. of Tech., Pasadena, CA.

AN ALGORITHM FOR EXTRACTION OF PERIODIC SIGNALS FROM SPARSE, IRREGULARLY SAMPLED DATA

J. Z. Wilcox *In its* The Telecommunications and Data Acquisition Report 15 Nov. 1994 p 12-28 (For primary document see N95-17279 04-32)
(RTOP 314-40-22-12-03)
Avail: CASI HC A03/MF A03

Temporal gaps in discrete sampling sequences produce spurious Fourier components at the intermodulation frequencies of an oscillatory signal and the temporal gaps, thus significantly complicating spectral analysis of such sparsely sampled data. A new fast Fourier transform (FFT)-based algorithm has been developed, suitable for spectral analysis of sparsely sampled data with a relatively small number of oscillatory components buried in background noise. The algorithm's principal idea has its origin in the so-called 'clean' algorithm used to sharpen images of scenes corrupted by atmospheric and sensor aperture effects. It identifies as the signal's 'true' frequency that oscillatory component which, when passed through the same sampling sequence as the original data, produces a Fourier image that is the best match to the original Fourier space. The algorithm has generally met with succession trials with simulated data with a low signal-to-noise ratio, including those of a type similar to hourly residuals for Earth orientation parameters extracted from VLBI data. For eight oscillatory components in the diurnal and semidiurnal bands, all components with an amplitude-noise ratio greater than 0.2 were successfully extracted for all sequences and duty cycles (greater than 0.1) tested; the amplitude-noise ratios of the extracted signals were as low as 0.05 for high duty cycles and long sampling sequences. When, in addition to these high frequencies, strong low-frequency components are present in the data, the low-frequency components are generally eliminated first, by employing a version of the algorithm that searches for non-integer multiples of the discrete FET minimum frequency. Author

N95-17282*# Jet Propulsion Lab., California Inst. of Tech., Pasadena, CA.

SPACE VLBI TELECOMMUNICATION CHARACTERISTICS, PROTECTION CRITERIA, AND FREQUENCY SHARING

B. O. Gutierrez-Luaces and D. F. Bishop *In its* The Telecommunications and Data Acquisition Report 15 Nov. 1994 p 29-45 (For primary document see N95-17279 04-32)
(RTOP 315-90-31-00-02)
Avail: CASI HC A03/MF A03

A brief description of the technical characteristics of space VLBI is made, emphasizing the VLBI cross-correlation process. The signal-to-noise ratio of the cross-correlation process should be maintained as large as possible for the duration of the observation. Protection of this process from unwanted interference is a primary objective. The telecommunication radio links required in a space VLBI system are identified and characterized. Maximum bandwidths are suggested, as well as the minimum carrier frequencies required for the telemetering and the phase-transfer radio links. Planned space VLBI system models-Radioastron (Russia), VLBI Space Observatory Project (VSOP) (Japan), and the DSN orbiting VLBI subnet. (United States)--are taken as a baseline to determine the interference criteria. It is concluded that existing interference criteria for near-Earth research satellites are suitable for the protection of the space VLBI systems planned. Author

N95-17283*# Jet Propulsion Lab., California Inst. of Tech., Pasadena, CA.

RADIO-PLANETARY FROM TIE FROM PHOBOS-2 VLBI DATA

C. E. Hildebrand, B. A. Iijima, P. M. Kroger, W. M. Folkner, and C. D. Edwards *In its* The Telecommunications and Data Acquisition Report 15 Nov. 1994 p 46-82 (For primary document see N95-17279 04-32)
(RTOP 310-10-60-50)
Avail: CASI HC A03/MF A03

In an ongoing effort to improve the knowledge of the relative orientation (the 'frame tie') of the planetary ephemeris reference frame used in deep navigation and a second reference frame that is defined by the coordinates of a set of extragalactic radio sources, VLBI observations of the Soviet Phobos-2 spacecraft and nearby (in angle) radio sources were obtained at two epochs in 1989, shortly after the spacecraft entered orbit about Mars. The frame tie is an important systematic error source affecting both interplanetary navigation and the process of improving the theory of the Earth's orientation. The data from a single Phobos-2 VLBI session measure one component of the direction vector from Earth to Mars in the frame of the extragalactic radio sources (the 'radio frame'). The radio frame has been shown to be stable and internally consistent with an accuracy of 5 nrad. The planetary ephemeris reference frame has an internal consistency of approximately 15 nrad. The planetary and radio source reference frames were aligned prior to 1989 and measurements of occulations of the radio source 3C273 by the Moon. The Phobos-2 VLBI measurements provide improvement in the accuracy of two of the three angles describing a general rotation between the planetary and radio reference frames. A complete set of measurements is not available because data acquisition was terminated prematurely by loss of spacecraft. The analysis of the two Phobos-2 VLBI data sets indicates that, in the directions of the two rotation components determined by these data, the JPL planetary ephemeris DE200 is aligned with the radio frame as adopted by the International Earth Rotation Service within an accuracy of 20-40 nrad, depending on direction. The limiting errors in the solutions for these offsets are spacecraft trajectory (20 nrad), instrumental biases (19 nrad), and dependence of quasar coordinates on observing frequency (24 nrad). Author

N95-17284*# Jet Propulsion Lab., California Inst. of Tech., Pasadena, CA.

CLOSED-LOOP CARRIER PHASE SYNCHRONIZATION TECHNIQUES MOTIVATED BY LIKELIHOOD FUNCTIONS

H. Tsou, S. Hinedi, and M. Simon *In its* The Telecommunications and Data Acquisition Report 15 Nov. 1994 p 83-104 (For primary

document see N95-17279 04-32)
(RTOP 314-30-61-02-04)
Avail: CASI HC A03/MF A03

This article reexamines the notion of closed-loop carrier phase synchronization motivated by the theory of maximum a posteriori phase estimation with emphasis on the development of new structures based on both maximum-likelihood and average-likelihood functions. The criterion of performance used for comparison of all the closed-loop structures discussed is the mean-squared phase error for a fixed-loop bandwidth. Author

N95-17285*# California Inst. of Tech., Pasadena, CA.
ON THE APPLICATION OF UNDER-DECIMATED FILTER BANKS c33
Y.-P. Lin and P. P. Vaidyanathan *In* JPL, The Telecommunications and Data Acquisition Report 15 Nov. 1994 p 105-128 (For primary document see N95-17279 04-32)
(RTOP 315-91-40-20-35)
Avail: CASI HC A03/MF A03

Maximally decimated filter banks have been extensively studied in the past. A filter bank is said to be under-decimated if the number of channels is more than the decimation ratio in the subbands. A maximally decimated filter bank is well known for its application in subband coding. Another application of maximally decimated filter banks is in block filtering. Convolution through block filtering has the advantages that parallelism is increased and data are processed at a lower rate. However, the computational complexity is comparable to that of direct convolution. More recently, another type of filter bank convolver has been developed. In this scheme, the convolution is performed in the subbands. Quantization and bit allocation of subband signals are based on signal variance, as in subband coding. Consequently, for a fixed rate, the result of convolution is more accurate than is direct convolution. This type of filter bank convolver also enjoys the advantages of block filtering, parallelism, and a lower working rate. Nevertheless, like block filtering, there is no computational saving. In this article, under-decimated systems are introduced to solve the problem. The new system is decimated only by half the number of channels. Two types of filter banks can be used in the under-decimated system: the discrete Fourier transform (DFT) filter banks and the cosine modulated filter banks. They are well known for their low complexity. In both cases, the system is approximately alias free, and the overall response is equivalent to a tunable multilevel filter. Properties of the DFT filter banks and the cosine modulated filter banks can be exploited to simultaneously achieve parallelism, computational saving, and a lower working rate. Furthermore, for both systems, the implementation cost of the analysis or synthesis bank is comparable to that of one prototype filter plus some low-complexity modulation matrices. The individual analysis and synthesis filters have complex coefficients in the DFT filter banks but have real coefficients in the cosine modulated filter banks. Author

N95-17286*# Jet Propulsion Lab., California Inst. of Tech., Pasadena, CA.
A SIMPLIFIED INTEGER COSINE TRANSFORM AND ITS APPLICATION IN IMAGE COMPRESSION c64
M. Costa and K. Tong *In its* The Telecommunications and Data Acquisition Report 15 Nov. 1994 p 129-139 (For primary document see N95-17279 04-32)
(RTOP 310-30-71-83-04)
Avail: CASI HC A03/MF A03

A simplified version of the integer cosine transform (ICT) is described. For practical reasons, the transform is considered jointly with the quantization of its coefficients. It differs from conventional ICT algorithms in that the combined factors for normalization and quantization are approximated by powers of two. In conventional algorithms, the normalization/quantization stage typically requires as many integer divisions as the number of transform coefficients. By restricting the factors to powers of two, these divisions can be performed by variable shifts in the binary representation of the coefficients, with speed and cost advantages to the hardware implementation of the algorithm. The error introduced by the factor approximations is compensated for in the inverse ICT operation, executed with floating point precision. The simplified ICT algorithm has potential applications in image-compression systems with disparate cost and speed requirements in the encoder and decoder ends. For example, in deep space image telemetry, the image processors on board the spacecraft could take advantage of the simplified, faster encoding operation, which would be adjusted on the ground, with high-precision arithmetic. A dual application is found in compressed video broadcasting. Here, a fast, high-performance processor at the transmitter would precompensate for the factor approximations in the inverse ICT operation, to be performed in real time, at a large number of low-cost receivers. Author

N95-17287*# Jet Propulsion Lab., California Inst. of Tech., Pasadena, CA.
ADAPTIVE LINE ENHANCERS FOR FAST ACQUISITION c61
H.-G. Yeh and T. M. Nguyen *In its* The Telecommunications and Data Acquisition Report 15 Nov. 1994 p 140-159 (For primary document see N95-17279 04-32)
(RTOP 315-91-10-13-08)
Avail: CASI HC A03/MF A03

Three adaptive line enhancer (ALE) algorithms and architectures - namely, conventional ALE, ALE with double filtering, and ALE with coherent accumulation - are investigated for fast carrier acquisition in the time domain. The advantages of these algorithms are their simplicity, flexibility, robustness, and applicability to general situations including the Earth-to-space uplink carrier acquisition and tracking of the spacecraft. In the acquisition mode, these algorithms act as bandpass filters; hence, the carrier-to-noise ratio (CNR) is improved for fast acquisition. In the tracking mode, these algorithms simply act as lowpass filters to improve signal-to-noise ratio; hence, better tracking performance is obtained. It is not necessary to have a priori knowledge of the received signal parameters, such as CNR, Doppler, and carrier sweeping rate. The implementation of these algorithms is in the time domain (as opposed to the frequency domain, such as the fast Fourier transform (FFT)). The carrier frequency estimation can be updated in real time at each time sample (as opposed to the batch processing of the FFT). The carrier frequency to be acquired can be time varying, and the noise can be non-Gaussian, nonstationary, and colored. Author

N95-17288*# Jet Propulsion Lab., California Inst. of Tech., Pasadena, CA.
ANTENNA NOISE TEMPERATURES OF THE 34-METER BEAM-WAVEGUIDE ANTENNA WITH HORNS OF DIFFERENT GAINS INSTALLED AT F1
T. Y. Otoshi, P. R. Lee, and M. M. Franco *In its* The Telecommunications and Data Acquisition Report 15 Nov. 1994 p 160-180 (For primary document see N95-17279 04-32)
(RTOP 310-20-65-86-08)
Avail: CASI HC A03/MF A03

This article presents a set of theoretical and measured zenith-antenna noise temperatures at 8.45 GHz for the DSS-13 34-m beam-waveguide antenna when horns of different gains are installed at F1. The methodology for calculations is shown in detail. The major differences between calculated and measured values are attributed to changes in subreflector support leg scattering when illuminated by the various horns. Author

N95-17289*# Jet Propulsion Lab., California Inst. of Tech., Pasadena, CA.
LOW-COMPLEXITY WAVELET FILTER DESIGN FOR IMAGE COMPRESSION c33
E. Majani *In its* The Telecommunications and Data Acquisition Report 15 Nov. 1994 p 181-200 (For primary document see N95-17279 04-32)
(RTOP 315-91-40-20-36)
Avail: CASI HC A03/MF A03

Image compression algorithms based on the wavelet transform are an increasingly attractive and flexible alternative to other algorithms based on block orthogonal transforms. While the design of orthogonal wavelet filters has been studied in significant depth, the design of nonorthogonal wavelet filters, such as linear-phase (LP) filters, has not yet reached that point. Of particular interest are wavelet transforms with low complexity at the encoder. In this article, we present known and new parameterizations of the two families of LP perfect reconstruction (PR) filters. The first family is that of all PR LP filters with finite impulse response (FIR), with equal complexity at the encoder and decoder. The second family is one of LP PR filters, which are FIR at the encoder and infinite impulse response (IIR) at the decoder, i.e., with controllable encoder complexity. These parameterizations are used to optimize the subband/wavelet transform coding gain, as defined for nonorthogonal wavelet transforms. Optimal LP wavelet filters are given

for low levels of encoder complexity, as well as their corresponding integer approximations, to allow for applications limited to using integer arithmetic. These optimal LP filters yield larger coding gains than orthogonal filters with an equivalent complexity. The parameterizations described in this article can be used for the optimization of any other appropriate objective function. Author

N95-17290*# Jet Propulsion Lab., California Inst. of Tech., Pasadena, CA.

A PRELIMINARY OPTICAL VISIBILITY MODEL c74

K. Cowles and B. M. Levine *In its* The Telecommunications and Data Acquisition Report 15 Nov. 1994 p 201-209 (For primary document see N95-17279 04-32)

(RTOP 315-91-40-20-29)

Avail: CASI HC A02/MF A03

A model is being created to describe the effect of weather on optical communications links between space and ground sites. This article describes the process by which the model is developed and gives preliminary results for two sites. The results indicate nighttime attenuation of optical transmission at five wavelengths. It is representative of a sampling of nights at Table Mountain Observatory from January to June and Mount Lemmon Observatory from May and June. The results are designed to predict attenuation probabilities for optical communications links. Author

N95-17291*# Jet Propulsion Lab., California Inst. of Tech., Pasadena, CA.

FIELD VERIFICATION OF THE WIND TUNNEL COEFFICIENTS c02

W. K. Gawronski and J. A. Mellstrom *In its* The Telecommunications and Data Acquisition Report 15 Nov. 1994 p 210-220 (For primary document see N95-17279 04-32)

(RTOP 314-40-52-01-02)

Avail: CASI HC A03/MF A03

Accurate information about wind action on antennas is required for reliable prediction of antenna pointing errors in windy weather and for the design of an antenna controller with wind disturbance rejection properties. The wind tunnel data obtained 3 years ago using a scaled antenna model serves as an antenna industry standard, frequently used for the first purpose. The accuracy of the wind tunnel data has often been challenged, since they have not yet been tested in a field environment (full-aized antenna, real wind, actual terrain, etc.). The purpose of this investigation was to obtain selected field measurements and compare them with the available wind tunnel data. For this purpose, wind steady-state torques of the DSS-13 antenna were measured, and dimensionless wind torque coefficients were obtained for a variety of yaw and elevation angles. The results showed that the differences between the wind tunnel torque coefficients and the field torque coefficients were less than 10 percent of their values. The wind-gusting action on the antenna was characterized by the power spectra of the antenna encoder and the antenna torques. The spectra showed that wind gusting primarily affects the antenna principal modes. Author

N95-17292*# Jet Propulsion Lab., California Inst. of Tech., Pasadena, CA.

TRACKING THE GALILEO SPACECRAFT WITH THE DSCC GALILEO TELEMETRY PROTOTYPE c17

T. T. Pham, S. Shambayati, D. E. Hardi, and S. G. Finley *In its* The Telecommunications and Data Acquisition Report 15 Nov. 1994 p 221-235 (For primary document see N95-17279 04-32)

(RTOP 314-30-61-02-10)

Avail: CASI HC A03/MF A03

On day of the year 062, 1994, a prototype of the Deep Space Communications Complex Galileo Telemetry subsystem successfully tracked and processed signals from the Galileo spacecraft, under fully suppressed-carrier modulation. The demonstration took place at Goldstone, employing the 70-m antenna and the 34-m high-efficiency antenna. This article presents the findings from that demonstration. Specific issues are the system performance in terms of signal-to-noise (SNR) degradation and the arraying gain. Validation of the test results is via symbol-error-rate measurement and the standard symbol SNR. The analysis is also extended to include characterization of the signal received from Galileo. Author

N95-17293*# Jet Propulsion Lab., California Inst. of Tech., Pasadena, CA.

COMPUTATION OF REFLECTED AND TRANSMITTED HORN RADIATION PATTERNS FOR A DICHROIC PLATE

J. C. Chen *In its* The Telecommunications and Data Acquisition Report 15 Nov. 1994 p 236-254 (For primary document see N95-17279 04-32)

(RTOP 315-91-40-20-26)

Avail: CASI HC A03/MF A03

A previous dichroic plate analysis has assumed that an ideal uniform plane wave illuminates the dichroic plate at a single angle of incidence. In fact, a horn radiates energy at the dichroic plate and illuminates it at many different angles. To model the horn and dichroic plate system, the horn pattern is represented as a group of plane waves traveling in different directions. The details of this analysis are presented this article. The calculated and measured reflected radiation patterns show good agreement. The noise temperature predicted from the horn pattern model is shown to be more accurate than that from a simple plane-wave model. Author

N95-17294*# Jet Propulsion Lab., California Inst. of Tech., Pasadena, CA.

X-/Ka-BAND DICHROIC PLATE NOISE TEMPERATURE REDUCTION

W. Veruttipong and P. Lee *In its* The Telecommunications and Data Acquisition Report 15 Nov. 1994 p 255-261 (For primary document see N95-17279 04-32)

(RTOP 315-91-40-20-26)

Avail: CASI HC A02/MF A03

The X-/Ka-band (8.4 GHz/32.0 GHz) dichroic plate installed as DSS 13 contributes an estimated 3 K to the system noise temperature at 32.0 GHz. Approximately 1 percent of the Ka-band incident field is reflected by the plate into the 300-K environment of the DSS-13 pedestal room. A low-cost, easily implemented method of reducing the noise temperature is presented. Using a curved reflector, the reflected field can be re-focused into an 80-K cold load, reducing the noise temperature contribution of the dichroic plate by about 2 K. Author

N95-17295*# Jet Propulsion Lab., California Inst. of Tech., Pasadena, CA.

A MODEL FOR ANALYSIS OF TDA BUDGET ALLOCATION

D. S. Remer (Harvey Mudd Coll., Claremont, CA.) and H. R. Buchanan *In its* The Telecommunications and Data Acquisition Report 15 Nov. 1994 p 262-267 (For primary document see N95-17279 04-32)

(RTOP 314-40-31-30-03)

Avail: CASI HC A02/MF A03

There is an ever-increasing need to achieve greater efficiency in the operation of the Deep Space Network (DSN), i.e., increased productivity at reduced cost. One of the tools used in the course of a planning workshop on this subject was a methodology for budget allocation applicable to long-range planning. This article presents a model for analysis of the TDA budget allocation. For the 1994 through 1999 period, the percentage of the total TDA budget allocated to capacity and capability is being cut in half, whereas the percentage spent on efficiency of delivery will be increasing. Author

N95-17296*# Jet Propulsion Lab., California Inst. of Tech., Pasadena, CA.

RF OPTICS STUDY FOR DSS-43 ULTRACONE IMPLEMENTATION

P. Lee and W. Veruttipong *In its* The Telecommunications and Data Acquisition Report 15 Nov. 1994 p 268-281 (For primary document see N95-17279 04-32)

(RTOP 314-30-61-02-17)

Avail: CASI HC A03/MF A03

The Ultracone feed system will be implemented on DSS 43 to support the S-band (2.3 GHz) Galileo contingency mission. The feed system will be installed in the host country's cone, which is normally used for radio astronomy, VLBI, and holography. The design must retain existing radio-astronomy capabilities, which could be impaired by shadowing from the large S-band feed horn. Computer calculations were completed to estimate system performance and shadowing effects for various configurations of the host country's cone feed systems. Also, the DSS-43 system performance using higher gain S-band horns was analyzed. A new

S-band horn design with improved return loss and cross-polarization characteristics is presented. Author

N95-17297*# Jet Propulsion Lab., California Inst. of Tech., Pasadena, CA.

JPL-ANTOPT ANTENNA STRUCTURE OPTIMIZATION PROGRAM

D. M. Strain *In its* The Telecommunications and Data Acquisition Report 15 Nov. 1994 p 282-292 (For primary document see N95-17279 04-32)

(RTOP 314-30-55-02-07)

Avail: CASI HC A03/MF A03

New antenna path-length error and pointing-error structure optimization codes were recently added to the MSC/NASTRAN structural analysis computer program. Path-length and pointing errors are important measured of structure-related antenna performance. The path-length and pointing errors are treated as scalar displacements for statics loading cases. These scalar displacements can be subject to constraint during the optimization process. Path-length and pointing-error calculations supplement the other optimization and sensitivity capabilities of NASTRAN. The analysis and design functions were implemented as 'DMAP ALTERs' to the Design Optimization (SOL 200) Solution Sequence of MSC-NASTRAN, Version 67.5. Author

N95-17301 National Defence Research Establishment, Linkoeping (Sweden). Huvudavdelning foer Informationsteknologi.

MULTISTATIC RADAR, MSR Annual Report, 1992 - 1993 [MULTISTATISK RADAR, MSR, ARSRAPPORT 1992/93]

A. Nelander and H. Ottersten Dec. 1993 17 p In SWEDISH

(PB94-190709; FOA-A-30090-8.4,3.3) Avail: Issuing Activity

The report covers the activities performed within project multistatic radar (MSR) during the fiscal year 1992/1993. References to current work and project seminars are listed. The reference list also includes work during fiscal years 1991/1992 and 1990/1991. During 1993 the MSR project has been complemented by contract work for the Defense Materiel Administration on Antenna Integrated Microwave Techniques (AIMT). Starting with fiscal year 1993/1994, the MSR work is included and reported in the AIMT program under the title AIMT multistatic radar principles. The work on antenna techniques is continued under the new title AIMT digital array antennas. NTIS

N95-17336 Massachusetts Inst. of Tech., Lexington. Lincoln Lab.

DOCUMENTATION OF 9-PAC BEACON TARGET DETECTOR PROCESSING FUNCTION

Jeffrey L. Gertz and Gabriel R. Elkin 26 Jul. 1994 104 p Limited Reproducibility: More than 20% of this document may be affected by microfiche quality

(Contracts DTFA01-93-Z-02012; F19628-90-C-0002)

(AD-A283090; ATC-220) Avail: Issuing Activity (Defense Technical Information Center (DTIC))

This project report documents the algorithms and flow of the beacon target detector (BTD) processing function incorporated as part of the ASR-9 processor augmentation card (9-PAC). The BTD function combines replies that arise from the same aircraft to form beacon targets, and sends these beacon targets to the 9-PAC merge process where they are combined with primary radar reports. The 9-PAC BTD process was designed to solve two problems with the ASR-9 array signal processor (ASP) BTD: identifying and removing false beacon targets due to reflections and preventing merging or splitting of targets due to reply overlap and garble. The BTD reflection processing algorithm marks each beacon target as either real or false, and provides this information to the 9-PAC merge process. Discrete Mode A reflection false targets are identified when duplicate code reports satisfying stringent conditions are located. In order to find nondiscrete Mode A code reflection false targets, the BTD builds an automated, dynamic reflector database based on the geography of pairs of discrete real and false targets. DTIC

N95-17436 Naval Postgraduate School, Monterey, CA.

AN ANALYSIS OF THE EFFECTS OF FEEDLINE AND GROUND SCREEN NOISE CURRENTS ON A CONICAL MONOPOLE RECEIVING ANTENNA M.S. Thesis

Thomas D. Gehrki Jun. 1994 46 p Limited Reproducibility: More than 20% of this document may be affected by microfiche quality

(AD-A283401) Avail: Issuing Activity (Defense Technical Information Center (DTIC))

Excessive electromagnetic interference/radio frequency interference (EMI/RFI) degrades the capability of the Naval Security Group (NSG) high frequency direction finding (HFDF) sites to receive signals of interest (SOI). These sites use a circularly disposed antenna array (CDAA) to receive signals in the 2 to 30 MHz frequency range. A conical monopole (CM), an antenna whose bandwidth matches the CDAA's, may provide a solution to the EMI/RFI problem through separation and isolation. Semiremotely locating the CM away from EMI/RFI sources achieves the former, while its independence from the noisy RF distribution system accomplishes the latter. This thesis analyzed the susceptibility of the CM to EMI/RFI currents that might be injected onto the feedline from equipment in the building at the center of the CDAA. The Numerical Electromagnetics Code (NEC) was used to model the CM and its buried feedline at the Imperial Beach CDAA site. The numerical model was used to validate proposed limits for the maximum allowable EMI/RFI current on incidental conductors and grounds at receiving sites. A maximum of two microamps of EMI current has been suggested to ensure that no appreciable degradation of SOI reception occurred. The NEC CM model predicted that the two microamp current limit would be adequate for SOI reception on the CM examined. Experimental measurements obtained at the Imperial Beach HFDF site partially validated these results and demonstrated that the CDAA response to the two microamp EMI/RFI limit is within the expected levels. DTIC

N95-17450 Phillips Lab., Kirtland AFB, NM.

RADIATION ELECTRODYNAMICS OF THE PHOTO-ELECTRON CLOUD PRODUCED BY AN ARBITRARY PHOTON PULSE INCIDENT ON A PLANAR EMITTING SURFACE IN VACUUM Final Report, 1 Sep. 1990 - 31 Aug. 1992

David Dietz Jun. 1994 136 p Limited Reproducibility: More than 20% of this document may be affected by microfiche quality

(AD-A282153; AD-E202066; PL-TR-94-1004) Avail: CASI HC A07

The electromagnetic radiation field produced by the cloud of accelerating electrons induced at a planar photoelectron emitting surface in vacuum by a photon pulse of arbitrary time profile incident upon that surface is derived analytically in the nonrelativistic, small-spot-size regime. This derivation provides scaling relations for the radiated fields explicit in the pulse and surface parameters. Electron cloud dynamics are discussed and integral expressions for the electric and magnetic fields at large but finite (i.e., 'finitely-remote') distances from the cloud are derived. The fields are calculated by directly summing contributions over individual electron trajectories, using exact small-spot retarded times, rather than by the usual technique of first forming the electron charge and current densities and integrating them. The resulting integral representation of the finitely-remote fields are correct to first order in v/c and are valid for all time and for somewhat spatially extended charge clouds. These finitely-remote fields are then used to compute asymptotic radiation fields in the limit of the field point going to infinity in a suitable fashion. From these asymptotic radiation quantities in which all the integrations have been fully carried out are then derived. Illustrations of the general results for some sample pulses (constant, linear ramp, triangular, parabolic, and sq sin) are provided. DTIC

N95-17453 National Defence Research Establishment, Linkoeping (Sweden). Huvudavdelning foer Informationsteknologi.

PRELIMINARY STUDY OF AN ACTIVE MILLIMETER WAVE SENSOR [FOERSTUDIE ANGAENDE AKTIV MILLIMETER VAGSSENSOR]

U. Dahlgren, H. Hentzell, J. Kjellgren, H. Zirath, and B. Albinsson Oct. 1993 40 p In SWEDISH Prepared in cooperation with Chalmers Univ. of Technology, Goeteborg, Sweden

(PB94-189206; FOA-C-30734-3.2) Avail: Issuing Activity (National Technical Information Service (NTIS))

In seekers and battlefield radar, the millimeter wave technology will be of large importance in the future. The short wavelength makes it possible to use the high transmittivity and coherence of a microwave radar. In imaging millimeter wave systems, one could realize a real time signal processing capability similar to an optical sensor array. Further, the resolution of a millimeter wave system is higher for a given aperture size, compared with a typical microwave system. One important reason for this is the development of HEMT transistors which could be used as amplifiers to

several hundreds of gigahertz. In both digital and low frequency analog technology, the size is reducing and the speed is increasing. One technology to do this is the multilayer technology used in Multichip Modules and gate arrays. The authors suggest that fully integrated millimeter wave sensor with antennas and HEMT-transistors can be realized with a similar technology. If an array of millimeter wave sensors is fed by an optical system, it would be possible to realize a real time radar camera with 1000 pixels where each pixel corresponds to an angle of 0.5 deg. NTIS

N95-17455 National Defence Research Establishment, Linkoeping (Sweden). Huvudavdelning foer Informationsteknologi.
SUPERRESOLUTION IN A JAMMED RADAR SIGNAL ENVIRONMENT [SUPERUPPLOESNING VID RADARSPANING I STOERD SIGNALMILJOE. HUVUDPROJEKT LUFTFOERSVAR]
O. Carlstedt Dec. 1993 72 p In SWEDISH
(PB94-190758; FOA-C-30740-8.4,3.3) Avail: Issuing Activity (National Technical Information Service (NTIS))

For radar surveillance of air targets flying close together super resolution with array antennas can be a possible method to separate targets within the main antenna lobe. A system based on an algorithm of type Parametric Target Model fitting has been simulated and evaluated for some cases of electronic jamming and target configuration. A target configuration can include both radar quiet but illuminated targets and active jammers. NTIS

N95-17480# Department of the Navy, Washington, DC.
CENTER-FED MULTIFILAR HELIX ANTENNA Patent Application
Edwin H. Wood, inventor (to Navy) 2 May 1994 18 p
(AD-D016390; US-Patent-Appl-SN-230459) Avail: CASI HC A03/MF A01

An antenna system including a phasing circuit for producing balanced, phase displaced, signals for connection to an antenna. The antenna comprises, for each set of balanced phase signals, a pair of antenna elements disposed serially along a helical path. A transmission line, connected to each of the phasing circuit terminals, drives each antenna element pair at a center location by being connected to the proximate ends of each pair. The antenna has a omnidirectional radiation pattern, a wide band width, a good front-to-back ratio and can be constructed in a compact form. DTIC

N95-17482 Department of the Navy, Washington, DC.
SIMULTANEOUS DETERMINATION OF INCOMING MICROWAVE FREQUENCY AND ANGLE-OF-ARRIVAL Patent Application
Nickolas P. Vlannes, inventor (to Navy) 4 May 1994 51 p Limited Reproducibility: More than 20% of this document may be affected by microfiche quality
(AD-D016392; US-Patent-Appl-SN-245284; Navy-Case-73971) Avail: CASI HC A04

Incoming signals radiated to an array of antennas are processed within a signal surveillance system by adding signal outputs of two antennas at a common frequency. Separation of the added signal outputs according to frequency and comparison of power level measurement thereof provides signal phase difference data from which frequency and direction of the incoming signals are simultaneously determined. DTIC

N95-17501 Phillips Lab., Kirtland AFB, NM.
RADIAL ACCELETRON, A NEW LOW IMPEDANCE HPM SOURCE Final Report, Nov. 1991 - Oct. 1992
M. J. Arman and Kyle J. Hendricks Mar. 1994 21 p Limited Reproducibility: More than 20% of this document may be affected by microfiche quality
(AD-A282008; AD-E202012; PL-TR-93-1092) Avail: Issuing Activity (Defense Technical Information Center (DTIC))

This report explores and analyzes using transit-time effects in a coaxial geometry to develop a low-impedance high power microwave (HPM) source that uses no external magnetic field and no confining foils. This source works in the 1-20 GHz range and has a power output of no less than 1 GW. The input is a low-voltage dc pulse of only 350 kV or less with a flat top of approximately 200 ns. The dc pulse is launched into a coaxial structure comprised of the diode, the oscillator, and the buncher. Strong impedance mismatch between the diode section and the body of the device provides enough reflection to have a well defined coaxial cavity of high Q to support cavity characteristic modes. Electrons emitted from the inner conductor of the structure accelerate toward the anode interacting with a selected characteristic mode of the structure, usually losing kinetic energy to the mode, until the RF fields are strong enough to optimize, thus leading to saturation. The source offers significant improvements in power, repetition rate, size, and efficiency because of the coaxial structure. The diode impedance may be reduced to a few ohms thus allowing larger input and output powers. With no foils to erode, the only thing limiting the repetition rate is the vacuum ability and, with no external magnetic field required, the device is simple, lightweight, and inexpensive. Because of the strong bunching, the efficiency is high and, as with all transit-time oscillators, the signal is stable and monochromatic. The device may be used as a buncher or as an oscillator. DTIC

N95-17502# Helsinki Univ. of Technology, Espoo (Finland). Electromagnetics Lab.
STATIC IMAGE METHOD FOR THE INTERACTION OF TWO CO-AXIAL CONDUCTING PROLATE SPHEROIDS
J. C. E. Sten Mar. 1994 13 p
(PB94-197696; ISBN-951-22-1616-7) Avail: CASI HC A03/MF A01

An image solution was recently found for the electrostatic problem of a point charge located on the axis of revolution of a conducting prolate spheroid. The image theory in this paper is applied to account for the reaction of two co-axial conducting prolate spheroids subject for a homogeneous axial electric field. Integral equations are given for the image dipole moment density functions in each spheroid. A similar integral equation based method is given for calculating the capacitance. NTIS

N95-17649# Instituto de Pesquisas Espaciais, Sao Paulo (Brazil). Lab. de Computacao de Matematica Aplicada.
PHONOLOGIC-GRAPHEMIC TRANSCODIFIER FOR PORTUGUESE LANGUAGE SPOKEN IN BRAZIL (PLB)
Francisco Jose FragadaSilva, Osamu Saotome, and Carlos Alberto deOliveira 1994 13 p Presented at the 11th Brazilian Symposium of Artifical Intelligence, Fortaleza, Brazil, 17-20 Oct. 1994
(INPE-5575-PRE/1803) Avail: CASI HC A03/MF A01

An automatic speech-to-text transformer system, suited to unlimited vocabulary, is presented. The basic acoustic unit considered are the allophones of the phonemes corresponding to the Portuguese language spoken in Brazil (PLB). The input to the system is a phonetic sequence, from a former step of isolated word recognition of slowly spoken speech. In a first stage, the system eliminates phonetic elements that don't belong to PLB. Using knowledge sources such as phonetics, phonology, orthography, and PLB specific lexicon, the output is a sequence of written words, ordered by probabilistic criterion that constitutes the set of graphemic possibilities to that input sequence. Pronunciation differences of some regions of Brazil are considered, but only those that cause differences in phonological transcription, because those of phonetic level are absorbed, during the transformation to phonological level. In the final stage, all possible written words are analyzed for orthography and grammar point of view, to eliminate the incorrect ones. Author

N95-17651*# Florida Univ., Gainesville, FL. Dept. of Electrial Engineering.
SYNTHETIC APERTURE RADAR TARGET DETECTION, FEATURE EXTRACTION, AND IMAGE FORMATION TECHNIQUES Final Report, Sep. 1993 - Sep. 1994
Jian Li Sep. 1994 119 p Sponsored by AFOSR; NSF; and Goeran Gustafsson Foundation Prepared for Ohio Aerospace Inst., Wright-Patterson AFB, OH
(Contract NCC3-319)
(NASA-CR-197485; NAS 1.26:197485) Avail: CASI HC A06/MF A02

This report presents new algorithms for target detection, feature extraction, and image formation with the synthetic aperture radar (SAR) technology. For target detection, we consider target detection with SAR and coherent subtraction. We also study how the image false alarm rates are related to the target template false alarm rates when target templates are used for target detection. For feature extraction from SAR images, we present a computationally efficient eigenstructure-based 2D-MODE algorithm for two-dimensional frequency estimation. For SAR image formation, we present a robust parametric data model for estimating high resolution range signatures of radar targets and for forming high resolution SAR images. Author

N95-17665*# Notre Dame Univ., IN. Dept. of Electrical Engineering.
ERROR CONTROL TECHNIQUES FOR SATELLITE AND SPACE COMMUNICATIONS Annual Status Report
Daniel J. Costello, Jr. Nov. 1994 123 p
(Grant NAG5-557)
(NASA-CR-197459; NAS 1.26:197459) Avail: CASI HC A06/MF A02

The unequal error protection capabilities of convolutional and trellis codes are studied. In certain environments, a discrepancy in the amount of error protection placed on different information bits is desirable. Examples of environments which have data of varying importance are a number of speech coding algorithms, packet switched networks, multi-user systems, embedded coding systems, and high definition television. Encoders which provide more than one level of error protection to information bits are called unequal error protection (UEP) codes. In this work, the effective free distance vector, d, is defined as an alternative to the free distance as a primary performance parameter for UEP convolutional and trellis encoders. For a given (n, k), convolutional encoder, G, the effective free distance vector is defined as the k-dimensional vector d = (d(sub 0), d(sub 1), ..., d(sub k-1)), where d(sub j), the j(exp th) effective free distance, is the lowest Hamming weight among all code sequences that are generated by input sequences with at least one '1' in the j(exp th) position. It is shown that, although the free distance for a code is unique to the code and independent of the encoder realization, the effective distance vector is dependent on the encoder realization. Derived from text

N95-17672# California Univ., Berkeley. Lawrence Berkeley Lab, CA.
TRANSVERSE MODE COUPLING INSTABILITY WITH A DOUBLE RF SYSTEM
Yong Ho Chin Jun. 1994 3 p Presented at the 4th European Particle Accelerator Conference, London, England, 27 Jun. - 1 Jul. 1994
(Contract DE-AC03-76SF-00098)
(DE94-017972; LBL-35957; CONF-940618-56) Avail: CASI HC A01/MF A01

Effects on a transverse mode coupling instability in a storage ring by a strongly deformed rf bucket in a double rf system are studied. An eigenvalue equation, respectively the vanishing of the determinant of an infinite matrix, is derived from a Hamiltonian formalism. Truncation of th is determinant permits solution of the problem on a computer, and a code MOSDRF has been written which finds the complex mode frequencies. The stability limits are determined by equating the imaginary part of the solution to the radiation damping rate. The theory was applied to LEP with third higher-harmonic cavities, and the results were compared with those obtained by the Multi-particle simulation program FEDBAK. They agree well, and show that the threshold current will be reduced rather than improved. DOE

N95-17696 Department of the Navy, Washington, DC.
SELF-INITIALIZING CIRCUIT LINK Patent
Anthony E. Spezio, inventor (to Navy), Saurabh Dalal, inventor (to Navy), Edward M. Alexander, inventor (to Navy), and Hal L. Levitt, inventor (to Navy) 21 Jun. 1994 5 p Filed 30 Jun. 1993
(AD-D016363; US-Patent-5,323,126; US-Patent-Appl-SN-083776;
US-Patent-Class-333-109) Avail: US Patent and Trademark Office

A circuit link, and method for using link, for self initializing any device operatively connected to the link. An input signal is split into two portions, one of which is delayed so that the undelayed signal can transverse the circuit link before the delayed signal. A pair of quadrature splitters are operatively connected to one another to split and combine the undelayed and delayed signals in their turns, and recombine them in their turns, in a manner effective to cause one of the circuit link's outputs to be nonzero responsive to the delayed signal, and zero responsive to the undelayed signal, with the opposite result on the other circuit output. The undelayed signal is thus available to initialize any device requiring initialization, and the delayed signal, unperturbed by any such device, is thus available for use as the circuit link's ultimate output. The circuit is especially useful with frequency selective limiters (FSL's), which are commonly used as channelizers in multichannel communication systems, and which are ineffective before initialization. DTIC

N95-17697 Department of the Navy, Washington, DC.
HIGH SPEED METHOD FOR PREDICTING RADIO-WAVE PROPAGATION Patent
Herbert V. Hitney, inventor (to Navy) 5 Apr. 1994 11 p Filed 12 Feb. 1992
(AD-D016369; US-Patent-5,301,127; US-Patent-Appl-SN-834916;
US-Patent-Class-364-525) Avail: US Patent and Trademark Office

Radio-wave propagation is rapidly predicted by a hybrid computational method that uses Ray Optics techniques to calculate radio field strength above a limiting radio-wave ray, Parabolic Equation techniques to calculate radio field strength below the limiting radiowave ray and below a predetermined altitude, and a newly created Extended Optics method to compute radio field strength in an area of the atmosphere below the limiting radio-wave ray and above the predetermined altitude. Rays in the extended optics area are initialized from the elevation angle that rays traced through the parabolic equation area make with the predetermined altitude. Where reflected, direct or origin created rays do not exist within the parabolic equation area, the elevation angle for the ray that does exist at the farthest range (optical limit) is used to initiate ray tracing in the extended optics area for ranges beyond the optical limit. DTIC

N95-17926# Argonne National Lab., IL.
ELECTROMAGNETIC FIELD MEASUREMENTS ON A mm-WAVE LINEAR ACCELERATOR
P. Matthews, Y. Kang, T. Berenc, R. Kustom, T. Willke (Illinois Univ., Chicago, IL.), and A. Feinerman (Illinois Univ., Chicago, IL.) 1994 4 p Presented at the 4th European Particle Accelerator Conference, London, England, 27 Jun. - 1 Jul. 1994
(Contract W-31-109-eng-38)
(DE94-015092; ANL/ASD/CP-83412; CONF-940618-15) Avail: CASI HC A01/MF A01

Field strength measurements for the determination of the R/Q of a mm-wave, 50-MeV electron linear accelerator using perturbational techniques are described. The perturbation is achieved using optical fibers coated with a thin metallic film to form a hollow cylinder. The perturbational form factors for such a geometry are approximated using several simple analytical expressions which are compared to a finite difference calculation as well as experimental results on a known cavity. DOE

N95-15991*# Bologna Univ. (Italy). Inst. di Glottologia.
CPP-TRS(C): ON USING VISUAL COGNITIVE SYMBOLS TO ENHANCE COMMUNICATION EFFECTIVENESS
Graziella Tonfoni *In* NASA. Johnson Space Center, ISMCR 1994: Topical Workshop on Virtual Reality. Proceedings of the Fourth International Symposium on Measurement and Control in Robotics Nov. 1994 p 136-142 (For primary document see N95-15972 04-63)
Avail: CASI HC A02/MF A02

N95-16268# Nanjing Univ. of Aeronautics and Astronautics, Nanjing, Jiangsu (China). Dept. of Electronic Engineering.
LINEAR PREDICTION DATA EXTRAPOLATION SUPERRESOLUTION RADAR IMAGING
Zhaoda Zhu, Zhenru Ye, and Xiaoqing Wu *In its* Joint Proceedings on Aeronautics and Astronautics (JPAA) 125-130 (SEE N95-16249 04-01) May 1993 Sponsored by the Aeronautical Science Foundation of China (For primary document see N95-16249 04-01)
Avail: CASI HC A02/MF A03

N95-16269# Nanjing Univ. of Aeronautics and Astronautics, Nanjing, Jiangsu (China). Dept. of Electronic Engineering.
DETECTING THE NUMBER OF TARGETS IN SPATIALLY COLORED NOISE USING SAMPLED APERTURE RADARS
Zhaoda Zhu and Zhishun She *In its* Joint Proceedings on Aeronautics and Astronautics (JPAA) May 1993 p 131-136 See also A91-30858 Sponsored by the Aeronautical Science Foundation of China (For primary document see N95-16249 04-01)
Avail: CASI HC A02/MF A03

N95-16270# Nanjing Univ. of Aeronautics and Astronautics, Nanjing, Jiangsu (China). Dept. of Electronic Engineering.
FAST ACQUISITION OF BURST DIRECT SEQUENCE SPREAD SPECTRUM SIGNALS THROUGH SATELLITE CHANNELS
Shuyao Yang *In its* Joint Proceedings on Aeronautics and Astronautics (JPAA) May 1993 p 137-146 See also A93-20859 (For primary document see N95-16249 04-01)
Avail: CASI HC A02/MF A03

N95-17198*# Jet Propulsion Lab., California Inst. of Tech., Pasadena, CA.
INTERNATIONAL DATA TRANSFER FOR SPACE VERY LONG BASELINE INTERFEROMETRY
Alexandria B. Wiercigroch *In* NASA. Goddard Space Flight Center, Third International Symposium on Space Mission Operations and Ground Data Systems, Part 1 Nov. 1994 p 169-175 (For primary document see N95-17179 04-17)
Avail: CASI HC A02/MF A06

N95-17210*# Jet Propulsion Lab., California Inst. of Tech., Pasadena, CA.
GALILEO MISSION PLANNING FOR LOW GAIN ANTENNA BASED OPERATIONS
R. Gershman, K. L. Buxbaum, J. M. Ludwinski, and B. G. Paczkowski *In* NASA. Goddard Space Flight Center, Third International Symposium on Space Mission Operations and Ground Data Systems, Part 1 Nov. 1994 p 279-286 (For primary document see N95-17179 04-17)
Avail: CASI HC A02/MF A06

N95-17214*# National Aeronautics and Space Administration, Washington, DC.
ACCURACY ANALYSIS OF TDRSS DEMAND FORECASTS
Daniel C. Stern, Allen J. Levine (National Aeronautics and Space Administration. Goddard Space Flight Center, Greenbelt, MD.), and Karl J. Pitt (Mitre Corp., Greenbelt, MD.) *In* NASA. Goddard Space Flight Center, Third International Symposium on Space Mission Operations and Ground Data Systems, Part 1 Nov. 1994 p 311-318 (For primary document see N95-17179 04-17)
Avail: CASI HC A02/MF A06

N95-17584*# National Aeronautics and Space Administration. Goddard Space Flight Center, Greenbelt, MD.
RE-ENGINEERING NASCOM'S NETWORK MANAGEMENT ARCHITECTURE
Brian C. Drake and David Messent (Computer Sciences Corp., Lanham, MD.) *In its* Third International Symposium on Space Mission Operations and Ground Data Systems, Part 2 Nov. 1994 p 1133-1141 (For primary document see N95-17531 04-17)
Avail: CASI HC A02/MF A06

N95-17585*# National Aeronautics and Space Administration, Washington, DC.
RE-ENGINEERING NASA'S SPACE COMMUNICATIONS TO REMAIN VIABLE IN A CONSTRAINED FISCAL ENVIRONMENT
Rhoda Shaller Hornstein, Donald J. Hei, Jr. (National Aeronautics and Space Administration. Goddard Space Flight Center, Greenbelt, MD.), Angelita C. Kelly (National Aeronautics and Space Administration. Goddard Space Flight Center, Greenbelt, MD.), Patricia C. Lightfoot (National Aeronautics and Space Administration. Goddard Space Flight Center, Greenbelt, MD.), Holland T. Bell (National Aeronautics and Space Administration. Wallops Flight Facility, Wallops Island, VA.), Izeller E. Cureton-Snead (Jet Propulsion Lab., California Inst. of Tech., Pasadena, CA.), William J. Hurd (Jet Propulsion Lab., California Inst. of Tech., Pasadena, CA.), and Charles H. Scales (National Aeronautics and Space Administration. Marshall Space Flight Center, Huntsville, AL.) *In* NASA. Goddard Space Flight Center, Third International Symposium on Space Mission Operations and Ground Data Systems, Part 2 Nov. 1994 p 1143-1150 (For primary document see N95-17531 04-17)
Avail: CASI HC A02/MF A06

33 ELECTRONICS AND ELECTRICAL ENGINEERING

Includes test equipment and maintainability; components, e.g., tunnel diodes and transistors; microminiaturization; and integrated circuitry.

For related information see also *60 Computer Operations and Hardware* and *76 Solid-State Physics.*

N95-16089# Illinois Univ., Urbana, IL. Coordinated Science Lab.
TIMING AND AREA OPTIMIZATION FOR VLSI CIRCUIT AND LAYOUT
Wei-Tong Chuang 10 May 1994 111 p
(Contract N00014-90-J-1270)
(AD-A281081; UILU-ENG-94-2216; DAC-46) Avail: CASI HC A06/MF A02

This thesis considers two problems in computer-aided design of VLSI circuits: (1) discrete gate sizing and (2) timing-driven placement improvement. The discrete gate-sizing problem is described as follows. A standard cell library typically contains several versions of any given gate type, each of which has a different gate size. We consider the problem of choosing optimal gate sizes from the library to minimize a cost function (such as total circuit area) while meeting the timing constraints imposed on the circuit. After presenting an efficient solution algorithm for combinational circuits, we examine the problem of minimizing the area of a synchronous sequential circuit for a given clock period specification. This is done by appropriately selecting a size for each gate in the circuit and by adjusting the delays between the central clock distribution node and individual flip-flops. Existing methods treat these two problems separately, which may lead to very suboptimal solutions in some cases. We develop a novel unified approach to tackle them simultaneously. We also address the problem of making this work applicable to very large synchronous sequential circuits by partitioning these circuits to reduce the computational complexity.

DTIC

N95-16110 Naval Postgraduate School, Monterey, CA.
A VLSI INTERFACE FOR THE NM24CF04 SERIAL-ACCESS FERROELECTRIC MEMORY M.S. Thesis
James H. Dickerson Mar. 1994 113 p Limited Reproducibility: More than 20% of this document may be affected by microfiche quality
(AD-A281535) Avail: Issuing Activity (Defense Technical Information Center (DTIC))

The goal of this research project was to design a VLSI implementation of the required digital circuitry to utilize ferroelectric memory as a portion of main microprocessor memory. An interface between National Semiconductor's NM24CF04, a nonvolatile, serial-access, ferroelectric memory device, and Intel's 8086 microprocessor was designed and implemented using SSI/MSI technology in a previous study. This thesis discusses the redesign of the previously designed circuit for VLSI implementation. The layout was accomplished using the Magic graphical layout editor and tested using the Esim event driven logic-level simulator.

DTIC

N95-16130# Massachusetts Inst. of Tech., Lexington. Lincoln Lab.
FREQUENCY MULTIPLIER ANALYSIS AND DESIGN USING PUNCH-THROUGH VARACTOR DIODES
P. H. Williams 8 Aug. 1994 46 p
(Contract F19628-90-C-0002)
(AD-A284963; TR-1003; ESC-TR-94-079) Avail: CASI HC A03/MF A01

Punch-through varactor diode frequency multipliers, a type of nonlinear reactive multiplier, can be 100% efficient, theoretically. This report presents a model of a punch-through diode and then analyzes it in the frequency domain. By restricting the currents that can flow, the analysis can be reduced to a finite set of equations for any order multiplier. Next, assuming that the diode loss is low enough, diode equations for the specific cases of a doubler and a tripler are developed. The report then adds the necessary circuit elements to give lumped-element circuit designs and design equations for both doublers and triplers. Finally, sample circuits are built using these designs, and design equations are shown along with their performance.

DTIC

N95-16136 Stanford Univ., CA.
VLSI CIRCUITS FOR HIGH SPEED DATA CONVERSION Final Report, 18 Mar. 1991 - 17 Mar. 1994
Bruce A. Wooley 16 May 1994 11 p Limited Reproducibility: More than 20% of this document may be affected by microfiche quality
(Contract DAAL03-91-G-0088)
(AD-A281556; ARO-28387.11-EL) Avail: Issuing Activity (Defense Technical Information Center (DTIC))

The focus of research has been the study of fundamental issues in the design and testing of data conversion interfaces for high performance VLSI signal processing and communications systems. Because of the increased speed and density that accompany the continuing scaling of VLSI technologies, digital means of processing, communicating, and storing information are rapidly displacing their analog counterparts across a broadening spectrum of applications. In such systems, the limitations on system performance generally occur at the interfaces between the digital representation of information and the analog environment in which the system is embedded. Specific results of this research include the design and implementation of low-power BiCMOS comparators and sample-and-hold amplifiers operating at clock rates as high as 200 MHz, the design and integration of a 12-bit, 5 MHz CMOS A/D converter employing a two-step architecture and a novel self-calibrating comparator, the design and integration of an optoelectronic communications receiver front-end in a GaAs-on-Si technology, the initiation of research into the use of an active silicon substrate probe card for fully testing high-performance mixed-signal circuits at the wafer level, and a preliminary study of means for correcting dynamic errors in high-performance A/D converters. DTIC

N95-16137# Arizona Univ., Tucson, AZ. Dept. of Mathematics.
ULTRASHORT PULSE EFFECTS IN SEMICONDUCTOR AMPLIFIERS AND IN DISPERSIVE MEDIA Final Report, 1 Dec. 1990 - 31 Mar. 1994
J. Moloney, R. A. Indik, S. W. Koch, and A. C. Newell 31 Mar. 1994 4 p
(Grant AF-AFOSR-0074-91)
(AD-A284925; AFOSR-94-0620TR) Avail: CASI HC A01/MF A01

The researchers developed a code for integrating envelope equations derived from scalar Maxwell's equations for a scalar field coupled to the SCB equations. This code can handle plane wave (one dimensional) and a single transverse dimension (two dimensional). At this time, the codes are being used to study the behavior of ultrashort pulses propagating in the nonlinear medium. The case of a semiconductor amplifier has been the focus. They have been able to integrate the plane wave equations for considerably longer propagation distances than had been possible previously due to the efficiency of the algorithm. In so doing, they have predicted novel effects such as pulse compression, the appearance of an adiabatic following behavior, and spontaneous pulse breakup for very high gain amplifiers. In addition they have made a study of the interactions in such an amplifier of simultaneous ultrashort strong pulses at different frequencies. This is relevant to the ability of such a device to be used with frequency multiplexing. DTIC

N95-16159# Georgia Tech Research Inst., Atlanta, GA.
CHARACTERISTICS OF PHASE-CORRECTING FRESNEL ZONE PLATES AND ELLIPTICAL WAVEGUIDES Final Report, 1 May 1991 - 31 Dec. 1994
James C. Wiltse Feb. 1994 73 p
(Contract DAAL03-91-G-0114)
(AD-A281385; ARO-28516.5-EL) Avail: CASI HC A04/MF A01

The primary area of activity has been concentrated on the investigations relating to Fresnel zone plate antennas. A secondary effort has dealt with the characteristics of propagation in waveguides of elliptical cross section. In both cases, applications at microwave and millimeter-wavelengths have been emphasized. Thorough literature searches were conducted, and the results are given in Appendices A and B. The zone plate work has dealt with both transmission and reflection types, and has included considering the off-axis-fed cases. In the latter case, the plate may consist of elliptical zones, rather than the usual circular configuration. In general, the characteristics studied include far-field patterns, focal region fields, off-axis performance, bandwidth, and aberrations. In the case of propagation in elliptical waveguides, the attenuation and modal properties were studied for enclosed metal waveguides, coaxial transmission lines, and various surface waveguides. DTIC

N95-16283# InnovASIC, Inc., Albuquerque, NM.
SUPPORT FOR DEVELOPMENT OF A CUSTOM VLSI AND FPGA LOGIC CHIPS BASED ON A VHDL TOP-DOWN DESIGN APPROACH
1994 11 p Prepared for Los Alamos National Lab., NM
(Contract W-7405-eng-36)
(DE94-013608; LA-Sub-94-32) Avail: CASI HC A03/MF A01

The objective of this contract was to perform the beginning stages of development for two Application Specific integrated Circuits: CMOS-1 and CMOS-2D. This work includes specification writing, behavioral modeling, and beginning design. In addition, the design work is required to be done in the VHSIC Hardware Description Language (VHDL). InnovASIC, Inc. completed all the tasks required of this contract. The specifications were written, VHDL for CMOS-1 was completed, a behavioral model of CMOS-2D was written, and a system simulation was performed. DOE

N95-16357# Sandia National Labs., Albuquerque, NM.
HOW CLEAN IS CLEAN: NON-DESTRUCTIVE/DIRECT METHODS OF FLUX, RESIDUE DETECTION
C. S. Welch (College of William and Mary, Hampton, VA.), U. Ray (Bell Telephone Labs., Inc., Princeton, NJ.), B. R. Stallard, R. D. Watkins, M. W. Koch, and M. M. Moya 1994 26 p Presented at the International Conference on Solder Fluxes and Pastes, Atlanta, GA, 1-3 Jun. 1994
(Contract DE-AC04-94AL-85000)
(DE94-013439; SAND-94-1263C; CONF-9406189-1) Avail: CASI HC A03/MF A01

The feasibility of three different non-destructive and direct methods of evaluating PCB (printed circuit boards) cleanliness was demonstrated. The detection limits associated with each method were established. In addition, the pros and cons of these methods as routine quality control inspection tools were discussed. OSEE (Optically Stimulated Electron Emission) was demonstrated to be a sensitive technique for detection of low levels of flux residues on insulating substances. However, future work including development of rugged OSEE instrumentation will determine whether the PCB industry can accept this technique in a production environment. FTIR (Fourier Transform Infrared) microscopy is a well established technique with well known characteristics. The inability of FTIR to discriminate an organic contaminant from an organic substrate limits its usefulness as a PCB line inspection tool, but it will still remain a technique for the QC/QA laboratory. One advantage of FTIR over the other two techniques described here is its ability to identify the chemical nature of the residue, which is important in Failure Mode Analysis. Optical imaging using sophisticated pattern recognition algorithms was found to be limited to high concentrations of residue. Further work on improved sensor techniques is necessary. DOE

N95-16394 Rochester Univ., NY.
PICOSECOND SILICON METAL-SEMICONDUCTOR-METAL PHOTODIODE Report, 11-16 Jul. 1993
Thomas Y. Hsiang, Sotiris Alexandrou, Chia-Chi Wang, Mark Y. Liu, and Stephen Y. Chou 16 Jul. 1993 5 p Limited Reproducibility: More than 20% of this document may be affected by microfiche quality
(Contract DAAL03-92-G-0112)
(AD-A281548; ARO-30407.4.EL-URI) Avail: Issuing Activity (Defense Technical Information Center (DTIC))

The ultrafast characteristics of crystalline-silicon metal-semiconductor-metal (MSM) photodiodes with finger widths and spacings down to 200 nm, subjected to femtosecond optical pulse excitations, was measured with a subpicosecond electro-optic sampling system. Electrical responses with full-width at half-maximum (FWHM) as short as 3.7 ps, at a corresponding 3 dB bandwidth of 110 GHz, were generated by violet-light excitation. These diodes are the fastest silicon photodetectors reported to date. Detailed bias and light-intensity dependence of the diode response has been measured. These results are used to obtain the velocity-field relation of electrons in silicon and to demonstrate the ideal transit-time-limited response of the diodes. DTIC

N95-16410 Georgia Tech Research Inst., Atlanta, GA.
ANALOG MICROCIRCUIT FAULT PREDICTION Final Report
Richard M. Ingle, John H. Bordelon, Michael J. Willis, and C. D. Stokes Apr. 1994 95 p Limited Reproducibility: More than 20% of this document may be affected by microfiche quality

(Contract F30602-88-D-0025)
(AD-A281958; RL-TR-94-75) Avail: Issuing Activity (Defense Technical Information Center (DTIC))

This report documents an effort to determine the feasibility of constructing a realistic fault set for a given analog microcircuit from the information provided by a microcircuit yield simulator program. A methodology for this was developed and demonstrated using a simple PMOS process. The fault set which was generated demonstrates that it is possible to define how process defects affect electrical performance through the use of high level circuit models. The fault set can be ranked by probability of occurrence, and is suitable for use by a circuit simulation program. DTIC

N95-16425# Midwest Research Inst., Golden, CO. National Renewable Energy Lab.
RESEARCH ON STABLE, HIGH-EFFICIENCY AMORPHOUS-SILICON MULTIJUNCTION MODULES
M. Ghosh, F. Kampas, and J. Xi Jul. 1994 13 p
(Contract DE-AC36-83CH-10093)
(DE94-011839; NREL/TP-411-6854) Avail: CASI HC A03/MF A01

This report describes work performed on same-band-gap, amorphous-silicon, tandem-junction 1 cm(exp 2) devices and 900 cm(exp 2) modules. The same band-gap, amorphous-silicon, tandem-junction structure is of interest because it suffers from less light-induced degradation than the single-junction structure. The tandem-junction structure is more complex than the single-junction structure in that the interface between the two junctions, the so-called 'tunnel junction', must enable the efficient recombination of holes from one junction with electrons from the other junction without absorbing a significant amount of light. The topics covered in this report include the deposition of the various amorphous silicon thin-film layers with the required electrical properties and uniformity for modules, deposition of nonsemiconductor layers for the front and back contact with the requisite optical properties, preparation and characterization of tunnel junctions and small-area devices, and preparation and characterization of modules. DOE

N95-16516# Rome Lab., Griffiss AFB, NY.
WAVES VHDL INTERFACE
James P. Hanna Jun. 1994 68 p
(AD-A285208; RL-TR-94-76) Avail: CASI HC A04/MF A01

The Waveform and Vector Exchange Specification (WAVES) is the Industry standard representation for digital stimulus and response for both the design and test communities. The VHSIC Hardware Description Language (VHDL) is the Industry standard language for the design, modeling, and simulation of digital electronics. Together VHDL and WAVES provide powerful support for top-down design and test methodologies and concurrent engineering practices. Although the syntax of WAVES is a subset of VHDL, no special support for using WAVES in a VHDL environment is defined within the language. This report will introduce and describe a VHDL package that was developed at Rome Laboratory to provide a software interface to support the use of WAVES in a VHDL environment. This VHDL package is referred to as the WAVES VHDL interface and has been proposed as a standard practice for a top-down design and test methodology using WAVES and VHDL. This report is not intended to provide a tutorial on VHDL or WAVES. It is assumed that the reader has an adequate understanding of the VHDL language and some modeling techniques. Further, it is assumed that the reader has an understanding of the WAVES language and can follow a simple Level 1 dataset description. DTIC

N95-16522# Army Research Lab., Aberdeen Proving Ground, MD.
AN ECONOMICAL SYSTEM FOR MEASURING, MONITORING, AND CONTROLLING THE RATE OF REPETITIVE EVENTS
Thomas Kottke Sep. 1994 49 p
(AD-A285219) Avail: CASI HC A03/MF A01

An integrated hardware/software system that can economically measure, monitor, and control the frequencies of repetitive events is presented. A user-adjustable counting interval allows high-resolution frequency measurements to be obtained for repetitive events with frequencies that range from tens of hertz to several kilohertz. The flexibility of this system is further enhanced by the inclusion of microprocessor control that allows both frequency values and trends to be determined and displayed. An assortment of digital inputs and outputs is available to interface this system with external devices such as alarms and frequency feedback controllers. Schematic diagrams, circuit descriptions, printed circuit board masks, and a parts lists of the hardware are included. Sample software that can be used to drive the microprocessor is also presented and discussed. DTIC

N95-16539# Department of the Navy, Washington, DC.
PROCESS OF MAKING A BISTABLE PHOTOCONDUCTIVE COMPONENT Patent Application
Randy Rousch, inventor (to Navy), Michael S. Mazzola, inventor (to Navy), and David C. Stoudt, inventor (to Navy) 5 Apr. 1994 18 p
(AD-D016449; US-Patent-Appl-SN-223350) Avail: CASI HC A03/MF A01

Semi-insulating gallium arsenide wafers manufactured with varying silicon density shallow donors are copper compensated by heating to temperature of at least 550 deg C to thermally diffuse the copper into the wafers and thereby provide deep copper acceptors in the wafer. Higher annealing temperatures are employed for higher concentrations of silicon in the wafers and the thermal diffusion is accomplished in the presence of copper, and in some instances, in the presence of varying quantities of arsenic. The copper compensated, silicon doped, gallium arsenide wafers obtained have the electrical property characteristic capability of being used as photoconductive switching components. In one aspect of the invention the silicon doped gallium arsenide wafer is sealed in a quartz ampoule in the presence of solid copper and solid arsenic and heated to the annealing temperature. In another aspect of the invention, the copper and arsenic are flowed as vapors over the silicon doped gallium arsenide wafer disposed in a reaction tube within a diffusion furnace, while the wafer is heated to the annealing temperature. DTIC

N95-16561*# National Aeronautics and Space Administration. Lyndon B. Johnson Space Center, Houston, TX.
PRIMARY BATTERY DESIGN AND SAFETY GUIDELINES HANDBOOK
Bobby J. Bragg, John E. Casey (Lockheed Engineering and Sciences Co., Houston, TX.), and J. Barry Trout (Lockheed Engineering and Sciences Co., Houston, TX.) Dec. 1994 81 p
(NASA-RP-1353; S-787; NAS 1.61:1353) Avail: CASI HC A05/MF A01

This handbook provides engineers and safety personnel with guidelines for the safe design or selection and use of primary batteries in spaceflight programs. Types of primary batteries described are silver oxide zinc alkaline, carbon-zinc, zinc-air alkaline, manganese dioxide-zionc alkaline, mercuric oxide-zinc alkaline, and lithium anode cells. Along with typical applications, the discussions of the individual battery types include electrochemistry, construction, capacities and configurations, and appropriate safety measures. A chapter on general battery safety covers hazard sources and controls applicable to all battery types. Guidelines are given for qualification and acceptance testing that should precede space applications. Permissible failure levels for NASA applications are discussed. Author

N95-16814# L and W Research, Inc., Wallington, CT.
HIGH BRIGHTNESS CATHODES FOR MICROFOCUS X-RAY GENERATORS Final Report
S. P. Renwick, H. J. Hansen, C. H. Shaughnessy, and P. H. Leek 27 Jun. 1994 19 p
(Contract F33615-91-C-5658)
(AD-A285256; WL-TR-94-4096) Avail: CASI HC A03/MF A01

Nondestructive inspection techniques such as Computed Tomography (CT) and Backscatter Imaging Tomography (BIT) have advanced to the point where detectors and image processors have reached a plateau in performance. Further improvement in the inspection techniques must come from better X-ray sources. Microfocus X-ray sources offer this improved performance due to their small X-ray spot size, which is generally on the order of tens of microns. The small spot approximates a point source, which reduces geometric distortions of the image. The sources currently available, however, frequently do not meet industrial user maintenance and ease-of-use standards, especially with regard to beam stability and electron emitter lifetime. By using new emitter materials, careful electron gun design, and proper high-vacuum construction techniques, we have developed a high-energy (360 keV), low-maintenance microfocus X-ray source with the improved performance required to meet these demands. DTIC

N95-16832 Sandia National Labs., Albuquerque, NM.
A NEW MANUFACTURING METHOD FOR THE FORMATION OF GATED FIELD EMISSION STRUCTURES

J. G. Fleming, R. Walko, and D. King 1994 4 p Presented at the 7th International Vacuum Microelectronics Conference, Grenoble (France), 7 Jul. 1994 Limited Reproducibility: More than 20% of this document may be affected by microfiche quality
(Contract DE-AC04-94AL-85000)
(DE94-015287; SAND-94-1825C; CONF-9407101-1) Avail: CASI HC A01

Functioning, matrixed, field emission devices have been fabricated using a modification of standard integrated circuit fabrication techniques. The emitter-to-gate spacing is fixed by the thickness of a deposited oxide and not by photolithographic techniques. Modeling of the emitted electron trajectories using a two dimensional, Poisson solver, finite difference code indicates that much of the current runs perpendicular to plane of the part. Functioning triode structures have been fabricated using this approach. Emission current, to a collector electrically and physically separated from the matrixed array follows Fowler-Nordheim behavior. DOE

N95-16834# California Univ., Santa Barbara, CA. Dept. of Electrical and Computer Engineering.
THE IMPACT OF LOW TEMPERATURE MATERIALS ON THE BREAKDOWN AND NOISE PROPERTIES OF GaAs AND InP BASED HEMT'S AND FET'S Final Report, 1 Nov. 1990 - 30 Apr. 1994
Umesh K. Mishra 30 Apr. 1994 50 p
(Grant AF-AFOSR-0111-91)
(AD-A285176; AFOSR-94-0592TR) Avail: CASI HC A03/MF A01

The breakdown voltage in GaAs field effect transistors (FET) has been the fundamental limitation of power performance in these devices. Previous studies have identified the high electric field at the drain edge of the gate metal as the cause of breakdown. At the start of this project, we successfully demonstrated that a low-temperature-grown GaAs (LTG-GaAs) surface 'insulator' dramatically improved the breakdown voltage in a GaAs MISFET. Subsequent device studies have concentrated on the use of LTG-GaAs as a surface passivation layer in GaAs MESFET's due to the potential shortcomings of a MESFET in its RF performance. Despite the early success, very little was known about the relevant electrical properties of LTG-GaAs. To better understand why LTG-GaAs works, what are its device limitations, and how device performance can be further improved, an extensive study of the material properties of LTG-GaAs has been carried out in parallel with device fabrication and testing. In this report, the results from our investigations will be split into two sections. The first section will discuss issues related to the fundamental understanding of LTG-GaAs, the second with device results using LTG-GaAs surface layers. DTIC

N95-16915 Lawrence Livermore National Lab., Livermore, CA.
PERFORMANCE CHARACTERIZATION OF PHOTONIC LINKS IN CRYOGENIC ENVIRONMENTS FOR ADVANCED SIGNAL PROCESSING APPLICATIONS
K. McCammon, J. Morse, D. Masquelier, C. McConaghey, H. Garrett, K. Hugenberg, M. Lowry, E. Track (Hypres, Inc., Elmsford, NY.), and L. Bunz (Hypres, Inc., Elmsford, NY.) Jan. 1994 7 p Presented at the 4th Annual ARPA Symposium on Photonics Systems for Antenna Applications, Monterey, CA, 18-21 Jan. 1994 Limited Reproducibility: More than 20% of this document may be affected by microfiche quality
(Contract W-7405-eng-48)
(DE94-015561; UCRL-JC-115712-Rev-1; CONF-940194-1-Rev-1) Avail: Issuing Activity (Department of Energy (DOE))

Low temperature experiments have been conducted to characterize the performance of high speed photodetectors and LiNbO3 optical modulators in cryogenic environments down to 4.2 K. Metal-semiconductor-metal (MSM) photodiodes fabricated from GaAs and InGaAs have been characterized. Results demonstrate that both the responsivity and bandwidth depend on temperature. Specific modulator parameters quantified at cryogenic temperatures include bandwidth, V(pi) (half wave voltage), optical loss and package stability. The successful operation of MSM photodiodes and LiNbO3 modulators at cryogenic temperatures enables a high sensitivity fiber optic approach to superconducting circuit interfaces. DOE

N95-16920 Los Alamos National Lab., NM.
PERFORMANCE EVALUATION OF POLYANILINE AS AN ACTIVE MATERIAL FOR ELECTROCHEMICAL CAPACITORS
A. Rudge, J. Davey, F. Uribe, J. Landeros, Jr., and S. Gottesfeld 1994 17 p Presented at the 185th Electrochemical Society Meeting, San Francisco, CA, 22-27 May 1994 Limited Reproducibility: More than 20% of this document may be affected by microfiche quality
(Contract W-7405-eng-36)
(DE94-016283; LA-UR-94-2385; CONF-940529-19) Avail: Issuing Activity (Department of Energy (DOE))

This paper describes experiments which evaluate the performance of polyaniline (PAni) as an active material in electrochemical capacitors. We have performed constant current multicycle tests on prototype symmetric devices where the same conducting polymer serves as the active material on both electrodes. When electropolymerized at high current density in aqueous acid solution, PAni exhibits a micro-morphology consisting of a network of interwoven fibrils with high porosity. Thick PAni layers (less than 250 micrometers) of the material can thus be electropolymerized onto a planar metal substrate without affecting the fast dynamics of the charge-discharge process. The aqueous PAni electrochemical capacitors exhibit rather low energy content because of limitations on the maximum applied voltage. However, due to their optimized morphology and the high conductivity of the aqueous acid solution, they exhibit relatively high power density. The PAni capacitor exhibits excellent cycle life (more than 25,000 cycles), provided the requirements on restricted cell voltage are met. This is a key result in the evaluation of conducting polymers as active materials in electrochemical capacitors. Scanning electron microscopy and impedance spectroscopy are used to provide information on this system. DOE

N95-16925 Lawrence Livermore National Lab., Livermore, CA.
A HIGH AVERAGE POWER ELECTRO-OPTIC SWITCH USING KTP
C. A. Ebbers, W. M. Cook, and S. P. Velsko Apr. 1994 22 p Limited Reproducibility: More than 20% of this document may be affected by microfiche quality
(Contract W-7405-eng-48)
(DE94-016416; UCRL-ID-117079) Avail: CASI HC A03

High damage threshold, high thermal conductivity, and small thermo-optic coefficients make KTiOPO4 (KTP) an attractive material for use in a high average power Q-switch. However, electro-chromic damage and refractive index homogeneity have prevented the utilization of KTP in such a device in the past. This work shows that electro-chromic damage is effectively suppressed using capacitive coupling, and a KTP crystal can be Q-switched for 1.5 x 10(exp 9) shots without any detectable electro-chromic damage. In addition, KTP with the high uniformity and large aperture size needed for a KTP electro-optic Q-switch can be obtained from flux crystals grown at constant temperature. A thermally compensated, dual crystal KTP Q-switch, which successfully produced 50 mJ pulses with a pulse width of 8 ns (FWHM), has been constructed. In addition, in off-line testing the Q-switch showed less than 7 percent depolarization at an average power loading of 3.2 kW/sq cm. DOE

N95-16932 Los Alamos National Lab., NM.
CHARACTERIZATION OF MULTIPORT SOLID STATE IMAGERS AT MEGAHERTZ DATA RATES
G. J. Yates, C. R. Pena, and B. T. Turko 1994 10 p Presented at the Annual Meeting of the Society of Photo-Optical Instrumentation Engineers, San Diego, CA, 24-29 Jul. 1994 Limited Reproducibility: More than 20% of this document may be affected by microfiche quality
(Contract W-7405-eng-36)
(DE94-016095; LA-UR-94-2562; CONF-940723-8) Avail: CASI HC A02

Test results obtained from two recently developed multiport Charge-Coupled Devices (CCD's) operated at pixel rates in the 10-100 MHz range will be presented. The CCD's were evaluated in Los Alamos National Laboratory's High Speed Solid State Imager Test Station (HSTS) which features PC-based programmable clock waveform generation (Tektronix DAS 9200) and synchronously clocked Digital Sampling Oscilloscopes (DSO's) (LeCroy 9424/9314 series) for CCD pixel data acquisition, analysis and storage. The HSTS also provided special designed optical pinhole array test patterns in the 5-50 micron diameter range for use with Xenon Strobe and pulsed laser light sources to simultaneously provide multiple single-pixel illumination patterns to study CCD point-spread-function (PSF) and pixel smear characteristics. The two CCD's tested, EEV model CCD-13 and EG&G Reticon model HSO512J, are both 512 x 512 pixel arrays with eight (8) and sixteen (16) video output ports respectively. Both devices are generically Frame Transfer CCD's (FT CCD's) designed for parallel bi-directional vertical readout to augment their multiport design for increased pixel rates over common single port serial readout

architecture. Although both CCD' were tested similarly, differences in their designs precluded normalization or any direct comparisons of test results. Rate dependent parameters investigated include S/N, PSF, and MTF. The performance observed for the two imagers at various pixel rates from selected typical output ports is discussed. DOE

N95-16945# Argonne National Lab., IL.
GIANT FLUX CREEP THROUGH THE SURFACE BARRIERS AND THE IRREVERSIBILITY LINE IN HIGH T(SUB c) SUPERCONDUCTORS
L. Burlachkov (Bar-Ilan Univ., Ramat-Gan, Israel.), V. B. Geshkenbein (Academy of Sciences, USSR, Moscow, USSR.), and A. E. Koshelev (Academy of Sciences of the Ukraine, Kharkov.) May 1994 3 p Presented at the Meeting on Materials and Mechanisms of Superconductivity: High Temperature Superconductors, Grenoble, France, 4-9 Jul. 1994
(Contract W-31-109-eng-38)
(DE94-013991; ANL/MSD/CP-82480; CONF-940701-8) Avail: CASI HC A01/MF A01

Magnetic flux relaxation over the surface barrier in high temperature superconductors are investigated. Vortex dynamics controlled by the penetration both of pancake vortices and vortex lines are discussed. The penetration field H(sub p) for pancakes decay is exponentially with temperature. The size of the magnetization loop is determined by the decay of H(sub p) during the process of relaxation, but its shape remains unchanged. The irreversibility line associated with the pancake penetration is given by H(sub irr) (proportional to) exp(- 2T/T(sub o)), and may lie both above and below the melting line. DOE

N95-16947# Department of the Navy, Washington, DC.
ALUMINUM PERMANGANATE BATTERY Patent Application
Catherine Marsh, inventor (to Navy) and Stuart L. Licht, inventor (to Navy) 30 Nov. 1993 21 p
(AD-D016337; US-Patent-Appl-SN-168788; Navy-Case-73986) Avail: CASI HC A03/MF A01

A battery is provided comprising an aluminum anode, an aqueous solution of permanganate as the cathodic species and a second electrode capable of reducing permanganate. Such a battery system is characterized by its high energy density and low polarization losses when operating at high temperatures in a strong caustic electrolyte, i.e., high concentration of hydroxyl ions. A variety of anode and electrocatalyst materials are suitable for the efficient oxidation-reduction process and are elucidated. DTIC

N95-16948# Department of the Navy, Washington, DC.
ALUMINUM-FERRICYANIDE BATTERY Patent Application
Catherine Marsh, inventor (to Navy) and Stuart L. Licht, inventor (to Navy) 29 Nov. 1993 20 p
(AD-D016338; US-Patent-Appl-SN-168787; Navy-Case-74011) Avail: CASI HC A03/MF A01

A battery capable of producing high current densities with high charge capacity is described which includes an aluminum anode, a ferricyanide electrolyte and a second electrode capable of reducing ferricyanide electrolyte which is either dissolved in an alkaline solution or alkaline seawater solution. The performance of the battery is enhanced by high temperature and high electrolyte flow rates. DTIC

N95-16949# Department of the Navy, Washington, DC.
IMPROVED DUAL FLOW ALUMINUM HYDROGEN PEROXIDE BATTERY Patent Application
Catherine Marsh, inventor (to Navy), Stuart L. Licht, inventor (to Navy), and Donna Matthews, inventor (to Navy) 30 Nov. 1993 19 p
(AD-D016339; US-Patent-Appl-SN-168789; Navy-Case-74990) Avail: CASI HC A03/MF A01

A novel dual flow battery configuration is provided comprising an aqueous hydrogen peroxide catholyte, an aqueous anolyte, a porous solid electrocatalyst capable of reducing said hydrogen peroxide and separating said anolyte, and an aluminum anode positioned within said anolyte. Separation of catholyte and anolyte chambers prevents hydrogen peroxide poisoning of the aluminum anode. DTIC

N95-16950 Department of the Navy, Washington, DC.
AN ELASTOMERIC ELECTRICAL CONNECTOR Patent Application
Joseph E. Laska, inventor (to Navy), John Y. Oakley, inventor (to Navy), and Francis R. Reinert, inventor (to Navy) 16 Aug. 1993 20 p Limited Reproducibility: More than 20% of this document may be affected by microfiche quality
(AD-D016340; US-Patent-Appl-SN-107431; Navy-Case-73688) Avail: CASI HC A03

An elastic device that provides solderless, pressure contact, electrical connections between leads or leads and terminals at an interface. The elastic device comprises elastomeric material, such as monel, embedded in the silicone. The elastic device is particularly suited to provide electrical connections between an interface that is brought together by a connector and which is separable in response to an impulse that may be created by an explosion produced by a pyrotechnic device. DTIC

N95-16951# Helsinki Univ. of Technology, Espoo (Finland). Lab. of Electromechanics.
COMBINATION OF POWER ELECTRONIC MODELS WITH THE TWO-DIMENSIONAL FINITE ELEMENT ANALYSIS OF ELECTRICAL MACHINES Thesis
J. Vaeaenaenen Apr. 1994 91 p
(PB94-197720; ISBN-951-22-2050-4) Avail: CASI HC A05/MF A01

An analysis method for power electronic drives of electrical machines is presented. The machine is modeled by a two dimensional finite element method which allows the presence of magnetically nonlinear materials and the motion of the rotor. The power electronic device connected to the machine is modeled by a nonlinear circuit model. The field and the circuit equations are coupled together as a system of equations. The power electronic circuit can have a general topology given by a net-list type input file. Specific attention is paid to the numerical stability and efficiency of the combined field-circuit formulation. The computational efficiency and the numerical reliability of the method is investigated with the aid of theoretical cases. According to results, the inclusion of the nonlinear circuit model does not increase the computational costs significantly, provided that the sparsity of the system equations is preserved. The method is tested with three practical examples. The results obtained by the method are compared with the measured ones. The first example is a permanent magnet generator feeding a diode-rectifier. In the second example, a filter circuit is added in parallel with the rectifier. The third example is a cage-induction motor fed by a static frequency converter. The computed results agree well with the measured ones. NTIS

N95-16963# Argonne National Lab., IL.
SAFETY CHARACTERISTICS OF LITHIUM-ALLOY/METAL SULFIDE BATTERIES
G. L. Henriksen, D. R. Vissers, and A. A. Chilenskas 1994 6 p Presented at the 7th International Meeting on Lithium Batteries, Cambridge, MA, 15-20 May 1994
(Contract W-31-109-eng-38)
(DE94-013867; ANL/CMT/CP-82291; CONF-940568-4) Avail: CASI HC A02/MF A01

A battery using a Li-Al negative electrode, a molten LiCl-LiBr-KBr electrolyte, a FeS2 or a FeS positive electrode, and a stable chalcogenide-based ceramic sealant is under development. Full-size bipolar Li-Al/FeS and Li-Al/FeS2 cells (13 cm dia) and four cell stacks are being built and tested for electric-vehicle use. Chemical hazards, toxicity, thermal hazards, and hazards from electrical abuse are analyzed. The safety tests that have been conducted to date, including crash tests, are discussed; although they have not been extensive, they indicate that these batteries are inherently safe. A table of the preliminary hazard assessment is included. DOE

N95-17139 Georgia Inst. of Tech., Atlanta, GA. Computer Engineering Research Lab.
GUIDANCE, NAVIGATION, AND CONTROL DIGITAL EMULATION TECHNOLOGY LABORATORY Final Report
12 Jul. 1994 17 p Limited Reproducibility: More than 20% of this document may be affected by microfiche quality
(Contract DASG60-89-C-0142)
(AD-A282722; FR-0142-94-001) Avail: Issuing Activity (Defense Technical Information Center (DTIC))

The tasks of a speed test on the rad-hard FPU chip developed by Harris and the development of an FPA Test System are reviewed. Georgia Tech got three hardened chips from Harris: FPU 1, FPU 2, and FPU 3. The third chip (FPU 3) gave erroneous results at any frequency. This may

have been caused by inserting the chip into the socket incorrectly due to an incorrect pin diagram. FPU 2 was also inserted into the socket incorrectly; however, it did not stay in that configuration for very long and the only damage was a disabling of the fourth bit on the chip output. This was remedied by modifying the test software to mask out that bit. A commercial chip was designed on the Genesil silicon Compiler and fabricated by NCR using their 1.25 micron CMOS process. The rad-hard FPU chips were designed using a new version of the Genesil silicon compiler. The hardened chips, in a non-active mode, use about half the power of the commercial FPU chip. Tests were separated into 10 categories: logical, shift, integer addition, integer multiplication, floating point addition, floating point multiplication, pack exponent and float, generate speed, round or truncate a result, and sign manipulation. The FPA test system is being developed to analyze the characteristics and quality of an FPA sensor. It allows a user to study the effectiveness of the FPA sensor when using various signal and image processing functions. The primary features supported by the Georgia Tech system are the ability to: (1) interface a wide range of FPA's using a specification defined by USASSDC; (2) display the raw FPA image live on a color monitor to enable a user to visually locate bad detectors, and to compare and characterize the quality of an FPA sensor; (3) select or program any of the four signal/image filters provided (non-uniformity compensation, temporal filtering, spatial filtering, and thresholding); and (4) display the intermediate filtered frame outputs in real time, at a refresh rate that does not strain the eyes. Derived from text

N95-17433 Massachusetts Inst. of Tech., Cambridge. Research Lab. of Electronics.

FEMTOSECOND STUDIES OF CARRIER DYNAMICS IN COMPOUND SEMICONDUCTORS Annual Report, 1 Jan. 1993 - 31 May 1994

James G. Fujimoto 28 Jul. 1994 8 p Limited Reproducibility: More than 20% of this document may be affected by microfiche quality

(Contract N00014-91-J-1956)

(AD-A282871) Avail: CASI HC A02

The objective is to develop and combine state of the art femtosecond measurement techniques with advanced solid state theoretical techniques to study carrier dynamics in semiconductors. This program is a collaborative effort between investigators at the Massachusetts Institute of Technology and the University of Florida. Experimental efforts at MIT focus on the development and application of new femtosecond techniques for measuring ultrafast processes in compound semiconductors and devices. Studies include investigation of both nonlinear index and absorption and gain dynamics in bulk semiconductors and devices. The work at the University of Florida focuses on developing new approaches for studying ultrafast carrier dynamics of carriers in semiconductors and predicting transient behavior as it impacts on device performance. Investigations use full band structure calculation combined with techniques for numerically solving the Boltzmann and quantum transport equations for both electron and hole distributions. DTIC

N95-17463 Department of the Navy, Washington, DC.

TRENCHED BIPOLAR TRANSISTOR STRUCTURES Patent

Alvin M. Goodman, inventor (to Navy) and Max N. Yoder, inventor (to Navy) 10 May 1994 10 p Filed 22 Nov. 1991

(AD-D016406; US-Patent-5,311,055; US-Patent-Appl-SN-796553; US-Patent-Class-257-593) Avail: US Patent and Trademark Office

Both homojunction and heterojunction bipolar transistor structures are fabricated in unique trenched configurations so as to better utilize their surface areas by employing both the vertical and horizontal portions of their base regions with equal effectiveness. An important advantage of the unique trenched configurations is that the base region of each trenched structure is of precisely the same thickness throughout-both vertical and horizontal portions. Consequently, the transit time for charge carriers to diffuse across the base region and the base transport factor are uniform because of the uniform base thickness. Moreover, the parasitic capacitance region of each trenched structure beneath base metallization contacts is only a small portion of the entire base-collector junction region. Accordingly, the RC time constant of each trenched structure is very low and the high frequency response gain of the heterojunction trenched bipolar transistor structure is an order of magnitude higher than its conventional heterojunction bipolar transistor counterpart. DTIC

N95-17469 Technische Univ., Delft (Netherlands). Faculteit der Elektrotechniek

FREQUENCY DOMAIN ANALYSIS FOR NONLINEAR ELECTRONIC CIRCUITS Ph.D. Thesis

E. Kleihorst 14 Mar. 1994 238 p Prepared in cooperation with Philips Gloeilampenfabrieken N.V., Eindhoven, Netherlands

(PB94-201365; ISBN-90-74445-09-8) Copyright Avail: Issuing Activity

The thesis deals with an extension of the harmonic balance method. It is done as one would build a circuit analysis program. First, a general overview of network topology is given which can be used to set up the linearized network equations. A view on the solution methods for linearized electrical networks is given. Nonlinear elements and the devices which are implemented in the program are discussed. A brief overview is given of solution methods of the nonlinear algebraic equations used in the direct current (DC) algorithm and in the frequency and time domain analysis. The integration procedure to be used for the solution of on the subject of nonlinear alternating current (AC) analysis. The usefulness of the described method is shown on the basis of come circuit examples. Finally, a special numerical integration method is developed and a method based on harmonic balance is described which is able to calculate the harmonic distortion in case of small signal analysis. NTIS

N95-17478 Department of the Navy, Washington, DC.

MULTILAYER MICROELECTRONIC PHOTOMULTIPLIER DEVICE WITH A STACKED SERIES OF DYNODE AND INSULATING LAYERS Patent

Randy L. Shimabukuro, inventor (to Navy) and Stephen D. Russell, inventor (to Navy) 26 Apr. 1994 15 p Filed 16 Feb. 1993

(AD-D016377; US-Patent-5,306,904; US-Patent-Appl-SN-019414; US-Patent-Class-250-207) Avail: US Patent and Trademark Office

A multilayer microelectronic photomultiplier device is fabricated by discrete procedures to provide a photo-cathodeanode and dynode chain arrangement which is analogous in operation to conventional photomultiplier tubes. This multilayer microelectronic photomultiplier device provides for low level photon detection and realizes the advantages of high reliability, small size and fast response, plus lower cost, weight and power consumption compared to conventional photomultiplier tubes. In addition, the fabrication on an SOI substrate permits integration of logic and control circuitry with detectors. The insulating substrate also permits the integration of an on-chip high voltage supply and may easily be extended to a plurality of detectors with high packing densities due to the inherently stacked geometry offering improved performance and design flexibility. DTIC

N95-17481 Department of the Navy, Washington, DC.

BaF2/GaAs ELECTRONIC COMPONENTS Patent Application

Francisco Santiago, inventor (to Navy) and Tak-Kin Chu, inventor (to Navy) 19 May 1994 23 p Limited Reproducibility: More than 20% of this document may be affected by microfiche quality

(AD-D016391; US-Patent-Appl-SN-246206; Navy-Case-75860) Avail: CASI HC A03

Metal insulator semiconductor field effect transistors (MISFET's), charge coupled devices (CCD's), and capacitors based on an epitaxial barium fluoride (BF2) insulator layer deposited directly onto a single crystal gallium arsenide (GaAs) substrate is discussed in this report. DTIC

N95-17487# Greenwich Univ., London (England). School of Biological and Chemical Sciences.

PREPARATION AND INVESTIGATION OF IMPROVED LOW VOLTAGE ELECTRON EXCITABLE PHOSPHORS Final Report

A. Vecht, D. W. Smith, and S. S. Chadha Jul. 1994 64 p

(Contract DAJA45-92-C-0007)

(AD-A284265; R/D-6812-EE-0) Avail: CASI HC A04/MF A01

In the final report, we describe the work carried out on the investigation and development of low voltage phosphors for field emission displays. The standard blue-green ZnO:Zn was improved considerably and now yields very high luminance. New methods were developed which produced good, saturated green zinc gallate phosphor. A novel, narrow band calcium titanate red phosphor has been synthesized, as well as a broader band zinc magnesium oxide blue emitter. The synthesis and characteristics of these materials are described and analysed. Future work is suggested. Samples of all good phosphors were supplied to Fort Monmouth, as well as seven US firms. DTIC

N95-17691 Helsinki Univ. of Technology, Espoo (Finland). Lab. of Electromechanics.
CALORIMETRIC METHODS FOR LOSS MEASUREMENTS OF SMALL CAGE INDUCTION MOTORS M.S. Thesis - Chalmers Univ. of Technology
J. Lindstroem 1994 78 p Limited Reproducibility: More than 20% of this document may be affected by microfiche quality
(PB94-184439; ISBN-951-22-1998-0) Avail: Issuing Activity (National Technical Information Service (NTIS))

The report deals with the possibility of making more accurate power loss measurements of induction machines by the use of calorimetric methods. A brief summary of the losses in cage induction machines points out the complexity of the loss composition. The input-output method and the differential method are described in detail. The basic idea of calorimetric measurements of an electrical machine is presented and different methods, measuring equipment and measuring problematics are described. A detailed description of the balance method shows that it is the most convenient way of handling the problem, and a construction of a balance calorimeter for the 37 kW motor is made. NTIS

N95-16045*# National Aeronautics and Space Administration. Lyndon B. Johnson Space Center, Houston, TX.
KAPTON WIRE CONCERNS FOR AEROSPACE VEHICLES
J. VanLaak *In* NASA. Lewis Research Center, First NASA Workshop on Wiring for Space Applications Sep. 1994 p 11-17 (For primary document see N95-16044 04-20)
Avail: CASI HC A02/MF A02

N95-16046*# Rockwell International Corp., Downey, CA.
ORBITER KAPTON WIRE OPERATIONAL REQUIREMENTS AND EXPERIENCE
R. V. Peterson *In* NASA. Lewis Research Center, First NASA Workshop on Wiring for Space Applications Sep. 1994 p 19-41 (For primary document see N95-16044 04-20)
Avail: CASI HC A03/MF A02

N95-16047*# National Aeronautics and Space Administration. White Sands Test Facility, NM.
WSTF ELECTRICAL ARC PROJECTS
Larry Linley *In* NASA. Lewis Research Center, First NASA Workshop on Wiring for Space Applications Sep. 1994 p 43-60 (For primary document see N95-16044 04-20)
Avail: CASI HC A03/MF A02

N95-16048*# Naval Research Lab., Washington, DC.
PROBLEMS WITH AGING WIRING IN NAVAL AIRCRAFT
Frank J. Campbell *In* NASA. Lewis Research Center, First NASA Workshop on Wiring for Space Applications Sep. 1994 p 61-71 (For primary document see N95-16044 04-20)
Avail: CASI HC A03/MF A02

N95-16049*# Sverdrup Technology, Inc., Cleveland, OH.
KAPTON PYROLYSIS ON SPACE STATION FREEDOM'S SOLAR ARRAY FLEXIBLE CURRENT CARRIER
Thomas J. Stueber *In* NASA. Lewis Research Center, First NASA Workshop on Wiring for Space Applications Sep. 1994 p 73-80 (For primary document see N95-16044 04-20)
Avail: CASI HC A02/MF A02

N95-16053*# Auburn Univ., AL. Space Power Inst.
A STUDY OF ELECTRIC TRANSMISSION LINES FOR USE ON THE LUNAR SURFACE
Krista L. Gaustad, Lloyd B. Gordon, and Jennifer R. Weber *In* NASA. Lewis Research Center, First NASA Workshop on Wiring for Space Applications Sep. 1994 p 115-124 (For primary document see N95-16044 04-20)
Avail: CASI HC A02/MF A02

N95-16054*# National Aeronautics and Space Administration. Lewis Research Center, Cleveland, OH.
KAPTON PYROLYSIS, THE SPACE ENVIRONMENT AND WIRING REQUIREMENTS
Dale C. Ferguson *In its* First NASA Workshop on Wiring for Space Applications Sep. 1994 p 125-131 (For primary document see N95-16044 04-20)
Avail: CASI HC A02/MF A02

N95-16056*# Wright Lab., Wright-Patterson AFB, OH.
NEW INSULATION CONSTRUCTIONS FOR AEROSPACE WIRING APPLICATIONS
George Slenski *In* NASA. Lewis Research Center, First NASA Workshop on Wiring for Space Applications Sep. 1994 p 143-162 (For primary document see N95-16044 04-20)
Avail: CASI HC A03/MF A02

N95-16057*# Foster-Miller Associates, Inc., Waltham, MA.
HIGH PERFORMANCE DIELECTRIC MATERIALS DEVELOPMENT
Joe Piche, Ted Kirchner, and K. Jayaraj *In* NASA. Lewis Research Center, First NASA Workshop on Wiring for Space Applications Sep. 1994 p 173-180 (For primary document see N95-16044 04-20)
Avail: CASI HC A02/MF A02

N95-16271# Kazan Aviation Inst. (USSR).
METHOD OF CALCULATING THE OPTIMAL RADIOELECTRONIC EQUIPMENT DESIGN
Yu. P. Ermolaev *In* Nanjing Univ. of Aeronautics and Astronautics, Joint Proceedings on Aeronautics and Astronautics (JPAA) May 1993 p 147-151 (For primary document see N95-16249 04-01)
Avail: CASI HC A01/MF A03

N95-16278# Nanjing Univ. of Aeronautics and Astronautics, Nanjing, Jiangsu (China). Dept. of Automatic Control.
THE COMPUTER ANALYSIS OF THE PREDICTION OF AIRCRAFT ELECTRICAL POWER SUPPLY SYSTEM RELIABILITY
Xinhua Mu, Yangguang Yan, and Jibing Pen *In its* Joint Proceedings on Aeronautics and Astronautics (JPAA) May 1993 p 191-197 See also A92-37958 (For primary document see N95-16249 04-01)
Avail: CASI HC A02/MF A03

N95-17224*# National Aeronautics and Space Administration. Goddard Space Flight Center, Greenbelt, MD.
NICKEL CADMIUM BATTERY OPERATIONS AND PERFORMANCE
Gopalakrishna Rao, Jill Prettyman-Lukoschek (Loral AeroSys, Seabrook, MD.), Richard Calvin (Martin Marietta Services, Inc., Greenbelt, MD.), Thomas Berry (Allied-Signal Technical Services Corp., Columbia, MD.), Robert Bote (Allied-Signal Technical Services Corp., Columbia, MD.), and Mark Toft (Jackson and Tull, Inc., Seabrook, MD.) *In its* Third International Symposium on Space Mission Operations and Ground Data Systems, Part 1 Nov. 1994 p 399-408 (For primary document see N95-17179 04-17)
Avail: CASI HC A02/MF A06

N95-17285*# California Inst. of Tech., Pasadena, CA.
ON THE APPLICATION OF UNDER-DECIMATED FILTER BANKS
Y.-P. Lin and P. P. Vaidyanathan *In* JPL, The Telecommunications and Data Acquisition Report 15 Nov. 1994 p 105-128 (For primary document see N95-17279 04-32)
(RTOP 315-91-40-20-35)
Avail: CASI HC A03/MF A03

N95-17289*# Jet Propulsion Lab., California Inst. of Tech., Pasadena, CA.
LOW-COMPLEXITY WAVELET FILTER DESIGN FOR IMAGE COMPRESSION
E. Majani *In its* The Telecommunications and Data Acquisition Report 15 Nov. 1994 p 181-200 (For primary document see N95-17279 04-32)
(RTOP 315-91-40-20-36)
Avail: CASI HC A03/MF A03

34 FLUID MECHANICS AND HEAT TRANSFER

Includes boundary layers; hydrodynamics; fluidics; mass transfer; and ablation cooling.

For related information see also *02 Aerodynamics* and *77 Thermodynamics and Statistical Physics.*

N95-15966*# Old Dominion Univ., Norfolk, VA. Inst. for Computational and Applied Mechanics.

RADIATIVE INTERACTIONS IN CHEMICALLY REACTING COMPRESSIBLE NOZZLE FLOWS USING MONTE CARLO SIMULATIONS Progress Report, Jan. - Jun. 1994

J. Liu and Surendra N. Tiwari Sep. 1994 54 p Presented at the 6th AIAA/ASME Joint Thermophysics and Heat Transfer Conference, Colorado Springs, CO, 20-23 Jun. 1994

(Grant NAG1-363)

(NASA-CR-197133; NAS 1.26:197133; ODU/ICAM-94-102; AIAA Paper 94-2092) Avail: CASI HC A04/MF A01

The two-dimensional spatially elliptic Navier-Stokes equations have been used to investigate the radiative interactions in chemically reacting compressible flows of premixed hydrogen and air in an expanding nozzle. The radiative heat transfer term in the energy equation is simulated using the Monte Carlo method (MCM). The nongray model employed is based on the statistical narrow band model with an exponential-tailed inverse intensity distribution. The spectral correlation has been considered in the Monte Carlo formulations. Results obtained demonstrate that the effect of radiation on the flow field is minimal but its effect on the wall heat transfer is significant. Extensive parametric studies are conducted to investigate the effects of equivalence ratio, wall temperature, inlet flow temperature, and the nozzle size on the radiative and conductive wall fluxes. Author

N95-15969*# National Aeronautics and Space Administration. Lewis Research Center, Cleveland, OH.

NONLINEAR INSTABILITY OF A UNI-DIRECTIONAL TRANSVERSELY SHEARED MEAN FLOW

David W. Wundrow (NYMA, Inc., Brook Park, OH.) and Marvin E. Goldstein Nov. 1994 35 p

(Contract NAS3-25266; RTOP 505-90-51)

(NASA-TM-106779; E-9232; NAS 1.15:106779) Avail: CASI HC A03/MF A01

It is well known that the presence of a weak cross flow in an otherwise two-dimensional shear flow results in a spanwise variation in the mean streamwise velocity profile that can lead to an amplification of certain three-dimensional disturbances through a kind of resonant-interaction mechanism (Goldstein and Wundrow 1994). The spatial evolution of an initially linear, finite-growth-rate, instability wave in such a spanwise-varying shear flow is considered, The base flow, which is governed by the three-dimensional parabolized Navier-Stokes equations, is initiated by imposing a spanwise- periodic cross-flow velocity on an otherwise two-dimensional shear flow at some fixed streamwise location. The resulting mean-flow distortion initially grows with increasing streamwise distance, reaches a maximum and eventually decays through the action of viscosity. This decay, which coincides with the viscous spread of of the shear layer, means that the local growth rate of the instability wave will eventually decrease as the wave propagates downstream. Nonlinear effects can then become important within a thin spanwise-modulated critical layer once the local instability-wave amplitude and growth rate become sufficiently large and small, respectively. The amplitude equation that describes this stage of evolution is shown to be a generalization of the one obtained by Goldstein and Choi (1989) who considered the related problem of the interaction of two oblique modes in a two-dimensional shear layer. Author

N95-16064 Institute of Sound and Vibration Research, Southampton (England). Fluid Dynamics and Acoustics Group.

ACTIVE AND PASSIVE ACOUSTIC BUBBLE SIZING

A. D. Phelps, T. G. Leighton, M. F. Schneider, and P. R. White Oct. 1994 17 p Sponsored by Natural Environment Research Council

(ISVR-TR-237) Copyright Avail: Issuing Activity (Inst. of Sound and Vibration Research, Univ. of Southampton, Southampton SO9 5NH, England)

This report presents the results from the research associated with a two year NERC (Natural Environment Research Council) contract funded under the SIDAL scheme. The aim of the project was to investigate methods of sizing bubbles at the moment of entrainment by passive detection of the corresponding acoustic emission, and again to actively size the existing population at a later time. The technique for measuring this so-called 'old-age' population involves sizing bubbles by means of the two frequency insonation method, and the success of examining the subharmonic sum-and-difference coupling is reported. In addition, results are presented from investigations into the variation of the subharmonic response with differing excitation amplitude and step size between successive interrogating signals, and examinations into the reproducibility of the response. Work has also been done on the passive sizing of bubbles upon entrainment with the Gabor transform technique, which gives a fast and accurate representation of the bubble's resonant frequency, of the time at which entrainment occurs, and of the amplitude of the signal. Author

N95-16070*# Institute for Computer Applications in Science and Engineering, Hampton, VA.

A MODIFIED RESTRICTED EULER EQUATION FOR TURBULENT FLOWS WITH MEAN VELOCITY GRADIENTS Final Report

Sharath S. Girimaji and Charles G. Speziale (Boston Univ., MA.) Hampton, VA NASA Sep. 1994 19 p Submitted for publication

(Contract NAS1-19480; RTOP 505-90-52-01)

(NASA-CR-194979; NAS 1.26:194979; ICASE-94-76) Avail: CASI HC A03/MF A01

The restricted Euler equation captures many important features of the behavior of the velocity gradient tensor observed in direct numerical simulations (DNS) of isotropic turbulence. However, in slightly more complex flows the agreement is not good, especially in regions of low dissipation. In this paper, it is demonstrated that the Reynolds-averaged restricted Euler equation violates the balance of mean momentum for virtually all homogeneous turbulent flows with only two major exceptions: isotropic and homogeneously-sheared turbulence. A new model equation which overcomes this shortcoming and is more widely applicable is suggested. This modele is derived from the Navier-Stokes equation with a restricted Euler type approximation made on the fluctuating velocity gradient field. Analytical solutions of the proposed modified restricted Euler equation appear to be difficult to obtain. Hence, a strategy for numerically calculating the velocity gradient tensor is developed. Preliminary calculations tend to indicate that the modified restricted Euler equation captures many important aspects of the behavior of the fluctuating velocity gradients in anisotropic homogeneous turbulence. Author

N95-16071*# Institute for Computer Applications in Science and Engineering, Hampton, VA.

ON THE PREDICTION OF FREE TURBULENT JETS WITH SWIRL USING A QUADRATIC PRESSURE-STRAIN MODEL Final Report

Bassam A. Younis (City Univ., London, England.), Thomas B. Gatski (National Aeronautics and Space Administration. Langley Research Center, Hampton, VA.), and Charles G. Speziale (Boston Univ., MA.) Hampton, VA NASA Aug. 1994 27 p Submitted for publication

(Contract NAS1-19480; RTOP 505-90-52-01)

(NASA-CR-194964; NAS 1.26:194964; ICASE-94-70) Avail: CASI HC A03/MF A01

Data from free turbulent jets both with and without swirl are used to assess the performance of the pressure-strain model of Speziale, Sarkar and Gatski which is quadratic in the Reynolds stresses. Comparative predictions are also obtained with the two versions of the Launder, Reece and Rodi model which are linear in the same terms. All models are used as part of a complete second-order closure based on the solution of differential transport equations for each non-zero component of the Reynolds stress tensor together with an equation for the scalar energy dissipation rate. For non-swirling jets, the quadratic model underestimates the measured spreading rate of the plane jet but yields a better prediction for the axisymmetric case without resolving the plane jet/round jet anomaly. For the swirling axisymmetric jet, the same model accurately reproduces the effects of swirl on both the mean flow and the turbulence structure in sharp contrast with the linear models which yield results that are in serious error. The reasons for these differences are discussed. Author

N95-16156 Stanford Univ., CA. Dept. of Mathematics.
NON-LINEAR WAVES IN GAS DYNAMICS AND MECHANICS Final Report
Tai-Ping Liu 29 Apr. 1994 5 p Limited Reproducibility: More than 20% of this document may be affected by microfiche quality
(Contract DAAL03-91-G-0017)
(AD-A281376; ARO-28548.10-MA) Avail: Issuing Activity (Defense Technical Information Center (DTIC))

Nonlinear wave propagation in gas flows, MHD, combustions, elasticity, multiphase flows, etc. is studied. Shock waves which are either more or less compressive than the classical gas shocks are shown to be nonlinearly stable, but in the sense distinct from each other. This resolves the longstanding paradox on their physical admissibility by pointing out the sensitive role of dissipations. The phenomenon of nonequilibrium is systematically studied. The problem of zero relaxation limit is resolved for models in mechanics and phase transition. DTIC

N95-16163# Massachusetts Inst. of Tech., Cambridge. Turbine Lab.
UNSTEADY FLOW PHENOMENA IN DISCRETE PASSAGE DIFFUSERS FOR CENTRIFUGAL COMPRESSORS Final Report, 8 Jul. 1990 - 8 Jan. 1994
V. Filipenco, J. M. Johnston, and E. M. Greitzer 6 May 1994 39 p
(Contract DAAL03-90-G-0138)
(AD-A281412; ARO-27627.3-EG) Avail: CASI HC A03/MF A01

Research is described on the fluid dynamic behavior of high performance diffusers for centrifugal compressors, with particular application to small gas turbine engine applications. Using a unique swirl generator, experiments have been carried out to define the performance and stall onset behavior of a modern discrete passage diffuser as a function of inlet conditions. Two diffusers were examined, one with 30 passages and one with 38 passages. Inlet blockage and axial asymmetry were varied over Mach numbers up to unity and over a range of inlet swirl angles. Diffuser pressure recovery and operating range were calculated using traverse measurements made upstream of the diffuser. It was found that the performance of the diffuser under different inlet conditions could be expressed to a high degree of accuracy as a single curve of nondimensional static pressure recovery coefficient, based on availability averaged inlet stagnation pressure, and momentum-averaged inlet flow angle. Unsteady pressure measurements showed that the diffuser entered rotating stall at reduced flow rates. No long wavelength stall precursor was determined from the measurements. DTIC

N95-16211# Lawrence Livermore National Lab., Livermore, CA.
FILTER EFFICIENCY AND PRESSURE DROP CALCULATIONS THROUGH TWO AND THREE DIMENSIONAL FIBER ARRAYS
W. Bergman, I. Corey, and D. Speck Apr. 1994 9 p Presented at the 1994 American Filtration and Separation Society National Meeting, Chicago, IL, 9-11 May 1994
(Contract W-7405-eng-48)
(DE94-014111; UCRL-JC-116246; CONF-9405145-3) Avail: CASI HC A02/MF A01

We have used a commercially available fluid dynamics code, NEKTON version 2.85, and the Langevin particle equation of motion to compute the particle capture efficiency and pressure drop through selected two- and three-dimensional fiber arrays. The approach we used was to first compute the air velocity vector field throughout a defined region containing the fiber matrix. The particle capture in the fiber matrix is then computed by superimposing the Langevin particle equation of motion over the flow velocity field. Using the Langevin equation combines the particle Brownian motion, inertia and interception mechanisms in a single equation. In contrast, most previous investigations treat the different capture mechanisms separately. We have computed the particle capture efficiency and the pressure drop through a 2-D and two 3-D fiber matrix elements. DOE

N95-16239 Naval Postgraduate School, Monterey, CA.
NATURAL CONVECTION COOLING OF A THREE BY THREE ARRAY OF LEADLESS CHIP CARRIER PACKAGES IN A DIELECTRIC LIQUID M.S. Thesis
Joseph M. Bradley 24 Mar. 1994 132 p Limited Reproducibility: More than 20% of this document may be affected by microfiche quality
(AD-A282298) Avail: CASI HC A07

Liquid cooling of a three-by-three array of commercially available leadless chip carrier packages mounted on a ceramic substrate was examined. Baseline data were obtained for cooling with pure dielectric liquids. The effects of addition of high thermal conductivity ceramic powder to the liquid were next examined, both for natural and forced circulation conditions. Vertical and horizontal orientations were studied for two different ceramic particle types and two different particle sizes for each ceramic. For a range of chip power levels, chip, substrate, and cold plate temperatures were measured. Interpretations for these data are provided. A numerical model was developed for the vertical geometry and compared to the measurements obtained. DTIC

N95-16388*# Massachusetts Inst. of Tech., Cambridge. Computational Aerospace Sciences Lab.
VISUALIZATION OF UNSTEADY COMPUTATIONAL FLUID DYNAMICS Final Technical Report
Robert Haimes Nov. 1994 140 p
(Grant NAG2-884)
(NASA-CR-197461; NAS 1.26:197461) Avail: CASI HC A07/MF A02

A brief summary of the computer environment used for calculating three dimensional unsteady Computational Fluid Dynamic (CFD) results is presented. This environment requires a super computer as well as massively parallel processors (MPP's) and clusters of workstations acting as a single MPP (by concurrently working on the same task) provide the required computational bandwidth for CFD calculations of transient problems. The cluster of reduced instruction set computers (RISC) is a recent advent based on the low cost and high performance that workstation vendors provide. The cluster, with the proper software can act as a multiple instruction/multiple data (MIMD) machine. A new set of software tools is being designed specifically to address visualizing 3D unsteady CFD results in these environments. Three user's manuals for the parallel version of Visual3, pV3, revision 1.00 make up the bulk of this report. CASI

N95-16407*# National Aeronautics and Space Administration. Lewis Research Center, Cleveland, OH.
MODELING OF WALL-BOUNDED COMPLEX FLOWS AND FREE SHEAR FLOWS
Tsan-Hsing Shih, Jiang Zhu, and John L. Lumley (Cornell Univ., Ithaca, NY.) Feb. 1994 10 p Presented at the ASME Fluids Engineering Conference, Symposium on Boundary Layer and Free Shear Flows, Lake Tahoe, NV, 19-23 Jun. 1994 Sponsored in part by ONR
(Contracts NCC3-233; RTOP 505-90-5K; F49620-92-J-0038; AF-AFOSR-0226-89)
(NASA-TM-106513; E-8624; ICOMP-94-3; NAS 1.15:106513; CMOTT-94-1)
Avail: CASI HC A02/MF A01

Various wall-bounded flows with complex geometries and free shear flows have been studied with a newly developed realizable Reynolds stress algebraic equation model. The model development is based on the invariant theory in continuum mechanics. This theory enables us to formulate a general constitutive relation for the Reynolds stresses. Pope was the first to introduce this kind of constitutive relation to turbulence modeling. In our study, realizability is imposed on the truncated constitutive relation to determine the coefficients so that, unlike the standard k-E eddy viscosity model, the present model will not produce negative normal stresses in any situations of rapid distortion. The calculations based on the present model have shown an encouraging success in modeling complex turbulent flows. Author

N95-16417# General Electric Co., Schenectady, NY. Atomic Power Lab.
COLLOIDAL PARTICLE DEPOSITION IN TURBULENT FLOW
D. S. Morton May 1994 24 p
(Contract DE-AC12-76SN-00052)
(DE94-013375; KAPL-4773) Avail: CASI HC A03/MF A01

A theoretical analysis is presented which describes the initial deposition of monodispersed spherical colloidal particles from a steady fully developed turbulent flow onto conduit walls. When the net particle-conduit electrical interaction potential is attractive, particle deposition is shown to be often governed by turbulent hydrodynamics. When the net particle-conduit electrical interaction potential possess a repulsive maximum, particle deposition to first order is uniform and depends solely on electrical interaction effects. The developed theoretical model specialized to orifice deposition with the use of Harwell Flow 3D turbulence modelling software qualitatively described the deposition of 0.5 (mu)m silica particles onto glass orifices from an

aqueous suspension. The effect of the electrical double layer on the rate of colloidal particle deposition in laminar flow has been described by Spielman and Friedlander, Dahneke, Bowen et al. and Bowen and Epstein. This article describes the extension of their work to colloidal particle deposition under steady fully developed turbulent flow conditions. This article also reports the results of orifice particle deposition experiments which were conducted to qualitatively investigate the developed theoretical model. DOE

N95-16438# New Mexico Univ., Albuquerque, NM. Dept. of Mechanical Engineering.

DYNAMICAL SYSTEM PREDICTION OF THE SCALAR FIELD IN A TURBULENT CHANNEL FLOW Final Report, 1 Nov. 1990 - 31 Jan. 1994

C. R. Truman and Rick I. Zadoks 31 Mar. 1994 18 p

(Grant AF-AFOSR-0071-91)

(AD-A285519; AFOSR-94-0633TR) Avail: CASI HC A03/MF A01

The importance of large-scale (or coherent) structure to optical propagation through turbulent shear flow has been demonstrated. Direct simulations of low-Reynolds-number flows which include a passive scalar as well as experimental data have been examined. A passive scalar in the simulations is related to refractive-index fluctuations, while a heated jet was used in the experiment. Large fluctuations associated with large-scale turbulent structure produce a majority of the optical phase error. A low-order dynamical model for the near-wall region of a turbulent channel flow was developed. These predictions illustrate the importance of the dynamics of the turbulent shear flow to optical phase error. Techniques to use limited data to estimate the effect of large-scale structure upon optical propagation were developed. A round turbulent jet was also studied using a large eddy simulation as well as experimental data. Temperature at several locations and jitter in an optical beam propagated through the flow can be measured simultaneously in an experimental facility constructed at the Air Force Phillips Laboratory. A low-dimensional dynamical model for the round jet with passive scalar to be developed in subsequent work will be compared with this experimental data. DTIC

N95-16595# Cambridge Univ., Cambridge (England). Dept. of Engineering.

INVESTIGATIONS ON THE SENSITIVITY OF THE COMPUTER CODE TURBO-2D

B. Amon (Erlangen-Nuremberg Univ., Germany.) Dec. 1994 56 p

(ISSN 0309-6513)

(CUED/A-THERMO/TR-61) Avail: CASI HC A04/MF A01

The two-dimensional computer model TURBO-2D for the calculation of two-phase flow was used to calculate the cold injection of fuel into a model chamber. Investigations of the influence of the input parameter on its sensitivity relative to the obtained results were made. In addition to that calculations were performed and compared using experimental injection pressure data and corresponding averaged injection parameter. Author

N95-16616# Arizona State Univ., Tempe, AZ. Dept. of Mechanical and Aerospace Engineering.

EXPERIMENTAL AND THEORETICAL STUDIES OF WAKES IN STRATIFIED FLOWS Annual Report

Don L. Boyer and Harindra J. Fernando 30 Sep. 1994 5 p

(Contract N00014-90-J-4063)

(AD-A285305) Avail: CASI HC A01/MF A01

The long range goal of this research is to obtain, by laboratory experimentation and associated theoretical analysis an increased understanding of the dynamics of stratified flow past three-dimentional obstacles. Emphasis is given to such phenomena as blocking, flow separation, vortex shedding, lee-wave generation, unsteady characteristics of the free stream, and lift and drag on the obstacles in question. The near term objective of the research is to study the dynamics of simple body shapes (e.g., spheres) free to move in the vicinity of bounding surfaces under the action of oscillatory background motions. This objective was motivated by the recently expressed Navy interest in the motion of cobbles within and beyond the surf zone. Derived from text

N95-16736# North Carolina State Univ., Raleigh, NC. Dept. of Mechanical and Aerospace Engineering.

TIME ACCURATE COMPUTATION OF UNSTEADY INLET FLOWS WITH A DYNAMIC FLOW ADAPTIVE MESH Final Report, 15 Mar. 1992 - 30 Jun. 1994

D. S. McRae and Rusty A. Benson 7 Sep. 1994 52 p

(Contract F49620-92-J-0189)

(AD-A285498; AFOSR-94-0625TR) Avail: CASI HC A04/MF A01

Research has been performed to obtain very accurate dynamic simulations of supersonic inlet unstart using CFD codes and a dynamic solution adaptive mesh algorithm developed at NCSU. The codes use Runge-Kutta time differencing and Advective Upwind Split Method spatial differencing in finite volume form. Other changes have been incorporated to improve the time accuracy when the computational mesh is dynamically adapted. Solutions have been obtained and animated for unstart of generic 2-D mixed compressions and fully supersonic inlets. Analysis of results revealed that laminar viscous flow unstart occurs by a separation/oblique shock mechanism rather than movement of a normal shock. Turbulent flow simulations reveal that initial shock motion occurs initially but then reverts to the separation/oblique shock mechanisms. 3-D steady and unsteady simulations are presented and conclusions drawn concerning the role of separation in inlet unstart. DTIC

N95-16828*# National Aeronautics and Space Administration. Langley Research Center, Hampton, VA.

APPLICATIONS OF AUTOMATIC DIFFERENTIATION IN CFD

A. Carle (Rice Univ., Houston, TX.), L. L. Green, P. A. Newman, and C. H. Bischof (Argonne National Lab., IL.) 1994 13 p Presented at the 24th International Fluid Dynamics, Plasma Dynamics and Laser Conference, Colorado Springs, CO, 20-23 Jun. 1994

(Contract W-31-109-eng-38)

(NASA-TM-109948; NAS 1.15:109948; DE94-013400; ANL/MCS/CP-82980; CONF-940662-1) Avail: CASI HC A03/MF A01

Automated multidisciplinary design of aircraft requires the optimization of complex performance objectives with respect to a number of design parameters and constraints. The effect of these independent design variables on the system performance criteria can be quantified in terms of sensitivity derivatives for the individual discipline simulation codes. Typical advanced CFD codes do not provide such derivatives as part of a flow solution. These derivatives are expensive to obtain by divided differences from perturbed solutions, and may be unreliable, particularly for noisy functions. In this paper, automatic differentiation has been investigated as a means of extending iterative CFD codes with sensitivity derivatives. In particular, the ADIFOR automatic differentiator has been applied to the 3-D, thin-layer Navier-Stokes, multigrid flow solver called TLNS3D coupled with the WTCO wing grid generator. Results of a sequence of efforts in which TLNS3D has been successfully augmented to compute a variety of sensitivities are presented. It is shown that sensitivity derivatives can be obtained accurately and efficiently using ADIFOR, although significant advances are necessary for the efficiency of ADIFOR-generated derivative code to become truly competitive with hand-differentiated code. DOE

N95-16855*# National Aeronautics and Space Administration. Lewis Research Center, Cleveland, OH.

ON BI-GRID LOCAL MODE ANALYSIS OF SOLUTION TECHNIQUES FOR 3-D EULER AND NAVIER-STOKES EQUATIONS

S. O. Ibraheem (Old Dominion Univ., Norfolk, VA.) and A. O. Demuren Oct. 1994 51 p

(Contract NCC3-233; RTOP 505-90-5K)

(NASA-TM-106749; ICOMP-94-6; E-9165; NAS 1.15:106749) Avail: CASI HC A04/MF A01

A procedure is presented for utilizing a bi-grid stability analysis as a practical tool for predicting multigrid performance in a range of numerical methods for solving Euler and Navier-Stokes equations. Model problems based on the convection, diffusion and Burger's equation are used to illustrate the superiority of the bi-grid analysis as a predictive tool for multigrid performance in comparison to the smoothing factor derived from conventional von Neumann analysis. For the Euler equations, bi-grid analysis is presented for three upwind difference based factorizations, namely Spatial, Eigenvalue and Combination splits, and two central difference based factorizations, namely LU and ADI methods. In the former, both the Steger-Warming and van Leer flux-vector splitting methods are considered.

For the Navier-Stokes equations, only the Beam-Warming (ADI) central difference scheme is considered. In each case, estimates of multigrid convergence rates from the bi-grid analysis are compared to smoothing factors obtained from single-grid stability analysis. Effects of grid aspect ratio and flow skewness are examined. Both predictions are compared with practical multigrid convergence rates for 2-D Euler and Navier-Stokes solutions based on the Beam-Warming central scheme. Author

N95-16903*# National Aeronautics and Space Administration. Lewis Research Center, Cleveland, OH.
APPLICATION OF THE SPACE-TIME CONSERVATION ELEMENT AND SOLUTION ELEMENT METHOD TO SHOCK-TUBE PROBLEM
Xiao-Yen Wang (Colorado Univ., Boulder, CO.), Chuen-Yen Chow (Colorado Univ., Boulder, CO.), and Sin-Chung Chang Dec. 1994 37 p
(RTOP 505-62-52)
(NASA-TM-106806; E-9288; NAS 1.15:106806) Avail: CASI HC A03/MF A01

An Euler solver based on the method of space-time conservation element and solution element is in this paper to simulate shock-tube flows involving shock waves, contact discontinuities, expansion waves and their intersections. Seven test problems are considered to examine the capability of this method. The numerical results, when compared with exact solutions and/or numerical solutions by other methods, indicate that the present method can accurately resolve strong shock and contact discontinuities without using any ad hoc techniques which are used only at the neighborhood of a discontinuity. Author

N95-17165 Georgia Inst. of Tech., Atlanta, GA. School of Aerospace Engineering.
A NEW APPROACH TO VALIDATE SUBGRID MODELS IN COMPLEX HIGH REYNOLDS NUMBER FLOWS Semiannual Report, Oct. 1993 - May 1994
Suresh Menon May 1994 49 p Limited Reproducibility: More than 20% of this document may be affected by microfiche quality
(Contract N00014-93-1-0342)
(AD-A282340) Avail: Issuing Activity (Defense Technical Information Center (DTIC))

This second semi-annual report summarizes the progress made in the last six months. The overall objectives of this research are to develop new methods to evaluate subgrid models and then to utilize these methods to improve the chosen subgrid models. The subgrid models investigated in this research are chosen primarily for application in high Reynolds number complex flows. Preliminary studies of these models have been completed. A priori analysis using data from direct numerical simulations (DNS) homogeneous isotropic flows was carried out, and then the models were implemented in large-eddy simulation (LES) codes and further evaluated. Two types of analysis methods have been developed so far. The first method uses information in Fourier (spectral) space and evaluates the interscale energy transfer as a function of the wavenumbers resolved in the LES. The second, uses information in the physical space and uses cross correlation analysis to investigate the behavior of subgrid models. The physical space analysis method will be the primary analysis tool for the next year's study, since the next phase of research will focus on complex flows such as flows past rearward facing steps and swirling flows. DTIC

N95-17268*# High Technology Corp., Hampton, VA.
STABILITY OF SEPARATING SUBSONIC BOUNDARY LAYERS
Jamal A. Masad and Ali H. Nayfeh (Virginia Polytechnic Inst. and State Univ., Blacksburg, VA.) NASA Dec. 1994 152 p
(Contracts NAS1-19299; NAS1-19610; RTOP 538-05-15-01)
(NASA-CR-4638; NAS 1.26:4638) Avail: CASI HC A08/MF A02

The primary and subharmonic instabilities of separating compressible subsonic two-dimensional boundary layers in the presence of a two-dimensional roughness element on a flat plate are investigated. The roughness elements considered are humps and forward- and backward-facing steps. The use of cooling and suction to control these instabilities is studied. The similarities and differences between the instability characteristics of separating boundary layers and those of the boundary layer over a flat plate with a zero pressure gradient are pointed out and discussed. The theoretical results agree qualitatively and quantitatively with the experimental data of Dovgal and Kozlov. Cooling and suction decrease the growth rates of primary and subharmonic waves in the attached-flow regions but increase them in the separated-flow regions. Author

N95-17386*# NYMA, Inc., Brook Park, OH. Engineering Services Div.
SMALL-AMPLITUDE DISTURBANCES IN TURBOMACHINE FLOWS WITH SWIRL Final Report
David W. Wundrow Cleveland, OH NASA Nov. 1994 21 p
(Contract NAS3-27186; RTOP 505-90-53)
(NASA-CR-195406; E-9257; NAS 1.26:195406) Avail: CASI HC A03/MF A01

A method is proposed for determining the response of the steady swirling potential flow past a blade row in an axial turbomachine to the most general type of 'nonacoustic' incident disturbance. The method is based on Goldstein's decomposition of the disturbance velocity and only requires solving a linear inhomogeneous wave equation. It is believed that numerical solutions to this wave equation can be obtained more efficiently and will be more accurate than corresponding solutions to the linearized compressible Euler equations. Author (revised)

N95-17418*# California Univ., Los Angeles, CA.
IN-FLIGHT IMAGING OF TRANSVERSE GAS JETS INJECTED INTO TRANSONIC AND SUPERSONIC CROSSFLOWS: DESIGN AND DEVELOPMENT M.S. Thesis, Mar. 1993
Kon-Sheng Charles Wang Nov. 1994 88 p
(Contract NCC2-374; RTOP 505-68-53)
(NASA-CR-186031; H-2027; NAS 1.26:186031) Avail: CASI HC A05/MF A01

The design and development of an airborne flight-test experiment to study nonreacting gas jets injected transversely into transonic and supersonic crossflows is presented. Free-stream/crossflow Mach numbers range from 0.8 to 2.0. Planar laser-induced fluorescence (PLIF) of an iodine-seeded nitrogen jet is used to visualize the jet flow. Time-dependent images are obtained with a high-speed intensified video camera synchronized to the laser pulse rate. The entire experimental assembly is configured compactly inside a unique flight-test-fixture (FTF) mounted under the fuselage of the F-104G research aircraft, which serves as a 'flying wind tunnel' at NASA Dryden Flight Research Center. The aircraft is flown at predetermined speeds and altitudes to permit a perfectly expanded (or slightly underexpanded) gas jet to form just outside the FTF at each free-stream Mach number. Recorded gas jet images are then digitized to allow analysis of jet trajectory, spreading, and mixing characteristics. Comparisons will be made with analytical and numerical predictions. This study shows the viability of applying highly sophisticated groundbased flow diagnostic techniques to flight-test vehicle platforms that can achieve a wide range of thermo/fluid dynamic conditions. Realistic flow environments, high enthalpies, unconstrained flowfields, and moderate operating costs are also realized, in contrast to traditional wind-tunnel testing. Author

N95-17506 Miami Univ., FL.
SURFACTANT ADSORPTION BY SUB-MILLIMETER SIZE BUBBLES: QUANTIFICATION AND MODELLING Final Technical Report
Richard A. Skop Jul. 1994 7 p Limited Reproducibility: More than 20% of this document may be affected by microfiche quality
(Contract N00014-91-J-1771)
(AD-A282405) Avail: Issuing Activity (Defense Technical Information Center (DTIC))

Bubbles rising through seawater scavenge surface-active organic materials from the water column. The scavenging process in turn has a strong influence on the dynamics of the underlying bubble. The rate at which a surfactant is adsorbed by a bubble involves the ambient concentration of the material, the adsorption potential for the material, the bubble skin saturation limit, the surface area of the bubble, the collision kinetics and the diffusion rate, and the void fraction of the bubble cloud. Our objective was to quantify these factors and to develop and verify a model of the bubble scavenging process. DTIC

N95-17523# Argonne National Lab., IL.
TRANSIENT FLOWS AND PRESSURE WAVES IN PIPES
X. Q. Wang, J. G. Sun, and W. T. Sha 1994 14 p Presented at the Pressure Vessel and Piping Conference, Minneapolis, MN, 19-23 Jun. 1994

(Contract W-31-109-eng-38)
(DE94-012650; ANL/ET/CP-81529; CONF-940613-18) Avail: CASI HC A03/MF A01

Transient laminar flows and pressure-wave propagations in pipes connected with components, commonly known as water hammer, are analyzed. The system studied consists of a constant-pressure vessel, a uniform circular pipe, a valve between them, and a receiver vessel. A pressure-wave equation and a linearized velocity equation are derived from the equations of mass and momentum conservation. Waveform distortion due to viscous dissipation and pipe-wall elastic expansion is characterized by a dimensionless transmission number, K. The coefficients of the damping of the pressure waves were found to be related to the roots of the Bessel function J(sub 0). An exact solution of the pressure-wave equation was obtained numerically. The relationship between the distortion of a traveling wave and the transmission number K was studied. The problem is also calculated with a general-purpose computer code, COMMIX, which solves the exact mass conservation equation and Navier-Stokes equations. The COMMIX calculational results agreed well with the analytical solutions. DOE

N95-17617 Colorado Univ., Boulder, CO.
NONLINEAR PROBLEMS IN FLUID DYNAMICS AND INVERSE SCATTERING. PROPAGATION AND CAPTURING OF SINGULARITIES IN PROBLEMS OF FLUID DYNAMICS AND INVERSE SCATTERING
Annual Report, 10 Jan. 1993 - 30 Sep. 1994
Gregory Beylkin 31 Jul. 1994 3 p Limited Reproducibility: More than 20% of this document may be affected by microfiche quality
(Contract N00014-94-1-0194)
(AD-A282873; Rept-153-4619) Avail: Issuing Activity (Defense Technical Information Center (DTIC))

Research investigations and development of the fast adaptive algorithms using orthonormal bases with controlled localization in the time-frequency domain (e.g. wavelets) have been successful and several new algorithms have been developed. Among the results is the unequally spaced fast Fourier transform (USFFT) algorithm and a new approach to numerical homogenization. DTIC

N95-17656*# National Aeronautics and Space Administration. Lewis Research Center, Cleveland, OH.
EFFECTS OF ARTIFICIAL VISCOSITY ON THE ACCURACY OF HIGH-REYNOLDS-NUMBER KAPPA-EPSILON TURBULENCE MODEL
Tawit Chitsomboon Nov. 1994 20 p
(Contract NCC3-233; RTOP 505-90-5K)
(NASA-TM-106781; ICOMP-94-28; E-9234; NAS 1.15:106781) Avail: CASI HC A03/MF A01

Wall functions, as used in the typical high Reynolds number k-epsilon turbulence model, can be implemented in various ways. A least disruptive method (to the flow solver) is to directly solve for the flow variables at the grid point next to the wall while prescribing the values of k and epsilon. For the centrally-differenced finite-difference scheme employing artificial viscocity (AV) as a stabilizing mechanism, this methodology proved to be totally useless. This is because the AV gives rise to a large error at the wall due to too steep a velocity gradient resulting from the use of a coarse grid as required by the wall function methodology. This error can be eliminated simply by extrapolating velocities at the wall, instead of using the physical values of the no-slip velocities (i.e. the zero value). The applicability of the technique used in this paper is demonstrated by solving a flow over a flat plate and comparing the results with those of experiments. It was also observed that AV gives rise to a velocity overshoot (about 1 percent) near the edge of the boundary layer. This small velocity error, however, can yield as much as 10 percent error in the momentum thickness. A method which integrates the boundary layer up to only the edge of the boundary (instead of infinity) was proposed and demonstrated to give better results than the standard method. Author

N95-17708# Wisconsin Univ., Madison, WI.
[MULTI-DIMENSIONAL SHOCK CAPTURING]
Marshall Slemrod 1994 3 p
(Contract N00014-93-1-0015)
(AD-A282986) Avail: CASI HC A01/MF A01

The author has worked on two aspects of multidimensional shock capturing. The first project has been a multifaceted effort to understand dynamic liquid-vapor interface propagation from a kinetic point of view. The phenomenon was modeled via a Boltzmann like cluster dynamics model. Clusters represent groupings of molecules of various cluster sizes which can collide elastically and inelastically. The inelastic collisions can produce coagulation of clusters or fragmentation of a cluster. A fluid made of only small cluster sizes would represent a dilute vapor while one containing very large cluster sizes would be a metastable supersaturated vapor. The model via various scaling limits gives sets of equations describing vapor flow in various transition regimes. Numerical experiments were performed modeling vapor to saturated vapor phase change encountered when a dilute vapor encounters a rigid wall. DTIC

N95-17910# Oak Ridge National Lab., TN.
SIMULATION OF THE SEMATECH GRAVIMETRIC MASS FLOWMETER CALIBRATOR
R. F. Lind, J. O. Hylton, C. J. Remenyik (Tennessee Univ., Knoxville, TN.), and C. L. Carnal (Tennessee Technological Univ., Cookeville, TN.) 1994 7 p Presented at the SCSC 1993: Summer Computer Simulation Conference, Boston, MA, 19-21 Jul. 1993
(Contract DE-AC05-84OR-21400)
(DE94-018698; CONF-930765-4) Avail: CASI HC A02/MF A01

Many different processes in the fabrication of microelectronic circuits require precise metering of process gas flows. A facility is being designed at Oak Ridge National Laboratory (ORNL) to provide calibration of high-precision gas flowmeters for the Semiconductor Manufacturing Technology (SEMATECH) consortium. To provide proof-of-principle and to aid in the design of the facility, a digital computer simulation was developed. The gravimetric mass flowmeter is a new and unique apparatus that has been proposed for use as a primary calibration standard. The basic operating principles suggest that system dynamics and control will influence measurement accuracy and precision. Hence, a simulation of high fidelity was required because of the precision and accuracy specifications of the proposed facility. This paper describes the mathematical model development and software implementation using the Advanced Continuous Simulation Language (ACSL). Results obtained establish the feasibility of the proposed calibration facility. DOE

N95-16250# Nanjing Univ. of Aeronautics and Astronautics, Nanjing, Jiangsu (China). Research Inst. of Helicopter Technique.
INVESTIGATION OF DYNAMIC INFLOW'S INFLUENCE ON ROTOR CONTROL DERIVATIVES
Xiaogu Zhang and Jinsong Bao *In its* Joint Proceedings on Aeronautics and Astronautics (JPAA) May 1993 p 1-10 Sponsored by the Aeronautical Science Foundation of China (For primary document see N95-16249 04-01)
Avail: CASI HC A02/MF A03

N95-16253# Nanjing Univ. of Aeronautics and Astronautics, Nanjing, Jiangsu (China). Dept. of Power Engineering.
EXPERIMENTAL INVESTIGATION OF TURBULENT SEPARATED-REATTACHMENT FLOW BY USING LDV
Junfei Yin and Shaozhi Yu *In its* Joint Proceedings on Aeronautics and Astronautics (JPAA) May 1993 p 23-32 (For primary document see N95-16249 04-01)
Avail: CASI HC A02/MF A03

N95-16254# Nanjing Univ. of Aeronautics and Astronautics, Nanjing, Jiangsu (China). Dept. of Power Engineering.
IMPROVED METHOD FOR ESTIMATION OF THE MAXIMUM INSTANTANEOUS DISTORTION VALUES
Dewang Liang and Shiying Zhang *In its* Joint Proceedings on Aeronautics and Astronautics (JPAA) May 1993 p 33-42 See also A92-49076 (For primary document see N95-16249 04-01)
Avail: CASI HC A02/MF A03

N95-16255# Kazan Aviation Inst. (USSR).
SURFACE HEAT TRANSFER IN A CHANNEL WITH POROUS INSERT
Yu. F. Gortyshov *In* Nanjing Univ. of Aeronautics and Astronautics, Joint Proceedings on Aeronautics and Astronautics (JPAA) May 1993 p 43-47 (For primary document see N95-16249 04-01)
Avail: CASI HC A01/MF A03

N95-16322# Wright Lab., Wright-Patterson AFB, OH.
AN ENGINEERING CODE TO ANALYZE HYPERSONIC THERMAL MANAGEMENT SYSTEMS
Valerie J. VanGriethuysen and Clark E. Wallace (Science Applications International Corp., Torrance, CA.) *In* JHU The 1993 JANNAF Propulsion Meeting, Volume 1 Nov. 1993 p 319-333 (For primary document see N95-16312 04-20)
(Contract F33615-91-C-2169)
Avail: CPIA, 10630 Little Patuxent Pkwy., Suite 202, Columbia, MD 21044-3200 HC

N95-16461*# National Aeronautics and Space Administration. Langley Research Center, Hampton, VA.
APPLICATIONS OF AUTOMATIC DIFFERENTIATION IN COMPUTATIONAL FLUID DYNAMICS
Lawrence L. Green, A. Carle (Rice Univ., Houston, TX.), C. Bischof (Argonne National Lab., IL.), Kara J. Haigler, and Perry A. Newman *In its* The Role of Computers in Research and Development at Langley Research Center Oct. 1994 p 168-180 (For primary document see N95-16453 04-62)
Avail: CASI HC A03/MF A06

N95-17847# Deutsche Forschungsanstalt fuer Luft- und Raumfahrt, Brunswick (Germany). Inst. fuer Entwurfsaerodynamik.
2-D AIRFOIL TESTS INCLUDING SIDE WALL BOUNDARY LAYER MEASUREMENTS
W. Bartelheimer, K. H. Horstmann, and W. Puffert-Meissner *In* AGARD, A Selection of Experimental Test Cases for the Validation of CFD Codes, Volume 2 Aug. 1994 11 p (For primary document see N95-17846 04-02)
Copyright Avail: CASI HC A03/MF A06

N95-17867# Deutsche Forschungsanstalt fuer Luft- und Raumfahrt, Goettingen (Germany). Inst. fuer Stroemungsmechanik.
THREE-DIMENSIONAL BOUNDARY LAYER AND FLOW FIELD DATA OF AN INCLINED PROLATE SPHEROID
H.-P. Kreplin *In* AGARD, A Selection of Experimental Test Cases for the Validation of CFD Codes, Volume 2 Aug. 1994 12 p (For primary document see N95-17846 04-02)
Copyright Avail: CASI HC A03/MF A06

N95-17869# Office National d'Etudes et de Recherches Aerospatiales, Paris (France).
ELLIPSOID-CYLINDER MODEL
D. Barberis *In* AGARD, A Selection of Experimental Test Cases for the Validation of CFD Codes, Volume 2 Aug. 1994 11 p (For primary document see N95-17846 04-02)
Copyright Avail: CASI HC A03/MF A06

N95-17871# Office National d'Etudes et de Recherches Aerospatiales, Paris (France).
TEST DATA ON A NON-CIRCULAR BODY FOR SUBSONIC, TRANSONIC AND SUPERSONIC MACH NUMBERS
P. Champigny *In* AGARD, A Selection of Experimental Test Cases for the Validation of CFD Codes, Volume 2 Aug. 1994 11 p (For primary document see N95-17846 04-02)
Copyright Avail: CASI HC A03/MF A06

35 INSTRUMENTATION AND PHOTOGRAPHY

Includes remote sensors; measuring instruments and gages; detectors; cameras and photographic supplies; and holography.

For aerial photography see *43 Earth Resources and Remote Sensing*. For related information see also *06 Aircraft Instrumentation*, and *19 Spacecraft Instrumentation*.

N95-16074# National Inst. of Standards and Technology, Gaithersburg, MD.
USE OF THE ELECTRONIC BALANCE FOR HIGHLY ACCURATE DIRECT MASS MEASUREMENTS WITHOUT THE USE OF EXTERNAL MASS STANDARDS
R. M. Schoonover and F. E. Jones May 1994 20 p
(PB94-187713; NISTIR-5423) Avail: CASI HC A03/MF A01

The object of the paper is to show how to make highly accurate mass measurements using an appropriate electronic balance without the use of external mass standards. The method eliminates the need for a set of external mass standards and, therefore the need to have these mass standards calibrated periodically at a standards laboratory. Traceability to NIST can be achieved by periodic calibration of the built-in mass standard of the balance by a standards laboratory and by self-verification of balance linearity and function. The method benefits the user with lower cost and a higher measurement rate. Presented here is a detailed analysis of the method, a determination of measurement uncertainty, and the traceability path. Lastly, the method is illustrated by specific examples including the calculation of uncertainty. Author

N95-16242 Massachusetts Inst. of Tech., Cambridge.
SHAPED STRAIN SENSORS FOR INTELLIGENT STRUCTURES Final Report, 1 Nov. 1991 - 31 Jan. 1994
Mark S. Anderson and Edward Crawley 3 Jun. 1994 113 p Limited Reproducibility: More than 20% of this document may be affected by microfiche quality
(Contract F49620-92-J-0010)
(AD-A282333; AFOSR-94-0456TR) Avail: CASI HC A06

Tbe design of sensors for use in the control of intelligent structures is investigated. It is found that certain spatially averaging strain sensors can be used to satisfy these requirements. The output and transfer function characteristics of spatially averaging sensors with arbitrary weightings are derived for both sinusoidal and exponential strain fields. An interpretation of shaped sensor behavior is given which explains how the rolloff of shaped sensors can occur for a simulated pinned-pinned beam with collocated Barrett and point sensors. Experiments using clamped-free beams fitted with different spatially averaging strain sensors are conducted to verify the predicted rolloff rate of the sensor transfer function. Results of the tests indicate that the sensor's rolloff can be predicted if the sensors (in the experiment) can be implemented properly. In order to investigate the possibility of using an array of spatially averaging sensors to estimate global structural shape, the dynamic mode shapes of pinned-pinned and clamped-free beams are also estimated using a variety of sensor weightings and integration rules. DTIC

N95-16247# Defence Science and Technology Organization, Melbourne (Australia).
DESIGN OF THERMOCOUPLE PROBES FOR MEASUREMENT OF ROCKET EXHAUST PLUME TEMPERATURES
R. C. Warren Jun. 1994 40 p
(AD-A285423; DSTO-TR-0006; DODA-AR-008-651) Avail: CASI HC A03/MF A01

This paper summarizes a literature survey on high temperature measurement and describes the design of probes used in plume measurements. There were no cases reported of measurements in extreme environments such as exist in solid rocket exhausts, but there were a number of thermocouple designs which had been used under less extreme conditions and which could be further developed. Tungsten-rhenium(W-Rh) thermocouples had the combined properties of strength at high temperatures, high thermoelectric emf, and resistance to chemical attack. A shielded probe was required, both to protect the thermocouple junction, and to minimise radiative heat losses. After some experimentation, a twin shielded design made from molybdenum gave acceptable results. Corrections for thermal conduction losses were made based on a method obtained from the literature. Radiation losses were minimized with this probe design, and corrections for these losses were too complex and unreliable to be included. DTIC

N95-16804# EG and G Energy Measurements, Inc., Las Vegas, NV.
EVALUATION OF A NEW MINIATURE TEMPERATURE DATA LOGGER: HERPETOLOGICAL REVIEW
J. M. Mueller and D. L. Rakestraw 1994 6 p
(Contract DE-AC08-93NV-11265)
(DE94-013561; EGG-11265-1063) Avail: CASI HC A02/MF A01

Peterson and Dorcas described the advantages of using data loggers to measure variation in the environment. We used a new, miniature

temperature data logger to measure the temperatures of nests and hibernacula of desert tortoises (Gopherus agassizii). Here we report on the accuracy, reliability, and ease of use of these data loggers. Reference to a company or product name does not imply approval or recommendation of the product by the US Department of Energy to the exclusion of others that may be suitable. Quoted costs are from a published price list. DOE

N95-16910*# Purdue Univ., West Lafayette, IN.
LASER INDUCED FLUORESCENCE MEASUREMENTS AND MODELING OF NITRIC OXIDE IN HIGH-PRESSURE PREMIXED FLAMES Final Report
John R. Reisel and Normand M. Laurendeau Cleveland, OH NASA Dec. 1994 240 p
(Grant NAG3-1038; RTOP 537-02-20)
(NASA-CR-195404; E-9248; NAS 1.26:195404) Avail: CASI HC A11/MF A03

Laser-induced fluorescence (LIF) has been applied to the quantitative measurement of nitric oxide (NO) in premixed, laminar, high-pressure flames. Their chemistry was also studied using three current kinetics schemes to determine the predictive capabilities of each mechanism with respect to NO concentrations. The flames studied were low-temperature (1600 less than T less than 1850K) C2H6/O2/N2 and C2H6/O2/N2 flames, and high temperature (2100 less than T less than 2300K) C2H6/O2/N2 flames. Laser-saturated fluorescence (LSF) was initially used to measure the NO concentrations. However, while the excitation transition was well saturated at atmospheric pressure, the fluorescence behavior was basically linear with respect to laser power at pressures above 6 atm. Measurements and calculations demonstrated that the fluorescence quenching rate variation is negligible for LIF measurements of NO at a given pressure. Therefore, linear LIF was used to perform quantitative measurements of NO concentration in these high-pressure flames. The transportability of a calibration factor from one set of flame conditions to another also was investigated by considering changes in the absorption and quenching environment for different flame conditions. The feasibility of performing LIF measurements of (NO) in turbulent flames was studied; the single-shot detection limit was determined to be 2 ppm. Author

N95-17170 National Defence Research Establishment, Linkoeping (Sweden). Huvudavdelning foer Informationsteknologi.
FEASIBILITY STUDY CONCERNING AN ACTIVE MILLIMETERWAVE SENSOR [REALISERBARHETSSTUDIE AVSEENDE EN AKTIV MILLIMETERVAGSSENSOR]
J. Svedin, U. Dahlgren, H. Johansson, H. Zirath, and O. J. Hagel Jan. 1994 39 p In SWEDISH Prepared in cooperation with Chalmers Univ. of Technology, Goeteborg, Sweden and Industrial Microelectronics Center, Linkoeping, Oestergoetland, Sweden
(PB94-190691; FOA-C-30747-3.2) Avail: Issuing Activity (National Technical Information Service (NTIS))

The report gives a brief summary of attained results within the above mentioned project, phases MMS1.1 and MMS1.2b. A number of integrated, active millimeter wave sensors intended for imaging applications and built on relatively thick layers of BCB (benzotyclobutene) substrates have been designed, simulated, and manufactured for use at 35 GHz. A millimeter wave sensor manufactured using a hybrid technology (MMS1.2b) has been characterized. It comprises a rectangular microstrip patch attenna and a HEMT based mixer working in a resistive mode. This sensor has demonstrated a conversion loss at best around 8 dB at 35 GHz, and a 3 dB bandwidth of approximately 500 MHz. NTIS

N95-17307# California Univ., Berkeley. Lawrence Berkeley Lab, CA.
SIMULATING THE ENERGY PERFORMANCE OF HOLOGRAPHIC GLAZINGS
K. Papamichael, L. Beltran, R. Furler, E. S. Lee, S. Selkowitz, and M. Rubin Mar. 1994 9 p Presented at the SPIE 13: International Symposium on Optical Materials Technology for Energy Efficiency and Solar Energy Conversion, Freiburg, Germany, 18-22 Apr. 1994
(Contract DE-AC03-76SF-00098)
(DE94-013110; LBL-35382; CONF-9404167-1) Avail: CASI HC A02/MF A01

The light diffraction properties of holographic diffractive structures present an opportunity to improve the daylight performance in side-lit office spaces by redirecting and reflecting sunlight off the ceiling, providing adequate daylight illumination up to 30 ft (9.14 m) from the window wall. Prior studies of prototypical holographic glazings, installed above conventional 'view' windows, have shown increased daylight levels over a deeper perimeter area than clear glass, for selected sun positions. We report on the simulation of the energy performance of prototypical holographic glazings assuming a commercial office building in the inland Los Angeles climate. The simulation of the energy performance involved determination of both luminous and thermal performance. Since the optical complexity of holographic glazings prevented the use of conventional algorithms for the simulation of their luminous performance, we used a newly developed method that combines experimentally determined directional workplace illuminance coefficients with computer-based analytical routines to determine a comprehensive set of daylight factors for many sun positions. These daylight factors were then used within the DOE-2.1D energy simulation program to determine hourly daylight and energy performance over the course of an entire year for four window orientations. Since the prototypical holographic diffractive structures considered were applied on single pane clear glass, we also simulated the performance of hypothetical glazings, assuming the daylight performance of the prototype holographic glazings and the thermal performance of double-pane and low-e glazings. Finally, we addressed various design and implementation issues towards potential performance improvement. DOE

N95-17376 Department of the Navy, Washington, DC.
MAGNETOSTRICTIVE TORQUE SENSOR Patent
Howard T. Savage, inventor (to Navy), Arthur E. Clark, inventor (to Navy), Marilyn Wun-Fogle, inventor (to Navy), Lawrence T. Kabacoff, inventor (to Navy), and Antonio Hernando, inventor (to Navy) 31 May 1994 6 p Filed 23 Oct. 1992
(AD-D016376; US-Patent-5,315,881; US-Patent-Appl-SN-965329; US-Patent-Class-73-862.333) Avail: US Patent and Trademark Office

Magnetostrictive wire having a low surface-to-volume ratio established by a constant nonplanar cross-section is helically deformed into contact with a shaft under a stress maintaining the wire in fixed relation to the shaft surface. Magnetic anisotropy is imparted to the wire by twist thereof about its cross-sectional axis while the wire is being helically deformed into contact with the shaft surface to form a torque sensor through which accurate torque detection is achieved. DTIC

N95-17380# Lawrence Livermore National Lab., Livermore, CA.
PHYSICAL AND CHEMICAL SENSOR TECHNOLOGIES DEVELOPED AT LAWRENCE LIVERMORE NATIONAL LABORATORY
J. W. Balch, D. Ciarlo, J. Folta, R. Glass, K. Hagans, F. Milanovich, and S. Sheem 10 Aug. 1993 10 p Presented at the Sensors Expo Conference, Philadelphia, PA, 26-28 Oct. 1993
(Contract W-7405-eng-48)
(DE94-012231; UCRL-JC-114823; CONF-9310146-2) Avail: CASI HC A02/MF A01

The increasing emphasis on environmental issues, waste reduction, and improved efficiency for industrial processes has mandated the development of new chemical and physical sensors for field or in-plant use. The Lawrence Livermore National Laboratory (LLNL) has developed a number of technologies for sensing physical and chemical properties. Physical sensors of pressure, temperature, acceleration, acoustic vibration spectra, and ionizing radiation have been developed. Sensors developed at LLNL for chemical species include inorganic solvents, heavy metal ions', and gaseous atoms and compounds. Primary sensing technologies we have employed have been based on optical fibers, semiconductor optical or radiation detectors, electrochemical activity, micromachined electromechanical (MEMs) structures, or chemical separation technologies. The complexities of these sensor systems range from single detectors to more advanced micro-instruments on-a-chip. For many of the sensors we have developed the necessary intelligent electronic support systems for both local and remote sensing applications. Each of these sensor technologies are briefly described in the remaining sections of this paper. DOE

N95-17428 Department of the Navy, Washington, DC.
MAGNETOSTRICTIVE TRANSDUCER SYSTEM HAVING A THREE DUAL-STRIP FIBER OPTIC MAGNETOSTRICTIVE TRANSDUCERS BONDED INTO A SINGLE FIBER MACH-ZEHNDER INTERFEROMETER Patent

Frank Bucholtz, inventor (to Navy), Kee P. Koo, inventor (to Navy), and Dominique M. Dagenais, inventor (to Navy) 19 Apr. 1994 10 p Filed 29 Jan. 1993
(AD-D016373; US-Patent-5,305,075; US-Patent-Appl-SN-012140; US-Patent-Class-356-345) Avail: US Patent and Trademark Office

The fiber-optic magnetostrictive transducer system consists of a sensing element having three dual-strip fiber optic magnetostrictive transducers bonded into a single fiber Mach-Zehnder interferometer operating single mode mounted in a symmetrical orthogonal geometry. The dual-strip fiber optic magnetostrictive transducers have predictable and consistent reproducibility and are comprised of a pair of field annealed metallic glass strips bonded to a coil of optical fiber. This structure is in turn mounted on a bobbin structure where the fiber ribbon is attached to the bobbin only at the two ends of the bobbin. This reduces the possible loading of the transducer due to friction between the optical fiber and the surface of the mounting structure and at the same time provide a long sensing fiber in contact with the magnetostrictive element for high sensitivity. The symmetrical orthogonal arrangement of the transducers minimizes magnetic crosstalk and the strip form of the transducer elements maintain high directional sensitivity. DTIC

N95-17522# Lawrence Livermore National Lab., Livermore, CA.
MINIATURE, VACUUM COMPATIBLE 1024 (TIMES) 1024 CCD CAMERA FOR X RAY, ULTRAVIOLET, OR OPTICAL IMAGING
A. D. Conder, J. Dunn, and B. K. F. Young May 1994 5 p Presented at the 10th Topical Conference on High-Temperature Plasma Diagnostics, Rochester, NY, 8-12 May 1994
(Contract W-7405-eng-48)
(DE94-012235; UCRL-JC-117170; CONF-940552-4) Avail: CASI HC A01/MF A01

We have developed a very compact (60 (times) 60 (times) 75 mm(exp 3)), vacuum compatible, large format (25(times) 25 mm(exp 2), 1024 (times) 1024 pixels) CCD camera for digital imaging of visible and ultraviolet radiation, soft to penetrating x-rays (less than 20 keV), and charged particles. This camera provides a suitable replacement for film with a linear response, dynamic range and intrinsic signal-to-noise response superior than current x-ray film, and provides real-time access to the data. The spatial resolution of the camera (less than 25 micrometer) is similar to typical digitization slit or step sizes used in processing film data. This new large format CCD camera has immediate applications as the recording device for steak cameras or gated microchannel plate diagnostic, or when used directly as the detector for x-ray, XUV, or optical signals. This is especially important in studying high-energy plasmas produced in pulse-power, ICF, and high powered laser-plasma experiments, as well as other medical and industrial applications. DOE

N95-17895*# Case Western Reserve Univ., Cleveland, OH. Electronics Design Center.
THE DEVELOPMENT OF A SOLID-STATE HYDROGEN SENSOR FOR ROCKET ENGINE LEAKAGE DETECTION Final Technical Report
Chung-Chiun Liu 1994 8 p
(Grant NAG3-1149)
(NASA-CR-197567; NAS 1.26:197567) Avail: CASI HC A02/MF A01

Hydrogen propellant leakage poses significant operational problems in the rocket propulsion industry as well as for space exploratory applications. Vigorous efforts have been devoted to minimizing hydrogen leakage in assembly, test, and launch operations related to hydrogen propellant. The objective has been to reduce the operational cost of assembling and maintaining hydrogen delivery systems. Specifically, efforts have been made to develop a hydrogen leak detection system for point-contact measurement. Under the auspices of Lewis Research Center, the Electronics Design Center at Case Western Reserve University, Cleveland, Ohio, has undertaken the development of a point-contact hydrogen gas sensor with potential applications to the hydrogen propellant industry. We envision a sensor array consisting of numbers of discrete hydrogen sensors that can be located in potential leak sites. Silicon-based microfabrication and micromachining techniques are used in the fabrication of these sensor prototypes. Evaluations of the sensor are carried out in-house at Case Western Reserve University as well as at Lewis Research Center and GenCorp Aerojet, Sacramento, California. The hydrogen gas sensor is not only applicable in a hydrogen propulsion system, but also usable in many other civilian and industrial settings. This includes vehicles or facility use, or in the production of hydrogen gas. Dual space and commercial uses of these point-contacted hydrogen sensors are feasible and will directly meet the needs and objectives of NASA as well as various industrial segments. Derived from text

N95-16273# Kazan Aviation Inst. (USSR).
THEORY OF ONE-DIMENSIONAL AND TWO-DIMENSIONAL DISTRIBUTED SENSORS FOR MEASURING THE SPATIAL CHARACTERISTICS OF THERMOPHYSICAL AND HYDRODYNAMIC FIELDS
Yu. K. Evdokimov and M. P. Vyaselev *In* Nanjing Univ. of Aeronautics and Astronautics, Joint Proceedings on Aeronautics and Astronautics (JPAA) 157-160 (SEE N95-16249 04-01) May 1993 (For primary document see N95-16249 04-01)
Avail: CASI HC A01/MF A03

N95-17208*# National Aeronautics and Space Administration. Goddard Space Flight Center, Greenbelt, MD.
LESSONS LEARNED SUPPORTING ONBOARD SOLID-STATE RECORDERS
Jeff Shi (RMS Technologies, Inc., Landover, MD.), Tony Mao (RMS Technologies, Inc., Landover, MD.), Tim Clotworthy (RMS Technologies, Inc., Landover, MD.), and Gerald Grebowsky *In its* Third International Symposium on Space Mission Operations and Ground Data Systems, Part 1 Nov. 1994 p 257-264 (For primary document see N95-17179 04-17)
Avail: CASI HC A02/MF A06

36 LASERS AND MASERS

Includes parametric amplifiers.
For related information see also *76 Solid-State Physics*.

N95-16166# Yale Univ., New Haven, CT. Dept. of Applied Physics.
HIGH-INTENSITY AND HIGH ENERGY LASER INTERACTIONS WITH SINGLE DROPLETS Final Report, 1 Feb. 1991 - 31 Mar. 1994
Richard K. Chang 29 Apr. 1994 24 p
(Contract DAAL03-91-G-0042)
(AD-A281415; ARO-28489.11-GS) Avail: CASI HC A03/MF A01

Our research accomplishments have been in five main areas: (1) third-order sum frequency generation in the volume of the droplet and the role of phase-matching condition with droplet-cavity modes which are standing waves; (2) retention of acoustic phonons generated by stimulated Brillouin scattering (SBS) and the role of these long-lived acoustic waves and photons in 'seeding' the SBS during the subsequent input-laser pulse; (3) stimulated low-frequency scattering from anisotropic molecules in droplets and the effect of the low-frequency scattering process in causing the elastic scattering spectrum and the stimulated Raman scattering (SRS) spectrum to be asymmetrically broadened; (4) resonance Raman enhancement of the SRS gain coefficient with the intent to increase the sensitivity of SRS to minor species in the droplet; and (5) the use of population inverted laser-dye molecules to provide extra gain for SRS from minor species in the droplet. DTIC

N95-16353# Arizona Univ., Tucson, AZ. Optical Sciences Center.
THEORY OF CARRIER HEATING THROUGH INJECTION PUMPING AND LASING IN SEMICONDUCTOR MICROCAVITY LASERS
F. Jahnke and S. W. Koch 1 Sep. 1993 4 p Repr. from Optics Letters, v. 18, no. 17 p 1438-1440
(Contract DAAL03-90-G-0329)
(AD-A281795; ARO-30482.9-PH) Avail: CASI HC A01/MF A01

Nonequilibrium carrier distributions in microcavity lasers are computed by solution of a quantum Boltzmann equation that includes carrier-carrier-phonon, and carrier-photon scattering as well as the pump process. A significant heating of the carrier plasma is observed as a consequence of the Pauli blocking of carrier injection and the removal of cold carriers through the process of stimulated recombination. DTIC

N95-16486# Oak Ridge National Lab., TN.
A CO2 LASER POLARIMETER FOR MEASUREMENT OF PLASMA CURRENT PROFILE IN ALCATOR C-MOD

C. H. Ma, D. P. Hutchinson, R. K. Richards, J. Irby (Massachusetts Inst. of Tech., Cambridge.), and T. Luke (Massachusetts Inst. of Tech., Cambridge.) 1994 13 p Presented at the 10th Topical Conference on High-Temperature Plasma Diagnostics, Rochester, NY, 8-12 May 1994
(Contract DE-AC05-84OR-21400)
(DE94-014017; CONF-940552-10) Avail: CASI HC A03/MF A01

A multichannel infrared polarimeter system for measurement of the plasma current profile in Alcator C-Mod has been designed, constructed, and tested. The system utilizes a cw CO2 laser at a wavelength of 10.6 microns. An electro-optic polarization-modulation technique has been used to achieve the high sensitivity required for the measurement. The recent results of the measurements as well as the feasibility of its application on ITER are presented. DOE

N95-16548# Aerospace Corp., El Segundo, CA. Technology Operations.
A AgGaSe2 OPTICAL PARAMETRIC OSCILLATOR PUMPED BY A RAMAN-SHIFTED YAG LASER Report, Sep. 1990 - Oct. 1991
Sherwin T. Amimoto, Rolf W. Gross, M. Jupina, J. Machan, and Lissa S. Garman-DuVall 2 Sep. 1994 14 p
(Contract F04701-88-C-0089)
(AD-A284743; TR-0090(5930-07)-2; SMC-TR-94-34) Avail: CASI HC A03/MF A01

The operation of a AgGaSe2, infrared parametric oscillator pumped by a Raman-shifted YAG laser at 1.9 micrometers is reported. Output energies up to 1.2 mJ were measured near 4.5 micrometers with a photon conversion efficiency of 10%. Phase matching is possible to produce outputs over the 2.3 to 12.0 micrometer region. Fluence thresholds as low as 0.031 J/sq cm were measured using an 8-ns pump pulse. The thresholds were shown to be cavity-length dependent in agreement with theory. No optical damage was observed at fluences up to 0.18 J/sq cm at the 1.9 micrometers pump wavelength. DTIC

N95-16917 Sandia National Labs., Albuquerque, NM.
TUNABLE UV SOURCE FOR UV FLUORESCENCE REMOTE SENSING
R. D. Mead (Aculight Corp., Bellevue, WA.), D. D. Lowenthal (Aculight Corp., Bellevue, WA.), T. D. Raymond, W. J. Alford, A. V. Smith, and M. S. Johnson 1994 5 p Presented at the 1994 Caliope Interim Technical Review, Oakland, CA, 26-28 Apr. 1994 Limited Reproducibility: More than 20% of this document may be affected by microfiche quality
(Contract DE-AC04-94AL-85000)
(DE94-015745; SAND-94-1436C; CONF-9404162-9) Avail: CASI HC A01

Efficient generation of ultraviolet radiation tunable over the 240-410 nm range has been achieved in a system suitable for ultraviolet (UV) fluorescence remote sensing. Light from an Optical Parametric Oscillator/Amplifier turning in the 0.7-2.1 micrometer range is mixed with the second or third harmonic from a Nd:YAG laser, to obtain up to 30 mJ of broadly tunable output in the ultraviolet. DOE

N95-16929 Lawrence Livermore National Lab., Livermore, CA.
FAST ELECTRONS, FILAMENTED LASER LIGHT, AND THE FAST IGNITOR
W. L. Kruer and S. C. Wilks Feb. 1994 11 p Presented at the 11th International Workshop on Laser Interaction and Related Plasma Phenomena, Monterey, CA, 25-29 Oct. 1993 Limited Reproducibility: More than 20% of this document may be affected by microfiche quality
(Contract W-7405-eng-48)
(DE94-015898; UCRL-JC-114062; CONF-931048-16) Avail: CASI HC A03

We report on the absorption of laser energy that results when an ultra-intense laser pulse is incident onto a sharp vacuum-plasma boundary, where the initial shelf density of the plasma is much greater than the critical density, n(sub cr). It is found that 2-D effects greatly increase the amount of absorption into hot electrons, over the amount predicted using 1-D theory. In particular, a scaling for the absorption as a function of density, for a fixed laser intensity, implies that the absorption will be of order 30 percent for densities well in excess of The interaction is studied using both 1- and 2- dimensional particle-in-cell (PIC) 100 n(sub cr) simulations. The 1-D results agree quite well with a simple scaling of JxB heating, where the laser electric field penetrates a skin depth into the overdense plasma and subsequently heats electrons. In 2-D, when the laser is incident at an angle, the absorption is seen to increase substantially due to a form of resonant absorption that occurs in steep density profiles. We find that the inclusion of kinetic and multi-dimensional effects are crucial to obtaining a complete picture of the interaction. The ability of ultra-intense lasers to produce acceptable amounts of hot electrons necessary for the fast ignitor fusion concept will also be assessed. DOE

N95-17168# Lawrence Livermore National Lab., Livermore, CA.
PROPERTIES OF Ce:LiSrAlF6 AND Ce:LiCaAlF6 ULTRAVIOLET LASERS
C. D. Marshall, S. A. Payne, J. A. Speth, J. B. Tassano, W. F. Krupke, G. J. Quarles (Lightning Optical Corp., Tarpon Springs, FL.), V. Castillo (Lightning Optical Corp., Tarpon Springs, FL.), and B. H. T. Chai (University of Central Florida, Orlando, FL.) Jan. 1994 14 p Presented at the OE/LASE 1994: Conference on Optics, Electro-Optics, and Laser Applications in Science and Engineering, Los Angeles, CA, 22-29 Jan. 1994
(Contract W-7405-eng-48)
(DE94-013737; UCRL-JC-114987; CONF-940142-41) Avail: CASI HC A03/MF A01

The ultraviolet laser properties of LiSrAlF6 doped with trivalent cerium (Ce:LiSAF) and LiCaAlF6 (Ce:LiCAF) are reported. Polarized absorption, emission and excited state absorption cross sections for both Ce:LiSAF and Ce:LiCAF were determined for 266 mn pump and 290 nm laser emission wavelengths. The single exponential emission lifetime was measured to be 28 +/- 2 and 25 +/- 2 ns for Ce:LiSAF and Ce:LiCAF, respectively. The gain was found to be highest when the probe was polarized parallel to the optic axis of the crystal due to the anisotropic nature of the excited state absorption. The excited state absorption is ascribed to a transition from the 5d orbital of Ce(3+) to the conduction band of the host. Laser slope efficiencies of up to 29% and 21% were for Ce:LiSAF and Ce:LiCAF when the 266 nm pulsed pump beam was parallel to the optic or c-axis. These are the highest law slope efficiencies yet observed for any known solid-state ultraviolet laser material. When the pump beam was polarized perpendicular to the optic axis of the crystals, the gain and laser efficiencies dropped by up to an order of magnitude. The magnitude of pump-induced solarization was found to be highly variable for different crystals, and to have insignificant impact on the laser performance when favorable, crystals were utilized. DOE

N95-17302 Department of the Navy, Washington, DC.
WAVELENGTH DISPERSIVE GAIN ELEMENT FOR A TUNABLE LASER Patent
Richard Scheps, inventor (to Navy) 26 Apr. 1994 17 p Filed 20 May 1993
(AD-D016381; US-Patent-5,307,358; US-Patent-Appl-SN-067504; US-Patent-Class-372-20) Avail: US Patent and Trademark Office

A tunable laser is described in which the gain element is fabricated to produce wavelength dispersion within the laser resonator cavity. Specifically, the laser gain element has Brewster angled entrance and exit faces which allow it to operate as a wavelength dispersive element while simultaneously performing the functions of an optical gain element within a laser cavity. Wavelength tuning is effected by angular rotation of one of the end reflective elements in the cavity. By using suitable dispersive materials for the laser gain element no additional tuning elements are required providing high efficiency, low threshold laser operation for a variety of optical excitation methods. The laser gain element replaces other discrete intracavity laser tuning means required for tunable lasers, including prisms, diffraction gratings, and birefringent filter elements. Solid state crystalline laser gain elements which are doped with impurity ions for laser operation are highly suitable for this type of laser, as are ion doped glasses or other amorphous materials. In addition, a suitable laser gain element can be constructed of a hollow fluid-containing cell where the cell is fabricated in the shape of a Brewster dispersing prism and the cell is filled with a laser gain fluid such as a dye solution or a chelate solution. Optical exciting means and geometries are discussed, as are the conditions for minimizing astigmatism introduced by the prism. DTIC

N95-17303# Naval Postgraduate School, Monterey, CA.
SIMULATIONS OF AN FEL PRODUCING COHERENT X RAYS UTILIZING THE SLAC LINAC M.S. Thesis
Joseph B. Hall Jun. 1994 45 p
(AD-A283524) Avail: CASI HC A03/MF A01

Due to its tunability and high efficiency, the free electron laser (FEL) has proven to be a versatile coherent light source for a variety of applications

in science, industry, and defense. This unique capability provides the scientific community with its first realistic source for an x ray laser. This thesis will initially consider the basics of the FEL and its applications as a defensive weapon. In a technological era where the missile has maximized its physical capabilities to the point that defensive missiles are physically incapable of achieving a kill in protection of the fleet, speed of light weapons are the next logical step in defense. Next we shall explore the theory behind the free electron laser and the amplification of a beam of light by transferring energy from an electron beam. In conclusion, we examine the proposal to utilize the Stanford Linear Accelerator Center (SLAC) linac as an electron beam source for a high power x ray FEL. Compressing the electron pulse to sub-picosecond length yields a peak current of 2500 amps. An electron beam energy of 7 GeV would result in a radiation wavelength of 4 nm and peak optical power in the gigawatt range. In order to examine this proposal, single-mode phase space simulations are run to look at the effectiveness of electron bunching and the onset of saturation. Longitudinal multimode simulations show coherence development and the trapped-particle instability. Transverse multimode simulations examine the effects of optical guiding and mode distortion. DTIC

N95-17337 Old Dominion Univ., Norfolk, VA. Dept. of Physics.
SDIO/IST ULTRASHORT WAVELENGTH. MOSSBAUER AND GAMMA RAY STUDIES FOR GRASERS Final Report, period ending 30 Apr. 1994
Gilbert R. Hoy Jun. 1994 17 p Limited Reproducibility: More than 20% of this document may be affected by microfiche quality
(Contract N00014-90-K-2003)
(AD-A283091) Avail: Issuing Activity (Defense Technical Information Center (DTIC))

Ideas of making gamma-ray lasers and focusing gamma rays have fascinated scientists for many years. Over the past 30 years a number of important scientific and technological advances have been made which motivated the research whose results are presented here. Such developments included: the discovery of the Mossbauer Effect, the ability to fabricate perfect single crystals, the ability to structure materials on an atomic scale, the development of synchrotron radiation facilities, and the experimental realization of the consequences of the so-called dynamical theory of x-ray diffraction. Although the consequences of the dynamical theory using x radiation have been thoroughly explored, relatively little research has been done using gamma radiation. The dynamical theory predicts that radiation can pass through perfect single crystals that are 100 times thicker than one would normally expect. A specific goal of the proposed research was to search for this anomalous transmission effect using gamma radiation. This was to be accomplished by making measurements on radioactively doped single crystals. The general goal in proposing this research was to begin to provide a foundation of experimental evidence in this new field of gamma-ray optics which may lead to technical advances that parallel those in atomic, optical, and solid state physics, e.g., focusing, lasers, enhanced or inhibited spontaneous emission, coupled atom-cavity modes, and superradiance. DTIC

N95-17464 Department of the Navy, Washington, DC.
METHOD OF RAPID SAMPLE HANDLING FOR LASER PROCESSING Patent
Stephen D. Russell, inventor (to Navy), Douglas A. Sexton, inventor (to Navy), and Eugene P. Kelley, inventor (to Navy) 21 Jun. 1994 8 p Filed 31 Mar. 1992
(AD-D016408; US-Patent-5,323,013; US-Patent-Appl-SN-861409) Avail: US Patent and Trademark Office

A method of rapid sample handling in a production environment for laser processing of individual microelectronic die is particularly suited for handling partially fabricated die and die which are susceptible to mechanical and electrostatic damage, such as backside illuminated CCD's requiring backside dopant activation and laser texturing of sidewalls. Securing a die within a modified sample holder provides for electrostatic and mechanical protection during laser processing. Placing the modified die holder onto a feeder base portion that engages a tractor-feed translation subsystem protects the die during a translation and positioning of the die below and aligned with a laser processing structure. A window holder is engaged with the die holder to seal the die in a processing chamber and to assure an appropriate pressurizing with a gaseous ambient for a desired processing. Illuminating, repetitively if desired, the die in the chamber with a laser beam of appropriate size, laser fluence, repetition rate and number of pulses processes the die. Next, the processed die is translated from beneath laser processing structure while the next die is correctly positioned for processing. DTIC

N95-17498# Sandia National Labs., Albuquerque, NM.
PHASE-LOCKED ARRAYS OF VERTICAL-CAVITY SURFACE-EMITTING LASERS
M. E. Warren, G. R. Hadley, K. L. Lear, P. L. Gourley, G. A. Vawter, J. C. Zolper, T. M. Brennan, and B. E. Hammons May 1994 26 p
(Contract DE-AC04-94AL-85000)
(DE94-014941; SAND-94-1125) Avail: CASI HC A03/MF A01

Vertical Cavity Surface-Emitting Lasers (VCSEL's) are of increasing interest to the photonics community because of their surface-emitting structure, simple fabrication and packaging, wafer-level testability and potential for low cost. Scaling VCSEL's to higher power outputs requires increasing the device area, which leads to transverse mode control difficulties if devices become larger than 10-15 microns. One approach to increasing the device size while maintaining a well controlled transverse mode profile is to form coupled or phase-locked, two-dimensional arrays of VCSEL's that are individually single-transverse mode. The authors have fabricated and characterized both photopumped and electrically injected two-dimensional VCSEL arrays with apertures over 100 microns wide. Their work has led to an increased understanding of these devices and they have developed new types of devices, including hybrid semiconductor/dielectric mirror VCSEL arrays, VCSEL arrays with etched trench, self-aligned, gold grid contacts and arrays with integrated phase-shifters to correct the far-field pattern. DOE

N95-17500 Phillips Lab., Kirtland AFB, NM.
THERMAL EFFECTS IN END-HEATED LASER RODS: A TIME-DEPENDENT MODEL AND DIAGNOSTIC Final Report, Feb. - Nov. 1993
Dana C. Kopf May 1994 98 p Limited Reproducibility: More than 20% of this document may be affected by microfiche quality
(AD-A282007; AD-E202015; PL-TR-93-1079) Avail: CASI HC A05

Unwanted heat generated in optically-pumped solid-state lasers causes thermal gradients, strain, and thermal expansion which in turn results in a nonuniform optical path difference (OPD) increase across the gain media. This ultimately results in poor beam quality. An interferometric based diagnostic for experimentally determining the time-dependent OPD change in an optically heated media was developed. This device is demonstrated by heating a glass (BK7) window with a CO2 laser, effectively simulating high power end-pumping in a rod. Temporal OPD changes are measured by automated counting of interference fringes as they are generated by the thermal effects. A two-dimensional, time dependent model is developed to describe the radial temperature distribution in a cylinder, the stress and strain distributions, the thermal expansion, and the associated OPD change caused by a Gaussian heat source. This compared to the experimental data for the BK7 window to determine the validity of the approximations and its usefulness for other systems. Good agreement between the model and experiment, within 10% was observed. DTIC

N95-17627 Lawrence Livermore National Lab., Livermore, CA.
DEVELOPMENT OF X-RAY LASER ARCHITECTURAL COMPONENTS
A. S. Wan, L. B. DaSilva, J. C. Moreno, R. C. Cauble, E. A. Chandler, H. E. Dalhed, S. B. Libby, R. W. Mayle, J. Nilsen, and R. P. Ratowsky et al Jun. 1994 11 p Presented at the 4th International Colloquium on X-Ray Lasers, Williamsburg, VA, 16-20 May 1994 Limited Reproducibility: More than 20% of this document may be affected by microfiche quality
(Contract W-7405-eng-48)
(DE94-016446; UCRL-JC-117488; CONF-940592-1) Avail: CASI HC A03

This paper describes the recent experimental and computational development of short-pulse, enhanced-coherence, and high-brilliance x-ray lasers (XRL's). The authors will describe the development of an XRL cavity by injecting laser photons back into an amplifying XRL plasma. Using a combination of LASNEX/GLF/SPECTRE-BEAM3 codes, they obtained good agreement with experimental results. They will describe the adaptive spatial filtering technique used to design small-aperture shaped XRL's with near diffraction-limited output. Finally they will discuss issues concerning the development of high-brilliance XRL architecture, with emphasis on scaling the XRL aperture. Combining these advances in XRL

architectural components allows them to develop a short-pulse, high-brilliance, coherent XRL suitable for applications in areas such as biological holography, plasma interferometry, and nonlinear optics. DOE

N95-17635 Lawrence Livermore National Lab., Livermore, CA.
AN X RAY TECHNIQUE FOR PRECISION LASER BEAM SYNCHRONIZATION
O. L. Landen, R. A. Lerche, R. G. Hay, B. A. Hammel, D. Kalantar, and M. D. Cable 2 May 1994 15 p Presented at the 10th Topical Conference on High-Temperature Plasma Diagnostics, Rochester, NY, 8-12 May 1994 Limited Reproducibility: More than 20% of this document may be affected by microfiche quality
(Contract W-7405-eng-48)
(DE94-016449; UCRL-JC-115599; CONF-940552-18) Avail: CASI HC A03

A new x-ray technique for recording the relative arrival times of multiple laser beams at a common target with better than +/- 10 ps accuracy has been implemented at the Nova laser facility. 100 ps, 3(omega) Nova beam are focused to separate locations on a gold ribbon target viewed from the side. The measurement consists of using well characterized re-entrant x ray streak cameras for 1-dimensional streaked imaging of the greater than 3 keV x rays emanating from these isolated laser plasmas. After making the necessary correction for the differential laser, x ray and electron transit times involved, timing offsets as low as +/- 7 ps are resolved, and on subsequent shots, corrected for, verified and independently checked. This level of synchronization proved critical in meeting the power balance requirements for indirectly-driven pulse-shaped Nova implosions. DOE

N95-17680# Oak Ridge National Lab., TN.
DESIGN OF A CO2-LASER THOMSON SCATTERING ION-TAIL DIAGNOSTIC FOR ALCATOR C-MOD
R. K. Richards, D. P. Hutchinson, and C. H. Ma 1994 12 p Presented at the 10th Topical Conference on High-Temperature Plasma Diagnostics, Rochester, NY, 8-12 May 1994
(Contract DE-AC05-84OR-21400)
(DE94-018056; CONF-940552-30) Avail: CASI HC A03/MF A01

A CO2-laser Thomson scattering diagnostic ha s been designed for the measurement of the ICRH-produced ion tail on Alcator C-Mod. The plasma parameters and port access require that the detection of scattered radiation be made at small angles, typically one degree or less. The receiver system consists of five heterodyne detectors and the source laser produces an energy of 10 Joules per pulse with a 1 to 5 microsecond pulse length. The scattering system is currently being installed on the Alcator C-Mod experiment. Details of the diagnostic, calculations of the expected measurements, and application of the diagnostic for ITER are presented. DOE

N95-17688# Lawrence Livermore National Lab., Livermore, CA.
BEAM CHARACTERISTICS OF A LARGE-BORE COPPER LASER WITH A RADIATIVELY COOLED PLASMA
J. J. Chang, C. D. Boley, W. A. Molander, B. E. Warner, and M. W. Martinez (Martin Marietta Energy Systems, Inc., Livermore, CA.) 18 Jan. 1994 10 p Presented at the OE/LASE 1994: Conference on Optics, Electro-Optics, and Laser Applications in Science and Engineering, Los Angeles, CA, 22-29 Jan. 1994
(Contract W-7405-eng-48)
(DE94-015139; UCRL-JC-114954; CONF-940142-42) Avail: CASI HC A02/MF A01

In a large-bore copper vapor laser (CVL), excessive gas heating at the axial region of the discharge lowers its efficiency by thermally populating the metastable lower laser levels. The associated lower gas density also lengthens the discharge field-diffusion time, leading to weaker axial pumping and undesired beam characteristics. The authors' laboratory has developed a novel approach to circumvent this obstacle by cooling the plasma radiatively via a series of segmented metal plates (septa) placed vertically along the length of the tube. This improved tube design significantly lowers the average gas temperature and shortens the radial delay. A 27% increase in laser power was observed with the addition of septa. The authors have characterized the beam intensity profile, spatial and temporal pulse variation, and beam polarization through extensive laboratory measurements. A detailed computational model of the laser has been used to characterize and interpret the laboratory results. DOE

N95-17689# Lawrence Livermore National Lab., Livermore, CA.
HIGH-AVERAGE-POWER, DIODE-PUMPED SOLID STATE LASERS FOR ENERGY AND INDUSTRIAL APPLICATIONS
W. F. Krupke 2 Mar. 1994 12 p Presented at the 6th International Symposium on Advanced Nuclear Energy Research, Mito, Japan, 23-25 Mar. 1994
(Contract W-7405-eng-48)
(DE94-015142; UCRL-JC-115511; CONF-9403144-1) Avail: CASI HC A03/MF A01

Progress at LLNL in the development high-average-power diode-pumped solid state lasers is summarized, including the development of enabling technologies. DOE

N95-17698 Department of the Navy, Washington, DC.
RARE EARTH ION DOPED CW CASCADE FIBER LASER Patent
Leon Esterowitz, inventor (to Navy) and Roger E. Allen, inventor (to Navy) 17 May 1994 8 p Filed 30 Oct. 1992
(AD-D016370; US-Patent-5,313,477; US-Patent-Appl-SN-968890; US-Patent-Class-372-6) Avail: US Patent and Trademark Office

A continuous wave (CW) activator ion doped fiber laser is presented which lases at a normally self-terminating laser transition at a slope efficiency greater than that achieved by a self-terminating fiber laser. Two laser transitions, one corresponding to a self-terminating laser transition and the other to a transition out of the lower level of the self-terminating transition, are simultaneously stimulated in the activator ion doped fiber. Through simultaneous lasing of the two wavelengths corresponding to these transitions, the lower level of the self-terminating transition is sufficiently depopulated so that CW operation is achieved. DTIC

N95-17729# California Univ., Berkeley. Lawrence Berkeley Lab, CA.
ADVANCES IN ULTRAFAST SCANNING PROBE MICROSCOPY
S. Weiss, D. Botkin, D. F. Ogletree, M. Salmeron, and D. S. Chemla May 1994 5 p Presented at the 9th International Conference on Ultrafast Phenomena, Dana Point, CA, 1-5 May 1994 Prepared in cooperation with California Univ., Berkeley, CA
(Contract DE-AC03-76SF-00098)
(DE94-018180; LBL-35220; CONF-940593-14) Avail: CASI HC A01/MF A01

We review the development of the ultrafast scanning tunneling microscope. Experimental results on the tunneling gap response to a short voltage pulse excitation are presented. DOE

N95-17887# California Univ., Berkeley. Lawrence Berkeley Lab, CA.
ULTRAFAST SCANNING PROBE MICROSCOPY
D. Botkin, S. Weiss, D. F. Ogletree, M. Salmeron, and D. S. Chemla Jan. 1994 7 p Presented at the OE/LASE 1994: Conference on Optics, Electro-Optics, and Laser Applications in Science and Engineering, Los Angeles, CA, 22-29 Jan. 1994
(Contract DE-AC03-76SF-00098)
(DE94-018186; LBL-35089; CONF-940142-46) Avail: CASI HC A02/MF A01

The authors have developed a general technique which combines the temporal resolution of ultrafast laser spectroscopy with the spatial resolution of scanned probe microscopy (SPM). Using this technique with scanning tunneling microscopy (STM), they have obtained simultaneous 2 ps time resolution and 50 (angstrom) spatial resolution. This improves the time resolution currently attainable with STM by nine orders of magnitude. The potential of this powerful technique for studying ultrafast dynamical phenomena on surfaces with atomic resolution is discussed. DOE

N95-17239*# Allied-Signal Aerospace Co., Seabrook, MD.
ADVANCED TECHNOLOGIES IN THE ASI MLRO TOWARDS A NEW GENERATION LASER RANGING SYSTEM
Thomas Varghese and Giuseppe Bianco (Italian Space Agency, Matera.) *In* NASA. Goddard Space Flight Center, Third International Symposium on Space Mission Operations and Ground Data Systems, Part 1 Nov. 1994 p 525-530 (For primary document see N95-17179 04-17)
Avail: CASI HC A02/MF A06

37 MECHANICAL ENGINEERING

Includes auxiliary systems (nonpower); machine elements and processes; and mechanical equipment.

N95-16031*# Florida State Univ., Tallahassee, FL. College of Engineering.

LUNAR SURFACE OPERATIONS. VOLUME 3: ROBOTIC ARM FOR LUNAR SURFACE VEHICLE Annual Report

William Shields, Salah Feteih, and Patrick Hollis Jul. 1993 122 p
(Contract NASw-4435)
(NASA-CR-195553-Vol-3; NAS 1.26:195553-Vol-3) Avail: CASI HC A06/MF A02

A robotic arm for a lunar surface vehicle that can help in handling cargo and equipment, and remove obstacles from the path of the vehicle is defined as a support to NASA's intention to establish a lunar based colony by the year 2010. Its mission would include, but not limited to the following: exploration, lunar sampling, replace and remove equipment, and setup equipment (e.g. microwave repeater stations). Performance objectives for the robotic arm include a reach of 3 m, accuracy of 1 cm, arm mass of 100 kg, and lifting capability of 50 kg. The end effectors must grip various sizes and shapes of cargo; push, pull, turn, lift, or lower various types of equipment; and clear a path on the lunar surface by shoveling, sweeping aside, or gripping the obstacle present in the desired path. The arm can safely complete a task within a reasonable amount of time; the actual time is dependent upon the task to be performed. The positioning of the arm includes a manual backup system such that the arm can be safely stored in case of failure. Remote viewing and proximity and positioning sensors are incorporated in the design of the arm. The following specific topic are addressed in this report: mission and requirements, system design and integration, mechanical structure, modified wrist, structure-to-end-effector interface, end-effectors, and system controls. CASI

N95-16139# Mechanical Technology, Inc., Latham, NY.

TWIN DISC GEAR TOOTH SIMULATOR Final Report, 30 Jun. 1986 - 30 Dec. 1993

Martin W. Eusepi and James F. Dill May 1994 125 p
(Contract F33615-86-C-2622)
(AD-A284927; MTI-94-TR-28; WL-TR-94-2055) Avail: CASI HC A06/MF A02

This report describes the results of an effort to develop a disc on disc test rig for evaluating lubricant load capacity. The goal of the program has been to develop a reliable disc on disc (or Twin Disc) test rig capable of providing more reliable and lower cost evaluation of lubricant load capacity than the Ryder gear test which is currently used. Disc rigs have been evaluated for this application in the past, but have failed to provide scuffing results which are comparable to those found in gear tests. The unique feature of the rig designed and evaluated under this program is a drive system design which varies the disc to disc sliding and rolling speeds in a fixed manner to simulate the combined rolling and sliding motion found in a gear tooth contact. Other features include a drive system design which insures that the same points on each disc always contact each other as they rotate, and material selection and heating system design for operation with experimental lubricants at temperatures up to 700 deg F. DTIC

N95-16224# Los Alamos National Lab., NM.

OPTICAL WHEEL-ROTATION SENSOR

L. Veeser, P. Rodriguez, P. Forman, and M. Deeter (National Inst. of Standards and Technology, Boulder, CO.) 1994 6 p Presented at the 10th Optical Fibre Sensors Conference, Glasgow, Scotland, 11-13 Oct. 1994
(Contract W-7405-eng-36)
(DE94-011719; LA-UR-94-1310; CONF-9410103-2) Avail: CASI HC A02/MF A01

We describe a fiber-optic rotation sensor based on diffraction of light in a magneto-optic crystal, bismuth iron garnet (BIG). Exploitation of this effect permits the construction of a sensor requiring no polarization elements or lenses. DOE

N95-16543# Department of the Navy, Washington, DC.

DIFFUSION WELD TEST FIXTURE Patent Application

Wendell Maciejewski, inventor (to Navy), Roger Tyron, inventor (to Navy), George Kavarnos, inventor (to Navy), Elizabeth McLaughlin, inventor (to Navy), and Kurt Janecek, inventor (to Navy) 9 Jun. 1994 23 p
(AD-D016450; US-Patent-Appl-SN-268341) Avail: CASI HC A03/MF A01

A weld joint test fixture for testing the strength of a weld joining several members forming a test specimen is provided. The fixture includes a base which supports the test specimen and an attachment for applying a testing force to the test specimen while the test specimen is supported by the base. The fixture further includes holding elements attached to the base for holding the test specimen on the base during the application of the testing force. The holding elements preferably engage one of the members forming the test specimen without engaging another of the members. The fixture may also include the holding elements being designed to oppose the testing force substantially only by forces directed in a plane parallel to the applied testing force. DTIC

N95-16636# Southwest Research Inst., San Antonio, TX. Belvoir Fuels and Lubricants Research Facility.

BENCH WEAR AND SINGLE-CYLINDER ENGINE EVALUATIONS OF HIGH-TEMPERATURE LUBRICANTS FOR US ARMY GROUND VEHICLES Interim Report, Jan. 1990 - Sep. 1993

Paul I. Lacey, Edwin A. Frame, and Douglas M. Yost Sep. 1994 220 p
(Contracts DAAK70-87-C-0043; DAAK70-92-C-0059)
(AD-A285399; BFLRF-291) Avail: CASI HC A10/MF A03

High-temperature lubricant (HTL) requirements for future U.S. Army ground vehicles were investigated. A single-cylinder diesel engine (SCE-903) was successfully modified to operate at increased cylinder liner temperatures and to serve as an evaluation tool for HTL's. Oil D, one of six lubricants evaluated, completed 200 test hours at an average cylinder wall temperature of 247 deg C and an oil sump temperature of 166 deg C with only minor oil degradation. However, improved piston cleanliness is desired. A wide range of bench scale wear techniques have been developed to highlight different lubricant performance characteristics, with particular emphasis on high-temperature operation and oxidation. Based on the bench tests, Oil D would be expected to have inadequate high-temperature, long-term wear protection. Oil D passed the Allison C-4 graphite clutch friction test. DTIC

N95-16900*# Michigan State Univ., East Lansing, MI. Dept. of Mechanical Engineering.

AN INVESTIGATION OF FLUID FLOW DURING INDUCTION STROKE OF A WATER ANALOG MODEL OF AN IC ENGINE USING AN INNOVATIVE OPTICAL VELOCIMETRY CONCEPT: LIPA Final Report

Bernd Stier and R. E. Falco Aug. 1994 285 p
(Grant NAG1-1106)
(NASA-CR-197451; NAS 1.26:197451) Avail: CASI HC A13/MF A03

Optical measurements on an axisymmetrical quartz component engine research model were made to evaluate the flow field encountered during induction. The measurement technique is LIPA (Laser Induced Photochemical Anemometry), a non-intrusive velocimetry concept that provides an investigator of fluid flow with a tool to attain planar information about three-dimensional velocity and vorticity vectors in a single measurement step. The goal of this investigation is to further develop this measurement technique and apply it to study the induction stroke of a water analog model of a four-stroke internal combustion engine. The research conducted in the water analog model is a fundamental scientific inquiry into the flow fields that develop in the induction stroke of an engine at idling engine speeds. As this is the first investigation of its kind using LIPA technique, our goal has been to quantify, in a preliminary manner, the flow field features that develop during the intake stroke. In the process a more comprehensive understanding of the flow field features was developed, and tied to the quantification. The study evaluated the flow field of the intake stroke by estimating fields of velocity and vorticity. On the basis of these data, information about fluid dynamics during induction at engine speeds of 10, 20, and 30 RPM (corresponding to 170, 340, and 510 RPM respectively, when air is the flowing medium) for three different valve lifts was obtained. The overall development of the flow field, its energy content (kinetic, fluctuation) for the different settings of the engine parameters, vorticity information, and cyclic variations have been quantified. These have been discussed in terms of mixing performance. Author

N95-16907*# National Aeronautics and Space Administration. Lewis Research Center, Cleveland, OH.

A REVIEW OF TRANSMISSION DIAGNOSTICS RESEARCH AT NASA LEWIS RESEARCH CENTER

James J. Zakajsek Dec. 1994 24 p

(RTOP 505-62-36)

(NASA-TM-106746; E-9158; NAS 1.15:106746) Avail: CASI HC A03/MF A01

This paper presents a summary of the transmission diagnostics research work conducted at NASA Lewis Research Center over the last four years. In 1990, the Transmission Health and Usage Monitoring Research Team at NASA Lewis conducted a survey to determine the critical needs of the diagnostics community. Survey results indicated that experimental verification of gear and bearing fault detection methods, improved fault detection in planetary systems, and damage magnitude assessment and prognostics research were all critical to a highly reliable health and usage monitoring system. In response to this, a variety of transmission fault detection methods were applied to experimentally obtained fatigue data. Failure modes of the fatigue data include a variety of gear pitting failures, tooth wear, tooth fracture, and bearing spalling failures. Overall results indicate that, of the gear fault detection techniques, no one method can successfully detect all possible failure modes. The more successful methods need to be integrated into a single more reliable detection technique. A recently developed method, NA4, in addition to being one of the more successful gear fault detection methods, was also found to exhibit damage magnitude estimation capabilities. Author

N95-17162# Pennsylvania State Univ., University Park, PA. Dept. of Mechanical Engineering.

AN IN-CYLINDER STUDY OF THE PARTICULATE/NO(x) TRADE-OFF IN A DI DIESEL ENGINE

T. A. Litzinger, D. A. Santavicca, and R. J. Santoro 1994 29 p

(Contract DE-AS04-87AL-42880)

(DE94-014599; DOE/AL-42880/T1) Avail: CASI HC A03/MF A01

The goal of the work performed during the contract period was to establish the ability to study soot and NO within the combustion chamber of a DI diesel engine and to couple these measurements with actual exhaust emissions. This work was motivated by the need to obtain a more complete understanding of the particulate/NO(x) trade-off, observed in diesel engines, to aid engine designers in meeting emissions limits. In order to achieve the desired goal, an optically accessible DI diesel engine was designed and constructed. Also, planar imaging methods for imaging soot and NO were developed in laboratory flames and were then applied to the engine. For the study of soot, planar Mie scattering was used and a polarization ratio method was investigated to distinguish soot from fuel droplets. The Mie scattering technique proved to be well suited for the engine, and extensive results were obtained. In order to observe NO, planar laser induced fluorescence was used and it was successfully applied in the engine. In addition to these techniques, high speed combustion photography and shadowgraph photography were applied to obtain general characteristics of the combustion process. As a final diagnostic, actual engine emissions were measured. This report begins with a brief discussion of the problem under investigation and a summary of other studies of the NO(x)/particulate trade-off. Following these sections is a summary of the accomplishments and results from the present study. DOE

N95-17169# Midwest Research Inst., Golden, CO. National Renewable Energy Lab.

ANALYSIS OF A TWO-BLADED, TEETERING-HUB TURBINE USING THE ADAMS (TM) SOFTWARE

A. D. Wright, R. O. Osgood, and D. J. Malcolm (Lynette, R. and Associates, Redmond, WA.) May 1994 10 p Presented at the American Wind Energy Association Annual Conference and Exhibition, Minneapolis, MN, 9-13 May 1994

(Contract DE-AC36-83CH-10093)

(DE94-006922; NREL/TP-442-6477; CONF-940548-1) Avail: CASI HC A02/MF A01

A major goal of the federal wind energy program is the rapid development and validation of structural models to determine loads and response for a wide variety of different wind turbine configurations operating under extreme conditions. Such codes are crucial to the successful design of future advanced wind turbines. In cooperation with R. Lynette & Associates the Wind Technology Division at NREL has developed a full system dynamics model of the AWT-26 PI machine, using the Automatic Dynamic analysis of Mechanical Systems (ADAMS) software from Mechanical Dynamics, Inc. In this paper, we show validation of sub-models by comparisons with modal test data. We describe the most important system modes involved in this structure and demonstrate how the ADAMS model can be used to tune the structure to avoid interactions. We also identify questions that remain unanswered by ADAMS in modeling this turbine and recommend future directions that DOE code development activities should take. DOE

N95-17263*# National Aeronautics and Space Administration. Lewis Research Center, Cleveland, OH.

ATOMIC OXYGEN DURABILITY EVALUATION OF THE FLEXIBLE BATTEN FOR THE PHOTOVOLTAIC ARRAY MAST ON SPACE STATION

Curtis R. Stidham (NYMA, Inc., Brook Park, OH.), Sharon K. Rutledge, Edward A. Sechkar (Cleveland State Univ., OH.), David S. Flaherty (Cleveland State Univ., OH.), David M. Roig (Cleveland State Univ., OH.), and Jonathan L. Edwards (Ohio Aerospace Inst., Brook Park.) Dec. 1994 24 p Presented at the 1995 International Solar Energy Conference, Lahaina, HI, 19-24 Mar. 1995; sponsored by ASME, JSME, and JSES

(Contract NAS3-27186; RTOP 233-01-OE)

(NASA-TM-106798; E-9270; NAS 1.15:106798) Avail: CASI HC A03/MF A01

A test program was conducted at the National Aeronautics and Space Administration's Lewis Research Center (LeRC) to evaluate the long term low Earth orbital (LEO) atomic oxygen (AO) durability of a flexible (fiberglass-epoxy composite) batten. The flexible batten is a component used to provide structural rigidity in the photovoltaic array mast on Space Station. The mast is used to support and articulate the photovoltaic array, therefore, the flexible batten must be preloaded for the 15 year lifetime of an array blanket. Development hardware and composite materials were evaluated in ground testing facilities for AO durability and dynamic retraction-deployment cyclic loading representative of expected full life in-space application. The CV1144 silicone (AO protective) coating was determined to provide adequate protection against AO degradation of the composite material and provided fiber containment, thus the structural integrity of the flexible batten was maintained. Both silicone coated and uncoated flexible battens maintained load carrying capabilities. Results of the testing did indicate that the CV1144 silicone protective coating was oxidized by AO reactions to form a brittle glassy (SiO_2) skin that formed cracking patterns on all sides of the coated samples. The cracking was observed in samples that were mechanically stressed as well as samples in non-stressed conditions. The oxidized silicon was observed to randomly spall in small localized areas, on the flexible battens that underwent retraction-deployment cycling. Some darkening of the silicon, attributed to vacuum ultraviolet (VUV) radiation, was observed. Author

N95-17335 Army Engineer Waterways Experiment Station, Vicksburg, MS. Structures Lab.

A MODEL FOR ASSESSMENT OF DYNAMIC INTERACTION BETWEEN MAGNETICALLY LEVITATED VEHICLES AND THEIR SUPPORTING GUIDEWAYS Final Report

James C. Ray and Mostafiz R. Chowdhury Jul. 1994 75 p Limited Reproducibility: More than 20% of this document may be affected by microfiche quality

(AD-A283088; WES/TR/SL-94-15) Avail: CASI HC A04

This report describes the development and verification of an analytical model to study the dynamic interaction between a moving maglev-type vehicle and its supporting flexible guideway, referred to as vehicle/guideway interaction (VGI). The theoretical basis and computer coding for the model are described in detail. For verification purposes, the model is applied to a very simple case study and compared to a closed-form solution to the same problem. The results compared very closely, indicating that the model provides an accurate VGI analysis tool. To demonstrate the use of the model, it is applied to an actual Maglev system. The result from this analysis also compared very closely to those from similar analyses using different analytical methods. The VGI model has two distinct applications: it can be used to accurately predict the vehicle ride quality to be expected from a given vehicle and guideway design and to accurately predict the dynamic deflections and stresses experienced throughout the guideway structure as a result of a vehicle passage. Ride quality results are necessary

to design a vehicle suspension system and to determine the guideway stiffness required to meet specific ride quality criteria. Dynamic structural analyses are necessary to produce safe, economical, and accurate guideway designs. DTIC

N95-17364# General Electric Environmental Services, Inc., Lebanon, PA.
COAL-FUELED DIESEL TECHNOLOGY DEVELOPMENT EMISSIONS CONTROL
W. VanKleunen, S. Kaldor, E. Gal, M. Mengel, and M. Arnold Jan. 1994 622 p
(Contract DE-AC21-88MC-23174)
(DE94-004096; DOE/MC-23174/3699) Avail: CASI HC A99/MF A06

General Electric Environmental Services, Inc. (GEESI), Emissions Control program activity ranged from control concept testing of 10 CFM slipstream from a coal-water-slurry (CWS) fuel single cylinder research diesel engine to the design, installation, and operation of a full-size emissions control system for a full-size CWS fuel diesel engine designed for locomotive operation. Early 10 CFM slipstream testing program activity was performed to determine emissions characteristics and to evaluate emissions control concepts such a barrier filtration, granular bed filtration, and cyclone particulate collection for reduction of particulate and gaseous emissions. Use of sorbent injection into the engine exhaust gas upstream of the barrier filter or use of sorbent media in the granular bed filter were found to provide reduction of exhaust gas SO2 and NO(x) in addition to collection of ash particulate. Emergence of the use of barrier filtration as a most practical emissions control concept disclosed a need to improve cleanability of the filter media in order to avoid reduction of turbocharger performance by excessive barrier filter pressure drop. The next progression of program activity, after the slipstream feasibility state, was 500 CFM cold flow testing of control system concepts. The successful completion of 500 CFM cold flow testing of the envelope filter led to a subsequent progression to a similar configuration envelope filter designed to operate at 500 CFM hot gas flow from the CWS fuel research diesel engine in the GETS engine test laboratory. This envelope filter included the design aspect proven by cold flow testing as well as optimization of the selection of the installed filter media. DOE

N95-17366 Sandia National Labs., Albuquerque, NM.
DECENTRALIZED SLIDING MODE CONTROL OF NONLINEAR FLEXIBLE ROBOTS
G. G. Parker, R. D. Robinett, D. J. Segalman, and D. J. Inman (Virginia Polytechnic Inst., Blacksburg, VA.) 1994 18 p Presented at the 2nd International Conference on Motion and Vibration Control, Yokohama, Japan, 31 Aug. - 3 Sep. 1994 Limited Reproducibility: More than 20% of this document may be affected by microfiche quality
(Contract DE-AC04-94AL-85000)
(DE94-013790; SAND-94-0337C; CONF-940849-1) Avail: CASI HC A03

A technique using augmented sliding mode control for robust, real-time control of flexible multiple link robots is presented. For the purpose of controller design, the n-link, n-joint robot is subdivided into n single joint, single link subsystems. A sliding surface for each subsystem is specified so as to be globally, asymptotically stable. Each sliding surface contains rigid-body angular velocity, angular displacement, and flexible body generalized velocities. The flexible body generalized accelerations are treated as disturbances during the controller design. This has the advantage of not requiring explicit equations for the flexible body motion. The result is n single input, single output controllers acting at the n joints of the robot, controlling rigid body angular displacement and providing damping for flexible body modes. Furthermore, the n controllers can be operated in parallel so that computation speed is independent of the number of links, affording real-time, robust control. DOE

N95-17430 Carnegie-Mellon Univ., Pittsburgh, PA. Robotics Inst.
ON PERFORMABILITY THEORY AND THE INVERSE SLIDING PROBLEM
Wesley H. Huang Mar. 1994 19 p Limited Reproducibility: More than 20% of this document may be affected by microfiche quality
(AD-A282847; CMU-RI-TR-94-05) Avail: CASI HC A03

For a given robot, we would like to know its capabilities and limitations. The question of what tasks a robot is capable of executing has been asked with increasing frequency as researchers explore the central issues of robotics. The theory that would answer this question is referred to here as performability theory. One approach to performability theory is to examine the mechanics of the robot and the task. However, a complete model of the mechanics of a real robot and its environment quickly becomes intractable. The inverse sliding problem involves simple mechanics; it deals with a planar world in which objects are free to translate and rotate but are subject to the forces of Coulomb friction. The problem is to determine the initial translational and rotational velocities required for an object to slide to a given final configuration. A solution is presented to a portion of the inverse sliding problem, which is proposed as the basis for a physically realistic yet simple world in which we can start to formulate the basic ideas of performability theory. DTIC

N95-17461 Department of the Navy, Washington, DC.
METHOD AND APPARATUS FOR REDUCING AXIAL THRUST IN CENTRIFUGAL PUMPS Patent
Alan S. Palmer, inventor (to Navy), John W. Henry, IV, inventor (to Navy), and John P. Kerr, inventor (to Navy) 14 Jun. 1994 6 p Filed 21 Sep. 1992
(AD-D016404; US-Patent-5,320,482; US-Patent-Appl-SN-947593; US-Patent-Class-415-104) Avail: US Patent and Trademark Office

A control stator comprising a plurality of stationary vanes, ribs, or cavities is provided in a centrifugal pump having a shrouded impeller. The function of the control stator is to slow the swirl of fluid in the cavity between the casing and the impeller front shroud and thereby provide a very cost effective solution to the problem of excess axial thrust. The control stator is a simple, inexpensive non-rotating part that can be affixed in an existing space in the pump casing between the casing wall and the front shroud of the impeller. DTIC

N95-17621# Naval Postgraduate School, Monterey, CA. Dept. of Mechanical Engineering.
REPEATABILITY IN REDUNDANT MANIPULATOR SYSTEMS
Ranjan Mukherjee 22 Feb. 1994 39 p
(AD-A282957; NPS-ME-94-003) Avail: CASI HC A03/MF A01

Terrestrial manipulators with more DOF than the dimension of the workspace and space manipulators with as many manipulator DOF as the dimension of the workspace are both redundant systems. An interesting problem of such redundant systems has been the repeatability problem due to the presence of nonholonomic constraints. We show, contrary to the existing belief, that integrability of the nonholonomic constraints is not a necessary condition for the repeatability of the configuration variables. There exist certain trajectories in the independent configuration variable space that are like 'holonomic loops' along which the redundant manipulators exhibit repeatable motion. We present a simple method based on optimization techniques for designing repeatable trajectories for free-flying space manipulators and terrestrial manipulators under pseudoinverse control. DTIC

N95-17716# Allied-Signal Aerospace Co., Kansas City, MO.
ELECTRON BEAM WELD DEVELOPMENT ON A FILTER PACK ASSEMBLY
J. P. Dereskiewicz Jun. 1994 48 p
(Contract DE-AC04-76DP-00613)
(DE94-015867; KCP-613-5431) Avail: CASI HC A03/MF A01

A continuous electron beam welding procedure was developed to replace the manual gas tungsten arc welding procedure on the Filter Pack Assembly. A statistical study was used to evaluate the feasibility of electron beam welding 6061-T6 aluminum covers to A356 cast weldments throughout the joint tolerance range specified on product drawings. Peak temperature exposures were not high enough to degrade the heat sensitive electrical components inside the cast weldment. Actual weldments with alodine coating on the weld joint area were successfully cleaned using a nonmetallic fiberglass brush cleaning method. DOE

N95-17717# Lawrence Livermore National Lab., Livermore, CA.
WPH-6112A THERMAL EXPANSION TEST OF PRESS TUBULATION
D. D. Kautz, R. L. Sites, and W. R. Cobb 26 May 1994 10 p
(Contract W-7405-eng-48)
(DE94-015946; UCRL-ID-117530) Avail: CASI HC A02/MF A01

We recently performed the WPH-6112A thermal expansion test of the lower portion of the PRESS program tubulation. The objective of the test was to determine whether the tubulation welds could withstand typical

stresses from a 1200 C thermal cycle. Test components failed in two areas: (1) the friction welded Monel to Vanadium tube fitting at the dissimilar metal interface and fell against the outer vanadium tube wall causing it to fail, and (2) the thin-walled, outer stainless steel tubing failed by cracking at the weld. Both failures were due to irregular occurrences for this system. We feel that the strength of all weldments is adequate to withstand the normal thermal stresses from a 1200 C cycle without failing prematurely. DOE

N95-17725# Yankee Scientific, Inc., Medfield, MA.
NONPOWERED INSTANT WATER HEATER Final Report, Mar. - Oct. 1993
Eric C. Guyer Aug. 1994 45 p
(Contract DAAK60-93-C-0022)
(AD-A285459; Natick-TR-94/028) Avail: CASI HC A03/MF A01

The technical feasibility of a nonpowered instantaneous water heater based on the use of a condensing steam ejector pump has been established by test of a commercially available ejector. Using steam at approximately 25 PSIG pressure, it has been demonstrated that water can be simultaneously heated and pumped to pressures up to two times the steam pressure. The overall system concept is that of a lightweight, portable heater package that is fired with a constant-run, manually-controlled burner. The concept can accommodate the operation of a constant-run burner with only intermittent water delivery, as in a kitchen use, by recirculation of heated water back to the supply tank/barrel. With outlet water pressure greater than the inlet steam pressure, the unit can incorporate automatic feed of makeup water to the steam generator. The system concept can be implemented in a range of outputs. At 100,000 Btu/hr burner output and 50% efficiency, system capability would be at about 0.8 GPM continuously with a 100 deg F temperature rise, 1.5 GPM continuously with about a 50 deg rise, or 1.5 GPM intermittently at 100 F rise and 50%/50% on-off delivery duty cycle. DTIC

N95-17928# Cambridge Univ., Cambridge (England). Dept. of Engineering.
STUDY OF THE FOLDING AND DEPLOYMENT ASPECTS OF A COLLAPSIBLE RIB TENSIONED SURFACE (CRTS) ANTENNA REFLECTOR
Z. You and S. Pellegrino 15 Mar. 1994 50 p
(ESTEC Order 125396) (ISSN 0309-7447)
(CUED/D-STRUCT/TR-144) Avail: CASI HC A03/MF A01

This report presents the results of a study on the folding and deployment of the CRTS antenna reflector, a novel concept under development by the European Space Technology Centre (ESTEC). The CRTS reflector consists of three elements: a parabolic membrane, a series of foldable ribs, and an expandable hub. The present, generic investigation of the folding and deployment properties of the CRTS reflector has focussed mainly on a small scale, symmetric reflector. The study was divided into two separate phases. The key aims of the first phase were: to identify suitable packaging techniques; to demonstrate their feasibility; and to examine related critical issues, such as the possibility of rib interference during deployment, or possible damage of the membrane. The key aim of the second phase was to obtain an understanding of the deployment process, for a selected packaging technique, in order to analyze the duration of deployment and the stresses induced in the membrane and in the ribs. All of these objectives have been achieved and key results have been validated experimentally. Three packaging methods for CRTS reflectors have been identified and analyzed in detail. Each method is based on a folding pattern whose geometry has been fully worked out and hence can be implemented without difficulty. A trade-off between the three packaging methods has been carried out. Two selected folding schemes have been tested experimentally and a folding apparatus has been developed for the selected packaging scheme, which involves a zig-zag folding of each rib. The scheme is the best in terms of ease of implementation and is joint best in terms of packaging efficiency. A simple folding apparatus has been developed to implement this packaging scheme and, with it, the folding operation has been repeated many times on a 1 m model reflector. Deployment tests have been carried out on the model, packaged in this way. A detailed experimental investigation of the large displacement, large rotation behavior of a rib has been carried out, leading to a full characterization of the moment/rotation relationship of the rib. Numerical investigations of the deployment process have been carried out with the ABAQUS finite element package. Also, an analytical technique has been developed especially for this study. Deployment experiments on small scale ribs with a single fold have proved to be a most valuable tool in assessing the validity of these numerical models. Author

N95-16267# Nanjing Univ. of Aeronautics and Astronautics, Nanjing, Jiangsu (China). Research Inst. of Vibration Engineering.
RESEARCHES ON GEAR FAULT DIAGNOSIS TECHNIQUES
Ming Bao and Chunsheng Zhao *In its* Joint Proceedings on Aeronautics and Astronautics (JPAA) May 1993 p 118-123 See also A93-20811 (For primary document see N95-16249 04-01)
Avail: CASI HC A02/MF A03

N95-16280# Nanjing Univ. of Aeronautics and Astronautics, Nanjing, Jiangsu (China). Dept. of Mechanical Engineering.
AN IMPROVED POSITION/FORCE CONTROL OF MANIPULATORS
Xiaoxi Huang, Sicong Li, and Jianying Zhu *In its* Joint Proceedings on Aeronautics and Astronautics (JPAA) May 1993 p 209-213 (For primary document see N95-16249 04-01)
Avail: CASI HC A01/MF A03

N95-16349# Marotta Scientific Controls, Inc., Montville, NJ.
A LIFTING BALL VALVE FOR CRYOGENIC FLUID APPLICATIONS
Joseph M. Cardin, Robert H. Reinicke, and Stephen D. Bruneau *In* JHU, The 1993 JANNAF Propulsion Meeting, Volume 2 Nov. 1993 p 297-312 (For primary document see N95-16324 04-20)
Avail: CASI HC A03/MF A04

38 QUALITY ASSURANCE AND RELIABILITY

Includes product sampling procedures and techniques; and quality control.

N95-16421 Stanford Univ., CA. Dept. of Operations Research.
EFFICIENT ESTIMATION OF THE MEAN TIME BETWEEN FAILURES IN NON-REGENERATIVE DEPENDABILITY MODELS
Peter W. Glynn, Philip Heidelberger, Victor Nicola, and Perwez Shahabuddin Aug. 1993 8 p Limited Reproducibility: More than 20% of this document may be affected by microfiche quality
(Contract DAAL03-91-G-0319)
(AD-A281563; ARO-29412.3-MA-SDI) Avail: Issuing Activity (Defense Technical Information Center (DTIC))

In this paper we discuss fast simulation techniques for estimating the steady-state mean time between failures (MTBF) in non-Markovian models of highly dependable systems. The key is to use a ratio representation of the MTBF, in which the denominator is closely related to the probability of a rare event and is therefore amenable to estimation using importance sampling. A simulation methodology based on splitting and batch means, used for steady-state estimation in non-regenerative systems, can then be employed. Experiments using this methodology yield good results. DTIC

N95-16538# Ames Lab., IA.
SUPPORT MINIMIZED INVERSION OF ACOUSTIC AND ELASTIC WAVE SCATTERING Ph.D. Thesis
A. Safaeinili 24 Apr. 1994 109 p
(Contract W-7405-eng-82)
(DE94-014233; IS-T-1672) Avail: CASI HC A06/MF A02

This report discusses the following topics on support minimized inversion of acoustic and elastic wave scattering: minimum support inversion; forward modeling of elastodynamic wave scattering; minimum support linearized acoustic inversion; support minimized nonlinear acoustic inversion without absolute phase; and support minimized nonlinear elastic inversion. DOE

N95-16870# Little (Arthur D.), Inc., Cambridge, MA.
VECTOR MAGNETOMETRY AND LIGHTWAVE DEFECT IMAGING SENSOR TECHNOLOGIES FOR INTERNAL PIPE INSPECTION SYSTEMS: PHASE 1 AND 2 FEASIBILITY STUDY, CONCEPTUAL DESIGN, AND PROTOTYPE DEVELOPMENT Final Report, Mar. 1991 - Jul. 1993
Steven Carroll, Thomas Fowler, Edward Peters, Wendy Power, and Michael Reed 5 Jan. 1994 104 p

(Contract GRI-5089-271-20931)
(PB94-194198; ADL-66163; GRI-93/0442) Avail: CASI HC A06/MF A02

The Gas Research Institute (GRI) has been sponsoring the development of a vehicle and sensors for an integrated nondestructive internal inspection system for natural gas distribution pipes. Arthur D. Little has developed two sensor technologies; Vector Magnetometry (VM) and Lightwave Defect Imaging (LDI) for the system.The Vector Magnetometry sensor utilizes multiple arrays of miniature detection coils (fluxgate magnetometer elements): a three-axis array measures both the amplitude and phase of the magnetic leakage field that occurs in the vicinity of pipe wall defects. This technology is applicable to both cast iron and steel pipe. Derived from text

N95-17360# Sandia National Labs., Albuquerque, NM.
THE APPLICATION OF NON-DESTRUCTIVE TECHNIQUES TO THE TESTING OF A WIND TURBINE BLADE
H. Sutherland, A. Beattie, B. Hansche, W. Musial (National Renewable Energy Lab., Golden, CO.), J. Allread (National Renewable Energy Lab., Golden, CO.), J. Johnson (National Renewable Energy Lab., Golden, CO.), and M. Summers (United Technologies Corp., West Palm Beach, FL.) Jun. 1994 61 p
(Contract DE-AC04-94AL-85000)
(DE95-000323; SAND-93-1380) Avail: CASI HC A04/MF A01

NonDestructive Testing (NDT), also called NonDestructive Evaluation (NDE), is commonly used to monitor structures before, during, and after testing. This paper reports on the use of two NDT techniques to monitor the behavior of a typical wind turbine blade during a quasi-static test-to-failure. The two NDT techniques used were acoustic emission and coherent optical. The former monitors the acoustic energy produced by the blade as it is loaded. The latter uses electron shearography to measure the differences in surface displacements between two load states. Typical results are presented to demonstrate the ability of these two techniques to locate and monitor both high damage regions and flaws in the blade structure. Furthermore, this experiment highlights the limitations in the techniques that must be addressed before one or both can be transferred, with a high probability of success, to the inspection and monitoring of turbine blades during the manufacturing process and under normal operating conditions. DOE

N95-17385*# National Aeronautics and Space Administration. Lewis Research Center, Cleveland, OH.
STATISTICAL ANALYSIS OF MICROGRAVITY EXPERIMENT PERFORMANCE USING THE DEGREES OF SUCCESS SCALE
Bernadette Upshaw (Raytheon Co., Brook Park, OH.), Ying-Hsin Andrew Liou (Cleveland State Univ., OH.), and Daniel P. Morilak Nov. 1994 13 p Presented at the Symposium on Analysis and Optimization, Panama City, FL, 7-9 Sep. 1994; sponsored by NASA, AIAA, USAF, and ISSMO
(Contract NAS3-26764; RTOP 323-42-04)
(NASA-TM-106791; E-9251; NAS 1.15:106791; AIAA Paper 94-4311)
Avail: CASI HC A03/MF A01

This paper describes an approach to identify factors that significantly influence microgravity experiment performance. Investigators developed the 'degrees of success' scale to provide a numerical representation of success. A degree of success was assigned to 293 microgravity experiments. Experiment information including the degree of success rankings and factors for analysis was compiled into a database. Through an analysis of variance, nine significant factors in microgravity experiment performance were identified. The frequencies of these factors are presented along with the average degree of success at each level. A preliminary discussion of the relationship between the significant factors and the degree of success is presented. Author

N95-17507 Northrop Corp., Pico Rivera, CA. B-2 Div.
EDDY CURRENT FOR DETECTING SECOND LAYER CRACKS UNDER INSTALLED FASTENERS Final Report, 1 Oct. 1991 - 1 Nov. 1993
William R. Sheppard Apr. 1994 64 p Limited Reproducibility: More than 20% of this document may be affected by microfiche quality
(Contract F33615-91-C-5660)
(AD-A282412; WL-TR-94-4006) Avail: CASI HC A04

The detection of second layer Cracks Under Fasteners (CUF) persists as an Air Force Logistics need. This work seeks to extend technology developed for detecting cracks in aluminum alloy substructure below graphite-epoxy skins, to structures with an aluminum first layer. Improvements to the design of the Northrop Low Frequency Eddy Current Array (LFECA) system are identified to improve sensitivity to CUFs in aluminum-over-aluminum structures. The probe core shape, dimensions, and coil configurations were optimized for detection with installed fasteners and metallic skin. A multiparameter analysis algorithm is applied to enable flaw discrimination from centering variations, edge responses and other sources of noise. The study also quantifies the capabilities and limitations of the LFECA system. DTIC

N95-16338*# National Aeronautics and Space Administration. Goddard Space Flight Center, Greenbelt, MD.
NONDESTRUCTIVE EXAMINATION OF THE TRMM RCS PROPELLANT TANKS
James M. Free *In* JHU, The 1993 JANNAF Propulsion Meeting, Volume 2 Nov. 1993 p 169-179 (For primary document see N95-16324 04-20)
Avail: CASI HC A03/MF A04

N95-17237*# National Aeronautics and Space Administration. Goddard Space Flight Center, Greenbelt, MD.
PRODUCTION AND QUALITY ASSURANCE AUTOMATION IN THE GODDARD SPACE FLIGHT CENTER FLIGHT DYNAMICS FACILITY
K. B. Chapman (Computer Sciences Corp., Lanham, MD.), C. M. Cox (Computer Sciences Corp., Lanham, MD.), C. W. Thomas (Computer Sciences Corp., Lanham, MD.), O. O. Cuevas, and R. M. Beckman *In its* Third International Symposium on Space Mission Operations and Ground Data Systems, Part 1 Nov. 1994 p 509-516 (For primary document see N95-17179 04-17)
(Contract NAS5-31500)
Avail: CASI HC A02/MF A06

39 STRUCTURAL MECHANICS

Includes structural element design and weight analysis; fatigue; and thermal stress.

For applications see *05 Aircraft Design, Testing and Performance* and *18 Spacecraft Design, Testing and Performance.*

N95-15953# CSA Engineering, Inc., Palo Alto, CA.
GUIDE TO ASIAC COMPUTER PROGRAMS Final Report, Feb. 1991 - Jan. 1994
Gordon R. Negaard Jul. 1994 35 p
(Contract F33615-90-C-3211)
(AD-A285354; WL-TR-94-3127) Avail: CASI HC A03/MF A01

ASIAC is an on-site contractor to the Structures Division of the Wright Laboratory's Flight Dynamics Directorate. In analyzing and solving aerospace structures technical problems, ASIAC utilizes approximately ninety structural analysis computer codes. The computer programs range from small codes, designed for special purposes, to large general purpose structural mechanics codes. These computer programs can be useful tools to a designer or manufacturer to use to calculate internal mechanical and thermal stresses, predict structural strength, stiffness, weight, fatigue life, or to design for minimum weight and maximum life. This handbook discusses the capabilities of each program and provides guidance in selecting a code to meet an individual need. DTIC

N95-16068*# Pennsylvania State Univ., University Park, PA.
DAMAGE-MITIGATING CONTROL OF SPACE PROPULSION SYSTEMS FOR HIGH PERFORMANCE AND EXTENDED LIFE Final Report
Asok Ray and Min-Kuang Wu Cleveland, OH NASA Mar. 1994 95 p
(Grant NAG3-1240; RTOP 584-03-11)
(NASA-CR-194470; E-8605; NAS 1.26:194470) Avail: CASI HC A05/MF A01

A major goal in the control of complex mechanical system such as spacecraft rocket engine's advanced aircraft, and power plants is to achieve high performance with increased reliability, component durability, and maintainability. The current practice of decision and control systems synthesis focuses on improving performance and diagnostic capabilities under constraints that often do not adequately represent the materials degradation.

In view of the high performance requirements of the system and availability of improved materials, the lack of appropriate knowledge about the properties of these materials will lead to either less than achievable performance due to overly conservative design, or over-straining of the structure leading to unexpected failures and drastic reduction of the service life. The key idea in this report is that a significant improvement in service life could be achieved by a small reduction in the system dynamic performance. The major task is to characterize the damage generation process, and then utilize this information in a mathematical form to synthesize a control law that would meet the system requirements and simultaneously satisfy the constraints that are imposed by the material and structural properties of the critical components. The concept of damage mitigation is introduced for control of mechanical systems to achieve high performance with a prolonged life span. A model of fatigue damage dynamics is formulated in the continuous-time setting, instead of a cycle-based representation, for direct application to control systems synthesis. An optimal control policy is then formulated via nonlinear programming under specified constraints of the damage rate and accumulated damage. The results of simulation experiments for the transient upthrust of a bipropellant rocket engine are presented to demonstrate efficacy of the damage-mitigating control concept. Author

N95-16072*# Applied Research Associates, Inc., Raleigh, NC.
PORTABLE PARALLEL STOCHASTIC OPTIMIZATION FOR THE DESIGN OF AEROPROPULSION COMPONENTS Final Report
Robert H. Sues and G. S. Rhodes Cleveland, OH NASA Oct. 1994 62 p Original contains color illustrations
(Contract NAS3-26839; RTOP 324-01-00)
(NASA-CR-195312; E-8725; NAS 1.26:195312) Avail: CASI HC A04/MF A01; 2 functional color pages

This report presents the results of Phase 1 research to develop a methodology for performing large-scale Multi-disciplinary Stochastic Optimization (MSO) for the design of aerospace systems ranging from aeropropulsion components to complete aircraft configurations. The current research recognizes that such design optimization problems are computationally expensive, and require the use of either massively parallel or multiple-processor computers. The methodology also recognizes that many operational and performance parameters are uncertain, and that uncertainty must be considered explicitly to achieve optimum performance and cost. The objective of this Phase 1 research was to initialize the development of an MSO methodology that is portable to a wide variety of hardware platforms, while achieving efficient, large-scale parallelism when multiple processors are available. The first effort in the project was a literature review of available computer hardware, as well as review of portable, parallel programming environments. The first effort was to implement the MSO methodology for a problem using the portable parallel programming language, Parallel Virtual Machine (PVM). The third and final effort was to demonstrate the example on a variety of computers, including a distributed-memory multiprocessor, a distributed-memory network of workstations, and a single-processor workstation. Results indicate the MSO methodology can be well-applied towards large-scale aerospace design problems. Nearly perfect linear speedup was demonstrated for computation of optimization sensitivity coefficients on both a 128-node distributed-memory multiprocessor (the Intel iPSC/860) and a network of workstations (speedups of almost 19 times achieved for 20 workstations). Very high parallel efficiencies (75 percent for 31 processors and 60 percent for 50 processors) were also achieved for computation of aerodynamic influence coefficients on the Intel. Finally, the multi-level parallelization strategy that will be needed for large-scale MSO problems was demonstrated to be highly efficient. The same parallel code instructions were used on both platforms, demonstrating portability. There are many applications for which MSO can be applied, including NASA's High-Speed-Civil Transport, and advanced propulsion systems. The use of MSO will reduce design and development time and testing costs dramatically. Author

N95-16102# Army Research Lab., Watertown, MA. Materials Directorate.
SPECIAL HYBRID STRESS FINITE ELEMENTS FOR THE ANALYSIS OF INTERFACE STRESS DISTRIBUTION IN ADHESIVE JOINTS Final Report
Erik Saether and Kristen Weight May 1994 78 p
(AD-A281612; ARL-TR-449) Avail: CASI HC A05/MF A01

The widespread application of adhesively bonded joints has necessitated the development of methodology to predict ultimate static joint strength and service life under cyclic loading. Due to the complexity of mathematically modeling adhesive joint response, analytical treatments are limited to highly idealized joint configurations simplified assumed stress states, applied loading, and material behavior. To overcome these limitations, a specialized finite element-based numerical approach is investigated wherein special 2-D and 3-D layered finite elements are formulated to improve the computational efficiency and accuracy of determining stresses in adhesive joints. The hybrid stress technique is used to explicitly enforce stress equilibrium throughout the element domain and stress continuity conditions at layer interfaces. The emphasis of this research is to explore a variety of possible element configurations to assess element performance. The optimum 2-D and 3-D element formulations demonstrate improved performance compared to standard displacement-based finite elements in predicting joint stresses. DTIC

N95-16245# Army Research Lab., Aberdeen Proving Ground, MD.
CONSIDERATIONS IN THE EXPERIMENTAL DETERMINATION OF CONSTITUTIVE PARAMETERS FOR FINITE STRAIN PLASTICITY Final Report
Norris J. Huffington, Jr. Sep. 1994 19 p
(DA Proj. 1L1-62618-AH-80)
(AD-A285410; ARL-TR-576) Avail: CASI HC A03/MF A01

Various experimental procedures for measurement of quasi-static constitutive parameters for finite strain elastoplasticity are discussed in relation to counterpart finite element analyses of specimen deformation. It is concluded that the usefulness of such analyses is limited by the assumption made in the formulation of current computer codes. DTIC

N95-16416*# National Aeronautics and Space Administration. Lewis Research Center, Cleveland, OH.
COMPUTATIONAL SIMULATION OF THE FORMATION AND MATERIAL BEHAVIOR OF ICE
Michael T. Tong (Sverdrup Technology, Inc., Brook Park, OH.), Surendra N. Singhal (Sverdrup Technology, Inc., Brook Park, OH.), and Christos C. Chamis Nov. 1994 14 p Presented at the 1994 Energy Technology Conference and Exhibition, Materials, Design and Analysis Symposium, New Orleans, LA, 23-26 Jan. 1994; sponsored by ASME
(Contract NAS3-25266; RTOP 505-63-5B)
(NASA-TM-106702; E-9064; NAS 1.15:106702) Avail: CASI HC A03/MF A01

Computational methods are described for simulating the formation and the material behavior of ice in prevailing transient environments. The methodology developed at the NASA Lewis Research Center was adopted. A three dimensional finite-element heat transfer analyzer was used to predict the thickness of ice formed under prevailing environmental conditions. A multi-factor interaction model for simulating the material behavior of time-variant ice layers is presented. The model, used in conjunction with laminated composite mechanics, updates the material properties of an ice block as its thickness increases with time. A sample case of ice formation in a body of water was used to demonstrate the methodology. The results showed that the formation and the material behavior of ice can be computationally simulated using the available composites technology. Author

N95-16502# Naval Postgraduate School, Monterey, CA.
EXPERIMENTAL STUDY OF SPATIALLY INCOMPLETE STRUCTURAL SYSTEM IDENTIFICATION M.S. Thesis
Vincent C. Gomes Mar. 1994 189 p
(AD-A280905) Avail: CASI HC A09/MF A02

A frequency domain transformation is the basis for a general approach to the identification of finite element modeling errors. The transformation provides information as to the location of modeling errors and provides the error matrices of stiffness, mass, and damping. The transformation is shown to have the unique property of directly revealing that the process of instrumenting an actual structure with a finite number of response transducers defines a reduced order system, with an attendant set of singular frequencies responsible for the nonlinear distortion imposed on the corrective parameters of stiffness, mass, and damping. Actual test data demonstrating this phenomenon will be presented. DTIC

N95-16577*# National Aeronautics and Space Administration. Marshall Space Flight Center, Huntsville, AL.

MEASUREMENT OF RESIDUAL FLEXIBILITY FOR SUBSTRUCTURES HAVING PROMINENT FLEXIBLE INTERFACES

Michael L. Tinker and Paul S. Bookout 1994 18 p Presented at the 35th AIAA Structures, Structural Dynamics and Materials Conference, Hilton Head, SC, 18-20 Apr. 1994

(RTOP 546-99-00)

(NASA-TM-110074; NAS 1.15:110074) Avail: CASI HC A03/MF A01

Verification of a dynamic model of a constrained structure requires a modal survey test of the physical structure and subsequent modification of the model to obtain the best agreement possible with test data. Constrained-boundary or fixed-base testing has historically been the most common approach for verifying constrained mathematical models, since the boundary conditions of the test article are designed to match the actual constraints in service. However, there are difficulties involved with fixed-base testing, in some cases making the approach impractical. It is not possible to conduct a truly fixed-base test due to coupling between the test article and the fixture. In addition, it is often difficult to accurately simulate the actual boundary constraints, and the cost of designing and constructing the fixture may be prohibitive. For use when fixed-base testing proves impractical or undesirable, alternate free-boundary test methods have been investigated, including the residual flexibility technique. The residual flexibility approach has been treated analytically in considerable detail and has had limited frequency response measurements for the method. This concern is well-justified for a number of reasons. First, residual flexibilities are very small numbers, typically on the order of 1.0E-6 in/lb for translational diagonal terms, and orders of magnitude smaller for off-diagonal values. This poses difficulty in obtaining accurate and noise-free measurements, especially for points removed from the excitation source. A second difficulty encountered in residual measurements lies in obtaining a clean residual function in the process of subtracting synthesized modal data from a measured response function. Inaccuracies occur since modes are not subtracted exactly, but only to the accuracy of the curve fits for each mode; these errors are compounded with increasing distance from the excitation point. In this paper, the residual flexibility method is applied to a simple structure in both test and analysis. Measured and predicted residual functions are compared, and regions of poor data in the measured curves are described. It is found that for accurate residual measurements, frequency response functions having prominent stiffness lines in the acceleration/force format are needed. The lack of such stiffness lines increases measurement errors. Interface drive point frequency respose functions for shuttle orbiter payloads exhibit dominant stiffness lines, making the residual test approach a good candidate for payload modal tests when constrained tests are inappropriate. Difficulties in extracting a residual flexibility value from noisy test data are discussed. It is shown that use of a weighted second order least-squares curve fit of the measured residual function allows identification of residual flexibility that compares very well with predictions for the simple structure. This approach also provides an estimate of second order residual mass effects. Author (revised)

N95-16588*# Toledo Univ., OH. Dept. of Mechanical Engineering.

FPCAS2D USER'S GUIDE, VERSION 1.0 Final Report

Milind A. Bakhle Cleveland, OH NASA Dec. 1994 58 p

(Grant NAG3-1234; RTOP 538-03-11)

(NASA-CR-195413; E-9299; NAS 1.26:195413) Avail: CASI HC A04/MF A01

The FPCAS2D computer code has been developed for aeroelastic stability analysis of bladed disks such as those in fans, compressors, turbines, propellers, or propfans. The aerodynamic analysis used in this code is based on the unsteady two-dimensional full potential equation which is solved for a cascade of blades. The structural analysis is based on a two degree-of-freedom rigid typical section model for each blade. Detailed explanations of the aerodynamic analysis, the numerical algorithms, and the aeroelastic analysis are not given in this report. This guide can be used to assist in the preparation of the input data required by the FPCAS2D code. A complete description of the input data is provided in this report. In addition, four test cases, including inputs and outputs, are provided. Author

N95-16601# Army Armament Research, Development and Engineering Center, Watervliet, NY.

THE EFFECTS OF FATIGUE LOADING FREQUENCY ON FATIGUE LIFE OF HIGH-STRENGTH PRESSURE VESSEL STEELS Final Report

Robert R. Fujczak Jun. 1994 23 p

(AD-A285301; ARCCB-TR-94023) Avail: CASI HC A03/MF A01

Bend specimens of high-strength pressure vessel steel were tested in bending fatigue to failure at 1.5, 15, 30, arid 75 Hz fatigue loading frequencies. In the 1.5 to 15 Hz range, there was no discernible difference in the frequency effect on fatigue life. However, in the 30 to 75 Hz range, there was a definite increase in fatigue life compared to the lower range of frequency. The average increase in fatigue over the stress range was a factor of 10 greater than the life at the lower frequency range. This factor increased at lower stresses decreased at higher stresses, but even at the highest stresses tested, the increase was significant, about 5 to 1. This indicates that the frequency effect is more effective at high-cycle fatigue and diminishes with low-cycle fatigue. A model for fatigue life deterioration caused by superimposition of loads under different frequencies is introduced. DTIC

N95-16785# Illinois Univ., Champaign, IL.

EFFECTS OF PRIOR DUCTILE TEARING ON CLEAVAGE FRACTURE TOUGHNESS IN THE TRANSITION REGION Final Report, Jun. 1992 - Nov. 1993

R. H. Dodds, Jr., M. Tang, and T. L. Anderson Dec. 1993 44 p

(Contract N61533-92-K-0030)

(AD-A281298; CARDIVNSWC-TR-61-CR-93/04) Avail: CASI HC A03/MF A01

Previous work by the authors described a micromechanics fracture model to correct measured J sub c-values for the mechanistic effects of large-scale yielding. This new work extends the model to also include the influence of ductile crack extension prior to cleavage. Ductile crack extensions of 10-15 times the initial crack tip opening displacement at initiation are considered in plane-strain, finite element computations. The finite element results demonstrate a significant elevation in crack-tip constraint due to macroscopic 'sharpening' of the extending tip relative to the-blunt tip at the initiation of growth. However this effect is offset partially by the additional plastic deformation associated with the increased applied J required to grow the crack. The initial a/W ratio, tearing modulus, strain hardening exponent and specimen size interact in a complex manner to define the evolving near-tip conditions for cleavage fracture. The paper explores development of the new model, provides necessary graphs and procedures for its application and demonstrates the effects of the model on fracture data sets for two pressure vessel steels (A533B and A515). DTIC

N95-16803# Oak Ridge National Lab., TN.

INVESTIGATION OF RESIDUAL STRESSES IN A MULTIPASS WELD IN 1 IN. STAINLESS STEEL PLATE

S. Spooner, J. A. FernandezBaca, S. A. David, C. R. Hubbard, T. M. Holden (Atomic Energy of Canada Ltd., Chalk River, Ontario.), and J. H. Root (Atomic Energy of Canada Ltd., Chalk River, Ontario.) 1994 5 p Presented at the 4th International Conference on Residual Stress (ICRS-4), Baltimore, MD, Jun. 1994

(Contract DE-AC05-84OR-21400)

(DE94-013277; CONF-940692-5) Avail: CASI HC A01/MF A01

Residual stresses and strains were measured in two welded 25-mm thick plates of type 304 stainless steel by the neutron diffraction technique. The filler metal was type 308 stainless steel and the weld zone had a two phase microstructure in which the austenitic phase lattice parameter differs from the base metal. In these circumstances strain-free samples were taken from the weld zone area for analysis of the lattice parameters and ferrite content using neutron powder diffraction. Corrections for lattice parameter variation were applied permitting the calculation of residual strains and stresses in weld zone, heat affected zone (HAZ), and base metal. One of the two welds was examined without stress relief and the other was given a stress relief treatment consisting of vibration at a frequency below the resonant condition during welding. In both plates the largest residual stress component (longitudinal) is found in the fusion zone near the boundary between the weld zone and the heat affected zone. This longitudinal component is 400 +/- 50 MPa in tension. The normal stresses are generally close to zero although large fluctuations are found in the

weld zone. The transverse stresses are as high as 200 MPa in the weld zone and decrease to 50 MPa +/- 40 MPa. The lattice parameter variation was equivalent to 5 x 10(exp -4) compressive strain and the ferrite content approached 9 percent at the center of the weld zone. Variations in residual stresses with thickness through the base metal plate were small. The treated plate and untreated plate showed nearly identical patterns of stress distribution. Differences in the measured stresses between vibratory-stress-relief treated and untreated plates fall within error bars of the stress determination in these particular 25 mm thick 300-type stainless steel plates. DOE

N95-16843# Naval Surface Warfare Center, Dahlgren, VA.
PENETRATION OF SOLID AND LAYERED TARGETS BY GAS GUN-LAUNCHED STEEL CUBES Final Report, period ending Jun. 1994
Willis Mock, Jr. and William H. Holt Jul. 1994 48 p
(AD-A285143; NSWCDD/TR-93/429) Avail: CASI HC A03/MF A01

A series of 14 impact experiments has been performed in which solid and layered targets nominally 3 x 3-in. by 0.5-in. thick have been impacted by 0.5-in. steel cubes in a flat-faced orientation. The number of target layers varied from one to five. The areal density of the targets ranged from 3.6 to 11.1 gm/sq cm. Three experiments were performed at an impact velocity ranging from 2000 to 2500 ft/sec and eleven experiments were performed at a velocity of approximately 3100 ft/sec. Target perforation did not occur in six of the higher velocity experiments. For these experiments, the number of target layers was either one or two. Target perforation occurred in five of the higher velocity experiments; the number of target layers was either three, four, or five for these experiments. Target failure consisted of one or more of the following types: cratering, shear bands, shear plugging, fracture, plate bending, petalling, and fiber breaking. DTIC

N95-16911*# National Aeronautics and Space Administration. Lewis Research Center, Cleveland, OH.
OPTIMIZATION OF ADAPTIVE INTRAPLY HYBRID FIBER COMPOSITES WITH RELIABILITY CONSIDERATIONS
Michael C. Shiao (NYMA, Inc., Brook Park, OH.) and Christos C. Chamis Dec. 1994 16 p Presented at 1994 North American Conference on Smart Structures and Materials, Orlando, FL, 13-18 Feb. 1994; sponsored by IEEE
(Contract NAS3-27186; RTOP 505-62-10)
(NASA-TM-106632; E-8933; NAS 1.15:106632) Avail: CASI HC A03/MF A01

The reliability with bounded distribution parameters (mean, standard deviation) was maximized and the reliability-based cost was minimized for adaptive intra-ply hybrid fiber composites by using a probabilistic method. The probabilistic method accounts for all naturally occurring uncertainties including those in constituent material properties, fabrication variables, structure geometry, and control-related parameters. Probabilistic sensitivity factors were computed and used in the optimization procedures. For actuated change in the angle of attack of an airfoil-like composite shell structure with an adaptive torque plate, the reliability was maximized to 0.9999 probability, with constraints on the mean and standard deviation of the actuation material volume ratio (percentage of actuation composite material in a ply) and the actuation strain coefficient. The reliability-based cost was minimized for an airfoil-like composite shell structure with an adaptive skin and a mean actuation material volume ratio as the design parameter. At a O.9-mean actuation material volume ratio, the minimum cost was obtained. Author

N95-16939# National Renewable Energy Lab., Golden, CO.
STRUCTURAL EFFECTS OF UNSTEADY AERODYNAMIC FORCES ON HORIZONTAL-AXIS WIND TURBINES
M. S. Miller and D. E. Shipley Aug. 1994 9 p Presented at the AIAA Region 5 Student Conference, Saint Louis, MO, 8-11 Apr. 1992 Prepared in cooperation with Colorado Univ., Boulder, CO
(Contract DE-AC36-83CH-10093)
(DE94-011863; NREL/TP-441-7078; CONF-9204294-1) Avail: CASI HC A02/MF A01

Due to its renewable nature and abundant resources, wind energy has the potential to fulfill a large portion of this nation's energy needs. The simplest means of utilizing wind energy is through the use of downwind, horizontal-axis wind turbines (HAWT) with fixed-pitch rotors. This configuration regulates the peak power by allowing the rotor blade to aerodynamically stall. The stall point, the point of maximum coefficient of lift, is currently predicted using data obtained from wind tunnel tests. Unfortunately, these tests do not accurately simulate conditions encountered in the field. Flow around the tower and nacelle coupled with inflow turbulence and rotation of the turbine blades create unpredicted aerodynamic forces. Dynamic stall is hypothesized to occur. Such aerodynamic loads are transmitted into the rotor and tower causing structural resonance that drastically reduces the design lifetime of the wind turbine. The current method of alleviating this problem is to structurally reinforce the tower and blades. However, this adds unneeded mass and, therefore, cost to the turbines. A better understanding of the aerodynamic forces and the manner in which they affect the structure would allow for the design of more cost effective and durable wind turbines. Data compiled by the National Renewable Energy Laboratory (NREL) for a downwind HAWT with constant chord, untwisted, fixed-pitch rotors is analyzed. From these data, the actual aerodynamic characteristics of the rotor are being portrayed and the potential effects upon the structure can for the first time be fully analyzed. Based upon their understanding, solutions to the problem of structural resonance are emerging. DOE

N95-17258*# National Aeronautics and Space Administration. Lewis Research Center, Cleveland, OH.
CORRELATION OF FINITE ELEMENT FREE VIBRATION PREDICTIONS USING RANDOM VIBRATION TEST DATA M.S. Thesis - Cleveland State Univ.
Jeffrey A. Chambers Nov. 1994 145 p
(NASA-TM-106787; E-9243; NAS 1.15:106787) Avail: CASI HC A07/MF A02

Finite element analysis is regularly used during the engineering cycle of mechanical systems to predict the response to static, thermal, and dynamic loads. The finite element model (FEM) used to represent the system is often correlated with physical test results to determine the validity of analytical results provided. Results from dynamic testing provide one means for performing this correlation. One of the most common methods of measuring accuracy is by classical modal testing, whereby vibratory mode shapes are compared to mode shapes provided by finite element analysis. The degree of correlation between the test and analytical mode shapes can be shown mathematically using the cross orthogonality check. A great deal of time and effort can be exhausted in generating the set of test acquired mode shapes needed for the cross orthogonality check. In most situations response data from vibration tests are digitally processed to generate the mode shapes from a combination of modal parameters, forcing functions, and recorded response data. An alternate method is proposed in which the same correlation of analytical and test acquired mode shapes can be achieved without conducting the modal survey. Instead a procedure is detailed in which a minimum of test information, specifically the acceleration response data from a random vibration test, is used to generate a set of equivalent local accelerations to be applied to the reduced analytical model at discrete points corresponding to the test measurement locations. The static solution of the analytical model then produces a set of deformations that once normalized can be used to represent the test acquired mode shapes in the cross orthogonality relation. The method proposed has been shown to provide accurate results for both a simple analytical model as well as a complex space flight structure. Author

N95-17270*# National Aeronautics and Space Administration. Lewis Research Center, Cleveland, OH.
PROBABILISTIC SIMULATION OF STRESS CONCENTRATION IN COMPOSITE LAMINATES
C. C. Chamis, P. L. N. Murthy, and D. G. Liaw (Sverdrup Technology, Inc., Brook Park, OH.) Dec. 1994 19 p Presented at the 34th Structures, Structural Dynamics, and Materials Conference, La Jolla, CA, 19-22 Apr. 1993; sponsored by AIAA, ASME, ASCE, AHS, and ASC
(Contract NAS3-25266; RTOP 510-02-12)
(NASA-TM-106712; E-9077; NAS 1.15:106712) Avail: CASI HC A03/MF A01

A computational methodology is described to probabilistically simulate the stress concentration factors (SCF's) in composite laminates. This new approach consists of coupling probabilistic composite mechanics with probabilistic finite element structural analysis. The composite mechanics is used to probabilistically describe all the uncertainties inherent in composite

material properties, whereas the finite element is used to probabilistically describe the uncertainties associated with methods to experimentally evaluate SCF's, such as loads, geometry, and supports. The effectiveness of the methodology is demonstrated by using is to simulate the SCF's in three different composite laminates. Simulated results match experimental data for probability density and for cumulative distribution functions. The sensitivity factors indicate that the SCF's are influenced by local stiffness variables, by load eccentricities, and by initial stress fields. Author

N95-17272*# Southwest Research Inst., San Antonio, TX.
SIGNIFICANT ISSUES IN PROOF TESTING: A CRITICAL APPRAISAL Interim Report
G. G. Chell, R. C. McClung, D. A. Russell (Rockwell International Corp., Canoga Park, CA.), K. J. Chang (Rockwell International Corp., Canoga Park, CA.), and B. Donnelly (Rockwell International Corp., Canoga Park, CA.) Washington NASA Sep. 1994 104 p
(Contract NAS8-39380)
(NASA-CR-4628; M-757; NAS 1.26:4628) Avail: CASI HC A06/MF A02

Issues which impact on the interpretation and quantification of proof test benefits are reviewed. The importance of each issue in contributing to the extra quality assurance conferred by proof testing components is discussed, particularly with respect to the application of advanced fracture mechanics concepts to enhance the flaw screening capability of a proof test analysis. Items covered include the role in proof testing of elastic-plastic fracture mechanics, ductile instability analysis, deterministic versus probabilistic analysis, single versus multiple cycle proof testing, and non-destructive examination (NDE). The effects of proof testing on subsequent service life are reviewed, particularly with regard to stress redistribution and changes in fracture behavior resulting from the overload. The importance of proof test conditions are also addressed, covering aspects related to test temperature, simulation of service environments, test media and the application of real-time NDE. The role of each issue in a proof test methodology is assessed with respect to its ability to: promote proof test practice to a state-of-the-art; aid optimization of proof test design; and increase awareness and understanding of outstanding issues. Author

N95-17417*# National Aeronautics and Space Administration. Hugh L. Dryden Flight Research Center, Edwards, CA.
THERMOCRYOGENIC BUCKLING AND STRESS ANALYSES OF A PARTIALLY FILLED CRYOGENIC TANK SUBJECTED TO CYLINDRICAL STRIP HEATING
William L. Ko Washington Nov. 1994 70 p
(RTOP 505-70-63)
(NASA-TM-4579; H-1955; NAS 1.15:4579) Avail: CASI HC A04/MF A01

Thermocryogenic buckling and stress analyses were conducted on a horizontally oriented cryogenic tank using the finite element method. The tank is a finite-length circular cylindrical shell with its two ends capped with hemispherical shells. The tank is subjected to cylindrical strip heating in the region above the liquid-cryogen fill level and to cryogenic cooling below the fill level (i.e., under thermocryogenic loading). The effects of cryogen fill level on the buckling temperature and thermocryogenic stress field were investigated in detail. Both the buckling temperature and stress magnitudes were relatively insensitive to the cryogen fill level. The buckling temperature, however, was quite sensitive to the radius-to-thickness ratio. A mechanical stress analysis of the tank also was conducted when the tank was under: (1) cryogen liquid pressure loading; (2) internal pressure loading; and (3) tank-wall inertia loading. Deformed shapes of the cryogenic tanks under different loading conditions were shown, and high-stress domains were mapped on the tank wall for the strain-gage installations. The accuracies of solutions from different finite element models were compared. Author

N95-17439# Sandia National Labs., Albuquerque, NM.
AN ANALYSIS OF SMOOTHED PARTICLE HYDRODYNAMICS
J. W. Swegle, S. W. Attaway, M. W. Heinstein, F. J. Mello, and D. L. Hicks (Michigan Technological Univ., Houghton, MI.) Mar. 1994 142 p
(Contract DE-AC04-94AL-85000)
(DE94-013817; SAND-93-2513) Avail: CASI HC A07/MF A02

SPH (Smoothed Particle Hydrodynamics) is a gridless Lagrangian technique which is appealing as a possible alternative to numerical techniques currently used to analyze high deformation impulsive loading events. In the present study, the SPH algorithm has been subjected to detailed testing and analysis to determine its applicability in the field of solid dynamics. An important result of the work is a rigorous von Neumann stability analysis which provides a simple criterion for the stability or instability of the method in terms of the stress state and the second derivative of the kernel function. Instability, which typically occurs only for solids in tension, results not from the numerical time integration algorithm, but because the SPH algorithm creates an effective stress with a negative modulus. The analysis provides insight into possible methods for removing the instability. Also, SPH has been coupled into the transient dynamics finite element code PRONTO, and a weighted residual derivation of the SPH equations has been obtained. DOE

N95-17490*# National Aeronautics and Space Administration. Hugh L. Dryden Flight Research Center, Edwards, CA.
SHEAR BUCKLING ANALYSIS OF A HAT-STIFFENED PANEL
William L. Ko and Raymond H. Jackson Washington Nov. 1994 20 p
(RTOP 505-63-40)
(NASA-TM-4644; H-2019; NAS 1.15:4644) Avail: CASI HC A03/MF A01

A buckling analysis was performed on a hat-stiffened panel subjected to shear loading. Both local buckling and global buckling were analyzed. The global shear buckling load was found to be several times higher than the local shear buckling load. The classical shear buckling theory for a flat plate was found to be useful in predicting the local shear buckling load of the hat-stiffened panel, and the predicted local shear buckling loads thus obtained compare favorably with the results of finite element analysis. Author

N95-17492*# Colorado Univ., Boulder, CO. Dept. of Aerospace Engineering Sciences.
ERROR ESTIMATION AND ADAPTIVE MESH REFINEMENT FOR PARALLEL ANALYSIS OF SHELL STRUCTURES
Scott C. Keating, Carlos A. Felippa, and K. C. Park Nov. 1994 42 p
Original contains color illustrations
(Contract NAS1-756)
(NASA-CR-197500; NAS 1.26:197500; CU-CAS-94-23) Avail: CASI HC A03/MF A01; 3 functional color pages

The formulation and application of element-level, element-independent error indicators is investigated. This research culminates in the development of an error indicator formulation which is derived based on the projection of element deformation onto the intrinsic element displacement modes. The qualifier 'element-level' means that no information from adjacent elements is used for error estimation. This property is ideally suited for obtaining error values and driving adaptive mesh refinements on parallel computers where access to neighboring elements residing on different processors may incur significant overhead. In addition such estimators are insensitive to the presence of physical interfaces and junctures. An error indicator qualifies as 'element-independent' when only visible quantities such as element stiffness and nodal displacements are used to quantify error. Error evaluation at the element level and element independence for the error indicator are highly desired properties for computing error in production-level finite element codes. Four element-level error indicators have been constructed. Two of the indicators are based on variational formulation of the element stiffness and are element-dependent. Their derivations are retained for developmental purposes. The second two indicators mimic and exceed the first two in performance but require no special formulation of the element stiffness mesh refinement which we demonstrate for two dimensional plane stress problems. The parallelizing of substructures and adaptive mesh refinement is discussed and the final error indicator using two-dimensional plane-stress and three-dimensional shell problems is demonstrated. Author

N95-17510 Army Research Lab., Watertown, MA. Materials Directorate.
USER-DEFINED SUBROUTINE FOR IMPLEMENTATION OF SPECIAL FINITE ELEMENTS IN ABAQUS FOR THE ANALYSIS OF ADHESIVE JOINTS Final Report
Erik Saether and Kristen Weight May 1994 114 p Limited Reproducibility. More than 20% of this document may be affected by microfiche quality
(AD-A282431; ARL-TR-450) Avail: Issuing Activity (Defense Technical Information Center (DTIC))

A user-defined subroutine has been developed to implement special

2-D and 3-D layered continuum elements in the commercial finite element program ABAQUS. These elements are specially configured to accurately predict interface stresses in adhesively bonded joints and are formulated using the hybrid stress technique to explicitly enforce stress equilibrium throughout the element domain and stress continuity conditions at layer interfaces. This report details the use of developed special 'adhesive elements' in ABAQUS for elastostatic analysis together with several numerical examples which demonstrate an improved accuracy and convergence behavior over conventional displacement-based elements. Sample input and output datasets and the complete FORTRAN subroutine which performs all element computations are presented in separate appendices. DTIC

N95-17658*# National Aeronautics and Space Administration. Lewis Research Center, Cleveland, OH.

THERMAL ANALYSIS OF A FUNCTIONALLY GRADED MATERIAL SUBJECT TO A THERMAL GRADIENT USING THE BOUNDARY ELEMENT METHOD

Robert K. Goldberg and Dale A. Hopkins Dec. 1994 15 p Presented at the International Conference on Composites Engineering, New Orleans, LA, 28-31 Aug. 1994; sponsored by International Community on Composites Engineering

(RTOP 505-63-12)

(NASA-TM-106801; E-9277; NAS 1.15:106801) Avail: CASI HC A03/MF A01

The boundary element method is utilized in this study to conduct thermal analysis of functionally graded composites, materials in which the internal microstructure or properties are explicitly tailored in order to obtain an optimal response, on the micromechanical (constituent) scale. A unique feature of the boundary element formulations used here is the use of circular shape functions to convert the two-dimensional integrations of the composite fibers to one dimensional integrations. Using the computer code BEST-CMS, the through the thickness temperature profiles are computed for a representative material with varying numbers of fibers and fiber spacing in the thickness direction. The computed temperature profiles are compared to those obtained using an alternate analytical theory which explicitly couples the heterogeneous microstructure to the global analysis. The boundary element results compared favorably to the analytical calculations, with discrepancies that are explainable based on the boundary element formulation. The results serve both to demonstrate the ability of the boundary element method to analyze these types of materials, and to verify the accuracy of the analytical theory. Author

N95-17675# Oak Ridge National Lab., TN.

MODELING OF THERMAL STRESSES IN WELDS

T. Zacharia and G. A. Aramayo 1993 9 p Presented at the American Welding Society International Conference on Modeling and Control of Joining Processes, Orlando, FL, 8-10 Dec. 1993

(Contract DE-AC05-84OR-21400)

(DE94-018046; CONF-931234-10) Avail: CASI HC A02/MF A01

The transient stress distribution in a Sigmajig test specimen resulting from mechanical and thermal loading was calculated for a Type 316 stainless steel specimen using finite element analysis. The study attempted to resolve the relationship between the dynamic stress distribution, particularly near the trailing edge of the pool, and the observed cracking behavior in the test specimen. The initiation and propagation of the crack during welding was visually monitored using a stroboscopic vision system. The numerical results were used to understand the initiation and propagation of hot-cracks during controlled welding of a specimen subjected to external restraint. DOE

N95-17701*# National Aeronautics and Space Administration. Lewis Research Center, Cleveland, OH.

STRUCTURAL OPTIMIZATION WITH APPROXIMATE SENSITIVITIES

S. N. Patnaik (Ohio Aerospace Inst., Brook Park.), D. A. Hopkins, and R. Coroneos Washington Apr. 1994 16 p

(RTOP 505-63-5B)

(NASA-TM-4553; E-8226; NAS 1.15:4553) Avail: CASI HC A03/MF A01

Computational efficiency in structural optimization can be enhanced if the intensive computations associated with the calculation of the sensitivities, that is, gradients of the behavior constraints, are reduced. Approximation to gradients of the behavior constraints that can be generated with small amount of numerical calculations is proposed. Structural optimization with these approximate sensitivities produced correct optimum solution. Approximate gradients performed well for different nonlinear programming methods, such as the sequence of unconstrained minimization technique, method of feasible directions, sequence of quadratic programming, and sequence of linear programming. Structural optimization with approximate gradients can reduce by one third the CPU time that would otherwise be required to solve the problem with explicit closed-form gradients. The proposed gradient approximation shows potential to reduce intensive computation that has been associated with traditional structural optimization. Author

N95-16259# Nanjing Univ. of Aeronautics and Astronautics, Nanjing, Jiangsu (China). Dept. of Aircraft Engineering.

A CONSISTENT LARGE DEFLECTION THEORY OF COMPOSITE SANDWICH SHELLS

Jinfu Zhu *In its* Joint Proceedings on Aeronautics and Astronautics (JPAA) May 1993 p 67-73 See also A93-20816 (For primary document see N95-16249 04-01)

Avail: CASI HC A02/MF A03

N95-16260# Nanjing Univ. of Aeronautics and Astronautics, Nanjing, Jiangsu (China). Research Inst. of Vibration Engineering.

A SUPER-ELEMENT SIMPLIFIED ANALYSIS FOR VIBRATION SYSTEMS OF COMPLEX STRUCTURES

Guoping Chen and Demao Zhu *In its* Joint Proceedings on Aeronautics and Astronautics (JPAA) 74-80 (SEE N95-16249 04-01) May 1993 See also A92-27903 (For primary document see N95-16249 04-01)

Avail: CASI HC A02/MF A03

N95-16261# Nanjing Univ. of Aeronautics and Astronautics, Nanjing, Jiangsu (China). Research Inst. of Vibration Engineering.

NUMERICAL ANALYSIS ON PERIODIC RESPONSE OF NONSMOOTH DYNAMIC SYSTEMS

Haiyan Hu *In its* Joint Proceedings on Aeronautics and Astronautics (JPAA) May 1993 p 81-88 Sponsored by the Aeronautical Science Foundation of China (For primary document see N95-16249 04-01)

Avail: CASI HC A02/MF A03

N95-16262# Nanjing Univ. of Aeronautics and Astronautics, Nanjing, Jiangsu (China). Research Inst. of Vibration Engineering.

A NEW REGULARIZATION APPROACH IN STRUCTURAL SYSTEM IDENTIFICATION

Lingmi Zhang and Baiqing He *In its* Joint Proceedings on Aeronautics and Astronautics (JPAA) May 1993 p 89-93 (For primary document see N95-16249 04-01)

Avail: CASI HC A01/MF A03

N95-16263# Nanjing Univ. of Aeronautics and Astronautics, Nanjing, Jiangsu (China). Dept. of Aircraft Engineering.

THERMOELASTICITY ANALYSIS OF LAMINATED PLATES AND SHELLS USING HYBRID-STRESS ELEMENTS

Shu Li and Liangxin Sun *In its* Joint Proceedings on Aeronautics and Astronautics (JPAA) May 1993 p 94-102 See also N91-43506 Sponsored by the Aeronautical Science Foundation of China (For primary document see N95-16249 04-01)

Avail: CASI HC A02/MF A03

42 GEOSCIENCES (GENERAL)

No abstracts in this category.

43 EARTH RESOURCES AND REMOTE SENSING

Includes remote sensing of earth resources by aircraft and spacecraft; photogrammetry; and aerial photography.

For instrumentation see *35 Instrumentation and Photography.*

N95-16215# Pacific Northwest Lab., Richland, WA.
INFRARED SIGNATURES FOR REMOTE SENSING
R. S. McDowell, S. W. Sharpe, and J. F. Kelly Apr. 1994 9 p Presented at the 1994 Caliope Interim Technical Review, Oakland, CA, 26-28 Apr. 1994
(Contract DE-AC06-76RL-01830)
(DE94-014222; PNL-SA-24200; CONF-9404162-8) Avail: CASI HC A02/MF A01

PNL's capabilities for infrared and near-infrared spectroscopy include tunable-diode-laser (TDL) systems covering 300-3,000 cm(exp -1) at less than 10 MHz bandwidth; a Bruker Fourier-transform infrared (FTIR) spectrometer for the near- to far-infrared at 50 MHz resolution; and a stable line-tunable, 12 w CW CO2 laser. PNL also has a beam expansion source with a 12 cm slit, which provides a 3 m effective path for gases at approximately 10 K, giving a Doppler width of typically 10 MHz; and long-path static gas cells (to 100 m). In applying this equipment to signatures work, the authors emphasize the importance of high spectral resolution for detecting and identifying atmospheric interferences; for identifying the optimum analytical frequencies; for deriving, by spectroscopic analysis, the molecular parameters needed for modeling; and for obtaining data on species and/or bands that are not in existing databases. As an example of such spectroscopy, the authors have assigned and analyzed the C-Cl stretching region of CCl4 at 770-800 cm(exp -1). This is an important potential signature species whose IR absorption has remained puzzling because of the natural isotopic mix, extensive hot-band structure, and a Fermi resonance involving a nearby combination band. Instrument development projects include the IR sniffer, a small high-sensitivity, high-discrimination (Doppler-limited) device for fence-line or downwind monitoring that is effective even in regions of atmospheric absorption; preliminary work has achieved sensitivities at the low-ppb level. Other work covers trace species detection with TDL's, and FM-modulated CO2 laser LIDAR. The authors are planning a field experiment to interrogate the Hanford tank farm for signature species from Rattlesnake Mountain, a standoff of ca. 15 km, to be accompanied by simultaneous ground-truthing at the tanks. DOE

N95-16547# Naval Research Lab., Bay Saint Louis, MS.
DIGITAL MAPPING, CHARTING, AND GEODESY ANALYSIS PROGRAM TECHNICAL REVIEW OF INTERIM TERRAIN ANALYSIS DATA SET PROTOTYPE 1 Final Report
Kevin Shaw, Hillary Mesick, Steven Kuder, Danette Coughlan, and Paulo Richard 12 Aug. 1994 19 p
(AD-A284742; NRL/MR/7441-94-7550) Avail: CASI HC A03/MF A01

The Digital Mapping, Charting, and Geodesy Analysis Program has performed a technical review of the interim terrain analysis data set (TADS). This review focuses on general prototype quality issues, individual features, and product specification errors and concerns. TADS uses the interim terrain data (ITD) product, so particular attention is given to the quality and quantity of information found in the ITD database. A conclusions section completes this product review. DTIC

N95-16895*# Montana Univ., Missoula, MT. School of Forestry.
FIFE DATA ANALYSIS: TESTING BIOME-BGC PREDICTIONS FOR GRASSLANDS Final Technical Report, 15 Aug. 1992 - 14 Aug. 1994
E. Raymond Hunt, Jr. 14 Aug. 1994 24 p Original contains color illustrations
(Grant NAG5-2065)
(NASA-CR-197522; NAS 1.26:197522) Avail: CASI HC A03/MF A01; 5 functional color pages

The First International Satellite Land Surface Climatology Project (ISLSCP) Field Experiment (FIFE) was conducted in a 15 km by 15 km research area located 8 km south of Manhattan, Kansas. The site consists primarily of native tallgrass prairie mixed with gallery oak forests and croplands. The objectives of FIFE are to better understand the role of biology in controlling the interactions between the land and the atmosphere, and to determine the value of remotely sensed data for estimating climatological parameters. The goals of FIFE are twofold: the upscale integration of models, and algorithm development for satellite remote sensing. The specific objectives of the field campaigns carried out in 1987 and 1989 were the simultaneous acquisition of satellite, atmospheric, and surface data; and the understanding of the processes controlling surface energy and mass exchange. Collected data were used to study the dynamics of various ecosystem processes (photosynthesis, evaporation and transpiration, autotrophic and heterotrophic respiration, etc.). Modelling terrestrial ecosystems at scales larger than that of a homogeneous plot led to the development of simple, generalized models of biogeochemical cycles that can be accurately applied to different biomes through the use of remotely sensed data. A model was developed called BIOME-BGC (for BioGeochemical Cycles) from a coniferous forest ecosystem model, FOREST-BGC, where a biome is considered a combination of a life forms in a specified climate. A predominately C4-photosynthetic grassland is probably the most different from a coniferous forest possible, hence the FIFE site was an excellent study area for testing BIOME-BGC. The transition from an essentially one-dimensional calculation to three-dimensional, landscape scale simulations requires the introduction of such factors as meteorology, climatology, and geomorphology. By using remotely sensed geographic information data for important model inputs, process-based ecosystem simulations at a variety of scales are possible. The second objective of this study is concerned with determining the accuracy of the estimated fluxes from BIOME-BGC, when extrapolated spatially over the entire 15-km by 15-km FIFE site. To accomplish this objective, a topographically distributed map of soil depth at the FIFE site was developed. These spatially-distributed fluxes were then tested with data from aircraft by eddy-flux correlation obtained during the FIFE experiment.
Author (revised)

N95-17372 Electronic Imaging Center, Saint Paul, MN.
FULL COLOR RECORDER Final Report, Jun. 1990 - Mar. 1994
Dean Beilke and William Rozzi Jan. 1994 152 p Limited Reproducibility: More than 20% of this document may be affected by microfiche quality
(Contract DACA76-90-C-0006)
(AD-A282278) Avail: Issuing Activity (Defense Technical Information Center (DTIC))

The U.S. Army Topographic Engineering Center (TEC) initiated this program to keep abreast of new and promising color image processing and printing methods that could be used by the Army. In 1990, new nonimpact printing technologies and derived products were rapidly emerging alongside high speed digital image processing capabilities. Linking these two areas held the promise of creating highly flexible digital demand color printing which had not been imagined 10 years earlier. This report studies the feasibility of creating a full color recorder system from available technologies, hardware, and software. Research and development under this contract produced results which have been adopted by the Army into the baseline QRMP system, a system designed to provide troops real-time terrain graphic images in the field. This final report documents the rationale, history, processes, technologies, and results of this program. DTIC

N95-17375 Argialas (Demetre P.), Athens (Greece).
STEPS TOWARD TERRAIN KNOWLEDGE ACQUISITION Interim Report No. 2
Demetre P. Argialas Jul. 1994 10 p Limited Reproducibility: More than 20% of this document may be affected by microfiche quality
(Contract DAJA45-93-C-0015)
(AD-A282667; R/D-6958-EN-09) Avail: Issuing Activity (Defense Technical Information Center (DTIC))

Progress was made towards identifying, representing, formalizing, and implementing aspects of terrain related knowledge relevant to drainage courses and the alluvial fan associated landforms including the representation of information related to physiographic information, e.g., basin and range. The relevant conceptual knowledge is being structured in the form of rules and objects. Opportunistic problem solving seems to fit this photointerpretation problem better that a forward or backward search of the state space. The appended objects and rules show examples related to knowledge representation of selected drainage courses (gorge, wash, ravine) as well as of alluvial fan morphology, physiography, and regional context. There are are also examples of rule executions (firings) for wash and ravine. DTIC

N95-17511 RAND Corp., Santa Monica, CA.
THE NEW MAP GRAPHICS IN RSAS 5.0
Bruce W. Bennett and Mark Hoyer 1993 49 p Limited Reproducibility: More than 20% of this document may be affected by microfiche quality
(AD-A282432) Avail: Issuing Activity (Defense Technical Information Center (DTIC))

The RAND Strategy Assessment System (RSAS) is a global warfare analysis system developed over the last decade for the Director of Net Assessment in the Office of the Secretary of Defense. RSAS Map has two major objectives: (1) Replace the former RSAS graphics package, Map Tool, with a new package that uses the current display standard (X Windows) and the current communications standard (ToolTalk) to make it more usable and easier to maintain than its predecessor; and (2) Provide a more visual interface for understanding theater military forces and their operations to make the RSAS easier to use. RSAS Map includes several components. The background maps are derived from a map server built around the Navy's Caricature map graphics program. The map server provides an interface. The map server allows the user to choose the area and resolution to be displayed, and can add several features (e.g., rivers) and employ a large number of map projections. DTIC

N95-17625 Mitre Corp., Bedford, MA.
ANALYSIS OF COMPRESSION TECHNIQUES FOR COMMON MAPPING STANDARD (CMS) RASTER DATA Final Report
Nancy J. Markuson Jul. 1994 40 p Limited Reproducibility: More than 20% of this document may be affected by microfiche quality
(Contract F19628-94-C-0001)
(AD-A283396; MTR-93B0000091) Avail: Issuing Activity (Defense Technical Information Center (DTIC))

Current Common Mapping Standard (CMS) data, produced for the Mission Support System (MSSII) and other fielded systems, are in a spatially and color-reduced format, but are uncompressed. The next generation of CMS data must satisfy the functional, performance, and quality requirements of a wide variety of systems from the mission planning, theater battle management (TBM), intelligence, and aircraft communities. Previous studies have indicated that a vector quantization (VQ) compression approach, combined with spatial downsampling and color reduction, can be implemented to achieve high quality compressed map products. The investigations described in this report use the previous studies as a base for this follow-on VQ compression analysis; further research has been performed in order to define a spatial reduction and VQ compression approach that can support both ground and airborne systems. The report recommends an approach to be used in the reduction and compression of the next generation CMS data that will satisfy the requirements of spatial density, displayed and printed image quality, image format, and performance for CMS systems. DTIC

N95-17894# Instituto de Pesquisas Espaciais, Sao Paulo (Brazil).
DETECTION OF DEFORESTATION IN THE AMAZON FOREST USING NOAA/AVHRR IMAGES AND THE GEOGRAPHIC INFORMATION SYSTEM SGI: METHODOLOGY AND TEST OF A POTENTIAL ALARM SYSTEM M.S. Thesis [DETECCAO DE DESMATAMENTOS NA FLORESTA AMAZONICA ATRAVES DE IMAGENS AVHRR/NOAA E DO SISTEMA DE INFORMACOES GEOGRAFICAS SGI: METODOLOGIA DE TESTE DE UM SISTEMA POTENCIAL DE ALERTA]
Angelica CarvalhoDiMaioMantovani Dec. 1993 126 p In PORTUGESE
(INPE-5580-TDI/543) Avail: CASI HC A07/MF A02

The rapid change in the Amazon forest cover has been causing a global concern in association with its impact to the environment. This work describes the results obtained from a low-cost methodology developed to locate new deforestation in the Amazon tropical forest. It combines automatic classification of the Advanced Very High Resolution Radiometer (NOAA/AVHRR) images and a geographic information system (GIS). Full resolution and geometrically corrected AVHRR channel 3 (3.5 micron to 3.9 micron) images of different dates were automatically compared in digital form. Changes in the original cover of the vegetation are detected in any two different images, and their locations were determined through the GIS. Tests in the northern region of the state of Mato Grosso were presented indicating the possibility of using AVHRR imagery operationally to detect new deforestation. Results comparing deforestation in the AVHRR channel 3 with corresponding high resolution Landsat-Thematic Mapper (TM) images indicated 49.1 percent and 56.5 percent of AVHRR correct location for 216 and 221 polygons of deforestation with different sizes, for two pairs of images, September 1989 and September 1990, and July 1990 and September 1990, respectively. Eighty-two percent and 90 percent of correct locations were obtained for the 50 TM polygons with deforestation greater than 3.1 sq km for the same pairs of images. Author

N95-17903# Pacific Northwest Lab., Richland, WA.
ON THE MEASUREMENT OF MOMENTUM FLUX PROFILES USING A FIVE-BEAM 915-MHz WIND PROFILER
W. J. Shaw and S. Zhong Aug. 1994 4 p Presented at the 3rd International Symposium on Tropospheric Profiling: Needs and Technologies, Hamburg, Germany, 30 Aug. - 2 Sep. 1994
(Contract DE-AC06-76RL-01830)
(DE94-018448; PNL-SA-24641; CONF-9408118-2) Avail: CASI HC A01/MF A01

The advent in the last few decades of surface-based remote sensing systems, including wind profiling radars, is revolutionizing meteorology. The concurrent advances in computer technology and numerical methods have spurred the development of new data assimilation techniques to manage the high temporal and spatial density of information that these systems now provide. The capabilities of wind profiling radars to measure profiles of the mean wind vector are now well established, although improvements, such as the removal of spurious wind readings caused by migrating birds, are still being made. When these radars are coupled with acoustic transducers to track vertically propagating sound pulses (the Radio Acoustic Sounding System, or RASS mode), they do a creditable job of providing temperature profiles as well, although generally to a lower attitude than they can measure the wind. While most of the attention devoted to wind profiler technology has been focused on mean wind and temperature observations, these systems can also measure velocity variances with the same Doppler spectra that are used to obtain the mean wind. In a five-beam system where the two pairs of off-zenith beams are coplanar, with the vertical, it is possible in principle to use profiles of the velocity variances to obtain estimates of the momentum flux profile. For a system with RASS capability, it is also theoretically possible to obtain a profile of the heat flux. Angevine et al. have attempted to use these techniques to obtain momentum and heat flux profiles in the atmospheric boundary layer. By compositing data from approximately two weeks, they were able to show a plausible diurnal variation in heat flux and a realistic profile of momentum flux. DOE

44 ENERGY PRODUCTION AND CONVERSION

Includes specific energy conversion systems, e.g., fuel cells; global sources of energy; geophysical conversion; and windpower.

For related information see also *07 Aircraft Propulsion and Power, 20 Spacecraft Propulsion and Power,* and *28 Propellants and Fuels.*

N95-15944# National Renewable Energy Lab., Golden, CO.
THE ROLE OF POINT DEFECTS AND DEFECT COMPLEXES IN SILICON DEVICE PROCESSING: SUMMARY REPORT AND PAPERS
Bhushan Sopori and Teh Y. Tan Aug. 1994 118 p The 3rd Workshop was held in Vail, CO, 16-18 Aug. 1993
(Contract DE-AC36-83CH-10093)
(DE94-011873; NREL/TP-413-7061; CONF-9308193-Summ) Avail: CASI HC A06/MF A02

This report is the summary of the third workshop on the role of point defects and defect complexes in silicon device processing. The workshop was organized: (1) to discuss recent progress in the material quality produced by photovoltaic Si manufacturers; (2) to foster the understanding of point defect issues in Si device processing; (3) to review the effects of inhomogeneities on large- area solar cell performance; (4) to discuss how to improve Si solar cell processing; and (5) to develop a new understanding of gettering, defect passivation, and defect annihilation. Separate abstracts were prepared for the individual papers, for the database. DOE

N95-15963*# Virginia Polytechnic Inst. and State Univ., Blacksburg, VA. Dept. of Mechanical Engineering.
HEAT TRANSFER MEASUREMENTS FOR STIRLING MACHINE CYLINDERS Final Report

Alan A. Kornhauser, B. C. Kafka, D. L. Finkbeiner, and F. C. Cantelmi
Aug. 1994 95 p
(Grant NAG3-1285)
(NASA-CR-197128; NAS 1.26: 197128) Avail: CASI HC A05/MF A01

The primary purpose of this study was to measure the effects of inflow-produced heat turbulence on heat transfer in Stirling machine cylinders. A secondary purpose was to provide new experimental information on heat transfer in gas springs without inflow. The apparatus for the experiment consisted of a varying-volume piston-cylinder space connected to a fixed volume space by an orifice. The orifice size could be varied to adjust the level of inflow-produced turbulence, or the orifice plate could be removed completely so as to merge the two spaces into a single gas spring space. Speed, cycle mean pressure, overall volume ratio, and varying volume space clearance ratio could also be adjusted. Volume, pressure in both spaces, and local heat flux at two locations were measured. The pressure and volume measurements were used to calculate area averaged heat flux, heat transfer hysteresis loss, and other heat transfer-related effects. Experiments in the one space arrangement extended the range of previous gas spring tests to lower volume ratio and higher nondimensional speed. The tests corroborated previous results and showed that analytic models for heat transfer and loss based on volume ratio approaching 1 were valid for volume ratios ranging from 1 to 2, a range covering most gas springs in Stirling machines. Data from experiments in the two space arrangement were first analyzed based on lumping the two spaces together and examining total loss and averaged heat transfer as a function of overall nondimensional parameter. Heat transfer and loss were found to be significantly increased by inflow-produced turbulence. These increases could be modeled by appropriate adjustment of empirical coefficients in an existing semi-analytic model. An attempt was made to use an inverse, parameter optimization procedure to find the heat transfer in each of the two spaces. This procedure was successful in retrieving this information from simulated pressure-volume data with artificially generated noise, but it failed with the actual experimental data. This is evidence that the models used in the parameter optimization procedure (and to generate the simulated data) were not correct. Data from the surface heat flux sensors indicated that the primary shortcoming of these models was that they assumed turbulence levels to be constant over the cycle. Sensor data in the varying volume space showed a large increase in heat flux, probably due to turbulence, during the expansion stroke. Author

N95-16067*# Jet Propulsion Lab., California Inst. of Tech., Pasadena, CA.
RESULTS OF THE 1994 NASA/JPL BALLOON FLIGHT SOLAR CELL CALIBRATION PROGRAM
B. E. Anspaugh and R. S. Weiss 1 Oct. 1994 24 p Sponsored by NASA, Washington
(NASA-CR-197248; JPL-Publ-94-22; NAS 1.26:197248) Avail: CASI HC A03/MF A01

The 1994 solar cell calibration balloon flight was completed on August 6, 1994. All objectives of the flight program were met. Thirty-seven modules were carried to an altitude of 119,000 ft (36.6 km). Data telemetered from the modules was corrected to 28 C and to 1 AU. The calibrated cells have been returned to the 6 participants and can now be used as reference standards in simulator testing of cells and arrays. Author

N95-16303 Hawaii Natural Energy Inst., Honolulu, HI.
MOLTEN SALT TECHNIQUES FOR EXCESS HEAT PRODUCTION AND THE LOADING ISSUE Interim Report
Bor Y. Liaw 12 Jul. 1994 8 p Limited Reproducibility: More than 20% of this document may be affected by microfiche quality
(Contract N00014-92-J-1673)
(AD-A282462) Avail: Issuing Activity (Defense Technical Information Center (DTIC))

An interesting molten salt technique for elevated-temperature excess heat production has recently been reported, promising great potential for commercial applications. This technique shows improved efficiency due to a high-temperature operation, high-grade heat production, and fast kinetics in metal-hydrogen reactions. This paper gives an overview of our work in molten salt electrolysis experiments using Ti and Pd as anodes in deuteride melts, in which substantial excess heat was found. This paper also presents some preliminary results using Ni and steel as anodes for electrolysis in hydride melts. Because the deuterium loading in Pd is considered a critical parameter for excess heat production, this paper will discuss this aspect and extend to elevated-temperature conditions. DTIC

N95-16435# Midwest Research Inst., Golden, CO. National Renewable Energy Lab.
AVAILABILITY OF DIRECT NORMAL RADIATION FOR SOLAR FURNACE PROCESSING: A CASE STUDY
C. E. Bingham Apr. 1994 7 p Presented at the SOLAR 1994: American Solar Energy Society Conference, San Jose, CA, 25-30 Jun. 1994
(Contract DE-AC36-83CH-10093)
(DE94-006907; NREL/TP-471-6233; CONF-9406134-2) Avail: CASI HC A02/MF A01

Predicting the availability of direct normal solar radiation is important for scheduling tests and estimating economics of solar furnaces. This paper looks at historical hourly average direct normal data to predict seasonal trends and report historical availability. Data collected at the Solar Radiation Research Laboratory (SRRL), located within 100 meters of the National Renewable Energy Laboratory's, (NREL's) High-Flux Solar Furnace (HFSF), are analyzed to determine availability of the furnace for testing and processing samples. The design of NREL's solar furnace allows considerable flexibility in processing samples under solar radiation levels of 100-1100 W/m(exp 2). Flux levels of 1-2000 W/cm(exp 2) can be delivered and controlled. Different processes pose different requirements for both incident flux and time. The historical data for this site show how often the hourly average direct normal solar radiation is above a certain threshold over the period 1981 to 1992. Results also show how many tests could have been completed (or samples processed) using five-minute data from 1992. DOE

N95-16437# Midwest Research Inst., Golden, CO.
STRUCTURAL TESTING OF THE NORTH WIND 250 COMPOSITE ROTOR JOINT
W. Musial, H. Link, and C. Coleman (Northern Power Systems, Inc., Moretown, VT.) May 1994 12 p Presented at the American Wind Energy Association Annual Conference and Exhibition, Minneapolis, MN, 9-13 May 1994
(Contract DE-AC36-83CH-10093)
(DE94-006923; NREL/TP-441-6619; CONF-940548-4) Avail: CASI HC A03/MF A01

The North Wind 250 wind turbine is under development at Northern Power Systems (NPS) in Moretown, VT. The turbine uses a unique, flow-through, teetered-rotor design. This design eliminates structural discontinuities at the blade/hub interface by fabricating the rotor as one continuous structural element. To accomplish this, the two blade spars are joined at the center of the rotor using a proprietary bonding technique. Fatigue tests were conducted on the full-scale rotor joint at the National Renewable Energy Laboratory (NREL). Subsequent tests are now underway to test the full-scale rotor and hub assembly to verify the design assumptions. The test articles were mounted in dedicated test fixtures. For the joint test, a constant moment was generated across the joint and parent material. Hydraulic actuators applied sinusoidal loading to the test article at levels equivalent to 90% of the extreme wind load for over one million cycles. When the loading was increased to 112% of the extreme wind load, the joint failed by buckling. Strain levels were monitored at 14 locations inside and outside of the blade joint during the test. The tests were used to qualify this critical element of the rotor for field testing and to provide information needed to improve the structural design of the joint. DOE

N95-16506# Pennsylvania State Univ., University Park, PA. Dept. of Physics.
ANISOTROPIC HEAT EXCHANGERS/STACK CONFIGURATIONS FOR THERMOACOUSTIC HEAT ENGINES Summary Report, 1 Oct. 1993 - 31 May 1994
Julian D. Maynard 21 Jun. 1994 8 p
(Contract N00014-93-1-1127)
(AD-A280974) Avail: CASI HC A02/MF A01

The goal of this project is to explore novel configurations of heat exchangers and the stack (heat pumping) section of thermoacoustic heat engines. The approach will be to use anisotropic systems, such as made

possible by glass capillary array technology. A part of the project will involve the development of high power drives and acoustic resonators for testing the new systems. DTIC

N95-16541# Department of Energy, Washington, DC. Office of the Deputy Assistant Secretary for Advanced Research and Special Technologies.

FUEL CELL SYSTEMS PROGRAM PLAN, FISCAL YEAR 1994

1994 37 p

(DE94-014301; DOE/FE-0311P) Avail: CASI HC A03/MF A01

The goal of the fuel cell program is to increase energy efficiency and economic effectiveness through development and commercialization of fuel cell systems which operate on fossil fuels in multiple end use sectors. DOE is participating with the private sector in sponsoring development of molten carbonate fuel cells and solid oxide fuel cells for application in the utility, commercial, and industrial sectors. Commercialization of phosphoric acid fuel cells is well underway. Besides the introduction, this document is divided into: goal/objectives, program strategy, technology description, technical status, program description/implementation, coordinated fuel cell activities, and international activities. DOE

N95-16544 Pechan (E. H.) and Associates, Inc., Durham, NC.

LANDFILL GAS ENERGY UTILIZATION: TECHNICAL AND NONTECHNICAL CONSIDERATIONS Report, Sep. 1992 - Mar. 1994

J. G. Pacey (EMCON Associates, San Jose, CA.), M. R. J. Doorn, and S. A. Thorneloe (Environmental Protection Agency, Research Triangle Park, NC.) Mar. 1994 5 p Presented at the 17th SWANA's Annual Landfill Gas Symposium, Long Beach, CA, 22-24 Mar. 1994 See also PB91-197061, PB92-137520, PB92-203116, and PB94-132180 Limited Reproducibility: More than 20% of this document may be affected by microfiche quality

(Contract EPA-68-D1-0146)

(PB94-189651; EPA/600/A-94/139) Avail: CASI HC A01

The paper discusses technical issues associated with the use of landfill gas (LFG) compared with natural gas, which is the primary fuel used for energy conversion equipment such as internal combustion engines, gas turbines, and fuel cells. LFG is a medium-heating-value fuel containing trace constituents that require gas pretreatment and energy equipment modifications to operate successfully. There are more than 100 LFG-to-energy projects in the U.S., and their developers and operators have found different ways to minimize the potential problems associated with LFG utilization. The paper also gives an overview of developers and operators of these projects, data of European projects, nontechnical issues such as project barriers and incentives, the relationship between LFG delivery and energy output, active landfill gas developers, and insights on project decision making. NTIS

N95-16575*# Auburn Univ., AL. Space Power Inst.

ANALYSIS OF SPACE ENVIRONMENT DAMAGE TO SOLAR CELL ASSEMBLIES FROM LDEF EXPERIMENT A0171-GSFC TEST PLATE Final Report, 21 Jul. 1993 - 19 Aug. 1994

David C. Hill and M. Frank Rose 2 Sep. 1994 92 p

(Contract NAS8-39131)

(NASA-CR-196523; NAS 1.26:196523) Avail: CASI HC A05/MF A01

The results of the postflight analysis of the solar cell assemblies from the LDEF (Long Duration Exposure facility) experiment A0171 is provided in this NASA sponsored research project. The following data on this research are provided as follows: (1) solar cell description, including, substrate composition and thickness, crystal orientation, anti-reflective coating composition and thickness; (2) preflight characteristics of the solar cell assemblies with respect to current and voltage; and (3) post-flight characteristics of the solar cell assemblies with respect to voltage and current. These solar cell assemblies are part of the Goddard Space Flight Center test plate which was designed to test the space environment effects (radiation, atomic oxygen, thermal cycling, meteoroid and debris) on conductively coated solar cell coversheets, various electrical bond materials, solar cell performance, and other material properties where feasible.

Derived from text

N95-16831*# Jet Propulsion Lab., California Inst. of Tech., Pasadena, CA.

PHOTOVOLTAIC POWER CONDITIONERS: DEVELOPMENT, EVOLUTION, AND THE NEXT GENERATION

A. Bulawka (Department of Energy, Washington, DC.), S. Krauthamer, R. Das, and W. Bower (Sandia National Labs., Albuquerque, NM.) 1994 7 p Presented at the 29th Intersociety Energy Conversion Engineering Conference, Monterey, CA, 7-12 Aug. 1994 Sponsored by NASA, Washington

(Contract DE-AC04-94AL-85000)

(NASA-CR-197005; NAS 1.26:197005; DE94-015284; SAND-94-1492C; CONF-94012-16) Avail: CASI HC A02/MF A01

Market-place acceptance of utility-connected photovoltaic (PV) power generation systems and their accelerated installation into residential and commercial applications are heavily dependent upon the ability of their power conditioning subsystems (PCS) to meet high reliability, low cost, and high performance goals. Many PCS development efforts have taken place over the last 15 years, and those efforts have resulted in substantial PCS hardware improvements. These improvements, however, have generally fallen short of meeting many reliability, cost and performance goals. Continuously evolving semiconductor technology developments, coupled with expanded market opportunities for power processing, offer a significant promise of improving PCS reliability, cost and performance, as they are integrated into future PCS designs. This paper revisits past and present development efforts in PCS design, identifies the evolutionary improvements and describes the new opportunities for PCS designs. The new opportunities are arising from the increased availability and capability of semiconductor switching components, smart power devices, and power integrated circuits (PICS). DOE

N95-16861*# National Aeronautics and Space Administration. Lewis Research Center, Cleveland, OH.

NICKEL HYDROGEN BATTERIES: AN OVERVIEW

John J. Smithrick and Patricia M. ODonnell Nov. 1994 13 p Presented at the 33rd Aerospace Sciences Meeting and Exhibit, Reno, NV, 9-12 Jan. 1995; sponsored by AIAA

(RTOP 233-01-0B)

(NASA-TM-106795; E-9259; NAS 1.15:106795; AIAA Paper 95-0026)

Copyright Avail: CASI HC A03/MF A01

This paper on nickel hydrogen batteries is an overview of the various nickel hydrogen battery design options, technical accomplishments, validation test results and trends. There is more than one nickel hydrogen battery design, each having its advantage for specific applications. The major battery designs are individual pressure vessel (IPV), common pressure vessel (CPV), bipolar and low pressure metal hydride. State-of-the-art (SOA) nickel hydrogen batteries are replacing nickel cadmium batteries in almost all geosynchronous orbit (GEO) applications requiring power above 1 kW. However, for the more severe low earth orbit (LEO) applications (greater than 30,000 cycles), the current cycle life of 4000 to 10,000 cycles at 60 percent DOD should be improved. A LeRC innovative advanced design IPV nickel hydrogen cell led to a breakthrough in cycle life enabling LEO applications at deep depths of discharge (DOD). A trend for some future satellites is to increase the power level to greater than 6 kW. Another trend is to decrease the power to less than 1 kW for small low cost satellites. Hence, the challenge is to reduce battery mass,volume, and cost. A key is to develop a light weight nickel electrode and alternate battery designs. A common pressure vessel (CPV) nickel hydrogen battery is emerging as a viable alternative to the IPV design. It has the advantage of reduced mass, volume and manufacturing costs. A 10 Ah CPV battery has successfully provided power on the relatively short lived Clementine Spacecraft. A bipolar nickel hydrogen battery design has been demonstrated (15,000 LEO cycles, 40 percent DOD). The advantage is also a significant reduction in volume, a modest reduction in mass, and like most bipolar designs, features a high pulse power capability. A low pressure aerospace nickel metal hydride battery cell has been developed and is on the market. It is a prismatic design which has the advantage of a significant reduction in volume and a reduction in manufacturing cost. Author

N95-16916 Pacific Northwest Lab., Richland, WA.

COATINGS FOR LARGE-AREA LOW-COST SOLAR CONCENTRATORS AND REFLECTORS

P. M. Martin, J. D. Affinito, M. E. Gross, and W. D. Bennett Jul. 1994 7 p Presented at the Annual Meeting of the Society of Photo-Optical Instrumentation Engineers, San Diego, CA, 24-29 Jul. 1994 Limited Reproducibility: More than 20% of this document may be affected by

microfiche quality
(Contract DE-AC06-76RL-01830)
(DE94-015735; PNL-SA-24444; CONF-940723-12) Avail: CASI HC A02

Seven years ago, Pacific Northwest Laboratory constructed a large-optics coating facility to develop and fabricate high-performance multilayer laser-mirror coatings on large substrates. With the reduction of DOD funding for the development of optical coatings for large optics, new applications for this chamber were sought. In addition to new DOD applications, the facility is now being used to fabricate multilayer enhanced-metal reflectors for low-cost large-area solar concentrators using both magnetron-sputtered metal and dielectric coatings, with future extension to vacuum-evaporated polymer coatings. Other new applications include: Ti/Ti:Al lamellar composites on flexible webs; EMI cladding for heater wire; EMI-shielding coatings on flexible webs; microwave-absorbing coatings on flexible webs; heat mirrors; bulk micromachining; and protective coatings on cylindrical substrates and webs. The facility has also been established as a DOD user facility for development and experimentation in large-area optical coatings. This paper describes important changes in the large-optics coating chamber and additional deposition equipment that has been added to pursue these new non-DOD technological areas. Solar reflectors and the resulting new coatings will be described. Future work and new technological areas being pursued will also be discussed. DOE

N95-16940# Georgia Inst. of Tech., Atlanta, GA.
DEVELOPMENT OF HIGH-EFFICIENCY, THIN-FILM CdTe SOLAR CELLS
A. Rohatgi, H. C. Chou, S. Kamra, and A. Bhat Sep. 1994 82 p Prepared for National Renewable Energy Lab., Golden, CO
(Contract DE-AC36-83CH-10093)
(DE94-011885; NREL/TP-451-7065) Avail: CASI HC A05/MF A01

Polycrystalline thin film CdTe solar cells are one of the leading candidates for terrestrial photovoltaic applications. Theoretical calculations project an efficiency of 27% for single crystal, single junction CdTe cells, and the practically achievable efficiency for polycrystalline CdTe cells is 18-20%. Polycrystalline CdTe cells made by different groups show a significant variation in short circuit currents, open circuit voltages, and cell efficiencies. A better understanding of carrier loss and transport mechanism is crucial for explaining these differences, improving the yield, and bridging the gap between current and practically achievable limits in CdTe cell efficiencies. The goal of this program is to improve the understanding of the loss mechanisms in thin film CdS/CdTe solar cells and to improve their efficiency by characterizing the properties of the films as well as the finished devices. DOE

N95-16954 Naval Postgraduate School, Monterey, CA. Dept. of Physics.
THERMOACOUSTIC PIN STACKS Summary Report
Robert M. Keolian 6 Jul. 1994 3 p Limited Reproducibility: More than 20% of this document may be affected by microfiche quality
(AD-A282267) Avail: CASI HC A01

The construction and testing of a new stack geometry for thermoacoustic engines, called a pin stack, has been started. The stack is at the heart of a class of heat engines that use sound to deliver refrigeration, or use a temperature difference to generate sound. Calculations show that the pin stack should make useful improvements in engine efficiency. About 2000 wires will be hand sewn in a hexagonal lattice between the hot and cold heat exchangers in a sound source using low pressure neon gas between 300 K and 77 K. DTIC

N95-16957# North Carolina Univ., Chapel Hill, NC.
RECOMBINATION AND METASTABILITY IN AMORPHOUS SILICON AND SILICON-GERMANIUM ALLOYS
M. Silver, D. X. Han, K. D. Wang, and M. Kemp Jul. 1994 35 p Prepared for National Renewable Energy Lab., Golden, CO
(Contract DE-AC36-83CH-10093)
(DE94-011837; NREL/TP-451-6491) Avail: CASI HC A03/MF A01

Electroluminescence-spectra- and transient-current measurements were taken before and after light-soaking a-Si:H p-i-n structures. For the first time, we were able to distinguish between bulk- and junction-controlled recombination. We found that in buffered p-b-i-n structures, the main-band luminescence was more pronounced than that in simple p-i-n structures. The enhancement of the main-band luminescence relates with an increase of the open-circuit voltage. This is evidence that the recombination takes place near the p-i interface, and the quality of the p-i interface is very important in solar cell performance. We also found that for thick p-i-n cells (greater than or equal to 2 microns), the luminescence contains more high-energy photons (1.1-1.2 eV) than does that for thin cells. Furthermore, the high-energy recombination is more efficient in creating metastable defects than is the low-energy recombination. Consequently, the thinner the i-layer, the less the light-induced effects. The results of repetition rate and reverse bias effects on forward-bias current imply that the junctions recover faster than the bulk when subjected to excess carriers caused by the bias. By including the coulomb interaction, we made progress on a microscopic model for radiative recombination. DOE

N95-17298 International Bank for Reconstruction and Development, Washington, DC.
SOLAR ENERGY: LESSONS FROM THE PACIFIC ISLAND EXPERIENCE
A. Liebenthal, S. Mathur, and H. Wade 1994 68 p Limited Reproducibility: More than 20% of this document may be affected by microfiche quality
(World-Bank-TP-244; ISBN-0-8213-2802-6) Copyright Avail: CASI HC A04

The experiences of several Pacific island countries provides a clear indication that in small, remote villages, off-the-shelf solar photovoltaic (PV) technologies are providing reliable power at costs less than those of the more commonly used diesel systems for households running a few electric lights and a TV/VCR. The report also confirms another point made repeatedly in the authors' recent energy sector work: appropriate technical choices need to be complemented by effective institutional approaches. The Pacific island experience demonstrated that the success of solar PV programs depended not merely on the choice of technology but on adequate training of maintenance personnel, good fee collection systems, and careful financial management. The report indicates that for solar PV systems installed in areas where managerial and technical expertise is scarce, ownership and maintenance of the systems by local, cooperatively owned utilities appears to be the soundest option. NTIS

N95-17521# Solarex Corp., Newtown, PA.
RESEARCH ON STABLE, HIGH-EFFICIENCY, AMORPHOUS SILICON MULTIJUNCTION MODULES
R. R. Arya, M. Bennett, L. Chen, B. Fieselmann, Y. Li, N. Maley, J. Newton, R. Podlesny, and L. Yang Jun. 1994 44 p Prepared for Midwest Research Inst., Golden, CO
(Contract DE-AC36-83CH-10093)
(DE94-011826; NREL/TP-411-6841) Avail: CASI HC A03/MF A01

This report describes work performed during the period 1 July 1992 through 30 June 1993. During this period, major improvements were achieved in the stabilized conversion efficiency of triple-junction modules. These resulted in the demonstration of triple-junction initial conversion efficiency of 11.3% and stabilized conversion efficiency of approximately 9%. Significant advances were made in the deposition of a-Si:H intrinsic layers that led to higher open-circuit voltage and improved stability. Thin microcrystalline n-layers were developed and scaled up for the recombination junctions in triple-junction modules that resulted in higher open-circuit voltage and fill factors. These improvements resulted in the demonstration of a-Si/a-Si/a-SiGe triple-junction modules with initial conversion efficiencies as high as 11.35% and 'stabilized' efficiencies of about 9%. DOE

45 ENVIRONMENT POLLUTION

Includes atmospheric, noise, thermal, and water pollution.

N95-16209# Department of Energy, Washington, DC.
GLOBAL WARMING POTENTIALS, PART 7
31 May 1994 21 p
(DE94-014066; DOE/PO-0015-Pt-7) Avail: CASI HC A03/MF A01

This document provides methods to account for the different effects of different gases on the atmosphere. It discusses the rationale and uses for simplified measures to represent human-related effects on climate and provides a brief introduction to a major index, the global warming potential (GWP) index. Appendix 7.A analyzes the science underlying the development of indices for concerns about climate, which is still evolving, evaluates the usefulness of currently available indices, and presents the state of the art for numerical indices and their uncertainties. For concerns about climate,

the Intergovernmental Panel on Climate Change (IPCC) has been instrumental in examining relative indices for comparing the radiative influences of greenhouse gases. The IPCC developed the concept of GWP's to provide a simple representation of the relative effects on climate resulting from a unit mass emission of a greenhouse gas. Alternative measures and variations on the definition of GWP's have also been considered and reported. DOE

N95-16212# Princeton Univ., NJ.
SIMULATIONS OF THE GLOBAL CARBON CYCLE AND ANTHROPOGENIC CO2 TRANSIENT
J. L. Sarmiento 1994 15 p
(Contract DE-FG02-90ER-61052)
(DE94-014165; DOE/ER-61052/3) Avail: CASI HC A03/MF A01

This research focuses on improving the understanding of the anthropogenic carbon dioxide transient using observations and models of the past and present. In addition, an attempt is made to develop an ability to predict the future of the carbon cycle in response to continued anthropogenic perturbations and climate change. Three aspects of the anthropogenic carbon budget were investigated: (1) the globally integrated budget at the present time; (2) the time history of the carbon budget; and (3) the spatial distribution of carbon fluxes. One of the major activities of this study was the participation in the model comparison study of Enting, et al. carried out in preparation for the IPCC 1994 report. DOE

N95-16213# SRI International Corp., Menlo Park, CA.
NOVEL MASS SPECTROMETRIC INSTRUMENT FOR GASEOUS AND PARTICULATE CHARACTERIZATION AND MONITORING
M. J. Coggiola Feb. 1994 15 p
(Contract DE-AC21-92MC-29116)
(DE94-014168; DOE/MC-29116/3799) Avail: CASI HC A03/MF A01

SRI International will develop a unique new instrument that will be capable of providing real-time (less than 1 minute), quantitative, chemical characterization of gaseous and particulate pollutants generated from DOE waste cleanup activities. The instrument will be capable of detecting and identifying volatile organic compounds, polynuclear aromatic hydrocarbons, heavy metals, and transuranic species released during waste cleanup activities. The instrument will be unique in its ability to detect and quantify in real-time these diverse pollutants in both vapor and particulate form. The instrument to be developed under this program will consist of several major components: (1) an isokinetic sampler capable of operating over a wide range of temperatures (up to 500 K) and flow rates; (2) a high pressure to low pressure transition and sampling region that efficiently separates particles from vapor-phase components for separate, parallel analyses; (3) two small mass spectrometers, one optimized for organic analysis using a unique field ionization source and one optimized for particulate characterization using thermal pyrolysis and electron-impact ionization (EI); and (4) a powerful personal computer for control and data acquisition. Initially, the instrument will be developed for targeted use in conjunction with the K-1435 Toxic Substances Control Act (TSCA) incinerator at the Oak Ridge National Laboratory K-25 site. Ultimately, the instrument will be designed to operate in the field at any cleanup site, located close to the stack or process vent, providing the plant operations personnel with real-time information and alarm capabilities. In addition, this instrument will be very broadly applicable for cleanup or sampling, for example, any time contaminated soil is moved or disturbed. DOE

N95-16386# Consultec Scientific, Inc., Knoxville, TN.
ASSESSMENT OF RESEARCH NEEDS FOR ADVANCED HETEROGENEOUS CATALYSTS FOR ENERGY APPLICATIONS, VOLUME 1
G. A. Mills Apr. 1994 28 p
(Contract DE-FG02-92ER-30201)
(DE94-015889; DOE/ER-30201-H1-Vol-1) Avail: CASI HC A03/MF A01

This report assesses the direction, technical content, and priority of research needs judged to provide the best chance of yielding new and improved heterogeneous catalysts for energy-related applications over a period of 5-20 years. It addresses is sues of energy conservation, alternate fuels and feedstocks, and the economics and applications that could alleviate pollution from energy processes. Recommended goals are defined in 3 major, closely linked research thrusts: (1) catalytic science; (2) environmental protection by catalysis; and(3) industrial catalytic applications. This volume provides a comprehensive executive summary, including research recommendations. DOE

N95-16545 Air Force Inst. of Tech., Wright-Patterson AFB, OH. School of Engineering.
SIMULATION OF HYDROLOGIC INFLUENCES ON WETLAND ECOSYSTEM SUCCESSION M.S. Thesis
Robert A. Pompilio Sep. 1994 128 p Limited Reproducibility: More than 20% of this document may be affected by microfiche quality
(AD-A284737; AFIT/GEE/ENV/94S-19) Avail: CASI HC A07

This research focuses on the development of a simulation model to determine the affects of hydrological influences on a wetland ecosystem. The model allows perturbations to the inputs of various wetland data which in turn influences the successional development of the ecosystem. This research consisted of converting a grassland ecosystem model to one which simulates wetland conditions. The critical factor in determining the success of wetland creation is the hydrology of the system. There are four of the areas of the original model which are affected by the hydrology. The model measures the health or success of the ecosystem through the measurement of the systems gross plant production, the respiration, and the net primary production of biomass. Altering the auxiliary variables of water level and the rate of flow through the system explicitly details the effects hydrologic influences have on those production rates. Ten case tests depicting exogenous perturbations of the hydrology were run to identify these affects. Although the tests dealt with the fluctuation of water through the system, any one of the auxiliary variables in the model could be changed to reflect site specific data. DTIC

N95-16557# Westinghouse Savannah River Co., Aiken, SC.
METEOROLOGICAL MONITORING PROGRAM
H. A. Hancock, Jr., ed. 1994 103 p
(Contract DE-AC09-89SR-18035)
(DE94-017810; WSRC-TR-93-0106) Avail: CASI HC A06/MF A02

The purpose of this technical report is to provide a comprehensive, detailed overview of the meteorological monitoring program at the Savannah River Site (SRS) near Aiken, South Carolina. The principle function of the program is to provide current, accurate meteorological data as input for calculating the transport and diffusion of any unplanned release of an atmospheric pollutant. The report is recommended for meteorologists, technicians, or any personnel who require an in-depth understanding of the meteorological monitoring program. DOE

N95-16881# Environmental Protection Agency, Research Triangle Park, NC. Air and Energy Engineering Research Lab.
ALTERNATIVES FOR OZONE-DEPLETING REFRIGERANTS Report, Oct. 1991 - Apr. 1993
N. Dean Smith and Krich Ratanaphruks (Acurex Corp., Research Triangle Park, NC.) 1993 6 p Presented at the Conference on Environmental Commerce, Chattanooga, TN, 17-20 Oct. 1993
(Contract EPA-68-D0-0141)
(PB94-190857; EPA/600/A-94/117) Avail: CASI HC A02/MF A01

The paper gives the results of tests of 2 of 11 compounds and several mixtures selected for intensive evaluation from about 40 new synthesized compounds that may serve as environmentally safe and effective refrigerant alternatives over the long term. The two compounds are: 1.1, 1.2, 3.3,-hexafluoropropane (HFC-236ea), a potential alternative for CFC-114; and 1.1, 2.2, 3-pentafluoropropane (HFC-245ca), a potential alternative for CFC-11. These two compounds have zero ozone depletion potential, low global warning potential, and thermophysical properties closely matching those of the chlorofluorocarbons (CFC's) they may replace. Limited toxicity tests to date reveal no adverse toxic effects. Flammability tests of HFC-236ea and HFC-245ca show the former to be marginally flammable depending on humidity and ignition source energy. Both compounds have been shown to be thermally and hydrolytically stable, miscible with the new polyolester lubricants, and compatible with numerous construction materials commonly used in refrigeration. Derived from text

N95-17304# Rijksinstituut voor Volksgezondheid en Milieuhygieene, Bilthoven (Netherlands).
ENERGY AND EMISSIONS OF CO2, NOx AND SO2 IN THE SCENARIO OF THE 3RD NATIONAL ENVIRONMENTAL EVALUATION, 1993 [ENERGIE EN EMISSIES VAN CO2, NOX EN SO2 IN DE SCENARIO'S VAN DE DERDE NATIONALE MILIEUVERKENNING]
R. Albers, ed., M. vanSchaaijk (Centraal Planbureau, The Hague, Netherlands.), W. Groot (Centraal Planbureau, The Hague, Netherlands.), O. V. Hilten (Netherlands Energy Research Foundation, Petten.), P. Kroon (Netherlands Energy Research Foundation, Petten.), M. Beeldman (Netherlands Energy Research Foundation, Petten.), and M. Rouw (Netherlands Energy Research Foundation, Petten.) Jun. 1993 99 p In DUTCH
(PB94-194792; RIVM-251701011) Avail: CASI HC A05/MF A02

In 1993 Dutch environmental policy was evaluated. Part of this evaluation was an outlook on the energy consumption, the energy supply, and the energy related emissions of CO2, NOx, and SO2. The main conclusions are: The use of energy will grow between 1990 and 2000 depending on economic growth and energy price level. Closely connected with the energy consumption the emission of CO2 will rise in most scenarios up to the year 2000. The emission of the acid components SO2 and NOx will decline. The goal for SO2 emission will likely be reached. This is not the case for the emission of NOx. Traffic is the main sector responsible for not reaching this goal. NTIS

N95-17348# Lamont-Doherty Geological Inst., Palisades, NY.
GLOBAL CLIMATE CHANGE MODEL NATURAL CLIMATE VARIATION: PALEOCLIMATE DATA BASE, PROBABILITIES AND ASTRONOMIC PREDICTORS
G. Kukla and J. Gavin May 1994 592 p Prepared for Pacific Northwest Lab., Richland, WA
(Contract DE-AC06-76RL-01830)
(DE94-013956; PNL-9418) Avail: CASI HC A25/MF A06

This report was prepared at the Lamont-Doherty Geological Observatory of Columbia University at Palisades, New York, under subcontract to Pacific Northwest Laboratory it is a part of a larger project of global climate studies which supports site characterization work required for the selection of a potential high-level nuclear waste repository and forms part of the Performance Assessment Scientific Support (PASS) Program at PNL. The work under the PASS Program is currently focusing on the proposed site at Yucca Mountain, Nevada, and is under the overall direction of the Yucca Mountain Project Office US Department of Energy, Las Vegas, Nevada. The final results of the PNL project will provide input to global atmospheric models designed to test specific climate scenarios which will be used in the site specific modeling work of others. The primary purpose of the data bases compiled and of the astronomic predictive models is to aid in the estimation of the probabilities of future climate states. The results will be used by two other teams working on the global climate study under contract to PNL. They are located at and the University of Maine in Orono, Maine, and the Applied Research Corporation in College Station, Texas. This report presents the results of the third year's work on the global climate change models and the data bases describing past climates. DOE

N95-17363# National Ocean Service, Rockville, MD. Coastal Monitoring and Bioeffects Assessment Div.
SOUTH FLORIDA ENVIRONMENTAL QUALITY. NATIONAL STATUS AND TRENDS PROGRAM FOR MARINE ENVIRONMENTAL QUALITY
A. Y. Cantillo, T. P. OConnor, and G. G. Lauenstein Dec. 1993 92 p
(PB94-173408; NOAA-TM-NOS-ORCA-75) Avail: CASI HC A05/MF A01

Florida Bay has undergone environmental change caused by man-made reduction of freshwater flow from the Everglades. The reduction in the freshwater flow resulted from the construction of drainage canals built to meet agricultural requirements and the demand for dry land by the increasing population of South Florida. This document is a summary of the environmental conditions of Florida Bay, Biscayne Bay, and the southern portion of the Gulf Coast of Florida; the levels of contaminants found at the NOAA National Status and Trends (NS&T) Program sites in the area; and how these levels compare with those found in other NS&T sites nationwide. NTIS

N95-17394 Oregon State Univ., Corvallis, OR.
A PROCEDURE FOR ESTIMATING THE CARBON BUDGET OF TERRESTRIAL ECOSYSTEMS IN THE FORMER SOVIET UNION BY GEOGRAPHIC INFORMATION SYSTEM ANALYSIS AND CLASSIFICATION OF AVHRR DERIVED GLOBAL VEGETATION INDEX Ph.D. Thesis
Greg G. Gaston 1993 180 p
Avail: Univ. Microfilms Order No. DA9413716

The purpose of this research was to develop methods for using geographic information system (GIS) analysis and unsupervised classification of global vegetation index (GVI) images to improve carbon budget estimates of the former Soviet Union (FSU). A GIS was used to locate the geographic distribution and estimate the area of agricultural lands in the FSU. Climatic factors were used to isolate agricultural lands suitable for no-till management. The effects of various tillage practices on the carbon cycle were estimated. Four years average, monthly maximum value GVI composites were clustered on the basis of timing, magnitude, and duration of 'greenness' as recorded by the normalized difference of vegetation index (NDVI). The resulting 42 image classes were identified by a variety of quantitative and qualitative methods including expert assessment by scientists with extensive field experience in the FSU and analysis of temporal NDVI response curves. The image classes appear to accurately delineate vegetation/landcover regions. The percent agricultural land, percent forest cover, and percent natural nonforest was estimated for each image class. Equivalent ecosystems described in the Bazilevich carbon data base were used to calculate the carbon cycle parameters forest and natural nonforest ecosystems. Carbon estimates for agricultural lands were calculated from production data. Comparisons between areal estimates of land cover from this research and reported statistics are very good. For example, forested land was estimated at 876 million hectares (MHa); forest statistical data from the FSU estimate 'commercial' forests to be 814 MHa. Total agricultural lands are estimated in research to be 211 MHa, the same as reported by the USDA and very close to the 217 MHz reported by statistics from the FSU. Results from carbon budget analysis include: (1) Complete conversion of all climatically suitable lands to no-till management would sequester over 3 gigatons (Gt) of carbon in the agricultural soils of the FSU. (2) Phytomass and net primary productivity (NPP) estimates for forest and nonforest ecosystems compare well with carbon budget estimates that used maps to identify carbon quantifiable regions. Dissert. Abstr.

N95-17399 Technische Univ., Delft (Netherlands). Lab. for Process Equipment.
CALCIUM PHOSPHATE PRECIPITATION IN A FLUIDIZED BED Ph.D. Thesis
M. M. Seckler 1994 184 p
(PB94-201407) Copyright Avail: Issuing Activity

The objectives of this thesis are: (1) to gain insight into the fundamental processes occurring in a fluidized bed for phosphorus removal from wastewater; (2) to optimize the phosphorus removal efficiency; and (3) to find ways of minimizing the detrimental effect of impurities normally present in wastewaters. NTIS

N95-17636 Lawrence Livermore National Lab., Livermore, CA.
ABSTRACTS AND PROGRAM PROCEEDINGS OF THE 1994 MEETING OF THE INTERNATIONAL SOCIETY FOR ECOLOGICAL MODELLING NORTH AMERICAN CHAPTER
J. R. Kercher Jun. 1994 40 p Meeting held in Knoxville, TN, 7-11 Aug. 1994 Limited Reproducibility: More than 20% of this document may be affected by microfiche quality
(Contract W-7405-eng-48)
(DE94-016456; CONF-940894) Avail: CASI HC A03

This document contains information about the 1994 meeting of the International Society for Ecological Modelling North American Chapter. The topics discussed include: (1) extinction risk assessment modelling; (2) ecological risk analysis of uranium mining; (3) impacts of pesticides; (4) demography, habitats; (5) atmospheric deposition; and (6) climate change. DOE

N95-17684# Environmental Protection Agency, Washington, DC.
PROCEEDINGS OF THE FIRST NATIONAL CONFERENCE ON CLIMATE CHANGE AND WATER RESOURCES MANAGEMENT

Thomas M. Ballentine and Eugene Z. Stakhiv Dec. 1993 411 p Conference held in Albuquerque, NM, 4-7 Nov. 1991
(AD-A281172; IWR-93-R-17) Avail: CASI HC A18/MF A04

The idea to hold this conference was developed from a belief on the part of the organizers that too little attention has been given to the views and needs of water managers in the ongoing public discourse on adaptation to potential global warming. This volume contains papers presented at the conference by scientists and water resource managers whose collected perspectives represent the best current thinking on the subject. The first of two plenary sessions framed the debate and discussion of response to climate change as it may be influenced by developing scientific, political, economic, institutional, environmental, and associated issues, conditions, and determinants. The papers presented and the ensuing discussion addressed the important scientific debate on questions surrounding whether or not mankind is causing global warming and, if so, how are policy, business, and political decisions being influenced. The papers presented at the second session addressed questions concerning assessments based on General Circulation Models (GCM's), attempts to improve accuracy in predictions generated by the models, and the relavence of model outputs to practical engineering solutions. The closing panel discussion addressed climate change and water resources management. Derived from text

N95-17718# Lawrence Livermore National Lab., Livermore, CA.
NATURAL AND ARTIFICIAL NOBEL GAS HYDROLOGIC TRACERS
G. B. Hudson Jun. 1994 30 p
(Contract W-7405-eng-48)
(DE94-016010; UCRL-ID-117543) Avail: CASI HC A03/MF A01

Noble gas isotopes provide opportunities for ground water tracing. Both naturally occurring tracers and artificially injected tracers can be used. The equilibration of water with the earth's atmosphere records the temperature and atmospheric pressure during ground water recharge. This temperature/pressure record can be used to distinguish cold recharge from warmer recharge with a resolution of 1-2 C temperature and 500m in altitude. The radioactive decay of U and Th produce large concentrations of 4He in old ground water and this 4He signature can be useful in tracing the small addition of old water (more than 10,000 yr.) to young water (less than 100 yr.). The decay of 3H present either from nuclear testing or cosmic ray interactions leads to detectable amounts of 3He in young ground water (less than 50 yr.). By measuring both 3H and 3He, the mean age of the 3H in the water can be calculated. In addition to these natural tracers, isotopically enriched noble gas isotopes are readily available at low cost and can be used as non-hazardous water tracers. This inert, persistent, and harmless tracing technique can be used in many situations at a cost of about one dollar per million gallons of water traced. DOE

N95-17740 University of Southern California, Los Angeles, CA. Dept. of Biological Sciences.
FLOW OVER ABRUPT TOPOGRAPHY: THE APPLICATION OF PATTERNS IN NUTRIENT AND PRODUCTIVITY IN REFLECTING PHYSICAL PROCESSES Final Technical Report, 15 Nov. 1988 - 31 Mar. 1994
Richard C. Dugdale and Frances P. Wilkerson 20 Jun. 1994 6 p
Limited Reproducibility: More than 20% of this document may be affected by microfiche quality
(Contract N00014-89-J-1423)
(AD-A280813) Avail: CASI HC A02

This project was part of an interdisciplinary study designed to investigate all aspects of seamount oceanography on the local and mesoscale level. The seamount selected for study was Fieberling Guyot a deep topographical feature that rises to within 430 m from the surface, located at 32 deg 25'N, 127 deg 47'W, just over 1000 km west of San Diego. In addition the biological components of the program chose to study, for comparison, two more shallow near-shore features, Northeast Bank and Sixtymile Bank, that were visited on cruises out to Fieberling Guyot. During the 3 field years (cruises in September 1989, 1990 and 1991) we made near-surface (i.e. the euphotic zone to approximately 100 m depth) measurements of nutrients (nitrate, nitrite, ammonium, silicate and phosphate) an new, regenerated and total productivity of the phytoplankton. The nutrient measurements using nanomolar analysis made it possible to clearly delineate the nitracline to be closely positioned near the chlorophyll maximum at about 110 m. The productivity measurements made using stable isotopes (13C labelled bicarbonate and 15N labelled nitrate and ammonium) showed ammonium uptake to exceed nitrate uptake with rates typical of oligotrophic waters (i.e. % new prodn. of 9%). There was interannular variability with higher nutrients and productivity in 1991. The shallow Banks showed more nutrients and productivity as apparently, topographically induced physical events there advect sufficient nutrients into the photic zone for a phytoplankton response, unlike at Fieberling. DTIC

N95-17908# Oak Ridge National Lab., TN. Environmental Sciences Div.
MODELLING INTERACTIONS OF CARBON DIOXIDE, FORESTS, AND CLIMATE
Robert J. Luxmoore and Dennis D. Baldocchi (National Oceanic and Atmospheric Administration, Oak Ridge, TN.) 1994 54 p Presented at the IPCC International Workshop on Biotic Feedbacks in the Global Climate System, Woods Hole, MA, 25-29 Oct. 1992
(Contract DE-AC05-84OR-21400)
(DE94-018694; CONF-9210354-2) Avail: CASI HC A04/MF A01

Atmospheric carbon dioxide is rising and forests and climate is changing. This combination of fact and premise may be evaluated at a range of temporal and spatial scales with the aid of computer simulators describing the interrelationships between forest vegetation, litter and soil characteristics, and appropriate meteorological variables. Some insights on the effects of climate on the transfers of carbon and the converse effect of carbon transfer on climate are discussed as a basis for assessing the significance of feedbacks between vegetation and climate under conditions of rising atmospheric carbon dioxide. Three main classes of forest models are reviewed. These are physiologically-based models, forest succession simulators based on the JABOWA model, and ecosystem-carbon budget models that use compartment transfer rates with empirically estimated coefficients. Some regression modeling approaches are also outlined. Energy budget models applied to forests and grasslands are also reviewed. This review presents examples of forest models; a comprehensive discussion of all available models is not undertaken. DOE

N95-17920# Lawrence Livermore National Lab., Livermore, CA.
CERES, PHASES 1 AND 2 Progress Report
W. P. Dannevik, J. Ambrosiano, J. Kercher, J. E. Penner, and W. Emanuel (Oak Ridge National Lab., TN.) 27 May 1994 61 p
(Contract W-7405-eng-48)
(DE94-014730; UCRL-ID-116573-Phase-1-2) Avail: CASI HC A04/MF A01

The CERES project represents a long-term commitment of LLNL's Global Climate Research Division to the EPA. The goal is to build an Earth System Model (ESM) with the ability in the near future to assist EPA in carrying out its responsibilities in the environmental policy and assessment arena, with particular emphasis on the terrestrial ecosystem components of the Earth system. There are two complementary aspects of the CERES development plan. The first is to provide a computational framework and modeling infrastructure for ESM development. The goal is to create an 'open architecture' enabling submodels from different research groups studying terrestrial ecosystems to become part of a fully-coupled model of the Earth's climate system. The second goal is to contribute fundamentally to understanding of the terrestrial component of the Earth system by developing advanced models. During this first phase of the CERES project, these two activities have been somewhat separate; the software engineering and framework building activity having been done in parallel with terrestrial model development. These two activities are merging as the framework becomes more mature, with robust software tools, and with a growing complement of tuned and benchmarked submodels and as the ecosystem models become fully incorporated into the ESM modeling framework. Two appendices contain the following papers: (1) 'Research Recommendations to the EPA in Support of Earth System Modeling Activities,' LLNL CERES project report; and (2) 'Progress Report on Terrestrial Model Development: Research in Support of the CERES Earth System Modeling Project,' LLNL CERES project report. DOE

N95-17922# Lawrence Livermore National Lab., Livermore, CA.
FEM3C, AN IMPROVED THREE-DIMENSIONAL HEAVY-GAS DISPERSION MODEL: USER'S MANUAL
S. T. Chan Mar. 1994 88 p
(Contract W-7405-eng-48)
(DE94-014731; UCRL-MA-116567) Avail: CASI HC A05/MF A01

FEM3C is another upgraded version of FEM3 (a three-dimensional Finite Element Model), which was developed primarily for simulating the atmospheric dispersion of heavier-than-air gas (or heavy gas) releases, based on solving the fully three-dimensional, time-dependent conservation equations of mass, momentum, energy, and species of an inert gas or a pollutant in the form of vapor/droplets. A generalized anelastic approximation, together with the ideal gas law for the density of the gas/air mixture, is invoked to preclude sound waves and allow large density variations in both space and time. The numerical algorithm utilizes a modified Galerkin finite element method to discretize spatially the time-dependent conservation equations of mass, momentum, energy, and species. A consistent pressure Poisson equation is formed and solved separately from the time-dependent equations, which are sequentially solved and integrated in time via a modified forward Euler method. The model can handle instantaneous source, finite-duration, and continuous releases. Also, it is capable of treating terrain and obstructions. Besides a K-theory model using similarity functions, an advanced turbulence model based on solving the k - (var epsilon) transport equations is available as well. Imbedded in the code are also options for solving the Boussinesq equations. In this report, an overview of the model is given, user's guides for using the model are provided, and example problems are presented to illustrate the usage of the model. DOE

46 GEOPHYSICS

Includes aeronomy; upper and lower atmosphere studies; ionospheric and magnetospheric physics; and geomagnetism.

For space radiation see *93 Space Radiation*.

N95-15965*# Michigan Univ., Ann Arbor, MI. Dept. of Atmospheric, Oceanic and Space Sciences.

SEPAC CO-INVESTIGATOR SUPPORT Final Report, 1 Sep. 1990 - 30 Jun. 1994

1994 7 p

(Contract NAS8-38772)

(NASA-CR-196527; NAS 1.26:196527) Avail: CASI HC A02/MF A01

Mission preparation and support, data reduction and analysis, and modelling of beam phenomenon activities are described with respect to the Space Experiments with Particle Accelerators (SEPAC) project. The SEPAC Electron Beam Accelerator was used in observing the life time and drift velocity of ionization streaks in the upper atmosphere by ground based radars. A second active source, the plasma contactor (PC) electrically neutralized the shuttle orbiter during beam injections. Several observations of plasma density enhancements were correlated with orbiter crossings of the magnetic meridian of the Jicamarca, Peru radar located near the magnetic equator. One of several successful experiments was the artificial aurora experiment in which downward directed electron beam pulses were observed by the onboard AEPI camera. Theoretical and modelling efforts focused on phenomena related to electron beam and plasma cloud injection from spacecraft. CASI

N95-16284# EG and G Energy Measurements, Inc., Santa Barbara, CA. Special Technologies Lab.

SITE CHARACTERIZATION AT THE RABBIT VALLEY GEOPHYSICAL PERFORMANCE EVALUATION RANGE

S Koppenjan, and M. Martinez 1994 68 p Presented at the Symposium on the Application of Geophysics to Environmental and Engineering Problems, Boston, MA, 27-31 Mar. 1994

(Contract DE-AC08-93NV-11265)

(DE94-013550; EGG-11265-3004; CONF-940353-6) Avail: CASI HC A04/MF A01

The United States Department of Energy (US DOE) is developing a Geophysical Performance Evaluation Range (GPER) at Rabbit Valley located 30 miles west of Grand Junction, Colorado. The purpose of the range is to provide a test area for geophysical instruments and survey procedures. Assessment of equipment accuracy and resolution is accomplished through the use of static and dynamic physical models. These models include targets with fixed configurations and targets that can be re-configured to simulate specific specifications. Initial testing (1991) combined with the current tests at the Rabbit Valley GPER will establish baseline data and will provide performance criteria for the development of geophysical technologies and techniques. The US DOE's Special Technologies Laboratory (STL) staff has conducted a Ground Penetrating Radar (GPR) survey of the site with its stepped FM-CW GPR. Additionally, STL contracted several other geophysical tests. These include an airborne GPR survey incorporating a 'chirped' FM-CW GPR system and a magnetic survey with a surfaced-towed magnetometer array unit Ground-based and aerial video and still frame pictures were also acquired. STL compiled and analyzed all of the geophysical maps and created a site characterization database. This paper discusses the results of the multi-sensor geophysical studies performed at Rabbit Valley and the future plans for the site. DOE

N95-16432*# Texas Univ. at Dallas, Richardson, TX. Center for Space Studies.

ION DRIFT METER RESEARCH Final Technical Report, 1 Jan. 1992 - 31 Dec. 1993

Roderick A. Heelis 1994 5 p

(Grant NAG5-306)

(NASA-CR-197124; NAS 1.26:197124; UTD-23253-961) Avail: CASI HC A01/MF A01

The final activity period for the DE project has been particularly productive. This period has seen the final delivery of geophysical data sets to the National Space Science Data Center, the granting of three Ph.D. degrees from cumulative work on the project, the operation of automatic data access and display routines for the data, and an increased effort in research and publication of the data. As before the research activities, largely devoted to studies involving the dynamics of the ionosphere, utilize data from the IDM and the RPA and thus the work is not easily attributable to one or the other of these separately funded efforts. In this final report we provide brief descriptions of the work accomplished in the final phase of the program. The Dynamics Explorer program has provided a significant opportunity for much of the community to participate in the data analysis and interpretation. The data, now residing in the national space science data center, are a great legacy that should continue to yield important results for many years. Author

N95-16521# Naval Postgraduate School, Monterey, CA.

RADAR OBSERVATIONS OF FIELD-ALIGNED PLASMA PROPAGATIONS ASSOCIATED WITH NASA'S PMG EXPERIMENT M.S. Thesis

Darren M. Olson Sep. 1994 90 p

(AD-A285218) Avail: CASI HC A05/MF A01

NASA's Plasma Motor Generator (PMG) tethered satellite mission was launched in June 1993 to verify the ability of hollow cathode plasma sources to couple electric currents from an electrodynamic tether into the ambient ionospheric plasma. This large-scale coupling process resulted in turbulent plasma signatures associated with the orbiting plasma generator, which propagated over great distances along the earth's geomagnetic field lines. VHF radars in Hilo, Hawaii and Jicamarca, Peru recorded observations of these field-aligned disturbances as part of the experiment. Based on analysis of these radar observations and tracking data of PMG's orbit, the effective propagation velocity of these traveling plasma waveforms was calculated to be of the order of 1000 meters per second. Detection of these disturbances, associated with PMG's passage overhead, supports the existence of a phantom current loop allowing current flow along the magnetic field lines of the earth and into the lower ionosphere from either end of an electrodynamic tether. DTIC

N95-16537# Los Alamos National Lab., NM.

GEOSYNCHRONOUS ORBIT MAGNETOPAUSE CROSSINGS

D. J. McComas, R. C. Elphic, M. B. Moldwin, and M. F. Thomsen 1994 5 p Presented at the 8th International Symposium on Solar Terrestrial Physics, Sendai, Japan, 6-10 Jun. 1994

(Contract W-7405-eng-36)

(DE94-014817; LA-UR-94-1610; CONF-9406192-2) Avail: CASI HC A01/MF A01

In this study we extend the analysis of magnetopause crossings observed with Magnetospheric Plasma Analyzer measurements to examine a much larger statistical data set. This study examines 39 maiznetosheath/LLBL intervals from 79 spacecraft-months of observations: these observations were taken from a survey of data from the start of each spacecraft mission and extending through March 1993. In contrast to the previous findings, we find no evidence for a significant dawn/dusk asymmetry in geosynchronous magnetopause crossings. DOE

N95-16735# Bristol Univ. (England).
LONG TERM MODELLING OF PERMAFROST DYNAMICS Final Technical Report
K. Fawcett and M. G. Anderson Jul. 1994 88 p
(Contract DAJA45-92-C-0011)
(AD-A285315; R/D-6477-EN-01) Avail: CASI HC A05/MF A01

The PERIMOVE model is capable of simulating moisture and heat transfers within soil profiles. In addition, the simulation of these processes formed the basis for the prediction of the volume changes that moisture redistribution and freezing create within soil profiles and the resulting movement of material and loss of soil strength during freezing and thawing cycles. In order to aid the development and validation of the model a suite of data sources have been identified and assembled. These have enabled model testing at each stage of development. Areas of further work are suggested. DTIC

N95-16872# Army Engineer Waterways Experiment Station, Vicksburg, MS. Geotechnical Lab.
NORMALIZATION AND PREDICTION OF GEOTECHNICAL PROPERTIES USING THE CONE PENETROMETER TEST (CPT) Final Report
Richard S. Olsen Aug. 1994 322 p
(AD-A285193; WES/TR/GL-94-29) Avail: CASI HC A14/MF A03

This research was to develop techniques for (1) stress normalization of CPT measurements (and geotechnical properties) and (2) CPT prediction of geotechnical properties using cone and sleeve friction resistance values. Stress normalization allows a variable geotechnical property to be reduced to an equivalent value at a standard confining stress. A new concept, the Stress Focus, was identified which provides a basis for understanding soil strength as a function of confining stress. This study demonstrated that sand friction angles for different initial relative densities converge to a Stress Focus at high confining stress (approximately 100 atm), where the strength behavior is similar to that of a sedimentary rock. Dilation of dense sands decreases with increased confining stress until the Stress Focus is reached, as confirmed using historic high pressure triaxial test data as well with CPT measurements from laboratory chamber tests and uniform soil layers. The paths of convergence to the Stress Focus are exponentially related to confining stress and are the basis for development of CPT cone and sleeve friction resistance normalization techniques. The overburden stress at the Stress Focus is soil type dependent. The stress exponent for SPT normalization was shown to be equal to the CPT derived stress exponent. CPT correlations to geotechnical properties were established using both CPT cone resistance and friction ratio. DTIC

N95-16927# Los Alamos National Lab., NM.
KINETIC EFFECTS NEAR THE MAGNETOPAUSE
S. P. Gary, D. Winske, M. E. McKean (California Univ., San Diego, CA.), S. A. Fuselier (Lockheed Missiles and Space Co., Palo Alto, CA.), and R. E. Denton (Dartmouth Coll., Hanover, NH.) 24 Mar. 1994 19 p Presented at the Chapman Conference on Physics of the Magnetopause, San Diego, CA, 14-18 Mar. 1994
(Contract W-7405-eng-36)
(DE94-009333; LA-UR-94-1057; CONF-940393-1) Avail: CASI HC A03/MF A01

Boundary conditions for magnetopause processes such as reconnection can be understood by studying the properties of magnetosheath plasma as it flows toward this transition. This manuscript reviews the role of electromagnetic ion cyclotron instabilities in constraining ion temperature anisotropies in the magnetosheath. Linear Vlasov theory and hybrid computer simulations have demonstrated that the inverse correlation between the proton anisotropy and the parallel proton (beta) observed from AMPTE/CCE in the subsolar sheath is due to wave-particle scattering by ion cyclotron anisotropy instabilities. Recent research on this topic is reviewed and the application of this inverse correlation to a successful bounded anisotropy model of proton temperatures in the sheath is described. DOE

N95-16981* National Aeronautics and Space Administration, Washington, DC.
FORECASTING EARTHQUAKES (Videotape)
1994 Videotape: 11 min. 20 sec. playing time, in color, with sound
(NASA-TM-110112; NASA-ASR-270; NONP-NASA-VT-95-35012) Avail: CASI VHS A02/BETA A22

In this video there are scenes of damage from the Northridge Earthquake and interviews with Dr. Andrea Donnelan, Geophysics at JPL, and Dr. Jim Dolan, earthquake geologist from Cal. Tech. The interviews discuss earthquake forecasting by tracking changes in the earth's crust using antenna receiving signals from a series of satellites called the Global Positioning System (GPS). JPL

N95-17362# Sandia National Labs., Albuquerque, NM.
APPLICATION OF NMR SHOCK BAROMETER TO NATURALLY SHOCKED MINERALS
R. T. Cygan and M. B. Boslough Jul. 1994 33 p
(Contract DE-AC04-94AL-85000)
(DE95-000326; SAND-94-1497) Avail: CASI HC A03/MF A01

The shock-loading of natural materials by an impact, such as a comet or meteorite, can result in the formation of modified and altered phases in the target rock. In order to characterize the resulting material and to evaluate the extent of shock modification, the authors have used nuclear magnetic resonance (NMR) spectroscopy to examine several natural and experimentally shocked minerals. NMR spectroscopy is used to characterize the formation of high pressure silica polymorphs and amorphous material associated with the shocked Coconino Sandstone from Meteor Crater, Arizona. Five samples of the sandstone were obtained from several locations at the crater to represent a range of shock conditions associated with the hypervelocity impact of a 30 meter-diameter meteorite. The NMR spectra for these powdered materials exhibit peaks assigned to quartz, coesite, stishovite, and glass. A new resonance, identified as a densified form of amorphous silica with silicon in tetrahedra with one hydroxyl group, is observed for two of the moderately shocked samples. Experimental shock-loading of dry and water-saturated Coconino Sandstone powders provides shock-metamorphosed material that exhibit broadening of NMR resonances with increasing shock pressure, but no evidence of the new dense silica phase. DOE

N95-17446 Air Force Inst. of Tech., Wright-Patterson AFB, OH.
A LATITUDINAL SURVEY OF MIDDLE ATMOSPHERIC WATER VAPOR REVEALED BY SHIPBOARD MICROWAVE SPECTROSCOPY M.S. Thesis
Mark L. Schrader May 1994 143 p Limited Reproducibility: More than 20% of this document may be affected by microfiche quality
(AD-A282000; AFIT/CI/CIA-94-036) Avail: Issuing Activity (Defense Technical Information Center (DTIC))

Water vapor is one of the most important greenhouse gases and is an important tracer of atmospheric motions in the middle atmosphere. It also plays an important role in the chemistry of the middle atmosphere and through its photodissociation by solar radiation, it is the major source of hydrogen escaping to space. Ground-based microwave measurements conducted in the 1980s have provided a fair understanding of the seasonal variation of mesospheric water vapor in the northern hemisphere mid-latitudes, but the global distribution of water vapor in the middle atmosphere is only beginning to be revealed by space-based measurements. DTIC

N95-17471# Moscow State Univ. (Russia). Inst. of Nuclear Physics.
CHARACTERISTICS OF MULTIPLE AURORAL INVERTED-V STRUCTURES AND THE PROBLEM OF MAGNETOSPHERIC PLASMA STRATIFICATION
E. E. Antonova, M. V. Stepanova, M. V. Teltzov, and B. A. Tverskoy 1993 32 p
(DE94-622233; INP-MSU-93-4-296; NIIYaF-MGU-93-4-296) Avail: CASI HC A03/MF A01 (US Sales Only)

The concept of hot stratification of magnetospheric plasma is presented. The stratification mechanism is based on the assumption that in the center of plasma sheet the pressure is approximately isotropic and under steady state conditions the gradient and curvature drift currents play the principal role. The number of formed structures is determined by the parameter of stratification. DOE

N95-17647# Instituto de Pesquisas Espaciais, Sao Paulo (Brazil).
EQUATORIAL AIRGLOW STUDIES VIA ROCKET EXPERIMENT Ph.D. Thesis [AEROLUMINESCENCIA DA REGIAO EQUATORIAL: ESTUDO VIA EXPERIMENTO DE FOGUETE]
Stella Maris Ludovic Melo Oct. 1994 209 p In PORTUGESE
(INPE-5589-TDI/551) Avail: CASI HC A10/MF A03

A rocket payload designed to measure mesospheric sodium, hydroxyl, and oxygen nightglow emissions, in addition to electron density and temperature, was launched from Alcantara Launch Center (2.3 deg S, 44.4 deg W), at 2352 LST on May 31, 1992. At the time of the launch, a sodium Lidar and a multichannel tilting filter photometer were operated at the same site, giving vertical profiles of atmospheric sodium density and OH (9-4) rotational temperature, respectively. The height profiles of the emission intensities of the atomic oxygen OI557.7 nm and molecular oxygen A (0-0) band are used to obtain the atomic oxygen density profiles. The results show the validity for the equatorial region of the empirical parameters proposed by McDade et al. The measured OH Meinel (8-3) band emission rates are considerably higher than expected from the OH excitation models proposed by McDade et al. The influence of the transition probabilities adopted are discussed, and new quenching parameters are introduced to explain the present data. The simultaneously measured profiles of NaD line emission and atomic sodium density are used to determine O3 concentrations. The H concentrations are then calculated from O and O3 concentrations. The derived H concentrations are much higher than those measured by others techniques or suggested by recent models. However, this difference can be attributed to the uncertainty in the value adopted for the branching ratio of the reaction which produces excited Na. Although the technique used is an indirect optical one, this is the first simultaneous measurement of the vertical profiles of O, O3, and H in the equatorial region. Author

47 METEOROLOGY AND CLIMATOLOGY

Includes weather forecasting and modification.

N95-16235 Air Force Inst. of Tech., Wright-Patterson AFB, OH.
AN IMPROVED NEUTRAL WIND MODEL WITH PREDICTIVE CAPABILITIES M.S. Thesis
Kathlene R. Dowdy 1993 87 p Limited Reproducibility: More than 20% of this document may be affected by microfiche quality
(AD-A282283; AFIT/CI/CIA-94-030) Avail: Issuing Activity (Defense Technical Information Center (DTIC))

It has been noted that one of the more essential ingredients of any model of the F2 region of the ionosphere is an accurate estimate of the meridional neutral winds. Inaccurate neutral wind values can drastically change the model's results. Since direct measurements have been difficult to make on a global scale, obtaining wind values has been a difficult problem. A servo model was developed at Utah State University to calculate the meridional neutral winds from the height of the F2 peak. This model incorporated the Mass Spectrometer Incoherent Scatter model to represent the neutral atmosphere and the International Reference Ionosphere to depict the height of the F2 peak. The servo model was designed to allow the input of F2 peak heights if desired. DTIC

N95-16290 Technische Univ., Delft (Netherlands).
LARGE-EDDY SIMULATION OF CUMULUS CONVECTION Ph.D. Thesis
J. W. M. Cuijpers 31 Jan. 1994 159 p Limited Reproducibility: More than 20% of this document may be affected by microfiche quality
(PB94-191368; ISBN-90-9006737-X) Copyright Avail: CASI HC A08

A study of the structure and nature of the physical processes, such as shear, buoyancy, condensation, and momentum and radiative transport, involved in the development and maintenance of cumulus clouds was performed. Models describing the processes were developed utilizing data obtained in a study conducted near Puerto Rico in December 1972 and in the Global Atmospheric Research Program Atlantic Tropical Experiment (GATE) June to September 1974. The models indicated that data obtained in the Puerto Rico study could be explained on the basis of shear and buoyancy processes occuring in the boundary layer and data obtained in the GATE experiment could be explained by buoyancy processes in the boundary layer. NTIS

N95-16398# Argonne National Lab., IL. Mathematics and Computer Science Div.
SENSITIVITY ANALYSIS OF NUMERICALLY-SIMULATED CONVECTIVE STORMS USING DIRECT AND ADJOINT METHODS
S. K. Park (Oklahoma Univ., Norman, OK.), K. K. Droegemeier (Oklahoma Univ., Norman, OK.), C. Bischof, and T. Knauff 1994 4 p Presented at the 6th Conference on Mesoscale Processes, Portland, OR, 18-22 Jul. 1994
(Contract W-31-109-eng-38)
(DE94-013399; ANL/MCS/CP-82981; CONF-940769-4) Avail: CASI HC A01/MF A01

The goal of this project is to evaluate the sensitivity of numerically modeled convective storms to control parameters such as the initial conditions, boundary conditions, environment, and various physical and computational parameters. In other words, the authors seek the gradient of the solution vector with respect to specified parameters. One can use two approaches to accomplish this task. In the first or so-called brute force method, one uses a fully nonlinear model to generate a control forecast starting from a specified initial state. Then, a number of other forecasts are made in which chosen parameters (e.g., initial conditions) are systematically varied. The obvious drawback is that a large number of full model predictions are needed to examine the effects of only a single parameter. The authors describe herein an alternative, essentially automated method (ADIFOR, or Automatic DIfferentiation of FORtran) for obtaining the solution gradient that bypasses the adjoint altogether yet provides even more information about the gradient. (ADIFOR, like the adjoint technique, is constrained by the linearity assumption.) Applied to a 1-D moist cloud model, the authors assess the utility of ADIFOR relative to the brute force approach and evaluate the validity of the tangent linear approximation in the context of deep convection. DOE

N95-16551# Naval Research Lab., Bay Saint Louis, MS.
MIXED-LAYER HINDCASTS CONDUCTED AT OWS VICTOR WITH INITIALIZATION FROM SYNTHETIC PROFILES/MIXED-LAYER HINDCASTS CONDUCTED WITH BTs TAKEN DURING 1990 WITH ATMOSPHERIC FORCING FROM NOGAPS Final Report
Paul J. Martin and Richard A. Allard 30 Aug. 1994 26 p
(AD-A284749; NRL/FR/7322-93-9439) Avail: CASI HC A03/MF A01

Mixed-layer hindcasts were conducted with data from Ocean Weathership Station Victor (164 deg E, 34 deg N) to investigate the question of whether the near-surface thermal structure of synthetic temperature profiles that are determined from observations of sea-surface height (SSH) and sea-surface temperature (SST) can be improved by mixed-layer hindcasting. Synthetic profiles were calculated at Victor based on the SSH and SST of observed deep temperature profiles. Mixed-layer hindcasts were initialized from the synthetic profiles, forced with wind stresses and heat fluxes calculated from 3-h meteorological observations at Victor, and integrated up to the time the observed profiles were taken. Hindcast durations ranged from 12 to 120 h. The mixed-layer depths (MLD's) of the synthetic and hindcast profiles were compared with the MLD's of the observed profiles, and mean and root-mean-square (rms) MLD errors were calculated on a monthly and annual basis. Overall, the rms MLD error of the hindcast profiles was lower than that of the synthetic profiles. However, the improvement was due mainly to the shallow MLD bias of the synthetic profiles relative to the observed MLD's in the fall and winter. For May through August, when we expected the hindcasts to show the most skill, the rms MLD error of the hindcasts was generally worse than that of the synthetic profiles. An inspection of the individual hindcasts in June and July showed a number of instances where the observed MLD was deeper than would be expected during light winds and strong heating, and shallower than would be expected when the winds were stronger. DTIC

N95-16802# Titan Systems, Inc., Princeton, NJ. Research and Technology Div.
THE SMALL-SCALE STRUCTURE OF DISPERSING CLOUDS IN THE ATMOSPHERE Technical Report, 1 Jun. 1992 - 31 May 1994
R. I. Sykes and Robert S. Gabruk Jul. 1994 17 p
(Contract DAAL03-92-C-0020)
(AD-A285493) Avail: CASI HC A03/MF A01

The fractal properties of a plume dispersing in a turbulent velocity field have been examined using Large-Eddy Simulation results for neutral and convective boundary layers. A fractal generation technique has been developed that correctly matches a specified mean and variance distribution for the plume. The spatial correlation scale of the fractal realizations can also be specified, and the one-point probability density function can be chosen as clipped normal or lognormal. Realizations generated with the fractal technique show reasonably close resemblance to the LES results. The small-scale structure of the plume is further analyzed using multifractal

techniques, and a the generation methodology is extended to incorporate unequal partitioning of the random variance during the refinement process. This procedure corresponds to the localization of small-scale energy in the turbulent cascade process which leads to an intermittent dissipation field. The multifractal spectrum of the dissipation field can be adjusted to match observations and the LES calculation results. The visual appearance of the dissipation field from the fractal/multifractal model is much more intermittent than the fractal realization, and the concentration field shows more localized small-scale fluctuations. These features give better correspondence to the LES realizations. DTIC

N95-16961# Applied Research Corp., College Station, TX.
REGIONAL FORECASTING WITH GLOBAL ATMOSPHERIC MODELS
T. J. Crowley, G. R. North, and N. R. Smith May 1994 328 p Prepared for Pacific Northwest Lab., Richland, WA
(Contract DE-AC06-76RL-01830)
(DE94-013863; PNL-9416) Avail: CASI HC A15/MF A03

This report was prepared by the Applied Research Corporation (ARC), College Station, Texas, under subcontract to Pacific Northwest Laboratory (PNL) as part of a global climate studies task. The task supports site characterization work required for the selection of a potential high-level nuclear waste repository and is part of the Performance Assessment Scientific Support (PASS) Program at PNL. The work is under the overall direction of the Office of Civilian Radioactive Waste Management (OCRWM), US Department of Energy Headquarters, Washington, DC. The scope of the report is to present the results of the third year's work on the atmospheric modeling part of the global climate studies task. The development testing of computer models and initial results are discussed. The appendices contain several studies that provide supporting information and guidance to the modeling work and further details on computer model development. Complete documentation of the models, including user information, will be prepared under separate reports and manuals. DOE

N95-17164# Air Force Inst. of Tech., Wright-Patterson AFB, OH.
AN AIR MASS TRANSFORMATION MODEL FOR COASTAL ENVIRONMENTS M.S. Thesis
Craig T. Sloan 1994 93 p
(AD-A281790; AFIT/CI/CIA-94-028) Avail: CASI HC A05/MF A01

Frequently during winter, cold fronts move through the Gulf of Mexico region. Several days after the passage of the cold front, return flow develops along the Gulf Coast advecting modified continental polar air over the Gulf Coast States. An operational air mass transformation (AMT) model has been developed to forecast the thermodynamic structure of the planetary boundary layer (PBL) at coastal locations during these return flow events. This document includes a return flow description; methodology; a minimum temperature study; and air mass transformation model results.
Author (revised)

N95-17259# Colorado State Univ., Fort Collins, CO. Dept. of Atmospheric Science.
SUMMARY OF 1994 ATLANTIC TROPICAL CYCLONE ACTIVITY AND VERIFICATION OF AUTHOR'S SEASONAL PREDICTION, 1
William M. Gray 30 Nov. 1994 21 p
Avail: CASI HC A03/MF A01

This paper summarizes the tropical cyclone (TC) activity which occurred in the Atlantic Basin during 1994 and verifies the author's seasonal forecast of this activity which was initially issued on 19 November of last year with updates on 5 June and 4 August of this year. The 1994 hurricane season was unusual in view of (1) the very suppressed activity during the height of the season, between late August and early November, and (2) the very active November when two hurricanes formed. There were a total of seven named storms (average 9.3) and three hurricanes (average 5.7) which lasted a total of seven days (average is 23). There were no major (intense) hurricanes of Saffir/Simpson category 3-4-5 (average is 2.1 intense hurricanes with 4.5 average intense storm days). The seasonal total of named storm days was 28 or, 61 percent of average. Net tropical cyclone (NTC) activity was only 37% of the average of the last 45 years. Three systems, tropical storms Alberto, Beryl and Gordon, affected the US southeast coast; Alberto brought devastating floods to western central Georgia. The author's extended range forecast, issued on 19 November of last year, called for a slightly above average hurricane season; this 9-11 month lead time forecast did not verify. The anticipated end of the unusually long running El Nino (since 1990) did not occur as expected. El Nino-like conditions persisted through the 1994 hurricane season and continued the suppression of hurricane activity as has occurred during each of the last four seasons. In addition, very high and unexpected surface pressure values developed over the western Atlantic during most of the 1994 season. The author's early June and early August updated forecasts, by contrast, showed considerable forecast skill. They accommodated the continuance of the El Nino and, in part, the higher surface pressure. They called for diminished overall hurricane conditions of only 70% and 50% percent of climatology. But hurricane activity was lighter yet. This lack of hurricane activity during 1994 was primarily the result of three factors: (1) strong and persistent high surface pressure conditions which occurred this year in the Caribbean basin and western Atlantic; (2) easterly lower stratospheric QBO winds; and (3) continued warm equatorial Pacific El Nino conditions. North Africa's West Sahel rainfall conditions were near average for this year and not thought to have been a significant factor in this year's diminished hurricane activity. Author

N95-17260# Colorado State Univ., Fort Collins, CO. Dept. of Atmospheric Science.
EXTENDED RANGE FORECAST OF ATLANTIC SEASONAL HURRICANE ACTIVITY FOR 1995, 2
William M. Gray 30 Nov. 1994 10 p Sponsored by NSF and NOAA
Avail: CASI HC A02/MF A01

This paper presents details of a 6-11 month extended range seasonal forecast of the tropical cyclone activity likely to occur in the Atlantic Ocean basin during 1995. This forecast is based on new research by the author and his colleagues which allows estimates of next season's Atlantic tropical cyclone activity to be made by late November of the prior year. The forecast scheme is based on a 10-month forward extrapolation of the Quasi-Biennial Oscillation (QBO) of equatorial stratospheric zonal winds, two measures of Western Sahel rainfall through mid-November 1994, an extended range forecast of El Nino conditions for August to October 1995 and an extended range forecast of Western Sahel rainfall amount for next season. Information through mid-November 1994 indicates that 1995 Atlantic hurricane activity is likely to be above average with 8 hurricanes (average 5.7), 12 named storms (average 9.3), 65 named storm days, 35 hurricane days (average 23), 3 intense (category 3-4-5) hurricanes (average 2.1), 8 intense hurricane days and a hurricane destruction potential (HDP) of 100 (average 68). Collectively, net tropical cyclone activity is expected to be 140 percent of the long period average. The 1995 season should be much more active than the four recent 1991 through 1994 hurricane seasons, and especially in the tropical regions at latitudes south of 25 deg N where only two short lived hurricane have occurred during the last four years. The character of 1995 season should tend toward that of the two recent hurricane seasons of 1988 and 1989 which produced a total of five intense or major hurricanes and 19 intense hurricane days. The probability of hurricane destruction along the US coastline and within the Caribbean basin for 1995 is projected to be higher than the mean probability for the last 45 years and distinctly higher than the probabilities for the last four years. It is expected that the long running 1990-1994 El Nino-like equatorial Pacific warm water conditions will finally dissipate by next summer and that comparatively cool surface water conditions will return to the east and central equatorial Pacific during next season's hurricane season. This trend should enhance hurricane activity over that of the last four years. It is also expected that the Western Sahel region of Africa will experience somewhat above average rainfall with total amounts ranking among the fourth or fifth highest since 1970. This upward trend in rainfall should also enhance the probability of intense hurricane activity for next year. Author

N95-17339 Naval Research Lab., Monterey, CA.
IMPACT OF PHYSICAL PROCESSES ON MARITIME FRONTOGENESIS Ph.D. Thesis
William T. Thompson Jun. 1994 243 p Limited Reproducibility: More than 20% of this document may be affected by microfiche quality
(AD-A283105) Avail: Issuing Activity (Defense Technical Information Center (DTIC))

A hydrostatic primitive equation model initialized in a highly baroclinically unstable state was used to simulate maritime cyclogenesis and frontogenesis. In order to identify boundary layer physical processes important in maritime frontogenesis, several different simulations were performed. An adiabatic and inviscid simulation provided the control for these experiments. The

two different boundary layer parameterizations used were a K-theory parameterization and a second-order closure scheme. Results indicated that strong warm and cold fronts formed in the adiabatic and inviscid case but that the near-surface wind speed and vertical motion fields were unrealistic. In the K-theory simulation, the results were somewhat more realistic but convergence and vorticity were weaker. Results from the second-order closure simulation demonstrated that turbulent mixing of momentum was most important in producing the frontogenetic (and frontolytic) effects of the transverse secondary circulation. DTIC

N95-17443 Air Force Inst. of Tech., Wright-Patterson AFB, OH. School of Engineering.

METEOROLOGICAL FACTORS THAT AFFECT THE FORMATION AN PREDICTION OF AIRCRAFT ICING M.S. Thesis

Christopher S. Bjorkman 1994 126 p Limited Reproducibility: More than 20% of this document may be affected by microfiche quality

(AD-A281984; AFIT/CI/CIA-94-029) Avail: Issuing Activity (Defense Technical Information Center (DTIC))

This thesis reviewed factors which influence aircraft icing, verified previous NACA data, and assessed forecasting techniques. Analysis of RAOB's (upper air soundings) and PIREP's (pilot reports) compiled by NOAA/FSL were required to have occurred within one hour of RAOB ascent and within 50 miles of the RAOB location. The results of this study compared favorably to those of NACA. Icing reports appeared to occur within a distinct range from 0 C to -20 C and with a 1 C dew point depression. While not as distinct, stability is related to the type of icing. Current forecast rules were found to be valid and suggestions for improvement are provided. DTIC

N95-17488 Air Force Inst. of Tech., Wrighi-Patterson AFB, OH.

THE EFFECTS OF THE HORIZONTAL RESOLUTION OF THE BOUNDARY FORCING SEA SURFACE TEMPERATURE FIELD ON THE FSU SPECTRAL MODEL M.S. Thesis

Brent D. Hickel Sep. 1994 66 p Limited Reproducibility: More than 20% of this document may be affected by microfiche quality

(AD-A284273; AFIT/CI/CIA-94-124) Avail: Issuing Activity (Defense Technical Information Center (DTIC))

This study examines the effects of higher wavenumbers in the boundary forcing sea surface temperature field (SST) on the output from an atmospheric model. The model is the FSU global spectral model employing triangular truncation at 170 wavenumbers for a horizontal resolution of .7 deg latitude by .7 deg longitude. Boundary forcing is provided by a fine scale SST, a smoothed version of that SST and a combination field where a region bounded by 200 deg N to 55 deg N by 120 deg E to 150 deg E from the fine scale SST is patched into the smoothed SST field. The results indicate that inclusion of higher wavenumbers in the boundary forcing SST significantly impacts the behavior of the atmospheric model. The areas downstream from regions of strong spatial gradient in the SST field, such as the Kuroshio and Gulf Stream have the largest differences. Geopotential height differences at 500 mb between the fine and smoothed SST model runs are as high as 230 meters. Pacific typhoon intensity is better modeled using the high resolution SST. The boundary forcing becomes increasingly important as the model integration progresses. The effects of the initial atmospheric conditions are tested and are clearly smaller than the impact of the fine scale SST. It is conjectured that medium range, 5-14 day forecasts will be greatly improved if the best resolution observed SST is used. We conclude that coupled ocean-atmosphere models will be negatively impacted if a low resolution ocean model is coupled to a higher resolution atmospheric model. DTIC

N95-17504# Helsinki Univ. of Technology, Espoo (Finland). Lab. of Computer and Information Science.

OPERATIONAL CLOUD CLASSIFIER BASED ON A SELF-ORGANIZED FEATURE MAP

K. Valkealahti, J. Iivarinen, A. Visa, and O. Simula Dec. 1993 25 p

(PB94-197852; ISBN-951-22-1789-9) Avail: CASI HC A03/MF A01

A segmentation and classification method for NOAA weather satellite images has been developed. The method is trainable by examples and hence, it is adaptive to changing circumstances. The method has been tested on hundreds of images. The existing problem is to get relible reference results. It is too early to publish classification rates as a whole but some results already exist. The authors wish to thank the Technology Development Center of Finland for financial support and the Finnish Meteorological Institute for the interesting application problem. NTIS

N95-17529 Royal Netherlands Meteorological Inst., De Bilt. Section of Climate Scenarios and Ozone.

MODELLING DAILY PRECIPITATION AS A FUNCTION OF TEMPERATURE FOR CLIMATE CHANGE IMPACT STUDIES

A. M. G. Klein Tank and T. A. Buishand 1993 38 p Sponsored by Dutch National Research Program on Global Air Pollution and Climate Change

(ISSN 0169-1651)

(KNMI-WR-93-02; ISBN-90-369-2039-6) Copyright Avail: Issuing Activity

A method is presented to derive times series of daily precipitation and temperature in a possible future climate at a certain location from the observed time series of these variables. The method considers the relation between daily precipitation and temperature. From this relation a temperature dependent factor F is obtained which gives the relative change in precipitation due to a given temperature perturbation. Multiplication of the observed daily amounts with this factor yields a consistent scenario for daily precipitation and temperature. The number of rain days does not change in this method. The observed precipitation-temperature relation for rain days at De Bilt (The Netherlands) is examined. This relation is described by a non-linear regression model using spline functions to reproduce the non-monotonous change of the mean amount with temperature. The standard deviation on the daily amounts increases with temperature, but the coefficient of variation is almost constant. This supports the use of a factor to transform the observed amounts toward a possible future climate. For a temperature increase the factor F derived from the model is generally greater than 1. F is, however, less than 1 when the daily mean temperature is around 12 C. The effect of a constant temperature increase of 3 C on the mean precipitation amounts at De Bilt was studied with different versions of the model. During winter the monthly mean precipitation amounts increase by about 20% when seasonal variation in the precipitation-temperature relation is ignored. For a seasonally varying model the increase in mean winter precipitation amounts to 27%. The changes in the monthly means are much smaller for the other seasons. The increase in annual mean precipitation ranges between 7% and 9% for the various models fitted to the observed precipitation-temperature relation. This is consistent with the change in global mean precipitation predicted by present day general circulation models in case of a temperature increase of 3 C. Author

N95-17686 Mesoscale Environmental Simulations and Operations, Inc., Troy, NY.

A THREE DIMENSIONAL MESOSCALE ATMOSPHERIC SIMULATION SYSTEM FOR USE IN VARIOUS MOBILE BATTLEFIELD ENVIRONMENTS. PHASE 2: TRANSITION TO AN OPERATIONAL FORECAST SYSTEM Final Report, 15 Sep. 1990 - 15 Mar. 1993

John W. Zack, Kenneth T. Waight, III, Steven H. Young, Mary D. Bousquet, and Pamela E. Price May 1994 137 p Limited Reproducibility: More than 20% of this document may be affected by microfiche quality

(Contract DAAD07-90-C-0134)

(AD-A281223; ArmySBIR2-0393-Phase-2; ARL-CR-98-Phase-2) Avail: CASI HC A07

A self-contained mesoscale numerical weather prediction system which can generate real-time or historical simulations on a high performance moderate-cost workstation computer was developed and tested in this project. The system is designed to: (1) ingest a variety of atmospheric data types; (2) combine the diverse mixture of ingested data into a dynamically consistent initialization dataset for the numerical model; (3) generate a mesoscale numerical simulation; (4) display the output from the simulation in a variety of graphicl and tabular formats; and (5) be easily used and reconfigured through a graphical user interface. The system was created by porting a version of the Mesoscale Atmospheric Simulation System (MASS) from a supercomputer to a Standent 750 vector processing workstation, and then configuring it to perform all the functions of a numerical weather prediction system within the workstation environment. The system was tested by executing 36 simulations with real-time atmospheric data and performing a subjective and objective verification. In addition to the generation of real-time mesoscale simulations for military applications, it is envisioned that the workstation-based mesoscale simulation system could

have a considerable number of applications in the private sector including the generation of tailored local forecasts for business and government operations that are weather sensitive. DTIC

N95-17709# Naval Command, Control and Ocean Surveillance Center, San Diego, CA. Research, Development, Technology and Evaluation Div.
PROPAGATION IN THE EVAPORATION DUCT. MODEL PREDICTIONS AND COMPARISONS TO DATA Final Report
R. A. Paulas Mar. 1994 46 p
(AD-A283012; NCCOSC/RDT/E-TR-1644) Avail: CASI HC A03/MF A01

In 1972, a series of radio propagation measurements in the 1- to 40-GHz frequency range was performed in the eastern Mediterranean. A 35.2-km over-the-horizon propagation path was established between the islands of Naxos and Mykonos in the Aegean Sea. During the November measurement period, surface meteorological measurements were made and used to characterize evaporation ducting conditions on both islands, Ornos Beach on Mykonos and the Greek Weather Service on Naxos. These data have been quantitatively analyzed with the Engineer's Refractive Effects Prediction System (EREPS), the Radio Physical Optics (RPO) propagation model assuming horizontal homogeneity of the evaporation duct as characterized by the Mykonos meteorological data, and RPO utilizing the data at both Mykonos and Naxos to provide range-varying refractive structure. Comparisons of predicted propagation loss by the three approaches to the observed data show the influences of the EREPS single-mode assumption, surface-layer stability, and range-varying evaporation ducting. DTIC

N95-17715# Hughes STX, Inc., Lexington, MA.
AN INVESTIGATION OF SMALL-SCALE VARIATIONS IN CLOUD CLIMATOLOGY INDUCED BY TOPOGRAPHY AND MONTHLY MEAN WINDS
James H. Willand, Albert R. Boehm, and Gary Gray 21 Jan. 1994 47 p
(Contract F19628-93-C-0051)
(AD-A283274; AD-E202113; PL-TR-94-2014; SR-3) Avail: CASI HC A03/MF A01

This report is an assessment of the use of vector mean wind components and terrain heights to indicate the occurrence of terrain-induced small-scale cloud amount conditions. DTIC

N95-17743# Columbia Univ., Palisades, NY. Earth Observatory.
RECENT CHANGES OF WEATHER PATTERNS IN NORTH AMERICA
G. J. Kukla and T. Karl 1994 9 p
(Contract DE-FG02-85ER-60372)
(DE94-016115; DOE/ER-60372/9) Avail: CASI HC A02/MF A01

This report contains information dealing with climatic change in North America. Results gathered from present and previous DOE contracts are discussed. These include: usage of the Historical Climatology Network, characteristics of recent climate change, impacts of increasing anthropogenic greenhouse gases, seasonal trends, geographic and seasonal distribution of temperature anomalies, paleoclimates, weather pattern differences between eastern and western regions, daily temperature variations, general circulation models, and results of oceanic circulation. DOE

N95-17927 National Oceanic and Atmospheric Administration, Boulder, CO. Space Environment Lab.
VERIFICATION OF NOAA SPACE ENVIRONMENT LABORATORY FORECASTS, 1 JANUARY - 31 DECEMBER 1993
K. A. Doggett Aug. 1994 71 p Limited Reproducibility: More than 20% of this document may be affected by microfiche quality
(PB95-104162; N0AA-TM-ERL-SEL-84) Avail: CASI HC A04

This summary report compiles verification statistics for the primary forecasts issued by the National Oceanic and Atmospheric Administration (NOAA) Space Environment Laboratory (SEL). The following forecasts are evaluated: probability forecasts of M-class, Chi-class, and Proton flares expected for each of the next three days; integer-value forecasts of 10.7 cm Solar Flux, Fredericksburg A-Index, and Planetary A-Index for each of the next seven days; and next-day probability forecasts of geomagnetic activity levels at middle latitudes. This report covers forecasts made during 1 January to 31 December 1993. Three levels of verification information are presented to accommodate different verification users. The first level presents an overview of forecast performance, concentrating on a few key verification measures and the ways in which these measures evolve over time. The second level offers several verification measures and diagrams to provide a detailed evaluation of each forecast. The third level focuses on the performance of individual forecasters. NTIS

48 OCEANOGRAPHY

Includes biological, dynamic, and physical oceanography; and marine resources.

For related information see also *43 Earth Resources and Remote Sensing.*

N95-16006*# National Aeronautics and Space Administration. Goddard Space Flight Center, Greenbelt, MD.
SeaWIFS TECHNICAL REPORT SERIES. VOLUME 21: THE HERITAGE OF SeaWIFS. A RETROSPECTIVE ON THE CZCS NIMBUS EXPERIMENT TEAM (NET) PROGRAM
James G. Acker (Hughes STX, Inc., Lanham, MD.), Stanford B. Hooker, ed., and Elaine R. Firestone, ed. (General Sciences Corp., Laurel, MD.) Sep. 1994 46 p
(NASA-TM-104566-Vol-21; Rept-94B00140-Vol-21; NAS 1.15:104566-Vol-21) Avail: CASI HC A03/MF A01

The Sea-viewing Wide Field-of-view Sensor (SeaWiFS) mission is based on the scientific heritage of the Coastal Zone Color Scanner (CZCS), a proof-of-concept instrument carried on the National Aeronautics and Space Administration (NASA) NIMBUS-7 environmental satellite for the purpose of measuring upwelling radiance from the ocean surface. The CZCS mission provided the first observations of ocean color from space, and over the mission lifetime of 1978-1986, allowed oceanographers an initial opportunity to observe the variable patterns of global biological productivity. One of the key elements of the CZCS mission was the formation of the CZCS NIMBUS Experiment Team (NET), a group of optical physicists and biological oceanographers. The CZCS NET was designated to validate the accuracy of the CZCS radiometric measurements and to connect the instrument's measurements to standard measures of oceanic biological productivity and optical seawater clarity. In the period following the cessation of CZCS observations, some of the insight and experience gained by the CZCS NET activity has dissipated as several proposed follow-on sensors failed to achieve active status. The Sea WiFS mission will be the first dedicated orbital successor to CZCS it in turn precedes observations by the Moderate Resolution Imaging Spectroradiometer (MODIS) of the Earth Observing System (EOS). Since the CZCS NET experience is an important model for Sea WiFS and MODIS surface truth efforts, this document is intended to provide a comprehensive review of the validation of oceanographic data for the first orbital ocean color sensor mission. This document also summarizes the history of the CZCS NET activities. The references listed in the Bibliography are a listing of published scientific research which relied upon the CZCS BET algorithms, or research which was conducted on the basis of CZCS mission elements. Author

N95-16062# Oregon State Univ., Corvallis, OR. Coll. of Oceanic and Atmospheric Sciences.
MARINE BOUNDARY-LAYER PARAMETERIZATIONS FOR LARGE-SCALE MODELS Final Report, 12 Feb. 1991 - 30 Apr. 1994
L. Mahrt, M. Ek, J. Sun, and M. Frech 19 Apr. 1994 235 p
(Contract F19628-91-K-0002)
(AD-A282402; PL-TR-94-2128) Avail: CASI HC A11/MF A03

This report describes work on the PL atmospheric boundary-layer model conducted under contract number F19628-91-K-0002 from the Phillips Laboratory. This model was developed to provide turbulence parameterization schemes for a global numerical weather prediction model. In this report, boundary-layer nonlocal turbulent mixing is reexamined, and a nonlocal momentum mixing formulation is presented. The boundary-layer cloud formulation, that accounts for turbulent and subgrid-mesoscale moisture variations, is extended to include enhanced cloud mixing using moist conservative variables. Observational data and results from model simulations are used to examine the complex land-surface/atmosphere interactions and the potential for cloud development. Exchange coefficients for subgrid fluxes are shown to depend significantly on grid size in the presence mesoscale motion induced by surface heterogeneity. Tower and aircraft-measured fluxes over heterogeneous terrain are analyzed to show the spatial variation of surface fluxes and the effect on the surface exchange

coefficients for area-averaged fluxes. The classical bulk aerodynamic method for estimating surface fluxes in terms of surface radiative temperature is examined. A new sea-surface roughness formulation includes the effects of aerodynamically smooth and rough flow, and wave age in terms of a simple wind tendency relation. DTIC

N95-16078 Maryland Univ., College Park, MD. Center for Automation Research.

ESTIMATION OF VEHICLE DYNAMICS FROM MONOCULAR NOISY IMAGES

Yi-Sheng Yao and Rama Chellappa Nov. 1993 22 p Limited Reproducibility: More than 20% of this document may be affected by microfiche quality

(Contract DAAH04-93-G-0419)

(AD-A281458; CAR-TR-692; CS-TR-3172; ARO-32365.1-MA) Avail: CASI HC A03

This paper presents a new model-based egomotion estimation algorithm for an autonomous vehicle navigating through rough terrain. Due to the uneven terrain, the vehicle undergoes bouncing, pitch and roll motion. To reliably accomplish other tasks such as tracking and obstacle avoidance using visual inputs, it is essential to consider these disturbances. In this paper, two vehicle models available in the literature are used for egomotion estimation. The Half Vehicle Model (HVM) takes into account the bouncing and pitch motion of the vehicle, and the Full Vehicle Model (FVM) also considers the roll motion. The dynamics of the vehicle are formulated using standard equations of motion. Assuming that depth information is known for some landmarks in the scene (e.g., obtained from a laser range finder), a feature-based approach is proposed to estimate vehicle motion parameters such as the vertical movement of the center of mass and the instantaneous angular velocity. An Iterated Extended Kalman Filter (IEKF) is used for recursive parameter estimation. Simulation results for both known and unknown terrain are presented. DTIC

N95-16079 Massachusetts Inst. of Tech., Cambridge.

SENSITIVITY STUDY OF THE SPEM MODEL TO THE ASSIMILATION OF SYNOP DATASETS USING TWO ASSIMILATION SCHEMES. 1: NUDGING. 2: THE KALMAN FILTER/SMOOTHER M.S. Thesis Final Report, 1 May - 31 Dec. 1993

Paola Malanotte-Rizzoli 31 Dec. 1993 2 p Limited Reproducibility: More than 20% of this document may be affected by microfiche quality

(Contract N00014-93-1-0754)

(AD-A281459) Avail: CASI HC A01

From CTD surveys taken two months apart during the 1981 Ocean Tomography experiment southwest of Bermuda, a time-dependent ocean state is estimated that evolves from the first survey to the second survey. Mesoscale motions in this region are modelled by quasi-geostrophic dynamics. The model domain is a doubly periodic 600km x 600km square centered at 26 deg N, 70 deg W. The oceanic density field is expanded in terms of a horizontal Fourier series with vertical modes. Freely propagating Rossby waves in the first and second baroclinic modes are fit to the data in a least-squares sense at the two survey times. Linear dynamics are first used to evolve the ocean state to fit both surveys. Weakly nonlinear interactions between the waves are then allowed and are found to do a better job. The wave-wave interactions enable Rossby waves in the barotropic mode to enter into the baroclinic Rossby wave evolution as unknown control variables which can then be estimated. DTIC

N95-16103# Army Cold Regions Research and Engineering Lab., Hanover, NH.

EXPERIMENTAL AND NUMERICAL ANALYSIS OF FLOATING ICE BEAM IMPACT FORCES AGAINST A SLOPED STRUCTURE

Barry A. Coutermarsh Mar. 1994 45 p

(AD-A280752; CRREL-94-2) Avail: CASI HC A03/MF A01

Floating ice impact forces are of concern where structures are built in ice-susceptible waters. Bridge piers, ice control structures, or icebreakers are a few examples where the ability to predict the expected ice impact force would be of great help in the design process. Experiments were performed to determine the response of a floating ice beam to a vertically applied force. The data were used to calibrate a numerical finite element model of the floating ice. The ice was characterized as a linear elastic material in the numerical analysis, and the calibration data were used to assess this assumption as well as to develop a fluid influence coefficient matrix to simulate the dynamic influence of the fluid beneath the ice beam. Finally, a scale model study was performed to determine actual impact forces generated by a floating ice beam against a 45 deg sloped structure. The numerical model developed was then compared to the actual data. The numerical model does well at predicting impact forces for all the beams at low velocity and the force from the thicker ice beams at all velocities. Both the numerical and experimental forces show the same trends and appear to level off and approach a constant value with increasing beam length. The discrepancies between numerical predictions and experimental results are thought to be caused by damage in the experimental ice beams which is not accounted for in the numerical model. Author

N95-16118# Army Engineer Waterways Experiment Station, Vicksburg, MS. Environmental Lab.

THREE-DIMENSIONAL EUTROPHICATION MODEL OF CHESAPEAKE BAY. VOLUME 1: MAIN REPORT Final Report

Carl F. Cerco and Thomas M. Cole May 1994 658 p

(AD-A280760; WES/TR/EL-94-4-Vol-1) Avail: CASI HC A99/MF A06

A three-dimensional, time-variable, eutrophication model, CE-QUAL-ICM, was applied to Chesapeake Bay. The model incorporated 22 state variables that included physical properties, multiple forms of algae, carbon, nitrogen, phosphorus, silica, and dissolved oxygen. The model was part of a larger package that included a three-dimensional hydrodynamic model and a benthic sediment diagenesis model. The model was initially applied to a three-year period, 1984-1986. The model successfully simulated water-column and sediment processes that affected water quality. Phenomena simulated include formation of the spring algal bloom subsequent to the annual peak in nutrient runoff, onset and breakup of summer anoxia, and coupling of organic particle deposition with sediment-water nutrient and oxygen fluxes. The model was next applied in a 30-year simulation of water quality, 1959-1988. The model indicated long-term trends in water quality and affirmed the role of stratification in determining anoxia. Final application of the model was in a series of nutrient load-reduction sensitivity analyses. The study demonstrated that complex eutrophication problems can be addressed with coupled three-dimensional hydrodynamic and water quality models. DTIC

N95-16124# Mississippi State Univ., Bay Saint Louis, MS. Center for Air Sea Technology.

STUDENT RESEARCH PROJECTS, 1993

Patrick Perrin, Dongmei Wu, Zhifan Zhu, Chandrashekar Ramanathan, and Julia Hodges 20 Sep. 1994 45 p

(Contract N00014-92-J-4109)

(AD-A284954; CAST-TN-04-94) Avail: CASI HC A03/MF A01

Eleven 1994 student research projects were sponsored by the Mississippi State University Center for Air Sea Technology. This technical note describes these projects which include an intelligent support system for scientific databases, error pattern identification, scientific visualization of environmental data, object-oriented prototype database, test and evaluation of the CAST (Center for Air Sea Technology) Model Evaluation System, enhancement of the Naval Interactive Data Analysis System, remote user enhancements to NEONS (Navy Environmental Operational Nowcasting System), using Oracle to implement a geophysical database, and enhancements to the CMES (CAST Model Evaluation System). DTIC

N95-16125# Mississippi State Univ., Bay Saint Louis, MS. Center for Air Sea Technology.

OBJECTIVE FEATURE IDENTIFICATION AND TRACKING: A REVIEW

Ranjit M. Passi and Harsh Anand 15 Sep. 1994 39 p

(Contracts N00014-92-J-4109; N00014-92-J-4112)

(AD-A284955; CAST-TR-94-4) Avail: CASI HC A03/MF A01

Remote sensing of the oceans via satellites is providing useful data that can be used for realtime input into and verification of the numerical ocean models. To make an optimum use of these data, efficient methods are being developed to handle vast amounts of data and provide their quick analyses and summaries in the form of mesoscale features. Identification, isolation and tracking of mesoscale features plays an important role in numerical ocean modeling. Of late, there has been considerable interest in designing algorithms to automatically detect such oceanographic features as temperature fronts and eddies. This report provides a literature review of recent approaches and efforts on objective feature identification (OFI) as it pertains to oceanographic applications. Most of the OFI work in

oceanography has been done on characterizing the Gulf Stream (GS); and since the GS incorporates all the mesoscale feature complexities that one may desire to resolve, the literature reviewed here pertains to this feature entirely. It is felt that the work cited is quite representative and is applicable to other geographical features of interest. DTIC

N95-16141# Gulf Weather Corp., Bay Saint Louis, MS.
METADATA DATABASE FOR AUTOMATED OCEANOGRAPHIC IMAGERY Final Report, Oct. 1993 - Mar. 1994
Robert Pickett, Frank Schatzle, James Corbin, Ramesh Krishnamagaru, and Valentine Anantharaj 29 Apr. 1994 32 p
(Contract N00014-93-C-0240)
(AD-A284932) Avail: CASI HC A03/MF A01

Investigation revealed that the primary means of satellite imagery interpretation is by manual. The methodology is cumbersome and the number of 'things of interest' is large, making it highly manpower intensive. The anticipated rapid increase in satellite systems and sensors and the increasing requirements for satellite remotely sensed data to support oceanographic and meteorological models and fleet support applications, particularly in the near-shore coastal zone, indicates that the situation will continue to worsen. The only long term solution is an integrated system of automated tools for satellite data interpretation. There are a number of automated satellite image analysis algorithms available today and others under development. This report provides the generic design for a metadata database system based on 'object-oriented' software, that will provide the 'user-friendly' system for making satellite data analysis tools available to Navy operational and research oceanographers and meteorologists. DTIC

N95-16168# Washington Univ., Seattle, WA.
THE FIFTH INTERNATIONAL CONGRESS ON THE HISTORY OF OCEANOGRAPHY
Keith R. Benson and Philip F. Rehbock 26 May 1994 89 p Meeting held in La Jolla, CA, 7-14 Jul. 1993
(Contract N00014-93-1-0665)
(AD-A281507) Avail: CASI HC A05/MF A01

Over one-hundred fifty historians and oceanographers gathered to discuss their common interests in the history of oceanography. There were one hundred six papers delivered during the week by scholars coming to Scripps Institution of Oceanography from all over the world. DTIC

N95-16414 Coast Guard Research and Development Center, Groton, CT.
FLORIDA GULF STREAM DATA (FLDA) CURRENT STUDY Final Report, Apr. 1992 - Mar. 1994
B. D. Perkins and R. L. Marsee (Analysis and Technology, Inc., New London, CT.) Mar. 1994 286 p Limited Reproducibility: More than 20% of this document may be affected by microfiche quality
(Contract N66604-93-D-1119)
(AD-A281965; CGR/DC-08/94; USCG-D-10-94) Avail: CASI HC A13

The Surveillance Systems Branch of the U.S. Coast Guard Research and Development Center and the Naval Undersea Warfare Center, New London Detachment (NUWCNL) had conducted an earlier study of the Coast Guard Computer Assisted Search Planning (CASP) program's southern Gulf Stream Florida Data (FLDA) environmental file. The study found errors in the FLDA environmental file data. The tasking for this project was to replace the corrupted (old) FLDA files with reconstructed (new) data files derived from data obtained in the original research by Nova University. The derived data files were created by merging Nova University Gulf Stream transect current data onto background data from Atlas of Pilot Charts. The data was then divided into 12 monthly sets and verified for continuity and accuracy. The 12 new monthly FLDA data sets were then prepared for transfer to the Coast Guard Operations Systems Center (OSC) computer. DTIC

N95-16610# Oak Ridge National Lab., TN. Carbon Dioxide Information Analysis Center.
A COASTAL HAZARDS DATA BASE FOR THE US GULF COAST
R. C. Daniels, ed. Jun. 1994 124 p
(Contract DE-AC05-84OR-21400)
(DE94-014573; ORNL/CDIAC-60; NDP-043B; ESDP-4101) Avail: CASI HC A06/MF A02

This document describes the contents of a digital data base that may be used to identify coastlines along the US Gulf Coast at risk to sea-level rise. The data base integrates point, line, and polygon data for the US Gulf Coast into 0.25 deg latitude by 0.25 deg longitude grid cells and into 1:2,000,000 digitized line segments that can be used by raster or vector geographic information systems (GIS) as well as by non-GIS data base systems. Each coastal grid cell and line segment contains data on elevation, geology, geomorphology, sea-level trends, shoreline displacement (erosion/accretion), tidal ranges, and wave heights. To allow for the identification of coastlines at risk from sea-level rise, 7 of the 22 original data variables in this data base were classified by vulnerability and used to create 7 relative risk variables. These relative risk variables range in value from 1 to 5 and may be used to calculate a coastal vulnerability index for each grid cell and/or line segment. The data for these 29 variables (i.e., the 22 original variables and 7 risk variables) have been placed into the following data formats: (1) Gridded polygon data for the 22 original data variables. Data include elevation, geology, geomorphology, sea-level trends, shoreline displacement (erosion/accretion), tidal ranges, and wave heights; (2) Gridded polygon data for the seven classified risk variables. The risk variables are classified versions of: mean coastal elevation, geology, geomorphology, local subsidence trend, mean shoreline displacement, maximum tidal range, and maximum significant wave height; (3) 1:2,000,000 line segment data containing the 29 data variables (the 22 original data variables and the seven classified risk variables); (4) Supplemental point data for the stations used in calculating the sea-level trend and tidal range data sets; and (5) Supplemental line segment data containing a 1:2,000,000 digitized coastline of the US Gulf Coast as defined by this document. DOE

N95-17277 Hawaii Univ., Honolulu, HI.
VARIATION OF THE THERMOHALINE STRUCTURE IN THE WESTERN EQUATORIAL PACIFIC UPPER OCEAN Ph.D. Thesis
Toshiaki Shinoda 1993 207 p
Avail: Univ. Microfilms Order No. DA9416073

Processes which control the upper ocean thermohaline structure in the western equatorial Pacific are examined using the available hydrographic data, surface forcing data, and a simple mixed layer model. A thick isothermal layer is frequently found in the region of the South Equatorial Current. Analyses of surface forcing data have indicated that the thick isothermal layer in the western equatorial Pacific is found during periods of light precipitation, strong winds, and downward Ekman pumping in the central Pacific. These results are consistent with the subduction mechanism hypothesized by Lukas and Lindstrom. A Lagrangian mixed layer model is used to investigate the hypothesis. The one-dimensional bulk mixed layer model is integrated along the trajectories derived from a nonlinear 1 1/2 layer reduced gravity model forced with actual wind fields. This simple model is able to simulate the isothermal layer and its variation. The subduction mechanism is evident in the model results. During the period of strong South Equatorial Current, the warm and salty mixed layer waters in the central Pacific are subducted below the fresh shallow mixed layer in the western Pacific. However, the subduction mechanism is not evident when upwelling Rossby waves reach the western equatorial Pacific or when a remarkable deepening of the mixed layer occurs due to the strong wind and light precipitation in the western equatorial Pacific.
Dissert. Abstr.

N95-17395 Oregon State Univ., Corvallis, OR.
LONG-TERM MOMENTUM AND HEAT BALANCES AND TURBULENT MIXING IN THE UPPER EQUATORIAL PACIFIC OCEAN Ph.D. Thesis
Shusheng Luan 1993 170 p
Avail: Univ. Microfilms Order No. DA9413740

The unique properties of high shear, low R(sub i), zero inertial rotation, and strong diurnal variations of the upper equatorial ocean provide an ideal setting for testing models of turbulent mixing. Initially, we utilize inverse methods to construct the long-term balances of zonal momentum and heat in the upper 200 meters of the equatorial Pacific Ocean at 152 deg W from meteorological and oceanic data. Then we use the time-independent forcing terms obtained from inverse analysis to drive a simple critical-R(sub i) model of turbulence, modified by excluding the bulk Richardson number mixing and adding a background diffusion of constant diffusivity. The modeled steady-state velocity, temperature, turbulent fluxes, and diffusivities are consistent with analysis. However, strong transient behavior of the model with a time scale of 100 days due to vertical advection underscores the importance of spin-up of a turbulence model before investigating effects of

time-varying surface forcing. When solar radiation is allowed to vary diurnally, the simulated diurnal cycle of turbulent mixing has two prominent phases: during the day, the solar insolation creates stratification that interrupts the strong turbulent transfers between the westward wind and the eastward EUC core; during the night, the surface cooling reestablishes their interaction through a 100-m deep water column. The diurnal cycle of turbulent dissipation compares well to the Tropic Heat 1984 measurements. The model uses only a local gradient Richardson number criterion to parameterize mixing. Model tests show that the inclusion of a bulk Richardson number criterion (as used in previous model simulations) distorts the turbulent mixing on both the steady and diurnally varying cases. The model periodically (7 days on average) results in an intense mixing event, then allows the gradual build-up of shear until the next catastrophic mixing event (even when all forcing terms are time-independent). The model produces smaller mean vertical gradients and highly intermittent time series of modeled velocity and temperature near the surface. It seems inconsistent to include both the bulk and the gradient Richardson number as mixing criteria in a model of turbulence. Dissert. Abstr.

N95-17396 Oregon State Univ., Corvallis, OR.
ON THE PROPAGATION OF NEAR-INERTIAL MOTION FROM THE OCEANIC MIXED LAYER Ph.D. Thesis
Vassilis Androklis Zervakis 1994 163 p
Avail: Univ. Microfilms Order No. DA9413766

The radiation of wind-generated inertial currents from the mixed-layers in the form of near-inertial internal waves is the subject of this study. Particular attention is paid to the time scales characteristic of the energy exchange between mixed-layer and pycnocline. For this purpose, a three-dimensional, beta-plane, linear model is developed. The numerical results are interpreted using analytical tools. The model is initialized by mixed-layer inertial oscillations set by a propagating atmospheric front. We demonstrate the importance of the propagation direction of the front in determining the decay of the mixed-layer inertial currents. The exchange of energy between mixed-layer and pycnocline is found to be due to modal interference and modal departure. The model is assessed by comparison to observations of near-inertial oscillations from the OCEAN-STORMS experiment. A slab mixed-layer model, force by a local wind time-series is used to isolate three events of local generation for detailed analysis. The transfer of energy from the mixed-layer to the pycnocline occurs approximately at times predicted by analytical theory. However, while the observed waves propagate vertically as 'beams', the modeled waves remain at the top of the pycnocline. The frequency of the modeled currents is similar to the observed, ranging from slightly subinertial to 1.05 f with the phase propagating upwards. Assuming linear dynamics we develop a time-dependent body friction coefficient simulating the loss of mixed-layer inertial energy to near-inertial internal gravity waves, for use in the traditional slab mixed-layer model. The new decay coefficient is a function of latitude, stratification, and horizontal wavenumber of forcing. Comparison of the slab model results with OCEAN-STORMS observations reveals a better agreement using the new parameterization, than the traditional method. This result suggests that the dominate sink of mixed-layer inertial energy during the experiment was inertial pumping, and that the horizontal scales of the forcing were large. Author

N95-17477 National Oceanic and Atmospheric Administration, Honolulu, HI. International Information Center.
TSUNAMI NEWSLETTER, VOLUME 26 Report No. 1, Jul. 1994
Jul. 1994 31 p Limited Reproducibility: More than 20% of this document may be affected by microfiche quality
(AD-A282751) Avail: CASI HC A03

This is the July 1994 edition (vol. 26) of the Tsunami Newletter published semi-annually by the International Tsunami Information Center in Honolulu, Hawaii. This newsletter is distributed worldwide. The news events in this volume consist of earthquake and tsunami reports from various parts of the world, seismic and geological data from the Japan Sea, corrections for national contacts list, IDNDR Report (International Decade for Natural Disaster Reduction) for their May 1994 Conference, INTERNET information and addresses, information regarding educational programs and national and area reports, meeting announcements, publication announcements, maps, and topical updates within the organization itself. CASI

N95-17505 Kansas Univ. Center for Research, Inc., Lawrence, KS. Radar Systems and Remote Sensing Lab.
ANALYSIS OF A THREE-BEAM RADAR AS AN INSTRUMENT FOR DETERMINING OCEAN WAVE HEIGHTS AND VECTOR SLOPES
Christopher T. Evans Jun. 1994 202 p Limited Reproducibility: More than 20% of this document may be affected by microfiche quality
(Contract N00014-89-J-3221)
(AD-A282342; CRINC/RSL-TR-8621-5) Avail: CASI HC A10

The Vector Slope Gauge (VSG) is a 35-GHz FM-CW scatterometer that has the unique capability of simultaneously (nearly) measuring the range and backscattered power to three points on the ocean surface. With three ranges and knowledge of the experimental geometry, the wave height at each footprint can be obtained. The three footprints form a plane surface which enable two orthogonal slope components to be obtained. Obtaining the slope of ocean waves is important because it is correlated with the backscattered power. By obtaining the vector slope, one does not have to make any assumptions about the linearity or long-crestedness of the ocean waves. With a time series record of ocean wave heights and slopes, one can learn a great deal about the ocean surface. Spectral analysis of the recorded time series yields information about the wave height power spectral density, the mean wave direction vs. frequency, and the directional width spectrum. The results from the VSG are similar to those obtained from a pitch-and-roll buoy. In addition, since the slope distribution of ocean waves is nearly normal, the moments of a bivariate normal distribution can be used to fit an ellipse to the wave slopes. DTIC

N95-17615# Science Applications International Corp., Raleigh, NC.
STRAITS OF FLORIDA PHYSICAL OCEANOGRAPHIC FIELD STUDY. VOLUME 1: EXECUTIVE SUMMARY. VOLUME 2: TECHNICAL REPORT. VOLUME 3: DATA REPORT Final Report
1992 315 p
(Contract DI-14-35-0001-30493)
(PB94-175031; OCS/MMS-92/0024-Vol-1-2) Avail: CASI HC A14/MF A03

The specific objectives of the study were two-fold: (1) to acquire data sets which provide initial and boundary conditions for a numerical circulation model as well as information which can be used for model validation and verification and (2) to develop an improved understanding of primary circulation patterns in the study area and the responsible forcing mechanisms. The overall rational for the Straits of Florida (SoF) project, which these objectives support, is development of a numerical circulation model which will provide improved input to and hence reliability of the Oil Spill Risk Assessment (OSRA) model results. OSRA is used to provide a probabilistic characterization of potential adverse impacts of activities linked directly to offshore oil and gas development, production, and transportation. NTIS

N95-17624 Naval Postgraduate School, Monterey, CA.
AN OBSERVATIONAL STUDY OF LONG WAVES IN THE EQUATORIAL PACIFIC OCEAN DURING THE 1991-1993 EL NINO M.S. Thesis
Todd W. Sitler Jun. 1994 160 p Limited Reproducibility: More than 20% of this document may be affected by microfiche quality
(AD-A283380) Avail: CASI HC A08

Long waves in the equatorial Pacific Ocean during the 1991-1993 El Nino event were examined using temperature, current, and wind time series from the Tropical Oceans-Global Atmosphere Tropical Atmosphere-Ocean (TOGA-TAO) moored buoy array. Numerous episodes of long wave activity were detected. The most prominent episodes were associated with eastward propagating equatorial Kelvin waves and with westward propagating tropical instability waves and mixed Rossby-gravity waves. Equatorial Kelvin waves, which were generated by westerly wind events in the western and central Pacific, were evident in the data between 2 deg N to 5 deg S and from 170 deg W to 110 deg W. These Kelvin waves, which were most pronounced from 75 to 300 m, had periods of 40 to 70 days, eastward phase speeds of 1.9 to 6.5 m/s, and zonal wavelengths on the order of 10,000 km. These waves were most evident in the Northern Hemisphere fall and winter. The period of greatest Kelvin wave activity was August 1991-May 1992, during the peak phase of the 1991-1993 El Nino event. DTIC

51 LIFE SCIENCES (GENERAL)

N95-15961*# North Carolina Univ., Raleigh, NC. Dept. of Soil Science.
REGULATION OF NITROGEN UPTAKE AND ASSIMILATION: EFFECTS OF NITROGEN SOURCE AND ROOT-ZONE AND AERIAL ENVIRONMENT ON GROWTH AND PRODUCTIVITY OF SOYBEAN Final Technical Report
C. David Raper, Jr. 1 Oct. 1994 20 p
(Contract NCC2-101)
(NASA-CR-197098; NAS 1.26:197098) Avail: CASI HC A03/MF A01

The interdependence of root and shoot growth produces a functional equilibrium as described in quantitative terms by numerous authors. It was noted that bean seedlings grown in a constant environment tended to have a constant distribution pattern of dry matter between roots and leaves characteristic of the set of environmental conditions. Disturbing equilibrium resulted in a change in relative growth of roots and leaves until the original ratio was restored. To define a physiological basis for regulation of nitrogen uptake within the balance between root and shoot activities, the authors combined a partioning scheme and a utilization priority assumption in which: (1) all carbon enters the plant through photosynthesis in leaves and all nitrogen enters the plant through active uptake by roots, (2) nitrogen uptake by roots and secretion into the xylem for transport to the shoots are active processes, (3) availability of exogenous nitrogen determines concentration of soluble carbohydrates within the roots, (4) leaves are a source and a sink for carbohydrates, and (5) the requirement for nitrogen by leaf growth is proportionally greater during initiation and early expansion than during later expansion. Derived from text

N95-16034*# Colorado Univ., Boulder, CO. Dept. of Aerospace Engineering Sciences.
BioServe SPACE TECHNOLOGIES: A NASA CENTER FOR THE COMMERCIAL DEVELOPMENT OF SPACE Annual Report
1992 55 p Prepared in cooperation with Kansas State Univ., Manhattan, KS
(Grant NAGw-1197)
(NASA-CR-196983; NAS 1.26:196983) Avail: CASI HC A04/MF A01

BioServe Space Technologies, a NASA Center for the Commercial Development of Space (CCDS), was established in 1987. As is characteristic of each CCDS designated by NASA, the goals of this commercial center are aimed at stimulating high technology research that takes advantage of the space environment and at leading in the development of new products and services which have commercial potential or that contribute to possible new commercial ventures. BioServe's efforts in these areas focus upon space life science studies and the development of enabling devices that will facilitate ground-based experiments as well as the conversion of such to the microgravity environment. A direct result of BioServe's hardware development and life sciences studies is the training of the next generation of bioengineers who will be knowledgeable and comfortable working with the challenges of the space frontier. Derived from text

N95-16164# Pittsburgh Univ., Pittsburgh, PA.
INVESTIGATION OF PRESSURE REGULATION IN AN ARCHAEBACTERIAL ENZYME Final Report, 1 Feb. 1991 - 31 Jan. 1994
Alan J. Russell 25 Mar. 1994 8 p
(Contract DAAL03-91-G-0034)
(AD-A281413; ARO-28011.2-LS) Avail: CASI HC A02/MF A01

Initial studies focused on the purification of the hydrogenase from Methanococcus jannaschii. The hydrogenase was characterized, N-terminal sequenced, and its amino acid content was compared to other hydrogenases. Researchers then constructed a library of genomic DNA from Methanococcus jannaschii. The genomic library, with over 1 million independent representatives, was cloned into bacteriophage lambda. The DNA from the organism has been found to be methylated, preventing classic enzyme treatments for gene library synthesis. A gene library has been synthesized by mechanical shearing, and the fragment size is approximately 8-15 kb. Another driving force for the production of the library was the independent discovery of a remarkably thermostable protease which retains activity at 135 C. The protease was partially purified. The partially purified sample was used for the studies to determine which class of protease it may be. DTIC

N95-16429*# Old Dominion Univ., Norfolk, VA. Dept. of Biological Sciences.
ROOT GROWTH AND DEVELOPMENT IN RESPONSE TO CO2 ENRICHMENT Final Report, 2 Jul. 1992 - 15 Oct. 1994
Frank P. Day, Jr. 15 Oct. 1994 5 p
(Grant NAG10-0110)
(NASA-CR-196154; NAS 1.26:196154) Avail: CASI HC A01/MF A01

A non-destructive technique (minirhizotron observation tubes) was used to assess the effects of CO2 enrichment on root growth and development in experimental plots in a scrub oak-palmetto community at the Kennedy Space Center. Potential effects of CO2 enrichment on plants have a global significance in light of concerns over increasing CO2 concentrations in the Earth's atmosphere. The study at Kennedy Space Center focused on aboveground physiological responses (photosynthetic efficiency and water use efficiency), effects on process rates (litter decomposition and nutrient turnover), and belowground responses of the plants. Belowground dynamics are an exceptionally important component of total plant response but are frequently ignored due to methodological difficulties. Most methods used to examine root growth and development are destructive and, therefore, severely compromise results. Minirhizotrons allow nondestructive observation and quantification of the same soil volume and roots through time. Root length density and root phenology were evaluated for CO2 effects with this nondestructive technique. Derived from text

N95-16599# Virginia Univ., Charlottesville, VA. Dept. of Biology.
CONTROL OF CIRCADIAN BEHAVIOR BY TRANSPLANTED SUPRACHIASMATIC NUCLEI Final Report, 1 Mar. 1993 - 28 Feb. 1994
Michael Menaker 2 Sep. 1994 15 p
(Contract F49620-93-1-0185)
(AD-A285233; AFOSR-94-0588TR) Avail: CASI HC A03/MF A01

Over the past three years we have focused our research efforts on the study of the properties of the suprachiasmatic nucleus (SCN) of the tau mutant hamster. In general we have sought to understand how this mutation, which changes the period of circadian rhythmicity from about 2.4 hours in wild-type animals to near 20 hours in homozygous mutants, affects the SCN itself and how it affects the locomotor behavior which is driven by the SCN. Specifically we have used SCN lesions, which abolish behavioral rhythmicity, followed by transplantation of fetal or neonatal donor SCN, which restores rhythmicity, to ask which components of rhythmic behavior are intrinsic to the SCN and which may depend on its interaction with other structures. We have also studied the free running locomotor rhythms of mutant and wild-type hamsters and compared their responses to constant darkness, constant light and to phase shifting light pulses as a first step toward discovering whether the profound differences that exist in the parameters can all be accounted for by changes in the SCN. DTIC

N95-16737# Aerospace Medical Association, Alexandria, VA.
AEROSPACE MEDICAL ASSOCIATION 63RD ANNUAL SCIENTI FIC MEETING PROGRAM Abstracts Only
14 May 1992 132 p Meeting held in Miami Beach, FL, 10-14 May 1992
Avail: CASI HC A07/MF A02

Abstracts submitted by the authors of slide, poster, and panel sessions are presented. They cover aerospace medicine topics in the following areas: gravitaional physiology related to space flight; simulation of microgravity using centrifuges and parabolic flight; motion sickness and space adaptation syndrome; medical techniques in microgravity; medical hardware developed for use in space flight environments; physiological constraints on aerobraking; aircraft control and navigation; anti gravity suits; pilot aging; the effect of long missions on flight crews; and psychological aspects of personnel selection and training. For individual titles, see N95-16738 through N95-16782.

N95-16738*# National Aeronautics and Space Administration. Lyndon B. Johnson Space Center, Houston, TX.
THE EFFECT OF DIFFERENCES IN TIME TO DETECTION OF CIRCULATING MICROBUBBLES ON THE RISK OF DECOMPRESSION SICKNESS Abstract Only c52
K. V. Kumar (Krug Life Sciences, Inc., Houston, TX.), J. H. Gilbert (Krug

Life Sciences, Inc., Houston, TX.), M. R. Powell, and J. M. Waligora *In* Aerospace Medical Association, Aerospace Medical Association 63rd Annual Scientific Meeting Program 14 May 1992 1 p (For primary document see N95-16737 04-51)
Avail: CASI HC A01/MF A02

Circulating microbubbles (CMB) are frequently detected prior to the appearance of symptoms of Decompression Sickness (DCS). It is difficult to analyze the effect of CMB on symptoms due to differences in the time to detection of CMB. This paper uses survival analysis models to evaluate the risk of symptoms in the presence of CMB. Methods: Information on 81 exposures to an altitude of 6,400 m (6.5 psi) for a period of three hours, with simulated extravehicular activities, was examined. The presence or absence of CMB was included as a time dependent covariate of the Cox proportional hazards regression model. Using this technique, the subgroup of exposures with CMB was analyzed further. Mean (S.D.) time in minutes to onset of CMB and symptoms were 125 (63) and 165 (33) respectively, following the three hours exposure. The risk of symptoms (17/81) increased 14 times in the presence of CMB, after controlling for variations in time to detection of CMB. Further, the risk was lower when time to detection of CMB was greater than 60 minutes (risk ratio = 0.96; 95 percent confidence intervals = 0.94 - 0.99 0.99 P less than 0.01) compared to CMB before 60 minutes at altitude. Conclusions: Survival analysis showed that individual risk of DCS changes significantly due to variations in time to detection of CMB. This information is important in evaluating the risk of DCS in the presence of CMB. Author

N95-16739*# National Aeronautics and Space Administration. Lyndon B. Johnson Space Center, Houston, TX.
VARIABILITY IN HOFFMANN AND TENDON REFLEXES IN HEALTHY MALE SUBJECTS Abstract Only **c52**
E. Good (Humana Hospital, Webster, TX.), S. Do (Baylor Coll. of Medicine, Houston, TX.), and M. Jaweed *In* Aerospace Medical Association, Aerospace Medical Association 63rd Annual Scientific Meeting Program 14 May 1992 1 p (For primary document see N95-16737 04-51)
Avail: CASI HC A01/MF A02

There is a time dependent decrease in amplitude of H- and T-reflexes during Zero-G exposure and subsequently an increase in the amplitude of the H-reflex 2-4 hours after return to a 1-G environment. These alterations have been attributed to the adaptation of the human neurosensory system to gravity. The Hoffman reflex (H-reflex) is an acknowledged method to determine the integrity of the monosynaptic reflex arc. However deep tendon reflexes (DTR's or T-reflexes), elicited by striking the tendon also utilize the entire reflex arc. The objective of this study was to compare the variability in latency and amplitude of the two reflexes in healthy subjects. Methods: Nine healthy male subjects, 27-43 years in age, 161-175 cm in height plus 60-86 Kg in weight, underwent weekly testing for four weeks with a Dan-Tec EMG counterpoint EMG system. Subjects were studied prone and surface EMG electrodes were placed on the right and left soleus muscles. The H-reflex was obtained by stimulating the tibial nerve in the politeal fossa with a 0.2 msec square wave pulse delivered at 2 Hz until the maximum H-reflex was obtained. The T-reflex was invoked by tapping the achilles tendon with a self triggering reflex hammer connected to the EMG system. The latencies and amplitudes for the H- and T-reflexes were measured. Results: These data indicate that the amplitudes of these reflexes varied considerably. However, latencies to invoked responses were consistent. The latency of the T-reflex was approximately 3-5 msec longer than the H-reflex. Conclusion: The T-reflex is easily obtained, requires less time, and is more comfortable to perform. Qualitative data can be obtained by deploying self triggering, force plated reflex hammers both in the 1-G and Zero-G environment. Author

N95-16740*# National Aeronautics and Space Administration. Ames Research Center, Moffett Field, CA.
THE PSYCHOPHYSICAL FUNCTION FOR PERCEIVED GRAVITATIONAL-INERTIAL FORCE DOES NOT DEPEND ON THE ORIENTATION OF THE OTOLITH ORGANS Abstract Only **c52**
M. Cohen, R. Welch, and C. DeRoshia *In* Aerospace Medical Association, Aerospace Medical Association 63rd Annual Scientific Meeting Program 14 May 1992 1 p (For primary document see N95-16737 04-51)
Avail: CASI HC A01/MF A02

It has generally been believed that the perceived intensity of a gravitational-inertial force depends on both the magnitude and orientation of the force with respect to the otolith organs, as does the elevator illusion. In this study, we examine the perceived intensity of Gz force and the elevator illusion as a function of the applied force and the orientation of the subject's head. Methods: Each of 7 male subjects was seated upright in a swinging chair mounted in the Ames 20-G Human Centrifuge while he set a visual target to his apparent horizon and judged the perceived intensity of Gz forces by cross-modal matches on a hand dynamometer. Plateau Gz levels were 1.00 1.25, 1.50, 2.00, 2.25, and 2.50; a 30 second ramp to plateau was used in all cases, and the duration of exposure at each plateau was 120 seconds. All measures were obtained both with the subject's head erect and pitched forward 30 degrees. Results: Although the elevator illusion changed with head orientation ($F(6,60) = 7.56$; p less than 0.001) the perceived intensity of Gz was essentially the same for both orientations of the head ($F(6,60) = 0.61$; p greater than 50). Conclusions: The results of this experiment suggest that the perceived intensity of gravitational-inertial force does not depend on otolith mechanisms in the same way as does the elevator illusion and that somesthetic, tactile, and other proprioceptive inputs are important for the psychophysical function. Author

N95-16741*# National Aeronautics and Space Administration. Lyndon B. Johnson Space Center, Houston, TX.
USE OF INJECTABLE PROMETHAZINE TO DECREASE SYMPTOM SCORES OF SPACE MOTION SICKNESS Abstract Only **c52**
B. G. Beck and A. E. Nicogossian *In* Aerospace Medical Association, Aerospace Medical Association 63rd Annual Scientific Meeting Program 14 May 1992 1 p (For primary document see N95-16737 04-51)
Avail: CASI HC A01/MF A02

Space motion sickness (SMS) has been a problem affecting approximately 74 percent of first time shuttle flyers. Promethazine injections have been used for 29 cases of SMS to decrease the severity of their illness. Although reported to be effective in reducing symptoms in 27 of the 29 cases, there has been no proof of its efficacy. Methods: Retrospective analysis of medical debriefs examining the symptom scores for nausea, vomiting, decreased appetite, and stomach awareness were performed. Each symptom is rated on a mild = 1, moderate = 2, severe = 3 system for each flight day. Crewmember scores for the first three flight days on an initial flight in which injectable promethazine had not been used were compared to scores in a later flight in which the promethazine was utilized. Scores were also compared in a similar group of crewmembers who did not use promethazine. Results: There was a decrease in median scores for all symptoms except nausea, however, it was significant ($p = 0.14$) only for the vomiting scores. This significant decrease was not seen in the control group. Conclusions: Injectable promethazine has been associated with a significant decrease in vomiting compared to earlier flights in which injectable promethazine was not used. Author

N95-16742*# National Aeronautics and Space Administration. Ames Research Center, Moffett Field, CA.
COMPARISON OF SALINE AND FLUDROCORTISONE AS FLUID-LOADING COUNTERMEASURES FOLLOWING EXPOSURE TO SIMULATED MICROGRAVITY Abstract Only **c52**
J. Vernikos, D. A. Ludwig (National Aeronautics and Space Administration. John F. Kennedy Space Center, Cocoa Beach, FL.), and V. A. Convertino (National Aeronautics and Space Administration. John F. Kennedy Space Center, Cocoa Beach, FL.) *In* Aerospace Medical Association, Aerospace Medical Association 63rd Annual Scientific Meeting Program 14 May 1992 1 p (For primary document see N95-16737 04-51)
Avail: CASI HC A01/MF A02

Saline loading (SL) within hours of reentry is currently used as a countermeasure against postflight orthostatic hypotension in astronauts. However, its effects on blood volume expansion is not quantified and its effectiveness has proved marginal at best. The purposes of the present study were: (1) to quantify the effects of SL on plasma volume and orthostatic tolerance following exposure to simulated microgravity and (2) to compare these effects with the use of a pharacological fluid expander, fludrcortisone (F). Method: Eleven men (30-45 yr.) underwent a 15-minute stand test before and immediately after 7 days of head-down bedrest (BR). Five subjects ingested SL (8 g salt tablets with 1 liter of water) 2 hours before standing at the end of BR while the other 6 subjects received 0.2 mg oral doses of F at 0800 and 2200 hours the day before and 0800 hours the day the subjects got out of bed (i.e., 2 hours before standing).

Plasma volume (PV) was measured before BR on day 7 of BR and after the final SL and F treatments just before the post-BR stand test. Blood pressure and heart rate were measured continuously during the stand tests. Results: BR decreased PV from 40.7 plus or minus 1.9 mml/kg to 35.9 plus or minus 1.1 ml/kg (minus 11.8 percent P less than 0.05). Following SL, PV remained at 36.4 plus or minus 1.5 ml/kg while F returned PV to 39.1 plus or minus 1.8 ml/kg. The post BR stand test was completed without syncopal symptoms by 5 of 6 F subjects but only 2 of 5 SL subjects. Conclusions: SL may be ineffective in restoring PV to preflight levels and may provide inadequate protection against postflight orthostatic hypotension. In contrast, F may provide a promising countermeasure since it restored PV and reduced the incidence of syncope following exposure to simulated microgravity in the present study. Author

N95-16743*# National Aeronautics and Space Administration. John F. Kennedy Space Center, Cocoa Beach, FL.

SKELETAL MUSCLE RESPONSES TO UNLOADING IN HUMANS Abstract Only **c52**

G. Dudley (Bionetics Corp., Cocoa Beach, FL.), P. Tesch, B. Hather, G. Adams, and P. Buchanan *In* Aerospace Medical Association, Aerospace Medical Association 63rd Annual Scientific Meeting Program 14 May 1992 1 p Prepared in cooperation with Karolinska Inst., Stockholm, Sweden (For primary document see N95-16737 04-51)

(Contract NAS10-11624)

Avail: CASI HC A01/MF A02

This study examined the effects of unloading on skeletal muscle structure. Method: Eight subjects walked on crutches for six weeks with a 110 cm elevated sole on the right shoe. This removed weight bearing by the left lower limb. Magnetic resonance imaging of both lower limbs and biopsies of the left m. vastus laterallis (VL) were used to study muscle structure. Results: Unloading decreased (P less than 0.05) muscle cross-sectional areas (CSA) of the knee extensors 16 percent. The knee flexors showed about 1/2 of this response (-7 percent, P less than 0.05). The three vasti muscles each showed decreases (P less than 0.05) of about 15 percent. M. rectus femoris did not change. Mean fiber CSA in VL decreased (P less than 0.05) 14 percent with type 2 and type 1 fibers showing reductions of 15 and 11 percent respectively. The ankle extensors showed a 20 percent decrease (P less than 0.05) in CSA. The reduction for the 'fast' m. gastrocnemius was 27 percent compared to the 18 percent decrease for the 'slow' soleus. Summary: The results suggest that decreases in muscle CSA are determined by the relative change in impact loading history because atrophy was (1) greater in extensor than flexor muscles, (2) at least as great in fast as compared to slow muscles or fibers, and (3) not dependent on single or multi-joint function. They also suggest that the atrophic responses to unloading reported for lower mammals are quantitatively but not qualitatively similar to those of humans. Author

N95-16744*# National Aeronautics and Space Administration. Ames Research Center, Moffett Field, CA.

INTRAMUSCULAR PRESSURE: A BETTER TOOL THAN EMG TO OPTIMIZE EXERCISE FOR LONG-DURATION SPACE FLIGHT Abstract Only **c52**

A. R. Hargens, R. E. Ballard, M. Aratow, A. Crenshaw, J. Styf, N. Kahan, and D. E. Watenpaugh *In* Aerospace Medical Association, Aerospace Medical Association 63rd Annual Scientific Meeting Program 14 May 1992 1 p (For primary document see N95-16737 04-51)

Avail: CASI HC A01/MF A02

A serious problem experienced by astronauts during long-duration space flight is muscle atrophy. In order to develop countermeasures for this problem, a simple method for monitoring in vivo function of specific muscles is needed. Previous studies document that both intramuscular pressure (IMP) and electromyography (EMG) provide quantitative indices of muscle contraction force during isometric exercise. However, at present there are no data available concerning the usefulness of IMP versus EMG during dynamic exercise. Methods: IMP (Myopress catheter) and surface EMG activity were measured continuously and simultaneously in the tibalis anterior (TA) and soleus (SOL) muscles of 9 normal male volunteers (28-54 years). These parameters were recorded during both concentric and eccentric exercises which consisted of plantarflexon and dorsiflexon of the ankle joint. A Lido Active Isokinetic Dynamometer concurrently recorded ankle joint torque and position. Results: Intramuscular pressure correlated linearly with contraction force for both SOL (r exp 2 = 0.037) and TA (R exp 2 = 0.716 and r exp 2 = 0.802, respectively). During eccentric exercises, SOL and TA IMP also correlated linearly with contraction force (r(exp 2) = 0.883 and r(exp 2) = 0.904 respectively), but SOL and TA EMG correlated poorly with force (r(exp 2) = 0.489 and r(exp 2) = 0.702 respectively). Conclusion: IMP measurement provides a better index of muscle contraction force than EMG during concentric and eccentric exercise. IMP reflects intrinsic mechanical properties of individual muscles, such as length tension relationships. Although invasive, IMP provides a more powerful tool and EMG for developing exercise hardware and protocols for astronauts exposed to long-duration space flight. Author

N95-16745*# National Aeronautics and Space Administration. Lyndon B. Johnson Space Center, Houston, TX.

CATECHOLAMINERGIC RESPONSES TO STRESSFUL MOTION STIMULI, SCOPOLAMINE PLUS AMPHETAMINE, AND DEXAMETHASONE Abstract Only **c52**

R. L. Kohl and W. E. Chelen *In* Aerospace Medical Association, Aerospace Medical Association 63rd Annual Scientific Meeting Program 14 May 1992 1 p Prepared in cooperation with National Academy of Sciences - National Research Council, Houston, TX (For primary document see N95-16737 04-51)

(Contract NAS9-17267; RTOP 199-16-11-08)

Avail: CASI HC A01/MF A02

Peripheral levels of epinephrine (EPI) and neoepinephrine (NE) generally rise following stressful motion stimuli. Effective anti-motion sickness drugs, scopolamine plus, d-amphetamine (S/D) and dexamthasone (DEX) modulate release of EPI and NE. This modulation may be of etiological relevance. Methods: Severe nausea was induced by exposure to coriolis simulation using a rotating chair. Chronic administration of S/D (0.4 and 5 mg/da) DEX (3 mg/day) and placebo preceded coriolis simulation. EPI and NE were measured immediately before and after simulation. A double-blind crossover design was used. Results: Nausea-induced elevations of EPI (2.5 fold, p less than .01) and NE were not diminished upon repeated exposure and adaptation to the stressor. Subjects with more pronounced elevations of EPI following simulation displayed higher resistance to stressful motion (p less .05). Alteration of peripheral catechlomaine levels following drug suggested that motion sickness was not mediated by peripheral catechlolamine receptor simulation. EPI and NE levels were 2.8 and 3.6-fold higher (p less than .03 and .01) after nausea without DEX treatment. DEX loading halved pre-stress levels of EPI and NE (p less than .05). Conclusions: Marked differences were noted in individual responses to drug and systematic responses of EPI and NE. It is possible that the responses of EPI to motion sickness may predict resistance to stressful motion and represent a peripheral manifestation of some as yet unknown central event of etiologic relevance. Author

N95-16746*# National Aeronautics and Space Administration. John F. Kennedy Space Center, Cocoa Beach, FL.

HEAT STRESS AND A COUNTERMEASURE IN THE SHUTTLE RESCUEMAN'S SUIT Abstract Only **c52**

D. F. Doerr, H. Reed, and V. A. Convertino *In* Aerospace Medical Association, Aerospace Medical Association 63rd Annual Scientific Meeting Program 14 May 1992 1 p (For primary document see N95-16737 04-51)

Avail: CASI HC A01/MF A02

Rescue of the astronaut flight crew from a contingency landing may risk exposure of the rescue crew to toxic propellants spilling from potentially ruptured tanks in the crew module area. An Aquala dry diver's suit has been in service by the rescue team to preclude exposure, especially in the water rescue scenario. Heat stress has become a factor of concern in recent years when older and less physically-fit team members work in this suit. Methods: Field testing was initiated using fully instrumented rescue men in a simulated scenario to determine the extent of heat stress. Two tests were accomplished, one in the normal (N) configuration and one with a proposed cooling countermeasure, the Steele vest (S). Results: Heat stress was high as indicated by average rectal temperatures (Tre) of 38.28 degrees C(100.9 degrees F) after the 45 minute protocol. Slopes of the regression equations describing the increase in Tre with time were greater (P less than 0.05) with N (0.073 plus or minus .008) compared to S (0.060 plus or minus .007). Projection of time to the 38.89 degree C (102 degree F) limit was increased by 15.3 percent with the vest. Mean skin temperature (Tsk) was higher (P less than 0.05) in N (38.33 plus or minus

.11 degrees C) compared to S (34.33 plus or minus .39 degrees C). Average heart rate was higher (P less than 0.05 in N than S. Sweat loss, as measured by weight loss, was more (P less than 0.05) for N (1.09 plus or minus .09 kg versus 0.77 plus or minus .06 kg). Air usage, while slightly less for S, was not statistically different. Conclusion: The use of the cool vest provided significant relief from thermal stress in spite of the addition of 3.4 kg (7.5 pounds) weight and some loss in mobility. Author

N95-16747*# National Aeronautics and Space Administration. Lyndon B. Johnson Space Center, Houston, TX.

A NEW MODEL FOR ESTIMATING TOTAL BODY WATER FROM BIOELECTRICAL RESISTANCE Abstract Only **c52**

S. F. Siconolfi and K. T. Kear (Krug Life Sciences, Inc., Houston, TX.) *In* Aerospace Medical Association, Aerospace Medical Association 63rd Annual Scientific Meeting Program 14 May 1992 1 p (For primary document see N95-16737 04-51)

Avail: CASI HC A01/MF A02

Estimation of total body water (T) from bioelectrical resistance (R) is commonly done by stepwise regression models with height squared over R, H(exp 2)/R, age, sex, and weight (W). Polynomials of H(exp 2)/R have not been included in these models. We examined the validity of a model with third order polynomials and W. Methods: T was measured with oxygen-18 labled water in 27 subjects. R at 50 kHz was obtained from electrodes placed on the hand and foot while subjects were in the supine position. A stepwise regression equation was developed with 13 subjects (age 31.5 plus or minus 6.2 years, T 38.2 plus or minus 6.6 L, W 65.2 plus or minus 12.0 kg). Correlations, standard error of estimates and mean differences were computed between T and estimated T's from the new (N) model and other models. Evaluations were completed with the remaining 14 subjects (age 32.4 plus or minus 6.3 years, T 40.3 plus or minus 8 L, W 70.2 plus or minus 12.3 kg) and two of its subgroups (high and low) Results: A regression equation was developed from the model. The only significant mean difference was between T and one of the earlier models. Conclusion: Third order polynomials in regression models may increase the accuracy of estimating total body water. Evaluating the model with a larger population is needed. Author (revised)

N95-16748*# Kentucky Univ., Lexington, KY. Center for Biomedical Engineering.

SPECTRAL COMPONENTS OF HUMAN CARDIOVASCULAR RESPONSES TO STEP CHANGES IN LOWER BODY NEGATIVE PRESSURE (LBNP) BEFORE AND AFTER 22 HOUR OF 6 DEG HEAD DOWN BED REST Abstract Only **c52**

C. F. Knapp, J. M. Evans, K. J. Grande, C. D. Murphy, and A. R. Patwardhan *In* Aerospace Medical Association, Aerospace Medical Association 63rd Annual Scientific Meeting Program 14 May 1992 1 p (For primary document see N95-16737 04-51)

(Grant NAG9-298)

Avail: CASI HC A01/MF A02

Changes in autonomic outflow to peripheral organs during the development of bedrest induced orthostatic intolerance have not been determined. Recent studies have indicated that spectral analysis provides an indirect assessment of these changes. Eight male subjects were studied before and after 22 hours of 6 degree head down bedrest plus Lasix (40 mg. P.P.). Cardiovascular spectra (using an autoregressive technique) were determined for heart rate (HR, ECG), arterial pressure (AP, Finapres), radial artery flow (RF, Hokansen) and respiration rate (RR, BoMed). Spectra were obtained from 2.5 minute segments during control, lower body negative pressure (minus 10, 20, 30, 40, 50 mmHg) and recovery. Bedrest increased HR spectra power in the low frequency (.001 to .041 Hz) range, increased RF power in the low and mid (.04 to .18 Hz) range and increased AP power in the high (.18 to .50 Hz) frequency range. Increasing levels of lower body negative pressure decreased HR power and increased RF power in the high frequency range and decreased AP power in the low frequency range. Since spectral power of HR in the high frequency range has been shown to indicate parasympathetically mediated regulation and power in the low and mid frequency ranges indicates a sympathetic / parasympathetic mixture, then both bedrest and lower body negative pressure appeared to shift sympathetic / parasympathetic balance toward sympathetic regulation of HR. The interpretation of the spectral content of AP and RF with respect to their autonomic origins remains unclear. Author

N95-16749*# National Aeronautics and Space Administration. Lyndon B. Johnson Space Center, Houston, TX.

MAGNETIC RESONANCE IMAGING (MRI) OF SKELETAL MUSCLES IN ASTRONAUTS AFTER 9 DAYS OF SPACE FLIGHT Abstract Only **c52**

M. Jaweed, P. Narayana (Texas Univ. Health Science Center, Houston, TX.), J. Slopis (Texas Univ. Health Science Center, Houston, TX.), I. Butler (Texas Univ. Health Science Center, Houston, TX.), V. Schneider, A. LeBlanc (Baylor Univ., Houston, TX.), L. Fotedar (Krug Life Sciences, Inc., Houston, TX.), and D. Bacon (Humana Hospital, Webster, TX.) *In* Aerospace Medical Association, Aerospace Medical Association 63rd Annual Scientific Meeting Program 14 May 1992 1 p (For primary document see N95-16737 04-51)

Avail: CASI HC A01/MF A02

Skylab data indicated that prolonged exposure of human subjects to microgravity environment causes significant muscle atrophy accompanied by reduced muscle strength and fatigue resistance. The objective of this study was to determine decrements in muscle size, if any, in the soleus and gastrocnemius muscles of male and female astronauts after 9 days of space flight. Methods: Eight astronauts, one female and seven male, between the ages of 31 and 59 years 59-84 kg in body weight were examined by MRI 2-3 times preflight within 16 days before launch, and 2 days, (n=6) and seven days (n=3) after landing. The right leg muscles (gastroc-soleus) were imaged with a lower extremity coil in magnets operating at 1.0 or 1.5 Tsela. The imaging protocol consisted of spin echo with a Tr of 0.70 - 1.5 sec. Thirty to forty 3-5 mm thick slices were acquired in 256 x 128 or 256 x 256 matrices. Acquisition time lasted 20-40 minutes. Multiple slices were measured by computerized planimetry. Results: Compared to the preflight, the cross-sectoral areas (CSA) of the soleus, gastrocnemius, and the leg, at 2 days after landing were reduced (at least p less than 0.05) 8.9 percent, 13.2 percent, and 9.5 percent respectively. The soleus and the leg of three astronauts evaluated at 7 days postflight did not show full recovery compared to the preflight values. Conclusions: It is concluded that l9-days of space flight may cause significant decreases in CSA of the leg muscles. The factors responsible for this loss need further determination. Author

N95-16750*# National Aeronautics and Space Administration. Lyndon B. Johnson Space Center, Houston, TX.

RESULTS OF AN INTERNATIONAL SPACE CREW DEBRIEF Abstract Only **c52**

P. A. Santy (Texas Univ., Galveston, TX.), A. W. Holland, L. Looper, and R. Marcondes-North *In* Aerospace Medical Association, Aerospace Medical Association 63rd Annual Scientific Meeting Program 14 May 1992 1 p (For primary document see N95-16737 04-51)

Avail: CASI HC A01/MF A02

In order to identify potential multi-cultural and multinational problems for future International Space Station Freedom crew, a crew debrief questionnaire was developed for U.S. astronauts who flew on shuttle missions with one or more crew members from other countries. Methods: From 1981-90, a total of 20 U.S. astronauts flew on international space missions. Debriefs were mailed to all 20 with instructions not to identify themselves or their specific mission. The debrief focused primarily on preflight training and post flight incidents of misunderstanding, miscommunication, and interpersonal friction among crewmembers. Astronauts were also asked to rate the impact of the incident to the mission (low, medium, high). Results: Ten astronauts responded, but only nine responses were able to be scored, for a return rate of 45 percent. 42 incidents were reported, 9 in the preflight period, 26 inflight, and 7 in the postflight period. Most of the incidents were rated at a low or medium impact, but 5 of the inflight incidents were rated at a 'high' mission impact. A number of causes for the problems were listed, and are discussed. Conclusions: The debrief respondents provide useful and timely recommendations on preflight training which might help facilitate the integration of multinational crews and prevent multi-cultural or multinational factors from interfering with mission operations. Author

N95-16751*# National Aeronautics and Space Administration. Ames Research Center, Moffett Field, CA.

PHYSIOLOGICAL CONSTRAINTS ON DECELERATION DURING THE AEROCAPTURE OF MANNED VEHICLES Abstract Only **c52**

J. E. Lyne *In* Aerospace Medical Association, Aerospace Medical

Association 63rd Annual Scientific Meeting Program 14 May 1992 1 p (For primary document see N95-16737 04-51)
Avail: CASI HC A01/MF A02

The peak deceleration load allowed for aerobraking of manned vehicles is a critical parameter in planning future excursions to Mars. However, considerable variation exists in the limits used by various investigators. The goal of this study was to determine the most appropriate level for this limit. Methods: Since previous U.S. space flights have been limited to 84 days duration, Soviet flight results were examined. Published details of Soviet entry trajectories were not available. However, personal communication with Soviet cosmonauts suggested that peak entry loads of 5-6 G had been encountered upon return from 8 months in orbit. Soyuz entry capsule's characteristics were established and the capsule's entry trajectory was numerically calculated. The results confirm a peak load of 5 to 6 G. Results: Although the Soviet flights were of shorter duration than expected Mars missions, evidence exists that the deceleration experience is applicable. G tolerance has been shown to stabilize after 1 to 3 months in space if adequate countermeasures are used. The calculated Soyuz deceleration histories are graphically compared with those expected for Mars aerobraking. Conclusions: Previous spaceflight experience supports the use of a 5 G limit for the aerocapture of a manned vehicle at Mars. Author

N95-16752*# National Aeronautics and Space Administration. Lyndon B. Johnson Space Center, Houston, TX.
BLOOD VOLUME AND ORTHOSTATIC RESPONSES OF MEN AND WOMEN TO A 13-DAY BEDREST Abstract Only **c52**
S. Fortney, T. Driscoll (Baylor Univ., Houston, TX.), L. Steinmann, and C. Alfrey (Baylor Univ., Houston, TX.) *In* Aerospace Medical Association, Aerospace Medical Association 63rd Annual Scientific Meeting Program 14 May 1992 1 p Prepared in cooperation with Krug Life Sciences, Inc., Houston, TX (For primary document see N95-16737 04-51)
Avail: CASI HC A01/MF A02

Changes in blood volume during space flight are thought to contribute to decrements in postflight orthostatic function. The purpose of this study was to determine whether gender affects red cell mass and plasma volume during a short exposure to simulated microgravity, and whether gender differences in orthostatic tolerance ensure. Methods: Ten men (31.5 plus or minus 5.2 years, STD) and eleven normally menstruating women (33.3) plus or minus 6.0 STD) underwent 13 days of 6 degree head-down bedrest. Plasma volume (Iodine 125 labeled human serum albumin) and red cell mass (Carbon 51 labeled red blood cells) were measured before bedrest and on bedrest day 13. On the same days, orthostatic tolerance (OT) was determined as the maximal pressure during a presyncopalimited lower body negative pressure test. Results: Plasma volume (PV) and red cell mass (RCM) decreased in both groups with a greater PV decrease (P less than 0.05) in men (6.3 plus or minus 0.7 ml/kg) than in women (4.1 plus or minus 0.6 ml/kg). Decreases in red cell mass were similar (1.7 plus or minus 0.2 ml/kg in men and 1.7 plus or minus 0.2 ml/kg in women). OT was similar for men and women before bedrest (minus 78 plus or minus 6 mmHg in men versus minus 70 plus or minus 4 mmHg in women) and decreased by a similar degree (by an average of 11 mmHg in both groups) after bedrest. The changes in OT did not correlate with changes in plasma volume during bedrest (r(exp 2) = 0.002). Conclusion: Thus, although female hormones may protect PV during bedrest, they do no appear to offer an advantage in terms of loss of orthostatic function. Author

N95-16753*# National Aeronautics and Space Administration. Lyndon B. Johnson Space Center, Houston, TX.
EFFECT OF ANTIORTHOSTATIC BEDREST (BR) ON GASTROINTESTINAL MOTILITY (GIM) OF NORMAL SUBJECTS Abstract Only **c52**
L. Putcha, R. P. Hunter (Krug Life Sciences, Inc., Houston, TX.), K. J. Tietze (Baylor Univ., Houston, TX.), and N. M. Cintron *In* Aerospace Medical Association, Aerospace Medical Association 63rd Annual Scientific Meeting Program 14 May 1992 1 p (For primary document see N95-16737 04-51)
Avail: CASI HC A01/MF A02

The combined effects of postural changes, fluid shifts and diuresis associated with the absence of the gravity vector may decrease gastrointestinal motility (GIM) during space flight. GIM can be estimated from the mouth to cecum transit time (MCTT) of orally administered lactulose (LAC); this test is used to assess changes in GIM in normal subjects and in patients with GI pathology and related disease conditions. Since bedrest (BR) mimics some of the physiological changes that occur during space flight, the effect of ten days of BR on GIM was evaluated from the MCTT of LAC. Methods: Subjects were 12 nonsmoking males between the ages of 35 and 50. After an 8-10 hour fast, subjects ingested Cephulac (registered) (20 g solution) with a low-fiber breakfast on four different days (45, 30, 25, and 20) before BR and on three separate days (4, 7, and 10) during BR. Breath-H2 concentrations were measured before and at 10 minute intervals for 4 hours after breakfast using a Quintron breathalyzer and MCTT was determined from these data. Results: MCTT ranged between 10 and 122 minutes during ambulation and 80 to 120 minutes during BR with means of 79 minutes and 122 minutes respectively. Conclusion: Mean MCTT during BR was 54 percent longer than during ambulation, suggesting that absorption and availability of orally administered medications and nutrients may be delayed or impaired as a result of decreased GIM during bedrest. Author

N95-16754*# National Aeronautics and Space Administration. Lyndon B. Johnson Space Center, Houston, TX.
CHANGES IN LEFT VENTRICULAR FUNCTION AS DETERMINED BY THE MULTI-WIRE GAMMA CAMERA AT NEAR PRESYNCOPAL LEVELS OF LOWER BODY NEGATIVE PRESSURE Abstract Only **c52**
R. Pintner (Krug Life Sciences, Inc., Houston, TX.), S. Fortney, S. Mulvagh (Universities Space Research Association, Houston, TX.), and J. Lacy (Baylor Univ., Houston, TX.) *In* Aerospace Medical Association, Aerospace Medical Association 63rd Annual Scientific Meeting Program 14 May 1992 1 p (For primary document see N95-16737 04-51)
Avail: CASI HC A01/MF A02

At presyncopal levels of lower body negative pressure (LBNP), we have frequently observed electrocardiographic responses that may be due to changes in cardiac position and/or shape, but could be indicative of altered myocardial function. To further investigate this, we evaluated cardiac function using a nuclear imaging technique in 21 healthy subjects (17 men and 4 women) after 30 minutes of supine rest and near the end of a presyncopal-limited LBNP exposure (LBNP averaged 65 plus or minus 3 mmHg at injection). Cardiac first pass images were obtained with a Multi-Wire Gamma Camera following an intravenous bolus injection of 30-50 millicurries of Tantalum-178. Manual blood pressures and electrocardiograms were obtained throughout the 3 minute graded LBNP protocol. Between rest and injection during LBNP, heart rate increased (P less than 0.01) from 67 plus or minus 3 beats per minute to 99 plus or minus beats per minute, systolic blood pressure decreased (P less than 0.01) from 110 plus or minus 3 mmHg to 107 plus or minus 3 mmHg and left ventricular ejection fraction (EF) decreased (P less than 0.01) from 0.57 plus or minus 0.02 to 0.48 plus or minus 0.02. During LBNP, ST segment depression of at least 0.5 mm occurred in 7 subjects. Subjects with ST depression had greater reductions (P = 0.05) in EF than subjects without ST depression (0.15 plus or minus 0.07 versus 0.005 plus or minus 0.03), but also tolerated greater levels (P less than 0.05) of negative pressure (88 plus or minus mmHg versus 69 plus or minus 5 mmHg). There was a significant relationship between presyncopal LBNP level and EF (R(exp 2) = 0.50, P less than 0.05). Our findings suggest there may be a decrease in systolic myocardial function at high levels of LBNP. Author

N95-16755*# National Aeronautics and Space Administration. Lyndon B. Johnson Space Center, Houston, TX.
COMPARISONS OF THREE ANTI-G SUIT CONFIGURATIONS DURING LONG DURATION, LOW ONSET, +Gz Abstract Only **c54**
B. J. Stegmann (Krug Life Sciences, Inc., San Antonio, TX.), R. W. Krutz (Krug Life Sciences, Inc., San Antonio, TX.), R. R. Burton (Air Force Systems Command, Brooks AFB, TX.), and C. F. Sawin *In* Aerospace Medical Association, Aerospace Medical Association 63rd Annual Scientific Meeting Program 14 May 1992 1 p (For primary document see N95-16737 04-51)
Avail: CASI HC A01/MF A02

Little physiologic data exist on the effects of long duration, low onset, hypergravity (+G). Space shuttle crewmembers are subjected to low +G forces (less than +3G) for upwards of 30 minutes during reentry. A similar reentry profile is predicted for the National Aerospace Plane (NASP). The physiologic effects of this acceleration stress are compounded by the loss of body water experienced during microgravity. Currently, a standard 5

bladder anti-G suit is being used during shuttle reentry. There have been complaints of discomfort using this suit, mainly due to the abdominal bladder. This study compared the effectiveness of three anti-G suit configurations in volume depleted subjects during a simulated space shuttle reentry profile. Methods: Seven male subjects were given intravenous Lasix in a dose from 20-40 mg to induce a total body weight loss of 3 plus or minus 1.5 percent. Approximately six hours after the injection, the subjects donned one of three anti-G suits - a standard 5 bladder anti-G suit, an extended coverage anti-G suit (the advanced technology anti-G suit or ATAGS), or an extended coverage anti-G suit without an abdominal bladder (the reentry anti-G suit or REAGS). All subjects were exposed to a simulated space shuttle reentry profile. Non-invasive eye-level blood pressure (ELBP) was monitored throughout the +G exposure. When systolic ELBP dropped below 70 mmHg, the anti-G suit was inflated in 0.5 psig increments to the pressure required to maintain 70 mmHg ELBP. Each subject rode with all three suits. Comparisons were made between the final pressure required in each suit to maintain ELBP and subjective reports of comfort. Results: The mean final suit pressure required to maintain ELBP was 1.1 psi, in both the ATAGS and REAGS versus 1.8 psi in the standard suit. In addition, the subjects rated the REAGS suit highest on the comfort scale, citing the absence of the abdominal bladder as the main reason. Conclusions: Overall, the REAGS suit was the superior anti-G suit during long duration, low onset +G. This is based on its ability to maintain ELBP and still remain comfortable when inflated for prolonged periods of time. Author

N95-16756*# National Aeronautics and Space Administration. Lyndon B. Johnson Space Center, Houston, TX.

ACHILLES TENDON REFLEX (ATR) IN RESPONSE TO SHORT EXPOSURES OF MICROGRAVITY AND HYPERGRAVITY Abstract Only **c52**

M. Fujii and M. Jaweed *In* Aerospace Medical Association, Aerospace Medical Association 63rd Annual Scientific Meeting Program 14 May 1992 1 p (For primary document see N95-16737 04-51)
Avail: CASI HC A01/MF A02

Previous studies indicate that latency and amplitude of the Achilles tendon reflex (ATR) are reduced after exposure to microgravity for 28 days. The objective of this study was to quantitatively measure the latency of ATR during brief (20 sec) exposure to microgravity in KC-135 parabolic flights. Methods: The ATR was elicited in ten men during parabolic flight with the ankle held neutrally, planarflexed, and dorsiflexed. During flight, the ATR was elicited during the zero G and 1.8 G phases. Postflight testing was performed flying back to the airfield. Latencies to onset of the ATR were calculated and analyses of variance were performed to determine the effect of gravity and ankle position on latency. Result: The mean latencies for zero-G, 1.8-G and postflight with the ankle in the neutral position were 32.7 plus or minus 0.5 ms, and 33.1 plus or minus 0.7 ms respectively, which were not significantly different. There was a trend toward prolongation of latencies postflight. The mean latency for those who were motion sick was 32.1 plus or minus 0.1 ms compared to 34.0 plus or minus 0.3 ms for those who were not sick. Conclusions: These studies indicate that neither the level of gravity nor ankle position significantly affected the latency of the ATR. Author

N95-16757*# National Aeronautics and Space Administration. Lyndon B. Johnson Space Center, Houston, TX.

PREDICTION OF SPACE SICKNESS IN ASTRONAUTS FROM PREFLIGHT FLUID, ELECTROLYTE, AND CARDIOVASCULAR VARIABLES AND WEIGHTLESS ENVIRONMENTAL TRAINING FACILITY (WETF) TRAINING Abstract Only **c52**

K. Simanonok, E. Mosely, and J. Charles *In* Aerospace Medical Association, Aerospace Medical Association 63rd Annual Scientific Meeting Program 14 May 1992 1 p (For primary document see N95-16737 04-51)
Avail: CASI HC A01/MF A02

Nine preflight variables related to fluid, electrolyte, and cardiovascular status from 64 first-time Shuttle crewmembers were differentially weighted by discrimination analysis to predict the incidence and severity of each crewmember's space sickness as rated by NASA flight surgeons. The nine variables are serum uric acid, red cell count, environmental temperature at the launch site, serum phosphate, urine osmolality, serum thyroxine, sitting systolic blood pressure, calculated blood volume, and serum chloride. Using two methods of cross-validation on the original samples (jackknife and a stratefied random subsample), these variables enable the prediction of space sickness incidence (NONE or SICK) with 80 percent sickness and space severity (NONE, MILD, MODERATE, of SEVERE) with 59 percent success by one method of cross-validation and 67 percent by another method. Addition of a tenth variable, hours spent in the Weightlessness Environment Training Facility (WETF) did not improve the prediction of space sickness incidences but did improve the prediction of space sickness severity to 66 percent success by the first method of cross-validation of original samples and to 71 percent by the second method. Results to date suggest the presence of predisposing physiologic factors to space sickness that implicate fluid shift etiology. The data also suggest that prior exposure to fluid shift during WETF training may produce some circulatory pre-adaption to fluid shifts in weightlessness that results in a reduction of space sickness severity. Author

N95-16758*# National Aeronautics and Space Administration. Lyndon B. Johnson Space Center, Houston, TX.

DARK FOCUS OF ACCOMMODATION AS DEPENDENT AND INDEPENDENT VARIABLES IN VISUAL DISPLAY TECHNOLOGY Abstract Only **c52**

Sherrie Jones (Naval Training Systems Center, Orlando, FL.), Robert Kennedy (Essex Corp., Orlando, FL.), and Deborah Harm *In* Aerospace Medical Association, Aerospace Medical Association 63rd Annual Scientific Meeting Program 14 May 1992 1 p (For primary document see N95-16737 04-51)
Avail: CASI HC A01/MF A02

When independent stimuli are available for accommodation, as in the dark or under low contrast conditions, the lens seeks its resting position. Individual differences in resting positions are reliable, under autonomic control, and can change with visual task demands. We hypothesized that motion sickness in a flight simulator might result in dark focus changes. Method: Subjects received training flights in three different Navy flight simulators. Two were helicopter simulators entailed CRT presentation using infinity optics, one involved a dome presentation of a computer graphic visual projection system. Results: In all three experiments there were significant differences between dark focus activity before and after simulator exposure when comparisons were made between sick and not-sick pilot subjects. In two of these experiments, the average shift in dark focus for the sick subjects was toward increased myopia when each subject was compared to his own baseline. In the third experiment, the group showed an average shift outward of small amount and the subjects who were sick showed significantly less outward movement than those who were symptom free. Conclusions: Although the relationship is not a simple one, dark focus changes in simulator sickness imply parasympathetic activity. Because changes can occur in relation to endogenous and exogenous events, such measurement may have useful applications as dependent measures in studies of visually coupled systems, virtual reality systems, and space adaptation syndrome. Author

N95-16759*# National Aeronautics and Space Administration, Washington, DC.

REVIEW OF PERFORMANCE, MEDICAL, AND OPERATIONAL DATA ON PILOT AGING ISSUES Abstract Only **c52**

J. H. Stoklosa *In* Aerospace Medical Association, Aerospace Medical Association 63rd Annual Scientific Meeting Program 14 May 1992 1 p (For primary document see N95-16737 04-51)
Avail: CASI HC A01/MF A02

An extensive review of the literature and studies relating to performance, medical, operational, and legal data regarding pilot aging issues was performed in order to determine what evidence there is, if any, to support mandatory pilot retirement. Popular misconceptions about aging, including the failure to distinguish between the normal aging process and disease processes that occur more frequently in older individuals, continue to contribute to much of the misunderstanding and controversy that surround this issue. Results: Review of medical data related to the pilot aging issue indicate that recent improvement in medical diagnostics and treatment technology have made it possible to identify to a high degree individuals who are at risk for developing sudden incapacitating illness and for treating those with disqualifying medical conditions. Performance studies revealed that after controlling for the presence of disease states, older pilots are able to perform as well as younger pilots on many performance tasks. Review of accident data showed that older, healthy pilots do not have higher accident rates than younger pilots, and indeeed, evidence suggests

that older pilots have an advantage in the cockpit due to higher experience levels. The Man-Machine-Mission-Environment interface of factors can be managed through structured, supervised, and enhanced operations, maintenance, flight reviews, and safety procedures in order to ensure safe and productive operations by reducing the margin of error and by increasing the margin of safety. Conclusions: There is no evidence indicating any specific age as an arbitrary cut-off point for pilots to perform their fight duties. A combination of regular medical screening, performance evaluation, enhanced operational maintenance, and safety procedures can most effectively ensure a safe pilot population than can a mandatory retirement policy based on arbitrary age restrictions. Author

N95-16760*# National Aeronautics and Space Administration. Ames Research Center, Moffett Field, CA.

ALERTNESS MANAGEMENT IN TWO-PERSON LONG-HAUL FLIGHT OPERATIONS Abstract Only **c53**

M. R. Rosekind and P. H. Gander (San Jose State Univ., Moffett Field, CA.) *In* Aerospace Medical Association, Aerospace Medical Association 63rd Annual Scientific Meeting Program 14 May 1992 1 p (For primary document see N95-16737 04-51)

Avail: CASI HC A01/MF A02

Long-haul flight operations involve cumulative sleep loss, circadian disruption, and extended and irregular duty schedules. These factors reduce pilot alertness and performance on the flightdeck. Conceptually and operationally, alertness management in flight operations can be divided into preventive strategies and operational countermeasures. Preventive strategies are utilized prior to a duty period to mitigate or reduce the effects of sleep loss, circadian disruption and fatigue during subsequent flight operations. Operational countermeasures are used during operations as acute techniques for maintaining performance and alertness. Results from previous NASA Ames field studies document the sleep loss and circadian disruption in three-person long-haul flying and illustrate the application of preventive strategies and operational countermeasures. One strategy that can be used in both a preventive and operational manner is strategic napping. The application and effectiveness of strategic napping in long-haul operations will be discussed. Finally, long-haul flying in two-person highly automated aircraft capable of extended range operations will create new challenges to maintaining pilot alertness and performance. Alertness management issues in this flight environment will be explored. Author

N95-16761*# National Aeronautics and Space Administration. Lyndon B. Johnson Space Center, Houston, TX.

RESULTS OF THE PSYCHIATRIC, SELECT-OUT EVALUATION OF US ASTRONAUT APPLICATIONS Abstract Only **c53**

D. M. Faulk (Texas Univ., Galveston, TX.), P. A. Santy (National Aeronautics and Space Administration. Lyndon B. Johnson Space Center, Houston, TX.), A. W. Holland (National Aeronautics and Space Administration. Lyndon B. Johnson Space Center, Houston, TX.), and R. Marsh (Texas Univ., Galveston, TX.) *In* Aerospace Medical Association, Aerospace Medical Association 63rd Annual Scientific Meeting Program 14 May 1992 1 p (For primary document see N95-16737 04-51)

Avail: CASI HC A01/MF A02

The psychiatric exclusion criteria for astronauts are based on NASA Medical Psychiatric Standards for space flight. Until recently, there were no standardized methods to evaluate disqualifying psychopathology in astronaut applicants. Method: One hundred and six astronaut applicants who had passed the intitial screening were evaluated for Axis 1 and Axis 2 DSM-3-R diagnoses using the NASA structured psychiatric interview. The interview consisted of three parts: (1) an unstructured portion for obtaining biographical and historical information, (2) the schedule for effective disorders-lifetime version (SASDL), specially modified to include all disqualifying Axis 1 mental disorders; and, (3) the personality assessment schedule (PAS) also modified to evaluate for Axis 2 disorders. Results: Nine of 106 candidates (8.5 percent) met diagnostic criteria for six Axis 1 disorders (including V code) or Axis 2 disorders. Two of these disorders were disqualifying for the applicants. 'Near' diagnoses (where applicants met at least 50 percent of the listed criteria) were assessed to demonstrate that clinicians using the interview were able to overcome applicants' reluctance to report symptomatomatology. Conclusion: The use of the NASA structured interview was effective in identifying past and present psychopathology in a group of highly motivated astronaut applicants. This was the first time a structured psychiatric interview had been used in such a setting for this purpose. Author

N95-16762*# National Aeronautics and Space Administration. Lyndon B. Johnson Space Center, Houston, TX.

VALIDATION OF ASTRONAUT PSYCHOLOGICAL SELECT-IN CRITERIA Abstract Only **c53**

R. M. Rose (Texas Univ., Galveston, TX.), R. L. Helmreich (Texas Univ., Austin, TX.), T. McFadden, P. A. Santy, and A. W. Holland *In* Aerospace Medical Association, Aerospace Medical Association 63rd Annual Scientific Meeting Program 14 May 1992 1 p (For primary document see N95-16737 04-51)

Avail: CASI HC A01/MF A02

An optional astronaut selection strategy would select-in individuals on the basis of personality attributes associated with superior performance. Method: A test battery, the Astronaut Personal Characteristics Inventory (ASTROPCI) was developed which assesses positive and negative components of achievement, motivation, and interpersonal orientations and skills. The battery was administered to one hundred three astronaut candidates and sixty-six current U.S. Shuttle astronauts. To determine performance, a series of conceptual areas related to space flight performance were defined. Astronauts rated their peers on each of these dimensions. Ratings were obtained on all eighty-four current astronauts (excluding those selected in 1990). In addition to peer ratings, supervisor assessments of the same dimensions were obtained for each astronaut. Results: Cluster and factor analysis techniques were employed to isolate subgroups of astronauts. Those astronauts with both high achievement needs and interpersonal skills were most often rated among the top five by their peers and least often rated among the lowest five. A number of scales discriminated between astronauts rated high and low on one or more performance dimensions. Conclusions: The results parallel findings from the personality assessment of individuals in other demanding professions, including aircraft pilots and research scientists, suggesting that personality factors are significant determinants to performance in the space environment. Author

N95-16763*# National Aeronautics and Space Administration. Lyndon B. Johnson Space Center, Houston, TX.

PSYCHOLOGICAL TRAINING OF NASA ASTRONAUTS FOR EXTENDED MISSIONS Abstract Only **c53**

A. W. Holland *In* Aerospace Medical Association, Aerospace Medical Association 63rd Annual Scientific Meeting Program 14 May 1992 1 p (For primary document see N95-16737 04-51)

Avail: CASI HC A01/MF A02

The success of operational teams working in remote and hostile environments rests in large part on adequate preparation of those teams prior to emplacement in field settings. Psychological training, directed at the maintenance of crew health and performance becomes increasingly important as space missions grow in duration and complexity. Methods: Topics to be discussed include: the conceptual framework of psychological training; needs analysis; content and delivery options; methods of assessing training efficacy; use of testbeds and analogies and the relationship of training to crew selection and real-time support activities. Results and Conclusions: This paper will discuss the psychological training approach being developed at the NASA/JSC Behavior and Performance Laboratory. This approach will be compared and contrasted with those underway in the U.S. Department of Defense and in other space agencies. Author

N95-16764*# National Aeronautics and Space Administration. Ames Research Center, Moffett Field, CA.

HUMAN PERFORMANCE IN THE MODERN COCKPIT Abstract Only **c53**

R. K. Dismukes and M. M. Cohen *In* Aerospace Medical Association, Aerospace Medical Association 63rd Annual Scientific Meeting Program 14 May 1992 1 p (For primary document see N95-16737 04-51)

Avail: CASI HC A01/MF A02

This panel was organized by the Aerospace Human Factors Committee to illustrate behavioral research on the perceptual, cognitive, and group processes that determine crew effectiveness in modern cockpits. Crew reactions to the introduction of highly automated systems in the cockpit will be reported on. Automation can improve operational capabilities and efficiency and can reduce some types of human error, but may also introduce

entirely new opportunities for error. The problem solving and decision making strategies used by crews led by captains with various personality profiles will be discussed. Also presented will be computational approaches to modeling the cognitive demands of cockpit operations and the cognitive capabilities and limitations of crew members. Factors contributing to aircrew deviations from standard operating procedures and misuse of checklist, often leading to violations, incidents, or accidents will be examined. The mechanisms of visual perception pilots use in aircraft control and the implications of these mechanisms for effective design of visual displays will be discussed. Author (revised)

N95-16765*# National Aeronautics and Space Administration. Ames Research Center, Moffett Field, CA.

CREW DECISION MAKING UNDER STRESS Abstract Only **c53**

J. Orasanu *In* Aerospace Medical Association, Aerospace Medical Association 63rd Annual Scientific Meeting Program 14 May 1992 1 p (For primary document see N95-16737 04-51)

Avail: CASI HC A01/MF A02

Flight crews must make decisions and take action when systems fail or emergencies arise during flight. These situations may involve high stress. Full-missiion flight simulation studies have shown that crews differ in how effectively they cope in these circumstances, judged by operational errors and crew coordination. The present study analyzed the problem solving and decision making strategies used by crews led by captains fitting three different personality profiles. Our goal was to identify more and less effective strategies that could serve as the basis for crew selection or training. Methods: Twelve 3-member B-727 crews flew a 5-leg mission simulated flight over 1 1/2 days. Two legs included 4 abnormal events that required decisions during high workload periods. Transcripts of videotapes were analyzed to describe decision making strategies. Crew performance (errors and coordination) was judged on-line and from videotapes by check airmen. Results: Based on a median split of crew performance errors, analyses to date indicate a difference in general strategy between crews who make more or less errors. Higher performance crews showed greater situational awareness - they responded quickly to cues and interpreted them appropriately. They requested more decision relevant information and took into account more constraints. Lower performing crews showed poorer situational awareness, planning, constraint sensitivity, and coordination. The major difference between higher and lower performing crews was that poorer crews made quick decisions and then collected information to confirm their decision. Conclusion: Differences in overall crew performance were associated with differences in situational awareness, information management, and decision strategy. Captain personality profiles were associated with these differences, a finding with implications for crew selection and training. Author

N95-16766*# National Aeronautics and Space Administration. Ames Research Center, Moffett Field, CA.

COGNITION AND PROCEDURE REPRESENTATIONAL REQUIREMENTS FOR PREDICTIVE HUMAN PERFORMANCE MODELS Abstract Only **c53**

K. Corker *In* Aerospace Medical Association, Aerospace Medical Association 63rd Annual Scientific Meeting Program 14 May 1992 1 p (For primary document see N95-16737 04-51)

Avail: CASI HC A01/MF A02

Models and modeling environments for human performance are becoming significant contributors to early system design and analysis procedures. Issues of levels of automation, physical environment, informational environment, and manning requirements are being addressed by such man/machine analysis systems. The research reported here investigates the close interaction between models of human cognition and models that described procedural performance. We describe a methodology for the decomposition of aircrew procedures that supports interaction with models of cognition on the basis of procedures observed; that serves to identify cockpit/avionics information sources and crew information requirements; and that provides the structure to support methods for function allocation among crew and aiding systems. Our approach is to develop an object-oriented, modular, executable software representation of the aircrew, the aircraft, and the procedures necessary to satisfy flight-phase goals. We then encode in a time-based language, taxonomies of the conceptual, relational, and procedural constraints among the cockpit avionics and control system and the aircrew. We have designed and implemented a goals/procedures hierarchic representation sufficient to describe procedural flow in the cockpit. We then execute the procedural representation in simulation software and calculate the values of the flight instruments, aircraft state variables and crew resources using the constraints available from the relationship taxonomies. The system provides a flexible, extensible, manipulative and executable representation of aircrew and procedures that is generally applicable to crew/procedure task-analysis. The representation supports developed methods of intent inference, and is extensible to include issues of information requirements and functional allocation. We are attempting to link the procedural representation to models of cognitive functions to establish several intent inference methods including procedural backtracking with concurrent search, temporal reasoning, and constraint checking for partial ordering of procedures. Finally, the representation is being linked to models of human decision making processes that include heuristic, propositional and prescriptive judgement models that are sensitive to the procedural content in which the valuative functions are being performed. Author

N95-16767*# National Aeronautics and Space Administration. Ames Research Center, Moffett Field, CA.

BEYOND THE COCKPIT: THE VISUAL WORLD AS A FLIGHT INSTRUMENT Abstract Only **c54**

W. W. Johnson, M. K. Kaiser, and D. C. Foyle *In* Aerospace Medical Association, Aerospace Medical Association 63rd Annual Scientific Meeting Program 14 May 1992 1 p (For primary document see N95-16737 04-51)

Avail: CASI HC A01/MF A02

The use of cockpit instruments to guide flight control is not always an option (e.g., low level rotorcraft flight). Under such circumstances the pilot must use out-the-window information for control and navigation. Thus it is important to determine the basis of visually guided flight for several reasons: (1) to guide the design and construction of the visual displays used in training simulators; (2) to allow modeling of visibility restrictions brought about by weather, cockpit constraints, or distortions introduced by sensor systems; and (3) to aid in the development of displays that augment the cockpit window scene and are compatible with the pilot's visual extraction of information from the visual scene. The authors are actively pursuing these questions. We have on-going studies using both low-cost, lower fidelity flight simulators, and state-of-the-art helicopter simulation research facilities. Research results will be presented on: (1) the important visual scene information used in altitude and speed control; (2) the utility of monocular, stereo, and hyperstereo cues for the control of flight; (3) perceptual effects due to the differences between normal unaided daylight vision, and that made available by various night vision devices (e.g., light intensifying goggles and infra-red sensor displays); and (4) the utility of advanced contact displays in which instrument information is made part of the visual scene, as on a 'scene linked' head-up display (e.g., displaying altimeter information on a virtual billboard located on the ground). Author

N95-16768*# National Aeronautics and Space Administration. Lyndon B. Johnson Space Center, Houston, TX.

SPACE MEDICINE RESEARCH: NEEDS FOR THE 21ST CENTURY Abstract Only **c52**

L. J. Pepper *In* Aerospace Medical Association, Aerospace Medical Association 63rd Annual Scientific Meeting Program 14 May 1992 1 p (For primary document see N95-16737 04-51)

Avail: CASI HC A01/MF A02

Space medicine research in the 21st century will continue to focus on the four major areas including: (1) expansion of the current incomplete knowledge base of clinical and subclinical physiological changes due to microgravity; (2) development of countermeasures to extend the capabilities of the human performance envelope in extended duration flights; (3) development of novel methods for delivering all aspects of a comprehensive health care system in extreme remote conditions: and (4) further research and application of systems for biological materials processing. New space transportation vehicles will place unique physiologic and human factors demands on the human system, while providing better access to platforms for materials processing. Success in meeting the demands in each of the noted research areas will require an extensive, interactive team approach. Personnel from the medical research,operational, developmental, and basic science communities will be essential to success. Author

N95-16769*# National Aeronautics and Space Administration, Washington, DC.

SLS-1: THE FIRST DEDICATED LIFE SCIENCES SHUTTLE FLIGHT Abstract Only **c16**

Robert W. Phillips *In* Aerospace Medical Association, Aerospace Medical Association 63rd Annual Scientific Meeting Program 14 May 1992 1 p (For primary document see N95-16737 04-51)

Avail: CASI HC A01/MF A02

Spacelab Life Sciences 1 was the first space laboratory dedicated to life science research. It was launched into orbit in early June 1991 aboard the space shuttle Columbia. The data from this flight have greatly expanded our knowledge of the effects of microgravity on human physiology as data were collected in-flight, not just pre and post. Principal goals of the mission were the measurement of rapid and semichronic (8 days) changes in the cardiovascular and cardiopulmonary systems during the flight and then to measure the rate of readaptation following return to Earth. Results from the four teams involved in that research will be presented in this panel. In addition to the cardiovascular-cardiopulmonary research, extensive metabolic studies encompassed fluid, electrolyte and energy balance, renal function, hematology and musculoskeletal changes. Finally, the crew participated in several neurovestibular studies. Overall, the mission was an outstanding success and has provided much new information on the lability of human responses to the space environment. Author

N95-16770*# National Aeronautics and Space Administration. Lyndon B. Johnson Space Center, Houston, TX.

EFFECTS OF WEIGHTLESSNESS ON HUMAN BAROREFLEX FUNCTION Abstract Only **c52**

Janice M. Fritsch and Dwain L. Eckberg *In* Aerospace Medical Association, Aerospace Medical Association 63rd Annual Scientific Meeting Program 14 May 1992 1 p Prepared in cooperation with Veterans Administration Hospital, Richmond, VA (For primary document see N95-16737 04-51)

Avail: CASI HC A01/MF A02

Impaired cardiovascular function, characterized by orthostatic intolerance and reduced exercise capacity, is a result of space travel. We hypothesized that postflight baroreflex dysfunction may contribute. We studied the vagally mediated carotid baroreceptor-cardiac reflex response of 6 astronauts before, during, and after the ten day SLS-I mission. A series of R-waves triggered pressure and suction steps (from 40 to minus 65 mmHg) were delivered to a neck chamber during held expirtation. Resulting R-R interval changes were plotted against carotid distending pressure (systolic - neck pressure), and curve parameters calculated. After an initial rise, the operational point declined consistently during the flight and reached a nadir on landing day, but had recovered to preflight levels by L + 4. Slope and range of the response declined throughout the flight, were slightly recovered by the time measurements were made on landing day, but still were reduced on L + 4. These data indicate that space flight results in a significant impairment of the carotid baroreceptor cardiac reflex response. Author

N95-16771*# National Aeronautics and Space Administration. Lyndon B. Johnson Space Center, Houston, TX.

DYNAMICS OF THE G-EXCESS ILLUSION Abstract Only **c52**

K. A. Baylor (Naval Aerospace Medical Research Lab., Pensacola, FL.), M. Reschke, F. E. Guedry (University of West Florida, Pensacola, FL.), B. J. McGrath (Naval Aerospace Medical Research Lab., Pensacola, FL.), and A. H. Rupert (Naval Aerospace Medical Research Lab., Pensacola, FL.) *In* Aerospace Medical Association, Aerospace Medical Association 63rd Annual Scientific Meeting Program 14 May 1992 1 p (For primary document see N95-16737 04-51)

Avail: CASI HC A01/MF A02

The G-excess illusion is increasingly recognized as a cause of aviation mishaps especially when pilots perform high-speed, steeply banked turns at low altitudes. Centrifuge studies of this illusion have examined the perception of subject orientation and/or target displacement during maintained hypergravity with the subject's head held stationary. The transient illusory perceptions produced by moving the head in hypergravity are difficult to study onboard centrifuges because the high angular velocity ensures the presence of strong Coriolis cross-coupled semicircular canal effects that mask immediate transient otolith-organ effects. The present study reports perceptions following head movements in hypergravity produced by high-speed aircraft maintaining a banked attitude with low angular velocity to minimize cross-coupled effects. Methods: Fourteen subjects flew on the NASA KC-135 and were exposed to resultant gravity forces of 1.3, 1.5, and 1.8 G for 3 minute periods. On command, seated subjects made controlled head movements in roll, pitch, and yaw at 30 second intervals both in the dark and with faint targets at a distance of 5 feet. Results: head movement produced transient perception of target displacement and velocity at levels as low as 1.3 G. Reports of target velocity without appropriate corresponding displacement were common. At 1.8 G when yaw head movements were made from a face down position, 4 subjects reported oscillatory rotational target displacement with fast and slow alternating components suggestive of torsional nystagmus. Head movements evoked symptoms of nausea in most subjects, with 2 subjects and 1 observer vomiting. Conclusions: The transient percepts present conflicting signals, which introduced confusion in target and subject orientation. Repeated head movements in hypergravity generate nausea by mechanisms distinct from cross-coupled Coriolis effects. Author

N95-16772*# National Aeronautics and Space Administration. Lyndon B. Johnson Space Center, Houston, TX.

MEDICAL CARE CAPABILITIES FOR SPACE STATION FREEDOM: A PHASE APPROACH Abstract Only **c18**

C. R. Doarn (Krug Life Sciences, Inc., Houston, TX.) and C. W. Lloyd *In* Aerospace Medical Association, Aerospace Medical Association 63rd Annual Scientific Meeting Program 14 May 1992 1 p (For primary document see N95-16737 04-51)

Avail: CASI HC A01/MF A02

As a result of Congressional mandate Space Station Freedom (SSF) was restructured. This restructuring activity has affected the capabilities for providing medical care on board the station. This presentation addresses the health care facility to be built and used on the orbiting space station. This unit, named the Health Maintenance Facility (HMF) is based on and modeled after remote, terrestrial medical facilities. It will provide a phased approach to health care for the crews of SSF. Beginning with a stabilization and transport phase, HMF will expand to provide the most advanced state of the art therapeutic and diagnostic capabilities. This presentation details the capabilities of such a phased HMF. As Freedom takes form over the next decade there will be ever-increasing engineering and scientific developmental activities. The HMF will evolve with this process until it eventually reaches a mature, complete stand-alone health care facility that provides a foundation to support interplanetary travel. As man's experience in space continues to grow so will the ability to provide advanced health care for Earth-orbital and exploratory missions as well. Author

N95-16773*# Krug Life Sciences, Inc., Houston, TX.

A PROTOTYPE CREW MEDICAL RESTRAINT SYSTEM (CMRS) FOR SPACE STATION FREEDOM Abstract Only **c54**

S. L. Johnston, F. T. Eichstadt, and R. D. Billica *In* Aerospace Medical Association, Aerospace Medical Association 63rd Annual Scientific Meeting Program 14 May 1992 1 p Sponsored by NASA. Lyndon B. Johnson Space Center, Houston, TX (For primary document see N95-16737 04-51)

Avail: CASI HC A01/MF A02

The Crew Medical Restrain System (CMRS) is a prototype system designed and developed for use as a universally deployable medical restraint/workstation on Space Station Freedom (SSF), the Shuttle Transportation System (STS), and the Assured Crew Rescue Vehicle (ACRV) for support of an ill or injured crewmember requiring stabilization and transportation to Earth. The CMRS will support all medical capabilities of the Health Maintenance Facility (HMF) by providing a restraint/interface system for all equipment (advance life support packs, defibrillator, ventilator, portable oxygen supply, IV pump, transport monitor, transport aspirator, and intervenous fluids delivery system) and personnel (patient and crew medical officers). It must be functional within the STS, ACRV, and all SSF habitable volumes. The CMRS will allow for medical capabilities within CPR, ACLS and ATLS standards of care. This must all be accomplished for a worst case transport time scenario of 24 hours from SSF to a definitive medical care facility on Earth. A presentation of the above design prototype with its subsequent one year SSF/HMF and STS/ACRV high fidelity mock-up ground based simulation testing will be given. Also, parabolic flight and underwater Weightless Test Facility evaluations will be demonstrated for various medical contingencies. The final design configuration to date will be discussed with future space program impact considerations. Author

N95-16774*# Krug Life Sciences, Inc., Houston, TX.
DELIVERY OF CARDIOPULMONARY RESUSCITATION IN THE MICROGRAVITY ENVIRONMENT Abstract Only **c52**
M. R. Barratt and R. D. Billica *In* Aerospace Medical Association, Aerospace Medical Association 63rd Annual Scientific Meeting Program 14 May 1992 1 p Sponsored by NASA. Lyndon B. Johnson Space Center, Houston, TX (For primary document see N95-16737 04-51)
Avail: CASI HC A01/MF A02

The microgravity environment presents several challenges for delivering effective cardiopulmonary resuscitation (CPR). Chest compressions must be driven by muscular force rather than by the weight of the rescuer's upper torso. Airway stabilization is influenced by the neutral body posture. Rescuers will consist of crew members of varying sizes and degrees of physical deconditioning from space flight. Several methods of CPR designed to accommodate these factors were tested in the one G environment, in parabolic flight, and on a recent shuttle flight. Methods: Utilizing study participants of varying sizes, different techniques of CPR delivery were evaluated using a recording CPR manikin to assess adequacy of compressive force and frequency. Under conditions of parabolic flight, methods tested included conventional positioning of rescuer and victim, free floating 'Heimlich type' compressions, straddling the patient with active and passive restraints, and utilizing a mechanical cardiac compression assist device (CCAD). Multiple restrain systems and ventilation methods were also assessed. Results: Delivery of effective CPR was possible in all configurations tested. Reliance on muscular force alone was quickly fatiguing to the rescuer. Effectiveness of CPR was dependent on technique, adequate restraint of the rescuer and patient, and rescuer size and preference. Free floating CPR was adequate but rapidly fatiguing. The CCAD was able to provide adequate compressive force but positioning was problematic. Conclusions: Delivery of effective CPR in microgravity will be dependent on adequate resuer and patient restraint, technique, and rescuer size and preference. Free floating CPR may be employed as a stop gap method until patient restraint is available. Development of an adequate CCAD would be desirable to compensate for the effects of deconditioning. Author

N95-16775*# National Aeronautics and Space Administration. Lyndon B. Johnson Space Center, Houston, TX.
ADVANCED CARDIAC LIFE SUPPORT (ACLS) UTILIZING MAN-TENDED CAPABILITY (MTC) HARDWARE ONBOARD SPACE STATION FREEDOM Abstract Only **c54**
M. Smith, M. Barratt, and C. Lloyd *In* Aerospace Medical Association, Aerospace Medical Association 63rd Annual Scientific Meeting Program 14 May 1992 1 p Prepared in cooperation with Krug Life Sciences, Inc., Houston, TX (For primary document see N95-16737 04-51)
Avail: CASI HC A01/MF A02

Because of the time and distance involved in returning a patient from space to a definitive medical care facility, the capability for Advanced Cardiac Life Support (ACLS) exists onboard Space Station Freedom. Methods: In order to evaluate the effectiveness of terrestrial ACLS protocols in microgravity, a medical team conducted simulations during parabolic flights onboard the KC-135 aircraft. The hardware planned for use during the MTC phase of the space station was utilized to increase the fidelity of the scenario and to evaluate the prototype equipment. Based on initial KC-135 testing of CPR and ACLS, changes were made to the ventricular fibrillation algorithm in order to accommodate the space environment. Other constraints to delivery of ACLS onboard the space station include crew size, minimum training, crew deconditioning, and limited supplies and equipment. Results: The delivery of ACLS in microgravity is hindered by the environment, but should be adequate. Factors specific to microgravity were identified for inclusion in the protocol including immediate restraint of the patient and early intubation to insure airway. External cardiac compressions of adequate force and frequency were administered using various methods. The more significant limiting factors appear to be crew training, crew size, and limited supplies. Conclusions: Although ACLS is possible in the microgravity environment, future evaluations are necessary to further refine the protocols. Proper patient and medical officer restraint is crucial prior to advanced procedures. Also emphasis should be placed on early intubation for airway management and drug administration. Preliminary results and further testing will be utilized in the design of medical hardware, determination of crew training, and medical operations for space station and beyond. Author

N95-16776*# Krug Life Sciences, Inc., Houston, TX.
A SURGICAL SUPPORT SYSTEM FOR SPACE STATION FREEDOM Abstract Only **c18**
M. R. Campbell, R. D. Billica, and S. L. Johnston *In* Aerospace Medical Association, Aerospace Medical Association 63rd Annual Scientific Meeting Program 14 May 1992 1 p Sponsored by NASA. Lyndon B. Johnson Space Center, Houston, TX (For primary document see N95-16737 04-51)
Avail: CASI HC A01/MF A02

Surgical techniques in microgravity are being developed for the Health Maintenance Facility (HMF) on Space Station Freedom (SSF). This will be a presentation of the proposed surgical capabilities and ongoing hardware and procedural investigations. Methods: Procedures and prototype hardware, which include a medical restraint system, a surgical overhead isolation canopy, a suction device, and a regional laminar flow device were evaluated. This was accomplished by realistic sterile surgical simulations involving both mannequins and animals during KC-135 parabolic flight and in a high fidelity ground based HMF mockup. Results: Animal surgery in the environment of microgravity allowed the observation of unique arterial and venous bleeding characteristics for the first time. The ability to control bleeding and to prevent cabin atmosphere contamination was also demonstrated. Conclusions: The procedures and prototype hardware tested provided valuable information and should be investigated and developed further. The use of standard surgical techniques are possible in microgravity if the principles of personnel and supply restraint and operative field containment are adhered to. Author

N95-16777*# National Aeronautics and Space Administration. Lyndon B. Johnson Space Center, Houston, TX.
MEDICINE ON MARS: REMOTE MEDICAL CARE AND THE SPACE EXPLORATION INITIATIVE Abstract Only **c52**
S. C. Simmons and R. D. Billica *In* Aerospace Medical Association, Aerospace Medical Association 63rd Annual Scientific Meeting Program (SEE N95-16737 04-51) 14 May 1992 Prepared in cooperation wiht Krug Life Sciences, Inc., Houston, TX (For primary document see N95-16737 04-51)
Avail: CASI HC A01/MF A02

Mars exploration missions as described in the Synthesis Group report will involve extended exposures of crew members to remote, hazardous environments for up to 100 days. Maintenance of crew health and performance will be critical to ensure mission success. Because of the great distances between the Earth and Mars, round trip telecommunication will take from seven to forty minutes and immediate return to Earth will not be feasible: an autonomous medical care system that integrates preventive, occupational, and environmental aspects of health care and provides diagnostic and treatment capabilities will be necessary. Providing medical care for Mars explorers will pose some unique technical and engineering challenges. Medical care equipment will need to be designed to be modular and portable to ensure that it is interchangeable between vehicle and planetary surface elements. Miniaturization will be necessary to reduce mass and volume. Computerized systems that automatically acquire and manage medical information and provide medical references (literature), decision support, and automated medical record keeping will be a crucial part of a Martian medical care system. Medical care will also rely on remote consultation with Earth-based specialists. This presentation will provide an overview of the health and medical concerns associated with Mars exploration missions and will describe some specific concepts for Mars medical care systems. Author

N95-16778*# National Aeronautics and Space Administration. Ames Research Center, Moffett Field, CA.
ARTIFICIAL GRAVITY: HOW MUCH, HOW OFTEN, HOW LONG? Abstract Only **c54**
R. Burton (Air Force Systems Command, Brooks AFB, TX.) and J. Vernikos *In* Aerospace Medical Association, Aerospace Medical Association 63rd Annual Scientific Meeting Program 14 May 1992 1 p Prepared in cooperation with Aerospace Medical Research Labs., Brooks AFB, TX (For primary document see N95-16737 04-51)
Avail: CASI HC A01/MF A02

The argument is not overwhelming for the need to provide a continuous 1G environment using tethers or other means of spinning a spacecraft in order to maintain crew health in planetary exploration. Even on Earth, we

spend a maximum of 16 hours in 1G (upright). Sporadic evidence over the years has suggested that somewhere between 30-minutes and 4-hours of 1G may suffice to prevent the deconditioning effects of bedrest (orthostatic intolerance and the rise in calcium excretion). However, it is not known what the minimum requirements are, whether they vary for different physiological systems and whether passive zero gravity or the enhancement of the effects of activity conducted in an increased G field are more effective. It is similarly not known what the optimal duration and frequency of the G stimulus is, and how time of day might alter its effectiveness. Since acceleration level and duration appear to be physiologically interactive, it seems feasible to hypothesize that periodic acceleration exposures to greater than 1G levels provided by some on-board centrifuge, would suffice and should be explored. Author

N95-16779*# National Aeronautics and Space Administration. Ames Research Center, Moffett Field, CA.

THE EFFECT OF INTERMITTENT STANDING OR WALKING DURING HEAD DOWN TILT BEDREST ON PEAK O2 CONSUMPTION Abstract Only **c52**

A. C. Ertl, A. S. Dearborn, and J. Vernikos *In* Aerospace Medical Association, Aerospace Medical Association 63rd Annual Scientific Meeting Program 14 May 1992 1 p (For primary document see N95-16737 04-51)

Avail: CASI HC A01/MF A02

The cardiovascular aspect of bedrest deconditioning is manifested by decreases in peak O2 uptake (VO(sub 2 peak)) during minimal exercise. The effect of intermittent standing (+G(z)) or walking (+G(z)W) during 4 days of 7 degree Head Down Tilt bedrest (HDT) on VO(sub 2 peak) was evaluated. Methods: Five protocols were performed by eight male subjects; control (C) consisting of complete bedrest, and 15 minute periods to total 2 or 4 hours daily of standing (+G(z)(exp 2) and +G(z)(exp 4) respectively) or walking at 3.0 MPH (+G(z)W2 and +G(z)W4 respectively). Subjects performed VO(sub 2 peak) tests prior to and on the final day of HDT. VO(sub 2 peak) was determined using open circuit indirect calorimetry during supine leg cycling ergometry. After a 5 minute warmup, three 2 minute incremental loads of 33 W previously determined to elicit VO(sub 2 peak) were given and the subject cycled to volitional fatigue. Results: The C protocol VO(sub 2 peak) decreased by 16 percent (2.71 plus or minus 0.16 to 2.27 plus or minus 0.14 L/min) and 11 percent in +G(z)(exp 4) (2.72 plus or minus 0.15 to 2.43 plus or minus 0.14 L/min). With +G(z)W2 VO(sub 2 peak) decreased by 9 percent (2.71 plus or minus 0.17 to 2.46 plus or minus 0.14 L/min) and with +G(z)W4, VO(sub 2 peak) decreased by 10 percent (2.71 plus or minus 0.14 to 2.43 plus or minus 0.14 L/min). VO(sub 2 peak) in all protocols decreased with HDT (P less than 0.05). The decrease in C VO(sub 2 peak) was significantly greater (P less than 0.05) than the decreases in either +G(z) or +G(z)W protocols. Conclusion: The deconditioning that occurs after only 4 days of HDT was demonstrated by decreases in VO(sub 2 peak). Intermittent +G(z) or +G(z)W attenuated, but did not prevent, the decrease in VO(sub 2 peak) with HDT. Author

N95-16780*# National Aeronautics and Space Administration. Ames Research Center, Moffett Field, CA.

PERIODIC UPRIGHT POSTURE NEGATES THE SUPPRESSION OF NEUROENDOCRINE RESPONSE TO HEAD DOWN BEDREST Abstract Only **c52**

C. E. Wade, J. Vernikos, J. Evans, and D. OHara *In* Aerospace Medical Association, Aerospace Medical Association 63rd Annual Scientific Meeting Program 14 May 1992 1 p (For primary document see N95-16737 04-51)

Avail: CASI HC A01/MF A02

Head down bedrest (HDT) decreases plasma neurohormone levels, attaining a nadir within four hours. The present study evaluates the effect of periodic standing or exercises (+G(z)) on this acute suppression of plasma neurohormones. Methods: Nine male subjects (mean plus or minus SE age 37 plus or minus 2 yr; height 182 plus or minus 2 cm; weight 83 plus or minus 3 kg) were admitted to the Human Research Facility on three occasions separated by one month. Subjects were assigned to head down tilt (minus 6 degrees) or 15-minutes of standing or moderate exercise at the end of each hour. Initially during an ambulatory period, subjects were placed in a supine position for 45-min and a control blood sample obtained. The next day following 4 hours of HDT with or without standing or exercise a blood sample was taken 45-min (3 3/4 hours into HDT) after the preceding stand or exercise. Blood was withdrawn and all plasma samples frozen for determination of neurohormone levels within the same assay. Plasma aldosterone, Plasma Renin Activity (PRA) vasopressin (AVP) and cortisol levels were measured by radioimmunoassay. Norepinephrine (NE) and epinephrine (E) levels were measured by electrochemical detection following HPLC. Values were compared by ANOVA, P less than 0.05. Results: Control levels following 45-min supine were not different between treatments. HDT suppressed plasma aldosterone (13.9 plus or minus 3.7 to 6.6 plus or minus 0.7 ng/dl) and NE levels (299 plus or minus 35 to 217 plus or minus 23 pg/dl), E (69 plus or minus 15 to 65 plus or minus 21 pg/ml), and PRA (0.64 plus or minus 0.13 to 0.58 plus or minus 0.17 ngAI/m/hr) were not significantly altered. Standing or exercise negated the decrease in aldosterone and NE levels due to HDT. Conclusions: Periodic upright posture (+G(z)) with or without exercise for 15-min out of each hour negates the acute suppression of aldosterone and NE associated with HDT. Author

N95-16781*# National Aeronautics and Space Administration. Ames Research Center, Moffett Field, CA.

THE EFFICACY OF PERIODIC +Gz EXPOSURE IN THE PREVENTION OF BEDREST INDUCED ORTHOSTATIC INTOLERANCE Abstract Only **c52**

D. A. Ludwig (North Carolina Univ., Greensboro, NC.), J. Vernikos, M. R Duvoisin (National Aeronautics and Space Administration. John F. Kennedy Space Center, Cocoa Beach, FL.), and J. L. Stinn *In* Aerospace Medical Association, Aerospace Medical Association 63rd Annual Scientific Meeting Program 14 May 1992 1 p (For primary document see N95-16737 04-51)

Avail: CASI HC A01/MF A02

What is the most efficient dosage of periodic exposure to positive 1G(z) during microgravity to maintain a functional upright position after returning to a positive 1G(z) environment? The answer has implications for the type of countermeasures astronauts will be required to perform during long term space flight. Methods: Nine males were subjected to four different positive 1G exposure protocols plus a control protocol ('zero G(z)') during four days of continuous bedrest. The four positive 1G(z) exposures consisted of periodic standing or walking, each for a total period of two or four hours. Each subject was returned for bedrest on five different occasions over a period of approximately one year to obtain data on each of the nine subjects across all four positive 1G(z) treatments and the control. A 30 min tilt test was used to measure orthostatic response during pre and post bedrest. Results: In terms of survival rate (percentage of subjects who did not faint after 30 sec of tilt), four hours of intermittent standing was the only protocol that maintained a rate comparable to pre bedrest levels (87.5 percent). Although the other three positive 1G(z) protocols performed better than the 'zero G(z) control (22.2 percent), only the four hour standing returned post bedrest survival rates to pre bedrest levels. Conclusions: The results will need to be evaluated with regards to a variety of other physiological systems which are known to decondition during microgravitry. Author

N95-16782*# National Aeronautics and Space Administration. Ames Research Center, Moffett Field, CA.

THE VALUE OF THE 4-DAY HEADDOWN BEDREST MODEL FOR SCREENING COUNTERMEASURES Abstract Only **c52**

J. Vernikos, L. Keil, A. C. Ertl, C. E. Wade, J. E. Greenleaf, D. OHara, and D. Ludwig (North Carolina Univ., Greensboro, NC.) *In* Aerospace Medical Association, Aerospace Medical Association 63rd Annual Scientific Meeting Program 14 May 1992 1 p (For primary document see N95-16737 04-51)

Avail: CASI HC A01/MF A02

In order to evaluate the benefits of periodic exposure to the +G(z) vector as a countermeasure to the physiological responses to minus 6 degree head down bedrest (HDT), we considered a two-tiered approach: (a) to use 4 days HDT as a quick and inexpensive means of screening countermeasures, (b) to use a 60 day HDT to validate the most promising candidates. The approach and results of a 4 day study are described here. Methods: Nine males were admitted to our Human Research Facility for one ambulatory control day followed by 4 days HDT and were released on the next day after completion of a peak oxygen consumption test (VO(sub 2 peak)). A battery of tests was selected and standardized to evaluate the known early effects of HDT on plasma volume, early bone

markers, orthostatic tolerance, physical performance, and fluid and electrolytes and their hormone regulation. Fluid sodium (Na) and potassium (K) intake and output in the urine were monitored throughout. Plasma volume was determined with a modified Evans Blue method and orthostatic tolerance with a 60 degree head-up tilt test for 30 minutes - both of which were determined on the ambulatory control day and on day 4 of HDT. Immediately after completion of the tilt test subjects were returned to the minus 6 degree position until the next morning when a VO(sub 2 peak) (horizontal ergometer) was done. This was compared to a similar control test determined on 2 separate occasions before subject admission. Results: Four hours after going HDT produced significant decreases (p less than 0.05) in the circulating concentration of fluid and electrolyte regulating hormones. Plasma volume, orthostatic tolerance and VO(sub 2 peak) changed significantly after 4 days HDT. There was also the expected natriuresis on day 1 of HDT but no significant diuresis. The consistency of the pre-bedrest VO(sub 2 peak) tilt tests and plasma volumes was remarkable. Conclusions: The 4 day HDT model seems highly promising for screening a variety of countermeasures alone and in combination before validating their benefits in extended bedrest or flight experiments. Author

N95-16801 California Univ., Davis, CA. Dept. of Veterinary Pharmacology.
FAILURE OF OZONE AND NITROGEN DIOXIDE TO ENHANCE LUNG TUMOR DEVELOPMENT IN HAMSTERS
H. Witschi, M. A. Breider, and H. M. Schuller Sep. 1993 43 p Prepared in cooperation with Tennessee Univ., Knoxville, TN
(Contract HEI-RFPA-87-4)
(PB94-182854; HEI/RR-60/93) Copyright Avail: Issuing Activity

The authors tested the hypothesis that ozone and nitrogen dioxide modulate the development of respiratory tract tumors, in particular neuroendocrine cell tumors, in Syrian golden hamsters. The animals received subcutaneous injections of the carcinogen N-diethylnitrosamine (20 mg/kg) twice a week while being exposed continuously to an atmosphere of 0.8 parts per million (ppm) of ozone or 15 ppm nitrogen dioxide. Animals were killed 16 weeks or 24 to 32 weeks after the beginning of the treatment. For positive controls, animals were treated with N-diethylnitrosamine and exposed to 65 percent oxygen. Ozone delayed the incidence of tumors in the lung periphery. Ozone also seemed to mitigate development of hepatoxic lesions mediated by N-diethylnitrosamine. The role of ozone and nitrogen dioxide as possible additional risks in the pathogenesis of lung cancer in animals continues to remain uncertain. Derived from text

N95-17666 Army Medical Research Inst. of Chemical Defense, Aberdeen Proving Ground, MD.
A STUDY TO DETERMINE THE CRITICAL CHARACTERISTICS FOR MICE IN A NEWLY DESIGNED WHOLE BODY TOXIC GAS EXPOSURE MODULE Final Technical Report, 8 Mar. - 18 Jul. 1993
Holcombe H. Hurt, Alfred M. Sciuto, and Richard R. Stotts Dec. 1993 21 p Limited Reproducibility: More than 20% of this document may be affected by microfiche quality
(AD-A285085; USAMRICD-TR-93-04) Avail: CASI HC A03

This project was undertaken to answer questions involved in optimizing the use of a newly designed whole body exposure chamber. To accomplish these objectives, individual groups were given 10-, 20-, and 30-minute whole body exposures to moderate concentrations (near LCT 50 concentrations) of phosgene. Survival rates were recorded at 24 hours. Pertinent conclusions were based on the survival rates and were as follows: (1) The LC50 for 20-minute exposures was found to be in the range of 21 to 27 mg per cubic meter; (2) Spatial homogeneity of the chamber gas concentration was satisfactory; and (3) Ten-minute exposures at higher concentrations of phosgene resulted in survival rates which were consistently reproducible as thirty minute exposures at lower concentrations. Author

N95-17714# Air Force Inst. of Tech., Wright-Patterson AFB, OH.
CARBON MONOXIDE DOES NOT MODULATE PULMONARY VASCULAR REACTIVITY IN ISOLATED RAT LUNGS M.S. Thesis
James M. Cantrell Jul. 1994 62 p
(AD-A283190; AFIT/CI/CIA-94-108) Avail: CASI HC A04/MF A01

Recent studies have demonstrated that the gas nitric oxide (NO), when inhaled in low concentrations, acts as a vasodilator in the pulmonary vasculature. Due to the physical and chemical similarities between NO and carbon monoxide (CO), we speculated that acute, low concentration exposure to CO would have similar effects in the isolated rat lung. Therefore, the purpose of this study was to determine the role of CO (200 and 1000 ppm) in modulating hypoxia and angiotensin 2 induced pulmonary vasoconstriction, using isolated salt-perfused (Earle's salt solution; + 4 g% Ficoll) lungs of male Sprague Dawley rats (CON). Pulmonary hypertensive rats (ALT), induced by simulated altitude exposure (15,000 ft; 4572 m; 430 mm Hg for 32-48 days) , were also used to determine the effects of CO in a remodeled pulmonary vascular bed. DTIC

52 AEROSPACE MEDICINE

Includes physiological factors; biological effects of radiation; and effects of weightlessness on man and animals.

N95-16105# Naval Health Research Center, San Diego, CA. Physiological Performance and Operational Medicine.
AN ANNOTATED BIBLIOGRAPHY OF HEAT TOLERANCE: REGARDING GENDER DIFFERENCES
M. Katherine Canine (Geo-Centers, Inc., Fort Washington, MD.), Toniann Derion (Public Health Service, Washington, DC.), Jay H. Heaney (San Diego State Univ., San Diego, CA.), and Robert Pozos 15 Mar. 1994 52 p (Proj. M00-96)
(AD-A280755; NHRC-TD-93-1A) Avail: CASI HC A04/MF A01

The purpose of this technical report is to provide an overview of the literature on the similarities and differences between men and women in their physiological responses to heat stress. Studies that compare thermoregulation in physically fit and sedentary females, as well as research examining the effect of the menstrual cycle on thermal physiology, are included. For each study review, a brief synopsis of the methodology and a summary of relevant results are provided. It was the intent of this report to provide a literature resource, not a review paper, regarding gender differences in thermoregulation during heat exposure. DTIC

N95-16112# North Carolina Univ., Chapel Hill, NC. Dept. of Chemistry.
EXTRACELLULAR IONIC COMPOSITION ALTERS KINETICS OF VESICULAR RELEASE OF CATECHOLAMINES AND QUANTAL SIZE DURING EXOCYTOSIS AT ADRENAL MEDULLARY CELLS Technical Report, Jun. 1993 - Jun. 1994
Jeffrey A. Jankowski, Jennifer M. Finnegan, and R. M. Wightman 5 Jul. 1994 33 p
(Contract N00014-91-J-1784)
(AD-A281613; TR-4) Avail: CASI HC A03/MF A01

The temporal resolution of carbon-fiber microelectrodes has been exploited to examine the plasticity of quantal secretory events at individual adrenal medullary cells. The size of individual quantal events monitored by amperometric oxidation of released catecholamines was found to be dependent on the extracellular ionic composition, the secretagogue, and the order of depolarization delivery. Release was observed with either exposure to 60 mM K+ in the presence of Ca2+ or exposure to 3 mM Ba2+ in the solutions of different pH, and without external Ca2+. Ba2+ was demonstrated to induce Ca2+ independent exocytotic release for an extended period of time (greater than 4 min) relative to release induced by K+ (approximately 30 s), which is Ca2+ dependent. In all cases, simultaneous changes of intracellular divalent cations, monitored by fura-2 fluorescence, accompanied quantal release and had a similar time course. Exocytosis caused by Ba2+ in Ca2+ free medium had a large mean spike area at pH 8.2 than at pH 7.4. When Ba2+ induced spikes measured at pH 7.4 were compared, the spikes in Ca2+ free medium were found to be broader and shorter, but had the same area. Release induced by K+ after exposure to Ba2+ was comprised of larger quantal events when compared to preceding K+ stimulations. Finally, spikes obtained with Ba2+ exposure at an extracellular pH of 5.5 had a different shape than those obtained in more basic solutions. These changes in spike size and shape are consistent with the interactions between catecholamines and other intravesicular components. DTIC

N95-16132# Army Aeromedical Research Lab., Fort Rucker, AL.
AVIATION EPIDEMIOLOGY DATA REGISTER: AGE-SPECIFIC MEDICAL AND NONMEDICAL ATTRITION RATES AMONG FORT RUCKER CIVILIAN AVIATORS Final Report

Kevin T. Mason and Samuel G. Shannon Jul. 1994 19 p
(DA Proj. 301-62787-A-878)
(AD-A284970; USAARL-94-35) Avail: CASI HC A03/MF A01

An epidemiological analysis of the coronary angiography outcomes of Fort Rucker civilian aviators could not be completed without first conducting an analysis of attrition from aviation service due to medical and nonmedical causes. Longitudinal data on flying duty medical examinations and aeromedical boards conducted on Fort Rucker area civilian aviators was reviewed using the U.S. Army Aviation Epidemiology Data Register (AEDR). The AEDR records of 847 Fort Rucker civilian aviators were reviewed over nine calendar years from 1985 to 1993. By the end of 1992, 528 (62.3 percent) remained in aviation service, 251 (29.6 percent) were lost to nonmedical attrition, and 68 (8.1 percent) were lost to medical attrition. Of the 847, 196 (23.14 percent) had operational military affiliation (dual-status service as civilians and reserve component aviators), while 651 (76.86 percent) did not. Controlling for age, there was a higher risk for nonmedical and medical attrition among those without operational military affiliation (chi(exp 2, sub Mantel-Haenszel), p less than 0.0001). Medical attrition was uncommon up to 50 years of age. Cardiovascular disease accounted for three-fourths of the cases of medical attrition. Overall, there was a threefold higher rate of medical attrition among those without operational military affiliation. DTIC

N95-16135# International Society for Optical Engineering, Bellingham, WA.
COMPUTATIONAL VISION BASED ON NEUROBIOLOGY Final Report, Jun. 1993 - Jun. 1994
Teri B. Lawton, ed. 10 Aug. 1994 254 p Conference held at Pacific Grove, CA, 6-9 Jul. 1993
(Contract F49620-93-1-0274)
(AD-A284472; AFOSR-94-0523TR) Avail: CASI HC A12/MF A03

Biological systems use multiple object attributes to construct a 3D perception from an initial 2D representation. This report explores computational vision models that are based on neurobiology. Each of the fundamental levels of analysis needed for high level pattern recognition are addressed to provide new insights into the different processing modules. Papers detail methods for reconstructing 3D images from partial information, for correcting image defects, or for effectively extracting/analyzing/interpreting images of neurobiological and biomedical interest. DTIC

N95-16151# Naval Aerospace Medical Research Lab., Pensacola, FL.
MATHEMATICAL MODEL FOR INTERACTION OF CANALS AND OTOLITHS IN PERCEPTION OF ORIENTATION, TRANSLATION, AND ROTATION Final Report
James D. Grissett Dec. 1993 23 p
(Proj. MR0-4101)
(AD-A280897; NAMRL-SR-93-5) Avail: CASI HC A03/MF A01

A computer model with six degrees of freedom was developed in which linear acceleration along each axis is detected and directed along two channels. Output of one channel is perceived as a signal that was generated by gravity, produces no perception of translation, and is used to determine body orientation with respect to earth-vertical. Output of the other channel is perceived as a signal generated by transient linear acceleration and produces a perception of translational motion. Attenuation of signals in these channels is controlled by computations that compare the angular velocity signal generated by the canals with the angular velocity of the input linear acceleration vector. The difference between these velocities serves as an error signal that increases the attenuation of the orientation channel and decreases the attenuation of the translation channel. Orientation channel outputs attenuate orthogonal canal signals that provide angular sensation and ocular reflexes. The model computes the following results that are consistent with empirical data reported in the literature: (1) For off-vertical rotation: bias and modulation components of nystagmus, faster decay of postrotatory nystagmus, attenuation of postrotatory turning sensations, and perceived conical translation; (2) For pendular centrifuge: vertical ascent and tumbling during deceleration; (3) For nonpendular centrifuge: delay in perception of roll; and (4) For passive roll: no delay in perception. DTIC

N95-16152# Naval Health Research Center, San Diego, CA.
EVENT-RELATED BRAIN POTENTIALS AS PREDICTORS OF TARGET DETECTION PERFORMANCE IN A MOVING WATERFALL DISPLAY SIMULATING PASSIVE BROAD-BAND SONAR MONITORING
S. Hillyard, P. Johnston, and Scott Makeig Mar. 1994 41 p
(AD-A280900; NHRC-93-33) Avail: CASI HC A03/MF A01

Fifteen subjects performed in a visual target detection task that took place in a simulated broad-band, sonar monitoring display. Over a one-hour test session, subjects attempted to detect two types of targets presented at an average rate of three/minute on a continuously updated waterfall display. Event-related brain potentials were recorded in response to the two classes of targets (growing lines of lighted pixels that simulated an acoustic source in the surroundings and briefly flashed vertical lines) as well as to two types of irrelevant 'probe' stimuli (occasional tone pips and diffuse flashes of the video screen). ERP amplitudes were significantly related to target detection performance in several ways. A late positive component (P300) was enlarged in response to correctly detected targets, particularly in subjects who were performing with a high level of accuracy. Specific ERP components elicited by both targets and irrelevant probes during the first 6 minutes of the session were found to be predictive of subsequent performance accuracy during the hour-long session in subjects studied under alert and drowsy conditions. These findings suggest the application of ERP measures to evaluate fitness for duty of operators in task situations requiring a high level of vigilance, such as radar and sonar operators, air traffic controllers, etc. DTIC

N95-16228# Army Research Inst. of Environmental Medicine, Natick, MA. Altitude Physiology and Medicine Div.
EVALUATION OF A NEWLY-DESIGNED, DYNAMIC KNEE EXTENSION DEVICE FOR THE STUDY OF MUSCLE FATIGUE IN HUMANS Final Report, 1 Sep. 1993 - 2 Sep. 1994
Charles S. Fulco, Steven F. Lewis (Boston Univ., MA.), Peter N. Frykman, Robert Boushel (Boston Univ., MA.), Sinclair Smith, Lindsay Gibson, Allen Cymerman, and Kent B. Pandolf 2 Sep. 1994 40 p
(AD-A284974; USARIEM-TR-94-18) Avail: CASI HC A03/MF A01

A device utilizing a simple pulley system was developed to study muscle fatigue during dynamic, submaximal exercise isolated to the knee-extensor muscles of one or both legs. The purposes of this study were to determine the following: (1) oxygen consumption requirements for various submaximal and maximal power outputs and to compare these data to values obtained from published reports using modified bicycle ergometers (criterion devices), (2) intraindividual test-retest variability, and (3) muscle fatigability during exercise. On each of 2 separate days, 8 male volunteers (mean age 18.6 + or - 0.3 yr (SE), weight 79.5 + or 5.1 kg, and height 179.1 + or - 2.0 cm) performed a graded, intermittent (4 min bouts) exercise test using the knee-extensor muscles of one leg to determine one-legged peak oxygen consumption. Maximal voluntary contractions (MVC) were obtained at the beginning, at 2 min, and at the end of each exercise bout as a means to monitor rate of muscle fatigue. The slope and intercept of the relationship of the increase in power output and oxygen consumption were 13.80 ml O2/watt and 470 ml/min, respectively, with r2 = 0.96. These values for slope and intercept are similar to those reported previously: slopes 13.10 and 14.70 ml O2/watt; intercepts, 400 and 471 ml/min; and r2 = 0.99. Also, there was minimal intra-individual variation (r2 = 0.90) in oxygen consumption values for identical power outputs. Test-retest oxygen consumption values did not differ from a line of identity. Stepwise accelerations in muscle fatigability were discernable with small increments in exercise intensity and elapsed exercise time. Our device represents a low-cost, expanded capability alternative compared to previous units utilizing modified bicycle ergometers as a testing mode. DTIC

N95-16297# Air Force Inst. of Tech., Wright-Patterson AFB, OH.
A PROPOSAL TO STUDY GENDER DIFFERENCES IN THE RATES OF DECOMPRESSION SICKNESS M.S. Thesis
Gregg A. Bendrick May 1994 50 p
(AD-A281854; AFIT/CI/CIA-94-049) Avail: CASI HC A03/MF A01

Decompression sickness is the clinical syndrome associated with evolution of nitrogen bubbles in the blood and body tissues upon exposure to an acute reduction in barometric pressure. Because nitrogen is more soluble in fatty substances than in water, adiposity has long been considered a risk factor for the development of decompression sickness. Due to the physiologic differences between the sexes, women have an average eight

percent more body fat than men, so it is possible that women have a greater likelihood of developing decompression sickness. Several studies in the scientific literature seem to support this hypothesis, but they have been associated with such drawbacks as selection and reporting bias, retrospective approach, and the lack of an objective diagnostic modality for the syndrome of decompression sickness. DTIC

N95-16360# Air Force Inst. of Tech., Wright-Patterson AFB, OH.
CHARACTERIZATION OF THE FAST-PHASE COMPONENT OF THE VESTIBULO-OCULAR RESPONSE M.S. Thesis
Rebecca Schultz May 1994 52 p
(AD-A281830; AFIT/CI/CIA-94-043) Avail: CASI HC A04/MF A01

The vestibular system can be tested by recording eye-movement responses to whole-body angular acceleration. The resulting vestibulo-ocular reflex (VOR) has two components. The slow-phase component is a compensating movement in the same direction as the stimulus, while the fast-phase component is a refixation movement usually in the opposite direction of the stimulus. The slow-phase signal is extracted and evaluated to determine the condition of the vestibular system. Currently the fast-phase component is not used for diagnostic purposes. Normal subjects were tested and the extracted fast-phase signal was characterized using parameters such as amplitude, velocity and duration of each fast eye movement. Derived from text

N95-16378 Michigan State Univ., East Lansing, MI. Dept. of Pediatrics and Human Development.
THE ROLE OF CHEMICAL INHIBITION OF GAP JUNCTIONAL INTERCELLULAR COMMUNICATION IN TOXICOLOGY Annual Technical Report, 14 May 1993 - 15 May 1994
James E. Trosko 14 Jun. 1994 206 p Limited Reproducibility: More than 20% of this document may be affected by microfiche quality
(Contract F49620-92-J-0293)
(AD-A282452; AFOSR-94-0421TR) Avail: Issuing Activity (Defense Technical Information Center (DTIC))

Gap junctional intercellular communication (GJIC) is the biological process which regulates homostatic control of cell proliferation, differentiation, and adaptive functions of differentiated cells. Disruption of GJIC by toxic chemicals, either at the level of gene expression or protein function, has been correlated with teratogenesis, tumor promotion, reproductive and neurotoxicities. The mechanisms by which various epigenetic toxicants or oncogenes inhibit GJIC have been studied. Modulation of phosphorylation of one gap junction protein (cx43) by two different tumor promoters (phorbol esters, DDT) has been shown to be different, yet the end result (inhibition of GJIC) is the common end point. Preliminary evidence has linked the toxic-chemical modification of the gap junction protein phosphorylation paths with altered trafficking of the protein within the cell. DTIC

N95-16405# Army Aeromedical Research Lab., Fort Rucker, AL.
AVIATION EPIDEMIOLOGY DATA REGISTER: CORONARY ANGIOGRAPHY OUTCOMES OF CIVILIAN AVIATORS FLYING US AIRCRAFT
Kevin T. Mason and Samuel G. Shannon Aug. 1994 26 p
(AD-A285191) Avail: CASI HC A03/MF A01

All Army aviators participate in a cardiovascular disease screening program. Five percent of Army aviators are civilian. The U.S. Army Aviation Center requested a review of cardiovascular disease screening outcomes among this subgroup of aviators. The AEDR was queried to determine the coronary angiography outcomes of civilian aviators who failed levels 1 and 2 of cardiovascular disease screening program during the period 1988 to 1992. Among 847 civilian aviators, 364 failed level 1 cardiovascular disease screening due to elevated risk factors for coronary artery disease. Among the 364, 289 passed level 2 screening with a normal exercise treadmill tent and a normal cardiac fluoroscopy. The remaining 75 failed level 2 by having an abnormal exercise treadmill tent and/or an abnormal cardiac fluoroscopy. These 75 were referred for further diagnostic testing in levels 3 and 4. Of the 55 aviators undergoing coronary angiography, 17 had normal coronary arteries, 14 had uncomplicated minimal coronary artery disease, 3 had complicated minimal coronary artery disease, and 21 had significant coronary artery occlusions. Eight other aviators had advanced heart conditions other than coronary artery disease, such as cardiomyopathy. Of 36 aviators with documented significant cardiovascular disease, 32 (88.9 percent) denied symptoms when their disease was detected by the screening program. They were referred for clinical, and in some cases, emergent care. DTIC

N95-16412*# National Aeronautics and Space Administration. Langley Research Center, Hampton, VA.
KINETICS MODEL FOR INITIATION AND PROMOTION FOR DESCRIBING TUMOR PREVALENCE FROM HZE RADIATION
Francis A. Cucinotta and John W. Wilson Dec. 1994 19 p
(RTOP 199-45-16-11)
(NASA-TP-3479; L-17404; NAS 1.60:3479) Avail: CASI HC A03/MF A01

A kinetics model for cellular repair and misrepair for multiple radiation-induced lesions (mutation-inactivation) is coupled to a two-mutation model of initiation and promotion in tissue to provide a parametric description of tumor prevalence in the Harderian gland in a mouse. Dose-response curves are described for gamma-rays and relativistic ions. The effects of nuclear fragmentation are also considered for high-energy proton and alpha particle exposures The model described provides a parametric description of age-dependent cancer induction for a wide range of radiation fields. We also consider the two hypotheses that radiation acts either solely as an initiator or as both initiator and promoter and make model calculations for fractionation exposures from gamma-rays and relativistic Fe ions. For fractionated Fe exposures, an inverse dose-rate effect is provided by a promotion hypothesis using a mutation rate for promotion typical of single-gene mutations. Author

N95-16423# Puerto Rico Univ., San Juan. Inst. of Neurobiology.
CHARACTERIZATION OF NEUROTROPHIC AND NEUROTROPIC INTERACTIONS BETWEEN NEURONS AND THEIR MUSCLE AND NERVE TARGETS Final Report, 1 Sep. 1990 - 30 Nov. 1993
Damien Kuffler 14 Feb. 1994 12 p
(Contract DAAL03-90-G-0189)
(AD-A281846; ARO-28095.4-LS-SAH) Avail: CASI HC A03/MF A01

The broad aim of the work carried out under the support of this grant was to examine the factors involved in promoting and directing axon regeneration. How do injured nerves find and recognize their targets and reestablish the correct types of synaptic contacts with them? Cultures have been established of adult sensory and motor neurons, as well as intact muscle fibers. These cells survive for weeks in vitro and the neurons extend processes. In electrophysiological experiments we have characterized several membrane properties of the neurons. The peripheral nerve tube, as well as isolated intact muscle fibers, have been shown to release trophic factors that promote and modify process outgrowth from the sensory neurons, and one of the trophic factors is being characterized. An extracellular matrix molecule that independently also promote process outgrowth has been isolated and characterized. A novel role of macrophages, as directors of process growth, has been shown. Preliminary experiments demonstrate that factors released from peripheral nerve can direct process outgrowth by means of diffusible concentration gradients DTIC

N95-16444# Minnesota Univ., Minneapolis, MN.
HEMOGLOBIN-BASED BLOOD SUBSTITUTES AND ENHANCED SUSCEPTIBILITY TO BACTERIAL INFECTIONS Final Report, 17 Jan. 1991 - 9 Feb. 1994
John R. Mahoney and John W. Eaton 8 Mar. 1994 26 p
(Contract DAMD17-91-Z-1009)
(AD-A281023) Avail: CASI HC A03/MF A01

Chemically modified human hemoglobin is currently being studied as a potential blood substitute for use in military and emergency medical applications. We have tested one form of modified hemoglobin, DBBF-Hb, against normal Hb in order to determine its ability to promote hemoglobin-driven bacterial infections. Using an experimental model of E. coli peritonitis we have determined that DBBF-Hb is equally likely as unmodified Hb (on a mole to mole basis) to lead to a fatal outcome in this model. Further investigations were undertaken to elucidate the molecular mechanism of these hemoglobin-driven bacterial infections. The strains of E. coli that exhibit the hemoglobin-adjuvant effect are resistant to phagocytosis by peritoneal macrophages. This feature may explain why hemoglobin is necessary (nutritional iron) but not sufficient for the promotion of E. coli infections. We are currently examining the composition of the outer membrane proteins in the hemoglobin-adjuvant strains. In addition,

using a molecular biological approach, we are attempting to clone the gene(s) responsible for the hemoglobin adjuvant phenotype in E. coli. Further understanding of the mechanism of hemoglobin driven bacterial infections may enable the rational design of a safe blood substitute. DTIC

N95-16481# Toronto Univ. (Ontario). Dept. of Psychology.
CELL CULTURE AND TRANSPLANTATION OF THE SUPRACHIASMATIC CIRCADIAN PACEMAKER Annual Report, 30 Sep. 1992 - 29 Sep. 1993
Martin R. Ralph 29 Sep. 1993 5 p
(Contract F49620-92-J-0517)
(AD-A280977; AFOSR-94-0374TR) Avail: CASI HC A01/MF A01

The general aim of the research supported by AFOSR is to understand how circadian rhythms in mammals are generated and controlled. We have used a variety of techniques to ask such questions as: (1) How does photic information reach and affect the clock? (2) What is the nature of the electrical events in pacemaker cells responsible for the generation and expression of rhythmicity? (3) What are the biochemical components of the pacemaker system? In particular, we have used the tau (period) mutation in the golden hamster, to pursue experiments designed to eventually identify mammalian circadian pacemaker cells. DTIC

N95-16484# Dalhousie Univ., Halifax (Nova Scotia). Dept. of Psychology.
NEUROPHYSIOLOGICAL ANALYSIS OF CIRCADIAN RHYTHM ENTRAINMENT Annual Technical Report, 1 Jun. - 31 Dec. 1993
Benjamin Rusak 24 May 1994 9 p
(Contract F49620-93-1-0089)
(AD-A280981; AFOSR-94-0372TR) Avail: CASI HC A02/MF A01

Loss of melatonin secretion in hamsters can alter the rhythm of melatonin sensitivity in the suprachiasmatic nuclei (SCN) as tested in an in-vitro slice preparation. The effect on melatonin sensitivity depended on whether pinealectomy or brief constant light exposure was used to reduce melatonin levels, with constant light increasing sensitivity and pinealectomy decreasing it. The same treatments also eliminated or reduced the amplitude of the firing-rate rhythms monitored in the SCN slice preparation. These results imply a role for pineal melatonin in the maintenance of the normal amplitude of the SCN pacemaker's output rhythms. Serotonin and melatonin were determined to suppress photic responses of SCN cells and intergeniculate leaflet cells studied in vivo. Serotonin appears to act at both targets via a receptor that is similar to the serotonin-1A receptor type, while melatonin acts via a non-serotonergic receptor. Gastrin-releasing peptide (GRP) causes increased firing of about 50% of SCN cells tested in a slice preparation; the proportion of responsive cells depends on the circadian phase tested. GRB injected into the SCN in vivo causes phase-dependent phase shifts that resemble those caused by light pulses. DTIC

N95-16491# Army Medical Research Inst. of Chemical Defense, Aberdeen Proving Ground, MD.
DEVELOPMENT OF AN IN VITRO MODEL ASSAY SYSTEM FOR THE EVALUATION OF THE EFFECTS OF TOXIC CHEMICALS ON HUMAN AIRWAYS Final Report, 1988 - 1993
James L. Ellis and Margaret G. Filbert Mar. 1994 16 p
(AD-A285074; USAMRICD-TR-94-02) Avail: CASI HC A02/MF A01

The ability of the anticholinesterase agent soman to contract human bronchi was examined. Soman (1-2 uM) had variable effects on human bronchi that had not been stimulated with an electric field stimulator (EFS). In bronchi continuously stimulated by EFS (0.5 Hz, 1 ms, 12 V), soman produced contractions in all tissues examined (12 preparations from 9 humans). In tissues stimulated by EFS, the beta-adrenoreceptor agonist isoproterenol produced relaxations that were greater in magnitude than the contractions produced by soman. The duration of the isoproterenol induced relaxations was variable. Of 12 preparations studied, 3 showed no reversal of the relaxation within 120 min, 6 showed a slow reversal with a reversal time of 106 +/- 6 min and 3 showed rapid reversal with a 50 percent reversal time of 14 min. In the latter group the duration of the relaxation produced by isoproterenol was doubled (28 +/- 2 min) by the M2 muscarinic receptor antagonist AFDX 116 (10 uM). These results show that the isolated human bronchus is a useful model for studying the effects of toxic chemical agents such as soman on the airways. The data obtained with isoproterenol suggest that beta-2 agonists may be useful adjuncts for treating the effects of anticholinesterase agents. DTIC

N95-16515# Arizona Univ., Tucson, AZ.
THE CHRONIC EFFECTS ON JP-8 JET FUEL EXPOSURE ON THE LUNGS Final Technical Report, 1 Apr. 1991 - 31 Mar. 1994
Mark L. Witten 2 Jun. 1994 12 p
(Grant AF-AFOSR-0199-91)
(AD-A280982; AFOSR-94-0382TR) Avail: CASI HC A03/MF A01

There are four major findings from the three years of work devoted to the effects of chronic JP-8 jet fuel exposure on the lungs and secondary organs. These findings are the following chronic exposure to JP-8 jet fuel alters pulmonary function and lung structures with an acute response with as little as seven days of low dose, approximately 500 mg/m3, exposure to JP-8 jet fuel; chronic exposure to JP-8 jet fuel increased liver, spleen, and kidney weights compared to controls. Microscopic evaluation of liver sections were normal; however, kidney and spleen had histological changes consistent with organic solvent exposure. There is a correlation between JP-8 jet fuel exposure-induced decreases in lung Substance P levels and lung neutral endopeptidase levels. Chronic exposure to JP-8 jet fuel caused a decrease in lung Substance P levels with a corresponding increase in lung neutral endopeptidase levels; and, there is a recovery process in the 56 day low dose JP-8 jet fuel-exposed lungs as marked by a return to baseline and longitudinal control 99mTcDTPA values. The 99mTcDTPA data was very consistent with our pathologic findings of very little lung injury in the 56 day low dose JP-8 jet fuel-exposed rats. We speculate that this finding indicates that there is a 'threshold' level of JP-8 jet fuel exposure that the lungs' defense mechanism(s) can tolerate. DTIC

N95-16619# Naval Health Research Center, San Diego, CA.
SKIN BLOOD FLOW AND BIOELECTRICAL IMPEDANCE Final Report, Jul. 1989 - Sep. 1990
Marcie B. Beckett, James A. Hodgdon, Wanda Woods, and Brian W. Appleton 14 Jun. 1994 20 p
(NR Proj. M00-001)
(AD-A285475; NHRC-94-17) Avail: CASI HC A03/MF A01

This study was performed to determine the effect of changes in skin blood flow (SBF) on bioelectrical resistance (RES). Twenty-three men had their left hand repeatedly immersed (1 min) and removed from water (3 min) for a total of 12 min in order to manipulate SBF in the contralateral (right) limbs where RES electrodes were located. Tests were completed at three water temperatures (5, 15, and 350C) in constant ambient air temperature (25 +/- 1 deg C). SBF was monitored on the middle finger of the right hand using a laser-Doppler flowmeter, and skin temperature on the dorsal right hand (Th) and foot (Tf). Time series analysis revealed cyclic SBF and RES responses were inversely correlated at all water temperatures ($r = -0.38$ to -0.64; p less than 0.05). Tb and Tf were not correlated with SBF for any test. During hand immersion in 5, 15, and 350C water, SBF decreased by 36, 20, and 4%, respectively, while RES increased by 3.5, 2.0, and 0.7 ohms, respectively. When incorporated into existing bioimpedance (BIA) prediction equations, the largest RES difference observed (3.5 ohms) translated into a difference of 0.4% body fat and 0.4 L body water. Changes in SBF of the magnitude observed in this study appear to have a relatively small impact on BIA prediction of body water and composition. DTIC

N95-16796# Chicago Univ., Chicago, IL. Dept. of Medicine.
PHASE-SHIFTING EFFECTS OF LIGHT AND ACTIVITY ON THE HUMAN CIRCADIAN CLOCK Final Report, 1 Mar. 1993 - 28 Feb. 1994
Eve VanCauter 28 Feb. 1994 19 p
(Contract F49620-93-1-0188)
(AD-A281204; AFOSR-94-0399TR) Avail: CASI HC A03/MF A01

While still preliminary, the findings from this study have provided two important novel observations (1) an overall elevation of TSH levels is a biological concomitant of the 'jet lag syndrome'; (2) exposure to dark/sleep is capable of exerting immediate phase-shifting effects of human rhythms. DTIC

N95-16809# Army Research Inst. of Environmental Medicine, Natick, MA.
INCREASED SKIN BLOOD FLOW AND ENHANCED HEAT LOSS IN

HUMANS AFTER NIACIN INGESTION
Lou A. Stephenson and Margaret A. Kolka Jun. 1994 52 p
(AD-A281124; USARIEM-T94-16) Avail: CASI HC A04/MF A01

Healthy, young subjects were studied in three separate series of studies characterizing nicotinic acid (NA) ingestion (5 mg/kg): (1) at rest, seated (T sub a = 30 C, rh = 23%) at 0800 h and again between 1800 and 2100 h; (2) at rest (R) and during seated exercise (X, T sub a = 29 C, rh = 30%); and (3) during upright exercise when wearing a protective clothing system (T sub a = 28 C, rh = 30%). NA treatment resulted in decreased T sub es, bar-T su b sk, SkBF, FBF, heart rate, and cutaneous vascular conductance (CVC) (P less than or equal to 0.05). NA decreased mean arterial pressure at rest. Subjects had no difficulty completing seated or upright exercise in either control or NA experiments. The pharmacological manipulation of skin blood flow at rest and during moderate exercise effectively increased sensible heat flux during seated as well as upright exercise. NA ingestion also increased sensible heat flux from individuals dressed in chemical protective clothing. These experiments show that pharmacologic manipulation of skin blood flow by NA ingestion should be done cautiously, especially when NA will be used repeatedly or in novel circumstances. DTIC

N95-16847# Virginia Univ., Charlottesville, VA. Dept. of Biology.
PHOTORECEPTORS REGULATING CIRCADIAN BEHAVIOR: A MOUSE MODEL Annual Report, 15 Mar. 1993 - 14 Mar. 1994
Russell G. Foster 14 Mar. 1994 15 p
(Contract F49620-92-J-0205)
(AD-A285157; AFOSR-94-0605TR) Avail: CASI HC A03/MF A01

In the rd mouse the absence of rod cells and the progressive loss of cones does not result in a decrease in circadian phase shifting responses to light. By contrast, rd mice are unable to perform simple visual tasks. In addition, rodless transgenic mice, and mice homozygous for the rds mutation, show unattenuated circadian responses to light. Collectively these data suggest that cone cells lacking outer segments are sufficient to maintain normal circadian responses to light, or there may be some unidentified photoreceptor within the retina. An action spectrum for circadian responses to light in rd mice, and molecular analysis of retinally degenerate mice and blind mole rat eyes, suggests the involvement of a green cone opsin in mammalian photoentrainment. DTIC

N95-16851# Scripps Clinic and Research Foundation, La Jolla, CA.
MOLECULAR APPROACH TO HYPOTHALAMIC RHYTHMS Annual Report, 15 Mar. 1993 - 14 Mar. 1994
J. G. Sutcliffe 14 Mar. 1994 41 p
(Contract F49620-92-J-0188)
(AD-A285164; AFOSR-94-0606TR) Avail: CASI HC A03/MF A01

The suprachiasmatic nucleus (SCN) of the hypothalamus is the anatomical seat of the mammalian endogenous biological clock which regulates the temporal expression of hormonal and behavioral circadian rhythms. Light, serotonin and melatonin are the dominant stimuli which affect the phase of the endogenous clock. The grantee has devised strategies to identify molecules that mediate the action of these stimuli within the SCN. The grantee has identified a novel receptor for serotonin, the 5-HT7 receptor, and determined its amino acid structure. Its pharmacological ligand binding properties have been measured and a unique profile of agonists and antagonists defined. These allowed demonstration that the 5-HT7 receptor mediated circadian activity of cultured SCN. The receptor has been shown to couple to activation of adenylyl cyclase and to be synthesized by neurons of the subparaventricular zone immediately dorsal to the SCN. Molecules whose expression within the SCN is activated by light entraining cues have also been identified. DTIC

N95-16871# Texas Univ. Health Science Center, Houston, TX.
INVESTIGATION OF LASER-INDUCED RETINAL DAMAGE: WAVELENGTH AND PULSEWIDTH DEPENDENT MECHANISMS Final Technical Report, 1 Apr. 1991 - 31 Mar. 1994
Randolph D. Glickman 31 Aug. 1994 20 p
(Grant AF-AFOSR-0208-91)
(AD-A285186; UTHSCSA-OPH-94-01; AFOSR-94-0621TR) Avail: CASI HC A03/MF A01

This research was initiated to develop biochemical and cellular assays of laser damage in ocular tissue. Photochemical damage was identified by evidence of oxidative reactions resulting from free radicals generated by the interaction of laser and incoherent light with ocular tissue components. Melanin contained in retinal pigment epithelial (RPE) cells formed a free radical during illumination and rapidly oxidized ascorbic acid (AA). RPE cells have a high capacity for utilizing AA; the cells have different transporters for AA and its oxidized form, dehydro-L-ascorbic acid (DHA), and efficiently reduce DHA to AA. The kinetics and specificity of these transporters were measured in these studies. In the absence of AA or other antioxidants, light-activated melanin promoted the formation of hydroperoxides of the fatty acid, linoleic acid. Thus, if intracellular antioxidants become depleted, the melanin radical may mediate some aspects of photochemical damage such as lipid peroxidation. Other assays of laser damage were investigated. Following laser exposure, release of K+ ions from RPE cells could be demonstrated, but the measured changes were small and inconsistent. Efflux of the cytoplasmic enzyme, lactate dehydrogenase, showed more promise as an assay for thermal or photodisruptive laser bioeffects. DTIC

N95-17174# Walter Reed Army Medical Center, Washington, DC.
COMPARISON OF WORK OF BREATHING DURING MECHANICAL VENTILATION USING ASSIST CONTROL AND INTERMITTENT MANDATORY VENTILATION Final Report, 15 Mar. 1992 - 30 Sep. 1993
Ronald K. Poropatich 19 Jul. 1994 6 p
(Contract MIPR-92MM2539)
(AD-A285516) Avail: CASI HC A02/MF A01

Request termination of MIPR 92MM2539, titled: Comparison of Work of Breathing During Mechanical Ventilation Using Assist Control and Intermittent Mandatory Ventilation. Since initiation of the above study in March 1992, only 2 patients have been enrolled. Difficulties in enrollment has been due to patients not tolerating the various ventilatory settings, as well as the metabolic cart (which measures the exhaled carbon dioxide and oxygen consumption) having too large a range in measured variables. This latter fact may be related to the difficulties encountered in tolerating the ventilator changes. DTIC

N95-17300 National Defence Research Establishment, Stockholm (Sweden). Huvudavdelning foer Maensklig Prestation och Funktion.
MENTAL EFFECTS OF CAFFEINE IN FATIGUED MEN AND WOMEN [KOFFEIN SOM ETT MEDEL MOT TROETTHET]
L. Linde Jan. 1994 29 p In SWEDISH
(PB94-190683; FOA-C-50105-5.1) Avail: Issuing Activity

The purpose of the present experiments was to investigate the effect of caffeine in subjective experience and in performance of cognitive tasks among men and women during vigil. In experiment 1: eight male and eight female subjects were randomly assigned to either a caffeine or a placebo condition. 150 mg caffeine was given at midnight and at 4 p.m. In experiment 2: nine female and nine male subjects were assigned randomly to either a placebo or caffeine treatment. 200 mg caffeine was given at 5 a.m. It is suggested (1) that effects of caffeine in fatigued subjects may not be revealed directly in the level of performance but in the experienced effort of performing a task, and (2) that there might be sex differences in the reaction to caffeine possibly due to different arousal patterns in men and women. It is also suggested that the results may be interpreted in terms of compensatory arousal mechanism. NTIS

N95-17342# Chicago Univ., Chicago, IL. Dept. of Medicine.
BASIC MECHANISMS AND IMPLICATIONS OF NON-PHOTIC ENTRAINMENT OF CIRCADIAN RHYTHMICITY Annual Report, 1 Sep. 1992 - 31 Aug. 1993
Eve VanCauter 30 Aug. 1993 5 p
(Contract F49620-92-J-0347)
(AD-A283180; AFOSR-94-0451TR) Avail: CASI HC A01/MF A01

The studies showed that afternoon exposure to exercise increases TSH levels and tends to delay the onset of nocturnal TSH secretion on the following night. Analysis of the melatonin levels is under progress. Studies examining the effects of carbohydrate intake on vigilance and performance were performed. A new computerized data collection and analysis system was used to determine the phase shifting effects of light pulses of varying intensity on the free-running circadian rhythm of locomotor activity in both young and old hamsters. It was demonstrated that old hamsters are about 20 times less sensitive to the effects of light on the circadian clock, despite there being little if any effect of age on the amount of light being transmitted through the eyes. DTIC

N95-17703* National Aeronautics and Space Administration, Washington, DC.
AEROSPACE MEDICINE AND BIOLOGY: A CONTINUING BIBLIOGRAPHY WITH INDEXES (SUPPLEMENT 396)
Jan. 1995 187 p
(NASA-SP-7011(396); NAS 1.21:7011(396)) Avail: CASI HC A09
This publication is a cumulative index to the abstracts contained in the Supplements 385 through 395 of Aerospace Medicine and Biology: A Continuing Bibliography. It includes seven indexes: subject, personal author, corporate source, foreign technology, contract number, report number, and accession number. Author

N95-15975*# Alaska Univ., Fairbanks, AK. Arctic Region Supercomputing Center.
SIMULATION OF ARTHROSCOPIC SURGERY USING MRI DATA
Geoffrey Heller and Jon Genetti *In* NASA. Johnson Space Center, ISMCR 1994: Topical Workshop on Virtual Reality. Proceedings of the Fourth International Symposium on Measurement and Control in Robotics Nov. 1994 p 21-26 Sponsored by Cray Research Inc. and Corps of Engineers (For primary document see N95-15972 04-63)
Avail: CASI HC A02/MF A02

N95-15976*# Padua Univ. (Italy). Dept. of Innovation in Mechanics and Management.
MULTIMODAL CORRELATION AND INTRAOPERATIVE MATCHING OF VIRTUAL MODELS IN NEUROSURGERY
Enrico Ceresole, Michele DalSasso, and Aldo Rossi *In* NASA. Johnson Space Center, ISMCR 1994: Topical Workshop on Virtual Reality. Proceedings of the Fourth International Symposium on Measurement and Control in Robotics Nov. 1994 p 27-30 (For primary document see N95-15972 04-63)
Avail: CASI HC A01/MF A02

N95-16738*# National Aeronautics and Space Administration. Lyndon B. Johnson Space Center, Houston, TX.
THE EFFECT OF DIFFERENCES IN TIME TO DETECTION OF CIRCULATING MICROBUBBLES ON THE RISK OF DECOMPRESSION SICKNESS Abstract Only
K. V. Kumar (Krug Life Sciences, Inc., Houston, TX.), J. H. Gilbert (Krug Life Sciences, Inc., Houston, TX.), M. R. Powell, and J. M. Waligora *In* Aerospace Medical Association, Aerospace Medical Association 63rd Annual Scientific Meeting Program 14 May 1992 1 p (For primary document see N95-16737 04-51)
Avail: CASI HC A01/MF A02

N95-16739*# National Aeronautics and Space Administration. Lyndon B. Johnson Space Center, Houston, TX.
VARIABILITY IN HOFFMANN AND TENDON REFLEXES IN HEALTHY MALE SUBJECTS Abstract Only
E. Good (Humana Hospital, Webster, TX.), S. Do (Baylor Coll. of Medicine, Houston, TX.), and M. Jaweed *In* Aerospace Medical Association, Aerospace Medical Association 63rd Annual Scientific Meeting Program 14 May 1992 1 p (For primary document see N95-16737 04-51)
Avail: CASI HC A01/MF A02

N95-16740*# National Aeronautics and Space Administration. Ames Research Center, Moffett Field, CA.
THE PSYCHOPHYSICAL FUNCTION FOR PERCEIVED GRAVITATIONAL-INERTIAL FORCE DOES NOT DEPEND ON THE ORIENTATION OF THE OTOLITH ORGANS Abstract Only
M. Cohen, R. Welch, and C. DeRoshia *In* Aerospace Medical Association, Aerospace Medical Association 63rd Annual Scientific Meeting Program 14 May 1992 1 p (For primary document see N95-16737 04-51)
Avail: CASI HC A01/MF A02

N95-16741*# National Aeronautics and Space Administration. Lyndon B. Johnson Space Center, Houston, TX.
USE OF INJECTABLE PROMETHAZINE TO DECREASE SYMPTOM SCORES OF SPACE MOTION SICKNESS Abstract Only
B. G. Beck and A. E. Nicogossian *In* Aerospace Medical Association, Aerospace Medical Association 63rd Annual Scientific Meeting Program 14 May 1992 1 p (For primary document see N95-16737 04-51)
Avail: CASI HC A01/MF A02

N95-16742*# National Aeronautics and Space Administration. Ames Research Center, Moffett Field, CA.
COMPARISON OF SALINE AND FLUDROCORTISONE AS FLUID-LOADING COUNTERMEASURES FOLLOWING EXPOSURE TO SIMULATED MICROGRAVITY Abstract Only
J. Vernikos, D. A. Ludwig (National Aeronautics and Space Administration. John F. Kennedy Space Center, Cocoa Beach, FL.), and V. A. Convertino (National Aeronautics and Space Administration. John F. Kennedy Space Center, Cocoa Beach, FL.) *In* Aerospace Medical Association, Aerospace Medical Association 63rd Annual Scientific Meeting Program 14 May 1992 1 p (For primary document see N95-16737 04-51)
Avail: CASI HC A01/MF A02

N95-16743*# National Aeronautics and Space Administration. John F. Kennedy Space Center, Cocoa Beach, FL.
SKELETAL MUSCLE RESPONSES TO UNLOADING IN HUMANS Abstract Only
G. Dudley (Bionetics Corp., Cocoa Beach, FL.), P. Tesch, B. Hather, G. Adams, and P. Buchanan *In* Aerospace Medical Association, Aerospace Medical Association 63rd Annual Scientific Meeting Program 14 May 1992 1 p Prepared in cooperation with Karolinska Inst., Stockholm, Sweden (For primary document see N95-16737 04-51)
(Contract NAS10-11624)
Avail: CASI HC A01/MF A02

N95-16744*# National Aeronautics and Space Administration. Ames Research Center, Moffett Field, CA.
INTRAMUSCULAR PRESSURE: A BETTER TOOL THAN EMG TO OPTIMIZE EXERCISE FOR LONG-DURATION SPACE FLIGHT Abstract Only
A. R. Hargens, R. E. Ballard, M. Aratow, A. Crenshaw, J. Styf, N. Kahan, and D. E. Watenpaugh *In* Aerospace Medical Association, Aerospace Medical Association 63rd Annual Scientific Meeting Program 14 May 1992 1 p (For primary document see N95-16737 04-51)
Avail: CASI HC A01/MF A02

N95-16745*# National Aeronautics and Space Administration. Lyndon B. Johnson Space Center, Houston, TX.
CATECHOLAMINERGIC RESPONSES TO STRESSFUL MOTION STIMULI, SCOPOLAMINE PLUS AMPHETAMINE, AND DEXAMETHASONE Abstract Only
R. L. Kohl and W. E. Chelen *In* Aerospace Medical Association, Aerospace Medical Association 63rd Annual Scientific Meeting Program 14 May 1992 1 p Prepared in cooperation with National Academy of Sciences - National Research Council, Houston, TX (For primary document see N95-16737 04-51)
(Contract NAS9-17267; RTOP 199-16-11-08)
Avail: CASI HC A01/MF A02

N95-16746*# National Aeronautics and Space Administration. John F. Kennedy Space Center, Cocoa Beach, FL.
HEAT STRESS AND A COUNTERMEASURE IN THE SHUTTLE RESCUEMAN'S SUIT Abstract Only
D. F. Doerr, H. Reed, and V. A. Convertino *In* Aerospace Medical Association, Aerospace Medical Association 63rd Annual Scientific Meeting Program 14 May 1992 1 p (For primary document see N95-16737 04-51)
Avail: CASI HC A01/MF A02

N95-16747*# National Aeronautics and Space Administration. Lyndon B. Johnson Space Center, Houston, TX.
A NEW MODEL FOR ESTIMATING TOTAL BODY WATER FROM BIOELECTRICAL RESISTANCE Abstract Only
S. F. Siconolfi and K. T. Kear (Krug Life Sciences, Inc., Houston, TX.) *In* Aerospace Medical Association, Aerospace Medical Association 63rd Annual Scientific Meeting Program 14 May 1992 1 p (For primary document see N95-16737 04-51)
Avail: CASI HC A01/MF A02

N95-16748*# Kentucky Univ., Lexington, KY. Center for Biomedical Engineering.
SPECTRAL COMPONENTS OF HUMAN CARDIOVASCULAR RESPONSES TO STEP CHANGES IN LOWER BODY NEGATIVE PRESSURE (LBNP) BEFORE AND AFTER 22 HOUR OF 6 DEG HEAD DOWN BED REST Abstract Only
C. F. Knapp, J. M. Evans, K. J. Grande, C. D. Murphy, and A. R. Patwardhan *In* Aerospace Medical Association, Aerospace Medical Association 63rd Annual Scientific Meeting Program 14 May 1992 1 p (For primary document see N95-16737 04-51)
(Grant NAG9-298)
Avail: CASI HC A01/MF A02

N95-16749*# National Aeronautics and Space Administration. Lyndon B. Johnson Space Center, Houston, TX.
MAGNETIC RESONANCE IMAGING (MRI) OF SKELETAL MUSCLES IN ASTRONAUTS AFTER 9 DAYS OF SPACE FLIGHT Abstract Only
M. Jaweed, P. Narayana (Texas Univ. Health Science Center, Houston, TX.), J. Slopis (Texas Univ. Health Science Center, Houston, TX.), I. Butler (Texas Univ. Health Science Center, Houston, TX.), V. Schneider, A. LeBlanc (Baylor Univ., Houston, TX.), L. Fotedar (Krug Life Sciences, Inc., Houston, TX.), and D. Bacon (Humana Hospital, Webster, TX.) *In* Aerospace Medical Association, Aerospace Medical Association 63rd Annual Scientific Meeting Program 14 May 1992 1 p (For primary document see N95-16737 04-51)
Avail: CASI HC A01/MF A02

N95-16750*# National Aeronautics and Space Administration. Lyndon B. Johnson Space Center, Houston, TX.
RESULTS OF AN INTERNATIONAL SPACE CREW DEBRIEF Abstract Only
P. A. Santy (Texas Univ., Galveston, TX.), A. W. Holland, L. Looper, and R. Marcondes-North *In* Aerospace Medical Association, Aerospace Medical Association 63rd Annual Scientific Meeting Program 14 May 1992 1 p (For primary document see N95-16737 04-51)
Avail: CASI HC A01/MF A02

N95-16751*# National Aeronautics and Space Administration. Ames Research Center, Moffett Field, CA.
PHYSIOLOGICAL CONSTRAINTS ON DECELERATION DURING THE AEROCAPTURE OF MANNED VEHICLES Abstract Only
J. E. Lyne *In* Aerospace Medical Association, Aerospace Medical Association 63rd Annual Scientific Meeting Program 14 May 1992 1 p (For primary document see N95-16737 04-51)
Avail: CASI HC A01/MF A02

N95-16752*# National Aeronautics and Space Administration. Lyndon B. Johnson Space Center, Houston, TX.
BLOOD VOLUME AND ORTHOSTATIC RESPONSES OF MEN AND WOMEN TO A 13-DAY BEDREST Abstract Only
S. Fortney, T. Driscoll (Baylor Univ., Houston, TX.), L. Steinmann, and C. Alfrey (Baylor Univ., Houston, TX.) *In* Aerospace Medical Association, Aerospace Medical Association 63rd Annual Scientific Meeting Program 14 May 1992 1 p Prepared in cooperation with Krug Life Sciences, Inc., Houston, TX (For primary document see N95-16737 04-51)
Avail: CASI HC A01/MF A02

N95-16753*# National Aeronautics and Space Administration. Lyndon B. Johnson Space Center, Houston, TX.
EFFECT OF ANTIORTHOSTATIC BEDREST (BR) ON GASTROINTESTINAL MOTILITY (GIM) OF NORMAL SUBJECTS Abstract Only
L. Putcha, R. P. Hunter (Krug Life Sciences, Inc., Houston, TX.), K. J. Tietze (Baylor Univ., Houston, TX.), and N. M. Cintron *In* Aerospace Medical Association, Aerospace Medical Association 63rd Annual Scientific Meeting Program 14 May 1992 1 p (For primary document see N95-16737 04-51)
Avail: CASI HC A01/MF A02

N95-16754*# National Aeronautics and Space Administration. Lyndon B. Johnson Space Center, Houston, TX.
CHANGES IN LEFT VENTRICULAR FUNCTION AS DETERMINED BY THE MULTI-WIRE GAMMA CAMERA AT NEAR PRESYNCOPAL LEVELS OF LOWER BODY NEGATIVE PRESSURE Abstract Only
R. Pintner (Krug Life Sciences, Inc., Houston, TX.), S. Fortney, S. Mulvagh (Universities Space Research Association, Houston, TX.), and J. Lacy (Baylor Univ., Houston, TX.) *In* Aerospace Medical Association, Aerospace Medical Association 63rd Annual Scientific Meeting Program 14 May 1992 1 p (For primary document see N95-16737 04-51)
Avail: CASI HC A01/MF A02

N95-16756*# National Aeronautics and Space Administration. Lyndon B. Johnson Space Center, Houston, TX.
ACHILLES TENDON REFLEX (ATR) IN RESPONSE TO SHORT EXPOSURES OF MICROGRAVITY AND HYPERGRAVITY Abstract Only
M. Fujii and M. Jaweed *In* Aerospace Medical Association, Aerospace Medical Association 63rd Annual Scientific Meeting Program 14 May 1992 1 p (For primary document see N95-16737 04-51)
Avail: CASI HC A01/MF A02

N95-16757*# National Aeronautics and Space Administration. Lyndon B. Johnson Space Center, Houston, TX.
PREDICTION OF SPACE SICKNESS IN ASTRONAUTS FROM PREFLIGHT FLUID, ELECTROLYTE, AND CARDIOVASCULAR VARIABLES AND WEIGHTLESS ENVIRONMENTAL TRAINING FACILITY (WETF) TRAINING Abstract Only
K. Simanonok, E. Mosely, and J. Charles *In* Aerospace Medical Association, Aerospace Medical Association 63rd Annual Scientific Meeting Program 14 May 1992 1 p (For primary document see N95-16737 04-51)
Avail: CASI HC A01/MF A02

N95-16758*# National Aeronautics and Space Administration. Lyndon B. Johnson Space Center, Houston, TX.
DARK FOCUS OF ACCOMMODATION AS DEPENDENT AND INDEPENDENT VARIABLES IN VISUAL DISPLAY TECHNOLOGY Abstract Only
Sherrie Jones (Naval Training Systems Center, Orlando, FL.), Robert Kennedy (Essex Corp., Orlando, FL.), and Deborah Harm *In* Aerospace Medical Association, Aerospace Medical Association 63rd Annual Scientific Meeting Program 14 May 1992 1 p (For primary document see N95-16737 04-51)
Avail: CASI HC A01/MF A02

N95-16759*# National Aeronautics and Space Administration, Washington, DC.
REVIEW OF PERFORMANCE, MEDICAL, AND OPERATIONAL DATA ON PILOT AGING ISSUES Abstract Only
J. H. Stoklosa *In* Aerospace Medical Association, Aerospace Medical Association 63rd Annual Scientific Meeting Program 14 May 1992 1 p (For primary document see N95-16737 04-51)
Avail: CASI HC A01/MF A02

N95-16768*# National Aeronautics and Space Administration. Lyndon B. Johnson Space Center, Houston, TX.
SPACE MEDICINE RESEARCH: NEEDS FOR THE 21ST CENTURY Abstract Only
L. J. Pepper *In* Aerospace Medical Association, Aerospace Medical Association 63rd Annual Scientific Meeting Program 14 May 1992 1 p (For primary document see N95-16737 04-51)
Avail: CASI HC A01/MF A02

N95-16770*# National Aeronautics and Space Administration. Lyndon B. Johnson Space Center, Houston, TX.
EFFECTS OF WEIGHTLESSNESS ON HUMAN BAROREFLEX FUNCTION Abstract Only
Janice M. Fritsch and Dwain L. Eckberg *In* Aerospace Medical Association, Aerospace Medical Association 63rd Annual Scientific Meeting Program 14 May 1992 1 p Prepared in cooperation with Veterans Administration Hospital, Richmond, VA (For primary document see N95-16737 04-51)
Avail: CASI HC A01/MF A02

N95-16771*# National Aeronautics and Space Administration. Lyndon B. Johnson Space Center, Houston, TX.
DYNAMICS OF THE G-EXCESS ILLUSION Abstract Only
K. A. Baylor (Naval Aerospace Medical Research Lab., Pensacola, FL.), M. Reschke, F. E. Guedry (University of West Florida, Pensacola, FL.), B. J. McGrath (Naval Aerospace Medical Research Lab., Pensacola, FL.), and A. H. Rupert (Naval Aerospace Medical Research Lab., Pensacola, FL.) *In* Aerospace Medical Association, Aerospace Medical Association 63rd Annual Scientific Meeting Program 14 May 1992 1 p (For primary document see N95-16737 04-51)
Avail: CASI HC A01/MF A02

N95-16774*# Krug Life Sciences, Inc., Houston, TX.
DELIVERY OF CARDIOPULMONARY RESUSCITATION IN THE MICROGRAVITY ENVIRONMENT Abstract Only
M. R. Barratt and R. D. Billica *In* Aerospace Medical Association, Aerospace Medical Association 63rd Annual Scientific Meeting Program 14 May 1992 1 p Sponsored by NASA. Lyndon B. Johnson Space Center, Houston, TX (For primary document see N95-16737 04-51)
Avail: CASI HC A01/MF A02

N95-16777*# National Aeronautics and Space Administration. Lyndon B. Johnson Space Center, Houston, TX.
MEDICINE ON MARS: REMOTE MEDICAL CARE AND THE SPACE EXPLORATION INITIATIVE Abstract Only
S. C. Simmons and R. D. Billica *In* Aerospace Medical Association, Aerospace Medical Association 63rd Annual Scientific Meeting Program (SEE N95-16737 04-51) 14 May 1992 Prepared in cooperation wiht Krug Life Sciences, Inc., Houston, TX (For primary document see N95-16737 04-51)
Avail: CASI HC A01/MF A02

N95-16779*# National Aeronautics and Space Administration. Ames Research Center, Moffett Field, CA.
THE EFFECT OF INTERMITTENT STANDING OR WALKING DURING HEAD DOWN TILT BEDREST ON PEAK O2 CONSUMPTION Abstract Only
A. C. Ertl, A. S. Dearborn, and J. Vernikos *In* Aerospace Medical Association, Aerospace Medical Association 63rd Annual Scientific Meeting Program 14 May 1992 1 p (For primary document see N95-16737 04-51)
Avail: CASI HC A01/MF A02

N95-16780*# National Aeronautics and Space Administration. Ames Research Center, Moffett Field, CA.
PERIODIC UPRIGHT POSTURE NEGATES THE SUPPRESSION OF NEUROENDOCRINE RESPONSE TO HEAD DOWN BEDREST Abstract Only
C. E. Wade, J. Vernikos, J. Evans, and D. OHara *In* Aerospace Medical Association, Aerospace Medical Association 63rd Annual Scientific Meeting Program 14 May 1992 1 p (For primary document see N95-16737 04-51)
Avail: CASI HC A01/MF A02

N95-16781*# National Aeronautics and Space Administration. Ames Research Center, Moffett Field, CA.
THE EFFICACY OF PERIODIC +Gz EXPOSURE IN THE PREVENTION OF BEDREST INDUCED ORTHOSTATIC INTOLERANCE Abstract Only
D. A. Ludwig (North Carolina Univ., Greensboro, NC.), J. Vernikos, M. R Duvoisin (National Aeronautics and Space Administration. John F. Kennedy Space Center, Cocoa Beach, FL.), and J. L. Stinn *In* Aerospace Medical Association, Aerospace Medical Association 63rd Annual Scientific Meeting Program 14 May 1992 1 p (For primary document see N95-16737 04-51)
Avail: CASI HC A01/MF A02

N95-16782*# National Aeronautics and Space Administration. Ames Research Center, Moffett Field, CA.
THE VALUE OF THE 4-DAY HEADDOWN BEDREST MODEL FOR SCREENING COUNTERMEASURES Abstract Only
J. Vernikos, L. Keil, A. C. Ertl, C. E. Wade, J. E. Greenleaf, D. OHara, and D. Ludwig (North Carolina Univ., Greensboro, NC.) *In* Aerospace Medical Association, Aerospace Medical Association 63rd Annual Scientific Meeting Program 14 May 1992 1 p (For primary document see N95-16737 04-51)
Avail: CASI HC A01/MF A02

53 BEHAVIORAL SCIENCES

Includes psychological factors; individual and group behavior; crew training and evaluation; and psychiatric research.

N95-15959 University of Central Florida, Orlando, FL.
SITUATIONAL AWARENESS IN COMPLEX SYSTEMS Final Report, 1 Feb. 1993 - 31 Jan. 1994
Richard D. Gilson 31 Jan. 1994 336 p Limited Reproducibility: More than 20% of this document may be affected by microfiche quality
(Contract F49620-93-1-0132)
(AD-A281448; AFOSR-94-0418TR) Avail: Issuing Activity (Defense Technical Information Center (DTIC))

Decisions, whose appropriateness depends on knowledge and rules, are expected more or less effectively depending on the psychomotor skills of the operator. If these are sequential rather than parallel processes, and it seems to me that they must be even though they may be carried out very quickly, then in some cases we may be able to infer decision from action, and gestalt from decision, as long as we understand that the cognitive centroid of the individual operator is idiosyncratic and unknowable to some degree. Training can help to improve perception: it can also help to standardize the decisions taken in a given situation. The comprehension and integration of sensed data can also be improved by training, practice and criticism. The changes brought about by carefully targeted training can be observed and can also help us to underlying processes. DTIC

N95-16010# Yale Univ., New Haven, CT.
PRESENTATIONS OF SHAPE IN OBJECT RECOGNITION AND LONG-TERM VISUAL MEMORY Annual Report, 15 Jan. 1993 - 14 Jan. 1994
Michael J. Tarr 5 Apr. 1994 22 p
(Contract F49620-92-J-0169)
(AD-A281336; AFOSR-94-0413TR) Avail: CASI HC A03/MF A01

A wide range of psychophysical experiments investigating the mechanisms and representations underlying human object recognition have been conducted. In particular, the focus of this research has been an approach in which object recognition is mediated by at least two systems, one based on an explicit qualitative encoding of viewpoint-invariant features and one based on a metrically specific encoding of shape. Within the literature, this dichotomy has been most often associated with measures of the effect of viewpoint on recognition performance. For the most part, the common assumption has been that viewpoint-dependent patterns of performance are the signature of one recognition mechanism, while viewpoint-invariant patterns of performance are the signature of another recognition mechanism. Reinforcing this distinction, viewpoint-dependent mechanisms have been more broadly associated with metrically specific representations sensitive to a range of image-based properties, for example, size, handedness, color, or illumination, while viewpoint invariant mechanisms have been more broadly associated with coarsely-coded representations insensitive to image based properties. To this point, the majority of work on this project has focused only on the former in recognition tasks where perceivers must discriminate between visually similar objects (e.g., a within-category or subordinate-level judgment). During the past year we have continued this line of research, but have extended our approach to include recognition tasks using objects that are relatively dissimilar in that they may be differentiated by a small number of quantitatively different parts (e.g., a between-category or entry-level judgment). DTIC

N95-16138# California Univ., Irvine, CA. Center for the Neurobiology of Learning and Memory.
SYNAPTIC PLASTICITY AND MEMORY FORMATION Annual Report, 1 Jun. 1993 - 31 May 1994
Gary Lynch 31 May 1994 5 p
(Contract F49620-92-J-0307)
(AD-A284926; AFOSR-94-0619TR) Avail: CASI HC A01/MF A01

Work described in past progress reports led to the conclusion that the

postsynaptic glutamate receptors which mediate fast, excitatory transmission in mammalian brain are the sites at which the changes responsible for LTP occur. Moreover, pharmacological and physiological experiments indicated that the nature of the change involved a modification of receptor channel kinetics. Modelling studies, incorporating this information into a biologically realistic simulation of the receptor, resulted in a specific hypothesis about which the channel opens and closes (see Progress Report, 1992-1993). During the past year, experimental work was carried out to test this hypothesis. This involved hippocampal slices in which fast, excitatory responses were isolated by pharmacologically blocking inhibitory conductances and post-synaptic spiking. The synaptic responses in those 'disinhibited' slices are simple reflections, modified by dendritic filtering, of AMPA receptor mediated currents. DTIC

N95-16140# Navy Computer and Telecommunications Station, Pensacola, FL.
DEVELOPMENT OF THE OMPAT NEUROPSYCHOLOGICAL/PSYCHOMOTOR PERFORMANCE EVALUATION AND OMPAT DATA AND TIMING SUPPORT PROGRAMS Final Report, 15 Nov. 1990 - 31 Dec. 1993
Kathryn P. Winter and Dennis L. Reeves 31 Dec. 1993 42 p
(Contract MIPR91-MM-1504)
(AD-A284928) Avail: CASI HC A03/MF A01

The objectives of this project have been: (1) to create a millisecond accuracy software timer module that could be incorporated into OMPAT and other testing programs; (2) to construct a set of automated, i.e., 'computerized' OMPAT Level I neuropsychological and psychomotor tests with documentation that provide a standardized, clinically relevant, and rapid method for assessment of nervous system integrity; and (3) to construct a version of UTCPAB that incorporates the software timer. DTIC

N95-16244# Utah Univ., Salt Lake City, UT. Dept. of Psychology.
STUDIES OF NOVEL POPOUT Annual Report, 15 Aug. 1992 - 14 Aug. 1994
William A. Johnston, Irene S. Schwarting, and Kevin J. Hawley 5 Aug. 1994 22 p
(Contract F49620-92-J-0473)
(AD-A285237; AFOSR-94-0590TR) Avail: CASI HC A03/MF A01

Familiar arrays of objects are perceived better than novel arrays, indicating a perceptual bias toward expected inputs. Yet a novel object in an otherwise familiar array attracts attention, indicating a perceptual bias toward unexpected inputs. These phenomena describe a highly adaptive system but pose a paradox: How can the mind be biased simultaneously toward both what it most expects and what it least expects? Our research on novel popout illuminates the empirical boundaries of this stability/plasticity dilemma, and our computational model, called mismatch theory, provides a resolution. In this report we summarize the last two years of research on novel popout and the evolution of mismatch theory. Among other findings, we cite evidence that novel popout represents an automatic and conceptually-driven form of attention capture and that it is not attributable exclusively to simple feature analysis. We argue that the data undermine certain widespread concepts of attention but are in accord with mismatch theory. The general idea behind mismatch theory is that because the processing of expected inputs can be knowledge-based or conceptually-driven data-driven processing can be inhibited for expected inputs and thereby dedicated to any unexpected inputs. Mismatch theory accommodates our findings and resolves the stability/plasticity dilemma without appealing to the concept of attention as a special gate-keeping device between preattentive and post-attentive processing. Instead, no distinction is drawn between pre-attention and post-attention, and attention is viewed as an emergent phenomenon of ordinary perceptual processes. DTIC

N95-16298# Air Force Inst. of Tech., Wright-Patterson AFB, OH.
THE EFFECTS OF TARGET ORIENTATION ON THE DYNAMIC CONTRAST SENSITIVITY FUNCTION M.S. Thesis
Craig A. Croxton 1994 122 p
(AD-A281855; AFIT/CI/CIA-94-035) Avail: CASI HC A06/MF A02

Much research has been accomplished on the effects of target motion on visual acuity. Research has also been accomplished on the effects of target orientation on visual acuity. The contrast sensitivity function (CSF) also had been studied as a predictor of visual performance under dynamic conditions. However, no previous studies have combined these areas of research and examined the effect of target orientation on the Dynamic Contrast Sensitivity Function (DCSF). DTIC

N95-16299# Air Force Inst. of Tech., Wright-Patterson AFB, OH.
TRAINING VISUAL PATTERN RECOGNITION: USING WORKED EXAMPLES TO AID SCHEMA ACQUISITION M.S. Thesis
Karin L. Nagel Aug. 1993 97 p
(AD-A281859; AFIT/CI/CIA-94-013) Avail: CASI HC A05/MF A02

One challenge faced by those involved in the provision of training is to find methods of instruction which retain flexibility, and therefore provide efficient transfer of skills and the ability to adapt to similiar situations in the future. A goal of this thesis is to provoke the reader to think about the learner's mental software when faced with a task requiring recognition in a dynamic, cluttered visual domain that demands flexibility. For example, how does a quarterback learn to recognize and react appropriately to so many defensive patterns, even ones that he has not seen before? This paper briefly reviews some of the literature pertaining to vision research which illustrates how quickly one can recognize features in a scene. Next, this paper addresses features of perceptual learning, specifically Treisman's feature integration theory, and also reviews the cognitive literature relevant to training for transfer, flexibility and adaptability and applies it to the domain of visual pattern recognition. Particular attention will be given to the role of models, schema or principles in transfer, as well as the role of examples in facilitating schema acquisition and hence transfer. The current study investigated whether the use of worked examples aids in schema development, which is believed to be one possible explanation for flexibility in novel situations. DTIC

N95-16301# Air Force Inst. of Tech., Wright-Patterson AFB, OH.
MENTAL ROTATION WITH AND WITHOUT A CONCURRENT TASK: MODERATING EFFECTS OF VISUOSPATIAL ABILITY M.S. Thesis
Paul K. Daly Apr. 1994 119 p
(AD-A281866; AFIT/CI/CIA-94-074) Avail: CASI HC A06/MF A02

Men (N = 25) and women (N = 27) rated as either high or low in visuospatial ability as assessed on a battery of visuospatial tests (Card Rotations, Mental Rotations, Minnesota Paper Form Board), performed a computer-administered task requiring the mental rotation of abstract geometric shapes presented sequentially, either alone or with a concurrent task of repeating sets of six random digits. Gender and skill-level effects were found. Men were faster than women, and high visuospatial subjects were faster than low. Individual performance did not significantly differ between the single- and dual-task conditions, either in terms of mean response time or rate of mental rotation. DTIC

N95-16368# New York Univ., New York, NY. Dept. of Psychology.
VISUAL NEURAL DEVELOPMENT AND CHROMATIC ABERRATION Final Report, 15 Mar. 1992 - 14 Mar. 1994
Laurence T. Maloney 14 Mar. 1994 4 p
(Contract F49620-92-J-0187)
(AD-A285064; AFOSR-94-0562TR) Avail: CASI HC A01/MF A01

The purpose of the research undertaken was to develop computational techniques and psychophysical methods for investigating the internal representation of visual information (shape, depth and color) in human observers. Some of the equipment needed was not available in Summer 1992. A no-cost one-year extension was requested and granted, and work on the project continued through March 1994. The following is a list of publications and presentations supported in whole or in part by the grant. A list of personnel is also included. DTIC

N95-16377 Hahnemann Medical Coll. and Hospital, Philadelphia, PA. Dept. of Mental Health Sciences.
LOCUS COERULEUS, VIGILANCE AND STRESS: BRAIN MECHANISMS OF ADAPTIVE BEHAVIORAL RESPONSIVENESS Annual Technical Report, 31 Dec. 1992 - 30 Dec. 1993
Gary Aston-Jones 8 Jul. 1994 9 p Limited Reproducibility: More than 20% of this document may be affected by microfiche quality
(Contract F49620-93-1-0099)
(AD-A282450; AFOSR-94-0471TR) Avail: CASI HC A02

We have recorded electrical activity from more than 200 neurons in the locus coeruleus (LC) in two behaving monkeys during the last year. We have made significant technical advances (e.g., use of 10

micrometers-diameter microwires for recordings, increased accuracy of electrode penetrations) which have increased the quality and quantity of data obtained. Results confirm our preliminary findings of the last period, i.e., LC neurons vary activity physically and tonically during a vigilance task indicating a role for the LC system in regulating attentional lability and adaptive responsiveness to urgent stimuli. Moreover, extensive analysis of reversal performance reveals that LC neurons may have a close relationship with cognitive processes underlying stimulus analysis and decision making. Finally, this analysis also reveals that LC neurons alter their responsiveness to stimuli after reversal of cue meaning in advance of corresponding alterations in behavioral responsiveness, indicating that LC neurons may play an important role in early learning processes, helping to 'entrain' other brain systems to respond adaptively to new significant stimuli. DTIC

N95-16433# Air Force Inst. of Tech., Wright-Patterson AFB, OH.
AVIATION SPATIAL ORIENTATION IN RELATIONSHIP TO HEAD POSITION, ATTITUDE INTERPRETATION, AND CONTROL M.S. Thesis
Daryl R. Smith 16 Jun. 1994 112 p
(AD-A281869; AFIT/CI/CIA-94-087) Avail: CASI HC A06/MF A02

Aircraft instrument design theory assumes pilots maintain head alignment with the aircraft during turn and bank maneuvers. As a result, the outside view through the windscreen is thought to be of a moving horizon. The attitude indicator used in today's aircraft displays moving horizon symbology thought to accurately represent pilot spatial orientation. Recently, an optokinetic collic neck reflex was documented which indicates that pilots align their heads with the horizon rather than the axis of the aircraft while manually flying the aircraft. If this is the case, then pilots orient about a fixed rather than moving horizon, implying current attitude instruments inaccurately present spatial information. The purpose of this study was to determine if the optokinetic collic neck reflex has an affect upon pilots while monitoring the autopilot and if so, what that affect is in relation to manual flight. Findings will help determine if the optokinetic collic reflex is transferrable to other flight crewmembers. DTIC

N95-16518# Carnegie-Mellon Univ., Pittsburgh, PA. School of Computer Science.
THE GOMS FAMILY OF ANALYSIS TECHNIQUES: TOOLS FOR DESIGN AND EVALUATION
Bonnie E. John and David E. Kieras 24 Aug. 1994 53 p
(Contracts N00014-89-J-1975; N00014-92-J-1173)
(AD-A285211; CMU-CS-94-181) Avail: CASI HC A04/MF A01

Since the seminal Card, Moran, & Newell (1983) book, 'The Psychology of Human-Computer Interaction,' the concept of the GOMS model has been one of the few widely known theoretical concepts in human-computer interaction. This concept has spawned much research to verify and extend the original concept and has been used in real-world design and evaluation situations. The original presentation of the GOMS concept left substantial room for interpretation and subsequent researchers and practitioners have applied the idea in a variety of ways. While this variety shows that the GOMS concept is fruitful, there is some confusion about the GOMS concept and the various approaches that share this label yet appear to be radically different. This paper synthesizes the previous work on GOMS to provide an integrated view of GOMS models and how they can be used in design. The major variants of GOMS that have matured sufficiently to be used in real-world design and evaluation situations are described and related to the original GOMS proposal and to each other. A single example is used to illustrate all of the techniques. Guidance is provided to practitioners who wish to use GOMS for their design and evaluation problems, and examples of actual applications of GOMS techniques are presented. DTIC

N95-16520# Army Aeromedical Research Lab., Fort Rucker, AL.
VISUAL PERCEPTION IN THE FIELD-OF-VIEW OF PARTIAL BINOCULAR OVERLAP HELMET-MOUNTED DISPLAYS Final Report
Victor Klymenko, Robert W. Verona, Howard H. Beasley, John S. Martin, and William E. McLean Aug. 1994 26 p
(DA Proj. 3M1-62787-A-879)
(AD-A285213; USAARL-94-40) Avail: CASI HC A03/MF A01

Because of limitations in the size of the field-of-view (FOV) available in helmet-mounted displays (HMD) using the full overlap display mode, where the entire FOV is binocular, partial binocular overlaps displays, which can be convergent or divergent, have been proposed. One consequence of this is a perceptual effect known as luning, which is a subjective darkening in the monocular regions of the FOV, which can in some cases cause fragmentation of the FOV into three regions. A concern is, the possible effect on target identification in the monocular regions, particularly in areas affected by luning. We review data we have collected in our binocular vision lab on the effect of display mode one aspects of visual perception. DTIC

N95-16615# Institute for Human Factors TNO, Soesterberg (Netherlands).
SUBSET-SELECTIVITY AND DISTRACTOR MATCHING IN VISUAL CONJUNCTION SEARCH
N. A. Kaptein and J. Theeuwes 25 Apr. 1994 49 p
(AD-A285137; IZF-1994-B-9; TDCK-94-0049) Avail: CASI HC A03/MF A01

In search for a conjunction of color and orientation, Theeuwes, Kaptein and Van der Heijden obtained target absent responses that were in some conditions faster and in other conditions slower than target present responses. In addition, target absent search function slopes were shallower than target present slopes. These findings cannot be explained by present conjunction search theories. Since in the same study Theeuwes et al. demonstrated subset-selectivity in conjunction search, the interdependence of the fast absent responses and subset-selective search needed to be assessed. The present study shows that subset-selective search is independent of the occurrence of fast absent responses. Experiment 1 replicated the findings of Theeuwes et al. Experiment 2 showed that the fast absents were not the result of a response bias. The results of Experiments 3 and 4 showed that the fast absents can be explained by a weak, parallel distractor matching process that enables responding 'target absent' if all relevant distractor elements are similar. Since this process is easily disturbed, the absence of a sameness-signal can not be used for 'target present' decisions. It is argued that both subset-selective search and distractor matching may have occurred unnoticed in previously reported experiments. DTIC

N95-16817# Organisatie voor Toegepast Natuurwetenschappelijk Onderzoek, Soesterberg (Netherlands). Human Factors Research Inst.
PERCEPTUAL SELECTIVITY FOR COLOR AND FORM: ON THE NATURE OF THE INTERFERENCE EFFECT Interim Report
J. Theeuwes 10 May 1994 23 p
(AD-A285338; TNO-TM-1994-B-11; TDCK-94-0053) Avail: CASI HC A03/MF A01

Previous research has shown that search for a shape singleton is disrupted by the presence of an irrelevant color singleton (Theeuwes, 1991b, 1992). These findings have been treated as evidence for the hypothesis that, irrespective of a goal-directed attentional set on part of the observer, attention is unintentionally captured by the most salient singleton. This hypothesis was tested in two experiments in which subjects searched multi-element displays for a shape singleton. Subjects reported the Letter that always appeared inside the target shape singleton (a green diamond). On some trials an irrelevant color singleton was present which contained a Letter that was compatible or incompatible with the Letter inside the target shape. As reported earlier, the presence of an irrelevant color singleton distracted goal-directed search for the shape singleton. The finding that the identity of the Letter inside the distractor affected responding to the Letter inside the target shape, provides support for the hypothesis that attention is captured by the most salient singleton. The identity of the Letter inside the distractor can only affect responding when it is assumed that attention is involuntarily drawn to the Location of the distracting singleton. DTIC

N95-16822# Organisatie voor Toegepast Natuurwetenschappelijk Onderzoek, Delft (Netherlands). Hoofdgroep Maatschappelijke Technologie.
PARALLEL SEARCH FOR A CONJUNCTION OF SHAPE AND CONTRAST POLARITY
J. Theeuwes and F. L. Kooi 1994 15 p
(AD-A285344; TNO-TM-1994-B-6; TDCK-94-0045) Avail: CASI HC A03/MF A01

When a target object embedded in an array of other objects can be distinguished along a single feature dimension (e.g., colour or shape), it can be detected in parallel. When a target object is defined by a conjunction

of stimulus features, search has to be conducted serially, indicating that the visual system is incapable of conducting a parallel search over two stimulus dimensions simultaneously. Earlier research has shown that there are two exceptions to this finding. one dimension can be searched in parallel if the other dimension is stereoscopic depth (Nakayama & Silverman, 1986), or relative motion (McLeod, Driver & Crisp, 1988). We report a third exception: if one dimension involves contrast polarity, another dimension (shape) can be searched in parallel. The neurophysiological implications are discussed. DTIC

N95-16835# Organisatie voor Toegepast Natuurwetenschappelijk Onderzoek, Delft (Netherlands). Hoofdgroep Maatschappelijke Technologie.

A FRAMEWORK FOR THE ANALYSIS OF COGNITIVE TASKS

E. J. Merkelback and J. M. Schraagen 1994 38 p

(AD-A285345; TNO-TM-1994-B-13; TDCK-94-0063) Avail: CASI HC A03/MF A01

The goal of this study was to examine similarities and differences between various types of cognitive task analysis and, if possible, to infer some framework in which the areas for further research should become clear. The result of this study is a framework which integrates three views on cognitive task analysis: task, knowledge and cognitive modelling. For each view, prototypical task analysis techniques are presented respectively: Hierarchical Task Analysis (HTA), Knowledge Analysis and Documentation System (KADS) and Goals Operators Methods and Selection rules (GOMS). The task modelling view and the cognitive modelling view are already known in the cognitive task analysis domain. The task modelling view concentrates on the decomposition of tasks into goals and subgoals. The cognitive modelling view concentrates on the cognitive performance of the task. The knowledge modelling view, however, is a relativeLy new element in the research area of cognitive task analysis. Within the knowledge modelling view, it is recommended by the framework to gain information about the requirements of the task. Those requirements can have a strong influence on the cognitive performance of the task and, therefore, within the framework of cognitive task analysis, it is advised to examine task requirements before starting to analyze the cognitive performance of the task. Further research in this area is therefore necessary to bridge the gap between one sight of the camp, the task modelling view, and the other side of the camp, the cognitive modelling view. An interesting work of research could be to invent a way in which task requirements are acquired in such a way that they, together with the task's goals, can easily be used to make predictions about cognitive performance. DTIC

N95-17175# Michigan Univ., Ann Arbor, MI. Intense Energy Beam Interaction Lab.

ESTIMATING THE BENEFITS OF PERSONNEL SELECTION AND CLASSIFICATION: AN EXTENSION OF THE BROGDEN TABLE Interim Technical Paper, Apr. 1993 - Mar. 1994

William E. Alley and Melody M. Darby Oct. 1994 25 p

(AF Proj. 7719)

(AD-A285674; AL/HR-TP-1994-0010) Avail: CASI HC A03/MF A01

A Monte Carlo study was done to estimate the standardized performance gain (Sigma units) for personnel who have been optimally selected and classified as a function of the number of alternative job assignments, the applicant rejection rate, the validity of the performance estimates, and the intercorrelation among the estimates. The study extended the number of job assignment categories considered to 500 based on a general solution provided by Brogden for up to 10 jobs. Results indicated that adding job categories with zero applicant rejection improved expected performance from 0.0 Sigma units with 1 job to 3.03 Sigma units with 500 jobs. For the highest level of applicant rejection (90%), corresponding gains were 1.75 a units and 3.78 or units respectively. Implications for use of the table were discussed. DTIC

N95-17447 Air Force Inst. of Tech., Wright-Patterson AFB, OH.

CAFFEINE'S INFLUENCE ON CRITICAL FREQUENCY THRESHOLDS M.S. Thesis

John P. Simeroth 11 May 1994 120 p Limited Reproducibility: More than 20% of this document may be affected by microfiche quality

(AD-A282005; AFIT/CI/CIA-94-069) Avail: CASI HC A06

Caffeine's effect on the visual system was investigated. Twelve male and twelve female subjects (aged 18- 25 years) were measured for Critical Flicker Frequency (CFF) thresholds at 15 levels of retinal illuminance (-1.0 to 3.0 log trolands) in each of four caffeine dosage conditions (0, 200mg, 400mg, 600mg). Variables of interest included dosage, gender, left and right eye differences and time after ingestion. Significant results were found for dosage ($p=.000$), gender ($p=.001$) and eye differences ($p=.000$). Interactions were found for gender and dosage ($p=.000$), and gender and eye differences ($p=.043$). DTIC

N95-17530# Washington Univ., Saint Louis, MO. Dept. of Psychology.

BLINKS, SACCADES, AND FIXATION PAUSES DURING VIGILANCE TASK PERFORMANCE. 1: TIME ON TASK Final Report

John A. Stern, Donna Boyer, David Schroeder (Civil Aeromedical Inst., Oklahoma City, OK.), Mark Touchstone (Civil Aeromedical Inst., Oklahoma City, OK.), and Nikolai Stoliarov (State Scientific Research Inst. for Civil Aviation, Moscow, Russia.) Washington Dec. 1994 44 p

(Contract DTFA02-91-C-91056)

(DOT/FAA/AM-94/26) Avail: CASI HC A03/MF A01

In the future, operators of complex equipment will spend more time monitoring computer controlled devices rather than having hands-on control of such equipment. The operator intervenes in system operation under 'unusual' conditions or when there is a computer malfunction. The latter occurs relatively seldom. The operator's task thus becomes a 'vigilance' task, one requiring attention to monitoring equipment with little need for action. An individual's ability to maintain vigilance is easily compromised, with time-on-task (TOT) a major detractor of performance. The question asked in this research was: Can gaze control measures be used to reflect, and hopefully to predict, periods of impaired vigilance? The results of this study clearly demonstrate that a number of aspects of eye movements and eye blinks show significant TOT effects. These effects are, we believe, more likely to be associated with short periods of attentional lapses or 'microsleep'; than with more tonic changes in alertness level. The literature dealing with such measures as indicants of 'fatigue' and/or 'time-on-task' effects is reviewed in considerable detail. The study evaluated aspects of blinking and eye movements in subjects performing the Thackray and Touchstone ATC simulation task. Subjects performed the task for a 2-hour period on 3 separate occasions. Significant increases in blink frequency, blink closing duration, blink flurries, eye closures and fixation pause were obtained as well as similar effects for derivative measures. Though the current data was collected through electrodes attached to the participant, much of the information can be acquired with remote monitoring technologies. This makes possible the application of such measures in a field setting where subjects are required to work on a display terminal. Additional exploration of this approach and the new technologies should provide the information needed to develop strategies and approaches that will enhance operator reliability. Author

N95-17655# Texas Technological Univ., Lubbock, TX. Dept. of Industrial Engineering.

SITUATION AWARENESS INFORMATION REQUIREMENTS FOR EN ROUTE AIR TRAFFIC CONTROL Final Report

Mica R. Endsley and Mark D. Rodgers (Civil Aeromedical Inst., Oklahoma City, OK.) Washington Dec. 1994 37 p Sponsored by FAA

(DOT/FAA/AM-94/27) Avail: CASI HC A03/MF A01

Situation awareness is presented as a fundamental requirement for effective air traffic control, forming the basis for controller decision making and performance. To develop a better understanding of the role of situation awareness in air traffic control, an analysis was performed to determine the specific situation awareness information requirements for air traffic control. This was conducted as a goal-directed task analysis in which the major goals, subgoals, decisions, and associated situation awareness information requirements for enroute air traffic control (ATC) were delineated based on elicitation from eight experienced air traffic control specialists (ATCS's). This effort was supported by available task analyses and video-tapes of simulated ATC tasks. A determination of the major situation awareness information requirements for enroute ATC was developed from this analysis, providing a foundation for future system development which seeks to enhance controller situation awareness and provides a basis for the development of situation awareness measures for air traffic control. Author

N95-16760*# National Aeronautics and Space Administration. Ames Research Center, Moffett Field, CA.
ALERTNESS MANAGEMENT IN TWO-PERSON LONG-HAUL FLIGHT OPERATIONS Abstract Only
M. R. Rosekind and P. H. Gander (San Jose State Univ., Moffett Field, CA.) *In* Aerospace Medical Association, Aerospace Medical Association 63rd Annual Scientific Meeting Program 14 May 1992 1 p (For primary document see N95-16737 04-51)
Avail: CASI HC A01/MF A02

N95-16761*# National Aeronautics and Space Administration. Lyndon B. Johnson Space Center, Houston, TX.
RESULTS OF THE PSYCHIATRIC, SELECT-OUT EVALUATION OF US ASTRONAUT APPLICATIONS Abstract Only
D. M. Faulk (Texas Univ., Galveston, TX.), P. A. Santy (National Aeronautics and Space Administration. Lyndon B. Johnson Space Center, Houston, TX.), A. W. Holland (National Aeronautics and Space Administration. Lyndon B. Johnson Space Center, Houston, TX.), and R. Marsh (Texas Univ., Galveston, TX.) *In* Aerospace Medical Association, Aerospace Medical Association 63rd Annual Scientific Meeting Program 14 May 1992 1 p (For primary document see N95-16737 04-51)
Avail: CASI HC A01/MF A02

N95-16762*# National Aeronautics and Space Administration. Lyndon B. Johnson Space Center, Houston, TX.
VALIDATION OF ASTRONAUT PSYCHOLOGICAL SELECT-IN CRITERIA Abstract Only
R. M. Rose (Texas Univ., Galveston, TX.), R. L. Helmreich (Texas Univ., Austin, TX.), T. McFadden, P. A. Santy, and A. W. Holland *In* Aerospace Medical Association, Aerospace Medical Association 63rd Annual Scientific Meeting Program 14 May 1992 1 p (For primary document see N95-16737 04-51)
Avail: CASI HC A01/MF A02

N95-16763*# National Aeronautics and Space Administration. Lyndon B. Johnson Space Center, Houston, TX.
PSYCHOLOGICAL TRAINING OF NASA ASTRONAUTS FOR EXTENDED MISSIONS Abstract Only
A. W. Holland *In* Aerospace Medical Association, Aerospace Medical Association 63rd Annual Scientific Meeting Program 14 May 1992 1 p (For primary document see N95-16737 04-51)
Avail: CASI HC A01/MF A02

N95-16764*# National Aeronautics and Space Administration. Ames Research Center, Moffett Field, CA.
HUMAN PERFORMANCE IN THE MODERN COCKPIT Abstract Only
R. K. Dismukes and M. M. Cohen *In* Aerospace Medical Association, Aerospace Medical Association 63rd Annual Scientific Meeting Program 14 May 1992 1 p (For primary document see N95-16737 04-51)
Avail: CASI HC A01/MF A02

N95-16765*# National Aeronautics and Space Administration. Ames Research Center, Moffett Field, CA.
CREW DECISION MAKING UNDER STRESS Abstract Only
J. Orasanu *In* Aerospace Medical Association, Aerospace Medical Association 63rd Annual Scientific Meeting Program 14 May 1992 1 p (For primary document see N95-16737 04-51)
Avail: CASI HC A01/MF A02

N95-16766*# National Aeronautics and Space Administration. Ames Research Center, Moffett Field, CA.
COGNITION AND PROCEDURE REPRESENTATIONAL REQUIREMENTS FOR PREDICTIVE HUMAN PERFORMANCE MODELS Abstract Only
K. Corker *In* Aerospace Medical Association, Aerospace Medical Association 63rd Annual Scientific Meeting Program 14 May 1992 1 p (For primary document see N95-16737 04-51)
Avail: CASI HC A01/MF A02

54 MAN/SYSTEM TECHNOLOGY AND LIFE SUPPORT

Includes human engineering; biotechnology; and space suits and protective clothing.

For related information see also *16 Space Transportation.*

N95-16119# Michigan Univ., Ann Arbor, MI. Div. of Research Development and Administration.
THE EPIC ARCHITECTURE FOR MODELING HUMAN INFORMATION-PROCESSING AND PERFORMANCE: A BRIEF INTRODUCTION Interim Report, 1 Jan. 1992 - 1 Apr. 1994
David E. Kieras and David E. Meyer 1 Apr. 1994 21 p
(Contract N00014-92-J-1173)
(AD-A280762; DRDA-TR-94/ONR-EPIC-1) Avail: CASI HC A03/MF A01

EPIC (Executive Process-Interactive Control) is a human information-processing architecture that is especially suited for modeling multiple-task performance. The EPIC architecture includes peripheral sensory-motor processors surrounding a production-rule cognitive processor, and is being used to construct precise computational models for basic multiple-task situations. Some of these models are briefly illustrated here to demonstrate how EPIC applies to multiple-task performance, and helps clarify some basic properties of human performance. Additional applications of EPIC to modeling human-computer interaction are briefly summarized.
DTIC

N95-16145# Army Aeromedical Research Lab., Fort Rucker, AL.
WHOLE-BODY VIBRATION ASSESSMENT OF THE PALLETIZED LOAD SYSTEM Final Report
Al W. Moran, Bradley S. Erickson, Tammy L. Simmons, and Barclay P. Butler Jul. 1994 105 p
(AD-A285181; USAARL-94-33) Avail: CASI HC A06/MF A02

An evaluation of all new tactical vehicles and aircraft is required to assess potential whole-body vibration (WBV) health hazards to crewmembers. As requested by the U.S. Army Environmental Hygiene Agency, a health hazard assessment (HHA) was performed by the U.S. Army Aeromedical Research Laboratory (USAARL) on the Palletized Load System (PLS) truck. The PLS was tested on five cross-country courses at Aberdeen Proving Ground, MD, by the U.S. Army Combat System Test Activity in coordination with the Response and Tolerance Branch of USAARL. The PLS was tested with speeds ranging from 3 to 20 mph. The results of these tests show that, for the worst-case scenario for each course, the lowest tolerances for WBV were on course 5. Less severe WBV occurred on courses 1 and 3, which had near equal tolerances, followed by course 4. Finally, the highest tolerances for WBV exposure were on course 2. The results also show that both driver and passenger were exposed to a Hazard Severity-Category III (marginal), with a Hazard Probability-Level C (occasional).
DTIC

N95-16147# Army Aeromedical Research Lab., Fort Rucker, AL.
WHOLE-BODY VIBRATION ASSESSMENT OF THE M1070 HEAVY EQUIPMENT TRANSPORTER, VOLUME 1
Tammy L. Simmons, Barclay P. Butler, Nabih M. Alem, and Bradley S. Erickson Aug. 1994 29 p
(AD-A285199; USAARL-94-41-Vol-1) Avail: CASI HC A03/MF A01

An evaluation of all new tactical vehicles and aircraft is required to assess potential whole-body vibration (WBV) health hazards to crewmembers. As requested by the U.S. Army Environmental Hygiene Agency (USAEHA), a health hazard assessment (HHA) was performed by the U.S. Army Aeromedical Research Laboratory (USAARL) on the M1070 Heavy Equipment Transporter System (HETS). The HETS was tested on three cross-country courses at Aberdeen Proving Ground (APG), MD, by the U.S. Army Combat Systems Test Activity (USACSTA), in coordination with the Response and Tolerance Branch of USAARL. The M1070 HETS was tested with a M1000 trailer in a loaded and unloaded configuration. The loaded configuration was obtained by placing an M1 tank on the bed of the M1000 trailer. The unloaded configuration consisted of a M1070 tractor with an empty M1000 trailer. While operating the HETS in its intended operational environment, the front passenger was exposed to an

overall risk assessment code of 5. This consisted of an overall assignment of hazard severity category IV and hazard probability level D. DTIC

N95-16418*# Arizona Univ., Tucson, AZ. Dept. of Aerospace and Mechanical Engineering.

THERMAL CONTROL SYSTEMS FOR LOW-TEMPERATURE HEAT REJECTION ON A LUNAR BASE Annual Progress Report

K. R. Sridhar, Matthias Gottmann, and Ashok Nanjundan Nov. 1993 80 p

(Grant NAG5-1572)

(NASA-CR-197486; NAS 1.26:197486) Avail: CASI HC A05/MF A01

One of the important issues in the design of a lunar base is the thermal control system (TCS) used to reject low-temperature heat from the base. The TCS ensures that the base and the components inside are maintained within an acceptable temperature range. The temperature of the lunar surface peaks at 400 K during the 336-hour lunar day. Under these circumstances, direct dissipation of waste heat from the lunar base using passive radiators would be impractical. Thermal control systems based on thermal storage, shaded radiators, and heat pumps have been proposed. Based on proven technology, innovation, realistic complexity, reliability, and near-term applicability, a heat pump-based TCS was selected as a candidate for early missions. In this report, Rankine-cycle heat pumps and absorption heat pumps (ammonia water and lithium bromide-water) have been analyzed and optimized for a lunar base cooling load of 100 kW. Author

N95-16553 Logicon Technical Services, Inc., Dayton, OH.

VISUAL ACUITY VERSUS FIELD-OF-VIEW AND LIGHT LEVEL FOR NIGHT VISION GOGGLES (NVG) Final Report, Nov. 1993 - Apr. 1994

Harry L. Task, Mary M. Donohue-Perry, and Sharon A. Davis May 1994 18 p Limited Reproducibility: More than 20% of this document may be affected by microfiche quality

(AF Proj. 7184)

(AD-A284750; AL/CF-TR-1994-0076) Avail: CASI HC A03

Parameters typically used to characterize night vision goggles (NVG) are visual acuity (resolution) and field-of-view (FOV). An increase in FOV is accomplished by providing higher magnification of the image intensifier tube. However, increased magnification means that the pixels will subtend a larger angle, thus leading to lower NVG visual acuity. An inverse relationship between visual acuity and field-of-view is expected based upon this optical/geometrical relationship. This relationship should be examined as production of NVG resolution quality increases. A trade-off study examining FOV and resolution was conducted with three observers having 20/20 corrected Snellen acuity. The NVGs had fields-of-view of 40, 47, and 52 degrees, respectively. Five levels of ambient scene illumination (corresponding to output luminance levels of 0.01, 0.03, 0.08, 0.26, and 1.4 ft-L) were provided by a 2856K light source. The targets used in the study were 95+% contrast square wave targets ranging in size from 45 cycles/degree to 5 cycles/degree. A walk-back method of adjustment was employed. The results indicate that the geometric relationship between field-of-view and visual acuity is valid. DTIC

N95-16813# Carnegie-Mellon Univ., Pittsburgh, PA. School of Computer Science.

INTEGRATING HUMAN FACTORS WITH SOFTWARE ENGINEERING PRACTICES

William E. Hefley, Elizabeth A. Buie (Computer Sciences Corp., Laurel, MD.), Gene F. Lynch (Tektronix, Inc., Beaverton, OR.), Michael J. Muller (Boulder, CO. Bolder, CO.), Douglas G. Hoecker (Westinghouse Science and Technology Center, Pittsburgh, PA.), Jim Carter (Saskatchewan Univ., Saskatoon.), and J. Thomas Roth (Ergonomics and Safety Technology, Inc., Pittsburgh, PA.) 29 Jul. 1994 11 p Presented at the 38th Annual Meeting of the Human Factors and Ergonomics Society, Nashville, TN, Oct. 1994 See also CMU-HCII-94-103 Submitted for publication

(AD-A285210; CMU-CS-94-175; CMU-HCII-94-103) Avail: CASI HC A03/MF A01

The design and development of human-computer interaction (HCI) has been evolving into a full engineering discipline for achieving system usability-developing systems that support their users in accomplishing their tasks with effectiveness, efficiency, and satisfaction. Advances have been occuring both in user interface engineering, focusing on the processes being used to develop artifacts, and in usability engineering, focusing on the products being developed. Large proportions of these systems are heavily software intensive. System engineering activities must therefore integrate HCI engineering with software engineering to achieve usability in software-intensive systems. This effort can take advantage of successful HCI engineering efforts, which have focused on human factors and HCI methods. DTIC

N95-16821# Organisatie voor Toegepast Natuurwetenschappelijk Onderzoek, Delft (Netherlands). Hoofdgroep Maatschappelijke Technologie.

ENERGY EXPENDITURE, PHYSICAL WORK LOAD AND POSTURAL CONTROL DURING WALKING ON A MOVING PLATFORM

A. H. Wertheim, R. Heus, and T. G. Vrijkotte 1994 30 p

(AD-A285343; TNO-TM-1994-B-8; TDCK-94-0048) Avail: CASI HC A03/MF A01

An experiment was performed in which subjects were required to walk on a treadmill inside a moving ship motion simulator (SMS). Ventilatory measures of energy consumption, heart rate, and measures of postural control were taken and compared to a condition in which the SMS did not move. Eleven SMS movement conditions were investigated, two of which consisted of pure one dimensional sinusoidal movements (vertical motion or roll), two of simulated ship movements, and seven of various combinations of (large or small) vertical, pitch and roll movements, derived from these simulated ship motion profiles. The results showed that energy expenditure was largest in conditions which included either large pitch movements, or Large roll components in combination with pitch. Energy expenditure was intermediate in all other conditions which included Large roll movements. Effects of the particular vertical motions used in the present study, were not observed. in this particular study, physiological task toad (expressed in terms of ventilatory parameters) was shown to increase on average with 15 percent during SMS movements. Heart rate appeared to be a less reliable measure of energy expenditure. Movement induced interruptions (MII,s) of the walking task-a measure of postural control-were most frequent in conditions which included a large roll component. The relevance of this work with respect to the development of work load criteria at sea, for the estimation of a crew's operational capacity, and for ship building design are given, together with some recommendations for further research. DTIC

N95-16875# Dayton Univ. Research Inst., OH.

AN EMPIRICAL APPROACH TO VISUAL DISPLAY PREFERENCE BASED UPON MODULATION TRANSFER FUNCTION AND LUMINANCE Final Report, Sep. 1992 - Jul. 1993

Ronald J. Evans Aug. 1994 80 p

(Contract F33615-90-C-0005)

(AD-A285450; AL/HR-TR-1994-0107) Avail: CASI HC A05/MF A01

The purpose of the present study was to develop a three-dimensional preference space for displays as a function of the display modulation transfer function (MTF) and average display luminance. For any MTF-luminance combination, then, the goal was to generate a point in the third dimension denoting the preference for that pair. A paired comparison experiment was conducted where, on individual trials, observers viewed side-by-side images varying in MTF (5 levels) and average luminance (4 levels). The 5 X 4 = 20 combinations of MTF and luminance could be thought of as 20 filters. Preferences on individual trials were cumulated into empirical preference probability matrices which denoted the probability of preferring any one of the 20 filters over any of the 20 filters. A psychological model of preference, the Bradley-Terry-Luce (BTL) Model was then fit to the matrices in order to estimate a scale value or preference for each of the 20 filters or points in the three-dimensional space. Regression techniques (R(2)=.98) were used to generate a preference surface in the three-dimensional space, from which the preference for any display could be predicted. Additional analyses indicated that not only did ratings differ significantly based upon changes in MTF and luminance, but ratings change significantly (P less than .001) as a function of using different scenery in the images. Finally, in predictive equations generated from the data, changes in MTF area (measured in percent contrast x cycles per degree of visual angle) tended to have about three times as much effect on preference as did changes in luminance (measured in foot lamberts). DTIC

N95-16894*# Georgia Tech Research Inst., Atlanta, GA. School of Textile and Fiber Engineering.

DESIGN AND TECHNICAL SUPPORT FOR DEVELOPMENT OF A MOLDED FABRIC SPACE SUIT JOINT Final Report, 1 Oct. 1992 - 31 Dec. 1994

L. Howard Olson 21 Dec. 1994 6 p

(Grant NAG2-806; Proj. E27-666)

(NASA-CR-197521; NAS 1.26:197521) Avail: CASI HC A02/MF A01

NASA Ames Research Center has under design a new joint or element for use in a space suit. The design concept involves molding a fabric to a geometry developed at Ames. Unusual characteristics of this design include the need to produce a fabric molding draw ratio on the order of thirty percent circumferentially on the surface. Previous work done at NASA on molded fabric joints has shown that standard, NASA qualified polyester fabrics as are currently available in the textile industry for use in suits have a maximum of about fifteen percent draw ratio. NASA has done the fundamental design for a prototype joint and of a mold which would impart the correct shape to the fabric support layer of the joint. NASA also has the capability to test a finished product for suitability and reliability. Responsibilities resting with Georgia Tech in the design effort for this project are textile related, namely fiber selection, fabric design to achieve the properties of the objective design, and determining production means and sources for the fabrics. The project goals are to produce a prototype joint using the NASA design for evaluation of effectiveness by NASA, and to establish the sources and specifications which would allow reliable and repeatable production of the joint. Author

N95-16953# Technische Univ., Delft (Netherlands).

EFFICIENCY IN WORK BEHAVIOUR: A DESIGN APPROACH FOR MODERN TOOLS Ph.D. Thesis

F. R. H. Zijlstra 23 Nov. 1993 189 p

(PB94-197761; ISBN-90-6275-918-1) Avail: CASI HC A09/MF A02

The study described in the book aims at presenting a scientific contribution to the (re)design of modern tools, i.e. personal computers. Some general principles of behavior economics are described and the concepts of psychological costs and psychological efficiency are developed. Certain theoretical viewpoints on mental effort are looked at. Several methods and instruments for measuring mental workload and mental effort are discussed. The validity of the Rating Scale Mental Effort (RSME) is explicitly examined in a laboratory study. A study is described in which the RSME is applied in an interface evaluation study. This study aims at collecting empirical evidence for the validity of the Action Facilitation Approach (AFA). The results contain several leads for designers and can therefore be seen as an illustration of the necessity of an interdisciplinary approach to system design. NTIS

N95-16966# Chicago Univ., Chicago, IL. Dept. of Computer Science.

QUALITATIVE VISION AND ACTION Annual Report

R. J. Firby and Michael J. Swain 23 Apr. 1994 34 p

(Contract N00014-93-1-0332)

(AD-A282697) Avail: CASI HC A03/MF A01

The objective of the Animate Agent Project is to understand both the basic motor and visual skill required to support robot behavior in a mixed man-machine environment and the planning techniques reuired to combine and coordinate those skills. As mobile robots and other complex machines are deployed in the world, the will come into contact with human beings and will have to be able to function in environments designed primarily for human use. It is imperative that the machines be capable of interacting with these environments and the people within them effectively and cooperatively. Our approach is built around a robot architecture that uses reactive planning, active perception and behavioral ocntr. The RAP reactive execution system selects actions to execute at run time based on an agent's goals and an understanding of the immediate situation. Making action decisions after situations actually unfold ensures that the decisions are based on what is really happening and gives tremendous flexibility in the face of bad information, actuator failure, and unexpected events. Derived from text

N95-17468 Technische Univ., Delft (Netherlands). Faculteit der Werktuigbouwkunde en Maritieme Techniek.

TOWARDS A HUMAN OPERATOR MODEL OF THE NAVIGATOR Ph.D. Thesis

R. Papenhuijzen 15 Feb. 1994 187 p

(PB94-197985; ISBN-90-370-0096-7) Copyright Avail: Issuing Activity

The study is aimed at investigating the feasibility of a general purpose human operator model of the navigator. Maneuvering issues in the realm of fairway design and fairway regulation and legislation are met in sea navigation as well as in inland waterway navigation. Consequently, it was decided that the field of application of the navigator model to spring from the study should range from navigating large deep-sea vessels to steering small inland vessels. The common factor is that practically always the waterway is more or less confined in relation to the dimensions and maneuvering characteristics of the vessel concerned. Further, for a human operator model of the navigator to be of any practical relevance, it is necessary that a variety of strategic and tactical aspects of the navigator's behavior be covered by the navigator model, in a clearly distinguished way. To be more precise, explicit modeling of planning, control and state estimation behavior is expected to be indispensable. An isolated navigator model, not coupled or fit to be coupled to suitable models of a ship and a fairway, is of no use. And what is more, it would be impossible for such a model to come into existence, every possibility to test or validate it being excluded. So, building a prototype navigator model inevitably implies the creation of a testing environment to complement it, thus arriving at a complete navigation simulation facility. NTIS

N95-17484# Army Aeromedical Research Lab., Fort Rucker, AL.

APACHE HELICOPTER SEAT CUSHION EVALUATION Final Report

Barclay P. Butler and Nabih M. Alem Jul. 1994 61 p

(AD-A284300; USAARL-94-32) Avail: CASI HC A04/MF A01

Two prototypes of the AH-64 pilot seat cushions were evaluated against the standard cushion set by each of a group of 12 AH-64 instructor pilots after being exposed to simulated AH-64 vibration signatures for a period of 1 hour. Objective indications of vibration attenuation were obtained by measuring transfer functions across each cushion. Subjective pilot preferences also were obtained after each ride using a questionnaire. Results of the objective measurements indicate both the air-filled and the foam-filled prototypes reduced low-frequency transmission of vibration better than the standard cushions. Subjective responses indicate significant improvement in comfort and vibration absorption for the seat back and bottom cushions of both prototypes over the standard cushion set. DTIC

N95-15984*# Tokyo Metropolitan Univ. (Japan). Precision and Intelligence Lab.

A VIRTUAL WORK SPACE FOR BOTH HANDS MANIPULATION WITH COHERENCY BETWEEN KINESTHETIC AND VISUAL SENSATION

Masahiro Ishii, P. Sukanya, and Makoto Sato *In* NASA. Johnson Space Center, ISMCR 1994: Topical Workshop on Virtual Reality. Proceedings of the Fourth International Symposium on Measurement and Control in Robotics Nov. 1994 p 84-90 (For primary document see N95-15972 04-63)

Avail: CASI HC A02/MF A02

N95-16755*# National Aeronautics and Space Administration. Lyndon B. Johnson Space Center, Houston, TX.

COMPARISONS OF THREE ANTI-G SUIT CONFIGURATIONS DURING LONG DURATION, LOW ONSET, +Gz Abstract Only

B. J. Stegmann (Krug Life Sciences, Inc., San Antonio, TX.), R. W. Krutz (Krug Life Sciences, Inc., San Antonio, TX.), R. R. Burton (Air Force Systems Command, Brooks AFB, TX.), and C. F. Sawin *In* Aerospace Medical Association, Aerospace Medical Association 63rd Annual Scientific Meeting Program 14 May 1992 1 p (For primary document see N95-16737 04-51)

Avail: CASI HC A01/MF A02

N95-16767*# National Aeronautics and Space Administration. Ames Research Center, Moffett Field, CA.

BEYOND THE COCKPIT: THE VISUAL WORLD AS A FLIGHT INSTRUMENT Abstract Only

W. W. Johnson, M. K. Kaiser, and D. C. Foyle *In* Aerospace Medical Association, Aerospace Medical Association 63rd Annual Scientific Meeting Program 14 May 1992 1 p (For primary document see N95-16737 04-51)

Avail: CASI HC A01/MF A02

N95-16773*# Krug Life Sciences, Inc., Houston, TX.
A PROTOTYPE CREW MEDICAL RESTRAINT SYSTEM (CMRS) FOR SPACE STATION FREEDOM Abstract Only
S. L. Johnston, F. T. Eichstadt, and R. D. Billica *In* Aerospace Medical Association, Aerospace Medical Association 63rd Annual Scientific Meeting Program 14 May 1992 1 p Sponsored by NASA. Lyndon B. Johnson Space Center, Houston, TX (For primary document see N95-16737 04-51)
Avail: CASI HC A01/MF A02

N95-16775*# National Aeronautics and Space Administration. Lyndon B. Johnson Space Center, Houston, TX.
ADVANCED CARDIAC LIFE SUPPORT (ACLS) UTILIZING MAN-TENDED CAPABILITY (MTC) HARDWARE ONBOARD SPACE STATION FREEDOM Abstract Only
M. Smith, M. Barratt, and C. Lloyd *In* Aerospace Medical Association, Aerospace Medical Association 63rd Annual Scientific Meeting Program 14 May 1992 1 p Prepared in cooperation with Krug Life Sciences, Inc., Houston, TX (For primary document see N95-16737 04-51)
Avail: CASI HC A01/MF A02

N95-16778*# National Aeronautics and Space Administration. Ames Research Center, Moffett Field, CA.
ARTIFICIAL GRAVITY: HOW MUCH, HOW OFTEN, HOW LONG? Abstract Only
R. Burton (Air Force Systems Command, Brooks AFB, TX.) and J. Vernikos *In* Aerospace Medical Association, Aerospace Medical Association 63rd Annual Scientific Meeting Program 14 May 1992 1 p Prepared in cooperation with Aerospace Medical Research Labs., Brooks AFB, TX (For primary document see N95-16737 04-51)
Avail: CASI HC A01/MF A02

55 SPACE BIOLOGY

Includes exobiology; planetary biology; and extraterrestrial life.

No abstracts in this category.

59 MATHEMATICAL AND COMPUTER SCIENCES (GENERAL)

N95-16898*# Institute for Computer Applications in Science and Engineering, Hampton, VA.
ICASE Semiannual Report, 1 Apr. - 30 Sep. 1994
NASA Oct. 1994 122 p
(Contracts NAS1-19480; NAS1-18605; NAS1-18107; NAS1-17070; NAS1-17130; NAS1-15810; NAS1-16394; NAS1-14101; NAS1-14472; RTOP 505-90-52-01)
(NASA-CR-195001; NAS 1.26:195001) Avail: CASI HC A06/MF A02
This report summarizes research conducted at the Institute for Computer Applications in Science and Engineering in the areas of (1) applied and numerical mathematics, including numerical analysis and algorithm development; (2) theoretical and computational research in fluid mechanics in selected areas of interest, including acoustics and combustion; (3) experimental research in transition and turbulence and aerodynamics involving Langley facilities and scientists; and (4) computer science.
Author (revised)

60 COMPUTER OPERATIONS AND HARDWARE

Includes hardware for computer graphics, firmware, and data processing.
For components see *33 Electronics and Electrical Engineering.*

N95-16618# California Univ., Berkeley, CA. Dept. of Electrical Engineering and Computer Science.
ANATOMY OF A SILICON COMPILER
Robert W. Brodersen, ed. 4 Oct. 1994 376 p
(Contract N00039-87-C-0182)
(AD-A285395) Avail: CASI HC A17/MF A03
Part 1 - framework and design entry; Part 2 - silicon assembly; Part 3- verification and testing; Part 4 - behavioral synthesis; Part 5 - applications.
DTIC

N95-16876# Texas Univ., El Paso, TX. Dept. of Electrical Engineering.
INVESTIGATION OF MODULARLY CONFIGURED ATTACHED PROCESSORS WITH INTELLIGENT MEMORIES Semiannual Report, 1 Apr. - 31 Sep. 1994
30 Sep. 1994 42 p
(Contract N00014-93-1-1343)
(AD-A285454) Avail: CASI HC A03/MF A01
A new architecture for high-performance parallel attached processors is described in this paper. Based on this architecture, an attached processor can be implemented as multiple memory-to-memory pipelines, each being constructed with a class of fundamental components. The unique features are that the attached processor can be configured to match a set algorithm and its memory controllers can be programmed to fit the access patterns required by the algorithms. As a result, high utilization of the processing logic for the given sets of algorithms can be obtained. An example based on matrix multiplication is used for illustration. Finally, design issues related to the implementation of the attached processor based on an MCM technology are discussed.
DTIC

N95-17400* National Aeronautics and Space Administration. Pasadena Office, CA.
HIGHLY PARALLEL RECONFIGURABLE COMPUTER ARCHITECTURE FOR ROBOTIC COMPUTATION HAVING PLURAL PROCESSOR CELLS EACH HAVING RIGHT AND LEFT ENSEMBLES OF PLURAL PROCESSORS Patent
Amir Fijany, inventor (to NASA) (Jet Propulsion Lab., California Inst. of Tech., Pasadena, CA.) and Antal K. Bejczy, inventor (to NASA) (Jet Propulsion Lab., California Inst. of Tech., Pasadena, CA.) 1 Nov. 1994 12 p Filed 10 Jun. 1991
(NASA-Case-NPO-17632-1-CU; US-Patent-5,361,367; US-Patent-Appl-SN-712796; US-Patent-Class-395-800; US-Patent-Class-395-375; US-Patent-Class-364-DIG.1; US-Patent-Class-364-231.9; Int-Patent-Class-G06F-9/00; Int-Patent-Class-G06F-15/16) Avail: US Patent and Trademark Office
In a computer having a large number of single-instruction multiple data (SIMD) processors, each of the SIMD processors has two sets of three individual processor elements controlled by a master control unit and interconnected among a plurality of register file units where data is stored. The register files input and output data in synchronism with a minor cycle clock under control of two slave control units controlling the register file units connected to respective ones of the two sets of processor elements. Depending upon which ones of the register file units are enabled to store or transmit data during a particular minor clock cycle, the processor elements within an SIMD processor are connected in rings or in pipeline arrays, and may exchange data with the internal bus or with neighboring SIMD processors through interface units controlled by respective ones of the two slave control units.
Official Gazette of the U.S. Patent and Trademark Office

N95-16477*# National Aeronautics and Space Administration. Langley Research Center, Hampton, VA.
HARDWARE DESCRIPTION LANGUAGES
Jerry H. Tucker *In its* The Role of Computers in Research and Development at Langley Research Center Oct. 1994 p 536-545 (For primary document see N95-16453 04-62)
Avail: CASI HC A02/MF A06

N95-17558*# Vitrociset S.p.A., Rome (Italy).
TOWARDS AN INTEGRAL COMPUTER ENVIRONMENT SUPPORTING SYSTEM OPERATIONS ANALYSIS AND CONCEPTUAL DESIGN
E. Barro, A. DelBufalo, and F. Rossi *In* NASA. Goddard Space Flight Center, Third International Symposium on Space Mission Operations and Ground Data Systems, Part 2 Nov. 1994 p 905-913 (For primary document see N95-17531 04-17)
Avail: CASI HC A02/MF A06

61 COMPUTER PROGRAMMING AND SOFTWARE

Includes computer programs, routines, alogorithms, and specific applications, e.g., CAD/CAM.

N95-15995# Naval Postgraduate School, Monterey, CA.
MULTIGRID METHODS IN NETWORK OPTIMIZATION: OVERVIEW AND APPRAISAL M.S. Thesis
Javier Nieto Mar. 1994 161 p
(AD-A280992) Avail: CASI HC A08/MF A02

Multigrid methods have been traditionally applied to the solution of certain partial differential equations. However, applications in control theory, optimization, pattern recognition, computational tomography, and particle physics are beginning to appear. This thesis analyzes the application of multigrid methodology to optimization problems. The work is centered on networks. Transportation problems are chosen frequently as reference because they have been the object of some multigrid research. The goal is to establish a basis for development of multigrid-based algorithms. Optimality conditions in linear programming and networks are reviewed, and a compilation of various multilevel approaches in optimization is presented. Emphasis is on the recent scaling techniques; they add some special insights into solving large network problems efficiently using progressive level of detail. An analysis of the difficulties that these problems present to the multigrid approach reveals that perhaps some abstraction is appropriate when interpreting multigrid components applied to optimization problems (in particular, the concept of grid itself). The idea of implicit ordering is developed and associated with the effectiveness of the multigrid method. These concepts are applied to identify problems that can be solved using multigrid. Finally, suggestions for the development of future multigrid-based algorithms are provided. DTIC

N95-15997# Naval Postgraduate School, Monterey, CA.
INTEGRATING COMPUTERS INTO CALCULUS INSTRUCTION M.S. Thesis
Jon L. Christensen and Brian E. Pierson Mar. 1994 109 p
(AD-A280996) Avail: CASI HC A06/MF A02

Visualization is key in helping a student understand the fundamentals of calculus. The new generation of computer literate students, raised in a video-based environment, will expect more than the traditional chalkboard methods in assisting them in this visualization. By integrating computers into the classroom and developing software to assist in mathematics instruction, we can enhance student comprehension of, and ability to apply, mathematics in solving real world problems of interest to the military. As evidenced by the success of both the Apple Macintosh and Windows software, mouse driven, graphical user interfaces (GUI's) represent a powerful and frequently-used tool in the computing environment. GUI's improve the visual capabilities in computing software, simplify program execution, and reduce the time required to become proficient with the software. When designed correctly, the GUI-based software can significantly improve the way in which people interact with computers. This thesis lays the framework and develops multiplatform GUI software modules needed for the instruction of calculus. DTIC

N95-16003# Rome Lab., Griffiss AFB, NY.
PARALLEL IMPLEMENTATION OF THE TERRAIN MASKING ALGORITHM Report, May 1991 - Dec. 1993
Milissa M. Benincasa Mar. 1994 73 p
(AD-A281017; RL-TR-94-34) Avail: CASI HC A04/MF A01

The terrain masking algorithm is a key algorithm used in battle management and mission planning in choosing the optimal location site for mobile radar and jammer systems. This algorithm calculates the region of clear line-of-sight at a particular altitude for an emitting device. Currently, to calculate the site for one radar or jammer system it can take up to eight hours running on a uniprocessor system. This is unacceptable because it increases the time and cost involved in the planning of a successful mission strategy. A solution to this problem is to utilize a parallel architecture and modify the existing sequential version of the terrain masking algorithm so that it can effectively execute in parallel. The approach presented uses the transputer architecture for executing the algorithm. This architecture was selected because it allows the simulation of a number of MIMD message passing architecture topologies, without having to drastically rewrite the parallel implementation of the algorithm. The approach for parallelizing the terrain masking algorithm involves reverse engineering the sequential version. The algorithm decomposition involved defining the data dependencies inherent in the sequential version so that the data can be properly partitioned for parallel execution. DTIC

N95-16004# Clarkson Univ., Potsdam, NY. Dept. of Electrical and Computer Engineering.
COMMUNICATION NETWORK SOFTWARE ANALYSIS Final Technical Report, Jun. 1992 - Dec. 1993
Robert A. Meyer and David A. Perreault Jun. 1994 18 p Prepared in cooperation with Boston Univ., MA
(Contract F30602-92-C-0083)
(AD-A281019; RL-TR-94-67) Avail: CASI HC A03/MF A01

Synchronous (or simultaneous) program execution (SPE) is a technique that allows the same program to run synchronously on geographically separated computers. However, the results generated appear to the user at the different sites as if the users are sitting in front of the same computer. The difference between the SPE technique and the distributed systems techniques is that with the SPE technique the same execution takes place at each computer, while with distributed systems techniques, parts of one program execute on different computers. The SPE technique can be used in reducing communications in cases such as computer conferencing. The SPE technique is based on the creation of a shell running at each computer and the transmission of messages between the shells. Only a low bandwidth line connects the computer systems. The shell is constructed at each computer system, in software, and resides between the operating system and the executing program and between the entering inputs and the operating systems. This paper presents and analyzes Petri nets that model the synchronization of simultaneous program execution between two computers. The analysis of the Petri nets indicates proper operation of the system. DTIC

N95-16040# Rochester Univ., NY. Dept. of Computer Science.
PROPERTIES OF MULTIHEAD TWO-WAY PROBABILISTIC FINITE AUTOMATA
Ioan I. Macarie Aug. 1994 21 p Revised
(Grant NSF CDA-88-22724)
(TR-477) Avail: CASI HC A03/MF A01

We present properties of multihead two-way probabilistic finite automata that parallel those of their deterministic and nondeterministic counterparts. We define multihead probabilistic finite automata with log-space constructible transition probabilities, and we describe a simple technique to simulate these automata by standard log-space probabilistic Turning machines. Next, we represent log-space probabilistic complexity classes as proper hierarchies based on corresponding multihead two-way probabilistic finite automata, and we show their (deterministic log-space) reducibility to the second levels of these hierarchies. We relate the number of heads of a multihead probabilistic finite automaton to the bandwidth of its configuration transition matrix for an input string; partially based on this relation, we find an apparently easier log-space complete problem for PL (the class of languages recognized by log-space unbounded-error probabilistic Turning machines), and we investigate possibilities for a space-efficient deterministic simulation of probabilistic automata. Author

N95-16088*# Illinois Univ., Urbana, IL. Coordinated Science Lab.
A GRAPHICAL ENVIRONMENT FOR OBJECT-ORIENTED SIMULATION MODEL ENVIRONMENT M.S. Thesis
Daniel Paul Olson 15 Jun. 1994 48 p Sponsored by NASA. Langley

Research Center, ONR and Computer Sciences Corp.
(NASA-CR-196887; NAS 1.26:196887; AD-A281080; UILU-ENG-94-2225; CRHC-94-11) Avail: CASI HC A03/MF A01

This thesis contains an overview of the work that has been done to develop GRIND (a graphical interface for DEPEND), which is also a design environment and code generator. GRIND's major features are described, and a general tutorial shows how to use the tool to create simulation models. Three models that were constructed using GRIND are presented to illustrate the utility of the tool. Remarks on how the work can be extended are included. DTIC

N95-16107 Wright Lab., Wright-Patterson AFB, OH.
DETAILED EXAMPLE OF USING PIWG ON THE SUN WORKSTATION AND THE DEC VAX COMPUTER Final Report, 6-18 Jun. 1993
Steven A. Davidson Dec. 1993 125 p Limited Reproducibility: More than 20% of this document may be affected by microfiche quality
(AF Proj. 2853)
(AD-A281528; WL-TR-94-1049) Avail: CASI HC A06

This report is a laboratory user's guide for evaluating performance of ADA compilers using the Association of Computing Machinery's (ACM) Performance Issues Working Group (PIWG) benchmarking test suite. The report covers the August 1, 1990 version PIWG suite. Part 1 of the report presents a detailed step-by-step instruction for installing these tests on a SUN workstation using a UNIX operating system, and performing an evaluation of a SPARCAda compiler. Part 2 of the report covers installation and execution of costs on the Wright Laboratory WL/AAAF VAX/4000 cluster. Results include recommendations for future work: optimization for avionics' functions by identification, selection, and execution of test subsets appropriate to specific functions, such as navigation, weapon delivery, and electronic warfare; modification of UNIX script files so that execution is completely automatic; computation of averages and variabilities of test results; and adding graphics to show comparisons of various Ada compilers. DTIC

N95-16149# Naval Postgraduate School, Monterey, CA.
A SURVEY OF THE SOFTWARE REUSE ENVIRONMENT: A STUDY FOR THE NSRS M.S. Thesis
Edward G. Bryant Mar. 1994 96 p
(AD-A280867) Avail: CASI HC A05/MF A01

This study investigates the needs of software developers in the area of software reuse. The study formulates recommendations on how a software repository can meet the needs of the software development community. The Naval Software Reuse System (NSRS) is the focus of this research and the findings are intended for their use. The study focuses on eight core questions that are the central issues for the NSRS. On the basis of these eight core questions, a survey was developed that elicited the opinions of Department of the Navy software developers. The analysis of the survey provides conclusions for seven of the eight core questions. These conclusions lead to recommendations that for the most part are completely within the control of Naval Computers and Telecommunications Station (NCTS) Washington, the agency presently building the NSRS. DTIC

N95-16153# Naval Postgraduate School, Monterey, CA. Dept. of Computer Science.
AUTOMATION SUPPORT FOR CONCURRENT SOFTWARE ENGINEERING Interim Technical Report
Salah Badr and M. S. Luqi 1994 23 p
(Contract ARO-MIPR-145-91)
(AD-A281372; ARO-28328.16-MA) Avail: CASI HC A03/MF A01

This paper presents an evolution control system that provides automated assistance for the software evolution process in an uncertain environment where designer-tasks and their properties are always changing. We view an evolution control system (ECS) as the agent that keeps track of proposed, ongoing, and completed changes to a software system. It provides automated assistance to the software evolution manager to help him/her make the right decisions. It automatically propagates change consequences by constructing the set of possibly affected modules. It also coordinates change implementation activities within the design team in a way that supports team work and maintains system integrity as well as adapting itself to the dynamic nature of the evolution process where new changes arrive randomly and ongoing modifications are themselves subject to change as more information becomes available. DTIC

N95-16154 Naval Postgraduate School, Monterey, CA. Dept. of Computer Science.
SOFTWARE MERGE: SEMANTICS OF COMBINING CHANGES TO PROGRAMS Interim Technical Report
Valdis Berzins 1994 30 p Limited Reproducibility: More than 20% of this document may be affected by microfiche quality
(Contract ARO-MIPR-145-91)
(AD-A281373; ARO-28328.15-MA) Avail: CASI HC A03

We present a language-independent semantic model of the process of combining changes to programs. This model extends the domains used in denotational semantics (complete partial orders) to Boolean algebras, and represents incompatible modifications as well as compatible extensions. The model is used to define the intended semantics of change merging operations on programs and to establish some general properties of software merging. We determine conditions under which changes to subprograms of a software system can be merged independently and illustrate cases where this is not possible. DTIC

N95-16167# Boeing Co., Seattle, WA. Defense and Space Group.
STARS CONCEPTUAL FRAMEWORK FOR REUSE PROCESS (CFRP). VOLUME 1: DEFINITION, VERSION 3.0
25 Oct. 1993 97 p Prepared for Air Force Systems Command, Hanscom AFB, MA
(Contract F19628-93-C-0130)
(AD-A281506) Avail: CASI HC A05/MF A02

This document supercedes an earlier Conceptual Framework for Reuse Process (CFRP) definition document and describes a new version of the CFRP. The document has been retitled to more directly reflect its CFRP subject matter, but the version sequencing has been retained. DTIC

N95-16219# Los Alamos National Lab., NM.
AN INVESTIGATION OF GENETIC OPERATORS FOR CONTINUOUS PARAMETER SPACE
T. Grossman and Y. Davidor (Weizmann Inst. of Science, Rehovot, Israel.) Mar. 1994 11 p Presented at the 3rd International Conference on Evolutionary Computation: Parallel Problem Solving From Nature, Jerusalem, Israel, 9-14 Oct. 1994
(Contract W-7405-eng-36)
(DE94-009364; LA-UR-94-895; CONF-941058-1) Avail: CASI HC A03/MF A01

The success of a genetic optimization algorithm in continuous parameter space depends on the recombination (crossover) operators that it uses. We consider a wide spectrum of such operators within a unified framework and study their relative importance in the search process. We consider four basic types of recombination operators which cover the relevant exploration potential of a continuous space: interpolation, extrapolation, exchange, and mutation. Each of these basic types may have several variants. We characterize the various operators and their variants by their spatial sampling properties and examine their contributions to the search by applying different mixtures of the operators in several benchmark problems. The results suggest that the optimal mixture of operators may depend on the problem. But, in general, all basic types are needed for efficient optimization. DOE

N95-16220# Lawrence Livermore National Lab., Livermore, CA.
SORTING AND HARDWARE ASSISTED RENDERING FOR VOLUME VISUALIZATION
C. Stein, B. Becker, and N. Max Mar. 1994 10 p Presented at the Visualization 1994, Washington, DC, 17-21 Oct. 1994
(Contract W-7405-eng-48)
(DE94-010204; UCRL-JC-116229; CONF-941085-2) Avail: CASI HC A02/MF A01

We present some techniques for volume rendering unstructured data. Interpolation between vertex colors and opacities is performed using hardware assisted texture mapping, and color is integrated for use with a volume rendering system. We also present an O(n(exp 2)) method for sorting n arbitrarily shaped convex polyhedra prior to visualization. It generalizes the Newell, Newell and Sancha sort for polygons to 3-D volume elements. DOE

N95-16223# Los Alamos National Lab., NM.
FAST STEREOSCOPIC IMAGES WITH RAY-TRACED VOLUME RENDERING
S. J. Adelson and C. D. Hansen 1994 18 p Presented at the Visualization 1994, Washington, DC, 17-21 Oct. 1994
(Contract W-7405-eng-36)
(DE94-011703; LA-UR-94-1250; CONF-941085-3) Avail: CASI HC A03/MF A01

One of the drawbacks of standard volume rendering techniques is that is it often difficult to comprehend the three-dimensional structure of the volume from a single frame; this is especially true in cases where there is no solid surface. Generally, several frames must be generated and viewed sequentially, using motion parallax to relay depth. Another option is to generate a single spectroscopic pair, resulting in clear and unambiguous depth information in both static and moving images. Methods have been developed which take advantage of the coherence between the two halves of a stereo pair for polygon rendering and ray-tracing, generating the second half of the pair in significantly less time than that required to completely render a single image. This paper reports the results of implementing these techniques with parallel ray-traced volume rendering. In tests with different data types, the time savings is in the range of 70 to 80%. DOE

N95-16234 Software Options, Inc., Cambridge, MA.
IMPROVING PRODUCTIVITY IN THE DEVELOPMENT OF LARGE SOFTWARE SYSTEMS Final Report
17 Feb. 1994 6 p Limited Reproducibility: More than 20% of this document may be affected by microfiche quality
(Contract N00014-85-C-0710)
(AD-A282270) Avail: CASI HC A02

The project began with a re-examination of the roles and boundaries of programming languages and environments. The belief was that present technology was a result of historical drift rather than technical foresight. The expectation was that a fresh look at modern hardware and programming practices would result in significantly better languages and environments. The results would, for example, reduce redundant effort and increase automation of implicit tasks, in order to allow the programmer to focus on the content of a problem. These are vague and lofty goals but our plan was specific and concrete. We developed appropriate formal underpinnings on which we based the implementation of infrastructures for developing languages and environments. We used the infrastructures to design and implement a new language and environment, called E-L. DTIC

N95-16236 Massachusetts Inst. of Tech., Cambridge. Artificial Intelligence Lab.
EXAMPLE BASED IMAGE ANALYSIS AND SYNTHESIS
David Beymer, Amnon Shashua, and Tomaso Poggio Nov. 1993 22 p Limited Reproducibility: More than 20% of this document may be affected by microfiche quality
(Contracts N00014-91-J-1270; N00014-92-J-1879)
(AD-A282285; AI-M-1431) Avail: Issuing Activity (Defense Technical Information Center (DTIC))

Image analysis and graphics synthesis can be achieved with learning techniques using direct image examples without physically-based, 3D models. In our technique: (1) the mapping from novel images to a vector of 'pose' and 'expression' parameters can be learned from a small set of example images using a function approximation technique that we call an analysis network and (2) the inverse mapping from input 'pose' and 'expression' parameters to output images can be synthesized from a small set of example images and used to produce new images using a similar synthesis network. The techniques described here have several applications in computer graphics, special effects, interactive multimedia, and very low bandwidth teleconferencing. DTIC

N95-16306 Carnegie-Mellon Univ., Pittsburgh, PA. School of Computer Science.
A STRUCTURED TCP IN STANDARD ML
Edoardo S. Biagioni Jul. 1994 19 p Limited Reproducibility: More than 20% of this document may be affected by microfiche quality
(Contract F19628-91-C-0168; ARPA Order 8313)
(AD-A282711; CMU-CS-94-171) Avail: CASI HC A03

This paper describes the design of an implementation of the Transmission Control Protocol using an extension of the Standard ML (SML) language. SML supports higher-order functions, modularity, and type-safe module composition. We find that by using SML we can achieve good structure and good performance simultaneously. Good structure includes a modular decomposition of the protocol stack and of the TCP implementation, a control structure that imposes a total ordering on all events and processes them synchronously, and a test structure that allows component testing to catch problems before system integration. Strategies that help achieve good performance include using fast algorithms, using language constructs that make it easy to stage function evaluation, and language implementation features such as compacting garbage collection. DTIC

N95-16358# Sandia National Labs., Albuquerque, NM.
MAGENCO: A MAP GENERALIZATION CONTROLLER FOR ARC/INFO
J. H. Ganter and J. W. Cashwell 1994 12 p Presented at the 14th Annual Environmental Systems Research Institute (ESRI) Users Conference, Palm Springs, CA, 23-27 May 1994
(Contract DE-AC04-94AL-85000)
(DE94-013440; SAND-94-0919C; CONF-9405164-2) Avail: CASI HC A03/MF A01

The Arc/Info GENERALIZE command implements the Douglas-Peucker algorithm, a well-regarded approach that preserves line 'character' while reducing the number of points according to a tolerance parameter supplied by the user. The authors have developed an Arc Macro Language (AML) interface called MAGENCO that allows the user to browse workspaces, select a coverage, extract a sample from this coverage, then apply various tolerances to the sample. The results are shown in multiple display windows that are arranged around the original sample for quick visual comparison. The user may then return to the whole coverage and apply the chosen tolerance. They analyze the ergonomics of line simplification, explain the design (which includes an animated demonstration of the Douglas-Peucker algorithm), and discuss key points of the MAGENCO implementation. DOE

N95-16446# Carnegie-Mellon Univ., Pittsburgh, PA. Dept. of Computer Science.
PROCEDURE CALLS ARE THE ASSEMBLY LANGUAGE OF SOFTWARE INTERCONNECTION: CONNECTORS DESERVE FIRST-CLASS STATUS
Mary Shaw Jan. 1994 7 p Presented at the Workshop on Studies of Software Design, May 1993 Sponsored by DOD and Siemens Corporate Research Submitted for publication
(AD-A281026; CMU-CS-94-107; CMU/SEI-94-TR-2; ESC-TR-94-002)
Avail: CASI HC A02/MF A01

Software designers compose systems from components written in some programming language. They regularly describe systems using abstract patterns and sophisticated relations among components. However, the configuration tools at their disposal restrict them to composition mechanisms directly supported by the programming language. To remedy this lack of expressiveness, we must elevate the relations among components to first-class entities of the system, entitled to their own specifications and abstractions. DTIC

N95-16447# Carnegie-Mellon Univ., Pittsburgh, PA. Dept. of Computer Science.
VERIFICATION OF ARITHMETIC FUNCTIONS WITH BINARY MOMENT DIAGRAMS
Randal E. Bryant and Yirng-An Chen 31 May 1994 40 p
(Contract F33615-93-1-1330)
(AD-A281028; CMU-CS-94-160) Avail: CASI HC A03/MF A01

Binary moment diagrams (BMD's) provide a canonical representations for linear functions similar to the way binary decision diagrams (BDD's) represent Boolean functions. Within the class of linear functions, we can embed arbitrary functions from Boolean variables to real, rational, or integer values. BMD's can thus model the functionality of data path circuits operating over word level data. Many important functions, including integer multiplication, that cannot be represented efficiently at the bit level with BDD's have simple representations at the word level with BMD's. Furthermore, BMD's can represent Boolean functions with around the same complexity as BDD's. We propose a hierarchical approach to verifying arithmetic circuits; here basic building blocks are first shown to implement

a word-level specification. The overall circuit functionality is then verified at the word level. Multipliers with word sizes of up to 62 bits have been verified by this technique. DTIC

N95-16452# Brown Univ., Providence, RI. Dept. of Computer Science.
THE COMPLEXITY OF PDL WITH INTERLEAVING
Alain J. Mayer and Larry J. Stockmeyer 30 Jun. 1994 13 p
(Contract N00014-91-J-1613)
(AD-A281044) Avail: CASI HC A03/MF A01

To provide a logic for reasoning about concurrently executing programs, Abrahamson has defined an extension of propositional dynamic logic (PDL) by allowing interleaving as an operator for combining programs, in addition to the regular PDL operators union, concatenation, and star. We show that the satisfiability problem for interleaving PDL is complete for deterministic double-exponential time, and that this problem requires time double-exponential in cn/log n for some positive constant c. Moreover, this lower bound holds even when restricted to formulas where each program appearing in the formula has the form a sub 1 vertical line a sub 2 vertical line ... vertical line a sub k where vertical line denotes the interleaving operator and where a sub 1, ..., a sub k are regular programs, i.e., programs built from atomic programs using only the regular operators. Another consequence of the method used to prove this result is that the equivalence problem for regular expressions with interleaving requires space 2(cn/log n). DTIC

N95-16490# Carnegie-Mellon Univ., Pittsburgh, PA. Software Engineering Inst.
MATURITY QUESTIONNAIRE Final Report
David Zubrow, William Hayes, Jane Siegel, and Dennis Goldenson Jun. 1994 53 p
(Contract F19628-89-C-0003)
(AD-A285073; CMU/SEI-94-SR-7) Avail: CASI HC A04/MF A01

This package contains a copy of the software process maturity questionnaire. It is intended for those interested in performing and learning about software process appraisals. This version differs in several important ways from its predecessor, A Method for Assessing the Software Capability of Contractors (CMU/SEI-87-TR-23). The most important difference is that this questionnaire is not an appraisal method itself; rather, it is one component that is used in different appraisal methods. DTIC

N95-16503# Carnegie-Mellon Univ., Pittsburgh, PA. Software Engineering Inst.
SOFTWARE COST AND SCHEDULE ESTIMATING: A PROCESS IMPROVEMENT INITIATIVE Final Report
Robert E. Park, Wolfhart B. Goethert, and J. T. Webb May 1994 100 p
(Contract F19628-90-C-0003)
(AD-A280915; CMU/SEI-94-SR-03) Avail: CASI HC A05/MF A02

This report describes efforts that have been initiated by the Software Engineering Institute to improve the practice of software cost and schedule estimating. These efforts involve support and participation from both industry and government. They are motivated by the Capability Maturity Model, which identifies the key roles estimating and cost management play in establishing repeatable software processes. Products from the initiative will include templates, criteria, and guidelines for establishing defined estimating processes, training materials, and examples for teaching good estimating practice, and evaluations of the abilities of contemporary cost models to meet today's estimating needs. DTIC

N95-16504# Carnegie-Mellon Univ., Pittsburgh, PA. Software Engineering Inst.
THE SEI AND NAWC: WORKING TOGETHER TO ESTABLISH A SOFTWARE MEASUREMENT PROGRAM Final Report
James A. Rozum Dec. 1993 99 p
(Contract F19628-90-C-0003)
(AD-A280916; CMU/SEI-93-TR-07; ESC-TR-93-184) Avail: CASI HC A05/MF A02

In 1990, the Software Engineering Institute (SEI) and the then Naval Air Development Center (NADC) in Warminster, Pennsylvania (now Naval Air Warfare Center, Aircraft Division, Warminster) signed an agreement to jointly develop a software measurement program for NADC - Warminster. To help with that development, a software measurement process action team (SMPAT) was formed with members from the SEI and NADC. The SMPAT's responsibility was to plan, develop, and assist in the implementation of the measurement program. The purpose of this technical report is to document and make available to the software community the process and methods used, experience gained, and some lessons learned in establishing the software measurement program at NADC. This report is meant to help organization that desire to start a software measurement program or have been struggling with such a program by providing an example of one organization that has also struggled to establish a software measurement program. To help an organization, real-life examples of how software measures were defined, collected, and used to improve the management process are included. DTIC

N95-16511# Washington Univ., Seattle, WA.
COMMUNICATING SITUATION AWARENESS IN VIRTUAL ENVIRONMENTS Interim Report, 15 May 1993 - 14 May 1994
Maxwell J. Wells Aug. 1994 60 p
(Contract F49620-93-1-0339)
(AD-A285239; AFOSR-94-0604TR) Avail: CASI HC A04/MF A01

The report documents the first year of work on a four-year project titled Communicating Situation Awareness in Virtual Environments. Included in the report are references to the fifteen papers that were produced, and descriptions of eleven of the research projects that were started. In addition, there is a description of a workshop on virtual reality which was hosted at the University of Washington, and which was attended by 10 federal labs. Other work performed during the period and described in the report includes the conceptual and software development of a virtual world (the Towering Inferno) for performing experimental manipulations, and the detailed design of a virtual reality testbed. As a part of the infrastructure for this line of research, a knowledge base was also developed. This knowledge base is structured to be compatible with ongoing efforts for electronic storage and retrieval of information. Ten objectives of the research effort are detailed. The report provides substantive evidence that the project is on schedule, and making effective use of the available facilities and support. DTIC

N95-16536# Lawrence Livermore National Lab., Livermore, CA.
THE SOFTWARE TECHNOLOGY CENTER AT LAWRENCE LIVERMORE NATIONAL LABORATORY: SOFTWARE ENGINEERING TECHNOLOGY TRANSFER IN A SCIENTIFIC R/D LABORATORY
L. Zucconi Dec. 1993 6 p Presented at the 4th IEEE Workshop on Software Engineering Technology Transfer, Dallas, TX, 28-29 Apr. 1994
(Contract W-7405-eng-48)
(DE94-014794; UCRL-JC-115839; CONF-9404185-1) Avail: CASI HC A02/MF A01

Software engineering technology transfer for productivity and quality improvement can be difficult to initiate and sustain in a non-profit research laboratory where the concepts of profit and loss do not exist. In this experience report, the author discusses the approach taken to establish and maintain a software engineering technology transfer organization at a large R/D laboratory. DOE

N95-16574*# Research Inst. for Computing and Information Systems, Houston, TX.
A SURVEY OF PROGRAM SLICING FOR SOFTWARE ENGINEERING
Jon Beck (West Virginia Univ., Morgantown, VA.) 5 Apr. 1993 45 p
(Contract NCC9-16; RICIS Proj. RB-10)
(NASA-CR-193116; NAS 1.26:193116) Avail: CASI HC A03/MF A01

This research concerns program slicing which is used as a tool for program maintainence of software systems. Program slicing decreases the level of effort required to understand and maintain complex software systems. It was first designed as a debugging aid, but it has since been generalized into various tools and extended to include program comprehension, module cohesion estimation, requirements verification, dead code elimination, and maintainence of several software systems, including reverse engineering, parallelization, portability, and reuse component generation. This paper seeks to address and define terminology, theoretical concepts, program representation, different program graphs, developments in static slicing, dynamic slicing, and semantics and mathematical models. Applications for conventional slicing are presented, along with a prognosis of future work in this field. CASI

N95-16586*# Stanford Univ., CA. Dept. of Computer Science.
OPEN ARCHITECTURES FOR FORMAL REASONING AND DEDUCTIVE TECHNOLOGIES FOR SOFTWARE DEVELOPMENT Final Technical Report, 1 May 1991 - 31 Jul. 1994
John McCarthy, Zohar Manna, Ian Mason, Amir Pnueli, Carolyn Talcott, and Richard Waldinger 31 Jul. 1994 16 p
(Grant NAG2-703)
(NASA-CR-197528; NAS 1.26:197528) Avail: CASI HC A03/MF A01

The objective of this project is to develop an open architecture for formal reasoning systems. One goal is to provide a framework with a clear semantic basis for specification and instantiation of generic components; construction of complex systems by interconnecting components; and for making incremental improvements and tailoring to specific applications. Another goal is to develop methods for specifying component interfaces and interactions to facilitate use of existing and newly built systems as 'off the shelf' components, thus helping bridge the gap between producers and consumers of reasoning systems. In this report we summarize results in several areas: our data base of reasoning systems; a theory of binding structures; a theory of components of open systems; a framework for specifying components of open reasoning system; and an analysis of the integration of rewriting and linear arithmetic modules in Boyer-Moore using the above framework. Author

N95-16587*# National Aeronautics and Space Administration. Goddard Space Flight Center, Greenbelt, MD.
MODIS TECHNICAL REPORT SERIES. VOLUME 4: MODIS DATA ACCESS USER'S GUIDE: SCAN CUBE FORMAT
Virginia L. Kalb and Thomas E. Goff (Research and Data Systems, Inc., Greenbelt, MD.) Nov. 1994 65 p
(Contract NAS5-31331; RTOP 920-00-00)
(NASA-TM-104594-Vol-4; Rept-95B00013-Vol-4; NAS 1.15:104594-Vol-4) Avail: CASI HC A04/MF A01

The software described in this document provides I/O functions to be used with Moderate Resolution Spectroradiometer (MODIS) level 1 and 2 data, and could be easily extended to other data sources. This data is in a scan cube data format: a 3-dimensional ragged array containing multiple bands which have resolutions ranging from 250 to 1000 meters. The complexity of the data structure is handled internally by the library. The I/O calls allow the user to access any pixel in any band through 'C' structure syntax. The high MODIS data volume (approaching half a terabyte per day) has been a driving factor in the library design. To avoid recopying data for user access, all I/O is performed through dynamic 'C' pointer manipulation. This manual contains background material on MODIS, several coding examples of library usage, in-depth discussions of each function, reference 'man' type pages, and several appendices with details of the included files used to customize a user's data product for use with the library. Author

N95-16602# Carnegie-Mellon Univ., Pittsburgh, PA. Dept. of Computer Science.
CONTROL TRANSFER IN OPERATING SYSTEM KERNELS Ph.D. Thesis
Richard Powell Draves, Jr. 13 May 1994 140 p Sponsored in cooperation with Fannie and John Hertz Foundation Fellowship and Microsoft Corp.
(Contract MDA972-90-C-0035; ARPA Order 7330)
(AD-A281135; CMU-CS-94-142) Avail: CASI HC A07/MF A02

Control transfer is the fundamental activity in an operating system kernel. The resource management functionality and application programmer interfaces of an operating system may be delegated to other system components, but the kernel must manage control transfer. The current trend towards increased modularity in operating systems only increases the importance of control transfer. The thesis is that a programming language abstraction, continuations, can be adapted for use in operating system kernels to achieve increased flexibility and performance for control transfer. The flexibility that continuations provide allows the kernel designer when necessary to choose implementation performance over convenience, without affecting the design of the rest of the kernel. The continuation abstraction generalizes existing operating system control transfer optimizations. This dissertation also makes two practical contributions, an interface for machine-independent control transfer management inside the kernel and a recipe for converting an existing operating system kernel to use continuations. The control transfer interface exposes enough functionality to let continuation-using code be machine-independent without sacrificing performance. It provides more functionality than the current state of the art, while still hiding the machine-dependent details of control transfer, such as switching register state and changing address spaces. The recipe provides a set of techniques and advice for converting existing code and writing new code with continuations. Taken together, these contributions form a blueprint for putting continuations into practice. The author has implemented continuations in the Mach 3.0 kernel from Carnegie Mellon University. This dissertation reports the performance improvements observed in that environment. DTIC

N95-16605# Helsinki Univ. of Technology, Espoo (Finland). Dept. of Computer Science.
ICONF: AN INCREMENTAL CONSTRAINT FACILITY IN A FEATURE MODELLING SYSTEM
K. Lagus, T. Laakko, and M. Maentylae 1994 19 p
(PB94-197654; TKO-B114) Avail: CASI HC A03/MF A01

The article describes how an incremental feature-based produce modeling system can utilize an incremental constraint facility (ICONF). A constraint is a relationship that the system should maintain. In ICONF, constraints may be defined, added, browsed and deleted incrementally by the user during the modelling, with immediately displayed consequences. Constraint definitions may also be embedded in feature and part class definitions, and inherited. In the feature modelling system , new part and feature classes can be created by translating them from prototype instances. Interactively created constraints for a part instance can automatically be saved to form constraint definitions in the new part class. NTIS

N95-16607# Software Productivity Consortium, Herndon, VA.
MIL-STD-498 SOFTWARE DEVELOPMENT AND DOCUMENTATION, VERSION 01.00.00
Perry R. DeWeese Jul. 1994 38 p See also AD-M000371 Prepared for Virginia Center of Excellance for Software Reuse and Technology Transfer, Herndon
(Contract MDA972-92-J-1018)
(AD-A282003; SPC-94032-CMC) Avail: CASI HC A03/MF A01

MIL-STD-498 is a standard for the software development process. It is applicable throughout the system acquisition cycle and any life cycle process model. The standard establishes uniform requirements for acquiring, developing, modifying, and documenting software in weapon systems and automated information systems. MIL-STD-498 will provide DOD a single standard for software development, it will cover both MCCR and AIS software, and is expected to be completed by 30 June 1994. For the first time in DOD's history, all software acquisition and development related requirements will be in one place. MIL-STD-498 will also provide a customer/supplier consensus based standard that will provide a transition to commercial software standard. DOD and industry are working with ISO to ensure consistency with ISO 12207 Information Technology Software Life Cycle Process. DTIC

N95-16626# RADEX, Inc., Bedford, MA.
CMCAM: A HIGH PERFORMANCE CM-5 LATTICE GAS SIMULATOR Scientific Report No. 4
G. P. Seeley 30 Dec. 1993 22 p
(Contract F19628-93-C-0023; AF Proj. 7659)
(AD-A281063; RXR-93121; PL-TR-93-2264) Avail: CASI HC A03/MF A01

CMCAM, an extendable lattice-gas simulation program for the Thinking Machines Corporation CM-5 supercomputer is described. CMCAM manipulates the vector processing accelerator units present on each CM-5 processing node using GCC/DPEAC, a macro package for issuing assembler instructions from a C program. The system is able to run several lattice gas rules and extract time and space averaged data for further processing. X-Window graphics are built into the code for remote display of 2-D hydrodynamic flows. An example case of 2-D flow past a flat plate obstacle is described. Performance results show that lattice gas simulations can be run at update rates of 550 million sites/second on a 256 node partition. This report contains detailed information on the implementation methodology used on the CM-5 and may be useful for persons interested in implementing other high-performance computations on the CM-5 that use the vector units directly. DTIC

N95-16632# Carnegie-Mellon Univ., Pittsburgh, PA. Dept. of Computer Science.

EXTENDING PROGRAMMING BY DEMONSTRATION WITH HIERARCHICAL EVENT HISTORIES

David S. Kosbie and Brad A. Myers May 1994 19 p

(Contract F33615-90-C-1465; ARPA Order 7597)

(AD-A281186; CMU-CS-94-156) Avail: CASI HC A03/MF A01

Programming by demonstration, or PBD, is an exciting and developing branch of human-computer interaction (HCI) research. With PBD techniques, end-users can add functionality to their environments without programming in the conventional sense. Virtually all research into PBD, however, presumes that the event history is a linear sequence of user actions. This paper challenges that notion by introducing hierarchical event histories, a new approach which represents some of the end-user's task structure directly in the event history. PBD systems can then take advantage of this structure to operate more correctly and in more situations. To assist programmers in generating structured histories, we also present Hieractors, a new model that provides a simple and clear syntax for describing arbitrary, high-level application behaviors. DTIC

N95-16634# Edgewood Research Development and Engineering Center, Aberdeen Proving Ground, MD.

REAL-TIME DATA COLLECTION PROGRAMS AND SOURCE CODE FOR A COMMERCIAL PASSIVE FTIR REMOTE SENSOR Final Report, Sep. 1992 - Jul. 1993

Robert Kroutil, Michael Housky (MIDAC Corp., Irvine, CA.), and Gary S. Small (Ohio Univ., Athens.) Aug. 1994 221 p

(DARPA Order 8304; DA Proj. 101-62622-A-553)

(AD-A284976; ERDEC-TR-128) Avail: CASI HC A10/MF A03

Computer programs for data collection and analysis of interferograms from a commercial Fourier Transform Infrared sensor were developed. Programs written in C language for an IBM PC using the DOS operating system allow one to collect and display data in a variety of formats useful for the environmental monitoring of vapor clouds. Software is described that enables the user to execute signal processing algorithms for the real-time analysis of interferograms. The programs collect data from the commercial interferometer and detect a vapor species using digital filters and pattern recognition methods. Source code and documentation describing all program functions are provided. DTIC

N95-16818 Carnegie-Mellon Univ., Pittsburgh, PA. Dept. of Computer Science.

INTERACTIVE SKETCHING FOR THE EARLY STAGES OF USER INTERFACE DESIGN

James A. Landay and Brad A. Myers 22 Jul. 1994 19 p Limited Reproducibility: More than 20% of this document may be affected by microfiche quality

(Contract N66001-94-C-6037; ARPA Order B326)

(AD-A285339; CMU-CS-94-176) Avail: CASI HC A03

Current interactive user interface construction tools are often more of a hindrance than a benefit during the early stages of user interface design. These tools take too much time to use and force designers to specify more of the design details than they wish to at this early stage. Most interface designers, especially those who have a background in graphic design, prefer to sketch early interface ideas on paper or on a white-board. We are developing an interactive tool that allows designers to quickly sketch an interface using an electronic pad and stylus. Our tool preserves the important properties of paper: A rough drawing can be produced very quickly and the medium is very flexible. However, unlike a paper sketch this electronic sketch can easily be exercised and modified. In addition, our system allows designers to examine, annotate, and edit a complete history of the design. When the designer is satisfied with this early prototype, the system can transform the sketch into a complete, finished interface in a specified look-and-feel. This transformation takes place with the guidance of the designer. By supporting the early design phases of the software life-cycle, our tool should both ease the prototyping of user interfaces and improve the speed with which a final interface can be created. DTIC

N95-16819# Carnegie-Mellon Univ., Pittsburgh, PA. Dept. of Computer Science.

COMPILING POLYMORPHISM USING INTENSIONAL TYPE ANALYSIS

Robert Harper and Greg Morrisett 2 Sep. 1994 26 p

(Contract F19628-91-C-0168; ARPA Order 8313)

(AD-A285340; CMU-CS-94-185) Avail: CASI HC A03/MF A01

Types have been used to describe the size and shape of data structures at compile time. In polymorphic languages or languages with abstract types, this is not possible since the types of some objects are not known at compile time. Consequently, most implementations of polymorphic languages box data (i.e., represent an object as a pointer), leading to inefficiencies. We introduce a new compilation method for polymorphic languages that avoids the problems associated with boxing data. The fundamental idea is to relax the requirement that code selection for primitive, polymorphic operations, such as pairing and projection, must be performed at compile time. Instead, we allow such operations to defer code selection until link- or even run-time when the types of the values are known. We formalize our approach as a translation into an explicitly-typed, predicative polymorphic delta-calculus with intensional polymorphism. By intensional polymorphism, we mean that constructors and terms can be constructed via structural recursion on types. The form of intensional analysis that we provide is sufficiently strong to perform non-trivial type-based code selection, but it is sufficiently weak that termination of operations that analyze types is assured. DTIC

N95-16850# Carnegie-Mellon Univ., Pittsburgh, PA. Dept. of Computer Science.

ONLINE PERFORMANCE-IMPROVEMENT ALGORITHMS Ph.D. Thesis

Prasad Chalasani Aug. 1994 107 p

(Grant NSF CCR-93-57793)

(AD-A285162; CMU-CS-94-179) Avail: CASI HC A06/MF A02

The results presented in this thesis contribute to two areas of computer science: machine learning and on-line algorithms. One limitation of current theoretical approaches to learning is that most of them involve function approximation, i.e., the learner improves the accuracy of its approximation to an unknown function as it sees more samples of the function. This thesis presents algorithms for improving performance at other tasks, such as navigation and paging. Specifically, these algorithms are online algorithms whose competitiveness improves when repeatedly applied to the same problem. The design of such algorithms is a new challenge in the area of online algorithms: the algorithms must not only be competitive on each application, but must also acquire useful information to improve their future competitiveness. We present a general framework based on task systems for studying such algorithms. DTIC

N95-16852# Sierra Monolithics, Inc., Redondo Beach, CA.

NON-VOLATILE, RAD-HARD RANDOM ACCESS MEMORY (RAM) ON GaAs

1993 10 p

(Contract N00014-91-C-0019)

(AD-A285170) Avail: CASI HC A02/MF A01

This short discussion summarizes the preliminary test results obtained with the first round of Sierra Monolithics RAM cells fabricated on GaAs by Honeywell. The RAM cell consists of a Hall effect sensor in the form of a 20 micron N- implanted square with ohmic connections at the four corners and a drive coil with four turns surrounding the Hall sensor. The basic program plan was to evaluate the characteristics of the RAM cell and then implement the appropriate read and write supporting circuits around it to make a full memory element. Thus in the first round of fabrication no supporting circuitry was fabricated with the basic cell. DTIC

N95-16874# Physics and Electronics Lab. TNO, The Hague (Netherlands).

ASSESSMENT OF BENEFITS AND DRAWBACKS OF USING FUZZY LOGIC, ESPECIALLY IN FIRE CONTROL SYSTEMS Final Report

N. M. DeReus Mar. 1994 39 p

(AD-A285428; FEL-93-A158; TDCK-93-2438) Avail: CASI HC A03/MF A01

Recently, many applications of fuzzy logic are emerging. More and more popular articles are published, reviewing the field of applications or reviewing the theory. The purpose of this report is to give a common sense introduction to the possibilities of fuzzy logic. One of the most important areas where fuzzy logic is used is that of systems where the input as well as output are not fuzzy but just numbers. For such systems it is shown that the fuzzy approach actually is a function approximation

method, often allowing more insight than different methods. Even in application areas that may not seem fuzzy at first sight, possibilities appear to exist. This is the reason for this surveying literature study on fuzzy logic applications in general and fire control applications in particular. DTIC

N95-16883# Rochester Univ., NY. Dept. of Computer Science.
ACTIONS AND EVENTS IN INTERVAL TEMPORAL LOGIC
James F. Allen and George Ferguson Jul. 1994 61 p Submitted for publication
(Contracts N00014-92-J-1512; F30602-91-C-0010; NSF IRI-90-03841)
(TR-521) Avail: CASI HC A04/MF A01

We present a representation of events and action based on interval temporal logic that is significantly more expressive and more natural than most previous AI approaches. The representation is motivated by work in natural language semantics and discourse, temporal logic, and AI planning and plan recognition. The formal basis of the representation is presented in detail, from the axiomatization of time periods to the relationship between actions and events and their effects. The power of the representation is illustrated by applying it to the axiomatization and solution of several standard problems from the AI literature on action and change. An approach to the frame problem based on explanation closure is shown to be both powerful and natural when combined with our representational framework. We also discuss features of the logic that are beyond the scope of many traditional representations, and describe our approach to difficult problems such as external events and simultaneous actions. Author

N95-16906*# National Aeronautics and Space Administration. Lewis Research Center, Cleveland, OH.
A WORKSTATION BASED SIMULATOR FOR TEACHING COMPRESSIBLE AERODYNAMICS
Thomas J. Benson Dec. 1994 15 p Presented at the 33rd Aerospace Sciences Meeting, Reno, NV, 9-12 Jan. 1995; sponsored by AIAA
(RTOP 505-62-52)
(NASA-TM-106799; E-9275; NAS 1.15:106799; AIAA Paper 95-0070)
Avail: CASI HC A03/MF A01

A workstation-based interactive flow simulator has been developed to aid in the teaching of undergraduate compressible aerodynamics. By solving the equations found in NACA 1135, the simulator models three basic fluids problems encountered in supersonic flow: flow past a compression corner, flow past two wedges in series, and flow past two opposed wedges. The study can vary the geometry or flow conditions through a graphical user interface and the new conditions are calculated immediately. Various graphical formats present the results of the flow calculations to the student. The simulator includes interactive questions and answers to aid in both the use of the tool and to develop an understanding of some of the complexities of compressible aerodynamics. A series of help screens make the simulator easy to learn and use. Author

N95-16923 Argonne National Lab., IL.
TRAPEZOIDAL RULE QUADRATURE ALGORITHMS FOR MIMD DISTRIBUTED MEMORY COMPUTERS
J. N. Lyness and S. E. Plowman (Liverpool Univ., England.) 1994 10 p Limited Reproducibility: More than 20% of this document may be affected by microfiche quality
(Contract W-31-109-eng-38)
(DE94-016369; ANL/MCS/PP-78200) Avail: CASI HC A02

An approach to multi-dimensional quadrature, designed to exploit parallel architectures, is described. This involves transforming the integral in such a way that an accurate result is given by the trapezoidal rule; and by evaluating the resulting sum in a manner which may be efficiently implemented on parallel architectures. This approach is to be implemented in the Liverpool NAG transputer library. DOE

N95-17172 Adaptive Solutions, Inc., Beaverton, OR.
HIGH PERFORMANCE HARDWARE AND SOFTWARE FOR PATTERN RECOGNITION AND IMAGE PROCESSING Status Report, 1 May - 31 Aug. 1994
Wendell A. Henry 31 Aug. 1994 6 p Limited Reproducibility: More than 20% of this document may be affected by microfiche quality
(Contract N00014-93-C-0234)
(AD-A284264) Avail: CASI HC A02

Effort on the Phase 1 tasks was completed during this reporting period. The hardware design of the CNAPS/PC board was completed and five (5) prototype boards were fabricated. Debugging of the boards was completed and several of the CNAPS/PC boards have been sent to various customer's sites for Beta Testing. The Beta Testing of the CNAPS/PC has been progressing well. The port of the CNAPS Control software for execution of CNAPS code on the CNAPS/PC hardware has been completed. This software has been sent with the CNAPS/PC hardware to various customer's sites for Beta Testing. The port of the CNAPS-C compiler, its preprocessor, and the CPL assembler to Windows/NT has been completed. This software is ready for Beta Testing. The Phase 1 deliveries were shipped on August 31, 1994 to the destination specified in the contract. At the time of this report, the project has expenditures and committments totaling 100% of the funds allocated for Phase 1 of the contract authorization of additional funding to the amount of $292,215.00 for the Phase 2 tasks has been received. The contract stipulates $492,893.00 for the completion of the Phase 2 tasks, therefore, an additional $200,678.00 of funding must be authorized to complete the Phase 2 tasks. DTIC

N95-17176# Army Construction Engineering Research Lab., Champaign, IL.
AN ASSESSMENT OF SIMULATION SYSTEMS APPLICABLE TO BUSINESS PROCESS REENGINEERING AT ARMY DIRECTORATES OF PUBLIC WORKS Final Report
Edgar S. Neely, James H. Johnson, and Mark J. Orth Sep. 1994 32 p
(DA Proj. 4A1-62784-AT-41)
(AD-A285696; USACERL-FF-TR-94/31) Avail: CASI HC A03/MF A01

All agencies of the Federal Government, including Army Directorates of Public Works (DPW's), are starting to apply business reengineering to improve current processes and reduce resource requirements. Currently, these Directorates have no way of forecasting and examining effects of proposed changes. The objective of this research was to evaluate and select a marketed simulation system that is optimal for use by DPW's during business reengineering planning and operations analyses. Seven simulation systems were evaluated and three were selected for detailed analysis and testing. Based on the documentation and available tutorial, ease of use, and capabilities, PROMODEL is recommended for use in DPW business process reengineering. DTIC

N95-17261# Rochester Univ., NY. Dept. of Computer Science.
ON SERIALIZABLE LANGUAGES
Mitsunori Ogihara Jun. 1994 20 p
(Grants NSF INT-91-16781; JSPS ENG-207)
(TR-519) Avail: CASI HC A03/MF A01

Cai and Furst introduced the notion of bottleneck Turing machines and showed that the languages recognized by width-5 bottleneck Turing machines are exactly those in PSPACE. Computational power of bottleneck Turing machines with width fewer than 5 is investigated. It is shown that width-2 bottleneck Turing machines capture polynomial-time many-one closure of nearly near-testable sets. For languages recognized by bottleneck Turing machines with intermediate width 3 and 4, some lower- and upper-bounds are shown. Author

N95-17264*# National Aeronautics and Space Administration. Lewis Research Center, Cleveland, OH.
INTERACTIVE COMPUTER GRAPHICS APPLICATIONS FOR COMPRESSIBLE AERODYNAMICS
Thomas J. Benson Dec. 1994 17 p Presented at the 33rd Aerospace Sciences Meeting, Reno, NV, 9-12 Jan. 1995; sponsored by AIAA
(RTOP 505-62-52)
(NASA-TM-106802; E-9279; NAS 1.15:106802; AIAA Paper 95-0119)
Avail: CASI HC A03/MF A01

Three computer applications have been developed to solve inviscid compressible fluids problems using interactive computer graphics. The first application is a compressible flow calculator which solves for isentropic flow, normal shocks, and oblique shocks or centered expansions produced by two dimensional ramps. The second application couples the solutions generated by the first application to a more graphical presentation of the results to produce a desk top simulator of three compressible flow problems: 1) flow past a single compression ramp; 2) flow past two ramps in series; and 3) flow past two opposed ramps. The third application extends the results of the second to produce a design tool which solves for the flow through supersonic external or mixed compression inlets. The applications

were originally developed to run on SGI or IBM workstations running GL graphics. They are currently being extended to solve additional types of flow problems and modified to operate on any X-based workstation.
Author

N95-17324*# National Center for Atmospheric Research, Boulder, CO.
AN INTERACTIVE INTERFACE FOR NCAR GRAPHICS Final Report, Jul. 1991 - Jul. 1994
Bill Buzbee, Bob Lackman, and Ethan Alpert Sep. 1994 218 p
(Contracts NAS5-32337; RTOP 656-65-07; USRA-C-5555-15)
(NASA-CR-189383; NAS 1.26:189383) Avail: CASI HC A10/MF A03

The NCAR Graphics package has been a valuable research tool for over 20 years. As a low level Fortran library, however, it was difficult to use for nonprogramming researchers. With this grant and NSF support, an interactive interface has been created which greatly facilitates use of the package by researchers of diverse computer skill levels. Author

N95-17327*# Colorado Univ., Boulder, CO. Dept. of Aerospace Engineering.
A LAND-SURFACE TESTBED FOR EOSDIS Final Report, 1994
William Emery and Tim Kelley 6 Sep. 1994 55 p
(Contracts NAS5-32337; RTOP 656-65-07; USRA-C-5555-07)
(NASA-CR-189392; NAS 1.26:189392) Avail: CASI HC A04/MF A01

The main objective of the Testbed project was to deliver satellite images via the Internet to scientific and educational users free of charge. The main method of operations was to store satellite images on a low cost tape library system, visually browse the raw satellite data, access the raw data filed, navigate the imagery through 'C' programming and X-Windows interface software, and deliver the finished image to the end user over the Internet by means of file transfer protocol methods. The conclusion is that the distribution of satellite imagery by means of the Internet is feasible, and the archiving of large data sets can be accomplished with low cost storage systems allowing multiple users. Author

N95-17338 Computational Logic, Inc., Austin, TX.
A COMPUTATIONAL LOGIC FOR APPLICATIVE COMMON LISP Final Report
Bob Boyer, Matt Kaufmann, and J. Moore 1994 25 p Limited Reproducibility: More than 20% of this document may be affected by microfiche quality
(Contract N00014-91-C-0130)
(AD-A283103) Avail: Issuing Activity (Defense Technical Information Center (DTIC))

We summarize results in automated reasoning under this contract. The development of the Boyer-Moor 'Nqthm' theorem prover was supported in part for approximately 20 years by the Office of Naval Research. The long range objective of this research has been to enable programmers to produce software that is mathematically proven to meet its specifications by using mechanical theorem-proving programs that check proofs. DTIC

N95-17355 Rutherford Appleton Lab., Chilton (England). Energy Research Unit.
ENGINEERING DESIGN TOOLS FOR WIND DIESEL SYSTEMS. VOLUME 2: JODYMOD DYNAMIC WIND DIESEL SIMULATION SOFTWARE PACKAGE. MODEL VERIFICATION Final Report, 1 Oct. 1990 - 30 Sep. 1993
P. Lundsager, H. Bindner, D. Infield, A. Scotney, and K. Uhlen Jan. 1994 40 p Prepared in cooperation with Risoe National Lab., Roskilde, Denmark; Elektrisitetsforsyningens Forskningsinstit., Trondheim, Norway; Netherlands Energy Research Foundation, Petten; and Commission of the European Communities, Brussels, Belgium
(PB95-104519; RAL-94-002-Vol-2) Avail: Issuing Activity (National Technical Information Service (NTIS))

A design tools software package for wind diesel systems has been developed. The complete package includes modeling of both dynamic and logistic aspects of system operation and runs on a PC. This report contains the verification of the dynamic model JODYMOD (JOule DYnamic MODular MODel) and a validation against measured results from two different wind diesel systems. NTIS

N95-17356 Rutherford Appleton Lab., Chilton (England). Energy Research Unit.
ENGINEERING DESIGN TOOLS FOR WIND DIESEL SYSTEMS. VOLUME 3: JODYMOD DYNAMIC SIMULATION SOFTWARE PACKAGE. MODEL DESCRIPTION Final Report, 1 Oct. 1990 - 30 Sep. 1993
P. Lundsager, H. Bindner, D. Infield, A. Scotney, and K. Uhlen Jan. 1994 214 p Prepared in cooperation with Risoe National Lab., Roskilde, Denmark; Elektrisitetsforsyningens Forskningsinst., Trondheim, Norway; Netherlands Energy Research Foundation, Petten; and Commission of the European Communities, Brussels, Belgium
(PB95-104527; RAL-94-003-Vol-3) Avail: Issuing Activity (National Technical Information Service (NTIS))

A design tools software package for wind diesel systems has been developed. The complete package includes modeling of both dynamic and logistic aspects of system operation and runs on a PC. This report contains the technical description of the dynamic model JODYMOD (JOule DYnamic MODular MODel) developed by the project. NTIS

N95-17410# National Defence Research Establishment, Stockholm (Sweden). Dept. of Weapon Systems.
IS-LAB: A TOOL FOR DEVELOPING INTERACTIVE PROGRAMS FOR SIMULATION AND ANALYSIS. USER'S GUIDE
I. Karasalo and D. Tollefsen Jan. 1994 130 p Prepared in cooperation with Royal Inst. of Tech., Stockholm, Sweden
(PB94-184710; FOA-C-20956-2.2) Avail: CASI HC A07/MF A02

IS-Lab is a software package for supporting the design and use of programs for scientific computing, in particular when such computing requires a general-purpose programming language like FORTRAN or C as an essential tool. IS-Lab is implemented in a UNIX operating system environment. A basic capability of IS-Lab is to collect a set of subprograms, written in FORTRAN or C, into a program controlled by commands entered from the keyboard or alternatively as high-level programs from script files. The commands and the associated command action subprogram names are specified in a simple notation by supplying a command tree file. IS-Lab provides a default set of commands and subprograms for basic general data handling and numerical analysis primitives, including handlers for scalar and matrix variables, a parser/interpreter for arithmetic expressions in such variables, and functions for simple textual and graphic output. This default command set may be used on its own as a platform for a large body of simulation and analysis tasks. User-supplied commands are inserted as extensions of the default command set. NTIS

N95-17420*# National Aeronautics and Space Administration. Lewis Research Center, Cleveland, OH.
FLEXIBLE METHOD FOR INTER-OBJECT COMMUNICATION IN C++
Brian P. Curlett and Jack J. Gould Nov. 1994 26 p
(RTOP 505-69-50)
(NASA-TM-106315; E-9196; NAS 1.15:106315) Avail: CASI HC A03/MF A01

A method has been developed for organizing and sharing large amounts of information between objects in C++ code. This method uses a set of object classes to define variables and group them into tables. The variable tables presented here provide a convenient way of defining and cataloging data, as well as a user-friendly input/output system, a standardized set of access functions, mechanisms for ensuring data integrity, methods for interprocessor data transfer, and an interpretive language for programming relationships between parameters. The object-oriented nature of these variable tables enables the use of multiple data types, each with unique attributes and behavior. Because each variable provides its own access methods, redundant table lookup functions can be bypassed, thus decreasing access times while maintaining data integrity. In addition, a method for automatic reference counting was developed to manage memory safely.
Author

N95-17432 Carnegie-Mellon Univ., Pittsburgh, PA. Robotics Inst.
GEOMETRIC SENSING OF KNOWN PLANAR SHAPES
Yan-Bin Jia and Michael Erdmann Jul. 1994 50 p Limited Reproducibility: More than 20% of this document may be affected by microfiche quality
(Grants NSF IRI-90-10686; NSF IRI-91-57643; NSF IRI-92-13993)
(AD-A282854; CMU-RI-TR-94-24) Avail: CASI HC A03

Industrial assembly involves sensing the pose (orientation and position) of a part. Efficient and reliable sensing strategies can be developed for an

assembly task if the shape of the part is known in advance. We investigate two problems of determining the pose of a polygonal part of known shape. In the first problem, the part has a continuum of possible poses, while in the second problem, it has a finite number of possible poses. More specifically, the first problem involves determining the pose of a convex n-gon from a set of m supporting cones, that is, cones with both sides supporting the polygon. An algorithm with running time O(nm) which almost always reduces to O(n + m log n) is presented to solve for all possible poses of the polygon. As a consequence, the polygon inscription problem of finding all possible poses for a convex n-gon inscribed in another convex n-gon can be solved within the same asymptotic time bound. We prove that the number of possible poses cannot exceed 6n, given m greater than or equal 2 supporting cones with distinct vertices. Experiments demonstrate that two supporting cones are sufficient to determine the real pose of the n-gon in most cases. Our results imply that sensing in practice can be carried out by obtaining viewing angles of a planar part at multiple exterior sites in the plane. As a conclusion, we generalize this and other sensing methods into a scheme named sensing by inscription. DTIC

N95-17445 Air Force Inst. of Tech., Wright-Patterson AFB, OH.
MULTIVARIATE SAMPLING WITH EXPLICIT CORRELATION INDUCTION FOR PRACTICAL SIMULATION AND OPTIMIZATION STUDIES Ph.D. Thesis
Raymond R. Hill 1994 51 p Limited Reproducibility: More than 20% of this document may be affected by microfiche quality
(AD-A281998; AFIT/CI/CIA-94-021D) Avail: CASI HC A04

The goals of this research are to develop a methodology for generating values of multivariate random variables with specified marginal distributions and a specified population correlation structure, to demonstrate the use of this methodology in generating synthetic optimization problems, and to conduct a computational study where the influence of the population correlation structure on the performance of optimization solution methods is assessed. DTIC

N95-17460 Naval Postgraduate School, Monterey, CA.
CORRECTIVE SOFTWARE MANAGEMENT: THE SUCCESS OF THE EPLRS PROGRAM M.S. Thesis
Terrence Cummings Mar. 1994 124 p Limited Reproducibility: More than 20% of this document may be affected by microfiche quality
(AD-A282430) Avail: Issuing Activity (Defense Technical Information Center (DTIC))

Software development in weapon systems is extremely challenging and has become a significant source of problems in DOD programs. The purpose of this thesis is to identify and document strategies and techniques for program offices to use in managing these software problems. This thesis documents the success of the Enhanced Position Location Reporting System in applying corrective software management actions to specific problems encountered. Lessons learned have been drawn from the analysis and generalized for application to other DOD programs. The principal finding is that an effective software corrective action plan requires a focused effort devoted to identifying and correcting all software deficiencies. This is accomplished before further developmental work requiring software is attempted. The thesis concludes that an astute program office should be prepared to implement and manage this type of software corrective action plan. Two primary recommendations are for the development of a DOD policy on the management of software corrective action and the development of a DOD model for software corrective action by program offices. DTIC

N95-17470 Technische Univ., Delft (Netherlands).
SMALL SAMPLE BEHAVIOR OF MULTI-LAYER FEEDFORWARD NETWORK CLASSIFIERS: THEORETICAL AND PRACTICAL ASPECTS Ph.D. Thesis
M. A. Kraaijveld 30 Nov. 1993 206 p Sponsored by Nederlandse Organisatie voor Wetenschappelijk Onderzoek
(PB94-201415; ISBN-90-6275-934-3) Copyright Avail: Issuing Activity

Multi-layer feedforward network classifiers have become very popular tools for pattern recognition during the last decade. In the first part of the thesis, a number of theoretical issues on this topic are investigated. A review of the literature on small sample problems in pattern recognition is presented, followed by a discussion of an elegant mathematical framework to study small sample problems. This framework, known as the Vapnik-Chervonenkis theory, is applied to the class of multi-layer feedforward network classifiers in order to characterize their small sample properties. Moreover, the influence of the training procedure on the small sample behavior of the multi-layer network classifier is investigated. The second part of the thesis is concerned with a number of practical aspects of training a multi-layer feedforward network classifier. The problem of the stopping criterion of an iterative learning procedure is studied. Some issues on the learning speed of a class of iterative learning procedures are investigated. NTIS

N95-17514# Oak Ridge National Lab., TN.
AUTOMATED ESTIMATING SYSTEM (AES) VERSION 6.0: USER'S MANUAL
D. A. Holder, ed. and R. K. Schwarz, ed. Jun. 1994 196 p Revised
(Contract DE-AC05-84OT-21400)
(DE94-013636; K/CSD/TM-64-Rev-5) Avail: CASI HC A09/MF A03

This document describes Version 6.0 of the Automated Estimating System (AES), a personal computer-based software package. The AES is designed to aid in the creation, updating, and reporting of project cost estimates for the Estimating and Scheduling Engineering Department of Central Engineering Services of Martin Marietta Energy Systems, Inc. AES provides formatted input screens to guide the user through the estimate creation/update process and provides several standardized reports that allow cost to be sorted and summarized in many different formats and at several levels of aggregation. DOE

N95-17515# Westinghouse Savannah River Co., Aiken, SC.
REVIEWS OF COMPUTING TECHNOLOGY: SOFTWARE OVERVIEW
W. R. Hartshorn and A. L. Johnson Jan. 1994 50 p
(Contract DE-AC09-89SR-18035)
(DE94-013662; WSRC-IM-90-83-14) Avail: CASI HC A03/MF A01

The Savannah River Site Computing Architecture states that the site computing environment will be standards-based, data-driven, and workstation-oriented. Larger server systems deliver needed information to users in a client-server relationship. Goals of the Architecture include utilizing computing resources effectively, maintaining a high level of data integrity, developing a robust infrastructure, and storing data in such a way as to promote accessibility and usability. This document describes the current storage environment at Savannah River Site (SRS) and presents some of the problems that will be faced and strategies that are planned over the next few years. DOE

N95-17628 Rutherford Appleton Lab., Chilton (England). Energy Research Unit.
ENGINEERING DESIGN TOOLS FOR WIND DIESEL SYSTEMS. VOLUME 4: JODYMOD DYNAMIC WIND DIESEL SIMULATION SOFTWARE PACKAGE. PROGRAM DOCUMENTATION Final Report, 1 Oct. 1990 - 30 Sep. 1993
H. Bindner, P. Lundsager, D. Infield, A. Scotney, and K. Uhlen Jan. 1994 150 p Prepared in cooperation with Risoe National Lab., Roskilde, Denmark; Elektrisitetsforsyningens Forskningsinst., Trondheim, Norway; Netherlands Energy Research Foundation, Petten; and Commission of the European Communities, Brussels, Belgium
(PB95-104535; RAL-94-004-Vol-4) Avail: Issuing Activity (National Technical Information Service (NTIS))

A design tools software package for wind diesel systems has been developed. The complete package includes modeling of both dynamic and logistic aspects of system operation and runs on a PC. This report is the Program Documentation for the User Interface software for the dynamic simulation program. NTIS

N95-17629 Rutherford Appleton Lab., Chilton (England). Energy Research Unit.
ENGINEERING DESIGN TOOLS FOR WIND DIESEL SYSTEMS. VOLUME 5: JODYMOD DYNAMIC WIND DIESEL SIMULATION SOFTWARE PACKAGE. USER'S GUIDE Final Report, 1 Oct. 1990 - 30 Sep. 1993
H. Bindner, P. Lundsager, D. Infield, A. Scotney, and K. Uhlen Jan. 1994 70 p Prepared in cooperation with Risoe National Lab., Roskilde, Denmark; Elektrisitetsforsyningens Forskningsinst., Trondheim, Norway; Netherlands Energy Research Foundation, Petten; and Commission of the European Communities, Brussels, Belgium

(PB95-104543; RAL-94-005-Vol-5) Avail: Issuing Activity (National Technical Information Service (NTIS))

A design tools software package for wind diesel systems has been developed. The complete package includes modeling of both dynamic and logistic aspects of system operation and runs on a PC. This report is the User's Guide for the software for dynamic simulation. NTIS

N95-17678# Oak Ridge National Lab., TN.

XPVM: A GRAPHICAL CONSOLE AND MONITOR FOR PVM

J. A. Kohl 1994 5 p Presented at the Scalable High Performance Computing Conference, Knoxville, TN, 23 May 1994

(Contract DE-AC05-84OR-21400)

(DE94-018050; CONF-9405100-12) Avail: CASI HC A01/MF A01

As technology continues to spawn new supercomputing platforms and more powerful workstation environments, it becomes increasingly important to integrate and apply these diverse collections of computers together to extract. the best performance possible. PVM (Parallel Virtual Machine) is gaining wide popularity as a means for realizing the computing power of these heterogeneous systems. PVM is a software package that permits a heterogeneous collection of serial, parallel and vector computers, hooked together by a network, to appear as one large distributed memory computer. One of the primary difficulties in designing applications for distributed computer systems is identifying precisely what is happening inside a program, as multiple threads of control interact to solve a problem. Often it is useful to provide the user with feedback as to the state of the system, including the individual tasks executing on it. XPVM is a graphical interface to PVM that provides such information, to monitor executions and assist in debugging and tuning the performance of PVM programs. XPVM can be used in real time, to observe program activity as it happens, or it can play back saved traces of PVM program executions, for detailed post-mortem analysis. DOE

N95-17732 Newcastle-upon-Tyne Univ., Newcastle (England).

BEHAVIOURAL MODELLING OF FORMAL DOCUMENTS AND ACTIVE INSTRUMENTS

B. N. Rossiter, K. G. Huntley, and M. A. Heather Dec. 1993 20 p Prepared in cooperation with Northumbria Univ., Newcastle-upon-Tyne, England

(PB95-104378; TRS-465) Avail: Issuing Activity (National Technical Information Service (NTIS))

Active documents have dynamical prescriptive and inferential properties. Electronic publishing has greater functionality for achieving these, because there are some difficulties which arise when the physical reality of documents is not available. For consistent operations, a systems analysis of the activity is needed with representations like entity-life histories. Careful attention has to be paid to the choice of a platform language, which needs to be strong on behavioral characteristics. Active documents play a key role in legal transactions, and the law is an important customer of electronic publishing. As an illustration, a fully-worked example is given of an implementation for a bill of lading which has been designed using an object-oriented graphical approach. NTIS

N95-17733 Rutherford Appleton Lab., Chilton (England).

ENGINEERING DESIGN TOOLS FOR WIND DIESEL SYSTEMS. VOLUME 1: EXECUTIVE SUMMARY Final Report, 1 Oct. 1990 - 30 Sep. 1993

D. Infield, A. Scotney, P. Lundsager, H. Bindner, and J. Pierik Jan. 1994 56 p Prepared in cooperation with Risoe National Lab., Roskilde, Denmark

(Proj. CEC-JOUR-0078)

(PB95-104501; RAL-94-001-Vol-1) Avail: Issuing Activity (National Technical Information Service (NTIS))

The report describes work undertaken to develop a user-friendly software package to assist the designers of wind diesel systems. These tools comprise two basic modules: a logistic modeling package for overall system performance assessment, and a modular dynamic model for investigating the electro-mechanical stability of designs. As an executive summary, the volume provides an assessment of the project. Project management issues are discussed, and the widespread dissemination of results is demonstrated. A full list of resulting publications is included. Details are given of a consortium agreement between the partners involved in the project, and a contractual agreement to facilitate public access to the software package. Details of how and where to obtain copies of the software and documentation are provided. NTIS

N95-17734 Rutherford Appleton Lab., Chilton (England). Energy Research Unit.

ENGINEERING DESIGN TOOLS FOR WIND DIESEL SYSTEMS. VOLUME 6: LOGISTIC PACKAGE. USER DOCUMENTATION Final Report

D. Infield, A. Scotney, P. Lundsager, H. Bindner, and J. Pierik 1994 550 p Prepared in cooperation with Risoe National Lab., Roskilde, Denmark; Elektrisitetsforsyningens Forskningsinst., Trondheim, Norway; Netherlands Energy Research Foundation, Petten; and Commission of the European Communities, Brussels, Belgium

(PB95-104550; RAL-94-006-Vol-6) Avail: Issuing Activity (National Technical Information Service (NTIS))

This document is the user manual for the European Wind Diesel Logistic Modelling Package (WDL). The main text constitutes a guide to the integrated user environment. This logistic design tools package aids the design and assessment of Wind Diesel systems. The new combined software package offers to the user a comprehensive integrated environment, from which to create simulation specifications and access simulation results. This Shell is designed for user-friendliness. It is 'menu-driven' throughout, with on-line help available at most points. A range of functions are also supported to aid the user. These include: data synthesis routines, functions to partially generate component specifications, etc. NTIS

N95-17735 Rutherford Appleton Lab., Chilton (England). Energy Research Unit.

ENGINEERING DESIGN TOOLS FOR WIND DIESEL SYSTEMS. VOLUME 7: LOGISTIC PACKAGE. VALIDATION REPORT Final Report

D. Infield, A. Scotney, P. Lundsager, H. Bindner, and J. Pierik 1994 213 p Prepared in cooperation with Risoe National Lab., Roskilde, Denmark; Elektrisitetsforsyningens Forskningsinst., Trondheim, Norway; Netherlands Energy Research Foundation, Petten; and Commission of the European Communities, Brussels, Belgium

(PB95-104568; RAL-94-007-Vol-7) Avail: Issuing Activity (National Technical Information Service (NTIS))

The report describes software specifically developed to assist the designers of wind diesel systems. It deals specifically with the validation of the logistic modeling package known as WDLTOOLS. As the package consists of user interface (Shell) giving access to the six embedded models, the detail of this report will be concerned with the validation of the individual models. Where feasible, the individual models have been run for the appropriate wind diesel system with measured input data describing the system load and the wind speed experienced by the system. NTIS

N95-17746# Virtual Image Labs., Inc., Silver Spring, MD.

ICCanvas 3D VISUALIZATION TOOL FOR WINDOWS (TM). SOFTWARE USER'S MANUAL Technical Report, 30 Sep. 1992 - 1 Jul. 1994

Ernie Wright 1 Oct. 1994 32 p

(Contract DNA001-92-C-0173)

(AD-A285603; DNA-TR-94-58) Avail: CASI HC A03/MF A01

The ICCanvas 3D visualization program was developed to simplify the study and communication of the results of complex meteorological models and other 3D simulations by exploiting the increasing graphics capabilities of microcomputers. The program allows you to use your personal computer to view level surfaces on structured 3D data, much of which may have been produced by large hydrocodes running on workstations and supercomputers. ICCanvas has been used by DNA to display density distributions of dust and water vapor in 3D simulations of nuclear blast clouds. Together with sophisticated 3D rendering applications, ICCanvas has helped to produce high-quality animated views of the development of a blast cloud featuring footprint projections and multiple semitransparent surfaces. DTIC

N95-16272# Kazan Aviation Inst. (USSR).

GENERALIZED METHOD OF SOLVING TOPOLOGICAL OPTIMIZATION PROBLEMS FOR ELECTRICAL AIRPLANE EQUIPMENT SYSTEMS IN COMPUTER-AIDED DESIGN

V. S. Tereshchuk *In* Nanjing Univ. of Aeronautics and Astronautics,

Joint Proceedings on Aeronautics and Astronautics (JPAA) May 1993 p 152-156 (For primary document see N95-16249 04-01)
Avail: CASI HC A01/MF A03

N95-16454*# National Aeronautics and Space Administration. Langley Research Center, Hampton, VA.
SOFTWARE ENGINEERING FROM A LANGLEY PERSPECTIVE
Susan Voigt *In its* The Role of Computers in Research and Development at Langley Research Center Oct. 1994 p 21-42 (For primary document see N95-16453 04-62)
Avail: CASI HC A03/MF A06

N95-16455*# Naval Surface Warfare Center, Virginia Beach, VA.
MODEL-BASED SOFTWARE PROCESS IMPROVEMENT
Brenda T. Zettervall *In* NASA. Langley Research Center, The Role of Computers in Research and Development at Langley Research Center Oct. 1994 p 68-84 (For primary document see N95-16453 04-62)
Avail: CASI HC A03/MF A06

N95-16457*# National Aeronautics and Space Administration. Langley Research Center, Hampton, VA.
A SOFTWARE TOOL FOR DATAFLOW GRAPH SCHEDULING
Robert L. Jones, III *In its* The Role of Computers in Research and Development at Langley Research Center Oct. 1994 p 106-113 (For primary document see N95-16453 04-62)
Avail: CASI HC A02/MF A06

N95-16468*# National Aeronautics and Space Administration. Langley Research Center, Hampton, VA.
DATA VISUALIZATION AND ANIMATION LAB (DVAL) OVERVIEW
Kathy Stacy and Bill vonOfenheim *In its* The Role of Computers in Research and Development at Langley Research Center Oct. 1994 p 292-315 (For primary document see N95-16453 04-62)
Avail: CASI HC A03/MF A06

N95-16469*# National Aeronautics and Space Administration. Langley Research Center, Hampton, VA.
DATA VISUALIZATION AND ANIMATION LAB (DVAL): APPLICATIONS
Kurt Severance and Mike Weisenborn *In its* The Role of Computers in Research and Development at Langley Research Center Oct. 1994 p 292-316 (For primary document see N95-16453 04-62)
Avail: CASI HC A03/MF A06

N95-16478*# Institute for Computer Applications in Science and Engineering, Hampton, VA.
HIGH PERFORMANCE FORTRAN
Piyush Mehrotra *In* NASA. Langley Research Center, The Role of Computers in Research and Development at Langley Research Center Oct. 1994 p 546-561 (For primary document see N95-16453 04-62)
Avail: CASI HC A03/MF A06

N95-16480*# National Aeronautics and Space Administration. Langley Research Center, Hampton, VA.
EPISTEMOLOGY, SOFTWARE ENGINEERING AND FORMAL METHODS
C. Michael Holloway *In its* The Role of Computers in Research and Development at Langley Research Center Oct. 1994 p 570-595 (For primary document see N95-16453 04-62)
Avail: CASI HC A03/MF A06

N95-17192*# Institute of Space Research, Moscow (USSR).
FAST COMPUTATIONAL SCHEME OF IMAGE COMPRESSION FOR 32-BIT MICROPROCESSORS
Leonid Kasperovich *In* NASA. Goddard Space Flight Center, Third International Symposium on Space Mission Operations and Ground Data Systems, Part 1 Nov. 1994 p 119-123 (For primary document see N95-17179 04-17)
Avail: CASI HC A01/MF A06

N95-17287*# Jet Propulsion Lab., California Inst. of Tech., Pasadena, CA.
ADAPTIVE LINE ENHANCERS FOR FAST ACQUISITION
H.-G. Yeh and T. M. Nguyen *In its* The Telecommunications and Data Acquisition Report 15 Nov. 1994 p 140-159 (For primary document see N95-17279 04-32)
(RTOP 315-91-10-13-08)
Avail: CASI HC A03/MF A03

N95-17533*# European Space Agency. European Space Operations Center, Darmstadt (Germany). Flight Control Systems Dept.
SCOSII OL: A DEDICATED LANGUAGE FOR MISSION OPERATIONS
Andrea Baldi, Dennis Elgaard (Computer Resources International A/S, Denmark.), Steen Lynenskjold (Computer Resources International A/S, Denmark.), and Mauro Pecchioli *In* NASA. Goddard Space Flight Center, Third International Symposium on Space Mission Operations and Ground Data Systems, Part 2 Nov. 1994 p 689-696 (For primary document see N95-17531 04-17)
Avail: CASI HC A02/MF A06

N95-17538*# Jet Propulsion Lab., California Inst. of Tech., Pasadena, CA.
A SOFTWARE ARCHITECTURE FOR AUTOMATING OPERATIONS PROCESSES
Kevin J. Miller *In* NASA. Goddard Space Flight Center, Third International Symposium on Space Mission Operations and Ground Data Systems, Part 2 Nov. 1994 p 729-734 (For primary document see N95-17531 04-17)
Avail: CASI HC A02/MF A06

N95-17540*# Jet Propulsion Lab., California Inst. of Tech., Pasadena, CA.
SEQ-GEN: A COMPREHENSIVE MULTIMISSION SEQUENCING SYSTEM
Jose Salcedo and Thomas J. Starbird *In* NASA. Goddard Space Flight Center, Third International Symposium on Space Mission Operations and Ground Data Systems, Part 2 Nov. 1994 p 741-748 (For primary document see N95-17531 04-17)
Avail: CASI HC A02/MF A06

N95-17560*# National Aeronautics and Space Administration. Goddard Space Flight Center, Greenbelt, MD.
KNOWLEDGE-BASED CRITIQUING OF GRAPHICAL USER INTERFACES WITH CHIMES
Jianping Jiang (Computer Technology Associates, Inc., Rockville, MD.), Elizabeth D. Murphy (Computer Technology Associates, Inc., Rockville, MD.), Leslie E. Carter (Computer Technology Associates, Inc., Rockville, MD.), and Walter F. Truszkowski *In its* Third International Symposium on Space Mission Operations and Ground Data Systems, Part 2 Nov. 1994 p 923-928 (For primary document see N95-17531 04-17)
Avail: CASI HC A02/MF A06

N95-17564*# Telos Corp., Pasadena, CA.
SOFTWARE INTERFACE VERIFIER
Tomas J. Soderstrom, Laura A. Krall, Sharon A. Hope, and Brian S. Zupke *In* NASA. Goddard Space Flight Center, Third International Symposium on Space Mission Operations and Ground Data Systems, Part 2 Nov. 1994 p 953-960 (For primary document see N95-17531 04-17)
Avail: CASI HC A02/MF A06

N95-17566*# National Aeronautics and Space Administration. Goddard Space Flight Center, Greenbelt, MD.
A PROVEN APPROACH FOR MORE EFFECTIVE SOFTWARE DEVELOPMENT AND MAINTENANCE
Rose Pajerski, Dana Hall (Science Applications International Corp., McLean, VA.), and Craig Sinclair (Science Applications International Corp., McLean, VA.) *In its* Third International Symposium on Space Mission Operations and Ground Data Systems, Part 2 Nov. 1994 p 975-983 (For primary document see N95-17531 04-17)
Avail: CASI HC A02/MF A06

N95-17567*# European Space Agency. European Space Operations Center, Darmstadt (Germany).
XMM INSTRUMENT ON-BOARD SOFTWARE MAINTENANCE CONCEPT
N. Peccia and F. Giannini (European Space Agency. European Space Research and Technology Center, ESTEC, Noordwijk, Netherlands.) *In* NASA. Goddard Space Flight Center, Third International Symposium on

Space Mission Operations and Ground Data Systems, Part 2 Nov. 1994 p 985-992 (For primary document see N95-17531 04-17)
Avail: CASI HC A02/MF A06

N95-17569*# National Aeronautics and Space Administration. Goddard Space Flight Center, Greenbelt, MD.
SOFTWARE PROCESS ASSESSMENT (SPA)
Linda H. Rosenberg (Unisys Corp., Lanham, MD.), Sylvia B. Sheppard, and Scott A. Butler (Maryland Univ., College Park, MD.) *In its* Third International Symposium on Space Mission Operations and Ground Data Systems, Part 2 Nov. 1994 p 1001-1008 (For primary document see N95-17531 04-17)
Avail: CASI HC A02/MF A06

N95-17571*# Computer Resources International A/S (Denmark).
SCOS 2: AN OBJECT ORIENTED SOFTWARE DEVELOPMENT APPROACH
Martin Symonds, Steen Lynenskjold, and Christian Mueller *In* NASA. Goddard Space Flight Center, Third International Symposium on Space Mission Operations and Ground Data Systems, Part 2 Nov. 1994 p 1015-1022 (For primary document see N95-17531 04-17)
Avail: CASI HC A02/MF A06

N95-17580*# National Aeronautics and Space Administration. Goddard Space Flight Center, Greenbelt, MD.
A GENERAL MISSION INDEPENDENT SIMULATOR (GMIS) AND SIMULATOR CONTROL PROGRAM (SCP)
Paul L. Baker (Global Science and Technology, Inc., Greenbelt, MD.), J. Michael Moore, and John Rosenberger (Computer Technology Associates, Inc., Rockville, MD.) *In its* Third International Symposium on Space Mission Operations and Ground Data Systems, Part 2 Nov. 1994 p 1093-1100 (For primary document see N95-17531 04-17)
Avail: CASI HC A02/MF A06

N95-17587*# National Aeronautics and Space Administration. Goddard Space Flight Center, Greenbelt, MD.
TRANSPORTABLE PAYLOAD OPERATIONS CONTROL CENTER REUSABLE SOFTWARE: BUILDING BLOCKS FOR QUALITY GROUND DATA SYSTEMS
Ron Mahmot, John T. Koslosky, Edward Beach (Computer Sciences Corp., Lanham, MD.), and Barbara Schwarz (Integral Systems, Inc., Lanham, MD.) *In its* Third International Symposium on Space Mission Operations and Ground Data Systems, Part 2 Nov. 1994 p 1161-1169 (For primary document see N95-17531 04-17)
Avail: CASI HC A02/MF A06

N95-17597*# European Space Agency. European Space Operations Center, Darmstadt (Germany).
USE OF DATA DESCRIPTION LANGUAGES IN THE INTERCHANGE OF DATA
M. Pignede, B. Real-Planells, and S. R. Smith (Logica Ltd., London, England.) *In* NASA. Goddard Space Flight Center, Third International Symposium on Space Mission Operations and Ground Data Systems, Part 2 Nov. 1994 p 1243-1251 (For primary document see N95-17531 04-17)
Avail: CASI HC A02/MF A06

N95-17602*# European Space Agency. European Space Operations Center, Darmstadt (Germany).
ATOS: INTEGRATION OF ADVANCED TECHNOLOGY SOFTWARE WITHIN DISTRIBUTED SPACECRAFT MISSION OPERATIONS SYSTEMS
M. Jones, J. Wheadon, W. OMullane, D. Whitgift (Logica Ltd., London, England.), K. Poulter (Logica Ltd., London, England.), M. Niezette (Space Applications Services, Brussels, Belgium.), R. Timmermans (Space Applications Services, Brussels, Belgium.), Ivan Rodriguez (Universidad Politecnica de Madrid, Spain.), and R. Romero (Universidad Politecnica de Madrid, Spain.) *In* NASA. Goddard Space Flight Center, Third International Symposium on Space Mission Operations and Ground Data Systems, Part 2 Nov. 1994 p 1289-1296 (For primary document see N95-17531 04-17)
Avail: CASI HC A02/MF A06

62 COMPUTER SYSTEMS

Includes computer networks and special application computer systems.

N95-15940 California Univ., Berkeley, CA. Computer Science Div.
NETWORK INTERFACE SPECIFICATION FOR THE T1 MICROPROCESSOR
Timothy J. Callahan May 1994 63 p Limited Reproducibility: More than 20% of this document may be affected by microfiche quality
(Contract N00014-92-J-1672; NSF CDA-87-22788)
(AD-A283392; UCB/CSD-94-823) Avail: Issuing Activity (Defense Technical Information Center (DTIC))

The overall performance of a multicomputer depends heavily on the interface between the software and the communication hardware. As pointed out in von Eicken's thesis, this communication architecture should be versatile in that it be able to support a variety of different communication models, including shared memory, dataflow, and send&receive; it should support an efficient implementation of each model; and it should be incremental in that it shouldn't interface with the computation performance of the processor. Active Messages communication architectures have been shown to satisfy these criteria. Software implementation of Active Messages have reduced communication overhead by over an order of magnitude to near the minimum possible given existing of an Active Message communication architecture, resulting in another order of magnitude reduction in communication overhead. The Active Message communication architecture defined in this report is an extension to the MIPS-II instruction set architecture. The resulting architecture features data transfer directly to/from processor registers, hardware dispatch directly to Active Message handlers (along with limited context preservation), automatic atomicity of handlers, cheap synchronization operations, and hardware support for multicast.
DTIC

N95-15946# Oak Ridge National Lab., TN.
A NEW COMMUNICATION SCHEME FOR THE NEUTRON DIFFUSION NODAL METHOD IN A DISTRIBUTED COMPUTING ENVIRONMENT
B. L. Kirk and Y. Azmy 1994 9 p Presented at the Topical Meeting on Advances in Reactor Physics, Knoxville, TN, 11-14 Apr. 1994
(Contract DE-AC05-84OR-21400)
(DE94-017907; CONF-940407-23) Avail: CASI HC A02/MF A01

A modified scheme is developed for solving the two-dimensional nodal diffusion equations on distributed memory computers. The scheme is aimed at minimizing the volume of communication among processors while maximizing the tasks in parallel. Results show a significant improvement in parallel efficiency on the Intel iPSC/860 hypercube compared to previous algorithms.
DOE

N95-16060# Syracuse Univ., NY. Northeast Parallel Architectures Center.
PARALLEL SOFTWARE BENCHMARKS FOR HIGH PERFORMANCE BMC3/IS SYSTEMS Final Report, Apr. 1992 - May 1993
Salim Hariri, Geoffrey C. Fox, Balaji Thiagarajan, and Manish Parashar May 1994 119 p
(Contract F30602-92-C-0063)
(AD-A282329; RL-TR-94-77) Avail: CASI HC A06/MF A02

This final technical report summarizes research accomplished under the Expert Science and Engineering (ES and E) program by the Northeast Parallel Architectures Center at Syracuse University. This 13-month research endeavor, entitled 'Parallel Software Benchmarks for BMC3/IS Systems,' examined issues in developing parallel software and tools that can be used in a parallel/distributed computing environment. These issues were evaluated via the development and application of benchmarks over a wide range of applications. Moreover, a hierarchical set of tool criteria to evaluate and benchmark different tools for parallel/distributed computing was also developed. This report gives a description of the process, benchmarks, criteria and a multi-target tracker implementation using various parallel software tools.
DTIC

N95-16061# Maryland Univ., College Park, MD.
ROBUST ROUTING IN DYNAMIC NETWORKS, PART 2 Final Technical Report

Ashok K. Agrawala Apr. 1994 540 p
(Contract F30602-90-C-0010)
(AD-A282396; RL-TR-94-37-Pt-2) Avail: CASI HC A23/MF A04

The goal of various control schemes used in a network is to assure a continued good performance as the load and other network characteristics change. Many of the flow and congestion control schemes are designed with assumed network dynamics. In order to get a better understanding of the network dynamics a tool was designed that can be used to monitor the detailed end-to-end behavior of a path of Internet for extended periods of time. The transit times and loss characteristics are observed by probe packets that are sent at regular intervals. Traditionally the flow control techniques used in the networks have been designed assuming a stochastic behavior for the load as well as the components of the network. In this research the approach has been to model a network and its connections using deterministic modeling techniques as far as possible, invoking stochastic assumptions only when deterministic assumptions cannot be justified or the lack of information makes it essential. A new version of Maryland Routing Simulator (MaRS) with improved front end has been completed and distributed through FTP. It has been copied by over 250 sites. DTIC

N95-16082 Rochester Univ., NY. Dept. of Computer Science.
THE SEARCH FOR LOST CYCLES: A NEW APPROACH TO PARALLEL PROGRAM PERFORMANCE EVALUATION
Mark E. Crovella and Thomas J. LeBlanc Dec. 1993 24 p Limited Reproducibility: More than 20% of this document may be affected by microfiche quality
(Contract N00014-92-J-1801; ARPA Order 8930)
(AD-A281467; TR-479) Avail: CASI HC A03

Traditional performance debugging and tuning of parallel programs is based on the 'measure-modify' approach, in which detailed measurements of program executions are used to guide incremental changes to the program that result in better performance. Unfortunately, the performance of a parallel algorithm is often related to its implementation, input data, and machine characteristics in surprising ways, and the measure-modify approach is unsuited to exploring these relationships fully: it is too heavily dependent on experimentation and measurement, which is impractical for studying the large number of variables that can affect parallel program performance. In this paper we argue that the problem of selecting the best implementation of a parallel algorithm requires a new approach to parallel program performance evaluation, one with a greater balance between measurement and modeling. We first present examples that demonstrate that different parallelizations of a program may be necessary to achieve the best possible performance as one varies the input data, machine architecture, or number of processors used. We then present an approach to performance evaluation based on lost cycles analysis, which involves measurement and modeling of all sources of overhead in a parallel program. We describe a measurement tool for lost cycles analysis that we have incorporated into the runtime environment for Fortran programs on the Kendall Square KSR1, and use this tool to analyze the performance tradeoffs among implementations of 2D FFT and parallel subgraph isomorphism. DTIC

N95-16083 Rochester Univ., NY. Dept. of Computer Science.
CAN HIGH BANDWIDTH AND LATENCY JUSTIFY LARGE CACHE BLOCKS IN SCALABLE MULTIPROCESSORS?
Ricardo Bianchini and Thomas J. LeBlanc Jan. 1994 30 p Limited Reproducibility: More than 20% of this document may be affected by microfiche quality
(Contract N00014-92-J-1801; ARPA Order 8930)
(AD-A281468; TR-486) Avail: CASI HC A03

An important architectural design decision affecting the performance of coherent caches in shared-memory multiprocessors is the choice of block size. There are two primary factors that influence this choice: the reference behavior of application programs and the remote access bandwidth and latency of the machine. Several studies have shown that increasing the block size can lower the miss rate and reduce the number of invalidations. However, increasing the block size can also increase the miss rate by, for example, increasing false sharing or the number of cache evictions. Large cache blocks can also generate network contention. Given that we anticipate enormous increases in both network bandwidth and latency in large-scale, shared-memory multiprocessors, the question arises as to what effect these increases will have on the choice of block size. We use analytical modeling and execution-driven simulation of parallel programs on a large-scale shared-memory machine to examine the relationship between cache block size and application performance as a function of remote access bandwidth and latency. We show that even under assumptions of high remote access bandwidth, the best application performance usually results from using cache blocks between 32 and 128 bytes in size. DTIC

N95-16113# Rochester Univ., NY. Dept. of Computer Science.
SOFTWARE CACHE COHERENCE FOR LARGE SCALE MULTIPROCESSORS
Leonidas I. Kontothanassis and Michael L. Scott Mar. 1994 20 p
(Contract N00014-92-J-1801; ARPA Order 8930)
(AD-A281628; TR-513) Avail: CASI HC A03/MF A01

Shared memory provides an attractive and intuitive programming model that makes good use of programmer time and effort. Shared memory however requires a coherence mechanism to allow caching for performance and to ensure that processors do not use stale data in their caches. We evaluate several algorithmic and architectural alternatives in the design space of non-cache coherent, nonuniform memory access (NCC-NUMA) machines with a globally-accessible physical address space. We present a new adaptive algorithm for software cache coherence that reduces interprocessor communication and scales to large numbers of processors; we compare it to existing software and hardware coherence schemes. We also evaluate the tradeoffs among various write policies (write-through, write-back, write-through with a write-collect buffer) and the effect on performance of using remote memory access. Finally, we observe that certain simple program changes can greatly improve performance. For example, we find that the use of reader-writer locks, synchronization variable relocation, and data structure padding and alignment can allow a protocol to avoid significant amounts of coherence overhead. DTIC

N95-16115 Rome Lab., Griffiss AFB, NY.
THE SURVIVABLE DISTRIBUTED COMPUTING ENVIRONMENT
Patrick M. Hurley and Scott M. Huse Jun. 1994 18 p Limited Reproducibility: More than 20% of this document may be affected by microfiche quality
(AD-A281637; RL-TR-94-29) Avail: Issuing Activity (Defense Technical Information Center (DTIC))

Distributed computer systems support several key attributes that are essential for the development and execution of command and control (C2) applications. Since C2 applications need to become more survivable, more dispersed, and better able to quickly adapt to new threats, we are seeking to provide an architecture for a survivable distributed computing environment (SDCE). In essence, the SDCE will be a base upon which survivable distributed applications can be built. This base must be flexible enough to incorporate advances in technology. It must also be tailorable to the needs of specific C2 applications, and well structured for ease of maintenance. Hence, this base must be capable of evolving with the needs of C2 systems and their supporting technologies. The approach that was used in this effort was to utilize existing technologies such as the Mach microkernel, along with the CRONUS and/or ISIS distributed computing environments to provide many of the SDCE requirements. DTIC

N95-16116 Rome Lab., Griffiss AFB, NY.
SUMMARY REPORT, 1992
Vaugh T. Combs, Gary L. Craig, Francis A. DiLego, Jr., Jerry L. Dussauly, and David J. Gray Mar. 1994 49 p Limited Reproducibility: More than 20% of this document may be affected by microfiche quality
(AF Proj. 5581)
(AD-A281639; RL-TR-94-35) Avail: CASI HC A03

The 1992 distributed systems evaluation environment (DISE) summary report is a progress report on the activity of the Rome Laboratory in-house work in distributed processing systems. In addition to the progress report, there are six condensed reports on the individual research, development, and application projects currently under way within the in-house group. The reports included are: Resource Management in Support of Application Management, Distributed-Parallel Effort, Distributed Image Compression in ISIS, Information Exchange using Cooperative Communicating Networks, The Survivable Distributed Computing Environment, and Weak Consistency and Recovery in a Command and Control Environment. DTIC

N95-16222# California Univ., Berkeley. Lawrence Berkeley Lab, CA.
ACCOUNTABILITY FOR NETWORK BACKUP FAILURES
W. H. Benson Feb. 1994 6 p Presented at the 12th Annual Pacific Northwest Software Quality Conference, Portland, OR, 17-19 Oct. 1994
(Contract DE-AC03-76SF-00098)
(DE94-011365; LBL-35282; CONF-9410102-1) Avail: CASI HC A02/MF A01

Regular hard disk backups for workstations are widely recommended. The necessity of backups is something most people would rather not think about. This attitude has two consequences. When people do subscribe to automated network backups, they expect the system to perform at a high level of reliability and that their files will be there for them when they need them. Second, they usually fail to appreciate that reliability is a shared responsibility. Although ostensibly their only responsibility is to keep the computer powered on overnight, there are actually many more opportunities for failure within the user's jurisdiction than in other parts of the infrastructure. High reliability is almost a sine qua non for backups. We describe a strategy for enhancing reliability based on the principle of accountability. This strategy involves monitoring the system, gathering statistics, detecting problems, anticipating problems, troubleshooting, and finally determining where failure occurred within the infrastructure and who should be accountable. We describe a specific backup system in a specific network environment to illustrate the value of accountability. This system, macdumps, backs up Macintosh disks over an AppleTalk network. The original software was written by Dan Tappan of BBN in the early years of the Mac and is available by ftp for noncommercial use. It has proven reliable and robust. Despite the high quality of the fundamental software, there are still many opportunities for failure within the infrastructure. We first discuss accountability in the context of network backups, then briefly describe how the backup system operates, the components of the infrastructure, types of failures experienced, and then summarize our experience. DOE

N95-16237 Massachusetts Inst. of Tech., Cambridge. Artificial Intelligence Lab.
PARTIAL EVALUATION FOR SCIENTIFIC COMPUTING: THE SUPERCOMPUTER TOOLKIT EXPERIENCE
Andrew Berlin and Rajeev Surati May 1994 11 p Limited Reproducibility: More than 20% of this document may be affected by microfiche quality
(Contract N00014-92-J-4097; NSF MIP-90-01651)
(AD-A282286; AI-M-1487) Avail: Issuing Activity (Defense Technical Information Center (DTIC))

We describe the key role played by partial evaluation in the Supercomputer Toolkit, a parallel computing system for scientific applications that effectively exploits the vast amount of parallelism exposed by partial evaluation. The Supercomputer Toolkit parallel processor and its associated partial evaluation-based compiler have been used extensively by scientists at M.I.T., and have made possible recent results in astrophysics showing that the motion of the planets in our solar system is chaotically unstable. DTIC

N95-16453*# National Aeronautics and Space Administration. Langley Research Center, Hampton, VA.
THE ROLE OF COMPUTERS IN RESEARCH AND DEVELOPMENT AT LANGLEY RESEARCH CENTER
Carol D. Wieseman, comp. Oct. 1994 605 p Workshop held in Hampton, VA, 15-16 Jun. 1994; sponsored by NASA, Washington
(RTOP 505-90-53)
(NASA-CP-10159; NAS 1.55:10159) Avail: CASI HC A99/MF A06

This document is a compilation of presentations given at a workshop on the role of computers in research and development at the Langley Research Center. The objectives of the workshop were to inform the Langley Research Center community of the current software systems and software practices in use at Langley. The workshop was organized in 10 sessions: Software Engineering; Software Engineering Standards, methods, and CASE tools; Solutions of Equations; Automatic Differentiation; Mosaic and the World Wide Web; Graphics and Image Processing; System Design Integration; CAE Tools; Languages; and Advanced Topics. For individual titles, see N95-16454 through N95-16480.

N95-16454*# National Aeronautics and Space Administration. Langley Research Center, Hampton, VA.
SOFTWARE ENGINEERING FROM A LANGLEY PERSPECTIVE **c61**
Susan Voigt *In its* The Role of Computers in Research and Development at Langley Research Center Oct. 1994 p 21-42 (For primary document see N95-16453 04-62)
Avail: CASI HC A03/MF A06

A brief introduction to software engineering is presented. The talk is divided into four sections beginning with the question 'What is software engineering', followed by a brief history of the progression of software engineering at the Langley Research Center in the context of an expanding computing environment. Several basic concepts and terms are introduced, including software development life cycles and maturity levels. Finally, comments are offered on what software engineering means for the Langley Research Center and where to find more information on the subject. Author (revised)

N95-16455*# Naval Surface Warfare Center, Virginia Beach, VA.
MODEL-BASED SOFTWARE PROCESS IMPROVEMENT **c61**
Brenda T. Zettervall *In* NASA. Langley Research Center, The Role of Computers in Research and Development at Langley Research Center Oct. 1994 p 68-84 (For primary document see N95-16453 04-62)
Avail: CASI HC A03/MF A06

The activities of a field test site for the Software Engineering Institute's software process definition project are discussed. Products tested included the improvement model itself, descriptive modeling techniques, the CMM level 2 framework document, and the use of process definition guidelines and templates. The software process improvement model represents a five stage cyclic approach for organizational process improvement. The cycles consist of the initiating, diagnosing, establishing, acting, and leveraging phases. CASI

N95-16456*# National Aeronautics and Space Administration. Langley Research Center, Hampton, VA.
A STUDY OF SOFTWARE STANDARDS USED IN THE AVIONICS INDUSTRY **c06**
Kelly J. Hayhurst *In its* The Role of Computers in Research and Development at Langley Research Center Oct. 1994 p 85-105 (For primary document see N95-16453 04-62)
Avail: CASI HC A03/MF A06

Within the past decade, software has become an increasingly common element in computing systems. In particular, the role of software used in the aerospace industry, especially in life- or safety-critical applications, is rapidly expanding. This intensifies the need to use effective techniques for achieving and verifying the reliability of avionics software. Although certain software development processes and techniques are mandated by government regulating agencies, no one methodology has been shown to consistently produce reliable software. The knowledge base for designing reliable software simply has not reached the maturity of its hardware counterpart. In an effort to increase our understanding of software, the Langley Research Center conducted a series of experiments over 15 years with the goal of understanding why and how software fails. As part of this program, the effectiveness of current industry standards for the development of avionics is being investigated. This study involves the generation of a controlled environment to conduct scientific experiments on software processes. Derived from text

N95-16457*# National Aeronautics and Space Administration. Langley Research Center, Hampton, VA.
A SOFTWARE TOOL FOR DATAFLOW GRAPH SCHEDULING **c61**
Robert L. Jones, III *In its* The Role of Computers in Research and Development at Langley Research Center Oct. 1994 p 106-113 (For primary document see N95-16453 04-62)
Avail: CASI HC A02/MF A06

A graph-theoretic design process and software tool is presented for selecting a multiprocessing scheduling solution for a class of computational problems. The problems of interest are those that can be described using a dataflow graph and are intended to be executed repetitively on multiple processors. The dataflow paradigm is very useful in exposing the parallelism inherent in algorithms. It provides a graphical and mathematical model which describes a partial ordering of algorithm tasks based on data precedence. Author

N95-16458*# National Aeronautics and Space Administration. Langley Research Center, Hampton, VA.
RAPID SOLUTION OF LARGE-SCALE SYSTEMS OF EQUATIONS
Olaf O. Storaasli *In its* The Role of Computers in Research and Development at Langley Research Center Oct. 1994 p 130-146 (For primary document see N95-16453 04-62)
Avail: CASI HC A03/MF A06

The analysis and design of complex aerospace structures requires the rapid solution of large systems of linear and nonlinear equations, eigenvalue extraction for buckling, vibration and flutter modes, structural optimization and design sensitivity calculation. Computers with multiple processors and vector capabilities can offer substantial computational advantages over traditional scalar computer for these analyses. These computers fall into two categories: shared memory computers and distributed memory computers. This presentation covers general-purpose, highly efficient algorithms for generation/assembly or element matrices, solution of systems of linear and nonlinear equations, eigenvalue and design sensitivity analysis and optimization. All algorithms are coded in FORTRAN for shared memory computers and many are adapted to distributed memory computers. The capability and numerical performance of these algorithms will be addressed. Author

N95-16459*# Lockheed Engineering and Sciences Co., Hampton, VA.
SOLUTION OF MATRIX EQUATIONS USING SPARSE TECHNIQUES
Majdi Baddourah *In* NASA. Langley Research Center, The Role of Computers in Research and Development at Langley Research Center Oct. 1994 p 147-155 (For primary document see N95-16453 04-62)
Avail: CASI HC A02/MF A06

The solution of large systems of matrix equations is key to the solution of a large number of scientific and engineering problems. This talk describes the sparse matrix solver developed at Langley which can routinely solve in excess of 263,000 equations in 40 seconds on one Cray C-90 processor. It appears that for large scale structural analysis applications, sparse matrix methods have a significant performance advantage over other methods. Derived from text

N95-16460*# National Aeronautics and Space Administration. Langley Research Center, Hampton, VA.
EQUATION SOLVERS FOR DISTRIBUTED-MEMORY COMPUTERS
Olaf O. Storaasli *In its* The Role of Computers in Research and Development at Langley Research Center Oct. 1994 p 156-166 (For primary document see N95-16453 04-62)
Avail: CASI HC A03/MF A06

A large number of scientific and engineering problems require the rapid solution of large systems of simultaneous equations. The performance of parallel computers in this area now dwarfs traditional vector computers by nearly an order of magnitude. This talk describes the major issues involved in parallel equation solvers with particular emphasis on the Intel Paragon, IBM SP-1 and SP-2 processors. Derived from text

N95-16461*# National Aeronautics and Space Administration. Langley Research Center, Hampton, VA.
APPLICATIONS OF AUTOMATIC DIFFERENTIATION IN COMPUTATIONAL FLUID DYNAMICS **c34**
Lawrence L. Green, A. Carle (Rice Univ., Houston, TX.), C. Bischof (Argonne National Lab., IL.), Kara J. Haigler, and Perry A. Newman *In its* The Role of Computers in Research and Development at Langley Research Center Oct. 1994 p 168-180 (For primary document see N95-16453 04-62)
Avail: CASI HC A03/MF A06

Automatic differentiation (AD) is a powerful computational method that provides for computing exact sensitivity derivatives (SD) from existing computer programs for multidisciplinary design optimization (MDO) or in sensitivity analysis. A pre-compiler AD tool for FORTRAN programs called ADIFOR has been developed. The ADIFOR tool has been easily and quickly applied by NASA Langley researchers to assess the feasibility and computational impact of AD in MDO with several different FORTRAN programs. These include a state-of-the-art three dimensional multigrid Navier-Stokes flow solver for wings or aircraft configurations in transonic turbulent flow. With ADIFOR the user specifies sets of independent and dependent variables with an existing computer code. ADIFOR then traces the dependency path throughout the code, applies the chain rule to formulate derivative expressions, and generates new code to compute the required SD matrix. The resulting codes have been verified to compute exact non-geometric and geometric SD for a variety of cases. in less time than is required to compute the SD matrix using centered divided differences. Author (revised)

N95-16462*# National Aeronautics and Space Administration. Langley Research Center, Hampton, VA.
AUTOMATIC DIFFERENTIATION FOR DESIGN SENSITIVITY ANALYSIS OF STRUCTURAL SYSTEMS USING MULTIPLE PROCESSORS
Duc T. Nguyen (Old Dominion Univ., Norfolk, VA.), Olaf O. Storaasli, Jiangning Qin (Old Dominion Univ., Norfolk, VA.), and Ramzi Qamar (Old Dominion Univ., Norfolk, VA.) *In its* The Role of Computers in Research and Development at Langley Research Center Oct. 1994 p 181-211 (For primary document see N95-16453 04-62)
Avail: CASI HC A03/MF A06

An automatic differentiation tool (ADIFOR) is incorporated into a finite element based structural analysis program for shape and non-shape design sensitivity analysis of structural systems. The entire analysis and sensitivity procedures are parallelized and vectorized for high performance computation. Small scale examples to verify the accuracy of the proposed program and a medium scale example to demonstrate the parallel vector performance on multiple CRAY C90 processors are included. Author (revised)

N95-16463*# Lockheed Engineering and Sciences Co., Hampton, VA.
INTRODUCTION TO THE WORLD WIDE WEB AND MOSAIC
Jim Youngblood *In* NASA. Langley Research Center, The Role of Computers in Research and Development at Langley Research Center Oct. 1994 p 213-223 (For primary document see N95-16453 04-62)
Avail: CASI HC A03/MF A06

This tutorial provides an introduction to some of the terminology related to the use of the World Wide Web and Mosaic. It is assumed that the user has some prior computer experience. References are included to other sources of additional information. Author

N95-16464*# National Aeronautics and Space Administration. Langley Research Center, Hampton, VA.
USE OF WORLD WIDE WEB AND NCSA MCSAIC AT LANGLEY **c82**
Michael Nelson *In its* The Role of Computers in Research and Development at Langley Research Center Oct. 1994 p 224-236 (For primary document see N95-16453 04-62)
Avail: CASI HC A03/MF A06

A brief history of the use of the World Wide Web at Langley Research Center is presented along with architecture of the Langley Web. Benefits derived from the Web and some Langley projects that have employed the World Wide Web are discussed. Derived from text

N95-16465*# National Aeronautics and Space Administration. Langley Research Center, Hampton, VA.
HOW TO USE THE WWW TO DISTRIBUTE STI **c82**
Donna G. Roper *In its* The Role of Computers in Research and Development at Langley Research Center Oct. 1994 p 237-245 (For primary document see N95-16453 04-62)
Avail: CASI HC A02/MF A06

This presentation explains how to use the World Wide Web (WWW) to distribute scientific and technical information as hypermedia. WWW clients and servers use the HyperText Transfer Protocol (HTTP) to transfer documents containing links to other text, graphics, video, and sound. The standard language for these documents is the HyperText MarkUp Language (HTML). These are simply text files with formatting codes that contain layout information and hyperlinks. HTML documents can be created with any text editor or with one of the publicly available HTML editors or convertors. HTML can also include links to available image formats. This presentation is available online. The URL is http://sti.larc.nasa. (followed by) gov/demos/workshop/introtext.html. Author (revised)

N95-16466*# Institute for Computer Applications in Science and Engineering, Hampton, VA.
IMAGE TOOLS FOR UNIX
David C. Banks *In* NASA. Langley Research Center, The Role of Computers in Research and Development at Langley Research Center

Oct. 1994 p 247-265 (For primary document see N95-16453 04-62)
Avail: CASI HC A03/MF A06

This talk features two simple and useful tools for digital image processing in the UNIX environment. They are xv and pbmplus. The xv image viewer which runs under the X window system reads images in a number of different file formats and writes them out in different formats. The view area supports a pop-up control panel. The 'algorithms' menu lets you blur an image. The xv control panel also activates the color editor which displays the image's color map (if one exists). The xv image viewer is available through the internet. The pbmplus package is a set of tools designed to perform image processing from within a UNIX shell. The acronym 'pbm' stands for portable bit map. Like xv, the pbm plus tool can convert images from and to many different file formats. The source code and manual pages for pbmplus are also available through the internet. This software is in the public domain. Author (revised)

N95-16467*# Hampton Univ., VA.
FROM COMPUTER IMAGES TO VIDEO PRESENTATION: ENHANCING TECHNOLOGY TRANSFER c82
Sherilee F. Beam *In* NASA. Langley Research Center, The Role of Computers in Research and Development at Langley Research Center Oct. 1994 p 266-271 (For primary document see N95-16453 04-62)
Avail: CASI HC A02/MF A06

With NASA placing increased emphasis on transferring technology to outside industry, NASA researchers need to evaluate many aspects of their efforts in this regard. Often it may seem like too much self-promotion to many researchers. However, industry's use of video presentations in sales, advertising, public relations and training should be considered. Today, the most typical presentation at NASA is through the use of vu-graphs (overhead transparencies) which can be effective for text or static presentations. For full blown color and sound presentations, however, the best method is videotape. In fact, it is frequently more convenient due to its portability and the availability of viewing equipment. This talk describes techniques for creating a video presentation through the use of a combined researcher and video professional team. Author (revised)

N95-16468*# National Aeronautics and Space Administration. Langley Research Center, Hampton, VA.
DATA VISUALIZATION AND ANIMATION LAB (DVAL) OVERVIEW c61
Kathy Stacy and Bill vonOfenheim *In its* The Role of Computers in Research and Development at Langley Research Center Oct. 1994 p 292-315 (For primary document see N95-16453 04-62)
Avail: CASI HC A03/MF A06

The general capabilities of the Langley Research Center Data Visualization and Animation Laboratory is described. These capabilities include digital image processing, 3-D interactive computer graphics, data visualization and analysis, video-rate acquisition and processing of video images, photo-realistic modeling and animation, video report generation, and color hardcopies. A specialized video image processing system is also discussed. CASI

N95-16469*# National Aeronautics and Space Administration. Langley Research Center, Hampton, VA.
DATA VISUALIZATION AND ANIMATION LAB (DVAL): APPLICATIONS c61
Kurt Severance and Mike Weisenborn *In its* The Role of Computers in Research and Development at Langley Research Center Oct. 1994 p 292-316 (For primary document see N95-16453 04-62)
Avail: CASI HC A03/MF A06

A wide variety of software tools has been successfully used to visualize, analyze and present computational and experimental data at Langley Research Center. These tools can be categorized according to five primary uses: (1) 2-D image analysis, (2) conventional 3-D visualization, (3) volume visualization, (4) photo-realistic rendering, or (5) special purpose applications. Software is accessible in each of these categories for Langley personnel, and training or consultation can be arranged with the Data Visualization and Animation laboratory staff. Author (revised)

N95-16470*# National Aeronautics and Space Administration. Langley Research Center, Hampton, VA.
THE DESIGN MANAGER'S AID FOR INTELLIGENT DECOMPOSITION (DeMAID)
James L. Rogers *In its* The Role of Computers in Research and Development at Langley Research Center Oct. 1994 p 317-350 (For primary document see N95-16453 04-62)
Avail: CASI HC A03/MF A06

Before the design of new complex systems such as large space platforms can begin, the possible interactions among subsystems and their parts must be determined. Once this is completed, the proposed system can be decomposed to identify its hierarchical structure. The design manager's aid for intelligent decomposition (DeMAID) is a knowledge based system for ordering the sequence of modules and identifying a possible multilevel structure for design. Although DeMAID requires an investment of time to generate and refine the list of modules for input, it could save considerable money and time in the total design process, particularly in new design problems where the ordering of the modules has not been defined. Author (revised)

N95-16471*# National Aeronautics and Space Administration. Langley Research Center, Hampton, VA.
RDD-100 AND THE SYSTEMS ENGINEERING PROCESS
Robert D. Averill *In its* The Role of Computers in Research and Development at Langley Research Center Oct. 1994 p 351-376 (For primary document see N95-16453 04-62)
Avail: CASI HC A03/MF A06

An effective systems engineering approach applied through the project life cycle can help Langley produce a better product. This paper demonstrates how an enhanced systems engineering process for in-house flight projects assures that each system will achieve its goals with quality performance and within planned budgets and schedules. This paper also describes how the systems engineering process can be used in combination with available software tools. Derived from text

N95-16472*# National Aeronautics and Space Administration. Langley Research Center, Hampton, VA.
COMPUTER TOOLS FOR SYSTEMS ENGINEERING AT LaRC
J. Milam Walters *In its* The Role of Computers in Research and Development at Langley Research Center Oct. 1994 p 377-384 (For primary document see N95-16453 04-62)
Avail: CASI HC A02/MF A06

The Systems Engineering Office (SEO) has been established to provide life cycle systems engineering support to Langley research Center projects. over the last two years, the computing market has been reviewed for tools which could enhance the effectiveness and efficiency of activities directed towards this mission. A group of interrelated applications have been procured, or are under development including a requirements management tool, a system design and simulation tool, and project and engineering data base. This paper will review the current configuration of these tools and provide information on future milestones and directions. Author

N95-16473*# National Aeronautics and Space Administration. Langley Research Center, Hampton, VA.
ELECTRONIC ENGINEERING NOTEBOOK: A SOFTWARE ENVIRONMENT FOR RESEARCH EXECUTION, DOCUMENTATION AND DISSEMINATION
Dan Moerder *In its* The Role of Computers in Research and Development at Langley Research Center Oct. 1994 p 443-469 (For primary document see N95-16453 04-62)
Avail: CASI HC A03/MF A06

The electronic engineering notebook (EEN) consists of a free form research notebook, implemented in a commercial package for distributed hypermedia, which includes utilities for graphics capture, formatting and display of LaTex constructs, and interfaces to the host operating system. The latter capability consists of an information computer-aided software engineering (CASE) tool and a means to associate executable scripts with source objects. The EEN runs on Sun and HP workstations. The EEN, in day-to-day use can be used in much the same manner as the sort of research notes most researchers keep during development of projects. Graphics can be pasted in, equations can be entered via LaTex, etc. In addition, the fact that the EEN is hypermedia permits easy management of 'context', e.g., derivations and data can contain easily formed links to other supporting derivations and data. The CASE tool also permits development and maintenance of source code directly in the notebook, with access to its derivations and data. Author (revised)

N95-16474*# National Aeronautics and Space Administration. Langley Research Center, Hampton, VA.

MATLAB AS A ROBUST CONTROL DESIGN TOOL **c63**

Irene M. Gregory *In its* The Role of Computers in Research and Development at Langley Research Center Oct. 1994 p 485-496 (For primary document see N95-16453 04-62)

Avail: CASI HC A03/MF A06

This presentation introduces Matlab as a tool used in flight control research. The example used to illustrate some of the capabilities of this software is a robust controller designed for a single stage to orbit air breathing vehicles's ascent to orbit. The global requirements of the controller are to stabilize the vehicle and follow a trajectory in the presence of atmospheric disturbances and strong dynamic coupling between airframe and propulsion. Author (revised)

N95-16475*# National Aeronautics and Space Administration. Langley Research Center, Hampton, VA.

SIMULATION OF THE COUPLED MULTI-SPACECRAFT CONTROL TESTBED AT THE MARSHALL SPACE FLIGHT CENTER **c63**

Dave Ghosh and Raymond C. Montgomery *In its* The Role of Computers in Research and Development at Langley Research Center Oct. 1994 p 497-517 (For primary document see N95-16453 04-62)

Avail: CASI HC A03/MF A06

The capture and berthing of a controlled spacecraft using a robotic manipulator is an important technology for future space missions and is presently being considered as a backup option for direct docking of the Space Shuttle to the Space Station during assembly missions. The dynamics and control of spacecraft configurations that are manipulator-coupled with each spacecraft having independent attitude control systems is not well understood and NASA is actively involved in both analytic research on this three dimensional control problem for manipulator coupled active spacecraft and experimental research using a two dimensional ground based facility at the Marshall Space Flight Center (MSFC). This paper first describes the MSFC testbed and then describes a two link arm simulator that has been developed to facilitate control theory development and test planning. The motion of the arms and the payload is controlled by motors located at the shoulder, elbow, and wrist. Author

N95-16476*# Institute for Computer Applications in Science and Engineering, Hampton, VA.

OBJECT-ORIENTED NUMERICAL COMPUTING C++

John VanRosendale *In* NASA. Langley Research Center, The Role of Computers in Research and Development at Langley Research Center Oct. 1994 p 519-535 (For primary document see N95-16453 04-62)

Avail: CASI HC A03/MF A06

An object oriented language is one allowing users to create a set of related types and then intermix and manipulate values of these related types. This paper discusses object oriented numerical computing using C++. CASI

N95-16477*# National Aeronautics and Space Administration. Langley Research Center, Hampton, VA.

HARDWARE DESCRIPTION LANGUAGES **c60**

Jerry H. Tucker *In its* The Role of Computers in Research and Development at Langley Research Center Oct. 1994 p 536-545 (For primary document see N95-16453 04-62)

Avail: CASI HC A02/MF A06

Hardware description languages are special purpose programming languages. They are primarily used to specify the behavior of digital systems and are rapidly replacing traditional digital system design techniques. This is because they allow the designer to concentrate on how the system should operate rather than on implementation details. Hardware description languages allow a digital system to be described with a wide range of abstraction, and they support top down design techniques. A key feature of any hardware description language environment is its ability to simulate the modeled system. The two most important hardware description languages are Verilog and VHDL. Verilog has been the dominant language for the design of application specific integrated circuits (ASIC's). However, VHDL is rapidly gaining in popularity. Author (revised)

N95-16478*# Institute for Computer Applications in Science and Engineering, Hampton, VA.

HIGH PERFORMANCE FORTRAN **c61**

Piyush Mehrotra *In* NASA. Langley Research Center, The Role of Computers in Research and Development at Langley Research Center Oct. 1994 p 546-561 (For primary document see N95-16453 04-62)

Avail: CASI HC A03/MF A06

High performance FORTRAN is a set of extensions for FORTRAN 90 designed to allow specification of data parallel algorithms. The programmer annotates the program with distribution directives to specify the desired layout of data. The underlying programming model provides a global name space and a single thread of control. Explicitly parallel constructs allow the expression of fairly controlled forms of parallelism in particular data parallelism. Thus the code is specified in a high level portable manner with no explicit tasking or communication statements. The goal is to allow architecture specific compilers to generate efficient code for a wide variety of architectures including SIMD, MIMD shared and distributed memory machines. Author

N95-16479*# National Aeronautics and Space Administration. Langley Research Center, Hampton, VA.

CURRENT RESEARCH ACTIVITIES AT THE NASA-SPONSORED ILLINOIS COMPUTING LABORATORY OF AEROSPACE SYSTEMS AND SOFTWARE

Kathryn A. Smith *In its* The Role of Computers in Research and Development at Langley Research Center Oct. 1994 p 563-569 (For primary document see N95-16453 04-62)

Avail: CASI HC A02/MF A06

The Illinois Computing Laboratory of Aerospace Systems and Software (ICLASS) was established to: (1) pursue research in the areas of aerospace computing systems, software and applications of critical importance to NASA, and (2) to develop and maintain close contacts between researchers at ICLASS and at various NASA centers to stimulate interaction and cooperation, and facilitate technology transfer. Current ICLASS activities are in the areas of parallel architectures and algorithms, reliable and fault tolerant computing, real time systems, distributed systems, software engineering and artificial intelligence. Author (revised)

N95-16480*# National Aeronautics and Space Administration. Langley Research Center, Hampton, VA.

EPISTEMOLOGY, SOFTWARE ENGINEERING AND FORMAL METHODS **c61**

C. Michael Holloway *In its* The Role of Computers in Research and Development at Langley Research Center Oct. 1994 p 570-595 (For primary document see N95-16453 04-62)

Avail: CASI HC A03/MF A06

One of the most basic questions anyone can ask is, 'How do I know that what I think I know is true?' The study of this question is called epistemology. Traditionally, epistemology has been considered to be of legitimate interest only to philosophers, theologians, and three year old children who respond to every statement by asking, 'Why?' Software engineers need to be interested in the subject, however, because a lack of sufficient understanding of epistemology contributes to many of the current problems in the field. Author

N95-16529# Colorado State Univ., Fort Collins, CO. Dept. of Computer Science.

PROCEEDINGS OF THE INTERNATIONAL CONFERENCE ON PARALLEL ARCHITECTURES AND COMPILATION TECHNIQUES

Michel Cosnard, Guang R. Gao, and Gabriel M. Silberman 26 Aug. 1994 378 p Conference held in Montreal, Quebec, 24-26 Aug. 1994

(Contract N00014-94-I-0198)

(AD-A285258) Avail: CASI HC A17/MF A03

Contents: Part 1- High Performance Architectures; Part 2- Code Generation for Multithreaded and Dataflow Architectures; Part 3- Memory and Cachelssues; Part 4- Distributed Memory Machines; Part 5- Multi-Level Parallelism; Part 6- Compiling for Parallel Machines; and Part 7- Logic Languages. DTIC

N95-16603# Carnegie-Mellon Univ., Pittsburgh, PA. Dept. of Computer Science.

ON-LINE SCHEDULING ON PARALLEL MACHINES Ph.D. Thesis

Jiri Sgall May 1994 119 p
(Grant NSF CCR-91-19319)
(AD-A281136; CMU-CS-94-144) Avail: CASI HC A06/MF A02

Given a parallel machine with processors arranged in some particular network topology (e.g., on a mesh machine the processors are arranged in a rectangular grid), we have to execute different parallel jobs. Each job requires some part of the machine (e.g., a mesh of a smaller size), and can be executed on any subset of processors with that network topology. Each job will run for some fixed time, regardless of when we execute it. But we do not know the running times in advance, the only way to determine the running time of a job is to execute it. Scheduling may also be constrained by dependencies between jobs; it may be the case that a job cannot be started until some other jobs have finished. Our task is to schedule a given set of jobs so that all constraints are satisfied and the total time is as small as possible. The author claims that in this model efficient on-line scheduling is possible on a variety of different parallel machines, including PRAMs, hypercubes, and mesh machines. However, the efficiency depends on various factors, including the presence of dependencies, the combinatorial complexity of the network topology, randomization, the use of virtualization, and the maximal size of jobs. DTIC

N95-16826# Carnegie-Mellon Univ., Pittsburgh, PA. Dept. of Computer Science.
DOME: DISTRIBUTED OBJECT MIGRATION ENVIRONMENT
Adam Beguelin, Erik Seligman, and Michael Starkey May 1994 27 p
(AD-A281134; CMU-CS-94-153) Avail: CASI HC A03/MF A01

Dome is an object based parallel programming environment for heterogeneous distributed networks of machines. This paper gives a brief overview of Dome. We show that Dome programs are easy to write. A description of the load balancing performed in Dome is presented along with performance measurements on a cluster of DEC Alpha workstations connected by a DEC Gigaswitch. A Dome program is compared with a sequential version and one written in PVM. We also present an overview of architecture independent checkpoint and restart in Dome. DTIC

N95-16830 Sandia National Labs., Albuquerque, NM.
ACTIVE MESSAGES VERSUS EXPLICIT MESSAGE PASSING UNDER SUNMOS
R. Riesen, S. R. Wheat, and A. B. Maccabe (New Mexico Univ., Albuquerque, NM.) 1994 7 p Presented at the Intel Supercomputing Users Group Meeting, San Diego, CA, 25-29 Jun. 1994 Limited Reproducibility: More than 20% of this document may be affected by microfiche quality
(Contract DE-AC04-94AL-85000)
(DE94-015278; SAND-94-1582C; CONF-9406205-3) Avail: CASI HC A02

In the past few years much effort has been devoted to finding faster and more convenient ways to exchange data between nodes of massively parallel distributed memory machines. One such approach, taken by Thorsten von Eicken et al. is called Active Messages. The idea is to hide message passing latency and continue to compute while data is being sent and delivered. The authors have implemented Active Messages under SUNMOS for the Intel Paragon and performed various experiments to determine their efficiency and utility. In this paper they concentrate on the subset of the Active Message layer that is used by the implementation of the Split-C library. They compare performance to explicit message passing under SUNMOS and explore new ways to support Split-C without Active Messages. They also compare the implementation to the original one on the Thinking Machines CM-5 and try to determine what the effects of low latency and low band-width versus high latency and high bandwidth are on user codes. DOE

N95-16901# National Aeronautical Lab., Bangalore (India). Flosolver Unit.
FLOSOLVER PARALLEL COMPUTERS: 1986-1994
Jul. 1994 30 p Original contains color illustrations
(NAL Proj. I-8-119)
(NAL-SP-9409) Avail: CASI HC A03/MF A01

This document is a technical account of the history of Flosolver development at NAL - starting with the early development using Intel's 8086/8087 and ending with a narrative on the successful parallelization of the T-80 weather prediction code on Flosolver Mk3 based on the i860 processor. The document also discusses system software, future plans and the financial details related to India's first parallel computer. Author

N95-17138# Technische Univ., Delft (Netherlands).
PARALLEL PARSING Ph.D. Thesis [PARALLEL ONTLEDEN]
J. P. M. deVreught 29 Jun. 1993 160 p
(PB94-191392; ISBN-90-9006256-4) Copyright Avail: CASI HC A08/MF A02

The thesis begins by forming one coherent theory on parsing context-free grammars in which three algorithms are described, first in the slow parallel case and then in the fast parallel case. Everything is tied up to essentially three similar partial parse relations. The presentation of each variant is kept as closely in line with the others as possible. It then goes on to describe a sharpest upper bound for the derivation length of acyclic context-free grammars and, almost as a corollary, its implication on acyclic noncircular attribute grammars. The next chapter covers the slow parallel decorating of all parses simultaneously. The bulk of the final chapter is on a parallel dag contraction algorithm. Working on such an algorithm is quite difficult because of the requirement of low time complexity. There is very little room to maneuver; even trivial steps must be analyzed on their contribution to the overall time complexity. NTIS

N95-17374 Quality Decision Management, Inc., North Andover, MA.
GROUPWARE SYSTEM FOR MULTIDISCIPLINARY PARTICIPATION Final Report, Jun. 1992 - Mar. 1994
D. A. Jeffrey, Dorothy S. Rhodes, and Richard C. Byron May 1994 82 p Limited Reproducibility: More than 20% of this document may be affected by microfiche quality
(Contract F41624-92-C-5006)
(AD-A282525; AL/HR-TR-1994-0061) Avail: Issuing Activity (Defense Technical Information Center (DTIC))

Quality Decision Management, Inc. (QDM) has developed a methodology and information architecture that support multidisciplinary participation and communication for geographically distributed community of individuals and workgroups. The system is an automated environment, based on management methods and workgroup technologies, that improves the effectiveness of workgroup communication and coordination, increases awareness of process and improves the efficiency of their execution, and provides users with feedback and status metrics. Through this research, we have demonstrated and utilized the synergy between workgroup technologies and management theories. Our work has resulted in a custom software solution for our pilot environment and in a widely applicable system that has been commercialized by QDM and is now available worldwide. The organization-wide benefits made possible by this system have been realized by our clients in both the public and private sectors. DTIC

N95-17516# Sandia National Labs., Albuquerque, NM.
ATM-TEST: A WORKSTATION-BASED SOFTWARE SUITE FOR TESTING ASYNCHRONOUS TRANSFER MODE (ATM) NETWORKS
T. D. Tarman Jun. 1994 25 p
(Contract DE-AC04-94AL-85000)
(DE94-013813; SAND-94-1547) Avail: CASI HC A03/MF A01

The design of a software package that provides a variety of Asynchronous Transfer Mode (ATM) test functions is presented here. These functions include cell capture, protocol decode for Transmission Control Protocol/Internet Protocol (TCP/IP) services, removal of cells (to support testing of an ATM system under cell loss conditions), and echo functions. This package is currently written to operate on the Sun Microsystems SPARCstation 10/SunOS 4.1.3 environment with a Fore Systems SBA-100 Sbus ATM adapter (140 Mbit/s TAXI interface), and the DEC 5000/240 running ULTRIX 4.2A with a Fore Systems TCA-100 TurboChannel adapter. Application scenarios and performance measurements of this software package on these host environments are presented here. DOE

N95-17638 Sandia National Labs., Albuquerque, NM.
TEST APPLICATIONS FOR HETEROGENEOUS REAL-TIME NETWORK TESTBED
R. F. Mines and E. W. Knightly Jul. 1994 18 p Presented at the 9th ACM SIGPLAN Conference on Object-Oriented Programming System, Languages and Applications, Portland, OR, 27 Oct. 1994 Limited Reproducibility: More than 20% of this document may be affected by

microfiche quality
(Contract DE-AC04-76DP-00789)
(DE94-016480; SAND-94-8227; CONF-941071-2) Avail: CASI HC A03

This paper investigates several applications for a heterogeneous real-time network testbed. The network is heterogeneous in terms of network devices, technologies, protocols, and algorithms. The network is real-time in that its services can provide per-connection end-to-end performance guarantees. Although different parts of the network use different algorithms, all components have the necessary mechanisms to provide performance guarantees: admission control and priority scheduling. Three applications for this network are described in this paper: a video conferencing tool, a tool for combustion modeling using distributed computing, and an MPEG video archival system. Each has minimum performance requirements that must be provided by the network. By analyzing these applications, we provide insights to the traffic characteristics and performance requirements of practical real-time loads. DOE

N95-17676# Oak Ridge National Lab., TN.
PARALLEL FAST FOURIER TRANSFORMS FOR NON POWER OF TWO DATA
B. D. Semeraro 1994 6 p Presented at the Intel Supercomputing Users Group Meeting, San Diego, CA, 25-29 Jun. 1994
(Contract DE-AC05-84OR-21400)
(DE94-018047; CONF-9406205-4) Avail: CASI HC A02/MF A01

This report deals with parallel algorithms for computing discrete Fourier transforms of real sequences of length N not equal to a power of two. The method described is an extension of existing power of two transforms to sequences with N a product of small primes. In particular, this implementation requires N = 2(sup p)3(sup q)5(sup r). The communication required is the same as for a transform of length N = 2(sup p). The algorithm presented is intended for use in the solution of partial differential equations, or in any situation in which a large number of forward and backward transforms must be performed and in which the Fourier Coefficients need not be ordered. This implementation is a one dimensional FFT but the techniques are applicable to multidimensional transforms as well. The algorithm has been implemented on a 128 node Intel Ipsc/860. DOE

N95-17741 Brown Univ., Providence, RI. Dept. of Computer Science.
CONTROLLING MEMORY ACCESS CONCURRENCY IN EFFICIENT FAULT-TOLERANT PARALLEL ALGORITHMS
Paris C. Kanellakis, Dimitrios Michailidis, and Alex A. Shvartsman 16 May 1994 33 p Limited Reproducibility: More than 20% of this document may be affected by microfiche quality
(Contract N00014-91-J-1613)
(AD-A280909) Avail: Issuing Activity (Defense Technical Information Center (DTIC))

The CRCW PRAM under dynamic fail-stop (no restart) processor behavior is a fault-prone multiprocessor model for which it is possible to both guarantee reliability and preserve efficiency. To handle dynamic faults some redundancy is necessary in the form of many processors concurrently performing a common read or write task. In this paper we show how to significantly decrease this concurrency by bounding it in terms of the number of actual processor faults. We describe a low concurrency, efficient and fault-tolerant algorithm for the Write-All primitive: 'using less than or equal to N processors, write 1's into N locations'. This primitive can serve as the basis for efficient fault-tolerant simulations of algorithms written for fault-free PRAM's on fault-prone PRAM's. For any dynamic failure pattern F, our algorithm has total write concurrency less than or equal to /F/ and total read concurrency less than or equal to 7/F/log N, where /F/ is the number of processor faults (for example, there is no concurrency in a run without failures); note that, previous algorithms used Omega(N log N) concurrency even in the absence of faults. We also describe a technique for limiting the per step concurrency and present an optimal fault-tolerant EREW PRAM algorithm for Write-All, when all processor faults are initial. DTIC

63 CYBERNETICS

Includes feedback and control theory, artificial intelligence, robotics and expert systems.

For related information see also *54 Man/System Technology and Life Support.*

N95-15952# California Univ., Los Angeles, CA.
DIGITAL ADAPTIVE AND OPTIMAL CONTROL OF DISTRIBUTED SYSTEMS Final Report, 1 Oct. 1990 - 31 Dec. 1993
J. S. Gibson 31 Dec. 1993 57 p
(Grant AF-AFOSR-0016-91)
(AD-A285352; AFOSR-94-0584TR) Avail: CASI HC A04/MF A01

Research on optimal and adaptive control and adaptive identification of distributed systems has been performed. Most of the research has focused on digital control and identification methods, to allow for real-time implementation. The main applications have been identification and control of flexible structures. Both new mathematical theory and new numerical methods have been primary objectives and results of the research. Experimental application of the new methods for adaptive identification and disturbance rejection has been carried out. DTIC

N95-15972*# National Aeronautics and Space Administration. Lyndon B. Johnson Space Center, Houston, TX.
ISMCR 1994: TOPICAL WORKSHOP ON VIRTUAL REALITY. PROCEEDINGS OF THE FOURTH INTERNATIONAL SYMPOSIUM ON MEASUREMENT AND CONTROL IN ROBOTICS
Nov. 1994 153 p Workshop held in Houston, TX, 30 Nov. - 3 Dec. 1994; cosponsored by ISA, IEEE, and AIAA
(NASA-CP-10163; S-788; NAS 1.55:10163; LC-94-69310; ISBN-0-9627116-1-6) Avail: CASI HC A08/MF A02

This symposium on measurement and control in robotics included sessions on: (1) rendering, including tactile perception and applied virtual reality; (2) applications in simulated medical procedures and telerobotics; (3) tracking sensors in a virtual environment; (4) displays for virtual reality applications; (5) sensory feedback including a virtual environment application with partial gravity simulation; and (6) applications in education, entertainment, technical writing, and animation. For individual titles, see N95-15973 through N95-15992.

N95-15973*# Tokyo Metropolitan Univ. (Japan).
VIBRATORY TACTILE DISPLAY FOR TEXTURES
Yasushi Ikei, Akihisa Ikeno, and Shuichi Fukuda *In* NASA. Johnson Space Center, ISMCR 1994: Topical Workshop on Virtual Reality. Proceedings of the Fourth International Symposium on Measurement and Control in Robotics Nov. 1994 p 3-10 (For primary document see N95-15972 04-63)
Avail: CASI HC A02/MF A02

We have developed a tactile display that produces vibratory stimulus to a fingertip in contact with a vibrating tactor matrix. The display depicts tactile surface textures while the user is exploring a virtual object surface. A piezoelectric actuator drives the individual tactor in accordance with both the finger movement and the surface texture being traced. Spatiotemporal display control schemes were examined for presenting the fundamental surface texture elements. The temporal duration of vibratory stimulus was experimentally optimized to simulate the adaptation process of cutaneous sensation. The selected duration time for presenting a single line edge agreed with the time threshold of tactile sensation. Then spatial stimulus disposition schemes were discussed for representation of other edge shapes. As an alternative means not relying on amplitude control, a method of augmented duration at the edge was investigated. Spatial resolution of the display was measured for the lines presented both in perpendicular and parallel to a finger axis. Discrimination of texture density was also measured on random dot textures. Author

N95-15974*# Research Triangle Inst., Research Triangle Park, NC. Virtual Reality Group.
APPLIED VIRTUAL REALITY AT THE RESEARCH TRIANGLE INSTITUTE
R. Jorge Montoya *In* NASA. Johnson Space Center, ISMCR 1994: Topical Workshop on Virtual Reality. Proceedings of the Fourth International

Symposium on Measurement and Control in Robotics Nov. 1994 p 11-18 (For primary document see N95-15972 04-63)
Avail: CASI HC A02/MF A02

Virtual Reality (VR) is a way for humans to use computers in visualizing, manipulating and interacting with large geometric data bases. This paper describes a VR infrastructure and its application to marketing, modeling, architectural walk through, and training problems. VR integration techniques used in these applications are based on a uniform approach which promotes portability and reusability of developed modules. For each problem, a 3D object data base is created using data captured by hand or electronically. The object's realism is enhanced through either procedural or photo textures. The virtual environment is created and populated with the data base using software tools which also support interactions with and immersivity in the environment. These capabilities are augmented by other sensory channels such as voice recognition, 3D sound, and tracking. Four applications are presented: a virtual furniture showroom, virtual reality models of the North Carolina Global TransPark, a walk through the Dresden Fraunenkirche, and the maintenance training simulator for the National Guard.

Author (revised)

N95-15975*# Alaska Univ., Fairbanks, AK. Arctic Region Supercomputing Center.

SIMULATION OF ARTHROSCOPIC SURGERY USING MRI DATA c52

Geoffrey Heller and Jon Genetti *In* NASA. Johnson Space Center, ISMCR 1994: Topical Workshop on Virtual Reality. Proceedings of the Fourth International Symposium on Measurement and Control in Robotics Nov. 1994 p 21-26 Sponsored by Cray Research Inc. and Corps of Engineers (For primary document see N95-15972 04-63)
Avail: CASI HC A02/MF A02

With the availability of Magnetic Resonance Imaging (MRI) technology in the medical field and the development of powerful graphics engines in the computer world the possibility now exists for the simulation of surgery using data obtained from an actual patient. This paper describes a surgical simulation system which will allow a physician or a medical student to practice surgery on a patient without ever entering an operating room. This could substantially lower the cost of medial training by providing an alternative to the use of cadavers. This project involves the use of volume data acquired by MRI which are converted to polygonal form using a corrected marching cubes algorithm. The data are then colored and a simulation of surface response based on springy structures is performed in real time. Control for the system is obtained through the use of an attached analog-to-digital unit. A remote electronic device is described which simulates an imaginary tool having features in common with both arthroscope and laparoscope.

Author

N95-15976*# Padua Univ. (Italy). Dept. of Innovation in Mechanics and Management.

MULTIMODAL CORRELATION AND INTRAOPERATIVE MATCHING OF VIRTUAL MODELS IN NEUROSURGERY c52

Enrico Ceresole, Michele DalSasso, and Aldo Rossi *In* NASA. Johnson Space Center, ISMCR 1994: Topical Workshop on Virtual Reality. Proceedings of the Fourth International Symposium on Measurement and Control in Robotics Nov. 1994 p 27-30 (For primary document see N95-15972 04-63)
Avail: CASI HC A01/MF A02

The multimodal correlation between different diagnostic exams, the intraoperative calibration of pointing tools and the correlation of the patient's virtual models with the patient himself, are some examples, taken from the biomedical field, of a unique problem: determine the relationship linking representation of the same object in different reference frames. Several methods have been developed in order to determine this relationship, among them, the surface matching method is one that gives the patient minimum discomfort and the errors occurring are compatible with the required precision. The surface matching method has been successfully applied to the multimodal correlation of diagnostic exams such as CT, MR, PET and SPECT. Algorithms for automatic segmentation of diagnostic images have been developed to extract the reference surfaces from the diagnostic exams, whereas the surface of the patient's skull has been monitored, in our approach, by means of a laser sensor mounted on the end effector of an industrial robot. An integrated system for virtual planning and real time execution of surgical procedures has been realized. Author (revised)

N95-15977*# Monash Univ., Clayton (Australia). Dept. of Computer Science.

VIRTUAL REALITY AND TELEROBOTICS APPLICATIONS OF AN ADDRESS RECALCULATION PIPELINE

Matthew Regan and Ronald Pose *In* NASA. Johnson Space Center, ISMCR 1994: Topical Workshop on Virtual Reality. Proceedings of the Fourth International Symposium on Measurement and Control in Robotics Nov. 1994 p 31-36 Sponsored by Australian Research Council (For primary document see N95-15972 04-63)
Avail: CASI HC A02/MF A02

The technology described in this paper was designed to reduce latency to user interactions in immersive virtual reality environments. It is also ideally suited to telerobotic applications such as interaction with remote robotic manipulators in space or in deep sea operations. in such circumstances the significant latency is observed response to user stimulus which is due to communications delays, and the disturbing jerkiness due to low and unpredictable frame rates on compressed video user feedback or computationally limited virtual worlds, can be masked by our techniques. The user is provided with highly responsive visual feedback independent of communication or computational delays in providing physical video feedback or in rendering virtual world images. Virtual and physical environments can be combined seamlessly using these techniques.

Author (revised)

N95-15978*# Jet Propulsion Lab., California Inst. of Tech., Wrightwood, CA.

USING VIRTUAL REALITY FOR SCIENCE MISSION PLANNING: A MARS PATHFINDER CASE c12

Jacqueline H. Kim, Richard J. Weidner, and Allan L. Sacks *In* NASA. Johnson Space Center, ISMCR 1994: Topical Workshop on Virtual Reality. Proceedings of the Fourth International Symposium on Measurement and Control in Robotics Nov. 1994 p 37-46 (For primary document see N95-15972 04-63)
Avail: CASI HC A02/MF A02

NASA's Mars Pathfinder Project requires a Ground Data System (GDS) that supports both engineering and scientific payloads with reduced mission operations staffing, and short planning schedules. Also, successful surface operation of the lander camera requires efficient mission planning and accurate pointing of the camera. To meet these challenges, a new software strategy that integrates virtual reality technology with existing navigational ancillary information and image processing capabilities. The result is an interactive workstation based applications software that provides a high resolution, 3-dimensial, stereo display of Mars as if it were viewed through the lander camera. The design, implementation strategy and parametric specification phases for the development of this software were completed, and the prototype tested. When completed, the software will allow scientists and mission planners to access simulated and actual scenes of Mars' surface. The perspective from the lander camera will enable scientists to plan activities more accurately and completely. The application will also support the sequence and command generation process and will allow testing and verification of camera pointing commands via simulation.

Author (revised)

N95-15979*# National Aeronautics and Space Administration. Lyndon B. Johnson Space Center, Houston, TX.

COORDINATED CONTROL OF A DUAL-ARM DEXTEROUS ROBOT USING FULL IMMERSION TELEPRESENCE AND VIRTUAL REALITY

Larry Li, Brian Cox (Lockheed Engineering and Sciences Co., Houston, TX.), Susan Shelton (Lockheed Engineering and Sciences Co., Houston, TX.), and Myron Diftler (Lockheed Engineering and Sciences Co., Houston, TX.) *In its* ISMCR 1994: Topical Workshop on Virtual Reality. Proceedings of the Fourth International Symposium on Measurement and Control in Robotics Nov. 1994 p 47-56 (For primary document see N95-15972 04-63)
Avail: CASI HC A02/MF A02

Telepresence is an approach to teleoperation that provides egocentric, intuitive interactions between an operator and a remote environment. This approach takes advantage of the natural cognitive and sensory motor skills of an on-board crew and effectively transfers them to a slave robot. A dual alarm dexterous robot operating under telepresence control has been developed and initial evaluations of the system performing candidate EVA, IVA and planetary geological tasks were conducted. The results of

our evaluation showed that telepresence control is very effective in transferring the operator's skills to the slave robot. However, the results also showed that, due to the kinematic and dynamics inconsistencies between the operator and the robot, a limited amount of intelligent automation is also required to carry out some to the tasks. Therefore, several enhancements have been made to the original system to increase the automated capabilities of the control system without losing the benefits of telepresence. Author

N95-15980*# GreyStone Technology, Inc., San Diego, CA.
AN APPLICATIONS-ORIENTED APPROACH TO THE DEVELOPMENT OF VIRTUAL ENVIRONMENTS
Michael X. Crowe *In* NASA. Johnson Space Center, ISMCR 1994: Topical Workshop on Virtual Reality. Proceedings of the Fourth International Symposium on Measurement and Control in Robotics Nov. 1994 p 57-63 (For primary document see N95-15972 04-63)
Avail: CASI HC A02/MF A02

The field of Virtual Reality (VR) is diverse, ranging in scope from research into fundamental enabling technologies to the building of full-scale entertainment facilities. However, the concept of virtual reality means many things to many people. Ideally, a definition of VR should derive from how it can provide solutions to existing challenges in building advanced human computer interfaces. The measure of success for VR lies in its ability to enhance the assimilation of complex information, whether to aid in difficult decision making processes, or to recreate real experiences in a compelling way. This philosophy is described using an example from a VR-based advertising project. The common and unique elements of this example are explained, though the fundamental development process is the same for all virtual environments that support information transfer. In short, this development approach is an applications oriented approach that begins by establishing and prioritizing user requirements and seeks to add value to the information transfer process through the appropriate use of VR technology. Author (revised)

N95-15981*# Texas A&M Univ., College Station, TX. Hypermedia Research Lab.
A SPECIFICATION OF 3D MANIPULATION IN VIRTUAL ENVIRONMENTS
S. Augustine Su and Richard Furuta *In* NASA. Johnson Space Center, ISMCR 1994: Topical Workshop on Virtual Reality. Proceedings of the Fourth International Symposium on Measurement and Control in Robotics Nov. 1994 p 64-68 (For primary document see N95-15972 04-63)
(Grant NSF IRI-94-96187)
Avail: CASI HC A01/MF A02

In this paper we discuss the modeling of three basic kinds of 3-D manipulations in the context of a logical hand device and our virtual panel architecture. The logical hand device is a useful software abstraction representing hands in virtual environments. The virtual panel architecture is the 3-D component of the 2-D window systems. Both of the abstractions are intended to form the foundation for adaptable 3-D manipulation. Author

N95-15982*# ATR Communication Systems Research Labs., Kyoto (Japan).
TELE HYPER VIRTUALITY
Nobuyoshi Terashima *In* NASA. Johnson Space Center, ISMCR 1994: Topical Workshop on Virtual Reality. Proceedings of the Fourth International Symposium on Measurement and Control in Robotics Nov. 1994 p 71-75 (For primary document see N95-15972 04-63)
Avail: CASI HC. A01/MF A02

In the future, remote images sent over communication lines will be reproduced in virtual reality (VR). This form of virtual telecommunications, which will allow observers to engage in an activity as though it were real, is the focus of considerable attention. Taken a step further, real and unreal objects will be placed in a single space to create an extremely realistic environment. Here, imaginary and other life forms as well as people and animals in remote locations will gather via telecommunication lines that create a common environment where life forms can work and interact together. Words, gestures, diagrams and other forms of communication will be used freely in performing work. Actual construction of a system based on this new concept will not only provide people with experiences that would have been impossible in the past, but will also inspire new applications in which people will function in environments where it would have been difficult if not impossible for them to function until now. This paper describes Tele Hyper Virtuality concept, its definition, applications, the key technologies to accomplish it and future prospects. Author

N95-15983*# Padua Univ. (Italy). Dept. of Innovation in Mechanics and Management.
SURFACE MATCHING FOR CORRELATION OF VIRTUAL MODELS: THEORY AND APPLICATION
Roberto Caracciolo, Francesco Fanton, and Alessandro Gasparetto *In* NASA. Johnson Space Center, ISMCR 1994: Topical Workshop on Virtual Reality. Proceedings of the Fourth International Symposium on Measurement and Control in Robotics Nov. 1994 p 76-83 (For primary document see N95-15972 04-63)
Avail: CASI HC A02/MF A02

Virtual reality can enable a robot user to off line generate and test in a virtual environment a sequence of operations to be executed by the robot in an assembly cell. Virtual models of objects are to be correlated to the real entities they represent by means of a suitable transformation. A solution to the correlation problem, which is basically a problem of 3-dimensional adjusting, has been found exploiting the surface matching theory. An iterative algorithm has been developed, which matches the geometric surface representing the shape of the virtual model of an object, with a set of points measured on the surface in the real world. A peculiar feature of the algorithm is to work also if there is no one-to-one correspondence between the measured points and those representing the surface model. Furthermore the problem of avoiding convergence to local minima is solved, by defining a starting point of states ensuring convergence to the global minimum. The developed algorithm has been tested by simulation. Finally, this paper proposes a specific application, i.e., correlating a robot cell, equipped for biomedical use with its virtual representation. Author

N95-15984*# Tokyo Metropolitan Univ. (Japan). Precision and Intelligence Lab.
A VIRTUAL WORK SPACE FOR BOTH HANDS MANIPULATION WITH COHERENCY BETWEEN KINESTHETIC AND VISUAL SENSATION c54
Masahiro Ishii, P. Sukanya, and Makoto Sato *In* NASA. Johnson Space Center, ISMCR 1994: Topical Workshop on Virtual Reality. Proceedings of the Fourth International Symposium on Measurement and Control in Robotics Nov. 1994 p 84-90 (For primary document see N95-15972 04-63)
Avail: CASI HC A02/MF A02

This paper describes the construction of a virtual work space for tasks performed by two handed manipulation. We intend to provide a virtual environment that encourages users to accomplish tasks as they usually act in a real environment. Our approach uses a three dimensional spatial interface device that allows the user to handle virtual objects by hand and be able to feel some physical properties such as contact, weight, etc. We investigated suitable conditions for constructing our virtual work space by simulating some basic assembly work, a face and fit task. We then selected the conditions under which the subjects felt most comfortable in performing this task and set up our virtual work space. Finally, we verified the possibility of performing more complex tasks in this virtual work space by providing simple virtual models and then let the subjects create new models by assembling these components. The subjects can naturally perform assembly operations and accomplish the task. Our evaluation shows that this virtual work space has the potential to be used for performing tasks that require two-handed manipulation or cooperation between both hands in a natural manner. Author (revised)

N95-15985*# Tokyo Univ. (Japan). Inst. of Industrial Science.
MASTER-SLAVE SYSTEM WITH FORCE FEEDBACK BASED ON DYNAMICS OF VIRTUAL MODEL
Shuji Nojima and Hideki Hashimoto *In* NASA. Johnson Space Center, ISMCR 1994: Topical Workshop on Virtual Reality. Proceedings of the Fourth International Symposium on Measurement and Control in Robotics Nov. 1994 p 93-100 (For primary document see N95-15972 04-63)
Avail: CASI HC A02/MF A02

A master-slave system can extend manipulating and sensing capabilities of a human operator to a remote environment. But the master-slave system has two serious problems: one is the mechanically large impedance of the system; the other is the mechanical complexity of the slave for complex

remote tasks. These two problems reduce the efficiency of the system. If the slave has local intelligence, it can help the human operator by using its good points like fast calculation and large memory. The authors suggest that the slave is a dextrous hand with many degrees of freedom able to manipulate an object of known shape. It is further suggested that the dimensions of the remote work space be shared by the human operator and the slave. The effect of the large impedance of the system can be reduced in a virtual model, a physical model constructed in a computer with physical parameters as if it were in the real world. A method to determine the damping parameter dynamically for the virtual model is proposed. Experimental results show that this virtual model is better than the virtual model with fixed damping. Author (revised)

N95-15986*# Northwestern Univ., Evanston, IL. Dept. of Mechanical Engineering.

PHYSICS-BASED APPROACH TO HAPTIC DISPLAY

J. Michael Brown and J. Edward Colgate *In* NASA. Johnson Space Center, ISMCR 1994: Topical Workshop on Virtual Reality. Proceedings of the Fourth International Symposium on Measurement and Control in Robotics Nov. 1994 p 101-106 (For primary document see N95-15972 04-63)

(Grants NSF MSS-90-22513; NSF IRI-92-13234)

Avail: CASI HC A02/MF A02

This paper addresses the implementation of complex multiple degree of freedom virtual environments for haptic display. We suggest that a physics based approach to rigid body simulation is appropriate for hand tool simulation, but that currently available simulation techniques are not sufficient to guarantee successful implementation. We discuss the desirable features of a virtual environment simulation, specifically highlighting the importance of stability guarantees. Author

N95-15987*# CM Research, Houston, TX.

THERMAL FEEDBACK IN VIRTUAL REALITY AND TELEROBOTIC SYSTEMS

Mike Zerkus, Bill Becker, Jon Ward, and Lars Halvorsen *In* NASA. Johnson Space Center, ISMCR 1994: Topical Workshop on Virtual Reality. Proceedings of the Fourth International Symposium on Measurement and Control in Robotics Nov. 1994 p 107-113 (For primary document see N95-15972 04-63)

Avail: CASI HC A02/MF A02

A new concept has been developed that allows temperature to be part of the virtual world. The Displaced Temperature Sensing System (DTSS) can 'display' temperature in a virtual reality system.The DTSS can also serve as a feedback device for telerobotics. For virtual reality applications the virtual world software would be required to have a temperature map of its world. By whatever means (magnetic tracker, ultrasound tracker, etc.) the hand and fingers, which have been instrumented with thermodes, would be tracked. The temperature associated with the current position would be transmitted to the DRSS via a serial data link. The DTSS would provide that temperature to the fingers. For telerobotic operation the function of the DTSS is to transmit a temperature from a remote location to the fingers where the temperature can be felt. Author

N95-15988*# National Aeronautics and Space Administration. Lyndon B. Johnson Space Center, Houston, TX.

VIRTUAL ENVIRONMENT APPLICATION WITH PARTIAL GRAVITY SIMULATION

David M. Ray and Michael N. VanChau *In its* ISMCR 1994: Topical Workshop on Virtual Reality. Proceedings of the Fourth International Symposium on Measurement and Control in Robotics Nov. 1994 p 114-122 (For primary document see N95-15972 04-63)

Avail: CASI HC A02/MF A02

To support manned missions to the surface of Mars and missions requiring manipulation of payloads and locomotion in space, a training facility is required to simulate the conditions of both partial and microgravity. A partial gravity simulator (Pogo) which uses pneumatic suspension is being studied for use in virtual reality training. Pogo maintains a constant partial gravity simulation with a variation of simulated body force between 2.2 and 10 percent, depending on the type of locomotion inputs. this paper is based on the concept and application of a virtual environment system with Pogo including a head-mounted display and glove. The reality engine consists of a high end SGI workstation and PC's which drive Pogo's sensors and data acquisition hardware used for tracking and control. The tracking system is a hybrid of magnetic and optical trackers integrated for this application. Author (revised)

N95-15989*# Avian Graphics, Ltd., League City, TX.

APPLYING VIRTUAL REALITY TO COMMERCIAL EDUTAINMENT

F. Grissom, Sharon P. Goza, and S. Michael Goza *In* NASA. Johnson Space Center, ISMCR 1994: Topical Workshop on Virtual Reality. Proceedings of the Fourth International Symposium on Measurement and Control in Robotics Nov. 1994 p 125-127 (For primary document see N95-15972 04-63)

Avail: CASI HC A01/MF A02

Virtual reality (VR) when defined as a computer generated, immersive, three dimensional graphics environment which provides varying degrees of interactivity, remains an expensive, highly specialized application, yet to find its way into the school, home, or business. As a novel approach to a theme park-type attraction, though, its use can be justified. This paper describes how a virtual reality 'tour of the human digestive system' was created for the Omniplex Science Museum of Oklahoma City, Oklahoma. The customers main objectives were: (1) to educate; (2) to entertain; (3) to draw visitors; and (4) to generate revenue. The 'Edutainment' system ultimately delivered met these goals. As more such systems come into existence the resulting library of licensable programs will greatly reduce development costs to individual institutions. Author

N95-15990*# Nottingham Univ. (England). Dept. of Computer Science.

A WORKOUT FOR VIRTUAL BODYBUILDERS (DESIGN ISSUES FOR EMBODIMENT IN MULTI-ACTOR VIRTUAL ENVIRONMENTS)

Steve Benford, John Bowers (Manchester Univ., England.), Lennart E. Fahlen (Swedish Inst. of Computer Science, Stockholm, Sweden.), Chris Greenhalgh, and Dave Snowdon *In* NASA. Johnson Space Center, ISMCR 1994: Topical Workshop on Virtual Reality. Proceedings of the Fourth International Symposium on Measurement and Control in Robotics Nov. 1994 p 128-135 (For primary document see N95-15972 04-63)

Avail: CASI HC A02/MF A02

This paper explores the issue of user embodiment within collaborative virtual environments. By user embodiment we mean the provision of users with appropriate body images so as to represent them to others and also to themselves. By collaborative virtual environments we mean multi-user virtual reality systems which support cooperative work (although we argue that the results of our exploration may also be applied to other kinds of collaborative systems). The main part of the paper identifies a list of embodiment design issues including: presence, location, identity, activity, availability, history of activity, viewpoint, action point, gesture, facial expression, voluntary versus involuntary expression, degree of presence, reflecting capabilities, manipulating the user's view of others, representation across multiple media, autonomous and distributed body parts, truthfulness and efficiency. Following this, we show how these issues are reflected in our own DIVE and MASSIVE prototype collaborative virtual environments. Author

N95-15991*# Bologna Univ. (Italy). Inst. di Glottologia.

CPP-TRS(C): ON USING VISUAL COGNITIVE SYMBOLS TO ENHANCE COMMUNICATION EFFECTIVENESS c32

Graziella Tonfoni *In* NASA. Johnson Space Center, ISMCR 1994: Topical Workshop on Virtual Reality. Proceedings of the Fourth International Symposium on Measurement and Control in Robotics Nov. 1994 p 136-142 (For primary document see N95-15972 04-63)

Avail: CASI HC A02/MF A02

Communicative Positioning Program/Text Representation Systems (CPP-TRS) is a visual language based on a system of 12 canvasses, 10 signals and 14 symbols. CPP-TRS is based on the fact that every communication action is the result of a set of cognitive processes and the whole system is based on the concept that you can enhance communication by visually perceiving text. With a simple syntax, CPP-TRS is capable of representing meaning and intention as well as communication functions visually. Those are precisely invisible aspects of natural language that are most relevant to getting the global meaning of a text. CPP-TRS reinforces natural language in human machine interaction systems. It complements natural language by adding certain important elements that are not represented by natural language by itself. These include communication intention and function of the text expressed by the sender, as well as the

role the reader is supposed to play. The communication intention and function of a text and the reader's role are invisible in natural language because neither specific words nor punctuation conveys them sufficiently and unambiguously; they are therefore non-transparent. Author (revised)

N95-15992*# National Aeronautics and Space Administration. Lyndon B. Johnson Space Center, Houston, TX.
SCRIPTING HUMAN ANIMATIONS IN A VIRTUAL ENVIRONMENT
Michael E. Goldsby (Lockheed Engineering and Sciences Co., Houston, TX.), Abhilash K. Pandya (Lockheed Engineering and Sciences Co., Houston, TX.), and James C. Maida *In its* ISMCR 1994: Topical Workshop on Virtual Reality. Proceedings of the Fourth International Symposium on Measurement and Control in Robotics Nov. 1994 p 143-150 (For primary document see N95-15972 04-63)
Avail: CASI HC A02/MF A02

The current deficiencies of virtual environment (VE) are well known: annoying lag time in drawing the current view, drastically simplified environments to reduce that time lag, low resolution and narrow field of view. Animation scripting is an application of VE technology which can be carried out successfully despite these deficiencies. The final product is a smoothly moving high resolution animation displaying detailed models. In this system, the user is represented by a human computer model with the same body proportions. Using magnetic tracking, the motions of the model's upper torso, head and arms are controlled by the user's movements (18 degrees of freedom). The model's lower torso and global position and orientation are controlled by a spaceball and keypad (12 degrees of freedom). Using this system human motion scripts can be extracted from the user's movements while immersed in a simplified virtual environment. Recorded data is used to define key frames; motion is interpolated between them and post processing adds a more detailed environment. The result is a considerable savings in time and a much more natural-looking movement of a human figure in a smooth and seamless animation. Author (revised)

N95-16011# Integrated Systems, Inc., Santa Clara, CA.
ADAPTIVE CONTROL OF NONLINEAR FLEXIBLE SYSTEMS Final Report, 1 Feb. 1991 - 31 Mar. 1994
Robert L. Kosut and M. G. Kabuli 26 May 1994 53 p
(Contract DAAL03-91-C-0011)
(AD-A281337; ISI-5923-1; ARO-28350.2-EG) Avail: CASI HC A04/MF A01

The objective is the development of adaptive control methods which can significantly improve closed-loop performance for a broad class of nonlinear flexible systems. Towards this end, a nonlinear controller, applicable to a broad class of nonlinear systems, was devised. The controller consists of a feedforward signal generator which incorporates a model estimate together with a global feedback linearizer. There is an inner feedback controller which modifies control action in accordance with output errors between the feedforward ideal output and the actual sensed output. The adaptive scheme studied uses measured data to update the model in the feedforward signal generator. It was discovered in many simulations that this two-level approach to adaptive feedback linearization can perform significantly better than feedback linearizers using an observer network.
DTIC

N95-16077 Physical Optics Corp., Torrance, CA.
A HIGHLY FUNCTIONAL DECISION PARADIGM BASED ON NONLINEAR ADAPTIVE GENETIC ALGORITHM Final Report, 10 Aug. 1993 - 9 Feb. 1994
Dai H. Kim 20 Apr. 1994 71 p Limited Reproducibility: More than 20% of this document may be affected by microfiche quality
(Contract DAAH04-93-C-0047)
(AD-A281457; ARO-31432.1-EL-SBI) Avail: CASI HC A04

In response to DOD Army solicitation A93-023, POC (Physical Optics Corporation) proposed a new type of processing module that is superior to any other type of computing method. The greatest advantage of POC's processing module is it combines the ability of a human to adapt to changing facts with the constant, uniform behavior, predictability, speed, large information storage capacity and non-emotional responses of machines. This proposed highly dimensional decision module is based on the genetic algorithm (GA). In Phase 1 of this program, POC successfully demonstrated a universal decision making method based on GAs and fuzzy rules. The algorithm of this decision making method can be used for multi-sensor feature space data, high dimensionality, and dynamically changing environments. In addition, the algorithm provides the capability to build a nonlinear adaptive system that incorporates many of the properties of human cognitive method. The multidimensional (10 dimensions) function demonstration of the optimization algorithm in Phase 1 has fully proved the feasibility of POC's high dimensionality decision making approach. Based on these results, POC believes that the high dimensionality decision module can be fully implemented with existing optic or electronic components in Phase 2.
DTIC

N95-16095 Yale Univ., New Haven, CT. Dept. of Computer Science.
[THE YALE KNOWLEDGE-BASED PLANNING PROJECT] Final Report
Drew McDermott and Gregory Hager 1994 8 p Limited Reproducibility: More than 20% of this document may be affected by microfiche quality
(Contract N00014-91-J-1577)
(AD-A281505) Avail: Issuing Activity (Defense Technical Information Center (DTIC))

The object of the Yale Knowledge-Based Planning Project is to find a unified theory of robot planning and sensing. We achieved several results in this direction, including the development of an architecture for a reactive planner, the implementation and testing of a theory of map making by a mobile robot, the development of an algorithm for reasoning about constraints on image hypotheses, and preliminary work on high-speed visual tracking. Our overall model of planning is this: An agent must be continuously executing plans in order to make progress on its goals. These plans are driven by sensors, and can normally cope with deviations from expected results without intervention from the planner. When intervention is required, the planner starts from scratch, generating plans and then revising them on the basis of their projected results. The projector contains a probabilistic model of the world that allows the planner to forecast probable errors. Our work on sensing has focused on these areas: (1) theoretical foundations for set-based decision-making algorithms; (2) visual tracking and vision-based control of servo systems; and (3) comparison of set-based and statistically-based estimation.
DTIC

N95-16170# Tennessee State Univ., Nashville, TN.
LARGE SCALE CONTROL AND DISTRIBUTED COMPUTING SYSTEMS UNDER STOCHASTIC STRUCTURAL PERTURBATIONS Final Report, 15 Dec. 1992 - 14 Dec. 1993
G. S. Ladde and S. Sathananthan 9 Mar. 1994 4 p
(Contract DAAH04-93-G-0024)
(AD-A281550; ARO-30986.6-MA-H) Avail: CASI HC A01/MF A01

The research was directed to initiate a study of large-scale hereditary/nonhereditary control and distributed systems under randomly varying structural perturbations. Error estimates between the stochastic and corresponding deterministic systems, numerical methods, and diagonalization and stability are investigated.
DTIC

N95-16246# Air Force Inst. of Tech., Wright-Patterson AFB, OH. School of Engineering.
EXPLOITING IB ASSIGNMENTS FOR APPROXIMATING MARGINAL PROBABILITIES
Solomon E. Shimony and Eugene Santos, Jr. 28 Sep. 1994 28 p
(AD-A285419; AFIT/EN/TR-94-06) Avail: CASI HC A03/MF A01

Computing marginal probabilities (whether prior or posterior) in Bayesian belief networks is a hard problem. This paper discusses deterministic approximation schemes that work by adding up the probability mass in a small number of value assignments to the network variables. Under certain assumptions, the probability mass in the union of these assignments is sufficient to obtain a good approximation. Such methods are especially useful for highly-connected networks, where the maximum clique size or the cutset size make the standard algorithms intractable. In considering assignments, it is not necessary to assign values to variables that are independent of (d-separated from) the evidence and query nodes. In many cases, however, there is a finer independence structure not evident from the topology, but dependent on the conditional distributions of the nodes. We note that independence-based (IB) assignments, which were originally proposed as theory of abductive explanations, take advantage of such independence, and thus contain fewer assigned variables. As a result, the probability mass in each assignment is greater than in the respective complete assignment. Thus, fewer IB assignments are sufficient, and a good approximation can be obtained more efficiently. IB assignments can

be used for efficiently approximating posterior node probabilities even in cases which do not obey the rather strict skewness assumptions used in previous research. Two algorithms for finding the high probability IB assignments are suggested: one by doing a best-first heuristic search, and another by special-purpose integer linear. Experimental results show that this approach is feasible for highly connected belief networks. DTIC

N95-16287# Pacific Northwest Lab., Richland, WA.
BRACING MICRO/MACRO MANIPULATORS CONTROL
J. Y. Lew and W. J. Book (Georgia Inst. of Tech., Atlanta, GA.) May 1994 8 p Presented at the Institute of Electrical and Electronics Engineers (IEEE) International Conference on Robotics, San Diego, CA, 8-13 May 1994
(Contract DE-AC06-76RL-01830)
(DE94-014434; PNL-SA-24223; CONF-940550-13) Avail: CASI HC A02/MF A01

This paper proposes a bracing strategy for micro/macro manipulators. The bracing micro/macro manipulator can provide advantages in accurate positioning, large work-space, and contact-task capability however, in exchange for improvement in performance one must accept the complex control problem along with the complex dynamics. This research develops a control scheme for a bracing manipulator which makes multiple contacts with the environment. Experimental results show the feasibility of the proposed ideas for real world applications. DOE

N95-16361# Oak Ridge National Lab., TN.
STOCHASTIC APPROXIMATION METHODS FOR FUSION-RULE ESTIMATION IN MULTIPLE SENSOR SYSTEMS
N. S. V. Rao 1994 13 p Presented at the 12th Symposium on Energy Engineering Sciences, Argonne, IL, 27-29 Apr. 1994
(Contract DE-AC05-84OR-21400)
(DE94-013629; CONF-9404137-4) Avail: CASI HC A03/MF A01

A system of N sensors S(sub 1), S(sub 2), ..., S(sub N) is considered; corresponding to an object with parameter x an element of (Re)(sup d), sensor S(sub i) yields output y(sup i) an element of (Re)(sup d) according to an unknown probability distribution p(sub i)(y(sup i) (vertical bar) x). A training l-sample (x(sub 1),y(sub 1)), (x(sub 2),y(sub 2)), ...,(x(sub l), y(sub l)) is given where y(sub i) = (y(sub i, sup (1)), y(sub i, sup (2)), ...,y(sub i, sup (N))) and y(sub i)(sup (j)) is the output of S(sub j) in response to input X(sub i). The problem is to estimate a fusion rule f : (Re)(sup Nd) yields (Re)(sup d), based on the sample, such that the expected square error l(f) is to be minimized over a family of fusion rules Lambda based on the given l-sample. Let f(sub *) an element of Lambda minimize l(f); f(sub *) cannot be computed since the underlying probability distributions are unknown. Three stochastic approximation methods are presented to compute (circumflex over f), such that under suitable conditions, for sufficiently large sample, P(l(circumflex over f) - l(f(sub *)) is greater than epsilon) is less than delta for arbitrarily specified epsilon greater than 0 and delta, 0 less than delta less than 1. The three methods are based on Robbins-Monro style algorithms, empirical risk minimization, and regression estimation algorithms. DOE

N95-16372# Naval Postgraduate School, Monterey, CA.
GRAPHICAL SIMULATION OF ARTICULATED RIGID BODY SYSTEM KINEMATICS WITH COLLISION DETECTION M.S. Thesis
John R. Goetz 23 Mar. 1994 82 p
(AD-A281842) Avail: CASI HC A05/MF A01

The area of concern addressed by this thesis is the development of a 3-D visual simulation to aid in the testing of ground detection and foot placement algorithms for an articulated walking robot's foot pads on uneven terrain. Several collision detection algorithms and terrain mapping techniques were studied to determine which approach would lend itself readily to the rapid detection of initial ground contact and the required orientation needed to place each foot firmly on the ground. As a result of these studies; a real-time, realistic and aesthetically pleasing graphical simulation for the testing of control software for articulated walking machines has been developed which utilizes the Silicon Graphics 3-D visual simulation toolkit, Performer. Not only is rapid ground contact sensing and foot orientation possible, it is accomplished without using extraneous data structures making the algorithm generic enough to use on any terrain model. Author

N95-16390 Minnesota Univ., Minneapolis, MN. Dept. of Computer Science.
REAL-TIME SIMULATION OF LARGE-SCALE MULTIBODY SYSTEMS USING AUTOMATED EQUATION DECOUPLING TECHNIQUES Final Report, 28 Sep. 1992 - 27 Dec. 1993
Linda R. Petzold and Roger A. Wehage 14 Jun. 1994 12 p Limited Reproducibility: More than 20% of this document may be affected by microfiche quality
(Contract DAAL03-92-G-0409)
(AD-A281544; ARO-30980.1-MA) Avail: CASI HC A03

A method for formulating highly optimized vehicle models using symbolic analysis has been developed. The vehicle model makes extensive use of computations which can be precomputed in advance of the real-time simulation. The new approach has been used at TARDEC for the efficient simulation of several military vehicles. DTIC

N95-16550# Army Armament Research, Development and Engineering Center, Watervliet, NY.
SERVO CONTROL USING SWITCHES FOR DISCRETE POSITIONAL FEEDBACK Final Report
Ronald L. Racicot May 1994 31 p
(AD-A284747; ARCCB-TR-94021) Avail: CASI HC A03/MF A01

This report describes an approach for providing and/or assisting in the positional control of a one degree-of-freedom servo-mechanism using switches. The switches, positioned along the path of a moving mechanism, can also be simulated using continuous feedback sensors for certain applications. Real time feedback of the discrete time at which each switch is tripped during motion is provided to the controller. Based on this time-position information, constant motor forces to be applied between switches are determined to sustain and complete the required repositioning task. A definitive control procedure is not presented here, but rather a promising one that may have important applications as we have found in our work. Also, the method is not intended to compete with more sophisticated and complicated approaches using higher component quality and quantity and computer power. On the contrary, one of the intended goals is to go somewhat the other way to make use of existing or even less expensive components. The main contribution that we make to this overall control technique is to introduce and use probability and statistical concepts in determining the switch locations and the required real time motor forces. A probabilistic approach is needed because of the uncertainty in the actual position and velocities of the mechanism as it travels between switches. These uncertainties in turn are derived from uncertainties in the disturbing forces that are encountered during any given motion cycle. In this report, we develop the theory for a statistically-based approach for control using switches. We then verify the results using simulation and experimentation. In our experimental work, we applied our techniques to the ramming mechanism of a large caliber tank autoloader with excellent results. DTIC

N95-16609# Pacific Northwest Lab., Richland, WA.
PROCEEDINGS OF THE NEURAL NETWORK WORKSHOP FOR THE HANFORD COMMUNITY
P. E. Keller Jan. 1994 101 p Workshop held in Richland, WA, 26 Jan. 1994
(Contract DE-AC06-76RL-01830)
(DE94-014567; PNL-SA-24393; CONF-940157) Avail: CASI HC A06/MF A02

These proceedings were generated from a series of presentations made at the Neural Network Workshop for the Hanford Community. The abstracts and viewgraphs of each presentation are reproduced in these proceedings. This workshop was sponsored by the Computing and Information Sciences Department in the Molecular Science Research Center (MSRC) at the Pacific Northwest Laboratory (PNL). Artificial neural networks constitute a new information processing technology that is destined within the next few years, to provide the world with a vast array of new products. A major reason for this is that artificial neural networks are able to provide solutions to a wide variety of complex problems in a much simpler fashion than is possible using existing techniques. In recognition of these capabilities, many scientists and engineers are exploring the potential application of this new technology to their fields of study. An artificial neural network (ANN) can be a software simulation, an electronic circuit, optical system, or even an electro-chemical system designed to emulate some of the

brain's rudimentary structure as well as some of the learning processes that are believed to take place in the brain. For a very wide range of applications in science, engineering, and information technology, ANN's offer a complementary and potentially superior approach to that provided by conventional computing and conventional artificial intelligence. This is because, unlike conventional computers, which have to be programmed, ANN's essentially learn from experience and can be trained in a straightforward fashion to carry out tasks ranging from the simple to the highly complex. DOE

N95-16631# Naval Command, Control and Ocean Surveillance Center, San Diego, CA.
EVOLVING NEURAL NETWORK PATTERN CLASSIFIERS
J. R. McDonnell, D. E. Waagen, and W. C. Page May 1994 13 p
(AD-A281181) Avail: CASI HC A03/MF A01

This work investigates the application of evolutionary programming for automatically configuring neural network architectures for pattern classification tasks. The evolutionary programming search procedure implements a parallel nonlinear regression technique and represents a powerful method for evaluating a multitude of neural network model hypotheses. The evolutionary programming search is augmented with the Solis & Wets random optimization method thereby maintaining the integrity of the stochastic search while taking into account empirical information about the response surface. A network architecture is proposed which is motivated by the structures generated in projection pursuit regression and the cascade-correlation learning architecture. Results are given for the three-bit parity, normally distributed data, and the T-C classifier problems. DTIC

N95-16820# Carnegie-Mellon Univ., Pittsburgh, PA. Dept. of Computer Science.
LEARNING ONE MORE THING
Sebastian Thrun and Tom M. Mitchell Sep. 1994 22 p
(Contract F33615-93-1-1330; NSF IRI-93-13367)
(AD-A285342; CMU-CS-94-184) Avail: CASI HC A03/MF A01

Most research on machine learning has focused on scenarios in which a learner faces a single, isolated learning risk. The life-long learning framework assumes instead that the learner encounters a multitude of related learning tasks over its lifetime, providing the opportunity for the transfer of knowledge. This paper studies life-long learning in the context of binary classification. It presents the invariance approach, in which knowledge is transferred via a learned model of the invariance of the domain. Results on learning to recognize objects from color images demonstrate superior generalization capabilities if invariances are learned and used to bias subsequent learning. DTIC

N95-16823# Department of the Navy, Washington, DC.
SELF-ORGANIZING NEURAL NETWORK FOR CLASSIFYING PATTERN SIGNATURES WITH A POSTERIORI CONDITIONAL CLASS PROBABILITY Patent Application
George W. Rogers, inventor (to Navy) and Jeffrey L. Solka, inventor (to Navy) 29 Aug. 1992 20 p
(AD-D016455; US-Patent-Appl-SN-936369) Avail: CASI HC A03/MF A01

The invention relates generally to neural networks, and more particularly to a self-organizing neural network and method for adaptively training and processing same in order to classify pattern signatures and provide the 'a posteriori' conditional class probability that the pattern signature is from a selected class with which the neural network was adaptively trained. DTIC

N95-16864# Massachusetts Inst. of Tech., Cambridge.
WORKSHOP ON FORMAL MODELS FOR INTELLIGENT CONTROL Final Report, 1 Sep. - 31 Dec. 1993
Sanjoy K. Mitter Apr. 1994 16 p
(Contract DAAH04-93-G-0500)
(AD-A281399; ARO-32483.1-MA-CF) Avail: CASI HC A03/MF A01

A workshop on Formal Models for Intelligent Control, jointly funded by the Army Office (ARO) and the National Aeronautics and Space Administration (NASA), and jointly sponsored by the Center for Intelligent Control Systems (CICS) and the University of California at Berkeley's Intelligent Machines and Robotics Laboratory, was held at M.I.T. during 30 September--2 October 1993. The workshop brought together a large number of researchers and specialists from universities, the government, and industry, providing a stage for interesting presentations as well as lively discussion. A number of papers discussed genera l characteristics of intelligent control systems, and several presented case studies. DTIC

N95-16967# Army Construction Engineering Research Lab., Champaign, IL.
USING NEURAL NETWORKS TO CORRELATE SATELLITE IMAGERY AND GROUND-TRUTH DATA Final Report
Xiping Wu and James D. Westervelt Aug. 1994 55 p
(AD-A285486; CERL-SR-EC-94/28) Avail: CASI HC A04/MF A01

Current approaches to evaluating the condition of natural resources on Army training and testing lands are statistically based and attempt to generate rational mathematical formulae that characterize the relationship between satellite imagery and ground-truth data. Even in the hands of a well trained image processing expert, the application of standard image processing tools can yield varying results. Army land managers need an alternate approach for correlating satellite imagery to ground-truth measurements. This approach can be found in the application of neural networks. This report presents the research results of using neural networks as a computational tool to correlate ground-truth data with satellite imagery for Hohenfels, Germany, and to turn the imagery into maps of the installation. DTIC

N95-17369 International Neural Network Society, Washington, DC.
THE 1994 INTERNATIONAL NEURAL NETWORK SOCIETY ANNUAL MEETING, VOLUME 3
9 Jun. 1994 812 p Meeting held in San Diego, CA, 5-9 Jun. 1994
Limited Reproducibility: More than 20% of this document may be affected by microfiche quality
(AD-A281736) Avail: CASI HC A99

Contents of volume 3 cover signal processing, pattern recognition, and supervised learning. DTIC

N95-17370 International Neural Network Society, Washington, DC.
THE 1994 INTERNATIONAL NEURAL NETWORK SOCIETY ANNUAL MEETING, VOLUME 4
9 Jun. 1994 861 p Meeting held in San Diego, CA, 5-9 Jun. 1994
Limited Reproducibility: More than 20% of this document may be affected by microfiche quality
(AD-A281737) Avail: CASI HC A99

Contents of volume 4 cover associative memory, unsupervised learning, biological vision, circuits and system neuroscience, links to cognitive science and artificial intelligence, speech and language, cognitive neuroscience, and neurodynamics and chaos. CASI

N95-17381# Northeast Consortium for Engineering Education, Port Royal, VA.
O-Plan2 VERSUS SIPE-2: A GENERAL COMPARISON Final Report, Feb. 1993 - Feb. 1994
Carla Ludlow Jul. 1994 40 p
(Contract F30602-93-C-0017; AF Proj. 5581)
(AD-A285531; RL-TR-94-96) Avail: CASI HC A03/MF A01

This report addresses strengths and limitations detected in SIPE-2 and O-Plan2 as a result of some experiments that were performed at Rome Laboratory using those generative planners. The main objective of the project was to provide an understanding of generative planners and familiarization with O-Plan2 and SIPE-2. A comparison between O-Plan2 and SIPE-2 was a secondary objective, mainly a subproduct of the experimentation with both planners. DTIC

N95-17383*# Ohio State Univ., Columbus. Cognitive Systems Engineering Lab.
BREAKING DOWN BARRIERS IN COOPERATIVE FAULT MANAGEMENT: TEMPORAL AND FUNCTIONAL INFORMATION DISPLAYS Final Report
Scott S. Potter and David D. Woods Oct. 1994 141 p
(Grant NAG9-390; OSU Proj. RF-727376)
(NASA-CR-197450; NAS 1.26:197450; CSEL-1994-TR-02) Avail: CASI HC A07/MF A02

At the highest level, the fundamental question addressed by this research

is how to aid human operators engaged in dynamic fault management. In dynamic fault management there is some underlying dynamic process (an engineered or physiological process referred to as the monitored process - MP) whose state changes over time and whose behavior must be monitored and controlled. In these types of applications (dynamic, real-time systems), a vast array of sensor data is available to provide information on the state of the MP. Faults disturb the MP and diagnosis must be performed in parallel with responses to maintain process integrity and to correct the underlying problem. These situations frequently involve time pressure, multiple interacting goals, high consequences of failure, and multiple interleaved tasks. Derived from text

N95-17458 Naval Postgraduate School, Monterey, CA.
BACK-PROPAGATION NEURAL NETWORKS IN ADAPTIVE CONTROL OF UNKNOWN NONLINEAR SYSTEMS M.S. Thesis
Alpay Cakarcan Jun. 1994 84 p Limited Reproducibility: More than 20% of this document may be affected by microfiche quality
(AD-A282414) Avail: CASI HC A05

The objective of this thesis research is to develop a Back-Propagation Neural Network (BNN) to control certain classes of unknown nonlinear systems and explore the network's capabilities. The structure of the Direct Model Reference Adaptive Controller (DMRAC) for Linear Time Invariant (LTI) systems with unknown parameters is first analyzed and then is extended to nonlinear systems by using BNN. Nonminimum phase systems, both linear and nonlinear. have also been considered. The analysis of the experiments shows that the BNN DMRAC gives satisfactory results for the representative nonlinear systems considered, while the conventional least-squares estimator DMRAC fails. Based on the analysis and experimental findings, some general conditions are shown to be required to ensure that this technique is satisfactory. These conditions are presented and discussed. It has been found that further research needs to be done for the nonminimum phase case in order to guarantee stability and tracking. Also, to establish this as a more general and significant control technique, further research is required to develop more specific rules and guidelines for the BNN design and training. DTIC

N95-17459 State Univ. of New York, Buffalo, NY. Dept. of Electrical and Computer Engineering.
OBJECT RECOGNITION USING MULTI-LAYER HOPFIELD NEURAL NETWORK
Susan S. Young, Peter D. Scott, and Nasser M. Nasrabadi 1994 6 p Limited Reproducibility: More than 20% of this document may be affected by microfiche quality
(Contract N00014-91-C-0257)
(AD-A282417) Avail: CASI HC A02

An object recognition approach based on concurrent coarse-and-fine matching using a multi-layer Hopfield neural network is presented. The proposed network consists of several cascaded single layer Hopfield networks, each encoding object features at a distinct resolution, with bidirectional interconnections linking adjacent layers. The interconnection weights between nodes associating adjacent layers are structured to favor node pairs for which model translation and rotation, when viewed at the two corresponding resolutions, are consistent. This inter-layer feedback feature of the algorithm reinforces the usual intra-layer matching process in conventional single layer Hopfield nets in order to compute the model-object match which is most consistent across several resolution levels. The performance of the algorithm is demonstrated in cases of images containing single and multiple occluded objects. These results are compared with recognition results obtained using a single layer Hopfield network. DTIC

N95-17465 Department of the Navy, Washington, DC.
FEEDBACK SYSTEM FOR REMOTELY OPERATED VEHICLES Patent
Hobart R. Everett, Jr., inventor (to Navy) and Judy M. Nieusma, inventor (to Navy) 3 May 1994 9 p Filed 26 Nov. 1991
(AD-D016409; US-Patent-5,309,140; US-Patent-Appl-SN-800341; US-Patent-Class-340-466) Avail: US Patent and Trademark Office

The present invention is a system for providing an output corresponding to the speed of a remote vehicle, comprising: a speed transducer mounted on the vehicle for providing a first output corresponding to the speed of the vehicle; a first data processor operably coupled to receive the first output from the speed transducer means for providing an ASCII coded output; a second data processor operably coupled to receive the ASCII coded output from the first data processor for providing an output transducer control output; and an output transducer operably coupled to receive the control output from the second data processor for providing an output having an amplitude proportional to the speed of the vehicle. DTIC

N95-17634# SRI International Corp., Menlo Park, CA.
REPRESENTATION, MODELING AND RECOGNITION OF OUTDOOR SCENES Annual Report No. 1, Mar. 1992 - Mar. 1993
Martin A. Fischler and Robert C. Bolles Nov. 1993 75 p
(Contract DACA76-92-C-0008)
(AD-A283257; TEC-0046) Avail: CASI HC A04/MF A01

The primary goal was to advance the state-of-the-art in scene interpretation for autonomous systems that operate in natural terrain. In particular, techniques are being developed for representing knowledge about complex cultural and natural environments so that a computer vision system can successfully plan, navigate, recognize and manipulate objects, and answer questions or make decisions relevant to this knowledge. The initial results are centered on the development of representations and associated methods for rapidly modeling natural terrain (from image sequences) at a level of organization higher than that of the conventional dense array of depths. This work will provide the essential advance needed to turn raw geometric measurements into timely information usable by robotic navigation and planning systems. Work is also progressing on two additional problems: modeling compact 3-D objects from their projected 2-D contours, and the problem of recognizing important classes of natural and man-made objects, especially roads, trees, and rocks. DTIC

N95-17915# Sandia National Labs., Albuquerque, NM.
OPTIMAL TRAJECTORIES FOR FLEXIBLE-LINK MANIPULATOR SLEWING USING RECURSIVE QUADRATIC PROGRAMMING: EXPERIMENTAL VERIFICATION
G. G. Parker, G. R. Eisler, and J. T. Feddema 1994 6 p Presented at the 5th International Symposium on Robotics and Manufacturing, Maui, HI, 14-18 Aug. 1994
(Contract DE-AC04-94AL-85000)
(DE94-018741; SAND-94-2072C; CONF-940859-25) Avail: CASI HC A02/MF A01

Procedures for trajectory planning and control of flexible link robots are becoming increasingly important to satisfy performance requirements of hazardous waste removal efforts. It has been shown that utilizing link flexibility in designing open loop joint commands can result in improved performance as opposed to damping vibration throughout a trajectory. The efficient use of link compliance is exploited in this work. Specifically, experimental verification of minimum time, straight line tracking using a two-link planar flexible robot is presented. A numerical optimization process, using an experimentally verified modal model, is used for obtaining minimum time joint torque and angle histories. The optimal joint states are used as commands to the proportional-derivative servo actuated joints. These commands are precompensated for the nonnegligible joint servo actuator dynamics. Using the precompensated joint commands, the optimal joint angles are tracked with such fidelity that the tip tracking error is less than 2.5 cm. DOE

N95-17921*# California Inst. of Tech., Pasadena, CA.
MULTIVARIATE STATISTICAL ANALYSIS SOFTWARE TECHNOLOGIES FOR ASTROPHYSICAL RESEARCH INVOLVING LARGE DATA SETS Final Technical Report, 1991 - 1994
S. G. Djorgovski 12 Nov. 1994 206 p
(Contracts NAS5-32337; NAS5-31348; RTOP 656-65-07; USRA-C-5555-32)
(NASA-CR-197499; NAS 1.26:197499) Avail: CASI HC A10/MF A03

We developed a package to process and analyze the data from the digital version of the Second Palomar Sky Survey. This system, called SKICAT, incorporates the latest in machine learning and expert systems software technology, in order to classify the detected objects objectively and uniformly, and facilitate handling of the enormous data sets from digital sky surveys and other sources. The system provides a powerful, integrated environment for the manipulation and scientific investigation of catalogs from virtually any source. It serves three principal functions: image catalog construction, catalog management, and catalog analysis. Through use of the GID3* Decision Tree artificial induction software, SKICAT automates the process of classifying objects within CCD and digitized

plate images. To exploit these catalogs, the system also provides tools to merge them into a large, complex database which may be easily queried and modified when new data or better methods of calibrating or classifying become available. The most innovative feature of SKICAT is the facility it provides to experiment with and apply the latest in machine learning technology to the tasks of catalog construction and analysis. SKICAT provides a unique environment for implementing these tools for any number of future scientific purposes. Initial scientific verification and performance tests have been made using galaxy counts and measurements of galaxy clustering from small subsets of the survey data, and a search for very high redshift quasars. All of the tests were successful and produced new and interesting scientific results. Attachments to this report give detailed accounts of the technical aspects of the SKICAT system, and of some of the scientific results achieved to date. We also developed a user-friendly package for multivariate statistical analysis of small and moderate-size data sets, called STATPROG. The package was tested extensively on a number of real scientific applications and has produced real, published results. Author

N95-16474*# National Aeronautics and Space Administration. Langley Research Center, Hampton, VA.
MATLAB AS A ROBUST CONTROL DESIGN TOOL
Irene M. Gregory *In its* The Role of Computers in Research and Development at Langley Research Center Oct. 1994 p 485-496 (For primary document see N95-16453 04-62)
Avail: CASI HC A03/MF A06

N95-16475*# National Aeronautics and Space Administration. Langley Research Center, Hampton, VA.
SIMULATION OF THE COUPLED MULTI-SPACECRAFT CONTROL TESTBED AT THE MARSHALL SPACE FLIGHT CENTER
Dave Ghosh and Raymond C. Montgomery *In its* The Role of Computers in Research and Development at Langley Research Center Oct. 1994 p 497-517 (For primary document see N95-16453 04-62)
Avail: CASI HC A03/MF A06

N95-17534*# MATRA Marconi Space, Toulouse (France).
DIAMS REVISITED: TAMING THE VARIETY OF KNOWLEDGE IN FAULT DIAGNOSIS EXPERT SYSTEMS
M. Haziza, S. Ayache, J.-M. Brenot, D. Cayrac, and D.-P. Vo *In* NASA. Goddard Space Flight Center, Third International Symposium on Space Mission Operations and Ground Data Systems, Part 2 Nov. 1994 p 697-706 Sponsored by Cap Gemini Innovation; Westfield College; Sintef Delab; Eritel; and ITMI (For primary document see N95-17531 04-17)
(ESPRIT Proj. 6083)
Avail: CASI HC A02/MF A06

64 NUMERICAL ANALYSIS

Includes iteration, difference equations, and numerical approximation.

N95-15948# Rochester Univ., NY. Dept. of Computer Science.
DECREASING THE BANDWIDTH OF A TRANSITION MATRIX
Ioan I. Macarie Apr. 1994 8 p
(Grant NSF CDA-88-22724)
(TR-505) Avail: CASI HC A02/MF A01

Adapting the competitions method of Freivalds to the setting of unbounded-error probabilistic computation, we prove that, for any epsilon element of (0,1), Band-Mat-Inv(n epsilon) is log-space complete for the class of languages recognized by log-space unbounded-error probabilistic Turing machines (PL). This extends the result of Jung that Band-Mat-Inv(n) is log-space complete for PL, and may open new possibilities for space-efficient deterministic simulation of space-bounded probabilistic Turing machines. Author

N95-15949# Rochester Univ., NY. Dept. of Computer Science.
A GENERAL METHOD TO DETERMINE INVARIANTS
Irene Rothe, Klaus Voss, Herbert Suesse (Friedrich-Schiller Univ., Jena, Germany.), and Joerg Rothe (Friedrich-Schiller Univ., Jena, Germany.) 25 Apr. 1994 26 p Sponsored by German Academic Exchange Service
(Grant NSF CCR-89-57604)
(TR-503) Avail: CASI HC A03/MF A01

The determination of invariant characteristics is an important problem in pattern recognition. Many invariants are known: Hu's moment invariants are invariant to shifts, to changes of scale, and to rotations; Arbter's Fourier descriptors to affine transformations; Wang's invariant moments to affine transformations; the two well-known 5-points invariants to projective transformations, etc. This paper shows that all these results, which were obtained independently and by different methods, derive from a common basic principle that allows the determination of new invariants as well. Author

N95-15950# Rochester Univ., NY. Dept. of Computer Science.
NP-SETS ARE Co-NP-IMMUNE RELATIVE TO A RANDOM ORACLE
Nikolai K. Vereshchagin (Institute of New Technologies, Moscow, USSR.) Apr. 1994 14 p Sponsored by American Mathematical Society; Soviet Union Aid Fund; International Science Foundation; and NAS-NRC
(Grant NSF CCR-89-57604)
(TR-501) Avail: CASI HC A03/MF A01

We prove that the class NP has Co-NP-immune sets and the class Co-NP- has NP-immune sets relative to a random oracle. Author

N95-15951# Rochester Univ., NY. Dept. of Computer Science.
ON P-SELECTIVITY AND CLOSENESS
Rajesh P. N. Rao Apr. 1994 13 p
(Grants NSF CDA-88-22724; NSF CCR-89-57604)
(TR-499) Avail: CASI HC A03/MF A01

P/poly, the class of sets with polynomial size circuits, has been the subject of considerable study in complexity theory. Two important subclasses of P/poly are the class of sparse sets and the class of P-selective sets. A large number of results have been proved about both these classes but it has been observed that despite their similarity, proofs about one class generally do not translate easily to proofs regarding the other class. In this note, we propose to resolve this asymmetry by investigating the class PSEL-close of sets that are polynomially close to P-selective sets; by definition, PSEL-close includes both sparse sets and P-selective sets, thereby providing a unifying platform for proving results applicable to both. Intuitively, PSEL-close is the class of sets that can in a certain sense be approximated by P-selective sets. We prove several results separating PSEL-close from known classes within and including P/poly, and establish its location optimally in the extended low hierarchy. We illustrate the naturalness and usefulness of the class by examining the question of whether sets hard for NP or E can be PSEL-close; several well-known results are obtained as immediate corollaries. Author

N95-16022# Rochester Univ., NY. Dept. of Computer Science.
ON COMPUTING THE MINIMAL LABELS IN TIME POINT ALGEBRA NETWORKS
Alfonso Gerevini (Trento Univ., Italy.) and Lenhart Schubert Mar. 1994 10 p Submitted for publication Sponsored by CNR and MAIA
(Contract F30602-91-C-0010)
(TR-495) Avail: CASI HC A02/MF A01

We analyze the problem of computing the minimal labels for a network of temporal relations in the Point Algebra. van Beek proposes an algorithm for accomplishing this task which takes O(max(n cubed, n squared times m)) time (for n points and m does not equal relations). We show that the proof of the corectness of this algorithm given by van Beek and Cohen is faulty, and we provide a new proof showing that the algorithm is indeed correct. Author

N95-16108 California Inst. of Tech., Pasadena, CA.
NONLINEAR PROBLEMS AND NUMERICAL METHOD IN DIFFERENTIAL EQUATIONS AND APPLIED PHENOMENA Final Report, 23 Jan. 1989 - 31 May 1993
Donald S. Cohen 22 Jul. 1993 6 p Limited Reproducibility: More than 20% of this document may be affected by microfiche quality
(Contract DAAL03-89-K-0014)
(AD-A281531; ARO-25874.1-MA) Avail: Issuing Activity (Defense Technical Information Center (DTIC))

By extension from our previous work on so called Case 2 diffusion, models have been developed to account for several kinds of anomalous

non-Fickian diffusion. We have applied them to various problems arising from the uses of certain modern polymeric materials in novel applications in pharmaceutical devices, separating membranes for controlled gaseous and liquid mixing, and methods of adhesive bonding. In addition to the formulation in which important parameter groupings were identified, analytical, asymptotic, and numerical methods were modified or devised to study the problems. DTIC

N95-16127# Pittsburgh Univ., Pittsburgh, PA. Inst. for Computational Mathematics and Applications.
A POSTERIORI ERROR ESTIMATION NEW APPROACH
Patrick J. Rabier 7 Sep. 1994 20 p
(Contract N00014-90-J-1025)
(AD-A284960; ICMA-94-188) Avail: CASI HC A03/MF A01

An approach to a posteriori estimation in finite element problems is developed via minimization of a functional depending upon element boundary data and local estimates. Author (DTIC)

N95-16128# Pittsburgh Univ., Pittsburgh, PA. Inst. for Computational Mathematics and Applications.
GLOBAL SUBJECTIVITY OF SUBMERSIONS VIA CONTRACTIBILITY OF THE FIBERS
Patrick J. Rabier 7 Sep. 1994 26 p
(Contract N00014-90-J-1025)
(AD-A284961; ICMA-94-189) Avail: CASI HC A03/MF A01

We give a sufficient condition for a C(sup 1) submersion F: X implies Y, X and Y real Banach spaces to be surjective with contractible fibers F(sup -1)(y). Roughly speaking, this condition 'interpolates' two well-known but uncorrelated hypotheses corresponding to the two extreme cases: Hadamard's criterion when Y is congruent to X and F is a local diffeomorphism, and the Palais-Smale condition when Y is congruent to the set of Reals. These results may be viewed as a global variant of the implicit function theorem, which unlike the local one does not require split kernels. They are derived from a deformation theorem tailored to fit functionals with a norm-like nondifferentiability. Author (DTIC)

N95-16169 Stanford Univ., CA. Dept. of Operations Research.
A LYAPUNOV BOUND FOR SOLUTIONS OF POISSON'S EQUATION
Peter W. Glynn and Sean P. Meyn Aug. 1993 26 p Limited Reproducibility: More than 20% of this document may be affected by microfiche quality
(Contract DAAL03-91-G-0101)
(AD-A281536; TR-93-14; ARO-29412.4-MA-SDI) Avail: Issuing Activity (Defense Technical Information Center (DTIC))

We consider psi-irreducible Markov processes evolving in discrete or continuous time, on a general state space. We develop a Lyapunov function criterion that permits one to obtain explicit bounds on the solution to Poisson's equation and, in particular, obtain conditions under which the solution is square integrable. These results are applied to obtain sufficient conditions that guarantee the validity of a functional central limit theorem for the Markov process. As a second consequence of the bounds obtained, a perturbation theory for Markov processes is developed which gives conditions under which both the solution to Poisson's equation and the invariant probability for the process are continuous functions of its transition kernel. The techniques are illustrated with applications to queueing theory and autoregressive processes. DTIC

N95-16221# Lawrence Livermore National Lab., Livermore, CA.
VISUALIZING 3D VELOCITY FIELDS NEAR CONTOUR SURFACES
N. Max, R. Crawfis, and C. Grant Mar. 1994 9 p Presented at the Visualization 1994, Washington, DC, 17-21 Oct. 1994
(Contract W-7405-eng-48)
(DE94-010205; UCRL-JC-116231; CONF-941085-1) Avail: CASI HC A02/MF A01

Vector field rendering is difficult in 3D because the vector icons overlap and hide each other. We propose four different techniques for visualizing vector fields only near surfaces. The first uses motion blurred particles in a thickened region around the surface. The second uses a voxel grid to contain integral curves of the vector field. The third uses many antialiased lines through the surface, and the fourth uses hairs sprouting from the surface and then bending in the direction of the vector field. All the methods use the graphite pipeline, allowing real time rotation and interaction, and the first two methods can animate the texture to move in the flow determined by the velocity field. DOE

N95-16291# Institut des Hautes Etudes Scientifiques, Bures-sur-Yvette (France).
COARSE GEOMETRY OF FOLIATIONS
S. Hurder (Illinois Univ., Chicago, IL.) Feb. 1994 54 p
(Grant NSF DMS-91-03297)
(PB94-192309; IHES/M/94/14) Avail: CASI HC A04/MF A01

Coarse geometry is an approach for exploring the 'structure at infinity' of open manifolds. Compact manifolds look like points in coarse geometry, and continuity is replaced by global Lipshitz estimates on maps. The contents of the document expand on three lectures given by the author at the International Symposium on the Geometric Theory of Foliations: (1) Beyond Volume Growth, which discussed the ideas of coarse geometry, introduced the entropy of metric spaces and applied these ideas to recurrence properties of the leaves of foliations (sections 2, 3 and 4); (2) Dimensions of Ends, which discussed coarse cohomology, coronas and coarse entropy (sections 5, 6 and 7); and (3) Coarse Families Produce Fine Invariants, which discussed the construction of foliation fundamental classes, and their application to spectral geometry and the proof of the Foliation Novikov Conjecture (section 8, 9 and 10). NTIS

N95-16292# Institut des Hautes Etudes Scientifiques, Bures-sur-Yvette (France).
CLASSICAL SOLUTIONS OF THE PRANDTL-REUSS EQUATIONS OF PERFECT ELASTO-PLASTICITY
S. B. Kuksin Mar. 1994 12 p
(PB94-192333; IHES/M/94/17) Avail: CASI HC A03/MF A01

We study the elasticity domain for an antiplane deformation of a perfect elasto-plastic medium, which is described by the Prandtl-Reuss equations. We prove that a boundary of this domain can be found by solving a system of nonlinear functional equations. In the simplest case of simple shear deformations, this system of equations is studied in detail. NTIS

N95-16293# Institut des Hautes Etudes Scientifiques, Bures-sur-Yvette (France).
QUASICONFORMAL MAPPINGS, OPERATORS ON HILBERT SPACE, AND LOCAL FORMULAE FOR CHARACTERISTIC CLASSES
A. Connes, D. Sullivan, and N. Teleman Feb. 1994 28 p
(PB94-192366; IHES/M/94/15) Avail: CASI HC A03/MF A01

Local formulae are given for the characteristic classes of a quasiconformal manifold using the subspace of exact forms in the Hilbert space of middle dimensional forms. The method applies to combinatorial manifolds and all topological manifolds except certain ones in dimension four. NTIS

N95-16294# Institut des Hautes Etudes Scientifiques, Bures-sur-Yvette (France).
SOME FUNDAMENTAL TECHNIQUES IN THE THEORY OF INTEGRABLE SYSTEMS
P. Cartier (Ecole Normale Superieure, Paris, France.) Mar. 1994 42 p
(PB94-192390; IHES/M/94/23) Avail: CASI HC A03/MF A01

The importance of Poisson brackets in classical mechanics was gradually recognized by Lagrange, Poisson and Jacobi. The original remark was as follows: if two mechanical quantities F and G are constants of motion for a certain dynamical system, then a suitable linear combination of products of first-order derivatives of F by similar ones for G, is another constant of motion. We assume that F and G are expressed as functions of positions and velocities of the various parts of the system. In these lectures, we intend to give an introduction to the various aspects of Poisson brackets. Our purpose has been to lay down the differential-geometric foundations for the use of Poisson brackets in the subsequent parts, where the emphasis is on the dynamical systems. Contents include: (1) analytical mechanics and differential geometry; (2) Poisson manifolds and symplectic manifolds; (3) Poisson manifolds and tensor calculus; (4) symplectic foliations on Poisson manifolds; and (5) the momentum map. NTIS

N95-16295# Institut des Hautes Etudes Scientifiques, Bures-sur-Yvette (France).
UNIQUENESS AND FREE INTERPOLATION FOR LOGARITHMIC POTENTIALS AND THE CAUCHY PROBLEM FOR THE LAPLACE EQUATION IN (R2)
A. Aleksandrov, J. Bourgain, M. Giesecke, V. Havin, and Y. Vymenets Mar. 1994 54 p
(PB94-192408; IHES/M/94/24) Avail: CASI HC A04/MF A01

The Cauchy problem for the Laplace equation is solved. Relations of (H1) to classes Alpha, A, and A1 are given for solvable sets and free interpolation by analytic functions. It is proved that classes S(sub k, sup a)(= S(sub k)) coincide (k = 0,1,2). A third section (after the introduction) proves that S(sub 0) = S(sub 1) = S(sub 2) = Por. CASI

N95-16367# Institut des Hautes Etudes Scientifiques, Bures-sur-Yvette (France).
SINGULARITIES OF SMOOTH MAPS IN A SPACE WITH A FIXED CONE
B. Z. Shapiro Mar. 1994 18 p
(PB94-192358; IHES/M/94/20) Avail: CASI HC A03/MF A01

The authors consider germs of smooth maps f : (R(sup l), 0) yields (R(sup n), C) where C is the standard nondegenerate cone of some signature, and classify their singularities under the actions of two natural groups of diffeomorphisms preserving C. Occurring singularities are subdivided into 3 classes: regular, semiregular, and irregular. In the regular case, the classification of singularities is reduced to the classification of the usual singularities of germs of functions. The authors present the list of simple semiregular singularities and also analyze the first nontrivial irregular singularity. NTIS

N95-16376 Carnegie-Mellon Univ., Pittsburgh, PA.
COMPUTATIONAL METHODS FOR MICROSTRUCTURE COVOLUME TECHNIQUES OF DISCRETIZATION Final Technical Report, 1 Jan. 1992 - 31 Mar. 1994
Roy A. Nicolaides 31 May 1994 5 p Limited Reproducibility: More than 20% of this document may be affected by microfiche quality
(Contract F49620-92-J-0133)
(AD-A282449; AFOSR-94-0428TR) Avail: Issuing Activity (Defense Technical Information Center (DTIC))

This work covers one of the basic computational issues in materials science, which is that of devising algorithms for computing microstructure. Finite element discretizations are used to approximate a standard energy density functional. Grid effects are found to affect the solutions in some cases and suitable remedies are investigated. Covolume methods are a second topic of research. Three dimensional error estimates are obtained. A new and optimal Voronoi-Delaunay mesh generator is given. DTIC

N95-16379 Maryland Univ., College Park, MD. Inst. for Physical Science and Technology.
VALIDATION OF RECIPES FOR THE RECOVERY OF STRESSES AND DERIVATIVES BY A COMPUTER-BASED APPROACH
I. Babuska, T. Strouboulis, S. K. Gangaraj, and C. S. Upadhyay May 1994 94 p Limited Reproducibility: More than 20% of this document may be affected by microfiche quality
(Contract N00014-90-J-1030)
(AD-A282712) Avail: CASI HC A05

We present a methodology for checking the local quality of recipes for the recovery of stresses or derivatives from finite element solutions of linear elliptic problems. The methodology accounts precisely for the factors which affect the local quality of the recovered quantities, namely, the geometry of the grid, the polynomial degree and the type of the elements, the coefficients of the differential equation, and the class of solutions of interest. We give examples of how the methodology can be used to obtain precise conclusions about the quality of a class of recipes, based on least-squares patch-recovery, in the interior of complex grids, like the ones employed in engineering computations. By using this approach we were able to discover recipes which are much more robust than the ones which are currently in use in the various finite element codes. DTIC

N95-16395 New Orleans Univ., LA. Dept. of Mathematics.
A STEPSIZE CONTROL STRATEGY FOR STIFF SYSTEMS OF ORDINARY DIFFERENTIAL EQUATIONS
Peter K. Moore and Linda R. Petzold Feb. 1994 22 p Limited Reproducibility: More than 20% of this document may be affected by microfiche quality
(Contract DAAL03-92-G-0247)
(AD-A281551; TR-94-08; ARO-29850.2-MA) Avail: Issuing Activity (Defense Technical Information Center (DTIC))

In solving stiff systems of ordinary differential equations using BDF methods, Jacobians needed for quasi-Newton iteration are frequently computed using finite differences. Round-off errors in the finite-difference approximation can lead to Newton failures forcing the code to choose its time steps based on stability rather than accuracy considerations. When standard stepsize control is used the code can experience thrashing which increases the total number of time steps, Jacobian evaluations, and function evaluations. We investigate this situation, explaining some surprising time step selection behavior produced by the standard control mechanism. A new control mechanism is proposed which attempts to find and use a stability stepsize. A comparison of the new strategy with the standard strategy and with two PI controllers introduced earlier is made using the stiff test set. DTIC

N95-16517# Rensselaer Polytechnic Inst., Troy, NY. Dept. of Computer Science.
NUMERICAL METHODS FOR SINGULARLY PERTURBED DIFFERENTIAL EQUATIONS WITH APPLICATIONS Final Report, 1 Apr. 1993 - 31 Mar. 1994
Joseph E. Flaherty 20 Jun. 1994 22 p
(Contract F49620-93-1-0218)
(AD-A285209; AFOSR-94-0583TR) Avail: CASI HC A03/MF A01

During this one-year project, we continued our research on the development, analysis, and application of serial and parallel adaptive computational strategies for solving transient and steady partial differential systems. We concentrated on high-order methods and adaptive approaches that unite mesh refinement and coarsening (h-refinement), order variation (p-refinement), and mesh motion (r-refinement). Parallel computational techniques involved load-balancing and load-redistribution strategies for implementing these adaptive methods on distributed-memory MIMD computers. In particular, we have developed migration strategies that exchange finite elements between neighboring spatial domains of different processors. Effective load balancing in an adaptive setting requires speedy procedures since balancing must be performed frequently. Migration offers several advantages in this regard since it (1) has a low unit cost, (2) can take advantage of locality, and (3) can improve communications volumes. Procedures tested in two dimensional situations are being extended to three dimensions and preliminary methods. DTIC

N95-16535# Lawrence Livermore National Lab., Livermore, CA.
AVOIDING BDF STABILITY BARRIERS IN THE MOL SOLUTION OF ADVECTION-DOMINATED PROBLEMS
A. C. Hindmarsh Apr. 1994 4 p Presented at the World Congress on Computational and Applied Mathematics, Atlanta, GA, 11-15 Jul. 1994
(Contract W-7405-eng-48)
(DE94-014793; UCRL-JC-116618; CONF-940719-6) Avail: CASI HC A01/MF A01

In the Method of Lines treatment of advection-dominated PDE problems, the resulting ODE system is typically characterized by weakly damped but strongly oscillatory modes. When a Backward Differentiation Formula (BDF) method is used on such a system, the step size may be unduly limited by the absolute stability region if the order is three or more. Existing BDF codes, which are heavily used in MOL applications generally, often perform poorly in this situation. The scaled derivatives that the BDF solver normally carries for error control purposes are also used for order selection, but until now no BDF solver has included a direct attempt to detect the presence of this stability limit. In an earlier paper, we analyze the scaled derivatives arising in the case where the numerical solution is completely dominated by a fixed, mildly damped, oscillatory mode, and this leads to a procedure for detecting the stability limit. The procedure is applied to the norms of the scaled derivatives of the solution and gives a value for the size of the dominant characteristic root. Stand-alone tests of the procedure on data from a simple ODE of size 2 were very encouraging. Here we use that procedure to form an algorithmic addition to the order selection scheme of the Adams/BDF solver VODE, whereby the order is reduced when a stability limitation is detected with BDF. This algorithm has been installed

in an experimental version of VODE. We use a simple advection-diffusion PDE in one space dimension to test the algorithm. In the tests so far, the order is successfully reduced at appropriate times, resulting in considerable savings over the unaltered solver. DOE

N95-16596*# Institute for Computer Applications in Science and Engineering, Hampton, VA.
AN ANALYSIS OF SPECTRAL ENVELOPE-REDUCTION VIA QUADRATIC ASSIGNMENT PROBLEMS Final Report
Alan George (Waterloo Univ., Ontario.) and Alex Pothen (Old Dominion Univ., Norfolk, VA.) Oct. 1994 26 p Submitted for publication
(Contracts NAS1-19480; RTOP 505-90-52-01; DE-FG02-91ER-25095; DE-FG05-94ER-25216; NSF CCR-90-24954; NSERC-OGP-0008111)
(NASA-CR-194992; NAS 1.26:194992; ICASE-94-81) Avail: CASI HC A03/MF A01

A new spectral algorithm for reordering a sparse symmetric matrix to reduce its envelope size was described. The ordering is computed by associating a Laplacian matrix with the given matrix and then sorting the components of a specified eigenvector of the Laplacian. In this paper, we provide an analysis of the spectral envelope reduction algorithm. We described related 1- and 2-sum problems; the former is related to the envelope size, while the latter is related to an upper bound on the work involved in an envelope Cholesky factorization scheme. We formulate the latter two problems as quadratic assignment problems, and then study the 2-sum problem in more detail. We obtain lower bounds on the 2-sum by considering a projected quadratic assignment problem, and then show that finding a permutation matrix closest to an orthogonal matrix attaining one of the lower bounds justifies the spectral envelope reduction algorithm. The lower bound on the 2-sum is seen to be tight for reasonably 'uniform' finite element meshes. We also obtain asymptotically tight lower bounds for the envelope size for certain classes of meshes. Author

N95-16611# Front Range Scientific Computation, Inc., Denver, CO.
SIXTH COPPER MOUNTAIN CONFERENCE ON MULTIGRID METHODS Abstracts Only
1994 108 p Conference held in Copper Mountain, CO, 4-9 Apr. 1993
(Contract DE-FG03-93ER-25157)
(DE94-014595; CONF-9304164-Absts) Avail: CASI HC A06/MF A02

During the 5-day meeting, 112 half-hour talks on current research topics were presented. Session topics included: (1) fluids; (2) domain decomposition; (3) iterative methods; (4) Basics 1 and 2; (5) adaptive methods; (6) nonlinear filtering; (7) CFD 1, 2, and 3; (8) applications; (9) transport; (10) algebraic solvers; (10) supercomputing; and (11) student paper winners. DOE

N95-16798# Wake Forest Univ., Winston-Salem, NC. Dept. of Mathematics.
LEAST SQUARES COMPUTATIONS IN SCIENCE AND ENGINEERING Final Report, 1 Feb. 1991 - 31 Jan. 1994
Robert J. Plemmons Feb. 1994 18 p
(Grant AF-AFOSR-0163-91)
(AD-A281213; AFOSR-94-0392TR) Avail: CASI HC A03/MF A01

Least squares computations constitute a fundamental tool in science and engineering. The reason is that they play a critical role in fitting numerical models to real world observations. This AFOSR supported research effort has been concerned with the design and testing of new algorithms for least squares computations and optimization in science and engineering. The objectives were to mathematically develop, test, and analyze fast numerical algorithms for the efficient solution to problems on modern high performance computers. The focus of this project was the application of scientific computing technology in the area of signal and image processing. Very many problems lead to over determined systems of linear or nonlinear equations that are often solved by least squares or related optimization methods. Generally, the problems are accompanied by constraints, such as bound constraints, and the observations are corrupted by noise. The project has involved the application of scientific computing in the area of computational linear and nonlinear least squares methods with particular applications in image and signal processing, where recovering images is often an ill-posed inverse problem. Additional work included control computations associated with adaptive optics. DTIC

N95-16869*# Institute for Computer Applications in Science and Engineering, Hampton, VA.
THE ALGEBRAIC MULTIGRID PROJECTION FOR EIGENVALUE PROBLEMS; BACKROTATIONS AND MULTIGRID FIXED POINTS Final Report
Sorin Costiner (Weizmann Inst. of Science, Rehovot, Israel.) and Shlomo Taasan (Weizmann Inst. of Science, Rehovot, Israel.) NASA Oct. 1994 19 p Submitted for publication Sponsored by Charles H. Revson Foundation
(Contract NAS1-19480; RTOP 505-90-52-01)
(NASA-CR-194990; NAS 1.26:194990; ICASE-94-82) Avail: CASI HC A03/MF A01

The periods of the theorem for the algebraic multigrid projection (MGP) for eigenvalue problems, and of the multigrid fixed point theorem for multigrid cycles combining MGP with backrotations, are presented. The MGP and the backrotations are central eigenvector separation techniques for multigrid eigenvalue algorithms. They allow computation on coarse levels of eigenvalues of a given eigenvalue problem, and are efficient tools in the computation of eigenvectors. Author

N95-16885*# National Aeronautics and Space Administration. Lewis Research Center, Cleveland, OH.
NEW DEVELOPMENTS IN THE METHOD OF SPACE-TIME CONSERVATION ELEMENT AND SOLUTION ELEMENT-APPLICATIONS TO TWO-DIMENSIONAL TIME-MARCHING PROBLEMS
Sin-Chung Chang, Xiao-Yen Wang (Colorado Univ., Boulder, CO.), and Chuen-Yen Chow (Colorado Univ., Boulder, CO.) Dec. 1994 124 p
(RTOP 505-62-52)
(NASA-TM-106758; E-9180; NAS 1.15:106758) Avail: CASI HC A06/MF A02

A new numerical discretization method for solving conservation laws is being developed. This new approach differs substantially in both concept and methodology from the well-established methods, i.e., finite difference, finite volume, finite element, and spectral methods. It is motivated by several important physical/numerical considerations and designed to avoid several key limitations of the above traditional methods. As a result of the above considerations, a set of key principles for the design of numerical schemes was put forth in a previous report. These principles were used to construct several numerical schemes that model a 1-D time-dependent convection-diffusion equation. These schemes were then extended to solve the time-dependent Euler and Navier-Stokes equations of a perfect gas. It was shown that the above schemes compared favorably with the traditional schemes in simplicity, generality, and accuracy. In this report, the 2-D versions of the above schemes, except the Navier-Stokes solver, are constructed using the same set of design principles. Their constructions are simplified greatly by the use of a nontraditional space-time mesh. Its use results in the simplest stencil possible, i.e., a tetrahedron in a 3-D space-time with a vertex at the upper time level and other three at the lower time level. Because of the similarity in their design, each of the present 2-D solvers virtually shares with its 1-D counterpart the same fundamental characteristics. Moreover, it is shown that the present Euler solver is capable of generating highly accurate solutions for a famous 2-D shock reflection problem. Specifically, both the incident and the reflected shocks can be resolved by a single data point without the presence of numerical oscillations near the discontinuity. Author

N95-16896*# Institute for Computer Applications in Science and Engineering, Hampton, VA.
MULTIGRID TECHNIQUES FOR NONLINEAR EIGENVALUE PROBEMS: SOLUTIONS OF A NONLINEAR SCHROEDINGER EIGENVALUE PROBLEM IN 2D AND 3D Final Report
Sorin Costiner (Weizmann Inst. of Science, Rehovot, Israel.) and Shlomo Taasan (Weizmann Inst. of Science, Rehovot, Israel.) Nov. 1994 41 p Submitted for publication Sponsored in part by Charles H. Revson Foundation
(Contract NAS1-19480; RTOP 505-90-52-01)
(NASA-CR-194999; NAS 1.26:194999; ICASE-94-91) Avail: CASI HC A03/MF A01

This paper presents multigrid (MG) techniques for nonlinear eigenvalue problems (EP) and emphasizes an MG algorithm for a nonlinear Schrodinger EP. The algorithm overcomes the mentioned difficulties combining the following techniques: an MG projection coupled with backrotations for

separation of solutions and treatment of difficulties related to clusters of close and equal eigenvalues; MG subspace continuation techniques for treatment of the nonlinearity; an MG simultaneous treatment of the eigenvectors at the same time with the nonlinearity and with the global constraints. The simultaneous MG techniques reduce the large number of self consistent iterations to only a few or one MG simultaneous iteration and keep the solutions in a right neighborhood where the algorithm converges fast. Author

N95-16897*# Institute for Computer Applications in Science and Engineering, Hampton, VA.

ALGORITHMS FOR BILEVEL OPTIMIZATION Final Report

Natalia Alexandrov and J. E. Dennis, Jr. NASA Sep. 1994 13 p Submitted for publication

(Contract NAS1-19480; RTOP 505-90-52-01)

(NASA-CR-194980; NAS 1.26:194980; ICASE-94-77) Avail: CASI HC A03/MF A01

General multilevel nonlinear optimization problems arise in design of complex systems and can be used as a means of regularization for multi-criteria optimization problems. Here, for clarity in displaying our ideas, we restrict ourselves to general bi-level optimization problems, and we present two solution approaches. Both approaches use a trust-region globalization strategy, and they can be easily extended to handle the general multilevel problem. We make no convexity assumptions, but we do assume that the problem has a nondegenerate feasible set. We consider necessary optimality conditions for the bi-level problem formulations and discuss results that can be extended to obtain multilevel optimization formulations with constraints at each level. Author

N95-16904*# Institute for Computer Applications in Science and Engineering, Hampton, VA.

ON THE REMOVAL OF BOUNDARY ERRORS CAUSED BY RUNGE-KUTTA INTEGRATION OF NON-LINEAR PARTIAL DIFFERENTIAL EQUATIONS Final Report

Saul Abarbanel (Tel-Aviv Univ., Ramat-Aviv, Tel-Aviv, Israel.), David Gottlieb (Brown Univ., Providence, RI.), and Mark H. Carpenter (National Aeronautics and Space Administration. Langley Research Center, Hampton, VA.) Hampton, VA NASA Sep. 1994 10 p Submitted for publication

(Contracts NAS1-19480; RTOP 505-90-52-01; N00014-91-J-4016; AF-AFOSR-0090-93; NSF DMS-92-11820)

(NASA-CR-194989; NAS 1.26:194989; ICASE-94-79) Avail: CASI HC A02/MF A01

It has been previously shown that the temporal integration of hyperbolic partial differential equations (PDE's) may, because of boundary conditions, lead to deterioration of accuracy of the solution. A procedure for removal of this error in the linear case has been established previously. In the present paper we consider hyperbolic (PDE's) (linear and non-linear) whose boundary treatment is done via the SAT-procedure. A methodology is present for recovery of the full order of accuracy, and has been applied to the case of a 4th order explicit finite difference scheme. Author

N95-17266*# Institute for Computer Applications in Science and Engineering, Hampton, VA.

MULTIRESOLUTION REPRESENTATION AND NUMERICAL ALGORITHMS: A BRIEF REVIEW Final Report

Amiram Harten (Tel-Aviv Univ., Ramat-Aviv, Tel-Aviv, Israel.) Hampton, VA NASA Oct. 1994 34 p Presented at the Parallel Numerical Algorithms Workshop, Hampton, VA, 22 May 1994

(Contracts NAS1-18605; NAS1-19480; RTOP 505-90-52-01)

(NASA-CR-194949; NAS 1.26:194949; ICASE-94-59) Avail: CASI HC A03/MF A01

In this paper we review recent developments in techniques to represent data in terms of its local scale components. These techniques enable us to obtain data compression by eliminating scale-coefficients which are sufficiently small. This capability for data compression can be used to reduce the cost of many numerical solution algorithms by either applying it to the numerical solution operator in order to get an approximate sparse representation, or by applying it to the numerical solution itself in order to reduce the number of quantities that need to be computed. Author

N95-17267*# Florida State Univ., Tallahassee, FL.

SPECTRAL SOLUTION OF THE VISCOUS BLUNT BODY PROBLEM. 2: MULTIDOMAIN APPROXIMATION Final Report

David A. Kopriva (Florida State Univ., Tallahassee, FL.) Hampton, VA NASA Aug. 1994 29 p Submitted for publication

(Contracts NAS1-19480; NAG1-862; RTOP 505-90-52-01; DE-FC05-85ER-25000)

(NASA-CR-194971; NAS 1.26:194971; ICASE-94-73) Avail: CASI HC A03/MF A01

We present steady solutions of high speed viscous flows over blunt bodies using a multidomain Chebyshev spectral collocation method. The region with the shock layer is divided into subdomains so that internal layers can be well-resolved. In the interiors of the subdomains, the solution is approximated by Chebyshev collocation. At interfaces between subdomains, the advective terms are upwinded and the viscous terms are treated by a penalty method. The method is applied to five flows, the Mach number range 5-25 and Reynolds number range 2,000 - 83,000, based on nose radius. Results are compared to experimental data and to a finite difference result. Author

N95-17306# Argonne National Lab., IL. Mathematics and Computer Science Div.

COMPUTATIONAL DIFFERENTIATION AND MULTIDISCIPLINARY DESIGN

C. Bischof and A. Griewank (Technische Univ., Dresden, German D.R..) 1993 26 p Presented at the SIAM Symposium on Inverse Problems and Optimal Design in Industry, Philadelphia, PA, 8-9 Jul. 1993

(Contract W-31-109-eng-38)

(DE94-013393; ANL/MCS/CP-82805; CONF-9307183-1) Avail: CASI HC A03/MF A01

Multidisciplinary design optimization (MDO) by means of formal sensitivity analysis requires that each single-discipline analysis code supply not only the output functions for the (usually constrained) optimization process and other discipline analysis inputs, but also the derivatives of all of these output functions with respect to its input variables. Computational differentiation techniques and automatic differentiation tools enable MDO by providing accurate and efficient derivatives of computer programs with little human effort. We discuss the principles behind automatic differentiation and give a brief overview of automatic differentiation tools and how they can be employed judiciously, for example, for sparse Jacobians and to exploit parallelism. We show how, and under what circumstances, automatic differentiation applied to iterative solvers delivers the mathematically desired derivatives. We then show how derivatives that can now be feasibly obtained by computational differentiation techniques can lead to improved solution schemes for nonlinear coupled systems and multidisciplinary design optimization. DOE

N95-17333# State Univ. of New York, Stony Brook, NY.

FIFTH INTERNATIONAL CONFERENCE ON HYPERBOLIC PROBLEMS: THEORY, NUMERICS, APPLICATIONS Abstracts Only

Remi Abgrall, Roumen Anguelov, Greg Baker, Fumioki Asakura, and Paul Arminjon 25 Jul. 1994 98 p Conference held in Stony Brook, NY, 13-17 Jun. 1994

(Contract N00014-94-1-0367)

(AD-A283078) Avail: CASI HC A05/MF A02

Abstracts presented include the following: On Genuinely Multidimensional Upwinding in the Finite Volume Context; A Method with Automatic Error Control for Numerical Solution of the Wave Equation; Two-Dimensional Finite Volume Extension of the Nessyahu-Tadmor Scheme for Conservation Laws; The Initial Boundary Value Problem for the Hyperbolic System of Conservation Laws; Singularities and Interfacial Patterns in Hele-Shaw Flows; Wave Processes in a Three Phase System of a Collapsing Bubble Near a Compliant Wall; Multidimensional Algorithms for Relativistic Hydrodynamics; Roe-Type Riemann Solver for Magnetohydrodynamics; and Eulerian Formulation of the MHD Riemann Problem. CASI

N95-17431 Maryland Univ., College Park, MD.

A MODEL STUDY OF ELEMENT RESIDUAL ESTIMATORS FOR LINEAR ELLIPTIC PROBLEMS: THE QUALITY OF THE ESTIMATORS IN THE INTERIOR OF MESHES OF TRIANGLES AND QUADRILATERALS

I. Babuska, T. Strouboulis (Texas A&M Univ., College Station, TX.), C. S. Upadhyay (Texas A&M Univ., College Station, TX.), and S. K. Gangaraj

(Texas A&M Univ., College Station, TX.) May 1994 97 p Limited Reproducibility: More than 20% of this document may be affected by microfiche quality
(Contract N00014-90-J-1030; NSF CCR-88-20279; NSF MSS-90-25110)
(AD-A282849; TN-BN-1171) Avail: CASI HC A05

We presented a model study of a posteriori error estimators in the interior of finite element meshes using a computer-based methodology. In this paper we investigate further the quality of element-residual error estimators. We analyzed several versions of the element-residual estimator and based on this study we propose recipes for robust estimators. DTIC

N95-17618 Carnegie-Mellon Univ., Pittsburgh, PA. Dept. of Computer Science.
REAL-TIME SYMBOLIC MODEL CHECKING FOR DISCRETE TIME MODELS
Sergio V. Campos and Edmund M. Clarke 2 May 1994 20 p Limited Reproducibility: More than 20% of this document may be affected by microfiche quality
(Contract MDA972-90-C-0035)
(AD-A282878; CMU-CS-94-146) Avail: CASI HC A03

A BDD-based symbolic model checking algorithm is extended to handle real-time properties using the 'bounded until' operator. We believe that this algorithm which is based on discrete time is able to handle many real-time properties that arise in practical problems. One example of such a property is 'priority inversion.' This is a serious problem that can make real-time systems unpredictable in subtle ways. Our work discusses this problem and presents one possible solution. The solution is formalized and verified using the modified algorithm. We also propose another extension to the model checking algorithm. Timed transition graphs (TTG's) are transition graphs in which events may take non-unit time to occur. The time it takes for a transition in a TTG to happen is determined by a time interval. This allows the construction of smaller and more realistic models. A symbolic model checking algorithm is given for formulas using the bounded until operator in TTG models. DTIC

N95-17713# State Univ. of New York, Stony Brook, NY.
REPORT ON THE 5TH INTERNATIONAL CONFERENCE ON NONLINEAR HYPERBOLIC PROBLEMS
James Glimm and Qiang Zhang 12 Jul. 1994 4 p Conference held in Stony Brook, NY, 13-17 Jun. 1994
(AD-A283077) Avail: CASI HC A01/MF A01

The conference demonstrated that hyperbolic problems and conservation laws play an important role in many areas including industrial applications and the studying of elasto-plastic materials. Among the various topics covered in the conference, we mention: the big bang theory, general relativity, critical phenomena, deformation and fracture of solids, shock wave interactions, numerical simulation in three dimensions, the level set method, multidimensional Riemann problem, application of the front tracking in petroleum reservoir simulations, global solution of the Navier-Stokes equations in high dimensions, recent progress in granular flow, and the study of elastic plastic materials. Derived from text

N95-17916# Pacific Northwest Lab., Richland, WA.
TRIGONOMETRIC FUNCTIONS OF NONLINEAR QUANTITIES
D. W. Wester Aug. 1994 35 p
(Contract DE-AC06-76RL-01830)
(DE94-018794; PNL-10073) Avail: CASI HC A03/MF A01

Trigonometric functions of nonlinear quantities are introduced. Functions of the form (line integral)(x(sup a)), (line integral)(x(sup y)), and (line integral)(sup n)(x(sup a)) are reported, where (line integral) is a trigonometric function such as cos, sin, tan, cot, sec, or csc; x is a variable; a is a constant; y is a variable; and n is a constant. Sums, products and quotients of these functions are defined. Trigonometric functions of nonlinear quantities involving constants to variable powers also are mentioned. Possible applications to quantum mechanics, gravity, and a final theory of matter are discussed. DOE

N95-16274# Kazan Aviation Inst. (USSR).
METHODS OF WAVE-FRONT IDENTIFICATION BY CONTROL IMAGES
G. L. Degtyarev, A. V. Makhanko, and S. M. Chernyavskii *In* Nanjing Univ. of Aeronautics and Astronautics, Joint Proceedings on Aeronautics and Astronautics (JPAA) May 1993 p 161-168 (For primary document see N95-16249 04-01)
Avail: CASI HC A02/MF A03

N95-16276# Kazan Aviation Inst. (USSR).
PROBLEM OF CONSTRUCTING THE LYAPUNOV'S FUNCTIONS IN LUMPED PARAMETER SYSTEMS
T. K. Sirazetdinov *In* Nanjing Univ. of Aeronautics and Astronautics, Joint Proceedings on Aeronautics and Astronautics (JPAA) May 1993 p 179-183 (For primary document see N95-16249 04-01)
Avail: CASI HC A01/MF A03

N95-17286*# Jet Propulsion Lab., California Inst. of Tech., Pasadena, CA.
A SIMPLIFIED INTEGER COSINE TRANSFORM AND ITS APPLICATION IN IMAGE COMPRESSION
M. Costa and K. Tong *In its* The Telecommunications and Data Acquisition Report 15 Nov. 1994 p 129-139 (For primary document see N95-17279 04-32)
(RTOP 310-30-71-83-04)
Avail: CASI HC A03/MF A03

65 STATISTICS AND PROBABILITY

Includes data sampling and smoothing; Monte Carlo method; and stochastic processes.

N95-16039# Rochester Univ., NY. Dept. of Computer Science.
ON THE STRUCTURE OF LOG-SPACE PROBABILISTIC COMPLEXITY CLASSES
Ioan I. Macarie Jul. 1994 25 p
(Grant NSF CDA-88-22724)
(TR-506) Avail: CASI HC A03/MF A01

We investigate hierarchical properties and log-space reductions of languages recognized by log-space probabilistic Turing machines, Arthur-Merlin games and Games against Nature with log-space probabilistic verifiers. For each log-space complexity class, we decompose it into a hierarchy based on corresponding multihead two-way finite automata and we (eventually) prove the separation of the hierarchy levels (even over one letter alphabet); furthermore, we show log-space reductions of each log-space complexity class to low levels of its corresponding hierarchy. We find probabilistic (and 'probabilistic+nondeterministic') variants of Savitch's maze threading problem which are log-space complete for PL (and respectively P) and can be recognized by two-head one-way and one-way one-counter finite automata with probabilistic (probabilistic and nondeterministic) states. Author

N95-16422# Air Force Inst. of Tech., Wright-Patterson AFB, OH.
A COMBINED BIASED-ROBUST ESTIMATOR FOR DEALING WITH INFLUENCE AND COLLINEARITY IN REGRESSION
James R. Simpson 1993 29 p
(AD-A281793; AFIT/CI/CIA-94-078) Avail: CASI HC A03/MF A01

Regression analysis is a statistical tool that has earned widespread use in nearly all areas of endeavor seeking to fit a model to a set of data. Although there are several methods of estimating the model parameters, the least squares method is used most often because of its general acceptance, elegant statistical properties and ease of computation. Unfortunately, the mathematical elegance that makes least squares so popular depends on a number of fairly strong and many times unrealistic assumptions. The assumption that makes least squares so attractive in terms of hypothesis testing and confidence intervals on the parameter estimates is that the distribution of the errors is normal or Gaussian. This assumption can be violated if one or more sufficiently outlying observations are present in the data, resulting in less than optimal estimates of the parameters. The second problem that can ruin the accuracy of least squares estimates is correlated regressors. Highly correlated regressors can cause large variances in the estimates of the coefficients, sometimes resulting in incorrect levels of magnitude or even incorrect signs for the coefficients. The objective of this research is to develop a biased-robust regression estimator and determine how the method performs in the presence of

nonnormal errors (outliers) and multicollinear regressor variables. To accomplish this major objective a number of investigative questions must be answered. DTIC

N95-16546# Stanford Univ., CA. Dept. of Statistics.
NONASYMPTOTIC FORMULAE FOR THE DISTRIBUTION OF THE MAXIMUM OF SMOOTH GAUSSIAN PROCESSES
J. Diebolt and C. Posse 11 Aug. 1994 28 p
(Contract N00014-92-J-1264)
(AD-A284741) Avail: CASI HC A03/MF A01

We derive an integral formula for the density of the maximum of smooth Gaussian processes. This expression induces explicit lower and upper bounds which are in general asymptotic to the density. Our constructive approach relies on a geometric representation of Gaussian processes involving a unit speed parameterized curve embedded in the unit sphere. DTIC

N95-17341# Air Force Inst. of Tech., Wright-Patterson AFB, OH.
BAYESIAN NONPARAMETRIC ESTIMATION VIA GIBBS SAMPLING FOR COHERENT SYSTEMS WITH REDUNDANCY Ph.D. Thesis
Kevin Lawson 13 Jul. 1994 67 p
(AD-A283173; AFIT/CI/CIA-94-028D) Avail: CASI HC A04/MF A01

We consider a coherent system S consisting of m independent components for which we do not know the distributions of the components' lifelengths. If we know the structure function of the system, then we can estimate the distribution of the system lifelength by estimating the distributions of the system lifelengths of the individual components. Suppose that we can collect data under the autopsy model, wherein a system is run until a failure occurs and then the status (functioning or dead) of each component is obtained. This test is repeated n times. The autopsy statistics consist of the age of the system at the time of breakdown and the set of parts that are dead by the time of breakdown. Using the structure function and the recorded status of the components, we then classify the failure time of each component. We develop a nonparametric Bayesian estimate of the distributions of the component lifelengths and then use this to obtain an estimate of the distribution of the lifelength of the system. The procedure is applicable to machine-test settings wherein the machines have redundant designs. A parametric procedure is also given. Author (DTIC)

N95-17377 Carnegie-Mellon Univ., Pittsburgh, PA. Robotics Inst.
HIDDEN MARKOV MODEL FOR GESTURE RECOGNITION
Jie Yang and Yangsheng Xu May 1994 27 p Limited Reproducibility: More than 20% of this document may be affected by microfiche quality
(AD-A282845; CMU-RI-TR-94-10) Avail: CASI HC A03

This report presents a method for developing a gesture-based system using a multidimensional hidden Markov model (HMM). Instead of using geometric features, gestures are converted into sequential symbols. HMM's are employed to represent the gestures and their parameters are learned from the training data. Based on the most likely performance criterion, the gestures can be recognized through evaluating the trained HMM's. We have developed a prototype system to demonstrate the feasibility of the proposed method. The system achieved 99.78% accuracy for an isolated recognition task with nine gestures. Encouraging results were also obtained from experiments of continuous gesture recognition. The proposed method is applicable to any gesture represented by a multidimensional signal, and will be a valuable tool in telerobotics and human computer interfaces. DTIC

N95-17426 Stanford Univ., CA. Dept. of Operations Research.
LIKELIHOOD RATIO GRADIENT ESTIMATION FOR STOCHASTIC RECURSIONS
Peter W. Glynn and Pierre LEcuyer Nov. 1993 41 p Limited Reproducibility: More than 20% of this document may be affected by microfiche quality
(Contract DAAL03-91-G-0319)
(AD-A281408; TR-93-20; ARO-29412.5-MA-SDI) Avail: CASI HC A03

In this paper, we develop mathematical machinery for verifying that a broad class of general state space Markov chains reacts smoothly to certain types of perturbations in the underlying transition structure. Our main result provide conditions under which the stationary probability measure of an ergodic Harris recurrent Markov chain is differentiable in a certain strong sense. The approach is based on likelihood ratio change of measure arguments, and leads directly to a likelihood ratio gradient estimator that can be used to numerically calculate the resulting derivatives: (1) Harris recurrent Markov chain; (2) Likelihood ratio; (3) Gradient estimation; and (4) Regeneration. DTIC

N95-17429 Carnegie-Mellon Univ., Pittsburgh, PA. Robotics Inst.
HIDDEN MARKOV MODEL FOR CONTROL STRATEGY LEARNING
Jie Yang and Yangsheng Xu May 1994 22 p Limited Reproducibility: More than 20% of this document may be affected by microfiche quality
(AD-A282846; CMU-RI-TR-94-11) Avail: CASI HC A03

This report presents a method for learning a control strategy using the hidden Markov model (HMM), i.e., developing a feedback controller based on HMM's. The HMM is a parametric model for nonstationary pattern recognition and is feasible to characterize a doubly stochastic process involving observable actions and a hidden decision pattern. The control strategy is encoded by HMMs through a training process. The trained models are then employed to control the system. The proposed method has been investigated by simulations of a linear system and an inverted pendulum system. The HMM-based controller provides a novel way to learn control strategy and to model the human decision making process. DTIC

N95-17526# Helsinki Univ. of Technology, Espoo (Finland). Inst. of Mathematics.
CELLULAR AUTOMATA FOR CONTOUR DYNAMICS
K. Eloranta Mar. 1994 34 p
(PB94-197613; RR-A-331) Avail: CASI HC A03/MF A01

The dynamics of deterministic partially permutive cellular automata in two dimensions is considered. In particular, the authors lay out the design principles and analyze the dynamic of generalized voter-type rules. They provide a two parameter model class of cellular automata which exhibit annealing, diffusive and critical domain behavior. They analyze the dynamics rigorously in certain cases and also show that all types of behavior are very close to their idea counterparts observed in probabilistic models based on strong independence assumptions. This is further evidence that the statistical mechanics extends to cover also this class of purely deterministic dynamics. NTIS

66 SYSTEMS ANALYSIS

Includes mathematical modeling; network analysis; and operations research.

N95-17211*# National Aeronautics and Space Administration. Marshall Space Flight Center, Huntsville, AL.
A DISTRIBUTED PLANNING CONCEPT FOR SPACE STATION PAYLOAD OPERATIONS
Jeff Hagopian, Theresa Maxwell, and Tracey Reed *In* NASA. Goddard Space Flight Center, Third International Symposium on Space Mission Operations and Ground Data Systems, Part 1 Nov. 1994 p 287-294 (For primary document see N95-17179 04-17)
Avail: CASI HC A02/MF A06

N95-17217*# Deutsche Forschungs- und Versuchsanstalt fuer Luft- und Raumfahrt, Oberpfaffenhofen (Germany).
GEOSTATIONARY SATELLITE POSITIONING BY DLR/GSOC OPERATIONS AND MANAGEMENT METHODS
Peter Brittinger *In* NASA. Goddard Space Flight Center, Third International Symposium on Space Mission Operations and Ground Data Systems, Part 1 Nov. 1994 p 339-346 (For primary document see N95-17179 04-17)
Avail: CASI HC A02/MF A06

N95-17218*# Martin Marietta Corp., Denver, CO.
MAGELLAN PROJECT: EVOLVING ENHANCED OPERATIONS EFFICIENCY TO MAXIMIZE SCIENCE VALUE
Allan R. Cheuvront, James C. Neuman, and J. Franklin McKinney *In* NASA. Goddard Space Flight Center, Third International Symposium on Space Mission Operations and Ground Data Systems, Part 1 Nov. 1994

p 347-354 Sponsored by JPL (For primary document see N95-17179 04-17)
Avail: CASI HC A02/MF A06

N95-17219*# European Space Agency. Ulysses Office, Pasadena, CA.
GRAND MISSION VERSUS SMALL OPS TEAM: CAN WE HAVE BOTH?
Raul Garcia-Perez *In* NASA. Goddard Space Flight Center, Third International Symposium on Space Mission Operations and Ground Data Systems, Part 1 Nov. 1994 p 355-360 (For primary document see N95-17179 04-17)
Avail: CASI HC A02/MF A06

N95-17220*# Johns Hopkins Univ., Laurel, MD. Applied Physics Lab.
THE ROLE OF MISSION OPERATIONS IN SPACECRAFT INTEGRATION AND TEST
Raymond J. Harvey *In* NASA. Goddard Space Flight Center, Third International Symposium on Space Mission Operations and Ground Data Systems, Part 1 Nov. 1994 p 361-369 (For primary document see N95-17179 04-17)
Avail: CASI HC A02/MF A06

N95-17221*# European Space Agency. European Space Research and Technology Center, ESTEC, Noordwijk (Netherlands).
PAYLOAD OPERATIONS MANAGEMENT OF A PLANNED EUROPEAN SL-MISSION EMPLOYING ESTABLISHMENTS OF ESA AND NATIONAL AGENCIES
Rolf Joensson and Karl L. Mueller (Deutsche Forschungsanstalt fuer Luft- und Raumfahrt, Cologne, Germany.) *In* NASA. Goddard Space Flight Center, Third International Symposium on Space Mission Operations and Ground Data Systems, Part 1 Nov. 1994 p 371-376 (For primary document see N95-17179 04-17)
Avail: CASI HC A02/MF A06

N95-17222*# Stanford Telecommunications, Inc., Reston, VA.
EVALUATING SPACE NETWORK (SN) SCHEDULING OPERATIONS CONCEPTS THROUGH STATISTICAL ANALYSIS
Carl Kwadrat and Nadine Happell *In* NASA. Goddard Space Flight Center, Third International Symposium on Space Mission Operations and Ground Data Systems, Part 1 Nov. 1994 p 377-388 (For primary document see N95-17179 04-17)
Avail: CASI HC A03/MF A06

N95-17225*# Loral AeroSys, Seabrook, MD.
MISSION OPERATIONS MANAGEMENT
David A. Rocco *In* NASA. Goddard Space Flight Center, Third International Symposium on Space Mission Operations and Ground Data Systems, Part 1 Nov. 1994 p 409-416 (For primary document see N95-17179 04-17)
Avail: CASI HC A02/MF A06

N95-17226*# Allied-Signal Technical Services Corp., Columbia, MD.
GRTS OPERATIONS MONITOR/CONTROL SYSTEM
Richard A. Rohrer *In* NASA. Goddard Space Flight Center, Third International Symposium on Space Mission Operations and Ground Data Systems, Part 1 Nov. 1994 p 417-423 (For primary document see N95-17179 04-17)
Avail: CASI HC A02/MF A06

N95-17227*# National Aeronautics and Space Administration. Marshall Space Flight Center, Huntsville, AL.
INTERNATIONAL SPACE STATION ALPHA USER PAYLOAD OPERATIONS CONCEPT
Ronald A. Schlagheck, William B. Crysel (Boeing Defense and Space Group, Huntsville, AL.), Elaine F. Duncan, and James W. Rider (Teledyne Brown Engineering, Huntsville, AL.) *In* NASA. Goddard Space Flight Center, Third International Symposium on Space Mission Operations and Ground Data Systems, Part 1 Nov. 1994 p 425-433 (For primary document see N95-17179 04-17)
Avail: CASI HC A02/MF A06

N95-17228*# Jet Propulsion Lab., California Inst. of Tech., Pasadena, CA.
SHARED MISSION OPERATIONS CONCEPT
Gary L. Spradlin, Richard P. Rudd, and Susan H. Linick *In* NASA. Goddard Space Flight Center, Third International Symposium on Space Mission Operations and Ground Data Systems, Part 1 Nov. 1994 p 435-442 (For primary document see N95-17179 04-17)
Avail: CASI HC A02/MF A06

N95-17229*# Jet Propulsion Lab., California Inst. of Tech., Pasadena, CA.
MARS PATHFINDER MISSION OPERATIONS CONCEPTS
Francis M. Sturms, Jr., William C. Dias, Albert Y. Nakata, and Wallace S. Tai *In* NASA. Goddard Space Flight Center, Third International Symposium on Space Mission Operations and Ground Data Systems, Part 1 Nov. 1994 p 443-450 (For primary document see N95-17179 04-17)
Avail: CASI HC A02/MF A06

N95-17230*# MATRA Marconi Space, Toulouse (France).
TOWARDS A NEW GENERATION OF MISSION PLANNING SYSTEMS: FLEXIBILITY AND PERFORMANCE
A. Gasquet, Y. Parrod, and A. DeSaintVincent *In* NASA. Goddard Space Flight Center, Third International Symposium on Space Mission Operations and Ground Data Systems, Part 1 Nov. 1994 p 453-460 (For primary document see N95-17179 04-17)
Avail: CASI HC A02/MF A06

N95-17232*# Centre National d'Etudes Spatiales, Toulouse (France).
A PC BASED TOOL FOR MISSION PLAN PRODUCTION
Jean-Pierre Joli and Clet Yven *In* NASA. Goddard Space Flight Center, Third International Symposium on Space Mission Operations and Ground Data Systems, Part 1 Nov. 1994 p 467-471 (For primary document see N95-17179 04-17)
Avail: CASI HC A01/MF A06

N95-17233*# European Space Agency. European Space Operations Center, Darmstadt (Germany).
TOWARDS A CLASS LIBRARY FOR MISSION PLANNING
Oliver Pujo, Simon T. Smith (Cray Systems, Bristol, England.), Paul Starkey (Cray Systems, Bristol, England.), and Thilo Wolff *In* NASA. Goddard Space Flight Center, Third International Symposium on Space Mission Operations and Ground Data Systems, Part 1 Nov. 1994 p 473-480 (For primary document see N95-17179 04-17)
Avail: CASI HC A02/MF A06

N95-17234*# National Aeronautics and Space Administration. Goddard Space Flight Center, Greenbelt, MD.
AUTONOMOUS MISSION PLANNING AND SCHEDULING: INNOVATIVE, INTEGRATED, RESPONSIVE
Charisse Sary (Computer Sciences Corp., Beltsville, MD.), Simon Liu (Computer Sciences Corp., Beltsville, MD.), Larry Hull, and Randy Davis (Colorado Univ., Boulder, CO.) *In its* Third International Symposium on Space Mission Operations and Ground Data Systems, Part 1 Nov. 1994 p 481-488 (For primary document see N95-17179 04-17)
Avail: CASI HC A02/MF A06

N95-17235*# Deutsche Forschungsanstalt fuer Luft- und Raumfahrt, Wessling (Germany).
A MISSION PLANNING CONCEPT AND MISSION PLANNING SYSTEM FOR FUTURE MANNED SPACE MISSIONS
Martin Wickler *In* NASA. Goddard Space Flight Center, Third International Symposium on Space Mission Operations and Ground Data Systems, Part 1 Nov. 1994 p 489-497 (For primary document see N95-17179 04-17)
Avail: CASI HC A02/MF A06

N95-17236*# OAO Corp., Altadena, CA.
OPERATIONS AUTOMATION
Charles Thomas Boreham *In* NASA. Goddard Space Flight Center, Third International Symposium on Space Mission Operations and Ground Data Systems, Part 1 Nov. 1994 p 501-505 (For primary document

see N95-17179 04-17)
Avail: CASI HC A01/MF A06

N95-17240*# Deutsche Forschungsanstalt fuer Luft- und Raumfahrt, Oberpfaffenhofen (Germany).
THE SEQUENCE OF EVENTS GENERATOR: A POWERFUL TOOL FOR MISSION OPERATIONS
Hubertus Wobbe and Armin Braun *In* NASA. Goddard Space Flight Center, Third International Symposium on Space Mission Operations and Ground Data Systems, Part 1 Nov. 1994 p 531-537 (For primary document see N95-17179 04-17)
Avail: CASI HC A02/MF A06

N95-17241*# California Univ., Berkeley, CA. Center for EUV Astrophysics.
DESIGNING AN AUTONOMOUS ENVIRONMENT FOR MISSION CRITICAL OPERATION OF THE EUVE SATELLITE
Annadiana Abedini and Roger F. Malina *In* NASA. Goddard Space Flight Center, Third International Symposium on Space Mission Operations and Ground Data Systems, Part 1 Nov. 1994 p 541-546 (For primary document see N95-17179 04-17)
(Contracts NAS5-29298; NCC2-838)
Avail: CASI HC A02/MF A06

N95-17242*# Jet Propulsion Lab., California Inst. of Tech., Pasadena, CA.
INCREASES IN EFFICIENCY AND ENHANCEMENTS TO THE MARS OBSERVER NON-STORED COMMANDING PROCESS
Robert N. Brooks, Jr. and J. Leigh Torgerson *In* NASA. Goddard Space Flight Center, Third International Symposium on Space Mission Operations and Ground Data Systems, Part 1 Nov. 1994 p 547-558 (For primary document see N95-17179 04-17)
Avail: CASI HC A03/MF A06

N95-17244*# Jet Propulsion Lab., California Inst. of Tech., Pasadena, CA.
MISSION OPERATIONS DATA ANALYSIS TOOLS FOR MARS OBSERVER GUIDANCE AND CONTROL
Edwin P. Kan *In* NASA. Goddard Space Flight Center, Third International Symposium on Space Mission Operations and Ground Data Systems, Part 1 Nov. 1994 p 569-576 (For primary document see N95-17179 04-17)
Avail: CASI HC A02/MF A06

N95-17548*# Johns Hopkins Univ., Laurel, MD. Applied Physics Lab.
COST EFFICIENT OPERATIONS FOR DISCOVERY CLASS MISSIONS
G. E. Cameron, J. A. Landshof, and G. W. Whitworth *In* NASA. Goddard Space Flight Center, Third International Symposium on Space Mission Operations and Ground Data Systems, Part 2 Nov. 1994 p 809-816 (For primary document see N95-17531 04-17)
Avail: CASI HC A02/MF A06

N95-17549*# Rutherford Appleton Lab., Chilton (England).
GROUND STATION SUPPORT FOR SMALL SCIENTIFIC SATELLITES
R. Holdaway, E. Dunford, and P. H. McPherson *In* NASA. Goddard Space Flight Center, Third International Symposium on Space Mission Operations and Ground Data Systems, Part 2 Nov. 1994 p 817-824 (For primary document see N95-17531 04-17)
Avail: CASI HC A02/MF A06

N95-17552*# Computer Technology Associates, Inc., McLean, VA. Space Systems.
SMALL SATELLITE SPACE OPERATIONS
Keith Reiss *In* NASA. Goddard Space Flight Center, Third International Symposium on Space Mission Operations and Ground Data Systems, Part 2 Nov. 1994 p 847-853 (For primary document see N95-17531 04-17)
Avail: CASI HC A02/MF A06

N95-17555*# National Aeronautics and Space Administration. Goddard Space Flight Center, Greenbelt, MD.
AN AGENT-ORIENTED APPROACH TO AUTOMATED MISSION OPERATIONS
Walt Truszkowski and Jide Odubiyi (Loral AeroSys, Seabrook, MD.) *In its* Third International Symposium on Space Mission Operations and Ground Data Systems, Part 2 Nov. 1994 p 879-887 Sponsored by NASA, Washington (For primary document see N95-17531 04-17)
Avail: CASI HC A02/MF A06

N95-17572*# National Aeronautics and Space Administration. Goddard Space Flight Center, Greenbelt, MD.
EVALUATING MODELING TOOLS FOR THE EDOS
Gordon Knoble, Frederick McCaleb, Tanweer Aslam (Computer Sciences Corp., Lanham, MD.), and Paul Nester (Computer Sciences Corp., Lanham, MD.) *In its* Third International Symposium on Space Mission Operations and Ground Data Systems, Part 2 Nov. 1994 p 1025-1030 (For primary document see N95-17531 04-17)
Avail: CASI HC A02/MF A06

N95-17586*# National Space Development Agency, Tokyo (Japan). Tracking and Data Acquisition Dept.
A SYSTEM STUDY FOR SATELLITE OPERATION AND CONTROL IN NEXT GENERATION
K. Nakayama, T. Shigeta, T. Gotanda (LTCB Systems Co. Ltd., Japan.), K. Yamamoto (LTCB Systems Co. Ltd., Japan.), and Y. Yokokawa (LTCB Systems Co. Ltd., Japan.) *In* NASA. Goddard Space Flight Center, Third International Symposium on Space Mission Operations and Ground Data Systems, Part 2 Nov. 1994 p 1151-1157 (For primary document see N95-17531 04-17)
Avail: CASI HC A02/MF A06

N95-17593*# Jet Propulsion Lab., California Inst. of Tech., Pasadena, CA.
STANDARD PROTOCOL STACK FOR MISSION CONTROL
Adrian J. Hooke *In* NASA. Goddard Space Flight Center, Third International Symposium on Space Mission Operations and Ground Data Systems, Part 2 Nov. 1994 p 1213-1220 (For primary document see N95-17531 04-17)
Avail: CASI HC A02/MF A06

N95-17598*# National Aeronautics and Space Administration. Goddard Space Flight Center, Greenbelt, MD.
CROSS SUPPORT OVERVIEW AND OPERATIONS CONCEPT FOR FUTURE SPACE MISSIONS
William Stallings and Jean-Francois Kaufeler (European Space Agency. European Space Operations Center, Darmstadt, Germany.) *In its* Third International Symposium on Space Mission Operations and Ground Data Systems, Part 2 Nov. 1994 p 1253-1260 (For primary document see N95-17531 04-17)
Avail: CASI HC A02/MF A06

N95-17603*# National Aeronautics and Space Administration. Goddard Space Flight Center, Greenbelt, MD.
THE NASA MISSION OPERATIONS AND CONTROL ARCHITECTURE PROGRAM
Paul J. Ondrus, Richard D. Carper (Science Applications International Corp., McLean, VA.), and Alan J. Jeffries (Science Applications International Corp., McLean, VA.) *In its* Third International Symposium on Space Mission Operations and Ground Data Systems, Part 2 Nov. 1994 p 1297-1303 (For primary document see N95-17531 04-17)
Avail: CASI HC A02/MF A06

N95-17605*# Tokyo Univ., Sagamihara (Japan). Inst. of Space and Astronautical Science.
ARCHITECTURE OF A DISTRIBUTED MULTIMISSION OPERATIONS SYSTEM
Takahiro Yamada *In* NASA. Goddard Space Flight Center, Third International Symposium on Space Mission Operations and Ground Data Systems, Part 2 Nov. 1994 p 1317-1324 (For primary document see N95-17531 04-17)
Avail: CASI HC A02/MF A06

N95-17606*# National Aeronautics and Space Administration. Goddard Space Flight Center, Greenbelt, MD.
RE-ENGINEERING THE MISSION LIFE CYCLE WITH ABC AND IDEF
Daniel Mandl, Michael Rackley, and Jay Karlin (Viable Systems, Inc., Germantown, MD.) *In its* Third International Symposium on Space Mission Operations and Ground Data Systems, Part 2 Nov. 1994 p 1327-1334 (For primary document see N95-17531 04-17)
Avail: CASI HC A02/MF A06

N95-17608*# National Aeronautics and Space Administration. Goddard Space Flight Center, Greenbelt, MD.
THE REQUIREMENTS GENERATION SYSTEM: A TOOL FOR MANAGING MISSION REQUIREMENTS
Sylvia B. Sheppard *In its* Third International Symposium on Space Mission Operations and Ground Data Systems, Part 2 Nov. 1994 p 1345-1351 (For primary document see N95-17531 04-17)
Avail: CASI HC A02/MF A06

N95-17609*# Massachusetts Inst. of Tech., Lexington. Lincoln Lab.
AN OPPORTUNITY ANALYSIS SYSTEM FOR SPACE SURVEILLANCE EXPERIMENTS WITH THE MSX
Ramaswamy Sridharan, Gary Duff, Tony Hayes, and Andy Wiseman *In* NASA. Goddard Space Flight Center, Third International Symposium on Space Mission Operations and Ground Data Systems, Part 2 Nov. 1994 p 1353-1360 (For primary document see N95-17531 04-17)
Avail: CASI HC A02/MF A06

N95-17610*# Jet Propulsion Lab., California Inst. of Tech., Pasadena, CA.
MATRIX EVALUATION OF SCIENCE OBJECTIVES
Randii R. Wessen *In* NASA. Goddard Space Flight Center, Third International Symposium on Space Mission Operations and Ground Data Systems, Part 2 Nov. 1994 p 1361-1368 (For primary document see N95-17531 04-17)
Avail: CASI HC A02/MF A06

N95-17611*# National Aeronautics and Space Administration. Goddard Space Flight Center, Greenbelt, MD.
A NEW SYSTEMS ENGINEERING APPROACH TO STREAMLINED SCIENCE AND MISSION OPERATIONS FOR THE FAR ULTRAVIOLET SPECTROSCOPIC EXPLORER (FUSE)
Madeline J. Butler, George Sonneborn, and Dorothy C. Perkins *In its* Third International Symposium on Space Mission Operations and Ground Data Systems, Part 2 Nov. 1994 p 1371-1376 (For primary document see N95-17531 04-17)
Avail: CASI HC A02/MF A06

N95-17612*# Loral AeroSys, Landover, MD.
RISK REDUCTION METHODOLOGIES AND TECHNOLOGIES FOR THE EARTH OBSERVING SYSTEM (EOS) OPERATIONS CENTER (EOC)
Richard K. Hudson and Nelson V. Pingitore *In* NASA. Goddard Space Flight Center, Third International Symposium on Space Mission Operations and Ground Data Systems, Part 2 Nov. 1994 p 1377-1381 (For primary document see N95-17531 04-17)
Avail: CASI HC A01/MF A06

N95-17613*# National Aeronautics and Space Administration. Goddard Space Flight Center, Greenbelt, MD.
EDOS OPERATIONS CONCEPT AND DEVELOPMENT APPROACH
G. Knoble, C. Garman, G. Alcott, C. Ramchandani (Computer Sciences Corp., Lanham, MD.), and J. Silvers (Computer Sciences Corp., Lanham, MD.) *In its* Third International Symposium on Space Mission Operations and Ground Data Systems, Part 2 Nov. 1994 p 1383-1390 (For primary document see N95-17531 04-17)
Avail: CASI HC A02/MF A06

N95-17614*# Johns Hopkins Univ., Laurel, MD. Applied Physics Lab.
CONCURRENT ENGINEERING: SPACECRAFT AND MISSION OPERATIONS SYSTEM DESIGN
J. A. Landshof, R. J. Harvey, and M. H. Marshall *In* NASA. Goddard Space Flight Center, Third International Symposium on Space Mission Operations and Ground Data Systems, Part 2 Nov. 1994 p 1391-1397 (For primary document see N95-17531 04-17)
Avail: CASI HC A02/MF A06

67 THEORETICAL MATHEMATICS

Includes topology and number theory.

No abstracts in this category.

70 PHYSICS (GENERAL)

For precision time and time interval (PTTI) see *35 Instrumentation and Photography;* for geophysics, astrophysics or solar physics see *46 Geophysics, 90 Astrophysics,* or *92 Solar Physics.*

N95-16162# North Carolina Univ., Chapel Hill, NC. Dept. of Chemistry.
CYCLIC VOLTAMMETRIC ANALYSIS OF FERROCENE ALKANETHIOL MONOLAYER ELECTRODE KINETICS BASED ON MARCUS THEORY
Interim Report, May 1993 - Jun. 1994
Leonard Tender, Michael T. Carter, and Royce W. Murray 1 Jul. 1994 40 p
(Contract N00014-90-J-1230)
(AD-A281411; TR-59) Avail: CASI HC A03/MF A01

Theory for electrode kinetics of surface-immobilized monolayers in cyclic voltammetry is developed based on the Marcus free energy-rate relation. Numerical calculations show that when the applied over-potential exceeds about 30% of the reorganizational energy of the electrode reaction, voltammetry predicted from Marcus theory differs from that based on classical Butler-Volmer kinetics with regard to waveshape, peak currents and their dependence on potential sweep rate, and variation of peak potential with potential sweep rate. Estimates of the standard rate constant, k(sup o), can be made from E peak data without exact knowledge of reorganizational energies. Examples are given of evaluating k(sup o) for monolayers of ferrocene alkanethiols chemisorbed on Au(111) electrodes, when the monolayers are highly ordered and kinetically monodisperse, and when they are somewhat disordered and kinetically disperse on bulk gold electrodes at room and 150 K temperatures. DTIC

N95-16288# Los Alamos National Lab., NM.
MUON(+) SR STUDIES OF MAGNETIC PROPERTIES OF BORON CARBIDE SUPERCONDUCTORS
L. P. Le, R. H. Heffner, G. J. Nieuwenhuys (Leiden Univ., Netherlands.), P. C. Canfield (Ames Lab., IA.), A. Amato, R. Feyerherm, and F. N Gygax 2 Jun. 1994 6 p Presented at the International Conference on Strongly Correlated Electron Systems, Amsterdam, Netherlands, 15-18 Aug. 1994
(Contract W-7405-eng-36)
(DE94-014440; LA-UR-94-1965; CONF-940863-2) Avail: CASI HC A02/MF A01

Positive-muon spin rotation (mu(sup +)SR) has been carried out in the recently discovered rare-earth boron carbide superconductors RNi2B2C, R = Ho, Er and Tm. For R = Ho and Er zero-field mu(sup +)SR measurements showed a well-defined internal field below the Neel temperatures (T(sub N) equivalent to 5.5 K) coexisting with the superconducting state down to 0.1 K. The observed temperature dependence of the order parameter in R = Ho is consistent with a 2-dimensional Ising model. For R = Tm a spontaneous internal field appears above 30 K, whose magnitude saturates below about 3 K at a value corresponding to a rare earth moment much smaller than for Ho and Er. Transverse-field mu(sup +)SR measurements in R = Tm showed a superconducting penetration depth A = 1,200 Angstrom. The temperature dependence of lambda is consistent with conventional s-wave pairing. DOE

N95-16856 Institute of Sound and Vibration Research, Southampton (England). Fluid Dynamics and Acoustics Group.
EVALUATION OF SEA LOSS FACTORS USING INPUT POWER

MODULATION
F. J. Fahy Nov. 1994 16 p
(ISVR-TR-240) Copyright Avail: Issuing Activity

It is demonstrated how, in principle, a power modulation technique may be used to evaluate the dissipation and coupling loss factors of an SEA model of two coupled subsystems. The power is injected into one subsystem only, and need not be quantified. Author

N95-17449 Northeastern Univ., Boston, MA. Dept. of Electrical Engineering.
EFFECT OF COULOMB COLLISIONS, LANDAU DAMPING AND PARTICLE TRAPPING ON LINEAR AND NONLINEAR ION ACOUSTIC WAVES
Chung Chan and Zhi-Jian Jin 30 Dec. 1993 16 p Limited Reproducibility: More than 20% of this document may be affected by microfiche quality
(Contract F19628-92-K-0011)
(AD-A282009; PL-TR-93-2236; SR-1) Avail: CASI HC A03

We have performed a series of experiments to study the damping effect of the ion acoustic waves. The experimental results have been analyzed both qualitatively and quantitatively based on the theory by Basu and Jasperse. The analysis shows that the theoretical and experimental results agree very well under certain conditions. Author (DTIC)

N95-17467# Helsinki Univ. of Technology, Espoo (Finland). Dept. of Technical Physics.
NONSTATIONARY THEORY OF MODE COMPETITION IN GYROTRONS WITH ALLOWANCE FOR INHOMOGENEITY OF THE GUIDING MAGNETIC FIELD
O. Dumbrajs 1994 20 p
(PB94-197621; TKK-F-A725) Avail: CASI HC A03/MF A01

High-power millimeter wave generators can induce electron cyclotron waves in a plasma which can fulfill many functions (plasma breakdown, heating, current drive) in fusion plasma reactors including both tokamak and stellarator concepts. All these applications require tons of megawatts of power in the frequency range 100-300 GHz and power 0.5-1.5 MW per unit. Among various microwave sources, gyrotrons are the most developed source. Because of the heat losses in resonator walls at such high frequencies and powers, oversized cavities must be used. In such cavities, the mode competition becomes a severe problem. The most advanced theory of mode competition in gyrotrons in the nonstationary nonlinear theory. In the present paper, the authors extend this theory by allowing for inhomogeneity of the guiding magnetic field. The importance of this generalized theory is illustrated in the case of a 3 MW 140 GHz gyrotron with a coaxial cavity working in the TE(21,13) mode. NTIS

N95-17731 Rutherford Appleton Lab., Chilton (England).
CRITICAL AND PARAMAGNETIC SPIN DYNAMICS IN AN ANTIFERROMAGNETICALLY COUPLED HEISENBERG MAGNET: RESULTS FOR RbMnF3
A. Cuccoli, S. W. Lovesey, and V. Tognetti Jun. 1994 27 p Prepared in cooperation with Florence Univ., Italy
(PB95-104329; RAL-94-066) Avail: Issuing Activity (National Technical Information Service (NTIS))

Results are provided for the spin-spin response function of a three dimensional, antiferromagnetically coupled Heisenberg magnet, covering a range of temperatures from critical temperature to deep in the paramagnetic phase. The wave vectors considered span the Brillouin zone. Damping rates are given at the zone center and the antiferromagnetic ordering wave vector, w, together with copious numerical results for the full response function. The calculations are based on the nonlinear, integral-differential equations obtained from so-called coupled-mode theory. In a confrontation between experimental and theoretical findings for RbMnF3 nearly all aspects have a positive outcome. NTIS

N95-17750 Rutherford Appleton Lab., Chilton (England).
TIME-DEPENDENT SPIN CORRELATIONS IN THE HEISENBERG MAGNET AT INFINITE TEMPERATURE
S. W. Lovesey, E. Engdahl, A. Cuccoli, V. Tognetti, and E. Balcar Jun. 1994 20 p Prepared in cooperation with Florence Univ., Italy
(PB95-104303; RAL-94-068) Avail: Issuing Activity (National Technical Information Service (NTIS))

A coupled-mode theory of spin fluctuations in the d-dimensional Heisenberg magnet at infinite temperature is used to predict the time-dependence of various spin correlation functions. The real-space spin autocorrelation function is shown to have a long-time behavior approx (l/t)(sup d/theta) where theta = (4 + d)/2. Properties at intermediate values of the time are extracted from the theory by numerical analysis. In this time window, the reciprocal-lattice spin autocorrelation function, G(q,t), is, to a good approximation, an exponential function of time. The decay rate is proportional to q(sub alpha), where q is the wave vector. Analysis of our numerical data indicates that, the exponent alpha depends weakly on d, and it is significantly different from the value 2 which is compatible with a spin diffusion model. In the asymptotic limit, defined by q approaches to 0, t approaches to infinity and q(sup 2)t approaches to 0, G (q,t) is a function of a single variable = (t(q(sup theta))). This result rules against the validity of a diffusion model also in the asymptotic limit. NTIS

N95-17930# Helsinki Univ. of Technology, Espoo (Finland). Dept. of Technical Physics.
THERMAL NOISE IN BIOMAGNETIC MEASUREMENTS
J. Nenonen, J. Montonen, and T. Katila Dec. 1993 30 p
(PB95-104360; TKK-F-A677) Avail: CASI HC A03/MF A01

Superconducting quantum interference devices (SQUID's) allow detection of very weak magnetic fields with an unprecedented accuracy. Since SQUID sensors provide highest accuracy in measurements of low-frequency fields, they have proved invaluable in studies of magnetic signals produced by electrical activation in human heart and brain. In the present report, the role of thermal magnetic noise in biomagnetic measurements is considered in detail. The authors present quantitative theoretical estimations based on a phenomenological model of thermal agitation of electric charge in conductors. NTIS

71 ACOUSTICS

Includes sound generation, transmission and attenuation.
For noise pollution see *45 Environmental Pollution.*

N95-16226# Army Aeromedical Research Lab., Fort Rucker, AL.
THE ASSESSMENT OF THE AH-64D, LONGBOW, MAST-MOUNTED ASSEMBLY NOISE HAZARD FOR MAINTENANCE PERSONNEL Final Report
Ben T. Mozo and Elmaree Gordon Jul. 1994 40 p
(AD-A284971; USAARL-94-37) Avail: CASI HC A03/MF A01

Noise levels around the AH-64 helicopter exceed safe limits. Maintenance personnel are required to wear hearing protection to reduce hazard to hearing while performing maintenance procedures. This evaluation was directed at determining the contribution to noise levels by the auxiliary power unit (APU), auxiliary ground power unit (AGPU), environmental control system (ECS), and mast mounted assembly (MMA) at a variety of maintenance positions and establish protection capabilities of standard protectors for those noise levels. DTIC

N95-16248# Ohio State Univ., Columbus. Dept. of Speech and Hearing Science.
DEMODULATION PROCESSES IN AUDITORY PERCEPTION Annual Report, 1 Jun. 1993 - 31 May 1994
Lawrence L. Feth 1 Aug. 1994 29 p
(Contract F49620-93-1-0299)
(AD-A285427; AFOSR-94-0627TR) Avail: CASI HC A03/MF A01

The long range goal of this project is the understanding of human auditory processing of information conveyed by complex, time-varying signals such as speech, music or important environmental sounds. Our work is guided by the assumption that human auditory communication is a 'modulation - demodulation' process. That is, we assume that sound sources produce a complex stream of sound pressure waves with information encoded as variations (modulations) of the signal amplitude and frequency. The listeners task then is one of demodulation. Much of past. psychoacoustics work has been based in what we characterize as 'spectrum picture processing.' Complex sounds are Fourier analyzed to produce an amplitude-by-frequency 'picture' and the perception process is modeled as if the listener were analyzing the spectral picture. This approach leads to studies such as 'profile analysis' and the power-spectrum model of masking.

Our approach leads us to investigate time-varying, complex sounds. We refer to them as dynamic signals and we have developed auditory signal processing models to help guide our experimental work. DTIC

N95-16401*# Missouri Univ., Rolla, MO. Dept. of Mechanical and Aerospace Engineering and Engineering Mechanics.
DUCTED FAN ACOUSTIC RADIATION INCLUDING THE EFFECTS OF NONUNIFORM MEAN FLOW AND ACOUSTIC TREATMENT Final Technical Report, 31 Aug. 1981 - 30 Jun. 1993
Walter Eversman and Indranil Danda Roy Jul. 1993 80 p
(Grant NAG3-178)
(NASA-CR-197449; NAS 1.26:197449) Avail: CASI HC A05/MF A01

Forward and aft acoustic propagation and radiation from a ducted fan is modeled using a finite element discretization of the acoustic field equations. The fan noise source is introduced as equivalent body forces representing distributed blade loading. The flow in and around the nacelle is assumed to be nonuniform, reflecting the effects of forward flight and flow into the inlet. Refraction due to the fan exit jet shear layer is not represented. Acoustic treatment on the inlet and exhaust duct surfaces provides a mechanism for attenuation. In a region enclosing the fan a pressure formulation is used with the assumption of locally uniform flow. Away from the fan a velocity potential formulation is used and the flow is assumed nonuniform but irrotational. A procedure is developed for matching the two regions by making use of local duct modal amplitudes as transition state variables and determining the amplitudes by enforcing natural boundary conditions at the interface between adjacent regions in which pressure and velocity potential are used. Simple models of rotor alone and rotor/exit guide vane generated noise are used to demonstrate the calculation of the radiated acoustic field and to show the effect of acoustic treatment. The model has been used to assess the success of four techniques for acoustic lining optimization in reducing far field noise. Author

N95-16413 Iowa Univ., Iowa City, IA. Dept. of Physics and Astronomy.
EFFECTIVE REFLECTION COEFFICIENTS FOR THE MEAN ACOUSTIC FIELD BETWEEN TWO ROUGH INTERFACES
David H. Berman 14 Feb. 1994 24 p Sponsored by NRL Limited Reproducibility: More than 20% of this document may be affected by microfiche quality
(AD-A281962) Avail: Issuing Activity (Defense Technical Information Center (DTIC))

A formalism is presented which demonstrates that the mean Green's function for the acoustic field between two rough interfaces can be expressed as a Green's function associated with two flat interfaces with effective reflection coefficients. This result incorporates all orders of the fluctuations in the half-space scattering amplitudes associated with each interface considered separately. From the mean Green's function modal attenuations can be found. To lowest order in the surface height fluctuations it is shown that it is not sufficient to use mean half-space scattering amplitudes as effective reflection coefficients. The formalism is designed to provide approximations for the Green's function in layered media which are based on previously developed approximations for half-space scattering amplitudes. DTIC

N95-16614 Strasbourg Univ. (France). Ultrasound and Complex Fluid Dynamics Lab.
NON-LINEAR ACOUSTICS IN FLUIDS AND GELS Final Report [ACOUSTIQUE NON LINEAIRE DANS LES FLUIDES ET LES GELS]
A. Moussaid and N. Herrmann 1994 28 p In FRENCH Sponsored by Direction des Recherches, Etudes et Techniques and Centre de Documentation de l'Armement
(PB94-201308) Avail: Issuing Activity (National Technical Information Service (NTIS))

The authors report here on a survey of the literature concerning the determination of the non-linearity B/A parameter, for a study of non-linear acoustics in liquids and gels. Their ultimate goal is to find materials with properties suited to non-linear acoustics and the fabrication of parametric antennas. They found little chance of obtaining high non-linearity coefficients with simple liquids under normal conditions. The many measurements and theoretical tests have failed to produce any notable values. Models of static and dynamic liquid/gas diphasic media predict low speeds of under 200 m/s, and very large non-linearity parameters of 100,000. Experimental difficulties explain the scarcity of measurements. The experimentally neglected area of non-Newtonian materials is considered. Current publications focus primarily on medical applications, ultrasound imagery, and the positive and negative effects of a large B/A in an ultrasound wave field. The authors also describe an experimental setup to measure ultrasound speed under pressure, and run preliminary tests on a few model materials. NTIS

N95-16810# Johns Hopkins Univ., Baltimore, MD. Dept. of Mechanical Engineering.
THERMO-FLUID MECHANIC STUDY OF THERMOACOUSTIC DEVICES Summary Report, 1 Oct. 1993 - 31 May 1994
A. Prosperetti, C. Herman, and O. Knio 27 Jun. 1994 39 p
(Contract N00014-94-J-0063)
(AD-A281130) Avail: CASI HC A03/MF A01

The work summarized is divided into three parts. In Part 1 the development of a simplified model of thermoacoustic devices is described and the results of its preliminary analysis documented. In Part 2 the results so far obtained in an experimental program designed for the visualization of flow and heat transfer in a thermoacoustic stack are described. Part 3 deals with the progress on a full Navier-Stokes numerical simulation of flow and heat transfer processes in the stack. DTIC

N95-16811# Army Aeromedical Research Lab., Fort Rucker, AL.
DIRECT COMPARISON OF TWO STATISTICAL METHODS FOR DETERMINATION OF EVOKED-POTENTIAL THRESHOLDS
Ted L. Langford and James H. Patterson, Jr. Jul. 1994 20 p
(AD-A285182; USAARL-94-38) Avail: CASI HC A03/MF A01

Several statistical procedures have been proposed as objective methods for determining evoked-potential thresholds. Data have been presented to support each of the methods, but there have not been direct comparisons using the same data. The goal of the present study was to evaluate correlation and variance ratio statistics using common data. A secondary goal was to evaluate the utility of a derived potential for determining thresholds. Chronic, bipolar electrodes were stereotaxically implanted in the inferior colliculi of six chinchillas. Evoked potentials were obtained at 0.25, 0.5, 1.0, 2.0, 4.0 and 8.0 kHz using 12-ms tone bursts and 12-ms tone bursts superimposed on 120-ms pedestal tones which were of the same frequency as the bursts, but lower in amplitude by 15 dB. Alternate responses were averaged in blocks of 200 to 4000 depending on the size of the response. Correlations were calculated for the pairs of averages. A response was deemed present if the correlation coefficient reached the 0.05 level of significance in 4000 or fewer averages. Threshold was defined as the mean of the level at which the correlation was significant and a level 5 dB below that at which it was not. Variance ratios were calculated as described by Elberling and Don (1984) using the same data. Averaged tone burst and tone burst-plus pedestal data were differenced and the resulting waveforms subjected to the same statistical analyses described above. All analyses yielded thresholds which were essentially the same as those obtained using behavioral methods. When the difference between stimulus durations is taken into account, however, evoked-potential methods produced lower thresholds than behavioral methods. DTIC

N95-16812# Defence Science and Technology Organization, Melbourne (Australia).
MODELS TO ESTIMATE HIGH FREQUENCY ACOUSTIC SCATTERING DUE TO THERMAL FINE- AND MICRO-STRUCTURE OF THE OCEAN
R. A. Thuraisingham Jun. 1994 53 p
(AD-A285456; DSTO-RR-0001; DODA-AR-008-638) Avail: CASI HC A04/MF A01

Existing models to obtain intensity and phase changes of sound due to thermal fluctuations in the ocean, such as that developed by Chernov, are limited in their application. They are valid only for an isotropic medium and where the range is much greater than the correlation distance of the fluctuations. Extensions to short range and for an anisotropic medium are described here, both for the stochastic wave and ray models. Theoretical expressions obtained for acoustic fluctuations are easily evaluated. Numerical estimates are provided using stochastic wave and ray models for certain parameters of range, frequency and temperature variation, of interest in target strength measurements. These estimates indicate acoustic fluctuations for an anisotropic medium are always higher than for an isotropic media. For a range of 100 m, frequency of 100 kHz and temperature fluctuation of 0.007 C deg, the root mean square relative intensities and the root

mean square phase fluctuations are on the average higher by a factor of 6, where the vertical correlation lengths are the same and the radial correlation length is about 50 times larger. Closed form expressions in the deterministic ray approximation are given to evaluate intensity and phase changes due to the mean temperature gradient. The validity of the deterministic ray theory results is discussed. Results from the stochastic wave and ray models are examined for the applicability of the stochastic ray model at high frequencies. DTIC

N95-16848*# Pennsylvania State Univ., State College, PA. Applied Research Lab.

ACTIVE MINIMIZATION OF ENERGY DENSITY IN THREE-DIMENSIONAL ENCLOSURES Performance Report, Dec. 1993 - Dec. 1994

Scott D. Sommerfeldt 23 Nov. 1994 8 p

(Grant NAG1-1557)

(NASA-CR-197213; NAS 1.26:197213) Avail: CASI HC A02/MF A01

The objective of this research project is to further investigate and develop a novel approach for actively controlling the sound field in enclosures. Typically the acoustic field in an enclosure has been controlled by minimizing the sum of the squared pressures from several microphones distributed throughout the enclosure. The approach being investigated in this project involves minimizing the acoustic energy density at the sensor locations, rather than the squared pressure. Previous research in a simple one-dimensional enclosure showed that improved global attenuation of the acoustic field is often obtained by minimizing the energy density, rather than the pressure. The current project builds on the previous research by extending the method of controlling the acoustic energy density to three-dimensional enclosures. The results will establish if improved control can still be expected in a more general enclosure. Pending successful results, the method could be applied to control problems such as attenuating the acoustic noise in an aircraft fuselage, an automobile cabin, or other general enclosures. The research project was set up as a two-year project designed to achieve both numerical and experimental results. The primary focus of the first year of research (now being completed) was on the analytical/numerical modeling of the method of controlling the acoustic energy density. During the second year, the research focuses on experimental verification of the approach and extending our understanding of the method. Derived from text

N95-17177# Naval Undersea Warfare Center, Newport, RI.

REVISIONS TO AN EMPIRICAL SURFACE LOSS MODEL USING A CORRECTION FOR pH-DEPENDENT ATTENUATION Final Report

Raymond J. Christian, David G. Williams, and David G. Browning 29 Sep. 1994 22 p Presented at the 127th Meeting of the Acoustical Society of America, Cambridge, MA, Jun. 1994

(NUWC Proj. B96420)

(AD-A285714; NUWC-NPT-TD-10715) Avail: CASI HC A02/MF A01

This document contains the presentation entitled 'Revisions to an Empirical Surface Loss Model Using a Correction for pH-Dependent Attenuation,' presented at the 127th meeting of the Acoustical Society of America, 7 June 1994, Cambridge, Massachusetts. DTIC

72 ATOMIC AND MOLECULAR PHYSICS

Includes atomic structure, electron properties, and molecular spectra.

N95-15945# Fermi National Accelerator Lab., Batavia, IL.

EXPERIMENTAL ISSUES IN HIGH-SENSITIVITY CHARM EXPERIMENTS

J. A. Appel Jul. 1994 12 p Presented at CHARM2000 Workshop, 7 Jun. 1994

(Contract DE-AC02-76CH-03000)

(DE94-015544; FNAL/C-94/193) Avail: CASI HC A03/MF A01

Progress in the exploration of charm physics at fixed target experiments has been prodigious over the last 15 years. The issue before the CHARM2000 Workshop is whether and how this progress can be continued beyond the next fixed target run. An equivalent of 10(exp 8) fully reconstructed charm decays has been selected as a worthy goal. Underlying all this is the list of physics questions which can be answered by pursuing charm in this way. This paper reviews the experimental issues associated with making this next step. It draws heavily on the experience gathered over the period of rapid progress and, at the end, poses the questions of what is needed and what choices may need to be made. DOE

N95-15956# National Lab. for High Energy Physics, Tsukuba (Japan).

PROCEEDINGS OF THE WORKSHOP ON CHARACTERIZATION OF MOLECULAR ASSEMBLIES

Toyoko Imae, ed. (Nagoya Univ., Aichi, Japan.) and Michihiro Furusaka, ed. Aug. 1993 55 p Workshop held in Tsukuba, Japan, 15-16 Mar. 1993

(DE94-753477; KEK-Proc-93-11; CONF-9303269) Avail: CASI HC A04/MF A01

A molecular condensation system shows the different physical characteristic properties from those of the component molecules, therefore, this workshop was to offer the place of discussion on the future of the research on molecular assembly states from wide visual field. The workshop was held on March 15 and 16, 1993 at the National Laboratory for High Energy Physics (KEK). Lectures were given on the future plan of pulsed neutron sources and present state of Wink, characterization by small angle neutron scattering of molecular assemblies that dodecyl dimethylamine oxide constructs, microscopic and macroscopic structures of new surface active molecules, characterization of phospholipid molecular assembly state, crystalline molecular complex formed in surfactant and additives, small angle neutron scattering for phase separation and critical phenomena of micro-emulsion, structural research on hydrophilic composite lipid, associative behavior of bile acid salts in aqueous solution, phase separation and morphology of surfactant system, characterization of macroscopic structure in polymers by ultrasmall angle X-ray scattering and dynamic light scattering, and research on light scattering of glass-forming polymers. DOE

N95-16018# Cornell Univ., Ithaca, NY. Lab. of Atomic and Solid State Physics.

RESONANT CHARGE TRANSFER IN HYPERTHERMAL ATOMIC AND MOLECULAR ION-SURFACE COLLISIONS Annual Report, 1 Jan. 1993 - 1 Apr. 1994

B. H. Cooper 14 Apr. 1994 30 p

(Contract AF-AFOSR-0137-91)

(AD-A281369; AFOSR-94-0390TR) Avail: CASI HC A03/MF A01

We are investigating the interactions of hyperthermal energy (few to several hundred eV) atomic ions with metal surfaces, focusing on ion-surface charge exchange processes. For Li+ scattering from alkali-covered Cu(001), we have measured branching ratios for Li+, Li-, and ground- and excited-state Li(0) in the scattered flux. These results are interpreted using a state-of-the art multichannel charge transfer code. Using this code, we have gained important insights into the dynamics of multichannel charge transfer processes. We are extending these studies to higher-lying excited states of Li, excited state formation in Na scattering, and multichannel charge transfer in O scattering. For Na+ scattering from clean Cu(001) we have observed trajectory-dependent charge transfer in which the charge transfer probability is dependent on the collisional history of the particle; evidence is found for modification of the neutralization due to defect formation that can occur in certain types of collisions with the surface. DTIC

N95-16059# Joint Inst. for Nuclear Research, Dubna (USSR). Lab. of Neutron Physics.

INELASTIC NEUTRON SCATTERING AND ANTIFERROMAGNETIC FLUCTUATIONS IN HIGH TEMPERATURE SUPERCONDUCTORS

V. L. Aksenov and V. V. Kabanov (Paris XIII Univ., Villetaneuse, France.) 1993 14 p Submitted for publication

(DE94-623269; JINR-E-17-93-366) Avail: CASI HC A03/MF A01 (US Sales Only)

The results important for the understanding of the superconducting pairing mechanism obtained with the help of the magnetic inelastic scattering of nonpolarized and polarized neutrons as well as with the magnetic inelastic scattering on 4 f-crystal field excitations are discussed. Measurements of the transition linewidth between 4 f levels of Tm split by crystal fields in (Y, Tm) Ba Cu O compounds are analyzed in the frame of the spin-wave approximation and the phenomenological theory of an antiferromagnetic Fermi liquid. It is shown that in the insulating state the main contribution to the linewidth arises from the one-magnon processes and the gap in the spectrum of magnetic excitations is rather small ((Delta) less than 100 K).

In the superconducting state the main contribution to the linewidth arises from the zone center magnetic fluctuations and the temperature dependence of the linewidth is determined by the static spin susceptibility. DOE

N95-16098 California Univ., Santa Barbara, CA.
BEEM 94. THE FIFTH ANNUAL WORKSHOP ON BALLISTIC ELECTRON EMISSION MICROSCOPY
24 Jan. 1994 44 p Workshop held in Mohonk, NY, 24 Jan. 1994 Limited Reproducibility: More than 20% of this document may be affected by microfiche quality
(AD-A281522) Avail: CASI HC A03

Partial contents are: electron transport across interfaces and surfaces: an overview; BEEM studies of strain-tuned semiconductor interfaces; transport studies in semiconductor heterostructures using BEEM; spectroscopic studies of quantum wells and wires using an STM; BEEM in pinholes of NiS2 films on n-Si(111)-7x7: determination of the impact ionization quantum yield in Si; low-temperature UHV BEEM of epitaxial CoSi2/Si(111); interfacial barrier studies of epitaxial CoGa on n-type (100) GaAs with BEEM; BEEM on Au/Si(111)7x7 and Au/CaF2/Si(111)7x7; temperature dependence of Schottky barriers as probed by BEEM; nanoscopic barrier height distributions at metal/semiconductor interfaces and observation of critical lengths; BEEM studies of reversed-biased Schottky diodes; ballistic models applied to low-temperature BEEM measurements of Au/Si interfaces; and electron inelastic mean free path and spatial resolution of BEEM. DTIC

N95-16121# Brookhaven National Lab., Upton, NY.
RHIC SPIN: THE FIRST POLARIZED PROTON COLLIDER
T. Roser 1994 5 p Presented at the Intersections of Particle and Nuclear Physics, St. Petersburg, FL, 31 May - 6 Jun. 1994
(Contract DE-AC02-76CH-00016)
(DE94-013760; BNL-60490; CONF-940514-1) Avail: CASI HC A01/MF A01

The very successful program of QCD and electroweak tests at the high energy hadron colliders have shown that the perturbative QCD has progressed towards becoming a 'precision' theory. At the same time, it has been shown that with the help of Siberian Snakes it is feasible to accelerate polarized protons to high enough energies where the proven methods of collider physics can be used to probe the spin content of the proton but also where fundamental tests of the spin effects in the standard model are possible. With Siberian Snakes the Relativistic Heavy Ion Collider (RHIC) will be the first collider to allow for 250 GeV on 250 GeV polarized proton collisions. DOE

N95-16155 Akron Univ., Akron, OH.
SMART MATERIALS BASED UPON OLIGOMERIC MOLECULES Final Report, 15 Mar. 1991 - 14 Mar. 1994
Darrell H. Reneker, Roderic P. Quirk, and Wayne L. Mattice Jun. 1994 12 p Limited Reproducibility: More than 20% of this document may be affected by microfiche quality
(Contract DAAL03-91-G-0047)
(AD-A281374; ARO-28747.1-MS-SM) Avail: Issuing Activity (Defense Technical Information Center (DTIC))

Macromolecular smart materials and structures were designed and characterized. The designs were based on oligomeric modules, each of which is responsible for a particular function in the smart material, or in the structure of which it is a part. Liquid crystals and block copolymers were also characterized for potential use as modules. Computer modeling of molecular architecture and motion was used to identify oligomers that can provide useful functions in a smart molecule system. Networks of oligomers, polymers, and block copolymers with well defined structures were identified and synthesized. Functional groups at specific locations were used to create the networks. Molecular scale assemblies were attached to mica or graphite and observed by atomic force microscopy or scanning tunneling microscopy. Rubbery networks containing strain sensitive chromophores were characterized by optical spectroscopy. Functions performed by the various oligomers that were examined include attachment of the oligomer to a graphite or mica surface, incorporation of a chromophore into an elastomeric network, piezochromic effects, formation of bonds that can be broken predictably by forces that do not break the backbone chain, and maintenance of a force transmitting connection between a reinforcing fiber and the polymer matrix in the presence of high strain. DTIC

N95-16241 Georgia Univ., Athens. Dept. of Chemistry.
ELECTROCHEMICAL ATOMIC LAYER PROCESSING
Choong K. Rhee, Baoming M. Huang, Elvin M. Wilmer, Sajan Thomas, and John L. Stickney 25 Jun. 1994 32 p Limited Reproducibility: More than 20% of this document may be affected by microfiche quality
(Contract N00014-91-J-1919)
(AD-A282330; TR-13) Avail: CASI HC A03

Atomic layer processing with electrochemical control is discussed. A method for the electrodeposition of compound semiconductors based on the principles of atomic layer epitaxy (ALE) is reported, with specific reference to the formation of ZnTe. This method is referred to as electrochemical atomic layer epitaxy (ECALE). A number of II-VI compounds have been formed using this method, including: CdTe, CdSe, CdS, ZnTe, ZnSe, ZnS, and HgSe. Initial studies of GaAs and PbSe have also been pursued. A computer-controlled electrochemical flow deposition system is described. The system has been constructed to form thin films of the compounds listed above using the ECALE methodology. In addition, an analogous digital electrochemical etching procedure has been developed and used to etch CdTe substrates. The etching cycle consists of oxidizing off the top atomic layer of Cd atoms at a relatively positive potential, followed by reducing off the top layer of Te atoms at a relatively negative potential. Atomic force microscopy (AFM) has been used to image the resulting features. ECALE and the digital electrochemical etching process are both based on selecting potentials where an atomic layer of an element is deposited, or removed, in a surface limited reaction. The potentials used are referred to as underpotentials in the electrochemical literature. The atomic layer deposition process is referred to as underpotential deposition (UPD). DTIC

N95-16309# Fermi National Accelerator Lab., Batavia, IL.
MEASUREMENT OF THE B MESON DIFFERENTIAL CROSS-SECTIONS IN p(-p) COLLISIONS AT THE SQUARE ROOT OF s = 1.8 TeV USING THE EXCLUSIVE DECAYS B(+-) YIELDS J/(PSI)K(+-) AND B(EXP 0) YIELDS J/(PSI)K(EXP *0)
Jun. 1994 5 p Presented at the 27th International Conference on High Energy Physics, Glasgow, Scotland, 21-27 Jul. 1994
(Contract DE-AC02-76CH-03000)
(DE94-015185; FNAL/C-94/141-E; CONF-940722-14) Avail: CASI HC A01/MF A01

This paper presents the first measurement of the differential B(+-) and B(exp 0) cross-sections, d(sigma)/dp(sub (Tau)), in p(anti p) collisions at the square root = 1.8 TeV. The data sample used represents an integrated luminosity of 19.3 +/- 0.8 pb(exp -1) accumulated by the Collider Detector at Fermilab (CDF). The cross-sections are measured over the p(sub T) range 6-15 GeV/c in the central pseudorapidity region (vert bar)(eta)(vert bar)less than 1 by fully reconstructing the B meson decays B(+-) (yields) J/(psi)K(+-) and B(exp 0) (yields) J/(psi)K*(exp 0), where the J/(psi) is required to decay to two muons, and the K*(exp 0) is required to decay to K(+-)(pi)(-+). The measured absolute normalization and shape of the cross-section as a function of p(sub (Tau)) are compared to the theoretical QCD prediction calculated at next-to-leading order. DOE

N95-16310 Fermi National Accelerator Lab., Batavia, IL.
PRODUCTION ASYMMETRIES IN x(SUB F) AND P(SUB t)(EXP 2) FOR D(+-) MESONS
Jul. 1994 10 p Limited Reproducibility: More than 20% of this document may be affected by microfiche quality
(Contract DE-AC02-76CH-03000)
(DE94-015546; FNAL/C-94/185-E) Avail: CASI HC A02

Non-zero asymmetries have been reported in x(sub f) distributions of leading and non-leading charmed mesons produced from hadronic beams. Production models have also been proposed that would explain these asymmetries and make predictions on how these asymmetries will depend on P(sub t)(sup 2). The authors present differences in leading and non-leading D charged meson production as a doubly differential function of both P(sub t)(sup 2) and x(sub f). This information is from the preliminary analysis of 1/3 of the data from Fermilab experiment E791. It was taken during the 1991-2 fixed target run using a 500 GeV/c (pi)(-) beam incident on a segmented target. DOE

N95-16402# Fermi National Accelerator Lab., Batavia, IL.
CP VIOLATION MEASUREMENTS IN NEUTRAL KAON SYSTEM AT FERMILAB
Yee Bob Hsiung Jul. 1994 11 p Presented at the 29th Moriond Meeting on Quantum Chromodynamics and High Energy Hadronic Interactions, Les Arcs, France, 12-26 Mar. 1994
(Contract DE-AC02-76CH-03000)
(DE94-016526; FNAL/C-94/214; CONF-940327-9) Avail: CASI HC A03/MF A01

Current results on the direct CP-violation measurements (var epsilon)(prime)/(var epsilon) in neutral kaon system at Fermilab (E731) in US are reviewed. The method used also allowed precise determinations of several other kaon decay parameters, (Delta)m, (Delta)(Phi) and (Phi)(sub (plus minus)) for stringent test on CPT invariance. New results of rare kaon decays from E799-I for K(sub L) (yields) (pi)(sup 0)e(sup +)e(sup (minus)), (pi)(sup 0)(mu)(sup +)(mu)(sup (minus)), (pi)(sup 0)v(bar v) and e(sup +)e(sup (minus))e(sup +)e(sup (minus)) are also presented here. We then discuss the current status of the new KTeV experiment and the future prospects of the possible kaon experiments at Fermilab Main Injector. DOE

N95-16403# Oak Ridge National Lab., TN.
DETERMINATION OF ION TEMPERATURES FROM ZEEMAN BROADENED SPECTRAL LINES IN THE EDGE OF TORE SUPRA
C. C. Klepper, R. C. Isler, S. J. Tobin, J. T. Hogan, and W. R. Hess (Commissariat a l'Energie Atomique, Saint-Paul-les-Durance, France.) 1994 5 p Presented at the European Conference on Controlled Fusion and Plasma Physics, Marseilles, France, 26 Jun. - 1 Jul. 1994 Prepared in cooperation with Princeton Univ., NJ
(Contracts DE-AC05-84OR-21400; DE-AC02-76CH-03073)
(DE94-018112; CONF-940635-12) Avail: CASI HC A01/MF A01

The authors have examined a (sup 3)P (yields) (sup 3)S multiplet of C III in Tore Supra in order to assess the possibility of determining the ion temperatures from transitions where the Zeeman effect cannot be neglected compared to the Doppler broadening. The preliminary studies lead them to believe that with good quality data the temperatures can be determined within about 20% in the 20-30 eV range and within about 50% in the neighborhood of 5 eV by fitting the entire multiplet rather than a semi-isolated feature, even though certain parameters important for the analysis, such as polarization effects of the optics, are not well characterized. In order to quantify these conclusions more precisely, future work will concentrate on developing numerical fitting routines and on examining the validity of the assumption that the distribution function for low ionization stages is Maxwellian. DOE

N95-16411 North Carolina Univ., Chapel Hill, NC. Dept. of Chemistry.
EFFECT OF ION-ELECTRODE CONTACT ON THE ENERGETICS OF THE HETEROGENEOUS ELECTRON TRANSFER
Xin-Fu Xia and Max L. Berkowitz Jul. 1994 16 p Sponsored by ONR
Limited Reproducibility: More than 20% of this document may be affected by microfiche quality
(AD-A281959) Avail: Issuing Activity (Defense Technical Information Center (DTIC))

Using molecular dynamics computer simulation technique we studied the effect of the ion-electrode contact on the energetics of electron transfer reactions. We observed that when the solvation shell of the ion undergoes large changes due to the ion transfer from the bulk to the interface, the energetics of the reaction at the interface differs substantially from the energetics of the reaction in bulk. DTIC

N95-16430# Argonne National Lab., IL.
ATOMIC TRANSPORT OF OXYGEN
J. L. Routbort and G. W. Tomlins 15 Jun. 1994 19 p Presented at the 7th Europhysical Conference on Defects in Insulating Materials, Lyon, France, 5-9 Jul. 1994
(Contract W-31-109-eng-38)
(DE94-013332; ANL/ET/CP-83016; CONF-940785-1) Avail: CASI HC A03/MF A01

Atomic transport of oxygen in nonstoichiometric oxides is an extremely important topic which overlaps science and technology. In many cases the diffusion of oxygen controls sintering, grain growth, and creep. High oxygen diffusivity is critical for efficient operation of many fuel cells. Additionally, oxygen diffusivities are an essential ingredient in any point defect model. Secondary Ion Mass Spectrometry (SIMS) is the most accurate modern technique to measure oxygen tracer diffusion. This paper briefly reviews the principles and applications of SIMS for the measurement of oxygen transport. Case studies are taken from recent work on ZnO and some high-temperature superconductors. DOE

N95-16482# Minnesota Univ., Minneapolis, MN. Dept. of Chemical Engineering and Materials Science.
NANOSCALE IMAGING OF MOLECULAR ADSORPTION Technical Report, 1 May 1993 - 30 Jun. 1994
Heng Cai, Andrew C. Hillier, Kevin R. Franklin, C. C. Nunn, and Michael D. Ward 23 Jun. 1994 17 p
(Contract N00014-93-1-0563)
(AD-A280979; TR-4-ONR) Avail: CASI HC A03/MF A01

The adsorption of organic molecular species onto highly ordered, chemically well defined substrates may provide insights into the intermolecular interactions, molecular recognition, and aggregation phenomena responsible for the formation of organic thin film and solid state assemblies. The advent of scanning probe microscopy, particularly the atomic force microscope, now provides a method for observation of these adsorption processes on the molecular level. We herein report atomic force microscope observations of the adsorption of anions of the organic di-acid 5-benzoyl-4-hydroxy 2-methoxybenzenesulfonic acid from aqueous solution onto the (0001) surface of hydrotalcite, a layered anionic clay. This adsorption process is believed to mimic the ion exchange reactions that commonly occur within the layers of hydrotalcite. Atomic force microscope images reveal that the coverage of the adsorbed anions depends upon the total charge of the anion (1- or 2-). This is due to electroneutrality requirements associated with coulombic interactions between the cationic hydrotalcite surface and the anionic molecules. The AFM data, along with consideration of coulombic interactions and hydrogen bonding between three-fold clay hydroxyl sites and the sulfonate moiety on the anions, enables tentative assignment of the orientation of the anions with respect to the hydrotalcite surface. DTIC

N95-16487# Argonne National Lab., IL.
STUDIES OF D-Li NEUTRON SOURCE: AN OVERVIEW
I. Gomes and D. L. Smith Jun. 1994 24 p
(Contract W-31-109-eng-38)
(DE94-014032; ANL/FPP/TM-267) Avail: CASI HC A03/MF A01

The construction of a neutron source facility able to reproduce the radiation environment predicted for a fusion reactor can be considered a very important milestone for the fusion program. Such a neutron source should allow materials testing over a wide range of neutron flux and neutron fluence. To date, none of the existing facilities reproduce the neutron flux with the energy spectrum of a fusion reactor. As a result, the major part of the required material database is obtained by extrapolations which may not be as reliable as needed to predict the real performance of those materials under fusion reactor conditions. As an example, the effect of the gas production, transmutation, atomic displacement, and other nuclear responses on the ductility and swelling and perhaps other properties as well must be analyzed in samples which have undergone reactor conditions environment. This study is focused on the neutronics analysis of a D-Li neutron source. Neutron induced nuclear responses and neutron transport are calculated with the aim at defining the expected performance of a D-Li neutron source. The first section describes the differences in the magnitude of the neutron flux when material is present or not inside the test cell. The second section deals with nuclear responses such as DPA, helium production, and nuclear heating. In the third section, calculations of the available volume above a threshold DPA value are presented. Section four presents results for the gamma-ray flux distribution. A brief discussion about tritium generation in the lithium jet is given in section five, and the conclusions are summarized in section six. DOE

N95-16493# California Inst. of Tech., Pasadena, CA. Chemical Physics Lab.
RESONANCE ENHANCED MULTIPHOTON IONIZATION OF MOLECULES AND MOLECULAR FRAGMENTS Final Technical Report, 1 Jun. 1990 - 31 Mar. 1994
Vincent McKoy 31 Mar. 1994 31 p

(Grant AF-AFOSR-0241-90)
(AD-A285076; AFOSR-94-0570TR) Avail: CASI HC A03/MF A01

We have completed studies of ion rotational distributions produced by resonance enhanced multiphoton ionization of excited states of molecules and by single-photon ionization of ground states of jet-cooled molecules by coherent VUV radiation. The objective of this effort was to provide a robust analysis and prediction of key spectral features of interest in related experimental studies and technological applications of these laser-driven ionization techniques. Specific achievements include: identification of underlying mechanisms for anomalous behavior of ion rotational distributions in laser ionization of molecules and molecular fragments, development of schemes for exploiting such anomalous behavior to achieve state-selective production of ions, and providing needed insight into the underlying dynamics of state-resolved molecular photoionization. Author (DTIC)

N95-16496 Florida Univ., Gainesville, FL. Dept. of Chemistry.
DEVELOPMENT OF PRACTICAL MO TECHNIQUES FOR PREDICTION OF THE PROPERTIES AND BEHAVIOR OF MATERIALS Final Report, 1 Feb. 1992 - 31 Jan. 1994
Michael J. Dewar 31 Jan. 1994 3 p Limited Reproducibility: More than 20% of this document may be affected by microfiche quality
(AF Proj. 2303)
(AD-A285079; AFOSR-94-0564TR) Avail: CASI HC A01

Our previous semiempirical treatments have been based on the ZDO approximations introduced by Pople, MNDO and AMI using the best of these (NDDO). Although there were good reasons to believe that the ZDO approximation is wholly unacceptable, we were forced to use it in order to obtain a treatment of practical value, i.e. one that could be applied directly to the molecules of interest to organic chemists rather than to meaninglessly simplified 'models', using generally available computers. Although the resulting treatments proved remarkably successful and have led to major developments in chemical theory, in particular in studies of reaction mechanisms. The situation has, however, changed dramatically in recent years with almost incredible increase in computing power of minicomputers due to the invention of the integrated circuit. The primary purpose of the research supported by this grant was to make use of the greatly improved computing facilities now available to us to develop a semiempirical treatment based on a full LCAO SCF MO approximation, i.e. one in which overlap is retained. Author (DTIC)

N95-16523# Florida Univ., Gainesville, FL.
METASTABILITY IN MOLECULES Annual Report, 1993
Rodney J. Bartlett 8 Sep. 1994 13 p
(Contract F49620-92-J-0141)
(AD-A285223; AFOSR-94-0598TR) Avail: CASI HC A03/MF A01

Synthesis and detonation of energetic materials involves several critical oxidation processes and associated intermediates. Carbonyl oxide, and its cyclic isomeric form, dioxirane, are two key compounds in such processes. Carbonyl oxide has never been observed experimentally, though it is one of the most discussed compounds awaiting detection. We performed high level coupled-cluster CCSD(T) calculations to characterize carbonyl oxide. These studies employed recently developed open-shell analytical gradients methods for CCSD(T), without which structures and vibrational frequencies would be difficult to obtain. The Delta H sub f deg (298) for carbonyl oxide is found to be 30.2 kcal/mol, while the barrier to isomerization to dioxirane is 19.2 kcal/mol. CCSD(T) vibrational frequencies of both species are presented to facilitate identification along with the 18 O isotope shifts. Shifts as high as 45 /cm permit experimental discrimination between the two forms. Carbonyl oxide is found to be far more zwitterionic than lower level theoretical studies would suggest, in line with the viewpoint of synthetic chemists. DTIC

N95-16629# South Carolina Univ., Columbia, SC.
THIRD HARMONIC GENERATION STUDY OF ALPHA-THIOPHENE OLIGOMERS: MONOMER TO OCTAMER
Lap-Tak Cheng, James M. Tour, Ruilian Wu, and Peter V. Bedworth 28 Jun. 1994 18 p
(Contract N00014-89-J-3062)
(AD-A281177; TR-35) Avail: CASI HC A03/MF A01

The second hyperpolarizabilities, (gamma(-3 omega, omega, omega, omega)), of alpha-thiophene oligomers up to the octamer have been measured with third-harmonic generation experiments. Measurements in THF solutions with 1.91 micrometer fundamental radiation found significantly lower nonlinearity and conjugation length dependence in comparison with reported results obtained from DC electric field-induced second-harmonic generation and degenerate four-wave mixing measurements. A previously reported nonlinearity saturation for the extended oligomers was also not evident in the current study. DTIC

N95-16784# South Carolina Univ., Columbia, SC. Dept. of Chemistry.
ITERATIVE DIVERGENT/CONVERGENT DOUBLING APPROACH TO LINEAR CONJUGATED OLIGOMERS. A RAPID ROUTE TO A 128 A LONG POTENTIAL MOLECULAR WIRE
James M. Tour, Jeffrey S. Schumm, and Darren L. Pearson 28 Jun. 1994 10 p
(Contract N00014-89-J-3062)
(AD-A281295; TR-29-ONR) Avail: CASI HC A02/MF A01

Described is the synthesis of oligo (2-ethylphenylene ethynylene)s and oligo (2-(3'ethylheptyl) phenylene ethynylene)s via an iterative divergent convergent approach. Synthesized were the monomer, dimer, tetramer, and octamer of the ethyl derivative and the monomer, dimer, tetramer, octamer, and 16-mer of the ethylheptyl derivative. The 16-mer is 128 A long. At each stage in the iteration, the length of the framework doubles. Only three sets of reaction conditions are needed for the entire iterative synthetic sequence; an iodination, a protodesilylation, and a Pd/Cu-catalyzed cross coupling. The oligomers were characterized spectroscopically and by mass spectrometry. The optical properties are presented which show the stage of optical absorbance saturation. The size exclusion chromatography values for the number average weights, relative to polystyrene, illustrate the tremendous differences in the hydrodynamic volume of these rigid rod oligomers verses the random coils of polystyrene. These differences become quite apparent at the octamer stage. These oligomers may act as molecular wires in molecular electronic devices and they also serve as useful models for understanding related bulk polymers. DTIC

N95-16797# Case Western Reserve Univ., Cleveland, OH. Dept. of Macromolecular Science.
ISOMORPHISM WITHIN THE HEXAGONAL COLUMNAR MESOPHASE OF MOLECULAR AND MACROMOLECULAR SELF- AND CO-ASSEMBLED COLUMNS CONTAINING TAPERED GROUPS
Dimitris Tomazos, Ron Out, James Heck, Gary Johansson, and Virgil Percec 30 Jun. 1994 47 p
(Contract N00014-89-J-1828)
(AD-A281205; Rept-3) Avail: CASI HC A03/MF A01

The phase behavior of binary mixtures of self assembled tapering molecules based on monoesters of oligooxyethylene glycol and 3,4,5-tris ((4-n-dodecan-1-yloxy) benzyloxy) benzoic acid, their corresponding polymethacrylates, and of 4'-methyl (benzp-15-crown) -3,4,5-tris ((4-n-dodecan 1-yloxy) benzyloxy) benzoate within their hexagonalcolumnar mesophase (Phi(sub h)) is described. The binary blends between molecular tapers co-assemble into a single supramolecular column resulting in isomorphism within their Phi(sub h) mesophase over the entire range of composition. The binary blends between polymetharylates containing tapered side groups co-assemble into a single phi(sub h) phase only when the columns of the parent polymers are of similar diameters. This results in binary mixtures which are isomorphic within the Phi sub h mesophase over the entire composition range. When the diameters of the columns formed by the parent polymers are dissimilar, isomorphic mixtures are obtained only over a narrow range of composition. Binary mixtures between molecular tapers and macromolecular systems containing tapered side groups co-assemble into a single column to the extent that intercalation of the molecular taper, within the column formed by the macromolecular system containing tapered side groups, is permissible. In all systems increased intra-columnar interactions can be induced by complexation of LiCF3SO3 by the oligooxyethylenic receptors and specific crown ether receptors and NaCF3SO3 as the third component are non-isomorphic within their Phi(sub h) phase due to preferentialcomplexation of the alkali metal cation by the column of the crown ether containing the molecular taper. This results in two columns of dissimilar diameters, which are isomorphic in the Phi(sub h) phase only within a limited range of composition. DTIC

N95-16799# South Carolina Univ., Columbia, SC. Dept. of Chemistry.
SYNTHESIS AND PROPERTIES OF SOLUBLE OLIGO- AND POLYPHENYLENES. A REVIEW

James M. Tour 28 Jun. 1994 24 p
(Contract N00014-89-J-3062)
(AD-A281293; TR-33-ONR) Avail: CASI HC A03/MF A01

An overview of the synthetic routes and material properties of soluble oligo- and polyphenylenes is presented with comparisons of the soluble materials to the insoluble poly(p-phenylene) (PPP). Covered are main chain phenylene oligomers and polymers; not copolymers that contain non-phenylene units. The specific classes of compounds discussed are poly(o-phenylenes), poly(m-phenylenes), and substituted polyphenylenes consisting of alkyl-, aryl-, carbonyl-, alkoxy-, nitro-, halo-, fused aromatic-, and ladder-containing moieties. DTIC

N95-16840# Fermi National Accelerator Lab., Batavia, IL.
TESTS OF STRUCTURE FUNCTIONS USING LEPTONS AT CDF: W ASYMMETRY AND DRELL-YAN PRODUCTION
Jun. 1994 17 p Presented at the 27th International Conference on High Energy Physics, Glasgow, England, 21-27 Jul. 1994
(Contract DE-AC02-76CH-03000)
(DE94-015727; FNAL/C-94/146-E; CONF-940722-17) Avail: CASI HC A03/MF A01

The charge asymmetry as a function of lepton rapidity, A(y(sub l)), has been measured at square root of s = 1.8 TeV for the absolute value of y(sub l) less than 1.8, using the W decays to electrons and muons recorded by CDF during the 1992-1993 run of the Tevatron Collider. The luminosity used, approximately 20 pb(exp -1), and detector improvements resulted in a seven fold increase in statistics relative to the 1988-1989 data. The increased statistics in the 1992-1993 data allow for discrimination between sets of modern parton distribution functions. The results of this analysis demonstrate the value of collider data in the measurement of the proton's structure. In addition, the Drell-Yan cross section has been measured using approximately 4 pb(exp -1) of dielectron and approximately 2.5 pb(exp -1) of dimuon data taken during the 1988-1989 run. These measurements probe the quark distributions to x less than 0.01 at high Q(exp 2) where nonperturbative effects are minimal. Studies of Drell-Yan production in the approximately 20 pb(exp -1) data from the 1992-1993 run are currently underway. DOE

N95-16868# Fermi National Accelerator Lab., Batavia, IL.
MEASUREMENT OF THE B(SUB s) MESON LIFETIME AT CDF
Jun. 1994 16 p Presented at the 27th International Conference on High Energy Physics, Glasgow, England, 21-27 Jul. 1994
(Contract DE-AC02-76CH-03000)
(DE94-015381; FNAL/C-94/138-E; CONF-940722-15) Avail: CASI HC A03/MF A01

Proton-antiproton collision data corresponding to a total integrated luminosity of (approximately) 21 pb(exp -1) were collected with the CDF detector at the Fermilab Tevatron collider during 1992-1993. The lifetime of the B(sub s) meson is measured using events from the semileptonic decay B(sub s) (yields) (ell)(+)(nu)D(sub s)(exp -X) and from the exclusive decay B(sub s) (yields) J/(psi)(phi). For the semileptonic decay channel, 76 (ell)(+)D(sub s)(exp -) signal events are selected where the D(sub s) is identified via the decay D(sub s)(exp -) (yields) (phi)(psi)(exp -), (phi) (yields) K(+)K(exp -). From this sample the B(sub s) meson lifetime is determined to be (tau)(sub s) = 1.42(sub -0.23)(exp +0.27) (stat.)(sub -0.11)(exp +0.11) (syst.) ps. In the J/(psi)(phi) channel, 11 events are used and the lifetime is found to be (tau)(sub s) = 1.74(sub-0.60)(exp +0.90) (stat.)(sub-0.07)(exp +0.07) (syst.) ps. DOE

N95-16914 Fermi National Accelerator Lab., Batavia, IL.
JET STUDIES AT CDF AND DO COLLABORATIONS
P. Bartalini Jun. 1994 8 p Presented at the 29th Moriond Meeting on Quantum Chromodynamics and High Energy Hadronic Interactions, Les Arcs (France), 12-26 Mar. 1994 Limited Reproducibility: More than 20% of this document may be affected by microfiche quality
(Contract DE-AC02-76CH-03000)
(DE94-015537; FNAL/C-94/180-E; CONF-940327-7) Avail: CASI HC A02

Both CDF and D0 collaborations measure inclusive jet cross section, energy flow and observe color coherence effects in (bar p)p collisions at (radical)s = 1800 GeV. The results on new compositeness limit using inclusive jet cross section and energy flow within a jet are described. Data are in good agreement with next to leading order QCD calculations. Color coherence effects are demonstrated by measuring spatial correlations between soft and leading jets in multi jet events. DOE

N95-16924 Argonne National Lab., IL.
A-DEPENDENT EFFECTS IN HIGH P(SUB T) REACTIONS
T. Fields 1994 6 p Presented at the Intersections of Particle and Nuclear Physics, St. Petersburg, FL, 31 May - 6 Jun. 1994 Limited Reproducibility: More than 20% of this document may be affected by microfiche quality
(Contract W-31-109-eng-38)
(DE94-016385; ANL-HEP-CP-94-40; CONF-940514-9) Avail: CASI HC A02

A brief summary of A-dependent effects which have been observed in various high energy scattering processes from nuclear targets is given. Reactions which are discussed include dijet production, dihadron production, Drell-Yan, deep inelastic muon scattering, and low-P(sub t) hadron production. The data are described in terms of multiple scattering of a fast parton in nuclear matter. Some suggestions for future work are given. DOE

N95-16931 Los Alamos National Lab., NM.
MODELING MESONS WITH RELATIVISTIC WAVE EQUATIONS
A. J. Sommerer (Iowa Univ., Iowa City, IA.), A. A. El-Hady (Iowa Univ., Iowa City, IA.), J. R. Spence (Iowa Univ., Iowa City, IA.), J. P. Vary (Iowa Univ., Iowa City, IA.), and C. Benesh (Rice Univ., Houston, TX.) 1994 5 p Presented at the 14th International Conference on Few Body Problems in Physics, Williamsburg, VA, 26-31 May 1994 Limited Reproducibility: More than 20% of this document may be affected by microfiche quality
(Contract W-7405-eng-36)
(DE94-016057; LA-UR-94-2327; CONF-9405132-7) Avail: CASI HC A01

We use two relativistic quasi-potential equations to fit meson spectra. A global fit of 45 mesons is achieved with an rams deviation from experiment of 43 MeV, and we compare meson two-photon decay widths calculated using the model wave functions with experimentally measured widths. We give an example calculation of in-medium (high temperature) effects that may be incorporated in the models. DOE

N95-16933 Los Alamos National Lab., NM.
CENTRIFUGAL SPACE-CHARGE FORCE FOR BUNCHED BEAMS
B. E. Carlsten and T. O. Raubenheimer (Stanford Linear Accelerator Center, CA.) 1994 4 p Presented at the 17th International LINAC Conference, Tsukuba, Japan, 21-26 Aug. 1994 Limited Reproducibility: More than 20% of this document may be affected by microfiche quality
(Contract W-7405-eng-36)
(DE94-016097; LA-UR-94-2560; CONF-9408125-1) Avail: CASI HC A01

In 1990, E. Lee showed for a DC beam that the effect of the centrifugal space-charge force (CSCF) on an electron's transverse motion in a end is cancelled to lowest order by the effect of the potential depression of the beam. However, this cancellation does not in general occur when the beam is bunched. We solve for the harmonic scalar and vector potentials and explicitly find the energy-independent transverse and longitudinal space-charge forces. We make estimates of the emittance growth as a function of bend angle and path length resulting from these forces. DOE

N95-16943# Stanford Linear Accelerator Center, CA.
QCD OF DIFFERENT FLAVORS WITH THE SLD DETECTORS
M. D. Hildreth May 1994 6 p Presented at the 29th Moriond Meeting on Quantum Chromodynamics and High Energy Hadronic Interactions, Les Arcs, France, 19-26 Mar. 1994
(Contracts DE-FG02-91ER-40676; DE-FG03-92ER-40701; DE-FG03-91ER-40618; DE-FG02-91ER-40672; DE-FG02-91ER-40677; DE-AC03-76SF-00098; DE-FG02-91ER-40672; DE-FG02-92ER-40715; DE-AC02-76ER-03069; DE-FG06-85ER-40226)
(DE94-013800; SU-SLAC-PUB-6505; CONF-940327-3) Avail: CASI HC A02/MF A01

We have exploited the unique capabilities of the SLD detector at the SLC to tag very pure samples of heavy and light quarks in Z(degree) decays with high efficiency in order to study the QCD of different quark flavors. Here, we present two measurements. First, we find the difference between the average charged multiplicity of Z(sup 0)(yields)b(bar b) and Z(sup 0)(yields) hadrons to be (bar n)(sub b)(minus)(bar n)(sub b)=2.24

(plus minus)0.30(stat)(plus minus)0.33(syst) tracks per event. From this, we have derived (bar n)(sub b) (minus)(bar n)(sub uds) = 3.31 (plus minus)0.41 (plus minus)0.79. Comparing this measurement with those at lower center-of-mass energies, we find no evidence that (bar n)(sub b)(minus)(bar n)(sub uds) depends on energy. This result is in agreement with a precise prediction of perturbative QCD, and supports the notion that QCD remains asymptotical free down to the scale M(sub b)(sup 2). Second, by comparing the jet rates in flavor-tag samples of uds, c, and b quarks, we find (alpha)(sub s)(uds)/(alpha)(sub s)(all) = 0.99 (plus minus) 0.03(stat) (plus minus)0.05(syst), (alpha)(sub s)(c)/(alpha) (sub s)(all) = 1.05(plus minus)0.11(stat)(plus minus)0.21(syst), and (alpha)(sub s)(b)/(alpha) (sub s)(all) = 1.02(plus minus)0.04(stat)(plus minus) 0.07(syst). DOE

N95-16959# Oak Ridge National Lab., TN.
MASS SPECTROMETRY STUDIES OF THE IONIZATION OF ORGANIC MOLECULES BY SLOW POSITRONS
L. D. Hulett, Jr., Jun Xu, T. A. Lewis, O. H. Crawford, and S. A. McLuckey 1994 4 p Presented at the 10th International Conference on Positron Annihilation, Beijing, China, 23-29 May 1994
(Contract DE-AC05-84OR-21400)
(DE94-013838; CONF-9405170-1) Avail: CASI HC A01/MF A01

The dissociative ionization of organic molecules, induced by positrons having energies below positronium thresholds (0.5-3 eV), has been studied. The ionization-fragmentation yields increase as positron energies decrease. The energies required for dissociative ionization are supplied by the annihilation processes. Fragmentation occurs by breakage of C-C single bonds in preference to double or triple bonds. DOE

N95-16960# Fermi National Accelerator Lab., Batavia, IL.
LIMIT ON THE RARE DECAY B YIELDS MUON(+)MUON(-) K(+-)
27 May 1994 4 p Presented at the 27th International Conference on High Energy Physics, Glasgow, Scotland, 21-27 Jul. 1994
(Contract DE-AC02-76CH-03000)
(DE94-013851; FNAL/C-94/145-E; CONF-940722-1) Avail: CASI HC A01/MF A01

We report on a search for flavor-changing neutral current decays of B mesons into (mu)(mu)K(sup +-) using data obtained in the Collider Detector at Fermilab (CDF) 1992-1993 data taking run. To reduce the amount of background in our data we use precise tracking information from the CDF silicon vertex detector to pinpoint the location of the decay vertex of the B candidate, and accept only events which have a large decay time. We compare this data to a B meson signal obtained in a similar fashion, but where the muon pears originate from (psi) decays, and calculate the relative branching ratios. In absence of any indication of flavor-changing neutral current decay we set an upper limit on the branching ratio of 3.2 x 10(exp -1), which is consistent with Standard Model expectations but leaves little room for non-standard physics. DOE

N95-16962# Argonne National Lab., IL.
SMALL ANGLE NEUTRON SCATTERING FROM NANOCRYSTALLINE Pd AND Cu COMPACTED AT ELEVATED TEMPERATURES
P. G. Sanders (Northwestern Univ., Evanston, IL.), J. R. Weertman (Northwestern Univ., Evanston, IL.), J. G. Barker (National Inst. of Standards and Technology, Gaithersburg, MD.), and R. W. Siegel May 1994 7 p Presented at the Spring Meeting of the Materials Research Society, San Francisco, CA, 4-8 Apr. 1994
(Contracts W-31-109-eng-38; DE-FG02-86ER-45229)
(DE94-013865; ANL/MSD/CP-81312; CONF-940411-35) Avail: CASI HC A02/MF A01

Nanocrystalline (n-) Cu and Pd, prepared by inert gas condensation and in situ room temperature (RT) and elevated temperature (warm) compactions, have been studied by small angle neutron scattering (SANS). Previous work on RT compacted and subsequently annealed n-Pd seemed to show that all the scattering could be accounted for by a distribution of pores. Analysis of more extensive SANS measurements, together with results of prompt gamma activation analysis, indicates that the SANS can be explained by the presence of pores and hydrogen. Warm compaction reduces the hydrogen impurity level, while increasing the bulk density and decreasing the pore size. This can lead to a dramatic hardness increase in these materials. DOE

N95-17153# Los Alamos National Lab., NM.
A MEASUREMENT OF THE MICHEL PARAMETER (RHO) IN MUON DECAY
R. E. Mischke, J. F. Amann, and R. D. Bolton et al 1994 11 p Presented at the 27th International Conference on High Energy Physics, Glasgow, Scotland, 21-27 Jul. 1994
(Contract W-7405-eng-36)
(DE94-014423; LA-UR-94-2201; CONF-940722-5) Avail: CASI HC A03/MF A01

An improved measurement of the Michel parameter (rho) in normal muon decay has been made using the MEGA positron spectrometer. Muons were stopped in the center of a large solenoid (1.5 T nominal field) and the momenta of positrons with energies over about 35 MeV were measured with a precision of about 0.6 MeV/c FWHM. There are over 15 million events in each spectrum taken for three operating configurations. The previous result has a precision of delta rho/rho = 0.003 based on a sample of about 1 million events in the positron energy spectrum. The present experiment expects to improve the precision by a factor of three to six, depending on the level of systematic uncertainties. The improved result is a precise test of the standard model of electroweak interactions for a purely leptonic process. It also provides a better constraint on the mixing angle in a left-right symmetric extension to the standard model. DOE

N95-17154# Los Alamos National Lab., NM.
FIRST RESULTS FROM SAGE 2
J. N. Abdurashitov (Academy of Sciences, USSR, Moscow, USSR.), E. L. Faizov (Academy of Sciences, USSR, Moscow, USSR.), and V. N. Gavrin (Academy of Sciences, USSR, Moscow, USSR.) 1994 9 p Presented at the Intersections of Particle and Nuclear Physics, St. Petersburg, FL, 31 May - 6 Jun. 1994
(Contract W-7405-eng-36)
(DE94-014431; LA-UR-94-1982; CONF-940514-2) Avail: CASI HC A02/MF A01

The Russian-American Gallium solar neutrino Experiment (SAGE) began the second phase of operation (SAGE 2) in September of 1992. Monthly measurements of the integral flux of solar neutrinos have been made with 55 tons of gallium. The K-peak results of the first five runs of SAGE 2 give a capture rate of 76(sub -18)(sup +21) (stat) (sub -7)(sup +5) (sys) SNU. Combined with the SAGE 1 result, the capture rate is 74(sub -12)(sup +13) (stat) (sub -7)(sup +5) (sys) SNU. This represents only 56% to 60% of the capture rate predicted by different standard solar models. DOE

N95-17158# Los Alamos National Lab., NM.
A SEARCH FOR MUONS YIELDS e GAMMA AT THE LEVEL OF 10(EXP -13)
R. E. Mischke, J. F. Amann, and D. Barlow (California Univ., Los Angeles, CA.) 1994 10 p Presented at the 27th International Conference on High Energy Physics, Glasgow, Scotland, 21-27 Jul. 1994
(Contract W-7405-eng-36)
(DE94-014488; LA-UR-94-2202; CONF-940722-4) Avail: CASI HC A02/MF A01

The MEGA experiment is a search for the decay mu yields e gamma, for which the present upper limit for the branching ratio is 4.9 x 10(exp -11). The observation of this decay would indicate the existence of physics outside the standard model of electroweak interactions. The experiment employs highly modular, fast detectors, state-of-the-art electronics, and a staged trigger with on-line filters. The detectors are contained in a 1.5 T solenoidal field produced by a superconducting magnet. Positrons are confined to the central region and are measured by a set of thin multiwire proportional chambers (MWPC's) with a designed energy resolution of 350 keV FWHM and angular resolution of 1 deg FWHM. Photons are measured by one of three layers of pair spectrometers in the outer region. The total photon detection efficiency is about 6%; the expected photon energy resolution is 1.7 MeV FWHM and the angular resolution is 10 deg FWHM. The time resolution between the photon and electron is 0.8 ns FWHM. About 10(exp 8) events that passed the on-line filters were recorded during the 1993 run. These data should have a branching ratio sensitivity approximately fifteen times better than the present limit. The measured resolutions are approaching the design values. DOE

N95-17351 Science Research Council, Daresbury (England).
PHOTON BEAM STUDIES OF MAGNETIC MATERIALS
S. W. Lovesey Jun. 1994 117 p
(PB95-104279; RAL-94-052) Avail: Issuing Activity (National Technical Information Service (NTIS))

The past decade has seen a surge of activity in the use of photon beam techniques to study magnetic properties of materials. By and large, in this period the experimental work has been accomplished with beams produced by electron synchrotron facilities. To date, it is fair to say that the surge of activity is underpinned by improvements in instrument performance, enjoyed at synchrotron sources, rather than outstanding intellectual advances. In consequence, improvements in the intensity at the sample, and the provision of good beams of polarized photons, which enable polarization induced discrimination effects to be exploited as a means of increasing the signal-to-noise, are particularly significant in the use for magnetic studies of photon beam techniques. NTIS

N95-17353 Science Research Council, Daresbury (England).
MULTILEPTON SUSY SIGNALS FROM R-PARITY VIOLATION AT THE TEVATRON (REVISED)
V. Barger, M. S. Berger, P. Ohmann, and R. J. N. Phillips Jun. 1994 21 p Prepared in cooperation with Wisconsin Univ., Madison, WI
(Contract DE-AC02-76ER-00881)
(PB95-104311; RAL-94-047-Rev) Avail: Issuing Activity (National Technical Information Service (NTIS))

The expected trilepton signals from p(- P) to chi (sub 1, sup +,-) chi(sub 2, sup 0) to (chi(sub 1, sup 0)l(sup +,-)nu)(chi(sub 1, sup 0)l'(sup +)l' (sup -)) will be converted into hadronically quiet multilepton signals, if the two final chi(sub 1, sup 0) have leptonic R-parity-violating (RPV) decays chi(sub 1, sup 0) to ll'nu. The authors make illustrative calculations of the acceptance for these spectacular RPV signals, and point out that distinctive multilepton signals are possible even when the R-conserving trilepton signals are blocked by the spoiler mode chi(sub 2, sup 0) to h(sup 0)chi(sub 1, sup 0). Other channels can also give quiet multileptons from RPV. The authors investigate these signals in the context of supersymmetric models with radiative electroweak symmetry breaking, using examples in the low-tan beta lambda(sub t) fixed-point region. NTIS

N95-17354 Science Research Council, Daresbury (England).
PARTON DISTRIBUTIONS OF THE PROTON
A. D. Martin, W. J. Stirling, and R. G. Roberts Jun. 1994 47 p Prepared in cooperation with Durham Univ., England
(PB95-104337; RAL-94-055) Avail: Issuing Activity (National Technical Information Service (NTIS))

To obtain improved parton densities of the proton, we present a new global analysis of deep-inelastic and related data including, in particular, the recent measurements of F2 at HERA, of the asymmetry of the rapidity distributions of W(+ or -) production at the FNAL p(- p) collider and of the asymmetry in Drell-Yan production in pp and pn collisions. We also incorporate data to determine the flavor dependence of the quark sea distributions. We find that the behavior of the partons at small x is consistent with the precocious onset of BFKL leading log(1/x) dynamics. We discuss the ambiguities remaining in the gluon distribution. We present improved predictions for W boson (and t quark) production at the FNAL p(-p) collider. NTIS

N95-17358# Louisiana State Univ., Baton Rouge, LA.
RESEARCH IN ELEMENTARY PARTICLE PHYSICS
Lai-Him Chan, R. Haymaker, R. Imlay, R. McNeil, W. Metcalf, and R. Svoboda 1994 188 p
(Contract DE-FG05-91ER-40617)
(DE94-019219; DOE/ER-40617/182) Avail: CASI HC A09/MF A02

This report discusses the following topics: Low-energy particle dynamics; QCD dynamics on the lattice; lattice QCD Vacuum; phenomenology & cosmology; the ZEUS Experiment at HERA; neutrino physics at LAMPF; non-accelerator physics; and SSC activity. DOE

N95-17520# Tokyo Univ., Tanashi (Japan). Inst. for Nuclear Study.
COMPOSITE-MODEL VIEW OF THE LL-BAR(GAMMA)(GAMMA) EVENTS AT LEP
Keiichi Akama and Hidezumi Terazawa Sep. 1993 14 p
(DE94-753312; INS-1006) Avail: CASI HC A03/MF A01 (US Sales Only)

We examine phenomenological consistency of composite-model pictures for the ll-bar(gamma)(gamma) events at LEP: the picture with an extra boson and that with an excited lepton. It turns out that the former is inconsistent with the Bhabha scattering data while the latter is consistent with the existing experimental data as far as the excited lepton is lighter than 200 GeV. DOE

N95-17630# Naval Surface Warfare Center, Silver Spring, MD.
XAFS INVESTIGATION OF STRUCTURE AND VALENCY OF NICKEL IN SOME OXYCOMPOUNDS Technical Report No. 4
A. N. Mansour and C. A. Melendres 4 Aug. 1994 10 p
(Contract N00014-94-WX-23074)
(AD-A283193) Avail: CASI HC A02/MF A01

Preliminary to using XAFS spectroscopy for 'in-situ' structural determinations in an electrochemical cell, it has been used to study a number of standard samples for subsequent use as references for the identification of electrochemically prepared (ECP) phases. Namely, the Ni valency and local atomic structure in chemically prepared (CP) alpha-Ni(OH)2, beta-Ni(OH)2, Ni2O3, Ni3O2(OH)4, beta-NiOOH, gamma-NiOOH, NiO2, and NiKIO6 and ECP gamma-NiOOH. Presented are XANES spectra of Ni k-edge, Fourier transforms of k(exp 3)-weighted Ni K-edge EXAFS, and summary of Ni local structure in some oxycompounds. CASI

N95-17669# Stanford Linear Accelerator Center, CA.
BARYOGENESIS AND STANDARD MODEL CP VIOLATION
P. Huet Aug. 1994 5 p Presented at the Meeting of the Division of Particles and Fields of the American Physical Society, Albuquerque, NM, 2-6 Aug. 1994
(Contract DE-AC03-76SF-00515)
(DE94-017935; SU-SLAC-PUB-6631; CONF-940816-1) Avail: CASI HC A01/MF A01

The standard model possesses a natural source of CP violation contained in the phase of the CKM matrix. Whether the latter participated to the making of the matter-antimatter asymmetry of the observable universe is a fundamental question which has been addressed only recently. The generation of a CP observable occurs through interference of quantum paths along which a sequence of flavor mixings and chirality flips take place. The coherence of this phenomenon in the primeval plasma is limited by the fast quark-gluon interactions. At the electroweak era, this phenomenon of decoherence forbids a successful baryogenesis based on the sole CP violation of the CKM matrix. DOE

N95-17683# Brookhaven National Lab., Upton, NY.
SEARCH FOR THE PRESENCE OF H PARTICLES IN A NEUTRAL BEAM
M. May 1994 2 p Presented at the International Conference on Hypernuclear and Strange Particle Physics, Vancouver, British Columbia, 4-8 Jul. 1994
(Contract DE-AC02-76CH-00016)
(DE94-013526; BNL-60475; CONF-940725-2) Avail: CASI HC A01/MF A01

If the H particle exists and is relatively long lived, it will occur as a component of neutral secondary beams. In an experiment at the Brookhaven National Laboratory Alternate Gradient Synchroton, the apparatus of an existing rare kaon decay experiment (designed to search for K(sub L) yields mu(e)) was modified to search for H particles. Derived from text

N95-17687# Oak Ridge National Lab., TN.
ELECTRICAL BREAKDOWN AND OPTICAL EMISSION PROPERTIES OF HIGH PRESSURE PULSED RF GAS DISCHARGES
S. R. Hunter (Pellissippi International, Oak Ridge, TN.), G. S. Hurst (Pellissippi International, Oak Ridge, TN.), W. A. Gibson (Consultec Scientific, Inc., Knoxville, TN.), J. E. Turner, and R. N. Hamm 1994 7 p Presented at the 7th International Symposium on Gaseous Dielectrics, Knoxville, TN, 24-28 Apr. 1994
(Contract DE-AC05-84OR-21400)
(DE94-012731; CONF-940414-3) Avail: CASI HC A02/MF A01

A fundamentally new technique for the measurement of the number of subexcitation electrons produced by the passage of ionizing radiation through a gas has been developed by us during the past few years. The new

detector is based on the digital characterization of the electrons in the particle track produced by the ionizing radiation where the charged particle track is registered by measuring the number of electrons found in given subvolumes of the gas in the ionization chamber. The track is thus characterized by a set of integers in each volume element, from which parameters such as the track length and energy can be measured. We have specifically developed this technique for use in the field of microdosimetry, where the study of the fluctuations in the energy deposition in the charged particle track on the order of the molecular to cellular dimensions is important in understanding the chemical and biological effects of ionizing radiation. If the charged particle is a recoil nucleus produced by a neutron interaction, the energy deposited and the linear energy transfer can be inferred from this information, allowing the detector to act as neutron spectrometer. In this paper the experimental apparatus used to make these measurements and the optical and pulsed RF electric field optimization we have performed are described. Images of particle tracks produced by alpha and beta particles, and recoil protons from the interaction of high energy neutrons with hydrogenous materials, are also presented to illustrate the sensitivity and track imaging resolution. The quality of the information gained from the detector is a very sensitive function of the gas mixture constituents, purities and pressures used in the chamber, along with the magnitude, duration, and frequency of the pulsed RF electric field. DOE

N95-17692 Case Western Reserve Univ., Cleveland, OH. Dept. of Macromolecular Science.

CHIRAL RECOGNITION IN MOLECULAR AND MACROMOLECULAR PAIRS OF LIQUID CRYSTALS OF (2R, 3S)- AND (2S, 3S)-2-FLUORO-3-METHYLPENTYL-4'-(11-VINYLOXYUNDECA YLOXY)BIPHENYL-4-CARBOXYLATE DIASTEREOMERS

V. Percec, H. Oda, P. L. Rinaldi, and D. R. Hensley 30 Jun. 1994 42 p Limited Reproducibility: More than 20% of this document may be affected by microfiche quality

(Contract N00014-89-J-1828)

(AD-A281770; TR-1) Avail: CASI HC A03

(2R, 3S)-2-Fluoro-3-methylpentyl 4'-(11-vinyloxyundecanyloxy)biphenyl-4-carboxylate (15) (2R 92%ee) and (2S, 3S)-2-fluoro-3-methylpentyl 4'-(11-vinyloxyundecanyloxy)biphenyl-4-carboxylate (16) (2S 96%ee) diastereomers and their corresponding homopolymers and copolymers with well defined molecular weight and narrow molecular weight distribution were synthesized and characterized. The phase behaviors of 15 and poly (15) are identical to those of 16 and poly(16) respectively. The phase behavior of the two diastereomeric polymers can be compared only by superimposing the dependence of their thermal transition temperatures as a function of molecular weight. Both monomers display enantiotropic S(sub A), monotropic S(sub C) and crystalline phases, while the corresponding polymers exhibit enantiotropic S(sub A), S(sub C) and S(sub X)(unidentified smectic) mesophases. The phase behavior of the binary mixtures of 15 with 16 and poly(15) with poly(16) shows that they are miscible and therefore isomorphic within all their mesophases and over the entire range of compositions. DTIC

N95-17720# California Univ., Berkeley. Lawrence Berkeley Lab, CA.

STRONG WW SCATTERING AT PHOTON LINEAR COLLIDERS

M. S. Berger (Wisconsin Univ., Madison, WI.) and M. S. Chanowitz Jun. 1994 14 p Presented at the Workshop on Gamma-Gamma Colliders, Berkeley, CA, 28-31 Mar. 1994

(Contracts DE-AC03-76SF-00098; DE-AC02-76ER-00881)

(DE94-018183; LBL-35746; CONF-940351-3) Avail: CASI HC A03/MF A01

We investigate the possibility of observing strong interactions of longitudinally polarized weak vector bosons in the process (gamma)(gamma) (yields) ZZ at a photon linear collider. We make use of polarization of the photon beams and cuts on the decay products of the Z bosons to enhance the signal relative to the background of transversely polarized ZZ pairs. We find that the background overwhelms the signal unless there are strong resonant effects, as for instance from a technicolor analogue of the hadronic f(sub 2) (1270) meson. DOE

N95-17727# Los Alamos National Lab., NM.

NEUTRINO OSCILLATION STUDIES AT LAMPF

W. C. Louis 1994 7 p Presented at the Neutrino 1994: 16th International Conference on Neutrino Physics and Astrophysics, Eilat, Israel, 29 May - 3 Jun. 1994

(Contract W-7405-eng-36)

(DE94-018098; LA-UR-94-2761; CONF-9405216-1) Avail: CASI HC A02/MF A01

A search for (anti v)(sub (mu)) (yields) (anti v)(sub e) oscillations has been made by the Liquid Scintillator Neutrino Detector experiment at LAMPF after an initial month and a half run. The experiment observes eight events consistent with the reaction (anti v)(sub e)p (yields) e(sup +)n followed by np (yields) d(gamma) (2.2 MeV). The total estimated background is 0.9 +/- 0.2 events. DOE

N95-17739# Tokyo Univ., Tanashi (Japan). Inst. for Nuclear Study.

DELAYED ANNIHILATION OF ANTIPROTONS IN HELIUM GAS

S. N. Nakamura (Tokyo Univ., Japan.), R. S. Hayano (Tokyo Univ., Japan.), M. Iwasaki (Tokyo Univ., Japan.), K. Shigaki (Tokyo Univ., Japan.), E. Widmann, T. Yamazaki, H. Daniel (Technische Univ., Munich, Germany.), T. vonEgidy (Technische Univ., Munich, Germany.), T. Hartmann (Technische Univ., Munich, Germany.), and P. Hofmann (Technische Univ., Munich, Germany.) et al Nov. 1993 28 p Prepared in cooperation with European Organization for Nuclear Research, Geneva, Switzerland

(DE94-753405; INS-1013) Avail: CASI HC A03/MF A01

The delayed annihilation of antiprotons, which was recently discovered in liquid He-4 at KEK, has been studied at CERN in gas-phase He-4 and He-3. The annihilation time spectra in gas He-4 at various pressures were found to be similar to that for liquid He-4. The observed average lifetime in the region t greater than 1(mu)sec for 3 atm He-4 was about 3.2 microseconds, while for 3 atm He-3 gas it was 2.8 microseconds, i.e. shorter by 15 %. The time spectra show a growth-decay type function, which is indicative of the presence of a series of metastable states. For He-4 and He-3 they have nearly identical shapes, differing only in the time scale by 14 (+-) 3 %. These observations are qualitatively consistent with the atomic model of p-bare(sup -)He(sup ++) proposed by Condo. The time spectra were found to be sensitive to the presence of small amounts (as small as 20 ppm) of H-2. No evidence was seen for delayed annihilation in gaseous Ne. DOE

N95-17889# California Univ., Berkeley. Lawrence Berkeley Lab, CA.

FLAVOR SYMMETRIES AND FERMION MASSES Ph.D. Thesis

A. Rasin Apr. 1994 100 p

(Contract DE-AC03-76SF-00098)

(DE94-018192; LBL-35586) Avail: CASI HC A05/MF A02

We introduce several ways in which approximate flavor symmetries act on fermions and which are consistent with observed fermion masses and mixings. Flavor changing interactions mediated by new scalars appear as a consequence of approximate flavor symmetries. We discuss the experimental limits on masses of the new scalars, and show that the masses can easily be of the order of weak scale. Some implications for neutrino physics are also discussed. Such flavor changing interactions would easily erase any primordial baryon asymmetry. We show that this situation can be saved by simply adding a new charged particle with its own asymmetry. The neutrality of the Universe, together with sphaleron processes, then ensures a survival of baryon asymmetry. Several topics on flavor structure of the supersymmetric grand unified theories are discussed. First, we show that the successful predictions for the Kobayashi-Maskawa mixing matrix elements, V(sub ub)/V(sub cb) = (radical)m(sub u)/m(sub c) and V(sub td)/V(sub ts) = (radical)m(sub d)/m(sub s), are a consequence of a large class of models, rather than specific properties of a few models. Second, we discuss how the recent observation of the decay (beta) (yields) s(gamma) constrains the parameter space when the ratio of the vacuum expectation values of the two Higgs doublets, tan(Beta), is large. Finally, we discuss the flavor structure of proton decay. We observe a surprising enhancement of the branching ratio for the muon mode in SO(10) models compared to the same mode in the SU(5) model. DOE

N95-17899# Argonne National Lab., IL.

NEW SHOWER MAXIMUM TRIGGER FOR ELECTRONS AND PHOTONS AT CDF

D. Amidei (Michigan Univ., Ann Arbor, MI.), K. Burkett (Michigan Univ., Ann Arbor, MI.), D. Gerdes (Michigan Univ., Ann Arbor, MI.), C. Miao (Michigan Univ., Ann Arbor, MI.), D. Wolinski (Michigan Univ., Ann Arbor, MI.), K.

Byrum, J. Dawson, L. Nodulman, and A. B. Wicklund 28 Jul. 1994 5 p Presented at the Meeting of the Division of Particles and Fields of the American Physical Society, Albuquerque, NM, 2-6 Aug. 1994
(Contract W-31-109-eng-38)
(DE94-018376; ANL-HEP-CP-94-43; CONF-940816-3) Avail: CASI HC A01/MF A01

For the 1994 Tevatron collider run, CDF has upgraded the electron and photo trigger hardware to make use of shower position and size information from the central shower maximum detector. For electrons, the upgrade has resulted in a 50 percent reduction in backgrounds while retaining approximately 90 percent of the signal. The new trigger also eliminates the background to photon triggers from single-phototube spikes. DOE

N95-17918# Sandia National Labs., Albuquerque, NM.
FIELD-INDUCED MINIGAP AND TRANSPORT WITH IN-PLANE MAGNETIC FIELDS IN DOUBLE QUANTUM WELLS
S. K. Lyo, J. A. Simmons, and N. E. Harff 1994 14 p Presented at the 22d International Conference on Physics of Semiconductors, Vancouver, British Columbia, 15-19 Aug. 1994
(Contract DE-AC04-94AL-85000)
(DE94-018893; SAND-94-2066C; CONF-9408155-2) Avail: CASI HC A03/MF A01

Theory and data are presented for the in-plane conductance in the presence of a minigap induced by an in-plane magnetic field B in a strongly coupled thin double-quantum-well structure. The conductance is calculated using a linear response theory by treating the effect of impurity scattering on the self-energy part of the Green's function in a self-consistent way. A maximum and a minimum are obtained for the B-dependent conductance in agreement with the data. Similarities between this structure and previously studied vicinal Si-inversion layers are pointed out. DOE

N95-17932# Fermi National Accelerator Lab., Batavia, IL.
SEARCH FOR FIRST AND SECOND GENERATION LEPTOQUARKS AT D(NULL)
D. Norman (Texas A&M Univ., College Station, TX.) Aug. 1994 7 p Presented at the Meeting of the Division of Particles and Fields of the American Physical Society, Albuquerque, NM, 2-6 Aug. 1994
(Contract DE-AC02-76CH-03000)
(DE94-018992; FNAL/C-94/267-E; CONF-940816-5) Avail: CASI HC A02/MF A01

A search for first and second generation leptoquarks has been done with the D(null) detector at Fermilab's p(bar p) collider with (radical)s = 1.8 TeV. 95 percent C.L. mass limits for first generation scalar leptoquarks have been recently published. The number for the total integrated luminosity used in the first generation leptoquark analysis has changed (via a change in the total inelastic cross section) since the publication. The new limits are 130 GeV/c(sup 2) and 116 GeV/c(sup 2) for a respective 100 percent and 50 percent decay branching ratio of the leptoquark to electron. The preliminary upper limit on the cross section from the search for second generation scalar leptoquarks has set limits on the mass of the second generation leptoquark of 97 GeV/c(sup 2) for 100 percent branching to muons and 80 GeV/c(sup 2) for 50 percent branching. In contrast with leptoquark detection thresholds at e(+)e(-) and e-p machines, these limits are independent of the unknown coupling of the leptoquark to leptons and quarks. DOE

73 NUCLEAR AND HIGH-ENERGY PHYSICS

Includes elementary and nuclear particles; and reactor theory. For space radiation see *93 Space Radiation*.

N95-16030# Argonne National Lab., IL.
MECHANISMS OF BEAM-HALO FORMATION IN HIGH-INTENSITY LINACS
C. L. Bohn and J. R. Delayen 1994 6 p Presented at the International Conference on Accelerated-Driven Transmutation Technologies and Applications, Las Vegas, NV, 25-28 Jul. 1994
(Contract W-31-109-eng-38)
(DE94-016316; ANL/TD/CP-83128; CONF-9407103-16) Avail: CASI HC A02/MF A01

An rms-mismatched beam with space-charge forces can evolve rapidly, and during the course of evolution its emittance grows and a diffuse halo forms. The halo is of particular concern for long-term operation of linacs such as those envisioned for accelerator transmutation of waste (ATW) because too much particle impingement on the accelerating structures would cause enough radioactivation to prohibit routine hands-on maintenance. Thus, halo suppression is a design consideration for these linacs. In this paper, the authors summarize both the physical processes associated with the rapid evolution of the rms-mismatched beam and a semianalytic formalism which was recently developed to account for them. They also provide representative results derived from the formalism. DOE

N95-16172# Los Alamos National Lab., NM.
THE LANL-BOEING APLE/HPO FLYING-WIRE BEAM-PROFILE MONITOR Status and Test Report
M. Wilke, D. Barlow, C. Fortgang, J. Gilpatrick, R. Meyer, A. Rendon, D. Warren, and R. Greegor (Boeing Co., Seattle, WA.) Jul. 1994 33 p
(Contract W-7405-eng-36)
(DE94-014255; LA-12732-SR) Avail: CASI HC A03/MF A01

The High-Power Oscillator (HPO) demonstration of the Average Power Laser Experiment (APLE) is a collaboration by Los Alamos National Laboratory and Boeing to demonstrate a 10 kW average power, 10 (mu)m free electron laser (FEL). As part of the collaboration, Los Alamos National Laboratory (LANL) is responsible for many of the electron beam diagnostics in the linac, transport, and laser sections. Because of the high duty factor and power of the electron beam, special diagnostics are required. This report describes the flying wire diagnostic required to monitor the beam profile during high-power, high-duty operation. The authors describe the diagnostic and prototype tests on the Los Alamos APLE Prototype Experiment (APEX) FEL. They also describe the current status of the flying wires being built for APLE. DOE

N95-16210# Brookhaven National Lab., Upton, NY.
STUDY OF THE EFFECT OF THE SPACE CHARGE USING SYNCH
A. F. Haffmans, D. Maletic, and A. G. Ruggiero 25 Apr. 1994 40 p
(Contract DE-AC02-76CH-00016)
(DE94-014086; BNL-60521) Avail: CASI HC A03/MF A01

The interparticle repulsion, or space charge, limits the density of charged-particle beams that can be obtained in storage rings. In this report the authors study the effect of increasing the space charge, with an exact computation of the lattice parameters using SYNCH. Systematically increasing the ion density by decreasing the emittance with cooling techniques lowers the betatron tune, until the lower half-integral stopband resonance -- also induced by the beam -- is reached. In the simple model described in the report, the amount of 'cooling' is limited by the encountered stopband of the lattice. Therefore, machines with a higher tune and larger periodicity are better suited to store beams with high space charge. DOE

N95-16217# Los Alamos National Lab., NM.
ONLINE DIAGNOSES OF HIGH CURRENT-DENSITY BEAMS
J. D. Gilpatrick 1994 4 p Presented at the 4th European Particle Accelerator Conference, London, England, 27 Jun. - 1 Jul. 1994
(Contract W-7405-eng-36)
(DE94-014420; LA-UR-94-2125; CONF-940618-8) Avail: CASI HC A01/MF A01

Los Alamos National Laboratory has proposed several CW-proton-beam facilities for production of tritium or transmutation of nuclear waste with beam-current densities greater than 5 mA/mm(exp 2). The primary beam-diagnostics instrumentation requirement for these facilities is provision of sufficient beam information to understand and minimize beam-loss. To accomplish this task, the beam-diagnostics instrumentation must measure beam parameters such as the centroids and profiles, total integrated current, and particle loss. Noninterceptive techniques must be used for diagnosis of high-intensity CW beam at low energies due to the large quantity of power deposited in an interceptive diagnostic device by the beam. Transverse and longitudinal centroid measurements have been developed for bunched beams by measuring and processing image currents on the accelerator walls. Transverse beam-profile measurement-techniques have also been developed using the interaction of the particle beam with the background gases near the beam region. This paper will discuss these noninterceptive diagnostic techniques. DOE

N95-16308# Argonne National Lab., IL. Advanced Photon Source Accelerator Systems Div.

FIELD CONFIGURATION OF BEAM EXCITED MODES IN THE ADVANCED PHOTON SOURCE (APS) STORAGE RING WAVEGUIDES

S. O. Brauer, R. L. Kustom, and P. L. E. Uslenghi 1994 8 p Presented at the International Symposium on Electromagnetic Environments and Consequences, Bordeaux, France, 30 May - 3 Jun. 1994

(Contract W-31-109-eng-38)

(DE94-015096; ANL/APS/CP-83263; CONF-940531-2) Avail: CASI HC A02/MF A01

Argonne National Laboratory (ANL) is in the process of building a positron accelerator and storage ring, the Advanced Photo source (APS). The RF system for the APS storage ring uses 16 cylindrical TM010-like, reentrant cavities operating at 351.93 MHz to resupply energy lost by the beam due to synchrotron radiation. The stored beam will have approximately 60 bunches, 5 mA per bunch, for a total beam current of 300 mA. Calculations of the threshold current for coupled-bench instabilities in the storage ring have indicated that several beam-induced higher-order modes (HOM's) will reduce the threshold for beam stability and therefore should be damped. Previous data taken using a pillbox cavity showed that it is likely that some of these modes couple, through the coupling loop, from the storage ring cavity into the waveguide. This study investigates the electric and magnetic field configuration of each HOM present in the waveguide. A pillbox and a prototype storage ring cavity, together with various WR2300 waveguide components, are used to obtain the measurements needed for the determination of the mode configuration of the HOM's at the frequencies of interest. To avoid the development of beam instabilities due to the existence of these HOM's in the RF cavity, damping of the modes will be required. The HOM's present in the RF cavity coupling into the loop coupler and traveling through the coupler into the waveguide, may allow damping of some of the HOM's by insertion of dampers into the waveguide adjacent to each cavity. DOE

N95-16937 Los Alamos National Lab., NM. Meson Physics Facility.

PROGRESS AT LAMPF Progress Report, 1992 - 1993

C. M. Hoffman, ed. 25 Jul. 1994 241 p Limited Reproducibility: More than 20% of this document may be affected by microfiche quality

(Contract W-7405-eng-36)

(DE94-016210; LA-UR-94-2614) Avail: CASI HC A11

This Progress Report describes the operation of the Los Alamos Meson Physics Facility (LAMPF) and the research programs carried out there for the years 1992 and 1993. The accelerator operated for over 100 days in 1992, providing beams of H(+), H(-), and polarized H(-), for a rich and varied research program in nuclear physics. The accelerator had only fair beam availability in 1992 (for example, the average H(+) beam availability was 72 percent, caused largely by problems in the 201-MHz rf system. A major effort was expended to address these problems before the 1993 run. These efforts were rewarded by good beam availability in 1993 and few problems with the 201-MHz system. LAMPF operated remarkably smoothly during 1993, in the midst of a period of great uncertainty in the future of the facility and the downsizing of MP Division, which led to the loss of a large number of key people to positions elsewhere in the Laboratory. The H(+) intensity had to be held to no more than (approximately) 800(mu)A because of a vacuum leak in the A2 target. Nevertheless, the accelerator operated very reliably and the summer run in 1993 proved to be extremely productive. This report discusses the research conducted on: nuclear and particle physics; atomic physics; radiation effects; materials science; astrophysics; and theoretical physics. DOE

N95-17361# Sandia National Labs., Albuquerque, NM.

REENTRY SAFETY FOR THE TOPAZ 2 SPACE REACTOR: ISSUES AND ANALYSES

L. W. Connell and L. C. Trost Mar. 1994 27 p

(Contract DE-AC04-94AL-85000)

(DE95-000325; SAND-94-0484) Avail: CASI HC A03/MF A01

This report documents the reentry safety analyses conducted for the TOPAZ II Nuclear Electric Propulsion Space Test Program (NEPSTP). Scoping calculations were performed on the reentry aerothermal breakup and ground footprint of reactor core debris. The calculations were used to assess the risks associated with radiologically cold reentry accidents and to determine if constraints should be placed on the core configuration for such accidents. Three risk factors were considered: inadvertent criticality upon reentry impact, atmospheric dispersal of U-235 fuel, and the Special Nuclear Material Safeguards risks. Results indicate that the risks associated with cold reentry are very low regardless of the core configuration. Core configuration constraints were therefore not established for radiologically cold reentry accidents. DOE

N95-17475# Maryland Univ., College Park, MD.

BEAMS 92: PROCEEDINGS

D. Mosher, ed. and G. Cooperstein, ed. 1993 713 p Presented at the 9th International Conference on High Power Particle Beams, Washington, DC, 25-29 May 1992

(Contract DE-FG05-92ER-54160)

(DE94-014784; DOE/ER-54160/1-Vol-2; CONF-920515-Vol-2) Avail: CASI HC A99/MF A06

This report contains papers on the following topics: ion beam papers; electron beam papers; and these papers have been indexed separately elsewhere. DOE

N95-17499 AstroTerra Corp., San Diego, CA.

HIGH CURRENT DENSITY SHEET-LIKE ELECTRON BEAM GENERATOR

Cora Chow-Miller, Eric Korevaar, and John Schuster 1994 37 p Limited Reproducibility: More than 20% of this document may be affected by microfiche quality

(Contract N00014-93-C-0177)

(AD-A281975) Avail: Issuing Activity (Defense Technical Information Center (DTIC))

Sheet electron beams are very desirable for coupling to the evanescent waves in small millimeter wave slow-wave circuits to achieve higher powers. In particular, they are critical for operation of the free-electron-laser-like Orotron. The program was a systematic effort to establish a solid technology base for such a sheet-like electron emitter system that will facilitate the detailed studies of beam propagation stability. Specifically, the effort involved the design and test of a novel electron gun using Lanthanum hexaboride (LaB6) as the thermionic cathode material. Three sets of experiments were performed to measure beam propagation as a function of collector current, beam voltage, and heating power. The design demonstrated its reliability by delivering 386.5 hours of operation throughout the weeks of experimentation. In addition, the cathode survived two venting and pump down cycles without being poisoned or losing its emission characteristics. A current density of 10.7 A/sq cm. was measured while operating at 50 W of ohmic heating power. Preliminary results indicate that the nearby presence of a metal plate can stabilize the beam. DTIC

N95-17503# Helsinki Univ. of Technology, Otaniemi (Finland). Dept. of Technical Physics.

APPLYING STEP PRINCIPLES TO PRODUCT MODELS IN HIGH ENERGY PHYSICS RESEARCH

M. Dach, N. Hoimyr, J. Saarela, and J. Vuoskoski 1994 20 p

(PB94-197704; TKK-F-A724) Avail: CASI HC A03/MF A01

STEP (STandard for the Exchange of Product model data) is a new International Standard to exchange and represent product model data. It uses an object-flavored data specification language to specify the representation of the data. This report describes how the STEP principles can be applied to product models in high energy physics research. We present the design and implementation of a program where STEP principles were applied to detector models used by the GEANT detector simulation package. The design and implementation of the program were carried out using object-oriented technology. Possible applications which can profit from this program are discussed briefly. NTIS

N95-17519# Joint Inst. for Nuclear Research, Dubna (USSR). Lab. of Nuclear Reactions.

HEAVY ION PHYSICS

R. Kalpakchieva, comp. and E. A. Cherepanov, comp. 1993 192 p Presented at the International School Seminar on Heavy Ion Physics, Dubna, Russia, 10-15 May 1993

(DE94-623321; JINR-E-7-93-126; CONF-9305203) Avail: CASI HC A09/MF A02 (US Sales Only)

The international school-seminar on heavy ion physics had been organized in Dubna in may of 1993. The scientific program of reports covers the following main topics: (1) synthesis and properties of heavy

nuclei; (2) synthesis and investigation of properties of exotic nuclei; (3) experiments with radioactive nuclear beams; and (4) interaction between complex nuclei at low and intermediate energies. It also includes reports on the following: (1) laser spectroscopy and exotic nuclear beams; (2) some application of heavy ion beams for the problems of solid state physics; (3) construction of multidetector facilities; and (4) developing of heavy ion accelerator complexes. DOE

N95-17619 Wright Lab., Wright-Patterson AFB, OH.
DIGITAL LOGIC AND RECONFIGURABLE INTERCONNECTS USING ALUMINUM GALLIUM ARSENIDE ELECTRO-OPTIC FREDKIN GATES Final Report
James G. Grote Jun. 1994 302 p Limited Reproducibility: More than 20% of this document may be affected by microfiche quality
(AD-A282880; WL-TR-94-5028) Avail: Issuing Activity (Defense Technical Information Center (DTIC))

This report describes digital logic operations and reconfigurable optical interconnects realized from aluminum gallium arsenide (AlGaAs) electro-optic Fredkin gates. The Fredkin gates fabricated for this effort were channel waveguide type passive and active AlGaAs zero-gap directional couplers (ZGDC's). The first AND logic gate reported in the open literature using AlGaAs ZGDC's is demonstrated along with a reconfigurable optical interconnect. Models predicting the refractive index of AlGaAs versus Al concentration and wavelength are treated. A model for predicting the electro-optic coefficient of AlGaAs versus Al concentration and wavelength is developed. Models for predicting the interaction length and switching voltage are optimized for AlGaAs. Fabrication techniques for AlGaAs ZGDC's are formulated. The performance of the actual AlGaAs ZGDC's fabricated for this effort fit the models exceptionally well. Correlation of experimental and theoretical results yielded a mole fraction of Al of 30% for the core and 35% for the cladding. A refractive index of 3.420 for 30% Al and 3.388 for 35% Al at lambda = 827 nm were determined. A linear EO coefficient of r sub 41 = -1.49 pm/V at lambda = 827 nm was inferred for the core layer. A switching voltage of 7.6 VDC was achieved for an AlGaAs ZGDC with a 5000 micrometers interaction channel length. DTIC

N95-17670# California Univ., Berkeley. Lawrence Berkeley Lab, CA.
MEASUREMENTS OF COLLECTIVE EFFECTS IN THE ALS
J. M. Byrd and J. N. Corlett Jun. 1994 3 p Presented at the 4th European Particle Accelerator Conference, London, England, 27 Jun. - 1 Jul. 1994
(Contract DE-AC03-76SF-00098)
(DE94-017966; LBL-34954; CONF-940618-71) Avail: CASI HC A01/MF A01

The Advanced Light Source (ALS) is a newly commissioned 1.5 GeV third generation synchrotron radiation facility. We present a summary of measurements single and multibunch collective effects in the ALS storage ring and correlations with the expected impedance. Longitudinal and transverse coupled-bunch (CB) oscillations are characterized using measurements of beam spectrum, transverse beam size in dispersive regions, and undulator spectral width. Single bunch transverse head-tail damping rate and frequency shift are used to develop a model of the transverse broadband impedance. To date, storage ring performance is limited by longitudinal coupled-bunch oscillations No deleterious single-bunch effects up to 20 mA have been observed. DOE

N95-17671# California Univ., Berkeley. Lawrence Berkeley Lab, CA.
EXPERIMENTAL CHARACTERIZATION OF ALS UNDULATOR RADIATION
P. Heimann, D. Mossessian, A. Warwick, E. Gullikson, C. Wang, S. Marks, H. Padmore, and B. Kincaid 15 Jul. 1994 13 p Presented at the International Meeting on Synchrotron Radiation Instrumentation, Stony Brook, NY, 18-22 Jul. 1994
(Contract DE-AC03-76SF-00098)
(DE94-017967; LBL-35886; CONF-940714-17) Avail: CASI HC A03/MF A01

The radiation from the 5 cm period undulator at the Advanced Light Source (ALS) has been characterized using a transmission grating spectrometer. Spectral and angular distributions of radiation were measured for deflection parameter K values between 0.45 and 2.12 at low storage ring current (0.1-0.5 mA). From the calibration of the spectrometer, the absolute flux density of the undulator harmonics has been determined together with the spectral linewidth. The electron the beam emittance was determined by analyzing the angular distribution of the red-shifted fundamental. Comparison has been made with radiation calculations based upon the measured magnetic field data of the undulator. Including field errors, electron beam emittance and energy spread, good agreement is found between theoretically and experimentally determined harmonic widths and peak brightness. DOE

N95-17721# Los Alamos National Lab., NM.
TOKAMAK TRANSMUTATION OF (NUCLEAR) WASTE (TTW): PARAMETRIC STUDIES
E. T. Cheng (TSI Research, Inc., Solana Beach, CA.), R. A. Krakowski, and Y. K. M. Peng (Oak Ridge National Lab., TN.) 1994 9 p Presented at the 11th Topical Meeting on the Technology of Fusion Energy, New Orleans, LA, 19-24 Jun. 1994
(Contract W-7405-eng-36)
(DE94-012891; LA-UR-94-1624; CONF-940630-7) Avail: CASI HC A02/MF A01

Radioactive waste generated as part of the commercial-power and defense nuclear programs can be either stored or transmuted. The latter treatment requires a capital-intensive neutron source and is reserved for particularly hazardous and long-lived actinide and fission-product waste. A comparative description of fusion-based transmutation is made on the basis of rudimentary estimates of ergonic performance and transmutation capacities versus inventories for both ultra-low aspect-ratio (spherical torus, ST) and conversional (aspect-ratio) tokamak fusion-power-core drivers. The parametric systems studies reported herein provides a preamble to more-detailed, cost-based systems analyses. DOE

N95-17886# California Univ., Berkeley. Lawrence Berkeley Lab, CA.
Z(PRIME) PHENOMENOLOGY: CONSTRAINTS FROM LOW-ENERGY MEASUREMENTS, AND DETAILED STUDY AT TeV-SCALE LEPTON AND HADRON COLLIDERS Ph.D. Thesis
M. H. Austern May 1994 70 p
(Contract DE-AC03-76SF-00098)
(DE94-018185; LBL-35710) Avail: CASI HC A04/MF A01

In this dissertation, I discuss the phenomenology of new massive neutral gauge bosons, or Z(prime) bosons, concentrating on experimental tests by which the properties of a Z(prime) boson could be determined. In Chapter 1, I briefly review the Standard Model of elementary particle physics, and discuss the motivation for extending it. I review some of the extensions to the Standard Model that predict the existence of Z(prime) bosons, and present a general, model-independent parameterization of the Z(prime)s properties, as well as a simpler parameterization that applies to the most important class of models. In Chapter 2, I discuss present-day limits on the existence of Z(prime) bosons, both from direct searches, and from indirect higher-order tests. In Chapter 3, I discuss the production and discovery of a Z(prime) at a future hadron collider, such as the CERN Large Hadron Collider (LHC). Discovery of a Z(prime) at the LHC may be possible if its mass is less than 5 TeV. I also discuss the experimental tests of its properties that could be performed at such a collider, emphasizing the measurement of leptonic asymmetries. Finally, the Chapter 4, I discuss the experimental tests that could be performed at an e(+)e(-) collider with (radical)s = M(sub Z(prime)). I include several higher-order effects, such as initial-state radiation and beamstrahlung, whose inclusion is necessary for a realistic description of the experimental environment at a very high energy e(+)e(-) collider. The combination of leptonic and hadronic experiments permits the measurement of all of the parameters. DOE

N95-17888# California Univ., Berkeley. Lawrence Berkeley Lab, CA.
PHYSICS AT HIGH ENERGY PHOTON PHOTON COLLIDERS
M. S. Chanowitz Jun. 1994 18 p Presented at the Workshop on Gamma-Gamma Colliders, Berkeley, CA, 28-31 Mar. 1994
(Contract DE-AC03-76SF-00098)
(DE94-018191; LBL-35776; CONF-940351-2) Avail: CASI HC A03/MF A01

I review the physics prospects for high energy photon photon colliders, emphasizing results presented at the LBL Gamma Gamma Collider Workshop. Advantages and difficulties are reported for studies of QCD, the electroweak gauge sector, supersymmetry, and electroweak symmetry breaking. DOE

N95-17890# California Univ., Berkeley. Lawrence Berkeley Lab, CA.
CLOSED ORBIT DISTORTION FROM PARASITIC COLLISIONS IN PEP-2
M. A. Furman Jun. 1994 3 p Presented at the 4th European Particle Accelerator Conference, London, England, 27 Jun. - 1 Jul. 1994
(Contract DE-AC03-76SF-00098)
(DE94-018203; LBL-34958; CONF-940618-69) Avail: CASI HC A01/MF A01

The dipole force on the beams caused by the parasitic collisions (PC's) induces closed orbit distortions in the interaction region (IR): 'typical' bunches (those far away from the ion-clearing gap), collide center-on-center with a small horizontal crossing angle; 'pacman' bunches (those close to the gap) not only collide at an angle, but their centers are displaced as well; and the orbit separation between the beams at the PCs is different from nominal. We evaluate these effects as a function of horizontal tune in first-order approximation. This analysis yields one set of constraints that are absolutely necessary, although far from sufficient, for reliable operation. We conclude that the crossing angle and orbit displacements are small except for tune values very close to the integer (above or below), and that fractional tunes greater than or approximately equal to 0.35 are favored. DOE

N95-17891# California Univ., Berkeley. Lawrence Berkeley Lab, CA.
BEAM-BEAM TUNE SHIFT AND DYNAMICAL BETA FUNCTION IN PEP-2
M. A. Furman Jun. 1994 3 p Presented at the 4th European Particle Accelerator Conference, London, England, 27 Jun. - 1 Jul. 1994
(Contract DE-AC03-76SF-00098)
(DE94-018207; LBL-34957; CONF-940618-75) Avail: CASI HC A01/MF A01

We present the calculation of the beam-beam tune shift and dynamical beta function for PEP-2 as a function of the fractional tune and the beam separation at the parasitic collision (PC) points. We do the calculation both for 'typical' and for 'pacman' bunches taking into account all the PC's. DOE

N95-17901# Argonne National Lab., IL.
MEASUREMENTS OF X RAY SPECTRAL FLUX AND INTENSITY DISTRIBUTION OF APS/CHESS UNDULATOR RADIATION
P. Ilinski, W. Yun, B. Lai, E. Gluskin, and Z. Cai 1994 11 p Presented at the International Meeting on Synchrotron Radiation Instrumentation, Stony Brook, NY, 18-22 Jul. 1994
(Contract W-31-109-eng-38)
(DE94-018384; ANL/XFD/CP-83940; CONF-940714-23) Avail: CASI HC A03/MF A01

Absolute radiation flux and polarization measurements of the APS undulators may have to be made under high thermal loading conditions. A method that may circumvent the high-heat-load problem was tested during a recent APS/CHESS undulator run. The technique makes use of a Si(Li) energy-dispersive detector to measure 5-35 keV x rays scattered from a well-defined He gas volume at controlled pressure. DOE

N95-17902# Argonne National Lab., IL.
BEAM PARAMETER MEASUREMENTS FOR THE APS LINAC SYSTEM
Y. L. Qian, W. Berg, R. Fuja, A. Grelick, K. Ko, T. Russell, W. Wesolowski, and M. White 1994 4 p Presented at the 17th International Linac Conference, Tsukuba, Japan
(Contract W-31-109-eng-38)
(DE94-018396; ANL/ASD/CP-83968; CONF-9408125-20) Avail: CASI HC A01/MF A01

The linac system is the first part of the injector for the Advanced Photon source (APS) 7-GeV storage ring. The determination of beam emittance, optimization of beam energy and energy spread, focusing, condition, and other parameters is important for positron production and for injection of positrons from the linac into the positron accumulator ring. Diagnostic lines have been incorporated into the linac design to allow measurement of critical beam parameters. Commissioning of the linac system began in October 1993. Beam parameters measurements have been made, and the results are discussed in this paper. DOE

N95-17914# Sandia National Labs., Albuquerque, NM.
RECENT ADVANCES IN THE DEVELOPMENT OF HIGH AVERAGE POWER INDUCTION ACCELERATORS FOR INDUSTRIAL AND ENVIRONMENTAL APPLICATIONS
E. L. Neau 1994 3 p Presented at the 9th International Meeting on Radiation Processing: Dedicated to the Dissemination and Advancement of the Technology of Industrial Radiation Processing, Istanbul, Turkey, 11-16 Sep. 1994
(Contract DE-AC04-94AL-85000)
(DE94-018734; SAND-94-2352C; CONF-940908-1) Avail: CASI HC A01/MF A01

Short-pulse accelerator technology developed during the early 1960's through the late 1980's is being extended to high average power systems capable of use in industrial and environmental applications. Processes requiring high dose levels and/or high volume throughput will require systems with beam power levels from several hundreds of kilowatts to megawatts. Beam accelerating potentials can range from less than 1 MeV to as much as 10 MeV depending on the type of beam, depth of penetration required, and the density of the product being treated. This paper addresses the present status of a family of high average power systems, with output beam power levels up to 200 kW, now in operation that use saturable core switches to achieve output pulse widths of 50 to 80 nanoseconds. Inductive adders and field emission cathodes are used to generate beams of electrons or x rays at up to 2.5 MeV over areas of 1000 sq cm. Similar high average power technology is being used at less than or equal to 1 MeV to drive repetitive ion beam sources for treatment of material surfaces over 100's of sq cm. DOE

N95-17924# Argonne National Lab., IL.
HIGH ENERGY PHYSICS DIVISION RESEARCH ACTIVITIES Semiannual Report, 1 Jul. - 31 Dec. 1993
R. Wagner, P. Moonier, P. Schoessow, and R. Talaga May 1994 90 p
(Contract W-31-109-eng-38)
(DE94-015024; ANL-HEP-TR-94-34) Avail: CASI HC A05/MF A01

This report describes the research conducted in the High Energy Physics Division of Argonne National Laboratory during the period of July 1, 1993-December 31, 1993. Topics covered here include experimental and theoretical particle physics, advanced accelerator physics, detector development, and experimental facilities research. Lists of division publications and colloquia are included. DOE

N95-17931# Fermi National Accelerator Lab., Batavia, IL.
BEAM POSITION CORRECTION IN THE FERMILAB LINAC
K. L. Junck and E. McCrory Aug. 1994 4 p Presented at the 17th International LINAC Conference, Tsukuba, Japan, 21-26 Aug. 1994
(Contract DE-AC02-76CH-03000)
(DE94-018984; FNAL/C-94/250; CONF-9408125-29) Avail: CASI HC A01/MF A01

Orbit correction has long been an essential feature of circular accelerators, storage rings, multipass linacs, and linear colliders. In a drift tube linear accelerator (DTL) such as the H- Linac at Fermilab, beam position monitors (BPMs) and dipole corrector magnets can only be located in between accelerating tanks. Within a tank many drift tubes (from 20 to 60) each house a quadrupole magnet to provide strong transverse focusing of the beam. With good alignment of the drift tubes and quadrupoles and a sufficiently large diameter for the drift tubes, beam position is not typically a major concern. In the Fermilab DTL, 95 percent of the beam occupies only 35 percent of the available physical aperture (4.4 cm). The recent upgrade of the Fermilab Linac from a final energy of 200 MeV to 400 MeV has been achieved by replacing four 201.25 MHz drift tube linac tanks with seven 805 MHz side-coupled cavity modules (the high energy portion of the linac or HEL). In order to achieve this increase in energy within the existing enclosure, an accelerating gradient is required that is a factor of 3 larger than that found in the DTL. This in turn required that the physical aperture through which the beam must pass be significantly reduced. In addition, the lattice of the side-coupled structure provides significantly less transverse focusing than the DTL. Therefore in the early portion of the HEL the beam occupies over 95 percent of the available physical aperture (3.0 cm). In order to prevent beam loss and the creation of excess radiation, the ability to correct beam position throughout the HEL is of importance. An orbit smoothing algorithm commonly used in the correction of closed orbits of circular machines has been implemented to

achieve a global least-squares minimization of beam position errors. In order to accommodate several features of this accelerator a refinement in the algorithm has been made to increase its robustness and utilize correctors of varying strengths. DOE

N95-17933*# National Aeronautics and Space Administration. Lewis Research Center, Cleveland, OH.
OVERVIEW OF SPACE POWER ELECTRONIC'S TECHNOLOGY UNDER THE CSTI HIGH CAPACITY POWER PROGRAM
Gene E. Schwarze 1994 8 p Presented at the 7th Symposium on Space Nuclear Power Systems, Albuquerque, NM, 7-11 Jan. 1990
(Contract DE-AI03-86SF-16310)
(NASA-TM-110110; NAS 1.15:110110; DE94-051198; CONF-900109-28)
Avail: CASI HC A02/MF A01

The Civilian Space Technology Initiative (CSTI) is a NASA Program targeted at the development of specific technologies in the areas of transportation, operations and science. Each of these three areas consists of major elements and one of the operation's elements is the High Capacity Power element. The goal of this element is to develop the technology base needed to meet the long duration, high capacity power requirements for future NASA initiatives. The High Capacity Power element is broken down into several subelements that includes energy conversion in the areas of the free piston Stirling power converter and thermoelectrics, thermal management, power management, system diagnostics, and environmental compatibility and system's lifetime. A recent overview of the CSTI High capacity Power element and a description of each of the program's subelements is given by Winter (1989). The goals of the Power Management subelement are twofold. The first is to develop, test, and demonstrate high temperature, radiation-resistant power and control components and circuits that will be needed in the Power Conditioning, Control and Transmission (PCCT) subsystem of a space nuclear power system. The results obtained under this goal will also be applicable to the instrumentation and control subsystem of a space nuclear reactor. These components and circuits must perform reliably for lifetimes of 7-10 years. The second goal is to develop analytical models for use in computer simulations of candidate PCCT subsystems. Circuits which will be required for a specific PCCT subsystem will be designed and built to demonstrate their performance and, also, to validate the analytical models and simulations. The tasks under the Power Management subelement will now be described in terms of objectives, approach and present status of work. DOE

74 OPTICS

Includes light phenomena; and optical devices.
For lasers see *36 Lasers and Masers.*

N95-15947# Michigan Univ., Ann Arbor, MI. Dept. of Physics.
DEVELOPMENT AND APPLICATIONS OF THE POSITRON MICROSCOPE
1994 5 p
(Contract DE-FG02-90ER-12103)
(DE94-017918; DOE/ER-12103/1) Avail: CASI HC A01/MF A01

Progress on the positron microscope has moved forward in three main areas: Hardware construction and detailed optical design; auxiliary projects, partially supported by the larger Michigan positron physics group, to make intense positron sources and to make and test transmission remoderators; and three papers written on experimental and theoretical aspects of positron microscope applications. DOE

N95-15954# Army Research Lab., Adelphi, MD.
NON-INTRUSIVE MISSILE CONTROL SURFACE MONITOR SYSTEM
Progress Report, Oct. 1991 - Sep. 1992
David J. DeTroye and Vincent J. Ellis Oct. 1994 13 p
(AD-A285356; ARL-TR-505) Avail: CASI HC A03/MF A01

The non-intrusive missile control surface monitor system uses optical technologies for nonintrusive monitoring of various aspects of the movements of a missile control surface (or any control surface) that is undergoing electromagnetic testing. The system comprises a laser source, an optical detector positioned opposite the laser source, an attenuator assembly, which is a framed translucent grey-scale shaded window positioned between the laser source and the detector, and means for recording output signals derived from the detector. The attenuator assembly is an electromagnetically transparent member, mounted on the missile control surface. The attenuator assembly moves in concert with the missile control surface and yet does not affect the electromagnetic signature of the missile. Generated laser beams project on the grey-scale shaded window. The grey-scale shading affects the intensity of the directed laser beams (the darker areas attenuate more light and the lighter areas allow more light to pass through). Accordingly, data are obtained by optical detecting of the different light intensities passing through the translucent grey-scale shaded window, which are directly related in synchronization with the movements of the attenuator assembly and, therefore, the missile control surface. DTIC

N95-15958 Rochester Univ., NY. Inst. of Optics.
ARO-URI CENTER FOR OPTO-ELECTRONIC SYSTEMS RESEARCH
Final Report, 1 Oct. 1986 - 30 Jun. 1993
Nicholas George Dec. 1993 51 p Limited Reproducibility: More than 20% of this document may be affected by microfiche quality
(Contract DAAL03-86-G-0202)
(AD-A281447; ARO-24628.3-PH-UIF) Avail: CASI HC A04

Through the establishment of the ARO-URI Center for Opto-Electronic Systems Research in The Institute of Optics of the University of Rochester and the subject grant, we have supported the fellowship program of 38 Ph.D. scholars. The key research interests have been in the areas of lasers, optical system design, signal processing, remote sensing, source analysis, integrated optics, and diffraction and propagation theory. The majority of these exceptional scholars have completed their Ph.D. research and have gone on to work in industry or academia. The few remaining students are completing their work and should be finished within one year. Included in this final report of the Fellowship Grant is a listing of the scholars who were supported along with their thesis title, advisor, and current place of employment. Finally, a listing of each of the thesis abstracts is given. DTIC

N95-15960* National Aeronautics and Space Administration. Pasadena Office, CA.
ELECTRIC-OPTIC RESONANT PHASE MODULATOR Patent
Chien-Chung Chen, inventor (to NASA) (Jet Propulsion Lab., California Inst. of Tech., Pasadena, CA.), Deborah L. Robinson, inventor (to NASA) (Jet Propulsion Lab., California Inst. of Tech., Pasadena, CA.), and Hamid Hemmati, inventor (to NASA) (Jet Propulsion Lab., California Inst. of Tech., Pasadena, CA.) 13 Sep. 1994 15 p Filed 26 Feb. 1992
(NASA-Case-NPO-18702-1-CU; US-Patent-5,347,392;
US-Patent-Appl-SN-842300; US-Patent-Class-359-279;
US-Patent-Class-359-183; US-Patent-Class-372-18; US-Patent-Class-372-95;
Int-Patent-Class-G03H-1/02; Int-Patent-Class-G08B-5/23;
Int-Patent-Class-H01S-3/10) Avail: US Patent and Trademark Office

An electro-optic resonant cavity is used to achieve phase modulation with lower driving voltages. Laser damage thresholds are inherently higher than with previously used integrated optics due to the utilization of bulk optics. Phase modulation is achieved at higher speeds with lower driving voltages than previously obtained with non-resonant electro-optic phase modulators. The instant scheme uses a data locking dither approach as opposed to the conventional sinusoidal locking schemes. In accordance with a disclosed embodiment, a resonant cavity modulator has been designed to operate at a data rate in excess of 100 Mbps. By carefully choosing the cavity finesse and its dimension, it is possible to control the pulse switching time to within 4 ns and to limit the required switching voltage to within 10 V. Experimentally, the resonant cavity can be maintained on resonance with respect to the input laser signal by monitoring the fluctuation of output intensity as the cavity is switched. This cavity locking scheme can be applied by using only the random data sequence, and without the need of additional dithering of the cavity. Compared to waveguide modulators, the resonant cavity has a comparable modulating voltage requirement. Because of its bulk geometry, resonant cavity modulator has the potential of accommodating higher throughput power. Furthermore, mode matching into a bulk device is easier and typically can be achieved with higher efficiency. On the other hand, unlike waveguide modulators which are essentially traveling wave devices, the resonant cavity modulator requires that the cavity be maintained in resonance with respect to the incoming laser signal. An additional control loop is incorporated into the modulator to maintain the cavity on resonance.
Official Gazette of the U.S. Patent and Trademark Office

N95-15999# Army Construction Engineering Research Lab., Champaign, IL. Energy and Utilities Systems Div.
PERFORMANCE OF SPECULAR REFLECTORS USED FOR LIGHTING ENHANCEMENT Final Report
Daiva E. Edgar Jun. 1994 43 p
(DA Proj. 4A1-62784-AT-45)
(AD-A281004; CERL-TR-FE-94/13) Avail: CASI HC A03/MF A01

Since lighting accounts for about 20 to 30 percent of the total utility bill on Army installations, many installations try to lower lighting costs by retrofitting or upgrading to more efficient lighting systems. This study evaluated the effectiveness of specular reflectors used to enhance the effectiveness of two-lamp fixtures, which are claimed to enhance light levels of such fixtures by 50 to 100 percent, reducing the number of lamps required to light a given area. Light levels and light distribution of two-lamp fixtures were measured before and after installation of specular reflectors to measure the change in lighting intensity, and to see if the use of reflectors changed the fixture spacing criteria. It was found that reflectors increased the ambient light levels from 9 to 34 percent, but did not increase the spacing criteria. It is recommended that specular reflectors be considered for two-lamp lighting applications not constrained by maximum spacing criteria, where illumination falls below recommended or desired levels. DTIC

N95-16009 Naval Command, Control and Ocean Surveillance Center, San Diego, CA.
A QUASI-SINGLE MODE OPTICAL FIBER FOR LONG-HAUL TRANSMISSION IN SEVERE BENDING ENVIRONMENTS
Neil Kamikawa and Ching-Ten Chang Jun. 1994 8 p Limited Reproducibility: More than 20% of this document may be affected by microfiche quality
(AD-A281313) Avail: CASI HC A02

We investigated the feasibility of a quasi-single mode optical fiber for low bending losses in long-haul transmission at 1550 nm. The advantage of a quasi-single mode fiber is that for comparable bending losses the relative index difference, delta, can be smaller than the delta in a single-mode fiber. We demonstrated that a quasi-single mode fiber with delta = 0.72 percent and single-mode cutoff wavelength, lambda sub c, equal to 1630 nm exhibits bending losses as low as the losses in a single-mode fiber with delta = 0.93 percent and lambda sub c = 1259 nm. Modal noise and modal dispersion effects in the quasi-single mode fiber also were tested and found to be minimal. This paper describes the matched-clad, quasi-single mode fiber and presents the test results. DTIC

N95-16015# California Inst. of Tech., Pasadena, CA.
SYSTEMATIC OPTIMIZATION OF SECOND ORDER NONLINEAR OPTICAL MATERIALS Annual Report, 1 May 1993 - 30 Apr. 1994
Seth Marder 14 Jun. 1994 23 p
(Contract F49620-93-1-0314)
(AD-A281350; AFOSR-TR-94-0410) Avail: CASI HC A03/MF A01

We have developed new compounds with a thiophene bridge and acceptors that gain aromaticity, such as 3-phenyl-5-isoxazolone and diphenylthiobarbituric acid. These compounds have a large second-order nonlinearity roughly ten times that of the common dye Disperse-Red and good thermal stability and are therefore promising candidates for electro-optic poled polymer applications. DTIC

N95-16133# Electronics Research Lab., Salisbury (Australia).
PRELIMINARY INVESTIGATION OF AN INTEGRATED OPTIC SAMPLER FOR HF SIGNALS
Anthony C. Lindsay Apr. 1994 39 p
(AD-A284285; ERL-0828-RN; DODA-AR-008-869) Avail: CASI HC A03/MF A01

A compact, rugged, and inexpensive optical sampling system has been constructed. The aperture time of the sampler is estimated to be 75 ps, and sampling rates of 100 MHz and 250 MHz have been demonstrated. The performance of the demonstrator can be enhanced to gigahertz sampling rates without a substantial increase in cost. DTIC

N95-16157# North Carolina State Univ., Raleigh, NC. Dept. of Physics.
DEVELOPMENT OF AN ANALYTICAL PHOTON SCANNING TUNNELING MICROSCOPE Final Report, 1 Mar. 1991 - 28 Feb. 1994
Michael A. Paesler 9 May 1994 6 p
(Contract DAAL03-91-G-0053)
(AD-A281382; ARO-28313.1-PH) Avail: CASI HC A02/MF A01

We have made significant progress in designing, constructing, and using a novel device called the near-field scanning optical microscope, or NSOM. The microscope is one of a family of instruments which use either small apertures or finely sharpened probes to scan the surface of a sample and thereby construct an image of that surface. Since demonstrating the utility of the microscope, we have subsequently built a number of other NSOM's incorporating a variety of illumination modes and signal transduction methods in imaging surfaces and taking optical spectra of features on these surfaces. Theoretical efforts to model the optical throughput of the probe have been undertaken, and the initial results have been published. DTIC

N95-16161# New Mexico State Univ., Las Cruces, NM. Physical Science Lab.
FRACTAL AGGREGATE RANDOM MEDIA ANALYSIS AND APPLICATIONS Final Report, 15 Jul. 1991 - 14 Jul. 1994
Kung-Hau Ding 7 Mar. 1994 41 p
(Contract DAAL03-91-G-0229)
(AD-A281410; ARO-29107.1-GS-SAH) Avail: CASI HC A03/MF A01

The research performed during the period of July 1991 to September 1993 was focused on the theoretical formulations and numerical simulations of electromagnetic wave interaction with random fractal clusters and electromagnetic wave propagation and scattering in media with adhesive scatterers, and their applications in atmospheric aerosols and random media consisting of aggregated particles. The first major accomplishment in this period is the development of a fractal-based aggregated model and a rigorous T-matrix approach for studying the light scattering and absorption by agglomerated particles. We have simulated the structure of random clusters, determined the fractal dimension, and investigated their optical properties. The second major accomplishment is the development of a sticky particle model for simulating a random medium consisting of aggregated particles. We have studied the propagation and scattering of waves in such random media and performed computer simulations to determine the cluster size distribution and the fractal dimension for agglomerates. DTIC

N95-16296# Naval Research Lab., Washington, DC.
SYSTEM DESIGN, IMPLEMENTATION, AND EVALUATION OF THE OPTICAL BROADBAND CORRELATOR
R. D. Griffin 20 Sep. 1994 29 p
(AD-A285406; NRL/MR/5620-94-7612) Avail: CASI HC A03/MF A01

This report describes the design, implementation, and evaluation of an acousto-optical wide band correlator that is integrated into a digital signal processing system testbed. The report compares the correlator's measured performance with various theoretical performance measures, one of which compares the optical system with an equivalent efficient digital correlator. This measured performance of the optical system was 20 to 70 times that of a VAX 6410 using an FFT correlation algorithm and a vector processor, even though the electronic interface system limited the performance of the optical system to less than one-half percent of its potential. DTIC

N95-16366# Lawrence Livermore National Lab., Livermore, CA.
OVERVIEW OF PHOTONICS RESEARCH AT LAWRENCE LIVERMORE NATIONAL LABORATORY
F. Roeske, B. Deri, S. Dijaili, H. Lee, M. Lowry, C. McConaghy, F. Patterson, M. Pocha, and T. Strand May 1994 14 p Presented at the Society of Photo-Optical Instrumentation Engineers Conference on Intelligent Information Systems, Orlando, FL, 4-8 Apr. 1994
(Contract W-7405-eng-48)
(DE94-014055; UCRL-JC-115911; CONF-940449-13) Avail: CASI HC A03/MF A01

Much of Lawrence Livermore National Laboratory's (LLNL) expertise in photonics was acquired in the execution of the Nuclear Testing mission. As LLNL refocuses its resources into areas that have dual benefit for the nation, their photonics program is beginning to apply these unique capabilities to key national issues involving high-speed communications, while retaining the expertise to apply the technology to defense missions. Much of the exciting work being done at LLNL will have applications in photonics systems and experiments to be used in space. The authors will describe research being conducted in the following areas: high-speed, 50 ohm, phased-matched

modulators and their applications to digital links; promising new research on flat-panel displays that will be full color, fast response, very thin, and have a very high resolution; all optical switches that are extremely fast, integrable and do not have the latency problems that exist with current optical switches; semiconductor optical amplifiers that are monolithically integrable, more flexible and less expensive than existing fiber amplifiers; novel, semiconductor waveguide devices; and automated packaging techniques that will lower the cost of photonics components. Much of this research can directly benefit the development of space systems where reliability, size and cost are important considerations. Additional applications in commercial communications and in military system qualifies the photonics research at LLNL as multi-use technology. DOE

N95-16443# Rome Lab., Griffiss AFB, NY.
LOG-POLAR OPTICAL COORDINATE TRANSFORMATION WITH APPLICATIONS FOR AUTOMATIC PATTERN RECOGNITION Technical Report, Sep. 1990 - Sep. 1993
Christopher W. Keefer, Mark A. Getbehead, and Wesley E. Foor May 1994 24 p
(AF Proj. 4600)
(AD-A281022; RL-TR-94-22) Avail: CASI HC A03/MF A01

An important task in machine vision and target recognition is the rapid estimation of the orientation and size of an object with respect to a reference. An optical image processing system is described which converts in-plane rotation and size variations into shift properties using log-polar coordinate transforms. The optical system consists of a binary optical element, which performs the log-polar coordinate transform of the input image, a Fourier transform lens, a Michelson interferometer, and a CCD camera for collecting the scale/rotation invariant output. The Michelson interferometer produces two identical patterns on the polar axis to prevent wraparound effects of the coordinate transform. Results are presented in terms of capability in estimating the rotation and size of simple images and discriminating between similar in-class and out-of-class images using the output of a binary phase-only correlator. DTIC

N95-16494# Massachusetts Inst. of Tech., Lexington. Lincoln Lab.
APPLICATION OF FOURIER-SPACE IMAGE-RESTORATION TECHNIQUES TO TURBULENCE COMPENSATION AND SPARSE-APERTURE IMAGING
Ronald R. Parenti 1 Jun. 1994 86 p
(Contract F19628-90-C-0002)
(AD-A285077; TR-996; ESC-TR-93-347) Avail: CASI HC A05/MF A01

Image reconstruction is important in any application in which the sensing apparatus or the intervening medium significantly corrupts the recorded data. Deconvolution processes are the oldest and best understood, and for many practical problems Fourier domain deconvolution is the method of choice because acceptable results can usually be obtained with a minimum of computational effort. This report describes two practical applications of the Fourier deconvolution process in which detailed knowledge of the system's instantaneous optical transfer function is effectively utilized. In the first example, speckle imagery is combined with wavefront-sensor data to produce diffraction-limited images of celestial objects; the results are shown to compare favorably with the output of a fully operational adaptive optics system, the second application involves a sparse-aperture collection system that could be incorporated into a lightweight space telescope; this discussion includes an assessment of the practical utility of sparse-aperture receivers in a realistic signal-to-noise environment. DTIC

N95-16524# Rochester Univ., NY. Dept. of Chemistry.
NONLINEAR OPTICAL RESPONSE OF CONDINED EXCITIONS IN MOLECULAR AND SEMICONDUCTOR NANOSTRUCTURES Annual Report, 1 Oct. 1992 - 30 Sep. 1993
Shaul Mukamel 30 Sep. 1993 6 p
(Contract F49620-93-1-0055)
(AD-A285225; AFOSR-94-0587TR) Avail: CASI HC A02/MF A01

A dynamical theory that connects electronic motions and the nonlinear optical response of conjugated polyenes is developed by introducing the concept of electronic normal modes. A novel picture for the mechanism of optical nonlinearities is obtained by identifying the few dominant modes. This quasiparticle electron-hole representation established a close analogy with small semiconductor particles (quantum dots), and is very different for the traditional approach based on the electronic eigenstates. The effective conjugation length (coherence size), which controls the scaling and saturation of the static third order susceptibility X(3) with the number of double bonds, is related to the coherence of the relative motion of electron-hole pairs created upon optical excitation. DTIC

N95-16528# University of Southern California, Los Angeles, CA. Dept. of Chemistry.
DEVELOPMENT OF DEVICE QUALITY NONLINEAR OPTICAL MATERIALS AND DEFINITION OF MECHANISMS OF OPTICAL NONLINEARITY Final Report, 1 Jun. 1991 - 31 May 1994
Larry R. Dalton 1 Sep. 1994 104 p
(Contract F49620-91-C-0270)
(AD-A285255; AFOSR-94-0611TR) Avail: CASI HC A06/MF A02

The following objectives were defined and pursued: (1) Synthesis of chromophores characterized by large hyperpolarizability and good thermal stability; (2) covalent coupling of nonlinear optical chromophores to polymer matrices; (3) lattice hardening reactions which permit locking-in of electric field poling-induced macroscopic noncentrosymmetric order; (4) definition of mechanisms of optical nonlinearity and development of improved instrumentation to effect such characterization; and (5) exploration of methods of enhancing optical nonlinearity and electromagnetic field intensities within-materials (e.g., exploration of cascading effects and morphological resonances). Substantial success was achieved in each of these areas with more than sixty publications resulting from AFOSR support. DTIC

N95-16620# Picotronix, Inc., Ann Arbor, MI.
PICOSECOND OPTOELECTRONIC AND-GATE Final Report, Mar. - Aug. 1993
Steven L. Williamson Aug. 1994 32 p
(Contract F30602-93-C-0067)
(AD-A285672; RL-TR-94-108) Avail: CASI HC A03/MF A01

Logic gates based on conventional high speed detectors are limited by the recovery time, which can be over a hundred pico seconds. High speed direct detection with picosecond response near 0.85 mm has been successfully demonstrated in LT grown GaAs structures using interdigitated electrodes. These can form the key element in an optical AND GATE used for demultiplexing digital data at rates of up to 100 G bits. In this project, new materials based on LT grown InGaAs are developed and tested for their suitability at the 1.3 and 1.5 mm wavelengths, where single mode fiber capable of supporting such rates operates. The results to date extend pico second range responses to around 1.06 mm, but basic physical properties still preclude full extension to the desired wavelengths allowed by the range of transparency. Successful applications have resulted at the shorter wavelengths, and the results of these studies will facilitate the on-going material development needed to further extend the range of this new device technology. DTIC

N95-16733# Brimrose Corp. of America, Baltimore, MD.
A NOVEL OPTIC BISTABLE DEVICE WITH VERY LOW THRESHOLD INTENSITY USING PHOTOREFRACTIVE FILMS Final Report
Sean X. Wang, Yuankun Sun, Sudhir B. Trivedi, and Guifang Li 13 Aug. 1994 25 p
(Contract F49620-93-C-0070)
(AD-A285310; AFOSR-94-0593TR) Avail: CASI HC A03/MF A01

Brimrose Corporation of America reports the successful completion of the SBIR Phase I research in low-threshold intensity optical bistable devices using photorefractive nonlinearity. A thin photorefractive film optical bistable device was proposed in the Phase I proposal. The feasibility of this device was theoretically investigated. The theoretical feasibility study formulates the materials requirements in such a kind of configuration for Phase II research. In addition, we have proposed and investigated another configuration of optical bistable devices that do not require advanced photorefractive materials, namely, the self-pumped phase conjugator. We have successfully demonstrated a low-threshold optical bistable operation in a KNSBN:CU crystal. To the best of our knowledge, the threshold of 650 mW/sq. cm is the lowest of its kind to be achieved so far. DTIC

N95-16787# California Inst. of Tech., Pasadena, CA.
MATERIALS FOR SECOND AND THIRD ORDER NONLINEAR OPTICAL APPLICATIONS Annual Report, 1 Jun. 1993 - 31 May 1994

Seth Marder 14 Jun. 1994 11 p
(Contract F49620-92-J-0278)
(AD-A281304; AFOSR-94-0409TR) Avail: CASI HC A03/MF A01

We have developed a new synthesis of aldehyde precursors to second and third-order nonlinear optical materials. In this procedure, aldehydes with extended conjugation can be conveniently prepared in one step from organolithium reagents and vinylogous amides. We have also synthesized some donor-acceptor substituted thiophenevinylene oligomers that display enhanced optical nonlinearities and that have been incorporated into poled polymer. Although the compounds had large nonlinearities, insolubility precluded incorporating large amounts of the compounds into the host-guest polymer systems. Finally we have synthesized a series of compounds that have allowed us to map out the behavior of the first hyperpolarizability as a function of ground-state polarization and bond length alternation. The ground-state polarization was monitored by infrared spectroscopy using the local vibrational modes of a functional group on the end of the molecule as a probe. DTIC

N95-16795# Carnegie-Mellon Univ., Pittsburgh, PA. Dept. of Computer Science.
SENSOR PLACEMENT DESIGN FOR OBJECT POSE DETERMINATION WITH THREE LIGHT-STRIPE RANGE FINDERS
Keiichi Kemmotsu and Takeo Kanade 10 May 1994 25 p
(Contract F33615-90-C-1465; ARPA Order 7597)
(AD-A281199; CMU-CS-94-152) Avail: CASI HC A03/MF A01

The pose of a polyhedral object can be determined with range data obtained from a set of simple light-stripe range sensors. However, localization results are highly dependent on sensor placement. This paper presents a method for designing an optimal sensor placement of three light-stripe sensors with which to determine the pose of an arbitrarily positioned object. We evaluate a sensor placement on the basis of average performance measures over the whole state space of object pose by a Monte Carlo method. An optimal sensor placement is then selected by another Monte Carlo method which searches for a maximal score function of the performance measures over the whole state of sensor placements. DTIC

N95-16815 Naval Command, Control and Ocean Surveillance Center, San Diego, CA. Research, Development, Technology and Evaluation.
DEVELOPMENT AND FABRICATION OF THE FIBER OPTIC MicroCable (TM) Final Report, period ending Jun. 1993
J. H. Dombrowski, W. A. Kerr, III, and S. J. Cowen Oct. 1993 65 p
Limited Reproducibility: More than 20% of this document may be affected by microfiche quality
(AD-A285266; NRAD-TR-1620) Avail: CASI HC A04

This report describes the development and fabrication of the Fiber Optic MicroCable (TM) (FOMC (TM)). The research into and selection of raw materials, fabrication components, and fabrication methods are discussed in Part 1. Part 2 consists of process instructions relevant to plant operation. FOMC manufacturing system setup procedure and operation checks, shutdown, as well as problems one can expect to encounter are discussed in Part 2. This report concludes with clean-up procedures of the FOMC manufacturing system. DTIC

N95-16965# Optoelectronics Industry Development Association, Mountain View, CA.
OPTOELECTRIC TECHNOLOGY ROADMAP: CONCLUSIONS AND RECOMMENDATIONS Final Report
Ron Nelson 1 May 1994 62 p
(Contract DAAL03-92-G-0279)
(AD-A281664; ARO-30437.1-EL) Avail: CASI HC A04/MF A01

This report sets forth the major recommendations of the Optoelectronics Industry Development Association (OIDA) to improve the competitiveness of North American optoelectronics industry. The report summarizes an effort to determine the greatest market opportunities and key technical barriers, and to identify the highest priorities for improving the competitiveness of the industry. DTIC

N95-17143 Arizona Univ., Tucson, AZ. Optical Sciences Center.
NEW MECHANISMS AND NEW MATERIALS FOR ORGANIC OPTICAL NONLINEARITY Annual Report, 2 Jun. 1993 - 1 Jun. 1994
N. Peyghambarian, S. Mazumdar, and N. Armstrong 1 Jun. 1994 12 p
Limited Reproducibility: More than 20% of this document may be affected by microfiche quality
(Contract F49620-93-1-0199)
(AD-A282781; AFOSR-94-0432TR) Avail: CASI HC A03

In order to be photorefractive, a material has to combine photogeneration, photoconductivity, trapping and electro-optic (EO) properties. For our work we have developed a guest/host polymer composite based on the photoconducting polymer poly(N-vinylcarbazole) (PVK). Photosensitivity in the visible was provided by the charge transfer (CT) complex that PVK forms with 2,4,7-trinitro 9 fluorenone (TNF). The azo dye 2,5-dimethyl 4 (p-nitrophenylazo) anisole (DMNPAA) was used as the EO active chromophore. We added N-ethylcarbazole (ECZ) as an additional plasticizer to further decrease the glass transition temperature of the material. This guarantees good alignment of the nonlinear optical chromophores in an externally applied electric field, necessary to obtain a macroscopic EO effect in the material. DTIC

N95-17271*# National Aeronautics and Space Administration. Langley Research Center, Hampton, VA.
NUMERICAL APERTURE LIMITS ON EFFICIENT BALL LENS COUPLING OF LASER DIODES TO SINGLE-MODE FIBERS WITH DEFOCUS TO BALANCE SPHERICAL ABERRATION
R. Gale Wilson Nov. 1994 15 p
(RTOP 586-03-11-11)
(NASA-TM-4578; L-17340; NAS 1.15:4578) Avail: CASI HC A03/MF A01

The potential capabilities and limitations of single ball lenses for coupling laser diode radiation to single-mode optical fibers have been analyzed; parameters important to optical communications were specifically considered. These parameters included coupling efficiency, effective numerical apertures, lens radius, lens refractive index, wavelength, magnification in imaging the laser diode on the fiber, and defocus to counterbalance spherical aberration of the lens. Limiting numerical apertures in object and image space were determined under the constraint that the lens perform to the Rayleigh criterion of 0.25-wavelength (Strehl ratio = 0.80). The spherical aberration-defocus balance to provide an optical path difference of 0.25 wavelength units was shown to define a constant coupling efficiency (i.e., 0.56). The relative numerical aperture capabilities of the ball lens were determined for a set of wavelengths and associated fiber-core diameters of particular interest for single-mode fiber-optic communication. The results support general continuing efforts in the optical fiber communications industry to improve coupling links within such systems with emphasis on manufacturing simplicity, system packaging flexibility, relaxation of assembly alignment tolerances, cost reduction of opto-electronic components and long term reliability and stability. Author

N95-17334# Army Aeromedical Research Lab., Fort Rucker, AL.
FACTORS AFFECTING THE VISUAL FRAGMENTATION OF THE FIELD-OF-VIEW IN PARTIAL BINOCULAR OVERLAP DISPLAYS *Final Report*
Victor Klymenko, Robert W. Verona, Howard H. Beasley, John S. Martin, and William E. McLean (Universal Energy Systems, Inc., Daleville, AL.)
Jun. 1994 55 p
(DA Proj. 3E1-62787-A-879)
(AD-A283081; USAARL-94-29) Avail: CASI HC A04/MF A01

Small fields-of-view (FOV) are detrimental to the visual tasks required of military pilots. In order to increase the extent of the visual world available to U.S. Army helicopter pilots using helmet mounted displays (HMD), without incurring increases in size or weight or losses in central resolution, an unusual method of display - partial binocular overlap - has been proposed. Two flanking monocular regions and a central binocular overlap region constitute the FOV in partial binocular overlap displays. DTIC

N95-17340# Air Force Inst. of Tech., Wright-Patterson AFB, OH.
SPATIAL INFORMATION CONTENT ANALYSIS OF WIENER SPECTRA FROM POLARIZED WATERWAVE IMAGERY Ph.D. Thesis
Jan A. North 15 Mar. 1994 35 p
(AD-A283171; AFIT/CI/CIA-94-101) Avail: CASI HC A03/MF A01

This study proposes to analyze the correlation sensitivity of spatial Wiener spectra derived from polarized (Stokes' parameter) imagery of both synthetic and measured waterwave scenes. The intent is to evaluate the utility of polarized imagery in the extraction of spatial information content (to include texture) from scenes containing waterwaves, one of many spatially

correlated natural features that can be described by Wiener spectra. This study will first enhance an existing simulation model to support the comparison of the spatial performance of an imaging system through the creation of synthetic polarized images of waterwave scenes and their spatial spectra. Second, this model will be tailored to a specific imaging system: differentially polarized 4-lens 35-mm photography. Third, a parametric exploration of the model will be used to predict the polarized imaging conditions that optimize spatial information content. Fourth, a polarized 4-lens camera system will collect representative imagery containing waterwave scenes under natural conditions. Finally, the synthetic and measured polarized image spectra will be analyzed and compared in order to validate the simulation model, calibrate the imaging system, and ultimately provide the basis for the utility evaluation. DTIC

N95-17409 National Defence Research Establishment, Stockholm (Sweden). Dept. of Weapon Systems, Effects and Protection.

THE m-LINE METHOD FOR OPTICAL CHARACTERISATION OF POLYMER WAVEGUIDES [M-LINJEMETODEN FOER OPTISK KARAKTERISERING AV POLYMERA VAGLEDARMATERIAL]

J. Lindstroem and M. Lindgren Sep. 1993 34 p In SWEDISH Limited Reproducibility: More than 20% of this document may be affected by microfiche quality

(PB94-184611; FOA-C-20941-2.6) Avail: Issuing Activity (National Technical Information Service (NTIS))

Nonlinear optical materials in the shape of thin films are often used in applications as well as experiments to determine material properties. This report describes an experimental method to determine material parameters as refractive index, refractive index anisotropy, and thickness of a thin film with the so called m-line method. We derive the theoretical expressions for propagations of electromagnetic waves in thin films that are used to evaluate measured data. The method is tested on a polymer, common in the production of waveguides, by matching analytical expressions for the optical mode dispersion with experimental data by using the method of nonlinear least squares. NTIS

N95-17441 National Inst. of Standards and Technology, Boulder, CO. Electronics and Electrical Engineering Lab.

OPTICAL FIBER SENSORS: ACCELERATING APPLICATIONS IN NAVY SHIPS

G. W. Day, P. S. Lovely, H. K. Whitesel (Naval Surface Warfare Center, Annapolis, MD.), and R. K. Hickernell May 1994 105 p Limited Reproducibility: More than 20% of this document may be affected by microfiche quality

(PB94-186848; NISTIR-5018) Avail: CASI HC A06

The Navy needs new sensors for shipboard machinery monitoring and control, condition-based maintenance, and damage assessment. Optical fiber sensors are strongly preferred because of their immunity to electrical disturbances, as well as potential size, weight, and performance advantages. But despite well over a decade of development and promise, relatively few optical fiber sensors available today can meet the Navy's needs with acceptable performance and cost. This report examines the reasons and recommends strategies to help the Navy achieve its goals. Some of the recommendations confirm approaches that the Navy is already implementing. Optical fiber sensors have very valuable potential advantages, but those that the Navy can use may remain too expensive to be deployed if the Navy uses traditional methods of writing specifications and soliciting development and procurement bids. For this reason, the study focuses on cooperation with industry and promoting commercial off-the-shelf and dual-use technology. Author

N95-17483 Technische Univ., Delft (Netherlands).

GREY-SCALE MEASUREMENTS IN MULTI-DIMENSIONAL DIGITIZED IMAGES Ph.D. Thesis

L. J. vanVliet 5 Oct. 1993 256 p Sponsored by Netherlands Project Team for Computer Science Research and Imagenetics

(Grant NWO-900-538-016)

(PB94-195492; ISBN-90-6275-904-1) Copyright Avail: Issuing Activity

In this thesis we propose new methods for estimating properties of analog objects in properly sampled multi-dimensional grey-scale images. We focus only on point measurements and object measurements. The theory for most measurements holds irrespective of the image dimension. For practical purposes, we have emphasized properties related to 2D and 3D images. Chapter 1 introduces the field of image analysis. In Chapter 2, attention is paid to image formation using an 'ideal' optical system. As an example we have chosen a microscope, an optical instrument for which diffraction limited optics are widely available. Chapter 3 deals with the systematic errors of second derivative operators applied to low-pass filtered curved edges. In chapter 4 combinations-of-Gaussians for edge localization are studied. Chapter 5 explains curvature estimation of isophotes. Chapter 6 introduces object measurements by estimating 2D area and 3D volume. Chapter 7 presents a method for the estimation of 2D edge length (contour length) and 3D surface area. Chapter 8 gives a short description of 3D length estimators. In Chapter 9 we discuss a shape descriptor: bending energy. NTIS

N95-17489# Surveillance Research Lab., Salisbury (Australia).

TESTING AND CHARACTERIZATION OF THE CYCLOPS HgCdTe FOCAL PLANE DETECTOR ARRAY

G. V. Poropat Aug. 1993 28 p

(AD-A284279; SRL-0114-RN; DODA-AR-008-154) Avail: CASI HC A03/MF A01

Optoelectronics Division has developed an advanced technology demonstrator utilizing an infrared focal plane detector array to assess the feasibility of using passive infrared sensors for ADF applications. To model the performance of the sensor the characteristics of the focal plane detector array have been measured. The measurement of the characteristics of large scale detector arrays and the testing of these arrays present problems which are not encountered with single element infrared detectors. Optoelectronics Division has gained considerable experience in these processes during the development of the 'Cyclops' technology demonstrator. The procedures used in characterizing the HgCdTe focal plane detector array and the results obtained are described. DTIC

N95-17695# Department of the Navy, Washington, DC.

ULTRA HIGH BIT RATE ALL OPTICAL COMMUNICATION SYSTEM Patent Application

Irl N. Duling, inventor (to Navy) and Ronald D. Easman, inventor (to Navy) 25 Jan. 1994 36 p

(AD-D016359; US-Patent-Appl-SN-196074) Avail: CASI HC A03/MF A01

A system that uses all optical elements for transmission, regeneration and reception of solitons in point-to-point, broadcast, ring and multi-user trunk type communication systems. Soliton pulses from an optical clock source are modulated by optical data pulses in an optical modulator producing a modulated channel of data pulses. Several channels are combined by an optical multiplexer into a network optical bit stream. This stream is carried by an optical fiber and one or more of optical regenerators which recover the system clock and regenerate the signal with the recovered system clock rather than just amplifying the signal. Each of the regenerators can, in addition to regenerating the data, act as part of a data drop or insert node in a ring network where the node can synchronously remove data from or insert data into the stream. Intermediate nodes can include packet drop/replace nodes if the network is a packet type network. DTIC

N95-17707# University of Central Florida, Orlando, FL. Center for Research in Electro-Optics and Lasers.

MEASUREMENT OF MODULATION TRANSFER FUNCTION OF FOCAL PLANE ARRAYS AND IMAGING SYSTEMS Final Report

Glenn D. Boreman 11 May 1994 39 p

(Contract DAAL01-93-K-0067)

(AD-A282976) Avail: CASI HC A03/MF A01

A method for measuring the modulation transfer function (MTF) of focal-plane arrays (FPA's) has been developed which uses the statistical properties of laser speckle. The entire area of the focal plane is characterized, and no optics are required for target projection. The random nature of the test pattern avoids phasing effects between the target and the detector-array structure, which greatly relaxes alignment tolerances as compared to other methods. The technique is applicable to arrays that have intentional nonlinearity of response, as well as to those arrays that are inherently linear. The test can be performed on any focal-plane configuration, either one dimensional (1D) or two dimensional (2D). The data processing is usually performed by an off-line computer. However, the test is also useful for real-time diagnostics, to facilitate adjustment of

focal-plane operating parameters. In the real-time case, the necessary signal processing can be performed on a digital oscilloscope. DTIC

N95-16275# Nanjing Univ. of Aeronautics and Astronautics, Nanjing, Jiangsu (China). Dept. of Test and Measurement Engineering.
THE COMBINATION PROBE OF OPTICAL FIBERS AND ITS APPLICATIONS
Baoqi Tao and Weixuan Li *In its* Joint Proceedings on Aeronautics and Astronautics (JPAA) May 1993 p 169-178 (For primary document see N95-16249 04-01)
Avail: CASI HC A02/MF A03

N95-17290*# Jet Propulsion Lab., California Inst. of Tech., Pasadena, CA.
A PRELIMINARY OPTICAL VISIBILITY MODEL
K. Cowles and B. M. Levine *In its* The Telecommunications and Data Acquisition Report 15 Nov. 1994 p 201-209 (For primary document see N95-17279 04-32)
(RTOP 315-91-40-20-29)
Avail: CASI HC A02/MF A03

75 PLASMA PHYSICS

Includes magnetohydrodynamics and plasma fusion.

For ionospheric plasmas see *46 Geophysics*. For space plasmas see *90 Astrophysics*.

N95-15941*# Iowa Univ., Iowa City, IA. Dept. of Physics and Astronomy.
ANALYSIS OF PLASMA MEASUREMENTS FOR THE GEOTAIL MISSION Annual Report, 1 Oct. 1993 - 30 Sep. 1994
Louis A. Frank 1994 13 p
(Grant NAG5-2371)
(NASA-CR-197020; NAS 1.26:197020) Avail: CASI HC A03/MF A01

Data processing and research efforts for the period October 1993 to September 1994 are reported. Routine data processing includes the production of color spectrograms and computing of quantitative plasma parameters such as the plasma number density, bulk flow velocity, temperature, and pressure. In addition, specialized analysis software is being developed for specific and general applications. Research activities include the measurement of plasmas from the Geotail spacecraft; the processing of the measurements from a hot plasma analyzer to compute one minute averages of plasma densities, temperatures, and velocities for a substantial part of the Geotail deep tail mission; and, a preliminary survey of the magnetotail for geocentric radial distances of 10 to 210 earth radii. The topology of the magnetotail with its various regions and boundaries is determined by a complex interaction with the fields and plasmas of the solar wind. Observations of the rotation of the magnetic field in the solar wind show that it is well correlated with repeated transitions at Geotail from the magnetotail lobe to a magnetosheath-like boundary layer. CASI

N95-16063 Texas Univ., Austin, TX.
PAPERS PRESENTED AT THE TENTH TOPICAL CONFERENCE ON HIGH-TEMPERATURE PLASMA DIAGNOSTICS
1994 253 p Conference held in Rochester, NY, 8-12 May 1994
Limited Reproducibility: More than 20% of this document may be affected by microfiche quality
(Contract DE-FG03-94ER-54241)
(DE94-015854; DOE/ER-54241/131; FRCR-446; CONF-940552) Avail: CASI HC A12

This report contains papers on the following topics: (1) effects of limited spatial resolution on fluctuation measurements; (2) vertical viewing of electron-cyclotron radiation in Text-U; (3) measurement of temperature fluctuations from electron-cyclotron emission; (4) a varying cross section magnetic coil diagnostic used in digital feedback control of plasma position in Text-Upgrade; (5) high-sensitivity, high resolution measurements of radiated power on Text-U; (6) wave launching as a diagnostic tool to investigate plasma turbulence; (7) edge parameters from an energy analyzer and particle transport on Text-U; (8) initial results from a charge exchange q-Diagnostic on Text-U; (9) a method for neutral spectra analysis taking ripple-trapped particle losses into account; (10) application of a three sample volume(sup S(k,(omega))) estimate to optical measurements of turbulence on Text; (11) initial operation of the 2D Firsis on Text-Upgrade; (12) horizontal-view interferometer on Text-Upgrade; (13) plasma potential measurements on Text-Upgrade with A 2 MeV heavy ion beam; (14) fluctuation measurements using the 2 MeV heavy ion beam probe on Text-U; (15) the time domain triple probe method; a phase contrast imaging system for Text-U; and (16) development of rugged corner cube detectors for the Text-U-Fir interferometer. DOE

N95-16122# Cornell Univ., Ithaca, NY. School of Applied and Engineering Physics.
RUNAWAY ELECTRONS BEAMS IN ITER DISRUPTIONS
H. H. Fleischmann 1993 50 p
(Contract DE-FG02-92ER-54183)
(DE94-013788; DOE/ER-54183/1) Avail: CASI HC A03/MF A01

In agreement with the initial projections, the potential generation of runaway beams in disruptions of ITER discharges was performed. This analysis was based on the best-available present projections of plasma parameters existing in large-tokamak disruptions. Using these parameters, the potential contributions from various basic mechanisms for the generation of runway electrons were estimated. The envisioned mechanisms included: (1) the well-known Dreicer process (assuming an evaporation of the runways from the thermal distribution); (2) the seeding of runaway beams resulting from the potential presence of trapped high-temperature electrons from the original discharge still remaining in the disruption plasma at time of reclosure of the magnetic surfaces; and (3) the generation of runaway beams through avalanche exponentiation of low-level seed runaways resulting via close collisions of existing runaways with cold plasma electrons. Finally, the prospective behavior of the any generated runaway beams -- in particular during their decay -- as well as their potential avoidance and/or damage controlled extraction through the use of magnetic perturbation fields also was considered in some detail. DOE

N95-16216# Sandia National Labs., Albuquerque, NM.
CONTROL OF A LARGE VACUUM WAVE PRECURSOR ON THE SABRE VOLTAGE ADDER MITL AND EXTRACTION ION DIODE
M. E. Cuneo, D. L. Hanson, J. W. Poukey, P. R. Menge, M. E. Savage, J. R. Smith (Titan Technologies, Albuquerque, NM.), and M. A. Bernard (Ktech Corp., Albuquerque, NM.) 1994 5 p Presented at the 10th International Conference on High Power Particle Beams, San Diego, CA, 20-24 Jun. 1994
(Contract DE-AC04-94AL-85000)
(DE94-014280; SAND-93-2766C; CONF-940634-4) Avail: CASI HC A01/MF A01

SABRE is a ten-cavity magnetically insulated voltage adder (6MV, 300 kA) used to study ion beam production in high voltage extraction applied-B ion diodes. Observations indicate that the machine power initially propagates in a large-amplitude vacuum wave prior to electron emission. This vacuum wave 'precursor' has an important impact on the turn-on and impedance history of ion diodes. Some typical precursor characteristics are shown using transmission line, diode, and beam current and voltage data and are compared to TWOQUICK simulations. Two techniques are under investigation to control the precursor and its effects on diode performance. A plasma opening switch (POS) has been used to erode the precursor. Field enhancing inserts are also planned to decrease the macroscopic field required for electron emission from the cathode. This will limit the distance over which vacuum and insulated waves separate by propagation at different velocities. Experimental data from the POS technique and TWOQUICK simulations of the insert technique are presented and discussed. DOE

N95-16218# Los Alamos National Lab., NM.
INITIAL DESIGN OF A 1 MEGAWATT AVERAGE, 150 KILOVOLT PULSE MODULATOR FOR AN INDUSTRIAL PLASMA SOURCE ION IMPLANTATION PROCESSOR
W. A. Reass and D. Deb (Litton Industries, San Carlos, CA.) 1994 5 p Presented at the 21st International Power Modulator Symposium, Costa Mesa, CA, 28-30 Jun. 1994
(Contract W-7405-eng-36)
(DE94-014421; LA-UR-94-2126; CONF-940678-3) Avail: CASI HC A01/MF A01

Plasma Source Ion Implantation (PSII) is a materials surface modification

process which can be used to improve performance characteristics of manufacturing tooling and products. Since improvements can be realized in surface hardness, reduced friction, wear, galling, and increased resistance to corrosion, PSII is applicable to a broad spectrum of manufactured items. In PSII, the object to be implanted is placed in a weakly ionized plasma and pulsed to a high negative voltage. The plasma ions are accelerated into the object's surface, thereby changing its' chemical and physical composition. The plasma dynamic load impedance is highly variable, dependent on implant object area, plasma density, and material composition. The modulator load impedance may be a few tens of ohms and a few thousand picofarads early in time. Late in time, the load may appear as 20,000 Ohms and 100 picofarads. The modulator system must accommodate any process changes, in addition to (frequent) initial 'start-up' object arcs (from impurities). To implant the required ion densities in a minimum of time, multi-kilohertz rep-rates are often required. An evolutionary design approach was utilized to design a cost-effective and reliable modulator system with components of established performance, suitable for a manufacturing environment. This paper, in addition to presenting the anticipated modulator design required for the PSII application, will review similar modulator topologies and determine operational lifetime characteristics. Further improvements in system electrical efficiency can also be realized with incremental design modifications to the high voltage switch tubes. Development options for upgraded switch tubes of higher efficiency will also be presented. DOE

N95-16243# Illinois Univ., Urbana, IL. Dept. of Mechanical and Industrial Engineering.

ARCJET PLASMA MODELING WITH EXPERIMENTAL VALIDATION

Annual Technical Report, 30 Jul. 1993 - 1 Sep. 1994

Herman Krier, Rodney L. Burton, Thomas W. Megli, Scott A. Bufton, and Nicholas T. Tiliakos 1 Sep. 1994 84 p

(Contract F49620-92-J-0448)

(AD-A285234; UILU-ENG-94-4011) Avail: CASI HC A05/MF A01

We report for the first time thermal non-equilibrium (separate electron and gas temperatures) numerical results for a hydrazine arcjet. All viscous flow properties are considered, assuming laminar axisymmetric flow. The model includes anode temperature distribution, and the electrical conductivity is coupled to the flow properties, allowing for a self-consistent current distribution. The numerical solution algorithm employs the compressible form of the PISO algorithm to solve the continuity and momentum equations. Run time is a few hours on a Convex C240 Mainframe with a 44 x 24 grid. Numerical results are presented for low power hydrogen and hydrazine thrusters. Preliminary results of quadruple electrostatic probe measurements at the exit plane of a 1 kW hydrazine arcjet, including ne and Te profiles, are presented. The quadruple probe model includes the effects of Te and Ne gradients across the probe volume to extract Te and Ne radial profiles from the asymmetric raw probe data. A time-of-flight electrostatic probe technique for measuring heavy particle velocities is described which, when coupled with the quadruple probe data can yield radial profiles of Ne(r), Te(r), Ti(r) and Ui(r). Experimental investigations of the energy deposition processes in the nozzle and constrictor regions of a 1-2 kill hydrazine arcjet are being performed. Electron number density and electron temperature measurements, using an array of flush-mounted Langmuir probes, will be made in the boundary layer. DTIC

N95-16285# Los Alamos National Lab., NM.

SYSTEM DESIGN AND OPERATION OF A 100 KILOVOLT, 2 KILOHERTZ PULSE MODULATOR FOR PLASMA SOURCE ION IMPLANTATION

W. A. Reass 1994 5 p Presented at the 21st International Power Modulator Symposium, Costa Mesa, CA, 28-30 Jun. 1994

(Contract W-7405-eng-36)

(DE94-014424; LA-UR-94-2193; CONF-940678-1) Avail: CASI HC A01/MF A01

This paper describes the electrical design and operation of a high power modulator system implemented for the Los Alamos Plasma Source Ion Implantation (PSII) facility. To test the viability of the PSII process for various automotive components, the modulator must accept wide variations of load impedance. Components have varying area and composition which must be processed with different plasmas. Additionally, the load impedance may change by large factors during the typical 20 uS pulse, due to plasma displacement currents and sheath growth. As a preliminary design to test the system viability for automotive component implantation, suitable for a manufacturing environment, circuit topology must be able to directly scale to high power versions, for increased component through-put. We have chosen an evolutionary design approach with component families of characterized performance, which should result in a reliable modulator system with component lifetimes. The modulator utilizes a pair of Litton L-3408 hollow beam amplifier tubes as switching elements in a 'hot-deck' configuration. Internal to the main of planar triode hot deck, an additional pair decks, configured in a totem pole circuit, provide input drive to the L-3408 mod-anodes. The modulator can output over 2 amps average current (at 100 kV) with 1 kW of modanode drive. Diagnostic electronics monitor the load and stops pulses for 100 mS when a load arcs occur. This paper, in addition to providing detailed engineering design information, will provide operational characteristics and reliability data that direct the design to the higher power, mass production line capable modulators. DOE

N95-16286# Los Alamos National Lab., NM.

ION BEAM GENERATION AND PROPAGATION FOR PLASMA PROCESSING APPLICATIONS

R. J. Faehl and D. J. Rej Jun. 1994 4 p Presented at the 10th International Conference on High Power Particle Beams, San Diego, CA, 20-24 Jun. 1994

(Contract W-7405-eng-36)

(DE94-014428; LA-UR-94-2176; CONF-940634-8) Avail: CASI HC A01/MF A01

Intense ion beams are being employed at Los Alamos to deposit thin films. Extraction geometry magnetically-insulated ion diodes (MID) are used to generate ion beams with currents up to 35 kA at 450 kV in a one-half microsecond long pulse. Multidimensional electromagnetic particle-in-cell (PIC) simulations have been performed to model the generation, extraction, and focusing of proton beams in realistic geometries. A ballistically focused MID has been studied to achieve the high deposition rates needed to form ablation plumes that preserve stoichiometric ratios. A high density waist with a diameter less than 8 cm is calculated near the geometrical focus. Extraction efficiency, beam divergence downstream of the aperture, and neutralization issues have been studied with the simulations. DOE

N95-16307# Argonne National Lab., IL.

PLASMA DISRUPTION MODELING AND SIMULATION

A. Hassanein Jun. 1994 9 p Presented at the 11th Topical Meeting on the Technology of Fusion Energy, New Orleans, LA, 19-24 Jun. 1994

(Contract W-31-109-eng-38)

(DE94-015095; ANL/TD/CP-82096; CONF-940630-34) Avail: CASI HC A02/MF A01

Disruptions in tokamak reactors are considered a limiting factor to successful operation and a reliable design. The behavior of plasma-facing components during a disruption is critical to the overall integrity of the reactor. Erosion of plasma facing-material (PFM) surfaces due to thermal energy dump during the disruption can severely limit the lifetime of these components and thus diminish the economic feasibility of the reactor.Initially, the incident plasma particles will deposit their energy directly on the PFM surface, heating it to a very high temperature where ablation occurs. Models for plasma-material interactions have been developed and used to predict material thermal evolution during the disruption. Within a few microseconds after the start of the disruption, enough material is vaporized to intercept most of the incoming plasma particles. Models for plasma-vapor interactions are necessary to predict vapor cloud expansion and hydrodynamics. Continuous heating of the vapor cloud above the material surface by the incident plasma particles will excite, ionize, and cause vapor atoms to emit thermal radiation. Accurate models for radiation transport in the vapor are essential for calculating the net radiated flux to the material surface which determines the final erosion thickness and consequently component lifetime. A comprehensive model that takes into account various stages of plasma-material interaction has been developed and used to predict erosion rates during reactor disruption, as well during induced disruption in laboratory experiments. Differences between various simulation experiments and reactor conditions are discussed. A two-dimensional radiation transport model has been developed to particularly simulate the effect of small test samples used in laboratory disruption experiments. DOE

N95-16554# Lawrence Livermore National Lab., Livermore, CA.

DEVELOPMENT OF A RADIATIVE DIVERTOR FOR DIII-D

S. L. Allen, N. H. Brooks (Sandia National Labs., Albuquerque, NM.), R. B. Campbell (Sandia National Labs., Albuquerque, NM.), M. E. Fenstermacher, D. N. Hill, A. W. Hyatt, D. Knoll (Oak Ridge National Lab., TN.), C. J. Lasnier, E. A. Lazarus (Idaho National Engineering Lab., Idaho Falls, ID.), and A. W. Leonard (Idaho National Engineering Lab., Idaho Falls, ID.) et al
Jul. 1994 18 p Presented at the 11th International Conference on Plasma Surface Interactions in Controlled Fusion Devices, Mito (Japan), 23-27 May 1994
(Contracts DE-AC03-89ER-51114; DE-AC05-84OR-21400; W-7405-eng-48; DE-AC04-76DP-00789; DE-AC07-76ID-01570)
(DE94-016522; GA-A-21714; CONF-940580-11) Avail: CASI HC A03/MF A01

We have used experiments and modeling to develop a new radiative divertor configuration for DIII-D. Gas puffing experiments with the existing open divertor have shown the creation of a localized (approximately 10 cm diameter) radiation zone which results in substantial reduction (3-10) in the divertor heat flux while tau(sub E) remains approximately 2 times ITER-89P scaling. However, n(sub e) increases with D(sub 2) puffing, and Z(sub eff) increases with neon puffing. Divertor structures are required to minimize the effects on the core plasma. The UEDGE fluid code, benchmarked with DIII-D data, and the DEGAS neutrals transport code are used to estimate the effectiveness of divertor configurations; slots reduce the core ionization more than baffles. The overall divertor shape is set by confinement studies which indicate that high triangularity (delta approximately equal to 0.8) is important for high tau(sub E)VH-modes. Results from engineering feasibility studies, including diagnostic access, will be presented. DOE

N95-16555# General Atomics Co., San Diego, CA.
ACTIVE SILICON X RAY FOR MEASURING ELECTRON TEMPERATURE
R. T. Snider Jul. 1994 12 p Presented at the 10th Topical Conference on High-Temperature Plasma Diagnostics, Rochester, NY, 8-12 May 1994
(Contract DE-AC03-89ER-51114)
(DE94-017521; GA-A-21694; CONF-940552-26) Avail: CASI HC A03/MF A01

Silicon diodes are commonly used for x-ray measurements in the soft x-ray region between a few hundred eV and 20 keV. Recent work by Cho has shown that the charge collecting region in an underbiased silicon detector is the depletion depth plus some contribution from a region near the depleted region due to charge-diffusion. The depletion depth can be fully characterized as a function of the applied bias voltage and is roughly proportional to the square root of the bias voltage. We propose a technique to exploit this effect to use the silicon within the detector as an actively controlled x-ray filter. With reasonable silicon manufacturing methods, a silicon diode detector can be constructed in which the sensitivity of the collected charge to the impinging photon energy spectrum can be changed dynamically in the visible to above the 20 keV range. This type of detector could be used to measure the electron temperature in, for example, a tokamak plasma by sweeping the applied bias voltage during a plasma discharge. The detector samples different parts of the energy spectrum during the bias sweep, and the data collected contains enough information to determine the electron temperature. Benefits and limitations of this technique will be discussed along with comparisons to similar methods for measuring electron temperature and other applications of an active silicon x-ray filter. DOE

N95-16617# Texas Univ., Austin, TX. Applied Research Lab.
PLASMA SOUND SOURCE BASIC RESEARCH Annual Summary Report, Jun. 1993 - May 1994
20 Sep. 1994 4 p
(Contracts N00014-94-1-0150; N00014-94-1-0018)
(AD-A285394) Avail: CASI HC A01/MF A01

The basic research component of this ONR sponsored program is focused on three areas of research: (1) Dielectric breakdown of salt water; (2) A study of the electrical and acoustic properties of multiple gap electrodes; and (3) Development of detailed model of the plasma arc and, if possible, the coupling of this model to the non-spherical bubble formation in the initial stages of the arc formation and energy delivery. DTIC

N95-16827# Oak Ridge National Lab., TN.
FUSION MATERIALS: TECHNICAL EVALUATION OF THE TECHNOLOGY OF VANDIUM ALLOYS FOR USE AS BLANKET STRUCTURAL MATERIALS IN FUSION POWER SYSTEMS
Aug. 1993 47 p
(Contract DE-AC05-84OR-21400)
(DE94-013194; DOE/ER-0313-100; ORNL/M-3576) Avail: CASI HC A03/MF A01

The Committee's evaluation of vanadium alloys as a structural material for fusion reactors was constrained by limited data and time. The design of the International Thermonuclear Experimental Reactor is still in the concept stage, so meaningful design requirements were not available. The data on the effect of environment and irradiation on vanadium alloys were sparse, and interpolation of these data were made to select the V-5Cr-5Ti alloy. With an aggressive, fully funded program it is possible to qualify a vanadium alloy as the principal structural material for the ITER blanket in the available 5 to 8-year window. However, the data base for V-5Cr-5Ti is limited and will require an extensive development and test program. Because of the chemical reactivity of vanadium the alloy will be less tolerant of system failures, accidents, and off-normal events than most other candidate blanket structural materials and will require more careful handling during fabrication of hardware. Because of the cost of the material more stringent requirements on processes, and minimal historical working experience, it will cost an order of magnitude to qualify a vanadium alloy for ITER blanket structures than other candidate materials. The use of vanadium is difficult and uncertain; therefore, other options should be explored more thoroughly before a final selection of vanadium is confirmed. The Committee views the risk as being too high to rely solely on vanadium alloys. In viewing the state and nature of the design of the ITER blanket as presented to the Committee, it is obvious that there is a need to move toward integrating fabrication, welding, and materials engineers into the ITER design team. If the vanadium alloy option is to be pursued, a large program needs to be started immediately. The commitment of funding and other resources needs to be firm and consistent with a realistic program plan. DOE

N95-16919 General Atomics Co., San Diego, CA.
POLOIDAL ROTATION AND THE EVOLUTION OF H-MODE AND VH-MODE PROFILES
F. L. Hinton, G. M. Staebler, and Y. B. Kim Dec. 1993 6 p Presented at the IAEA Meeting on H-Mode Physics, Naka, Japan, 15-17 Nov. 1993 Limited Reproducibility: More than 20% of this document may be affected by microfiche quality
(Contracts DE-FG03-92ER-54150; DE-AC03-89ER-51114)
(DE94-015858; GA-A-21523; CONF-9311147-9) Avail: CASI HC A02

The physics which determines poloidal rotation, and its role in the development of profiles during H- and VH-modes, is discussed. A simple phenomenological transport model, which incorporates the (rvec E) x (rvec B) flow shear suppression of turbulence, is shown to predict profile evolution similar to that observed experimentally during H-mode and VH-mode. DOE

N95-16921 North Carolina Univ., Asheville, NC. Dept. of Physics.
ALPHA PARTICLE KINETICS IN IGNITED FUSION PLASMAS: DESIGN APPLICATIONS FOR A CO2 LASER THOMSON SCATTERING EXPERIMENT
C. A. Bennett May 1994 5 p Presented at the 9th Topical Conference on High-Temperature Plasma Diagnostics, Santa Fe, NM, 15-19 Mar. 1992 Limited Reproducibility: More than 20% of this document may be affected by microfiche quality
(Contract DE-FG05-89ER-53288)
(DE94-016297; CONF-920362-49) Avail: CASI HC A01

Technical achievements during the initial budget phase of this study consists of work accomplished under the following categories: (1) Hot Cell Notch Filter; and (2) System Integration. In the two week period just prior to the 1993 shutdown of ATF, the authors were able to make the planned scattering measurement. The experiment was a complete success, and the feasibility of the approach was unambiguously demonstrated. The measurements have been reported in a separate article. DOE

N95-16936 Los Alamos National Lab., NM.
INTENSE ION BEAM OPTIMIZATION AND CHARACTERIZATION WITH THERMAL IMAGING
H. A. Davis, R. R. Bartsch, D. J. Rej, and W. J. Waganaar 1994 7 p Presented at the 10th International Conference on High Power Particle Beams, San Diego, CA, 20-24 Jun. 1994 Limited Reproducibility: More than 20% of this document may be affected by microfiche quality
(Contract W-7405-eng-36)
(DE94-016184; LA-UR-94-2438; CONF-940634-13) Avail: CASI HC A02

The authors have developed thermal imaging of beam targets to optimize and characterize intense ion beams. The technique, which measures the beam energy-density distribution on each machine firing, has been used to rapidly develop and characterize two very different beams: a 400 kV beam used to study materials processing, and an 80 kV beam use for magnetic fusion diagnostics. DOE

N95-16958# Oak Ridge National Lab., TN.
DIFFERENTIAL PHASE REFLECTOMETRY FOR EDGE PROFILE MEASUREMENTS ON TFTR
G. R. Hanson, J. B. Wilgen, T. S. Bigelow, A. C. England, M. Murakami, D. A. Rasmussen, I. Collazo (Georgia Inst. of Tech., Atlanta, GA.), and J. R. Wilson (Princeton Univ., NJ.) 1994 12 p Presented at the 10th Topical Conference on High-Tmperature Plasma Diagnostics, Rochester, NY, 8-12 May 1994
(Contract DE-AC05-84OR-21400)
(DE94-013837; CONF-940552-9) Avail: CASI HC A03/MF A01

Edge electron density profile measurements, including the scrape-off layer, have been made during ICRF heating with the two-frequency differential phase reflectometer installed in an ICRF antenna on TFTR. This system probes the plasma using the extraordinary mode with two signals swept from 90 to 118 GHz while maintaining a fixed difference frequency of 125 MHz. The extraordinary mode is used to obtain density profiles in the range of 1 x 10(exp 11) to 3 x 10(exp 13) cm(exp -3) in high-field (4.5 to 4.9 T) full size (R(sub 0) = 2.62 m, a = .96 m) TFTR plasmas. The reflectometer launcher is located in an ICRF antenna and views the plasma through a small penetration in the center of the Faraday shield. A 26 m long overmoded waveguide run connects the launcher to the reflectometer microwave electronics. Profile measurements made with this reflectometer system will be presented along with a discussion of the characteristics of this differential phase reflectometer and data analysis. DOE

N95-17155# Los Alamos National Lab., NM.
A COMPARISON OF STEADY-STATE ARIES AND PULSED PULSAR TOKAMAK POWER PLANTS
C. G. Bathke 1994 7 p Presented at the 11th Topical Meeting on the Technology of Fusion Energy, New Orleans, LA, 19-24 Jun. 1994
(Contract W-7405-eng-36)
(DE94-014441; LA-UR-94-1957; CONF-940630-13) Avail: CASI HC A02/MF A01

The multi-institutional ARIES study has completed a series of three steady-state and two pulsed cost-optimized conceptual designs of commercial tokamak fusion power plants that vary the level of assumed advances in technology and physics. The cost benefits of various design options are compared quantitatively. Possible means to improve the economic competitiveness of fusion are suggested. DOE

N95-17347# Oak Ridge National Lab., TN.
FIRST MEASUREMENTS OF ICRF AND EDGE/SOL PLASMA INTERACTIONS ON TORE SUPRA
C. E. Thomas, Jr., J. H. Harris, and G. R. Haste et al 1994 17 p Presented at the 11th International Conference on Plasma Surface Interactions in Controlled Fusion Devices, Mito, Japan, 23-27 May 1994
(Contract DE-AC05-84OR-21400)
(DE94-019320; CONF-940580-20) Avail: CASI HC A03/MF A01

Heat fluxes considerably larger than anticipated appear to be incident on the lateral protection of the TORE SUPRA Ion Cyclotron Range of Frequencies (ICRF) antennas. The antenna lateral protection shows overheating for power levels greater than 2 MW in dipole mode or 1 MW in monopole mode. A possible cause for overheating is a dc sheath voltage created on the antenna structure by the ICRF. DOE

N95-17365 Los Alamos National Lab., NM.
DETERMINATION OF THE NUCLEAR-INDUCED ELECTRICAL CONDUCTIVITY IN A NUCLEAR-DRIVEN MHD DEVICE
L. Bitteker 1994 6 p Presented at the 29th Intersociety Energy Conversion Engineering Conference, Monterey, CA, 7-12 Aug. 1994 Limited Reproducibility: More than 20% of this document may be affected by microfiche quality
(Contract W-7405-eng-36)
(DE94-013137; LA-UR-94-1852; CONF-940812-6) Avail: CASI HC A02

The continual need for more efficient energy conversion techniques for space, sea, and terrestrial systems has renewed interest in nuclear-driven magnetohydrodynamic (MHD) energy conversion. The concept of nuclear-driven MHD energy conversion utilizes a flow seeded with a neutron absorbing species. The energy released in neutron absorption or fission processes is used to ionize the flow and enhance electrical conductivity. Research into the use of He-3/He-4 mixtures in the 1960's and 1970's suggested the enhancement is insufficient for MHD purposes. However, new calculations suggest a region of conditions not previously considered may provide significant conductivity enhancement. Specifically, at densities less than standard atmospheric density and neutron flux greater than 1 x 10(exp 12)/cm(exp 2) s, conductivity greater than 10 mho/m may be achievable. These calculations also suggest conductivity's of several hundred mho/m may be possible for an achievable range of conditions. Additionally, the nuclear-induced conductivity is strongly density dependent and weakly temperature dependent. Therefore, higher flow velocities and hence higher power densities than those used in traditional MHD channels utilizing thermal ionization are possible. In order to confirm these promising calculations, a series of experiments has been proposed. DOE

N95-17367 Oak Ridge National Lab., TN.
PROSPECTS FOR TOROIDAL FUSION REACTORS
J. Sheffield and J. D. Galambos 1994 6 p Presented at the 11th Topical Meeting on the Technology of Fusion Energy, New Orleans, LA, 19-24 Jun. 1994 Limited Reproducibility: More than 20% of this document may be affected by microfiche quality
(Contract DE-AC05-84OR-21400)
(DE94-014020; CONF-940630-12) Avail: CASI HC A02

Work on the International Thermonuclear Experimental Reactor (ITER) tokamak has refined understanding of the realities of a deuterium-tritium (D-T) burning magnetic fusion reactor. An ITER-like tokamak reactor using ITER costs and performance would lead to a cost of electricity (COE) of about 130 mills/kWh. Advanced tokamak physics to be tested in the Toroidal Physics Experiment (TPX), coupled with moderate components in engineering, technology, and unit costs, should lead to a COE comparable with best existing fission systems around 60 mills/kWh. However, a larger unit size, approximately 2000 MW(e), is favored for the fusion system. Alternative toroidal configurations to the conventional tokamak, such as the stellarator, reversed-field pinch, and field-reversed configuration, offer some potential advantage, but are less well developed, and have their own challenges. DOE

N95-17382# Naval Research Lab., Washington, DC. Plasma Physics Div.
TRANSPORT EFFICIENCY STUDIES FOR LIGHT-ION INERTIAL CONFINEMENT FUSION Interim Report
D. V. Rose (JAYCOR, Vienna, VA.), P. F. Ottinger, and C. L. Olson (Sandia National Labs., Albuquerque, NM.) 30 Sep. 1994 51 p
(Contract DE-AC04-94AL-85000)
(AD-A285675; NRL/MR/6770-94-7609; SNL-FAO-AI-7233) Avail: CASI HC A04/MF A01

The proposed Laboratory Microfusion Facility (LMF) will require greater than or equal to 10 MJ of 30 MeV lithium ions to be transported and focused onto high-gain, high-yield inertial confinement fusion targets. The light-ion LMF approach used a multimodular system with individual ion extraction diodes as beam sources. Several transport schemes are being considered to deliver the individual ion beams to the centrally located target. Previous work P.F. Ottinger, D.V. Rose, and C.L. Olson, J. Appl. Phys. 75, 4402 (1994) examined the effect of time-of-flight bunching on energy transport efficiency, eta sub t, under realistic constraints on diode operation, beam transport, and packing. Target design considerations suggest that the instantaneous power efficiency, gamma sub t, be maximized near peak power. Because of time-of-flight bunching, peak power occurs at the

end of the power pulse for LMF designs. This work examines the effect of power efficiency tuning on eta sub t for three transport schemes. Results indicate that tuning the power pulse to maximize eta sub t, at about three-quarters through the pulse provides high power efficiency at the end of the pulse while still maintaining high eta sub t. In addition to power efficiency tuning, effects on eta sub t from variations of the diode impedance model and the diode voltage waveform are also examined. DTIC

N95-17442 Air Force Inst. of Tech., Wright-Patterson AFB, OH. School of Engineering.
THERMAL CHARACTERISTICS AND HEAT TRANSFER IN AN ELECTROTHERMAL LIGHT GAS GUN M.S. Thesis
R. J. Tegtmeyer 1994 215 p Limited Reproducibility: More than 20% of this document may be affected by microfiche quality
(AD-A281980; AFIT/CI/CIA-94-086) Avail: Issuing Activity (Defense Technical Information Center (DTIC))

In the electrothermal gun concept, the high enthalpy, low molecular weight, and high relative sound speed of a hot hydrogen plasma is used to impart high velocities to projectiles. While the plasma accelerates the projectile out of the gun barrel, it also transfers heat energy to the barrel walls and suffers from viscous dissipation. This thesis calculates the radiative, convective and conductive heat transfer processes and viscous effects. A study of plasma opacity is also presented, showing the gas in the barrel to be optically thick in most operating regimes, thus allowing the use of Rosseland diffusion theory. Finally, the overall energy loss is determined and a comparison of results to MACH 2 computer code presented. DTIC

N95-17497# General Atomics Co., San Diego, CA.
D3-D RESEARCH OPERATIONS Annual Report
R. J. LaHaye, ed. May 1994 130 p Prepared for Oak Ridge National Lab., TN
(Contracts DE-AC03-89ER-51114; DE-AC05-84OR-21400; W-7405-eng-48) (DE94-014934; GA-A-21645) Avail: CASI HC A07/MF A02

The DIII-D tokamak research program is carried out by General Atomics (GA) for the U.S. Department of Energy (DOE). The DIII-D is the most flexible tokamak in the world. The primary goal of the DIII-D tokamak research program is to provide data to develop a conceptual physics blueprint for a commercially attractive electrical demonstration plant (DEMO) that would open a path to fusion power commercialization. In doing so, the DIII-D program provides physics and technology R&D outputs to aid the Tokamak Physics Experiment (TPX) and the International Thermonuclear Experimental Reactor (ITER). Specific DIII-D objectives include the steady-state sustainment of plasma current as well as demonstrating techniques for microwave heating, divertor heat removal, fuel exhaust and tokamak plasma control. The DIII-D program is addressing these objectives in an integrated fashion with high beta and with good confinement. The long-range plan is organized into two major thrusts; the development of an advanced divertor and the development of advanced tokamak concepts. These two thrusts have a common goal: an improved DEMO reactor with lower cost and smaller size than the present DEMO which can be extrapolated from the conventional ITER operational scenario. In order to prepare for the long-range program, in FY93 the DIII-D research program concentrated on three major areas: Divertor and Boundary Physics, Advanced Tokamak Studies, and Tokamak Physics. The major goals of the Divertor and Boundary Physics studies are the control of impurities, efficient heat removal and understanding the strong role that the edge plasma plays in the global energy confinement of the plasma. The advanced tokamak studies initiated the investigation into new techniques for improving energy confinement, controlling particle fueling and increasing plasma beta. The major goal of the Tokamak Physics Studies is the understanding of energy and particle transport in a reactor relevant plasma. DOE

N95-17517# Australian Inst. of Nuclear Science and Engineering, Lucas Heights (Australia).
AINSE PLASMA SCIENCE AND TECHNOLOGY CONFERENCE AND ELIZABETH AND FREDERICK WHITE WORKSHOP ON FUNDAMENTAL PROBLEMS IN THE PHYSICS OF MAGNETICALLY CONFINED PLASMAS: CONFERENCE HANDBOOK
1993 80 p Conference and workshop were held in Canberra, Australia, 12-15 Jul. 1993
(DE94-622051; INIS-mf-13853; CONF-9307177) Avail: CASI HC A05/MF A01 (US Sales Only)

The handbook contains abstracts of papers and posters presented at the conference. The main topics relate to plasma physics and fusion, plasma processing and uses as well as specific fusion devices and experiments. Eighty-four out of ninety-two presentations were considered to be in the INIS subject scope and have been separately indexed. DOE

N95-17623 Science Research Lab., Inc., Somerville, MA.
MULTI-BEAM LASER INTERFEROMETER FOR PLASMA DENSITY MEASUREMENTS IN A PLASMA EROSION OPENING SWITCH (PEOS) Technical Report, 25 Aug. 1992 - 30 Nov. 1993
Stephen F. Fulghum 1 Jul. 1994 97 p Limited Reproducibility: More than 20% of this document may be affected by microfiche quality
(Contract DNA001-92-C-0098)
(AD-A283209; SRL-11-F-1993; DNA-TR-93-147) Avail: CASI HC A05

Science Research Laboratory has designed and fabricated a wide-bandwidth, highly sensitive, optical diagnostic for the simultaneous measurement of electron density and neutral gas density in plasma opening switches. The system uses two Mach-Zehnder interferometers, installed on a common support structure, to probe the refractive index of the plasma at 532 nm and 1064 nm along a common, 1-meter line-of-sight. Measurements at two wavelengths permit the effects of free electrons to be deconvolved from the effects of neutral gas species. The diagnostic is sensitive to fringe shifts of from 2 x 10(exp -5) waves to 0.2 waves at bandwidths of up to 100 MHz. This allows the measurement of electron density path integrals from 5 x 10(exp 12)/sq cm to 5 x 10(exp 16)/sq cm with risetimes below 5 ns. The completed system was installed and tested on the HAWK facility at the Naval Research Laboratory in September 1993. Data is presented on the temporal history of the electron and neutral density path integrals in HAWK. DTIC

N95-17640 General Atomics Co., San Diego, CA.
EFFECT OF LOW DENSITY H-MODE OPERATION ON EDGE AND DIVERTOR PLASMA PARAMETERS
R. Maingi (Oak Ridge Associated Universities, Inc., TN.), P. K. Mioduszewski (Oak Ridge National Lab., TN.), J. W. Cuthbertson (Sandia National Labs., Albuquerque, NM.), D. N. Hill (Lawrence Livermore National Lab., Livermore, CA.), D. L. Hillis (Oak Ridge National Lab., TN.), J. T. Hogan (Oak Ridge National Lab., TN.), C. C. Klepper (Oak Ridge National Lab., TN.), C. J. Lasnier (Lawrence Livermore National Lab., Livermore, CA.), D. K. Lee (Oak Ridge National Lab., TN.), and A. W. Leonard (California Univ., Los Angeles, CA.) et al Jul. 1994 18 p Presented at the 11th International Conference on Plasma Surface Interactions in Controlled Fusion Devices, Mito, Japan, 23-27 May 1994 Limited Reproducibility: More than 20% of this document may be affected by microfiche quality
(Contracts DE-AC03-89ER-51114; DE-AC05-84OR-21400; W-7405-eng-48) (DE94-016521; GA-A-21705; CONF-940580-10) Avail: CASI HC A03

We present a study of the impact of H-mode operation at low density on divertor plasma parameters on the D3-D tokamak. The line-average density in H-mode was scanned by variation of the particle exhaust rate, using the recently installed divertor cryo-condensation pump. The maximum decrease (50 percent) in line-average electron density was accompanied by a factor of 2 increase in the edge electron temperature, and 10 percent and 20 percent reductions in the measured core and divertor radiated power, respectively. The measured total power to the inboard divertor target increased by a factor of 3, with the major contribution coming from a factor of 5 increase in the peak heat flux very close to the inner strike point. The measured increase in power at the inboard divertor target was approximately equal to the measured decrease in core and divertor radiation. DOE

N95-17643 Wisconsin Univ., Madison, WI. Plasma Physics Research.
FLUCTUATION MEASUREMENTS AT c/(OMEGA)(SUB pe) SPATIAL SCALES IN A TOKAMAK
E. J. Haines, I. H. Tan, and S. C. Prager Jul. 1994 34 p Limited Reproducibility: More than 20% of this document may be affected by microfiche quality
(Contract DE-FG02-85ER-53198)
(DE94-016771; DOE/ER-53198/243) Avail: CASI HC A03

Magnetic and electrostatic fluctuations have been measured at the short scale length of the collisionless skin depth (c/(omega)(sub pe) using small magnetic and electrostatic probes in the Tokapole 2 tokamak. For certain conditions and at high frequency (MHz range) the amplitude is observed

to increase as wavelength is decreased toward the c/(omega)(sub pe) scale. Wavelength dependence is inferred from measurements with probes of varying sizes. The amplitude of the turbulence at the c/(omega)(sub pe) scale is smaller than the dominant low frequency turbulence, and is thus not relevant to transport in Tokapole 2. Comparison with theoretical treatments of c/(omega)(sub pe) turbulence is discussed. DOE

N95-17644 New York Univ., New York, NY. Inst. of Mathematical Sciences.

GLOBAL CONFINEMENT ANALYSIS

K. S. Riedel 22 Jul. 1994 5 p Limited Reproducibility: More than 20% of this document may be affected by microfiche quality

(Contract DE-FG02-92ER-54157)

(DE94-016820; DOE/ER-54157/3) Avail: CASI HC A01

A brief description of the task: (1) Analyze confinement databases to development predictions for ITER, and identify and quantify major sources of confinement uncertainty; (2) Determine the parametric dependencies of the temperature and density profiles for reactor relevant plasmas. DOE

N95-17674# Oak Ridge National Lab., TN.

ITER DESIGN: PHYSICS BASIS FOR SIZE, CONFINEMENT CAPABILITY POWER LEVELS AND BURN CONTROL

N. A. Uckan, J. Hogan, W. Houlberg, J. Galambos, L. J. Perkins (Lawrence Livermore National Lab., Livermore, CA.), S. Haney (Lawrence Livermore National Lab., Livermore, CA.), D. Post (Princeton Univ., NJ.), and S. Kaye (Princeton Univ., NJ.) 1994 4 p Presented at the 11th Topical Meeting on the Technology of Fusion Energy, New Orleans, LA, 19-24 Jun. 1994

(Contract DE-AC05-84OR-21400)

(DE94-018041; CONF-940630-46) Avail: CASI HC A01/MF A01

The ITER-EDA(93) design has been analyzed to evaluate the physics basis for: (1) size and design trade-off issues; (2) confinement capability; (3) power levels; and (4) burn control. DOE

N95-17677# Oak Ridge National Lab., TN.

MEASUREMENTS AND MODELING OF IMPURITY SOURCE DISTRIBUTIONS FROM THE TORE SUPRA OUTBOARD PUMP LIMITER

C. C. Klepper, J. T. Hogan, S. J. Tobin, R. C. Isler, D. Guilhem (Association Euratom-CEA, Saint Paul-les-Durance, France.), W. R. Hess (Association Euratom-CEA, Saint Paul-les-Durance, France.), and P. Monier-Garbet (Association Euratom-CEA, Saint Paul-les-Durance, France.) 1994 15 p Presented at the 11th International Conference on Plasma Surface Interactions in Controlled Fusion Devices, Mito, Japan, 23-27 May 1994

(Contract DE-AC05-84OR-21400)

(DE94-018049; CONF-940580-16) Avail: CASI HC A03/MF A01

An experiment has been carried out to study impurity generation processes on an inertial limiter on Tore Supra. It is part of a plan to assemble a more detailed integrated picture of impurity generation at the inner wall, the outboard and vertical pump limiters, and the heating and current drive antennas. A system has been implemented to permit quantitative measurement of impurity sources from the outboard limiter in Tore Supra. Data are presented for a representative case in which the limiter is isolated as much as possible from connection with other Tore Supra plasma-facing components. The data are compared with results from the Monte-Carlo SOL impurity transport code BBQ, in an attempt to identify the mechanism for impurity release. Evidence of chemical sputtering as an important impurity source is seen. DOE

N95-17896# General Atomics Co., San Diego, CA.

TWO PHASE LIQUID HELIUM FLOW TESTING TO SIMULATE THE OPERATION OF A CRYOCONDENSATION PUMP IN THE D3-D TOKAMAK

G. J. Laughon, C. B. Baxi, G. L. Campbell, M. A. Mahdavi, C. C. Makariou, J. P. Smith, M. J. Schaffer, K. M. Schaubel, and M. M. Menon (Oak Ridge National Lab., TN.) Jun. 1994 4 p Presented at the 15th International Cryogenic Engineering Conference, Genoa, Italy, 7-10 Jun. 1994

(Contracts DE-AC03-89ER-51114; DE-AC05-84OR-21400)

(DE94-018345; GA-A-21735; CONF-940615-3) Avail: CASI HC A01/MF A01

A liquid helium-cooled cryocondensation pump has been installed in the D3-D tokamak fusion energy research experiment at General Atomics. The pump is located within the tokamak vacuum chamber beneath the divertor baffle plates and is utilized for plasma density and contamination control. Two-phase helium flows through the pump at 5 to 10 g/s utilizing the heat transfer and constant temperature characteristics of boiling liquid . helium. The pump is designed for a pumping speed of 32,000 1/s. Extensive testing was performed with a prototypical pump test fixture. Several pump geometries (simple tube, coaxial flow plug, and coaxial slotted insert) were tested, in an iterative process, to determine which was the most satisfactory for stable cryocondensation pumping. Results from the different tests illustrating the temperature distribution and flow characteristics for each configuration are presented. DOE

N95-17897# General Atomics Co., San Diego, CA.

MEASUREMENTS OF NON-AXISYMMETRIC EFFECTS IN THE D3-D DIVERTOR

T. E Evans,, A. W. Leonard, T. W. Petrie, M. J. Schaffer, C. J. Lasnier (Lawrence Livermore National Lab., Livermore, CA.), D. N. Hill (Lawrence Livermore National Lab., Livermore, CA.), and M. E. Fenstermacher (Lawrence Livermore National Lab., Livermore, CA.) Jul. 1994 16 p Presented at the 11th International Conference on Plasma Surface Interactions in Controlled Fusion Devices, Mito, Japan, 23-27 May 1994

(Contracts DE-AC03-89ER-51114; DE-AC05-84OR-21400; W-7405-eng-48)

(DE94-018346; GA-A-21707; CONF-940580-17) Avail: CASI HC A03/MF A01

Non-stationary toroidal asymmetries are observed in the D3-D divertor heat flux and scrape-off lay er (SOL) currents. Using the present D3-D diagnostics asymmetries are seen much less frequently in single-null H-modes (less than 5 percent) than in double-null H-modes (greater than 5 percent). Divertor heat flux asymmetries are characterized by toroidal variations in the radial profile (i.e., multiple or bifurcated peaks at some toroidal locations and single peaks at others) while SOL currents sometimes have a strongly bipolar toroidal structure. SOL current asymmetries are particularly large during Edge Localized Modes (ELM's). In some cases heat flux variations of as much as a factor of two are seen. The measurements reported here indicate that these asymmetries are best described by a model in which non-axisymmetric radial magnetic perturbations create magnetic islands in the plasma boundary and scrape-off layer which then cause toroidal variation in the divertor heat flux and the scrape-off layer currents. DOE

N95-17900# Argonne National Lab., IL.

PRODUCTION OF HIGH PROTON FRACTIONS FROM ECR SOURCES BY PLASMA MODIFICATION

D. Spence and C. L. Fink 1994 2 p Presented at the 17th International LINAC Conference, Tsukuba, Japan, 21-26 Aug. 1994

(Contract W-31-109-eng-38)

(DE94-018381; ANL/TD/CP-83977; CONF-9408125-15) Avail: CASI HC A01/MF A01

A program has been initiated to increase the proton fractions extracted from ECR sources by modifying the atom concentration in the source using minor additives to the plasma. A progress report is given. DOE

N95-17907# Oak Ridge National Lab., TN.

STATUS OF THE US STELLARATOR REACTOR STUDY

J. F. Lyon, K. Gulec (Tennessee Univ., Knoxville, TN.), R. L. Miller (Los Alamos National Lab., NM.), and L. El-Guebaly (Wisconsin Univ., Madison, WI.) 1994 17 p Presented at the International Atomic Energy Agency (IAEA) Meeting on Fusion Reactor Design and Technology, Los Angeles, CA, 13-17 Sep. 1993

(Contract DE-AC05-84OR-21400)

(DE94-018693; CONF-9309274-3) Avail: CASI HC A03/MF A01

Stellarators have significant operational advantages over tokamaks as ignited steady-state reactors. This scoping study, which uses an integrated cost-minimization code that incorporates costing and reactor component models self-consistently with a 1-D energy transport calculation, shows that a torsatron reactor could also be competitive with a tokamak reactor. The projected cost of electricity (COE) estimated using the ARIES costing algorithms is 62.5 mill/kW(e)h in constant 1992 dollars for a 1-GW(e) Compact Torsatron reactor reference case. The COE is relatively insensitive (less than 10 percent variation) over a wide range of assumptions including variations in the maximum field allowed on the coils, the coil elongation, the shape of the density profile, the beta limit, the confinement multiplier,

and the presence of a large loss region for alpha particles. The largest variations in the COE occur for variations in the electrical power output demanded and the plasma-coil separation ratio. DOE

N95-17929# Helsinki Univ. of Technology, Espoo (Finland). Nuclear Engineering Lab.
INVESTIGATION OF THE EFFECT OF ALFVEN RESONANCE ABSORPTION ON FAST WAVE CURRENT DRIVE IN ITER
M. J. Alava, J. A. Heikkinen, and T. Hellsten (Royal Inst. of Tech., Stockholm, Sweden.) 1994 21 p
(PB95-104352; TKK-F-A717) Avail: CASI HC A03/MF A01

The use of frequencies below the ion cyclotron frequency of minority ion species or second harmonic of majority species has been proposed for fast wave current drive in order to reduce or to avoid ion cyclotron damping. For these scenarios, the Alfven resonance can appear on the high field side of a tokamak. The presence of this resonance causes parasitic absorption competing with the electron Landau damping and transit time magnetic pumping responsible for the fast wave current drive. In the present study, the mode conversion at the Alfven resonance is shown to be of the order of 5 to 10 percent in the current drive scenarios for the planned International Thermonuclear Experimental Reactor (ITER) experiment. However, if the single pass absorption in the center can be made sufficiently high, the conversion at the Alfven resonance becomes negligible. NTIS

76 SOLID-STATE PHYSICS

Includes superconductivity.

For related information, see also *33 Electronics and Electrical Engineering* and *36 Lasers and Masers.*

N95-15942# Sandia National Labs., Albuquerque, NM.
CRYSTALLINE SILICON PROCESSING
P. A. Basore 13 Jul. 1994 15 p Presented at the 1994 Photovoltaic Systems Workshop, Albuquerque, NM, 13 Jul. 1994
(Contract DE-AC04-94AL-85000)
(DE94-016552; SAND-94-1898C; CONF-9407110-1) Avail: CASI HC A03/MF A01

This presentation (consisting of vugraphs) first provides the background motivation for Sandia's effort for the development of improved crystalline silicon solar cells. It then discusses specific results and progress, and concludes with a brief discussion of options for next year. DOE

N95-16012# Massachusetts Inst. of Tech., Cambridge. Research Lab. of Electronics.
SURFACE AND DEFECT EXCITATIONS IN COVALENTLY BONDED SOLIDS Final Report, 1 Feb. 1990 - 28 Feb. 1994
John Joannopoulos 29 Jun. 1994 170 p
(Contract N00014-90-J-1370)
(AD-A281338) Avail: CASI HC A08/MF A02

Research completed during the period 1 Feb. 1990 - 28 Feb. 1994 is summarized in the following included papers: 'Ab Initio Statistical Mechanics of Structural Phase Transition'; 'Ab Initio Molecular Dynamics: Analytically Continued Energy Functionals and Insights into Iterative Solutions'; 'Ab Initio Theory of the Si(111)-(7x7) Surface Reconstruction: A Challenge for Massively Parallel Computation'; 'Hardness and Softness in the Ab Initio Study of Polyatomic Systems'; 'Tip-Surface Interactions in Scanning Tunneling Microscopy'; 'Wavelets in Electronic Structure Calculations'; 'Oxygen Complexes in Silicon'; 'Ab Initio Molecular-Dynamics Techniques Extended to Large-Length-Scale Systems'; 'Oxygen-Induced Broken-Bond Defect in Silicon'; 'Mixed-Basis Pseudopotential Method Applied to Iterative Diagonalization Techniques'; 'Scanning-Tunneling-Microscopy Signatures and Chemical Identifications of the (110) Surface of Si-doped GaAs'; 'Accurate Theoretical Analysis of Photonic Band-Gap Materials'; 'Chemical Softness and Impurity Segregation at Grain Boundaries'; 'Local Softness, Scanning Tunneling Microscopy, and Surface Reactivity'; and 'Iterative Minimization Techniques for Ab Initio Total-Energy Calculations: Molecular Dynamics and Conjugate Gradients'. CASI

N95-16043# Pittsburgh Univ., Pittsburgh, PA. Surface Science Center.
AN UNEXPECTED ADSORPTION SITE EXCLUSION PROCESS ON Si(100)-(2x1) Annual Report, 1 Jun. 1993 - 31 May 1994
John T. Yates, Jr. 5 Aug. 1994 6 p
(Contract F49620-93-1-0341)
(AD-A284950; AFOSR-94-0551TR) Avail: CASI HC A02/MF A01

STM studies are being carried out on Si(100)-(2x1) single crystal surfaces to understand the statistical site distribution of H atoms and Cl atoms. Procedures for producing the clean Si(100) surface with wide terraces have been devised, and preliminary studies have been carried out using three other measurement techniques. DTIC

N95-16081 North Carolina Univ., Charlotte, NC.
INTERNATIONAL WORKSHOP ON LIGHT EMISSION AND ELECTRONIC PROPERTIES OF NANOSCALE SILICON Final Report, 25 Jan. 1993 - 24 Jan. 1994
Raphael Tsu Apr. 1994 95 p Workshop held in Charlotte, NC, 1-3 Feb. 1993 Limited Reproducibility: More than 20% of this document may be affected by microfiche quality
(Contract DAAH04-93-G-0058)
(AD-A281464; ARO-30955.1-EL-CF) Avail: Issuing Activity (Defense Technical Information Center (DTIC))

This workshop assembled significant recent research in electronic transport and luminescence in nanoscale silicon structures, together with a diverse selection of fabrication techniques, in order to begin to address the critical physics and fabrication issues in using this exciting new material for optoelectronic applications. DTIC

N95-16084 North Carolina State Univ., Raleigh, NC.
INTERFACE PROPERTIES OF WIDE BANDGAP SEMICONDUCTOR STRUCTURES Semiannual Technical Report, 1 Jan. - 30 Jun. 1994
Robert F. Davis, Salah Bedair, Jerry Bernholc, Jeffrey T. Glass, and R. J. Nemanich Jun. 1994 63 p Limited Reproducibility: More than 20% of this document may be affected by microfiche quality
(Contract N00014-92-J-1477)
(AD-A281469) Avail: CASI HC A04

The structure and electronic properties of 1x1 and 2x1 H-terminated and clean C(100)2x1 surfaces have been calculated with ab initio molecular dynamics. A negative electron affinity was found for these surfaces; a positive electron affinity was found for the C(100) surface. In related growth calculations for ALE of diamond, the desorption of the HF molecule was found to be critical for H- and F-based growth mechanisms. Ni3Si and Ni substrates were compared for the deposition of diamond films under the same conditions. Diamond (C) particles were obtained on the Ni3Si, but only diamond-like C and graphite on the latter. C films deposited on via CVD. Field emission showed very high stability as well as high current densities. Step bunching occurred at the outset of the initial stage of SiC growth using C2H4Si2H6 ratios of 1, 2 or 10 and gas source (GS) MBE. Subsequent growth occurred via island formation (C2H4-rich) or step-flow (1:1 ratio). Beta-SiC or 6H-SiC deposited using high or 1:1 C/Si ratios, respectively. DTIC

N95-16106 Oregon Univ., Eugene, OR. Inst. of Theoretical Science.
[ELECTRON TRANSPORT AND TUNNELING EXPERIMENTS] Final Technical Report
James M. Valles, Jr. 7 Oct. 1993 19 p Limited Reproducibility: More than 20% of this document may be affected by microfiche quality
(Contract N00014-92-J-1344)
(AD-A281527) Avail: Issuing Activity (Defense Technical Information Center (DTIC))

This final technical report describes the results of electron transport and tunneling experiments on high sheet resistance ultrathin normal metal and superconducting films. DTIC

N95-16111# Carnegie-Mellon Univ., Pittsburgh, PA.
WORKSHOP ON EPITAXY, INTERFACES, DEFECTS AND PROCESSING OF ELECTRONIC AND PHOTONIC MATERIALS Final Report, 16 Sep. 1991 - 14 Sep. 1992
S. Mahajan 11 May 1994 9 p
(Contract DAAL03-91-G-0332)
(AD-A281595; ARO-29614.1-MS-CF) Avail: CASI HC A02/MF A01

A Workshop on 'Epitaxy, Interfaces, Defects, and Processing of Electronic

and Photonic Materials' was held in Pittsburgh, 4-7 November 1991. The following three topic areas were discussed in detail: fundamental aspects of two- and three-dimensional epitaxial growth, especially during heteroepitaxy involving misfits, and generation of defects; atomic structure of interfaces and defects; and growth and processing of electronic and photonic materials using novel concepts. Scientific issues were delineated and approaches or techniques to address these issues were also discussed in detail. DTIC

N95-16114# North Carolina Agricultural and Technical State Univ., Greensboro, NC. Dept. of Electrical Engineering.
LPEE GROWTH AND CHARACTERIZATION OF In(x)Ga(1-x)As(y)Sb(1 y) LATTICE MATCHED TO GaSb AND InAs FOR PHOTODETECTORS Final Report, 15 Sep. 1989 - 31 Oct. 1993
Shanthi N. Iyer and Ali A. Fadl Jun. 1994 111 p
(Contract DAAL03-89-G-0115)
(AD-A281631) Avail: CASI HC A06/MF A02

The optical characteristics of liquid phase electroepitaxial (LPEE) grown undoped and doped GaSb and GaInAsSb epilayers of different compositions were the subject of detailed investigations. The temperature and intensity dependences of the low temperature photoluminescence (PL) spectra of these alloys were studied as a function of the alloy compositions to determine the nature of the recombination processes. In Te-doped GaSb epilayers, the PL spectra become increasingly complicated due to the presence of additional transitions associated with deeper acceptor levels. A systematic and quantitative evaluation of the effects of compensation in GaSb has been examined as a function of Te concentration in the layers and growth temperature, under both low and high excitation conditions. Photoreflectance spectroscopy has been assembled for the characterization of semiconductor band structure and surface. Electrical transport characteristics of Au-n-GaSb Schottky diodes were investigated on the LPEE grown epilayers as a function of the growth temperature of the grown layers. Well behaved p-n homojunctions with forward onset voltage of 0.5 V were fabricated on LPEE grown GaSb layers by Zn diffusion in an open tube configuration. The room temperature electrical characteristics of these junctions were studied in detail. DTIC

N95-16134# Auburn Univ., AL. Dept. of Materials Engineering.
SINGLE CRYSTAL FILMS AND WAVEGUIDES OF ORGANIC MATERIALS: PREPARATION AND NONLINEAR OPTICAL PROPERTIES Annual Report, 1 Apr. 1993 - 31 Mar. 1994
Mrinal Thakur 31 Mar. 1994 5 p
(Contract F49620-93-1-0216)
(AD-A284471; AFOSR-94-0506TR) Avail: CASI HC A01/MF A01

The objective of this program is to establish a generic method for the growth of thin single crystal films of important organic nonlinear optical materials and measurement of their nonlinear optical properties. Through the last year's effort we have successfully prepared single crystal films of three organic materials which are: (1) (N-(4-Nitrophenyl)-L-prolinol) abbreviated as NPP, (2) 2-cyclooctylamino- 5-nitropyridine, abbreviated as COANP, and (3) 4'-N, N-dimethylamino- 4-N-methylstilbazolium toluene-p-sulfonate, abbreviated as DAST. These materials have very large second order susceptibilities. Both NPP and COANP have an amphiphillic molecular structure, while DAST is an organic molecular salt. The single crystal films were prepared by a method called the shear method, with appropriate choice of the growth conditions. The shear method involves crystal growth at an interface and was originally applied to the growth of polydiacetylene films. Our results show that using the principles involved in the shear method, if the growth conditions are properly optimized for each compound, then molecules other than diacetylene are possible to organize as single crystal films. The only major condition that needs to be satisfied for this method to be applicable is that the molecule must be of an elongated shape with polar chemical groups at one or both ends. DTIC

N95-16158# Arizona State Univ., Tempe, AZ. Center for Solid State Electronics Research.
QUANTUM TRANSPORT IN SEMICONDUCTOR DEVICES Final Report
David K. Ferry 30 Jun. 1994 19 p
(Contract DAAL03-91-G-0067)
(AD-A281383; ARO-28461.11-EL) Avail: CASI HC A03/MF A01

This program concentrated on research investigating quantum effects which become important in ultra-small semiconductor devices, and the manner in which these effects may limit downscaling of individual feature sizes. The major concentrations of the program were on: (1) tunneling-in gated semiconductor structures, an effect which has been found to be important in normal high-electron mobility transistors (HEMT's) with gate lengths of less than or equal to 0.025 micrometer; (2) the role played by slab and interface phonon modes in transport within small semiconductor devices; and (3) modeling of quantum effects in MESFET devices as a general tool for approaching the inclusion of such effects in dynamic semiconductor device models. DTIC

N95-16238 Georgia Univ., Athens. Dept. of Chemistry.
PREPARATION OF Au SINGLE CRYSTALS FOR STUDY OF THE ECALE DEPOSITION OF CdTe Technical Report No. 15
Laura B. Goetting, Baoming M. Huang, Tedd E. Lister, and John L. Stickney 25 Jun. 1994 49 p Limited Reproducibility: More than 20% of this document may be affected by microfiche quality
(Contract N00014-91-J-1919)
(AD-A282294) Avail: Issuing Activity (Defense Technical Information Center (DTIC))

A sequence of questions concerning the preparation of atomically flat Au surfaces is addressed. In addition, the formation of a 1/2 monolayer Te adlayer of a Au(100) is discussed. The 1/2 coverage of Au(100)-Te surface is desired as a first step in the electrodeposition of CdTe by the ECALE methodology. The use of oxidation/reduction cycles (ORC's) to clean the Au(100) surface is shown to be counterproductive, if atomically flat planes are also desired. Roughening results from the ORC's as the surface reconstructs at low potentials, then unreconstructs at high potentials. The reconstructed surface contains excess surface atoms, such that upon lifting of the reconstruction, monoatomically high Au islands are formed on the surface. It is also shown that treatment in a mM I(-) solution results in the formation of ordered iodine adlattices on each of the low index planes. In addition, electrochemical annealing is facilitated, resulting in removal of previously formed Au islands, and formation of large, atomically flat terraces. Te can be deposited directly on these I coated surfaces, displacing the I and forming thin films of bulk Te. The excess, bulk Te can then be removed either reductively or oxidatively to form ordered atomic layers of Te with coverages near 1/2. DTIC

N95-16311# Sandia National Labs., Albuquerque, NM.
RELIABILITY IMPLICATIONS OF DEFECTS IN HIGH TEMPERATURE ANNEALED Si/SiO2/Si STRUCTURES
W. L. Warren, D. M. Fleetwood, M. R. Shaneyfelt, P. S. Winokur, R. A. B. Devine (Centre National d'Etudes des Telecommunications, Meylan, France.), D. Mathiot (Centre National d'Etudes des Telecommunications, Meylan, France.), I. H. Wilson (Chinese Univ. of Hong Kong, Shatin.), and J. B. Xu (Chinese Univ. of Hong Kong, Shatin.) 1994 10 p Presented at the Spring Meeting of the Materials Research Society, San Francisco, CA, 4-8 Apr. 1994
(Contract DE-AC04-94AL-85000)
(DE94-015765; SAND-94-1726C; CONF-940411-44) Avail: CASI HC A02/MF A01

High-temperature post-oxidation annealing of poly-Si/SiO2/Si structures such as metal-oxide-semiconductor capacitors and metal-oxide-semiconductor field effect transistors is known to result in enhanced radiation sensitivity, increased 1/f noise, and low field breakdown. The authors have studied the origins of these effects from a spectroscopic standpoint using electron paramagnetic resonance (EPR) and atomic force microscopy. One result of high temperature annealing is the generation of three types of paramagnetic defect centers, two of which are associated with the oxide close to the Si/SiO2 interface (oxygen-vacancy centers) and the third with the bulk Si substrate (oxygen-related donors). In all three cases, the origin of the defects may be attributed to out-diffusion of O from the SiO2 network into the Si substrate with associated reduction of the oxide. The authors present a straightforward model for the interfacial region which assumes the driving force for O out-diffusion is the chemical potential difference of the O in the two phases SiO2 and the Si substrate). Experimental evidence is provided to show that enhanced hole trapping and interface-trap and border-trap generation in irradiated high-temperature annealed Si/SiO2/Si systems are all related either directly, or indirectly, to the presence of oxygen vacancies. DOE

N95-16359# EG and G Energy Measurements, Inc., Goleta, CA.
ELEMENTAL IMPURITY ANALYSIS OF MERCURIC IODIDE BY ICP/MS
E. S. Cross, E. Mroz (Los Alamos National Lab., NM.), and J. A. Olivares (Los Alamos National Lab., NM.) 1994 6 p Presented at the Pittsburgh Conference on Analytical Chemistry and Applied Spectroscopy, Chicago, IL, 1 Mar. 1994
(Contract DE-AC08-93NV-11265)
(DE94-013553; EGG-11265-2045; CONF-9403129-1) Avail: CASI HC A02/MF A01

A method has been developed to analyze mercuric iodide (HgI2) for elemental contamination using Inductively Coupled Plasma/Mass Spectroscopy (ICP/MS). This paper discusses the ICP/MS method, the effectiveness of purification schemes for removing impurities from HgI2, as well as preliminary correlations between HgI2 detector performance and elemental contamination levels. The purified HgI2 is grown into a single crystals by physical vapor transport. The crystals are cut into slices and they are fabricated into room temperature radiation detectors and photocells. Crystals that produce good resolution gamma detector do not necessarily make good resolution photocells or x-ray detectors. Many factors other than elemental impurities may contribute to these differences in performance. DOE

N95-16365# Hughes Research Labs., Malibu, CA.
MODIFICATION OF 2-6 AND 3-5 MATERIALS USING ION BEAMS Final Report, 1 Apr. 1991 - 31 May 1994
Roger G. Williams and O. K. Wu Jun. 1994 25 p
(Contract DAAL03-91-C-0001)
(AD-A281839; ARO-26708.9-EL) Avail: CASI HC A03/MF A01

A major part of this program involved characterization of 2-6 materials and device structures, primarily HgCdTe. The results of this research benefitted MBE growth of HgCdTe for infrared detector technology. The primary industry beneficiary of these results has been Santa Barbara Research Center (SBRC), but because of a collaborative agreement that began at the end of 1992 with Rockwell, their Science Center may also have benefitted. Both SBRC and Rockwell manufacture IR detector systems for the US government. The 3-5 work done on this program benefitted Hughes directly, and other industry through other ARO contracts and our joint publications. Also AT&T (Bell Labs/Pearton) and Hughes collaborate on programs like MMIC, in which 3-5 technology is used substantially. DTIC

N95-16385# Brookhaven National Lab., Upton, NY.
SCINTILLATION MECHANISM AND RADIATION DAMAGE IN Ce(x)La(1-x)F3 CRYSTALS
A. J. Wojtowicz (Purkyne Univ., Brno, Czechoslovakia.), D. Wisniewski (Purkyne Univ., Brno, Czechoslovakia.), A. Lempicki (Boston Univ., MA.), C. Brecher (Boston Univ., MA.), R. H. Bartram (Connecticut Univ., Storrs, CT.), C. Woody, and P. Levy 1994 7 p Presented at the Spring Meeting of the Materials Research Society, San Francisco, CA, 4-8 Apr. 1994
(Contracts DE-AC02-76CH-00016; DE-FG02-90ER-61033)
(DE94-015848; BNL-60593; CONF-940411-43) Avail: CASI HC A02/MF A01

Recent spectroscopic and radiation damage experiments on a series of Ce(x)La(1-x)F3 crystals suggest that the scintillation light output is limited by an unusual quenching mechanism, which also plays a major role in minimizing radiation-induced damage. The intensity of the radiation-induced absorptions is a strong function of the Ce content x, reaching a maximum for x = 0.03 and a minimum for x = 1. This peculiar dependence appears to be due to the influence of deep-lying Ce levels on both scintillation mechanism and radiation damage. The authors suggest that various charge transfer processes can explain many aspects of the performance of Ce(x)La(1-x)F3 scintillators. DOE

N95-16389# Los Alamos National Lab., NM.
NON-FERMI LIQUID SCALING IN UPd(x)Cu(5-x)(x = 1,1.5)
M. C. Aronson (Michigan Univ., Ann Arbor, MI.), R. Osborn (Argonne National Lab., IL.), R. A. Robinson, and J. W. Lynn (National Inst. of Standards and Technology, Gaithersburg, MD.) 28 Jun. 1994 9 p Presented at the International Conference on Strongly Correlated Electron Systems, Amsterdam, Netherlands, 15-18 Aug. 1994
(Contract W-7405-eng-36)
(DE94-016072; LA-UR-94-2272; CONF-940863-3) Avail: CASI HC A02/MF A01

We have determined the inelastic magnetic response S((omega)) of UPd(x)Cu(5-x) (X=1,1.5) for temperatures from 0.3 to 300 K and energies between 05 and 400 meV using the neutron time of flight technique. S((omega)) is virtually identical in the two compound, displaying marginal Fermi Liquid scaling over the entire range of temperatures, as well as scale invariant energetics. DOE

N95-16391 Virginia Univ., Charlottesville, VA. Dept. of Electrical Engineering.
MONTE CARLO SIMULATION OF MERCURY CADMIUM TELLURIDE Final Report, 1 Apr. 1991 - 31 May 1994
Michael Shur Jul. 1994 5 p Limited Reproducibility: More than 20% of this document may be affected by microfiche quality
(Contract DAAL03-91-G-0048)
(AD-A281546; ARO-28347.5-EL) Avail: CASI HC A01

Mercury cadmium telluride (MCT) has a very large electron mobility and exhibits a non-ohmic behavior in relatively small electric fields. The goal of this project was to reach the understanding of electron transport properties of narrow band gap semiconductors, with emphasis on high-field behavior. Even though the primary material of interest was MCT, we also investigated indium antimonide. Researchers derived expressions for scattering rates for electrons in MCT which accounted for correct wave functions for narrow band gap materials, and performed the Monte-Carlo simulation of Hg(0.205)Cd(0.795)Te at 77 K for different doping levels. DTIC

N95-16396 Minnesota Univ., Minneapolis, MN.
SEMICONDUCTOR HETEROJUNCTION ENGINEERING Final Report
A. Franciosi 4 Mar. 1994 8 p Limited Reproducibility: More than 20% of this document may be affected by microfiche quality
(Contract DAAL03-90-G-0001)
(AD-A281553; ARO-26761.12-EL) Avail: Issuing Activity (Defense Technical Information Center (DTIC))

The purpose of the research was to explore the microscopic mechanisms that determine interface parameters in semiconductor heterojunctions and develop new methods to tune such interface parameters. We found that while in most isovalent heterojunctions the interface parameters are primarily dependent on the properties of the bulk semiconductor constituents, in heterovalent heterojunctions with polar orientation the interface parameters can be controlled by modifying the local interface environment. Changes in the relative abundance of the different elemental constituents at the interface, for example, produced unprecedented changes in the band alignment across the interface. Even in isovalent heterojunctions, we succeeded in modifying the band offsets through fabrication of thin heterovalent interface layers within the interface region. The resulting system of inequivalent, neutral heterovalent interfaces can be used to control the band alignment across the overall structure. Among the systems of interest for which we have obtained unprecedented modifications of the interface parameters, we mention AlAs/GaAs, CdTe/GaAs, and ZnSe/GaAs heterostructures, all of which have important applications in optoelectronic devices ranging from lasers to light emitting diodes and photodetectors. DTIC

N95-16399# Department of the Navy, Washington, DC.
METHOD FOR INTRINSICALLY DOPED III-A AND V-A COMPOUNDS AND PRODUCTS THEREOF Patent Application
Mark E. Twigg, inventor (to Navy), Mohammad Fatemi, inventor (to Navy), and Brian Tadayon, inventor (to Navy) 12 Apr. 1994 17 p
(AD-D016324; US-Patent-Appl-SN-226586; Navy-Case-75507) Avail: CASI HC A03/MF A01

An amorphous compound is changed to single crystal structure by heating at an elevated temperature in an inert atmosphere or in an atmosphere of a forming gas. The amorphous compound is composed of at least one Group III-A element of the Periodic Table and at least on Group V-A element, the amorphous compound having an excess over stoichiometric amount of at least one Group V-A element. The single crystal phase compound, intrinsically doped with at least one element from Group V-A, has the properties of high conductivity for a semiconductor without using any extrinsic dopant and a non-alloyed ohmic contact with a metal. Author (DTIC)

N95-16408# Argonne National Lab., IL.
FLUX IMAGING OF HIGH TEMPERATURE SUPERCONDUCTOR SINGLE CRYSTALS AND Ag SHEATHED WIRES
G. W. Crabtree, U. Welp, T. A. Gardiner, B. W. Veal, J. Fendrich, and V. K. Vlasko-Vlasov (Academy of Sciences of the Ukraine, Kharkov.) May 1994 5 p Presented at the International Workshop on Superconductivity: Critical Current of High-Temperature Superconductors and Related Topics, Kyoto, Japan, 6-9 Jun. 1994
(Contract W-31-109-eng-38)
(DE94-013874; ANL/MSD/CP-83115; CONF-940651-5) Avail: CASI HC A01/MF A01

The flux imaging technique is described and examples of its use are given, including measuring the critical current anisotropy in single crystals, demonstrating instabilities of the interface between oppositely polarized regions of flux, and evaluating the performance of powder-in-tube wires. DOE

N95-16424# Siemens Solar Industries, Camarillo, CA.
PV CZ SILICON MANUFACTURING TECHNOLOGY IMPROVEMENTS
T. Jester Jun. 1994 14 p Prepared for Midwest Research Inst., Golden, CO
(Contract DE-AC36-83CH-10093)
(DE94-011818; NREL/TP-411-6634) Avail: CASI HC A03/MF A01

This report describes work performed under a 3-year contract to demonstrate signficant cost reductions and improvements in manufacturing technology. The work focused an near-term projects for implementation in the Siemens Solar Industries (SSI) Czochralski (CZ) manufacturing facility in Camarillo, California, and was undertaken to increase the commercial viability and volume of photovoltaic manufacturing by evaluating the most significant cost categories and then lowering the cost of each Rem through experimentation, materials refinement, and better industrial engineering. During this reporting period, several significant improvements were achieved. (1) The crystal-growing operation improved with an increase in growth capacity. Higher growing throughput was demonstrated with larger crucibles, higher polysilicon packing density, and higher pull speeds. (2) The operation was completely converted to wire-saw wafer processing. The wire saws yield over 40% more wafers per inch in production. The capacity improvement generated by wire saws increased overall manufacturing volume by more than 40% without additional expenses in crystal growth. (3) Cell processing improvements focused on better understanding of the contact paste and firing processes. (4) Module designs for lower material and labor costs began with the focus on a new junction box, larger modules with larger cells, and less costly framing technique. CFC usage was completely eliminated in the SSI manufacturing facility during this phase of the contract. DOE

N95-16445# Minnesota Univ., Minneapolis, MN. Dept. of Chemical Engineering and Materials Science.
ATOMIC FORCE MICROSCOPY OF THE ELECTROCHEMICAL NUCLEATION AND GROWTH OF MOLECULAR CRYSTALS Report, 1 May 1993 - 30 Jun. 1994
Andrew C. Miller and Michael D. Ward 30 Jun. 1994 2 p
(Contract N00014-93-1-0563)
(AD-A281024; TR-5) Avail: CASI HC A01/MF A01

The atomic force microscope (AFM) was employed to examine the nanoscale morphology, surface topography, and growth and dissolution characteristics of single crystals of a series of organic charge transfer salts, specifically those comprising the tetracyanoquinodimethane (TCNQ) acceptor and tetrathiafulvalene (TTF), tetramethyltetraselenafulvalene (TMTSF), and bis-(ethylenedithiolo)tetrathiafulvalene (BEDT-TTF) donors. The dynamics of electrocrystallization were studied in situ on specific exposed crystal faces of these salts while the supersaturation was controlled by the applied electrochemical potential. Results indicate that the growth modes and the distribution and orientation of topographic features can be correlated with the strength and direction of solid state intermolecular bonding. In general, the nanoscale topographic structure resembled the macroscopic morphology, suggesting self-similarity across the length scales examined. DTIC

N95-16498# Hughes Research Labs., Malibu, CA.
LIQUID CRYSTAL MATERIALS FOR LASER BEAM STEERING Final Report, Sep. 1992 - Aug. 1994
Shin-Tson Wu and J. D. Margerum Aug. 1994 18 p
(Contract F49620-92-C-0071)
(AD-A285089; AFOSR-94-0548TR) Avail: CASI HC A03/MF A01

Several new liquid crystal compounds have been developed for laser beam steering application. The asymmetric diakyl diphenyl-diacetylenes exhibit a low melting temperature, wide nematic range, high birefringence, low viscosity and small heat fusion enthalpy. They are excellent host materials for forming eutectic mixtures except for the small dielectric anisotropy. To enhance dielectric anisotropy, some polar diphenyl-diacetylenes and tolanes, and a new series of the nitro-azo-benzene dyes have been considered. Among these polar compounds, the nitro-azo-benzene dyes exhibit a mesogenic phase with melting temperature at about 80 deg C huge dielectric anisotropy, excellent solubility and relatively low viscosity. The solubility and viscosity of these dyes are about one order to an asymmetric diphenyl-diacetylene binary mixture reduces its threshold voltage from 3.5 to 1.7 V sub rms. Author (DTIC)

N95-16508# Minnesota Univ., Minneapolis, MN. Dept. of Chemical Engineering and Materials Science.
SNAPSHOTS OF CRYSTAL GROWTH: NANOCLUSTERS OF ORGANIC CONDUCTORS ON Au(111) SURFACES Technical Report No. 2, 1 May 1993 - 30 Jun. 1994
J. H. Schott and M. D. Ward 23 Jun. 1994 18 p
(Contract N00014-93-1-0563)
(AD-A280976; TR-2-ONR) Avail: CASI HC A03/MF A01

Mono- and multilayer crystalline nanoclusters of tetra-hiafulvalene-tetracyanoquinodimethane ((TTF) (TCNO)), a low-dimensional organic conductor in the bulk form, can be formed readily on Au(111) surfaces by vapor phase sublimation under ambient conditions. Scanning tunneling microscopy of monolayer (TTF)(TCNQ) films reveals a two-dimensional density of states (DOS) that is consistent with the arrangement of TTF and TCNO molecules in the ac face of bulk (TTF)(TCNO), in which the molecular planes are nearly parallel to the Au(111) substrate. In contrast, clusters with thicknesses corresponding to two or three molecular layers exhibit a transformation to a highly anisotropic DOS that can be attributed to interlayer molecular overlap in segregated TTF and TCNQ molecular chains along the c-axis, which can be described as 'molecular wires'. The orientation of the crystalline (TTF)(TCNO) clusters is preserved throughout the crystal growth sequence, leading to meso- and macroscopic (TTF)(TCNO) needles that are oriented perpendicular to the Au(111) substrate. These studies provide visualization of crystal growth from the initial stages of nucleation to macroscopic crystals, and a revealing example of the changes in electronic structure that occur during the evolution of molecular (TTF)(TCNQ) nuclei into a bulk crystalline phase. DTIC

N95-16510# Ames Lab., IA.
THE RELATIONSHIP OF STRUCTURE TO SUPERCONDUCTIVITY IN THE Pr-Ba-Cu-O SYSTEM Ph.D. Thesis
P. Minseo 10 May 1994 75 p
(Contract W-7405-eng-82)
(DE94-014231; IS-T-1707) Avail: CASI HC A04/MF A01

The relation of structure to lack of superconductivity in Pr-Ba-Cu-O was systematically investigated. First, the phase equilibria of this system was studied to find the processing parameters which maximize the cation-site ordering between Pr and Ba ions. Second, a comparative study between superconducting Nd-Ba-Cu-O and nonsuperconducting Pr-Ba-Cu-O was performed by forming solid-solution Nd-Pr-Ba-Cu-O. The relation between structure and superconductivity in Nd(1-x)Pr(x)Ba2Cu3O(7-delta) is investigated. T sub c decreases monotonically with increasing x and superconductivity disappears at around x = 0.3 to 0.4. T sub c is enhanced by 10 K when the sample is processed at an oxygen partial pressure (PO2) of 0.01 atm, followed by oxygenation at 450 C. Depression of T sub c as a function of x and PO2 is explained in terms of a charge-transfer model. It is suggested that destruction of superconductivity in the RE(1-x)Pr(x)Ba2Cu3O(7-delta) (RE=rare-earth) system can be viewed as disruption of four-fold planar coordinated Cu ions in the chain-site due to permanent occupation of extra Pr ions on Ba sites. DOE

N95-16525# Pennsylvania State Univ., University Park, PA. Dept. of Physics.
INNOVATIVE ACOUSTIC TECHNIQUES FOR STUDYING NEW MATERIALS AND NEW DEVELOPMENTS IN SOLID STATE PHYSICS
Summary Report, 1 Oct. 1993 - 31 May 1994
Julian D. Maynard 21 Jun. 1994 13 p
(Contracts N00014-92-J-1186; N00014-93-1-0779)
(AD-A280986) Avail: CASI HC A03/MF A01

The goals of this project involve the use of innovative acoustic techniques to study new materials and new developments in solid state physics. Major accomplishments include (a) the preparation and publication of a number of papers and book chapters, (b) the measurement and new analysis of more samples of aluminum quasicrystal and its cubic approximant to eliminate the possibility of sample artifacts, (c) the use of resonant ultrasound to measure acoustic attenuation and determine the effects of heat treatment on ceramics, (d) the extension of our technique for measuring even lower (possibly the lowest) infrared optical absorption coefficient, and (e) the measurement of the effects of disorder on the propagation of a nonlinear pulse, and (f) the observation of statistical effects in measurements of individual bond breaking events in fracture. DTIC

N95-16526# North Dakota State Univ., Fargo, ND.
LOW TEMPERATURE SYNTHESIS OF SEMICONDUCTOR MATERIALS
Annual Report, 15 Aug. 1992 - 14 Aug. 1993
Philip Boudjouk 14 Sep. 1993 13 p
(Contract F49620-92-J-0431)
(AD-A285230; AFOSR-94-0601TR) Avail: CASI HC A03/MF A01

The results of one year's effort to produce single source precursors that will generate high yields of semiconductor materials consisting of elements from groups 14 and 16 are summarized in this report. Laboratory studies demonstrate that compounds in which bonds between group 14 and 16 elements exist and in which remaining valences are occupied with phenyl groups are excellent sources of phase pure binary compounds such as tin sulfide, tin selenide and tin telluride. Mechanistic studies reveal that phenyl migration is the dominant reaction pathway allowing formation of the target compounds at temperatures as low as 300 deg C. DTIC

N95-16527# Case Western Reserve Univ., Cleveland, OH.
PSEUDOMORPHIC STABILIZATION OF DIAMOND ON NON-DIAMOND SUBSTRATES Final Report, 1 Mar. 1989 - 30 Apr. 1993
Alberto Argoitia, John C. Angus, Long Wang, and Walter R. Lambrecht 16 Sep. 1994 13 p
(Contract N00014-89-J-1631)
(AD-A285231) Avail: CASI HC A03/MF A01

First principles electronic structure calculations and high resolution transmission electron microscopy were used to study the interface of diamond with beryllium oxide (BeO) and cubic boron nitride (c-BN). These are the tetrahedrally coordinated, covalently bonded solids that are most closely lattice-matched to diamond. The theoretical results indicate that diamond should adhere strongly to both BeO and c-BN. Diamond deposited on the Be terminated (0001) surfaces of BeO by hot-filament assisted deposition showed local epitaxy of isolated diamond crystals. Parallel epitaxy of diamond films was achieved on the B terminated (111) surfaces of c-BN. DTIC

N95-16532# North Carolina State Univ., Raleigh, NC. Dept. of Materials Science and Engineering.
ATOMIC LAYER EPITAXY OF GROUP 4 MATERIALS: SURFACE PROCESSES, THIN FILMS, DEVICES AND THEIR CHARACTERIZATION
Semiannual Technical Report, 1 Jan. - 30 Jun. 1994
Robert F. Davis Jun. 1994 45 p
(Contract N00014-90-J-1427)
(AD-A280987) Avail: CASI HC A03/MF A01

The viability of Si2Cl6, C2H2 and C2H4 as precursors for chemically self-limiting ALE of SiC has been investigated via XPS and LEED. Si2Cl6 readily adsorbs in a self-limiting manner on a Si(100) surface; however, neither hydrocarbon will adsorb or react with a Cl-terminated Si surface to 475 deg C. Conversely, partial chlorination of Si(100) saturated with C2H2 and C2H4 does occur and implies that Si2Cl6 will adsorb/react with a hydrocarbon terminated surface. Layer-by-layer growth of Beta-SiC on Si(100) or 6H-SiC has been achieved with a carrier concentration of approx. 10(exp 17)/cu cm. P-type doping with Al has allowed the achievement of hole concentrations of 4 x 10(exp 18) - 2 10(exp 20)/cu cm. Efforts to produce an HBT using Beta-SiC emitters is described. Ni3Si has been employed for the deposition of diamond because of the close lattice match. Under the same growth conditions, diamond particles were obtained on the Ni3Si, but only diamond-like C and graphite on pure Ni substrates. Evidence of oriented particles was observed. REED and TEM of cerium oxide films grown on Si(111) substrates has revealed the formation of a dual amorphous layer of CeOx and SiO2 at the Si interface followed by a layer of CeO2. Post annealing in dry oxygen caused the CeOx layer to disappear and the SiO2 layer to thicken. D(sub it) = 6 x 10(exp 11)/sq cm and Q sub f = 5 x 10(exp 11)/sq cm. The structure exhibits a high capacitance due to the large dielectric constant of CeO2 and has electrical properties comparable with those of other reported gate insulators on Si. DTIC

N95-16533# North Carolina State Univ., Raleigh, NC. Dept. of Materials Science and Engineering.
NITRIDE SEMICONDUCTORS FOR ULTRAVIOLET DETECTION
Semiannual Technical Report, 1 Jan. 1994 - 30 Jun. 1994
R. F. Davis, K. Linthicum, B. Perry, C. Wang, and W. Weeks Jun. 1994 26 p
(Contract N00014-92-J-1720)
(AD-A280988) Avail: CASI HC A03/MF A01

Monocrystalline GaN thin films have been grown on vicinal alpha(6H)-SiC(0001) and sapphire(0001) wafers via organometallic vapor phase epitaxy (OMVPE) using a cold-wall, vertical barrel reactor with triethylgallium (TEG) and ammonia. Chemical, analytical and microstructural studies revealed epitaxial films of high microstructural quality. The surface morphologies and photoluminescence spectroscopy (PL) spectra of GaN films on both substrates are presented and described. Specifically, the PL data revealed donor bound exciton emission at 357.6nm for films thicker than 1 mm. Two other emission peaks at 375-378 nm and 540 nm were common to all films tested. Hall effect measurements showed that the unintentionally doped films were highly n-type with a mobility of approximately 40 sq cm/V(dot)s. The new method for the growth of the III-V compounds, namely, the use on an ammonia cracker cell to minimize film damage and increase growth rate has been designed and ordered. Preliminary studies of the use of AlN as a candidate insulator material has been conducted via the fabrication of an MIS structure. I-V and high frequency C-V measurements revealed a 13.4 MV/cm breakdown field and a dielectric constant of approx. 14. Operation of the MIS devices at 300 deg C made only a slight reduction in the breakdown field to 13 MV/cm. DTIC

N95-16598*# Analatom, Inc., Westlake, OH.
THEORETICAL STUDY OF CATHODE SURFACES AND HIGH-TEMPERATURE SUPERCONDUCTORS Final Technical Report
Wolfgang Mueller Oct. 1994 88 p
(Contract NAS3-25085; RTOP 235-01-0A)
(NASA-CR-195407; E-9264; NAS 1.26:195407) Avail: CASI HC A05/MF A01

The surface-dipole properties of model cathode surfaces have been investigated with relativistic scattered-wave cluster calculations. Work-function/coverage curves have been derived from these data by employing the depolarization model of interacting surface dipoles. Accurate values have been obtained for the minimum work functions of several low-work-function surfaces. In the series BaO on bcc W, hcp Os, and fcc Pt, BaO/Os shows a lower and BaO/Pt a higher work function than BaO/W, which is attributed to the different substrate crystal structures involved. Results are also presented on the electronic structure of the high-temperature superconductor YBa2Cu3O7, which has been investigated with fully relativistic calculations for the first time. Author

N95-16623# Cornell Univ., Ithaca, NY.
GROWTH, CHARACTERIZATION AND APPLICATIONS OF BETA-BARIUM BORATE AND RELATED CRYSTALS Final Report, 1 Aug. 1990 - 31 Oct. 1993
C. L. Tang 31 Oct. 1993 120 p
(Contract N00014-90-J-4107)
(AD-A281047) Avail: CASI HC A06/MF A02

Emphasis of our program during the past three years has been on improving the size and quality of beta-barium borate (BBO) crystal; developing the growth recipe for lithium triborate crystal (LBO); automation of the growth process of BBO and LBO; characterization of LBO; developing

optical parametric oscillators using BBO, LBO, and new nonlinear crystals such as KTiOPO4 (KTP), KTA (arsenate), C(Cs)TA, and R(Rb)TA; and helping to establish commercial sources of BBO and LBO crystals and optical parametric oscillator making use of these new crystals. Significant progress has been made in all these areas and is summarized. DTIC

N95-16789 Indiana Univ., Bloomington, IN. Dept. of Chemistry.
DESIGN AND SYNTHESIS OF ORGANIC SUPERCONDUCTORS (FY92 URI/RIP) Annual Report, 1 Oct. 1992 - 30 Sep. 1993
Lawrence K. Montgomery 29 Oct. 1993 8 p Limited Reproducibility: More than 20% of this document may be affected by microfiche quality
(Contract F49620-92-J-0534)
(AD-A281308; AFOSR-94-0403TR) Avail: CASI HC A02

A number of mixed-valence (2:1), conducting salts of bis(ethylenedithio) tetraselena fulvalene (BETS) have been prepared. Four (GaCl4, SbF6, CF3SO3 and CuN(CN)2Br) have been characterized in detail (X-ray crystallography, DC resistivity from 300-10 K, RF penetration depth measurements (0.5K), pressure studies from 0.5-5 kbar at 4K, and tight-binding band calculations). The salts are highly metallic to low temperatures but do not exhibit superconductivity under the experimental conditions explored. The synthesis of a new synthetic metal precursor, bis(ethylenedithio) tetrathionaphthalene (BEDT-TTN), is about three-quarters completed. Spin density wave (SDW) and charge density wave (CDW) phenomena of three organic superconductors (k-(BEDT-TTF)CuN(CN)2Cl, (TMTSF)2PF6, and (TMTSF)2ReO4, where BEDTTTF is bis(ethylenedithio) tetrathiafulvalene and TMTSF is tetramethyl tetraselena fulvalene) have been studied in collaboration with Professor J.W. Brill (Department of Physics, University of Kentucky). The three organic metals avert the SDW and CDW transitions under pressure and become superconductors. DTIC

N95-16805# Oak Ridge National Lab., TN.
FIRST PRINCIPLES SIMULATION OF MATERIALS PROPERTIES
W. A. Shelton, G. M. Stocks, F. J. Pinski (Cincinnati Univ., OH.), R. G. Jordan (Florida Atlantic Univ., Boca Raton, FL.), Y. Liu (Florida Atlantic Univ., Boca Raton, FL.), L. L. Qui (Florida Atlantic Univ., Boca Raton, FL.), J. B. Staunton (Warwick Univ., Coventry, England.), D. D. Johnson (Sandia National Labs., Livermore, CA.), and B. Ginatempo (Messina Univ., Italy.) 1994 8 p Presented at the Scalable High Performance Computing Conference, Knoxville, TN, 23 May 1994
(Contract DE-AC05-84OR-21400)
(DE94-013615; CONF-9405100-6) Avail: CASI HC A02/MF A01

We have developed a hybrid, parallel computer code for calculating the electronic structure of both ordered and substitutionally disordered materials. By using PVM3.3, we can integrate into our local computer environment multiple parallel and vector supercomputers as well as high performance workstations. Without this approach, calculations of materials properties of large systems would be otherwise untenable due to a lack of computer resources. For example, we have determined the short-range order intensity and its electronic origin for the Ag-Mg alloy system, including an estimate of the order-disorder (spinodal) temperature. DOE

N95-16806# Oak Ridge National Lab., TN.
THERMAL AND MECHANICAL BEHAVIOR OF Ba(1+x)Zr4P(6-2x)Si(2x)O24
S. Shanmugham (Tennessee Univ., Knoxville, TN.), K. L. More, D. P. Stinton, C. R. Hubbard, O. B. Cavin, W. O. Porter, and M. K. Ferber 1994 14 p Presented at the 96th Annual Meeting of the American Ceramic Society, Indianapolis, IN, 24-28 Apr. 1994
(Contract DE-AC05-84OR-21400)
(DE94-013620; CONF-940416-12) Avail: CASI HC A03/MF A01

Ba(1+x)Zr4P(6-2x)Si(2x)O24 or BS compounds (0 less than or equal to x less than or equal to 0.5) were synthesized by the sintering of powders formed by a solid-state reaction. Thermal and mechanical properties of BS were studied as a function of composition. It was found that the bulk linear thermal expansion varied with increasing x and was negative for BS with x = 0.5. Among the BS compositions investigated, BS with x = 0.375 had the highest flexural strength, Young's modulus, and hardness. DOE

N95-16849# Conductus, Inc., Sunnyvale, CA.
HTS SNS DEVICES ON LARGE-AREA SUBSTRATES BY SINGLE-SOURCE MOCVD Final Report, 4 Jun. 1993 - 28 Feb. 1994
J. K. Truman 18 May 1994 16 p
(Contract DASG60-93-C-0118)
(AD-A285159) Avail: CASI HC A03/MF A01

A novel, single-source metalorganic chemical vapor deposition (SSMOCVD) technique has shown exceptional promise for the growth of epitaxial oxide films and multilayers on large area substrates, as needed for the commercial-scale production of high temperature superconductor devices and circuits. In this contract the SSMOCVD technique was applied to growth of YBa2Cu3O(7-x) and CaRuO3 films and multilayers for the fabrication of superconductor-normal-superconductor Josephson junctions. A process was developed for the growth of epitaxial CaRuO3 films by SSMOCVD, which was the first reported growth of CaRuO3 by MOCVD. Also, a process was developed for the in situ growth of epitaxial YBa2Cu3O(7-x)/CaRuO3 multilayers by SSMOCVD. Finally, epitaxial SNS edge junctions were fabricated and tested which used a top YBCO/CaRuO3 bilayer grown in situ by SSMOCVD and a base SrTiO3/YBa2Cu3O(7-x) bilayer grown in situ by pulsed laser ablation. DTIC

N95-16867# Lawrence Livermore National Lab., Livermore, CA.
NEW YTTERBIUM-DOPED APATITE CRYSTALS FOR FLEXIBLE LASER DESIGN
S. A. Payne, L. D. DeLoach, L. K. Smith, W. F. Krupke, B. H. T. Chai (University of Central Florida, Orlando, FL.), and G. Loutts (University of Central Florida, Orlando, FL.) Mar. 1994 7 p Presented at the 9th Advanced Solid-State Lasers Meeting, Salt Lake City, UT, 7-10 Feb. 1994
(Contract W-7405-eng-48)
(DE94-015138; UCRL-JC-115149; CONF-940226-8) Avail: CASI HC A02/MF A01

A new class of Yb-lasers is summarized in this article. The apatite family of crystals has been found to impose favorable spectroscopic and laser properties on the Yb(exp 3+) activator ion. Crystals of Yb-doped Ca5(PO4)(sub 3)F, Sr5(PO4)(sub 3)F, Ca(x)Sr(5-x)(PO4)(sub 3)F, and Sr5(VO4)(sub 3)F, have been grown and investigated. Several useful laser crystals have been identified which offer a variety of fundamental laser parameters for designing diode-pumped systems. In general, this class of materials is characterized by high emission cross sections 3.6-13.1 x 10(exp - 20) sq cm, useful emission lifetimes (0.59-1.26 msec), a strong pump band (sigma)(sub abs) = 2.0-10.0 x 10(exp -20) sq cm and pump and extraction wavelengths near 900 and 1,045 nm, respectively. Efficient lasing has been demonstrated for several of the members of this class of materials, and high optical quality crystals have been grown by the Czochralski method. DOE

N95-16913 General Electric Co., Schenectady, NY.
PROPERTIES OF SEMICONDUCTING Ru2Ge3
Jean-Pierre Fleurial (California Inst. of Tech., Pasadena, CA.) and A. Borshchevsky (California Inst. of Tech., Pasadena, CA.) Sep. 1993 14 p Presented at the 12th International Conference on Thermoelectrics, Yohohama (Japan), 9-11 Nov. 1993 Limited Reproducibility: More than 20% of this document may be affected by microfiche quality
(Contract DE-AC12-76SN-00052)
(DE94-015361; KAPL-4766; CONF-9311224-1; UC-904) Avail: CASI HC A03/MF A01

Transport properties of large single crystalline samples of Ru2Ge3 grown from the melt have been investigated in a 25-1000 C temperature range. A diffusionless transition between 500 and 550 C from a high temperature tetragonal structure to a low temperature orthorhombic structure was clearly observed. Results showed that both the low temperature orthorhombic and the high temperature structural tetragonal phase are semiconductors. Some anisotropy of the transport coefficients was determined by measuring the samples in orientations parallel and perpendicular to the preferential direction of crystal growth. Large Seebeck coefficient up to 400 (mu)VK(exp -1) and low thermal conductivity as low as 20 x 10(exp -1) Wcm(exp -1)K(exp -1) were achieved for the low temperature orthorhombic phase. Difficulties in preparing heavily doped samples and low Hall mobilities have limited values for the maximum figure of merit to 0.5 x 10(exp -3) K(exp -1) at 500 C. DOE

N95-16918 Brookhaven National Lab., Upton, NY.
POSITRON ANNIHILATION STUDIES OF DEFECTS IN MOLECULAR BEAM EPITAXY GROWN 3 TO 5 LAYERS
M. T. Umlor, D. J. Keeble, P. Asoka-Kumar, K. G. Lynn, and P. W. Cooke

1994 16 p Presented at the 6th International Workshop on Slow-Positron Beam Techniques for Solids and Surfaces (SLOPOS6), Makuhari, Japan, 18-22 May 1994 Limited Reproducibility: More than 20% of this document may be affected by microfiche quality
(Contract DE-AC02-76CH-00016)
(DE94-015823; BNL-60605; CONF-9405198-3) Avail: CASI HC A03

A summary of recent positron annihilation experiments on molecular beam epitaxy (MBE) grown 3-5 layers is presented. Variable energy positron beam measurements on Al(0.32)Ga(0.68)As undoped and Si doped have been completed. Positron trapping at a open volume defect in Al(0.32)Ga(0.68):Si for temperatures from 300 to 25 K in the dark was observed. The positron trap was lost after 1.3 eV illumination at 25K. These results indicate an open volume defect is associated with the local structure of the deep donor state of the DX center. Stability of MBE GaAs to thermal annealing was investigated over the temperature range of 230 to 700 C. Proximity wafer furnace anneals in flowing argon were used. Samples grown above 450 C were shown to be stable but for sample below this temperature an anneal induced vacancy related defect was produced for anneals between 400 and 500 C. The nature of the defect was shown to be different for material grown at 350 and 230 C. Activation energies of 2.5 eV to 2.3 eV were obtained from isochronal anneal experiments for samples grown at 350 and 230 C, respectively. DOE

N95-16928 Florida Univ., Gainesville, FL. Dept. of Electrical Engineering.
INVESTIGATION OF A NORMAL INCIDENCE HIGH-PERFORMANCE p-TYPE STRAINED LAYER In(0.3)Ga(0.7)As/In(0.52)Al(0 48)As QUANTUM WELL INFRARED PHOTODETECTOR Semiannual Report No. 2, 16 Jan. - 15 Jul. 1994
Max N. Yoder 15 Jul. 1994 34 p Limited Reproducibility: More than 20% of this document may be affected by microfiche quality
(Contract N00014-93-1-0827)
(AD-A282720) Avail: Issuing Activity (Defense Technical Information Center (DTIC))

During this reporting period, we have made excellent progress towards the program goals. A significant achievement was made in the development of a new compressionally strained p-type GaAs/InGaAs QWIP grown on GaAs by MBE. This new QWIP achieved two color detection with detective peaks at 8.9 microns and 8.4 microns in the LWIR band and 5.5 microns in the MWIR band. This detector is under background limited performance (BLIP) at temperatures up to 70 K. The measured responsivity were found to be 24 mA/W and 45 mA/W for the two LWIR peaks respectively, while a responsivity of 13 mA/W was found for the MWIR peak; all at T=75 K. Additional characterization on the tensile strain InGaAs/InAlAs on InP P-QWIP has been performed and the results are summarized in this report. Currently, we are investigating other possible p-type QWIP structures with different performance parameters. These include a new dual strained InGaAs/InAlAs p-type QWIP. Additional consideration is being given towards the reliability of p-type contacts and the strained layer material for these QWIP structures. DTIC

N95-16946# Argonne National Lab., IL.
AC SUSCEPTIBILITY AND CRITICAL CURRENT IN THE ORGANIC SUPERCONDUCTOR (KAPPA)-(ET)2Cu(NCS)2
M. A. Gonzalez (Universidad Complutense, Madrid, Spain.), M. Velez (Universidad Complutense, Madrid, Spain.), J. L. Vicent (Universidad Complutense, Madrid, Spain.), J. Schleuter, J. M. Williams, and G. W. Crabtree May 1994 3 p Presented at the Meeting on Materials and Mechanisms of Superconductivity: High Temperature Superconductors, Grenoble, France, 4-9 Jul. 1994
(Contract W-31-109-eng-38)
(DE94-013997; ANL/MSD/CP-83110; CONF-940701-6) Avail: CASI HC A01/MF A01

The AC susceptibility (X(prime), X(double prime)) has been measured in a single crystal of the organic superconductor kappa-(ET)(sub 2)Cu(NCS)(sub 2) (T(sub C) = 9.5 K) as a function of the DC magnetic field, for several frequencies (10 (sup 2) Hz less than f less than 10(sup 4) Hz) and different AC fields (l(mu)T less than h(sub dc) <300(mu)T) at fixed temperatures. DOE

N95-16952# Technische Univ., Delft (Netherlands). Interfaculty Reactor Inst.
APPLICATIONS OF POSITRON DEPTH PROFILING Ph.D. Thesis [TOEPASSINGEN VAN POSITRON DIEPTE-PROFILTERING]
R. A. Hakvoort 23 Dec. 1993 194 p
(PB94-197753; ISBN-90-73861-15-2) Copyright Avail: CASI HC A09/MF A03

In this thesis, some contributions of the positron-depth profiling technique to materials science are described. A review of this technique is presented in chapters 1 and 2, while chapter 3 deals with the Delft Variable Energy Positron Beam and some techniques employed for acquiring additional information on the materials examined. Positron-annihilation measurements on neon-implanted steel is reported in chapter 4. Chapter 5 reported void creation in silicon by helium implantation. By positron measurements the density of vacancy-type defects present in amorphous silicon prepared by ion implantation has been estimated at 1.2 at.%, as described in chapter 6. Chapter 7 reported on measurements of other types of amorphous silicon. Epitaxial cobalt disilicide prepared by cobalt out diffusion has been studied in chapter 8. Finally, chapter 9 reported on positron-annihilation experiments on low-pressure CVD silicon-nitride films. In conclusion, the positron depth-profiling technique is able to give valuable information on specific problems in materials science. NTIS

N95-17137 Duke Univ., Durham, NC. Dept. of Chemistry.
SYNTHESIS AND CHARACTERIZATION OF NEOPENTYL INDIUM COMPOUNDS: X-RAY CRYSTAL STRUCTURES OF ((Me3CCH2)2InAs(SiMe3)2)2 AND ((Me3CCH2)2InAs(SiMe3)2In (CH2CMe3)2Cl)
18 Jul. 1994 24 p Limited Reproducibility: More than 20% of this document may be affected by microfiche quality
(Contract N00014-89-J-1545)
(AD-A282766; DU/DC/TR-43) Avail: Issuing Activity (Defense Technical Information Center (DTIC))

A major impetus for main group chemists lies in the desire for new precursors to ceramic and electronic materials. As investigators of groups 13-15 compounds, our interest can be attributed to the quest for new precursors to semiconducting materials such as GaAs and InP. An important aspect of this research is ascertaining the fundamental chemistry of these systems in order to synthesize the most efficient precursors for a specific method of deposition. Research in our laboratory has primarily focused on the use of dehalosilylation and salt elimination reactions to form the group 13-15 bonds. DTIC

N95-17156# Los Alamos National Lab., NM.
ASYMPTOTIC BEHAVIOR IN GRAIN GROWTH
D. T. Wu 1994 6 p Presented at the Spring Meeting of the Materials Research Society, San Francisco, CA, 4-8 Apr. 1994
(Contract W-7405-eng-36)
(DE94-014452; LA-UR-94-1919; CONF-940411-37) Avail: CASI HC A02/MF A01

Hillert's model of grain growth consists of a drift term in size space that leads asymptotically to a distribution function and a growth exponent not often observed. Later theories introduce a diffusion term that is either assumed to dominate the drift term or a correction to it. This paper shows that the lower order drift term alone determines asymptotic grain growth behavior. A possible conclusion is that experimental results may need to be reinterpreted. DOE

N95-17171 Duke Univ., Durham, NC. Dept. of Chemistry.
X-RAY CRYSTAL STRUCTURE OF A MONOMERIC TRIS(ARSINO)GALLANE, ((Me3Si)2As)3Ga)3Ga
Richard L. Wells, Mark F. Self, Ryan A. Baldwin, and Peter S. White 18 Jul. 1994 16 p Limited Reproducibility: More than 20% of this document may be affected by microfiche quality
(Contract N00014-89-J-1545)
(AD-A282343; DU/DC/TR-44) Avail: Issuing Activity (Defense Technical Information Center (DTIC))

Early effects in organogallium-arsenic synthetic chemistry centered on the utilization of alkane elimination reactions, as evidenced by the work of Coates and co-workers in the 1960. Through their efforts, they were able to isolate mono(arsino) gallanes and show that intermolecular As-Ga bonding to form four-coordinate gallium and arsenic dominates the structural

properties of these compounds. We desired to obtain sterically hindered arsinogallanes by this method. However, we discovered that the practicality of alkane elimination was severely diminished as the steric bulk of the substituents was increased. Subsequently, we employed a coupling reaction involving a lithium arsenide and a chlorogallane to successfully isolate the first example of a tris(arsino)galane which was shown by X-ray analysis to be a monomer containing three-coordinate gallium and arsenic. This coupling method was also used in the formation of the tris(arsino)gallanes synthesized in our laboratory. DTIC

N95-17349# Argonne National Lab., IL.
COLUMNAR DEFECT PINNING IN UNTWINNED SINGLE CRYSTAL YBa2Cu2O7
G. W. Crabtree, J. Fendrich, W. K. Kwok, and B. G. Glagola May 1994 3 p Presented at the Meeting on Materials and Mechanisms of Superconductivity: High Temperature Superconductors, Grenoble, France, 4-9 Jul. 1994
(Contract W-31-109-eng-38)
(DE94-013962; ANL/MSD/CP-83142; CONF-940701-3) Avail: CASI HC A01/MF A01

The pinning by columnar defects produced by 1.0 GeV U ion bombardment along the c-axis of an untwinned YBa2Cu3O7 single crystal is characterized. The accommodation angle is nearly 90(degrees) at low field, the resistivity anisotropy is reversed, and the onset of pinning occurs well into the fluctuation regime. The anisotropy and strength of the pinning are compared to that of twin boundaries. DOE

N95-17350# Argonne National Lab., IL.
SUPPRESSION OF SUPERCONDUCTIVITY IN ORTHORHOMBIC La(2-x)M(x)CuO4 (M = Ca,Sr)
B. Dabrowski (University of Northern Illinois, De Kalb, IL.), Z. Wang (University of Northern Illinois, De Kalb, IL.), J. D. Jorgensen, R. L. Hitterman, J. L. Wagner, B. A. Hunter, P. G. Radaelli, and D. G. Hinks May 1994 3 p Presented at the Meeting on Materials and Mechanisms of Superconductivity: High Temperature Superconductors, Grenoble, France, 4-9 Jul. 1994
(Contract W-31-109-eng-38)
(DE94-013963; ANL/MSD/CP-83143; CONF-940701-9) Avail: CASI HC A01/MF A01

We have extended the calcium solid-solubility limit in La(2-x)Ca(x)CuO4 to x = 0.2 using synthesis at high oxygen pressure. The superconducting transition temperature increases with doping to 34 K at x = 0.15 and is suppressed for x is greater than 0.15, similar to the Sr-substituted material. At a fixed doping level, the optimum superconducting properties (the highest (Tc)) are found for flat and square CuO2 planes. DOE

N95-17424 Houston Univ., TX.
INVESTIGATION OF NOVEL ELECTRICAL TRANSPORT PHENOMENA IN SEMIMETAL-SEMICONDUCTOR HETEROSTRUCTURES Final Report, 1 Sep. 1992 - 2 Mar. 1994
Terry D. Golding and John H. Miller 2 May 1994 7 p Limited Reproducibility: More than 20% of this document may be affected by microfiche quality
(Contract DAAL03-92-G-0385)
(AD-A281406; ARO-30772.7-MS) Avail: CASI HC A02

The Sb/GaSb system has been proposed as a unique new material which has significant potential for quantum transport studies, electronic devices, incorporating semimetal/semiconductor heterostructures, and for infrared optical and nonlinear optical applications requiring an indirect narrow band-gap material. Researchers have demonstrated the growth of both single Sb/GaSb heteroepitaxial layers and elementary GaSb/Sb/GaSb multilayer structures using MBE and MEE on GaSb (111) substrates. Magnetotransport measurements have yielded electron and hole mobilities in excess of 3 x 10(exp 4) sq cm/V(dot)s, which correspond to mean free paths of greater than 2 micrometers for both carrier types. Further studies are current underway to characterize the transport and optical properties of Sb/GaSb multilayer structures. DTIC

N95-17518# Academy of Sciences of the Ukraine, Kiev. Inst. Teoreticheskoj Fiziki.
POSSIBLE SUPERSTRUCTURES OF METALLIC IONS IN NONSTOICHIOMETRIC FULLERITES M(x) C(60)
V. M. Loktev and O. M. Tatarenko 1993 16 p
(DE94-622052; ITP-93-47) Avail: CASI HC A03/MF A01 (US Sales Only)

The ordered structures of alkali metal M=K,Rb,Cs atoms are considered in the M(x)C(60) systems for x less than 6 on the basis of symmetry analysis. Using the static concentration wave approach the x values and the corresponding vectors resulting in periodic structures are determined. The phase diagram that agrees qualitatively with the one observed experimentally is obtained. DOE

N95-17620 Aerospace Corp., El Segundo, CA. Technology Operations.
EVALUATION OF THE QUALITY OF SAPPHIRE USING X-RAY ROCKING CURVES AND DOUBLE-CRYSTAL X-RAY TOPOGRAPHY
P. M. Adams 1 May 1994 23 p Limited Reproducibility: More than 20% of this document may be affected by microfiche quality
(Contract F04701-93-C-0094)
(AD-A282905; TR-94(4935)-7; SMC-TR-94-32) Avail: Issuing Activity (Defense Technical Information Center (DTIC))

Single-crystal sapphire is a material with a wide range of applications as a result of its unique physical, optical, mechanical, and chemical properties. The quality of a sapphire crystal can influence its effectiveness in many applications. High-quality, near-perfect, single-crystal sapphire can be grown, but it is difficult to shape and polish because of its extreme hardness, and surface flaws and damage are commonly produced during fabrication. Since this damage may exist in a buried subsurface layer, it can be difficult to detect. X-ray rocking curves and x-ray topography are extremely sensitive to the level of defects and strains in single crystals. A number of sapphire substrates from several suppliers were examined using these techniques in order to determine how applicable they are for detecting defects in sapphire. A wide range in quality was found in sapphire received from different suppliers. Residual grinding/polishing damage was observed in many samples. Other defects observed included dislocations and mosaic structure and twinning in lower quality material. Rocking curves and double-crystal x-ray topography appear to be simple techniques for evaluating and determining the quality of sapphire. In particular, they are sensitive to subsurface damage and microscopic defects can be imaged at low to moderate magnification. DTIC

N95-17667# Oak Ridge National Lab., TN. Solid State Div.
STUDIES BY NEUTRON DIFFRACTION AND MUON SR OF FLUX LATTICE ORIENTATION, PINNING, MELTING AND DECOMPOSITION IN HIGH-T(SUB c) SUPERCONDUCTORS
E. M. Forgan (Birmingham Univ., England.), R. Cubitt (Birmingham Univ., England.), M. T. Wylie (Birmingham Univ., England.), S. L. Lee (Zurich Univ., Switzerland.), H. Keller (Zurich Univ., Switzerland.), D. M. Paul (Warwick Univ., Coventry, England.), M. Yethiraj, H. A. Mook, and P. H. Kess (Leiden Univ., Netherlands.) 1994 6 p Presented at the 7th IWCC International Workshop on Critical Currents in Superconductors, Alpbach, Austria, 24-27 Jan. 1994
(Contract DE-AC05-84OR-21400)
(DE94-017704; CONF-940122-5) Avail: CASI HC A02/MF A01

We review the results of recent microscopic measurements of flux line structures and their breakdown in the high-Tc superconductors BSCCO and YBCO. These results show clear effects of flux of lattice melting, dimensional crossover and pinning. The huge differences in behaviour of the flux lattice in these two materials can be understood theoretically. DOE

N95-17673# Brookhaven National Lab., Upton, NY.
CRYSTALLINE BEAMS: THE VERTICAL ZIGZAG
A. F. Haffmans, D. Maletic, and A. G. Ruggiero May 1994 22 p
(Contract DE-AC02-76CH-00016)
(DE94-017986; BNL-60743) Avail: CASI HC A03/MF A01

This note is the continuation of our comprehensive investigation of Crystalline Beams. After having determined the equations of motion and the conditions for the formation of the simplest configuration, i.e. the string, we study the possibility of storing an intense beam of charged particles in a storage ring where they form a vertical zigzag. We define the equilibrium configuration, and examine the confinement conditions. Subsequently, we derive the transfer matrix for motion through various elements of the storage ring. Finally we investigate the stability conditions for such a beam. DOE

N95-17705 Arizona Univ., Tucson, AZ. Dept. of Physics.
SCANNING TUNNELING MICROSCOPY OF 3 TO 5 SEMICONDUCTORS Final Report, 1 Mar. 1991 - 28 Feb. 1994
John D. Dow 6 Jun. 1994 7 p Limited Reproducibility: More than 20% of this document may be affected by microfiche quality
(Contract DAAL03-91-G-0054)
(AD-A281722; ARO-28508.7-EL) Avail: CASI HC A02

Scanning tunneling microscopy and theory were combined to create novel depressive quantum dots at room temperature on the (110) surfaces of InSb dots which merit further exploration as potential nanopixels for tiny-device lithography; develop a strained-layer superlattice model of high-temperature superconductivity; image, understand, and make models of single-atom-high steps on III-V surfaces; invent and exploit a new kind of spectroscopy of surface states of semiconductors, called tipology; and develop phenomenological models of a variety of surface phenomena.
Author (DTIC)

N95-17711# Puerto Rico Univ., Rio Piedras. Dept. of Physics.
UNDERPOTENTIAL DEPOSITION OF Cu ON Au(111): IMPLICATIONS OF THE HB MODEL
L. Blum and Dale A. Huckaby (Texas Christian Univ., Fort Worth, TX.) 4 May 1994 30 p Submitted for publication
(Contract N00014-90-J-1263)
(AD-A283028; TR-31-ONR) Avail: CASI HC A03/MF A01

In recent papers a model for the underpotential deposition of Cu on Au(111) in the presence of bisulfate ions was proposed. In this model it was assumed that the bisulfate ions formed a square root of 3 times square root of 3 template. This template leaves a honeycomb lattice of free sites for the adsorption of copper. The clear implication is that the first peak has 2/3 of a monolayer of Cu. The second peak corresponds to the replacement of the bisulfate by copper in the adlayer. We showed also that the broad foot of the first peak is due to a second order hard hexagon like transition, which is seen experimentally by Itaya and Kolb. The interpretation, based on the STM and LEED observations, that the first peak corresponds to only 1/3 of a monolayer, is consistent with our model if it is the bisulfate ion that is actually seen in those experiments.
DTIC

N95-17742# Lawrence Livermore National Lab., Livermore, CA.
THERMAL AND LASER CONDITIONING OF PRODUCTION AND RAPID-GROWTH KDP AND KD*P CRYSTALS
L. J. Atherton, F. Rainer, J. J. DeYoreo, I. M. Thomas, N. Zaitseva, and F. DeMarco 13 Jan. 1994 12 p Presented at the 25th Boulder Damage Symposium: Annual Symposium on Optical Materials for High-Power Lasers, Boulder, CO, 27-29 Oct. 1993 Submitted for publication
(Contract W-7405-eng-48)
(DE94-013738; UCRL-JC-115121; CONF-931054-11) Avail: CASI HC A03/MF A01

Large solid state lasers such as Beamlet and the proposed National Ignition Facility (NIF) require optical materials with extremely high damage thresholds. Potassium dihydrogen phosphate (KDP) and its deuterated analog (KD*P) both require some form of conditioning to reach the design fluence of these lasers. Both the bulk material and the crystal surfaces must have damage thresholds in excess of 16J/sq cm at 1053 nm and 11J/sq cm at 351 nm for 3-ns pulselengths. The use of ultrafiltration techniques has been demonstrated to produce bulk material with damage thresholds exceeding these requirements with the use of R:1 laser conditioning. More recent results at LLNL using large-area laser conditioning and thermal annealing are described for a variety of state-of-the-art KDP and KD*P crystals. Results on thermally annealed KD*P with a deuteration range of 60% to 80% are also presented, and compared to those of ordinary KDP.
DOE

N95-17898# Argonne National Lab., IL.
TEXTURE ANALYSIS OF CRITICAL CURRENT DENSITY IN Bi2Sr2CaCu2O(x) TAPES
A. C. Biondo (Illinois Inst. of Tech., Chicago, IL.), J. S. Kallend (Illinois Inst. of Tech., Chicago, IL.), C. T. Wu (Illinois Inst. of Tech., Chicago, IL.), W. L. Knapp, M. T. Lanagan, and K. C. Goretta Aug. 1994 16 p Presented at the 7th Conference on Superconductivity and Applications, Buffalo, NY, 7-9 Sep. 1994
(Contract W-31-109-eng-38)
(DE94-018375; ANL/ET/CP-83715; CONF-940926-1) Avail: CASI HC A03/MF A01

Ag-clad Bi2Sr2CaCu2O(x) tapes were fabricated by a powder-in-tube process. Transport critical current density J(sub c) data were obtained at 4.2 K. X ray diffraction data were used to quantify the texture of each superconductor core. J(sub c) and texture data were related by a geometric model based on J(sub c) anisotropy within individual grains. The model, which fit the data well, is applicable to strongly linked superconductors only.
DOE

N95-17906# Allied-Signal Aerospace Co., Kansas City, MO.
THIN FILM SUPERCONDUCTORS
B. Z. Rosenblum Aug. 1994 4 p
(Contract DE-AC04-76DP-00613)
(DE94-018585; KCP-613-5434) Avail: CASI HC A01/MF A01

This project was initiated to develop thin film superconductors and to incorporate them as elements of weapon safety. Although a vacuum system was modified and the materials procured for fabricating the components, few samples were produced because of a change in priorities and the lack of personnel resources. Literature search results are included.
DOE

N95-17917# Sandia National Labs., Albuquerque, NM.
STUDY OF CuPt-TYPE ORDERING AND DOPANT EFFECT OF In(0.5)Ga(0.5)P/GaAs USING SPECTROSCOPIC ELLIPSOMETRY
H. Lee (Illinois Univ., Urbana, IL.) and M. V. Klein (Illinois Univ., Urbana, IL.) 1994 5 p Presented at the 22d International Conference on Physics of Semiconductors, Vancouver, British Columbia, 15-19 Aug. 1994
(Contract DE-AC04-94AL-85000)
(DE94-018890; SAND-94-2100C; CONF-9408155-3) Avail: CASI HC A01/MF A01

The CuPt-type ordering and dopant effects of In(0.5)Ga(0.5)P/GaAs epitaxial layers have been studied using spectroscopic ellipsometry and transmission electron microscopy. The degree of ordering was estimated by both transmission electron diffraction and direct band edge, E(sub 0). Conventional lineshape fitting of E(sub 1), E(sub 1)+(Delta)(sub 1), and E(sub 2) gaps using the second derivative of pseudo dielectric functions shows that the peak position and oscillator strength of the E(sub 1) gap are basically a function of CuPt-type ordering whereas their broadening and phase depend mainly on carrier concentration. The decrease of E(sub 1) gap is explained in terms of CuPt-type ordering. In contrast to the E(sub 1) gap, all the lineshape parameters of the E(sub 2) gap depend mainly on CuPt-type ordering. This difference is discussed in terms of apparent 'CuAu-type ordering' or Y2 structure which was observed by transmission electron diffraction.
DOE

77 THERMODYNAMICS AND STATISTICAL PHYSICS

Includes quantum mechanics; theoretical physics; and Bose and Fermi statistics.

For related information see also *25 Inorganic and Physical Chemistry* and *34 Fluid Mechanics and Heat Transfer.*

N95-16075 Integrated System Assemblies Corp., Woburn, MA.
LIQUID COOLED HEAT SINK WITH THROUGH VIAS (LCHS) Final Report, Dec. 1992 - Sep. 1993
Charles W. Eichelberger and J. P. Kusior 30 Sep. 1993 31 p Limited Reproducibility: More than 20% of this document may be affected by microfiche quality
(Contract N00014-91-C-0219)
(AD-A281450) Avail: CASI HC A03

A Liquid Cooled Heat Sink with Through Electrical Vias was designed, fabricated and tested. The Heat Sink was designed for use in 3D stacks of high heat producing multichip modules. The report covers design considerations, the fabrication process and measured performance achieved. A special section compares the Heat Sink performance to an equivalent diamond heat sink. A second special section discusses the economics of high volume production of the Heat Sink. Important performance results

include: (1) Power Density of 5OW/cm(exp 2) with temperature rise of 15C; (2) 100 through vias per sq cm; and (3) Thickness of 1.25mm.

DTIC

N95-16428# Los Alamos National Lab., NM.

EXACT, E = 0, CLASSICAL AND QUANTUM SOLUTIONS FOR GENERAL POWER-LAW OSCILLATORS

M. M. Nieto and J. Daboul (Negev Univ., Beersheva, Israel.) 1994 12 p Presented at the Workshop on Harmonic Oscillators, Cocoyoc, Mexico, 23-25 Mar. 1994

(Contract W-7405-eng-36)

(DE94-014436; LA-UR-94-1949; CONF-9403139-1) Avail: CASI HC A03/MF A01

For zero energy, E = 0, we derive exact, classical and quantum solutions for all power-law oscillators with potentials V(r) = -(gamma)/r(sup (nu)), (gamma) greater than 0 and -(infinity) less than (nu) less than (infinity). When the angular momentum is non-zero, these solutions lead to the classical orbits (rho)(t) = (cos (mu)((var phi)(t) - (var phi)(sub 0)(t)) (sup 1/(mu)), with (mu) = (nu)/2 - 1 (ne) 0. For (nu) greater than 2, the orbits are bound and go through the origin. We calculate the periods and precessions of these bound orbits, and graph a number of specific examples. The unbound orbits are also discussed in detail. Quantum mechanically, this system is also exactly solvable. We find that when (nu) greater than 2 the solutions are normalizable (bound), as in the classical case. Also, there are normalizable discrete, yet unbound, state which correspond to unbound classical particles which reach infinity in a finite time. These and other interesting comparisons to the classical system will be discussed.

DOE

N95-16489# Princeton Univ., NJ. Dept. of Chemistry.

EXTRACTION OF HIGH QUALITY POTENTIAL SURFACES FROM LABORATORY DATA Annual Technical Report, 15 May 1993 - 14 May 1994

Herschel Rabitz 17 Aug. 1994 8 p

(Contract F49620-93-1-0300)

(AD-A285071; AFOSR-94-0514TR) Avail: CASI HC A02/MF A01

A new direct inversion algorithm is being developed, capable of taking high quality laboratory pump-probe data and directly inverting it to potential surface and optical coupling coefficient information. The algorithm is based on employing the laboratory data in a two-stage noniterative inversion. Inversion with simulated data shows that the developing algorithm is capable of being highly efficient and superior to any other available techniques.

Author (DTIC)

N95-16604# State Univ. of New York, Binghamton, NY. Dept. of Physics.

UNUSUAL INITIAL AND FINAL STATE EFFECTS IN QUANTUM CHROMODYNAMICS

C. A. Nelson Dec. 1993 10 p

(Contract DE-FG02-86ER-40291)

(DE94-015341; DOE/ER-40291/21) Avail: CASI HC A02/MF A01

The author has constructed a number of fundamental tests which can be used to probe discrete symmetries, and their possible violations, in the required 'new physics' beyond the standard model. On-going experiments with unpolarized e(-) e(+) collisions contain many events for the production-decay sequence e(-) e(+) (yields) Z(o), (gamma)(*) (yields) (tau)(-))(tau)(+) (yields) (A(sup -X)(B(sup +X). By inclusion of (rho) polarimetry observables such experiments enable two distinct tests for leptonic CP violation in (tau) (yields) (rho)(nu) decay (similarly in (tau) (yields) a(sub 1)(nu) decay) by generalization of the energy correlation function for Z(o), or (gamma)(*) (yields) (tau)(-)(tau)(+) (yields)((rho)(-) (nu))((rho)(+)(bar (nu)). In other research programs, the author is:(1) continuing to investigate the proposal that partons be identified with nearly degenerate, coherent quark-gluon 'jet' states; and (2) is investigating the novel consequences of the possible existence of q-bosons and of a related completeness relation for the q-analogue coherent states. This year the author has also written papers on the zeros of the q-analogue exponential function, and on the number and phase uncertainties of the q-analogue quantized field.

DOE

N95-16839 Direction des Recherches, Etudes et Techniques, Paris (France). Centre de Documentation de l'Armement.

STUDY OF THE STRUCTURING OF PURE MOLECULAR LIQUIDS Final Report [ETUDE DE LA STRUCTURATION DE LIQUIDES MOLECULAIRES PURS]

L. Letamendia, R. Duplessix, G. Nouchi, and C. Vaucamps 1994 48 p In FRENCH

(PB94-201316) Avail: Issuing Activity (National Technical Information Service (NTIS))

Recent experiments have shown that changes in the slope of specific heat variation as a function of temperature in liquids are not always regular. In this study, the authors consider the possibility that fluid structure can change with temperature, by shifting from one form to another. They study such molecular liquids as benzene, hexafluorobenzene, and quinoleine using Rayleigh-Brillouin and depolarized Rayleigh diffusion, and total intensity diffusion. The authors clearly found anomalies for all collective properties of the medium in the liquids studied, though purely molecular properties were undisturbed. The accidents observed occurred at the same temperatures, whatever the collective or intermolecular property under study. But it took some time (several hours) for them to manifest themselves, which suggests that molecular liquids are characterized by a long thermodynamic equilibrium. Results also show a disturbance in hydrodynamic state at accident temperatures, which are similar to those generated by long spatial correlation processes.

NTIS

N95-16877# Naval Surface Warfare Center, Bethesda, MD.

ANALYSIS OF INFRARED SCALING LAWS Final Report

Lou Massa and Peter O. Cervenka Mar. 1994 47 p

(NR Proj. RH2-1-C-17)

(AD-A285461; CARDIVNSWC-TR-94/004) Avail: CASI HC A03/MF A01

The scaling laws appropriate to the IR radiation from ships are displayed. The heat equation is rendered in dimensionless form so that its solutions manifestly apply to ships of arbitrary scale. The important variables for IR thermodynamic similarity are shown, viz. the dimensionless quantities, also called pi variables, associated with temperature, position, time, power per unit volume, and heat transfer coefficient. The purpose of scale modeling is to duplicate the ship values of these dimensionless quantities in the scale models studied. In so doing, the IR signals are duplicated as well and may be studied in a laboratory setting with all the advantages of repetition and control thus implied. Questions of compatibility of dimensionless variables are discussed. It is concluded that no apparent inherent incompatibilities among the dimensionless quantities relevant to the IR present themselves.

DTIC

N95-16944# Stanford Linear Accelerator Center, CA.

LIGHT-RAY OPERATORS AND THEIR APPLICATION IN QCD

B. Geyer (Leipzig Univ., German D.R..), D. Robaschik (Leipzig Univ., German D.R..), and D. Mueller May 1994 7 p Presented at the Workshop on Quantum Field Theoretical Aspects of High Energy Physics, Bad Frankenhausen, Germany, 20-24 Sep. 1993

(Contract DE-AC03-76SF-00515)

(DE94-013801; SU-SLAC-PUB-6495; CONF-9309386-1) Avail: CASI HC A02/MF A01

The nonperturbative parton distribution and wave functions are directly related to matrix elements of light-ray (nonlocal) operators. These operators are generalizations of the standard local operators known from the operator product expansions. The renormalization group equation for these operators leads to evolution equations for more general distribution amplitudes which include the Altarelli-Parisi and the Brodsky-Lepage equations as special cases. It is possible to derive the Altarelli-Parisi kernel as a limiting case of the extended Brodsky-Lepage kernel. As a new application of the operator product expansion, the virtual Compton scattering near forward direction is considered.

DOE

N95-17473# Academy of Sciences of the Ukraine, Kharkov. Inst. Radiofiziki i Ehlektroniki.

RELATIVISTIC EFFECT OF ENERGY INCREASE OF A PARTICLE MOVING FREELY IN VACUUM FROM THE QUANTUM FIELD THEORY POINT OF VIEW

G. N. Gestrina 1993 10 p

(DE94-622757; IRE-93-1) Avail: CASI HC A02/MF A01 (US Sales Only)

Einstein's formula connecting mass and velocity of a relativistic particle moving freely in vacuum is considered from the quantum field theory point of view with wing some supersymmetry ideas. DOE

N95-17474# Academy of Sciences of the Ukraine, Kiev. Inst. Teoreticheskoj Fiziki.
THE QUANTUM SOLITONS OF THE NONLINEAR (SIGMA)-MODEL WITH BROKEN CHIRAL SYMMETRY
A. P. Kostyuk, A. P. Kobushkin, N. M. Chepilko, and T. Okazaki 1993 16 p
(DE94-622758; ITP-93-44) Avail: CASI HC A03/MF A01 (US Sales Only)

It is proved that the quantum-mechanical consideration of global breathing of a hedgehog-like field configuration leads to the dynamically stable soliton solutions in the nonlinear (sigma)-model without the Skyrme term. Such solutions exist only when chiral symmetry of the model is broken. DOE

N95-17645 Texas Univ., Austin, TX. Inst. for Fusion Studies.
ELECTRON-NEUTRINO PHASE SEPARATION INSTABILITY
C. Lai and T. Tajima Jul. 1994 15 p Limited Reproducibility: More than 20% of this document may be affected by microfiche quality
(Contract DE-FG05-80ET-53088)
(DE94-016859; DOE/ET-53088/665; IFSR-665) Avail: CASI HC A03

Deduced from Weinberg-Salam electroweak theory, a Boltzmann equation and subsequent fluid equations are derived for the primordial electron-positron-neutrino-photon plasma. A collective instability that separates the phases of electrons (and positrons) and neutrinos (and anti-neutrinos) is discussed. Cosmological implications are mentioned. DOE

N95-17668# Stanford Linear Accelerator Center, CA.
PROBING VIOLATION OF QUANTUM MECHANICS IN THE K0-(BAR K)0 SYSTEM
P. Huet Aug. 1994 6 p Presented at the Meeting of the Division of Particles and Fields of the American Physical Society, Albuquerque, NM, 2-6 Aug. 1994
(Contract DE-AC03-76SF-00515)
(DE94-017934; SU-SLAC-PUB-6630; CONF-940816-2) Avail: CASI HC A02/MF A01

I present a recent study made in collaboration with M.E. Peskin, on the time dependence of a kaon beam propagating according to the '(alpha)(beta)(gamma)' generalization of quantum mechanics due to Ellis, Hagelin, Nanopoulos and Srednicki, in which CP- and CPT-violating signatures arise from the evolution of pure states to mixed states. The magnitude of two of its parameters (beta) and (gamma) are constrained on the basis of existing experimental data. New facilities such as (phi)-Factories are shown to be particularly adequate to study this generalization from quantum mechanics and to disentangle its parameters from other CPT violating perturbations of the kaon system. DOE

N95-17712 Puerto Rico Univ., Rio Piedras. Dept. of Physics.
THE SOLVATION THERMODYNAMIC FUNCTIONS IN THE MEAN SPHERICAL APPROXIMATION (MSA): BEHAVIOR NEAR THE SOLVENT CRITICAL REGION
L. Blum and Dong-Qing Wei 4 May 1994 28 p Limited Reproducibility: More than 20% of this document may be affected by microfiche quality
(Contract N00014-90-J-1263)
(AD-A283040; TR-32) Avail: CASI HC A03

Explicit expressions of the MSA solvation thermodynamic functions, the Gibbs free energy, energy enthalpy, entropy, apparent molar heat capacities, and partial molar volume are derived starting from the Helmholtz free energy. The thermodynamic consistency of the MSA solvation thermodynamic functions are discussed. Some limiting behaviors of the MSA solvation thermodynamic function are compared with the Born theory. The effect of explicit solvent structures in the MSA theory on the Gibbs and the Helmholtz free energy is given special attention. Model calculations of alkali and halide ions in water are carried out and compared with experimental data. The apparent molar heat capacities at constant volume and pressure and the partial molar volume are calculated along an isobaric line to the critical region of a dipolar liquid. A great deal of insight has been gained on the behavior of the solvation thermodynamic properties near the critical region of dipolar solvent. It helps to explain some of the recent experimental observations. Author (DTIC)

N95-17904# California Univ., Berkeley. Lawrence Berkeley Lab, CA.
STUDIES OF TRANSVERSE COHERENT BUNCH INSTABILITIES FOR THE ADVANCED LIGHT SOURCE (ALS)
M. Meddahi and J. Bengtsson 31 May 1994 47 p
(Contract DE-AC03-76SF-00098)
(DE94-018536; LBL-35703; CBP-017) Avail: CASI HC A03/MF A01

We have studied the transverse coherent bunch instabilities for the Advanced Light Source (ALS). We have in particular applied a Hamiltonian formalism to obtain the linearized averaged equations of motion (i.e. the one turn map) for the resistive wall effect to obtain the corresponding localized kick when the beta function is varying along the lattice. We have also included a 2-dimensional model for the transverse higher order cavity modes. In addition, we have used power series maps to represent the lattice which enabled us to include non-linear effects. These models have been implemented in a computer code and numerical simulations have been carried out for ALS. The model was successfully verified against analytical calculations in cases where they overlap. The non-linear effects from the lattice proved to be important, since they led to a qualitative change of the dynamics for the stored beam. We also studied the injection process in some detail and found that the non-linear effects also fundamentally change the injection dynamics. DOE

N95-17925# Argonne National Lab., IL.
THE THREE LOOP EQUATION OF STATE OF QED AT HIGH TEMPERATURE
C. Coriano and R. R. Parwani (Commissariat a l'Energie Atomique, Saclay, France.) May 1994 12 p
(Contract W-31-109-eng-38)
(DE94-015029; ANL-HEP-PR-94-02) Avail: CASI HC A03/MF A01

The authors present the three loop contribution (order e(sup 4)) to the pressure of Quantum Electrodynamics at high temperature for massless electrons. The calculations are performed in the imaginary time formalism. Dimensional regularization is used for the regulation of both the ultraviolet and infrared singularities, and also to prevent overcounting of diagrams during resummation. DOE

80 SOCIAL SCIENCES (GENERAL)

Includes educational matters.

N95-16007*# National Aeronautics and Space Administration, Washington, DC.
PRESIDENTIAL LEADERSHIP IN THE DEVELOPMENT OF THE US SPACE PROGRAM
Roger D. Launius, ed. and Howard E. McCurdy, ed. Jul. 1994 460 p Presented at the Historical Symposium on Presidential Leadership in the Space Program, Washington, DC, 27-28 Mar. 1993
(NASA-TM-110107; NASA-HHR-59; NAS 1.15:110107) Avail: CASI HC A20/MF A04

Papers presented at a historical symposium on Presidential leadership in the space program include the following: 'The Imperial Presidency in the History of Space Exploration'; 'The Reluctant Racer: Dwight D. Eisenhower and United States Space Policy'; 'Kennedy and the Decision to Go to the Moon'; 'Johnson, Project Apollo, and the Politics of Space Program Planning'; 'The Presidency, Congress, and the Deceleration of the U.S. Space Program in the 1970s'; 'Politics not Science: The U.S. Space Program in the Reagan and Bush Years'; 'Presidential Leadership and International Aspects of the Space Program'; 'National Leadership and Presidential Power'; and 'Epilogue: Beyond NASA Exceptionalism'. CASI

81 ADMINISTRATION AND MANAGEMENT

Includes management planning and research.

N95-16289# Technische Univ., Delft (Netherlands).
IMPROVING PRODUCTION SCHEDULES WITHOUT SCHEDULING Ph.D.

Thesis
E. P. Jansen 27 Sep. 1993 205 p
(PB94-191350; ISBN-90-9006355-2) Avail: CASI HC A10/MF A03

Developments in manufacturing and technology lead to the development of manufacturing systems that reduce the amount of decision making by those responsible for operating and supervising the manufacturing process. In this thesis, various techniques to fine tune schedules are presented and discussed. To support the Production Management System (PMS) and the Operator Management System (OMS), and hence the users of these systems, these techniques have been implemented in an Expert Management System (EMS). On requests by the PMS or OMS, and initiated by the user, the EMS investigates the indicated orders or jobs that are tardy. If one or more fine tuning techniques can be applied to improve the order or job's lead time, advice is generated and returned to the caller, that is either PMS or OMS. The thesis shows that it is possible to devise and to build a knowledge-based support system that is able to counsel on how to improve the lead time of a job, that uses idle periods of the resources and that does not need to re-schedule to achieve a lead time improvement. NTIS

N95-16633* National Aeronautics and Space Administration, Washington, DC.
CONTINUAL IMPROVEMENT: A BIBLIOGRAPHY WITH INDEXES, 1992-1993
Sep. 1994 168 p
(NASA-SP-7097(02); NAS 1.21:7097(02)) Avail: CASI HC A08

This bibliography lists 606 references to reports and journal articles entered into the NASA Scientific and Technical Information Database during 1992 to 1993. Topics cover the philosophy and history of Continual Improvement (CI), basic approaches and strategies for implementation, and lessons learned from public and private sector models. Entries are arranged according to the following categories: Leadership for Quality, Information and Analysis, Strategic Planning for CI, Human Resources Utilization, Management of Process Quality, Supplier Quality, Assessing Results, Customer Focus and Satisfaction, TQM Tools and Philosophies, and Applications. Indexes include subject, personal author, corporate source, contract number, report number, and accession number. Author

N95-17231*# National Aeronautics and Space Administration. Marshall Space Flight Center, Huntsville, AL.
GENERIC MISSION PLANNING AND SCHEDULING: THE AXAF SOLUTION
O. T. Guffin and M. Newhouse (Computer Sciences Corp., Huntsville, AL.) *In* NASA. Goddard Space Flight Center, Third International Symposium on Space Mission Operations and Ground Data Systems, Part 1 Nov. 1994 p 461-466 (For primary document see N95-17179 04-17)
Avail: CASI HC A02/MF A06

82 DOCUMENTATION AND INFORMATION SCIENCE

Includes information management; information storage and retrieval technology; technical writing; graphic arts; and micrography.

For computer documentation see *61 Computer Programming and Software.*

N95-15919*# National Aeronautics and Space Administration, Washington, DC.
FOURTH ANNUAL INTERNATIONAL ACQUISITIONS WORKSHOP: ACCESS TO MULTIPLE MEDIA WORLDWIDE
14 Sep. 1994 250 p Workshop held in Arlington, VA, 12-14 Sep. 1994; sponsored by AFSC, Central Intelligence Agency, Foreign Broadcast Information Service, and DTIC
(NASA-TM-109896; NAS 1.15:109896) Avail: CASI HC A11/MF A03

Topics discussed during the workshop include: (1) Multinational-Multiple media collections and activities spanning many countries; (2) Multiple media in North American trade and commerce; (3) African spotlight; (4) Europe-Multiple media in national libraries and services; (5) Scandinavian spotlight; (6) Internet update; (7) Multiple media in US federal agencies; (8) Open-source multiple media in US federal agencies; and (9) Multiple media at US federal technical agencies-NIST and NOAA. For individual titles, see N95-15920 through N95-15939.

N95-15920*# National Library of Australia, Canberra, Australian Capital Territory (Australia).
THE AUSTRIALIAN NATIONAL CHINESE JAPANESE KOREAN PROJECT
Linda Groom *In* NASA, Washington, Fourth Annual International Acquisitions Workshop: Access to Multiple Media Worldwide 14 Sep. 1994 2 p (For primary document see N95-15919 04-82)
Avail: CASI HC A01/MF A03

Providing access to Asian-language materials has always been a problem for libraries. There are particular difficulties in acquiring Asian materials, in cataloguing them and providing access, and in incorporating them in library systems. There is, however, an urgent and growing need for access to Asian materials. Part of the response of the Australian library community to the difficulties and to the increasing need has been the Australian National CJK (Chinese, Japanese and Korean) Project. The CJK Project is a co-operative project involving seven Australian universities and the National Library of Australia. Membership is expected to grow to include other Australian research libraries, some public research libraries and some overseas libraries. Derived from text

N95-15921*# Scientific and Technical Research Council of Turkey, Ankara. Informatics Div.
INFORMATICS IN TURKEY
Serhat Cakir *In* NASA, Washington, Fourth Annual International Aquisitions Workshop: Access to Multiple Media Worldwide 14 Sep. 1994 15 p (For primary document see N95-15919 04-82)
Avail: CASI HC A03/MF A03

In the last twenty years the rapid change in the informatics sector has had economic and social impact on private and government activities. The Supreme Council for Science and Technology of Turkey assigned highest priority to the informatics in its meeting in February 1993. With this advice TUBITAK (The Scientific and Technical Research Council of Turkey) intends to give a strong impulse to development of a research policy in this field. Derived from text

N95-15922*# International Trade Commission Library, Washington, DC. Acquisitions.
NAFTA LITERATURE AT THE INTERNATIONAL TRADE COMMISSION LIBRARY
Elizabeth A. Root *In* NASA, Washington, Fourth Annual International Acquisitions Workshop: Access to Multiple Media Worldwide 14 Sep. 1994 2 p (For primary document see N95-15919 04-82)
Avail: CASI HC A01/MF A03

Most of the US official materials regarding NAFTA originate in the Executive Office of the President, especially the Office of the United States Trade Representative. These materials can be purchased from the U.S.G.P.O. There were also numerous Congressional hearings; many of which are probably now out of print, government agencies and the public are welcome to make copies of the ones in the collections of the ITC libraries. One of the most important sources of materials available in electronic format is the National Trade Data Base, produced by the Department of Commerce. This is a collection of at least 120 separate files containing documents relating to trade. It includes several files specifically on NAFTA, including the text of the treaty. It is available as two CD-ROM's, issued monthly, or on Internet. Derived from text

N95-15923*# Bureau of the Census, Suitland, MD. Information and Research Services.
BUREAU OF THE CENSUS CENTER FOR INTERNATIONAL RESEARCH
Nina Pane Pinto *In* NASA, Washington, Fourth Annual International Acquisitions Worksh op: Access to Multiple Media Worldwide 14 Sep. 1994 2 p (For primary document see N95-15919 04-82)
Avail: CASI HC A01/MF A03

This paper describes the organization and activities of the Center for International Research at the Bureau of the Census. There is a formal publication exchange program with other government's statistical programs. This has resulted in the Center's collection being one of the world's largest in the area of international census and demographic information.

Foreign statistical publications are in three libraries, one being dedicated to the former Soviet Union and one to the Peoples Republic of China. In addition to the libraries there are two computerized data bases. The International data base is a source of demographic and socio-economic statistics for all countries of the world. The second data base is the HIV/AIDS Surveillance Data Base which contains information related to the publication and dissemination of the results of seroprevalence surveys.
Derived from text

N95-15924*# Botswana Univ., Gaborone. National Inst. of Development Research and Documentation.
ACQUIRING AND DISSEMINATING UNPUBLISHED ECONOMIC AND SOCIAL DEVELOPMENT MATERIALS IN AFRICA: THE CASE OF THE NATIONAL INSTITUTE OF DEVELOPMENT RESEARCH AND DOCUMENTATION UNIVERSITY OF BOTSWANA
Kate Kwafo-Akoto *In* NASA, Washington, Fourth Annual International Acquisitions Workshop: Access to Multiple Media Worldwide 14 Sep. 1994 15 p (For primary document see N95-15919 04-82)
Avail: CASI HC A03/MF A03

Generally in Africa, the identification and acquisition of both published and unpublished documents can be an extremely difficult task due, among other factors, to the unsatisfactory state of the publishing industry and the poor state of bibliographic control. This paper analyzes the various problems involved in the acquisition of documents in Africa and illustrates them with the author's personal experience as an acquisitions librarian working on an information project which necessitated travel to about 15 African countries.
Author

N95-15925*# National Technical Information Center and Library, Budapest, Pest (Hungary).
INFORMATION SYSTEM IN TRANSITION: THE HUNGARIAN SCENE
Gyorgy Stubnya and Akos Robert Herman *In* NASA, Washington, Fourth Annual International Acquisitions Workshop: Access to Multiple Media Worldwide 14 Sep. 1994 15 p (For primary document see N95-15919 04-82)
Avail: CASI HC A03/MF A03

Recent changes in political and economical conditions in eastern European countries are influencing the function and activities of the Hungarian Library and Information network. The National Technical Information Center and Library (OMIKK) is an active participant in this process of transition. In the first part of this paper, the general transformations of Hungarian libraries and information centers are analyzed and some predictions for future trends are presented. The second part is a short summary of the activities of OMIKK and its present and prospective role in the development of national information policy. Author (revised)

N95-15926*# Bureau Jupiter, The Hague, South Holland (Netherlands).
DOCUMENT DELIVERY BY THE JUPITER LIBRARY CONSORTIUM
Robert H. A. Wessels *In* NASA, Washington, Fourth Annual International Acquisitions Workshop: Access to Multiple Media Worldwide 14 Sep. 1994 21 p (For primary document see N95-15919 04-82)
Avail: CASI HC A03/MF A03

The Jupiter library consortium consists of 4 of the leading libraries in the Netherlands. During 1993 Jupiter received 600,000 requests for copies of journal articles, or 70 percent of all external article requests in the Netherlands. Over 90 percent of the requested documents were delivered from a collection of 40,000 current international journal subscriptions. Jupiter and its affiliate libraries are non-profit organizations belonging to, and serving, the scientific and technical research community. The usage of the current journal collection of the libraries was analyzed to improve the cost/benefit ratio. Author (revised)

N95-15927*# Center for Scientific Information and Documentation, Madrid, Madrid (Spain).
CINDOC, CSIC, AND SPANISH R AND D
Rosa delaViesca *In* NASA, Washington, Fourth Annual International Acquisitions Workshop: Access to Multiple Media Worldwide 14 Sep. 1994 21 p (For primary document see N95-15919 04-82)
Avail: CASI HC A03/MF A03

The organizational structure and functional activities of the Spanish Center for Scientific Information and Documentation (CINDOC) are discussed. The library holds 8,500 journals, including all the Spanish scientific journals; 16,000 books and 20 CD-ROM data bases. CINDOC creates and distributes its own data bases that include all the articles published in Spanish scientific journals.
Derived from text

N95-15928*# Technische Univ., Hanover (Germany). Technical Information Library.
THE TECHNICAL INFORMATION LIBRARY: TIB
Uwe Rosemann *In* NASA, Washington, Fourth Annual International Acquisitions Workshop: Access to Multiple Media Worldwide 14 Sep. 1994 19 p (For primary document see N95-15919 04-82)
Avail: CASI HC A03/MF A03

The Technische Informationsbibliothek Hannover (TIB) is the German national central library for all areas of technology and related sciences, especially chemistry, computer science, mathematics, and physics. The TIB acquires and makes available a comprehensive collection of conventional and non-conventional literature, especially foreign material, with particular emphasis on specialized new publications which are difficult to obtain or in difficult languages.
Author (revised)

N95-15929*# Royal Inst. of Tech., Stockholm (Sweden).
THE NATIONAL RESOURCE LIBRARY FOR SCIENCE AND TECHNOLOGY IN SWEDEN: A NORDIC MODEL OF COOPERATING TECHNOLOGY LIBRARIES
Gunnar Lagar *In* NASA, Washington, Fourth Annual International Acquisitions Workshop: Access to Multiple Media Worldwide 14 Sep. 1994 3 p (For primary document see N95-15919 04-82)
Avail: CASI HC A01/MF A03

The scope of this presentation is to give a state-of-the-art report on the present situation of Nordic technology libraries, to elaborate on a plan for national resource libraries in Sweden, and to share how the Royal Institute of Technology Library in Stockholm (KTHB) has fostered a network of cooperating libraries in order to optimize government funding for the system of resource libraries.
Author (revised)

N95-15930*# Tampere Univ. of Technology (Finland).
INFORMATION SOURCES IN SCIENCE AND TECHNOLOGY IN FINLAND
Arja-Riitta Haarala *In* NASA, Washington, Fourth Annual International Acquisitions Workshop: Access to Multiple Media Worldwide 14 Sep. 1994 4 p (For primary document see N95-15919 04-82)
Avail: CASI HC A01/MF A03

Finland poses some problems to be overcome in the field of scientific and technical information: a small user community which makes domestic systems costly; great distances within the country between users and suppliers of information; great distances to international data systems and large libraries abroad; and inadequate collections of scientific and technical information. The national bibliography Fennica includes all books and journals published in Finland. Data base services available in Finland include: reference data bases in science and technology; data banks for decision making such as statistical time series or legal proceedings; national bibliographies; and library catalogs.
Author (revised)

N95-15931*# Mitre Corp., Bedford, MA. Articial Intelligence Center.
THE FUTURE OF INTERACTION ON THE INTERNET
Mark T. Maybury *In* NASA, Washington, Fourth Annual International Acquisitions Workshop: Access to Multiple Media Worldwide 14 Sep. 1994 4 p (For primary document see N95-15919 04-82)
Avail: CASI HC A01/MF A03

The federated collection of heterogeneous computers we collectively term the Internet has been the force behind revolutionary change, both in terms of actual practice and imagination of what might be. The raw numbers are staggering: IP registrations are now ten times that of only five years ago; and between 1992 - 1993 the amount of information being transferred tripled. Changes in three key areas: knowledge discovery; intelligent information access; and collaboration on the Internet are discussed.
Author (revised)

N95-15932*# Cornell Univ., Ithaca, NY.
NETWORKED INFORMATION: MANAGEMENT ISSUES FOR THE ACQUISITIONS LIBRARIAN
Gregory Lawrence *In* NASA, Washington, Fourth Annual International

Acquisitions Workshop: Access to Multiple Media Worldwide 14 Sep. 1994 2 p (For primary document see N95-15919 04-82)
Avail: CASI HC A01/MF A03

Historically, libraries have been the depositories and public access points to both domestic and international government information. A change in the information seeking behavior of the public is driving a change in government information publishing and dissemination. Patrons who traditionally used libraries for access to printed government information have become familiar and comfortable with the electronic environment. These data users are showing an increased interest in certain types of government information in electronic format, including indexes, numeric files, statistics, and hypertext documents. Government response to increased demand for electronic information has led to a flurry of special initiatives, with the production of information products on diskette, CD-ROM, and dissemination via the Internet. Libraries, and acquisitions units in particular, are being challenged to provide consistent and timely management of the information. The rapidly developing communications infrastructure, which frequently redesigns access to the information environment, poses significant obstacles to, and the tremendous opportunities for, making large bodies of government information available to a broad base of users. Author

N95-15933*# Mitre Corp., McLean, VA.
ADDING TOOLS TO THE OPEN SOURCE TOOLBOX: THE INTERNET
Tricia Porth *In* NASA, Washington, Fourth Annual International Acquisitions Workshop: Access to Multiple Media Worldwide 14 Sep. 1994 3 p (For primary document see N95-15919 04-82)
Avail: CASI HC A01/MF A03

The Internet offers researchers additional sources of information not easily available from traditional sources such as print volumes or commercial data bases. Internet tools such as e-mail and file transfer protocol (ftp) speed up the way researchers communicate and transmit data. Mosaic, one of the newest additions to the Internet toolbox, allows users to combine tools such as ftp, gopher, wide area information server, and the world wide web with multimedia capabilities. Mosaic has quickly become a popular means of making information available on the Internet because it is versatile and easily customizable. Author

N95-15934*# Air Force Inst. of Tech., Wright-Patterson AFB, OH. Information Exploitation Div.
OPEN SOURCE SERVICE AGENT (OSSA) IN THE INTELLIGENCE COMMUNITY'S OPEN SOURCE ARCHITECTURE
Bruce F. Fiene *In* NASA, Washington, Fourth Annual International Acquisitions Workshop: Access to Multiple Media Worldwide 14 Sep. 1994 23 p (For primary document see N95-15919 04-82)
Avail: CASI HC A03/MF A03

The Community Open Source Program Office (COSPO) has developed an architecture for the intelligence community's new Open Source Information System (OSIS). The architecture is a multi-phased program featuring connectivity, interoperability, and functionality. OSIS is based on a distributed architecture concept. The system is designed to function as a virtual entity. OSIS will be a restricted (non-public), user configured network employing Internet communications. Privacy and authentication will be provided through firewall protection. Connection to OSIS can be made through any server on the Internet or through dial-up modems provided the appropriate firewall authentication system is installed on the client. Author (revised)

N95-15935*# Office of Naval Research, Arlington, VA.
ELECTRONIC ACCESS TO ONREUR/ONRAISIA S AND T REPORTS
Abstract Only
William McCluskey *In* NASA, Washington, Fourth Annual International Acquisitions Workshop: Access to Multiple Media Worldwide 14 Sep. 1994 1 p (For primary document see N95-15919 04-82)
Avail: CASI HC A01/MF A03

The Office of Naval Research maintains two foreign field offices in London, England and in Tokyo, Japan. These offices survey world-wide findings, trends and achievements in science and technology. These offices maintain liaison between U.S. Navy and foreign scientific research and development organizations conducting programs of naval interest. Expert personnel survey foreign scientific and technical activities, identify new directions and progress of potential interest, and report their findings. Report topics cover a broad range of basic scientific thrusts in mathematics, physics, chemistry, computer science, and oceanography, as well as advances in technologies such as electronics, materials, optics, and robotics. These unclassified reports will be made available via the Internet in 1995, replacing hard-copy publication. Author (revised)

N95-15936*# Department of Energy, Oak Ridge, TN. Office of Scientific and Technical Information.
DEPARTMENT OF ENERGY: OFFICE OF SCIENTIFIC AND TECHNICAL INFORMATION
Catherine Grissom *In* NASA, Washington, Fourth Annual International Acquisitions Workshop: Access to Multiple Media Worldwide 14 Sep. 1994 3 p (For primary document see N95-15919 04-82)
Avail: CASI HC A01/MF A03

The international acquisitions functions and activities of the Office of Scientific and Technical Information (OSTI) are described. There are four mechanisms for obtaining foreign information related to energy and nuclear science: The Energy Technology Data Exchange consisting of 14 member countries and 2 associate members; the International Nuclear Information System consisting of 86 countries and 17 international organizations; the Nuclear Energy Agency's 19 member countries provide reports for departmental scientists' use; bilateral agreements with countries such as Germany, the Nordic Consortium, and Australia result in records of foreign research in progress. Derived from text

N95-15937*# National Inst. of Standards and Technology, Gaithersburg, MD.
NUMERIC DATA DISTRIBUTION: THE VITAL ROLE OF DATA EXCHANGE IN TODAY'S WORLD
Malcolm W. Chase *In* NASA, Washington, Fourth Annual International Acquisitions Workshop: Access to Multiple Media Worldwide 14 Sep. 1994 2 p (For primary document see N95-15919 04-82)
Avail: CASI HC A01/MF A03

The major aim of the NIST standard Reference Data Program (SRD) is to provide critically evaluated numeric data to the scientific and technical community in a convenient and accessible form. A second aim of the program is to provide feedback into the experimental and theoretical programs to help raise the general standards of measurement. By communicating the experience gained in evaluating the world output of data in the physical sciences, NIST/SRD helps to advance the level of experimental techniques and improve the reliability of physical measurements. Author

N95-15938*# National Inst. of Standards and Technology, Gaithersburg, MD.
NATIONAL CENTER FOR STANDARDS AND CERTIFICATION INFORMATION: SERVICE AND PROGRAMS
JoAnne Overman *In* NASA, Washington, Fourth Annual International Acquisitions Workshop: Access to Multiple Media Worldwide 14 Sep. 1994 7 p (For primary document see N95-15919 04-82)
Avail: CASI HC A02/MF A03

The National Center for Standards and Certification Information (NCSCI) provides information on U.S., foreign and international voluntary standards, government regulations, and conformity assessment procedures for non-agricultural products. The Center serves as a referral service and focal point in the United States for information on standards and standards-related information. NCSCI staff respond to inquiries, maintain a reference collection of standards and standards-related documents, and serve as the U.S. inquiry point for information to and from foreign countries. Author (revised)

N95-15939*# National Oceanic and Atmospheric Administration, Washington, DC.
COLLECTION DEVELOPMENT AT THE NOAA CENTRAL LIBRARY
Abstract Only
Steve R. Quillen *In* NASA, Washington, Fourth Annual International Acquisitions Workshop: Access to Multiple Media Worldwide 14 Sep. 1994 1 p (For primary document see N95-15919 04-82)
Avail: CASI HC A01/MF A03

The National Oceanic and Atmospheric Administration (NOAA) Central Library collection, approximately one million volumes, incorporates the holdings of its predecessor agencies. Within the library, the collections are filed separately, based on their source and/or classification schemes. The

NOAA Central Library provides a variety of services to users, ranging from quick reference and interlibrary loan to in-depth research and online data bases. Author (revised)

N95-15957# Defense Technical Information Center, Alexandria, VA.
SOURCE HIERARCHY LIST. VOLUME 2: E THROUGH N Report, Nov. 1992 - Jun. 1994
Linda Stallard Jul. 1994 904 p See also AD-A256101, AD-A281100, and AD-AD281102
(AD-A281101; DTIC/TR-94/18-Vol-2; DTIC/TR-92/6-Vol-2) Avail: CASI HC A99/MF A10

This is the second of three volumes of an alphabetical listing of corporate authors as used for announcement of reports received by the Defense Technical Information Center (DTIC). Former names of organizations are included and displayed below the current source name used by DTIC. Cross reference direct the user from sub-element organizations to the major source level entry where they are also displayed. Major and sub-hierarchies are preceded and ended by a row of asterisks. The list is used in conjunction with and is not a replacement for DTIC's Source Header List, Volume 1, AD-A281 000, and Volume 2, AD-A281 001. It displays only those source names from the Source Header List to which hierarchical linkages are pertinent. DTIC

N95-15998# Defense Technical Information Center, Alexandria, VA.
SOURCE HEADER LIST. VOLUME 2: L THROUGH Z Report, Sep. 1992 - Jun. 1994
Claudine S. Long Jun. 1994 644 p See also AD-A256001 and AD-A281000
(AD-A281001; DTIC/TR-94/17-Vol-2; DTIC/TR-92/5-Vol-2) Avail: CASI HC A99/MF A06

This publication is the second of two volumes of an alphabetically arranged compilation of corporate author names used by the Defense Technical Information Center in the DTIC database system. Each source name is assigned a six-digit numeric code for computer input and retrieval purposes plus a four-digit alphanumeric geopolitical code and an alphanumeric type code. Source names displayed are included as data elements in the Technical Report, Work Unit Information System, and Independent Research and Development databases maintained by DTIC. DTIC

N95-16014 Keele Univ. (England).
SECOND INTERNATIONAL WORKING CONFERENCE ON COOPERATING KNOWLEDGE BASED SYSTEMS. VOLUME 1
17 Jun. 1994 119 p Conference held in Keele, England, 14-17 Jun. 1994 Limited Reproducibility: More than 20% of this document may be affected by microfiche quality
(AD-A281347) Avail: Issuing Activity (Defense Technical Information Center (DTIC))

Partial contents include: Session 1: Invited Paper; Session 2 Stream B: Coordination Strategies; Session 3 Stream A: Holonic Manufacturing Systems 1; Session 3 Stream B: Distributed Information Systems; Session 4 Stream A: Holonic Manufacturing Systems 2; Session 4 Stream B: Logic-based Approaches; Session 5 Stream A: Concurrent Engineering; and Session 5 Stream B: Communications and Protocol. DTIC

N95-16086 Defense Technical Information Center, Alexandria, VA.
DIRECTORY OF ORGANIZATIONAL TECHNICAL REPORT ACRONYM CODES (DOTRAC) Annual Report
Linda Stallard Jul. 1994 600 p See also AD-A237000 Limited Reproducibility: More than 20% of this document may be affected by microfiche quality
(AD-A281500; DTIC/TR-94/16; DTIC/TR-91/2) Avail: Issuing Activity (Defense Technical Information Center (DTIC))

This compilation is a guide to acronyms as assigned by the Defense Technical Information Center (DTIC). The listing contains entries from the Department of Defense (DOD), Federal Government, foreign military and non-government organizations. The acronyms reflect reports processed into the DTIC collection. In all instances the acronyms are those actually used by the organization itself. The listing is arranged in two parts, as follows: alphabetically by acronym, and alphabetically by full name of organization. The Appendix contains Standard Technical Report Number Update Notification Form 'STRN-UP'. DTIC

N95-16090# Defense Technical Information Center, Alexandria, VA.
SOURCE HIERARCHY LIST. VOLUME 3: O THROUGH Z Report, Nov. 1992 - Jun. 1994
Linda Stallard Jul. 1994 797 p Supersedes DTIC/TR-92/6-Vol-3 dated Oct. 1992, AD-A256102. See also Volume 1, AD-A281100 and Volume 2, AD-A281101
(AD-A281102; DTIC/TR-94/18-Vol-3; DTIC/TR-92/6-Vol-3) Avail: CASI HC A99/MF A10

This is the third of three volumes of an alphabetical listing of corporate authors as used for announcement of reports received in the Defense Technical Information Center (DTIC). Former names of organizations are included and displayed below the current source name used by DTIC. Cross references direct the user from subelement organizations to the major source level entry where they are also displayed. Major and subhierarchies are preceded and ended by a row of asterisks. This list is used in conjunction with and is not a replacement for DTIC's Source Header List, Volume 1, AD-A281000, and Volume 2, AD-A2810001. It displays only those source names from the Source Header List to which hierarchical linkages are pertinent. DTIC

N95-16093# North Dakota State Univ., Fargo, ND. Dept. of Computer Science and Operations Research.
GEOTRANS GEOGRAPHIC DECISION SUPPORT SYSTEM
K. E. Nygard and M. J. Haugrud May 1994 44 p Sponsored by DOT
(PB94-183670; NDSU-MPC-94-31) Avail: CASI HC A03/MF A01

A Geographical Information System (GIS) is a software environment that supports management, display, and analysis on high-quality maps and associated data. A GIS fundamentally extends the functionality of a database management system by supporting spatial data as well as attribute data. However, GIS functionality can be extended to include more advanced decision support features such a mathematical models, artificial intelligence inferencing techniques, statistical methodologies, spatial analysis and other decision-making aids. The authors use the term Geographical Decision Support System, or GDSS, to describe a GIS that is extended in this way. The GEOTRANS (GEographical Optimizer for TRANSportation) is an implementation of a GDSS for rural transportation. Algorithms and specialized data structures were developed to accomplish accurate and efficient solution of a suite of network flow optimization models for use in GEOTRANS. These include shortest path, assignment, transshipment, capacitated transshipment and facility location models. Author

N95-16282# CH2M/Hill, Inc., Reston, VA.
RISK-BASED DATA MANAGEMENT SYSTEM DESIGN SPECIFICATIONS AND IMPLEMENTATION PLAN FOR THE ALASKA OIL AND GAS CONSERVATION COMMISSION; THE MISSISSIPPI STATE OIL AND GAS BOARD; THE MONTANA BOARD OF OIL AND GAS CONSERVATION; AND THE NEBRASKA OIL AND GAS CONSERVATION COMMISSION, ATTACHMENT B
Sep. 1993 374 p Prepared in cooperation with Digital Design Group, Inc., Denver, CO
(Contract DE-FG22-91MT-91003)
(DE94-013189; DOE/MT-91003/T7-Attach-B) Avail: CASI HC A16/MF A03

The purpose of this document is to present design specifications and an implementation schedule for the development and implementation of Risk Based Data Management Systems (RBDMS's) in the states of Alaska, Mississippi, Montana, and Nebraska. The document presents detailed design information including a description of the system database structure, data dictionary, data entry and inquiry screen layouts, specifications for standard reports that will be produced by the system, functions and capabilities (including environmental risk analyses), and table relationships for each database table within the system. This design information provides a comprehensive blueprint of the system to be developed and presents the necessary detailed information for system development and implementation. A proposed schedule for development and implementation also is presented. The schedule presents timeframes for the development of system modules, training, implementation, and providing assistance to the states with data conversion from existing systems. However, the schedule will vary depending upon the timing of funding allocations from the United States Department of Energy (DOE) for the development and implementation phase of the project. For planning purposes, the schedule assumes that initiation of the

development and implementation phase will commence November 1, 1993, somewhat later than originally anticipated. DOE

N95-16305 Naval Postgraduate School, Monterey, CA.
VIDEOCONFERENCING AND ITS ROLE IN THE ARMY M.S. Thesis
William M. Churchwell Jun. 1994 88 p Limited Reproducibility: More than 20% of this document may be affected by microfiche quality
(AD-A282707) Avail: CASI HC A05

This thesis discusses the capabilities and the requirements for integrating videoconferencing technology into the Army's communication system. As the bandwidth requirements for videoconferencing are lowered and the bandwidth availability increases, it is becoming more feasible to incorporate a videoconferencing system into a commander's communication structure. The current family of videoconferencing equipment is reviewed and current standards that govern videoconferencing are examined. Videoconferencing systems are described in both a tactical and garrison environment with an emphasis on bandwidth requirements, survivability, and system security. Also, current tactical examples of videoconferencing use are discussed to provide insight as to the possible future uses of systems. Currently videoconferencing systems are used for staff planning, videomedicine, and videotraining. Finally, a projected videoconferencing architecture for a corps/division is analyzed with possible locations of the videoconferencing sites and communication systems that could link the videoconferencing sites together. A breakdown of possible users is provided to show that videoconferencing can play a successful support role in the Army.
Author (DTIC)

N95-16374 Defense Technical Information Center, Alexandria, VA.
DOD STINFO REGULATIONS AND FORMS. SELECTED TITLES Special Report, 1979 - 1994
Sharon L. Serzan and Forrest R. Frank Aug. 1994 416 p Limited Reproducibility: More than 20% of this document may be affected by microfiche quality
(AD-A282332; DTIC/TR-94-23) Avail: Issuing Activity (Defense Technical Information Center (DTIC))

This compendium of DOD scientific and technical information regulations and forms brings to a single document the most widely used DOD issuances which affect the collection and dissemination of scientific and technical information. This reference collection is provided as an aid to the operation and management of STI activities. It is not intended to be a substitute for the authoritative versions of these issuances and implementing DOD component instructions, handbooks, or policy letters. DTIC

N95-16382 Assistant Secretary of Defense (Communications Command Control and Intelligence), Washington, DC.
DATA ADMINISTRATION PROCEDURES
Mar. 1994 112 p Supersedes AD-A272700 Limited Reproducibility: More than 20% of this document may be affected by microfiche quality
(AD-A282718; DOD-8320.1-M) Avail: Issuing Activity (Defense Technical Information Center (DTIC))

This manual provides uniform procedures for implementation of the policies and concepts set forth in DOD Directive 8320.1 for DOD Data Administration. This manual supports the Defense Information Management (IM) Program. Successful execution of these procedures will help to ensure that DOD data can be identified, standardized, collected, distributed, used, and disposed of with accuracy and consistency, regardless of medium or intended use as described in DOD Directive 8000.1. It will also ensure the effective management of data, like other DOD resources, throughout its life-cycle. DTIC

N95-16400# National Defence Research Establishment, Linkoeping (Sweden). Huvudavdelning foer Informationsteknologi.
DIVISION OF INFORMATION SYSTEMS (FOA 37) Annual Report
K. Baeckstroem Nov. 1993 54 p See also PB92-125541
(PB94-190766; FOA-C-30739-3.4) Avail: CASI HC A04/MF A01

This report gives an overview of the work carried out at the Division of Information Systems (FOA 37) during FY 1992/93. Research projects covered include: Main Project Electronic Warfare (HPTK); Main Project Air Defense (HPLF); Spatial Information Analysis; Computer Vision; Autonomous Systems and Robotics; C3I Techniques; and Space Technology. NTIS

N95-16431# TRADOC Test and Experimentation Command, Fort Hunter Liggett, CA.
A PARSER FOR THE ISO 8211 DATA FORMAT
Michael McDonnell Jan. 1994 24 p
(AD-A281594; TEC-0045) Avail: CASI HC A03/MF A01

This report describes a library of functions that parse an ISO 8211 file and convert the parsed data into a form useful to other programs, which can then read user data from the file. The structure of ISO 8211 files will be defined and then it will be shown how these programs interpret data in those files. Finally, an example program will be presented that reads an ISO 8211 file by using this library. DTIC

N95-16441*# National Aeronautics and Space Administration. Goddard Space Flight Center, Greenbelt, MD.
NSSDC DATA LISTING
Richard Horowitz and Joseph H. King Oct. 1994 154 p
(NASA-TM-109986; NSSDC/WDC-A-R/S-94-09; NAS 1.15:109986) Avail: CASI HC A08/MF A02

This document identifies, in a highly summarized way, all the data held at the National Space Science Data Center (NSSDC). These data cover astrophysics and astronomy, solar and space physics, planetary and lunar, and Earth science disciplines. They are primarily but not exclusively from past and on-going NASA spaceflight missions. We first identify all the data electronically available through NSSDC's principal on-line (magnetic disk-based) and near-line (robotics jukebox-based) systems and then those data available on CD-ROM's. Finally, we identify all NSSDC-held data, the majority of which are still off line on magnetic tape, film, etc., but include the electronically accessible and CD-ROM-resident data of earlier sections. These comprehensive identifications are in the form of two listings, one for the majority of NSSDC-held data sets resulting from individual instruments flown on individual spacecraft and the other for the remainder of NSSDC-held data sets that do not adhere to this spacecraft/experiment/data set hierarchy. The latter listing is presented in two parts, one for the numerous source catalogs of the NSSDC-operated Astronomical Data Center and the other for the remainder. Author

N95-16845 Defense Technical Information Center, Alexandria, VA.
HANDBOOK FOR USERS Final Report
Mary J. Brewster and Charles E. Reed Oct. 1994 115 p Supersedes AD-A260738 and AD-A268726 Limited Reproducibility: More than 20% of this document may be affected by microfiche quality
(AD-A285148; DTIC/TR-95-1; AD-A260738; AD-A268726) Avail: CASI HC A06

This handbook is your guide to DTIC. It describes DTIC's products and services and provides users step by step instructions for completing all basic DTIC transactions such as registering for general and network services, and ordering and submitting technical reports. To assist the user, it includes examples of the required forms and several appendices containing commonly used abbreviations, telephone numbers and DTIC prices. DTIC

N95-16879# Wright Lab., Wright-Patterson AFB, OH.
PATTERN THEORETIC KNOWLEDGE DISCOVERY Final Report, Dec. 1993 - Aug. 1994
Jeffrey A. Goldman Aug. 1994 53 p
(AF Proj. 0100)
(AD-A285472; WL-TR-94-1093) Avail: CASI HC A04/MF A01

Among the future research directions of Knowledge Discovery in Databases is the ability to extract an overlying concept relating data objects that are useful to the investigator. Some of the current limitations involve the search complexity and what it means to be useful. The Pattern Theory research crosses over in a natural way to the aforementioned domain. The goal of this paper is threefold. First, we wish to present a new approach to the problem of learning by Discovery and robust pattern finding in general. Second, we will show its performance by exhibiting several learning curves. Third, from a practical standpoint, we wish to explore the current limitations of a Pattern Theoretic Discovery and Databases problem. Function decomposition is the central core of Pattern Theory. The development allows us to discuss the notion of patterns, and thus, the notion of useful, in a formal manner. DTIC

N95-16884# Naval Research Lab., Washington, DC.
AN INTEGRATED KNOWLEDGE ACQUISITION AND DATABASE MANAGEMENT SYSTEM
C. B. Barclay and J. A. Molnar 26 Aug. 1994 21 p
(AD-A285404; NRL/FR/5520-94-9733) Avail: CASI HC A03/MF A01

FISDM is a menu driven database interface that was developed to enhance the acquisition and management of knowledge acquired for Fault Isolation System Knowledge Bases. This software was of general purpose and could be accessed on any ASCII terminal. FISDMPro enhanced the basic FISDM software by providing a Graphical User Interface (GUI) and Expert System to aid knowledge base creation. FISDMPro was developed with the GUI development tool TAE (Transportable Application Engine). The Expert system portion of FISDMPro uses the C Language Integrated Production System (CLIPS) expert system engine, and rules were developed that govern the creation of the major components of a FIS knowledge base. The Interface now presents a graphical method of creating the knowledge base by simply defining modules as blocks and providing interconnections between the blocks. The interconnections are governed by the physical interrelations of the modules, and the expert system generates rules relating to the interconnections. A presentation of the capabilities is shown along with the discussion of the software dynamics. DTIC

N95-16922 Argonne National Lab., IL.
THE PASS PROJECT Progress Report
D. R. Quarrie (California Univ., Berkeley. Lawrence Berkeley Lab, CA.), C. T. Day (California Univ., Berkeley. Lawrence Berkeley Lab, CA.), and S. Loken (California Univ., Berkeley. Lawrence Berkeley Lab, CA.) 1994 4 p Presented at the Meeting on Computing in High-Energy Physics, San Francisco, CA, 21-27 Apr. 1994 Limited Reproducibility: More than 20% of this document may be affected by microfiche quality
(Contracts W-31-109-eng-38; DE-AC03-76SF-00098)
(DE94-016308; ANL-HEP-CP-94-37; CONF-940492-10) Avail: CASI HC A01

The PASS project has as its goal the implementation of solutions to the foreseen data access problems of the next generation of scientific experiments. It is in the process of transitioning from an exploratory phase, where the focus has been on understanding the requirements and available technologies to an implementation phase, where detailed design work is commencing on a common framework for scientific applications. DOE

N95-16971# Naval Postgraduate School, Monterey, CA.
KNOWLEDGE QUALITY FUNCTIONS FOR RULE DISCOVERY M.S. Thesis
Elizabeth S. Walters and Frank J. Bunn Sep. 1994 63 p
(AD-A285513) Avail: CASI HC A04/MF A01

The Department of Defense (DOD) possesses tremendous amounts of data stored in many large databases. Due to the size of these databases, humans are incapable of efficiently discovering interesting and useful patterns so an automated data-mining tool is necessary. Output in the form of production rules, ie., 'If y Then x,' is preferred because they are understandable by humans and support decision making processes. This thesis investigates the manner in which data-mining systems discover useful, interesting, but currently unavailable knowledge. The search and evaluation process, guided by a knowledge quality function, is the key task of a data-mining system. This thesis evaluates three knowledge quality functions taken from the literature. Each knowledge quality function discovers new and interesting sets of rules reflecting different characteristics of knowledge. DOD applications are suggested for each of the knowledge quality functions. DTIC

N95-16972# Naval Postgraduate School, Monterey, CA.
AN ANALYSIS OF INTERNET'S MBONE: A MEDIA CHOICE PERSPECTIVE M.S. Thesis
John R. Gambrino Sep. 1994 107 p
(AD-A285514) Avail: CASI HC A06/MF A02

This thesis examines the perceived effectiveness of Internet's Multicast Backbone (MBONE) compressed-motion video-teleconferencing system and analyzes its capabilities and limitations. The analysis follows the media richness model of media choice and discusses seven influences on a managers' media selection. This study expands the video-teleconferencing branch of the continuum of communication media to include compressed-motion video-teleconferencing and the distinguishing factors between systems. The study uses data gathered from the Monterey Bay Aquarium Research Institute's (MBARI) Internet conference experiment to compare MBONE versus face-to-face viewer perceptions of the different communication media and to support the theoretical analysis. The survey instrument used to gather data is presented in this thesis. Research results showed that the compressed motion video image of MBONE filtered and restricted the conveyance of some non-verbal cues and that feedback could be delayed in one-to-many situations. MBONE is found to be more effective for reducing uncertainty than resolving equivocal communication situations. This framework for analysis will enable those responsible for the selection of communication media within the Department of Defense (DOD) to have a basis for distinguishing between choices of video-teleconferencing systems. DTIC

N95-17166 RAND Corp., Santa Monica, CA.
DATA REARRANGEMENT AND REAL-TIME COMPUTATION
Philip N. Armstrong 1993 116 p Limited Reproducibility: More than 20% of this document may be affected by microfiche quality
(AD-A282349) Avail: Issuing Activity (Defense Technical Information Center (DTIC))

Data rearrangement is among the most prevalent and time-consuming tasks for which computers are used. Some idea of the prevalence of this task may be gained by observing that the memory input sequence is different from the memory output sequence in nearly every computer program. This report has been prepared to display special switching networks and memory systems that permit simultaneous storage and rearrangement of data so that the required difference between input and output data sequences can be accommodated without expenditure of time. DTIC

N95-17322*# Colorado Univ., Boulder, CO. Colorado Space Grant Consortium.
EXPERIMENTER'S LABORATORY FOR VISUALIZED INTERACTIVE SCIENCE Final Report
Elaine R. Hansen, Daniel R. Rodier, and Marjorie K. Klemp Dec. 1994 44 p
(Contracts NAS5-32337; RTOP 656-65-07; USRA-C-5555-14)
(NASA-CR-189391; NAS 1.26:189391) Avail: CASI HC A03/MF A01

ELVIS (Experimenter's Laboratory for Visualized Interactive Science) is an interactive visualization environment that enables scientists, students, and educators to visualize and analyze large, complex, and diverse sets of scientific data. It accomplishes this by presenting the data sets as 2-D, 3-D, color, stereo, and graphic images with movable and multiple light sources combined with displays of solid-surface, contours, wire-frame, and transparency. By simultaneously rendering diverse data sets acquired from multiple sources, formats, and resolutions and by interacting with the data through an intuitive, direct-manipulation interface, ELVIS provides an interactive and responsive environment for exploratory data analysis. Author

N95-17323*# Wisconsin Univ., Madison, WI.
McIDAS-eXplorer: A VERSION OF McIDAS FOR PLANETARY APPLICATIONS Final Report
Sanjay S. Limaye, R. Stephen Saunders, Lawrence A. Sromovsky, and Michael Martin 15 Sep. 1994 276 p
(Contracts NAS5-32337; NAS5-31347; RTOP 656-65-07; USRA-C-5555-08)
(NASA-CR-189382; NAS 1.26:189382) Avail: CASI HC A13/MF A03

McIDAS-eXplorer is a set of software tools developed for analysis of planetary data published by the Planetary Data System on CD-ROM's. It is built upon McIDAS-X, an environment which has been in use nearly two decades now for earth weather satellite data applications in research and routine operations. The environment allows convenient access, navigation, analysis, display, and animation of planetary data by utilizing the full calibration data accompanying the planetary data. Support currently exists for Voyager images of the giant planets and their satellites; Magellan radar images (F-MIDR and C-MIDR's, global map products (GxDR's), and altimetry data (ARCDR's)); Galileo SSI images of the earth, moon, and Venus; Viking Mars images and MDIM's as well as most earth based telescopic images of solar system objects (FITS). The NAIF/JPL SPICE kernels are used for image navigation when available. For data without the SPICE kernels (such as the bulk of the Voyager Jupiter and Saturn imagery and Pioneer Orbiter images of Venus), tools based on NAIF toolkit allow the

user to navigate the images interactively. Multiple navigation types can be attached to a given image (e.g., for ring navigation and planet navigation in the same image). Tools are available to perform common image processing tasks such as digital filtering, cartographic mapping, map overlays, and data extraction. It is also possible to have different planetary radii for an object such as Venus which requires a different radius for the surface and for the cloud level. A graphical user interface based on Tel-Tk scripting language is provided (UNIX only at present) for using the environment and also to provide on-line help. It is possible for end users to add applications of their own to the environment at any time. Author (revised)

N95-17325*# California Inst. of Tech., Pasadena, CA.
MULTIVARIATE STATISTICAL ANALYSIS SOFTWARE TECHNOLOGIES FOR ASTROPHYSICAL RESEARCH INVOLVING LARGE DATA BASES Final Technical Report, 1993-1994
S. George Djorgovski 12 Nov. 1994 208 p
(Contracts NAS5-32337; NAS5-31348; RTOP 656-65-07; USRA-C-5555-32)
(NASA-CR-189393; NAS 1.26:189393) Avail: CASI HC A10/MF A03

We developed a package to process and analyze the data from the digital version of the Second Palomar Sky Survey. This system, called SKICAT, incorporates the latest in machine learning and expert systems software technology, in order to classify the detected objects objectively and uniformly, and facilitate handling of the enormous data sets from digital sky surveys and other sources. The system provides a powerful, integrated environment for the manipulation and scientific investigation of catalogs from virtually any source. It serves three principal functions: image catalog construction, catalog management, and catalog analysis. Through use of the GID3* Decision Tree artificial induction software, SKICAT automates the process of classifying objects within CCD and digitized plate images. To exploit these catalogs, the system also provides tools to merge them into a large, complete database which may be easily queried and modified when new data or better methods of calibrating or classifying become available. The most innovative feature of SKICAT is the facility it provides to experiment with and apply the latest in machine learning technology to the tasks of catalog construction and analysis. SKICAT provides a unique environment for implementing these tools for any number of future scientific purposes. Initial scientific verification and performance tests have been made using galaxy counts and measurements of galaxy clustering from small subsets of the survey data, and a search for very high redshift quasars. All of the tests were successful, and produced new and interesting scientific results. Attachments to this report give detailed accounts of the technical aspects for multivariate statistical analysis of small and moderate-size data sets, called STATPROG. The package was tested extensively on a number of real scientific applications, and has produced real, published results. Author

N95-17326*# Illinois Univ. at Urbana-Champaign, Savoy, IL. National Center for Supercomputing Applications.
A DISTRIBUTED ANALYSIS AND VISUALIZATION SYSTEM FOR MODEL AND OBSERVATIONAL DATA Final Report, 31 Jul. 1991 - 31 Jul. 1994
Robert B. Wilhelmson 1 Sep. 1994 12 p
(Contracts NAS5-32337; RTOP 656-65-07; USRA-C-5555-06)
(NASA-CR-189386; NAS 1.26:189386; NRA-89-OSSA-21) Avail: CASI HC A03/MF A01

Software was developed with NASA support to aid in the analysis and display of the massive amounts of data generated from satellites, observational field programs, and from model simulations. This software was developed in the context of the PATHFINDER (Probing ATmospHeric Flows in an Interactive and Distributed EnviRonment) Project. The overall aim of this project is to create a flexible, modular, and distributed environment for data handling, modeling simulations, data analysis, and visualization of atmospheric and fluid flows. Software completed with NASA support includes GEMPAK analysis, data handling, and display modules for which collaborators at NASA had primary responsibility, and prototype software modules for three-dimensional interactive and distributed control and display as well as data handling, for which NSCA was responsible. Overall process control was handled through a scientific and visualization application builder from Silicon Graphics known as the Iris Explorer. In addition, the GEMPAK related work (GEMVIS) was also ported to the Advanced Visualization System (AVS) application builder. Many modules were developed to enhance those already available in Iris Explorer including HDF file support, improved visualization and display, simple lattice math, and the handling of metadata through development of a new grid datatype. Complete source and runtime binaries along with on-line documentation is available via the World Wide Web at: http://redrock.ncsa.uiuc.edu/PATHFINDER/pathre12/top/top.html. Author (revised)

N95-17328*# Space Telescope Science Inst., Baltimore, MD. Association of Universities for Research in Astronomy.
DEVELOPMENT OF A DATA REDUCTION EXPERT ASSISTANT Final Report, Jul. 1993 - Jun. 1994
Glenn E. Miller 5 Jul. 1994 29 p
(Contracts NAS5-32337; RTOP 656-65-07; USRA-C-5555-02)
(NASA-CR-189385; NAS 1.26:189385) Avail: CASI HC A03/MF A01

This report documents the development and deployment of the Data Reduction Expert Assistant (DRACO). The system was successfully applied to two astronomical research projects. The first was the removal of cosmic ray artifacts from Hubble Space Telescope (HST) Wide Field Planetary Camera data. The second was the reduction and calibration of low-dispersion CCD spectra taken from a ground-based telescope. This has validated our basic approach and demonstrated the applicability of this technology. This work has been made available to the scientific community in two ways. First, we have published the work in the scientific literature and presented papers at relevant conferences. Secondly, we have made the entire system (including documentation and source code) available to the community via the World Wide Web. Author

N95-17329*# Brandeis Univ., Waltham, MA. Dept. of Computer Science.
HIGH PERFORMANCE COMPRESSION OF SCIENCE DATA Final Report
James A. Storer and Martin Cohn Aug. 1994 17 p
(Contracts NAS5-32337; NAS5-31354; RTOP 656-65-07; USRA-C-5555-11)
(NASA-CR-189388; NAS 1.26:189388) Avail: CASI HC A03/MF A01

Two papers make up the body of this report. One presents a single-pass adaptive vector quantization algorithm that learns a codebook of variable size and shape entries; the authors present experiments on a set of test images showing that with no training or prior knowledge of the data, for a given fidelity, the compression achieved typically equals or exceeds that of the JPEG standard. The second paper addresses motion compensation, one of the most effective techniques used in the interframe data compression. A parallel block-matching algorithm for estimating interframe displacement of blocks with minimum error is presented. The algorithm is designed for a simple parallel architecture to process video in real time. Author

N95-17330*# Texas A&M Univ., College Station, TX. Dept. of Meteorology.
AN INTERACTIVE ENVIRONMENT FOR THE ANALYSIS OF LARGE EARTH OBSERVATION AND MODEL DATA SETS Final Report, 5 Jun. 1991 - 4 Jun. 1994
Kenneth P. Bowman, John E. Walsh (Illinois Univ., Urbana, IL.), and Robert B. Wilhelmson (Illinois Univ., Urbana, IL.) Sep. 1994 10 p
(Contracts NAS5-32337; RTOP 656-65-07; USRA-C-5555-03; USRA-C-5555-04)
(NASA-CR-189381; NAS 1.26:189381) Avail: CASI HC A02/MF A01

Envision is an interactive environment that provides researchers in the earth sciences convenient ways to manage, browse, and visualize large observed or model data sets. Its main features are support for the netCDF and HDF file formats, an easy to use X/Motif user interface, a client-server configuration, and portability to many UNIX workstations. The Envision package also provides new ways to view and change metadata in a set of data files. It permits a scientist to conveniently and efficiently manage large data sets consisting of many data files. It also provides links to popular visualization tools so that data can be quickly browsed. Envision is a public domain package, freely available to the scientific community. Envision software (binaries and source code) and documentation can be obtained from either of these servers: ftp://vista.atmos.uiuc.edu/pub/envision/ and ftp://csrp.tamu.edu/pub/envision/. Detailed descriptions of Envision capabilities and operations can be found in the User's Guide and Reference Manuals distributed with Envision software. Author (revised)

N95-17472# International Atomic Energy Agency, Vienna (Austria).
DIRECTORY OF IAEA DATABASES
Dec. 1993 124 p
(DE94-622696; INIS-mf-13856) Avail: CASI HC A06/MF A02 (US Sales Only)

This second edition of the Directory of IAEA Databases has been prepared within the Division of Scientific and Technical Information. Its main objective is to describe the computerized information sources available to staff members. This directory contains all databases produced at the IAEA, including databases stored on the mainframe, LAN's and PC's. All IAEA Division Directors have been requested to register the existence of their databases with NESI. For the second edition database owners were requested to review the existing entries for their databases and answer four additional questions. The four additional questions concerned the type of database (e.g. Bibliographic, Text, Statistical etc.), the category of database (e.g. Administrative, Nuclear Data etc.), the available documentation and the type of media used for distribution. In the individual entries on the following pages the answers to the first two questions (type and category) is always listed, but the answer to the second two questions (documentation and media) is only listed when information has been made available.
DOE

N95-17491*# Institute of Global Environment and Society, Inc., Calverton, MD. Center for Ocean-Land-Atmosphere Studies.
THE GRID ANALYSIS AND DISPLAY SYSTEM (GrADS) Final Report, 1 Sep. 1993 - 31 Aug. 1994
James L. Kinter, III Oct. 1994 8 p
(Contracts NAS5-32337; RTOP-656-65-07; USRA-C-5555-31)
(NASA-CR-189387; NAS 1.26:189387) Avail: CASI HC A02/MF A01

During the period 1 September 1993 - 31 August 1994, further development of the Grid Analysis and Display System (GrADS) was conducted at the Center for Ocean-Land-Atmosphere Studies (COLA) of the Institute of Global Environment and Society, Inc. (IGES) under subcontract 5555-31 from the University Space Research Association (USRA) administered by The Center of Excellence in Space Data and Information Sciences (CESDIS). This final report documents progress made under this subcontract and provides directions on how to access the software and documentation developed therein. A short description of GrADS is provided followed by summary of progress completed and a summary of the distribution of the software to date and the establishment of research collaborations. Author

N95-17633# Department of Defense, Washington, DC.
DEPARTMENT OF DEFENSE DICTIONARY OF MILITARY AND ASSOCIATED TERMS. INCLUDES US ACRONYMS AND ABBREVIATIONS AND NATO TERMS (ENGLISH ONLY)
23 Mar. 1994 504 p See also Joint-Pub-1-02
(AD-A283218; Joint-Pub-1-02(94); Joint-Pub-1-02) Avail: CASI HC A22/MF A04

This publication sets forth standard military terminology to govern the joint activities and performance of the Armed Forces of the United States in joint operations as well as the terminology basis for US military involvement in multinational and interagency operations. It provides military terminology for use by the Armed Forces in preparing their appropriate plans. It is not the intent of this publication to restrict the authority of the joint force commander (JFC) from organizing the force and executing the mission in a manner the JFC deems most appropriate to ensure unity of effort in the accomplishment of the overall mission. Derived from text

N95-17650# Instituto de Pesquisas Espaciais, Sao Paulo (Brazil). Div. de Processamento de Imagens.
ON THE IMPROVEMENT OF 1-LOOK SAR IMAGE SEGMENTATIONS WITH MATHEMATICAL MORPHOLOGY
Alejandro C. Frery and Ana Lucia BezerreaCandeias 1994 14 p Presented at the European Symposium on Satellite Remote Sensing, Rome, Italy, 26-30 Sep. 1994
(FAPESP Proj. 91/3532-2)
(INPE-5577-PRE/1805) Avail: CASI HC A03/MF A01

Synthetic aperture radar (SAR) images are an important source of information. This kind of imaging is little affected by adverse atmospheric conditions, such as rain, clouds, fog, etc., since it operates at frequencies other than the visible. Also, since the sensor is active and carries its own source of illumination, it can operate by night. The problem that arises with the use of this technology is a signal-dependent noise, called speckle. This kind of noise is common to all imaging devices that use coherent illumination, such as laser, microwaves, etc. One of the most useful techniques for image analysis is the segmentation. Using statistical modeling, two multiclass segmentation techniques for one-look and linear detection SAR images are derived: the maximum likelihood and the iterated conditional modes (ICM), both assuming multiplicative Rayleigh models for the data. Although the ICM segmentation yields significantly better results than the maximum likelihood segmentation, the one-look linear detection case is noisy enough to deserve some improvement. Mathematical morphology, a nonlinear approach to signal processing, is then used as a refinement technique in order to extract information. Author

N95-17652*# Maryland Univ., College Park, MD. Dept. of Computer Science.
AN INCREMENTAL DATABASE ACCESS METHOD FOR AUTONOMOUS INTEROPERABLE DATABASES Final Report
Nicholas Roussopoulos and Timos Sellis 31 Aug. 1994 18 p
(Contracts NAS5-32337; RTOP 656-65-07; USRA-C-5555-09)
(NASA-CR-189384; NAS 1.26:189384) Avail: CASI HC A03/MF A01

We investigated a number of design and performance issues of interoperable database management systems (DBMS's). The major results of our investigation were obtained in the areas of client-server database architectures for heterogeneous DBMS's, incremental computation models, buffer management techniques, and query optimization. We finished a prototype of an advanced client-server workstation-based DBMS which allows access to multiple heterogeneous commercial DBMS's. Experiments and simulations were then run to compare its performance with the standard client-server architectures. The focus of this research was on adaptive optimization methods of heterogeneous database systems. Adaptive buffer management accounts for the random and object-oriented access methods for which no known characterization of the access patterns exists. Adaptive query optimization means that value distributions and selectives, which play the most significant role in query plan evaluation, are continuously refined to reflect the actual values as opposed to static ones that are computed off-line. Query feedback is a concept that was first introduced to the literature by our group. We employed query feedback for both adaptive buffer management and for computing value distributions and selectivities. For adaptive buffer management, we use the page faults of prior executions to achieve more 'informed' management decisions. For the estimation of the distributions of the selectivities, we use curve-fitting techniques, such as least squares and splines, for regressing on these values. Author

N95-17660 Defense Technical Information Center, Alexandria, VA.
DROLS: AN INTRODUCTION TO SEARCHING (VIDEORECORDING) Final Report
Richard J. Wayman, Holly J. Wilson, and Christian M. Cupp 1 Apr. 1994 See also AD-M000339
(AD-M000338; DTIC-94/15-VR; NONP-DTIC-VT-94-14638) Avail: Issuing Activity (Defense Technical Information Center (DTIC))

The Defense RDT and E Online System (DROLS) training video is designed to tutor new and infrequent DROLS users in the basic operational skills needed to navigate the system. This video concentrates on building search strategies by employing the use of boolean operators, DTIC's thesaurus of controlled vocabulary, and inverted file browsing feature. The use of special search options such as truncation, hierarchy, and term weighting are also addressed. DTIC

N95-17710# Logistics Management Inst., Bethesda, MD.
DEPARTMENT OF DEFENSE ELECTRONIC DATA INTERCHANGE PROJECT BASELINE REPORT FOR FY 1994 Final Report
Morey M. Henderson and John B. Harris Jun. 1994 54 p
(Contract MDA903-90-C-0006)
(AD-A283015; LMI-PL311RD1) Avail: CASI HC A04/MF A01

Information about the Department of Defense Electronic Data Interchange (EDI) project portfolio for FY94 is presented. Information includes: the volume of paper forms to be converted to EDI, EDI project descriptions, and EDI standards being used by DOD projects. More than 60 EDI projects are described. These projects, reported by three military services and four

defense agencies, address the functional areas of procurement, contracting, transportation, supply, maintenance, fuels, and finance. DTIC

N95-16351# Naval Air Warfare Center, China Lake, CA. Weapons Div.
OVERVIEW OF TTCP AND AGARD PROPULSION ACTIVITIES
R. L. Derr and C. F. Markarian *In* JHU, The 1993 JANNAF Propulsion Meeting, Volume 2 Nov. 1993 p 331-343 (For primary document see N95-16324 04-20)
Avail: CASI HC A03/MF A04

N95-16464*# National Aeronautics and Space Administration. Langley Research Center, Hampton, VA.
USE OF WORLD WIDE WEB AND NCSA MCSAIC AT LANGLEY
Michael Nelson *In its* The Role of Computers in Research and Development at Langley Research Center Oct. 1994 p 224-236 (For primary document see N95-16453 04-62)
Avail: CASI HC A03/MF A06

N95-16465*# National Aeronautics and Space Administration. Langley Research Center, Hampton, VA.
HOW TO USE THE WWW TO DISTRIBUTE STI
Donna G. Roper *In its* The Role of Computers in Research and Development at Langley Research Center Oct. 1994 p 237-245 (For primary document see N95-16453 04-62)
Avail: CASI HC A02/MF A06

N95-16467*# Hampton Univ., VA.
FROM COMPUTER IMAGES TO VIDEO PRESENTATION: ENHANCING TECHNOLOGY TRANSFER
Sherilee F. Beam *In* NASA. Langley Research Center, The Role of Computers in Research and Development at Langley Research Center Oct. 1994 p 266-271 (For primary document see N95-16453 04-62)
Avail: CASI HC A02/MF A06

N95-17193*# National Aeronautics and Space Administration. Goddard Space Flight Center, Greenbelt, MD.
THE DEVELOPMENT AND OPERATION OF THE INTERNATIONAL SOLAR-TERRESTRIAL PHYSICS CENTRAL DATA HANDLING FACILITY
Kenneth Lehtonen *In its* Third International Symposium on Space Mission Operations and Ground Data Systems, Part 1 Nov. 1994 p 125-132 (For primary document see N95-17179 04-17)
Avail: CASI HC A02/MF A06

N95-17194*# Jet Propulsion Lab., California Inst. of Tech., Pasadena, CA.
ECONOMICAL GROUND DATA DELIVERY
Richard W. Markley, Russell H. Byrne, and Daniel E. Bromberg *In* NASA. Goddard Space Flight Center, Third International Symposium on Space Mission Operations and Ground Data Systems, Part 1 Nov. 1994 p 133-138 (For primary document see N95-17179 04-17)
Avail: CASI HC A02/MF A06

N95-17195*# National Aeronautics and Space Administration. Lyndon B. Johnson Space Center, Houston, TX.
NASA JOHNSON SPACE CENTER LIFE SCIENCES DATA SYSTEM
Hasan Rahman (Martin Marietta Corp., Houston, TX.) and Jeffery Cardenas *In* NASA. Goddard Space Flight Center, Third International Symposium on Space Mission Operations and Ground Data Systems, Part 1 Nov. 1994 p 139-147 (For primary document see N95-17179 04-17)
Avail: CASI HC A02/MF A06

N95-17197*# McDonnell-Douglas Space Systems Co., Cocoa Beach, FL.
SINGLE STAGE ROCKET TECHNOLOGY'S REAL TIME DATA SYSTEM
Steven D. Voglewede *In* NASA. Goddard Space Flight Center, Third International Symposium on Space Mission Operations and Ground Data Systems, Part 1 Nov. 1994 p 155-168 (For primary document see N95-17179 04-17)
Avail: CASI HC A03/MF A06

N95-17199*# Jet Propulsion Lab., California Inst. of Tech., Pasadena, CA.
ARACHNID: A PROTOTYPE OBJECT-ORIENTED DATABASE TOOL FOR DISTRIBUTED SYSTEMS
Herbert Younger, John OReilly (MIMD Systems, Inc., Palo Alto, CA.), and Bjorn Frogner (MIMD Systems, Inc., Palo Alto, CA.) *In* NASA. Goddard Space Flight Center, Third International Symposium on Space Mission Operations and Ground Data Systems, Part 1 Nov. 1994 p 177-183 (For primary document see N95-17179 04-17)
(Contract NAS7-1156)
Avail: CASI HC A02/MF A06

N95-17245*# National Aeronautics and Space Administration. Goddard Space Flight Center, Greenbelt, MD.
GENERIC TRENDING AND ANALYSIS SYSTEM
Lori Keehan and Jay Reese (Loral AeroSys, Seabrook, MD.) *In its* Third International Symposium on Space Mission Operations and Ground Data Systems, Part 1 Nov. 1994 p 577-582 (For primary document see N95-17179 04-17)
Avail: CASI HC A02/MF A06

N95-17536*# Deutsche Forschungsanstalt fuer Luft- und Raumfahrt, Cologne (Germany).
DEVELOPMENT OF USE OF AN OPERATIONAL PROCEDURE INFORMATION SYSTEM (OPIS) FOR FUTURE SPACE MISSIONS
N. Illmer, L. Mies, A. Schoen, and A. Jain (WIB G.m.b.H., Berlin, Germany.) *In* NASA. Goddard Space Flight Center, Third International Symposium on Space Mission Operations and Ground Data Systems, Part 2 Nov. 1994 p 713-717 (For primary document see N95-17531 04-17)
Avail: CASI HC A01/MF A06

N95-17557*# Jet Propulsion Lab., California Inst. of Tech., Pasadena, CA.
AUTOMATING TESTBED DOCUMENTATION AND DATABASE ACCESS USING WORLD WIDE WEB (WWW) TOOLS
Charles Ames, Brent Auernheimer (California State Univ., Fresno, CA.), and Young H. Lee *In* NASA. Goddard Space Flight Center, Third International Symposium on Space Mission Operations and Ground Data Systems, Part 2 Nov. 1994 p 899-904 (For primary document see N95-17531 04-17)
Avail: CASI HC A02/MF A06

N95-17563*# Centre National d'Etudes Spatiales, Toulouse (France).
ELISA, A DEMONSTRATOR ENVIRONMENT FOR INFORMATION SYSTEMS ARCHITECTURE DESIGN
Chantal Panem *In* NASA. Goddard Space Flight Center, Third International Symposium on Space Mission Operations and Ground Data Systems, Part 2 Nov. 1994 p 945-952 (For primary document see N95-17531 04-17)
Avail: CASI HC A02/MF A06

N95-17570*# National Aeronautics and Space Administration. Goddard Space Flight Center, Greenbelt, MD.
TAKING ADVANTAGE OF GROUND DATA SYSTEMS ATTRIBUTES TO ACHIEVE QUALITY RESULTS IN TESTING SOFTWARE
Clayton B. Sigman, John T. Koslosky, and Barbara H. Hageman (Integral Systems, Inc., Lanham, MD.) *In its* Third International Symposium on Space Mission Operations and Ground Data Systems, Part 2 Nov. 1994 p 1009-1014 (For primary document see N95-17531 04-17)
Avail: CASI HC A02/MF A06

N95-17575*# Computer Technology Associates, Inc., Rockville, MD.
THE ADVANCED ORBITING SYSTEMS TESTBED PROGRAM: RESULTS TO DATE
John F. Otranto and Penny A. Newsome *In* NASA. Goddard Space Flight Center, Third International Symposium on Space Mission Operations and Ground Data Systems, Part 2 Nov. 1994 p 1045-1054 Sponsored by NASA, Washington (For primary document see N95-17531 04-17)
Avail: CASI HC A02/MF A06

N95-17577*# National Aeronautics and Space Administration. Goddard Space Flight Center, Greenbelt, MD.
EVALUATION OF NASA'S END-TO-END DATA SYSTEMS USING DSDS+
Christopher Rouff, William Davenport, and Philip Message (Stanford Telecommunications, Inc., Seabrook, MD.) *In its* Third International Symposium on Space Mission Operations and Ground Data Systems, Part 2 Nov. 1994 p 1063-1069 (For primary document see N95-17531 04-17)
Avail: CASI HC A02/MF A06

N95-17588*# Jet Propulsion Lab., California Inst. of Tech., Pasadena, CA.
CUSTOMIZING THE JPL MULTIMISSION GROUND DATA SYSTEM: LESSONS LEARNED
Susan C. Murphy, John J. Louie, Ana Maria Guerrero, Daniel Hurley, and Dana Flora-Adams *In* NASA. Goddard Space Flight Center, Third International Symposium on Space Mission Operations and Ground Data Systems, Part 2 Nov. 1994 p 1171-1175 (For primary document see N95-17531 04-17)
Avail: CASI HC A01/MF A06

N95-17591*# McDonnell-Douglas Aerospace, Huntington Beach, CA. Space Station Div.
STANDARDIZING THE INFORMATION ARCHITECTURE FOR SPACECRAFT OPERATIONS
C. R. Easton *In* NASA. Goddard Space Flight Center, Third International Symposium on Space Mission Operations and Ground Data Systems, Part 2 Nov. 1994 p 1197-1204 (For primary document see N95-17531 04-17)
Avail: CASI HC A02/MF A06

N95-17604*# National Aeronautics and Space Administration. Goddard Space Flight Center, Greenbelt, MD.
RENAISSANCE ARCHITECTURE FOR GROUND DATA SYSTEMS
Dorothy C. Perkins and Lawrence B. Zeigenfuss *In its* Third International Symposium on Space Mission Operations and Ground Data Systems, Part 2 Nov. 1994 p 1305-1316 (For primary document see N95-17531 04-17)
Avail: CASI HC A03/MF A06

N95-17607*# Loral AeroSys, Seabrook, MD.
MO/DSD ONLINE INFORMATION SERVER AND GLOBAL INFORMATION REPOSITORY ACCESS
Diem Nguyen, Kam Ghaffarian, Keith Hogie (Computer Sciences Corp., Lanham, MD.), and William Mackey (Computer Sciences Corp., Lanham, MD.) *In* NASA. Goddard Space Flight Center, Third International Symposium on Space Mission Operations and Ground Data Systems, Part 2 Nov. 1994 p 1335-1342 (For primary document see N95-17531 04-17)
Avail: CASI HC A02/MF A06

83 ECONOMICS AND COST ANALYSIS

Includes cost effectiveness studies.

N95-15962# General Accounting Office, Washington, DC. National Security and International Affairs Div.
NASA CONTRACT MANGAGEMENT: IMPROVING THE USE OF DCAA'S AUDITING SERVICES. REPORT TO THE CHAIRMAN, COMMITTEE ON GOVERNMENT OPERATIONS, HOUSE OF REPRESENTATIVES
30 Sep. 1994 27 p
(GAO/NSIAD-94-229; B-257877) Avail: CASI HC A03/MF A01; GAO, PO Box 6015, Gaithersburg, MD 20884-6015 HC

The National Aeronautics and Space Administration's (NASA) management and use of audit support provided by the Department of Defense's (DOD) Defense Contract Audit Agency (DCAA) were reviewed. NASA relies extensively on DCAA to provide audit and financial advisory services on the billions of dollars of contracts NASA awards. This report assess NASA's (1) need for an enforcement mechanism to deter contractors from claiming unallowable costs, (2) use of DCAA proposal audit services, (3) involvement in audit planning, (4) oversight of contract audit and administration services, and (5) backlog of contracts awaiting closeout.
Author (revised)

84 LAW, POLITICAL SCIENCE AND SPACE POLICY

Includes NASA appropriation hearings; aviation law; space law and policy; international law; international cooperation; and patent policy.

No abstracts in this category.

85 URBAN TECHNOLOGY AND TRANSPORTATION

Includes applications of space technology to urban problems; technology transfer; technology assessment; and surface and mass transportation.

For related information see also *03 Air Transportation and Safety, 16 Space Transportation,* and *44 Energy Production and Conversion.*

No abstracts in this category.

88 SPACE SCIENCES (GENERAL)

No abstracts in this category.

89 ASTRONOMY

Includes radio, gamma-ray, and infrared astronomy, and astrometry.

N95-15964*# California Univ., Los Angeles, CA. Dept. of Physics and Space Sciences Center.
A RARE GAS OPTICS-FREE ABSOLUTE PHOTON FLUX AND ENERGY ANALYZER TO PROVIDE ABSOLUTE PHOTOIONIZATION RATES OF INFLOWING INTERSTELLAR NEUTRALS Final Report, 1 Dec. 1991 - 31 May 1994
Darrell L. Judge Nov. 1994 26 p
(Grant NAGw-2677)
(NASA-CR-197228; NAS 1.26:197228) Avail: CASI HC A03/MF A01

A prototype spectrometer has been developed for space applications requiring long term absolute EUV photon flux measurements. The energy spectrum of the incoming photons is transformed directly into an electron energy spectrum by taking advantage of the photoelectric effect in one of several rare gases at low pressures. Using an electron energy spectrometer, followed by an electron multiplier detector, pulses due to individual electrons are counted. The overall efficiency of this process can be made essentially independent of gain drifts in the signal path, and the secular degradation of optical components which is often a problem in other techniques is avoided. A very important feature of this approach is its freedom from the problem of overlapping spectral orders that plagues grating EUV spectrometers. An instrument with these features has not been flown before, but is essential to further advances in our understanding of solar EUV flux

dynamics, and the coupled dynamics of terrestrial and planetary atmospheres. The detailed characteristics of this optics-free spectrometer are presented in the publications section. Derived from text

N95-16021*# University of Southern California, Los Angeles, CA. Dept. of Physics.

A RARE GAS OPTICS-FREE ABSOLUTE PHOTON FLUX AND ENERGY ANALYZER FOR SOLAR AND PLANETARY OBSERVATIONS Final Technical Report, 1 Jan. 1991 - 31 Dec. 1993

Darrell L. Judge Nov. 1994 27 p

(Grant NAGw-2354)

(NASA-CR-197227; NAS 1.26:197227) Avail: CASI HC A03/MF A01

We have developed a prototype spectrometer for space applications requiring long term absolute EUV photon flux measurements. In this recently developed spectrometer, the energy spectrum of the incoming photons is transformed directly into an electron energy spectrum by taking advantage of the photoelectric effect in one of several rare gases at low pressures. Using an electron energy spectrometer, followed by an electron multiplier detector, pulses due to individual electrons are counted. The overall efficiency of this process can be made essentially independent of gain drifts in the signal path, and the secular degradation of optical components which is often a problem in other techniques is avoided. A very important feature of this approach is its freedom from the problem of overlapping spectral orders that plagues grating EUV spectrometers. An instrument with these features has not been flown before, but is essential to further advances in our understanding of solar EUV flux dynamics, and the coupled dynamics of terrestrial and planetary atmospheres. The detailed characteristics of this optics-free spectrometer are presented in the publications section. Derived from text

N95-16558*# National Aeronautics and Space Administration. Marshall Space Flight Center, Huntsville, AL.

NASA MARSHALL SPACE FLIGHT CENTER SOLAR OBSERVATORY REPORT, MARCH - MAY 1994

J. E. Smith Washington Dec. 1994 35 p

(NASA-TM-108471; NAS 1.15:108471) Avail: CASI HC A03/MF A01

This report provides a description of the NASA Marshall Space Flight Center's Solar Vector Magnetograph Facility and gives a summary of its observations and data reduction during March-May 1994. The systems that make up the facility are a magnetograph telescope, an H-alpha telescope, a Questar telescope, and a computer code. Author

N95-16854 Department of the Navy, Washington, DC.

SPACE-BASED ASTEROID DETECTION AND MONITORING SYSTEM Patent Application

William A. Shaffer, inventor (to Navy) and Martin J. McHugh, inventor (to Navy) 25 Jan. 1994 21 p Limited Reproducibility: More than 20% of this document may be affected by microfiche quality

(AD-D016329; US-Patent-Appl-SN-186075; Navy-Case-75384) Avail: Issuing Activity (Defense Technical Information Center (DTIC))

A satellite-borne system for the detection of near earth objects is presented. The system periodically captures two images of the celestial sphere about the earth using a pair of linear arrays of optical detectors oriented so that the detectors image lines on the celestial sphere that are separated at each pixel in azimuth by the same angle. The position of the linear detectors is varied for each orbit of the earth by the satellite such that the entire celestial sphere can be imaged. The images produced by the two detector arrays are temporarily stored in memory until they can be processed using frame difference signal processing techniques. The results from the frame difference signal processing are transmitted at a ground station for further processing. The processing on the ground can include object classification, orbit tracking (using a time sequence of differenced frames), and earth collision determination and warning. DTIC

N95-17494*# Computer Sciences Corp., Calverton, MD. System Sciences Div.

THE Mg 2 LINES AS DIAGNOSTIC OF PMS NATURE IN HERBIG Ae/Be STARS Final Report

1994 5 p

(NASA Order S-93073-E)

(NASA-CR-197518; NAS 1.26:197518) Avail: CASI HC A01/MF A01

The main objective of this program was to observe some newly discovered and previously unobserved Herbig Ae/Be (HAeBe) stars with IUE. A previous archival study suggested that there was a full range of profiles in the Mg II lines for these objects; ranging from the double peak emission to the narrow absorption lines. It has been found that by studying the IUE data of main sequence B and classical Be stars that the P Cygni profiles in the Mg II lines in HAeBe stars are truly unique and are the signature of accelerating winds in their extended circumstellar material. The arguement, for the purposes of this proposal, that the structure of the Mg II lines was a superior diagnostic of the dynamical activity and ultimately the PMS nature of these objects. This program was a follow up study of several interesting intermediate-mass stars with the goal of classifying these objects based on the shape of their MG II lines. A list of publications resulting from this research is included. Author

N95-17495*# Johns Hopkins Univ., Baltimore, MD. Dept. of Physics and Astronomy.

THE MASS AND DYNAMICS OF cD CLUSTERS WITH COOLING FLOWS. 1: ROSAT OBSERVATIONS OF A 496 Final Technical Report

Gerard A. Kriss 15 Dec. 1994 16 p

(Grant NAG5-1636)

(NASA-CR-197534; NAS 1.26:197534) Avail: CASI HC A03/MF A01

As part of a program to determine the mass distribution of cD galaxy clusters with cooling flows, we obtained a ROSAT image of the cluster A 496. The image reveals sharply peaked emission centered on the cD galaxy. Both the peaked cooling flow emission and the more extended emission filling the cluster are centered on the cD galaxy to within 15 sec . The surface brightness profile is consistent with previous Einstein observations. We measure spatially resolved spectra for the X-ray emission, and find a significant decline in temperature in the innermost 2 min to 4 min. We also find a gradient in absorption due to cold neutral gas, with an excess above the neutral hydrogen column due to our own galaxy in the inner 4 min. The excess absorption, however, is far below previously reported values. The surface brightness profile and the spatially resolved temperature profile are indicative of a cooling flow in the cluster. Cooling flow models fit to the X-ray spectra in the innermost 2 min yield a mass flow rate of 59 solar mass yr(exp -1). The spatially resolved temperature and surface brightness profiles are used to derive the mass distribution of the cluster both in the hot, X-ray emitting plasma and in the unseen dark matter that binds the cluster. To a radius of 1.0 Mpc we find a total cluster mass of 3.44 x 10(exp 14) solar mass ; the X-ray emitting gas mass of 0.75 x 10(exp 14) solar mass to this radius comprises 16 percent of the total cluster mass. Author

N95-17496*# Colorado Univ., Boulder, CO. Center for Astrophysics and Space Astronomy.

ROSAT DETECTION OF DIFFUSE HOT GAS IN THE EDGE-ON GALAXY NGC 4631

Q. David Wang, Rene A. M. Walterbos (New Mexico State Univ., Las Cruces, NM.), Michael F. Steakley (New Mexico State Univ., Las Cruces, NM.), Colin A. Norman (Johns Hopkins Univ., Baltimore, MD.), and Robert Braun (Netherlands Foundation for Research in Astronomy, Dwingelo, Netherlands.) 1994 25 p

(Grants NAG5-1924; NAG5-2014; NAG5-1y29; NSF AST-91-23777)

(NASA-CR-197535; NAS 1.26:197535) Avail: CASI HC A03/MF A01

ROSAT observation is presented of the edge-on spiral galaxy NGC 4631, a nearby Sc/SBd galaxy best known for its extended radio halo. Because of the low foreground Galactic X-ray-absorbing gas column density, N(sub H) approximately 1.4 x 10(exp 20)cm(exp -2), this observation is sensitive to gas of temperature greater than or equal to a few times 10(exp 5) K. A soft (approximately 0.25 keV) X-ray radiation out to more than 8 kpc above the midplane of the galaxy was detected. The strongest X-ray emission in the halo is above the central disk, a region of about 3 kpc radius which shows high star formation activity. The X-ray emission in the halo is bordered by two extended filaments of radio continuum emission. Diffuse X-ray emission from hot gas in the galaxy's disk was found. The spectrum of the radiation can be characterized by a thermal plasma with a temperature of 3 x 10(exp 6) K and a radiative cooling rate of approximately 8 x 10(exp 39) ergs s(exp -1). This rate is only a few percent of the estimated supernova energy release in the interstellar medium of the galaxy. Analysis of the X-ray spectrum shows evidence for the presence of a cooler (several times 10(exp 5) K) halo gas component that could consume a much larger fraction of the supernova energy. Strong evidence was

found for disk/halo interaction. Hot gas apparently blows out from supershells in the galaxy's disk at a rate of approximately 1 solar mass yr(exp -1). This outflow of hot gas drags magnetic field lines up in the halo and forms a magnetized gaseous halo. If the magnetic field lines are still anchored to the disk gas at large disk radii, the outflowing gas may be confined high above the disk by magnetic pressure. A strong X-ray source which coincides spatially with an H I supershell has been identified. However, the source is likely an extremely luminous X-ray binary with L(sub chi)(0.1 - 2 keV) approximately 5 x 10(exp 39) ergs s(exp -1), which makes it a stellar mass black hole candidate. Author

N95-17525# Lawrence Livermore National Lab., Livermore, CA.
ISSUES IN THE DESIGN AND OPTIMIZATION OF ADAPTIVE OPTICS AND LASER GUIDE STARS FOR THE KECK TELESCOPES
C. E. Max, D. T. Gavel, and S. S. Olivier et al Mar. 1994 14 p
Presented at the Society of Photo-Optical Instrumentation Engineers (SPIE) Conference, Kona Beach, HI, 13-18 Mar. 1994 Revised
(Contract W-7405-eng-48)
(DE94-012888; UCRL-JC-116505-Rev-1; CONF-940391-9-Rev-1) Avail: CASI HC A03/MF A01

We discuss issues in optimizing the design of adaptive optics and laser guide star systems for the Keck Telescope. The initial tip-tilt system will use Keck's chopping secondary mirror. We describe design constraints, choice of detector, and expected performance of this tip-tilt system as well as its sky coverage. The adaptive optics system is being optimized for wavelengths of 1-2.2 micro m. We are studying adaptive optics concepts which use a wavefront sensor with varying numbers of subaperatures, so as to respond to changing turbulence conditions. The goal is to be able to 'gang together' groups of deformable mirror subaperatures under software control, when conditions call for larger subaperatures. We present performance predictions as a function of sky coverage and the number of deformable mirror degrees of freedom. We analyze the predicted brightness of several candidate laser guide star systems, as a function of laser power and pulse format. These predictions are used to examine the resulting Strehl as a function of observing wavelength. We discuss laser waste heat and thermal management issues, and conclude with an overview of instruments under design to take advantage of the Keck adaptive optics system. DOE

N95-17528*# Columbia Univ., New York, NY. Astrophysics Lab.
A HIGH RESOLUTION LIQUID XENON IMAGING TELESCOPE FOR 0.3-10 MeV GAMMA-RAY ASTROPHYSICS: CONSTRUCTION AND INITIAL BALLOON FLIGHTS Annual Report, 1 Jan. - 31 Dec. 1994
Elena Aprile 31 Dec. 1994 54 p
(Grant NAGw-2013)
(NASA-CR-197556; NAS 1.26:197556; CAL-2260) Avail: CASI HC A04/MF A01

An instrument is described which will provide a direct image of gamma-ray line or continuum sources in the energy range 300 keV to 10 MeV. The use of this instrument to study the celestial distribution of the (exp 26)Al isotope by observing the 1.809 MeV deexcitation gamma-ray line is illustrated. The source location accuracy is 2' or better. The imaging telescope is a liquid xenon time projection chamber coupled with a coded aperture mask (LXe-CAT). This instrument will confirm and extend the COMPTEL observations from the Compton Gamma-Ray Observatory (CGRO) with an improved capability for identifying the actual Galactic source or sources of (exp 26)Al, which are currently not known with certainty. sources currently under consideration include red giants on the asymptotic giant branch (AGB), novae, Type 1b or Type 2 supernovae, Wolf-Rayet stars and cosmic-rays interacting in molecular clouds. The instrument could also identify a local source of the celestial 1.809 MeV gamma-ray line, such as a recent nearby supernova. Author

90 ASTROPHYSICS

Includes cosmology; celestial mechanics; space plasmas; and interstellar and interplanetary gases and dust.

For related information see also *75 Plasma Physics.*

N95-16020*# Lehigh Univ., Bethlehem, PA.
SHOCK AND THERMAL HISTORY OF IRON AND CHONDRITIC METEORITES Final Report, 1 Apr. 1989 - 31 Mar. 1993
Joseph I. Goldstein 20 Oct. 1994 4 p
(Grant NAG9-45)
(NASA-CR-197125; NAS 1.26:197125) Avail: CASI HC A01/MF A01

This research grant included a study of the shock and thermal history of iron and chondritic meteorites. The important research findings are to be found in the 20 publications that were published as a result of the research support. A complete bibliographic reference to all these papers is given. Derived from text

N95-16032*# Johns Hopkins Univ., Baltimore, MD. Center for Astrophysical Sciences.
DUST NEAR LUMINOUS ULTRAVIOLET STARS Final Report
Richard C. Henry 30 Sep. 1993 37 p
(Grant NAG5-1282)
(NASA-CR-197108; NAS 1.26:197108) Avail: CASI HC A03/MF A01

This report describes research activities related to the Infrared Astronomical Satellite (IRAS) sky survey. About 745 luminous stars were examined for the presence of interstellar dust heated by a nearby star. The 'cirrus' discovered by IRAS is thermal radiation from interstellar dust at moderate and high galactic latitudes. The IRAS locates the dust which must (at some level) scatter ultraviolet starlight, although it was expected that thermal emission would be found around virtually every star, most stars shown no detectable emission. And the emission found is not uniform. It is not that the star is embedded in 'an interstellar medium', but rather what is found are discrete clouds that are heated by starlight. An exception is the dearth of clouds near the very hottest stars, implying that the very hottest stars play an active role with respect to destroying or substantially modifying the dust clouds over time. The other possibility is simply that the hottest stars are located in regions lacking in dust, which is counter-intuitive. A bibliography of related journal articles is attached. CASI

N95-16600# Lockheed Missiles and Space Co., Palo Alto, CA. Space Sciences Lab.
RADIATION BELT DYNAMIC AND QUASI-STATIC MODELING BASED ON CRRES DATA Final Report, 1 May 1990 - 30 Jun. 1994
Y. T. Chiu, M. A. Rinaldi, W. E. Francis, R. M. Robinson, and R. W. Nightingale 30 Jun. 1994 92 p
(Contract F19628-90-C-0097)
(AD-A285282; PL-TR-94-2182) Avail: CASI HC A05/MF A01

This report summarizes achievements made in the subject contract. New results on modeling the outer magnetosphere have been derived in order to provide an interpretation of CRRES radiation belt data. New features of the outer radiation belt dynamic response to geomagnetic storms are characterized by using CRRES data. A CRRES outer-belt electron data base was chosen and quantitative determination of adiabatic and diffusive elements of the outer electron belt dynamic response to distinct geomagnetic disturbances were delineated. Scientific results of the subject contract were published in six articles in referred journals and books. DTIC

N95-17332 Onsala Space Observatory (Sweden).
FIRST DETECTION OF CO (j = 0 - 1) ADSORPTION AT COSMOLOGICAL DISTANCES (z = 0.247)
T. Wiklind and F. Combes 4 Apr. 1994 7 p
(PB94-184595) Avail: Issuing Activity (National Technical Information Service (NTIS))

We report the first detection of CO absorption lines in an intermediate redshift galaxy, at z = 0.24671. The background continuum source is the BL Lac object PKS 1413+135, which is likely to be situated in the nucleus of the spiral galaxy hosting the absorbing clouds. At least three CO(j = 0 - 1) components were detected. The lines are very narrow, down to 0.6 km/s. The filling factor of the absorbing clouds is large. The extent of the continuum source is unknown. NTIS

N95-17393 Hawaii Univ., Honolulu, HI.
INVESTIGATIONS OF ASTEROID FAMILY GEOLOGY Ph.D. Thesis
James Charles Granahan 1993 202 p
Avail: Univ. Microfilms Order No. DA9416048

An asteroid family is a collection of asteroids that have very similar proper orbital elements. These clusters are thought to be the products of an impact disruptive collision of an asteroid. This idea is used to test two recently proposed asteroid family taxonomies with the use of asteroid spectra. These asteroid family classification systems were tested by seeing if the asteroid family members would be geologically compatible if they were reassembled into one planetoid. The Zappala taxonomy was more accurate in classifying these 'genetic' asteroid families than the Williams taxonomy. By recreating the parent bodies of the asteroid families it is possible to reconstruct the recent geologic history of the asteroid belt. The Zappala dependent model shows fluctuations in the solar radial distribution of asteroid types through time while the Williams dependent model shows a nearly static solar radial distribution of asteroid belts through time. Infrared observations of the Eos asteroid family revealed a minimum of 10 new K asteroids indicating that the parent body of the Eos family was composed of CO/CV chrondrite like material instead of an igneous differentiated planetesimal. Crater count ages of 951 Gaspra indicate that it was the product of impact disruptive asteroid family forming processes. A multispectral synergistic mineralogic study of 951 Gaspra utilizing data from the SSI and NIMS Galileo instruments indicate mineralogic heterogeneities on its surface. This data set also indicates that the olivine/orthopyroxene abundances are significantly higher than ordinary chrondrite abundances. This multi-instrument study provides a spatially resolved spectral data set of an asteroid family member for comparison with earth-based spectral data sets. Dissert. Abstr.

N95-17422*# Johns Hopkins Univ., Baltimore, MD. Center for Astrophysical Sciences.
VOYAGER INVESTIGATION OF THE COSMIC DIFFUSE BACKGROUND: OBSERVATIONS OF ROCKET-STUDIED LOCATIONS WITH VOYAGER Final Technical Report
Richard C. Henry 1994 32 p
(Grant NAG5-2341)
(NASA-CR-197532; NAS 1.26:197532) Avail: CASI HC A03/MF A01

Attachments to this final report include 2 papers connected with the Voyager work: 'Voyager Observations of Dust Scattering Near the Coalsack Nebula' and 'Search for the Intergalactic Medium'. An appendix of 12 one-page write-ups prepared in connection with another program, UVISI, is also included. The one-page write-ups are: (1) Sky survey of UV point sources to 600 times fainter than previous (TD-1) survey; (2) Diffuse galactic light: starlight scattered from dust at high galactic latitude; (3) Optical properties of interstellar grains; (4) Fluorescence of molecular hydrogen in the interstellar medium; (5) Line emission from hot interstellar medium and/or hot halo of galaxy; (6) Integrated light of distant galaxies in the ultraviolet; (7) Intergalactic far-ultraviolet radiation field; (8) Radiation from recombining intergalactic medium; (9) Radiation from re-heating of intergalactic medium following recombination; (10) Radiation from radiative decay of dark matter candidates (neutrino, etc.); (11) Reflectivity of the asteroids in the Ultraviolet; and (12) Zodiacal light. CASI

91 LUNAR AND PLANETARY EXPLORATION

Includes planetology; and manned and unmanned flights.

For spacecraft design or space stations see *18 Spacecraft Design, Testing and Performance.*

N95-16176*# Lunar and Planetary Inst., Houston, TX.
MARS PATHFINDER LANDING SITE WORKSHOP Abstracts Only
Matthew Golombek, ed. (Jet Propulsion Lab., California Inst. of Tech., Pasadena, CA.) 1994 57 p Workshop held in Houston, TX, 18-19 Apr. 1994
(Contract NASw-4574)
(NASA-CR-196745; NAS 1.26:196745; LPI-TR-94-04) Avail: CASI HC A04/MF A01

The Mars Pathfinder Project is an approved Discovery-class mission that will place a lander and rover on the surface of the Red Planet in July 1997. The Mars Pathfinder Landing Site Workshop was designed to allow the Mars scientific community to provide input as to where to land Pathfinder on Mars. The workshop was attended by over 60 people from around the United States and from Europe. Over 20 landing sites were proposed at the workshop, and the scientific questions and problems concerning each were addressed. The workshop and the discussion that occured during and afterward have significantly improved the ability to select a scientifically exciting but safe landing site on Mars. For individual titles, see N95-16177 through N95-16208.

N95-16177*# Lockheed Engineering and Sciences Co., Houston, TX.
SAMPLING ELYSIUM LAVAS (13 DEG N, 203 DEG W) Abstract Only
Carlton C. Allen *In* Lunar and Planetary Inst., Mars Pathfinder Landing Site Workshop 1994 p 15-16 (For primary document see N95-16176 04-91)
Avail: CASI HC A01/MF A01

The proposed Pathfinder landing site presents the opportunity to determine chemical and mineralogical compositions of an Elysium lava flow. The flow is part of a geologic unit of planetary significance. The proposed site appears suitable for landing, and lava surfaces should be accessible to the Pathfinder instruments. By analogy to terrestrial flood basalts, any lava analyzed by Pathfinder is likely to be representative of the entire Elysium province. Derived from text

N95-16178*# Lunar and Planetary Inst., Houston, TX.
MARS PATHFINDER AND THE EXPLORATION OF SOUTHERN AMAZONIS PLANITIA Abstract Only
Nadine G. Barlow *In its* Mars Pathfinder Landing Site Workshop 1994 p 16-17 (For primary document see N95-16176 04-91)
Avail: CASI HC A01/MF A01

The southern region of Amazonis Planitia provides a variety of target terrains for a roving vehicle such as the Mars Pathfinder Mission. A landing site is proposed at 4 deg N latitude 162 deg W longitude. This area has a reference altitude of between 0 and -1 km and consists of relatively smooth Amazonian-aged deposits within the entire 100 x 200 km landing ellipse. The proposed landing site is within the Upper Member Medusae Fossae Formation deposits (Amu) and near the boundary with Middle Member Medusae Fossae Formation deposits (Amm) and Member 1 Arcadia Formation plains (Aa(sub 1)). Slightly further afield are 107-km-diameter Nicholson crater, its ejecta deposits, and knobby terrain of proposed Hesperian age (HNu). Depending on the exact landing site of the spacecraft and the traverse distance of the rover, these materials also may be sampled. Derived from text

N95-16179*# Oregon State Univ., Corvallis, OR. Coll. of Oceanic and Atmospheric Sciences.
METEOROLOGICAL OBSERVATIONS OF SYNOPTIC DISTURBANCES: SENSITIVITY TO LATITUDE Abstract Only
Jeff R. Barnes *In* Lunar and Planetary Inst., Mars Pathfinder Landing Site Workshop 1994 p 17 (For primary document see N95-16176 04-91)
Avail: CASI HC A01/MF A01

The Mars pathfinder MET experiment will make pressure, temperature, and wind measurements on the surface of Mars. The Viking Lander Meteorology Experiment measurements were marked by the presence of variations associated with synoptic weather disturbances throughout the fall and winter season. Numerical simulations of the Mars atmospheric circulation show that the winter midlatitudes are the center of activity for traveling disturbances of planetary scale, disturbances that have their fundamental origin in the baroclinic instability of the wintertime Mars atmospheric circulation. The studies are consistent with Viking observations in that the disturbances decay in amplitude toward lower latitudes. The further north the Mars Pathfinder is located, the more clearly it will be able to detect the signatures of the midlatitude weather system. A landing site close to 15 deg N should allow measurement of the weather disturbances, along with observations of the thermal tides, slope winds, and the relatively steady winds associated with the general circulation - the 'trade winds' of Mars. A landing site near 15 deg N would be significantly further equatorward than the Viking Lander 1 site, and thus would provide more of a view of tropical circulation processes. CASI

N95-16180*# San Juan Capistrano Research Inst., CA.
IMPLICATIONS OF HIGH-SPATIAL-RESOLUTION THERMAL INFRARED (TERMOSKAN) DATA FOR MARS LANDING SITE SELECTION Abstract Only
Bruce H. Betts *In* Lunar and Planetary Inst., Mars Pathfinder Landing Site Workshop 1994 p 17-18 (For primary document see N95-16176 04-91)
Avail: CASI HC A01/MF A01

Thermal infrared observations of Mars from spacecraft provide physical information about the upper thermal skin depth of the surface, which is on the order of a few centimeters in depth and thus very significant for lander site selection. The Termoskan instrument onboard the Soviet Phobos '88 spacecraft acquired the highest spatial-resolution thermal infrared data obtained for Mars, ranging in resolution from 300 m to 3 km per pixel. It simultaneously obtained broadband reflected solar flux data. Although the 6 deg N - 30 deg S Termoskan coverage only slightly overlaps the nominal Mars Pathfinder target range, the implications of Termoskan data for that overlap region and the extrapolations that can be made to other regions give important clues for optimal landing site selection. Derived from text

N95-16181*# Dartmouth Coll., Hanover, NH. Surficial Processes Lab.
A MARS PATHFINDER LANDING ON A RECENTLY DRAINED EPHEMERAL SEA: CERBERUS PLAINS, 6 DEG N, 188 DEG W Abstract Only
G. Robert Brakenridge *In* Lunar and Planetary Inst., Mars Pathfinder Landing Site Workshop 1994 p 19 (For primary document see N95-16176 04-91)
Avail: CASI HC A01/MF A01

Along a 500 km-wide belt extending between 202 deg and 180 deg W and lying astride the martian equator, moderately low-albedo, uncratered smooth plains exhibit low thermal inertia and potentially favorable conditions for the preservation of near-surface ice. The Cerberus Plains occupy a topographic trough as much as 2 km below the planetary datum, and the denser atmosphere at these altitudes would also favor long residence times for near-surface ice once emplaced. The plains have previously been interpreted as the result of young (late Amazonian) low viscosity lava flows or similarly youthful fluvial deposition. However, the plains are also included in maps of possibly extensive martian paleoseas or paleolakes. Ice emplaced as such seas dissipated could still be preserved under thin (a few tens of centimeters) sedimentary cover. In any case, and if a sea once existed, aqueous-born interstitial cementation, probably including hydrated iron oxides and sulfate minerals, would have been favored and is now susceptible to investigation by the Pathfinder alpha proton x-ray spectrometer and multispectral imager. Derived from text

N95-16182*# Arizona State Univ., Tempe, AZ. Dept. of Geology.
PHYSICAL PROPERTIES (PARTICLE SIZE, ROCK ABUNDANCE) FROM THERMAL INFRARED REMOTE OBSERVATIONS: IMPLICATIONS FOR MARS LANDING SITES Abstract Only
P. R. Christensen and Kenneth S. Edgett *In* Lunar and Planetary Inst., Mars Pathfinder Landing Site Workshop 1994 p 19-20 (For primary document see N95-16176 04-91)
Avail: CASI HC A01/MF A01

Critical to the assessment of potential sites for the 1997 Pathfinder landing is estimation of general physical properties of the martian surface. Surface properties have been studied using a variety of spacecraft and earth-based remote sensing observations, plus in situ studies at the Viking lander sites. Because of their value in identifying landing hazards and defining scientific objectives, we focus this discussion on thermal inertia and rock abundance derived from middle-infrared (6 to 30 microns) observations. Used in conjunction with other datasets, particularly albedo and Viking orbiter images, thermal inertia and rock abundance provide clues about the properties of potential Mars landing sites.
Derived from text

N95-16183*# National Air and Space Museum, Washington, DC. Center for Earth and Planetary Studies.
RATIONALE FOR A MARS PATHFINDER MISSION TO CHRYSE PLANITIA AND THE VIKING 1 LANDER Abstract Only
Robert A. Craddock *In* Lunar and Planetary Inst., Mars Pathfinder Landing Site Workshop 1994 p 20-21 (For primary document see N95-16176 04-91)
Avail: CASI HC A01/MF A01

Presently the landing site for Mars Pathfinder will be constrained to latitudes between 0 deg and 30 deg N to facilitate communication with earth and to allow the lander and rover solar arrays to generate the maximum possible power. The reference elevation of the site must also be below 0 km so that the descent parachute, a Viking derivative, has sufficient time to open and slow the lander to the correct terminal velocity. Although Mars has as much land surface area as the continental crust of the earth, such engineering constraints immediately limit the number of possible landing sites to only three broad areas: Amazonis, Chryse, and Isidis Planitia. Of these, both Chryse and Isidis Planitia stand out as the sites offering the most information to address several broad scientific topics.
Derived from text

N95-16184*# National Air and Space Museum, Washington, DC. Center for Earth and Planetary Studies.
RATIONALE FOR ISIDIS PLANITIA AS A BACK-UP LANDING SITE FOR THE MARS PATHFINDER MISSION Abstract Only
Robert A. Craddock *In* Lunar and Planetary Inst., Mars Pathfinder Landing Site Workshop 1994 p 21-22 (For primary document see N95-16176 04-91)
Avail: CASI HC A01/MF A01

The present engineering constraints imposed on the Mars Pathfinder mission leave only three broad regions available for site selection: Amazonis, Chryse, and Isidis Planitia. Because of the knowledge gained by the Viking 1 mission, Chryse Planitia would make an ideal primary landing site. Geological characteristics of Isidis Planitia are discussed with a view to making it a back-up landing site. CASI

N95-16185*# Brown Univ., Providence, RI. Dept. of Geological Sciences.
CHRYSE PLANITIA AS A MARS PATHFINDER LANDING SITE: THE IMPERATIVE OF BUILDING ON PREVIOUS GROUND TRUTH Abstract Only
Larry S. Crumpler *In* Lunar and Planetary Inst., Mars Pathfinder Landing Site Workshop 1994 p 23-24 (For primary document see N95-16176 04-91)
Avail: CASI HC A01/MF A01

Based on consideration of the geological characteristics of Chryse Planitia, the requirements for Mars Pathfinder landing sites, the nature of the mission, the scale of the observations to be made, and the need to build outward from previous experience, a new mission to Chryse Planitia offers several advantages that are difficult to ignore as well as offering a low-gamble/high-return mission scenario. Considering the need to ensure a successful mission, and to ensure the continued health of planetary exploration, the reasons for a new mission to Chryse Planitia are compelling. Results of 1:500,000 mapping, operational benefits of Chryse Planitia, science benefits of Chryse Planitia, and conclusions and site recommendations are discussed. Derived from text

N95-16186*# University of Northeast Louisiana, Monroe, LA. Dept. of Geosciences.
A HIGHLAND SAMPLE STRATEGY FOR PATHFINDER Abstract Only
Rene A. DeHon *In* Lunar and Planetary Inst., Mars Pathfinder Landing Site Workshop 1994 p 24-25 (For primary document see N95-16176 04-91)
Avail: CASI HC A01/MF A01

Potential landing sites are confined to latitudes between 0 deg and 30 deg N and surfaces below 0 km elevation. The landing ellipse is 100 x 200 km oriented N 74 deg E. The constraints essentially eliminate the slopes of Elysium Mons, Olympus Mons, Tharsis Ridge, Lunae Plaunum, all the southern highlands, and almost all the Noachian material of Arabia Terra. Those areas that remain as potential landing sites are chiefly lowland plains of Amazonis Chryse, Isidis, and Elysium Planitia. Any attempt to sample highland material further constrains the possible landing sites by eliminating areas of Hesperian or Amazonian lavas and sediments. One possible sampling strategy is to sample materials within those few 'highland' terrains that extend to low elevations. A second strategy is to sample materials at the mouth of an outflow channel that drains from the highlands. Potential landing sites include outflow channel material at the edge of

Chryse Planitia and highland materials bordering southern Amazonis Planitia. Derived from text

N95-16187*# Arizona State Univ., Tempe, AZ. Dept. of Geology.
OPPORTUNITY TO SAMPLE SOMETHING DIFFERENT: THE DARK, UNWEATHERED, MAFIC SANDS OF CERBERUS AND THE PATHFINDER 1997 MARS LANDING Abstract Only
Kenneth S. Edgett, Robert B. Singer (Arizona Univ., Tucson, AZ.), and P. E. Geissler (Arizona Univ., Tucson, AZ.) *In* Lunar and Planetary Inst., Mars Pathfinder Landing Site Workshop 1994 p 25 (For primary document see N95-16176 04-91)
Avail: CASI HC A01/MF A01

A very important surface component, typically described as 'dark gray material', was not seen at the Viking lander sites, but is common to all low-albedo regions on Mars. Dark material probably includes unaltered mafic volcanic and/or crustal rock and soil not coated by dust, weathering rinds, or varnish. A Pathfinder landing in Cerberus (9 deg N - 16 deg N, 194 deg W - 215 deg W) will guarantee examination of materials that are distinctly different from the two Viking lander sites. In situ study of dark material will provide vital ground truth for orbiter-based observations like those anticipated from Mars '94/'96 and Mars Global Surveyor.
Derived from text

N95-16188*# National Aeronautics and Space Administration. Ames Research Center, Moffett Field, CA.
EXOBIOLOGY SITE PRIORITIES FOR MARS PATHFINDER Abstract Only
Jack D. Farmer and David J. DesMarais *In* Lunar and Planetary Inst., Mars Pathfinder Landing Site Workshop 1994 p 26-27 (For primary document see N95-16176 04-91)
Avail: CASI HC A01/MF A01

The fact that life developed on the Earth within the first billion years of its history makes it quite plausible that life may have also developed on Mars. If life did develop on Mars, it undoubtedly left behind a fossil record. Such a fossil record is likely to be more accessible than either subsurface environments that may harbor life, or scattered 'oases' that may be present at the surface. Consequently, the post-Viking approach of Mars exobiology has shifted focus to search for evidence of an ancient martian biosphere. This has led to the emergence of a new subdiscipline of paleontology, herein termed 'exopaleontology', which deals with the exploration for fossils on other planets and whose core concepts derive from Earth-based Precambrian paleontology, microbial ecology, and sedimentology. Potential targets on Mars for subaqueous spring deposits, sedimentary cements, and evaporites are ancient terminal lake basins where hydrological systems could have endured for some time under arid conditions. Potential targets for the Mars Pathfinder mission include channeled impact craters and areas of deranged drainage associated with outflows in northwest Arabia and Xanthe Terra, where water may have ponded temporarily to form lakes. The major uncertainty of such targets is their comparatively younger age and the potentially short duration of hydrological activity compared to older paleolake basins found in the southern hemisphere. However, it has been suggested that cycles of catastrophic flooding associated with Tharsis volcanism may have sustained a large body of water, Oceanus Borealis, in the northern plains area until quite late in martian history. Although problematic, the shoreline areas of the proposed northern ocean provide potential targets for a Mars Pathfinder mission aimed at exploring for carbonates or other potentially fossiliferous marine deposits. Carbonates and evaporites possess characteristic spectra signatures in the near-infrared and should be detectable using rover-based spectroscopy and other methods for in situ mineralogical analysis. Derived from text

N95-16189*# Laboratoire de Meteorologie Dynamique, Paris (France).
MARS PATHFINDER METEOROLOGICAL OBSERVATIONS ON THE BASIS OF RESULTS OF AN ATMOSPHERIC GLOBAL CIRCULATION MODEL Abstract Only
Francois Forget, F. Hourdin, and O. Talagrand *In* Lunar and Planetary Inst., Mars Pathfinder Landing Site Workshop 1994 p 27-28 (For primary document see N95-16176 04-91)
Avail: CASI HC A01/MF A01

The Mars Pathfinder Meteorological Package (ASI/MET) will measure the local pressure, temperature, and winds at its future landing site, somewhere between the latitudes 0 deg N and 30 deg N. Comparable measurements have already been obtained at the surface of Mars by the Viking Landers at 22 deg N (VL1) and 48 deg N (VL2), providing much useful information on the martian atmosphere. In particular the pressure measurements contain very instructive information on the global atmospheric circulation. At the Laboratoire de Meteorologie Dynamique (LMD), we have analyzed and simulated these measurements with a martian atmospheric global circulation model (GCM), which was the first to simulate the martian atmospheric circulation over more than 1 year. The model is able to reproduce rather accurately many observed features of the martian atmosphere, including the long- and short-period oscillations of the surface pressure observed by the Viking landers. From a meteorological point of view, we think that a landing site located near or at the equator would be an interesting choice. Derived from text

N95-16190*# Jet Propulsion Lab., California Inst. of Tech., Pasadena, CA.
PATHFINDER LANDING SITES AT CANDIDATE SNC IMPACT EJECTION SITES Abstract Only
Matthew P. Golombek *In* Lunar and Planetary Inst., Mars Pathfinder Landing Site Workshop 1994 p 28-29 (For primary document see N95-16176 04-91)
Avail: CASI HC A01/MF A01

If Mars Pathfinder were able to land at a site on Mars from which the SNC meteorites were ejected by impact, the Pathfinder mission would essentially represent a very inexpensive sample return mission. Geologic units that contain four potential impact craters from which SNC meteorites could have been ejected from Mars are accessible to the Mars Pathfinder lander. Determining that SNC meteorites came from a particular spot on Mars raises the intriguing possibility of using Pathfinder as a sample return mission and providing a radiometric age for the considerably uncertain martian crater-age timescale. Pathfinder instruments are capable of determining if the rock type at the landing site is similar to that of one or more of the SNC meteorites, which would strengthen the hypothesis that the SNC meteorites did, in fact, come from Mars. Unfortunately, instrument observations from Pathfinder are probably not capable of determining if the geologic unit sampled by the lander is definitively the unit from which a SNC meteorite came from as opposed to Mars in general or perhaps a particular region on Mars. This abstract evaluates the possibility of landing at potential SNC ejection sites and the ability of Pathfinder to identify the landing site as the place from which an SNC meteorite came.
Derived from text

N95-16191*# Arizona State Univ., Tempe, AZ. Dept. of Geology.
STRATEGY FOR SELECTING MARS PATHFINDER LANDING SITES Abstract Only
Ronald Greeley and Ruslin O. Kuzmin (Academy of Sciences, USSR, Moscow, USSR.) *In* Lunar and Planetary Inst., Mars Pathfinder Landing Site Workshop 1994 p 29-30 (For primary document see N95-16176 04-91)
Avail: CASI HC A01/MF A01

A strategy for Pathfinder site selection must be developed that is fundamentally different from most previous considerations. At least two approaches can be identified. In one approach, the objective is to select a site representing a key geologic unit on Mars, i.e., a unit that is widespread, easily recognized, and used frequently as a datum in various investigations. The second approach is to select a site that potentially affords access to a wide variety of rock types. Because rover range is limited, rocks from a variety of sources must be assembled in a small area for sampling. Regardless of the approach taken in site selection, the Pathfinder site should include eolian deposits and provisions should be made to obtain measurements on soils. A recommended approach for selecting the Mars Pathfinder landing site is to identify a deltaic deposit, composed of sediments derived from sources of various ages and geologic units that shows evidence of eolian activity. The site should be located as close as possible to the part of the outwash where rapid deposition occurred because the likelihood of 'sorting' by size and composition increases with distance, decreasing the probability of heterogeneity. In addition, it is recommended that field operation tests be conducted to gain experience and insight into conducting science with Pathfinder. Derived from text

N95-16192*# Max-Planck-Inst. fuer Aeronomie, Katlenburg-Lindau (Germany).

OBSERVATIONS BY THE MARS 1994 ORBITER AND POSSIBLE CORRELATIONS WITH MARS PATHFINDER Abstract Only

H. Uwe Keller *In* Lunar and Planetary Inst., Mars Pathfinder Landing Site Workshop 1994 p 30 (For primary document see N95-16176 04-91)

Avail: CASI HC A01/MF A01

The Mars '94 spacecraft will still be operational when Mars Pathfinder begins its observations. While it will probably not be possible to detect the lander directly, the terrain, including the landing error ellipse, can be covered in high resolution (10 m) in various color bands. The stereo capability of the high resolution camera will provide a three-dimensional terrain map. The landing site of Pathfinder could possibly be chosen so that correlated observations of IMP and the remote sensing instruments onboard Mars '94 may be possible. We will discuss this scenario based on the presently adopted Mars '94 orbit and resulting enhancements stemming from correlations of data obtained by both spacecraft. Author

N95-16193*# Academy of Sciences (USSR), Moscow (USSR). Inst. of Geochemistry and Analytical Chemistry.

POTENTIAL LANDING SITES FOR MARS PATHFINDER Abstract Only

Ruslan O. Kuzmin, R. Landheim (Arizona State Univ., Tempe, AZ.), and Ronald Greeley (Arizona State Univ., Tempe, AZ.) *In* Lunar and Planetary Inst., Mars Pathfinder Landing Site Workshop 1994 p 30-31 (For primary document see N95-16176 04-91)

Avail: CASI HC A01/MF A01

In addition to a better understanding of the geological evolution of Mars, new techniques for processing available data have emerged, new data have been acquired, and the engineering approaches for placing spacecraft on the surface have evolved. Selection of the Mars Pathfinder landing site must take these issues into account, along with mission constraints. An advantage of Mars Pathfinder is the rover for sampling surface materials over a range of tens of meters. However, engineering constraints and the limited scientific payload of this mission require new approaches for landing site selection. One approach is to select sites exhibiting a wide variety of rocks near the lander. An alternative approach is to select sites in which the regional geology consists of a single rock type representing a key datum for the geological study of Mars, and is uniformly distributed within the landing ellipse. Derived from text

N95-16194*# Geological Survey, Menlo Park, CA.

A PERSPECTIVE OF LANDING-SITE SELECTION Abstract Only

Henry J. Moore *In* Lunar and Planetary Inst., Mars Pathfinder Landing Site Workshop 1994 p 31-32 (For primary document see N95-16176 04-91)

Avail: CASI HC A01/MF A01

The problems that now confront Mars Pathfinder are much the same as those that confronted Viking, but more and better information exists today. Like Viking, Mars Pathfinder must select a landing site compatible with lander and rover designs as evidenced by available data (Viking images, radar and thermal observations, albedo and color observations, visible-infrared spectra, etc.). Most regions at low elevations probably contain favorable sites, but some sites at low elevations with weak quasispecular echoes and low thermal inertias may be unfavorable. Derived from text

N95-16195*# Lunar and Planetary Inst., Houston, TX.

TARTARUS COLLES: A SAMPLING OF THE MARTIAN HIGHLANDS Abstract Only

Scott Murchie and Allan Treiman *In its* Mars Pathfinder Landing Site Workshop 1994 p 32-33 (For primary document see N95-16176 04-91)

Avail: CASI HC A01/MF A01

Several of the most fundamental issues about the geology of Mars can be addressed using information on composition and structure of the plateau plains ('highlands') that cover approximately half the planet. The units that compose the highlands are interpreted as a mixture of volcanic, fluvial, lacustrine, and impact ejecta deposits. A more precise inventory of differing of igneous and sedimentary lithologies in highland rock units would not only lead to a better understanding of how the plateau plains formed, but would also clarify the nature of the surface environment during the first 800 m.y. of martian history. Structural features including bedforms, joints, and small faults that are unresolved from orbit record a history of the emplacement and deformation of the highlands. In addition, weathering products present in this very ancient terrain represent a mineralogic record of past climate and of the pathways by which bedrock is altered chemically. Their similarity or dissimilarity to bright soils observed spectroscopically and in situ at the Viking Lander sites will be evidence for the relative roles of regional sources and global eolian transport in producing the widespread cover of 'dust.' Unfortunately, these issues are difficult to address in the plateau plains proper, because bedrock is covered by mobile sand and weathering products, which dominate both surface composition and remotely measurable spectral properties. However, the 'Tartarus Colles' site, located at 11.41 deg N, 197.69 deg W at an elevation of -1 km, provides an excellent opportunity to address the highland geology within the mission constraints of Mars Pathfinder. The site is mapped as unit HNu, and consists of knobby remnants of deeply eroded highlands. It contains rolling hills, but lacks steep escarpments and massifs common in most highland remnants, and is free of large channels that would have removed colluvium from eroded upper portions of the stratigraphic column. These characteristics indicate that variety of bedrock types from throughout the Noachian-Hesperian stratigraphic column may remain at the site.

Derived from text

N95-16196*# Jet Propulsion Lab., California Inst. of Tech., Pasadena, CA.

SCIENTIFIC RATIONALE FOR SELECTING NORTHERN EUMENIDES DORSUM (9 DEG - 11 DEG N LATITUDE, 159 DEG - 162 DEG LONGITUDE) AS A POTENTIAL MARS PATHFINDER LANDING SITE Abstract Only

Tim J. Parker *In* Lunar and Planetary Inst., Mars Pathfinder Landing Site Workshop 1994 p 34 (For primary document see N95-16176 04-91)

Avail: CASI HC A01/MF A01

The proposed site is the northernmost occurrence of the Medusae Fossae Formation (MFF), and lies at or below the -2 km contour. The MFF is the famous radar 'stealth' deposit that extends from south of Olympus Mons westward across southern Amazonis Planitia to southern Elysium Planitia. The MFF appears to be composed of some kind of wind-eroded friable material, the origin of which is very problematic. It appears to be a radar-absorbing material, whereas Mars' south polar layered deposits appear bright in the same scenes. Synthetic aperture radar images of young terrestrial ash deposits in the Andes also appear relatively bright. The MFF's radar signature appears to require a uniformly fine-grained material (on the order of dust-sized to fine sand-sized) at least several meters thick, in order not to transmit reflections off underlying terrain or internal reflective horizons. The proposed Pathfinder landing site lies on a relatively smooth, 'unmodified' portion of the MFF, more than 100 km away from its northern and western edges, which exhibit evidence of eolian etching in the form of closely spaced yardings. There are no large craters or steep slopes within a few hundred kilometers of the landing site. Derived from text

N95-16197*# Jet Propulsion Lab., California Inst. of Tech., Pasadena, CA.

SCIENTIFIC RATIONALE FOR SELECTING NORTHWEST ISIDIS PLANITIA (14 DEG - 17 DEG N LATITUDE, 278 DEG - 281 DEG LONGITUDE) AS A POTENTIAL MARS PATHFINDER LANDING SITE Abstract Only

Tim J. Parker and Jim W. Rice (Arizona State Univ., Tempe, AZ.) *In* Lunar and Planetary Inst., Mars Pathfinder Landing Site Workshop 1994 p 34-35 (For primary document see N95-16176 04-91)

Avail: CASI HC A01/MF A01

The northwest Isidis Basin offers a unique opportunity to land near a fretted terrain lowland/upland boundary that meets both the latitudinal and elevation requirements imposed on the spacecraft. The landing site lies east of erosional scarps and among remnant massif inselbergs of the Syrtis Major volcanic plains. The plains surface throughout Isidis exhibits abundant, low-relief mounds that are the local expression of the 'thumbprint terrain' that is common within a few hundred kilometers of the lowland/upland boundary. The massif inselbergs are not as numerous nor as massive as those fretted terrains to the northwest, so local slopes are not expected to be steep. Neither feature should pose a serious threat to the lander. Landing on or adjacent to one of these features would enhance the

science return and would help to pinpoint the landing site in Viking and subsequent orbiter images by offering views of landmarks beyond the local horizon. Derived from text

N95-16198*# Jet Propulsion Lab., California Inst. of Tech., Pasadena, CA.
CERBERUS PLAINS: A MOST EXCELLENT PATHFINDER LANDING SITE Abstract Only
Jeff B. Plescia *In* Lunar and Planetary Inst., Mars Pathfinder Landing Site Workshop 1994 p 35 (For primary document see N95-16176 04-91)
Avail: CASI HC A01/MF A01

The Cerberus Plains in southeastern Elysium and western Amazonis cover greater than 10(exp 5) sq km, extending an east-west distance of approximately 3000 km and a north-south distance of up to 700 km near 195 deg. Crater numbers are 89 plus or minus 15 craters greater than 1 km/10(exp 6) sq km, indicating a stratigraphic age of Upper Amazonian and an absolute age of 200-500 Ma. The material forming the surface is referred to as the Cerberus Formation. The two ideas postulated about the unit's origin are fluvial and volcanic. Regardless of which interpretation is correct, the Cerberus Plains is an important candidate for a pathfinder landing site because it represents the youngest major geologic event (be it fluvial or volcanic) on Mars. Derived from text

N95-16199*# Arizona State Univ., Tempe, AZ. Dept. of Geography.
MAJA VALLEY AND THE CHRYSE OUTFLOW COMPLEX SITES Abstract Only
Jim W. Rice *In* Lunar and Planetary Inst., Mars Pathfinder Landing Site Workshop 1994 p 36 (For primary document see N95-16176 04-91)
Avail: CASI HC A01/MF A01

This candidate landing site is located at 19 deg N, 53.5 deg W near the mouth of a major outflow channel. Maja Valles, and two 'valley network' channel systems, Maumee and Vedra Valles. The following objectives are to be analyzed in this region: (1) origin and paleohydrology of outflow and valley network channels; (2) fan delta complex composition (the deposit located in this area is one of the few identified at the mouth s of any channels on the planet); and (3) analysis of any paleolake sediments (carbonates, evaporites). The primary objectives of the Chryse Outflow Complex region (Ares, Tiu, Mawrth, Simud, and Shalbatana Valles) would be outflow channel dynamics (paleohydrology) of five different channel systems. Derived from text

N95-16200*# Arizona State Univ., Tempe, AZ. Dept. of Geography.
MARTE VALLES SITE Abstract Only
Jim W. Rice *In* Lunar and Planetary Inst., Mars Pathfinder Landing Site Workshop 1994 p 36 (For primary document see N95-16176 04-91)
Avail: CASI HC A01/MF A01

This site is located at 16 deg N, 177 deg W on the flood plains of Marte Valles, which is perhaps the youngest channel system on Mars. The young age of this channel warrants investigation because of climatic implications for fluvial activities in recent geologic time. The paucity of craters makes this an excellent site in terms of safety requirements. Some of the objectives stated previously for the Maja Valles region would also apply to this site (grab bag of rock types, etc.). Derived from text

N95-16201*# Max-Planck-Inst. fuer Chemie, Mainz (Germany).
ALPHA PROTON X RAY SPECTROMETER Abstract Only **c19**
Rudi Rieder, H. Waeke, and T. Economou (Chicago Univ., Chicago, IL.) *In* Lunar and Planetary Inst., Mars Pathfinder Landing Site Workshop 1994 p 36-37 (For primary document see N95-16176 04-91)
Avail: CASI HC A01/MF A01

Mars Pathfinder will carry an alpha-proton x ray spectrometer (APX) for the determination of the elemental chemical composition of Martian rocks and soils. The instrument will measure the concentration of all major and some minor elements, including C, N, and O at levels above typically 1 percent. Derived from text

N95-16202*# National Aeronautics and Space Administration. Ames Research Center, Moffett Field, CA.
ATMOSPHERE STRUCTURE AND METEOROLOGY INSTRUMENT FOR MARS PATHFINDER Abstract Only **c19**
Alvin Seiff (San Francisco State Univ., CA.) *In* Lunar and Planetary Inst., Mars Pathfinder Landing Site Workshop 1994 p 37 (For primary document see N95-16176 04-91)
Avail: CASI HC A01/MF A01

The MESUR Science Definition Team recommended that all MESUR probes, including Pathfinder, carry an ASI/MET experiment, in order that no opportunity be lost to characterize the atmosphere of Mars in passing through it. The experiment was thus included on Pathfinder from the start (February 1992), but on an essentially noninterference basis: It was to make no unusual demands on the spacecraft. A Science Advisory Team was appointed by NASA Headquarters in September 1993 first met on November 3rd to initiate formal science participation, and the level of activity has since been high. The instrument passed its Preliminary Design Review on February 28th. Derived from text

N95-16203*# National Aeronautics and Space Administration. Ames Research Center, Moffett Field, CA.
LANDING SITE CONSIDERATIONS FOR ATMOSPHERE STRUCTURE AND METEOROLOGY Abstract Only
Alvin Seiff (San Francisco State Univ., CA.), R. Haberle, and J. Murphy (San Francisco State Univ., CA.) *In* Lunar and Planetary Inst., Mars Pathfinder Landing Site Workshop 1994 p 38 (For primary document see N95-16176 04-91)
Avail: CASI HC A01/MF A01

The goal of the ASI/MET experiments is to extend our knowledge of Mars atmosphere structure and meteorology over that established by the Viking mission. The two in situ soundings of Mars atmosphere by Vikings 1 and 2 were highly similar, but radio occultations and infrared soundings have shown large variability in atmosphere structure on Mars with latitude, season, and terrain elevation. It would be of great interest to obtain an in situ sounding showing strong contrast in thermal structure with the Viking profiles. These would be expected to occur in the winter season, in the southern hemisphere, or at polar latitudes. These options are ruled out by Pathfinder Mission constraints, which place the entry in low, northern latitudes in mid summer, with small seasonal difference from the two Viking landers, and small latitude difference from Viking 1. Derived from text

N95-16204*# Arizona Univ., Tucson, AZ. Planetary Image Research Lab.
SURFACE SCIENCE CAPABILITIES FROM IMP SPECTRAL IMAGING Abstract Only
Robert B. Singer et al *In* Lunar and Planetary Inst., Mars Pathfinder Landing Site Workshop 1994 p 39-40 (For primary document see N95-16176 04-91)
Avail: CASI HC A01/MF A01

The Imager for Mars Pathfinder (IMP) had a single 12-position filter wheel for one of its two 'eyes'. Originally eight, and then nine, of these filters were optimized for surface science, and three narrow-band filters for atmospheric science. Because of some design revisions we will now have filter wheels on both sides. The wheels for right and left eyes are identical, 12 filter positions each, and rigidly linked to the same rotation shaft. There are now 13 surface filters, in addition to 5 for atmospheric observations. Details of all the filter positions are tabulated and approximate gaussian bandpasses for the 13 surface filters are shown. Derived from text

N95-16205*# Jet Propulsion Lab., California Inst. of Tech., Pasadena, CA.
GOLDSTONE RADAR CONTRIBUTIONS TO MARS PATHFINDER LANDING SAFETY Abstract Only
Martin A. Slade and R. F. Jurgens *In* Lunar and Planetary Inst., Mars Pathfinder Landing Site Workshop 1994 p 40 (For primary document see N95-16176 04-91)
Avail: CASI HC A01/MF A01

Goldstar radar can provide topography 'profiles', statistical surface roughness, and radar images within a few degrees of the sub-Earth point. Goldstone/Very Large Array (VLA) bistatic radar observations can image the whole disk of Mars with integration times on the order of ten min before pixel smearing occurs. Data from all these radar techniques can be useful for observing the local surface conditions relating to landing safety issues for Mars Pathfinder. Derived from text

N95-16206*# Arizona Univ., Tucson, AZ. Lunar and Planetary Lab.
IMAGER FOR MARS PATHFINDER (IMF) Abstract Only **c19**

Peter H. Smith *In* Lunar and Planetary Inst., Mars Pathfinder Landing Site Workshop 1994 p 40-41 (For primary document see N95-16176 04-91)
Avail: CASI HC A01/MF A01

The IMP camera is a near-surface sensing experiment with many capabilities beyond those normally associated with an imager. It is fully pointable in both elevation and azimuth with a protected, stowed position looking straight down. Stereo separation is provided with two optical paths; each has a 12-position filter wheel. The primary function of the camera, strongly tied to mission success, is to take a color panorama of the surrounding terrain. IMP requires approximately 120 images to give a complete downward hemisphere from the deployed position. IMP provides the geologist, and everyone else, a view of the local morphology with millimeter-tometer-scale resolution over a broad area. In addition to the general morphology of the scale, IMP has a large compliment of specially chosen filters to aid in both the identification of the mineral types and their degree of weathering. Derived from text

N95-16207*# Lunar and Planetary Inst., Houston, TX.
MELAS CHASMA: A MARS PATHFINDER VIEW OF VALLES MARINERIS Abstract Only
Allan H. Treiman and Scott Murchie *In its* Mars Pathfinder Landing Site Workshop 1994 p 41-42 (For primary document see N95-16176 04-91)
Avail: CASI HC A01/MF A01

A Mars Pathfinder landing site in Melas Chasma (Valles Marineris) would yield significant science return, but is outside present mission constraints. In Melas Chasma, Mars Pathfinder could investigate minimally altered basaltic material, sedimentary deposits, chemical weathering, tectonic features, the highland crust, equatorial weather, and Valles mists. Critical issues include the following: (1) nature and the origin of the Valles interior layered deposits, important for understanding water as a sedimentary and chemical agent, and for the past existence of of environments favorable for life; (2) compositions of little-altered basaltic sands, important for understanding magma genesis and weathering on Mars, and the martian meteorites; and (3) structure and composition of the highland crust, important for understanding Mars' early history . Derived from text

N95-16208*# Search for Extraterrestrial Intelligence Inst., Mountain View, CA.
CLIMATOLOGICAL TARGETS FOR MARS PATHFINDER Abstract Only
AAron P. Zent *In* Lunar and Planetary Inst., Mars Pathfinder Landing Site Workshop 1994 p 42-43 (For primary document see N95-16176 04-91)
Avail: CASI HC A01/MF A01

Four areas fit within the elevation and latitude constraints: Chryse, Elysium, Amazonis, and Isidis. There is geomorphic evidence that all have supported standing water. In some cases it would be difficult to pick a landing site that had no hope of teaching us about the climatic history of Mars. The southeast Elysium Basin provides an optimal target in which a variety of materials may be accessible in a near-shore environment. The albedo of the region is moderately low, and the thermal inertia is indicative of moderate rock coverage or some consolidation of fines, arguing that the site has not been covered with eolian dust deposits.
Derived from text

N95-16436*# National Aeronautics and Space Administration. Lyndon B. Johnson Space Center, Houston, TX.
CATALOG OF LUNAR AND MARS SCIENCE PAYLOADS
Nancy Ann Budden, ed. Aug. 1994 236 p
(NASA-RP-1345; S-777; NAS 1.61:1345) Avail: CASI HC A11/MF A03

This catalog collects and describes science payloads considered for future robotic and human exploration missions to the Moon and Mars. The science disciplines included are geosciences, meteorology, space physics, astronomy and astrophysics, life sciences, in-situ resource utilization, and robotic science. Science payload data is helpful for mission scientists and engineers developing reference architectures and detailed descriptions of mission organizations. One early step in advanced planning is formulating the science questions for each mission and identifying the instrumentation required to address these questions. The next critical element is to establish and quantify the supporting infrastructure required to deliver, emplace, operate, and maintain the science experiments with human crews or robots. This requires a comprehensive collection of up-to-date science payload information--hence the birth of this catalog. Divided into lunar and Mars sections, the catalog describes the physical characteristics of science instruments in terms of mass, volume, power and data requirements, mode of deployment and operation, maintenance needs, and technological readiness. It includes descriptions of science payloads for specific missions that have been studied in the last two years: the Scout Program, the Artemis Program, the First Lunar Outpost, and the Mars Exploration Program. Author

N95-16836* National Aeronautics and Space Administration. Lyndon B. Johnson Space Center, Houston, TX.
APOLLO 16: NOTHING SO HIDDEN (Videotape)
1972 Videotape: 28 min. 30 sec. playing time, in color, with sound
(NASA-TM-110104; NONP-NASA-VT-95-33955) Avail: CASI VHS A02/BETA A22

This film shows the landing and the three lunar traverses in the highland region of the moon, near the crater descartes. It includes an astronaut's eye view from the rover, lunar grand prix, discovery of the house-sized rock, lunar lift-off and eva 173,000 miles above the earth. Microphones and cameras in mission control record the emergency problem solving during the prelanding crisis and the reactions of scientists on earth as the astronauts explore the moon. JSC

N95-16837* National Aeronautics and Space Administration. Lyndon B. Johnson Space Center, Houston, TX.
APOLLO 17: ON THE SHOULDERS OF GIANTS (Videotape)
1973 Videotape: 28 min. 30 sec. playing time, in color, with sound
(NASA-TM-110105; NONP-NASA-VT-95-33956) Avail: CASI VHS A02/BETA A22

A documentary view of the Apollo 17 journey to Taurus-Littrow, the final lunar landing mission in the Apollo program is discussed. The film depicts the highlights of the mission and relates the Apollo program to Skylab, the Apollo-Soyuz linkup and the Space Shuttle. Author

N95-16838* National Aeronautics and Space Administration. Lyndon B. Johnson Space Center, Houston, TX.
NEW LOOK AT THE OLD MOON (Videotape)
1980 Videotape: 28 min. 30 sec. playing time, in color, with sound
(NASA-TM-110106; NONP-NASA-VT-95-33957) Avail: CASI VHS A02/BETA A22

The decade of 1969-1979 is seen as the time when lunar science emerged from the dark ages as a result of the geophysical and sample investigations made possible by the Apollo flights to the moon. After a brief summary of the Apollo missions and laboratory investigative techniques, the film treats the major epochs in lunar history uncovered by the investigations. Finally, the moon is depicted as having a practical role in the future of science and technology, as well as serving as the pattern for the future exploration of space. JSC

N95-16942* National Aeronautics and Space Administration. Lyndon B. Johnson Space Center, Houston, TX.
APOLLO 15: IN THE MOUNTAINS OF THE MOON (Videotape)
1971 Videotape: 28 min. playing time, in color, with sound
(NASA-TM-109988; NONP-NASA-VT-95-34903) Avail: CASI VHS A02/BETA A22

This video features the following: (1) extra vehicle activity (EVA); (2) the three traversed of the lunar surface; (3) film taken from the Lunar Rover; (4) hammer and feather tests of Galileo's theory on falling objects in gravity fields; (5) Worden's EVA; (6) subsatellite launching; (7) X-ray pulsar observations; and (8) splash down with one parachute collapsed.
JSC

N95-17392 Cornell Univ., Ithaca, NY.
RHEOLOGY AND STRUCTURE OF PLANETARY NEAR-SURFACE MATERIALS FROM LANDFORM TOPOGRAPHY Ph.D. Thesis
David Gerard Jankowski 1994 337 p
Avail: Univ. Microfilms Order No. DA9416729

The topography of landforms observed in spacecraft images of planetary bodies is used to infer the rheologies of the materials comprising them. Rheologic models are then used to infer information about the subsurface composition, structure, and physical state. A quantitative analysis of error

sources in one-dimensional planetary photoclinometry is presented. Slope errors are investigated for a variety of viewing and lighting geometries, slope angles, and slope orientations. The results can be broken down into nonsystematic errors, which affect each pixel element independently, and systematic errors, that may retain the general appearance of the topography while approximately scaling all relief by a multiplicative constant. Images of the Uranian satellite Ariel show flow features with morphologies suggesting the extrusion of ice in the solid state. Topographic profiles across a number of lows have been derived using photoclinometry. Using a simple model of extrusion, spreading, and cooling, the viscosity of the flow material is found to have been less than approximately 10(exp 16) poise, far lower than expected for H2O ice likely extrusion temperatures. Sharply reduced viscosities may have resulted from incorporation of ices like NH3 or CH4 in the Uranian satellites. Terrain softening is a distinct style of landform degradation observed in images of Mars. Morphometric measurements on the photoclinometrically-derived topographic profiles provide strong evidence that craters that have been designated 'softened' and 'unsoftened' by visual inspection are topographically distinct. A finite element model is used to test the hypothesis that softened terrain is the result of quasi-viscous relaxation of topography due to the creep deformation of subsurface ice. Model results indicate that the morphology of softened terrain is consistent with ice-rich permafrost relaxation in a layer no more than approximately 1 km deep. Lavinia Planitia, a low-lying plains region on Venus, has been observed to contain a system of deformation belts. Magellan altimetry and measurements on synthetic aperture radar images are used to characterize the topography of the region. The topography within an individual deformation belt is used to place an approximate lower limit on the Venusian thermal gradient at the time of deformation. Dissert. Abstr.

N95-17403*# California Univ., Los Angeles, CA. Inst. for Geophysics and Planetary Physics.

ANALYSIS OF MAGNETIC FIELD DATA FROM PIONEER VENUS ORBITER Final Technical Report, 1 Oct. 1987 - 30 Sep. 1994

Christopher T. Russell 20 Nov. 1994 32 p

(Grant NAG2-501)

(NASA-CR-197492; NAS 1.26:197492) Avail: CASI HC A03/MF A01

The subject grant (NAG 2-501) supported the analysis of magnetic field data from the Pioneer Venus orbiter for the period 10/1/87 to 9/30/94. During that period, 188 papers were contributed to scientific meetings that either analyzed the magnetometer data or used the data as part of the analysis of a scientific problem. Further, 107 papers were published in research journals and books. The magnetic moment of Venus was described. Venus was found to be essentially devoid of any intrinsic magnetic field. There was evidence though for the presence of lightning in the Venus atmosphere. The altitude distribution of impulsive signals in the night atmosphere was mapped and geographic clusters were found, most probably associated with local time ordering. A new means to create flux ropes in the ionosphere was postulated. On the nightside, ionospheric holes, ionospheric clouds, and tail rays were studied. The subsolar ionopause and the magnetic barrier were examined as was the altitude asymmetry of the ionopause, properties of the magnetosheath, and location of the bow shock upstream waves. CASI

N95-17653*# Kentucky Univ., Lexington, KY. Center for Applied Energy Research.

EVALUATION OF A PNEUMATIC MARTIAN SOIL SAMPLER CONCEPT Final Report

John L. Schaefer, James K. Neathery, and John M. Stencel 15 Dec. 1994 19 p

(Contract NCC2-5087)

(NASA-CR-197539; NAS 1.26:197539) Avail: CASI HC A03/MF A01

The pneumatic soil sampler concept was successfully demonstrated by penetrating a Martian simulant soil to a depth of 2 meters. Working gas pressure, composition, and pulsing were evaluated with the objective of minimizing gas usage. Also, the probe penetration force was investigated with the objective of minimizing probe weight. Gas and probe penetration force, while not yet optimized, are within the range which make the soil sampler concept feasible. While the tests described in this report did not answer all the questions and address all the variables associated with pneumatic soil sampling, valuable data experience and knowledge were gained which can be used to further develop the concept. Author

92 SOLAR PHYSICS

Includes solar activity, solar flares, solar radiation and sunspots. For related information see *93 Space Radiation*.

N95-16080 Louisiana State Univ., Baton Rouge, LA. Dept. of Physics and Astronomy.

SOLAR FLARES AND MAGNETOSPHERIC PARTICLES: INVESTIGATIONS BASED UPON THE ONR-602 AND ONR-604 EXPERIMENTS Performance Report

John P. Wefel and T. G. Guzik 23 Mar. 1994 8 p Limited Reproducibility: More than 20% of this document may be affected by microfiche quality

(Contract N00014-90-J-1466)

(AD-A281463) Avail: Issuing Activity (Defense Technical Information Center (DTIC))

This performance report covers work accomplished under ONR Grant N00014-90-J-1466 related to the radiation environment in near-Earth space. The goal of the research is to measure and describe, quantitatively, the Geospace radiation environment in which men and spacecraft must survive and function. The tools for this investigation are the data returned by the ONR-602 and ONR-604 experiments, both flown under the auspices of ONR and the Air Force Space Test Program, augmented by correlative databases of both space-based and ground-based data. The investigation involves data analysis, modeling and applications to a variety of space equipment and environments. This report builds upon the detailed Technical Report (Fall 1992) and the previous performance reports. For the current period, the principal effort was in further analysis of quiet-time particle access to the inner magnetosphere and in expanded solar energetic particle investigations. Derived from text

N95-17352 Science Research Council, Daresbury (England).

SOLAR NEUTRINO OSCILLATIONS

R. J. N. Phillips Jun. 1994 11 p Presented at the Conference on Non-Accelerator Particle Physics (ICNAPP-94), Bangalore, India, 2-9 Jan. 1994

(PB95-104295; RAL-94-017) Avail: Issuing Activity (National Technical Information Service (NTIS))

Standard Solar Models (SSM) predict the nu(sub e) with some uncertainties. Measurements by capture in (37)Cl, nu - e scattering and capture in (71)Ga with differing E(sub nu) thresholds, find three different deficits, where the first error is experimental, the second is from the SSM. These numbers suggest a differential suppression, with the top and bottom of the accessible range less suppressed than the middle. They pose the Solar Neutrino Problem 1994. Re-tuning the solar model gives no easy solution. A lower central temperature would suppress (8)B production and the nu - e rate, but to explain (37)Cl rates the (7)Be line must then be obliterated - a bit unlikely given that (8)B is made from (7)Be. Neutrino oscillations offer several possible explanations, that the author will briefly compare. NTIS

N95-17723# Louisiana State Univ., Baton Rouge, LA. Dept. of Physics and Astronomy.

SOLAR FLARES AND MAGNETOSPHERIC PARTICLES: INVESTIGATIONS BASED UPON THE ONR-602 AND ONR-604 EXPERIMENTS Quarterly Report No. 2

John P. Wefel and T. G. Guzik 19 May 1994 25 p

(Contract N00014-90-J-1466)

(AD-A283275) Avail: CASI HC A02/MF A01

This performance report covers work related to the radiation environment in near-earth space. The goal of the research is to measure and describe, quantitatively, the Geospace radiation environment in which men and spacecraft must survive and function. The tools for this investigation are the data returned by the ONR-602 and ONR-604 experiments, both flown under the auspices of ONR and the Air Force Space Test Program, augmented by correlative data bases of both space-based and ground-based data. The principal effort was in analysis of the full set of solar energetic particle (SEP) events, comparing CRRES measured spectra to model calculations and finalizing a manuscript on the 'trapped helium.'

Derived from text

N95-17736 National Geophysical Data Center, Boulder, CO.
SOLAR-GEOPHYSICAL DATA NUMBER 596, APRIL 1994. PART 1: (PROMPT REPORTS). DATA FOR MARCH, FEBRUARY 1994, AND LATE DATA
Helen E. Coffey, ed. Feb. 1994 119 p See also PB94-183555
Limited Reproducibility: More than 20% of this document may be affected by microfiche quality
(PB94-183548; SGD-596-Pt-1) Avail: CASI HC A06

Contents include the following for February 1994: Solar Active Regions; Sudden Ionospheric Disturbances; Solar Radio Spectral Observations: Solar Radioheliograph; Cosmic Ray Measurements by Neutron Monitor; Geomagnetic Indices; and Principal Magnetic Storms. Contents include the following for March 1994: Solar-Terrestrial Environment; Plots of GOES satellite X-rays, Particles and Magnetometer data with ground-based Boulder Magnetometer and Deep River Neutron Monitor; IUWDS Alert Periods (Advance and Worldwide); Solar Activity Indices; Solar Flares; Solar Radio Emission; and Stanford Mean Solar Magnetic Field. NTIS

N95-17737 National Geophysical Data Center, Boulder, CO.
SOLAR-GEOPHYSICAL DATA NUMBER 596, APRIL 1994. PART 2: (COMPREHENSIVE REPORTS). DATA FOR OCTOBER 1993, AND MISCELLANEOUS
Helen E. Coffey, ed. Apr. 1994 72 p See also PB94-183548
Limited Reproducibility: More than 20% of this document may be affected by microfiche quality
(PB94-183555; SGD-596-Pt-2) Avail: CASI HC A04

Contents include the following for October 1993: Solar Flares; Solar Radio Bursts at Fixed Frequencies; Solar X-ray Radiation from GOES Satellite Graphs; Mass Ejections from the Sun; Active Prominences and Filaments; and IMP-8 Solar Wind Plot. NTIS

93 SPACE RADIATION

Includes cosmic radiation; and inner and outer earth's radiation belts.

For biological effects of radiation see *52 Aerospace Medicine*. For theory see *73 Nuclear and High-Energy Physics*.

N95-16383*# Chicago Univ., Chicago, IL. Dept. of Astronomy and Astrophysics.
Na-22 DECAY GAMMA RAYS FROM CLASSICAL NOVAE Final Report, 15 May 1991 - 14 May 1993
James W. Truran 14 May 1993 5 p
(Grant NAG5-1565)
(NASA-CR-197454; NAS 1.26:197454) Avail: CASI HC A01/MF A01

NASA Grant NAG 5-1565 has provided support for a program of theoretical research in nuclear astrophysics and related areas, focusing upon the possibility of detecting gamma rays from nearby novae. Particular attention has been given to the evaluation of the theoretical expectations for gamma ray emission from four possible sources: (1) the positron decays of the unstable CNO and fluorine isotopes that are transported to the surface regions of the envelope in the earliest stages of the outbursts; (2) Be-7 decay gamma rays, (3) Na-22 decay gamma rays released in the later stages of the outbursts; and (4) Al-26 decay gamma rays from novae and their possible contribution to Galactic emission. The critical questions of (1) the frequency of occurrence of ONeMg-enriched novae; (2) the expected Galactic distribution of the novae that produce 26Al; and (3) the nature of the observed soft X-ray emission from classical novae, have also been addressed. Considerable progress in research has been achieved on many of these fronts. Brief summaries of the results of several research projects are presented. Author (revised)

N95-16912*# National Aeronautics and Space Administration. Langley Research Center, Hampton, VA.
PERFORMANCE STUDY OF GALACTIC COSMIC RAY SHIELD MATERIALS
Myung-Hee Y. Kim (College of William and Mary, Williamsburg, VA.), John W. Wilson, Sheila A. Thibeault, John E. Nealy, Francis F. Badavi (Christopher Newport Coll., Newport News, VA.), and Richard L. Kiefer (College of William and Mary, Williamsburg, VA.) Nov. 1994 38 p
(RTOP 199-45-16-11)
(NASA-TP-3473; L-17389; NAS 1.60:3473) Avail: CASI HC A03/MF A01

The space program is faced with two difficult radiation protection issues for future long-term operations. First, retrofit of shield material or conservatism in shield design is prohibitively expensive and often impossible. Second, shielding from the cosmic heavy ions is faced with limited knowledge on the physical properties and biological responses of these radiations. The current status of space shielding technology and its impact on radiation health is discussed herein in terms of conventional protection practice and a test biological response model. The impact of biological response on the selection of optimum materials for cosmic ray shielding is presented in terms of the transmission characteristics of the shield material. Although the systematics of nuclear cross sections are able to demonstrate the relation of exposure risk to shield-material composition, the current uncertainty in-nuclear cross sections will not allow an accurate evaluation of risk reduction. This paper presents a theoretical study of risk-related factors and a pilot experiment to study the effectiveness of choice of shield materials to reduce the risk in space operations. Author

N95-17421*# Smithsonian Astrophysical Observatory, Cambridge, MA.
VERY HIGH GAMMA RAY EXTENSION OF GRO OBSERVATIONS Final Report, 1 Jun. 1990 - 31 May 1994
Trevor C. Weekes Dec. 1994 35 p
(Grant NAG5-1381)
(NASA-CR-197489; NAS 1.26:197489) Avail: CASI HC A03/MF A01

The membership, progress, and invited talks, publications, and proceedings made by the Whipple Gamma Ray Collaboration is reported for june 1990 through May 1994. Progress was made in the following areas: the May 1994 Markarian Flare at Whipple and EGRET (Energetic Gamma Ray Experiment Telescope) energies; AGN's (Active Galactic Nuclei); bursts; supernova remnants; and simulations and energy spectra. CASI

N95-17527*# New Mexico State Univ., Las Cruces, NM. Dept. of Astronomy.
X-RAY EMISSION FROM THE EDGE-ON SPIRAL GALAXY NGC 4631 Final Report, 15 Mar. 1992 - 14 Jul. 1994
R. A. M. Walterbos 14 Jul. 1994 4 p
(Grant NAG5-1924)
(NASA-CR-197536; NAS 1.26:197436) Avail: CASI HC A01/MF A01

This grant supported research of the X-ray emission from the disk and halo of the edge-on spiral galaxy NGC 4631, using data from the ROSAT satellite. The data were obtained on the basis of a proposal submitted by the PI, which was highly ranked in the peer review. It is a pleasure to say that the goals of the project, imaging and spectroscopy of hot gas in the disk and halo of a vigorously star forming galaxy, have been achieved. The results of the project have been submitted for publication, and are in press. A list of the publications is included. Author

99 GENERAL

N95-16120# California Univ., Berkeley. Lawrence Berkeley Lab, CA.
LABORATORY DIRECTED RESEARCH AND DEVELOPMENT PROGRAM
Feb. 1994 97 p
(Contract DE-AC03-76SF-00098)
(DE94-011381; LBL-Pub-5382) Avail: CASI HC A05/MF A02

This report is compiled from annual reports submitted by principal investigators following the close of fiscal year 1993. This report describes the projects supported and summarizes their accomplishments. The program advances the Laboratory's core competencies, foundations, scientific capability, and permits exploration of exciting new opportunities. Reports are given from the following divisions: Accelerator and Fusion Research, Chemical Sciences, Earth Sciences, Energy and Environment, Engineering, Environment -- Health and Safety, Information and Computing Sciences, Life Sciences, Materials Sciences, Nuclear Science, Physics, and Structural Biology. DOE

N95-16581*# National Aeronautics and Space Administration. Goddard Space Flight Center, Greenbelt, MD.

SCIENTIFIC AND TECHNICAL PUBLISHING AT GODDARD SPACE FLIGHT CENTER IN FISCAL YEAR 1994

Nov. 1994 195 p
(NASA-TM-104614; Rept-95B00010; NAS 1.15:104614) Avail: CASI HC A09/MF A03

This publication is a compilation of scientific and technical material that was researched, written, prepared, and disseminated by the Center's scientists and engineers during FY94. It is presented in numerical order of the GSFC author's sponsoring technical directorate; i.e., Code 300 is the Office of Flight Assurance, Code 400 is the Flight Projects Directorate, Code 500 is the Mission Operations and Data Systems Directorate, Code 600 is the Space Sciences Directorate, Code 700 is the Engineering Directorate, Code 800 is the Suborbital Projects and Operations Directorate, and Code 900 is the Earth Sciences Directorate. The publication database contains publication or presentation title, author(s), document type, sponsor, and organizational code. This is the second annual compilation for the Center. Author

Typical Subject Index Listing

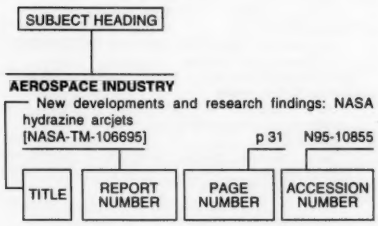

The subject heading is a key to the subject content of the document. Titles, report numbers, and accession numbers of pertinent documents are provided under each subject heading. When the title is insufficiently descriptive of the document content, a title extension is added, separated from the title by three hyphens. The report number helps to indicate the type of document cited (e.g., NASA report, NASA translation, NASA contractor report). The accession number is the number by which the document abstracts are arranged in this journal and by which the document is sold or requested. The page number helps you locate the citation in the abstract section. The titles, with title extensions if present, are arranged under each subject heading in ascending accession number order. The subject headings have been selected from the latest revision of the *NASA Thesaurus*.

A

A STARS
The Mg 2 lines as diagnostic of PMS nature in Herbig Ae/Be stars
[NASA-CR-197518] p 915 N95-17494
ABBREVIATIONS
Directory of Organizational Technical Report Acronym Codes (DOTRAC)
[AD-A281500] p 908 N95-16086
Department of Defense dictionary of military and associated terms. Includes US acronyms and abbreviations and NATO terms (English only)
[AD-A283218] p 912 N95-17633
ABERRATION
Visual neural development and chromatic aberration
[AD-A285064] p 826 N95-16368
ABLATION
Plasma disruption modeling and simulation
[DE94-015095] p 889 N95-16307
Thermal chemical energy of ablating silica surfaces in air breathing solid rocket engines p 714 N95-16316
Intense ion beam characterization and thermal modeling for beam materials processing
[DE94-016281] p 745 N95-16938
ABLATIVE MATERIALS
Thermal chemical energy of ablating silica surfaces in air breathing solid rocket engines p 714 N95-16316
ABRASION RESISTANCE
Evaluation of alternate F-14 wing lug coating
[AD-A283207] p 669 N95-17631
ABSORPTION
Revisions to an empirical surface loss model using a correction for pH-dependent attenuation
[AD-A285714] p 871 N95-17177
ABSORPTION CROSS SECTIONS
The chemistry and physics of transition metal clusters
[DE94-014012] p 734 N95-16364
Properties of Ce:LiSrAlF6 and Ce:LiCaAlF6 ultraviolet lasers
[DE94-013737] p 777 N95-17168
ABSORPTION SPECTRA
Infrared signatures for remote sensing
[DE94-014222] p 790 N95-16215
X-ray absorption spectra and structure of some nickel oxides (hydroxides)
[AD-A281305] p 735 N95-16788
New ytterbium-doped apatite crystals for flexible laser design
[DE94-015138] p 899 N95-16867
Chemical properties of the fullerenes
[AD-A282730] p 730 N95-17141
First detection of CO (j = 0 - 1) adsorption at cosmological distances (z = 0.247)
[PB94-184595] p 916 N95-17332
The Mg 2 lines as diagnostic of PMS nature in Herbig Ae/Be stars
[NASA-CR-197518] p 915 N95-17494
ABSORPTION SPECTROSCOPY
Atomic structure and valency of nickel in some of its oxycompounds
[AD-A281109] p 733 N95-16091
In-situ x-ray characterization of the electrolyte-solid interface
[AD-A281165] p 729 N95-16627
XAFS investigation of structure and valency of nickel in some oxycompounds
[AD-A283193] p 877 N95-17630
An XAFS study of the oxidation of structural iron in biotite mica by solutions containing Br2 or H2O2
[DE94-018721] p 733 N95-17912
ABSORPTIVITY
Effects of substrate temperature on metal colloid formation and on optical response in metal ion implanted silica
[DE94-013633] p 736 N95-16807
ABSTRACTS
ARO-URI Center for Opto-Electronic Systems Research
[AD-A281447] p 883 N95-15958
Proceedings of the Neural Network Workshop for the Hanford Community
[DE94-014567] p 856 N95-16609
Abstracts and program Proceedings of the 1994 Meeting of the International Society for Ecological Modelling North American Chapter
[DE94-016456] p 796 N95-17636
ACCELERATION (PHYSICS)
Summary report of mission acceleration measurements for STS-62, launched 4 March 1994
[NASA-TM-106773] p 750 N95-17893
ACCELEROMETERS
Summary report of mission acceleration measurements for STS-62, launched 4 March 1994
[NASA-TM-106773] p 750 N95-17893
ACCEPTABILITY
Use of the electronic balance for highly accurate direct mass measurements without the use of external mass standards
[PB94-187713] p 774 N95-16074
ACCEPTOR MATERIALS
Process of making a bistable photoconductive component
[AD-D016449] p 764 N95-16539
ACCIDENT INVESTIGATION
Annual review of aircraft accident data: US Air carrier operations, calendar year 1992
[PB95-100319] p 665 N95-17748
ACCRETION DISKS
ROSAT detection of diffuse hot gas in the edge-on galaxy NGC 4631
[NASA-CR-197535] p 915 N95-17496
X-ray emission from the edge-on spiral galaxy NGC 4631
[NASA-CR-197536] p 924 N95-17527
ACCURACY
Numeric data distribution: The vital role of data exchange in today's world p 907 N95-15937
Analysis of infrared scaling laws
[AD-A285461] p 903 N95-16877
ACETATES
Living radical polymerization of vinyl acetate
[AD-A280901] p 743 N95-16500
From living carbocationic to living radical polymerization
[AD-A280902] p 743 N95-16501
ACETYLENE
Atomic layer epitaxy of group 4 materials: Surface processes, thin films, devices and their characterization
[AD-A280987] p 898 N95-16532
Identification and temporal behavior of radical intermediates formed during the combustion and pyrolysis of gaseous fuels: Kinetic pathways to soot formation
[DE94-014681] p 731 N95-17163
ACIDITY
The stability of calibration standards for ICP/AES analysis: A two-year study
[DE94-013398] p 728 N95-16426
ACOUSTIC ATTENUATION
Innovative acoustic techniques for studying new materials and new developments in solid state physics
[AD-A280986] p 898 N95-16525
Active minimization of energy density in three-dimensional enclosures
[NASA-CR-197213] p 871 N95-16848
ACOUSTIC EMISSION
Active and passive acoustic bubble sizing
[ISVR-TR-237] p 769 N95-16064
ACOUSTIC MEASUREMENT
Formulation of probe-corrected time-domain planar near-field measurements
[AD-A281053] p 754 N95-16624
The application of non-destructive techniques to the testing of a wind turbine blade
[DE95-000323] p 784 N95-17360
ACOUSTIC PROPAGATION
Ducted fan acoustic radiation including the effects of nonuniform mean flow and acoustic treatment
[NASA-CR-197449] p 870 N95-16401
ACOUSTIC PROPERTIES
Plasma sound source basic research
[AD-A285394] p 890 N95-16617
ACOUSTIC SCATTERING
Effective reflection coefficients for the mean acoustic field between two rough interfaces
[AD-A281962] p 870 N95-16413
Support minimized inversion of acoustic and elastic wave scattering
[DE94-014233] p 783 N95-16538
Models to estimate high frequency acoustic scattering due to thermal fine- and micro-structure of the ocean
[AD-A285456] p 870 N95-16812
ACOUSTIC SOUNDING
On the measurement of momentum flux profiles using a five-beam 915-MHz wind profiler
[DE94-018448] p 791 N95-17903
ACOUSTIC VELOCITY
Thermal characteristics and heat transfer in an electrothermal light gas gun
[AD-A281980] p 892 N95-17442
ACOUSTICS
Effective reflection coefficients for the mean acoustic field between two rough interfaces
[AD-A281962] p 870 N95-16413
Anisotropic heat exchangers/stack configurations for thermoacoustic heat engines
[AD-A280974] p 792 N95-16506
Innovative acoustic techniques for studying new materials and new developments in solid state physics
[AD-A280986] p 898 N95-16525
Non-linear acoustics in fluids and gels
[PB94-201308] p 870 N95-16614
Thermo-fluid mechanic study of thermoacoustic devices
[AD-A281130] p 870 N95-16810
Active minimization of energy density in three-dimensional enclosures
[NASA-CR-197213] p 871 N95-16848
Thermoacoustic pin stacks
[AD-A282267] p 794 N95-16954

ACOUSTO-OPTICS
System design, implementation, and evaluation of the optical broadband correlator
[AD-A285406] p 884 N95-16296
ACQUISITION
NAFTA literature at the International Trade Commission library p 905 N95-15922
ACRYLATES
From living carbocationic to living radical polymerization
[AD-A280902] p 743 N95-16501
ACRYLIC RESINS
Vacuum deposited polymer/silver reflector material
[DE94-018729] p 748 N95-17913
ACTIVATED CARBON
An X-Ray Photoelectron Spectroscopy (XPS) study of activated carbons impregnated with some organocopper complexes
[AD-A282721] p 727 N95-16384
ACTIVATION ENERGY
Parametric study of shock-induced combustion in a hydrogen air system
[NASA-CR-197134] p 726 N95-15967
ACTIVE CONTROL
Energy decay and control for elastic and viscoelastic distributed parameter systems
[AD-A281312] p 726 N95-16008
A computational investigation of wake-induced airfoil flutter in incompressible flow and active flutter control
[AD-A281534] p 670 N95-16109
An improved position/force control of manipulators p 653 N95-16280
Integrated passive and active control of structures
[AD-A282684] p 708 N95-16304
Active load control during rolling maneuvers --- performed in the Langley Transonic Dynamics Tunnel
[NASA-TP-3455] p 669 N95-17397
A new communication protocol family for a distributed spacecraft control system p 703 N95-17590
Microgravity isolation system design: A case study
[NASA-TM-106804] p 654 N95-17657
Conducting polymers as corrosion resistant coatings
[DE94-018265] p 748 N95-17892
ACTIVE GALACTIC NUCLEI
Very high gamma ray extension of GRO observations
[NASA-CR-197489] p 924 N95-17421
ACTIVITY (BIOLOGY)
Molecular approach to hypothalamic rhythms
[AD-A285164] p 822 N95-16851
ACTUATORS
Structural integrity of intelligent materials and structures. Constitutive modeling of shape memory alloys
[AD-A281301] p 735 N95-16786
A comparison of different control methods for vibration suppression of flexible structures using piezoelectric actuators
[AD-A282958] p 710 N95-17622
New shower maximum trigger for electrons and photons at CDF
[DE94-018376] p 878 N95-17899
ADA (PROGRAMMING LANGUAGE)
Detailed example of using PIWG on the SUN workstation and the DEC VAX computer
[AD-A281528] p 834 N95-16107
Use of data description languages in the interchange of data p 704 N95-17597
ADAPTATION
Vibratory tactile display for textures p 851 N95-15973
SLS-1: The first dedicated life sciences shuttle flight p 676 N95-16769
Adaptive line enhancers for fast acquisition p 757 N95-17287
SEQ-POINTER: Next generation, planetary spacecraft remote sensing science observation design tool p 697 N95-17559
ADAPTIVE CONTROL
Digital adaptive and optimal control of distributed systems
[AD-A285352] p 851 N95-15952
Adaptive control of nonlinear flexible systems
[AD-A281337] p 855 N95-16011
Studies of novel popout
[AD-A285237] p 826 N95-16244
Approach to in-process tool wear monitoring in drilling: Application of Kalman filter theory p 653 N95-16279
Adaptive line enhancers for fast acquisition p 757 N95-17287
A feedforward control approach to the local navigation problem for autonomous vehicles
[AD-A282787] p 666 N95-17706
ADAPTIVE FILTERS
Mitre adaptive processing capability
[AD-A281078] p 755 N95-16825
ADAPTIVE OPTICS
Methods of wave-front identification by control images p 652 N95-16274
Least squares computations in science and engineering
[AD-A281213] p 862 N95-16798
Issues in the design and optimization of adaptive optics and laser guide stars for the Keck Telescopes
[DE94-012888] p 916 N95-17525
ADDITIVES
International Winterschool on Electronic Properties of Novel Materials: Progress in Fullerene Research
[AD-A282128] p 728 N95-16608
Rare earth ion doped CW cascade fiber laser
[AD-D016370] p 779 N95-17698
ADDUCTS
Methods development toward the measurement of polyaromatic hydrocarbon-DNA adducts by mass spectrometry
[PB94-182722] p 727 N95-16373
ADHESION
The effect of brush polydispersity on the interphase between end-grafted brushed and polymeric matrices
[AD-A280975] p 743 N95-16507
ADHESIVE BONDING
Special hybrid stress finite elements for the analysis of interface stress distribution in adhesive joints
[AD-A281612] p 785 N95-16102
User-defined subroutine for implementation of special finite elements in ABAQUS for the analysis of adhesive joints
[AD-A282431] p 788 N95-17510
Adhesion of silicon oxide to diamond
[AD-D016356] p 747 N95-17694
ADIPOSE TISSUES
Skin blood flow and bioelectrical impedance
[AD-A285475] p 821 N95-16619
ADSORBENTS
Nano-scale metal oxide particles as materials for air purification
[AD-A281394] p 729 N95-16791
ADSORPTION
An unexpected adsorption site exclusion process on Si(100)-(2x1)
[AD-A284950] p 894 N95-16043
Characterization of surfaces
[NASA-CR-196995] p 750 N95-16065
Reaction of methanol with porous silicon
[AD-A285518] p 728 N95-16406
Nanoscale imaging of molecular adsorption
[AD-A280979] p 873 N95-16482
Gas-surface interactions near dissociation threshold
[AD-A282726] p 730 N95-17140
Surfactant adsorption by sub-millimeter size bubbles: Quantification and modelling
[AD-A282405] p 772 N95-17506
ADVECTION
Avoiding BDF stability barriers in the MOL solution of advection-dominated problems
[DE94-014793] p 861 N95-16535
AERIAL RECONNAISSANCE
Multistatic radar, MSR
[PB94-190709] p 759 N95-17301
AEROACOUSTICS
Aeronautical enginnering: A cumulative index to a continuing bibliography (supplement 312)
[NASA-SP-7037(312)] p 654 N95-17702
AEROASSIST
Numerical optimization of synergetic maneuvers
[AD-A283398] p 656 N95-17435
AEROBRAKING
Physiological constraints on deceleration during the aerocapture of manned vehicles p 810 N95-16751
AEROCAPTURE
Physiological constraints on deceleration during the aerocapture of manned vehicles p 810 N95-16751
AERODYNAMIC CHARACTERISTICS
Joint Proceedings on Aeronautics and Astronautics (JPAA)
[ISBN-7-80-046602-7] p 649 N95-16249
An approach to aerodynamic characteristics of low radar cross-section fuselages p 649 N95-16251
FPCAS2D user's guide, version 1.0
[NASA-CR-195413] p 786 N95-16588
Twin engine afterbody model p 663 N95-17880
Investigation into the aerodynamic characteristics of a combat aircraft research model fitted with a forward swept wing p 664 N95-17884
AERODYNAMIC COEFFICIENTS
Error propagation equations for estimating the uncertainty in high-speed wind tunnel test results
[DE94-014136] p 671 N95-16509
Measurements on a two-dimensional aerofoil with high-lift devices p 657 N95-17848
Two-dimensional 16.5 percent thick supercritical airfoil NLR 7301 p 658 N95-17854
AERODYNAMIC CONFIGURATIONS
Optimum Design Methods for Aerodynamics
[AGARD-R-803] p 666 N95-16562
Single-pass method for the solution of inverse potential and rotational problems. Part 1: 2-D and quasi 3-D theory and application p 664 N95-16563
Single-pass method for the solution of inverse potential and rotational problems. Part 2: Fully 3-D potential theory and applications p 664 N95-16564
Optimum aerodynamic design via boundary control p 667 N95-16565
Residual-correction type and related computational methods for aerodynamic design. Part 1: Airfoil and wing design p 667 N95-16566
Tools for applied engineering optimization p 668 N95-16570
Automation of reverse engineering process in aircraft modeling and related optimization problems
[NASA-CR-197109] p 668 N95-16899
A selection of experimental test cases for the validation of CFD codes, volume 2
[AGARD-AR-303-VOL-2] p 657 N95-17846
AERODYNAMIC DRAG
An investigation of the transonic pressure drag coefficient for axi-symmetric bodies
[AD-A280990] p 654 N95-15994
Measurements on a two-dimensional aerofoil with high-lift devices p 657 N95-17848
AERODYNAMIC FORCES
Structural effects of unsteady aerodynamic forces on horizontal-axis wind turbines
[DE94-011863] p 787 N95-16939
Force and pressure data of an ogive-nosed slender body at high angles of attack and different Reynolds numbers p 661 N95-17868
Subsonic flow around US-orbiter model FALKE in the DNW p 663 N95-17877
AERODYNAMIC HEAT TRANSFER
An analysis code for the Rapid Engineering Estimation of Momentum and Energy Losses (REMEL)
[NASA-CR-191178] p 656 N95-16887
AERODYNAMIC HEATING
An engineering code to analyze hypersonic thermal management systems p 715 N95-16322
Numerical optimization of synergetic maneuvers
[AD-A283398] p 656 N95-17435
AERODYNAMIC INTERFERENCE
Wall-signature methods for high speed wind tunnel wall interference corrections p 650 N95-16257
2-D aileron effectiveness study p 658 N95-17851
Data from the GARTEur (AD) Action Group 02 airfoil CAST 7/DOA1 experiments p 659 N95-17856
Single-engine tail interference model p 663 N95-17879
Low speed propeller slipstream aerodynamic effects p 663 N95-17882
AERODYNAMIC LOADS
Residual-correction type and related computational methods for aerodynamic design. Part 2: Multi-point airfoil design p 667 N95-16567
Optimal shape design for aerodynamics p 667 N95-16568
Airfoil optimization by the one-shot method p 667 N95-16569
Aerodynamic shape optimization p 668 N95-16572
Active load control during rolling maneuvers --- performed in the Langley Transonic Dynamics Tunnel
[NASA-TP-3455] p 669 N95-17397
AERODYNAMIC NOISE
Ducted fan acoustic radiation including the effects of nonuniform mean flow and acoustic treatment
[NASA-CR-197449] p 870 N95-16401
AERODYNAMIC STABILITY
Investigation of dynamic inflow's influence on rotor control derivatives p 649 N95-16250
AERODYNAMIC STALLING
Structural effects of unsteady aerodynamic forces on horizontal-axis wind turbines
[DE94-011863] p 787 N95-16939
Aircraft accident report: Stall and loss of control on final approach, Atlantic Coast Airlines, Inc./United Express Flight 6291 Jetstream 4101, N304UE Columbus, OH, 7 January 1994
[PB94-910409] p 665 N95-17646
AERODYNAMICS
A workstation based simulator for teaching compressible aerodynamics
[NASA-TM-106799] p 839 N95-16906
Interactive computer graphics applications for compressible aerodynamics
[NASA-TM-106802] p 839 N95-17264
Aeronautical enginnering: A cumulative index to a continuing bibliography (supplement 312)
[NASA-SP-7037(312)] p 654 N95-17702
Low speed propeller slipstream aerodynamic effects p 663 N95-17882

AEROELASTICITY
Measurements of unsteady pressure and structural response for an elastic supercritical wing
[NASA-TP-3443] p 653 N95-16560
FPCAS2D user's guide, version 1.0
[NASA-CR-195413] p 786 N95-16588
AEROGELS
Computer modeling of organic aerogels, 93-SR-062
[DE94-016485] p 722 N95-17745
AEROMANEUVERING
Numerical optimization of synergetic maneuvers
[AD-A283398] p 656 N95-17435
AERONAUTICAL ENGINEERING
Aeronautical enginnering: A cumulative index to a continuing bibliography (supplement 312)
[NASA-SP-7037(312)] p 654 N95-17702
Aeronautical engineering: A continuing bibliography with indexes (supplement 311)
[NASA-SP-7037(311)] p 654 N95-17704
AEROSOLS
Fractal aggregate random media analysis and applications
[AD-A281410] p 884 N95-16161
AEROSPACE ENGINEERING
Development of the vibration test equipment for testing the products of aircraft and space technology with simulation of operating conditions p 651 N95-16266
Overview of TTCP and AGARD propulsion activities p 720 N95-16351
Optimum Design Methods for Aerodynamics
[AGARD-R-803] p 666 N95-16562
Tools for applied engineering optimization p 668 N95-16570
Graphite-reinforced polycyanate composites for space and missile applications
[AD-A285509] p 725 N95-16970
A new systems engineering approach to streamlined science and mission operations for the Far Ultraviolet Spectroscopic Explorer (FUSE) p 707 N95-17611
Concurrent engineering: Spacecraft and mission operations system design p 708 N95-17614
Overview of space power electronic's technology under the CSTI High Capacity Power Program
[NASA-TM-110110] p 883 N95-17933
AEROSPACE ENVIRONMENTS
Conceptual design study of a solar concentrator/support structure: A three dimensional finite element model p 718 N95-16342
Analysis of space environment damage to solar cell assemblies from LDEF experiment A0171-GSFC test plate
[NASA-CR-196523] p 793 N95-16575
Validation of astronaut psychological select-in criteria p 813 N95-16762
SLS-1: The first dedicated life sciences shuttle flight p 676 N95-16769
Medical care capabilities for Space Station Freedom: A phase approach p 710 N95-16772
Advanced Cardiac Life Support (ACLS) utilizing Man-Tended Capability (MTC) hardware onboard Space Station Freedom p 816 N95-16775
Artificial gravity: How much, how often, how long? p 816 N95-16778
Verification of NOAA Space Environment Laboratory forecasts, 1 January - 31 December 1993
[PB95-104162] p 803 N95-17927
AEROSPACE INDUSTRY
A study of software standards used in the avionics industry p 670 N95-16456
The global aircraft shape p 668 N95-16571
Review of the EUROPT Project AERO-0026 p 668 N95-16573
Military aviation maintenance industry in Western Europe: Concentration and internationalization
[PB94-189180] p 653 N95-17451
AEROSPACE MEDICINE
Aviation epidemiology data register: Age-specific medical and nonmedical attrition rates among Fort Rucker civilian aviators
[AD-A284970] p 818 N95-16132
Aerospace Medical Association 63rd Annual Scienti fic Meeting Program p 807 N95-16737
The effect of differences in time to detection of circulating microbubbles on the risk of decompression sickness p 807 N95-16738
Variability in Hoffmann and tendon reflexes in healthy male subjects p 808 N95-16739
The psychophysical function for perceived gravitational-inertial force does not depend on the orientation of the otolith organs p 808 N95-16740
Use of injectable promethazine to decrease symptom scores of Space Motion Sickness p 808 N95-16741
Comparison of saline and fludrocortisone as fluid-loading countermeasures following exposure to simulated microgravity p 808 N95-16742
Skeletal muscle responses to unloading in humans p 809 N95-16743
Intramuscular pressure: A better tool than EMG to optimize exercise for long-duration space flight p 809 N95-16744
Catecholaminergic responses to stressful motion stimuli, scopolamine plus amphetamine, and dexamethasone p 809 N95-16745
Heat stress and a countermeasure in the Shuttle rescueman's suit p 809 N95-16746
A new model for estimating total body water from bioelectrical resistance p 810 N95-16747
Spectral components of human cardiovascular responses to step changes in Lower Body Negative Pressure (LBNP) before and after 22 hour of 6 deg head down bed rest p 810 N95-16748
Magnetic Resonance Imaging (MRI) of skeletal muscles in astronauts after 9 days of space flight p 810 N95-16749
Results of an International Space Crew Debrief p 810 N95-16750
Physiological constraints on deceleration during the aerocapture of manned vehicles p 810 N95-16751
Blood volume and orthostatic responses of men and women to a 13-day bedrest p 811 N95-16752
Effect of antiorthostatic BedRest (BR) on GastroIntestinal Motility (GIM) of normal subjects p 811 N95-16753
Changes in left ventricular function as determined by the multi-wire gamma camera at near presyncopal levels of lower body negative pressure p 811 N95-16754
Comparisons of three anti-G suit configurations during long duration, low onset, +Gz p 811 N95-16755
Achilles Tendon Reflex (ATR) in response to short exposures of microgravity and hypergravity p 812 N95-16756
Prediction of space sickness in astronauts from preflight fluid, electrolyte, and cardiovascular variables and Weightless Environmental Training Facility (WETF) training p 812 N95-16757
Dark focus of accommodation as dependent and independent variables in visual display technology p 812 N95-16758
Review of performance, medical, and operational data on pilot aging issues p 812 N95-16759
Alertness management in two-person long-haul flight operations p 813 N95-16760
Results of the psychiatric, select-out evaluation of US astronaut applications p 813 N95-16761
Validation of astronaut psychological select-in criteria p 813 N95-16762
Psychological training of NASA astronauts for extended missions p 813 N95-16763
Human performance in the modern cockpit p 813 N95-16764
Crew decision making under stress p 814 N95-16765
Space medicine research: Needs for the 21st century p 814 N95-16768
SLS-1: The first dedicated life sciences shuttle flight p 676 N95-16769
Effects of weightlessness on human baroreflex function p 815 N95-16770
Dynamics of the G-excess illusion p 815 N95-16771
Medical care capabilities for Space Station Freedom: A phase approach p 710 N95-16772
A prototype Crew Medical Restraint System (CMRS) for Space Station Freedom p 815 N95-16773
Delivery of cardiopulmonary resuscitation in the microgravity environment p 816 N95-16774
Advanced Cardiac Life Support (ACLS) utilizing Man-Tended Capability (MTC) hardware onboard Space Station Freedom p 816 N95-16775
A surgical support system for Space Station Freedom p 710 N95-16776
Medicine on Mars: Remote medical care and the space exploration initiative p 816 N95-16777
Artificial gravity: How much, how often, how long? p 816 N95-16778
The effect of intermittent standing or walking during head down tilt bedrest on peak O2 consumption p 817 N95-16779
Periodic upright posture negates the suppression of neuroendocrine response to head down bedrest p 817 N95-16780
The efficacy of periodic +Gz exposure in the prevention of bedrest induced orthostatic intolerance p 817 N95-16781
The value of the 4-day headdown bedrest model for screening countermeasures p 817 N95-16782
Aerospace medicine and biology: A continuing bibliography with indexes (supplement 396)
[NASA-SP-7011(396)] p 823 N95-17703
AEROSPACE PLANES
Constrained minimization of smooth functions using a genetic algorithm
[NASA-TP-3329] p 709 N95-16902
AEROSPACE SYSTEMS
Proceedings of the 12th Annual Space Surveillance Workshop, volume 1
[AD-A285265] p 672 N95-16530
Towards cheaper control centers p 674 N95-17250
Towards an integral computer environment supporting system operations analysis and conceptual design p 686 N95-17558
The Advanced Orbiting Systems Testbed Program: Results to date p 700 N95-17575
The ESA standard for telemetry and telecommand packet utilisation: PUS p 704 N95-17595
Cross support overview and operations concept for future space missions p 705 N95-17598
AEROSPACE TECHNOLOGY TRANSFER
BioServe space technologies: A NASA Center for the Commercial Development of Space
[NASA-CR-196983] p 807 N95-16034
Revitalizing general aviation
[NASA-TM-110113] p 669 N95-16982
AEROSPACE VEHICLES
New insulation constructions for aerospace wiring applications p 712 N95-16056
AEROTHERMODYNAMICS
A model for preliminary facility design including simulation issues p 672 N95-16318
AFRICA
Acquiring and disseminating unpublished economic and social development materials in Africa: The case of the National Institute of Development Research and Documentation University of Botswana p 906 N95-15924
AFTERBODIES
An investigation of the transonic pressure drag coefficient for axi-symmetric bodies
[AD-A280990] p 654 N95-15994
Single-engine tail interference model p 663 N95-17879
Twin engine afterbody model p 663 N95-17880
AFTERBURNING
Single-engine tail interference model p 663 N95-17879
AGE FACTOR
Aviation epidemiology data register: Age-specific medical and nonmedical attrition rates among Fort Rucker civilian aviators
[AD-A284970] p 818 N95-16132
Kinetics model for initiation and promotion for describing tumor prevalence from HZE radiation
[NASA-TP-3479] p 820 N95-16412
AGGLOMERATION
Reduction and aggregation of silver in aqueous gelatin and silica suspensions
[DE94-013998] p 727 N95-16363
AGING (BIOLOGY)
Basic mechanisms and implications of non-photic entrainment of circadian rhythmicity
[AD-A283180] p 822 N95-17342
AGING (MATERIALS)
Problems with aging wiring in Naval aircraft p 711 N95-16048
AGREEMENTS
Department of Energy: Office of Scientific and Technical Information p 907 N95-15936
AGRICULTURE
A procedure for estimating the carbon budget of terrestrial ecosystems in the former Soviet Union by geographic information system analysis and classification of AVHRR derived global vegetation index p 796 N95-17394
AH-64 HELICOPTER
The assessment of the AH-64D, longbow, mast-mounted assembly noise hazard for maintenance personnel
[AD-A284971] p 869 N95-16226
AILERONS
2-D aileron effectiveness study p 658 N95-17851
AIR BREATHING ENGINES
Hypersonic air-breathing aeropropulsion facility test support requirements p 672 N95-16319
AIR DEFENSE
Division of Information Systems (FOA 37)
[PB94-190766] p 909 N95-16400
Assessment of benefits and drawbacks of using fuzzy logic, especially in fire control systems
[AD-A285428] p 838 N95-16874
AIR FILTERS
Filter efficiency and pressure drop calculations through two and three dimensional fiber arrays
[DE94-014111] p 770 N95-16211

AIR FLOW
Filter efficiency and pressure drop calculations through two and three dimensional fiber arrays
[DE94-014111] p 770 N95-16211
A selection of experimental test cases for the validation of CFD codes, volume 2
[AGARD-AR-303-VOL-2] p 657 N95-17846

AIR INTAKES
Numerical simulation of helicopter engine plume in forward flight
[NASA-CR-197488] p 655 N95-16589
Data acquisition and processing software for the Low Speed Wind Tunnel tests of the Jindivik auxiliary air intake
[AD-A285455] p 656 N95-17178

AIR LAND INTERACTIONS
An investigation of small-scale variations in cloud climatology induced by topography and monthly mean winds
[AD-A283274] p 803 N95-17715

AIR MASSES
An air mass transformation model for coastal environments
[AD-A281790] p 801 N95-17164

AIR POLLUTION
Novel mass spectrometric instrument for gaseous and particulate characterization and monitoring
[DE94-014168] p 795 N95-16213
Infrared signatures for remote sensing
[DE94-014222] p 790 N95-16215
Meteorological Monitoring Program
[DE94-017810] p 795 N95-16557
Energy and emissions of CO2, NOx and SO2 in the scenario of the 3rd national environmental evaluation, 1993
[PB94-194792] p 796 N95-17304

AIR PURIFICATION
Nano-scale metal oxide particles as materials for air purification
[AD-A281394] p 729 N95-16791

AIR QUALITY
Novel mass spectrometric instrument for gaseous and particulate characterization and monitoring
[DE94-014168] p 795 N95-16213

AIR TRAFFIC CONTROL
Solid state radar demonstration test results at the FAA Technical Center
[AD-A281520] p 752 N95-16097
Application of research techniques for documenting cognitive processes in air traffic control: Sector complexity and decision making
[AD-A282336] p 665 N95-16375
Modeling of Instrument Landing System (ILS) localizer signal on runway 25L at Los Angeles International Airport
[NASA-TM-4588] p 665 N95-17384
Federal Aviation Administration aviation system capital investment plan, 1993
[PB94-171956] p 654 N95-17512
Situation awareness information requirements for En Route Air Traffic Control
[DOT/FAA/AM-94/27] p 828 N95-17655

AIR TRAFFIC CONTROLLERS (PERSONNEL)
Application of research techniques for documenting cognitive processes in air traffic control: Sector complexity and decision making
[AD-A282336] p 665 N95-16375
Situation awareness information requirements for En Route Air Traffic Control
[DOT/FAA/AM-94/27] p 828 N95-17655

AIR WATER INTERACTIONS
Mixed-layer hindcasts conducted at OWS Victor with initialization from synthetic profiles/mixed-layer hindcasts conducted with BTs taken during 1990 with atmospheric forcing from NOGAPS
[AD-A284749] p 800 N95-16551
Variation of the thermohaline structure in the western equatorial Pacific upper ocean p 805 N95-17277
Analysis of a three-beam radar as an instrument for determining ocean wave heights and vector slopes
[AD-A282342] p 806 N95-17505

AIRBORNE EQUIPMENT
Generalized method of solving topological optimization problems for electrical airplane equipment systems in computer-aided design p 652 N95-16272

AIRBORNE RADAR
Using lidar tomography to characterize scattering in a turbulent media
[AD-A281014] p 751 N95-16002

AIRBORNE/SPACEBORNE COMPUTERS
Current research activities at the NASA-sponsored Illinois Computing Laboratory of Aerospace Systems and Software p 849 N95-16479
The SAX Italian scientific satellite. The on-board implemented automation as a support to the ground control capability p 695 N95-17551
XMM instrument on-board software maintenance concept p 699 N95-17567

AIRCRAFT ACCIDENT INVESTIGATION
A correlative investigation of simulated occupant motion and accident report in a helicopter crash
[AD-A285190] p 664 N95-16404
Aircraft accident report: Stall and loss of control on final approach, Atlantic Coast Airlines, Inc./United Express Flight 6291 Jetstream 4101, N304UE Columbus, OH, 7 January 1994
[PB94-910409] p 665 N95-17646

AIRCRAFT ACCIDENTS
Aircraft accident report: Stall and loss of control on final approach, Atlantic Coast Airlines, Inc./United Express Flight 6291 Jetstream 4101, N304UE Columbus, OH, 7 January 1994
[PB94-910409] p 665 N95-17646
Annual review of aircraft accident data: US Air carrier operations, calendar year 1992
[PB95-100319] p 665 N95-17748

AIRCRAFT ANTENNAS
A VHF/UHF antenna for the Precision Antenna Measurement System (PAMS)
[AD-A285673] p 754 N95-16621

AIRCRAFT COMMUNICATION
Spread spectrum applications in unmanned aerial vehicles
[AD-A281035] p 754 N95-16448

AIRCRAFT COMPARTMENTS
Generalized method of solving topological optimization problems for electrical airplane equipment systems in computer-aided design p 652 N95-16272

AIRCRAFT CONFIGURATIONS
Portable parallel stochastic optimization for the design of aeropropulsion components
[NASA-CR-195312] p 785 N95-16072
STOVL CFD model test case p 663 N95-17881

AIRCRAFT CONSTRUCTION MATERIALS
Shear buckling analysis of a hat-stiffened panel
[NASA-TM-4644] p 788 N95-17490

AIRCRAFT CONTROL
Human performance in the modern cockpit p 813 N95-16764

AIRCRAFT DESIGN
Joint Proceedings on Aeronautics and Astronautics (JPAA)
[ISBN-7-80-046602-7] p 649 N95-16249
An improved method of airfoil design p 649 N95-16252
Development of strength analysis methods and design model for aircraft constructions in Kazan Aviation Institute p 651 N95-16264
Evaluation of the dynamic stability characteristics of the NAL Light Transport Aircraft
[NAL-PD-CA-9217] p 671 N95-16392
Optimum Design Methods for Aerodynamics
[AGARD-R-803] p 666 N95-16562
Optimum aerodynamic design via boundary control p 667 N95-16565
Residual-correction type and related computational methods for aerodynamic design. Part 1: Airfoil and wing design p 667 N95-16566
Residual-correction type and related computational methods for aerodynamic design. Part 2: Multi-point airfoil design p 667 N95-16567
Optimal shape design for aerodynamics p 667 N95-16568
Airfoil optimization by the one-shot method p 667 N95-16569
Tools for applied engineering optimization p 668 N95-16570
The global aircraft shape p 668 N95-16571
Applications of automatic differentiation in CFD
[NASA-TM-109948] p 771 N95-16828
Multi-lab comparison on R-curve methodologies: Alloy 2024-T3
[NASA-CR-195004] p 736 N95-16860
Automation of reverse engineering process in aircraft modeling and related optimization problems
[NASA-CR-197109] p 668 N95-16899
Cooperative control theory and integrated flight and propulsion control
[NASA-CR-197493] p 671 N95-17404
Aeronautical engineering: A continuing bibliography with indexes (supplement 311)
[NASA-SP-7037(311)] p 654 N95-17704
OAT15A airfoil data p 659 N95-17857
Measurements of the flow over a low aspect-ratio wing in the Mach number range 0.6 to 0.87 for the purpose of validation of computational methods. Part 1: Wing design, model construction, surface flow. Part 2: Mean flow in the boundary layer and wake, 4 test cases p 660 N95-17860
Investigation into the aerodynamic characteristics of a combat aircraft research model fitted with a forward swept wing p 664 N95-17884

AIRCRAFT ENGINES
Portable parallel stochastic optimization for the design of aeropropulsion components
[NASA-CR-195312] p 785 N95-16072
Theoretical fundamentals of the aircraft GTE tests p 651 N95-16265
Hypersonic air-breathing aeropropulsion facility test support requirements p 672 N95-16319
The global aircraft shape p 668 N95-16571

AIRCRAFT EQUIPMENT
Bicarbonate of soda blasting technology for aircraft wheel depainting
[PB94-193323] p 654 N95-17466

AIRCRAFT GUIDANCE
Modeling of Instrument Landing System (ILS) localizer signal on runway 25L at Los Angeles International Airport
[NASA-TM-4588] p 665 N95-17384

AIRCRAFT ICING
Meteorological factors that affect the formation an prediction of aircraft icing
[AD-A281984] p 802 N95-17443

AIRCRAFT INDUSTRY
Development of processes, means, and theoretical principles of thin-walled detail plastic forming at Kazan Aviation Institute p 653 N95-16281

AIRCRAFT LANDING
Application of GPS/SINS/RA integrated system to aircraft approach landing p 653 N95-16277

AIRCRAFT MAINTENANCE
Problems with aging wiring in Naval aircraft p 711 N95-16048
Military aviation maintenance industry in Western Europe: Concentration and internationalization
[PB94-189180] p 653 N95-17451

AIRCRAFT MODELS
Linear prediction data extrapolation superresolution radar imaging p 651 N95-16268
Automation of reverse engineering process in aircraft modeling and related optimization problems
[NASA-CR-197109] p 668 N95-16899
Measurements on a two-dimensional aerofoil with high-lift devices p 657 N95-17848
Two-dimensional 16.5 percent thick supercritical airfoil NLR 7301 p 658 N95-17854
Low-speed surface pressure and boundary layer measurement data for the NLR 7301 airfoil section with trailing edge flap p 658 N95-17855
Data from the GARTEur (AD) Action Group 02 airfoil CAST 7/DOA1 experiments p 659 N95-17856
A supercritical airfoil experiment p 659 N95-17858
Two-dimensional high-lift airfoil data for CFD code validation p 659 N95-17859
Measurements of the flow over a low aspect-ratio wing in the Mach number range 0.6 to 0.87 for the purpose of validation of computational methods. Part 1: Wing design, model construction, surface flow. Part 2: Mean flow in the boundary layer and wake, 4 test cases p 660 N95-17860
Detailed study at supersonic speeds of the flow around delta wings p 660 N95-17861
Investigation into the aerodynamic characteristics of a combat aircraft research model fitted with a forward swept wing p 664 N95-17884

AIRCRAFT NOISE
The assessment of the AH-64D, longbow, mast-mounted assembly noise hazard for maintenance personnel
[AD-A284971] p 869 N95-16226

AIRCRAFT PARTS
Automation of reverse engineering process in aircraft modeling and related optimization problems
[NASA-CR-197109] p 668 N95-16899

AIRCRAFT PILOTS
Aviation epidemiology data register: Age-specific medical and nonmedical attrition rates among Fort Rucker civilian aviators
[AD-A284970] p 818 N95-16132
A correlative investigation of simulated occupant motion and accident report in a helicopter crash
[AD-A285190] p 664 N95-16404

AIRCRAFT POWER SUPPLIES
The computer analysis of the prediction of aircraft electrical power supply system reliability p 653 N95-16278

AIRCRAFT PRODUCTION
Low rate initial production in Army Aviation systems development
[AD-A281871] p 666 N95-16356
Composite chronicles: A study of the lessons learned in the development, production, and service of composite structures
[NASA-CR-4620] p 724 N95-16859

AIRCRAFT SAFETY
Aircraft accident report: Stall and loss of control on final approach, Atlantic Coast Airlines, Inc./United Express Flight 6291 Jetstream 4101, N304UE Columbus, OH, 7 January 1994
[PB94-910409] p 665 N95-17646

AIRCRAFT STRUCTURES
Development of strength analysis methods and design model for aircraft constructions in Kazan Aviation Institute p 651 N95-16264
Development of processes, means, and theoretical principles of thin-walled detail plastic forming at Kazan Aviation Institute p 653 N95-16281
The use of electrochemistry and ellipsometry for identifying and evaluating corrosion on aircraft
[AD-A285323] p 734 N95-16371
Rapid solution of large-scale systems of equations p 847 N95-16458
Composite chronicles: A study of the lessons learned in the development, production, and service of composite structures
[NASA-CR-4620] p 724 N95-16859

AIRFIELD SURFACE MOVEMENTS
Development of an Automated Airfield Dynamic Cone Penetrometer (AADCP) prototype and the evaluation of unsurfaced airfield seismic surveying using Spectral Analysis of Surface Waves (SASW) technology
[AD-A281985] p 672 N95-17444

AIRFOIL PROFILES
Measurements on a two-dimensional aerofoil with high-lift devices p 657 N95-17848
Investigation of the flow over a series of 14 percent-thick supercritical aerofoils with significant rear camber p 657 N95-17849
Surface pressure and wake drag measurements on the Boeing A4 airfoil in the IAR 1.5X1.5m Wind Tunnel Facility p 657 N95-17850
Low-speed surface pressure and boundary layer measurement data for the NLR 7301 airfoil section with trailing edge flap p 658 N95-17855

AIRFOILS
A computational investigation of wake-induced airfoil flutter in incompressible flow and active flutter control
[AD-A281534] p 670 N95-16109
An improved method of airfoil design p 649 N95-16252
Residual-correction type and related computational methods for aerodynamic design. Part 1: Airfoil and wing design p 667 N95-16566
Residual-correction type and related computational methods for aerodynamic design. Part 2: Multi-point airfoil design p 667 N95-16567
Optimal shape design for aerodynamics p 667 N95-16568
Airfoil optimization by the one-shot method p 667 N95-16569
Review of the EUROPT Project AERO-0026 p 668 N95-16573
2-D airfoil tests including side wall boundary layer measurements p 657 N95-17847
Measurements on a two-dimensional aerofoil with high-lift devices p 657 N95-17848
Surface pressure and wake drag measurements on the Boeing A4 airfoil in the IAR 1.5X1.5m Wind Tunnel Facility p 657 N95-17850
Investigation of an NLF(1)-0416 airfoil in compressible subsonic flow p 658 N95-17852
Experiments in the trailing edge flow of an NLR 7702 airfoil p 658 N95-17853
Two-dimensional 16.5 percent thick supercritical airfoil NLR 7301 p 658 N95-17854
Data from the GARTEur (AD) Action Group 02 airfoil CAST 7/DOA1 experiments p 659 N95-17856
OAT15A airfoil data p 659 N95-17857
Two-dimensional high-lift airfoil data for CFD code validation p 659 N95-17859

AIRFRAME MATERIALS
Static and dynamic friction behavior of candidate high temperature airframe seal materials
[NASA-TM-106571] p 722 N95-16905

AIRFRAMES
Cooperative control theory and integrated flight and propulsion control
[NASA-CR-197493] p 671 N95-17404
Experimental data on the aerodynamic interactions between a helicopter rotor and an airframe p 664 N95-17883

AIRLINE OPERATIONS
Aircraft accident report: Stall and loss of control on final approach, Atlantic Coast Airlines, Inc./United Express Flight 6291 Jetstream 4101, N304UE Columbus, OH, 7 January 1994
[PB94-910409] p 665 N95-17646

AIRPORTS
Modeling of Instrument Landing System (ILS) localizer signal on runway 25L at Los Angeles International Airport
[NASA-TM-4588] p 665 N95-17384

ALBEDO
Climatological targets for Mars Pathfinder p 922 N95-16208

ALDEHYDES
Materials for second and third order nonlinear optical applications
[AD-A281304] p 885 N95-16787

ALERTNESS
Locus coeruleus, vigilance and stress: Brain mechanisms of adaptive behavioral responsiveness
[AD-A282450] p 826 N95-16377
Alertness management in two-person long-haul flight operations p 813 N95-16760
Blinks, saccades, and fixation pauses during vigilance task performance. 1: Time on task
[DOT/FAA/AM-94/26] p 828 N95-17530

ALGEBRA
The algebraic multigrid projection for eigenvalue problems; backrotations and multigrid fixed points
[NASA-CR-194990] p 862 N95-16869

ALGORITHMS
A new communication scheme for the neutron diffusion nodal method in a distributed computing environment
[DE94-017907] p 844 N95-15946
Simulation of arthroscopic surgery using MRI data p 823 N95-15975
Multimodal correlation and intraoperative matching of virtual models in neurosurgery p 823 N95-15976
A specification of 3D manipulation in virtual environments p 853 N95-15981
Surface matching for correlation of virtual models: Theory and application p 853 N95-15983
On computing the minimal labels in time point algebra networks
[TR-495] p 859 N95-16022
Robust routing in dynamic networks, part 2
[AD-A282396] p 844 N95-16061
Ultrashort pulse effects in semiconductor amplifiers and in dispersive media
[AD-A284925] p 763 N95-16137
Evaluation of FEL image processing algorithm for 12-bit CCD-images as function of various atmospheric conditions
[AD-A285187] p 752 N95-16146
Generalized method of solving topological optimization problems for electrical airplane equipment systems in computer-aided design p 652 N95-16272
Theory of one-dimensional and two-dimensional distributed sensors for measuring the spatial characteristics of thermophysical and hydrodynamic fields p 652 N95-16273
Methods of wave-front identification by control images p 652 N95-16274
A software tool for dataflow graph scheduling p 843 N95-16457
Extraction of high quality potential surfaces from laboratory data
[AD-A285071] p 903 N95-16489
Optimum Design Methods for Aerodynamics
[AGARD-R-803] p 666 N95-16562
FPCAS2D user's guide, version 1.0
[NASA-CR-195413] p 786 N95-16588
An analysis of spectral envelope-reduction via quadratic assignment problems
[NASA-CR-194992] p 862 N95-16596
Online performance-improvement algorithms
[AD-A285162] p 838 N95-16850
The algebraic multigrid projection for eigenvalue problems; backrotations and multigrid fixed points
[NASA-CR-194990] p 862 N95-16869
Multigrid techniques for nonlinear eigenvalue problems: Solutions of a nonlinear Schroedinger eigenvalue problem in 2D and 3D
[NASA-CR-194999] p 862 N95-16896
Algorithms for bilevel optimization
[NASA-CR-194980] p 863 N95-16897
Trapezoidal rule quadrature algorithms for MIMD distributed memory computers
[DE94-016369] p 839 N95-16923
Statistical properties of an algorithm used for illicit substance detection by fast-neutron transmission
[DE94-013868] p 665 N95-16964
An algorithm for extraction of periodic signals from sparse, irregularly sampled data p 756 N95-17281
A simplified Integer Cosine Transform and its application in image compression p 757 N95-17286
Adaptive line enhancers for fast acquisition p 757 N95-17287
Low-complexity wavelet filter design for image compression p 757 N95-17289
An analysis of smoothed particle hydrodynamics
[DE94-013817] p 788 N95-17439
Eddy current for detecting second layer cracks under installed fasteners
[AD-A282412] p 784 N95-17507
Test applications for heterogeneous real-time network testbed
[DE94-016480] p 850 N95-17638
Report on the 5th International Conference on Nonlinear Hyperbolic Problems
[AD-A283077] p 864 N95-17713
Controlling memory access concurrency in efficient fault-tolerant parallel algorithms
[AD-A280909] p 851 N95-17741
Status of the US stellarator reactor study
[DE94-018693] p 893 N95-17907
Beam position correction in the Fermilab Linac
[DE94-018984] p 882 N95-17931

ALKALI METALS
Sonochemical synthesis of polysilylenes by reductive coupling of disubstituted dichlorosilanes with alkali metals
[AD-A280994] p 739 N95-15996
Possible superstructures of metallic ions in nonstoichiometric fullerites M(x) C(60)
[DE94-622052] p 901 N95-17516

ALKALINE BATTERIES
Aluminum-ferricyanide battery
[AD-D016338] p 766 N95-16948

ALKALINE EARTH COMPOUNDS
Encapsulated alkaline-earth organometallics as controlled sources of calcium, strontium, and barium ions
[AD-A281547] p 741 N95-16393

ALKANES
Cyclic voltammetric analysis of ferrocene alkanethiol monolayer electrode kinetics based on Marcus theory
[AD-A281411] p 868 N95-16162

ALKENES
Research on organofluorine chemistry for 700 F thermooxidative stability
[AD-A282767] p 731 N95-17142
Development of heterogeneous Wacker oxidation catalysts: The role of the support and the redox component
[PB94-201431] p 732 N95-17700

ALKYL COMPOUNDS
Mass spectral data of alkyl and cycloalkyl methylphosphonofluoridates
[AD-A285312] p 722 N95-16734
Synthesis and mesomorphic behavior of poly((2S, 3S)-(+)-2-chloro-3-methylpentyl xy)biphenyl-4-carboxylate s with ethyl and propyl alkyl groups
[AD-A281402] p 744 N95-16865
Volatile CVD precursors based on copper alkoxides and mixed group IIA-copper alkoxides
[AD-D016380] p 732 N95-17479

ALL-WEATHER AIR NAVIGATION
A PC-based interactive simulation of the F-111C Pave Tack system and related sensor, avionics and aircraft aspects
[AD-A285500] p 669 N95-16969

ALLOYING
The influence of tungsten alloying on the mechanical properties of tantalum
[DE94-010071] p 736 N95-17378

ALLYL COMPOUNDS
Synthesis and characterization of a new class of thermosetting resins: Allyl and propargyl substituted cyclopentadiene derivatives
[AD-A281976] p 746 N95-17485

ALPHA PARTICLES
Alpha proton x ray spectrometer p 710 N95-16201
Alpha particle kinetics in ignited fusion plasmas: Design applications for a CO2 laser Thomson scattering experiment
[DE94-016297] p 890 N95-16921

ALTERNATING CURRENT
The use of electrochemistry and ellipsometry for identifying and evaluating corrosion on aircraft
[AD-A285323] p 734 N95-16371
AC susceptibility and critical current in the organic superconductor (kappa)-(ET)2Cu(NCS)2
[DE94-013997] p 900 N95-16946
Test results of superconducting AC magnets for magnetic refrigeration experiment
[DE94-018695] p 751 N95-17909

ALTERNATIVES
Alternatives for ozone-depleting refrigerants
[PB94-190857] p 795 N95-16881

ALTITUDE
Evaluation of an autopilot based multimodelling
[PB94-190725] p 671 N95-17454

ALUMINIDES
Abstracts: Eighth Annual Conference on Fossil Energy Materials
[DE94-014053] p 725 N95-17368
Fundamental concepts relating local atomic arrangements, deformation, and fracture of intermetallic alloys
[AD-A282971] p 738 N95-17664
Selected properties of iron aluminides
[DE94-018057] p 738 N95-17726
Environmental effects on iron aluminide
[DE94-017900] p 739 N95-17747

ALUMINUM
Aluminum permanganate battery
[AD-D016337] p 766 N95-16947
Aluminum-ferricyanide battery
[AD-D016338] p 766 N95-16948
Improved dual flow aluminum hydrogen peroxide battery
[AD-D016339] p 766 N95-16949
Erosion effects on TVC vane heat transfer characteristics
[AD-A282006] p 721 N95-17448
Electron beam weld development on a Filter Pack Assembly
[DE94-015867] p 782 N95-17716

ALUMINUM ALLOYS
The use of electrochemistry and ellipsometry for identifying and evaluating corrosion on aircraft
[AD-A285276] p 734 N95-16370
Multi-lab comparison on R-curve methodologies: Alloy 2024-T3
[NASA-CR-195004] p 736 N95-16860
The mechanical property data base from an Air Force/industry cooperative test program on high temperature aluminum alloys
[AD-A282911] p 737 N95-17398
Analysis of the through-thickness micropore and constituent particle population gradients in the 7050-T7451 plate aluminum alloys
[AD-A282970] p 738 N95-17663
Fundamental concepts relating local atomic arrangements, deformation, and fracture of intermetallic alloys
[AD-A282971] p 738 N95-17664
Selected properties of iron aluminides
[DE94-018057] p 738 N95-17726
Forging of FeAl intermetallic compounds
[DE94-018124] p 739 N95-17728

ALUMINUM FLUORIDES
Properties of Ce:LiSrAlF6 and Ce:LiCaAlF6 ultraviolet lasers
[DE94-013737] p 777 N95-17168

ALUMINUM GALLIUM ARSENIDES
Digital logic and reconfigurable interconnects using aluminum gallium arsenide electro-optic Fredkin gates
[AD-A282880] p 881 N95-17619

ALUMINUM OXIDES
A preliminary attempt at sintering an ultrafine alumina powder using microwaves
[AD-A284978] p 734 N95-16229
Computer studies of the dynamic strength of ceramics
[DE94-010890] p 745 N95-17379
Multiphase ceramics for mechanical and structural reliability at low and elevated temperatures
[AD-A285497] p 746 N95-17438
Micromechanics of interfaces in metal matrix composites
[AD-A282404] p 725 N95-17457
Development of heterogeneous Wacker oxidation catalysts: The role of the support and the redox component
[PB94-201431] p 732 N95-17700

ALUMINUM SILICATES
Fundamental studies of polyphosphazene and polysiloxane polyelectrolytes for electrochemical devices
[AD-A281339] p 739 N95-16013

AMAZON REGION (SOUTH AMERICA)
Detection of deforestation in the Amazon forest using NOAA/AVHRR images and the geographic information system SGI: Methodology and test of a potential alarm system
[INPE-5580-TDI/543] p 791 N95-17894

AMBIENT TEMPERATURE
Prediction of space sickness in astronauts from preflight fluid, electrolyte, and cardiovascular variables and Weightless Environmental Training Facility (WETF) training p 812 N95-16757

AMINES
Research on organofluorine chemistry for 700 F thermooxidative stability
[AD-A282767] p 731 N95-17142

AMINO ACIDS
Molecular approach to hypothalamic rhythms
[AD-A285164] p 822 N95-16851

AMMONIUM COMPOUNDS
Synthesis and characterization of a new class of thermosetting resins: Allyl and propargyl substituted cyclopentadiene derivatives
[AD-A281976] p 746 N95-17485

AMORPHOUS MATERIALS
Method for intrinsically doped III-A and V-A compounds and products thereof
[AD-D016324] p 896 N95-16399
Shock initiation of crystalline boron in oxygen and fluorine compounds
[AD-A284266] p 730 N95-16955
Low-temperature fabrication of transparent silicon nitride
[DE94-014902] p 746 N95-17456

AMORPHOUS SILICON
Research on stable, high-efficiency amorphous-silicon multijunction modules
[DE94-011839] p 764 N95-16425
Applications of positron depth profiling
[PB94-197753] p 900 N95-16952
Recombination and metastability in amorphous silicon and silicon-germanium alloys
[DE94-011837] p 794 N95-16957
Research on stable, high-efficiency, amorphous silicon multijunction modules
[DE94-011826] p 794 N95-17521

AMPLIFICATION
Resist materials design: Base-catalyzed chemical amplification
[AD-A281805] p 741 N95-16354
Development of x-ray laser architectural components
[DE94-016446] p 778 N95-17627

AMPLIFIERS
Ultrashort pulse effects in semiconductor amplifiers and in dispersive media
[AD-A284925] p 763 N95-16137

ANALOG CIRCUITS
Analog microcircuit fault prediction
[AD-A281958] p 763 N95-16410

ANALOG SIMULATION
An investigation of fluid flow during induction stroke of a water analog model of an IC engine using an innovative optical velocimetry concept: LIPA
[NASA-CR-197451] p 780 N95-16900
Grey-scale measurements in multi-dimensional digitized images
[PB94-195492] p 887 N95-17483

ANALOG TO DIGITAL CONVERTERS
Simulation of arthroscopic surgery using MRI data p 823 N95-15975
VLSI circuits for high speed data conversion
[AD-A281556] p 763 N95-16136

ANALYSIS OF VARIANCE
Statistical analysis of microgravity experiment performance using the degrees of success scale
[NASA-TM-106791] p 784 N95-17385

ANGIOGRAPHY
Aviation epidemiology data register: Coronary angiography outcomes of civilian aviators flying US aircraft
[AD-A285191] p 820 N95-16405

ANGLE OF ATTACK
An approach to aerodynamic characteristics of low radar cross-section fuselages p 649 N95-16251
An improved method of airfoil design p 649 N95-16252
Residual-correction type and related computational methods for aerodynamic design. Part 2: Multi-point airfoil design p 667 N95-16567
Numerical simulation of transient vortex breakdown above a pitching delta wing
[AD-A281075] p 655 N95-16808
DLR-F4 wing body configuration p 660 N95-17863
DLR-F5: Test wing for CFD and applied aerodynamics p 660 N95-17864
Low aspect ratio wing experiment p 661 N95-17865
Wind tunnel investigations of the appearance of shocks in the windward region of bodies with circular cross section at angle of attack p 661 N95-17866
Three-dimensional boundary layer and flow field data of an inclined prolate spheroid p 661 N95-17867
Force and pressure data of an ogive-nosed slender body at high angles of attack and different Reynolds numbers p 661 N95-17868
Ellipsoid-cylinder model p 661 N95-17869

ANGLES (GEOMETRY)
Superspheroid geometries for radome analysis
[AD-A285405] p 753 N95-16233

ANGULAR DISTRIBUTION
Experimental characterization of ALS undulator radiation
[DE94-017967] p 881 N95-17671

ANGULAR MOMENTUM
Exact, E = 0, classical and quantum solutions for general power-law oscillators
[DE94-014436] p 903 N95-16428

ANGULAR VELOCITY
Optical wheel-rotation sensor
[DE94-011719] p 780 N95-16224
Dynamics of the G-excess illusion p 815 N95-16771

ANIONS
Spectroscopy of the transition state region in hydrogen transfer reactions
[AD-A285151] p 729 N95-16846

ANISOTROPY
Liquid crystal materials for laser beam steering
[AD-A285089] p 897 N95-16498
Snapshots of crystal growth: Nanoclusters of organic conductors on Au(111) surfaces
[AD-A280976] p 897 N95-16508

ANNEALING
Electromagnetic processing of refractory metal silicide/oxide composites
[AD-A281470] p 740 N95-16085
Reliability implications of defects in high temperature annealed Si/SiO2/Si structures
[DE94-015765] p 895 N95-16311
Process of making a bistable photoconductive component
[AD-D016449] p 764 N95-16539
Positron annihilation studies of defects in molecular beam epitaxy grown 3 to 5 layers
[DE94-015823] p 899 N95-16918
Forging of FeAl intermetallic compounds
[DE94-018124] p 739 N95-17728
Raman spectroscopy of C-irradiated graphite
[DE94-018705] p 733 N95-17911

ANNIHILATION REACTIONS
Mass spectrometry studies of the ionization of organic molecules by slow positrons
[DE94-013838] p 876 N95-16959
Delayed annihilation of antiprotons in helium gas
[DE94-753405] p 878 N95-17739

ANNUAL VARIATIONS
Summary of 1994 Atlantic tropical cyclone activity and verification of author's seasonal prediction, 1 p 801 N95-17259
A latitudinal survey of middle atmospheric water vapor revealed by shipboard microwave spectroscopy
[AD-A282000] p 799 N95-17446
Operational cloud classifier based on a self-organized feature map
[PB94-197852] p 802 N95-17504

ANODES
Improved dual flow aluminum hydrogen peroxide battery
[AD-D016339] p 766 N95-16949

ANOLYTES
Improved dual flow aluminum hydrogen peroxide battery
[AD-D016339] p 766 N95-16949

ANOMALIES
Space Shuttle main engine OPAD: The search for a hardware enhanced plume p 716 N95-16330
Study of the structuring of pure molecular liquids
[PB94-201316] p 903 N95-16839

ANTENNA ARRAYS
Detecting the number of targets in spatially colored noise using sampled aperture radars p 652 N95-16269
Demand access communications for TDRSS users p 677 N95-17187
Tracking the Galileo spacecraft with the DSCC Galileo Telemetry prototype p 708 N95-17292
An analysis of the effects of feedline and ground screen noise currents on a conical monopole receiving antenna
[AD-A283401] p 759 N95-17436
Superresolution in a jammed radar signal environment
[PB94-190758] p 760 N95-17455
Simultaneous determination of incoming microwave frequency and angle-of-arrival
[AD-D016392] p 760 N95-17482

ANTENNA DESIGN
Fast acquisition of burst direct sequence spread spectrum signals through satellite channels p 652 N95-16270
A simple EHF hemispheric coverage antenna
[AD-A285078] p 754 N95-16495
A VHF/UHF antenna for the Precision Antenna Measurement System (PAMS)
[AD-A285673] p 754 N95-16621
Galileo mission planning for Low Gain Antenna based operations p 682 N95-17210
Antenna noise temperatures of the 34-meter beam-waveguide antenna with horns of different gains installed at F1 p 757 N95-17288
Field verification of the wind tunnel coefficients p 664 N95-17291

Computation of reflected and transmitted horn radiation patterns for a dichroic plate p 758 N95-17293
X-/Ka-band dichroic plate noise temperature reduction p 758 N95-17294
RF optics study for DSS-43 ultracone implementation p 758 N95-17296
JPL-ANTOPT antenna structure optimization program p 759 N95-17297
Center-fed multifilar helix antenna
[AD-D016390] p 760 N95-17480
Study of the folding and deployment aspects of a Collapsible Rib Tensioned Surface (CRTS) antenna reflector
[CUED/D-STRUCT/TR-144] p 783 N95-17928

ANTENNA FEEDS
An analysis of the effects of feedline and ground screen noise currents on a conical monopole receiving antenna
[AD-A283401] p 759 N95-17436

ANTENNA RADIATION PATTERNS
Characteristics of phase-correcting fresnel zone plates and elliptical waveguides
[AD-A281385] p 763 N95-16159
A VHF/UHF antenna for the Precision Antenna Measurement System (PAMS)
[AD-A285673] p 754 N95-16621
Formulation of probe-corrected time-domain planar near-field measurements
[AD-A281053] p 754 N95-16624
Galileo mission planning for Low Gain Antenna based operations p 682 N95-17210
Antenna noise temperatures of the 34-meter beam-waveguide antenna with horns of different gains installed at F1 p 757 N95-17288
Computation of reflected and transmitted horn radiation patterns for a dichroic plate p 758 N95-17293
X-/Ka-band dichroic plate noise temperature reduction p 758 N95-17294
Center-fed multifilar helix antenna
[AD-D016390] p 760 N95-17480

ANTENNAS
First measurements of ICRF and edge/SOL plasma interactions on TORE SUPRA
[DE94-019320] p 891 N95-17347
Antenna dielectric sealing process characterization
[DE94-015864] p 747 N95-17690

ANTIFERROMAGNETISM
Inelastic neutron scattering and antiferromagnetic fluctuations in high temperature superconductors
[DE94-623269] p 871 N95-16059
Rietveld refinement of magnetic structures from pulsed-neutron-source powder-diffraction data
[DE94-016599] p 737 N95-17641
Critical and paramagnetic spin dynamics in an antiferromagnetically coupled Heisenberg magnet: Results for RbMnF3
[PB95-104329] p 869 N95-17731

ANTIMATTER
Baryogenesis and standard model CP violation
[DE94-017935] p 877 N95-17669

ANTIPROTONS
Multilepton SUSY signals from R-parity violation at the Tevatron (revised)
[PB95-104311] p 877 N95-17353
Delayed annihilation of antiprotons in helium gas
[DE94-753405] p 878 N95-17739

ANTIREFLECTION COATINGS
Analysis of space environment damage to solar cell assemblies from LDEF experiment A0171-GSFC test plate
[NASA-CR-196523] p 793 N95-16575
Coatings for large-area low-cost solar concentrators and reflectors
[DE94-015735] p 793 N95-16916

APERTURES
Methods of wave-front identification by control images p 652 N95-16274
Development of x-ray laser architectural components
[DE94-016446] p 778 N95-17627

APOLLO FLIGHTS
New look at the old Moon
[NASA-TM-110106] p 922 N95-16838

APOLLO SOYUZ TEST PROJECT
Apollo 17: On the shoulders of giants
[NASA-TM-110105] p 922 N95-16837

APOLLO 15 FLIGHT
Apollo 15: In the mountains of the Moon
[NASA-TM-109988] p 922 N95-16842

APOLLO 16 FLIGHT
Apollo 16: Nothing so hidden
[NASA-TM-110104] p 922 N95-16836

APOLLO 17 FLIGHT
Apollo 17: On the shoulders of giants
[NASA-TM-110105] p 922 N95-16837

APPLICATION SPECIFIC INTEGRATED CIRCUITS
Support for development of a custom VLSI and FPGA logic chips based on a VHDL top-down design approach
[DE94-013608] p 763 N95-16283
A second generation 50 Mbps VLSI level zero processing system prototype p 678 N95-17191
VLSI technology for smaller, cheaper, faster return link systems p 681 N95-17206

APPLICATIONS PROGRAMS (COMPUTERS)
Applied virtual reality at the Research Triangle Institute p 851 N95-15974
Using virtual reality for science mission planning: A Mars Pathfinder case p 673 N95-15978
Applying Virtual Reality to commercial Edutainment p 854 N95-15989
CPP-TRS(C): On using visual cognitive symbols to enhance communication effectiveness p 761 N95-15991
The search for lost cycles: A new approach to parallel program performance evaluation
[AD-A281467] p 845 N95-16082
Visualization of unsteady computational fluid dynamics
[NASA-CR-197461] p 770 N95-16388
Solution of matrix equations using sparse techniques p 847 N95-16459
Applications of automatic differentiation in computational fluid dynamics p 774 N95-16461
Automatic differentiation for design sensitivity analysis of structural systems using multiple processors p 847 N95-16462
Data Visualization and Animation Lab (DVAL): Applications p 843 N95-16469
Computer tools for systems engineering at LaRC p 848 N95-16472
Electronic Engineering Notebook: A software environment for research execution, documentation and dissemination p 848 N95-16473
Investigations on the sensitivity of the computer code TURBO-2D
[CUED/A-THERMO/TR-61] p 771 N95-16595
CMCAM: A high performance CM-5 lattice gas simulator
[AD-A281063] p 837 N95-16626
Extending programming by demonstration with hierarchical event histories
[AD-A281186] p 838 N95-16632
Real-time data collection programs and source code for a commercial passive FTIR remote sensor
[AD-A284976] p 838 N95-16634
An integrated knowledge acquisition and database management system
[AD-A285404] p 910 N95-16884
An analysis code for the Rapid Engineering Estimation of Momentum and Energy Losses (REMEL)
[NASA-CR-191178] p 656 N95-16887
The development and validation of command schedules for SeaWiFS p 690 N95-17249
The IUE Science Operations Ground System p 674 N95-17255
Interactive computer graphics applications for compressible aerodynamics
[NASA-TM-106802] p 839 N95-17264
Evaluation of current tropospheric mapping functions by Deep Space Network very long baseline interferometry p 756 N95-17280
JPL-ANTOPT antenna structure optimization program p 759 N95-17297
McIDAS-eXplorer: A version of McIDAS for planetary applications
[NASA-CR-189382] p 910 N95-17323
A distributed analysis and visualization system for model and observational data
[NASA-CR-189386] p 911 N95-17326
Development of a data reduction expert assistant
[NASA-CR-189385] p 911 N95-17328
An interactive environment for the analysis of large Earth observation and model data sets
[NASA-CR-189381] p 911 N95-17330
Engineering design tools for wind diesel systems. Volume 2: JODYMOD dynamic wind diesel simulation software package. Model verification
[PB95-104519] p 840 N95-17355
Engineering design tools for wind diesel systems. Volume 3: JODYMOD dynamic simulation software package. Model description
[PB95-104527] p 840 N95-17356
IS-Lab: A tool for developing interactive programs for simulation and analysis. User's guide
[PB94-184710] p 840 N95-17410
User-defined subroutine for implementation of special finite elements in ABAQUS for the analysis of adhesive joints
[AD-A282431] p 788 N95-17510
Automated Estimating System (AES) version 6.0: User's manual
[DE94-013636] p 841 N95-17514
ATM-test: A workstation-based software suite for testing Asynchronous Transfer Mode (ATM) networks
[DE94-013813] p 850 N95-17516
A software architecture for automating operations processes p 692 N95-17538
SEQ-GEN: A comprehensive multimission sequencing system p 693 N95-17540
Implementation of a low-cost, commercial orbit determination system p 673 N95-17544
Towards an integral computer environment supporting system operations analysis and conceptual design p 696 N95-17558
SEQ-REVIEW: A tool for reviewing and checking spacecraft sequences p 697 N95-17561
The ESA standard for telemetry and telecommand packet utilisation: PUS p 704 N95-17595
ATOS: Integration of advanced technology software within distributed Spacecraft Mission Operations Systems p 705 N95-17602
Engineering design tools for wind diesel systems. Volume 4: JODYMOD dynamic wind diesel simulation software package. Program documentation
[PB95-104535] p 841 N95-17628
Engineering design tools for wind diesel systems. Volume 5: JODYMOD dynamic wind diesel simulation software package. User's guide
[PB95-104543] p 841 N95-17629
Modeling of stress/strain behavior of fiber-reinforced ceramic matrix composites including stress redistribution
[NASA-TM-106789] p 725 N95-17659
Engineering design tools for wind diesel systems. Volume 1: Executive summary
[PB95-104501] p 842 N95-17733
Engineering design tools for wind diesel systems. Volume 6: Logistic package. User documentation
[PB95-104550] p 842 N95-17734
CHEETAH 1.0 user's manual
[DE94-014727] p 749 N95-17919

APPROACH CONTROL
Modeling of Instrument Landing System (ILS) localizer signal on runway 25L at Los Angeles International Airport
[NASA-TM-4588] p 665 N95-17384

APPROXIMATION
A posteriori error estimation new approach
[AD-A284960] p 860 N95-16127
Exploiting IB assignments for approximating marginal probabilities
[AD-A285419] p 855 N95-16246
Stochastic approximation methods for fusion-rule estimation in multiple sensor systems
[DE94-013629] p 856 N95-16361
Online performance-improvement algorithms
[AD-A285162] p 838 N95-16850
Structural optimization with approximate sensitivities
[NASA-TM-4553] p 789 N95-17701

AQUEOUS SOLUTIONS
Precision aqueous cleaner for RSRM p 715 N95-16326
Solubilization of hydrophobic substances into block copolymer micelles in aqueous media and their release
[AD-A281395] p 744 N95-16792
Performance evaluation of polyaniline as an active material for electrochemical capacitors
[DE94-016283] p 765 N95-16920
Aluminum permanganate battery
[AD-D016337] p 766 N95-16947
Improved dual flow aluminum hydrogen peroxide battery
[AD-D016339] p 766 N95-16949
Ion modulated electroactivity in thin-film polymers derived from bipyridyl and phenanthroline complexes of iron
[AD-A280704] p 747 N95-17682

ARC HEATING
Plasma sound source basic research
[AD-A285394] p 890 N95-16617

ARC JET ENGINES
ARCJET plasma modeling with experimental validation
[AD-A285234] p 889 N95-16243

ARCHAEBACTERIA
Investigation of pressure regulation in an archaebacterial enzyme
[AD-A281413] p 807 N95-16164

ARCHITECTURE (COMPUTERS)
Open Source Service Agent (OSSA) in the intelligence community's Open Source Architecture p 907 N95-15934
Network interface specification for the T1 microprocessor
[AD-A283392] p 844 N95-15940
Portable parallel stochastic optimization for the design of aeropropulsion components
[NASA-CR-195312] p 785 N95-16072

Can high bandwidth and latency justify large cache blocks in scalable multiprocessors?
[AD-A281468] p 845 N95-16083
Risk-Based Data Management System design specifications and implementation plan for the Alaska Oil and Gas Conservation Commission; the Mississippi State Oil and Gas Board; the Montana Board of Oil and Gas Conservation; and the Nebraska Oil and Gas Conservation Commission, attachment B
[DE94-013189] p 908 N95-16282
System design, implementation, and evaluation of the optical broadband correlator
[AD-A285406] p 884 N95-16296
Visualization of unsteady computational fluid dynamics
[NASA-CR-197461] p 770 N95-16388
The Role of Computers in Research and Development at Langley Research Center
[NASA-CP-10159] p 846 N95-16453
Software engineering from a Langley perspective
p 843 N95-16454
Equation solvers for distributed-memory computers
p 847 N95-16460
High Performance FORTRAN p 843 N95-16478
Current research activities at the NASA-sponsored Illinois Computing Laboratory of Aerospace Systems and Software p 849 N95-16479
Proceedings of the International Conference on Parallel Architectures and Compilation Techniques
[AD-A285258] p 849 N95-16529
Open architectures for formal reasoning and deductive technologies for software development
[NASA-CR-197528] p 837 N95-16586
Anatomy of a silicon compiler
[AD-A285395] p 832 N95-16618
Investigation of modularly configured attached processors with intelligent memories
[AD-A285454] p 832 N95-16876
Flosolver parallel computers: 1986-1994
[NAL-SP-9409] p 850 N95-16901
The PASS project
[DE94-016308] p 910 N95-16922
Use of a multimission system for cost effective support of planetary science data processing
p 678 N95-17190
CCS-MIP: Low cost Customizable Control Centre
p 674 N95-17254
Mini All-purpose Satellite Control Center (MASCC)
p 674 N95-17257
Highly parallel reconfigurable computer architecture for robotic computation having plural processor cells each having right and left ensembles of plural processors
[NASA-CASE-NPO-17632-1-CU] p 832 N95-17400
Reviews of computing technology: Software overview
[DE94-013662] p 841 N95-17515
ELISA, a demonstrator environment for information systems architecture design p 698 N95-17563
Integration of a satellite ground support system based on analysis of the satellite ground support domain
p 675 N95-17568
Evaluation of NASA's end-to-end data systems using DSDS+ p 700 N95-17577
Re-engineering Nascom's network management architecture p 702 N95-17584
Standardizing the information architecture for spacecraft operations p 703 N95-17591
A standard satellite control reference model
p 704 N95-17592
Mission Operations Centers (MOCs): Integrating key spacecraft ground data system components
p 675 N95-17601
ATOS: Integration of advanced technology software within distributed Spacecraft Mission Operations Systems p 705 N95-17602

ARITHMETIC
Verification of arithmetic functions with binary moment diagrams
[AD-A281028] p 835 N95-16447

ARRAYS
Object-oriented numerical computing C++
p 849 N95-16476

ARSENIC COMPOUNDS
X-ray crystal structure of a monomeric Tris(Arsino)Gallane, ((Me3Si)2As)3Ga)3Ga
[AD-A282343] p 900 N95-17171

ARTIFICIAL INTELLIGENCE
Master-slave system with force feedback based on dynamics of virtual model p 853 N95-15985
Second International Working Conference on Cooperating Knowledge Based Systems. Volume 1
[AD-A281347] p 908 N95-16014
Exploiting IB assignments for approximating marginal probabilities
[AD-A285419] p 855 N95-16246
Current research activities at the NASA-sponsored Illinois Computing Laboratory of Aerospace Systems and Software p 849 N95-16479
Structural integrity of intelligent materials and structures. Constitutive modeling of shape memory alloys
[AD-A281301] p 735 N95-16786
Workshop on Formal Models for Intelligent Control
[AD-A281399] p 857 N95-16864
Actions and events in interval temporal logic
[TR-521] p 839 N95-16883
Data link level interconnection of remote Fiber Distributed Data Interface Local Area Networks (FDDI LANs) through the Critical Data Link (CDL)
[AD-A284307] p 755 N95-17173
A mission planning concept and mission planning system for future manned space missions p 687 N95-17235
Multivariate statistical analysis software technologies for astrophysical research involving large data bases
[NASA-CR-189393] p 911 N95-17325
Identification of Artificial Intelligence (AI) applications for maintenance, monitoring, and control of airway facilities
[AD-A282479] p 665 N95-17373
O-Plan2 versus SIPE-2: A general comparison
[AD-A285531] p 857 N95-17381
Towards a human operator model of the navigator
[PB94-197985] p 831 N95-17468
An intelligent automated command and control system for spacecraft mission operations p 693 N95-17542
ATOS: Integration of advanced technology software within distributed Spacecraft Mission Operations Systems p 705 N95-17602

ARTIFICIAL SATELLITES
Mission planning for space based satellite surveillance experiments with the MSX p 673 N95-17212
The development and validation of command schedules for SeaWiFS p 690 N95-17249

ASCENT
Matlab as a robust control design tool
p 849 N95-16474

ASIA
The Austrialian National Chinese Japanese Korean Project p 905 N95-15920

ASPECT RATIO
Measurements of the flow over a low aspect-ratio wing in the Mach number range 0.6 to 0.87 for the purpose of validation of computational methods. Part 1: Wing design, model construction, surface flow. Part 2: Mean flow in the boundary layer and wake, 4 test cases
p 660 N95-17860

ASPHERICITY
Numerical aperture limits on efficient ball lens coupling of laser diodes to single-mode fibers with defocus to balance spherical aberration
[NASA-TM-4578] p 886 N95-17271

ASSAYING
Development of an in vitro model assay system for the evaluation of the effects of toxic chemicals on human airways
[AD-A285074] p 821 N95-16491

ASSESSMENTS
Abstracts and program Proceedings of the 1994 Meeting of the International Society for Ecological Modelling North American Chapter
[DE94-016456] p 796 N95-17636

ASSIMILATION
Regulation of nitrogen uptake and assimilation: Effects of nitrogen source and root-zone and aerial environment on growth and productivity of soybean
[NASA-CR-197098] p 807 N95-15961

ASTEROID BELTS
Investigations of asteroid family geology
p 917 N95-17393

ASTEROID MISSIONS
Cost efficient operations for Discovery class missions
p 695 N95-17548
Concurrent engineering: Spacecraft and mission operations system design p 708 N95-17614

ASTEROIDS
Space-based asteroid detection and monitoring system
[AD-D016329] p 915 N95-16854

ASTRONAUT TRAINING
Psychological training of NASA astronauts for extended missions p 813 N95-16763

ASTRONAUTS
Magnetic Resonance Imaging (MRI) of skeletal muscles in astronauts after 9 days of space flight
p 810 N95-16749
Results of the psychiatric, select-out evaluation of US astronaut applications p 813 N95-16761
Validation of astronaut psychological select-in criteria
p 813 N95-16762

ASTRONOMICAL CATALOGS
ARACHNID: A prototype object-oriented database tool for distributed systems p 680 N95-17199
Multivariate statistical analysis software technologies for astrophysical research involving large data bases
[NASA-CR-189393] p 911 N95-17325
Multivariate statistical analysis software technologies for astrophysical research involving large data sets
[NASA-CR-197499] p 858 N95-17921

ASTRONOMICAL INTERFEROMETRY
DSN co-observing operations to support space VLBI missions p 694 N95-17543

ASTRONOMICAL OBSERVATORIES
Advanced technologies in the ASI MLRO towards a new generation laser ranging system p 687 N95-17239

ASTRONOMICAL SATELLITES
The SAX Italian scientific satellite. The on-board implemented automation as a support to the ground control capability p 695 N95-17551

ASTRONOMICAL SPECTROSCOPY
A rare gas optics-free absolute photon flux and energy analyzer to provide absolute photoionization rates of inflowing interstellar neutrals
[NASA-CR-197228] p 914 N95-15964

ASYMMETRY
Production asymmetries in x(sub F) and P(sub t)(exp 2) for D(+-) mesons
[DE94-015546] p 872 N95-16310
Liquid crystal materials for laser beam steering
[AD-A285089] p 897 N95-16498
Geosynchronous orbit magnetopause crossings
[DE94-014817] p 798 N95-16537
Tests of structure functions using leptons at CDF: W asymmetry and Drell-Yan production
[DE94-015727] p 875 N95-16840
Baryogenesis and standard model CP violation
[DE94-017935] p 877 N95-17669
Flavor symmetries and fermion masses
[DE94-018192] p 878 N95-17889
Measurements of non-axisymmetric effects in the D3-D divertor
[DE94-018346] p 893 N95-17897

ASYMPTOTIC PROPERTIES
Asymptotic behavior in grain growth
[DE94-014452] p 900 N95-17156
Time-dependent spin correlations in the heisenberg magnet at infinite temperature
[PB95-104303] p 869 N95-17750

ATLANTIC OCEAN
Extended range forecast of Atlantic seasonal hurricane activity for 1995, 2 p 801 N95-17260

ATMOSPHERIC ATTENUATION
Using lidar tomography to characterize scattering in a turbulent media
[AD-A281014] p 751 N95-16002

ATMOSPHERIC BOUNDARY LAYER
Large-eddy simulation of cumulus convection
[PB94-191368] p 800 N95-16290
An air mass transformation model for coastal environments
[AD-A281790] p 801 N95-17164
Impact of physical processes on maritime frontogenesis
[AD-A283105] p 801 N95-17339

ATMOSPHERIC CHEMISTRY
Surface science capabilities from IMP spectral imaging
p 921 N95-16204
Spectroscopy of the transition state region in hydrogen transfer reactions
[AD-A285151] p 729 N95-16846
FEM3C, an improved three-dimensional heavy-gas dispersion model: User's manual
[DE94-014731] p 797 N95-17922

ATMOSPHERIC CIRCULATION
Mars Pathfinder meteorological observations on the basis of results of an atmospheric global circulation model p 919 N95-16189
An improved neutral wind model with predictive capabilities
[AD-A282283] p 800 N95-16235
An air mass transformation model for coastal environments
[AD-A281790] p 801 N95-17164
Impact of physical processes on maritime frontogenesis
[AD-A283105] p 801 N95-17339
A latitudinal survey of middle atmospheric water vapor revealed by shipboard microwave spectroscopy
[AD-A282000] p 799 N95-17446
Recent changes of weather patterns in North America
[DE94-016115] p 803 N95-17743
FEM3C, an improved three-dimensional heavy-gas dispersion model: User's manual
[DE94-014731] p 797 N95-17922

ATMOSPHERIC COMPOSITION
Fire protection engineering criteria: Electronic equipment installations
[AD-A285174] p 750 N95-16853
Modelling interactions of carbon dioxide, forests, and climate
[DE94-018694] p 797 N95-17908

ATMOSPHERIC CORRECTION
The three loop equation of state of QED at high temperature
[DE94-015029] p 904 N95-17925
ATMOSPHERIC EFFECTS
Matlab as a robust control design tool
p 849 N95-16474
ATMOSPHERIC GENERAL CIRCULATION MODELS
Mars Pathfinder meteorological observations on the basis of results of an atmospheric global circulation model p 919 N95-16189
ATMOSPHERIC MODELS
Marine boundary-layer parameterizations for large-scale models
[AD-A282402] p 803 N95-16062
An improved neutral wind model with predictive capabilities
[AD-A282283] p 800 N95-16235
Large-eddy simulation of cumulus convection
[PB94-191368] p 800 N95-16290
Sensitivity analysis of numerically-simulated convective storms using direct and adjoint methods
[DE94-013399] p 800 N95-16398
Regional forecasting with global atmospheric models
[DE94-013863] p 801 N95-16961
An air mass transformation model for coastal environments
[AD-A281790] p 801 N95-17164
Evaluation of current tropospheric mapping functions by Deep Space Network very long baseline interferometry
p 756 N95-17280
A preliminary optical visibility model
p 758 N95-17290
Impact of physical processes on maritime frontogenesis
[AD-A283105] p 801 N95-17339
Global climate change model natural climate variation: Paleoclimate data base, probabilities and astronomic predictors
[DE94-013956] p 796 N95-17348
The effects of the horizontal resolution of the boundary forcing sea surface temperature field on the FSU spectral model
[AD-A284273] p 802 N95-17488
The Grid Analysis and Display System (GrADS)
[NASA-CR-189387] p 912 N95-17491
CERES, phases 1 and 2
[DE94-014730] p 797 N95-17920
ATMOSPHERIC PHYSICS
Surface science capabilities from IMP spectral imaging
p 921 N95-16204
ATMOSPHERIC PRESSURE
Mars Pathfinder meteorological observations on the basis of results of an atmospheric global circulation model p 919 N95-16189
Atmosphere structure and meteorology instrument for Mars Pathfinder p 711 N95-16202
A proposal to study gender differences in the rates of decompression sickness
[AD-A281854] p 819 N95-16297
ATMOSPHERIC SCATTERING
Using lidar tomography to characterize scattering in a turbulent media
[AD-A281014] p 751 N95-16002
Fractal aggregate random media analysis and applications
[AD-A281410] p 884 N95-16161
ATMOSPHERIC SOUNDING
On the measurement of momentum flux profiles using a five-beam 915-MHz wind profiler
[DE94-018448] p 791 N95-17903
ATMOSPHERIC TEMPERATURE
Properties of semiconducting Ru2Ge3
[DE94-015361] p 899 N95-16913
Recent changes of weather patterns in North America
[DE94-016115] p 803 N95-17743
ATMOSPHERICS
Evaluation of FEL image processing algorithm for 12-bit CCD-images as function of various atmospheric conditions
[AD-A285187] p 752 N95-16146
The small-scale structure of dispersing clouds in the atmosphere
[AD-A285493] p 800 N95-16802
Mitre adaptive processing capability
[AD-A281078] p 755 N95-16825
ATOM CONCENTRATION
Production of high proton fractions from ECR sources by plasma modification
[DE94-018381] p 893 N95-17900
ATOMIC COLLISIONS
Resonant charge transfer in hyperthermal atomic and molecular ion-surface collisions
[AD-A281369] p 871 N95-16018
ATOMIC EXCITATIONS
Preparation and investigation of improved low voltage electron excitable phosphors
[AD-A284265] p 767 N95-17487
ATOMIC FORCE MICROSCOPY
Atomic force microscopy of the electrochemical nucleation and growth of molecular crystals
[AD-A281024] p 897 N95-16445
Nanoscale imaging of molecular adsorption
[AD-A280979] p 873 N95-16482
ATOMIC STRUCTURE
Atomic structure and valency of nickel in some of its oxycompounds
[AD-A281109] p 733 N95-16091
Atomic scale structure and chemistry of interfaces by Z-contrast imaging and electron energy loss spectroscopy in the stem
[DE94-013632] p 728 N95-16419
First principles simulation of materials properties
[DE94-013615] p 899 N95-16805
New ytterbium-doped apatite crystals for flexible laser design
[DE94-015138] p 899 N95-16867
XAFS investigation of structure and valency of nickel in some oxycompounds
[AD-A283193] p 877 N95-17630
ATROPHY
Skeletal muscle responses to unloading in humans
p 809 N95-16743
Intramuscular pressure: A better tool than EMG to optimize exercise for long-duration space flight
p 809 N95-16744
Magnetic Resonance Imaging (MRI) of skeletal muscles in astronauts after 9 days of space flight
p 810 N95-16749
ATTENUATION
Revisions to an empirical surface loss model using a correction for pH-dependent attenuation
[AD-A285714] p 871 N95-17177
ATTITUDE (INCLINATION)
Aviation spatial orientation in relationship to head position, attitude interpretation, and control
[AD-A281869] p 827 N95-16433
The psychophysical function for perceived gravitational-inertial force does not depend on the orientation of the otolith organs p 808 N95-16740
Dynamics of the G-excess illusion
p 815 N95-16771
The efficacy of periodic +Gz exposure in the prevention of bedrest induced orthostatic intolerance
p 817 N95-16781
Auroral interactions with ISSA
[NASA-TM-106794] p 709 N95-16862
Re-engineering NASA's space communications to remain viable in a constrained fiscal environment
p 702 N95-17585
ATTITUDE CONTROL
Aviation spatial orientation in relationship to head position, attitude interpretation, and control
[AD-A281869] p 827 N95-16433
Simulation of the coupled multi-spacecraft control testbed at the Marshall Space Flight Center
p 849 N95-16475
Magnetometer-only attitude and rate determination for a gyro-less spacecraft p 694 N95-17546
Study of simulation in microgravity environment
[PB95-104261] p 750 N95-17730
ATTITUDE INDICATORS
Aviation spatial orientation in relationship to head position, attitude interpretation, and control
[AD-A281869] p 827 N95-16433
AUDITORY PERCEPTION
Demodulation processes in auditory perception
[AD-A285427] p 869 N95-16248
AUDITORY SIGNALS
Demodulation processes in auditory perception
[AD-A285427] p 869 N95-16248
AURORAL ZONES
Characteristics of multiple auroral inverted-V structures and the problem of magnetospheric plasma stratification
[DE94-622233] p 799 N95-17471
AURORAS
Ion drift meter research
[NASA-CR-197124] p 798 N95-16432
Auroral interactions with ISSA
[NASA-TM-106794] p 709 N95-16862
AUSTENITE
Metallurgical examination of failed T-158 Cast Austempered Ductile Iron (CADI) track shoes
[AD-A282433] p 737 N95-17486
AUSTENITIC STAINLESS STEELS
Abstracts: Eighth Annual Conference on Fossil Energy Materials
[DE94-014053] p 725 N95-17368
AUSTRALIA
The Austrialian National Chinese Japanese Korean Project p 905 N95-15920
AUTOCORRELATION
Time-dependent spin correlations in the heisenberg magnet at infinite temperature
[PB95-104303] p 869 N95-17750
AUTOMATA THEORY
Decreasing the bandwidth of a transition matrix
[TR-505] p 859 N95-15948
NP-sets are Co-NP-immune relative to a random oracle
[TR-501] p 859 N95-15950
On the structure of log-space probabilistic complexity classes
[TR-506] p 864 N95-16039
Properties of multihead two-way probabilistic finite automata
[TR-477] p 833 N95-16040
Studies of novel popout
[AD-A285237] p 826 N95-16244
Towards a human operator model of the navigator
[PB94-197985] p 831 N95-17468
Cellular automata for contour dynamics
[PB94-197613] p 865 N95-17526
AUTOMATED GUIDEWAY TRANSIT VEHICLES
A model for assessment of dynamic interaction between magnetically levitated vehicles and their supporting guideways
[AD-A283068] p 781 N95-17335
AUTOMATIC CONTROL
Human performance in the modern cockpit
p 813 N95-16764
International Space Station Alpha user payload operations concept p 685 N95-17227
Operations automation p 687 N95-17236
The development and validation of command schedules for SeaWiFS p 690 N95-17249
Mini All-purpose Satellite Control Center (MASCC)
p 674 N95-17257
An intelligent automated command and control system for spacecraft mission operations p 693 N95-17542
An agent-oriented approach to automated mission operations p 696 N95-17555
Test/score/report: Simulation techniques for automating the test process p 675 N95-17581
AUTOMATIC PILOTS
Aviation spatial orientation in relationship to head position, attitude interpretation, and control
[AD-A281869] p 827 N95-16433
Evaluation of an autopilot based multimodelling
[PB94-190725] p 671 N95-17454
AUTOMATION
Coordinated control of a dual-arm dexterous robot using full immersion telepresence and virtual reality
p 852 N95-15979
AUTONOMIC NERVOUS SYSTEM
Spectral components of human cardiovascular responses to step changes in Lower Body Negative Pressure (LBNP) before and after 22 hour of 6 deg head down bed rest p 810 N95-16748
AUTONOMOUS NAVIGATION
Estimation of vehicle dynamics from monocular noisy images
[AD-A281458] p 804 N95-16078
The Yale Knowledge-Based Planning project
[AD-A281505] p 855 N95-16095
Autonomous weapon guidance
[AD-A282715] p 671 N95-16381
Division of Information Systems (FOA 37)
[PB94-190766] p 909 N95-16400
Representation, modeling and recognition of outdoor scenes
[AD-A283257] p 858 N95-17634
A feedforward control approach to the local navigation problem for autonomous vehicles
[AD-A282787] p 666 N95-17706
AUTONOMY
A workout for virtual bodybuilders (design issues for embodiment in multi-actor virtual environments)
p 854 N95-15990
The SAX Italian scientific satellite. The on-board implemented automation as a support to the ground control capability p 695 N95-17551
AVIONICS
The computer analysis of the prediction of aircraft electrical power supply system reliability
p 653 N95-16278
A study of software standards used in the avionics industry p 670 N95-16456
AXES OF ROTATION
Method and apparatus for reducing axial thrust in centrifugal pumps
[AD-D016404] p 782 N95-17461

AXIAL LOADS
A Lifting Ball Valve for cryogenic fluid applications p 720 N95-16349
AXISYMMETRIC BODIES
An investigation of the transonic pressure drag coefficient for axi-symmetric bodies
[AD-A280990] p 654 N95-15994
Pressure distributions on research wing W4 mounted on an axisymmetric body p 660 N95-17862
Ellipsoid-cylinder model p 661 N95-17869
AXISYMMETRIC FLOW
A simple EHF hemispheric coverage antenna
[AD-A285078] p 754 N95-16495
AXONS
Characterization of neurotrophic and neurotropic interactions between neurons and their muscle and nerve targets
[AD-A281846] p 820 N95-16423
AZIDES (INORGANIC)
Thermal dissociation of halogen azides
[AD-A285088] p 728 N95-16497
AZIDES (ORGANIC)
Thermal dissociation of halogen azides
[AD-A285088] p 728 N95-16497
AZIMUTH
Imager for Mars Pathfinder (IMF) p 711 N95-16206
AZO COMPOUNDS
Mobility measurement and computer simulation at specific sites in polystyrene solutions and gels
[AD-A281214] p 747 N95-17685

B

B STARS
The Mg 2 lines as diagnostic of PMS nature in Herbig Ae/Be stars
[NASA-CR-197518] p 915 N95-17494
BACKGROUND NOISE
An algorithm for extraction of periodic signals from sparse, irregularly sampled data p 756 N95-17281
BACKGROUND RADIATION
Voyager investigation of the cosmic diffuse background: Observations of rocket-studied locations with Voyager
[NASA-CR-197532] p 917 N95-17422
BACKSCATTERING
Using lidar tomography to characterize scattering in a turbulent media
[AD-A281014] p 751 N95-16002
High brightness cathodes for microfocus x-ray generators
[AD-A285256] p 764 N95-16814
Analysis of a three-beam radar as an instrument for determining ocean wave heights and vector slopes
[AD-A282342] p 806 N95-17505
Strong WW scattering at photon linear colliders
[DE94-018183] p 878 N95-17720
BACKWARD DIFFERENCING
Avoiding BDF stability barriers in the MOL solution of advection-dominated problems
[DE94-014793] p 861 N95-16535
BACKWARD WAVES
Slow wave vane structure with elliptical cross-section slots, an analysis
[NASA-CR-195352] p 755 N95-16886
BACTERIA
Investigation into the susceptibility of corrosion resistant alloys to biocorrosion
[AD-A281066] p 736 N95-16793
BACTERIAL DISEASES
Hemoglobin-based blood substitutes and enhanced susceptibility to bacterial infections
[AD-A281023] p 820 N95-16444
BACTERIOPHAGES
Investigation of pressure regulation in an archaebacterial enzyme
[AD-A281413] p 807 N95-16164
BALANCE
Use of the electronic balance for highly accurate direct mass measurements without the use of external mass standards
[PB94-187713] p 774 N95-16074
BALL BEARINGS
A Lifting Ball Valve for cryogenic fluid applications p 720 N95-16349
BALLISTIC MISSILES
Emerging national space launch programs: Economics and safeguards
[AD-A282107] p 672 N95-17427
BALLOON FLIGHT
Results of the 1994 NASA/JPL balloon flight solar cell calibration program
[NASA-CR-197248] p 792 N95-16067
A high resolution liquid xenon imaging telescope for 0.3-10 MeV gamma-ray astrophysics: Construction and initial balloon flights
[NASA-CR-197556] p 916 N95-17528
BANACH SPACE
Global subjectivity of submersions via contractibility of the fibers
[AD-A284961] p 860 N95-16128
BANDPASS FILTERS
Adaptive line enhancers for fast acquisition p 757 N95-17287
BANDWIDTH
Decreasing the bandwidth of a transition matrix
[TR-505] p 859 N95-15948
Properties of multihead two-way probabilistic finite automata
[TR-477] p 833 N95-16040
Can high bandwidth and latency justify large cache blocks in scalable multiprocessors?
[AD-A281468] p 845 N95-16083
Implementation of a real-time data processing system for radar bandwidth extrapolation and stretch
[AD-A281195] p 754 N95-16794
In-fibre Bragg gratings for millimetre-wave EW systems
[AD-A284283] p 755 N95-16956
Economical ground data delivery p 679 N95-17194
BARIUM
Encapsulated alkaline-earth organometallics as controlled sources of calcium, strontium, and barium ions
[AD-A281547] p 741 N95-16393
BARIUM COMPOUNDS
Growth, characterization and applications of beta-barium borate and related crystals
[AD-A281047] p 898 N95-16623
Columnar defect pinning in untwinned single crystal YBa2Cu2O7
[DE94-013962] p 901 N95-17349
BARIUM FLUORIDES
BaF2/GaAs electronic components
[AD-D016391] p 767 N95-17481
Precision machining and polishing of scintillating crystals for large calorimeters and hodoscopes
[DE94-012060] p 751 N95-17738
BARIUM OXIDES
The relationship of structure to superconductivity in the Pr-Ba-Cu-O system
[DE94-014231] p 897 N95-16510
Thermal and mechanical behavior of Ba(1+x)Zr4P(6-2x)Si(2x)O24
[DE94-013620] p 899 N95-16806
BARORECEPTORS
Effects of weightlessness on human baroreflex function p 815 N95-16770
BAROTROPIC FLOW
Sensitivity study of the SPEM model to the assimilation of synop datasets using two assimilation schemes. 1: Nudging. 2: The Kalman filter/smoother
[AD-A281459] p 804 N95-16079
BARYONS
Flavor symmetries and fermion masses
[DE94-018192] p 878 N95-17889
BASALT
Melas Chasma: A Mars Pathfinder view of Valles Marineris p 922 N95-16207
BASE FLOW
Numerical study of base pressure characteristic curve for a four-engine clustered nozzle configuration p 716 N95-16329
BASE PRESSURE
Numerical study of base pressure characteristic curve for a four-engine clustered nozzle configuration p 716 N95-16329
Investigation of the flow development on a highly swept canard/wing research model with segmented leading- and trailing-edge flaps p 662 N95-17876
BATTERY CHARGERS
A modular electric power system test bed for small spacecraft
[NASA-TM-106812] p 721 N95-17276
BAYES THEOREM
Exploiting IB assignments for approximating marginal probabilities
[AD-A285419] p 855 N95-16246
Bayesian nonparametric estimation via Gibbs sampling for coherent systems with redundancy
[AD-A283173] p 865 N95-17341
BAYS (TOPOGRAPHIC FEATURES)
South Florida environmental quality. National Status and Trends Program for marine environmental quality
[PB94-173408] p 796 N95-17363
BEAM CURRENTS
Online diagnoses of high current-density beams
[DE94-014420] p 879 N95-16217
BEAM INJECTION
SEPAC co-investigator support
[NASA-CR-196527] p 798 N95-15965
Mechanisms of beam-halo formation in high-intensity linacs
[DE94-016316] p 879 N95-16030
Beam parameter measurements for the APS linac system
[DE94-018396] p 882 N95-17902
BEAM INTERACTIONS
Beam-beam tune shift and dynamical beta function in PEP-2
[DE94-018207] p 882 N95-17891
BEAM WAVEGUIDES
Antenna noise temperatures of the 34-meter beam-waveguide antenna with horns of different gains installed at F1 p 757 N95-17288
X-/Ka-band dichroic plate noise temperature reduction p 758 N95-17294
BEAMFORMING
Multistatic radar, MSR
[PB94-190709] p 759 N95-17301
Production of high proton fractions from ECR sources by plasma modification
[DE94-018381] p 893 N95-17900
BEAMS (RADIATION)
Liquid crystal materials for laser beam steering
[AD-A285089] p 897 N95-16498
Beam position correction in the Fermilab Linac
[DE94-018984] p 882 N95-17931
BED REST
Comparison of saline and fludrocortisone as fluid-loading countermeasures following exposure to simulated microgravity p 808 N95-16742
Spectral components of human cardiovascular responses to step changes in Lower Body Negative Pressure (LBNP) before and after 22 hour of 6 deg head down bed rest p 810 N95-16748
Blood volume and orthostatic responses of men and women to a 13-day bedrest p 811 N95-16752
Effect of antiorthostatic BedRest (BR) on GastroIntestinal Motility (GIM) of normal subjects p 811 N95-16753
Artificial gravity: How much, how often, how long? p 816 N95-16778
The effect of intermittent standing or walking during head down tilt bedrest on peak O2 consumption p 817 N95-16779
Periodic upright posture negates the suppression of neuroendocrine response to head down bedrest p 817 N95-16780
The efficacy of periodic +Gz exposure in the prevention of bedrest induced orthostatic intolerance p 817 N95-16781
The value of the 4-day headdown bedrest model for screening countermeasures p 817 N95-16782
BELIEF NETWORKS
Exploiting IB assignments for approximating marginal probabilities
[AD-A285419] p 855 N95-16246
BENDING
A quasi-single mode optical fiber for long-haul transmission in severe bending environments
[AD-A281313] p 884 N95-16009
BENDING FATIGUE
The effects of fatigue loading frequency on fatigue life of high-strength pressure vessel steels
[AD-A285301] p 786 N95-16601
BENDING MOMENTS
Investigation of dynamic inflow's influence on rotor control derivatives p 649 N95-16250
BENZENE
The mechanism of the oligomerization of thiophene-based para-quinodimethanes
[DE94-014232] p 722 N95-16058
Synthesis of polyphenylenes and polynaphthalenes by thermolysis of enediyness and dialkynylbenzenes
[AD-A281294] p 743 N95-16783
Study of the structuring of pure molecular liquids
[PB94-201316] p 903 N95-16839
Mobility measurement and computer simulation at specific sites in polystyrene solutions and gels
[AD-A281214] p 747 N95-17685
BENZOIC ACID
The influence of the complexation of sodium and lithium triflate on the self-assembly of tubular-supramolecular architectures displaying a columnar mesophase based on taper-shaped monoesters of oligoethyleneoxide with 3,4,5-tris(p-(n-dodecan-l-yloxy)benzyloxy)benzoic acid and of their polymethacrylates
[AD-A281403] p 730 N95-16866
BERYLLIUM ALLOYS
Experimental heat treatment of beryllium copper alloy
[AD-A282714] p 734 N95-16380

BERYLLIUM OXIDES
Pseudomorphic stabilization of diamond on non-diamond substrates
[AD-A285231] p 898 N95-16527
BIAS
Studies of novel popout
[AD-A285237] p 826 N95-16244
BIBLIOGRAPHIES
Acquiring and disseminating unpublished economic and social development materials in Africa: The case of the National Institute of Development Research and Documentation University of Botswana
p 906 N95-15924
An annotated bibliography of heat tolerance: Regarding gender differences
[AD-A280755] p 818 N95-16105
Continual improvement: A bibliography with indexes, 1992-1993
[NASA-SP-7097(02)] p 905 N95-16633
Aeronautical enginnering: A cumulative index to a continuing bibliography (supplement 312)
[NASA-SP-7037(312)] p 654 N95-17702
Aerospace medicine and biology: A continuing bibliography with indexes (supplement 396)
[NASA-SP-7011(396)] p 823 N95-17703
Aeronautical engineering: A continuing bibliography with indexes (supplement 311)
[NASA-SP-7037(311)] p 654 N95-17704
Thin film superconductors
[DE94-018585] p 902 N95-17906
BINARY ALLOYS
Possible superstructures of metallic ions in nonstoichiometric fullerites M(x) C(60)
[DE94-622052] p 901 N95-17518
BINARY DATA
NP-sets are Co-NP-immune relative to a random oracle
[TR-501] p 859 N95-15950
On P-selectivity and closeness
[TR-499] p 859 N95-15951
BINARY DIGITS
Verification of arithmetic functions with binary moment diagrams
[AD-A281028] p 835 N95-16447
BINARY MIXTURES
Chiral recognition in molecular and macromolecular pairs of liquid crystals of (2R, 3S)- and (2S, 3S)-2-fluoro-3-methylpentyl-4'-(11-vinyloxyundeca iphenyl-4-carboxylate diastereomers
[AD-A281770] p 878 N95-17692
BINARY SYSTEMS (MATERIALS)
Polymeric precursors to binary inorganic materials
[AD-A281010] p 739 N95-16000
BINOCULAR VISION
Visual perception in the field-of-view of partial binocular overlap helmet-mounted displays
[AD-A285213] p 827 N95-16520
BINOCULARS
Visual perception in the field-of-view of partial binocular overlap helmet-mounted displays
[AD-A285213] p 827 N95-16520
Factors affecting the visual fragmentation of the field-of-view in partial binocular overlap displays
[AD-A283081] p 886 N95-17334
BIOACOUSTICS
Direct comparison of two statistical methods for determination of evoked-potential thresholds
[AD-A285182] p 870 N95-16811
BIOASSAY
Methods development toward the measurement of polyaromatic hydrocarbon-DNA adducts by mass spectrometry
[PB94-182722] p 727 N95-16373
BIOASTRONAUTICS
BioServe space technologies: A NASA Center for the Commercial Development of Space
[NASA-CR-196983] p 807 N95-16034
Aerospace medicine and biology: A continuing bibliography with indexes (supplement 396)
[NASA-SP-7011(396)] p 823 N95-17703
BIOCHEMISTRY
The role of chemical inhibition of gap junctional intercellular communication in toxicology
[AD-A282452] p 820 N95-16378
BIODEGRADATION
Root growth and development in response to CO2 enrichment
[NASA-CR-196154] p 807 N95-16429
Investigation into the susceptibility of corrosion resistant alloys to biocorrosion
[AD-A281066] p 736 N95-16793
BIOELECTRIC POTENTIAL
Direct comparison of two statistical methods for determination of evoked-potential thresholds
[AD-A285182] p 870 N95-16811
BIOELECTRICITY
Skin blood flow and bioelectrical impedance
[AD-A285475] p 821 N95-16619
A new model for estimating total body water from bioelectrical resistance p 810 N95-16747
BIOLOGICAL EFFECTS
Site characterization at the Rabbit Valley Geophysical Performance Evaluation Range
[DE94-013550] p 798 N95-16284
The role of chemical inhibition of gap junctional intercellular communication in toxicology
[AD-A282452] p 820 N95-16378
The chronic effects on JP-8 jet fuel exposure on the lungs
[AD-A280982] p 821 N95-16515
Investigation of laser-induced retinal damage: Wavelength and pulsewidth dependent mechanisms
[AD-A285186] p 822 N95-16871
Performance study of galactic cosmic ray shield materials
[NASA-TP-3473] p 924 N95-16912
Basic mechanisms and implications of non-photic entrainment of circadian rhythmicity
[AD-A283180] p 822 N95-17342
BIOLOGICAL MODELS (MATHEMATICS)
The EPIC architecture for modeling human information-processing and performance: A brief introduction
[AD-A280762] p 829 N95-16119
Mathematical model for interaction of canals and otoliths in perception of orientation, translation, and rotation
[AD-A280897] p 819 N95-16151
BIOMAGNETISM
Thermal noise in biomagnetic measurements
[PB95-104360] p 869 N95-17930
BIOPROCESSING
BioServe space technologies: A NASA Center for the Commercial Development of Space
[NASA-CR-196983] p 807 N95-16034
Space medicine research: Needs for the 21st century
p 814 N95-16768
BIOSPHERE
Exobiology site priorities for Mars Pathfinder
p 919 N95-16188
BIOTECHNOLOGY
Review of performance, medical, and operational data on pilot aging issues p 812 N95-16759
BIOTITE
An XAFS study of the oxidation of structural iron in biotite mica by solutions containing Br2 or H2O2
[DE94-018721] p 733 N95-17912
BIPOLAR TRANSISTORS
Atomic layer epitaxy of group 4 materials: Surface processes, thin films, devices and their characterization
[AD-A280987] p 898 N95-16532
Trenched bipolar transistor structures
[AD-D016406] p 767 N95-17463
BIREFRINGENCE
Liquid crystal materials for laser beam steering
[AD-A285089] p 897 N95-16498
BIT ERROR RATE
Telecommunications end-to-end systems monitoring on TOPEX/Poseidon: Tools and techniques
p 676 N95-17180
Ultra high bit rate all optical communication system
[AD-D016359] p 887 N95-17695
BLINKING
Blinks, saccades, and fixation pauses during vigilance task performance. 1: Time on task
[DOT/FAA/AM-94/26] p 828 N95-17530
BLOCK COPOLYMERS
Smart materials based upon oligomeric molecules
[AD-A281374] p 872 N95-16155
Solubilization of hydrophobic substances into block copolymer micelles in aqueous media and their release
[AD-A281395] p 744 N95-16792
BLOOD
Hemoglobin-based blood substitutes and enhanced susceptibility to bacterial infections
[AD-A281023] p 820 N95-16444
BLOOD FLOW
Skin blood flow and bioelectrical impedance
[AD-A285475] p 821 N95-16619
Increased skin blood flow and enhanced heat loss in humans after niacin ingestion
[AD-A281124] p 821 N95-16809
BLOOD VESSELS
Carbon monoxide does not modulate pulmonary vascular reactivity in isolated rat lungs
[AD-A283190] p 818 N95-17714
BLOOD VOLUME
Comparison of saline and fludrocortisone as fluid-loading countermeasures following exposure to simulated microgravity p 808 N95-16742
Blood volume and orthostatic responses of men and women to a 13-day bedrest p 811 N95-16752
Periodic upright posture negates the suppression of neuroendocrine response to head down bedrest
p 817 N95-16780
BLOWDOWN WIND TUNNELS
Free-jet testing at Mach 3.44 in GASL's aero/thermo test facility p 672 N95-16320
BLUNT BODIES
Parametric study of shock-induced combustion in a hydrogen air system
[NASA-CR-197134] p 726 N95-15967
Spectral solution of the viscous blunt body problem. 2: Multidomain approximation
[NASA-CR-194971] p 863 N95-17267
Ellipsoid-cylinder model p 661 N95-17869
BODIES OF REVOLUTION
Superspheroid geometries for radome analysis
[AD-A285405] p 753 N95-16233
BODY CENTERED CUBIC LATTICES
Theoretical study of cathode surfaces and high-temperature superconductors
[NASA-CR-195407] p 898 N95-16598
BODY FLUIDS
Skin blood flow and bioelectrical impedance
[AD-A285475] p 821 N95-16619
A new model for estimating total body water from bioelectrical resistance p 810 N95-16747
Comparisons of three anti-G suit configurations during long duration, low onset, +Gz p 811 N95-16755
BODY TEMPERATURE
An annotated bibliography of heat tolerance: Regarding gender differences
[AD-A280755] p 818 N95-16105
BODY-WING CONFIGURATIONS
Wing-body juncture flows
[AD-A281526] p 655 N95-16099
Aerodynamic shape optimization p 668 N95-16572
Review of the EUROPT Project AERO-0026
p 668 N95-16573
Pressure distributions on research wing W4 mounted on an axisymmetric body p 660 N95-17862
DLR-F4 wing body configuration p 660 N95-17863
BONDED JOINTS
Special hybrid stress finite elements for the analysis of interface stress distribution in adhesive joints
[AD-A281612] p 785 N95-16102
User-defined subroutine for implementation of special finite elements in ABAQUS for the analysis of adhesive joints
[AD-A282431] p 788 N95-17510
BONDING
Structural testing of the North Wind 250 composite rotor joint
[DE94-006923] p 792 N95-16437
BONES
The value of the 4-day headdown bedrest model for screening countermeasures p 817 N95-16782
BOOLEAN FUNCTIONS
Verification of arithmetic functions with binary moment diagrams
[AD-A281028] p 835 N95-16447
BOOSTER ROCKET ENGINES
The 1993 JANNAF Propulsion Meeting, volume 1
[CPIA-PUBL-602-VOL-1] p 713 N95-16312
Design margin testing of Peacekeeper solid rocket boosters p 713 N95-16313
BORATES
Growth, characterization and applications of beta-barium borate and related crystals
[AD-A281047] p 898 N95-16623
BORESIGHT ERROR
Superspheroid geometries for radome analysis
[AD-A285405] p 753 N95-16233
BORIDES
High current density sheet-like electron beam generator
[AD-A281975] p 880 N95-17499
BORON
Shock initiation of crystalline boron in oxygen and fluorine compounds
[AD-A284266] p 730 N95-16955
BORON CARBIDES
Muon(+) SR studies of magnetic properties of boron carbide superconductors
[DE94-014440] p 868 N95-16288
Computer studies of the dynamic strength of ceramics
[DE94-010890] p 745 N95-17379
BORON NITRIDES
Polymeric precursors to binary inorganic materials
[AD-A281010] p 739 N95-16000
Pseudomorphic stabilization of diamond on non-diamond substrates
[AD-A285231] p 898 N95-16527
BOROSILICATE GLASS
High-level waste borosilicate glass: A compendium of corrosion characteristics
[DE94-016636] p 739 N95-15943

Studies on improvement of oxidation resistivity of carbon materials by glass impregnation and SiC formation
[DE94-796529] p 724 N95-16833

BOSONS

Tests of structure functions using leptons at CDF: W asymmetry and Drell-Yan production
[DE94-015727] p 875 N95-16840
QCD of different flavors with the SLD detectors
[DE94-013800] p 875 N95-16943
Relativistic effect of energy increase of a particle moving freely in vacuum from the quantum field theory point of view
[DE94-622757] p 903 N95-17473
Composite-model view of the ll-bar(gamma)(gamma) events at LEP
[DE94-753312] p 877 N95-17520
Strong WW scattering at photon linear colliders
[DE94-018183] p 878 N95-17720
Z(prime) phenomenology: Constraints from low-energy measurements, and detailed study at TeV-scale lepton and hadron colliders
[DE94-018185] p 881 N95-17886

BOUNDARIES

A super-element simplified analysis for vibration systems of complex structures p 650 N95-16260
Fast electrons, filamented laser light, and the fast ignitor
[DE94-015898] p 777 N95-16929

BOUNDARY CONDITIONS

A consistent large deflection theory of composite sandwich shells p 650 N95-16259
Numerical study of base pressure characteristic curve for a four-engine clustered nozzle configuration p 716 N95-16329
Measurement of residual flexibility for substructures having prominent flexible interfaces
[NASA-TM-110074] p 786 N95-16577
On the removal of boundary errors caused by Runge-Kutta integration of non-linear partial differential equations
[NASA-CR-194989] p 863 N95-16904
Kinetic effects near the magnetopause
[DE94-009333] p 799 N95-16927
The effects of the horizontal resolution of the boundary forcing sea surface temperature field on the FSU spectral model
[AD-A284273] p 802 N95-17488
Effects of artificial viscosity on the accuracy of high-Reynolds-number kappa-epsilon turbulence model
[NASA-TM-106781] p 773 N95-17656
2-D airfoil tests including side wall boundary layer measurements p 657 N95-17847
Data from the GARTEur (AD) Action Group 02 airfoil CAST 7/DOA1 experiments p 659 N95-17856
Low aspect ratio wing experiment p 661 N95-17865
FEM3C, an improved three-dimensional heavy-gas dispersion model: User's manual
[DE94-014731] p 797 N95-17922

BOUNDARY ELEMENT METHOD

Thermal analysis of a functionally graded material subject to a thermal gradient using the boundary element method
[NASA-TM-106801] p 789 N95-17658

BOUNDARY LAYER COMBUSTION

Service and physical properties of liquid-jet fuels p 650 N95-16256

BOUNDARY LAYER CONTROL

Optimum aerodynamic design via boundary control p 667 N95-16565

BOUNDARY LAYER FLOW

Mach number, flow angle, and loss measurements downstream of a transonic fan-blade cascade
[AD-A280907] p 656 N95-16824
Stability of separating subsonic boundary layers
[NASA-CR-4638] p 772 N95-17268
Effects of artificial viscosity on the accuracy of high-Reynolds-number kappa-epsilon turbulence model
[NASA-TM-106781] p 773 N95-17656
Experiments in the trailing edge flow of an NLR 7702 airfoil p 658 N95-17853
Data from the GARTEur (AD) Action Group 02 airfoil CAST 7/DOA1 experiments p 659 N95-17856

BOUNDARY LAYER SEPARATION

Wing-body juncture flows
[AD-A281526] p 655 N95-16099
Experimental and theoretical studies of wakes in stratified flows
[AD-A285305] p 771 N95-16616
Time accurate computation of unsteady inlet flows with a dynamic flow adaptive mesh
[AD-A285498] p 771 N95-16736
Mach number, flow angle, and loss measurements downstream of a transonic fan-blade cascade
[AD-A280907] p 656 N95-16824
Stability of separating subsonic boundary layers
[NASA-CR-4638] p 772 N95-17268
Low-speed surface pressure and boundary layer measurement data for the NLR 7301 airfoil section with trailing edge flap p 658 N95-17855
Three-dimensional boundary layer and flow field data of an inclined prolate spheroid p 661 N95-17867
Ellipsoid-cylinder model p 661 N95-17869
Supersonic vortex flow around a missile body p 661 N95-17870
Test data on a non-circular body for subsonic, transonic and supersonic Mach numbers p 662 N95-17871
Experimental investigation of the vortex flow over a 76/60-deg double delta wing p 662 N95-17874
Wind tunnel test on a 65 deg delta wing with rounded leading edges: The International Vortex Flow Experiment p 662 N95-17875
Subsonic flow around US-orbiter model FALKE in the DNW p 663 N95-17877

BOUNDARY LAYER TRANSITION

Wind tunnel test on a 65 deg delta wing with a sharp or rounded leading edge: The international vortex flow experiment p 662 N95-17872

BOUNDARY LAYERS

Analysis of plasma measurements for the Geotail mission
[NASA-CR-197020] p 888 N95-15941
Nonlinear instability of a uni-directional transversely sheared mean flow
[NASA-TM-106779] p 769 N95-15969
Marine boundary-layer parameterizations for large-scale models
[AD-A282402] p 803 N95-16062
Aerodynamic shape optimization p 668 N95-16572
The small-scale structure of dispersing clouds in the atmosphere
[AD-A285493] p 800 N95-16802
2-D airfoil tests including side wall boundary layer measurements p 657 N95-17847
Low-speed surface pressure and boundary layer measurement data for the NLR 7301 airfoil section with trailing edge flap p 658 N95-17855
Measurements of the flow over a low aspect-ratio wing in the Mach number range 0.6 to 0.87 for the purpose of validation of computational methods. Part 1: Wing design, model construction, surface flow. Part 2: Mean flow in the boundary layer and wake, 4 test cases p 660 N95-17860

BOUNDARY LUBRICATION

Deformation behavior of thin lubricant films at elevated pressure
[AD-A281848] p 741 N95-16355

BOUNDARY VALUE PROBLEMS

Classical solutions of the Prandtl-Reuss equations of perfect elasto-plasticity
[PB94-192333] p 860 N95-16292
Validation of recipes for the recovery of stresses and derivatives by a computer-based approach
[AD-A282712] p 861 N95-16379

BOW WAVES

Analysis of magnetic field data from Pioneer Venus orbiter
[NASA-CR-197492] p 923 N95-17403

BRAGG CELLS

In-fibre Bragg gratings for millimetre-wave EW systems
[AD-A284283] p 755 N95-16956

BRAIN

Event-related brain potentials as predictors of target detection performance in a moving waterfall display simulating passive broad-band sonar monitoring
[AD-A280900] p 819 N95-16152
Locus coeruleus, vigilance and stress: Brain mechanisms of adaptive behavioral responsiveness
[AD-A282450] p 826 N95-16377

BRANCHING (MATHEMATICS)

Singularities of smooth maps in a space with a fixed cone
[PB94-192358] p 861 N95-16367

BRANCHING (PHYSICS)

Measurement of the B meson differential cross-sections in p(-p) collisions at the square root of s = 1.8 TeV using the exclusive decays B(+-) yields J/(psi)K(+-) and B(exp 0) yields J/(psi)K(exp *0)
[DE94-015185] p 872 N95-16309
CP violation measurements in neutral kaon system at Fermilab
[DE94-016526] p 873 N95-16402

BRAZING

Workshop on Characterizing Diamond Films, 3
[PB94-187663] p 747 N95-17722

BREADBOARD MODELS

Updated test results of a pumped monopropellant propulsion system p 713 N95-16315
Eddy current for detecting second layer cracks under installed fasteners
[AD-A282412] p 784 N95-17507

BREATHING APPARATUS

Comparison of work of breathing during mechanical ventilation using assist control and intermittent mandatory ventilation
[AD-A285516] p 822 N95-17174

BREMSSTRAHLUNG

Beams 92: Proceedings
[DE94-014784] p 880 N95-17475

BRIGHTNESS

Performance of specular reflectors used for lighting enhancement
[AD-A281004] p 884 N95-15999
High brightness cathodes for microfocus x-ray generators
[AD-A285256] p 764 N95-16814

BRIGHTNESS DISTRIBUTION

The mass and dynamics of cD clusters with cooling flows. 1: ROSAT observations of A 496
[NASA-CR-197534] p 915 N95-17495

BRILLOUIN EFFECT

High-intensity and high energy laser interactions with single droplets
[AD-A281415] p 776 N95-16166

BRILLOUIN ZONES

Possible superstructures of metallic ions in nonstoichiometric fullerites M(x) C(60)
[DE94-622052] p 901 N95-17518

BRITTLE MATERIALS

Life prediction for bridged fatigue cracks
[DE94-016000] p 724 N95-16930

BRITTLENESS

Effects of prior ductile tearing on cleavage fracture toughness in the transition region
[AD-A281298] p 786 N95-16785

BROADBAND AMPLIFIERS

System design, implementation, and evaluation of the optical broadband correlator
[AD-A285406] p 884 N95-16296

BROADCASTING

A low-cost transportable ground station for capture and processing of direct broadcast EOS satellite data p 680 N95-17200

BROKEN SYMMETRY

CP violation measurements in neutral kaon system at Fermilab
[DE94-016526] p 873 N95-16402
Multilepton SUSY signals from R-parity violation at the Tevatron (revised)
[PB95-104311] p 877 N95-17353
The quantum solitons of the nonlinear (sigma)-model with broken chiral symmetry
[DE94-622758] p 904 N95-17474
Probing violation of quantum mechanics in the K0-(bar K)0 system
[DE94-017934] p 904 N95-17668
Physics at high energy photon photon colliders
[DE94-018191] p 881 N95-17888

BRUSHES

The effect of brush polydispersity on the interphase between end-grafted brushed and polymeric matrices
[AD-A280975] p 743 N95-16507

BUBBLES

Phase segregation due to simultaneous migration and coalescence
[NASA-CR-196819] p 721 N95-16035
Active and passive acoustic bubble sizing
[ISVR-TR-237] p 769 N95-16064
The effect of differences in time to detection of circulating microbubbles on the risk of decompression sickness p 807 N95-16738
Revisions to an empirical surface loss model using a correction for pH-dependent attenuation
[AD-A285714] p 871 N95-17177
Surfactant adsorption by sub-millimeter size bubbles: Quantification and modelling
[AD-A282405] p 772 N95-17506
Low-speed surface pressure and boundary layer measurement data for the NLR 7301 airfoil section with trailing edge flap p 658 N95-17855

BUCKLING

Thermocryogenic buckling and stress analyses of a partially filled cryogenic tank subjected to cylindrical strip heating
[NASA-TM-4579] p 788 N95-17417
Shear buckling analysis of a hat-stiffened panel
[NASA-TM-4644] p 788 N95-17490

BUDGETS

Activities of the Space Studies Board
[NASA-CR-197105] p 672 N95-16033
A model for analysis of TDA budget allocation p 758 N95-17295

BUNCHING
Transport efficiency studies for light-ion inertial confinement fusion
[AD-A285675] p 891 N95-17382
BURNING RATE
The use of designed experiments in the process development of continuous propellant mixing p 717 N95-16334
Ignition propagation and heat effects of propellant chips embedded in castable inhibitor using a laser flux test bomb p 717 N95-16335

C

C (PROGRAMMING LANGUAGE)
Real-time data collection programs and source code for a commercial passive FTIR remote sensor
[AD-A284976] p 838 N95-16634
C++ (PROGRAMMING LANGUAGE)
Object-oriented numerical computing C++ p 849 N95-16476
Flexible method for inter-object communication in C++
[NASA-TM-106315] p 840 N95-17420
Applying STEP principles to product models in high energy physics research
[PB94-197704] p 880 N95-17503
Behavioural modelling of formal documents and active instruments
[PB95-104378] p 842 N95-17732
C-135 AIRCRAFT
Achilles Tendon Reflex (ATR) in response to short exposures of microgravity and hypergravity p 812 N95-16756
Advanced Cardiac Life Support (ACLS) utilizing Man-Tended Capability (MTC) hardware onboard Space Station Freedom p 816 N95-16775
CADMIUM TELLURIDES
Preparation of Au single crystals for study of the ECALE deposition of CdTe
[AD-A282294] p 895 N95-16238
Electrochemical atomic layer processing
[AD-A282330] p 872 N95-16241
Development of high-efficiency, thin-film CdTe solar cells
[DE94-011885] p 794 N95-16940
CAFFEINE
Mental effects of caffeine in fatigued men and women
[PB94-190683] p 822 N95-17300
Caffeine's influence on critical frequency thresholds
[AD-A282005] p 828 N95-17447
CALCIUM
Encapsulated alkaline-earth organometallics as controlled sources of calcium, strontium, and barium ions
[AD-A281547] p 741 N95-16393
CALCIUM FLUORIDES
New ytterbium-doped apatite crystals for flexible laser design
[DE94-015138] p 899 N95-16867
CALCIUM OXIDES
Suppression of superconductivity in orthorhombic La(2-x)M(x)CuO4 (M = Ca,Sr)
[DE94-013963] p 901 N95-17350
Volatile CVD precursors based on copper alkoxides and mixed group IIA-copper alkoxides
[AD-D016380] p 732 N95-17479
Preparation and investigation of improved low voltage electron excitable phosphors
[AD-A284265] p 767 N95-17487
CALCIUM PHOSPHATES
New ytterbium-doped apatite crystals for flexible laser design
[DE94-015138] p 899 N95-16867
Calcium phosphate precipitation in a fluidized bed
[PB94-201407] p 796 N95-17399
CALCULUS
Integrating computers into calculus instruction
[AD-A280996] p 833 N95-15997
CALIBRATING
Results of the 1994 NASA/JPL balloon flight solar cell calibration program
[NASA-CR-197248] p 792 N95-16067
Use of the electronic balance for highly accurate direct mass measurements without the use of external mass standards
[PB94-187713] p 774 N95-16074
An investigation of polynomial calibrations methods for wind tunnel balances p 650 N95-16258
The stability of calibration standards for ICP/AES analysis: A two-year study
[DE94-013398] p 728 N95-16426
Calorimetric methods for loss measurements of small cage induction motors
[PB94-184439] p 768 N95-17691
Simulation of the SEMATECH gravimetric mass flowmeter calibrator
[DE94-018698] p 773 N95-17910
CAMBER
Investigation of the flow over a series of 14 percent-thick supercritical aerofoils with significant rear camber p 657 N95-17849
CAMERAS
Evaluation of FEL image processing algorithm for 12-bit CCD-images as function of various atmospheric conditions
[AD-A285187] p 752 N95-16146
Imager for Mars Pathfinder (IMF) p 711 N95-16206
Miniature, vacuum compatible 1024 (times) 1024 CCD camera for x ray, ultraviolet, or optical imaging
[DE94-012235] p 776 N95-17522
CANARD CONFIGURATIONS
Experimental study at low supersonic speeds of a missile concept having opposing wraparound tails
[NASA-TM-4582] p 655 N95-16069
Wind tunnel test on a 65 deg delta wing with a sharp or rounded leading edge: The international vortex flow experiment p 662 N95-17872
Wind tunnel test on a 65 deg delta wing with rounded leading edges: The International Vortex Flow Experiment p 662 N95-17875
Investigation of the flow development on a highly swept canard/wing research model with segmented leading- and trailing-edge flaps p 662 N95-17876
CANCER
Kinetics model for initiation and promotion for describing tumor prevalence from HZE radiation
[NASA-TP-3479] p 820 N95-16412
CANTILEVER BEAMS
Correlation of finite element free vibration predictions using random vibration test data
[NASA-TM-106787] p 787 N95-17258
CAPACITANCE
Static image method for the interaction of two co-axial conducting prolate spheroids
[PB94-197696] p 760 N95-17502
CAPACITORS
Performance evaluation of polyaniline as an active material for electrochemical capacitors
[DE94-016283] p 765 N95-16920
BaF2/GaAs electronic components
[AD-D016391] p 767 N95-17481
CAPILLARY FLOW
Phase segregation due to simultaneous migration and coalescence
[NASA-CR-196819] p 721 N95-16035
CARBON
Carbon clusters studied by neutralization-reionization mass spectrometry
[AD-A281367] p 726 N95-16017
In situ laser activation of electrochemical kinetics at carbon electrodes
[AD-A280892] p 727 N95-16150
From living carbocationic to living radical polymerization
[AD-A280902] p 743 N95-16501
Studies on improvement of oxidation resistivity of carbon materials by glass impregnation and SiC formation
[DE94-796529] p 724 N95-16833
Chemical properties of the fullerenes
[AD-A282730] p 730 N95-17141
CARBON CYCLE
Simulations of the global carbon cycle and anthropogenic CO2 transient
[DE94-014165] p 795 N95-16212
A procedure for estimating the carbon budget of terrestrial ecosystems in the former Soviet Union by geographic information system analysis and classification of AVHRR derived global vegetation index p 796 N95-17394
CARBON DIOXIDE
Simulations of the global carbon cycle and anthropogenic CO2 transient
[DE94-014165] p 795 N95-16212
Root growth and development in response to CO2 enrichment
[NASA-CR-196154] p 807 N95-16429
Energy and emissions of CO2, NOx and SO2 in the scenario of the 3rd national environmental evaluation, 1993
[PB94-194792] p 796 N95-17304
Recent changes of weather patterns in North America
[DE94-016115] p 803 N95-17743
Modelling interactions of carbon dioxide, forests, and climate
[DE94-018694] p 797 N95-17908
CARBON DIOXIDE CONCENTRATION
Modelling interactions of carbon dioxide, forests, and climate
[DE94-018694] p 797 N95-17908
CARBON DIOXIDE LASERS
A CO2 laser polarimeter for measurement of plasma current profile in Alcator C-Mod
[DE94-014017] p 776 N95-16486
Thermal dissociation of halogen azides
[AD-A285088] p 728 N95-16497
Alpha particle kinetics in ignited fusion plasmas: Design applications for a CO2 laser Thomson scattering experiment
[DE94-016297] p 890 N95-16921
Thermal effects in end-heated laser rods: A time-dependent model and diagnostic
[AD-A282007] p 778 N95-17500
Design of a CO2-laser Thomson scattering ion-tail diagnostic for Alcator C-Mod
[DE94-018056] p 779 N95-17680
CARBON FIBERS
Supercritical fluid extraction: Preparing a superior mesophase precursor for carbon fibers
[AD-A284933] p 726 N95-16142
CARBON MONOXIDE
First detection of CO (j = 0 - 1) adsorption at cosmological distances (z = 0.247)
[PB94-184595] p 916 N95-17332
Carbon monoxide does not modulate pulmonary vascular reactivity in isolated rat lungs
[AD-A283190] p 818 N95-17714
CARBON STEELS
Applications of positron depth profiling
[PB94-197753] p 900 N95-16952
Characterization of the corrosion behavior of the carbon steel liner in Hanford site single-shell tanks
[DE94-016475] p 737 N95-17637
CARBONATES
Bicarbonate of soda blasting technology for aircraft wheel depainting
[PB94-193323] p 654 N95-17466
CARBONYL COMPOUNDS
Metastability in molecules
[AD-A285223] p 874 N95-16523
CARCINOGENS
Methods development toward the measurement of polyaromatic hydrocarbon-DNA adducts by mass spectrometry
[PB94-182722] p 727 N95-16373
CARDIAC OUTPUT
Effects of weightlessness on human baroreflex function p 815 N95-16770
CARDIOVASCULAR SYSTEM
Aviation epidemiology data register: Coronary angiography outcomes of civilian aviators flying US aircraft
[AD-A285191] p 820 N95-16405
Spectral components of human cardiovascular responses to step changes in Lower Body Negative Pressure (LBNP) before and after 22 hour of 6 deg head down bed rest p 810 N95-16748
Changes in left ventricular function as determined by the multi-wire gamma camera at near presyncopal levels of lower body negative pressure p 811 N95-16754
Prediction of space sickness in astronauts from preflight fluid, electrolyte, and cardiovascular variables and Weightless Environmental Training Facility (WETF) training p 812 N95-16757
SLS-1: The first dedicated life sciences shuttle flight p 676 N95-16769
Effects of weightlessness on human baroreflex function p 815 N95-16770
The effect of intermittent standing or walking during head down tilt bedrest on peak O2 consumption p 817 N95-16779
CARGO SPACECRAFT
International Space Station Alpha (ISSA) Integrated Traffic Model
[NASA-CR-197566] p 710 N95-17331
CARRIER FREQUENCIES
Adaptive line enhancers for fast acquisition p 757 N95-17287
CARRIER INJECTION
Theory of carrier heating through injection pumping and lasing in semiconductor microcavity lasers
[AD-A281795] p 776 N95-16353
CARRIER MOBILITY
Femtosecond studies of carrier dynamics in compound semiconductors
[AD-A282871] p 767 N95-17433
CARRIER TO NOISE RATIOS
Adaptive line enhancers for fast acquisition p 757 N95-17287
CASCADE CONTROL
Object recognition using multi-layer Hopfield neural network
[AD-A282417] p 858 N95-17459

CASCADE FLOW
Mach number, flow angle, and loss measurements downstream of a transonic fan-blade cascade
[AD-A280907] p 656 N95-16824
Small-amplitude disturbances in turbomachine flows with swirl
[NASA-CR-195406] p 772 N95-17386

CASSEGRAIN ANTENNAS
Antenna noise temperatures of the 34-meter beam-waveguide antenna with horns of different gains installed at F1 p 757 N95-17288

CASSINI MISSION
Process and methodology of developing Cassini G and C Telemetry Dictionary p 681 N95-17204
Matrix evaluation of science objectives p 707 N95-17610

CAST ALLOYS
Metallurgical examination of failed T-158 Cast Austempered Ductile Iron (CADI) track shoes
[AD-A282433] p 737 N95-17486

CASTING
Design and technical support for development of a molded fabric space suit joint
[NASA-CR-197521] p 831 N95-16894
Method of rapid sample handling for laser processing
[AD-D016408] p 778 N95-17464

CASTINGS
Forging of FeAl intermetallic compounds
[DE94-018124] p 739 N95-17728

CATALOGS
NSSDC data listing
[NASA-TM-109986] p 909 N95-16441

CATALOGS (PUBLICATIONS)
Source header list. Volume 2: L through Z
[AD-A281001] p 908 N95-15998
Source hierarchy list. Volume 3: O through Z
[AD-A281102] p 908 N95-16090
Catalog of lunar and Mars science payloads
[NASA-RP-1345] p 922 N95-16436
Scientific and technical publishing at Goddard Space Flight Center in Fiscal Year 1994
[NASA-TM-104614] p 925 N95-16581

CATALYSIS
Augmentation for research training: Surface-mediated photocatalysis
[AD-A281591] p 722 N95-16100
Well-defined polyphosphazenes by anionic polymerization of phosphoranimines
[AD-A281414] p 740 N95-16165
Resist materials design: Base-catalyzed chemical amplification
[AD-A281805] p 741 N95-16354
Assessment of research needs for advanced heterogeneous catalysts for energy applications, volume 1
[DE94-015889] p 795 N95-16386
Surftherm: A program to analyze thermochemical and kinetic data in gas-phase and surface chemical reaction mechanisms
[DE94-016145] p 733 N95-17744

CATALYSTS
Resist materials design: Base-catalyzed chemical amplification
[AD-A281805] p 741 N95-16354
Assessment of research needs for advanced heterogeneous catalysts for energy applications, volume 1
[DE94-015889] p 795 N95-16386
Assessment of research needs for advanced heterogeneous catalysts for energy applications, volume 2
[DE94-015890] p 727 N95-16387
Development of heterogeneous Wacker oxidation catalysts: The role of the support and the redox component
[PB94-201431] p 732 N95-17700

CATECHOLAMINE
Extracellular ionic composition alters kinetics of vesicular release of catecholamines and quantal size during exocytosis at adrenal medullary cells
[AD-A281613] p 818 N95-16112

CATHODES
Theoretical study of cathode surfaces and high-temperature superconductors
[NASA-CR-195407] p 898 N95-16598
High brightness cathodes for microfocus x-ray generators
[AD-A285256] p 764 N95-16814

CATHOLYTES
Improved dual flow aluminum hydrogen peroxide battery
[AD-D016339] p 766 N95-16949

CATIONS
Encapsulated alkaline-earth organometallics as controlled sources of calcium, strontium, and barium ions
[AD-A281547] p 741 N95-16393
Radical cations of quadricyclane and norbornadiene in polar ZSM-5 matrices: Radical cation photochemical transformations without photons
[DE94-014007] p 728 N95-16485
From living carbocationic to living radical polymerization
[AD-A280902] p 743 N95-16501

CAUCHY PROBLEM
Uniqueness and free interpolation for logarithmic potentials and the Cauchy problem for the Laplace equation in (R2)
[PB94-192408] p 861 N95-16295

CAVITIES
Radial acceletron, a new low impedance HPM source
[AD-A282008] p 760 N95-17501

CAVITY RESONATORS
Electric-optic resonant phase modulator
[NASA-CASE-NPO-18702-1-CU] p 883 N95-15960
Wavelength dispersive gain element for a tunable laser
[AD-D016381] p 777 N95-17302
Electromagnetic field measurements on a mm-wave linear accelerator
[DE94-015092] p 761 N95-17926

CD-ROM
NSSDC data listing
[NASA-TM-109986] p 909 N95-16441

CELESTIAL SPHERE
Space-based asteroid detection and monitoring system
[AD-D016329] p 915 N95-16854

CELLS (BIOLOGY)
The role of chemical inhibition of gap junctional intercellular communication in toxicology
[AD-A282452] p 820 N95-16378
Cell culture and transplantation of the suprachiasmatic circadian pacemaker
[AD-A280977] p 821 N95-16481
Investigation of laser-induced retinal damage: Wavelength and pulsewidth dependent mechanisms
[AD-A285186] p 822 N95-16871

CENSUS
Bureau of the Census Center for International Research p 905 N95-15923

CENTRAL PROCESSING UNITS
Re-engineering Nascom's network management architecture p 702 N95-17584

CENTRIFUGAL COMPRESSORS
Unsteady flow phenomena in discrete passage diffusers for centrifugal compressors
[AD-A281412] p 770 N95-16163

CENTRIFUGAL FORCE
Centrifugal space-charge force for bunched beams
[DE94-016097] p 875 N95-16933
Method and apparatus for reducing axial thrust in centrifugal pumps
[AD-D016404] p 782 N95-17461

CERAMIC BONDING
Characterization on defect solids
[NASA-CR-197540] p 746 N95-17654

CERAMIC COATINGS
Testing and evaluation of oxide-coated iridium/rhenium chambers p 719 N95-16346

CERAMIC MATRIX COMPOSITES
Cornell program for the design and synthesis of advanced materials
[AD-A281352] p 723 N95-16016
Chemical vapor infiltration of non-oxide ceramic matrix composites
[DE94-017770] p 723 N95-16225
Numerical methods for singularly perturbed differential equations with applications
[AD-A285209] p 861 N95-16517
Abstracts: Eighth Annual Conference on Fossil Energy Materials
[DE94-014053] p 725 N95-17368
Multiphase ceramics for mechanical and structural reliability at low and elevated temperatures
[AD-A285497] p 746 N95-17438
Modeling of stress/strain behavior of fiber-reinforced ceramic matrix composites including stress redistribution
[NASA-TM-106789] p 725 N95-17659
Mechanisms of mechanical fatigue in ceramics
[DE94-016040] p 747 N95-17719
Research and development of material/processing methods for the Continuous Fiber Ceramic Composites Program
[DE94-018569] p 725 N95-17905

CERAMICS
Electromagnetic processing of refractory metal silicide/oxide composites
[AD-A281470] p 740 N95-16085
Ceramic/metal composite circuit-board-level technology for Application Specific Electronic Modules (ASEMs)
[AD-A285066] p 741 N95-16369
Experimental studies of stress measurement by optical fluorescence
[AD-A282337] p 723 N95-16415
Atomic scale structure and chemistry of interfaces by Z-contrast imaging and electron energy loss spectroscopy in the stem
[DE94-013632] p 728 N95-16419
Processing, fabrication, characterization and device demonstration of high temperature superconducting ceramics
[AD-A285145] p 744 N95-16844
Epitaxial MOCVD of thin film ceramics for pyroelectric detectors
[AD-A281397] p 744 N95-16863
Modeling of chemical vapor infiltration for composite fabrication
[DE93-001715] p 724 N95-16926
Life prediction for bridged fatigue cracks
[DE94-016000] p 724 N95-16930
Superplasticity and superplastic forming of ceramics
[DE94-016172] p 745 N95-16935
Abstracts: Eighth Annual Conference on Fossil Energy Materials
[DE94-014053] p 725 N95-17368
Computer studies of the dynamic strength of ceramics
[DE94-010890] p 745 N95-17379
Low-temperature fabrication of transparent silicon nitride
[DE94-014902] p 746 N95-17456
Characterization on defect solids
[NASA-CR-197540] p 746 N95-17654
Mechanisms of mechanical fatigue in ceramics
[DE94-016040] p 747 N95-17719

CERIUM
Properties of Ce:LiSrAlF6 and Ce:LiCaAlF6 ultraviolet lasers
[DE94-013737] p 777 N95-17168

CERIUM COMPOUNDS
Scintillation mechanism and radiation damage in Ce(x)La(1-x)F3 crystals
[DE94-015848] p 896 N95-16385

CERTIFICATION
National Center for Standards and Certification Information: Service and programs p 907 N95-15938
Aircraft and sub-system certification by piloted simulation
[AGARD-AR-278] p 671 N95-17388

CESIUM
Possible superstructures of metallic ions in nonstoichiometric fullerites M(x) C(60)
[DE94-622052] p 901 N95-17518

CESIUM IODIDES
Precision machining and polishing of scintillating crystals for large calorimeters and hodoscopes
[DE94-012060] p 751 N95-17738

CHANGE DETECTION
Space Shuttle main engine OPAD: The search for a hardware enhanced plume p 716 N95-16330
Detection of deforestation in the Amazon forest using NOAA/AVHRR images and the geographic information system SGI: Methodology and test of a potential alarm system
[INPE-5580-TDI/543] p 791 N95-17894

CHANNEL FLOW
Dynamical system prediction of the scalar field in a turbulent channel flow
[AD-A285519] p 771 N95-16438

CHANNELS (DATA TRANSMISSION)
Fast acquisition of burst direct sequence spread spectrum signals through satellite channels p 652 N95-16270

CHARACTERIZATION
Intense ion beam optimization and characterization with thermal imaging
[DE94-016184] p 891 N95-16936
Intense ion beam characterization and thermal modeling for beam materials processing
[DE94-016281] p 745 N95-16938

CHARGE CARRIERS
Theory of carrier heating through injection pumping and lasing in semiconductor microcavity lasers
[AD-A281795] p 776 N95-16353
Trenched bipolar transistor structures
[AD-D016406] p 767 N95-17463

CHARGE COUPLED DEVICES
Evaluation of FEL image processing algorithm for 12-bit CCD-images as function of various atmospheric conditions
[AD-A285187] p 752 N95-16146

Imager for Mars Pathfinder (IMF) p 711 N95-16206
Characterization of multiport solid state imagers at megahertz data rates
[DE94-016095] p 765 N95-16932
Method of rapid sample handling for laser processing
[AD-D016408] p 778 N95-17464
BaF2/GaAs electronic components
[AD-D016391] p 767 N95-17481
Miniature, vacuum compatible 1024 (times) 1024 CCD camera for x ray, ultraviolet, or optical imaging
[DE94-012235] p 776 N95-17522
Measurements and modeling of impurity source distributions from the Tore Supra outboard pump limiter
[DE94-018049] p 893 N95-17677

CHARGE DISTRIBUTION
Nonlinear optical and charge distribution studies probing electric field effects in polymer thin films for second order nonlinear optics
[AD-A280980] p 742 N95-16483
Theoretical study of cathode surfaces and high-temperature superconductors
[NASA-CR-195407] p 898 N95-16598

CHARGE EXCHANGE
Resonant charge transfer in hyperthermal atomic and molecular ion-surface collisions
[AD-A281369] p 871 N95-16018

CHARGE TRANSFER
Scintillation mechanism and radiation damage in Ce(x)La(1-x)F3 crystals
[DE94-015848] p 896 N95-16385
Charge transfer processes on liquid/liquid interfaces: The status in 1994
[AD-A285067] p 729 N95-16635
New mechanisms and new materials for organic optical nonlinearity
[AD-A282781] p 886 N95-17143

CHARGED PARTICLES
Study of the effect of the space charge using SYNCH
[DE94-014086] p 879 N95-16210
Charging hydrogen into Ni in hydride-containing molten salts
[AD-A282335] p 730 N95-16973
Effect of Coulomb collisions, Landau damping and particle trapping on linear and nonlinear ion acoustic waves
[AD-A282009] p 869 N95-17449
D3-D research operations
[DE94-014934] p 892 N95-17497
Search for the presence of H particles in a neutral beam
[DE94-013526] p 877 N95-17683
Flavor symmetries and fermion masses
[DE94-018192] p 878 N95-17889
Field-induced minigap and transport with in-plane magnetic fields in double quantum wells
[DE94-018893] p 879 N95-17918

CHARM (PARTICLE PHYSICS)
Experimental issues in high-sensitivity charm experiments
[DE94-015544] p 871 N95-15945

CHASSIGNITES
Pathfinder landing sites at candidate SNC impact ejection sites p 919 N95-16190

CHEBYSHEV APPROXIMATION
Spectral solution of the viscous blunt body problem. 2: Multidomain approximation
[NASA-CR-194971] p 863 N95-17267

CHEMICAL ANALYSIS
Elemental impurity analysis of mercuric iodide by ICP/MS
[DE94-013553] p 896 N95-16359

CHEMICAL BONDS
Ligand field stabilization control of metal ion binding
[AD-A281011] p 726 N95-16001
New methods for treatment of electron correlation and surface dynamics (FY91 AASERT)
[AD-A285177] p 727 N95-16144
Synthesis and characterization of neopentyl indium compounds: X-ray crystal structures of ((Me3CCH2)2InAs(SiMe3)2)2 and ((Me3CCH2)2InAs(SiMe3)2In (CH2CMe3)2Cl)
[AD-A282766] p 900 N95-17137

CHEMICAL CLEANING
Precision aqueous cleaner for RSRM p 715 N95-16326

CHEMICAL COMPOSITION
Alpha proton x ray spectrometer p 710 N95-16201
Low temperature synthesis of semiconductor materials
[AD-A285230] p 898 N95-16526
Surface composition of a series of dimethylsiloxane urea, urethane segmented copolymers studied by electron spectroscopy for chemical analysis
[AD-A282872] p 745 N95-17434

CHEMICAL EFFECTS
Development of an in vitro model assay system for the evaluation of the effects of toxic chemicals on human airways
[AD-A285074] p 821 N95-16491

CHEMICAL ENGINEERING
Volatile CVD precursors based on copper alkoxides and mixed group IIA-copper alkoxides
[AD-D016380] p 732 N95-17479

CHEMICAL EXPLOSIONS
Mechanical effects in cookoff modeling
[DE94-014174] p 748 N95-16214
Statistical properties of an algorithm used for illicit substance detection by fast-neutron transmission
[DE94-013868] p 665 N95-16964

CHEMICAL INDICATORS
Kinetics and mechanism of chemical marker formation and water-activated heat generation
[AD-A281407] p 731 N95-17425

CHEMICAL PROPERTIES
Development of practical MO techniques for prediction of the properties and behavior of materials
[AD-A285079] p 874 N95-16496
Chemical properties of the fullerenes
[AD-A282730] p 730 N95-17141

CHEMICAL PROPULSION
The 1993 JANNAF Propulsion Meeting, volume 2
[CPIA-PUBL-602-VOL-2] p 715 N95-16324

CHEMICAL REACTIONS
Electrochemical synthesis of ultrathin film composite membranes
[AD-A285075] p 724 N95-16492
Thermal dissociation of halogen azides
[AD-A285088] p 728 N95-16497
New approaches to novel organosilanes
[AD-A285253] p 722 N95-16513
Synthesis and characterization of neopentyl indium compounds: X-ray crystal structures of ((Me3CCH2)2InAs(SiMe3)2)2 and ((Me3CCH2)2InAs(SiMe3)2In (CH2CMe3)2Cl)
[AD-A282766] p 900 N95-17137
X-ray crystal structure of a monomeric Tris(Arsino)Gallane, ((Me3Si)2As)3Ga)3Ga
[AD-A282343] p 900 N95-17171
Surftherm: A program to analyze thermochemical and kinetic data in gas-phase and surface chemical reaction mechanisms
[DE94-016145] p 733 N95-17744

CHEMICAL VAPOR INFILTRATION
Chemical vapor infiltration of non-oxide ceramic matrix composites
[DE94-017770] p 723 N95-16225
Modeling of chemical vapor infiltration for composite fabrication
[DE93-001715] p 724 N95-16926

CHEMISORPTION
Chemisorption energetics of superactive chlorine containing species on gallium arsenide surfaces
[AD-A281311] p 729 N95-16790

CHESAPEAKE BAY (US)
Three-dimensional eutrophication model of Chesapeake Bay. Volume 1: Main report
[AD-A280760] p 804 N95-16118

CHINA
The Austrialian National Chinese Japanese Korean Project p 905 N95-15920

CHIPS
The combination probe of optical fibers and its applications p 652 N95-16275
Ignition propagation and heat effects of propellant chips embedded in castable inhibitor using a laser flux test bomb p 717 N95-16335

CHIPS (ELECTRONICS)
Natural convection cooling of a three by three array of leadless chip carrier packages in a dielectric liquid
[AD-A282298] p 770 N95-16239
Support for development of a custom VLSI and FPGA logic chips based on a VHDL top-down design approach
[DE94-013608] p 763 N95-16283
Guidance, navigation, and control digital emulation technology laboratory
[AD-A282722] p 766 N95-17139
VLSI technology for smaller, cheaper, faster return link systems p 681 N95-17206

CHIRALITY
The quantum solitons of the nonlinear (sigma)-model with broken chiral symmetry
[DE94-622758] p 904 N95-17474
Baryogenesis and standard model CP violation
[DE94-017935] p 877 N95-17669

CHLORIDES
Nano-scale metal oxide particles as materials for air purification
[AD-A281394] p 729 N95-16791
Identification and temporal behavior of radical intermediates formed during the combustion and pyrolysis of gaseous fuels: Kinetic pathways to soot formation
[DE94-014681] p 731 N95-17163
Synthesis and characterization of a new class of thermosetting resins: Allyl and propargyl substituted cyclopentadiene derivatives
[AD-A281976] p 746 N95-17485
Development of heterogeneous Wacker oxidation catalysts: The role of the support and the redox component
[PB94-201431] p 732 N95-17700

CHLORINE
An unexpected adsorption site exclusion process on Si(100)-(2x1)
[AD-A284950] p 894 N95-16043
Chemisorption energetics of superactive chlorine containing species on gallium arsenide surfaces
[AD-A281311] p 729 N95-16790

CHLOROBENZENES
Identification and temporal behavior of radical intermediates formed during the combustion and pyrolysis of gaseous fuels: Kinetic pathways to soot formation
[DE94-014681] p 731 N95-17163

CHLOROCARBONS
Nano-scale metal oxide particles as materials for air purification
[AD-A281394] p 729 N95-16791

CHLOROFLUOROCARBONS
Alternatives for ozone-depleting refrigerants
[PB94-190857] p 795 N95-16881

CHLOROPHYLLS
Flow over abrupt topography: The application of patterns in nutrient and productivity in reflecting physical processes
[AD-A280813] p 797 N95-17740

CHLOROSILANES
Sonochemical synthesis of polysilylenes by reductive coupling of disubstituted dichlorosilanes with alkali metals
[AD-A280994] p 739 N95-15996

CHOLESKY FACTORIZATION
An analysis of spectral envelope-reduction via quadratic assignment problems
[NASA-CR-194992] p 862 N95-16596

CHOLINESTERASE
Development of an in vitro model assay system for the evaluation of the effects of toxic chemicals on human airways
[AD-A285074] p 821 N95-16491

CHONDRITES
Shock and thermal history of iron and chondritic meteorites
[NASA-CR-197125] p 916 N95-16020

CHROMIUM COMPOUNDS
Conducting polymers as corrosion resistant coatings
[DE94-018265] p 748 N95-17892

CHROMOPHORES
Design of new multi-functional electroactive polymers with emphasis on optical nonlinearity
[AD-A284983] p 741 N95-16230
Development of device quality nonlinear optical materials and definition of mechanisms of optical nonlinearity
[AD-A285255] p 885 N95-16528

CIRCADIAN RHYTHMS
Cell culture and transplantation of the suprachiasmatic circadian pacemaker
[AD-A280977] p 821 N95-16481
Neurophysiological analysis of circadian rhythm entrainment
[AD-A280981] p 821 N95-16484
Control of circadian behavior by transplanted suprachiasmatic nuclei
[AD-A285233] p 807 N95-16599
Alertness management in two-person long-haul flight operations p 813 N95-16760
Phase-shifting effects of light and activity on the human circadian clock
[AD-A281204] p 821 N95-16796
Photoreceptors regulating circadian behavior: A mouse model
[AD-A285157] p 822 N95-16847
Molecular approach to hypothalamic rhythms
[AD-A285164] p 822 N95-16851
Basic mechanisms and implications of non-photic entrainment of circadian rhythmicity
[AD-A283180] p 822 N95-17342

CIRCUIT BOARDS
How clean is clean: Non-destructive/direct methods of flux, residue detection
[DE94-013439] p 763 N95-16357
Guidance, navigation, and control digital emulation technology laboratory
[AD-A282722] p 766 N95-17139

CIRCUIT RELIABILITY
Analog microcircuit fault prediction
[AD-A281958] p 763 N95-16410
CIRCUITS
Frequency multiplier analysis and design using punch-through varactor diodes
[AD-A284963] p 762 N95-16130
HTS SNS devices on large-area substrates by single-source MOCVD
[AD-A285159] p 899 N95-16849
Combination of power electronic models with the two-dimensional finite element analysis of electrical machines
[PB94-197720] p 766 N95-16951
Frequency domain analysis for nonlinear electronic circuits
[PB94-201365] p 767 N95-17469
Self-initializing circuit link
[AD-D016363] p 761 N95-17696
Simulation of the SEMATECH gravimetric mass flowmeter calibrator
[DE94-018698] p 773 N95-17910
CIRCULAR CYLINDERS
Wind tunnel investigations of the appearance of shocks in the windward region of bodies with circular cross section at angle of attack p 661 N95-17866
Force and pressure data of an ogive-nosed slender body at high angles of attack and different Reynolds numbers p 661 N95-17868
CIRCULAR WAVEGUIDES
Fields and waves in elliptic waveguides
[AD-A285337] p 755 N95-16816
CIRCULATION
The effect of differences in time to detection of circulating microbubbles on the risk of decompression sickness p 807 N95-16738
CLADDING
Coatings for large-area low-cost solar concentrators and reflectors
[DE94-015735] p 793 N95-16916
CLASSICAL MECHANICS
Some fundamental techniques in the theory of integrable systems
[PB94-192390] p 860 N95-16294
CLASSIFICATIONS
Collection development at the NOAA Central Library p 907 N95-15939
Singularities of smooth maps in a space with a fixed cone
[PB94-192358] p 861 N95-16367
Learning one more thing
[AD-A285342] p 857 N95-16820
CLASSIFIERS
Small sample behavior of multi-layer feedforward network classifiers: Theoretical and practical aspects
[PB94-201415] p 841 N95-17470
Operational cloud classifier based on a self-organized feature map
[PB94-197852] p 802 N95-17504
CLEAN ENERGY
Hydrogen production by gasification of municipal solid waste
[DE94-016483] p 732 N95-17639
CLEAN FUELS
Assessment of research needs for advanced heterogeneous catalysts for energy applications, volume 2
[DE94-015890] p 727 N95-16387
CLEANERS
Precision aqueous cleaner for RSRM p 715 N95-16326
CLEANLINESS
How clean is clean: Non-destructive/direct methods of flux, residue detection
[DE94-013439] p 763 N95-16357
Bench wear and single-cylinder engine evaluations of high-temperature lubricants for US Army ground vehicles
[AD-A285399] p 780 N95-16636
CLEARANCES
Aircraft and sub-system certification by piloted simulation
[AGARD-AR-278] p 671 N95-17388
CLEAVAGE
Experimental application of methodologies to quantify the effect of constraint on JC for a 3-D flaw geometry
[AD-A285309] p 735 N95-16531
Effects of prior ductile tearing on cleavage fracture toughness in the transition region
[AD-A281298] p 786 N95-16785
CLIMATE
Global warming potentials, part 7
[DE94-014066] p 794 N95-16209
Recent changes of weather patterns in North America
[DE94-016115] p 803 N95-17743
Modelling interactions of carbon dioxide, forests, and climate
[DE94-018694] p 797 N95-17908
CLIMATE CHANGE
Global warming potentials, part 7
[DE94-014066] p 794 N95-16209
Simulations of the global carbon cycle and anthropogenic CO2 transient
[DE94-014165] p 795 N95-16212
Regional forecasting with global atmospheric models
[DE94-013863] p 801 N95-16961
Global climate change model natural climate variation: Paleoclimate data base, probabilities and astronomic predictors
[DE94-013956] p 796 N95-17348
Proceedings of the First National Conference on Climate Change and Water Resources Management
[AD-A281172] p 796 N95-17684
Recent changes of weather patterns in North America
[DE94-016115] p 803 N95-17743
CERES, phases 1 and 2
[DE94-014730] p 797 N95-17920
CLIMATOLOGY
Marte Valles site p 921 N95-16200
Climatological targets for Mars Pathfinder p 922 N95-16208
Florida Gulf Stream Data (FLDA) current study
[AD-A281965] p 805 N95-16414
Mixed-layer hindcasts conducted at OWS Victor with initialization from synthetic profiles/mixed-layer hindcasts conducted with BTs taken during 1990 with atmospheric forcing from NOGAPS
[AD-A284749] p 800 N95-16551
Summary of 1994 Atlantic tropical cyclone activity and verification of author's seasonal prediction, 1 p 801 N95-17259
Extended range forecast of Atlantic seasonal hurricane activity for 1995, 2 p 801 N95-17260
Recent changes of weather patterns in North America
[DE94-016115] p 803 N95-17743
CERES, phases 1 and 2
[DE94-014730] p 797 N95-17920
CLOCKS
Ultra high bit rate all optical communication system
[AD-D016359] p 887 N95-17695
CLOSED ECOLOGICAL SYSTEMS
BioServe space technologies: A NASA Center for the Commercial Development of Space
[NASA-CR-196983] p 807 N95-16034
CLOUD COVER
An investigation of small-scale variations in cloud climatology induced by topography and monthly mean winds
[AD-A283274] p 803 N95-17715
CLOUDS
The small-scale structure of dispersing clouds in the atmosphere
[AD-A285493] p 800 N95-16802
CLOUDS (METEOROLOGY)
Operational cloud classifier based on a self-organized feature map
[PB94-197852] p 802 N95-17504
CLUTTER
Clutter signal polarization in bistatic radar: Effect of antenna sidelobe clutter
[AD-A282300] p 753 N95-16240
Mitre adaptive processing capability
[AD-A281078] p 755 N95-16825
CMOS
Support for development of a custom VLSI and FPGA logic chips based on a VHDL top-down design approach
[DE94-013608] p 763 N95-15283
COAL DERIVED LIQUIDS
Coal-fueled diesel technology development emissions control
[DE94-004096] p 782 N95-17364
COAL UTILIZATION
Abstracts: Eighth Annual Conference on Fossil Energy Materials
[DE94-014053] p 725 N95-17368
COALESCING
Phase segregation due to simultaneous migration and coalescence
[NASA-CR-196819] p 721 N95-16035
COASTAL ZONE COLOR SCANNER
SeaWiFS technical report series. Volume 21: The heritage of SeaWiFS. A retrospective on the CZCS NIMBUS Experiment Team (NET) program
[NASA-TM-104566-VOL-21] p 803 N95-16006
COASTS
A coastal hazards data base for the US Gulf Coast
[DE94-014573] p 805 N95-16610
An air mass transformation model for coastal environments
[AD-A281790] p 801 N95-17164
South Florida environmental quality. National Status and Trends Program for marine environmental quality
[PB94-173408] p 796 N95-17363
COATING
Testing and evaluation of oxide-coated iridium/rhenium chambers p 719 N95-16346
Coatings for large-area low-cost solar concentrators and reflectors
[DE94-015735] p 793 N95-16916
Conducting polymers as corrosion resistant coatings
[DE94-018265] p 748 N95-17892
COATINGS
The use of electrochemistry and ellipsometry for identifying and evaluating corrosion on aircraft
[AD-A285276] p 734 N95-16370
COAXIAL CABLES
Static image method for the interaction of two co-axial conducting prolate spheroids
[PB94-197696] p 760 N95-17502
COAXIAL FLOW
Two phase liquid helium flow testing to simulate the operation of a cryocondensation pump in the D3-D tokamak
[DE94-018345] p 893 N95-17896
COCKPITS
Human performance in the modern cockpit p 813 N95-16764
Cognition and procedure representational requirements for predictive human performance models p 814 N95-16766
Beyond the cockpit: The visual world as a flight instrument p 814 N95-16767
Industry review of a crew-centered cockpit design process and toolset
[AD-A282966] p 669 N95-17661
CODERS
Error control techniques for satellite and space communications
[NASA-CR-197459] p 761 N95-17665
CODING
Low-complexity wavelet filter design for image compression p 757 N95-17289
Object recognition using multi-layer Hopfield neural network
[AD-A282417] p 858 N95-17459
Feedback system for remotely operated vehicles
[AD-D016409] p 858 N95-17465
The CCSDS return all frames Space Link Extension service p 705 N95-17599
COEFFICIENTS
Non-linear acoustics in fluids and gels
[PB94-201308] p 870 N95-16614
A high average power electro-optic switch using KTP
[DE94-016416] p 765 N95-16925
Multiresolution representation and numerical algorithms: A brief review
[NASA-CR-194949] p 863 N95-17266
COGNITION
Coordinated control of a dual-arm dexterous robot using full immersion telepresence and virtual reality p 852 N95-15979
Tele Hyper Virtuality p 853 N95-15982
A workout for virtual bodybuilders (design issues for embodiment in multi-actor virtual environments) p 854 N95-15990
CPP-TRS(C): On using visual cognitive symbols to enhance communication effectiveness p 761 N95-15991
Studies of novel popout
[AD-A285237] p 826 N95-16244
Exploiting IB assignments for approximating marginal probabilities
[AD-A285419] p 855 N95-16246
Demodulation processes in auditory perception
[AD-A285427] p 869 N95-16248
Epistemology, software engineering and formal methods p 843 N95-16480
The GOMS family of analysis techniques: Tools for design and evaluation
[AD-A285211] p 827 N95-16518
Open architectures for formal reasoning and deductive technologies for software development
[NASA-CR-197528] p 837 N95-16586
Cognition and procedure representational requirements for predictive human performance models p 814 N95-16766
A framework for the analysis of cognitive tasks
[AD-A285345] p 828 N95-16835
Pattern theoretic knowledge discovery
[AD-A285472] p 909 N95-16879
COGNITIVE PSYCHOLOGY
Presentations of shape in object recognition and long-term visual memory
[AD-A281336] p 825 N95-16010

The EPIC architecture for modeling human information-processing and performance: A brief introduction
[AD-A280762] p 829 N95-16119
Application of research techniques for documenting cognitive processes in air traffic control: Sector complexity and decision making
[AD-A282336] p 665 N95-16375
Efficiency in work behaviour: A design approach for modern tools
[PB94-197761] p 831 N95-16953
The 1994 International Neural Network Society Annual Meeting, volume 4
[AD-A281737] p 857 N95-17370

COHERENT LIGHT
Simulations of an FEL producing coherent x rays utilizing the SLAC LINAC
[AD-A283524] p 777 N95-17303

COLD FLOW TESTS
Coal-fueled diesel technology development emissions control
[DE94-004096] p 782 N95-17364

COLD FRONTS
An air mass transformation model for coastal environments
[AD-A281790] p 801 N95-17164

COLLECTION
Collection development at the NOAA Central Library
p 907 N95-15939

COLLINEARITY
A combined biased-robust estimator for dealing with influence and collinearity in regression
[AD-A281793] p 864 N95-16422

COLLISION AVOIDANCE
Graphical simulation of articulated rigid body system kinematics with collision detection
[AD-A281842] p 856 N95-16372

COLLISIONS
Measurement of the B meson differential cross-sections in p(-p) collisions at the square root of s = 1.8 TeV using the exclusive decays B(+-) yields J/(psi)K(+-) and B(exp 0) yields J/(psi)K(exp *0)
[DE94-015185] p 872 N95-16309
Unusual initial and final state effects in quantum chromodynamics
[DE94-015341] p 903 N95-16604
Space-based asteroid detection and monitoring system
[AD-D016329] p 915 N95-16854
Measurement of the B(sub s) meson lifetime at CDF
[DE94-015381] p 875 N95-16868
Closed orbit distortion from parasitic collisions in PEP-2
[DE94-018203] p 882 N95-17890
Beam-beam tune shift and dynamical beta function in PEP-2
[DE94-018207] p 882 N95-17891

COLLOCATION
Spectral solution of the viscous blunt body problem. 2: Multidomain approximation
[NASA-CR-194971] p 863 N95-17267

COLLOIDS
Colloidal particle deposition in turbulent flow
[DE94-013375] p 770 N95-16417

COLOR
Sorting and hardware assisted rendering for volume visualization
[DE94-010204] p 834 N95-16220
Detecting the number of targets in spatially colored noise using sampled aperture radars p 652 N95-16269
Subset-selectivity and distractor matching in visual conjunction search
[AD-A285137] p 827 N95-16615
Perceptual selectivity for color and form: On the nature of the interference effect
[AD-A285338] p 827 N95-16817
Learning one more thing
[AD-A285342] p 857 N95-16820
Jet studies at CDF and DO collaborations
[DE94-015537] p 875 N95-16914
Full color recorder
[AD-A282278] p 790 N95-17372
Re-engineering NASA's space communications to remain viable in a constrained fiscal environment
p 702 N95-17585

COLOR VISION
Visual neural development and chromatic aberration
[AD-A285064] p 826 N95-16368

COMBUSTION
Conceptual design of the Space Station combustion module
[NASA-TM-106788] p 675 N95-17419

COMBUSTION CHAMBERS
A model for preliminary facility design including simulation issues p 672 N95-16318
Test results from a simple, low-cost, pressure-fed liquid hydrogen/liquid oxygen rocket combustor
p 716 N95-16328
Structurally-compliant rocket engine combustion chamber: Experimental/analytical validation
p 718 N95-16337
Design, analysis, and fabrication of oxide-coated iridium/rhenium combustion chambers
p 719 N95-16347

COMBUSTION CHEMISTRY
Shock initiation of crystalline boron in oxygen and fluorine compounds
[AD-A284266] p 730 N95-16955
Identification and temporal behavior of radical intermediates formed during the combustion and pyrolysis of gaseous fuels: Kinetic pathways to soot formation
[DE94-014681] p 731 N95-17163
CHEETAH 1.0 user's manual
[DE94-014727] p 749 N95-17919

COMBUSTION EFFICIENCY
Combustor kinetic energy efficiency analysis of the hypersonic research engine data p 714 N95-16321
Test results from a simple, low-cost, pressure-fed liquid hydrogen/liquid oxygen rocket combustor
p 716 N95-16328
Experimental and analytical methods for the determination of connected-pipe ramjet and ducted rocket internal performance
[AGARD-AR-323] p 721 N95-17278

COMBUSTION PHYSICS
Parametric study of shock-induced combustion in a hydrogen air system
[NASA-CR-197134] p 726 N95-15967
Conceptual design of the Space Station combustion module
[NASA-TM-106788] p 675 N95-17419

COMBUSTION PRODUCTS
Laser induced fluorescence measurements and modeling of nitric oxide in high-pressure premixed flames
[NASA-CR-195404] p 775 N95-16910
An in-cylinder study of the particulate/NO(x) trade-off in a DI diesel engine
[DE94-014599] p 781 N95-17162
Coal-fueled diesel technology development emissions control
[DE94-004096] p 782 N95-17364

COMBUSTION STABILITY
Test results from a simple, low-cost, pressure-fed liquid hydrogen/liquid oxygen rocket combustor
p 716 N95-16328
Combustion instability phenomena of importance to liquid propellant engines
[AD-A284780] p 730 N95-16882

COMFORT
Comparisons of three anti-G suit configurations during long duration, low onset, +Gz p 811 N95-16755

COMMAND AND CONTROL
The survivable distributed computing environment
[AD-A281637] p 845 N95-16115
Summary Report, 1992 --- distributed systems evaluation environment
[AD-A281639] p 845 N95-16116
Videoconferencing and its role in the Army
[AD-A282707] p 909 N95-16305
Spread spectrum applications in unmanned aerial vehicles
[AD-A281035] p 754 N95-16448
Workshop on Formal Models for Intelligent Control
[AD-A281399] p 857 N95-16864
SCL: An off-the-shelf system for spacecraft control
p 688 N95-17243
Spacecraft command and control using expert systems p 693 N95-17539
SEQ-GEN: A comprehensive multimission sequencing system p 693 N95-17540
An intelligent automated command and control system for spacecraft mission operations p 693 N95-17542
Configurable technology development for reusable control and monitor ground systems
p 675 N95-17589
Standard protocol stack for mission control
p 704 N95-17593
The Space Communications Protocol Standards Program p 704 N95-17594
Packet utilisation definitions for the ESA XMM mission
p 704 N95-17596
Mission Operations Centers (MOCs): Integrating key spacecraft ground data system components
p 675 N95-17601

COMMAND GUIDANCE
SCL: An off-the-shelf system for spacecraft control
p 688 N95-17243
Mission operations data analysis tools for Mars Observer guidance and control p 689 N95-17244
Safety aspects of spacecraft commanding
p 689 N95-17248
The development and validation of command schedules for SeaWiFS p 690 N95-17249

COMMAND LANGUAGES
Extending programming by demonstration with hierarchical event histories
[AD-A281186] p 838 N95-16632
SCL: An off-the-shelf system for spacecraft control
p 688 N95-17243

COMMERCE
HTS SNS devices on large-area substrates by single-source MOCVD
[AD-A285159] p 899 N95-16849

COMMERCIAL AIRCRAFT
Annual review of aircraft accident data: US Air carrier operations, calendar year 1992
[PB95-100319] p 665 N95-17748
DLR-F4 wing body configuration p 660 N95-17863

COMMERCIAL ENERGY
Fuel cell systems program plan, fiscal year 1994
[DE94-014301] p 793 N95-16541
D3-D research operations
[DE94-014934] p 892 N95-17497

COMMERCIAL SPACECRAFT
Survey of United States commercial satellites in geosynchronous Earth orbit
[AD-A284969] p 708 N95-16131
A survey of commercially available expendable heavy lift launch vehicles
[AD-A282429] p 676 N95-17509

COMMUNICATING
Communicating situation awareness in virtual environments
[AD-A285239] p 836 N95-16511

COMMUNICATION CABLES
A quasi-single mode optical fiber for long-haul transmission in severe bending environments
[AD-A281313] p 884 N95-16009

COMMUNICATION EQUIPMENT
Re-engineering Nascom's network management architecture p 702 N95-17584

COMMUNICATION NETWORKS
Open Source Service Agent (OSSA) in the intelligence community's Open Source Architecture
p 907 N95-15934
High speed transport protocols: An attempt to find the best solution
[AD-A280989] p 751 N95-15993
Communication network software analysis
[AD-A281019] p 833 N95-16004
An introduction to intelligent networks
[AD-A284284] p 752 N95-16123
Detectability models and waveform design for multiple access Low-Probability-of-Intercept networks
[AD-A281864] p 753 N95-16300
Handbook for users
[AD-A285148] p 909 N95-16845
Third International Symposium on Space Mission Operations and Ground Data Systems, part 1
[NASA-CP-3281-PT-1] p 676 N95-17179
Communication network for decentralized remote tele-science during the Spacelab mission IML-2
p 676 N95-17181
S-band and Ku-band return service interference between TDRSS users p 677 N95-17183
Attempt of automated space network operations at ETS-VI experimental data relay system
p 677 N95-17184
End-to-end communication test on variable length packet structures utilizing AOS testbed
p 677 N95-17186
The GRO remote terminal system
p 678 N95-17188
Telemetry distribution and processing for the second German Spacelab Mission D-2 p 681 N95-17207
A preliminary optical visibility model
p 758 N95-17290
Center-fed multifilar helix antenna
[AD-D016390] p 760 N95-17480
NCCDS performance model p 675 N95-17576
The NASA Mission Operations and Control Architecture Program p 706 N95-17603
Renaissance architecture for Ground Data Systems
p 706 N95-17604
Architecture of a distributed multimission operations system p 706 N95-17605
EDOS operations concept and development approach
p 708 N95-17613

COMMUNICATION SATELLITES
Survey of United States commercial satellites in geosynchronous Earth orbit
[AD-A284969] p 708 N95-16131
The Sequence of Events generator: A powerful tool for mission operations p 688 N95-17240

The SILEX experiment system operations p 674 N95-17251
Efficient mission control for the 48-satellite Globalstar Constellation p 674 N95-17256
Analysis of space network loading p 701 N95-17578
Modeling ESA's TT/C systems p 701 N95-17579

COMPACTING
Small angle neutron scattering from nanocrystalline Pd and Cu compacted at elevated temperatures
[DE94-013865] p 876 N95-16962

COMPARATORS
VLSI circuits for high speed data conversion
[AD-A281556] p 763 N95-16136

COMPATIBILITY
Overview of space power electronic's technology under the CSTI High Capacity Power Program
[NASA-TM-110110] p 883 N95-17933

COMPENSATORS
Energy decay and control for elastic and viscoelastic distributed parameter systems
[AD-A281312] p 726 N95-16008

COMPETITION
Optoelectric technology roadmap: Conclusions and recommendations
[AD-A281664] p 886 N95-16965

COMPILERS
Detailed example of using PIWG on the SUN workstation and the DEC VAX computer
[AD-A281528] p 834 N95-16107
Partial evaluation for scientific computing: The supercomputer toolkit experience
[AD-A282286] p 846 N95-16237
Anatomy of a silicon compiler
[AD-A285395] p 832 N95-16618
Compiling polymorphism using intensional type analysis
[AD-A285340] p 838 N95-16819

COMPLETENESS
Decreasing the bandwidth of a transition matrix
[TR-505] p 859 N95-15948
On the structure of log-space probabilistic complexity classes
[TR-506] p 864 N95-16039

COMPLEX COMPOUNDS
Synthesis of tungsten nitrene complexes as precursors for tungsten nitride
[AD-A281592] p 740 N95-16101
An X-Ray Photoelectron Spectroscopy (XPS) study of activated carbons impregnated with some organocopper complexes
[AD-A282721] p 727 N95-16384

COMPLEX NUMBERS
A new approach to validate subgrid models in complex high Reynolds number flows
[AD-A282340] p 772 N95-17165

COMPLEX SYSTEMS
NP-sets are Co-NP-immune relative to a random oracle
[TR-501] p 859 N95-15950
On P-selectivity and closeness
[TR-499] p 859 N95-15951
Situational awareness in complex systems
[AD-A281448] p 825 N95-15959
A super-element simplified analysis for vibration systems of complex structures p 650 N95-16260
The Design Manager's Aid for Intelligent Decomposition (DeMAID) p 848 N95-16470
Open architectures for formal reasoning and deductive technologies for software development
[NASA-CR-197528] p 837 N95-16586
Algorithms for bilevel optimization
[NASA-CR-194980] p 863 N95-16897
Evaluating modeling tools for the EDOS p 700 N95-17572

COMPONENT RELIABILITY
Bayesian nonparametric estimation via Gibbs sampling for coherent systems with redundancy
[AD-A283173] p 865 N95-17341

COMPOSITE MATERIALS
Property control of (perfluorinated ionomer)/(inorganic oxide) composites by tailoring the nanoscale morphology
[AD-A281370] p 723 N95-16019
Anionically-conductive ultrathin film composite membranes
[AD-A284944] p 723 N95-16041
Electromagnetic processing of refractory metal silicide/oxide composites
[AD-A281470] p 740 N95-16085
US-Russian Workshop on Computer Synthesis of Structure and Properties of Advanced Composites
[AD-A281647] p 723 N95-16397
Electrochemical synthesis of ultrathin film composite membranes
[AD-A285075] p 724 N95-16492
Modeling of chemical vapor infiltration for composite fabrication
[DE93-001715] p 724 N95-16926
Cost-effective method for synthesizing innovative transducer materials for sensors and actuators
[AD-A282339] p 725 N95-16974
Effect of extrusion parameters on consolidation of tungsten-hafnium and tungsten-steel powders
[DE94-013270] p 737 N95-17513
Research and development of material/processing methods for the Continuous Fiber Ceramic Composites Program
[DE94-018569] p 725 N95-17905

COMPOSITE STRUCTURES
Service and physical properties of liquid-jet fuels p 650 N95-16256
A consistent large deflection theory of composite sandwich shells p 650 N95-16259
Thermoelasticity analysis of laminated plates and shells using hybrid-stress elements p 651 N95-16263
Failure analysis of 2D and 3D woven composites
[NASA-CR-197247] p 724 N95-16597
Composite chronicles: A study of the lessons learned in the development, production, and service of composite structures
[NASA-CR-4620] p 724 N95-16859
Optimization of adaptive intraply hybrid fiber composites with reliability considerations
[NASA-TM-106632] p 787 N95-16911
Atomic oxygen durability evaluation of the flexible batten for the photovoltaic array mast on Space Station
[NASA-TM-106798] p 781 N95-17263
Composite-model view of the ll-bar(gamma)(gamma) events at LEP
[DE94-753312] p 877 N95-17520

COMPOSITE WRAPPING
Filament overwrapped motor case technology p 720 N95-16350

COMPOSITION (PROPERTY)
Environmental effects on iron aluminide
[DE94-017900] p 739 N95-17747

COMPRESSED GAS
Electrical breakdown and optical emission properties of high pressure pulsed RF gas discharges
[DE94-012731] p 877 N95-17687

COMPRESSIBILITY
Study of the compression behavior of high performance fibers
[AD-A284959] p 723 N95-16126
Delivery of cardiopulmonary resuscitation in the microgravity environment p 816 N95-16774
Investigation of an NLF(1)-0416 airfoil in compressible subsonic flow p 658 N95-17852

COMPRESSIBLE FLOW
A workstation based simulator for teaching compressible aerodynamics
[NASA-TM-106799] p 839 N95-16906
An elastomeric electrical connector
[AD-D016340] p 766 N95-16950
A new approach to validate subgrid models in complex high Reynolds number flows
[AD-A282340] p 772 N95-17165
Small-amplitude disturbances in turbomachine flows with swirl
[NASA-CR-195406] p 772 N95-17386
Three dimensional compressible turbulent flow computations for a diffusing S-duct with/without vortex generators
[NASA-CR-195390] p 670 N95-17402
Investigation of an NLF(1)-0416 airfoil in compressible subsonic flow p 658 N95-17852

COMPRESSIBLE FLUIDS
Interactive computer graphics applications for compressible aerodynamics
[NASA-TM-106802] p 839 N95-17264

COMPRESSION LOADS
Shear buckling analysis of a hat-stiffened panel
[NASA-TM-4644] p 788 N95-17490

COMPRESSION RATIO
Analysis of compression techniques for Common Mapping Standard (CMS) raster data
[AD-A283396] p 791 N95-17625

COMPRESSIVE STRENGTH
Study of the compression behavior of high performance fibers
[AD-A284959] p 723 N95-16126
The mechanical property data base from an Air Force/industry cooperative test program on high temperature aluminum alloys
[AD-A282911] p 737 N95-17398
Development of an Automated Airfield Dynamic Cone Penetrometer (AADCP) prototype and the evaluation of unsurfaced airfield seismic surveying using Spectral Analysis of Surface Waves (SASW) technology
[AD-A281985] p 672 N95-17444

COMPTON EFFECT
Light-ray operators and their application in QCD
[DE94-013801] p 903 N95-16944

COMPUTATION
Least squares computations in science and engineering
[AD-A281213] p 862 N95-16798
Reviews of computing technology: Software overview
[DE94-013662] p 841 N95-17515

COMPUTATIONAL ASTROPHYSICS
Multivariate statistical analysis software technologies for astrophysical research involving large data bases
[NASA-CR-189393] p 911 N95-17325

COMPUTATIONAL CHEMISTRY
First principles simulation of materials properties
[DE94-013615] p 899 N95-16805

COMPUTATIONAL FLUID DYNAMICS
Nonlinear instability of a uni-directional transversely sheared mean flow
[NASA-TM-106779] p 769 N95-15969
Numerical simulation of supersonic compression corners and hypersonic inlet flows using the RPLUS2D code
[NASA-TM-106580] p 654 N95-16038
Computational fluid dynamics studies of nuclear rocket performance
[NASA-TM-105436] p 713 N95-16066
High altitude hypersonic flowfield radiation
[AD-A281386] p 655 N95-16160
Visualization of unsteady computational fluid dynamics
[NASA-CR-197461] p 770 N95-16388
Applications of automatic differentiation in computational fluid dynamics p 774 N95-16461
Optimum Design Methods for Aerodynamics
[AGARD-R-803] p 666 N95-16562
Experimental and theoretical studies of wakes in stratified flows
[AD-A285305] p 771 N95-16616
CMCAM: A high performance CM-5 lattice gas simulator
[AD-A281063] p 837 N95-16626
Time accurate computation of unsteady inlet flows with a dynamic flow adaptive mesh
[AD-A285498] p 771 N95-16736
Applications of automatic differentiation in CFD
[NASA-TM-109948] p 771 N95-16828
On bi-grid local mode analysis of solution techniques for 3-D Euler and Navier-Stokes equations
[NASA-TM-106749] p 771 N95-16855
New developments in the method of space-time conservation element and solution element-applications to two-dimensional time-marching problems
[NASA-TM-106758] p 862 N95-16885
Flosolver parallel computers: 1986-1994
[NAL-SP-9409] p 850 N95-16901
A new approach to validate subgrid models in complex high Reynolds number flows
[AD-A282340] p 772 N95-17165
Interactive computer graphics applications for compressible aerodynamics
[NASA-TM-106802] p 839 N95-17264
Fifth International Conference on Hyperbolic Problems: Theory, Numerics, Applications
[AD-A283078] p 863 N95-17333
Three dimensional compressible turbulent flow computations for a diffusing S-duct with/without vortex generators
[NASA-CR-195390] p 670 N95-17402
Transient flows and pressure waves in pipes
[DE94-012650] p 772 N95-17523
Effects of artificial viscosity on the accuracy of high-Reynolds-number kappa-epsilon turbulence model
[NASA-TM-106781] p 773 N95-17656
Computer modeling of organic aerogels, 93-SR-062
[DE94-016485] p 722 N95-17745
A selection of experimental test cases for the validation of CFD codes, volume 2
[AGARD-AR-303-VOL-2] p 657 N95-17846
Low-speed surface pressure and boundary layer measurement data for the NLR 7301 airfoil section with trailing edge flap p 658 N95-17855
Data from the GARTEur (AD) Action Group 02 airfoil CAST 7/DOA1 experiments p 659 N95-17856
A supercritical airfoil experiment p 659 N95-17858
Two-dimensional high-lift airfoil data for CFD code validation p 659 N95-17859
Measurements of the flow over a low aspect-ratio wing in the Mach number range 0.6 to 0.87 for the purpose of validation of computational methods. Part 1: Wing design, model construction, surface flow. Part 2: Mean flow in the boundary layer and wake, 4 test cases p 660 N95-17860
Detailed study at supersonic speeds of the flow around delta wings p 660 N95-17861
STOVL CFD model test case p 663 N95-17881
Low speed propeller slipstream aerodynamic effects p 663 N95-17882

FEM3C, an improved three-dimensional heavy-gas dispersion model: User's manual
[DE94-014731] p 797 N95-17922

COMPUTATIONAL GEOMETRY

Sorting and hardware assisted rendering for volume visualization
[DE94-010204] p 834 N95-16220
Geometric sensing of known planar shapes
[AD-A282854] p 840 N95-17432

COMPUTATIONAL GRIDS

Numerical study of base pressure characteristic curve for a four-engine clustered nozzle configuration
p 716 N95-16329
Computational methods for microstructure covolume techniques of discretization
[AD-A282449] p 861 N95-16376
An analysis of spectral envelope-reduction via quadratic assignment problems
[NASA-CR-194992] p 862 N95-16596
A coastal hazards data base for the US Gulf Coast
[DE94-014573] p 805 N95-16610
Time accurate computation of unsteady inlet flows with a dynamic flow adaptive mesh
[AD-A285498] p 771 N95-16736
On bi-grid local mode analysis of solution techniques for 3-D Euler and Navier-Stokes equations
[NASA-TM-106749] p 771 N95-16855
A new approach to validate subgrid models in complex high Reynolds number flows
[AD-A282340] p 772 N95-17165
Data rearrangement and real-time computation
[AD-A282349] p 910 N95-17166
Spectral solution of the viscous blunt body problem. 2: Multidomain approximation
[NASA-CR-194971] p 863 N95-17267
A model study of element residual estimators for linear elliptic problems: The quality of the estimators in the interior of meshes of triangles and quadrilaterals
[AD-A282849] p 863 N95-17431
The Grid Analysis and Display System (GrADS)
[NASA-CR-189387] p 912 N95-17491
Error estimation and adaptive mesh refinement for parallel analysis of shell structures
[NASA-CR-197500] p 788 N95-17492
FEM3C, an improved three-dimensional heavy-gas dispersion model: User's manual
[DE94-014731] p 797 N95-17922

COMPUTER AIDED DESIGN

A graphical environment for object-oriented simulation model environment
[NASA-CR-196887] p 833 N95-16088
Timing and area optimization for VLSI circuit and layout
[AD-A281081] p 762 N95-16089
Generalized method of solving topological optimization problems for electrical airplane equipment systems in computer-aided design p 652 N95-16272
Support for development of a custom VLSI and FPGA logic chips based on a VHDL top-down design approach
[DE94-013608] p 763 N95-16283
An engineering code to analyze hypersonic thermal management systems p 715 N95-16322
Structural analysis of solid-propellant rocket motors with and without flaws p 720 N95-16348
Electronic Engineering Notebook: A software environment for research execution, documentation and dissemination p 848 N95-16473
ICONF: An incremental constraint facility in a feature modelling system
[PB94-197654] p 837 N95-16605
Applications of automatic differentiation in CFD
[NASA-TM-109948] p 771 N95-16828
Analysis of a two-bladed, teetering-hub turbine using the ADAMS (tm) software
[DE94-006922] p 781 N95-17169
Computational differentiation and multidisciplinary design
[DE94-013393] p 863 N95-17306
Engineering design tools for wind diesel systems. Volume 3: JODYMOD dynamic simulation software package. Model description
[PB95-104527] p 840 N95-17356
Applying STEP principles to product models in high energy physics research
[PB94-197704] p 880 N95-17503
Engineering design tools for wind diesel systems. Volume 5: JODYMOD dynamic wind diesel simulation software package. User's guide
[PB95-104543] p 841 N95-17629
Engineering design tools for wind diesel systems. Volume 1: Executive summary
[PB95-104501] p 842 N95-17733
Engineering design tools for wind diesel systems. Volume 6: Logistic package. User documentation
[PB95-104550] p 842 N95-17734
Engineering design tools for wind diesel systems. Volume 7: Logistic package. Validation report
[PB95-104568] p 842 N95-17735

COMPUTER AIDED MANUFACTURING

Improving production schedules without scheduling
[PB94-191350] p 904 N95-16289
Liquefied metal jet program Automation and Robotics Research Institute (ARRI)
[AD-A285470] p 736 N95-16878

COMPUTER AIDED MAPPING

Digital mapping, charting, and geodesy analysis program technical review of interim terrain analysis data set prototype 1
[AD-A284742] p 790 N95-16547
Full color recorder
[AD-A282278] p 790 N95-17372

COMPUTER AIDED TOMOGRAPHY

Least squares computations in science and engineering
[AD-A281213] p 862 N95-16798
High brightness cathodes for microfocus x-ray generators
[AD-A285256] p 764 N95-16814

COMPUTER ANIMATION

Graphic Server: A real time system for displaying and monitoring telemetry data of several satellites
p 687 N95-17238

COMPUTER ASSISTED INSTRUCTION

Integrating computers into calculus instruction
[AD-A280996] p 833 N95-15997
Training visual pattern recognition: Using worked examples to aid schema acquisition
[AD-A281859] p 826 N95-16299
A workstation based simulator for teaching compressible aerodynamics
[NASA-TM-106799] p 839 N95-16906
On serializable languages
[TR-519] p 839 N95-17261

COMPUTER COMPONENTS

Re-engineering Nascom's network management architecture p 702 N95-17584

COMPUTER CONFERENCING

Communication network software analysis
[AD-A281019] p 833 N95-16004

COMPUTER DESIGN

Timing and area optimization for VLSI circuit and layout
[AD-A281081] p 762 N95-16089
A VLSI interface for the NM24CF04 serial-access ferroelectric memory
[AD-A281535] p 762 N95-16110
Anatomy of a silicon compiler
[AD-A285395] p 832 N95-16618
Investigation of modularly configured attached processors with intelligent memories
[AD-A285454] p 832 N95-16876
Flosolver parallel computers: 1986-1994
[NAL-SP-9409] p 850 N95-16901
High performance hardware and software for pattern recognition and image processing
[AD-A284264] p 839 N95-17172
Highly parallel reconfigurable computer architecture for robotic computation having plural processor cells each having right and left ensembles of plural processors
[NASA-CASE-NPO-17632-1-CU] p 832 N95-17400

COMPUTER GRAPHICS

ISMCR 1994: Topical Workshop on Virtual Reality. Proceedings of the Fourth International Symposium on Measurement and Control in Robotics
[NASA-CP-10163] p 851 N95-15972
Applying Virtual Reality to commercial Edutainment
p 854 N95-15989
CPP-TRS(C): On using visual cognitive symbols to enhance communication effectiveness
p 761 N95-15991
Scripting human animations in a virtual environment
p 855 N95-15992
Sorting and hardware assisted rendering for volume visualization
[DE94-010204] p 834 N95-16220
Visualizing 3D velocity fields near contour surfaces
[DE94-010205] p 860 N95-16221
Fast stereoscopic images with ray-traced volume rendering
[DE94-011703] p 835 N95-16223
Example based image analysis and synthesis
[AD-A282285] p 835 N95-16236
MAGENCO: A map generalization controller for Arc/Info
[DE94-013440] p 835 N95-16358
Visualization of unsteady computational fluid dynamics
[NASA-CR-197461] p 770 N95-16388
How to use the WWW to distribute STI
p 847 N95-16465
Image tools for UNIX p 847 N95-16466
From computer images to video presentation: Enhancing technology transfer p 848 N95-16467
Data Visualization and Animation Lab (DVAL): Applications p 843 N95-16469
Electronic Engineering Notebook: A software environment for research execution, documentation and dissemination p 848 N95-16473
Dark focus of accommodation as dependent and independent variables in visual display technology
p 812 N95-16758
Interactive sketching for the early stages of user interface design
[AD-A285339] p 838 N95-16818
A graphic system for telemetry monitoring and procedure performing at the Telecom SCC p 689 N95-17246
Interactive computer graphics applications for compressible aerodynamics
[NASA-TM-106802] p 839 N95-17264
An object-oriented graphical user interface for a reusable rocket engine intelligent control system
[NASA-TM-106750] p 721 N95-17274
Experimenter's Laboratory for Visualized Interactive Science
[NASA-CR-189391] p 910 N95-17322
An interactive interface for NCAR Graphics
[NASA-CR-189383] p 840 N95-17324
The Grid Analysis and Display System (GrADS)
[NASA-CR-189387] p 912 N95-17491
Using graphics and expert system technologies to support satellite monitoring at the NASA Goddard Space Flight Center p 674 N95-17535
Knowledge-based critiquing of graphical user interfaces with CHIMES p 697 N95-17560
XPVM: A graphical console and monitor for PVM
[DE94-018050] p 842 N95-17678
ICCanvas 3D visualization tool for Windows (tm). Software user's manual
[AD-A285603] p 842 N95-17746

COMPUTER INFORMATION SECURITY

Open Source Service Agent (OSSA) in the intelligence community's Open Source Architecture
p 907 N95-15934
The Space Communications Protocol Standards Program p 704 N95-17594

COMPUTER NETWORKS

The future of interaction on the Internet
p 906 N95-15931
Electronic access to ONREUR/ONRAISIA S and T reports p 907 N95-15935
Network interface specification for the T1 microprocessor
[AD-A283392] p 844 N95-15940
Accountability for network backup failures
[DE94-011365] p 846 N95-16222
A structured TCP in standard ML
[AD-A282711] p 835 N95-16306
ARACHNID: A prototype object-oriented database tool for distributed systems p 680 N95-17199
Multimission Telemetry Visualization (MTV) system: A mission applications project from JPL's Multimedia Communications Laboratory p 681 N95-17205
Back-propagation neural networks in adaptive control of unknown nonlinear systems
[AD-A282414] p 858 N95-17458
Object recognition using multi-layer Hopfield neural network
[AD-A282417] p 858 N95-17459
ATM-test: A workstation-based software suite for testing Asynchronous Transfer Mode (ATM) networks
[DE94-013813] p 850 N95-17516
Standard protocol stack for mission control
p 704 N95-17593
An incremental database access method for autonomous interoperable databases
[NASA-CR-189384] p 912 N95-17652
XPVM: A graphical console and monitor for PVM
[DE94-018050] p 842 N95-17678

COMPUTER PROGRAM INTEGRITY

A study of software standards used in the avionics industry p 670 N95-16456
Automatic differentiation for design sensitivity analysis of structural systems using multiple processors
p 847 N95-16462
The Software Technology Center at Lawrence Livermore National Laboratory: Software engineering technology transfer in a scientific R/D laboratory
[DE94-014794] p 836 N95-16536

COMPUTER PROGRAMMING

Improving productivity in the development of large software systems
[AD-A282270] p 835 N95-16234
Procedure calls are the assembly language of software interconnection: Connectors deserve first-class status
[AD-A281026] p 835 N95-16446
Software engineering from a Langley perspective
p 843 N95-16454

A study of software standards used in the avionics industry p 670 N95-16456
Equation solvers for distributed-memory computers p 847 N95-16460
Applications of automatic differentiation in computational fluid dynamics p 774 N95-16461
Electronic Engineering Notebook: A software environment for research execution, documentation and dissemination p 848 N95-16473
Object-oriented numerical computing C++ p 849 N95-16476
High Performance FORTRAN p 843 N95-16478
Current research activities at the NASA-sponsored Illinois Computing Laboratory of Aerospace Systems and Software p 849 N95-16479
Epistemology, software engineering and formal methods p 843 N95-16480
Software cost and schedule estimating: A process improvement initiative
[AD-A280915] p 836 N95-16503
The Software Technology Center at Lawrence Livermore National Laboratory: Software engineering technology transfer in a scientific R/D laboratory
[DE94-014794] p 836 N95-16536
A survey of program slicing for software engineering
[NASA-CR-193116] p 836 N95-16574
Open architectures for formal reasoning and deductive technologies for software development
[NASA-CR-197528] p 837 N95-16586
MIL-STD-498 software development and documentation, version 01.00.00
[AD-A282003] p 837 N95-16607
Anatomy of a silicon compiler
[AD-A285395] p 832 N95-16618
Extending programming by demonstration with hierarchical event histories
[AD-A281186] p 838 N95-16632
Integrating human factors with software engineering practices
[AD-A285210] p 830 N95-16813
Interactive sketching for the early stages of user interface design
[AD-A285339] p 838 N95-16818
Compiling polymorphism using intensional type analysis
[AD-A285340] p 838 N95-16819
Generic mission planning and scheduling: The AXAF solution p 686 N95-17231
CCS-MIP: Low cost Customizable Control Centre p 674 N95-17254
A computational logic for applicative common Lisp
[AD-A283103] p 840 N95-17338
Corrective software management: The success of the EPLRS program
[AD-A282430] p 841 N95-17460
A proven approach for more effective software development and maintenance p 698 N95-17566

COMPUTER PROGRAMS

Guide to ASIAC computer programs
[AD-A285354] p 784 N95-15953
Parallel software benchmarks for high performance BMC3/IS systems
[AD-A282329] p 844 N95-16060
Development of the OMPAT neuropsychological/psychomotor performance evaluation and OMPAT data and timing support programs
[AD-A284928] p 826 N95-16140
Metadata database for automated oceanographic imagery
[AD-A284932] p 805 N95-16141
Structural analysis of solid-propellant rocket motors with and without flaws p 720 N95-16348
Evaluation of the dynamic stability characteristics of the NAL Light Transport Aircraft
[NAL-PD-CA-9217] p 671 N95-16392
US-Russian Workshop on Computer Synthesis of Structure and Properties of Advanced Composites
[AD-A281647] p 723 N95-16397
The complexity of PDL with interleaving
[AD-A281044] p 836 N95-16452
Model-based software process improvement p 843 N95-16455
A study of software standards used in the avionics industry p 670 N95-16456
Introduction to the World Wide Web and Mosaic p 847 N95-16463
WAVES VHDL interface
[AD-A285208] p 764 N95-16516
An economical system for measuring, monitoring, and controlling the rate of repetitive events
[AD-A285219] p 764 N95-16522
FPCAS2D user's guide, version 1.0
[NASA-CR-195413] p 786 N95-16588
Investigations on the sensitivity of the computer code TURBO-2D
[CUED/A-THERMO/TR-61] p 771 N95-16595
MIL-STD-498 software development and documentation, version 01.00.00
[AD-A282003] p 837 N95-16607
Cognition and procedure representational requirements for predictive human performance models p 814 N95-16766
Data rearrangement and real-time computation
[AD-A282349] p 910 N95-17166
High performance hardware and software for pattern recognition and image processing
[AD-A284264] p 839 N95-17172
Table-driven configuration and formatting of telemetry data in the Deep Space Network p 677 N95-17185
Use of a multimission system for cost effective support of planetary science data processing p 678 N95-17190
Towards cheaper control centers p 674 N95-17250
On serializable languages
[TR-519] p 839 N95-17261
Erosion effects on TVC vane heat transfer characteristics
[AD-A282006] p 721 N95-17448
Corrective software management: The success of the EPLRS program
[AD-A282430] p 841 N95-17460
Demonstration of the Dynamic Flowgraph Methodology using the Titan 2 Space Launch Vehicle Digital Flight Control System
[NASA-CR-197517] p 675 N95-17493
Applying STEP principles to product models in high energy physics research
[PB94-197704] p 880 N95-17503
ATM-test: A workstation-based software suite for testing Asynchronous Transfer Mode (ATM) networks
[DE94-013813] p 850 N95-17516
The SAX Italian scientific satellite. The on-board implemented automation as a support to the ground control capability p 695 N95-17551
SEQ-POINTER: Next generation, planetary spacecraft remote sensing science observation design tool p 697 N95-17559
Integration of a satellite ground support system based on analysis of the satellite ground support domain p 675 N95-17568
Software Process Assessment (SPA) p 699 N95-17569
Taking advantage of ground data systems attributes to achieve quality results in testing software p 699 N95-17570
A General Mission Independent Simulator (GMIS) and Simulator Control Program (SCP) p 701 N95-17580
Surftherm: A program to analyze thermochemical and kinetic data in gas-phase and surface chemical reaction mechanisms
[DE94-016145] p 733 N95-17744
ICCanvas 3D visualization tool for Windows (tm). Software user's manual
[AD-A285603] p 842 N95-17746
Data from the GARTEur (AD) Action Group 02 airfoil CAST 7/DOA1 experiments p 659 N95-17856
OAT15A airfoil data p 659 N95-17857
Two-dimensional high-lift airfoil data for CFD code validation p 659 N95-17859

COMPUTER STORAGE DEVICES

A VLSI interface for the NM24CF04 serial-access ferroelectric memory
[AD-A281535] p 762 N95-16110
Non-volatile, rad-hard Random Access Memory (RAM) on GaAs
[AD-A285170] p 838 N95-16852

COMPUTER SYSTEMS DESIGN

Network interface specification for the T1 microprocessor
[AD-A283392] p 844 N95-15940
A graphical environment for object-oriented simulation model environment
[NASA-CR-196887] p 833 N95-16088
The survivable distributed computing environment
[AD-A281637] p 845 N95-16115
Summary Report, 1992 --- distributed systems evaluation environment
[AD-A281639] p 845 N95-16116
Risk-Based Data Management System design specifications and implementation plan for the Alaska Oil and Gas Conservation Commission; the Mississippi State Oil and Gas Board; the Montana Board of Oil and Gas Conservation; and the Nebraska Oil and Gas Conservation Commission, attachment B
[DE94-013189] p 908 N95-16282
Current research activities at the NASA-sponsored Illinois Computing Laboratory of Aerospace Systems and Software p 849 N95-16479
Control transfer in operating system kernels
[AD-A281135] p 837 N95-16602
Efficiency in work behaviour: A design approach for modern tools
[PB94-197761] p 831 N95-16953
A second generation 50 Mbps VLSI level zero processing system prototype p 678 N95-17191
ARACHNID: A prototype object-oriented database tool for distributed systems p 680 N95-17199
Production and quality assurance automation in the Goddard Space Flight Center Flight Dynamics Facility p 687 N95-17237
Designing an autonomous environment for mission critical operation of the EUVE satellite p 688 N95-17241
Generic trending and analysis system p 689 N95-17245
CCS-MIP: Low cost Customizable Control Centre p 674 N95-17254
A land-surface Testbed for EOSDIS
[NASA-CR-189392] p 840 N95-17327
Development of a prototype real-time automated filter for operational deep space navigation p 694 N95-17545
Embedded parallel processing based ground control systems for small satellite telemetry p 674 N95-17553
A system study for satellite operation and control in next generation p 702 N95-17586
On the measurement of momentum flux profiles using a five-beam 915-MHz wind profiler
[DE94-018448] p 791 N95-17903

COMPUTER SYSTEMS PERFORMANCE

Network interface specification for the T1 microprocessor
[AD-A283392] p 844 N95-15940
A new communication scheme for the neutron diffusion nodal method in a distributed computing environment
[DE94-017907] p 844 N95-15946
Control transfer in operating system kernels
[AD-A281135] p 837 N95-16602
SCOSII: ESA's new generation of mission control systems: The user's perspective p 674 N95-17537

COMPUTER SYSTEMS PROGRAMS

Communication network software analysis
[AD-A281019] p 833 N95-16004
A structured TCP in standard ML
[AD-A282711] p 835 N95-16306
The Role of Computers in Research and Development at Langley Research Center
[NASA-CP-10159] p 846 N95-16453
Current research activities at the NASA-sponsored Illinois Computing Laboratory of Aerospace Systems and Software p 849 N95-16479
Analysis of a two-bladed, teetering-hub turbine using the ADAMS (tm) software
[DE94-006922] p 781 N95-17169
The IUE Science Operations Ground System p 674 N95-17255
XMM instrument on-board software maintenance concept p 699 N95-17567
Taking advantage of ground data systems attributes to achieve quality results in testing software p 699 N95-17570
Modeling ESA's TT/C systems p 701 N95-17579
Engineering design tools for wind diesel systems. Volume 4: JODYMOD dynamic wind diesel simulation software package. Program documentation
[PB95-104535] p 841 N95-17628

COMPUTER TECHNIQUES

Applied virtual reality at the Research Triangle Institute p 851 N95-15974
Portable parallel stochastic optimization for the design of aeropropulsion components
[NASA-CR-195312] p 785 N95-16072
Joint Proceedings on Aeronautics and Astronautics (JPAA)
[ISBN-7-80-046602-7] p 649 N95-16249
The computer analysis of the prediction of aircraft electrical power supply system reliability p 653 N95-16278
Validation of recipes for the recovery of stresses and derivatives by a computer-based approach
[AD-A282712] p 861 N95-16379
Real-time simulation of large-scale multibody systems using automated equation decoupling techniques
[AD-A281544] p 856 N95-16390
A parser for the ISO 8211 data format
[AD-A281594] p 909 N95-16431
Rapid solution of large-scale systems of equations p 847 N95-16458
RDD-100 and the systems engineering process p 848 N95-16471
Computer tools for systems engineering at LaRC p 848 N95-16472
Real-time data collection programs and source code for a commercial passive FTIR remote sensor
[AD-A284976] p 838 N95-16634

Fast computational scheme of image compression for 32-bit microprocessors p 678 N95-17192
Debris/ice/TPS assessment and integrated photographic analysis of Shuttle Mission STS-64 on 9 August 1994
[NASA-TM-109206] p 676 N95-17262
Interactive computer graphics applications for compressible aerodynamics
[NASA-TM-106802] p 839 N95-17264
Identification of Artificial Intelligence (AI) applications for maintenance, monitoring, and control of airway facilities
[AD-A282479] p 665 N95-17373
Groupware system for multidisciplinary participation
[AD-A282525] p 850 N95-17374
A model study of element residual estimators for linear elliptic problems: The quality of the estimators in the interior of meshes of triangles and quadrilaterals
[AD-A282849] p 863 N95-17431
Department of Defense Electronic Data Interchange project baseline report for FY 1994
[AD-A283015] p 912 N95-17710

COMPUTER VISION
Estimation of vehicle dynamics from monocular noisy images
[AD-A281458] p 804 N95-16078
Computational vision based on neurobiology
[AD-A284472] p 819 N95-16135
Example based image analysis and synthesis
[AD-A282285] p 835 N95-16236
Training visual pattern recognition: Using worked examples to aid schema acquisition
[AD-A281859] p 826 N95-16299
Division of Information Systems (FOA 37)
[PB94-190766] p 909 N95-16400
Log-polar optical coordinate transformation with applications for automatic pattern recognition
[AD-A281022] p 885 N95-16443
Qualitative vision and action
[AD-A282697] p 831 N95-16966
The 1994 International Neural Network Society Annual Meeting, volume 4
[AD-A281737] p 857 N95-17370
Representation, modeling and recognition of outdoor scenes
[AD-A283257] p 858 N95-17634

COMPUTERIZED SIMULATION
Simulation of arthroscopic surgery using MRI data p 823 N95-15975
Surface matching for correlation of virtual models: Theory and application p 853 N95-15983
A virtual work space for both hands manipulation with coherency between kinesthetic and visual sensation p 831 N95-15984
Physics-based approach to haptic display p 854 N95-15986
Scripting human animations in a virtual environment p 855 N95-15992
Graphical simulation of articulated rigid body system kinematics with collision detection
[AD-A281842] p 856 N95-16372
Real-time simulation of large-scale multibody systems using automated equation decoupling techniques
[AD-A281544] p 856 N95-16390
Sensitivity analysis of numerically-simulated convective storms using direct and adjoint methods
[DE94-013399] p 800 N95-16398
Computational simulation of the formation and material behavior of ice
[NASA-TM-106702] p 785 N95-16416
Dynamical system prediction of the scalar field in a turbulent channel flow
[AD-A285519] p 771 N95-16438
RDD-100 and the systems engineering process p 848 N95-16471
Computer tools for systems engineering at LaRC p 848 N95-16472
Matlab as a robust control design tool p 849 N95-16474
Simulation of the coupled multi-spacecraft control testbed at the Marshall Space Flight Center p 849 N95-16475
The effect of brush polydispersity on the interphase between end-grafted brushed and polymeric matrices
[AD-A280975] p 743 N95-16507
Communicating situation awareness in virtual environments
[AD-A285239] p 836 N95-16511
Numerical simulation of helicopter engine plume in forward flight
[NASA-CR-197488] p 655 N95-16589
Investigations on the sensitivity of the computer code TURBO-2D
[CUED/A-THERMO/TR-61] p 771 N95-16595
Proceedings of the Neural Network Workshop for the Hanford Community
[DE94-014567] p 856 N95-16609
Cognition and procedure representational requirements for predictive human performance models p 814 N95-16766
Applications of automatic differentiation in CFD
[NASA-TM-109948] p 771 N95-16828
Flosolver parallel computers: 1986-1994
[NAL-SP-9409] p 850 N95-16901
A workstation based simulator for teaching compressible aerodynamics
[NASA-TM-106799] p 839 N95-16906
Kinetic effects near the magnetopause
[DE94-009333] p 799 N95-16927
A PC-based interactive simulation of the F-111C Pave Tack system and related sensor, avionics and aircraft aspects
[AD-A285500] p 669 N95-16969
A new approach to validate subgrid models in complex high Reynolds number flows
[AD-A282340] p 772 N95-17165
An assessment of simulation systems applicable to business process reengineering at Army Directorates of Public Works
[AD-A285696] p 839 N95-17176
Interactive computer graphics applications for compressible aerodynamics
[NASA-TM-106802] p 839 N95-17264
Engineering design tools for wind diesel systems. Volume 2: JODYMOD dynamic wind diesel simulation software package. Model verification
[PB95-104519] p 840 N95-17355
Engineering design tools for wind diesel systems. Volume 3: JODYMOD dynamic simulation software package. Model description
[PB95-104527] p 840 N95-17356
IS-Lab: A tool for developing interactive programs for simulation and analysis. User's guide
[PB94-184710] p 840 N95-17410
Back-propagation neural networks in adaptive control of unknown nonlinear systems
[AD-A282414] p 858 N95-17458
Frequency domain analysis for nonlinear electronic circuits
[PB94-201365] p 767 N95-17469
Demonstration of the Dynamic Flowgraph Methodology using the Titan 2 Space Launch Vehicle Digital Flight Control System
[NASA-CR-197517] p 675 N95-17493
Thermal effects in end-heated laser rods: A time-dependent model and diagnostic
[AD-A282007] p 778 N95-17500
Applying STEP principles to product models in high energy physics research
[PB94-197704] p 880 N95-17503
OOD/OOP experience in the Science Operations Center part of the ground system for X ray Timing Explorer mission p 675 N95-17565
Taking advantage of ground data systems attributes to achieve quality results in testing software p 699 N95-17570
Evaluating modeling tools for the EDOS p 700 N95-17572
Galileo spacecraft modeling for orbital operations p 700 N95-17574
Test/score/report: Simulation techniques for automating the test process p 675 N95-17581
Mobility measurement and computer simulation at specific sites in polystyrene solutions and gels
[AD-A281214] p 747 N95-17685
A three dimensional mesoscale atmospheric simulation system for use in various mobile battlefield environments. Phase 2: Transition to an operational forecast system
[AD-A281223] p 802 N95-17686
Study of simulation in microgravity environment
[PB95-104261] p 750 N95-17730
Computer modeling of organic aerogels, 93-SR-062
[DE94-016485] p 722 N95-17745
Low-speed surface pressure and boundary layer measurement data for the NLR 7301 airfoil section with trailing edge flap p 658 N95-17855
Data from the GARTEur (AD) Action Group 02 airfoil CAST 7/DOA1 experiments p 659 N95-17856
OAT15A airfoil data p 659 N95-17857
A supercritical airfoil experiment p 659 N95-17858
Two-dimensional high-lift airfoil data for CFD code validation p 659 N95-17859

COMPUTERS
The IUE Science Operations Ground System p 674 N95-17255
Reviews of computing technology: Software overview
[DE94-013662] p 841 N95-17515

CONCENTRATORS
Conceptual design study of a solar concentrator/support structure: A three dimensional finite element model p 718 N95-16342
Prediction of the response of a polyimide concentrator for solar thermal propulsion p 719 N95-16343

CONCURRENT ENGINEERING
Automation support for concurrent software engineering
[AD-A281372] p 834 N95-16153
WAVES VHDL interface
[AD-A285208] p 764 N95-16516
Groupware system for multidisciplinary participation
[AD-A282525] p 850 N95-17374
Re-engineering the mission life cycle with ABC and IDEF p 706 N95-17606
Concurrent engineering: Spacecraft and mission operations system design p 708 N95-17614

CONCURRENT PROCESSING
The complexity of PDL with interleaving
[AD-A281044] p 836 N95-16452

CONDENSING
Nonpowered instant water heater
[AD-A285459] p 783 N95-17725

CONDUCTING POLYMERS
Fundamental studies of polyphosphazene and polysiloxane polyelectrolytes for electrochemical devices
[AD-A281339] p 739 N95-16013
Anionically-conductive ultrathin film composite membranes
[AD-A284944] p 723 N95-16041
Electrochemical properties of lithium ion conducting solid polymer electrolytes
[AD-A281875] p 742 N95-16434
Performance evaluation of polyaniline as an active material for electrochemical capacitors
[DE94-016283] p 765 N95-16920
Conducting polymers as corrosion resistant coatings
[DE94-018265] p 748 N95-17892

CONDUCTIVE HEAT TRANSFER
Design of thermocouple probes for measurement of rocket exhaust plume temperatures
[AD-A285423] p 774 N95-16247
Surface heat transfer in a channel with porous insert p 650 N95-16255
Thermal characteristics and heat transfer in an electrothermal light gas gun
[AD-A281980] p 892 N95-17442

CONDUCTIVITY
Charge transfer processes on liquid/liquid interfaces: The status in 1994
[AD-A285067] p 729 N95-16635

CONDUCTORS
Self-assembly of low-dimensional conductors on Au(111) surfaces
[AD-A280936] p 734 N95-16505
Snapshots of crystal growth: Nanoclusters of organic conductors on Au(111) surfaces
[AD-A280976] p 897 N95-16508

CONES
Normalization and prediction of geotechnical properties using the Cone Penetrometer Test (CPT)
[AD-A285193] p 799 N95-16872

CONFERENCES
Proceedings of the Workshop on Characterization of Molecular Assemblies
[DE94-753477] p 871 N95-15956
ISMCR 1994: Topical Workshop on Virtual Reality. Proceedings of the Fourth International Symposium on Measurement and Control in Robotics
[NASA-CP-10163] p 851 N95-15972
Presidential leadership in the development of the US space program
[NASA-TM-110107] p 904 N95-16007
Second International Working Conference on Cooperating Knowledge Based Systems. Volume 1
[AD-A281347] p 908 N95-16014
First NASA Workshop on Wiring for Space Applications
[NASA-CP-10145] p 711 N95-16044
Papers presented at the Tenth Topical Conference on High-Temperature Plasma Diagnostics
[DE94-015854] p 888 N95-16063
BEEM 94. The Fifth Annual Workshop on Ballistic Electron Emission Microscopy
[AD-A281522] p 872 N95-16098
Computational vision based on neurobiology
[AD-A284472] p 819 N95-16135
The Fifth International Congress on the History of Oceanography
[AD-A281507] p 805 N95-16168
The 1993 JANNAF Propulsion Meeting, volume 1
[CPIA-PUBL-602-VOL-1] p 713 N95-16312
US-Russian Workshop on Computer Synthesis of Structure and Properties of Advanced Composites
[AD-A281647] p 723 N95-16397
Proceedings of the International Conference on Parallel Architectures and Compilation Techniques
[AD-A285258] p 849 N95-16529
Proceedings of the 12th Annual Space Surveillance Workshop, volume 1
[AD-A285265] p 672 N95-16530

Proceedings of the Neural Network Workshop for the Hanford Community
[DE94-014567] p 856 N95-16609
Sixth Copper Mountain Conference on Multigrid Methods
[DE94-014595] p 862 N95-16611
Proceedings of the 12th Space Surveillance Workshop, volume 2
[AD-A285115] p 672 N95-16842
Workshop on Formal Models for Intelligent Control
[AD-A281399] p 857 N95-16864
Third International Symposium on Space Mission Operations and Ground Data Systems, part 1
[NASA-CP-3281-PT-1] p 676 N95-17179
Fifth International Conference on Hyperbolic Problems: Theory, Numerics, Applications
[AD-A283078] p 863 N95-17333
Beams 92: Proceedings
[DE94-014784] p 880 N95-17475
AINSE Plasma Science and Technology Conference and Elizabeth and Frederick White Workshop on Fundamental Problems in the Physics of Magnetically Confined Plasmas: Conference handbook
[DE94-622051] p 892 N95-17517
Third International Symposium on Space Mission Operations and Ground Data Systems, part 2
[NASA-CP-3281-PT-2] p 691 N95-17531
Abstracts and program Proceedings of the 1994 Meeting of the International Society for Ecological Modelling North American Chapter
[DE94-016456] p 796 N95-17636
Proceedings of the First National Conference on Climate Change and Water Resources Management
[AD-A281172] p 796 N95-17684
Workshop on Characterizing Diamond Films, 3
[PB94-187663] p 747 N95-17722

CONFIGURATION MANAGEMENT
Automation support for concurrent software engineering
[AD-A281372] p 834 N95-16153
Procedure calls are the assembly language of software interconnection: Connectors deserve first-class status
[AD-A281026] p 835 N95-16446

CONFINEMENT
AINSE Plasma Science and Technology Conference and Elizabeth and Frederick White Workshop on Fundamental Problems in the Physics of Magnetically Confined Plasmas: Conference handbook
[DE94-622051] p 892 N95-17517
Global confinement analysis
[DE94-016820] p 893 N95-17644
ITER design: Physics basis for size, confinement capability power levels and burn control
[DE94-018041] p 893 N95-17674

CONFORMAL MAPPING
Optimum aerodynamic design via boundary control
p 667 N95-16565

CONGESTION
Robust routing in dynamic networks, part 2
[AD-A282396] p 844 N95-16061

CONGRESSIONAL REPORTS
NAFTA literature at the International Trade Commission library p 905 N95-15922

CONJUNCTIVA
Subset-selectivity and distractor matching in visual conjunction search
[AD-A285137] p 827 N95-16615

CONSERVATION EQUATIONS
Application of the space-time conservation element and solution element method to shock-tube problem
[NASA-TM-106806] p 772 N95-16903
FEM3C, an improved three-dimensional heavy-gas dispersion model: User's manual
[DE94-014731] p 797 N95-17922

CONSERVATION LAWS
New developments in the method of space-time conservation element and solution element-applications to two-dimensional time-marching problems
[NASA-TM-106758] p 862 N95-16885
Fifth International Conference on Hyperbolic Problems: Theory, Numerics, Applications
[AD-A283078] p 863 N95-17333
Report on the 5th International Conference on Nonlinear Hyperbolic Problems
[AD-A283077] p 864 N95-17713

CONSISTENCY
Composite-model view of the ll-bar(gamma)(gamma) events at LEP
[DE94-753312] p 877 N95-17520

CONSOLES
XPVM: A graphical console and monitor for PVM
[DE94-018050] p 842 N95-17678

CONSOLIDATION
Climatological targets for Mars Pathfinder
p 922 N95-16208

CONSTRAINTS
ICONF: An incremental constraint facility in a feature modelling system
[PB94-197654] p 837 N95-16605

CONSTRUCTION
Houston, I think we've got a satellite
[NASA-TM-109987] p 709 N95-16941
A high resolution liquid xenon imaging telescope for 0.3-10 MeV gamma-ray astrophysics: Construction and initial balloon flights
[NASA-CR-197556] p 916 N95-17528

CONTACTORS
Extended test of a xenon hollow cathode for a space plasma contactor
[NASA-CR-195402] p 720 N95-17265

CONTAMINANTS
Novel mass spectrometric instrument for gaseous and particulate characterization and monitoring
[DE94-014168] p 795 N95-16213
South Florida environmental quality. National Status and Trends Program for marine environmental quality
[PB94-173408] p 796 N95-17363
Bicarbonate of soda blasting technology for aircraft wheel depainting
[PB94-193323] p 654 N95-17466

CONTAMINATION
Space Shuttle reaction control system thruster metal nitrate removal and characterization
p 716 N95-16332
Elemental impurity analysis of mercuric iodide by ICP/MS
[DE94-013553] p 896 N95-16359
The analysis and minimization of oxygen contamination in the powder processing of molybdenum disilicide
[DE94-014234] p 735 N95-16540
Synthesis of pure RDX
[DE94-014356] p 749 N95-16542
Two phase liquid helium flow testing to simulate the operation of a cryocondensation pump in the D3-D tokamak
[DE94-018345] p 893 N95-17896

CONTEXT FREE LANGUAGES
Parallel parsing
[PB94-191392] p 850 N95-17138

CONTINUITY (MATHEMATICS)
Multigrid techniques for nonlinear eigenvalue probems: Solutions of a nonlinear Schroedinger eigenvalue problem in 2D and 3D
[NASA-CR-194999] p 862 N95-16896

CONTINUOUS RADIATION
Online diagnoses of high current-density beams
[DE94-014420] p 879 N95-16217

CONTINUOUS WAVE LASERS
Electric-optic resonant phase modulator
[NASA-CASE-NPO-18702-1-CU] p 883 N95-15960
Rare earth ion doped CW cascade fiber laser
[AD-D016370] p 779 N95-17698

CONTINUUMS
User-defined subroutine for implementation of special finite elements in ABAQUS for the analysis of adhesive joints
[AD-A282431] p 788 N95-17510

CONTOURS
An approach to aerodynamic characteristics of low radar cross-section fuselages p 649 N95-16251
Cellular automata for contour dynamics
[PB94-197613] p 865 N95-17526

CONTRACT MANAGEMENT
NASA contract mangagement: Improving the use of DCAA's auditing services. Report to the Chairman, Committee on Government Operations, House of Representatives
[GAO/NSIAD-94-229] p 914 N95-15962

CONTRACTION
Intramuscular pressure: A better tool than EMG to optimize exercise for long-duration space flight
p 809 N95-16744

CONTRACTORS
NASA contract mangagement: Improving the use of DCAA's auditing services. Report to the Chairman, Committee on Government Operations, House of Representatives
[GAO/NSIAD-94-229] p 914 N95-15962

CONTROL
A General Mission Independent Simulator (GMIS) and Simulator Control Program (SCP) p 701 N95-17580
ITER design: Physics basis for size, confinement capability power levels and burn control
[DE94-018041] p 893 N95-17674

CONTROL BOARDS
High performance hardware and software for pattern recognition and image processing
[AD-A284264] p 839 N95-17172
Multilayer microelectronic photomultiplier device with a stacked series of dynode and insulating layers
[AD-D016377] p 767 N95-17478

CONTROL EQUIPMENT
Configurable technology development for reusable control and monitor ground systems
p 675 N95-17589

CONTROL SIMULATION
An object-oriented graphical user interface for a reusable rocket engine intelligent control system
[NASA-TM-106750] p 721 N95-17274
Configurable technology development for reusable control and monitor ground systems
p 675 N95-17589

CONTROL SURFACES
Non-intrusive missile control surface monitor system
[AD-A285356] p 883 N95-15954
Active load control during rolling maneuvers --- performed in the Langley Transonic Dynamics Tunnel
[NASA-TP-3455] p 669 N95-17397

CONTROL SYSTEMS DESIGN
Sensor fault detection and diagnosis simulation of a helicopter engine in an intelligent control framework
[NASA-TM-106784] p 669 N95-15970
Adaptive control of nonlinear flexible systems
[AD-A281337] p 855 N95-16011
Robust routing in dynamic networks, part 2
[AD-A282396] p 844 N95-16061
An improved position/force control of manipulators
p 653 N95-16280
Space Shuttle reaction control system thruster metal nitrate removal and characterization
p 716 N95-16332
Matlab as a robust control design tool
p 849 N95-16474
Experimental validation of an integrated controls-structures design methodology for a class of flexible space structures
[NASA-TP-3462] p 709 N95-16857
Workshop on Formal Models for Intelligent Control
[AD-A281399] p 857 N95-16864
Qualitative vision and action
[AD-A282697] p 831 N95-16966
Decentralized sliding mode control of nonlinear flexible robots
[DE94-013790] p 782 N95-17366
Breaking down barriers in cooperative fault management: Temporal and functional information displays
[NASA-CR-197450] p 857 N95-17383
Aircraft and sub-system certification by piloted simulation
[AGARD-AR-278] p 671 N95-17388
Cooperative control theory and integrated flight and propulsion control
[NASA-CR-197493] p 671 N95-17404
Hidden Markov model for control strategy learning
[AD-A282846] p 865 N95-17429
Towards a human operator model of the navigator
[PB94-197985] p 831 N95-17468
Standard protocol stack for mission control
p 704 N95-17593
Microgravity isolation system design: A case study
[NASA-TM-106804] p 654 N95-17657

CONTROL THEORY
Digital adaptive and optimal control of distributed systems
[AD-A285352] p 851 N95-15952
Simulation of the coupled multi-spacecraft control testbed at the Marshall Space Flight Center
p 849 N95-16475
Servo control using switches for discrete positional feedback
[AD-A284747] p 856 N95-16550
Optimum aerodynamic design via boundary control
p 667 N95-16565
Decentralized sliding mode control of nonlinear flexible robots
[DE94-013790] p 782 N95-17366
Cooperative control theory and integrated flight and propulsion control
[NASA-CR-197493] p 671 N95-17404
Towards a human operator model of the navigator
[PB94-197985] p 831 N95-17468
Repeatability in redundant manipulator systems
[AD-A282957] p 782 N95-17621

CONTROLLERS
Space Shuttle reaction control system thruster metal nitrate removal and characterization
p 716 N95-16332
MAGENCO: A map generalization controller for Arc/Info
[DE94-013440] p 835 N95-16358
Study of simulation in microgravity environment
[PB95-104261] p 750 N95-17730
Overview of space power electronic's technology under the CSTI High Capacity Power Program
[NASA-TM-110110] p 883 N95-17933

CONVECTION
Large-eddy simulation of cumulus convection
[PB94-191368] p 800 N95-16290
Sensitivity analysis of numerically-simulated convective storms using direct and adjoint methods
[DE94-013399] p 800 N95-16398
CONVECTION CLOUDS
Sensitivity analysis of numerically-simulated convective storms using direct and adjoint methods
[DE94-013399] p 800 N95-16398
CONVECTION-DIFFUSION EQUATION
On bi-grid local mode analysis of solution techniques for 3-D Euler and Navier-Stokes equations
[NASA-TM-106749] p 771 N95-16855
New developments in the method of space-time conservation element and solution element-applications to two-dimensional time-marching problems
[NASA-TM-106758] p 862 N95-16885
CONVECTIVE FLOW
Surface heat transfer in a channel with porous insert
p 650 N95-16255
CONVECTIVE HEAT TRANSFER
Thermal characteristics and heat transfer in an electrothermal light gas gun
[AD-A281980] p 892 N95-17442
CONVERGENCE
Global subjectivity of submersions via contractibility of the fibers
[AD-A284961] p 860 N95-16128
Validation of recipes for the recovery of stresses and derivatives by a computer-based approach
[AD-A282712] p 861 N95-16379
User-defined subroutine for implementation of special finite elements in ABAQUS for the analysis of adhesive joints
[AD-A282431] p 788 N95-17510
CONVERGENT NOZZLES
Single-engine tail interference model
p 663 N95-17879
COOLING
Increased skin blood flow and enhanced heat loss in humans after niacin ingestion
[AD-A281124] p 821 N95-16809
COOLING FLOWS (ASTROPHYSICS)
The mass and dynamics of cD clusters with cooling flows. 1: ROSAT observations of A 496
[NASA-CR-197534] p 915 N95-17495
COOLING SYSTEMS
Thermal control systems for low-temperature heat rejection on a lunar base
[NASA-CR-197486] p 830 N95-16418
COORDINATE TRANSFORMATIONS
Log-polar optical coordinate transformation with applications for automatic pattern recognition
[AD-A281022] p 885 N95-16443
COORDINATES
Experimental investigation of turbulent separated-reattachment flow by using LDV
p 649 N95-16253
COORDINATION POLYMERS
X-ray crystal structure of a monomeric Tris(Arsino)Gallane, ((Me3Si)2As)3Ga)3Ga
[AD-A282343] p 900 N95-17171
COPOLYMERS
Synthesis and properties of soluble oligo- and polyphenylenes. A review
[AD-A281293] p 874 N95-16799
Surface composition of a series of dimethylsiloxane urea, urethane segmented copolymers studied by electron spectroscopy for chemical analysis
[AD-A282872] p 745 N95-17434
Chiral recognition in molecular and macromolecular pairs of liquid crystals of (2R, 3S)- and (2S, 3S)-2-fluoro-3-methylpentyl-4'-(11-vinyloxyundeca iphenyl-4-carboxylate diastereomers
[AD-A281770] p 878 N95-17692
COPPER
Sixth Copper Mountain Conference on Multigrid Methods
[DE94-014595] p 862 N95-16611
Small angle neutron scattering from nanocrystalline Pd and Cu compacted at elevated temperatures
[DE94-013865] p 876 N95-16962
Volatile CVD precursors based on copper alkoxides and mixed group IIA-copper alkoxides
[AD-D016380] p 732 N95-17479
Use of copper powder extinguishers on lithium fires
[AD-A283213] p 751 N95-17632
Beam characteristics of a large-bore copper laser with a radiatively cooled plasma
[DE94-015139] p 779 N95-17688
Underpotential deposition of Cu on Au(111): Implications of the HB model
[AD-A283028] p 902 N95-17711
COPPER ALLOYS
Experimental heat treatment of beryllium copper alloy
[AD-A282714] p 734 N95-16380
Non-Fermi liquid scaling in UPd(x)Cu(5-x)(x = 1,1.5)
[DE94-016072] p 896 N95-16389
COPPER COMPOUNDS
An X-Ray Photoelectron Spectroscopy (XPS) study of activated carbons impregnated with some organocopper complexes
[AD-A282721] p 727 N95-16384
AC susceptibility and critical current in the organic superconductor (kappa)-(ET)2Cu(NCS)2
[DE94-013997] p 900 N95-16946
COPPER OXIDES
The relationship of structure to superconductivity in the Pr-Ba-Cu-O system
[DE94-014231] p 897 N95-16510
Suppression of superconductivity in orthorhombic La(2-x)M(x)CuO4 (M = Ca,Sr)
[DE94-013963] p 901 N95-17350
CORIOLIS EFFECT
Catecholaminergic responses to stressful motion stimuli, scopolamine plus amphetamine, and dexamethasone
p 809 N95-16745
Dynamics of the G-excess illusion
p 815 N95-16771
CORNER FLOW
Numerical simulation of supersonic compression corners and hypersonic inlet flows using the RPLUS2D code
[NASA-TM-106580] p 654 N95-16038
CORONARY ARTERY DISEASE
Aviation epidemiology data register: Coronary angiography outcomes of civilian aviators flying US aircraft
[AD-A285191] p 820 N95-16405
CORRECTION
Wall-signature methods for high speed wind tunnel wall interference corrections p 650 N95-16257
CORRELATION
Surface matching for correlation of virtual models: Theory and application p 853 N95-15983
Log-(Chi(exp 2)) distribution of correlation times revisited
[AD-A281123] p 740 N95-16092
New methods for treatment of electron correlation and surface dynamics (FY91 AASERT)
[AD-A285177] p 727 N95-16144
Unusual initial and final state effects in quantum chromodynamics
[DE94-015341] p 903 N95-16604
Jet studies at CDF and DO collaborations
[DE94-015537] p 875 N95-16914
Correlation of finite element free vibration predictions using random vibration test data
[NASA-TM-106787] p 787 N95-17258
CORRELATION COEFFICIENTS
A new model for estimating total body water from bioelectrical resistance p 810 N95-16747
Direct comparison of two statistical methods for determination of evoked-potential thresholds
[AD-A285182] p 870 N95-16811
CORROSION
High-level waste borosilicate glass: A compendium of corrosion characteristics
[DE94-016636] p 739 N95-15943
Investigation into the susceptibility of corrosion resistant alloys to biocorrosion
[AD-A281066] p 736 N95-16793
Characterization of the corrosion behavior of the carbon steel liner in Hanford site single-shell tanks
[DE94-016475] p 737 N95-17637
Conducting polymers as corrosion resistant coatings
[DE94-018265] p 748 N95-17892
CORROSION PREVENTION
Conducting polymers as corrosion resistant coatings
[DE94-018265] p 748 N95-17892
CORROSION RESISTANCE
Investigation into the susceptibility of corrosion resistant alloys to biocorrosion
[AD-A281066] p 736 N95-16793
Corrosion inhibition in high temperature environment
[AD-D016372] p 738 N95-17699
Environmental effects on iron aluminide
[DE94-017900] p 739 N95-17747
Conducting polymers as corrosion resistant coatings
[DE94-018265] p 748 N95-17892
CORROSION TESTS
The use of electrochemistry and ellipsometry for identifying and evaluating corrosion on aircraft
[AD-A285276] p 734 N95-16370
The use of electrochemistry and ellipsometry for identifying and evaluating corrosion on aircraft
[AD-A285323] p 734 N95-16371
Characterization of the hydrogen induced cold cracking susceptibility at simulated weld zones in HSLA-100 steel
[PB94-174505] p 737 N95-17616
Environmental effects on iron aluminide
[DE94-017900] p 739 N95-17747
COSINE SERIES
A simplified Integer Cosine Transform and its application in image compression p 757 N95-17286
COSMIC DUST
Dust near luminous ultraviolet stars
[NASA-CR-197108] p 916 N95-16032
Voyager investigation of the cosmic diffuse background: Observations of rocket-studied locations with Voyager
[NASA-CR-197532] p 917 N95-17422
COSMIC RAYS
Kinetics model for initiation and promotion for describing tumor prevalence from HZE radiation
[NASA-TP-3479] p 820 N95-16412
Solar-geophysical data number 596, April 1994. Part 1: (Prompt reports). Data for March, February 1994, and late data
[PB94-183548] p 924 N95-17736
COSMOLOGY
Research in elementary particle physics
[DE94-019219] p 877 N95-17358
COST ANALYSIS
Liquid Cooled Heat Sink with Through Vias (LCHS)
[AD-A281450] p 902 N95-16075
PV CZ silicon manufacturing technology improvements
[DE94-011818] p 897 N95-16424
Towards cheaper control centers p 674 N95-17250
SCOS 2: ESA's new generation of mission control system p 674 N95-17253
Prospects for toroidal fusion reactors
[DE94-014020] p 891 N95-17367
Optical fiber sensors: Accelerating applications in Navy ships
[PB94-186848] p 887 N95-17441
Re-engineering the mission life cycle with ABC and IDEF p 706 N95-17606
COST EFFECTIVENESS
The National Resource Library for Science and Technology in Sweden: A Nordic model of cooperating technology libraries p 906 N95-15929
Information sources in science and technology in Finland p 906 N95-15930
NASA contract mangagement: Improving the use of DCAA's auditing services. Report to the Chairman, Committee on Government Operations, House of Representatives
[GAO/NSIAD-94-229] p 914 N95-15962
Plasma disruption modeling and simulation
[DE94-015095] p 889 N95-16307
PV CZ silicon manufacturing technology improvements
[DE94-011818] p 897 N95-16424
Optimum Design Methods for Aerodynamics
[AGARD-R-803] p 666 N95-16562
Review of the EUROPT Project AERO-0026
p 668 N95-16573
A comparison of steady-state ARIES and pulsed PULSAR tokamak power plants
[DE94-014441] p 891 N95-17155
Use of a multimission system for cost effective support of planetary science data processing
p 678 N95-17190
COST ESTIMATES
Software cost and schedule estimating: A process improvement initiative
[AD-A280915] p 836 N95-16503
Mars Pathfinder mission operations concepts
p 686 N95-17229
Prospects for toroidal fusion reactors
[DE94-014020] p 891 N95-17367
Automated Estimating System (AES) version 6.0: User's manual
[DE94-013636] p 841 N95-17514
Status of the US stellarator reactor study
[DE94-018693] p 893 N95-17907
COST REDUCTION
Applying Virtual Reality to commercial Edutainment
p 854 N95-15989
PV CZ silicon manufacturing technology improvements
[DE94-011818] p 897 N95-16424
Optimization of adaptive intraply hybrid fiber composites with reliability considerations
[NASA-TM-106632] p 787 N95-16911
Economical ground data delivery p 679 N95-17194
VLSI technology for smaller, cheaper, faster return link systems p 681 N95-17206
Operations automation p 687 N95-17236
Towards cheaper control centers p 674 N95-17250
Ground Station support for small scientific satellites
p 695 N95-17549
Advanced ground station architecture
p 674 N95-17556
Transportable Payload Operations Control Center reusable software: Building blocks for quality ground data systems p 703 N95-17587

The development of a solid-state hydrogen sensor for rocket engine leakage detection
[NASA-CR-197567] p 776 N95-17895
COULOMB COLLISIONS
Effect of Coulomb collisions, Landau damping and particle trapping on linear and nonlinear ion acoustic waves
[AD-A282009] p 869 N95-17449
COUNTERMEASURES
Comparison of saline and fludrocortisone as fluid-loading countermeasures following exposure to simulated microgravity p 808 N95-16742
The value of the 4-day headdown bedrest model for screening countermeasures p 817 N95-16782
COUPLED MODES
Transverse mode coupling instability with a double RF system
[DE94-017972] p 761 N95-17672
COUPLING
Radar observations of field-aligned plasma propagations associated with NASA's PMG experiment
[AD-A285218] p 798 N95-16521
COUPLING COEFFICIENTS
Extraction of high quality potential surfaces from laboratory data
[AD-A285071] p 903 N95-16489
Slow wave vane structure with elliptical cross-section slots, an analysis
[NASA-CR-195352] p 755 N95-16886
CRACK GEOMETRY
Mixed-mode I/III fracture toughness of a ferritic/martensitic stainless steel
[DE94-014492] p 736 N95-17159
CRACK INITIATION
Ductile fracture and failure criteria of structural steels
[AD-A280754] p 733 N95-16104
CRACK OPENING DISPLACEMENT
Effects of prior ductile tearing on cleavage fracture toughness in the transition region
[AD-A281298] p 786 N95-16785
Mechanisms of mechanical fatigue in ceramics
[DE94-016040] p 747 N95-17719
CRACK PROPAGATION
Guide to ASIAC computer programs
[AD-A285354] p 784 N95-15953
Global and near tip response of cracked solid propellant p 715 N95-16325
Experimental application of methodologies to quantify the effect of constraint on JC for a 3-D flaw geometry
[AD-A285309] p 735 N95-16531
Effects of prior ductile tearing on cleavage fracture toughness in the transition region
[AD-A281298] p 786 N95-16785
Multi-lab comparison on R-curve methodologies: Alloy 2024-T3
[NASA-CR-195004] p 736 N95-16860
The mechanical property data base from an Air Force/industry cooperative test program on high temperature aluminum alloys
[AD-A282911] p 737 N95-17398
Mechanisms of mechanical fatigue in ceramics
[DE94-016040] p 747 N95-17719
CRACK TIPS
Global and near tip response of cracked solid propellant p 715 N95-16325
Experimental application of methodologies to quantify the effect of constraint on JC for a 3-D flaw geometry
[AD-A285309] p 735 N95-16531
CRACKING (FRACTURING)
Ductile fracture and failure criteria of structural steels
[AD-A280754] p 733 N95-16104
Global and near tip response of cracked solid propellant p 715 N95-16325
Effects of prior ductile tearing on cleavage fracture toughness in the transition region
[AD-A281298] p 786 N95-16785
Mixed-mode I/III fracture toughness of a ferritic/martensitic stainless steel
[DE94-014492] p 736 N95-17159
Eddy current for detecting second layer cracks under installed fasteners
[AD-A282412] p 784 N95-17507
Modeling of stress/strain behavior of fiber-reinforced ceramic matrix composites including stress redistribution
[NASA-TM-106789] p 725 N95-17659
Mechanisms of mechanical fatigue in ceramics
[DE94-016040] p 747 N95-17719
CRACKS
Structural analysis of solid-propellant rocket motors with and without flaws p 720 N95-16348
Life prediction for bridged fatigue cracks
[DE94-016000] p 724 N95-16930
Eddy current for detecting second layer cracks under installed fasteners
[AD-A282412] p 784 N95-17507
CRASH LANDING
Aircraft accident report: Stall and loss of control on final approach, Atlantic Coast Airlines, Inc./United Express Flight 6291 Jetstream 4101, N304UE Columbus, OH, 7 January 1994
[PB94-910409] p 665 N95-17646
CRASHES
A correlative investigation of simulated occupant motion and accident report in a helicopter crash
[AD-A285190] p 664 N95-16404
CRATERS
Cerberus Plains: A most excellent Pathfinder landing site p 921 N95-16198
CREEP PROPERTIES
Giant flux creep through the surface barriers and the irreversibility line in high T(sub c) superconductors
[DE94-013991] p 766 N95-16945
Multiphase ceramics for mechanical and structural reliability at low and elevated temperatures
[AD-A285497] p 746 N95-17438
Fundamental concepts relating local atomic arrangements, deformation, and fracture of intermetallic alloys
[AD-A282971] p 738 N95-17664
Mechanisms of mechanical fatigue in ceramics
[DE94-016040] p 747 N95-17719
CREEP RUPTURE STRENGTH
Effect of heat treatment temperature on creep-rupture properties of Fe3Al-based alloys
[DE94-018054] p 738 N95-17679
CREEP STRENGTH
Fundamental concepts relating local atomic arrangements, deformation, and fracture of intermetallic alloys
[AD-A282971] p 738 N95-17664
CREW PROCEDURES (INFLIGHT)
Federal aviation regulations, part 91. General operating and flight rules. Change 5
[PB94-194883] p 665 N95-17476
Development of use of an Operational Procedure Information System (OPIS) for future space missions p 692 N95-17536
CREW WORKSTATIONS
Industry review of a crew-centered cockpit design process and toolset
[AD-A282966] p 669 N95-17661
CRITICAL FREQUENCIES
Na-22 decay gamma rays from classical novae
[NASA-CR-197454] p 924 N95-16383
Caffeine's influence on critical frequency thresholds
[AD-A282005] p 828 N95-17447
CROP GROWTH
Regulation of nitrogen uptake and assimilation: Effects of nitrogen source and root-zone and aerial environment on growth and productivity of soybean
[NASA-CR-197098] p 807 N95-15961
CROSS CORRELATION
Space VLBI telecommunication characteristics, protection criteria, and frequency sharing p 756 N95-17282
CROSS COUPLING
Synthesis of polyphenylenes and polynaphthalenes by thermolysis of enediyness and dialkynylbenzenes
[AD-A281294] p 743 N95-16783
CROSS FLOW
Nonlinear instability of a uni-directional transversely sheared mean flow
[NASA-TM-106779] p 769 N95-15969
Wall-signature methods for high speed wind tunnel wall interference corrections p 650 N95-16257
In-flight imaging of transverse gas jets injected into transonic and supersonic crossflows: Design and development
[NASA-CR-186031] p 772 N95-17418
CROSS SECTIONS
Strong WW scattering at photon linear colliders
[DE94-018183] p 878 N95-17720
Physics at high energy photon photon colliders
[DE94-018191] p 881 N95-17888
New shower maximum trigger for electrons and photons at CDF
[DE94-018376] p 878 N95-17899
Measurements of x ray spectral flux and intensity distribution of APS/CHESS undulator radiation
[DE94-018384] p 882 N95-17901
Search for first and second generation leptoquarks at D(null)
[DE94-018992] p 879 N95-17932
CROSSINGS
Geosynchronous orbit magnetopause crossings
[DE94-014817] p 798 N95-16537
Closed orbit distortion from parasitic collisions in PEP-2
[DE94-018203] p 882 N95-17890
CROSSLINKING
Detection of crosslink formation by 2 + 2 photocycloaddition in poly (vinyl cinnamate) by C-13 solid-state NMR
[AD-A281955] p 741 N95-16409
CRYOGENIC COOLING
Thermocryogenic buckling and stress analyses of a partially filled cryogenic tank subjected to cylindrical strip heating
[NASA-TM-4579] p 788 N95-17417
CRYOGENIC FLUID STORAGE
Thermocryogenic buckling and stress analyses of a partially filled cryogenic tank subjected to cylindrical strip heating
[NASA-TM-4579] p 788 N95-17417
CRYOGENIC FLUIDS
A Lifting Ball Valve for cryogenic fluid applications p 720 N95-16349
CRYOGENIC TEMPERATURE
Performance characterization of photonic links in cryogenic environments for advanced signal processing applications
[DE94-015561] p 765 N95-16915
CRYOGENICS
Cryogenic foil bearing turbopumps p 716 N95-16331
Performance characterization of photonic links in cryogenic environments for advanced signal processing applications
[DE94-015561] p 765 N95-16915
CRYSTAL DEFECTS
The role of point defects and defect complexes in silicon device processing: Summary report and papers
[DE94-011873] p 791 N95-15944
Workshop on Epitaxy, Interfaces, Defects and Processing of Electronic and Photonic Materials
[AD-A281595] p 894 N95-16111
Development of high-efficiency, thin-film CdTe solar cells
[DE94-011885] p 794 N95-16940
Evaluation of the quality of sapphire using x-ray rocking curves and double-crystal x-ray topography
[AD-A282905] p 901 N95-17620
Precision machining and polishing of scintillating crystals for large calorimeters and hodoscopes
[DE94-012060] p 751 N95-17738
CRYSTAL DISLOCATIONS
Columnar defect pinning in untwinned single crystal YBa2Cu2O7
[DE94-013962] p 901 N95-17349
CRYSTAL FIELD THEORY
Inelastic neutron scattering and antiferromagnetic fluctuations in high temperature superconductors
[DE94-623269] p 871 N95-16059
CRYSTAL GROWTH
Single crystal films and waveguides of organic materials: Preparation and nonlinear optical properties
[AD-A284471] p 895 N95-16134
PV CZ silicon manufacturing technology improvements
[DE94-011818] p 897 N95-16424
Atomic force microscopy of the electrochemical nucleation and growth of molecular crystals
[AD-A281024] p 897 N95-16445
Self-assembly of low-dimensional conductors on Au(111) surfaces
[AD-A280936] p 734 N95-16505
Snapshots of crystal growth: Nanoclusters of organic conductors on Au(111) surfaces
[AD-A280976] p 897 N95-16508
Growth, characterization and applications of beta-barium borate and related crystals
[AD-A281047] p 898 N95-16623
A high average power electro-optic switch using KTP
[DE94-016416] p 765 N95-16925
Asymptotic behavior in grain growth
[DE94-014452] p 900 N95-17156
Multiphase ceramics for mechanical and structural reliability at low and elevated temperatures
[AD-A285497] p 746 N95-17438
CRYSTAL LATTICES
X-ray crystal structure of a monomeric Tris(Arsino)Gallane, ((Me3Si)2As)3Ga)3Ga
[AD-A282343] p 900 N95-17171
CRYSTAL OPTICS
SDIO/IST ultrashort wavelength. Mossbauer and gamma ray studies for grasers
[AD-A283091] p 778 N95-17337
CRYSTAL STRUCTURE
Method for intrinsically doped III-A and V-A compounds and products thereof
[AD-D016324] p 896 N95-16399
Theoretical study of cathode surfaces and high-temperature superconductors
[NASA-CR-195407] p 898 N95-16598

Synthesis and characterization of neopentyl indium compounds: X-ray crystal structures of ((Me3CCH2)2InAs(SiMe3)2)2 and ((Me3CCH2)2InAs(SiMe3)2In (CH2CMe3)2Cl)
[AD-A282766] p 900 N95-17137
X-ray crystal structure of a monomeric Tris(Arsino)Gallane, ((Me3Si)2As)3Ga)3Ga
[AD-A282343] p 900 N95-17171
Possible superstructures of metallic ions in nonstoichiometric fullerites M(x) C(60)
[DE94-622052] p 901 N95-17518
Crystalline beams: The vertical zigzag
[DE94-017986] p 901 N95-17673

CRYSTAL SURFACES
An unexpected adsorption site exclusion process on Si(100)-(2x1)
[AD-A284950] p 894 N95-16043
Snapshots of crystal growth: Nanoclusters of organic conductors on Au(111) surfaces
[AD-A280976] p 897 N95-16508
Nitride semiconductors for ultraviolet detection
[AD-A280988] p 898 N95-16533
Precision machining and polishing of scintillating crystals for large calorimeters and hodoscopes
[DE94-012060] p 751 N95-17738
Thermal and laser conditioning of production and rapid-growth KDP and KD*P crystals
[DE94-013738] p 902 N95-17742

CRYSTALLINITY
Crystalline silicon processing
[DE94-016552] p 894 N95-15942
Proceedings of the Workshop on Characterization of Molecular Assemblies
[DE94-753477] p 871 N95-15956
Snapshots of crystal growth: Nanoclusters of organic conductors on Au(111) surfaces
[AD-A280976] p 897 N95-16508
Shock initiation of crystalline boron in oxygen and fluorine compounds
[AD-A284266] p 730 N95-16955
Crystalline beams: The vertical zigzag
[DE94-017986] p 901 N95-17673

CRYSTALS
Scintillation mechanism and radiation damage in Ce(x)La(1-x)F3 crystals
[DE94-015848] p 896 N95-16385
Structure of 4-methylpyridinium hydrogen sulfide
[NASA-TM-106778] p 731 N95-17387
Precision machining and polishing of scintillating crystals for large calorimeters and hodoscopes
[DE94-012060] p 751 N95-17738
Thermal and laser conditioning of production and rapid-growth KDP and KD*P crystals
[DE94-013738] p 902 N95-17742

CUBES (MATHEMATICS)
Simulation of arthroscopic surgery using MRI data
p 823 N95-15975

CULTURE TECHNIQUES
Cell culture and transplantation of the suprachiasmatic circadian pacemaker
[AD-A280977] p 821 N95-16481

CUMULUS CLOUDS
Large-eddy simulation of cumulus convection
[PB94-191368] p 800 N95-16290

CURIE TEMPERATURE
Relationships between ferroelectric 90 deg domain formation and electrical properties of chemically prepared Pb(Zr,Ti)O3 thin films
[DE94-015274] p 744 N95-16829

CURRENT DENSITY
Online diagnoses of high current-density beams
[DE94-014420] p 879 N95-16217
Processing, fabrication, characterization and device demonstration of high temperature superconducting ceramics
[AD-A285145] p 744 N95-16844
Performance evaluation of polyaniline as an active material for electrochemical capacitors
[DE94-016283] p 765 N95-16920
AC susceptibility and critical current in the organic superconductor (kappa)-(ET)2Cu(NCS)2
[DE94-013997] p 900 N95-16946
Aluminum-ferricyanide battery
[AD-D016338] p 766 N95-16948
Characteristics of multiple auroral inverted-V structures and the problem of magnetospheric plasma stratification
[DE94-622233] p 799 N95-17471
High current density sheet-like electron beam generator
[AD-A281975] p 880 N95-17499
Texture analysis of critical current density in Bi2Sr2CaCu2O(x) tapes
[DE94-018375] p 902 N95-17898

CURRENT DISTRIBUTION
ARCJET plasma modeling with experimental validation
[AD-A285234] p 889 N95-16243

CURRENT SHEETS
High current density sheet-like electron beam generator
[AD-A281975] p 880 N95-17499

CURVED PANELS
Shear buckling analysis of a hat-stiffened panel
[NASA-TM-4644] p 788 N95-17490

CUSHIONS
Apache helicopter seat cushion evaluation
[AD-A284300] p 831 N95-17484

CYANATES
AC susceptibility and critical current in the organic superconductor (kappa)-(ET)2Cu(NCS)2
[DE94-013997] p 900 N95-16946
Graphite-reinforced polycyanate composites for space and missile applications
[AD-A285509] p 725 N95-16970

CYCLES
Test results of superconducting AC magnets for magnetic refrigeration experiment
[DE94-018695] p 751 N95-17909

CYCLIC COMPOUNDS
Regiochemistry of polysilanes prepared by ring opening polymerization
[AD-A281041] p 742 N95-16450
Metastability in molecules
[AD-A285223] p 874 N95-16523

CYCLIC HYDROCARBONS
Radical cations of quadricyclane and norbornadiene in polar ZSM-5 matrices: Radical cation photochemical transformations without photons
[DE94-014007] p 728 N95-16485

CYCLIC LOADS
Computer modelling of cyclic deformation of high-temperature materials
[AD-A285212] p 735 N95-16519
Life prediction for bridged fatigue cracks
[DE94-016000] p 724 N95-16930

CYCLOGENESIS
Impact of physical processes on maritime frontogenesis
[AD-A283105] p 801 N95-17339

CYCLOTRON FREQUENCY
Investigation of the effect of Alfven resonance absorption on fast wave current drive in ITER
[PB95-104352] p 894 N95-17929

CYCLOTRON RESONANCE
Production of high proton fractions from ECR sources by plasma modification
[DE94-018381] p 893 N95-17900

CYCLOTRON RESONANCE DEVICES
Nonstationary theory of mode competition in gyrotrons with allowance for inhomogeneity of the guiding magnetic field
[PB94-197621] p 869 N95-17467

CYGNUS CONSTELLATION
The Mg 2 lines as diagnostic of PMS nature in Herbig Ae/Be stars
[NASA-CR-197518] p 915 N95-17494

CYLINDRICAL BODIES
Field configuration of beam excited modes in the Advanced Photon Source (APS) storage ring waveguides
[DE94-015096] p 880 N95-16308
Slow wave vane structure with elliptical cross-section slots, an analysis
[NASA-CR-195352] p 755 N95-16886
Wind tunnel investigations of the appearance of shocks in the windward region of bodies with circular cross section at angle of attack p 661 N95-17866
Force and pressure data of an ogive-nosed slender body at high angles of attack and different Reynolds numbers
p 661 N95-17868
Supersonic vortex flow around a missile body
p 661 N95-17870

CYLINDRICAL SHELLS
Heat transfer measurements for Stirling machine cylinders
[NASA-CR-197128] p 791 N95-15963
A consistent large deflection theory of composite sandwich shells p 650 N95-16259
Development of strength analysis methods and design model for aircraft constructions in Kazan Aviation Institute p 651 N95-16264

CYLINDRICAL TANKS
Thermocryogenic buckling and stress analyses of a partially filled cryogenic tank subjected to cylindrical strip heating
[NASA-TM-4579] p 788 N95-17417

CYTOLOGY
Extracellular ionic composition alters kinetics of vesicular release of catecholamines and quantal size during exocytosis at adrenal medullary cells
[AD-A281613] p 818 N95-16112

D

DAMAGE
Orbiter Kapton wire operational requirements and experience p 711 N95-16046
WSTF electrical arc projects p 711 N95-16047
Kapton pyrolysis on Space Station Freedom's solar array flexible current carrier p 712 N95-16049
Debris/ice/TPS assessment and integrated photographic analysis of Shuttle Mission STS-64 on 9 August 1994
[NASA-TM-109206] p 676 N95-17262

DAMAGE ASSESSMENT
Whole-body vibration assessment of the M1070 heavy equipment transporter, volume 1
[AD-A285199] p 829 N95-16147
A review of transmission diagnostics research at NASA Lewis Research Center
[ARL-TR-599] p 781 N95-16907
Optical fiber sensors: Accelerating applications in Navy ships
[PB94-186848] p 887 N95-17441

DAMPING
Transverse mode coupling instability with a double RF system
[DE94-017972] p 761 N95-17672

DATA ACQUISITION
The Technical Information Library: TIB
p 906 N95-15928
Information sources in science and technology in Finland p 906 N95-15930
Networked information: Management issues for the acquisitions librarian p 906 N95-15932
Department of Energy: Office of Scientific and Technical Information p 907 N95-15936
Using virtual reality for science mission planning: A Mars Pathfinder case p 673 N95-15978
Virtual environment application with partial gravity simulation p 854 N95-15988
Signal wave generator signals recorded by the Federal Outdoor Impact Laboratory's on-board Data Acquisition System
[PB94-186525] p 752 N95-16094
MODIS Technical Report Series. Volume 4: MODIS data access user's guide: Scan cube format
[NASA-TM-104594-VOL-4] p 837 N95-16587
Real-time data collection programs and source code for a commercial passive FTIR remote sensor
[AD-A284976] p 838 N95-16634
Evaluation of a new miniature temperature data logger: Herpetological review
[DE94-013561] p 774 N95-16804
An integrated knowledge acquisition and database management system
[AD-A285404] p 910 N95-16884
Characterization of multiport solid state imagers at megahertz data rates
[DE94-016095] p 765 N95-16932
Data acquisition and processing software for the Low Speed Wind Tunnel tests of the Jindivik auxiliary air intake
[AD-A285455] p 656 N95-17178
Multimission Telemetry Visualization (MTV) system: A mission applications project from JPL's Multimedia Communications Laboratory p 681 N95-17205
International Space Station Alpha user payload operations concept p 685 N95-17227
The Telecommunications and Data Acquisition Report
[NASA-CR-197249] p 755 N95-17279
Radio-planetary from tie from Phobos-2 VLBI data
p 756 N95-17283
Tracking the Galileo spacecraft with the DSCC Galileo Telemetry prototype p 708 N95-17292
Transportable Payload Operations Control Center reusable software: Building blocks for quality ground data systems p 703 N95-17587
Customizing the JPL Multimission Ground Data System: Lessons learned p 703 N95-17588
The NASA Mission Operations and Control Architecture Program p 706 N95-17603
Matrix evaluation of science objectives
p 707 N95-17610
Engineering design tools for wind diesel systems. Volume 7: Logistic package. Validation report
[PB95-104568] p 842 N95-17735

DATA BASE MANAGEMENT SYSTEMS
Risk-Based Data Management System design specifications and implementation plan for the Alaska Oil and Gas Conservation Commission; the Mississippi State Oil and Gas Board; the Montana Board of Oil and Gas Conservation; and the Nebraska Oil and Gas Conservation Commission, attachment B
[DE94-013189] p 908 N95-16282

An integrated knowledge acquisition and database management system
[AD-A285404] p 910 N95-16884
The PASS project
[DE94-016308] p 910 N95-16922
Data rearrangement and real-time computation
[AD-A282349] p 910 N95-17166
Directory of IAEA databases
[DE94-622696] p 912 N95-17472
An incremental database access method for autonomous interoperable databases
[NASA-CR-189384] p 912 N95-17652

DATA BASES
Bureau of the Census Center for International Research p 905 N95-15923
CINDOC, CSIC, and Spanish R and D p 906 N95-15927
Information sources in science and technology in Finland p 906 N95-15930
Adding tools to the open source toolbox: The Internet p 907 N95-15933
Collection development at the NOAA Central Library p 907 N95-15939
Student research projects, 1993
[AD-A284954] p 804 N95-16124
NSSDC data listing
[NASA-TM-109986] p 909 N95-16441
Radiation belt dynamic and quasi-static modeling based on CRRES data
[AD-A285282] p 916 N95-16600
A coastal hazards data base for the US Gulf Coast
[DE94-014573] p 805 N95-16610
Knowledge quality functions for rule discovery
[AD-A285513] p 910 N95-16971
ARACHNID: A prototype object-oriented database tool for distributed systems p 680 N95-17199
Autonomous mission planning and scheduling: Innovative, integrated, responsive p 686 N95-17234
Mini All-purpose Satellite Control Center (MASCC) p 674 N95-17257
Multivariate statistical analysis software technologies for astrophysical research involving large data bases
[NASA-CR-189393] p 911 N95-17325
Global climate change model natural climate variation: Paleoclimate data base, probabilities and astronomic predictors
[DE94-013956] p 796 N95-17348
Directory of IAEA databases
[DE94-622696] p 912 N95-17472
Automating testbed documentation and database access using World Wide Web (WWW) tools p 696 N95-17557
Engineering design tools for wind diesel systems. Volume 4: JODYMOD dynamic wind diesel simulation software package. Program documentation
[PB95-104535] p 841 N95-17628
DROLS: An introduction to searching (videorecording)
[AD-M000338] p 912 N95-17660
Engineering design tools for wind diesel systems. Volume 7: Logistic package. Validation report
[PB95-104568] p 842 N95-17735
A supercritical airfoil experiment p 659 N95-17858

DATA COMPRESSION
End-to-end communication test on variable length packet structures utilizing AOS testbed p 677 N95-17186
Fast computational scheme of image compression for 32-bit microprocessors p 678 N95-17192
Multiresolution representation and numerical algorithms: A brief review
[NASA-CR-194949] p 863 N95-17266
A simplified Integer Cosine Transform and its application in image compression p 757 N95-17286
Low-complexity wavelet filter design for image compression p 757 N95-17289
Analysis of compression techniques for Common Mapping Standard (CMS) raster data
[AD-A283396] p 791 N95-17625

DATA CONVERSION ROUTINES
A parser for the ISO 8211 data format
[AD-A281594] p 909 N95-16431

DATA CORRELATION
Using neural networks to correlate satellite imagery and ground-truth data
[AD-A285486] p 857 N95-16967
Data from the GARTEur (AD) Action Group 02 airfoil CAST 7/DOA1 experiments p 659 N95-17856

DATA LINKS
Spread spectrum applications in unmanned aerial vehicles
[AD-A281035] p 754 N95-16448
Data link level interconnection of remote Fiber Distributed Data Interface Local Area Networks (FDDI LANs) through the Critical Data Link (CDL)
[AD-A284307] p 755 N95-17173
Telecommunications end-to-end systems monitoring on TOPEX/Poseidon: Tools and techniques p 676 N95-17180
Attempt of automated space network operations at ETS-VI experimental data relay system p 677 N95-17184
The GRO remote terminal system p 678 N95-17188
Economical ground data delivery p 679 N95-17194
VLSI technology for smaller, cheaper, faster return link systems p 681 N95-17206
GRTS operations monitor/control system p 685 N95-17226
The SILEX experiment system operations p 674 N95-17251
Feedback system for remotely operated vehicles
[AD-D016409] p 858 N95-17465
Proposal for implementation of CCSDS standards for use with spacecraft engineering/housekeeping data p 705 N95-17600
EDOS operations concept and development approach p 708 N95-17613

DATA MANAGEMENT
Metadata database for automated oceanographic imagery
[AD-A284932] p 805 N95-16141
Data administration procedures
[AD-A282718] p 909 N95-16382
Third International Symposium on Space Mission Operations and Ground Data Systems, part 1
[NASA-CP-3281-PT-1] p 676 N95-17179
The development and operation of the international solar-terrestrial physics central data handling facility p 679 N95-17193
NASA Johnson Space Center Life Sciences Data System p 679 N95-17195
International Space Station Alpha user payload operations concept p 685 N95-17227
A mission planning concept and mission planning system for future manned space missions p 687 N95-17235
A distributed analysis and visualization system for model and observational data
[NASA-CR-189386] p 911 N95-17326
Development of a data reduction expert assistant
[NASA-CR-189385] p 911 N95-17328
An interactive environment for the analysis of large Earth observation and model data sets
[NASA-CR-189381] p 911 N95-17330
An agent-oriented approach to automated mission operations p 696 N95-17555
The CCSDS return all frames Space Link Extension service p 705 N95-17599
Proposal for implementation of CCSDS standards for use with spacecraft engineering/housekeeping data p 705 N95-17600
Multivariate statistical analysis software technologies for astrophysical research involving large data sets
[NASA-CR-197499] p 858 N95-17921

DATA PROCESSING
Analysis of plasma measurements for the Geotail mission
[NASA-CR-197020] p 888 N95-15941
Production asymmetries in x(sub F) and P(sub t)(exp 2) for D(+-) mesons
[DE94-015546] p 872 N95-16310
Proceedings of the Neural Network Workshop for the Hanford Community
[DE94-014567] p 856 N95-16609
Implementation of a real-time data processing system for radar bandwidth extrapolation and stretch
[AD-A281195] p 754 N95-16794
Measurement of the B(sub s) meson lifetime at CDF
[DE94-015381] p 875 N95-16868
Automation of reverse engineering process in aircraft modeling and related optimization problems
[NASA-CR-197109] p 668 N95-16899
The PASS project
[DE94-016308] p 910 N95-16922
Table-driven configuration and formatting of telemetry data in the Deep Space Network p 677 N95-17185
Overview on METEOSAT geometrical image data processing p 678 N95-17189
Use of a multimission system for cost effective support of planetary science data processing p 678 N95-17190
A second generation 50 Mbps VLSI level zero processing system prototype p 678 N95-17191
The development and operation of the international solar-terrestrial physics central data handling facility p 679 N95-17193
A processing centre for the CNES CE-GPS experimentation p 666 N95-17196
Telemetry distribution and processing for the second German Spacelab Mission D-2 p 681 N95-17207
Lessons learned supporting onboard solid-state recorders p 681 N95-17208
Experience with the EURECA Packet Telemetry and Packet Telecommand system p 682 N95-17209
Operations automation p 687 N95-17236
Designing an autonomous environment for mission critical operation of the EUVE satellite p 688 N95-17241
Mission operations data analysis tools for Mars Observer guidance and control p 689 N95-17244
Generic trending and analysis system p 689 N95-17245
The Pacor 2 expert system: A case-based reasoning approach to troubleshooting p 693 N95-17541
Development of a prototype real-time automated filter for operational deep space navigation p 694 N95-17545
Evaluation of NASA's end-to-end data systems using DSDS+ p 700 N95-17577
Configurable technology development for reusable control and monitor ground systems p 675 N95-17589
Architecture of a distributed multimission operations system p 706 N95-17605
Re-engineering the mission life cycle with ABC and IDEF p 706 N95-17606
A new systems engineering approach to streamlined science and mission operations for the Far Ultraviolet Spectroscopic Explorer (FUSE) p 707 N95-17611
Risk reduction methodologies and technologies for the Earth Observing System (EOS) Operations Center (EOC) p 707 N95-17612
EDOS operations concept and development approach p 708 N95-17613
OAT15A airfoil data p 659 N95-17857

DATA PROCESSING EQUIPMENT
A low-cost transportable ground station for capture and processing of direct broadcast EOS satellite data p 680 N95-17200
Test Telemetry And Command System (TTACS) p 680 N95-17202
Feedback system for remotely operated vehicles
[AD-D016409] p 858 N95-17465

DATA RECORDING
Lessons learned supporting onboard solid-state recorders p 681 N95-17208

DATA REDUCTION
SEPAC co-investigator support
[NASA-CR-196527] p 798 N95-15965
A comparison of signal-processing front ends for automatic speech recognition
[AD-A284962] p 752 N95-16129
NASA Marshall Space Flight Center Solar Observatory report, March - May 1994
[NASA-TM-108471] p 915 N95-16558
A distributed analysis and visualization system for model and observational data
[NASA-CR-189386] p 911 N95-17326
Development of a data reduction expert assistant
[NASA-CR-189385] p 911 N95-17328
Proposal for implementation of CCSDS standards for use with spacecraft engineering/housekeeping data p 705 N95-17600

DATA SMOOTHING
An analysis of smoothed particle hydrodynamics
[DE94-013817] p 788 N95-17439

DATA STORAGE
Knowledge quality functions for rule discovery
[AD-A285513] p 910 N95-16971
Data rearrangement and real-time computation
[AD-A282349] p 910 N95-17166
Lessons learned supporting onboard solid-state recorders p 681 N95-17208
Proposal for implementation of CCSDS standards for use with spacecraft engineering/housekeeping data p 705 N95-17600

DATA STRUCTURES
Extending programming by demonstration with hierarchical event histories
[AD-A281186] p 838 N95-16632
End-to-end communication test on variable length packet structures utilizing AOS testbed p 677 N95-17186
Towards a class library for mission planning p 686 N95-17233
Flexible method for inter-object communication in C++
[NASA-TM-106315] p 840 N95-17420
Engineering design tools for wind diesel systems. Volume 4: JODYMOD dynamic wind diesel simulation software package. Program documentation
[PB95-104535] p 841 N95-17628

DATA SYSTEMS
Telecommunications end-to-end systems monitoring on TOPEX/Poseidon: Tools and techniques p 676 N95-17180

Earth Observing System (EOS) Communication (Ecom) Modeling, Analysis, and Testbed (EMAT) activiy p 677 N95-17182
A second generation 50 Mbps VLSI level zero processing system prototype p 678 N95-17191
NASA Johnson Space Center Life Sciences Data System p 679 N95-17195
Single Stage Rocket Technology's real time data system p 679 N95-17197
Applications of massively parallel computers in telemetry processing p 680 N95-17201
Test Telemetry And Command System (TTACS) p 680 N95-17202
Multimission Telemetry Visualization (MTV) system: A mission applications project from JPL's Multimedia Communications Laboratory p 681 N95-17205
VLSI technology for smaller, cheaper, faster return link systems p 681 N95-17206
Evaluating Space Network (SN) scheduling operations concepts through statistical analysis p 684 N95-17222
Operations automation p 687 N95-17236
McIDAS-eXplorer: A version of McIDAS for planetary applications
[NASA-CR-189382] p 910 N95-17323
A land-surface Testbed for EOSDIS
[NASA-CR-189392] p 840 N95-17327
Corrective software management: The success of the EPLRS program
[AD-A282430] p 841 N95-17460
Third International Symposium on Space Mission Operations and Ground Data Systems, part 2
[NASA-CP-3281-PT-2] p 691 N95-17531
The Advanced Orbiting Systems Testbed Program: Results to date p 700 N95-17575
NCCDS performance model p 675 N95-17576
Evaluation of NASA's end-to-end data systems using DSDS+ p 700 N95-17577
Spacecraft Data Simulator for the test of level zero processing systems p 675 N95-17582
Transportable Payload Operations Control Center reusable software: Building blocks for quality ground data systems p 703 N95-17587
Customizing the JPL Multimission Ground Data System: Lessons learned p 703 N95-17588
The ESA standard for telemetry and telecommand packet utilisation: PUS p 704 N95-17595
Use of data description languages in the interchange of data p 704 N95-17597
Cross support overview and operations concept for future space missions p 705 N95-17598
The CCSDS return all frames Space Link Extension service p 705 N95-17599
Proposal for implementation of CCSDS standards for use with spacecraft engineering/housekeeping data p 705 N95-17600
Mission Operations Centers (MOCs): Integrating key spacecraft ground data system components p 675 N95-17601
Renaissance architecture for Ground Data Systems p 706 N95-17604
Matrix evaluation of science objectives p 707 N95-17610
A new systems engineering approach to streamlined science and mission operations for the Far Ultraviolet Spectroscopic Explorer (FUSE) p 707 N95-17611

DATA TRANSFER (COMPUTERS)
Data rearrangement and real-time computation
[AD-A282349] p 910 N95-17166
International data transfer for space very long baseline interferometry p 680 N95-17198
Applying STEP principles to product models in high energy physics research
[PB94-197704] p 880 N95-17503
Use of data description languages in the interchange of data p 704 N95-17597
Cross support overview and operations concept for future space missions p 705 N95-17598
Proposal for implementation of CCSDS standards for use with spacecraft engineering/housekeeping data p 705 N95-17600

DATA TRANSMISSION
High speed transport protocols: An attempt to find the best solution
[AD-A280989] p 751 N95-15993
An analysis of Internet's MBONE: A media choice perspective
[AD-A285514] p 910 N95-16972
Earth Observing System (EOS) Communication (Ecom) Modeling, Analysis, and Testbed (EMAT) activiy p 677 N95-17182
The GRO remote terminal system p 678 N95-17188
Fast computational scheme of image compression for 32-bit microprocessors p 678 N95-17192
Economical ground data delivery p 679 N95-17194
Multimission Telemetry Visualization (MTV) system: A mission applications project from JPL's Multimedia Communications Laboratory p 681 N95-17205
VLSI technology for smaller, cheaper, faster return link systems p 681 N95-17206
The SILEX experiment system operations p 674 N95-17251
Evaluation of NASA's end-to-end data systems using DSDS+ p 700 N95-17577
A standard satellite control reference model p 704 N95-17592
The Space Communications Protocol Standards Program p 704 N95-17594
Architecture of a distributed multimission operations system p 706 N95-17605

DECARBOXYLATION
Resist materials design: Base-catalyzed chemical amplification
[AD-A281805] p 741 N95-16354

DECELERATION
Physiological constraints on deceleration during the aerocapture of manned vehicles p 810 N95-16751

DECISION MAKING
Situational awareness in complex systems
[AD-A281448] p 825 N95-15959
An applications-oriented approach to the development of virtual environments p 853 N95-15980
A highly functional decision paradigm based on nonlinear adaptive genetic algorithm
[AD-A281457] p 855 N95-16077
GEOTRANS geographic decision support system
[PB94-183670] p 908 N95-16093
Improving production schedules without scheduling
[PB94-191350] p 904 N95-16289
Application of research techniques for documenting cognitive processes in air traffic control: Sector complexity and decision making
[AD-A282336] p 665 N95-16375
Crew decision making under stress p 814 N95-16765
Qualitative vision and action
[AD-A282697] p 831 N95-16966
Multi-objective decision-making under uncertainty: Fuzzy logic methods
[NASA-TM-106796] p 720 N95-17269
A model for analysis of TDA budget allocation p 758 N95-17295

DECODERS
Low-complexity wavelet filter design for image compression p 757 N95-17289

DECOMMUTATORS
Test/score/report: Simulation techniques for automating the test process p 675 N95-17581

DECOMPOSITION
On the structure of log-space probabilistic complexity classes
[TR-506] p 864 N95-16039
A new regularization approach in structural system identification p 651 N95-16262
Reaction of methanol with porous silicon
[AD-A285518] p 728 N95-16406
The Design Manager's Aid for Intelligent Decomposition (DeMAID) p 848 N95-16470
Single-pass method for the solution of inverse potential and rotational problems. Part 1: 2-D and quasi 3-D theory and application p 664 N95-16563

DECOMPRESSION SICKNESS
A proposal to study gender differences in the rates of decompression sickness
[AD-A281854] p 819 N95-16297
The effect of differences in time to detection of circulating microbubbles on the risk of decompression sickness p 807 N95-16738

DECONDITIONING
Delivery of cardiopulmonary resuscitation in the microgravity environment p 816 N95-16774
The effect of intermittent standing or walking during head down tilt bedrest on peak O2 consumption p 817 N95-16779

DECONTAMINATION
Augmentation for research training: Surface-mediated photocatalysis
[AD-A281591] p 722 N95-16100

DEEP SPACE
Development of a prototype real-time automated filter for operational deep space navigation p 694 N95-17545

DEEP SPACE NETWORK
Economical ground data delivery p 679 N95-17194
Galileo mission planning for Low Gain Antenna based operations p 682 N95-17210
Accuracy analysis of TDRSS demand forecasts p 683 N95-17214
The Telecommunications and Data Acquisition Report
[NASA-CR-197249] p 755 N95-17279
Evaluation of current tropospheric mapping functions by Deep Space Network very long baseline interferometry p 756 N95-17280
Space VLBI telecommunication characteristics, protection criteria, and frequency sharing p 756 N95-17282
A simplified Integer Cosine Transform and its application in image compression p 757 N95-17286
Tracking the Galileo spacecraft with the DSCC Galileo Telemetry prototype p 708 N95-17292
A model for analysis of TDA budget allocation p 758 N95-17295
Re-engineering the Multimission Command System at the Jet Propulsion Laboratory p 702 N95-17583

DEFECTS
Surface and defect excitations in covalently bonded solids
[AD-A281338] p 894 N95-16012
Researches on gear fault diagnosis techniques p 651 N95-16267
Reliability implications of defects in high temperature annealed Si/SiO2/Si structures
[DE94-015765] p 895 N95-16311
Vector magnetometry and lightwave defect imaging sensor technologies for internal pipe inspection systems: Phase 1 and 2 feasibility study, conceptual design, and prototype development
[PB94-194198] p 783 N95-16870
Positron annihilation studies of defects in molecular beam epitaxy grown 3 to 5 layers
[DE94-015823] p 899 N95-16918
The application of non-destructive techniques to the testing of a wind turbine blade
[DE95-000323] p 784 N95-17360
Characterization on defect solids
[NASA-CR-197540] p 746 N95-17654

DEFENSE PROGRAM
DOD STINFO regulations and forms. Selected titles
[AD-A282332] p 909 N95-16374
Data administration procedures
[AD-A282718] p 909 N95-16382
Department of Defense dictionary of military and associated terms. Includes US acronyms and abbreviations and NATO terms (English only)
[AD-A283218] p 912 N95-17633
Department of Defense Electronic Data Interchange project baseline report for FY 1994
[AD-A283015] p 912 N95-17710

DEFLECTION
A consistent large deflection theory of composite sandwich shells p 650 N95-16259

DEFOCUSING
Numerical aperture limits on efficient ball lens coupling of laser diodes to single-mode fibers with defocus to balance spherical aberration
[NASA-TM-4578] p 886 N95-17271

DEFORESTATION
Detection of deforestation in the Amazon forest using NOAA/AVHRR images and the geographic information system SGI: Methodology and test of a potential alarm system
[INPE-5580-TDI/543] p 791 N95-17894

DEFORMATION
Computer modelling of cyclic deformation of high-temperature materials
[AD-A285212] p 735 N95-16519
Superplasticity and superplastic forming of ceramics
[DE94-016172] p 745 N95-16935
An analysis of smoothed particle hydrodynamics
[DE94-013817] p 788 N95-17439
Error estimation and adaptive mesh refinement for parallel analysis of shell structures
[NASA-CR-197500] p 788 N95-17492

DEGRADATION
Materials degradation and fatigue under extreme conditions
[AD-A282969] p 746 N95-17662

DEGREES OF FREEDOM
Master-slave system with force feedback based on dynamics of virtual model p 853 N95-15985
Physics-based approach to haptic display p 854 N95-15986
Scripting human animations in a virtual environment p 855 N95-15992
A super-element simplified analysis for vibration systems of complex structures p 650 N95-16260
FPCAS2D user's guide, version 1.0
[NASA-CR-195413] p 786 N95-16588

DEICERS
Meteorological factors that affect the formation an prediction of aircraft icing
[AD-A281984] p 802 N95-17443

DEIONIZATION
Electric probe measurements in the plume of the UK-10 ion thruster
[AD-A282460] p 713 N95-16302

DELAY
Failure of ozone and nitrogen dioxide to enhance lung tumor development in hamsters
[PB94-182854] p 818 N95-16801
Self-initializing circuit link
[AD-D016363] p 761 N95-17696
Delayed annihilation of antiprotons in helium gas
[DE94-753405] p 878 N95-17739

DELTA CLIPPER
Single Stage Rocket Technology's real time data system p 679 N95-17197
Configurable technology development for reusable control and monitor ground systems p 675 N95-17589

DELTA WINGS
Numerical simulation of transient vortex breakdown above a pitching delta wing
[AD-A281075] p 655 N95-16808
Transonic Navier-Stokes calculations about a 65 deg delta wing
[NASA-CR-4635] p 656 N95-17273
Detailed study at supersonic speeds of the flow around delta wings p 660 N95-17861
Wind tunnel test on a 65 deg delta wing with a sharp or rounded leading edge: The international vortex flow experiment p 662 N95-17872
Delta-wing model p 662 N95-17873
Experimental investigation of the vortex flow over a 76/60-deg double delta wing p 662 N95-17874
Wind tunnel test on a 65 deg delta wing with rounded leading edges: The International Vortex Flow Experiment p 662 N95-17875
STOVL CFD model test case p 663 N95-17881

DEMODULATION
Demodulation processes in auditory perception
[AD-A285427] p 869 N95-16248

DEMOGRAPHY
Bureau of the Census Center for International Research p 905 N95-15923

DEMULTIPLEXING
Picosecond optoelectronic AND-GATE
[AD-A285672] p 885 N95-16620

DENSITY MEASUREMENT
Multi-beam laser interferometer for plasma density measurements in a Plasma Erosion Opening Switch (PEOS)
[AD-A283209] p 892 N95-17623

DEOXYRIBONUCLEIC ACID
Investigation of pressure regulation in an archaebacterial enzyme
[AD-A281413] p 807 N95-16164
Methods development toward the measurement of polyaromatic hydrocarbon-DNA adducts by mass spectrometry
[PB94-182722] p 727 N95-16373

DEPENDENT VARIABLES
Single-pass method for the solution of inverse potential and rotational problems. Part 2: Fully 3-D potential theory and applications p 664 N95-16564
Dark focus of accommodation as dependent and independent variables in visual display technology p 812 N95-16758

DEPLOYMENT
Foam inflated rigidized structures for space applications p 710 N95-16344
EURECA mission control experience and messages for the future p 690 N95-17252

DEPOLARIZATION
A high average power electro-optic switch using KTP
[DE94-016416] p 765 N95-16925

DEPOSITION
Ion beam generation and propagation for plasma processing applications
[DE94-014428] p 889 N95-16286
Colloidal particle deposition in turbulent flow
[DE94-013375] p 770 N95-16417
The deposition of electro-optic films on semiconductors
[AD-A285068] p 742 N95-16488
Low temperature deposition and characterization of N- and P-type silicon carbide thin films and associated ohmic and Schottky contacts
[AD-A281060] p 743 N95-16625
Underpotential deposition of Cu on Au(111): Implications of the HB model
[AD-A283028] p 902 N95-17711

DEPOSITS
Maja Valley and the Chryse outflow complex sites p 921 N95-16199
Melas Chasma: A Mars Pathfinder view of Valles Marineris p 922 N95-16207
Corrosion inhibition in high temperature environment
[AD-D016372] p 738 N95-17699

DEPTH
Recent advances in the development of high average power induction accelerators for industrial and environmental applications
[DE94-018734] p 882 N95-17914

DEPTH MEASUREMENT
Applications of positron depth profiling
[PB94-197753] p 900 N95-16952

DERIVATION
Investigation of dynamic inflow's influence on rotor control derivatives p 649 N95-16250

DESCENT
Mars Pathfinder mission operations concepts p 686 N95-17229

DESIGN ANALYSIS
Development and applications of the positron microscope
[DE94-017918] p 883 N95-15947
Portable parallel stochastic optimization for the design of aeropropulsion components
[NASA-CR-195312] p 785 N95-16072
Twin disc gear tooth simulator
[AD-A284927] p 780 N95-16139
An improved method of airfoil design p 649 N95-16252
Method of calculating the optimal radioelectronic equipment design p 652 N95-16271
Small turbojets: Designs and installations p 670 N95-16323
Model-based software process improvement p 843 N95-16455
Rapid solution of large-scale systems of equations p 847 N95-16458
Automatic differentiation for design sensitivity analysis of structural systems using multiple processors p 847 N95-16462
The Design Manager's Aid for Intelligent Decomposition (DeMAID) p 848 N95-16470
RDD-100 and the systems engineering process p 848 N95-16471
Matlab as a robust control design tool p 849 N95-16474
Natural frequency of uniform and optimized tetrahedral truss platforms
[NASA-TP-3461] p 709 N95-16559
Optimum Design Methods for Aerodynamics
[AGARD-R-803] p 666 N95-16562
Airfoil optimization by the one-shot method p 667 N95-16569
FPCAS2D user's guide, version 1.0
[NASA-CR-195413] p 786 N95-16588
Anatomy of a silicon compiler
[AD-A285395] p 832 N95-16618
Applications of automatic differentiation in CFD
[NASA-TM-109948] p 771 N95-16828
Nickel hydrogen batteries: An overview
[NASA-TM-106795] p 793 N95-16861
Algorithms for bilevel optimization
[NASA-CR-194980] p 863 N95-16897
On the application of under-decimated filter banks p 757 N95-17285
Low-complexity wavelet filter design for image compression p 757 N95-17289
JPL-ANTOPT antenna structure optimization program p 759 N95-17297
International Space Station Alpha (ISSA) Integrated Traffic Model
[NASA-CR-197566] p 710 N95-17331
Eddy current for detecting second layer cracks under installed fasteners
[AD-A282412] p 784 N95-17507
Issues in the design and optimization of adaptive optics and laser guide stars for the Keck Telescopes
[DE94-012888] p 916 N95-17525
SEQ-REVIEW: A tool for reviewing and checking spacecraft sequences p 697 N95-17561

DESIGN TO COST
Re-engineering the mission life cycle with ABC and IDEF p 706 N95-17606

DESORPTION
Reaction of methanol with porous silicon
[AD-A285518] p 728 N95-16406

DETECTION
Imager for Mars Pathfinder (IMF) p 711 N95-16206
Application of Fourier-space image-restoration techniques to turbulence compensation and sparse-aperture imaging
[AD-A285077] p 885 N95-16494
Search for first and second generation leptoquarks at D(null)
[DE94-018992] p 879 N95-17932

DETERIORATION
Problems with aging wiring in Naval aircraft p 711 N95-16048

DETERMINANTS
Validation of astronaut psychological select-in criteria p 813 N95-16762
Transverse mode coupling instability with a double RF system
[DE94-017972] p 761 N95-17672

DETONATION
CHEETAH 1.0 user's manual
[DE94-014727] p 749 N95-17919

DETONATION WAVES
Parametric study of shock-induced combustion in a hydrogen air system
[NASA-CR-197134] p 726 N95-15967

DEUTERIUM
Studies of D-Li neutron source: An overview
[DE94-014032] p 873 N95-16487

DEUTERIUM COMPOUNDS
Thermal and laser conditioning of production and rapid-growth KDP and KD*P crystals
[DE94-013738] p 902 N95-17742

DIAGNOSIS
Overview of space power electronic's technology under the CSTI High Capacity Power Program
[NASA-TM-110110] p 883 N95-17933

DIAGRAMS
Verification of arithmetic functions with binary moment diagrams
[AD-A281028] p 835 N95-16447

DIAMOND FILMS
Workshop on Characterizing Diamond Films, 3
[PB94-187663] p 747 N95-17722

DIAMONDS
Pseudomorphic stabilization of diamond on non-diamond substrates
[AD-A285231] p 898 N95-16527
Atomic layer epitaxy of group 4 materials: Surface processes, thin films, devices and their characterization
[AD-A280987] p 898 N95-16532
Adhesion of silicon oxide to diamond
[AD-D016356] p 747 N95-17694

DIATOMIC MOLECULES
Development of practical MO techniques for prediction of the properties and behavior of materials
[AD-A285079] p 874 N95-16496

DICHROISM
Computation of reflected and transmitted horn radiation patterns for a dichroic plate p 758 N95-17293
X-/Ka-band dichroic plate noise temperature reduction p 758 N95-17294

DICTIONARIES
Process and methodology of developing Cassini G and C Telemetry Dictionary p 681 N95-17204
Department of Defense dictionary of military and associated terms. Includes US acronyms and abbreviations and NATO terms (English only)
[AD-A283218] p 912 N95-17633

DIELECTRIC PROPERTIES
Plasma sound source basic research
[AD-A285394] p 890 N95-16617
Relationships between ferroelectric 90 deg domain formation and electrical properties of chemically prepared Pb(Zr,Ti)O3 thin films
[DE94-015274] p 744 N95-16829

DIELECTRICS
First NASA Workshop on Wiring for Space Applications
[NASA-CP-10145] p 711 N95-16044
A study of electric transmission lines for use on the lunar surface p 712 N95-16053
High temperature polymer dielectric film-wire insulation p 712 N95-16055
High performance dielectric materials development p 712 N95-16057
Natural convection cooling of a three by three array of leadless chip carrier packages in a dielectric liquid
[AD-A282298] p 770 N95-16239
Nonlinear optical and charge distribution studies probing electric field effects in polymer thin films for second order nonlinear optics
[AD-A280980] p 742 N95-16483
A simple EHF hemispheric coverage antenna
[AD-A285078] p 754 N95-16495
Liquid crystal materials for laser beam steering
[AD-A285089] p 897 N95-16498
Coatings for large-area low-cost solar concentrators and reflectors
[DE94-015735] p 793 N95-16916
Antenna dielectric sealing process characterization
[DE94-015864] p 747 N95-17690

DIELS-ALDER REACTIONS
Radical cations of quadricyclane and norbornadiene in polar ZSM-5 matrices: Radical cation photochemical transformations without photons
[DE94-014007] p 728 N95-16485

DIES
Method of rapid sample handling for laser processing
[AD-D016408] p 778 N95-17464
DIESEL ENGINES
Bench wear and single-cylinder engine evaluations of high-temperature lubricants for US Army ground vehicles
[AD-A285399] p 780 N95-16636
An in-cylinder study of the particulate/NO(x) trade-off in a DI diesel engine
[DE94-014599] p 781 N95-17162
Engineering design tools for wind diesel systems. Volume 2: JODYMOD dynamic wind diesel simulation software package. Model verification
[PB95-104519] p 840 N95-17355
Engineering design tools for wind diesel systems. Volume 3: JODYMOD dynamic simulation software package. Model description
[PB95-104527] p 840 N95-17356
Coal-fueled diesel technology development emissions control
[DE94-004096] p 782 N95-17364
Engineering design tools for wind diesel systems. Volume 4: JODYMOD dynamic wind diesel simulation software package. Program documentation
[PB95-104535] p 841 N95-17628
DIESEL FUELS
Alternatives to traditional transportation fuels: An overview
[DE94-014979] p 749 N95-17923
DIFFERENTIAL CALCULUS
Computational differentiation and multidisciplinary design
[DE94-013393] p 863 N95-17306
DIFFERENTIAL EQUATIONS
A modified restricted Euler equation for turbulent flows with mean velocity gradients
[NASA-CR-194979] p 769 N95-16070
Large scale control and distributed computing systems under stochastic structural perturbations
[AD-A281550] p 855 N95-16170
A stepsize control strategy for stiff systems of ordinary differential equations
[AD-A281551] p 861 N95-16395
Single-pass method for the solution of inverse potential and rotational problems. Part 2: Fully 3-D potential theory and applications p 664 N95-16564
Optimum aerodynamic design via boundary control p 667 N95-16565
Frequency domain analysis for nonlinear electronic circuits
[PB94-201365] p 767 N95-17469
DIFFERENTIAL GEOMETRY
Some fundamental techniques in the theory of integrable systems
[PB94-192390] p 860 N95-16294
Nonasymptotic formulae for the distribution of the maximum of smooth Gaussian processes
[AD-A284741] p 865 N95-16546
Single-pass method for the solution of inverse potential and rotational problems. Part 1: 2-D and quasi 3-D theory and application p 664 N95-16563
DIFFRACTION
Rietveld refinement of magnetic structures from pulsed-neutron-source powder-diffraction data
[DE94-016599] p 737 N95-17641
DIFFRACTION PROPAGATION
ARO-URI Center for Opto-Electronic Systems Research
[AD-A281447] p 883 N95-15958
DIFFRACTOMETERS
Rietveld refinement of magnetic structures from pulsed-neutron-source powder-diffraction data
[DE94-016599] p 737 N95-17641
DIFFUSE RADIATION
Chemical properties of the fullerenes
[AD-A282730] p 730 N95-17141
DIFFUSION
Nonlinear problems and numerical method in differential equations and applied phenomena
[AD-A281531] p 859 N95-16108
Atomic transport of oxygen
[DE94-013332] p 873 N95-16430
Study of the structuring of pure molecular liquids
[PB94-201316] p 903 N95-16839
DIFFUSIVITY
Atomic transport of oxygen
[DE94-013332] p 873 N95-16430
DIGESTIVE SYSTEM
Applying Virtual Reality to commercial Edutainment p 854 N95-15989
DIGITAL COMPUTERS
A PC-based interactive simulation of the F-111C Pave Tack system and related sensor, avionics and aircraft aspects
[AD-A285500] p 669 N95-16969
Guidance, navigation, and control digital emulation technology laboratory
[AD-A282722] p 766 N95-17139
DIGITAL DATA
Digital mapping, charting, and geodesy analysis program technical review of interim terrain analysis data set prototype 1
[AD-A284742] p 790 N95-16547
A coastal hazards data base for the US Gulf Coast
[DE94-014573] p 805 N95-16610
Overview on METEOSAT geometrical image data processing p 678 N95-17189
Grey-scale measurements in multi-dimensional digitized images
[PB94-195492] p 887 N95-17483
Analysis of compression techniques for Common Mapping Standard (CMS) raster data
[AD-A283396] p 791 N95-17625
DIGITAL ELECTRONICS
A VLSI interface for the NM24CF04 serial-access ferroelectric memory
[AD-A281535] p 762 N95-16110
WAVES VHDL interface
[AD-A285208] p 764 N95-16516
DIGITAL FILTERS
Wavelets, signal processing and matrix computations
[AD-A283832] p 755 N95-16841
On the application of under-decimated filter banks p 757 N95-17285
DIGITAL SIMULATION
Support for development of a custom VLSI and FPGA logic chips based on a VHDL top-down design approach
[DE94-013608] p 763 N95-16283
The new map graphics in RSAS 5.0
[AD-A282432] p 791 N95-17511
Simulation of the SEMATECH gravimetric mass flowmeter calibrator
[DE94-018698] p 773 N95-17910
DIGITAL SYSTEMS
Digital adaptive and optimal control of distributed systems
[AD-A285352] p 851 N95-15952
Papers presented at the Tenth Topical Conference on High-Temperature Plasma Diagnostics
[DE94-015854] p 888 N95-16063
Verification of arithmetic functions with binary moment diagrams
[AD-A281028] p 835 N95-16447
Hardware description languages p 832 N95-16477
DIGITAL TECHNIQUES
VLSI circuits for high speed data conversion
[AD-A281556] p 763 N95-16136
Detecting the number of targets in spatially colored noise using sampled aperture radars p 652 N95-16269
Data Visualization and Animation Lab (DVAL) overview p 843 N95-16468
Data Visualization and Animation Lab (DVAL): Applications p 843 N95-16469
DIMENSIONAL ANALYSIS
Visualization of unsteady computational fluid dynamics
[NASA-CR-197461] p 770 N95-16388
DIMENSIONAL MEASUREMENT
Numeric data distribution: The vital role of data exchange in today's world p 907 N95-15937
Theory of one-dimensional and two-dimensional distributed sensors for measuring the spatial characteristics of thermophysical and hydrodynamic fields p 652 N95-16273
Grey-scale measurements in multi-dimensional digitized images
[PB94-195492] p 887 N95-17483
DIMERIZATION
The mechanism of the oligomerization of thiophene-based para-quinodimethanes
[DE94-014232] p 722 N95-16058
DIPOLE MOMENTS
Theoretical study of cathode surfaces and high-temperature superconductors
[NASA-CR-195407] p 898 N95-16598
DIRECTIONAL COUPLERS
Development of device quality nonlinear optical materials and definition of mechanisms of optical nonlinearity
[AD-A285255] p 885 N95-16528
DIRECTORIES
Directory of Organizational Technical Report Acronym Codes (DOTRAC)
[AD-A281500] p 908 N95-16086
Directory of IAEA databases
[DE94-622696] p 912 N95-17472
DISASTERS
Tsunami newsletter, volume 26
[AD-A282751] p 806 N95-17477
DISCONTINUITY
Application of the space-time conservation element and solution element method to shock-tube problem
[NASA-TM-106806] p 772 N95-16903
DISCRETE COSINE TRANSFORM
Fast computational scheme of image compression for 32-bit microprocessors p 678 N95-17192
DISCRETE FUNCTIONS
Theory of one-dimensional and two-dimensional distributed sensors for measuring the spatial characteristics of thermophysical and hydrodynamic fields p 652 N95-16273
DISCRIMINANT ANALYSIS (STATISTICS)
Prediction of space sickness in astronauts from preflight fluid, electrolyte, and cardiovascular variables and Weightless Environmental Training Facility (WETF) training p 812 N95-16757
DISILICIDES
Processing - property relationship in advanced intermetallics
[AD-A285262] p 735 N95-16514
The analysis and minimization of oxygen contamination in the powder processing of molybdenum disilicide
[DE94-014234] p 735 N95-16540
DISK OPERATING SYSTEM (DOS)
Real-time data collection programs and source code for a commercial passive FTIR remote sensor
[AD-A284976] p 838 N95-16634
Use of data description languages in the interchange of data p 704 N95-17597
DISORDERS
Results of the psychiatric, select-out evaluation of US astronaut applications p 813 N95-16761
DISPERSING
The small-scale structure of dispersing clouds in the atmosphere
[AD-A285493] p 800 N95-16802
FEM3C, an improved three-dimensional heavy-gas dispersion model: User's manual
[DE94-014731] p 797 N95-17922
DISPERSIONS
Phase segregation due to simultaneous migration and coalescence
[NASA-CR-196819] p 721 N95-16035
DISPLACEMENT
Error estimation and adaptive mesh refinement for parallel analysis of shell structures
[NASA-CR-197500] p 788 N95-17492
DISPLACEMENT MEASUREMENT
Mechanisms of mechanical fatigue in ceramics
[DE94-016040] p 747 N95-17719
DISPLAY DEVICES
Image tools for UNIX p 847 N95-16466
Human performance in the modern cockpit p 813 N95-16764
An empirical approach to visual display preference based upon modulation transfer function and luminance
[AD-A285450] p 830 N95-16875
Breaking down barriers in cooperative fault management: Temporal and functional information displays
[NASA-CR-197450] p 857 N95-17383
The Grid Analysis and Display System (GrADS)
[NASA-CR-189387] p 912 N95-17491
DISSIPATION
Evaluation of SEA loss factors using input power modulation
[ISVR-TR-240] p 868 N95-16856
DISSOCIATION
Gas-surface interactions near dissociation threshold
[AD-A284945] p 726 N95-16042
DISTORTION
Methods of wave-front identification by control images p 652 N95-16274
Closed orbit distortion from parasitic collisions in PEP-2
[DE94-018203] p 882 N95-17890
DISTRIBUTED PARAMETER SYSTEMS
Energy decay and control for elastic and viscoelastic distributed parameter systems
[AD-A281312] p 726 N95-16008
A new communication protocol family for a distributed spacecraft control system p 703 N95-17590
DISTRIBUTED PROCESSING
Second International Working Conference on Cooperating Knowledge Based Systems. Volume 1
[AD-A281347] p 908 N95-16014
The survivable distributed computing environment
[AD-A281637] p 845 N95-16115
Summary Report, 1992 --- distributed systems evaluation environment
[AD-A281639] p 845 N95-16116
Large scale control and distributed computing systems under stochastic structural perturbations
[AD-A281550] p 855 N95-16170

Rapid solution of large-scale systems of equations p 847 N95-16458
Open architectures for formal reasoning and deductive technologies for software development [NASA-CR-197528] p 837 N95-16586
First principles simulation of materials properties [DE94-013615] p 899 N95-16805
DOME: Distributed Object Migration Environment [AD-A281134] p 850 N95-16826
ARACHNID: A prototype object-oriented database tool for distributed systems p 680 N95-17199
Autonomous mission planning and scheduling: Innovative, integrated, responsive p 686 N95-17234
Open solutions to distributed control in ground tracking stations p 674 N95-17554
Automating testbed documentation and database access using World Wide Web (WWW) tools p 696 N95-17557
XPVM: A graphical console and monitor for PVM [DE94-018050] p 842 N95-17678

DISTRIBUTION (PROPERTY)
Digital adaptive and optimal control of distributed systems [AD-A285352] p 851 N95-15952

DISTRIBUTION FUNCTIONS
Log-(Chi(exp 2)) distribution of correlation times revisited [AD-A281123] p 740 N95-16092
Determination of ion temperatures from Zeeman broadened spectral lines in the edge of Tore Supra [DE94-018112] p 873 N95-16403
Nonasymptotic formulae for the distribution of the maximum of smooth Gaussian processes [AD-A284741] p 865 N95-16546
Probabilistic simulation of stress concentration in composite laminates [NASA-TM-106712] p 787 N95-17270
Parton distributions of the proton [PB95-104337] p 877 N95-17354

DITHERS
Electric-optic resonant phase modulator [NASA-CASE-NPO-18702-1-CU] p 883 N95-15960

DIURNAL VARIATIONS
Long-term momentum and heat balances and turbulent mixing in the upper equatorial Pacific Ocean p 805 N95-17395
Recent changes of weather patterns in North America [DE94-016115] p 803 N95-17743

DIVERGENT NOZZLES
Single-engine tail interference model p 663 N95-17879

DIVERTERS
Development of a radiative divertor for DIII-D [DE94-016522] p 889 N95-16554
D3-D research operations [DE94-014934] p 892 N95-17497
Effect of low density H-mode operation on edge and divertor plasma parameters [DE94-016521] p 892 N95-17640
Measurements of non-axisymmetric effects in the D3-D divertor [DE94-018346] p 893 N95-17897

DIVING (UNDERWATER)
Heat stress and a countermeasure in the Shuttle rescueman's suit p 809 N95-16746

DOCUMENTATION
Document delivery by the Jupiter Library Consortium p 906 N95-15926
The Technical Information Library: TIB p 906 N95-15928
The National Resource Library for Science and Technology in Sweden: A Nordic model of cooperating technology libraries p 906 N95-15929

DOCUMENTS
Behavioural modelling of formal documents and active instruments [PB95-104378] p 842 N95-17732

DOMAINS
Relationships between ferroelectric 90 deg domain formation and electrical properties of chemically prepared Pb(Zr,Ti)O3 thin films [DE94-015274] p 744 N95-16829

DOPED CRYSTALS
LPEE growth and characterization of In(x)Ga(1-x)As(y)Sb(1-y) lattice matched to GaSb and InAs for photodetectors [AD-A281631] p 895 N95-16114
Method for intrinsically doped III-A and V-A compounds and products thereof [AD-D016324] p 896 N95-16399
New approaches to novel organosilanes [AD-A285253] p 722 N95-16513
Process of making a bistable photoconductive component [AD-D016449] p 764 N95-16539
New ytterbium-doped apatite crystals for flexible laser design [DE94-015138] p 899 N95-16867
Positron annihilation studies of defects in molecular beam epitaxy grown 3 to 5 layers [DE94-015823] p 899 N95-16918
Rare earth ion doped CW cascade fiber laser [AD-D016370] p 779 N95-17698

DOPPLER RADAR
Linear prediction data extrapolation superresolution radar imaging p 651 N95-16268

DOSAGE
The chronic effects on JP-8 jet fuel exposure on the lungs [AD-A280982] p 821 N95-16515
Recent advances in the development of high average power induction accelerators for industrial and environmental applications [DE94-018734] p 882 N95-17914

DOWNLINKING
Simplifying operations with an uplink/downlink integration toolkit p 697 N95-17562

DOWNWASH
Numerical simulation of helicopter engine plume in forward flight [NASA-CR-197488] p 655 N95-16589

DRAFTING (DRAWING)
Interactive sketching for the early stages of user interface design [AD-A285339] p 838 N95-16818

DRAG
Investigation of the influence of pylons and stores on the wing lower surface flow p 664 N95-17885

DRAG COEFFICIENTS
An investigation of the transonic pressure drag coefficient for axi-symmetric bodies [AD-A280990] p 654 N95-15994

DRAG MEASUREMENT
Surface pressure and wake drag measurements on the Boeing A4 airfoil in the IAR 1.5X1.5m Wind Tunnel Facility p 657 N95-17850

DRAG REDUCTION
An investigation of the transonic pressure drag coefficient for axi-symmetric bodies [AD-A280990] p 654 N95-15994

DRAINAGE
The impact of low temperature materials on the breakdown and noise properties of GaAs and InP based HEMT's and FET's [AD-A285176] p 765 N95-16834

DRAINAGE PATTERNS
Steps toward terrain knowledge acquisition [AD-A282667] p 790 N95-17375

DRAWINGS
Scripting human animations in a virtual environment p 855 N95-15992

DRIFT RATE
Ion drift meter research [NASA-CR-197124] p 798 N95-16432

DRILLING
Approach to in-process tool wear monitoring in drilling: Application of Kalman filter theory p 653 N95-16279
Ceramic/metal composite circuit-board-level technology for Application Specific Electronic Modules (ASEMs) [AD-A285066] p 741 N95-16369

DRIVES
Combination of power electronic models with the two-dimensional finite element analysis of electrical machines [PB94-197720] p 766 N95-16951

DROOPED AIRFOILS
Wind tunnel test on a 65 deg delta wing with a sharp or rounded leading edge: The international vortex flow experiment p 662 N95-17872

DROPS (LIQUIDS)
Phase segregation due to simultaneous migration and coalescence [NASA-CR-196819] p 721 N95-16035
High-intensity and high energy laser interactions with single droplets [AD-A281415] p 776 N95-16166

DRUGS
Synaptic plasticity and memory formation [AD-A284926] p 825 N95-16138
Catecholaminergic responses to stressful motion stimuli, scopolamine plus amphetamine, and dexamethasone p 809 N95-16745
Statistical properties of an algorithm used for illicit substance detection by fast-neutron transmission [DE94-013868] p 665 N95-16964

DUCT GEOMETRY
Three dimensional compressible turbulent flow computations for a diffusing S-duct with/without vortex generators [NASA-CR-195390] p 670 N95-17402

DUCTED FAN ENGINES
Ducted fan acoustic radiation including the effects of nonuniform mean flow and acoustic treatment [NASA-CR-197449] p 870 N95-16401

DUCTED ROCKET ENGINES
Experimental and analytical methods for the determination of connected-pipe ramjet and ducted rocket internal performance [AGARD-AR-323] p 721 N95-17278

DUCTILE-BRITTLE TRANSITION
Effects of prior ductile tearing on cleavage fracture toughness in the transition region [AD-A281298] p 786 N95-16785

DUCTILITY
Ductile fracture and failure criteria of structural steels [AD-A280754] p 733 N95-16104
Material and ballistic investigation of a tungsten-26 percent rhenium alloy [PB94-189156] p 734 N95-16420
Effects of prior ductile tearing on cleavage fracture toughness in the transition region [AD-A281298] p 786 N95-16785
Metallurgical examination of failed T-158 Cast Austempered Ductile Iron (CADI) track shoes [AD-A282433] p 737 N95-17486

DURABILITY
Structurally-compliant rocket engine combustion chamber: Experimental/analytical validation p 718 N95-16337

DYADICS
Duality transformations, green dyadics and plane-wave solutions for a class of bianisotropic media [PB94-197670] p 754 N95-16612
Electromagnetostatics in uniaxial bianisotropic media [PB94-197688] p 754 N95-16613

DYNAMIC CHARACTERISTICS
Computational fluid dynamics studies of nuclear rocket performance [NASA-TM-105436] p 713 N95-16066
Material and ballistic investigation of a tungsten-26 percent rhenium alloy [PB94-189156] p 734 N95-16420
Radiation belt dynamic and quasi-static modeling based on CRRES data [AD-A285282] p 916 N95-16600
Static and dynamic friction behavior of candidate high temperature airframe seal materials [NASA-TM-106571] p 722 N95-16905

DYNAMIC CONTROL
Simulation of the coupled multi-spacecraft control testbed at the Marshall Space Flight Center p 849 N95-16475

DYNAMIC LOADS
Matlab as a robust control design tool p 849 N95-16474
Computer studies of the dynamic strength of ceramics [DE94-010890] p 745 N95-17379
Modeling of thermal stresses in welds [DE94-018046] p 789 N95-17675

DYNAMIC MODELS
Quantum transport in semiconductor devices [AD-A281383] p 895 N95-16158
Investigation of dynamic inflow's influence on rotor control derivatives p 649 N95-16250
Approach to in-process tool wear monitoring in drilling: Application of Kalman filter theory p 653 N95-16279
Measurement of residual flexibility for substructures having prominent flexible interfaces [NASA-TM-110074] p 786 N95-16577
A model for assessment of dynamic interaction between magnetically levitated vehicles and their supporting guideways [AD-A283088] p 781 N95-17335

DYNAMIC PRESSURE
Improved method for estimation of the maximum instantaneous distortion values p 649 N95-16254

DYNAMIC RESPONSE
Energy decay and control for elastic and viscoelastic distributed parameter systems [AD-A281312] p 726 N95-16008
Shaped strain sensors for intelligent structures [AD-A282333] p 774 N95-16242
A new regularization approach in structural system identification p 651 N95-16262
Measurements of unsteady pressure and structural response for an elastic supercritical wing [NASA-TP-3443] p 653 N95-16560

DYNAMIC STABILITY
Evaluation of the dynamic stability characteristics of the NAL Light Transport Aircraft [NAL-PD-CA-9217] p 671 N95-16392

DYNAMIC STRUCTURAL ANALYSIS
Experimental and numerical analysis of floating ice beam impact forces against a sloped structure [AD-A280752] p 804 N95-16103

Experimental study of spatially incomplete structural system identification
[AD-A280905] p 785 N95-16502
A model for assessment of dynamic interaction between magnetically levitated vehicles and their supporting guideways
[AD-A283088] p 781 N95-17335

DYNAMIC TESTS
Investigation of dynamic inflow's influence on rotor control derivatives p 649 N95-16250
Correlation of finite element free vibration predictions using random vibration test data
[NASA-TM-106787] p 787 N95-17258

DYNAMICAL SYSTEMS
Cellular automata for contour dynamics
[PB94-197613] p 865 N95-17526

DYNAMICS EXPLORER SATELLITES
Ion drift meter research
[NASA-CR-197124] p 798 N95-16432

DYNODES
Multilayer microelectronic photomultiplier device with a stacked series of dynode and insulating layers
[AD-D016377] p 767 N95-17478

E

EARTH CRUST
Forecasting earthquakes
[NASA-TM-110112] p 799 N95-16981

EARTH MAGNETOSPHERE
Characteristics of multiple auroral inverted-V structures and the problem of magnetospheric plasma stratification
[DE94-622233] p 799 N95-17471
Solar flares and magnetospheric particles: Investigations based upon the ONR-602 and ONR-604 experiments
[AD-A283275] p 923 N95-17723

EARTH OBSERVING SYSTEM (EOS)
Earth Observing System (EOS) Communication (Ecom) Modeling, Analysis, and Testbed (EMAT) activiy p 677 N95-17182
A low-cost transportable ground station for capture and processing of direct broadcast EOS satellite data p 680 N95-17200
Evaluating modeling tools for the EDOS p 700 N95-17572
Evaluation of NASA's end-to-end data systems using DSDS+ p 700 N95-17577
Risk reduction methodologies and technologies for the Earth Observing System (EOS) Operations Center (EOC) p 707 N95-17612
EDOS operations concept and development approach p 708 N95-17613
CERES, phases 1 and 2
[DE94-014730] p 797 N95-17920

EARTH ORBITAL ENVIRONMENTS
Kapton pyrolysis on Space Station Freedom's solar array flexible current carrier p 712 N95-16049
Kapton pyrolysis, the space environment and wiring requirements p 712 N95-16054
Accuracy analysis of TDRSS demand forecasts p 683 N95-17214
Solar flares and magnetospheric particles: Investigations based upon the ONR-602 and ONR-604 experiments
[AD-A283275] p 923 N95-17723

EARTH ORBITAL RENDEZVOUS
EURECA mission control experience and messages for the future p 690 N95-17252

EARTH ORBITS
Efficient mission control for the 48-satellite Globalstar Constellation p 674 N95-17256
Space VLBI telecommunication characteristics, protection criteria, and frequency sharing p 756 N95-17282
An analysis of a single-burn algorithm for Low-Earth Orbit maintenance
[AD-A283418] p 721 N95-17626

EARTH ORIENTATION
An algorithm for extraction of periodic signals from sparse, irregularly sampled data p 756 N95-17281

EARTH RADIATION BUDGET
Nickel cadmium battery operations and performance p 685 N95-17224

EARTH RESOURCES
Activities of the Space Studies Board
[NASA-CR-197105] p 672 N95-16033
Using neural networks to correlate satellite imagery and ground-truth data
[AD-A285486] p 857 N95-16967

EARTH SCIENCES
Aeronautical engineering: A continuing bibliography with indexes (supplement 311)
[NASA-SP-7037(311)] p 654 N95-17704

EARTHQUAKES
Forecasting earthquakes
[NASA-TM-110112] p 799 N95-16981
Tsunami newsletter, volume 26
[AD-A282751] p 806 N95-17477

ECOLOGY
Simulation of hydrologic influences on wetland ecosystem succession
[AD-A284737] p 795 N95-16545
Abstracts and program Proceedings of the 1994 Meeting of the International Society for Ecological Modelling North American Chapter
[DE94-016456] p 796 N95-17636
Natural and artificial nobel gas hydrologic tracers
[DE94-016010] p 797 N95-17718

ECONOMIC ANALYSIS
Bureau of the Census Center for International Research p 905 N95-15923
Plasma disruption modeling and simulation
[DE94-015095] p 889 N95-16307
A comparison of steady-state ARIES and pulsed PULSAR tokamak power plants
[DE94-014441] p 891 N95-17155

ECONOMIC DEVELOPMENT
Acquiring and disseminating unpublished economic and social development materials in Africa: The case of the National Institute of Development Research and Documentation University of Botswana p 906 N95-15924

ECONOMIC IMPACT
Informatics in Turkey p 905 N95-15921

ECONOMICS
Emerging national space launch programs: Economics and safeguards
[AD-A282107] p 672 N95-17427

ECOSYSTEMS
Simulation of hydrologic influences on wetland ecosystem succession
[AD-A284737] p 795 N95-16545
FIFE data analysis: Testing BIOME-BGC predictions for grasslands
[NASA-CR-197522] p 790 N95-16895

EDDY CURRENTS
Nondestructive examination of the TRMM RCS propellant tanks p 718 N95-16338
Eddy current for detecting second layer cracks under installed fasteners
[AD-A282412] p 784 N95-17507

EDDY VISCOSITY
Experimental investigation of turbulent separated-reattachment flow by using LDV p 649 N95-16253
Modeling of wall-bounded complex flows and free shear flows
[NASA-TM-106513] p 770 N95-16407

EDGE DETECTION
Grey-scale measurements in multi-dimensional digitized images
[PB94-195492] p 887 N95-17483

EDUCATION
Applied virtual reality at the Research Triangle Institute p 851 N95-15974
Simulation of arthroscopic surgery using MRI data p 823 N95-15975
Integrating computers into calculus instruction
[AD-A280996] p 833 N95-15997
How to use the WWW to distribute STI p 847 N95-16465
Epistemology, software engineering and formal methods p 843 N95-16480
Results of an International Space Crew Debrief p 810 N95-16750
A workstation based simulator for teaching compressible aerodynamics
[NASA-TM-106799] p 839 N95-16906

EFFERENT NERVOUS SYSTEMS
Characterization of neurotrophic and neurotropic interactions between neurons and their muscle and nerve targets
[AD-A281846] p 820 N95-16423

EFFICIENCY
Magellan Project: Evolving enhanced operations efficiency to maximize science value p 684 N95-17218

EIGENVALUES
The algebraic multigrid projection for eigenvalue problems; backrotations and multigrid fixed points
[NASA-CR-194990] p 862 N95-16869
Multigrid techniques for nonlinear eigenvalue probems: Solutions of a nonlinear Schroedinger eigenvalue problem in 2D and 3D
[NASA-CR-194999] p 862 N95-16896
Correlation of finite element free vibration predictions using random vibration test data
[NASA-TM-106787] p 787 N95-17258
Transverse mode coupling instability with a double RF system
[DE94-017972] p 761 N95-17672

EIGENVECTORS
An analysis of spectral envelope-reduction via quadratic assignment problems
[NASA-CR-194992] p 862 N95-16596
The algebraic multigrid projection for eigenvalue problems; backrotations and multigrid fixed points
[NASA-CR-194990] p 862 N95-16869
Multigrid techniques for nonlinear eigenvalue probems: Solutions of a nonlinear Schroedinger eigenvalue problem in 2D and 3D
[NASA-CR-194999] p 862 N95-16896

EL NINO
An observational study of long waves in the equatorial Pacific Ocean during the 1991-1993 El Nino
[AD-A283380] p 806 N95-17624

ELASTIC DEFORMATION
Classical solutions of the Prandtl-Reuss equations of perfect elasto-plasticity
[PB94-192333] p 860 N95-16292
Deformation behavior of thin lubricant films at elevated pressure
[AD-A281848] p 741 N95-16355

ELASTIC PROPERTIES
Generic propellant transfer unit: A project update p 719 N95-16345
Structural integrity of intelligent materials and structures. Constitutive modeling of shape memory alloys
[AD-A281301] p 735 N95-16786

ELASTIC WAVES
Transient flows and pressure waves in pipes
[DE94-012650] p 772 N95-17523

ELASTOHYDRODYNAMICS
Deformation behavior of thin lubricant films at elevated pressure
[AD-A281848] p 741 N95-16355

ELASTOMERS
Smart materials based upon oligomeric molecules
[AD-A281374] p 872 N95-16155
An elastomeric electrical connector
[AD-D016340] p 766 N95-16950
Reaction and protection of electrical wire insulators in atomic-oxygen environments
[NASA-TM-106767] p 709 N95-17275

ELASTOPLASTICITY
Considerations in the experimental determination of constitutive parameters for finite strain plasticity
[AD-A285410] p 785 N95-16245
Classical solutions of the Prandtl-Reuss equations of perfect elasto-plasticity
[PB94-192333] p 860 N95-16292

ELASTOSTATICS
User-defined subroutine for implementation of special finite elements in ABAQUS for the analysis of adhesive joints
[AD-A282431] p 788 N95-17510

ELECTRIC ARCS
First NASA Workshop on Wiring for Space Applications
[NASA-CP-10145] p 711 N95-16044
WSTF electrical arc projects p 711 N95-16047

ELECTRIC BATTERIES
Aluminum permanganate battery
[AD-D016337] p 766 N95-16947
Aluminum-ferricyanide battery
[AD-D016338] p 766 N95-16948
Improved dual flow aluminum hydrogen peroxide battery
[AD-D016339] p 766 N95-16949
Nickel cadmium battery operations and performance p 685 N95-17224

ELECTRIC CHARGE
Electromagnetostatics in uniaxial bianisotropic media
[PB94-197688] p 754 N95-16613
Radial acceletron, a new low impedance HPM source
[AD-A282008] p 760 N95-17501

ELECTRIC CONDUCTORS
Field-induced minigap and transport with in-plane magnetic fields in double quantum wells
[DE94-018893] p 879 N95-17918

ELECTRIC CONNECTORS
An elastomeric electrical connector
[AD-D016340] p 766 N95-16950

ELECTRIC CONTACTS
Low temperature deposition and characterization of N- and P-type silicon carbide thin films and associated ohmic and Schottky contacts
[AD-A281060] p 743 N95-16625

ELECTRIC EQUIPMENT
Generalized method of solving topological optimization problems for electrical airplane equipment systems in computer-aided design p 652 N95-16272

ELECTRIC EQUIPMENT TESTS
A modular electric power system test bed for small spacecraft
[NASA-TM-106812] p 721 N95-17276

ELECTRIC FIELDS
Field configuration of beam excited modes in the Advanced Photon Source (APS) storage ring waveguides
[DE94-015096] p 880 N95-16308
Monte Carlo simulation of mercury cadmium telluride
[AD-A281546] p 896 N95-16391
Ion drift meter research
[NASA-CR-197124] p 798 N95-16432
Nonlinear optical and charge distribution studies probing electric field effects in polymer thin films for second order nonlinear optics
[AD-A280980] p 742 N95-16483
Electromagnetostatics in uniaxial bianisotropic media
[PB94-197688] p 754 N95-16613
The impact of low temperature materials on the breakdown and noise properties of GaAs and InP based HEMT's and FET's
[AD-A285176] p 765 N95-16834
Radiation electrodynamics of the photo-electron cloud produced by an arbitrary photon pulse incident on a planar emitting surface in vacuum
[AD-A282153] p 759 N95-17450
Static image method for the interaction of two co-axial conducting prolate spheroids
[PB94-197696] p 760 N95-17502
Poling dynamics and relaxation of polar order in guest/host polymers by second harmonic generation
[AD-A283291] p 748 N95-17724
ELECTRIC FILTERS
Elimination of electromagnetic interference to receivers and sensitive equipment generated by switching systems
[AD-A281643] p 752 N95-16117
ELECTRIC MOTOR VEHICLES
Safety characteristics of lithium-alloy/metal sulfide batteries
[DE94-013867] p 766 N95-16963
ELECTRIC POTENTIAL
Control of a large vacuum wave precursor on the SABRE voltage adder MITL and extraction ion diode
[DE94-014280] p 888 N95-16216
Analysis of space environment damage to solar cell assemblies from LDEF experiment A0171-GSFC test plate
[NASA-CR-196523] p 793 N95-16575
The impact of low temperature materials on the breakdown and noise properties of GaAs and InP based HEMT's and FET's
[AD-A285176] p 765 N95-16834
Performance characterization of photonic links in cryogenic environments for advanced signal processing applications
[DE94-015561] p 765 N95-16915
Performance evaluation of polyaniline as an active material for electrochemical capacitors
[DE94-016283] p 765 N95-16920
First measurements of ICRF and edge/SOL plasma interactions on TORE SUPRA
[DE94-019320] p 891 N95-17347
High current density sheet-like electron beam generator
[AD-A281975] p 880 N95-17499
ELECTRIC POWER
Calorimetric methods for loss measurements of small cage induction motors
[PB94-184439] p 768 N95-17691
ELECTRIC POWER TRANSMISSION
A study of electric transmission lines for use on the lunar surface p 712 N95-16053
ELECTRIC PROPULSION
ARCJET plasma modeling with experimental validation
[AD-A285234] p 889 N95-16243
ELECTRIC WIRE
Orbiter Kapton wire operational requirements and experience p 711 N95-16046
WSTF electrical arc projects p 711 N95-16047
Problems with aging wiring in Naval aircraft p 711 N95-16048
Space Station Freedom primary power wiring requirements p 712 N95-16051
Space Station Freedom secondary power wiring requirements p 712 N95-16052
High temperature polymer dielectric film-wire insulation p 712 N95-16055
New insulation constructions for aerospace wiring applications p 712 N95-16056
High performance dielectric materials development p 712 N95-16057
Flux imaging of high temperature superconductor single crystals and Ag sheathed wires
[DE94-013874] p 897 N95-16408
Reaction and protection of electrical wire insulators in atomic-oxygen environments
[NASA-TM-106767] p 709 N95-17275
ELECTRICAL FAULTS
Analog microcircuit fault prediction
[AD-A281958] p 763 N95-16410
Electrical breakdown and optical emission properties of high pressure pulsed RF gas discharges
[DE94-012731] p 877 N95-17687
ELECTRICAL GROUNDING
Elimination of electromagnetic interference to receivers and sensitive equipment generated by switching systems
[AD-A281643] p 752 N95-16117
ELECTRICAL INSULATION
First NASA Workshop on Wiring for Space Applications
[NASA-CP-10145] p 711 N95-16044
Orbiter Kapton wire operational requirements and experience p 711 N95-16046
WSTF electrical arc projects p 711 N95-16047
Problems with aging wiring in Naval aircraft p 711 N95-16048
Kapton pyrolysis on Space Station Freedom's solar array flexible current carrier p 712 N95-16049
Space Station Freedom primary power wiring requirements p 712 N95-16051
A study of electric transmission lines for use on the lunar surface p 712 N95-16053
High temperature polymer dielectric film-wire insulation p 712 N95-16055
New insulation constructions for aerospace wiring applications p 712 N95-16056
High performance dielectric materials development p 712 N95-16057
Reaction and protection of electrical wire insulators in atomic-oxygen environments
[NASA-TM-106767] p 709 N95-17275
ELECTRICAL MEASUREMENT
Extracellular ionic composition alters kinetics of vesicular release of catecholamines and quantal size during exocytosis at adrenal medullary cells
[AD-A281613] p 818 N95-16112
ELECTRICAL PROPERTIES
International Workshop on Light Emission and Electronic Properties of Nanoscale silicon
[AD-A281464] p 894 N95-16081
Interface properties of wide bandgap semiconductor structures
[AD-A281469] p 894 N95-16084
Research on stable, high-efficiency amorphous-silicon multijunction modules
[DE94-011839] p 764 N95-16425
Process of making a bistable photoconductive component
[AD-D016449] p 764 N95-16539
Relationships between ferroelectric 90 deg domain formation and electrical properties of chemically prepared Pb(Zr,Ti)O3 thin films
[DE94-015274] p 744 N95-16829
ELECTRICAL RESISTIVITY
ARCJET plasma modeling with experimental validation
[AD-A285234] p 889 N95-16243
Analysis of space environment damage to solar cell assemblies from LDEF experiment A0171-GSFC test plate
[NASA-CR-196523] p 793 N95-16575
Determination of the nuclear-induced electrical conductivity in a nuclear-driven MHD device
[DE94-013137] p 891 N95-17365
Ion modulated electroactivity in thin-film polymers derived from bipyridyl and phenanthroline complexes of iron
[AD-A280704] p 747 N95-17682
ELECTRIFICATION
Solar energy: Lessons from the Pacific island experience
[WORLD-BANK-TP-244] p 794 N95-17298
ELECTRO-OPTICAL EFFECT
Picosecond optoelectronic AND-GATE
[AD-A285672] p 885 N95-16620
ELECTRO-OPTICS
ARO-URI Center for Opto-Electronic Systems Research
[AD-A281447] p 883 N95-15958
Electric-optic resonant phase modulator
[NASA-CASE-NPO-18702-1-CU] p 883 N95-15960
Systematic optimization of second order nonlinear optical materials
[AD-A281350] p 884 N95-16015
International Workshop on Light Emission and Electronic Properties of Nanoscale silicon
[AD-A281464] p 894 N95-16081
Preliminary investigation of an integrated optic sampler for HF signals
[AD-A284285] p 884 N95-16133
Design of new multi-functional electroactive polymers with emphasis on optical nonlinearity
[AD-A284983] p 741 N95-16230
Overview of photonics research at Lawrence Livermore National Laboratory
[DE94-014055] p 884 N95-16366
The deposition of electro-optic films on semiconductors
[AD-A285068] p 742 N95-16488
Development of device quality nonlinear optical materials and definition of mechanisms of optical nonlinearity
[AD-A285255] p 885 N95-16528
A high average power electro-optic switch using KTP
[DE94-016416] p 765 N95-16925
Optoelectric technology roadmap: Conclusions and recommendations
[AD-A281664] p 886 N95-16965
New mechanisms and new materials for organic optical nonlinearity
[AD-A282781] p 886 N95-17143
Testing and characterization of the CYCLOPS HgCdTe focal plane detector array
[AD-A284279] p 887 N95-17489
Digital logic and reconfigurable interconnects using aluminum gallium arsenide electro-optic Fredkin gates
[AD-A282880] p 881 N95-17619
ELECTROACOUSTIC TRANSDUCERS
On the measurement of momentum flux profiles using a five-beam 915-MHz wind profiler
[DE94-018448] p 791 N95-17903
ELECTROCARDIOGRAPHY
Changes in left ventricular function as determined by the multi-wire gamma camera at near presyncopal levels of lower body negative pressure p 811 N95-16754
ELECTROCATALYSTS
The response of the Sandia robust wide range hydrogen sensor to H2-O2 mixtures
[DE94-013763] p 727 N95-16362
Aluminum permanganate battery
[AD-D016337] p 766 N95-16947
Improved dual flow aluminum hydrogen peroxide battery
[AD-D016339] p 766 N95-16949
ELECTROCHEMICAL CELLS
Charging hydrogen into Ni in hydride-containing molten salts
[AD-A282335] p 730 N95-16973
ELECTROCHEMICAL CORROSION
The use of electrochemistry and ellipsometry for identifying and evaluating corrosion on aircraft
[AD-A285276] p 734 N95-16370
The use of electrochemistry and ellipsometry for identifying and evaluating corrosion on aircraft
[AD-A285323] p 734 N95-16371
ELECTROCHEMISTRY
In situ laser activation of electrochemical kinetics at carbon electrodes
[AD-A280892] p 727 N95-16150
The use of electrochemistry and ellipsometry for identifying and evaluating corrosion on aircraft
[AD-A285276] p 734 N95-16370
The use of electrochemistry and ellipsometry for identifying and evaluating corrosion on aircraft
[AD-A285323] p 734 N95-16371
Electrochemical synthesis of ultrathin film composite membranes
[AD-A285075] p 724 N95-16492
In-situ x-ray characterization of the electrolyte-solid interface
[AD-A281165] p 729 N95-16627
Electro-separations: Efficient processing for the twenty-first century
[DE94-012656] p 732 N95-17524
Adhesion of silicon oxide to diamond
[AD-D016356] p 747 N95-17694
ELECTROCHROMISM
Nonlinear optical and charge distribution studies probing electric field effects in polymer thin films for second order nonlinear optics
[AD-A280980] p 742 N95-16483
ELECTRODE MATERIALS
Atomic structure and valency of nickel in some of its oxycompounds
[AD-A281109] p 733 N95-16091
Cyclic voltammetric analysis of ferrocene alkanethiol monolayer electrode kinetics based on Marcus theory
[AD-A281411] p 868 N95-16162
Molten salt techniques for excess heat production and the loading issue
[AD-A282462] p 792 N95-16303
XAFS spectra and the oxidation state of nickel in some of its oxycompounds
[AD-A281137] p 735 N95-16606
ELECTRODEPOSITION
Preparation of Au single crystals for study of the ECALE deposition of CdTe
[AD-A282294] p 895 N95-16238

Electrochemical atomic layer processing
[AD-A282330] p 872 N95-16241

ELECTRODES

In situ laser activation of electrochemical kinetics at carbon electrodes
[AD-A280892] p 727 N95-16150

Cyclic voltammetric analysis of ferrocene alkanethiol monolayer electrode kinetics based on Marcus theory
[AD-A281411] p 868 N95-16162

Effect of ion-electrode contact on the energetics of the heterogeneous electron transfer
[AD-A281959] p 873 N95-16411

Plasma sound source basic research
[AD-A285394] p 890 N95-16617

Picosecond optoelectronic AND-GATE
[AD-A285672] p 885 N95-16620

In-situ x-ray characterization of the electrolyte-solid interface
[AD-A281165] p 729 N95-16627

Charging hydrogen into Ni in hydride-containing molten salts
[AD-A282335] p 730 N95-16973

ELECTRODIALYSIS

Electro-separations: Efficient processing for the twenty-first century
[DE94-012656] p 732 N95-17524

ELECTRODYNAMICS

Radiation electrodynamics of the photo-electron cloud produced by an arbitrary photon pulse incident on a planar emitting surface in vacuum
[AD-A282153] p 759 N95-17450

Electro-separations: Efficient processing for the twenty-first century
[DE94-012656] p 732 N95-17524

ELECTROENCEPHALOGRAPHY

Event-related brain potentials as predictors of target detection performance in a moving waterfall display simulating passive broad-band sonar monitoring
[AD-A280900] p 819 N95-16152

ELECTROEPITAXY

LPEE growth and characterization of In(x)Ga(1-x)As(y)Sb(1-y) lattice matched to GaSb and InAs for photodetectors
[AD-A281631] p 895 N95-16114

ELECTROLUMINESCENCE

International Workshop on Light Emission and Electronic Properties of Nanoscale silicon
[AD-A281464] p 894 N95-16081

Recombination and metastability in amorphous silicon and silicon-germanium alloys
[DE94-011837] p 794 N95-16957

ELECTROLYSIS

Molten salt techniques for excess heat production and the loading issue
[AD-A282462] p 792 N95-16303

ELECTROLYTES

Fundamental studies of polyphosphazene and polysiloxane polyelectrolytes for electrochemical devices
[AD-A281339] p 739 N95-16013

Charge transfer processes on liquid/liquid interfaces: The status in 1994
[AD-A285067] p 729 N95-16635

Aluminum permanganate battery
[AD-D016337] p 766 N95-16947

Aluminum-ferricyanide battery
[AD-D016338] p 766 N95-16948

Ion modulated electroactivity in thin-film polymers derived from bipyridyl and phenanthroline complexes of iron
[AD-A280704] p 747 N95-17682

ELECTROMAGNETIC ABSORPTION

Synthesis of low band gap zwitterionic and planar conjugated pyrrole-derived polymers. Reversible optical absorbances from the UV to the near-IR
[AD-A281174] p 743 N95-16628

Synthesis of planar poly(p-phenylene) derivatives for maximization of extended pi-conjugation
[AD-A281179] p 743 N95-16630

ELECTROMAGNETIC FIELDS

Non-intrusive missile control surface monitor system
[AD-A285356] p 883 N95-15954

Electromagnetic processing of refractory metal silicide/oxide composites
[AD-A281470] p 740 N95-16085

Formulation of probe-corrected time-domain planar near-field measurements
[AD-A281053] p 754 N95-16624

Interaction of electromagnetic fields with magnetized plasmas
[AD-A285496] p 755 N95-16968

Electromagnetic field measurements on a mm-wave linear accelerator
[DE94-015092] p 761 N95-17926

ELECTROMAGNETIC INTERACTIONS

High-intensity and high energy laser interactions with single droplets
[AD-A281415] p 776 N95-16166

A Lifting Ball Valve for cryogenic fluid applications
p 720 N95-16349

Static image method for the interaction of two co-axial conducting prolate spheroids
[PB94-197696] p 760 N95-17502

ELECTROMAGNETIC INTERFERENCE

Electromagnetic interference tests
[AD-A281396] p 755 N95-16800

An analysis of the effects of feedline and ground screen noise currents on a conical monopole receiving antenna
[AD-A283401] p 759 N95-17436

ELECTROMAGNETIC MEASUREMENT

Formulation of probe-corrected time-domain planar near-field measurements
[AD-A281053] p 754 N95-16624

ELECTROMAGNETIC RADIATION

Optimum truncation of a Gaussian beam in the presence of random jitter
[AD-A284951] p 752 N95-16143

Interaction of electromagnetic fields with magnetized plasmas
[AD-A285496] p 755 N95-16968

The m-line method for optical characterisation of polymer waveguides
[PB94-184611] p 887 N95-17409

Radiation electrodynamics of the photo-electron cloud produced by an arbitrary photon pulse incident on a planar emitting surface in vacuum
[AD-A282153] p 759 N95-17450

Simultaneous determination of incoming microwave frequency and angle-of-arrival
[AD-D016392] p 760 N95-17482

Radial acceletron, a new low impedance HPM source
[AD-A282008] p 760 N95-17501

ELECTROMAGNETIC SHIELDING

Elimination of electromagnetic interference to receivers and sensitive equipment generated by switching systems
[AD-A281643] p 752 N95-16117

ELECTROMAGNETIC WAVE TRANSMISSION

Fractal aggregate random media analysis and applications
[AD-A281410] p 884 N95-16161

ELECTROMECHANICAL DEVICES

Electromagnetic interference tests
[AD-A281396] p 755 N95-16800

ELECTROMECHANICS

Engineering design tools for wind diesel systems. Volume 1: Executive summary
[PB95-104501] p 842 N95-17733

ELECTROMYOGRAPHY

Variability in Hoffmann and tendon reflexes in healthy male subjects p 808 N95-16739

Intramuscular pressure: A better tool than EMG to optimize exercise for long-duration space flight
p 809 N95-16744

ELECTRON AFFINITY

Interface properties of wide bandgap semiconductor structures
[AD-A281469] p 894 N95-16084

ELECTRON AVALANCHE

Runaway electrons beams in ITER disruptions
[DE94-013788] p 888 N95-16122

ELECTRON BEAM WELDING

Electron beam weld development on a Filter Pack Assembly
[DE94-015867] p 782 N95-17716

ELECTRON BEAMS

SEPAC co-investigator support
[NASA-CR-196527] p 798 N95-15965

Runaway electrons beams in ITER disruptions
[DE94-013788] p 888 N95-16122

The LANL-Boeing APLE/HPO flying-wire beam-profile monitor
[DE94-014255] p 879 N95-16172

Low voltage electron beam lithography
[AD-A281046] p 729 N95-16622

Beams 92: Proceedings
[DE94-014784] p 880 N95-17475

High current density sheet-like electron beam generator
[AD-A281975] p 880 N95-17499

Recent advances in the development of high average power induction accelerators for industrial and environmental applications
[DE94-018734] p 882 N95-17914

Electromagnetic field measurements on a mm-wave linear accelerator
[DE94-015092] p 761 N95-17926

ELECTRON CLOUDS

Radiation electrodynamics of the photo-electron cloud produced by an arbitrary photon pulse incident on a planar emitting surface in vacuum
[AD-A282153] p 759 N95-17450

ELECTRON COUNTERS

New shower maximum trigger for electrons and photons at CDF
[DE94-018376] p 878 N95-17899

ELECTRON DENSITY (CONCENTRATION)

A CO2 laser polarimeter for measurement of plasma current profile in Alcator C-Mod
[DE94-014017] p 776 N95-16486

Multi-beam laser interferometer for plasma density measurements in a Plasma Erosion Opening Switch (PEOS)
[AD-A283209] p 892 N95-17623

Effect of low density H-mode operation on edge and divertor plasma parameters
[DE94-016521] p 892 N95-17640

Theoretical studies of the strengths of matrix second phase particle interfaces
[AD-A280703] p 738 N95-17681

ELECTRON DENSITY PROFILES

Differential phase reflectometry for edge profile measurements on TFTR
[DE94-013837] p 891 N95-16958

ELECTRON DIFFRACTION

Runaway electrons beams in ITER disruptions
[DE94-013788] p 888 N95-16122

Study of CuPt-type ordering and dopant effect of In(0.5)Ga(0.5)P/GaAs using spectroscopic ellipsometry
[DE94-018890] p 902 N95-17917

ELECTRON EMISSION

BEEM 94. The Fifth Annual Workshop on Ballistic Electron Emission Microscopy
[AD-A281522] p 872 N95-16098

Control of a large vacuum wave precursor on the SABRE voltage adder MITL and extraction ion diode
[DE94-014280] p 888 N95-16216

How clean is clean: Non-destructive/direct methods of flux, residue detection
[DE94-013439] p 763 N95-16357

Extended test of a xenon hollow cathode for a space plasma contactor
[NASA-CR-195402] p 720 N95-17265

Preparation and investigation of improved low voltage electron excitable phosphors
[AD-A284265] p 767 N95-17487

ELECTRON ENERGY

Atomic scale structure and chemistry of interfaces by Z-contrast imaging and electron energy loss spectroscopy in the stem
[DE94-013632] p 728 N95-16419

Active silicon x ray for measuring electron temperature
[DE94-017521] p 890 N95-16555

Spectroscopy of the transition state region in hydrogen transfer reactions
[AD-A285151] p 729 N95-16846

ELECTRON GUNS

Development of a medium energy modulated electron gun for orbital experiments
[AD-A281021] p 675 N95-16005

High brightness cathodes for microfocus x-ray generators
[AD-A285256] p 764 N95-16814

ELECTRON IMPACT

Mass spectral data of alkyl and cycloalkyl methylphosphonofluoridates
[AD-A285312] p 722 N95-16734

ELECTRON MICROSCOPES

Development and applications of the positron microscope
[DE94-017918] p 883 N95-15947

Advances in ultrafast scanning probe microscopy
[DE94-018180] p 779 N95-17729

ELECTRON MICROSCOPY

BEEM 94. The Fifth Annual Workshop on Ballistic Electron Emission Microscopy
[AD-A281522] p 872 N95-16098

ELECTRON MOBILITY

Quantum transport in semiconductor devices
[AD-A281383] p 895 N95-16158

Monte Carlo simulation of mercury cadmium telluride
[AD-A281546] p 896 N95-16391

ELECTRON PARAMAGNETIC RESONANCE

Reliability implications of defects in high temperature annealed Si/SiO2/Si structures
[DE94-015765] p 895 N95-16311

ELECTRON SCATTERING

Atomic scale structure and chemistry of interfaces by Z-contrast imaging and electron energy loss spectroscopy in the stem
[DE94-013632] p 728 N95-16419

Low voltage electron beam lithography
[AD-A281046] p 729 N95-16622

First principles simulation of materials properties
[DE94-013615] p 899 N95-16805
Light-ray operators and their application in QCD
[DE94-013801] p 903 N95-16944

ELECTRON TRANSFER
BEEM 94. The Fifth Annual Workshop on Ballistic Electron Emission Microscopy
[AD-A281522] p 872 N95-16098
Electron transport and tunneling experiments
[AD-A281527] p 894 N95-16106
Cyclic voltammetric analysis of ferrocene alkanethiol monolayer electrode kinetics based on Marcus theory
[AD-A281411] p 868 N95-16162
Monte Carlo simulation of mercury cadmium telluride
[AD-A281546] p 896 N95-16391
Effect of ion-electrode contact on the energetics of the heterogeneous electron transfer
[AD-A281959] p 873 N95-16411
Electrochemical properties of lithium ion conducting solid polymer electrolytes
[AD-A281875] p 742 N95-16434
Ion modulated electroactivity in thin-film polymers derived from bipyridyl and phenanthroline complexes of iron
[AD-A280704] p 747 N95-17682

ELECTRON TUNNELING
Electron transport and tunneling experiments
[AD-A281527] p 894 N95-16106
Quantum transport in semiconductor devices
[AD-A281383] p 895 N95-16158
Advances in ultrafast scanning probe microscopy
[DE94-018180] p 779 N95-17729

ELECTRON-POSITRON PAIRS
Strong WW scattering at photon linear colliders
[DE94-018183] p 878 N95-17720

ELECTRONIC COUNTERMEASURES
Mitre adaptive processing capability
[AD-A281078] p 755 N95-16825

ELECTRONIC EQUIPMENT
Use of the electronic balance for highly accurate direct mass measurements without the use of external mass standards
[PB94-187713] p 774 N95-16074
Electromagnetic interference tests
[AD-A281396] p 755 N95-16800
Fire protection engineering criteria: Electronic equipment installations
[AD-A285174] p 750 N95-16853
An elastomeric electrical connector
[AD-D016340] p 766 N95-16950
Self-initializing circuit link
[AD-D016363] p 761 N95-17696

ELECTRONIC MODULES
Liquid Cooled Heat Sink with Through Vias (LCHS)
[AD-A281450] p 902 N95-16075
Ceramic/metal composite circuit-board-level technology for Application Specific Electronic Modules (ASEMs)
[AD-A285066] p 741 N95-16369

ELECTRONIC PACKAGING
Natural convection cooling of a three by three array of leadless chip carrier packages in a dielectric liquid
[AD-A282298] p 770 N95-16239

ELECTRONIC WARFARE
Parallel implementation of the terrain masking algorithm
[AD-A281017] p 833 N95-16003
Division of Information Systems (FOA 37)
[PB94-190766] p 909 N95-16400

ELECTRONS
New methods for treatment of electron correlation and surface dynamics (FY91 AASERT)
[AD-A285177] p 727 N95-16144
Fast electrons, filamented laser light, and the fast ignitor
[DE94-015898] p 777 N95-16929
Centrifugal space-charge force for bunched beams
[DE94-016097] p 875 N95-16933
A search for muons yields e gamma at the level of 10(exp -13)
[DE94-014488] p 876 N95-17158
Electron-neutrino phase separation instability
[DE94-016859] p 904 N95-17645
New shower maximum trigger for electrons and photons at CDF
[DE94-018376] p 878 N95-17899
The three loop equation of state of QED at high temperature
[DE94-015029] p 904 N95-17925

ELECTROPHORESIS
Characterization of surfaces
[NASA-CR-196995] p 750 N95-16065
Electro-separations: Efficient processing for the twenty-first century
[DE94-012656] p 732 N95-17524

ELECTROPHYSIOLOGY
Characterization of neurotrophic and neurotropic interactions between neurons and their muscle and nerve targets
[AD-A281846] p 820 N95-16423

ELECTROSTATIC PROBES
Fluctuation measurements at c/(omega)(sub pe) spatial scales in a tokamak
[DE94-016771] p 892 N95-17643

ELECTROSTATICS
Static image method for the interaction of two co-axial conducting prolate spheroids
[PB94-197696] p 760 N95-17502
Fluctuation measurements at c/(omega)(sub pe) spatial scales in a tokamak
[DE94-016771] p 892 N95-17643

ELECTROWEAK INTERACTIONS (FIELD THEORY)
RHIC spin: The first polarized proton collider
[DE94-013760] p 872 N95-16121
A measurement of the Michel parameter (rho) in muon decay
[DE94-014423] p 876 N95-17153
A search for muons yields e gamma at the level of 10(exp -13)
[DE94-014488] p 876 N95-17158
Multilepton SUSY signals from R-parity violation at the Tevatron (revised)
[PB95-104311] p 877 N95-17353
Physics at high energy photon photon colliders
[DE94-018191] p 881 N95-17888

ELECTROWEAK MODEL
A measurement of the Michel parameter (rho) in muon decay
[DE94-014423] p 876 N95-17153
Electron-neutrino phase separation instability
[DE94-016859] p 904 N95-17645

ELEMENTARY PARTICLE INTERACTIONS
Research in elementary particle physics
[DE94-019219] p 877 N95-17358

ELEMENTARY PARTICLES
High Energy Physics Division research activities
[DE94-015024] p 882 N95-17924

ELEVATION
Climatological targets for Mars Pathfinder p 922 N95-16208

ELEVATION ANGLE
High speed method for predicting radio-wave propagation
[AD-D016369] p 761 N95-17697

ELEVATOR ILLUSION
The psychophysical function for perceived gravitational-inertial force does not depend on the orientation of the otolith organs p 808 N95-16740

ELLIPSOMETRY
The use of electrochemistry and ellipsometry for identifying and evaluating corrosion on aircraft
[AD-A285276] p 734 N95-16370
The use of electrochemistry and ellipsometry for identifying and evaluating corrosion on aircraft
[AD-A285323] p 734 N95-16371
Study of CuPt-type ordering and dopant effect of In(0.5)Ga(0.5)P/GaAs using spectroscopic ellipsometry
[DE94-018890] p 902 N95-17917

ELLIPTIC DIFFERENTIAL EQUATIONS
A new communication scheme for the neutron diffusion nodal method in a distributed computing environment
[DE94-017907] p 844 N95-15946
Radiative interactions in chemically reacting compressible nozzle flows using Monte Carlo simulations
[NASA-CR-197133] p 769 N95-15966

ELLIPTICAL CYLINDERS
Ellipsoid-cylinder model p 661 N95-17869

ELLIPTICAL GALAXIES
The mass and dynamics of cD clusters with cooling flows. 1: ROSAT observations of A 496
[NASA-CR-197534] p 915 N95-17495

ELONGATION
Effect of extrusion parameters on consolidation of tungsten-hafnium and tungsten-steel powders
[DE94-013270] p 737 N95-17513
Status of the US stellarator reactor study
[DE94-018693] p 893 N95-17907

EMBEDDING
ICONF: An incremental constraint facility in a feature modelling system
[PB94-197654] p 837 N95-16605
An elastomeric electrical connector
[AD-D016340] p 766 N95-16950

EMISSION SPECTRA
Space Shuttle main engine OPAD: The search for a hardware enhanced plume p 716 N95-16330
Na-22 decay gamma rays from classical novae
[NASA-CR-197454] p 924 N95-16383
The stability of calibration standards for ICP/AES analysis: A two-year study
[DE94-013398] p 728 N95-16426
New ytterbium-doped apatite crystals for flexible laser design
[DE94-015138] p 899 N95-16867
Equatorial airglow studies via rocket experiment
[INPE-5589-TDI/551] p 799 N95-17647

EMITTANCE
Mechanisms of beam-halo formation in high-intensity linacs
[DE94-016316] p 879 N95-16030
Beam parameter measurements for the APS linac system
[DE94-018396] p 882 N95-17902

EMITTERS
High brightness cathodes for microfocus x-ray generators
[AD-A285256] p 764 N95-16814

EMPTYING
Generic propellant transfer unit: A project update p 719 N95-16345

ENCAPSULATING
Encapsulated alkaline-earth organometallics as controlled sources of calcium, strontium, and barium ions
[AD-A281547] p 741 N95-16393

ENCLOSURE
Active minimization of energy density in three-dimensional enclosures
[NASA-CR-197213] p 871 N95-16848

END EFFECTORS
Multimodal correlation and intraoperative matching of virtual models in neurosurgery p 823 N95-15976
Lunar surface operations. Volume 3: Robotic arm for lunar surface vehicle
[NASA-CR-195553-VOL-3] p 780 N95-16031
Bracing micro/macro manipulators control
[DE94-014434] p 856 N95-16287

END-TO-END DATA SYSTEMS
End-to-end communication test on variable length packet structures utilizing AOS testbed p 677 N95-17186
Evaluation of NASA's end-to-end data systems using DSDS+ p 700 N95-17577

ENDEAVOUR (ORBITER)
Houston, I think we've got a satellite
[NASA-TM-109987] p 709 N95-16941

ENERGETIC PARTICLES
Solar flares and magnetospheric particles: Investigations based upon the ONR-602 and ONR-604 experiments
[AD-A281463] p 923 N95-16080

ENERGY BUDGETS
Evaluation of SEA loss factors using input power modulation
[ISVR-TR-240] p 868 N95-16856

ENERGY CONSERVATION
Assessment of research needs for advanced heterogeneous catalysts for energy applications, volume 1
[DE94-015889] p 795 N95-16386
Assessment of research needs for advanced heterogeneous catalysts for energy applications, volume 2
[DE94-015890] p 727 N95-16387
Alternatives to traditional transportation fuels: An overview
[DE94-014979] p 749 N95-17923

ENERGY CONSUMPTION
Energy expenditure, physical work load and postural control during walking on a moving platform
[AD-A285343] p 830 N95-16821
Energy and emissions of CO2, NOx and SO2 in the scenario of the 3rd national environmental evaluation, 1993
[PB94-194792] p 796 N95-17304

ENERGY CONVERSION
Landfill gas energy utilization: Technical and nontechnical considerations
[PB94-189651] p 793 N95-16544
Determination of the nuclear-induced electrical conductivity in a nuclear-driven MHD device
[DE94-013137] p 891 N95-17365
Overview of space power electronic's technology under the CSTI High Capacity Power Program
[NASA-TM-110110] p 883 N95-17933

ENERGY CONVERSION EFFICIENCY
Research on stable, high-efficiency, amorphous silicon multijunction modules
[DE94-011826] p 794 N95-17521

ENERGY DISSIPATION
An analysis code for the Rapid Engineering Estimation of Momentum and Energy Losses (REMEL)
[NASA-CR-191178] p 656 N95-16887

ENERGY GAPS (SOLID STATE)
Interface properties of wide bandgap semiconductor structures
[AD-A281469] p 894 N95-16084
ENERGY OF FORMATION
Plasma sound source basic research
[AD-A285394] p 890 N95-16617
ENERGY POLICY
Alternatives to traditional transportation fuels: An overview
[DE94-014979] p 749 N95-17923
ENERGY SPECTRA
Very high gamma ray extension of GRO observations
[NASA-CR-197489] p 924 N95-17421
ENERGY STORAGE
Nickel hydrogen batteries: An overview
[NASA-TM-106795] p 793 N95-16861
ENERGY TECHNOLOGY
Department of Energy: Office of Scientific and Technical Information p 907 N95-15936
Assessment of research needs for advanced heterogeneous catalysts for energy applications, volume 2
[DE94-015890] p 727 N95-16387
Fuel cell systems program plan, fiscal year 1994
[DE94-014301] p 793 N95-16541
Solar energy: Lessons from the Pacific island experience
[WORLD-BANK-TP-244] p 794 N95-17298
Abstracts: Eighth Annual Conference on Fossil Energy Materials
[DE94-014053] p 725 N95-17368
Two phase liquid helium flow testing to simulate the operation of a cryocondensation pump in the D3-D tokamak
[DE94-018345] p 893 N95-17896
ENERGY TRANSFER
Papers presented at the Tenth Topical Conference on High-Temperature Plasma Diagnostics
[DE94-015854] p 888 N95-16063
Thermal dissociation of halogen azides
[AD-A285088] p 728 N95-16497
FIFE data analysis: Testing BIOME-BGC predictions for grasslands
[NASA-CR-197522] p 790 N95-16895
A new approach to validate subgrid models in complex high Reynolds number flows
[AD-A282340] p 772 N95-17165
Transport efficiency studies for light-ion inertial confinement fusion
[AD-A285675] p 891 N95-17382
Status of the US stellarator reactor study
[DE94-018693] p 893 N95-17907
ENGINE AIRFRAME INTEGRATION
Cooperative control theory and integrated flight and propulsion control
[NASA-CR-197493] p 671 N95-17404
ENGINE CONTROL
An object-oriented graphical user interface for a reusable rocket engine intelligent control system
[NASA-TM-106750] p 721 N95-17274
Cooperative control theory and integrated flight and propulsion control
[NASA-CR-197493] p 671 N95-17404
ENGINE DESIGN
Small turbojets: Designs and installations
p 670 N95-16323
Integrated modular engine configuration options
p 717 N95-16336
Investigations on the sensitivity of the computer code TURBO-2D
[CUED/A-THERMO/TR-61] p 771 N95-16595
An investigation of fluid flow during induction stroke of a water analog model of an IC engine using an innovative optical velocimetry concept: LIPA
[NASA-CR-197451] p 780 N95-16900
Thermoacoustic pin stacks
[AD-A282267] p 794 N95-16954
Experimental and analytical methods for the determination of connected-pipe ramjet and ducted rocket internal performance
[AGARD-AR-323] p 721 N95-17278
ENGINE INLETS
Three dimensional compressible turbulent flow computations for a diffusing S-duct with/without vortex generators
[NASA-CR-195390] p 670 N95-17402
ENGINE MONITORING INSTRUMENTS
SSME propellant path leak detection real-time
[NASA-CR-197032] p 748 N95-16029
An artificial neural network system for diagnosing gas turbine engine fuel faults
[DE94-013960] p 670 N95-17371
ENGINE TESTS
Theoretical fundamentals of the aircraft GTE tests
p 651 N95-16265
Scramjet testing guidelines p 670 N95-16317
Hypersonic air-breathing aeropropulsion facility test support requirements p 672 N95-16319
Free-jet testing at Mach 3.44 in GASL's aero/thermo test facility p 672 N95-16320
An in-cylinder study of the particulate/NO(x) trade-off in a DI diesel engine
[DE94-014599] p 781 N95-17162
ENGINEERING MANAGEMENT
STARS Conceptual Framework for Reuse Process (CFRP). Volume 1: Definition, version 3.0
[AD-A281506] p 834 N95-16167
Concurrent engineering: Spacecraft and mission operations system design p 708 N95-17614
ENGINEERS
Development of strength analysis methods and design model for aircraft constructions in Kazan Aviation Institute p 651 N95-16264
Scientific and technical publishing at Goddard Space Flight Center in Fiscal Year 1994
[NASA-TM-104614] p 925 N95-16581
Proceedings of the Neural Network Workshop for the Hanford Community
[DE94-014567] p 856 N95-16609
ICASE
[NASA-CR-195001] p 832 N95-16898
Selected properties of iron aluminides
[DE94-018057] p 738 N95-17726
ENRICHMENT
Root growth and development in response to CO2 enrichment
[NASA-CR-196154] p 807 N95-16429
ENTHALPY
Liquid crystal materials for laser beam steering
[AD-A285089] p 897 N95-16498
Study of the structuring of pure molecular liquids
[PB94-201316] p 903 N95-16839
The solvation thermodynamic functions in the Mean Spherical Approximation (MSA): Behavior near the solvent critical region
[AD-A283040] p 904 N95-17712
ENTRAINMENT
Active and passive acoustic bubble sizing
[ISVR-TR-237] p 769 N95-16064
Neurophysiological analysis of circadian rhythm entrainment
[AD-A280981] p 821 N95-16484
ENTROPY
Coarse geometry of foliations
[PB94-192309] p 860 N95-16291
The solvation thermodynamic functions in the Mean Spherical Approximation (MSA): Behavior near the solvent critical region
[AD-A283040] p 904 N95-17712
ENVIRONMENT EFFECTS
Three-dimensional eutrophication model of Chesapeake Bay. Volume 1: Main report
[AD-A280760] p 804 N95-16118
Global warming potentials, part 7
[DE94-014066] p 794 N95-16209
Simulations of the global carbon cycle and anthropogenic CO2 transient
[DE94-014165] p 795 N95-16212
Global climate change model natural climate variation: Paleoclimate data base, probabilities and astronomic predictors
[DE94-013956] p 796 N95-17348
ENVIRONMENT MANAGEMENT
Site characterization at the Rabbit Valley Geophysical Performance Evaluation Range
[DE94-013550] p 798 N95-16284
Energy and emissions of CO2, NOx and SO2 in the scenario of the 3rd national environmental evaluation, 1993
[PB94-194792] p 796 N95-17304
Proceedings of the First National Conference on Climate Change and Water Resources Management
[AD-A281172] p 796 N95-17684
ENVIRONMENT MODELS
Three-dimensional eutrophication model of Chesapeake Bay. Volume 1: Main report
[AD-A280760] p 804 N95-16118
Simulation of hydrologic influences on wetland ecosystem succession
[AD-A284737] p 795 N95-16545
FIFE data analysis: Testing BIOME-BGC predictions for grasslands
[NASA-CR-197522] p 790 N95-16895
Abstracts and program Proceedings of the 1994 Meeting of the International Society for Ecological Modelling North American Chapter
[DE94-016456] p 796 N95-17636
CERES, phases 1 and 2
[DE94-014730] p 797 N95-17920
ENVIRONMENT PROTECTION
Precision aqueous cleaner for RSRM
p 715 N95-16326
Assessment of research needs for advanced heterogeneous catalysts for energy applications, volume 1
[DE94-015889] p 795 N95-16386
Assessment of research needs for advanced heterogeneous catalysts for energy applications, volume 2
[DE94-015890] p 727 N95-16387
Physical and chemical sensor technologies developed at Lawrence Livermore National Laboratory
[DE94-012231] p 775 N95-17380
ENVIRONMENT SIMULATION
Physics-based approach to haptic display
p 854 N95-15986
Studies of D-Li neutron source: An overview
[DE94-014032] p 873 N95-16487
Reaction and protection of electrical wire insulators in atomic-oxygen environments
[NASA-TM-106767] p 709 N95-17275
ENVIRONMENTAL ENGINEERING
Simulating the energy performance of holographic glazings
[DE94-013110] p 775 N95-17307
ENVIRONMENTAL MONITORING
South Florida environmental quality. National Status and Trends Program for marine environmental quality
[PB94-173408] p 796 N95-17363
ENVIRONMENTAL TESTS
Design of thermocouple probes for measurement of rocket exhaust plume temperatures
[AD-A285423] p 774 N95-16247
Site characterization at the Rabbit Valley Geophysical Performance Evaluation Range
[DE94-013550] p 798 N95-16284
Atomic oxygen durability evaluation of the flexible batten for the photovoltaic array mast on Space Station
[NASA-TM-106798] p 781 N95-17263
ENZYMES
Investigation of pressure regulation in an archaebacterial enzyme
[AD-A281413] p 807 N95-16164
ENZYMOLOGY
Investigation of pressure regulation in an archaebacterial enzyme
[AD-A281413] p 807 N95-16164
EPIDEMIOLOGY
Aviation epidemiology data register: Age-specific medical and nonmedical attrition rates among Fort Rucker civilian aviators
[AD-A284970] p 818 N95-16132
EPINEPHRINE
Catecholaminergic responses to stressful motion stimuli, scopolamine plus amphetamine, and dexamethasone
p 809 N95-16745
EPITAXY
Workshop on Epitaxy, Interfaces, Defects and Processing of Electronic and Photonic Materials
[AD-A281595] p 894 N95-16111
Preparation of Au single crystals for study of the ECALE deposition of CdTe
[AD-A282294] p 895 N95-16236
Electrochemical atomic layer processing
[AD-A282330] p 872 N95-16241
The deposition of electro-optic films on semiconductors
[AD-A285068] p 742 N95-16488
Atomic layer epitaxy of group 4 materials: Surface processes, thin films, devices and their characterization
[AD-A280987] p 898 N95-16532
HTS SNS devices on large-area substrates by single-source MOCVD
[AD-A285159] p 899 N95-16849
Epitaxial MOCVD of thin film ceramics for pyroelectric detectors
[AD-A281397] p 744 N95-16863
Investigation of novel electrical transport phenomena in semimetal-semiconductor heterostructures
[AD-A281406] p 901 N95-17424
BaF2/GaAs electronic components
[AD-D016391] p 767 N95-17481
Study of CuPt-type ordering and dopant effect of In(0.5)Ga(0.5)P/GaAs using spectroscopic ellipsometry
[DE94-018890] p 902 N95-17917
EPOXY MATRIX COMPOSITES
Atomic oxygen durability evaluation of the flexible batten for the photovoltaic array mast on Space Station
[NASA-TM-106798] p 781 N95-17263
EPOXY RESINS
Conducting polymers as corrosion resistant coatings
[DE94-018265] p 748 N95-17892

EQUATIONS OF MOTION
Real-time simulation of large-scale multibody systems using automated equation decoupling techniques
[AD-A281544] p 856 N95-16390
Evaluation of the dynamic stability characteristics of the NAL Light Transport Aircraft
[NAL-PD-CA-9217] p 671 N95-16392
Crystalline beams: The vertical zigzag
[DE94-017986] p 901 N95-17673
Studies of transverse coherent bunch instabilities for the Advanced Light Source (ALS)
[DE94-018536] p 904 N95-17904

EQUATIONS OF STATE
Characterization on defect solids
[NASA-CR-197540] p 746 N95-17654
FEM3C, an improved three-dimensional heavy-gas dispersion model: User's manual
[DE94-014731] p 797 N95-17922
The three loop equation of state of QED at high temperature
[DE94-015029] p 904 N95-17925

EQUATORIAL ATMOSPHERE
Equatorial airglow studies via rocket experiment
[INPE-5589-TDI/551] p 799 N95-17647

EQUATORIAL REGIONS
Variation of the thermohaline structure in the western equatorial Pacific upper ocean p 805 N95-17277
Long-term momentum and heat balances and turbulent mixing in the upper equatorial Pacific Ocean p 805 N95-17395
An observational study of long waves in the equatorial Pacific Ocean during the 1991-1993 El Nino
[AD-A283380] p 806 N95-17624

EROSION
Plasma disruption modeling and simulation
[DE94-015095] p 889 N95-16307
Erosion effects on TVC vane heat transfer characteristics
[AD-A282006] p 721 N95-17448

ERROR ANALYSIS
A posteriori error estimation new approach
[AD-A284960] p 860 N95-16127
Performance of a fast frequency-hopped noncoherent MFSK receiver with non-ideal noise normalization combining over ricean fading channels with partial-band interference
[AD-A284989] p 753 N95-16232
Researches on gear fault diagnosis techniques p 651 N95-16267
Experimental study of spatially incomplete structural system identification
[AD-A280905] p 785 N95-16502
Error propagation equations for estimating the uncertainty in high-speed wind tunnel test results
[DE94-014136] p 671 N95-16509
A new model for estimating total body water from bioelectrical resistance p 810 N95-16747
Field verification of the wind tunnel coefficients p 664 N95-17291
Rheology and structure of planetary near-surface materials from landform topography p 922 N95-17392
A model study of element residual estimators for linear elliptic problems: The quality of the estimators in the interior of meshes of triangles and quadrilaterals
[AD-A282849] p 863 N95-17431
Error estimation and adaptive mesh refinement for parallel analysis of shell structures
[NASA-CR-197500] p 788 N95-17492

ERROR CORRECTING CODES
Error control techniques for satellite and space communications
[NASA-CR-197459] p 761 N95-17665

ERROR DETECTION CODES
Avoiding BDF stability barriers in the MOL solution of advection-dominated problems
[DE94-014793] p 861 N95-16535
On the application of under-decimated filter banks p 757 N95-17285
A simplified Integer Cosine Transform and its application in image compression p 757 N95-17286
JPL-ANTOPT antenna structure optimization program p 759 N95-17297

ERRORS
Human performance in the modern cockpit p 813 N95-16764
Experimental characterization of ALS undulator radiation
[DE94-017967] p 881 N95-17671

ERYTHROCYTES
Prediction of space sickness in astronauts from preflight fluid, electrolyte, and cardiovascular variables and Weightless Environmental Training Facility (WETF) training p 812 N95-16757

ESCHERICHIA
Hemoglobin-based blood substitutes and enhanced susceptibility to bacterial infections
[AD-A281023] p 820 N95-16444

ESTERS
Hydromining a full-scale class 1.1 solid rocket motor p 713 N95-16314

ESTIMATING
Efficient estimation of the mean time between failures in non-regenerative dependability models
[AD-A281563] p 783 N95-16421
A combined biased-robust estimator for dealing with influence and collinearity in regression
[AD-A281793] p 864 N95-16422
A model study of element residual estimators for linear elliptic problems: The quality of the estimators in the interior of meshes of triangles and quadrilaterals
[AD-A282849] p 863 N95-17431
Automated Estimating System (AES) version 6.0: User's manual
[DE94-013636] p 841 N95-17514

ETCHING
Microchannel formation in polyimide by heavy ion irradiation
[DE94-753315] p 740 N95-16073
Electrochemical atomic layer processing
[AD-A282330] p 872 N95-16241

ETHERS
Synthesis and characterization of a new class of thermosetting resins: Allyl and propargyl substituted cyclopentadiene derivatives
[AD-A281976] p 746 N95-17485

ETHYL COMPOUNDS
Iterative divergent/convergent doubling approach to linear conjugated oligomers. A rapid route to a 128 A long potential molecular wire
[AD-A281295] p 874 N95-16784
Synthesis and mesomorphic behavior of poly((2S, 3S)-(+)-2-chloro-3-methylpentyl xy)biphenyl-4-carboxylate s with ethyl and propyl alkyl groups
[AD-A281402] p 744 N95-16865

ETHYLENE COMPOUNDS
Isomorphism within the hexagonal columnar mesophase of molecular and macromolecular self- and co-assembled columns containing tapered groups
[AD-A281205] p 874 N95-16797
The influence of the complexation of sodium and lithium triflate on the self-assembly of tubular-supramolecular architectures displaying a columnar mesophase based on taper-shaped monoesters of oligoethyleneoxide with 3,4,5-tris(p-(n-dodecan-l-yloxy)benzyloxy)benzoic acid and of their polymethacrylates
[AD-A281403] p 730 N95-16866

ETHYLENE OXIDE
The influence of the complexation of sodium and lithium triflate on the self-assembly of tubular-supramolecular architectures displaying a columnar mesophase based on taper-shaped monoesters of oligoethyleneoxide with 3,4,5-tris(p-(n-dodecan-l-yloxy)benzyloxy)benzoic acid and of their polymethacrylates
[AD-A281403] p 730 N95-16866

EUCLIDEAN GEOMETRY
Single-pass method for the solution of inverse potential and rotational problems. Part 2: Fully 3-D potential theory and applications p 664 N95-16564

EULER EQUATIONS OF MOTION
A modified restricted Euler equation for turbulent flows with mean velocity gradients
[NASA-CR-194979] p 769 N95-16070
On bi-grid local mode analysis of solution techniques for 3-D Euler and Navier-Stokes equations
[NASA-TM-106749] p 771 N95-16855
New developments in the method of space-time conservation element and solution element-applications to two-dimensional time-marching problems
[NASA-TM-106758] p 862 N95-16885
Application of the space-time conservation element and solution element method to shock-tube problem
[NASA-TM-106806] p 772 N95-16903
Fifth International Conference on Hyperbolic Problems: Theory, Numerics, Applications
[AD-A283078] p 863 N95-17333
Magnetometer-only attitude and rate determination for a gyro-less spacecraft p 694 N95-17546

EURECA (ESA)
Experience with the EURECA Packet Telemetry and Packet Telecommand system p 682 N95-17209
EURECA mission control experience and messages for the future p 690 N95-17252

EUROPEAN SPACE AGENCY
Payload operations management of a planned European SL-Mission employing establishments of ESA and national agencies p 684 N95-17221
Modeling ESA's TT/C systems p 701 N95-17579

EUROPEAN SPACE PROGRAMS
The Sequence of Events generator: A powerful tool for mission operations p 688 N95-17240

EUTECTICS
Liquid crystal materials for laser beam steering
[AD-A285089] p 897 N95-16498

EUTROPHICATION
Three-dimensional eutrophication model of Chesapeake Bay. Volume 1: Main report
[AD-A280760] p 804 N95-16118
Flow over abrupt topography: The application of patterns in nutrient and productivity in reflecting physical processes
[AD-A280813] p 797 N95-17740

EVALUATION
High performance dielectric materials development p 712 N95-16057
Validation of astronaut psychological select-in criteria p 813 N95-16762
Performance evaluation of polyaniline as an active material for electrochemical capacitors
[DE94-016283] p 765 N95-16920

EVAPORATION
Characterization of the corrosion behavior of the carbon steel liner in Hanford site single-shell tanks
[DE94-016475] p 737 N95-17637

EVERGLADES (FL)
South Florida environmental quality. National Status and Trends Program for marine environmental quality
[PB94-173408] p 796 N95-17363

EVOKED RESPONSE (PSYCHOPHYSIOLOGY)
Direct comparison of two statistical methods for determination of evoked-potential thresholds
[AD-A285182] p 870 N95-16811

EXCITATION
Inelastic neutron scattering and antiferromagnetic fluctuations in high temperature superconductors
[DE94-623269] p 871 N95-16059
Laser induced fluorescence measurements and modeling of nitric oxide in high-pressure premixed flames
[NASA-CR-195404] p 775 N95-16910

EXCITONS
Nonlinear optical response of condined excitions in molecular and semiconductor nanostructures
[AD-A285225] p 885 N95-16524

EXCLUSION
Results of the psychiatric, select-out evaluation of US astronaut applications p 813 N95-16761
Iterative divergent/convergent doubling approach to linear conjugated oligomers. A rapid route to a 128 A long potential molecular wire
[AD-A281295] p 874 N95-16784

EXERCISE PHYSIOLOGY
Evaluation of a newly-designed, dynamic knee extension device for the study of muscle fatigue in humans
[AD-A284974] p 819 N95-16228
Basic mechanisms and implications of non-photic entrainment of circadian rhythmicity
[AD-A283180] p 822 N95-17342

EXHAUST DIFFUSERS
Unsteady flow phenomena in discrete passage diffusers for centrifugal compressors
[AD-A281412] p 770 N95-16163

EXHAUST EMISSION
An in-cylinder study of the particulate/NO(x) trade-off in a DI diesel engine
[DE94-014599] p 781 N95-17162
Coal-fueled diesel technology development emissions control
[DE94-004096] p 782 N95-17364
Corrosion inhibition in high temperature environment
[AD-D016372] p 738 N95-17699

EXHAUST GASES
Design of thermocouple probes for measurement of rocket exhaust plume temperatures
[AD-A285423] p 774 N95-16247
Numerical simulation of helicopter engine plume in forward flight
[NASA-CR-197488] p 655 N95-16589
An in-cylinder study of the particulate/NO(x) trade-off in a DI diesel engine
[DE94-014599] p 781 N95-17162

EXHAUST NOZZLES
Small turbojets: Designs and installations p 670 N95-16323

EXOBIOLOGY
Exobiology site priorities for Mars Pathfinder p 919 N95-16188
Aerospace medicine and biology: A continuing bibliography with indexes (supplement 396)
[NASA-SP-7011(396)] p 823 N95-17703

EXPANDABLE STRUCTURES
Study of the folding and deployment aspects of a Collapsible Rib Tensioned Surface (CRTS) antenna reflector
[CUED/D-STRUCT/TR-144] p 783 N95-17928
EXPENDABLE STAGES (SPACECRAFT)
Program test objectives milestone 3 --- Integrated Propulsion Technology Demonstrator
[NASA-CR-197030] p 666 N95-15971
EXPERIENCE
Epistemology, software engineering and formal methods p 843 N95-16480
Review of performance, medical, and operational data on pilot aging issues p 812 N95-16759
EXPERIMENT DESIGN
Experimental issues in high-sensitivity charm experiments
[DE94-015544] p 871 N95-15945
A study of software standards used in the avionics industry p 670 N95-16456
The value of the 4-day headdown bedrest model for screening countermeasures p 817 N95-16782
Experimental and analytical methods for the determination of connected-pipe ramjet and ducted rocket internal performance
[AGARD-AR-323] p 721 N95-17278
The m-line method for optical characterisation of polymer waveguides
[PB94-184611] p 887 N95-17409
EXPERT SYSTEMS
An integrated knowledge acquisition and database management system
[AD-A285404] p 910 N95-16884
Data link level interconnection of remote Fiber Distributed Data Interface Local Area Networks (FDDI LANs) through the Critical Data Link (CDL)
[AD-A284307] p 755 N95-17173
Third International Symposium on Space Mission Operations and Ground Data Systems, part 1
[NASA-CP-3281-PT-1] p 676 N95-17179
Grand mission versus small OPS team: Can we have both? p 684 N95-17219
SCL: An off-the-shelf system for spacecraft control p 688 N95-17243
Development of a data reduction expert assistant
[NASA-CR-189385] p 911 N95-17328
Identification of Artificial Intelligence (AI) applications for maintenance, monitoring, and control of airway facilities
[AD-A282479] p 665 N95-17373
O-Plan2 versus SIPE-2: A general comparison
[AD-A285531] p 857 N95-17381
Towards a human operator model of the navigator
[PB94-197985] p 831 N95-17468
DIAMS revisited: Taming the variety of knowledge in fault diagnosis expert systems p 692 N95-17534
Using graphics and expert system technologies to support satellite monitoring at the NASA Goddard Space Flight Center p 674 N95-17535
Spacecraft command and control using expert systems p 693 N95-17539
The Pacor 2 expert system: A case-based reasoning approach to troubleshooting p 693 N95-17541
ATOS: Integration of advanced technology software within distributed Spacecraft Mission Operations Systems p 705 N95-17602
Risk reduction methodologies and technologies for the Earth Observing System (EOS) Operations Center (EOC) p 707 N95-17612
Multivariate statistical analysis software technologies for astrophysical research involving large data sets
[NASA-CR-197499] p 858 N95-17921
EXPLORER SATELLITES
Nickel cadmium battery operations and performance p 685 N95-17224
EXPLOSIVES
The removal of heteroatoms from organic compounds by supercritical water
[AD-A281532] p 722 N95-16087
EXPOSURE
Kinetics model for initiation and promotion for describing tumor prevalence from HZE radiation
[NASA-TP-3479] p 820 N95-16412
The chronic effects on JP-8 jet fuel exposure on the lungs
[AD-A280982] p 821 N95-16515
The psychophysical function for perceived gravitational-inertial force does not depend on the orientation of the otolith organs p 808 N95-16740
Magnetic Resonance Imaging (MRI) of skeletal muscles in astronauts after 9 days of space flight p 810 N95-16749
Medicine on Mars: Remote medical care and the space exploration initiative p 816 N95-16777
Phase-shifting effects of light and activity on the human circadian clock
[AD-A281204] p 821 N95-16796
A study to determine the critical characteristics for mice in a newly designed whole body toxic gas exposure module
[AD-A285085] p 818 N95-17666
EXTINCTION
Abstracts and program Proceedings of the 1994 Meeting of the International Society for Ecological Modelling North American Chapter
[DE94-016456] p 796 N95-17636
EXTINGUISHING
Use of copper powder extinguishers on lithium fires
[AD-A283213] p 751 N95-17632
EXTRACTION
Supercritical fluid extraction: Preparing a superior mesophase precursor for carbon fibers
[AD-A284933] p 726 N95-16142
Extraction of high quality potential surfaces from laboratory data
[AD-A285071] p 903 N95-16489
EXTRAGALACTIC RADIO SOURCES
Radio-planetary from tie from Phobos-2 VLBI data p 756 N95-17283
EXTRAPOLATION
Linear prediction data extrapolation superresolution radar imaging p 651 N95-16268
Implementation of a real-time data processing system for radar bandwidth extrapolation and stretch
[AD-A281195] p 754 N95-16794
Extended range forecast of Atlantic seasonal hurricane activity for 1995, 2 p 801 N95-17260
EXTRAVEHICULAR ACTIVITY
The effect of differences in time to detection of circulating microbubbles on the risk of decompression sickness p 807 N95-16738
Houston, I think we've got a satellite
[NASA-TM-109987] p 709 N95-16941
Apollo 15: In the mountains of the Moon
[NASA-TM-109988] p 922 N95-16942
EXTREME ULTRAVIOLET EXPLORER SATELLITE
Nickel cadmium battery operations and performance p 685 N95-17224
Designing an autonomous environment for mission critical operation of the EUVE satellite p 688 N95-17241
EXTREME ULTRAVIOLET RADIATION
A rare gas optics-free absolute photon flux and energy analyzer to provide absolute photoionization rates of inflowing interstellar neutrals
[NASA-CR-197228] p 914 N95-15964
A rare gas optics-free absolute photon flux and energy analyzer for solar and planetary observations
[NASA-CR-197227] p 915 N95-16021
EXTREMELY HIGH FREQUENCIES
A simple EHF hemispheric coverage antenna
[AD-A285078] p 754 N95-16495
Feasibility study concerning an active millimeterwave sensor
[PB94-190691] p 775 N95-17170
Attempt of automated space network operations at ETS-VI experimental data relay system p 677 N95-17184
EXTREMELY LOW FREQUENCIES
Observations of ELF propagation at high latitudes during the sporadic-E conditions of November 1986
[AD-A284973] p 753 N95-16227
EXTREMELY LOW RADIO FREQUENCIES
Observations of ELF propagation at high latitudes during the sporadic-E conditions of November 1986
[AD-A284973] p 753 N95-16227
EXTRUDING
Effect of extrusion parameters on consolidation of tungsten-hafnium and tungsten-steel powders
[DE94-013270] p 737 N95-17513
EYE (ANATOMY)
Investigation of laser-induced retinal damage: Wavelength and pulsewidth dependent mechanisms
[AD-A285186] p 822 N95-16871
Blinks, saccades, and fixation pauses during vigilance task performance. 1: Time on task
[DOT/FAA/AM-94/26] p 828 N95-17530
EYE MOVEMENTS
Characterization of the fast-phase component of the vestibulo-ocular response
[AD-A281830] p 820 N95-16360
Blinks, saccades, and fixation pauses during vigilance task performance. 1: Time on task
[DOT/FAA/AM-94/26] p 828 N95-17530

F

F 2 REGION
An improved neutral wind model with predictive capabilities
[AD-A282283] p 800 N95-16235
F-111 AIRCRAFT
A PC-based interactive simulation of the F-111C Pave Tack system and related sensor, avionics and aircraft aspects
[AD-A285500] p 669 N95-16969
F-14 AIRCRAFT
Evaluation of alternate F-14 wing lug coating
[AD-A283207] p 669 N95-17631
F-15 AIRCRAFT
Development of a low-aspect ratio fin for flight research experiments
[NASA-TM-4596] p 656 N95-16858
FABRICATION
Liquid Cooled Heat Sink with Through Vias (LCHS)
[AD-A281450] p 902 N95-16075
International Workshop on Light Emission and Electronic Properties of Nanoscale silicon
[AD-A281464] p 894 N95-16081
PV CZ silicon manufacturing technology improvements
[DE94-011818] p 897 N95-16424
Development and fabrication of the fiber optic MicroCable (tm)
[AD-A285266] p 886 N95-16815
A new manufacturing method for the formation of gated field emission structures
[DE94-015287] p 764 N95-16832
Processing, fabrication, characterization and device demonstration of high temperature superconducting ceramics
[AD-A285145] p 744 N95-16844
Optimization of adaptive intraply hybrid fiber composites with reliability considerations
[NASA-TM-106632] p 787 N95-16911
Modeling of chemical vapor infiltration for composite fabrication
[DE93-001715] p 724 N95-16926
Low-temperature fabrication of transparent silicon nitride
[DE94-014902] p 746 N95-17456
FABRICS
Design and technical support for development of a molded fabric space suit joint
[NASA-CR-197521] p 831 N95-16894
FACTORIAL DESIGN
Cellular automata for contour dynamics
[PB94-197613] p 865 N95-17526
FAILURE
Failure of ozone and nitrogen dioxide to enhance lung tumor development in hamsters
[PB94-182854] p 818 N95-16801
Characterization of the corrosion behavior of the carbon steel liner in Hanford site single-shell tanks
[DE94-016475] p 737 N95-17637
FAILURE ANALYSIS
Continuing life test of a xenon hollow cathode for a space plasma contactor
[NASA-CR-195401] p 711 N95-15968
Ductile fracture and failure criteria of structural steels
[AD-A280754] p 733 N95-16104
Efficient estimation of the mean time between failures in non-regenerative dependability models
[AD-A281563] p 783 N95-16421
A study of software standards used in the avionics industry p 670 N95-16456
Failure analysis of 2D and 3D woven composites
[NASA-CR-197247] p 724 N95-16597
Breaking down barriers in cooperative fault management: Temporal and functional information displays
[NASA-CR-197450] p 857 N95-17383
Metallurgical examination of failed T-158 Cast Austempered Ductile Iron (CADI) track shoes
[AD-A282433] p 737 N95-17486
FAILURE MODES
A Lifting Ball Valve for cryogenic fluid applications p 720 N95-16349
A review of transmission diagnostics research at NASA Lewis Research Center
[ARL-TR-599] p 781 N95-16907
FAN BLADES
Ducted fan acoustic radiation including the effects of nonuniform mean flow and acoustic treatment
[NASA-CR-197449] p 870 N95-16401
Mach number, flow angle, and loss measurements downstream of a transonic fan-blade cascade
[AD-A280907] p 656 N95-16824
FAR FIELDS
Optimum truncation of a Gaussian beam in the presence of random jitter
[AD-A284951] p 752 N95-16143
Ducted fan acoustic radiation including the effects of nonuniform mean flow and acoustic treatment
[NASA-CR-197449] p 870 N95-16401

FAR UV SPECTROSCOPIC EXPLORER
A new systems engineering approach to streamlined science and mission operations for the Far Ultraviolet Spectroscopic Explorer (FUSE) p 707 N95-17611
FARMLANDS
FIFE data analysis: Testing BIOME-BGC predictions for grasslands
[NASA-CR-197522] p 790 N95-16895
FAST FOURIER TRANSFORMATIONS
Linear prediction data extrapolation superresolution radar imaging p 651 N95-16268
Least squares computations in science and engineering
[AD-A281213] p 862 N95-16798
Nonlinear problems in fluid dynamics and inverse scattering. Propagation and capturing of singularities in problems of fluid dynamics and inverse scattering
[AD-A282873] p 773 N95-17617
Parallel fast Fourier transforms for non power of two data
[DE94-018047] p 851 N95-17676
FAST NEUTRONS
Statistical properties of an algorithm used for illicit substance detection by fast-neutron transmission
[DE94-013868] p 665 N95-16964
FASTENERS
Eddy current for detecting second layer cracks under installed fasteners
[AD-A282412] p 784 N95-17507
FATIGUE (BIOLOGY)
Mental effects of caffeine in fatigued men and women
[PB94-190683] p 822 N95-17300
FATIGUE (MATERIALS)
Structural analysis of solid-propellant rocket motors with and without flaws p 720 N95-16348
Reaction and protection of electrical wire insulators in atomic-oxygen environments
[NASA-TM-106767] p 709 N95-17275
Mechanisms of mechanical fatigue in ceramics
[DE94-016040] p 747 N95-17719
FATIGUE LIFE
Damage-mitigating control of space propulsion systems for high performance and extended life
[NASA-CR-194470] p 784 N95-16068
The effects of fatigue loading frequency on fatigue life of high-strength pressure vessel steels
[AD-A285301] p 786 N95-16601
FATIGUE TESTS
Structural testing of the North Wind 250 composite rotor joint
[DE94-006923] p 792 N95-16437
FAULT DETECTION
Sensor fault detection and diagnosis simulation of a helicopter engine in an intelligent control framework
[NASA-TM-106784] p 669 N95-15970
SSME propellant path leak detection real-time
[NASA-CR-197032] p 748 N95-16029
A review of transmission diagnostics research at NASA Lewis Research Center
[ARL-TR-599] p 781 N95-16907
Significant issues in proof testing: A critical appraisal
[NASA-CR-4628] p 788 N95-17272
An artificial neural network system for diagnosing gas turbine engine fuel faults
[DE94-013960] p 670 N95-17371
Eddy current for detecting second layer cracks under installed fasteners
[AD-A282412] p 784 N95-17507
DIAMS revisited: Taming the variety of knowledge in fault diagnosis expert systems p 692 N95-17534
Using graphics and expert system technologies to support satellite monitoring at the NASA Goddard Space Flight Center p 674 N95-17535
FAULT TOLERANCE
The survivable distributed computing environment
[AD-A281637] p 845 N95-16115
An integrated knowledge acquisition and database management system
[AD-A285404] p 910 N95-16884
A modular electric power system test bed for small spacecraft
[NASA-TM-106812] p 721 N95-17276
Breaking down barriers in cooperative fault management: Temporal and functional information displays
[NASA-CR-197450] p 857 N95-17383
Controlling memory access concurrency in efficient fault-tolerant parallel algorithms
[AD-A280909] p 851 N95-17741
FEASIBILITY
Vector magnetometry and lightwave defect imaging sensor technologies for internal pipe inspection systems: Phase 1 and 2 feasibility study, conceptual design, and prototype development
[PB94-194198] p 783 N95-16870
FEASIBILITY ANALYSIS
SCOS 2: ESA's new generation of mission control system p 674 N95-17253
Testing and characterization of the CYCLOPS HgCdTe focal plane detector array
[AD-A284279] p 887 N95-17489
FEDERAL BUDGETS
Federal Aviation Administration aviation system capital investment plan, 1993
[PB94-171956] p 654 N95-17512
FEED SYSTEMS
RF optics study for DSS-43 ultracone implementation p 758 N95-17296
FEEDBACK
An incremental database access method for autonomous interoperable databases
[NASA-CR-189384] p 912 N95-17652
XPVM: A graphical console and monitor for PVM
[DE94-018050] p 842 N95-17678
FEEDBACK CONTROL
ISMCR 1994: Topical Workshop on Virtual Reality. Proceedings of the Fourth International Symposium on Measurement and Control in Robotics
[NASA-CP-10163] p 851 N95-15972
Virtual reality and telerobotics applications of an Address Recalculation Pipeline p 852 N95-15977
Coordinated control of a dual-arm dexterous robot using full immersion telepresence and virtual reality p 852 N95-15979
Master-slave system with force feedback based on dynamics of virtual model p 853 N95-15985
Thermal feedback in virtual reality and telerobotic systems p 854 N95-15987
Energy decay and control for elastic and viscoelastic distributed parameter systems
[AD-A281312] p 726 N95-16008
Adaptive control of nonlinear flexible systems
[AD-A281337] p 855 N95-16011
Papers presented at the Tenth Topical Conference on High-Temperature Plasma Diagnostics
[DE94-015854] p 888 N95-16063
An improved position/force control of manipulators p 653 N95-16280
Integrated passive and active control of structures
[AD-A282684] p 708 N95-16304
Servo control using switches for discrete positional feedback
[AD-A284747] p 856 N95-16550
Telemetry distribution and processing for the second German Spacelab Mission D-2 p 681 N95-17207
Closed-loop carrier phase synchronization techniques motivated by likelihood functions p 756 N95-17284
Cooperative control theory and integrated flight and propulsion control
[NASA-CR-197493] p 671 N95-17404
Hidden Markov model for control strategy learning
[AD-A282846] p 865 N95-17429
Back-propagation neural networks in adaptive control of unknown nonlinear systems
[AD-A282414] p 858 N95-17458
Feedback system for remotely operated vehicles
[AD-D016409] p 858 N95-17465
Simplifying operations with an uplink/downlink integration toolkit p 697 N95-17562
Microgravity isolation system design: A case study
[NASA-TM-106804] p 654 N95-17657
Simulation investigation on system identification of gas turbine
[PB95-104238] p 670 N95-17749
FEEDFORWARD CONTROL
Adaptive control of nonlinear flexible systems
[AD-A281337] p 855 N95-16011
Small sample behavior of multi-layer feedforward network classifiers: Theoretical and practical aspects
[PB94-201415] p 841 N95-17470
A feedforward control approach to the local navigation problem for autonomous vehicles
[AD-A282787] p 666 N95-17706
FEMALES
An annotated bibliography of heat tolerance: Regarding gender differences
[AD-A280755] p 818 N95-16105
Blood volume and orthostatic responses of men and women to a 13-day bedrest p 811 N95-16752
Mental effects of caffeine in fatigued men and women
[PB94-190683] p 822 N95-17300
FERMI LIQUIDS
Non-Fermi liquid scaling in UPd(x)Cu(5-x)(x = 1,1.5)
[DE94-016072] p 896 N95-16389
FERMI SURFACES
First principles simulation of materials properties
[DE94-013615] p 899 N95-16805
FERMIONS
Flavor symmetries and fermion masses
[DE94-018192] p 878 N95-17889
FERRITIC STAINLESS STEELS
Mixed-mode I/III fracture toughness of a ferritic/martensitic stainless steel
[DE94-014492] p 736 N95-17159
FERROCENES
Cyclic voltammetric analysis of ferrocene alkanethiol monolayer electrode kinetics based on Marcus theory
[AD-A281411] p 868 N95-16162
FERROELECTRICITY
A VLSI interface for the NM24CF04 serial-access ferroelectric memory
[AD-A281535] p 762 N95-16110
Relationships between ferroelectric 90 deg domain formation and electrical properties of chemically prepared Pb(Zr,Ti)O3 thin films
[DE94-015274] p 744 N95-16829
FIBER COMPOSITES
Study of the compression behavior of high performance fibers
[AD-A284959] p 723 N95-16126
Chemical vapor infiltration of non-oxide ceramic matrix composites
[DE94-017770] p 723 N95-16225
Filament overwrapped motor case technology p 720 N95-16350
Experimental studies of stress measurement by optical fluorescence
[AD-A282337] p 723 N95-16415
Development and fabrication of the fiber optic MicroCable (tm)
[AD-A285266] p 886 N95-16815
Optimization of adaptive intraply hybrid fiber composites with reliability considerations
[NASA-TM-106632] p 787 N95-16911
Micromechanics of interfaces in metal matrix composites
[AD-A282404] p 725 N95-17457
Thermal analysis of a functionally graded material subject to a thermal gradient using the boundary element method
[NASA-TM-106801] p 789 N95-17658
Modeling of stress/strain behavior of fiber-reinforced ceramic matrix composites including stress redistribution
[NASA-TM-106789] p 725 N95-17659
Research and development of material/processing methods for the Continuous Fiber Ceramic Composites Program
[DE94-018569] p 725 N95-17905
FIBER OPTICS
High speed transport protocols: An attempt to find the best solution
[AD-A280989] p 751 N95-15993
Optical wheel-rotation sensor
[DE94-011719] p 780 N95-16224
The combination probe of optical fibers and its applications p 652 N95-16275
Picosecond optoelectronic AND-GATE
[AD-A285672] p 885 N95-16620
Development and fabrication of the fiber optic MicroCable (tm)
[AD-A285266] p 886 N95-16815
In-fibre Bragg gratings for millimetre-wave EW systems
[AD-A284283] p 755 N95-16956
Magnetostrictive transducer system having a three dual-strip fiber optic magnetostrictive transducers bonded into a single fiber Mach-Zehnder interferometer
[AD-D016373] p 775 N95-17428
FIBER ORIENTATION
Life prediction for bridged fatigue cracks
[DE94-016000] p 724 N95-16930
FIBER PULLOUT
Micromechanics of interfaces in metal matrix composites
[AD-A282404] p 725 N95-17457
FIBER-MATRIX INTERFACES
Failure analysis of 2D and 3D woven composites
[NASA-CR-197247] p 724 N95-16597
FIBERS
Anionically-conductive ultrathin film composite membranes
[AD-A284944] p 723 N95-16041
Phase transformations, ultrastructure and properties of rigid-rod fibers
[AD-A285249] p 749 N95-16512
FIBERS (MATHEMATICS)
Global subjectivity of submersions via contractibility of the fibers
[AD-A284961] p 860 N95-16128
FIBRILLATION
Advanced Cardiac Life Support (ACLS) utilizing Man-Tended Capability (MTC) hardware onboard Space Station Freedom p 816 N95-16775
FIELD COILS
Status of the US stellarator reactor study
[DE94-018693] p 893 N95-17907

FIELD EFFECT TRANSISTORS
Reliability implications of defects in high temperature annealed Si/SiO2/Si structures
[DE94-015765] p 895 N95-16311
The response of the Sandia robust wide range hydrogen sensor to H2-O2 mixtures
[DE94-013763] p 727 N95-16362
The impact of low temperature materials on the breakdown and noise properties of GaAs and InP based HEMT's and FET's
[AD-A285176] p 765 N95-16834
An algorithm for extraction of periodic signals from sparse, irregularly sampled data p 756 N95-17281
BaF2/GaAs electronic components
[AD-D016391] p 767 N95-17481

FIELD EMISSION
A new manufacturing method for the formation of gated field emission structures
[DE94-015287] p 764 N95-16832

FIELD OF VIEW
Scripting human animations in a virtual environment p 855 N95-15992
Visual perception in the field-of-view of partial binocular overlap helmet-mounted displays
[AD-A285213] p 827 N95-16520
Visual acuity versus field-of-view and light level for Night Vision Goggles (NVG)
[AD-A284750] p 830 N95-16553
The development and validation of command schedules for SeaWiFS p 690 N95-17249
Factors affecting the visual fragmentation of the field-of-view in partial binocular overlap displays
[AD-A283081] p 886 N95-17334

FIELD THEORY (PHYSICS)
Research in elementary particle physics
[DE94-019219] p 877 N95-17358

FIGHTER AIRCRAFT
Investigation into the aerodynamic characteristics of a combat aircraft research model fitted with a forward swept wing p 664 N95-17884

FILAMENT WINDING
Recent advances in graphite/epoxy motor cases p 717 N95-16333
Filament overwrapped motor case technology p 720 N95-16350

FILE MAINTENANCE (COMPUTERS)
Software merge: Semantics of combining changes to programs
[AD-A281373] p 834 N95-16154
Accountability for network backup failures
[DE94-011365] p 846 N95-16222
A survey of program slicing for software engineering
[NASA-CR-193116] p 836 N95-16574

FILM COOLING
The prediction of nozzle performance and heat transfer in hydrogen/oxygen rocket engines with transpiration cooling, film cooling, and high area ratios p 718 N95-16339

FILM THICKNESS
Analysis of space environment damage to solar cell assemblies from LDEF experiment A0171-GSFC test plate
[NASA-CR-196523] p 793 N95-16575

FILTERS
An automatic repeater station for signal transmissions
[AD-D016454] p 754 N95-16549

FILTRATION
Coal-fueled diesel technology development emissions control
[DE94-004096] p 782 N95-17364

FINE STRUCTURE
An XAFS study of the oxidation of structural iron in biotite mica by solutions containing Br2 or H2O2
[DE94-018721] p 733 N95-17912

FINGERS
Vibratory tactile display for textures p 851 N95-15973
Thermal feedback in virtual reality and telerobotic systems p 854 N95-15987

FINITE DIFFERENCE THEORY
The prediction of nozzle performance and heat transfer in hydrogen/oxygen rocket engines with transpiration cooling, film cooling, and high area ratios p 718 N95-16339
A stepsize control strategy for stiff systems of ordinary differential equations
[AD-A281551] p 861 N95-16395
On the removal of boundary errors caused by Runge-Kutta integration of non-linear partial differential equations
[NASA-CR-194989] p 863 N95-16904

FINITE ELEMENT METHOD
Special hybrid stress finite elements for the analysis of interface stress distribution in adhesive joints
[AD-A281612] p 785 N95-16102
Experimental and numerical analysis of floating ice beam impact forces against a sloped structure
[AD-A280752] p 804 N95-16103
A posteriori error estimation new approach
[AD-A284960] p 860 N95-16127
Considerations in the experimental determination of constitutive parameters for finite strain plasticity
[AD-A285410] p 785 N95-16245
A super-element simplified analysis for vibration systems of complex structures p 650 N95-16260
Conceptual design study of a solar concentrator/support structure: A three dimensional finite element model p 718 N95-16342
Structural analysis of solid-propellant rocket motors with and without flaws p 720 N95-16348
Computational methods for microstructure covolume techniques of discretization
[AD-A282449] p 861 N95-16376
Validation of recipes for the recovery of stresses and derivatives by a computer-based approach
[AD-A282712] p 861 N95-16379
Automatic differentiation for design sensitivity analysis of structural systems using multiple processors p 847 N95-16462
Experimental study of spatially incomplete structural system identification
[AD-A280905] p 785 N95-16502
Numerical methods for singularly perturbed differential equations with applications
[AD-A285209] p 861 N95-16517
An analysis of spectral envelope-reduction via quadratic assignment problems
[NASA-CR-194992] p 862 N95-16596
Failure analysis of 2D and 3D woven composites
[NASA-CR-197247] p 724 N95-16597
Combination of power electronic models with the two-dimensional finite element analysis of electrical machines
[PB94-197720] p 766 N95-16951
Correlation of finite element free vibration predictions using random vibration test data
[NASA-TM-106787] p 787 N95-17258
Probabilistic simulation of stress concentration in composite laminates
[NASA-TM-106712] p 787 N95-17270
Thermocryogenic buckling and stress analyses of a partially filled cryogenic tank subjected to cylindrical strip heating
[NASA-TM-4579] p 788 N95-17417
A model study of element residual estimators for linear elliptic problems: The quality of the estimators in the interior of meshes of triangles and quadrilaterals
[AD-A282849] p 863 N95-17431
An analysis of smoothed particle hydrodynamics
[DE94-013817] p 788 N95-17439
Shear buckling analysis of a hat-stiffened panel
[NASA-TM-4644] p 788 N95-17490
Error estimation and adaptive mesh refinement for parallel analysis of shell structures
[NASA-CR-197500] p 788 N95-17492
User-defined subroutine for implementation of special finite elements in ABAQUS for the analysis of adhesive joints
[AD-A282431] p 788 N95-17510
Transient flows and pressure waves in pipes
[DE94-012650] p 772 N95-17523
Antenna dielectric sealing process characterization
[DE94-015864] p 747 N95-17690
FEM3C, an improved three-dimensional heavy-gas dispersion model: User's manual
[DE94-014731] p 797 N95-17922

FINITE VOLUME METHOD
Three dimensional compressible turbulent flow computations for a diffusing S-duct with/without vortex generators
[NASA-CR-195390] p 670 N95-17402

FINLAND
Information sources in science and technology in Finland p 906 N95-15930

FINS
Development of a low-aspect ratio fin for flight research experiments
[NASA-TM-4596] p 656 N95-16858

FIRE CONTROL
Assessment of benefits and drawbacks of using fuzzy logic, especially in fire control systems
[AD-A285428] p 838 N95-16874

FIRE EXTINGUISHERS
Combustion and fires in low gravity p 712 N95-16050
Fire protection engineering criteria: Electronic equipment installations
[AD-A285174] p 750 N95-16853
Use of copper powder extinguishers on lithium fires
[AD-A283213] p 751 N95-17632

FIRE FIGHTING
Combustion and fires in low gravity p 712 N95-16050
Use of copper powder extinguishers on lithium fires
[AD-A283213] p 751 N95-17632

FIRE PREVENTION
Combustion and fires in low gravity p 712 N95-16050
Fire protection engineering criteria: Electronic equipment installations
[AD-A285174] p 750 N95-16853

FIRES
Combustion and fires in low gravity p 712 N95-16050
Ceramic/metal composite circuit-board-level technology for Application Specific Electronic Modules (ASEMs)
[AD-A285066] p 741 N95-16369

FIRING (IGNITING)
Mechanical effects in cookoff modeling
[DE94-014174] p 748 N95-16214

FLAME PROPAGATION
Experimental study of premixed flames in intense isotropic turbulence
[DE94-016868] p 732 N95-17437

FLAME STABILITY
Experimental study of premixed flames in intense isotropic turbulence
[DE94-016868] p 732 N95-17437

FLAME TEMPERATURE
Laser induced fluorescence measurements and modeling of nitric oxide in high-pressure premixed flames
[NASA-CR-195404] p 775 N95-16910

FLAMMABILITY
Alternatives for ozone-depleting refrigerants
[PB94-190857] p 795 N95-16881
Fire protective coating and method for applying same to a structure
[AD-D016405] p 746 N95-17462

FLAT SURFACES
Preparation of Au single crystals for study of the ECALE deposition of CdTe
[AD-A282294] p 895 N95-16238

FLAVOR (PARTICLE PHYSICS)
QCD of different flavors with the SLD detectors
[DE94-013800] p 875 N95-16943

FLEXIBILITY
Measurement of residual flexibility for substructures having prominent flexible interfaces
[NASA-TM-110074] p 786 N95-16577
Towards a new generation of mission planning systems: Flexibility and performance p 686 N95-17230

FLEXIBLE BODIES
Digital adaptive and optimal control of distributed systems
[AD-A285352] p 851 N95-15952
Adaptive control of nonlinear flexible systems
[AD-A281337] p 855 N95-16011
Decentralized sliding mode control of nonlinear flexible robots
[DE94-013790] p 782 N95-17366

FLEXIBLE SPACECRAFT
Experimental validation of an integrated controls-structures design methodology for a class of flexible space structures
[NASA-TP-3462] p 709 N95-16857
A comparison of different control methods for vibration suppression of flexible structures using piezoelectric actuators
[AD-A282958] p 710 N95-17622

FLEXIBLE WINGS
Active load control during rolling maneuvers --- performed in the Langley Transonic Dynamics Tunnel
[NASA-TP-3455] p 669 N95-17397

FLEXORS
Skeletal muscle responses to unloading in humans p 809 N95-16743

FLICKER
Caffeine's influence on critical frequency thresholds
[AD-A282005] p 828 N95-17447

FLIGHT
Energy and Technology Review
[DE95-000321] p 710 N95-17359

FLIGHT CHARACTERISTICS
Evaluation of the dynamic stability characteristics of the NAL Light Transport Aircraft
[NAL-PD-CA-9217] p 671 N95-16392
STOVL CFD model test case p 663 N95-17881

FLIGHT CONDITIONS
Numerical simulation of helicopter engine plume in forward flight
[NASA-CR-197488] p 655 N95-16589

FLIGHT CONTROL
Aviation spatial orientation in relationship to head position, attitude interpretation, and control
[AD-A281869] p 827 N95-16433

Matlab as a robust control design tool p 849 N95-16474
Beyond the cockpit: The visual world as a flight instrument p 814 N95-16767
Workshop on Formal Models for Intelligent Control [AD-A281399] p 857 N95-16864
EURECA mission control experience and messages for the future p 690 N95-17252
Aircraft and sub-system certification by piloted simulation [AGARD-AR-278] p 671 N95-17388
Packet utilisation definitions for the ESA XMM mission p 704 N95-17596

FLIGHT CREWS
Aerospace Medical Association 63rd Annual Scienti fic Meeting Program p 807 N95-16737
Human performance in the modern cockpit p 813 N95-16764
Crew decision making under stress p 814 N95-16765
Cognition and procedure representational requirements for predictive human performance models p 814 N95-16766

FLIGHT ENVELOPES
Aircraft and sub-system certification by piloted simulation [AGARD-AR-278] p 671 N95-17388

FLIGHT INSTRUMENTS
Beyond the cockpit: The visual world as a flight instrument p 814 N95-16767

FLIGHT OPERATIONS
Alertness management in two-person long-haul flight operations p 813 N95-16760
Operations automation p 687 N95-17236
The Sequence of Events generator: A powerful tool for mission operations p 688 N95-17240
Increases in efficiency and enhancements to the Mars Observer non-stored commanding process p 688 N95-17242
Third International Symposium on Space Mission Operations and Ground Data Systems, part 2 [NASA-CP-3281-PT-2] p 691 N95-17531
SCOSII OL: A dedicated language for mission operations p 692 N95-17533
Using graphics and expert system technologies to support satellite monitoring at the NASA Goddard Space Flight Center p 674 N95-17535
Development of use of an Operational Procedure Information System (OPIS) for future space missions p 692 N95-17536
SCOSII: ESA's new generation of mission control systems: The user's perspective p 674 N95-17537
A software architecture for automating operations processes p 692 N95-17538
Cost efficient operations for Discovery class missions p 695 N95-17548
An agent-oriented approach to automated mission operations p 696 N95-17555
Test/score/report: Simulation techniques for automating the test process p 675 N95-17581
Transportable Payload Operations Control Center reusable software: Building blocks for quality ground data systems p 703 N95-17587
Renaissance architecture for Ground Data Systems p 706 N95-17604
Risk reduction methodologies and technologies for the Earth Observing System (EOS) Operations Center (EOC) p 707 N95-17612

FLIGHT PATHS
Beyond the cockpit: The visual world as a flight instrument p 814 N95-16767

FLIGHT PLANS
International Space Station Alpha user payload operations concept p 685 N95-17227

FLIGHT SAFETY
Review of performance, medical, and operational data on pilot aging issues p 812 N95-16759
Federal aviation regulations, part 91. General operating and flight rules. Change 5 [PB94-194883] p 665 N95-17476
Annual review of aircraft accident data: US Air carrier operations, calendar year 1992 [PB95-100319] p 665 N95-17748

FLIGHT SIMULATION
Aviation spatial orientation in relationship to head position, attitude interpretation, and control [AD-A281869] p 827 N95-16433
Crew decision making under stress p 814 N95-16765

FLIGHT SIMULATORS
ADST system test report for the rotary wing aircraft airnet aeromodel and weapon model merge with the ATAC 2 baseline [AD-A281580] p 666 N95-16171
Dark focus of accommodation as dependent and independent variables in visual display technology p 812 N95-16758
Aircraft and sub-system certification by piloted simulation [AGARD-AR-278] p 671 N95-17388

FLIGHT TEST INSTRUMENTS
Development of a medium energy modulated electron gun for orbital experiments [AD-A281021] p 675 N95-16005

FLIGHT TEST VEHICLES
Development of a low-aspect ratio fin for flight research experiments [NASA-TM-4596] p 656 N95-16858
In-flight imaging of transverse gas jets injected into transonic and supersonic crossflows: Design and development [NASA-CR-186031] p 772 N95-17418

FLIGHT TESTS
A VHF/UHF antenna for the Precision Antenna Measurement System (PAMS) [AD-A285673] p 754 N95-16621
Development of a low-aspect ratio fin for flight research experiments [NASA-TM-4596] p 656 N95-16858
Modeling of Instrument Landing System (ILS) localizer signal on runway 25L at Los Angeles International Airport [NASA-TM-4588] p 665 N95-17384

FLOATING
Delivery of cardiopulmonary resuscitation in the microgravity environment p 816 N95-16774

FLOATING POINT ARITHMETIC
A simplified Integer Cosine Transform and its application in image compression p 757 N95-17286

FLOOD PLAINS
Marte Valles site p 921 N95-16200

FLORIDA
Florida Gulf Stream Data (FLDA) current study [AD-A281965] p 805 N95-16414
South Florida environmental quality. National Status and Trends Program for marine environmental quality [PB94-173408] p 796 N95-17363
Straits of Florida physical oceanographic field study. Volume 1: Executive summary. Volume 2: Technical report. Volume 3: Data report [PB94-175031] p 806 N95-17615

FLOW CHARACTERISTICS
ARCJET plasma modeling with experimental validation [AD-A285234] p 889 N95-16243
Numerical study of base pressure characteristic curve for a four-engine clustered nozzle configuration p 716 N95-16329
A selection of experimental test cases for the validation of CFD codes, volume 2 [AGARD-AR-303-VOL-2] p 657 N95-17846
Experiments in the trailing edge flow of an NLR 7702 airfoil p 658 N95-17853
Delta-wing model p 662 N95-17873
STOVL CFD model test case p 663 N95-17881

FLOW DISTORTION
Improved method for estimation of the maximum instantaneous distortion values p 649 N95-16254

FLOW DISTRIBUTION
Radiative interactions in chemically reacting compressible nozzle flows using Monte Carlo simulations [NASA-CR-197133] p 769 N95-15966
Dynamical system prediction of the scalar field in a turbulent channel flow [AD-A285519] p 771 N95-16438
Residual-correction type and related computational methods for aerodynamic design. Part 1: Airfoil and wing design p 667 N95-16566
Airfoil optimization by the one-shot method p 667 N95-16569
Numerical simulation of helicopter engine plume in forward flight [NASA-CR-197488] p 655 N95-16589
Numerical simulation of transient vortex breakdown above a pitching delta wing [AD-A281075] p 655 N95-16808
Improved dual flow aluminum hydrogen peroxide battery [AD-D016339] p 766 N95-16949
Three-dimensional boundary layer and flow field data of an inclined prolate spheroid p 661 N95-17867
Force and pressure data of an ogive-nosed slender body at high angles of attack and different Reynolds numbers p 661 N95-17868
Pressure distribution measurements on an isolated TPS 441 nacelle p 663 N95-17878
Low speed propeller slipstream aerodynamic effects p 663 N95-17882

FLOW EQUATIONS
Fifth International Conference on Hyperbolic Problems: Theory, Numerics, Applications [AD-A283078] p 863 N95-17333

FLOW MEASUREMENT
Mach number, flow angle, and loss measurements downstream of a transonic fan-blade cascade [AD-A280907] p 656 N95-16824
Detailed study at supersonic speeds of the flow around delta wings p 660 N95-17861

FLOW RESISTANCE
Skin blood flow and bioelectrical impedance [AD-A285475] p 821 N95-16619

FLOW STABILITY
Nonlinear instability of a uni-directional transversely sheared mean flow [NASA-TM-106779] p 769 N95-15969
Stability of separating subsonic boundary layers [NASA-CR-4638] p 772 N95-17268

FLOW VELOCITY
Analysis of plasma measurements for the Geotail mission [NASA-CR-197020] p 888 N95-15941
Filter efficiency and pressure drop calculations through two and three dimensional fiber arrays [DE94-014111] p 770 N95-16211
Modeling of chemical vapor infiltration for composite fabrication [DE93-001715] p 724 N95-16926

FLOW VISUALIZATION
Data Visualization and Animation Lab (DVAL) overview p 843 N95-16468
Data Visualization and Animation Lab (DVAL): Applications p 843 N95-16469
In-flight imaging of transverse gas jets injected into transonic and supersonic crossflows: Design and development [NASA-CR-186031] p 772 N95-17418
Subsonic flow around US-orbiter model FALKE in the DNW p 663 N95-17877

FLOWMETERS
Simulation of the SEMATECH gravimetric mass flowmeter calibrator [DE94-018698] p 773 N95-17910

FLUENCE
Studies of D-Li neutron source: An overview [DE94-014032] p 873 N95-16487

FLUID DYNAMICS
Unsteady flow phenomena in discrete passage diffusers for centrifugal compressors [AD-A281412] p 770 N95-16163
An analysis code for the Rapid Engineering Estimation of Momentum and Energy Losses (REMEL) [NASA-CR-191178] p 656 N95-16887
An investigation of fluid flow during induction stroke of a water analog model of an IC engine using an innovative optical velocimetry concept: LIPA [NASA-CR-197451] p 780 N95-16900
Small-amplitude disturbances in turbomachine flows with swirl [NASA-CR-195406] p 772 N95-17386
Nonlinear problems in fluid dynamics and inverse scattering. Propagation and capturing of singularities in problems of fluid dynamics and inverse scattering [AD-A282873] p 773 N95-17617
Multi-dimensional shock capturing [AD-A282986] p 773 N95-17708

FLUID FLOW
An investigation of fluid flow during induction stroke of a water analog model of an IC engine using an innovative optical velocimetry concept: LIPA [NASA-CR-197451] p 780 N95-16900
A new approach to validate subgrid models in complex high Reynolds number flows [AD-A282340] p 772 N95-17165
Surftherm: A program to analyze thermochemical and kinetic data in gas-phase and surface chemical reaction mechanisms [DE94-016145] p 733 N95-17744
Computer modeling of organic aerogels, 93-SR-062 [DE94-016485] p 722 N95-17745

FLUID JETS
Combustion instability phenomena of importance to liquid propellant engines [AD-A284780] p 730 N95-16882

FLUIDIZED BED PROCESSORS
Liquefied metal jet program Automation and Robotics Research Institute (ARRI) [AD-A285470] p 736 N95-16878
Calcium phosphate precipitation in a fluidized bed [PB94-201407] p 796 N95-17399

FLUORESCENCE
Experimental studies of stress measurement by optical fluorescence [AD-A282337] p 723 N95-16415

Solubilization of hydrophobic substances into block copolymer micelles in aqueous media and their release
[AD-A281395] p 744 N95-16792
Tunable UV source for UV fluorescence remote sensing
[DE94-015745] p 777 N95-16917

FLUORINE
Chiral recognition in molecular and macromolecular pairs of liquid crystals of (2R, 3S)- and (2S, 3S)-2-fluoro-3-methylpentyl-4'-(11-vinyloxyundeca iphenyl-4-carboxylate diastereomers
[AD-A281770] p 878 N95-17692

FLUORINE COMPOUNDS
Research on organofluorine chemistry for 700 F thermooxidative stability
[AD-A282767] p 731 N95-17142
Critical and paramagnetic spin dynamics in an antiferromagnetically coupled Heisenberg magnet: Results for RbMnF3
[PB95-104329] p 869 N95-17731

FLUOROHYDROCARBONS
Property control of (perfluorinated ionomer)/(inorganic oxide) composites by tailoring the nanoscale morphology
[AD-A281370] p 723 N95-16019

FLUOROPOLYMERS
Anionically-conductive ultrathin film composite membranes
[AD-A284944] p 723 N95-16041
Reaction and protection of electrical wire insulators in atomic-oxygen environments
[NASA-TM-106767] p 709 N95-17275

FLUTTER
A computational investigation of wake-induced airfoil flutter in incompressible flow and active flutter control
[AD-A281534] p 670 N95-16109

FLUTTER ANALYSIS
A computational investigation of wake-induced airfoil flutter in incompressible flow and active flutter control
[AD-A281534] p 670 N95-16109

FLUX (RATE)
Studies of D-Li neutron source: An overview
[DE94-014032] p 873 N95-16487

FLUX DENSITY
A consistent large deflection theory of composite sandwich shells p 650 N95-16259
Active minimization of energy density in three-dimensional enclosures
[NASA-CR-197213] p 871 N95-16848
Intense ion beam optimization and characterization with thermal imaging
[DE94-016184] p 891 N95-16936

FLUX PINNING
Studies by neutron diffraction and muon SR of flux lattice orientation, pinning, melting and decomposition in high-T(sub c) superconductors
[DE94-017704] p 901 N95-17667

FOAMS
Foam inflated rigidized structures for space applications p 710 N95-16344

FOCAL PLANE DEVICES
Testing and characterization of the CYCLOPS HgCdTe focal plane detector array
[AD-A284279] p 887 N95-17489
Measurement of modulation transfer function of focal plane arrays and imaging systems
[AD-A282976] p 887 N95-17707

FOIL BEARINGS
Cryogenic foil bearing turbopumps p 716 N95-16331

FOLDING STRUCTURES
Study of the folding and deployment aspects of a Collapsible Rib Tensioned Surface (CRTS) antenna reflector
[CUED/D-STRUCT/TR-144] p 783 N95-17928

FOOTPRINTS
Analysis of a three-beam radar as an instrument for determining ocean wave heights and vector slopes
[AD-A282342] p 806 N95-17505

FORCE DISTRIBUTION
2-D aileron effectiveness study p 658 N95-17851

FORECASTING
Mixed-layer hindcasts conducted at OWS Victor with initialization from synthetic profiles/mixed-layer hindcasts conducted with BTs taken during 1990 with atmospheric forcing from NOGAPS
[AD-A284749] p 800 N95-16551
Forecasting earthquakes
[NASA-TM-110112] p 799 N95-16981
An assessment of simulation systems applicable to business process reengineering at Army Directorates of Public Works
[AD-A285696] p 839 N95-17176
Verification of NOAA Space Environment Laboratory forecasts, 1 January - 31 December 1993
[PB95-104162] p 803 N95-17927

FORESTS
FIFE data analysis: Testing BIOME-BGC predictions for grasslands
[NASA-CR-197522] p 790 N95-16895
Modelling interactions of carbon dioxide, forests, and climate
[DE94-018694] p 797 N95-17908

FORGING
Forging of FeAl intermetallic compounds
[DE94-018124] p 739 N95-17728

FORMALISM
Studies of transverse coherent bunch instabilities for the Advanced Light Source (ALS)
[DE94-018536] p 904 N95-17904

FORMAT
A parser for the ISO 8211 data format
[AD-A281594] p 909 N95-16431
Table-driven configuration and formatting of telemetry data in the Deep Space Network p 677 N95-17185

FORTRAN
Applications of automatic differentiation in computational fluid dynamics p 774 N95-16461
High Performance FORTRAN p 843 N95-16478
An interactive interface for NCAR Graphics
[NASA-CR-189383] p 840 N95-17324
IS-Lab: A tool for developing interactive programs for simulation and analysis. User's guide
[PB94-184710] p 840 N95-17410
Applying STEP principles to product models in high energy physics research
[PB94-197704] p 880 N95-17503

FOSSIL FUELS
Hydrogen production by gasification of municipal solid waste
[DE94-016483] p 732 N95-17639

FOSSILS
Exobiology site priorities for Mars Pathfinder p 919 N95-16188

FOURIER TRANSFORMATION
Real-time data collection programs and source code for a commercial passive FTIR remote sensor
[AD-A284976] p 838 N95-16634
An algorithm for extraction of periodic signals from sparse, irregularly sampled data p 756 N95-17281
On the application of under-decimated filter banks p 757 N95-17285
Adaptive line enhancers for fast acquisition p 757 N95-17287
Radial acceletron, a new low impedance HPM source
[AD-A282008] p 760 N95-17501

FRACTALS
Fractal aggregate random media analysis and applications
[AD-A281410] p 884 N95-16161
The small-scale structure of dispersing clouds in the atmosphere
[AD-A285493] p 800 N95-16802

FRACTIONATION
Supercritical fluid extraction: Preparing a superior mesophase precursor for carbon fibers
[AD-A284933] p 726 N95-16142

FRACTOGRAPHY
Forging of FeAl intermetallic compounds
[DE94-018124] p 739 N95-17728

FRACTURE MECHANICS
Cornell program for the design and synthesis of advanced materials
[AD-A281352] p 723 N95-16016
Ductile fracture and failure criteria of structural steels
[AD-A280754] p 733 N95-16104
Innovative acoustic techniques for studying new materials and new developments in solid state physics
[AD-A280986] p 898 N95-16525
Experimental application of methodologies to quantify the effect of constraint on JC for a 3-D flaw geometry
[AD-A285309] p 735 N95-16531
Penetration of solid and layered targets by gas gun-launched steel cubes
[AD-A285143] p 787 N95-16843
Significant issues in proof testing: A critical appraisal
[NASA-CR-4628] p 788 N95-17272
Multiphase ceramics for mechanical and structural reliability at low and elevated temperatures
[AD-A285497] p 746 N95-17438
Micromechanics of interfaces in metal matrix composites
[AD-A282404] p 725 N95-17457
Metallurgical examination of failed T-158 Cast Austempered Ductile Iron (CADI) track shoes
[AD-A282433] p 737 N95-17486
Modeling of stress/strain behavior of fiber-reinforced ceramic matrix composites including stress redistribution
[NASA-TM-106789] p 725 N95-17659
Mechanisms of mechanical fatigue in ceramics
[DE94-016040] p 747 N95-17719
Workshop on Characterizing Diamond Films, 3
[PB94-187663] p 747 N95-17722

FRACTURE STRENGTH
Cornell program for the design and synthesis of advanced materials
[AD-A281352] p 723 N95-16016
Experimental application of methodologies to quantify the effect of constraint on JC for a 3-D flaw geometry
[AD-A285309] p 735 N95-16531
Effects of prior ductile tearing on cleavage fracture toughness in the transition region
[AD-A281298] p 786 N95-16785
Multi-lab comparison on R-curve methodologies: Alloy 2024-T3
[NASA-CR-195004] p 736 N95-16860
Mixed-mode I/III fracture toughness of a ferritic/martensitic stainless steel
[DE94-014492] p 736 N95-17159
The mechanical property data base from an Air Force/industry cooperative test program on high temperature aluminum alloys
[AD-A282911] p 737 N95-17398
Characterization of the hydrogen induced cold cracking susceptibility at simulated weld zones in HSLA-100 steel
[PB94-174505] p 737 N95-17616
Forging of FeAl intermetallic compounds
[DE94-018124] p 739 N95-17728

FRACTURING
Structural analysis of solid-propellant rocket motors with and without flaws p 720 N95-16348
Penetration of solid and layered targets by gas gun-launched steel cubes
[AD-A285143] p 787 N95-16843
Multi-lab comparison on R-curve methodologies: Alloy 2024-T3
[NASA-CR-195004] p 736 N95-16860
Effect of heat treatment temperature on creep-rupture properties of Fe3Al-based alloys
[DE94-018054] p 738 N95-17679

FRAGMENTATION
Mass spectrometry studies of the ionization of organic molecules by slow positrons
[DE94-013838] p 876 N95-16959

FRAGMENTS
Resonance enhanced multiphoton ionization of molecules and molecular fragments
[AD-A285076] p 873 N95-16493

FRAMES (DATA PROCESSING)
The CCSDS return all frames Space Link Extension service p 705 N95-17599

FREDHOLM EQUATIONS
Static image method for the interaction of two co-axial conducting prolate spheroids
[PB94-197696] p 760 N95-17502

FREE BOUNDARIES
Measurement of residual flexibility for substructures having prominent flexible interfaces
[NASA-TM-110074] p 786 N95-16577

FREE CONVECTION
Natural convection cooling of a three by three array of leadless chip carrier packages in a dielectric liquid
[AD-A282298] p 770 N95-16239

FREE ELECTRON LASERS
Evaluation of FEL image processing algorithm for 12-bit CCD-images as function of various atmospheric conditions
[AD-A285187] p 752 N95-16146
The LANL-Boeing APLE/HPO flying-wire beam-profile monitor
[DE94-014255] p 879 N95-16172
Simulations of an FEL producing coherent x rays utilizing the SLAC LINAC
[AD-A283524] p 777 N95-17303

FREE ENERGY
Effect of ion-electrode contact on the energetics of the heterogeneous electron transfer
[AD-A281959] p 873 N95-16411
The solvation thermodynamic functions in the Mean Spherical Approximation (MSA): Behavior near the solvent critical region
[AD-A283040] p 904 N95-17712

FREE FLOW
Parametric study of shock-induced combustion in a hydrogen air system
[NASA-CR-197134] p 726 N95-15967
Investigation of the flow over a series of 14 percent-thick supercritical aerofoils with significant rear camber p 657 N95-17849
OAT15A airfoil data p 659 N95-17857
Two-dimensional high-lift airfoil data for CFD code validation p 659 N95-17859

FREE JETS
On the prediction of free turbulent jets with swirl using a quadratic pressure-strain model
[NASA-CR-194964] p 769 N95-16071

FREE VIBRATION
Correlation of finite element free vibration predictions using random vibration test data
[NASA-TM-106787] p 787 N95-17258
FREEZING
Computational simulation of the formation and material behavior of ice
[NASA-TM-106702] p 785 N95-16416
FRENCH SATELLITES
CCS-MIP: Low cost Customizable Control Centre p 674 N95-17254
FREQUENCIES
An economical system for measuring, monitoring, and controlling the rate of repetitive events
[AD-A285219] p 764 N95-16522
The effects of fatigue loading frequency on fatigue life of high-strength pressure vessel steels
[AD-A285301] p 786 N95-16601
International mission planning for space Very Long Baseline Interferometry p 673 N95-17216
FREQUENCY ANALYZERS
In-fibre Bragg gratings for millimetre-wave EW systems
[AD-A284283] p 755 N95-16956
FREQUENCY CONTROL
An economical system for measuring, monitoring, and controlling the rate of repetitive events
[AD-A285219] p 764 N95-16522
FREQUENCY DIVISION MULTIPLE ACCESS
Detectability models and waveform design for multiple access Low-Probability-of-Intercept networks
[AD-A281864] p 753 N95-16300
FREQUENCY MEASUREMENT
An economical system for measuring, monitoring, and controlling the rate of repetitive events
[AD-A285219] p 764 N95-16522
FREQUENCY MODULATION
Evaluation of SEA loss factors using input power modulation
[ISVR-TR-240] p 868 N95-16856
FREQUENCY MULTIPLIERS
Frequency multiplier analysis and design using punch-through varactor diodes
[AD-A284963] p 762 N95-16130
FREQUENCY RESPONSE
Experimental study of spatially incomplete structural system identification
[AD-A280905] p 785 N95-16502
Measurement of residual flexibility for substructures having prominent flexible interfaces
[NASA-TM-110074] p 786 N95-16577
Frequency domain analysis for nonlinear electronic circuits
[PB94-201365] p 767 N95-17469
FREQUENCY SHIFT KEYING
Performance of a fast frequency-hopped noncoherent MFSK receiver with non-ideal noise normalization combining over ricean fading channels with partial-band interference
[AD-A284989] p 753 N95-16232
FRESNEL REGION
Characteristics of phase-correcting fresnel zone plates and elliptical waveguides
[AD-A281385] p 763 N95-16159
FRICTION
Deformation behavior of thin lubricant films at elevated pressure
[AD-A281848] p 741 N95-16355
FRICTION FACTOR
Static and dynamic friction behavior of candidate high temperature airframe seal materials
[NASA-TM-106571] p 722 N95-16905
FRONTS (METEOROLOGY)
Impact of physical processes on maritime frontogenesis
[AD-A283105] p 801 N95-17339
FUEL CELL POWER PLANTS
Fuel cell systems program plan, fiscal year 1994
[DE94-014301] p 793 N95-16541
FUEL CELLS
Atomic transport of oxygen
[DE94-013332] p 873 N95-16430
Fuel cell systems program plan, fiscal year 1994
[DE94-014301] p 793 N95-16541
FUEL COMBUSTION
Combustor kinetic energy efficiency analysis of the hypersonic research engine data p 714 N95-16321
An in-cylinder study of the particulate/NO(x) trade-off in a DI diesel engine
[DE94-014599] p 781 N95-17162
Identification and temporal behavior of radical intermediates formed during the combustion and pyrolysis of gaseous fuels: Kinetic pathways to soot formation
[DE94-014681] p 731 N95-17163
FUEL CONSUMPTION
Alternatives to traditional transportation fuels: An overview
[DE94-014979] p 749 N95-17923
FUEL VALVES
A Lifting Ball Valve for cryogenic fluid applications p 720 N95-16349
FULLERENES
International Winterschool on Electronic Properties of Novel Materials: Progress in Fullerene Research
[AD-A282128] p 728 N95-16608
Chemical properties of the fullerenes
[AD-A282730] p 730 N95-17141
Possible superstructures of metallic ions in nonstoichiometric fullerites M(x) C(60)
[DE94-622052] p 901 N95-17518
FUNCTIONAL ANALYSIS
A posteriori error estimation new approach
[AD-A284960] p 860 N95-16127
SCOS 2: ESA's new generation of mission control system p 674 N95-17253
FUNCTIONAL DESIGN SPECIFICATIONS
Generalized method of solving topological optimization problems for electrical airplane equipment systems in computer-aided design p 652 N95-16272
SCOS 2: ESA's new generation of mission control system p 674 N95-17253
Customizing the JPL Multimission Ground Data System: Lessons learned p 703 N95-17588
FURANS
The mechanism of the oligomerization of thiophene-based para-quinodimethanes
[DE94-014232] p 722 N95-16058
FURLABLE ANTENNAS
Study of the folding and deployment aspects of a Collapsible Rib Tensioned Surface (CRTS) antenna reflector
[CUED/D-STRUCT/TR-144] p 783 N95-17928
FUSELAGES
An approach to aerodynamic characteristics of low radar cross-section fuselages p 649 N95-16251
Numerical simulation of helicopter engine plume in forward flight
[NASA-CR-197488] p 655 N95-16589
Wind tunnel investigations of the appearance of shocks in the windward region of bodies with circular cross section at angle of attack p 661 N95-17866
STOVL CFD model test case p 663 N95-17881
Investigation of the influence of pylons and stores on the wing lower surface flow p 664 N95-17885
FUSION REACTORS
Fusion materials: Technical evaluation of the technology of vandium alloys for use as blanket structural materials in fusion power systems
[DE94-013194] p 890 N95-16827
Differential phase reflectometry for edge profile measurements on TFTR
[DE94-013837] p 891 N95-16958
A comparison of steady-state ARIES and pulsed PULSAR tokamak power plants
[DE94-014441] p 891 N95-17155
Prospects for toroidal fusion reactors
[DE94-014020] p 891 N95-17367
D3-D research operations
[DE94-014934] p 892 N95-17497
FUZZY SYSTEMS
Workshop on Formal Models for Intelligent Control
[AD-A281399] p 857 N95-16864
Assessment of benefits and drawbacks of using fuzzy logic, especially in fire control systems
[AD-A285428] p 838 N95-16874
Multi-objective decision-making under uncertainty: Fuzzy logic methods
[NASA-TM-106796] p 720 N95-17269

G

GALACTIC CLUSTERS
The mass and dynamics of cD clusters with cooling flows. 1: ROSAT observations of A 496
[NASA-CR-197534] p 915 N95-17495
GALACTIC COSMIC RAYS
Performance study of galactic cosmic ray shield materials
[NASA-TP-3473] p 924 N95-16912
GALACTIC STRUCTURE
Dust near luminous ultraviolet stars
[NASA-CR-197108] p 916 N95-16032
GALILEO PROJECT
Galileo mission planning for Low Gain Antenna based operations p 682 N95-17210
Small scale sequence automation pays big dividends p 689 N95-17247
RF optics study for DSS-43 ultracone implementation p 758 N95-17296
GALILEO SPACECRAFT
Tracking the Galileo spacecraft with the DSCC Galileo Telemetry prototype p 708 N95-17292
Galileo spacecraft modeling for orbital operations p 700 N95-17574
Re-engineering the Multimission Command System at the Jet Propulsion Laboratory p 702 N95-17583
Customizing the JPL Multimission Ground Data System: Lessons learned p 703 N95-17588
GALLIUM ANTIMONIDES
LPEE growth and characterization of In(x)Ga(1-x)As(y)Sb(1-y) lattice matched to GaSb and InAs for photodetectors
[AD-A281631] p 895 N95-16114
GALLIUM ARSENIDES
Process of making a bistable photoconductive component
[AD-D016449] p 764 N95-16539
Chemisorption energetics of superactive chlorine containing species on gallium arsenide surfaces
[AD-A281311] p 729 N95-16790
The impact of low temperature materials on the breakdown and noise properties of GaAs and InP based HEMT's and FET's
[AD-A285176] p 765 N95-16834
Non-volatile, rad-hard Random Access Memory (RAM) on GaAs
[AD-A285170] p 838 N95-16852
Performance characterization of photonic links in cryogenic environments for advanced signal processing applications
[DE94-015561] p 765 N95-16915
Positron annihilation studies of defects in molecular beam epitaxy grown 3 to 5 layers
[DE94-015823] p 899 N95-16918
Investigation of a normal incidence high-performance p-type strained layer In(0.3)Ga(0.7)As/In(0.52)Al(0.48)As quantum well infrared photodetector
[AD-A282720] p 900 N95-16928
Synthesis and characterization of neopentyl indium compounds: X-ray crystal structures of ((Me3CCH2)2InAs(SiMe3)2)2 and ((Me3CCH2)2InAs(SiMe3)2In (CH2CMe3)2Cl)
[AD-A282766] p 900 N95-17137
X-ray crystal structure of a monomeric Tris(Arsino)Gallane, ((Me3Si)2As)3Ga)3Ga
[AD-A282343] p 900 N95-17171
BaF2/GaAs electronic components
[AD-D016391] p 767 N95-17481
GALLIUM COMPOUNDS
Nitride semiconductors for ultraviolet detection
[AD-A280988] p 898 N95-16533
X-ray crystal structure of a monomeric Tris(Arsino)Gallane, ((Me3Si)2As)3Ga)3Ga
[AD-A282343] p 900 N95-17171
GALLIUM ISOTOPES
First results from SAGE 2
[DE94-014431] p 876 N95-17154
GALLIUM SELENIDES
A AgGaSe2 optical parametric oscillator pumped by a Raman-shifted YAG laser
[AD-A284743] p 777 N95-16548
GAMMA RAY ASTRONOMY
Na-22 decay gamma rays from classical novae
[NASA-CR-197454] p 924 N95-16383
Very high gamma ray extension of GRO observations
[NASA-CR-197489] p 924 N95-17421
A high resolution liquid xenon imaging telescope for 0.3-10 MeV gamma-ray astrophysics: Construction and initial balloon flights
[NASA-CR-197556] p 916 N95-17528
GAMMA RAY BURSTS
Very high gamma ray extension of GRO observations
[NASA-CR-197489] p 924 N95-17421
GAMMA RAY LASERS
SDIO/IST ultrashort wavelength. Mossbauer and gamma ray studies for grasers
[AD-A283091] p 778 N95-17337
GAMMA RAY OBSERVATORY
The GRO remote terminal system p 678 N95-17188
Nickel cadmium battery operations and performance p 685 N95-17224
Very high gamma ray extension of GRO observations
[NASA-CR-197489] p 924 N95-17421
GAMMA RAY TELESCOPES
Very high gamma ray extension of GRO observations
[NASA-CR-197489] p 924 N95-17421
GAMMA RAYS
Na-22 decay gamma rays from classical novae
[NASA-CR-197454] p 924 N95-16383
Kinetics model for initiation and promotion for describing tumor prevalence from HZE radiation
[NASA-TP-3479] p 820 N95-16412

SDIO/IST ultrashort wavelength. Mossbauer and gamma ray studies for grasers
[AD-A283091] p 778 N95-17337
Very high gamma ray extension of GRO observations
[NASA-CR-197489] p 924 N95-17421
Composite-model view of the ll-bar(gamma)(gamma) events at LEP
[DE94-753312] p 877 N95-17520
Physics at high energy photon photon colliders
[DE94-018191] p 881 N95-17888

GARP ATLANTIC TROPICAL EXPERIMENT
Large-eddy simulation of cumulus convection
[PB94-191368] p 800 N95-16290

GAS CHROMATOGRAPHY
Methods development toward the measurement of polyaromatic hydrocarbon-DNA adducts by mass spectrometry
[PB94-182722] p 727 N95-16373

GAS COMPOSITION
A study to determine the critical characteristics for mice in a newly designed whole body toxic gas exposure module
[AD-A285085] p 818 N95-17666

GAS DENSITY
Multi-beam laser interferometer for plasma density measurements in a Plasma Erosion Opening Switch (PEOS)
[AD-A283209] p 892 N95-17623
Beam characteristics of a large-bore copper laser with a radiatively cooled plasma
[DE94-015139] p 779 N95-17688

GAS DETECTORS
Novel mass spectrometric instrument for gaseous and particulate characterization and monitoring
[DE94-014168] p 795 N95-16213
The response of the Sandia robust wide range hydrogen sensor to H2-O2 mixtures
[DE94-013763] p 727 N95-16362
Physical and chemical sensor technologies developed at Lawrence Livermore National Laboratory
[DE94-012231] p 775 N95-17380
Electrical breakdown and optical emission properties of high pressure pulsed RF gas discharges
[DE94-012731] p 877 N95-17687
The development of a solid-state hydrogen sensor for rocket engine leakage detection
[NASA-CR-197567] p 776 N95-17895

GAS DISCHARGES
Electrical breakdown and optical emission properties of high pressure pulsed RF gas discharges
[DE94-012731] p 877 N95-17687

GAS DYNAMICS
Non-linear waves in gas dynamics and mechanics
[AD-A281376] p 770 N95-16156
CMCAM: A high performance CM-5 lattice gas simulator
[AD-A281063] p 837 N95-16626

GAS FLOW
Modeling of chemical vapor infiltration for composite fabrication
[DE93-001715] p 724 N95-16926
Computer modeling of organic aerogels, 93-SR-062
[DE94-016485] p 722 N95-17745
Simulation of the SEMATECH gravimetric mass flowmeter calibrator
[DE94-018698] p 773 N95-17910

GAS GUNS
Penetration of solid and layered targets by gas gun-launched steel cubes
[AD-A285143] p 787 N95-16843

GAS HEATING
Beam characteristics of a large-bore copper laser with a radiatively cooled plasma
[DE94-015139] p 779 N95-17688

GAS INJECTION
In-flight imaging of transverse gas jets injected into transonic and supersonic crossflows: Design and development
[NASA-CR-186031] p 772 N95-17418

GAS LASERS
Characterization of multiport solid state imagers at megahertz data rates
[DE94-016095] p 765 N95-16932

GAS METERS
Simulation of the SEMATECH gravimetric mass flowmeter calibrator
[DE94-018698] p 773 N95-17910

GAS PIPES
Vector magnetometry and lightwave defect imaging sensor technologies for internal pipe inspection systems: Phase 1 and 2 feasibility study, conceptual design, and prototype development
[PB94-194198] p 783 N95-16870

GAS PRESSURE
Measurements of x ray spectral flux and intensity distribution of APS/CHESS undulator radiation
[DE94-018384] p 882 N95-17901

GAS TEMPERATURE
ARCJET plasma modeling with experimental validation
[AD-A285234] p 889 N95-16243

GAS TURBINE ENGINES
Theoretical fundamentals of the aircraft GTE tests
p 651 N95-16265
An artificial neural network system for diagnosing gas turbine engine fuel faults
[DE94-013960] p 670 N95-17371
Simulation investigation on system identification of gas turbine
[PB95-104238] p 670 N95-17749

GAS-SOLID INTERACTIONS
Gas-surface interactions near dissociation threshold
[AD-A284945] p 726 N95-16042
Gas-surface interactions near dissociation threshold
[AD-A282726] p 730 N95-17140

GASEOUS FUELS
Identification and temporal behavior of radical intermediates formed during the combustion and pyrolysis of gaseous fuels: Kinetic pathways to soot formation
[DE94-014681] p 731 N95-17163

GASES
Spectroscopy of the transition state region in hydrogen transfer reactions
[AD-A285151] p 729 N95-16846

GASIFICATION
Hydrogen production by gasification of municipal solid waste
[DE94-016483] p 732 N95-17639

GASOHOL (FUEL)
Alternatives to traditional transportation fuels: An overview
[DE94-014979] p 749 N95-17923

GASOLINE
Alternatives to traditional transportation fuels: An overview
[DE94-014979] p 749 N95-17923

GASTROINTESTINAL SYSTEM
Effect of antiorthostatic BedRest (BR) on GastroIntestinal Motility (GIM) of normal subjects
p 811 N95-16753

GATES (CIRCUITS)
Picosecond optoelectronic AND-GATE
[AD-A285672] p 885 N95-16620
Digital logic and reconfigurable interconnects using aluminum gallium arsenide electro-optic Fredkin gates
[AD-A282880] p 881 N95-17619

GEAR TEETH
Twin disc gear tooth simulator
[AD-A284927] p 780 N95-16139
A review of transmission diagnostics research at NASA Lewis Research Center
[ARL-TR-599] p 781 N95-16907

GEARS
Twin disc gear tooth simulator
[AD-A284927] p 780 N95-16139
Researches on gear fault diagnosis techniques
p 651 N95-16267

GELATINS
Reduction and aggregation of silver in aqueous gelatin and silica suspensions
[DE94-013998] p 727 N95-16363

GELS
Non-linear acoustics in fluids and gels
[PB94-201308] p 870 N95-16614
Structure-property relationships in sol-gel-derived thin films
[DE94-016149] p 744 N95-16934
Mobility measurement and computer simulation at specific sites in polystyrene solutions and gels
[AD-A281214] p 747 N95-17685

GENE EXPRESSION
The role of chemical inhibition of gap junctional intercellular communication in toxicology
[AD-A282452] p 820 N95-16378

GENERAL AVIATION AIRCRAFT
Revitalizing general aviation
[NASA-TM-110113] p 669 N95-16982
Annual review of aircraft accident data: US Air carrier operations, calendar year 1992
[PB95-100319] p 665 N95-17748

GENERAL OVERVIEWS
Survey of United States commercial satellites in geosynchronous Earth orbit
[AD-A284969] p 708 N95-16131
Composite chronicles: A study of the lessons learned in the development, production, and service of composite structures
[NASA-CR-4620] p 724 N95-16859

GENETIC ALGORITHMS
A highly functional decision paradigm based on nonlinear adaptive genetic algorithm
[AD-A281457] p 855 N95-16077
An investigation of genetic operators for continuous parameter space
[DE94-009364] p 834 N95-16219
Review of the EUROPT Project AERO-0026
p 668 N95-16573
Constrained minimization of smooth functions using a genetic algorithm
[NASA-TP-3329] p 709 N95-16902

GEOCHRONOLOGY
Marte Valles site p 921 N95-16200

GEODESY
Digital mapping, charting, and geodesy analysis program technical review of interim terrain analysis data set prototype 1
[AD-A284742] p 790 N95-16547

GEOGRAPHIC INFORMATION SYSTEMS
GEOTRANS geographic decision support system
[PB94-183670] p 908 N95-16093
A coastal hazards data base for the US Gulf Coast
[DE94-014573] p 805 N95-16610
A procedure for estimating the carbon budget of terrestrial ecosystems in the former Soviet Union by geographic information system analysis and classification of AVHRR derived global vegetation index
p 796 N95-17394
Detection of deforestation in the Amazon forest using NOAA/AVHRR images and the geographic information system SGI: Methodology and test of a potential alarm system
[INPE-5580-TDI/543] p 791 N95-17894

GEOLOGICAL SURVEYS
Imager for Mars Pathfinder (IMF) p 711 N95-16206
Site characterization at the Rabbit Valley Geophysical Performance Evaluation Range
[DE94-013550] p 798 N95-16284
Forecasting earthquakes
[NASA-TM-110112] p 799 N95-16981

GEOLOGY
Tsunami newsletter, volume 26
[AD-A282751] p 806 N95-17477

GEOMAGNETIC TAIL
Geosynchronous orbit magnetopause crossings
[DE94-014817] p 798 N95-16537

GEOMAGNETISM
Ion drift meter research
[NASA-CR-197124] p 798 N95-16432
Radiation belt dynamic and quasi-static modeling based on CRRES data
[AD-A285282] p 916 N95-16600
Magnetometer-only attitude and rate determination for a gyro-less spacecraft p 694 N95-17546

GEOMETRIC RECTIFICATION (IMAGERY)
Overview on METEOSAT geometrical image data processing p 678 N95-17189

GEOMETRICAL OPTICS
High speed method for predicting radio-wave propagation
[AD-D016369] p 761 N95-17697

GEOMORPHOLOGY
Climatological targets for Mars Pathfinder
p 922 N95-16208
A coastal hazards data base for the US Gulf Coast
[DE94-014573] p 805 N95-16610

GEOPHYSICS
Site characterization at the Rabbit Valley Geophysical Performance Evaluation Range
[DE94-013550] p 798 N95-16284

GEOSYNCHRONOUS ORBITS
Geostationary satellite positioning by DLR/GSOC operations and management methods
p 684 N95-17217

GEOTECHNICAL ENGINEERING
Normalization and prediction of geotechnical properties using the Cone Penetrometer Test (CPT)
[AD-A285193] p 799 N95-16872

GERMANIUM
New methods for treatment of electron correlation and surface dynamics (FY91 AASERT)
[AD-A285177] p 727 N95-16144
New approaches to novel organosilanes
[AD-A285253] p 722 N95-16513

GERMANIUM ALLOYS
Recombination and metastability in amorphous silicon and silicon-germanium alloys
[DE94-011837] p 794 N95-16957

GERMANY
The Technical Information Library: TIB
p 906 N95-15928

GLASS
Nonlinear problems and numerical method in differential equations and applied phenomena
[AD-A281531] p 859 N95-16108

GLASS TRANSITION TEMPERATURE
Thermoplastic and thermosetting high glass transition temperature matrix resins
[AD-A281508] p 740 N95-16096
GLIDE PATHS
Application of GPS/SINS/RA integrated system to aircraft approach landing p 653 N95-16277
GLOBAL AIR POLLUTION
Global warming potentials, part 7
[DE94-014066] p 794 N95-16209
Simulations of the global carbon cycle and anthropogenic CO2 transient
[DE94-014165] p 795 N95-16212
GLOBAL POSITIONING SYSTEM
Application of GPS/SINS/RA integrated system to aircraft approach landing p 653 N95-16277
Autonomous weapon guidance
[AD-A282715] p 671 N95-16381
Forecasting earthquakes
[NASA-TM-110112] p 799 N95-16981
A processing centre for the CNES CE-GPS experimentation p 666 N95-17196
GPS tides and datums
[AD-A282422] p 666 N95-17508
GLOBAL WARMING
Global warming potentials, part 7
[DE94-014066] p 794 N95-16209
Proceedings of the First National Conference on Climate Change and Water Resources Management
[AD-A281172] p 796 N95-17684
GLYCOLS
Isomorphism within the hexagonal columnar mesophase of molecular and macromolecular self- and co-assembled columns containing tapered groups
[AD-A281205] p 874 N95-16797
The influence of the complexation of sodium and lithium triflate on the self-assembly of tubular-supramolecular architectures displaying a columnar mesophase based on taper-shaped monoesters of oligoethyleneoxide with 3,4,5-tris(p-(n-dodecan-l-yloxy)benzyloxy)benzoic acid and of their polymethacrylates
[AD-A281403] p 730 N95-16866
GOAL THEORY
A framework for the analysis of cognitive tasks
[AD-A285345] p 828 N95-16835
GOGGLES
Visual acuity versus field-of-view and light level for Night Vision Goggles (NVG)
[AD-A284750] p 830 N95-16553
GOLD
Preparation of Au single crystals for study of the ECALE deposition of CdTe
[AD-A282294] p 895 N95-16238
Snapshots of crystal growth: Nanoclusters of organic conductors on Au(111) surfaces
[AD-A280976] p 897 N95-16508
Underpotential deposition of Cu on Au(111): Implications of the HB model
[AD-A283028] p 902 N95-17711
GOLD ISOTOPES
Self-assembly of low-dimensional conductors on Au(111) surfaces
[AD-A280936] p 734 N95-16505
GOVERNMENT PROCUREMENT
Federal Aviation Administration aviation system capital investment plan, 1993
[PB94-171956] p 654 N95-17512
Department of Defense Electronic Data Interchange project baseline report for FY 1994
[AD-A283015] p 912 N95-17710
GOVERNMENT/INDUSTRY RELATIONS
NASA contract mangagement: Improving the use of DCAA's auditing services. Report to the Chairman, Committee on Government Operations, House of Representatives
[GAO/NSIAD-94-229] p 914 N95-15962
From computer images to video presentation: Enhancing technology transfer p 848 N95-16467
Optical fiber sensors: Accelerating applications in Navy ships
[PB94-186848] p 887 N95-17441
GOVERNMENTS
Bureau of the Census Center for International Research p 905 N95-15923
Networked information: Management issues for the acquisitions librarian p 906 N95-15932
GRADIENTS
Modeling of chemical vapor infiltration for composite fabrication
[DE93-001715] p 724 N95-16926
Likelihood ratio gradient estimation for stochastic recursions
[AD-A281408] p 865 N95-17426
Beam position correction in the Fermilab Linac
[DE94-018984] p 882 N95-17931
GRAIN BOUNDARIES
Theoretical studies of the strengths of matrix second phase particle interfaces
[AD-A280703] p 738 N95-17681
GRAIN SIZE
Superplasticity and superplastic forming of ceramics
[DE94-016172] p 745 N95-16935
Asymptotic behavior in grain growth
[DE94-014452] p 900 N95-17156
Low-temperature fabrication of transparent silicon nitride
[DE94-014902] p 746 N95-17456
GRAMMARS
Parallel parsing
[PB94-191392] p 850 N95-17138
GRAND UNIFIED THEORY
Flavor symmetries and fermion masses
[DE94-018192] p 878 N95-17889
GRAPH THEORY
On computing the minimal labels in time point algebra networks
[TR-495] p 859 N95-16022
A software tool for dataflow graph scheduling p 843 N95-16457
Real-time symbolic model checking for discrete time models
[AD-A282878] p 864 N95-17618
GRAPHICAL USER INTERFACE
Integrating computers into calculus instruction
[AD-A280996] p 833 N95-15997
MAGENCO: A map generalization controller for Arc/Info
[DE94-013440] p 835 N95-16358
A workstation based simulator for teaching compressible aerodynamics
[NASA-TM-106799] p 839 N95-16906
Graphic Server: A real time system for displaying and monitoring telemetry data of several satellites p 687 N95-17238
An object-oriented graphical user interface for a reusable rocket engine intelligent control system
[NASA-TM-106750] p 721 N95-17274
Experimenter's Laboratory for Visualized Interactive Science
[NASA-CR-189391] p 910 N95-17322
An interactive interface for NCAR Graphics
[NASA-CR-189383] p 840 N95-17324
An interactive environment for the analysis of large Earth observation and model data sets
[NASA-CR-189381] p 911 N95-17330
Breaking down barriers in cooperative fault management: Temporal and functional information displays
[NASA-CR-197450] p 857 N95-17383
A software architecture for automating operations processes p 692 N95-17538
Knowledge-based critiquing of graphical user interfaces with CHIMES p 697 N95-17560
ELISA, a demonstrator environment for information systems architecture design p 698 N95-17563
Mission Operations Centers (MOCs): Integrating key spacecraft ground data system components p 675 N95-17601
A three dimensional mesoscale atmospheric simulation system for use in various mobile battlefield environments. Phase 2: Transition to an operational forecast system
[AD-A281223] p 802 N95-17686
Behavioural modelling of formal documents and active instruments
[PB95-104378] p 842 N95-17732
GRAPHITE
Raman spectroscopy of C-irradiated graphite
[DE94-018705] p 733 N95-17911
GRAPHITE-EPOXY COMPOSITES
Recent advances in graphite/epoxy motor cases p 717 N95-16333
Graphite-reinforced polycyanate composites for space and missile applications
[AD-A285509] p 725 N95-16970
GRAPHS (CHARTS)
Exact, E = 0, classical and quantum solutions for general power-law oscillators
[DE94-014436] p 903 N95-16428
Interactive sketching for the early stages of user interface design
[AD-A285339] p 838 N95-16818
GRASSLANDS
FIFE data analysis: Testing BIOME-BGC predictions for grasslands
[NASA-CR-197522] p 790 N95-16895
GRATINGS (SPECTRA)
In-fibre Bragg gratings for millimetre-wave EW systems
[AD-A284283] p 755 N95-16956
GRAVIMETRY
Simulation of the SEMATECH gravimetric mass flowmeter calibrator
[DE94-018698] p 773 N95-17910
GRAVITATIONAL EFFECTS
Phase segregation due to simultaneous migration and coalescence
[NASA-CR-196819] p 721 N95-16035
Combustion and fires in low gravity p 712 N95-16050
Variability in Hoffmann and tendon reflexes in healthy male subjects p 808 N95-16739
Achilles Tendon Reflex (ATR) in response to short exposures of microgravity and hypergravity p 812 N95-16756
GRAVITATIONAL PHYSIOLOGY
Virtual environment application with partial gravity simulation p 854 N95-15988
Mathematical model for interaction of canals and otoliths in perception of orientation, translation, and rotation
[AD-A280897] p 819 N95-16151
Aerospace Medical Association 63rd Annual Scienti fic Meeting Program p 807 N95-16737
The psychophysical function for perceived gravitational-inertial force does not depend on the orientation of the otolith organs p 808 N95-16740
Use of injectable promethazine to decrease symptom scores of Space Motion Sickness p 808 N95-16741
Comparison of saline and fludrocortisone as fluid-loading countermeasures following exposure to simulated microgravity p 808 N95-16742
Catecholaminergic responses to stressful motion stimuli, scopolamine plus amphetamine, and dexamethasone p 809 N95-16745
Physiological constraints on deceleration during the aerocapture of manned vehicles p 810 N95-16751
Blood volume and orthostatic responses of men and women to a 13-day bedrest p 811 N95-16752
Effect of antiorthostatic BedRest (BR) on GastroIntestinal Motility (GIM) of normal subjects p 811 N95-16753
Comparisons of three anti-G suit configurations during long duration, low onset, +Gz p 811 N95-16755
Achilles Tendon Reflex (ATR) in response to short exposures of microgravity and hypergravity p 812 N95-16756
Prediction of space sickness in astronauts from preflight fluid, electrolyte, and cardiovascular variables and Weightless Environmental Training Facility (WETF) training p 812 N95-16757
Space medicine research: Needs for the 21st century p 814 N95-16768
SLS-1: The first dedicated life sciences shuttle flight p 676 N95-16769
Effects of weightlessness on human baroreflex function p 815 N95-16770
Delivery of cardiopulmonary resuscitation in the microgravity environment p 816 N95-16774
Advanced Cardiac Life Support (ACLS) utilizing Man-Tended Capability (MTC) hardware onboard Space Station Freedom p 816 N95-16775
A surgical support system for Space Station Freedom p 710 N95-16776
Artificial gravity: How much, how often, how long? p 816 N95-16778
The effect of intermittent standing or walking during head down tilt bedrest on peak O2 consumption p 817 N95-16779
Periodic upright posture negates the suppression of neuroendocrine response to head down bedrest p 817 N95-16780
The efficacy of periodic +Gz exposure in the prevention of bedrest induced orthostatic intolerance p 817 N95-16781
The value of the 4-day headdown bedrest model for screening countermeasures p 817 N95-16782
GRAVITY WAVES
An observational study of long waves in the equatorial Pacific Ocean during the 1991-1993 El Nino
[AD-A283380] p 806 N95-17624
GRAY SCALE
Grey-scale measurements in multi-dimensional digitized images
[PB94-195492] p 887 N95-17483
GREEN'S FUNCTIONS
Effective reflection coefficients for the mean acoustic field between two rough interfaces
[AD-A281962] p 870 N95-16413
Electromagnetostatics in uniaxial bianisotropic media
[PB94-197688] p 754 N95-16613
GREENHOUSE EFFECT
Global warming potentials, part 7
[DE94-014066] p 794 N95-16209
Regional forecasting with global atmospheric models
[DE94-013863] p 801 N95-16961

GRID GENERATION (MATHEMATICS)
Sorting and hardware assisted rendering for volume visualization
[DE94-010204] p 834 N95-16220
Computational methods for microstructure covolume techniques of discretization
[AD-A282449] p 861 N95-16376
Numerical methods for singularly perturbed differential equations with applications
[AD-A285209] p 861 N95-16517
The Grid Analysis and Display System (GrADS)
[NASA-CR-189387] p 912 N95-17491
Error estimation and adaptive mesh refinement for parallel analysis of shell structures
[NASA-CR-197500] p 788 N95-17492

GROUND BASED CONTROL
Third International Symposium on Space Mission Operations and Ground Data Systems, part 1
[NASA-CP-3281-PT-1] p 676 N95-17179
SPOT4 Management Centre p 673 N95-17223
Autonomous mission planning and scheduling: Innovative, integrated, responsive p 686 N95-17234
Graphic Server: A real time system for displaying and monitoring telemetry data of several satellites
p 687 N95-17238
Designing an autonomous environment for mission critical operation of the EUVE satellite
p 688 N95-17241
Increases in efficiency and enhancements to the Mars Observer non-stored commanding process
p 688 N95-17242
A graphic system for telemetry monitoring and procedure performing at the Telecom SCC p 689 N95-17246
Towards cheaper control centers p 674 N95-17250
EURECA mission control experience and messages for the future p 690 N95-17252
CCS-MIP: Low cost Customizable Control Centre
p 674 N95-17254
Mini All-purpose Satellite Control Center (MASCC)
p 674 N95-17257
Third International Symposium on Space Mission Operations and Ground Data Systems, part 2
[NASA-CP-3281-PT-2] p 691 N95-17531
SEQ-GEN: A comprehensive multimission sequencing system p 693 N95-17540
An intelligent automated command and control system for spacecraft mission operations p 693 N95-17542
Cost efficient operations for Discovery class missions
p 695 N95-17548
Design of ground segments for small satellites
p 674 N95-17550
Small satellite space operations p 695 N95-17552
Embedded parallel processing based ground control systems for small satellite telemetry
p 674 N95-17553
An agent-oriented approach to automated mission operations p 696 N95-17555
Taking advantage of ground data systems attributes to achieve quality results in testing software
p 699 N95-17570
Solar and Heliospheric Observatory (SOHO) Experimenters' Operations Facility (EOF)
p 675 N95-17573
Transportable Payload Operations Control Center reusable software: Building blocks for quality ground data systems p 703 N95-17587
Customizing the JPL Multimission Ground Data System: Lessons learned p 703 N95-17588
Standardizing the information architecture for spacecraft operations p 703 N95-17591
Standard protocol stack for mission control
p 704 N95-17593
Cross support overview and operations concept for future space missions p 705 N95-17598
The NASA Mission Operations and Control Architecture Program p 706 N95-17603

GROUND OPERATIONAL SUPPORT SYSTEM
International Space Station Alpha user payload operations concept p 685 N95-17227
Efficient mission control for the 48-satellite Globalstar Constellation p 674 N95-17256
A General Mission Independent Simulator (GMIS) and Simulator Control Program (SCP) p 701 N95-17580
Configurable technology development for reusable control and monitor ground systems
p 675 N95-17589
Cross support overview and operations concept for future space missions p 705 N95-17598
Renaissance architecture for Ground Data Systems
p 706 N95-17604

GROUND STATE
Resonance enhanced multiphoton ionization of molecules and molecular fragments
[AD-A285076] p 873 N95-16493

GROUND STATIONS
A VHF/UHF antenna for the Precision Antenna Measurement System (PAMS)
[AD-A285673] p 754 N95-16621
Telecommunications end-to-end systems monitoring on TOPEX/Poseidon: Tools and techniques
p 676 N95-17180
The GRO remote terminal system
p 678 N95-17188
The development and operation of the international solar-terrestrial physics central data handling facility
p 679 N95-17193
Economical ground data delivery p 679 N95-17194
A processing centre for the CNES CE-GPS experimentation p 666 N95-17196
A low-cost transportable ground station for capture and processing of direct broadcast EOS satellite data
p 680 N95-17200
GRTS operations monitor/control system
p 685 N95-17226
Space VLBI telecommunication characteristics, protection criteria, and frequency sharing
p 756 N95-17282
Ground Station support for small scientific satellites
p 695 N95-17549
Small satellite space operations p 695 N95-17552
Open solutions to distributed control in ground tracking stations p 674 N95-17554
Advanced ground station architecture
p 674 N95-17556
Matrix evaluation of science objectives
p 707 N95-17610
A new systems engineering approach to streamlined science and mission operations for the Far Ultraviolet Spectroscopic Explorer (FUSE) p 707 N95-17611

GROUND SUPPORT EQUIPMENT
Ground equipment for the support of packet telemetry and telecommand p 681 N95-17203

GROUND SUPPORT SYSTEMS
Generic propellant transfer unit: A project update
p 719 N95-16345
Communication network for decentralized remote tele-science during the Spacelab mission IML-2
p 676 N95-17181
Single Stage Rocket Technology's real time data system p 679 N95-17197
Production and quality assurance automation in the Goddard Space Flight Center Flight Dynamics Facility
p 687 N95-17237
Designing an autonomous environment for mission critical operation of the EUVE satellite
p 688 N95-17241
Third International Symposium on Space Mission Operations and Ground Data Systems, part 2
[NASA-CP-3281-PT-2] p 691 N95-17531
Delivering spacecraft control centers with embedded knowledge-based systems: The methodology issue
p 674 N95-17532
SCOSII OL: A dedicated language for mission operations p 692 N95-17533
DIAMS revisited: Taming the variety of knowledge in fault diagnosis expert systems p 692 N95-17534
Using graphics and expert system technologies to support satellite monitoring at the NASA Goddard Space Flight Center p 674 N95-17535
SCOSII: ESA's new generation of mission control systems: The user's perspective p 674 N95-17537
Spacecraft command and control using expert systems p 693 N95-17539
SEQ-GEN: A comprehensive multimission sequencing system p 693 N95-17540
Cost efficient operations for Discovery class missions
p 695 N95-17548
Ground Station support for small scientific satellites
p 695 N95-17549
Design of ground segments for small satellites
p 674 N95-17550
ELISA, a demonstrator environment for information systems architecture design p 698 N95-17563
Software interface verifier p 698 N95-17564
OOD/OOP experience in the Science Operations Center part of the ground system for X ray Timing Explorer mission p 675 N95-17565
Integration of a satellite ground support system based on analysis of the satellite ground support domain
p 675 N95-17568
Taking advantage of ground data systems attributes to achieve quality results in testing software
p 699 N95-17570
Solar and Heliospheric Observatory (SOHO) Experimenters' Operations Facility (EOF)
p 675 N95-17573
The Advanced Orbiting Systems Testbed Program: Results to date p 700 N95-17575
Re-engineering Nascom's network management architecture p 702 N95-17584
ATOS: Integration of advanced technology software within distributed Spacecraft Mission Operations Systems p 705 N95-17602

GROUND TESTS
A model for preliminary facility design including simulation issues p 672 N95-16318
Hypersonic air-breathing aeropropulsion facility test support requirements p 672 N95-16319
Development of a low-aspect ratio fin for flight research experiments
[NASA-TM-4596] p 656 N95-16858
International Space Station Alpha user payload operations concept p 685 N95-17227
A modular electric power system test bed for small spacecraft
[NASA-TM-106812] p 721 N95-17276
Test/score/report: Simulation techniques for automating the test process p 675 N95-17581
Transportable Payload Operations Control Center reusable software: Building blocks for quality ground data systems p 703 N95-17587
Customizing the JPL Multimission Ground Data System: Lessons learned p 703 N95-17588

GROUND TRUTH
Using neural networks to correlate satellite imagery and ground-truth data
[AD-A285486] p 857 N95-16967
Field verification of the wind tunnel coefficients
p 664 N95-17291

GROUND-AIR-GROUND COMMUNICATION
Communication network for decentralized remote tele-science during the Spacelab mission IML-2
p 676 N95-17181
Efficient mission control for the 48-satellite Globalstar Constellation p 674 N95-17256

GULF OF MEXICO
An air mass transformation model for coastal environments
[AD-A281790] p 801 N95-17164
South Florida environmental quality. National Status and Trends Program for marine environmental quality
[PB94-173408] p 796 N95-17363

GULF STREAM
Objective feature identification and tracking: A review
[AD-A284955] p 804 N95-16125
Florida Gulf Stream Data (FLDA) current study
[AD-A281965] p 805 N95-16414

GULFS
A coastal hazards data base for the US Gulf Coast
[DE94-014573] p 805 N95-16610

GUN PROPELLANTS
The 1993 JANNAF Propulsion Meeting, volume 1
[CPIA-PUBL-602-VOL-1] p 713 N95-16312

GUSTS
Field verification of the wind tunnel coefficients
p 664 N95-17291

GYRATORS
Duality transformations, green dyadics and plane-wave solutions for a class of bianisotropic media
[PB94-197670] p 754 N95-16612

H

HABITUATION (LEARNING)
Learning one more thing
[AD-A285342] p 857 N95-16820

HADRONS
Experimental issues in high-sensitivity charm experiments
[DE94-015544] p 871 N95-15045
Production asymmetries in x(sub F) and P(sub t)(exp 2) for D(+-) mesons
[DE94-015546] p 872 N95-16310
QCD of different flavors with the SLD detectors
[DE94-013800] p 875 N95-16943
Delayed annihilation of antiprotons in helium gas
[DE94-753405] p 878 N95-17739
Z(prime) phenomenology: Constraints from low-energy measurements, and detailed study at TeV-scale lepton and hadron colliders
[DE94-018185] p 881 N95-17886

HAFNIUM ALLOYS
Effect of extrusion parameters on consolidation of tungsten-hafnium and tungsten-steel powders
[DE94-013270] p 737 N95-17513

HAFNIUM CARBIDES
Tribological properties of reactively sputtered nitrides and carbides of titanium, zirconium and hafnium
[DE94-014583] p 745 N95-17160

HAFNIUM COMPOUNDS
Tribological properties of reactively sputtered nitrides and carbides of titanium, zirconium and hafnium
[DE94-014583] p 745 N95-17160

HALL EFFECT
Non-volatile, rad-hard Random Access Memory (RAM) on GaAs
[AD-A285170] p 838 N95-16852
HALOGENS
Thermal dissociation of halogen azides
[AD-A285088] p 728 N95-16497
Chemisorption energetics of superactive chlorine containing species on gallium arsenide surfaces
[AD-A281311] p 729 N95-16790
HALOS
Mechanisms of beam-halo formation in high-intensity linacs
[DE94-016316] p 879 N95-16030
ROSAT detection of diffuse hot gas in the edge-on galaxy NGC 4631
[NASA-CR-197535] p 915 N95-17496
X-ray emission from the edge-on spiral galaxy NGC 4631
[NASA-CR-197536] p 924 N95-17527
HAMILTONIAN FUNCTIONS
Some fundamental techniques in the theory of integrable systems
[PB94-192390] p 860 N95-16294
Extraction of high quality potential surfaces from laboratory data
[AD-A285071] p 903 N95-16489
Time-dependent spin correlations in the heisenberg magnet at infinite temperature
[PB95-104303] p 869 N95-17750
Studies of transverse coherent bunch instabilities for the Advanced Light Source (ALS)
[DE94-018536] p 904 N95-17904
HAMMERS
Variability in Hoffmann and tendon reflexes in healthy male subjects p 808 N95-16739
HAMSTERS
Control of circadian behavior by transplanted suprachiasmatic nuclei
[AD-A285233] p 807 N95-16599
Failure of ozone and nitrogen dioxide to enhance lung tumor development in hamsters
[PB94-182854] p 818 N95-16801
HAND (ANATOMY)
A specification of 3D manipulation in virtual environments p 853 N95-15981
A virtual work space for both hands manipulation with coherency between kinesthetic and visual sensation p 831 N95-15984
HANDBOOKS
Primary battery design and safety guidelines handbook
[NASA-RP-1353] p 764 N95-16561
Handbook for users
[AD-A285148] p 909 N95-16845
HARD LANDING
Mars Pathfinder mission operations concepts p 686 N95-17229
HARDWARE
The development and operation of the international solar-terrestrial physics central data handling facility p 679 N95-17193
HARDWARE DESCRIPTION LANGUAGES
Hardware description languages p 832 N95-16477
WAVES VHDL interface
[AD-A285208] p 764 N95-16516
HARMONIC ANALYSIS
Frequency domain analysis for nonlinear electronic circuits
[PB94-201365] p 767 N95-17469
HARMONIC GENERATIONS
Third harmonic generation study of alpha-thiophene oligomers: Monomer to octamer
[AD-A281177] p 874 N95-16629
Tunable UV source for UV fluorescence remote sensing
[DE94-015745] p 777 N95-16917
Poling dynamics and relaxation of polar order in guest/host polymers by second harmonic generation
[AD-A283291] p 748 N95-17724
HARMONIC OSCILLATORS
Relativistic effect of energy increase of a particle moving freely in vacuum from the quantum field theory point of view
[DE94-622757] p 903 N95-17473
HAZARDS
The assessment of the AH-64D, longbow, mast-mounted assembly noise hazard for maintenance personnel
[AD-A284971] p 869 N95-16226
Generic propellant transfer unit: A project update p 719 N95-16345
A coastal hazards data base for the US Gulf Coast
[DE94-014573] p 805 N95-16610
Safety characteristics of lithium-alloy/metal sulfide batteries
[DE94-013867] p 766 N95-16963
HEAD DOWN TILT
Blood volume and orthostatic responses of men and women to a 13-day bedrest p 811 N95-16752
The effect of intermittent standing or walking during head down tilt bedrest on peak O2 consumption p 817 N95-16779
Periodic upright posture negates the suppression of neuroendocrine response to head down bedrest p 817 N95-16780
The value of the 4-day headdown bedrest model for screening countermeasures p 817 N95-16782
HEAD MOVEMENT
Dynamics of the G-excess illusion p 815 N95-16771
HEAD-UP DISPLAYS
Beyond the cockpit: The visual world as a flight instrument p 814 N95-16767
HEALTH
Space medicine research: Needs for the 21st century p 814 N95-16768
Medical care capabilities for Space Station Freedom: A phase approach p 710 N95-16772
A prototype Crew Medical Restraint System (CMRS) for Space Station Freedom p 815 N95-16773
Medicine on Mars: Remote medical care and the space exploration initiative p 816 N95-16777
Artificial gravity: How much, how often, how long? p 816 N95-16778
HEARING
The assessment of the AH-64D, longbow, mast-mounted assembly noise hazard for maintenance personnel
[AD-A284971] p 869 N95-16226
Direct comparison of two statistical methods for determination of evoked-potential thresholds
[AD-A285182] p 870 N95-16811
HEART FUNCTION
Spectral components of human cardiovascular responses to step changes in Lower Body Negative Pressure (LBNP) before and after 22 hour of 6 deg head down bed rest p 810 N95-16748
Changes in left ventricular function as determined by the multi-wire gamma camera at near presyncopal levels of lower body negative pressure p 811 N95-16754
HEAT AFFECTED ZONE
Characterization of the hydrogen induced cold cracking susceptibility at simulated weld zones in HSLA-100 steel
[PB94-174505] p 737 N95-17616
HEAT BALANCE
Long-term momentum and heat balances and turbulent mixing in the upper equatorial Pacific Ocean p 805 N95-17395
HEAT ENGINES
Anisotropic heat exchangers/stack configurations for thermoacoustic heat engines
[AD-A280974] p 792 N95-16506
Thermoacoustic pin stacks
[AD-A282267] p 794 N95-16954
HEAT EXCHANGERS
Materials characterization and design for solar-thermal propulsion p 718 N95-16340
Solar-powered rocket engine optimization for high specific impulse p 718 N95-16341
Anisotropic heat exchangers/stack configurations for thermoacoustic heat engines
[AD-A280974] p 792 N95-16506
HEAT FLUX
Development of a radiative divertor for DIII-D
[DE94-016522] p 889 N95-16554
First measurements of ICRF and edge/SOL plasma interactions on TORE SUPRA
[DE94-019320] p 891 N95-17347
Measurements of non-axisymmetric effects in the D3-D divertor
[DE94-018346] p 893 N95-17897
On the measurement of momentum flux profiles using a five-beam 915-MHz wind profiler
[DE94-018448] p 791 N95-17903
HEAT GENERATION
Molten salt techniques for excess heat production and the loading issue
[AD-A282462] p 792 N95-16303
Kinetics and mechanism of chemical marker formation and water-activated heat generation
[AD-A281407] p 731 N95-17425
HEAT MEASUREMENT
Charging hydrogen into Ni in hydride-containing molten salts
[AD-A282335] p 730 N95-16973
Calorimetric methods for loss measurements of small cage induction motors
[PB94-184439] p 768 N95-17691
HEAT OF FORMATION
Kinetics and mechanism of chemical marker formation and water-activated heat generation
[AD-A281407] p 731 N95-17425
HEAT PUMPS
Thermal control systems for low-temperature heat rejection on a lunar base
[NASA-CR-197486] p 830 N95-16418
HEAT RESISTANT ALLOYS
The mechanical property data base from an Air Force/industry cooperative test program on high temperature aluminum alloys
[AD-A282911] p 737 N95-17398
HEAT SINKS
Liquid Cooled Heat Sink with Through Vias (LCHS)
[AD-A281450] p 902 N95-16075
HEAT STORAGE
Thermal control systems for low-temperature heat rejection on a lunar base
[NASA-CR-197486] p 830 N95-16418
HEAT TOLERANCE
An annotated bibliography of heat tolerance: Regarding gender differences
[AD-A280755] p 818 N95-16105
Heat stress and a countermeasure in the Shuttle rescueman's suit p 809 N95-16746
HEAT TRANSFER
Heat transfer measurements for Stirling machine cylinders
[NASA-CR-197128] p 791 N95-15963
Service and physical properties of liquid-jet fuels p 650 N95-16256
An engineering code to analyze hypersonic thermal management systems p 715 N95-16322
The prediction of nozzle performance and heat transfer in hydrogen/oxygen rocket engines with transpiration cooling, film cooling, and high area ratios p 718 N95-16339
Materials characterization and design for solar-thermal propulsion p 718 N95-16340
Computational simulation of the formation and material behavior of ice
[NASA-TM-106702] p 785 N95-16416
Long term modelling of permafrost dynamics
[AD-A285315] p 799 N95-16735
Thermo-fluid mechanic study of thermoacoustic devices
[AD-A281130] p 870 N95-16810
Erosion effects on TVC vane heat transfer characteristics
[AD-A282006] p 721 N95-17448
Two phase liquid helium flow testing to simulate the operation of a cryocondensation pump in the D3-D tokamak
[DE94-018345] p 893 N95-17896
HEAT TRANSFER COEFFICIENTS
Analysis of infrared scaling laws
[AD-A285461] p 903 N95-16877
HEAT TRANSMISSION
Mechanical effects in cookoff modeling
[DE94-014174] p 748 N95-16214
HEAT TREATMENT
Experimental heat treatment of beryllium copper alloy
[AD-A282714] p 734 N95-16380
Method for intrinsically doped III-A and V-A compounds and products thereof
[AD-D016324] p 896 N95-16399
Effect of heat treatment temperature on creep-rupture properties of Fe3Al-based alloys
[DE94-018054] p 738 N95-17679
HEATING
Plasma disruption modeling and simulation
[DE94-015095] p 889 N95-16307
Measurements and modeling of impurity source distributions from the Tore Supra outboard pump limiter
[DE94-018049] p 893 N95-17677
Investigation of the effect of Alfven resonance absorption on fast wave current drive in ITER
[PB95-104352] p 894 N95-17929
HEAVY IONS
RHIC spin: The first polarized proton collider
[DE94-013760] p 872 N95-16121
Performance study of galactic cosmic ray shield materials
[NASA-TP-3473] p 924 N95-16912
Heavy ion physics
[DE94-623321] p 880 N95-17519
HEAVY LIFT LAUNCH VEHICLES
A survey of commercially available expendable heavy lift launch vehicles
[AD-A282429] p 676 N95-17509
HEAVY NUCLEI
Heavy ion physics
[DE94-623321] p 880 N95-17519
HEAVY WATER
Use of magnesium for recovering hydrogen isotopes from tritiated water
[DE94-014471] p 731 N95-17157

HEIGHT
Analysis of a three-beam radar as an instrument for determining ocean wave heights and vector slopes
[AD-A282342] p 808 N95-17505
GPS tides and datums
[AD-A282422] p 666 N95-17508
HELICAL ANTENNAS
Center-fed multifilar helix antenna
[AD-D016390] p 760 N95-17480
HELICOPTER ENGINES
Sensor fault detection and diagnosis simulation of a helicopter engine in an intelligent control framework
[NASA-TM-106784] p 669 N95-15970
Numerical simulation of helicopter engine plume in forward flight
[NASA-CR-197488] p 655 N95-16589
HELICOPTERS
A correlative investigation of simulated occupant motion and accident report in a helicopter crash
[AD-A285190] p 664 N95-16404
Experimental data on the aerodynamic interactions between a helicopter rotor and an airframe
p 664 N95-17883
HELIOSPHERE
Engineering Ulysses extended mission
p 673 N95-17213
HELIUM
Two phase liquid helium flow testing to simulate the operation of a cryocondensation pump in the D3-D tokamak
[DE94-018345] p 893 N95-17896
HELIUM ISOTOPES
Determination of the nuclear-induced electrical conductivity in a nuclear-driven MHD device
[DE94-013137] p 891 N95-17365
Delayed annihilation of antiprotons in helium gas
[DE94-753405] p 878 N95-17739
HELMET MOUNTED DISPLAYS
Visual perception in the field-of-view of partial binocular overlap helmet-mounted displays
[AD-A285213] p 827 N95-16520
Factors affecting the visual fragmentation of the field-of-view in partial binocular overlap displays
[AD-A283081] p 886 N95-17334
HEMOGLOBIN
Hemoglobin-based blood substitutes and enhanced susceptibility to bacterial infections
[AD-A281023] p 820 N95-16444
HETEROCYCLIC COMPOUNDS
Research on organofluorine chemistry for 700 F thermooxidative stability
[AD-A282767] p 731 N95-17142
HETEROGENEITY
Marine boundary-layer parameterizations for large-scale models
[AD-A282402] p 803 N95-16062
Assessment of research needs for advanced heterogeneous catalysts for energy applications, volume 1
[DE94-015889] p 795 N95-16386
Assessment of research needs for advanced heterogeneous catalysts for energy applications, volume 2
[DE94-015890] p 727 N95-16387
Test applications for heterogeneous real-time network testbed
[DE94-016480] p 850 N95-17638
Development of heterogeneous Wacker oxidation catalysts: The role of the support and the redox component
[PB94-201431] p 732 N95-17700
HETEROJUNCTION DEVICES
Atomic layer epitaxy of group 4 materials: Surface processes, thin films, devices and their characterization
[AD-A280987] p 898 N95-16532
HETEROJUNCTIONS
Semiconductor heterojunction engineering
[AD-A281553] p 896 N95-16396
Trenched bipolar transistor structures
[AD-D016406] p 767 N95-17463
HEURISTIC METHODS
Exploiting IB assignments for approximating marginal probabilities
[AD-A285419] p 855 N95-16246
HIERARCHIES
Source hierarchy list. Volume 3: O through Z
[AD-A281102] p 908 N95-16090
The Design Manager's Aid for Intelligent Decomposition (DeMAID) p 848 N95-16470
HIGGS BOSONS
Physics at high energy photon photon colliders
[DE94-018191] p 881 N95-17888
HIGH ALTITUDE
Energy and Technology Review
[DE95-000321] p 710 N95-17359
HIGH CURRENT
Aluminum-ferricyanide battery
[AD-D016338] p 766 N95-16948
High current density sheet-like electron beam generator
[AD-A281975] p 880 N95-17499
HIGH ELECTRON MOBILITY TRANSISTORS
The impact of low temperature materials on the breakdown and noise properties of GaAs and InP based HEMT's and FET's
[AD-A285176] p 765 N95-16834
Feasibility study concerning an active millimeterwave sensor
[PB94-190691] p 775 N95-17170
HIGH ENERGY ELECTRONS
Auroral interactions with ISSA
[NASA-TM-106794] p 709 N95-16862
HIGH ENERGY INTERACTIONS
CP violation measurements in neutral kaon system at Fermilab
[DE94-016526] p 873 N95-16402
High Energy Physics Division research activities
[DE94-015024] p 882 N95-17924
HIGH FREQUENCIES
Preliminary investigation of an integrated optic sampler for HF signals
[AD-A284285] p 884 N95-16133
Models to estimate high frequency acoustic scattering due to thermal fine- and micro-structure of the ocean
[AD-A285456] p 870 N95-16812
An analysis of the effects of feedline and ground screen noise currents on a conical monopole receiving antenna
[AD-A283401] p 759 N95-17436
Fluctuation measurements at c/(omega)(sub pe) spatial scales in a tokamak
[DE94-016771] p 892 N95-17643
HIGH GRAVITY ENVIRONMENTS
Aerospace Medical Association 63rd Annual Scienti fic Meeting Program p 807 N95-16737
Comparisons of three anti-G suit configurations during long duration, low onset, +Gz p 811 N95-16755
Dynamics of the G-excess illusion
p 815 N95-16771
HIGH IMPULSE
Solar-powered rocket engine optimization for high specific impulse p 718 N95-16341
HIGH POLYMERS
Well-defined polyphosphazenes by anionic polymerization of phosphoranimines
[AD-A281414] p 740 N95-16165
HIGH POWER LASERS
High-intensity and high energy laser interactions with single droplets
[AD-A281415] p 776 N95-16166
High-average-power, diode-pumped solid state lasers for energy and industrial applications
[DE94-015142] p 779 N95-17689
HIGH PRESSURE
Hydromining a full-scale class 1.1 solid rocket motor
p 713 N95-16314
Laser induced fluorescence measurements and modeling of nitric oxide in high-pressure premixed flames
[NASA-CR-195404] p 775 N95-16910
Twin engine afterbody model p 663 N95-17880
HIGH RESOLUTION
Papers presented at the Tenth Topical Conference on High-Temperature Plasma Diagnostics
[DE94-015854] p 888 N95-16063
Observations by the Mars 1994 orbiter and possible correlations with Mars Pathfinder p 920 N95-16192
Overview of photonics research at Lawrence Livermore National Laboratory
[DE94-014055] p 884 N95-16366
A high resolution liquid xenon imaging telescope for 0.3-10 MeV gamma-ray astrophysics: Construction and initial balloon flights
[NASA-CR-197556] p 916 N95-17528
Micro-UltraViolet Spectrograph (Micro-UVS)
[DE94-016704] p 732 N95-17642
HIGH REYNOLDS NUMBER
A new approach to validate subgrid models in complex high Reynolds number flows
[AD-A282340] p 772 N95-17165
Effects of artificial viscosity on the accuracy of high-Reynolds-number kappa-epsilon turbulence model
[NASA-TM-106781] p 773 N95-17656
Detailed study at supersonic speeds of the flow around delta wings p 660 N95-17861
HIGH SPEED
VLSI circuits for high speed data conversion
[AD-A281556] p 763 N95-16136
Error propagation equations for estimating the uncertainty in high-speed wind tunnel test results
[DE94-014136] p 671 N95-16509
Performance characterization of photonic links in cryogenic environments for advanced signal processing applications
[DE94-015561] p 765 N95-16915
Characterization of multiport solid state imagers at megahertz data rates
[DE94-016095] p 765 N95-16932
Re-engineering Nascom's network management architecture p 702 N95-17584
High speed method for predicting radio-wave propagation
[AD-D016369] p 761 N95-17697
Two-dimensional 16.5 percent thick supercritical airfoil NLR 7301 p 658 N95-17854
HIGH STRENGTH
The effects of fatigue loading frequency on fatigue life of high-strength pressure vessel steels
[AD-A285301] p 786 N95-16601
HIGH TEMPERATURE
High temperature polymer dielectric film-wire insulation
p 712 N95-16055
Thermoplastic and thermosetting high glass transition temperature matrix resins
[AD-A281508] p 740 N95-16096
Plasma disruption modeling and simulation
[DE94-015095] p 889 N95-16307
Reliability implications of defects in high temperature annealed Si/SiO2/Si structures
[DE94-015765] p 895 N95-16311
Processing, fabrication, characterization and device demonstration of high temperature superconducting ceramics
[AD-A285145] p 744 N95-16844
Properties of semiconducting Ru2Ge3
[DE94-015361] p 899 N95-16913
Life prediction for bridged fatigue cracks
[DE94-016000] p 724 N95-16930
Modeling mesons with relativistic wave equations
[DE94-016057] p 875 N95-16931
Aluminum-ferricyanide battery
[AD-D016338] p 766 N95-16948
The three loop equation of state of QED at high temperature
[DE94-015029] p 904 N95-17925
Overview of space power electronic's technology under the CSTI High Capacity Power Program
[NASA-TM-110110] p 883 N95-17933
HIGH TEMPERATURE ENVIRONMENTS
Corrosion inhibition in high temperature environment
[AD-D016372] p 738 N95-17699
HIGH TEMPERATURE GASES
ROSAT detection of diffuse hot gas in the edge-on galaxy NGC 4631
[NASA-CR-197535] p 915 N95-17496
X-ray emission from the edge-on spiral galaxy NGC 4631
[NASA-CR-197536] p 924 N95-17527
HIGH TEMPERATURE LUBRICANTS
Bench wear and single-cylinder engine evaluations of high-temperature lubricants for US Army ground vehicles
[AD-A285399] p 780 N95-16636
HIGH TEMPERATURE PLASMAS
Analysis of plasma measurements for the Geotail mission
[NASA-CR-197020] p 888 N95-15941
Papers presented at the Tenth Topical Conference on High-Temperature Plasma Diagnostics
[DE94-015854] p 888 N95-16063
Thermal characteristics and heat transfer in an electrothermal light gas gun
[AD-A281980] p 892 N95-17442
Characteristics of multiple auroral inverted-V structures and the problem of magnetospheric plasma stratification
[DE94-622233] p 799 N95-17471
HIGH TEMPERATURE SUPERCONDUCTORS
Inelastic neutron scattering and antiferromagnetic fluctuations in high temperature superconductors
[DE94-623269] p 871 N95-16059
Atomic transport of oxygen
[DE94-013332] p 873 N95-16430
The relationship of structure to superconductivity in the Pr-Ba-Cu-O system
[DE94-014231] p 897 N95-16510
Theoretical study of cathode surfaces and high-temperature superconductors
[NASA-CR-195407] p 898 N95-16598
HTS SNS devices on large-area substrates by single-source MOCVD
[AD-A285159] p 899 N95-16849
Giant flux creep through the surface barriers and the irreversibility line in high T(sub c) superconductors
[DE94-013991] p 766 N95-16945
Suppression of superconductivity in orthorhombic La(2-x)M(x)CuO4 (M = Ca,Sr)
[DE94-013963] p 901 N95-17350

Studies by neutron diffraction and muon SR of flux lattice orientation, pinning, melting and decomposition in high-T(sub c) superconductors
[DE94-017704] p 901 N95-17667
Thin film superconductors
[DE94-018585] p 902 N95-17906

HIGH VOLTAGES
Auroral interactions with ISSA
[NASA-TM-106794] p 709 N95-16862

HIGHLANDS
A highland sample strategy for Pathfinder p 918 N95-16186
Tartarus Colles: A sampling of the Martian highlands p 920 N95-16195
Melas Chasma: A Mars Pathfinder view of Valles Marineris p 922 N95-16207

HIGHWAYS
Signal wave generator signals recorded by the Federal Outdoor Impact Laboratory's on-board Data Acquisition System
[PB94-186525] p 752 N95-16094

HILBERT SPACE
Quasiconformal mappings, operators on Hilbert space, and local formulae for characteristic classes
[PB94-192366] p 860 N95-16293

HIPPOCAMPUS
Synaptic plasticity and memory formation
[AD-A284926] p 825 N95-16138

HISTORIES
Presidential leadership in the development of the US space program
[NASA-TM-110107] p 904 N95-16007
The Fifth International Congress on the History of Oceanography
[AD-A281507] p 805 N95-16168

HOLDERS
Method of rapid sample handling for laser processing
[AD-D016408] p 778 N95-17464

HOLLOW CATHODES
Continuing life test of a xenon hollow cathode for a space plasma contactor
[NASA-CR-195401] p 711 N95-15968
Radar observations of field-aligned plasma propagations associated with NASA's PMG experiment
[AD-A285218] p 798 N95-16521
Extended test of a xenon hollow cathode for a space plasma contactor
[NASA-CR-195402] p 720 N95-17265

HOLOGRAPHY
Simulating the energy performance of holographic glazings
[DE94-013110] p 775 N95-17307

HOMING DEVICES
Autonomous weapon guidance
[AD-A282715] p 671 N95-16381
Preliminary study of an active millimeter wave sensor
[PB94-189206] p 759 N95-17453

HOMOGENEOUS TURBULENCE
A modified restricted Euler equation for turbulent flows with mean velocity gradients
[NASA-CR-194979] p 769 N95-16070

HOMOJUNCTIONS
LPEE growth and characterization of In(x)Ga(1-x)As(y)Sb(1-y) lattice matched to GaSb and InAs for photodetectors
[AD-A281631] p 895 N95-16114
Trenched bipolar transistor structures
[AD-D016406] p 767 N95-17463

HOMOLOGY
Coarse geometry of foliations
[PB94-192309] p 860 N95-16291

HONEYCOMB STRUCTURES
Surface heat transfer in a channel with porous insert p 650 N95-16255

HORIZONTAL FLIGHT
Numerical simulation of helicopter engine plume in forward flight
[NASA-CR-197488] p 655 N95-16589

HORIZONTAL ORIENTATION
The effects of the horizontal resolution of the boundary forcing sea surface temperature field on the FSU spectral model
[AD-A284273] p 802 N95-17488

HORN ANTENNAS
Antenna noise temperatures of the 34-meter beam-waveguide antenna with horns of different gains installed at F1 p 757 N95-17288
Computation of reflected and transmitted horn radiation patterns for a dichroic plate p 758 N95-17293
RF optics study for DSS-43 ultracone implementation p 758 N95-17296

HORSESHOE VORTICES
Wing-body juncture flows
[AD-A281526] p 655 N95-16099

HUMAN BEHAVIOR
A workout for virtual bodybuilders (design issues for embodiment in multi-actor virtual environments) p 854 N95-15990

HUMAN CENTRIFUGES
The psychophysical function for perceived gravitational-inertial force does not depend on the orientation of the otolith organs p 808 N95-16740

HUMAN FACTORS ENGINEERING
Whole-body vibration assessment of the palletized load system
[AD-A285181] p 829 N95-16145
Whole-body vibration assessment of the M1070 heavy equipment transporter, volume 1
[AD-A285199] p 829 N95-16147
Human performance in the modern cockpit p 813 N95-16764
Space medicine research: Needs for the 21st century p 814 N95-16768
Integrating human factors with software engineering practices
[AD-A285210] p 830 N95-16813
An integrated knowledge acquisition and database management system
[AD-A285404] p 910 N95-16884
Third International Symposium on Space Mission Operations and Ground Data Systems, part 1
[NASA-CP-3281-PT-1] p 676 N95-17179
Simulating the energy performance of holographic glazings
[DE94-013110] p 775 N95-17307
Apache helicopter seat cushion evaluation
[AD-A284300] p 831 N95-17484
Situation awareness information requirements for En Route Air Traffic Control
[DOT/FAA/AM-94/27] p 828 N95-17655
Industry review of a crew-centered cockpit design process and toolset
[AD-A282966] p 669 N95-17661

HUMAN PATHOLOGY
Aviation epidemiology data register: Coronary angiography outcomes of civilian aviators flying US aircraft
[AD-A285191] p 820 N95-16405

HUMAN PERFORMANCE
The EPIC architecture for modeling human information-processing and performance: A brief introduction
[AD-A280762] p 829 N95-16119
Mental rotation with and without a concurrent task: Moderating effects of visuospatial ability
[AD-A281866] p 826 N95-16301
The GOMS family of analysis techniques: Tools for design and evaluation
[AD-A285211] p 827 N95-16518
Human performance in the modern cockpit p 813 N95-16764
Space medicine research: Needs for the 21st century p 814 N95-16768
Mental effects of caffeine in fatigued men and women
[PB94-190683] p 822 N95-17300
Caffeine's influence on critical frequency thresholds
[AD-A282005] p 828 N95-17447
Blinks, saccades, and fixation pauses during vigilance task performance. 1: Time on task
[DOT/FAA/AM-94/26] p 828 N95-17530
Situation awareness information requirements for En Route Air Traffic Control
[DOT/FAA/AM-94/27] p 828 N95-17655

HUMAN REACTIONS
Results of the psychiatric, select-out evaluation of US astronaut applications p 813 N95-16761

HUMAN RESOURCES
Estimating the benefits of personnel selection and classification: An extension of the Brogden table
[AD-A285674] p 828 N95-17175

HUMAN TOLERANCES
An annotated bibliography of heat tolerance: Regarding gender differences
[AD-A280755] p 818 N95-16105
The chronic effects on JP-8 jet fuel exposure on the lungs
[AD-A280982] p 821 N95-16515

HUMAN-COMPUTER INTERFACE
The future of interaction on the Internet p 906 N95-15931
Applied virtual reality at the Research Triangle Institute p 851 N95-15974
An applications-oriented approach to the development of virtual environments p 853 N95-15980
A specification of 3D manipulation in virtual environments p 853 N95-15981
CPP-TRS(C): On using visual cognitive symbols to enhance communication effectiveness p 761 N95-15991
MAGENCO: A map generalization controller for Arc/Info
[DE94-013440] p 835 N95-16358
Communicating situation awareness in virtual environments
[AD-A285239] p 836 N95-16511
The GOMS family of analysis techniques: Tools for design and evaluation
[AD-A285211] p 827 N95-16518
Open architectures for formal reasoning and deductive technologies for software development
[NASA-CR-197528] p 837 N95-16586
Extending programming by demonstration with hierarchical event histories
[AD-A281186] p 838 N95-16632
Integrating human factors with software engineering practices
[AD-A285210] p 830 N95-16813
An empirical approach to visual display preference based upon modulation transfer function and luminance
[AD-A285450] p 830 N95-16875
Qualitative vision and action
[AD-A282697] p 831 N95-16966
Groupware system for multidisciplinary participation
[AD-A282525] p 850 N95-17374
Hidden Markov model for gesture recognition
[AD-A282845] p 865 N95-17377
Breaking down barriers in cooperative fault management: Temporal and functional information displays
[NASA-CR-197450] p 857 N95-17383
The new map graphics in RSAS 5.0
[AD-A282432] p 791 N95-17511
Automating testbed documentation and database access using World Wide Web (WWW) tools p 696 N95-17557

HUNGARY
Information system in transition: The Hungarian Scene p 906 N95-15925

HURRICANES
Summary of 1994 Atlantic tropical cyclone activity and verification of author's seasonal prediction, 1 p 801 N95-17259
Extended range forecast of Atlantic seasonal hurricane activity for 1995, 2 p 801 N95-17260

HYBRID COMPOSITES
Optimization of adaptive intraply hybrid fiber composites with reliability considerations
[NASA-TM-106632] p 787 N95-16911

HYBRID COMPUTERS
Kinetic effects near the magnetopause
[DE94-009333] p 799 N95-16927

HYBRID PROPELLANT ROCKET ENGINES
Large-scale hybrid motor performance and designs for use in launch vehicle applications p 715 N95-16327

HYBRID PROPELLANTS
Large-scale hybrid motor performance and designs for use in launch vehicle applications p 715 N95-16327

HYDRAULIC JETS
Hydromining a full-scale class 1.1 solid rocket motor p 713 N95-16314

HYDRAZINES
ARCJET plasma modeling with experimental validation
[AD-A285234] p 889 N95-16243
Updated test results of a pumped monopropellant propulsion system p 713 N95-16315
Nondestructive examination of the TRMM RCS propellant tanks p 718 N95-16338

HYDRIDES
The response of the Sandia robust wide range hydrogen sensor to H2-O2 mixtures
[DE94-013763] p 727 N95-16362
Charging hydrogen into Ni in hydride-containing molten salts
[AD-A282335] p 730 N95-16973

HYDROCARBON FUEL PRODUCTION
Landfill gas energy utilization: Technical and nontechnical considerations
[PB94-189651] p 793 N95-16544

HYDROCARBONS
Atomic layer epitaxy of group 4 materials: Surface processes, thin films, devices and their characterization
[AD-A280987] p 898 N95-16532

HYDRODYNAMICS
Theory of one-dimensional and two-dimensional distributed sensors for measuring the spatial characteristics of thermophysical and hydrodynamic fields p 652 N95-16273
Plasma disruption modeling and simulation
[DE94-015095] p 889 N95-16307
Colloidal particle deposition in turbulent flow
[DE94-013375] p 770 N95-16417
Study of the structuring of pure molecular liquids
[PB94-201316] p 903 N95-16839
On the propagation of near-inertial motion from the oceanic mixed layer p 806 N95-17396

An analysis of smoothed particle hydrodynamics
[DE94-013817] p 788 N95-17439

HYDROFLUORIC ACID
Shock initiation of crystalline boron in oxygen and fluorine compounds
[AD-A284266] p 730 N95-16955

HYDROGEN
The response of the Sandia robust wide range hydrogen sensor to H2-O2 mixtures
[DE94-013763] p 727 N95-16362
Spectroscopy of the transition state region in hydrogen transfer reactions
[AD-A285151] p 729 N95-16846
Charging hydrogen into Ni in hydride-containing molten salts
[AD-A282335] p 730 N95-16973
A latitudinal survey of middle atmospheric water vapor revealed by shipboard microwave spectroscopy
[AD-A282000] p 799 N95-17446
Hydrogen production by gasification of municipal solid waste
[DE94-016483] p 732 N95-17639
The development of a solid-state hydrogen sensor for rocket engine leakage detection
[NASA-CR-197567] p 776 N95-17895
Alternatives to traditional transportation fuels: An overview
[DE94-014979] p 749 N95-17923

HYDROGEN BONDS
Self assembled spin coated and bulk films of a novel polydiacetylene as second order NLO polymers
[AD-A282271] p 742 N95-16427

HYDROGEN EMBRITTLEMENT
Characterization of the hydrogen induced cold cracking susceptibility at simulated weld zones in HSLA-100 steel
[PB94-174505] p 737 N95-17616
Characterization of the corrosion behavior of the carbon steel liner in Hanford site single-shell tanks
[DE94-016475] p 737 N95-17637

HYDROGEN FUELS
Hydrogen production by gasification of municipal solid waste
[DE94-016483] p 732 N95-17639

HYDROGEN OXYGEN ENGINES
Test results from a simple, low-cost, pressure-fed liquid hydrogen/liquid oxygen rocket combustor
p 716 N95-16328
The prediction of nozzle performance and heat transfer in hydrogen/oxygen rocket engines with transpiration cooling, film cooling, and high area ratios
p 718 N95-16339

HYDROGEN PEROXIDE
Improved dual flow aluminum hydrogen peroxide battery
[AD-D016339] p 766 N95-16949

HYDROGEN PLASMA
Thermal characteristics and heat transfer in an electrothermal light gas gun
[AD-A281980] p 892 N95-17442

HYDROGEN PRODUCTION
Hydrogen production by gasification of municipal solid waste
[DE94-016483] p 732 N95-17639

HYDROGEN RECOMBINATIONS
Computational fluid dynamics studies of nuclear rocket performance
[NASA-TM-105436] p 713 N95-16066

HYDROGEN SULFIDE
Structure of 4-methylpyridinium hydrogen sulfide
[NASA-TM-106778] p 731 N95-17387

HYDROLOGY
Simulation of hydrologic influences on wetland ecosystem succession
[AD-A284737] p 795 N95-16545
Natural and artificial nobel gas hydrologic tracers
[DE94-016010] p 797 N95-17718

HYDROLOGY MODELS
Simulation of hydrologic influences on wetland ecosystem succession
[AD-A284737] p 795 N95-16545

HYDROXIDES
Atomic structure and valency of nickel in some of its oxycompounds
[AD-A281109] p 733 N95-16091
X-ray absorption spectra and structure of some nickel oxides (hydroxides)
[AD-A281305] p 735 N95-16788

HYDROXYL RADICALS
Equatorial airglow studies via rocket experiment
[INPE-5589-TDI/551] p 799 N95-17647

HYPERBOLIC DIFFERENTIAL EQUATIONS
On the removal of boundary errors caused by Runge-Kutta integration of non-linear partial differential equations
[NASA-CR-194989] p 863 N95-16904
Fifth International Conference on Hyperbolic Problems: Theory, Numerics, Applications
[AD-A283078] p 863 N95-17333
Report on the 5th International Conference on Nonlinear Hyperbolic Problems
[AD-A283077] p 864 N95-17713

HYPERCUBE MULTIPROCESSORS
A new communication scheme for the neutron diffusion nodal method in a distributed computing environment
[DE94-017907] p 844 N95-15946

HYPERSONIC AIRCRAFT
Static and dynamic friction behavior of candidate high temperature airframe seal materials
[NASA-TM-106571] p 722 N95-16905

HYPERSONIC FLOW
High altitude hypersonic flowfield radiation
[AD-A281386] p 655 N95-16160
In-flight imaging of transverse gas jets injected into transonic and supersonic crossflows: Design and development
[NASA-CR-186031] p 772 N95-17418

HYPERSONIC INLETS
Numerical simulation of supersonic compression corners and hypersonic inlet flows using the RPLUS2D code
[NASA-TM-106580] p 654 N95-16038

HYPERSONIC SPEED
Parametric study of shock-induced combustion in a hydrogen air system
[NASA-CR-197134] p 726 N95-15967
Numerical simulation of supersonic compression corners and hypersonic inlet flows using the RPLUS2D code
[NASA-TM-106580] p 654 N95-16038
Scramjet testing guidelines p 670 N95-16317
Spectral solution of the viscous blunt body problem. 2: Multidomain approximation
[NASA-CR-194971] p 863 N95-17267

HYPERSONIC TEST APPARATUS
A model for preliminary facility design including simulation issues p 672 N95-16318
Hypersonic air-breathing aeropropulsion facility test support requirements p 672 N95-16319

HYPERSONIC VEHICLES
Ultraviolet emissions occurring about hypersonic vehicles in rarefied flows
[AD-A281452] p 655 N95-16076

HYPERSONIC WIND TUNNELS
Wall-signature methods for high speed wind tunnel wall interference corrections p 650 N95-16257
A model for preliminary facility design including simulation issues p 672 N95-16318
Hypersonic air-breathing aeropropulsion facility test support requirements p 672 N95-16319

HYPERSONICS
High altitude hypersonic flowfield radiation
[AD-A281386] p 655 N95-16160
An engineering code to analyze hypersonic thermal management systems p 715 N95-16322

HYPOTENSION
Comparison of saline and fludrocortisone as fluid-loading countermeasures following exposure to simulated microgravity p 808 N95-16742

HYPOTHALAMUS
Molecular approach to hypothalamic rhythms
[AD-A285164] p 822 N95-16851

HYPOTHESES
Failure of ozone and nitrogen dioxide to enhance lung tumor development in hamsters
[PB94-182854] p 818 N95-16801

I

ICE
A Mars Pathfinder landing on a recently drained ephemeral sea: Cerberus Plains, 6 deg N, 188 deg W
p 918 N95-16181

ICE ENVIRONMENTS
Computational simulation of the formation and material behavior of ice
[NASA-TM-106702] p 785 N95-16416

ICE FLOES
Experimental and numerical analysis of floating ice beam impact forces against a sloped structure
[AD-A280752] p 804 N95-16103

ICE FORMATION
Computational simulation of the formation and material behavior of ice
[NASA-TM-106702] p 785 N95-16416
Debris/ice/TPS assessment and integrated photographic analysis of Shuttle Mission STS-64 on 9 August 1994
[NASA-TM-109206] p 676 N95-17262
Meteorological factors that affect the formation an prediction of aircraft icing
[AD-A281984] p 802 N95-17443

IDEAL GAS
New developments in the method of space-time conservation element and solution element-applications to two-dimensional time-marching problems
[NASA-TM-106758] p 862 N95-16885

IDENTIFYING
The use of electrochemistry and ellipsometry for identifying and evaluating corrosion on aircraft
[AD-A285276] p 734 N95-16370
The use of electrochemistry and ellipsometry for identifying and evaluating corrosion on aircraft
[AD-A285323] p 734 N95-16371

IDENTITIES
A workout for virtual bodybuilders (design issues for embodiment in multi-actor virtual environments)
p 854 N95-15990

IGNITION
Alpha particle kinetics in ignited fusion plasmas: Design applications for a CO2 laser Thomson scattering experiment
[DE94-016297] p 890 N95-16921
Shock initiation of crystalline boron in oxygen and fluorine compounds
[AD-A284266] p 730 N95-16955

ILL-CONDITIONED PROBLEMS (MATHEMATICS)
A new regularization approach in structural system identification p 651 N95-16262
Evaluation of SEA loss factors using input power modulation
[ISVR-TR-240] p 868 N95-16856

ILLUMINANCE
Caffeine's influence on critical frequency thresholds
[AD-A282005] p 828 N95-17447

ILLUMINATING
Performance of specular reflectors used for lighting enhancement
[AD-A281004] p 884 N95-15999
Simulating the energy performance of holographic glazings
[DE94-013110] p 775 N95-17307
Superresolution in a jammed radar signal environment
[PB94-190758] p 760 N95-17455

ILLUSIONS
Dynamics of the G-excess illusion
p 815 N95-16771

IMAGE ANALYSIS
A general method to determine invariants
[TR-503] p 859 N95-15949
Metadata database for automated oceanographic imagery
[AD-A284932] p 805 N95-16141
Example based image analysis and synthesis
[AD-A282285] p 835 N95-16236
Data Visualization and Animation Lab (DVAL): Applications p 843 N95-16469
Debris/ice/TPS assessment and integrated photographic analysis of Shuttle Mission STS-64 on 9 August 1994
[NASA-TM-109206] p 676 N95-17262
Spatial information content analysis of Wiener spectra from polarized waterwave imagery
[AD-A283171] p 886 N95-17340
Grey-scale measurements in multi-dimensional digitized images
[PB94-195492] p 887 N95-17483

IMAGE CLASSIFICATION
Evolving neural network pattern classifiers
[AD-A281181] p 857 N95-16631
A procedure for estimating the carbon budget of terrestrial ecosystems in the former Soviet Union by geographic information system analysis and classification of AVHRR derived global vegetation index
p 796 N95-17394
Detection of deforestation in the Amazon forest using NOAA/AVHRR images and the geographic information system SGI: Methodology and test of a potential alarm system
[INPE-5580-TDI/543] p 791 N95-17894
Multivariate statistical analysis software technologies for astrophysical research involving large data sets
[NASA-CR-197499] p 858 N95-17921

IMAGE CORRELATORS
Log-polar optical coordinate transformation with applications for automatic pattern recognition
[AD-A281022] p 885 N95-16443

IMAGE FILTERS
Low-complexity wavelet filter design for image compression p 757 N95-17289
A preliminary optical visibility model
p 758 N95-17290

IMAGE INTENSIFIERS
Visual acuity versus field-of-view and light level for Night Vision Goggles (NVG)
[AD-A284750] p 830 N95-16553

IMAGE MOTION COMPENSATION
High performance compression of science data
[NASA-CR-189388] p 911 N95-17329
IMAGE PROCESSING
Using virtual reality for science mission planning: A Mars Pathfinder case p 673 N95-15978
SSME propellant path leak detection real-time
[NASA-CR-197032] p 748 N95-16029
Estimation of vehicle dynamics from monocular noisy images
[AD-A281458] p 804 N95-16078
Student research projects, 1993
[AD-A284954] p 804 N95-16124
Objective feature identification and tracking: A review
[AD-A284955] p 804 N95-16125
Computational vision based on neurobiology
[AD-A284472] p 819 N95-16135
Evaluation of FEL image processing algorithm for 12-bit CCD-images as function of various atmospheric conditions
[AD-A285187] p 752 N95-16146
Fast stereoscopic images with ray-traced volume rendering
[DE94-011703] p 835 N95-16223
Example based image analysis and synthesis
[AD-A282285] p 835 N95-16236
Joint Proceedings on Aeronautics and Astronautics (JPAA)
[ISBN-7-80-046602-7] p 649 N95-16249
Methods of wave-front identification by control images p 652 N95-16274
Log-polar optical coordinate transformation with applications for automatic pattern recognition
[AD-A281022] p 885 N95-16443
The Role of Computers in Research and Development at Langley Research Center
[NASA-CP-10159] p 846 N95-16453
Image tools for UNIX p 847 N95-16466
Data Visualization and Animation Lab (DVAL) overview p 843 N95-16468
Sensor placement design for object pose determination with three light-stripe range finders
[AD-A281199] p 886 N95-16795
Least squares computations in science and engineering
[AD-A281213] p 862 N95-16798
Learning one more thing
[AD-A285342] p 857 N95-16820
Space-based asteroid detection and monitoring system
[AD-D016329] p 915 N95-16854
An empirical approach to visual display preference based upon modulation transfer function and luminance
[AD-A285450] p 830 N95-16875
Using neural networks to correlate satellite imagery and ground-truth data
[AD-A285486] p 857 N95-16967
High performance hardware and software for pattern recognition and image processing
[AD-A284264] p 839 N95-17172
End-to-end communication test on variable length packet structures utilizing AOS testbed p 677 N95-17186
Fast computational scheme of image compression for 32-bit microprocessors p 678 N95-17192
Low-complexity wavelet filter design for image compression p 757 N95-17289
McIDAS-eXplorer: A version of McIDAS for planetary applications
[NASA-CR-189382] p 910 N95-17323
High performance compression of science data
[NASA-CR-189388] p 911 N95-17329
Full color recorder
[AD-A282278] p 790 N95-17372
Object recognition using multi-layer Hopfield neural network
[AD-A282417] p 858 N95-17459
Operational cloud classifier based on a self-organized feature map
[PB94-197852] p 802 N95-17504
SEQ-POINTER: Next generation, planetary spacecraft remote sensing science observation design tool p 697 N95-17559
On the improvement of 1-look SAR image segmentations with mathematical morphology
[INPE-5577-PRE/1805] p 912 N95-17650
IMAGE RECONSTRUCTION
Application of Fourier-space image-restoration techniques to turbulence compensation and sparse-aperture imaging
[AD-A285077] p 885 N95-16494
Overview on METEOSAT geometrical image data processing p 678 N95-17189
IMAGE RESOLUTION
Object recognition using multi-layer Hopfield neural network
[AD-A282417] p 858 N95-17459
GPS tides and datums
[AD-A282422] p 666 N95-17508
IMAGERY
Application of Fourier-space image-restoration techniques to turbulence compensation and sparse-aperture imaging
[AD-A285077] p 885 N95-16494
Non-linear acoustics in fluids and gels
[PB94-201308] p 870 N95-16614
IMAGES
Visual perception in the field-of-view of partial binocular overlap helmet-mounted displays
[AD-A285213] p 827 N95-16520
IMAGING RADAR
Linear prediction data extrapolation superresolution radar imaging p 651 N95-16268
IMAGING SPECTROMETERS
MODIS Technical Report Series. Volume 4: MODIS data access user's guide: Scan cube format
[NASA-TM-104594-VOL-4] p 837 N95-16587
IMAGING TECHNIQUES
Simulation of arthroscopic surgery using MRI data p 823 N95-15975
Virtual reality and telerobotics applications of an Address Recalculation Pipeline p 852 N95-15977
Tele Hyper Virtuality p 853 N95-15982
A virtual work space for both hands manipulation with coherency between kinesthetic and visual sensation p 831 N95-15984
Development of an analytical photon scanning tunneling microscope
[AD-A281382] p 884 N95-16157
Surface science capabilities from IMP spectral imaging p 921 N95-16204
Linear prediction data extrapolation superresolution radar imaging p 651 N95-16268
How clean is clean: Non-destructive/direct methods of flux, residue detection
[DE94-013439] p 763 N95-16357
Flux imaging of high temperature superconductor single crystals and Ag sheathed wires
[DE94-013874] p 897 N95-16408
Atomic scale structure and chemistry of interfaces by Z-contrast imaging and electron energy loss spectroscopy in the stem
[DE94-013632] p 728 N95-16419
Nanoscale imaging of molecular adsorption
[AD-A280979] p 873 N95-16482
Application of Fourier-space image-restoration techniques to turbulence compensation and sparse-aperture imaging
[AD-A285077] p 885 N95-16494
Magnetic Resonance Imaging (MRI) of skeletal muscles in astronauts after 9 days of space flight p 810 N95-16749
Changes in left ventricular function as determined by the multi-wire gamma camera at near presyncopal levels of lower body negative pressure p 811 N95-16754
High brightness cathodes for microfocus x-ray generators
[AD-A285256] p 764 N95-16814
Vector magnetometry and lightwave defect imaging sensor technologies for internal pipe inspection systems: Phase 1 and 2 feasibility study, conceptual design, and prototype development
[PB94-194198] p 783 N95-16870
Fast computational scheme of image compression for 32-bit microprocessors p 678 N95-17192
In-flight imaging of transverse gas jets injected into transonic and supersonic crossflows: Design and development
[NASA-CR-186031] p 772 N95-17418
Preliminary study of an active millimeter wave sensor
[PB94-189206] p 759 N95-17453
GPS tides and datums
[AD-A282422] p 666 N95-17508
Miniature, vacuum compatible 1024 (times) 1024 CCD camera for x ray, ultraviolet, or optical imaging
[DE94-012235] p 776 N95-17522
A high resolution liquid xenon imaging telescope for 0.3-10 MeV gamma-ray astrophysics: Construction and initial balloon flights
[NASA-CR-197556] p 916 N95-17528
IMPACT DAMAGE
Impact vulnerability of thermoplastic-matrix composites
[PB94-201274] p 745 N95-17305
IMPACT LOADS
Experimental and numerical analysis of floating ice beam impact forces against a sloped structure
[AD-A280752] p 804 N95-16103
Skeletal muscle responses to unloading in humans p 809 N95-16743
IMPACT STRENGTH
Impact vulnerability of thermoplastic-matrix composites
[PB94-201274] p 745 N95-17305
IMPACT TESTS
Signal wave generator signals recorded by the Federal Outdoor Impact Laboratory's on-board Data Acquisition System
[PB94-186525] p 752 N95-16094
Shotgun/drop-weight initiation of energetic materials
[AD-A285090] p 749 N95-16499
Impact vulnerability of thermoplastic-matrix composites
[PB94-201274] p 745 N95-17305
IMPEDANCE
Initial design of a 1 megawatt average, 150 kilovolt pulse modulator for an industrial plasma source ion implantation processor
[DE94-014421] p 888 N95-16218
System design and operation of a 100 kilovolt, 2 kilohertz pulse modulator for plasma source ion implantation
[DE94-014424] p 889 N95-16285
The use of electrochemistry and ellipsometry for identifying and evaluating corrosion on aircraft
[AD-A285276] p 734 N95-16370
Skin blood flow and bioelectrical impedance
[AD-A285475] p 821 N95-16619
Measurements of collective effects in the ALS
[DE94-017966] p 881 N95-17670
Electromagnetic field measurements on a mm-wave linear accelerator
[DE94-015092] p 761 N95-17926
IMPEDANCE MATCHING
Radial acceletron, a new low impedance HPM source
[AD-A282008] p 760 N95-17501
IMPEDANCE MEASUREMENT
The use of electrochemistry and ellipsometry for identifying and evaluating corrosion on aircraft
[AD-A285323] p 734 N95-16371
IMPINGEMENT
New methods for treatment of electron correlation and surface dynamics (FY91 AASERT)
[AD-A285177] p 727 N95-16144
IMPREGNATING
An X-Ray Photoelectron Spectroscopy (XPS) study of activated carbons impregnated with some organocopper complexes
[AD-A282721] p 727 N95-16384
Studies on improvement of oxidation resistivity of carbon materials by glass impregnation and SiC formation
[DE94-796529] p 724 N95-16833
IMPULSES
Informatics in Turkey p 905 N95-15921
IMPURITIES
Elemental impurity analysis of mercuric iodide by ICP/MS
[DE94-013553] p 896 N95-16359
Chemical properties of the fullerenes
[AD-A282730] p 730 N95-17141
Measurements and modeling of impurity source distributions from the Tore Supra outboard pump limiter
[DE94-018049] p 893 N95-17677
INCIDENT RADIATION
X-/Ka-band dichroic plate noise temperature reduction p 758 N95-17294
INCOMPRESSIBLE FLOW
A computational investigation of wake-induced airfoil flutter in incompressible flow and active flutter control
[AD-A281534] p 670 N95-16109
INDEXES (DOCUMENTATION)
Source hierarchy list. Volume 2: E through N
[AD-A281101] p 908 N95-15957
Scientific and technical publishing at Goddard Space Flight Center in Fiscal Year 1994
[NASA-TM-104614] p 925 N95-16581
Aeronautical enginnering: A cumulative index to a continuing bibliography (supplement 312)
[NASA-SP-7037(312)] p 654 N95-17702
Aerospace medicine and biology: A continuing bibliography with indexes (supplement 396)
[NASA-SP-7011(396)] p 823 N95-17703
Aeronautical engineering: A continuing bibliography with indexes (supplement 311)
[NASA-SP-7037(311)] p 654 N95-17704
INDIUM ANTIMONIDES
Scanning tunneling microscopy of 3 to 5 semiconductors
[AD-A281722] p 902 N95-17705
INDIUM ARSENIDES
Picosecond optoelectronic AND-GATE
[AD-A285672] p 885 N95-16620
Performance characterization of photonic links in cryogenic environments for advanced signal processing applications
[DE94-015561] p 765 N95-16915

INDIUM COMPOUNDS
Synthesis and characterization of neopentyl indium compounds: X-ray crystal structures of ((Me3CCH2)2InAs(SiMe3)2)2 and ((Me3CCH2)2InAs(SiMe3)2In (CH2CMe3)2Cl)
[AD-A282766] p 900 N95-17137
INDIUM GALLIUM ARSENIDES
LPEE growth and characterization of In(x)Ga(1-x)As(y)Sb(1-y) lattice matched to GaSb and InAs for photodetectors
[AD-A281631] p 895 N95-16114
INDUSTRIAL ENERGY
Fuel cell systems program plan, fiscal year 1994
[DE94-014301] p 793 N95-16541
INDUSTRIAL MANAGEMENT
An assessment of simulation systems applicable to business process reengineering at Army Directorates of Public Works
[AD-A285696] p 839 N95-17176
INDUSTRIES
Optoelectric technology roadmap: Conclusions and recommendations
[AD-A281664] p 886 N95-16965
Military aviation maintenance industry in Western Europe: Concentration and internationalization
[PB94-189180] p 653 N95-17451
INELASTIC SCATTERING
Inelastic neutron scattering and antiferromagnetic fluctuations in high temperature superconductors
[DE94-623269] p 871 N95-16059
A-dependent effects in high P(sub T) reactions
[DE94-016385] p 875 N95-16924
Parton distributions of the proton
[PB95-104337] p 877 N95-17354
INERTIAL CONFINEMENT FUSION
Transport efficiency studies for light-ion inertial confinement fusion
[AD-A285675] p 891 N95-17382
INERTIAL NAVIGATION
Application of GPS/SINS/RA integrated system to aircraft approach landing p 653 N95-16277
Autonomous weapon guidance
[AD-A282715] p 671 N95-16381
INFORMATION DISSEMINATION
Bureau of the Census Center for International Research p 905 N95-15923
CINDOC, CSIC, and Spanish R and D p 906 N95-15927
The Technical Information Library: TIB p 906 N95-15928
Information sources in science and technology in Finland p 906 N95-15930
Networked information: Management issues for the acquisitions librarian p 906 N95-15932
Electronic access to ONREUR/ONRAISIA S and T reports p 907 N95-15935
Department of Energy: Office of Scientific and Technical Information p 907 N95-15936
Numeric data distribution: The vital role of data exchange in today's world p 907 N95-15937
National Center for Standards and Certification Information: Service and programs p 907 N95-15938
Collection development at the NOAA Central Library p 907 N95-15939
Source header list. Volume 2: L through Z
[AD-A281001] p 908 N95-15998
Source hierarchy list. Volume 3: O through Z
[AD-A281102] p 908 N95-16090
Use of World Wide Web and NCSA Mcsaic at Langley p 847 N95-16464
How to use the WWW to distribute STI p 847 N95-16465
Data Visualization and Animation Lab (DVAL) overview p 843 N95-16468
ICASE
[NASA-CR-195001] p 832 N95-16898
A land-surface Testbed for EOSDIS
[NASA-CR-189392] p 840 N95-17327
MO/DSD online information server and global information repository access p 706 N95-17607
INFORMATION FLOW
Economical ground data delivery p 679 N95-17194
Software interface verifier p 698 N95-17564
Re-engineering NASA's space communications to remain viable in a constrained fiscal environment p 702 N95-17585
INFORMATION MANAGEMENT
Bureau of the Census Center for International Research p 905 N95-15923
Acquiring and disseminating unpublished economic and social development materials in Africa: The case of the National Institute of Development Research and Documentation University of Botswana p 906 N95-15924
Information system in transition: The Hungarian Scene p 906 N95-15925
Document delivery by the Jupiter Library Consortium p 906 N95-15926
CINDOC, CSIC, and Spanish R and D p 906 N95-15927
The Technical Information Library: TIB p 906 N95-15928
The National Resource Library for Science and Technology in Sweden: A Nordic model of cooperating technology libraries p 906 N95-15929
Information sources in science and technology in Finland p 906 N95-15930
The future of interaction on the Internet p 906 N95-15931
Networked information: Management issues for the acquisitions librarian p 906 N95-15932
Adding tools to the open source toolbox: The Internet p 907 N95-15933
DOD STINFO regulations and forms. Selected titles
[AD-A282332] p 909 N95-16374
Data administration procedures
[AD-A282718] p 909 N95-16382
Crew decision making under stress p 814 N95-16765
NASA Johnson Space Center Life Sciences Data System p 679 N95-17195
INFORMATION PROCESSING (BIOLOGY)
The EPIC architecture for modeling human information-processing and performance: A brief introduction
[AD-A280762] p 829 N95-16119
Computational vision based on neurobiology
[AD-A284472] p 819 N95-16135
INFORMATION RETRIEVAL
Source hierarchy list. Volume 2: E through N
[AD-A281101] p 908 N95-15957
The PASS project
[DE94-016308] p 910 N95-16922
Knowledge quality functions for rule discovery
[AD-A285513] p 910 N95-16971
A land-surface Testbed for EOSDIS
[NASA-CR-189392] p 840 N95-17327
Automating testbed documentation and database access using World Wide Web (WWW) tools p 696 N95-17557
MO/DSD online information server and global information repository access p 706 N95-17607
An incremental database access method for autonomous interoperable databases
[NASA-CR-189384] p 912 N95-17652
DROLS: An introduction to searching (videorecording)
[AD-M000338] p 912 N95-17660
INFORMATION SYSTEMS
Fourth Annual International Acquisitions Workshop: Access to Multiple Media Worldwide
[NASA-TM-109896] p 905 N95-15919
The Australian National Chinese Japanese Korean Project p 905 N95-15920
Informatics in Turkey p 905 N95-15921
NAFTA literature at the International Trade Commission library p 905 N95-15922
Information system in transition: The Hungarian Scene p 906 N95-15925
Open Source Service Agent (OSSA) in the intelligence community's Open Source Architecture p 907 N95-15934
Department of Energy: Office of Scientific and Technical Information p 907 N95-15936
National Center for Standards and Certification Information: Service and programs p 907 N95-15938
Collection development at the NOAA Central Library p 907 N95-15939
Division of Information Systems (FOA 37)
[PB94-190766] p 909 N95-16400
Cognition and procedure representational requirements for predictive human performance models p 814 N95-16766
Knowledge quality functions for rule discovery
[AD-A285513] p 910 N95-16971
Telecommunications end-to-end systems monitoring on TOPEX/Poseidon: Tools and techniques p 676 N95-17180
NASA Johnson Space Center Life Sciences Data System p 679 N95-17195
The Telecommunications and Data Acquisition Report
[NASA-CR-197249] p 755 N95-17279
Directory of IAEA databases
[DE94-622696] p 912 N95-17472
Development of use of an Operational Procedure Information System (OPIS) for future space missions p 692 N95-17536
Automating testbed documentation and database access using World Wide Web (WWW) tools p 696 N95-17557
ELISA, a demonstrator environment for information systems architecture design p 698 N95-17563
Standardizing the information architecture for spacecraft operations p 703 N95-17591
A standard satellite control reference model p 704 N95-17592
Use of data description languages in the interchange of data p 704 N95-17597
Architecture of a distributed multimission operations system p 706 N95-17605
INFORMATION THEORY
Detecting the number of targets in spatially colored noise using sampled aperture radars p 652 N95-16269
Pattern theoretic knowledge discovery
[AD-A285472] p 909 N95-16879
INFORMATION TRANSFER
An applications-oriented approach to the development of virtual environments p 853 N95-15980
Thermal feedback in virtual reality and telerobotic systems p 854 N95-15987
CPP-TRS(C): On using visual cognitive symbols to enhance communication effectiveness p 761 N95-15991
Overview of TTCP and AGARD propulsion activities p 720 N95-16351
Catalog of lunar and Mars science payloads
[NASA-RP-1345] p 922 N95-16436
NSSDC data listing
[NASA-TM-109986] p 909 N95-16441
Introduction to the World Wide Web and Mosaic p 847 N95-16463
From computer images to video presentation: Enhancing technology transfer p 848 N95-16467
Scientific and technical publishing at Goddard Space Flight Center in Fiscal Year 1994
[NASA-TM-104614] p 925 N95-16581
Open architectures for formal reasoning and deductive technologies for software development
[NASA-CR-197528] p 837 N95-16586
Department of Defense Electronic Data Interchange project baseline report for FY 1994
[AD-A283015] p 912 N95-17710
INFRARED ABSORPTION
Innovative acoustic techniques for studying new materials and new developments in solid state physics
[AD-A280986] p 898 N95-16525
INFRARED ASTRONOMY
Implications of high-spatial-resolution thermal infrared (Termoskan) data for Mars landing site selection p 918 N95-16180
Physical properties (particle size, rock abundance) from thermal infrared remote observations: Implications for Mars landing sites p 918 N95-16182
INFRARED ASTRONOMY SATELLITE
Dust near luminous ultraviolet stars
[NASA-CR-197108] p 916 N95-16032
INFRARED DETECTORS
Modification of 2-6 and 3-5 materials using ion beams
[AD-A281839] p 896 N95-16365
Real-time data collection programs and source code for a commercial passive FTIR remote sensor
[AD-A284976] p 838 N95-16634
Proceedings of the 12th Space Surveillance Workshop, volume 2
[AD-A285115] p 672 N95-16842
Testing and characterization of the CYCLOPS HgCdTe focal plane detector array
[AD-A284279] p 887 N95-17489
INFRARED IMAGERY
Detection of deforestation in the Amazon forest using NOAA/AVHRR images and the geographic information system SGI: Methodology and test of a potential alarm system
[INPE-5580-TDI/543] p 791 N95-17894
INFRARED INSTRUMENTS
Investigation of a normal incidence high-performance p-type strained layer In(0.3)Ga(0.7)As/In(0.52)Al(0.48)As quantum well infrared photodetector
[AD-A282720] p 900 N95-16928
INFRARED LASERS
A CO2 laser polarimeter for measurement of plasma current profile in Alcator C-Mod
[DE94-014017] p 776 N95-16486
INFRARED RADIATION
Physical properties (particle size, rock abundance) from thermal infrared remote observations: Implications for Mars landing sites p 918 N95-16182
Landing site considerations for atmosphere structure and meteorology p 921 N95-16203
Analysis of infrared scaling laws
[AD-A285461] p 903 N95-16877
Tunable UV source for UV fluorescence remote sensing
[DE94-015745] p 777 N95-16917
Investigation of novel electrical transport phenomena in semimetal-semiconductor heterostructures
[AD-A281406] p 901 N95-17424

INFRARED SIGNATURES
Infrared signatures for remote sensing
[DE94-014222] p 790 N95-16215
The Mg 2 lines as diagnostic of PMS nature in Herbig Ae/Be stars
[NASA-CR-197518] p 915 N95-17494
INFRARED SPACE OBSERVATORY (ISO)
Issues in the design and optimization of adaptive optics and laser guide stars for the Keck Telescopes
[DE94-012888] p 916 N95-17525
INFRARED SPECTROSCOPY
Infrared signatures for remote sensing
[DE94-014222] p 790 N95-16215
Reaction of methanol with porous silicon
[AD-A285518] p 728 N95-16406
Materials for second and third order nonlinear optical applications
[AD-A281304] p 885 N95-16787
Chemical properties of the fullerenes
[AD-A282730] p 730 N95-17141
INHIBITORS
Ignition propagation and heat effects of propellant chips embedded in castable inhibitor using a laser flux test bomb p 717 N95-16335
Control of molecular weights and polydispersities in radical polymerization of styrene in the presence of stable radicals
[AD-A281040] p 742 N95-16449
INHOMOGENEITY
Nonstationary theory of mode competition in gyrotrons with allowance for inhomogeneity of the guiding magnetic field
[PB94-197621] p 869 N95-17467
INITIATION
Shock initiation of crystalline boron in oxygen and fluorine compounds
[AD-A284266] p 730 N95-16955
INJECTION
Changes in left ventricular function as determined by the multi-wire gamma camera at near presyncopal levels of lower body negative pressure p 811 N95-16754
INJECTION LOCKING
Phase-locked arrays of vertical-cavity surface-emitting lasers
[DE94-014941] p 778 N95-17498
INLET FLOW
Numerical simulation of supersonic compression corners and hypersonic inlet flows using the RPLUS2D code
[NASA-TM-106580] p 654 N95-16038
Unsteady flow phenomena in discrete passage diffusers for centrifugal compressors
[AD-A281412] p 770 N95-16163
Improved method for estimation of the maximum instantaneous distortion values p 649 N95-16254
Time accurate computation of unsteady inlet flows with a dynamic flow adaptive mesh
[AD-A285498] p 771 N95-16736
Three dimensional compressible turbulent flow computations for a diffusing S-duct with/without vortex generators
[NASA-CR-195390] p 670 N95-17402
INLET NOZZLES
Combustor kinetic energy efficiency analysis of the hypersonic research engine data p 714 N95-16321
Small turbojets: Designs and installations p 670 N95-16323
INMARSAT SATELLITES
A processing centre for the CNES CE-GPS experimentation p 666 N95-17196
INORGANIC CHEMISTRY
Polymeric precursors to binary inorganic materials
[AD-A281010] p 739 N95-16000
INPUT/OUTPUT ROUTINES
Feedback system for remotely operated vehicles
[AD-D016409] p 858 N95-17465
Surftherm: A program to analyze thermochemical and kinetic data in gas-phase and surface chemical reaction mechanisms
[DE94-016145] p 733 N95-17744
INSERTS
Surface heat transfer in a channel with porous insert p 650 N95-16255
INSPECTION
How clean is clean: Non-destructive/direct methods of flux, residue detection
[DE94-013439] p 763 N95-16357
Vector magnetometry and lightwave defect imaging sensor technologies for internal pipe inspection systems: Phase 1 and 2 feasibility study, conceptual design, and prototype development
[PB94-194198] p 783 N95-16870
Debris/ice/TPS assessment and integrated photographic analysis of Shuttle Mission STS-64 on 9 August 1994
[NASA-TM-109206] p 676 N95-17262
INSTALLING
Photovoltaic power conditioners: Development, evolution, and the next generation
[NASA-CR-197005] p 793 N95-16831
INSTRUMENT LANDING SYSTEMS
Modeling of Instrument Landing System (ILS) localizer signal on runway 25L at Los Angeles International Airport
[NASA-TM-4588] p 665 N95-17384
INSULATION
Multilayer microelectronic photomultiplier device with a stacked series of dynode and insulating layers
[AD-D016377] p 767 N95-17478
Conducting polymers as corrosion resistant coatings
[DE94-018265] p 748 N95-17892
INSULATORS
BaF2/GaAs electronic components
[AD-D016391] p 767 N95-17481
INTEGERS
A simplified Integer Cosine Transform and its application in image compression p 757 N95-17286
INTEGRAL EQUATIONS
Trapezoidal rule quadrature algorithms for MIMD distributed memory computers
[DE94-016369] p 839 N95-16923
INTEGRATED CIRCUITS
Analog microcircuit fault prediction
[AD-A281958] p 763 N95-16410
Development of practical MO techniques for prediction of the properties and behavior of materials
[AD-A285079] p 874 N95-16496
A new manufacturing method for the formation of gated field emission structures
[DE94-015287] p 764 N95-16832
Feasibility study concerning an active millimeterwave sensor
[PB94-190691] p 775 N95-17170
Multilayer microelectronic photomultiplier device with a stacked series of dynode and insulating layers
[AD-D016377] p 767 N95-17478
INTEGRATED LIBRARY SYSTEMS
Risk-Based Data Management System design specifications and implementation plan for the Alaska Oil and Gas Conservation Commission; the Mississippi State Oil and Gas Board; the Montana Board of Oil and Gas Conservation; and the Nebraska Oil and Gas Conservation Commission, attachment B
[DE94-013189] p 908 N95-16282
Mini All-purpose Satellite Control Center (MASCC) p 674 N95-17257
INTEGRATED MISSION CONTROL CENTER
Towards cheaper control centers p 674 N95-17250
EURECA mission control experience and messages for the future p 690 N95-17252
SCOS 2: ESA's new generation of mission control system p 674 N95-17253
The IUE Science Operations Ground System p 674 N95-17255
Efficient mission control for the 48-satellite Globalstar Constellation p 674 N95-17256
Mini All-purpose Satellite Control Center (MASCC) p 674 N95-17257
Standardizing the information architecture for spacecraft operations p 703 N95-17591
Cross support overview and operations concept for future space missions p 705 N95-17598
ATOS: Integration of advanced technology software within distributed Spacecraft Mission Operations Systems p 705 N95-17602
The NASA Mission Operations and Control Architecture Program p 706 N95-17603
INTEGRATED OPTICS
ARO-URI Center for Opto-Electronic Systems Research
[AD-A281447] p 883 N95-15958
Electric-optic resonant phase modulator
[NASA-CASE-NPO-18702-1-CU] p 883 N95-15960
Preliminary investigation of an integrated optic sampler for HF signals
[AD-A284285] p 884 N95-16133
In-fibre Bragg gratings for millimetre-wave EW systems
[AD-A284283] p 755 N95-16956
Digital logic and reconfigurable interconnects using aluminum gallium arsenide electro-optic Fredkin gates
[AD-A282880] p 881 N95-17619
INTELLIGENCE
Open Source Service Agent (OSSA) in the intelligence community's Open Source Architecture p 907 N95-15934
INTELSAT SATELLITES
Houston, I think we've got a satellite
[NASA-TM-109987] p 709 N95-16941
INTERACTIONAL AERODYNAMICS
Wing-body juncture flows
[AD-A281526] p 655 N95-16099
A computational investigation of wake-induced airfoil flutter in incompressible flow and active flutter control
[AD-A281534] p 670 N95-16109
Single-engine tail interference model p 663 N95-17879
INTERACTIONS
Measurement of the B(sub s) meson lifetime at CDF
[DE94-015381] p 875 N95-16868
INTERCEPTION
Detectability models and waveform design for multiple access Low-Probability-of-Intercept networks
[AD-A281864] p 753 N95-16300
INTERCONTINENTAL BALLISTIC MISSILES
Design margin testing of Peacekeeper solid rocket boosters p 713 N95-16313
Hydromining a full-scale class 1.1 solid rocket motor p 713 N95-16314
INTERFACES
Network interface specification for the T1 microprocessor
[AD-A283392] p 844 N95-15940
Data link level interconnection of remote Fiber Distributed Data Interface Local Area Networks (FDDI LANs) through the Critical Data Link (CDL)
[AD-A284307] p 755 N95-17173
Grand mission versus small OPS team: Can we have both? p 684 N95-17219
INTERFACIAL ENERGY
Charge transfer processes on liquid/liquid interfaces: The status in 1994
[AD-A285067] p 729 N95-16635
INTERFACIAL TENSION
Measurement of residual flexibility for substructures having prominent flexible interfaces
[NASA-TM-110074] p 786 N95-16577
INTERFERENCE DRAG
Single-engine tail interference model p 663 N95-17879
INTERFEROMETERS
Real-time data collection programs and source code for a commercial passive FTIR remote sensor
[AD-A284976] p 838 N95-16634
INTERFEROMETRY
TDRS orbit determination by radio interferometry p 673 N95-17547
INTERGALACTIC MEDIA
Voyager investigation of the cosmic diffuse background: Observations of rocket-studied locations with Voyager
[NASA-CR-197532] p 917 N95-17422
INTERMETALLICS
Non-Fermi liquid scaling in UPd(x)Cu(5-x)(x = 1,1.5)
[DE94-016072] p 896 N95-16389
Processing - property relationship in advanced intermetallics
[AD-A285262] p 735 N95-16514
Life prediction for bridged fatigue cracks
[DE94-016000] p 724 N95-16930
Abstracts: Eighth Annual Conference on Fossil Energy Materials
[DE94-014053] p 725 N95-17368
Fundamental concepts relating local atomic arrangements, deformation, and fracture of intermetallic alloys
[AD-A282971] p 738 N95-17664
Forging of FeAl intermetallic compounds
[DE94-018124] p 739 N95-17728
INTERNAL COMBUSTION ENGINES
An investigation of fluid flow during induction stroke of a water analog model of an IC engine using an innovative optical velocimetry concept: LIPA
[NASA-CR-197451] p 780 N95-16900
INTERNAL PRESSURE
Experimental and analytical methods for the determination of connected-pipe ramjet and ducted rocket internal performance
[AGARD-AR-323] p 721 N95-17278
INTERNAL WAVES
On the propagation of near-inertial motion from the oceanic mixed layer p 806 N95-17396
INTERNATIONAL COOPERATION
Department of Energy: Office of Scientific and Technical Information p 907 N95-15936
National Center for Standards and Certification Information: Service and programs p 907 N95-15938
Results of an International Space Crew Debrief p 810 N95-16750
International data transfer for space very long baseline interferometry p 680 N95-17198
Aircraft and sub-system certification by piloted simulation
[AGARD-AR-278] p 671 N95-17388
Military aviation maintenance industry in Western Europe: Concentration and internationalization
[PB94-189180] p 653 N95-17451

INTERNATIONAL SPACE STATION
Assessment of the Space Station program p 709 N95-16352
Auroral interactions with ISSA [NASA-TM-106794] p 709 N95-16862
INTERNATIONAL TRADE
NAFTA literature at the International Trade Commission library p 905 N95-15922
INTERNETS
Fourth Annual International Acquisitions Workshop: Access to Multiple Media Worldwide [NASA-TM-109896] p 905 N95-15919
The future of interaction on the Internet p 906 N95-15931
Networked information: Management issues for the acquisitions librarian p 906 N95-15932
Adding tools to the open source toolbox: The Internet p 907 N95-15933
Robust routing in dynamic networks, part 2 [AD-A282396] p 844 N95-16061
Introduction to the World Wide Web and Mosaic p 847 N95-16463
Use of World Wide Web and NCSA Mcsaic at Langley p 847 N95-16464
How to use the WWW to distribute STI p 847 N95-16465
Image tools for UNIX p 847 N95-16466
An analysis of Internet's MBONE: A media choice perspective [AD-A285514] p 910 N95-16972
MO/DSD online information server and global information repository access p 706 N95-17607
INTERORBITAL TRAJECTORIES
Numerical optimization of synergetic maneuvers [AD-A283398] p 656 N95-17435
INTERPLANETARY NAVIGATION
Radio-planetary from tie from Phobos-2 VLBI data p 756 N95-17283
INTERPLANETARY SPACECRAFT
Magellan Project: Evolving enhanced operations efficiency to maximize science value p 684 N95-17218
Operations automation p 687 N95-17236
Matrix evaluation of science objectives p 707 N95-17610
INTERPOLATION
Uniqueness and free interpolation for logarithmic potentials and the Cauchy problem for the Laplace equation in (R2) [PB94-192408] p 861 N95-16295
Evaluation of an autopilot based multimodelling [PB94-190725] p 671 N95-17454
INTERPRETATION
Use of data description languages in the interchange of data p 704 N95-17597
INTERPROCESSOR COMMUNICATION
Network interface specification for the T1 microprocessor [AD-A283392] p 844 N95-15940
Communication network software analysis [AD-A281019] p 833 N95-16004
Software cache coherence for large scale multiprocessors [AD-A281628] p 845 N95-16113
The new map graphics in RSAS 5.0 [AD-A282432] p 791 N95-17511
Open solutions to distributed control in ground tracking stations p 674 N95-17554
INTERSTELLAR GAS
The mass and dynamics of cD clusters with cooling flows. 1: ROSAT observations of A 496 [NASA-CR-197534] p 915 N95-17495
ROSAT detection of diffuse hot gas in the edge-on galaxy NGC 4631 [NASA-CR-197535] p 915 N95-17496
INTERSTELLAR MATTER
Dust near luminous ultraviolet stars [NASA-CR-197108] p 916 N95-16032
First detection of CO (j = 0 - 1) adsorption at cosmological distances (z = 0.247) [PB94-184595] p 916 N95-17332
Voyager investigation of the cosmic diffuse background: Observations of rocket-studied locations with Voyager [NASA-CR-197532] p 917 N95-17422
X-ray emission from the edge-on spiral galaxy NGC 4631 [NASA-CR-197536] p 924 N95-17527
INTRAVENOUS PROCEDURES
Changes in left ventricular function as determined by the multi-wire gamma camera at near presyncopal levels of lower body negative pressure p 811 N95-16754
INVARIANCE
A general method to determine invariants [TR-503] p 859 N95-15949
Baryogenesis and standard model CP violation [DE94-017935] p 877 N95-17669
INVENTIONS
Development of practical MO techniques for prediction of the properties and behavior of materials [AD-A285079] p 874 N95-16496
Self-organizing neural network for classifying pattern signatures with a posteriori conditional class probability [AD-D016455] p 857 N95-16823
INVERSE KINEMATICS
On performability theory and the inverse sliding problem [AD-A282647] p 782 N95-17430
INVERSE SCATTERING
Support minimized inversion of acoustic and elastic wave scattering [DE94-014233] p 783 N95-16538
Nonlinear problems in fluid dynamics and inverse scattering. Propagation and capturing of singularities in problems of fluid dynamics and inverse scattering [AD-A282873] p 773 N95-17617
INVERSIONS
Extraction of high quality potential surfaces from laboratory data [AD-A285071] p 903 N95-16489
INVISCID FLOW
The prediction of nozzle performance and heat transfer in hydrogen/oxygen rocket engines with transpiration cooling, film cooling, and high area ratios p 718 N95-16339
Interactive computer graphics applications for compressible aerodynamics [NASA-TM-106802] p 839 N95-17264
IODIDES
Elemental impurity analysis of mercuric iodide by ICP/MS [DE94-013553] p 896 N95-16359
ION ACOUSTIC WAVES
Effect of Coulomb collisions, Landau damping and particle trapping on linear and nonlinear ion acoustic waves [AD-A282009] p 869 N95-17449
ION ATOM INTERACTIONS
Resonant charge transfer in hyperthermal atomic and molecular ion-surface collisions [AD-A281369] p 871 N95-16018
Effect of ion-electrode contact on the energetics of the heterogeneous electron transfer [AD-A281959] p 873 N95-16411
ION BEAMS
Mechanisms of beam-halo formation in high-intensity linacs [DE94-016316] p 879 N95-16030
Study of the effect of the space charge using SYNCH [DE94-014086] p 879 N95-16210
Control of a large vacuum wave precursor on the SABRE voltage adder MITL and extraction ion diode [DE94-014280] p 888 N95-16216
Ion beam generation and propagation for plasma processing applications [DE94-014428] p 889 N95-16286
Modification of 2-6 and 3-5 materials using ion beams [AD-A281839] p 896 N95-16365
Intense ion beam optimization and characterization with thermal imaging [DE94-016184] p 891 N95-16936
Intense ion beam characterization and thermal modeling for beam materials processing [DE94-016281] p 745 N95-16938
Transport efficiency studies for light-ion inertial confinement fusion [AD-A285675] p 891 N95-17382
Beams 92: Proceedings [DE94-014784] p 880 N95-17475
Heavy ion physics [DE94-623321] p 880 N95-17519
ION CURRENTS
Fundamental studies of polyphosphazene and polysiloxane polyelectrolytes for electrochemical devices [AD-A281339] p 739 N95-16013
ION CYCLOTRON RADIATION
Differential phase reflectometry for edge profile measurements on TFTR [DE94-013837] p 891 N95-16958
First measurements of ICRF and edge/SOL plasma interactions on TORE SUPRA [DE94-019320] p 891 N95-17347
Investigation of the effect of Alfven resonance absorption on fast wave current drive in ITER [PB95-104352] p 894 N95-17929
ION DENSITY (CONCENTRATION)
Study of the effect of the space charge using SYNCH [DE94-014086] p 879 N95-16210
Poloidal rotation and the evolution of H-mode and VH-mode profiles [DE94-015858] p 890 N95-16919
ION DISTRIBUTION
Resonance enhanced multiphoton ionization of molecules and molecular fragments [AD-A285076] p 873 N95-16493
ION ENGINES
Electric probe measurements in the plume of the UK-10 ion thruster [AD-A282460] p 713 N95-16302
ION EXCHANGING
Charge transfer processes on liquid/liquid interfaces: The status in 1994 [AD-A285067] p 729 N95-16635
ION IMPLANTATION
Initial design of a 1 megawatt average, 150 kilovolt pulse modulator for an industrial plasma source ion implantation processor [DE94-014421] p 888 N95-16218
System design and operation of a 100 kilovolt, 2 kilohertz pulse modulator for plasma source ion implantation [DE94-014424] p 889 N95-16285
Effects of substrate temperature on metal colloid formation and on optical response in metal ion implanted silica [DE94-013633] p 736 N95-16807
Applications of positron depth profiling [PB94-197753] p 900 N95-16952
ION IRRADIATION
Microchannel formation in polyimide by heavy ion irradiation [DE94-753315] p 740 N95-16073
Columnar defect pinning in untwinned single crystal YBa2Cu2O7 [DE94-013962] p 901 N95-17349
ION PROBES
Electric probe measurements in the plume of the UK-10 ion thruster [AD-A282460] p 713 N95-16302
ION PROPULSION
Extended test of a xenon hollow cathode for a space plasma contactor [NASA-CR-195402] p 720 N95-17265
ION TEMPERATURE
Determination of ion temperatures from Zeeman broadened spectral lines in the edge of Tore Supra [DE94-018112] p 873 N95-16403
Kinetic effects near the magnetopause [DE94-009333] p 799 N95-16927
IONIC COLLISIONS
Resonant charge transfer in hyperthermal atomic and molecular ion-surface collisions [AD-A281369] p 871 N95-16018
RHIC spin: The first polarized proton collider [DE94-013760] p 872 N95-16121
IONIZATION
Carbon clusters studied by neutralization-reionization mass spectrometry [AD-A281367] p 726 N95-16017
Determination of ion temperatures from Zeeman broadened spectral lines in the edge of Tore Supra [DE94-018112] p 873 N95-16403
Mass spectrometry studies of the ionization of organic molecules by slow positrons [DE94-013838] p 876 N95-16959
Gas-surface interactions near dissociation threshold [AD-A282726] p 730 N95-17140
IONIZATION POTENTIALS
The chemistry and physics of transition metal clusters [DE94-014012] p 734 N95-16364
IONIZING RADIATION
Performance study of galactic cosmic ray shield materials [NASA-TP-3473] p 924 N95-16912
IONOSPHERIC DISTURBANCES
Observations of ELF propagation at high latitudes during the sporadic-E conditions of November 1986 [AD-A284973] p 753 N95-16227
Radar observations of field-aligned plasma propagations associated with NASA's PMG experiment [AD-A285218] p 798 N95-16521
IONOSPHERIC DRIFT
Ion drift meter research [NASA-CR-197124] p 798 N95-16432
IONS
Effect of ion-electrode contact on the energetics of the heterogeneous electron transfer [AD-A281959] p 873 N95-16411
Raman spectroscopy of C-irradiated graphite [DE94-018705] p 733 N95-17911
IRIDIUM
Testing and evaluation of oxide-coated iridium/rhenium chambers p 719 N95-16346
Design, analysis, and fabrication of oxide-coated iridium/rhenium combustion chambers p 719 N95-16347

IRON
Selected properties of iron aluminides
[DE94-018057] p 738 N95-17726

IRON ALLOYS
Metallurgical examination of failed T-158 Cast Austempered Ductile Iron (CADI) track shoes
[AD-A282433] p 737 N95-17486
Selected properties of iron aluminides
[DE94-018057] p 738 N95-17726
Forging of FeAl intermetallic compounds
[DE94-018124] p 739 N95-17728
Environmental effects on iron aluminide
[DE94-017900] p 739 N95-17747

IRON COMPOUNDS
Ion modulated electroactivity in thin-film polymers derived from bipyridyl and phenanthroline complexes of iron
[AD-A280704] p 747 N95-17682

IRON CYANIDES
Aluminum-ferricyanide battery
[AD-D016338] p 766 N95-16948

IRON METEORITES
Shock and thermal history of iron and chondritic meteorites
[NASA-CR-197125] p 916 N95-16020

IRRADIATION
A study to determine the critical characteristics for mice in a newly designed whole body toxic gas exposure module
[AD-A285085] p 818 N95-17666
Raman spectroscopy of C-irradiated graphite
[DE94-018705] p 733 N95-17911

ISOMERIZATION
Mobility measurement and computer simulation at specific sites in polystyrene solutions and gels
[AD-A281214] p 747 N95-17685

ISOMERS
Carbon clusters studied by neutralization-reionization mass spectrometry
[AD-A281367] p 726 N95-16017

ISOMORPHISM
Isomorphism within the hexagonal columnar mesophase of molecular and macromolecular self- and co-assembled columns containing tapered groups
[AD-A281205] p 874 N95-16797

ISOTHERMAL LAYERS
Variation of the thermohaline structure in the western equatorial Pacific upper ocean p 805 N95-17277

ISOTOPIC LABELING
Natural and artificial nobel gas hydrologic tracers
[DE94-016010] p 797 N95-17718

ISOTROPIC TURBULENCE
A modified restricted Euler equation for turbulent flows with mean velocity gradients
[NASA-CR-194979] p 769 N95-16070
Experimental study of premixed flames in intense isotropic turbulence
[DE94-016868] p 732 N95-17437

ISOTROPY
Characteristics of multiple auroral inverted-V structures and the problem of magnetospheric plasma stratification
[DE94-622233] p 799 N95-17471

ITALIAN SPACE PROGRAM
The SAX Italian scientific satellite. The on-board implemented automation as a support to the ground control capability p 695 N95-17551

ITERATIVE SOLUTION
Numerical analysis on periodic response of nonsmooth dynamic systems p 650 N95-16261
A stepsize control strategy for stiff systems of ordinary differential equations
[AD-A281551] p 861 N95-16395
Sixth Copper Mountain Conference on Multigrid Methods
[DE94-014595] p 862 N95-16611
Multigrid techniques for nonlinear eigenvalue probems: Solutions of a nonlinear Schroedinger eigenvalue problem in 2D and 3D
[NASA-CR-194999] p 862 N95-16896
Combination of power electronic models with the two-dimensional finite element analysis of electrical machines
[PB94-197720] p 766 N95-16951
Computational differentiation and multidisciplinary design
[DE94-013393] p 863 N95-17306

IUE
The IUE Science Operations Ground System p 674 N95-17255

J

J INTEGRAL
Effects of prior ductile tearing on cleavage fracture toughness in the transition region
[AD-A281298] p 786 N95-16785
Multi-lab comparison on R-curve methodologies: Alloy 2024-T3
[NASA-CR-195004] p 736 N95-16860
Mixed-mode I/III fracture toughness of a ferritic/martensitic stainless steel
[DE94-014492] p 736 N95-17159

JAMMERS
Superresolution in a jammed radar signal environment
[PB94-190758] p 760 N95-17455

JAMMING
Mitre adaptive processing capability
[AD-A281078] p 755 N95-16825
Data link level interconnection of remote Fiber Distributed Data Interface Local Area Networks (FDDI LANs) through the Critical Data Link (CDL)
[AD-A284307] p 755 N95-17173

JAPAN
The Austrialian National Chinese Japanese Korean Project p 905 N95-15920
Space VLBI telecommunication characteristics, protection criteria, and frequency sharing p 756 N95-17282

JET ENGINE FUELS
Service and physical properties of liquid-jet fuels p 650 N95-16256

JET ENGINES
Pressure distribution measurements on an isolated TPS 441 nacelle p 663 N95-17878

JET FLOW
On the prediction of free turbulent jets with swirl using a quadratic pressure-strain model
[NASA-CR-194964] p 769 N95-16071
Modeling of wall-bounded complex flows and free shear flows
[NASA-TM-106513] p 770 N95-16407
Liquefied metal jet program Automation and Robotics Research Institute (ARRI)
[AD-A285470] p 736 N95-16878
Combustion instability phenomena of importance to liquid propellant engines
[AD-A284780] p 730 N95-16882
Jet studies at CDF and DO collaborations
[DE94-015537] p 875 N95-16914

JET IMPINGEMENT
Combustion instability phenomena of importance to liquid propellant engines
[AD-A284780] p 730 N95-16882

JET PROPULSION
Twin engine afterbody model p 663 N95-17880

JET PUMPS
Nonpowered instant water heater
[AD-A285459] p 783 N95-17725

JET VANES
Erosion effects on TVC vane heat transfer characteristics
[AD-A282006] p 721 N95-17448

JETSTREAM AIRCRAFT
Aircraft accident report: Stall and loss of control on final approach, Atlantic Coast Airlines, Inc./United Express Flight 6291 Jetstream 4101, N304UE Columbus, OH, 7 January 1994
[PB94-910409] p 665 N95-17646

JETTISONING
Mars Pathfinder mission operations concepts p 686 N95-17229

JINDIVIK TARGET AIRCRAFT
Data acquisition and processing software for the Low Speed Wind Tunnel tests of the Jindivik auxiliary air intake
[AD-A285455] p 656 N95-17178

JOURNALS
Document delivery by the Jupiter Library Consortium p 906 N95-15926

JP-8 JET FUEL
The chronic effects on JP-8 jet fuel exposure on the lungs
[AD-A280982] p 821 N95-16515

K

K-EPSILON TURBULENCE MODEL
Effects of artificial viscosity on the accuracy of high-Reynolds-number kappa-epsilon turbulence model
[NASA-TM-106781] p 773 N95-17656

KALMAN FILTERS
Sensitivity study of the SPEM model to the assimilation of synop datasets using two assimilation schemes. 1: Nudging. 2: The Kalman filter/smoother
[AD-A281459] p 804 N95-16079
Application of GPS/SINS/RA integrated system to aircraft approach landing p 653 N95-16277
Approach to in-process tool wear monitoring in drilling: Application of Kalman filter theory p 653 N95-16279
Autonomous weapon guidance
[AD-A282715] p 671 N95-16381
Assessment of benefits and drawbacks of using fuzzy logic, especially in fire control systems
[AD-A285428] p 838 N95-16874
Magnetometer-only attitude and rate determination for a gyro-less spacecraft p 694 N95-17546

KAONS
CP violation measurements in neutral kaon system at Fermilab
[DE94-016526] p 873 N95-16402
Probing violation of quantum mechanics in the K0-(bar K)0 system
[DE94-017934] p 904 N95-17668
Search for the presence of H particles in a neutral beam
[DE94-013526] p 877 N95-17683

KAPTON (TRADEMARK)
Kapton wire concerns for aerospace vehicles p 711 N95-16045
Orbiter Kapton wire operational requirements and experience p 711 N95-16046
Problems with aging wiring in Naval aircraft p 711 N95-16048
Kapton pyrolysis on Space Station Freedom's solar array flexible current carrier p 712 N95-16049
Kapton pyrolysis, the space environment and wiring requirements p 712 N95-16054

KELVIN WAVES
An observational study of long waves in the equatorial Pacific Ocean during the 1991-1993 El Nino
[AD-A283380] p 806 N95-17624

KERNEL FUNCTIONS
An analysis of smoothed particle hydrodynamics
[DE94-013817] p 788 N95-17439

KEVLAR (TRADEMARK)
Study of the compression behavior of high performance fibers
[AD-A284959] p 723 N95-16126

KINEMATICS
Real-time simulation of large-scale multibody systems using automated equation decoupling techniques
[AD-A281544] p 856 N95-16390

KINETIC ENERGY
Combustor kinetic energy efficiency analysis of the hypersonic research engine data p 714 N95-16321
Spectroscopy of the transition state region in hydrogen transfer reactions
[AD-A285151] p 729 N95-16846
An analysis code for the Rapid Engineering Estimation of Momentum and Energy Losses (REMEL)
[NASA-CR-191178] p 656 N95-16887

KINETICS
Real-time simulation of large-scale multibody systems using automated equation decoupling techniques
[AD-A281544] p 856 N95-16390
Kinetics model for initiation and promotion for describing tumor prevalence from HZE radiation
[NASA-TP-3479] p 820 N95-16412
Alpha particle kinetics in ignited fusion plasmas: Design applications for a CO2 laser Thomson scattering experiment
[DE94-016297] p 890 N95-16921

KIRCHHOFF LAW
Combination of power electronic models with the two-dimensional finite element analysis of electrical machines
[PB94-197720] p 766 N95-16951

KNEE (ANATOMY)
Simulation of arthroscopic surgery using MRI data p 823 N95-15975
Evaluation of a newly-designed, dynamic knee extension device for the study of muscle fatigue in humans
[AD-A284974] p 819 N95-16228
Skeletal muscle responses to unloading in humans p 809 N95-16743

KNOWLEDGE BASED SYSTEMS
Second International Working Conference on Cooperating Knowledge Based Systems. Volume 1
[AD-A281347] p 908 N95-16014
The Yale Knowledge-Based Planning project
[AD-A281505] p 855 N95-16095
Studies of novel popout
[AD-A285237] p 826 N95-16244
The Design Manager's Aid for Intelligent Decomposition (DeMAID) p 848 N95-16470

Communicating situation awareness in virtual environments
[AD-A285239] p 836 N95-16511
Learning one more thing
[AD-A285342] p 857 N95-16820
Qualitative vision and action
[AD-A282697] p 831 N95-16966
Towards a new generation of mission planning systems: Flexibility and performance p 686 N95-17230
Delivering spacecraft control centers with embedded knowledge-based systems: The methodology issue p 674 N95-17532
SCOSII OL: A dedicated language for mission operations p 692 N95-17533
SEQ-GEN: A comprehensive multimission sequencing system p 693 N95-17540
An agent-oriented approach to automated mission operations p 696 N95-17555
ATOS: Integration of advanced technology software within distributed Spacecraft Mission Operations Systems p 705 N95-17602

KNOWLEDGE REPRESENTATION
Use of World Wide Web and NCSA Mcsaic at Langley p 847 N95-16464
Pattern theoretic knowledge discovery
[AD-A285472] p 909 N95-16879
Actions and events in interval temporal logic
[TR-521] p 839 N95-16883
An integrated knowledge acquisition and database management system
[AD-A285404] p 910 N95-16884
Steps toward terrain knowledge acquisition
[AD-A282667] p 790 N95-17375

KONDO EFFECT
Non-Fermi liquid scaling in UPd(x)Cu(5-x)(x = 1,1.5)
[DE94-016072] p 896 N95-16389

L

LAGRANGE MULTIPLIERS
Constrained minimization of smooth functions using a genetic algorithm
[NASA-TP-3329] p 709 N95-16902

LAGRANGIAN FUNCTION
A consistent large deflection theory of composite sandwich shells p 650 N95-16259
An analysis of smoothed particle hydrodynamics
[DE94-013817] p 788 N95-17439

LAMINAR BOUNDARY LAYER
Three-dimensional boundary layer and flow field data of an inclined prolate spheroid p 661 N95-17867

LAMINAR FLOW
Stability of separating subsonic boundary layers
[NASA-CR-4638] p 772 N95-17268
Transient flows and pressure waves in pipes
[DE94-012650] p 772 N95-17523

LAMINATES
Thermoelasticity analysis of laminated plates and shells using hybrid-stress elements p 651 N95-16263
Computational simulation of the formation and material behavior of ice
[NASA-TM-106702] p 785 N95-16416
Probabilistic simulation of stress concentration in composite laminates
[NASA-TM-106712] p 787 N95-17270
Impact vulnerability of thermoplastic-matrix composites
[PB94-201274] p 745 N95-17305
Investigation of novel electrical transport phenomena in semimetal-semiconductor heterostructures
[AD-A281406] p 901 N95-17424
Fundamental concepts relating local atomic arrangements, deformation, and fracture of intermetallic alloys
[AD-A282971] p 738 N95-17664
Vacuum deposited polymer/silver reflector material
[DE94-018729] p 748 N95-17913

LAND USE
FIFE data analysis: Testing BIOME-BGC predictions for grasslands
[NASA-CR-197522] p 790 N95-16895

LANDAU DAMPING
Effect of Coulomb collisions, Landau damping and particle trapping on linear and nonlinear ion acoustic waves
[AD-A282009] p 869 N95-17449

LANDFILLS
Landfill gas energy utilization: Technical and nontechnical considerations
[PB94-189651] p 793 N95-16544

LANDFORMS
Steps toward terrain knowledge acquisition
[AD-A282667] p 790 N95-17375
Rheology and structure of planetary near-surface materials from landform topography p 922 N95-17392

LANDING AIDS
Joint Proceedings on Aeronautics and Astronautics (JPAA)
[ISBN-7-80-046602-7] p 649 N95-16249
Application of GPS/SINS/RA integrated system to aircraft approach landing p 653 N95-16277

LANDING SITES
Mars Pathfinder Landing Site Workshop
[NASA-CR-196745] p 917 N95-16176
Sampling Elysium lavas (13 deg N, 203 deg W) p 917 N95-16177
Mars Pathfinder and the exploration of southern Amazonis Planitia p 917 N95-16178
Meteorological observations of synoptic disturbances: Sensitivity to latitude p 917 N95-16179
Implications of high-spatial-resolution thermal infrared (Termoskan) data for Mars landing site selection p 918 N95-16180
A Mars Pathfinder landing on a recently drained ephemeral sea: Cerberus Plains, 6 deg N, 188 deg W p 918 N95-16181
Physical properties (particle size, rock abundance) from thermal infrared remote observations: Implications for Mars landing sites p 918 N95-16182
Rationale for a Mars Pathfinder mission to Chryse Planitia and the Viking 1 lander p 918 N95-16183
Rationale for Isidis Planitia as a back-up landing site for the Mars Pathfinder mission p 918 N95-16184
Chryse Planitia as a Mars Pathfinder landing site: The imperative of building on previous ground truth p 918 N95-16185
A highland sample strategy for Pathfinder p 918 N95-16186
Opportunity to sample something different: The dark, unweathered, mafic sands of Cerberus and the Pathfinder 1997 Mars landing p 919 N95-16187
Mars Pathfinder meteorological observations on the basis of results of an atmospheric global circulation model p 919 N95-16189
Pathfinder landing sites at candidate SNC impact ejection sites p 919 N95-16190
Strategy for selecting Mars Pathfinder landing sites p 919 N95-16191
Observations by the Mars 1994 orbiter and possible correlations with Mars Pathfinder p 920 N95-16192
Potential landing sites for Mars Pathfinder p 920 N95-16193
A perspective of landing-site selection p 920 N95-16194
Tartarus Colles: A sampling of the Martian highlands p 920 N95-16195
Scientific rationale for selecting northern Eumenides Dorsum (9 deg - 11 deg N latitude, 159 deg - 162 deg longitude) as a potential Mars Pathfinder landing site p 920 N95-16196
Scientific rationale for selecting northwest Isidis Planitia (14 deg - 17 deg N latitude, 278 deg - 281 deg longitude) as a potential Mars Pathfinder landing site p 920 N95-16197
Cerberus Plains: A most excellent Pathfinder landing site p 921 N95-16198
Maja Valley and the Chryse outflow complex sites p 921 N95-16199
Landing site considerations for atmosphere structure and meteorology p 921 N95-16203
Melas Chasma: A Mars Pathfinder view of Valles Marineris p 922 N95-16207
Climatological targets for Mars Pathfinder p 922 N95-16208
Development of an Automated Airfield Dynamic Cone Penetrometer (AADCP) prototype and the evaluation of unsurfaced airfield seismic surveying using Spectral Analysis of Surface Waves (SASW) technology
[AD-A281985] p 672 N95-17444

LANDSAT SATELLITES
MODIS Technical Report Series. Volume 4: MODIS data access user's guide: Scan cube format
[NASA-TM-104594-VOL-4] p 837 N95-16587

LANGEVIN FORMULA
Filter efficiency and pressure drop calculations through two and three dimensional fiber arrays
[DE94-014111] p 770 N95-16211

LANGUAGE PROGRAMMING
On serializable languages
[TR-519] p 839 N95-17261

LANGUAGES
Decreasing the bandwidth of a transition matrix
[TR-505] p 859 N95-15948
On the structure of log-space probabilistic complexity classes
[TR-506] p 864 N95-16039
SCOSII OL: A dedicated language for mission operations p 692 N95-17533
Phonologic-graphemic transcodifier for Portuguese Language spoken in Brazil (PLB)
[INPE-5575-PRE/1803] p 760 N95-17649

LANTHANUM
High current density sheet-like electron beam generator
[AD-A281975] p 880 N95-17499

LANTHANUM OXIDES
Suppression of superconductivity in orthorhombic La(2-x)M(x)CuO4 (M = Ca,Sr)
[DE94-013963] p 901 N95-17350

LAPLACE EQUATION
Uniqueness and free interpolation for logarithmic potentials and the Cauchy problem for the Laplace equation in (R2)
[PB94-192408] p 861 N95-16295

LAPLACE TRANSFORMATION
An analysis of spectral envelope-reduction via quadratic assignment problems
[NASA-CR-194992] p 862 N95-16596

LARGE SPACE STRUCTURES
Integrated passive and active control of structures
[AD-A282684] p 708 N95-16304
Experimental validation of an integrated controls-structures design methodology for a class of flexible space structures
[NASA-TP-3462] p 709 N95-16857

LASER APPLICATIONS
ARO-URI Center for Opto-Electronic Systems Research
[AD-A281447] p 883 N95-15958
Multimodal correlation and intraoperative matching of virtual models in neurosurgery p 823 N95-15976
Modification of the Naval Postgraduate School Lidar System
[AD-A284987] p 753 N95-16231
Method of rapid sample handling for laser processing
[AD-D016408] p 778 N95-17464
Measurement of modulation transfer function of focal plane arrays and imaging systems
[AD-A282976] p 887 N95-17707

LASER ARRAYS
Phase-locked arrays of vertical-cavity surface-emitting lasers
[DE94-014941] p 778 N95-17498

LASER BEAMS
Non-intrusive missile control surface monitor system
[AD-A285356] p 883 N95-15954
Optimum truncation of a Gaussian beam in the presence of random jitter
[AD-A284951] p 752 N95-16143
Liquid crystal materials for laser beam steering
[AD-A285089] p 897 N95-16498
Investigation of laser-induced retinal damage: Wavelength and pulsewidth dependent mechanisms
[AD-A285186] p 822 N95-16871
An x ray technique for precision laser beam synchronization
[DE94-016449] p 779 N95-17635
Beam characteristics of a large-bore copper laser with a radiatively cooled plasma
[DE94-015139] p 779 N95-17688

LASER CAVITIES
Theory of carrier heating through injection pumping and lasing in semiconductor microcavity lasers
[AD-A281795] p 776 N95-16353
Wavelength dispersive gain element for a tunable laser
[AD-D016381] p 777 N95-17302
Phase-locked arrays of vertical-cavity surface-emitting lasers
[DE94-014941] p 778 N95-17498
Development of x-ray laser architectural components
[DE94-016446] p 778 N95-17627

LASER DAMAGE
Investigation of laser-induced retinal damage: Wavelength and pulsewidth dependent mechanisms
[AD-A285186] p 822 N95-16871

LASER DOPPLER VELOCIMETERS
Experimental investigation of turbulent separated-reattachment flow by using LDV p 649 N95-16253

LASER GUIDE STARS
Issues in the design and optimization of adaptive optics and laser guide stars for the Keck Telescopes
[DE94-012888] p 916 N95-17525

LASER HEATING
Beam characteristics of a large-bore copper laser with a radiatively cooled plasma
[DE94-015139] p 779 N95-17688

LASER INDUCED FLUORESCENCE
Laser induced fluorescence measurements and modeling of nitric oxide in high-pressure premixed flames
[NASA-CR-195404] p 775 N95-16910

LASER INTERFEROMETRY
Multi-beam laser interferometer for plasma density measurements in a Plasma Erosion Opening Switch (PEOS)
[AD-A283209] p 892 N95-17623
Development of x-ray laser architectural components
[DE94-016446] p 778 N95-17627

LASER MATERIALS
New ytterbium-doped apatite crystals for flexible laser design
[DE94-015138] p 899 N95-16867
High-average-power, diode-pumped solid state lasers for energy and industrial applications
[DE94-015142] p 779 N95-17689
Rare earth ion doped CW cascade fiber laser
[AD-D016370] p 779 N95-17698
Thermal and laser conditioning of production and rapid-growth KDP and KD*P crystals
[DE94-013738] p 902 N95-17742

LASER MODE LOCKING
Phase-locked arrays of vertical-cavity surface-emitting lasers
[DE94-014941] p 778 N95-17498

LASER MODES
Rare earth ion doped CW cascade fiber laser
[AD-D016370] p 779 N95-17698

LASER OUTPUTS
Investigation of laser-induced retinal damage: Wavelength and pulsewidth dependent mechanisms
[AD-A285186] p 822 N95-16871
Laser induced fluorescence measurements and modeling of nitric oxide in high-pressure premixed flames
[NASA-CR-195404] p 775 N95-16910
Fast electrons, filamented laser light, and the fast ignitor
[DE94-015898] p 777 N95-16929
Characterization of multiport solid state imagers at megahertz data rates
[DE94-016095] p 765 N95-16932
Properties of Ce:LiSrAlF6 and Ce:LiCaAlF6 ultraviolet lasers
[DE94-013737] p 777 N95-17168
Thermal effects in end-heated laser rods: A time-dependent model and diagnostic
[AD-A282007] p 778 N95-17500
High-average-power, diode-pumped solid state lasers for energy and industrial applications
[DE94-015142] p 779 N95-17689

LASER PUMPING
A AgGaSe2 optical parametric oscillator pumped by a Raman-shifted YAG laser
[AD-A284743] p 777 N95-16548
Thermal effects in end-heated laser rods: A time-dependent model and diagnostic
[AD-A282007] p 778 N95-17500

LASER RANGE FINDERS
Advanced technologies in the ASI MLRO towards a new generation laser ranging system p 687 N95-17239

LASER RANGER/TRACKER
Advanced technologies in the ASI MLRO towards a new generation laser ranging system p 687 N95-17239

LASER SPECTROSCOPY
Heavy ion physics
[DE94-623321] p 880 N95-17519
Advances in ultrafast scanning probe microscopy
[DE94-018180] p 779 N95-17729
Ultrafast scanning probe microscopy
[DE94-018186] p 779 N95-17887

LASER TARGET INTERACTIONS
In situ laser activation of electrochemical kinetics at carbon electrodes
[AD-A280892] p 727 N95-16150
High-intensity and high energy laser interactions with single droplets
[AD-A281415] p 776 N95-16166

LASER WEAPONS
Simulations of an FEL producing coherent x rays utilizing the SLAC LINAC
[AD-A283524] p 777 N95-17303

LASERS
Resonance enhanced multiphoton ionization of molecules and molecular fragments
[AD-A285076] p 873 N95-16493
Shotgun/drop-weight initiation of energetic materials
[AD-A285090] p 749 N95-16499
Tunable UV source for UV fluorescence remote sensing
[DE94-015745] p 777 N95-16917
Fast electrons, filamented laser light, and the fast ignitor
[DE94-015898] p 777 N95-16929
An x ray technique for precision laser beam synchronization
[DE94-016449] p 779 N95-17635

LASING
Theory of carrier heating through injection pumping and lasing in semiconductor microcavity lasers
[AD-A281795] p 776 N95-16353

LATERAL CONTROL
Evaluation of an autopilot based multimodelling
[PB94-190725] p 671 N95-17454

LATITUDE
Meteorological observations of synoptic disturbances: Sensitivity to latitude p 917 N95-16179
Climatological targets for Mars Pathfinder p 922 N95-16208
Mars Pathfinder mission operations concepts p 686 N95-17229

LATTICE PARAMETERS
Study of the effect of the space charge using SYNCH
[DE94-014086] p 879 N95-16210

LATTICES
Thermoacoustic pin stacks
[AD-A282267] p 794 N95-16954

LAUNCH VEHICLES
Large-scale hybrid motor performance and designs for use in launch vehicle applications p 715 N95-16327
Integrated modular engine configuration options p 717 N95-16336
Emerging national space launch programs: Economics and safeguards
[AD-A282107] p 672 N95-17427

LAUNCHING
International mission planning for space Very Long Baseline Interferometry p 673 N95-17216
Mars Pathfinder mission operations concepts p 686 N95-17229
A survey of commercially available expendable heavy lift launch vehicles
[AD-A282429] p 676 N95-17509

LAVA
Sampling Elysium lavas (13 deg N, 203 deg W) p 917 N95-16177

LAYOUTS
Timing and area optimization for VLSI circuit and layout
[AD-A281081] p 762 N95-16089

LEAD (METAL)
New approaches to novel organosilanes
[AD-A285253] p 722 N95-16513

LEAD TITANATES
Epitaxial MOCVD of thin film ceramics for pyroelectric detectors
[AD-A281397] p 744 N95-16863

LEAD ZIRCONATE TITANATES
Cost-effective method for synthesizing innovative transducer materials for sensors and actuators
[AD-A282339] p 725 N95-16974

LEADERSHIP
Presidential leadership in the development of the US space program
[NASA-TM-110107] p 904 N95-16007

LEADING EDGE FLAPS
Investigation of the flow development on a highly swept canard/wing research model with segmented leading- and trailing-edge flaps p 662 N95-17876

LEADING EDGES
Transonic Navier-Stokes calculations about a 65 deg delta wing
[NASA-CR-4635] p 656 N95-17273
Two-dimensional high-lift airfoil data for CFD code validation p 659 N95-17859
Wind tunnel test on a 65 deg delta wing with a sharp or rounded leading edge: The international vortex flow experiment p 662 N95-17872
Wind tunnel test on a 65 deg delta wing with rounded leading edges: The International Vortex Flow Experiment p 662 N95-17875

LEAKAGE
SSME propellant path leak detection real-time
[NASA-CR-197032] p 748 N95-16029
Progress at LAMPF
[DE94-016210] p 880 N95-16937
Characterization of the corrosion behavior of the carbon steel liner in Hanford site single-shell tanks
[DE94-016475] p 737 N95-17637
Antenna dielectric sealing process characterization
[DE94-015864] p 747 N95-17690
The development of a solid-state hydrogen sensor for rocket engine leakage detection
[NASA-CR-197567] p 776 N95-17895

LEARNING CURVES
Pattern theoretic knowledge discovery
[AD-A285472] p 909 N95-16879

LEAST SQUARES METHOD
A combined biased-robust estimator for dealing with influence and collinearity in regression
[AD-A281793] p 864 N95-16422
Least squares computations in science and engineering
[AD-A281213] p 862 N95-16798
A preliminary optical visibility model p 758 N95-17290

LEAVES
Regulation of nitrogen uptake and assimilation: Effects of nitrogen source and root-zone and aerial environment on growth and productivity of soybean
[NASA-CR-197098] p 807 N95-15961

LEGAL LIABILITY
NASA contract mangagement: Improving the use of DCAA's auditing services. Report to the Chairman, Committee on Government Operations, House of Representatives
[GAO/NSIAD-94-229] p 914 N95-15962

LENSES
A simpie EHF hemispheric coverage antenna
[AD-A285078] p 754 N95-16495
Dark focus of accommodation as dependent and independent variables in visual display technology p 812 N95-16758
Numerical aperture limits on efficient ball lens coupling of laser diodes to single-mode fibers with defocus to balance spherical aberration
[NASA-TM-4578] p 886 N95-17271

LENTICULAR BODIES
Test data on a non-circular body for subsonic, transonic and supersonic Mach numbers p 662 N95-17871

LEPTONS
Tests of structure functions using leptons at CDF: W asymmetry and Drell-Yan production
[DE94-015727] p 875 N95-16840
Multilepton SUSY signals from R-parity violation at the Tevatron (revised)
[PB95-104311] p 877 N95-17353
Composite-model view of the ll-bar(gamma)(gamma) events at LEP
[DE94-753312] p 877 N95-17520
Z(prime) phenomenology: Constraints from low-energy measurements, and detailed study at TeV-scale lepton and hadron colliders
[DE94-018185] p 881 N95-17886
Search for first and second generation leptoquarks at D(null)
[DE94-018992] p 879 N95-17932

LESIONS
Kinetics model for initiation and promotion for describing tumor prevalence from HZE radiation
[NASA-TP-3479] p 820 N95-16412
Failure of ozone and nitrogen dioxide to enhance lung tumor development in hamsters
[PB94-182854] p 818 N95-16801

LIAPUNOV FUNCTIONS
A Lyapunov bound for solutions of Poisson's equation
[AD-A281536] p 860 N95-16169

LIBRARIES
Fourth Annual International Acquisitions Workshop: Access to Multiple Media Worldwide
[NASA-TM-109896] p 905 N95-15919
The Austrialian National Chinese Japanese Korean Project p 905 N95-15920
NAFTA literature at the International Trade Commission library p 905 N95-15922
Bureau of the Census Center for International Research p 905 N95-15923
Acquiring and disseminating unpublished economic and social development materials in Africa: The case of the National Institute of Development Research and Documentation University of Botswana p 906 N95-15924
Information system in transition: The Hungarian Scene p 906 N95-15925
Document delivery by the Jupiter Library Consortium p 906 N95-15926
CINDOC, CSIC, and Spanish R and D p 906 N95-15927
The Technical Information Library: TIB p 906 N95-15928
The National Resource Library for Science and Technology in Sweden: A Nordic model of cooperating technology libraries p 906 N95-15929
Information sources in science and technology in Finland p 906 N95-15930
Networked information: Management issues for the acquisitions librarian p 906 N95-15932
National Center for Standards and Certification Information: Service and programs p 907 N95-15938
Collection development at the NOAA Central Library p 907 N95-15939

LIE GROUPS
Some fundamental techniques in the theory of integrable systems
[PB94-192390] p 860 N95-16294

LIFE (DURABILITY)
Continuing life test of a xenon hollow cathode for a space plasma contactor
[NASA-CR-195401] p 711 N95-15968
MIL-STD-498 software development and documentation, version 01.00.00
[AD-A282003] p 837 N95-16607
Performance evaluation of polyaniline as an active material for electrochemical capacitors
[DE94-016283] p 765 N95-16920
Life prediction for bridged fatigue cracks
[DE94-016000] p 724 N95-16930
Evaluation of NASA's end-to-end data systems using DSDS+ p 700 N95-17577

LIFE CYCLE COSTS
Software engineering from a Langley perspective p 843 N95-16454
RDD-100 and the systems engineering process p 848 N95-16471
Computer tools for systems engineering at LaRC p 848 N95-16472
Aerodynamic shape optimization p 668 N95-16572
Transportable Payload Operations Control Center reusable software: Building blocks for quality ground data systems p 703 N95-17587

LIFE SCIENCES
BioServe space technologies: A NASA Center for the Commercial Development of Space
[NASA-CR-196983] p 807 N95-16034
SLS-1: The first dedicated life sciences shuttle flight p 676 N95-16769
Medical care capabilities for Space Station Freedom: A phase approach p 710 N95-16772
NASA Johnson Space Center Life Sciences Data System p 679 N95-17195
Aerospace medicine and biology: A continuing bibliography with indexes (supplement 396)
[NASA-SP-7011(396)] p 823 N95-17703

LIFE SUPPORT SYSTEMS
A prototype Crew Medical Restraint System (CMRS) for Space Station Freedom p 815 N95-16773
Advanced Cardiac Life Support (ACLS) utilizing Man-Tended Capability (MTC) hardware onboard Space Station Freedom p 816 N95-16775
Molecular approach to hypothalamic rhythms
[AD-A285164] p 822 N95-16851
Aerospace medicine and biology: A continuing bibliography with indexes (supplement 396)
[NASA-SP-7011(396)] p 823 N95-17703

LIFT
Measurements on a two-dimensional aerofoil with high-lift devices p 657 N95-17848

LIFT DRAG RATIO
An approach to aerodynamic characteristics of low radar cross-section fuselages p 649 N95-16251
Residual-correction type and related computational methods for aerodynamic design. Part 2: Multi-point airfoil design p 667 N95-16567
The global aircraft shape p 668 N95-16571
Aerodynamic shape optimization p 668 N95-16572

LIGANDS
Ligand field stabilization control of metal ion binding
[AD-A281011] p 726 N95-16001

LIGHT (VISIBLE RADIATION)
Phase-shifting effects of light and activity on the human circadian clock
[AD-A281204] p 821 N95-16796
Tunable UV source for UV fluorescence remote sensing
[DE94-015745] p 777 N95-16917
Basic mechanisms and implications of non-photic entrainment of circadian rhythmicity
[AD-A283180] p 822 N95-17342
Miniature, vacuum compatible 1024 (times) 1024 CCD camera for x ray, ultraviolet, or optical imaging
[DE94-012235] p 776 N95-17522

LIGHT AMPLIFIERS
Overview of photonics research at Lawrence Livermore National Laboratory
[DE94-014055] p 884 N95-16366
Wavelength dispersive gain element for a tunable laser
[AD-D016381] p 777 N95-17302

LIGHT BEAMS
Investigation of laser-induced retinal damage: Wavelength and pulsewidth dependent mechanisms
[AD-A285186] p 822 N95-16871
Fast electrons, filamented laser light, and the fast ignitor
[DE94-015898] p 777 N95-16929

LIGHT EMISSION
International Workshop on Light Emission and Electronic Properties of Nanoscale silicon
[AD-A281464] p 894 N95-16081
Electrical breakdown and optical emission properties of high pressure pulsed RF gas discharges
[DE94-012731] p 877 N95-17687

LIGHT EMITTING DIODES
Numerical aperture limits on efficient ball lens coupling of laser diodes to single-mode fibers with defocus to balance spherical aberration
[NASA-TM-4578] p 886 N95-17271

LIGHT GAS GUNS
Thermal characteristics and heat transfer in an electrothermal light gas gun
[AD-A281980] p 892 N95-17442

LIGHT IONS
Transport efficiency studies for light-ion inertial confinement fusion
[AD-A285675] p 891 N95-17382

LIGHT SCATTERING
Fractal aggregate random media analysis and applications
[AD-A281410] p 884 N95-16161
The combination probe of optical fibers and its applications p 652 N95-16275
Alpha particle kinetics in ignited fusion plasmas: Design applications for a CO2 laser Thomson scattering experiment
[DE94-016297] p 890 N95-16921

LIGHT SCATTERING METERS
Non-intrusive missile control surface monitor system
[AD-A285356] p 883 N95-15954

LIGHT SOURCES
Measurements of collective effects in the ALS
[DE94-017966] p 881 N95-17670
Experimental characterization of ALS undulator radiation
[DE94-017967] p 881 N95-17671
Studies of transverse coherent bunch instabilities for the Advanced Light Source (ALS)
[DE94-018536] p 904 N95-17904

LIGHT TRANSMISSION
Innovative acoustic techniques for studying new materials and new developments in solid state physics
[AD-A280986] p 898 N95-16525
Synthesis of low band gap zwitterionic and planar conjugated pyrrole-derived polymers. Reversible optical absorbances from the UV to the near-IR
[AD-A281174] p 743 N95-16628
Ultra high bit rate all optical communication system
[AD-D016359] p 887 N95-17695

LIGHT TRANSPORT AIRCRAFT
Evaluation of the dynamic stability characteristics of the NAL Light Transport Aircraft
[NAL-PD-CA-9217] p 671 N95-16392

LIGHTNING
Analysis of magnetic field data from Pioneer Venus orbiter
[NASA-CR-197492] p 923 N95-17403

LIKELIHOOD RATIO
Likelihood ratio gradient estimation for stochastic recursions
[AD-A281408] p 865 N95-17426

LINE OF SIGHT
Parallel implementation of the terrain masking algorithm
[AD-A281017] p 833 N95-16003

LINE SPECTRA
Determination of ion temperatures from Zeeman broadened spectral lines in the edge of Tore Supra
[DE94-018112] p 873 N95-16403
Adaptive line enhancers for fast acquisition p 757 N95-17287
First detection of CO (j = 0 - 1) adsorption at cosmological distances (z = 0.247)
[PB94-184595] p 916 N95-17332
The Mg 2 lines as diagnostic of PMS nature in Herbig Ae/Be stars
[NASA-CR-197518] p 915 N95-17494
Raman spectroscopy of C-irradiated graphite
[DE94-018705] p 733 N95-17911

LINEAR ACCELERATORS
Mechanisms of beam-halo formation in high-intensity linacs
[DE94-016316] p 879 N95-16030
Beam parameter measurements for the APS linac system
[DE94-018396] p 882 N95-17902
Electromagnetic field measurements on a mm-wave linear accelerator
[DE94-015092] p 761 N95-17926
Beam position correction in the Fermilab Linac
[DE94-018984] p 882 N95-17931

LINEAR ARRAYS
Space-based asteroid detection and monitoring system
[AD-D016329] p 915 N95-16854
Testing and characterization of the CYCLOPS HgCdTe focal plane detector array
[AD-A284279] p 887 N95-17489

LINEAR EQUATIONS
A new regularization approach in structural system identification p 651 N95-16262
Rapid solution of large-scale systems of equations p 847 N95-16458

LINEAR PREDICTION
Linear prediction data extrapolation superresolution radar imaging p 651 N95-16268

LINEAR PROGRAMMING
Multigrid methods in network optimization: Overview and appraisal
[AD-A280992] p 833 N95-15995
Timing and area optimization for VLSI circuit and layout
[AD-A281081] p 762 N95-16089
Multivariate sampling with explicit correlation induction for practical simulation and optimization studies
[AD-A281998] p 841 N95-17445
Structural optimization with approximate sensitivities
[NASA-TM-4553] p 788 N95-17701

LINEAR SYSTEMS
Effect of Coulomb collisions, Landau damping and particle trapping on linear and nonlinear ion acoustic waves
[AD-A282009] p 869 N95-17449
Back-propagation neural networks in adaptive control of unknown nonlinear systems
[AD-A282414] p 858 N95-17458

LINEAR TRANSFORMATIONS
Duality transformations, green dyadics and plane-wave solutions for a class of bianisotropic media
[PB94-197670] p 754 N95-16612

LININGS
Characterization of the corrosion behavior of the carbon steel liner in Hanford site single-shell tanks
[DE94-016475] p 737 N95-17637

LINKAGES
Data link level interconnection of remote Fiber Distributed Data Interface Local Area Networks (FDDI LANs) through the Critical Data Link (CDL)
[AD-A284307] p 755 N95-17173

LIQUEFIED GASES
A high resolution liquid xenon imaging telescope for 0.3-10 MeV gamma-ray astrophysics: Construction and initial balloon flights
[NASA-CR-197556] p 916 N95-17528

LIQUID ATOMIZATION
Combustion instability phenomena of importance to liquid propellant engines
[AD-A284780] p 730 N95-16882

LIQUID COOLING
Natural convection cooling of a three by three array of leadless chip carrier packages in a dielectric liquid
[AD-A282298] p 770 N95-16239

LIQUID CRYSTALS
Supercritical fluid extraction: Preparing a superior mesophase precursor for carbon fibers
[AD-A284933] p 726 N95-16142
Smart materials based upon oligomeric molecules
[AD-A281374] p 872 N95-16155
Liquid crystal materials for laser beam steering
[AD-A285089] p 897 N95-16498
Chiral recognition in molecular and macromolecular pairs of liquid crystals of (2R, 3S)- and (2S, 3S)-2-fluoro-3-methylpentyl-4'-(11-vinyloxyundeca iphenyl-4-carboxylate diastereomers
[AD-A281770] p 878 N95-17692

LIQUID HELIUM
Two phase liquid helium flow testing to simulate the operation of a cryocondensation pump in the D3-D tokamak
[DE94-018345] p 893 N95-17896

LIQUID HYDROGEN
Cryogenic foil bearing turbopumps p 716 N95-16331

LIQUID INJECTION
Combustion instability phenomena of importance to liquid propellant engines
[AD-A284780] p 730 N95-16882

LIQUID METALS
Liquefied metal jet program Automation and Robotics Research Institute (ARRI)
[AD-A285470] p 736 N95-16878

LIQUID OXYGEN
Large-scale hybrid motor performance and designs for use in launch vehicle applications p 715 N95-16327
Cryogenic foil bearing turbopumps p 716 N95-16331

LIQUID PHASE EPITAXY
LPEE growth and characterization of In(x)Ga(1-x)As(y)Sb(1-y) lattice matched to GaSb and InAs for photodetectors
[AD-A281631] p 895 N95-16114

LIQUID PROPELLANT ROCKET ENGINES
The 1993 JANNAF Propulsion Meeting, volume 2
[CPIA-PUBL-602-VOL-2] p 715 N95-16324
Nondestructive examination of the TRMM RCS propellant tanks p 718 N95-16338
Combustion instability phenomena of importance to liquid propellant engines
[AD-A284780] p 730 N95-16882
The development of a solid-state hydrogen sensor for rocket engine leakage detection
[NASA-CR-197567] p 776 N95-17895

LIQUID ROCKET PROPELLANTS
The 1993 JANNAF Propulsion Meeting, volume 2
[CPIA-PUBL-602-VOL-2] p 715 N95-16324
Nondestructive examination of the TRMM RCS propellant tanks p 718 N95-16338
Thermocryogenic buckling and stress analyses of a partially filled cryogenic tank subjected to cylindrical strip heating
[NASA-TM-4579] p 788 N95-17417

LIQUID-LIQUID INTERFACES
Charge transfer processes on liquid/liquid interfaces: The status in 1994
[AD-A285067] p 729 N95-16635

LIQUID-SOLID INTERFACES
Characterization of surfaces
[NASA-CR-196995] p 750 N95-16065
In-situ x-ray characterization of the electrolyte-solid interface
[AD-A281165] p 729 N95-16627
Materials degradation and fatigue under extreme conditions
[AD-A282969] p 746 N95-17662

LIQUID-VAPOR INTERFACES
Active and passive acoustic bubble sizing
[ISVR-TR-237] p 769 N95-16064
Multi-dimensional shock capturing
[AD-A282986] p 773 N95-17708

LIQUIDS
Study of the structuring of pure molecular liquids
[PB94-201316] p 903 N95-16839
Materials degradation and fatigue under extreme conditions
[AD-A282969] p 746 N95-17662

LISP (PROGRAMMING LANGUAGE)
A computational logic for applicative common Lisp
[AD-A283103] p 840 N95-17338

LISTS
Source hierarchy list. Volume 2: E through N
[AD-A281101] p 908 N95-15957
Source header list. Volume 2: L through Z
[AD-A281001] p 908 N95-15998
Source hierarchy list. Volume 3: O through Z
[AD-A281102] p 908 N95-16090
Scientific and technical publishing at Goddard Space Flight Center in Fiscal Year 1994
[NASA-TM-104614] p 925 N95-16581
ICASE
[NASA-CR-195001] p 832 N95-16898

LITERATURE
The Technical Information Library: TIB
p 906 N95-15928

LITHIUM
Electrochemical properties of lithium ion conducting solid polymer electrolytes
[AD-A281875] p 742 N95-16434
Studies of D-Li neutron source: An overview
[DE94-014032] p 873 N95-16487
The influence of the complexation of sodium and lithium triflate on the self-assembly of tubular-supramolecular architectures displaying a columnar mesophase based on taper-shaped monoesters of oligoethyleneoxide with 3,4,5-tris(p-(n-dodecan-l-yloxy)benzyloxy)benzoic acid and of their polymethacrylates
[AD-A281403] p 730 N95-16866
Transport efficiency studies for light-ion inertial confinement fusion
[AD-A285675] p 891 N95-17382
Use of copper powder extinguishers on lithium fires
[AD-A283213] p 751 N95-17632

LITHIUM ALLOYS
Safety characteristics of lithium-alloy/metal sulfide batteries
[DE94-013867] p 766 N95-16963

LITHIUM BORATES
Growth, characterization and applications of beta-barium borate and related crystals
[AD-A281047] p 898 N95-16623

LITHIUM NIOBATES
Performance characterization of photonic links in cryogenic environments for advanced signal processing applications
[DE94-015561] p 765 N95-16915

LITHIUM SULFUR BATTERIES
Safety characteristics of lithium-alloy/metal sulfide batteries
[DE94-013867] p 766 N95-16963

LITHOGRAPHY
Low voltage electron beam lithography
[AD-A281046] p 729 N95-16622

LOADS (FORCES)
Twin disc gear tooth simulator
[AD-A284927] p 780 N95-16139
An investigation of polynomial calibrations methods for wind tunnel balances p 650 N95-16258
Diffusion weld test fixture
[AD-D016450] p 780 N95-16543
Field verification of the wind tunnel coefficients
p 664 N95-17291
Thermocryogenic buckling and stress analyses of a partially filled cryogenic tank subjected to cylindrical strip heating
[NASA-TM-4579] p 788 N95-17417

LOCAL AREA NETWORKS
Data link level interconnection of remote Fiber Distributed Data Interface Local Area Networks (FDDI LANs) through the Critical Data Link (CDL)
[AD-A284307] p 755 N95-17173
SCOS 2: ESA's new generation of mission control system p 674 N95-17253
Open solutions to distributed control in ground tracking stations p 674 N95-17554

LOCOMOTION
Effect of antiorthostatic BedRest (BR) on GastroIntestinal Motility (GIM) of normal subjects
p 811 N95-16753

LOCOMOTIVES
Coal-fueled diesel technology development emissions control
[DE94-004096] p 782 N95-17364

LOG PERIODIC ANTENNAS
A VHF/UHF antenna for the Precision Antenna Measurement System (PAMS)
[AD-A285673] p 754 N95-16621

LOGIC CIRCUITS
Multilayer microelectronic photomultiplier device with a stacked series of dynode and insulating layers
[AD-D016377] p 767 N95-17478
Digital logic and reconfigurable interconnects using aluminum gallium arsenide electro-optic Fredkin gates
[AD-A282880] p 881 N95-17619

LOGIC DESIGN
Timing and area optimization for VLSI circuit and layout
[AD-A281081] p 762 N95-16089
Support for development of a custom VLSI and FPGA logic chips based on a VHDL top-down design approach
[DE94-013608] p 763 N95-16283
Proceedings of the International Conference on Parallel Architectures and Compilation Techniques
[AD-A285258] p 849 N95-16529
Workshop on Formal Models for Intelligent Control
[AD-A281399] p 857 N95-16864
Multi-objective decision-making under uncertainty: Fuzzy logic methods
[NASA-TM-106796] p 720 N95-17269

LOGISTICS
Engineering design tools for wind diesel systems. Volume 1: Executive summary
[PB95-104501] p 842 N95-17733
Engineering design tools for wind diesel systems. Volume 6: Logistic package. User documentation
[PB95-104550] p 842 N95-17734
Engineering design tools for wind diesel systems. Volume 7: Logistic package. Validation report
[PB95-104568] p 842 N95-17735

LOGISTICS MANAGEMENT
Department of Defense Electronic Data Interchange project baseline report for FY 1994
[AD-A283015] p 912 N95-17710

LONG DURATION SPACE FLIGHT
Intramuscular pressure: A better tool than EMG to optimize exercise for long-duration space flight
p 809 N95-16744
Magnetic Resonance Imaging (MRI) of skeletal muscles in astronauts after 9 days of space flight
p 810 N95-16749
Physiological constraints on deceleration during the aerocapture of manned vehicles p 810 N95-16751
Psychological training of NASA astronauts for extended missions p 813 N95-16763
Artificial gravity: How much, how often, how long?
p 816 N95-16778
The efficacy of periodic +Gz exposure in the prevention of bedrest induced orthostatic intolerance
p 817 N95-16781

LOSSES
Photoreceptors regulating circadian behavior: A mouse model
[AD-A285157] p 822 N95-16847
Evaluation of SEA loss factors using input power modulation
[ISVR-TR-240] p 868 N95-16856
Progress at LAMPF
[DE94-016210] p 880 N95-16937
Revisions to an empirical surface loss model using a correction for pH-dependent attenuation
[AD-A285714] p 871 N95-17177

LOW ASPECT RATIO
Development of a low-aspect ratio fin for flight research experiments
[NASA-TM-4596] p 656 N95-16858

LOW ASPECT RATIO WINGS
An approach to aerodynamic characteristics of low radar cross-section fuselages p 649 N95-16251
Low aspect ratio wing experiment
p 661 N95-17865

LOW CARBON STEELS
Characterization of the hydrogen induced cold cracking susceptibility at simulated weld zones in HSLA-100 steel
[PB94-174505] p 737 N95-17616

LOW COST
Coatings for large-area low-cost solar concentrators and reflectors
[DE94-015735] p 793 N95-16916
CCS-MIP: Low cost Customizable Control Centre
p 674 N95-17254
Implementation of a low-cost, commercial orbit determination system p 673 N95-17544
Cost efficient operations for Discovery class missions
p 695 N95-17548
Ground Station support for small scientific satellites
p 695 N95-17549
Design of ground segments for small satellites
p 674 N95-17550
Small satellite space operations p 695 N95-17552
Micro-UltraViolet Spectrograph (Micro-UVS)
[DE94-016704] p 732 N95-17642

LOW CURRENTS
Experimental characterization of ALS undulator radiation
[DE94-017967] p 881 N95-17671

LOW FREQUENCIES
Fluctuation measurements at c/(omega)(sub pe) spatial scales in a tokamak
[DE94-016771] p 892 N95-17643
Thermal noise in biomagnetic measurements
[PB95-104360] p 869 N95-17930

LOW PRESSURE
Selective area platinum film deposition
[AD-D016355] p 747 N95-17693

LOW SPEED
Re-engineering Nascom's network management architecture p 702 N95-17584
Two-dimensional 16.5 percent thick supercritical airfoil NLR 7301 p 658 N95-17854
Low-speed surface pressure and boundary layer measurement data for the NLR 7301 airfoil section with trailing edge flap p 658 N95-17855
Force and pressure data of an ogive-nosed slender body at high angles of attack and different Reynolds numbers
p 661 N95-17868
Low speed propeller slipstream aerodynamic effects
p 663 N95-17882

LOW SPEED WIND TUNNELS
Data acquisition and processing software for the Low Speed Wind Tunnel tests of the Jindivik auxiliary air intake
[AD-A285455] p 656 N95-17178
Low speed propeller slipstream aerodynamic effects
p 663 N95-17882

LOW TEMPERATURE
Liquid crystal materials for laser beam steering
[AD-A285089] p 897 N95-16498
Design and synthesis of organic superconductors (FY92 URI/RIP)
[AD-A281308] p 899 N95-16789
The impact of low temperature materials on the breakdown and noise properties of GaAs and InP based HEMT's and FET's
[AD-A285176] p 765 N95-16834
Properties of semiconducting Ru2Ge3
[DE94-015361] p 899 N95-16913
Performance characterization of photonic links in cryogenic environments for advanced signal processing applications
[DE94-015561] p 765 N95-16915
Low-temperature fabrication of transparent silicon nitride
[DE94-014902] p 746 N95-17456

LOW VOLTAGE
Low voltage electron beam lithography
[AD-A281046] p 729 N95-16622
Preparation and investigation of improved low voltage electron excitable phosphors
[AD-A284265] p 767 N95-17487
LOWER BODY NEGATIVE PRESSURE
Spectral components of human cardiovascular responses to step changes in Lower Body Negative Pressure (LBNP) before and after 22 hour of 6 deg head down bed rest p 810 N95-16748
Blood volume and orthostatic responses of men and women to a 13-day bedrest p 811 N95-16752
LUBRICANTS
Twin disc gear tooth simulator
[AD-A284927] p 780 N95-16139
Deformation behavior of thin lubricant films at elevated pressure
[AD-A281848] p 741 N95-16355
Materials degradation and fatigue under extreme conditions
[AD-A282969] p 746 N95-17662
LUGS
Evaluation of alternate F-14 wing lug coating
[AD-A283207] p 669 N95-17631
LUMINAIRES
Performance of specular reflectors used for lighting enhancement
[AD-A281004] p 884 N95-15999
LUMINANCE
An empirical approach to visual display preference based upon modulation transfer function and luminance
[AD-A285450] p 830 N95-16875
LUMINOSITY
Measurement of the B meson differential cross-sections in p(-p) collisions at the square root of s = 1.8 TeV using the exclusive decays B(+-) yields J/(psi)K(+-) and B(exp 0) yields J/(psi)K(exp *0)
[DE94-015185] p 872 N95-16309
Na-22 decay gamma rays from classical novae
[NASA-CR-197454] p 924 N95-16383
Measurement of the B(sub s) meson lifetime at CDF
[DE94-015381] p 875 N95-16868
LUMINOUS INTENSITY
The combination probe of optical fibers and its applications p 652 N95-16275
LUMPED PARAMETER SYSTEMS
Problem of constructing the Lyapunov's functions in lumped parameter systems p 653 N95-16276
LUNAR BASES
A study of electric transmission lines for use on the lunar surface p 712 N95-16053
Thermal control systems for low-temperature heat rejection on a lunar base
[NASA-CR-197486] p 830 N95-16418
Catalog of lunar and Mars science payloads
[NASA-RP-1345] p 922 N95-16436
LUNAR CRATERS
Apollo 16: Nothing so hidden
[NASA-TM-110104] p 922 N95-16836
LUNAR ENVIRONMENT
A study of electric transmission lines for use on the lunar surface p 712 N95-16053
LUNAR EVOLUTION
New look at the old Moon
[NASA-TM-110106] p 922 N95-16838
LUNAR EXPLORATION
Apollo 16: Nothing so hidden
[NASA-TM-110104] p 922 N95-16836
New look at the old Moon
[NASA-TM-110106] p 922 N95-16838
LUNAR EXPLORATION SYSTEM FOR APOLLO
Apollo 15: In the mountains of the Moon
[NASA-TM-109988] p 922 N95-16942
LUNAR LANDING
Apollo 16: Nothing so hidden
[NASA-TM-110104] p 922 N95-16836
Apollo 17: On the shoulders of giants
[NASA-TM-110105] p 922 N95-16837
LUNAR LAUNCH
Apollo 16: Nothing so hidden
[NASA-TM-110104] p 922 N95-16836
LUNAR PHOTOGRAPHY
Apollo 16: Nothing so hidden
[NASA-TM-110104] p 922 N95-16836
LUNAR PROGRAMS
New look at the old Moon
[NASA-TM-110106] p 922 N95-16838
LUNAR ROCKS
Apollo 16: Nothing so hidden
[NASA-TM-110104] p 922 N95-16836
LUNAR SURFACE
Thermal control systems for low-temperature heat rejection on a lunar base
[NASA-CR-197486] p 830 N95-16418
LUNAR SURFACE VEHICLES
Lunar surface operations. Volume 3: Robotic arm for lunar surface vehicle
[NASA-CR-195553-VOL-3] p 780 N95-16031
LUNAR TRAJECTORIES
Apollo 16: Nothing so hidden
[NASA-TM-110104] p 922 N95-16836
LUNGS
Failure of ozone and nitrogen dioxide to enhance lung tumor development in hamsters
[PB94-182854] p 818 N95-16801
Carbon monoxide does not modulate pulmonary vascular reactivity in isolated rat lungs
[AD-A283190] p 818 N95-17714

M

MACH NUMBER
Unsteady flow phenomena in discrete passage diffusers for centrifugal compressors
[AD-A281412] p 770 N95-16163
Scramjet testing guidelines p 670 N95-16317
Error propagation equations for estimating the uncertainty in high-speed wind tunnel test results
[DE94-014136] p 671 N95-16509
Mach number, flow angle, and loss measurements downstream of a transonic fan-blade cascade
[AD-A280907] p 656 N95-16824
Comparison of computational and experimental results for a supercritical airfoil
[NASA-TM-4601] p 656 N95-16908
2-D aileron effectiveness study p 658 N95-17851
Investigation of an NLF(1)-0416 airfoil in compressible subsonic flow p 658 N95-17852
OAT15A airfoil data p 659 N95-17857
Measurements of the flow over a low aspect-ratio wing in the Mach number range 0.6 to 0.87 for the purpose of validation of computational methods. Part 1: Wing design, model construction, surface flow. Part 2: Mean flow in the boundary layer and wake, 4 test cases
p 660 N95-17860
Pressure distributions on research wing W4 mounted on an axisymmetric body p 660 N95-17862
DLR-F4 wing body configuration p 660 N95-17863
Low aspect ratio wing experiment
p 661 N95-17865
MACH-ZEHNDER INTERFEROMETERS
Magnetostrictive transducer system having a three dual-strip fiber optic magnetostrictive transducers bonded into a single fiber Mach-Zehnder interferometer
[AD-D016373] p 775 N95-17428
Multi-beam laser interferometer for plasma density measurements in a Plasma Erosion Opening Switch (PEOS)
[AD-A283209] p 892 N95-17623
MACHINE LEARNING
Learning one more thing
[AD-A285342] p 857 N95-16820
Online performance-improvement algorithms
[AD-A285162] p 838 N95-16850
Pattern theoretic knowledge discovery
[AD-A285472] p 909 N95-16879
The 1994 International Neural Network Society Annual Meeting, volume 3
[AD-A281736] p 857 N95-17369
The 1994 International Neural Network Society Annual Meeting, volume 4
[AD-A281737] p 857 N95-17370
Hidden Markov model for gesture recognition
[AD-A282845] p 865 N95-17377
Hidden Markov model for control strategy learning
[AD-A282846] p 865 N95-17429
Small sample behavior of multi-layer feedforward network classifiers: Theoretical and practical aspects
[PB94-201415] p 841 N95-17470
MACHINE TOOLS
Approach to in-process tool wear monitoring in drilling: Application of Kalman filter theory p 653 N95-16279
Development of processes, means, and theoretical principles of thin-walled detail plastic forming at Kazan Aviation Institute p 653 N95-16281
Cost-effective method for synthesizing innovative transducer materials for sensors and actuators
[AD-A282339] p 725 N95-16974
MACHINING
Precision machining and polishing of scintillating crystals for large calorimeters and hodoscopes
[DE94-012060] p 751 N95-17738
MACROMOLECULES
Log-(Chi(exp 2)) distribution of correlation times revisited
[AD-A281123] p 740 N95-16092
Living radical polymerization. 1: Possibilities and limitations
[AD-A281042] p 742 N95-16451
Isomorphism within the hexagonal columnar mesophase of molecular and macromolecular self- and co-assembled columns containing tapered groups
[AD-A281205] p 874 N95-16797
Chiral recognition in molecular and macromolecular pairs of liquid crystals of (2R, 3S)- and (2S, 3S)-2-fluoro-3-methylpentyl-4'-(11-vinyloxyundeca iphenyl-4-carboxylate diastereomers
[AD-A281770] p 878 N95-17692
MAGELLAN PROJECT (NASA)
Magellan Project: Evolving enhanced operations efficiency to maximize science value
p 684 N95-17218
MAGELLAN SPACECRAFT (NASA)
Magellan Project: Evolving enhanced operations efficiency to maximize science value
p 684 N95-17218
MAGMA
Melas Chasma: A Mars Pathfinder view of Valles Marineris p 922 N95-16207
MAGNESIUM
Use of magnesium for recovering hydrogen isotopes from tritiated water
[DE94-014471] p 731 N95-17157
MAGNESIUM OXIDES
The deposition of electro-optic films on semiconductors
[AD-A285068] p 742 N95-16488
Nano-scale metal oxide particles as materials for air purification
[AD-A281394] p 729 N95-16791
Preparation and investigation of improved low voltage electron excitable phosphors
[AD-A284265] p 767 N95-17487
MAGNETIC COILS
Papers presented at the Tenth Topical Conference on High-Temperature Plasma Diagnostics
[DE94-015854] p 888 N95-16063
MAGNETIC COOLING
Test results of superconducting AC magnets for magnetic refrigeration experiment
[DE94-018695] p 751 N95-17909
MAGNETIC EFFECTS
Ion beam generation and propagation for plasma processing applications
[DE94-014428] p 889 N95-16286
MAGNETIC FIELD CONFIGURATIONS
Field configuration of beam excited modes in the Advanced Photon Source (APS) storage ring waveguides
[DE94-015096] p 880 N95-16308
Rietveld refinement of magnetic structures from pulsed-neutron-source powder-diffraction data
[DE94-016599] p 737 N95-17641
MAGNETIC FIELD RECONNECTION
Kinetic effects near the magnetopause
[DE94-009333] p 799 N95-16927
MAGNETIC FIELDS
Ion drift meter research
[NASA-CR-197124] p 798 N95-16432
Electromagnetostatics in uniaxial bianisotropic media
[PB94-197688] p 754 N95-16613
Analysis of magnetic field data from Pioneer Venus orbiter
[NASA-CR-197492] p 923 N95-17403
Radiation electrodynamics of the photo-electron cloud produced by an arbitrary photon pulse incident on a planar emitting surface in vacuum
[AD-A282153] p 759 N95-17450
Nonstationary theory of mode competition in gyrotrons with allowance for inhomogeneity of the guiding magnetic field
[PB94-197621] p 869 N95-17467
Test results of superconducting AC magnets for magnetic refrigeration experiment
[DE94-018695] p 751 N95-17909
Field-induced minigap and transport with in-plane magnetic fields in double quantum wells
[DE94-018893] p 879 N95-17918
Thermal noise in biomagnetic measurements
[PB95-104360] p 869 N95-17930
MAGNETIC FLUX
Flux imaging of high temperature superconductor single crystals and Ag sheathed wires
[DE94-013874] p 897 N95-16408
Giant flux creep through the surface barriers and the irreversibility line in high T(sub c) superconductors
[DE94-013991] p 766 N95-16945
AC susceptibility and critical current in the organic superconductor (kappa)-(ET)2Cu(NCS)2
[DE94-013997] p 900 N95-16946
MAGNETIC LEVITATION VEHICLES
A model for assessment of dynamic interaction between magnetically levitated vehicles and their supporting guideways
[AD-A283088] p 781 N95-17335

MAGNETIC MATERIALS
Photon beam studies of magnetic materials
[PB95-104279] p 877 N95-17351
Test results of superconducting AC magnets for magnetic refrigeration experiment
[DE94-018695] p 751 N95-17909

MAGNETIC MEASUREMENT
Vector magnetometry and lightwave defect imaging sensor technologies for internal pipe inspection systems: Phase 1 and 2 feasibility study, conceptual design, and prototype development
[PB94-194198] p 783 N95-16870
Magnetometer-only attitude and rate determination for a gyro-less spacecraft p 694 N95-17546
Thermal noise in biomagnetic measurements
[PB95-104360] p 869 N95-17930

MAGNETIC MOMENTS
Analysis of magnetic field data from Pioneer Venus orbiter
[NASA-CR-197492] p 923 N95-17403

MAGNETIC PERMEABILITY
AC susceptibility and critical current in the organic superconductor (kappa)-(ET)2Cu(NCS)2
[DE94-013997] p 900 N95-16946

MAGNETIC PROPERTIES
Photon beam studies of magnetic materials
[PB95-104279] p 877 N95-17351

MAGNETIC RELAXATION
Muon(+) SR studies of magnetic properties of boron carbide superconductors
[DE94-014440] p 868 N95-16288
Giant flux creep through the surface barriers and the irreversibility line in high T(sub c) superconductors
[DE94-013991] p 766 N95-16945

MAGNETIC RESONANCE
Simulation of arthroscopic surgery using MRI data
p 823 N95-15975
Magnetic Resonance Imaging (MRI) of skeletal muscles in astronauts after 9 days of space flight
p 810 N95-16749

MAGNETIC STORMS
Radiation belt dynamic and quasi-static modeling based on CRRES data
[AD-A285282] p 916 N95-16600
Verification of NOAA Space Environment Laboratory forecasts, 1 January - 31 December 1993
[PB95-104162] p 803 N95-17927

MAGNETIC SUSPENSION
A model for assessment of dynamic interaction between magnetically levitated vehicles and their supporting guideways
[AD-A283088] p 781 N95-17335

MAGNETIC TAPES
NSSDC data listing
[NASA-TM-109986] p 909 N95-16441

MAGNETIC TRANSDUCERS
Magnetostrictive transducer system having a three dual-strip fiber optic magnetostrictive transducers bonded into a single fiber Mach-Zehnder interferometer
[AD-D016373] p 775 N95-17428

MAGNETO-OPTICS
Optical wheel-rotation sensor
[DE94-011719] p 780 N95-16224

MAGNETOHYDRODYNAMIC GENERATORS
Determination of the nuclear-induced electrical conductivity in a nuclear-driven MHD device
[DE94-013137] p 891 N95-17365

MAGNETOHYDRODYNAMIC STABILITY
Kinetic effects near the magnetopause
[DE94-009333] p 799 N95-16927
Electron-neutrino phase separation instability
[DE94-016859] p 904 N95-17645

MAGNETOHYDRODYNAMIC WAVES
Investigation of the effect of Alfven resonance absorption on fast wave current drive in ITER
[PB95-104352] p 894 N95-17929

MAGNETOHYDRODYNAMICS
Determination of the nuclear-induced electrical conductivity in a nuclear-driven MHD device
[DE94-013137] p 891 N95-17365

MAGNETOMETERS
NASA Marshall Space Flight Center Solar Observatory report, March - May 1994
[NASA-TM-108471] p 915 N95-16558
Magnetometer-only attitude and rate determination for a gyro-less spacecraft p 694 N95-17546

MAGNETOPAUSE
Geosynchronous orbit magnetopause crossings
[DE94-014817] p 798 N95-16537
Kinetic effects near the magnetopause
[DE94-009333] p 799 N95-16927

MAGNETOSHEATH
Kinetic effects near the magnetopause
[DE94-009333] p 799 N95-16927
Analysis of magnetic field data from Pioneer Venus orbiter
[NASA-CR-197492] p 923 N95-17403

MAGNETOSPHERES
Analysis of plasma measurements for the Geotail mission
[NASA-CR-197020] p 888 N95-15941
Solar flares and magnetospheric particles: Investigations based upon the ONR-602 and ONR-604 experiments
[AD-A281463] p 923 N95-16080

MAGNETOSPHERIC INSTABILITY
Geosynchronous orbit magnetopause crossings
[DE94-014817] p 798 N95-16537

MAGNETOSTRICTION
Magnetostrictive torque sensor
[AD-D016376] p 775 N95-17376
Magnetostrictive transducer system having a three dual-strip fiber optic magnetostrictive transducers bonded into a single fiber Mach-Zehnder interferometer
[AD-D016373] p 775 N95-17428

MAGNETRON SPUTTERING
Coatings for large-area low-cost solar concentrators and reflectors
[DE94-015735] p 793 N95-16916

MAGNETRONS
Slow wave vane structure with elliptical cross-section slots, an analysis
[NASA-CR-195352] p 755 N95-16886

MAGNETS
Critical and paramagnetic spin dynamics in an antiferromagnetically coupled Heisenberg magnet: Results for RbMnF3
[PB95-104329] p 869 N95-17731
Time-dependent spin correlations in the heisenberg magnet at infinite temperature
[PB95-104303] p 869 N95-17750
Beam position correction in the Fermilab Linac
[DE94-018984] p 882 N95-17931

MAGNIFICATION
Numerical aperture limits on efficient ball lens coupling of laser diodes to single-mode fibers with defocus to balance spherical aberration
[NASA-TM-4578] p 886 N95-17271

MAGNONS
Critical and paramagnetic spin dynamics in an antiferromagnetically coupled Heisenberg magnet: Results for RbMnF3
[PB95-104329] p 869 N95-17731

MAIN SEQUENCE STARS
The Mg 2 lines as diagnostic of PMS nature in Herbig Ae/Be stars
[NASA-CR-197518] p 915 N95-17494

MAINTAINABILITY
Damage-mitigating control of space propulsion systems for high performance and extended life
[NASA-CR-194470] p 784 N95-16068

MAINTENANCE
The assessment of the AH-64D, longbow, mast-mounted assembly noise hazard for maintenance personnel
[AD-A284971] p 869 N95-16226
Identification of Artificial Intelligence (AI) applications for maintenance, monitoring, and control of airway facilities
[AD-A282479] p 665 N95-17373
XMM instrument on-board software maintenance concept p 699 N95-17567

MALES
An annotated bibliography of heat tolerance: Regarding gender differences
[AD-A280755] p 818 N95-16105
Comparison of saline and fludrocortisone as fluid-loading countermeasures following exposure to simulated microgravity p 808 N95-16742
Intramuscular pressure: A better tool than EMG to optimize exercise for long-duration space flight
p 809 N95-16744
Blood volume and orthostatic responses of men and women to a 13-day bedrest p 811 N95-16752
The effect of intermittent standing or walking during head down tilt bedrest on peak O2 consumption
p 817 N95-16779
The efficacy of periodic +Gz exposure in the prevention of bedrest induced orthostatic intolerance
p 817 N95-16781
Mental effects of caffeine in fatigued men and women
[PB94-190683] p 822 N95-17300

MAMMALS
Molecular approach to hypothalamic rhythms
[AD-A285164] p 822 N95-16851

MAN ENVIRONMENT INTERACTIONS
Simulations of the global carbon cycle and anthropogenic CO2 transient
[DE94-014165] p 795 N95-16212
South Florida environmental quality. National Status and Trends Program for marine environmental quality
[PB94-173408] p 796 N95-17363

MAN MACHINE SYSTEMS
Coordinated control of a dual-arm dexterous robot using full immersion telepresence and virtual reality
p 852 N95-15979
A highly functional decision paradigm based on nonlinear adaptive genetic algorithm
[AD-A281457] p 855 N95-16077
MAGENCO: A map generalization controller for Arc/Info
[DE94-013440] p 835 N95-16358
Towards a human operator model of the navigator
[PB94-197985] p 831 N95-17468
Industry review of a crew-centered cockpit design process and toolset
[AD-A282966] p 669 N95-17661
Aerospace medicine and biology: A continuing bibliography with indexes (supplement 396)
[NASA-SP-7011(396)] p 823 N95-17703

MANAGEMENT ANALYSIS
GEOTRANS geographic decision support system
[PB94-183670] p 908 N95-16093
Software Process Assessment (SPA)
p 699 N95-17569

MANAGEMENT INFORMATION SYSTEMS
Groupware system for multidisciplinary participation
[AD-A282525] p 850 N95-17374

MANAGEMENT METHODS
Situational awareness in complex systems
[AD-A281448] p 825 N95-15959
Alertness management in two-person long-haul flight operations p 813 N95-16760
Geostationary satellite positioning by DLR/GSOC operations and management methods
p 684 N95-17217
Groupware system for multidisciplinary participation
[AD-A282525] p 850 N95-17374
Corrective software management: The success of the EPLRS program
[AD-A282430] p 841 N95-17460

MANAGEMENT PLANNING
Software cost and schedule estimating: A process improvement initiative
[AD-A280915] p 836 N95-16503
The SEI and NAWC: Working together to establish a software measurement program
[AD-A280916] p 836 N95-16504
Continual improvement: A bibliography with indexes, 1992-1993
[NASA-SP-7097(02)] p 905 N95-16633
Joint operations planning for space surveillance missions on the MSX satellite p 673 N95-17215
A model for analysis of TDA budget allocation
p 758 N95-17295
Corrective software management: The success of the EPLRS program
[AD-A282430] p 841 N95-17460
Proceedings of the First National Conference on Climate Change and Water Resources Management
[AD-A281172] p 796 N95-17684

MANAGEMENT SYSTEMS
Automation support for concurrent software engineering
[AD-A281372] p 834 N95-16153
An engineering code to analyze hypersonic thermal management systems p 715 N95-16322
Computer tools for systems engineering at LaRC
p 848 N95-16472
Third International Symposium on Space Mission Operations and Ground Data Systems, part 1
[NASA-CP-3281-PT-1] p 676 N95-17179
Payload operations management of a planned European SL-Mission employing establishments of ESA and national agencies p 684 N95-17221
SPOT4 Management Centre p 673 N95-17223
Mission operations management p 685 N95-17225
Towards a new generation of mission planning systems: Flexibility and performance p 686 N95-17230
Re-engineering NASA's space communications to remain viable in a constrained fiscal environment
p 702 N95-17585
Packet utilisation definitions for the ESA XMM mission
p 704 N95-17596
Mission Operations Centers (MOCs): Integrating key spacecraft ground data system components
p 675 N95-17601
Overview of space power electronic's technology under the CSTI High Capacity Power Program
[NASA-TM-110110] p 883 N95-17933

MANGANESE ALLOYS
Critical and paramagnetic spin dynamics in an antiferromagnetically coupled Heisenberg magnet: Results for RbMnF3
[PB95-104329] p 869 N95-17731

MANGANESE COMPOUNDS
Aluminum permanganate battery
[AD-D016337] p 766 N95-16947

MANIFOLDS (MATHEMATICS)
Coarse geometry of foliations
[PB94-192309] p 860 N95-16291
Quasiconformal mappings, operators on Hilbert space, and local formulae for characteristic classes
[PB94-192366] p 860 N95-16293
Some fundamental techniques in the theory of integrable systems
[PB94-192390] p 860 N95-16294
MANIPULATORS
Physics-based approach to haptic display
p 854 N95-15986
Bracing micro/macro manipulators control
[DE94-014434] p 856 N95-16287
Simulation of the coupled multi-spacecraft control testbed at the Marshall Space Flight Center
p 849 N95-16475
Repeatability in redundant manipulator systems
[AD-A282957] p 782 N95-17621
Optimal trajectories for flexible-link manipulator slewing using recursive quadratic programming: Experimental verification
[DE94-018741] p 858 N95-17915
MANNED MARS MISSIONS
Catalog of lunar and Mars science payloads
[NASA-RP-1345] p 922 N95-16436
Physiological constraints on deceleration during the aerocapture of manned vehicles p 810 N95-16751
Medicine on Mars: Remote medical care and the space exploration initiative p 816 N95-16777
MANNED SPACE FLIGHT
Virtual environment application with partial gravity simulation p 854 N95-15988
Activities of the Space Studies Board
[NASA-CR-197105] p 672 N95-16033
A mission planning concept and mission planning system for future manned space missions p 687 N95-17235
MANPOWER
Estimating the benefits of personnel selection and classification: An extension of the Brogden table
[AD-A285674] p 828 N95-17175
MANUFACTURING
System design and operation of a 100 kilovolt, 2 kilohertz pulse modulator for plasma source ion implantation
[DE94-014424] p 889 N95-16285
Filament overwrapped motor case technology
p 720 N95-16350
Development and fabrication of the fiber optic MicroCable (tm)
[AD-A285266] p 886 N95-16815
A new manufacturing method for the formation of gated field emission structures
[DE94-015287] p 764 N95-16832
MANY BODY PROBLEM
Real-time simulation of large-scale multibody systems using automated equation decoupling techniques
[AD-A281544] p 856 N95-16390
MAPS
GEOTRANS geographic decision support system
[PB94-183670] p 908 N95-16093
Analysis of compression techniques for Common Mapping Standard (CMS) raster data
[AD-A283396] p 791 N95-17625
MARINE BIOLOGY
The Fifth International Congress on the History of Oceanography
[AD-A281507] p 805 N95-16168
MARINE CHEMISTRY
Three-dimensional eutrophication model of Chesapeake Bay. Volume 1: Main report
[AD-A280760] p 804 N95-16118
MARINE ENVIRONMENTS
South Florida environmental quality. National Status and Trends Program for marine environmental quality
[PB94-173408] p 796 N95-17363
Flow over abrupt topography: The application of patterns in nutrient and productivity in reflecting physical processes
[AD-A280813] p 797 N95-17740
MARINE METEOROLOGY
Mixed-layer hindcasts conducted at OWS Victor with initialization from synthetic profiles/mixed-layer hindcasts conducted with BTs taken during 1990 with atmospheric forcing from NOGAPS
[AD-A284749] p 800 N95-16551
Impact of physical processes on maritime frontogenesis
[AD-A283105] p 801 N95-17339
Propagation in the evaporation duct. Model predictions and comparisons to data
[AD-A283012] p 803 N95-17709
MARINE PROPULSION
Simulation investigation on system identification of gas turbine
[PB95-104238] p 670 N95-17749
MARKARIAN GALAXIES
Very high gamma ray extension of GRO observations
[NASA-CR-197489] p 924 N95-17421
MARKERS
The value of the 4-day headdown bedrest model for screening countermeasures p 817 N95-16782
Kinetics and mechanism of chemical marker formation and water-activated heat generation
[AD-A281407] p 731 N95-17425
MARKET RESEARCH
Optoelectric technology roadmap: Conclusions and recommendations
[AD-A281664] p 886 N95-16965
MARKETING
Applied virtual reality at the Research Triangle Institute p 851 N95-15974
An applications-oriented approach to the development of virtual environments p 853 N95-15980
From computer images to video presentation: Enhancing technology transfer p 848 N95-16467
MARKOV CHAINS
Likelihood ratio gradient estimation for stochastic recursions
[AD-A281408] p 865 N95-17426
MARKOV PROCESSES
A Lyapunov bound for solutions of Poisson's equation
[AD-A281536] p 860 N95-16169
Hidden Markov model for gesture recognition
[AD-A282845] p 865 N95-17377
Hidden Markov model for control strategy learning
[AD-A282846] p 865 N95-17429
MARS (PLANET)
Exobiology site priorities for Mars Pathfinder
p 919 N95-16188
Pathfinder landing sites at candidate SNC impact ejection sites p 919 N95-16190
Observations by the Mars 1994 orbiter and possible correlations with Mars Pathfinder p 920 N95-16192
Potential landing sites for Mars Pathfinder
p 920 N95-16193
A perspective of landing-site selection
p 920 N95-16194
Tartarus Colles: A sampling of the Martian highlands
p 920 N95-16195
Scientific rationale for selecting northern Eumenides Dorsum (9 deg - 11 deg N latitude, 159 deg - 162 deg longitude) as a potential Mars Pathfinder landing site
p 920 N95-16196
MARS ATMOSPHERE
Meteorological observations of synoptic disturbances: Sensitivity to latitude p 917 N95-16179
Mars Pathfinder meteorological observations on the basis of results of an atmospheric global circulation model p 919 N95-16189
Atmosphere structure and meteorology instrument for Mars Pathfinder p 711 N95-16202
Landing site considerations for atmosphere structure and meteorology p 921 N95-16203
Mars Pathfinder mission operations concepts
p 686 N95-17229
MARS EXPLORATION
Using virtual reality for science mission planning: A Mars Pathfinder case p 673 N95-15978
Mars Pathfinder Landing Site Workshop
[NASA-CR-196745] p 917 N95-16176
Mars Pathfinder and the exploration of southern Amazonis Planitia p 917 N95-16178
Rationale for a Mars Pathfinder mission to Chryse Planitia and the Viking 1 lander p 918 N95-16183
Chryse Planitia as a Mars Pathfinder landing site: The imperative of building on previous ground truth
p 918 N95-16185
A highland sample strategy for Pathfinder
p 918 N95-16186
Catalog of lunar and Mars science payloads
[NASA-RP-1345] p 922 N95-16436
Medicine on Mars: Remote medical care and the space exploration initiative p 816 N95-16777
MARS LANDING
Mars Pathfinder Landing Site Workshop
[NASA-CR-196745] p 917 N95-16176
Sampling Elysium lavas (13 deg N, 203 deg W)
p 917 N95-16177
Mars Pathfinder and the exploration of southern Amazonis Planitia p 917 N95-16178
Implications of high-spatial-resolution thermal infrared (Termoskan) data for Mars landing site selection
p 918 N95-16180
A Mars Pathfinder landing on a recently drained ephemeral sea: Cerberus Plains, 6 deg N, 188 deg W
p 918 N95-16181
Physical properties (particle size, rock abundance) from thermal infrared remote observations: Implications for Mars landing sites p 918 N95-16182
Rationale for a Mars Pathfinder mission to Chryse Planitia and the Viking 1 lander p 918 N95-16183
Rationale for Isidis Planitia as a back-up landing site for the Mars Pathfinder mission p 918 N95-16184
Chryse Planitia as a Mars Pathfinder landing site: The imperative of building on previous ground truth
p 918 N95-16185
A highland sample strategy for Pathfinder
p 918 N95-16186
Opportunity to sample something different: The dark, unweathered, mafic sands of Cerberus and the Pathfinder 1997 Mars landing p 919 N95-16187
Strategy for selecting Mars Pathfinder landing sites
p 919 N95-16191
Potential landing sites for Mars Pathfinder
p 920 N95-16193
Scientific rationale for selecting northern Eumenides Dorsum (9 deg - 11 deg N latitude, 159 deg - 162 deg longitude) as a potential Mars Pathfinder landing site
p 920 N95-16196
Scientific rationale for selecting northwest Isidis Planitia (14 deg - 17 deg N latitude, 278 deg - 281 deg longitude) as a potential Mars Pathfinder landing site
p 920 N95-16197
Goldstone radar contributions to Mars Pathfinder landing safety p 921 N95-16205
Melas Chasma: A Mars Pathfinder view of Valles Marineris p 922 N95-16207
MARS OBSERVER
Increases in efficiency and enhancements to the Mars Observer non-stored commanding process
p 688 N95-17242
Mission operations data analysis tools for Mars Observer guidance and control p 689 N95-17244
Customizing the JPL Multimission Ground Data System: Lessons learned p 703 N95-17588
MARS PHOTOGRAPHS
Observations by the Mars 1994 orbiter and possible correlations with Mars Pathfinder p 920 N95-16192
A perspective of landing-site selection
p 920 N95-16194
MARS PROBES
Mars Pathfinder Landing Site Workshop
[NASA-CR-196745] p 917 N95-16176
Atmosphere structure and meteorology instrument for Mars Pathfinder p 711 N95-16202
MARS SURFACE
Using virtual reality for science mission planning: A Mars Pathfinder case p 673 N95-15978
Virtual environment application with partial gravity simulation p 854 N95-15988
Mars Pathfinder Landing Site Workshop
[NASA-CR-196745] p 917 N95-16176
Mars Pathfinder and the exploration of southern Amazonis Planitia p 917 N95-16178
A Mars Pathfinder landing on a recently drained ephemeral sea: Cerberus Plains, 6 deg N, 188 deg W
p 918 N95-16181
Physical properties (particle size, rock abundance) from thermal infrared remote observations: Implications for Mars landing sites p 918 N95-16182
Rationale for a Mars Pathfinder mission to Chryse Planitia and the Viking 1 lander p 918 N95-16183
Rationale for Isidis Planitia as a back-up landing site for the Mars Pathfinder mission p 918 N95-16184
Chryse Planitia as a Mars Pathfinder landing site: The imperative of building on previous ground truth
p 918 N95-16185
A highland sample strategy for Pathfinder
p 918 N95-16186
Opportunity to sample something different: The dark, unweathered, mafic sands of Cerberus and the Pathfinder 1997 Mars landing p 919 N95-16187
Exobiology site priorities for Mars Pathfinder
p 919 N95-16188
Pathfinder landing sites at candidate SNC impact ejection sites p 919 N95-16190
Strategy for selecting Mars Pathfinder landing sites
p 919 N95-16191
Observations by the Mars 1994 orbiter and possible correlations with Mars Pathfinder p 920 N95-16192
Potential landing sites for Mars Pathfinder
p 920 N95-16193
A perspective of landing-site selection
p 920 N95-16194
Tartarus Colles: A sampling of the Martian highlands
p 920 N95-16195
Scientific rationale for selecting northern Eumenides Dorsum (9 deg - 11 deg N latitude, 159 deg - 162 deg longitude) as a potential Mars Pathfinder landing site
p 920 N95-16196
Scientific rationale for selecting northwest Isidis Planitia (14 deg - 17 deg N latitude, 278 deg - 281 deg longitude) as a potential Mars Pathfinder landing site
p 920 N95-16197
Cerberus Plains: A most excellent Pathfinder landing site p 921 N95-16198

Maja Valley and the Chryse outflow complex sites
p 921 N95-16199
Marte Valles site p 921 N95-16200
Melas Chasma: A Mars Pathfinder view of Valles Marineris p 922 N95-16207
Climatological targets for Mars Pathfinder
p 922 N95-16208

MARS SURFACE SAMPLES
Opportunity to sample something different: The dark, unweathered, mafic sands of Cerberus and the Pathfinder 1997 Mars landing p 919 N95-16187
Pathfinder landing sites at candidate SNC impact ejection sites p 919 N95-16190
Strategy for selecting Mars Pathfinder landing sites
p 919 N95-16191
Evaluation of a pneumatic Martian soil sampler concept
[NASA-CR-197539] p 923 N95-17653

MARS VOLCANOES
Cerberus Plains: A most excellent Pathfinder landing site p 921 N95-16198

MARTENSITIC STAINLESS STEELS
Mixed-mode I/III fracture toughness of a ferritic/martensitic stainless steel
[DE94-014492] p 736 N95-17159

MASS
Micro-UltraViolet Spectrograph (Micro-UVS)
[DE94-016704] p 732 N95-17642

MASS DISTRIBUTION
Use of the electronic balance for highly accurate direct mass measurements without the use of external mass standards
[PB94-187713] p 774 N95-16074
The effect of brush polydispersity on the interphase between end-grafted brushed and polymeric matrices
[AD-A280975] p 743 N95-16507
The mass and dynamics of cD clusters with cooling flows. 1: ROSAT observations of A 496
[NASA-CR-197534] p 915 N95-17495

MASS SPECTRA
CP violation measurements in neutral kaon system at Fermilab
[DE94-016526] p 873 N95-16402
Mass spectral data of alkyl and cycloalkyl methylphosphonofluoridates
[AD-A285312] p 722 N95-16734
Mass spectrometry studies of the ionization of organic molecules by slow positrons
[DE94-013838] p 876 N95-16959

MASS SPECTROSCOPY
Novel mass spectrometric instrument for gaseous and particulate characterization and monitoring
[DE94-014168] p 795 N95-16213
Elemental impurity analysis of mercuric iodide by ICP/MS
[DE94-013553] p 896 N95-16359
Methods development toward the measurement of polyaromatic hydrocarbon-DNA adducts by mass spectrometry
[PB94-182722] p 727 N95-16373
Mass spectrometry studies of the ionization of organic molecules by slow positrons
[DE94-013838] p 876 N95-16959

MASS TRANSFER
Design, analysis, and fabrication of oxide-coated iridium/rhenium combustion chambers
p 719 N95-16347

MASSIVELY PARALLEL PROCESSORS
Portable parallel stochastic optimization for the design of aeropropulsion components
[NASA-CR-195312] p 785 N95-16072
Visualization of unsteady computational fluid dynamics
[NASA-CR-197461] p 770 N95-16388
Active messages versus explicit message passing under SUNMOS
[DE94-015278] p 850 N95-16830
Applications of massively parallel computers in telemetry processing p 680 N95-17201

MATCHED FILTERS
System design, implementation, and evaluation of the optical broadband correlator
[AD-A285406] p 884 N95-16296

MATERIAL BALANCE
Use of the electronic balance for highly accurate direct mass measurements without the use of external mass standards
[PB94-187713] p 774 N95-16074

MATERIALS TESTS
Materials characterization and design for solar-thermal propulsion p 718 N95-16340
Design, analysis, and fabrication of oxide-coated iridium/rhenium combustion chambers
p 719 N95-16347

MATHEMATICAL LOGIC
A general method to determine invariants
[TR-503] p 859 N95-15949
On the structure of log-space probabilistic complexity classes
[TR-506] p 864 N95-16039
The complexity of PDL with interleaving
[AD-A281044] p 836 N95-16452
Epistemology, software engineering and formal methods p 843 N95-16480
Open architectures for formal reasoning and deductive technologies for software development
[NASA-CR-197528] p 837 N95-16586

MATHEMATICAL MODELS
Radiative interactions in chemically reacting compressible nozzle flows using Monte Carlo simulations
[NASA-CR-197133] p 769 N95-15966
Parametric study of shock-induced combustion in a hydrogen air system
[NASA-CR-197134] p 726 N95-15967
Marine boundary-layer parameterizations for large-scale models
[AD-A282402] p 803 N95-16062
Experimental and numerical analysis of floating ice beam impact forces against a sloped structure
[AD-A280752] p 804 N95-16103
Three-dimensional eutrophication model of Chesapeake Bay. Volume 1: Main report
[AD-A280760] p 804 N95-16118
Rough surface models implemented within the split-step parabolic equation algorithm
[AD-A280843] p 753 N95-16148
Simulations of the global carbon cycle and anthropogenic CO2 transient
[DE94-014165] p 795 N95-16212
Mechanical effects in cookoff modeling
[DE94-014174] p 748 N95-16214
An improved neutral wind model with predictive capabilities
[AD-A282283] p 800 N95-16235
ARCJET plasma modeling with experimental validation
[AD-A285234] p 889 N95-16243
Considerations in the experimental determination of constitutive parameters for finite strain plasticity
[AD-A285410] p 785 N95-16245
Joint Proceedings on Aeronautics and Astronautics (JPAA)
[ISBN-7-80-046602-7] p 649 N95-16249
An investigation of polynomial calibrations methods for wind tunnel balances p 650 N95-16258
A super-element simplified analysis for vibration systems of complex structures p 650 N95-16260
Researches on gear fault diagnosis techniques
p 651 N95-16267
Theory of one-dimensional and two-dimensional distributed sensors for measuring the spatial characteristics of thermophysical and hydrodynamic fields p 652 N95-16273
Bracing micro/macro manipulators control
[DE94-014434] p 856 N95-16287
Conceptual design study of a solar concentrator/support structure: A three dimensional finite element model
p 718 N95-16342
Evaluation of the dynamic stability characteristics of the NAL Light Transport Aircraft
[NAL-PD-CA-9217] p 671 N95-16392
US-Russian Workshop on Computer Synthesis of Structure and Properties of Advanced Composites
[AD-A281647] p 723 N95-16397
Sensitivity analysis of numerically-simulated convective storms using direct and adjoint methods
[DE94-013399] p 800 N95-16398
Modeling of wall-bounded complex flows and free shear flows
[NASA-TM-106513] p 770 N95-16407
A software tool for dataflow graph scheduling
p 843 N95-16457
Experimental study of spatially incomplete structural system identification
[AD-A280905] p 785 N95-16502
The GOMS family of analysis techniques: Tools for design and evaluation
[AD-A285211] p 827 N95-16518
Measurement of residual flexibility for substructures having prominent flexible interfaces
[NASA-TM-110074] p 786 N95-16577
Numerical simulation of helicopter engine plume in forward flight
[NASA-CR-197488] p 655 N95-16589
Long term modelling of permafrost dynamics
[AD-A285315] p 799 N95-16735
The effect of differences in time to detection of circulating microbubbles on the risk of decompression sickness p 807 N95-16738
A new model for estimating total body water from bioelectrical resistance p 810 N95-16747
Structural integrity of intelligent materials and structures. Constitutive modeling of shape memory alloys
[AD-A281301] p 735 N95-16786
Least squares computations in science and engineering
[AD-A281213] p 862 N95-16798
Thermo-fluid mechanic study of thermoacoustic devices
[AD-A281130] p 870 N95-16810
Models to estimate high frequency acoustic scattering due to thermal fine- and micro-structure of the ocean
[AD-A285456] p 870 N95-16812
On bi-grid local mode analysis of solution techniques for 3-D Euler and Navier-Stokes equations
[NASA-TM-106749] p 771 N95-16855
Slow wave vane structure with elliptical cross-section slots, an analysis
[NASA-CR-195352] p 755 N95-16886
Algorithms for bilevel optimization
[NASA-CR-194980] p 863 N95-16897
Constrained minimization of smooth functions using a genetic algorithm
[NASA-TP-3329] p 709 N95-16902
Modeling of chemical vapor infiltration for composite fabrication
[DE93-001715] p 724 N95-16926
Combination of power electronic models with the two-dimensional finite element analysis of electrical machines
[PB94-197720] p 766 N95-16951
Asymptotic behavior in grain growth
[DE94-014452] p 900 N95-17156
A new approach to validate subgrid models in complex high Reynolds number flows
[AD-A282340] p 772 N95-17165
Data rearrangement and real-time computation
[AD-A282349] p 910 N95-17166
Correlation of finite element free vibration predictions using random vibration test data
[NASA-TM-106787] p 787 N95-17258
A preliminary optical visibility model
p 758 N95-17290
Computation of reflected and transmitted horn radiation patterns for a dichroic plate p 758 N95-17293
International Space Station Alpha (ISSA) Integrated Traffic Model
[NASA-CR-197566] p 710 N95-17331
A model for assessment of dynamic interaction between magnetically levitated vehicles and their supporting guideways
[AD-A283088] p 781 N95-17335
An analysis of smoothed particle hydrodynamics
[DE94-013817] p 788 N95-17439
Erosion effects on TVC vane heat transfer characteristics
[AD-A282006] p 721 N95-17448
Evaluation of an autopilot based multimodelling
[PB94-190725] p 671 N95-17454
Back-propagation neural networks in adaptive control of unknown nonlinear systems
[AD-A282414] p 858 N95-17458
Nonstationary theory of mode competition in gyrotrons with allowance for inhomogeneity of the guiding magnetic field
[PB94-197621] p 869 N95-17467
Towards a human operator model of the navigator
[PB94-197985] p 831 N95-17468
Frequency domain analysis for nonlinear electronic circuits
[PB94-201365] p 767 N95-17469
Small sample behavior of multi-layer feedforward network classifiers: Theoretical and practical aspects
[PB94-201415] p 841 N95-17470
Grey-scale measurements in multi-dimensional digitized images
[PB94-195492] p 887 N95-17483
The Grid Analysis and Display System (GrADS)
[NASA-CR-189387] p 912 N95-17491
Demonstration of the Dynamic Flowgraph Methodology using the Titan 2 Space Launch Vehicle Digital Flight Control System
[NASA-CR-197517] p 675 N95-17493
Thermal effects in end-heated laser rods: A time-dependent model and diagnostic
[AD-A282007] p 778 N95-17500
Modelling daily precipitation as a function of temperature for climate change impact studies
[KNMI-WR-93-02] p 802 N95-17529
Calorimetric methods for loss measurements of small cage induction motors
[PB94-184439] p 768 N95-17691
Structural optimization with approximate sensitivities
[NASA-TM-4553] p 789 N95-17701
Multi-dimensional shock capturing
[AD-A282986] p 773 N95-17708

The solvation thermodynamic functions in the Mean Spherical Approximation (MSA): Behavior near the solvent critical region
[AD-A283040] p 904 N95-17712
Study of simulation in microgravity environment
[PB95-104261] p 750 N95-17730
Computer modeling of organic aerogels, 93-SR-062
[DE94-016485] p 722 N95-17745

MATHEMATICAL PROGRAMMING
Evolving neural network pattern classifiers
[AD-A281181] p 857 N95-16631
Error estimation and adaptive mesh refinement for parallel analysis of shell structures
[NASA-CR-197500] p 788 N95-17492

MATHIEU FUNCTION
Fields and waves in elliptic waveguides
[AD-A285337] p 755 N95-16816

MATRICES (MATHEMATICS)
Decreasing the bandwidth of a transition matrix
[TR-505] p 859 N95-15948
Solution of matrix equations using sparse techniques p 847 N95-16459
An analysis of spectral envelope-reduction via quadratic assignment problems
[NASA-CR-194992] p 862 N95-16596
Wavelets, signal processing and matrix computations
[AD-A283832] p 755 N95-16841
Transverse mode coupling instability with a double RF system
[DE94-017972] p 761 N95-17672
Crystalline beams: The vertical zigzag
[DE94-017986] p 901 N95-17673

MATRIX MATERIALS
Thermoplastic and thermosetting high glass transition temperature matrix resins
[AD-A281508] p 740 N95-16096
Chemical vapor infiltration of non-oxide ceramic matrix composites
[DE94-017770] p 723 N95-16225
Life prediction for bridged fatigue cracks
[DE94-016000] p 724 N95-16930
Research and development of material/processing methods for the Continuous Fiber Ceramic Composites Program
[DE94-018569] p 725 N95-17905

MATRIX METHODS
Solution of matrix equations using sparse techniques p 847 N95-16459

MATTER (PHYSICS)
A-dependent effects in high P(sub T) reactions
[DE94-016385] p 875 N95-16924
Baryogenesis and standard model CP violation
[DE94-017935] p 877 N95-17669

MAXIMA
Nonasymptotic formulae for the distribution of the maximum of smooth Gaussian processes
[AD-A284741] p 865 N95-16546

MAXIMUM ENTROPY METHOD
Researches on gear fault diagnosis techniques p 651 N95-16267

MAXIMUM LIKELIHOOD ESTIMATES
Closed-loop carrier phase synchronization techniques motivated by likelihood functions p 756 N95-17284

MAXWELL EQUATION
Ultrashort pulse effects in semiconductor amplifiers and in dispersive media
[AD-A284925] p 763 N95-16137
Combination of power electronic models with the two-dimensional finite element analysis of electrical machines
[PB94-197720] p 766 N95-16951

MEAN SQUARE VALUES
Closed-loop carrier phase synchronization techniques motivated by likelihood functions p 756 N95-17284

MEASURE AND INTEGRATION
Numeric data distribution: The vital role of data exchange in today's world p 907 N95-15937

MEASURING INSTRUMENTS
Z(prime) phenomenology: Constraints from low-energy measurements, and detailed study at TeV-scale lepton and hadron colliders
[DE94-018185] p 881 N95-17886

MECHANICAL MEASUREMENT
Magnetostrictive torque sensor
[AD-D016376] p 775 N95-17376

MECHANICAL PROPERTIES
Guide to ASIAC computer programs
[AD-A285354] p 784 N95-15953
Development of the vibration test equipment for testing the products of aircraft and space technology with simulation of operating conditions p 651 N95-16266
Materials characterization and design for solar-thermal propulsion p 718 N95-16340
US-Russian Workshop on Computer Synthesis of Structure and Properties of Advanced Composites
[AD-A281647] p 723 N95-16397
Phase transformations, ultrastructure and properties of rigid-rod fibers
[AD-A285249] p 749 N95-16512
Processing - property relationship in advanced intermetallics
[AD-A285262] p 735 N95-16514
Studies on improvement of oxidation resistivity of carbon materials by glass impregnation and SiC formation
[DE94-796529] p 724 N95-16833
Graphite-reinforced polycyanate composites for space and missile applications
[AD-A285509] p 725 N95-16970
The influence of tungsten alloying on the mechanical properties of tantalum
[DE94-010071] p 736 N95-17378
Computer studies of the dynamic strength of ceramics
[DE94-010890] p 745 N95-17379
Selected properties of iron aluminides
[DE94-018057] p 738 N95-17726

MEDICAL EQUIPMENT
Cell culture and transplantation of the suprachiasmatic circadian pacemaker
[AD-A280977] p 821 N95-16481
Review of performance, medical, and operational data on pilot aging issues p 812 N95-16759
A prototype Crew Medical Restraint System (CMRS) for Space Station Freedom p 815 N95-16773
Medicine on Mars: Remote medical care and the space exploration initiative p 816 N95-16777

MEDICAL PERSONNEL
Advanced Cardiac Life Support (ACLS) utilizing Man-Tended Capability (MTC) hardware onboard Space Station Freedom p 816 N95-16775

MEDICAL SERVICES
Aerospace Medical Association 63rd Annual Scienti fic Meeting Program p 807 N95-16737
Medical care capabilities for Space Station Freedom: A phase approach p 710 N95-16772
A prototype Crew Medical Restraint System (CMRS) for Space Station Freedom p 815 N95-16773
A surgical support system for Space Station Freedom p 710 N95-16776
Medicine on Mars: Remote medical care and the space exploration initiative p 816 N95-16777

MEDITERRANEAN SEA
Propagation in the evaporation duct. Model predictions and comparisons to data
[AD-A283012] p 803 N95-17709

MELTING
Studies by neutron diffraction and muon SR of flux lattice orientation, pinning, melting and decomposition in high-T(sub c) superconductors
[DE94-017704] p 901 N95-17667

MEMBRANES
Anionically-conductive ultrathin film composite membranes
[AD-A284944] p 723 N95-16041
Characterization of neurotrophic and neurotropic interactions between neurons and their muscle and nerve targets
[AD-A281846] p 820 N95-16423
Electrochemical synthesis of ultrathin film composite membranes
[AD-A285075] p 724 N95-16492
Fundamental studies in oxidation-reduction in relation to water photolysis
[DE94-014598] p 731 N95-17161
Morphology and dynamics of membrane systems
[PB94-184660] p 745 N95-17299

MEMORY
Presentations of shape in object recognition and long-term visual memory
[AD-A281336] p 825 N95-16010
Synaptic plasticity and memory formation
[AD-A284926] p 825 N95-16138
The 1994 International Neural Network Society Annual Meeting, volume 4
[AD-A281737] p 857 N95-17370

MEMORY (COMPUTERS)
A VLSI interface for the NM24CF04 serial-access ferroelectric memory
[AD-A281535] p 762 N95-16110
Software cache coherence for large scale multiprocessors
[AD-A281628] p 845 N95-16113
Rapid solution of large-scale systems of equations p 847 N95-16458
Equation solvers for distributed-memory computers p 847 N95-16460
High Performance FORTRAN p 843 N95-16478
Proceedings of the International Conference on Parallel Architectures and Compilation Techniques
[AD-A285258] p 849 N95-16529
Active messages versus explicit message passing under SUNMOS
[DE94-015278] p 850 N95-16830
Investigation of modularly configured attached processors with intelligent memories
[AD-A285454] p 832 N95-16876
The PASS project
[DE94-016308] p 910 N95-16922
Trapezoidal rule quadrature algorithms for MIMD distributed memory computers
[DE94-016369] p 839 N95-16923
Data rearrangement and real-time computation
[AD-A282349] p 910 N95-17166
Reviews of computing technology: Software overview
[DE94-013662] p 841 N95-17515
Controlling memory access concurrency in efficient fault-tolerant parallel algorithms
[AD-A280909] p 851 N95-17741

MENTAL HEALTH
Results of the psychiatric, select-out evaluation of US astronaut applications p 813 N95-16761
Psychological training of NASA astronauts for extended missions p 813 N95-16763

MENTAL PERFORMANCE
Development of the OMPAT neuropsychological/psychomotor performance evaluation and OMPAT data and timing support programs
[AD-A284928] p 826 N95-16140
Event-related brain potentials as predictors of target detection performance in a moving waterfall display simulating passive broad-band sonar monitoring
[AD-A280900] p 819 N95-16152
Mental rotation with and without a concurrent task: Moderating effects of visuospatial ability
[AD-A281866] p 826 N95-16301
A framework for the analysis of cognitive tasks
[AD-A285345] p 828 N95-16835
Efficiency in work behaviour: A design approach for modern tools
[PB94-197761] p 831 N95-16953
Mental effects of caffeine in fatigued men and women
[PB94-190683] p 822 N95-17300
Situation awareness information requirements for En Route Air Traffic Control
[DOT/FAA/AM-94/27] p 828 N95-17655

MERCURY CADMIUM TELLURIDES
Modification of 2-6 and 3-5 materials using ion beams
[AD-A281839] p 896 N95-16365
Monte Carlo simulation of mercury cadmium telluride
[AD-A281546] p 896 N95-16391
Testing and characterization of the CYCLOPS HgCdTe focal plane detector array
[AD-A284279] p 887 N95-17489

MERCURY COMPOUNDS
Elemental impurity analysis of mercuric iodide by ICP/MS
[DE94-013553] p 896 N95-16359

MERGING ROUTINES
Software merge: Semantics of combining changes to programs
[AD-A281373] p 834 N95-16154

MERIDIONAL FLOW
An improved neutral wind model with predictive capabilities
[AD-A282283] p 800 N95-16235

MESOMETEOROLOGY
A three dimensional mesoscale atmospheric simulation system for use in various mobile battlefield environments. Phase 2: Transition to an operational forecast system
[AD-A281223] p 802 N95-17686

MESONS
Measurement of the B meson differential cross-sections in p(-p) collisions at the square root of s = 1.8 TeV using the exclusive decays B(+-) yields J/(psi)K(+-) and B(exp 0) yields J/(psi)K(exp *0)
[DE94-015185] p 872 N95-16309
Production asymmetries in x(sub F) and P(sub t)(exp 2) for D(+-) mesons
[DE94-015546] p 872 N95-16310
Measurement of the B(sub s) meson lifetime at CDF
[DE94-015381] p 875 N95-16868
Modeling mesons with relativistic wave equations
[DE94-016057] p 875 N95-16931
Progress at LAMPF
[DE94-016210] p 880 N95-16937
Limit on the rare decay B yields muon(+)muon(-) K(+-)
[DE94-013851] p 876 N95-16960
Strong WW scattering at photon linear colliders
[DE94-018183] p 878 N95-17720

MESOSCALE PHENOMENA
Marine boundary-layer parameterizations for large-scale models
[AD-A282402] p 803 N95-16062
Sensitivity study of the SPEM model to the assimilation of synop datasets using two assimilation schemes. 1: Nudging. 2: The Kalman filter/smoother
[AD-A281459] p 804 N95-16079

Objective feature identification and tracking: A review
[AD-A284955] p 804 N95-16125
A three dimensional mesoscale atmospheric simulation system for use in various mobile battlefield environments. Phase 2: Transition to an operational forecast system
[AD-A281223] p 802 N95-17686
Flow over abrupt topography: The application of patterns in nutrient and productivity in reflecting physical processes
[AD-A280813] p 797 N95-17740

MESOSPHERE
A latitudinal survey of middle atmospheric water vapor revealed by shipboard microwave spectroscopy
[AD-A282000] p 799 N95-17446
Equatorial airglow studies via rocket experiment
[INPE-5589-TDI/551] p 799 N95-17647

MESSAGE PROCESSING
Network interface specification for the T1 microprocessor
[AD-A283392] p 844 N95-15940
Re-engineering Nascom's network management architecture p 702 N95-17584

MESSAGES
Active messages versus explicit message passing under SUNMOS
[DE94-015278] p 850 N95-16830

METAL BONDING
Characterization on defect solids
[NASA-CR-197540] p 746 N95-17654

METAL CLUSTERS
The chemistry and physics of transition metal clusters
[DE94-014012] p 734 N95-16364

METAL CUTTING
Approach to in-process tool wear monitoring in drilling: Application of Kalman filter theory p 653 N95-16279

METAL FATIGUE
The mechanical property data base from an Air Force/industry cooperative test program on high temperature aluminum alloys
[AD-A282911] p 737 N95-17398

METAL FILMS
Electron transport and tunneling experiments
[AD-A281527] p 894 N95-16106
In-situ x-ray characterization of the electrolyte-solid interface
[AD-A281165] p 729 N95-16627
Underpotential deposition of Cu on Au(111): Implications of the HB model
[AD-A283028] p 902 N95-17711

METAL FOAMS
Solar-powered rocket engine optimization for high specific impulse p 718 N95-16341

METAL HYDRIDES
Nickel hydrogen batteries: An overview
[NASA-TM-106795] p 793 N95-16861

METAL IONS
Ligand field stabilization control of metal ion binding
[AD-A281011] p 726 N95-16001
Encapsulated alkaline-earth organometallics as controlled sources of calcium, strontium, and barium ions
[AD-A281547] p 741 N95-16393
Electrochemical properties of lithium ion conducting solid polymer electrolytes
[AD-A281875] p 742 N95-16434
Effects of substrate temperature on metal colloid formation and on optical response in metal ion implanted silica
[DE94-013633] p 736 N95-16807
Possible superstructures of metallic ions in nonstoichiometric fullerites M(x) C(60)
[DE94-622052] p 901 N95-17518
Rare earth ion doped CW cascade fiber laser
[AD-D016370] p 779 N95-17698

METAL MATRIX COMPOSITES
Micromechanics of interfaces in metal matrix composites
[AD-A282404] p 725 N95-17457
Theoretical studies of the strengths of matrix second phase particle interfaces
[AD-A280703] p 738 N95-17681

METAL OXIDE SEMICONDUCTORS
Reliability implications of defects in high temperature annealed Si/SiO2/Si structures
[DE94-015765] p 895 N95-16311

METAL OXIDES
Design, analysis, and fabrication of oxide-coated iridium/rhenium combustion chambers p 719 N95-16347

METAL PLATES
Microchannel formation in polyimide by heavy ion irradiation
[DE94-753315] p 740 N95-16073
Investigation of residual stresses in a multipass weld in 1 in. stainless steel plate
[DE94-013277] p 786 N95-16803
Analysis of the through-thickness micropore and constituent particle population gradients in the 7050-T7451 plate aluminum alloys
[AD-A282970] p 738 N95-17663

METAL POWDER
A preliminary attempt at sintering an ultrafine alumina powder using microwaves
[AD-A284978] p 734 N95-16229
Effect of extrusion parameters on consolidation of tungsten-hafnium and tungsten-steel powders
[DE94-013270] p 737 N95-17513
Use of copper powder extinguishers on lithium fires
[AD-A283213] p 751 N95-17632

METAL PROPELLANTS
Erosion effects on TVC vane heat transfer characteristics
[AD-A282006] p 721 N95-17448

METAL SURFACES
Resonant charge transfer in hyperthermal atomic and molecular ion-surface collisions
[AD-A281369] p 871 N95-16018
Effect of ion-electrode contact on the energetics of the heterogeneous electron transfer
[AD-A281959] p 873 N95-16411

METAL VAPOR LASERS
Beam characteristics of a large-bore copper laser with a radiatively cooled plasma
[DE94-015139] p 779 N95-17688

METAL VAPORS
Volatile CVD precursors based on copper alkoxides and mixed group IIA-copper alkoxides
[AD-D016380] p 732 N95-17479

METAL WORKING
Development of processes, means, and theoretical principles of thin-walled detail plastic forming at Kazan Aviation Institute p 653 N95-16281

METALLOGRAPHY
Effect of extrusion parameters on consolidation of tungsten-hafnium and tungsten-steel powders
[DE94-013270] p 737 N95-17513
Analysis of the through-thickness micropore and constituent particle population gradients in the 7050-T7451 plate aluminum alloys
[AD-A282970] p 738 N95-17663
Effect of heat treatment temperature on creep-rupture properties of Fe3Al-based alloys
[DE94-018054] p 738 N95-17679

METALORGANIC CHEMICAL VAPOR DEPOSITION
Synthesis of tungsten nitrene complexes as precursors for tungsten nitride
[AD-A281592] p 740 N95-16101
HTS SNS devices on large-area substrates by single-source MOCVD
[AD-A285159] p 899 N95-16849
Epitaxial MOCVD of thin film ceramics for pyroelectric detectors
[AD-A281397] p 744 N95-16863
Chemical vapor deposition of high T(sub c) superconducting films in a microgravity environment
[NASA-CR-197527] p 750 N95-16880

METALS
Bicarbonate of soda blasting technology for aircraft wheel depainting
[PB94-193323] p 654 N95-17466

METASTABLE STATE
Thermal dissociation of halogen azides
[AD-A285088] p 728 N95-16497
Metastability in molecules
[AD-A285223] p 874 N95-16523
Recombination and metastability in amorphous silicon and silicon-germanium alloys
[DE94-011837] p 794 N95-16957

METEORITE CRATERS
Application of NMR shock barometer to naturally shocked minerals
[DE95-000326] p 799 N95-17362

METEORITIC DAMAGE
Analysis of space environment damage to solar cell assemblies from LDEF experiment A0171-GSFC test plate
[NASA-CR-196523] p 793 N95-16575

METEOROLOGICAL PARAMETERS
Mars Pathfinder meteorological observations on the basis of results of an atmospheric global circulation model p 919 N95-16189
Availability of direct normal radiation for solar furnace processing: A case study
[DE94-006907] p 792 N95-16435
Meteorological Monitoring Program
[DE94-017810] p 795 N95-16557
Evaluation of current tropospheric mapping functions by Deep Space Network very long baseline interferometry p 756 N95-17280
Meteorological factors that affect the formation an prediction of aircraft icing
[AD-A281984] p 802 N95-17443
A three dimensional mesoscale atmospheric simulation system for use in various mobile battlefield environments. Phase 2: Transition to an operational forecast system
[AD-A281223] p 802 N95-17686
Propagation in the evaporation duct. Model predictions and comparisons to data
[AD-A283012] p 803 N95-17709
ICCanvas 3D visualization tool for Windows (tm). Software user's manual
[AD-A285603] p 842 N95-17746

METEOROLOGY
Atmosphere structure and meteorology instrument for Mars Pathfinder p 711 N95-16202
Landing site considerations for atmosphere structure and meteorology p 921 N95-16203
Meteorological Monitoring Program
[DE94-017810] p 795 N95-16557
Summary of 1994 Atlantic tropical cyclone activity and verification of author's seasonal prediction, 1 p 801 N95-17259
Extended range forecast of Atlantic seasonal hurricane activity for 1995, 2 p 801 N95-17260
On the measurement of momentum flux profiles using a five-beam 915-MHz wind profiler
[DE94-018448] p 791 N95-17903

METEOSAT SATELLITE
Overview on METEOSAT geometrical image data processing p 678 N95-17189

METHANE
Landfill gas energy utilization: Technical and nontechnical considerations
[PB94-189651] p 793 N95-16544

METHODOLOGY
Operational cloud classifier based on a self-organized feature map
[PB94-197852] p 802 N95-17504
Calorimetric methods for loss measurements of small cage induction motors
[PB94-184439] p 768 N95-17691

METHYL ALCOHOL
Reaction of methanol with porous silicon
[AD-A285518] p 728 N95-16406

METHYL COMPOUNDS
Study of the compression behavior of high performance fibers
[AD-A284959] p 723 N95-16126
Regiochemistry of polysilanes prepared by ring opening polymerization
[AD-A281041] p 742 N95-16450
From living carbocationic to living radical polymerization
[AD-A280902] p 743 N95-16501
Mass spectral data of alkyl and cycloalkyl methylphosphonofluoridates
[AD-A285312] p 722 N95-16734
Synthesis and mesomorphic behavior of poly((2S, 3S)-(+)-2-chloro-3-methylpentyl xy)biphenyl-4-carboxylate s with ethyl and propyl alkyl groups
[AD-A281402] p 744 N95-16865
Reaction and protection of electrical wire insulators in atomic-oxygen environments
[NASA-TM-106767] p 709 N95-17275
Chiral recognition in molecular and macromolecular pairs of liquid crystals of (2R, 3S)- and (2S, 3S)-2-fluoro-3-methylpentyl-4'-(11-vinyloxyundeca iphenyl-4-carboxylate diastereomers
[AD-A281770] p 878 N95-17692

METHYL POLYSILOXANES
Surface composition of a series of dimethylsiloxane urea, urethane segmented copolymers studied by electron spectroscopy for chemical analysis
[AD-A282872] p 745 N95-17434

MICA
An XAFS study of the oxidation of structural iron in biotite mica by solutions containing Br2 or H2O2
[DE94-018721] p 733 N95-17912

MICE
Kinetics model for initiation and promotion for describing tumor prevalence from HZE radiation
[NASA-TP-3479] p 820 N95-16412
Photoreceptors regulating circadian behavior: A mouse model
[AD-A285157] p 822 N95-16847
A study to determine the critical characteristics for mice in a newly designed whole body toxic gas exposure module
[AD-A285085] p 818 N95-17666

MICROCHANNELS
Microchannel formation in polyimide by heavy ion irradiation
[DE94-753315] p 740 N95-16073

MICROCLIMATOLOGY
An investigation of small-scale variations in cloud climatology induced by topography and monthly mean winds
[AD-A283274] p 803 N95-17715
MICROCOMPUTERS
ICCanvas 3D visualization tool for Windows (tm). Software user's manual
[AD-A285603] p 842 N95-17746
MICROELECTRONICS
Method of calculating the optimal radioelectronic equipment design p 652 N95-16271
Analog microcircuit fault prediction
[AD-A281958] p 763 N95-16410
Method of rapid sample handling for laser processing
[AD-D016408] p 778 N95-17464
Multilayer microelectronic photomultiplier device with a stacked series of dynode and insulating layers
[AD-D016377] p 767 N95-17478
Spacecraft Data Simulator for the test of level zero processing systems p 675 N95-17582
Simulation of the SEMATECH gravimetric mass flowmeter calibrator
[DE94-018698] p 773 N95-17910
MICROGRAVITY
Virtual environment application with partial gravity simulation p 854 N95-15988
Combustion and fires in low gravity
p 712 N95-16050
Aerospace Medical Association 63rd Annual Scienti fic Meeting Program p 807 N95-16737
Variability in Hoffmann and tendon reflexes in healthy male subjects p 808 N95-16739
Comparison of saline and fludrocortisone as fluid-loading countermeasures following exposure to simulated microgravity p 808 N95-16742
Magnetic Resonance Imaging (MRI) of skeletal muscles in astronauts after 9 days of space flight
p 810 N95-16749
Blood volume and orthostatic responses of men and women to a 13-day bedrest p 811 N95-16752
Comparisons of three anti-G suit configurations during long duration, low onset, +Gz p 811 N95-16755
Achilles Tendon Reflex (ATR) in response to short exposures of microgravity and hypergravity
p 812 N95-16756
Space medicine research: Needs for the 21st century
p 814 N95-16768
SLS-1: The first dedicated life sciences shuttle flight
p 676 N95-16769
Delivery of cardiopulmonary resuscitation in the microgravity environment p 816 N95-16774
Advanced Cardiac Life Support (ACLS) utilizing Man-Tended Capability (MTC) hardware onboard Space Station Freedom p 816 N95-16775
A surgical support system for Space Station Freedom
p 710 N95-16776
Artificial gravity: How much, how often, how long?
p 816 N95-16778
The efficacy of periodic +Gz exposure in the prevention of bedrest induced orthostatic intolerance
p 817 N95-16781
Chemical vapor deposition of high T(sub c) superconducting films in a microgravity environment
[NASA-CR-197527] p 750 N95-16880
Statistical analysis of microgravity experiment performance using the degrees of success scale
[NASA-TM-106791] p 784 N95-17385
Conceptual design of the Space Station combustion module
[NASA-TM-106788] p 675 N95-17419
Microgravity isolation system design: A case study
[NASA-TM-106804] p 654 N95-17657
Study of simulation in microgravity environment
[PB95-104261] p 750 N95-17730
Summary report of mission acceleration measurements for STS-62, launched 4 March 1994
[NASA-TM-106773] p 750 N95-17893
MICROINSTRUMENTATION
Physical and chemical sensor technologies developed at Lawrence Livermore National Laboratory
[DE94-012231] p 775 N95-17380
MICROMECHANICS
Cornell program for the design and synthesis of advanced materials
[AD-A281352] p 723 N95-16016
Micromechanics of interfaces in metal matrix composites
[AD-A282404] p 725 N95-17457
Thermal analysis of a functionally graded material subject to a thermal gradient using the boundary element method
[NASA-TM-106801] p 789 N95-17658
Modeling of stress/strain behavior of fiber-reinforced ceramic matrix composites including stress redistribution
[NASA-TM-106789] p 725 N95-17659
MICROPOROSITY
Analysis of the through-thickness micropore and constituent particle population gradients in the 7050-T7451 plate aluminum alloys
[AD-A282970] p 738 N95-17663
MICROPROCESSORS
Network interface specification for the T1 microprocessor
[AD-A283392] p 844 N95-15940
MICROSCOPY
Advances in ultrafast scanning probe microscopy
[DE94-018180] p 779 N95-17729
Ultrafast scanning probe microscopy
[DE94-018186] p 779 N95-17887
MICROSTRIP ANTENNAS
Feasibility study concerning an active millimeterwave sensor
[PB94-190691] p 775 N95-17170
MICROSTRUCTURE
Proceedings of the Workshop on Characterization of Molecular Assemblies
[DE94-753477] p 871 N95-15956
Cornell program for the design and synthesis of advanced materials
[AD-A281352] p 723 N95-16016
Property control of (perfluorinated ionomer)/(inorganic oxide) composites by tailoring the nanoscale morphology
[AD-A281370] p 723 N95-16019
Electromagnetic processing of refractory metal silicide/oxide composites
[AD-A281470] p 740 N95-16085
Ductile fracture and failure criteria of structural steels
[AD-A280754] p 733 N95-16104
Computational methods for microstructure covolume techniques of discretization
[AD-A282449] p 861 N95-16376
Phase transformations, ultrastructure and properties of rigid-rod fibers
[AD-A285249] p 749 N95-16512
Processing - property relationship in advanced intermetallics
[AD-A285262] p 735 N95-16514
Failure analysis of 2D and 3D woven composites
[NASA-CR-197247] p 724 N95-16597
Investigation of residual stresses in a multipass weld in 1 in. stainless steel plate
[DE94-013277] p 786 N95-16803
Models to estimate high frequency acoustic scattering due to thermal fine- and micro-structure of the ocean
[AD-A285456] p 870 N95-16812
Superplasticity and superplastic forming of ceramics
[DE94-016172] p 745 N95-16935
Analysis of the through-thickness micropore and constituent particle population gradients in the 7050-T7451 plate aluminum alloys
[AD-A282970] p 738 N95-17663
Fundamental concepts relating local atomic arrangements, deformation, and fracture of intermetallic alloys
[AD-A282971] p 738 N95-17664
Forging of FeAl intermetallic compounds
[DE94-018124] p 739 N95-17728
Raman spectroscopy of C-irradiated graphite
[DE94-018705] p 733 N95-17911
MICROWAVE ANTENNAS
Characteristics of phase-correcting fresnel zone plates and elliptical waveguides
[AD-A281385] p 763 N95-16159
JPL-ANTOPT antenna structure optimization program
p 759 N95-17297
MICROWAVE EQUIPMENT
In-fibre Bragg gratings for millimetre-wave EW systems
[AD-A284283] p 755 N95-16956
MICROWAVE FREQUENCIES
Antenna noise temperatures of the 34-meter beam-waveguide antenna with horns of different gains installed at F1 p 757 N95-17288
Simultaneous determination of incoming microwave frequency and angle-of-arrival
[AD-D016392] p 760 N95-17482
MICROWAVE OSCILLATORS
Slow wave vane structure with elliptical cross-section slots, an analysis
[NASA-CR-195352] p 755 N95-16886
MICROWAVE SENSORS
Feasibility study concerning an active millimeterwave sensor
[PB94-190691] p 775 N95-17170
MICROWAVE SPECTRA
A latitudinal survey of middle atmospheric water vapor revealed by shipboard microwave spectroscopy
[AD-A282000] p 799 N95-17446
MICROWAVE TRANSMISSION
Simultaneous determination of incoming microwave frequency and angle-of-arrival
[AD-D016392] p 760 N95-17482
Propagation in the evaporation duct. Model predictions and comparisons to data
[AD-A283012] p 803 N95-17709
MICROWAVES
A preliminary attempt at sintering an ultrafine alumina powder using microwaves
[AD-A284978] p 734 N95-16229
Preliminary study of an active millimeter wave sensor
[PB94-189206] p 759 N95-17453
Beams 92: Proceedings
[DE94-014784] p 880 N95-17475
Radial acceletron, a new low impedance HPM source
[AD-A282008] p 760 N95-17501
MIDCOURSE GUIDANCE
Autonomous weapon guidance
[AD-A282715] p 671 N95-16381
MIDLATITUDE ATMOSPHERE
An improved neutral wind model with predictive capabilities
[AD-A282283] p 800 N95-16235
MILITARY AIRCRAFT
Military aviation maintenance industry in Western Europe: Concentration and internationalization
[PB94-189180] p 653 N95-17451
MILITARY AVIATION
Low rate initial production in Army Aviation systems development
[AD-A281871] p 666 N95-16356
MILITARY OPERATIONS
Detectability models and waveform design for multiple access Low-Probability-of-Intercept networks
[AD-A281864] p 753 N95-16300
Videoconferencing and its role in the Army
[AD-A282707] p 909 N95-16305
MILITARY TECHNOLOGY
Optical fiber sensors: Accelerating applications in Navy ships
[PB94-186848] p 887 N95-17441
MILITARY VEHICLES
Bench wear and single-cylinder engine evaluations of high-temperature lubricants for US Army ground vehicles
[AD-A285399] p 780 N95-16636
MILLIMETER WAVES
In-fibre Bragg gratings for millimetre-wave EW systems
[AD-A284283] p 755 N95-16956
Feasibility study concerning an active millimeterwave sensor
[PB94-190691] p 775 N95-17170
Preliminary study of an active millimeter wave sensor
[PB94-189206] p 759 N95-17453
High current density sheet-like electron beam generator
[AD-A281975] p 880 N95-17499
Electromagnetic field measurements on a mm-wave linear accelerator
[DE94-015092] p 761 N95-17926
MIMD (COMPUTERS)
Visualization of unsteady computational fluid dynamics
[NASA-CR-197461] p 770 N95-16388
Trapezoidal rule quadrature algorithms for MIMD distributed memory computers
[DE94-016369] p 839 N95-16923
MINERALOGY
Investigations of asteroid family geology
p 917 N95-17393
MINIATURE ELECTRONIC EQUIPMENT
Evaluation of a new miniature temperature data logger: Herpetological review
[DE94-013561] p 774 N95-16804
MINICOMPUTERS
Development of practical MO techniques for prediction of the properties and behavior of materials
[AD-A285079] p 874 N95-16496
MINIMA
Constrained minimization of smooth functions using a genetic algorithm
[NASA-TP-3329] p 709 N95-16902
MIRRORS
Methods of wave-front identification by control images
p 652 N95-16274
The combination probe of optical fibers and its applications p 652 N95-16275
MIS (SEMICONDUCTORS)
BaF2/GaAs electronic components
[AD-D016391] p 767 N95-17481
MISSILE BODIES
Supersonic vortex flow around a missile body
p 661 N95-17870

MISSILE CONFIGURATIONS
Experimental study at low supersonic speeds of a missile concept having opposing wraparound tails
[NASA-TM-4582] p 655 N95-16069
Superspheroid geometries for radome analysis
[AD-A285405] p 753 N95-16233
Evaluation of an autopilot based multimodelling
[PB94-190725] p 671 N95-17454
A selection of experimental test cases for the validation of CFD codes, volume 2
[AGARD-AR-303-VOL-2] p 657 N95-17846

MISSILE CONTROL
Non-intrusive missile control surface monitor system
[AD-A285356] p 883 N95-15954
Experimental study at low supersonic speeds of a missile concept having opposing wraparound tails
[NASA-TM-4582] p 655 N95-16069
Evaluation of an autopilot based multimodelling
[PB94-190725] p 671 N95-17454

MISSILE DEFENSE
An opportunity analysis system for space surveillance experiments with the MSX p 707 N95-17609

MISSILE DETECTION
An opportunity analysis system for space surveillance experiments with the MSX p 707 N95-17609

MISSILE SYSTEMS
Autonomous weapon guidance
[AD-A282715] p 671 N95-16381

MISSILE TRACKING
An opportunity analysis system for space surveillance experiments with the MSX p 707 N95-17609

MISSILES
Graphite-reinforced polycyanate composites for space and missile applications
[AD-A285509] p 725 N95-16970
Mission planning for space based satellite surveillance experiments with the MSX p 673 N95-17212
Evaluation of an autopilot based multimodelling
[PB94-190725] p 671 N95-17454

MISSION PLANNING
Using virtual reality for science mission planning: A Mars Pathfinder case p 673 N95-15978
Potential landing sites for Mars Pathfinder p 920 N95-16193
Melas Chasma: A Mars Pathfinder view of Valles Marineris p 922 N95-16207
Catalog of lunar and Mars science payloads
[NASA-RP-1345] p 922 N95-16436
Results of an International Space Crew Debrief p 810 N95-16750
Galileo mission planning for Low Gain Antenna based operations p 682 N95-17210
Mission planning for space based satellite surveillance experiments with the MSX p 673 N95-17212
Engineering Ulysses extended mission p 673 N95-17213
Joint operations planning for space surveillance missions on the MSX satellite p 673 N95-17215
International mission planning for space Very Long Baseline Interferometry p 673 N95-17216
The role of mission operations in spacecraft integration and test p 684 N95-17220
Mission operations management p 685 N95-17225
Shared mission operations concept p 685 N95-17228
Mars Pathfinder mission operations concepts p 686 N95-17229
Towards a new generation of mission planning systems: Flexibility and performance p 686 N95-17230
Generic mission planning and scheduling: The AXAF solution p 686 N95-17231
A PC based tool for mission plan production p 686 N95-17232
Towards a class library for mission planning p 686 N95-17233
Autonomous mission planning and scheduling: Innovative, integrated, responsive p 686 N95-17234
A mission planning concept and mission planning system for future manned space missions p 687 N95-17235
The Sequence of Events generator: A powerful tool for mission operations p 688 N95-17240
Small scale sequence automation pays big dividends p 689 N95-17247
EURECA mission control experience and messages for the future p 690 N95-17252
SCOS 2: ESA's new generation of mission control system p 674 N95-17253
Third International Symposium on Space Mission Operations and Ground Data Systems, part 2
[NASA-CP-3281-PT-2] p 691 N95-17531
A software architecture for automating operations processes p 692 N95-17538
Towards an integral computer environment supporting system operations analysis and conceptual design p 696 N95-17558
Analysis of space network loading p 701 N95-17578
ATOS: Integration of advanced technology software within distributed Spacecraft Mission Operations Systems p 705 N95-17602
Renaissance architecture for Ground Data Systems p 706 N95-17604
The Requirements Generation System: A tool for managing mission requirements p 707 N95-17608
Matrix evaluation of science objectives p 707 N95-17610
Concurrent engineering: Spacecraft and mission operations system design p 708 N95-17614

MIXING
The use of designed experiments in the process development of continuous propellant mixing p 717 N95-16334

MIXING CIRCUITS
Feasibility study concerning an active millimeterwave sensor
[PB94-190691] p 775 N95-17170

MOBILE COMMUNICATION SYSTEMS
Efficient mission control for the 48-satellite Globalstar Constellation p 674 N95-17256

MOBILITY
Mobility measurement and computer simulation at specific sites in polystyrene solutions and gels
[AD-A281214] p 747 N95-17685

MODAL RESPONSE
Shaped strain sensors for intelligent structures
[AD-A282333] p 774 N95-16242
Correlation of finite element free vibration predictions using random vibration test data
[NASA-TM-106787] p 787 N95-17258

MODEL REFERENCE ADAPTIVE CONTROL
Back-propagation neural networks in adaptive control of unknown nonlinear systems
[AD-A282414] p 858 N95-17458

MODELS
Model-based software process improvement p 843 N95-16455
Radiation belt dynamic and quasi-static modeling based on CRRES data
[AD-A285282] p 916 N95-16600

MODULARITY
Cognition and procedure representational requirements for predictive human performance models p 814 N95-16766

MODULATION
Demodulation processes in auditory perception
[AD-A285427] p 869 N95-16248
Development of device quality nonlinear optical materials and definition of mechanisms of optical nonlinearity
[AD-A285255] p 885 N95-16528
Catecholaminergic responses to stressful motion stimuli, scopolamine plus amphetamine, and dexamethasone p 809 N95-16745

MODULATION TRANSFER FUNCTION
An empirical approach to visual display preference based upon modulation transfer function and luminance
[AD-A285450] p 830 N95-16875
Measurement of modulation transfer function of focal plane arrays and imaging systems
[AD-A282976] p 887 N95-17707

MODULATORS
Electric-optic resonant phase modulator
[NASA-CASE-NPO-18702-1-CU] p 883 N95-15960
Initial design of a 1 megawatt average, 150 kilovolt pulse modulator for an industrial plasma source ion implantation processor
[DE94-014421] p 888 N95-16218
System design and operation of a 100 kilovolt, 2 kilohertz pulse modulator for plasma source ion implantation
[DE94-014424] p 889 N95-16285
Ultra high bit rate all optical communication system
[AD-D016359] p 887 N95-17695

MODULES
The Design Manager's Aid for Intelligent Decomposition (DeMAID) p 848 N95-16470
Research on stable, high-efficiency, amorphous silicon multijunction modules
[DE94-011826] p 794 N95-17521
Beam position correction in the Fermilab Linac
[DE94-018984] p 882 N95-17931

MOISTURE CONTENT
Long term modelling of permafrost dynamics
[AD-A285315] p 799 N95-16735

MOLECULAR BEAM EPITAXY
Modification of 2-6 and 3-5 materials using ion beams
[AD-A281839] p 896 N95-16365
Low temperature deposition and characterization of N- and P-type silicon carbide thin films and associated ohmic and Schottky contacts
[AD-A281060] p 743 N95-16625
Positron annihilation studies of defects in molecular beam epitaxy grown 3 to 5 layers
[DE94-015823] p 899 N95-16918
Investigation of novel electrical transport phenomena in semimetal-semiconductor heterostructures
[AD-A281406] p 901 N95-17424

MOLECULAR BIOLOGY
Hemoglobin-based blood substitutes and enhanced susceptibility to bacterial infections
[AD-A281023] p 820 N95-16444

MOLECULAR CHAINS
Self assembled spin coated and bulk films of a novel polydiacetylene as second order NLO polymers
[AD-A282271] p 742 N95-16427
Iterative divergent/convergent doubling approach to linear conjugated oligomers. A rapid route to a 128 A long potential molecular wire
[AD-A281295] p 874 N95-16784

MOLECULAR CLOUDS
First detection of CO (j = 0 - 1) adsorption at cosmological distances (z = 0.247)
[PB94-184595] p 916 N95-17332

MOLECULAR CLUSTERS
Carbon clusters studied by neutralization-reionization mass spectrometry
[AD-A281367] p 726 N95-16017
Multi-dimensional shock capturing
[AD-A282986] p 773 N95-17708

MOLECULAR COLLISIONS
Resonant charge transfer in hyperthermal atomic and molecular ion-surface collisions
[AD-A281369] p 871 N95-16018
Mass spectrometry studies of the ionization of organic molecules by slow positrons
[DE94-013838] p 876 N95-16959

MOLECULAR DIFFUSION
Study of the structuring of pure molecular liquids
[PB94-201316] p 903 N95-16839

MOLECULAR DYNAMICS
Surface and defect excitations in covalently bonded solids
[AD-A281338] p 894 N95-16012
Interface properties of wide bandgap semiconductor structures
[AD-A281469] p 894 N95-16084
Log-(Chi(exp 2)) distribution of correlation times revisited
[AD-A281123] p 740 N95-16092
Effect of ion-electrode contact on the energetics of the heterogeneous electron transfer
[AD-A281959] p 873 N95-16411
Morphology and dynamics of membrane systems
[PB94-184660] p 745 N95-17299
Computer modeling of organic aerogels, 93-SR-062
[DE94-016485] p 722 N95-17745

MOLECULAR ELECTRONICS
Iterative divergent/convergent doubling approach to linear conjugated oligomers. A rapid route to a 128 A long potential molecular wire
[AD-A281295] p 874 N95-16784

MOLECULAR INTERACTIONS
The chemistry and physics of transition metal clusters
[DE94-014012] p 734 N95-16364
Nanoscale imaging of molecular adsorption
[AD-A280979] p 873 N95-16482

MOLECULAR ORBITALS
Development of practical MO techniques for prediction of the properties and behavior of materials
[AD-A285079] p 874 N95-16496

MOLECULAR SPECTRA
First detection of CO (j = 0 - 1) adsorption at cosmological distances (z = 0.247)
[PB94-184595] p 916 N95-17332

MOLECULAR STRUCTURE
Proceedings of the Workshop on Characterization of Molecular Assemblies
[DE94-753477] p 871 N95-15956
Smart materials based upon oligomeric molecules
[AD-A281374] p 872 N95-16155
Atomic force microscopy of the electrochemical nucleation and growth of molecular crystals
[AD-A281024] p 897 N95-16445
Living radical polymerization. 1: Possibilities and limitations
[AD-A281042] p 742 N95-16451
Development of practical MO techniques for prediction of the properties and behavior of materials
[AD-A285079] p 874 N95-16496
The relationship of structure to superconductivity in the Pr-Ba-Cu-O system
[DE94-014231] p 897 N95-16510
Nonlinear optical response of condined excitions in molecular and semiconductor nanostructures
[AD-A285225] p 885 N95-16524

Iterative divergent/convergent doubling approach to linear conjugated oligomers. A rapid route to a 128 A long potential molecular wire
[AD-A281295] p 874 N95-16784
Isomorphism within the hexagonal columnar mesophase of molecular and macromolecular self- and co-assembled columns containing tapered groups
[AD-A281205] p 874 N95-16797
The influence of the complexation of sodium and lithium triflate on the self-assembly of tubular-supramolecular architectures displaying a columnar mesophase based on taper-shaped monoesters of oligoethyleneoxide with 3,4,5-tris(p-(n-dodecan-l-yloxy)benzyloxy)benzoic acid and of their polymethacrylates
[AD-A281403] p 730 N95-16866
Structure of 4-methylpyridinium hydrogen sulfide
[NASA-TM-106778] p 731 N95-17387
Chiral recognition in molecular and macromolecular pairs of liquid crystals of (2R, 3S)- and (2S, 3S)-2-fluoro-3-methylpentyl-4'-(11-vinyloxyundeca iphenyl-4-carboxylate diastereomers
[AD-A281770] p 878 N95-17692

MOLECULAR WEIGHT
Control of molecular weights and polydispersities in radical polymerization of styrene in the presence of stable radicals
[AD-A281040] p 742 N95-16449
Surface composition of a series of dimethylsiloxane urea, urethane segmented copolymers studied by electron spectroscopy for chemical analysis
[AD-A282872] p 745 N95-17434

MOLECULES
The mechanism of the oligomerization of thiophene-based para-quinodimethanes
[DE94-014232] p 722 N95-16058
Resonance enhanced multiphoton ionization of molecules and molecular fragments
[AD-A285076] p 873 N95-16493
Thermal dissociation of halogen azides
[AD-A285088] p 728 N95-16497
Metastability in molecules
[AD-A285223] p 874 N95-16523

MOLTEN SALT ELECTROLYTES
Molten salt techniques for excess heat production and the loading issue
[AD-A282462] p 792 N95-16303

MOLTEN SALTS
Molten salt techniques for excess heat production and the loading issue
[AD-A282462] p 792 N95-16303
Charging hydrogen into Ni in hydride-containing molten salts
[AD-A282335] p 730 N95-16973

MOLYBDENUM ALLOYS
Computer modelling of cyclic deformation of high-temperature materials
[AD-A285212] p 735 N95-16519

MOLYBDENUM COMPOUNDS
Processing - property relationship in advanced intermetallics
[AD-A285262] p 735 N95-16514
The analysis and minimization of oxygen contamination in the powder processing of molybdenum disilicide
[DE94-014234] p 735 N95-16540

MOMENTUM
A modified restricted Euler equation for turbulent flows with mean velocity gradients
[NASA-CR-194979] p 769 N95-16070
On the measurement of momentum flux profiles using a five-beam 915-MHz wind profiler
[DE94-018448] p 791 N95-17903

MOMENTUM TRANSFER
Long-term momentum and heat balances and turbulent mixing in the upper equatorial Pacific Ocean
p 805 N95-17395

MONEL (TRADEMARK)
WPH-6112A thermal expansion test of PRESS tubulation
[DE94-015946] p 782 N95-17717

MONITORS
The LANL-Boeing APLE/HPO flying-wire beam-profile monitor
[DE94-014255] p 879 N95-16172
Beam position correction in the Fermilab Linac
[DE94-018984] p 882 N95-17931

MONOMERS
X-ray crystal structure of a monomeric Tris(Arsino)Gallane, ((Me3Si)2As)3Ga)3Ga
[AD-A282343] p 900 N95-17171
Chiral recognition in molecular and macromolecular pairs of liquid crystals of (2R, 3S)- and (2S, 3S)-2-fluoro-3-methylpentyl-4'-(11-vinyloxyundeca iphenyl-4-carboxylate diastereomers
[AD-A281770] p 878 N95-17692

MONOMOLECULAR FILMS
Cyclic voltammetric analysis of ferrocene alkanethiol monolayer electrode kinetics based on Marcus theory
[AD-A281411] p 868 N95-16162
Underpotential deposition of Cu on Au(111): Implications of the HB model
[AD-A283028] p 902 N95-17711

MONOPOLE ANTENNAS
An analysis of the effects of feedline and ground screen noise currents on a conical monopole receiving antenna
[AD-A283401] p 759 N95-17436

MONOPROPELLANTS
Updated test results of a pumped monopropellant propulsion system p 713 N95-16315

MONTE CARLO METHOD
Radiative interactions in chemically reacting compressible nozzle flows using Monte Carlo simulations
[NASA-CR-197133] p 769 N95-15966
Monte Carlo simulation of mercury cadmium telluride
[AD-A281546] p 896 N95-16391
Sensor placement design for object pose determination with three light-stripe range finders
[AD-A281199] p 886 N95-16795
Estimating the benefits of personnel selection and classification: An extension of the Brogden table
[AD-A285674] p 828 N95-17175
Measurements and modeling of impurity source distributions from the Tore Supra outboard pump limiter
[DE94-018049] p 893 N95-17677

MOON
Apollo 16: Nothing so hidden
[NASA-TM-110104] p 922 N95-16836
New look at the old Moon
[NASA-TM-110106] p 922 N95-16838
Radio-planetary from tie from Phobos-2 VLBI data
p 756 N95-17283

MORPHOLOGY
Imager for Mars Pathfinder (IMF) p 711 N95-16206
Performance evaluation of polyaniline as an active material for electrochemical capacitors
[DE94-016283] p 765 N95-16920
Structure-property relationships in sol-gel-derived thin films
[DE94-016149] p 744 N95-16934
Morphology and dynamics of membrane systems
[PB94-184660] p 745 N95-17299

MOSSBAUER EFFECT
SDIO/IST ultrashort wavelength. Mossbauer and gamma ray studies for grasers
[AD-A283091] p 778 N95-17337

MOTION PERCEPTION
Computational vision based on neurobiology
[AD-A284472] p 819 N95-16135
Mathematical model for interaction of canals and otoliths in perception of orientation, translation, and rotation
[AD-A280897] p 819 N95-16151
An improved position/force control of manipulators
p 653 N95-16280
The effects of target orientation on the dynamic contrast sensitivity function
[AD-A281855] p 826 N95-16298

MOTION SICKNESS
Use of injectable promethazine to decrease symptom scores of Space Motion Sickness p 808 N95-16741
Catecholaminergic responses to stressful motion stimuli, scopolamine plus amphetamine, and dexamethasone
p 809 N95-16745
Prediction of space sickness in astronauts from preflight fluid, electrolyte, and cardiovascular variables and Weightless Environmental Training Facility (WETF) training p 812 N95-16757
Dark focus of accommodation as dependent and independent variables in visual display technology
p 812 N95-16758

MOTION SIMULATION
ISMCR 1994: Topical Workshop on Virtual Reality. Proceedings of the Fourth International Symposium on Measurement and Control in Robotics
[NASA-CP-10163] p 851 N95-15972
Scripting human animations in a virtual environment
p 855 N95-15992

MOTION SIMULATORS
Energy expenditure, physical work load and postural control during walking on a moving platform
[AD-A285343] p 830 N95-16821

MOTIVATION
Validation of astronaut psychological select-in criteria
p 813 N95-16762

MSM (SEMICONDUCTORS)
Picosecond silicon metal-semiconductor-metal photodiode
[AD-A281548] p 763 N95-16394
Performance characterization of photonic links in cryogenic environments for advanced signal processing applications
[DE94-015561] p 765 N95-16915

MTBF
Efficient estimation of the mean time between failures in non-regenerative dependability models
[AD-A281563] p 783 N95-16421

MULTICHANNEL COMMUNICATION
Self-initializing circuit link
[AD-D016363] p 761 N95-17696

MULTIGRID METHODS
Multigrid methods in network optimization: Overview and appraisal
[AD-A280992] p 833 N95-15995
Sixth Copper Mountain Conference on Multigrid Methods
[DE94-014595] p 862 N95-16611
Multigrid techniques for nonlinear eigenvalue problems: Solutions of a nonlinear Schroedinger eigenvalue problem in 2D and 3D
[NASA-CR-194999] p 862 N95-16896

MULTIMEDIA
Fourth Annual International Acquisitions Workshop: Access to Multiple Media Worldwide
[NASA-TM-109896] p 905 N95-15919
How to use the WWW to distribute STI
p 847 N95-16465
Data Visualization and Animation Lab (DVAL): Applications p 843 N95-16469
Multimission Telemetry Visualization (MTV) system: A mission applications project from JPL's Multimedia Communications Laboratory p 681 N95-17205

MULTIPHOTON ABSORPTION
Resonance enhanced multiphoton ionization of molecules and molecular fragments
[AD-A285076] p 873 N95-16493

MULTIPLE ACCESS
Fourth Annual International Acquisitions Workshop: Access to Multiple Media Worldwide
[NASA-TM-109896] p 905 N95-15919
The Australian National Chinese Japanese Korean Project p 905 N95-15920
Demand access communications for TDRSS users
p 677 N95-17187

MULTIPLEXING
A standard satellite control reference model
p 704 N95-17592
The Space Communications Protocol Standards Program p 704 N95-17594

MULTIPLIERS
Verification of arithmetic functions with binary moment diagrams
[AD-A281028] p 835 N95-16447

MULTIPROCESSING (COMPUTERS)
Portable parallel stochastic optimization for the design of aeropropulsion components
[NASA-CR-195312] p 785 N95-16072
Can high bandwidth and latency justify large cache blocks in scalable multiprocessors?
[AD-A281468] p 845 N95-16083
Software cache coherence for large scale multiprocessors
[AD-A281628] p 845 N95-16113
A software tool for dataflow graph scheduling
p 843 N95-16457
Investigation of modularly configured attached processors with intelligent memories
[AD-A285454] p 832 N95-16876
Controlling memory access concurrency in efficient fault-tolerant parallel algorithms
[AD-A280909] p 851 N95-17741

MULTIPROGRAMMING
Control transfer in operating system kernels
[AD-A281135] p 837 N95-16602

MULTISTATIC RADAR
Clutter signal polarization in bistatic radar: Effect of antenna sidelobe clutter
[AD-A282300] p 753 N95-16240
Multistatic radar, MSR
[PB94-190709] p 759 N95-17301

MULTIVARIATE STATISTICAL ANALYSIS
Multivariate statistical analysis software technologies for astrophysical research involving large data bases
[NASA-CR-189393] p 911 N95-17325
Multivariate sampling with explicit correlation induction for practical simulation and optimization studies
[AD-A281998] p 841 N95-17445
Multivariate statistical analysis software technologies for astrophysical research involving large data sets
[NASA-CR-197499] p 858 N95-17921

MUON SPIN ROTATION
Muon(+) SR studies of magnetic properties of boron carbide superconductors
[DE94-014440] p 868 N95-16288

MUONS
A-dependent effects in high P(sub T) reactions
[DE94-016385] p 875 N95-16924
A measurement of the Michel parameter (rho) in muon decay
[DE94-014423] p 876 N95-17153
A search for muons yields e gamma at the level of 10(exp -13)
[DE94-014488] p 876 N95-17158
Studies by neutron diffraction and muon SR of flux iattice orientation, pinning, melting and decomposition in high-T(sub c) superconductors
[DE94-017704] p 901 N95-17667
Search for first and second generation leptoquarks at D(null)
[DE94-018992] p 879 N95-17932

MUSCLES
Evaluation of a newly-designed, dynamic knee extension device for the study of muscle fatigue in humans
[AD-A284974] p 819 N95-16228
Characterization of neurotrophic and neurotropic interactions between neurons and their muscle and nerve targets
[AD-A281846] p 820 N95-16423
Variability in Hoffmann and tendon reflexes in healthy male subjects p 808 N95-16739

MUSCULAR FATIGUE
Evaluation of a newly-designed, dynamic knee extension device for the study of muscle fatigue in humans
[AD-A284974] p 819 N95-16228

MUSCULAR FUNCTION
Skeletal muscle responses to unloading in humans p 809 N95-16743
Intramuscular pressure: A better tool than EMG to optimize exercise for long-duration space flight p 809 N95-16744

MUSCULAR STRENGTH
Magnetic Resonance Imaging (MRI) of skeletal muscles in astronauts after 9 days of space flight p 810 N95-16749

MUSCULOSKELETAL SYSTEM
Skeletal muscle responses to unloading in humans p 809 N95-16743
Magnetic Resonance Imaging (MRI) of skeletal muscles in astronauts after 9 days of space flight p 810 N95-16749

MUSIC
Demodulation processes in auditory perception
[AD-A285427] p 869 N95-16248

MYOCARDIUM
Changes in left ventricular function as determined by the multi-wire gamma camera at near presyncopal levels of lower body negative pressure p 811 N95-16754

N

N-TYPE SEMICONDUCTORS
Low temperature deposition and characterization of N- and P-type silicon carbide thin films and associated ohmic and Schottky contacts
[AD-A281060] p 743 N95-16625

NACELLES
Ducted fan acoustic radiation including the effects of nonuniform mean flow and acoustic treatment
[NASA-CR-197449] p 870 N95-16401
Pressure distribution measurements on an isolated TPS 441 nacelle p 663 N95-17878
Low speed propeller slipstream aerodynamic effects p 663 N95-17882

NAKHLITES
Pathfinder landing sites at candidate SNC impact ejection sites p 919 N95-16190

NARROWBAND
Surface science capabilities from IMP spectral imaging p 921 N95-16204

NASA PROGRAMS
NASA contract mangagement: Improving the use of DCAA's auditing services. Report to the Chairman, Committee on Government Operations, House of Representatives
[GAO/NSIAD-94-229] p 914 N95-15962
SeaWiFS technical report series. Volume 21: The heritage of SeaWiFS. A retrospective on the CZCS NIMBUS Experiment Team (NET) program
[NASA-TM-104566-VOL-21] p 803 N95-16006
Activities of the Space Studies Board
[NASA-CR-197105] p 672 N95-16033
BioServe space technologies: A NASA Center for the Commercial Development of Space
[NASA-CR-196983] p 807 N95-16034
Assessment of the Space Station program p 709 N95-16352
NSSDC data listing
[NASA-TM-109986] p 909 N95-16441
Psychological training of NASA astronauts for extended missions p 813 N95-16763
ICASE
[NASA-CR-195001] p 832 N95-16898

NASA SPACE PROGRAMS
Presidential leadership in the development of the US space program
[NASA-TM-110107] p 904 N95-16007
Operations automation p 687 N95-17236

NASCOM NETWORK
Earth Observing System (EOS) Communication (Ecom) Modeling, Analysis, and Testbed (EMAT) activiy p 677 N95-17182
Spacecraft Data Simulator for the test of level zero processing systems p 675 N95-17582
Re-engineering Nascom's network management architecture p 702 N95-17584

NATIONAL AIRSPACE SYSTEM
Identification of Artificial Intelligence (AI) applications for maintenance, monitoring, and control of airway facilities
[AD-A282479] p 665 N95-17373
Federal Aviation Administration aviation system capital investment plan, 1993
[PB94-171956] p 654 N95-17512

NATURAL GAS
Vector magnetometry and lightwave defect imaging sensor technologies for internal pipe inspection systems: Phase 1 and 2 feasibility study, conceptual design, and prototype development
[PB94-194198] p 783 N95-16870
Natural and artificial nobel gas hydrologic tracers
[DE94-016010] p 797 N95-17718
Alternatives to traditional transportation fuels: An overview
[DE94-014979] p 749 N95-17923

NATURAL LANGUAGE (COMPUTERS)
CPP-TRS(C): On using visual cognitive symbols to enhance communication effectiveness p 761 N95-15991

NATURAL LANGUAGE PROCESSING
Parallel parsing
[PB94-191392] p 850 N95-17138
The 1994 International Neural Network Society Annual Meeting, volume 4
[AD-A281737] p 857 N95-17370

NAUSEA
Catecholaminergic responses to stressful motion stimuli, scopolamine plus amphetamine, and dexamethasone p 809 N95-16745

NAVIER-STOKES EQUATION
Radiative interactions in chemically reacting compressible nozzle flows using Monte Carlo simulations
[NASA-CR-197133] p 769 N95-15966
Nonlinear instability of a uni-directional transversely sheared mean flow
[NASA-TM-106779] p 769 N95-15969
A modified restricted Euler equation for turbulent flows with mean velocity gradients
[NASA-CR-194979] p 769 N95-16070
The prediction of nozzle performance and heat transfer in hydrogen/oxygen rocket engines with transpiration cooling, film cooling, and high area ratios p 718 N95-16339
On bi-grid local mode analysis of solution techniques for 3-D Euler and Navier-Stokes equations
[NASA-TM-106749] p 771 N95-16855
Comparison of computational and experimental results for a supercritical airfoil
[NASA-TM-4601] p 656 N95-16908
Three dimensional compressible turbulent flow computations for a diffusing S-duct with/without vortex generators
[NASA-CR-195390] p 670 N95-17402
Transient flows and pressure waves in pipes
[DE94-012650] p 772 N95-17523

NAVIGATION
Beyond the cockpit: The visual world as a flight instrument p 814 N95-16767
Online performance-improvement algorithms
[AD-A285162] p 838 N95-16850

NAVIGATION INSTRUMENTS
Guidance, navigation, and control digital emulation technology laboratory
[AD-A282722] p 766 N95-17139

NAVIGATORS
Towards a human operator model of the navigator
[PB94-197985] p 831 N95-17468

NAVY
Electronic access to ONREUR/ONRAISIA S and T reports p 907 N95-15935
Optical fiber sensors: Accelerating applications in Navy ships
[PB94-186848] p 887 N95-17441

NEAR FIELDS
Development of an analytical photon scanning tunneling microscope
[AD-A281382] p 884 N95-16157
Formulation of probe-corrected time-domain planar near-field measurements
[AD-A281053] p 754 N95-16624

NEAR INFRARED RADIATION
A quasi-single mode optical fiber for long-haul transmission in severe bending environments
[AD-A281313] p 884 N95-16009

NEBULAE
Dust near luminous ultraviolet stars
[NASA-CR-197108] p 916 N95-16032
Voyager investigation of the cosmic diffuse background: Observations of rocket-studied locations with Voyager
[NASA-CR-197532] p 917 N95-17422

NECK (ANATOMY)
Effects of weightlessness on human baroreflex function p 815 N95-16770

NEGATIVE ELECTRON AFFINITY
Interface properties of wide bandgap semiconductor structures
[AD-A281469] p 894 N95-16084

NEOPLASMS
The role of chemical inhibition of gap junctional intercellular communication in toxicology
[AD-A282452] p 820 N95-16378

NERVES
Characterization of neurotrophic and neurotropic interactions between neurons and their muscle and nerve targets
[AD-A281846] p 820 N95-16423
Investigation of laser-induced retinal damage: Wavelength and pulsewidth dependent mechanisms
[AD-A285186] p 822 N95-16871

NERVOUS SYSTEM
Development of the OMPAT neuropsychological/psychomotor performance evaluation and OMPAT data and timing support programs
[AD-A284928] p 826 N95-16140

NETHERLANDS
Document delivery by the Jupiter Library Consortium p 906 N95-15926
Energy and emissions of CO2, NOx and SO2 in the scenario of the 3rd national environmental evaluation, 1993
[PB94-194792] p 796 N95-17304

NETWORK ANALYSIS
Multigrid methods in network optimization: Overview and appraisal
[AD-A280992] p 833 N95-15995
Communication network software analysis
[AD-A281019] p 833 N95-16004
Detectability models and waveform design for multiple access Low-Probability-of-Intercept networks
[AD-A281864] p 753 N95-16300
Frequency domain analysis for nonlinear electronic circuits
[PB94-201365] p 767 N95-17469
Analysis of space network loading p 701 N95-17578

NETWORK CONTROL
An introduction to intelligent networks
[AD-A284284] p 752 N95-16123
Evaluating Space Network (SN) scheduling operations concepts through statistical analysis p 684 N95-17222
Back-propagation neural networks in adaptive control of unknown nonlinear systems
[AD-A282414] p 858 N95-17458
NCCDS performance model p 675 N95-17576

NEURAL NETS
Visual neural development and chromatic aberration
[AD-A285064] p 826 N95-16368
Proceedings of the Neural Network Workshop for the Hanford Community
[DE94-014567] p 856 N95-16609
Evolving neural network pattern classifiers
[AD-A281181] p 857 N95-16631
A novel optic bistable device with very low threshold intensity using photorefractive films
[AD-A285310] p 885 N95-16733
Learning one more thing
[AD-A285342] p 857 N95-16820
Self-organizing neural network for classifying pattern signatures with a posteriori conditional class probability
[AD-D016455] p 857 N95-16823
Using neural networks to correlate satellite imagery and ground-truth data
[AD-A285486] p 857 N95-16967
The 1994 International Neural Network Society Annual Meeting, volume 3
[AD-A281736] p 857 N95-17369

The 1994 International Neural Network Society Annual Meeting, volume 4
[AD-A281737] p 857 N95-17370
An artificial neural network system for diagnosing gas turbine engine fuel faults
[DE94-013960] p 670 N95-17371
Back-propagation neural networks in adaptive control of unknown nonlinear systems
[AD-A282414] p 858 N95-17458
Object recognition using multi-layer Hopfield neural network
[AD-A282417] p 858 N95-17459

NEUROLOGY
Development of the OMPAT neuropsychological/psychomotor performance evaluation and OMPAT data and timing support programs
[AD-A284928] p 826 N95-16140
Locus coeruleus, vigilance and stress: Brain mechanisms of adaptive behavioral responsiveness
[AD-A282450] p 826 N95-16377
The 1994 International Neural Network Society Annual Meeting, volume 4
[AD-A281737] p 857 N95-17370

NEURONS
Locus coeruleus, vigilance and stress: Brain mechanisms of adaptive behavioral responsiveness
[AD-A282450] p 826 N95-16377
Characterization of neurotrophic and neurotropic interactions between neurons and their muscle and nerve targets
[AD-A281846] p 820 N95-16423
Molecular approach to hypothalamic rhythms
[AD-A285164] p 822 N95-16851

NEUROPHYSIOLOGY
Computational vision based on neurobiology
[AD-A284472] p 819 N95-16135
Synaptic plasticity and memory formation
[AD-A284926] p 825 N95-16138
Characterization of the fast-phase component of the vestibulo-ocular response
[AD-A281830] p 820 N95-16360
Locus coeruleus, vigilance and stress: Brain mechanisms of adaptive behavioral responsiveness
[AD-A282450] p 826 N95-16377
Neurophysiological analysis of circadian rhythm entrainment
[AD-A280981] p 821 N95-16484
Parallel search for a conjunction of shape and contrast polarity
[AD-A285344] p 827 N95-16822

NEUTRAL BEAMS
Search for the presence of H particles in a neutral beam
[DE94-013526] p 877 N95-17683

NEUTRAL CURRENTS
Limit on the rare decay B yields muon(+)muon(-) K(+-)
[DE94-013851] p 876 N95-16960
Solar neutrino oscillations
[PB95-104295] p 923 N95-17352

NEUTRINOS
Research in elementary particle physics
[DE94-019219] p 877 N95-17358
Electron-neutrino phase separation instability
[DE94-016859] p 904 N95-17645
Neutrino oscillation studies at LAMPF
[DE94-018098] p 878 N95-17727
Flavor symmetries and fermion masses
[DE94-018192] p 878 N95-17889

NEUTRON DIFFRACTION
Proceedings of the Workshop on Characterization of Molecular Assemblies
[DE94-753477] p 871 N95-15956
Studies by neutron diffraction and muon SR of flux lattice orientation, pinning, melting and decomposition in high-T(sub c) superconductors
[DE94-017704] p 901 N95-17667

NEUTRON IRRADIATION
Statistical properties of an algorithm used for illicit substance detection by fast-neutron transmission
[DE94-013868] p 665 N95-16964

NEUTRON RADIOGRAPHY
Statistical properties of an algorithm used for illicit substance detection by fast-neutron transmission
[DE94-013868] p 665 N95-16964

NEUTRON SCATTERING
Inelastic neutron scattering and antiferromagnetic fluctuations in high temperature superconductors
[DE94-623269] p 871 N95-16059
Processing, fabrication, characterization and device demonstration of high temperature superconducting ceramics
[AD-A285145] p 744 N95-16844
Small angle neutron scattering from nanocrystalline Pd and Cu compacted at elevated temperatures
[DE94-013865] p 876 N95-16962

NEUTRON SOURCES
Proceedings of the Workshop on Characterization of Molecular Assemblies
[DE94-753477] p 871 N95-15956
Studies of D-Li neutron source: An overview
[DE94-014032] p 873 N95-16487
Tokamak Transmutation of (nuclear) Waste (TTW): Parametric studies
[DE94-012891] p 881 N95-17721

NEUTRONS
A new communication scheme for the neutron diffusion nodal method in a distributed computing environment
[DE94-017907] p 844 N95-15946
Non-Fermi liquid scaling in UPd(x)Cu(5-x)(x = 1,1.5)
[DE94-016072] p 896 N95-16389

NEWTON METHODS
A stepsize control strategy for stiff systems of ordinary differential equations
[AD-A281551] p 861 N95-16395

NEWTON-RAPHSON METHOD
Demonstration of the Dynamic Flowgraph Methodology using the Titan 2 Space Launch Vehicle Digital Flight Control System
[NASA-CR-197517] p 675 N95-17493

NICKEL
Atomic structure and valency of nickel in some of its oxycompounds
[AD-A281109] p 733 N95-16091
XAFS spectra and the oxidation state of nickel in some of its oxycompounds
[AD-A281137] p 735 N95-16606
Charging hydrogen into Ni in hydride-containing molten salts
[AD-A282335] p 730 N95-16973
XAFS investigation of structure and valency of nickel in some oxycompounds
[AD-A283193] p 877 N95-17630

NICKEL ALLOYS
Cornell program for the design and synthesis of advanced materials
[AD-A281352] p 723 N95-16016
Computer modelling of cyclic deformation of high-temperature materials
[AD-A285212] p 735 N95-16519
X-ray absorption spectra and structure of some nickel oxides (hydroxides)
[AD-A281305] p 735 N95-16788

NICKEL CADMIUM BATTERIES
Nickel cadmium battery operations and performance
p 685 N95-17224

NICKEL HYDROGEN BATTERIES
Nickel hydrogen batteries: An overview
[NASA-TM-106795] p 793 N95-16861

NICKEL OXIDES
Atomic structure and valency of nickel in some of its oxycompounds
[AD-A281109] p 733 N95-16091
XAFS spectra and the oxidation state of nickel in some of its oxycompounds
[AD-A281137] p 735 N95-16606
X-ray absorption spectra and structure of some nickel oxides (hydroxides)
[AD-A281305] p 735 N95-16788
XAFS investigation of structure and valency of nickel in some oxycompounds
[AD-A283193] p 877 N95-17630

NICOTINIC ACID
Increased skin blood flow and enhanced heat loss in humans after niacin ingestion
[AD-A281124] p 821 N95-16809

NIGHT
A preliminary optical visibility model
p 758 N95-17290

NIGHT VISION
Visual acuity versus field-of-view and light level for Night Vision Goggles (NVG)
[AD-A284750] p 830 N95-16553

NIGHTGLOW
Equatorial airglow studies via rocket experiment
[INPE-5589-TDI/551] p 799 N95-17647

NIOBATES
The deposition of electro-optic films on semiconductors
[AD-A285068] p 742 N95-16488

NITRATES
Space Shuttle reaction control system thruster metal nitrate removal and characterization
p 716 N95-16332

NITRIC OXIDE
Laser induced fluorescence measurements and modeling of nitric oxide in high-pressure premixed flames
[NASA-CR-195404] p 775 N95-16910

NITRIDES
Synthesis of tungsten nitrene complexes as precursors for tungsten nitride
[AD-A281592] p 740 N95-16101
Nitride semiconductors for ultraviolet detection
[AD-A280988] p 898 N95-16533
Tribological properties of reactively sputtered nitrides and carbides of titanium, zirconium and hafnium
[DE94-014583] p 745 N95-17160

NITROGEN
Regulation of nitrogen uptake and assimilation: Effects of nitrogen source and root-zone and aerial environment on growth and productivity of soybean
[NASA-CR-197098] p 807 N95-15961
Space Shuttle reaction control system thruster metal nitrate removal and characterization
p 716 N95-16332

NITROGEN COMPOUNDS
Structure of 4-methylpyridinium hydrogen sulfide
[NASA-TM-106778] p 731 N95-17387

NITROGEN DIOXIDE
Gas-surface interactions near dissociation threshold
[AD-A284945] p 726 N95-16042
Failure of ozone and nitrogen dioxide to enhance lung tumor development in hamsters
[PB94-182854] p 818 N95-16801

NITROGEN OXIDES
Gas-surface interactions near dissociation threshold
[AD-A282726] p 730 N95-17140
An in-cylinder study of the particulate/NO(x) trade-off in a DI diesel engine
[DE94-014599] p 781 N95-17162
Energy and emissions of CO2, NOx and SO2 in the scenario of the 3rd national environmental evaluation, 1993
[PB94-194792] p 796 N95-17304

NITROSYL CHLORIDES
Gas-surface interactions near dissociation threshold
[AD-A282726] p 730 N95-17140

NOISE (SOUND)
The assessment of the AH-64D, longbow, mast-mounted assembly noise hazard for maintenance personnel
[AD-A284971] p 869 N95-16226

NOISE GENERATORS
Ducted fan acoustic radiation including the effects of nonuniform mean flow and acoustic treatment
[NASA-CR-197449] p 870 N95-16401

NOISE INTENSITY
The assessment of the AH-64D, longbow, mast-mounted assembly noise hazard for maintenance personnel
[AD-A284971] p 869 N95-16226

NOISE REDUCTION
Mitre adaptive processing capability
[AD-A281078] p 755 N95-16825
X-/Ka-band dichroic plate noise temperature reduction
p 758 N95-17294

NOISE TEMPERATURE
Antenna noise temperatures of the 34-meter beam-waveguide antenna with horns of different gains installed at F1 p 757 N95-17288
Computation of reflected and transmitted horn radiation patterns for a dichroic plate p 758 N95-17293
X-/Ka-band dichroic plate noise temperature reduction
p 758 N95-17294

NOISE THRESHOLD
Direct comparison of two statistical methods for determination of evoked-potential thresholds
[AD-A285182] p 870 N95-16811

NONDESTRUCTIVE TESTS
Nondestructive examination of the TRMM RCS propellant tanks p 718 N95-16338
How clean is clean: Non-destructive/direct methods of flux, residue detection
[DE94-013439] p 763 N95-16357
Significant issues in proof testing: A critical appraisal
[NASA-CR-4628] p 788 N95-17272
The application of non-destructive techniques to the testing of a wind turbine blade
[DE95-000323] p 784 N95-17360

NONEQUILIBRIUM FLOW
High altitude hypersonic flowfield radiation
[AD-A281386] p 655 N95-16160

NONINTRUSIVE MEASUREMENT
Non-intrusive missile control surface monitor system
[AD-A285356] p 883 N95-15954
An investigation of fluid flow during induction stroke of a water analog model of an IC engine using an innovative optical velocimetry concept: LIPA
[NASA-CR-197451] p 780 N95-16900

NONLINEAR EQUATIONS
Rapid solution of large-scale systems of equations
p 847 N95-16458
Frequency domain analysis for nonlinear electronic circuits
[PB94-201365] p 767 N95-17469

NONLINEAR OPTICS
ARO-URI Center for Opto-Electronic Systems Research
[AD-A281447] p 883 N95-15958
Systematic optimization of second order nonlinear optical materials
[AD-A281350] p 884 N95-16015
Single crystal films and waveguides of organic materials: Preparation and nonlinear optical properties
[AD-A284471] p 895 N95-16134
High-intensity and high energy laser interactions with single droplets
[AD-A281415] p 776 N95-16166
Design of new multi-functional electroactive polymers with emphasis on optical nonlinearity
[AD-A284983] p 741 N95-16230
Detection of crosslink formation by 2 + 2 photocycloaddition in poly (vinyl cinnamate) by C-13 solid-state NMR
[AD-A281955] p 741 N95-16409
Self assembled spin coated and bulk films of a novel polydiacetylene as second order NLO polymers
[AD-A282271] p 742 N95-16427
Nonlinear optical and charge distribution studies probing electric field effects in polymer thin films for second order nonlinear optics
[AD-A280980] p 742 N95-16483
Nonlinear optical response of condined excitions in molecular and semiconductor nanostructures
[AD-A285225] p 885 N95-16524
Development of device quality nonlinear optical materials and definition of mechanisms of optical nonlinearity
[AD-A285255] p 885 N95-16528
Growth, characterization and applications of beta-barium borate and related crystals
[AD-A281047] p 898 N95-16623
Third harmonic generation study of alpha-thiophene oligomers: Monomer to octamer
[AD-A281177] p 874 N95-16629
Materials for second and third order nonlinear optical applications
[AD-A281304] p 885 N95-16787
New mechanisms and new materials for organic optical nonlinearity
[AD-A282781] p 886 N95-17143
The m-line method for optical characterisation of polymer waveguides
[PB94-184611] p 887 N95-17409
Poling dynamics and relaxation of polar order in guest/host polymers by second harmonic generation
[AD-A283291] p 748 N95-17724

NONLINEAR PROGRAMMING
Structural optimization with approximate sensitivities
[NASA-TM-4553] p 789 N95-17701

NONLINEAR SYSTEMS
Adaptive control of nonlinear flexible systems
[AD-A281337] p 855 N95-16011
A highly functional decision paradigm based on nonlinear adaptive genetic algorithm
[AD-A281457] p 855 N95-16077
Numerical analysis on periodic response of nonsmooth dynamic systems p 650 N95-16261
Computational differentiation and multidisciplinary design
[DE94-013393] p 863 N95-17306
O-Plan2 versus SIPE-2: A general comparison
[AD-A285531] p 857 N95-17381
Effect of Coulomb collisions, Landau damping and particle trapping on linear and nonlinear ion acoustic waves
[AD-A282009] p 869 N95-17449
Back-propagation neural networks in adaptive control of unknown nonlinear systems
[AD-A282414] p 858 N95-17458
Nonstationary theory of mode competition in gyrotrons with allowance for inhomogeneity of the guiding magnetic field
[PB94-197621] p 869 N95-17467
Frequency domain analysis for nonlinear electronic circuits
[PB94-201365] p 767 N95-17469
2-D aileron effectiveness study p 658 N95-17851

NONLINEARITY
Nonlinear instability of a uni-directional transversely sheared mean flow
[NASA-TM-106779] p 769 N95-15969
Non-linear waves in gas dynamics and mechanics
[AD-A281376] p 770 N95-16156
Problem of constructing the Lyapunov's functions in lumped parameter systems p 653 N95-16276
Non-linear acoustics in fluids and gels
[PB94-201308] p 870 N95-16614
A novel optic bistable device with very low threshold intensity using photorefractive films
[AD-A285310] p 885 N95-16733
Multigrid techniques for nonlinear eigenvalue probems: Solutions of a nonlinear Schroedinger eigenvalue problem in 2D and 3D
[NASA-CR-194999] p 862 N95-16896
Algorithms for bilevel optimization
[NASA-CR-194980] p 863 N95-16897
On the removal of boundary errors caused by Runge-Kutta integration of non-linear partial differential equations
[NASA-CR-194989] p 863 N95-16904
Combination of power electronic models with the two-dimensional finite element analysis of electrical machines
[PB94-197720] p 766 N95-16951
Investigation of novel electrical transport phenomena in semimetal-semiconductor heterostructures
[AD-A281406] p 901 N95-17424
The quantum solitons of the nonlinear (sigma)-model with broken chiral symmetry
[DE94-622758] p 904 N95-17474
Modelling daily precipitation as a function of temperature for climate change impact studies
[KNMI-WR-93-02] p 802 N95-17529
Trigonometric functions of nonlinear quantities
[DE94-018794] p 864 N95-17916

NONUNIFORM FLOW
Ducted fan acoustic radiation including the effects of nonuniform mean flow and acoustic treatment
[NASA-CR-197449] p 870 N95-16401

NONUNIFORMITY
Testing and characterization of the CYCLOPS HgCdTe focal plane detector array
[AD-A284279] p 887 N95-17489

NORMS
Avoiding BDF stability barriers in the MOL solution of advection-dominated problems
[DE94-014793] p 861 N95-16535

NORTH AMERICA
Optoelectric technology roadmap: Conclusions and recommendations
[AD-A281664] p 886 N95-16965

NORTH ATLANTIC TREATY ORGANIZATION (NATO)
Overview of TTCP and AGARD propulsion activities p 720 N95-16351

NOVAE
Na-22 decay gamma rays from classical novae
[NASA-CR-197454] p 924 N95-16383

NOZZLE DESIGN
A model for preliminary facility design including simulation issues p 672 N95-16318

NOZZLE EFFICIENCY
Combustor kinetic energy efficiency analysis of the hypersonic research engine data p 714 N95-16321
The prediction of nozzle performance and heat transfer in hydrogen/oxygen rocket engines with transpiration cooling, film cooling, and high area ratios p 718 N95-16339

NOZZLE FLOW
Radiative interactions in chemically reacting compressible nozzle flows using Monte Carlo simulations
[NASA-CR-197133] p 769 N95-15966
Numerical study of base pressure characteristic curve for a four-engine clustered nozzle configuration p 716 N95-16329
The prediction of nozzle performance and heat transfer in hydrogen/oxygen rocket engines with transpiration cooling, film cooling, and high area ratios p 718 N95-16339

NUCLEAR ASTROPHYSICS
Na-22 decay gamma rays from classical novae
[NASA-CR-197454] p 924 N95-16383

NUCLEAR ELECTRIC PROPULSION
Reentry safety for the Topaz 2 Space Reactor: Issues and analyses
[DE95-000325] p 880 N95-17361

NUCLEAR ENERGY
Determination of the nuclear-induced electrical conductivity in a nuclear-driven MHD device
[DE94-013137] p 891 N95-17365

NUCLEAR FISSION
Determination of the nuclear-induced electrical conductivity in a nuclear-driven MHD device
[DE94-013137] p 891 N95-17365

NUCLEAR FUEL REPROCESSING
Use of magnesium for recovering hydrogen isotopes from tritiated water
[DE94-014471] p 731 N95-17157

NUCLEAR MAGNETIC RESONANCE
Structure-property relationships in sol-gel-derived thin films
[DE94-016149] p 744 N95-16934
Synthesis and characterization of neopentyl indium compounds: X-ray crystal structures of ((Me3CCH2)2InAs(SiMe3)2)2 and ((Me3CCH2)2InAs(SiMe3)2In (CH2CMe3)2Cl)
[AD-A282766] p 900 N95-17137
Application of NMR shock barometer to naturally shocked minerals
[DE95-000326] p 799 N95-17362

NUCLEAR PARTICLES
Progress at LAMPF
[DE94-016210] p 880 N95-16937

NUCLEAR PHYSICS
Progress at LAMPF
[DE94-016210] p 880 N95-16937
High Energy Physics Division research activities
[DE94-015024] p 882 N95-17924

NUCLEAR POWER PLANTS
A comparison of steady-state ARIES and pulsed PULSAR tokamak power plants
[DE94-014441] p 891 N95-17155
D3-D research operations
[DE94-014934] p 892 N95-17497

NUCLEAR PROPULSION
Computational fluid dynamics studies of nuclear rocket performance
[NASA-TM-105436] p 713 N95-16066

NUCLEATION
Atomic force microscopy of the electrochemical nucleation and growth of molecular crystals
[AD-A281024] p 897 N95-16445

NUCLEI (CYTOLOGY)
Neurophysiological analysis of circadian rhythm entrainment
[AD-A280981] p 821 N95-16484
Control of circadian behavior by transplanted suprachiasmatic nuclei
[AD-A285233] p 807 N95-16599

NUCLEONS
A-dependent effects in high P(sub T) reactions
[DE94-016385] p 875 N95-16924

NUMERICAL ANALYSIS
Numerical analysis on periodic response of nonsmooth dynamic systems p 650 N95-16261
Object-oriented numerical computing C++ p 849 N95-16476
Optimum Design Methods for Aerodynamics
[AGARD-R-803] p 666 N95-16562
Optimal shape design for aerodynamics p 667 N95-16568
Review of the EUROPT Project AERO-0026 p 668 N95-16573
Application of the space-time conservation element and solution element method to shock-tube problem
[NASA-TM-106806] p 772 N95-16903
On the measurement of momentum flux profiles using a five-beam 915-MHz wind profiler
[DE94-018448] p 791 N95-17903

NUMERICAL CONTROL
Approach to in-process tool wear monitoring in drilling: Application of Kalman filter theory p 653 N95-16279
Production and quality assurance automation in the Goddard Space Flight Center Flight Dynamics Facility p 687 N95-17237
Designing an autonomous environment for mission critical operation of the EUVE satellite p 688 N95-17241
Small scale sequence automation pays big dividends p 689 N95-17247
Development of a prototype real-time automated filter for operational deep space navigation p 694 N95-17545
Embedded parallel processing based ground control systems for small satellite telemetry p 674 N95-17553
Test/score/report: Simulation techniques for automating the test process p 675 N95-17581

NUMERICAL DATA BASES
Numeric data distribution: The vital role of data exchange in today's world p 907 N95-15937

NUMERICAL FLOW VISUALIZATION
Visualizing 3D velocity fields near contour surfaces
[DE94-010205] p 860 N95-16221

NUMERICAL STABILITY
A stepsize control strategy for stiff systems of ordinary differential equations
[AD-A281551] p 861 N95-16395

NUMERICAL WEATHER FORECASTING
Marine boundary-layer parameterizations for large-scale models
[AD-A282402] p 803 N95-16062
An air mass transformation model for coastal environments
[AD-A281790] p 801 N95-17164

A three dimensional mesoscale atmospheric simulation system for use in various mobile battlefield environments. Phase 2: Transition to an operational forecast system
[AD-A281223] p 802 N95-17686

NUSSELT NUMBER
Heat transfer measurements for Stirling machine cylinders
[NASA-CR-197128] p 791 N95-15963

O

OBJECT PROGRAMS
Student research projects, 1993
[AD-A284954] p 804 N95-16124
Flexible method for inter-object communication in C++
[NASA-TM-106315] p 840 N95-17420

OBJECT-ORIENTED PROGRAMMING
Student research projects, 1993
[AD-A284954] p 804 N95-16124
Object-oriented numerical computing C++
p 849 N95-16476
Cognition and procedure representational requirements for predictive human performance models
p 814 N95-16766
DOME: Distributed Object Migration Environment
[AD-A281134] p 850 N95-16826
Towards a class library for mission planning
p 686 N95-17233
Safety aspects of spacecraft commanding
p 689 N95-17248
Flexible method for inter-object communication in C++
[NASA-TM-106315] p 840 N95-17420
Applying STEP principles to product models in high energy physics research
[PB94-197704] p 880 N95-17503
SEQ-REVIEW: A tool for reviewing and checking spacecraft sequences p 697 N95-17561
OOD/OOP experience in the Science Operations Center part of the ground system for X ray Timing Explorer mission p 675 N95-17565
SCOS 2: An object oriented software development approach p 699 N95-17571
Standardizing the information architecture for spacecraft operations p 703 N95-17591
Behavioural modelling of formal documents and active instruments
[PB95-104378] p 842 N95-17732

OBSERVATORIES
The IUE Science Operations Ground System
p 674 N95-17255

OBSTACLE AVOIDANCE
Estimation of vehicle dynamics from monocular noisy images
[AD-A281458] p 804 N95-16078

OCCULTATION
Landing site considerations for atmosphere structure and meteorology p 921 N95-16203
Shotgun/drop-weight initiation of energetic materials
[AD-A285090] p 749 N95-16499

OCEAN BOTTOM
Virtual reality and telerobotics applications of an Address Recalculation Pipeline p 852 N95-15977

OCEAN CURRENTS
On the propagation of near-inertial motion from the oceanic mixed layer p 806 N95-17396
GPS tides and datums
[AD-A282422] p 666 N95-17508
Straits of Florida physical oceanographic field study. Volume 1: Executive summary. Volume 2: Technical report. Volume 3: Data report
[PB94-175031] p 806 N95-17615

OCEAN DYNAMICS
Long-term momentum and heat balances and turbulent mixing in the upper equatorial Pacific Ocean
p 805 N95-17395

OCEAN MODELS
Sensitivity study of the SPEM model to the assimilation of synop datasets using two assimilation schemes. 1: Nudging. 2: The Kalman filter/smoother
[AD-A281459] p 804 N95-16079
Student research projects, 1993
[AD-A284954] p 804 N95-16124
Objective feature identification and tracking: A review
[AD-A284955] p 804 N95-16125
Florida Gulf Stream Data (FLDA) current study
[AD-A281965] p 805 N95-16414
Mixed-layer hindcasts conducted at OWS Victor with initialization from synthetic profiles/mixed-layer hindcasts conducted with BTs taken during 1990 with atmospheric forcing from NOGAPS
[AD-A284749] p 800 N95-16551
Models to estimate high frequency acoustic scattering due to thermal fine- and micro-structure of the ocean
[AD-A285456] p 870 N95-16812
Variation of the thermohaline structure in the western equatorial Pacific upper ocean p 805 N95-17277
Long-term momentum and heat balances and turbulent mixing in the upper equatorial Pacific Ocean
p 805 N95-17395
The effects of the horizontal resolution of the boundary forcing sea surface temperature field on the FSU spectral model
[AD-A284273] p 802 N95-17488
The Grid Analysis and Display System (GrADS)
[NASA-CR-189387] p 912 N95-17491

OCEAN SURFACE
SeaWiFS technical report series. Volume 21: The heritage of SeaWiFS. A retrospective on the CZCS NIMBUS Experiment Team (NET) program
[NASA-TM-104566-VOL-21] p 803 N95-16006
The effects of the horizontal resolution of the boundary forcing sea surface temperature field on the FSU spectral model
[AD-A284273] p 802 N95-17488
Analysis of a three-beam radar as an instrument for determining ocean wave heights and vector slopes
[AD-A282342] p 806 N95-17505
GPS tides and datums
[AD-A282422] p 666 N95-17508

OCEAN TEMPERATURE
Variation of the thermohaline structure in the western equatorial Pacific upper ocean p 805 N95-17277
Straits of Florida physical oceanographic field study. Volume 1: Executive summary. Volume 2: Technical report. Volume 3: Data report
[PB94-175031] p 806 N95-17615

OCEANOGRAPHIC PARAMETERS
Student research projects, 1993
[AD-A284954] p 804 N95-16124
Metadata database for automated oceanographic imagery
[AD-A284932] p 805 N95-16141
Florida Gulf Stream Data (FLDA) current study
[AD-A281965] p 805 N95-16414

OCEANOGRAPHY
The Fifth International Congress on the History of Oceanography
[AD-A281507] p 805 N95-16168
Straits of Florida physical oceanographic field study. Volume 1: Executive summary. Volume 2: Technical report. Volume 3: Data report
[PB94-175031] p 806 N95-17615
Flow over abrupt topography: The application of patterns in nutrient and productivity in reflecting physical processes
[AD-A280813] p 797 N95-17740

OCEANS
Objective feature identification and tracking: A review
[AD-A284955] p 804 N95-16125

OCULOMOTOR NERVES
Characterization of the fast-phase component of the vestibulo-ocular response
[AD-A281830] p 820 N95-16360

OILS
Bicarbonate of soda blasting technology for aircraft wheel depainting
[PB94-193323] p 654 N95-17466

OLIGOMERS
Smart materials based upon oligomeric molecules
[AD-A281374] p 872 N95-16155
Third harmonic generation study of alpha-thiophene oligomers: Monomer to octamer
[AD-A281177] p 874 N95-16629
Iterative divergent/convergent doubling approach to linear conjugated oligomers. A rapid route to a 128 A long potential molecular wire
[AD-A281295] p 874 N95-16784
Synthesis and properties of soluble oligo- and polyphenylenes. A review
[AD-A281293] p 874 N95-16799

OMNIDIRECTIONAL ANTENNAS
Center-fed multifilar helix antenna
[AD-D016390] p 760 N95-17480

ON-LINE SYSTEMS
Sensor fault detection and diagnosis simulation of a helicopter engine in an intelligent control framework
[NASA-TM-106784] p 669 N95-15970
NSSDC data listing
[NASA-TM-109986] p 909 N95-16441
Introduction to the World Wide Web and Mosaic
p 847 N95-16463
Use of World Wide Web and NCSA Mcsaic at Langley
p 847 N95-16464
How to use the WWW to distribute STI
p 847 N95-16465
Image tools for UNIX p 847 N95-16466
Online performance-improvement algorithms
[AD-A285162] p 838 N95-16850
Automating testbed documentation and database access using World Wide Web (WWW) tools
p 696 N95-17557
The CCSDS return all frames Space Link Extension service p 705 N95-17599
MO/DSD online information server and global information repository access p 706 N95-17607
The Requirements Generation System: A tool for managing mission requirements p 707 N95-17608
DROLS: An introduction to searching (videorecording)
[AD-M000338] p 912 N95-17660

ONBOARD DATA PROCESSING
Lessons learned supporting onboard solid-state recorders p 681 N95-17208
The SAX Italian scientific satellite. The on-board implemented automation as a support to the ground control capability p 695 N95-17551
Galileo spacecraft modeling for orbital operations
p 700 N95-17574
Packet utilisation definitions for the ESA XMM mission
p 704 N95-17596
Proposal for implementation of CCSDS standards for use with spacecraft engineering/housekeeping data
p 705 N95-17600

OPERATING SYSTEMS (COMPUTERS)
Control transfer in operating system kernels
[AD-A281135] p 837 N95-16602
Flexible method for inter-object communication in C++
[NASA-TM-106315] p 840 N95-17420

OPERATIONS
Architecture of a distributed multimission operations system p 706 N95-17605

OPERATOR PERFORMANCE
Event-related brain potentials as predictors of target detection performance in a moving waterfall display simulating passive broad-band sonar monitoring
[AD-A280900] p 819 N95-16152
Efficiency in work behaviour: A design approach for modern tools
[PB94-197761] p 831 N95-16953

OPERATORS (MATHEMATICS)
An investigation of genetic operators for continuous parameter space
[DE94-009364] p 834 N95-16219
The complexity of PDL with interleaving
[AD-A281044] p 836 N95-16452
Light-ray operators and their application in QCD
[DE94-013801] p 903 N95-16944

OPERATORS (PERSONNEL)
Situational awareness in complex systems
[AD-A281448] p 825 N95-15959
Breaking down barriers in cooperative fault management: Temporal and functional information displays
[NASA-CR-197450] p 857 N95-17383

OPTICAL BISTABILITY
A novel optic bistable device with very low threshold intensity using photorefractive films
[AD-A285310] p 885 N95-16733

OPTICAL COMMUNICATION
ARO-URI Center for Opto-Electronic Systems Research
[AD-A281447] p 883 N95-15958
High speed transport protocols: An attempt to find the best solution
[AD-A280989] p 751 N95-15993
A quasi-single mode optical fiber for long-haul transmission in severe bending environments
[AD-A281313] p 884 N95-16009
Preliminary investigation of an integrated optic sampler for HF signals
[AD-A284285] p 884 N95-16133
A novel optic bistable device with very low threshold intensity using photorefractive films
[AD-A285310] p 885 N95-16733
The SILEX experiment system operations
p 674 N95-17251
A preliminary optical visibility model
p 758 N95-17290
Ultra high bit rate all optical communication system
[AD-D016359] p 887 N95-17695

OPTICAL CORRELATORS
System design, implementation, and evaluation of the optical broadband correlator
[AD-A285406] p 884 N95-16296

OPTICAL COUPLING
Extraction of high quality potential surfaces from laboratory data
[AD-A285071] p 903 N95-16489
Numerical aperture limits on efficient ball lens coupling of laser diodes to single-mode fibers with defocus to balance spherical aberration
[NASA-TM-4578] p 886 N95-17271

Digital logic and reconfigurable interconnects using aluminum gallium arsenide electro-optic Fredkin gates
[AD-A282880] p 881 N95-17619

OPTICAL DATA PROCESSING

Ultra high bit rate all optical communication system
[AD-D016359] p 887 N95-17695

OPTICAL FIBERS

A quasi-single mode optical fiber for long-haul transmission in severe bending environments
[AD-A281313] p 884 N95-16009
The combination probe of optical fibers and its applications p 652 N95-16275
In-fibre Bragg gratings for millimetre-wave EW systems
[AD-A284283] p 755 N95-16956
Numerical aperture limits on efficient ball lens coupling of laser diodes to single-mode fibers with defocus to balance spherical aberration
[NASA-TM-4578] p 886 N95-17271
Optical fiber sensors: Accelerating applications in Navy ships
[PB94-186848] p 887 N95-17441

OPTICAL MATERIALS

Systematic optimization of second order nonlinear optical materials
[AD-A281350] p 884 N95-16015
Workshop on Epitaxy, Interfaces, Defects and Processing of Electronic and Photonic Materials
[AD-A281595] p 894 N95-16111
Single crystal films and waveguides of organic materials: Preparation and nonlinear optical properties
[AD-A284471] p 895 N95-16134
Design of new multi-functional electroactive polymers with emphasis on optical nonlinearity
[AD-A284983] p 741 N95-16230
Detection of crosslink formation by 2 + 2 photocycloaddition in poly (vinyl cinnamate) by C-13 solid-state NMR
[AD-A281955] p 741 N95-16409
Self assembled spin coated and bulk films of a novel polydiacetylene as second order NLO polymers
[AD-A282271] p 742 N95-16427
Development of device quality nonlinear optical materials and definition of mechanisms of optical nonlinearity
[AD-A285255] p 885 N95-16528
Growth, characterization and applications of beta-barium borate and related crystals
[AD-A281047] p 898 N95-16623
Synthesis of low band gap zwitterionic and planar conjugated pyrrole-derived polymers. Reversible optical absorbances from the UV to the near-IR
[AD-A281174] p 743 N95-16628
Third harmonic generation study of alpha-thiophene oligomers: Monomer to octamer
[AD-A281177] p 874 N95-16629
Materials for second and third order nonlinear optical applications
[AD-A281304] p 885 N95-16787
Effects of substrate temperature on metal colloid formation and on optical response in metal ion implanted silica
[DE94-013633] p 736 N95-16807
New mechanisms and new materials for organic optical nonlinearity
[AD-A282781] p 886 N95-17143
The m-line method for optical characterisation of polymer waveguides
[PB94-184611] p 887 N95-17409
Poling dynamics and relaxation of polar order in guest/host polymers by second harmonic generation
[AD-A283291] p 748 N95-17724
Thermal and laser conditioning of production and rapid-growth KDP and KD*P crystals
[DE94-013738] p 902 N95-17742

OPTICAL MEASUREMENT

Modification of the Naval Postgraduate School Lidar System
[AD-A284987] p 753 N95-16231
Space Shuttle main engine OPAD: The search for a hardware enhanced plume p 716 N95-16330
Sensor placement design for object pose determination with three light-stripe range finders
[AD-A281199] p 886 N95-16795
An investigation of fluid flow during induction stroke of a water analog model of an IC engine using an innovative optical velocimetry concept: LIPA
[NASA-CR-197451] p 780 N95-16900
Differential phase reflectometry for edge profile measurements on TFTR
[DE94-013837] p 891 N95-16958
Measurement of modulation transfer function of focal plane arrays and imaging systems
[AD-A282976] p 887 N95-17707

OPTICAL MEASURING INSTRUMENTS

Non-intrusive missile control surface monitor system
[AD-A285356] p 883 N95-15954
Optical wheel-rotation sensor
[DE94-011719] p 780 N95-16224
Space-based asteroid detection and monitoring system
[AD-D016329] p 915 N95-16854

OPTICAL MICROSCOPES

Development and applications of the positron microscope
[DE94-017918] p 883 N95-15947
Development of an analytical photon scanning tunneling microscope
[AD-A281382] p 884 N95-16157

OPTICAL PATHS

Imager for Mars Pathfinder (IMF) p 711 N95-16206
Thermal effects in end-heated laser rods: A time-dependent model and diagnostic
[AD-A282007] p 778 N95-17500

OPTICAL PROPERTIES

Single crystal films and waveguides of organic materials: Preparation and nonlinear optical properties
[AD-A284471] p 895 N95-16134
Innovative acoustic techniques for studying new materials and new developments in solid state physics
[AD-A280986] p 898 N95-16525
Iterative divergent/convergent doubling approach to linear conjugated oligomers. A rapid route to a 128 A long potential molecular wire
[AD-A281295] p 874 N95-16784
New ytterbium-doped apatite crystals for flexible laser design
[DE94-015138] p 899 N95-16867

OPTICAL PUMPING

Phase-locked arrays of vertical-cavity surface-emitting lasers
[DE94-014941] p 778 N95-17498

OPTICAL RADAR

Using lidar tomography to characterize scattering in a turbulent media
[AD-A281014] p 751 N95-16002
Infrared signatures for remote sensing
[DE94-014222] p 790 N95-16215
Modification of the Naval Postgraduate School Lidar System
[AD-A284987] p 753 N95-16231

OPTICAL RANGE FINDERS

Sensor placement design for object pose determination with three light-stripe range finders
[AD-A281199] p 886 N95-16795

OPTICAL SCANNERS

Development of an analytical photon scanning tunneling microscope
[AD-A281382] p 884 N95-16157
Space-based asteroid detection and monitoring system
[AD-D016329] p 915 N95-16854
Effect of heat treatment temperature on creep-rupture properties of Fe3Al-based alloys
[DE94-018054] p 738 N95-17679

OPTICAL TRACKING

The Yale Knowledge-Based Planning project
[AD-A281505] p 855 N95-16095

OPTICAL TRANSFER FUNCTION

Application of Fourier-space image-restoration techniques to turbulence compensation and sparse-aperture imaging
[AD-A285077] p 885 N95-16494

OPTICAL WAVEGUIDES

Single crystal films and waveguides of organic materials: Preparation and nonlinear optical properties
[AD-A284471] p 895 N95-16134
Design of new multi-functional electroactive polymers with emphasis on optical nonlinearity
[AD-A284983] p 741 N95-16230
The m-line method for optical characterisation of polymer waveguides
[PB94-184611] p 887 N95-17409

OPTIMAL CONTROL

Digital adaptive and optimal control of distributed systems
[AD-A285352] p 851 N95-15952
Microgravity isolation system design: A case study
[NASA-TM-106804] p 654 N95-17657
A feedforward control approach to the local navigation problem for autonomous vehicles
[AD-A282787] p 666 N95-17706

OPTIMIZATION

Portable parallel stochastic optimization for the design of aeropropulsion components
[NASA-CR-195312] p 785 N95-16072
Numerical analysis on periodic response of nonsmooth dynamic systems p 650 N95-16261
Method of calculating the optimal radioelectronic equipment design p 652 N95-16271
Solar-powered rocket engine optimization for high specific impulse p 718 N95-16341
Stochastic approximation methods for fusion-rule estimation in multiple sensor systems
[DE94-013629] p 856 N95-16361
Optimum Design Methods for Aerodynamics
[AGARD-R-803] p 666 N95-16562
Optimum aerodynamic design via boundary control p 667 N95-16565
Optimal shape design for aerodynamics p 667 N95-16568
Airfoil optimization by the one-shot method p 667 N95-16569
Tools for applied engineering optimization p 668 N95-16570
The global aircraft shape p 668 N95-16571
Aerodynamic shape optimization p 668 N95-16572
Review of the EUROPT Project AERO-0026 p 668 N95-16573
Algorithms for bilevel optimization
[NASA-CR-194980] p 863 N95-16897
Constrained minimization of smooth functions using a genetic algorithm
[NASA-TP-3329] p 709 N95-16902
Optimization of adaptive intraply hybrid fiber composites with reliability considerations
[NASA-TM-106632] p 787 N95-16911
JPL-ANTOPT antenna structure optimization program p 759 N95-17297
Computational differentiation and multidisciplinary design
[DE94-013393] p 863 N95-17306
Structural optimization with approximate sensitivities
[NASA-TM-4553] p 789 N95-17701
Beam position correction in the Fermilab Linac
[DE94-018984] p 882 N95-17931

OPTOELECTRONIC DEVICES

International Workshop on Light Emission and Electronic Properties of Nanoscale silicon
[AD-A281464] p 894 N95-16081

ORBIT CALCULATION

Production and quality assurance automation in the Goddard Space Flight Center Flight Dynamics Facility p 687 N95-17237
Evaluation of current tropospheric mapping functions by Deep Space Network very long baseline interferometry p 756 N95-17280
Implementation of a low-cost, commercial orbit determination system p 673 N95-17544
TDRS orbit determination by radio interferometry p 673 N95-17547

ORBIT DECAY

An analysis of a single-burn algorithm for Low-Earth Orbit maintenance
[AD-A283418] p 721 N95-17626

ORBITAL MANEUVERS

Numerical optimization of synergetic maneuvers
[AD-A283398] p 656 N95-17435
Optimal transfer and swing-orbits in the two- and three-body problems
[INPE-5572-TAE/022] p 673 N95-17648

ORBITAL MECHANICS

Optimal transfer and swing-orbits in the two- and three-body problems
[INPE-5572-TAE/022] p 673 N95-17648

ORBITAL POSITION ESTIMATION

TDRS orbit determination by radio interferometry p 673 N95-17547

ORDER-DISORDER TRANSFORMATIONS

Electron transport and tunneling experiments
[AD-A281527] p 894 N95-16106
First principles simulation of materials properties
[DE94-013615] p 899 N95-16805

ORGANIC CHARGE TRANSFER SALTS

Atomic force microscopy of the electrochemical nucleation and growth of molecular crystals
[AD-A281024] p 897 N95-16445

ORGANIC CHEMISTRY

Carbon clusters studied by neutralization-reionization mass spectrometry
[AD-A281367] p 726 N95-16017
Radical cations of quadricyclane and norbornadiene in polar ZSM-5 matrices: Radical cation photochemical transformations without photons
[DE94-014007] p 728 N95-16485

ORGANIC COMPOUNDS

The removal of heteroatoms from organic compounds by supercritical water
[AD-A281532] p 722 N95-16087
Augmentation for research training: Surface-mediated photocatalysis
[AD-A281591] p 722 N95-16100
Self-assembly of low-dimensional conductors on Au(111) surfaces
[AD-A280936] p 734 N95-16505

New approaches to novel organosilanes
[AD-A285253] p 722 N95-16513
Mass spectral data of alkyl and cycloalkyl methylphosphonofluoridates
[AD-A285312] p 722 N95-16734
ORGANIC MATERIALS
Single crystal films and waveguides of organic materials: Preparation and nonlinear optical properties
[AD-A284471] p 895 N95-16134
Design of new multi-functional electroactive polymers with emphasis on optical nonlinearity
[AD-A284983] p 741 N95-16230
ORGANIC SOLIDS
Nanoscale imaging of molecular adsorption
[AD-A280979] p 873 N95-16482
ORGANIC SUPERCONDUCTORS
Design and synthesis of organic superconductors (FY92 URI/RIP)
[AD-A281308] p 899 N95-16789
AC susceptibility and critical current in the organic superconductor (kappa)-(ET)2Cu(NCS)2
[DE94-013997] p 900 N95-16946
ORGANIZATIONS
Source hierarchy list. Volume 2: E through N
[AD-A281101] p 908 N95-15957
Source header list. Volume 2: L through Z
[AD-A281001] p 908 N95-15998
Directory of Organizational Technical Report Acronym Codes (DOTRAC)
[AD-A281500] p 908 N95-16086
Source hierarchy list. Volume 3: O through Z
[AD-A281102] p 908 N95-16090
Payload operations management of a planned European SL-Mission employing establishments of ESA and national agencies p 684 N95-17221
ORGANOMETALLIC COMPOUNDS
An X-Ray Photoelectron Spectroscopy (XPS) study of activated carbons impregnated with some organocopper complexes
[AD-A282721] p 727 N95-16384
Encapsulated alkaline-earth organometallics as controlled sources of calcium, strontium, and barium ions
[AD-A281547] p 741 N95-16393
Living radical polymerization of vinyl acetate
[AD-A280901] p 743 N95-16500
Chemical vapor deposition of high T(sub c) superconducting films in a microgravity environment
[NASA-CR-197527] p 750 N95-16880
ORTHOGRAPHY
Phonologic-graphemic transcodifier for Portuguese Language spoken in Brazil (PLB)
[INPE-5575-PRE/1803] p 760 N95-17649
ORTHOSTATIC TOLERANCE
Comparison of saline and fludrocortisone as fluid-loading countermeasures following exposure to simulated microgravity p 808 N95-16742
Blood volume and orthostatic responses of men and women to a 13-day bedrest p 811 N95-16752
The value of the 4-day headdown bedrest model for screening countermeasures p 817 N95-16782
OSCILLATING FLOW
A computational investigation of wake-induced airfoil flutter in incompressible flow and active flutter control
[AD-A281534] p 670 N95-16109
OSCILLATIONS
Avoiding BDF stability barriers in the MOL solution of advection-dominated problems
[DE94-014793] p 861 N95-16535
Solar neutrino oscillations
[PB95-104295] p 923 N95-17352
On the propagation of near-inertial motion from the oceanic mixed layer p 806 N95-17396
Neutrino oscillation studies at LAMPF
[DE94-018098] p 878 N95-17727
OSCILLATORS
The LANL-Boeing APLE/HPO flying-wire beam-profile monitor
[DE94-014255] p 879 N95-16172
Exact, E = 0, classical and quantum solutions for general power-law oscillators
[DE94-014436] p 903 N95-16428
OSCILLOSCOPES
Characterization of multiport solid state imagers at megahertz data rates
[DE94-016095] p 765 N95-16932
OSMOSIS
Characterization of surfaces
[NASA-CR-196995] p 750 N95-16065
OTOLITH ORGANS
Mathematical model for interaction of canals and otoliths in perception of orientation, translation, and rotation
[AD-A280897] p 819 N95-16151
The psychophysical function for perceived gravitational-inertial force does not depend on the orientation of the otolith organs p 808 N95-16740
OXIDATION
Testing and evaluation of oxide-coated iridium/rhenium chambers p 719 N95-16346
XAFS spectra and the oxidation state of nickel in some of its oxycompounds
[AD-A281137] p 735 N95-16606
Bench wear and single-cylinder engine evaluations of high-temperature lubricants for US Army ground vehicles
[AD-A285399] p 780 N95-16636
Research on organofluorine chemistry for 700 F thermooxidative stability
[AD-A282767] p 731 N95-17142
Development of heterogeneous Wacker oxidation catalysts: The role of the support and the redox component
[PB94-201431] p 732 N95-17700
Environmental effects on iron aluminide
[DE94-017900] p 739 N95-17747
An XAFS study of the oxidation of structural iron in biotite mica by solutions containing Br2 or H2O2
[DE94-018721] p 733 N95-17912
OXIDATION RESISTANCE
Design, analysis, and fabrication of oxide-coated iridium/rhenium combustion chambers p 719 N95-16347
Studies on improvement of oxidation resistivity of carbon materials by glass impregnation and SiC formation
[DE94-796529] p 724 N95-16833
OXIDATION-REDUCTION REACTIONS
Aluminum permanganate battery
[AD-D016337] p 766 N95-16947
Aluminum-ferricyanide battery
[AD-D016338] p 766 N95-16948
Fundamental studies in oxidation-reduction in relation to water photolysis
[DE94-014598] p 731 N95-17161
Ion modulated electroactivity in thin-film polymers derived from bipyridyl and phenanthroline complexes of iron
[AD-A280704] p 747 N95-17682
Development of heterogeneous Wacker oxidation catalysts: The role of the support and the redox component
[PB94-201431] p 732 N95-17700
OXIDE FILMS
HTS SNS devices on large-area substrates by single-source MOCVD
[AD-A285159] p 899 N95-16849
Preparation and investigation of improved low voltage electron excitable phosphors
[AD-A284265] p 767 N95-17487
OXIDES
Property control of (perfluorinated ionomer)/(inorganic oxide) composites by tailoring the nanoscale morphology
[AD-A281370] p 723 N95-16019
Metastability in molecules
[AD-A285223] p 874 N95-16523
OXYGEN
The analysis and minimization of oxygen contamination in the powder processing of molybdenum disilicide
[DE94-014234] p 735 N95-16540
Failure of ozone and nitrogen dioxide to enhance lung tumor development in hamsters
[PB94-182854] p 818 N95-16801
Shock initiation of crystalline boron in oxygen and fluorine compounds
[AD-A284266] p 730 N95-16955
Equatorial airglow studies via rocket experiment
[INPE-5589-TDI/551] p 799 N95-17647
OXYGEN ATOMS
Surface and defect excitations in covalently bonded solids
[AD-A281338] p 894 N95-16012
Atomic transport of oxygen
[DE94-013332] p 873 N95-16430
Atomic oxygen durability evaluation of the flexible batten for the photovoltaic array mast on Space Station
[NASA-TM-106798] p 781 N95-17263
Reaction and protection of electrical wire insulators in atomic-oxygen environments
[NASA-TM-106767] p 709 N95-17275
OXYGEN CONSUMPTION
Evaluation of a newly-designed, dynamic knee extension device for the study of muscle fatigue in humans
[AD-A284974] p 819 N95-16228
The effect of intermittent standing or walking during head down tilt bedrest on peak O2 consumption p 817 N95-16779
The value of the 4-day headdown bedrest model for screening countermeasures p 817 N95-16782
Energy expenditure, physical work load and postural control during walking on a moving platform
[AD-A285343] p 830 N95-16821
OXYGEN RECOMBINATION
Gas-surface interactions near dissociation threshold
[AD-A284945] p 726 N95-16042
OZONE
Failure of ozone and nitrogen dioxide to enhance lung tumor development in hamsters
[PB94-182854] p 818 N95-16801
Fire protection engineering criteria: Electronic equipment installations
[AD-A285174] p 750 N95-16853
Equatorial airglow studies via rocket experiment
[INPE-5589-TDI/551] p 799 N95-17647
OZONE DEPLETION
Alternatives for ozone-depleting refrigerants
[PB94-190857] p 795 N95-16881

P

P-I-N JUNCTIONS
Recombination and metastability in amorphous silicon and silicon-germanium alloys
[DE94-011837] p 794 N95-16957
P-N JUNCTIONS
LPEE growth and characterization of In(x)Ga(1-x)As(y)Sb(1-y) lattice matched to GaSb and InAs for photodetectors
[AD-A281631] p 895 N95-16114
P-TYPE SEMICONDUCTORS
Low temperature deposition and characterization of N- and P-type silicon carbide thin films and associated ohmic and Schottky contacts
[AD-A281060] p 743 N95-16625
PACIFIC ISLANDS
Solar energy: Lessons from the Pacific island experience
[WORLD-BANK-TP-244] p 794 N95-17298
PACIFIC OCEAN
Variation of the thermohaline structure in the western equatorial Pacific upper ocean p 805 N95-17277
Long-term momentum and heat balances and turbulent mixing in the upper equatorial Pacific Ocean p 805 N95-17395
An observational study of long waves in the equatorial Pacific Ocean during the 1991-1993 El Nino
[AD-A283380] p 806 N95-17624
PACKET SWITCHING
Data rearrangement and real-time computation
[AD-A282349]* p 910 N95-17166
PACKET TRANSMISSION
End-to-end communication test on variable length packet structures utilizing AOS testbed p 677 N95-17186
Ground equipment for the support of packet telemetry and telecommand p 681 N95-17203
Experience with the EURECA Packet Telemetry and Packet Telecommand system p 682 N95-17209
The Advanced Orbiting Systems Testbed Program: Results to date p 700 N95-17575
The ESA standard for telemetry and telecommand packet utilisation: PUS p 704 N95-17595
PACKETS (COMMUNICATION)
End-to-end communication test on variable length packet structures utilizing AOS testbed p 677 N95-17186
Process and methodology of developing Cassini G and C Telemetry Dictionary p 681 N95-17204
Experience with the EURECA Packet Telemetry and Packet Telecommand system p 682 N95-17209
The Pacor 2 expert system: A case-based reasoning approach to troubleshooting p 693 N95-17541
Spacecraft Data Simulator for the test of level zero processing systems p 675 N95-17582
The ESA standard for telemetry and telecommand packet utilisation: PUS p 704 N95-17595
Packet utilisation definitions for the ESA XMM mission p 704 N95-17596
Proposal for implementation of CCSDS standards for use with spacecraft engineering/housekeeping data p 705 N95-17600
PAINTS
Bicarbonate of soda blasting technology for aircraft wheel depainting
[PB94-193323] p 654 N95-17466
PAIR PRODUCTION
Multilepton SUSY signals from R-parity violation at the Tevatron (revised)
[PB95-104311] p 877 N95-17353
PALEONTOLOGY
Exobiology site priorities for Mars Pathfinder p 919 N95-16188
PALLADIUM
Small angle neutron scattering from nanocrystalline Pd and Cu compacted at elevated temperatures
[DE94-013865] p 876 N95-16962

PALLADIUM COMPOUNDS
Development of heterogeneous Wacker oxidation catalysts: The role of the support and the redox component
[PB94-201431] p 732 N95-17700
PANEL METHOD (FLUID DYNAMICS)
A computational investigation of wake-induced airfoil flutter in incompressible flow and active flutter control
[AD-A281534] p 670 N95-16109
PARABOLAS
Intense ion beam characterization and thermal modeling for beam materials processing
[DE94-016281] p 745 N95-16938
PARABOLIC BODIES
Conceptual design study of a solar concentrator/support structure: A three dimensional finite element model
p 718 N95-16342
PARABOLIC DIFFERENTIAL EQUATIONS
Rough surface models implemented within the split-step parabolic equation algorithm
[AD-A280843] p 753 N95-16148
PARABOLIC FLIGHT
Achilles Tendon Reflex (ATR) in response to short exposures of microgravity and hypergravity
p 812 N95-16756
Dynamics of the G-excess illusion
p 815 N95-16771
Delivery of cardiopulmonary resuscitation in the microgravity environment p 816 N95-16774
A surgical support system for Space Station Freedom
p 710 N95-16776
PARABOLIC REFLECTORS
Conceptual design study of a solar concentrator/support structure: A three dimensional finite element model
p 718 N95-16342
PARACHUTE DESCENT
Mars Pathfinder mission operations concepts
p 686 N95-17229
PARALLEL COMPUTERS
Equation solvers for distributed-memory computers
p 847 N95-16460
On-line scheduling on parallel machines
[AD-A281136] p 849 N95-16603
Flosolver parallel computers: 1986-1994
[NAL-SP-9409] p 850 N95-16901
Highly parallel reconfigurable computer architecture for robotic computation having plural processor cells each having right and left ensembles of plural processors
[NASA-CASE-NPO-17632-1-CU] p 832 N95-17400
XPVM: A graphical console and monitor for PVM
[DE94-018050] p 842 N95-17678
PARALLEL PROCESSING (COMPUTERS)
A new communication scheme for the neutron diffusion nodal method in a distributed computing environment
[DE94-017907] p 844 N95-15946
Parallel implementation of the terrain masking algorithm
[AD-A281017] p 833 N95-16003
Parallel software benchmarks for high performance BMC3/IS systems
[AD-A282329] p 844 N95-16060
Portable parallel stochastic optimization for the design of aeropropulsion components
[NASA-CR-195312] p 785 N95-16072
Partial evaluation for scientific computing: The supercomputer toolkit experience
[AD-A282286] p 846 N95-16237
Rapid solution of large-scale systems of equations
p 847 N95-16458
Solution of matrix equations using sparse techniques
p 847 N95-16459
Equation solvers for distributed-memory computers
p 847 N95-16460
Automatic differentiation for design sensitivity analysis of structural systems using multiple processors
p 847 N95-16462
Proceedings of the International Conference on Parallel Architectures and Compilation Techniques
[AD-A285258] p 849 N95-16529
On-line scheduling on parallel machines
[AD-A281136] p 849 N95-16603
CMCAM: A high performance CM-5 lattice gas simulator
[AD-A281063] p 837 N95-16626
Active messages versus explicit message passing under SUNMOS
[DE94-015278] p 850 N95-16830
Online performance-improvement algorithms
[AD-A285162] p 838 N95-16850
Investigation of modularly configured attached processors with intelligent memories
[AD-A285454] p 832 N95-16876
Flosolver parallel computers: 1986-1994
[NAL-SP-9409] p 850 N95-16901
Trapezoidal rule quadrature algorithms for MIMD distributed memory computers
[DE94-016369] p 839 N95-16923
Parallel parsing
[PB94-191392] p 850 N95-17138
Applications of massively parallel computers in telemetry processing p 680 N95-17201
Highly parallel reconfigurable computer architecture for robotic computation having plural processor cells each having right and left ensembles of plural processors
[NASA-CASE-NPO-17632-1-CU] p 832 N95-17400
Cellular automata for contour dynamics
[PB94-197613] p 865 N95-17526
Embedded parallel processing based ground control systems for small satellite telemetry
p 674 N95-17553
Parallel fast Fourier transforms for non power of two data
[DE94-018047] p 851 N95-17676
XPVM: A graphical console and monitor for PVM
[DE94-018050] p 842 N95-17678
PARALLEL PROGRAMMING
Portable parallel stochastic optimization for the design of aeropropulsion components
[NASA-CR-195312] p 785 N95-16072
The search for lost cycles: A new approach to parallel program performance evaluation
[AD-A281467] p 845 N95-16082
Software cache coherence for large scale multiprocessors
[AD-A281628] p 845 N95-16113
DOME: Distributed Object Migration Environment
[AD-A281134] p 850 N95-16826
PARAMETER IDENTIFICATION
Erosion effects on TVC vane heat transfer characteristics
[AD-A282006] p 721 N95-17448
PARAMETERIZATION
Marine boundary-layer parameterizations for large-scale models
[AD-A282402] p 803 N95-16062
An investigation of genetic operators for continuous parameter space
[DE94-009364] p 834 N95-16219
PARAMETRIC AMPLIFIERS
A AgGaSe2 optical parametric oscillator pumped by a Raman-shifted YAG laser
[AD-A284743] p 777 N95-16548
Growth, characterization and applications of beta-barium borate and related crystals
[AD-A281047] p 898 N95-16623
Tunable UV source for UV fluorescence remote sensing
[DE94-015745] p 777 N95-16917
PARASITES
Closed orbit distortion from parasitic collisions in PEP-2
[DE94-018203] p 882 N95-17890
Beam-beam tune shift and dynamical beta function in PEP-2
[DE94-018207] p 882 N95-17891
PARSING ALGORITHMS
A parser for the ISO 8211 data format
[AD-A281594] p 909 N95-16431
Parallel parsing
[PB94-191392] p 850 N95-17138
Use of data description languages in the interchange of data p 704 N95-17597
PARTIAL DIFFERENTIAL EQUATIONS
Problem of constructing the Lyapunov's functions in lumped parameter systems p 653 N95-16276
Numerical methods for singularly perturbed differential equations with applications
[AD-A285209] p 861 N95-16517
Avoiding BDF stability barriers in the MOL solution of advection-dominated problems
[DE94-014793] p 861 N95-16535
On the removal of boundary errors caused by Runge-Kutta integration of non-linear partial differential equations
[NASA-CR-194989] p 863 N95-16904
Parallel fast Fourier transforms for non power of two data
[DE94-018047] p 851 N95-17676
PARTIAL PRESSURE
The response of the Sandia robust wide range hydrogen sensor to H2-O2 mixtures
[DE94-013763] p 727 N95-16362
PARTICLE ACCELERATION
Radial acceletron, a new low impedance HPM source
[AD-A282008] p 760 N95-17501
PARTICLE ACCELERATORS
SEPAC co-investigator support
[NASA-CR-196527] p 798 N95-15965
Radial acceletron, a new low impedance HPM source
[AD-A282008] p 760 N95-17501
High Energy Physics Division research activities
[DE94-015024] p 882 N95-17924
PARTICLE BEAMS
Online diagnoses of high current-density beams
[DE94-014420] p 879 N95-16217
Radial acceletron, a new low impedance HPM source
[AD-A282008] p 760 N95-17501
High Energy Physics Division research activities
[DE94-015024] p 882 N95-17924
PARTICLE COLLISIONS
Parton distributions of the proton
[PB95-104337] p 877 N95-17354
Surfactant adsorption by sub-millimeter size bubbles: Quantification and modelling
[AD-A282405] p 772 N95-17506
Theoretical studies of the strengths of matrix second phase particle interfaces
[AD-A280703] p 738 N95-17681
PARTICLE DECAY
Experimental issues in high-sensitivity charm experiments
[DE94-015544] p 871 N95-15945
Measurement of the B meson differential cross-sections in p(-p) collisions at the square root of s = 1.8 TeV using the exclusive decays B(+-) yields J/(psi)K(+-) and B(exp 0) yields J/(psi)K(exp *0)
[DE94-015185] p 872 N95-16309
Tests of structure functions using leptons at CDF: W asymmetry and Dreil-Yan production
[DE94-015727] p 875 N95-16840
QCD of different flavors with the SLD detectors
[DE94-013800] p 875 N95-16943
Limit on the rare decay B yields muon(+)muon(-) K(+-)
[DE94-013851] p 876 N95-16960
A measurement of the Michel parameter (rho) in muon decay
[DE94-014423] p 876 N95-17153
A search for muons yields e gamma at the level of 10(exp -13)
[DE94-014488] p 876 N95-17158
Search for the presence of H particles in a neutral beam
[DE94-013526] p 877 N95-17683
PARTICLE DIFFUSION
A new communication scheme for the neutron diffusion nodal method in a distributed computing environment
[DE94-017907] p 844 N95-15946
Surfactant adsorption by sub-millimeter size bubbles: Quantification and modelling
[AD-A282405] p 772 N95-17506
PARTICLE INTERACTIONS
Light-ray operators and their application in QCD
[DE94-013801] p 903 N95-16944
Solar neutrino oscillations
[PB95-104295] p 923 N95-17352
PARTICLE MOTION
Filter efficiency and pressure drop calculations through two and three dimensional fiber arrays
[DE94-014111] p 770 N95-16211
PARTICLE PRODUCTION
Experimental issues in high-sensitivity charm experiments
[DE94-015544] p 871 N95-15945
A-dependent effects in high P(sub T) reactions
[DE94-016385] p 875 N95-16924
Z(prime) phenomenology: Constraints from low-energy measurements, and detailed study at TeV-scale lepton and hadron colliders
[DE94-018185] p 881 N95-17886
PARTICLE SIZE DISTRIBUTION
Analysis of the through-thickness micropore and constituent particle population gradients in the 7050-T7451 plate aluminum alloys
[AD-A282970] p 738 N95-17663
PARTICLE SPIN
High Energy Physics Division research activities
[DE94-015024] p 882 N95-17924
PARTICLE TRACKS
Electrical breakdown and optical emission properties of high pressure pulsed RF gas discharges
[DE94-012731] p 877 N95-17687
PARTICULATES
Novel mass spectrometric instrument for gaseous and particulate characterization and monitoring
[DE94-014168] p 795 N95-16213
PARTONS
Tests of structure functions using leptons at CDF: W asymmetry and Dreil-Yan production
[DE94-015727] p 875 N95-16840
A-dependent effects in high P(sub T) reactions
[DE94-016385] p 875 N95-16924
Light-ray operators and their application in QCD
[DE94-013801] p 903 N95-16944
Parton distributions of the proton
[PB95-104337] p 877 N95-17354

PASSIVITY
Reaction of methanol with porous silicon
[AD-A285518] p 728 N95-16406
PATIENTS
A prototype Crew Medical Restraint System (CMRS) for Space Station Freedom p 815 N95-16773
Advanced Cardiac Life Support (ACLS) utilizing Man-Tended Capability (MTC) hardware onboard Space Station Freedom p 816 N95-16775
PATTERN METHOD (FORECASTING)
Summary of 1994 Atlantic tropical cyclone activity and verification of author's seasonal prediction, 1
p 801 N95-17259
Extended range forecast of Atlantic seasonal hurricane activity for 1995, 2 p 801 N95-17260
PATTERN RECOGNITION
A general method to determine invariants
[TR-503] p 859 N95-15949
Presentations of shape in object recognition and long-term visual memory
[AD-A281336] p 825 N95-16010
Student research projects, 1993
[AD-A284954] p 804 N95-16124
Computational vision based on neurobiology
[AD-A284472] p 819 N95-16135
Training visual pattern recognition: Using worked examples to aid schema acquisition
[AD-A281859] p 826 N95-16299
Log-polar optical coordinate transformation with applications for automatic pattern recognition
[AD-A281022] p 885 N95-16443
Evolving neural network pattern classifiers
[AD-A281181] p 857 N95-16631
Learning one more thing
[AD-A285342] p 857 N95-16820
Self-organizing neural network for classifying pattern signatures with a posteriori conditional class probability
[AD-D016455] p 857 N95-16823
Online performance-improvement algorithms
[AD-A285162] p 838 N95-16850
Pattern theoretic knowledge discovery
[AD-A285472] p 909 N95-16879
High performance hardware and software for pattern recognition and image processing
[AD-A284264] p 839 N95-17172
The 1994 International Neural Network Society Annual Meeting, volume 3
[AD-A281736] p 857 N95-17369
Hidden Markov model for gesture recognition
[AD-A282845] p 865 N95-17377
Hidden Markov model for control strategy learning
[AD-A282846] p 865 N95-17429
Object recognition using multi-layer Hopfield neural network
[AD-A282417] p 858 N95-17459
Small sample behavior of multi-layer feedforward network classifiers: Theoretical and practical aspects
[PB94-201415] p 841 N95-17470
Representation, modeling and recognition of outdoor scenes
[AD-A283257] p 858 N95-17634
Synthetic aperture radar target detection, feature extraction, and image formation techniques
[NASA-CR-197485] p 760 N95-17651
PAYLOAD CONTROL
A General Mission Independent Simulator (GMIS) and Simulator Control Program (SCP) p 701 N95-17580
Test/score/report: Simulation techniques for automating the test process p 675 N95-17581
Transportable Payload Operations Control Center reusable software: Building blocks for quality ground data systems p 703 N95-17587
A new systems engineering approach to streamlined science and mission operations for the Far Ultraviolet Spectroscopic Explorer (FUSE) p 707 N95-17611
PAYLOADS
Using virtual reality for science mission planning: A Mars Pathfinder case p 673 N95-15978
Virtual environment application with partial gravity simulation p 854 N95-15988
Catalog of lunar and Mars science payloads
[NASA-RP-1345] p 922 N95-16436
Payload operations management of a planned European SL-Mission employing establishments of ESA and national agencies p 684 N95-17221
International Space Station Alpha user payload operations concept p 685 N95-17227
A survey of commercially available expendable heavy lift launch vehicles
[AD-A282429] p 676 N95-17509
An opportunity analysis system for space surveillance experiments with the MSX p 707 N95-17609
Matrix evaluation of science objectives
p 707 N95-17610
PENETRATION
Material and ballistic investigation of a tungsten-26 percent rhenium alloy
[PB94-189156] p 734 N95-16420
Penetration of solid and layered targets by gas gun-launched steel cubes
[AD-A285143] p 787 N95-16843
Development of an Automated Airfield Dynamic Cone Penetrometer (AADCP) prototype and the evaluation of unsurfaced airfield seismic surveying using Spectral Analysis of Surface Waves (SASW) technology
[AD-A281985] p 672 N95-17444
Recent advances in the development of high average power induction accelerators for industrial and environmental applications
[DE94-018734] p 882 N95-17914
PENETROMETERS
Normalization and prediction of geotechnical properties using the Cone Penetrometer Test (CPT)
[AD-A285193] p 799 N95-16872
Development of an Automated Airfield Dynamic Cone Penetrometer (AADCP) prototype and the evaluation of unsurfaced airfield seismic surveying using Spectral Analysis of Surface Waves (SASW) technology
[AD-A281985] p 672 N95-17444
PEPTIDES
Ligand field stabilization control of metal ion binding
[AD-A281011] p 726 N95-16001
PERCEPTION
Studies of novel popout
[AD-A285237] p 826 N95-16244
PERFORMANCE
Towards a new generation of mission planning systems: Flexibility and performance p 686 N95-17230
PERFORMANCE PREDICTION
The search for lost cycles: A new approach to parallel program performance evaluation
[AD-A281467] p 845 N95-16082
The EPIC architecture for modeling human information-processing and performance: A brief introduction
[AD-A280762] p 829 N95-16119
The computer analysis of the prediction of aircraft electrical power supply system reliability
p 653 N95-16278
Analog microcircuit fault prediction
[AD-A281958] p 763 N95-16410
Efficient estimation of the mean time between failures in non-regenerative dependability models
[AD-A281563] p 783 N95-16421
Cognition and procedure representational requirements for predictive human performance models
p 814 N95-16766
On bi-grid local mode analysis of solution techniques for 3-D Euler and Navier-Stokes equations
[NASA-TM-106749] p 771 N95-16855
Summary of 1994 Atlantic tropical cyclone activity and verification of author's seasonal prediction, 1
p 801 N95-17259
Extended range forecast of Atlantic seasonal hurricane activity for 1995, 2 p 801 N95-17260
Evaluating modeling tools for the EDOS
p 700 N95-17572
NCCDS performance model p 675 N95-17576
PERFORMANCE TESTS
New insulation constructions for aerospace wiring applications p 712 N95-16056
High performance dielectric materials development
p 712 N95-16057
The search for lost cycles: A new approach to parallel program performance evaluation
[AD-A281467] p 845 N95-16082
Solid state radar demonstration test results at the FAA Technical Center
[AD-A281520] p 752 N95-16097
Detailed example of using PIWG on the SUN workstation and the DEC VAX computer
[AD-A281528] p 834 N95-16107
ADST system test report for the rotary wing aircraft airnet aeromodel and weapon model merge with the ATAC 2 baseline
[AD-A281580] p 666 N95-16171
Site characterization at the Rabbit Valley Geophysical Performance Evaluation Range
[DE94-013550] p 798 N95-16284
Cryogenic foil bearing turbopumps
p 716 N95-16331
Assessment of research needs for advanced heterogeneous catalysts for energy applications, volume 2
[DE94-015890] p 727 N95-16387
Primary battery design and safety guidelines handbook
[NASA-RP-1353] p 764 N95-16561
Bench wear and single-cylinder engine evaluations of high-temperature lubricants for US Army ground vehicles
[AD-A285399] p 780 N95-16636
Aerospace Medical Association 63rd Annual Scienti fic Meeting Program p 807 N95-16737
Review of performance, medical, and operational data on pilot aging issues p 812 N95-16759
Evaluation of a new miniature temperature data logger: Herpetological review
[DE94-013561] p 774 N95-16804
Performance evaluation of polyaniline as an active material for electrochemical capacitors
[DE94-016283] p 765 N95-16920
Thermoacoustic pin stacks
[AD-A282267] p 794 N95-16954
The role of mission operations in spacecraft integration and test p 684 N95-17220
Apache helicopter seat cushion evaluation
[AD-A284300] p 831 N95-17484
Testing and characterization of the CYCLOPS HgCdTe focal plane detector array
[AD-A284279] p 887 N95-17489
ATM-test: A workstation-based software suite for testing Asynchronous Transfer Mode (ATM) networks
[DE94-013813] p 850 N95-17516
Blinks, saccades, and fixation pauses during vigilance task performance. 1: Time on task
[DOT/FAA/AM-94/26] p 828 N95-17530
Use of copper powder extinguishers on lithium fires
[AD-A283213] p 751 N95-17632
Evaluation of a pneumatic Martian soil sampler concept
[NASA-CR-197539] p 923 N95-17653
PERIODIC FUNCTIONS
Numerical analysis on periodic response of nonsmooth dynamic systems p 650 N95-16261
PERIODICALS
Tsunami newsletter, volume 26
[AD-A282751] p 806 N95-17477
PERIPHERAL CIRCULATION
Increased skin blood flow and enhanced heat loss in humans after niacin ingestion
[AD-A281124] p 821 N95-16809
PERMAFROST
Long term modelling of permafrost dynamics
[AD-A285315] p 799 N95-16735
PERMANGANATES
Aluminum permanganate battery
[AD-D016337] p 766 N95-16947
PERMEABILITY
Surface heat transfer in a channel with porous insert
p 650 N95-16255
Duality transformations, green dyadics and plane-wave solutions for a class of bianisotropic media
[PB94-197670] p 754 N95-16612
PERMITTIVITY
Duality transformations, green dyadics and plane-wave solutions for a class of bianisotropic media
[PB94-197670] p 754 N95-16612
PERSONAL COMPUTERS
Integrating computers into calculus instruction
[AD-A280996] p 833 N95-15997
Efficiency in work behaviour: A design approach for modern tools
[PB94-197761] p 831 N95-16953
High performance hardware and software for pattern recognition and image processing
[AD-A284264] p 839 N95-17172
Small satellite space operations p 695 N95-17552
PERSONALITY
A workout for virtual bodybuilders (design issues for embodiment in multi-actor virtual environments)
p 854 N95-15990
Validation of astronaut psychological select-in criteria
p 813 N95-16762
Human performance in the modern cockpit
p 813 N95-16764
Crew decision making under stress
p 814 N95-16765
PERSONNEL
Shared mission operations concept
p 685 N95-17228
PERSONNEL DEVELOPMENT
Estimating the benefits of personnel selection and classification: An extension of the Brogden table
[AD-A285674] p 828 N95-17175
PERSONNEL MANAGEMENT
Development of strength analysis methods and design model for aircraft constructions in Kazan Aviation Institute p 651 N95-16264
SPOT4 Management Centre p 673 N95-17223
PERSONNEL SELECTION
Aerospace Medical Association 63rd Annual Scienti fic Meeting Program p 807 N95-16737
Psychological training of NASA astronauts for extended missions p 813 N95-16763
Crew decision making under stress
p 814 N95-16765

Estimating the benefits of personnel selection and classification: An extension of the Brogden table
[AD-A285674] p 828 N95-17175

PERTURBATION
Airfoil optimization by the one-shot method
p 667 N95-16569
Likelihood ratio gradient estimation for stochastic recursions
[AD-A281408] p 865 N95-17426
Measurements of non-axisymmetric effects in the D3-D divertor
[DE94-018346] p 893 N95-17897
Electromagnetic field measurements on a mm-wave linear accelerator
[DE94-015092] p 761 N95-17926

PERTURBATION THEORY
A Lyapunov bound for solutions of Poisson's equation
[AD-A281536] p 860 N95-16169
Numerical methods for singularly perturbed differential equations with applications
[AD-A285209] p 861 N95-16517
Small-amplitude disturbances in turbomachine flows with swirl
[NASA-CR-195406] p 772 N95-17386

PETRI NETS
Communication network software analysis
[AD-A281019] p 833 N95-16004

PETROLEUM PRODUCTS
Assessment of research needs for advanced heterogeneous catalysts for energy applications, volume 1
[DE94-015889] p 795 N95-16386

PHARMACOLOGY
Increased skin blood flow and enhanced heat loss in humans after niacin ingestion
[AD-A281124] p 821 N95-16809

PHASE CHANGE MATERIALS
Synthesis and characterization of a new class of thermosetting resins: Allyl and propargyl substituted cyclopentadiene derivatives
[AD-A281976] p 746 N95-17485

PHASE DIAGRAMS
Possible superstructures of metallic ions in nonstoichiometric fullerites M(x) C(60)
[DE94-622052] p 901 N95-17518

PHASE ERROR
Dynamical system prediction of the scalar field in a turbulent channel flow
[AD-A285519] p 771 N95-16438
Closed-loop carrier phase synchronization techniques motivated by likelihood functions p 756 N95-17284

PHASE LOCKED SYSTEMS
Phase-locked arrays of vertical-cavity surface-emitting lasers
[DE94-014941] p 778 N95-17498

PHASE MODULATION
Electric-optic resonant phase modulator
[NASA-CASE-NPO-18702-1-CU] p 883 N95-15960

PHASE SEPARATION (MATERIALS)
Phase segregation due to simultaneous migration and coalescence
[NASA-CR-196819] p 721 N95-16035

PHASE SHIFT
Analysis of a three-beam radar as an instrument for determining ocean wave heights and vector slopes
[AD-A282342] p 806 N95-17505

PHASE STABILITY (MATERIALS)
Synthesis and characterization of a new class of thermosetting resins: Allyl and propargyl substituted cyclopentadiene derivatives
[AD-A281976] p 746 N95-17485

PHASE TRANSFORMATIONS
Surface and defect excitations in covalently bonded solids
[AD-A281338] p 894 N95-16012
Phase transformations, ultrastructure and properties of rigid-rod fibers
[AD-A285249] p 749 N95-16512
Application of NMR shock barometer to naturally shocked minerals
[DE95-000326] p 799 N95-17362
Synthesis and characterization of a new class of thermosetting resins: Allyl and propargyl substituted cyclopentadiene derivatives
[AD-A281976] p 746 N95-17485

PHASED ARRAYS
Demand access communications for TDRSS users
p 677 N95-17187

PHENOLIC RESINS
Fire protective coating and method for applying same to a structure
[AD-D016405] p 746 N95-17462

PHENOLOGY
Root growth and development in response to CO2 enrichment
[NASA-CR-196154] p 807 N95-16429

PHENOMENOLOGY
Poloidal rotation and the evolution of H-mode and VH-mode profiles
[DE94-015858] p 890 N95-16919
Research in elementary particle physics
[DE94-019219] p 877 N95-17358
Z(prime) phenomenology: Constraints from low-energy measurements, and detailed study at TeV-scale lepton and hadron colliders
[DE94-018185] p 881 N95-17886

PHENYLS
Low temperature synthesis of semiconductor materials
[AD-A285230] p 898 N95-16526
Synthesis of polyphenylenes and polynaphthalenes by thermolysis of enediyness and dialkynylbenzenes
[AD-A281294] p 743 N95-16783
Synthesis and properties of soluble oligo- and polyphenylenes. A review
[AD-A281293] p 874 N95-16799

PHILOSOPHY
Epistemology, software engineering and formal methods p 843 N95-16480

PHOBOS
Radio-planetary from tie from Phobos-2 VLBI data
p 756 N95-17283

PHONEMES
Phonologic-graphemic transcodifier for Portuguese Language spoken in Brazil (PLB)
[INPE-5575-PRE/1803] p 760 N95-17649

PHONETICS
Phonologic-graphemic transcodifier for Portuguese Language spoken in Brazil (PLB)
[INPE-5575-PRE/1803] p 760 N95-17649

PHOSPHATES
Prediction of space sickness in astronauts from preflight fluid, electrolyte, and cardiovascular variables and Weightless Environmental Training Facility (WETF) training p 812 N95-16757
Nano-scale metal oxide particles as materials for air purification
[AD-A281394] p 729 N95-16791
Thermal and laser conditioning of production and rapid-growth KDP and KD*P crystals
[DE94-013738] p 902 N95-17742

PHOSPHAZENE
Polymeric precursors to binary inorganic materials
[AD-A281010] p 739 N95-16000
Fundamental studies of polyphosphazene and polysiloxane polyelectrolytes for electrochemical devices
[AD-A281339] p 739 N95-16013
Well-defined polyphosphazenes by anionic polymerization of phosphoranimines
[AD-A281414] p 740 N95-16165

PHOSPHORS
Preparation and investigation of improved low voltage electron excitable phosphors
[AD-A284265] p 767 N95-17487

PHOSPHORUS
Calcium phosphate precipitation in a fluidized bed
[PB94-201407] p 796 N95-17399

PHOSPHORUS OXIDES
Thermal and mechanical behavior of Ba(1+x)Zr4P(6-2x)Si(2x)O24
[DE94-013620] p 899 N95-16806

PHOTOABSORPTION
The chemistry and physics of transition metal clusters
[DE94-014012] p 734 N95-16364

PHOTOCHEMICAL REACTIONS
Detection of crosslink formation by 2 + 2 photocycloaddition in poly (vinyl cinnamate) by C-13 solid-state NMR
[AD-A281955] p 741 N95-16409
Radical cations of quadricyclane and norbornadiene in polar ZSM-5 matrices: Radical cation photochemical transformations without photons
[DE94-014007] p 728 N95-16485
International Winterschool on Electronic Properties of Novel Materials: Progress in Fullerene Research
[AD-A282128] p 728 N95-16608
Investigation of laser-induced retinal damage: Wavelength and pulsewidth dependent mechanisms
[AD-A285186] p 822 N95-16871
Mobility measurement and computer simulation at specific sites in polystyrene solutions and gels
[AD-A281214] p 747 N95-17685

PHOTOCONDUCTIVITY
Process of making a bistable photoconductive component
[AD-D016449] p 764 N95-16539

PHOTOCONDUCTORS
Resist materials design: Base-catalyzed chemical amplification
[AD-A281805] p 741 N95-16354

PHOTODETACHMENT
Spectroscopy of the transition state region in hydrogen transfer reactions
[AD-A285151] p 729 N95-16846

PHOTODIODES
Picosecond silicon metal-semiconductor-metal photodiode
[AD-A281548] p 763 N95-16394
Performance characterization of photonic links in cryogenic environments for advanced signal processing applications
[DE94-015561] p 765 N95-16915

PHOTODISSOCIATION
Gas-surface interactions near dissociation threshold
[AD-A282726] p 730 N95-17140
A latitudinal survey of middle atmospheric water vapor revealed by shipboard microwave spectroscopy
[AD-A282000] p 799 N95-17446

PHOTOELECTRIC EFFECT
A rare gas optics-free absolute photon flux and energy analyzer for solar and planetary observations
[NASA-CR-197227] p 915 N95-16021

PHOTOELECTRON SPECTROSCOPY
Spectroscopy of the transition state region in hydrogen transfer reactions
[AD-A285151] p 729 N95-16846

PHOTOELECTRONS
Radiation electrodynamics of the photo-electron cloud produced by an arbitrary photon pulse incident on a planar emitting surface in vacuum
[AD-A282153] p 759 N95-17450

PHOTOEXCITATION
Gas-surface interactions near dissociation threshold
[AD-A284945] p 726 N95-16042

PHOTOGEOLOGY
Rheology and structure of planetary near-surface materials from landform topography p 922 N95-17392

PHOTOGRAMMETRY
Rheology and structure of planetary near-surface materials from landform topography p 922 N95-17392

PHOTOGRAPHS
Debris/ice/TPS assessment and integrated photographic analysis of Shuttle Mission STS-64 on 9 August 1994
[NASA-TM-109206] p 676 N95-17262

PHOTOGRAPHY
Spatial information content analysis of Wiener spectra from polarized waterwave imagery
[AD-A283171] p 886 N95-17340

PHOTOIONIZATION
A rare gas optics-free absolute photon flux and energy analyzer to provide absolute photoionization rates of inflowing interstellar neutrals
[NASA-CR-197228] p 914 N95-15964
Resonance enhanced multiphoton ionization of molecules and molecular fragments
[AD-A285076] p 873 N95-16493

PHOTOLUMINESCENCE
International Workshop on Light Emission and Electronic Properties of Nanoscale silicon
[AD-A281464] p 894 N95-16081
LPEE growth and characterization of In(x)Ga(1-x)As(y)Sb(1-y) lattice matched to GaSb and InAs for photodetectors
[AD-A281631] p 895 N95-16114
Nitride semiconductors for ultraviolet detection
[AD-A280988] p 898 N95-16533

PHOTOLYSIS
Fundamental studies in oxidation-reduction in relation to water photolysis
[DE94-014598] p 731 N95-17161

PHOTOMETERS
LPEE growth and characterization of In(x)Ga(1-x)As(y)Sb(1-y) lattice matched to GaSb and InAs for photodetectors
[AD-A281631] p 895 N95-16114
Picosecond silicon metal-semiconductor-metal photodiode
[AD-A281548] p 763 N95-16394
Performance characterization of photonic links in cryogenic environments for advanced signal processing applications
[DE94-015561] p 765 N95-16915
Investigation of a normal incidence high-performance p-type strained layer In(0.3)Ga(0.7)As/In(0.52)Al(0.48)As quantum well infrared photodetector
[AD-A282720] p 900 N95-16928

PHOTOMULTIPLIER TUBES
Multilayer microelectronic photomultiplier device with a stacked series of dynode and insulating layers
[AD-D016377] p 767 N95-17478

PHOTON BEAMS
Photon beam studies of magnetic materials
[PB95-104279] p 877 N95-17351
Strong WW scattering at photon linear colliders
[DE94-018183] p 878 N95-17720

PHOTONICS
Overview of photonics research at Lawrence Livermore National Laboratory
[DE94-014055] p 884 N95-16366
PHOTONS
A rare gas optics-free absolute photon flux and energy analyzer to provide absolute photoionization rates of inflowing interstellar neutrals
[NASA-CR-197228] p 914 N95-15964
Field configuration of beam excited modes in the Advanced Photon Source (APS) storage ring waveguides
[DE94-015096] p 880 N95-16308
A search for muons yields e gamma at the level of 10(exp -13)
[DE94-014488] p 876 N95-17158
Radiation electrodynamics of the photo-electron cloud produced by an arbitrary photon pulse incident on a planar emitting surface in vacuum
[AD-A282153] p 759 N95-17450
Strong WW scattering at photon linear colliders
[DE94-018183] p 878 N95-17720
Physics at high energy photon photon colliders
[DE94-018191] p 881 N95-17888
New shower maximum trigger for electrons and photons at CDF
[DE94-018376] p 878 N95-17899
Beam parameter measurements for the APS linac system
[DE94-018396] p 882 N95-17902
PHOTOOXIDATION
Augmentation for research training: Surface-mediated photocatalysis
[AD-A281591] p 722 N95-16100
PHOTORECEPTORS
Photoreceptors regulating circadian behavior: A mouse model
[AD-A285157] p 822 N95-16847
PHOTOSYNTHESIS
Regulation of nitrogen uptake and assimilation: Effects of nitrogen source and root-zone and aerial environment on growth and productivity of soybean
[NASA-CR-197098] p 807 N95-15961
Flow over abrupt topography: The application of patterns in nutrient and productivity in reflecting physical processes
[AD-A280813] p 797 N95-17740
PHOTOVOLTAIC CELLS
A modular electric power system test bed for small spacecraft
[NASA-TM-106812] p 721 N95-17276
Energy and Technology Review
[DE95-000321] p 710 N95-17359
PHOTOVOLTAIC CONVERSION
Photovoltaic power conditioners: Development, evolution, and the next generation
[NASA-CR-197005] p 793 N95-16831
Solar energy: Lessons from the Pacific island experience
[WORLD-BANK-TP-244] p 794 N95-17298
Energy and Technology Review
[DE95-000321] p 710 N95-17359
PHYSICAL CHEMISTRY
Development of practical MO techniques for prediction of the properties and behavior of materials
[AD-A285079] p 874 N95-16496
PHYSICAL EXERCISE
Evaluation of a newly-designed, dynamic knee extension device for the study of muscle fatigue in humans
[AD-A284974] p 819 N95-16228
Intramuscular pressure: A better tool than EMG to optimize exercise for long-duration space flight
p 809 N95-16744
Effects of weightlessness on human baroreflex function p 815 N95-16770
The effect of intermittent standing or walking during head down tilt bedrest on peak O2 consumption
p 817 N95-16779
Periodic upright posture negates the suppression of neuroendocrine response to head down bedrest
p 817 N95-16780
The efficacy of periodic +Gz exposure in the prevention of bedrest induced orthostatic intolerance
p 817 N95-16781
Basic mechanisms and implications of non-photic entrainment of circadian rhythmicity
[AD-A283180] p 822 N95-17342
PHYSICAL PROPERTIES
Selected properties of iron aluminides
[DE94-018057] p 738 N95-17726
PHYSICAL WORK
Energy expenditure, physical work load and postural control during walking on a moving platform
[AD-A285343] p 830 N95-16821
PHYSIOLOGICAL EFFECTS
Regulation of nitrogen uptake and assimilation: Effects of nitrogen source and root-zone and aerial environment on growth and productivity of soybean
[NASA-CR-197098] p 807 N95-15961
The chronic effects on JP-8 jet fuel exposure on the lungs
[AD-A280982] p 821 N95-16515
Subset-selectivity and distractor matching in visual conjunction search
[AD-A285137] p 827 N95-16615
Comparisons of three anti-G suit configurations during long duration, low onset, +Gz p 811 N95-16755
Phase-shifting effects of light and activity on the human circadian clock
[AD-A281204] p 821 N95-16796
Caffeine's influence on critical frequency thresholds
[AD-A282005] p 828 N95-17447
PHYSIOLOGICAL FACTORS
Space medicine research: Needs for the 21st century
p 814 N95-16768
PHYSIOLOGICAL RESPONSES
Root growth and development in response to CO2 enrichment
[NASA-CR-196154] p 807 N95-16429
Aerospace Medical Association 63rd Annual Scienti fic Meeting Program p 807 N95-16737
Spectral components of human cardiovascular responses to step changes in Lower Body Negative Pressure (LBNP) before and after 22 hour of 6 deg head down bed rest p 810 N95-16748
Changes in left ventricular function as determined by the multi-wire gamma camera at near presyncopal levels of lower body negative pressure p 811 N95-16754
Effects of weightlessness on human baroreflex function p 815 N95-16770
The value of the 4-day headdown bedrest model for screening countermeasures p 817 N95-16782
Performance study of galactic cosmic ray shield materials
[NASA-TP-3473] p 924 N95-16912
Caffeine's influence on critical frequency thresholds
[AD-A282005] p 828 N95-17447
PHYSIOLOGICAL TESTS
Blinks, saccades, and fixation pauses during vigilance task performance. 1: Time on task
[DOT/FAA/AM-94/26] p 828 N95-17530
PHYTOPLANKTON
Flow over abrupt topography: The application of patterns in nutrient and productivity in reflecting physical processes
[AD-A280813] p 797 N95-17740
PIERCING
Material and ballistic investigation of a tungsten-26 percent rhenium alloy
[PB94-189156] p 734 N95-16420
PIEZOELECTRIC CERAMICS
Cost-effective method for synthesizing innovative transducer materials for sensors and actuators
[AD-A282339] p 725 N95-16974
PIEZOELECTRIC GAGES
A comparison of different control methods for vibration suppression of flexible structures using piezoelectric actuators
[AD-A282958] p 710 N95-17622
PILOT ERROR
Aircraft accident report: Stall and loss of control on final approach, Atlantic Coast Airlines, Inc./United Express Flight 6291 Jetstream 4101, N304UE Columbus, OH, 7 January 1994
[PB94-910409] p 665 N95-17646
PILOT INDUCED OSCILLATION
Aircraft and sub-system certification by piloted simulation
[AGARD-AR-278] p 671 N95-17388
PILOT PERFORMANCE
Alertness management in two-person long-haul flight operations p 813 N95-16760
Crew decision making under stress
p 814 N95-16765
Cognition and procedure representational requirements for predictive human performance models
p 814 N95-16766
Aircraft and sub-system certification by piloted simulation
[AGARD-AR-278] p 671 N95-17388
PILOTLESS AIRCRAFT
Spread spectrum applications in unmanned aerial vehicles
[AD-A281035] p 754 N95-16448
PINNING
Columnar defect pinning in untwinned single crystal YBa2Cu2O7
[DE94-013962] p 901 N95-17349
PIONEER VENUS 1 SPACECRAFT
Analysis of magnetic field data from Pioneer Venus orbiter
[NASA-CR-197492] p 923 N95-17403
PIPE FLOW
Colloidal particle deposition in turbulent flow
[DE94-013375] p 770 N95-16417
Transient flows and pressure waves in pipes
[DE94-012650] p 772 N95-17523
PIPES (TUBES)
Vector magnetometry and lightwave defect imaging sensor technologies for internal pipe inspection systems: Phase 1 and 2 feasibility study, conceptual design, and prototype development
[PB94-194198] p 783 N95-16870
Transient flows and pressure waves in pipes
[DE94-012650] p 772 N95-17523
WPH-6112A thermal expansion test of PRESS tubulation
[DE94-015946] p 782 N95-17717
PISTON THEORY
Multi-dimensional shock capturing
[AD-A282986] p 773 N95-17708
PISTONS
Heat transfer measurements for Stirling machine cylinders
[NASA-CR-197128] p 791 N95-15963
PITCH (INCLINATION)
Numerical simulation of transient vortex breakdown above a pitching delta wing
[AD-A281075] p 655 N95-16808
PITCHING MOMENTS
Measurements on a two-dimensional aerofoil with high-lift devices p 657 N95-17848
PITTING
A review of transmission diagnostics research at NASA Lewis Research Center
[ARL-TR-599] p 781 N95-16907
PIXELS
Characterization of multiport solid state imagers at megahertz data rates
[DE94-016095] p 765 N95-16932
PLAINS
A Mars Pathfinder landing on a recently drained ephemeral sea: Cerberus Plains, 6 deg N, 188 deg W
p 918 N95-16181
PLANAR STRUCTURES
Synthesis of planar poly(p-phenylene) derivatives for maximization of extended pi-conjugation
[AD-A281179] p 743 N95-16630
PLANE WAVES
Ultrashort pulse effects in semiconductor amplifiers and in dispersive media
[AD-A284925] p 763 N95-16137
Duality transformations, green dyadics and plane-wave solutions for a class of bianisotropic media
[PB94-197670] p 754 N95-16612
PLANETARY COMPOSITION
Opportunity to sample something different: The dark, unweathered, mafic sands of Cerberus and the Pathfinder 1997 Mars landing p 919 N95-16187
Tartarus Colles: A sampling of the Martian highlands
p 920 N95-16195
Rheology and structure of planetary near-surface materials from landform topography p 922 N95-17392
PLANETARY CRUSTS
Opportunity to sample something different: The dark, unweathered, mafic sands of Cerberus and the Pathfinder 1997 Mars landing p 919 N95-16187
PLANETARY ENVIRONMENTS
Medicine on Mars: Remote medical care and the space exploration initiative p 816 N95-16777
PLANETARY GEOLOGY
Sampling Elysium lavas (13 deg N, 203 deg W)
p 917 N95-16177
Mars Pathfinder and the exploration of southern Amazonis Planitia p 917 N95-16178
A Mars Pathfinder landing on a recently drained ephemeral sea: Cerberus Plains, 6 deg N, 188 deg W
p 918 N95-16181
Rationale for Isidis Planitia as a back-up landing site for the Mars Pathfinder mission p 918 N95-16184
Opportunity to sample something different: The dark, unweathered, mafic sands of Cerberus and the Pathfinder 1997 Mars landing p 919 N95-16187
Exobiology site priorities for Mars Pathfinder
p 919 N95-16188
Tartarus Colles: A sampling of the Martian highlands
p 920 N95-16195
Cerberus Plains: A most excellent Pathfinder landing site p 921 N95-16198
Rheology and structure of planetary near-surface materials from landform topography p 922 N95-17392
Investigations of asteroid family geology
p 917 N95-17393

PLANETARY MAGNETOTAILS
Analysis of magnetic field data from Pioneer Venus orbiter
[NASA-CR-197492] p 923 N95-17403
PLANETARY MAPPING
Observations by the Mars 1994 orbiter and possible correlations with Mars Pathfinder p 920 N95-16192
PLANETARY METEOROLOGY
Meteorological observations of synoptic disturbances: Sensitivity to latitude p 917 N95-16179
McIDAS-eXplorer: A version of McIDAS for planetary applications
[NASA-CR-189382] p 910 N95-17323
PLANETARY STRUCTURE
Rheology and structure of planetary near-surface materials from landform topography p 922 N95-17392
PLANETARY SURFACES
Medicine on Mars: Remote medical care and the space exploration initiative p 816 N95-16777
PLANETARY WAVES
An observational study of long waves in the equatorial Pacific Ocean during the 1991-1993 El Nino
[AD-A283380] p 806 N95-17624
PLANNING
C-Plan2 versus SIPE-2: A general comparison
[AD-A285531] p 857 N95-17381
PLANT DESIGN
D3-D research operations
[DE94-014934] p 892 N95-17497
PLANT ROOTS
Regulation of nitrogen uptake and assimilation: Effects of nitrogen source and root-zone and aerial environment on growth and productivity of soybean
[NASA-CR-197098] p 807 N95-15961
Root growth and development in response to CO2 enrichment
[NASA-CR-196154] p 807 N95-16429
PLANTS (BOTANY)
Regulation of nitrogen uptake and assimilation: Effects of nitrogen source and root-zone and aerial environment on growth and productivity of soybean
[NASA-CR-197098] p 807 N95-15961
PLASMA BUBBLES
Plasma sound source basic research
[AD-A285394] p 890 N95-16617
PLASMA CLOUDS
SEPAC co-investigator support
[NASA-CR-196527] p 798 N95-15965
PLASMA CONTROL
Continuing life test of a xenon hollow cathode for a space plasma contactor
[NASA-CR-195401] p 711 N95-15968
Runaway electrons beams in ITER disruptions
[DE94-013788] p 888 N95-16122
Control of a large vacuum wave precursor on the SABRE voltage adder MITL and extraction ion diode
[DE94-014280] p 888 N95-16216
Development of a radiative divertor for DIII-D
[DE94-016522] p 889 N95-16554
Extended test of a xenon hollow cathode for a space plasma contactor
[NASA-CR-195402] p 720 N95-17265
AINSE Plasma Science and Technology Conference and Elizabeth and Frederick White Workshop on Fundamental Problems in the Physics of Magnetically Confined Plasmas: Conference handbook
[DE94-622051] p 892 N95-17517
Global confinement analysis
[DE94-016820] p 893 N95-17644
ITER design: Physics basis for size, confinement capability power levels and burn control
[DE94-018041] p 893 N95-17674
PLASMA CURRENTS
System design and operation of a 100 kilovolt, 2 kilohertz pulse modulator for plasma source ion implantation
[DE94-014424] p 889 N95-16285
A CO2 laser polarimeter for measurement of plasma current profile in Alcator C-Mod
[DE94-014017] p 776 N95-16486
PLASMA DECAY
Runaway electrons beams in ITER disruptions
[DE94-013788] p 888 N95-16122
PLASMA DENSITY
Analysis of plasma measurements for the Geotail mission
[NASA-CR-197020] p 888 N95-15941
SEPAC co-investigator support
[NASA-CR-196527] p 798 N95-15965
Multi-beam laser interferometer for plasma density measurements in a Plasma Erosion Opening Switch (PEOS)
[AD-A283209] p 892 N95-17623
Global confinement analysis
[DE94-016820] p 893 N95-17644
Two phase liquid helium flow testing to simulate the operation of a cryocondensation pump in the D3-D tokamak
[DE94-018345] p 893 N95-17896
PLASMA DIAGNOSTICS
Papers presented at the Tenth Topical Conference on High-Temperature Plasma Diagnostics
[DE94-015854] p 888 N95-16063
Electric probe measurements in the plume of the UK-10 ion thruster
[AD-A282460] p 713 N95-16302
Determination of ion temperatures from Zeeman broadened spectral lines in the edge of Tore Supra
[DE94-018112] p 873 N95-16403
A CO2 laser polarimeter for measurement of plasma current profile in Alcator C-Mod
[DE94-014017] p 776 N95-16486
Active silicon x ray for measuring electron temperature
[DE94-017521] p 890 N95-16555
Differential phase reflectometry for edge profile measurements on TFTR
[DE94-013837] p 891 N95-16958
Beams 92: Proceedings
[DE94-014784] p 880 N95-17475
Miniature, vacuum compatible 1024 (times) 1024 CCD camera for x ray, ultraviolet, or optical imaging
[DE94-012235] p 776 N95-17522
Multi-beam laser interferometer for plasma density measurements in a Plasma Erosion Opening Switch (PEOS)
[AD-A283209] p 892 N95-17623
Design of a CO2-laser Thomson scattering ion-tail diagnostic for Alcator C-Mod
[DE94-018056] p 779 N95-17680
Measurements of non-axisymmetric effects in the D3-D divertor
[DE94-018346] p 893 N95-17897
PLASMA DRIFT
Poloidal rotation and the evolution of H-mode and VH-mode profiles
[DE94-015858] p 890 N95-16919
PLASMA GENERATORS
Radar observations of field-aligned plasma propagations associated with NASA's PMG experiment
[AD-A285218] p 798 N95-16521
PLASMA HEATING
Theory of carrier heating through injection pumping and lasing in semiconductor microcavity lasers
[AD-A281795] p 776 N95-16353
Differential phase reflectometry for edge profile measurements on TFTR
[DE94-013837] p 891 N95-16958
PLASMA INTERACTIONS
Interaction of electromagnetic fields with magnetized plasmas
[AD-A285496] p 755 N95-16968
First measurements of ICRF and edge/SOL plasma interactions on TORE SUPRA
[DE94-019320] p 891 N95-17347
PLASMA LAYERS
Characteristics of multiple auroral inverted-V structures and the problem of magnetospheric plasma stratification
[DE94-622233] p 799 N95-17471
PLASMA PHYSICS
Development of a radiative divertor for DIII-D
[DE94-016522] p 889 N95-16554
AINSE Plasma Science and Technology Conference and Elizabeth and Frederick White Workshop on Fundamental Problems in the Physics of Magnetically Confined Plasmas: Conference handbook
[DE94-622051] p 892 N95-17517
PLASMA RADIATION
Interaction of electromagnetic fields with magnetized plasmas
[AD-A285496] p 755 N95-16968
PLASMA TURBULENCE
Papers presented at the Tenth Topical Conference on High-Temperature Plasma Diagnostics
[DE94-015854] p 888 N95-16063
Poloidal rotation and the evolution of H-mode and VH-mode profiles
[DE94-015858] p 890 N95-16919
Interaction of electromagnetic fields with magnetized plasmas
[AD-A285496] p 755 N95-16968
PLASMAS (PHYSICS)
Analysis of plasma measurements for the Geotail mission
[NASA-CR-197020] p 888 N95-15941
Papers presented at the Tenth Topical Conference on High-Temperature Plasma Diagnostics
[DE94-015854] p 888 N95-16063
Ion beam generation and propagation for plasma processing applications
[DE94-014428] p 889 N95-16286
Plasma disruption modeling and simulation
[DE94-015095] p 889 N95-16307
Auroral interactions with ISSA
[NASA-TM-106794] p 709 N95-16862
Alpha particle kinetics in ignited fusion plasmas: Design applications for a CO2 laser Thomson scattering experiment
[DE94-016297] p 890 N95-16921
Fast electrons, filamented laser light, and the fast ignitor
[DE94-015898] p 777 N95-16929
Interaction of electromagnetic fields with magnetized plasmas
[AD-A285496] p 755 N95-16968
Thermal characteristics and heat transfer in an electrothermal light gas gun
[AD-A281980] p 892 N95-17442
Beams 92: Proceedings
[DE94-014784] p 880 N95-17475
AINSE Plasma Science and Technology Conference and Elizabeth and Frederick White Workshop on Fundamental Problems in the Physics of Magnetically Confined Plasmas: Conference handbook
[DE94-622051] p 892 N95-17517
Development of x-ray laser architectural components
[DE94-016446] p 778 N95-17627
Effect of low density H-mode operation on edge and divertor plasma parameters
[DE94-016521] p 892 N95-17640
Global confinement analysis
[DE94-016820] p 893 N95-17644
Electron-neutrino phase separation instability
[DE94-016859] p 904 N95-17645
Baryogenesis and standard model CP violation
[DE94-017935] p 877 N95-17669
Design of a CO2-laser Thomson scattering ion-tail diagnostic for Alcator C-Mod
[DE94-018056] p 779 N95-17680
Beam characteristics of a large-bore copper laser with a radiatively cooled plasma
[DE94-015139] p 779 N95-17688
Production of high proton fractions from ECR sources by plasma modification
[DE94-018381] p 893 N95-17900
PLASTIC COATINGS
Characterization of surfaces
[NASA-CR-196995] p 750 N95-16065
PLASTIC DEFORMATION
Considerations in the experimental determination of constitutive parameters for finite strain plasticity
[AD-A285410] p 785 N95-16245
Thermoelasticity analysis of laminated plates and shells using hybrid-stress elements p 651 N95-16263
Development of processes, means, and theoretical principles of thin-walled detail plastic forming at Kazan Aviation Institute p 653 N95-16281
Classical solutions of the Prandtl-Reuss equations of perfect elasto-plasticity
[PB94-192333] p 860 N95-16292
PLASTIC PROPERTIES
Synaptic plasticity and memory formation
[AD-A284926] p 825 N95-16138
PLASTICS
Fire protective coating and method for applying same to a structure
[AD-D016405] p 746 N95-17462
PLATES (STRUCTURAL MEMBERS)
Thermoelasticity analysis of laminated plates and shells using hybrid-stress elements p 651 N95-16263
Impact vulnerability of thermoplastic-matrix composites
[PB94-201274] p 745 N95-17305
PLATINUM
Selective area platinum film deposition
[AD-D016355] p 747 N95-17693
PLAYBACKS
Lessons learned supporting onboard solid-state recorders p 681 N95-17208
PLUMES
Design of thermocouple probes for measurement of rocket exhaust plume temperatures
[AD-A285423] p 774 N95-16247
Space Shuttle main engine OPAD: The search for a hardware enhanced plume p 716 N95-16330
Numerical simulation of helicopter engine plume in forward flight
[NASA-CR-197488] p 655 N95-16589
PNEUMATIC EQUIPMENT
Evaluation of a pneumatic Martian soil sampler concept
[NASA-CR-197539] p 923 N95-17653
POINT DEFECTS
The role of point defects and defect complexes in silicon device processing: Summary report and papers
[DE94-011873] p 791 N95-15944

POINT SOURCES
Static image method for the interaction of two co-axial conducting prolate spheroids
[PB94-197696] p 760 N95-17502
POINT TO POINT COMMUNICATION
Data link level interconnection of remote Fiber Distributed Data Interface Local Area Networks (FDDI LANs) through the Critical Data Link (CDL)
[AD-A284307] p 755 N95-17173
POINTING CONTROL SYSTEMS
A specification of 3D manipulation in virtual environments p 853 N95-15981
Experimental validation of an integrated controls-structures design methodology for a class of flexible space structures
[NASA-TP-3462] p 709 N95-16857
The SILEX experiment system operations p 674 N95-17251
POINTS (MATHEMATICS)
Surface matching for correlation of virtual models: Theory and application p 853 N95-15983
Methods of wave-front identification by control images p 652 N95-16274
The algebraic multigrid projection for eigenvalue problems; backrotations and multigrid fixed points
[NASA-CR-194990] p 862 N95-16869
POISSON EQUATION
A Lyapunov bound for solutions of Poisson's equation
[AD-A281536] p 860 N95-16169
Some fundamental techniques in the theory of integrable systems
[PB94-192390] p 860 N95-16294
POLAR REGIONS
Observations of ELF propagation at high latitudes during the sporadic-E conditions of November 1986
[AD-A284973] p 753 N95-16227
POLAR SUBSTORMS
Ion drift meter research
[NASA-CR-197124] p 798 N95-16432
POLARIMETERS
A CO2 laser polarimeter for measurement of plasma current profile in Alcator C-Mod
[DE94-014017] p 776 N95-16486
POLARIMETRY
Unusual initial and final state effects in quantum chromodynamics
[DE94-015341] p 903 N95-16604
POLARITY
Parallel search for a conjunction of shape and contrast polarity
[AD-A285344] p 827 N95-16822
POLARIZATION (CHARGE SEPARATION)
Fundamental studies in oxidation-reduction in relation to water photolysis
[DE94-014598] p 731 N95-17161
Poling dynamics and relaxation of polar order in guest/host polymers by second harmonic generation
[AD-A283291] p 748 N95-17724
POLARIZATION (SPIN ALIGNMENT)
Third harmonic generation study of alpha-thiophene oligomers: Monomer to octamer
[AD-A281177] p 874 N95-16629
POLARIZATION (WAVES)
Clutter signal polarization in bistatic radar: Effect of antenna sidelobe clutter
[AD-A282300] p 753 N95-16240
Spatial information content analysis of Wiener spectra from polarized waterwave imagery
[AD-A283171] p 886 N95-17340
POLICIES
Informatics in Turkey p 905 N95-15921
Information system in transition: The Hungarian Scene p 906 N95-15925
CINDOC, CSIC, and Spanish R and D p 906 N95-15927
The future of interaction on the Internet p 906 N95-15931
Networked information: Management issues for the acquisitions librarian p 906 N95-15932
Adding tools to the open source toolbox: The Internet p 907 N95-15933
Data administration procedures
[AD-A282718] p 909 N95-16092
Review of performance, medical, and operational data on pilot aging issues p 812 N95-16759
POLISHING
Precision machining and polishing of scintillating crystals for large calorimeters and hodoscopes
[DE94-012060] p 751 N95-17738
POLITICS
Presidential leadership in the development of the US space program
[NASA-TM-110107] p 904 N95-16007
POLLUTION CONTROL
Assessment of research needs for advanced heterogeneous catalysts for energy applications, volume 2
[DE94-015890] p 727 N95-16387
Coal-fueled diesel technology development emissions control
[DE94-004096] p 782 N95-17364
POLLUTION MONITORING
Novel mass spectrometric instrument for gaseous and particulate characterization and monitoring
[DE94-014168] p 795 N95-16213
Infrared signatures for remote sensing
[DE94-014222] p 790 N95-16215
Meteorological Monitoring Program
[DE94-017810] p 795 N95-16557
POLYACETYLENE
Self assembled spin coated and bulk films of a novel polydiacetylene as second order NLO polymers
[AD-A282271] p 742 N95-16427
POLYBUTADIENE
Large-scale hybrid motor performance and designs for use in launch vehicle applications p 715 N95-16327
POLYCRYSTALS
Development of high-efficiency, thin-film CdTe solar cells
[DE94-011885] p 794 N95-16940
Asymptotic behavior in grain growth
[DE94-014452] p 900 N95-17156
POLYESTERS
Design and technical support for development of a molded fabric space suit joint
[NASA-CR-197521] p 831 N95-16894
Vacuum deposited polymer/silver reflector material
[DE94-018729] p 748 N95-17913
POLYGONS
Geometric sensing of known planar shapes
[AD-A282854] p 840 N95-17432
POLYHEDRONS
Sorting and hardware assisted rendering for volume visualization
[DE94-010204] p 834 N95-16220
POLYIMIDE RESINS
Thermoplastic and thermosetting high glass transition temperature matrix resins
[AD-A281508] p 740 N95-16096
POLYIMIDES
Microchannel formation in polyimide by heavy ion irradiation
[DE94-753315] p 740 N95-16073
Thermoplastic and thermosetting high glass transition temperature matrix resins
[AD-A281508] p 740 N95-16096
Prediction of the response of a polyimide concentrator for solar thermal propulsion p 719 N95-16343
Selective area platinum film deposition
[AD-D016355] p 747 N95-17693
POLYMER BLENDS
Log-(Chi(exp 2)) distribution of correlation times revisited
[AD-A281123] p 740 N95-16092
POLYMER CHEMISTRY
Systematic optimization of second order nonlinear optical materials
[AD-A281350] p 884 N95-16015
Resist materials design: Base-catalyzed chemical amplification
[AD-A281805] p 741 N95-16354
Living radical polymerization. 1: Possibilities and limitations
[AD-A281042] p 742 N95-16451
Synthesis of polyphenylenes and polynaphthalenes by thermolysis of enediyness and dialkynylbenzenes
[AD-A281294] p 743 N95-16783
POLYMER MATRIX COMPOSITES
The effect of brush polydispersity on the interphase between end-grafted brushed and polymeric matrices
[AD-A280975] p 743 N95-16507
Development of device quality nonlinear optical materials and definition of mechanisms of optical nonlinearity
[AD-A285255] p 885 N95-16528
POLYMER PHYSICS
Nonlinear problems and numerical method in differential equations and applied phenomena
[AD-A281531] p 859 N95-16108
Synthesis of low band gap zwitterionic and planar conjugated pyrrole-derived polymers. Reversible optical absorbances from the UV to the near-IR
[AD-A281174] p 743 N95-16628
Morphology and dynamics of membrane systems
[PB94-184660] p 745 N95-17299
POLYMERIC FILMS
Property control of (perfluorinated ionomer)/(inorganic oxide) composites by tailoring the nanoscale morphology
[AD-A281370] p 723 N95-16019
Anionically-conductive ultrathin film composite membranes
[AD-A284944] p 723 N95-16041
Characterization of surfaces
[NASA-CR-196995] p 750 N95-16065
Self assembled spin coated and bulk films of a novel polydiacetylene as second order NLO polymers
[AD-A282271] p 742 N95-16427
Nonlinear optical and charge distribution studies probing electric field effects in polymer thin films for second order nonlinear optics
[AD-A280980] p 742 N95-16483
Atomic oxygen durability evaluation of the flexible batten for the photovoltaic array mast on Space Station
[NASA-TM-106798] p 781 N95-17263
Surface composition of a series of dimethylsiloxane urea, urethane segmented copolymers studied by electron spectroscopy for chemical analysis
[AD-A282872] p 745 N95-17434
Ion modulated electroactivity in thin-film polymers derived from bipyridyl and phenanthroline complexes of iron
[AD-A280704] p 747 N95-17682
Poling dynamics and relaxation of polar order in guest/host polymers by second harmonic generation
[AD-A283291] p 748 N95-17724
POLYMERIZATION
Sonochemical synthesis of polysilylenes by reductive coupling of disubstituted dichlorosilanes with alkali metals
[AD-A280994] p 739 N95-15996
Polymeric precursors to binary inorganic materials
[AD-A281010] p 739 N95-16000
Anionically-conductive ultrathin film composite membranes
[AD-A284944] p 723 N95-16041
The mechanism of the oligomerization of thiophene-based para-quinodimethanes
[DE94-014232] p 722 N95-16058
Well-defined polyphosphazenes by anionic polymerization of phosphoranimines
[AD-A281414] p 740 N95-16165
Control of molecular weights and polydispersities in radical polymerization of styrene in the presence of stable radicals
[AD-A281040] p 742 N95-16449
Regiochemistry of polysilanes prepared by ring opening polymerization
[AD-A281041] p 742 N95-16450
Living radical polymerization. 1: Possibilities and limitations
[AD-A281042] p 742 N95-16451
Living radical polymerization of vinyl acetate
[AD-A280901] p 743 N95-16500
From living carbocationic to living radical polymerization
[AD-A280902] p 743 N95-16501
Synthesis of low band gap zwitterionic and planar conjugated pyrrole-derived polymers. Reversible optical absorbances from the UV to the near-IR
[AD-A281174] p 743 N95-16628
Synthesis of planar poly(p-phenylene) derivatives for maximization of extended pi-conjugation
[AD-A281179] p 743 N95-16630
Synthesis of polyphenylenes and polynaphthalenes by thermolysis of enediyness and dialkynylbenzenes
[AD-A281294] p 743 N95-16783
Iterative divergent/convergent doubling approach to linear conjugated oligomers. A rapid route to a 128 A long potential molecular wire
[AD-A281295] p 874 N95-16784
Synthesis and mesomorphic behavior of poly((2S, 3S)-(+)-2-chloro-3-methylpentyl xy)biphenyl-4-carboxylate s with ethyl and propyl alkyl groups
[AD-A281402] p 744 N95-16865
POLYMETHYL METHACRYLATE
Shotgun/drop-weight initiation of energetic materials
[AD-A285090] p 749 N95-16499
Solubilization of hydrophobic substances into block copolymer micelles in aqueous media and their release
[AD-A281395] p 744 N95-16792
POLYMORPHISM
Compiling polymorphism using intensional type analysis
[AD-A285340] p 838 N95-16819
POLYNOMIALS
On P-selectivity and closeness
[TR-499] p 859 N95-15951
An investigation of polynomial calibrations methods for wind tunnel balances p 650 N95-16258
A new model for estimating total body water from bioelectrical resistance p 810 N95-16747

POLYPHENYLS
Regiochemistry of polysilanes prepared by ring opening polymerization
[AD-A281041] p 742 N95-16450
Synthesis of planar poly(p-phenylene) derivatives for maximization of extended pi-conjugation
[AD-A281179] p 743 N95-16630
Synthesis and mesomorphic behavior of poly((2S, 3S)-(+)-2-chloro-3-methylpentyl
xy)biphenyl-4-carboxylate s with ethyl and propyl alkyl groups
[AD-A281402] p 744 N95-16865
Chiral recognition in molecular and macromolecular pairs of liquid crystals of (2R, 3S)- and (2S, 3S)-2-fluoro-3-methylpentyl-4'-(11-vinyloxyundeca iphenyl-4-carboxylate diastereomers
[AD-A281770] p 878 N95-17692
POLYPYRROLES
Anionically-conductive ultrathin film composite membranes
[AD-A284944] p 723 N95-16041
POLYSILANES
Sonochemical synthesis of polysilylenes by reductive coupling of disubstituted dichlorosilanes with alkali metals
[AD-A280994] p 739 N95-15996
Regiochemistry of polysilanes prepared by ring opening polymerization
[AD-A281041] p 742 N95-16450
POLYSILOXANES
Fundamental studies of polyphosphazene and polysiloxane polyelectrolytes for electrochemical devices
[AD-A281339] p 739 N95-16013
Reaction and protection of electrical wire insulators in atomic-oxygen environments
[NASA-TM-106767] p 709 N95-17275
POLYSTYRENE
Control of molecular weights and polydispersities in radical polymerization of styrene in the presence of stable radicals
[AD-A281040] p 742 N95-16449
Solubilization of hydrophobic substances into block copolymer micelles in aqueous media and their release
[AD-A281395] p 744 N95-16792
Mobility measurement and computer simulation at specific sites in polystyrene solutions and gels
[AD-A281214] p 747 N95-17685
POLYURETHANE RESINS
Evaluation of alternate F-14 wing lug coating
[AD-A283207] p 669 N95-17631
Conducting polymers as corrosion resistant coatings
[DE94-018265] p 748 N95-17892
POPULATIONS
Multivariate sampling with explicit correlation induction for practical simulation and optimization studies
[AD-A281998] p 841 N95-17445
POROSITY
Surface heat transfer in a channel with porous insert
p 650 N95-16255
Reaction of methanol with porous silicon
[AD-A285518] p 728 N95-16406
Structure-property relationships in sol-gel-derived thin films
[DE94-016149] p 744 N95-16934
POROUS MATERIALS
Surface heat transfer in a channel with porous insert
p 650 N95-16255
Service and physical properties of liquid-jet fuels
p 650 N95-16256
POSEIDON SATELLITE
Telecommunications end-to-end systems monitoring on TOPEX/Poseidon: Tools and techniques
p 676 N95-17180
POSITION (LOCATION)
On P-selectivity and closeness
[TR-499] p 859 N95-15951
Tele Hyper Virtuality p 853 N95-15982
GEOTRANS geographic decision support system
[PB94-183670] p 908 N95-16093
Perceptual selectivity for color and form: On the nature of the interference effect
[AD-A285338] p 827 N95-16817
The new map graphics in RSAS 5.0
[AD-A282432] p 791 N95-17511
A high resolution liquid xenon imaging telescope for 0.3-10 MeV gamma-ray astrophysics: Construction and initial balloon flights
[NASA-CR-197556] p 916 N95-17528
Measurements of non-axisymmetric effects in the D3-D divertor
[DE94-018346] p 893 N95-17897
POSITION ERRORS
Beam position correction in the Fermilab Linac
[DE94-018984] p 862 N95-17931
POSITION SENSING
Servo control using switches for discrete positional feedback
[AD-A284747] p 856 N95-16550
Geometric sensing of known planar shapes
[AD-A282854] p 840 N95-17432
POSITIONING
Delivery of cardiopulmonary resuscitation in the microgravity environment p 816 N95-16774
A PC based tool for mission plan production
p 686 N95-17232
POSITIONING DEVICES (MACHINERY)
Servo control using switches for discrete positional feedback
[AD-A284747] p 856 N95-16550
POSITRON ANNIHILATION
Positron annihilation studies of defects in molecular beam epitaxy grown 3 to 5 layers
[DE94-015823] p 899 N95-16918
Applications of positron depth profiling
[PB94-197753] p 900 N95-16952
POSITRONS
Development and applications of the positron microscope
[DE94-017918] p 883 N95-15947
Na-22 decay gamma rays from classical novae
[NASA-CR-197454] p 924 N95-16383
Applications of positron depth profiling
[PB94-197753] p 900 N95-16952
Mass spectrometry studies of the ionization of organic molecules by slow positrons
[DE94-013838] p 876 N95-16959
Electron-neutrino phase separation instability
[DE94-016859] p 904 N95-17645
POSTURE
Scripting human animations in a virtual environment
p 855 N95-15992
Periodic upright posture negates the suppression of neuroendocrine response to head down bedrest
p 817 N95-16780
Energy expenditure, physical work load and postural control during walking on a moving platform
[AD-A285343] p 830 N95-16821
POTASSIUM
The deposition of electro-optic films on semiconductors
[AD-A285068] p 742 N95-16488
POTASSIUM PHOSPHATES
Thermal and laser conditioning of production and rapid-growth KDP and KD*P crystals
[DE94-013738] p 902 N95-17742
POTENTIAL ENERGY
A consistent large deflection theory of composite sandwich shells p 650 N95-16259
POTENTIAL FLOW
Single-pass method for the solution of inverse potential and rotational problems. Part 1: 2-D and quasi 3-D theory and application p 664 N95-16563
Small-amplitude disturbances in turbomachine flows with swirl
[NASA-CR-195406] p 772 N95-17386
POTENTIAL THEORY
Single-pass method for the solution of inverse potential and rotational problems. Part 2: Fully 3-D potential theory and applications p 664 N95-16564
POWDER (PARTICLES)
Surface heat transfer in a channel with porous insert
p 650 N95-16255
Low-temperature fabrication of transparent silicon nitride
[DE94-014902] p 746 N95-17456
Preparation and investigation of improved low voltage electron excitable phosphors
[AD-A284265] p 767 N95-17487
Rietveld refinement of magnetic structures from pulsed-neutron-source powder-diffraction data
[DE94-016599] p 737 N95-17641
POWDER METALLURGY
The analysis and minimization of oxygen contamination in the powder processing of molybdenum disilicide
[DE94-014234] p 735 N95-16540
Effect of extrusion parameters on consolidation of tungsten-hafnium and tungsten-steel powders
[DE94-013270] p 737 N95-17513
POWER CONDITIONING
Photovoltaic power conditioners: Development, evolution, and the next generation
[NASA-CR-197005] p 793 N95-16831
Overview of space power electronic's technology under the CSTI High Capacity Power Program
[NASA-TM-110110] p 883 N95-17933
POWER CONVERTERS
Overview of space power electronic's technology under the CSTI High Capacity Power Program
[NASA-TM-110110] p 883 N95-17933
POWER LINES
Space Station Freedom primary power wiring requirements p 712 N95-16051
A study of electric transmission lines for use on the lunar surface p 712 N95-16053
POWER LOSS
Calorimetric methods for loss measurements of small cage induction motors
[PB94-184439] p 768 N95-17691
POWER SPECTRA
Simultaneous determination of incoming microwave frequency and angle-of-arrival
[AD-D016392] p 760 N95-17482
POWERED LIFT AIRCRAFT
STOVL CFD model test case p 663 N95-17881
PRASEODYMIUM COMPOUNDS
The relationship of structure to superconductivity in the Pr-Ba-Cu-O system
[DE94-014231] p 897 N95-16510
PRECESSION
Exact, E = 0, classical and quantum solutions for general power-law oscillators
[DE94-014436] p 903 N95-16428
PRECIPITATION (CHEMISTRY)
Calcium phosphate precipitation in a fluidized bed
[PB94-201407] p 796 N95-17399
PRECIPITATION (METEOROLOGY)
Modelling daily precipitation as a function of temperature for climate change impact studies
[KNMI-WR-93-02] p 802 N95-17529
PRECIPITATION HARDENING
Experimental heat treatment of beryllium copper alloy
[AD-A282714] p 734 N95-16380
PRECISION
Approach to in-process tool wear monitoring in drilling: Application of Kalman filter theory p 653 N95-16279
Development of processes, means, and theoretical principles of thin-walled detail plastic forming at Kazan Aviation Institute p 653 N95-16281
PREDICTION ANALYSIS TECHNIQUES
The computer analysis of the prediction of aircraft electrical power supply system reliability
p 653 N95-16278
Efficient estimation of the mean time between failures in non-regenerative dependability models
[AD-A281563] p 783 N95-16421
Availability of direct normal radiation for solar furnace processing: A case study
[DE94-006907] p 792 N95-16435
Failure analysis of 2D and 3D woven composites
[NASA-CR-197247] p 724 N95-16597
Cognition and procedure representational requirements for predictive human performance models
p 814 N95-16766
Auroral interactions with ISSA
[NASA-TM-106794] p 709 N95-16862
Normalization and prediction of geotechnical properties using the Cone Penetrometer Test (CPT)
[AD-A285193] p 799 N95-16872
An empirical approach to visual display preference based upon modulation transfer function and luminance
[AD-A285450] p 830 N95-16875
Laser induced fluorescence measurements and modeling of nitric oxide in high-pressure premixed flames
[NASA-CR-195404] p 775 N95-16910
High speed method for predicting radio-wave propagation
[AD-D016369] p 761 N95-17697
PREDICTIONS
The future of interaction on the Internet
p 906 N95-15931
On the prediction of free turbulent jets with swirl using a quadratic pressure-strain model
[NASA-CR-194964] p 769 N95-16071
Space medicine research: Needs for the 21st century
p 814 N95-16768
Life prediction for bridged fatigue cracks
[DE94-016000] p 724 N95-16930
PREFORMS
Cost-effective method for synthesizing innovative transducer materials for sensors and actuators
[AD-A282339] p 725 N95-16974
PREMIXED FLAMES
Laser induced fluorescence measurements and modeling of nitric oxide in high-pressure premixed flames
[NASA-CR-195404] p 775 N95-16910
Experimental study of premixed flames in intense isotropic turbulence
[DE94-016868] p 732 N95-17437
PRESENTATION
From computer images to video presentation: Enhancing technology transfer p 848 N95-16467
Data Visualization and Animation Lab (DVAL) overview
p 843 N95-16468

PRESSURE
Investigation of the influence of pylons and stores on the wing lower surface flow p 664 N95-17885
PRESSURE DISTRIBUTION
An improved method of airfoil design p 649 N95-16252
Improved method for estimation of the maximum instantaneous distortion values p 649 N95-16254
Wall-signature methods for high speed wind tunnel wall interference corrections p 650 N95-16257
Measurements of unsteady pressure and structural response for an elastic supercritical wing [NASA-TP-3443] p 653 N95-16560
Residual-correction type and related computational methods for aerodynamic design. Part 1: Airfoil and wing design p 667 N95-16566
Aerodynamic shape optimization p 668 N95-16572
Review of the EUROPT Project AERO-0026 p 668 N95-16573
Investigations on the sensitivity of the computer code TURBO-2D [CUED/A-THERMO/TR-61] p 771 N95-16595
2-D airfoil tests including side wall boundary layer measurements p 657 N95-17847
Measurements on a two-dimensional aerofoil with high-lift devices p 657 N95-17848
2-D aileron effectiveness study p 658 N95-17851
Two-dimensional 16.5 percent thick supercritical airfoil NLR 7301 p 658 N95-17854
Low-speed surface pressure and boundary layer measurement data for the NLR 7301 airfoil section with trailing edge flap p 658 N95-17855
Measurements of the flow over a low aspect-ratio wing in the Mach number range 0.6 to 0.87 for the purpose of validation of computational methods. Part 1: Wing design, model construction, surface flow. Part 2: Mean flow in the boundary layer and wake, 4 test cases p 660 N95-17860
Detailed study at supersonic speeds of the flow around delta wings p 660 N95-17861
Pressure distributions on research wing W4 mounted on an axisymmetric body p 660 N95-17862
DLR-F5: Test wing for CFD and applied aerodynamics p 660 N95-17864
Wind tunnel investigations of the appearance of shocks in the windward region of bodies with circular cross section at angle of attack p 661 N95-17866
Force and pressure data of an ogive-nosed slender body at high angles of attack and different Reynolds numbers p 661 N95-17868
Pressure distribution measurements on an isolated TPS 441 nacelle p 663 N95-17878
PRESSURE DRAG
An investigation of the transonic pressure drag coefficient for axi-symmetric bodies [AD-A280990] p 654 N95-15994
PRESSURE EFFECTS
Investigation of pressure regulation in an archaebacterial enzyme [AD-A281413] p 807 N95-16164
Mechanical effects in cookoff modeling [DE94-014174] p 748 N95-16214
Deformation behavior of thin lubricant films at elevated pressure [AD-A281848] p 741 N95-16355
Normalization and prediction of geotechnical properties using the Cone Penetrometer Test (CPT) [AD-A285193] p 799 N95-16872
Materials degradation and fatigue under extreme conditions [AD-A282969] p 746 N95-17662
PRESSURE GRADIENTS
On the prediction of free turbulent jets with swirl using a quadratic pressure-strain model [NASA-CR-194964] p 769 N95-16071
Experimental investigation of turbulent separated-reattachment flow by using LDV p 649 N95-16253
Airfoil optimization by the one-shot method p 667 N95-16569
Tools for applied engineering optimization p 668 N95-16570
Mach number, flow angle, and loss measurements downstream of a transonic fan-blade cascade [AD-A280907] p 656 N95-16824
Poloidal rotation and the evolution of H-mode and VH-mode profiles [DE94-015858] p 890 N95-16919
Investigation of the flow over a series of 14 percent-thick supercritical aerofoils with significant rear camber p 657 N95-17849
PRESSURE MEASUREMENT
Data acquisition and processing software for the Low Speed Wind Tunnel tests of the Jindivik auxiliary air intake [AD-A285455] p 656 N95-17178
Measurements on a two-dimensional aerofoil with high-lift devices p 657 N95-17848
Surface pressure and wake drag measurements on the Boeing A4 airfoil in the IAR 1.5X1.5m Wind Tunnel Facility p 657 N95-17850
Pressure distribution measurements on an isolated TPS 441 nacelle p 663 N95-17878
PRESSURE RATIO
Error propagation equations for estimating the uncertainty in high-speed wind tunnel test results [DE94-014136] p 671 N95-16509
PRESSURE REDUCTION
A proposal to study gender differences in the rates of decompression sickness [AD-A281854] p 819 N95-16297
PRESSURE SENSORS
Single-engine tail interference model p 663 N95-17879
PRESSURE SUITS
Comparisons of three anti-G suit configurations during long duration, low onset, +Gz p 811 N95-16755
PRESSURE VESSELS
The effects of fatigue loading frequency on fatigue life of high-strength pressure vessel steels [AD-A285301] p 786 N95-16601
Nickel hydrogen batteries: An overview [NASA-TM-106795] p 793 N95-16861
PRESSURIZING
Updated test results of a pumped monopropellant propulsion system p 713 N95-16315
PRIMARY BATTERIES
Primary battery design and safety guidelines handbook [NASA-RP-1353] p 764 N95-16561
PRIMITIVE EQUATIONS
Impact of physical processes on maritime frontogenesis [AD-A283105] p 801 N95-17339
PRINTED CIRCUITS
How clean is clean: Non-destructive/direct methods of flux, residue detection [DE94-013439] p 763 N95-16357
PRINTERS (DATA PROCESSING)
Full color recorder [AD-A282278] p 790 N95-17372
PRIORITIES
Informatics in Turkey p 905 N95-15921
PRIVACY
Open Source Service Agent (OSSA) in the intelligence community's Open Source Architecture p 907 N95-15934
PROBABILITY DENSITY FUNCTIONS
Improved method for estimation of the maximum instantaneous distortion values p 649 N95-16254
The small-scale structure of dispersing clouds in the atmosphere [AD-A285493] p 800 N95-16802
Statistical properties of an algorithm used for illicit substance detection by fast-neutron transmission [DE94-013868] p 665 N95-16964
PROBABILITY THEORY
Decreasing the bandwidth of a transition matrix [TR-505] p 859 N95-15948
On the structure of log-space probabilistic complexity classes [TR-506] p 864 N95-16039
Exploiting IB assignments for approximating marginal probabilities [AD-A285419] p 855 N95-16246
Self-organizing neural network for classifying pattern signatures with a posteriori conditional class probability [AD-D016455] p 857 N95-16823
An empirical approach to visual display preference based upon modulation transfer function and luminance [AD-A285450] p 830 N95-16875
Extended range forecast of Atlantic seasonal hurricane activity for 1995, 2 p 801 N95-17260
A preliminary optical visibility model p 758 N95-17290
Verification of NOAA Space Environment Laboratory forecasts, 1 January - 31 December 1993 [PB95-104162] p 803 N95-17927
PROBES
Design of thermocouple probes for measurement of rocket exhaust plume temperatures [AD-A285423] p 774 N95-16247
Eddy curreni for detecting second layer cracks under installed fasteners [AD-A282412] p 784 N95-17507
PROBLEM SOLVING
Decreasing the bandwidth of a transition matrix [TR-505] p 859 N95-15948
A general method to determine invariants [TR-503] p 859 N95-15949
On P-selectivity and closeness [TR-499] p 859 N95-15951

On the structure of log-space probabilistic complexity classes [TR-506] p 864 N95-16039
Equation solvers for distributed-memory computers p 847 N95-16480
Optimum Design Methods for Aerodynamics [AGARD-R-803] p 666 N95-16562
Review of the EUROPT Project AERO-0026 p 668 N95-16573
Crew decision making under stress p 814 N95-16765
A framework for the analysis of cognitive tasks [AD-A285345] p 828 N95-16835
Multivariate sampling with explicit correlation induction for practical simulation and optimization studies [AD-A281998] p 841 N95-17445
PROCEDURES
Mission operations management p 685 N95-17225
Re-engineering NASA's space communications to remain viable in a constrained fiscal environment p 702 N95-17585
PROCESS CONTROL (INDUSTRY)
Breaking down barriers in cooperative fault management: Temporal and functional information displays [NASA-CR-197450] p 857 N95-17383
PROCUREMENT MANAGEMENT
Federal Aviation Administration aviation system capital investment plan, 1993 [PB94-171956] p 654 N95-17512
Department of Defense Electronic Data Interchange project baseline report for FY 1994 [AD-A283015] p 912 N95-17710
PROCUREMENT POLICY
Low rate initial production in Army Aviation systems development [AD-A281871] p 666 N95-16356
PRODUCT DEVELOPMENT
Physics-based approach to haptic display p 854 N95-15986
Method of calculating the optimal radioelectronic equipment design p 652 N95-16271
Design and technical support for development of a molded fabric space suit joint [NASA-CR-197521] p 831 N95-16894
Eddy current for detecting second layer cracks under installed fasteners [AD-A282412] p 784 N95-17507
PRODUCTION ENGINEERING
Studies on improvement of oxidation resistivity of carbon materials by glass impregnation and SiC formation [DE94-796529] p 724 N95-16833
PRODUCTION MANAGEMENT
Improving production schedules without scheduling [PB94-191350] p 904 N95-16289
PRODUCTION PLANNING
Improving production schedules without scheduling [PB94-191350] p 904 N95-16289
PRODUCTIVITY
Development of processes, means, and theoretical principles of thin-walled detail plastic forming at Kazan Aviation Institute p 653 N95-16281
The global aircraft shape p 668 N95-16571
Flow over abrupt topography: The application of patterns in nutrient and productivity in reflecting physical processes [AD-A280813] p 797 N95-17740
PROGRAM VERIFICATION (COMPUTERS)
Parallel software benchmarks for high performance BMC3/IS systems [AD-A282329] p 844 N95-16060
The search for lost cycles: A new approach to parallel program performance evaluation [AD-A281467] p 845 N95-16082
Detailed example of using PIWG on the SUN workstation and the DEC VAX computer [AD-A281528] p 834 N95-16107
The SEI and NAWC: Working together to establish a software measurement program [AD-A280916] p 836 N95-16504
A survey of program slicing for software engineering [NASA-CR-193116] p 836 N95-16574
Engineering design tools for wind diesel systems. Volume 2: JODYMOD dynamic wind diesel simulation software package. Model verification [PB95-104519] p 840 N95-17355
ATM-test: A workstation-based software suite for testing Asynchronous Transfer Mode (ATM) networks [DE94-013813] p 850 N95-17516
Software interface verifier p 698 N95-17564
A proven approach for more effective software development and maintenance p 698 N95-17566
Engineering design tools for wind diesel systems. Volume 7: Logistic package. Validation report [PB95-104568] p 842 N95-17735

PROGRAMMERS
High Performance FORTRAN p 843 N95-16478
PROGRAMMING ENVIRONMENTS
Portable parallel stochastic optimization for the design of aeropropulsion components
[NASA-CR-195312] p 785 N95-16072
A graphical environment for object-oriented simulation model environment
[NASA-CR-196887] p 833 N95-16088
Improving productivity in the development of large software systems
[AD-A282270] p 835 N95-16234
DOME: Distributed Object Migration Environment
[AD-A281134] p 850 N95-16826
PROGRAMMING LANGUAGES
Improving productivity in the development of large software systems
[AD-A282270] p 835 N95-16234
A structured TCP in standard ML
[AD-A282711] p 835 N95-16306
Procedure calls are the assembly language of software interconnection: Connectors deserve first-class status
[AD-A281026] p 835 N95-16446
Hardware description languages p 832 N95-16477
Proceedings of the International Conference on Parallel Architectures and Compilation Techniques
[AD-A285258] p 849 N95-16529
Compiling polymorphism using intensional type analysis
[AD-A285340] p 838 N95-16819
PROGRESS
International Winterschool on Electronic Properties of Novel Materials: Progress in Fullerene Research
[AD-A282128] p 728 N95-16608
PROJECT MANAGEMENT
NASA contract mangagement: Improving the use of DCAA's auditing services. Report to the Chairman, Committee on Government Operations, House of Representatives
[GAO/NSIAD-94-229] p 914 N95-15962
Activities of the Space Studies Board
[NASA-CR-197105] p 672 N95-16033
The Role of Computers in Research and Development at Langley Research Center
[NASA-CP-10159] p 846 N95-16453
The Design Manager's Aid for Intelligent Decomposition (DeMAID) p 848 N95-16470
RDD-100 and the systems engineering process p 848 N95-16471
Computer tools for systems engineering at LaRC p 848 N95-16472
Electronic Engineering Notebook: A software environment for research execution, documentation and dissemination p 848 N95-16473
Review of the EUROPT Project AERO-0026 p 668 N95-16573
Results of an International Space Crew Debrief p 810 N95-16750
An integrated knowledge acquisition and database management system
[AD-A285404] p 910 N95-16884
An assessment of simulation systems applicable to business process reengineering at Army Directorates of Public Works
[AD-A285696] p 839 N95-17176
The development and operation of the international solar-terrestrial physics central data handling facility p 679 N95-17193
A model for analysis of TDA budget allocation p 758 N95-17295
SCOS 2: An object oriented software development approach p 699 N95-17571
Test/score/report: Simulation techniques for automating the test process p 675 N95-17581
Transportable Payload Operations Control Center reusable software: Building blocks for quality ground data systems p 703 N95-17587
The Requirements Generation System: A tool for managing mission requirements p 707 N95-17608
PROJECT PLANNING
Fuel cell systems program plan, fiscal year 1994
[DE94-014301] p 793 N95-16541
A distributed planning concept for Space Station payload operations p 682 N95-17211
PROJECTILES
Shotgun/drop-weight initiation of energetic materials
[AD-A285090] p 749 N95-16499
PROLATE SPHEROIDS
Static image method for the interaction of two co-axial conducting prolate spheroids
[PB94-197696] p 760 N95-17502
Three-dimensional boundary layer and flow field data of an inclined prolate spheroid p 661 N95-17867
PROMETHAZINE
Use of injectable promethazine to decrease symptom scores of Space Motion Sickness p 808 N95-16741
PROP-FAN TECHNOLOGY
FPCAS2D user's guide, version 1.0
[NASA-CR-195413] p 786 N95-16588
PROPAGATION MODES
Nonstationary theory of mode competition in gyrotrons with allowance for inhomogeneity of the guiding magnetic field
[PB94-197621] p 869 N95-17467
PROPARGYL GROUPS
Identification and temporal behavior of radical intermediates formed during the combustion and pyrolysis of gaseous fuels: Kinetic pathways to soot formation
[DE94-014681] p 731 N95-17163
Synthesis and characterization of a new class of thermosetting resins: Allyl and propargyl substituted cyclopentadiene derivatives
[AD-A281976] p 746 N95-17485
PROPELLANT CHEMISTRY
Synthesis of pure RDX
[DE94-014356] p 749 N95-16542
PROPELLANT COMBUSTION
Mechanical effects in cookoff modeling
[DE94-014174] p 748 N95-16214
PROPELLANT PROPERTIES
The use of designed experiments in the process development of continuous propellant mixing p 717 N95-16334
PROPELLANT TANKS
Nondestructive examination of the TRMM RCS propellant tanks p 718 N95-16338
PROPELLANT TRANSFER
Generic propellant transfer unit: A project update p 719 N95-16345
PROPELLANTS
Hydromining a full-scale class 1.1 solid rocket motor p 713 N95-16314
Prediction of the response of a polyimide concentrator for solar thermal propulsion p 719 N95-16343
Testing and evaluation of oxide-coated iridium/rhenium chambers p 719 N95-16346
Shotgun/drop-weight initiation of energetic materials
[AD-A285090] p 749 N95-16499
Heat stress and a countermeasure in the Shuttle rescueman's suit p 809 N95-16746
PROPELLER FANS
FPCAS2D user's guide, version 1.0
[NASA-CR-195413] p 786 N95-16588
PROPELLER SLIPSTREAMS
Low speed propeller slipstream aerodynamic effects p 663 N95-17882
PROPRIOCEPTION
The psychophysical function for perceived gravitational-inertial force does not depend on the orientation of the otolith organs p 808 N95-16740
PROPULSION
The 1993 JANNAF Propulsion Meeting, volume 1
[CPIA-PUBL-602-VOL-1] p 713 N95-16312
Design margin testing of Peacekeeper solid rocket boosters p 713 N95-16313
Updated test results of a pumped monopropellant propulsion system p 713 N95-16315
Integrated modular engine configuration options p 717 N95-16336
Overview of TTCP and AGARD propulsion activities p 720 N95-16351
Re-engineering the Multimission Command System at the Jet Propulsion Laboratory p 702 N95-17583
PROPULSION SYSTEM CONFIGURATIONS
Damage-mitigating control of space propulsion systems for high performance and extended life
[NASA-CR-194470] p 784 N95-16068
Small turbojets: Designs and installations p 670 N95-16323
Integrated modular engine configuration options p 717 N95-16336
Materials characterization and design for solar-thermal propulsion p 718 N95-16340
The global aircraft shape p 668 N95-16571
PROPULSION SYSTEM PERFORMANCE
Damage-mitigating control of space propulsion systems for high performance and extended life
[NASA-CR-194470] p 784 N95-16068
Joint Proceedings on Aeronautics and Astronautics (JPAA)
[ISBN-7-80-046602-7] p 649 N95-16249
Service and physical properties of liquid-jet fuels p 650 N95-16256
Theoretical fundamentals of the aircraft GTE tests p 651 N95-16265
Large-scale hybrid motor performance and designs for use in launch vehicle applications p 715 N95-16327
Integrated modular engine configuration options p 717 N95-16336
Materials characterization and design for solar-thermal propulsion p 718 N95-16340
Experimental and analytical methods for the determination of connected-pipe ramjet and ducted rocket internal performance
[AGARD-AR-323] p 721 N95-17278
Cooperative control theory and integrated flight and propulsion control
[NASA-CR-197493] p 671 N95-17404
PROTECTION
The assessment of the AH-64D, longbow, mast-mounted assembly noise hazard for maintenance personnel
[AD-A284971] p 869 N95-16226
PROTECTIVE COATINGS
Design, analysis, and fabrication of oxide-coated iridium/rhenium combustion chambers p 719 N95-16347
Tribological properties of reactively sputtered nitrides and carbides of titanium, zirconium and hafnium
[DE94-014583] p 745 N95-17160
Atomic oxygen durability evaluation of the flexible batten for the photovoltaic array mast on Space Station
[NASA-TM-106798] p 781 N95-17263
Fire protective coating and method for applying same to a structure
[AD-D016405] p 746 N95-17462
Evaluation of alternate F-14 wing lug coating
[AD-A283207] p 669 N95-17631
PROTEINS
Ligand field stabilization control of metal ion binding
[AD-A281011] p 726 N95-16001
PROTOCOL (COMPUTERS)
Adding tools to the open source toolbox: The Internet p 907 N95-15933
Virtual reality and telerobotics applications of an Address Recalculation Pipeline p 852 N95-15977
High speed transport protocols: An attempt to find the best solution
[AD-A280989] p 751 N95-15993
A structured TCP in standard ML
[AD-A282711] p 835 N95-16306
The Role of Computers in Research and Development at Langley Research Center
[NASA-CP-10159] p 846 N95-16453
How to use the WWW to distribute STI p 847 N95-16465
An analysis of Internet's MBONE: A media choice perspective
[AD-A285514] p 910 N95-16972
Open solutions to distributed control in ground tracking stations p 674 N95-17554
Re-engineering Nascom's network management architecture p 702 N95-17584
A new communication protocol family for a distributed spacecraft control system p 703 N95-17590
Standardizing the information architecture for spacecraft operations p 703 N95-17591
A standard satellite control reference model p 704 N95-17592
Standard protocol stack for mission control p 704 N95-17593
The Space Communications Protocol Standards Program p 704 N95-17594
Proposal for implementation of CCSDS standards for use with spacecraft engineering/housekeeping data p 705 N95-17600
Test applications for heterogeneous real-time network testbed
[DE94-016480] p 850 N95-17638
PROTON BEAMS
RHIC spin: The first polarized proton collider
[DE94-013760] p 872 N95-16121
Ion beam generation and propagation for plasma processing applications
[DE94-014428] p 889 N95-16286
Production of high proton fractions from ECR sources by plasma modification
[DE94-018381] p 893 N95-17900
PROTON-PROTON REACTIONS
RHIC spin: The first polarized proton collider
[DE94-013760] p 872 N95-16121
PROTONS
Alpha proton x ray spectrometer p 710 N95-16201
Tests of structure functions using leptons at CDF: W asymmetry and Drell-Yan production
[DE94-015727] p 875 N95-16840
Multilepton SUSY signals from R-parity violation at the Tevatron (revised)
[PB95-104311] p 877 N95-17353
Parton distributions of the proton
[PB95-104337] p 877 N95-17354
Production of high proton fractions from ECR sources by plasma modification
[DE94-018381] p 893 N95-17900
PROTOTYPES
A prototype Crew Medical Restraint System (CMRS) for Space Station Freedom p 815 N95-16773

Advanced Cardiac Life Support (ACLS) utilizing Man-Tended Capability (MTC) hardware onboard Space Station Freedom p 816 N95-16775
A surgical support system for Space Station Freedom p 710 N95-16776
Interactive sketching for the early stages of user interface design
[AD-A285339] p 838 N95-16818
Vector magnetometry and lightwave defect imaging sensor technologies for internal pipe inspection systems: Phase 1 and 2 feasibility study, conceptual design, and prototype development
[PB94-194198] p 783 N95-16870

PROVING
Significant issues in proof testing: A critical appraisal
[NASA-CR-4628] p 788 N95-17272
Real-time symbolic model checking for discrete time models
[AD-A282878] p 864 N95-17618

PSYCHOACOUSTICS
Demodulation processes in auditory perception
[AD-A285427] p 869 N95-16248

PSYCHOLOGICAL EFFECTS
Results of an International Space Crew Debrief p 810 N95-16750

PSYCHOLOGICAL FACTORS
Psychological training of NASA astronauts for extended missions p 813 N95-16763

PSYCHOLOGICAL TESTS
Results of the psychiatric, select-out evaluation of US astronaut applications p 813 N95-16761
Validation of astronaut psychological select-in criteria p 813 N95-16762

PSYCHOLOGY
Development of the OMPAT neuropsychological/psychomotor performance evaluation and OMPAT data and timing support programs
[AD-A284928] p 826 N95-16140

PSYCHOMOTOR PERFORMANCE
Situational awareness in complex systems
[AD-A281448] p 825 N95-15959
Development of the OMPAT neuropsychological/psychomotor performance evaluation and OMPAT data and timing support programs
[AD-A284928] p 826 N95-16140

PSYCHOPHYSICS
Presentations of shape in object recognition and long-term visual memory
[AD-A281336] p 825 N95-16010

PSYCHOPHYSIOLOGY
Subset-selectivity and distractor matching in visual conjunction search
[AD-A285137] p 827 N95-16615

PUBLIC RELATIONS
From computer images to video presentation: Enhancing technology transfer p 848 N95-16467

PULMONARY CIRCULATION
Carbon monoxide does not modulate pulmonary vascular reactivity in isolated rat lungs
[AD-A283190] p 818 N95-17714

PULMONARY FUNCTIONS
The chronic effects on JP-8 jet fuel exposure on the lungs
[AD-A280982] p 821 N95-16515

PULSE COMMUNICATION
Preliminary investigation of an integrated optic sampler for HF signals
[AD-A284285] p 884 N95-16133

PULSE DURATION
A high average power electro-optic switch using KTP
[DE94-016416] p 765 N95-16925

PULSE MODULATION
Initial design of a 1 megawatt average, 150 kilovolt pulse modulator for an industrial plasma source ion implantation processor
[DE94-014421] p 888 N95-16218
System design and operation of a 100 kilovolt, 2 kilohertz pulse modulator for plasma source ion implantation
[DE94-014424] p 889 N95-16285

PULSE RADAR
Solid state radar demonstration test results at the FAA Technical Center
[AD-A281520] p 752 N95-16097
Detecting the number of targets in spatially colored noise using sampled aperture radars p 652 N95-16269

PULSED LASERS
Thermal dissociation of halogen azides
[AD-A285088] p 728 N95-16497
Investigation of laser-induced retinal damage: Wavelength and pulsewidth dependent mechanisms
[AD-A285186] p 822 N95-16871
Fast electrons, filamented laser light, and the fast ignitor
[DE94-015898] p 777 N95-16929
Characterization of multiport solid state imagers at megahertz data rates
[DE94-016095] p 765 N95-16932

PULSED RADIATION
Reduction and aggregation of silver in aqueous gelatin and silica suspensions
[DE94-013998] p 727 N95-16363

PURIFICATION
Elemental impurity analysis of mercuric iodide by ICP/MS
[DE94-013553] p 896 N95-16359

PYLONS
Investigation of the influence of pylons and stores on the wing lower surface flow p 664 N95-17885

PYRIDINES
Structure of 4-methylpyridinium hydrogen sulfide
[NASA-TM-106778] p 731 N95-17387

PYROELECTRICITY
Epitaxial MOCVD of thin film ceramics for pyroelectric detectors
[AD-A281397] p 744 N95-16863

PYROLYSIS
Kapton pyrolysis on Space Station Freedom's solar array flexible current carrier p 712 N95-16049
Kapton pyrolysis, the space environment and wiring requirements p 712 N95-16054
Identification and temporal behavior of radical intermediates formed during the combustion and pyrolysis of gaseous fuels: Kinetic pathways to soot formation
[DE94-014681] p 731 N95-17163

PYROLYTIC GRAPHITE
Raman spectroscopy of C-irradiated graphite
[DE94-018705] p 733 N95-17911

PYROLYTIC MATERIALS
WSTF electrical arc projects p 711 N95-16047

PYRROLES
Synthesis of low band gap zwitterionic and planar conjugated pyrrole-derived polymers. Reversible optical absorbances from the UV to the near-IR
[AD-A281174] p 743 N95-16628

Q

Q FACTORS
Radial acceletron, a new low impedance HPM source
[AD-A282008] p 760 N95-17501

Q SWITCHED LASERS
A high average power electro-optic switch using KTP
[DE94-016416] p 765 N95-16925

QUADRATIC EQUATIONS
Superspheroid geometries for radome analysis
[AD-A285405] p 753 N95-16233

QUADRATIC PROGRAMMING
Automation of reverse engineering process in aircraft modeling and related optimization problems
[NASA-CR-197109] p 668 N95-16899
Structural optimization with approximate sensitivities
[NASA-TM-4553] p 789 N95-17701
Optimal trajectories for flexible-link manipulator slewing using recursive quadratic programming: Experimental verification
[DE94-018741] p 858 N95-17915

QUADRATURE AMPLITUDE MODULATION
On the application of under-decimated filter banks p 757 N95-17285

QUADRATURES
Trapezoidal rule quadrature algorithms for MIMD distributed memory computers
[DE94-016369] p 839 N95-16923

QUADRUPOLES
Beam position correction in the Fermilab Linac
[DE94-018984] p 882 N95-17931

QUALITY
Significant issues in proof testing: A critical appraisal
[NASA-CR-4628] p 788 N95-17272

QUALITY CONTROL
Method of calculating the optimal radioelectronic equipment design p 652 N95-16271
How clean is clean: Non-destructive/direct methods of flux, residue detection
[DE94-013439] p 763 N95-16357
Maturity questionnaire
[AD-A285073] p 836 N95-16490
Continual improvement: A bibliography with indexes, 1992-1993
[NASA-SP-7097(02)] p 905 N95-16633
Design and technical support for development of a molded fabric space suit joint
[NASA-CR-197521] p 831 N95-16894
Production and quality assurance automation in the Goddard Space Flight Center Flight Dynamics Facility p 687 N95-17237
Significant issues in proof testing: A critical appraisal
[NASA-CR-4628] p 788 N95-17272
SEQ-REVIEW: A tool for reviewing and checking spacecraft sequences p 697 N95-17561
A proven approach for more effective software development and maintenance p 698 N95-17566
Software Process Assessment (SPA) p 699 N95-17569
Taking advantage of ground data systems attributes to achieve quality results in testing software p 699 N95-17570
Evaluation of the quality of sapphire using x-ray rocking curves and double-crystal x-ray topography
[AD-A282905] p 901 N95-17620

QUANTUM CHROMODYNAMICS
RHIC spin: The first polarized proton collider
[DE94-013760] p 872 N95-16121
Measurement of the B meson differential cross-sections in p(-p) collisions at the square root of s = 1.8 TeV using the exclusive decays B(+-) yields J/(psi)K(+-) and B(exp 0) yields J/(psi)K(exp *0)
[DE94-015185] p 872 N95-16309
Unusual initial and final state effects in quantum chromodynamics
[DE94-015341] p 903 N95-16604
Jet studies at CDF and DO collaborations
[DE94-015537] p 875 N95-16914
QCD of different flavors with the SLD detectors
[DE94-013800] p 875 N95-16943
Light-ray operators and their application in QCD
[DE94-013801] p 903 N95-16944
Research in elementary particle physics
[DE94-019219] p 877 N95-17358
Physics at high energy photon photon colliders
[DE94-018191] p 881 N95-17888

QUANTUM ELECTRODYNAMICS
The three loop equation of state of QED at high temperature
[DE94-015029] p 904 N95-17925

QUANTUM ELECTRONICS
Quantum transport in semiconductor devices
[AD-A281383] p 895 N95-16158

QUANTUM MECHANICS
Exact, E = 0, classical and quantum solutions for general power-law oscillators
[DE94-014436] p 903 N95-16428
Probing violation of quantum mechanics in the K0-(bar K)0 system
[DE94-017934] p 904 N95-17668
Trigonometric functions of nonlinear quantities
[DE94-018794] p 864 N95-17916

QUANTUM THEORY
Relativistic effect of energy increase of a particle moving freely in vacuum from the quantum field theory point of view
[DE94-622757] p 903 N95-17473

QUANTUM WELLS
Investigation of a normal incidence high-performance p-type strained layer In(0.3)Ga(0.7)As/In(0.52)Al(0.48)As quantum well infrared photodetector
[AD-A282720] p 900 N95-16928
Field-induced minigap and transport with in-plane magnetic fields in double quantum wells
[DE94-018893] p 879 N95-17918

QUARK PARTON MODEL
QCD of different flavors with the SLD detectors
[DE94-013800] p 875 N95-16943

QUARKS
QCD of different flavors with the SLD detectors
[DE94-013800] p 875 N95-16943
Search for first and second generation leptoquarks at D(null)
[DE94-018992] p 879 N95-17932

QUERY LANGUAGES
An incremental database access method for autonomous interoperable databases
[NASA-CR-189384] p 912 N95-17652

QUEUEING THEORY
Multivariate sampling with explicit correlation induction for practical simulation and optimization studies
[AD-A281998] p 841 N95-17445

QUOTIENTS
Trigonometric functions of nonlinear quantities
[DE94-018794] p 864 N95-17916

R

RADAR ABSORBERS
Interaction of electromagnetic fields with magnetized plasmas
[AD-A285496] p 755 N95-16968

RADAR ASTRONOMY
The Telecommunications and Data Acquisition Report
[NASA-CR-197249] p 755 N95-17279

RADAR BEACONS
Documentation of 9-PAC Beacon Target Detector processing function
[AD-A283090] p 759 N95-17336
RADAR CROSS SECTIONS
An approach to aerodynamic characteristics of low radar cross-section fuselages p 649 N95-16251
RADAR DETECTION
Clutter signal polarization in bistatic radar: Effect of antenna sidelobe clutter
[AD-A282300] p 753 N95-16240
RADAR ECHOES
Investigation of a normal incidence high-performance p-type strained layer In(0.3)Ga(0.7)As/In(0.52)Al(0.48)As quantum well infrared photodetector
[AD-A282720] p 900 N95-16928
RADAR FILTERS
Mitre adaptive processing capability
[AD-A281078] p 755 N95-16825
RADAR IMAGERY
Goldstone radar contributions to Mars Pathfinder landing safety p 921 N95-16205
On the improvement of 1-look SAR image segmentations with mathematical morphology
[INPE-5577-PRE/1805] p 912 N95-17650
Synthetic aperture radar target detection, feature extraction, and image formation techniques
[NASA-CR-197485] p 760 N95-17651
RADAR SCANNING
Using lidar tomography to characterize scattering in a turbulent media
[AD-A281014] p 751 N95-16002
RADAR SIGNATURES
Synthetic aperture radar target detection, feature extraction, and image formation techniques
[NASA-CR-197485] p 760 N95-17651
RADAR TARGETS
Superresolution in a jammed radar signal environment
[PB94-190758] p 760 N95-17455
RADAR TRACKING
Radar observations of field-aligned plasma propagations associated with NASA's PMG experiment
[AD-A285218] p 798 N95-16521
Implementation of a real-time data processing system for radar bandwidth extrapolation and stretch
[AD-A281195] p 754 N95-16794
Analysis of a three-beam radar as an instrument for determining ocean wave heights and vector slopes
[AD-A282342] p 806 N95-17505
RADAR TRANSMITTERS
Solid state radar demonstration test results at the FAA Technical Center
[AD-A281520] p 752 N95-16097
RADIANCE
Optimum truncation of a Gaussian beam in the presence of random jitter
[AD-A284951] p 752 N95-16143
RADIATION BELTS
Radiation belt dynamic and quasi-static modeling based on CRRES data
[AD-A285282] p 916 N95-16600
RADIATION DAMAGE
Scintillation mechanism and radiation damage in Ce(x)La(1-x)F3 crystals
[DE94-015848] p 896 N95-16385
RADIATION DETECTORS
Physical and chemical sensor technologies developed at Lawrence Livermore National Laboratory
[DE94-012231] p 775 N95-17380
RADIATION DISTRIBUTION
Kinetics model for initiation and promotion for describing tumor prevalence from HZE radiation
[NASA-TP-3479] p 820 N95-16412
Radiation electrodynamics of the photo-electron cloud produced by an arbitrary photon pulse incident on a planar emitting surface in vacuum
[AD-A282153] p 759 N95-17450
RADIATION DOSAGE
Radiation belt dynamic and quasi-static modeling based on CRRES data
[AD-A285282] p 916 N95-16600
RADIATION EFFECTS
Microchannel formation in polyimide by heavy ion irradiation
[DE94-753315] p 740 N95-16073
Reliability implications of defects in high temperature annealed Si/SiO2/Si structures
[DE94-015765] p 895 N95-16311
Reduction and aggregation of silver in aqueous gelatin and silica suspensions
[DE94-013998] p 727 N95-16363
Kinetics model for initiation and promotion for describing tumor prevalence from HZE radiation
[NASA-TP-3479] p 820 N95-16412
Basic mechanisms and implications of non-photic entrainment of circadian rhythmicity
[AD-A283180] p 822 N95-17342
Delayed annihilation of antiprotons in helium gas
[DE94-753405] p 878 N95-17739
RADIATION HARDENING
Non-volatile, rad-hard Random Access Memory (RAM) on GaAs
[AD-A285170] p 838 N95-16852
RADIATION MEASUREMENT
First results from SAGE 2
[DE94-014431] p 876 N95-17154
Electrical breakdown and optical emission properties of high pressure pulsed RF gas discharges
[DE94-012731] p 877 N95-17687
RADIATION MEASURING INSTRUMENTS
The combination probe of optical fibers and its applications p 652 N95-16275
A VHF/UHF antenna for the Precision Antenna Measurement System (PAMS)
[AD-A285673] p 754 N95-16621
RADIATION PROTECTION
Performance study of galactic cosmic ray shield materials
[NASA-TP-3473] p 924 N95-16912
RADIATION SPECTRA
High altitude hypersonic flowfield radiation
[AD-A281386] p 655 N95-16160
RADIATIVE HEAT TRANSFER
Thermal characteristics and heat transfer in an electrothermal light gas gun
[AD-A281980] p 892 N95-17442
RADIATIVE RECOMBINATION
Recombination and metastability in amorphous silicon and silicon-germanium alloys
[DE94-011837] p 794 N95-16957
RADICALS
Living radical polymerization. 1: Possibilities and limitations
[AD-A281042] p 742 N95-16451
Synthesis and mesomorphic behavior of poly((2S, 3S)-(+)-2-chloro-3-methylpentyl xy)biphenyl-4-carboxylate s with ethyl and propyl alkyl groups
[AD-A281402] p 744 N95-16865
Identification and temporal behavior of radical intermediates formed during the combustion and pyrolysis of gaseous fuels: Kinetic pathways to soot formation
[DE94-014681] p 731 N95-17163
Volatile CVD precursors based on copper alkoxides and mixed group IIA-copper alkoxides
[AD-D016380] p 732 N95-17479
RADIO ALTIMETERS
Application of GPS/SINS/RA integrated system to aircraft approach landing p 653 N95-16277
RADIO ASTRONOMY
The IUE Science Operations Ground System p 674 N95-17255
RF optics study for DSS-43 ultracone implementation p 758 N95-17296
First detection of CO (j = 0 - 1) adsorption at cosmological distances (z = 0.247)
[PB94-184595] p 916 N95-17332
DSN co-observing operations to support space VLBI missions p 694 N95-17543
RADIO COMMUNICATION
S-band and Ku-band return service interference between TDRSS users p 677 N95-17183
Advanced ground station architecture p 674 N95-17556
RADIO DIRECTION FINDERS
An analysis of the effects of feedline and ground screen noise currents on a conical monopole receiving antenna
[AD-A283401] p 759 N95-17436
RADIO EMISSION
ROSAT detection of diffuse hot gas in the edge-on galaxy NGC 4631
[NASA-CR-197535] p 915 N95-17496
RADIO EQUIPMENT
Method of calculating the optimal radioelectronic equipment design p 652 N95-16271
An automatic repeater station for signal transmissions
[AD-D016454] p 754 N95-16549
Electromagnetic interference tests
[AD-A281396] p 755 N95-16800
RADIO FILTERS
Mitre adaptive processing capability
[AD-A281078] p 755 N95-16825
RADIO FREQUENCIES
Field configuration of beam excited modes in the Advanced Photon Source (APS) storage ring waveguides
[DE94-015096] p 880 N95-16308
Spectral components of human cardiovascular responses to step changes in Lower Body Negative Pressure (LBNP) before and after 22 hour of 6 deg head down bed rest p 810 N95-16748
Progress at LAMPF
[DE94-016210] p 880 N95-16937
Interaction of electromagnetic fields with magnetized plasmas
[AD-A285496] p 755 N95-16968
Transverse mode coupling instability with a double RF system
[DE94-017972] p 761 N95-17672
RADIO FREQUENCY HEATING
First measurements of ICRF and edge/SOL plasma interactions on TORE SUPRA
[DE94-019320] p 891 N95-17347
RADIO FREQUENCY INTERFERENCE
Elimination of electromagnetic interference to receivers and sensitive equipment generated by switching systems
[AD-A281643] p 752 N95-16117
Performance of a fast frequency-hopped noncoherent MFSK receiver with non-ideal noise normalization combining over ricean fading channels with partial-band interference
[AD-A284989] p 753 N95-16232
S-band and Ku-band return service interference between TDRSS users p 677 N95-17183
RADIO NAVIGATION
The Telecommunications and Data Acquisition Report
[NASA-CR-197249] p 755 N95-17279
RADIO OBSERVATION
Solar-geophysical data number 596, April 1994. Part 1: (Prompt reports). Data for March, February 1994, and late data
[PB94-183548] p 924 N95-17736
RADIO RECEIVERS
Elimination of electromagnetic interference to receivers and sensitive equipment generated by switching systems
[AD-A281643] p 752 N95-16117
A low-cost transportable ground station for capture and processing of direct broadcast EOS satellite data p 680 N95-17200
Advanced ground station architecture p 674 N95-17556
RADIO RECEPTION
An analysis of the effects of feedline and ground screen noise currents on a conical monopole receiving antenna
[AD-A283401] p 759 N95-17436
RADIO SIGNALS
An automatic repeater station for signal transmissions
[AD-D016454] p 754 N95-16549
RADIO TELESCOPES
International mission planning for space Very Long Baseline Interferometry p 673 N95-17216
DSN co-observing operations to support space VLBI missions p 694 N95-17543
RADIO TRANSMISSION
Development of a medium energy modulated electron gun for orbital experiments
[AD-A281021] p 675 N95-16005
Rough surface models implemented within the split-step parabolic equation algorithm
[AD-A280843] p 753 N95-16148
Observations of ELF propagation at high latitudes during the sporadic-E conditions of November 1986
[AD-A284973] p 753 N95-16227
High speed method for predicting radio-wave propagation
[AD-D016369] p 761 N95-17697
RADIO TRANSMITTERS
Advanced ground station architecture p 674 N95-17556
RADIO WAVES
Evaluation of current tropospheric mapping functions by Deep Space Network very long baseline interferometry p 756 N95-17280
High speed method for predicting radio-wave propagation
[AD-D016369] p 761 N95-17697
RADIOACTIVE DECAY
High-level waste borosilicate glass: A compendium of corrosion characteristics
[DE94-016636] p 739 N95-15943
Natural and artificial nobel gas hydrologic tracers
[DE94-016010] p 797 N95-17718
RADIOACTIVE WASTES
High-level waste borosilicate glass: A compendium of corrosion characteristics
[DE94-016636] p 739 N95-15943
Online diagnoses of high current-density beams
[DE94-014420] p 879 N95-16217
Regional forecasting with global atmospheric models
[DE94-013863] p 801 N95-16961

Global climate change model natural climate variation: Paleoclimate data base, probabilities and astronomic predictors
[DE94-013956] p 796 N95-17348
Tokamak Transmutation of (nuclear) Waste (TTW): Parametric studies
[DE94-012891] p 881 N95-17721

RADIOACTIVITY
Heavy ion physics
[DE94-623321] p 880 N95-17519

RADIOIMMUNOASSAY
Periodic upright posture negates the suppression of neuroendocrine response to head down bedrest
p 817 N95-16780

RADIOSONDES
Modification of the Naval Postgraduate School Lidar System
[AD-A284987] p 753 N95-16231

RADOMES
Superspheroid geometries for radome analysis
[AD-A285405] p 753 N95-16233

RAIN FORESTS
Detection of deforestation in the Amazon forest using NOAA/AVHRR images and the geographic information system SGI: Methodology and test of a potential alarm system
[INPE-5580-TDI/543] p 791 N95-17894

RAMAN SPECTRA
High-intensity and high energy laser interactions with single droplets
[AD-A281415] p 776 N95-16166

RAMAN SPECTROSCOPY
Raman spectroscopy of C-irradiated graphite
[DE94-018705] p 733 N95-17911

RAMJET ENGINES
The 1993 JANNAF Propulsion Meeting, volume 1
[CPIA-PUBL-602-VOL-1] p 713 N95-16312
Thermal chemical energy of ablating silica surfaces in air breathing solid rocket engines p 714 N95-16316
Free-jet testing at Mach 3.44 in GASL's aero/thermo test facility p 672 N95-16320
Experimental and analytical methods for the determination of connected-pipe ramjet and ducted rocket internal performance
[AGARD-AR-323] p 721 N95-17278

RANDOM ACCESS MEMORY
Non-volatile, rad-hard Random Access Memory (RAM) on GaAs
[AD-A285170] p 838 N95-16852

RANDOM VARIABLES
Multivariate sampling with explicit correlation induction for practical simulation and optimization studies
[AD-A281998] p 841 N95-17445

RANDOM VIBRATION
Development of the vibration test equipment for testing the products of aircraft and space technology with simulation of operating conditions p 651 N95-16266
Correlation of finite element free vibration predictions using random vibration test data
[NASA-TM-106787] p 787 N95-17258

RANGEFINDING
Advanced technologies in the ASI MLRO towards a new generation laser ranging system p 687 N95-17239

RANKINE CYCLE
Thermal control systems for low-temperature heat rejection on a lunar base
[NASA-CR-197486] p 830 N95-16418

RARE EARTH ALLOYS
Rare earth ion doped CW cascade fiber laser
[AD-D016370] p 779 N95-17698

RARE GASES
A rare gas optics-free absolute photon flux and energy analyzer to provide absolute photoionization rates of inflowing interstellar neutrals
[NASA-CR-197228] p 914 N95-15964
A rare gas optics-free absolute photon flux and energy analyzer for solar and planetary observations
[NASA-CR-197227] p 915 N95-16021
Natural and artificial nobel gas hydrologic tracers
[DE94-016010] p 797 N95-17718

RAREFIED GAS DYNAMICS
Ultraviolet emissions occurring about hypersonic vehicles in rarefied flows
[AD-A281452] p 655 N95-16076

RATES (PER TIME)
Picosecond optoelectronic AND-GATE
[AD-A285672] p 885 N95-16620
Characterization of multiport solid state imagers at megahertz data rates
[DE94-016095] p 765 N95-16932
Spacecraft Data Simulator for the test of level zero processing systems p 675 N95-17582
Ultra high bit rate all optical communication system
[AD-D016359] p 887 N95-17695

RATINGS
Validation of astronaut psychological select-in criteria
p 813 N95-16762

RAY TRACING
Fast stereoscopic images with ray-traced volume rendering
[DE94-011703] p 835 N95-16223
Superspheroid geometries for radome analysis
[AD-A285405] p 753 N95-16233
Models to estimate high frequency acoustic scattering due to thermal fine- and micro-structure of the ocean
[AD-A285456] p 870 N95-16812
High speed method for predicting radio-wave propagation
[AD-D016369] p 761 N95-17697

RDX
Synthesis of pure RDX
[DE94-014356] p 749 N95-16542

REACTING FLOW
Radiative interactions in chemically reacting compressible nozzle flows using Monte Carlo simulations
[NASA-CR-197133] p 769 N95-15966

REACTION KINETICS
Computational fluid dynamics studies of nuclear rocket performance
[NASA-TM-105436] p 713 N95-16066
In situ laser activation of electrochemical kinetics at carbon electrodes
[AD-A280892] p 727 N95-16150
Control of molecular weights and polydispersities in radical polymerization of styrene in the presence of stable radicals
[AD-A281040] p 742 N95-16449
Living radical polymerization. 1: Possibilities and limitations
[AD-A281042] p 742 N95-16451
Development of practical MO techniques for prediction of the properties and behavior of materials
[AD-A285079] p 874 N95-16496
Kinetics and mechanism of chemical marker formation and water-activated heat generation
[AD-A281407] p 731 N95-17425
Development of heterogeneous Wacker oxidation catalysts: The role of the support and the redox component
[PB94-201431] p 732 N95-17700
Surftherm: A program to analyze thermochemical and kinetic data in gas-phase and surface chemical reaction mechanisms
[DE94-016145] p 733 N95-17744

REACTION TIME
Perceptual selectivity for color and form: On the nature of the interference effect
[AD-A285338] p 827 N95-16817
Parallel search for a conjunction of shape and contrast polarity
[AD-A285344] p 827 N95-16822

REACTIVITY
In situ laser activation of electrochemical kinetics at carbon electrodes
[AD-A280892] p 727 N95-16150
The chemistry and physics of transition metal clusters
[DE94-014012] p 734 N95-16364

REACTOR CORES
Reentry safety for the Topaz 2 Space Reactor: Issues and analyses
[DE95-000325] p 880 N95-17361

REACTOR DESIGN
A comparison of steady-state ARIES and pulsed PULSAR tokamak power plants
[DE94-014441] p 891 N95-17155

REACTOR MATERIALS
Fusion materials: Technical evaluation of the technology of vandium alloys for use as blanket structural materials in fusion power systems
[DE94-013194] p 890 N95-16827

REACTOR SAFETY
Reentry safety for the Topaz 2 Space Reactor: Issues and analyses
[DE95-000325] p 880 N95-17361

REACTOR TECHNOLOGY
Use of magnesium for recovering hydrogen isotopes from tritiated water
[DE94-014471] p 731 N95-17157

REAL TIME OPERATION
Sensor fault detection and diagnosis simulation of a helicopter engine in an intelligent control framework
[NASA-TM-106784] p 669 N95-15970
Simulation of arthroscopic surgery using MRI data
p 823 N95-15975
Multimodal correlation and intraoperative matching of virtual models in neurosurgery p 823 N95-15976
Tele Hyper Virtuality p 853 N95-15982
SSME propellant path leak detection real-time
[NASA-CR-197032] p 748 N95-16029
Methods of wave-front identification by control images
p 652 N95-16274
Approach to in-process tool wear monitoring in drilling: Application of Kalman filter theory p 653 N95-16279
Real-time data collection programs and source code for a commercial passive FTIR remote sensor
[AD-A284976] p 838 N95-16634
Implementation of a real-time data processing system for radar bandwidth extrapolation and stretch
[AD-A281195] p 754 N95-16794
Data rearrangement and real-time computation
[AD-A282349] p 910 N95-17166
Single Stage Rocket Technology's real time data system p 679 N95-17197
Multimission Telemetry Visualization (MTV) system: A mission applications project from JPL's Multimedia Communications Laboratory p 681 N95-17205
Telemetry distribution and processing for the second German Spacelab Mission D-2 p 681 N95-17207
Lessons learned supporting onboard solid-state recorders p 681 N95-17208
The role of mission operations in spacecraft integration and test p 684 N95-17220
Graphic Server: A real time system for displaying and monitoring telemetry data of several satellites
p 687 N95-17238
Towards cheaper control centers p 674 N95-17250
The SILEX experiment system operations
p 674 N95-17251
The IUE Science Operations Ground System
p 674 N95-17255
Mini All-purpose Satellite Control Center (MASCC)
p 674 N95-17257
Adaptive line enhancers for fast acquisition
p 757 N95-17287
Preliminary study of an active millimeter wave sensor
[PB94-189206] p 759 N95-17453
Development of a prototype real-time automated filter for operational deep space navigation
p 694 N95-17545
Re-engineering the Multimission Command System at the Jet Propulsion Laboratory p 702 N95-17583
A system study for satellite operation and control in next generation p 702 N95-17586
Configurable technology development for reusable control and monitor ground systems
p 675 N95-17589
Mission Operations Centers (MOCs): Integrating key spacecraft ground data system components
p 675 N95-17601
A new systems engineering approach to streamlined science and mission operations for the Far Ultraviolet Spectroscopic Explorer (FUSE) p 707 N95-17611
Risk reduction methodologies and technologies for the Earth Observing System (EOS) Operations Center (EOC)
p 707 N95-17612
Real-time symbolic model checking for discrete time models
[AD-A282878] p 864 N95-17618
Test applications for heterogeneous real-time network testbed
[DE94-016480] p 850 N95-17638
XPVM: A graphical console and monitor for PVM
[DE94-018050] p 842 N95-17678

RECIPROCATION
Updated test results of a pumped monopropellant propulsion system p 713 N95-16315

RECOGNITION
A workout for virtual bodybuilders (design issues for embodiment in multi-actor virtual environments)
p 854 N95-15990

RECOMBINATION REACTIONS
Fundamental studies in oxidation-reduction in relation to water photolysis
[DE94-014598] p 731 N95-17161

RECONNAISSANCE AIRCRAFT
Spread spectrum applications in unmanned aerial vehicles
[AD-A281035] p 754 N95-16448

RECORDS MANAGEMENT
Source header list. Volume 2: L through Z
[AD-A281001] p 908 N95-15998
Source hierarchy list. Volume 3: O through Z
[AD-A281102] p 908 N95-16090
Risk-Based Data Management System design specifications and implementation plan for the Alaska Oil and Gas Conservation Commission; the Mississippi State Oil and Gas Board; the Montana Board of Oil and Gas Conservation; and the Nebraska Oil and Gas Conservation Commission, attachment B
[DE94-013189] p 908 N95-16282

RECOVERABLE LAUNCH VEHICLES
Program test objectives milestone 3 — Integrated Propulsion Technology Demonstrator
[NASA-CR-197030] p 666 N95-15971

RECRYSTALLIZATION
Processing - property relationship in advanced intermetallics
[AD-A285262] p 735 N95-16514
RECURSIVE FUNCTIONS
NP-sets are Co-NP-immune relative to a random oracle
[TR-501] p 859 N95-15950
RED GIANT STARS
A high resolution liquid xenon imaging telescope for 0.3-10 MeV gamma-ray astrophysics: Construction and initial balloon flights
[NASA-CR-197556] p 916 N95-17528
REDUNDANCY
Repeatability in redundant manipulator systems
[AD-A282957] p 782 N95-17621
REDUNDANT COMPONENTS
Bayesian nonparametric estimation via Gibbs sampling for coherent systems with redundancy
[AD-A283173] p 865 N95-17341
REFERENCE SYSTEMS
Numeric data distribution: The vital role of data exchange in today's world p 907 N95-15937
REFLECTANCE
Effective reflection coefficients for the mean acoustic field between two rough interfaces
[AD-A281962] p 870 N95-16413
REFLECTED WAVES
Computation of reflected and transmitted horn radiation patterns for a dichroic plate p 758 N95-17293
REFLECTORS
Performance of specular reflectors used for lighting enhancement
[AD-A281004] p 884 N95-15999
A simple EHF hemispheric coverage antenna
[AD-A285078] p 754 N95-16495
Coatings for large-area low-cost solar concentrators and reflectors
[DE94-015735] p 793 N95-16916
Vacuum deposited polymer/silver reflector material
[DE94-018729] p 748 N95-17913
Study of the folding and deployment aspects of a Collapsible Rib Tensioned Surface (CRTS) antenna reflector
[CUED/D-STRUCT/TR-144] p 783 N95-17928
REFLEXES
Variability in Hoffmann and tendon reflexes in healthy male subjects p 808 N95-16739
Achilles Tendon Reflex (ATR) in response to short exposures of microgravity and hypergravity p 812 N95-16756
Effects of weightlessness on human baroreflex function p 815 N95-16770
REFRACTION
Effects of substrate temperature on metal colloid formation and on optical response in metal ion implanted silica
[DE94-013633] p 736 N95-16807
REFRACTIVITY
New mechanisms and new materials for organic optical nonlinearity
[AD-A282781] p 886 N95-17143
Numerical aperture limits on efficient ball lens coupling of laser diodes to single-mode fibers with defocus to balance spherical aberration
[NASA-TM-4578] p 886 N95-17271
The m-line method for optical characterisation of polymer waveguides
[PB94-184611] p 887 N95-17409
REFRACTORY COATINGS
Micromechanics of interfaces in metal matrix composites
[AD-A282404] p 725 N95-17457
REFRACTORY MATERIALS
Materials characterization and design for solar-thermal propulsion p 718 N95-16340
Computer modelling of cyclic deformation of high-temperature materials
[AD-A285212] p 735 N95-16519
Static and dynamic friction behavior of candidate high temperature airframe seal materials
[NASA-TM-106571] p 722 N95-16905
REFRACTORY METALS
Electromagnetic processing of refractory metal silicide/oxide composites
[AD-A281470] p 740 N95-16085
Solar-powered rocket engine optimization for high specific impulse p 718 N95-16341
Design, analysis, and fabrication of oxide-coated iridium/rhenium combustion chambers p 719 N95-16347
REFRIGERANTS
Alternatives for ozone-depleting refrigerants
[PB94-190857] p 795 N95-16881
REFRIGERATING
Test results of superconducting AC magnets for magnetic refrigeration experiment
[DE94-018695] p 751 N95-17909
REFRIGERATORS
Thermo-fluid mechanic study of thermoacoustic devices
[AD-A281130] p 870 N95-16810
REGENERATIVE FUEL CELLS
Energy and Technology Review
[DE95-000321] p 710 N95-17359
REGENERATORS
Ultra high bit rate all optical communication system
[AD-D016359] p 887 N95-17695
REGRESSION ANALYSIS
A combined biased-robust estimator for dealing with influence and collinearity in regression
[AD-A281793] p 864 N95-16422
A new model for estimating total body water from bioelectrical resistance p 810 N95-16747
Modelling daily precipitation as a function of temperature for climate change impact studies
[KNMI-WR-93-02] p 802 N95-17529
REGULATIONS
National Center for Standards and Certification Information: Service and programs p 907 N95-15938
Application of GPS/SINS/RA integrated system to aircraft approach landing p 653 N95-16277
DOD STINFO regulations and forms. Selected titles
[AD-A282332] p 909 N95-16374
Evaluation of the dynamic stability characteristics of the NAL Light Transport Aircraft
[NAL-PD-CA-9217] p 671 N95-16392
Review of performance, medical, and operational data on pilot aging issues p 812 N95-16759
Federal aviation regulations, part 91. General operating and flight rules. Change 5
[PB94-194883] p 665 N95-17476
REINFORCING FIBERS
Study of the compression behavior of high performance fibers
[AD-A284959] p 723 N95-16126
Micromechanics of interfaces in metal matrix composites
[AD-A282404] p 725 N95-17457
Fire protective coating and method for applying same to a structure
[AD-D016405] p 746 N95-17462
RELATIVISTIC EFFECTS
Relativistic effect of energy increase of a particle moving freely in vacuum from the quantum field theory point of view
[DE94-622757] p 903 N95-17473
RELAY SATELLITES
Attempt of automated space network operations at ETS-VI experimental data relay system p 677 N95-17184
GRTS operations monitor/control system p 685 N95-17226
RELIABILITY
Numeric data distribution: The vital role of data exchange in today's world p 907 N95-15937
Problems with aging wiring in Naval aircraft p 711 N95-16048
Damage-mitigating control of space propulsion systems for high performance and extended life
[NASA-CR-194470] p 784 N95-16068
Reliability implications of defects in high temperature annealed Si/SiO2/Si structures
[DE94-015765] p 895 N95-16311
Photovoltaic power conditioners: Development, evolution, and the next generation
[NASA-CR-197005] p 793 N95-16831
Optimization of adaptive intraply hybrid fiber composites with reliability considerations
[NASA-TM-106632] p 787 N95-16911
RELIABILITY ANALYSIS
The computer analysis of the prediction of aircraft electrical power supply system reliability p 653 N95-16278
The SEI and NAWC: Working together to establish a software measurement program
[AD-A280916] p 836 N95-16504
Bayesian nonparametric estimation via Gibbs sampling for coherent systems with redundancy
[AD-A283173] p 865 N95-17341
Statistical analysis of microgravity experiment performance using the degrees of success scale
[NASA-TM-106791] p 784 N95-17385
RELIABILITY ENGINEERING
The computer analysis of the prediction of aircraft electrical power supply system reliability p 653 N95-16278
RELIEF MAPS
The new map graphics in RSAS 5.0
[AD-A282432] p 791 N95-17511
REMOTE CONTROL
A specification of 3D manipulation in virtual environments p 853 N95-15981
Thermal feedback in virtual reality and telerobotic systems p 854 N95-15987
Bracing micro/macro manipulators control
[DE94-014434] p 856 N95-16287
Telemetry distribution and processing for the second German Spacelab Mission D-2 p 681 N95-17207
Feedback system for remotely operated vehicles
[AD-D016409] p 858 N95-17465
DSN co-observing operations to support space VLBI missions p 694 N95-17543
Solar and Heliospheric Observatory (SOHO) Experimenters' Operations Facility (EOF) p 675 N95-17573
Re-engineering the Multimission Command System at the Jet Propulsion Laboratory p 702 N95-17583
REMOTE MANIPULATOR SYSTEM
ISMCR 1994: Topical Workshop on Virtual Reality. Proceedings of the Fourth International Symposium on Measurement and Control in Robotics
[NASA-CP-10163] p 851 N95-15972
Virtual reality and telerobotics applications of an Address Recalculation Pipeline p 852 N95-15977
Master-slave system with force feedback based on dynamics of virtual model p 853 N95-15985
An improved position/force control of manipulators p 653 N95-16280
REMOTE SENSING
SeaWiFS technical report series. Volume 21: The heritage of SeaWiFS. A retrospective on the CZCS NIMBUS Experiment Team (NET) program
[NASA-TM-104566-VOL-21] p 803 N95-16006
Objective feature identification and tracking: A review
[AD-A284955] p 804 N95-16125
Survey of United States commercial satellites in geosynchronous Earth orbit
[AD-A284969] p 708 N95-16131
Imager for Mars Pathfinder (IMF) p 711 N95-16206
Infrared signatures for remote sensing
[DE94-014222] p 790 N95-16215
FIFE data analysis: Testing BIOME-BGC predictions for grasslands
[NASA-CR-197522] p 790 N95-16895
Tunable UV source for UV fluorescence remote sensing
[DE94-015745] p 777 N95-16917
Physical and chemical sensor technologies developed at Lawrence Livermore National Laboratory
[DE94-012231] p 775 N95-17380
SEQ-POINTER: Next generation, planetary spacecraft remote sensing science observation design tool p 697 N95-17559
On the measurement of momentum flux profiles using a five-beam 915-MHz wind profiler
[DE94-018448] p 791 N95-17903
REMOTE SENSORS
Real-time data collection programs and source code for a commercial passive FTIR remote sensor
[AD-A284976] p 838 N95-16634
The development and validation of command schedules for SeaWiFS p 690 N95-17249
REMOVAL
Bicarbonate of soda blasting technology for aircraft wheel depainting
[PB94-193323] p 654 N95-17466
REPEATERS
An automatic repeater station for signal transmissions
[AD-D016454] p 754 N95-16549
REPORTS
Laboratory Directed Research and Development Program
[DE94-011381] p 924 N95-16120
ICASE
[NASA-CR-195001] p 832 N95-16898
RESCUE OPERATIONS
Florida Gulf Stream Data (FLDA) current study
[AD-A281965] p 805 N95-16414
Heat stress and a countermeasure in the Shuttle rescueman's suit p 809 N95-16746
A prototype Crew Medical Restraint System (CMRS) for Space Station Freedom p 815 N95-16773
RESEARCH
Student research projects, 1993
[AD-A284954] p 804 N95-16124
RESEARCH AND DEVELOPMENT
Electronic access to ONREUR/ONRAISIA S and T reports p 907 N95-15935
Crystalline silicon processing
[DE94-016552] p 894 N95-15942
Activities of the Space Studies Board
[NASA-CR-197105] p 672 N95-16033
Laboratory Directed Research and Development Program
[DE94-011381] p 924 N95-16120

The Software Technology Center at Lawrence Livermore National Laboratory: Software engineering technology transfer in a scientific R/D laboratory
[DE94-014794] p 836 N95-16536
ICASE
[NASA-CR-195001] p 832 N95-16898
Physical and chemical sensor technologies developed at Lawrence Livermore National Laboratory
[DE94-012231] p 775 N95-17380
AINSE Plasma Science and Technology Conference and Elizabeth and Frederick White Workshop on Fundamental Problems in the Physics of Magnetically Confined Plasmas: Conference handbook
[DE94-622051] p 892 N95-17517
Electro-separations: Efficient processing for the twenty-first century
[DE94-012656] p 732 N95-17524

RESEARCH FACILITIES
The National Resource Library for Science and Technology in Sweden: A Nordic model of cooperating technology libraries p 906 N95-15929
Information sources in science and technology in Finland p 906 N95-15930
Development of strength analysis methods and design model for aircraft constructions in Kazan Aviation Institute p 651 N95-16264
The Role of Computers in Research and Development at Langley Research Center
[NASA-CP-10159] p 846 N95-16453
Software engineering from a Langley perspective p 843 N95-16454
A study of software standards used in the avionics industry p 670 N95-16456
Use of World Wide Web and NCSA Mcsaic at Langley p 847 N95-16464
From computer images to video presentation: Enhancing technology transfer p 848 N95-16467
Data Visualization and Animation Lab (DVAL): Applications p 843 N95-16469
The Software Technology Center at Lawrence Livermore National Laboratory: Software engineering technology transfer in a scientific R/D laboratory
[DE94-014794] p 836 N95-16536
A VHF/UHF antenna for the Precision Antenna Measurement System (PAMS)
[AD-A285673] p 754 N95-16621
Space medicine research: Needs for the 21st century p 814 N95-16768
ICASE
[NASA-CR-195001] p 832 N95-16898

RESEARCH MANAGEMENT
Electronic Engineering Notebook: A software environment for research execution, documentation and dissemination p 848 N95-16473
The Software Technology Center at Lawrence Livermore National Laboratory: Software engineering technology transfer in a scientific R/D laboratory
[DE94-014794] p 836 N95-16536

RESEARCH PROJECTS
Laboratory Directed Research and Development Program
[DE94-011381] p 924 N95-16120
D3-D research operations
[DE94-014934] p 892 N95-17497

RESERVES
Hydrogen production by gasification of municipal solid waste
[DE94-016483] p 732 N95-17639

RESIDUAL STRESS
Experimental studies of stress measurement by optical fluorescence
[AD-A282337] p 723 N95-16415
Investigation of residual stresses in a multipass weld in 1 in. stainless steel plate
[DE94-013277] p 786 N95-16803

RESIDUES
How clean is clean: Non-destructive/direct methods of flux, residue detection
[DE94-013439] p 763 N95-16357

RESIN MATRIX COMPOSITES
Impact vulnerability of thermoplastic-matrix composites
[PB94-201274] p 745 N95-17305

RESINS
Foam inflated rigidized structures for space applications p 710 N95-16344
Graphite-reinforced polycyanate composites for space and missile applications
[AD-A285509] p 725 N95-16970

RESISTORS
Resist materials design: Base-catalyzed chemical amplification
[AD-A281805] p 741 N95-16354

RESONANCE
Resonance enhanced multiphoton ionization of molecules and molecular fragments
[AD-A285076] p 873 N95-16493
Investigation of the effect of Alfven resonance absorption on fast wave current drive in ITER
[PB95-104352] p 894 N95-17929

RESONANCE SCATTERING
Photon beam studies of magnetic materials
[PB95-104279] p 877 N95-17351

RESONANT FREQUENCIES
Active and passive acoustic bubble sizing
[ISVR-TR-237] p 769 N95-16064
Natural frequency of uniform and optimized tetrahedral truss platforms
[NASA-TP-3461] p 709 N95-16559

RESONATORS
Anisotropic heat exchangers/stack configurations for thermoacoustic heat engines
[AD-A280974] p 792 N95-16506

RESOURCE ALLOCATION
An assessment of simulation systems applicable to business process reengineering at Army Directorates of Public Works
[AD-A285696] p 839 N95-17176
A mission planning concept and mission planning system for future manned space missions p 687 N95-17235
A model for analysis of TDA budget allocation p 758 N95-17295

RESOURCES MANAGEMENT
Risk-Based Data Management System design specifications and implementation plan for the Alaska Oil and Gas Conservation Commission; the Mississippi State Oil and Gas Board; the Montana Board of Oil and Gas Conservation; and the Nebraska Oil and Gas Conservation Commission, attachment B
[DE94-013189] p 908 N95-16282
Proceedings of the First National Conference on Climate Change and Water Resources Management
[AD-A281172] p 796 N95-17684

RESPIRATION
Energy expenditure, physical work load and postural control during walking on a moving platform
[AD-A285343] p 830 N95-16821

RESPIRATORY SYSTEM
Comparison of work of breathing during mechanical ventilation using assist control and intermittent mandatory ventilation
[AD-A285516] p 822 N95-17174

RESPONSE BIAS
Subset-selectivity and distractor matching in visual conjunction search
[AD-A285137] p 827 N95-16615

RESUSCITATION
Delivery of cardiopulmonary resuscitation in the microgravity environment p 816 N95-16774
Advanced Cardiac Life Support (ACLS) utilizing Man-Tended Capability (MTC) hardware onboard Space Station Freedom p 816 N95-16775

RETENTION (PSYCHOLOGY)
Synaptic plasticity and memory formation
[AD-A284926] p 825 N95-16138

RETINA
Investigation of laser-induced retinal damage: Wavelength and pulsewidth dependent mechanisms
[AD-A285186] p 822 N95-16871
Caffeine's influence on critical frequency thresholds
[AD-A282005] p 828 N95-17447

RETIREMENT
Review of performance, medical, and operational data on pilot aging issues p 812 N95-16759

REUSABLE ROCKET ENGINES
An object-oriented graphical user interface for a reusable rocket engine intelligent control system
[NASA-TM-106750] p 721 N95-17274

REVENUE
Applying Virtual Reality to commercial Edutainment p 854 N95-15989

REVERSE ENGINEERING
A survey of program slicing for software engineering
[NASA-CR-193116] p 836 N95-16574
Automation of reverse engineering process in aircraft modeling and related optimization problems
[NASA-CR-197109] p 668 N95-16899

REYNOLDS NUMBER
Transonic Navier-Stokes calculations about a 65 deg delta wing
[NASA-CR-4635] p 656 N95-17273
2-D aileron effectiveness study p 658 N95-17851
Two-dimensional 16.5 percent thick supercritical airfoil NLR 7301 p 658 N95-17854
OAT15A airfoil data p 659 N95-17857
Pressure distributions on research wing W4 mounted on an axisymmetric body p 660 N95-17862
Three-dimensional boundary layer and flow field data of an inclined prolate spheroid p 661 N95-17867
Force and pressure data of an ogive-nosed slender body at high angles of attack and different Reynolds numbers p 661 N95-17868

REYNOLDS STRESS
On the prediction of free turbulent jets with swirl using a quadratic pressure-strain model
[NASA-CR-194964] p 769 N95-16071

RHENIUM
Testing and evaluation of oxide-coated iridium/rhenium chambers p 719 N95-16346
Design, analysis, and fabrication of oxide-coated iridium/rhenium combustion chambers p 719 N95-16347

RHENIUM ALLOYS
Material and ballistic investigation of a tungsten-26 percent rhenium alloy
[PB94-189156] p 734 N95-16420

RHEOLOGY
Rheology and structure of planetary near-surface materials from landform topography p 922 N95-17392

RHYTHM (BIOLOGY)
Molecular approach to hypothalamic rhythms
[AD-A285164] p 822 N95-16851

RIBONUCLEIC ACIDS
Molecular approach to hypothalamic rhythms
[AD-A285164] p 822 N95-16851

RICHARDSON NUMBER
Long-term momentum and heat balances and turbulent mixing in the upper equatorial Pacific Ocean p 805 N95-17395

RIGID STRUCTURES
Physics-based approach to haptic display p 854 N95-15986

RING CURRENTS
Experimental characterization of ALS undulator radiation
[DE94-017967] p 881 N95-17671

RISK
Kapton wire concerns for aerospace vehicles p 711 N95-16045
The effect of differences in time to detection of circulating microbubbles on the risk of decompression sickness p 807 N95-16738
Heat stress and a countermeasure in the Shuttle rescueman's suit p 809 N95-16746
Review of performance, medical, and operational data on pilot aging issues p 812 N95-16759
Fusion materials: Technical evaluation of the technology of vandium alloys for use as blanket structural materials in fusion power systems
[DE94-013194] p 890 N95-16827
Performance study of galactic cosmic ray shield materials
[NASA-TP-3473] p 924 N95-16912

ROBOT ARMS
Virtual reality and telerobotics applications of an Address Recalculation Pipeline p 852 N95-15977
Coordinated control of a dual-arm dexterous robot using full immersion telepresence and virtual reality p 852 N95-15979
Master-slave system with force feedback based on dynamics of virtual model p 853 N95-15985
Lunar surface operations. Volume 3: Robotic arm for lunar surface vehicle
[NASA-CR-195553-VOL-3] p 780 N95-16031
An improved position/force control of manipulators p 653 N95-16280
Simulation of the coupled multi-spacecraft control testbed at the Marshall Space Flight Center p 849 N95-16475
Repeatability in redundant manipulator systems
[AD-A282957] p 782 N95-17621

ROBOT CONTROL
Coordinated control of a dual-arm dexterous robot using full immersion telepresence and virtual reality p 852 N95-15979
Lunar surface operations. Volume 3: Robotic arm for lunar surface vehicle
[NASA-CR-195553-VOL-3] p 780 N95-16031
Qualitative vision and action
[AD-A282697] p 831 N95-16966
Decentralized sliding mode control of nonlinear flexible robots
[DE94-013790] p 782 N95-17366
Repeatability in redundant manipulator systems
[AD-A282957] p 782 N95-17621

ROBOT DYNAMICS
Lunar surface operations. Volume 3: Robotic arm for lunar surface vehicle
[NASA-CR-195553-VOL-3] p 780 N95-16031
On performability theory and the inverse sliding problem
[AD-A282847] p 782 N95-17430
Repeatability in redundant manipulator systems
[AD-A282957] p 782 N95-17621

ROBOT SENSORS
The Yale Knowledge-Based Planning project
[AD-A281505] p 855 N95-16095

Stochastic approximation methods for fusion-rule estimation in multiple sensor systems
[DE94-013629] p 856 N95-16361
Geometric sensing of known planar shapes
[AD-A282854] p 840 N95-17432

ROBOTICS
ISMCR 1994: Topical Workshop on Virtual Reality. Proceedings of the Fourth International Symposium on Measurement and Control in Robotics
[NASA-CP-10163] p 851 N95-15972
Using virtual reality for science mission planning: A Mars Pathfinder case p 673 N95-15978
A virtual work space for both hands manipulation with coherency between kinesthetic and visual sensation p 831 N95-15984
Activities of the Space Studies Board
[NASA-CR-197105] p 672 N95-16033
The Yale Knowledge-Based Planning project
[AD-A281505] p 855 N95-16095
Joint Proceedings on Aeronautics and Astronautics (JPAA)
[ISBN-7-80-046602-7] p 649 N95-16249
An improved position/force control of manipulators p 653 N95-16280
Division of Information Systems (FOA 37)
[PB94-190766] p 909 N95-16400
Liquefied metal jet program Automation and Robotics Research Institute (ARRI)
[AD-A285470] p 736 N95-16878
Qualitative vision and action
[AD-A282697] p 831 N95-16966
Highly parallel reconfigurable computer architecture for robotic computation having plural processor cells each having right and left ensembles of plural processors
[NASA-CASE-NPO-17632-1-CU] p 832 N95-17400
On performability theory and the inverse sliding problem
[AD-A282847] p 782 N95-17430
Representation, modeling and recognition of outdoor scenes
[AD-A283257] p 858 N95-17634
A feedforward control approach to the local navigation problem for autonomous vehicles
[AD-A282787] p 666 N95-17706

ROBOTS
Multimodal correlation and intraoperative matching of virtual models in neurosurgery p 823 N95-15976
Surface matching for correlation of virtual models: Theory and application p 853 N95-15983
Stochastic approximation methods for fusion-rule estimation in multiple sensor systems
[DE94-013629] p 856 N95-16361
Graphical simulation of articulated rigid body system kinematics with collision detection
[AD-A281842] p 856 N95-16372
Decentralized sliding mode control of nonlinear flexible robots
[DE94-013790] p 782 N95-17366
Optimal trajectories for flexible-link manipulator slewing using recursive quadratic programming: Experimental verification
[DE94-018741] p 858 N95-17915

ROBUSTNESS (MATHEMATICS)
Tools for applied engineering optimization p 668 N95-16570
The algebraic multigrid projection for eigenvalue problems; backrotations and multigrid fixed points
[NASA-CR-194990] p 862 N95-16869

ROCKET ENGINE CASES
Filament overwrapped motor case technology p 720 N95-16350

ROCKET ENGINE DESIGN
Program test objectives milestone 3 — Integrated Propulsion Technology Demonstrator
[NASA-CR-197030] p 666 N95-15971
Large-scale hybrid motor performance and designs for use in launch vehicle applications p 715 N95-16327
Test results from a simple, low-cost, pressure-fed liquid hydrogen/liquid oxygen rocket combustor p 716 N95-16328
Integrated modular engine configuration options p 717 N95-16336
Structurally-compliant rocket engine combustion chamber: Experimental/analytical validation p 718 N95-16337
Solar-powered rocket engine optimization for high specific impulse p 718 N95-16341

ROCKET ENGINES
Structurally-compliant rocket engine combustion chamber: Experimental/analytical validation p 718 N95-16337
Solar-powered rocket engine optimization for high specific impulse p 718 N95-16341

ROCKET EXHAUST
Design of thermocouple probes for measurement of rocket exhaust plume temperatures
[AD-A285423] p 774 N95-16247
Electric probe measurements in the plume of the UK-10 ion thruster
[AD-A282460] p 713 N95-16302

ROCKET NOZZLES
Computational fluid dynamics studies of nuclear rocket performance
[NASA-TM-105436] p 713 N95-16066
The prediction of nozzle performance and heat transfer in hydrogen/oxygen rocket engines with transpiration cooling, film cooling, and high area ratios p 718 N95-16339

ROCKET SOUNDING
Equatorial airglow studies via rocket experiment
[INPE-5589-TDI/551] p 799 N95-17647

ROCKET-BORNE INSTRUMENTS
Development of a medium energy modulated electron gun for orbital experiments
[AD-A281021] p 675 N95-16005

ROCKS
Physical properties (particle size, rock abundance) from thermal infrared remote observations: Implications for Mars landing sites p 918 N95-16182
Alpha proton x ray spectrometer p 710 N95-16201

RODS
Phase transformations, ultrastructure and properties of rigid-rod fibers
[AD-A285249] p 749 N95-16512
Photoreceptors regulating circadian behavior: A mouse model
[AD-A285157] p 822 N95-16847
Thermal effects in end-heated laser rods: A time-dependent model and diagnostic
[AD-A282007] p 778 N95-17500

ROLL
Active load control during rolling maneuvers — performed in the Langley Transonic Dynamics Tunnel
[NASA-TP-3455] p 669 N95-17397

ROLLING MOMENTS
Experimental study at low supersonic speeds of a missile concept having opposing wraparound tails
[NASA-TM-4582] p 655 N95-16069

ROOT-MEAN-SQUARE ERRORS
Mixed-layer hindcasts conducted at OWS Victor with initialization from synthetic profiles/mixed-layer hindcasts conducted with BTs taken during 1990 with atmospheric forcing from NOGAPS
[AD-A284749] p 800 N95-16551

ROTARY WING AIRCRAFT
ADST system test report for the rotary wing aircraft airnet aeromodel and weapon model merge with the ATAC 2 baseline
[AD-A281580] p 666 N95-16171
Experimental data on the aerodynamic interactions between a helicopter rotor and an airframe p 664 N95-17883

ROTARY WINGS
Experimental data on the aerodynamic interac'ions between a helicopter rotor and an airframe p 664 N95-17883

ROTATING BODIES
A Lifting Ball Valve for cryogenic fluid applications p 720 N95-16349

ROTATING PLASMAS
Analysis of plasma measurements for the Geotail mission
[NASA-CR-197020] p 888 N95-15941

ROTATING STALLS
Unsteady flow phenomena in discrete passage diffusers for centrifugal compressors
[AD-A281412] p 770 N95-16163

ROTATION
Mathematical model for interaction of canals and otoliths in perception of orientation, translation, and rotation
[AD-A280897] p 819 N95-16151
Optical wheel-rotation sensor
[DE94-011719] p 780 N95-16224
Poloidal rotation and the evolution of H-mode and VH-mode profiles
[DE94-015858] p 890 N95-16919

ROTOR AERODYNAMICS
Investigation of dynamic inflow's influence on rotor control derivatives p 649 N95-16250

ROTOR BLADES
Investigation of dynamic inflow's influence on rotor control derivatives p 649 N95-16250

ROTOR BODY INTERACTIONS
Experimental data on the aerodynamic interactions between a helicopter rotor and an airframe p 664 N95-17883

ROTORS
A Lifting Ball Valve for cryogenic fluid applications p 720 N95-16349
Numerical simulation of helicopter engine plume in forward flight
[NASA-CR-197488] p 655 N95-16589
Structural effects of unsteady aerodynamic forces on horizontal-axis wind turbines
[DE94-011863] p 787 N95-16939

ROVING VEHICLES
Mars Pathfinder and the exploration of southern Amazonis Planitia p 917 N95-16178

RUBIDIUM COMPOUNDS
Critical and paramagnetic spin dynamics in an antiferromagnetically coupled Heisenberg magnet: Results for RbMnF3
[PB95-104329] p 869 N95-17731

RULES
Cellular automata for contour dynamics
[PB94-197613] p 865 N95-17526

RUN TIME (COMPUTERS)
On-line scheduling on parallel machines
[AD-A281136] p 849 N95-16603

RUNGE-KUTTA METHOD
On the removal of boundary errors caused by Runge-Kutta integration of non-linear partial differential equations
[NASA-CR-194989] p 863 N95-16904

RUNWAYS
Modeling of Instrument Landing System (ILS) localizer signal on runway 25L at Los Angeles International Airport
[NASA-TM-4588] p 665 N95-17384

RURAL LAND USE
A procedure for estimating the carbon budget of terrestrial ecosystems in the former Soviet Union by geographic information system analysis and classification of AVHRR derived global vegetation index p 796 N95-17394

RUSSIAN FEDERATION
Development of strength analysis methods and design model for aircraft constructions in Kazan Aviation Institute p 651 N95-16264
Space VLBI telecommunication characteristics, protection criteria, and frequency sharing p 756 N95-17282

S

SAFETY
Combustion and fires in low gravity p 712 N95-16050
Goldstone radar contributions to Mars Pathfinder landing safety p 921 N95-16205
Primary battery design and safety guidelines handbook
[NASA-RP-1353] p 764 N95-16561
Safety characteristics of lithium-alloy/metal sulfide batteries
[DE94-013867] p 766 N95-16963
Risk reduction methodologies and technologies for the Earth Observing System (EOS) Operations Center (EOC) p 707 N95-17612

SAFETY DEVICES
Combustion and fires in low gravity p 712 N95-16050

SAFETY FACTORS
Signal wave generator signals recorded by the Federal Outdoor Impact Laboratory's on-board Data Acquisition System
[PB94-186525] p 752 N95-16094
The global aircraft shape p 668 N95-16571
Review of performance, medical, and operational data on pilot aging issues p 812 N95-16759
Safety aspects of spacecraft commanding p 689 N95-17248
Aircraft and sub-system certification by piloted simulation
[AGARD-AR-278] p 671 N95-17388

SAFETY MANAGEMENT
Primary battery design and safety guidelines handbook
[NASA-RP-1353] p 764 N95-16561
Safety aspects of spacecraft commanding p 689 N95-17248

SALINITY
Variation of the thermohaline structure in the western equatorial Pacific upper ocean p 805 N95-17277
Straits of Florida physical oceanographic field study. Volume 1: Executive summary. Volume 2: Technical report. Volume 3: Data report
[PB94-175031] p 806 N95-17615

SALTS
Plasma sound source basic research
[AD-A285394] p 890 N95-16617

SAMPLED DATA SYSTEMS
An algorithm for extraction of periodic signals from sparse, irregularly sampled data p 756 N95-17281

SAMPLERS
Preliminary investigation of an integrated optic sampler for HF signals
[AD-A284285] p 884 N95-16133
Novel mass spectrometric instrument for gaseous and particulate characterization and monitoring
[DE94-014168] p 795 N95-16213
Evaluation of a pneumatic Martian soil sampler concept
[NASA-CR-197539] p 923 N95-17653
SAMPLING
Evaluation of a pneumatic Martian soil sampler concept
[NASA-CR-197539] p 923 N95-17653
SANDS
Opportunity to sample something different: The dark, unweathered, mafic sands of Cerberus and the Pathfinder 1997 Mars landing p 919 N95-16187
SANDSTONES
Application of NMR shock barometer to naturally shocked minerals
[DE95-000326] p 799 N95-17362
SANDWICH STRUCTURES
A consistent large deflection theory of composite sandwich shells p 650 N95-16259
SAPPHIRE
Evaluation of the quality of sapphire using x-ray rocking curves and double-crystal x-ray topography
[AD-A282905] p 901 N95-17620
SATELLITE ATTITUDE CONTROL
Mission operations data analysis tools for Mars Observer guidance and control p 689 N95-17244
SATELLITE COMMUNICATION
Survey of United States commercial satellites in geosynchronous Earth orbit
[AD-A284969] p 708 N95-16131
Fast acquisition of burst direct sequence spread spectrum signals through satellite channels p 652 N95-16270
Telecommunications end-to-end systems monitoring on TOPEX/Poseidon: Tools and techniques p 676 N95-17180
Attempt of automated space network operations at ETS-VI experimental data relay system p 677 N95-17184
Demand access communications for TDRSS users p 677 N95-17187
The GRO remote terminal system p 678 N95-17188
Accuracy analysis of TDRSS demand forecasts p 683 N95-17214
The SILEX experiment system operations p 674 N95-17251
Simplifying operations with an uplink/downlink integration toolkit p 697 N95-17562
Modeling ESA's TT/C systems p 701 N95-17579
The ESA standard for telemetry and telecommand packet utilisation: PUS p 704 N95-17595
SATELLITE CONTROL
A PC based tool for mission plan production p 686 N95-17232
Graphic Server: A real time system for displaying and monitoring telemetry data of several satellites p 687 N95-17238
A graphic system for telemetry monitoring and procedure performing at the Telecom SCC p 689 N95-17246
Mini All-purpose Satellite Control Center (MASCC) p 674 N95-17257
ELISA, a demonstrator environment for information systems architecture design p 698 N95-17563
Taking advantage of ground data systems attributes to achieve quality results in testing software p 699 N95-17570
A system study for satellite operation and control in next generation p 702 N95-17586
A standard satellite control reference model p 704 N95-17592
SATELLITE DESIGN
Survey of United States commercial satellites in geosynchronous Earth orbit
[AD-A284969] p 708 N95-16131
Efficient mission control for the 48-satellite Globalstar Constellation p 674 N95-17256
A system study for satellite operation and control in next generation p 702 N95-17586
SATELLITE GROUND SUPPORT
Simplifying operations with an uplink/downlink integration toolkit p 697 N95-17562
Integration of a satellite ground support system based on analysis of the satellite ground support domain p 675 N95-17568
NCCDS performance model p 675 N95-17576
SATELLITE IMAGERY
Metadata database for automated oceanographic imagery
[AD-A284932] p 805 N95-16141
Using neural networks to correlate satellite imagery and ground-truth data
[AD-A285486] p 857 N95-16967
A land-surface Testbed for EOSDIS
[NASA-CR-189392] p 840 N95-17327
Operational cloud classifier based on a self-organized feature map
[PB94-197852] p 802 N95-17504
SATELLITE INSTRUMENTS
The development and validation of command schedules for SeaWiFS p 690 N95-17249
SATELLITE NETWORKS
S-band and Ku-band return service interference between TDRSS users p 677 N95-17183
Attempt of automated space network operations at ETS-VI experimental data relay system p 677 N95-17184
Demand access communications for TDRSS users p 677 N95-17187
Economical ground data delivery p 679 N95-17194
Accuracy analysis of TDRSS demand forecasts p 683 N95-17214
SATELLITE OBSERVATION
Objective feature identification and tracking: A review
[AD-A284955] p 804 N95-16125
FIFE data analysis: Testing BIOME-BGC predictions for grasslands
[NASA-CR-197522] p 790 N95-16895
Overview on METEOSAT geometrical image data processing p 678 N95-17189
The development and validation of command schedules for SeaWiFS p 690 N95-17249
SEQ-POINTER: Next generation, planetary spacecraft remote sensing science observation design tool p 697 N95-17559
SATELLITE ORBITS
Implementation of a low-cost, commercial orbit determination system p 673 N95-17544
SATELLITE TRACKING
Objective feature identification and tracking: A review
[AD-A284955] p 804 N95-16125
Accuracy analysis of TDRSS demand forecasts p 683 N95-17214
TDRS orbit determination by radio interferometry p 673 N95-17547
SATELLITE TRANSMISSION
Earth Observing System (EOS) Communication (Ecom) Modeling, Analysis, and Testbed (EMAT) activiy p 677 N95-17182
End-to-end communication test on variable length packet structures utilizing AOS testbed p 677 N95-17186
The GRO remote terminal system p 678 N95-17188
Simplifying operations with an uplink/downlink integration toolkit p 697 N95-17562
SCALARS
Dynamical system prediction of the scalar field in a turbulent channel flow
[AD-A285519] p 771 N95-16438
Electromagnetostatics in uniaxial bianisotropic media
[PB94-197688] p 754 N95-16613
Flavor symmetries and fermion masses
[DE94-018192] p 878 N95-17889
Search for first and second generation leptoquarks at D(null)
[DE94-018992] p 879 N95-17932
SCALE MODELS
Analysis of infrared scaling laws
[AD-A285461] p 903 N95-16877
Erosion effects on TVC vane heat transfer characteristics
[AD-A282006] p 721 N95-17448
SCALING LAWS
Analysis of infrared scaling laws
[AD-A285461] p 903 N95-16877
SCANNERS
MODIS Technical Report Series. Volume 4: MODIS data access user's guide: Scan cube format
[NASA-TM-104594-VOL-4] p 837 N95-16587
Full color recorder
[AD-A282278] p 790 N95-17372
Advances in ultrafast scanning probe microscopy
[DE94-018180] p 779 N95-17729
Ultrafast scanning probe microscopy
[DE94-018186] p 779 N95-17887
SCANNING ELECTRON MICROSCOPY
Atomic scale structure and chemistry of interfaces by Z-contrast imaging and electron energy loss spectroscopy in the stem
[DE94-013632] p 728 N95-16419
Self-assembly of low-dimensional conductors on Au(111) surfaces
[AD-A280936] p 734 N95-16505
SCANNING TUNNELING MICROSCOPY
Surface and defect excitations in covalently bonded solids
[AD-A281338] p 894 N95-16012
Self-assembly of low-dimensional conductors on Au(111) surfaces
[AD-A280936] p 734 N95-16505
Scanning tunneling microscopy of 3 to 5 semiconductors
[AD-A281722] p 902 N95-17705
Ultrafast scanning probe microscopy
[DE94-018186] p 779 N95-17887
SCATTERING
Antenna noise temperatures of the 34-meter beam-waveguide antenna with horns of different gains installed at F1 p 757 N95-17288
Rietveld refinement of magnetic structures from pulsed-neutron-source powder-diffraction data
[DE94-016599] p 737 N95-17641
SCAVENGING
Surfactant adsorption by sub-millimeter size bubbles: Quantification and modelling
[AD-A282405] p 772 N95-17506
SCENE ANALYSIS
Representation, modeling and recognition of outdoor scenes
[AD-A283257] p 858 N95-17634
SCHEDULES
Using virtual reality for science mission planning: A Mars Pathfinder case p 673 N95-15978
RDD-100 and the systems engineering process p 848 N95-16471
SCHEDULING
Improving production schedules without scheduling
[PB94-191350] p 904 N95-16289
Availability of direct normal radiation for solar furnace processing: A case study
[DE94-006907] p 792 N95-16435
A software tool for dataflow graph scheduling p 843 N95-16457
Software cost and schedule estimating: A process improvement initiative
[AD-A280915] p 836 N95-16503
On-line scheduling on parallel machines
[AD-A281136] p 849 N95-16603
A distributed planning concept for Space Station payload operations p 682 N95-17211
Joint operations planning for space surveillance missions on the MSX satellite p 673 N95-17215
Evaluating Space Network (SN) scheduling operations concepts through statistical analysis p 684 N95-17222
Generic mission planning and scheduling: The AXAF solution p 686 N95-17231
Autonomous mission planning and scheduling: Innovative, integrated, responsive p 686 N95-17234
A mission planning concept and mission planning system for future manned space missions p 687 N95-17235
Production and quality assurance automation in the Goddard Space Flight Center Flight Dynamics Facility p 687 N95-17237
The Sequence of Events generator: A powerful tool for mission operations p 688 N95-17240
SCHLIEREN PHOTOGRAPHY
Wind tunnel investigations of the appearance of shocks in the windward region of bodies with circular cross section at angle of attack p 661 N95-17866
SCHOTTKY DIODES
LPEE growth and characterization of In(x)Ga(1-x)As(y)Sb(1-y) lattice matched to GaSb and InAs for photodetectors
[AD-A281631] p 895 N95-16114
The development of a solid-state hydrogen sensor for rocket engine leakage detection
[NASA-CR-197567] p 776 N95-17895
SCIENTIFIC SATELLITES
The SAX Italian scientific satellite. The on-board implemented automation as a support to the ground control capability p 695 N95-17551
SCIENTIFIC VISUALIZATION
Student research projects, 1993
[AD-A284954] p 804 N95-16124
Sorting and hardware assisted rendering for volume visualization
[DE94-010204] p 834 N95-16220
Visualizing 3D velocity fields near contour surfaces
[DE94-010205] p 860 N95-16221
Fast stereoscopic images with ray-traced volume rendering
[DE94-011703] p 835 N95-16223
Visualization of unsteady computational fluid dynamics
[NASA-CR-197461] p 770 N95-16388
Data Visualization and Animation Lab (DVAL) overview p 843 N95-16468
Data Visualization and Animation Lab (DVAL): Applications p 843 N95-16469

Graphic Server: A real time system for displaying and monitoring telemetry data of several satellites p 687 N95-17238
Experimenter's Laboratory for Visualized Interactive Science
[NASA-CR-189391] p 910 N95-17322
McIDAS-eXplorer: A version of McIDAS for planetary applications
[NASA-CR-189382] p 910 N95-17323
An interactive interface for NCAR Graphics
[NASA-CR-189383] p 840 N95-17324
A distributed analysis and visualization system for model and observational data
[NASA-CR-189386] p 911 N95-17326
An interactive environment for the analysis of large Earth observation and model data sets
[NASA-CR-189381] p 911 N95-17330

SCIENTISTS
From computer images to video presentation: Enhancing technology transfer p 848 N95-16467
Scientific and technical publishing at Goddard Space Flight Center in Fiscal Year 1994
[NASA-TM-104614] p 925 N95-16581
Proceedings of the Neural Network Workshop for the Hanford Community
[DE94-014567] p 856 N95-16609
ICASE
[NASA-CR-195001] p 832 N95-16898

SCINTILLATION
Scintillation mechanism and radiation damage in Ce(x)La(1-x)F3 crystals
[DE94-015848] p 896 N95-16385
Precision machining and polishing of scintillating crystals for large calorimeters and hodoscopes
[DE94-012060] p 751 N95-17738

SCINTILLATION COUNTERS
Scintillation mechanism and radiation damage in Ce(x)La(1-x)F3 crystals
[DE94-015848] p 896 N95-16385
Neutrino oscillation studies at LAMPF
[DE94-018098] p 878 N95-17727

SEA LEVEL
A coastal hazards data base for the US Gulf Coast
[DE94-014573] p 805 N95-16610

SEA STATES
Models to estimate high frequency acoustic scattering due to thermal fine- and micro-structure of the ocean
[AD-A285456] p 870 N95-16812

SEA SURFACE TEMPERATURE
SeaWiFS technical report series. Volume 21: The heritage of SeaWiFS. A retrospective on the CZCS NIMBUS Experiment Team (NET) program
[NASA-TM-104566-VOL-21] p 803 N95-16006
Mixed-layer hindcasts conducted at OWS Victor with initialization from synthetic profiles/mixed-layer hindcasts conducted with BTs taken during 1990 with atmospheric forcing from NOGAPS
[AD-A284749] p 800 N95-16551
The effects of the horizontal resolution of the boundary forcing sea surface temperature field on the FSU spectral model
[AD-A284273] p 802 N95-17488

SEA WATER
Surfactant adsorption by sub-millimeter size bubbles: Quantification and modelling
[AD-A282405] p 772 N95-17506

SEALING
Antenna dielectric sealing process characterization
[DE94-015864] p 747 N95-17690

SEAMOUNTS
Flow over abrupt topography: The application of patterns in nutrient and productivity in reflecting physical processes
[AD-A280813] p 797 N95-17740

SEARCH PROFILES
DROLS: An introduction to searching (videorecording)
[AD-M000338] p 912 N95-17660

SEARCHING
Knowledge quality functions for rule discovery
[AD-A285513] p 910 N95-16971

SEATS
A correlative investigation of simulated occupant motion and accident report in a helicopter crash
[AD-A285190] p 664 N95-16404
Apache helicopter seat cushion evaluation
[AD-A284300] p 831 N95-17484

SECONDARY ION MASS SPECTROMETRY
Atomic transport of oxygen
[DE94-013332] p 873 N95-16430

SECRETIONS
Extracellular ionic composition alters kinetics of vesicular release of catecholamines and quantal size during exocytosis at adrenal medullary cells
[AD-A281613] p 818 N95-16112

SECURITY
DOD STINFO regulations and forms. Selected titles
[AD-A282332] p 909 N95-16374

SEDIMENTS
Three-dimensional eutrophication model of Chesapeake Bay. Volume 1: Main report
[AD-A280760] p 804 N95-16118
Maja Valley and the Chryse outflow complex sites p 921 N95-16199

SEGMENTS
Production asymmetries in x(sub F) and P(sub t)(exp 2) for D(+-) mesons
[DE94-015546] p 872 N95-16310

SELECTIVE DISSEMINATION OF INFORMATION
DOD STINFO regulations and forms. Selected titles
[AD-A282332] p 909 N95-16374

SELENIUM
New approaches to novel organosilanes
[AD-A285253] p 722 N95-16513

SELF CONSISTENT FIELDS
Development of practical MO techniques for prediction of the properties and behavior of materials
[AD-A285079] p 874 N95-16496

SELF ORGANIZING SYSTEMS
Self-organizing neural network for classifying pattern signatures with a posteriori conditional class probability
[AD-D016455] p 857 N95-16823

SEMANTICS
Software merge: Semantics of combining changes to programs
[AD-A281373] p 834 N95-16154
Open architectures for formal reasoning and deductive technologies for software development
[NASA-CR-197528] p 837 N95-16586
Use of data description languages in the interchange of data p 704 N95-17597

SEMICIRCULAR CANALS
Mathematical model for interaction of canals and otoliths in perception of orientation, translation, and rotation
[AD-A280897] p 819 N95-16151
Dynamics of the G-excess illusion p 815 N95-16771

SEMICONDUCTING FILMS
Electrochemical atomic layer processing
[AD-A282330] p 872 N95-16241
Method for intrinsically doped III-A and V-A compounds and products thereof
[AD-D016324] p 896 N95-16399
Low temperature deposition and characterization of N- and P-type silicon carbide thin films and associated ohmic and Schottky contacts
[AD-A281060] p 743 N95-16625
Selective area platinum film deposition
[AD-D016355] p 747 N95-17693

SEMICONDUCTOR DEVICES
Interface properties of wide bandgap semiconductor structures
[AD-A281469] p 894 N95-16084
Quantum transport in semiconductor devices
[AD-A281383] p 895 N95-16158
Overview of photonics research at Lawrence Livermore National Laboratory
[DE94-014055] p 884 N95-16366
Femtosecond studies of carrier dynamics in compound semiconductors
[AD-A282871] p 767 N95-17433
Adhesion of silicon oxide to diamond
[AD-D016356] p 747 N95-17694
Field-induced minigap and transport with in-plane magnetic fields in double quantum wells
[DE94-018893] p 879 N95-17918

SEMICONDUCTOR DIODES
Active silicon x ray for measuring electron temperature
[DE94-017521] p 890 N95-16555

SEMICONDUCTOR JUNCTIONS
Research on stable, high-efficiency amorphous-silicon multijunction modules
[DE94-011839] p 764 N95-16425

SEMICONDUCTOR LASERS
Theory of carrier heating through injection pumping and lasing in semiconductor microcavity lasers
[AD-A281795] p 776 N95-16353
The SILEX experiment system operations p 674 N95-17251

SEMICONDUCTORS (MATERIALS)
Augmentation for research training: Surface-mediated photocatalysis
[AD-A281591] p 722 N95-16100
Workshop on Epitaxy, Interfaces, Defects and Processing of Electronic and Photonic Materials
[AD-A281595] p 894 N95-16111
LPEE growth and characterization of In(x)Ga(1-x)As(y)Sb(1-y) lattice matched to GaSb and InAs for photodetectors
[AD-A281631] p 895 N95-16114
Ultrashort pulse effects in semiconductor amplifiers and in dispersive media
[AD-A284925] p 763 N95-16137
Electrochemical atomic layer processing
[AD-A282330] p 872 N95-16241
Modification of 2-6 and 3-5 materials using ion beams
[AD-A281839] p 896 N95-16365
Monte Carlo simulation of mercury cadmium telluride
[AD-A281546] p 896 N95-16391
Semiconductor heterojunction engineering
[AD-A281553] p 896 N95-16396
The deposition of electro-optic films on semiconductors
[AD-A285068] p 742 N95-16488
New approaches to novel organosilanes
[AD-A285253] p 722 N95-16513
Nonlinear optical response of condined excitions in molecular and semiconductor nanostructures
[AD-A285225] p 885 N95-16524
Low temperature synthesis of semiconductor materials
[AD-A285230] p 898 N95-16526
Nitride semiconductors for ultraviolet detection
[AD-A280988] p 898 N95-16533
Process of making a bistable photoconductive component
[AD-D016449] p 764 N95-16539
Properties of semiconducting Ru2Ge3
[DE94-015361] p 899 N95-16913
Femtosecond studies of carrier dynamics in compound semiconductors
[AD-A282871] p 767 N95-17433
BaF2/GaAs electronic components
[AD-D016391] p 767 N95-17481
Selective area platinum film deposition
[AD-D016355] p 747 N95-17693
Scanning tunneling microscopy of 3 to 5 semiconductors
[AD-A281722] p 902 N95-17705
Simulation of the SEMATECH gravimetric mass flowmeter calibrator
[DE94-018698] p 773 N95-17910

SEMIEMPIRICAL EQUATIONS
Natural frequency of uniform and optimized tetrahedral truss platforms
[NASA-TP-3461] p 709 N95-16559

SENSITIVITY
Applications of automatic differentiation in computational fluid dynamics p 774 N95-16461
Automatic differentiation for design sensitivity analysis of structural systems using multiple processors p 847 N95-16462
Investigations on the sensitivity of the computer code TURBO-2D
[CUED/A-THERMO/TR-61] p 771 N95-16595

SENSORIMOTOR PERFORMANCE
The EPIC architecture for modeling human information-processing and performance: A brief introduction
[AD-A280762] p 829 N95-16119
Mental rotation with and without a concurrent task: Moderating effects of visuospatial ability
[AD-A281866] p 826 N95-16301

SENSORS
Theory of one-dimensional and two-dimensional distributed sensors for measuring the spatial characteristics of thermophysical and hydrodynamic fields p 652 N95-16273
Optical fiber sensors: Accelerating applications in Navy ships
[PB94-186848] p 887 N95-17441

SENSORY FEEDBACK
ISMCR 1994: Topical Workshop on Virtual Reality. Proceedings of the Fourth International Symposium on Measurement and Control in Robotics
[NASA-CP-10163] p 851 N95-15972

SENSORY PERCEPTION
Characterization of the fast-phase component of the vestibulo-ocular response
[AD-A281830] p 820 N95-16360

SEPAC (PAYLOAD)
SEPAC co-investigator support
[NASA-CR-196527] p 798 N95-15965

SEPARATED FLOW
Experimental investigation of turbulent separated-reattachment flow by using LDV p 649 N95-16253
Numerical simulation of helicopter engine plume in forward flight
[NASA-CR-197488] p 655 N95-16589

SEPARATION
Modeling of wall-bounded complex flows and free shear flows
[NASA-TM-106513] p 770 N95-16407

SEQUENCING
The Sequence of Events generator: A powerful tool for mission operations p 688 N95-17240

Small scale sequence automation pays big dividends p 689 N95-17247
Galileo spacecraft modeling for orbital operations p 700 N95-17574

SEQUENTIAL CONTROL
Online performance-improvement algorithms [AD-A285162] p 838 N95-16850
Structural optimization with approximate sensitivities [NASA-TM-4553] p 789 N95-17701

SERVICE LIFE
Problems with aging wiring in Naval aircraft p 711 N95-16048
Space Station Freedom primary power wiring requirements p 712 N95-16051
Damage-mitigating control of space propulsion systems for high performance and extended life [NASA-CR-194470] p 784 N95-16068
Service and physical properties of liquid-jet fuels p 650 N95-16256
Computer modelling of cyclic deformation of high-temperature materials [AD-A285212] p 735 N95-16519
Bayesian nonparametric estimation via Gibbs sampling for coherent systems with redundancy [AD-A283173] p 865 N95-17341

SERVOCONTROL
Servo control using switches for discrete positional feedback [AD-A284747] p 856 N95-16550

SERVOMECHANISMS
Master-slave system with force feedback based on dynamics of virtual model p 853 N95-15985
Servo control using switches for discrete positional feedback [AD-A284747] p 856 N95-16550

SET THEORY
On P-selectivity and closeness [TR-499] p 859 N95-15951
Uniqueness and free interpolation for logarithmic potentials and the Cauchy problem for the Laplace equation in (R2) [PB94-192408] p 861 N95-16295

SEX FACTOR
An annotated bibliography of heat tolerance: Regarding gender differences [AD-A280755] p 818 N95-16105
A proposal to study gender differences in the rates of decompression sickness [AD-A281854] p 819 N95-16297
Mental rotation with and without a concurrent task: Moderating effects of visuospatial ability [AD-A281866] p 826 N95-16301

SHAPE MEMORY ALLOYS
Structural integrity of intelligent materials and structures. Constitutive modeling of shape memory alloys [AD-A281301] p 735 N95-16786

SHAPES
Measurement of the B meson differential cross-sections in p(-p) collisions at the square root of s = 1.8 TeV using the exclusive decays B(+-) yields J/(psi)K(+-) and B(exp 0) yields J/(psi)K(exp *0) [DE94-015185] p 872 N95-16309
Optimum aerodynamic design via boundary control p 667 N95-16565
Residual-correction type and related computational methods for aerodynamic design. Part 1: Airfoil and wing design p 667 N95-16566
Optimal shape design for aerodynamics p 667 N95-16568
Airfoil optimization by the one-shot method p 667 N95-16569
The global aircraft shape p 668 N95-16571
Review of the EUROPT Project AERO-0026 p 668 N95-16573
Perceptual selectivity for color and form: On the nature of the interference effect [AD-A285338] p 827 N95-16817
Parallel search for a conjunction of shape and contrast polarity [AD-A285344] p 827 N95-16822

SHARP LEADING EDGES
Wind tunnel test on a 65 deg delta wing with a sharp or rounded leading edge: The international vortex flow experiment p 662 N95-17872
Delta-wing model p 662 N95-17873
Experimental investigation of the vortex flow over a 76/60-deg double delta wing p 662 N95-17874

SHEAR FLOW
Nonlinear instability of a uni-directional transversely sheared mean flow [NASA-TM-106779] p 769 N95-15969
Modeling of wall-bounded complex flows and free shear flows [NASA-TM-106513] p 770 N95-16407
Dynamical system prediction of the scalar field in a turbulent channel flow [AD-A285519] p 771 N95-16438

SHEAR PROPERTIES
Classical solutions of the Prandtl-Reuss equations of perfect elasto-plasticity [PB94-192333] p 860 N95-16292

SHEAR STRENGTH
The mechanical property data base from an Air Force/industry cooperative test program on high temperature aluminum alloys [AD-A282911] p 737 N95-17398

SHEAR STRESS
On the prediction of free turbulent jets with swirl using a quadratic pressure-strain model [NASA-CR-194964] p 769 N95-16071
Considerations in the experimental determination of constitutive parameters for finite strain plasticity [AD-A285410] p 785 N95-16245
Experimental investigation of turbulent separated-reattachment flow by using LDV p 649 N95-16253
Deformation behavior of thin lubricant films at elevated pressure [AD-A281848] p 741 N95-16355
Penetration of solid and layered targets by gas gun-launched steel cubes [AD-A285143] p 787 N95-16843
Normalization and prediction of geotechnical properties using the Cone Penetrometer Test (CPT) [AD-A285193] p 799 N95-16872
An analysis code for the Rapid Engineering Estimation of Momentum and Energy Losses (REMEL) [NASA-CR-191178] p 656 N95-16887
Shear buckling analysis of a hat-stiffened panel [NASA-TM-4644] p 788 N95-17490

SHEATHS
First measurements of ICRF and edge/SOL plasma interactions on TORE SUPRA [DE94-019320] p 891 N95-17347

SHELL THEORY
A consistent large deflection theory of composite sandwich shells p 650 N95-16259
Structural integrity of intelligent materials and structures. Constitutive modeling of shape memory alloys [AD-A281301] p 735 N95-16786

SHELLS (STRUCTURAL FORMS)
Thermoelasticity analysis of laminated plates and shells using hybrid-stress elements p 651 N95-16263

SHERGOTTITES
Pathfinder landing sites at candidate SNC impact ejection sites p 919 N95-16190

SHIELDING
Performance study of galactic cosmic ray shield materials [NASA-TP-3473] p 924 N95-16912

SHIPS
Analysis of infrared scaling laws [AD-A285461] p 903 N95-16877
Optical fiber sensors: Accelerating applications in Navy ships [PB94-186848] p 887 N95-17441

SHOCK HEATING
Parametric study of shock-induced combustion in a hydrogen air system [NASA-CR-197134] p 726 N95-15967

SHOCK LOADS
Shock and thermal history of iron and chondritic meteorites [NASA-CR-197125] p 916 N95-16020
Application of NMR shock barometer to naturally shocked minerals [DE95-000326] p 799 N95-17362

SHOCK TUBES
Application of the space-time conservation element and solution element method to shock-tube problem [NASA-TM-106806] p 772 N95-16903

SHOCK WAVE INTERACTION
Numerical simulation of supersonic compression corners and hypersonic inlet flows using the RPLUS2D code [NASA-TM-106580] p 654 N95-16038
Mach number, flow angle, and loss measurements downstream of a transonic fan-blade cascade [AD-A280907] p 656 N95-16824

SHOCK WAVES
Non-linear waves in gas dynamics and mechanics [AD-A281376] p 770 N95-16156
Time accurate computation of unsteady inlet flows with a dynamic flow adaptive mesh [AD-A285498] p 771 N95-16736
Application of the space-time conservation element and solution element method to shock-tube problem [NASA-TM-106806] p 772 N95-16903
Shock initiation of crystalline boron in oxygen and fluorine compounds [AD-A284266] p 730 N95-16955
Multi-dimensional shock capturing [AD-A282986] p 773 N95-17708
Investigation of the flow over a series of 14 percent-thick supercritical aerofoils with significant rear camber p 657 N95-17849
Wind tunnel investigations of the appearance of shocks in the windward region of bodies with circular cross section at angle of attack p 661 N95-17866

SHOES
Metallurgical examination of failed T-158 Cast Austempered Ductile Iron (CADI) track shoes [AD-A282433] p 737 N95-17486

SHRINKAGE
Ceramic/metal composite circuit-board-level technology for Application Specific Electronic Modules (ASEMs) [AD-A285066] p 741 N95-16369

SHUTDOWNS
Development and fabrication of the fiber optic MicroCable (tm) [AD-A285266] p 886 N95-16815

SIDELOBES
Clutter signal polarization in bistatic radar: Effect of antenna sidelobe clutter [AD-A282300] p 753 N95-16240
Superresolution in a jammed radar signal environment [PB94-190758] p 760 N95-17455

SIGNAL DISTORTION
Clutter signal polarization in bistatic radar: Effect of antenna sidelobe clutter [AD-A282300] p 753 N95-16240

SIGNAL FADING
Performance of a fast frequency-hopped noncoherent MFSK receiver with non-ideal noise normalization combining over ricean fading channels with partial-band interference [AD-A284989] p 753 N95-16232

SIGNAL GENERATORS
Signal wave generator signals recorded by the Federal Outdoor Impact Laboratory's on-board Data Acquisition System [PB94-186525] p 752 N95-16094

SIGNAL PROCESSING
A comparison of signal-processing front ends for automatic speech recognition [AD-A284962] p 752 N95-16129
Preliminary investigation of an integrated optic sampler for HF signals [AD-A284285] p 884 N95-16133
VLSI circuits for high speed data conversion [AD-A281556] p 763 N95-16136
Joint Proceedings on Aeronautics and Astronautics (JPAA) [ISBN-7-80-046602-7] p 649 N95-16249
Detecting the number of targets in spatially colored noise using sampled aperture radars p 652 N95-16269
Fast acquisition of burst direct sequence spread spectrum signals through satellite channels p 652 N95-16270
System design, implementation, and evaluation of the optical broadband correlator [AD-A285406] p 884 N95-16296
An automatic repeater station for signal transmissions [AD-D016454] p 754 N95-16549
Anatomy of a silicon compiler [AD-A285395] p 832 N95-16618
Real-time data collection programs and source code for a commercial passive FTIR remote sensor [AD-A284976] p 838 N95-16634
Least squares computations in science and engineering [AD-A281213] p 862 N95-16798
Mitre adaptive processing capability [AD-A281078] p 755 N95-16825
Wavelets, signal processing and matrix computations [AD-A283832] p 755 N95-16841
Space-based asteroid detection and monitoring system [AD-D016329] p 915 N95-16854
Performance characterization of photonic links in cryogenic environments for advanced signal processing applications [DE94-015561] p 765 N95-16915
Guidance, navigation, and control digital emulation technology laboratory [AD-A282722] p 766 N95-17139
Fast computational scheme of image compression for 32-bit microprocessors p 678 N95-17192
Closed-loop carrier phase synchronization techniques motivated by likelihood functions p 756 N95-17284
On the application of under-decimated filter banks p 757 N95-17285
Tracking the Galileo spacecraft with the DSCC Galileo Telemetry prototype p 708 N95-17292
RF optics study for DSS-43 ultracone implementation p 758 N95-17296

Documentation of 9-PAC Beacon Target Detector processing function
[AD-A283090] p 759 N95-17336
The 1994 International Neural Network Society Annual Meeting, volume 3
[AD-A281736] p 857 N95-17369
Preliminary study of an active millimeter wave sensor
[PB94-189206] p 759 N95-17453
Software interface verifier p 698 N95-17564
Self-initializing circuit link
[AD-D016363] p 761 N95-17696

SIGNAL TO NOISE RATIOS
A comparison of signal-processing front ends for automatic speech recognition
[AD-A284962] p 752 N95-16129
Detecting the number of targets in spatially colored noise using sampled aperture radars p 652 N95-16269
Fast acquisition of burst direct sequence spread spectrum signals through satellite channels p 652 N95-16270
Application of Fourier-space image-restoration techniques to turbulence compensation and sparse-aperture imaging
[AD-A285077] p 885 N95-16494
An algorithm for extraction of periodic signals from sparse, irregularly sampled data p 756 N95-17281
Space VLBI telecommunication characteristics, protection criteria, and frequency sharing p 756 N95-17282
Closed-loop carrier phase synchronization techniques motivated by likelihood functions p 756 N95-17284
Adaptive line enhancers for fast acquisition p 757 N95-17287
Tracking the Galileo spacecraft with the DSCC Galileo Telemetry prototype p 708 N95-17292

SIGNATURES
Singularities of smooth maps in a space with a fixed cone
[PB94-192358] p 861 N95-16367
The use of electrochemistry and ellipsometry for identifying and evaluating corrosion on aircraft
[AD-A285323] p 734 N95-16371
Self-organizing neural network for classifying pattern signatures with a posteriori conditional class probability
[AD-D016455] p 857 N95-16823
Apache helicopter seat cushion evaluation
[AD-A284300] p 831 N95-17484

SIGNS AND SYMPTOMS
The effect of differences in time to detection of circulating microbubbles on the risk of decompression sickness p 807 N95-16738
Use of injectable promethazine to decrease symptom scores of Space Motion Sickness p 808 N95-16741
Comparison of saline and fludrocortisone as fluid-loading countermeasures following exposure to simulated microgravity p 808 N95-16742
Dark focus of accommodation as dependent and independent variables in visual display technology p 812 N95-16758

SILANES
Characterization of surfaces
[NASA-CR-196995] p 750 N95-16065

SILICATES
Structure-property relationships in sol-gel-derived thin films
[DE94-016149] p 744 N95-16934

SILICIDES
Electromagnetic processing of refractory metal silicide/oxide composites
[AD-A281470] p 740 N95-16085
Epitaxial MOCVD of thin film ceramics for pyroelectric detectors
[AD-A281397] p 744 N95-16863

SILICON
Surface and defect excitations in covalently bonded solids
[AD-A281338] p 894 N95-16012
An unexpected adsorption site exclusion process on Si(100)-(2x1)
[AD-A284950] p 894 N95-16043
International Workshop on Light Emission and Electronic Properties of Nanoscale silicon
[AD-A281464] p 894 N95-16081
New methods for treatment of electron correlation and surface dynamics (FY91 AASERT)
[AD-A285177] p 727 N95-16144
Picosecond silicon metal-semiconductor-metal photodiode
[AD-A281548] p 763 N95-16394
Reaction of methanol with porous silicon
[AD-A285518] p 728 N95-16406
PV CZ silicon manufacturing technology improvements
[DE94-011818] p 897 N95-16424
New approaches to novel organosilanes
[AD-A285253] p 722 N95-16513
Active silicon x ray for measuring electron temperature
[DE94-017521] p 890 N95-16555
Analysis of space environment damage to solar cell assemblies from LDEF experiment A0171-GSFC test plate
[NASA-CR-196523] p 793 N95-16575
Anatomy of a silicon compiler
[AD-A285395] p 832 N95-16618

SILICON ALLOYS
Recombination and metastability in amorphous silicon and silicon-germanium alloys
[DE94-011837] p 794 N95-16957

SILICON CARBIDES
Atomic layer epitaxy of group 4 materials: Surface processes, thin films, devices and their characterization
[AD-A280987] p 898 N95-16532
Low temperature deposition and characterization of N- and P-type silicon carbide thin films and associated ohmic and Schottky contacts
[AD-A281060] p 743 N95-16625
Computer studies of the dynamic strength of ceramics
[DE94-010890] p 745 N95-17379

SILICON COMPOUNDS
Crystalline silicon processing
[DE94-016552] p 894 N95-15942

SILICON DIOXIDE
Thermal chemical energy of ablating silica surfaces in air breathing solid rocket engines p 714 N95-16316
Reduction and aggregation of silver in aqueous gelatin and silica suspensions
[DE94-013998] p 727 N95-16363
The analysis and minimization of oxygen contamination in the powder processing of molybdenum disilicide
[DE94-014234] p 735 N95-16540
Effects of substrate temperature on metal colloid formation and on optical response in metal ion implanted silica
[DE94-013633] p 736 N95-16807
Application of NMR shock barometer to naturally shocked minerals
[DE95-000326] p 799 N95-17362
Adhesion of silicon oxide to diamond
[AD-D016356] p 747 N95-17694
Computer modeling of organic aerogels, 93-SR-062
[DE94-016485] p 722 N95-17745

SILICON JUNCTIONS
Research on stable, high-efficiency, amorphous silicon multijunction modules
[DE94-011826] p 794 N95-17521

SILICON NITRIDES
Applications of positron depth profiling
[PB94-197753] p 900 N95-16952
Computer studies of the dynamic strength of ceramics
[DE94-010890] p 745 N95-17379
Low-temperature fabrication of transparent silicon nitride
[DE94-014902] p 746 N95-17456

SILICON OXIDES
Analysis of space environment damage to solar cell assemblies from LDEF experiment A0171-GSFC test plate
[NASA-CR-196523] p 793 N95-16575
Thermal and mechanical behavior of Ba(1+x)Zr4P(6-2x)Si(2x)O24
[DE94-013620] p 899 N95-16806
Structure-property relationships in sol-gel-derived thin films
[DE94-016149] p 744 N95-16934
Adhesion of silicon oxide to diamond
[AD-D016356] p 747 N95-17694

SILICON POLYMERS
Fundamental studies of polyphosphazene and polysiloxane polyelectrolytes for electrochemical devices
[AD-A281339] p 739 N95-16013

SILICONES
An elastomeric electrical connector
[AD-D016340] p 766 N95-16950
Atomic oxygen durability evaluation of the flexible batten for the photovoltaic array mast on Space Station
[NASA-TM-106798] p 781 N95-17263
Reaction and protection of electrical wire insulators in atomic-oxygen environments
[NASA-TM-106767] p 709 N95-17275
Antenna dielectric sealing process characterization
[DE94-015864] p 747 N95-17690

SILVER
Reduction and aggregation of silver in aqueous gelatin and silica suspensions
[DE94-013998] p 727 N95-16363

SILVER ALLOYS
A AgGaSe2 optical parametric oscillator pumped by a Raman-shifted YAG laser
[AD-A284743] p 777 N95-16548

SIMD (COMPUTERS)
Applications of massively parallel computers in telemetry processing p 680 N95-17201
Highly parallel reconfigurable computer architecture for robotic computation having plural processor cells each having right and left ensembles of plural processors
[NASA-CASE-NPO-17632-1-CU] p 832 N95-17400

SIMULATION
A correlative investigation of simulated occupant motion and accident report in a helicopter crash
[AD-A285190] p 664 N95-16404
A surgical support system for Space Station Freedom p 710 N95-16776
Probabilistic simulation of stress concentration in composite laminates
[NASA-TM-106712] p 787 N95-17270
Modeling ESA's TT/C systems p 701 N95-17579
Simulation of the SEMATECH gravimetric mass flowmeter calibrator
[DE94-018698] p 773 N95-17910

SIMULATORS
Twin disc gear tooth simulator
[AD-A284927] p 780 N95-16139
A General Mission Independent Simulator (GMIS) and Simulator Control Program (SCP) p 701 N95-17580
Spacecraft Data Simulator for the test of level zero processing systems p 675 N95-17582
Modelling interactions of carbon dioxide, forests, and climate
[DE94-018694] p 797 N95-17908

SIMULTANEOUS EQUATIONS
Equation solvers for distributed-memory computers p 847 N95-16460

SINGLE CRYSTALS
An unexpected adsorption site exclusion process on Si(100)-(2x1)
[AD-A284950] p 894 N95-16043
Single crystal films and waveguides of organic materials: Preparation and nonlinear optical properties
[AD-A284471] p 895 N95-16134
Preparation of Au single crystals for study of the ECALE deposition of CdTe
[AD-A282294] p 895 N95-16238
Method for intrinsically doped III-A and V-A compounds and products thereof
[AD-D016324] p 896 N95-16399
Flux imaging of high temperature superconductor single crystals and Ag sheathed wires
[DE94-013874] p 897 N95-16408
Atomic force microscopy of the electrochemical nucleation and growth of molecular crystals
[AD-A281024] p 897 N95-16445
Growth, characterization and applications of beta-barium borate and related crystals
[AD-A281047] p 898 N95-16623
Processing, fabrication, characterization and device demonstration of high temperature superconducting ceramics
[AD-A285145] p 744 N95-16844
Properties of semiconducting Ru2Ge3
[DE94-015361] p 899 N95-16913
Columnar defect pinning in untwinned single crystal YBa2Cu2O7
[DE94-013962] p 901 N95-17349
BaF2/GaAs electronic components
[AD-D016391] p 767 N95-17481
Evaluation of the quality of sapphire using x-ray rocking curves and double-crystal x-ray topography
[AD-A282905] p 901 N95-17620

SINGLE STAGE ROCKET VEHICLES
Configurable technology development for reusable control and monitor ground systems p 675 N95-17589

SINGLE STAGE TO ORBIT VEHICLES
Matlab as a robust control design tool p 849 N95-16474

SINGULARITY (MATHEMATICS)
Singularities of smooth maps in a space with a fixed cone
[PB94-192358] p 861 N95-16367

SINTERING
A preliminary attempt at sintering an ultrafine alumina powder using microwaves
[AD-A284978] p 734 N95-16229

SISO (CONTROL SYSTEMS)
Decentralized sliding mode control of nonlinear flexible robots
[DE94-013790] p 782 N95-17366

SITE SELECTION
Mars Pathfinder Landing Site Workshop
[NASA-CR-196745] p 917 N95-16176
Sampling Elysium lavas (13 deg N, 203 deg W) p 917 N95-16177
Mars Pathfinder and the exploration of southern Amazonis Planitia p 917 N95-16178
Meteorological observations of synoptic disturbances: Sensitivity to latitude p 917 N95-16179

Implications of high-spatial-resolution thermal infrared (Termoskan) data for Mars landing site selection
p 918 N95-16180
A Mars Pathfinder landing on a recently drained ephemeral sea: Cerberus Plains, 6 deg N, 188 deg W
p 918 N95-16181
Physical properties (particle size, rock abundance) from thermal infrared remote observations: Implications for Mars landing sites
p 918 N95-16182
Rationale for a Mars Pathfinder mission to Chryse Planitia and the Viking 1 lander
p 918 N95-16183
Rationale for Isidis Planitia as a back-up landing site for the Mars Pathfinder mission
p 918 N95-16184
Chryse Planitia as a Mars Pathfinder landing site: The imperative of building on previous ground truth
p 918 N95-16185
A highland sample strategy for Pathfinder
p 918 N95-16186
Strategy for selecting Mars Pathfinder landing sites
p 919 N95-16191
Potential landing sites for Mars Pathfinder
p 920 N95-16193
A perspective of landing-site selection
p 920 N95-16194
Scientific rationale for selecting northern Eumenides Dorsum (9 deg - 11 deg N latitude, 159 deg - 162 deg longitude) as a potential Mars Pathfinder landing site
p 920 N95-16196
Scientific rationale for selecting northwest Isidis Planitia (14 deg - 17 deg N latitude, 278 deg - 281 deg longitude) as a potential Mars Pathfinder landing site
p 920 N95-16197

SITTING POSITION
The psychophysical function for perceived gravitational-inertial force does not depend on the orientation of the otolith organs
p 808 N95-16740
Catecholaminergic responses to stressful motion stimuli, scopolamine plus amphetamine, and dexamethasone
p 809 N95-16745

SIZE DETERMINATION
Active and passive acoustic bubble sizing
[ISVR-TR-237] p 769 N95-16064

SKIN (ANATOMY)
Skin blood flow and bioelectrical impedance
[AD-A285475] p 821 N95-16619
Increased skin blood flow and enhanced heat loss in humans after niacin ingestion
[AD-A281124] p 821 N95-16809

SKIN FRICTION
An analysis code for the Rapid Engineering Estimation of Momentum and Energy Losses (REMEL)
[NASA-CR-191178] p 656 N95-16887

SKIN TEMPERATURE (BIOLOGY)
Heat stress and a countermeasure in the Shuttle rescueman's suit
p 809 N95-16746

SKULL
Multimodal correlation and intraoperative matching of virtual models in neurosurgery
p 823 N95-15976

SKY SURVEYS (ASTRONOMY)
Dust near luminous ultraviolet stars
[NASA-CR-197108] p 916 N95-16032
Multivariate statistical analysis software technologies for astrophysical research involving large data bases
[NASA-CR-189393] p 911 N95-17325
Voyager investigation of the cosmic diffuse background: Observations of rocket-studied locations with Voyager
[NASA-CR-197532] p 917 N95-17422
Multivariate statistical analysis software technologies for astrophysical research involving large data sets
[NASA-CR-197499] p 858 N95-17921

SLEEP
Alertness management in two-person long-haul flight operations
p 813 N95-16760
Phase-shifting effects of light and activity on the human circadian clock
[AD-A281204] p 821 N95-16796

SLENDER BODIES
Force and pressure data of an ogive-nosed slender body at high angles of attack and different Reynolds numbers
p 661 N95-17868

SLEWING
Optimal trajectories for flexible-link manipulator slewing using recursive quadratic programming: Experimental verification
[DE94-018741] p 858 N95-17915

SLIDING
On performability theory and the inverse sliding problem
[AD-A282847] p 782 N95-17430

SLOPES
Analysis of a three-beam radar as an instrument for determining ocean wave heights and vector slopes
[AD-A282342] p 806 N95-17505

SLOTS
Slow wave vane structure with elliptical cross-section slots, an analysis
[NASA-CR-195352] p 755 N95-16886

SMALL SCIENTIFIC SATELLITES
Cost efficient operations for Discovery class missions
p 695 N95-17548
Ground Station support for small scientific satellites
p 695 N95-17549
Design of ground segments for small satellites
p 674 N95-17550
Small satellite space operations
p 695 N95-17552

SMART STRUCTURES
Smart materials based upon oligomeric molecules
[AD-A281374] p 872 N95-16155
Shaped strain sensors for intelligent structures
[AD-A282333] p 774 N95-16242
Structural integrity of intelligent materials and structures. Constitutive modeling of shape memory alloys
[AD-A281301] p 735 N95-16786
A comparison of different control methods for vibration suppression of flexible structures using piezoelectric actuators
[AD-A282958] p 710 N95-17622

SNELLEN TESTS
Visual acuity versus field-of-view and light level for Night Vision Goggles (NVG)
[AD-A284750] p 830 N95-16553

SODIUM
The influence of the complexation of sodium and lithium triflate on the self-assembly of tubular-supramolecular architectures displaying a columnar mesophase based on taper-shaped monoesters of oligoethyleneoxide with 3,4,5-tris(p-(n-dodecan-l-yloxy)benzyloxy)benzoic acid and of their polymethacrylates
[AD-A281403] p 730 N95-16866
Equatorial airglow studies via rocket experiment
[INPE-5589-TDI/551] p 799 N95-17647

SODIUM 22
Na-22 decay gamma rays from classical novae
[NASA-CR-197454] p 924 N95-16383

SOFTWARE ENGINEERING
Informatics in Turkey
p 905 N95-15921
Parallel implementation of the terrain masking algorithm
[AD-A281017] p 833 N95-16003
Parallel software benchmarks for high performance BMC3/IS systems
[AD-A282329] p 844 N95-16060
A survey of the software reuse environment: A study for the NSRS
[AD-A280867] p 834 N95-16149
Automation support for concurrent software engineering
[AD-A281372] p 834 N95-16153
Software merge: Semantics of combining changes to programs
[AD-A281373] p 834 N95-16154
STARS Conceptual Framework for Reuse Process (CFRP). Volume 1: Definition, version 3.0
[AD-A281506] p 834 N95-16167
Procedure calls are the assembly language of software interconnection: Connectors deserve first-class status
[AD-A281026] p 835 N95-16446
The Role of Computers in Research and Development at Langley Research Center
[NASA-CP-10159] p 846 N95-16453
Software engineering from a Langley perspective
p 843 N95-16454
Model-based software process improvement
p 843 N95-16455
A study of software standards used in the avionics industry
p 670 N95-16456
A software tool for dataflow graph scheduling
p 843 N95-16457
Rapid solution of large-scale systems of equations
p 847 N95-16458
Solution of matrix equations using sparse techniques
p 847 N95-16459
Equation solvers for distributed-memory computers
p 847 N95-16460
Applications of automatic differentiation in computational fluid dynamics
p 774 N95-16461
Automatic differentiation for design sensitivity analysis of structural systems using multiple processors
p 847 N95-16462
RDD-100 and the systems engineering process
p 848 N95-16471
Computer tools for systems engineering at LaRC
p 848 N95-16472
Electronic Engineering Notebook: A software environment for research execution, documentation and dissemination
p 848 N95-16473
Hardware description languages
p 832 N95-16477
Current research activities at the NASA-sponsored Illinois Computing Laboratory of Aerospace Systems and Software
p 849 N95-16479
Epistemology, software engineering and formal methods
p 843 N95-16480
Maturity questionnaire
[AD-A285073] p 836 N95-16490
Software cost and schedule estimating: A process improvement initiative
[AD-A280915] p 836 N95-16503
The SEI and NAWC: Working together to establish a software measurement program
[AD-A280916] p 836 N95-16504
The Software Technology Center at Lawrence Livermore National Laboratory: Software engineering technology transfer in a scientific R/D laboratory
[DE94-014794] p 836 N95-16536
A survey of program slicing for software engineering
[NASA-CR-193116] p 836 N95-16574
Open architectures for formal reasoning and deductive technologies for software development
[NASA-CR-197528] p 837 N95-16586
MIL-STD-498 software development and documentation, version 01.00.00
[AD-A282003] p 837 N95-16607
Anatomy of a silicon compiler
[AD-A285395] p 832 N95-16618
Integrating human factors with software engineering practices
[AD-A285210] p 830 N95-16813
Interactive sketching for the early stages of user interface design
[AD-A285339] p 838 N95-16818
Investigation of modularly configured attached processors with intelligent memories
[AD-A285454] p 832 N95-16876
Data acquisition and processing software for the Low Speed Wind Tunnel tests of the Jindivik auxiliary air intake
[AD-A285455] p 656 N95-17178
The development and operation of the international solar-terrestrial physics central data handling facility
p 679 N95-17193
Generic mission planning and scheduling: The AXAF solution
p 686 N95-17231
CCS-MIP: Low cost Customizable Control Centre
p 674 N95-17254
IS-Lab: A tool for developing interactive programs for simulation and analysis. User's guide
[PB94-184710] p 840 N95-17410
Corrective software management: The success of the EPLRS program
[AD-A282430] p 841 N95-17460
Reviews of computing technology: Software overview
[DE94-013662] p 841 N95-17515
ATM-test: A workstation-based software suite for testing Asynchronous Transfer Mode (ATM) networks
[DE94-013813] p 850 N95-17516
Knowledge-based critiquing of graphical user interfaces with CHIMES
p 697 N95-17560
OOD/OOP experience in the Science Operations Center part of the ground system for X ray Timing Explorer mission
p 675 N95-17565
A proven approach for more effective software development and maintenance
p 698 N95-17566
Software Process Assessment (SPA)
p 699 N95-17569
Taking advantage of ground data systems attributes to achieve quality results in testing software
p 699 N95-17570
SCOS 2: An object oriented software development approach
p 699 N95-17571
Configurable technology development for reusable control and monitor ground systems
p 675 N95-17589
ATOS: Integration of advanced technology software within distributed Spacecraft Mission Operations Systems
p 705 N95-17602
CERES, phases 1 and 2
[DE94-014730] p 797 N95-17920

SOFTWARE RELIABILITY
The survivable distributed computing environment
[AD-A281637] p 845 N95-16115
Accountability for network backup failures
[DE94-011365] p 846 N95-16222
The SEI and NAWC: Working together to establish a software measurement program
[AD-A280916] p 836 N95-16504
A proven approach for more effective software development and maintenance
p 698 N95-17566
XMM instrument on-board software maintenance concept
p 699 N95-17567
Software Process Assessment (SPA)
p 699 N95-17569
SCOS 2: An object oriented software development approach
p 699 N95-17571

SOFTWARE REUSE
A survey of the software reuse environment: A study for the NSRS
[AD-A280867] p 834 N95-16149
STARS Conceptual Framework for Reuse Process (CFRP). Volume 1: Definition, version 3.0
[AD-A281506] p 834 N95-16167
Towards a class library for mission planning
p 686 N95-17233
SCL: An off-the-shelf system for spacecraft control
p 688 N95-17243
SCOS 2: An object oriented software development approach p 699 N95-17571
Transportable Payload Operations Control Center reusable software: Building blocks for quality ground data systems p 703 N95-17587

SOFTWARE TOOLS
The future of interaction on the Internet
p 906 N95-15931
Networked information: Management issues for the acquisitions librarian p 906 N95-15932
Adding tools to the open source toolbox: The Internet
p 907 N95-15933
Open Source Service Agent (OSSA) in the intelligence community's Open Source Architecture
p 907 N95-15934
Applied virtual reality at the Research Triangle Institute p 851 N95-15974
A specification of 3D manipulation in virtual environments p 853 N95-15981
Parallel software benchmarks for high performance BMC3/IS systems
[AD-A282329] p 844 N95-16060
Partial evaluation for scientific computing: The supercomputer toolkit experience
[AD-A282286] p 846 N95-16237
Visualization of unsteady computational fluid dynamics
[NASA-CR-197461] p 770 N95-16388
Software engineering from a Langley perspective
p 843 N95-16454
Model-based software process improvement
p 843 N95-16455
A software tool for dataflow graph scheduling
p 843 N95-16457
Applications of automatic differentiation in computational fluid dynamics p 774 N95-16461
Automatic differentiation for design sensitivity analysis of structural systems using multiple processors
p 847 N95-16462
Use of World Wide Web and NCSA Mcsaic at Langley
p 847 N95-16464
How to use the WWW to distribute STI
p 847 N95-16465
Image tools for UNIX p 847 N95-16466
Data Visualization and Animation Lab (DVAL): Applications p 843 N95-16469
The Design Manager's Aid for Intelligent Decomposition (DeMAID) p 848 N95-16470
RDD-100 and the systems engineering process
p 848 N95-16471
Computer tools for systems engineering at LaRC
p 848 N95-16472
Electronic Engineering Notebook: A software environment for research execution, documentation and dissemination p 848 N95-16473
Matlab as a robust control design tool
p 849 N95-16474
Object-oriented numerical computing C++
p 849 N95-16476
Hardware description languages p 832 N95-16477
High Performance FORTRAN p 843 N95-16478
Epistemology, software engineering and formal methods p 843 N95-16480
Tools for applied engineering optimization
p 668 N95-16570
A survey of program slicing for software engineering
[NASA-CR-193116] p 836 N95-16574
Open architectures for formal reasoning and deductive technologies for software development
[NASA-CR-197528] p 837 N95-16586
An integrated knowledge acquisition and database management system
[AD-A285404] p 910 N95-16884
High performance hardware and software for pattern recognition and image processing
[AD-A284264] p 839 N95-17172
An assessment of simulation systems applicable to business process reengineering at Army Directorates of Public Works
[AD-A285696] p 839 N95-17176
Data acquisition and processing software for the Low Speed Wind Tunnel tests of the Jindivik auxiliary air intake
[AD-A285455] p 656 N95-17178
A PC based tool for mission plan production
p 686 N95-17232
Production and quality assurance automation in the Goddard Space Flight Center Flight Dynamics Facility
p 687 N95-17237
The Sequence of Events generator: A powerful tool for mission operations p 688 N95-17240
Small scale sequence automation pays big dividends
p 689 N95-17247
The IUE Science Operations Ground System
p 674 N95-17255
Interactive computer graphics applications for compressible aerodynamics
[NASA-TM-106802] p 839 N95-17264
X-/Ka-band dichroic plate noise temperature reduction
p 758 N95-17294
Experimenter's Laboratory for Visualized Interactive Science
[NASA-CR-189391] p 910 N95-17322
McIDAS-eXplorer: A version of McIDAS for planetary applications
[NASA-CR-189382] p 910 N95-17323
An interactive interface for NCAR Graphics
[NASA-CR-189383] p 840 N95-17324
Engineering design tools for wind diesel systems. Volume 2: JODYMOD dynamic wind diesel simulation software package. Model verification
[PB95-104519] p 840 N95-17355
Engineering design tools for wind diesel systems. Volume 3: JODYMOD dynamic simulation software package. Model description
[PB95-104527] p 840 N95-17356
IS-Lab: A tool for developing interactive programs for simulation and analysis. User's guide
[PB94-184710] p 840 N95-17410
The Grid Analysis and Display System (GrADS)
[NASA-CR-189387] p 912 N95-17491
Demonstration of the Dynamic Flowgraph Methodology using the Titan 2 Space Launch Vehicle Digital Flight Control System
[NASA-CR-197517] p 675 N95-17493
The new map graphics in RSAS 5.0
[AD-A282432] p 791 N95-17511
SEQ-POINTER: Next generation, planetary spacecraft remote sensing science observation design tool
p 697 N95-17559
Knowledge-based critiquing of graphical user interfaces with CHIMES p 697 N95-17560
SEQ-REVIEW: A tool for reviewing and checking spacecraft sequences p 697 N95-17561
Simplifying operations with an uplink/downlink integration toolkit p 697 N95-17562
ELISA, a demonstrator environment for information systems architecture design p 698 N95-17563
Software interface verifier p 698 N95-17564
A proven approach for more effective software development and maintenance p 698 N95-17566
Taking advantage of ground data systems attributes to achieve quality results in testing software
p 699 N95-17570
Evaluating modeling tools for the EDOS
p 700 N95-17572
Solar and Heliospheric Observatory (SOHO) Experimenters' Operations Facility (EOF)
p 675 N95-17573
Galileo spacecraft modeling for orbital operations
p 700 N95-17574
Evaluation of NASA's end-to-end data systems using DSDS+ p 700 N95-17577
Modeling ESA's TT/C systems p 701 N95-17579
Engineering design tools for wind diesel systems. Volume 4: JODYMOD dynamic wind diesel simulation software package. Program documentation
[PB95-104535] p 841 N95-17628
Engineering design tools for wind diesel systems. Volume 5: JODYMOD dynamic wind diesel simulation software package. User's guide
[PB95-104543] p 841 N95-17629
Engineering design tools for wind diesel systems. Volume 1: Executive summary
[PB95-104501] p 842 N95-17733
Engineering design tools for wind diesel systems. Volume 6: Logistic package. User documentation
[PB95-104550] p 842 N95-17734
Engineering design tools for wind diesel systems. Volume 7: Logistic package. Validation report
[PB95-104568] p 842 N95-17735
CERES, phases 1 and 2
[DE94-014730] p 797 N95-17920

SOHO MISSION
Solar and Heliospheric Observatory (SOHO) Experimenters' Operations Facility (EOF)
p 675 N95-17573

SOI (SEMICONDUCTORS)
Multilayer microelectronic photomultiplier device with a stacked series of dynode and insulating layers
[AD-D016377] p 767 N95-17478

SOIL MAPPING
Development of an Automated Airfield Dynamic Cone Penetrometer (AADCP) prototype and the evaluation of unsurfaced airfield seismic surveying using Spectral Analysis of Surface Waves (SASW) technology
[AD-A281985] p 672 N95-17444

SOIL MECHANICS
Normalization and prediction of geotechnical properties using the Cone Penetrometer Test (CPT)
[AD-A285193] p 799 N95-16872

SOIL SCIENCE
Long term modelling of permafrost dynamics
[AD-A285315] p 799 N95-16735

SOILS
Opportunity to sample something different: The dark, unweathered, mafic sands of Cerberus and the Pathfinder 1997 Mars landing p 919 N95-16187
Alpha proton x ray spectrometer p 710 N95-16201
Normalization and prediction of geotechnical properties using the Cone Penetrometer Test (CPT)
[AD-A285193] p 799 N95-16872
Evaluation of a pneumatic Martian soil sampler concept
[NASA-CR-197539] p 923 N95-17653
Modelling interactions of carbon dioxide, forests, and climate
[DE94-018694] p 797 N95-17908

SOL-GEL PROCESSES
Testing and evaluation of oxide-coated iridium/rhenium chambers p 719 N95-16346
Structure-property relationships in sol-gel-derived thin films
[DE94-016149] p 744 N95-16934

SOLAR ACTIVITY EFFECTS
Engineering Ulysses extended mission
p 673 N95-17213

SOLAR ARRAYS
Results of the 1994 NASA/JPL balloon flight solar cell calibration program
[NASA-CR-197248] p 792 N95-16067
Atomic oxygen durability evaluation of the flexible batten for the photovoltaic array mast on Space Station
[NASA-TM-106798] p 781 N95-17263

SOLAR CELLS
Crystalline silicon processing
[DE94-016552] p 894 N95-15942
The role of point defects and defect complexes in silicon device processing: Summary report and papers
[DE94-011873] p 791 N95-15944
Results of the 1994 NASA/JPL balloon flight solar cell calibration program
[NASA-CR-197248] p 792 N95-16067
PV CZ silicon manufacturing technology improvements
[DE94-011818] p 897 N95-16424
Analysis of space environment damage to solar cell assemblies from LDEF experiment A0171-GSFC test plate
[NASA-CR-196523] p 793 N95-16575
Development of high-efficiency, thin-film CdTe solar cells
[DE94-011885] p 794 N95-16940
Recombination and metastability in amorphous silicon and silicon-germanium alloys
[DE94-011837] p 794 N95-16957
Solar energy: Lessons from the Pacific island experience
[WORLD-BANK-TP-244] p 794 N95-17298

SOLAR COLLECTORS
Conceptual design study of a solar concentrator/support structure: A three dimensional finite element model
p 718 N95-16342
Prediction of the response of a polyimide concentrator for solar thermal propulsion p 719 N95-16343
Foam inflated rigidized structures for space applications p 710 N95-16344
Coatings for large-area low-cost solar concentrators and reflectors
[DE94-015735] p 793 N95-16916
Vacuum deposited polymer/silver reflector material
[DE94-018729] p 748 N95-17913

SOLAR ENERGY
Prediction of the response of a polyimide concentrator for solar thermal propulsion p 719 N95-16343

SOLAR FLARES
Solar flares and magnetospheric particles: Investigations based upon the ONR-602 and ONR-604 experiments
[AD-A281463] p 923 N95-16080
Solar flares and magnetospheric particles: Investigations based upon the ONR-602 and ONR-604 experiments
[AD-A283275] p 923 N95-17723
Solar-geophysical data number 596, April 1994. Part 1: (Prompt reports). Data for March, February 1994, and late data
[PB94-183548] p 924 N95-17736

Solar-geophysical data number 596, April 1994. Part 2: (Comprehensive reports). Data for October 1993, and miscellaneous
[PB94-183555] p 924 N95-17737
Verification of NOAA Space Environment Laboratory forecasts, 1 January - 31 December 1993
[PB95-104162] p 803 N95-17927

SOLAR FURNACES
Availability of direct normal radiation for solar furnace processing: A case study
[DE94-006907] p 792 N95-16435

SOLAR GENERATORS
Photovoltaic power conditioners: Development, evolution, and the next generation
[NASA-CR-197005] p 793 N95-16831

SOLAR INSTRUMENTS
NASA Marshall Space Flight Center Solar Observatory report, March - May 1994
[NASA-TM-108471] p 915 N95-16558

SOLAR MAGNETIC FIELD
Analysis of plasma measurements for the Geotail mission
[NASA-CR-197020] p 888 N95-15941
Solar-geophysical data number 596, April 1994. Part 1: (Prompt reports). Data for March, February 1994, and late data
[PB94-183548] p 924 N95-17736

SOLAR NEUTRINOS
First results from SAGE 2
[DE94-014431] p 876 N95-17154
Solar neutrino oscillations
[PB95-104295] p 923 N95-17352

SOLAR OBSERVATORIES
NASA Marshall Space Flight Center Solar Observatory report, March - May 1994
[NASA-TM-108471] p 915 N95-16558

SOLAR PHYSICS
Solar-geophysical data number 596, April 1994. Part 1: (Prompt reports). Data for March, February 1994, and late data
[PB94-183548] p 924 N95-17736
Solar-geophysical data number 596, April 1994. Part 2: (Comprehensive reports). Data for October 1993, and miscellaneous
[PB94-183555] p 924 N95-17737

SOLAR POWERED AIRCRAFT
Solar-powered rocket engine optimization for high specific impulse p 718 N95-16341
Energy and Technology Review
[DE95-000321] p 710 N95-17359

SOLAR PROMINENCES
Solar-geophysical data number 596, April 1994. Part 1: (Prompt reports). Data for March, February 1994, and late data
[PB94-183548] p 924 N95-17736
Solar-geophysical data number 596, April 1994. Part 2: (Comprehensive reports). Data for October 1993, and miscellaneous
[PB94-183555] p 924 N95-17737

SOLAR PROPULSION
The 1993 JANNAF Propulsion Meeting, volume 2
[CPIA-PUBL-602-VOL-2] p 715 N95-16324
Energy and Technology Review
[DE95-000321] p 710 N95-17359

SOLAR RADIATION
A rare gas optics-free absolute photon flux and energy analyzer to provide absolute photoionization rates of inflowing interstellar neutrals
[NASA-CR-197228] p 914 N95-15964
Availability of direct normal radiation for solar furnace processing: A case study
[DE94-006907] p 792 N95-16435
A latitudinal survey of middle atmospheric water vapor revealed by shipboard microwave spectroscopy
[AD-A282000] p 799 N95-17446
Solar flares and magnetospheric particles: Investigations based upon the ONR-602 and ONR-604 experiments
[AD-A283275] p 923 N95-17723

SOLAR RADIO BURSTS
Solar-geophysical data number 596, April 1994. Part 2: (Comprehensive reports). Data for October 1993, and miscellaneous
[PB94-183555] p 924 N95-17737

SOLAR RADIO EMISSION
Solar-geophysical data number 596, April 1994. Part 1: (Prompt reports). Data for March, February 1994, and late data
[PB94-183548] p 924 N95-17736
Verification of NOAA Space Environment Laboratory forecasts, 1 January - 31 December 1993
[PB95-104162] p 803 N95-17927

SOLAR REFLECTORS
Coatings for large-area low-cost solar concentrators and reflectors
[DE94-015735] p 793 N95-16916
Vacuum deposited polymer/silver reflector material
[DE94-018729] p 748 N95-17913

SOLAR SPECTROMETERS
A rare gas optics-free absolute photon flux and energy analyzer for solar and planetary observations
[NASA-CR-197227] p 915 N95-16021

SOLAR STORMS
Solar-geophysical data number 596, April 1994. Part 1: (Prompt reports). Data for March, February 1994, and late data
[PB94-183548] p 924 N95-17736

SOLAR SYSTEM
Activities of the Space Studies Board
[NASA-CR-197105] p 672 N95-16033
Engineering Ulysses extended mission p 673 N95-17213

SOLAR SYSTEM EVOLUTION
Investigations of asteroid family geology p 917 N95-17393

SOLAR THERMAL PROPULSION
Materials characterization and design for solar-thermal propulsion p 718 N95-16340
Prediction of the response of a polyimide concentrator for solar thermal propulsion p 719 N95-16343

SOLAR WIND
Analysis of plasma measurements for the Geotail mission
[NASA-CR-197020] p 888 N95-15941
Geosynchronous orbit magnetopause crossings
[DE94-014817] p 798 N95-16537
Analysis of magnetic field data from Pioneer Venus orbiter
[NASA-CR-197492] p 923 N95-17403
Solar-geophysical data number 596, April 1994. Part 2: (Comprehensive reports). Data for October 1993, and miscellaneous
[PB94-183555] p 924 N95-17737

SOLAR X-RAYS
Solar-geophysical data number 596, April 1994. Part 2: (Comprehensive reports). Data for October 1993, and miscellaneous
[PB94-183555] p 924 N95-17737

SOLID ELECTROLYTES
Electrochemical properties of lithium ion conducting solid polymer electrolytes
[AD-A281875] p 742 N95-16434

SOLID PROPELLANT COMBUSTION
Ignition propagation and heat effects of propellant chips embedded in castable inhibitor using a laser flux test bomb p 717 N95-16335

SOLID PROPELLANT IGNITION
Ignition propagation and heat effects of propellant chips embedded in castable inhibitor using a laser flux test bomb p 717 N95-16335

SOLID PROPELLANT ROCKET ENGINES
The 1993 JANNAF Propulsion Meeting, volume 1
[CPIA-PUBL-602-VOL-1] p 713 N95-16312
Design margin testing of Peacekeeper solid rocket boosters p 713 N95-16313
Hydromining a full-scale class 1.1 solid rocket motor p 713 N95-16314
Thermal chemical energy of ablating silica surfaces in air breathing solid rocket engines p 714 N95-16316
The 1993 JANNAF Propulsion Meeting, volume 2
[CPIA-PUBL-602-VOL-2] p 715 N95-16324
Recent advances in graphite/epoxy motor cases p 717 N95-16333
Structural analysis of solid-propellant rocket motors with and without flaws p 720 N95-16348
Filament overwrapped motor case technology p 720 N95-16350

SOLID PROPELLANTS
Global and near tip response of cracked solid propellant p 715 N95-16325

SOLID ROCKET PROPELLANTS
The 1993 JANNAF Propulsion Meeting, volume 2
[CPIA-PUBL-602-VOL-2] p 715 N95-16324
The use of designed experiments in the process development of continuous propellant mixing p 717 N95-16334
Ignition propagation and heat effects of propellant chips embedded in castable inhibitor using a laser flux test bomb p 717 N95-16335

SOLID STATE
Characterization of multiport solid state imagers at megahertz data rates
[DE94-016095] p 765 N95-16932
Evaluation of NASA's end-to-end data systems using DSDS+ p 700 N95-17577

SOLID STATE DEVICES
Solid state radar demonstration test results at the FAA Technical Center
[AD-A281520] p 752 N95-16097
Lessons learned supporting onboard solid-state recorders p 681 N95-17208
Femtosecond studies of carrier dynamics in compound semiconductors
[AD-A282871] p 767 N95-17433

SOLID STATE LASERS
New ytterbium-doped apatite crystals for flexible laser design
[DE94-015138] p 899 N95-16867
Properties of Ce:LiSrAlF6 and Ce:LiCaAlF6 ultraviolet lasers
[DE94-013737] p 777 N95-17168
Thermal effects in end-heated laser rods: A time-dependent model and diagnostic
[AD-A282007] p 778 N95-17500
High-average-power, diode-pumped solid state lasers for energy and industrial applications
[DE94-015142] p 779 N95-17689

SOLID WASTES
Bicarbonate of soda blasting technology for aircraft wheel depainting
[PB94-193323] p 654 N95-17466
Hydrogen production by gasification of municipal solid waste
[DE94-016483] p 732 N95-17639

SOLID-SOLID INTERFACES
BEEM 94. The Fifth Annual Workshop on Ballistic Electron Emission Microscopy
[AD-A281522] p 872 N95-16098
Semiconductor heterojunction engineering
[AD-A281553] p 896 N95-16396
Characterization on defect solids
[NASA-CR-197540] p 746 N95-17654

SOLIDS
An analysis of smoothed particle hydrodynamics
[DE94-013817] p 788 N95-17439
Characterization on defect solids
[NASA-CR-197540] p 746 N95-17654

SOLITARY WAVES
The quantum solitons of the nonlinear (sigma)-model with broken chiral symmetry
[DE94-622758] p 904 N95-17474
Ultra high bit rate all optical communication system
[AD-D016359] p 887 N95-17695

SOLUBILITY
Charge transfer processes on liquid/liquid interfaces: The status in 1994
[AD-A285067] p 729 N95-16635
Solubilization of hydrophobic substances into block copolymer micelles in aqueous media and their release
[AD-A281395] p 744 N95-16792
Chemical properties of the fullerenes
[AD-A282730] p 730 N95-17141

SOLVATION
The solvation thermodynamic functions in the Mean Spherical Approximation (MSA): Behavior near the solvent critical region
[AD-A283040] p 904 N95-17712

SOLVENTS
Precision aqueous cleaner for RSRM p 715 N95-16326
The solvation thermodynamic functions in the Mean Spherical Approximation (MSA): Behavior near the solvent critical region
[AD-A283040] p 904 N95-17712

SONAR
Event-related brain potentials as predictors of target detection performance in a moving waterfall display simulating passive broad-band sonar monitoring
[AD-A280900] p 819 N95-16152

SOOT
An in-cylinder study of the particulate/NO(x) trade-off in a DI diesel engine
[DE94-014599] p 781 N95-17162
Identification and temporal behavior of radical intermediates formed during the combustion and pyrolysis of gaseous fuels: Kinetic pathways to soot formation
[DE94-014681] p 731 N95-17163

SOUND FIELDS
Effective reflection coefficients for the mean acoustic field between two rough interfaces
[AD-A281962] p 870 N95-16413
Formulation of probe-corrected time-domain planar near-field measurements
[AD-A281053] p 754 N95-16624
Active minimization of energy density in three-dimensional enclosures
[NASA-CR-197213] p 871 N95-16848

SOUND GENERATORS
Anisotropic heat exchangers/stack configurations for thermoacoustic heat engines
[AD-A280974] p 792 N95-16506

SOUND PRESSURE
Demodulation processes in auditory perception
[AD-A285427] p 869 N95-16248

SOUND TRANSDUCERS
On the measurement of momentum flux profiles using a five-beam 915-MHz wind profiler
[DE94-018448] p 791 N95-17903
SOUND TRANSMISSION
Demodulation processes in auditory perception
[AD-A285427] p 869 N95-16248
SOUND WAVES
Ducted fan acoustic radiation including the effects of nonuniform mean flow and acoustic treatment
[NASA-CR-197449] p 870 N95-16401
Support minimized inversion of acoustic and elastic wave scattering
[DE94-014233] p 783 N95-16538
Active minimization of energy density in three-dimensional enclosures
[NASA-CR-197213] p 871 N95-16848
SOUNDING ROCKETS
Development of a medium energy modulated electron gun for orbital experiments
[AD-A281021] p 675 N95-16005
SOURCE PROGRAMS
Open Source Service Agent (OSSA) in the intelligence community's Open Source Architecture
p 907 N95-15934
Object-oriented numerical computing C++
p 849 N95-16476
Real-time data collection programs and source code for a commercial passive FTIR remote sensor
[AD-A284976] p 838 N95-16634
SOUTHERN HEMISPHERE
Landing site considerations for atmosphere structure and meteorology p 921 N95-16203
SOUTHERN OSCILLATION
An observational study of long waves in the equatorial Pacific Ocean during the 1991-1993 El Nino
[AD-A283380] p 806 N95-17624
SOVIET SPACECRAFT
Radio-planetary from tie from Phobos-2 VLBI data
p 756 N95-17283
SOYUZ SPACECRAFT
Physiological constraints on deceleration during the aerocapture of manned vehicles p 810 N95-16751
SPACE ADAPTATION SYNDROME
Aerospace Medical Association 63rd Annual Scienti fic Meeting Program p 807 N95-16737
Prediction of space sickness in astronauts from preflight fluid, electrolyte, and cardiovascular variables and Weightless Environmental Training Facility (WETF) training p 812 N95-16757
Dark focus of accommodation as dependent and independent variables in visual display technology
p 812 N95-16758
SPACE CAPSULES
Study of simulation in microgravity environment
[PB95-104261] p 750 N95-17730
SPACE CHARGE
Mechanisms of beam-halo formation in high-intensity linacs
[DE94-016316] p 879 N95-16030
Study of the effect of the space charge using SYNCH
[DE94-014086] p 879 N95-16210
Centrifugal space-charge force for bunched beams
[DE94-016097] p 875 N95-16933
SPACE COMMERCIALIZATION
BioServe space technologies: A NASA Center for the Commercial Development of Space
[NASA-CR-196983] p 807 N95-16034
SPACE COMMUNICATION
The Telecommunications and Data Acquisition Report
[NASA-CR-197249] p 755 N95-17279
Tracking the Galileo spacecraft with the DSCC Galileo Telemetry prototype p 708 N95-17292
Advanced ground station architecture
p 674 N95-17556
Re-engineering NASA's space communications to remain viable in a constrained fiscal environment
p 702 N95-17585
Standard protocol stack for mission control
p 704 N95-17593
The Space Communications Protocol Standards Program p 704 N95-17594
Error control techniques for satellite and space communications
[NASA-CR-197459] p 761 N95-17665
SPACE DEBRIS
Analysis of space environment damage to solar cell assemblies from LDEF experiment A0171-GSFC test plate
[NASA-CR-196523] p 793 N95-16575
Debris/ice/TPS assessment and integrated photographic analysis of Shuttle Mission STS-64 on 9 August 1994
[NASA-TM-109206] p 676 N95-17262
SPACE ENVIRONMENT SIMULATION
Virtual environment application with partial gravity simulation p 854 N95-15988
Catecholaminergic responses to stressful motion stimuli, scopolamine plus amphetamine, and dexamethasone
p 809 N95-16745
SPACE EXPLORATION
Presidential leadership in the development of the US space program
[NASA-TM-110107] p 904 N95-16007
Activities of the Space Studies Board
[NASA-CR-197105] p 672 N95-16033
Foam inflated rigidized structures for space applications p 710 N95-16344
Artificial gravity: How much, how often, how long?
p 816 N95-16778
New look at the old Moon
[NASA-TM-110106] p 922 N95-16838
SPACE FLIGHT
SLS-1: The first dedicated life sciences shuttle flight
p 676 N95-16769
SPACE HABITATS
Catalog of lunar and Mars science payloads
[NASA-RP-1345] p 922 N95-16436
SPACE LOGISTICS
International Space Station Alpha (ISSA) Integrated Traffic Model
[NASA-CR-197566] p 710 N95-17331
SPACE MISSIONS
Landing site considerations for atmosphere structure and meteorology p 921 N95-16203
NSSDC data listing
[NASA-TM-109986] p 909 N95-16441
Psychological training of NASA astronauts for extended missions p 813 N95-16763
Third International Symposium on Space Mission Operations and Ground Data Systems, part 1
[NASA-CP-3281-PT-1] p 676 N95-17179
Grand mission versus small OPS team: Can we have both? p 684 N95-17219
Mission operations management p 685 N95-17225
Mars Pathfinder mission operations concepts
p 686 N95-17229
A mission planning concept and mission planning system for future manned space missions p 687 N95-17235
Re-engineering the Multimission Command System at the Jet Propulsion Laboratory p 702 N95-17583
Standard protocol stack for mission control
p 704 N95-17593
The Space Communications Protocol Standards Program p 704 N95-17594
The Requirements Generation System: A tool for managing mission requirements p 707 N95-17608
SPACE NAVIGATION
Development of a prototype real-time automated filter for operational deep space navigation
p 694 N95-17545
SPACE PERCEPTION
Computational vision based on neurobiology
[AD-A284472] p 819 N95-16135
SPACE PLASMAS
Continuing life test of a xenon hollow cathode for a space plasma contactor
[NASA-CR-195401] p 711 N95-15968
Characteristics of multiple auroral inverted-V structures and the problem of magnetospheric plasma stratification
[DE94-622233] p 799 N95-17471
SPACE POWER REACTORS
Reentry safety for the Topaz 2 Space Reactor: Issues and analyses
[DE95-000325] p 880 N95-17361
SPACE SHUTTLE BOOSTERS
Design margin testing of Peacekeeper solid rocket boosters p 713 N95-16313
Precision aqueous cleaner for RSRM
p 715 N95-16326
SPACE SHUTTLE MAIN ENGINE
SSME propellant path leak detection real-time
[NASA-CR-197032] p 748 N95-16029
Space Shuttle main engine OPAD: The search for a hardware enhanced plume p 716 N95-16330
SPACE SHUTTLE MISSIONS
Summary report of mission acceleration measurements for STS-62, launched 4 March 1994
[NASA-TM-106773] p 750 N95-17893
SPACE SHUTTLE ORBITERS
SEPAC co-investigator support
[NASA-CR-196527] p 798 N95-15965
Orbiter Kapton wire operational requirements and experience p 711 N95-16046
SPACE SHUTTLE PAYLOADS
Statistical analysis of microgravity experiment performance using the degrees of success scale
[NASA-TM-106791] p 784 N95-17385
SPACE SHUTTLES
Ultraviolet emissions occurring about hypersonic vehicles in rarefied flows
[AD-A281452] p 655 N95-16076
Space Shuttle reaction control system thruster metal nitrate removal and characterization
p 716 N95-16332
Simulation of the coupled multi-spacecraft control testbed at the Marshall Space Flight Center
p 849 N95-16475
Comparisons of three anti-G suit configurations during long duration, low onset, +Gz p 811 N95-16755
SLS-1: The first dedicated life sciences shuttle flight
p 676 N95-16769
Apollo 17: On the shoulders of giants
[NASA-TM-110105] p 922 N95-16837
Houston, I think we've got a satellite
[NASA-TM-109987] p 709 N95-16941
Debris/ice/TPS assessment and integrated photographic analysis of Shuttle Mission STS-64 on 9 August 1994
[NASA-TM-109206] p 676 N95-17262
SPACE STATION FREEDOM
Space Station Freedom primary power wiring requirements p 712 N95-16051
Space Station Freedom secondary power wiring requirements p 712 N95-16052
Medical care capabilities for Space Station Freedom: A phase approach p 710 N95-16772
A surgical support system for Space Station Freedom
p 710 N95-16776
Conceptual design of the Space Station combustion module
[NASA-TM-106788] p 675 N95-17419
SPACE STATION PAYLOADS
A distributed planning concept for Space Station payload operations p 682 N95-17211
SPACE STATION POWER SUPPLIES
Kapton pyrolysis on Space Station Freedom's solar array flexible current carrier p 712 N95-16049
SPACE STATION STRUCTURES
Atomic oxygen durability evaluation of the flexible batten for the photovoltaic array mast on Space Station
[NASA-TM-106798] p 781 N95-17263
SPACE STATIONS
Continuing life test of a xenon hollow cathode for a space plasma contactor
[NASA-CR-195401] p 711 N95-15968
Activities of the Space Studies Board
[NASA-CR-197105] p 672 N95-16033
Simulation of the coupled multi-spacecraft control testbed at the Marshall Space Flight Center
p 849 N95-16475
Results of an International Space Crew Debrief
p 810 N95-16750
Houston, I think we've got a satellite
[NASA-TM-109987] p 709 N95-16941
International Space Station Alpha user payload operations concept p 685 N95-17227
International Space Station Alpha (ISSA) Integrated Traffic Model
[NASA-CR-197566] p 710 N95-17331
SPACE SUITS
Design and technical support for development of a molded fabric space suit joint
[NASA-CR-197521] p 831 N95-16894
SPACE SURVEILLANCE
Proceedings of the 12th Space Surveillance Workshop, volume 2
[AD-A285115] p 672 N95-16842
SPACE SURVEILLANCE (GROUND BASED)
Proceedings of the 12th Annual Space Surveillance Workshop, volume 1
[AD-A285265] p 672 N95-16530
SPACE SURVEILLANCE (SPACEBORNE)
Proceedings of the 12th Annual Space Surveillance Workshop, volume 1
[AD-A285265] p 672 N95-16530
Proceedings of the 12th Space Surveillance Workshop, volume 2
[AD-A285115] p 672 N95-16842
Mission planning for space based satellite surveillance experiments with the MSX p 673 N95-17212
Joint operations planning for space surveillance missions on the MSX satellite p 673 N95-17215
An opportunity analysis system for space surveillance experiments with the MSX p 707 N95-17609
SPACE TRANSPORTATION
International Space Station Alpha (ISSA) Integrated Traffic Model
[NASA-CR-197566] p 710 N95-17331
SPACE TRANSPORTATION SYSTEM
Debris/ice/TPS assessment and integrated photographic analysis of Shuttle Mission STS-64 on 9 August 1994
[NASA-TM-109206] p 676 N95-17262

SPACE TRANSPORTATION SYSTEM FLIGHTS
A distributed planning concept for Space Station payload operations p 682 N95-17211
Debris/ice/TPS assessment and integrated photographic analysis of Shuttle Mission STS-64 on 9 August 1994
[NASA-TM-109206] p 676 N95-17262
SPACE-TIME FUNCTIONS
Application of the space-time conservation element and solution element method to shock-tube problem
[NASA-TM-106806] p 772 N95-16903
SPACEBORNE ASTRONOMY
Space-based asteroid detection and monitoring system
[AD-D016329] p 915 N95-16854
Engineering Ulysses extended mission p 673 N95-17213
Generic mission planning and scheduling: The AXAF solution p 686 N95-17231
SPACEBORNE EXPERIMENTS
SEPAC co-investigator support
[NASA-CR-196527] p 798 N95-15965
Mission planning for space based satellite surveillance experiments with the MSX p 673 N95-17212
Engineering Ulysses extended mission p 673 N95-17213
Joint operations planning for space surveillance missions on the MSX satellite p 673 N95-17215
Statistical analysis of microgravity experiment performance using the degrees of success scale
[NASA-TM-106791] p 784 N95-17385
An opportunity analysis system for space surveillance experiments with the MSX p 707 N95-17609
SPACEBORNE TELESCOPES
International mission planning for space Very Long Baseline Interferometry p 673 N95-17216
SPACECRAFT ANTENNAS
Galileo mission planning for Low Gain Antenna based operations p 682 N95-17210
Study of the folding and deployment aspects of a Collapsible Rib Tensioned Surface (CRTS) antenna reflector
[CUED/D-STRUCT/TR-144] p 783 N95-17928
SPACECRAFT CHARGING
Continuing life test of a xenon hollow cathode for a space plasma contactor
[NASA-CR-195401] p 711 N95-15968
Auroral interactions with ISSA
[NASA-TM-106794] p 709 N95-16862
SPACECRAFT COMMUNICATION
Third International Symposium on Space Mission Operations and Ground Data Systems, part 1
[NASA-CP-3281-PT-1] p 676 N95-17179
Communication network for decentralized remote tele-science during the Spacelab mission IML-2 p 676 N95-17181
Earth Observing System (EOS) Communication (Ecom) Modeling, Analysis, and Testbed (EMAT) activiy p 677 N95-17182
S-band and Ku-band return service interference between TDRSS users p 677 N95-17183
Table-driven configuration and formatting of telemetry data in the Deep Space Network p 677 N95-17185
Experience with the EURECA Packet Telemetry and Packet Telecommand system p 682 N95-17209
Evaluating Space Network (SN) scheduling operations concepts through statistical analysis p 684 N95-17222
The Pacor 2 expert system: A case-based reasoning approach to troubleshooting p 693 N95-17541
The Advanced Orbiting Systems Testbed Program: Results to date p 700 N95-17575
NCCDS performance model p 675 N95-17576
SPACECRAFT COMPONENTS
SEQ-REVIEW: A tool for reviewing and checking spacecraft sequences p 697 N95-17561
Mission Operations Centers (MOCs): Integrating key spacecraft ground data system components p 675 N95-17601
SPACECRAFT CONFIGURATIONS
Simulation of the coupled multi-spacecraft control testbed at the Marshall Space Flight Center p 849 N95-16475
An analysis of a single-burn algorithm for Low-Earth Orbit maintenance
[AD-A283418] p 721 N95-17626
SPACECRAFT CONSTRUCTION MATERIALS
First NASA Workshop on Wiring for Space Applications
[NASA-CP-10145] p 711 N95-16044
Kapton wire concerns for aerospace vehicles p 711 N95-16045
Orbiter Kapton wire operational requirements and experience p 711 N95-16046
Recent advances in graphite/epoxy motor cases p 717 N95-16333
SPACECRAFT CONTROL
Simulation of the coupled multi-spacecraft control testbed at the Marshall Space Flight Center p 849 N95-16475
Third International Symposium on Space Mission Operations and Ground Data Systems, part 1
[NASA-CP-3281-PT-1] p 676 N95-17179
Increases in efficiency and enhancements to the Mars Observer non-stored commanding process p 688 N95-17242
SCL: An off-the-shelf system for spacecraft control p 688 N95-17243
Safety aspects of spacecraft commanding p 689 N95-17248
SCOS 2: ESA's new generation of mission control system p 674 N95-17253
Third International Symposium on Space Mission Operations and Ground Data Systems, part 2
[NASA-CP-3281-PT-2] p 691 N95-17531
Spacecraft command and control using expert systems p 693 N95-17539
SEQ-GEN: A comprehensive multimission sequencing system p 693 N95-17540
An intelligent automated command and control system for spacecraft mission operations p 693 N95-17542
Magnetometer-only attitude and rate determination for a gyro-less spacecraft p 694 N95-17546
SCOS 2: An object oriented software development approach p 699 N95-17571
A new communication protocol family for a distributed spacecraft control system p 703 N95-17590
Standardizing the information architecture for spacecraft operations p 703 N95-17591
Standard protocol stack for mission control p 704 N95-17593
Packet utilisation definitions for the ESA XMM mission p 704 N95-17596
Cross support overview and operations concept for future space missions p 705 N95-17598
The NASA Mission Operations and Control Architecture Program p 706 N95-17603
Renaissance architecture for Ground Data Systems p 706 N95-17604
Architecture of a distributed multimission operations system p 706 N95-17605
A new systems engineering approach to streamlined science and mission operations for the Far Ultraviolet Spectroscopic Explorer (FUSE) p 707 N95-17611
SPACECRAFT DESIGN
Combustion and fires in low gravity p 712 N95-16050
A survey of commercially available expendable heavy lift launch vehicles
[AD-A282429] p 676 N95-17509
Concurrent engineering: Spacecraft and mission operations system design p 708 N95-17614
SPACECRAFT DOCKING
Simulation of the coupled multi-spacecraft control testbed at the Marshall Space Flight Center p 849 N95-16475
SPACECRAFT ENVIRONMENTS
Summary report of mission acceleration measurements for STS-62, launched 4 March 1994
[NASA-TM-106773] p 750 N95-17893
SPACECRAFT GLOW
Gas-surface interactions near dissociation threshold
[AD-A284945] p 726 N95-16042
Ultraviolet emissions occurring about hypersonic vehicles in rarefied flows
[AD-A281452] p 655 N95-16076
SPACECRAFT INSTRUMENTS
Engineering Ulysses extended mission p 673 N95-17213
A new systems engineering approach to streamlined science and mission operations for the Far Ultraviolet Spectroscopic Explorer (FUSE) p 707 N95-17611
SPACECRAFT LAUNCHING
Program test objectives milestone 3 --- Integrated Propulsion Technology Demonstrator
[NASA-CR-197030] p 666 N95-15971
Emerging national space launch programs: Economics and safeguards
[AD-A282107] p 672 N95-17427
A survey of commercially available expendable heavy lift launch vehicles
[AD-A282429] p 676 N95-17509
SPACECRAFT MAINTENANCE
CCS-MIP: Low cost Customizable Control Centre p 674 N95-17254
SPACECRAFT MODELS
Safety aspects of spacecraft commanding p 689 N95-17248
Galileo spacecraft modeling for orbital operations p 700 N95-17574
A standard satellite control reference model p 704 N95-17592
SPACECRAFT MODULES
Heat stress and a countermeasure in the Shuttle rescueman's suit p 809 N95-16746
SPACECRAFT ORBITS
Radio-planetary from tie from Phobos-2 VLBI data p 756 N95-17283
SPACECRAFT PERFORMANCE
The role of mission operations in spacecraft integration and test p 684 N95-17220
Generic trending and analysis system p 689 N95-17245
Safety aspects of spacecraft commanding p 689 N95-17248
SPACECRAFT POWER SUPPLIES
Nickel hydrogen batteries: An overview
[NASA-TM-106795] p 793 N95-16861
A modular electric power system test bed for small spacecraft
[NASA-TM-106812] p 721 N95-17276
SPACECRAFT PROPULSION
Damage-mitigating control of space propulsion systems for high performance and extended life
[NASA-CR-194470] p 784 N95-16068
SPACECRAFT REENTRY
Reentry safety for the Topaz 2 Space Reactor: Issues and analyses
[DE95-000325] p 880 N95-17361
SPACECRAFT STRUCTURES
A comparison of different control methods for vibration suppression of flexible structures using piezoelectric actuators
[AD-A282958] p 710 N95-17622
SPACECRAFT TRACKING
Third International Symposium on Space Mission Operations and Ground Data Systems, part 1
[NASA-CP-3281-PT-1] p 676 N95-17179
Mission planning for space based satellite surveillance experiments with the MSX p 673 N95-17212
Advanced technologies in the ASI MLRO towards a new generation laser ranging system p 687 N95-17239
Space VLBI telecommunication characteristics, protection criteria, and frequency sharing p 756 N95-17282
Radio-planetary from tie from Phobos-2 VLBI data p 756 N95-17283
Tracking the Galileo spacecraft with the DSCC Galileo Telemetry prototype p 708 N95-17292
RF optics study for DSS-43 ultracone implementation p 758 N95-17296
Open solutions to distributed control in ground tracking stations p 674 N95-17554
Advanced ground station architecture p 674 N95-17556
SPACECRAFT TRAJECTORIES
An analysis of a single-burn algorithm for Low-Earth Orbit maintenance
[AD-A283418] p 721 N95-17626
SPACECREWS
Virtual environment application with partial gravity simulation p 854 N95-15988
Aerospace Medical Association 63rd Annual Scienti fic Meeting Program p 807 N95-16737
Use of injectable promethazine to decrease symptom scores of Space Motion Sickness p 808 N95-16741
Heat stress and a countermeasure in the Shuttle rescueman's suit p 809 N95-16746
Results of an International Space Crew Debrief p 810 N95-16750
Comparisons of three anti-G suit configurations during long duration, low onset, +Gz p 811 N95-16755
Prediction of space sickness in astronauts from preflight fluid, electrolyte, and cardiovascular variables and Weightless Environmental Training Facility (WETF) training p 812 N95-16757
Psychological training of NASA astronauts for extended missions p 813 N95-16763
Medical care capabilities for Space Station Freedom: A phase approach p 710 N95-16772
A prototype Crew Medical Restraint System (CMRS) for Space Station Freedom p 815 N95-16773
Delivery of cardiopulmonary resuscitation in the microgravity environment p 816 N95-16774
Medicine on Mars: Remote medical care and the space exploration initiative p 816 N95-16777
Artificial gravity: How much, how often, how long? p 816 N95-16778
SPACELAB
SLS-1: The first dedicated life sciences shuttle flight p 676 N95-16769
Communication network for decentralized remote tele-science during the Spacelab mission IML-2 p 676 N95-17181
Telemetry distribution and processing for the second German Spacelab Mission D-2 p 681 N95-17207

Payload operations management of a planned European SL-Mission employing establishments of ESA and national agencies p 684 N95-17221

SPACING

A new manufacturing method for the formation of gated field emission structures
[DE94-015287] p 764 N95-16832

SPAIN

CINDOC, CSIC, and Spanish R and D p 906 N95-15927

SPATIAL DISTRIBUTION

Mental rotation with and without a concurrent task: Moderating effects of visuospatial ability
[AD-A281866] p 826 N95-16301

Spatial information content analysis of Wiener spectra from polarized waterwave imagery
[AD-A283171] p 886 N95-17340

SPATIAL RESOLUTION

Vibratory tactile display for textures p 851 N95-15973

Papers presented at the Tenth Topical Conference on High-Temperature Plasma Diagnostics
[DE94-015854] p 888 N95-16063

SPECIFIC HEAT

Prediction of the response of a polyimide concentrator for solar thermal propulsion p 719 N95-16343

Study of the structuring of pure molecular liquids
[PB94-201316] p 903 N95-16839

SPECIFIC IMPULSE

Solar-powered rocket engine optimization for high specific impulse p 718 N95-16341

SPECIFICATIONS

ELISA, a demonstrator environment for information systems architecture design p 698 N95-17563

SPECKLE PATTERNS

On the improvement of 1-look SAR image segmentations with mathematical morphology
[INPE-5577-PRE/1805] p 912 N95-17650

Measurement of modulation transfer function of focal plane arrays and imaging systems
[AD-A282976] p 887 N95-17707

SPECTRA

Surface science capabilities from IMP spectral imaging p 921 N95-16204

Resonance enhanced multiphoton ionization of molecules and molecular fragments
[AD-A285076] p 873 N95-16493

An analysis of spectral envelope-reduction via quadratic assignment problems
[NASA-CR-194992] p 862 N95-16596

SPECTRAL METHODS

Spectral solution of the viscous blunt body problem. 2: Multidomain approximation
[NASA-CR-194971] p 863 N95-17267

SPECTRAL RESOLUTION

Infrared signatures for remote sensing
[DE94-014222] p 790 N95-16215

SPECTROGRAPHS

Micro-UltraViolet Spectrograph (Micro-UVS)
[DE94-016704] p 732 N95-17642

SPECTROMETERS

Alpha proton x ray spectrometer p 710 N95-16201

The stability of calibration standards for ICP/AES analysis: A two-year study
[DE94-013398] p 728 N95-16426

Experimental characterization of ALS undulator radiation
[DE94-017967] p 881 N95-17671

SPECTRORADIOMETERS

MODIS Technical Report Series. Volume 4: MODIS data access user's guide: Scan cube format
[NASA-TM-104594-VOL-4] p 837 N95-16587

SPECTROSCOPIC ANALYSIS

Infrared signatures for remote sensing
[DE94-014222] p 790 N95-16215

Methods development toward the measurement of polyaromatic hydrocarbon-DNA adducts by mass spectrometry
[PB94-182722] p 727 N95-16373

Atomic scale structure and chemistry of interfaces by Z-contrast imaging and electron energy loss spectroscopy in the stem
[DE94-013632] p 728 N95-16419

Nitride semiconductors for ultraviolet detection
[AD-A280988] p 898 N95-16533

SPECTROSCOPY

Spectroscopy of the transition state region in hydrogen transfer reactions
[AD-A285151] p 729 N95-16846

Study of CuPt-type ordering and dopant effect of In(0.5)Ga(0.5)P/GaAs using spectroscopic ellipsometry
[DE94-018890] p 902 N95-17917

SPECTRUM ANALYSIS

Researches on gear fault diagnosis techniques p 651 N95-16267

Spectral components of human cardiovascular responses to step changes in Lower Body Negative Pressure (LBNP) before and after 22 hour of 6 deg head down bed rest p 810 N95-16748

Study of the structuring of pure molecular liquids
[PB94-201316] p 903 N95-16839

An algorithm for extraction of periodic signals from sparse, irregularly sampled data p 756 N95-17281

Adaptive line enhancers for fast acquisition p 757 N95-17287

Spatial information content analysis of Wiener spectra from polarized waterwave imagery
[AD-A283171] p 886 N95-17340

Development of an Automated Airfield Dynamic Cone Penetrometer (AADCP) prototype and the evaluation of unsurfaced airfield seismic surveying using Spectral Analysis of Surface Waves (SASW) technology
[AD-A281985] p 672 N95-17444

SPECULAR REFLECTION

Performance of specular reflectors used for lighting enhancement
[AD-A281004] p 884 N95-15999

SPEECH RECOGNITION

A comparison of signal-processing front ends for automatic speech recognition
[AD-A284962] p 752 N95-16129

Anatomy of a silicon compiler
[AD-A285395] p 832 N95-16618

The 1994 International Neural Network Society Annual Meeting, volume 4
[AD-A281737] p 857 N95-17370

Phonologic-graphemic transcodifier for Portuguese Language spoken in Brazil (PLB)
[INPE-5575-PRE/1803] p 760 N95-17649

SPEED REGULATORS

Method and apparatus for reducing axial thrust in centrifugal pumps
[AD-D016404] p 782 N95-17461

Simulation investigation on system identification of gas turbine
[PB95-104238] p 670 N95-17749

SPHERICAL COORDINATES

Single-pass method for the solution of inverse potential and rotational problems. Part 2: Fully 3-D potential theory and applications p 664 N95-16564

SPHEROIDS

Superspheroid geometries for radome analysis
[AD-A285405] p 753 N95-16233

SPIN DYNAMICS

RHIC spin: The first polarized proton collider
[DE94-013760] p 872 N95-16121

Critical and paramagnetic spin dynamics in an antiferromagnetically coupled Heisenberg magnet: Results for RbMnF3
[PB95-104329] p 869 N95-17731

SPIN-LATTICE RELAXATION

Materials degradation and fatigue under extreme conditions
[AD-A282969] p 746 N95-17662

SPIN-SPIN COUPLING

Critical and paramagnetic spin dynamics in an antiferromagnetically coupled Heisenberg magnet: Results for RbMnF3
[PB95-104329] p 869 N95-17731

Time-dependent spin correlations in the heisenberg magnet at infinite temperature
[PB95-104303] p 869 N95-17750

SPIRAL GALAXIES

First detection of CO (j = 0 - 1) adsorption at cosmological distances (z = 0.247)
[PB94-184595] p 916 N95-17332

ROSAT detection of diffuse hot gas in the edge-on galaxy NGC 4631
[NASA-CR-197535] p 915 N95-17496

X-ray emission from the edge-on spiral galaxy NGC 4631
[NASA-CR-197536] p 924 N95-17527

SPLINE FUNCTIONS

Modelling daily precipitation as a function of temperature for climate change impact studies
[KNMI-WR-93-02] p 802 N95-17529

SPRAYED COATINGS

Fire protective coating and method for applying same to a structure
[AD-D016405] p 746 N95-17462

SPREAD SPECTRUM TRANSMISSION

Performance of a fast frequency-hopped noncoherent MFSK receiver with non-ideal noise normalization combining over ricean fading channels with partial-band interference
[AD-A284989] p 753 N95-16232

Fast acquisition of burst direct sequence spread spectrum signals through satellite channels p 652 N95-16270

Spread spectrum applications in unmanned aerial vehicles
[AD-A281035] p 754 N95-16448

SQUEEZED STATES (QUANTUM THEORY)

Light-ray operators and their application in QCD
[DE94-013801] p 903 N95-16944

SQUID (DETECTORS)

Thermal noise in biomagnetic measurements
[PB95-104360] p 869 N95-17930

STABILITY

Problem of constructing the Lyapunov's functions in lumped parameter systems p 653 N95-16276

New approaches to novel organosilanes
[AD-A285253] p 722 N95-16513

Avoiding BDF stability barriers in the MOL solution of advection-dominated problems
[DE94-014793] p 861 N95-16535

Chemical vapor deposition of high T(sub c) superconducting films in a microgravity environment
[NASA-CR-197527] p 750 N95-16880

Radio-planetary from tie from Phobos-2 VLBI data p 756 N95-17283

Research on stable, high-efficiency, amorphous silicon multijunction modules
[DE94-011826] p 794 N95-17521

Studies of transverse coherent bunch instabilities for the Advanced Light Source (ALS)
[DE94-018536] p 904 N95-17904

STABILITY DERIVATIVES

Evaluation of the dynamic stability characteristics of the NAL Light Transport Aircraft
[NAL-PD-CA-9217] p 671 N95-16392

Error propagation equations for estimating the uncertainty in high-speed wind tunnel test results
[DE94-014136] p 671 N95-16509

STABILITY TESTS

FPCAS2D user's guide, version 1.0
[NASA-CR-195413] p 786 N95-16588

STABILIZATION

Pseudomorphic stabilization of diamond on non-diamond substrates
[AD-A285231] p 898 N95-16527

A prototype Crew Medical Restraint System (CMRS) for Space Station Freedom p 815 N95-16773

Delivery of cardiopulmonary resuscitation in the microgravity environment p 816 N95-16774

The influence of the complexation of sodium and lithium triflate on the self-assembly of tubular-supramolecular architectures displaying a columnar mesophase based on taper-shaped monoesters of oligoethyleneoxide with 3,4,5-tris(p-(n-dodecan-l-yloxy)benzyloxy)benzoic acid and of their polymethacrylates
[AD-A281403] p 730 N95-16866

STABILIZERS (FLUID DYNAMICS)

Twin engine afterbody model p 663 N95-17880

STAINLESS STEELS

Investigation into the susceptibility of corrosion resistant alloys to biocorrosion
[AD-A281066] p 736 N95-16793

Investigation of residual stresses in a multipass weld in 1 in. stainless steel plate
[DE94-013277] p 786 N95-16803

Modeling of thermal stresses in welds
[DE94-018046] p 789 N95-17675

STANDARD DEVIATION

Optimization of adaptive intraply hybrid fiber composites with reliability considerations
[NASA-TM-106632] p 787 N95-16911

STANDARD MODEL (PARTICLE PHYSICS)

A measurement of the Michel parameter (rho) in muon decay
[DE94-014423] p 876 N95-17153

Baryogenesis and standard model CP violation
[DE94-017935] p 877 N95-17669

STANDARDIZATION

The value of the 4-day headdown bedrest model for screening countermeasures p 817 N95-16782

Standardizing the information architecture for spacecraft operations p 703 N95-17591

A standard satellite control reference model p 704 N95-17592

Standard protocol stack for mission control p 704 N95-17593

The Space Communications Protocol Standards Program p 704 N95-17594

Cross support overview and operations concept for future space missions p 705 N95-17598

The CCSDS return all frames Space Link Extension service p 705 N95-17599

STANDARDS

Numeric data distribution: The vital role of data exchange in today's world p 907 N95-15937

National Center for Standards and Certification Information: Service and programs p 907 N95-15938

Use of the electronic balance for highly accurate direct mass measurements without the use of external mass standards
[PB94-187713] p 774 N95-16074
Software engineering from a Langley perspective
p 843 N95-16454
A study of software standards used in the avionics industry p 670 N95-16456
Field verification of the wind tunnel coefficients
p 664 N95-17291
Aircraft and sub-system certification by piloted simulation
[AGARD-AR-278] p 671 N95-17388

STAR FORMATION
ROSAT detection of diffuse hot gas in the edge-on galaxy NGC 4631
[NASA-CR-197535] p 915 N95-17496

STATIC FIRING
Test results from a simple, low-cost, pressure-fed liquid hydrogen/liquid oxygen rocket combustor
p 716 N95-16328

STATIC FRICTION
Static and dynamic friction behavior of candidate high temperature airframe seal materials
[NASA-TM-106571] p 722 N95-16905

STATIONKEEPING
An analysis of a single-burn algorithm for Low-Earth Orbit maintenance
[AD-A283418] p 721 N95-17626

STATISTICAL ANALYSIS
Improved method for estimation of the maximum instantaneous distortion values p 649 N95-16254
Direct comparison of two statistical methods for determination of evoked-potential thresholds
[AD-A285182] p 870 N95-16811
Evaluating Space Network (SN) scheduling operations concepts through statistical analysis
p 684 N95-17222
Object recognition using multi-layer Hopfield neural network
[AD-A282417] p 858 N95-17459
Small sample behavior of multi-layer feedforward network classifiers: Theoretical and practical aspects
[PB94-201415] p 841 N95-17470
Operational cloud classifier based on a self-organized feature map
[PB94-197852] p 802 N95-17504

STATISTICAL CORRELATION
System design, implementation, and evaluation of the optical broadband correlator
[AD-A285406] p 884 N95-16296

STATORS
A Lifting Ball Valve for cryogenic fluid applications
p 720 N95-16349
Method and apparatus for reducing axial thrust in centrifugal pumps
[AD-D016404] p 782 N95-17461

STEADY FLOW
Experimental and theoretical studies of wakes in stratified flows
[AD-A285305] p 771 N95-16616
Small-amplitude disturbances in turbomachine flows with swirl
[NASA-CR-195406] p 772 N95-17386

STEAM
Nonpowered instant water heater
[AD-A285459] p 783 N95-17725

STEELS
Ductile fracture and failure criteria of structural steels
[AD-A280754] p 733 N95-16104
Experimental application of methodologies to quantify the effect of constraint on JC for a 3-D flaw geometry
[AD-A285309] p 735 N95-16531
The effects of fatigue loading frequency on fatigue life of high-strength pressure vessel steels
[AD-A285301] p 786 N95-16601
Effects of prior ductile tearing on cleavage fracture toughness in the transition region
[AD-A281298] p 786 N95-16785
Penetration of solid and layered targets by gas gun-launched steel cubes
[AD-A285143] p 787 N95-16843
Conducting polymers as corrosion resistant coatings
[DE94-018265] p 748 N95-17892

STEERING
Liquid crystal materials for laser beam steering
[AD-A285089] p 897 N95-16498

STELLAR ENVELOPES
The Mg 2 lines as diagnostic of PMS nature in Herbig Ae/Be stars
[NASA-CR-197518] p 915 N95-17494

STELLAR LUMINOSITY
A preliminary optical visibility model
p 758 N95-17290

STELLAR MASS EJECTION
Solar-geophysical data number 596, April 1994. Part 2: (Comprehensive reports). Data for October 1993, and miscellaneous
[PB94-183555] p 924 N95-17737

STELLAR MODELS
First results from SAGE 2
[DE94-014431] p 876 N95-17154

STELLARATORS
Status of the US stellarator reactor study
[DE94-018693] p 893 N95-17907

STEP RECOVERY DIODES
Frequency multiplier analysis and design using punch-through varactor diodes
[AD-A284963] p 762 N95-16130

STEREOCHEMISTRY
Chiral recognition in molecular and macromolecular pairs of liquid crystals of (2R, 3S)- and (2S, 3S)-2-fluoro-3-methylpentyl-4'-(11-vinyloxyundeca iphenyl-4-carboxylate diastereomers
[AD-A281770] p 878 N95-17692

STEREOSCOPY
Fast stereoscopic images with ray-traced volume rendering
[DE94-011703] p 835 N95-16223

STIRLING CYCLE
Overview of space power electronic's technology under the CSTI High Capacity Power Program
[NASA-TM-110110] p 883 N95-17933

STIRLING ENGINES
Heat transfer measurements for Stirling machine cylinders
[NASA-CR-197128] p 791 N95-15963

STOCHASTIC PROCESSES
Portable parallel stochastic optimization for the design of aeropropulsion components
[NASA-CR-195312] p 785 N95-16072
Large scale control and distributed computing systems under stochastic structural perturbations
[AD-A281550] p 855 N95-16170
Stochastic approximation methods for fusion-rule estimation in multiple sensor systems
[DE94-013629] p 856 N95-16361
Nonasymptotic formulae for the distribution of the maximum of smooth Gaussian processes
[AD-A284741] p 865 N95-16546
Likelihood ratio gradient estimation for stochastic recursions
[AD-A281408] p 865 N95-17426

STORAGE RINGS (PARTICLE ACCELERATORS)
Study of the effect of the space charge using SYNCH
[DE94-014086] p 879 N95-16210
Field configuration of beam excited modes in the Advanced Photon Source (APS) storage ring waveguides
[DE94-015096] p 880 N95-16308
Measurements of collective effects in the ALS
[DE94-017966] p 881 N95-17670
Experimental characterization of ALS undulator radiation
[DE94-017967] p 881 N95-17671
Transverse mode coupling instability with a double RF system
[DE94-017972] p 761 N95-17672
Crystalline beams: The vertical zigzag
[DE94-017986] p 901 N95-17673

STORMS (METEOROLOGY)
Sensitivity analysis of numerically-simulated convective storms using direct and adjoint methods
[DE94-013399] p 800 N95-16398

STRAIN DISTRIBUTION
Shaped strain sensors for intelligent structures
[AD-A282333] p 774 N95-16242

STRAIN ENERGY METHODS
A consistent large deflection theory of composite sandwich shells p 650 N95-16259
Failure analysis of 2D and 3D woven composites
[NASA-CR-197247] p 724 N95-16597

STRAIN GAGES
Shaped strain sensors for intelligent structures
[AD-A282333] p 774 N95-16242

STRAIN MEASUREMENT
Shaped strain sensors for intelligent structures
[AD-A282333] p 774 N95-16242

STRAIN RATE
Material and ballistic investigation of a tungsten-26 percent rhenium alloy
[PB94-189156] p 734 N95-16420

STRAITS
Straits of Florida physical oceanographic field study. Volume 1: Executive summary. Volume 2: Technical report. Volume 3: Data report
[PB94-175031] p 806 N95-17615

STRAKES
Experimental investigation of the vortex flow over a 76/60-deg double delta wing p 662 N95-17874

STRATIFICATION
On the propagation of near-inertial motion from the oceanic mixed layer p 806 N95-17396

STRATIFIED FLOW
Experimental and theoretical studies of wakes in stratified flows
[AD-A285305] p 771 N95-16616

STRATIGRAPHY
Cerberus Plains: A most excellent Pathfinder landing site p 921 N95-16198
Normalization and prediction of geotechnical properties using the Cone Penetrometer Test (CPT)
[AD-A285193] p 799 N95-16872

STRESS (PHYSIOLOGY)
Catecholaminergic responses to stressful motion stimuli, scopolamine plus amphetamine, and dexamethasone
p 809 N95-16745
Mental effects of caffeine in fatigued men and women
[PB94-190683] p 822 N95-17300

STRESS (PSYCHOLOGY)
Locus coeruleus, vigilance and stress: Brain mechanisms of adaptive behavioral responsiveness
[AD-A282450] p 826 N95-16377

STRESS ANALYSIS
Special hybrid stress finite elements for the analysis of interface stress distribution in adhesive joints
[AD-A281612] p 785 N95-16102
Validation of recipes for the recovery of stresses and derivatives by a computer-based approach
[AD-A282712] p 861 N95-16379
Modeling of wall-bounded complex flows and free shear flows
[NASA-TM-106513] p 770 N95-16407
Thermocryogenic buckling and stress analyses of a partially filled cryogenic tank subjected to cylindrical strip heating
[NASA-TM-4579] p 788 N95-17417
An analysis of smoothed particle hydrodynamics
[DE94-013817] p 788 N95-17439
Thermal effects in end-heated laser rods: A time-dependent model and diagnostic
[AD-A282007] p 778 N95-17500
Modeling of thermal stresses in welds
[DE94-018046] p 789 N95-17675

STRESS CONCENTRATION
Probabilistic simulation of stress concentration in composite laminates
[NASA-TM-106712] p 787 N95-17270
Metallurgical examination of failed T-158 Cast Austempered Ductile Iron (CADI) track shoes
[AD-A282433] p 737 N95-17486

STRESS CORROSION CRACKING
Characterization of the hydrogen induced cold cracking susceptibility at simulated weld zones in HSLA-100 steel
[PB94-174505] p 737 N95-17616
Characterization of the corrosion behavior of the carbon steel liner in Hanford site single-shell tanks
[DE94-016475] p 737 N95-17637

STRESS DISTRIBUTION
Special hybrid stress finite elements for the analysis of interface stress distribution in adhesive joints
[AD-A281612] p 785 N95-16102
Experimental studies of stress measurement by optical fluorescence
[AD-A282337] p 723 N95-16415
Significant issues in proof testing: A critical appraisal
[NASA-CR-4628] p 788 N95-17272
Modeling of stress/strain behavior of fiber-reinforced ceramic matrix composites including stress redistribution
[NASA-TM-106789] p 725 N95-17659
Modeling of thermal stresses in welds
[DE94-018046] p 789 N95-17675

STRESS FUNCTIONS
Thermoelasticity analysis of laminated plates and shells using hybrid-stress elements p 651 N95-16263

STRESS INTENSITY FACTORS
Multi-lab comparison on R-curve methodologies: Alloy 2024-T3
[NASA-CR-195004] p 736 N95-16860

STRESS MEASUREMENT
Experimental studies of stress measurement by optical fluorescence
[AD-A282337] p 723 N95-16415
Normalization and prediction of geotechnical properties using the Cone Penetrometer Test (CPT)
[AD-A285193] p 799 N95-16872

STRESS RELAXATION
Giant flux creep through the surface barriers and the irreversibility line in high T(sub c) superconductors
[DE94-013991] p 766 N95-16945

STRESS TENSORS
On the prediction of free turbulent jets with swirl using a quadratic pressure-strain model
[NASA-CR-194964] p 769 N95-16071
A consistent large deflection theory of composite sandwich shells p 650 N95-16259

STRESS-STRAIN RELATIONSHIPS
Considerations in the experimental determination of constitutive parameters for finite strain plasticity
[AD-A285410] p 785 N95-16245
Modeling of stress/strain behavior of fiber-reinforced ceramic matrix composites including stress redistribution
[NASA-TM-106789] p 725 N95-17659
STRINGS
Crystalline beams: The vertical zigzag
[DE94-017986] p 901 N95-17673
STRONTIUM
Encapsulated alkaline-earth organometallics as controlled sources of calcium, strontium, and barium ions
[AD-A281547] p 741 N95-16393
STRONTIUM OXIDES
Suppression of superconductivity in orthorhombic La(2-x)M(x)CuO4 (M = Ca,Sr)
[DE94-013963] p 901 N95-17350
Volatile CVD precursors based on copper alkoxides and mixed group IIA-copper alkoxides
[AD-D016380] p 732 N95-17479
STRUCTURAL ANALYSIS
Guide to ASIAC computer programs
[AD-A285354] p 784 N95-15953
A super-element simplified analysis for vibration systems of complex structures p 650 N95-16260
A new regularization approach in structural system identification p 651 N95-16262
Structural analysis of solid-propellant rocket motors with and without flaws p 720 N95-16348
Solution of matrix equations using sparse techniques p 847 N95-16459
Automatic differentiation for design sensitivity analysis of structural systems using multiple processors p 847 N95-16462
The Design Manager's Aid for Intelligent Decomposition (DeMAID) p 848 N95-16470
FPCAS2D user's guide, version 1.0
[NASA-CR-195413] p 786 N95-16588
Analysis of a two-bladed, teetering-hub turbine using the ADAMS (tm) software
[DE94-006922] p 781 N95-17169
Probabilistic simulation of stress concentration in composite laminates
[NASA-TM-106712] p 787 N95-17270
JPL-ANTOPT antenna structure optimization program p 759 N95-17297
Error estimation and adaptive mesh refinement for parallel analysis of shell structures
[NASA-CR-197500] p 788 N95-17492
Aeronautical engineering: A continuing bibliography with indexes (supplement 311)
[NASA-SP-7037(311)] p 654 N95-17704
Measurements on a two-dimensional aerofoil with high-lift devices p 657 N95-17848
STRUCTURAL DESIGN
A Lifting Ball Valve for cryogenic fluid applications p 720 N95-16349
Rapid solution of large-scale systems of equations p 847 N95-16458
Natural frequency of uniform and optimized tetrahedral truss platforms
[NASA-TP-3461] p 709 N95-16559
Measurement of residual flexibility for substructures having prominent flexible interfaces
[NASA-TM-110074] p 786 N95-16577
Experimental validation of an integrated controls-structures design methodology for a class of flexible space structures
[NASA-TP-3462] p 709 N95-16857
Graphite-reinforced polycyanate composites for space and missile applications
[AD-A285509] p 725 N95-16970
STRUCTURAL FAILURE
Structural integrity of intelligent materials and structures. Constitutive modeling of shape memory alloys
[AD-A281301] p 735 N95-16786
STRUCTURAL RELIABILITY
Multiphase ceramics for mechanical and structural reliability at low and elevated temperatures
[AD-A285497] p 746 N95-17438
STRUCTURAL STRAIN
Structurally-compliant rocket engine combustion chamber: Experimental/analytical validation p 718 N95-16337
STRUCTURAL VIBRATION
Integrated passive and active control of structures
[AD-A282684] p 708 N95-16304
STRUCTURAL WEIGHT
Guide to ASIAC computer programs
[AD-A285354] p 784 N95-15953
STRUCTURED PROGRAMMING
A structured TCP in standard ML
[AD-A282711] p 835 N95-16306
Flexible method for inter-object communication in C++
[NASA-TM-106315] p 840 N95-17420
STUDENTS
ARO-URI Center for Opto-Electronic Systems Research
[AD-A281447] p 883 N95-15958
A workstation based simulator for teaching compressible aerodynamics
[NASA-TM-106799] p 839 N95-16906
SUBCRITICAL FLOW
An improved method of airfoil design p 649 N95-16252
SUBLIMATION
Self-assembly of low-dimensional conductors on Au(111) surfaces
[AD-A280936] p 734 N95-16505
Snapshots of crystal growth: Nanoclusters of organic conductors on Au(111) surfaces
[AD-A280976] p 897 N95-16508
SUBROUTINE LIBRARIES (COMPUTERS)
Towards a class library for mission planning p 686 N95-17233
SUBROUTINES
Demonstration of the Dynamic Flowgraph Methodology using the Titan 2 Space Launch Vehicle Digital Flight Control System
[NASA-CR-197517] p 675 N95-17493
User-defined subroutine for implementation of special finite elements in ABAQUS for the analysis of adhesive joints
[AD-A282431] p 788 N95-17510
A standard satellite control reference model p 704 N95-17592
SUBSONIC FLOW
Three dimensional compressible turbulent flow computations for a diffusing S-duct with/without vortex generators
[NASA-CR-195390] p 670 N95-17402
Investigation of an NLF(1)-0416 airfoil in compressible subsonic flow p 658 N95-17852
Measurements of the flow over a low aspect-ratio wing in the Mach number range 0.6 to 0.87 for the purpose of validation of computational methods. Part 1: Wing design, model construction, surface flow. Part 2: Mean flow in the boundary layer and wake, 4 test cases p 660 N95-17860
Pressure distributions on research wing W4 mounted on an axisymmetric body p 660 N95-17862
Three-dimensional boundary layer and flow field data of an inclined prolate spheroid p 661 N95-17867
Ellipsoid-cylinder model p 661 N95-17869
Delta-wing model p 662 N95-17873
Wind tunnel test on a 65 deg delta wing with rounded leading edges: The International Vortex Flow Experiment p 662 N95-17875
Investigation of the flow development on a highly swept canard/wing research model with segmented leading- and trailing-edge flaps p 662 N95-17876
Subsonic flow around US-orbiter model FALKE in the DNW p 663 N95-17877
SUBSONIC SPEED
Measurements of the flow over a low aspect-ratio wing in the Mach number range 0.6 to 0.87 for the purpose of validation of computational methods. Part 1: Wing design, model construction, surface flow. Part 2: Mean flow in the boundary layer and wake, 4 test cases p 660 N95-17860
DLR-F4 wing body configuration p 660 N95-17863
Low aspect ratio wing experiment p 661 N95-17865
Test data on a non-circular body for subsonic, transonic and supersonic Mach numbers p 662 N95-17871
Wind tunnel test on a 65 deg delta wing with a sharp or rounded leading edge: The international vortex flow experiment p 662 N95-17872
SUBSTITUTES
Synthesis and characterization of a new class of thermosetting resins: Allyl and propargyl substituted cyclopentadiene derivatives
[AD-A281976] p 746 N95-17485
SUBSTRATES
Pseudomorphic stabilization of diamond on non-diamond substrates
[AD-A285231] p 898 N95-16527
Relationships between ferroelectric 90 deg domain formation and electrical properties of chemically prepared Pb(Zr,Ti)O3 thin films
[DE94-015274] p 744 N95-16829
HTS SNS devices on large-area substrates by single-source MOCVD
[AD-A285159] p 899 N95-16849
Coatings for large-area low-cost solar concentrators and reflectors
[DE94-015735] p 793 N95-16916
Selective area platinum film deposition
[AD-D016355] p 747 N95-17693
Adhesion of silicon oxide to diamond
[AD-D016356] p 747 N95-17694
Vacuum deposited polymer/silver reflector material
[DE94-018729] p 748 N95-17913
SUBSTRUCTURES
Measurement of residual flexibility for substructures having prominent flexible interfaces
[NASA-TM-110074] p 786 N95-16577
SULFATES
Investigation into the susceptibility of corrosion resistant alloys to biocorrosion
[AD-A281066] p 736 N95-16793
Underpotential deposition of Cu on Au(111): Implications of the HB model
[AD-A283028] p 902 N95-17711
SULFIDATION
Environmental effects on iron aluminide
[DE94-017900] p 739 N95-17747
SULFONATES
Property control of (perfluorinated ionomer)/(inorganic oxide) composites by tailoring the nanoscale morphology
[AD-A281370] p 723 N95-16019
SULFONIC ACID
Study of the compression behavior of high performance fibers
[AD-A284959] p 723 N95-16126
SULFUR DIOXIDES
Energy and emissions of CO2, NOx and SO2 in the scenario of the 3rd national environmental evaluation, 1993
[PB94-194792] p 796 N95-17304
SULFUR HEXAFLUORIDE
Thermal dissociation of halogen azides
[AD-A285088] p 728 N95-16497
Shock initiation of crystalline boron in oxygen and fluorine compounds
[AD-A284266] p 730 N95-16955
SULFUR OXIDES
Corrosion inhibition in high temperature environment
[AD-D016372] p 738 N95-17699
SUMPS
Bench wear and single-cylinder engine evaluations of high-temperature lubricants for US Army ground vehicles
[AD-A285399] p 780 N95-16636
SUNLIGHT
Simulating the energy performance of holographic glazings
[DE94-013110] p 775 N95-17307
SUPERCOMPUTERS
Partial evaluation for scientific computing: The supercomputer toolkit experience
[AD-A282286] p 846 N95-16237
Active messages versus explicit message passing under SUNMOS
[DE94-015278] p 850 N95-16830
SUPERCONDUCTING FILMS
Electron transport and tunneling experiments
[AD-A281527] p 894 N95-16106
Chemical vapor deposition of high T(sub c) superconducting films in a microgravity environment
[NASA-CR-197527] p 750 N95-16880
Thin film superconductors
[DE94-018585] p 902 N95-17906
SUPERCONDUCTING MAGNETS
Test results of superconducting AC magnets for magnetic refrigeration experiment
[DE94-018695] p 751 N95-17909
SUPERCONDUCTING SUPER COLLIDER
Research in elementary particle physics
[DE94-019219] p 877 N95-17358
SUPERCONDUCTIVITY
Inelastic neutron scattering and antiferromagnetic fluctuations in high temperature superconductors
[DE94-623269] p 871 N95-16059
Electron transport and tunneling experiments
[AD-A281527] p 894 N95-16106
Muon(+) SR studies of magnetic properties of boron carbide superconductors
[DE94-014440] p 868 N95-16288
The relationship of structure to superconductivity in the Pr-Ba-Cu-O system
[DE94-014231] p 897 N95-16510
International Winterschool on Electronic Properties of Novel Materials: Progress in Fullerene Research
[AD-A282128] p 728 N95-16608
Design and synthesis of organic superconductors (FY92 URI/RIP)
[AD-A281308] p 899 N95-16789
Processing, fabrication, characterization and device demonstration of high temperature superconducting ceramics
[AD-A285145] p 744 N95-16844

Suppression of superconductivity in orthorhombic La(2-x)M(x)CuO4 (M = Ca,Sr)
[DE94-013963] p 901 N95-17350

SUPERCONDUCTORS (MATERIALS)
Muon(+) SR studies of magnetic properties of boron carbide superconductors
[DE94-014440] p 868 N95-16288

SUPERCRITICAL AIRFOILS
Comparison of computational and experimental results for a supercritical airfoil
[NASA-TM-4601] p 656 N95-16908
A supercritical airfoil experiment p 659 N95-17858

SUPERCRITICAL FLUIDS
The removal of heteroatoms from organic compounds by supercritical water
[AD-A281532] p 722 N95-16087
Supercritical fluid extraction: Preparing a superior mesophase precursor for carbon fibers
[AD-A284933] p 726 N95-16142

SUPERCRITICAL WINGS
Measurements of unsteady pressure and structural response for an elastic supercritical wing
[NASA-TP-3443] p 653 N95-16560

SUPERHIGH FREQUENCIES
S-band and Ku-band return service interference between TDRSS users p 677 N95-17183
Investigation of the effect of Alfven resonance absorption on fast wave current drive in ITER
[PB95-104352] p 894 N95-17929

SUPERNOVA REMNANTS
Very high gamma ray extension of GRO observations
[NASA-CR-197489] p 924 N95-17421

SUPERPLASTIC FORMING
Superplasticity and superplastic forming of ceramics
[DE94-016172] p 745 N95-16935

SUPERPLASTICITY
Superplasticity and superplastic forming of ceramics
[DE94-016172] p 745 N95-16935

SUPERSONIC COMBUSTION RAMJET ENGINES
Scramjet testing guidelines p 670 N95-16317
Combustor kinetic energy efficiency analysis of the hypersonic research engine data p 714 N95-16321

SUPERSONIC FLOW
In-flight imaging of transverse gas jets injected into transonic and supersonic crossflows: Design and development
[NASA-CR-186031] p 772 N95-17418
Detailed study at supersonic speeds of the flow around delta wings p 660 N95-17861
Wind tunnel investigations of the appearance of shocks in the windward region of bodies with circular cross section at angle of attack p 661 N95-17866
Supersonic vortex flow around a missile body p 661 N95-17870

SUPERSONIC INLETS
Time accurate computation of unsteady inlet flows with a dynamic flow adaptive mesh
[AD-A285498] p 771 N95-16736

SUPERSONIC SPEED
Numerical simulation of supersonic compression corners and hypersonic inlet flows using the RPLUS2D code
[NASA-TM-106580] p 654 N95-16038
Experimental study at low supersonic speeds of a missile concept having opposing wraparound tails
[NASA-TM-4582] p 655 N95-16069
Detailed study at supersonic speeds of the flow around delta wings p 660 N95-17861
Test data on a non-circular body for subsonic, transonic and supersonic Mach numbers p 662 N95-17871
Wind tunnel test on a 65 deg delta wing with a sharp or rounded leading edge: The international vortex flow experiment p 662 N95-17872

SUPERSONIC TRANSPORTS
Aerodynamic shape optimization p 668 N95-16572
Multi-lab comparison on R-curve methodologies: Alloy 2024-T3
[NASA-CR-195004] p 736 N95-16860

SUPERSONIC WIND TUNNELS
Free-jet testing at Mach 3.44 in GASL's aero/thermo test facility p 672 N95-16320

SUPERSYMMETRY
Multilepton SUSY signals from R-parity violation at the Tevatron (revised)
[PB95-104311] p 877 N95-17353
Relativistic effect of energy increase of a particle moving freely in vacuum from the quantum field theory point of view
[DE94-622757] p 903 N95-17473
Physics at high energy photon photon colliders
[DE94-018191] p 881 N95-17888
Flavor symmetries and fermion masses
[DE94-018192] p 878 N95-17889

SUPINE POSITION
Effect of antiorthostatic BedRest (BR) on GastroIntestinal Motility (GIM) of normal subjects p 811 N95-16753
Periodic upright posture negates the suppression of neuroendocrine response to head down bedrest p 817 N95-16780

SUPPORT SYSTEMS
GEOTRANS geographic decision support system
[PB94-183670] p 908 N95-16093
Student research projects, 1993
[AD-A284954] p 804 N95-16124
Improving production schedules without scheduling
[PB94-191350] p 904 N95-16289
A surgical support system for Space Station Freedom p 710 N95-16776
International Space Station Alpha user payload operations concept p 685 N95-17227
Evaluating modeling tools for the EDOS p 700 N95-17572
Analysis of space network loading p 701 N95-17578

SUPPORTS
Atomic oxygen durability evaluation of the flexible batten for the photovoltaic array mast on Space Station
[NASA-TM-106798] p 781 N95-17263

SURFACE CRACKS
Experimental application of methodologies to quantify the effect of constraint on JC for a 3-D flaw geometry
[AD-A285309] p 735 N95-16531
Raman spectroscopy of C-irradiated graphite
[DE94-018705] p 733 N95-17911

SURFACE DEFECTS
Structural analysis of solid-propellant rocket motors with and without flaws p 720 N95-16348

SURFACE DIFFUSION
Trenched bipolar transistor structures
[AD-D016406] p 767 N95-17463

SURFACE EMITTING LASERS
Phase-locked arrays of vertical-cavity surface-emitting lasers
[DE94-014941] p 778 N95-17498

SURFACE ENERGY
FIFE data analysis: Testing BIOME-BGC predictions for grasslands
[NASA-CR-197522] p 790 N95-16895

SURFACE FINISHING
Antenna dielectric sealing process characterization
[DE94-015864] p 747 N95-17690
Electron beam weld development on a Filter Pack Assembly
[DE94-015867] p 782 N95-17716

SURFACE GEOMETRY
Trenched bipolar transistor structures
[AD-D016406] p 767 N95-17463

SURFACE LAYERS
An X-Ray Photoelectron Spectroscopy (XPS) study of activated carbons impregnated with some organocopper complexes
[AD-A282721] p 727 N95-16384
Variation of the thermohaline structure in the western equatorial Pacific upper ocean p 805 N95-17277

SURFACE NAVIGATION
Towards a human operator model of the navigator
[PB94-197985] p 831 N95-17468

SURFACE PROPERTIES
Surface matching for correlation of virtual models: Theory and application p 853 N95-15983
Surface and defect excitations in covalently bonded solids
[AD-A281338] p 894 N95-16012
Interface properties of wide bandgap semiconductor structures
[AD-A281469] p 894 N95-16084
Physical properties (particle size, rock abundance) from thermal infrared remote observations: Implications for Mars landing sites p 918 N95-16182
Semiconductor heterojunction engineering
[AD-A281553] p 896 N95-16396
Auroral interactions with ISSA
[NASA-TM-106794] p 709 N95-16862
Revisions to an empirical surface loss model using a correction for pH-dependent attenuation
[AD-A285714] p 871 N95-17177
Scanning tunneling microscopy of 3 to 5 semiconductors
[AD-A281722] p 902 N95-17705

SURFACE REACTIONS
Resonant charge transfer in hyperthermal atomic and molecular ion-surface collisions
[AD-A281369] p 871 N95-16018
Gas-surface interactions near dissociation threshold
[AD-A284945] p 726 N95-16042
Augmentation for research training: Surface-mediated photocatalysis
[AD-A281591] p 722 N95-16100
In situ laser activation of electrochemical kinetics at carbon electrodes
[AD-A280892] p 727 N95-16150
Effect of ion-electrode contact on the energetics of the heterogeneous electron transfer
[AD-A281959] p 873 N95-16411
Self-assembly of low-dimensional conductors on Au(111) surfaces
[AD-A280936] p 734 N95-16505
Chemisorption energetics of superactive chlorine containing species on gallium arsenide surfaces
[AD-A281311] p 729 N95-16790
Giant flux creep through the surface barriers and the irreversibility line in high T(sub c) superconductors
[DE94-013991] p 766 N95-16945
Gas-surface interactions near dissociation threshold
[AD-A282726] p 730 N95-17140
Fundamental studies in oxidation-reduction in relation to water photolysis
[DE94-014598] p 731 N95-17161
Morphology and dynamics of membrane systems
[PB94-184660] p 745 N95-17299
Surfactant adsorption by sub-millimeter size bubbles: Quantification and modelling
[AD-A282405] p 772 N95-17506
Surftherm: A program to analyze thermochemical and kinetic data in gas-phase and surface chemical reaction mechanisms
[DE94-016145] p 733 N95-17744

SURFACE ROUGHNESS
Goldstone radar contributions to Mars Pathfinder landing safety p 921 N95-16205
Effective reflection coefficients for the mean acoustic field between two rough interfaces
[AD-A281962] p 870 N95-16413
Stability of separating subsonic boundary layers
[NASA-CR-4638] p 772 N95-17268
Precision machining and polishing of scintillating crystals for large calorimeters and hodoscopes
[DE94-012060] p 751 N95-17738

SURFACE ROUGHNESS EFFECTS
Rough surface models implemented within the split-step parabolic equation algorithm
[AD-A280843] p 753 N95-16148

SURFACE STABILITY
Reaction of methanol with porous silicon
[AD-A285518] p 728 N95-16406

SURFACE TEMPERATURE
Thermal control systems for low-temperature heat rejection on a lunar base
[NASA-CR-197486] p 830 N95-16418
Giant flux creep through the surface barriers and the irreversibility line in high T(sub c) superconductors
[DE94-013991] p 766 N95-16945

SURFACE TREATMENT
Initial design of a 1 megawatt average, 150 kilovolt pulse modulator for an industrial plasma source ion implantation processor
[DE94-014421] p 888 N95-16218
Preparation of Au single crystals for study of the ECALE deposition of CdTe
[AD-A282294] p 895 N95-16238

SURFACE VEHICLES
Estimation of vehicle dynamics from monocular noisy images
[AD-A281458] p 804 N95-16078

SURFACE WAVES
Development of an Automated Airfield Dynamic Cone Penetrometer (AADCP) prototype and the evaluation of unsurfaced airfield seismic surveying using Spectral Analysis of Surface Waves (SASW) technology
[AD-A281985] p 672 N95-17444

SURFACES
New methods for treatment of electron correlation and surface dynamics (FY91 AASERT)
[AD-A285177] p 727 N95-16144
Extraction of high quality potential surfaces from laboratory data
[AD-A285071] p 903 N95-16489

SURFACTANTS
Proceedings of the Workshop on Characterization of Molecular Assemblies
[DE94-753477] p 871 N95-15956
Surfactant adsorption by sub-millimeter size bubbles: Quantification and modelling
[AD-A282405] p 772 N95-17506

SURGERY
Simulation of arthroscopic surgery using MRI data p 823 N95-15975
Multimodal correlation and intraoperative matching of virtual models in neurosurgery p 823 N95-15976
A surgical support system for Space Station Freedom p 710 N95-16776

SURVEILLANCE
Implementation of a real-time data processing system for radar bandwidth extrapolation and stretch
[AD-A281195] p 754 N95-16794
Superresolution in a jammed radar signal environment
[PB94-190758] p 760 N95-17455

SURVEILLANCE RADAR
Solid state radar demonstration test results at the FAA Technical Center
[AD-A281520] p 752 N95-16097
Documentation of 9-PAC Beacon Target Detector processing function
[AD-A283090] p 759 N95-17336

SURVEYS
Bureau of the Census Center for International Research p 905 N95-15923
Electronic access to ONREUR/ONRAISIA S and T reports p 907 N95-15935
A survey of the software reuse environment: A study for the NSRS
[AD-A280867] p 834 N95-16149
Maturity questionnaire
[AD-A285073] p 836 N95-16490
Assessment of benefits and drawbacks of using fuzzy logic, especially in fire control systems
[AD-A285428] p 838 N95-16874
A review of transmission diagnostics research at NASA Lewis Research Center
[ARL-TR-599] p 781 N95-16907
An assessment of simulation systems applicable to business process reengineering at Army Directorates of Public Works
[AD-A285696] p 839 N95-17176
A survey of commercially available expendable heavy lift launch vehicles
[AD-A282429] p 676 N95-17509
Industry review of a crew-centered cockpit design process and toolset
[AD-A282966] p 669 N95-17661

SWEAT COOLING
The prediction of nozzle performance and heat transfer in hydrogen/oxygen rocket engines with transpiration cooling, film cooling, and high area ratios p 718 N95-16339

SWEDEN
The National Resource Library for Science and Technology in Sweden: A Nordic model of cooperating technology libraries p 906 N95-15929

SWEPT FORWARD WINGS
Investigation into the aerodynamic characteristics of a combat aircraft research model fitted with a forward swept wing p 664 N95-17884

SWEPT WINGS
Investigation of the flow development on a highly swept canard/wing research model with segmented leading- and trailing-edge flaps p 662 N95-17876

SWEPTBACK WINGS
Measurements of the flow over a low aspect-ratio wing in the Mach number range 0.6 to 0.87 for the purpose of validation of computational methods. Part 1: Wing design, model construction, surface flow. Part 2: Mean flow in the boundary layer and wake, 4 test cases p 660 N95-17860
Pressure distributions on research wing W4 mounted on an axisymmetric body p 660 N95-17862
DLR-F4 wing body configuration p 660 N95-17863
DLR-F5: Test wing for CFD and applied aerodynamics p 660 N95-17864
Delta-wing model p 662 N95-17873
Wind tunnel test on a 65 deg delta wing with rounded leading edges: The International Vortex Flow Experiment p 662 N95-17875

SWINGBY TECHNIQUE
Optimal transfer and swing-orbits in the two- and three-body problems
[INPE-5572-TAE/022] p 673 N95-17648

SWIRLING
On the prediction of free turbulent jets with swirl using a quadratic pressure-strain model
[NASA-CR-194964] p 769 N95-16071
Small-amplitude disturbances in turbomachine flows with swirl
[NASA-CR-195406] p 772 N95-17386

SWITCHES
Servo control using switches for discrete positional feedback
[AD-A284747] p 856 N95-16550
Picosecond optoelectronic AND-GATE
[AD-A285672] p 885 N95-16620
A high average power electro-optic switch using KTP
[DE94-016416] p 765 N95-16925
Recent advances in the development of high average power induction accelerators for industrial and environmental applications
[DE94-018734] p 882 N95-17914

SWITCHING CIRCUITS
Elimination of electromagnetic interference to receivers and sensitive equipment generated by switching systems
[AD-A281643] p 752 N95-16117
Demonstration of the Dynamic Flowgraph Methodology using the Titan 2 Space Launch Vehicle Digital Flight Control System
[NASA-CR-197517] p 675 N95-17493

SYMBOLS
CPP-TRS(C): On using visual cognitive symbols to enhance communication effectiveness p 761 N95-15991

SYMMETRY
Chiral recognition in molecular and macromolecular pairs of liquid crystals of (2R, 3S)- and (2S, 3S)-2-fluoro-3-methylpentyl-4'-(11-vinyloxyundeca iphenyl-4-carboxylate diastereomers
[AD-A281770] p 878 N95-17692

SYNAPSES
Synaptic plasticity and memory formation
[AD-A284926] p 825 N95-16138

SYNCHRONISM
Closed-loop carrier phase synchronization techniques motivated by likelihood functions p 756 N95-17284
ATM-test: A workstation-based software suite for testing Asynchronous Transfer Mode (ATM) networks
[DE94-013813] p 850 N95-17516
An x ray technique for precision laser beam synchronization
[DE94-016449] p 779 N95-17635

SYNCHRONOUS METEOROLOGICAL SATELLITE
Energy expenditure, physical work load and postural control during walking on a moving platform
[AD-A285343] p 830 N95-16821

SYNCHRONOUS PLATFORMS
Geostationary satellite positioning by DLR/GSOC operations and management methods p 684 N95-17217
The SILEX experiment system operations p 674 N95-17251
Mini All-purpose Satellite Control Center (MASCC) p 674 N95-17257

SYNCHROTRON RADIATION
Measurements of collective effects in the ALS
[DE94-017966] p 881 N95-17670

SYNOPTIC METEOROLOGY
Meteorological observations of synoptic disturbances: Sensitivity to latitude p 917 N95-16179

SYNTAX
Use of data description languages in the interchange of data p 704 N95-17597

SYNTHESIS (CHEMISTRY)
Synthesis of tungsten nitrene complexes as precursors for tungsten nitride
[AD-A281592] p 740 N95-16101
Synthesis of pure RDX
[DE94-014356] p 749 N95-16542
Materials for second and third order nonlinear optical applications
[AD-A281304] p 885 N95-16787
Design and synthesis of organic superconductors (FY92 URI/RIP)
[AD-A281308] p 899 N95-16789
Synthesis and properties of soluble oligo- and polyphenylenes. A review
[AD-A281293] p 874 N95-16799
X-ray crystal structure of a monomeric Tris(Arsino)Gallane, ((Me3Si)2As)3Ga)3Ga
[AD-A282343] p 900 N95-17171

SYNTHETIC APERTURE RADAR
Linear prediction data extrapolation superresolution radar imaging p 651 N95-16268
Detecting the number of targets in spatially colored noise using sampled aperture radars p 652 N95-16269
On the improvement of 1-look SAR image segmentations with mathematical morphology
[INPE-5577-PRE/1805] p 912 N95-17650
Synthetic aperture radar target detection, feature extraction, and image formation techniques
[NASA-CR-197485] p 760 N95-17651

SYNTHETIC APERTURES
Numerical aperture limits on efficient ball lens coupling of laser diodes to single-mode fibers with defocus to balance spherical aberration
[NASA-TM-4578] p 886 N95-17271

SYNTHETIC METALS
Design and synthesis of organic superconductors (FY92 URI/RIP)
[AD-A281308] p 899 N95-16789

SYSTEM FAILURES
Accountability for network backup failures
[DE94-011365] p 846 N95-16222
Bayesian nonparametric estimation via Gibbs sampling for coherent systems with redundancy
[AD-A283173] p 865 N95-17341

SYSTEM IDENTIFICATION
A new regularization approach in structural system identification p 651 N95-16262
Experimental study of spatially incomplete structural system identification
[AD-A280905] p 785 N95-16502

SYSTEMS ANALYSIS
Efficient estimation of the mean time between failures in non-regenerative dependability models
[AD-A281563] p 783 N95-16421
Qualitative vision and action
[AD-A282697] p 831 N95-16966
Demonstration of the Dynamic Flowgraph Methodology using the Titan 2 Space Launch Vehicle Digital Flight Control System
[NASA-CR-197517] p 675 N95-17493
Towards an integral computer environment supporting system operations analysis and conceptual design p 696 N95-17558
XMM instrument on-board software maintenance concept p 699 N95-17567
Integration of a satellite ground support system based on analysis of the satellite ground support domain p 675 N95-17568
Evaluating modeling tools for the EDOS p 700 N95-17572
Engineering design tools for wind diesel systems. Volume 1: Executive summary
[PB95-104501] p 842 N95-17733

SYSTEMS ENGINEERING
ARO-URI Center for Opto-Electronic Systems Research
[AD-A281447] p 883 N95-15958
Program test objectives milestone 3 --- Integrated Propulsion Technology Demonstrator
[NASA-CR-197030] p 666 N95-15971
Twin disc gear tooth simulator
[AD-A284927] p 780 N95-16139
Generalized method of solving topological optimization problems for electrical airplane equipment systems in computer-aided design p 652 N95-16272
The computer analysis of the prediction of aircraft electrical power supply system reliability p 653 N95-16278
Risk-Based Data Management System design specifications and implementation plan for the Alaska Oil and Gas Conservation Commission; the Mississippi State Oil and Gas Board; the Montana Board of Oil and Gas Conservation; and the Nebraska Oil and Gas Conservation Commission, attachment B
[DE94-013189] p 908 N95-16282
System design, implementation, and evaluation of the optical broadband correlator
[AD-A285406] p 884 N95-16296
Updated test results of a pumped monopropellant propulsion system p 713 N95-16315
The Role of Computers in Research and Development at Langley Research Center
[NASA-CP-10159] p 846 N95-16453
RDD-100 and the systems engineering process p 848 N95-16471
Computer tools for systems engineering at LaRC p 848 N95-16472
Hardware description languages p 832 N95-16477
Efficiency in work behaviour: A design approach for modern tools
[PB94-197761] p 831 N95-16953
An assessment of simulation systems applicable to business process reengineering at Army Directorates of Public Works
[AD-A285696] p 839 N95-17176
Third International Symposium on Space Mission Operations and Ground Data Systems, part 1
[NASA-CP-3281-PT-1] p 676 N95-17179
VLSI technology for smaller, cheaper, faster return link systems p 681 N95-17206
Mars Pathfinder mission operations concepts p 686 N95-17229
A modular electric power system test bed for small spacecraft
[NASA-TM-106812] p 721 N95-17276
Cooperative control theory and integrated flight and propulsion control
[NASA-CR-197493] p 671 N95-17404
Conceptual design of the Space Station combustion module
[NASA-TM-106788] p 675 N95-17419
Towards a human operator model of the navigator
[PB94-197985] p 831 N95-17468
Towards an integral computer environment supporting system operations analysis and conceptual design p 696 N95-17558
Evaluation of NASA's end-to-end data systems using DSDS+ p 700 N95-17577
Re-engineering NASA's space communications to remain viable in a constrained fiscal environment p 702 N95-17585
Packet utilisation definitions for the ESA XMM mission p 704 N95-17596

Matrix evaluation of science objectives
p 707 N95-17610
A new systems engineering approach to streamlined science and mission operations for the Far Ultraviolet Spectroscopic Explorer (FUSE) p 707 N95-17611
EDOS operations concept and development approach
p 708 N95-17613
Concurrent engineering: Spacecraft and mission operations system design p 708 N95-17614
Simulation investigation on system identification of gas turbine
[PB95-104238] p 670 N95-17749

SYSTEMS INTEGRATION
Metadata database for automated oceanographic imagery
[AD-A284932] p 805 N95-16141
Liquefied metal jet program Automation and Robotics Research Institute (ARRI)
[AD-A285470] p 736 N95-16878

SYSTEMS SIMULATION
A graphical environment for object-oriented simulation model environment
[NASA-CR-196887] p 833 N95-16088

T

TABLES (DATA)
Table-driven configuration and formatting of telemetry data in the Deep Space Network p 677 N95-17185

TACHOMETERS
Optical wheel-rotation sensor
[DE94-011719] p 780 N95-16224

TACTILE DISCRIMINATION
Vibratory tactile display for textures
p 851 N95-15973
A virtual work space for both hands manipulation with coherency between kinesthetic and visual sensation
p 831 N95-15984

TACTILE SENSORS (ROBOTICS)
ISMCR 1994: Topical Workshop on Virtual Reality. Proceedings of the Fourth International Symposium on Measurement and Control in Robotics
[NASA-CP-10163] p 851 N95-15972

TAIL ASSEMBLIES
Single-engine tail interference model
p 663 N95-17879
Twin engine afterbody model p 663 N95-17880

TAKEOFF
STOVL CFD model test case p 663 N95-17881

TANK TRUCKS
Metallurgical examination of failed T-158 Cast Austempered Ductile Iron (CADI) track shoes
[AD-A282433] p 737 N95-17486

TANTALUM ALLOYS
The influence of tungsten alloying on the mechanical properties of tantalum
[DE94-010071] p 736 N95-17378

TARGET ACQUISITION
Detecting the number of targets in spatially colored noise using sampled aperture radars p 652 N95-16269
Dynamics of the G-excess illusion
p 815 N95-16771
Perceptual selectivity for color and form: On the nature of the interference effect
[AD-A285338] p 827 N95-16817
Adaptive line enhancers for fast acquisition
p 757 N95-17287
An opportunity analysis system for space surveillance experiments with the MSX p 707 N95-17609
Synthetic aperture radar target detection, feature extraction, and image formation techniques
[NASA-CR-197485] p 760 N95-17651

TARGET MASKING
Parallel implementation of the terrain masking algorithm
[AD-A281017] p 833 N95-16003

TARGET RECOGNITION
Event-related brain potentials as predictors of target detection performance in a moving waterfall display simulating passive broad-band sonar monitoring
[AD-A280900] p 819 N95-16152
Log-polar optical coordinate transformation with applications for automatic pattern recognition
[AD-A281022] p 885 N95-16443
Implementation of a real-time data processing system for radar bandwidth extrapolation and stretch
[AD-A281195] p 754 N95-16794
Sensor placement design for object pose determination with three light-stripe range finders
[AD-A281199] p 886 N95-16795
Mission planning for space based satellite surveillance experiments with the MSX p 673 N95-17212
Documentation of 9-PAC Beacon Target Detector processing function
[AD-A283090] p 759 N95-17336

TARGETS
Climatological targets for Mars Pathfinder
p 922 N95-16208
Production asymmetries in x(sub F) and P(sub t)(exp 2) for D(+-) mesons
[DE94-015546] p 872 N95-16310
Perceptual selectivity for color and form: On the nature of the interference effect
[AD-A285338] p 827 N95-16817
Parallel search for a conjunction of shape and contrast polarity
[AD-A285344] p 827 N95-16822
Proceedings of the 12th Space Surveillance Workshop, volume 2
[AD-A285115] p 672 N95-16842
Penetration of solid and layered targets by gas gun-launched steel cubes
[AD-A285143] p 787 N95-16843
A-dependent effects in high P(sub T) reactions
[DE94-016385] p 875 N95-16924
Intense ion beam optimization and characterization with thermal imaging
[DE94-016184] p 891 N95-16936
Progress at LAMPF
[DE94-016210] p 880 N95-16937
Intense ion beam characterization and thermal modeling for beam materials processing
[DE94-016281] p 745 N95-16938
Superresolution in a jammed radar signal environment
[PB94-190758] p 760 N95-17455
An x ray technique for precision laser beam synchronization
[DE94-016449] p 779 N95-17635

TASK COMPLEXITY
Application of research techniques for documenting cognitive processes in air traffic control: Sector complexity and decision making
[AD-A282336] p 665 N95-16375

TASK PLANNING (ROBOTICS)
The Yale Knowledge-Based Planning project
[AD-A281505] p 855 N95-16095
On performability theory and the inverse sliding problem
[AD-A282847] p 782 N95-17430

TASKS
Estimating the benefits of personnel selection and classification: An extension of the Brogden table
[AD-A285674] p 828 N95-17175

TAXONOMY
Investigations of asteroid family geology
p 917 N95-17393

TDR SATELLITES
S-band and Ku-band return service interference between TDRSS users p 677 N95-17183
Demand access communications for TDRSS users
p 677 N95-17187
The GRO remote terminal system
p 678 N95-17188
Accuracy analysis of TDRSS demand forecasts
p 683 N95-17214
GRTS operations monitor/control system
p 685 N95-17226
TDRS orbit determination by radio interferometry
p 673 N95-17547

TECHNICAL WRITING
Scientific and technical publishing at Goddard Space Flight Center in Fiscal Year 1994
[NASA-TM-104614] p 925 N95-16581
ICASE
[NASA-CR-195001] p 832 N95-16898

TECHNOLOGIES
Informatics in Turkey p 905 N95-15921
Electronic access to ONREUR/ONRAISIA S and T reports p 907 N95-15935
AINSE Plasma Science and Technology Conference and Elizabeth and Frederick White Workshop on Fundamental Problems in the Physics of Magnetically Confined Plasmas: Conference handbook
[DE94-622051] p 892 N95-17517

TECHNOLOGY ASSESSMENT
An introduction to intelligent networks
[AD-A284284] p 752 N95-16123
Optoelectric technology roadmap: Conclusions and recommendations
[AD-A281664] p 886 N95-16965
Solar energy: Lessons from the Pacific island experience
[WORLD-BANK-TP-244] p 794 N95-17298
High-average-power, diode-pumped solid state lasers for energy and industrial applications
[DE94-015142] p 779 N95-17689

TECHNOLOGY TRANSFER
Use of World Wide Web and NCSA Mosaic at Langley
p 847 N95-16464
From computer images to video presentation: Enhancing technology transfer p 848 N95-16467
Current research activities at the NASA-sponsored Illinois Computing Laboratory of Aerospace Systems and Software p 849 N95-16479
The Software Technology Center at Lawrence Livermore National Laboratory: Software engineering technology transfer in a scientific R/D laboratory
[DE94-014794] p 836 N95-16536

TECHNOLOGY UTILIZATION
The future of interaction on the Internet
p 906 N95-15931
Program test objectives milestone 3 --- Integrated Propulsion Technology Demonstrator
[NASA-CR-197030] p 666 N95-15971
Videoconferencing and its role in the Army
[AD-A282707] p 909 N95-16305
Foam inflated rigidized structures for space applications p 710 N95-16344
Overview of photonics research at Lawrence Livermore National Laboratory
[DE94-014055] p 884 N95-16366
Revitalizing general aviation
[NASA-TM-110113] p 669 N95-16982
Optical fiber sensors: Accelerating applications in Navy ships
[PB94-186848] p 887 N95-17441
Small sample behavior of multi-layer feedforward network classifiers: Theoretical and practical aspects
[PB94-201415] p 841 N95-17470
Electro-separations: Efficient processing for the twenty-first century
[DE94-012656] p 732 N95-17524
Mission Operations Centers (MOCs): Integrating key spacecraft ground data system components
p 675 N95-17601

TECTONICS
Melas Chasma: A Mars Pathfinder view of Valles Marineris p 922 N95-16207
Evaluation of current tropospheric mapping functions by Deep Space Network very long baseline interferometry
p 756 N95-17280

TEFLON (TRADEMARK)
Space Shuttle reaction control system thruster metal nitrate removal and characterization
p 716 N95-16332

TELECOMMUNICATION
Tele Hyper Virtuality p 853 N95-15982
Telecommunications end-to-end systems monitoring on TOPEX/Poseidon: Tools and techniques
p 676 N95-17180
Geostationary satellite positioning by DLR/GSOC operations and management methods
p 684 N95-17217
Mini All-purpose Satellite Control Center (MASCC)
p 674 N95-17257
The Telecommunications and Data Acquisition Report
[NASA-CR-197249] p 755 N95-17279
Space VLBI telecommunication characteristics, protection criteria, and frequency sharing
p 756 N95-17282
NCCDS performance model p 675 N95-17576
The Requirements Generation System: A tool for managing mission requirements p 707 N95-17608

TELECONFERENCING
Videoconferencing and its role in the Army
[AD-A282707] p 909 N95-16305
An analysis of Internet's MBONE: A media choice perspective
[AD-A285514] p 910 N95-16972

TELEMETRY
Telecommunications end-to-end systems monitoring on TOPEX/Poseidon: Tools and techniques
p 676 N95-17180
Earth Observing System (EOS) Communication (Ecom) Modeling, Analysis, and Testbed (EMAT) activiy
p 677 N95-17182
Table-driven configuration and formatting of telemetry data in the Deep Space Network p 677 N95-17185
Use of a multimission system for cost effective support of planetary science data processing
p 678 N95-17190
A second generation 50 Mbps VLSI level zero processing system prototype p 678 N95-17191
A low-cost transportable ground station for capture and processing of direct broadcast EOS satellite data
p 680 N95-17200
Applications of massively parallel computers in telemetry processing p 680 N95-17201
Test Telemetry And Command System (TTACS)
p 680 N95-17202
Ground equipment for the support of packet telemetry and telecommand p 681 N95-17203
Process and methodology of developing Cassini G and C Telemetry Dictionary p 681 N95-17204
Multimission Telemetry Visualization (MTV) system: A mission applications project from JPL's Multimedia Communications Laboratory p 681 N95-17205

VLSI technology for smaller, cheaper, faster return link systems p 681 N95-17206
Telemetry distribution and processing for the second German Spacelab Mission D-2 p 681 N95-17207
Experience with the EURECA Packet Telemetry and Packet Telecommand system p 682 N95-17209
Galileo mission planning for Low Gain Antenna based operations p 682 N95-17210
Graphic Server: A real time system for displaying and monitoring telemetry data of several satellites p 687 N95-17238
Mission operations data analysis tools for Mars Observer guidance and control p 689 N95-17244
Generic trending and analysis system p 689 N95-17245
A graphic system for telemetry monitoring and procedure performing at the Telecom SCC p 689 N95-17246
A simplified Integer Cosine Transform and its application in image compression p 757 N95-17286
Tracking the Galileo spacecraft with the DSCC Galileo Telemetry prototype p 708 N95-17292
The Pacor 2 expert system: A case-based reasoning approach to troubleshooting p 693 N95-17541
Simplifying operations with an uplink/downlink integration toolkit p 697 N95-17562
OOD/OOP experience in the Science Operations Center part of the ground system for X ray Timing Explorer mission p 675 N95-17565
Galileo spacecraft modeling for orbital operations p 700 N95-17574
The Advanced Orbiting Systems Testbed Program: Results to date p 700 N95-17575
Test/score/report: Simulation techniques for automating the test process p 675 N95-17581
Configurable technology development for reusable control and monitor ground systems p 675 N95-17589
A new communication protocol family for a distributed spacecraft control system p 703 N95-17590
The ESA standard for telemetry and telecommand packet utilisation: PUS p 704 N95-17595
Packet utilisation definitions for the ESA XMM mission p 704 N95-17596
The CCSDS return all frames Space Link Extension service p 705 N95-17599
Risk reduction methodologies and technologies for the Earth Observing System (EOS) Operations Center (EOC) p 707 N95-17612
EDOS operations concept and development approach p 708 N95-17613

TELEOPERATORS
ISMCR 1994: Topical Workshop on Virtual Reality. Proceedings of the Fourth International Symposium on Measurement and Control in Robotics
[NASA-CP-10163] p 851 N95-15972
Coordinated control of a dual-arm dexterous robot using full immersion telepresence and virtual reality p 852 N95-15979
Master-slave system with force feedback based on dynamics of virtual model p 853 N95-15985
Thermal feedback in virtual reality and telerobotic systems p 854 N95-15987

TELEPHONES
Handbook for users
[AD-A285148] p 909 N95-16845

TELEPHONY
An introduction to intelligent networks
[AD-A284284] p 752 N95-16123

TELEROBOTICS
Virtual reality and telerobotics applications of an Address Recalculation Pipeline p 852 N95-15977
Coordinated control of a dual-arm dexterous robot using full immersion telepresence and virtual reality p 852 N95-15979
Thermal feedback in virtual reality and telerobotic systems p 854 N95-15987
Telemetry distribution and processing for the second German Spacelab Mission D-2 p 681 N95-17207

TELESCOPES
NASA Marshall Space Flight Center Solar Observatory report, March - May 1994
[NASA-TM-108471] p 915 N95-16558
Issues in the design and optimization of adaptive optics and laser guide stars for the Keck Telescopes
[DE94-012868] p 916 N95-17525
A high resolution liquid xenon imaging telescope for 0.3-10 MeV gamma-ray astrophysics: Construction and initial balloon flights
[NASA-CR-197556] p 916 N95-17528

TELLURIUM
New approaches to novel organosilanes
[AD-A285253] p 722 N95-16513

TEMPERATURE CONTROL
Natural convection cooling of a three by three array of leadless chip carrier packages in a dielectric liquid
[AD-A282296] p 770 N95-16239
An engineering code to analyze hypersonic thermal management systems p 715 N95-16322
Thermal control systems for low-temperature heat rejection on a lunar base
[NASA-CR-197486] p 830 N95-16418
Overview of space power electronic's technology under the CSTI High Capacity Power Program
[NASA-TM-110110] p 883 N95-17933

TEMPERATURE DEPENDENCE
Muon(+) SR studies of magnetic properties of boron carbide superconductors
[DE94-014440] p 868 N95-16288
Positron annihilation studies of defects in molecular beam epitaxy grown 3 to 5 layers
[DE94-015823] p 899 N95-16918
Modeling mesons with relativistic wave equations
[DE94-016057] p 875 N95-16931
Modelling daily precipitation as a function of temperature for climate change impact studies
[KNMI-WR-93-02] p 802 N95-17529
Recent changes of weather patterns in North America
[DE94-016115] p 803 N95-17743

TEMPERATURE DISTRIBUTION
Landing site considerations for atmosphere structure and meteorology p 921 N95-16203
ARCJET plasma modeling with experimental validation
[AD-A285234] p 889 N95-16243
Charging hydrogen into Ni in hydride-containing molten salts
[AD-A282335] p 730 N95-16973
The effects of the horizontal resolution of the boundary forcing sea surface temperature field on the FSU spectral model
[AD-A284273] p 802 N95-17488

TEMPERATURE EFFECTS
Mechanical effects in cookoff modeling
[DE94-014174] p 748 N95-16214
Global and near tip response of cracked solid propellant p 715 N95-16325
Innovative acoustic techniques for studying new materials and new developments in solid state physics
[AD-A280986] p 898 N95-16525
Skin blood flow and bioelectrical impedance
[AD-A285475] p 821 N95-16619
Picosecond optoelectronic AND-GATE
[AD-A285672] p 885 N95-16620
Effects of substrate temperature on metal colloid formation and on optical response in metal ion implanted silica
[DE94-013633] p 736 N95-16807
Static and dynamic friction behavior of candidate high temperature airframe seal materials
[NASA-TM-106571] p 722 N95-16905
Modeling mesons with relativistic wave equations
[DE94-016057] p 875 N95-16931
Thermal effects in end-heated laser rods: A time-dependent model and diagnostic
[AD-A282007] p 778 N95-17500
Modelling daily precipitation as a function of temperature for climate change impact studies
[KNMI-WR-93-02] p 802 N95-17529
Materials degradation and fatigue under extreme conditions
[AD-A282969] p 746 N95-17662
Effect of heat treatment temperature on creep-rupture properties of Fe3Al-based alloys
[DE94-018054] p 738 N95-17679
Environmental effects on iron aluminide
[DE94-017900] p 739 N95-17747

TEMPERATURE GRADIENTS
Computational simulation of the formation and material behavior of ice
[NASA-TM-106702] p 785 N95-16416
Thermoacoustic pin stacks
[AD-A282267] p 794 N95-16954
Thermal analysis of a functionally graded material subject to a thermal gradient using the boundary element method
[NASA-TM-106801] p 789 N95-17658

TEMPERATURE MEASUREMENT
Papers presented at the Tenth Topical Conference on High-Temperature Plasma Diagnostics
[DE94-015854] p 888 N95-16063
Design of thermocouple probes for measurement of rocket exhaust plume temperatures
[AD-A285423] p 774 N95-16247
Evaluation of a new miniature temperature data logger: Herpetological review
[DE94-013561] p 774 N95-16804
Calorimetric methods for loss measurements of small cage induction motors
[PB94-184439] p 768 N95-17691

TEMPERATURE MEASURING INSTRUMENTS
Evaluation of a new miniature temperature data logger: Herpetological review
[DE94-013561] p 774 N95-16804

TEMPERATURE PROFILES
Mixed-layer hindcasts conducted at OWS Victor with initialization from synthetic profiles/mixed-layer hindcasts conducted with BTs taken during 1990 with atmospheric forcing from NOGAPS
[AD-A284749] p 800 N95-16551
Modeling of chemical vapor infiltration for composite fabrication
[DE93-001715] p 724 N95-16926
The mass and dynamics of cD clusters with cooling flows. 1: ROSAT observations of A 496
[NASA-CR-197534] p 915 N95-17495

TEMPERATURE SENSORS
Thermal feedback in virtual reality and telerobotic systems p 854 N95-15987

TEMPORAL DISTRIBUTION
Breaking down barriers in cooperative fault management: Temporal and functional information displays
[NASA-CR-197450] p 857 N95-17383

TEMPORAL LOGIC
On computing the minimal labels in time point algebra networks
[TR-495] p 859 N95-16022
Actions and events in interval temporal logic
[TR-521] p 839 N95-16883
Real-time symbolic model checking for discrete time models
[AD-A282878] p 864 N95-17618

TEMPORAL RESOLUTION
Ultrafast scanning probe microscopy
[DE94-018186] p 779 N95-17887

TENDONS
Variability in Hoffmann and tendon reflexes in healthy male subjects p 808 N95-16739
Achilles Tendon Reflex (ATR) in response to short exposures of microgravity and hypergravity p 812 N95-16756

TENSILE PROPERTIES
The mechanical property data base from an Air Force/industry cooperative test program on high temperature aluminum alloys
[AD-A282911] p 737 N95-17398

TENSILE STRENGTH
Experimental heat treatment of beryllium copper alloy
[AD-A282714] p 734 N95-16380

TENSILE TESTS
Global and near tip response of cracked solid propellant p 715 N95-16325

TENSOR ANALYSIS
Single-pass method for the solution of inverse potential and rotational problems. Part 1: 2-D and quasi 3-D theory and application p 664 N95-16563

TENSORS
Some fundamental techniques in the theory of integrable systems
[PB94-192390] p 860 N95-16294

TERMINAL BALLISTICS
Material and ballistic investigation of a tungsten-26 percent rhenium alloy
[PB94-189156] p 734 N95-16420

TERMINAL GUIDANCE
Autonomous weapon guidance
[AD-A282715] p 671 N95-16381

TERMINOLOGY
Introduction to the World Wide Web and Mosaic p 847 N95-16463
A survey of program slicing for software engineering
[NASA-CR-193116] p 836 N95-16574
Department of Defense dictionary of military and associated terms. Includes US acronyms and abbreviations and NATO terms (English only)
[AD-A283218] p 912 N95-17633

TERRAIN
Parallel implementation of the terrain masking algorithm
[AD-A281017] p 833 N95-16003
Estimation of vehicle dynamics from monocular noisy images
[AD-A281458] p 804 N95-16078
Observations by the Mars 1994 orbiter and possible correlations with Mars Pathfinder p 920 N95-16192
Tartarus Colles: A sampling of the Martian highlands p 920 N95-16195
Scientific rationale for selecting northwest Isidis Planitia (14 deg - 17 deg N latitude, 278 deg - 281 deg longitude) as a potential Mars Pathfinder landing site p 920 N95-16197
Graphical simulation of articulated rigid body system kinematics with collision detection
[AD-A281842] p 856 N95-16372
Full color recorder
[AD-A282278] p 790 N95-17372

An investigation of small-scale variations in cloud climatology induced by topography and monthly mean winds
[AD-A283274] p 803 N95-17715

TERRAIN ANALYSIS
Site characterization at the Rabbit Valley Geophysical Performance Evaluation Range
[DE94-013550] p 798 N95-16284
Digital mapping, charting, and geodesy analysis program technical review of interim terrain analysis data set prototype 1
[AD-A284742] p 790 N95-16547
FIFE data analysis: Testing BIOME-BGC predictions for grasslands
[NASA-CR-197522] p 790 N95-16895
Steps toward terrain knowledge acquisition
[AD-A282667] p 790 N95-17375
Rheology and structure of planetary near-surface materials from landform topography p 922 N95-17392
Representation, modeling and recognition of outdoor scenes
[AD-A283257] p 858 N95-17634

TEST FACILITIES
Continuing life test of a xenon hollow cathode for a space plasma contactor
[NASA-CR-195401] p 711 N95-15968
Development of the vibration test equipment for testing the products of aircraft and space technology with simulation of operating conditions p 651 N95-16266
Non-linear acoustics in fluids and gels
[PB94-201308] p 870 N95-16614
Experimental and analytical methods for the determination of connected-pipe ramjet and ducted rocket internal performance
[AGARD-AR-323] p 721 N95-17278

TEST FIRING
Program test objectives milestone 3 --- Integrated Propulsion Technology Demonstrator
[NASA-CR-197030] p 666 N95-15971

TEST STANDS
Diffusion weld test fixture
[AD-D016450] p 780 N95-16543
Experimental validation of an integrated controls-structures design methodology for a class of flexible space structures
[NASA-TP-3462] p 709 N95-16857

TETHERED SATELLITES
Radar observations of field-aligned plasma propagations associated with NASA's PMG experiment
[AD-A285218] p 798 N95-16521

TETHERLINES
Artificial gravity: How much, how often, how long?
p 816 N95-16778

TEXTILES
Design and technical support for development of a molded fabric space suit joint
[NASA-CR-197521] p 831 N95-16894

TEXTS
CPP-TRS(C): On using visual cognitive symbols to enhance communication effectiveness
p 761 N95-15991

TEXTURES
Vibratory tactile display for textures
p 851 N95-15973
Applied virtual reality at the Research Triangle Institute p 851 N95-15974
Texture analysis of critical current density in Bi2Sr2CaCu2O(x) tapes
[DE94-018375] p 902 N95-17898

THEOREM PROVING
On computing the minimal labels in time point algebra networks
[TR-495] p 859 N95-16022
A computational logic for applicative common Lisp
[AD-A283103] p 840 N95-17338

THEOREMS
NP-sets are Co-NP-immune relative to a random oracle
[TR-501] p 859 N95-15950
Nonstationary theory of mode competition in gyrotrons with allowance for inhomogeneity of the guiding magnetic field
[PB94-197621] p 869 N95-17467
Cellular automata for contour dynamics
[PB94-197613] p 865 N95-17526

THEORETICAL PHYSICS
High Energy Physics Division research activities
[DE94-015024] p 882 N95-17924

THERMAL ANALYSIS
ARCJET plasma modeling with experimental validation
[AD-A285234] p 889 N95-16243
Synthesis of polyphenylenes and polynaphthalenes by thermolysis of enediynes and dialkynylbenzenes
[AD-A281294] p 743 N95-16783
Thermal analysis of a functionally graded material subject to a thermal gradient using the boundary element method
[NASA-TM-106801] p 789 N95-17658

THERMAL CONDUCTIVITY
A high average power electro-optic switch using KTP
[DE94-016416] p 765 N95-16925
Workshop on Characterizing Diamond Films, 3
[PB94-187663] p 747 N95-17722

THERMAL CYCLING TESTS
WPH-6112A thermal expansion test of PRESS tubulation
[DE94-015946] p 782 N95-17717

THERMAL DECOMPOSITION
Polymeric precursors to binary inorganic materials
[AD-A281010] p 739 N95-16000

THERMAL DIFFUSION
Testing and evaluation of oxide-coated iridium/rhenium chambers p 719 N95-16346
Process of making a bistable photoconductive component
[AD-D016449] p 764 N95-16539
Diffusion weld test fixture
[AD-D016450] p 780 N95-16543

THERMAL DISSOCIATION
Thermal dissociation of halogen azides
[AD-A285088] p 728 N95-16497

THERMAL EMISSION
Dust near luminous ultraviolet stars
[NASA-CR-197108] p 916 N95-16032

THERMAL ENERGY
Plasma disruption modeling and simulation
[DE94-015095] p 889 N95-16307
Solar-powered rocket engine optimization for high specific impulse p 718 N95-16341
Thermal and laser conditioning of production and rapid-growth KDP and KD*P crystals
[DE94-013738] p 902 N95-17742

THERMAL EXPANSION
Thermal and mechanical behavior of Ba(1+x)Zr4P(6-2x)Si(2x)O24
[DE94-013620] p 899 N95-16806
Relationships between ferroelectric 90 deg domain formation and electrical properties of chemically prepared Pb(Zr,Ti)O3 thin films
[DE94-015274] p 744 N95-16829
WPH-6112A thermal expansion test of PRESS tubulation
[DE94-015946] p 782 N95-17717

THERMAL FATIGUE
Structurally-compliant rocket engine combustion chamber: Experimental/analytical validation
p 718 N95-16337

THERMAL INSULATION
Thermal chemical energy of ablating silica surfaces in air breathing solid rocket engines p 714 N95-16316

THERMAL MAPPING
Models to estimate high frequency acoustic scattering due to thermal fine- and micro-structure of the ocean
[AD-A285456] p 870 N95-16812
Intense ion beam optimization and characterization with thermal imaging
[DE94-016184] p 891 N95-16936
Operational cloud classifier based on a self-organized feature map
[PB94-197852] p 802 N95-17504

THERMAL NOISE
Thermal noise in biomagnetic measurements
[PB95-104360] p 869 N95-17930

THERMAL PLASMAS
ROSAT detection of diffuse hot gas in the edge-on galaxy NGC 4631
[NASA-CR-197535] p 915 N95-17496

THERMAL PROTECTION
Thermal chemical energy of ablating silica surfaces in air breathing solid rocket engines p 714 N95-16316

THERMAL RADIATION
High altitude hypersonic flowfield radiation
[AD-A281386] p 655 N95-16160
Plasma disruption modeling and simulation
[DE94-015095] p 889 N95-16307
Analysis of infrared scaling laws
[AD-A285461] p 903 N95-16877

THERMAL SHOCK
Testing and evaluation of oxide-coated iridium/rhenium chambers p 719 N95-16346

THERMAL STABILITY
High performance dielectric materials development
p 712 N95-16057
Thermoplastic and thermosetting high glass transition temperature matrix resins
[AD-A281508] p 740 N95-16096
Performance study of galactic cosmic ray shield materials
[NASA-TP-3473] p 924 N95-16912
Research on organofluorine chemistry for 700 F thermooxidative stability
[AD-A282767] p 731 N95-17142

THERMAL STRESSES
Guide to ASIAC computer programs
[AD-A285354] p 784 N95-15953
Shock and thermal history of iron and chondritic meteorites
[NASA-CR-197125] p 916 N95-16020
Heat stress and a countermeasure in the Shuttle rescueman's suit p 809 N95-16746
Modeling of thermal stresses in welds
[DE94-018046] p 789 N95-17675
WPH-6112A thermal expansion test of PRESS tubulation
[DE94-015946] p 782 N95-17717

THERMIONIC DIODES
Control of a large vacuum wave precursor on the SABRE voltage adder MITL and extraction ion diode
[DE94-014280] p 888 N95-16216

THERMIONIC EMISSION
High current density sheet-like electron beam generator
[AD-A281975] p 880 N95-17499

THERMISTORS
Evaluation of a new miniature temperature data logger: Herpetological review
[DE94-013561] p 774 N95-16804

THERMOCHEMICAL PROPERTIES
Design, analysis, and fabrication of oxide-coated iridium/rhenium combustion chambers
p 719 N95-16347

THERMOCHEMISTRY
Thermal chemical energy of ablating silica surfaces in air breathing solid rocket engines p 714 N95-16316
Surftherm: A program to analyze thermochemical and kinetic data in gas-phase and surface chemical reaction mechanisms
[DE94-016145] p 733 N95-17744

THERMOCOUPLES
Design of thermocouple probes for measurement of rocket exhaust plume temperatures
[AD-A285423] p 774 N95-16247

THERMODYNAMIC EQUILIBRIUM
Study of the structuring of pure molecular liquids
[PB94-201316] p 903 N95-16839

THERMODYNAMIC PROPERTIES
Anisotropic heat exchangers/stack configurations for thermoacoustic heat engines
[AD-A280974] p 792 N95-16506
Single-pass method for the solution of inverse potential and rotational problems. Part 1: 2-D and quasi 3-D theory and application p 664 N95-16563
Single-pass method for the solution of inverse potential and rotational problems. Part 2: Fully 3-D potential theory and applications p 664 N95-16564
Structural integrity of intelligent materials and structures. Constitutive modeling of shape memory alloys
[AD-A281301] p 735 N95-16788
Thermoacoustic pin stacks
[AD-A282267] p 794 N95-16954

THERMODYNAMICS
Theory of one-dimensional and two-dimensional distributed sensors for measuring the spatial characteristics of thermophysical and hydrodynamic fields p 652 N95-16273
Design, analysis, and fabrication of oxide-coated iridium/rhenium combustion chambers
p 719 N95-16347
The solvation thermodynamic functions in the Mean Spherical Approximation (MSA): Behavior near the solvent critical region
[AD-A283040] p 904 N95-17712
CHEETAH 1.0 user's manual
[DE94-014727] p 749 N95-17919

THERMOELASTICITY
Thermoelasticity analysis of laminated plates and shells using hybrid-stress elements p 651 N95-16263

THERMOELECTRICITY
Thermal feedback in virtual reality and telerobotic systems p 854 N95-15987

THERMONUCLEAR REACTIONS
Tokamak Transmutation of (nuclear) Waste (TTW): Parametric studies
[DE94-012891] p 881 N95-17721

THERMOPHYSICAL PROPERTIES
Alternatives for ozone-depleting refrigerants
[PB94-190857] p 795 N95-16881

THERMOPLASTIC RESINS
Thermoplastic and thermosetting high glass transition temperature matrix resins
[AD-A281508] p 740 N95-16096
Impact vulnerability of thermoplastic-matrix composites
[PB94-201274] p 745 N95-17305

THERMOREGULATION
An annotated bibliography of heat tolerance: Regarding gender differences
[AD-A280755] p 818 N95-16105
Increased skin blood flow and enhanced heat loss in humans after niacin ingestion
[AD-A281124] p 821 N95-16809

THERMOSETTING RESINS
Thermoplastic and thermosetting high glass transition temperature matrix resins
[AD-A281508] p 740 N95-16096
Synthesis and characterization of a new class of thermosetting resins: Allyl and propargyl substituted cyclopentadiene derivatives
[AD-A281976] p 746 N95-17485

THICK FILMS
Ceramic/metal composite circuit-board-level technology for Application Specific Electronic Modules (ASEMs)
[AD-A285066] p 741 N95-16369

THICKNESS
A new manufacturing method for the formation of gated field emission structures
[DE94-015287] p 764 N95-16832

THIN AIRFOILS
Wing-body juncture flows
[AD-A281526] p 655 N95-16099

THIN FILMS
Anionically-conductive ultrathin film composite membranes
[AD-A284944] p 723 N95-16041
Synthesis of tungsten nitrene complexes as precursors for tungsten nitride
[AD-A281592] p 740 N95-16101
Electron transport and tunneling experiments
[AD-A281527] p 894 N95-16106
Single crystal films and waveguides of organic materials: Preparation and nonlinear optical properties
[AD-A284471] p 895 N95-16134
Electrochemical atomic layer processing
[AD-A282330] p 872 N95-16241
Ion beam generation and propagation for plasma processing applications
[DE94-014428] p 889 N95-16286
Prediction of the response of a polyimide concentrator for solar thermal propulsion p 719 N95-16343
Deformation behavior of thin lubricant films at elevated pressure
[AD-A281848] p 741 N95-16355
Research on stable, high-efficiency amorphous-silicon multijunction modules
[DE94-011839] p 764 N95-16425
Nonlinear optical and charge distribution studies probing electric field effects in polymer thin films for second order nonlinear optics
[AD-A280980] p 742 N95-16483
The deposition of electro-optic films on semiconductors
[AD-A285068] p 742 N95-16488
Electrochemical synthesis of ultrathin film composite membranes
[AD-A285075] p 724 N95-16492
Atomic layer epitaxy of group 4 materials: Surface processes, thin films, devices and their characterization
[AD-A280987] p 898 N95-16532
Nitride semiconductors for ultraviolet detection
[AD-A280988] p 898 N95-16533
Theoretical study of cathode surfaces and high-temperature superconductors
[NASA-CR-195407] p 898 N95-16598
Low temperature deposition and characterization of N- and P-type silicon carbide thin films and associated ohmic and Schottky contacts
[AD-A281060] p 743 N95-16625
A novel optic bistable device with very low threshold intensity using photorefractive films
[AD-A285310] p 885 N95-16733
Relationships between ferroelectric 90 deg domain formation and electrical properties of chemically prepared Pb(Zr,Ti)O3 thin films
[DE94-015274] p 744 N95-16829
Epitaxial MOCVD of thin film ceramics for pyroelectric detectors
[AD-A281397] p 744 N95-16863
Structure-property relationships in sol-gel-derived thin films
[DE94-016149] p 744 N95-16934
Intense ion beam characterization and thermal modeling for beam materials processing
[DE94-016281] p 745 N95-16938
Development of high-efficiency, thin-film CdTe solar cells
[DE94-011885] p 794 N95-16940
Applications of positron depth profiling
[PB94-197753] p 900 N95-16952
The m-line method for optical characterisation of polymer waveguides
[PB94-184611] p 887 N95-17409
Volatile CVD precursors based on copper alkoxides and mixed group IIA-copper alkoxides
[AD-D016380] p 732 N95-17479
Preparation and investigation of improved low voltage electron excitable phosphors
[AD-A284265] p 767 N95-17487
Ion modulated electroactivity in thin-film polymers derived from bipyridyl and phenanthroline complexes of iron
[AD-A280704] p 747 N95-17682
Thin film superconductors
[DE94-018585] p 902 N95-17906

THIN WALLED SHELLS
Development of strength analysis methods and design model for aircraft constructions in Kazan Aviation Institute p 651 N95-16264

THIN WALLS
Development of processes, means, and theoretical principles of thin-walled detail plastic forming at Kazan Aviation Institute p 653 N95-16281
Testing and evaluation of oxide-coated iridium/rhenium chambers p 719 N95-16346

THIOLS
Cyclic voltammetric analysis of ferrocene alkanethiol monolayer electrode kinetics based on Marcus theory
[AD-A281411] p 868 N95-16162

THOMSON SCATTERING
Alpha particle kinetics in ignited fusion plasmas: Design applications for a CO2 laser Thomson scattering experiment
[DE94-016297] p 890 N95-16921
Design of a CO2-laser Thomson scattering ion-tail diagnostic for Alcator C-Mod
[DE94-018056] p 779 N95-17680

THREADS
High Performance FORTRAN p 843 N95-16478

THREE BODY PROBLEM
Optimal transfer and swing-orbits in the two- and three-body problems
[INPE-5572-TAE/022] p 673 N95-17648

THREE DIMENSIONAL BODIES
Surface matching for correlation of virtual models: Theory and application p 853 N95-15983
A virtual work space for both hands manipulation with coherency between kinesthetic and visual sensation p 831 N95-15984

THREE DIMENSIONAL BOUNDARY LAYER
Three-dimensional boundary layer and flow field data of an inclined prolate spheroid p 661 N95-17867

THREE DIMENSIONAL FLOW
Wing-body juncture flows
[AD-A281526] p 655 N95-16099
Numerical study of base pressure characteristic curve for a four-engine clustered nozzle configuration p 716 N95-16329
Three dimensional compressible turbulent flow computations for a diffusing S-duct with/without vortex generators
[NASA-CR-195390] p 670 N95-17402
Test data on a non-circular body for subsonic, transonic and supersonic Mach numbers p 662 N95-17871
Low speed propeller slipstream aerodynamic effects p 663 N95-17882

THREE DIMENSIONAL MODELS
Conceptual design study of a solar concentrator/support structure: A three dimensional finite element model p 718 N95-16342
ICONF: An incremental constraint facility in a feature modelling system
[PB94-197654] p 837 N95-16605
Modeling of chemical vapor infiltration for composite fabrication
[DE93-001715] p 724 N95-16926
Grey-scale measurements in multi-dimensional digitized images
[PB94-195492] p 887 N95-17483
A three dimensional mesoscale atmospheric simulation system for use in various mobile battlefield environments. Phase 2: Transition to an operational forecast system
[AD-A281223] p 802 N95-17686

THRESHOLD CURRENTS
Transverse mode coupling instability with a double RF system
[DE94-017972] p 761 N95-17672

THRESHOLDS (PERCEPTION)
Direct comparison of two statistical methods for determination of evoked-potential thresholds
[AD-A285182] p 870 N95-16811

THRUST CHAMBERS
Testing and evaluation of oxide-coated iridium/rhenium chambers p 719 N95-16346

THRUST VECTOR CONTROL
Erosion effects on TVC vane heat transfer characteristics
[AD-A282006] p 721 N95-17448

THRUSTORS
ARCJET plasma modeling with experimental validation
[AD-A285234] p 889 N95-16243
Space Shuttle reaction control system thruster metal nitrate removal and characterization p 716 N95-16332
Extended test of a xenon hollow cathode for a space plasma contactor
[NASA-CR-195402] p 720 N95-17265

TIDES
GPS tides and datums
[AD-A282422] p 666 N95-17508

TIME DEPENDENCE
Vibratory tactile display for textures p 851 N95-15973
Sensitivity study of the SPEM model to the assimilation of synop datasets using two assimilation schemes. 1: Nudging. 2: The Kalman filter/smoother
[AD-A281459] p 804 N95-16079
Demodulation processes in auditory perception
[AD-A285427] p 869 N95-16248
Picosecond optoelectronic AND-GATE
[AD-A285672] p 885 N95-16620
The effect of differences in time to detection of circulating microbubbles on the risk of decompression sickness p 807 N95-16738
Variability in Hoffmann and tendon reflexes in healthy male subjects p 808 N95-16739
On the removal of boundary errors caused by Runge-Kutta integration of non-linear partial differential equations
[NASA-CR-194989] p 863 N95-16904
Demonstration of the Dynamic Flowgraph Methodology using the Titan 2 Space Launch Vehicle Digital Flight Control System
[NASA-CR-197517] p 675 N95-17493
Thermal effects in end-heated laser rods: A time-dependent model and diagnostic
[AD-A282007] p 778 N95-17500
Probing violation of quantum mechanics in the K0-(bar K)0 system
[DE94-017934] p 904 N95-17668
Time-dependent spin correlations in the heisenberg magnet at infinite temperature
[PB95-104303] p 869 N95-17750

TIME DIVISION MULTIPLEXING
Telemetry distribution and processing for the second German Spacelab Mission D-2 p 681 N95-17207

TIME LAG
Scripting human animations in a virtual environment p 855 N95-15992
Shock initiation of crystalline boron in oxygen and fluorine compounds
[AD-A284266] p 730 N95-16955
Evaluation of current tropospheric mapping functions by Deep Space Network very long baseline interferometry p 756 N95-17280

TIME MARCHING
A stepsize control strategy for stiff systems of ordinary differential equations
[AD-A281551] p 861 N95-16395
New developments in the method of space-time conservation element and solution element-applications to two-dimensional time-marching problems
[NASA-TM-106758] p 862 N95-16885

TIME MEASUREMENT
Radio-planetary from tie from Phobos-2 VLBI data p 756 N95-17283

TIME RESPONSE
Blinks, saccades, and fixation pauses during vigilance task performance. 1: Time on task
[DOT/FAA/AM-94/26] p 828 N95-17530

TIME SERIES ANALYSIS
Skin blood flow and bioelectrical impedance
[AD-A285475] p 821 N95-16619
Modelling daily precipitation as a function of temperature for climate change impact studies
[KNMI-WR-93-02] p 802 N95-17529

TIME SIGNALS
Preliminary study of an active millimeter wave sensor
[PB94-189206] p 759 N95-17453

TIN
Corrosion inhibition in high temperature environment
[AD-D016372] p 738 N95-17699

TIN COMPOUNDS
Low temperature synthesis of semiconductor materials
[AD-A285230] p 898 N95-16526

TIN OXIDES
Preparation and investigation of improved low voltage electron excitable phosphors
[AD-A284265] p 767 N95-17487

Corrosion inhibition in high temperature environment
[AD-D016372] p 738 N95-17699

TIN TELLURIDES
Low temperature synthesis of semiconductor materials
[AD-A285230] p 898 N95-16526

TITANIUM ALLOYS
Micromechanics of interfaces in metal matrix composites
[AD-A282404] p 725 N95-17457
Fundamental concepts relating local atomic arrangements, deformation, and fracture of intermetallic alloys
[AD-A282971] p 738 N95-17664

TITANIUM CARBIDES
Tribological properties of reactively sputtered nitrides and carbides of titanium, zirconium and hafnium
[DE94-014583] p 745 N95-17160

TITANIUM NITRIDES
Tribological properties of reactively sputtered nitrides and carbides of titanium, zirconium and hafnium
[DE94-014583] p 745 N95-17160

TITANIUM OXIDES
Development of heterogeneous Wacker oxidation catalysts: The role of the support and the redox component
[PB94-201431] p 732 N95-17700

TOKAMAK DEVICES
Runaway electrons beams in ITER disruptions
[DE94-013788] p 888 N95-16122
Plasma disruption modeling and simulation
[DE94-015095] p 889 N95-16307
Determination of ion temperatures from Zeeman broadened spectral lines in the edge of Tore Supra
[DE94-018112] p 873 N95-16403
Development of a radiative divertor for DIII-D
[DE94-016522] p 889 N95-16554
Active silicon x ray for measuring electron temperature
[DE94-017521] p 890 N95-16555
Differential phase reflectometry for edge profile measurements on TFTR
[DE94-013837] p 891 N95-16958
A comparison of steady-state ARIES and pulsed PULSAR tokamak power plants
[DE94-014441] p 891 N95-17155
Prospects for toroidal fusion reactors
[DE94-014020] p 891 N95-17367
D3-D research operations
[DE94-014934] p 892 N95-17497
Effect of low density H-mode operation on edge and divertor plasma parameters
[DE94-016521] p 892 N95-17640
Fluctuation measurements at c/(omega)(sub pe) spatial scales in a tokamak
[DE94-016771] p 892 N95-17643
Tokamak Transmutation of (nuclear) Waste (TTW): Parametric studies
[DE94-012891] p 881 N95-17721
Two phase liquid helium flow testing to simulate the operation of a cryocondensation pump in the D3-D tokamak
[DE94-018345] p 893 N95-17896
Status of the US stellarator reactor study
[DE94-018693] p 893 N95-17907

TOLUENE
Supercritical fluid extraction: Preparing a superior mesophase precursor for carbon fibers
[AD-A284933] p 726 N95-16142
Identification and temporal behavior of radical intermediates formed during the combustion and pyrolysis of gaseous fuels: Kinetic pathways to soot formation
[DE94-014681] p 731 N95-17163

TOMOGRAPHY
Using lidar tomography to characterize scattering in a turbulent media
[AD-A281014] p 751 N95-16002
Sensitivity study of the SPEM model to the assimilation of synop datasets using two assimilation schemes. 1: Nudging. 2: The Kalman filter/smoother
[AD-A281459] p 804 N95-16079

TOOLING
Cost-effective method for synthesizing innovative transducer materials for sensors and actuators
[AD-A282339] p 725 N95-16974

TOOLS
Physics-based approach to haptic display
p 854 N95-15986

TOPEX
Telecommunications end-to-end systems monitoring on TOPEX/Poseidon: Tools and techniques
p 676 N95-17180

TOPOGRAPHY
Goldstone radar contributions to Mars Pathfinder landing safety p 921 N95-16205
Imager for Mars Pathfinder (IMF) p 711 N95-16206
Site characterization at the Rabbit Valley Geophysical Performance Evaluation Range
[DE94-013550] p 798 N95-16284
Rheology and structure of planetary near-surface materials from landform topography p 922 N95-17392
The new map graphics in RSAS 5.0
[AD-A282432] p 791 N95-17511
Flow over abrupt topography: The application of patterns in nutrient and productivity in reflecting physical processes
[AD-A280813] p 797 N95-17740
Raman spectroscopy of C-irradiated graphite
[DE94-018705] p 733 N95-17911

TOPOLOGY
Generalized method of solving topological optimization problems for electrical airplane equipment systems in computer-aided design p 652 N95-16272

TORQUE
Magnetostrictive torque sensor
[AD-D016376] p 775 N95-17376

TORQUEMETERS
Magnetostrictive torque sensor
[AD-D016376] p 775 N95-17376

TORSO
Scripting human animations in a virtual environment
p 855 N95-15992

TORUSES
Foam inflated rigidized structures for space applications p 710 N95-16344

TOTAL QUALITY MANAGEMENT
Continual improvement: A bibliography with indexes, 1992-1993
[NASA-SP-7097(02)] p 905 N95-16633
Increases in efficiency and enhancements to the Mars Observer non-stored commanding process
p 688 N95-17242

TOUCH
Vibratory tactile display for textures
p 851 N95-15973

TOUGHNESS
Multiphase ceramics for mechanical and structural reliability at low and elevated temperatures
[AD-A285497] p 746 N95-17438

TOXIC HAZARDS
A study to determine the critical characteristics for mice in a newly designed whole body toxic gas exposure module
[AD-A285085] p 818 N95-17666

TOXICITY
The role of chemical inhibition of gap junctional intercellular communication in toxicology
[AD-A282452] p 820 N95-16378
Development of an in vitro model assay system for the evaluation of the effects of toxic chemicals on human airways
[AD-A285074] p 821 N95-16491
Heat stress and a countermeasure in the Shuttle rescueman's suit p 809 N95-16746
Alternatives for ozone-depleting refrigerants
[PB94-190857] p 795 N95-16881
A study to determine the critical characteristics for mice in a newly designed whole body toxic gas exposure module
[AD-A285085] p 818 N95-17666

TOXICITY AND SAFETY HAZARD
The removal of heteroatoms from organic compounds by supercritical water
[AD-A281532] p 722 N95-16087

TOXICOLOGY
The role of chemical inhibition of gap junctional intercellular communication in toxicology
[AD-A282452] p 820 N95-16378

TOXINS AND ANTITOXINS
The role of chemical inhibition of gap junctional intercellular communication in toxicology
[AD-A282452] p 820 N95-16378

TRACE ELEMENTS
Natural and artificial nobel gas hydrologic tracers
[DE94-016010] p 797 N95-17718

TRACKING STATIONS
Open solutions to distributed control in ground tracking stations p 674 N95-17554

TRAFFIC
Signal wave generator signals recorded by the Federal Outdoor Impact Laboratory's on-board Data Acquisition System
[PB94-186525] p 752 N95-16094

TRAILING EDGE FLAPS
Low-speed surface pressure and boundary layer measurement data for the NLR 7301 airfoil section with trailing edge flap p 658 N95-17855
Two-dimensional high-lift airfoil data for CFD code validation p 659 N95-17859
Investigation of the flow development on a highly swept canard/wing research model with segmented leading- and trailing-edge flaps p 662 N95-17876

TRAILING EDGES
Experiments in the trailing edge flow of an NLR 7702 airfoil p 658 N95-17853

TRAINING DEVICES
DROLS: An introduction to searching (videorecording)
[AD-M000338] p 912 N95-17660

TRAINING SIMULATORS
Beyond the cockpit: The visual world as a flight instrument p 814 N95-16767

TRAJECTORIES
Optimal trajectories for flexible-link manipulator slewing using recursive quadratic programming: Experimental verification
[DE94-018741] p 858 N95-17915

TRAJECTORY ANALYSIS
Physiological constraints on deceleration during the aerocapture of manned vehicles p 810 N95-16751
An analysis of a single-burn algorithm for Low-Earth Orbit maintenance
[AD-A283418] p 721 N95-17626

TRAJECTORY CONTROL
Matlab as a robust control design tool
p 849 N95-16474
Optimal trajectories for flexible-link manipulator slewing using recursive quadratic programming: Experimental verification
[DE94-018741] p 858 N95-17915

TRAJECTORY OPTIMIZATION
Numerical optimization of synergetic maneuvers
[AD-A283398] p 656 N95-17435
An analysis of a single-burn algorithm for Low-Earth Orbit maintenance
[AD-A283418] p 721 N95-17626

TRAJECTORY PLANNING
Optimal trajectories for flexible-link manipulator slewing using recursive quadratic programming: Experimental verification
[DE94-018741] p 858 N95-17915

TRANSDUCERS
Feedback system for remotely operated vehicles
[AD-D016409] p 858 N95-17465

TRANSFER ORBITS
Numerical optimization of synergetic maneuvers
[AD-A283398] p 656 N95-17435
Optimal transfer and swing-orbits in the two- and three-body problems
[INPE-5572-TAE/022] p 673 N95-17648

TRANSFORMATIONS (MATHEMATICS)
A general method to determine invariants
[TR-503] p 859 N95-15949
An improved method of airfoil design
p 649 N95-16252
Quasiconformal mappings, operators on Hilbert space, and local formulae for characteristic classes
[PB94-192366] p 860 N95-16293
Wavelets, signal processing and matrix computations
[AD-A283832] p 755 N95-16841
Multiresolution representation and numerical algorithms: A brief review
[NASA-CR-194949] p 863 N95-17266
Low-complexity wavelet filter design for image compression p 757 N95-17289

TRANSISTORS
Support for development of a custom VLSI and FPGA logic chips based on a VHDL top-down design approach
[DE94-013608] p 763 N95-16283

TRANSIT TIME
Robust routing in dynamic networks, part 2
[AD-A282396] p 844 N95-16061
Effect of antiorthostatic BedRest (BR) on GastroIntestinal Motility (GIM) of normal subjects
p 811 N95-16753
Trenched bipolar transistor structures
[AD-D016406] p 767 N95-17463
Radial acceletron, a new low impedance HPM source
[AD-A282008] p 760 N95-17501

TRANSITION FLIGHT
STOVL CFD model test case p 663 N95-17881

TRANSITION FLOW
Experimental investigation of the vortex flow over a 76/60-deg double delta wing p 662 N95-17874

TRANSITION METALS
The chemistry and physics of transition metal clusters
[DE94-014012] p 734 N95-16364

TRANSITION TEMPERATURE
The relationship of structure to superconductivity in the Pr-Ba-Cu-O system
[DE94-014231] p 897 N95-16510

TRANSLATING
Compiling polymorphism using intensional type analysis
[AD-A285340] p 838 N95-16819

TRANSLATIONAL MOTION
Mathematical model for interaction of canals and otoliths in perception of orientation, translation, and rotation
[AD-A280897] p 819 N95-16151

TRANSMISSION
Static image method for the interaction of two co-axial conducting prolate spheroids
[PB94-197696] p 760 N95-17502
TRANSMISSION EFFICIENCY
The ESA standard for telemetry and telecommand packet utilisation: PUS p 704 N95-17595
TRANSMISSION ELECTRON MICROSCOPY
Study of CuPt-type ordering and dopant effect of In(0.5)Ga(0.5)P/GaAs using spectroscopic ellipsometry
[DE94-018890] p 902 N95-17917
TRANSMISSION LINES
Control of a large vacuum wave precursor on the SABRE voltage adder MITL and extraction ion diode
[DE94-014280] p 888 N95-16216
Center-fed multifilar helix antenna
[AD-D016390] p 760 N95-17480
TRANSMISSION LOSS
A quasi-single mode optical fiber for long-haul transmission in severe bending environments
[AD-A281313] p 884 N95-16009
TRANSMISSION RATE (COMMUNICATIONS)
High speed transport protocols: An attempt to find the best solution
[AD-A280989] p 751 N95-15993
TRANSMISSIONS (MACHINE ELEMENTS)
A review of transmission diagnostics research at NASA Lewis Research Center
[ARL-TR-599] p 781 N95-16907
TRANSMITTER RECEIVERS
An automatic repeater station for signal transmissions
[AD-D016454] p 754 N95-16549
TRANSMUTATION
Tokamak Transmutation of (nuclear) Waste (TTW): Parametric studies
[DE94-012891] p 881 N95-17721
TRANSOCEANIC COMMUNICATION
The GRO remote terminal system
p 678 N95-17188
TRANSONIC FLOW
An investigation of the transonic pressure drag coefficient for axi-symmetric bodies
[AD-A280990] p 654 N95-15994
Mach number, flow angle, and loss measurements downstream of a transonic fan-blade cascade
[AD-A280907] p 656 N95-16824
Comparison of computational and experimental results for a supercritical airfoil
[NASA-TM-4601] p 656 N95-16908
Transonic Navier-Stokes calculations about a 65 deg delta wing
[NASA-CR-4635] p 656 N95-17273
2-D airfoil tests including side wall boundary layer measurements p 657 N95-17847
Investigation of an NLF(1)-0416 airfoil in compressible subsonic flow p 658 N95-17852
OAT15A airfoil data p 659 N95-17857
DLR-F5: Test wing for CFD and applied aerodynamics p 660 N95-17864
Wind tunnel test on a 65 deg delta wing with rounded leading edges: The International Vortex Flow Experiment p 662 N95-17875
Investigation of the flow development on a highly swept canard/wing research model with segmented leading- and trailing-edge flaps p 662 N95-17876
TRANSONIC SPEED
Measurements of unsteady pressure and structural response for an elastic supercritical wing
[NASA-TP-3443] p 653 N95-16560
Two-dimensional 16.5 percent thick supercritical airfoil NLR 7301 p 658 N95-17854
DLR-F4 wing body configuration p 660 N95-17863
Low aspect ratio wing experiment p 661 N95-17865
Test data on a non-circular body for subsonic, transonic and supersonic Mach numbers p 662 N95-17871
Wind tunnel test on a 65 deg delta wing with a sharp or rounded leading edge: The international vortex flow experiment p 662 N95-17872
TRANSONIC WIND TUNNELS
Wall-signature methods for high speed wind tunnel wall interference corrections p 650 N95-16257
Comparison of computational and experimental results for a supercritical airfoil
[NASA-TM-4601] p 656 N95-16908
Single-engine tail interference model p 663 N95-17879
TRANSPARENCE
Low-temperature fabrication of transparent silicon nitride
[DE94-014902] p 746 N95-17456
TRANSPLANTATION
Cell culture and transplantation of the suprachiasmatic circadian pacemaker
[AD-A280977] p 821 N95-16481
Control of circadian behavior by transplanted suprachiasmatic nuclei
[AD-A285233] p 807 N95-16599
TRANSPORT AIRCRAFT
DLR-F4 wing body configuration p 660 N95-17863
TRANSPORT PROPERTIES
International Workshop on Light Emission and Electronic Properties of Nanoscale silicon
[AD-A281464] p 894 N95-16081
Space Shuttle main engine OPAD: The search for a hardware enhanced plume p 716 N95-16330
Atomic transport of oxygen
[DE94-013332] p 873 N95-16430
Electrochemical properties of lithium ion conducting solid polymer electrolytes
[AD-A281875] p 742 N95-16434
Properties of semiconducting Ru2Ge3
[DE94-015361] p 899 N95-16913
D3-D research operations
[DE94-014934] p 892 N95-17497
TRANSPORT THEORY
Femtosecond studies of carrier dynamics in compound semiconductors
[AD-A282871] p 767 N95-17433
TRANSPORTATION
GEOTRANS geographic decision support system
[PB94-183670] p 908 N95-16093
Overview of space power electronic's technology under the CSTI High Capacity Power Program
[NASA-TM-110110] p 883 N95-17933
TRANSPORTATION NETWORKS
Multigrid methods in network optimization: Overview and appraisal
[AD-A280992] p 833 N95-15995
TRANSPORTER
Whole-body vibration assessment of the M1070 heavy equipment transporter, volume 1
[AD-A285199] p 829 N95-16147
TRANSPUTERS
Embedded parallel processing based ground control systems for small satellite telemetry
p 674 N95-17553
TRANSVERSE OSCILLATION
Measurements of collective effects in the ALS
[DE94-017966] p 881 N95-17670
TRAPPED MAGNETIC FIELDS
Runaway electrons beams in ITER disruptions
[DE94-013788] p 888 N95-16122
TRAPPING
Effect of Coulomb collisions, Landau damping and particle trapping on linear and nonlinear ion acoustic waves
[AD-A282009] p 869 N95-17449
TRAVELING WAVE TUBES
Slow wave vane structure with elliptical cross-section slots, an analysis
[NASA-CR-195352] p 755 N95-16886
TREADMILLS
Energy expenditure, physical work load and postural control during walking on a moving platform
[AD-A285343] p 830 N95-16821
TRELLIS CODING
Error control techniques for satellite and space communications
[NASA-CR-197459] p 761 N95-17665
TREND ANALYSIS
Generic trending and analysis system
p 689 N95-17245
TRENDS
Information system in transition: The Hungarian Scene
p 906 N95-15925
Electronic access to ONREUR/ONRAISIA S and T reports p 907 N95-15935
TRIBOLOGY
Bench wear and single-cylinder engine evaluations of high-temperature lubricants for US Army ground vehicles
[AD-A285399] p 780 N95-16636
Tribological properties of reactively sputtered nitrides and carbides of titanium, zirconium and hafnium
[DE94-014583] p 745 N95-17160
TRIGGER CIRCUITS
New shower maximum trigger for electrons and photons at CDF
[DE94-018376] p 878 N95-17899
TRIGONOMETRIC FUNCTIONS
Trigonometric functions of nonlinear quantities
[DE94-018794] p 864 N95-17916
TRITIUM
Use of magnesium for recovering hydrogen isotopes from tritiated water
[DE94-014471] p 731 N95-17157
TROPOSPHERE
Evaluation of current tropospheric mapping functions by Deep Space Network very long baseline interferometry
p 756 N95-17280
TRUCKS
Whole-body vibration assessment of the palletized load system
[AD-A285181] p 829 N95-16145
TRUSSES
Natural frequency of uniform and optimized tetrahedral truss platforms
[NASA-TP-3461] p 709 N95-16559
TSUNAMI WAVES
Tsunami newsletter, volume 26
[AD-A282751] p 806 N95-17477
TUMORS
Kinetics model for initiation and promotion for describing tumor prevalence from HZE radiation
[NASA-TP-3479] p 820 N95-16412
Failure of ozone and nitrogen dioxide to enhance lung tumor development in hamsters
[PB94-182854] p 818 N95-16801
TUNABLE LASERS
Wavelength dispersive gain element for a tunable laser
[AD-D016381] p 777 N95-17302
Simulations of an FEL producing coherent x rays utilizing the SLAC LINAC
[AD-A283524] p 777 N95-17303
TUNGSTEN
The influence of tungsten alloying on the mechanical properties of tantalum
[DE94-010071] p 736 N95-17378
Adhesion of silicon oxide to diamond
[AD-D016356] p 747 N95-17694
TUNGSTEN ALLOYS
Material and ballistic investigation of a tungsten-26 percent rhenium alloy
[PB94-189156] p 734 N95-16420
The influence of tungsten alloying on the mechanical properties of tantalum
[DE94-010071] p 736 N95-17378
Effect of extrusion parameters on consolidation of tungsten-hafnium and tungsten-steel powders
[DE94-013270] p 737 N95-17513
TUNGSTEN COMPOUNDS
Synthesis of tungsten nitrene complexes as precursors for tungsten nitride
[AD-A281592] p 740 N95-16101
TUNNEL JUNCTIONS
Research on stable, high-efficiency amorphous-silicon multijunction modules
[DE94-011839] p 764 N95-16425
TURBINE BLADES
Structural testing of the North Wind 250 composite rotor joint
[DE94-006923] p 792 N95-16437
Structural effects of unsteady aerodynamic forces on horizontal-axis wind turbines
[DE94-011863] p 787 N95-16939
Analysis of a two-bladed, teetering-hub turbine using the ADAMS (tm) software
[DE94-006922] p 781 N95-17169
The application of non-destructive techniques to the testing of a wind turbine blade
[DE95-000323] p 784 N95-17360
TURBINE PUMPS
Cryogenic foil bearing turbopumps
p 716 N95-16331
TURBOJET ENGINES
Small turbojets: Designs and installations
p 670 N95-16323
TURBOMACHINE BLADES
Small-amplitude disturbances in turbomachine flows with swirl
[NASA-CR-195406] p 772 N95-17386
TURBOSHAFTS
Sensor fault detection and diagnosis simulation of a helicopter engine in an intelligent control framework
[NASA-TM-106784] p 669 N95-15970
TURBULENCE
Marine boundary-layer parameterizations for large-scale models
[AD-A282402] p 803 N95-16062
Dynamical system prediction of the scalar field in a turbulent channel flow
[AD-A285519] p 771 N95-16438
Application of Fourier-space image-restoration techniques to turbulence compensation and sparse-aperture imaging
[AD-A285077] p 885 N95-16494
Laser induced fluorescence measurements and modeling of nitric oxide in high-pressure premixed flames
[NASA-CR-195404] p 775 N95-16910
Structural effects of unsteady aerodynamic forces on horizontal-axis wind turbines
[DE94-011863] p 787 N95-16939
Experiments in the trailing edge flow of an NLR 7702 airfoil p 658 N95-17853

TURBULENCE EFFECTS
Heat transfer measurements for Stirling machine cylinders
[NASA-CR-197128] p 791 N95-15963
TURBULENCE MODELS
Modeling of wall-bounded complex flows and free shear flows
[NASA-TM-106513] p 770 N95-16407
Colloidal particle deposition in turbulent flow
[DE94-013375] p 770 N95-16417
Transonic Navier-Stokes calculations about a 65 deg delta wing
[NASA-CR-4635] p 656 N95-17273
Long-term momentum and heat balances and turbulent mixing in the upper equatorial Pacific Ocean
p 805 N95-17395
A supercritical airfoil experiment p 659 N95-17858
TURBULENT BOUNDARY LAYER
Numerical simulation of supersonic compression corners and hypersonic inlet flows using the RPLUS2D code
[NASA-TM-106580] p 654 N95-16038
Experimental investigation of turbulent separated-reattachment flow by using LDV
p 649 N95-16253
Experimental and theoretical studies of wakes in stratified flows
[AD-A285305] p 771 N95-16616
On the propagation of near-inertial motion from the oceanic mixed layer p 806 N95-17396
Three-dimensional boundary layer and flow field data of an inclined prolate spheroid p 661 N95-17867
TURBULENT DIFFUSION
Large-eddy simulation of cumulus convection
[PB94-191368] p 800 N95-16290
TURBULENT FLOW
A modified restricted Euler equation for turbulent flows with mean velocity gradients
[NASA-CR-194979] p 769 N95-16070
Experimental investigation of turbulent separated-reattachment flow by using LDV
p 649 N95-16253
Numerical study of base pressure characteristic curve for a four-engine clustered nozzle configuration
p 716 N95-16329
Modeling of wall-bounded complex flows and free shear flows
[NASA-TM-106513] p 770 N95-16407
Colloidal particle deposition in turbulent flow
[DE94-013375] p 770 N95-16417
Dynamical system prediction of the scalar field in a turbulent channel flow
[AD-A285519] p 771 N95-16438
Time accurate computation of unsteady inlet flows with a dynamic flow adaptive mesh
[AD-A285498] p 771 N95-16736
The small-scale structure of dispersing clouds in the atmosphere
[AD-A285493] p 800 N95-16802
Three dimensional compressible turbulent flow computations for a diffusing S-duct with/without vortex generators
[NASA-CR-195390] p 670 N95-17402
TURBULENT JETS
On the prediction of free turbulent jets with swirl using a quadratic pressure-strain model
[NASA-CR-194964] p 769 N95-16071
Dynamical system prediction of the scalar field in a turbulent channel flow
[AD-A285519] p 771 N95-16438
Combustion instability phenomena of importance to liquid propellant engines
[AD-A284780] p 730 N95-16882
TURBULENT MIXING
Marine boundary-layer parameterizations for large-scale models
[AD-A282402] p 803 N95-16062
Long-term momentum and heat balances and turbulent mixing in the upper equatorial Pacific Ocean
p 805 N95-17395
TURBULENT WAKES
A supercritical airfoil experiment p 659 N95-17858
TURING MACHINES
Decreasing the bandwidth of a transition matrix
[TR-505] p 859 N95-15948
NP-sets are Co-NP-immune relative to a random oracle
[TR-501] p 859 N95-15950
On the structure of log-space probabilistic complexity classes
[TR-506] p 864 N95-16039
Properties of multihead two-way probabilistic finite automata
[TR-477] p 833 N95-16040
The complexity of PDL with interleaving
[AD-A281044] p 836 N95-16452
On serializable languages
[TR-519] p 839 N95-17261
TWO BODY PROBLEM
Optimal transfer and swing-orbits in the two- and three-body problems
[INPE-5572-TAE/022] p 673 N95-17648
TWO DIMENSIONAL BODIES
2-D airfoil tests including side wall boundary layer measurements p 657 N95-17847
2-D aileron effectiveness study p 658 N95-17851
TWO DIMENSIONAL FLOW
Nonlinear instability of a uni-directional transversely sheared mean flow
[NASA-TM-106779] p 769 N95-15969
Numerical simulation of supersonic compression corners and hypersonic inlet flows using the RPLUS2D code
[NASA-TM-106580] p 654 N95-16038
New developments in the method of space-time conservation element and solution element-applications to two-dimensional time-marching problems
[NASA-TM-106758] p 862 N95-16885
Two-dimensional high-lift airfoil data for CFD code validation p 659 N95-17859
TWO DIMENSIONAL MODELS
Investigations on the sensitivity of the computer code TURBO-2D
[CUED/A-THERMO/TR-61] p 771 N95-16595
Long term modelling of permafrost dynamics
[AD-A285315] p 799 N95-16735
Combination of power electronic models with the two-dimensional finite element analysis of electrical machines
[PB94-197720] p 766 N95-16951
Grey-scale measurements in multi-dimensional digitized images
[PB94-195492] p 887 N95-17483
Thermal effects in end-heated laser rods: A time-dependent model and diagnostic
[AD-A282007] p 778 N95-17500
Measurements on a two-dimensional aerofoil with high-lift devices p 657 N95-17848
Investigation of the flow over a series of 14 percent-thick supercritical aerofoils with significant rear camber
p 657 N95-17849
Experiments in the trailing edge flow of an NLR 7702 airfoil p 658 N95-17853
Two-dimensional 16.5 percent thick supercritical airfoil NLR 7301 p 658 N95-17854
Low-speed surface pressure and boundary layer measurement data for the NLR 7301 airfoil section with trailing edge flap p 658 N95-17855
OAT15A airfoil data p 659 N95-17857
A supercritical airfoil experiment p 659 N95-17858
Two-dimensional high-lift airfoil data for CFD code validation p 659 N95-17859
TWO PHASE FLOW
Investigations on the sensitivity of the computer code TURBO-2D
[CUED/A-THERMO/TR-61] p 771 N95-16595
Two phase liquid helium flow testing to simulate the operation of a cryocondensation pump in the D3-D tokamak
[DE94-018345] p 893 N95-17896

U

U.S.S.R.
A procedure for estimating the carbon budget of terrestrial ecosystems in the former Soviet Union by geographic information system analysis and classification of AVHRR derived global vegetation index
p 796 N95-17394
ULTRAHIGH FREQUENCIES
A VHF/UHF antenna for the Precision Antenna Measurement System (PAMS)
[AD-A285673] p 754 N95-16621
S-band and Ku-band return service interference between TDRSS users p 677 N95-17183
ULTRASHORT PULSED LASERS
Ultrashort pulse effects in semiconductor amplifiers and in dispersive media
[AD-A284925] p 763 N95-16137
ULTRASONIC AGITATION
Sonochemical synthesis of polysilylenes by reductive coupling of disubstituted dichlorosilanes with alkali metals
[AD-A280994] p 739 N95-15996
ULTRASONIC RADIATION
Support minimized inversion of acoustic and elastic wave scattering
[DE94-014233] p 783 N95-16538
ULTRASONICS
Innovative acoustic techniques for studying new materials and new developments in solid state physics
[AD-A280986] p 898 N95-16525
Support minimized inversion of acoustic and elastic wave scattering
[DE94-014233] p 783 N95-16538
ULTRAVIOLET ASTRONOMY
Voyager investigation of the cosmic diffuse background: Observations of rocket-studied locations with Voyager
[NASA-CR-197532] p 917 N95-17422
ULTRAVIOLET EMISSION
Ultraviolet emissions occurring about hypersonic vehicles in rarefied flows
[AD-A281452] p 655 N95-16076
ULTRAVIOLET LASERS
Properties of Ce:LiSrAlF6 and Ce:LiCaAlF6 ultraviolet lasers
[DE94-013737] p 777 N95-17168
ULTRAVIOLET RADIATION
Detection of crosslink formation by 2 + 2 photocycloaddition in poly (vinyl cinnamate) by C-13 solid-state NMR
[AD-A281955] p 741 N95-16409
Tunable UV source for UV fluorescence remote sensing
[DE94-015745] p 777 N95-16917
Miniature, vacuum compatible 1024 (times) 1024 CCD camera for x ray, ultraviolet, or optical imaging
[DE94-012235] p 776 N95-17522
ULTRAVIOLET SPECTROMETERS
A rare gas optics-free absolute photon flux and energy analyzer to provide absolute photoionization rates of inflowing interstellar neutrals
[NASA-CR-197226] p 914 N95-15964
A rare gas optics-free absolute photon flux and energy analyzer for solar and planetary observations
[NASA-CR-197227] p 915 N95-16021
Micro-UltraViolet Spectrograph (Micro-UVS)
[DE94-016704] p 732 N95-17642
ULTRAVIOLET SPECTROSCOPY
Nitride semiconductors for ultraviolet detection
[AD-A280988] p 898 N95-16533
ULYSSES MISSION
Engineering Ulysses extended mission
p 673 N95-17213
Grand mission versus small OPS team: Can we have both? p 684 N95-17219
Re-engineering the Multimission Command System at the Jet Propulsion Laboratory p 702 N95-17583
Customizing the JPL Multimission Ground Data System: Lessons learned p 703 N95-17588
UNDERWATER ACOUSTICS
Revisions to an empirical surface loss model using a correction for pH-dependent attenuation
[AD-A285714] p 871 N95-17177
UNDERWATER COMMUNICATION
Development and fabrication of the fiber optic MicroCable (tm)
[AD-A285266] p 886 N95-16815
UNDERWATER TESTS
Characterization of the hydrogen induced cold cracking susceptibility at simulated weld zones in HSLA-100 steel
[PB94-174505] p 737 N95-17616
UNIQUENESS THEOREM
Uniqueness and free interpolation for logarithmic potentials and the Cauchy problem for the Laplace equation in (R2)
[PB94-192408] p 861 N95-16295
UNITED STATES
NAFTA literature at the International Trade Commission library p 905 N95-15922
Survey of United States commercial satellites in geosynchronous Earth orbit
[AD-A284969] p 708 N95-16131
Annual review of aircraft accident data: US Air carrier operations, calendar year 1992
[PB95-100319] p 665 N95-17748
UNIVERSITIES
The Australian National Chinese Japanese Korean Project p 905 N95-15920
UNIVERSITY PROGRAM
Laboratory Directed Research and Development Program
[DE94-011381] p 924 N95-16120
UNIX (OPERATING SYSTEM)
Image tools for UNIX p 847 N95-16466
IS-Lab: A tool for developing interactive programs for simulation and analysis. User's guide
[PB94-184710] p 840 N95-17410
Customizing the JPL Multimission Ground Data System: Lessons learned p 703 N95-17588
UNLOADING
Skeletal muscle responses to unloading in humans
p 809 N95-16743
UNSTEADY AERODYNAMICS
A computational investigation of wake-induced airfoil flutter in incompressible flow and active flutter control
[AD-A281534] p 670 N95-16109

Numerical simulation of transient vortex breakdown above a pitching delta wing
[AD-A281075] p 655 N95-16808
Structural effects of unsteady aerodynamic forces on horizontal-axis wind turbines
[DE94-011863] p 787 N95-16939

UNSTEADY FLOW
Unsteady flow phenomena in discrete passage diffusers for centrifugal compressors
[AD-A281412] p 770 N95-16163
Measurements of unsteady pressure and structural response for an elastic supercritical wing
[NASA-TP-3443] p 653 N95-16560
Experimental and theoretical studies of wakes in stratified flows
[AD-A285305] p 771 N95-16616
Time accurate computation of unsteady inlet flows with a dynamic flow adaptive mesh
[AD-A285498] p 771 N95-16736
A supercritical airfoil experiment p 659 N95-17858

UPLINKING
Simplifying operations with an uplink/downlink integration toolkit p 697 N95-17562

UPPER ATMOSPHERE RESEARCH SATELLITE (UARS)
Nickel cadmium battery operations and performance p 685 N95-17224

URANIUM ALLOYS
Non-Fermi liquid scaling in UPd(x)Cu(5-x)(x = 1,1.5)
[DE94-016072] p 896 N95-16389

URBAN PLANNING
GEOTRANS geographic decision support system
[PB94-183670] p 908 N95-16093

USER MANUALS (COMPUTER PROGRAMS)
Detailed example of using PIWG on the SUN workstation and the DEC VAX computer
[AD-A281528] p 834 N95-16107
Visualization of unsteady computational fluid dynamics
[NASA-CR-197461] p 770 N95-16388
Model-based software process improvement p 843 N95-16455
Image tools for UNIX p 847 N95-16466
MODIS Technical Report Series. Volume 4: MODIS data access user's guide: Scan cube format
[NASA-TM-104594-VOL-4] p 837 N95-16587
FPCAS2D user's guide, version 1.0
[NASA-CR-195413] p 786 N95-16588
IS-Lab: A tool for developing interactive programs for simulation and analysis. User's guide
[PB94-184710] p 840 N95-17410
Automated Estimating System (AES) version 6.0: User's manual
[DE94-013636] p 841 N95-17514
Engineering design tools for wind diesel systems. Volume 5: JODYMOD dynamic wind diesel simulation software package. User's guide
[PB95-104543] p 841 N95-17629
Engineering design tools for wind diesel systems. Volume 6: Logistic package. User documentation
[PB95-104550] p 842 N95-17734
Surftherm: A program to analyze thermochemical and kinetic data in gas-phase and surface chemical reaction mechanisms
[DE94-016145] p 733 N95-17744
ICCanvas 3D visualization tool for Windows (tm). Software user's manual
[AD-A285603] p 842 N95-17746
CHEETAH 1.0 user's manual
[DE94-014727] p 749 N95-17919
FEM3C, an improved three-dimensional heavy-gas dispersion model: User's manual
[DE94-014731] p 797 N95-17922

USER REQUIREMENTS
An applications-oriented approach to the development of virtual environments p 853 N95-15980
Method of calculating the optimal radioelectronic equipment design p 652 N95-16271
Risk-Based Data Management System design specifications and implementation plan for the Alaska Oil and Gas Conservation Commission; the Mississippi State Oil and Gas Board; the Montana Board of Oil and Gas Conservation; and the Nebraska Oil and Gas Conservation Commission, attachment B
[DE94-013189] p 908 N95-16282
Bench wear and single-cylinder engine evaluations of high-temperature lubricants for US Army ground vehicles
[AD-A285399] p 760 N95-16636
Knowledge-based critiquing of graphical user interfaces with CHIMES p 697 N95-17560
ELISA, a demonstrator environment for information systems architecture design p 698 N95-17563
The Space Communications Protocol Standards Program p 704 N95-17594
The ESA standard for telemetry and telecommand packet utilisation: PUS p 704 N95-17595

UTILITIES
Solar energy: Lessons from the Pacific island experience
[WORLD-BANK-TP-244] p 794 N95-17298

V

V/STOL AIRCRAFT
Cooperative control theory and integrated flight and propulsion control
[NASA-CR-197493] p 671 N95-17404
STOVL CFD model test case p 663 N95-17881

VACANCIES (CRYSTAL DEFECTS)
Applications of positron depth profiling
[PB94-197753] p 900 N95-16952

VACUUM
Control of a large vacuum wave precursor on the SABRE voltage adder MITL and extraction ion diode
[DE94-014280] p 888 N95-16216
Progress at LAMPF
[DE94-016210] p 880 N95-16937
Radiation electrodynamics of the photo-electron cloud produced by an arbitrary photon pulse incident on a planar emitting surface in vacuum
[AD-A282153] p 759 N95-17450
Relativistic effect of energy increase of a particle moving freely in vacuum from the quantum field theory point of view
[DE94-622757] p 903 N95-17473
Vacuum deposited polymer/silver reflector material
[DE94-018729] p 748 N95-17913

VACUUM CHAMBERS
Two phase liquid helium flow testing to simulate the operation of a cryocondensation pump in the D3-D tokamak
[DE94-018345] p 893 N95-17896

VACUUM DEPOSITION
Vacuum deposited polymer/silver reflector material
[DE94-018729] p 748 N95-17913

VACUUM SYSTEMS
Thin film superconductors
[DE94-018585] p 902 N95-17906

VALENCE
Atomic structure and valency of nickel in some of its oxycompounds
[AD-A281109] p 733 N95-16091
XAFS investigation of structure and valency of nickel in some oxycompounds
[AD-A283193] p 877 N95-17630

VALLEYS
Maja Valley and the Chryse outflow complex sites p 921 N95-16199

VALVES
An investigation of fluid flow during induction stroke of a water analog model of an IC engine using an innovative optical velocimetry concept: LIPA
[NASA-CR-197451] p 780 N95-16900

VANADIUM
WPH-6112A thermal expansion test of PRESS tubulation
[DE94-015946] p 782 N95-17717

VANADIUM ALLOYS
Fusion materials: Technical evaluation of the technology of vandium alloys for use as blanket structural materials in fusion power systems
[DE94-013194] p 890 N95-16827

VANES
Slow wave vane structure with elliptical cross-section slots, an analysis
[NASA-CR-195352] p 755 N95-16886

VAPOR DEPOSITION
Pseudomorphic stabilization of diamond on non-diamond substrates
[AD-A285231] p 898 N95-16527
Development of high-efficiency, thin-film CdTe solar cells
[DE94-011885] p 794 N95-16940
Volatile CVD precursors based on copper alkoxides and mixed group IIA-copper alkoxides
[AD-D016380] p 732 N95-17479
Selective area platinum film deposition
[AD-D016355] p 747 N95-17693
Workshop on Characterizing Diamond Films, 3
[PB94-187663] p 747 N95-17722

VAPOR PHASE EPITAXY
Nitride semiconductors for ultraviolet detection
[AD-A280988] p 898 N95-16533

VAPOR PHASES
Delayed annihilation of antiprotons in helium gas
[DE94-753405] p 878 N95-17739
Surftherm: A program to analyze thermochemical and kinetic data in gas-phase and surface chemical reaction mechanisms
[DE94-016145] p 733 N95-17744

VAPORIZING
Plasma disruption modeling and simulation
[DE94-015095] p 889 N95-16307

VARACTOR DIODES
Frequency multiplier analysis and design using punch-through varactor diodes
[AD-A284963] p 762 N95-16130

VARIABILITY
Variability in Hoffmann and tendon reflexes in healthy male subjects p 808 N95-16739

VARIANCE (STATISTICS)
Direct comparison of two statistical methods for determination of evoked-potential thresholds
[AD-A285182] p 870 N95-16811

VASOCONSTRICTION
Carbon monoxide does not modulate pulmonary vascular reactivity in isolated rat lungs
[AD-A283190] p 818 N95-17714

VASOCONSTRICTOR DRUGS
Carbon monoxide does not modulate pulmonary vascular reactivity in isolated rat lungs
[AD-A283190] p 818 N95-17714

VECTOR PROCESSING (COMPUTERS)
CMCAM: A high performance CM-5 lattice gas simulator
[AD-A281063] p 837 N95-16626

VECTOR QUANTIZATION
High performance compression of science data
[NASA-CR-189388] p 911 N95-17329
Analysis of compression techniques for Common Mapping Standard (CMS) raster data
[AD-A283396] p 791 N95-17625

VEGETATION
A procedure for estimating the carbon budget of terrestrial ecosystems in the former Soviet Union by geographic information system analysis and classification of AVHRR derived global vegetation index p 796 N95-17394

VEGETATION GROWTH
Root growth and development in response to CO2 enrichment
[NASA-CR-196154] p 807 N95-16429

VEGETATIVE INDEX
A procedure for estimating the carbon budget of terrestrial ecosystems in the former Soviet Union by geographic information system analysis and classification of AVHRR derived global vegetation index p 796 N95-17394

VELOCITY DISTRIBUTION
A modified restricted Euler equation for turbulent flows with mean velocity gradients
[NASA-CR-194979] p 769 N95-16070
Filter efficiency and pressure drop calculations through two and three dimensional fiber arrays
[DE94-014111] p 770 N95-16211
Visualizing 3D velocity fields near contour surfaces
[DE94-010205] p 860 N95-16221
Ion drift meter research
[NASA-CR-197124] p 798 N95-16432
Single-pass method for the solution of inverse potential and rotational problems. Part 1: 2-D and quasi 3-D theory and application p 664 N95-16563
Residual-correction type and related computational methods for aerodynamic design. Part 1: Airfoil and wing design p 667 N95-16566
Residual-correction type and related computational methods for aerodynamic design. Part 2: Multi-point airfoil design p 667 N95-16567
Straits of Florida physical oceanographic field study. Volume 1: Executive summary. Volume 2: Technical report. Volume 3: Data report
[PB94-175031] p 806 N95-17615

VELOCITY MEASUREMENT
Optical wheel-rotation sensor
[DE94-011719] p 780 N95-16224
An investigation of fluid flow during induction stroke of a water analog model of an IC engine using an innovative optical velocimetry concept: LIPA
[NASA-CR-197451] p 780 N95-16900

VENTILATION
Comparison of work of breathing during mechanical ventilation using assist control and intermittent mandatory ventilation
[AD-A285516] p 822 N95-17174

VENUS (PLANET)
Analysis of magnetic field data from Pioneer Venus orbiter
[NASA-CR-197492] p 923 N95-17403

VENUS ATMOSPHERE
Analysis of magnetic field data from Pioneer Venus orbiter
[NASA-CR-197492] p 923 N95-17403

VERBAL COMMUNICATION
Phonologic-graphemic transcodifier for Portuguese Language spoken in Brazil (PLB)
[INPE-5575-PRE/1803] p 760 N95-17649

VERTICAL LANDING
STOVL CFD model test case p 663 N95-17881
VERTICAL MOTION
Energy expenditure, physical work load and postural control during walking on a moving platform
[AD-A285343] p 830 N95-16821
VERY HIGH FREQUENCIES
A VHF/UHF antenna for the Precision Antenna Measurement System (PAMS)
[AD-A285673] p 754 N95-16621
VERY LARGE ARRAY (VLA)
Goldstone radar contributions to Mars Pathfinder landing safety p 921 N95-16205
VERY LARGE SCALE INTEGRATION
Timing and area optimization for VLSI circuit and layout
[AD-A281081] p 762 N95-16089
A VLSI interface for the NM24CF04 serial-access ferroelectric memory
[AD-A281535] p 762 N95-16110
VLSI circuits for high speed data conversion
[AD-A281556] p 763 N95-16136
Support for development of a custom VLSI and FPGA logic chips based on a VHDL top-down design approach
[DE94-013608] p 763 N95-16283
A second generation 50 Mbps VLSI level zero processing system prototype p 678 N95-17191
VLSI technology for smaller, cheaper, faster return link systems p 681 N95-17206
VERY LONG BASE INTERFEROMETRY
International data transfer for space very long baseline interferometry p 680 N95-17198
International mission planning for space Very Long Baseline Interferometry p 673 N95-17216
The Telecommunications and Data Acquisition Report
[NASA-CR-197249] p 755 N95-17279
Evaluation of current tropospheric mapping functions by Deep Space Network very long baseline interferometry p 756 N95-17280
An algorithm for extraction of periodic signals from sparse, irregularly sampled data p 756 N95-17281
Space VLBI telecommunication characteristics, protection criteria, and frequency sharing p 756 N95-17282
Radio-planetary from tie from Phobos-2 VLBI data p 756 N95-17283
RF optics study for DSS-43 ultracone implementation p 758 N95-17296
DSN co-observing operations to support space VLBI missions p 694 N95-17543
VERY LOW FREQUENCIES
Development of a medium energy modulated electron gun for orbital experiments
[AD-A281021] p 675 N95-16005
VESTIBULAR TESTS
Characterization of the fast-phase component of the vestibulo-ocular response
[AD-A281830] p 820 N95-16360
VHSIC (CIRCUITS)
Hardware description languages p 832 N95-16477
WAVES VHDL interface
[AD-A285208] p 764 N95-16516
VIBRATION
Optimum truncation of a Gaussian beam in the presence of random jitter
[AD-A284951] p 752 N95-16143
Whole-body vibration assessment of the palletized load system
[AD-A285181] p 829 N95-16145
Whole-body vibration assessment of the M1070 heavy equipment transporter, volume 1
[AD-A285199] p 829 N95-16147
Materials for second and third order nonlinear optical applications
[AD-A281304] p 885 N95-16787
VIBRATION DAMPING
A comparison of different control methods for vibration suppression of flexible structures using piezoelectric actuators
[AD-A282958] p 710 N95-17622
VIBRATION EFFECTS
Whole-body vibration assessment of the palletized load system
[AD-A285181] p 829 N95-16145
Whole-body vibration assessment of the M1070 heavy equipment transporter, volume 1
[AD-A285199] p 829 N95-16147
A super-element simplified analysis for vibration systems of complex structures p 650 N95-16260
VIBRATION ISOLATORS
Microgravity isolation system design: A case study
[NASA-TM-106804] p 654 N95-17657
VIBRATION MEASUREMENT
Development of the vibration test equipment for testing the products of aircraft and space technology with simulation of operating conditions p 651 N95-16266
Evaluation of SEA loss factors using input power modulation
[ISVR-TR-240] p 868 N95-16856
Apache helicopter seat cushion evaluation
[AD-A284300] p 831 N95-17484
VIBRATION PERCEPTION
Whole-body vibration assessment of the palletized load system
[AD-A285181] p 829 N95-16145
VIBRATION TESTS
Vibratory tactile display for textures p 851 N95-15973
Development of the vibration test equipment for testing the products of aircraft and space technology with simulation of operating conditions p 651 N95-16266
Correlation of finite element free vibration predictions using random vibration test data
[NASA-TM-106787] p 787 N95-17258
Apache helicopter seat cushion evaluation
[AD-A284300] p 831 N95-17484
VIBRATIONAL SPECTRA
Development of the vibration test equipment for testing the products of aircraft and space technology with simulation of operating conditions p 651 N95-16266
Researches on gear fault diagnosis techniques p 651 N95-16267
VIBRATIONAL STATES
Dynamical system prediction of the scalar field in a turbulent channel flow
[AD-A285519] p 771 N95-16438
VIDEO COMMUNICATION
Videoconferencing and its role in the Army
[AD-A282707] p 909 N95-16305
VIDEO COMPRESSION
Virtual reality and telerobotics applications of an Address Recalculation Pipeline p 852 N95-15977
An analysis of Internet's MBONE: A media choice perspective
[AD-A285514] p 910 N95-16972
A simplified Integer Cosine Transform and its application in image compression p 757 N95-17286
High performance compression of science data
[NASA-CR-189388] p 911 N95-17329
VIDEO TAPES
From computer images to video presentation: Enhancing technology transfer p 848 N95-16467
Data Visualization and Animation Lab (DVAL) overview p 843 N95-16468
VIEWING
Mission operations management p 685 N95-17225
VIKING LANDER SPACECRAFT
A perspective of landing-site selection p 920 N95-16194
Mars Pathfinder mission operations concepts p 686 N95-17229
VIKING LANDER 1
Rationale for a Mars Pathfinder mission to Chryse Planitia and the Viking 1 lander p 918 N95-16183
VIKING MARS PROGRAM
Landing site considerations for atmosphere structure and meteorology p 921 N95-16203
VINYL POLYMERS
Detection of crosslink formation by 2 + 2 photocycloaddition in poly (vinyl cinnamate) by C-13 solid-state NMR
[AD-A281955] p 741 N95-16409
Living radical polymerization of vinyl acetate
[AD-A280901] p 743 N95-16500
VINYL RADICAL
Living radical polymerization of vinyl acetate
[AD-A280901] p 743 N95-16500
From living carbocationic to living radical polymerization
[AD-A280902] p 743 N95-16501
Chiral recognition in molecular and macromolecular pairs of liquid crystals of (2R, 3S)- , and (2S, 3S)-2-fluoro-3-methylpentyl-4'-(11-vinyloxyundeca iphenyl-4-carboxylate diastereomers
[AD-A281770] p 878 N95-17692
VIRTUAL REALITY
ISMCR 1994: Topical Workshop on Virtual Reality. Proceedings of the Fourth International Symposium on Measurement and Control in Robotics
[NASA-CP-10163] p 851 N95-15972
Vibratory tactile display for textures p 851 N95-15973
Applied virtual reality at the Research Triangle Institute p 851 N95-15974
Simulation of arthroscopic surgery using MRI data p 823 N95-15975
Multimodal correlation and intraoperative matching of virtual models in neurosurgery p 823 N95-15976
Virtual reality and telerobotics applications of an Address Recalculation Pipeline p 852 N95-15977
Using virtual reality for science mission planning: A Mars Pathfinder case p 673 N95-15978
Coordinated control of a dual-arm dexterous robot using full immersion telepresence and virtual reality p 852 N95-15979
An applications-oriented approach to the development of virtual environments p 853 N95-15980
A specification of 3D manipulation in virtual environments p 853 N95-15981
Tele Hyper Virtuality p 853 N95-15982
Surface matching for correlation of virtual models: Theory and application p 853 N95-15983
A virtual work space for both hands manipulation with coherency between kinesthetic and visual sensation p 831 N95-15984
Master-slave system with force feedback based on dynamics of virtual model p 853 N95-15985
Physics-based approach to haptic display p 854 N95-15986
Thermal feedback in virtual reality and telerobotic systems p 854 N95-15987
Virtual environment application with partial gravity simulation p 854 N95-15988
Applying Virtual Reality to commercial Edutainment p 854 N95-15989
A workout for virtual bodybuilders (design issues for embodiment in multi-actor virtual environments) p 854 N95-15990
Scripting human animations in a virtual environment p 855 N95-15992
Communicating situation awareness in virtual environments
[AD-A285239] p 836 N95-16511
VISCOELASTIC DAMPING
Energy decay and control for elastic and viscoelastic distributed parameter systems
[AD-A281312] p 726 N95-16008
Integrated passive and active control of structures
[AD-A282684] p 708 N95-16304
VISCOELASTICITY
Energy decay and control for elastic and viscoelastic distributed parameter systems
[AD-A281312] p 726 N95-16008
VISCOSITY
Effects of artificial viscosity on the accuracy of high-Reynolds-number kappa-epsilon turbulence model
[NASA-TM-106781] p 773 N95-17656
VISCOUS DRAG
An analysis code for the Rapid Engineering Estimation of Momentum and Energy Losses (REMEL)
[NASA-CR-191178] p 656 N95-16887
VISCOUS FLOW
Time accurate computation of unsteady inlet flows with a dynamic flow adaptive mesh
[AD-A285498] p 771 N95-16736
Spectral solution of the viscous blunt body problem. 2: Multidomain approximation
[NASA-CR-194971] p 863 N95-17267
Three dimensional compressible turbulent flow computations for a diffusing S-duct with/without vortex generators
[NASA-CR-195390] p 670 N95-17402
Investigation of the flow over a series of 14 percent-thick supercritical aerofoils with significant rear camber p 657 N95-17849
Measurements of the flow over a low aspect-ratio wing in the Mach number range 0.6 to 0.87 for the purpose of validation of computational methods. Part 1: Wing design, model construction, surface flow. Part 2: Mean flow in the boundary layer and wake, 4 test cases p 660 N95-17860
VISIBILITY
A preliminary optical visibility model p 758 N95-17290
VISION
Subset-selectivity and distractor matching in visual conjunction search
[AD-A285137] p 827 N95-16615
VISUAL ACUITY
The effects of target orientation on the dynamic contrast sensitivity function
[AD-A281855] p 826 N95-16298
Visual acuity versus field-of-view and light level for Night Vision Goggles (NVG)
[AD-A284750] p 830 N95-16553
VISUAL AIDS
An empirical approach to visual display preference based upon modulation transfer function and luminance
[AD-A285450] p 830 N95-16875
VISUAL DISCRIMINATION
Coordinated control of a dual-arm dexterous robot using full immersion telepresence and virtual reality p 852 N95-15979
A virtual work space for both hands manipulation with coherency between kinesthetic and visual sensation p 831 N95-15984

A workout for virtual bodybuilders (design issues for embodiment in multi-actor virtual environments)
p 854 N95-15990
CPP-TRS(C): On using visual cognitive symbols to enhance communication effectiveness
p 761 N95-15991
Training visual pattern recognition: Using worked examples to aid schema acquisition
[AD-A281859] p 826 N95-16299

VISUAL FIELDS
Factors affecting the visual fragmentation of the field-of-view in partial binocular overlap displays
[AD-A283081] p 886 N95-17334

VISUAL FLIGHT
Beyond the cockpit: The visual world as a flight instrument p 814 N95-16767

VISUAL FLIGHT RULES
Federal aviation regulations, part 91. General operating and flight rules. Change 5
[PB94-194883] p 665 N95-17476

VISUAL PERCEPTION
ISMCR 1994: Topical Workshop on Virtual Reality. Proceedings of the Fourth International Symposium on Measurement and Control in Robotics
[NASA-CP-10163] p 851 N95-15972
Presentations of shape in object recognition and long-term visual memory
[AD-A281336] p 825 N95-16010
The effects of target orientation on the dynamic contrast sensitivity function
[AD-A281855] p 826 N95-16298
Mental rotation with and without a concurrent task: Moderating effects of visuospatial ability
[AD-A281866] p 826 N95-16301
Visual neural development and chromatic aberration
[AD-A285064] p 826 N95-16368
Visual perception in the field-of-view of partial binocular overlap helmet-mounted displays
[AD-A285213] p 827 N95-16520
Subset-selectivity and distractor matching in visual conjunction search
[AD-A285137] p 827 N95-16615
Beyond the cockpit: The visual world as a flight instrument p 814 N95-16767
Dynamics of the G-excess illusion
p 815 N95-16771
Perceptual selectivity for color and form: On the nature of the interference effect
[AD-A285338] p 827 N95-16817
Parallel search for a conjunction of shape and contrast polarity
[AD-A285344] p 827 N95-16822
A framework for the analysis of cognitive tasks
[AD-A285345] p 828 N95-16835
An empirical approach to visual display preference based upon modulation transfer function and luminance
[AD-A285450] p 830 N95-16875
Factors affecting the visual fragmentation of the field-of-view in partial binocular overlap displays
[AD-A283081] p 886 N95-17334

VISUAL TASKS
Event-related brain potentials as predictors of target detection performance in a moving waterfall display simulating passive broad-band sonar monitoring
[AD-A280900] p 819 N95-16152
Training visual pattern recognition: Using worked examples to aid schema acquisition
[AD-A281859] p 826 N95-16299
Dark focus of accommodation as dependent and independent variables in visual display technology
p 812 N95-16758
Photoreceptors regulating circadian behavior: A mouse model
[AD-A285157] p 822 N95-16847

VITRIFICATION
High-level waste borosilicate glass: A compendium of corrosion characteristics
[DE94-016636] p 739 N95-15943

VOICE COMMUNICATION
Demodulation processes in auditory perception
[AD-A285427] p 869 N95-16248

VOIDS
Applications of positron depth profiling
[PB94-197753] p 900 N95-16952

VOLTAGE CONVERTERS (DC TO DC)
Space Station Freedom secondary power wiring requirements p 712 N95-16052
A modular electric power system test bed for small spacecraft
[NASA-TM-106812] p 721 N95-17276

VOLTAGE REGULATORS
A modular electric power system test bed for small spacecraft
[NASA-TM-106812] p 721 N95-17276

VORTEX BREAKDOWN
Numerical simulation of transient vortex breakdown above a pitching delta wing
[AD-A281075] p 655 N95-16808

VORTEX GENERATORS
Mach number, flow angle, and loss measurements downstream of a transonic fan-blade cascade
[AD-A280907] p 656 N95-16824
Three dimensional compressible turbulent flow computations for a diffusing S-duct with/without vortex generators
[NASA-CR-195390] p 670 N95-17402

VORTEX SHEDDING
Experimental and theoretical studies of wakes in stratified flows
[AD-A285305] p 771 N95-16616

VORTICES
Dynamical system prediction of the scalar field in a turbulent channel flow
[AD-A285519] p 771 N95-16438
The small-scale structure of dispersing clouds in the atmosphere
[AD-A285493] p 800 N95-16802
Numerical simulation of transient vortex breakdown above a pitching delta wing
[AD-A281075] p 655 N95-16808
A new approach to validate subgrid models in complex high Reynolds number flows
[AD-A282340] p 772 N95-17165
Transonic Navier-Stokes calculations about a 65 deg delta wing
[NASA-CR-4635] p 656 N95-17273
Three dimensional compressible turbulent flow computations for a diffusing S-duct with/without vortex generators
[NASA-CR-195390] p 670 N95-17402
Ellipsoid-cylinder model p 661 N95-17869
Supersonic vortex flow around a missile body
p 661 N95-17870
Test data on a non-circular body for subsonic, transonic and supersonic Mach numbers p 662 N95-17871
Wind tunnel test on a 65 deg delta wing with a sharp or rounded leading edge: The international vortex flow experiment p 662 N95-17872
Delta-wing model p 662 N95-17873
Experimental investigation of the vortex flow over a 76/60-deg double delta wing p 662 N95-17874
Wind tunnel test on a 65 deg delta wing with rounded leading edges: The International Vortex Flow Experiment
p 662 N95-17875
Investigation of the flow development on a highly swept canard/wing research model with segmented leading- and trailing-edge flaps p 662 N95-17876
Subsonic flow around US-orbiter model FALKE in the DNW p 663 N95-17877

VOYAGER PROJECT
Shared mission operations concept
p 685 N95-17228

VOYAGER 1 SPACECRAFT
Voyager investigation of the cosmic diffuse background: Observations of rocket-studied locations with Voyager
[NASA-CR-197532] p 917 N95-17422

VOYAGER 2 SPACECRAFT
Voyager investigation of the cosmic diffuse background: Observations of rocket-studied locations with Voyager
[NASA-CR-197532] p 917 N95-17422

W

WAFERS
Process of making a bistable photoconductive component
[AD-D016449] p 764 N95-16539

WAKEFULNESS
Alertness management in two-person long-haul flight operations p 813 N95-16760

WAKES
Experimental and theoretical studies of wakes in stratified flows
[AD-A285305] p 771 N95-16616
Surface pressure and wake drag measurements on the Boeing A4 airfoil in the IAR 1.5X1.5m Wind Tunnel Facility p 657 N95-17850

WALKING
Graphical simulation of articulated rigid body system kinematics with collision detection
[AD-A281842] p 856 N95-16372
The effect of intermittent standing or walking during head down tilt bedrest on peak O2 consumption
p 817 N95-16779
The efficacy of periodic + Gz exposure in the prevention of bedrest induced orthostatic intolerance
p 817 N95-16781
Energy expenditure, physical work load and postural control during walking on a moving platform
[AD-A285343] p 830 N95-16821

WALKING MACHINES
Graphical simulation of articulated rigid body system kinematics with collision detection
[AD-A281842] p 856 N95-16372

WALL FLOW
Wall-signature methods for high speed wind tunnel wall interference corrections p 650 N95-16257
Modeling of wall-bounded complex flows and free shear flows
[NASA-TM-106513] p 770 N95-16407
Effects of artificial viscosity on the accuracy of high-Reynolds-number kappa-epsilon turbulence model
[NASA-TM-106781] p 773 N95-17656
2-D airfoil tests including side wall boundary layer measurements p 657 N95-17847
Data from the GARTEur (AD) Action Group 02 airfoil CAST 7/DOA1 experiments p 659 N95-17856
A supercritical airfoil experiment p 659 N95-17858

WAR GAMES
ADST system test report for the rotary wing aircraft airnet aeromodel and weapon model merge with the ATAC 2 baseline
[AD-A281580] p 666 N95-16171

WARNING SYSTEMS
Detection of deforestation in the Amazon forest using NOAA/AVHRR images and the geographic information system SGI: Methodology and test of a potential alarm system
[INPE-5580-TDI/543] p 791 N95-17894

WASTE DISPOSAL
The removal of heteroatoms from organic compounds by supercritical water
[AD-A281532] p 722 N95-16087
Regional forecasting with global atmospheric models
[DE94-013863] p 801 N95-16961
Global climate change model natural climate variation: Paleoclimate data base, probabilities and astronomic predictors
[DE94-013956] p 796 N95-17348

WASTE HEAT
Thermal control systems for low-temperature heat rejection on a lunar base
[NASA-CR-197486] p 830 N95-16418

WASTE TREATMENT
Regional forecasting with global atmospheric models
[DE94-013863] p 801 N95-16961

WASTE UTILIZATION
Site characterization at the Rabbit Valley Geophysical Performance Evaluation Range
[DE94-013550] p 798 N95-16284
Landfill gas energy utilization: Technical and nontechnical considerations
[PB94-189651] p 793 N95-16544

WASTE WATER
Calcium phosphate precipitation in a fluidized bed
[PB94-201407] p 796 N95-17399

WASTES
Generic propellant transfer unit: A project update
p 719 N95-16345

WATER
The removal of heteroatoms from organic compounds by supercritical water
[AD-A281532] p 722 N95-16087
Computational simulation of the formation and material behavior of ice
[NASA-TM-106702] p 785 N95-16416
Plasma sound source basic research
[AD-A285394] p 890 N95-16617
Skin blood flow and bioelectrical impedance
[AD-A285475] p 821 N95-16619
An investigation of fluid flow during induction stroke of a water analog model of an IC engine using an innovative optical velocimetry concept: LIPA
[NASA-CR-197451] p 780 N95-16900
Fundamental studies in oxidation-reduction in relation to water photolysis
[DE94-014598] p 731 N95-17161
GPS tides and datums
[AD-A282422] p 666 N95-17508
Nonpowered instant water heater
[AD-A285459] p 783 N95-17725

WATER COLOR
SeaWiFS technical report series. Volume 21: The heritage of SeaWiFS. A retrospective on the CZCS NIMBUS Experiment Team (NET) program
[NASA-TM-104566-VOL-21] p 803 N95-16006

WATER CONSUMPTION
Root growth and development in response to CO2 enrichment
[NASA-CR-196154] p 807 N95-16429

WATER HAMMER
Transient flows and pressure waves in pipes
[DE94-012650] p 772 N95-17523

WATER HEATING
Nonpowered instant water heater
[AD-A285459] p 783 N95-17725
WATER QUALITY
Three-dimensional eutrophication model of Chesapeake Bay. Volume 1: Main report
[AD-A280760] p 804 N95-16118
South Florida environmental quality. National Status and Trends Program for marine environmental quality
[PB94-173408] p 796 N95-17363
WATER RESOURCES
Proceedings of the First National Conference on Climate Change and Water Resources Management
[AD-A281172] p 796 N95-17684
WATER SPLITTING
Use of magnesium for recovering hydrogen isotopes from tritiated water
[DE94-014471] p 731 N95-17157
WATER TREATMENT
Calcium phosphate precipitation in a fluidized bed
[PB94-201407] p 796 N95-17399
WATER VAPOR
A latitudinal survey of middle atmospheric water vapor revealed by shipboard microwave spectroscopy
[AD-A282000] p 799 N95-17446
WATER WAVES
Spatial information content analysis of Wiener spectra from polarized waterwave imagery
[AD-A283171] p 886 N95-17340
Analysis of a three-beam radar as an instrument for determining ocean wave heights and vector slopes
[AD-A282342] p 806 N95-17505
An observational study of long waves in the equatorial Pacific Ocean during the 1991-1993 El Nino
[AD-A283380] p 806 N95-17624
WAVE DIFFRACTION
Simulating the energy performance of holographic glazings
[DE94-013110] p 775 N95-17307
WAVE DISPERSION
High current density sheet-like electron beam generator
[AD-A281975] p 880 N95-17499
WAVE EQUATIONS
Ultrashort pulse effects in semiconductor amplifiers and in dispersive media
[AD-A284925] p 763 N95-16137
Slow wave vane structure with elliptical cross-section slots, an analysis
[NASA-CR-195352] p 755 N95-16886
Modeling mesons with relativistic wave equations
[DE94-016057] p 875 N95-16931
WAVE INTERACTION
Parametric study of shock-induced combustion in a hydrogen air system
[NASA-CR-197134] p 726 N95-15967
Sensitivity study of the SPEM model to the assimilation of synop datasets using two assimilation schemes. 1: Nudging. 2: The Kalman filter/smoother
[AD-A281459] p 804 N95-16079
WAVE PROPAGATION
Development of a medium energy modulated electron gun for orbital experiments
[AD-A281021] p 675 N95-16005
Rough surface models implemented within the split-step parabolic equation algorithm
[AD-A280843] p 753 N95-16148
Non-linear waves in gas dynamics and mechanics
[AD-A281376] p 770 N95-16156
Characteristics of phase-correcting fresnel zone plates and elliptical waveguides
[AD-A281385] p 763 N95-16159
On the propagation of near-inertial motion from the oceanic mixed layer p 806 N95-17396
Transient flows and pressure waves in pipes
[DE94-012650] p 772 N95-17523
High speed method for predicting radio-wave propagation
[AD-D016369] p 761 N95-17697
Propagation in the evaporation duct. Model predictions and comparisons to data
[AD-A283012] p 803 N95-17709
WAVE REFLECTION
Effective reflection coefficients for the mean acoustic field between two rough interfaces
[AD-A281962] p 870 N95-16413
WAVE-PARTICLE INTERACTIONS
Fractal aggregate random media analysis and applications
[AD-A281410] p 884 N95-16161
WAVEFORMS
Signal wave generator signals recorded by the Federal Outdoor Impact Laboratory's on-board Data Acquisition System
[PB94-186525] p 752 N95-16094
Characterization of multiport solid state imagers at megahertz data rates
[DE94-016095] p 765 N95-16932
WAVEGUIDE ANTENNAS
Field verification of the wind tunnel coefficients p 664 N95-17291
WAVEGUIDES
Characteristics of phase-correcting fresnel zone plates and elliptical waveguides
[AD-A281385] p 763 N95-16159
Field configuration of beam excited modes in the Advanced Photon Source (APS) storage ring waveguides
[DE94-015096] p 880 N95-16308
A simple EHF hemispheric coverage antenna
[AD-A285078] p 754 N95-16495
Fields and waves in elliptic waveguides
[AD-A285337] p 755 N95-16816
WAVELET ANALYSIS
Wavelets, signal processing and matrix computations
[AD-A283832] p 755 N95-16841
Low-complexity wavelet filter design for image compression p 757 N95-17289
WEAPON SYSTEMS
ADST system test report for the rotary wing aircraft airnet aeromodel and weapon model merge with the ATAC 2 baseline
[AD-A281580] p 666 N95-16171
Low rate initial production in Army Aviation systems development
[AD-A281871] p 666 N95-16356
MIL-STD-498 software development and documentation, version 01.00.00
[AD-A282003] p 837 N95-16607
Assessment of benefits and drawbacks of using fuzzy logic, especially in fire control systems
[AD-A285428] p 838 N95-16874
WEAPONS DELIVERY
A PC-based interactive simulation of the F-111C Pave Tack system and related sensor, avionics and aircraft aspects
[AD-A285500] p 669 N95-16969
WEAPONS DEVELOPMENT
Low rate initial production in Army Aviation systems development
[AD-A281871] p 666 N95-16356
WEAR
Static and dynamic friction behavior of candidate high temperature airframe seal materials
[NASA-TM-106571] p 722 N95-16905
A review of transmission diagnostics research at NASA Lewis Research Center
[ARL-TR-599] p 781 N95-16907
WEAR RESISTANCE
Tribological properties of reactively sputtered nitrides and carbides of titanium, zirconium and hafnium
[DE94-014583] p 745 N95-17160
WEAR TESTS
Approach to in-process tool wear monitoring in drilling: Application of Kalman filter theory p 653 N95-16279
Bench wear and single-cylinder engine evaluations of high-temperature lubricants for US Army ground vehicles
[AD-A285399] p 780 N95-16636
Tribological properties of reactively sputtered nitrides and carbides of titanium, zirconium and hafnium
[DE94-014583] p 745 N95-17160
Extended test of a xenon hollow cathode for a space plasma contactor
[NASA-CR-195402] p 720 N95-17265
Evaluation of alternate F-14 wing lug coating
[AD-A283207] p 669 N95-17631
WEATHER
A preliminary optical visibility model p 758 N95-17290
Field verification of the wind tunnel coefficients p 664 N95-17291
Recent changes of weather patterns in North America
[DE94-016115] p 803 N95-17743
WEATHER FORECASTING
Regional forecasting with global atmospheric models
[DE94-013863] p 801 N95-16961
Summary of 1994 Atlantic tropical cyclone activity and verification of author's seasonal prediction, 1 p 801 N95-17259
Extended range forecast of Atlantic seasonal hurricane activity for 1995, 2 p 801 N95-17260
Meteorological factors that affect the formation an prediction of aircraft icing
[AD-A281984] p 802 N95-17443
Operational cloud classifier based on a self-organized feature map
[PB94-197852] p 802 N95-17504
WEATHERING
High-level waste borosilicate glass: A compendium of corrosion characteristics
[DE94-016636] p 739 N95-15943
WEIGHT INDICATORS
An investigation of polynomial calibrations methods for wind tunnel balances p 650 N95-16258
WEIGHTLESSNESS
Virtual environment application with partial gravity simulation p 854 N95-15988
Variability in Hoffmann and tendon reflexes in healthy male subjects p 808 N95-16739
Achilles Tendon Reflex (ATR) in response to short exposures of microgravity and hypergravity p 812 N95-16756
Prediction of space sickness in astronauts from preflight fluid, electrolyte, and cardiovascular variables and Weightless Environmental Training Facility (WETF) training p 812 N95-16757
Effects of weightlessness on human baroreflex function p 815 N95-16770
Artificial gravity: How much, how often, how long? p 816 N95-16778
WELDABILITY
Characterization of the hydrogen induced cold cracking susceptibility at simulated weld zones in HSLA-100 steel
[PB94-174505] p 737 N95-17616
WELDED JOINTS
Diffusion weld test fixture
[AD-D016450] p 780 N95-16543
Investigation of residual stresses in a multipass weld in 1 in. stainless steel plate
[DE94-013277] p 786 N95-16803
Modeling of thermal stresses in welds
[DE94-018046] p 789 N95-17675
Electron beam weld development on a Filter Pack Assembly
[DE94-015867] p 782 N95-17716
WPH-6112A thermal expansion test of PRESS tubulation
[DE94-015946] p 782 N95-17717
WELDING
Modeling of thermal stresses in welds
[DE94-018046] p 789 N95-17675
WETLANDS
Simulation of hydrologic influences on wetland ecosystem succession
[AD-A284737] p 795 N95-16545
WETTING
Characterization of surfaces
[NASA-CR-196995] p 750 N95-16065
WHEELS
Bicarbonate of soda blasting technology for aircraft wheel depainting
[PB94-193323] p 654 N95-17466
WHITE NOISE
Closed-loop carrier phase synchronization techniques motivated by likelihood functions p 756 N95-17284
WIND DIRECTION
Structural effects of unsteady aerodynamic forces on horizontal-axis wind turbines
[DE94-011863] p 787 N95-16939
Field verification of the wind tunnel coefficients p 664 N95-17291
On the measurement of momentum flux profiles using a five-beam 915-MHz wind profiler
[DE94-018448] p 791 N95-17903
WIND TUNNEL APPARATUS
An investigation of polynomial calibrations methods for wind tunnel balances p 650 N95-16258
WIND TUNNEL CALIBRATION
Free-jet testing at Mach 3.44 in GASL's aero/thermo test facility p 672 N95-16320
Error propagation equations for estimating the uncertainty in high-speed wind tunnel test results
[DE94-014136] p 671 N95-16509
WIND TUNNEL MODELS
Comparison of computational and experimental results for a supercritical airfoil
[NASA-TM-4601] p 656 N95-16908
WIND TUNNEL TESTS
Experimental study at low supersonic speeds of a missile concept having opposing wraparound tails
[NASA-TM-4582] p 655 N95-16069
An approach to aerodynamic characteristics of low radar cross-section fuselages p 649 N95-16251
Wall-signature methods for high speed wind tunnel wall interference corrections p 650 N95-16257
Hypersonic air-breathing aeropropulsion facility test support requirements p 672 N95-16319
Free-jet testing at Mach 3.44 in GASL's aero/thermo test facility p 672 N95-16320
Error propagation equations for estimating the uncertainty in high-speed wind tunnel test results
[DE94-014136] p 671 N95-16509
Measurements of unsteady pressure and structural response for an elastic supercritical wing
[NASA-TP-3443] p 653 N95-16560

Structural effects of unsteady aerodynamic forces on horizontal-axis wind turbines
[DE94-011863] p 787 N95-16939
Data acquisition and processing software for the Low Speed Wind Tunnel tests of the Jindivik auxiliary air intake
[AD-A285455] p 656 N95-17178
Field verification of the wind tunnel coefficients p 664 N95-17291
Active load control during rolling maneuvers — performed in the Langley Transonic Dynamics Tunnel
[NASA-TP-3455] p 669 N95-17397
A selection of experimental test cases for the validation of CFD codes, volume 2
[AGARD-AR-303-VOL-2] p 657 N95-17846
2-D airfoil tests including side wall boundary layer measurements p 657 N95-17847
Measurements on a two-dimensional aerofoil with high-lift devices p 657 N95-17848
Investigation of the flow over a series of 14 percent-thick supercritical aerofoils with significant rear camber p 657 N95-17849
Surface pressure and wake drag measurements on the Boeing A4 airfoil in the IAR 1.5X1.5m Wind Tunnel Facility p 657 N95-17850
2-D aileron effectiveness study p 658 N95-17851
Investigation of an NLF(1)-0416 airfoil in compressible subsonic flow p 658 N95-17852
Experiments in the trailing edge flow of an NLR 7702 airfoil p 658 N95-17853
Two-dimensional 16.5 percent thick supercritical airfoil NLR 7301 p 658 N95-17854
Low-speed surface pressure and boundary layer measurement data for the NLR 7301 airfoil section with trailing edge flap p 658 N95-17855
Data from the GARTEur (AD) Action Group 02 airfoil CAST 7/DOA1 experiments p 659 N95-17856
OAT15A airfoil data p 659 N95-17857
A supercritical airfoil experiment p 659 N95-17858
Two-dimensional high-lift airfoil data for CFD code validation p 659 N95-17859
Measurements of the flow over a low aspect-ratio wing in the Mach number range 0.6 to 0.87 for the purpose of validation of computational methods. Part 1: Wing design, model construction, surface flow. Part 2: Mean flow in the boundary layer and wake, 4 test cases p 660 N95-17860
Detailed study at supersonic speeds of the flow around delta wings p 660 N95-17861
Pressure distributions on research wing W4 mounted on an axisymmetric body p 660 N95-17862
DLR-F4 wing body configuration p 660 N95-17863
DLR-F5: Test wing for CFD and applied aerodynamics p 660 N95-17864
Low aspect ratio wing experiment p 661 N95-17865
Wind tunnel investigations of the appearance of shocks in the windward region of bodies with circular cross section at angle of attack p 661 N95-17866
Three-dimensional boundary layer and flow field data of an inclined prolate spheroid p 661 N95-17867
Force and pressure data of an ogive-nosed slender body at high angles of attack and different Reynolds numbers p 661 N95-17868
Ellipsoid-cylinder model p 661 N95-17869
Supersonic vortex flow around a missile body p 661 N95-17870
Test data on a non-circular body for subsonic, transonic and supersonic Mach numbers p 662 N95-17871
Wind tunnel test on a 65 deg delta wing with a sharp or rounded leading edge: The international vortex flow experiment p 662 N95-17872
Delta-wing model p 662 N95-17873
Experimental investigation of the vortex flow over a 76/60-deg double delta wing p 662 N95-17874
Wind tunnel test on a 65 deg delta wing with rounded leading edges: The International Vortex Flow Experiment p 662 N95-17875
Investigation of the flow development on a highly swept canard/wing research model with segmented leading- and trailing-edge flaps p 662 N95-17876
Subsonic flow around US-orbiter model FALKE in the DNW p 663 N95-17877
Low speed propeller slipstream aerodynamic effects p 663 N95-17882

WIND TUNNEL WALLS
Wall-signature methods for high speed wind tunnel wall interference corrections p 650 N95-16257
Surface pressure and wake drag measurements on the Boeing A4 airfoil in the IAR 1.5X1.5m Wind Tunnel Facility p 657 N95-17850
2-D aileron effectiveness study p 658 N95-17851
Data from the GARTEur (AD) Action Group 02 airfoil CAST 7/DOA1 experiments p 659 N95-17856
OAT15A airfoil data p 659 N95-17857
A supercritical airfoil experiment p 659 N95-17858
Two-dimensional high-lift airfoil data for CFD code validation p 659 N95-17859

WIND TUNNELS
STOVL CFD model test case p 663 N95-17881

WIND TURBINES
Structural testing of the North Wind 250 composite rotor joint
[DE94-006923] p 792 N95-16437
Structural effects of unsteady aerodynamic forces on horizontal-axis wind turbines
[DE94-011863] p 787 N95-16939
Analysis of a two-bladed, teetering-hub turbine using the ADAMS (tm) software
[DE94-006922] p 781 N95-17169
Engineering design tools for wind diesel systems. Volume 2: JODYMOD dynamic wind diesel simulation software package. Model verification
[PB95-104519] p 840 N95-17355
Engineering design tools for wind diesel systems. Volume 3: JODYMOD dynamic simulation software package. Model description
[PB95-104527] p 840 N95-17356
The application of non-destructive techniques to the testing of a wind turbine blade
[DE95-000323] p 784 N95-17360
Engineering design tools for wind diesel systems. Volume 4: JODYMOD dynamic wind diesel simulation software package. Program documentation
[PB95-104535] p 841 N95-17628

WIND VELOCITY
Atmosphere structure and meteorology instrument for Mars Pathfinder p 711 N95-16202
An investigation of small-scale variations in cloud climatology induced by topography and monthly mean winds
[AD-A283274] p 803 N95-17715
On the measurement of momentum flux profiles using a five-beam 915-MHz wind profiler
[DE94-018448] p 791 N95-17903

WINDOWS (APERTURES)
Simulating the energy performance of holographic glazings
[DE94-013110] p 775 N95-17307
Issues in the design and optimization of adaptive optics and laser guide stars for the Keck Telescopes
[DE94-012888] p 916 N95-17525

WINDOWS (COMPUTER PROGRAMS)
A graphical environment for object-oriented simulation model environment
[NASA-CR-196887] p 833 N95-16088
The new map graphics in RSAS 5.0
[AD-A282432] p 791 N95-17511
ICCanvas 3D visualization tool for Windows (tm). Software user's manual
[AD-A285603] p 842 N95-17746

WINDPOWER UTILIZATION
Structural effects of unsteady aerodynamic forces on horizontal-axis wind turbines
[DE94-011863] p 787 N95-16939
Analysis of a two-bladed, teetering-hub turbine using the ADAMS (tm) software
[DE94-006922] p 781 N95-17169
Engineering design tools for wind diesel systems. Volume 2: JODYMOD dynamic wind diesel simulation software package. Model verification
[PB95-104519] p 840 N95-17355
Engineering design tools for wind diesel systems. Volume 3: JODYMOD dynamic simulation software package. Model description
[PB95-104527] p 840 N95-17356
Engineering design tools for wind diesel systems. Volume 4: JODYMOD dynamic wind diesel simulation software package. Program documentation
[PB95-104535] p 841 N95-17628
Engineering design tools for wind diesel systems. Volume 5: JODYMOD dynamic wind diesel simulation software package. User's guide
[PB95-104543] p 841 N95-17629
Engineering design tools for wind diesel systems. Volume 1: Executive summary
[PB95-104501] p 842 N95-17733
Engineering design tools for wind diesel systems. Volume 6: Logistic package. User documentation
[PB95-104550] p 842 N95-17734
Engineering design tools for wind diesel systems. Volume 7: Logistic package. Validation report
[PB95-104568] p 842 N95-17735

WINDS ALOFT
An improved neutral wind model with predictive capabilities
[AD-A282283] p 800 N95-16235

WING FLAPS
Low-speed surface pressure and boundary layer measurement data for the NLR 7301 airfoil section with trailing edge flap p 658 N95-17855

WING LOADING
Active load control during rolling maneuvers — performed in the Langley Transonic Dynamics Tunnel
[NASA-TP-3455] p 669 N95-17397
2-D aileron effectiveness study p 658 N95-17851

WING OSCILLATIONS
A computational investigation of wake-induced airfoil flutter in incompressible flow and active flutter control
[AD-A281534] p 670 N95-16109

WINGS
Aerodynamic shape optimization p 668 N95-16572
Investigation of the influence of pylons and stores on the wing lower surface flow p 664 N95-17885

WIRE
Kapton wire concerns for aerospace vehicles p 711 N95-16045
Thermoacoustic pin stacks
[AD-A282267] p 794 N95-16954
Magnetostrictive torque sensor
[AD-D016376] p 775 N95-17376

WIRING
First NASA Workshop on Wiring for Space Applications
[NASA-CP-10145] p 711 N95-16044
Problems with aging wiring in Naval aircraft p 711 N95-16048
Space Station Freedom primary power wiring requirements p 712 N95-16051
Space Station Freedom secondary power wiring requirements p 712 N95-16052
Kapton pyrolysis, the space environment and wiring requirements p 712 N95-16054
New insulation constructions for aerospace wiring applications p 712 N95-16056

WOOD
Development of processes, means, and theoretical principles of thin-walled detail plastic forming at Kazan Aviation Institute p 653 N95-16281

WORDS (LANGUAGE)
Tele Hyper Virtuality p 853 N95-15982
CPP-TRS(C): On using visual cognitive symbols to enhance communication effectiveness p 761 N95-15991

WORKLOADS (PSYCHOPHYSIOLOGY)
The EPIC architecture for modeling human information-processing and performance: A brief introduction
[AD-A280762] p 829 N95-16119
Application of research techniques for documenting cognitive processes in air traffic control: Sector complexity and decision making
[AD-A282336] p 665 N95-16375
Crew decision making under stress p 814 N95-16765
Energy expenditure, physical work load and postural control during walking on a moving platform
[AD-A285343] p 830 N95-16821
Efficiency in work behaviour: A design approach for modern tools
[PB94-197761] p 831 N95-16953
Situation awareness information requirements for En Route Air Traffic Control
[DOT/FAA/AM-94/27] p 828 N95-17655

WORKSTATIONS
Electronic Engineering Notebook: A software environment for research execution, documentation and dissemination p 848 N95-16473
A workstation based simulator for teaching compressible aerodynamics
[NASA-TM-106799] p 839 N95-16906
XPVM: A graphical console and monitor for PVM
[DE94-018050] p 842 N95-17678

WOVEN COMPOSITES
Failure analysis of 2D and 3D woven composites
[NASA-CR-197247] p 724 N95-16597

X

X RAY ABSORPTION
Atomic structure and valency of nickel in some of its oxycompounds
[AD-A281109] p 733 N95-16091
X-ray absorption spectra and structure of some nickel oxides (hydroxides)
[AD-A281305] p 735 N95-16788

X RAY ANALYSIS
XAFS spectra and the oxidation state of nickel in some of its oxycompounds
[AD-A281137] p 735 N95-16606

X RAY ASTRONOMY
Activities of the Space Studies Board
[NASA-CR-197105] p 672 N95-16033
The mass and dynamics of cD clusters with cooling flows. 1: ROSAT observations of A 496
[NASA-CR-197534] p 915 N95-17495

ROSAT detection of diffuse hot gas in the edge-on galaxy NGC 4631
[NASA-CR-197535] p 915 N95-17496
X-ray emission from the edge-on spiral galaxy NGC 4631
[NASA-CR-197536] p 924 N95-17527

X RAY ASTROPHYSICS FACILITY
Generic mission planning and scheduling: The AXAF solution p 686 N95-17231

X RAY DETECTORS
Active silicon x ray for measuring electron temperature
[DE94-017521] p 890 N95-16555

X RAY DIFFRACTION
Synthesis and characterization of neopentyl indium compounds: X-ray crystal structures of ((Me3CCH2)2InAs(SiMe3)2)2 and ((Me3CCH2)2InAs(SiMe3)2In (CH2CMe3)2Cl)
[AD-A282766] p 900 N95-17137
Evaluation of the quality of sapphire using x-ray rocking curves and double-crystal x-ray topography
[AD-A282905] p 901 N95-17620
Texture analysis of critical current density in Bi2Sr2CaCu2O(x) tapes
[DE94-018375] p 902 N95-17898

X RAY LASERS
Simulations of an FEL producing coherent x rays utilizing the SLAC LINAC
[AD-A283524] p 777 N95-17303
Development of x-ray laser architectural components
[DE94-016446] p 778 N95-17627

X RAY SOURCES
High brightness cathodes for microfocus x-ray generators
[AD-A285256] p 764 N95-16814
The mass and dynamics of cD clusters with cooling flows. 1: ROSAT observations of A 496
[NASA-CR-197534] p 915 N95-17495
X-ray emission from the edge-on spiral galaxy NGC 4631
[NASA-CR-197536] p 924 N95-17527

X RAY SPECTRA
The mass and dynamics of cD clusters with cooling flows. 1: ROSAT observations of A 496
[NASA-CR-197534] p 915 N95-17495
ROSAT detection of diffuse hot gas in the edge-on galaxy NGC 4631
[NASA-CR-197535] p 915 N95-17496
X-ray emission from the edge-on spiral galaxy NGC 4631
[NASA-CR-197536] p 924 N95-17527
Measurements of x ray spectral flux and intensity distribution of APS/CHESS undulator radiation
[DE94-018384] p 882 N95-17901

X RAY SPECTROSCOPY
XAFS investigation of structure and valency of nickel in some oxycompounds
[AD-A283193] p 877 N95-17630
Measurements of x ray spectral flux and intensity distribution of APS/CHESS undulator radiation
[DE94-018384] p 882 N95-17901

X RAY TIMING EXPLORER
OOD/OOP experience in the Science Operations Center part of the ground system for X ray Timing Explorer mission p 675 N95-17565

X RAYS
Alpha proton x ray spectrometer p 710 N95-16201
High brightness cathodes for microfocus x-ray generators
[AD-A285256] p 764 N95-16814
Miniature, vacuum compatible 1024 (times) 1024 CCD camera for x ray, ultraviolet, or optical imaging
[DE94-012235] p 776 N95-17522
An x ray technique for precision laser beam synchronization
[DE94-016449] p 779 N95-17635
Measurements of x ray spectral flux and intensity distribution of APS/CHESS undulator radiation
[DE94-018384] p 882 N95-17901
Recent advances in the development of high average power induction accelerators for industrial and environmental applications
[DE94-018734] p 882 N95-17914

XENON
Continuing life test of a xenon hollow cathode for a space plasma contactor
[NASA-CR-195401] p 711 N95-15968
Electric probe measurements in the plume of the UK-10 ion thruster
[AD-A282460] p 713 N95-16302
Characterization of multiport solid state imagers at megahertz data rates
[DE94-016095] p 765 N95-16932
Extended test of a xenon hollow cathode for a space plasma contactor
[NASA-CR-195402] p 720 N95-17265
A high resolution liquid xenon imaging telescope for 0.3-10 MeV gamma-ray astrophysics: Construction and initial balloon flights
[NASA-CR-197556] p 916 N95-17528

Y

YAG LASERS
A AgGaSe2 optical parametric oscillator pumped by a Raman-shifted YAG laser
[AD-A284743] p 777 N95-16548

YBCO SUPERCONDUCTORS
Flux imaging of high temperature superconductor single crystals and Ag sheathed wires
[DE94-013874] p 897 N95-16408
Chemical vapor deposition of high T(sub c) superconducting films in a microgravity environment
[NASA-CR-197527] p 750 N95-16880

YIELD POINT
A high average power electro-optic switch using KTP
[DE94-016416] p 765 N95-16925

YTTRIUM
Processing, fabrication, characterization and device demonstration of high temperature superconducting ceramics
[AD-A285145] p 744 N95-16844

YTTRIUM COMPOUNDS
Columnar defect pinning in untwinned single crystal YBa2Cu2O7
[DE94-013962] p 901 N95-17349

YTTRIUM OXIDES
Multiphase ceramics for mechanical and structural reliability at low and elevated temperatures
[AD-A285497] p 746 N95-17438
Micromechanics of interfaces in metal matrix composites
[AD-A282404] p 725 N95-17457

Z

ZEEMAN EFFECT
Determination of ion temperatures from Zeeman broadened spectral lines in the edge of Tore Supra
[DE94-018112] p 873 N95-16403

ZEOLITES
Radical cations of quadricyclane and norbornadiene in polar ZSM-5 matrices: Radical cation photochemical transformations without photons
[DE94-014007] p 728 N95-16485

ZETA PINCH
Beams 92: Proceedings
[DE94-014784] p 880 N95-17475

ZINC OXIDES
Preparation and investigation of improved low voltage electron excitable phosphors
[AD-A284265] p 767 N95-17487

ZINC TELLURIDES
Electrochemical atomic layer processing
[AD-A282330] p 872 N95-16241

ZIRCONIUM CARBIDES
Tribological properties of reactively sputtered nitrides and carbides of titanium, zirconium and hafnium
[DE94-014583] p 745 N95-17160

ZIRCONIUM NITRIDES
Tribological properties of reactively sputtered nitrides and carbides of titanium, zirconium and hafnium
[DE94-014583] p 745 N95-17160

ZIRCONIUM OXIDES
Testing and evaluation of oxide-coated iridium/rhenium chambers p 719 N95-16346
Thermal and mechanical behavior of Ba(1+x)Zr4P(6-2x)Si(2x)O24
[DE94-013620] p 899 N95-16806

Typical Personal Author Index Listing

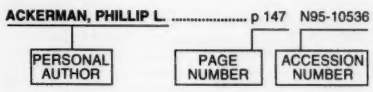

Listings in this index are arranged alphabetically by personal author. The page number helps you locate the citation in the abstract section. The accession number denotes the number by which the citation is identified.

A

ABARBANEL, SAUL ..... p 863 N95-16904
ABDURASHITOV, J. N. ..... p 876 N95-17154
ABEDINI, ANNADIANA ..... p 688 N95-17241
ABGRALL, REMI ..... p 863 N95-17333
ABSIL, L. H. J. ..... p 658 N95-17853
ACKER, JAMES G. ..... p 803 N95-16006
ADACHI, MASAKAZU ..... p 724 N95-16833
ADAMS, G. ..... p 809 N95-16740
ADAMS, P. M. ..... p 901 N95-17620
ADELSON, S. J. ..... p 835 N95-16223
ADKISSON, LORI ..... p 665 N95-17373
AFFINITO, J. ..... p 748 N95-17913
AFFINITO, J. D. ..... p 793 N95-16916
AGRAWALA, ASHOK K. ..... p 844 N95-16061
AGUILERA, CHRISTINE ..... p 697 N95-17562
AHUJA, J. K. ..... p 726 N95-15967
AKAMA, KEIICHI ..... p 877 N95-17520
AKSAY, ILHAN A. ..... p 744 N95-16844
AKSENOV, V. L. ..... p 871 N95-16059
ALAVA, M. J. ..... p 894 N95-17929
ALBERS, R. ..... p 796 N95-17304
ALBINSSON, B. ..... p 759 N95-17453
ALCOTT, G. ..... p 708 N95-17613
ALEKSANDROV, A. ..... p 861 N95-16295
ALEM, NABIH M. ..... p 829 N95-16147
p 664 N95-16404
p 831 N95-17484
ALEXANDER, EDWARD M. ..... p 761 N95-17696
ALEXANDER, SCOTT ..... p 702 N95-17583
ALEXANDROU, SOTIRIS ..... p 763 N95-16394
ALEXANDROV, NATALIA ..... p 863 N95-16897
ALFORD, W. J. ..... p 777 N95-16917
ALFREY, C. ..... p 811 N95-16752
ALHAMBRA, EDGAR M. ..... p 734 N95-16229
ALLAIRE, P. E. ..... p 654 N95-17657
ALLARD, RICHARD A. ..... p 800 N95-16551
ALLEN, CARLTON C. ..... p 917 N95-16177
ALLEN, CHRISTOPHER W. ..... p 739 N95-16000
ALLEN, JAMES F. ..... p 839 N95-16883
ALLEN, JERRY M. ..... p 655 N95-16069
ALLEN, ROGER E. ..... p 779 N95-17698
ALLEN, S. L. ..... p 889 N95-16554
ALLEY, WILLIAM E. ..... p 828 N95-17175
ALLREAD, J. ..... p 784 N95-17360
ALMANZA, JOE ..... p 666 N95-16171
ALPERT, ETHAN ..... p 840 N95-17324
ALTUNIN, VALERY I. ..... p 694 N95-17543
AMANN, J. F. ..... p 876 N95-17153
p 876 N95-17158
AMARNATH, A. ..... p 732 N95-17524
AMATO, A. ..... p 868 N95-16288
AMBROSIANO, J. ..... p 797 N95-17920
AMES, CHARLES ..... p 696 N95-17557
AMIDEI, D. ..... p 878 N95-17899
AMIMOTO, SHERWIN T. ..... p 777 N95-16548
AMON, B. ..... p 771 N95-16595
AMONETTE, J. E. ..... p 733 N95-17912
ANAND, HARSH ..... p 804 N95-16125
ANANTATMULA, R. P. ..... p 737 N95-17637
ANANTHARAJ, VALENTINE ..... p 805 N95-16141
ANDERSON, BERNHARD H. ..... p 654 N95-16038
ANDERSON, M. G. ..... p 799 N95-16735
ANDERSON, MARK S. ..... p 774 N95-16242
ANDERSON, T. L. ..... p 786 N95-16785
ANDERSON, T. S. ..... p 736 N95-16807
ANDERSON, WILLIAM E. ..... p 730 N95-16882
ANDRAS, MARIA T. ..... p 731 N95-17387
ANGUELOV, ROUMEN ..... p 863 N95-17333
ANGUS, JOHN C. ..... p 898 N95-16527
ANKENY, ALAN E. ..... p 669 N95-17631
ANNIS, B. K. ..... p 733 N95-17911
ANSPAUGH, B. E. ..... p 792 N95-16067
ANTONOVA, E. E. ..... p 799 N95-17471
APOSTOLAKIS, G. ..... p 675 N95-17493
APPEL, J. A. ..... p 871 N95-15945
APPLETON, BRIAN W. ..... p 821 N95-16619
APRILE, ELENA ..... p 916 N95-17528
ARAMAYO, G. A. ..... p 789 N95-17675
ARATOW, M. ..... p 809 N95-16744
ARCHAMBAUD, J. P. ..... p 659 N95-17856
p 659 N95-17857
ARGIALAS, DEMETRE P. ..... p 790 N95-17375
ARGOITIA, ALBERTO ..... p 898 N95-16527
ARMAN, M. J. ..... p 760 N95-17501
ARMINJON, PAUL ..... p 863 N95-17333
ARMSTRONG, N. ..... p 886 N95-17143
ARMSTRONG, PHILIP N. ..... p 910 N95-17166
ARNOLD, M. ..... p 782 N95-17364
ARONSON, M. C. ..... p 896 N95-16389
ARQUILLA, RICHARD ..... p 674 N95-17255
ARYA, R. R. ..... p 794 N95-17521
ARYA, V. K. ..... p 718 N95-16337
ASAKURA, FUMIOKI ..... p 863 N95-17333
ASHILL, P. R. ..... p 657 N95-17849
ASLAM, TANWEER ..... p 700 N95-17572
ASOKA-KUMAR, P. ..... p 899 N95-16918
ASTON-JONES, GARY ..... p 826 N95-16377
ATHERTON, L. J. ..... p 902 N95-17742
ATTAWAY, S. W. ..... p 788 N95-17439
AUCIELLO, ORLANDO H. ..... p 742 N95-16488
AUERNHEIMER, BRENT ..... p 696 N95-17557
AURICCHIO, F. ..... p 735 N95-16786
AUSTERN, M. H. ..... p 881 N95-17886
AUSTIN, JEFFREY G. ..... p 656 N95-16824
AVERILL, ROBERT D. ..... p 848 N95-16471
AYACHE, S. ..... p 674 N95-17532
p 692 N95-17534
AZMY, Y. ..... p 844 N95-15946

B

BABUSKA, I. ..... p 861 N95-16379
p 863 N95-17431
BACHMANN, KLAUS J. ..... p 742 N95-16488
BACON, D. ..... p 810 N95-16749
BADAVI, FRANCIS F. ..... p 924 N95-16912
BADDOURAH, MAJDI ..... p 847 N95-16459
BADR, SALAH ..... p 834 N95-16153
BAECKLUND, K. ..... p 653 N95-17451
BAECKSTROEM, K. ..... p 909 N95-16400
BAER, M. R. ..... p 748 N95-16214
BAEZ, ANASTACIO N. ..... p 721 N95-17276
BAIR, SCOTT ..... p 741 N95-16355
BAIZE, LIONEL ..... p 674 N95-17250
BAKER, D. F. ..... p 694 N95-17546
BAKER, GREG ..... p 863 N95-17333
BAKER, PAUL L. ..... p 701 N95-17580
BAKHLE, MILIND A. ..... p 786 N95-16588
BALCAR, E. ..... p 869 N95-17750
BALCH, J. W. ..... p 775 N95-17380
BALDI, ANDREA ..... p 692 N95-17533
p 703 N95-17590
BALDOCCHI, DENNIS D. ..... p 797 N95-17908
BALDWIN, RYAN A. ..... p 900 N95-17171
BALLARD, R. E. ..... p 809 N95-16744
BALLENTINE, THOMAS M. ..... p 796 N95-17684
BANCROFT, DOUGLAS ..... p 754 N95-16549
BANKS, DAVID C. ..... p 847 N95-16466
BAO, JINSONG ..... p 649 N95-16250
BAO, MING ..... p 651 N95-16267
BARBERIS, D. ..... p 661 N95-17869
p 661 N95-17870
p 662 N95-17873
BARCLAY, C. B. ..... p 910 N95-16884
BARGER, V. ..... p 877 N95-17353
BARKER, J. G. ..... p 876 N95-16962
BARLOW, D. ..... p 879 N95-16172
p 876 N95-17158
BARLOW, NADINE G. ..... p 917 N95-16178
BARNABAS, M. V. ..... p 728 N95-16485
BARNES, JEFF R. ..... p 917 N95-16179
BARRATT, M. ..... p 816 N95-16775
BARRATT, M. R. ..... p 816 N95-16774
BARRIOS, AMALIA E. ..... p 753 N95-16148
BARRO, E. ..... p 696 N95-17558
BARTALINI, P. ..... p 875 N95-16914
BARTELHEIMER, W. ..... p 657 N95-17847
BARTLETT, RODNEY J. ..... p 874 N95-16523
BARTRAM, R. H. ..... p 896 N95-16385
BARTSCH, R. R. ..... p 891 N95-16936
BASORE, P. A. ..... p 894 N95-15942
BATES, J. K. ..... p 739 N95-15943
BATHKE, C. G. ..... p 891 N95-17155
BAUMERT, W. ..... p 663 N95-17878
BAXI, C. B. ..... p 893 N95-17896
BAYLOR, K. A. ..... p 815 N95-16771
BEACH, EDWARD ..... p 703 N95-17587
BEALE, DAVID G. ..... p 664 N95-16404
BEAM, SHERILEE F. ..... p 848 N95-16467
BEASLEY, HOWARD H. ..... p 827 N95-16520
p 886 N95-17334
BEATTIE, A. ..... p 784 N95-17360
BECK, B. G. ..... p 808 N95-16741
BECK, JON ..... p 836 N95-16574
BECKER, B. ..... p 834 N95-16220
BECKER, BILL ..... p 854 N95-15987
BECKETT, MARCIE B. ..... p 821 N95-16619
BECKMAN, R. M. ..... p 687 N95-17237
BEDAIR, SALAH ..... p 894 N95-16084
BEDAT, B. ..... p 732 N95-17437
BEDWORTH, PETER V. ..... p 874 N95-16629
BEELDMAN, M. ..... p 796 N95-17304
BEGUELIN, ADAM ..... p 850 N95-16826
BEILKE, DEAN ..... p 790 N95-17372
BEITHER, J. ..... p 751 N95-17632
BEJCZY, ANTAL K. ..... p 832 N95-17400
BELL, HOLLAND T. ..... p 702 N95-17585
BELTRAN, L. ..... p 775 N95-17307
BENARD, D. J. ..... p 728 N95-16497
BENDRICK, GREGG A. ..... p 819 N95-16297
BENESH, C. ..... p 875 N95-16931
BENFORD, STEVE ..... p 854 N95-15990
BENGTSSON, J. ..... p 904 N95-17904
BENICEWICZ, B. C. ..... p 748 N95-17892
BENINCASA, MILISSA M. ..... p 833 N95-16003
BENJAMIN, TED ..... p 674 N95-17556
BENNETT, BRUCE W. ..... p 791 N95-17511
BENNETT, C. A. ..... p 890 N95-16921
BENNETT, M. ..... p 794 N95-17521
BENNETT, M. J. ..... p 739 N95-17747
BENNETT, TOBY ..... p 678 N95-17191
p 680 N95-17200
p 681 N95-17206
BENNETT, W. ..... p 748 N95-17913
BENNETT, W. D. ..... p 793 N95-16916
BENSON, KEITH R. ..... p 805 N95-16168
BENSON, RUSTY A. ..... p 771 N95-16736
BENSON, THOMAS J. ..... p 713 N95-16066
p 839 N95-16906
p 839 N95-17264
BENSON, W. H. ..... p 846 N95-16222
BERENC, T. ..... p 761 N95-17926
BERG, JEREMY M. ..... p 726 N95-16001
BERG, W. ..... p 882 N95-17902
BERGER, M. S. ..... p 877 N95-17353
p 878 N95-17720
BERGMAN, W. ..... p 770 N95-16211
BERKOWITZ, MAX L. ..... p 873 N95-16411
BERLIN, ANDREW ..... p 846 N95-16237
BERMAN, DAVID H. ..... p 870 N95-16413
BERNARD, M. A. ..... p 888 N95-16216

BERNHOLC, JERRY ..... p 894 N95-16084
BERRIER, BOBBY L. ..... p 663 N95-17879
BERRY, THOMAS ..... p 685 N95-17224
BERTACHINIDEALMEIDAPRADO, ANTONIO FERNANDO ..... p 673 N95-17648
BERZINS, VALDIS ..... p 834 N95-16154
BESMANN, T. M. ..... p 723 N95-16225
p 724 N95-16926
BESS, PHILIP K. ..... p 754 N95-16448
BETTS, BRUCE H. ..... p 918 N95-16180
BETZEN, V. R. ..... p 713 N95-16313
BEYLKIN, GREGORY ..... p 773 N95-17617
BEYMER, DAVID ..... p 835 N95-16236
BEZERREACANDEIAS, ANA LUCIA ..... p 912 N95-17650
BHAT, A. ..... p 794 N95-16940
BI, NAI-PEI ..... p 664 N95-17883
BIAGIONI, EDOARDO S. ..... p 835 N95-16306
BIANCHINI, RICARDO ..... p 845 N95-16083
BIANCO, GIUSEPPE ..... p 687 N95-17239
BIESIADECKI, JEFF ..... p 702 N95-17583
BIGELOW, T. S. ..... p 891 N95-16958
BIHARI, B. ..... p 742 N95-16427
BILLICA, R. D. ..... p 815 N95-16773
p 816 N95-16774
p 710 N95-16776
p 816 N95-16777
BINDNER, H. ..... p 840 N95-17355
p 840 N95-17356
p 841 N95-17628
p 841 N95-17629
p 842 N95-17733
p 842 N95-17734
p 842 N95-17735
BINGHAM, C. E. ..... p 792 N95-16435
BIONDO, A. C. ..... p 902 N95-17898
BISCHOF, C. ..... p 800 N95-16398
p 774 N95-16461
p 863 N95-17306
BISCHOF, C. H. ..... p 771 N95-16828
BISHOP, D. F. ..... p 756 N95-17282
BITTEKER, L. ..... p 891 N95-17365
BJORKMAN, CHRISTOPHER S. ..... p 802 N95-17443
BLAIR, M. ..... p 710 N95-16344
BLUM, FRANK D. ..... p 740 N95-16092
BLUM, L. ..... p 902 N95-17711
p 904 N95-17712
BODEN, J. A. ..... p 752 N95-16146
BODONYL, RICHARD J. ..... p 655 N95-16099
BOEHM, ALBERT R. ..... p 803 N95-17715
BOHN, C. L. ..... p 879 N95-16030
BOLEY, C. D. ..... p 779 N95-17688
BOLLES, ROBERT C. ..... p 858 N95-17634
BOLTON, DOUGLAS E., JR. ..... p 717 N95-16335
BOLTON, R. D. ..... p 876 N95-17153
BOOK, W. J. ..... p 856 N95-16287
BOOKOUT, PAUL S. ..... p 786 N95-16577
BORDELON, JOHN H. ..... p 763 N95-16410
BOREHAM, CHARLES THOMAS ..... p 687 N95-17236
BOREMAN, GLENN D. ..... p 887 N95-17707
BORSHCHEVSKY, A. ..... p 899 N95-16913
BOSLOUGH, M. B. ..... p 799 N95-17362
BOTE, ROBERT ..... p 685 N95-17224
BOTKIN, D. ..... p 779 N95-17729
p 779 N95-17887
BOUDJOUK, PHILIP ..... p 722 N95-16513
p 898 N95-16526
BOURGAIN, J. ..... p 861 N95-16295
BOUSHEL, ROBERT ..... p 819 N95-16228
BOUSQUET, MARY D. ..... p 802 N95-17686
BOWDEN, FRED D. ..... p 669 N95-16969
BOWEN, BARRY C. ..... p 676 N95-17262
BOWER, W. ..... p 793 N95-16831
BOWERS, JOHN ..... p 854 N95-15990
BOWMAN, KENNETH P. ..... p 911 N95-17330
BOYER, BOB ..... p 840 N95-17338
BOYER, DON L. ..... p 771 N95-16616
BOYER, DONNA ..... p 828 N95-17530
BOYER, JEFFREY S. ..... p 697 N95-17559
BRADLEY, C. R. ..... p 739 N95-15943
BRADLEY, JOSEPH M. ..... p 770 N95-16239
BRAGG, BOBBY J. ..... p 764 N95-16561
BRAKENRIDGE, G. ROBERT ..... p 918 N95-16181
BRAUER, S. O. ..... p 880 N95-16308
BRAUN, ARMIN ..... p 688 N95-17240
BRAUN, ROBERT ..... p 915 N95-17496
BRECHER, C. ..... p 896 N95-16385
BREIDER, M. A. ..... p 818 N95-16801
BRENNAN, T. M. ..... p 778 N95-17498
BRENOT, J.-M. ..... p 692 N95-17534
BREWSTER, MARY J. ..... p 909 N95-16845
BRILEY, G. L. ..... p 717 N95-16336
BRINKER, C. J. ..... p 744 N95-16934
BRITTINGER, PETER ..... p 684 N95-17217
BRIZZOLARA, R. A. ..... p 735 N95-16606
BRIZZOLARE, R. A. ..... p 733 N95-16091
BROCKMANN, THORSTEN W. ..... p 743 N95-16628
BRODERSEN, ROBERT W. ..... p 832 N95-16618
BROMBERG, DANIEL E. ..... p 679 N95-17194
BRONSON, ARTURO ..... p 740 N95-16085
BROOKS, N. H. ..... p 889 N95-16554
BROOKS, ROBERT N., JR. ..... p 688 N95-17242
BROWN, C. ..... p 752 N95-16094
BROWN, J. MICHAEL ..... p 854 N95-15986
BROWNING, DAVID G. ..... p 871 N95-17177
BROWNING, N. D. ..... p 728 N95-16419
BROWNING, R. ..... p 729 N95-16622
BRUNE, G. W. ..... p 659 N95-17859
BRUNEAU, STEPHEN D. ..... p 720 N95-16349
BRYANT, EDWARD G. ..... p 834 N95-16149
BRYANT, RANDAL E. ..... p 835 N95-16447
BUCHANAN, H. R. ..... p 758 N95-17295
BUCHANAN, P. ..... p 809 N95-16743
BUCHOLTZ, FRANK ..... p 775 N95-17428
BUCKLEY, BRIAN ..... p 688 N95-17243
BUDDEN, NANCY ANN ..... p 922 N95-16436
BUETEFISCH, K. A. ..... p 662 N95-17875
BUFTON, SCOTT A. ..... p 889 N95-16243
BUIE, ELIZABETH A. ..... p 830 N95-16813
BUISHAND, T. A. ..... p 802 N95-17529
BULAWKA, A. ..... p 793 N95-16831
BUNN, FRANK J. ..... p 910 N95-16971
BUNTINE, W. L. ..... p 716 N95-16330
BUNZ, L. ..... p 765 N95-16915
BURKETT, K. ..... p 878 N95-17899
BURLACHKOV, L. ..... p 766 N95-16945
BURNS, H. D., JR. ..... p 715 N95-16326
BURNS, R. ..... p 751 N95-17632
BURTON, R. ..... p 816 N95-16778
BURTON, R. R. ..... p 811 N95-16755
BURTON, RODNEY L. ..... p 889 N95-16243
p 730 N95-16955
p 747 N95-17690
BUSBY, M. L. ..... p 829 N95-16145
BUTLER, BARCLAY P. ..... p 829 N95-16147
p 664 N95-16404
p 831 N95-17484
BUTLER, I. ..... p 810 N95-16749
BUTLER, MADELINE J. ..... p 707 N95-17611
BUTLER, SCOTT A. ..... p 699 N95-17569
BUTTON, ROBERT M. ..... p 721 N95-17276
BUXBAUM, K. L. ..... p 682 N95-17210
BUZBEE, BILL ..... p 840 N95-17324
BYERS, C. H. ..... p 732 N95-17524
BYRD, J. M. ..... p 881 N95-17670
BYRNE, RUSSELL H. ..... p 679 N95-17194
BYRON, RICHARD C. ..... p 850 N95-17374
BYRUM, K. ..... p 878 N95-17899

C

CABLE, M. D. ..... p 779 N95-17635
CAI, HENG ..... p 873 N95-16482
CAI, Z. ..... p 882 N95-17901
CAKARCAN, ALPAY ..... p 858 N95-17458
CAKIR, SERHAT ..... p 905 N95-15921
CALANCHE, BRUNO J. ..... p 676 N95-17180
CALEDONIA, GEORGE E. ..... p 655 N95-16076
CALEF, D. ..... p 722 N95-17745
CALLAHAN, TIMOTHY J. ..... p 844 N95-15940
CALVIN, RICHARD ..... p 685 N95-17224
CAMERON, G. E. ..... p 695 N95-17548
CAMERON, J. F. ..... p 741 N95-16354
CAMPBELL, FRANK J. ..... p 711 N95-16048
CAMPBELL, G. L. ..... p 893 N95-17896
CAMPBELL, J. A. ..... p 717 N95-16334
CAMPBELL, M. R. ..... p 710 N95-16776
CAMPBELL, R. B. ..... p 889 N95-16554
CAMPILLO, B. ..... p 739 N95-17728
CAMPOS, SERGIO V. ..... p 864 N95-17618
CANFIELD, P. C. ..... p 868 N95-16288
CANINE, M. KATHERINE ..... p 818 N95-16105
CANTELMI, F. C. ..... p 791 N95-15963
CANTILLO, A. Y. ..... p 796 N95-17363
CANTRELL, GIDGET ..... p 709 N95-17275
CANTRELL, JAMES M. ..... p 818 N95-17714
CARACCIOLO, ROBERTO ..... p 853 N95-15983
CARDENAS, JEFFERY ..... p 679 N95-17195
CARDIN, JOSEPH M. ..... p 720 N95-16349
CARLE, A. ..... p 774 N95-16461
p 771 N95-16828
CARLSTEDT, O. ..... p 760 N95-17455
CARLSTEN, B. E. ..... p 875 N95-16933
CARNAL, C. L. ..... p 773 N95-17910
CARPENTER, MARK H. ..... p 863 N95-16904
CARPER, RICHARD D. ..... p 706 N95-17603
CARROLL, STEVEN ..... p 783 N95-16870
CARTER, EMILY A. ..... p 727 N95-16144
CARTER, JIM ..... p 830 N95-16813
CARTER, LESLIE E. ..... p 697 N95-17560
CARTER, MICHAEL T. ..... p 868 N95-16162
CARTIER, P. ..... p 860 N95-16294
CARVALHODIMAIOMANTOVANI, ANGELICA ..... p 791 N95-17894
CASEY, JOHN E. ..... p 764 N95-16561
CASHWELL, J. W. ..... p 835 N95-16358
CASTILLO, V. ..... p 777 N95-17168
CAUBLE, R. C. ..... p 778 N95-17627
CAUL-TOSKIN, ATHENA R. ..... p 754 N95-16794
CAVIN, O. B. ..... p 899 N95-16806
CAYRAC, D. ..... p 674 N95-17532
p 692 N95-17534
CERCO, CARL F. ..... p 804 N95-16118
CERESOLE, ENRICO ..... p 823 N95-15976
CERVENKA, PETER O. ..... p 903 N95-16877
CHADHA, S. S. ..... p 767 N95-17487
CHAI, B. H. T. ..... p 899 N95-16867
p 777 N95-17168
CHALASANI, PRASAD ..... p 838 N95-16850
CHALLA, M. S. ..... p 694 N95-17546
CHAMBERS, JEFFREY A. ..... p 787 N95-17258
CHAMIS, C. C. ..... p 787 N95-17270
CHAMIS, CHRISTOS C. ..... p 785 N95-16416
p 787 N95-16911
p 725 N95-17659
CHAMPAGNE, V. ..... p 737 N95-17486
CHAMPIGNY, P. ..... p 662 N95-17871
CHAN, CHUNG ..... p 869 N95-17449
CHAN, H. M. ..... p 746 N95-17438
CHAN, LAI-HIM ..... p 877 N95-17358
CHAN, S. T. ..... p 797 N95-17922
CHANDLER, E. A. ..... p 778 N95-17627
p 722 N95-17745
CHANG, CHING-TEN ..... p 884 N95-16009
CHANG, J. J. ..... p 779 N95-17688
CHANG, K. J. ..... p 788 N95-17272
CHANG, P. ..... p 745 N95-17160
CHANG, RICHARD K. ..... p 776 N95-16166
CHANG, SIN-CHUNG ..... p 862 N95-16885
p 772 N95-16903
CHANOWITZ, M. S. ..... p 878 N95-17720
p 881 N95-17888
CHAPMAN, DEAN R. ..... p 655 N95-16160
CHAPMAN, K. B. ..... p 687 N95-17237
CHARLES, J. ..... p 812 N95-16757
CHASE, MALCOLM W. ..... p 907 N95-15937
CHAVIAROPOULOS, P. ..... p 664 N95-16563
p 664 N95-16564
CHELEN, W. E. ..... p 809 N95-16745
CHELL, G. G. ..... p 788 N95-17272
CHELLAPPA, RAMA ..... p 804 N95-16078
CHEMLA, D. S. ..... p 779 N95-17729
p 779 N95-17887
CHEN, A. S. C. ..... p 654 N95-17466
CHEN, CHIEN-CHUNG ..... p 883 N95-15960
CHEN, GUOPING ..... p 650 N95-16260
CHEN, H. ..... p 731 N95-17163
CHEN, J. C. ..... p 758 N95-17293
CHEN, L. ..... p 794 N95-17521
CHEN, WEI ..... p 746 N95-17456
CHEN, XIN ..... p 745 N95-17434
CHEN, YIRNG-AN ..... p 835 N95-16447
CHENG, E. T. ..... p 881 N95-17721
CHENG, LAP-TAK ..... p 874 N95-16629
CHENG, R. K. ..... p 732 N95-17437
CHEPILKO, N. M. ..... p 904 N95-17474
CHEREPANOV, E. A. ..... p 880 N95-17519
CHERNYAVSKII, S. M. ..... p 652 N95-16274
CHEUVRONT, ALLAN R. ..... p 684 N95-17218
CHILENSKAS, A. A. ..... p 766 N95-16963
CHIN, V. D. ..... p 658 N95-17851
CHIN, YONG HO ..... p 761 N95-17672
CHISHOLM, M. F. ..... p 728 N95-16419
CHITSOMBOON, TAWIT ..... p 773 N95-17656
CHIU, Y. T. ..... p 916 N95-16600
CHLEBORAD, O. W. ..... p 713 N95-16314
CHO, SOO-YONG ..... p 670 N95-17402
CHOU, H. C. ..... p 794 N95-16940
CHOU, STEPHEN Y. ..... p 763 N95-16394
CHOUDHARY, ABDUR RAHIM ..... p 675 N95-17565
CHOW-MILLER, CORA ..... p 880 N95-17499
CHOW, BRIAN G. ..... p 672 N95-17427
CHOW, CHUEN-YEN ..... p 862 N95-16885
p 772 N95-16903
CHOWDHURY, MOSTAFIZ R. ..... p 781 N95-17335
CHRIST, UWE ..... p 676 N95-17181
CHRISTENSEN, JON L. ..... p 833 N95-15997
CHRISTENSEN, P. R. ..... p 918 N95-16182
CHRISTENSEN, PAUL E. ..... p 717 N95-16333
CHRISTIAN, RAYMOND J. ..... p 871 N95-17177
CHU, TAK-KIN ..... p 767 N95-17481
CHUANG, WEI-TONG ..... p 762 N95-16089
CHURCHWELL, WILLIAM M. ..... p 909 N95-16305
CIARLO, D. ..... p 775 N95-17380
CINTRON, N. M. ..... p 811 N95-16753
CLARK, ARTHUR E. ..... p 775 N95-17376
CLARK, E. L. ..... p 671 N95-16509

CLARKE, DAVID R. p 723 N95-16415
CLARKE, EDMUND M. p 864 N95-17618
CLAYTON, CLIVE R. p 736 N95-16793
CLEMONS, K. T. p 717 N95-16334
CLOTWORTHY, TIM p 681 N95-17208
COBB, W. R. p 782 N95-17717
COFFEY, HELEN E. p 924 N95-17736
p 924 N95-17737
COGGIOLA, M. J. p 795 N95-16213
COHEN, DONALD S. p 859 N95-16108
COHEN, M. p 808 N95-16740
COHEN, M. M. p 813 N95-16764
COHN, MARTIN p 911 N95-17329
COLE, THOMAS M. p 804 N95-16118
COLEMAN, C. p 792 N95-16437
COLGATE, J. EDWARD p 854 N95-15986
COLLAZO, I. p 891 N95-16958
COLTRIN, M. E. p 733 N95-17744
COMBES, F. p 916 N95-17332
COMBS, VAUGH T. p 845 N95-16116
COMPTON, JOEL P. p 720 N95-16350
CONAWAY, B. p 677 N95-17186
CONDER, A. D. p 776 N95-17522
CONNELL, L. W. p 880 N95-17361
CONNES, A. p 860 N95-16293
CONVERTINO, V. A. p 808 N95-16742
p 809 N95-16746
COOK, W. M. p 765 N95-16925
COOKE, P. W. p 899 N95-16918
COOPER, A. E. p 716 N95-16330
COOPER, B. H. p 871 N95-16018
COOPERSTEIN, G. p 880 N95-17475
CORBIN, JAMES p 805 N95-16141
COREY, I. p 770 N95-16211
CORIANO, C. p 904 N95-17925
CORKER, K. p 814 N95-16766
CORLETT, J. N. p 881 N95-17670
CORNWELL, MICHAEL D. p 714 N95-16316
CORONEOS, R. p 789 N95-17701
CORRIGAN, JIM p 673 N95-17544
COSNARD, MICHEL p 849 N95-16529
COSTA, M. p 757 N95-17286
COSTELLO, DANIEL J., JR. p 761 N95-17665
COSTINER, SORIN p 862 N95-16869
p 862 N95-16896
COUGHLAN, DANETTE p 790 N95-16547
COUTERMARSH, BARRY A. p 804 N95-16103
COVA, P. J. p 713 N95-16314
COWEN, S. J. p 886 N95-16815
COWLES, K. p 758 N95-17290
COX, B. p 747 N95-17719
COX, B. N. p 724 N95-16930
COX, BRIAN p 852 N95-15979
COX, C. M. p 687 N95-17237
COX, NAGIN p 702 N95-17583
CRABTREE, G. W. p 897 N95-16408
p 900 N95-16946
p 901 N95-17349
CRADDOCK, ROBERT A. p 918 N95-16183
p 918 N95-16184
CRAIG, GARY L. p 845 N95-16116
CRAIG, KENNETH H. p 753 N95-16148
CRAWFIS, R. p 860 N95-16221
CRAWFORD, O. H. p 876 N95-16959
CRAWFORD, R. A. p 748 N95-16029
CRAWLEY, EDWARD p 774 N95-16242
CRENSHAW, A. p 809 N95-16744
CRESCI, D. p 672 N95-16320
CROSS, E. S. p 896 N95-16359
CROVELLA, MARK E. p 845 N95-16082
CROWE, MICHAEL X. p 853 N95-15980
CROWLEY, T. J. p 801 N95-16961
CROXTON, CRAIG A. p 826 N95-16298
CRUMPLER, LARRY S. p 918 N95-16185
CRYSEL, WILLIAM B. p 685 N95-17227
CUBITT, R. p 901 N95-17667
CUCCOLI, A. p 869 N95-17731
p 869 N95-17750
CUCINOTTA, FRANCIS A. p 820 N95-16412
CUEVAS, O. O. p 687 N95-17237
CUIJPERS, J. W. M. p 800 N95-16290
CUMMINGS, TERRENCE p 841 N95-17460
CUNEO, M. E. p 888 N95-16216
CUNNANE, J. C. p 739 N95-15943
CUPP, CHRISTIAN M. p 912 N95-17660
CURETON-SNEAD, IZELLER E. p 702 N95-17585
CURLETT, BRIAN P. p 840 N95-17420
CUTHBERTSON, J. W. p 892 N95-17640
CYGAN, R. T. p 799 N95-17362
CYMERMAN, ALLEN p 819 N95-16228

D

DABOUL, J. p 903 N95-16428
DABROWSKI, B. p 901 N95-17350
DACH, M. p 880 N95-17503
DACRES, CHESTER M. p 734 N95-16370
p 734 N95-16371
DAGENAIS, DOMINIQUE M. p 775 N95-17428
DAHLGREN, U. p 775 N95-17170
p 759 N95-17453
DALAL, SAURABH p 761 N95-17696
DALHED, H. E. p 778 N95-17627
DALSASSO, MICHELE p 823 N95-15976
DALTON, LARRY R. p 741 N95-16230
p 885 N95-16528
DALY, PAUL K. p 826 N95-16301
DANFORTH, S. C. p 746 N95-17456
DANIEL, H. p 878 N95-17739
DANIELS, R. C. p 805 N95-16610
DANIELSON, M. J. p 737 N95-17637
DANNEVIK, W. P. p 797 N95-17920
DAPP, TIMOTHY L. p 746 N95-17462
DARBY, MELODY M. p 828 N95-17175
DARGAN, JOHN L. p 671 N95-16381
DARWIN, R. p 751 N95-17632
DAS, R. p 793 N95-16831
DASILVA, L. B. p 778 N95-17627
DAVENPORT, WILLIAM p 700 N95-17577
DAVEY, J. p 765 N95-16920
DAVID, S. A. p 786 N95-16803
DAVIDOR, Y. p 834 N95-16219
DAVIDSON, STEVEN A. p 834 N95-16107
DAVIES, MIKE p 669 N95-16969
DAVIS, C. L. p 719 N95-16345
DAVIS, DON p 680 N95-17200
DAVIS, H. A. p 891 N95-16936
p 745 N95-16938
DAVIS, J. BRADLEY p 676 N95-17262
DAVIS, R. F. p 898 N95-16533
DAVIS, RANDY p 686 N95-17234
DAVIS, ROBERT F. p 894 N95-16084
p 898 N95-16532
p 743 N95-16625
DAVIS, ROBERT H. p 721 N95-16035
DAVIS, SHARON A. p 830 N95-16553
DAWSON, J. p 878 N95-17899
DAY, C. T. p 910 N95-16922
DAY, FRANK P., JR. p 807 N95-16429
DAY, G. W. p 887 N95-17441
DEARBORN, A. S. p 817 N95-16779
DEB, D. p 888 N95-16218
DEBOER, P. C. p 713 N95-16302
DECHANT, LAWRENCE J. p 656 N95-16887
DEDOUSSIS, V. p 664 N95-16563
p 664 N95-16564
DEETER, M. p 780 N95-16224
DEGTYAREV, G. L. p 649 N95-16249
p 652 N95-16274
DEHON, RENE A. p 918 N95-16186
DEJONG, A. L. p 722 N95-16734
DEKEN, L. R. p 720 N95-16348
DELAROSA, M. J. p 718 N95-16340
DELAVIESCA, ROSA p 906 N95-15927
DELAYEN, J. R. p 879 N95-16030
DELBUFALO, A. p 696 N95-17558
DELFRATE, JOHN H. p 656 N95-16858
DELLACORTE, C. p 722 N95-16905
DELOACH, L. D. p 899 N95-16867
DELOACH, STEPHEN R. p 666 N95-17508
DELOMBARD, RICHARD p 750 N95-17893
DEMARCO, F. p 902 N95-17742
DEMELENNE, B. p 674 N95-17251
DEMUREN, A. O. p 771 N95-16855
DENNIS, J. E., JR. p 863 N95-16897
DENTON, R. E. p 799 N95-16927
DEOLIVEIRA, CARLOS ALBERTO p 760 N95-17649
DERESKIEWICZ, J. P. p 782 N95-17716
DEREUS, N. M. p 838 N95-16874
DERI, B. p 884 N95-16366
DERION, TONIANN p 818 N95-16105
DEROSHIA, C. p 808 N95-16740
DERR, R. L. p 720 N95-16351
DESAI, VISHAL p 677 N95-17182
DESAINTVINCENT, A. p 686 N95-17230
DESMARAIS, DAVID J. p 919 N95-16188
DETROYE, DAVID J. p 883 N95-15954
DEUTSCHMANN, J. p 694 N95-17546
DEVAN, J. H. p 739 N95-17747
DEVINE, R. A. B. p 895 N95-16311
DEVREUGHT, J. P. M. p 850 N95-17138
DEWAR, MICHAEL J. p 874 N95-16498
DEWEESE, C. D. p 715 N95-16326
DEWEESE, PERRY R. p 837 N95-16607
DEYOREO, J. J. p 902 N95-17742
DIAS, WILLIAM C. p 686 N95-17229
DICKERSON, JAMES H. p 762 N95-16110
DIEBOLT, J. p 865 N95-16546
DIEKMANN, FRANK J. p 678 N95-17189
DIETZ, DAVID p 759 N95-17450
DIETZ, G. p 658 N95-17852
DIFTLER, MYRON p 852 N95-15979
DIJAILI, S. p 884 N95-16366
DILEGO, FRANCIS A., JR. p 845 N95-16116
DILL, JAMES F. p 780 N95-16139
DIMANLIG, ARSENIO C. B. p 655 N95-16589
DIMOS, D. p 744 N95-16829
DING, KUNG-HAU p 884 N95-16161
DING, YI p 730 N95-16973
DISMUKES, R. K. p 813 N95-16764
DJORGOVSKI, S. G. p 858 N95-17921
DJORGOVSKI, S. GEORGE p 911 N95-17325
DO, S. p 808 N95-16739
DOAN, P. A. p 715 N95-16326
DOARN, C. R. p 710 N95-16772
DODDS, R. H., JR. p 735 N95-16531
p 786 N95-16785
DOERR, D. F. p 809 N95-16746
DOGGETT, K. A. p 803 N95-17927
DOMBROWSKI, J. H. p 886 N95-16815
DOMINIK, C. J. p 658 N95-17851
DONNELLY, B. p 788 N95-17272
DONOHUE-PERRY, MARY M. p 830 N95-16553
DONTAS, KEJITAN p 665 N95-17373
DOORN, M. R. J. p 793 N95-16544
DOUARD, STEPHANE p 687 N95-17238
DOW, JOHN D. p 902 N95-17705
DOWDY, KATHLENE R. p 800 N95-16235
DOWLING, JASON p 681 N95-17206
DRAKE, BRIAN C. p 702 N95-17584
DRAVES, RICHARD POWELL, JR. p 837 N95-16602
DRAVID, V. P. p 728 N95-16419
DREGALIN, A. F. p 650 N95-16256
DRESSLER, G. A. p 716 N95-16328
DRINGENBURG, NICK p 736 N95-16878
DRISCOLL, T. p 811 N95-16752
DROEGEMEIER, K. K. p 800 N95-16398
DUBOIS, PATRICK p 736 N95-16878
DUDLEY, G. p 809 N95-16743
DUESBERY, M. S. p 735 N95-16519
DUFF, GARY p 707 N95-17609
DUFFY, K. P. p 749 N95-16499
DUGDALE, RICHARD C. p 797 N95-17740
DULING, IRL N. p 887 N95-17695
DUMBRAJS, O. p 869 N95-17467
DUNCAN, ELAINE F. p 685 N95-17227
DUNFORD, E. p 695 N95-17549
DUNN, J. p 776 N95-17522
DUPLESSIX, R. p 903 N95-16839
DUQUE, EARL P. N. p 655 N95-16589
DURAJ, STAN A. p 731 N95-17387
DURAND, JEAN-CLAUDE p 666 N95-17196
DUSSAULY, JERRY L. p 845 N95-16116
DUVOISIN, M. R p 817 N95-16781
DUYAR, AHMET p 669 N95-15970

E

EASMAN, RONALD D. p 887 N95-17695
EASTON, C. R. p 703 N95-17591
EATON, JOHN W. p 820 N95-16444
EATOUGH, M. O. p 744 N95-16829
EBBERS, C. A. p 765 N95-16925
ECCLI, D. B. p 713 N95-16314
ECKBERG, DWAIN L. p 815 N95-16770
ECKSTROM, CLINTON V. p 653 N95-16560
ECONOMOU, T. p 710 N95-16201
EDGAR, DAIVA E. p 884 N95-15999
EDGETT, KENNETH S. p 918 N95-16182
p 919 N95-16187
EDWARDS, C. D. p 756 N95-17283
EDWARDS, JONATHAN L. p 781 N95-17263
EGGLESTON, DEBRA S. p 713 N95-16312
p 715 N95-16324
EGUCHI, KIYOHISA p 724 N95-16833
EICHELBERGER, CHARLES W. p 902 N95-16075
EICHSTADT, F. T. p 815 N95-16773
EISLER, G. R. p 858 N95-17915
EK, M. p 803 N95-16062
EL-BOUSHI, MEKKI p 697 N95-17561
EL-GHAZAWI, TAREK A. p 680 N95-17201
EL-GUEBALY, L. p 893 N95-17907
EL-HADY, A. A. p 875 N95-16931
ELGAARD, DENNIS p 692 N95-17533
ELKIN, GABRIEL R. p 759 N95-17336
ELLIOTT, KENNY B. p 709 N95-16857
ELLIS, JAMES L. p 821 N95-16491
ELLIS, VINCENT J. p 883 N95-15954
ELORANTA, K. p 865 N95-17526
ELPHIC, R. C. p 798 N95-16537
ELSENAAR, A. p 662 N95-17872
EMANUEL, W. p 797 N95-17920
EMERY, WILLIAM p 840 N95-17327
ENDSLEY, MICA R. p 828 N95-17655
ENGDAHL, E. p 869 N95-17750
ENGLAND, A. C. p 891 N95-16958

ERDMANN, MICHAEL p 840 N95-17432
ERICKSON, BRADLEY S. p 829 N95-16145
p 829 N95-16147
ERMOLAEV, YU. P. p 652 N95-16271
ERTL, A. C. p 817 N95-16779
p 817 N95-16782
ESCH, H. p 661 N95-17866
ESTEROWITZ, LEON p 779 N95-17698
ESTEY, P. p 715 N95-16327
EUSEPI, MARTIN W. p 780 N95-16139
EVANS, CHRISTOPHER T. p 806 N95-17505
EVANS, J. p 817 N95-16780
EVANS, J. M. p 810 N95-16748
EVANS, RONALD J. p 830 N95-16875
EVANS, T. E. p 893 N95-17897
EVDOKIMOV, YU. K. p 652 N95-16273
EVERETT, HOBART R., JR. p 858 N95-17465
EVERSMAN, WALTER p 870 N95-16401

F

FADL, ALI A. p 895 N95-16114
FAEHL, R. J. p 889 N95-16286
FAHLEN, LENNART E. p 854 N95-15990
FAHY, F. J. p 868 N95-16856
FAIZOV, E. L. p 876 N95-17154
FALCO, R. E. p 780 N95-16900
FALLON, DANIEL S. p 753 N95-16240
FANTON, FRANCESCO p 853 N95-15983
FANWICK, PHILLIP E. p 731 N95-17387
FARMER, JACK D. p 919 N95-16188
FATEMI, MOHAMMAD p 896 N95-16399
FAULK, D. M. p 813 N95-16761
FAWCETT, K. p 799 N95-16735
FEDDEMA, J. T. p 858 N95-17915
FEINERMAN, A. p 761 N95-17926
FELDMAN, A. p 747 N95-17722
FELIPPA, CARLOS A. p 788 N95-17492
FENDRICH, J. p 897 N95-16408
p 901 N95-17349
FENSTERMACHER, M. E. p 889 N95-16554
p 893 N95-17897
FERBER, M. K. p 899 N95-16806
FERGUSON, DALE C. p 712 N95-16054
FERGUSON, GEORGE p 839 N95-16883
FERNANDEZBACA, J. A. p 786 N95-16803
FERNANDO, HARINDRA J. p 771 N95-16616
FERRANTI, RICHARD L. p 752 N95-16097
FERRI, P. p 690 N95-17252
FERRI, PAOLO p 682 N95-17209
FERRY, DAVID K. p 895 N95-16158
FETEIH, SALAH p 780 N95-16031
FETH, LAWRENCE L. p 869 N95-16248
FEUERSTEIN, MARK G. p 710 N95-17622
FEYERHERM, R. p 868 N95-16288
FIELDS, T. p 875 N95-16924
FIENE, BRUCE F. p 907 N95-15934
FIESELMANN, B. p 794 N95-17521
FIJANY, AMIR p 832 N95-17400
FILBERT, MARGARET G. p 821 N95-16491
FILIPENCO, V. p 770 N95-16163
FINK, C. L. p 893 N95-17900
FINKBEINER, D. L. p 791 N95-15963
FINLEY, S. G. p 708 N95-17292
FINNEGAN, JENNIFER M. p 818 N95-16112
FIRBY, R. J. p 831 N95-16966
FIRESTONE, ELAINE R. p 803 N95-16006
FIRMIN, M. C. P. p 660 N95-17860
FISCHLER, MARTIN A. p 858 N95-17634
FISHMAN, T. p 673 N95-17212
FLAHERTY, DAVID S. p 781 N95-17263
FLAHERTY, JOSEPH E. p 861 N95-16517
FLEETWOOD, D. M. p 895 N95-16311
FLEISCHMANN, H. H. p 888 N95-16122
FLEMING, J. G. p 764 N95-16832
FLEURIAL, JEAN-PIERRE p 899 N95-16913
FLITTIE, K. J. p 715 N95-16327
FLORA-ADAMS, DANA p 703 N95-17588
FLORES, O. p 739 N95-17728
FOGEL, ALVIN J. p 680 N95-17202
FOGG, DAVID A. p 669 N95-16969
FOLK, JOHN p 677 N95-17186
FOLKNER, W. M. p 756 N95-17283
FOLTA, J. p 775 N95-17380
FONG, WAI p 677 N95-17186
FOOR, WESLEY E. p 885 N95-16443
FORGAN, E. M. p 901 N95-17667
FORGET, FRANCOIS p 919 N95-16189
FORMAN, MICHAEL L. p 674 N95-17553
FORMAN, P. p 780 N95-16224
FORTGANG, C. p 879 N95-16172
FORTNEY, S. p 811 N95-16752
p 811 N95-16754
FOSSUM, ERIC p 742 N95-16450
FOSTER, RUSSELL G. p 822 N95-16847
FOTEDAR, L. p 810 N95-16749
FOWLER, THOMAS p 783 N95-16870
FOX, GEOFFREY C. p 844 N95-16060
FOX, MARYE A. p 722 N95-16100
FOYLE, D. C. p 814 N95-16767
FRAGADASILVA, FRANCISCO JOSE p 760 N95-17649
FRAME, EDWIN A. p 780 N95-16636
FRANCIOSI, A. p 896 N95-16396
FRANCIS, W. E. p 916 N95-16600
FRANCO, M. M. p 757 N95-17288
FRANK, FORREST R. p 909 N95-16374
FRANK, LOUIS A. p 888 N95-15941
FRANKLIN, KEVIN R. p 873 N95-16482
FRECH, M. p 803 N95-16062
FRECHET, J. M. p 741 N95-16354
FREE, JAMES M. p 718 N95-16338
FRERY, ALEJANDRO C. p 912 N95-17650
FRIED, L. E. p 749 N95-17919
FRIEDMAN, ROBERT p 712 N95-16050
FRITSCH, JANICE M. p 815 N95-16770
FROGNER, BJORN p 680 N95-17199
FRYKMAN, PETER N. p 819 N95-16228
FUCHS, B. A. p 751 N95-17738
FUJA, R. p 882 N95-17902
FUJCZAK, ROBERT R. p 786 N95-16601
FUJII, M. p 812 N95-16756
FUJII, ROKURO p 724 N95-16833
FUJIMOTO, JAMES G. p 767 N95-17433
FUKUDA, SHUICHI p 851 N95-15973
FULCO, CHARLES S. p 819 N95-16228
FULGHUM, STEPHEN F. p 892 N95-17623
FULKER, J. L. p 660 N95-17862
FURLER, R. p 775 N95-17307
FURMAN, M. A. p 882 N95-17890
p 882 N95-17891
FURUSAKA, MICHIHIRO p 871 N95-15956
FURUTA, RICHARD p 853 N95-15981
FUSELIER, S. A. p 799 N95-16927

G

GABRUK, ROBERT S. p 800 N95-16802
GAL, E. p 782 N95-17364
GALAMBOS, J. p 893 N95-17674
GALAMBOS, J. D. p 891 N95-17367
GALFORD, G. R. p 718 N95-16337
GAMBRINO, JOHN R. p 910 N95-16972
GANDER, P. H. p 813 N95-16760
GANGARAJ, S. K. p 861 N95-16379
p 863 N95-17431
GANTER, J. H. p 835 N95-16358
GAO, GUANG R. p 849 N95-16529
GARCIA-PEREZ, RAUL p 684 N95-17219
GARDELLA, JOSEPH A., JR. p 745 N95-17434
GARDINER, T. A. p 897 N95-16408
GARDNER, PAUL A. p 721 N95-17626
GARDNER, STEVEN R. p 721 N95-17448
GARINO, T. J. p 744 N95-16829
GARMAN-DUVALL, LISSA S. p 777 N95-16548
GARMAN, C. p 708 N95-17613
GARRETT, H. p 765 N95-16915
GARY, S. P. p 799 N95-16927
GASPARETTO, ALESSANDRO p 853 N95-15983
GASQUET, A. p 686 N95-17230
GASTON, GREG G. p 796 N95-17394
GATES, ROBERT E. p 710 N95-17331
GATSKI, THOMAS B. p 769 N95-16071
GAUSTAD, KRISTA L. p 712 N95-16053
GAVEL, D. T. p 916 N95-17525
GAVIN, J. p 796 N95-17348
GAVITT, K. R. p 716 N95-16328
GAVRIN, V. N. p 876 N95-17154
GAWRONSKI, W. K. p 664 N95-17291
GAYNOR, T. L. p 666 N95-15971
GEHRKI, THOMAS D. p 759 N95-17436
GEISSLER, P. E. p 919 N95-16187
GELLES, D. S. p 736 N95-17159
GENETTI, JON p 823 N95-15975
GEORGE, ALAN p 862 N95-16596
GEORGE, NICHOLAS p 883 N95-15958
GERBERICH, WILLIAM W. p 725 N95-17457
GERDES, D. p 878 N95-17899
GEREVINI, ALFONSO p 859 N95-16022
GERSHMAN, R. p 682 N95-17210
GERTZ, JEFFREY L. p 759 N95-17336
GESHKENBEIN, V. B. p 766 N95-16945
GESTRINA, G. N. p 903 N95-17473
GETBEHEAD, MARK A. p 885 N95-16443
GETTO, WOLF p 752 N95-16123
GEYER, B. p 903 N95-16944
GHAFFARIAN, KAM p 706 N95-17607
GHONIEM, N. M. p 719 N95-16347
GHOSH, DAVE p 849 N95-16475
GHOSH, M. p 764 N95-16425
GHUMAN, PARMINDER p 681 N95-17206
GIANNINI, F. p 699 N95-17567
GIBSON, J. S. p 851 N95-15952
GIBSON, LINDSAY p 819 N95-16228
GIBSON, W. A. p 877 N95-17687
GIEROW, PAUL ARMIN p 719 N95-16343
GIESE, R. W. p 727 N95-16373
GIESECKE, M. p 861 N95-16295
GILBERT, J. H. p 807 N95-16738
GILPATRICK, J. p 879 N95-16172
GILPATRICK, J. D. p 879 N95-16217
GILSON, RICHARD D. p 825 N95-15959
GINATEMPO, B. p 899 N95-16805
GIRIMAJI, SHARATH S. p 769 N95-16070
GLAD, T. J. p 713 N95-16314
GLAGOLA, B. G. p 901 N95-17349
GLASS, J. A., JR. p 728 N95-16406
GLASS, JEFFREY T. p 894 N95-16084
GLASS, R. p 775 N95-17380
GLICKMAN, RANDOLPH D. p 822 N95-16871
GLIMM, JAMES p 864 N95-17713
GLUSKIN, E. p 882 N95-17901
GLYNN, A. p 747 N95-17685
GLYNN, PETER W. p 860 N95-16169
p 783 N95-16421
p 865 N95-17426
GOETHERT, WOLFHART B. p 836 N95-16503
GOETTING, LAURA B. p 895 N95-16238
GOETZ, JOHN R. p 856 N95-16372
GOFF, THOMAS E. p 837 N95-16587
GOLDBERG, ROBERT K. p 789 N95-17658
GOLDEN, CONSTANCE p 704 N95-17592
GOLDENSON, DENNIS p 836 N95-16490
GOLDING, TERRY D. p 901 N95-17424
GOLDMAN, JEFFREY A. p 909 N95-16879
GOLDSBY, MICHAEL E. p 855 N95-15992
GOLDSTEIN, JOSEPH I. p 916 N95-16020
GOLDSTEIN, MARVIN E. p 769 N95-15969
GOLDSTONE, J. A. p 737 N95-17641
GOLOMBEK, MATTHEW p 917 N95-16176
GOLOMBEK, MATTHEW P. p 919 N95-16190
GOMES, I. p 873 N95-16487
GOMES, VINCENT C. p 785 N95-16502
GONZALEZ, M. A. p 900 N95-16946
GOOD, ANDREW p 673 N95-17215
GOOD, E. p 808 N95-16739
GOODEN, J. H. M. p 658 N95-17855
GOODMAN, ALVIN M. p 767 N95-17463
GORDON, EDWARD M. p 731 N95-17387
GORDON, ELMAREE p 869 N95-16226
GORDON, JULIE p 675 N95-17582
GORDON, LLOYD B. p 712 N95-16053
GORETTA, K. C. p 902 N95-17898
GORTYSHOV, YU. F. p 650 N95-16255
GOTANDA, T. p 702 N95-17586
GOTTESFELD, S. p 765 N95-16920
GOTTLIEB, DAVID p 863 N95-16904
GOTTMANN, MATTHIAS p 830 N95-16418
GOULD, JACK J. p 840 N95-17420
GOURDIN, W. H. p 736 N95-17378
GOURLEY, P. L. p 778 N95-17498
GOZA, S. MICHAEL p 854 N95-15989
GOZA, SHARON P. p 854 N95-15989
GRAHAM, M. E. p 745 N95-17160
GRANAHAN, JAMES CHARLES p 917 N95-17393
GRANDE, K. J. p 810 N95-16748
GRANT, C. p 860 N95-16221
GRAY, DAVID J. p 845 N95-16116
GRAY, GARY p 803 N95-17715
GRAY, WILLIAM M. p 801 N95-17259
p 801 N95-17260
GREBER, ISAAC p 670 N95-17402
GREBOWSKY, GERALD p 681 N95-17208
GREEGOR, R. p 879 N95-16172
GREELEY, RONALD p 919 N95-16191
p 920 N95-16193
GREEN, L. L. p 771 N95-16828
GREEN, LAWRENCE L. p 774 N95-16461
GREEN, WILLIAM B. p 678 N95-17190
GREENHALGH, CHRIS p 854 N95-15990
GREENLEAF, J. E. p 817 N95-16782
GREGG, WATSON W. p 690 N95-17249
GREGORY, IRENE M. p 849 N95-16474
GREITZER, E. M. p 770 N95-16163
GREITZER, F. L. p 670 N95-17371
GRELICK, A. p 882 N95-17902
GRESZTA, D. p 739 N95-15996
GRESZTA, DOROTA p 742 N95-16451
GRIESER, WILLIAM H. p 693 N95-17539
GRIEWANK, A. p 863 N95-17306
GRIFFIN, R. D. p 884 N95-16296
GRISSETT, JAMES D. p 819 N95-16151
GRISSOM, CATHERINE p 907 N95-15936
GRISSOM, F. p 854 N95-15989
GRODSINSKY, C. M. p 654 N95-17657
GROOM, LINDA p 905 N95-15920

GROOT, W. ..... p 796 N95-17304
GROSS, M. ..... p 748 N95-17913
GROSS, M. E. ..... p 793 N95-16916
GROSS, R. J. ..... p 748 N95-16214
GROSS, ROLF W. ..... p 777 N95-16548
GROSSMAN, T. ..... p 834 N95-16219
GROTE, JAMES G. ..... p 881 N95-17619
GU, ALSTON L. ..... p 716 N95-16331
GU, S. H. ..... p 748 N95-17724
GUAN, H. W. ..... p 748 N95-17724
GUARRO, S. ..... p 675 N95-17493
GUEDRY, F. E. ..... p 815 N95-16771
GUERRERO, ANA MARIA ..... p 697 N95-17562
p 703 N95-17588
GUFFIN, O. T. ..... p 686 N95-17231
GUILHEM, D. ..... p 893 N95-17677
GULEC, K. ..... p 893 N95-17907
GULLIKSON, E. ..... p 881 N95-17671
GUNTERMANN, P. ..... p 658 N95-17852
GUO, TEN-HUEI ..... p 721 N95-17274
GUPTA, SANDEEP ..... p 709 N95-16857
GUTIERREZ-LUACES, B. O. ..... p 756 N95-17282
GUTTMAN, J. A. ..... p 665 N95-16375
GUYER, ERIC C. ..... p 783 N95-17725
GUZIK, T. G. ..... p 923 N95-16080
p 923 N95-17723
GYGAX, F. N ..... p 868 N95-16288

H

HAARALA, ARJA-RIITTA ..... p 906 N95-15930
HAAS, OTTO ..... p 742 N95-16434
HABERLE, R. ..... p 921 N95-16203
HADCOCK, RICHARD N. ..... p 724 N95-16859
HADLEY, G. R. ..... p 778 N95-17498
HAFFMANS, A. F. ..... p 879 N95-16210
p 901 N95-17673
HAGANS, K. ..... p 775 N95-17380
HAGEL, O. J. ..... p 775 N95-17170
HAGEMAN, BARBARA H. ..... p 699 N95-17570
p 675 N95-17581
HAGER, GREGORY ..... p 855 N95-16095
HAGOPIAN, JEFF ..... p 682 N95-17211
HAIGLER, KARA J. ..... p 774 N95-16461
HAIMES, ROBERT ..... p 770 N95-16388
HAINES, E. J. ..... p 892 N95-17643
HAKVOORT, R. A. ..... p 900 N95-16952
HALL, DANA ..... p 698 N95-17566
HALL, JOSEPH B. ..... p 777 N95-17303
HALVORSEN, LARS ..... p 854 N95-15987
HAMM, R. N. ..... p 877 N95-17687
HAMMEL, B. A. ..... p 779 N95-17635
HAMMOND, AHMAD ..... p 711 N95-16044
HAMMONS, B. E. ..... p 778 N95-17498
HAMPTON, R. D. ..... p 654 N95-17657
HAN, BUZHANG ..... p 650 N95-16258
HAN, D. X. ..... p 794 N95-16957
HAN, S. O. T. H. ..... p 658 N95-17854
HANCOCK, H. A., JR. ..... p 795 N95-16557
HAND, LAWRENCE A. ..... p 659 N95-17858
HANEY, S. ..... p 893 N95-17674
HANNA, JAMES P. ..... p 764 N95-16516
HANNSGEN, KENNETH B. ..... p 726 N95-16008
HANSCHE, B. ..... p 784 N95-17360
HANSEN, C. D. ..... p 835 N95-16223
HANSEN, ELAINE R. ..... p 910 N95-17322
HANSEN, H. J. ..... p 764 N95-16814
HANSEN, THORKILD B. ..... p 754 N95-16624
HANSON, D. L. ..... p 888 N95-16216
HANSON, G. R. ..... p 891 N95-16958
HANUSA, TIMOTHY P. ..... p 741 N95-16393
HAPPELL, NADINE ..... p 684 N95-17222
HARBAUGH, RANDY ..... p 675 N95-17601
HARDI, D. E. ..... p 708 N95-17292
HARDWICK, D. A. ..... p 735 N95-16514
HARDY, TERRY L. ..... p 720 N95-17269
HARFF, N. E. ..... p 879 N95-17918
HARGENS, A. R. ..... p 809 N95-16744
HARIRI, SALIM ..... p 844 N95-16060
HARM, DEBORAH ..... p 812 N95-16758
HARMER, M. P. ..... p 746 N95-17438
HARMON, T. J. ..... p 717 N95-16336
HARPER, M. K. ..... p 665 N95-16964
HARPER, ROBERT ..... p 838 N95-16819
HARRELL, LINDA ..... p 677 N95-17183
HARRIS, J. H. ..... p 891 N95-17347
HARRIS, JOHN B. ..... p 912 N95-17710
HARRIS, JONATHAN C. ..... p 678 N95-17191
HARTEN, AMIRAM ..... p 863 N95-17266
HARTMANN, K. ..... p 661 N95-17868
p 662 N95-17875
HARTMANN, T. ..... p 878 N95-17739
HARTSHORN, W. R. ..... p 841 N95-17515
HARVEY, R. J. ..... p 708 N95-17614
HARVEY, RAYMOND J. ..... p 684 N95-17220
HASHIMOTO, HIDEKI ..... p 853 N95-15985
HASSANEIN, A. ..... p 889 N95-16307
HASTE, G. R. ..... p 891 N95-17347
HATHER, B. ..... p 809 N95-16743
HAUGRUD, M. J. ..... p 908 N95-16093
HAVIN, V. ..... p 861 N95-16295
HAW, JAMES F. ..... p 741 N95-16409
HAWLEY, KEVIN J. ..... p 826 N95-16244
HAY, R. G. ..... p 779 N95-17635
HAYANO, R. S. ..... p 878 N95-17739
HAYES, T. M. ..... p 729 N95-16627
HAYES, TONY ..... p 707 N95-17609
HAYES, WILLIAM ..... p 836 N95-16490
HAYHURST, KELLY J. ..... p 670 N95-16456
HAYMAKER, R. ..... p 877 N95-17358
HAZIZA, M. ..... p 674 N95-17532
p 692 N95-17534
HAZRA, TUSHAR K. ..... p 674 N95-17553
HE, BAIQING ..... p 651 N95-16262
HE, NING ..... p 653 N95-16279
HEAD, N. C. ..... p 674 N95-17253
HEADLEY, T. J. ..... p 744 N95-16829
HEALD, S. M. ..... p 733 N95-17912
HEANEY, JAY H. ..... p 818 N95-16105
HEATHER, M. A. ..... p 842 N95-17732
HECK, J. L., JR. ..... p 751 N95-17738
HECK, JAMES ..... p 874 N95-16797
p 730 N95-16866
HEELIS, RODERICK A. ..... p 798 N95-16432
HEFFNER, R. H. ..... p 868 N95-16288
HEFLEY, WILLIAM E. ..... p 830 N95-16813
HEI, DONALD J., JR. ..... p 702 N95-17585
HEIDELBERGER, PHILIP ..... p 783 N95-16421
HEIKKINEN, J. A. ..... p 894 N95-17929
HEIMANN, P. ..... p 881 N95-17671
HEINSTEIN, M. W. ..... p 788 N95-17439
HELL, WOLFGANG ..... p 681 N95-17203
HELLER, GEOFFREY ..... p 823 N95-15975
HELLSTEN, T. ..... p 894 N95-17929
HELMREICH, R. L. ..... p 813 N95-16762
HEMBREE, D. M., JR. ..... p 733 N95-17911
HEMMATI, HAMID ..... p 883 N95-15960
HENDERSON, MOREY M. ..... p 912 N95-17710
HENDRICKS, KYLE J. ..... p 760 N95-17501
HENRIKSEN, G. L. ..... p 766 N95-16963
HENRY, JOHN W., IV ..... p 782 N95-17461
HENRY, RICHARD C. ..... p 916 N95-16032
p 917 N95-17422
HENRY, WENDELL A. ..... p 839 N95-17172
HENSLEY, D. R. ..... p 878 N95-17692
HENTZELL, H. ..... p 759 N95-17453
HEPP, ALOYSIUS F. ..... p 731 N95-17387
HERMAN, AKOS ROBERT ..... p 906 N95-15925
HERMAN, C. ..... p 870 N95-16810
HERNANDO, ANTONIO ..... p 775 N95-17376
HERRMANN, N. ..... p 870 N95-16614
HESS, W. R. ..... p 873 N95-16403
p 893 N95-17677
HEUS, R. ..... p 830 N95-16821
HEUSER, WILLIAM RANDY ..... p 674 N95-17554
HIBINO, YUTAKA ..... p 740 N95-16073
HICKEL, BRENT D. ..... p 802 N95-17488
HICKERNELL, R. K. ..... p 887 N95-17441
HICKS, D. L. ..... p 788 N95-17439
HILDEBRAND, C. E. ..... p 756 N95-17283
HILDRETH, M. D. ..... p 875 N95-16943
HILL, D. N. ..... p 889 N95-16554
p 892 N95-17640
p 893 N95-17897
HILL, DAVID C. ..... p 793 N95-16575
HILL, RAYMOND R. ..... p 841 N95-17445
HILL, THOMAS J. ..... p 712 N95-16051
HILLIER, ANDREW C. ..... p 873 N95-16482
HILLIS, D. L. ..... p 892 N95-17640
HILLYARD, S. ..... p 819 N95-16152
HILTEN, O. V. ..... p 796 N95-17304
HINDMARSH, A. C. ..... p 861 N95-16535
HINEDI, S. ..... p 756 N95-17284
HINKS, D. G. ..... p 901 N95-17350
HINTON, F. L. ..... p 890 N95-16919
HIRTH, J. P. ..... p 736 N95-17159
HITNEY, HERBERT V. ..... p 761 N95-17697
HITTERMAN, R. L. ..... p 901 N95-17350
HO, TAI ..... p 745 N95-17434
HOADLEY, SHERWOOD T. ..... p 669 N95-17397
HOBBS, M. L. ..... p 748 N95-16214
HODGDON, JAMES A. ..... p 821 N95-16619
HODGES, JULIA ..... p 804 N95-16124
HOECKER, DOUGLAS G. ..... p 830 N95-16813
HOFFMAN, C. M. ..... p 880 N95-16937
HOFFMAN, JOE D. ..... p 718 N95-16339
HOFMANN, P. ..... p 878 N95-17739
HOGAN, J. ..... p 893 N95-17674
HOGAN, J. T. ..... p 873 N95-16403
p 892 N95-17640
p 893 N95-17677
HOGIE, KEITH ..... p 706 N95-17607
HOIMYR, N. ..... p 880 N95-17503
HOLDAWAY, R. ..... p 695 N95-17549
HOLDEN, T. M. ..... p 786 N95-16803
HOLDENER, F. R. ..... p 751 N95-17738
HOLDER, D. A. ..... p 841 N95-17514
HOLLAND, A. W. ..... p 810 N95-16750
p 813 N95-16761
p 813 N95-16762
p 813 N95-16763
HOLLIS, PATRICK ..... p 780 N95-16031
HOLLOWAY, C. MICHAEL ..... p 843 N95-16480
HOLLY, S. ..... p 747 N95-17722
HOLT, WILLIAM H. ..... p 787 N95-16843
HOOKE, ADRIAN J. ..... p 704 N95-17593
p 704 N95-17594
HOOKER, STANFORD B. ..... p 803 N95-16006
HOOPER, WILLIAM P. ..... p 751 N95-16002
HOOSE, K. V. ..... p 714 N95-16321
HOPE, SHARON A. ..... p 698 N95-17564
HOPKINS, D. A. ..... p 789 N95-17701
HOPKINS, DALE A. ..... p 789 N95-17658
HORI, SHOUJI ..... p 724 N95-16833
HORNSTEIN, RHODA SHALLER ..... p 702 N95-17585
HOROWITZ, RICHARD ..... p 909 N95-16441
HORSTMANN, K. H. ..... p 657 N95-17847
HOULBERG, W. ..... p 893 N95-17674
HOURDIN, F. ..... p 919 N95-16189
HOUSER, THOMAS ..... p 722 N95-16087
HOUSKY, MICHAEL ..... p 838 N95-16634
HOWARD, P. ..... p 674 N95-17253
HOY, GILBERT R. ..... p 778 N95-17337
HOYER, MARK ..... p 791 N95-17511
HRKACH, J. ..... p 739 N95-15996
HSIANG, THOMAS Y. ..... p 763 N95-16394
HSIUNG, YEE BOB ..... p 873 N95-16402
HSU, DAVID S. ..... p 747 N95-17693
HU, HAIYAN ..... p 650 N95-16261
HUA, D. ..... p 744 N95-16934
HUANG, BAOMING M. ..... p 895 N95-16238
p 872 N95-16241
HUANG, WESLEY H. ..... p 782 N95-17430
HUANG, XIAOXI ..... p 653 N95-16280
HUBBARD, C. R. ..... p 786 N95-16803
p 899 N95-16806
HUCKABY, DALE A. ..... p 902 N95-17711
HUDSON, G. B. ..... p 797 N95-17718
HUDSON, RICHARD K. ..... p 707 N95-17612
HUEBNER, H. ..... p 690 N95-17252
HUESCHEN, RICHARD M. ..... p 665 N95-17384
HUET, P. ..... p 904 N95-17668
p 877 N95-17669
HUFF, D. R. ..... p 728 N95-16426
HUFF, E. A. ..... p 728 N95-16426
HUFFINGTON, NORRIS J., JR. ..... p 785 N95-16245
HUGENBERG, K. ..... p 765 N95-16915
HUGHES, PETER M. ..... p 674 N95-17535
HUGHES, R. C. ..... p 727 N95-16362
HULETT, L. D., JR. ..... p 876 N95-16959
HULL, LARRY ..... p 686 N95-17234
HUNG, CHING-CHEH ..... p 709 N95-17275
HUNT, E. RAYMOND, JR. ..... p 790 N95-16895
HUNT, LAWERENCE D. ..... p 708 N95-16131
HUNTER, B. A. ..... p 901 N95-17350
HUNTER, R. P. ..... p 811 N95-16753
HUNTER, S. R. ..... p 877 N95-17687
HUNTLEY, K. G. ..... p 842 N95-17732
HUPP, JOSEPH T. ..... p 747 N95-17682
HURD, WILLIAM J. ..... p 702 N95-17585
HURDER, S. ..... p 860 N95-16291
HURLEY, DANIEL ..... p 703 N95-17588
HURLEY, PATRICK M. ..... p 845 N95-16115
HURST, G. S. ..... p 877 N95-17687
HURST, J. K. ..... p 731 N95-17161
HURT, HOLCOMBE H. ..... p 818 N95-17666
HUSE, SCOTT M. ..... p 845 N95-16115
HUTCHENS, D. E. ..... p 715 N95-16326
HUTCHINSON, D. P. ..... p 776 N95-16486
p 779 N95-17680
HYATT, A. W. ..... p 889 N95-16554
HYLTON, J. O. ..... p 773 N95-17910

I

IBRAHEEM, S. O. ..... p 771 N95-16855
IIJIMA, B. A. ..... p 756 N95-17283
IIVARINEN, J. ..... p 802 N95-17504
IKEDA, SHIGERU ..... p 724 N95-16833
IKEI, YASUSHI ..... p 851 N95-15973
IKENO, AKIHISA ..... p 851 N95-15973
ILINSKI, P. ..... p 882 N95-17901
ILLI, O. J., JR. ..... p 670 N95-17371
ILLMER, N. ..... p 692 N95-17536
IMAE, TOYOKO ..... p 871 N95-15956
IMLAY, R. ..... p 877 N95-17358

INCOLLINGO, MARCO ..... p 676 N95-17181
INDIK, R. A. ..... p 763 N95-16137
INFIELD, D. ..... p 840 N95-17355
p 840 N95-17356
p 841 N95-17628
p 841 N95-17629
p 842 N95-17733
p 842 N95-17734
p 842 N95-17735
INGLE, RICHARD M. ..... p 763 N95-16410
INMAN, D. J. ..... p 782 N95-17366
IRBY, J. ..... p 776 N95-16486
ISHIHARA, KIYOOMI ..... p 677 N95-17184
ISHII, MASAHIRO ..... p 831 N95-15984
ISHIKAWA, NIRO ..... p 740 N95-16073
ISLER, R. C. ..... p 873 N95-16403
p 893 N95-17677
IWASAKI, HIDETOSHI ..... p 753 N95-16232
IWASAKI, M. ..... p 878 N95-17739
IYER, SHANTHI N. ..... p 895 N95-16114

J

JACKSON, KATHERINE ..... p 669 N95-17661
JACKSON, RAYMOND H. ..... p 788 N95-17490
JAHNKE, F. ..... p 776 N95-16353
JAIN, A. ..... p 692 N95-17536
JAMESON, ANTONY ..... p 667 N95-16565
JANECEK, KURT ..... p 780 N95-16543
JANG, Q. ..... p 719 N95-16347
JANKOVSKY, R. S. ..... p 718 N95-16337
JANKOWSKI, C. R., JR. ..... p 752 N95-16129
JANKOWSKI, DAVID GERARD ..... p 922 N95-17392
JANKOWSKI, JEFFREY A. ..... p 818 N95-16112
JANSEN, E. P. ..... p 904 N95-16289
JANUS, RAY ..... p 669 N95-16969
JAWEED, M. ..... p 808 N95-16739
p 810 N95-16749
p 812 N95-16756
JAYARAJ, K. ..... p 712 N95-16057
JEFFREY, D. A. ..... p 850 N95-17374
JEFFRIES, ALAN ..... p 704 N95-17594
JEFFRIES, ALAN J. ..... p 706 N95-17603
JELLINEK, J. ..... p 734 N95-16364
JENKINS, M. W. ..... p 727 N95-16362
JESTER, T. ..... p 897 N95-16424
JIA, YAN-BIN ..... p 840 N95-17432
JIANG, JIANPING ..... p 697 N95-17560
JIANG, X. ..... p 750 N95-17730
JIN, ZHI-JIAN ..... p 869 N95-17449
JOANNOPOULOS, J. D. ..... p 738 N95-17681
JOANNOPOULOS, JOHN ..... p 894 N95-16012
JOE, CHESTER ..... p 697 N95-17562
JOENSSON, ROLF ..... p 684 N95-17221
JOHANSSON, GARY ..... p 874 N95-16797
JOHANSSON, H. ..... p 775 N95-17170
JOHN, BONNIE E. ..... p 827 N95-16518
JOHN, JENS A. ..... p 743 N95-16783
JOHNSON, A. L. ..... p 841 N95-17515
JOHNSON, D. D. ..... p 899 N95-16805
JOHNSON, INGMAR ..... p 650 N95-16258
JOHNSON, J. ..... p 784 N95-17360
JOHNSON, JAMES H. ..... p 839 N95-17176
JOHNSON, M. S. ..... p 777 N95-16917
JOHNSON, W. W. ..... p 814 N95-16767
JOHNSTON, G. P. ..... p 745 N95-16938
JOHNSTON, J. M. ..... p 770 N95-16163
JOHNSTON, P. ..... p 819 N95-16152
JOHNSTON, S. L. ..... p 815 N95-16773
p 710 N95-16776
JOHNSTON, WILLIAM A. ..... p 826 N95-16244
JOLI, JEAN-PIERRE ..... p 686 N95-17232
JONAS, JIRI ..... p 746 N95-17662
JONES, D. J. ..... p 657 N95-17850
JONES, F. E. ..... p 774 N95-16074
JONES, M. ..... p 674 N95-17253
p 705 N95-17602
JONES, R. H. ..... p 736 N95-17159
JONES, ROBERT L. ..... p 738 N95-17699
JONES, ROBERT L., III ..... p 843 N95-16457
JONES, SHERRIE ..... p 812 N95-16758
JONGEWARD, GARY A. ..... p 709 N95-16862
JORDAN, R. G. ..... p 899 N95-16805
JORGENSEN, J. D. ..... p 901 N95-17350
JOSHI, SURESH M. ..... p 709 N95-16857
JUAREZ, J. ..... p 739 N95-17728
JUDGE, DARRELL L. ..... p 914 N95-15964
p 915 N95-16021
JUNCK, K. L. ..... p 882 N95-17931
JUPINA, M. ..... p 777 N95-16548
JURGENS, R. F. ..... p 921 N95-16205

K

KABACOFF, LAWRENCE T. ..... p 775 N95-17376
KABANOV, V. V. ..... p 871 N95-16059
KABULI, M. G. ..... p 855 N95-16011
KACYNSKI, KENNETH J. ..... p 718 N95-16339
KAFKA, B. C. ..... p 791 N95-15963
KAHAN, N. ..... p 809 N95-16744
KAISER, M. K. ..... p 814 N95-16767
KALANTAR, D. ..... p 779 N95-17635
KALB, VIRGINIA L. ..... p 837 N95-16587
KALDOR, S. ..... p 782 N95-17364
KALLEND, J. S. ..... p 902 N95-17898
KALPAKCHIEVA, R. ..... p 880 N95-17519
KAMIKAWA, NEIL ..... p 884 N95-16009
KAMPAS, F. ..... p 764 N95-16425
KAMRA, S. ..... p 794 N95-16940
KAN, EDWIN P. ..... p 681 N95-17204
p 689 N95-17244
KANADE, TAKEO ..... p 886 N95-16795
KANELLAKIS, PARIS C. ..... p 851 N95-17741
KANG, Y. ..... p 761 N95-17926
KANGAS, L. J. ..... p 670 N95-17371
KANNAN, S. M. ..... p 671 N95-16392
KAPOOR, D. ..... p 737 N95-17513
KAPOOR, KAMLESH ..... p 654 N95-16038
KAPOOR, S. ..... p 727 N95-16363
KAPTEIN, N. A. ..... p 827 N95-16615
KARASALO, I. ..... p 840 N95-17410
KARAYAKAYLAR, SELCUK ..... p 755 N95-17173
KARL, T. ..... p 803 N95-17743
KARLIN, JAY ..... p 706 N95-17606
KARNA, ANITA ..... p 665 N95-17373
KARNA, KAMAL ..... p 665 N95-17373
KASPEROVICH, LEONID ..... p 678 N95-17192
KATAN, J. R. ..... p 753 N95-16227
KATILA, T. ..... p 869 N95-17930
KATNIK, GREGORY N. ..... p 676 N95-17262
KATZ, DONALD ..... p 665 N95-17373
KAUFELER, JEAN-FRANCOIS ..... p 704 N95-17595
p 705 N95-17598
KAUFELER, P. ..... p 674 N95-17537
KAUFMANN, MATT ..... p 840 N95-17338
KAUTZ, D. D. ..... p 782 N95-17717
KAVARNOS, GEORGE ..... p 780 N95-16543
KAWAKAMI, KOICHI ..... p 740 N95-16073
KAYE, S. ..... p 893 N95-17674
KAZAROFF, J. M. ..... p 718 N95-16337
KEAR, K. T. ..... p 810 N95-16747
KEATING, SCOTT C. ..... p 788 N95-17492
KEEBLE, D. J. ..... p 899 N95-16918
KEEFER, CHRISTOPHER W. ..... p 885 N95-16443
KEEHAN, LORI ..... p 689 N95-17245
KEEN, J. M. ..... p 715 N95-16326
KEIL, L. ..... p 817 N95-16782
KELLER, H. ..... p 901 N95-17667
KELLER, H. UWE ..... p 920 N95-16192
KELLER, P. E. ..... p 856 N95-16609
KELLEY, EUGENE P. ..... p 778 N95-17464
KELLEY, TIM ..... p 840 N95-17327
KELLY, ALONZO ..... p 666 N95-17706
KELLY, ANGELITA C. ..... p 702 N95-17585
KELLY, J. F. ..... p 790 N95-16215
KEMMOTSU, KEIICHI ..... p 886 N95-16795
KEMP, M. ..... p 794 N95-16957
KENNEDY, ROBERT ..... p 812 N95-16758
KENNEPOHL, P. ..... p 727 N95-16363
KEOLIAN, ROBERT M. ..... p 794 N95-16954
KERCHER, J. ..... p 797 N95-17920
KERCHER, J. R. ..... p 796 N95-17636
KERN, R. D. ..... p 731 N95-17163
KERR, JOHN P. ..... p 782 N95-17461
KERR, W. A., III ..... p 886 N95-16815
KERREBROCK, JACK L. ..... p 709 N95-16352
KESS, P. H. ..... p 901 N95-17667
KEYTE, K. ..... p 674 N95-17253
KIEFER, RICHARD L. ..... p 924 N95-16912
KIERAS, DAVID E. ..... p 829 N95-16119
p 827 N95-16518
KIM, DAI H. ..... p 855 N95-16077
KIM, H. K. ..... p 739 N95-15996
KIM, JACQUELINE H. ..... p 673 N95-15978
KIM, MYUNG-HEE Y. ..... p 924 N95-16912
KIM, SUK C. ..... p 713 N95-16066
KIM, W. H. ..... p 742 N95-16427
KIM, Y. B. ..... p 890 N95-16919
KIM, Y. H. ..... p 747 N95-17685
KIM, Y. S. ..... p 747 N95-17685
KINCAID, B. ..... p 881 N95-17671
KING, D. ..... p 764 N95-16832
KING, JOSEPH H. ..... p 909 N95-16441
KINGON, ANGUS I. ..... p 742 N95-16488
KINTER, JAMES L., III ..... p 912 N95-17491
KIOCK, R. ..... p 663 N95-17878
KIRCHMEIER, ROBERT L. ..... p 731 N95-17142
KIRCHNER, TED ..... p 712 N95-16057
KIRK, B. L. ..... p 844 N95-15946
KJELLGREN, J. ..... p 759 N95-17453
KLABUNDE, KENNETH J. ..... p 729 N95-16791
KLEIHORST, E. ..... p 767 N95-17469
KLEIN, C. A. ..... p 747 N95-17722
KLEIN, M. V. ..... p 902 N95-17917
KLEM, M. D. ..... p 716 N95-16328
KLEMP, MARJORIE K. ..... p 910 N95-17322
KLEPPER, C. C. ..... p 873 N95-16403
p 892 N95-17640
p 893 N95-17677
KLYMENKO, VICTOR ..... p 827 N95-16520
p 886 N95-17334
KNAPP, C. F. ..... p 810 N95-16748
KNAPP, W. L. ..... p 902 N95-17898
KNAUFF, T. ..... p 800 N95-16398
KNICKELBEIN, M. B. ..... p 734 N95-16364
KNIGHTLY, E. W. ..... p 850 N95-17638
KNIO, O. ..... p 870 N95-16810
KNOBLE, G. ..... p 708 N95-17613
KNOBLE, GORDON ..... p 680 N95-17201
p 700 N95-17572
KNOLL, D. ..... p 889 N95-16554
KNOSPE, C. R. ..... p 654 N95-17657
KNOX, CHARLES E. ..... p 665 N95-17384
KO, K. ..... p 882 N95-17902
KO, WILLIAM L. ..... p 788 N95-17417
p 788 N95-17490
KOBERSTEIN, JEFFERY T. ..... p 743 N95-16507
KOBUSHKIN, A. P. ..... p 904 N95-17474
KOCH, M. W. ..... p 763 N95-16357
KOCH, S. W. ..... p 763 N95-16137
p 776 N95-16353
KODALI, N. B. ..... p 742 N95-16427
KOEBERLEIN, ERNEST, III ..... p 681 N95-17205
KOHL, J. A. ..... p 842 N95-17678
KOHL, R. L. ..... p 809 N95-16745
KOHLSTEDT, DAVID L. ..... p 725 N95-17457
KOLKA, MARGARET A. ..... p 821 N95-16809
KOMAKI, YOSHIHIDE ..... p 740 N95-16073
KONISHI, SATOSHI ..... p 731 N95-17157
KONTOTHANASSIS, LEONIDAS I. ..... p 845 N95-16113
KOO, KEE P. ..... p 775 N95-17428
KOOI, F. L. ..... p 827 N95-16822
KOONTZ, S. ..... p 672 N95-16320
KOPF, DANA C. ..... p 778 N95-17500
KOPPENJAN, S. ..... p 798 N95-16284
KOPRIVA, DAVID A. ..... p 863 N95-17267
KOREVAAR, ERIC ..... p 880 N95-17499
KORNHAUSER, ALAN A. ..... p 791 N95-15963
KOSBIE, DAVID S. ..... p 838 N95-16632
KOSHELEV, A. E. ..... p 766 N95-16945
KOSLOSKY, JOHN T. ..... p 699 N95-17570
p 675 N95-17581
p 703 N95-17587
KOSMAHL, HENRY G. ..... p 755 N95-16886
KOSS, D. A. ..... p 733 N95-16104
KOSTYUK, A. P. ..... p 904 N95-17474
KOSUT, ROBERT L. ..... p 855 N95-16011
KOTTKE, THOMAS ..... p 764 N95-16522
KOZHEVNIKOV, YU. V. ..... p 651 N95-16265
KRAAIJVELD, M. A. ..... p 841 N95-17470
KRAKOWSKI, R. A. ..... p 881 N95-17721
KRALL, LAURA A. ..... p 698 N95-17564
KRAUTHAMER, S. ..... p 793 N95-16831
KRECH, ROBERT H. ..... p 655 N95-16076
KREPLIN, H.-P. ..... p 661 N95-17867
KRIER, HERMAN ..... p 889 N95-16243
p 730 N95-16955
KRISHNAMAGARU, RAMESH ..... p 805 N95-16141
KRISS, GERARD A. ..... p 915 N95-17495
KROGER, P. M. ..... p 756 N95-17283
KROON, P. ..... p 796 N95-17304
KROUTIL, ROBERT ..... p 838 N95-16634
KRUCK, MARY ..... p 666 N95-16171
KRUER, W. L. ..... p 777 N95-16929
KRUPKE, W. F. ..... p 899 N95-16867
p 777 N95-17168
p 779 N95-17689
KRUSE, W. ..... p 681 N95-17207
KRUTZ, R. W. ..... p 811 N95-16755
KUDER, STEVEN ..... p 790 N95-16547
KUFFLER, DAMIEN ..... p 820 N95-16423
KUIPER, THOMAS B. ..... p 694 N95-17543
KUKLA, G. ..... p 796 N95-17348
KUKLA, G. J. ..... p 803 N95-17743
KUKSIN, S. B. ..... p 860 N95-16292
KULWICKI, PHILIP ..... p 669 N95-17661
KUMAR, J. ..... p 742 N95-16427
KUMAR, K. V. ..... p 807 N95-16738
KUMAR, SATISH ..... p 723 N95-16126
KUMMEL, ANDREW C. ..... p 729 N95-16790
KUNKLE, D. M. ..... p 713 N95-16314
KURTKAYA, MEHMET ..... p 669 N95-15970
KURUVILA, G. ..... p 667 N95-16569

KUSIOR, J. P. ..... p 902 N95-16075
KUSTIN, KENNETH ..... p 731 N95-17425
KUSTOM, R. ..... p 761 N95-17926
KUSTOM, R. L. ..... p 880 N95-16308
KUTSCHENREUTER, P. ..... p 670 N95-16317
KUZMIN, RUSLAN O. ..... p 920 N95-16193
KUZMIN, RUSLIN O. ..... p 919 N95-16191
KWADRAT, CARL ..... p 684 N95-17222
KWAFO-AKOTO, KATE ..... p 906 N95-15924
KWOK, W. K. ..... p 901 N95-17349

L

LAAKKO, T. ..... p 837 N95-16605
LABBE, X. ..... p 673 N95-17223
LABEZIN, CHRISTIAN ..... p 674 N95-17254
LABRUJERE, TH. E. ..... p 667 N95-16566
p 667 N95-16567
LABRUNE, YVES ..... p 673 N95-17223
LACEY, PAUL I. ..... p 780 N95-16636
LACKMAN, BOB ..... p 840 N95-17324
LACKRITZ, HILARY S. ..... p 742 N95-16483
LACY, J. ..... p 811 N95-16754
LADD, A. J. C. ..... p 722 N95-17745
LADDE, G. S. ..... p 855 N95-16170
LAFERLA, R. ..... p 719 N95-16347
LAGAR, GUNNAR ..... p 906 N95-15929
LAGUS, K. ..... p 837 N95-16605
LAHAYE, R. J. ..... p 892 N95-17497
LAI, B. ..... p 882 N95-17901
LAI, C. ..... p 904 N95-17645
LAKE, MARK S. ..... p 709 N95-16559
LAM, S. S. ..... p 656 N95-17178
LAMBA, JAYDEEP S. ..... p 743 N95-16630
LAMBRECHT, WALTER R. ..... p 898 N95-16527
LANAGAN, M. T. ..... p 902 N95-17898
LANDAY, JAMES A. ..... p 838 N95-16818
LANDEN, O. L. ..... p 779 N95-17635
LANDEROS, J., JR. ..... p 765 N95-16920
LANDHEIM, R. ..... p 920 N95-16193
LANDSHOF, J. A. ..... p 695 N95-17548
p 708 N95-17614
LANGFORD, TED L. ..... p 870 N95-16811
LANYI, G. E. ..... p 756 N95-17280
LARDUINAT, ELIANE ..... p 675 N95-17573
LARRSON, GUS ..... p 701 N95-17578
LARSON, A. C. ..... p 737 N95-17641
LASKA, JOSEPH E. ..... p 766 N95-16950
LASNIER, C. J. ..... p 889 N95-16554
p 892 N95-17640
p 893 N95-17897
LASSILA, D. H. ..... p 736 N95-17378
LAUB, CHARLES F. ..... p 743 N95-16507
LAUENSTEIN, G. G. ..... p 796 N95-17363
LAUG, K. K. ..... p 718 N95-16342
LAUGHON, G. J. ..... p 893 N95-17896
LAUNIUS, ROGER D. ..... p 904 N95-16007
LAURENDEAU, NORMAND M. ..... p 775 N95-16910
LAWLESS, D. ..... p 727 N95-16363
LAWRENCE, GREGORY ..... p 906 N95-15932
LAWSON, A. C. ..... p 737 N95-17641
LAWSON, KEVIN ..... p 865 N95-17341
LAWTON, TERI B. ..... p 819 N95-16135
LAZARIS, KONSTANTINOS A. ..... p 751 N95-15993
LAZARUS, E. A. ..... p 889 N95-16554
LE, L. P. ..... p 868 N95-16288
LEAR, K. L. ..... p 778 N95-17498
LEBLANC, A. ..... p 810 N95-16749
LEBLANC, M. M. ..... p 736 N95-17378
LEBLANC, THOMAS J. ..... p 845 N95-16082
p 845 N95-16083
LECUYER, PIERRE ..... p 865 N95-17426
LEE, D. K. ..... p 892 N95-17640
LEE, E. S. ..... p 775 N95-17307
LEE, H. ..... p 884 N95-16366
p 902 N95-17917
LEE, J. C. ..... p 754 N95-16495
LEE, P. ..... p 758 N95-17294
p 758 N95-17296
LEE, P. R. ..... p 757 N95-17288
LEE, S. L. ..... p 901 N95-17667
LEE, YOUNG H. ..... p 696 N95-17557
LEEK, P. H. ..... p 764 N95-16814
LEHMAN, EDWARD ..... p 669 N95-17661
LEHTONEN, KENNETH ..... p 679 N95-17193
LEIGHTON, T. G. ..... p 769 N95-16064
LEISHMAN, J. G. ..... p 664 N95-17883
LEMPICKI, A. ..... p 896 N95-16385
LEONARD, A. W. ..... p 889 N95-16554
p 892 N95-17640
p 893 N95-17897
LEONARD, JOSEPH T. ..... p 751 N95-17632
LERCHE, R. A. ..... p 779 N95-17635
LESTER, D. M. ..... p 710 N95-16344
LETAMENDIA, L. ..... p 903 N95-16839
LEVINE, ALLEN J. ..... p 683 N95-17214
LEVINE, B. M. ..... p 758 N95-17290
LEVITT, D. S. ..... p 675 N95-17568
LEVITT, HAL L. ..... p 761 N95-17696
LEVY, MOISES ..... p 750 N95-16880
LEVY, P. ..... p 896 N95-16385
LEVY, YORAM ..... p 754 N95-16549
LEW, J. Y. ..... p 856 N95-16287
LEWIS, STEVEN F. ..... p 819 N95-16228
LEWIS, T. A. ..... p 876 N95-16959
LI, GUIFANG ..... p 885 N95-16733
LI, HUA-XIN ..... p 736 N95-17159
LI, JIAN ..... p 760 N95-17651
LI, LARRY ..... p 852 N95-15979
LI, SHU ..... p 651 N95-16263
LI, SICONG ..... p 653 N95-16280
LI, W. ..... p 668 N95-16899
LI, WEIXUAN ..... p 652 N95-16275
LI, Y. ..... p 794 N95-17521
LIANG, DEWANG ..... p 649 N95-16254
LIANG, S. H. ..... p 727 N95-16384
LIAW, BOR Y. ..... p 792 N95-16303
p 730 N95-16973
LIAW, D. G. ..... p 787 N95-17270
LIBBY, S. B. ..... p 778 N95-17627
LICHT, STUART L. ..... p 766 N95-16947
p 766 N95-16948
p 766 N95-16949
LIEBENTHAL, A. ..... p 794 N95-17298
LIGHTFOOT, PATRICIA C. ..... p 702 N95-17585
LIMAYE, SANJAY S. ..... p 910 N95-17323
LIN, Y.-P. ..... p 757 N95-17285
LIND, R. F. ..... p 773 N95-17910
LINDE, L. ..... p 822 N95-17300
LINDELL, I. V. ..... p 754 N95-16612
p 754 N95-16613
LINDGREN, M. ..... p 887 N95-17409
LINDSAY, ANTHONY C. ..... p 884 N95-16133
p 755 N95-16956
LINDSTROEM, J. ..... p 887 N95-17409
p 768 N95-17691
LINICK, SUSAN H. ..... p 685 N95-17228
LINK, H. ..... p 792 N95-16437
LINK, R. E. ..... p 735 N95-16531
LINLEY, LARRY ..... p 711 N95-16047
LINTHICUM, K. ..... p 898 N95-16533
LIOU, YING-HSIN ANDREW ..... p 784 N95-17385
LIPPMANN, R. P. ..... p 752 N95-16129
LISTER, TEDD E. ..... p 895 N95-16238
LITT, JONATHAN ..... p 669 N95-15970
LITT, JONATHAN S. ..... p 721 N95-17274
LITZINGER, T. A. ..... p 781 N95-17162
LIU, B. ..... p 752 N95-16094
LIU, C. T. ..... p 715 N95-16325
LIU, CHUNG-CHIUN ..... p 776 N95-17895
LIU, J. ..... p 769 N95-15966
LIU, JIANYE ..... p 653 N95-16277
LIU, MARK Y. ..... p 763 N95-16394
LIU, SIMON ..... p 686 N95-17234
LIU, TAI-PING ..... p 770 N95-16156
LIU, Y. ..... p 899 N95-16805
LLOYD, C. ..... p 816 N95-16775
LLOYD, C. W. ..... p 710 N95-16772
LOKEN, S. ..... p 910 N95-16922
LOKTEV, V. M. ..... p 901 N95-17518
LONDENBERG, W. KELLY ..... p 656 N95-17273
LONG, CLAUDINE S. ..... p 908 N95-15998
LOOPER, L. ..... p 810 N95-16750
LOU, Y. ..... p 750 N95-17730
LOUAT, N. P. ..... p 735 N95-16519
LOUBEYRE, JEAN PHILIPPE ..... p 689 N95-17246
LOUIE, JOHN J. ..... p 697 N95-17562
p 703 N95-17588
LOUIS, W. C. ..... p 878 N95-17727
LOUTTS, G. ..... p 899 N95-16867
LOVELY, P. S. ..... p 887 N95-17441
LOVESEY, S. W. ..... p 877 N95-17351
p 869 N95-17731
p 869 N95-17750
LOWDEN, R. A. ..... p 723 N95-16225
LOWENTHAL, D. D. ..... p 777 N95-16917
LOWRY, M. ..... p 884 N95-16366
p 765 N95-16915
LU, G. ..... p 747 N95-17722
LUAN, SHUSHENG ..... p 805 N95-17395
LUCZAK, EDWARD C. ..... p 674 N95-17535
LUDLOW, CARLA ..... p 857 N95-17381
LUDWIG, D. ..... p 817 N95-16782
LUDWIG, D. A. ..... p 808 N95-16742
p 817 N95-16781
LUDWINSKI, J. M. ..... p 682 N95-17210
LUE, J. W. ..... p 751 N95-17909
LUEVANO, ANNETTA J. ..... p 738 N95-17663
LUHMAN, THOMAS S. ..... p 744 N95-16844
LUKASZEWICZ, V. ..... p 722 N95-16905
LUKE, T. ..... p 776 N95-16486
LUMLEY, JOHN L. ..... p 770 N95-16407
LUNDSAGER, P. ..... p 840 N95-17355
p 840 N95-17356
p 841 N95-17628
p 841 N95-17629
p 842 N95-17733
p 842 N95-17734
p 842 N95-17735
LUQI, M. S. ..... p 834 N95-16153
LUTON, J. N. ..... p 751 N95-17909
LUXMOORE, ROBERT J. ..... p 797 N95-17908
LYNCH, F. T. ..... p 658 N95-17851
LYNCH, GARY ..... p 825 N95-16138
LYNCH, GENE F. ..... p 830 N95-16813
LYNE, J. E. ..... p 810 N95-16751
LYNENSKJOLD, S. ..... p 674 N95-17253
LYNENSKJOLD, STEEN ..... p 692 N95-17533
p 699 N95-17571
LYNESS, J. N. ..... p 839 N95-16923
LYNN, J. W. ..... p 896 N95-16389
LYNN, K. G. ..... p 899 N95-16918
LYO, S. K. ..... p 879 N95-17918
LYON, J. F. ..... p 893 N95-17907
LYON, L. A. ..... p 747 N95-17682

M

MA, C. H. ..... p 776 N95-16486
p 779 N95-17680
MACARIE, IOAN I. ..... p 859 N95-15948
p 864 N95-16039
p 833 N95-16040
MACCABE, A. B. ..... p 850 N95-16830
MACCORMACK, ROBERT W. ..... p 655 N95-16160
MACDONALD, S. A. ..... p 741 N95-16354
MACE, GUY ..... p 674 N95-17550
MACHAN, J. ..... p 777 N95-16548
MACIEJEWSKI, WENDELL ..... p 780 N95-16543
MACKEY, WILLIAM ..... p 706 N95-17607
MAENTYLAE, M. ..... p 837 N95-16605
MAGHAMI, PEIMAN G. ..... p 709 N95-16857
MAGRUDER, R. H., III ..... p 736 N95-16807
MAHAJAN, S. ..... p 894 N95-16111
MAHDAVI, M. A. ..... p 893 N95-17896
MAHMOT, RON ..... p 703 N95-17587
MAHONEY, JOHN R. ..... p 820 N95-16444
MAHRT, L. ..... p 803 N95-16062
MAIDA, JAMES C. ..... p 855 N95-15992
MAINGI, R. ..... p 892 N95-17640
MAJANI, E. ..... p 757 N95-17289
MAKARIOU, C. C. ..... p 893 N95-17896
MAKEIG, SCOTT ..... p 819 N95-16152
MAKHANKO, A. V. ..... p 652 N95-16274
MALANOTTE-RIZZOLI, PAOLA ..... p 804 N95-16079
MALCOLM, D. J. ..... p 781 N95-17169
MALDAGUE, PIERRE F. ..... p 697 N95-17561
MALETIC, D. ..... p 879 N95-16210
p 901 N95-17673
MALEY, N. ..... p 794 N95-17521
MALGHAN, S. G. ..... p 746 N95-17456
MALINA, ROGER F. ..... p 688 N95-17241
MALLO, GARY ..... p 753 N95-16231
MALONEY, LAURENCE T. ..... p 826 N95-16368
MANDL, DANIEL ..... p 706 N95-17606
MANNA, ZOHAR ..... p 837 N95-16586
MANNING, EVAN ..... p 677 N95-17185
MANSOUR, A. N. ..... p 733 N95-16091
p 735 N95-16606
p 735 N95-16788
p 877 N95-17630
MANTEL, B. ..... p 668 N95-16573
MAO, TONY ..... p 681 N95-17208
MARCHYWKA, MICHAEL J. ..... p 747 N95-17694
MARCONDES-NORTH, R. ..... p 810 N95-16750
MARDARE, D. ..... p 743 N95-16500
MARDARE, DANIELA ..... p 742 N95-16449
p 742 N95-16451
MARDER, SETH ..... p 884 N95-16015
p 885 N95-16787
MARGERUM, J. D. ..... p 897 N95-16498
MARKARIAN, C. F. ..... p 720 N95-16351
MARKLEY, RICHARD W. ..... p 679 N95-17194
MARKS, S. ..... p 881 N95-17671
MARKUSON, NANCY J. ..... p 791 N95-17625
MARSEE, R. L. ..... p 805 N95-16414
MARSH, CATHERINE ..... p 766 N95-16947
p 766 N95-16948
p 766 N95-16949
MARSH, R. ..... p 813 N95-16761
MARSHALL, C. D. ..... p 777 N95-17168
MARSHALL, M. H. ..... p 708 N95-17614
MARTELLI, ANDREA ..... p 695 N95-17551
MARTIN, A. D. ..... p 877 N95-17354
MARTIN, CHARLES R. ..... p 723 N95-16041
p 724 N95-16492

MARTIN, JOHN S. p 827 N95-16520
p 886 N95-17334
MARTIN, MICHAEL p 910 N95-17323
MARTIN, P. p 748 N95-17913
MARTIN, P. L. p 735 N95-16514
MARTIN, P. M. p 793 N95-16916
MARTIN, PAUL J. p 800 N95-16551
MARTIN, V. p 745 N95-17305
MARTINEZ, L. p 739 N95-17728
MARTINEZ, M. p 798 N95-16284
MARTINEZ, M. W. p 779 N95-17688
MARTUCH, ROBERT A. p 731 N95-17387
MASAD, JAMAL A. p 772 N95-17268
MASELAND, J. E. J. p 662 N95-17874
MASON, IAN p 837 N95-16586
MASON, KEVIN T. p 818 N95-16132
p 820 N95-16405
MASQUELIER, D. p 765 N95-16915
MASSA, LOU p 903 N95-16877
MASTERS, W. C. p 694 N95-17545
MASUD, A. p 735 N95-16786
MATEER, GEORGE G. p 659 N95-17858
MATHIAS, L. J. p 746 N95-17485
MATHIOT, D. p 895 N95-16311
MATHUR, S. p 794 N95-17298
MATSUMOTO, YASUYO p 740 N95-16073
MATSUO, KANJI p 724 N95-16833
MATSUURA, YUKI p 740 N95-16073
MATTHEWS, DONNA p 766 N95-16949
MATTHEWS, P. p 761 N95-17926
MATTICE, WAYNE L. p 872 N95-16155
MATYJASZEWSKI, K. p 743 N95-16500
MATYJASZEWSKI, KRZYSZTOF p 739 N95-15996
p 740 N95-16165
p 742 N95-16449
p 742 N95-16450
p 742 N95-16451
p 743 N95-16501
MAURITZ, KENNETH A. p 723 N95-16019
MAX, C. E. p 916 N95-17525
MAX, N. p 834 N95-16220
p 860 N95-16221
MAXWELL, THERESA p 682 N95-17211
MAY, M. p 877 N95-17683
MAYBEE, JEFFREY C. p 713 N95-16315
MAYBURY, MARK T. p 906 N95-15931
MAYER, ALAIN J. p 836 N95-16452
MAYLE, R. W. p 778 N95-17627
MAYNARD, JULIAN D. p 792 N95-16506
p 898 N95-16525
MAZIASZ, P. J. p 738 N95-17679
MAZUMDAR, S. p 886 N95-17143
MAZZOLA, MICHAEL S. p 764 N95-16539
MCCALEB, FREDERICK p 700 N95-17572
MCCAMMON, K. p 765 N95-16915
MCCARTHY, JOHN p 837 N95-16586
MCCARTNEY, P. A. p 716 N95-16332
MCCLUNG, R. C. p 788 N95-17272
MCCLUSKEY, WILLIAM p 907 N95-15935
MCCOMAS, D. J. p 798 N95-16537
MCCONAGHEY, C. p 765 N95-16915
MCCONAGHY, C. p 884 N95-16366
MCCREERY, RICHARD L. p 727 N95-16150
MCCRORY, E. p 882 N95-17931
MCCURDY, HOWARD E. p 904 N95-16007
MCDERMOTT, DREW p 855 N95-16095
MCDONALD, M. A. p 660 N95-17860
MCDONNELL, J. R. p 857 N95-16631
MCDONNELL, MICHAEL p 909 N95-16431
MCDOWELL, R. S. p 790 N95-16215
MCELWEE-WHITE, LISA p 740 N95-16101
MCFADDEN, T. p 813 N95-16762
MCGIBBON, A. J. p 728 N95-16419
MCGIBBON, M. M. p 728 N95-16419
MCGOVERN, JANET L. p 669 N95-17631
MCGRATH, B. J. p 815 N95-16771
MCGRATH, JAMES E. p 740 N95-16096
MCHUGH, MARTIN J. p 915 N95-16854
MCKAMEY, C. G. p 738 N95-17679
MCKEAN, M. E. p 799 N95-16927
MCKINNEY, J. FRANKLIN p 684 N95-17218
MCKOY, VINCENT p 873 N95-16493
MCLAFFERTY, FRED W. p 726 N95-16017
MCLAUGHLIN, BRUCE A. p 700 N95-17574
MCLAUGHLIN, ELIZABETH p 780 N95-16543
MCLEAN, WILLIAM E. p 827 N95-16520
p 886 N95-17334
MCLUCKEY, S. A. p 876 N95-16959
MCNEIL, R. p 877 N95-17358
MCOMBER, ROBERT p 677 N95-17187
MCPHERSON, P. H. p 695 N95-17549
MCRAE, D. S. p 771 N95-16736
MEAD, R. D. p 777 N95-16917
MEDDAHI, M. p 904 N95-17904
MEDLER, LAWRENCE P. p 666 N95-16356
MEGLI, THOMAS W. p 889 N95-16243
MEHROTRA, PIYUSH p 843 N95-16478
MEISEL, D. p 727 N95-16363
MELENDRES, C. A. p 733 N95-16091
p 735 N95-16606
p 735 N95-16788
p 877 N95-17630
MELLO, F. J. p 788 N95-17439
MELLOR, A. M. p 749 N95-16499
MELLSTROM, J. A. p 664 N95-17291
MELO, STELLA MARIS LUDOVICO p 799 N95-17647
MENAKER, MICHAEL p 807 N95-16599
MENGE, P. R. p 888 N95-16216
MENGEL, M. p 782 N95-17364
MENON, M. M. p 893 N95-17896
MENON, SURESH p 772 N95-17165
MERKELBACK, E. J. p 828 N95-16835
MERRILL, WALTER C. p 721 N95-17274
MESICK, HILLARY p 790 N95-16547
MESSAGE, PHILIP p 700 N95-17577
MESSENT, DAVID p 702 N95-17584
METCALF, W. p 877 N95-17358
MEYER, DAVID E. p 829 N95-16119
MEYER, R. p 879 N95-16172
MEYER, ROBERT A. p 833 N95-16004
MEYN, SEAN P. p 860 N95-16169
MIAO, C. p 878 N95-17899
MICHAEL, K. p 677 N95-17186
MICHAILIDIS, DIMITRIOS p 851 N95-17741
MICKLICH, B. J. p 665 N95-16964
MIES, L. p 692 N95-17536
MIGNOSI, A. p 659 N95-17856
MIHAL, JOSEPH J., JR. p 676 N95-17509
MIKO, J. p 677 N95-17186
MILANOVICH, F. p 775 N95-17380
MILLER, ANDREW C. p 897 N95-16445
MILLER, G. A. p 746 N95-17438
MILLER, GLENN E. p 911 N95-17328
MILLER, J. E. p 749 N95-16499
MILLER, JEFFREY L. p 708 N95-16131
MILLER, JOHN H. p 901 N95-17424
MILLER, KEVIN J. p 692 N95-17538
p 697 N95-17562
MILLER, M. S. p 787 N95-16939
MILLER, R. L. p 893 N95-17907
MILLER, WARNER H. p 677 N95-17186
MILLS, G. A. p 795 N95-16386
p 727 N95-16387
MILLS, ROBERT F. p 753 N95-16300
MINES, R. F. p 850 N95-17638
MINSEO, P. p 897 N95-16510
MIODUSZEWSKI, P. K. p 892 N95-17640
MIRCHANDANI, CHANDRU p 675 N95-17582
MISCHKE, R. E. p 676 N95-17153
p 876 N95-17158
MISHRA, UMESH K. p 765 N95-16834
MITAL, SUBODH K. p 725 N95-17659
MITCHELL, TOM M. p 857 N95-16820
MITTER, SANJOY K. p 857 N95-16864
MOCK, WILLIS, JR. p 787 N95-16843
MOERDER, DAN p 848 N95-16473
MOERDER, DANIEL D. p 709 N95-16902
MOFFAT, H. K. p 733 N95-17744
MOGFORD, R. H. p 665 N95-16375
MOIR, I. R. M. p 657 N95-17848
MOLANDER, W. A. p 779 N95-17688
MOLDWIN, M. B. p 798 N95-16537
MOLNAR, J. A. p 910 N95-16884
MOLONEY, J. p 763 N95-16137
MONIER-GARBET, P. p 893 N95-17677
MONTGOMERY, LAWRENCE K. p 899 N95-16789
MONTGOMERY, RAYMOND C. p 849 N95-16475
MONTONEN, J. p 869 N95-17930
MONTOYA, R. JORGE p 851 N95-15974
MOODY, R. p 742 N95-16427
MOOK, H. A. p 901 N95-17667
MOONIER, P. p 882 N95-17924
MOORE, HENRY J. p 920 N95-16194
MOORE, J. p 840 N95-17338
MOORE, J. MICHAEL p 701 N95-17580
MOORE, JAMES D. p 719 N95-16343
MOORE, PETER K. p 861 N95-16395
MOORE, ROBERT B. p 723 N95-16019
MORAN, AL W. p 829 N95-16145
MORE, K. L. p 899 N95-16806
MORENO, D. J. p 727 N95-16362
MORENO, J. C. p 778 N95-17627
MORILAK, DANIEL P. p 784 N95-17385
p 675 N95-17419
MORRIS, D. E. p 722 N95-16905
MORRISETT, GREG p 838 N95-16819
MORSE, J. p 765 N95-16915
MORTON, D. S. p 770 N95-16417
MOSELY, E. p 812 N95-16757
MOSHER, D. p 880 N95-17475
MOSSESSIAN, D. p 881 N95-17671
MOUSSAID, A. p 870 N95-16614
MOYA, M. M. p 763 N95-16357
MOZO, BEN T. p 869 N95-16226
MROZ, E. p 896 N95-16359
MU, XINHUA p 653 N95-16278
MUELLER, CHRISTIAN p 699 N95-17571
MUELLER, D. p 903 N95-16944
MUELLER, J. M. p 774 N95-16804
MUELLER, KARL L. p 684 N95-17221
MUELLER, WOLFGANG p 898 N95-16598
MUKAMEL, SHAUL p 885 N95-16524
MUKHERJEE, RANJAN p 782 N95-17621
MULLER, MICHAEL J. p 830 N95-16813
MULVAGH, S. p 811 N95-16754
MUNK, P. p 744 N95-16792
MURAKAMI, M. p 891 N95-16958
MURCHIE, SCOTT p 920 N95-16195
p 922 N95-16207
MURPHY, C. D. p 810 N95-16748
MURPHY, E. E. p 665 N95-16375
MURPHY, ELIZABETH D. p 697 N95-17560
MURPHY, J. p 921 N95-16203
MURPHY, SUSAN C. p 697 N95-17562
p 702 N95-17583
p 703 N95-17588
MURRAY, ROYCE W. p 868 N95-16162
MURTHY, P. L. N. p 787 N95-17270
MURTHY, PAPPU L. N. p 725 N95-17659
MUSGRAVE, JEFFREY L. p 721 N95-17274
MUSIAL, W. p 792 N95-16437
p 784 N95-17360
MUTHIAH, J. p 746 N95-17485
MYERS, BRAD A. p 838 N95-16632
p 838 N95-16818
MYERS, C. R. p 675 N95-17568

N

NAGEL, KARIN L. p 826 N95-16299
NAIRUS, JOHN G. p 712 N95-16055
NAKAMURA, OSAMU p 724 N95-16833
NAKAMURA, S. N. p 878 N95-17739
NAKATA, ALBERT Y. p 686 N95-17229
NAKAYAMA, K. p 702 N95-17586
NANJUNDAN, ASHOK p 830 N95-16418
NANZETTA, KATHY p 681 N95-17206
NARAYANA, P. p 810 N95-16749
NASRABADI, NASSER M. p 858 N95-17459
NATANSON, G. A. p 694 N95-17546
NAYFEH, ALI H. p 772 N95-17268
NEALY, JOHN E. p 924 N95-16912
NEATHERY, JAMES K. p 923 N95-17653
NEAU, E. L. p 882 N95-17914
NEELY, EDGAR S. p 839 N95-17176
NEGAARD, GORDON R. p 784 N95-15953
NELANDER, A. p 759 N95-17301
NELSON, BILL p 689 N95-17247
NELSON, C. A. p 903 N95-16604
NELSON, MICHAEL p 847 N95-16464
NELSON, RON p 886 N95-16965
NEMANICH, R. J. p 894 N95-16084
NEMANICH, ROBERT J. p 743 N95-16625
NENONEN, J. p 869 N95-17930
NESTER, PAUL p 700 N95-17572
NEUBERT, VERNON H. p 708 N95-16304
NEUMAN, JAMES C. p 684 N95-17218
NEUMARK, DANIEL M. p 729 N95-16846
NEWELL, A. C. p 763 N95-16137
NEWHOUSE, M. p 686 N95-17231
NEWMAN, P. A. p 771 N95-16828
NEWMAN, PERRY A. p 774 N95-16461
NEWSOME, PENNY A. p 700 N95-17575
NEWTON, J. p 794 N95-17521
NGUYEN, DIEM p 675 N95-17582
p 706 N95-17607
NGUYEN, DUC T. p 847 N95-16462
NGUYEN, T. M. p 757 N95-17287
NI, YONGXI p 653 N95-16277
NICHOLSON, JOHN C. p 656 N95-17435
NICKUM, WILLIAM G. p 674 N95-17553
NICOGOSSIAN, A. E. p 808 N95-16741
NICOLA, VICTOR p 783 N95-16421
NICOLAIDES, ROY A. p 861 N95-16376
NIEH, T. G. p 745 N95-16935
NIESERT, C. P. p 741 N95-16354
NIETO, JAVIER p 833 N95-15995
NIETO, M. M. p 903 N95-16428
NIEUSMA, JUDY M. p 858 N95-17465
NIEUWENHUYS, G. J. p 868 N95-16288
NIEZETTE, M. p 705 N95-17602
NIGHTINGALE, R. W. p 916 N95-16600
NILSEN, ERIK N. p 700 N95-17574
NILSEN, J. p 778 N95-17627
NISHIMURA, Y. p 657 N95-17850
NODULMAN, L. p 878 N95-17899

NOJIMA, SHUJI ..... p 853 N95-15985
NOLL, KATHRYN E. ..... p 734 N95-16380
NORCROSS, SCOTT ..... p 693 N95-17539
NORMAN, COLIN A. ..... p 915 N95-17496
NORMAN, D. ..... p 879 N95-17932
NORTH, G. R. ..... p 801 N95-16961
NORTH, JAN A. ..... p 886 N95-17340
NOUCHI, G. ..... p 903 N95-16839
NOVICK, A. H. ..... p 665 N95-16964
NUNN, C. C. ..... p 873 N95-16482
NYBLOM, K. ..... p 653 N95-17451
NYE, H. R. ..... p 704 N95-17596
NYGARD, K. E. ..... p 908 N95-16093

O

OAKLEY, JOHN Y. ..... p 766 N95-16950
OCONNOR, ROBERT D. ..... p 740 N95-16092
OCONNOR, T. P. ..... p 796 N95-17363
ODA, H. ..... p 878 N95-17692
ODONNELL, PATRICIA M. ..... p 793 N95-16861
ODUBIYI, JIDE ..... p 696 N95-17555
OGIHARA, MITSUNORI ..... p 839 N95-17261
OGLETREE, D. F. ..... p 779 N95-17729
p 779 N95-17887
OHARA, D. ..... p 817 N95-16780
p 817 N95-16782
OHMANN, P. ..... p 877 N95-17353
OHRINER, E. K. ..... p 737 N95-17513
OKAZAKI, T. ..... p 904 N95-17474
OKUNO, KENJI ..... p 731 N95-17157
OLFENBUTTEL, R. F. ..... p 654 N95-17466
OLIVARES, J. A. ..... p 896 N95-16359
OLIVIER, S. S. ..... p 916 N95-17525
OLSEN, MIKE ..... p 661 N95-17865
OLSEN, RICHARD S. ..... p 799 N95-16872
OLSON, C. L. ..... p 891 N95-17382
OLSON, DANIEL PAUL ..... p 833 N95-16088
OLSON, DARREN M. ..... p 798 N95-16521
OLSON, L. HOWARD ..... p 831 N95-16894
OLYSLAGER, F. ..... p 754 N95-16612
OMULLANE, W. ..... p 705 N95-17602
ONDRUS, PAUL J. ..... p 706 N95-17603
ORASANU, J. ..... p 814 N95-16765
OREILLY, JOHN ..... p 680 N95-17199
ORTH, MARK J. ..... p 839 N95-17176
OSBORN, R. ..... p 896 N95-16389
OSBORNE, D. H., JR. ..... p 736 N95-16807
OSGOOD, R. O. ..... p 781 N95-17169
OSKARSSON, H. ..... p 734 N95-16420
OTOSHI, T. Y. ..... p 757 N95-17288
OTRANTO, JOHN F. ..... p 700 N95-17575
OTSUKI, SHINICHI ..... p 724 N95-16833
OTTERSTEN, H. ..... p 759 N95-17301
OTTINGER, P. F. ..... p 891 N95-17382
OUELETTE, R. ..... p 751 N95-17632
OUT, RON ..... p 874 N95-16797
OVERFELT, P. L. ..... p 753 N95-16233
OVERMAN, JOANNE ..... p 907 N95-15938

P

PACE, MARCO ..... p 703 N95-17590
PACEY, J. G. ..... p 793 N95-16544
PACZKOWSKI, B. G. ..... p 682 N95-17210
PADMORE, H. ..... p 881 N95-17671
PAESLER, MICHAEL A. ..... p 884 N95-16157
PAGE, W. C. ..... p 857 N95-16631
PAGORIA, P. F. ..... p 749 N95-16542
PAJERSKI, ROSE ..... p 698 N95-17566
PALMER, ALAN S. ..... p 782 N95-17461
PAMADI, BANDU N. ..... p 709 N95-16902
PAN, JIAZHENG ..... p 649 N95-16251
PAN, LIANGXIAN ..... p 653 N95-16279
PANAHANDEH, M. ..... p 735 N95-16786
PANDE, J. BRADLEY ..... p 718 N95-16341
PANDOLF, KENT B. ..... p 819 N95-16228
PANDYA, ABHILASH K. ..... p 855 N95-15992
PANEM, CHANTAL ..... p 698 N95-17563
PANKUCH, M. ..... p 733 N95-16091
p 735 N95-16606
PAPAILIOU, K. D. ..... p 664 N95-16563
p 664 N95-16564
PAPAMICHAEL, K. ..... p 775 N95-17307
PAPENHUIJZEN, R. ..... p 831 N95-17468
PARASHAR, MANISH ..... p 844 N95-16060
PARENTI, RONALD R. ..... p 885 N95-16494
PARK, K. C. ..... p 788 N95-17492
PARK, ROBERT E. ..... p 836 N95-16503
PARK, S. K. ..... p 800 N95-16398
PARKER, G. G. ..... p 782 N95-17366
p 858 N95-17915
PARKER, TIM J. ..... p 920 N95-16196
p 920 N95-16197
PARKS, E. K. ..... p 734 N95-16364
PARROD, Y. ..... p 686 N95-17230
PARWANI, R. R. ..... p 904 N95-17925
PASSCHIER, D. M. ..... p 658 N95-17853
PASSI, RANJIT M. ..... p 804 N95-16125
PATNAIK, S. N. ..... p 789 N95-17701
PATT, FREDERICK S. ..... p 690 N95-17249
PATTERSON, F. ..... p 884 N95-16366
PATTERSON, JAMES H., JR. ..... p 870 N95-16811
PATWARDHAN, A. R. ..... p 810 N95-16748
PAUL, D. M. ..... p 901 N95-17667
PAULAS, R. A. ..... p 803 N95-17709
PAVLOFF, MICHAEL S. ..... p 673 N95-17547
PAXSON, DANIEL E. ..... p 721 N95-17274
PAYNE, S. A. ..... p 899 N95-16867
p 777 N95-17168
PEARSON, DARREN L. ..... p 874 N95-16784
PEASE, R. F. ..... p 729 N95-16622
PECCHIOLI, M. ..... p 674 N95-17537
PECCHIOLI, MAURO ..... p 692 N95-17533
PECCIA, N. ..... p 689 N95-17248
p 699 N95-17567
PECHENIK, A. ..... p 746 N95-17456
PEDRAZA, D. F. ..... p 733 N95-17911
PELLEGRINO, S. ..... p 783 N95-17928
PEN, JIBING ..... p 653 N95-16278
PENA, C. R. ..... p 765 N95-16932
PENDER, SHAW EXUM ..... p 681 N95-17205
PENDLEY, R. D. ..... p 675 N95-17568
PENG, Y. K. M. ..... p 881 N95-17721
PENNER, J. E. ..... p 797 N95-17920
PENNYCOOK, S. J. ..... p 728 N95-16419
PEPI, M. ..... p 737 N95-17486
PEPPER, L. J. ..... p 814 N95-16768
PERCEC, V. ..... p 744 N95-16865
p 878 N95-17692
PERCEC, VIRGIL ..... p 874 N95-16797
p 730 N95-16866
PERIAUX, J. ..... p 668 N95-16573
PERKINS, B. D. ..... p 805 N95-16414
PERKINS, DOROTHY C. ..... p 706 N95-17604
p 707 N95-17611
PERKINS, L. J. ..... p 893 N95-17674
PERREAULT, DAVID A. ..... p 833 N95-16004
PERRIN, PATRICK ..... p 804 N95-16124
PERRY, B. ..... p 898 N95-16533
PETERS, EDWARD ..... p 783 N95-16870
PETERSON, R. V. ..... p 711 N95-16046
PETRIE, T. W. ..... p 893 N95-17897
PETZOLD, LINDA R. ..... p 856 N95-16390
p 861 N95-16395
PEYGHAMBARIAN, N. ..... p 886 N95-17143
PHAM, T. T. ..... p 708 N95-17292
PHELPS, A. D. ..... p 769 N95-16064
PHILLIPS, MARY A. ..... p 737 N95-17398
PHILLIPS, R. J. N. ..... p 923 N95-17352
p 877 N95-17353
PHILLIPS, ROBERT W. ..... p 676 N95-16769
PICHE, JOE ..... p 712 N95-16057
PICKETT, ROBERT ..... p 805 N95-16141
PIERIK, J. ..... p 842 N95-17733
p 842 N95-17734
p 842 N95-17735
PIERLUISSI, JOSEPH ..... p 740 N95-16085
PIERSON, BRIAN E. ..... p 833 N95-15997
PIETRAS, JOHN ..... p 705 N95-17599
PIGNEDE, M. ..... p 704 N95-17597
PINGITORE, NELSON V. ..... p 707 N95-17612
PINSKI, F. J. ..... p 899 N95-16805
PINTNER, R. ..... p 811 N95-16754
PINTO, NINA PANE ..... p 905 N95-15923
PIRMAN, S. R. ..... p 730 N95-16955
PIRONNEAU, O. ..... p 667 N95-16568
PITT, KARL J. ..... p 683 N95-17214
PITTS, RONALD E. ..... p 674 N95-17255
PLEMMONS, ROBERT J. ..... p 862 N95-16798
PLESCIA, JEFF B. ..... p 921 N95-16198
PLOWMAN, S. E. ..... p 839 N95-16923
PNUELI, AMIR ..... p 837 N95-16586
POCHA, M. ..... p 884 N95-16366
PODLESNY, R. ..... p 794 N95-17521
POGGIO, TOMASO ..... p 835 N95-16236
POIRIER, J. L. ..... p 753 N95-16240
POLLMEIER, V. M. ..... p 694 N95-17545
POMPILIO, ROBERT A. ..... p 795 N95-16545
PORAT, ZEEV ..... p 742 N95-16434
POROPAT, G. V. ..... p 887 N95-17489
POROPATICH, RONALD K. ..... p 822 N95-17174
PORR, W. C., JR. ..... p 735 N95-16531
PORTER, W. O. ..... p 899 N95-16806
PORTH, TRICIA ..... p 907 N95-15933
POSE, RONALD ..... p 852 N95-15977
POSSE, C. ..... p 865 N95-16546
POST, D. ..... p 893 N95-17674
POTHEN, ALEX ..... p 862 N95-16596
POTHIER, B. ..... p 737 N95-17486
POTOTZKY, ANTHONY S. ..... p 669 N95-17397
POTTER, SCOTT S. ..... p 857 N95-17383
POTTER, WILLIAM ..... p 675 N95-17573
POUKEY, J. W. ..... p 888 N95-16216
POULTER, K. ..... p 705 N95-17602
POWELL, E. S. ..... p 672 N95-16318
POWELL, M. R. ..... p 807 N95-16738
POWER, WENDY ..... p 783 N95-16870
POWERS, M. ..... p 677 N95-17186
POWERS, W. T. ..... p 716 N95-16330
POZOS, ROBERT ..... p 818 N95-16105
PRAGER, S. C. ..... p 892 N95-17643
PRETTYMAN-LUKOSCHEK, JILL ..... p 685 N95-17224
PRICE, PAMELA E. ..... p 802 N95-17686
PRIEST, JOHN ..... p 736 N95-16878
PRITCHARD, JIM ..... p 680 N95-17201
PRIYONO, EDDY ..... p 654 N95-15994
PROSPERETTI, A. ..... p 870 N95-16810
PRZYSTUPA, MAREK A. ..... p 738 N95-17663
PSZOLLA, H. ..... p 662 N95-17875
PUFFERT-MEISSNER, W. ..... p 657 N95-17847
PUJO, OLIVER ..... p 686 N95-17233
PURASINGHE, R. ..... p 718 N95-16342
PURDY, ANDREW ..... p 732 N95-17479
PURVIS, CAROLYN K. ..... p 709 N95-16862
PUTCHA, L. ..... p 811 N95-16753

Q

QAMAR, RAMZI ..... p 847 N95-16462
QIAN, Y. L. ..... p 882 N95-17902
QIN, JIANGNING ..... p 847 N95-16462
QUARLES, G. J. ..... p 777 N95-17168
QUARRIE, D. R. ..... p 910 N95-16922
QUAST, A. ..... p 663 N95-17877
QUI, L. L. ..... p 899 N95-16805
QUILLEN, STEVE R. ..... p 907 N95-15939
QUIRK, RODERIC P. ..... p 872 N95-16155

R

RABENAU, E. ..... p 681 N95-17207
RABIER, PATRICK J. ..... p 860 N95-16127
p 860 N95-16128
RABITZ, HERSCHEL ..... p 903 N95-16489
RACICOT, RONALD L. ..... p 856 N95-16550
RACKLEY, MICHAEL ..... p 706 N95-17606
RADAELLI, P. G. ..... p 901 N95-17350
RADESPIEL, R. ..... p 663 N95-17877
RAHMAN, HASAN ..... p 679 N95-17195
RAINER, F. ..... p 902 N95-17742
RAITT, W. J. ..... p 675 N95-16005
RAKESTRAW, D. L. ..... p 774 N95-16804
RALPH, MARTIN R. ..... p 821 N95-16481
RAMAN, N. K. ..... p 744 N95-16934
RAMANATHAN, CHANDRASHEKAR
p 804 N95-16124
RAMCHANDANI, C. ..... p 708 N95-17613
RAO, GOPALAKRISHNA ..... p 685 N95-17224
RAO, N. S. V. ..... p 856 N95-16361
RAO, RAJESH P. N. ..... p 859 N95-15951
RAPER, C. DAVID, JR. ..... p 807 N95-15961
RASH, JAMES L. ..... p 676 N95-17179
p 691 N95-17531
RASIN, A. ..... p 878 N95-17889
RASMUSSEN, D. A. ..... p 891 N95-16958
RATANAPHRUKS, KRICH ..... p 795 N95-16881
RATNER, M. A. ..... p 739 N95-16013
RATNER, MARK A. ..... p 747 N95-17682
RATOWSKY, R. P. ..... p 778 N95-17627
RAUBENHEIMER, T. O. ..... p 875 N95-16933
RAVIKUMAR, V. ..... p 728 N95-16419
RAY, ASOK ..... p 784 N95-16066
RAY, DAVID M. ..... p 854 N95-15988
RAY, JAMES C. ..... p 781 N95-17335
RAY, U. ..... p 763 N95-16357
RAYMOND, T. D. ..... p 777 N95-16917
REAL-PLANELLS, B. ..... p 704 N95-17597
REASS, W. A. ..... p 888 N95-16218
p 889 N95-16285
REDEKER, G. ..... p 660 N95-17863
REED, BRIAN D. ..... p 719 N95-16346
REED, CHARLES E. ..... p 909 N95-16845
REED, H. ..... p 809 N95-16746
REED, MICHAEL ..... p 783 N95-16870
REED, TRACEY ..... p 682 N95-17211
REESE, JAY ..... p 689 N95-17245
REEVE, T. ..... p 670 N95-17371
REEVE, TIM ..... p 702 N95-17583
REEVES, DENNIS L. ..... p 826 N95-16140
REGAN, MATTHEW ..... p 852 N95-15977
REHBOCK, PHILIP F. ..... p 805 N95-16168
REINERT, FRANCIS R. ..... p 766 N95-16950
REINICKE, ROBERT H. ..... p 720 N95-16349

REISEL, JOHN R. p 775 N95-16910
REISLER, HANNA p 726 N95-16042
p 730 N95-17140
REISS, KEITH p 695 N95-17552
REJ, D. J. p 889 N95-16286
p 891 N95-16936
p 745 N95-16938
REMENYIK, C. J. p 773 N95-17910
REMER, D. S. p 758 N95-17295
RENDON, A. p 879 N95-16172
RENEKER, DARRELL H. p 872 N95-16155
RENWICK, S. P. p 764 N95-16814
RESCHKE, M. p 815 N95-16771
RESSLER, ELLIOT L. p 754 N95-16549
REYNOLDS, ANTHONY P. p 736 N95-16860
RHATIGAN, JENNIFER L. p 675 N95-17419
RHEE, CHOONG K. p 872 N95-16241
RHODES, DOROTHY S. p 850 N95-17374
RHODES, G. S. p 785 N95-16072
RICE, JIM W. p 920 N95-16197
p 921 N95-16199
p 921 N95-16200
RICHARD, PAULO p 790 N95-16547
RICHARDS, R. K. p 776 N95-16486
p 779 N95-17680
RICHMOND, ERIC p 675 N95-17576
RICHWINE, DAVID M. p 656 N95-16858
RICKER, R. E. p 737 N95-17616
RIDER, JAMES W. p 685 N95-17227
RIEDEL, K. S. p 893 N95-17644
RIEDER, RUDI p 710 N95-16201
RIESEN, R. p 850 N95-16830
RIGDON, MICHAEL p 725 N95-16970
RILEY, S. J. p 734 N95-16364
RINALDI, M. A. p 916 N95-16600
RINALDI, P. L. p 878 N95-17692
RIVERA, JORGE E. p 676 N95-17262
RIVERS, MELISSA B. p 656 N95-16908
ROBASCHIK, D. p 903 N95-16944
ROBERTS, R. G. p 877 N95-17354
ROBINETT, R. D. p 782 N95-17366
ROBINSON, DEBORAH L. p 883 N95-15960
ROBINSON, E. p 673 N95-17212
ROBINSON, R. A. p 896 N95-16389
p 737 N95-17641
ROBINSON, R. M. p 916 N95-16600
ROCCO, DAVID A. p 685 N95-17225
RODDE, A. M. p 659 N95-17857
RODGERS, C. p 670 N95-16323
RODGERS, MARK D. p 828 N95-17655
RODIER, DANIEL R. p 910 N95-17322
RODRIGUEZ, D. L. p 658 N95-17851
RODRIGUEZ, IVAN p 705 N95-17602
RODRIGUEZ, J. L. p 727 N95-16362
RODRIGUEZ, P. p 780 N95-16224
ROESKE, F. p 884 N95-16366
ROGERS, GEORGE W. p 857 N95-16823
ROGERS, JAMES L. p 848 N95-16470
ROGERS, MELISSA J. B. p 750 N95-17893
ROGERS, R., III p 732 N95-17639
ROHATGI, A. p 794 N95-16940
ROHN, DENNIS W. p 675 N95-17419
ROHRER, RICHARD A. p 685 N95-17226
ROIG, DAVID M. p 781 N95-17263
ROMANOSKI, G. R. p 733 N95-17911
ROMERO, R. p 705 N95-17602
ROOT, ELIZABETH A. p 905 N95-15922
ROOT, J. H. p 786 N95-16803
ROPER, DONNA G. p 847 N95-16465
ROSE, D. V. p 891 N95-17382
ROSE, M. FRANK p 793 N95-16575
ROSE, R. M. p 813 N95-16762
ROSEKIND, M. R. p 813 N95-16760
ROSEMANN, UWE p 906 N95-15928
ROSENBERG, LINDA H. p 699 N95-17569
ROSENBERGER, JOHN p 701 N95-17580
ROSENBLUM, B. Z. p 902 N95-17906
ROSER, T. p 872 N95-16121
ROSKE-HOFSTRAND, R. J. p 665 N95-16375
ROSSI, ALDO p 823 N95-15976
ROSSI, F. p 696 N95-17558
ROSSITER, B. N. p 842 N95-17732
ROTH, J. R. p 755 N95-16968
ROTH, J. THOMAS p 830 N95-16813
ROTH, KARLIN R. p 663 N95-17881
ROTHE, IRENE p 859 N95-15949
ROTHE, JOERG p 859 N95-15949
ROUFF, CHRISTOPHER p 700 N95-17577
ROUNTREE, MICHAEL p 669 N95-17661
ROUSCH, RANDY p 764 N95-16539
ROUSSEL, A. p 673 N95-17223
ROUSSOPOULOS, NICHOLAS p 912 N95-17652
ROUTBORT, J. L. p 873 N95-16430
ROUW, M. p 796 N95-17304
ROY, INDRANIL DANDA p 870 N95-16401
ROZUM, JAMES A. p 836 N95-16504
ROZZI, WILLIAM p 790 N95-17372
RUBIN, M. p 775 N95-17307
RUDD, RICHARD P. p 685 N95-17228
RUDGE, A. p 765 N95-16920
RUGGIERO, A. G. p 879 N95-16210
p 901 N95-17673
RUIZ, C. L. p 745 N95-16938
RUPERT, A. H. p 815 N95-16771
RUSAK, BENJAMIN p 821 N95-16484
RUSSELL, ALAN J. p 807 N95-16164
RUSSELL, CHRISTOPHER T. p 923 N95-17403
RUSSELL, D. A. p 788 N95-17272
RUSSELL, STEPHEN D. p 778 N95-17464
p 767 N95-17478
RUSSELL, T. p 882 N95-17902
RUTLEDGE, SHARON K. p 781 N95-17263

S

SAARELA, J. p 880 N95-17503
SACKS, ALLAN L. p 673 N95-15978
SAETHER, ERIK p 785 N95-16102
p 788 N95-17510
SAFAEINILI, A. p 783 N95-16538
SAGALOVSKY, L. p 665 N95-16964
SAKURAI, TSUTOMU p 740 N95-16073
SALAS, M. D. p 667 N95-16569
SALCEDO, JOSE p 693 N95-17540
SALEEM, D. J. p 753 N95-16227
SALMERON, M. p 779 N95-17729
p 779 N95-17887
SAMSONOV, A. E. p 713 N95-16313
SAMUELSSON, I. p 663 N95-17882
SANDERS, P. G. p 876 N95-16962
SANDFORD, MAYNARD C. p 653 N95-16560
SANK, V. p 677 N95-17186
SANTAVICCA, D. A. p 781 N95-17162
SANTIAGO, FRANCISCO p 767 N95-17481
SANTORO, R. J. p 781 N95-17162
SANTORO, ROBERT J. p 730 N95-16882
SANTOS, EUGENE, JR. p 855 N95-16246
SANTY, P. A. p 810 N95-16750
p 813 N95-16761
p 813 N95-16762
SAOTOME, OSAMU p 760 N95-17649
SARMA, BIMAL K. p 750 N95-16880
SARMIENTO, J. L. p 795 N95-16212
SARVER-VERHEY, TIMOTHY R. p 711 N95-15968
p 720 N95-17265
SARY, CHARISSE p 686 N95-17234
p 693 N95-17541
SASS, STEPHEN L. p 723 N95-16016
SATER, JANET M. p 725 N95-16970
SATHANANTHAN, S. p 855 N95-16170
SATO, MAKOTO p 831 N95-15984
SAULSBERRY, R. L. p 716 N95-16332
SAUNDERS, R. STEPHEN p 910 N95-17323
SAUS, JOSEPH R. p 721 N95-17274
SAVAGE, HOWARD T. p 775 N95-17376
SAVAGE, M. E. p 888 N95-16216
SAWIN, C. F. p 811 N95-16755
SAWYER, C. R. p 712 N95-16052
SCALES, CHARLES H. p 702 N95-17585
SCHAEFER, JOHN L. p 923 N95-17653
SCHAFFER, M. J. p 893 N95-17896
p 893 N95-17897
SCHATZLE, FRANK p 805 N95-16141
SCHAUBEL, K. M. p 893 N95-17896
SCHEIDKER, E. J. p 675 N95-17568
SCHEPS, RICHARD p 777 N95-17302
SCHIERMAN, JOHN D. p 671 N95-17404
SCHLAGHECK, RONALD A. p 685 N95-17227
SCHLEUTER, J. p 900 N95-16946
SCHLOSSER, HERBERT p 746 N95-17654
SCHMIDLLAP, F. A. p 745 N95-16938
SCHMIDT, DAVID K. p 671 N95-17404
SCHNEIBEL, J. H. p 738 N95-17726
p 739 N95-17728
SCHNEIDER, M. F. p 769 N95-16064
SCHNEIDER, V. p 810 N95-16749
SCHOEN, A. p 692 N95-17536
SCHOESSOW, P. p 882 N95-17924
SCHOONOVER, R. M. p 774 N95-16074
SCHOTT, J. H. p 734 N95-16505
p 897 N95-16508
SCHRAAGEN, J. M. p 828 N95-16835
SCHRADER, MARK L. p 799 N95-17446
SCHROEDER, DAVID p 828 N95-17530
SCHUBERT, LENHART p 859 N95-16022
SCHULLER, H. M. p 818 N95-16801
SCHULTZ, REBECCA p 820 N95-16360
SCHULZ, KLAUS-JUERGEN p 676 N95-17181
SCHUMM, JEFFREY S. p 874 N95-16784
SCHUSTER, JOHN p 880 N95-17499
SCHWAN, K. P. p 672 N95-16530
p 672 N95-16842
SCHWARTING, IRENE S. p 826 N95-16244
SCHWARZ, BARBARA p 703 N95-17587
SCHWARZ, R. K. p 841 N95-17514
SCHWARZE, GENE E. p 883 N95-17933
SCHWENK, E. B. p 737 N95-17637
SCHWENTERLY, S. W. p 751 N95-17909
SCIUTO, ALFRED M. p 818 N95-17666
SCOTNEY, A. p 840 N95-17355
p 840 N95-17356
p 841 N95-17628
p 841 N95-17629
p 842 N95-17733
p 842 N95-17734
p 842 N95-17735
SCOTT, A. D. p 733 N95-17912
SCOTT, MICHAEL L. p 845 N95-16113
SCOTT, PETER D. p 858 N95-17459
SECHKAR, EDWARD A. p 781 N95-17263
SECKLER, M. M. p 796 N95-17399
SEEGMILLER, H. LEE p 659 N95-17858
p 661 N95-17865
SEELEY, G. P. p 837 N95-16626
SEGALMAN, D. J. p 782 N95-17366
SEHGAL, R. p 744 N95-16934
SEIDEL, DAVID A. p 653 N95-16560
SEIFF, ALVIN p 711 N95-16202
p 921 N95-16203
SELF, MARK F. p 900 N95-17171
SELIGMAN, ERIK p 850 N95-16826
SELKOWITZ, S. p 775 N95-17307
SELLIS, TIMOS p 912 N95-17652
SEMERARO, B. D. p 851 N95-17676
SERPONE, N. p 727 N95-16363
SERZAN, SHARON L. p 909 N95-16374
SEVERANCE, KURT p 843 N95-16469
SEXTON, DOUGLAS A. p 778 N95-17464
SGALL, JIRI p 849 N95-16603
SHA, W. T. p 772 N95-17523
SHAFFER, WILLIAM A. p 915 N95-16854
SHAHABUDDIN, PERWEZ p 783 N95-16421
SHAMBAYATI, S. p 708 N95-17292
SHANEYFELT, M. R. p 895 N95-16311
SHANMUGHAM, S. p 899 N95-16806
SHANNON, K. p 735 N95-16540
SHANNON, SAMUEL G. p 818 N95-16132
p 820 N95-16405
SHAPIRO, B. Z. p 861 N95-16367
SHARPE, S. W. p 790 N95-16215
SHASHUA, AMNON p 835 N95-16236
SHAUGHNESSY, C. H. p 764 N95-16814
SHAW, KEVIN p 790 N95-16547
SHAW, MARY p 835 N95-16446
SHAW, ROBERT J. p 654 N95-16038
SHAW, W. J. p 791 N95-17903
SHE, ZHISHUN p 652 N95-16269
SHEEM, S. p 775 N95-17380
SHEFFIELD, J. p 891 N95-17367
SHELTON, SUSAN p 852 N95-15979
SHELTON, W. A. p 899 N95-16805
SHEPPARD, SYLVIA B. p 699 N95-17569
p 707 N95-17608
SHEPPARD, WILLIAM R. p 784 N95-17507
SHI, JEFF p 678 N95-17191
p 681 N95-17208
p 675 N95-17582
SHIAO, MICHAEL C. p 787 N95-16911
SHIELDS, A. L. p 736 N95-17378
SHIELDS, WILLIAM p 780 N95-16031
SHIGAKI, K. p 878 N95-17739
SHIGEMOTO, TAKEO p 742 N95-16449
SHIGETA, T. p 702 N95-17586
SHIH, TSAN-HSING p 770 N95-16407
SHIMABUKURO, RANDY L. p 767 N95-17478
SHIMONY, SOLOMON E. p 855 N95-16246
SHINODA, TOSHIAKI p 805 N95-17277
SHIOYAMA, HIROSHI p 724 N95-16833
SHIPLEY, D. E. p 787 N95-16939
SHIRAH, GREGORY W. p 674 N95-17535
SHORT, NICHOLAS M., JR. p 680 N95-17200
SHREEVE, JEANNE M. p 731 N95-17142
SHRIVER, D. F. p 739 N95-16013
SHUR, MICHAEL p 896 N95-16391
SHURMER, I. p 674 N95-17537
SHVARTSMAN, ALEX A. p 851 N95-17741
SICONOLFI, S. F. p 810 N95-16747
SIEGEL, JANE p 836 N95-16490
SIEGEL, R. W. p 876 N95-16962
SIGMAN, CLAYTON B. p 699 N95-17570
p 675 N95-17581
SIHVOLA, A. H. p 754 N95-16613
SIKKA, V. K. p 737 N95-17513
SILBERMAN, GABRIEL M. p 849 N95-16529
SILVER, M. p 794 N95-16957
SILVERS, J. p 708 N95-17613
SIMANONOK, K. p 812 N95-16757
SIMEROTH, JOHN P. p 828 N95-17447

SIMMONS, J. A. p 879 N95-17918
SIMMONS, M. J. p 660 N95-17861
SIMMONS, S. C. p 816 N95-16777
SIMMONS, TAMMY L. p 829 N95-16145
p 829 N95-16147
SIMON, M. p 756 N95-17284
SIMONS, MARK p 701 N95-17578
SIMPSON, JAMES R. p 864 N95-16422
SIMULA, O. p 802 N95-17504
SINCLAIR, CRAIG p 698 N95-17566
SINGER, ROBERT B. p 919 N95-16187
p 921 N95-16204
SINGHAL, SURENDRA N. p 785 N95-16416
SIRAZETDINOV, T. K. p 653 N95-16276
SITES, R. L. p 782 N95-17717
SITLER, TODD W. p 806 N95-17624
SKLOSS, TIMOTHY W. p 741 N95-16409
SKOMOROKHOV, V. I. p 650 N95-16256
SKOP, RICHARD A. p 772 N95-17506
SLADE, MARTIN A. p 921 N95-16205
SLATER, D. C. p 732 N95-17642
SLEMROD, MARSHALL p 773 N95-17708
SLENSKI, GEORGE p 712 N95-16056
SLOAN, CRAIG T. p 801 N95-17164
SLOPIS, J. p 810 N95-16749
SMALL, GARY S. p 838 N95-16634
SMITH, A. V. p 777 N95-16917
SMITH, ALLAN L. p 730 N95-17141
SMITH, C. W. p 715 N95-16325
SMITH, CHARLES p 736 N95-16878
SMITH, D. L. p 873 N95-16487
p 665 N95-16964
SMITH, D. W. p 767 N95-17487
SMITH, DAN p 674 N95-17256
SMITH, DARYL R. p 827 N95-16433
SMITH, J. E. p 915 N95-16558
SMITH, J. P. p 893 N95-17896
SMITH, J. R. p 888 N95-16216
SMITH, KATHRYN A. p 849 N95-16479
SMITH, L. A. p 654 N95-17466
SMITH, L. K. p 899 N95-16867
SMITH, L. M. p 748 N95-16029
SMITH, M. p 816 N95-16775
SMITH, N. DEAN p 795 N95-16881
SMITH, N. R. p 801 N95-16961
SMITH, PETER H. p 711 N95-16206
SMITH, S. R. p 704 N95-17597
SMITH, SIMON T. p 686 N95-17233
SMITH, SINCLAIR p 819 N95-16228
SMITHRICK, JOHN J. p 793 N95-16861
SNIDER, R. T. p 890 N95-16555
SNOHA, D. J. p 737 N95-17486
SNOWDON, DAVE p 854 N95-15990
SNYDER, DAVID B. p 709 N95-16862
SOBIECZKY, H. p 660 N95-17864
SODERSTROM, TOMAS J. p 698 N95-17564
SOGABE, TOSHIAKI p 724 N95-16833
SOLKA, JEFFREY L. p 857 N95-16823
SOLOMON, JEFF p 681 N95-17206
SOMMERER, A. J. p 875 N95-16931
SOMMERFELDT, SCOTT D. p 871 N95-16848
SONNEBORN, GEORGE p 707 N95-17611
SOPORI, BHUSHAN p 791 N95-15944
SORATHIA, USMAN A. p 746 N95-17462
SORENSEN, ERIK MOSE p 682 N95-17209
SOVERS, O. J. p 756 N95-17280
SPECIALE, NICK p 678 N95-17191
SPECK, D. p 770 N95-16211
SPEECE, ROBERT F. p 676 N95-17262
SPENCE, D. p 893 N95-17900
SPENCE, J. R. p 875 N95-16931
SPETH, J. A. p 777 N95-17168
SPEZIALE, CHARLES G. p 769 N95-16070
p 769 N95-16071
SPEZIO, ANTHONY E. p 761 N95-17696
SPOONER, S. p 786 N95-16803
SPRADLIN, GARY L. p 685 N95-17228
SPROUL, W. D. p 745 N95-17160
SRIDHAR, K. R. p 830 N95-16418
SRIDHARAN, R. p 673 N95-17212
SRIDHARAN, RAMASWAMY p 707 N95-17609
SROMOVSKY, LAWRENCE A. p 910 N95-17323
STACY, KATHY p 843 N95-16468
STAEBLER, G. M. p 890 N95-16919
STAKHIV, EUGENE Z. p 796 N95-17684
STALLARD, B. R. p 763 N95-16357
STALLARD, LINDA p 908 N95-15957
p 908 N95-16086
p 908 N95-16090
STALLINGS, WILLIAM p 705 N95-17598
STANDLEY, SHAUN p 673 N95-17213
STANEWSKY, E. p 659 N95-17856
STANNILAND, D. p 662 N95-17876
p 664 N95-17884
p 664 N95-17885
STARBIRD, THOMAS J. p 693 N95-17540
p 697 N95-17561
STARKEY, MICHAEL p 850 N95-16826
STARKEY, PAUL p 686 N95-17233
STARR, T. L. p 724 N95-16926
STAUNTON, J. B. p 899 N95-16805
STAVNES, MARK W. p 711 N95-16044
STEAKLEY, MICHAEL F. p 915 N95-17496
STEGMANN, B. J. p 811 N95-16755
STEIN, C. p 834 N95-16220
STEINBERG, D. J. p 745 N95-17379
STEINETZ, B. M. p 722 N95-16905
STEINMANN, L. p 811 N95-16752
STELIOUDAKIS, EMMANUEL p 752 N95-16117
STEN, J. C. E. p 760 N95-17502
STENCEL, JOHN M. p 923 N95-17653
STEPANOVA, M. V. p 799 N95-17471
STEPHENSON, LOU A. p 821 N95-16809
STERN, DANIEL C. p 683 N95-17214
STERN, JOHN A. p 828 N95-17530
STERN, S. A. p 732 N95-17642
STICKNEY, JOHN L. p 895 N95-16238
p 872 N95-16241
STIDHAM, CURTIS R. p 781 N95-17263
STIER, BERND p 780 N95-16900
STINN, J. L. p 817 N95-16781
STINTON, D. P. p 723 N95-16225
p 899 N95-16806
STIRLING, W. J. p 877 N95-17354
STOBBE-KREEMERS, A. W. p 732 N95-17700
STOCKMEYER, LARRY J. p 836 N95-16452
STOCKS, G. M. p 899 N95-16805
STODDARD, F. J. p 716 N95-16328
STOFFEL, A. WILLIAM p 693 N95-17542
STOKES, C. D. p 763 N95-16410
STOKES, GRANT p 673 N95-17215
STOKLOSA, J. H. p 812 N95-16759
STOLIAROV, NIKOLAI p 828 N95-17530
STOLOFF, MICHAEL p 705 N95-17599
STORAASLI, OLAF O. p 847 N95-16458
p 847 N95-16460
p 847 N95-16462
STORER, JAMES A. p 911 N95-17329
STOREY, BRETT p 669 N95-17661
STOTTS, RICHARD R. p 818 N95-17666
STOUDT, DAVID C. p 764 N95-16539
STOUDT, M. R. p 737 N95-17616
STOUFFLET, B. p 668 N95-16573
STRAIN, D. M. p 759 N95-17297
STRAND, T. p 884 N95-16366
STROUBOULIS, T. p 861 N95-16379
p 863 N95-17431
STUBBS, ROBERT M. p 713 N95-16066
STUBNYA, GYORGY p 906 N95-15925
STUEBER, THOMAS J. p 712 N95-16049
STURMS, FRANCIS M., JR. p 686 N95-17229
STYF, J. p 809 N95-16744
SU, M. p 670 N95-17749
SU, S. AUGUSTINE p 853 N95-15981
SUARD, NORBERT p 666 N95-17196
SUES, ROBERT H. p 785 N95-16072
SUESSE, HERBERT p 859 N95-15949
SUGAWARA, MASAYUKI p 677 N95-17184
SUKANYA, P. p 831 N95-15984
SULLIVAN, D. p 860 N95-16293
SUMMERS, M. p 784 N95-17360
SUN, J. p 803 N95-16062
SUN, J. G. p 772 N95-17523
SUN, LIANGXIN p 651 N95-16263
SUN, YUANKUN p 885 N95-16733
SUNG, CHONG S. p 747 N95-17685
SURATI, RAJEEV p 846 N95-16237
SUTCLIFFE, J. G. p 822 N95-16851
SUTER, BRUCE W. p 755 N95-16841
SUTHERLAND, H. p 784 N95-17360
SVEDIN, J. p 775 N95-17170
SVOBODA, R. p 877 N95-17358
SWAIN, MICHAEL J. p 831 N95-16966
SWEGLE, J. W. p 788 N95-17439
SWETITS, J. p 668 N95-16899
SWINK, DON G. p 713 N95-16315
SYKES, R. I. p 800 N95-16802
SYMONDS, MARTIN p 699 N95-17571
SZAKAL, DONNA p 675 N95-17601
SZODRUCH, JOACHIM p 659 N95-17858
SZWEDA, A. p 725 N95-17905

T

TAASAN, SHLOMO p 667 N95-16569
p 862 N95-16869
p 862 N95-16896
TACHIKAWA, ENZO p 740 N95-16073
TADAYON, BRIAN p 896 N95-16399
TAI, WALLACE S. p 686 N95-17229
TAJIMA, T. p 904 N95-17645
TALAGA, R. p 882 N95-17924
TALAGRAND, O. p 919 N95-16189
TALCOTT, CAROLYN p 837 N95-16586
TAN, I. H. p 892 N95-17643
TAN, TEH Y. p 791 N95-15944
TANG, C. L. p 898 N95-16623
TANG, M. p 786 N95-16785
TANK, A. M. G. KLEIN p 802 N95-17529
TAO, BAOQI p 652 N95-16275
TARMAN, T. D. p 850 N95-17516
TARR, MICHAEL J. p 825 N95-16010
TASK, HARRY L. p 830 N95-16553
TASSANO, J. B. p 777 N95-17168
TATARENKO, O. M. p 901 N95-17518
TEGTMEYER, R. J. p 892 N95-17442
TELEMAN, N. p 860 N95-16293
TELTZOV, M. V. p 799 N95-17471
TENDER, LEONARD p 868 N95-16162
TERASHIMA, NOBUYOSHI p 853 N95-15982
TERAZAWA, HIDEZUMI p 877 N95-17520
TERESHCHUK, V. S. p 652 N95-16272
TESCH, P. p 809 N95-16743
THAKUR, MRINAL p 895 N95-16134
THALER, BARRY J. p 741 N95-16369
THEEUWES, J. p 827 N95-16615
p 827 N95-16817
p 827 N95-16822
THIAGARAJAN, BALAJI p 844 N95-16060
THIBEAULT, SHEILA A. p 924 N95-16912
THIES, MARK C. p 726 N95-16142
THOMAS, C. E., JR. p 891 N95-17347
THOMAS, C. W. p 687 N95-17237
THOMAS, EDWIN L. p 749 N95-16512
THOMAS, I. M. p 902 N95-17742
THOMAS, SAJAN p 872 N95-16241
THOMPSON, A. M. p 746 N95-17438
THOMPSON, LYNN p 666 N95-16171
THOMPSON, STEVEN R. p 737 N95-17398
THOMPSON, WILLIAM T. p 801 N95-17339
THOMSEN, M. F. p 798 N95-16537
THORNELOE, S. A. p 793 N95-16544
THRUN, SEBASTIAN p 857 N95-16820
THURAISINGHAM, R. A. p 870 N95-16812
TIETZE, K. J. p 811 N95-16753
TILIAKOS, NICHOLAS T. p 889 N95-16243
TIMMERMANS, R. p 705 N95-17602
TINKER, MICHAEL L. p 786 N95-16577
TIWARI, SURENDRA N. p 769 N95-15966
p 726 N95-15967
TOBIN, S. J. p 873 N95-16403
p 893 N95-17677
TOFT, MARK p 685 N95-17224
TOGNETTI, V. p 869 N95-17731
p 869 N95-17750
TOLLEFSEN, D. p 840 N95-17410
TOMAZOS, DIMITRIS p 874 N95-16797
p 730 N95-16866
TOMLINS, G. W. p 873 N95-16430
TONFONI, GRAZIELLA p 761 N95-15991
TONG, K. p 757 N95-17286
TONG, MICHAEL T. p 785 N95-16416
TORGERSON, J. LEIGH p 688 N95-17242
TORTORELLI, P. F. p 739 N95-17747
TOUCHSTONE, MARK p 828 N95-17530
TOUR, JAMES M. p 743 N95-16628
p 874 N95-16629
p 743 N95-16630
p 743 N95-16783
p 874 N95-16784
p 874 N95-16799
TRACK, E. p 765 N95-16915
TREIMAN, ALLAN p 920 N95-16195
TREIMAN, ALLAN H. p 922 N95-16207
TRIFUNAC, A. D. p 728 N95-16485
TRIVEDI, SUDHIR B. p 885 N95-16733
TROENDLY, GREGORY M. p 674 N95-17553
TROSKO, JAMES E. p 820 N95-16378
TROST, L. C. p 880 N95-17361
TROUT, J. BARRY p 764 N95-16561
TRUMAN, C. R. p 771 N95-16438
TRUMAN, J. K. p 899 N95-16849
TRURAN, JAMES W. p 924 N95-16383
TRUSZKOWSKI, WALT p 696 N95-17555
TRUSZKOWSKI, WALTER F. p 697 N95-17560
TSAI, C. Y. p 672 N95-16320
TSOU, H. p 756 N95-17284
TSU, RAPHAEL p 894 N95-16081
TUCKER, JERRY H. p 832 N95-16477
TUFFIAS, R. H. p 718 N95-16340
p 719 N95-16347
TURKO, B. T. p 765 N95-16932
TURNER, G. D. p 733 N95-17912
TURNER, J. E. p 877 N95-17687
TURNER, MARK A. p 670 N95-16109
TUTTLE, B. A. p 744 N95-16829
TVERSKOY, B. A. p 799 N95-17471
TWIGG, MARK E. p 896 N95-16399

TYRON, ROGER ..... p 780 N95-16543

U

UCKAN, N. A. ..... p 893 N95-17674
UHLEN, K. ..... p 840 N95-17355
p 840 N95-17356
p 841 N95-17628
p 841 N95-17629
UHRIG, HANS ..... p 705 N95-17599
UHRLAUB, DAVID R. ..... p 675 N95-17589
ULVESTAD, JAMES S. ..... p 673 N95-17216
UMLOR, M. T. ..... p 899 N95-16918
UNGAR, GORAN ..... p 730 N95-16866
UPADHYAY, C. S. ..... p 861 N95-16379
p 863 N95-17431
UPSHAW, BERNADETTE ..... p 784 N95-17385
URETSKII, YA. S. ..... p 651 N95-16266
URIBE, F. ..... p 765 N95-16920
USLENGHI, P. L. E. ..... p 880 N95-16308

V

VAEAENAENEN, J. ..... p 766 N95-16951
VAIDYANATHAN, P. P. ..... p 757 N95-17285
VAKHITOV, M. V. ..... p 651 N95-16264
VALKEALAHTI, K. ..... p 802 N95-17504
VALLES, JAMES M., JR. ..... p 894 N95-16106
VALLONE, ANTONIO ..... p 675 N95-17576
VALVANO, JOE ..... p 678 N95-17188
VANALSTINE, JAMES M. ..... p 750 N95-16065
VANCAUTER, EVE ..... p 821 N95-16796
p 822 N95-17342
VANCHAU, MICHAEL N. ..... p 854 N95-15988
VANDAM, CORNELIS P. ..... p 655 N95-16589
VANDENBERG, B. ..... p 658 N95-17855
VANDERVELDEN, A. ..... p 668 N95-16570
p 668 N95-16571
p 668 N95-16572
VANGAASBECK, JAMES ..... p 688 N95-17243
VANGRIETHUYSEN, VALERIE J. ..... p 715 N95-16322
VANKLEUNEN, W. ..... p 782 N95-17364
VANLAAK, J. ..... p 711 N95-16045
VANROSENDALE, JOHN ..... p 849 N95-16476
VANSCHAAIJK, M. ..... p 796 N95-17304
VANVLIET, L. J. ..... p 887 N95-17483
VANYSEK, PETR ..... p 729 N95-16635
VARGHESE, THOMAS ..... p 687 N95-17239
VARY, J. P. ..... p 875 N95-16931
VASSALLO, ENRICO ..... p 701 N95-17579
VAUCAMPS, C. ..... p 903 N95-16839
VAWTER, G. A. ..... p 778 N95-17498
VEAL, B. W. ..... p 897 N95-16408
VECHT, A. ..... p 767 N95-17487
VEESER, L. ..... p 780 N95-16224
VELAZQUEZ, C. S. ..... p 742 N95-16434
VELEZ, M. ..... p 900 N95-16946
VELSKO, S. P. ..... p 765 N95-16925
VERESHCHAGIN, NIKOLAI K. ..... p 859 N95-15950
VERHAAGEN, N. G. ..... p 662 N95-17874
VERNIKOS, J. ..... p 808 N95-16742
p 816 N95-16778
p 817 N95-16779
p 817 N95-16780
p 817 N95-16781
p 817 N95-16782
VERONA, ROBERT W. ..... p 827 N95-16520
p 886 N95-17334
VERUTTIPONG, W. ..... p 758 N95-17294
p 758 N95-17296
VICENT, J. L. ..... p 900 N95-16946
VICKERS, J. H. ..... p 715 N95-16326
VIELCANET, P. ..... p 673 N95-17223
VIELCANET, PIERRE ..... p 674 N95-17254
VIGGH, H. ..... p 673 N95-17212
VISA, A. ..... p 802 N95-17504
VISBAL, MIGUEL R. ..... p 655 N95-16808
VISSER, H. J. ..... p 755 N95-16816
VISSERS, D. R. ..... p 766 N95-16963
VLANNES, NICKOLAS P. ..... p 760 N95-17482
VLASKO-VLASOV, V. K. ..... p 897 N95-16408
VO, D.-P. ..... p 692 N95-17534
VO, H.-D. H. ..... p 752 N95-16129
VOGLEWEDE, STEVEN D. ..... p 679 N95-17197
VOIGT, J. A. ..... p 744 N95-16829
VOIGT, SUSAN ..... p 843 N95-16454
VONDREELE, R. B. ..... p 737 N95-17641
VONEGIDY, T. ..... p 878 N95-17739
VONOFENHEIM, BILL ..... p 843 N95-16468
VOSS, KLAUS ..... p 859 N95-15949
VOSTEEN, LOUIS F. ..... p 724 N95-16859
VOUROS, P. ..... p 727 N95-16373
VRIJKOTTE, T. G. ..... p 830 N95-16821
VUOSKOSKI, J. ..... p 880 N95-17503
VYASELEV, M. P. ..... p 652 N95-16273
VYMENETS, Y. ..... p 861 N95-16295

W

WAAGEN, D. E. ..... p 857 N95-16631
WADE, C. E. ..... p 817 N95-16780
p 817 N95-16782
WADE, H. ..... p 794 N95-17298
WADSWORTH, J. ..... p 745 N95-16935
WAEKE, H. ..... p 710 N95-16201
WAGANAAR, W. J. ..... p 891 N95-16936
p 745 N95-16938
WAGNER, J. L. ..... p 901 N95-17350
WAGNER, R. ..... p 882 N95-17924
WAHLS, RICHARD A. ..... p 656 N95-16908
WAIGHT, KENNETH T., III ..... p 802 N95-17686
WALDINGER, RICHARD ..... p 837 N95-16586
WALIGORA, J. M. ..... p 807 N95-16738
WALKO, R. ..... p 764 N95-16832
WALLACE, CLARK E. ..... p 715 N95-16322
WALLACE, TIM L. ..... p 716 N95-16330
WALSH, JOHN E. ..... p 911 N95-17330
WALTERBOS, R. A. M. ..... p 924 N95-17527
WALTERBOS, RENE A. M. ..... p 915 N95-17496
WALTERS, ELIZABETH S. ..... p 910 N95-16971
WALTERS, J. MILAM ..... p 848 N95-16472
WALZ, JOSEPH E. ..... p 709 N95-16857
WAN, A. S. ..... p 778 N95-17627
WANG, C. ..... p 898 N95-16533
p 881 N95-17671
WANG, C. H. ..... p 748 N95-17724
WANG, CHIA-CHI ..... p 763 N95-16394
WANG, K. D. ..... p 794 N95-16957
WANG, KON-SHENG CHARLES ..... p 772 N95-17418
WANG, LONG ..... p 898 N95-16527
WANG, Q. DAVID ..... p 915 N95-17496
WANG, SEAN X. ..... p 885 N95-16733
WANG, TEN-SEE ..... p 716 N95-16329
WANG, X. Q. ..... p 772 N95-17523
WANG, XIAO-YEN ..... p 862 N95-16885
p 772 N95-16903
WANG, YIFEI ..... p 649 N95-16251
WANG, YILI ..... p 722 N95-16058
WANG, Z. ..... p 901 N95-17350
WARD, JON ..... p 854 N95-15987
WARD, M. D. ..... p 734 N95-16505
p 897 N95-16508
WARD, MICHAEL D. ..... p 897 N95-16445
p 873 N95-16482
WARNER, B. E. ..... p 779 N95-17688
WARNER, M. J. ..... p 710 N95-16344
WARREN, D. ..... p 879 N95-16172
WARREN, DANIEL E. ..... p 754 N95-16621
WARREN, M. E. ..... p 778 N95-17498
WARREN, R. C. ..... p 774 N95-16247
WARREN, W. L. ..... p 895 N95-16311
WARWICK, A. ..... p 881 N95-17671
WASKEY, J. P. ..... p 735 N95-16531
WATANABE, M. ..... p 742 N95-16434
WATENPAUGH, D. E. ..... p 809 N95-16744
WATKINS, R. D. ..... p 763 N95-16357
WATSON, CAROLYN B. ..... p 655 N95-16069
WAYMAN, RICHARD J. ..... p 912 N95-17660
WEBB, J. T. ..... p 836 N95-16503
WEBBER, S. E. ..... p 744 N95-16792
WEBER, JENNIFER R. ..... p 712 N95-16053
WECHSLER, G. ..... p 737 N95-17486
WEEKES, TREVOR C. ..... p 924 N95-17421
WEEKS, R. A. ..... p 736 N95-16807
WEEKS, W. ..... p 898 N95-16533
WEERTMAN, J. R. ..... p 876 N95-16962
WEFEL, JOHN P. ..... p 923 N95-16080
p 923 N95-17723
WEHAGE, ROGER A. ..... p 856 N95-16390
WEI, DONG-QING ..... p 904 N95-17712
WEIDNER, RICHARD J. ..... p 673 N95-15978
WEIGHT, KRISTEN ..... p 785 N95-16102
p 788 N95-17510
WEINBERG, AARON ..... p 677 N95-17187
WEINTRAUB, DAVID ..... p 672 N95-17444
WEISENBORN, MIKE ..... p 843 N95-16469
WEISS, R. S. ..... p 792 N95-16067
WEISS, S. ..... p 779 N95-17729
p 779 N95-17887
WELCH, C. S. ..... p 763 N95-16357
WELCH, DAVE ..... p 705 N95-17600
WELCH, R. ..... p 808 N95-16740
WELLING, JOHN ..... p 681 N95-17206
WELLS, MAXWELL J. ..... p 836 N95-16511
WELLS, RICHARD L. ..... p 900 N95-17171
WELP, U. ..... p 897 N95-16408
WERKING, R. D. ..... p 675 N95-17568
WERT, J. A. ..... p 738 N95-17664
WERTHEIM, A. H. ..... p 830 N95-16821
WESOLOWSKI, W. ..... p 882 N95-17902
WESSELS, ROBERT H. A. ..... p 906 N95-15926
WESSEN, RANDII R. ..... p 707 N95-17610
WESTER, D. W. ..... p 864 N95-17916
WESTERVELT, JAMES D. ..... p 857 N95-16967
WETTLAUFER, BRIAN ..... p 672 N95-16319
WHEADON, J. ..... p 705 N95-17602
WHEAT, S. R. ..... p 850 N95-16830
WHEELER, ROBERT L. ..... p 726 N95-16008
WHETSEL, ELWIN ..... p 736 N95-16878
WHITAKER, K. W. ..... p 716 N95-16330
WHITCOMB, JOHN D. ..... p 724 N95-16597
WHITE, C. W. ..... p 736 N95-16807
WHITE, M. ..... p 882 N95-17902
WHITE, P. R. ..... p 769 N95-16064
WHITE, PETER S. ..... p 900 N95-17171
WHITEHEAD, JOHN C. ..... p 713 N95-16315
WHITESEL, H. K. ..... p 887 N95-17441
WHITGIFT, D. ..... p 705 N95-17602
WHITWORTH, G. W. ..... p 695 N95-17548
WICKLER, MARTIN ..... p 687 N95-17235
WICKLUND, A. B. ..... p 878 N95-17899
WIDMANN, E. ..... p 878 N95-17739
WIERCIGROCH, ALEXANDRIA B. ..... p 680 N95-17198
WIESEMAN, CAROL D. ..... p 846 N95-16453
WIGHTMAN, R. M. ..... p 818 N95-16112
WIKLIND, T. ..... p 916 N95-17332
WILCOX, J. Z. ..... p 756 N95-17281
WILGEN, J. B. ..... p 891 N95-16958
WILHELMSON, ROBERT B. ..... p 911 N95-17326
p 911 N95-17330
WILKE, M. ..... p 879 N95-16172
WILKERSON, FRANCES P. ..... p 797 N95-17740
WILKS, S. C. ..... p 777 N95-16929
WILLAND, JAMES H. ..... p 803 N95-17715
WILLIAMS, DAVID G. ..... p 871 N95-17177
WILLIAMS, J. M. ..... p 900 N95-16946
WILLIAMS, P. H. ..... p 762 N95-16130
WILLIAMS, ROGER G. ..... p 896 N95-16365
WILLIAMSON, STEVEN L. ..... p 885 N95-16620
WILLIS, MICHAEL J. ..... p 763 N95-16410
WILLKE, T. ..... p 761 N95-17926
WILLMS, R. S. ..... p 731 N95-17157
WILLSON, C. G. ..... p 741 N95-16354
WILMER, ELVIN M. ..... p 872 N95-16241
WILS, E. R. J. ..... p 722 N95-16734
WILSON, C. T. ..... p 751 N95-17909
WILSON, HOLLY J. ..... p 912 N95-17660
WILSON, I. H. ..... p 895 N95-16311
WILSON, J. R. ..... p 891 N95-16958
WILSON, JOHN W. ..... p 820 N95-16412
p 924 N95-16912
WILSON, R. GALE ..... p 886 N95-17271
WILSON, WILLIAM G. ..... p 717 N95-16333
WILTSE, JAMES C. ..... p 763 N95-16159
WIMMER, W. ..... p 690 N95-17252
WING, DAVID J. ..... p 663 N95-17880
WINOKUR, P. S. ..... p 895 N95-16311
WINSKE, D. ..... p 799 N95-16927
WINTER, KATHRYN P. ..... p 826 N95-16140
WIRKANDER, S. L. ..... p 671 N95-17454
WISEMAN, A. ..... p 673 N95-17212
WISEMAN, ANDY ..... p 707 N95-17609
WISNIEWSKI, D. ..... p 896 N95-16385
WITHROW, S. P. ..... p 733 N95-17911
WITSCHI, H. ..... p 818 N95-16801
WITTEN, MARK L. ..... p 821 N95-16515
WITTIG, CURT ..... p 726 N95-16042
p 730 N95-17140
WOBBE, HUBERTUS ..... p 688 N95-17240
WOJTOWICZ, A. J. ..... p 896 N95-16385
WOLFF, THILO ..... p 686 N95-17233
WOLINSKI, D. ..... p 878 N95-17899
WOLKEN, PAMELA R. ..... p 694 N95-17543
WONG, EDMOND ..... p 721 N95-17274
WONG, M. K. ..... p 717 N95-16334
WOOD, EDWIN H. ..... p 760 N95-17480
WOODS-VEDELER, JESSICA A. ..... p 669 N95-17397
WOODS, DAVID D. ..... p 857 N95-17383
WOODS, WANDA ..... p 821 N95-16619
WOODWARD, ROBERT H. ..... p 690 N95-17249
WOODY, C. ..... p 896 N95-16385
WOOLEY, BRUCE A. ..... p 763 N95-16136
WOOSTER, T. T. ..... p 742 N95-16434
WOVCHKO, E. A. ..... p 728 N95-16406
WRIGHT, A. D. ..... p 781 N95-17169
WRIGHT, ERNIE ..... p 842 N95-17746
WROBLESKI, D. A. ..... p 748 N95-17892
WU, C. T. ..... p 902 N95-17898
WU, D. T. ..... p 900 N95-17156
WU, DONGMEI ..... p 804 N95-16124
WU, K. CHAUNCEY ..... p 709 N95-16559
WU, MIN-KUANG ..... p 784 N95-16068
WU, O. K. ..... p 896 N95-16365
WU, RUILIAN ..... p 874 N95-16629
WU, SHIN-TSON ..... p 897 N95-16498

WU, XIAOQING ..... p 651 N95-16268
WU, XIPING ..... p 857 N95-16967
WUEST, C. R. ..... p 751 N95-17738
WUN-FOGLE, MARILYN ..... p 775 N95-17376
WUNDROW, DAVID W. ..... p 769 N95-15969
p 772 N95-17386
WYLIE, M. T. ..... p 901 N95-17667

X

XI, J. ..... p 764 N95-16425
XIA, XIN-FU ..... p 873 N95-16411
XU, J. B. ..... p 895 N95-16311
XU, JUN ..... p 876 N95-16959
XU, YANGSHENG ..... p 865 N95-17377
p 865 N95-17429

Y

YAGHJIAN, ARTHUR D. ..... p 754 N95-16624
YAMADA, TAKAHIRO ..... p 706 N95-17605
YAMAMOTO, K. ..... p 702 N95-17586
YAMAZAKI, T. ..... p 878 N95-17739
YAN, YANGGUANG ..... p 653 N95-16278
YANG, JIE ..... p 865 N95-17377
p 865 N95-17429
YANG, L. ..... p 794 N95-17521
YANG. SHUYAO ..... p 652 N95-16270
YANOVSKY, YURI G. ..... p 723 N95-16397
YAO, YI-SHENG ..... p 804 N95-16078
YASTROP, G. ..... p 665 N95-16375
YATES, G. J. ..... p 765 N95-16932
YATES, J. T., JR. ..... p 728 N95-16406
YATES, JOHN T., JR. ..... p 894 N95-16043
YAU, M. ..... p 675 N95-17493
YE, ZHENRU ..... p 651 N95-16268
YEH, H.-G. ..... p 757 N95-17287
YEH, PEN-SHU ..... p 677 N95-17186
YERGANIAN, S. S. ..... p 747 N95-17690
YETHIRAJ, M. ..... p 901 N95-17667
YIN, JUNFEI ..... p 649 N95-16253
YODER, MAX N. ..... p 900 N95-16928
p 767 N95-17463
YOKOKAWA, Y. ..... p 702 N95-17586
YORK, JAMES L. ..... p 717 N95-16333
YOST, DOUGLAS M. ..... p 780 N95-16636
YOU, Z. ..... p 783 N95-17928
YOUNG, B. K. F. ..... p 776 N95-17522
YOUNG, M. F. ..... p 713 N95-16314
YOUNG, STEVEN H. ..... p 802 N95-17686
YOUNG, SUSAN S. ..... p 858 N95-17459
YOUNGBLOOD, JIM ..... p 847 N95-16463
YOUNGER, HERBERT ..... p 680 N95-17199
YOUNIS, BASSAM A. ..... p 769 N95-16071
YU, SHAOZHI ..... p 649 N95-16253
YUAN, XIN ..... p 653 N95-16277
YUEN, JOSEPH H. ..... p 755 N95-17279
YUN, W. ..... p 882 N95-17901
YURA, H. T. ..... p 752 N95-16143
YVEN, CLET ..... p 686 N95-17232

Z

ZACHARIA, T. ..... p 789 N95-17675
ZACK, JOHN W. ..... p 802 N95-17686
ZADOKS, RICK I. ..... p 771 N95-16438
ZAITSEVA, N. ..... p 902 N95-17742
ZAKAJSEK, JAMES J. ..... p 781 N95-16907
ZAKIROV, I. M. ..... p 653 N95-16281
ZAOUCHE, GERARD ..... p 674 N95-17257
ZAWACKI, STEVEN J. ..... p 697 N95-17561
ZEIGENFUSS, LAWRENCE B. ..... p 706 N95-17604
ZENT, AARON P. ..... p 922 N95-16208
ZERKUS, MIKE ..... p 854 N95-15987
ZERVAKIS, VASSILIS ANDROKLIS
p 806 N95-17396
ZETTERVALL, BRENDA T. ..... p 843 N95-16455
ZHANG, CAIWEN ..... p 649 N95-16251
p 649 N95-16252
ZHANG, JIMIN ..... p 738 N95-17663
ZHANG, LINGMI ..... p 651 N95-16262
ZHANG, QIANG ..... p 864 N95-17713
ZHANG, QIWEI ..... p 650 N95-16257
ZHANG, SHIYING ..... p 649 N95-16254
ZHANG, XIAOGU ..... p 649 N95-16250
ZHANG, YOUZHEN ..... p 653 N95-16279
ZHAO, CHUNSHENG ..... p 651 N95-16267
ZHAO, J. ..... p 746 N95-17438
ZHENG, Q. ..... p 744 N95-16865
ZHONG, S. ..... p 791 N95-17903
ZHU, DEMAO ..... p 650 N95-16260
ZHU, JIANG ..... p 770 N95-16407
ZHU, JIANYING ..... p 649 N95-16249
p 653 N95-16280
ZHU, JINFU ..... p 650 N95-16259
ZHU, ZHAODA ..... p 651 N95-16268
p 652 N95-16269
ZHU, ZHIFAN ..... p 804 N95-16124
ZIJLSTRA, F. R. H. ..... p 831 N95-16953
ZILLIG, DAVID ..... p 677 N95-17187
p 674 N95-17556
ZILLIG, DAVID J. ..... p 678 N95-17188
ZIRATH, H. ..... p 775 N95-17170
p 759 N95-17453
ZOLPER, J. C. ..... p 778 N95-17498
ZUBROW, DAVID ..... p 836 N95-16490
ZUCCONI, L. ..... p 836 N95-16536
ZUHR, R. A. ..... p 736 N95-16807
ZUPKE, BRIAN S. ..... p 698 N95-17564

Typical Corporate Source Index Listing

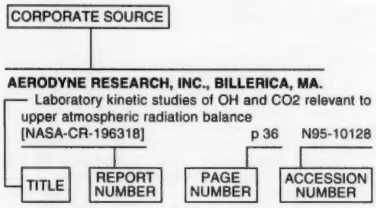

Listings in this index are arranged alphabetically by corporate source. The title of the document provides the user with a brief description of the subject matter. The report number helps to indicate the type of document cited (e.g., NASA report, translation, NASA contractor report). The accession number denotes the number by which the citation is identified. The page number helps you locate the citation in the abstract section. The titles are arranged under each corporate source in ascending accession number order.

A

ACADEMIA SINICA, BEIJING (CHINA).
Study of simulation in microgravity environment
[PB95-104261] p 750 N95-17730

ACADEMY OF SCIENCES OF THE UKRAINE, KHARKOV.
Relativistic effect of energy increase of a particle moving freely in vacuum from the quantum field theory point of view
[DE94-622757] p 903 N95-17473

ACADEMY OF SCIENCES OF THE UKRAINE, KIEV.
The quantum solitons of the nonlinear (sigma)-model with broken chiral symmetry
[DE94-622758] p 904 N95-17474
Possible superstructures of metallic ions in nonstoichiometric fullerites M(x) C(60)
[DE94-622052] p 901 N95-17518

ACADEMY OF SCIENCES (USSR), MOSCOW (USSR).
Potential landing sites for Mars Pathfinder
p 920 N95-16193
US-Russian Workshop on Computer Synthesis of Structure and Properties of Advanced Composites
[AD-A281647] p 723 N95-16397

ADAPTIVE SOLUTIONS, INC., BEAVERTON, OR.
High performance hardware and software for pattern recognition and image processing
[AD-A284264] p 839 N95-17172

ADVANCED TECHNOLOGY AND RESEARCH, INC., LAUREL, MD.
Signal wave generator signals recorded by the Federal Outdoor Impact Laboratory's on-board Data Acquisition System
[PB94-186525] p 752 N95-16094

ADVISORY GROUP FOR AEROSPACE RESEARCH AND DEVELOPMENT, NEUILLY-SUR-SEINE (FRANCE).
Optimum Design Methods for Aerodynamics
[AGARD-R-803] p 666 N95-16562
Experimental and analytical methods for the determination of connected-pipe ramjet and ducted rocket internal performance
[AGARD-AR-323] p 721 N95-17278
Aircraft and sub-system certification by piloted simulation
[AGARD-AR-278] p 671 N95-17388
A selection of experimental test cases for the validation of CFD codes, volume 2
[AGARD-AR-303-VOL-2] p 657 N95-17846

AEROJET-GENERAL CORP., SACRAMENTO, CA.
Hydromining a full-scale class 1.1 solid rocket motor
p 713 N95-16314
The use of designed experiments in the process development of continuous propellant mixing
p 717 N95-16334

AERONAUTICAL RESEARCH INST. OF SWEDEN, BROMMA.
Low speed propeller slipstream aerodynamic effects
p 663 N95-17882

AEROSPACE CORP., EL SEGUNDO, CA.
Optimum truncation of a Gaussian beam in the presence of random jitter
[AD-A284951] p 752 N95-16143
Electric probe measurements in the plume of the UK-10 ion thruster
[AD-A282460] p 713 N95-16302
A AgGaSe2 optical parametric oscillator pumped by a Raman-shifted YAG laser
[AD-A284743] p 777 N95-16548
Evaluation of the quality of sapphire using x-ray rocking curves and double-crystal x-ray topography
[AD-A282905] p 901 N95-17620

AEROSPACE MEDICAL ASSOCIATION, ALEXANDRIA, VA.
Aerospace Medical Association 63rd Annual Scienti fic Meeting Program p 807 N95-16737

AEROSPACE MEDICAL RESEARCH LABS., BROOKS AFB, TX.
Artificial gravity: How much, how often, how long?
p 816 N95-16778

AGENCY OF INDUSTRIAL SCIENCE AND TECHNOLOGY, OSAKA (JAPAN).
Studies on improvement of oxidation resistivity of carbon materials by glass impregnation and SiC formation
[DE94-796529] p 724 N95-16833

AIR FORCE CIVIL ENGINEERING CENTER, TYNDALL AFB, FL.
Fire protection engineering criteria: Electronic equipment installations
[AD-A285174] p 750 N95-16853

AIR FORCE INST. OF TECH., WRIGHT-PATTERSON AFB, OH.
Open Source Service Agent (OSSA) in the intelligence community's Open Source Architecture
p 907 N95-15934
An improved neutral wind model with predictive capabilities
[AD-A282283] p 800 N95-16235
Exploiting IB assignments for approximating marginal probabilities
[AD-A285419] p 855 N95-16246
A proposal to study gender differences in the rates of decompression sickness
[AD-A281854] p 819 N95-16297
The effects of target orientation on the dynamic contrast sensitivity function
[AD-A281855] p 826 N95-16298
Training visual pattern recognition: Using worked examples to aid schema acquisition
[AD-A281859] p 826 N95-16299
Detectability models and waveform design for multiple access Low-Probability-of-Intercept networks
[AD-A281864] p 753 N95-16300
Mental rotation with and without a concurrent task: Moderating effects of visuospatial ability
[AD-A281866] p 826 N95-16301
Characterization of the fast-phase component of the vestibulo-ocular response
[AD-A281830] p 820 N95-16360
A combined biased-robust estimator for dealing with influence and collinearity in regression
[AD-A281793] p 864 N95-16422
Aviation spatial orientation in relationship to head position, attitude interpretation, and control
[AD-A281869] p 827 N95-16433
Simulation of hydrologic influences on wetland ecosystem succession
[AD-A284737] p 795 N95-16545
Wavelets, signal processing and matrix computations
[AD-A283832] p 755 N95-16841
An air mass transformation model for coastal environments
[AD-A281790] p 801 N95-17164
Spatial information content analysis of Wiener spectra from polarized waterwave imagery
[AD-A283171] p 886 N95-17340
Bayesian nonparametric estimation via Gibbs sampling for coherent systems with redundancy
[AD-A283173] p 865 N95-17341
Thermal characteristics and heat transfer in an electrothermal light gas gun
[AD-A281980] p 892 N95-17442
Meteorological factors that affect the formation an prediction of aircraft icing
[AD-A281984] p 802 N95-17443
Development of an Automated Airfield Dynamic Cone Penetrometer (AADCP) prototype and the evaluation of unsurfaced airfield seismic surveying using Spectral Analysis of Surface Waves (SASW) technology
[AD-A281985] p 672 N95-17444
Multivariate sampling with explicit correlation induction for practical simulation and optimization studies
[AD-A281998] p 841 N95-17445
A latitudinal survey of middle atmospheric water vapor revealed by shipboard microwave spectroscopy
[AD-A282000] p 799 N95-17446
Caffeine's influence on critical frequency thresholds
[AD-A282005] p 828 N95-17447
The effects of the horizontal resolution of the boundary forcing sea surface temperature field on the FSU spectral model
[AD-A284273] p 802 N95-17488
Carbon monoxide does not modulate pulmonary vascular reactivity in isolated rat lungs
[AD-A283190] p 818 N95-17714

AIRCRAFT RESEARCH ASSOCIATION LTD., BEDFORD (ENGLAND).
Investigation of the flow development on a highly swept canard/wing research model with segmented leading- and trailing-edge flaps p 662 N95-17876
Investigation into the aerodynamic characteristics of a combat aircraft research model fitted with a forward swept wing p 664 N95-17884
Investigation of the influence of pylons and stores on the wing lower surface flow p 664 N95-17885

AKRON UNIV., AKRON, OH.
Smart materials based upon oligomeric molecules
[AD-A281374] p 872 N95-16155

ALABAMA UNIV., HUNTSVILLE, AL.
Characterization of surfaces
[NASA-CR-196995] p 750 N95-16065

ALASKA UNIV., FAIRBANKS, AK.
Simulation of arthroscopic surgery using MRI data
p 823 N95-15975

ALENIA SPAZIO S.P.A., TURIN (ITALY).
The SAX Italian scientific satellite. The on-board implemented automation as a support to the ground control capability p 695 N95-17551

ALLIED-SIGNAL AEROSPACE CO., KANSAS CITY, MO.
Antenna dielectric sealing process characterization
[DE94-015864] p 747 N95-17690
Electron beam weld development on a Filter Pack Assembly
[DE94-015867] p 782 N95-17716
Thin film superconductors
[DE94-018585] p 902 N95-17906

ALLIED-SIGNAL AEROSPACE CO., SEABROOK, MD.
Advanced technologies in the ASI MLRO towards a new generation laser ranging system p 687 N95-17239

ALLIED-SIGNAL AEROSPACE CO., TORRANCE, CA.
Cryogenic foil bearing turbopumps
p 716 N95-16331
ALLIED-SIGNAL TECHNICAL SERVICES CORP., COLUMBIA, MD.
GRTS operations monitor/control system
p 685 N95-17226
ALLIED-SIGNAL TECHNICAL SERVICES CORP., LANHAM, MD.
Proposal for implementation of CCSDS standards for use with spacecraft engineering/housekeeping data
p 705 N95-17600
AMERICAN ROCKET CO., VENTURA, CA.
Large-scale hybrid motor performance and designs for use in launch vehicle applications p 715 N95-16327
AMES LAB., IA.
The mechanism of the oligomerization of thiophene-based para-quinodimethanes
[DE94-014232] p 722 N95-16058
The relationship of structure to superconductivity in the Pr-Ba-Cu-O system
[DE94-014231] p 897 N95-16510
Support minimized inversion of acoustic and elastic wave scattering
[DE94-014233] p 783 N95-16538
The analysis and minimization of oxygen contamination in the powder processing of molybdenum disilicide
[DE94-014234] p 735 N95-16540
ANALATOM, INC., WESTLAKE, OH.
Theoretical study of cathode surfaces and high-temperature superconductors
[NASA-CR-195407] p 898 N95-16598
ANALEX CORP., BROOK PARK, OH.
Slow wave vane structure with elliptical cross-section slots, an analysis
[NASA-CR-195352] p 755 N95-16886
ANALYTICAL SERVICES AND MATERIALS, INC., HAMPTON, VA.
Composite chronicles: A study of the lessons learned in the development, production, and service of composite structures
[NASA-CR-4620] p 724 N95-16859
Multi-lab comparison on R-curve methodologies: Alloy 2024-T3
[NASA-CR-195004] p 736 N95-16860
APPLIED RESEARCH ASSOCIATES, INC., RALEIGH, NC.
Portable parallel stochastic optimization for the design of aeropropulsion components
[NASA-CR-195312] p 785 N95-16072
APPLIED RESEARCH CORP., COLLEGE STATION, TX.
Regional forecasting with global atmospheric models
[DE94-013863] p 801 N95-16961
APPLIED THERMAL SCIENCES, ORONO, ME.
Combustor kinetic energy efficiency analysis of the hypersonic research engine data p 714 N95-16321
ARGIALAS (DEMETRE P.), ATHENS (GREECE).
Steps toward terrain knowledge acquisition
[AD-A282667] p 790 N95-17375
ARGONNE NATIONAL LAB., IL.
Mechanisms of beam-halo formation in high-intensity linacs
[DE94-016316] p 879 N95-16030
Plasma disruption modeling and simulation
[DE94-015095] p 889 N95-16307
Field configuration of beam excited modes in the Advanced Photon Source (APS) storage ring waveguides
[DE94-015096] p 880 N95-16308
Reduction and aggregation of silver in aqueous gelatin and silica suspensions
[DE94-013998] p 727 N95-16363
The chemistry and physics of transition metal clusters
[DE94-014012] p 734 N95-16364
Sensitivity analysis of numerically-simulated convective storms using direct and adjoint methods
[DE94-013399] p 800 N95-16398
Flux imaging of high temperature superconductor single crystals and Ag sheathed wires
[DE94-013874] p 897 N95-16408
The stability of calibration standards for ICP/AES analysis: A two-year study
[DE94-013398] p 728 N95-16426
Atomic transport of oxygen
[DE94-013332] p 873 N95-16430
Radical cations of quadricyclane and norbornadiene in polar ZSM-5 matrices: Radical cation photochemical transformations without photons
[DE94-014007] p 728 N95-16485
Studies of D-Li neutron source: An overview
[DE94-014032] p 873 N95-16487
The PASS project
[DE94-016308] p 910 N95-16922
Trapezoidal rule quadrature algorithms for MIMD distributed memory computers
[DE94-016369] p 839 N95-16923
A-dependent effects in high P(sub T) reactions
[DE94-016385] p 875 N95-16924
Giant flux creep through the surface barriers and the irreversibility line in high T(sub c) superconductors
[DE94-013991] p 766 N95-16945
AC susceptibility and critical current in the organic superconductor (kappa)-(ET)2Cu(NCS)2
[DE94-013997] p 900 N95-16946
Small angle neutron scattering from nanocrystalline Pd and Cu compacted at elevated temperatures
[DE94-013865] p 876 N95-16962
Safety characteristics of lithium-alloy/metal sulfide batteries
[DE94-013867] p 766 N95-16963
Statistical properties of an algorithm used for illicit substance detection by fast-neutron transmission
[DE94-013868] p 665 N95-16964
Tribological properties of reactively sputtered nitrides and carbides of titanium, zirconium and hafnium
[DE94-014583] p 745 N95-17160
Computational differentiation and multidisciplinary design
[DE94-013393] p 863 N95-17306
Columnar defect pinning in untwinned single crystal YBa2Cu2O7
[DE94-013962] p 901 N95-17349
Suppression of superconductivity in orthorhombic La(2-x)M(x)CuO4 (M = Ca,Sr)
[DE94-013963] p 901 N95-17350
Transient flows and pressure waves in pipes
[DE94-012650] p 772 N95-17523
Texture analysis of critical current density in Bi2Sr2CaCu2O(x) tapes
[DE94-018375] p 902 N95-17898
New shower maximum trigger for electrons and photons at CDF
[DE94-018376] p 878 N95-17899
Production of high proton fractions from ECR sources by plasma modification
[DE94-018381] p 893 N95-17900
Measurements of x ray spectral flux and intensity distribution of APS/CHESS undulator radiation
[DE94-018384] p 882 N95-17901
Beam parameter measurements for the APS linac system
[DE94-018396] p 882 N95-17902
High Energy Physics Division research activities
[DE94-015024] p 882 N95-17924
The three loop equation of state of QED at high temperature
[DE94-015029] p 904 N95-17925
Electromagnetic field measurements on a mm-wave linear accelerator
[DE94-015092] p 761 N95-17926
ARIZONA STATE UNIV., TEMPE, AZ.
Quantum transport in semiconductor devices
[AD-A281383] p 895 N95-16158
Physical properties (particle size, rock abundance) from thermal infrared remote observations: Implications for Mars landing sites p 918 N95-16182
Opportunity to sample something different: The dark, unweathered, mafic sands of Cerberus and the Pathfinder 1997 Mars landing p 919 N95-16187
Strategy for selecting Mars Pathfinder landing sites
p 919 N95-16191
Maja Valley and the Chryse outflow complex sites
p 921 N95-16199
Marte Valles site p 921 N95-16200
Experimental and theoretical studies of wakes in stratified flows
[AD-A285305] p 771 N95-16616
ARIZONA UNIV., TUCSON, AZ.
Ultrashort pulse effects in semiconductor amplifiers and in dispersive media
[AD-A284925] p 763 N95-16137
Surface science capabilities from IMP spectral imaging
p 921 N95-16204
Imager for Mars Pathfinder (IMF) p 711 N95-16206
Theory of carrier heating through injection pumping and lasing in semiconductor microcavity lasers
[AD-A281795] p 776 N95-16353
Thermal control systems for low-temperature heat rejection on a lunar base
[NASA-CR-197486] p 830 N95-16418
The chronic effects on JP-8 jet fuel exposure on the lungs
[AD-A280982] p 821 N95-16515
New mechanisms and new materials for organic optical nonlinearity
[AD-A282781] p 886 N95-17143
Scanning tunneling microscopy of 3 to 5 semiconductors
[AD-A281722] p 902 N95-17705
ARMY AEROMEDICAL RESEARCH LAB., FORT RUCKER, AL.
Aviation epidemiology data register: Age-specific medical and nonmedical attrition rates among Fort Rucker civilian aviators
[AD-A284970] p 818 N95-16132
Whole-body vibration assessment of the palletized load system
[AD-A285181] p 829 N95-16145
Whole-body vibration assessment of the M1070 heavy equipment transporter, volume 1
[AD-A285199] p 829 N95-16147
The assessment of the AH-64D, longbow, mast-mounted assembly noise hazard for maintenance personnel
[AD-A284971] p 869 N95-16226
A correlative investigation of simulated occupant motion and accident report in a helicopter crash
[AD-A285190] p 664 N95-16404
Aviation epidemiology data register: Coronary angiography outcomes of civilian aviators flying US aircraft
[AD-A285191] p 820 N95-16405
Visual perception in the field-of-view of partial binocular overlap helmet-mounted displays
[AD-A285213] p 827 N95-16520
Direct comparison of two statistical methods for determination of evoked-potential thresholds
[AD-A285182] p 870 N95-16811
Factors affecting the visual fragmentation of the field-of-view in partial binocular overlap displays
[AD-A283081] p 886 N95-17334
Apache helicopter seat cushion evaluation
[AD-A284300] p 831 N95-17484
ARMY ARMAMENT RESEARCH, DEVELOPMENT AND ENGINEERING CENTER, WATERVLIET, NY.
Experimental heat treatment of beryllium copper alloy
[AD-A282714] p 734 N95-16380
Servo control using switches for discrete positional feedback
[AD-A284747] p 856 N95-16550
The effects of fatigue loading frequency on fatigue life of high-strength pressure vessel steels
[AD-A285301] p 786 N95-16601
ARMY COLD REGIONS RESEARCH AND ENGINEERING LAB., HANOVER, NH.
Experimental and numerical analysis of floating ice beam impact forces against a sloped structure
[AD-A280752] p 804 N95-16103
ARMY CONSTRUCTION ENGINEERING RESEARCH LAB., CHAMPAIGN, IL.
Performance of specular reflectors used for lighting enhancement
[AD-A281004] p 884 N95-15999
Using neural networks to correlate satellite imagery and ground-truth data
[AD-A285486] p 857 N95-16967
An assessment of simulation systems applicable to business process reengineering at Army Directorates of Public Works
[AD-A285696] p 839 N95-17176
ARMY ENGINEER WATERWAYS EXPERIMENT STATION, VICKSBURG, MS.
Three-dimensional eutrophication model of Chesapeake Bay. Volume 1: Main report
[AD-A280760] p 804 N95-16118
Normalization and prediction of geotechnical properties using the Cone Penetrometer Test (CPT)
[AD-A285193] p 799 N95-16872
A model for assessment of dynamic interaction between magnetically levitated vehicles and their supporting guideways
[AD-A283088] p 781 N95-17335
ARMY MEDICAL RESEARCH INST. OF CHEMICAL DEFENSE, ABERDEEN PROVING GROUND, MD.
Development of an in vitro model assay system for the evaluation of the effects of toxic chemicals on human airways
[AD-A285074] p 821 N95-16491
A study to determine the critical characteristics for mice in a newly designed whole body toxic gas exposure module
[AD-A285085] p 818 N95-17666
ARMY RESEARCH INST. OF ENVIRONMENTAL MEDICINE, NATICK, MA.
Evaluation of a newly-designed, dynamic knee extension device for the study of muscle fatigue in humans
[AD-A284974] p 819 N95-16228
Increased skin blood flow and enhanced heat loss in humans after niacin ingestion
[AD-A281124] p 821 N95-16809
ARMY RESEARCH LAB., ABERDEEN PROVING GROUND, MD.
Considerations in the experimental determination of constitutive parameters for finite strain plasticity
[AD-A285410] p 785 N95-16245

An economical system for measuring, monitoring, and controlling the rate of repetitive events
[AD-A285219] p 764 N95-16522

ARMY RESEARCH LAB., ADELPHI, MD.
Non-intrusive missile control surface monitor system
[AD-A285356] p 883 N95-15954

ARMY RESEARCH LAB., CLEVELAND, OH.
Sensor fault detection and diagnosis simulation of a helicopter engine in an intelligent control framework
[NASA-TM-106784] p 669 N95-15970

ARMY RESEARCH LAB., WATERTOWN, MA.
Special hybrid stress finite elements for the analysis of interface stress distribution in adhesive joints
[AD-A281612] p 785 N95-16102
Metallurgical examination of failed T-158 Cast Austempered Ductile Iron (CADI) track shoes
[AD-A282433] p 737 N95-17486
User-defined subroutine for implementation of special finite elements in ABAQUS for the analysis of adhesive joints
[AD-A282431] p 788 N95-17510

ARMY TEST AND EVALUATION COMMAND, ABERDEEN PROVING GROUND, MD.
Electromagnetic interference tests
[AD-A281396] p 755 N95-16800

ARMY TOPOGRAPHIC ENGINEERING CENTER, FORT BELVOIR, VA.
GPS tides and datums
[AD-A282422] p 666 N95-17508

ARNOLD ENGINEERING DEVELOPMENT CENTER, ARNOLD AFS, TN.
A model for preliminary facility design including simulation issues p 672 N95-16318
Hypersonic air-breathing aeropropulsion facility test support requirements p 672 N95-16319

ASSISTANT SECRETARY OF DEFENSE (COMMUNICATIONS COMMAND CONTROL AND INTELLIGENCE), WASHINGTON, DC.
Data administration procedures
[AD-A282718] p 909 N95-16382

ASTROTERRA CORP., SAN DIEGO, CA.
High current density sheet-like electron beam generator
[AD-A281975] p 880 N95-17499

ATLANTIC RESEARCH CORP., GAINESVILLE, VA.
Filament overwrapped motor case technology p 720 N95-16350

ATR COMMUNICATION SYSTEMS RESEARCH LABS., KYOTO (JAPAN).
Tele Hyper Virtuality p 853 N95-15982

AUBURN UNIV., AL.
A study of electric transmission lines for use on the lunar surface p 712 N95-16053
Single crystal films and waveguides of organic materials: Preparation and nonlinear optical properties
[AD-A284471] p 895 N95-16134
Analysis of space environment damage to solar cell assemblies from LDEF experiment A0171-GSFC test plate
[NASA-CR-196523] p 793 N95-16575

AUSTRALIAN INST. OF NUCLEAR SCIENCE AND ENGINEERING, LUCAS HEIGHTS (AUSTRALIA).
AINSE Plasma Science and Technology Conference and Elizabeth and Frederick White Workshop on Fundamental Problems in the Physics of Magnetically Confined Plasmas: Conference handbook
[DE94-622051] p 892 N95-17517

AVIAN GRAPHICS, LTD., LEAGUE CITY, TX.
Applying Virtual Reality to commercial Edutainment p 854 N95-15989

AVIONS MARCEL DASSAULT-BREGUET AVIATION, SAINT-CLOUD (FRANCE).
Review of the EUROPT Project AERO-0026 p 668 N95-16573

B

BATTELLE COLUMBUS LABS., OH.
Bicarbonate of soda blasting technology for aircraft wheel depainting
[PB94-193323] p 654 N95-17466

BERKELEY APPLIED SCIENCE AND ENGINEERING, INC., SAN FRANCISCO, CA.
Structural integrity of intelligent materials and structures. Constitutive modeling of shape memory alloys
[AD-A281301] p 735 N95-16786

BOEING AEROSPACE AND ELECTRONICS CO., HUNTSVILLE, AL.
Space Station Freedom secondary power wiring requirements p 712 N95-16052

BOEING CO., SEATTLE, WA.
STARS Conceptual Framework for Reuse Process (CFRP). Volume 1: Definition, version 3.0
[AD-A281506] p 834 N95-16167

BOEING COMMERCIAL AIRPLANE CO., SEATTLE, WA.
Two-dimensional high-lift airfoil data for CFD code validation p 659 N95-17859

BOEING DEFENSE AND SPACE GROUP, SEATTLE, WA.
Processing, fabrication, characterization and device demonstration of high temperature superconducting ceramics
[AD-A285145] p 744 N95-16844

BOLOGNA UNIV. (ITALY).
CPP-TRS(C): On using visual cognitive symbols to enhance communication effectiveness p 761 N95-15991

BOOZ-ALLEN AND HAMILTON, INC., HOUSTON, TX.
International Space Station Alpha (ISSA) Integrated Traffic Model
[NASA-CR-197566] p 710 N95-17331

BOSTON UNIV., MA.
Communication network software analysis
[AD-A281019] p 833 N95-16004

BOTSWANA UNIV., GABORONE.
Acquiring and disseminating unpublished economic and social development materials in Africa: The case of the National Institute of Development Research and Documentation University of Botswana p 906 N95-15924

BRANDEIS UNIV., WALTHAM, MA.
High performance compression of science data
[NASA-CR-189388] p 911 N95-17329
Kinetics and mechanism of chemical marker formation and water-activated heat generation
[AD-A281407] p 731 N95-17425

BRIMROSE CORP. OF AMERICA, BALTIMORE, MD.
A novel optic bistable device with very low threshold intensity using photorefractive films
[AD-A285310] p 885 N95-16733

BRISTOL UNIV. (ENGLAND).
Long term modelling of permafrost dynamics
[AD-A285315] p 799 N95-16735

BROOKHAVEN NATIONAL LAB., UPTON, NY.
RHIC spin: The first polarized proton collider
[DE94-013760] p 872 N95-16121
Study of the effect of the space charge using SYNCH
[DE94-014086] p 879 N95-16210
Scintillation mechanism and radiation damage in Ce(x)La(1-x)F3 crystals
[DE94-015848] p 896 N95-16385
Positron annihilation studies of defects in molecular beam epitaxy grown 3 to 5 layers
[DE94-015823] p 899 N95-16918
Crystalline beams: The vertical zigzag
[DE94-017986] p 901 N95-17673
Search for the presence of H particles in a neutral beam
[DE94-013526] p 877 N95-17683

BROWN UNIV., PROVIDENCE, RI.
Chryse Planitia as a Mars Pathfinder landing site: The imperative of building on previous ground truth p 918 N95-16185
The complexity of PDL with interleaving
[AD-A281044] p 836 N95-16452
Controlling memory access concurrency in efficient fault-tolerant parallel algorithms
[AD-A280909] p 851 N95-17741

BUREAU JUPITER, THE HAGUE, SOUTH HOLLAND (NETHERLANDS).
Document delivery by the Jupiter Library Consortium p 906 N95-15926

BUREAU OF THE CENSUS, SUITLAND, MD.
Bureau of the Census Center for International Research p 905 N95-15923

C

CALIFORNIA INST. OF TECH., PASADENA, CA.
Systematic optimization of second order nonlinear optical materials
[AD-A281350] p 884 N95-16015
Nonlinear problems and numerical method in differential equations and applied phenomena
[AD-A281531] p 859 N95-16108
Resonance enhanced multiphoton ionization of molecules and molecular fragments
[AD-A285076] p 873 N95-16493
Materials for second and third order nonlinear optical applications
[AD-A281304] p 885 N95-16787
On the application of under-decimated filter banks p 757 N95-17285
Multivariate statistical analysis software technologies for astrophysical research involving large data bases
[NASA-CR-189393] p 911 N95-17325
Multivariate statistical analysis software technologies for astrophysical research involving large data sets
[NASA-CR-197499] p 858 N95-17921

CALIFORNIA STATE UNIV., LOS ANGELES, CA.
Conceptual design study of a solar concentrator/support structure: A three dimensional finite element model p 718 N95-16342

CALIFORNIA UNIV., BERKELEY, CA.
Network interface specification for the T1 microprocessor
[AD-A283392] p 844 N95-15940
Anatomy of a silicon compiler
[AD-A285395] p 832 N95-16618
Spectroscopy of the transition state region in hydrogen transfer reactions
[AD-A285151] p 729 N95-16846
Designing an autonomous environment for mission critical operation of the EUVE satellite p 688 N95-17241
Advances in ultrafast scanning probe microscopy
[DE94-018180] p 779 N95-17729

CALIFORNIA UNIV., BERKELEY. LAWRENCE BERKELEY LAB, CA.
Laboratory Directed Research and Development Program
[DE94-011381] p 924 N95-16120
Accountability for network backup failures
[DE94-011365] p 846 N95-16222
Simulating the energy performance of holographic glazings
[DE94-013110] p 775 N95-17307
Experimental study of premixed flames in intense isotropic turbulence
[DE94-016868] p 732 N95-17437
Measurements of collective effects in the ALS
[DE94-017966] p 881 N95-17670
Experimental characterization of ALS undulator radiation
[DE94-017967] p 881 N95-17671
Transverse mode coupling instability with a double RF system
[DE94-017972] p 761 N95-17672
Strong WW scattering at photon linear colliders
[DE94-018183] p 878 N95-17720
Advances in ultrafast scanning probe microscopy
[DE94-018180] p 779 N95-17729
Z(prime) phenomenology: Constraints from low-energy measurements, and detailed study at TeV-scale lepton and hadron colliders
[DE94-018185] p 881 N95-17886
Ultrafast scanning probe microscopy
[DE94-018186] p 779 N95-17887
Physics at high energy photon photon colliders
[DE94-018191] p 881 N95-17888
Flavor symmetries and fermion masses
[DE94-018192] p 878 N95-17889
Closed orbit distortion from parasitic collisions in PEP-2
[DE94-018203] p 882 N95-17890
Beam-beam tune shift and dynamical beta function in PEP-2
[DE94-018207] p 882 N95-17891
Studies of transverse coherent bunch instabilities for the Advanced Light Source (ALS)
[DE94-018536] p 904 N95-17904

CALIFORNIA UNIV., DAVIS, CA.
Numerical simulation of helicopter engine plume in forward flight
[NASA-CR-197488] p 655 N95-16589
Failure of ozone and nitrogen dioxide to enhance lung tumor development in hamsters
[PB94-182854] p 818 N95-16801

CALIFORNIA UNIV., IRVINE, CA.
Synaptic plasticity and memory formation
[AD-A284926] p 825 N95-16138

CALIFORNIA UNIV., LOS ANGELES, CA.
Digital adaptive and optimal control of distributed systems
[AD-A285352] p 851 N95-15952
A rare gas optics-free absolute photon flux and energy analyzer to provide absolute photoionization rates of inflowing interstellar neutrals
[NASA-CR-197228] p 914 N95-15964
New methods for treatment of electron correlation and surface dynamics (FY91 AASERT)
[AD-A285177] p 727 N95-16144
Analysis of magnetic field data from Pioneer Venus orbiter
[NASA-CR-197492] p 923 N95-17403
In-flight imaging of transverse gas jets injected into transonic and supersonic crossflows: Design and development
[NASA-CR-186031] p 772 N95-17418
Demonstration of the Dynamic Flowgraph Methodology using the Titan 2 Space Launch Vehicle Digital Flight Control System
[NASA-CR-197517] p 675 N95-17493

Analysis of the through-thickness micropore and constituent particle population gradients in the 7050-T7451 plate aluminum alloys
[AD-A282970] p 738 N95-17663

CALIFORNIA UNIV., SAN DIEGO, LA JOLLA, CA.
Chemisorption energetics of superactive chlorine containing species on gallium arsenide surfaces
[AD-A281311] p 729 N95-16790

CALIFORNIA UNIV., SANTA BARBARA, CA.
BEEM 94. The Fifth Annual Workshop on Ballistic Electron Emission Microscopy
[AD-A281522] p 872 N95-16098
Experimental studies of stress measurement by optical fluorescence
[AD-A282337] p 723 N95-16415
The impact of low temperature materials on the breakdown and noise properties of GaAs and InP based HEMT's and FET's
[AD-A285176] p 765 N95-16834

CAMBRIDGE UNIV., CAMBRIDGE (ENGLAND).
Investigations on the sensitivity of the computer code TURBO-2D
[CUED/A-THERMO/TR-61] p 771 N95-16595
Study of the folding and deployment aspects of a Collapsible Rib Tensioned Surface (CRTS) antenna reflector
[CUED/D-STRUCT/TR-144] p 783 N95-17928

CARNEGIE-MELLON UNIV., PITTSBURGH, PA.
Sonochemical synthesis of polysilylenes by reductive coupling of disubstituted dichlorosilanes with alkali metals
[AD-A280994] p 739 N95-15996
Workshop on Epitaxy, Interfaces, Defects and Processing of Electronic and Photonic Materials
[AD-A281595] p 894 N95-16111
Well-defined polyphosphazenes by anionic polymerization of phosphoranimines
[AD-A281414] p 740 N95-16165
A structured TCP in standard ML
[AD-A282711] p 835 N95-16306
Computational methods for microstructure covolume techniques of discretization
[AD-A282449] p 861 N95-16376
Procedure calls are the assembly language of software interconnection: Connectors deserve first-class status
[AD-A281026] p 835 N95-16446
Verification of arithmetic functions with binary moment diagrams
[AD-A281028] p 835 N95-16447
Control of molecular weights and polydispersities in radical polymerization of styrene in the presence of stable radicals
[AD-A281040] p 742 N95-16449
Regiochemistry of polysilanes prepared by ring opening polymerization
[AD-A281041] p 742 N95-16450
Living radical polymerization. 1: Possibilities and limitations
[AD-A281042] p 742 N95-16451
Maturity questionnaire
[AD-A285073] p 836 N95-16490
Living radical polymerization of vinyl acetate
[AD-A280901] p 743 N95-16500
From living carbocationic to living radical polymerization
[AD-A280902] p 743 N95-16501
Software cost and schedule estimating: A process improvement initiative
[AD-A280915] p 836 N95-16503
The SEI and NAWC: Working together to establish a software measurement program
[AD-A280916] p 836 N95-16504
The GOMS family of analysis techniques: Tools for design and evaluation
[AD-A285211] p 827 N95-16518
Control transfer in operating system kernels
[AD-A281135] p 837 N95-16602
On-line scheduling on parallel machines
[AD-A281136] p 849 N95-16603
Extending programming by demonstration with hierarchical event histories
[AD-A281186] p 838 N95-16632
Sensor placement design for object pose determination with three light-stripe range finders
[AD-A281199] p 886 N95-16795
Integrating human factors with software engineering practices
[AD-A285210] p 830 N95-16813
Interactive sketching for the early stages of user interface design
[AD-A285339] p 838 N95-16818
Compiling polymorphism using intensional type analysis
[AD-A285340] p 838 N95-16819
Learning one more thing
[AD-A285342] p 857 N95-16820
DOME: Distributed Object Migration Environment
[AD-A281134] p 850 N95-16826
Online performance-improvement algorithms
[AD-A285162] p 838 N95-16850
Hidden Markov model for gesture recognition
[AD-A282845] p 865 N95-17377
Hidden Markov model for control strategy learning
[AD-A282846] p 865 N95-17429
On performability theory and the inverse sliding problem
[AD-A282847] p 782 N95-17430
Geometric sensing of known planar shapes
[AD-A282854] p 840 N95-17432
Real-time symbolic model checking for discrete time models
[AD-A282878] p 864 N95-17618
A feedforward control approach to the local navigation problem for autonomous vehicles
[AD-A282787] p 666 N95-17706

CASE WESTERN RESERVE UNIV., CLEVELAND, OH.
Pseudomorphic stabilization of diamond on non-diamond substrates
[AD-A285231] p 898 N95-16527
Isomorphism within the hexagonal columnar mesophase of molecular and macromolecular self- and co-assembled columns containing tapered groups
[AD-A281205] p 874 N95-16797
Synthesis and mesomorphic behavior of poly((2S, 3S)-(+)-2-chloro-3-methylpentyl
xy)biphenyl-4-carboxylate s with ethyl and propyl alkyl groups
[AD-A281402] p 744 N95-16865
The influence of the complexation of sodium and lithium triflate on the self-assembly of tubular-supramolecular architectures displaying a columnar mesophase based on taper-shaped monoesters of oligoethyleneoxide with 3,4,5-tris(p-(n-dodecan-l-yloxy)benzyloxy)benzoic acid and of their polymethacrylates
[AD-A281403] p 730 N95-16866
Three dimensional compressible turbulent flow computations for a diffusing S-duct with/without vortex generators
[NASA-CR-195390] p 670 N95-17402
Chiral recognition in molecular and macromolecular pairs of liquid crystals of (2R, 3S)- and (2S, 3S)-2-fluoro-3-methylpentyl-4'-(11-vinyloxyundeca iphenyl-4-carboxylate diastereomers
[AD-A281770] p 878 N95-17692
The development of a solid-state hydrogen sensor for rocket engine leakage detection
[NASA-CR-197567] p 776 N95-17895

CCG ASSOCIATES, INC., SILVER SPRING, MD.
Identification of Artificial Intelligence (AI) applications for maintenance, monitoring, and control of airway facilities
[AD-A282479] p 665 N95-17373

CENTER FOR SCIENTIFIC INFORMATION AND DOCUMENTATION, MADRID, MADRID (SPAIN).
CINDOC, CSIC, and Spanish R and D
p 906 N95-15927

CENTRE NATIONAL D'ETUDES SPATIALES, TOULOUSE (FRANCE).
A processing centre for the CNES CE-GPS experimentation p 666 N95-17196
SPOT4 Management Centre p 673 N95-17223
A PC based tool for mission plan production
p 686 N95-17232
Graphic Server: A real time system for displaying and monitoring telemetry data of several satellites
p 687 N95-17238
A graphic system for telemetry monitoring and procedure performing at the Telecom SCC p 689 N95-17246
Towards cheaper control centers p 674 N95-17250
Mini All-purpose Satellite Control Center (MASCC)
p 674 N95-17257
ELISA, a demonstrator environment for information systems architecture design p 698 N95-17563

CENTRE NATIONAL DE LA RECHERCHE SCIENTIFIQUE, PARIS (FRANCE).
Morphology and dynamics of membrane systems
[PB94-184660] p 745 N95-17299

CHALMERS UNIV. OF TECHNOLOGY, GOETEBORG (SWEDEN).
Feasibility study concerning an active millimeterwave sensor
[PB94-190691] p 775 N95-17170
Preliminary study of an active millimeter wave sensor
[PB94-189206] p 759 N95-17453

CM RESEARCH, HOUSTON, TX.
Thermal feedback in virtual reality and telerobotic systems p 854 N95-15987

CHICAGO UNIV., CHICAGO, IL.
Na-22 decay gamma rays from classical novae
[NASA-CR-197454] p 924 N95-16383
Phase-shifting effects of light and activity on the human circadian clock
[AD-A281204] p 821 N95-16796
Qualitative vision and action
[AD-A282697] p 831 N95-16966
Basic mechanisms and implications of non-photic entrainment of circadian rhythmicity
[AD-A283180] p 822 N95-17342

CH2M/HILL, INC., RESTON, VA.
Risk-Based Data Management System design specifications and implementation plan for the Alaska Oil and Gas Conservation Commission; the Mississippi State Oil and Gas Board; the Montana Board of Oil and Gas Conservation; and the Nebraska Oil and Gas Conservation Commission, attachment B
[DE94-013189] p 908 N95-16282

CLARKSON UNIV., POTSDAM, NY.
Communication network software analysis
[AD-A281019] p 833 N95-16004

CLEMSON UNIV., SC.
Supercritical fluid extraction: Preparing a superior mesophase precursor for carbon fibers
[AD-A284933] p 726 N95-16142

CLEVELAND STATE UNIV., OH.
Characterization on defect solids
[NASA-CR-197540] p 746 N95-17654

COAST GUARD RESEARCH AND DEVELOPMENT CENTER, GROTON, CT.
Florida Gulf Stream Data (FLDA) current study
[AD-A281965] p 805 N95-16414

COLORADO STATE UNIV., FORT COLLINS, CO.
Anionically-conductive ultrathin film composite membranes
[AD-A284944] p 723 N95-16041
Electrochemical synthesis of ultrathin film composite membranes
[AD-A285075] p 724 N95-16492
Proceedings of the International Conference on Parallel Architectures and Compilation Techniques
[AD-A285258] p 849 N95-16529
Summary of 1994 Atlantic tropical cyclone activity and verification of author's seasonal prediction, 1
p 801 N95-17259
Extended range forecast of Atlantic seasonal hurricane activity for 1995, 2 p 801 N95-17260

COLORADO UNIV., BOULDER, CO.
BioServe space technologies: A NASA Center for the Commercial Development of Space
[NASA-CR-196983] p 807 N95-16034
Phase segregation due to simultaneous migration and coalescence
[NASA-CR-196819] p 721 N95-16035
Structural effects of unsteady aerodynamic forces on horizontal-axis wind turbines
[DE94-011863] p 787 N95-16939
Experimenter's Laboratory for Visualized Interactive Science
[NASA-CR-189391] p 910 N95-17322
A land-surface Testbed for EOSDIS
[NASA-CR-189392] p 840 N95-17327
Error estimation and adaptive mesh refinement for parallel analysis of shell structures
[NASA-CR-197500] p 788 N95-17492
ROSAT detection of diffuse hot gas in the edge-on galaxy NGC 4631
[NASA-CR-197535] p 915 N95-17496
Nonlinear problems in fluid dynamics and inverse scattering. Propagation and capturing of singularities in problems of fluid dynamics and inverse scattering
[AD-A282873] p 773 N95-17617

COLUMBIA UNIV., NEW YORK, NY.
A high resolution liquid xenon imaging telescope for 0.3-10 MeV gamma-ray astrophysics: Construction and initial balloon flights
[NASA-CR-197556] p 916 N95-17528

COLUMBIA UNIV., PALISADES, NY.
Recent changes of weather patterns in North America
[DE94-016115] p 803 N95-17743

COMMISSION OF THE EUROPEAN COMMUNITIES, BRUSSELS (BELGIUM).
Engineering design tools for wind diesel systems. Volume 2: JODYMOD dynamic wind diesel simulation software package. Model verification
[PB95-104519] p 840 N95-17355
Engineering design tools for wind diesel systems. Volume 3: JODYMOD dynamic simulation software package. Model description
[PB95-104527] p 840 N95-17356
Engineering design tools for wind diesel systems. Volume 4: JODYMOD dynamic wind diesel simulation software package. Program documentation
[PB95-104535] p 841 N95-17628
Engineering design tools for wind diesel systems. Volume 5: JODYMOD dynamic wind diesel simulation software package. User's guide
[PB95-104543] p 841 N95-17629
Engineering design tools for wind diesel systems. Volume 6: Logistic package. User documentation
[PB95-104550] p 842 N95-17734

Engineering design tools for wind diesel systems. Volume 7: Logistic package. Validation report
[PB95-104568] p 842 N95-17735

COMPAGNIE INTERNATIONALE DE SERVICE EN INFORMATIQUE, TOULOUSE (FRANCE).
CCS-MIP: Low cost Customizable Control Centre p 674 N95-17254

COMPUTATIONAL LOGIC, INC., AUSTIN, TX.
A computational logic for applicative common Lisp
[AD-A283103] p 840 N95-17338

COMPUTER RESOURCES INTERNATIONAL A/S (DENMARK).
SCOS 2: An object oriented software development approach p 699 N95-17571

COMPUTER SCIENCES CORP., CALVERTON, MD.
The Mg 2 lines as diagnostic of PMS nature in Herbig Ae/Be stars
[NASA-CR-197518] p 915 N95-17494

COMPUTER SCIENCES CORP., LANHAM, MD.
The IUE Science Operations Ground System p 674 N95-17255
The Pacor 2 expert system: A case-based reasoning approach to troubleshooting p 693 N95-17541
Integration of a satellite ground support system based on analysis of the satellite ground support domain p 675 N95-17568

COMPUTER TECHNOLOGY ASSOCIATES, INC., MCKEE CITY, NJ.
Application of research techniques for documenting cognitive processes in air traffic control: Sector complexity and decision making
[AD-A282336] p 665 N95-16375

COMPUTER TECHNOLOGY ASSOCIATES, INC., MCLEAN, VA.
Small satellite space operations p 695 N95-17552

COMPUTER TECHNOLOGY ASSOCIATES, INC., ROCKVILLE, MD.
The Advanced Orbiting Systems Testbed Program: Results to date p 700 N95-17575

CONDUCTUS, INC., SUNNYVALE, CA.
HTS SNS devices on large-area substrates by single-source MOCVD
[AD-A285159] p 899 N95-16849

CONNECTICUT UNIV., STORRS, CT.
The effect of brush polydispersity on the interphase between end-grafted brushed and polymeric matrices
[AD-A280975] p 743 N95-16507
Mobility measurement and computer simulation at specific sites in polystyrene solutions and gels
[AD-A281214] p 747 N95-17685

CONSULTEC SCIENTIFIC, INC., KNOXVILLE, TN.
Assessment of research needs for advanced heterogeneous catalysts for energy applications, volume 1
[DE94-015889] p 795 N95-16386
Assessment of research needs for advanced heterogeneous catalysts for energy applications, volume 2
[DE94-015890] p 727 N95-16387

CORNELL UNIV., ITHACA, NY.
Networked information: Management issues for the acquisitions librarian p 906 N95-15932
Cornell program for the design and synthesis of advanced materials
[AD-A281352] p 723 N95-16016
Carbon clusters studied by neutralization-reionization mass spectrometry
[AD-A281367] p 726 N95-16017
Resonant charge transfer in hyperthermal atomic and molecular ion-surface collisions
[AD-A281369] p 871 N95-16018
Runaway electrons beams in ITER disruptions
[DE94-013788] p 888 N95-16122
Resist materials design: Base-catalyzed chemical amplification
[AD-A281805] p 741 N95-16354
Growth, characterization and applications of beta-barium borate and related crystals
[AD-A281047] p 898 N95-16623
Rheology and structure of planetary near-surface materials from landform topography p 922 N95-17392

CSA ENGINEERING, INC., PALO ALTO, CA.
Guide to ASIAC computer programs
[AD-A285354] p 784 N95-15953

D

DACCO SCI, INC., COLUMBIA, MD.
The use of electrochemistry and ellipsometry for identifying and evaluating corrosion on aircraft
[AD-A285276] p 734 N95-16370
The use of electrochemistry and ellipsometry for identifying and evaluating corrosion on aircraft
[AD-A285323] p 734 N95-16371

DALHOUSIE UNIV., HALIFAX (NOVA SCOTIA).
Neurophysiological analysis of circadian rhythm entrainment
[AD-A280981] p 821 N95-16484

DARTMOUTH COLL., HANOVER, NH.
A Mars Pathfinder landing on a recently drained ephemeral sea: Cerberus Plains, 6 deg N, 188 deg W p 918 N95-16181

DAVID SARNOFF RESEARCH CENTER, PRINCETON, NJ.
Ceramic/metal composite circuit-board-level technology for Application Specific Electronic Modules (ASEMs)
[AD-A285066] p 741 N95-16369

DAYTON UNIV. RESEARCH INST., OH.
An empirical approach to visual display preference based upon modulation transfer function and luminance
[AD-A285450] p 830 N95-16875

DEFENCE RESEARCH AGENCY, BEDFORD (ENGLAND).
Investigation of the flow over a series of 14 percent-thick supercritical aerofoils with significant rear camber p 657 N95-17849
Detailed study at supersonic speeds of the flow around delta wings p 660 N95-17861
Pressure distributions on research wing W4 mounted on an axisymmetric body p 660 N95-17862

DEFENCE RESEARCH AGENCY, FARNBOROUGH, HAMPSHIRE (ENGLAND).
Measurements on a two-dimensional aerofoil with high-lift devices p 657 N95-17848
Measurements of the flow over a low aspect-ratio wing in the Mach number range 0.6 to 0.87 for the purpose of validation of computational methods. Part 1: Wing design, model construction, surface flow. Part 2: Mean flow in the boundary layer and wake, 4 test cases p 660 N95-17860

DEFENCE RESEARCH ESTABLISHMENT OTTAWA, OTTAWA (ONTARIO).
An X-Ray Photoelectron Spectroscopy (XPS) study of activated carbons impregnated with some organocopper complexes
[AD-A282721] p 727 N95-16384

DEFENCE SCIENCE AND TECHNOLOGY ORGANIZATION, MELBOURNE (AUSTRALIA).
Design of thermocouple probes for measurement of rocket exhaust plume temperatures
[AD-A285423] p 774 N95-16247
Models to estimate high frequency acoustic scattering due to thermal fine- and micro-structure of the ocean
[AD-A285456] p 870 N95-16812
Data acquisition and processing software for the Low Speed Wind Tunnel tests of the Jindivik auxiliary air intake
[AD-A285455] p 656 N95-17178

DEFENSE TECHNICAL INFORMATION CENTER, ALEXANDRIA, VA.
Source hierarchy list. Volume 2: E through N
[AD-A281101] p 908 N95-15957
Source header list. Volume 2: L through Z
[AD-A281001] p 908 N95-15998
Directory of Organizational Technical Report Acronym Codes (DOTRAC)
[AD-A281500] p 908 N95-16086
Source hierarchy list. Volume 3: O through Z
[AD-A281102] p 908 N95-16090
DOD STINFO regulations and forms. Selected titles
[AD-A282332] p 909 N95-16374
Handbook for users
[AD-A285148] p 909 N95-16845
DROLS: An introduction to searching (videorecording)
[AD-M000338] p 912 N95-17660

DELAVAN, INC., WEST DES MOINES, IA.
Thermal chemical energy of ablating silica surfaces in air breathing solid rocket engines p 714 N95-16316

DEPARTMENT OF DEFENSE, WASHINGTON, DC.
Department of Defense dictionary of military and associated terms. Includes US acronyms and abbreviations and NATO terms (English only)
[AD-A283218] p 912 N95-17633

DEPARTMENT OF ENERGY, OAK RIDGE, TN.
Department of Energy: Office of Scientific and Technical Information p 907 N95-15936

DEPARTMENT OF ENERGY, WASHINGTON, DC.
High-level waste borosilicate glass: A compendium of corrosion characteristics
[DE94-016636] p 739 N95-15943
Global warming potentials, part 7
[DE94-014066] p 794 N95-16209
Fuel cell systems program plan, fiscal year 1994
[DE94-014301] p 793 N95-16541

DEPARTMENT OF THE NAVY, WASHINGTON, DC.
Method for intrinsically doped III-A and V-A compounds and products thereof
[AD-D016324] p 896 N95-16399
Process of making a bistable photoconductive component
[AD-D016449] p 764 N95-16539
Diffusion weld test fixture
[AD-D016450] p 780 N95-16543
An automatic repeater station for signal transmissions
[AD-D016454] p 754 N95-16549
Self-organizing neural network for classifying pattern signatures with a posteriori conditional class probability
[AD-D016455] p 857 N95-16823
Space-based asteroid detection and monitoring system
[AD-D016329] p 915 N95-16854
Aluminum permanganate battery
[AD-D016337] p 766 N95-16947
Aluminum-ferricyanide battery
[AD-D016338] p 766 N95-16948
Improved dual flow aluminum hydrogen peroxide battery
[AD-D016339] p 766 N95-16949
An elastomeric electrical connector
[AD-D016340] p 766 N95-16950
Wavelength dispersive gain element for a tunable laser
[AD-D016381] p 777 N95-17302
Magnetostrictive torque sensor
[AD-D016376] p 775 N95-17376
Magnetostrictive transducer system having a three dual-strip fiber optic magnetostrictive transducers bonded into a single fiber Mach-Zehnder interferometer
[AD-D016373] p 775 N95-17428
Method and apparatus for reducing axial thrust in centrifugal pumps
[AD-D016404] p 782 N95-17461
Fire protective coating and method for applying same to a structure
[AD-D016405] p 746 N95-17462
Trenched bipolar transistor structures
[AD-D016406] p 767 N95-17463
Method of rapid sample handling for laser processing
[AD-D016408] p 778 N95-17464
Feedback system for remotely operated vehicles
[AD-D016409] p 858 N95-17465
Multilayer microelectronic photomultiplier device with a stacked series of dynode and insulating layers
[AD-D016377] p 767 N95-17478
Volatile CVD precursors based on copper alkoxides and mixed group IIA-copper alkoxides
[AD-D016380] p 732 N95-17479
Center-fed multifilar helix antenna
[AD-D016390] p 760 N95-17480
BaF2/GaAs electronic components
[AD-D016391] p 767 N95-17481
Simultaneous determination of incoming microwave frequency and angle-of-arrival
[AD-D016392] p 760 N95-17482
Selective area platinum film deposition
[AD-D016355] p 747 N95-17693
Adhesion of silicon oxide to diamond
[AD-D016356] p 747 N95-17694
Ultra high bit rate all optical communication system
[AD-D016359] p 887 N95-17695
Self-initializing circuit link
[AD-D016363] p 761 N95-17696
High speed method for predicting radio-wave propagation
[AD-D016369] p 761 N95-17697
Rare earth ion doped CW cascade fiber laser
[AD-D016370] p 779 N95-17698
Corrosion inhibition in high temperature environment
[AD-D016372] p 738 N95-17699

DEUTSCHE AIRBUS G.M.B.H., BREMEN (GERMANY).
Tools for applied engineering optimization p 668 N95-16570
The global aircraft shape p 668 N95-16571
Aerodynamic shape optimization p 668 N95-16572

DEUTSCHE FORSCHUNGS- UND VERSUCHSANSTALT FUER LUFT- UND RAUMFAHRT, OBERPFAFFENHOFEN (GERMANY).
Geostationary satellite positioning by DLR/GSOC operations and management methods p 684 N95-17217

DEUTSCHE FORSCHUNGSANSTALT FUER LUFT- UND RAUMFAHRT, BRUNSWICK (GERMANY).
2-D airfoil tests including side wall boundary layer measurements p 657 N95-17847
DLR-F4 wing body configuration p 660 N95-17863
Subsonic flow around US-orbiter model FALKE in the DNW p 663 N95-17877
Pressure distribution measurements on an isolated TPS 441 nacelle p 663 N95-17878

DEUTSCHE FORSCHUNGSANSTALT FUER LUFT- UND RAUMFAHRT, COLOGNE (GERMANY).
Development of use of an Operational Procedure Information System (OPIS) for future space missions p 692 N95-17536

Wind tunnel investigations of the appearance of shocks in the windward region of bodies with circular cross section at angle of attack p 661 N95-17866

DEUTSCHE FORSCHUNGSANSTALT FUER LUFT- UND RAUMFAHRT, GOETTINGEN (GERMANY).

DLR-F5: Test wing for CFD and applied aerodynamics p 660 N95-17864

Three-dimensional boundary layer and flow field data of an inclined prolate spheroid p 661 N95-17867

Force and pressure data of an ogive-nosed slender body at high angles of attack and different Reynolds numbers p 661 N95-17868

Wind tunnel test on a 65 deg delta wing with rounded leading edges: The International Vortex Flow Experiment p 662 N95-17875

DEUTSCHE FORSCHUNGSANSTALT FUER LUFT- UND RAUMFAHRT, OBERPFAFFENHOFEN (GERMANY).

The Sequence of Events generator: A powerful tool for mission operations p 688 N95-17240

DEUTSCHE FORSCHUNGSANSTALT FUER LUFT- UND RAUMFAHRT, WESSLING (GERMANY).

A mission planning concept and mission planning system for future manned space missions p 687 N95-17235

DIGITAL DESIGN GROUP, INC., DENVER, CO.

Risk-Based Data Management System design specifications and implementation plan for the Alaska Oil and Gas Conservation Commission; the Mississippi State Oil and Gas Board; the Montana Board of Oil and Gas Conservation; and the Nebraska Oil and Gas Conservation Commission, attachment B
[DE94-013189] p 908 N95-16282

DIRECTION DES RECHERCHES, ETUDES ET TECHNIQUES, PARIS (FRANCE).

Study of the structuring of pure molecular liquids
[PB94-201316] p 903 N95-16839

Morphology and dynamics of membrane systems
[PB94-184660] p 745 N95-17299

DOW CORNING CORP., MIDLAND, MI.

Research and development of material/processing methods for the Continuous Fiber Ceramic Composites Program
[DE94-018569] p 725 N95-17905

DREXEL UNIV., PHILADELPHIA, PA.

Chemical properties of the fullerenes
[AD-A282730] p 730 N95-17141

DUKE UNIV., DURHAM, NC.

Synthesis and characterization of neopentyl indium compounds: X-ray crystal structures of ((Me3CCH2)2InAs(SiMe3)2)2 and ((Me3CCH2)2InAs(SiMe3)2In (CH2CMe3)2Cl)
[AD-A282766] p 900 N95-17137

X-ray crystal structure of a monomeric Tris(Arsino)Gallane, ((Me3Si)2As)3Ga)3Ga
[AD-A282343] p 900 N95-17171

DURHAM UNIV. (ENGLAND).

Parton distributions of the proton
[PB95-104337] p 877 N95-17354

E

ECOLE NATIONALE SUPERIEURE D'ARTS ET METIERS, BORDEAUX (FRANCE).

Impact vulnerability of thermoplastic-matrix composites
[PB94-201274] p 745 N95-17305

EDGEWOOD RESEARCH DEVELOPMENT AND ENGINEERING CENTER, ABERDEEN PROVING GROUND, MD.

Real-time data collection programs and source code for a commercial passive FTIR remote sensor
[AD-A284976] p 838 N95-16634

EG AND G ENERGY MEASUREMENTS, INC., GOLETA, CA.

Elemental impurity analysis of mercuric iodide by ICP/MS
[DE94-013553] p 896 N95-16359

EG AND G ENERGY MEASUREMENTS, INC., LAS VEGAS, NV.

Evaluation of a new miniature temperature data logger: Herpetological review
[DE94-013561] p 774 N95-16804

EG AND G ENERGY MEASUREMENTS, INC., SANTA BARBARA, CA.

Site characterization at the Rabbit Valley Geophysical Performance Evaluation Range
[DE94-013550] p 796 N95-16284

ELECTRONIC IMAGING CENTER, SAINT PAUL, MN.

Full color recorder
[AD-A282278] p 790 N95-17372

ELECTRONICS RESEARCH LAB., SALISBURY (AUSTRALIA).

An introduction to intelligent networks
[AD-A284284] p 752 N95-16123

Preliminary investigation of an integrated optic sampler for HF signals
[AD-A284285] p 884 N95-16133

In-fibre Bragg gratings for millimetre-wave EW systems
[AD-A284283] p 755 N95-16956

A PC-based interactive simulation of the F-111C Pave Tack system and related sensor, avionics and aircraft aspects
[AD-A285500] p 669 N95-16969

ELEKTRISITETSFORSYNINGENS FORSKNINGSINST., TRONDHEIM (NORWAY).

Engineering design tools for wind diesel systems. Volume 2: JODYMOD dynamic wind diesel simulation software package. Model verification
[PB95-104519] p 840 N95-17355

Engineering design tools for wind diesel systems. Volume 3: JODYMOD dynamic simulation software package. Model description
[PB95-104527] p 840 N95-17356

Engineering design tools for wind diesel systems. Volume 4: JODYMOD dynamic wind diesel simulation software package. Program documentation
[PB95-104535] p 841 N95-17628

Engineering design tools for wind diesel systems. Volume 5: JODYMOD dynamic wind diesel simulation software package. User's guide
[PB95-104543] p 841 N95-17629

Engineering design tools for wind diesel systems. Volume 6: Logistic package. User documentation
[PB95-104550] p 842 N95-17734

Engineering design tools for wind diesel systems. Volume 7: Logistic package. Validation report
[PB95-104568] p 842 N95-17735

ENERGY INFORMATION ADMINISTRATION, WASHINGTON, DC.

Alternatives to traditional transportation fuels: An overview
[DE94-014979] p 749 N95-17923

ENVIRONMENTAL PROTECTION AGENCY, CINCINNATI, OH.

Bicarbonate of soda blasting technology for aircraft wheel depainting
[PB94-193323] p 654 N95-17466

ENVIRONMENTAL PROTECTION AGENCY, RESEARCH TRIANGLE PARK, NC.

Alternatives for ozone-depleting refrigerants
[PB94-190857] p 795 N95-16881

ENVIRONMENTAL PROTECTION AGENCY, WASHINGTON, DC.

Proceedings of the First National Conference on Climate Change and Water Resources Management
[AD-A281172] p 796 N95-17684

EUROPEAN ORGANIZATION FOR NUCLEAR RESEARCH, GENEVA (SWITZERLAND).

Delayed annihilation of antiprotons in helium gas
[DE94-753405] p 878 N95-17739

EUROPEAN SPACE AGENCY, REDU (BELGIUM).

The SILEX experiment system operations p 674 N95-17251

EUROPEAN SPACE AGENCY. EUROPEAN SPACE OPERATIONS CENTER, DARMSTADT (GERMANY).

Communication network for decentralized remote tele-science during the Spacelab mission IML-2 p 676 N95-17181

Overview on METEOSAT geometrical image data processing p 678 N95-17189

Ground equipment for the support of packet telemetry and telecommand p 681 N95-17203

Experience with the EURECA Packet Telemetry and Packet Telecommand system p 682 N95-17209

Engineering Ulysses extended mission p 673 N95-17213

Towards a class library for mission planning p 686 N95-17233

Safety aspects of spacecraft commanding p 689 N95-17248

EURECA mission control experience and messages for the future p 690 N95-17252

SCOS 2: ESA's new generation of mission control system p 674 N95-17253

SCOSII OL: A dedicated language for mission operations p 692 N95-17533

SCOSII: ESA's new generation of mission control systems: The user's perspective p 674 N95-17537

XMM instrument on-board software maintenance concept p 699 N95-17567

Modeling ESA's TT/C systems p 701 N95-17579

A new communication protocol family for a distributed spacecraft control system p 703 N95-17590

The ESA standard for telemetry and telecommand packet utilisation: PUS p 704 N95-17595

Packet utilisation definitions for the ESA XMM mission p 704 N95-17596

Use of data description languages in the interchange of data p 704 N95-17597

The CCSDS return all frames Space Link Extension service p 705 N95-17599

ATOS: Integration of advanced technology software within distributed Spacecraft Mission Operations Systems p 705 N95-17602

EUROPEAN SPACE AGENCY. EUROPEAN SPACE RESEARCH AND TECHNOLOGY CENTER, ESTEC, NOORDWIJK (NETHERLANDS).

Payload operations management of a planned European SL-Mission employing establishments of ESA and national agencies p 684 N95-17221

EUROPEAN SPACE AGENCY. ULYSSES OFFICE, PASADENA, CA.

Grand mission versus small OPS team: Can we have both? p 684 N95-17219

F

FAIRFAX MATERIALS RESEARCH, INC., ALEXANDRIA, VA.

Computer modelling of cyclic deformation of high-temperature materials
[AD-A285212] p 735 N95-16519

FEDERAL AVIATION ADMINISTRATION, WASHINGTON, DC.

Federal aviation regulations, part 91. General operating and flight rules. Change 5
[PB94-194883] p 665 N95-17476

Federal Aviation Administration aviation system capital investment plan, 1993
[PB94-171956] p 654 N95-17512

FERMI NATIONAL ACCELERATOR LAB., BATAVIA, IL.

Experimental issues in high-sensitivity charm experiments
[DE94-015544] p 871 N95-15945

Measurement of the B meson differential cross-sections in p(-p) collisions at the square root of s = 1.8 TeV using the exclusive decays B(+-) yields J/(psi)K(+-) and B(exp 0) yields J/(psi)K(exp *0)
[DE94-015185] p 872 N95-16309

Production asymmetries in x(sub F) and P(sub t)(exp 2) for D(+-) mesons
[DE94-015546] p 872 N95-16310

CP violation measurements in neutral kaon system at Fermilab
[DE94-016526] p 873 N95-16402

Tests of structure functions using leptons at CDF: W asymmetry and Drell-Yan production
[DE94-015727] p 875 N95-16840

Measurement of the B(sub s) meson lifetime at CDF
[DE94-015381] p 875 N95-16868

Jet studies at CDF and DO collaborations
[DE94-015537] p 875 N95-16914

Limit on the rare decay B yields muon(+)muon(-) K(+-)
[DE94-013851] p 876 N95-16960

Beam position correction in the Fermilab Linac
[DE94-018984] p 882 N95-17931

Search for first and second generation leptoquarks at D(null)
[DE94-018992] p 879 N95-17932

FLORENCE UNIV. (ITALY).

Critical and paramagnetic spin dynamics in an antiferromagnetically coupled Heisenberg magnet: Results for RbMnF3
[PB95-104329] p 869 N95-17731

Time-dependent spin correlations in the heisenberg magnet at infinite temperature
[PB95-104303] p 869 N95-17750

FLORIDA STATE UNIV., TALLAHASSEE, FL.

Lunar surface operations. Volume 3: Robotic arm for lunar surface vehicle
[NASA-CR-195553-VOL-3] p 780 N95-16031

Spectral solution of the viscous blunt body problem. 2: Multidomain approximation
[NASA-CR-194971] p 863 N95-17267

FLORIDA UNIV., GAINESVILLE, FL.

Development of practical MO techniques for prediction of the properties and behavior of materials
[AD-A285079] p 874 N95-16496

Metastability in molecules
[AD-A285223] p 874 N95-16523

Investigation of a normal incidence high-performance p-type strained layer In(0.3)Ga(0.7)As/In(0.52)Al(0.48)As quantum well infrared photodetector
[AD-A282720] p 900 N95-16928

Synthetic aperture radar target detection, feature extraction, and image formation techniques
[NASA-CR-197485] p 760 N95-17651

FOSTER-MILLER ASSOCIATES, INC., WALTHAM, MA.

High performance dielectric materials development p 712 N95-16057

FRONT RANGE SCIENTIFIC COMPUTATION, INC., DENVER, CO.

Sixth Copper Mountain Conference on Multigrid Methods
[DE94-014595] p 862 N95-16611

G

GENERAL ACCOUNTING OFFICE, WASHINGTON, DC.
NASA contract mangagement: Improving the use of DCAA's auditing services. Report to the Chairman, Committee on Government Operations, House of Representatives
[GAO/NSIAD-94-229] p 914 N95-15962

GENERAL APPLIED SCIENCE LABS., INC., RONKONKOMA, NY.
Free-jet testing at Mach 3.44 in GASL's aero/thermo test facility p 672 N95-16320

GENERAL ATOMICS CO., SAN DIEGO, CA.
Active silicon x ray for measuring electron temperature
[DE94-017521] p 890 N95-16555
Poloidal rotation and the evolution of H-mode and VH-mode profiles
[DE94-015858] p 890 N95-16919
D3-D research operations
[DE94-014934] p 892 N95-17497
Effect of low density H-mode operation on edge and divertor plasma parameters
[DE94-016521] p 892 N95-17640
Two phase liquid helium flow testing to simulate the operation of a cryocondensation pump in the D3-D tokamak
[DE94-018345] p 893 N95-17896
Measurements of non-axisymmetric effects in the D3-D divertor
[DE94-018346] p 893 N95-17897

GENERAL ELECTRIC CO., CINCINNATI, OH.
Scramjet testing guidelines p 670 N95-16317

GENERAL ELECTRIC CO., SCHENECTADY, NY.
Colloidal particle deposition in turbulent flow
[DE94-013375] p 770 N95-16417
Properties of semiconducting Ru2Ge3
[DE94-015361] p 899 N95-16913

GENERAL ELECTRIC ENVIRONMENTAL SERVICES, INC., LEBANON, PA.
Coal-fueled diesel technology development emissions control
[DE94-004096] p 782 N95-17364

GEOLOGICAL SURVEY, MENLO PARK, CA.
A perspective of landing-site selection p 920 N95-16194

GEORGIA INST. OF TECH., ATLANTA, GA.
Deformation behavior of thin lubricant films at elevated pressure
[AD-A281848] p 741 N95-16355
Development of high-efficiency, thin-film CdTe solar cells
[DE94-011885] p 794 N95-16940
Guidance, navigation, and control digital emulation technology laboratory
[AD-A282722] p 766 N95-17139
A new approach to validate subgrid models in complex high Reynolds number flows
[AD-A282340] p 772 N95-17165

GEORGIA TECH RESEARCH INST., ATLANTA, GA.
Study of the compression behavior of high performance fibers
[AD-A284959] p 723 N95-16126
Characteristics of phase-correcting fresnel zone plates and elliptical waveguides
[AD-A281385] p 763 N95-16159
Analog microcircuit fault prediction
[AD-A281958] p 763 N95-16410
Design and technical support for development of a molded fabric space suit joint
[NASA-CR-197521] p 831 N95-16894

GEORGIA UNIV., ATHENS.
Preparation of Au single crystals for study of the ECALE deposition of CdTe
[AD-A282294] p 895 N95-16238
Electrochemical atomic layer processing
[AD-A282330] p 872 N95-16241

GREENWICH UNIV., LONDON (ENGLAND).
Preparation and investigation of improved low voltage electron excitable phosphors
[AD-A284265] p 767 N95-17487

GREYSTONE TECHNOLOGY, INC., SAN DIEGO, CA.
An applications-oriented approach to the development of virtual environments p 853 N95-15980

GULF WEATHER CORP., BAY SAINT LOUIS, MS.
Metadata database for automated oceanographic imagery
[AD-A284932] p 805 N95-16141

H

HAHNEMANN MEDICAL COLL. AND HOSPITAL, PHILADELPHIA, PA.
Locus coeruleus, vigilance and stress: Brain mechanisms of adaptive behavioral responsiveness
[AD-A282450] p 826 N95-16377

HAMPTON UNIV., VA.
From computer images to video presentation: Enhancing technology transfer p 848 N95-16467

HAWAII NATURAL ENERGY INST., HONOLULU, HI.
Molten salt techniques for excess heat production and the loading issue
[AD-A282462] p 792 N95-16303

HAWAII UNIV., HONOLULU, HI.
Variation of the thermohaline structure in the western equatorial Pacific upper ocean p 805 N95-17277
Investigations of asteroid family geology p 917 N95-17393

HAWAII UNIV., MANOA, HI.
Charging hydrogen into Ni in hydride-containing molten salts
[AD-A282335] p 730 N95-16973

HELSINKI UNIV. OF TECHNOLOGY, ESPOO (FINLAND).
ICONF: An incremental constraint facility in a feature modelling system
[PB94-197654] p 837 N95-16605
Duality transformations, green dyadics and plane-wave solutions for a class of bianisotropic media
[PB94-197670] p 754 N95-16612
Electromagnetostatics in uniaxial bianisotropic media
[PB94-197688] p 754 N95-16613
Combination of power electronic models with the two-dimensional finite element analysis of electrical machines
[PB94-197720] p 766 N95-16951
Nonstationary theory of mode competition in gyrotrons with allowance for inhomogeneity of the guiding magnetic field
[PB94-197621] p 869 N95-17467
Static image method for the interaction of two co-axial conducting prolate spheroids
[PB94-197696] p 760 N95-17502
Operational cloud classifier based on a self-organized feature map
[PB94-197852] p 802 N95-17504
Cellular automata for contour dynamics
[PB94-197613] p 865 N95-17526
Calorimetric methods for loss measurements of small cage induction motors
[PB94-184439] p 768 N95-17691
Investigation of the effect of Alfven resonance absorption on fast wave current drive in ITER
[PB95-104352] p 894 N95-17929
Thermal noise in biomagnetic measurements
[PB95-104360] p 869 N95-17930

HELSINKI UNIV. OF TECHNOLOGY, OTANIEMI (FINLAND).
Applying STEP principles to product models in high energy physics research
[PB94-197704] p 880 N95-17503

HERCULES AEROSPACE CO., MAGNA, UT.
Recent advances in graphite/epoxy motor cases p 717 N95-16333
Solar-powered rocket engine optimization for high specific impulse p 718 N95-16341

HIGH TECHNOLOGY CORP., HAMPTON, VA.
Stability of separating subsonic boundary layers
[NASA-CR-4638] p 772 N95-17268

HOUSTON UNIV., TX.
Investigation of novel electrical transport phenomena in semimetal-semiconductor heterostructures
[AD-A281406] p 901 N95-17424

HUGHES RESEARCH LABS., MALIBU, CA.
Modification of 2-6 and 3-5 materials using ion beams
[AD-A281839] p 896 N95-16365
Liquid crystal materials for laser beam steering
[AD-A285089] p 897 N95-16498

HUGHES STX, INC., GREENBELT, MD.
OOD/OOP experience in the Science Operations Center part of the ground system for X ray Timing Explorer mission p 675 N95-17565

HUGHES STX, INC., LEXINGTON, MA.
An investigation of small-scale variations in cloud climatology induced by topography and monthly mean winds
[AD-A283274] p 803 N95-17715

I

IBM FEDERAL SYSTEMS DIV., GAITHERSBURG, MD.
STARS Conceptual Framework for Reuse Process (CFRP). Volume 1: Definition, version 3.0
[AD-A281506] p 834 N95-16167

IDAHO UNIV., MOSCOW, ID.
Research on organofluorine chemistry for 700 F thermooxidative stability
[AD-A282767] p 731 N95-17142

ILLINOIS UNIV., CHAMPAIGN, IL.
Effects of prior ductile tearing on cleavage fracture toughness in the transition region
[AD-A281298] p 786 N95-16785

ILLINOIS UNIV., URBANA, IL.
A graphical environment for object-oriented simulation model environment
[NASA-CR-196887] p 833 N95-16088
Timing and area optimization for VLSI circuit and layout
[AD-A281081] p 762 N95-16089
ARCJET plasma modeling with experimental validation
[AD-A285234] p 889 N95-16243
Materials degradation and fatigue under extreme conditions
[AD-A282969] p 746 N95-17662

ILLINOIS UNIV., URBANA-CHAMPAIGN, IL.
Shock initiation of crystalline boron in oxygen and fluorine compounds
[AD-A284266] p 730 N95-16955

ILLINOIS UNIV. AT URBANA-CHAMPAIGN, SAVOY, IL.
A distributed analysis and visualization system for model and observational data
[NASA-CR-189386] p 911 N95-17326

INDIANA UNIV., BLOOMINGTON, IN.
Design and synthesis of organic superconductors (FY92 URI/RIP)
[AD-A281308] p 899 N95-16789

INDUSTRIAL MICROELECTRONICS CENTER, LINKOEPING, OESTERGOETLAND (SWEDEN).
Feasibility study concerning an active millimeterwave sensor
[PB94-190691] p 775 N95-17170

INNOVASIC, INC., ALBUQUERQUE, NM.
Support for development of a custom VLSI and FPGA logic chips based on a VHDL top-down design approach
[DE94-013608] p 763 N95-16283

INSTITUT DES HAUTES ETUDES SCIENTIFIQUES, BURES-SUR-YVETTE (FRANCE).
Coarse geometry of foliations
[PB94-192309] p 860 N95-16291
Classical solutions of the Prandtl-Reuss equations of perfect elasto-plasticity
[PB94-192333] p 860 N95-16292
Quasiconformal mappings, operators on Hilbert space, and local formulae for characteristic classes
[PB94-192366] p 860 N95-16293
Some fundamental techniques in the theory of integrable systems
[PB94-192390] p 860 N95-16294
Uniqueness and free interpolation for logarithmic potentials and the Cauchy problem for the Laplace equation in (R2)
[PB94-192408] p 861 N95-16295
Singularities of smooth maps in a space with a fixed cone
[PB94-192358] p 861 N95-16367

INSTITUTE FOR COMPUTER APPLICATIONS IN SCIENCE AND ENGINEERING, HAMPTON, VA.
A modified restricted Euler equation for turbulent flows with mean velocity gradients
[NASA-CR-194979] p 769 N95-16070
On the prediction of free turbulent jets with swirl using a quadratic pressure-strain model
[NASA-CR-194964] p 769 N95-16071
Image tools for UNIX p 847 N95-16466
Object-oriented numerical computing C++ p 849 N95-16476
High Performance FORTRAN p 843 N95-16478
An analysis of spectral envelope-reduction via quadratic assignment problems
[NASA-CR-194992] p 862 N95-16596
The algebraic multigrid projection for eigenvalue problems; backrotations and multigrid fixed points
[NASA-CR-194990] p 862 N95-16869
Multigrid techniques for nonlinear eigenvalue probems: Solutions of a nonlinear Schroedinger eigenvalue problem in 2D and 3D
[NASA-CR-194999] p 862 N95-16896
Algorithms for bilevel optimization
[NASA-CR-194980] p 863 N95-16897
ICASE
[NASA-CR-195001] p 832 N95-16898
On the removal of boundary errors caused by Runge-Kutta integration of non-linear partial differential equations
[NASA-CR-194989] p 863 N95-16904
Multiresolution representation and numerical algorithms: A brief review
[NASA-CR-194949] p 863 N95-17266

INSTITUTE FOR DEFENSE ANALYSES, ALEXANDRIA, VA.
Graphite-reinforced polycyanate composites for space and missile applications
[AD-A285509] p 725 N95-16970
INSTITUTE FOR HUMAN FACTORS TNO, SOESTERBERG (NETHERLANDS).
Subset-selectivity and distractor matching in visual conjunction search
[AD-A285137] p 827 N95-16615
INSTITUTE OF GLOBAL ENVIRONMENT AND SOCIETY, INC., CALVERTON, MD.
The Grid Analysis and Display System (GrADS)
[NASA-CR-189387] p 912 N95-17491
INSTITUTE OF SOUND AND VIBRATION RESEARCH, SOUTHAMPTON (ENGLAND).
Active and passive acoustic bubble sizing
[ISVR-TR-237] p 769 N95-16064
Evaluation of SEA loss factors using input power modulation
[ISVR-TR-240] p 868 N95-16856
INSTITUTE OF SPACE RESEARCH, MOSCOW (USSR).
Fast computational scheme of image compression for 32-bit microprocessors p 678 N95-17192
INSTITUTO DE PESQUISAS ESPACIAIS, SAO PAULO (BRAZIL).
Equatorial airglow studies via rocket experiment
[INPE-5589-TDI/551] p 799 N95-17647
Optimal transfer and swing-orbits in the two- and three-body problems
[INPE-5572-TAE/022] p 673 N95-17648
Phonologic-graphemic transcodifier for Portuguese Language spoken in Brazil (PLB)
[INPE-5575-PRE/1803] p 760 N95-17649
On the improvement of 1-look SAR image segmentations with mathematical morphology
[INPE-5577-PRE/1805] p 912 N95-17650
Detection of deforestation in the Amazon forest using NOAA/AVHRR images and the geographic information system SGI: Methodology and test of a potential alarm system
[INPE-5580-TDI/543] p 791 N95-17894
INTEGRATED SYSTEM ASSEMBLIES CORP., WOBURN, MA.
Liquid Cooled Heat Sink with Through Vias (LCHS)
[AD-A281450] p 902 N95-16075
INTEGRATED SYSTEMS, INC., SANTA CLARA, CA.
Adaptive control of nonlinear flexible systems
[AD-A281337] p 855 N95-16011
INTERFACE AND CONTROL SYSTEMS, WEST MELBOURNE, FL.
SCL: An off-the-shelf system for spacecraft control p 688 N95-17243
INTERNATIONAL ATOMIC ENERGY AGENCY, VIENNA (AUSTRIA).
Directory of IAEA databases
[DE94-622696] p 912 N95-17472
INTERNATIONAL BANK FOR RECONSTRUCTION AND DEVELOPMENT, WASHINGTON, DC.
Solar energy: Lessons from the Pacific island experience
[WORLD-BANK-TP-244] p 794 N95-17298
INTERNATIONAL NEURAL NETWORK SOCIETY, WASHINGTON, DC.
The 1994 International Neural Network Society Annual Meeting, volume 3
[AD-A281736] p 857 N95-17369
The 1994 International Neural Network Society Annual Meeting, volume 4
[AD-A281737] p 857 N95-17370
INTERNATIONAL SOCIETY FOR OPTICAL ENGINEERING, BELLINGHAM, WA.
Computational vision based on neurobiology
[AD-A284472] p 819 N95-16135
INTERNATIONAL TRADE COMMISSION LIBRARY, WASHINGTON, DC.
NAFTA literature at the International Trade Commission library p 905 N95-15922
IOWA UNIV., IOWA CITY, IA.
Analysis of plasma measurements for the Geotail mission
[NASA-CR-197020] p 888 N95-15941
Effective reflection coefficients for the mean acoustic field between two rough interfaces
[AD-A281962] p 870 N95-16413

J

JAPAN ATOMIC ENERGY RESEARCH INST., TOKYO (JAPAN).
Microchannel formation in polyimide by heavy ion irradiation
[DE94-753315] p 740 N95-16073
JET PROPULSION LAB., CALIFORNIA INST. OF TECH., PASADENA, CA.
Electric-optic resonant phase modulator
[NASA-CASE-NPO-18702-1-CU] p 883 N95-15960
Results of the 1994 NASA/JPL balloon flight solar cell calibration program
[NASA-CR-197248] p 792 N95-16067
Pathfinder landing sites at candidate SNC impact ejection sites p 919 N95-16190
Scientific rationale for selecting northern Eumenides Dorsum (9 deg - 11 deg N latitude, 159 deg - 162 deg longitude) as a potential Mars Pathfinder landing site p 920 N95-16196
Scientific rationale for selecting northwest Isidis Planitia (14 deg - 17 deg N latitude, 278 deg - 281 deg longitude) as a potential Mars Pathfinder landing site p 920 N95-16197
Cerberus Plains: A most excellent Pathfinder landing site p 921 N95-16198
Goldstone radar contributions to Mars Pathfinder landing safety p 921 N95-16205
Photovoltaic power conditioners: Development, evolution, and the next generation
[NASA-CR-197005] p 793 N95-16831
Telecommunications end-to-end systems monitoring on TOPEX/Poseidon: Tools and techniques p 676 N95-17180
Use of a multimission system for cost effective support of planetary science data processing p 678 N95-17190
Economical ground data delivery p 679 N95-17194
International data transfer for space very long baseline interferometry p 680 N95-17198
ARACHNID: A prototype object-oriented database tool for distributed systems p 680 N95-17199
Test Telemetry And Command System (TTACS) p 680 N95-17202
Process and methodology of developing Cassini G and C Telemetry Dictionary p 681 N95-17204
Multimission Telemetry Visualization (MTV) system: A mission applications project from JPL's Multimedia Communications Laboratory p 681 N95-17205
Galileo mission planning for Low Gain Antenna based operations p 682 N95-17210
International mission planning for space Very Long Baseline Interferometry p 673 N95-17216
Shared mission operations concept p 685 N95-17228
Mars Pathfinder mission operations concepts p 686 N95-17229
Increases in efficiency and enhancements to the Mars Observer non-stored commanding process p 688 N95-17242
Mission operations data analysis tools for Mars Observer guidance and control p 689 N95-17244
Small scale sequence automation pays big dividends p 689 N95-17247
The Telecommunications and Data Acquisition Report
[NASA-CR-197249] p 755 N95-17279
Evaluation of current tropospheric mapping functions by Deep Space Network very long baseline interferometry p 756 N95-17280
An algorithm for extraction of periodic signals from sparse, irregularly sampled data p 756 N95-17281
Space VLBI telecommunication characteristics, protection criteria, and frequency sharing p 756 N95-17282
Radio-planetary from tie from Phobos-2 VLBI data p 756 N95-17283
Closed-loop carrier phase synchronization techniques motivated by likelihood functions p 756 N95-17284
A simplified Integer Cosine Transform and its application in image compression p 757 N95-17286
Adaptive line enhancers for fast acquisition p 757 N95-17287
Antenna noise temperatures of the 34-meter beam-waveguide antenna with horns of different gains installed at F1 p 757 N95-17288
Low-complexity wavelet filter design for image compression p 757 N95-17289
A preliminary optical visibility model p 758 N95-17290
Field verification of the wind tunnel coefficients p 664 N95-17291
Tracking the Galileo spacecraft with the DSCC Galileo Telemetry prototype p 708 N95-17292
Computation of reflected and transmitted horn radiation patterns for a dichroic plate p 758 N95-17293
X-/Ka-band dichroic plate noise temperature reduction p 758 N95-17294
A model for analysis of TDA budget allocation p 758 N95-17295
RF optics study for DSS-43 ultracone implementation p 758 N95-17296
JPL-ANTOPT antenna structure optimization program p 759 N95-17297
Highly parallel reconfigurable computer architecture for robotic computation having plural processor cells each having right and left ensembles of plural processors
[NASA-CASE-NPO-17632-1-CU] p 832 N95-17400
A software architecture for automating operations processes p 692 N95-17538
SEQ-GEN: A comprehensive multimission sequencing system p 693 N95-17540
DSN co-observing operations to support space VLBI missions p 694 N95-17543
Development of a prototype real-time automated filter for operational deep space navigation p 694 N95-17545
Open solutions to distributed control in ground tracking stations p 674 N95-17554
Automating testbed documentation and database access using World Wide Web (WWW) tools p 696 N95-17557
SEQ-POINTER: Next generation, planetary spacecraft remote sensing science observation design tool p 697 N95-17559
SEQ-REVIEW: A tool for reviewing and checking spacecraft sequences p 697 N95-17561
Simplifying operations with an uplink/downlink integration toolkit p 697 N95-17562
Galileo spacecraft modeling for orbital operations p 700 N95-17574
Re-engineering the Multimission Command System at the Jet Propulsion Laboratory p 702 N95-17583
Customizing the JPL Multimission Ground Data System: Lessons learned p 703 N95-17588
Standard protocol stack for mission control p 704 N95-17593
Matrix evaluation of science objectives p 707 N95-17610
JET PROPULSION LAB., CALIFORNIA INST. OF TECH., WRIGHTWOOD, CA.
Using virtual reality for science mission planning: A Mars Pathfinder case p 673 N95-15978
JIAOTONG UNIV., SHANGHAI (CHINA).
Simulation investigation on system identification of gas turbine
[PB95-104238] p 670 N95-17749
JOHNS HOPKINS UNIV., BALTIMORE, MD.
Ligand field stabilization control of metal ion binding
[AD-A281011] p 726 N95-16001
Dust near luminous ultraviolet stars
[NASA-CR-197108] p 916 N95-16032
Thermo-fluid mechanic study of thermoacoustic devices
[AD-A281130] p 870 N95-16810
Voyager investigation of the cosmic diffuse background: Observations of rocket-studied locations with Voyager
[NASA-CR-197532] p 917 N95-17422
The mass and dynamics of cD clusters with cooling flows. 1: ROSAT observations of A 496
[NASA-CR-197534] p 915 N95-17495
JOHNS HOPKINS UNIV., COLUMBIA, MD.
The 1993 JANNAF Propulsion Meeting, volume 1
[CPIA-PUBL-602-VOL-1] p 713 N95-16312
The 1993 JANNAF Propulsion Meeting, volume 2
[CPIA-PUBL-602-VOL-2] p 715 N95-16324
JOHNS HOPKINS UNIV., LAUREL, MD.
The role of mission operations in spacecraft integration and test p 684 N95-17220
Cost efficient operations for Discovery class missions p 695 N95-17548
Concurrent engineering: Spacecraft and mission operations system design p 708 N95-17614
JOINT INST. FOR NUCLEAR RESEARCH, DUBNA (USSR).
Inelastic neutron scattering and antiferromagnetic fluctuations in high temperature superconductors
[DE94-623269] p 871 N95-16059
Heavy ion physics
[DE94-623321] p 880 N95-17519

K

KANSAS STATE UNIV., MANHATTAN, KS.
BioServe space technologies: A NASA Center for the Commercial Development of Space
[NASA-CR-196983] p 807 N95-16034
Nano-scale metal oxide particles as materials for air purification
[AD-A281394] p 729 N95-16791
KANSAS UNIV. CENTER FOR RESEARCH, INC., LAWRENCE, KS.
Analysis of a three-beam radar as an instrument for determining ocean wave heights and vector slopes
[AD-A282342] p 806 N95-17505
KAROLINSKA INST., STOCKHOLM (SWEDEN).
Skeletal muscle responses to unloading in humans p 809 N95-16743

KAZAN AVIATION INST. (USSR).
Joint Proceedings on Aeronautics and Astronautics (JPAA)
[ISBN-7-80-046602-7] p 649 N95-16249
Surface heat transfer in a channel with porous insert p 650 N95-16255
Service and physical properties of liquid-jet fuels p 650 N95-16256
Development of strength analysis methods and design model for aircraft constructions in Kazan Aviation Institute p 651 N95-16264
Theoretical fundamentals of the aircraft GTE tests p 651 N95-16265
Development of the vibration test equipment for testing the products of aircraft and space technology with simulation of operating conditions p 651 N95-16266
Method of calculating the optimal radioelectronic equipment design p 652 N95-16271
Generalized method of solving topological optimization problems for electrical airplane equipment systems in computer-aided design p 652 N95-16272
Theory of one-dimensional and two-dimensional distributed sensors for measuring the spatial characteristics of thermophysical and hydrodynamic fields p 652 N95-16273
Methods of wave-front identification by control images p 652 N95-16274
Problem of constructing the Lyapunov's functions in lumped parameter systems p 653 N95-16276
Development of processes, means, and theoretical principles of thin-walled detail plastic forming at Kazan Aviation Institute p 653 N95-16281

KEELE UNIV. (ENGLAND).
Second International Working Conference on Cooperating Knowledge Based Systems. Volume 1
[AD-A281347] p 908 N95-16014

KENTUCKY UNIV., LEXINGTON, KY.
Spectral components of human cardiovascular responses to step changes in Lower Body Negative Pressure (LBNP) before and after 22 hour of 6 deg head down bed rest p 810 N95-16748
Evaluation of a pneumatic Martian soil sampler concept
[NASA-CR-197539] p 923 N95-17653

KRUG LIFE SCIENCES, INC., HOUSTON, TX.
Blood volume and orthostatic responses of men and women to a 13-day bedrest p 811 N95-16752
A prototype Crew Medical Restraint System (CMRS) for Space Station Freedom p 815 N95-16773
Delivery of cardiopulmonary resuscitation in the microgravity environment p 816 N95-16774
Advanced Cardiac Life Support (ACLS) utilizing Man-Tended Capability (MTC) hardware onboard Space Station Freedom p 816 N95-16775
A surgical support system for Space Station Freedom p 710 N95-16776
Medicine on Mars: Remote medical care and the space exploration initiative p 816 N95-16777

L

L AND W RESEARCH, INC., WALLINGTON, CT.
High brightness cathodes for microfocus x-ray generators
[AD-A285256] p 764 N95-16814

LABORATOIRE DE METEOROLOGIE DYNAMIQUE, PARIS (FRANCE).
Mars Pathfinder meteorological observations on the basis of results of an atmospheric global circulation model p 919 N95-16189

LAMONT-DOHERTY GEOLOGICAL INST., PALISADES, NY.
Global climate change model natural climate variation: Paleoclimate data base, probabilities and astronomic predictors
[DE94-013956] p 796 N95-17348

LAWRENCE LIVERMORE NATIONAL LAB., LIVERMORE, CA.
Filter efficiency and pressure drop calculations through two and three dimensional fiber arrays
[DE94-014111] p 770 N95-16211
Sorting and hardware assisted rendering for volume visualization
[DE94-010204] p 834 N95-16220
Visualizing 3D velocity fields near contour surfaces
[DE94-010205] p 860 N95-16221
Overview of photonics research at Lawrence Livermore National Laboratory
[DE94-014055] p 884 N95-16366
Avoiding BDF stability barriers in the MOL solution of advection-dominated problems
[DE94-014793] p 861 N95-16535
The Software Technology Center at Lawrence Livermore National Laboratory: Software engineering technology transfer in a scientific R/D laboratory
[DE94-014794] p 836 N95-16536
Synthesis of pure RDX
[DE94-014356] p 749 N95-16542
Development of a radiative divertor for DIII-D
[DE94-016522] p 889 N95-16554
New ytterbium-doped apatite crystals for flexible laser design
[DE94-015138] p 899 N95-16867
Performance characterization of photonic links in cryogenic environments for advanced signal processing applications
[DE94-015561] p 765 N95-16915
A high average power electro-optic switch using KTP
[DE94-016416] p 765 N95-16925
Fast electrons, filamented laser light, and the fast ignitor
[DE94-015898] p 777 N95-16929
Superplasticity and superplastic forming of ceramics
[DE94-016172] p 745 N95-16935
Properties of Ce:LiSrAlF6 and Ce:LiCaAlF6 ultraviolet lasers
[DE94-013737] p 777 N95-17168
Energy and Technology Review
[DE95-000321] p 710 N95-17359
The influence of tungsten alloying on the mechanical properties of tantalum
[DE94-010071] p 736 N95-17378
Computer studies of the dynamic strength of ceramics
[DE94-010890] p 745 N95-17379
Physical and chemical sensor technologies developed at Lawrence Livermore National Laboratory
[DE94-012231] p 775 N95-17380
Miniature, vacuum compatible 1024 (times) 1024 CCD camera for x ray, ultraviolet, or optical imaging
[DE94-012235] p 776 N95-17522
Issues in the design and optimization of adaptive optics and laser guide stars for the Keck Telescopes
[DE94-012888] p 916 N95-17525
Development of x-ray laser architectural components
[DE94-016446] p 778 N95-17627
An x ray technique for precision laser beam synchronization
[DE94-016449] p 779 N95-17635
Abstracts and program Proceedings of the 1994 Meeting of the International Society for Ecological Modelling North American Chapter
[DE94-016456] p 796 N95-17636
Hydrogen production by gasification of municipal solid waste
[DE94-016483] p 732 N95-17639
Micro-UltraViolet Spectrograph (Micro-UVS)
[DE94-016704] p 732 N95-17642
Beam characteristics of a large-bore copper laser with a radiatively cooled plasma
[DE94-015139] p 779 N95-17688
High-average-power, diode-pumped solid state lasers for energy and industrial applications
[DE94-015142] p 779 N95-17689
WPH-6112A thermal expansion test of PRESS tubulation
[DE94-015946] p 782 N95-17717
Natural and artificial nobel gas hydrologic tracers
[DE94-016010] p 797 N95-17718
Precision machining and polishing of scintillating crystals for large calorimeters and hodoscopes
[DE94-012060] p 751 N95-17738
Thermal and laser conditioning of production and rapid-growth KDP and KD*P crystals
[DE94-013738] p 902 N95-17742
Computer modeling of organic aerogels, 93-SR-062
[DE94-016485] p 722 N95-17745
CHEETAH 1.0 user's manual
[DE94-014727] p 749 N95-17919
CERES, phases 1 and 2
[DE94-014730] p 797 N95-17920
FEM3C, an improved three-dimensional heavy-gas dispersion model: User's manual
[DE94-014731] p 797 N95-17922

LEHIGH UNIV., BETHLEHEM, PA.
Shock and thermal history of iron and chondritic meteorites
[NASA-CR-197125] p 916 N95-16020
Multiphase ceramics for mechanical and structural reliability at low and elevated temperatures
[AD-A285497] p 746 N95-17438

LITTLE (ARTHUR D.), INC., CAMBRIDGE, MA.
Vector magnetometry and lightwave defect imaging sensor technologies for internal pipe inspection systems: Phase 1 and 2 feasibility study, conceptual design, and prototype development
[PB94-194198] p 783 N95-16870

LOCKHEED ENGINEERING AND SCIENCES CO., HAMPTON, VA.
Solution of matrix equations using sparse techniques p 847 N95-16459
Introduction to the World Wide Web and Mosaic p 847 N95-16463

LOCKHEED ENGINEERING AND SCIENCES CO., HOUSTON, TX.
Sampling Elysium lavas (13 deg N, 203 deg W) p 917 N95-16177

LOCKHEED MISSILES AND SPACE CO., PALO ALTO, CA.
Radiation belt dynamic and quasi-static modeling based on CRRES data
[AD-A285282] p 916 N95-16600

LOGICON TECHNICAL SERVICES, INC., DAYTON, OH.
Visual acuity versus field-of-view and light level for Night Vision Goggles (NVG)
[AD-A284750] p 830 N95-16553

LOGISTICS MANAGEMENT INST., BETHESDA, MD.
Department of Defense Electronic Data Interchange project baseline report for FY 1994
[AD-A283015] p 912 N95-17710

LORAL AEROSYS, LANDOVER, MD.
Risk reduction methodologies and technologies for the Earth Observing System (EOS) Operations Center (EOC) p 707 N95-17612

LORAL AEROSYS, SEABROOK, MD.
Mission operations management p 685 N95-17225
Efficient mission control for the 48-satellite Globalstar Constellation p 674 N95-17256
MO/DSD online information server and global information repository access p 706 N95-17607

LORAL SPACE AND RANGE SYSTEMS, SUNNYVALE, CA.
A standard satellite control reference model p 704 N95-17592

LORAL SYSTEMS, INC., ORLANDO, FL.
ADST system test report for the rotary wing aircraft airnet aeromodel and weapon model merge with the ATAC 2 baseline
[AD-A281580] p 666 N95-16171

LOS ALAMOS NATIONAL LAB., NM.
The LANL-Boeing APLE/HPO flying-wire beam-profile monitor
[DE94-014255] p 879 N95-16172
Online diagnoses of high current-density beams
[DE94-014420] p 879 N95-16217
Initial design of a 1 megawatt average, 150 kilovolt pulse modulator for an industrial plasma source ion implantation processor
[DE94-014421] p 888 N95-16218
An investigation of genetic operators for continuous parameter space
[DE94-009364] p 834 N95-16219
Fast stereoscopic images with ray-traced volume rendering
[DE94-011703] p 835 N95-16223
Optical wheel-rotation sensor
[DE94-011719] p 780 N95-16224
Support for development of a custom VLSI and FPGA logic chips based on a VHDL top-down design approach
[DE94-013608] p 763 N95-16283
System design and operation of a 100 kilovolt, 2 kilohertz pulse modulator for plasma source ion implantation
[DE94-014424] p 889 N95-16285
Ion beam generation and propagation for plasma processing applications
[DE94-014428] p 889 N95-16286
Muon(+) SR studies of magnetic properties of boron carbide superconductors
[DE94-014440] p 868 N95-16288
Non-Fermi liquid scaling in UPd(x)Cu(5-x)(x = 1,1.5)
[DE94-016072] p 896 N95-16389
Exact, E = 0, classical and quantum solutions for general power-law oscillators
[DE94-014436] p 903 N95-16428
Geosynchronous orbit magnetopause crossings
[DE94-014817] p 798 N95-16537
Performance evaluation of polyaniline as an active material for electrochemical capacitors
[DE94-016283] p 765 N95-16920
Kinetic effects near the magnetopause
[DE94-009333] p 799 N95-16927
Modeling mesons with relativistic wave equations
[DE94-016057] p 875 N95-16931
Characterization of multiport solid state imagers at megahertz data rates
[DE94-016095] p 765 N95-16932
Centrifugal space-charge force for bunched beams
[DE94-016097] p 875 N95-16933
Intense ion beam optimization and characterization with thermal imaging
[DE94-016184] p 891 N95-16936
Progress at LAMPF
[DE94-016210] p 880 N95-16937

Intense ion beam characterization and thermal modeling for beam materials processing
[DE94-016281] p 745 N95-16938
A measurement of the Michel parameter (rho) in muon decay
[DE94-014423] p 876 N95-17153
First results from SAGE 2
[DE94-014431] p 876 N95-17154
A comparison of steady-state ARIES and pulsed PULSAR tokamak power plants
[DE94-014441] p 891 N95-17155
Asymptotic behavior in grain growth
[DE94-014452] p 900 N95-17156
Use of magnesium for recovering hydrogen isotopes from tritiated water
[DE94-014471] p 731 N95-17157
A search for muons yields e gamma at the level of 10(exp -13)
[DE94-014488] p 876 N95-17158
Determination of the nuclear-induced electrical conductivity in a nuclear-driven MHD device
[DE94-013137] p 891 N95-17365
Rietveld refinement of magnetic structures from pulsed-neutron-source powder-diffraction data
[DE94-016599] p 737 N95-17641
Tokamak Transmutation of (nuclear) Waste (TTW): Parametric studies
[DE94-012891] p 881 N95-17721
Neutrino oscillation studies at LAMPF
[DE94-018098] p 878 N95-17727
Conducting polymers as corrosion resistant coatings
[DE94-018265] p 748 N95-17892

LOUISIANA STATE UNIV., BATON ROUGE, LA.
Solar flares and magnetospheric particles: Investigations based upon the ONR-602 and ONR-604 experiments
[AD-A281463] p 923 N95-16080
Research in elementary particle physics
[DE94-019219] p 877 N95-17358
Solar flares and magnetospheric particles: Investigations based upon the ONR-602 and ONR-604 experiments
[AD-A283275] p 923 N95-17723

LUNAR AND PLANETARY INST., HOUSTON, TX.
Mars Pathfinder Landing Site Workshop
[NASA-CR-196745] p 917 N95-16176
Mars Pathfinder and the exploration of southern Amazonis Planitia p 917 N95-16178
Tartarus Colles: A sampling of the Martian highlands p 920 N95-16195
Melas Chasma: A Mars Pathfinder view of Valles Marineris p 922 N95-16207

M

MAROTTA SCIENTIFIC CONTROLS, INC., MONTVILLE, NJ.
A Lifting Ball Valve for cryogenic fluid applications p 720 N95-16349

MARTIN MARIETTA CORP., DENVER, CO.
Magellan Project: Evolving enhanced operations efficiency to maximize science value p 684 N95-17218

MARYLAND UNIV., COLLEGE PARK, MD.
Robust routing in dynamic networks, part 2
[AD-A282396] p 844 N95-16061
Estimation of vehicle dynamics from monocular noisy images
[AD-A281458] p 804 N95-16078
Validation of recipes for the recovery of stresses and derivatives by a computer-based approach
[AD-A282712] p 861 N95-16379
Cooperative control theory and integrated flight and propulsion control
[NASA-CR-197493] p 671 N95-17404
A model study of element residual estimators for linear elliptic problems: The quality of the estimators in the interior of meshes of triangles and quadrilaterals
[AD-A282849] p 863 N95-17431
Beams 92: Proceedings
[DE94-014784] p 880 N95-17475
An incremental database access method for autonomous interoperable databases
[NASA-CR-189384] p 912 N95-17652
Experimental data on the aerodynamic interactions between a helicopter rotor and an airframe p 664 N95-17883

MASSACHUSETTS INST. OF TECH., CAMBRIDGE.
Surface and defect excitations in covalently bonded solids
[AD-A281338] p 894 N95-16012
Sensitivity study of the SPEM model to the assimilation of synop datasets using two assimilation schemes. 1: Nudging. 2: The Kalman filter/smoother
[AD-A281459] p 804 N95-16079
Unsteady flow phenomena in discrete passage diffusers for centrifugal compressors
[AD-A281412] p 770 N95-16163
Example based image analysis and synthesis
[AD-A282285] p 835 N95-16236
Partial evaluation for scientific computing: The supercomputer toolkit experience
[AD-A282286] p 846 N95-16237
Shaped strain sensors for intelligent structures
[AD-A282333] p 774 N95-16242
Visualization of unsteady computational fluid dynamics
[NASA-CR-197461] p 770 N95-16388
Phase transformations, ultrastructure and properties of rigid-rod fibers
[AD-A285249] p 749 N95-16512
Proceedings of the 12th Annual Space Surveillance Workshop, volume 1
[AD-A285265] p 672 N95-16530
Workshop on Formal Models for Intelligent Control
[AD-A281399] p 857 N95-16864
Mission planning for space based satellite surveillance experiments with the MSX p 673 N95-17212
Joint operations planning for space surveillance missions on the MSX satellite p 673 N95-17215
Femtosecond studies of carrier dynamics in compound semiconductors
[AD-A282871] p 767 N95-17433
Theoretical studies of the strengths of matrix second phase particle interfaces
[AD-A280703] p 738 N95-17681

MASSACHUSETTS INST. OF TECH., LEXINGTON.
Solid state radar demonstration test results at the FAA Technical Center
[AD-A281520] p 752 N95-16097
A comparison of signal-processing front ends for automatic speech recognition
[AD-A284962] p 752 N95-16129
Frequency multiplier analysis and design using punch-through varactor diodes
[AD-A284963] p 762 N95-16130
Application of Fourier-space image-restoration techniques to turbulence compensation and sparse-aperture imaging
[AD-A285077] p 885 N95-16494
A simple EHF hemispheric coverage antenna
[AD-A285078] p 754 N95-16495
Proceedings of the 12th Space Surveillance Workshop, volume 2
[AD-A285115] p 672 N95-16842
Documentation of 9-PAC Beacon Target Detector processing function
[AD-A283090] p 759 N95-17336
An opportunity analysis system for space surveillance experiments with the MSX p 707 N95-17609

MASSACHUSETTS UNIV., LOWELL, MA.
Self assembled spin coated and bulk films of a novel polydiacetylene as second order NLO polymers
[AD-A282271] p 742 N95-16427

MATERIALS SYSTEMS, INC., CONCORD, MA.
Cost-effective method for synthesizing innovative transducer materials for sensors and actuators
[AD-A282339] p 725 N95-16974

MATRA MARCONI SPACE, TOULOUSE (FRANCE).
Towards a new generation of mission planning systems: Flexibility and performance p 686 N95-17230
Delivering spacecraft control centers with embedded knowledge-based systems: The methodology issue p 674 N95-17532
DIAMS revisited: Taming the variety of knowledge in fault diagnosis expert systems p 692 N95-17534
Design of ground segments for small satellites p 674 N95-17550

MAX-PLANCK-INST. FUER AERONOMIE, KATLENBURG-LINDAU (GERMANY).
Observations by the Mars 1994 orbiter and possible correlations with Mars Pathfinder p 920 N95-16192

MAX-PLANCK-INST. FUER CHEMIE, MAINZ (GERMANY).
Alpha proton x ray spectrometer p 710 N95-16201

MCDONNELL-DOUGLAS AEROSPACE, HUNTINGTON BEACH, CA.
Standardizing the information architecture for spacecraft operations p 703 N95-17591

MCDONNELL-DOUGLAS CORP., CAPE CANAVERAL, FL.
Configurable technology development for reusable control and monitor ground systems p 675 N95-17589

MCDONNELL-DOUGLAS CORP., LONG BEACH, CA.
2-D aileron effectiveness study p 658 N95-17851

MCDONNELL-DOUGLAS SPACE SYSTEMS CO., COCOA BEACH, FL.
Single Stage Rocket Technology's real time data system p 679 N95-17197

MECHANICAL TECHNOLOGY, INC., LATHAM, NY.
Twin disc gear tooth simulator
[AD-A284927] p 780 N95-16139

MESOSCALE ENVIRONMENTAL SIMULATIONS AND OPERATIONS, INC., TROY, NY.
A three dimensional mesoscale atmospheric simulation system for use in various mobile battlefield environments. Phase 2: Transition to an operational forecast system
[AD-A281223] p 802 N95-17686

MIAMI UNIV., FL.
Surfactant adsorption by sub-millimeter size bubbles: Quantification and modelling
[AD-A282405] p 772 N95-17506

MICHIGAN STATE UNIV., EAST LANSING, MI.
The role of chemical inhibition of gap junctional intercellular communication in toxicology
[AD-A282452] p 820 N95-16378
An investigation of fluid flow during induction stroke of a water analog model of an IC engine using an innovative optical velocimetry concept: LIPA
[NASA-CR-197451] p 780 N95-16900

MICHIGAN UNIV., ANN ARBOR, MI.
Development and applications of the positron microscope
[DE94-017918] p 883 N95-15947
SEPAC co-investigator support
[NASA-CR-196527] p 798 N95-15965
The EPIC architecture for modeling human information-processing and performance: A brief introduction
[AD-A280762] p 829 N95-16119
Estimating the benefits of personnel selection and classification: An extension of the Brogden table
[AD-A285674] p 828 N95-17175

MIDWEST RESEARCH INST., GOLDEN, CO.
PV CZ silicon manufacturing technology improvements
[DE94-011818] p 897 N95-16424
Research on stable, high-efficiency amorphous-silicon multijunction modules
[DE94-011839] p 764 N95-16425
Availability of direct normal radiation for solar furnace processing: A case study
[DE94-006907] p 792 N95-16435
Structural testing of the North Wind 250 composite rotor joint
[DE94-006923] p 792 N95-16437
Analysis of a two-bladed, teetering-hub turbine using the ADAMS (tm) software
[DE94-006922] p 781 N95-17169
Research on stable, high-efficiency, amorphous silicon multijunction modules
[DE94-011826] p 794 N95-17521

MINNESOTA UNIV., MINNEAPOLIS, MN.
Real-time simulation of large-scale multibody systems using automated equation decoupling techniques
[AD-A281544] p 856 N95-16390
Semiconductor heterojunction engineering
[AD-A281553] p 896 N95-16396
Hemoglobin-based blood substitutes and enhanced susceptibility to bacterial infections
[AD-A281023] p 820 N95-16444
Atomic force microscopy of the electrochemical nucleation and growth of molecular crystals
[AD-A281024] p 897 N95-16445
Nanoscale imaging of molecular adsorption
[AD-A280979] p 873 N95-16482
Self-assembly of low-dimensional conductors on Au(111) surfaces
[AD-A280936] p 734 N95-16505
Snapshots of crystal growth: Nanoclusters of organic conductors on Au(111) surfaces
[AD-A280976] p 897 N95-16508
Micromechanics of interfaces in metal matrix composites
[AD-A282404] p 725 N95-17457

MISSISSIPPI STATE UNIV., BAY SAINT LOUIS, MS.
Student research projects, 1993
[AD-A284954] p 804 N95-16124
Objective feature identification and tracking: A review
[AD-A284955] p 804 N95-16125

MISSOURI UNIV., ROLLA, MO.
Log-(Chi(exp 2)) distribution of correlation times revisited
[AD-A281123] p 740 N95-16092
Ducted fan acoustic radiation including the effects of nonuniform mean flow and acoustic treatment
[NASA-CR-197449] p 870 N95-16401

MITRE CORP., BEDFORD, MA.
The future of interaction on the Internet p 906 N95-15931
Mitre adaptive processing capability
[AD-A281078] p 755 N95-16825
TDRS orbit determination by radio interferometry p 673 N95-17547

Analysis of compression techniques for Common Mapping Standard (CMS) raster data
[AD-A283396] p 791 N95-17625

MITRE CORP., MCLEAN, VA.
Adding tools to the open source toolbox: The Internet
p 907 N95-15933

MONASH UNIV., CLAYTON (AUSTRALIA).
Virtual reality and telerobotics applications of an Address Recalculation Pipeline p 852 N95-15977

MONTANA UNIV., MISSOULA, MT.
FIFE data analysis: Testing BIOME-BGC predictions for grasslands
[NASA-CR-197522] p 790 N95-16895

MOSCOW STATE UNIV. (RUSSIA).
Characteristics of multiple auroral inverted-V structures and the problem of magnetospheric plasma stratification
[DE94-622233] p 799 N95-17471

N

NANJING UNIV. OF AERONAUTICS AND ASTRONAUTICS, NANJING, JIANGSU (CHINA).
Joint Proceedings on Aeronautics and Astronautics (JPAA)
[ISBN-7-80-046602-7] p 649 N95-16249
Investigation of dynamic inflow's influence on rotor control derivatives p 649 N95-16250
An approach to aerodynamic characteristics of low radar cross-section fuselages p 649 N95-16251
An improved method of airfoil design
p 649 N95-16252
Experimental investigation of turbulent separated-reattachment flow by using LDV
p 649 N95-16253
Improved method for estimation of the maximum instantaneous distortion values p 649 N95-16254
Wall-signature methods for high speed wind tunnel wall interference corrections p 650 N95-16257
An investigation of polynomial calibrations methods for wind tunnel balances p 650 N95-16258
A consistent large deflection theory of composite sandwich shells p 650 N95-16259
A super-element simplified analysis for vibration systems of complex structures p 650 N95-16260
Numerical analysis on periodic response of nonsmooth dynamic systems p 650 N95-16261
A new regularization approach in structural system identification p 651 N95-16262
Thermoelasticity analysis of laminated plates and shells using hybrid-stress elements p 651 N95-16263
Researches on gear fault diagnosis techniques
p 651 N95-16267
Linear prediction data extrapolation superresolution radar imaging p 651 N95-16268
Detecting the number of targets in spatially colored noise using sampled aperture radars p 652 N95-16269
Fast acquisition of burst direct sequence spread spectrum signals through satellite channels
p 652 N95-16270
The combination probe of optical fibers and its applications p 652 N95-16275
Application of GPS/SINS/RA integrated system to aircraft approach landing p 653 N95-16277
The computer analysis of the prediction of aircraft electrical power supply system reliability
p 653 N95-16278
Approach to in-process tool wear monitoring in drilling: Application of Kalman filter theory p 653 N95-16279
An improved position/force control of manipulators
p 653 N95-16280

NATIONAL ACADEMY OF SCIENCES - NATIONAL RESEARCH COUNCIL, HOUSTON, TX.
Catecholaminergic responses to stressful motion stimuli, scopolamine plus amphetamine, and dexamethasone
p 809 N95-16745

NATIONAL ACADEMY OF SCIENCES - NATIONAL RESEARCH COUNCIL, WASHINGTON, DC.
Activities of the Space Studies Board
[NASA-CR-197105] p 672 N95-16033
Assessment of the Space Station program
p 709 N95-16352

NATIONAL AERONAUTICAL LAB., BANGALORE (INDIA).
Evaluation of the dynamic stability characteristics of the NAL Light Transport Aircraft
[NAL-PD-CA-9217] p 671 N95-16392
Flosolver parallel computers: 1986-1994
[NAL-SP-9409] p 850 N95-16901

NATIONAL AERONAUTICS AND SPACE ADMINISTRATION, WASHINGTON, DC.
Fourth Annual International Acquisitions Workshop: Access to Multiple Media Worldwide
[NASA-TM-109896] p 905 N95-15919
Presidential leadership in the development of the US space program
[NASA-TM-110107] p 904 N95-16007
Continual improvement: A bibliography with indexes, 1992-1993
[NASA-SP-7097(02)] p 905 N95-16633
Review of performance, medical, and operational data on pilot aging issues p 812 N95-16759
SLS-1: The first dedicated life sciences shuttle flight
p 676 N95-16769
Forecasting earthquakes
[NASA-TM-110112] p 799 N95-16981
Revitalizing general aviation
[NASA-TM-110113] p 669 N95-16982
Accuracy analysis of TDRSS demand forecasts
p 683 N95-17214
Re-engineering NASA's space communications to remain viable in a constrained fiscal environment
p 702 N95-17585
Aeronautical enginnering: A cumulative index to a continuing bibliography (supplement 312)
[NASA-SP-7037(312)] p 654 N95-17702
Aerospace medicine and biology: A continuing bibliography with indexes (supplement 396)
[NASA-SP-7011(396)] p 823 N95-17703
Aeronautical engineering: A continuing bibliography with indexes (supplement 311)
[NASA-SP-7037(311)] p 654 N95-17704

NATIONAL AERONAUTICS AND SPACE ADMINISTRATION. AMES RESEARCH CENTER, MOFFETT FIELD, CA.
Exobiology site priorities for Mars Pathfinder
p 919 N95-16188
Atmosphere structure and meteorology instrument for Mars Pathfinder p 711 N95-16202
Landing site considerations for atmosphere structure and meteorology p 921 N95-16203
The psychophysical function for perceived gravitational-inertial force does not depend on the orientation of the otolith organs p 808 N95-16740
Comparison of saline and fludrocortisone as fluid-loading countermeasures following exposure to simulated microgravity p 808 N95-16742
Intramuscular pressure: A better tool than EMG to optimize exercise for long-duration space flight
p 809 N95-16744
Physiological constraints on deceleration during the aerocapture of manned vehicles p 810 N95-16751
Alertness management in two-person long-haul flight operations p 813 N95-16760
Human performance in the modern cockpit
p 813 N95-16764
Crew decision making under stress
p 814 N95-16765
Cognition and procedure representational requirements for predictive human performance models
p 814 N95-16766
Beyond the cockpit: The visual world as a flight instrument p 814 N95-16767
Artificial gravity: How much, how often, how long?
p 816 N95-16778
The effect of intermittent standing or walking during head down tilt bedrest on peak O2 consumption
p 817 N95-16779
Periodic upright posture negates the suppression of neuroendocrine response to head down bedrest
p 817 N95-16780
The efficacy of periodic +Gz exposure in the prevention of bedrest induced orthostatic intolerance
p 817 N95-16781
The value of the 4-day headdown bedrest model for screening countermeasures p 817 N95-16782
A supercritical airfoil experiment p 659 N95-17858
Low aspect ratio wing experiment
p 661 N95-17865
STOVL CFD model test case p 663 N95-17881

NATIONAL AERONAUTICS AND SPACE ADMINISTRATION. GODDARD SPACE FLIGHT CENTER, GREENBELT, MD.
SeaWiFS technical report series. Volume 21: The heritage of SeaWiFS. A retrospective on the CZCS NIMBUS Experiment Team (NET) program
[NASA-TM-104566-VOL-21] p 803 N95-16006
Nondestructive examination of the TRMM RCS propellant tanks p 718 N95-16338
NSSDC data listing
[NASA-TM-109986] p 909 N95-16441
Scientific and technical publishing at Goddard Space Flight Center in Fiscal Year 1994
[NASA-TM-104614] p 925 N95-16581
MODIS Technical Report Series. Volume 4: MODIS data access user's guide: Scan cube format
[NASA-TM-104594-VOL-4] p 837 N95-16587
Third International Symposium on Space Mission Operations and Ground Data Systems, part 1
[NASA-CP-3281-PT-1] p 676 N95-17179
Earth Observing System (EOS) Communication (Ecom) Modeling, Analysis, and Testbed (EMAT) activiy
p 677 N95-17182
End-to-end communication test on variable length packet structures utilizing AOS testbed
p 677 N95-17186
Demand access communications for TDRSS users
p 677 N95-17187
The GRO remote terminal system
p 678 N95-17188
A second generation 50 Mbps VLSI level zero processing system prototype p 678 N95-17191
The development and operation of the international solar-terrestrial physics central data handling facility
p 679 N95-17193
A low-cost transportable ground station for capture and processing of direct broadcast EOS satellite data
p 680 N95-17200
Applications of massively parallel computers in telemetry processing p 680 N95-17201
VLSI technology for smaller, cheaper, faster return link systems p 681 N95-17206
Lessons learned supporting onboard solid-state recorders p 681 N95-17208
Nickel cadmium battery operations and performance
p 685 N95-17224
Autonomous mission planning and scheduling: Innovative, integrated, responsive p 686 N95-17234
Production and quality assurance automation in the Goddard Space Flight Center Flight Dynamics Facility
p 687 N95-17237
Generic trending and analysis system
p 689 N95-17245
The development and validation of command schedules for SeaWiFS p 690 N95-17249
Third International Symposium on Space Mission Operations and Ground Data Systems, part 2
[NASA-CP-3281-PT-2] p 691 N95-17531
Using graphics and expert system technologies to support satellite monitoring at the NASA Goddard Space Flight Center p 674 N95-17535
An intelligent automated command and control system for spacecraft mission operations p 693 N95-17542
Magnetometer-only attitude and rate determination for a gyro-less spacecraft p 694 N95-17546
Embedded parallel processing based ground control systems for small satellite telemetry
p 674 N95-17553
An agent-oriented approach to automated mission operations p 696 N95-17555
Advanced ground station architecture
p 674 N95-17556
Knowledge-based critiquing of graphical user interfaces with CHIMES p 697 N95-17560
A proven approach for more effective software development and maintenance p 698 N95-17566
Software Process Assessment (SPA)
p 699 N95-17569
Taking advantage of ground data systems attributes to achieve quality results in testing software
p 699 N95-17570
Evaluating modeling tools for the EDOS
p 700 N95-17572
Solar and Heliospheric Observatory (SOHO) Experimenters' Operations Facility (EOF)
p 675 N95-17573
NCCDS performance model p 675 N95-17576
Evaluation of NASA's end-to-end data systems using DSDS+ p 700 N95-17577
Analysis of space network loading
p 701 N95-17578
A General Mission Independent Simulator (GMIS) and Simulator Control Program (SCP) p 701 N95-17580
Test/score/report: Simulation techniques for automating the test process p 675 N95-17581
Spacecraft Data Simulator for the test of level zero processing systems p 675 N95-17582
Re-engineering Nascom's network management architecture p 702 N95-17584
Transportable Payload Operations Control Center reusable software: Building blocks for quality ground data systems p 703 N95-17587
Cross support overview and operations concept for future space missions p 705 N95-17598
Mission Operations Centers (MOCs): Integrating key spacecraft ground data system components
p 675 N95-17601
The NASA Mission Operations and Control Architecture Program p 706 N95-17603
Renaissance architecture for Ground Data Systems
p 706 N95-17604
Re-engineering the mission life cycle with ABC and IDEF p 706 N95-17606
The Requirements Generation System: A tool for managing mission requirements p 707 N95-17608

A new systems engineering approach to streamlined science and mission operations for the Far Ultraviolet Spectroscopic Explorer (FUSE) p 707 N95-17611
EDOS operations concept and development approach p 708 N95-17613

NATIONAL AERONAUTICS AND SPACE ADMINISTRATION. HUGH L. DRYDEN FLIGHT RESEARCH CENTER, EDWARDS, CA.

Development of a low-aspect ratio fin for flight research experiments
[NASA-TM-4596] p 656 N95-16858
Thermocryogenic buckling and stress analyses of a partially filled cryogenic tank subjected to cylindrical strip heating
[NASA-TM-4579] p 788 N95-17417
Shear buckling analysis of a hat-stiffened panel
[NASA-TM-4644] p 788 N95-17490

NATIONAL AERONAUTICS AND SPACE ADMINISTRATION. JOHN F. KENNEDY SPACE CENTER, COCOA BEACH, FL.

Generic propellant transfer unit: A project update p 719 N95-16345
Skeletal muscle responses to unloading in humans p 809 N95-16743
Heat stress and a countermeasure in the Shuttle rescueman's suit p 809 N95-16746
Debris/ice/TPS assessment and integrated photographic analysis of Shuttle Mission STS-64 on 9 August 1994
[NASA-TM-109206] p 676 N95-17262

NATIONAL AERONAUTICS AND SPACE ADMINISTRATION. LYNDON B. JOHNSON SPACE CENTER, HOUSTON, TX.

ISMCR 1994: Topical Workshop on Virtual Reality. Proceedings of the Fourth International Symposium on Measurement and Control in Robotics
[NASA-CP-10163] p 851 N95-15972
Coordinated control of a dual-arm dexterous robot using full immersion telepresence and virtual reality p 852 N95-15979
Virtual environment application with partial gravity simulation p 854 N95-15988
Scripting human animations in a virtual environment p 855 N95-15992
Kapton wire concerns for aerospace vehicles p 711 N95-16045
Catalog of lunar and Mars science payloads
[NASA-RP-1345] p 922 N95-16436
Primary battery design and safety guidelines handbook
[NASA-RP-1353] p 764 N95-16561
The effect of differences in time to detection of circulating microbubbles on the risk of decompression sickness p 807 N95-16738
Variability in Hoffmann and tendon reflexes in healthy male subjects p 808 N95-16739
Use of injectable promethazine to decrease symptom scores of Space Motion Sickness p 808 N95-16741
Catecholaminergic responses to stressful motion stimuli, scopolamine plus amphetamine, and dexamethasone p 809 N95-16745
A new model for estimating total body water from bioelectrical resistance p 810 N95-16747
Magnetic Resonance Imaging (MRI) of skeletal muscles in astronauts after 9 days of space flight p 810 N95-16749
Results of an International Space Crew Debrief p 810 N95-16750
Blood volume and orthostatic responses of men and women to a 13-day bedrest p 811 N95-16752
Effect of antiorthostatic BedRest (BR) on GastroIntestinal Motility (GIM) of normal subjects p 811 N95-16753
Changes in left ventricular function as determined by the multi-wire gamma camera at near presyncopal levels of lower body negative pressure p 811 N95-16754
Comparisons of three anti-G suit configurations during long duration, low onset, +Gz p 811 N95-16755
Achilles Tendon Reflex (ATR) in response to short exposures of microgravity and hypergravity p 812 N95-16756
Prediction of space sickness in astronauts from preflight fluid, electrolyte, and cardiovascular variables and Weightless Environmental Training Facility (WETF) training p 812 N95-16757
Dark focus of accommodation as dependent and independent variables in visual display technology p 812 N95-16758
Results of the psychiatric, select-out evaluation of US astronaut applications p 813 N95-16761
Validation of astronaut psychological select-in criteria p 813 N95-16762
Psychological training of NASA astronauts for extended missions p 813 N95-16763
Space medicine research: Needs for the 21st century p 814 N95-16766
Effects of weightlessness on human baroreflex function p 815 N95-16770
Dynamics of the G-excess illusion p 815 N95-16771
Medical care capabilities for Space Station Freedom: A phase approach p 710 N95-16772
Advanced Cardiac Life Support (ACLS) utilizing Man-Tended Capability (MTC) hardware onboard Space Station Freedom p 816 N95-16775
Medicine on Mars: Remote medical care and the space exploration initiative p 816 N95-16777
Apollo 16: Nothing so hidden
[NASA-TM-110104] p 922 N95-16836
Apollo 17: On the shoulders of giants
[NASA-TM-110105] p 922 N95-16837
New look at the old Moon
[NASA-TM-110106] p 922 N95-16838
Houston, I think we've got a satellite
[NASA-TM-109987] p 709 N95-16941
Apollo 15: In the mountains of the Moon
[NASA-TM-109988] p 922 N95-16942
NASA Johnson Space Center Life Sciences Data System p 679 N95-17195

NATIONAL AERONAUTICS AND SPACE ADMINISTRATION. LANGLEY RESEARCH CENTER, HAMPTON, VA.

Experimental study at low supersonic speeds of a missile concept having opposing wraparound tails
[NASA-TM-4582] p 655 N95-16069
Kinetics model for initiation and promotion for describing tumor prevalence from HZE radiation
[NASA-TP-3479] p 820 N95-16412
The Role of Computers in Research and Development at Langley Research Center
[NASA-CP-10159] p 846 N95-16453
Software engineering from a Langley perspective p 843 N95-16454
A study of software standards used in the avionics industry p 670 N95-16456
A software tool for dataflow graph scheduling p 843 N95-16457
Rapid solution of large-scale systems of equations p 847 N95-16458
Equation solvers for distributed-memory computers p 847 N95-16460
Applications of automatic differentiation in computational fluid dynamics p 774 N95-16461
Automatic differentiation for design sensitivity analysis of structural systems using multiple processors p 847 N95-16462
Use of World Wide Web and NCSA Mcsaic at Langley p 847 N95-16464
How to use the WWW to distribute STI p 847 N95-16465
Data Visualization and Animation Lab (DVAL) overview p 843 N95-16468
Data Visualization and Animation Lab (DVAL): Applications p 843 N95-16469
The Design Manager's Aid for Intelligent Decomposition (DeMAID) p 848 N95-16470
RDD-100 and the systems engineering process p 848 N95-16471
Computer tools for systems engineering at LaRC p 848 N95-16472
Electronic Engineering Notebook: A software environment for research execution, documentation and dissemination p 848 N95-16473
Matlab as a robust control design tool p 849 N95-16474
Simulation of the coupled multi-spacecraft control testbed at the Marshall Space Flight Center p 849 N95-16475
Hardware description languages p 832 N95-16477
Current research activities at the NASA-sponsored Illinois Computing Laboratory of Aerospace Systems and Software p 849 N95-16479
Epistemology, software engineering and formal methods p 843 N95-16480
Natural frequency of uniform and optimized tetrahedral truss platforms
[NASA-TP-3461] p 709 N95-16559
Measurements of unsteady pressure and structural response for an elastic supercritical wing
[NASA-TP-3443] p 653 N95-16560
Applications of automatic differentiation in CFD
[NASA-TM-109948] p 771 N95-16828
Experimental validation of an integrated controls-structures design methodology for a class of flexible space structures
[NASA-TP-3462] p 709 N95-16857
Constrained minimization of smooth functions using a genetic algorithm
[NASA-TP-3329] p 709 N95-16902
Comparison of computational and experimental results for a supercritical airfoil
[NASA-TM-4601] p 656 N95-16908
Performance study of galactic cosmic ray shield materials
[NASA-TP-3473] p 924 N95-16912
Numerical aperture limits on efficient ball lens coupling of laser diodes to single-mode fibers with defocus to balance spherical aberration
[NASA-TM-4578] p 886 N95-17271
Modeling of Instrument Landing System (ILS) localizer signal on runway 25L at Los Angeles International Airport
[NASA-TM-4588] p 665 N95-17384
Active load control during rolling maneuvers
[NASA-TP-3455] p 669 N95-17397
Single-engine tail interference model p 663 N95-17879
Twin engine afterbody model p 663 N95-17880

NATIONAL AERONAUTICS AND SPACE ADMINISTRATION. LEWIS RESEARCH CENTER, CLEVELAND, OH.

Nonlinear instability of a uni-directional transversely sheared mean flow
[NASA-TM-106779] p 769 N95-15969
Sensor fault detection and diagnosis simulation of a helicopter engine in an intelligent control framework
[NASA-TM-106784] p 669 N95-15970
Numerical simulation of supersonic compression corners and hypersonic inlet flows using the RPLUS2D code
[NASA-TM-106580] p 654 N95-16038
First NASA Workshop on Wiring for Space Applications
[NASA-CP-10145] p 711 N95-16044
Combustion and fires in low gravity p 712 N95-16050
Space Station Freedom primary power wiring requirements p 712 N95-16051
Kapton pyrolysis, the space environment and wiring requirements p 712 N95-16054
Computational fluid dynamics studies of nuclear rocket performance
[NASA-TM-105436] p 713 N95-16066
Test results from a simple, low-cost, pressure-fed liquid hydrogen/liquid oxygen rocket combustor p 716 N95-16328
Structurally-compliant rocket engine combustion chamber: Experimental/analytical validation p 718 N95-16337
The prediction of nozzle performance and heat transfer in hydrogen/oxygen rocket engines with transpiration cooling, film cooling, and high area ratios p 718 N95-16339
Testing and evaluation of oxide-coated iridium/rhenium chambers p 719 N95-16346
Modeling of wall-bounded complex flows and free shear flows
[NASA-TM-106513] p 770 N95-16407
Computational simulation of the formation and material behavior of ice
[NASA-TM-106702] p 785 N95-16416
Airfoil optimization by the one-shot method p 667 N95-16569
On bi-grid local mode analysis of solution techniques for 3-D Euler and Navier-Stokes equations
[NASA-TM-106749] p 771 N95-16855
Nickel hydrogen batteries: An overview
[NASA-TM-106795] p 793 N95-16861
Auroral interactions with ISSA
[NASA-TM-106794] p 709 N95-16862
New developments in the method of space-time conservation element and solution element-applications to two-dimensional time-marching problems
[NASA-TM-106758] p 862 N95-16885
Application of the space-time conservation element and solution element method to shock-tube problem
[NASA-TM-106806] p 772 N95-16903
Static and dynamic friction behavior of candidate high temperature airframe seal materials
[NASA-TM-106571] p 722 N95-16905
A workstation based simulator for teaching compressible aerodynamics
[NASA-TM-106799] p 839 N95-16906
A review of transmission diagnostics research at NASA Lewis Research Center
[ARL-TR-599] p 781 N95-16907
Optimization of adaptive intraply hybrid fiber composites with reliability considerations
[NASA-TM-106632] p 787 N95-16911
Correlation of finite element free vibration predictions using random vibration test data
[NASA-TM-106787] p 787 N95-17258
Atomic oxygen durability evaluation of the flexible batten for the photovoltaic array mast on Space Station
[NASA-TM-106798] p 781 N95-17263
Interactive computer graphics applications for compressible aerodynamics
[NASA-TM-106802] p 839 N95-17264

Multi-objective decision-making under uncertainty: Fuzzy logic methods
[NASA-TM-106796] p 720 N95-17269
Probabilistic simulation of stress concentration in composite laminates
[NASA-TM-106712] p 787 N95-17270
An object-oriented graphical user interface for a reusable rocket engine intelligent control system
[NASA-TM-106750] p 721 N95-17274
Reaction and protection of electrical wire insulators in atomic-oxygen environments
[NASA-TM-106767] p 709 N95-17275
A modular electric power system test bed for small spacecraft
[NASA-TM-106812] p 721 N95-17276
Statistical analysis of microgravity experiment performance using the degrees of success scale
[NASA-TM-106791] p 784 N95-17385
Structure of 4-methylpyridinium hydrogen sulfide
[NASA-TM-106778] p 731 N95-17387
Conceptual design of the Space Station combustion module
[NASA-TM-106788] p 675 N95-17419
Flexible method for inter-object communication in C++
[NASA-TM-106315] p 840 N95-17420
Effects of artificial viscosity on the accuracy of high-Reynolds-number kappa-epsilon turbulence model
[NASA-TM-106781] p 773 N95-17656
Microgravity isolation system design: A case study
[NASA-TM-106804] p 654 N95-17657
Thermal analysis of a functionally graded material subject to a thermal gradient using the boundary element method
[NASA-TM-106801] p 789 N95-17658
Modeling of stress/strain behavior of fiber-reinforced ceramic matrix composites including stress redistribution
[NASA-TM-106789] p 725 N95-17659
Structural optimization with approximate sensitivities
[NASA-TM-4553] p 789 N95-17701
Summary report of mission acceleration measurements for STS-62, launched 4 March 1994
[NASA-TM-106773] p 750 N95-17893
Overview of space power electronic's technology under the CSTI High Capacity Power Program
[NASA-TM-110110] p 883 N95-17933

NATIONAL AERONAUTICS AND SPACE ADMINISTRATION. MARSHALL SPACE FLIGHT CENTER, HUNTSVILLE, AL.
Precision aqueous cleaner for RSRM p 715 N95-16326
Numerical study of base pressure characteristic curve for a four-engine clustered nozzle configuration p 716 N95-16329
Space Shuttle main engine OPAD: The search for a hardware enhanced plume p 716 N95-16330
NASA Marshall Space Flight Center Solar Observatory report, March - May 1994
[NASA-TM-108471] p 915 N95-16558
Measurement of residual flexibility for substructures having prominent flexible interfaces
[NASA-TM-110074] p 786 N95-16577
A distributed planning concept for Space Station payload operations p 682 N95-17211
International Space Station Alpha user payload operations concept p 685 N95-17227
Generic mission planning and scheduling: The AXAF solution p 686 N95-17231

NATIONAL AERONAUTICS AND SPACE ADMINISTRATION. PASADENA OFFICE, CA.
Electric-optic resonant phase modulator
[NASA-CASE-NPO-18702-1-CU] p 883 N95-15960
Highly parallel reconfigurable computer architecture for robotic computation having plural processor cells each having right and left ensembles of plural processors
[NASA-CASE-NPO-17632-1-CU] p 832 N95-17400

NATIONAL AERONAUTICS AND SPACE ADMINISTRATION. WHITE SANDS TEST FACILITY, NM.
WSTF electrical arc projects p 711 N95-16047
Space Shuttle reaction control system thruster metal nitrate removal and characterization p 716 N95-16332

NATIONAL AEROSPACE LAB., AMSTERDAM (NETHERLANDS).
Residual-correction type and related computational methods for aerodynamic design. Part 1: Airfoil and wing design p 667 N95-16566
Residual-correction type and related computational methods for aerodynamic design. Part 2: Multi-point airfoil design p 667 N95-16567
Two-dimensional 16.5 percent thick supercritical airfoil NLR 7301 p 658 N95-17854
Low-speed surface pressure and boundary layer measurement data for the NLR 7301 airfoil section with trailing edge flap p 658 N95-17855
Wind tunnel test on a 65 deg delta wing with a sharp or rounded leading edge: The international vortex flow experiment p 662 N95-17872

NATIONAL AIR AND SPACE MUSEUM, WASHINGTON, DC.
Rationale for a Mars Pathfinder mission to Chryse Planitia and the Viking 1 lander p 918 N95-16183
Rationale for Isidis Planitia as a back-up landing site for the Mars Pathfinder mission p 918 N95-16184

NATIONAL CENTER FOR ATMOSPHERIC RESEARCH, BOULDER, CO.
An interactive interface for NCAR Graphics
[NASA-CR-189383] p 840 N95-17324

NATIONAL DEFENCE RESEARCH ESTABLISHMENT, LINKOEPING (SWEDEN).
Division of Information Systems (FOA 37)
[PB94-190766] p 909 N95-16400
Feasibility study concerning an active millimeterwave sensor
[PB94-190691] p 775 N95-17170
Multistatic radar, MSR
[PB94-190709] p 759 N95-17301
Preliminary study of an active millimeter wave sensor
[PB94-189206] p 759 N95-17453
Superresolution in a jammed radar signal environment
[PB94-190758] p 760 N95-17455

NATIONAL DEFENCE RESEARCH ESTABLISHMENT, STOCKHOLM (SWEDEN).
Material and ballistic investigation of a tungsten-26 percent rhenium alloy
[PB94-189156] p 734 N95-16420
Mental effects of caffeine in fatigued men and women
[PB94-190683] p 822 N95-17300
The m-line method for optical characterisation of polymer waveguides
[PB94-184611] p 887 N95-17409
IS-Lab: A tool for developing interactive programs for simulation and analysis. User's guide
[PB94-184710] p 840 N95-17410
Military aviation maintenance industry in Western Europe: Concentration and internationalization
[PB94-189180] p 653 N95-17451
Evaluation of an autopilot based multimodelling
[PB94-190725] p 671 N95-17454

NATIONAL GEOPHYSICAL DATA CENTER, BOULDER, CO.
Solar-geophysical data number 596, April 1994. Part 1: (Prompt reports). Data for March, February 1994, and late data
[PB94-183548] p 924 N95-17736
Solar-geophysical data number 596, April 1994. Part 2: (Comprehensive reports). Data for October 1993, and miscellaneous
[PB94-183555] p 924 N95-17737

NATIONAL INST. OF STANDARDS AND TECHNOLOGY, BOULDER, CO.
Optical fiber sensors: Accelerating applications in Navy ships
[PB94-186848] p 887 N95-17441

NATIONAL INST. OF STANDARDS AND TECHNOLOGY, GAITHERSBURG, MD.
Numeric data distribution: The vital role of data exchange in today's world p 907 N95-15937
National Center for Standards and Certification Information: Service and programs p 907 N95-15938
Use of the electronic balance for highly accurate direct mass measurements without the use of external mass standards
[PB94-187713] p 774 N95-16074
Low-temperature fabrication of transparent silicon nitride
[DE94-014902] p 746 N95-17456
Characterization of the hydrogen induced cold cracking susceptibility at simulated weld zones in HSLA-100 steel
[PB94-174505] p 737 N95-17616
Workshop on Characterizing Diamond Films, 3
[PB94-187663] p 747 N95-17722

NATIONAL LAB. FOR HIGH ENERGY PHYSICS, TSUKUBA (JAPAN).
Proceedings of the Workshop on Characterization of Molecular Assemblies
[DE94-753477] p 871 N95-15956

NATIONAL LIBRARY OF AUSTRALIA, CANBERRA, AUSTRALIAN CAPITAL TERRITORY (AUSTRALIA).
The Australian National Chinese Japanese Korean Project p 905 N95-15920

NATIONAL OCEAN SERVICE, ROCKVILLE, MD.
South Florida environmental quality. National Status and Trends Program for marine environmental quality
[PB94-173408] p 796 N95-17363

NATIONAL OCEANIC AND ATMOSPHERIC ADMINISTRATION, BOULDER, CO.
Verification of NOAA Space Environment Laboratory forecasts, 1 January - 31 December 1993
[PB95-104162] p 803 N95-17927

NATIONAL OCEANIC AND ATMOSPHERIC ADMINISTRATION, HONOLULU, HI.
Tsunami newsletter, volume 26
[AD-A282751] p 806 N95-17477

NATIONAL OCEANIC AND ATMOSPHERIC ADMINISTRATION, WASHINGTON, DC.
Collection development at the NOAA Central Library p 907 N95-15939

NATIONAL RENEWABLE ENERGY LAB., GOLDEN, CO.
The role of point defects and defect complexes in silicon device processing: Summary report and papers
[DE94-011873] p 791 N95-15944
Structural effects of unsteady aerodynamic forces on horizontal-axis wind turbines
[DE94-011863] p 787 N95-16939
Development of high-efficiency, thin-film CdTe solar cells
[DE94-011885] p 794 N95-16940
Recombination and metastability in amorphous silicon and silicon-germanium alloys
[DE94-011837] p 794 N95-16957

NATIONAL RESEARCH COUNCIL OF CANADA, OTTAWA (ONTARIO).
Surface pressure and wake drag measurements on the Boeing A4 airfoil in the IAR 1.5X1.5m Wind Tunnel Facility p 657 N95-17850

NATIONAL SPACE DEVELOPMENT AGENCY, TOKYO (JAPAN).
A system study for satellite operation and control in next generation p 702 N95-17586

NATIONAL SPACE DEVELOPMENT AGENCY, TSUKUBA (JAPAN).
Attempt of automated space network operations at ETS-VI experimental data relay system p 677 N95-17184

NATIONAL TECHNICAL INFORMATION CENTER AND LIBRARY, BUDAPEST, PEST (HUNGARY).
Information system in transition: The Hungarian Scene p 906 N95-15925

NATIONAL TECHNICAL UNIV., ATHENS (GREECE).
Single-pass method for the solution of inverse potential and rotational problems. Part 1: 2-D and quasi 3-D theory and application p 664 N95-16563
Single-pass method for the solution of inverse potential and rotational problems. Part 2: Fully 3-D potential theory and applications p 664 N95-16564

NATIONAL TRANSPORTATION SAFETY BOARD, WASHINGTON, DC.
Aircraft accident report: Stall and loss of control on final approach, Atlantic Coast Airlines, Inc./United Express Flight 6291 Jetstream 4101, N304UE Columbus, OH, 7 January 1994
[PB94-910409] p 665 N95-17646
Annual review of aircraft accident data: US Air carrier operations, calendar year 1992
[PB95-100319] p 665 N95-17748

NAVAL AEROSPACE MEDICAL RESEARCH LAB., PENSACOLA, FL.
Mathematical model for interaction of canals and otoliths in perception of orientation, translation, and rotation
[AD-A280897] p 819 N95-16151

NAVAL AIR WARFARE CENTER, CHINA LAKE, CA.
Superspheroid geometries for radome analysis
[AD-A285405] p 753 N95-16233
Overview of TTCP and AGARD propulsion activities p 720 N95-16351

NAVAL AIR WARFARE CENTER, WARMINSTER, PA.
Evaluation of alternate F-14 wing lug coating
[AD-A283207] p 669 N95-17631

NAVAL COMMAND, CONTROL AND OCEAN SURVEILLANCE CENTER, SAN DIEGO, CA.
A quasi-single mode optical fiber for long-haul transmission in severe bending environments
[AD-A281313] p 884 N95-16009
Rough surface models implemented within the split-step parabolic equation algorithm
[AD-A280843] p 753 N95-16148
Evolving neural network pattern classifiers
[AD-A281181] p 857 N95-16631
Development and fabrication of the fiber optic MicroCable (tm)
[AD-A285266] p 886 N95-16815
Propagation in the evaporation duct. Model predictions and comparisons to data
[AD-A283012] p 803 N95-17709

NAVAL HEALTH RESEARCH CENTER, SAN DIEGO, CA.
An annotated bibliography of heat tolerance: Regarding gender differences
[AD-A280755] p 818 N95-16105
Event-related brain potentials as predictors of target detection performance in a moving waterfall display simulating passive broad-band sonar monitoring
[AD-A280900] p 819 N95-16152
Skin blood flow and bioelectrical impedance
[AD-A285475] p 821 N95-16619

NAVAL POSTGRADUATE SCHOOL, MONTEREY, CA.
High speed transport protocols: An attempt to find the best solution
[AD-A280989] p 751 N95-15993
An investigation of the transonic pressure drag coefficient for axi-symmetric bodies
[AD-A280990] p 654 N95-15994
Multigrid methods in network optimization: Overview and appraisal
[AD-A280992] p 833 N95-15995
Integrating computers into calculus instruction
[AD-A280996] p 833 N95-15997
A computational investigation of wake-induced airfoil flutter in incompressible flow and active flutter control
[AD-A281534] p 670 N95-16109
A VLSI interface for the NM24CF04 serial-access ferroelectric memory
[AD-A281535] p 762 N95-16110
Elimination of electromagnetic interference to receivers and sensitive equipment generated by switching systems
[AD-A281643] p 752 N95-16117
Survey of United States commercial satellites in geosynchronous Earth orbit
[AD-A284969] p 708 N95-16131
A survey of the software reuse environment: A study for the NSRS
[AD-A280867] p 834 N95-16149
Automation support for concurrent software engineering
[AD-A281372] p 834 N95-16153
Software merge: Semantics of combining changes to programs
[AD-A281373] p 834 N95-16154
A preliminary attempt at sintering an ultrafine alumina powder using microwaves
[AD-A284978] p 734 N95-16229
Modification of the Naval Postgraduate School Lidar System
[AD-A284987] p 753 N95-16231
Performance of a fast frequency-hopped noncoherent MFSK receiver with non-ideal noise normalization combining over ricean fading channels with partial-band interference
[AD-A284989] p 753 N95-16232
Natural convection cooling of a three by three array of leadless chip carrier packages in a dielectric liquid
[AD-A282298] p 770 N95-16239
Videoconferencing and its role in the Army
[AD-A282707] p 909 N95-16305
Low rate initial production in Army Aviation systems development
[AD-A281871] p 666 N95-16356
Graphical simulation of articulated rigid body system kinematics with collision detection
[AD-A281842] p 856 N95-16372
Spread spectrum applications in unmanned aerial vehicles
[AD-A281035] p 754 N95-16448
Experimental study of spatially incomplete structural system identification
[AD-A280905] p 785 N95-16502
Radar observations of field-aligned plasma propagations associated with NASA's PMG experiment
[AD-A285218] p 798 N95-16521
Mach number, flow angle, and loss measurements downstream of a transonic fan-blade cascade
[AD-A280907] p 656 N95-16824
Thermoacoustic pin stacks
[AD-A282267] p 794 N95-16954
Knowledge quality functions for rule discovery
[AD-A285513] p 910 N95-16971
An analysis of Internet's MBONE: A media choice perspective
[AD-A285514] p 910 N95-16972
Data link level interconnection of remote Fiber Distributed Data Interface Local Area Networks (FDDI LANs) through the Critical Data Link (CDL)
[AD-A284307] p 755 N95-17173
Simulations of an FEL producing coherent x rays utilizing the SLAC LINAC
[AD-A283524] p 777 N95-17303
Numerical optimization of synergetic maneuvers
[AD-A283398] p 656 N95-17435
An analysis of the effects of feedline and ground screen noise currents on a conical monopole receiving antenna
[AD-A283401] p 759 N95-17436
Erosion effects on TVC vane heat transfer characteristics
[AD-A282006] p 721 N95-17448
Back-propagation neural networks in adaptive control of unknown nonlinear systems
[AD-A282414] p 858 N95-17458
Corrective software management: The success of the EPLRS program
[AD-A282430] p 841 N95-17460
A survey of commercially available expendable heavy lift launch vehicles
[AD-A282429] p 676 N95-17509
Repeatability in redundant manipulator systems
[AD-A282957] p 782 N95-17621
A comparison of different control methods for vibration suppression of flexible structures using piezoelectric actuators
[AD-A282958] p 710 N95-17622
An observational study of long waves in the equatorial Pacific Ocean during the 1991-1993 El Nino
[AD-A283380] p 806 N95-17624
An analysis of a single-burn algorithm for Low-Earth Orbit maintenance
[AD-A283418] p 721 N95-17626

NAVAL RESEARCH LAB., BAY SAINT LOUIS, MS.
Digital mapping, charting, and geodesy analysis program technical review of interim terrain analysis data set prototype 1
[AD-A284742] p 790 N95-16547
Mixed-layer hindcasts conducted at OWS Victor with initialization from synthetic profiles/mixed-layer hindcasts conducted with BTs taken during 1990 with atmospheric forcing from NOGAPS
[AD-A284749] p 800 N95-16551

NAVAL RESEARCH LAB., MONTEREY, CA.
Impact of physical processes on maritime frontogenesis
[AD-A283105] p 801 N95-17339

NAVAL RESEARCH LAB., WASHINGTON, DC.
Using lidar tomography to characterize scattering in a turbulent media
[AD-A281014] p 751 N95-16002
Problems with aging wiring in Naval aircraft
p 711 N95-16048
System design, implementation, and evaluation of the optical broadband correlator
[AD-A285406] p 884 N95-16296
Implementation of a real-time data processing system for radar bandwidth extrapolation and stretch
[AD-A281195] p 754 N95-16794
An integrated knowledge acquisition and database management system
[AD-A285404] p 910 N95-16884
Transport efficiency studies for light-ion inertial confinement fusion
[AD-A285675] p 891 N95-17382
Use of copper powder extinguishers on lithium fires
[AD-A283213] p 751 N95-17632

NAVAL SURFACE WARFARE CENTER, BETHESDA, MD.
Experimental application of methodologies to quantify the effect of constraint on JC for a 3-D flaw geometry
[AD-A285309] p 735 N95-16531
Analysis of infrared scaling laws
[AD-A285461] p 903 N95-16877

NAVAL SURFACE WARFARE CENTER, DAHLGREN, VA.
Penetration of solid and layered targets by gas gun-launched steel cubes
[AD-A285143] p 787 N95-16843

NAVAL SURFACE WARFARE CENTER, SILVER SPRING, MD.
Atomic structure and valency of nickel in some of its oxycompounds
[AD-A281109] p 733 N95-16091
X-ray absorption spectra and structure of some nickel oxides (hydroxides)
[AD-A281305] p 735 N95-16788
XAFS investigation of structure and valency of nickel in some oxycompounds
[AD-A283193] p 877 N95-17630

NAVAL SURFACE WARFARE CENTER, VIRGINIA BEACH, VA.
Model-based software process improvement
p 843 N95-16455

NAVAL SURFACE WEAPONS CENTER, SILVER SPRING, MD.
XAFS spectra and the oxidation state of nickel in some of its oxycompounds
[AD-A281137] p 735 N95-16606

NAVAL UNDERSEA WARFARE CENTER, NEWPORT, RI.
Observations of ELF propagation at high latitudes during the sporadic-E conditions of November 1986
[AD-A284973] p 753 N95-16227
Revisions to an empirical surface loss model using a correction for pH-dependent attenuation
[AD-A285714] p 871 N95-17177

NAVY COMPUTER AND TELECOMMUNICATIONS STATION, PENSACOLA, FL.
Development of the OMPAT neuropsychological/psychomotor performance evaluation and OMPAT data and timing support programs
[AD-A284926] p 826 N95-16140

NEBRASKA UNIV., LINCOLN, NE.
Poling dynamics and relaxation of polar order in guest/host polymers by second harmonic generation
[AD-A283291] p 748 N95-17724

NETHERLANDS ENERGY RESEARCH FOUNDATION, PETTEN.
Engineering design tools for wind diesel systems. Volume 2: JODYMOD dynamic wind diesel simulation software package. Model verification
[PB95-104519] p 840 N95-17355
Engineering design tools for wind diesel systems. Volume 3: JODYMOD dynamic simulation software package. Model description
[PB95-104527] p 840 N95-17356
Engineering design tools for wind diesel systems. Volume 4: JODYMOD dynamic wind diesel simulation software package. Program documentation
[PB95-104535] p 841 N95-17628
Engineering design tools for wind diesel systems. Volume 5: JODYMOD dynamic wind diesel simulation software package. User's guide
[PB95-104543] p 841 N95-17629
Engineering design tools for wind diesel systems. Volume 6: Logistic package. User documentation
[PB95-104550] p 842 N95-17734
Engineering design tools for wind diesel systems. Volume 7: Logistic package. Validation report
[PB95-104568] p 842 N95-17735

NEW MEXICO STATE UNIV., LAS CRUCES, NM.
Fractal aggregate random media analysis and applications
[AD-A281410] p 884 N95-16161
X-ray emission from the edge-on spiral galaxy NGC 4631
[NASA-CR-197536] p 924 N95-17527

NEW MEXICO UNIV., ALBUQUERQUE, NM.
Dynamical system prediction of the scalar field in a turbulent channel flow
[AD-A285519] p 771 N95-16438

NEW ORLEANS UNIV., LA.
A stepsize control strategy for stiff systems of ordinary differential equations
[AD-A281551] p 861 N95-16395
Identification and temporal behavior of radical intermediates formed during the combustion and pyrolysis of gaseous fuels: Kinetic pathways to soot formation
[DE94-014681] p 731 N95-17163

NEW YORK UNIV., NEW YORK, NY.
Visual neural development and chromatic aberration
[AD-A285064] p 826 N95-16368
Global confinement analysis
[DE94-016820] p 893 N95-17644

NEWCASTLE-UPON-TYNE UNIV., NEWCASTLE (ENGLAND).
Behavioural modelling of formal documents and active instruments
[PB95-104378] p 842 N95-17732

NORTH CAROLINA AGRICULTURAL AND TECHNICAL STATE UNIV., GREENSBORO, NC.
LPEE growth and characterization of In(x)Ga(1-x)As(y)Sb(1-y) lattice matched to GaSb and InAs for photodetectors
[AD-A281631] p 895 N95-16114

NORTH CAROLINA STATE UNIV., RALEIGH, NC.
Interface properties of wide bandgap semiconductor structures
[AD-A281469] p 894 N95-16084
Development of an analytical photon scanning tunneling microscope
[AD-A281382] p 884 N95-16157
The deposition of electro-optic films on semiconductors
[AD-A285068] p 742 N95-16488
Atomic layer epitaxy of group 4 materials: Surface processes, thin films, devices and their characterization
[AD-A280987] p 898 N95-16532
Nitride semiconductors for ultraviolet detection
[AD-A280988] p 898 N95-16533
Low temperature deposition and characterization of N- and P-type silicon carbide thin films and associated ohmic and Schottky contacts
[AD-A281060] p 743 N95-16625
Time accurate computation of unsteady inlet flows with a dynamic flow adaptive mesh
[AD-A285498] p 771 N95-16736

NORTH CAROLINA UNIV., ASHEVILLE, NC.
Alpha particle kinetics in ignited fusion plasmas: Design applications for a CO2 laser Thomson scattering experiment
[DE94-016297] p 890 N95-16921

NORTH CAROLINA UNIV., CHAPEL HILL, NC.
Extracellular ionic composition alters kinetics of vesicular release of catecholamines and quantal size during exocytosis at adrenal medullary cells
[AD-A281613] p 818 N95-16112

Cyclic voltammetric analysis of ferrocene alkanethiol monolayer electrode kinetics based on Marcus theory
[AD-A281411] p 868 N95-16162

Effect of ion-electrode contact on the energetics of the heterogeneous electron transfer
[AD-A281959] p 873 N95-16411

Electrochemical properties of lithium ion conducting solid polymer electrolytes
[AD-A281875] p 742 N95-16434

Recombination and metastability in amorphous silicon and silicon-germanium alloys
[DE94-011837] p 794 N95-16957

NORTH CAROLINA UNIV., CHARLOTTE, NC.

International Workshop on Light Emission and Electronic Properties of Nanoscale silicon
[AD-A281464] p 894 N95-16081

NORTH CAROLINA UNIV., RALEIGH, NC.

Regulation of nitrogen uptake and assimilation: Effects of nitrogen source and root-zone and aerial environment on growth and productivity of soybean
[NASA-CR-197098] p 807 N95-15961

NORTH DAKOTA STATE UNIV., FARGO, ND.

GEOTRANS geographic decision support system
[PB94-183670] p 908 N95-16093

New approaches to novel organosilanes
[AD-A285253] p 722 N95-16513

Low temperature synthesis of semiconductor materials
[AD-A285230] p 898 N95-16526

NORTHEAST CONSORTIUM FOR ENGINEERING EDUCATION, PORT ROYAL, VA.

O-Plan2 versus SIPE-2: A general comparison
[AD-A285531] p 857 N95-17381

NORTHEASTERN UNIV., BOSTON, MA.

Methods development toward the measurement of polyaromatic hydrocarbon-DNA adducts by mass spectrometry
[PB94-182722] p 727 N95-16373

Effect of Coulomb collisions, Landau damping and particle trapping on linear and nonlinear ion acoustic waves
[AD-A282009] p 869 N95-17449

NORTHROP CORP., PICO RIVERA, CA.

Eddy current for detecting second layer cracks under installed fasteners
[AD-A282412] p 784 N95-17507

NORTHUMBRIA UNIV., NEWCASTLE-UPON-TYNE (ENGLAND).

Behavioural modelling of formal documents and active instruments
[PB95-104378] p 842 N95-17732

NORTHWESTERN UNIV., EVANSTON, IL.

Physics-based approach to haptic display
p 854 N95-15986

Fundamental studies of polyphosphazene and polysiloxane polyelectrolytes for electrochemical devices
[AD-A281339] p 739 N95-16013

Tribological properties of reactively sputtered nitrides and carbides of titanium, zirconium and hafnium
[DE94-014583] p 745 N95-17160

Ion modulated electroactivity in thin-film polymers derived from bipyridyl and phenanthroline complexes of iron
[AD-A280704] p 747 N95-17682

NOTRE DAME UNIV., IN.

Error control techniques for satellite and space communications
[NASA-CR-197459] p 761 N95-17665

NOTTINGHAM UNIV. (ENGLAND).

A workout for virtual bodybuilders (design issues for embodiment in multi-actor virtual environments)
p 854 N95-15990

NYMA, INC., BROOK PARK, OH.

Continuing life test of a xenon hollow cathode for a space plasma contactor
[NASA-CR-195401] p 711 N95-15968

Small-amplitude disturbances in turbomachine flows with swirl
[NASA-CR-195406] p 772 N95-17386

O

OAK RIDGE NATIONAL LAB., TN.

A new communication scheme for the neutron diffusion nodal method in a distributed computing environment
[DE94-017907] p 844 N95-15946

Chemical vapor infiltration of non-oxide ceramic matrix composites
[DE94-017770] p 723 N95-16225

Stochastic approximation methods for fusion-rule estimation in multiple sensor systems
[DE94-013629] p 856 N95-16361

Determination of ion temperatures from Zeeman broadened spectral lines in the edge of Tore Supra
[DE94-018112] p 873 N95-16403

Atomic scale structure and chemistry of interfaces by Z-contrast imaging and electron energy loss spectroscopy in the stem
[DE94-013632] p 728 N95-16419

A CO2 laser polarimeter for measurement of plasma current profile in Alcator C-Mod
[DE94-014017] p 776 N95-16486

A coastal hazards data base for the US Gulf Coast
[DE94-014573] p 805 N95-16610

Investigation of residual stresses in a multipass weld in 1 in. stainless steel plate
[DE94-013277] p 786 N95-16803

First principles simulation of materials properties
[DE94-013615] p 899 N95-16805

Thermal and mechanical behavior of Ba(1+x)Zr4P(6-2x)Si(2x)O24
[DE94-013620] p 899 N95-16806

Effects of substrate temperature on metal colloid formation and on optical response in metal ion implanted silica
[DE94-013633] p 736 N95-16807

Fusion materials: Technical evaluation of the technology of vandium alloys for use as blanket structural materials in fusion power systems
[DE94-013194] p 890 N95-16827

Modeling of chemical vapor infiltration for composite fabrication
[DE93-001715] p 724 N95-16926

Differential phase reflectometry for edge profile measurements on TFTR
[DE94-013837] p 891 N95-16958

Mass spectrometry studies of the ionization of organic molecules by slow positrons
[DE94-013838] p 876 N95-16959

First measurements of ICRF and edge/SOL plasma interactions on TORE SUPRA
[DE94-019320] p 891 N95-17347

Prospects for toroidal fusion reactors
[DE94-014020] p 891 N95-17367

Abstracts: Eighth Annual Conference on Fossil Energy Materials
[DE94-014053] p 725 N95-17368

Low-temperature fabrication of transparent silicon nitride
[DE94-014902] p 746 N95-17456

D3-D research operations
[DE94-014934] p 892 N95-17497

Effect of extrusion parameters on consolidation of tungsten-hafnium and tungsten-steel powders
[DE94-013270] p 737 N95-17513

Automated Estimating System (AES) version 6.0: User's manual
[DE94-013636] p 841 N95-17514

Electro-separations: Efficient processing for the twenty-first century
[DE94-012656] p 732 N95-17524

Studies by neutron diffraction and muon SR of flux lattice orientation, pinning, melting and decomposition in high-T(sub c) superconductors
[DE94-017704] p 901 N95-17667

ITER design: Physics basis for size, confinement capability power levels and burn control
[DE94-018041] p 893 N95-17674

Modeling of thermal stresses in welds
[DE94-018046] p 789 N95-17675

Parallel fast Fourier transforms for non power of two data
[DE94-018047] p 851 N95-17676

Measurements and modeling of impurity source distributions from the Tore Supra outboard pump limiter
[DE94-018049] p 893 N95-17677

XPVM: A graphical console and monitor for PVM
[DE94-018050] p 842 N95-17678

Effect of heat treatment temperature on creep-rupture properties of Fe3Al-based alloys
[DE94-018054] p 738 N95-17679

Design of a CO2-laser Thomson scattering ion-tail diagnostic for Alcator C-Mod
[DE94-018056] p 779 N95-17680

Electrical breakdown and optical emission properties of high pressure pulsed RF gas discharges
[DE94-012731] p 877 N95-17687

Selected properties of iron aluminides
[DE94-018057] p 738 N95-17726

Forging of FeAl intermetallic compounds
[DE94-018124] p 739 N95-17728

Environmental effects on iron aluminide
[DE94-017900] p 739 N95-17747

Status of the US stellarator reactor study
[DE94-018693] p 893 N95-17907

Modelling interactions of carbon dioxide, forests, and climate
[DE94-018694] p 797 N95-17908

Test results of superconducting AC magnets for magnetic refrigeration experiment
[DE94-018695] p 751 N95-17909

Simulation of the SEMATECH gravimetric mass flowmeter calibrator
[DE94-018698] p 773 N95-17910

Raman spectroscopy of C-irradiated graphite
[DE94-018705] p 733 N95-17911

OAO CORP., ALTADENA, CA.

Operations automation p 687 N95-17236

OFFICE NATIONAL D'ETUDES ET DE RECHERCHES AEROSPATIALES, PARIS (FRANCE).

Ellipsoid-cylinder model p 661 N95-17869

Supersonic vortex flow around a missile body
p 661 N95-17870

Test data on a non-circular body for subsonic, transonic and supersonic Mach numbers p 662 N95-17871

Delta-wing model p 662 N95-17873

OFFICE NATIONAL D'ETUDES ET DE RECHERCHES AEROSPATIALES, TOULOUSE (FRANCE).

Data from the GARTEur (AD) Action Group 02 airfoil CAST 7/DOA1 experiments p 659 N95-17856

OAT15A airfoil data p 659 N95-17857

OFFICE OF NAVAL RESEARCH, ARLINGTON, VA.

Electronic access to ONREUR/ONRAISIA S and T reports p 907 N95-15935

OHIO AEROSPACE INST., WRIGHT-PATTERSON AFB, OH.

Synthetic aperture radar target detection, feature extraction, and image formation techniques
[NASA-CR-197485] p 760 N95-17651

OHIO STATE UNIV., COLUMBUS.

Wing-body juncture flows
[AD-A281526] p 655 N95-16099

In situ laser activation of electrochemical kinetics at carbon electrodes
[AD-A280892] p 727 N95-16150

Demodulation processes in auditory perception
[AD-A285427] p 869 N95-16248

Breaking down barriers in cooperative fault management: Temporal and functional information displays
[NASA-CR-197450] p 857 N95-17383

OLD DOMINION UNIV., NORFOLK, VA.

Radiative interactions in chemically reacting compressible nozzle flows using Monte Carlo simulations
[NASA-CR-197133] p 769 N95-15986

Parametric study of shock-induced combustion in a hydrogen air system
[NASA-CR-197134] p 726 N95-15967

Root growth and development in response to CO2 enrichment
[NASA-CR-196154] p 807 N95-16429

Automation of reverse engineering process in aircraft modeling and related optimization problems
[NASA-CR-197109] p 668 N95-16899

SDIO/IST ultrashort wavelength. Mossbauer and gamma ray studies for grasers
[AD-A283091] p 778 N95-17337

ONSALA SPACE OBSERVATORY (SWEDEN).

First detection of CO (j = 0 - 1) adsorption at cosmological distances (z = 0.247)
[PB94-184595] p 916 N95-17332

OPTOELECTRONICS INDUSTRY DEVELOPMENT ASSOCIATION, MOUNTAIN VIEW, CA.

Optoelectric technology roadmap: Conclusions and recommendations
[AD-A281664] p 886 N95-16965

OREGON GRADUATE INST. OF SCIENCE AND TECHNOLOGY, BEAVERTON, OR.

Fundamental studies in oxidation-reduction in relation to water photolysis
[DE94-014598] p 731 N95-17161

OREGON STATE UNIV., CORVALLIS, OR.

Marine boundary-layer parameterizations for large-scale models
[AD-A282402] p 803 N95-16082

Meteorological observations of synoptic disturbances: Sensitivity to latitude p 917 N95-16179

A procedure for estimating the carbon budget of terrestrial ecosystems in the former Soviet Union by geographic information system analysis and classification of AVHRR derived global vegetation index
p 796 N95-17394

Long-term momentum and heat balances and turbulent mixing in the upper equatorial Pacific Ocean
p 805 N95-17395

On the propagation of near-inertial motion from the oceanic mixed layer p 806 N95-17396

OREGON UNIV., EUGENE, OR.

Electron transport and tunneling experiments
[AD-A281527] p 894 N95-16106

ORGANISATIE VOOR TOEGEPAST NATUURWETENSCHAPPELIJK ONDERZOEK, DELFT (NETHERLANDS).

Energy expenditure, physical work load and postural control during walking on a moving platform
[AD-A285343] p 830 N95-16821

Parallel search for a conjunction of shape and contrast polarity
[AD-A285344] p 827 N95-16822
A framework for the analysis of cognitive tasks
[AD-A285345] p 828 N95-16835
ORGANISATIE VOOR TOEGEPAST NATUURWETENSCHAPPELIJK ONDERZOEK, SOESTERBERG (NETHERLANDS).
Perceptual selectivity for color and form: On the nature of the interference effect
[AD-A285338] p 827 N95-16817
ORGANISATIE VOOR TOEGEPAST NATUURWETENSCHAPPELIJK ONDERZOEK, THE HAGUE (NETHERLANDS).
Fields and waves in elliptic waveguides
[AD-A285337] p 755 N95-16816

P

PACIFIC NORTHWEST LAB., RICHLAND, WA.
Infrared signatures for remote sensing
[DE94-014222] p 790 N95-16215
Bracing micro/macro manipulators control
[DE94-014434] p 856 N95-16287
Proceedings of the Neural Network Workshop for the Hanford Community
[DE94-014567] p 856 N95-16609
Coatings for large-area low-cost solar concentrators and reflectors
[DE94-015735] p 793 N95-16916
Regional forecasting with global atmospheric models
[DE94-013863] p 801 N95-16961
Mixed-mode I/III fracture toughness of a ferritic/martensitic stainless steel
[DE94-014492] p 736 N95-17159
Global climate change model natural climate variation: Paleoclimate data base, probabilities and astronomic predictors
[DE94-013956] p 796 N95-17348
An artificial neural network system for diagnosing gas turbine engine fuel faults
[DE94-013960] p 670 N95-17371
On the measurement of momentum flux profiles using a five-beam 915-MHz wind profiler
[DE94-018448] p 791 N95-17903
An XAFS study of the oxidation of structural iron in biotite mica by solutions containing Br2 or H2O2
[DE94-018721] p 733 N95-17912
Vacuum deposited polymer/silver reflector material
[DE94-018729] p 748 N95-17913
Trigonometric functions of nonlinear quantities
[DE94-018794] p 864 N95-17916
PADUA UNIV. (ITALY).
Multimodal correlation and intraoperative matching of virtual models in neurosurgery p 823 N95-15976
Surface matching for correlation of virtual models: Theory and application p 853 N95-15983
PARIS VI UNIV. (FRANCE).
Optimal shape design for aerodynamics p 667 N95-16568
PECHAN (E. H.) AND ASSOCIATES, INC., DURHAM, NC.
Landfill gas energy utilization: Technical and nontechnical considerations
[PB94-189651] p 793 N95-16544
PENNSYLVANIA STATE UNIV., STATE COLLEGE, PA.
Active minimization of energy density in three-dimensional enclosures
[NASA-CR-197213] p 871 N95-16848
PENNSYLVANIA STATE UNIV., UNIVERSITY PARK, PA.
Damage-mitigating control of space propulsion systems for high performance and extended life
[NASA-CR-194470] p 784 N95-16068
Ductile fracture and failure criteria of structural steels
[AD-A280754] p 733 N95-16104
Integrated passive and active control of structures
[AD-A282684] p 708 N95-16304
Anisotropic heat exchangers/stack configurations for thermoacoustic heat engines
[AD-A280974] p 792 N95-16506
Innovative acoustic techniques for studying new materials and new developments in solid state physics
[AD-A280986] p 898 N95-16525
Combustion instability phenomena of importance to liquid propellant engines
[AD-A284780] p 730 N95-16882
An in-cylinder study of the particulate/NO(x) trade-off in a DI diesel engine
[DE94-014599] p 781 N95-17162
PHILIPS GLOEILAMPENFABRIEKEN N.V., EINDHOVEN (NETHERLANDS).
Frequency domain analysis for nonlinear electronic circuits
[PB94-201365] p 767 N95-17469
PHILLIPS LAB., KIRTLAND AFB, NM.
Radiation electrodynamics of the photo-electron cloud produced by an arbitrary photon pulse incident on a planar emitting surface in vacuum
[AD-A282153] p 759 N95-17450
Thermal effects in end-heated laser rods: A time-dependent model and diagnostic
[AD-A282007] p 778 N95-17500
Radial acceletron, a new low impedance HPM source
[AD-A282008] p 760 N95-17501
PHYSICAL OPTICS CORP., TORRANCE, CA.
A highly functional decision paradigm based on nonlinear adaptive genetic algorithm
[AD-A281457] p 855 N95-16077
PHYSICAL SCIENCES, INC., ANDOVER, MA.
Ultraviolet emissions occurring about hypersonic vehicles in rarefied flows
[AD-A281452] p 655 N95-16076
PHYSICS AND ELECTRONICS LAB. TNO, THE HAGUE (NETHERLANDS).
Evaluation of FEL image processing algorithm for 12-bit CCD-images as function of various atmospheric conditions
[AD-A285187] p 752 N95-16146
Assessment of benefits and drawbacks of using fuzzy logic, especially in fire control systems
[AD-A285428] p 838 N95-16874
PICOTRONIX, INC., ANN ARBOR, MI.
Picosecond optoelectronic AND-GATE
[AD-A285672] p 885 N95-16620
PITTSBURGH UNIV., PITTSBURGH, PA.
An unexpected adsorption site exclusion process on Si(100)-(2x1)
[AD-A284950] p 894 N95-16043
A posteriori error estimation new approach
[AD-A284960] p 860 N95-16127
Global subjectivity of submersions via contractibility of the fibers
[AD-A284961] p 860 N95-16128
Investigation of pressure regulation in an archaebacterial enzyme
[AD-A281413] p 807 N95-16164
Reaction of methanol with porous silicon
[AD-A285518] p 728 N95-16406
PRINCETON UNIV., NJ.
Simulations of the global carbon cycle and anthropogenic CO2 transient
[DE94-014165] p 795 N95-16212
Determination of ion temperatures from Zeeman broadened spectral lines in the edge of Tore Supra
[DE94-018112] p 873 N95-16403
Extraction of high quality potential surfaces from laboratory data
[AD-A285071] p 903 N95-16489
Optimum aerodynamic design via boundary control p 667 N95-16565
PRINS MAURITS LAB. TNO, RIJSWIJK (NETHERLANDS).
Mass spectral data of alkyl and cycloalkyl methylphosphonofluoridates
[AD-A285312] p 722 N95-16734
PUERTO RICO UNIV., RIO PIEDRAS.
Underpotential deposition of Cu on Au(111): Implications of the HB model
[AD-A283028] p 902 N95-17711
The solvation thermodynamic functions in the Mean Spherical Approximation (MSA): Behavior near the solvent critical region
[AD-A283040] p 904 N95-17712
PUERTO RICO UNIV., SAN JUAN.
Characterization of neurotrophic and neurotropic interactions between neurons and their muscle and nerve targets
[AD-A281846] p 820 N95-16423
PURDUE UNIV., WEST LAFAYETTE, IN.
Nonlinear optical and charge distribution studies probing electric field effects in polymer thin films for second order nonlinear optics
[AD-A280980] p 742 N95-16483
Laser induced fluorescence measurements and modeling of nitric oxide in high-pressure premixed flames
[NASA-CR-195404] p 775 N95-16910

Q

QUALITY DECISION MANAGEMENT, INC., NORTH ANDOVER, MA.
Groupware system for multidisciplinary participation
[AD-A282525] p 850 N95-17374

R

RADEX, INC., BEDFORD, MA.
CMCAM: A high performance CM-5 lattice gas simulator
[AD-A281063] p 837 N95-16626
RAND CORP., SANTA MONICA, CA.
Data rearrangement and real-time computation
[AD-A282349] p 910 N95-17166
Emerging national space launch programs: Economics and safeguards
[AD-A282107] p 672 N95-17427
The new map graphics in RSAS 5.0
[AD-A282432] p 791 N95-17511
RENSSELAER POLYTECHNIC INST., TROY, NY.
Numerical methods for singularly perturbed differential equations with applications
[AD-A285209] p 861 N95-16517
In-situ x-ray characterization of the electrolyte-solid interface
[AD-A281165] p 729 N95-16627
RESEARCH INST. FOR COMPUTING AND INFORMATION SYSTEMS, HOUSTON, TX.
A survey of program slicing for software engineering
[NASA-CR-193116] p 836 N95-16574
RESEARCH TRIANGLE INST., RESEARCH TRIANGLE PARK, NC.
Applied virtual reality at the Research Triangle Institute p 851 N95-15974
RIJKSINSTITUUT VOOR VOLKSGEZONDHEID EN MILIEUHYGIEENE, BILTHOVEN (NETHERLANDS).
Energy and emissions of CO2, NOx and SO2 in the scenario of the 3rd national environmental evaluation, 1993
[PB94-194792] p 796 N95-17304
RISOE NATIONAL LAB., ROSKILDE (DENMARK).
Engineering design tools for wind diesel systems. Volume 2: JODYMOD dynamic wind diesel simulation software package. Model verification
[PB95-104519] p 840 N95-17355
Engineering design tools for wind diesel systems. Volume 3: JODYMOD dynamic simulation software package. Model description
[PB95-104527] p 840 N95-17356
Engineering design tools for wind diesel systems. Volume 4: JODYMOD dynamic wind diesel simulation software package. Program documentation
[PB95-104535] p 841 N95-17628
Engineering design tools for wind diesel systems. Volume 5: JODYMOD dynamic wind diesel simulation software package. User's guide
[PB95-104543] p 841 N95-17629
Engineering design tools for wind diesel systems. Volume 1: Executive summary
[PB95-104501] p 842 N95-17733
Engineering design tools for wind diesel systems. Volume 6: Logistic package. User documentation
[PB95-104550] p 842 N95-17734
Engineering design tools for wind diesel systems. Volume 7: Logistic package. Validation report
[PB95-104568] p 842 N95-17735
ROCHESTER UNIV., NY.
Decreasing the bandwidth of a transition matrix
[TR-505] p 859 N95-15948
A general method to determine invariants
[TR-503] p 859 N95-15949
NP-sets are Co-NP-immune relative to a random oracle
[TR-501] p 859 N95-15950
On P-selectivity and closeness
[TR-499] p 859 N95-15951
ARO-URI Center for Opto-Electronic Systems Research
[AD-A281447] p 883 N95-15958
On computing the minimal labels in time point algebra networks
[TR-495] p 859 N95-16022
On the structure of log-space probabilistic complexity classes
[TR-506] p 864 N95-16039
Properties of multihead two-way probabilistic finite automata
[TR-477] p 833 N95-16040
The search for lost cycles: A new approach to parallel program performance evaluation
[AD-A281467] p 845 N95-16082
Can high bandwidth and latency justify large cache blocks in scalable multiprocessors?
[AD-A281468] p 845 N95-16083
Software cache coherence for large scale multiprocessors
[AD-A281628] p 845 N95-16113
Picosecond silicon metal-semiconductor-metal photodiode
[AD-A281548] p 763 N95-16394

Nonlinear optical response of condined excitions in molecular and semiconductor nanostructures
[AD-A285225] p 885 N95-16524
Actions and events in interval temporal logic
[TR-521] p 839 N95-16883
On serializable languages
[TR-519] p 839 N95-17261

ROCKET RESEARCH CORP., REDMOND, WA.
Updated test results of a pumped monopropellant propulsion system p 713 N95-16315

ROCKWELL INTERNATIONAL CORP., CANOGA PARK, CA.
Integrated modular engine configuration options p 717 N95-16336

ROCKWELL INTERNATIONAL CORP., DOWNEY, CA.
Program test objectives milestone 3
[NASA-CR-197030] p 666 N95-15971
Orbiter Kapton wire operational requirements and experience p 711 N95-16046

ROCKWELL INTERNATIONAL CORP., THOUSAND OAKS, CA.
Life prediction for bridged fatigue cracks
[DE94-016000] p 724 N95-16930
Mechanisms of mechanical fatigue in ceramics
[DE94-016040] p 747 N95-17719

ROCKWELL INTERNATIONAL SCIENCE CENTER, THOUSAND OAKS, CA.
Thermal dissociation of halogen azides
[AD-A285088] p 728 N95-16497
Processing - property relationship in advanced intermetallics
[AD-A285262] p 735 N95-16514

ROME LAB., GRIFFISS AFB, NY.
Parallel implementation of the terrain masking algorithm
[AD-A281017] p 833 N95-16003
The survivable distributed computing environment
[AD-A281637] p 845 N95-16115
Summary Report, 1992
[AD-A281639] p 845 N95-16116
Log-polar optical coordinate transformation with applications for automatic pattern recognition
[AD-A281022] p 885 N95-16443
WAVES VHDL interface
[AD-A285208] p 764 N95-16516
A VHF/UHF antenna for the Precision Antenna Measurement System (PAMS)
[AD-A285673] p 754 N95-16621

ROME LAB., HANSCOM AFB, MA.
Clutter signal polarization in bistatic radar: Effect of antenna sidelobe clutter
[AD-A282300] p 753 N95-16240
Formulation of probe-corrected time-domain planar near-field measurements
[AD-A281053] p 754 N95-16624

ROYAL INST. OF TECH., STOCKHOLM (SWEDEN).
The National Resource Library for Science and Technology in Sweden: A Nordic model of cooperating technology libraries p 906 N95-15929
IS-Lab: A tool for developing interactive programs for simulation and analysis. User's guide
[PB94-184710] p 840 N95-17410

ROYAL NETHERLANDS METEOROLOGICAL INST., DE BILT.
Modelling daily precipitation as a function of temperature for climate change impact studies
[KNMI-WR-93-02] p 802 N95-17529

RUTHERFORD APPLETON LAB., CHILTON (ENGLAND).
Engineering design tools for wind diesel systems. Volume 2: JODYMOD dynamic wind diesel simulation software package. Model verification
[PB95-104519] p 840 N95-17355
Engineering design tools for wind diesel systems. Volume 3: JODYMOD dynamic simulation software package. Model description
[PB95-104527] p 840 N95-17356
Ground Station support for small scientific satellites p 695 N95-17549
Engineering design tools for wind diesel systems. Volume 4: JODYMOD dynamic wind diesel simulation software package. Program documentation
[PB95-104535] p 841 N95-17628
Engineering design tools for wind diesel systems. Volume 5: JODYMOD dynamic wind diesel simulation software package. User's guide
[PB95-104543] p 841 N95-17629
Critical and paramagnetic spin dynamics in an antiferromagnetically coupled Heisenberg magnet: Results for RbMnF3
[PB95-104329] p 869 N95-17731
Engineering design tools for wind diesel systems. Volume 1: Executive summary
[PB95-104501] p 842 N95-17733
Engineering design tools for wind diesel systems. Volume 6: Logistic package. User documentation
[PB95-104550] p 842 N95-17734
Engineering design tools for wind diesel systems. Volume 7: Logistic package. Validation report
[PB95-104568] p 842 N95-17735
Time-dependent spin correlations in the heisenberg magnet at infinite temperature
[PB95-104303] p 869 N95-17750

S

SAN JUAN CAPISTRANO RESEARCH INST., CA.
Implications of high-spatial-resolution thermal infrared (Termoskan) data for Mars landing site selection p 918 N95-16180

SANDIA NATIONAL LABS., ALBUQUERQUE, NM.
Crystalline silicon processing
[DE94-016552] p 894 N95-15942
Mechanical effects in cookoff modeling
[DE94-014174] p 748 N95-16214
Control of a large vacuum wave precursor on the SABRE voltage adder MITL and extraction ion diode
[DE94-014280] p 888 N95-16216
Reliability implications of defects in high temperature annealed Si/SiO2/Si structures
[DE94-015765] p 895 N95-16311
How clean is clean: Non-destructive/direct methods of flux, residue detection
[DE94-013439] p 763 N95-16357
MAGENCO: A map generalization controller for Arc/Info
[DE94-013440] p 835 N95-16358
The response of the Sandia robust wide range hydrogen sensor to H2-O2 mixtures
[DE94-013763] p 727 N95-16362
Error propagation equations for estimating the uncertainty in high-speed wind tunnel test results
[DE94-014136] p 671 N95-16509
Relationships between ferroelectric 90 deg domain formation and electrical properties of chemically prepared Pb(Zr,Ti)O3 thin films
[DE94-015274] p 744 N95-16829
Active messages versus explicit message passing under SUNMOS
[DE94-015278] p 850 N95-16830
A new manufacturing method for the formation of gated field emission structures
[DE94-015287] p 764 N95-16832
Tunable UV source for UV fluorescence remote sensing
[DE94-015745] p 777 N95-16917
Structure-property relationships in sol-gel-derived thin films
[DE94-016149] p 744 N95-16934
The application of non-destructive techniques to the testing of a wind turbine blade
[DE95-000323] p 784 N95-17360
Reentry safety for the Topaz 2 Space Reactor: Issues and analyses
[DE95-000325] p 880 N95-17361
Application of NMR shock barometer to naturally shocked minerals
[DE95-000326] p 799 N95-17362
Decentralized sliding mode control of nonlinear flexible robots
[DE94-013790] p 782 N95-17366
An analysis of smoothed particle hydrodynamics
[DE94-013817] p 788 N95-17439
Phase-locked arrays of vertical-cavity surface-emitting lasers
[DE94-014941] p 778 N95-17498
ATM-test: A workstation-based software suite for testing Asynchronous Transfer Mode (ATM) networks
[DE94-013813] p 850 N95-17516
Test applications for heterogeneous real-time network testbed
[DE94-016480] p 850 N95-17638
Surftherm: A program to analyze thermochemical and kinetic data in gas-phase and surface chemical reaction mechanisms
[DE94-016145] p 733 N95-17744
Recent advances in the development of high average power induction accelerators for industrial and environmental applications
[DE94-018734] p 882 N95-17914
Optimal trajectories for flexible-link manipulator slewing using recursive quadratic programming: Experimental verification
[DE94-018741] p 858 N95-17915
Study of CuPt-type ordering and dopant effect of In(0.5)Ga(0.5)P/GaAs using spectroscopic ellipsometry
[DE94-018890] p 902 N95-17917
Field-induced minigap and transport with in-plane magnetic fields in double quantum wells
[DE94-018893] p 879 N95-17918

SATELLITE OPERATIONAL SERVICES G.M.B.H., GILCHING (GERMANY).
Telemetry distribution and processing for the second German Spacelab Mission D-2 p 681 N95-17207

SCIENCE APPLICATIONS INTERNATIONAL CORP., MCLEAN, VA.
The Space Communications Protocol Standards Program p 704 N95-17594

SCIENCE APPLICATIONS INTERNATIONAL CORP., RALEIGH, NC.
Straits of Florida physical oceanographic field study. Volume 1: Executive summary. Volume 2: Technical report. Volume 3: Data report
[PB94-175031] p 806 N95-17615

SCIENCE RESEARCH COUNCIL, DARESBURY (ENGLAND).
Photon beam studies of magnetic materials
[PB95-104279] p 877 N95-17351
Solar neutrino oscillations
[PB95-104295] p 923 N95-17352
Multilepton SUSY signals from R-parity violation at the Tevatron (revised)
[PB95-104311] p 877 N95-17353
Parton distributions of the proton
[PB95-104337] p 877 N95-17354

SCIENCE RESEARCH LAB., INC., SOMERVILLE, MA.
Multi-beam laser interferometer for plasma density measurements in a Plasma Erosion Opening Switch (PEOS)
[AD-A283209] p 892 N95-17623

SCIENTIFIC AND TECHNICAL RESEARCH COUNCIL OF TURKEY, ANKARA.
Informatics in Turkey p 905 N95-15921

SCRIPPS CLINIC AND RESEARCH FOUNDATION, LA JOLLA, CA.
Molecular approach to hypothalamic rhythms
[AD-A285164] p 822 N95-16851

SEARCH FOR EXTRATERRESTRIAL INTELLIGENCE INST., MOUNTAIN VIEW, CA.
Climatological targets for Mars Pathfinder p 922 N95-16208

SIEMENS SOLAR INDUSTRIES, CAMARILLO, CA.
PV CZ silicon manufacturing technology improvements
[DE94-011818] p 897 N95-16424

SIERRA MONOLITHICS, INC., REDONDO BEACH, CA.
Non-volatile, rad-hard Random Access Memory (RAM) on GaAs
[AD-A285170] p 838 N95-16852

SMITHSONIAN ASTROPHYSICAL OBSERVATORY, CAMBRIDGE, MA.
Very high gamma ray extension of GRO observations
[NASA-CR-197489] p 924 N95-17421

SOFTWARE OPTIONS, INC., CAMBRIDGE, MA.
Improving productivity in the development of large software systems
[AD-A282270] p 835 N95-16234

SOFTWARE PRODUCTIVITY CONSORTIUM, HERNDON, VA.
MIL-STD-498 software development and documentation, version 01.00.00
[AD-A282003] p 837 N95-16607

SOLAREX CORP., NEWTOWN, PA.
Research on stable, high-efficiency, amorphous silicon multijunction modules
[DE94-011826] p 794 N95-17521

SOUTH CAROLINA UNIV., COLUMBIA, SC.
Synthesis of low band gap zwitterionic and planar conjugated pyrrole-derived polymers. Reversible optical absorbances from the UV to the near-IR
[AD-A281174] p 743 N95-16628
Third harmonic generation study of alpha-thiophene oligomers: Monomer to octamer
[AD-A281177] p 874 N95-16629
Synthesis of planar poly(p-phenylene) derivatives for maximization of extended pi-conjugation
[AD-A281179] p 743 N95-16630
Synthesis of polyphenylenes and polynaphthalenes by thermolysis of enediyness and dialkynylbenzenes
[AD-A281294] p 743 N95-16783
Iterative divergent/convergent doubling approach to linear conjugated oligomers. A rapid route to a 128 A long potential molecular wire
[AD-A281295] p 874 N95-16784
Synthesis and properties of soluble oligo- and polyphenylenes. A review
[AD-A281293] p 874 N95-16799

SOUTHWEST RESEARCH INST., SAN ANTONIO, TX.
Bench wear and single-cylinder engine evaluations of high-temperature lubricants for US Army ground vehicles
[AD-A285399] p 780 N95-16636
Significant issues in proof testing: A critical appraisal
[NASA-CR-4628] p 788 N95-17272
Micro-UltraViolet Spectrograph (Micro-UVS)
[DE94-016704] p 732 N95-17642

SPACE TELESCOPE SCIENCE INST., BALTIMORE, MD.
Development of a data reduction expert assistant
[NASA-CR-189385] p 911 N95-17328
SPECTRA RESEARCH SYSTEMS, INC., HUNTSVILLE, AL.
Prediction of the response of a polyimide concentrator for solar thermal propulsion p 719 N95-16343
SPIRE CORP., BEDFORD, MA.
Epitaxial MOCVD of thin film ceramics for pyroelectric detectors
[AD-A281397] p 744 N95-16863
SRI INTERNATIONAL CORP., MENLO PARK, CA.
Novel mass spectrometric instrument for gaseous and particulate characterization and monitoring
[DE94-014168] p 795 N95-16213
Representation, modeling and recognition of outdoor scenes
[AD-A283257] p 858 N95-17634
STANFORD LINEAR ACCELERATOR CENTER, CA.
QCD of different flavors with the SLD detectors
[DE94-013800] p 875 N95-16943
Light-ray operators and their application in QCD
[DE94-013801] p 903 N95-16944
Probing violation of quantum mechanics in the K0-(bar K)0 system
[DE94-017934] p 904 N95-17668
Baryogenesis and standard model CP violation
[DE94-017935] p 877 N95-17669
STANFORD TELECOMMUNICATIONS, INC., RESTON, VA.
Evaluating Space Network (SN) scheduling operations concepts through statistical analysis
p 684 N95-17222
STANFORD TELECOMMUNICATIONS, INC., SEABROOK, MD.
S-band and Ku-band return service interference between TDRSS users p 677 N95-17183
STANFORD UNIV., CA.
Synthesis of tungsten nitrene complexes as precursors for tungsten nitride
[AD-A281592] p 740 N95-16101
VLSI circuits for high speed data conversion
[AD-A281556] p 763 N95-16136
Non-linear waves in gas dynamics and mechanics
[AD-A281376] p 770 N95-16156
High altitude hypersonic flowfield radiation
[AD-A281386] p 655 N95-16160
A Lyapunov bound for solutions of Poisson's equation
[AD-A281536] p 860 N95-16169
Efficient estimation of the mean time between failures in non-regenerative dependability models
[AD-A281563] p 783 N95-16421
Nonasymptotic formulae for the distribution of the maximum of smooth Gaussian processes
[AD-A284741] p 865 N95-16546
Open architectures for formal reasoning and deductive technologies for software development
[NASA-CR-197528] p 837 N95-16586
Low voltage electron beam lithography
[AD-A281046] p 729 N95-16622
Likelihood ratio gradient estimation for stochastic recursions
[AD-A281408] p 865 N95-17426
STATE UNIV. OF NEW YORK, BINGHAMTON, NY.
Unusual initial and final state effects in quantum chromodynamics
[DE94-015341] p 903 N95-16604
STATE UNIV. OF NEW YORK, BUFFALO, NY.
Surface composition of a series of dimethylsiloxane urea, urethane segmented copolymers studied by electron spectroscopy for chemical analysis
[AD-A282872] p 745 N95-17434
Object recognition using multi-layer Hopfield neural network
[AD-A282417] p 858 N95-17459
STATE UNIV. OF NEW YORK, STONY BROOK, NY.
Investigation into the susceptibility of corrosion resistant alloys to biocorrosion
[AD-A281066] p 736 N95-16793
Fifth International Conference on Hyperbolic Problems: Theory, Numerics, Applications
[AD-A283078] p 863 N95-17333
Report on the 5th International Conference on Nonlinear Hyperbolic Problems
[AD-A283077] p 864 N95-17713
STORM INTEGRATION, INC., HERNDON, VA.
Spacecraft command and control using expert systems p 693 N95-17539
STORM INTEGRATION, INC., SAN JOSE, CA.
Implementation of a low-cost, commercial orbit determination system p 673 N95-17544
STRASBOURG UNIV. (FRANCE).
Non-linear acoustics in fluids and gels
[PB94-201308] p 870 N95-16614
SUNDSTRAND POWER SYSTEMS, SAN DIEGO, CA.
Small turbojets: Designs and installations
p 670 N95-16323
SURVEILLANCE RESEARCH LAB., SALISBURY (AUSTRALIA).
Testing and characterization of the CYCLOPS HgCdTe focal plane detector array
[AD-A284279] p 887 N95-17489
SVERDRUP TECHNOLOGY, INC., ARNOLD AFS, TN.
Structural analysis of solid-propellant rocket motors with and without flaws p 720 N95-16348
SVERDRUP TECHNOLOGY, INC., BROOK PARK, OH.
An analysis code for the Rapid Engineering Estimation of Momentum and Energy Losses (REMEL)
[NASA-CR-191178] p 656 N95-16887
Extended test of a xenon hollow cathode for a space plasma contactor
[NASA-CR-195402] p 720 N95-17265
SVERDRUP TECHNOLOGY, INC., CLEVELAND, OH.
Kapton pyrolysis on Space Station Freedom's solar array flexible current carrier p 712 N95-16049
SYRACUSE UNIV., NY.
Parallel software benchmarks for high performance BMC3/IS systems
[AD-A282329] p 844 N95-16060

T

TAMPERE UNIV. OF TECHNOLOGY (FINLAND).
Information sources in science and technology in Finland p 906 N95-15930
TECHNISCHE HOCHSCHULE, AACHEN (GERMANY).
Investigation of an NLF(1)-0416 airfoil in compressible subsonic flow p 658 N95-17852
TECHNISCHE HOGESCHOOL, DELFT (NETHERLANDS).
Experiments in the trailing edge flow of an NLR 7702 airfoil p 658 N95-17853
Experimental investigation of the vortex flow over a 76/60-deg double delta wing p 662 N95-17874
TECHNISCHE UNIV., DELFT (NETHERLANDS).
Improving production schedules without scheduling
[PB94-191350] p 904 N95-16289
Large-eddy simulation of cumulus convection
[PB94-191368] p 800 N95-16290
Applications of positron depth profiling
[PB94-197753] p 900 N95-16952
Efficiency in work behaviour: A design approach for modern tools
[PB94-197761] p 831 N95-16953
Parallel parsing
[PB94-191392] p 850 N95-17138
Calcium phosphate precipitation in a fluidized bed
[PB94-201407] p 796 N95-17399
Towards a human operator model of the navigator
[PB94-197985] p 831 N95-17468
Frequency domain analysis for nonlinear electronic circuits
[PB94-201365] p 767 N95-17469
Small sample behavior of multi-layer feedforward network classifiers: Theoretical and practical aspects
[PB94-201415] p 841 N95-17470
Grey-scale measurements in multi-dimensional digitized images
[PB94-195492] p 887 N95-17483
Development of heterogeneous Wacker oxidation catalysts: The role of the support and the redox component
[PB94-201431] p 732 N95-17700
TECHNISCHE UNIV., HANOVER (GERMANY).
The Technical Information Library: TIB
p 906 N95-15928
TELOS CORP., PASADENA, CA.
Software interface verifier p 698 N95-17564
TELOS INFORMATION SYSTEMS, PASADENA, CA.
Table-driven configuration and formatting of telemetry data in the Deep Space Network p 677 N95-17185
TENNESSEE STATE UNIV., NASHVILLE, TN.
Large scale control and distributed computing systems under stochastic structural perturbations
[AD-A281550] p 855 N95-16170
TENNESSEE UNIV., KNOXVILLE, TN.
Failure of ozone and nitrogen dioxide to enhance lung tumor development in hamsters
[PB94-182854] p 818 N95-16801
Interaction of electromagnetic fields with magnetized plasmas
[AD-A285496] p 755 N95-16968
TENNESSEE UNIV., TULLAHOMA, TN.
SSME propellant path leak detection real-time
[NASA-CR-197032] p 748 N95-16029
TEXAS A&M UNIV., COLLEGE STATION, TX.
A specification of 3D manipulation in virtual environments p 853 N95-15981
Detection of crosslink formation by 2 + 2 photocycloaddition in poly (vinyl cinnamate) by C-13 solid-state NMR
[AD-A281955] p 741 N95-16409
Failure analysis of 2D and 3D woven composites
[NASA-CR-197247] p 724 N95-16597
An interactive environment for the analysis of large Earth observation and model data sets
[NASA-CR-189381] p 911 N95-17330
TEXAS INSTRUMENTS, INC., DALLAS.
Liquefied metal jet program Automation and Robotics Research Institute (ARRI)
[AD-A285470] p 736 N95-16878
TEXAS TECHNOLOGICAL UNIV., LUBBOCK, TX.
Situation awareness information requirements for En Route Air Traffic Control
[DOT/FAA/AM-94/27] p 828 N95-17655
TEXAS UNIV., AUSTIN, TX.
Papers presented at the Tenth Topical Conference on High-Temperature Plasma Diagnostics
[DE94-015854] p 888 N95-16063
Augmentation for research training: Surface-mediated photocatalysis
[AD-A281591] p 722 N95-16100
Plasma sound source basic research
[AD-A285394] p 890 N95-16617
Solubilization of hydrophobic substances into block copolymer micelles in aqueous media and their release
[AD-A281395] p 744 N95-16792
Electron-neutrino phase separation instability
[DE94-016859] p 904 N95-17645
TEXAS UNIV., EL PASO, TX.
Electromagnetic processing of refractory metal silicide/oxide composites
[AD-A281470] p 740 N95-16085
Investigation of modularly configured attached processors with intelligent memories
[AD-A285454] p 832 N95-16876
TEXAS UNIV. AT DALLAS, RICHARDSON, TX.
Ion drift meter research
[NASA-CR-197124] p 798 N95-16432
TEXAS UNIV. HEALTH SCIENCE CENTER, HOUSTON, TX.
Investigation of laser-induced retinal damage: Wavelength and pulsewidth dependent mechanisms
[AD-A285186] p 822 N95-16871
THIOKOL CORP., BRIGHAM CITY, UT.
Ignition propagation and heat effects of propellant chips embedded in castable inhibitor using a laser flux test bomb p 717 N95-16335
Foam inflated rigidized structures for space applications p 710 N95-16344
TITAN SYSTEMS, INC., PRINCETON, NJ.
The small-scale structure of dispersing clouds in the atmosphere
[AD-A285493] p 800 N95-16802
TOKYO METROPOLITAN UNIV. (JAPAN).
Vibratory tactile display for textures
p 851 N95-15973
A virtual work space for both hands manipulation with coherency between kinesthetic and visual sensation
p 831 N95-15984
TOKYO UNIV. (JAPAN).
Master-slave system with force feedback based on dynamics of virtual model p 853 N95-15985
TOKYO UNIV., SAGAMIHARA (JAPAN).
Architecture of a distributed multimission operations system p 706 N95-17605
TOKYO UNIV., TANASHI (JAPAN).
Composite-model view of the ll-bar(gamma)(gamma) events at LEP
[DE94-753312] p 877 N95-17520
Delayed annihilation of antiprotons in helium gas
[DE94-753405] p 878 N95-17739
TOLEDO UNIV., OH.
FPCAS2D user's guide, version 1.0
[NASA-CR-195413] p 786 N95-16588
TORONTO UNIV. (ONTARIO).
Cell culture and transplantation of the suprachiasmatic circadian pacemaker
[AD-A280977] p 821 N95-16481
TRADOC TEST AND EXPERIMENTATION COMMAND, FORT HUNTER LIGGETT, CA.
A parser for the ISO 8211 data format
[AD-A281594] p 909 N95-16431
TRW, INC., REDONDO BEACH, CA.
Design margin testing of Peacekeeper solid rocket boosters p 713 N95-16313

U

ULTRAMET CO., PACOIMA, CA.
Materials characterization and design for solar-thermal propulsion p 718 N95-16340

Design, analysis, and fabrication of oxide-coated iridium/rhenium combustion chambers
p 719 N95-16347

UNISYS CORP., RESTON, VA.
STARS Conceptual Framework for Reuse Process (CFRP). Volume 1: Definition, version 3.0
[AD-A281506] p 834 N95-16167

UNIVERSITY OF CENTRAL FLORIDA, ORLANDO, FL.
Situational awareness in complex systems
[AD-A281448] p 825 N95-15959
Measurement of modulation transfer function of focal plane arrays and imaging systems
[AD-A282976] p 887 N95-17707

UNIVERSITY OF NORTHEAST LOUISIANA, MONROE, LA.
A highland sample strategy for Pathfinder
p 918 N95-16186

UNIVERSITY OF NORTHERN ILLINOIS, DE KALB, IL.
Charge transfer processes on liquid/liquid interfaces: The status in 1994
[AD-A285067] p 729 N95-16635

UNIVERSITY OF SOUTHERN CALIFORNIA, DOWNEY, CA.
Gas-surface interactions near dissociation threshold
[AD-A282726] p 730 N95-17140

UNIVERSITY OF SOUTHERN CALIFORNIA, LOS ANGELES, CA.
A rare gas optics-free absolute photon flux and energy analyzer for solar and planetary observations
[NASA-CR-197227] p 915 N95-16021
Gas-surface interactions near dissociation threshold
[AD-A284945] p 726 N95-16042
Design of new multi-functional electroactive polymers with emphasis on optical nonlinearity
[AD-A284983] p 741 N95-16230
Development of device quality nonlinear optical materials and definition of mechanisms of optical nonlinearity
[AD-A285255] p 885 N95-16528
Flow over abrupt topography: The application of patterns in nutrient and productivity in reflecting physical processes
[AD-A280813] p 797 N95-17740

UNIVERSITY OF SOUTHERN MISSISSIPPI, HATTIESBURG, MS.
Property control of (perfluorinated ionomer)/(inorganic oxide) composites by tailoring the nanoscale morphology
[AD-A281370] p 723 N95-16019
Synthesis and characterization of a new class of thermosetting resins: Allyl and propargyl substituted cyclopentadiene derivatives
[AD-A281976] p 746 N95-17485

UNIVERSITY OF WESTERN MICHIGAN, KALAMAZOO, MI.
The removal of heteroatoms from organic compounds by supercritical water
[AD-A281532] p 722 N95-16087

UTAH STATE UNIV., LOGAN, UT.
Development of a medium energy modulated electron gun for orbital experiments
[AD-A281021] p 675 N95-16005

UTAH UNIV., SALT LAKE CITY, UT.
Studies of novel popout
[AD-A285237] p 826 N95-16244

V

VANDERBILT UNIV., NASHVILLE, TN.
Encapsulated alkaline-earth organometallics as controlled sources of calcium, strontium, and barium ions
[AD-A281547] p 741 N95-16393
Shotgun/drop-weight initiation of energetic materials
[AD-A285090] p 749 N95-16499

VEDA, INC., DAYTON, OHIO,
Industry review of a crew-centered cockpit design process and toolset
[AD-A282966] p 669 N95-17661

VERMONT UNIV., BURLINGTON, VT.
Polymeric precursors to binary inorganic materials
[AD-A281010] p 739 N95-16000

VETERANS ADMINISTRATION HOSPITAL, RICHMOND, VA.
Effects of weightlessness on human baroreflex function
p 815 N95-16770

VIGYAN RESEARCH ASSOCIATES, INC., HAMPTON, VA.
Transonic Navier-Stokes calculations about a 65 deg delta wing
[NASA-CR-4635] p 656 N95-17273

VIRGINIA CENTER OF EXCELLANCE FOR SOFTWARE REUSE AND TECHNOLOGY TRANSFER, HERNDON, VA.
MIL-STD-498 software development and documentation, version 01.00.00
[AD-A282003] p 837 N95-16607

VIRGINIA POLYTECHNIC INST. AND STATE UNIV., BLACKSBURG, VA.
Heat transfer measurements for Stirling machine cylinders
[NASA-CR-197128] p 791 N95-15963
Energy decay and control for elastic and viscoelastic distributed parameter systems
[AD-A281312] p 726 N95-16008
Thermoplastic and thermosetting high glass transition temperature matrix resins
[AD-A281508] p 740 N95-16096
Global and near tip response of cracked solid propellant
p 715 N95-16325

VIRGINIA UNIV., CHARLOTTESVILLE, VA.
Monte Carlo simulation of mercury cadmium telluride
[AD-A281546] p 896 N95-16391
Control of circadian behavior by transplanted suprachiasmatic nuclei
[AD-A285233] p 807 N95-16599
Photoreceptors regulating circadian behavior: A mouse model
[AD-A285157] p 822 N95-16847
Fundamental concepts relating local atomic arrangements, deformation, and fracture of intermetallic alloys
[AD-A282971] p 738 N95-17664

VIRTUAL IMAGE LABS., INC., SILVER SPRING, MD.
ICCanvas 3D visualization tool for Windows (tm). Software user's manual
[AD-A285603] p 842 N95-17746

VITROCISET S.P.A., ROME (ITALY).
Towards an integral computer environment supporting system operations analysis and conceptual design
p 696 N95-17558

W

WAKE FOREST UNIV., WINSTON-SALEM, NC.
Least squares computations in science and engineering
[AD-A281213] p 862 N95-16798

WALTER REED ARMY MEDICAL CENTER, WASHINGTON, DC.
Comparison of work of breathing during mechanical ventilation using assist control and intermittent mandatory ventilation
[AD-A285516] p 822 N95-17174

WASHINGTON UNIV., SAINT LOUIS, MO.
Blinks, saccades, and fixation pauses during vigilance task performance. 1: Time on task
[DOT/FAA/AM-94/26] p 828 N95-17530

WASHINGTON UNIV., SEATTLE, WA.
The Fifth International Congress on the History of Oceanography
[AD-A281507] p 805 N95-16168
Communicating situation awareness in virtual environments
[AD-A285239] p 836 N95-16511

WESTINGHOUSE HANFORD CO., RICHLAND, WA.
Characterization of the corrosion behavior of the carbon steel liner in Hanford site single-shell tanks
[DE94-016475] p 737 N95-17637

WESTINGHOUSE SAVANNAH RIVER CO., AIKEN, SC.
Meteorological Monitoring Program
[DE94-017810] p 795 N95-16557
Reviews of computing technology: Software overview
[DE94-013662] p 841 N95-17515

WIEN UNIV. (AUSTRIA).
International Winterschool on Electronic Properties of Novel Materials: Progress in Fullerene Research
[AD-A282128] p 728 N95-16608

WISCONSIN UNIV., MADISON, WI.
McIDAS-eXplorer: A version of McIDAS for planetary applications
[NASA-CR-189382] p 910 N95-17323
Multilepton SUSY signals from R-parity violation at the Tevatron (revised)
[PB95-104311] p 877 N95-17353
Fluctuation measurements at c/(omega)(sub pe) spatial scales in a tokamak
[DE94-016771] p 892 N95-17643
Multi-dimensional shock capturing
[AD-A282986] p 773 N95-17708

WISCONSIN UNIV., MILWAUKEE, WI.
Chemical vapor deposition of high T(sub c) superconducting films in a microgravity environment
[NASA-CR-197527] p 750 N95-16880

WRIGHT LAB., EGLIN AFB, FL.
Autonomous weapon guidance
[AD-A282715] p 671 N95-16381

WRIGHT LAB., WRIGHT-PATTERSON AFB, OH.
High temperature polymer dielectric film-wire insulation
p 712 N95-16055
New insulation constructions for aerospace wiring applications
p 712 N95-16056
Detailed example of using PIWG on the SUN workstation and the DEC VAX computer
[AD-A281528] p 834 N95-16107
An engineering code to analyze hypersonic thermal management systems
p 715 N95-16322
Numerical simulation of transient vortex breakdown above a pitching delta wing
[AD-A281075] p 655 N95-16808
Pattern theoretic knowledge discovery
[AD-A285472] p 909 N95-16879
The mechanical property data base from an Air Force/industry cooperative test program on high temperature aluminum alloys
[AD-A282911] p 737 N95-17398
Digital logic and reconfigurable interconnects using aluminum gallium arsenide electro-optic Fredkin gates
[AD-A282880] p 881 N95-17619

Y

YALE UNIV., NEW HAVEN, CT.
Presentations of shape in object recognition and long-term visual memory
[AD-A281336] p 825 N95-16010
The Yale Knowledge-Based Planning project
[AD-A281505] p 855 N95-16095
High-intensity and high energy laser interactions with single droplets
[AD-A281415] p 776 N95-16166

YANKEE SCIENTIFIC, INC., MEDFIELD, MA.
Nonpowered instant water heater
[AD-A285459] p 783 N95-17725

Typical Contract Number Index Listing

AF- AFOSR-0090-93 ..... p 173 N95-10812

CONTRACT NUMBER | PAGE NUMBER | ACCESSION NUMBER

Listings in this index are arranged alphanumerically by contract number. Under each contract number the accession numbers denoting documents that have been produced as a result of research done under that contract are arranged in ascending order. The page number helps to locate the citation in the abstract section. The accession number denotes the number by which the citation is identified.

AF PROJ. 0100 ..... p 909 N95-16879
AF PROJ. 2303 ..... p 874 N95-16496
AF PROJ. 2307 ..... p 655 N95-16808
AF PROJ. 2308 ..... p 730 N95-16882
AF PROJ. 2853 ..... p 834 N95-16107
AF PROJ. 3321 ..... p 754 N95-16621
AF PROJ. 4600 ..... p 753 N95-16240
p 885 N95-16443
AF PROJ. 5581 ..... p 845 N95-16116
p 857 N95-17381
AF PROJ. 670B ..... p 671 N95-16381
AF PROJ. 7184 ..... p 830 N95-16553
AF PROJ. 7659 ..... p 837 N95-16626
AF PROJ. 7719 ..... p 828 N95-17175
AF-AFOSR-0016-91 ..... p 851 N95-15952
AF-AFOSR-0071-91 ..... p 771 N95-16438
AF-AFOSR-0074-91 ..... p 763 N95-16137
AF-AFOSR-0078-91 ..... p 749 N95-16512
AF-AFOSR-0083-91 ..... p 726 N95-16008
AF-AFOSR-0084-91 ..... p 729 N95-16846
AF-AFOSR-0090-93 ..... p 863 N95-16904
AF-AFOSR-0111-91 ..... p 765 N95-16834
AF-AFOSR-0126-91 ..... p 746 N95-17438
AF-AFOSR-0137-91 ..... p 871 N95-16018
AF-AFOSR-0163-91 ..... p 862 N95-16798
AF-AFOSR-0189-91 ..... p 731 N95-17142
AF-AFOSR-0194-91 ..... p 723 N95-16126
AF-AFOSR-0199-91 ..... p 821 N95-16515
AF-AFOSR-0208-91 ..... p 822 N95-16871
AF-AFOSR-0213-91 ..... p 727 N95-16150
AF-AFOSR-0226-89 ..... p 770 N95-16407
AF-AFOSR-0241-90 ..... p 873 N95-16493
AF-AFOSR-0319-89 ..... p 755 N95-16968
AF-AFOSR-0336-91 ..... p 730 N95-16882
AF-AFOSR-0391-91 ..... p 667 N95-16565
ARO-MIPR-145-91 ..... p 834 N95-16153
p 834 N95-16154
ARPA ORDER A840 ..... p 741 N95-16369
ARPA ORDER B326 ..... p 838 N95-16818
ARPA ORDER 7330 ..... p 837 N95-16602
ARPA ORDER 7597 ..... p 838 N95-16632
p 886 N95-16795
ARPA ORDER 8313 ..... p 835 N95-16306
p 838 N95-16819
ARPA ORDER 8930 ..... p 845 N95-16082
p 845 N95-16083
p 845 N95-16113
ARPA ORDER 9328 ..... p 736 N95-16878
BRITE-EURAM-AERO-0026 ..... p 668 N95-16573
DA PROJ. 1L1-61102-AH-45 ..... p 669 N95-15970
p 721 N95-17274
DA PROJ. 1L1-62618-AH-80 ..... p 785 N95-16245
DA PROJ. 101-62622-A-553 ..... p 838 N95-16634
DA PROJ. 3E1-62787-A-879 ..... p 886 N95-17334
DA PROJ. 3M1-62787-A-879 ..... p 827 N95-16520
DA PROJ. 301-62787-A-878 ..... p 818 N95-16132
DA PROJ. 4A1-62784-AT-41 ..... p 839 N95-17176
DA PROJ. 4A1-62784-AT-45 ..... p 884 N95-15999
DAAB07-93-C-U009 ..... p 744 N95-16863
DAAB07-94-C-C009 ..... p 741 N95-16369
DAAD07-90-C-0134 ..... p 802 N95-17686
DAAE07-90-C-R059 ..... p 666 N95-17706
DAAH04-93-C-0015 ..... p 655 N95-16076
DAAH04-93-C-0047 ..... p 855 N95-16077
DAAH04-93-G-0024 ..... p 855 N95-16170
DAAH04-93-G-0058 ..... p 894 N95-16081
DAAH04-93-G-0405 ..... p 744 N95-16792
DAAH04-93-G-0419 ..... p 804 N95-16078
DAAH04-93-G-0500 ..... p 857 N95-16864
DAAH04-94-G-0090 ..... p 723 N95-16397
DAAK60-93-C-0022 ..... p 783 N95-17725
DAAK70-87-C-0043 ..... p 780 N95-16636
DAAK70-92-C-0059 ..... p 780 N95-16636
DAAL01-93-K-0067 ..... p 887 N95-17707
DAAL03-86-G-0202 ..... p 883 N95-15958
DAAL03-89-G-0115 ..... p 895 N95-16114
DAAL03-89-K-0014 ..... p 859 N95-16108
DAAL03-89-K-0061 ..... p 749 N95-16499
DAAL03-90-G-0001 ..... p 896 N95-16396
DAAL03-90-G-0028 ..... p 722 N95-16087
DAAL03-90-G-0031 ..... p 655 N95-16160
DAAL03-90-G-0044 ..... p 739 N95-16013
DAAL03-90-G-0121 ..... p 729 N95-16791
DAAL03-90-G-0138 ..... p 770 N95-16163
DAAL03-90-G-0186 ..... p 655 N95-16099
DAAL03-90-G-0189 ..... p 820 N95-16423
DAAL03-90-G-0194 ..... p 740 N95-16085
DAAL03-90-G-0329 ..... p 776 N95-16353
DAAL03-91-C-0001 ..... p 896 N95-16365
DAAL03-91-C-0011 ..... p 855 N95-16011
DAAL03-91-C-0034 ..... p 730 N95-17141
DAAL03-91-G-0005 ..... p 731 N95-17425
DAAL03-91-G-0008 ..... p 741 N95-16393
DAAL03-91-G-0017 ..... p 770 N95-16156
DAAL03-91-G-0034 ..... p 807 N95-16164
DAAL03-91-G-0042 ..... p 776 N95-16166
DAAL03-91-G-0047 ..... p 872 N95-16155
DAAL03-91-G-0048 ..... p 896 N95-16391
DAAL03-91-G-0053 ..... p 884 N95-16157
DAAL03-91-G-0054 ..... p 902 N95-17705
DAAL03-91-G-0067 ..... p 895 N95-16158
DAAL03-91-G-0088 ..... p 763 N95-16136
DAAL03-91-G-0101 ..... p 860 N95-16169
DAAL03-91-G-0114 ..... p 763 N95-16159
DAAL03-91-G-0126 ..... p 740 N95-16165
DAAL03-91-G-0130 ..... p 740 N95-16101
DAAL03-91-G-0140 ..... p 740 N95-16096
DAAL03-91-G-0229 ..... p 884 N95-16161
DAAL03-91-G-0319 ..... p 783 N95-16421
p 865 N95-17426
DAAL03-91-G-0332 ..... p 894 N95-16111
DAAL03-92-C-0020 ..... p 800 N95-16802
DAAL03-92-G-0089 ..... p 722 N95-16100
DAAL03-92-G-0112 ..... p 763 N95-16394
DAAL03-92-G-0194 ..... p 726 N95-16142
DAAL03-92-G-0247 ..... p 861 N95-16395
DAAL03-92-G-0279 ..... p 886 N95-16965
DAAL03-92-G-0385 ..... p 901 N95-17424
DAAL03-92-G-0409 ..... p 856 N95-16390
DACA76-89-C-0014 ..... p 666 N95-17706
DACA76-90-C-0006 ..... p 790 N95-17372
DACA76-92-C-0008 ..... p 858 N95-17634
DAJA45-92-C-0007 ..... p 767 N95-17487
DAJA45-92-C-0011 ..... p 799 N95-16735
DAJA45-93-C-0015 ..... p 790 N95-17375
DAMD17-91-Z-1009 ..... p 820 N95-16444
DARPA ORDER 8304 ..... p 838 N95-16634
DASG60-89-C-0142 ..... p 766 N95-17139
DASG60-93-C-0118 ..... p 899 N95-16849
DE-AC02-76CH-00016 ..... p 872 N95-16121
p 879 N95-16210
p 896 N95-16385
p 899 N95-16918
p 901 N95-17673
p 877 N95-17683
DE-AC02-76CH-03000 ..... p 871 N95-15945
p 872 N95-16309
p 872 N95-16310
p 873 N95-16402
p 875 N95-16840
p 875 N95-16868
p 875 N95-16914
p 876 N95-16960
p 882 N95-17931
p 879 N95-17932
DE-AC02-76CH-03073 ..... p 873 N95-16403
DE-AC02-76ER-00881 ..... p 877 N95-17353
p 878 N95-17720
DE-AC02-76ER-03069 ..... p 875 N95-16943
DE-AC03-76SF-00098 ..... p 924 N95-16120
p 846 N95-16222
p 910 N95-16922
p 875 N95-16943
p 775 N95-17307
p 732 N95-17437
p 881 N95-17670
p 881 N95-17671
p 761 N95-17672
p 878 N95-17720
p 779 N95-17729
p 881 N95-17886
p 779 N95-17887
p 881 N95-17888
p 878 N95-17889
p 882 N95-17890
p 882 N95-17891
p 904 N95-17904
DE-AC03-76SF-00515 ..... p 903 N95-16944
p 904 N95-17668
p 877 N95-17669
DE-AC03-89ER-51114 ..... p 889 N95-16554
p 890 N95-16555
p 890 N95-16919
p 892 N95-17497
p 892 N95-17640
p 893 N95-17896
p 893 N95-17897
DE-AC04-76DP-00613 ..... p 747 N95-17690
p 782 N95-17716
p 902 N95-17906
DE-AC04-76DP-00789 ..... p 889 N95-16554
p 850 N95-17638
DE-AC04-94AL-85000 ..... p 894 N95-15942
p 748 N95-16214
p 888 N95-16216
p 895 N95-16311
p 763 N95-16357
p 835 N95-16358
p 727 N95-16362
p 671 N95-16509
p 744 N95-16829
p 850 N95-16830
p 793 N95-16831
p 764 N95-16832
p 777 N95-16917
p 744 N95-16934
p 784 N95-17360
p 880 N95-17361
p 799 N95-17362
p 782 N95-17366
p 891 N95-17382
p 788 N95-17439
p 778 N95-17498
p 850 N95-17516
p 733 N95-17744
p 882 N95-17914
p 858 N95-17915
p 902 N95-17917
p 879 N95-17918
DE-AC05-84OR-21400 ..... p 844 N95-15946
p 723 N95-16225
p 856 N95-16361
p 873 N95-16403
p 728 N95-16419
p 776 N95-16486
p 889 N95-16554
p 805 N95-16610
p 786 N95-16803
p 899 N95-16805
p 899 N95-16806
p 736 N95-16807
p 890 N95-16827
p 724 N95-16926
p 891 N95-16958
p 876 N95-16959
p 891 N95-17347
p 891 N95-17367

DE-AC05-84OT-21400 p 841 N95-17514
DE-AC06-76RL-01830 p 790 N95-16215
p 856 N95-16287
p 856 N95-16609
p 793 N95-16916
p 801 N95-16961
p 736 N95-17159
p 796 N95-17348
p 670 N95-17371
p 791 N95-17903
p 733 N95-17912
p 748 N95-17913
p 864 N95-17916
DE-AC06-87RL-10930 p 737 N95-17637
DE-AC07-76ID-01570 p 889 N95-16554
DE-AC08-93NV-11265 p 798 N95-16284
p 896 N95-16359
p 774 N95-16804
DE-AC09-89SR-18035 p 795 N95-16557
p 841 N95-17515
DE-AC12-76SN-00052 p 770 N95-16417
p 899 N95-16913
DE-AC21-88MC-23174 p 782 N95-17364
DE-AC21-92MC-29116 p 795 N95-16213
DE-AC36-83CH-10093 p 791 N95-15944
p 897 N95-16424
p 764 N95-16425
p 792 N95-16435
p 792 N95-16437
p 787 N95-16939
p 794 N95-16940
p 794 N95-16957
p 781 N95-17169
p 794 N95-17521
DE-AI03-86SF-16310 p 883 N95-17933
DE-AS04-87AL-42880 p 781 N95-17162
DE-FC02-92CE-40993 p 725 N95-17905
DE-FC05-85ER-25000 p 863 N95-17267
DE-FG02-85ER-53198 p 892 N95-17643
DE-FG02-85ER-60372 p 803 N95-17743
DE-FG02-86ER-40291 p 903 N95-16604
DE-FG02-86ER-45229 p 876 N95-16962
DE-FG02-90ER-12103 p 883 N95-15947
DE-FG02-90ER-61033 p 896 N95-16385
DE-FG02-90ER-61052 p 795 N95-16212
DE-FG02-91ER-25095 p 862 N95-16596
DE-FG02-91ER-40672 p 875 N95-16943
p 875 N95-16943
DE-FG02-91ER-40676 p 875 N95-16943
DE-FG02-91ER-40677 p 875 N95-16943
DE-FG02-92ER-30201 p 795 N95-16386
p 727 N95-16387
DE-FG02-92ER-40715 p 875 N95-16943
DE-FG02-92ER-45475 p 728 N95-16419
DE-FG02-92ER-54157 p 893 N95-17644
DE-FG02-92ER-54183 p 888 N95-16122
DE-FG03-89ER-45400 p 724 N95-16930
p 747 N95-17719
DE-FG03-91ER-40618 p 875 N95-16943
DE-FG03-92ER-40701 p 875 N95-16943
DE-FG03-92ER-54150 p 890 N95-16919
DE-FG03-93ER-25157 p 862 N95-16611
DE-FG03-94ER-54241 p 888 N95-16063
DE-FG05-80ET-53088 p 904 N95-17645
DE-FG05-85ER-13400 p 731 N95-17163
DE-FG05-89ER-53288 p 890 N95-16921
DE-FG05-91ER-40617 p 877 N95-17358
DE-FG05-92ER-54160 p 880 N95-17475
DE-FG05-94ER-25216 p 862 N95-16596
DE-FG06-85ER-40226 p 875 N95-16940
DE-FG06-87ER-13664 p 731 N95-17161
DE-FG22-91MT-91003 p 908 N95-16282
DI-14-35-0001-30493 p 806 N95-17615
DNA001-92-C-0098 p 892 N95-17623
DNA001-92-C-0173 p 842 N95-17746
DTFA01-93-Z-02012 p 752 N95-16097
p 759 N95-17336
DTFA02-91-C-91056 p 828 N95-17530
DTFH61-91-Z-00002 p 752 N95-16094
EPA-68-C0-0003 p 654 N95-17466
EPA-68-D0-0141 p 795 N95-16881
EPA-68-D1-0146 p 793 N95-16544
ESPRIT PROJ. 6083 p 674 N95-17532
p 692 N95-17534
ESTEC ORDER 125396 p 783 N95-17928
FAPESP PROJ. 91/3532-2 p 912 N95-17650
F04611-92-C-0012 p 715 N95-16325
F04701-88-C-0089 p 713 N95-16302
p 777 N95-16548
F04701-91-C-0076 p 717 N95-16336
F04701-93-C-0094 p 752 N95-16143
p 901 N95-17620
F04704-92-C-0005 p 713 N95-16313
F19628-89-C-0003 p 836 N95-16490
F19628-90-C-0002 p 752 N95-16129
p 762 N95-16130
p 885 N95-16494
p 754 N95-16495
p 672 N95-16530
p 672 N95-16842
p 759 N95-17336
F19628-90-C-0003 p 836 N95-16503
p 836 N95-16504
F19628-90-C-0097 p 916 N95-16600
F19628-91-C-0168 p 835 N95-16306
p 838 N95-16819
F19628-91-K-0002 p 803 N95-16062
F19628-91-K-0037 p 675 N95-16005
F19628-92-K-0011 p 869 N95-17449
F19628-93-C-0023 p 837 N95-16626
F19628-93-C-0051 p 803 N95-17715
F19628-93-C-0130 p 834 N95-16167
F19628-94-C-0001 p 791 N95-17625
F29601-92-C-0076 p 719 N95-16343
F29601-92-C-0119 p 718 N95-16340
F30602-88-D-0025 p 763 N95-16410
F30602-90-C-0010 p 844 N95-16061
F30602-91-C-0010 p 859 N95-16022
p 839 N95-16883
F30602-92-C-0063 p 844 N95-16060
F30602-92-C-0083 p 833 N95-16004
F30602-93-C-0017 p 857 N95-17381
F30602-93-C-0067 p 885 N95-16620
F33615-86-C-2622 p 780 N95-16139
F33615-90-C-0005 p 830 N95-16875
F33615-90-C-1465 p 838 N95-16632
p 886 N95-16795
F33615-90-C-3205 p 708 N95-16304
F33615-90-C-3211 p 784 N95-15953
F33615-91-C-2169 p 715 N95-16322
F33615-91-C-5658 p 764 N95-16814
F33615-91-C-5660 p 784 N95-17507
F33615-92-C-5936 p 669 N95-17661
F33615-93-1-1330 p 835 N95-16447
p 857 N95-16820
F41624-92-C-5006 p 850 N95-17374
F49620-83-1-0343 p 723 N95-16041
F49620-90-C-0079 p 744 N95-16844
F49620-91-C-0027 p 735 N95-16514
F49620-91-C-0054 p 741 N95-16230
F49620-91-C-0270 p 885 N95-16528
F49620-92-C-0071 p 897 N95-16498
F49620-92-J-0010 p 774 N95-16242
F49620-92-J-0038 p 770 N95-16407
F49620-92-J-0133 p 861 N95-16376
F49620-92-J-0141 p 874 N95-16523
F49620-92-J-0168 p 730 N95-17140
F49620-92-J-0169 p 825 N95-16010
F49620-92-J-0187 p 826 N95-16368
F49620-92-J-0188 p 822 N95-16851
F49620-92-J-0189 p 771 N95-16736
F49620-92-J-0205 p 822 N95-16847
F49620-92-J-0230 p 726 N95-16042
F49620-92-J-0244 p 727 N95-16144
F49620-92-J-0278 p 885 N95-16787
F49620-92-J-0293 p 820 N95-16378
F49620-92-J-0307 p 825 N95-16138
F49620-92-J-0347 p 822 N95-17342
F49620-92-J-0431 p 898 N95-16526
F49620-92-J-0448 p 889 N95-16243
F49620-92-J-0473 p 826 N95-16244
F49620-92-J-0517 p 821 N95-16481
F49620-92-J-0534 p 899 N95-16789
F49620-93-C-0028 p 735 N95-16786
F49620-93-C-0070 p 885 N95-16733
F49620-93-1-0055 p 885 N95-16524
F49620-93-1-0089 p 821 N95-16484
F49620-93-1-0099 p 826 N95-16377
F49620-93-1-0132 p 825 N95-15959
F49620-93-1-0158 p 742 N95-16483
F49620-93-1-0176 p 729 N95-16790
F49620-93-1-0185 p 807 N95-16599
F49620-93-1-0188 p 821 N95-16796
F49620-93-1-0189 p 723 N95-16019
F49620-93-1-0199 p 886 N95-17143
F49620-93-1-0216 p 895 N95-16134
F49620-93-1-0218 p 861 N95-16517
F49620-93-1-0234 p 724 N95-16492
F49620-93-1-0235 p 723 N95-16016
F49620-93-1-0241 p 746 N95-17662
F49620-93-1-0245 p 738 N95-17664
F49620-93-1-0274 p 819 N95-16135
F49620-93-1-0299 p 869 N95-16248
F49620-93-1-0300 p 903 N95-16489
F49620-93-1-0314 p 884 N95-16015
F49620-93-1-0339 p 836 N95-16511
F49620-93-1-0341 p 894 N95-16043
F49620-94-C-0025 p 728 N95-16497
F49620-94-C-0042 p 734 N95-16370
p 734 N95-16371
GRI-5089-271-20931 p 783 N95-16870
HEI-RFPA-87-4 p 818 N95-16801
JSPS ENG-207 p 839 N95-17261
MDA903-89-C-0003 p 725 N95-16970
MDA903-90-C-0004 p 672 N95-17427
MDA903-90-C-0006 p 912 N95-17710
MDA972-90-C-0035 p 837 N95-16602
p 864 N95-17618
MDA972-92-J-1018 p 837 N95-16607
MDA972-93-C-0035 p 736 N95-16878
MIPR-92MM2539 p 822 N95-17174
MIPR91-MM-1504 p 826 N95-16140
NAGW-1197 p 807 N95-16034
NAGW-2013 p 916 N95-17528
NAGW-2354 p 915 N95-16021
NAGW-2677 p 914 N95-15964
NAG1-1106 p 780 N95-16900
NAG1-1324 p 724 N95-16597
NAG1-1557 p 871 N95-16848
NAG1-363 p 769 N95-15966
p 726 N95-15967
NAG1-862 p 863 N95-17267
NAG10-0110 p 807 N95-16429
NAG2-501 p 923 N95-17403
NAG2-703 p 837 N95-16586
NAG2-806 p 831 N95-16894
NAG2-884 p 770 N95-16388
NAG3-1038 p 775 N95-16910
NAG3-1149 p 776 N95-17895
NAG3-1198 p 669 N95-15970
NAG3-1234 p 786 N95-16588
NAG3-1240 p 784 N95-16068
NAG3-1274 p 750 N95-16880
NAG3-1285 p 791 N95-15963
NAG3-1313 p 746 N95-17654
NAG3-1389 p 721 N95-16035
NAG3-178 p 870 N95-16401
NAG3-998 p 671 N95-17404
NAG5-1Y29 p 915 N95-17496
NAG5-1282 p 916 N95-16032
NAG5-1381 p 924 N95-17421
NAG5-1440 p 675 N95-17493
NAG5-1565 p 924 N95-16383
NAG5-1572 p 830 N95-16418
NAG5-1636 p 915 N95-17495
NAG5-1924 p 915 N95-17496
p 924 N95-17527
NAG5-2014 p 915 N95-17496
NAG5-2065 p 790 N95-16895
NAG5-2341 p 917 N95-17422
NAG5-2371 p 888 N95-15941
NAG5-306 p 798 N95-16432
NAG5-557 p 761 N95-17665
NAG8-140 p 748 N95-16029
NAG8-955 p 750 N95-16065
NAG9-298 p 810 N95-16148
NAG9-390 p 857 N95-17383
NAG9-45 p 916 N95-16020
NAL PROJ. I-8-119 p 850 N95-16901
NAL PROJ. ID-8-117L p 671 N95-16392
NASA ORDER S-93073-E p 915 N95-17494
NASW-4435 p 780 N95-16031
NASW-4574 p 917 N95-16176
NASW-4627 p 672 N95-16033
NAS1-14101 p 832 N95-16898
NAS1-14472 p 832 N95-16898
NAS1-15810 p 832 N95-16898
NAS1-16394 p 832 N95-16898
NAS1-17070 p 832 N95-16898
NAS1-17130 p 832 N95-16898
NAS1-18107 p 832 N95-16898
NAS1-18450 p 672 N95-16320
NAS1-18585 p 656 N95-17273

NAS1-18605 ..... p 832 N95-16898
p 863 N95-17266
NAS1-19299 ..... p 772 N95-17268
NAS1-19317 ..... p 724 N95-16859
NAS1-19480 ..... p 769 N95-16070
p 769 N95-16071
p 862 N95-16596
p 862 N95-16869
p 862 N95-16896
p 863 N95-16897
p 832 N95-16898
p 863 N95-16904
p 863 N95-17266
p 863 N95-17267
NAS1-19610 ..... p 772 N95-17268
NAS1-19708 ..... p 736 N95-16860
NAS1-756 ..... p 788 N95-17492
NAS10-11624 ..... p 809 N95-16743
NAS15-10000 ..... p 710 N95-17331
NAS3-25085 ..... p 898 N95-16598
NAS3-252662-52 ..... p 713 N95-16066
NAS3-25266 ..... p 769 N95-15969
p 785 N95-16416
p 656 N95-16887
p 720 N95-17265
p 787 N95-17270
NAS3-25685 ..... p 722 N95-16905
NAS3-25776 ..... p 755 N95-16886
NAS3-26253 ..... p 719 N95-16347
NAS3-26764 ..... p 784 N95-17385
NAS3-26839 ..... p 785 N95-16072
NAS3-27186 ..... p 711 N95-15968
p 711 N95-16044
p 787 N95-16911
p 781 N95-17263
p 772 N95-17386
NAS5-27772 ..... p 675 N95-17573
NAS5-29298 ..... p 688 N95-17241
NAS5-31331 ..... p 837 N95-16587
NAS5-31347 ..... p 910 N95-17323
NAS5-31348 ..... p 911 N95-17325
p 858 N95-17921
NAS5-31354 ..... p 911 N95-17329
NAS5-31500 ..... p 687 N95-17237
p 694 N95-17546
NAS5-31739 ..... p 674 N95-17553
NAS5-32337 ..... p 910 N95-17322
p 910 N95-17323
p 840 N95-17324
p 911 N95-17325
p 911 N95-17326
p 840 N95-17327
p 911 N95-17328
p 911 N95-17329
p 911 N95-17330
p 912 N95-17491
p 912 N95-17652
p 858 N95-17921
NAS7-1156 ..... p 680 N95-17199
NAS8-37800 ..... p 717 N95-16334
NAS8-38100 ..... p 715 N95-16326
p 717 N95-16335
NAS8-38772 ..... p 798 N95-15965
NAS8-39131 ..... p 793 N95-16575
NAS8-39380 ..... p 788 N95-17272
NAS9-17267 ..... p 809 N95-16745
NCC1-68 ..... p 668 N95-16899
NCC2-101 ..... p 807 N95-15961
NCC2-374 ..... p 772 N95-17418
p 675 N95-17493
NCC2-5061 ..... p 655 N95-16589
NCC2-5087 ..... p 923 N95-17653
NCC2-838 ..... p 688 N95-17241
NCC3-181 ..... p 670 N95-17402
NCC3-233 ..... p 770 N95-16407
p 771 N95-16855
p 773 N95-17656
NCC3-319 ..... p 760 N95-17651
NCC3-365 ..... p 654 N95-17657
NCC8-47 ..... p 666 N95-15971
NCC9-16 ..... p 836 N95-16574
NOAA-50-DGNE-1-00138 ..... p 672 N95-16033
NR PROJ. M00-001 ..... p 821 N95-16619
NR PROJ. M51-007 ..... p 753 N95-16227
NR PROJ. RH2-1-C-17 ..... p 903 N95-16877
NR PROJ. RR0-3103 ..... p 751 N95-16002
NSERC-OGP-0008111 ..... p 862 N95-16596
NSF AST-91-23777 ..... p 915 N95-17496
NSF CCR-88-20279 ..... p 863 N95-17431
NSF CCR-89-57604 ..... p 859 N95-15949
p 859 N95-15950
p 859 N95-15951
NSF CCR-90-24954 ..... p 862 N95-16596
NSF CCR-91-19319 ..... p 849 N95-16603
NSF CCR-93-57793 ..... p 838 N95-16850
NSF CDA-87-22788 ..... p 844 N95-15940
NSF CDA-88-22724 ..... p 859 N95-15948
p 859 N95-15951
p 864 N95-16039
p 833 N95-16040
NSF DMS-91-03297 ..... p 860 N95-16291
NSF DMS-92-11820 ..... p 863 N95-16904
NSF INT-91-16781 ..... p 839 N95-17261
NSF IRI-90-03841 ..... p 839 N95-16883
NSF IRI-90-10686 ..... p 840 N95-17432
NSF IRI-91-57643 ..... p 840 N95-17432
NSF IRI-92-13234 ..... p 854 N95-15986
NSF IRI-92-13993 ..... p 840 N95-17432
NSF IRI-93-13367 ..... p 857 N95-16820
NSF IRI-94-96187 ..... p 853 N95-15981
NSF MIP-90-01651 ..... p 846 N95-16237
NSF MSS-90-22513 ..... p 854 N95-15986
NSF MSS-90-25110 ..... p 863 N95-17431
NUWC PROJ. B96420 ..... p 871 N95-17177
NWO-900-538-016 ..... p 887 N95-17483
N00014-85-C-0710 ..... p 835 N95-16234
N00014-89-F-0101 ..... p 737 N95-17616
N00014-89-J-1041 ..... p 739 N95-16000
N00014-89-J-1145 ..... p 747 N95-17685
N00014-89-J-1225 ..... p 746 N95-17485
N00014-89-J-1423 ..... p 797 N95-17740
N00014-89-J-1545 ..... p 900 N95-17137
p 900 N95-17171
N00014-89-J-1631 ..... p 898 N95-16527
N00014-89-J-1828 ..... p 874 N95-16797
p 744 N95-16865
p 730 N95-16866
p 878 N95-17692
N00014-89-J-1975 ..... p 827 N95-16518
N00014-89-J-3062 ..... p 743 N95-16628
p 874 N95-16629
p 743 N95-16630
p 743 N95-16783
p 874 N95-16784
p 874 N95-16799
N00014-89-J-3221 ..... p 806 N95-17505
N00014-90-J-1025 ..... p 860 N95-16127
p 860 N95-16128
N00014-90-J-1030 ..... p 861 N95-16379
p 863 N95-17431
N00014-90-J-1148 ..... p 742 N95-16427
N00014-90-J-1230 ..... p 868 N95-16162
N00014-90-J-1263 ..... p 902 N95-17711
p 904 N95-17712
N00014-90-J-1270 ..... p 762 N95-16089
N00014-90-J-1332 ..... p 729 N95-16627
N00014-90-J-1370 ..... p 894 N95-16012
N00014-90-J-1427 ..... p 898 N95-16532
N00014-90-J-1466 ..... p 923 N95-16080
p 923 N95-17723
N00014-90-J-1700 ..... p 726 N95-16001
N00014-90-J-1948 ..... p 726 N95-16017
N00014-90-J-4063 ..... p 771 N95-16616
N00014-90-J-4107 ..... p 898 N95-16623
N00014-90-K-2003 ..... p 778 N95-17337
N00014-91-C-0001 ..... p 713 N95-16312
p 715 N95-16324
N00014-91-C-0019 ..... p 838 N95-16852
N00014-91-C-0130 ..... p 840 N95-17338
N00014-91-C-0219 ..... p 902 N95-16075
N00014-91-C-0257 ..... p 858 N95-17459
N00014-91-J-1035 ..... p 747 N95-17682
N00014-91-J-1058 ..... p 729 N95-16635
N00014-91-J-1270 ..... p 835 N95-16236
N00014-91-J-1274 ..... p 740 N95-16092
N00014-91-J-1299 ..... p 738 N95-17663
N00014-91-J-1307 ..... p 742 N95-16488
N00014-91-J-1338 ..... p 741 N95-16354
N00014-91-J-1414 ..... p 733 N95-16104
N00014-91-J-1475 ..... p 741 N95-16409
N00014-91-J-1577 ..... p 855 N95-16095
N00014-91-J-1613 ..... p 836 N95-16452
p 851 N95-17741
N00014-91-J-1641 ..... p 728 N95-16406
N00014-91-J-1771 ..... p 772 N95-17506
N00014-91-J-1784 ..... p 818 N95-16112
N00014-91-J-1786 ..... p 743 N95-16507
N00014-91-J-1875 ..... p 723 N95-16415
N00014-91-J-1919 ..... p 895 N95-16238
p 872 N95-16241
N00014-91-J-1956 ..... p 767 N95-17433
N00014-91-J-4016 ..... p 863 N95-16904
N00014-92-J-1173 ..... p 829 N95-16119
p 827 N95-16518
N00014-92-J-1186 ..... p 898 N95-16525
N00014-92-J-1264 ..... p 865 N95-16546
N00014-92-J-1344 ..... p 894 N95-16106
N00014-92-J-1477 ..... p 894 N95-16084
N00014-92-J-1500 ..... p 743 N95-16625
N00014-92-J-1512 ..... p 839 N95-16883
N00014-92-J-1672 ..... p 844 N95-15940
N00014-92-J-1673 ..... p 792 N95-16303
N00014-92-J-1720 ..... p 730 N95-16973
N00014-92-J-1752 ..... p 898 N95-16533
N00014-92-J-1801 ..... p 738 N95-17681
p 845 N95-16082
p 845 N95-16083
p 845 N95-16113
N00014-92-J-1879 ..... p 835 N95-16236
N00014-92-J-1962 ..... p 725 N95-17457
N00014-92-J-1976 ..... p 667 N95-16565
N00014-92-J-1996 ..... p 729 N95-16622
N00014-92-J-4089 ..... p 736 N95-16793
N00014-92-J-4097 ..... p 846 N95-16237
N00014-92-J-4109 ..... p 804 N95-16124
p 804 N95-16125
N00014-92-J-4112 ..... p 804 N95-16125
N00014-93-C-0177 ..... p 880 N95-17499
N00014-93-C-0234 ..... p 839 N95-17172
N00014-93-C-0240 ..... p 805 N95-16141
N00014-93-WX-24290 ..... p 733 N95-16091
p 735 N95-16788
N00014-93-1-0015 ..... p 773 N95-17708
N00014-93-1-0058 ..... p 745 N95-17434
N00014-93-1-0332 ..... p 831 N95-16966
N00014-93-1-0342 ..... p 772 N95-17165
N00014-93-1-0563 ..... p 897 N95-16445
p 873 N95-16482
p 734 N95-16505
p 897 N95-16508
N00014-93-1-0654 ..... p 730 N95-16955
N00014-93-1-0665 ..... p 805 N95-16168
N00014-93-1-0754 ..... p 804 N95-16079
N00014-93-1-0779 ..... p 898 N95-16525
N00014-93-1-0827 ..... p 900 N95-16928
N00014-93-1-1127 ..... p 792 N95-16506
N00014-93-1-1343 ..... p 832 N95-16876
N00014-94-C-0019 ..... p 725 N95-16974
N00014-94-I-0101 ..... p 743 N95-16500
p 743 N95-16501
N00014-94-I-0198 ..... p 849 N95-16529
N00014-94-J-0063 ..... p 870 N95-16810
N00014-94-WX-23074 ..... p 877 N95-17630
N00014-94-1-0018 ..... p 890 N95-16617
N00014-94-1-0101 ..... p 739 N95-15996
p 742 N95-16449
p 742 N95-16450
p 742 N95-16451
N00014-94-1-0150 ..... p 890 N95-16617
N00014-94-1-0194 ..... p 773 N95-17617
N00014-94-1-0367 ..... p 863 N95-17333
N00039-87-C-0182 ..... p 832 N95-16618
N00060-86-C-4971 ..... p 720 N95-16350
N00173-93-P-6207 ..... p 672 N95-16033
N61339-91-D-0001 ..... p 666 N95-16171
N61533-92-K-0030 ..... p 786 N95-16785
N66001-94-C-6037 ..... p 838 N95-16818
N66604-93-D-1119 ..... p 805 N95-16414
N68171-94-M-5319 ..... p 728 N95-16608
OSU PROJ. RF-727376 ..... p 857 N95-17383
PROJ. CEC-JOUR-0078 ..... p 842 N95-17733
PROJ. E27-666 ..... p 831 N95-16894
PROJ. MR0-4101 ..... p 819 N95-16151
PROJ. M00-96 ..... p 818 N95-16105
RFA-85-2 ..... p 727 N95-16373
RICIS PROJ. RB-10 ..... p 836 N95-16574
RTOP 199-16-11-08 ..... p 809 N95-16745
RTOP 199-45-16-11 ..... p 820 N95-16412
p 924 N95-16912
RTOP 233-01-OC ..... p 721 N95-17276
RTOP 233-01-OE ..... p 781 N95-17263
RTOP 233-01-0A ..... p 731 N95-17387
RTOP 233-01-0B ..... p 793 N95-16861
RTOP 233-01-0E ..... p 709 N95-16862
RTOP 233-01-01-05 ..... p 709 N95-16857
RTOP 235-01-0A ..... p 898 N95-16598
p 755 N95-16886
RTOP 310-10-60-50 ..... p 756 N95-17283
RTOP 310-20-65-86-08 ..... p 757 N95-17288
RTOP 310-30-71-83-04 ..... p 757 N95-17286
RTOP 314-30-55-02-07 ..... p 759 N95-17297
RTOP 314-30-56-28-50 ..... p 756 N95-17280
RTOP 314-30-61-02-04 ..... p 756 N95-17284
RTOP 314-30-61-02-10 ..... p 708 N95-17292
RTOP 314-30-61-02-17 ..... p 758 N95-17296
RTOP 314-40-22-12-03 ..... p 756 N95-17281
RTOP 314-40-31-30-03 ..... p 758 N95-17295
RTOP 314-40-52-01-02 ..... p 664 N95-17291
RTOP 315-90-31-00-02 ..... p 756 N95-17282
RTOP 315-91-10-13-08 ..... p 757 N95-17287
RTOP 315-91-40-20-26 ..... p 758 N95-17293
p 758 N95-17294
RTOP 315-91-40-20-29 ..... p 758 N95-17290
RTOP 315-91-40-20-35 ..... p 757 N95-17285
RTOP 315-91-40-20-36 ..... p 757 N95-17289
RTOP 323-15-03 ..... p 711 N95-16044
RTOP 323-41-22 ..... p 720 N95-17269
RTOP 323-42-04 ..... p 784 N95-17385

RTOP 324-01-00 ..... p 785 N95-16072
RTOP 468-01-11 ..... p 721 N95-17274
RTOP 478-43-00 ..... p 711 N95-15968
RTOP 500-00-00 ..... p 676 N95-17179
p 691 N95-17531
RTOP 505-59-10-31 ..... p 656 N95-16908
RTOP 505-59-30-01 ..... p 655 N95-16069
RTOP 505-59-54-01 ..... p 656 N95-17273
RTOP 505-62-0X ..... p 669 N95-15970
RTOP 505-62-10 ..... p 787 N95-16911
RTOP 505-62-36 ..... p 781 N95-16907
RTOP 505-62-52 ..... p 713 N95-16066
p 862 N95-16885
p 772 N95-16903
p 839 N95-16906
p 839 N95-17264
p 670 N95-17402
RTOP 505-63-1A ..... p 722 N95-16905
RTOP 505-63-12 ..... p 789 N95-17658
p 725 N95-17659
RTOP 505-63-36-01 ..... p 669 N95-17397
RTOP 505-63-40 ..... p 788 N95-17490
RTOP 505-63-5B ..... p 785 N95-16416
p 789 N95-17701
RTOP 505-63-50-13 ..... p 653 N95-16560
RTOP 505-64-13-04 ..... p 665 N95-17384
RTOP 505-68-00 ..... p 656 N95-16858
RTOP 505-68-53 ..... p 772 N95-17418
RTOP 505-69-50 ..... p 656 N95-16887
p 840 N95-17420
RTOP 505-70-63 ..... p 788 N95-17417
RTOP 505-90-5K ..... p 770 N95-16407
p 771 N95-16855
p 773 N95-17656
RTOP 505-90-51 ..... p 769 N95-15969
RTOP 505-90-52-01 ..... p 769 N95-16070
p 769 N95-16071
p 862 N95-16596
p 862 N95-16869
p 862 N95-16896
p 863 N95-16897
p 832 N95-16898
p 863 N95-16904
p 863 N95-17266
p 863 N95-17267
RTOP 505-90-53 ..... p 846 N95-16453
p 772 N95-17386
RTOP 506-41-41 ..... p 709 N95-17275
RTOP 506-42-31 ..... p 720 N95-17265
RTOP 506-43-41-02 ..... p 709 N95-16559
RTOP 506-59-61-01 ..... p 709 N95-16902
RTOP 510-02-12 ..... p 787 N95-17270
RTOP 510-02-13-01 ..... p 724 N95-16859
RTOP 537-02-20 ..... p 775 N95-16910
RTOP 537-02-23 ..... p 654 N95-16038
RTOP 537-06-20-06 ..... p 736 N95-16860
RTOP 538-03-11 ..... p 786 N95-16588
RTOP 538-05-15-01 ..... p 772 N95-17268
RTOP 546-99-00 ..... p 786 N95-16577
RTOP 584-03-11 ..... p 784 N95-16068
RTOP 586-03-11-11 ..... p 886 N95-17271
RTOP 656-65-07 ..... p 910 N95-17322
p 910 N95-17323
p 840 N95-17324
p 911 N95-17325
p 911 N95-17326
p 840 N95-17327
p 911 N95-17328
p 911 N95-17329
p 911 N95-17330
p 912 N95-17652
p 858 N95-17921
RTOP 920-00-00 ..... p 837 N95-16587
RTOP 963-60-OD ..... p 750 N95-17893
RTOP 963-70-OH ..... p 654 N95-17657
RTOP-656-65-07 ..... p 912 N95-17491
USRA-C-5555-02 ..... p 911 N95-17328
USRA-C-5555-03 ..... p 911 N95-17330
USRA-C-5555-04 ..... p 911 N95-17330
USRA-C-5555-06 ..... p 911 N95-17326
USRA-C-5555-07 ..... p 840 N95-17327
USRA-C-5555-08 ..... p 910 N95-17323
USRA-C-5555-09 ..... p 912 N95-17652
USRA-C-5555-11 ..... p 911 N95-17329
USRA-C-5555-14 ..... p 910 N95-17322
USRA-C-5555-15 ..... p 840 N95-17324
USRA-C-5555-31 ..... p 912 N95-17491
USRA-C-5555-32 ..... p 911 N95-17325
p 858 N95-17921
W-31-109-ENG-38 ..... p 879 N95-16030
p 889 N95-16307
p 880 N95-16308
p 727 N95-16363
p 734 N95-16364
p 800 N95-16398
p 897 N95-16408
p 728 N95-16426
p 873 N95-16430
p 728 N95-16485
p 873 N95-16487
p 771 N95-16828
p 910 N95-16922
p 839 N95-16923
p 875 N95-16924
p 766 N95-16945
p 900 N95-16946
p 876 N95-16962
p 766 N95-16963
p 665 N95-16964
p 745 N95-17160
p 863 N95-17306
p 901 N95-17349
p 901 N95-17350
p 772 N95-17523
p 902 N95-17898
p 878 N95-17899
p 893 N95-17900
p 882 N95-17901
p 882 N95-17902
p 882 N95-17924
p 904 N95-17925
p 761 N95-17926
W-7405-ENG-36 ..... p 879 N95-16172
p 879 N95-16217
p 838 N95-16218
p 834 N95-16219
p 835 N95-16223
p 780 N95-16224
p 763 N95-16283
p 889 N95-16285
p 889 N95-16286
p 868 N95-16288
p 896 N95-16389
p 903 N95-16428
p 798 N95-16537
p 765 N95-16920
p 799 N95-16927
p 875 N95-16931
p 765 N95-16932
p 875 N95-16933
p 891 N95-16936
p 880 N95-16937
p 745 N95-16938
p 876 N95-17153
p 876 N95-17154
p 891 N95-17155
p 900 N95-17156
p 731 N95-17157
p 876 N95-17158
p 891 N95-17365
p 737 N95-17641
p 881 N95-17721
p 878 N95-17727
p 748 N95-17892
W-7405-ENG-48 ..... p 770 N95-16211
p 834 N95-16220
p 860 N95-16221
p 884 N95-16366
p 861 N95-16535
p 836 N95-16536
p 749 N95-16542
p 889 N95-16554
p 899 N95-16867
p 765 N95-16915
p 765 N95-16925
p 777 N95-16929
p 745 N95-16935
p 777 N95-17168
p 710 N95-17359
p 736 N95-17378
p 745 N95-17379
p 775 N95-17380
p 892 N95-17497
p 776 N95-17522
p 916 N95-17525
p 778 N95-17627
p 779 N95-17635
p 796 N95-17636
p 732 N95-17639
p 892 N95-17640
p 732 N95-17642
p 779 N95-17688
p 779 N95-17689
p 782 N95-17717
p 797 N95-17718
p 751 N95-17738
p 902 N95-17742
p 722 N95-17745
p 893 N95-17897
p 749 N95-17919
p 797 N95-17920
p 797 N95-17922
W-7405-ENG-82 ..... p 722 N95-16058
p 897 N95-16510
p 783 N95-16538
p 735 N95-16540

Typical Report Number Index Listing

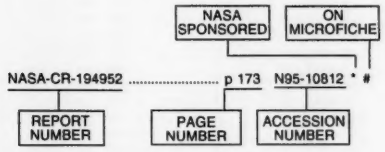

Listings in this index are arranged alphanumerically by report number. The accession number denotes the number by which the citation is identified. The page number helps to locate the citation in the abstract section. An asterisk (*) indicates that the item is a NASA report. A pound sign (#) indicates that the item is available on microfiche.

AD-A260738 ..... p 909 N95-16845
AD-A268726 ..... p 909 N95-16845
AD-A279759 ..... p 737 N95-17616 #
AD-A280703 ..... p 738 N95-17681
AD-A280704 ..... p 747 N95-17682
AD-A280752 ..... p 804 N95-16103 #
AD-A280754 ..... p 733 N95-16104 #
AD-A280755 ..... p 818 N95-16105 #
AD-A280760 ..... p 804 N95-16118 #
AD-A280762 ..... p 829 N95-16119 #
AD-A280813 ..... p 797 N95-17740
AD-A280843 ..... p 753 N95-16148 #
AD-A280867 ..... p 834 N95-16149 #
AD-A280892 ..... p 727 N95-16150 #
AD-A280897 ..... p 819 N95-16151 #
AD-A280900 ..... p 819 N95-16152 #
AD-A280901 ..... p 743 N95-16500 #
AD-A280902 ..... p 743 N95-16501 #
AD-A280905 ..... p 785 N95-16502 #
AD-A280907 ..... p 656 N95-16824 #
AD-A280909 ..... p 851 N95-17741
AD-A280915 ..... p 836 N95-16503 #
AD-A280916 ..... p 836 N95-16504 #
AD-A280936 ..... p 734 N95-16505
AD-A280974 ..... p 792 N95-16506 #
AD-A280975 ..... p 743 N95-16507 #
AD-A280976 ..... p 897 N95-16508 #
AD-A280977 ..... p 821 N95-16481 #
AD-A280979 ..... p 873 N95-16482 #
AD-A280980 ..... p 742 N95-16483 #
AD-A280981 ..... p 821 N95-16484 #
AD-A280982 ..... p 821 N95-16515 #
AD-A280986 ..... p 898 N95-16525 #
AD-A280987 ..... p 898 N95-16532 #
AD-A280988 ..... p 898 N95-16533 #
AD-A280989 ..... p 751 N95-15993 #
AD-A280990 ..... p 654 N95-15994 #
AD-A280992 ..... p 833 N95-15995 #
AD-A280994 ..... p 739 N95-15996 #
AD-A280996 ..... p 833 N95-15997 #
AD-A281001 ..... p 908 N95-15998 #
AD-A281004 ..... p 884 N95-15999 #
AD-A281010 ..... p 739 N95-16000 #
AD-A281011 ..... p 726 N95-16001 #
AD-A281014 ..... p 751 N95-16002 #
AD-A281017 ..... p 833 N95-16003 #
AD-A281019 ..... p 833 N95-16004 #
AD-A281021 ..... p 675 N95-16005 #
AD-A281022 ..... p 885 N95-16443 #
AD-A281023 ..... p 820 N95-16444 #
AD-A281024 ..... p 897 N95-16445 #
AD-A281026 ..... p 835 N95-16446 #
AD-A281028 ..... p 835 N95-16447 #
AD-A281035 ..... p 754 N95-16448 #
AD-A281040 ..... p 742 N95-16449 #
AD-A281041 ..... p 742 N95-16450 #
AD-A281042 ..... p 742 N95-16451 #
AD-A281044 ..... p 836 N95-16452 #
AD-A281046 ..... p 729 N95-16622 #
AD-A281047 ..... p 898 N95-16623 #
AD-A281053 ..... p 754 N95-16624 #
AD-A281060 ..... p 743 N95-16625 #
AD-A281063 ..... p 837 N95-16626 #
AD-A281066 ..... p 736 N95-16793 #
AD-A281075 ..... p 655 N95-16808 #
AD-A281078 ..... p 755 N95-16825 #
AD-A281080 ..... p 833 N95-16088 * #
AD-A281081 ..... p 762 N95-16089 #
AD-A281101 ..... p 908 N95-15957 #
AD-A281102 ..... p 908 N95-16090 #
AD-A281109 ..... p 733 N95-16091 #
AD-A281123 ..... p 740 N95-16092 #
AD-A281124 ..... p 821 N95-16809 #
AD-A281130 ..... p 870 N95-16810 #
AD-A281134 ..... p 850 N95-16826 #
AD-A281135 ..... p 837 N95-16602 #
AD-A281136 ..... p 849 N95-16603 #
AD-A281137 ..... p 735 N95-16606 #
AD-A281165 ..... p 729 N95-16627 #
AD-A281172 ..... p 796 N95-17684 #
AD-A281174 ..... p 743 N95-16628 #
AD-A281177 ..... p 874 N95-16629 #
AD-A281179 ..... p 743 N95-16630 #
AD-A281181 ..... p 857 N95-16631 #
AD-A281186 ..... p 838 N95-16632 #
AD-A281195 ..... p 754 N95-16794 #
AD-A281199 ..... p 886 N95-16795 #
AD-A281204 ..... p 821 N95-16796 #
AD-A281205 ..... p 874 N95-16797 #
AD-A281213 ..... p 862 N95-16798 #
AD-A281214 ..... p 747 N95-17685 #
AD-A281223 ..... p 802 N95-17686
AD-A281293 ..... p 874 N95-16799 #
AD-A281294 ..... p 743 N95-16783 #
AD-A281295 ..... p 874 N95-16784 #
AD-A281298 ..... p 786 N95-16785 #
AD-A281301 ..... p 735 N95-16786 #
AD-A281304 ..... p 885 N95-16787 #
AD-A281305 ..... p 735 N95-16788 #
AD-A281308 ..... p 899 N95-16789
AD-A281311 ..... p 729 N95-16790
AD-A281312 ..... p 726 N95-16008
AD-A281313 ..... p 884 N95-16009
AD-A281336 ..... p 825 N95-16010 #
AD-A281337 ..... p 855 N95-16011 #
AD-A281338 ..... p 894 N95-16012 #
AD-A281339 ..... p 739 N95-16013 #
AD-A281347 ..... p 908 N95-16014
AD-A281350 ..... p 884 N95-16015 #
AD-A281352 ..... p 723 N95-16016 #
AD-A281367 ..... p 726 N95-16017
AD-A281369 ..... p 871 N95-16018 #
AD-A281370 ..... p 723 N95-16019 #
AD-A281372 ..... p 834 N95-16153 #
AD-A281373 ..... p 834 N95-16154
AD-A281374 ..... p 872 N95-16155
AD-A281376 ..... p 770 N95-16156
AD-A281382 ..... p 884 N95-16157 #
AD-A281383 ..... p 895 N95-16158 #
AD-A281385 ..... p 763 N95-16159 #
AD-A281386 ..... p 655 N95-16160 #
AD-A281394 ..... p 729 N95-16791
AD-A281395 ..... p 744 N95-16792
AD-A281396 ..... p 755 N95-16800
AD-A281397 ..... p 744 N95-16863
AD-A281399 ..... p 857 N95-16864 #
AD-A281402 ..... p 744 N95-16865 #
AD-A281403 ..... p 730 N95-16866 #
AD-A281406 ..... p 901 N95-17424
AD-A281407 ..... p 731 N95-17425
AD-A281408 ..... p 865 N95-17426
AD-A281410 ..... p 884 N95-16161 #
AD-A281411 ..... p 868 N95-16162 #
AD-A281412 ..... p 770 N95-16163 #
AD-A281413 ..... p 807 N95-16164 #
AD-A281414 ..... p 740 N95-16165
AD-A281415 ..... p 776 N95-16166 #
AD-A281447 ..... p 883 N95-15958
AD-A281448 ..... p 825 N95-15959
AD-A281450 ..... p 902 N95-16075
AD-A281452 ..... p 655 N95-16076
AD-A281457 ..... p 855 N95-16077
AD-A281458 ..... p 804 N95-16078
AD-A281459 ..... p 804 N95-16079
AD-A281463 ..... p 923 N95-16080
AD-A281464 ..... p 894 N95-16081
AD-A281467 ..... p 845 N95-16082
AD-A281468 ..... p 845 N95-16083
AD-A281469 ..... p 894 N95-16084
AD-A281470 ..... p 740 N95-16085
AD-A281500 ..... p 908 N95-16086
AD-A281505 ..... p 855 N95-16095
AD-A281506 ..... p 834 N95-16167 #
AD-A281507 ..... p 805 N95-16168 #
AD-A281508 ..... p 740 N95-16096
AD-A281520 ..... p 752 N95-16097
AD-A281522 ..... p 872 N95-16098
AD-A281526 ..... p 655 N95-16099
AD-A281527 ..... p 894 N95-16106
AD-A281528 ..... p 834 N95-16107
AD-A281531 ..... p 859 N95-16108
AD-A281532 ..... p 722 N95-16087
AD-A281534 ..... p 670 N95-16109
AD-A281535 ..... p 762 N95-16110
AD-A281536 ..... p 860 N95-16169
AD-A281544 ..... p 856 N95-16390
AD-A281546 ..... p 896 N95-16391
AD-A281547 ..... p 741 N95-16393
AD-A281548 ..... p 763 N95-16394
AD-A281550 ..... p 855 N95-16170 #
AD-A281551 ..... p 861 N95-16395
AD-A281553 ..... p 896 N95-16396
AD-A281556 ..... p 763 N95-16136
AD-A281563 ..... p 783 N95-16421
AD-A281580 ..... p 666 N95-16171 #
AD-A281591 ..... p 722 N95-16100 #
AD-A281592 ..... p 740 N95-16101 #
AD-A281594 ..... p 909 N95-16431 #
AD-A281595 ..... p 894 N95-16111 #
AD-A281612 ..... p 785 N95-16102 #
AD-A281613 ..... p 818 N95-16112 #
AD-A281628 ..... p 845 N95-16113 #
AD-A281631 ..... p 895 N95-16114 #
AD-A281637 ..... p 845 N95-16115
AD-A281639 ..... p 845 N95-16116
AD-A281643 ..... p 752 N95-16117 #
AD-A281647 ..... p 723 N95-16397
AD-A281664 ..... p 886 N95-16965 #
AD-A281722 ..... p 902 N95-17705
AD-A281736 ..... p 857 N95-17369
AD-A281737 ..... p 857 N95-17370
AD-A281770 ..... p 878 N95-17692
AD-A281790 ..... p 801 N95-17164 #
AD-A281793 ..... p 864 N95-16422 #
AD-A281795 ..... p 776 N95-16353 #
AD-A281805 ..... p 741 N95-16354 #
AD-A281830 ..... p 820 N95-16360 #
AD-A281839 ..... p 896 N95-16365 #
AD-A281842 ..... p 856 N95-16372 #
AD-A281846 ..... p 820 N95-16423 #
AD-A281848 ..... p 741 N95-16355 #
AD-A281854 ..... p 819 N95-16297 #
AD-A281855 ..... p 826 N95-16298 #
AD-A281859 ..... p 826 N95-16299 #
AD-A281864 ..... p 753 N95-16300 #
AD-A281866 ..... p 826 N95-16301 #
AD-A281869 ..... p 827 N95-16433 #
AD-A281871 ..... p 666 N95-16356 #
AD-A281875 ..... p 742 N95-16434 #
AD-A281955 ..... p 741 N95-16409
AD-A281958 ..... p 763 N95-16410
AD-A281959 ..... p 873 N95-16411
AD-A281962 ..... p 870 N95-16413
AD-A281965 ..... p 805 N95-16414
AD-A281975 ..... p 880 N95-17499
AD-A281976 ..... p 746 N95-17485
AD-A281980 ..... p 892 N95-17442
AD-A281984 ..... p 802 N95-17443
AD-A281985 ..... p 672 N95-17444
AD-A281998 ..... p 841 N95-17445
AD-A282000 ..... p 799 N95-17446

AD-A282003 p 837 N95-16607 #
AD-A282005 p 828 N95-17447
AD-A282006 p 721 N95-17448
AD-A282007 p 778 N95-17500
AD-A282008 p 760 N95-17501
AD-A282009 p 869 N95-17449
AD-A282107 p 672 N95-17427
AD-A282128 p 728 N95-16608
AD-A282153 p 759 N95-17450
AD-A282267 p 794 N95-16954
AD-A282270 p 835 N95-16234
AD-A282271 p 742 N95-16427
AD-A282278 p 790 N95-17372
AD-A282283 p 800 N95-16235
AD-A282285 p 835 N95-16236
AD-A282286 p 846 N95-16237
AD-A282294 p 895 N95-16238
AD-A282298 p 770 N95-16239
AD-A282300 p 753 N95-16240
AD-A282329 p 844 N95-16060 #
AD-A282330 p 872 N95-16241
AD-A282332 p 909 N95-16374
AD-A282333 p 774 N95-16242
AD-A282335 p 730 N95-16973
AD-A282336 p 665 N95-16375
AD-A282337 p 723 N95-16415
AD-A282339 p 725 N95-16974
AD-A282340 p 772 N95-17165
AD-A282342 p 806 N95-17505
AD-A282343 p 900 N95-17171
AD-A282349 p 910 N95-17166
AD-A282396 p 844 N95-16061 #
AD-A282402 p 803 N95-16062 #
AD-A282404 p 725 N95-17457
AD-A282405 p 772 N95-17506
AD-A282412 p 784 N95-17507
AD-A282414 p 858 N95-17458
AD-A282417 p 858 N95-17459
AD-A282422 p 666 N95-17508
AD-A282429 p 676 N95-17509
AD-A282430 p 841 N95-17460
AD-A282431 p 788 N95-17510
AD-A282432 p 791 N95-17511
AD-A282433 p 737 N95-17486
AD-A282449 p 861 N95-16376
AD-A282450 p 826 N95-16377
AD-A282452 p 820 N95-16378
AD-A282460 p 713 N95-16302
AD-A282462 p 792 N95-16303
AD-A282479 p 665 N95-17373
AD-A282525 p 850 N95-17374
AD-A282667 p 790 N95-17375
AD-A282684 p 708 N95-16304
AD-A282697 p 831 N95-16966 #
AD-A282707 p 909 N95-16305
AD-A282711 p 835 N95-16306
AD-A282712 p 861 N95-16379
AD-A282714 p 734 N95-16380
AD-A282715 p 671 N95-16381
AD-A282718 p 909 N95-16382
AD-A282720 p 900 N95-16928
AD-A282721 p 727 N95-16384
AD-A282722 p 766 N95-17139
AD-A282726 p 730 N95-17140
AD-A282730 p 730 N95-17141
AD-A282751 p 806 N95-17477
AD-A282766 p 900 N95-17137
AD-A282767 p 731 N95-17142
AD-A282781 p 886 N95-17143
AD-A282787 p 666 N95-17706
AD-A282845 p 865 N95-17377
AD-A282846 p 865 N95-17429
AD-A282847 p 782 N95-17430
AD-A282849 p 863 N95-17431
AD-A282854 p 840 N95-17432
AD-A282871 p 767 N95-17433
AD-A282872 p 745 N95-17434
AD-A282873 p 773 N95-17617
AD-A282878 p 864 N95-17618
AD-A282880 p 881 N95-17619
AD-A282905 p 901 N95-17620
AD-A282911 p 737 N95-17398
AD-A282957 p 782 N95-17621 #
AD-A282958 p 710 N95-17622 #
AD-A282966 p 669 N95-17661 #
AD-A282969 p 746 N95-17662 #
AD-A282970 p 738 N95-17663 #
AD-A282971 p 738 N95-17664 #
AD-A282976 p 887 N95-17707 #
AD-A282986 p 773 N95-17708 #
AD-A283012 p 803 N95-17709 #
AD-A283015 p 912 N95-17710 #
AD-A283028 p 902 N95-17711 #
AD-A283040 p 904 N95-17712
AD-A283077 p 864 N95-17713 #
AD-A283078 p 863 N95-17333 #
AD-A283081 p 886 N95-17334 #
AD-A283088 p 781 N95-17335
AD-A283090 p 759 N95-17336
AD-A283091 p 778 N95-17337
AD-A283103 p 840 N95-17338
AD-A283105 p 801 N95-17339
AD-A283171 p 886 N95-17340 #
AD-A283173 p 865 N95-17341 #
AD-A283180 p 822 N95-17342 #
AD-A283190 p 818 N95-17714 #
AD-A283193 p 877 N95-17630 #
AD-A283207 p 669 N95-17631 #
AD-A283209 p 892 N95-17623
AD-A283213 p 751 N95-17632 #
AD-A283218 p 912 N95-17633 #
AD-A283257 p 858 N95-17634 #
AD-A283274 p 803 N95-17715 #
AD-A283275 p 923 N95-17723 #
AD-A283291 p 748 N95-17724 #
AD-A283380 p 806 N95-17624
AD-A283392 p 844 N95-15940
AD-A283396 p 791 N95-17625
AD-A283398 p 656 N95-17435
AD-A283401 p 759 N95-17436
AD-A283418 p 721 N95-17626
AD-A283524 p 777 N95-17303 #
AD-A283832 p 755 N95-16841 #
AD-A284264 p 839 N95-17172
AD-A284265 p 767 N95-17487 #
AD-A284266 p 730 N95-16955 #
AD-A284273 p 802 N95-17488
AD-A284279 p 887 N95-17489 #
AD-A284283 p 755 N95-16956 #
AD-A284284 p 752 N95-16123 #
AD-A284285 p 884 N95-16133 #
AD-A284300 p 831 N95-17484 #
AD-A284307 p 755 N95-17173
AD-A284471 p 895 N95-16134 #
AD-A284472 p 819 N95-16135 #
AD-A284737 p 795 N95-16545
AD-A284741 p 865 N95-16546 #
AD-A284742 p 790 N95-16547 #
AD-A284743 p 777 N95-16548 #
AD-A284747 p 856 N95-16550 #
AD-A284749 p 800 N95-16551 #
AD-A284750 p 830 N95-16553
AD-A284780 p 730 N95-16882
AD-A284925 p 763 N95-16137 #
AD-A284926 p 825 N95-16138 #
AD-A284927 p 780 N95-16139 #
AD-A284928 p 826 N95-16140 #
AD-A284932 p 805 N95-16141 #
AD-A284933 p 726 N95-16142 #
AD-A284944 p 723 N95-16041 #
AD-A284945 p 726 N95-16042 #
AD-A284950 p 894 N95-16043 #
AD-A284951 p 752 N95-16143 #
AD-A284954 p 804 N95-16124 #
AD-A284955 p 804 N95-16125 #
AD-A284959 p 723 N95-16126 #
AD-A284960 p 860 N95-16127 #
AD-A284961 p 860 N95-16128 #
AD-A284962 p 752 N95-16129 #
AD-A284963 p 762 N95-16130 #
AD-A284969 p 708 N95-16131 #
AD-A284970 p 818 N95-16132 #
AD-A284971 p 869 N95-16226 #
AD-A284973 p 753 N95-16227 #
AD-A284974 p 819 N95-16228 #
AD-A284976 p 838 N95-16634 #
AD-A284978 p 734 N95-16229 #
AD-A284983 p 741 N95-16230 #
AD-A284987 p 753 N95-16231 #
AD-A284989 p 753 N95-16232 #
AD-A285064 p 826 N95-16368 #
AD-A285066 p 741 N95-16369
AD-A285067 p 729 N95-16635 #
AD-A285068 p 742 N95-16488 #
AD-A285071 p 903 N95-16489 #
AD-A285073 p 836 N95-16490 #
AD-A285074 p 821 N95-16491 #
AD-A285075 p 724 N95-16492 #
AD-A285076 p 873 N95-16493 #
AD-A285077 p 885 N95-16494 #
AD-A285078 p 754 N95-16495 #
AD-A285079 p 874 N95-16496
AD-A285085 p 818 N95-17666
AD-A285086 p 728 N95-16497 #
AD-A285089 p 897 N95-16498 #
AD-A285090 p 749 N95-16499 #
AD-A285115 p 672 N95-16842
AD-A285137 p 827 N95-16615 #
AD-A285143 p 787 N95-16843 #
AD-A285145 p 744 N95-16844 #
AD-A285148 p 909 N95-16845
AD-A285151 p 729 N95-16846 #
AD-A285157 p 822 N95-16847 #
AD-A285159 p 899 N95-16849 #
AD-A285162 p 838 N95-16850 #
AD-A285164 p 822 N95-16851 #
AD-A285170 p 838 N95-16852 #
AD-A285174 p 750 N95-16853 #
AD-A285176 p 765 N95-16834 #
AD-A285177 p 727 N95-16144 #
AD-A285181 p 829 N95-16145 #
AD-A285182 p 870 N95-16811 #
AD-A285186 p 822 N95-16871 #
AD-A285187 p 752 N95-16146 #
AD-A285190 p 664 N95-16404 #
AD-A285191 p 820 N95-16405 #
AD-A285193 p 799 N95-16872 #
AD-A285199 p 829 N95-16147 #
AD-A285208 p 764 N95-16516 #
AD-A285209 p 861 N95-16517 #
AD-A285210 p 830 N95-16813 #
AD-A285211 p 827 N95-16518 #
AD-A285212 p 735 N95-16519 #
AD-A285213 p 827 N95-16520 #
AD-A285218 p 798 N95-16521 #
AD-A285219 p 764 N95-16522 #
AD-A285223 p 874 N95-16523 #
AD-A285225 p 885 N95-16524 #
AD-A285230 p 898 N95-16526 #
AD-A285231 p 898 N95-16527 #
AD-A285233 p 807 N95-16599 #
AD-A285234 p 889 N95-16243 #
AD-A285237 p 826 N95-16244 #
AD-A285239 p 836 N95-16511 #
AD-A285249 p 749 N95-16512 #
AD-A285253 p 722 N95-16513 #
AD-A285255 p 885 N95-16528 #
AD-A285256 p 764 N95-16814 #
AD-A285258 p 849 N95-16529 #
AD-A285262 p 735 N95-16514 #
AD-A285265 p 672 N95-16530 #
AD-A285266 p 886 N95-16815
AD-A285276 p 734 N95-16370 #
AD-A285282 p 916 N95-16600 #
AD-A285301 p 786 N95-16601 #
AD-A285305 p 771 N95-16616 #
AD-A285309 p 735 N95-16531 #
AD-A285310 p 885 N95-16733 #
AD-A285312 p 722 N95-16734 #
AD-A285315 p 799 N95-16735 #
AD-A285323 p 734 N95-16371 #
AD-A285337 p 755 N95-16816 #
AD-A285338 p 827 N95-16817 #
AD-A285339 p 838 N95-16818
AD-A285340 p 838 N95-16819 #
AD-A285342 p 857 N95-16820 #
AD-A285343 p 830 N95-16821 #
AD-A285344 p 827 N95-16822 #
AD-A285345 p 828 N95-16835 #
AD-A285352 p 851 N95-15952 #
AD-A285354 p 784 N95-15953 #
AD-A285356 p 883 N95-15954 #
AD-A285394 p 890 N95-16617 #
AD-A285395 p 832 N95-16618 #
AD-A285399 p 780 N95-16636 #
AD-A285404 p 910 N95-16884 #
AD-A285405 p 753 N95-16233 #
AD-A285406 p 884 N95-16296 #
AD-A285410 p 785 N95-16245 #
AD-A285419 p 855 N95-16246 #
AD-A285423 p 774 N95-16247 #
AD-A285427 p 869 N95-16248 #
AD-A285428 p 838 N95-16874 #
AD-A285450 p 830 N95-16875 #
AD-A285454 p 832 N95-16876 #
AD-A285455 p 656 N95-17178 #
AD-A285456 p 870 N95-16812 #
AD-A285459 p 783 N95-17725 #
AD-A285461 p 903 N95-16877 #
AD-A285470 p 736 N95-16878 #
AD-A285472 p 909 N95-16879 #
AD-A285475 p 821 N95-16619 #
AD-A285486 p 857 N95-16967 #
AD-A285493 p 800 N95-16802 #
AD-A285496 p 755 N95-16968 #
AD-A285497 p 746 N95-17438
AD-A285498 p 771 N95-16736 #
AD-A285500 p 669 N95-16969 #
AD-A285509 p 725 N95-16970 #
AD-A285513 p 910 N95-16971 #
AD-A285514 p 910 N95-16972 #
AD-A285516 p 822 N95-17174 #
AD-A285518 p 728 N95-16406 #
AD-A285519 p 771 N95-16438 #
AD-A285531 p 857 N95-17381 #
AD-A285603 p 842 N95-17746 #
AD-A285672 p 885 N95-16620 #
AD-A285673 p 754 N95-16621 #

AD-A285674 ..... p 828 N95-17175 #
AD-A285675 ..... p 891 N95-17382 #
AD-A285696 ..... p 839 N95-17176 #
AD-A285714 ..... p 871 N95-17177 #

AD-D016324 ..... p 896 N95-16399 #
AD-D016329 ..... p 915 N95-16854
AD-D016337 ..... p 766 N95-16947 #
AD-D016338 ..... p 766 N95-16948 #
AD-D016339 ..... p 766 N95-16949 #
AD-D016340 ..... p 766 N95-16950
AD-D016355 ..... p 747 N95-17693
AD-D016356 ..... p 747 N95-17694 #
AD-D016359 ..... p 887 N95-17695 #
AD-D016363 ..... p 761 N95-17696
AD-D016369 ..... p 761 N95-17697
AD-D016370 ..... p 779 N95-17698
AD-D016372 ..... p 738 N95-17699
AD-D016373 ..... p 775 N95-17428
AD-D016376 ..... p 775 N95-17376
AD-D016377 ..... p 767 N95-17478
AD-D016380 ..... p 732 N95-17479
AD-D016381 ..... p 777 N95-17302
AD-D016390 ..... p 760 N95-17480 #
AD-D016391 ..... p 767 N95-17481
AD-D016392 ..... p 760 N95-17482
AD-D016404 ..... p 782 N95-17461
AD-D016405 ..... p 746 N95-17462
AD-D016406 ..... p 767 N95-17463
AD-D016408 ..... p 778 N95-17464
AD-D016409 ..... p 858 N95-17465
AD-D016449 ..... p 764 N95-16539 #
AD-D016450 ..... p 780 N95-16543 #
AD-D016454 ..... p 754 N95-16549 #
AD-D016455 ..... p 857 N95-16823 #

AD-E202012 ..... p 760 N95-17501
AD-E202015 ..... p 778 N95-17500
AD-E202066 ..... p 759 N95-17450
AD-E202113 ..... p 803 N95-17715 #
AD-E501839 ..... p 725 N95-16970 #

AD-M000338 ..... p 912 N95-17660

ADL-66163 ..... p 783 N95-16870 #

ADST/WDL/TR-93-003274 ..... p 666 N95-16171 #

AFCESA/ETL-89-3 ..... p 750 N95-16853 #
AFCESA/ETL-93-5 ..... p 750 N95-16853 #

AFIT/CI/CIA-94-013D ..... p 672 N95-17444
AFIT/CI/CIA-94-013 ..... p 826 N95-16299 #
AFIT/CI/CIA-94-016 ..... p 753 N95-16300 #
AFIT/CI/CIA-94-021D ..... p 841 N95-17445
AFIT/CI/CIA-94-028D ..... p 865 N95-17341 #
AFIT/CI/CIA-94-028 ..... p 801 N95-17164 #
AFIT/CI/CIA-94-029 ..... p 802 N95-17443
AFIT/CI/CIA-94-030 ..... p 800 N95-16235
AFIT/CI/CIA-94-035 ..... p 826 N95-16298 #
AFIT/CI/CIA-94-036 ..... p 799 N95-17446
AFIT/CI/CIA-94-043 ..... p 820 N95-16360 #
AFIT/CI/CIA-94-049 ..... p 819 N95-16297 #
AFIT/CI/CIA-94-069 ..... p 828 N95-17447
AFIT/CI/CIA-94-074 ..... p 826 N95-16301 #
AFIT/CI/CIA-94-078 ..... p 864 N95-16422 #
AFIT/CI/CIA-94-086 ..... p 892 N95-17442
AFIT/CI/CIA-94-087 ..... p 827 N95-16433 #
AFIT/CI/CIA-94-101 ..... p 886 N95-17340 #
AFIT/CI/CIA-94-108 ..... p 818 N95-17714 #
AFIT/CI/CIA-94-124 ..... p 802 N95-17488

AFIT/EN-TR-94-04 ..... p 755 N95-16841 #

AFIT/EN/TR-94-06 ..... p 855 N95-16246 #

AFIT/GEE/ENV/94S-19 ..... p 795 N95-16545

AFOSR-TR-94-0410 ..... p 884 N95-16015 #

AFOSR-94-0372TR ..... p 821 N95-16484 #
AFOSR-94-0374TR ..... p 821 N95-16481 #
AFOSR-94-0382TR ..... p 821 N95-16515 #
AFOSR-94-0387TR ..... p 742 N95-16483 #
AFOSR-94-0389TR ..... p 727 N95-16150 #
AFOSR-94-0390TR ..... p 871 N95-16018 #
AFOSR-94-0391TR ..... p 726 N95-16008
AFOSR-94-0392TR ..... p 862 N95-16798 #
AFOSR-94-0396TR ..... p 729 N95-16790
AFOSR-94-0399TR ..... p 821 N95-16796 #
AFOSR-94-0403TR ..... p 899 N95-16789
AFOSR-94-0409TR ..... p 885 N95-16787 #
AFOSR-94-0411TR ..... p 735 N95-16786 #
AFOSR-94-0412TR ..... p 723 N95-16016 #
AFOSR-94-0413TR ..... p 825 N95-16010 #
AFOSR-94-0417TR ..... p 723 N95-16019 #
AFOSR-94-0418TR ..... p 825 N95-15959
AFOSR-94-0421TR ..... p 820 N95-16378
AFOSR-94-0428TR ..... p 861 N95-16376
AFOSR-94-0432TR ..... p 886 N95-17143
AFOSR-94-0446TR ..... p 746 N95-17662 #
AFOSR-94-0451TR ..... p 822 N95-17342 #
AFOSR-94-0455TR ..... p 731 N95-17142
AFOSR-94-0456TR ..... p 774 N95-16242
AFOSR-94-0458TR ..... p 730 N95-17140
AFOSR-94-0471TR ..... p 826 N95-16377
AFOSR-94-0472TR ..... p 738 N95-17664 #
AFOSR-94-0506TR ..... p 895 N95-16134 #
AFOSR-94-0512TR ..... p 728 N95-16497 #
AFOSR-94-0514TR ..... p 903 N95-16489 #
AFOSR-94-0523TR ..... p 819 N95-16135 #
AFOSR-94-0548TR ..... p 897 N95-16498 #
AFOSR-94-0549TR ..... p 741 N95-16230 #
AFOSR-94-0550TR ..... p 723 N95-16041 #
AFOSR-94-0551TR ..... p 894 N95-16043 #
AFOSR-94-0553TR ..... p 729 N95-16846 #
AFOSR-94-0560TR ..... p 723 N95-16126 #
AFOSR-94-0562TR ..... p 826 N95-16368 #
AFOSR-94-0564TR ..... p 874 N95-16496
AFOSR-94-0566TR ..... p 724 N95-16492 #
AFOSR-94-0567TR ..... p 735 N95-16514 #
AFOSR-94-0569TR ..... p 726 N95-16042 #
AFOSR-94-0570TR ..... p 873 N95-16493 #
AFOSR-94-0578TR ..... p 730 N95-16882
AFOSR-94-0583TR ..... p 861 N95-16517 #
AFOSR-94-0584TR ..... p 851 N95-15952 #
AFOSR-94-0586TR ..... p 727 N95-16144 #
AFOSR-94-0587TR ..... p 885 N95-16524 #
AFOSR-94-0588TR ..... p 807 N95-16599 #
AFOSR-94-0590TR ..... p 826 N95-16244 #
AFOSR-94-0592TR ..... p 765 N95-16834 #
AFOSR-94-0593TR ..... p 885 N95-16733 #
AFOSR-94-0594TR ..... p 755 N95-16968 #
AFOSR-94-0598TR ..... p 874 N95-16523 #
AFOSR-94-0599TR ..... p 722 N95-16513 #
AFOSR-94-0601TR ..... p 898 N95-16526 #
AFOSR-94-0602TR ..... p 744 N95-16844 #
AFOSR-94-0604TR ..... p 836 N95-16511 #
AFOSR-94-0605TR ..... p 822 N95-16847 #
AFOSR-94-0606TR ..... p 822 N95-16851 #
AFOSR-94-0607TR ..... p 734 N95-16370 #
AFOSR-94-0609TR ..... p 749 N95-16512 #
AFOSR-94-0611TR ..... p 885 N95-16528 #
AFOSR-94-0619TR ..... p 825 N95-16138 #
AFOSR-94-0620TR ..... p 763 N95-16137 #
AFOSR-94-0621TR ..... p 822 N95-16871 #
AFOSR-94-0623TR ..... p 746 N95-17438
AFOSR-94-0625TR ..... p 771 N95-16736 #
AFOSR-94-0627TR ..... p 869 N95-16248 #
AFOSR-94-0633TR ..... p 771 N95-16438 #
AFOSR-94-0640TR ..... p 734 N95-16371 #

AGARD-AR-278 ..... p 671 N95-17388 #
AGARD-AR-303-VOL-2 ..... p 657 N95-17846 #
AGARD-AR-323 ..... p 721 N95-17278 #

AGARD-R-803 ..... p 666 N95-16562 #

AI-M-1431 ..... p 835 N95-16236
AI-M-1487 ..... p 846 N95-16237

AIAA PAPER 91-3577 ..... p 713 N95-16066 * #
AIAA PAPER 94-0674 ..... p 726 N95-15967 * #
AIAA PAPER 94-2092 ..... p 769 N95-15966 * #
AIAA PAPER 94-2133 ..... p 656 N95-16858 * #
AIAA PAPER 94-4311 ..... p 784 N95-17385 * #
AIAA PAPER 95-0026 ..... p 793 N95-16861 * #
AIAA PAPER 95-0030 ..... p 721 N95-17276 * #
AIAA PAPER 95-0070 ..... p 839 N95-16906 * #
AIAA PAPER 95-0119 ..... p 839 N95-17264 * #
AIAA PAPER 95-0692 ..... p 675 N95-17419 * #

AL/CF-TR-1994-0063 ..... p 669 N95-17661 #
AL/CF-TR-1994-0076 ..... p 830 N95-16553

AL/HR-TP-1994-0010 ..... p 828 N95-17175 #

AL/HR-TR-1994-0061 ..... p 850 N95-17374
AL/HR-TR-1994-0107 ..... p 830 N95-16875 #

ANL-HEP-CP-94-37 ..... p 910 N95-16922
ANL-HEP-CP-94-40 ..... p 875 N95-16924
ANL-HEP-CP-94-43 ..... p 878 N95-17899 #

ANL-HEP-PR-94-02 ..... p 904 N95-17925 #

ANL-HEP-TR-94-34 ..... p 882 N95-17924 #

ANL/APS/CP-83263 ..... p 880 N95-16308 #

ANL/ASD/CP-83412 ..... p 761 N95-17926 #
ANL/ASD/CP-83968 ..... p 882 N95-17902 #

ANL/CHM/CP-81481 ..... p 727 N95-16363 #
ANL/CHM/CP-83188 ..... p 734 N95-16364 #

ANL/CHM/PP-77639 ..... p 728 N95-16485 #

ANL/CMT-ACL/CP-82364 ..... p 728 N95-16426 #

ANL/CMT/CP-82291 ..... p 766 N95-16963 #

ANL/ET/CP-81529 ..... p 772 N95-17523 #
ANL/ET/CP-83016 ..... p 873 N95-16430 #
ANL/ET/CP-83715 ..... p 902 N95-17898 #

ANL/FPP/TM-267 ..... p 873 N95-16487 #

ANL/MCS/CP-82805 ..... p 863 N95-17306 #
ANL/MCS/CP-82980 ..... p 771 N95-16828 * #
ANL/MCS/CP-82981 ..... p 800 N95-16398 #

ANL/MCS/PP-78200 ..... p 839 N95-16923

ANL/MSD/CP-81312 ..... p 876 N95-16962 #
ANL/MSD/CP-82480 ..... p 766 N95-16945 #
ANL/MSD/CP-83110 ..... p 900 N95-16946 #
ANL/MSD/CP-83115 ..... p 897 N95-16408 #
ANL/MSD/CP-83142 ..... p 901 N95-17349 #
ANL/MSD/CP-83143 ..... p 901 N95-17350 #

ANL/OTM/CR-8 ..... p 745 N95-17160 #

ANL/TD/CP-82096 ..... p 889 N95-16307 #
ANL/TD/CP-83128 ..... p 879 N95-16030 #
ANL/TD/CP-83205 ..... p 665 N95-16964 #
ANL/TD/CP-83977 ..... p 893 N95-17900 #

ANL/XFD/CP-83940 ..... p 882 N95-17901 #

ARCCB-TR-94018 ..... p 734 N95-16380
ARCCB-TR-94021 ..... p 856 N95-16550 #
ARCCB-TR-94023 ..... p 786 N95-16601 #

ARL-CR-98-PHASE-2 ..... p 802 N95-17686

ARL-TR-449 ..... p 785 N95-16102 #
ARL-TR-450 ..... p 788 N95-17510
ARL-TR-451 ..... p 737 N95-17486
ARL-TR-505 ..... p 883 N95-15954 #
ARL-TR-576 ..... p 785 N95-16245 #
ARL-TR-598 ..... p 721 N95-17274 * #
ARL-TR-599 ..... p 781 N95-16907 * #
ARL-TR-637 ..... p 669 N95-15970 * #

ARMYSBIR2-0393-PHASE-2 ..... p 802 N95-17686

ARO-24628.3-PH-UIF ..... p 883 N95-15958
ARO-25874.1-MA ..... p 859 N95-16108
ARO-26708.9-EL ..... p 896 N95-16365 #
ARO-26761.12-EL ..... p 896 N95-16396
ARO-27054.14-CH ..... p 739 N95-16013 #
ARO-27480.6-EG-SDI ..... p 655 N95-16160 #
ARO-27505.5-CH ..... p 722 N95-16087
ARO-27627.3-EG ..... p 770 N95-16163 #
ARO-27775.15-CH ..... p 729 N95-16791
ARO-28011.2-LS ..... p 807 N95-16164 #
ARO-28095.4-LS-SAH ..... p 820 N95-16423 #
ARO-28198.1-MS-SAH ..... p 740 N95-16085
ARO-28249.2-EG ..... p 655 N95-16099
ARO-28313.1-PH ..... p 884 N95-16157 #
ARO-28328.15-MA ..... p 834 N95-16154
ARO-28328.16-MA ..... p 834 N95-16153 #
ARO-28347.5-EL ..... p 896 N95-16391
ARO-28350.2-EG ..... p 855 N95-16011 #
ARO-28353.7-CH ..... p 740 N95-16101 #
ARO-28387.11-EL ..... p 763 N95-16136
ARO-28402.6-CH ..... p 741 N95-16393
ARO-28461.11-EL ..... p 895 N95-16158 #
ARO-28489.11-GS ..... p 776 N95-16166 #
ARO-28508.7-EL ..... p 902 N95-17705
ARO-28516.5-EL ..... p 763 N95-16159 #
ARO-28548.10-MA ..... p 770 N95-16156
ARO-28631.24-CH ..... p 740 N95-16165
ARO-28691.2-LS ..... p 731 N95-17425
ARO-28747.1-MS-SM ..... p 872 N95-16155
ARO-29107.1-GS-SAH ..... p 884 N95-16161 #
ARO-29412.3-MA-SDI ..... p 783 N95-16421
ARO-29412.4-MA-SDI ..... p 860 N95-16169
ARO-29412.5-MA-SDI ..... p 865 N95-17426
ARO-29548.8-CH-AAS ..... p 722 N95-16100 #
ARO-29614.1-MS-CF ..... p 894 N95-16111 #
ARO-29850.2-MA ..... p 861 N95-16395
ARO-30407.4.EL-URI ..... p 763 N95-16394
ARO-30437.1-EL ..... p 886 N95-16965 #
ARO-30482.9-PH ..... p 776 N95-16353 #
ARO-30772.7-MS ..... p 901 N95-17424
ARO-30955.1-EL-CF ..... p 894 N95-16081
ARO-30980.1-MA ..... p 856 N95-16390

ARO-30986.6-MA-H ..... p 855 N95-16170 #
ARO-31210.2-EG-SDI ..... p 655 N95-16076
ARO-31432.1-EL-SBI ..... p 855 N95-16077
ARO-32305.3-CH ..... p 744 N95-16792
ARO-32365.1-MA ..... p 804 N95-16078
ARO-32483.1-MA-CF ..... p 857 N95-16864 #
ARO-33007.1-MS-CF ..... p 723 N95-16397

ATC-220 ..... p 759 N95-17336
ATC-221 ..... p 752 N95-16097

B-257877 ..... p 914 N95-15962 #

BFLRF-291 ..... p 780 N95-16636 #

BNL-60475 ..... p 877 N95-17683 #
BNL-60490 ..... p 872 N95-16121 #
BNL-60521 ..... p 879 N95-16210 #
BNL-60593 ..... p 896 N95-16385 #
BNL-60605 ..... p 899 N95-16918
BNL-60743 ..... p 901 N95-17673 #

CAL-2260 ..... p 916 N95-17528 * #

CAR-TR-692 ..... p 804 N95-16078

CARDIVNSWC-TR-61-CR-93/04 . p 786 N95-16785 #
CARDIVNSWC-TR-94/004 ..... p 903 N95-16877 #

CARDIVNSWC/TR-61-94/25 ..... p 735 N95-16531 #

CAST-TN-04-94 ..... p 804 N95-16124 #

CAST-TR-94-4 ..... p 804 N95-16125 #

CBP-017 ..... p 904 N95-17904 #

CERL-SR-EC-94/28 ..... p 857 N95-16967 #

CERL-TR-FE-94/13 ..... p 884 N95-15999 #

CGR/DC-08/94 ..... p 805 N95-16414

CMOTT-94-1 ..... p 770 N95-16407 * #

CMU-CS-94-107 ..... p 835 N95-16446 #
CMU-CS-94-142 ..... p 837 N95-16602 #
CMU-CS-94-144 ..... p 849 N95-16603 #
CMU-CS-94-146 ..... p 864 N95-17618
CMU-CS-94-152 ..... p 886 N95-16795 #
CMU-CS-94-153 ..... p 850 N95-16826 #
CMU-CS-94-156 ..... p 838 N95-16632 #
CMU-CS-94-160 ..... p 835 N95-16447 #
CMU-CS-94-171 ..... p 835 N95-16306
CMU-CS-94-175 ..... p 830 N95-16813 #
CMU-CS-94-176 ..... p 838 N95-16818
CMU-CS-94-179 ..... p 838 N95-16850 #
CMU-CS-94-181 ..... p 827 N95-16518 #
CMU-CS-94-184 ..... p 857 N95-16820 #
CMU-CS-94-185 ..... p 838 N95-16819 #

CMU-HCII-94-103 ..... p 830 N95-16813 #

CMU-RI-TR-94-05 ..... p 782 N95-17430
CMU-RI-TR-94-10 ..... p 865 N95-17377
CMU-RI-TR-94-11 ..... p 865 N95-17429
CMU-RI-TR-94-17 ..... p 666 N95-17706
CMU-RI-TR-94-24 ..... p 840 N95-17432

CMU/SEI-93-TR-07 ..... p 836 N95-16504 #
CMU/SEI-94-SR-03 ..... p 836 N95-16503 #
CMU/SEI-94-SR-7 ..... p 836 N95-16490 #
CMU/SEI-94-TR-2 ..... p 835 N95-16446 #

CONF-900109-28 ..... p 883 N95-17933 * #
CONF-920362-49 ..... p 890 N95-16921
CONF-9204294-1 ..... p 787 N95-16939 #
CONF-920515-VOL-2 ..... p 880 N95-17475 #
CONF-9210354-2 ..... p 797 N95-17908 #
CONF-921101-143 ..... p 733 N95-17911 #
CONF-930304-33 ..... p 744 N95-16934
CONF-9303269 ..... p 871 N95-15956 #
CONF-9304164-ABSTS ..... p 862 N95-16611 #
CONF-9305203 ..... p 880 N95-17519 #
CONF-9307177 ..... p 892 N95-17517 #
CONF-9307183-1 ..... p 863 N95-17306 #
CONF-930765-4 ..... p 773 N95-17910 #
CONF-9308193-SUMM ..... p 791 N95-15944 #
CONF-930926-40 ..... p 751 N95-17909 #
CONF-9309274-3 ..... p 893 N95-17907 #
CONF-9309386-1 ..... p 903 N95-16944 #
CONF-930961-1 ..... p 724 N95-16926 #
CONF-931009-27 ..... p 736 N95-17159 #
CONF-9310146-2 ..... p 775 N95-17380 #
CONF-931048-16 ..... p 777 N95-16929
CONF-931054-11 ..... p 902 N95-17742 #

CONF-931108-105 ..... p 723 N95-16225 #
CONF-9311147-9 ..... p 890 N95-16919
CONF-9311224-1 ..... p 899 N95-16913
CONF-931234-10 ..... p 789 N95-17675 #
CONF-94012-16 ..... p 793 N95-16831 * #
CONF-940122-5 ..... p 901 N95-17667 #
CONF-940142-41 ..... p 777 N95-17168 #
CONF-940142-42 ..... p 779 N95-17688 #
CONF-940142-46 ..... p 779 N95-17887 #
CONF-940157 ..... p 856 N95-16609 #
CONF-940194-1-REV-1 ..... p 765 N95-16915
CONF-940226-8 ..... p 899 N95-16867 #
CONF-940286-5 ..... p 738 N95-17726 #
CONF-940286-6 ..... p 739 N95-17728 #
CONF-9403129-1 ..... p 896 N95-16359 #
CONF-9403139-1 ..... p 903 N95-16428 #
CONF-9403144-1 ..... p 779 N95-17689 #
CONF-940327-3 ..... p 875 N95-16943 #
CONF-940327-7 ..... p 875 N95-16914
CONF-940327-9 ..... p 873 N95-16402 #
CONF-940351-2 ..... p 881 N95-17888 #
CONF-940351-3 ..... p 878 N95-17720 #
CONF-940353-6 ..... p 798 N95-16284 #
CONF-940391-9-REV-1 ..... p 916 N95-17525 #
CONF-940393-1 ..... p 799 N95-16927 #
CONF-940399-1 ..... p 724 N95-16930
CONF-940407-23 ..... p 844 N95-15946 #
CONF-940411-19-REV-1 ..... p 751 N95-17738 #
CONF-940411-26 ..... p 728 N95-16419 #
CONF-940411-35 ..... p 876 N95-16962 #
CONF-940411-37 ..... p 900 N95-17156 #
CONF-940411-43 ..... p 896 N95-16385 #
CONF-940411-44 ..... p 895 N95-16311 #
CONF-9404137-4 ..... p 856 N95-16361 #
CONF-940414-3 ..... p 877 N95-17687 #
CONF-940416-12 ..... p 899 N95-16806 #
CONF-9404162-8 ..... p 790 N95-16215 #
CONF-9404162-9 ..... p 777 N95-16917
CONF-9404167-1 ..... p 775 N95-17307 #
CONF-9404179-1 ..... p 670 N95-17371 #
CONF-9404185-1 ..... p 836 N95-16536 #
CONF-940433-5 ..... p 732 N95-17524 #
CONF-940449-13 ..... p 884 N95-16366 #
CONF-940492-10 ..... p 910 N95-16922
CONF-9405100-12 ..... p 842 N95-17678 #
CONF-9405100-6 ..... p 899 N95-16805 #
CONF-9405132-7 ..... p 875 N95-16931
CONF-940514-1 ..... p 872 N95-16121 #
CONF-940514-2 ..... p 876 N95-17154 #
CONF-940514-9 ..... p 875 N95-16924
CONF-9405143-ABSTS ..... p 725 N95-17368
CONF-9405143-4 ..... p 739 N95-17747 #
CONF-9405143-5 ..... p 738 N95-17679 #
CONF-9405145-3 ..... p 770 N95-16211 #
CONF-9405164-2 ..... p 835 N95-16358 #
CONF-9405170-1 ..... p 876 N95-16959 #
CONF-9405179-1 ..... p 727 N95-16363 #
CONF-9405181-1 ..... p 734 N95-16364 #
CONF-9405198-3 ..... p 899 N95-16918
CONF-940521-1 ..... p 737 N95-17513 #
CONF-9405216-1 ..... p 878 N95-17727 #
CONF-940529-19 ..... p 765 N95-16920
CONF-940531-2 ..... p 880 N95-16308 #
CONF-940548-1 ..... p 781 N95-17169 #
CONF-940548-4 ..... p 792 N95-16437 #
CONF-940550-13 ..... p 856 N95-16287 #
CONF-940552-10 ..... p 776 N95-16486 #
CONF-940552-18 ..... p 779 N95-17635
CONF-940552-26 ..... p 890 N95-16555 #
CONF-940552-30 ..... p 779 N95-17680 #
CONF-940552-4 ..... p 776 N95-17522 #
CONF-940552-9 ..... p 891 N95-16958 #
CONF-940552 ..... p 888 N95-16063
CONF-940568-4 ..... p 766 N95-16963 #
CONF-940580-10 ..... p 892 N95-17640
CONF-940580-11 ..... p 889 N95-16554 #
CONF-940580-16 ..... p 893 N95-17677 #
CONF-940580-17 ..... p 893 N95-17897 #
CONF-940580-20 ..... p 891 N95-17347 #
CONF-940592-1 ..... p 778 N95-17627
CONF-940593-14 ..... p 779 N95-17729 #
CONF-940613-18 ..... p 772 N95-17523 #
CONF-9406134-2 ..... p 792 N95-16435 #
CONF-940615-3 ..... p 893 N95-17896 #
CONF-9406166-4 ..... p 727 N95-16362 #
CONF-9406176-2 ..... p 665 N95-16964 #
CONF-940618-15 ..... p 761 N95-17926 #
CONF-940618-56 ..... p 761 N95-17672 #
CONF-940618-69 ..... p 882 N95-17890 #
CONF-940618-71 ..... p 881 N95-17670 #
CONF-940618-75 ..... p 882 N95-17891 #
CONF-940618-8 ..... p 879 N95-16217 #
CONF-9406188-1 ..... p 671 N95-16509 #
CONF-9406189-1 ..... p 763 N95-16357 #
CONF-9406192-2 ..... p 798 N95-16537 #
CONF-9406205-3 ..... p 850 N95-16830

CONF-9406205-4 ..... p 851 N95-17676 #
CONF-9406220-1 ..... p 744 N95-16829
CONF-940630-12 ..... p 891 N95-17367
CONF-940630-13 ..... p 891 N95-17155 #
CONF-940630-14 ..... p 731 N95-17157 #
CONF-940630-34 ..... p 889 N95-16307 #
CONF-940630-46 ..... p 893 N95-17674 #
CONF-940630-7 ..... p 881 N95-17721 #
CONF-940634-13 ..... p 891 N95-16936
CONF-940634-14 ..... p 745 N95-16938
CONF-940634-4 ..... p 888 N95-16216 #
CONF-940634-8 ..... p 889 N95-16286 #
CONF-940635-12 ..... p 873 N95-16403 #
CONF-940641-1 ..... p 736 N95-16807 #
CONF-940651-5 ..... p 897 N95-16408 #
CONF-940662-1 ..... p 771 N95-16828 * #
CONF-940678-1 ..... p 889 N95-16285 #
CONF-940678-3 ..... p 888 N95-16218 #
CONF-940692-5 ..... p 786 N95-16803 #
CONF-940701-3 ..... p 901 N95-17349 #
CONF-940701-6 ..... p 900 N95-16946 #
CONF-940701-8 ..... p 766 N95-16945 #
CONF-940701-9 ..... p 901 N95-17350 #
CONF-9407101-1 ..... p 764 N95-16832
CONF-9407103-16 ..... p 879 N95-16030 #
CONF-940711-17 ..... p 732 N95-17437
CONF-9407110-1 ..... p 894 N95-15942 #
CONF-940714-17 ..... p 881 N95-17671 #
CONF-940714-23 ..... p 882 N95-17901 #
CONF-940719-6 ..... p 861 N95-16535 #
CONF-940722-14 ..... p 872 N95-16309 #
CONF-940722-15 ..... p 875 N95-16868 #
CONF-940722-17 ..... p 875 N95-16840 #
CONF-940722-1 ..... p 876 N95-16960 #
CONF-940722-4 ..... p 876 N95-17158 #
CONF-940722-5 ..... p 876 N95-17153 #
CONF-940723-12 ..... p 793 N95-16916
CONF-940723-27 ..... p 748 N95-17913 #
CONF-940723-8 ..... p 765 N95-16932
CONF-940725-2 ..... p 877 N95-17683 #
CONF-940769-4 ..... p 800 N95-16398 #
CONF-940776-5 ..... p 748 N95-16214 #
CONF-940785-1 ..... p 873 N95-16430 #
CONF-940790-1 ..... p 728 N95-16426 #
CONF-9408118-2 ..... p 791 N95-17903 #
CONF-940812-6 ..... p 891 N95-17365
CONF-9408125-15 ..... p 893 N95-17900 #
CONF-9408125-1 ..... p 875 N95-16933
CONF-9408125-20 ..... p 882 N95-17902 #
CONF-9408125-29 ..... p 882 N95-17931 #
CONF-9408131-3 ..... p 733 N95-17912 #
CONF-9408155-2 ..... p 879 N95-17918 #
CONF-9408155-3 ..... p 902 N95-17917 #
CONF-9408156-1 ..... p 748 N95-17892 #
CONF-940816-1 ..... p 877 N95-17669 #
CONF-940816-2 ..... p 904 N95-17668 #
CONF-940816-3 ..... p 878 N95-17899 #
CONF-940816-5 ..... p 879 N95-17932 #
CONF-940849-1 ..... p 782 N95-17366
CONF-940859-25 ..... p 858 N95-17915 #
CONF-940863-2 ..... p 868 N95-16288 #
CONF-940863-3 ..... p 896 N95-16389 #
CONF-940894 ..... p 796 N95-17636
CONF-940908-1 ..... p 882 N95-17914 #
CONF-940926-1 ..... p 902 N95-17898 #
CONF-940956-8 ..... p 736 N95-17378 #
CONF-940956-9 ..... p 745 N95-17379 #
CONF-9410102-1 ..... p 846 N95-16222 #
CONF-9410103-2 ..... p 780 N95-16224 #
CONF-9410165-2 ..... p 737 N95-17641
CONF-941058-1 ..... p 834 N95-16219 #
CONF-941071-2 ..... p 850 N95-17638
CONF-941085-1 ..... p 860 N95-16221 #
CONF-941085-2 ..... p 834 N95-16220 #
CONF-941085-3 ..... p 835 N95-16223 #

CPIA-PUBL-602-VOL-1 ..... p 713 N95-16312 #
CPIA-PUBL-602-VOL-2 ..... p 715 N95-16324 #

CRHC-94-11 ..... p 833 N95-16088 * #

CRINC/RSL-TR-8621-5 ..... p 806 N95-17505

CRREL-94-2 ..... p 804 N95-16103 #

CS-TR-3172 ..... p 804 N95-16078

CSEL-1994-TR-02 ..... p 857 N95-17383 * #

CU-CAS-94-23 ..... p 788 N95-17492 * #

CUED/A-THERMO/TR-61 ..... p 771 N95-16595 #

CUED/D-STRUCT/TR-144 ..... p 783 N95-17928 #

DAC-46 ..... p 762 N95-16089 #

DE93-001715 ..... p 724 N95-16926 #
DE94-004096 ..... p 782 N95-17364 #
DE94-006907 ..... p 792 N95-16435 #
DE94-006922 ..... p 781 N95-17169 #
DE94-006923 ..... p 792 N95-16437 #
DE94-009333 ..... p 799 N95-16927 #
DE94-009364 ..... p 834 N95-16219 #
DE94-010071 ..... p 736 N95-17378 #
DE94-010204 ..... p 834 N95-16220 #
DE94-010205 ..... p 860 N95-16221 #
DE94-010890 ..... p 745 N95-17379 #
DE94-011365 ..... p 846 N95-16222 #
DE94-011381 ..... p 924 N95-16120 #
DE94-011703 ..... p 835 N95-16223 #
DE94-011719 ..... p 780 N95-16224 #
DE94-011818 ..... p 897 N95-16424 #
DE94-011826 ..... p 794 N95-17521 #
DE94-011837 ..... p 794 N95-16957 #
DE94-011839 ..... p 764 N95-16425 #
DE94-011863 ..... p 787 N95-16939 #
DE94-011873 ..... p 791 N95-15944 #
DE94-011885 ..... p 794 N95-16940 #
DE94-012060 ..... p 751 N95-17738 #
DE94-012231 ..... p 775 N95-17380 #
DE94-012235 ..... p 776 N95-17522 #
DE94-012650 ..... p 772 N95-17523 #
DE94-012656 ..... p 732 N95-17524 #
DE94-012731 ..... p 877 N95-17687 #
DE94-012888 ..... p 916 N95-17525 #
DE94-012891 ..... p 881 N95-17721 #
DE94-013110 ..... p 775 N95-17307 #
DE94-013137 ..... p 891 N95-17365
DE94-013189 ..... p 908 N95-16282 #
DE94-013194 ..... p 890 N95-16827 #
DE94-013270 ..... p 737 N95-17513 #
DE94-013277 ..... p 786 N95-16803 #
DE94-013332 ..... p 873 N95-16430 #
DE94-013375 ..... p 770 N95-16417 #
DE94-013393 ..... p 863 N95-17306 #
DE94-013398 ..... p 728 N95-16426 #
DE94-013399 ..... p 800 N95-16398 #
DE94-013400 ..... p 771 N95-16828 * #
DE94-013439 ..... p 763 N95-16357 #
DE94-013440 ..... p 835 N95-16358 #
DE94-013526 ..... p 877 N95-17683 #
DE94-013550 ..... p 798 N95-16284 #
DE94-013553 ..... p 896 N95-16359 #
DE94-013561 ..... p 774 N95-16804 #
DE94-013608 ..... p 763 N95-16283 #
DE94-013615 ..... p 899 N95-16805 #
DE94-013620 ..... p 899 N95-16806 #
DE94-013629 ..... p 856 N95-16361 #
DE94-013632 ..... p 728 N95-16419 #
DE94-013633 ..... p 736 N95-16807 #
DE94-013636 ..... p 841 N95-17514 #
DE94-013662 ..... p 841 N95-17515 #
DE94-013737 ..... p 777 N95-17168 #
DE94-013738 ..... p 902 N95-17742 #
DE94-013760 ..... p 872 N95-16121 #
DE94-013763 ..... p 727 N95-16362 #
DE94-013788 ..... p 888 N95-16122 #
DE94-013790 ..... p 782 N95-17366
DE94-013800 ..... p 875 N95-16943 #
DE94-013801 ..... p 903 N95-16944 #
DE94-013813 ..... p 850 N95-17516 #
DE94-013817 ..... p 788 N95-17439 #
DE94-013837 ..... p 891 N95-16958 #
DE94-013838 ..... p 876 N95-16959 #
DE94-013851 ..... p 876 N95-16960 #
DE94-013863 ..... p 801 N95-16961 #
DE94-013865 ..... p 876 N95-16962 #
DE94-013867 ..... p 766 N95-16963 #
DE94-013868 ..... p 665 N95-16964 #
DE94-013874 ..... p 897 N95-16408 #
DE94-013956 ..... p 796 N95-17348 #
DE94-013960 ..... p 670 N95-17371 #
DE94-013962 ..... p 901 N95-17349 #
DE94-013963 ..... p 901 N95-17350 #
DE94-013991 ..... p 766 N95-16945 #
DE94-013997 ..... p 900 N95-16946 #
DE94-013998 ..... p 727 N95-16363 #
DE94-014007 ..... p 728 N95-16485 #
DE94-014012 ..... p 734 N95-16364 #
DE94-014017 ..... p 776 N95-16486 #
DE94-014020 ..... p 891 N95-17367
DE94-014032 ..... p 873 N95-16487 #
DE94-014053 ..... p 725 N95-17368
DE94-014055 ..... p 884 N95-16366 #
DE94-014066 ..... p 794 N95-16209 #
DE94-014086 ..... p 879 N95-16210 #
DE94-014111 ..... p 770 N95-16211 #
DE94-014136 ..... p 671 N95-16509 #
DE94-014165 ..... p 795 N95-16212 #
DE94-014168 ..... p 795 N95-16213 #
DE94-014174 ..... p 748 N95-16214 #
DE94-014222 ..... p 790 N95-16215 #
DE94-014231 ..... p 897 N95-16510 #
DE94-014232 ..... p 722 N95-16058 #
DE94-014233 ..... p 783 N95-16538 #
DE94-014234 ..... p 735 N95-16540 #
DE94-014255 ..... p 879 N95-16172 #
DE94-014280 ..... p 888 N95-16216 #
DE94-014301 ..... p 793 N95-16541 #
DE94-014356 ..... p 749 N95-16542 #
DE94-014420 ..... p 879 N95-16217 #
DE94-014421 ..... p 888 N95-16218 #
DE94-014423 ..... p 876 N95-17153 #
DE94-014424 ..... p 889 N95-16285 #
DE94-014428 ..... p 889 N95-16286 #
DE94-014431 ..... p 876 N95-17154 #
DE94-014434 ..... p 856 N95-16287 #
DE94-014436 ..... p 903 N95-16428 #
DE94-014440 ..... p 868 N95-16288 #
DE94-014441 ..... p 891 N95-17155 #
DE94-014452 ..... p 900 N95-17156 #
DE94-014471 ..... p 731 N95-17157 #
DE94-014488 ..... p 876 N95-17158 #
DE94-014492 ..... p 736 N95-17159 #
DE94-014567 ..... p 856 N95-16609 #
DE94-014573 ..... p 805 N95-16610 #
DE94-014583 ..... p 745 N95-17160 #
DE94-014595 ..... p 862 N95-16611 #
DE94-014598 ..... p 731 N95-17161 #
DE94-014599 ..... p 781 N95-17162 #
DE94-014681 ..... p 731 N95-17163 #
DE94-014727 ..... p 749 N95-17919 #
DE94-014730 ..... p 797 N95-17920 #
DE94-014731 ..... p 797 N95-17922 #
DE94-014784 ..... p 880 N95-17475 #
DE94-014793 ..... p 861 N95-16535 #
DE94-014794 ..... p 836 N95-16536 #
DE94-014817 ..... p 798 N95-16537 #
DE94-014902 ..... p 746 N95-17456 #
DE94-014934 ..... p 892 N95-17497 #
DE94-014941 ..... p 778 N95-17498 #
DE94-014979 ..... p 749 N95-17923 #
DE94-015024 ..... p 882 N95-17924 #
DE94-015029 ..... p 904 N95-17925 #
DE94-015092 ..... p 761 N95-17926 #
DE94-015095 ..... p 889 N95-16307 #
DE94-015096 ..... p 880 N95-16308 #
DE94-015138 ..... p 899 N95-16867 #
DE94-015139 ..... p 779 N95-17688 #
DE94-015142 ..... p 779 N95-17689 #
DE94-015185 ..... p 872 N95-16309 #
DE94-015274 ..... p 744 N95-16829
DE94-015278 ..... p 850 N95-16830
DE94-015284 ..... p 793 N95-16831 * #
DE94-015287 ..... p 764 N95-16832
DE94-015341 ..... p 903 N95-16604 #
DE94-015361 ..... p 899 N95-16913
DE94-015381 ..... p 875 N95-16868 #
DE94-015537 ..... p 875 N95-16914
DE94-015544 ..... p 871 N95-15945 #
DE94-015546 ..... p 872 N95-16310
DE94-015561 ..... p 765 N95-16915
DE94-015727 ..... p 875 N95-16840 #
DE94-015735 ..... p 793 N95-16916
DE94-015745 ..... p 777 N95-16917
DE94-015765 ..... p 895 N95-16311 #
DE94-015823 ..... p 899 N95-16918
DE94-015848 ..... p 896 N95-16385 #
DE94-015854 ..... p 888 N95-16063
DE94-015858 ..... p 890 N95-16919
DE94-015864 ..... p 747 N95-17690 #
DE94-015867 ..... p 782 N95-17716 #
DE94-015889 ..... p 795 N95-16386 #
DE94-015890 ..... p 727 N95-16387 #
DE94-015898 ..... p 777 N95-16929
DE94-015946 ..... p 782 N95-17717 #
DE94-016000 ..... p 724 N95-16930
DE94-016010 ..... p 797 N95-17718 #
DE94-016040 ..... p 747 N95-17719 #
DE94-016057 ..... p 875 N95-16931
DE94-016072 ..... p 896 N95-16389 #
DE94-016095 ..... p 765 N95-16932
DE94-016097 ..... p 875 N95-16933
DE94-016115 ..... p 803 N95-17743 #
DE94-016145 ..... p 733 N95-17744 #
DE94-016149 ..... p 744 N95-16934
DE94-016172 ..... p 745 N95-16935
DE94-016184 ..... p 891 N95-16936
DE94-016210 ..... p 880 N95-16937
DE94-016281 ..... p 745 N95-16938
DE94-016283 ..... p 765 N95-16920
DE94-016297 ..... p 890 N95-16921
DE94-016308 ..... p 910 N95-16922
DE94-016316 ..... p 879 N95-16030 #
DE94-016369 ..... p 839 N95-16923
DE94-016385 ..... p 875 N95-16924
DE94-016416 ..... p 765 N95-16925
DE94-016446 ..... p 778 N95-17627
DE94-016449 ..... p 779 N95-17635
DE94-016456 ..... p 796 N95-17636
DE94-016475 ..... p 737 N95-17637
DE94-016480 ..... p 850 N95-17638
DE94-016483 ..... p 732 N95-17639
DE94-016485 ..... p 722 N95-17745 #
DE94-016521 ..... p 892 N95-17640
DE94-016522 ..... p 889 N95-16554 #
DE94-016526 ..... p 873 N95-16402 #
DE94-016552 ..... p 894 N95-15942 #
DE94-016599 ..... p 737 N95-17641
DE94-016636 ..... p 739 N95-15943 #
DE94-016704 ..... p 732 N95-17642
DE94-016771 ..... p 892 N95-17643
DE94-016820 ..... p 893 N95-17644
DE94-016859 ..... p 904 N95-17645
DE94-016868 ..... p 732 N95-17437
DE94-017521 ..... p 890 N95-16555 #
DE94-017704 ..... p 901 N95-17667 #
DE94-017770 ..... p 723 N95-16225 #
DE94-017810 ..... p 795 N95-16557 #
DE94-017900 ..... p 739 N95-17747 #
DE94-017907 ..... p 844 N95-15946 #
DE94-017918 ..... p 883 N95-15947 #
DE94-017934 ..... p 904 N95-17668 #
DE94-017935 ..... p 877 N95-17669 #
DE94-017966 ..... p 881 N95-17670 #
DE94-017967 ..... p 881 N95-17671 #
DE94-017972 ..... p 761 N95-17672 #
DE94-017986 ..... p 901 N95-17673 #
DE94-018041 ..... p 893 N95-17674 #
DE94-018046 ..... p 789 N95-17675 #
DE94-018047 ..... p 851 N95-17676 #
DE94-018049 ..... p 893 N95-17677 #
DE94-018050 ..... p 842 N95-17678 #
DE94-018054 ..... p 738 N95-17679 #
DE94-018056 ..... p 779 N95-17680 #
DE94-018057 ..... p 738 N95-17726 #
DE94-018098 ..... p 878 N95-17727 #
DE94-018112 ..... p 873 N95-16403 #
DE94-018124 ..... p 739 N95-17728 #
DE94-018180 ..... p 779 N95-17729 #
DE94-018183 ..... p 878 N95-17720 #
DE94-018185 ..... p 881 N95-17886 #
DE94-018186 ..... p 779 N95-17887 #
DE94-018191 ..... p 881 N95-17888 #
DE94-018192 ..... p 878 N95-17889 #
DE94-018203 ..... p 882 N95-17890 #
DE94-018207 ..... p 882 N95-17891 #
DE94-018265 ..... p 748 N95-17892 #
DE94-018345 ..... p 893 N95-17896 #
DE94-018346 ..... p 893 N95-17897 #
DE94-018375 ..... p 902 N95-17898 #
DE94-018376 ..... p 878 N95-17899 #
DE94-018381 ..... p 893 N95-17900 #
DE94-018384 ..... p 882 N95-17901 #
DE94-018396 ..... p 882 N95-17902 #
DE94-018448 ..... p 791 N95-17903 #
DE94-018536 ..... p 904 N95-17904 #
DE94-018569 ..... p 725 N95-17905 #
DE94-018585 ..... p 902 N95-17906 #
DE94-018693 ..... p 893 N95-17907 #
DE94-018694 ..... p 797 N95-17908 #
DE94-018695 ..... p 751 N95-17909 #
DE94-018698 ..... p 773 N95-17910 #
DE94-018705 ..... p 733 N95-17911 #
DE94-018721 ..... p 733 N95-17912 #
DE94-018729 ..... p 748 N95-17913 #
DE94-018734 ..... p 882 N95-17914 #
DE94-018741 ..... p 858 N95-17915 #
DE94-018794 ..... p 864 N95-17916 #
DE94-018890 ..... p 902 N95-17917 #
DE94-018893 ..... p 879 N95-17918 #
DE94-018984 ..... p 882 N95-17931 #
DE94-018992 ..... p 879 N95-17932 #
DE94-019219 ..... p 877 N95-17358 #
DE94-019320 ..... p 891 N95-17347 #
DE94-051198 ..... p 883 N95-17933 * #
DE94-622051 ..... p 892 N95-17517 #
DE94-622052 ..... p 901 N95-17518 #
DE94-622233 ..... p 799 N95-17471 #
DE94-622696 ..... p 912 N95-17472 #
DE94-622757 ..... p 903 N95-17473 #
DE94-622758 ..... p 904 N95-17474 #
DE94-623269 ..... p 871 N95-16059 #
DE94-623321 ..... p 880 N95-17519 #
DE94-753312 ..... p 877 N95-17520 #
DE94-753315 ..... p 740 N95-16073 #
DE94-753405 ..... p 878 N95-17739 #
DE94-753477 ..... p 871 N95-15956 #
DE94-796529 ..... p 724 N95-16833 #
DE95-000321 ..... p 710 N95-17359 #
DE95-000323 ..... p 784 N95-17360 #
DE95-000325 ..... p 880 N95-17361 #
DE95-000326 ..... p 799 N95-17362 #

DNA-TR-93-147 ..... p 892 N95-17623
DNA-TR-94-58 ..... p 842 N95-17746 #

DOD-8320.1-M ..... p 909 N95-16382

DODA-AR-007-005 ..... p 669 N95-16969 #
DODA-AR-007-100 ..... p 656 N95-17178 #
DODA-AR-008-154 ..... p 887 N95-17489 #
DODA-AR-008-638 ..... p 870 N95-16812 #
DODA-AR-008-651 ..... p 774 N95-16247 #
DODA-AR-008-866 ..... p 752 N95-16123 #
DODA-AR-008-868 ..... p 755 N95-16956 #
DODA-AR-008-869 ..... p 884 N95-16133 #

DOE/AL-42880/T1 ..... p 781 N95-17162 #

DOE/CE-40993/T1 ..... p 725 N95-17905 #

DOE/EIA-0585-O ..... p 749 N95-17923 #

DOE/EM-0177-VOL-1 ..... p 739 N95-15943 #

DOE/ER-0313-100 ..... p 890 N95-16827 #
DOE/ER-12103/1 ..... p 883 N95-15947 #
DOE/ER-13400/13 ..... p 731 N95-17163 #
DOE/ER-13664/7 ..... p 731 N95-17161 #
DOE/ER-30201-H1-VOL-1 ..... p 795 N95-16386 #
DOE/ER-30201-H1-VOL-2 ..... p 727 N95-16387 #
DOE/ER-40291/21 ..... p 903 N95-16604 #
DOE/ER-40617/182 ..... p 877 N95-17358 #
DOE/ER-45400/T6 ..... p 747 N95-17719 #
DOE/ER-53198/243 ..... p 892 N95-17643
DOE/ER-54157/3 ..... p 893 N95-17644
DOE/ER-54160/1-VOL-2 ..... p 880 N95-17475 #
DOE/ER-54183/1 ..... p 888 N95-16122 #
DOE/ER-54241/131 ..... p 888 N95-16063
DOE/ER-60372/9 ..... p 803 N95-17743 #
DOE/ER-61052/3 ..... p 795 N95-16212 #

DOE/ET-53088/665 ..... p 904 N95-17645

DOE/FE-0311P ..... p 793 N95-16541 #

DOE/MC-23174/3699 ..... p 782 N95-17364 #
DOE/MC-29116/3799 ..... p 795 N95-16213 #

DOE/MT-91003/T7-ATTACH-B ... p 908 N95-16282 #

DOE/PO-0015-PT-7 ..... p 794 N95-16209 #

DOT/FAA/AM-94/26 ..... p 828 N95-17530 #
DOT/FAA/AM-94/27 ..... p 828 N95-17655 #

DOT/FAA/CT-TN92/41-I ..... p 665 N95-17373
DOT/FAA/CT-TN94/3 ..... p 665 N95-16375

DRDA-TR-94/ONR-EPIC-1 ..... p 829 N95-16119 #

DREO-1196 ..... p 727 N95-16384

DSTO-RR-0001 ..... p 870 N95-16812 #

DSTO-TR-0006 ..... p 774 N95-16247 #
DSTO-TR-0043 ..... p 656 N95-17178 #

DTIC-94/15-VR ..... p 912 N95-17660

DTIC/TR-91/2 ..... p 908 N95-16086
DTIC/TR-92/5-VOL-2 ..... p 908 N95-15998 #
DTIC/TR-92/6-VOL-2 ..... p 908 N95-15957 #
DTIC/TR-92/6-VOL-3 ..... p 908 N95-16090 #
DTIC/TR-94-23 ..... p 909 N95-16374
DTIC/TR-94/16 ..... p 908 N95-16086
DTIC/TR-94/17-VOL-2 ..... p 908 N95-15998 #
DTIC/TR-94/18-VOL-2 ..... p 908 N95-15957 #
DTIC/TR-94/18-VOL-3 ..... p 908 N95-16090 #
DTIC/TR-95-1 ..... p 909 N95-16845

DU/DC/TR-43 ..... p 900 N95-17137
DU/DC/TR-44 ..... p 900 N95-17171

E-6858 ..... p 713 N95-16066 * #
E-8079 ..... p 656 N95-16887 * #
E-8226 ..... p 789 N95-17701 * #
E-8605 ..... p 784 N95-16068 * #
E-8624 ..... p 770 N95-16407 * #
E-8725 ..... p 785 N95-16072 * #
E-8774 ..... p 722 N95-16905 * #
E-8840 ..... p 654 N95-16038 * #
E-8886 ..... p 755 N95-16886 * #
E-8933 ..... p 787 N95-16911 * #
E-9021 ..... p 711 N95-16044 * #
E-9064 ..... p 785 N95-16416 * #
E-9077 ..... p 787 N95-17270 * #
E-9158 ..... p 781 N95-16907 * #
E-9160 ..... p 670 N95-17402 * #
E-9165 ..... p 771 N95-16855 * #
E-9166 ..... p 721 N95-17274 * #
E-9180 ..... p 862 N95-16885 * #
E-9196 ..... p 840 N95-17420 * #
E-9210 ..... p 709 N95-17275 * #
E-9222 ..... p 750 N95-17893 * #
E-9231 ..... p 731 N95-17387 * #
E-9232 ..... p 769 N95-15969 * #
E-9234 ..... p 773 N95-17656 * #
E-9237 ..... p 669 N95-15970 * #
E-9243 ..... p 787 N95-17258 * #
E-9244 ..... p 675 N95-17419 * #
E-9245 ..... p 711 N95-15968 * #
E-9246 ..... p 720 N95-17265 * #
E-9248 ..... p 775 N95-16910 * #
E-9249 ..... p 725 N95-17659 * #
E-9251 ..... p 784 N95-17385 * #
E-9257 ..... p 772 N95-17386 * #
E-9258 ..... p 709 N95-16862 * #
E-9259 ..... p 793 N95-16861 * #
E-9263 ..... p 720 N95-17269 * #
E-9264 ..... p 898 N95-16598 * #
E-9270 ..... p 781 N95-17263 * #
E-9275 ..... p 839 N95-16906 * #
E-9277 ..... p 789 N95-17658 * #
E-9279 ..... p 839 N95-17264 * #
E-9282 ..... p 654 N95-17657 * #
E-9288 ..... p 772 N95-16903 * #
E-9299 ..... p 786 N95-16588 * #
E-9335 ..... p 721 N95-17276 * #

EGG-11265-1063 ..... p 774 N95-16804 #
EGG-11265-2045 ..... p 896 N95-16359 #
EGG-11265-3004 ..... p 798 N95-16284 #

EPA/600/A-94/117 ..... p 795 N95-16881 #
EPA/600/A-94/139 ..... p 793 N95-16544
EPA/600/R-94/127 ..... p 654 N95-17466

ERDEC-CR-086 ..... p 730 N95-17141

ERDEC-TR-128 ..... p 838 N95-16634 #

ERL-0656-RR ..... p 669 N95-16969 #
ERL-0825-RE ..... p 752 N95-16123 #
ERL-0827-RR ..... p 755 N95-16956 #
ERL-0828-RN ..... p 884 N95-16133 #

ESC-TR-93-184 ..... p 836 N95-16504 #
ESC-TR-93-347 ..... p 885 N95-16494 #
ESC-TR-93-364 ..... p 754 N95-16495 #
ESC-TR-94-002 ..... p 835 N95-16446 #
ESC-TR-94-079 ..... p 762 N95-16130 #
ESC-TR-94-081 ..... p 752 N95-16129 #
ESC-TR-94-083-VOL-1 ..... p 672 N95-16530 #
ESC-TR-94-091-VOL-2 ..... p 672 N95-16842

ESDP-4101 ..... p 805 N95-16610 #

ETDE/JP-MF-94796529 ..... p 724 N95-16833 #

FEL-93-A158 ..... p 838 N95-16874 #
FEL-93-A323 ..... p 752 N95-16146 #
FEL-93-B227 ..... p 755 N95-16816 #

FHWA/RD-93/038 ..... p 752 N95-16094 #

FNAL/C-94/138-E ..... p 875 N95-16868 #
FNAL/C-94/141-E ..... p 872 N95-16309 #
FNAL/C-94/145-E ..... p 876 N95-16960 #
FNAL/C-94/146-E ..... p 875 N95-16840 #
FNAL/C-94/180-E ..... p 875 N95-16914
FNAL/C-94/185-E ..... p 872 N95-16310
FNAL/C-94/193 ..... p 871 N95-15945 #
FNAL/C-94/214 ..... p 873 N95-16402 #
FNAL/C-94/250 ..... p 882 N95-17931 #
FNAL/C-94/267-E ..... p 879 N95-17932 #

FOA-A-30090-8.4,3.3 ..... p 759 N95-17301

FOA-C-10358-1.3 ..... p 653 N95-17451
FOA-C-20941-2.6 ..... p 887 N95-17409
FOA-C-20956-2.2 ..... p 840 N95-17410 #
FOA-C-20957-2.1 ..... p 671 N95-17454
FOA-C-20962-2.3 ..... p 734 N95-16420
FOA-C-30734-3.2 ..... p 759 N95-17453
FOA-C-30739-3.4 ..... p 909 N95-16400 #
FOA-C-30740-8.4,3.3 ..... p 760 N95-17455
FOA-C-30747-3.2 ..... p 775 N95-17170
FOA-C-50105-5.1 ..... p 822 N95-17300

FR-0142-94-001 ..... p 766 N95-17139
FR-60266 ..... p 744 N95-16863

FRCR-446 ..... p 888 N95-16063

GA-A-21523 ..... p 890 N95-16919
GA-A-21645 ..... p 892 N95-17497 #
GA-A-21694 ..... p 890 N95-16555 #
GA-A-21705 ..... p 892 N95-17640
GA-A-21707 ..... p 893 N95-17897 #
GA-A-21714 ..... p 889 N95-16554 #
GA-A-21735 ..... p 893 N95-17896 #

GAO/NSIAD-94-229 ..... p 914 N95-15962 #

GRI-93/0442 ..... p 783 N95-16870 #

H-1955 ..... p 788 N95-17417 * #
H-1993 ..... p 656 N95-16858 * #
H-2019 ..... p 788 N95-17490 * #
H-2027 ..... p 772 N95-17418 * #

HEI/RR-60/93 ..... p 818 N95-16801
HEI/RR-61/93 ..... p 727 N95-16373 #

ICASE-94-59 ..... p 863 N95-17266 * #
ICASE-94-70 ..... p 769 N95-16071 * #
ICASE-94-73 ..... p 863 N95-17267 * #
ICASE-94-76 ..... p 769 N95-16070 * #
ICASE-94-77 ..... p 863 N95-16897 * #
ICASE-94-79 ..... p 863 N95-16904 * #
ICASE-94-81 ..... p 862 N95-16596 * #
ICASE-94-82 ..... p 862 N95-16869 * #
ICASE-94-91 ..... p 862 N95-16896 * #

ICMA-94-188 ..... p 860 N95-16127 #
ICMA-94-189 ..... p 860 N95-16128 #

ICOMP-94-28 ..... p 773 N95-17656 * #
ICOMP-94-3 ..... p 770 N95-16407 * #
ICOMP-94-6 ..... p 771 N95-16855 * #

IDA-D-1454 ..... p 725 N95-16970 #

IDA/HQ-93-44719 ..... p 725 N95-16970 #

IFSR-665 ..... p 904 N95-17645

IHES/M/94/14 ..... p 860 N95-16291 #
IHES/M/94/15 ..... p 860 N95-16293 #
IHES/M/94/17 ..... p 860 N95-16292 #
IHES/M/94/20 ..... p 861 N95-16367 #
IHES/M/94/23 ..... p 860 N95-16294 #
IHES/M/94/24 ..... p 861 N95-16295 #

INIS-MF-13853 ..... p 892 N95-17517 #
INIS-MF-13856 ..... p 912 N95-17472 #

INP-MSU-93-4-296 ..... p 799 N95-17471 #

INPE-5572-TAE/022 ..... p 673 N95-17648 #
INPE-5575-PRE/1803 ..... p 760 N95-17649 #
INPE-5577-PRE/1805 ..... p 912 N95-17650 #
INPE-5580-TDI/543 ..... p 791 N95-17694 #
INPE-5589-TDI/551 ..... p 799 N95-17647 #

INS-1006 ..... p 877 N95-17520 #
INS-1013 ..... p 878 N95-17739 #

INT-PATENT-CLASS-G03H-1/02 . p 883 N95-15960 *
INT-PATENT-CLASS-G06F-15/16 p 832 N95-17400 *
INT-PATENT-CLASS-G06F-9/00 . p 832 N95-17400 *
INT-PATENT-CLASS-G08B-5/23 . p 883 N95-15960 *

INT-PATENT-CLASS-H01S-3/10 . p 883 N95-15960 *

IRE-93-1 ..... p 903 N95-17473 #

IS-T-1663 ..... p 735 N95-16540 #
IS-T-1672 ..... p 783 N95-16538 #
IS-T-1685 ..... p 722 N95-16058 #
IS-T-1707 ..... p 897 N95-16510 #

ISBN-0-8213-2802-6 ..... p 794 N95-17298
ISBN-0-9627116-1-6 ..... p 851 N95-15972 * #
ISBN-7-80-046602-7 ..... p 649 N95-16249 #
ISBN-90-369-2039-6 ..... p 802 N95-17529
ISBN-90-370-0096-7 ..... p 831 N95-17468
ISBN-90-6275-904-1 ..... p 887 N95-17483
ISBN-90-6275-918-1 ..... p 831 N95-16953 #
ISBN-90-6275-925-4 ..... p 732 N95-17700
ISBN-90-6275-934-3 ..... p 841 N95-17470
ISBN-90-73861-15-2 ..... p 900 N95-16952 #
ISBN-90-74445-09-8 ..... p 767 N95-17469
ISBN-90-9006256-4 ..... p 850 N95-17138 #
ISBN-90-9006355-2 ..... p 904 N95-16289 #
ISBN-90-9006737-X ..... p 800 N95-16290
ISBN-92-835-0755-X ..... p 721 N95-17278 #
ISBN-92-835-0757-6 ..... p 671 N95-17388 #
ISBN-92-836-1003-2 ..... p 657 N95-17846 #
ISBN-92-836-1007-5 ..... p 666 N95-16562 #

ISBN-951-22-1610-8 ..... p 754 N95-16613 #
ISBN-951-22-1616-7 ..... p 760 N95-17502 #
ISBN-951-22-1789-9 ..... p 802 N95-17504 #
ISBN-951-22-1998-0 ..... p 768 N95-17691
ISBN-951-22-2002-4 ..... p 754 N95-16612 #
ISBN-951-22-2050-4 ..... p 766 N95-16951 #

ISI-5923-1 ..... p 855 N95-16011 #

ISTIC-TR-93123 ..... p 670 N95-17749
ISTIC-TR-93128 ..... p 750 N95-17730

ISVR-TR-237 ..... p 769 N95-16064
ISVR-TR-240 ..... p 868 N95-16856

ITP-93-44 ..... p 904 N95-17474 #
ITP-93-47 ..... p 901 N95-17518 #

IWR-93-R-17 ..... p 796 N95-17684 #

IZF-1994-B-9 ..... p 827 N95-16615 #

JAERI-M-93-196 ..... p 740 N95-16073 #

JINR-E-17-93-366 ..... p 871 N95-16059 #
JINR-E-7-93-126 ..... p 880 N95-17519 #

JOINT-PUB-1-02(94) ..... p 912 N95-17633 #
JOINT-PUB-1-02 ..... p 912 N95-17633 #

JPL-PUBL-94-22 ..... p 792 N95-16067 * #

JPL-TDA-PR-42-119 ..... p 755 N95-17279 * #

K/CSD/TM-64-REV-5 ..... p 841 N95-17514 #

KAPL-4766 ..... p 899 N95-16913
KAPL-4773 ..... p 770 N95-16417 #

KCP-613-5318 ..... p 747 N95-17690 #
KCP-613-5431 ..... p 782 N95-17716 #
KCP-613-5434 ..... p 902 N95-17906 #

KEK-PROC-93-11 ..... p 871 N95-15956 #

KNMI-WR-93-02 ..... p 802 N95-17529

L-17053 ..... p 669 N95-17397 * #
L-17073 ..... p 653 N95-16560 * #
L-17221 ..... p 709 N95-16902 * #
L-17307 ..... p 709 N95-16559 * #
L-17330 ..... p 656 N95-16908 * #
L-17334 ..... p 665 N95-17384 * #
L-17337 ..... p 655 N95-16069 * #
L-17340 ..... p 886 N95-17271 * #
L-17358 ..... p 709 N95-16857 * #
L-17389 ..... p 924 N95-16912 * #
L-17404 ..... p 820 N95-16412 * #

LA-SUB-94-32 ..... p 763 N95-16283 #

LA-UR-94-1057 ..... p 799 N95-16927 #
LA-UR-94-1250 ..... p 835 N95-16223 #
LA-UR-94-1310 ..... p 780 N95-16224 #
LA-UR-94-1610 ..... p 798 N95-16537 #
LA-UR-94-1624 ..... p 881 N95-17721 #
LA-UR-94-1852 ..... p 891 N95-17365
LA-UR-94-1919 ..... p 900 N95-17156 #
LA-UR-94-1949 ..... p 903 N95-16428 #
LA-UR-94-1957 ..... p 891 N95-17155 #
LA-UR-94-1965 ..... p 868 N95-16288 #
LA-UR-94-1982 ..... p 876 N95-17154 #
LA-UR-94-2063 ..... p 731 N95-17157 #
LA-UR-94-2125 ..... p 879 N95-16217 #
LA-UR-94-2126 ..... p 888 N95-16218 #
LA-UR-94-2176 ..... p 889 N95-16286 #
LA-UR-94-2193 ..... p 889 N95-16285 #
LA-UR-94-2201 ..... p 876 N95-17153 #
LA-UR-94-2202 ..... p 876 N95-17158 #
LA-UR-94-2272 ..... p 896 N95-16389 #
LA-UR-94-2327 ..... p 875 N95-16931
LA-UR-94-2385 ..... p 765 N95-16920
LA-UR-94-2437 ..... p 745 N95-16938
LA-UR-94-2438 ..... p 891 N95-16936
LA-UR-94-2560 ..... p 875 N95-16933
LA-UR-94-2562 ..... p 765 N95-16932
LA-UR-94-2574 ..... p 737 N95-17641
LA-UR-94-2614 ..... p 880 N95-16937
LA-UR-94-2734 ..... p 748 N95-17892 #
LA-UR-94-2761 ..... p 878 N95-17727 #
LA-UR-94-895 ..... p 834 N95-16219 #

LA-12732-SR ..... p 879 N95-16172 #

LBL-PUB-5382 ..... p 924 N95-16120 #

LBL-34954 ..... p 881 N95-17670 #
LBL-34957 ..... p 882 N95-17891 #
LBL-34958 ..... p 882 N95-17890 #
LBL-35089 ..... p 779 N95-17887 #
LBL-35220 ..... p 779 N95-17729 #
LBL-35282 ..... p 846 N95-16222 #
LBL-35382 ..... p 775 N95-17307 #
LBL-35559 ..... p 732 N95-17437
LBL-35586 ..... p 878 N95-17889 #
LBL-35703 ..... p 904 N95-17904 #
LBL-35710 ..... p 881 N95-17886 #
LBL-35746 ..... p 878 N95-17720 #
LBL-35776 ..... p 881 N95-17888 #
LBL-35886 ..... p 881 N95-17671 #
LBL-35957 ..... p 761 N95-17672 #

LC-94-69310 ..... p 851 N95-15972 * #

LMI-PL311RD1 ..... p 912 N95-17710 #

LPI-TR-94-04 ..... p 917 N95-16176 * #

M-757 ..... p 788 N95-17272 * #

MITRE-MP-94B0000074 ..... p 755 N95-16825 #

MTI-94-TR-28 ..... p 780 N95-16139 #

MTR-93B0000091 ..... p 791 N95-17625

NAL-PD-CA-9217 ..... p 671 N95-16392 #

NAL-SP-9409 ..... p 850 N95-16901 #

NAMRL-SR-93-5 ..... p 819 N95-16151 #

NAS 1.15:104566-VOL-21 ..... p 803 N95-16006 * #
NAS 1.15:104594-VOL-4 ..... p 837 N95-16587 * #
NAS 1.15:104614 ..... p 925 N95-16581 * #
NAS 1.15:105436 ..... p 713 N95-16066 * #
NAS 1.15:106315 ..... p 840 N95-17420 * #
NAS 1.15:106513 ..... p 770 N95-16407 * #
NAS 1.15:106571 ..... p 722 N95-16905 * #
NAS 1.15:106580 ..... p 654 N95-16038 * #
NAS 1.15:106632 ..... p 787 N95-16911 * #
NAS 1.15:106702 ..... p 785 N95-16416 * #
NAS 1.15:106712 ..... p 787 N95-17270 * #
NAS 1.15:106746 ..... p 781 N95-16907 * #
NAS 1.15:106749 ..... p 771 N95-16855 * #
NAS 1.15:106750 ..... p 721 N95-17274 * #
NAS 1.15:106758 ..... p 862 N95-16885 * #
NAS 1.15:106767 ..... p 709 N95-17275 * #
NAS 1.15:106773 ..... p 750 N95-17893 * #
NAS 1.15:106778 ..... p 731 N95-17387 * #
NAS 1.15:106779 ..... p 769 N95-15969 * #
NAS 1.15:106781 ..... p 773 N95-17656 * #
NAS 1.15:106784 ..... p 669 N95-15970 * #
NAS 1.15:106787 ..... p 787 N95-17258 * #
NAS 1.15:106788 ..... p 675 N95-17419 * #
NAS 1.15:106789 ..... p 725 N95-17659 * #
NAS 1.15:106791 ..... p 784 N95-17385 * #
NAS 1.15:106794 ..... p 709 N95-16862 * #
NAS 1.15:106795 ..... p 793 N95-16861 * #
NAS 1.15:106796 ..... p 720 N95-17269 * #
NAS 1.15:106798 ..... p 781 N95-17263 * #
NAS 1.15:106799 ..... p 839 N95-16906 * #
NAS 1.15:106801 ..... p 789 N95-17658 * #
NAS 1.15:106802 ..... p 839 N95-17264 * #
NAS 1.15:106804 ..... p 654 N95-17657 * #
NAS 1.15:106806 ..... p 772 N95-16903 * #
NAS 1.15:106812 ..... p 721 N95-17276 * #
NAS 1.15:108471 ..... p 915 N95-16558 * #
NAS 1.15:109206 ..... p 676 N95-17262 * #
NAS 1.15:109896 ..... p 905 N95-15919 * #
NAS 1.15:109948 ..... p 771 N95-16828 * #
NAS 1.15:109986 ..... p 909 N95-16441 * #
NAS 1.15:110074 ..... p 786 N95-16577 * #
NAS 1.15:110107 ..... p 904 N95-16007 * #
NAS 1.15:110110 ..... p 883 N95-17933 * #
NAS 1.15:4553 ..... p 789 N95-17701 * #
NAS 1.15:4578 ..... p 886 N95-17271 * #
NAS 1.15:4579 ..... p 788 N95-17417 * #
NAS 1.15:4582 ..... p 655 N95-16069 * #
NAS 1.15:4588 ..... p 665 N95-17384 * #
NAS 1.15:4596 ..... p 656 N95-16858 * #
NAS 1.15:4601 ..... p 656 N95-16908 * #
NAS 1.15:4644 ..... p 788 N95-17490 * #
NAS 1.21:7011(396) ..... p 823 N95-17703 *
NAS 1.21:7037(311) ..... p 654 N95-17704 *
NAS 1.21:7037(312) ..... p 654 N95-17702 *
NAS 1.21:7097(02) ..... p 905 N95-16633 *
NAS 1.26: 197128 ..... p 791 N95-15963 * #
NAS 1.26:186031 ..... p 772 N95-17418 * #
NAS 1.26:189381 ..... p 911 N95-17330 * #
NAS 1.26:189382 ..... p 910 N95-17323 * #
NAS 1.26:189383 ..... p 840 N95-17324 * #

NAS 1.26:189384 ..... p 912 N95-17652 * #
NAS 1.26:189385 ..... p 911 N95-17328 * #
NAS 1.26:189386 ..... p 911 N95-17326 * #
NAS 1.26:189387 ..... p 912 N95-17491 * #
NAS 1.26:189388 ..... p 911 N95-17329 * #
NAS 1.26:189391 ..... p 910 N95-17322 * #
NAS 1.26:189392 ..... p 840 N95-17327 * #
NAS 1.26:189393 ..... p 911 N95-17325 * #
NAS 1.26:191178 ..... p 656 N95-16887 * #
NAS 1.26:193116 ..... p 836 N95-16574 * #
NAS 1.26:194470 ..... p 784 N95-16068 * #
NAS 1.26:194949 ..... p 863 N95-17266 * #
NAS 1.26:194964 ..... p 769 N95-16071 * #
NAS 1.26:194971 ..... p 863 N95-17267 * #
NAS 1.26:194979 ..... p 769 N95-16070 * #
NAS 1.26:194980 ..... p 863 N95-16897 * #
NAS 1.26:194989 ..... p 863 N95-16904 * #
NAS 1.26:194990 ..... p 862 N95-16869 * #
NAS 1.26:194992 ..... p 862 N95-16596 * #
NAS 1.26:194999 ..... p 862 N95-16896 * #
NAS 1.26:195001 ..... p 832 N95-16898 * #
NAS 1.26:195004 ..... p 736 N95-16860 * #
NAS 1.26:195312 ..... p 785 N95-16072 * #
NAS 1.26:195352 ..... p 755 N95-16886 * #
NAS 1.26:195390 ..... p 670 N95-17402 * #
NAS 1.26:195401 ..... p 711 N95-15968 * #
NAS 1.26:195402 ..... p 720 N95-17265 * #
NAS 1.26:195404 ..... p 775 N95-16910 * #
NAS 1.26:195406 ..... p 772 N95-17386 * #
NAS 1.26:195407 ..... p 898 N95-16598 * #
NAS 1.26:195413 ..... p 786 N95-16588 * #
NAS 1.26:195553-VOL-3 ..... p 780 N95-16031 * #
NAS 1.26:196154 ..... p 807 N95-16429 * #
NAS 1.26:196523 ..... p 793 N95-16575 * #
NAS 1.26:196527 ..... p 798 N95-15965 * #
NAS 1.26:196745 ..... p 917 N95-16176 * #
NAS 1.26:196819 ..... p 721 N95-16035 * #
NAS 1.26:196887 ..... p 833 N95-16088 * #
NAS 1.26:196983 ..... p 807 N95-16034 * #
NAS 1.26:196995 ..... p 750 N95-16065 * #
NAS 1.26:197005 ..... p 793 N95-16831 * #
NAS 1.26:197020 ..... p 888 N95-15941 * #
NAS 1.26:197030 ..... p 666 N95-15971 * #
NAS 1.26:197032 ..... p 748 N95-16029 * #
NAS 1.26:197098 ..... p 807 N95-15961 * #
NAS 1.26:197105 ..... p 672 N95-16033 * #
NAS 1.26:197108 ..... p 916 N95-16032 * #
NAS 1.26:197109 ..... p 668 N95-16899 * #
NAS 1.26:197124 ..... p 798 N95-16432 * #
NAS 1.26:197125 ..... p 916 N95-16020 * #
NAS 1.26:197133 ..... p 769 N95-15966 * #
NAS 1.26:197134 ..... p 726 N95-15967 * #
NAS 1.26:197213 ..... p 871 N95-16848 * #
NAS 1.26:197227 ..... p 915 N95-16021 * #
NAS 1.26:197228 ..... p 914 N95-15964 * #
NAS 1.26:197247 ..... p 724 N95-16597 * #
NAS 1.26:197248 ..... p 792 N95-16067 * #
NAS 1.26:197249 ..... p 755 N95-17279 * #
NAS 1.26:197436 ..... p 924 N95-17527 * #
NAS 1.26:197449 ..... p 870 N95-16401 * #
NAS 1.26:197450 ..... p 857 N95-17383 * #
NAS 1.26:197451 ..... p 780 N95-16900 * #
NAS 1.26:197454 ..... p 924 N95-16383 * #
NAS 1.26:197459 ..... p 761 N95-17665 * #
NAS 1.26:197461 ..... p 770 N95-16388 * #
NAS 1.26:197485 ..... p 760 N95-17651 * #
NAS 1.26:197486 ..... p 830 N95-16418 * #
NAS 1.26:197488 ..... p 655 N95-16589 * #
NAS 1.26:197489 ..... p 924 N95-17421 * #
NAS 1.26:197492 ..... p 923 N95-17403 * #
NAS 1.26:197493 ..... p 671 N95-17404 * #
NAS 1.26:197499 ..... p 858 N95-17921 * #
NAS 1.26:197500 ..... p 788 N95-17492 * #
NAS 1.26:197517 ..... p 675 N95-17493 * #
NAS 1.26:197518 ..... p 915 N95-17494 * #
NAS 1.26:197521 ..... p 831 N95-16894 * #
NAS 1.26:197522 ..... p 790 N95-16895 * #
NAS 1.26:197527 ..... p 750 N95-16880 * #
NAS 1.26:197528 ..... p 837 N95-16586 * #
NAS 1.26:197532 ..... p 917 N95-17422 * #
NAS 1.26:197534 ..... p 915 N95-17495 * #
NAS 1.26:197535 ..... p 915 N95-17496 * #
NAS 1.26:197539 ..... p 923 N95-17653 * #
NAS 1.26:197540 ..... p 746 N95-17654 * #
NAS 1.26:197556 ..... p 916 N95-17528 * #
NAS 1.26:197566 ..... p 710 N95-17331 * #
NAS 1.26:197567 ..... p 776 N95-17895 * #
NAS 1.26:4620 ..... p 724 N95-16859 * #
NAS 1.26:4628 ..... p 788 N95-17272 * #
NAS 1.26:4635 ..... p 656 N95-17273 * #
NAS 1.26:4638 ..... p 772 N95-17268 * #
NAS 1.55:10145 ..... p 711 N95-16044 * #
NAS 1.55:10159 ..... p 846 N95-16453 * #
NAS 1.55:10163 ..... p 851 N95-15972 * #
NAS 1.55:3281-PT-1 ..... p 676 N95-17179 * #
NAS 1.55:3281-PT-2 ..... p 691 N95-17531 * #

NAS 1.60-3329 p 709 N95-16902 * #
NAS 1.60:3443 p 653 N95-16560 * #
NAS 1.60:3455 p 669 N95-17397 * #
NAS 1.60:3461 p 709 N95-16559 * #
NAS 1.60:3462 p 709 N95-16857 * #
NAS 1.60:3473 p 924 N95-16912 * #
NAS 1.60:3479 p 820 N95-16412 * #
NAS 1.61:1345 p 922 N95-16436 * #
NAS 1.61:1353 p 764 N95-16561 * #

NASA-ASR-268 p 669 N95-16982 *
NASA-ASR-270 p 799 N95-16981 *

NASA-CASE-NPO-17632-1-CU p 832 N95-17400 *
NASA-CASE-NPO-18702-1-CU p 883 N95-15960 *

NASA-CP-10145 p 711 N95-16044 * #
NASA-CP-10159 p 846 N95-16453 * #
NASA-CP-10163 p 851 N95-15972 * #
NASA-CP-3281-PT-1 p 676 N95-17179 * #
NASA-CP-3281-PT-2 p 691 N95-17531 * #

NASA-CR-186031 p 772 N95-17418 * #
NASA-CR-189381 p 911 N95-17330 * #
NASA-CR-189382 p 910 N95-17323 * #
NASA-CR-189383 p 840 N95-17324 * #
NASA-CR-189384 p 912 N95-17652 * #
NASA-CR-189385 p 911 N95-17328 * #
NASA-CR-189386 p 911 N95-17326 * #
NASA-CR-189387 p 912 N95-17491 * #
NASA-CR-189388 p 911 N95-17329 * #
NASA-CR-189391 p 910 N95-17322 * #
NASA-CR-189392 p 840 N95-17327 * #
NASA-CR-189393 p 911 N95-17325 * #
NASA-CR-191178 p 656 N95-16887 * #
NASA-CR-193116 p 836 N95-16574 * #
NASA-CR-194470 p 784 N95-16068 * #
NASA-CR-194949 p 863 N95-17266 * #
NASA-CR-194964 p 769 N95-16071 * #
NASA-CR-194971 p 863 N95-17267 * #
NASA-CR-194979 p 769 N95-16070 * #
NASA-CR-194980 p 863 N95-16897 * #
NASA-CR-194989 p 863 N95-16904 * #
NASA-CR-194990 p 862 N95-16869 * #
NASA-CR-194992 p 862 N95-16596 * #
NASA-CR-194999 p 862 N95-16896 * #
NASA-CR-195001 p 832 N95-16898 * #
NASA-CR-195004 p 736 N95-16860 * #
NASA-CR-195312 p 785 N95-16072 * #
NASA-CR-195352 p 755 N95-16886 * #
NASA-CR-195390 p 670 N95-17402 * #
NASA-CR-195401 p 711 N95-15968 * #
NASA-CR-195402 p 720 N95-17265 * #
NASA-CR-195404 p 775 N95-16910 * #
NASA-CR-195406 p 772 N95-17386 * #
NASA-CR-195407 p 898 N95-16598 * #
NASA-CR-195413 p 786 N95-16588 * #
NASA-CR-195553-VOL-3 p 780 N95-16031 * #
NASA-CR-196154 p 807 N95-16429 * #
NASA-CR-196523 p 793 N95-16575 * #
NASA-CR-196527 p 798 N95-15965 * #
NASA-CR-196745 p 917 N95-16176 * #
NASA-CR-196819 p 721 N95-16035 * #
NASA-CR-196887 p 833 N95-16088 * #
NASA-CR-196983 p 807 N95-16034 * #
NASA-CR-196995 p 750 N95-16065 * #
NASA-CR-197005 p 793 N95-16831 * #
NASA-CR-197020 p 888 N95-15941 * #
NASA-CR-197030 p 666 N95-15971 * #
NASA-CR-197032 p 748 N95-16029 * #
NASA-CR-197098 p 807 N95-15961 * #
NASA-CR-197105 p 672 N95-16033 * #
NASA-CR-197108 p 916 N95-16032 * #
NASA-CR-197109 p 668 N95-16899 * #
NASA-CR-197124 p 798 N95-16432 * #
NASA-CR-197125 p 916 N95-16020 * #
NASA-CR-197128 p 791 N95-15963 * #
NASA-CR-197133 p 769 N95-15966 * #
NASA-CR-197134 p 726 N95-15967 * #
NASA-CR-197213 p 871 N95-16848 * #
NASA-CR-197227 p 915 N95-16021 * #
NASA-CR-197228 p 914 N95-15964 * #
NASA-CR-197247 p 724 N95-16597 * #
NASA-CR-197248 p 792 N95-16067 * #
NASA-CR-197249 p 755 N95-17279 * #
NASA-CR-197449 p 870 N95-16401 * #
NASA-CR-197450 p 857 N95-17383 * #
NASA-CR-197451 p 780 N95-16900 * #
NASA-CR-197454 p 924 N95-16383 * #
NASA-CR-197459 p 761 N95-17665 * #
NASA-CR-197461 p 770 N95-16386 * #
NASA-CR-197485 p 760 N95-17651 * #
NASA-CR-197486 p 830 N95-16418 * #
NASA-CR-197488 p 655 N95-16589 * #
NASA-CR-197489 p 924 N95-17421 * #
NASA-CR-197492 p 923 N95-17403 * #
NASA-CR-197493 p 671 N95-17404 * #
NASA-CR-197499 p 858 N95-17921 * #
NASA-CR-197500 p 788 N95-17492 * #
NASA-CR-197517 p 675 N95-17493 * #
NASA-CR-197518 p 915 N95-17494 * #
NASA-CR-197521 p 831 N95-16894 * #
NASA-CR-197522 p 790 N95-16895 * #
NASA-CR-197527 p 750 N95-16880 * #
NASA-CR-197528 p 837 N95-16586 * #
NASA-CR-197532 p 917 N95-17422 * #
NASA-CR-197534 p 915 N95-17495 * #
NASA-CR-197535 p 915 N95-17496 * #
NASA-CR-197536 p 924 N95-17527 * #
NASA-CR-197539 p 923 N95-17653 * #
NASA-CR-197540 p 746 N95-17654 * #
NASA-CR-197556 p 916 N95-17528 * #
NASA-CR-197566 p 710 N95-17331 * #
NASA-CR-197567 p 776 N95-17895 * #
NASA-CR-4620 p 724 N95-16859 * #
NASA-CR-4628 p 788 N95-17272 * #
NASA-CR-4635 p 656 N95-17273 * #
NASA-CR-4638 p 772 N95-17268 * #

NASA-HHR-59 p 904 N95-16007 * #

NASA-RP-1345 p 922 N95-16436 * #
NASA-RP-1353 p 764 N95-16561 * #

NASA-SP-7011(396) p 823 N95-17703 *
NASA-SP-7037(311) p 654 N95-17704 *
NASA-SP-7037(312) p 654 N95-17702 *
NASA-SP-7097(02) p 905 N95-16633 *

NASA-TM-104566-VOL-21 p 803 N95-16006 * #
NASA-TM-104594-VOL-4 p 837 N95-16587 * #
NASA-TM-104614 p 925 N95-16581 * #
NASA-TM-105436 p 713 N95-16066 * #
NASA-TM-106315 p 840 N95-17420 * #
NASA-TM-106513 p 770 N95-16407 * #
NASA-TM-106571 p 722 N95-16905 * #
NASA-TM-106580 p 654 N95-16038 * #
NASA-TM-106632 p 787 N95-16911 * #
NASA-TM-106702 p 785 N95-16416 * #
NASA-TM-106712 p 787 N95-17270 * #
NASA-TM-106746 p 781 N95-16907 * #
NASA-TM-106749 p 771 N95-16855 * #
NASA-TM-106750 p 721 N95-17274 * #
NASA-TM-106758 p 862 N95-16885 * #
NASA-TM-106767 p 709 N95-17275 * #
NASA-TM-106773 p 750 N95-17893 * #
NASA-TM-106778 p 731 N95-17387 * #
NASA-TM-106779 p 769 N95-15969 * #
NASA-TM-106781 p 773 N95-17656 * #
NASA-TM-106784 p 669 N95-15970 * #
NASA-TM-106787 p 787 N95-17258 * #
NASA-TM-106788 p 675 N95-17419 * #
NASA-TM-106789 p 725 N95-17659 * #
NASA-TM-106791 p 784 N95-17385 * #
NASA-TM-106794 p 709 N95-16862 * #
NASA-TM-106795 p 793 N95-16861 * #
NASA-TM-106796 p 720 N95-17269 * #
NASA-TM-106798 p 781 N95-17263 * #
NASA-TM-106799 p 839 N95-16906 * #
NASA-TM-106801 p 789 N95-17658 * #
NASA-TM-106802 p 839 N95-17264 * #
NASA-TM-106804 p 654 N95-17657 * #
NASA-TM-106806 p 772 N95-16903 * #
NASA-TM-106812 p 721 N95-17276 * #
NASA-TM-108471 p 915 N95-16558 * #
NASA-TM-109206 p 676 N95-17262 * #
NASA-TM-109896 p 905 N95-15919 * #
NASA-TM-109948 p 771 N95-16828 * #
NASA-TM-109986 p 909 N95-16441 * #
NASA-TM-109987 p 709 N95-16941 *
NASA-TM-109988 p 922 N95-16942 *
NASA-TM-110074 p 786 N95-16577 * #
NASA-TM-110104 p 922 N95-16836 *
NASA-TM-110105 p 922 N95-16837 *
NASA-TM-110106 p 922 N95-16838 *
NASA-TM-110107 p 904 N95-16007 * #
NASA-TM-110110 p 883 N95-17933 * #
NASA-TM-110112 p 799 N95-16981 *
NASA-TM-110113 p 669 N95-16982 *
NASA-TM-4553 p 789 N95-17701 * #
NASA-TM-4578 p 886 N95-17271 * #
NASA-TM-4579 p 788 N95-17417 * #
NASA-TM-4582 p 655 N95-16069 * #
NASA-TM-4588 p 665 N95-17384 * #
NASA-TM-4596 p 656 N95-16858 * #
NASA-TM-4601 p 656 N95-16908 * #
NASA-TM-4644 p 788 N95-17490 * #

NASA-TP-3329 p 709 N95-16902 * #
NASA-TP-3443 p 653 N95-16560 * #
NASA-TP-3455 p 669 N95-17397 * #
NASA-TP-3461 p 709 N95-16559 * #
NASA-TP-3462 p 709 N95-16857 * #
NASA-TP-3473 p 924 N95-16912 * #
NASA-TP-3479 p 820 N95-16412 * #

NATICK-TR-94/028 p 783 N95-17725 #

NAVY-CASE-73688 p 766 N95-16950
NAVY-CASE-73971 p 760 N95-17482
NAVY-CASE-73986 p 766 N95-16947 #
NAVY-CASE-74011 p 766 N95-16948 #
NAVY-CASE-74990 p 766 N95-16949 #
NAVY-CASE-75384 p 915 N95-16854
NAVY-CASE-75507 p 896 N95-16399 #
NAVY-CASE-75860 p 767 N95-17481

NAWC-WPNS-TP-8216 p 753 N95-16233 #

NAWCADWAR-93082-60 p 669 N95-17631 #

NCCOSC/RDT/E-TR-1644 p 803 N95-17709 #

NDP-043B p 805 N95-16610 #

NDSU-MPC-94-31 p 908 N95-16093 #

NHRC-TD-93-1A p 818 N95-16105 #

NHRC-93-33 p 819 N95-16152 #
NHRC-94-17 p 821 N95-16619 #

NIIYAF-MGU-93-4-296 p 799 N95-17471 #

NISTIR-5018 p 887 N95-17441
NISTIR-5408 p 737 N95-17616 #
NISTIR-5418 p 747 N95-17722
NISTIR-5423 p 774 N95-16074 #

NOAA-TM-NOS-ORCA-75 p 796 N95-17363 #

NONP-DTIC-VT-94-14638 p 912 N95-17660

NONP-NASA-SUPPL-DK-94-31624 p 724 N95-16597 * #

NONP-NASA-VT-95-33955 p 922 N95-16836 *
NONP-NASA-VT-95-33956 p 922 N95-16837 *
NONP-NASA-VT-95-33957 p 922 N95-16838 *
NONP-NASA-VT-95-34902 p 709 N95-16941 *
NONP-NASA-VT-95-34903 p 922 N95-16942 *
NONP-NASA-VT-95-35012 p 799 N95-16981 *
NONP-NASA-VT-95-35013 p 669 N95-16982 *

NPS-ME-94-003 p 782 N95-17621 #

NRA-89-OSSA-21 p 911 N95-17326 * #

NRAD-TD-2630 p 753 N95-16148 #

NRAD-TR-1620 p 886 N95-16815

NREL/TP-411-6634 p 897 N95-16424 #
NREL/TP-411-6841 p 794 N95-17521 #
NREL/TP-411-6854 p 764 N95-16425 #
NREL/TP-413-7061 p 791 N95-15944 #
NREL/TP-441-6619 p 792 N95-16437 #
NREL/TP-441-7078 p 787 N95-16939 #
NREL/TP-442-6477 p 781 N95-17169 #
NREL/TP-451-6491 p 794 N95-16957 #
NREL/TP-451-7065 p 794 N95-16940 #
NREL/TP-471-6233 p 792 N95-16435 #

NRL/FR/5520-94-9733 p 910 N95-16884 #
NRL/FR/7322-93-9439 p 800 N95-16551 #

NRL/MR/5320-94-7456 p 754 N95-16794 #
NRL/MR/5620-94-7612 p 884 N95-16296 #
NRL/MR/6180-94-7490 p 751 N95-17632 #
NRL/MR/6770-94-7609 p 891 N95-17382 #
NRL/MR/7220-94-7478 p 751 N95-16002 #
NRL/MR/7441-94-7550 p 790 N95-16547 #

NSSDC/WDC-A-R/S-94-09 p 909 N95-16441 * #

NSWCDD/TR-93/429 p 787 N95-16843 #

NTSB/AAR-94/07 p 665 N95-17646 #

NTSB/ARC-94/02 p 665 N95-17748 #

NUWC-NPT-TD-10715 p 871 N95-17177 #

NUWC-NPT-TR-10687 p 753 N95-16227 #

N0AA-TM-ERL-SEL-84 p 803 N95-17927

OCS/MMS-92/0024-VOL-1-2 p 806 N95-17615 #

ODU/ICAM-94-101 ..... p 726 N95-15967 * #
ODU/ICAM-94-102 ..... p 769 N95-15966 * #

ODURF-124303 ..... p 668 N95-16899 * #

ORNL/CDIAC-60 ..... p 805 N95-16610 #

ORNL/M-3576 ..... p 890 N95-16827 #
ORNL/M-3677 ..... p 725 N95-17368

ORNL/SUB-92-22041/01 ..... p 746 N95-17456 #

OSURF-768992/724639 ..... p 727 N95-16150 #

PB94-171956 ..... p 654 N95-17512 #
PB94-173408 ..... p 796 N95-17363 #
PB94-174505 ..... p 737 N95-17616 #
PB94-175031 ..... p 806 N95-17615 #
PB94-182722 ..... p 727 N95-16373 #
PB94-182854 ..... p 818 N95-16801
PB94-183548 ..... p 924 N95-17736
PB94-183555 ..... p 924 N95-17737
PB94-183670 ..... p 908 N95-16093 #
PB94-184439 ..... p 768 N95-17691
PB94-184595 ..... p 916 N95-17332
PB94-184611 ..... p 887 N95-17409
PB94-184660 ..... p 745 N95-17299
PB94-184710 ..... p 840 N95-17410 #
PB94-186525 ..... p 752 N95-16094 #
PB94-186848 ..... p 887 N95-17441
PB94-187663 ..... p 747 N95-17722
PB94-187713 ..... p 774 N95-16074 #
PB94-189156 ..... p 734 N95-16420
PB94-189180 ..... p 653 N95-17451
PB94-189206 ..... p 759 N95-17453
PB94-189651 ..... p 793 N95-16544
PB94-190683 ..... p 822 N95-17300
PB94-190691 ..... p 775 N95-17170
PB94-190709 ..... p 759 N95-17301
PB94-190725 ..... p 671 N95-17454
PB94-190758 ..... p 760 N95-17455
PB94-190766 ..... p 909 N95-16400 #
PB94-190857 ..... p 795 N95-16881 #
PB94-191350 ..... p 904 N95-16289 #
PB94-191368 ..... p 800 N95-16290
PB94-191392 ..... p 850 N95-17138 #
PB94-192309 ..... p 860 N95-16291 #
PB94-192333 ..... p 860 N95-16292 #
PB94-192358 ..... p 861 N95-16367 #
PB94-192366 ..... p 860 N95-16293 #
PB94-192390 ..... p 860 N95-16294 #
PB94-192408 ..... p 861 N95-16295 #
PB94-193323 ..... p 654 N95-17466
PB94-194198 ..... p 783 N95-16870 #
PB94-194792 ..... p 796 N95-17304 #
PB94-194883 ..... p 665 N95-17476 #
PB94-195492 ..... p 887 N95-17483
PB94-197613 ..... p 865 N95-17526 #
PB94-197621 ..... p 869 N95-17467 #
PB94-197654 ..... p 837 N95-16605 #
PB94-197670 ..... p 754 N95-16612 #
PB94-197688 ..... p 754 N95-16613 #
PB94-197696 ..... p 760 N95-17502 #
PB94-197704 ..... p 880 N95-17503 #
PB94-197720 ..... p 766 N95-16951 #
PB94-197753 ..... p 900 N95-16952 #
PB94-197761 ..... p 831 N95-16953 #
PB94-197852 ..... p 802 N95-17504 #
PB94-197985 ..... p 831 N95-17466
PB94-201274 ..... p 745 N95-17305
PB94-201308 ..... p 870 N95-16614
PB94-201316 ..... p 903 N95-16839
PB94-201365 ..... p 767 N95-17469
PB94-201407 ..... p 796 N95-17399
PB94-201415 ..... p 841 N95-17470
PB94-201431 ..... p 732 N95-17700
PB94-910409 ..... p 665 N95-17646 #
PB95-100319 ..... p 665 N95-17748 #
PB95-104162 ..... p 803 N95-17927
PB95-104238 ..... p 670 N95-17749
PB95-104261 ..... p 750 N95-17730
PB95-104279 ..... p 877 N95-17351
PB95-104295 ..... p 923 N95-17352
PB95-104303 ..... p 869 N95-17750
PB95-104311 ..... p 877 N95-17353
PB95-104329 ..... p 869 N95-17731
PB95-104337 ..... p 877 N95-17354
PB95-104352 ..... p 894 N95-17929 #
PB95-104360 ..... p 869 N95-17930 #
PB95-104378 ..... p 842 N95-17732
PB95-104501 ..... p 842 N95-17733
PB95-104519 ..... p 840 N95-17355
PB95-104527 ..... p 840 N95-17356
PB95-104535 ..... p 841 N95-17628
PB95-104543 ..... p 841 N95-17629
PB95-104550 ..... p 842 N95-17734
PB95-104568 ..... p 842 N95-17735

PL-TR-93-1079 ..... p 778 N95-17500
PL-TR-93-1092 ..... p 760 N95-17501
PL-TR-93-2236 ..... p 869 N95-17449
PL-TR-93-2264 ..... p 837 N95-16626 #
PL-TR-94-1004 ..... p 759 N95-17450
PL-TR-94-2014 ..... p 803 N95-17715 #
PL-TR-94-2128 ..... p 803 N95-16062 #
PL-TR-94-2182 ..... p 916 N95-16600 #

PML-1994-A24 ..... p 722 N95-16734 #

PNL-SA-22493 ..... p 736 N95-17159 #
PNL-SA-22914 ..... p 670 N95-17371 #
PNL-SA-24200 ..... p 790 N95-16215 #
PNL-SA-24223 ..... p 856 N95-16287 #
PNL-SA-24393 ..... p 856 N95-16609 #
PNL-SA-24444 ..... p 793 N95-16916
PNL-SA-24641 ..... p 791 N95-17903 #
PNL-SA-24678 ..... p 748 N95-17913 #
PNL-SA-24814 ..... p 733 N95-17912 #

PNL-10073 ..... p 864 N95-17916 #
PNL-9416 ..... p 801 N95-16961 #
PNL-9418 ..... p 796 N95-17348 #

PSI-1177/TR-1305 ..... p 655 N95-16076

R/D-6477-EN-01 ..... p 799 N95-16735 #
R/D-6812-EE-0 ..... p 767 N95-17487 #
R/D-6958-EN-09 ..... p 790 N95-17375
R/D-7294-CH-03 ..... p 728 N95-16608

RAL-94-001-VOL-1 ..... p 842 N95-17733
RAL-94-002-VOL-2 ..... p 840 N95-17355
RAL-94-003-VOL-3 ..... p 840 N95-17356
RAL-94-004-VOL-4 ..... p 841 N95-17628
RAL-94-005-VOL-5 ..... p 841 N95-17629
RAL-94-006-VOL-6 ..... p 842 N95-17734
RAL-94-007-VOL-7 ..... p 842 N95-17735
RAL-94-017 ..... p 923 N95-17352
RAL-94-047-REV ..... p 877 N95-17353
RAL-94-052 ..... p 877 N95-17351
RAL-94-055 ..... p 877 N95-17354
RAL-94-066 ..... p 869 N95-17731
RAL-94-068 ..... p 869 N95-17750

RAND/R-4179-USDP ..... p 672 N95-17427

REPT-153-4619 ..... p 773 N95-17617
REPT-26 ..... p 748 N95-17724 #
REPT-3 ..... p 874 N95-16797 #
REPT-53-2452 ..... p 723 N95-16041 #
REPT-63193-94U/P60099 ..... p 669 N95-17661 #
REPT-83-148 ..... p 735 N95-16786 #
REPT-94B00135-PT-1 ..... p 676 N95-17179 * #
REPT-94B00135-PT-2 ..... p 691 N95-17531 * #
REPT-94B00140-VOL-21 ..... p 803 N95-16006 * #
REPT-95B00010 ..... p 925 N95-16581 * #
REPT-95B00013-VOL-4 ..... p 837 N95-16587 * #

RIVM-251701011 ..... p 796 N95-17304 #

RL-TR-94-106 ..... p 753 N95-16240
RL-TR-94-108 ..... p 885 N95-16620 #
RL-TR-94-22 ..... p 885 N95-16443 #
RL-TR-94-29 ..... p 845 N95-16115
RL-TR-94-34 ..... p 833 N95-16003 #
RL-TR-94-35 ..... p 845 N95-16116
RL-TR-94-37-PT-2 ..... p 844 N95-16061 #
RL-TR-94-50 ..... p 675 N95-16005 #
RL-TR-94-67 ..... p 833 N95-16004 #
RL-TR-94-74 ..... p 754 N95-16624 #
RL-TR-94-75 ..... p 763 N95-16410
RL-TR-94-76 ..... p 764 N95-16516 #
RL-TR-94-77 ..... p 844 N95-16060 #
RL-TR-94-85 ..... p 754 N95-16621 #
RL-TR-94-96 ..... p 857 N95-17381 #

RR-A-331 ..... p 865 N95-17526 #

RXR-93121 ..... p 837 N95-16626 #

S-777 ..... p 922 N95-16436 * #
S-787 ..... p 764 N95-16561 * #
S-788 ..... p 851 N95-15972 * #

SAND-93-0208C ..... p 671 N95-16509 #
SAND-93-1380 ..... p 784 N95-17360 #
SAND-93-2513 ..... p 788 N95-17439 #
SAND-93-2766C ..... p 888 N95-16216 #
SAND-94-0047C ..... p 727 N95-16362 #
SAND-94-0219 ..... p 733 N95-17744 #
SAND-94-0337C ..... p 782 N95-17366
SAND-94-0484 ..... p 880 N95-17361 #
SAND-94-0919C ..... p 835 N95-16358 #
SAND-94-1125 ..... p 778 N95-17498 #
SAND-94-1263C ..... p 763 N95-16357 #
SAND-94-1436C ..... p 777 N95-16917
SAND-94-1492C ..... p 793 N95-16831 * #
SAND-94-1497 ..... p 799 N95-17362 #
SAND-94-1547 ..... p 850 N95-17516 #
SAND-94-1577C ..... p 748 N95-16214 #
SAND-94-1582C ..... p 850 N95-16830
SAND-94-1629C ..... p 744 N95-16829
SAND-94-1669C ..... p 744 N95-16934
SAND-94-1726C ..... p 895 N95-16311 #
SAND-94-1825C ..... p 764 N95-16832
SAND-94-1898C ..... p 894 N95-15942 #
SAND-94-2066C ..... p 879 N95-17918 #
SAND-94-2072C ..... p 858 N95-17915 #
SAND-94-2100C ..... p 902 N95-17917 #
SAND-94-2352C ..... p 882 N95-17914 #
SAND-94-8227 ..... p 850 N95-17638

SC71024.FR ..... p 728 N95-16497 #
SC71047.FR ..... p 735 N95-16514 #

SGD-596-PT-1 ..... p 924 N95-17736
SGD-596-PT-2 ..... p 924 N95-17737

SMC-TR-94-28 ..... p 713 N95-16302
SMC-TR-94-32 ..... p 901 N95-17620
SMC-TR-94-34 ..... p 777 N95-16548 #
SMC-TR-94-35 ..... p 752 N95-16143 #

SNL-FAO-AI-7233 ..... p 891 N95-17382 #

SPC-94032-CMC ..... p 837 N95-16607 #

SR-1 ..... p 869 N95-17449
SR-3 ..... p 803 N95-17715 #

SRL-0114-RN ..... p 887 N95-17489 #
SRL-11-F-1993 ..... p 892 N95-17623

SSD94D0335 ..... p 666 N95-15971 * #

STK-221-VOL-1 ..... p 672 N95-16530 #
STK-221-VOL-2 ..... p 672 N95-16842

SU-SLAC-PUB-6495 ..... p 903 N95-16944 #
SU-SLAC-PUB-6505 ..... p 875 N95-16943 #
SU-SLAC-PUB-6630 ..... p 904 N95-17668 #
SU-SLAC-PUB-6631 ..... p 877 N95-17669 #

TDCK-93-2434 ..... p 755 N95-16816 #
TDCK-93-2438 ..... p 838 N95-16874 #
TDCK-93-3418 ..... p 752 N95-16146 #
TDCK-94-0028 ..... p 722 N95-16734 #
TDCK-94-0045 ..... p 827 N95-16822 #
TDCK-94-0048 ..... p 830 N95-16821 #
TDCK-94-0049 ..... p 827 N95-16615 #
TDCK-94-0053 ..... p 827 N95-16817 #
TDCK-94-0063 ..... p 828 N95-16835 #

TEC-0045 ..... p 909 N95-16431 #
TEC-0046 ..... p 858 N95-17634 #

TKK-F-A677 ..... p 869 N95-17930 #
TKK-F-A717 ..... p 894 N95-17929 #
TKK-F-A724 ..... p 880 N95-17503 #
TKK-F-A725 ..... p 869 N95-17467 #

TKO-B114 ..... p 837 N95-16605 #

TN-BN-1171 ..... p 863 N95-17431

TNO-TM-1994-B-11 ..... p 827 N95-16817 #
TNO-TM-1994-B-13 ..... p 828 N95-16835 #
TNO-TM-1994-B-6 ..... p 827 N95-16822 #
TNO-TM-1994-B-8 ..... p 830 N95-16821 #

TOP-6-2-542 ..... p 755 N95-16800

TR-0090(5930-07)-2 ..... p 777 N95-16548 #
TR-057 ..... p 729 N95-16635 #
TR-1001 ..... p 754 N95-16495 #
TR-1002 ..... p 752 N95-16129 #
TR-1003 ..... p 762 N95-16130 #
TR-11 ..... p 739 N95-15996 #
TR-13 ..... p 872 N95-16241
TR-16-1 ..... p 742 N95-16451 #
TR-17 ..... p 743 N95-16500 #
TR-18 ..... p 743 N95-16501 #
TR-19 ..... p 742 N95-16450 #
TR-1 ..... p 735 N95-16606 #
TR-1 ..... p 878 N95-17692
TR-2-ONR ..... p 897 N95-16508 #
TR-20-ONR ..... p 747 N95-17682
TR-28 ..... p 743 N95-16628 #

TR-29-ONR ..... p 874 N95-16784 #
TR-3-ONR ..... p 734 N95-16505
TR-3-ONR ..... p 735 N95-16788 #
TR-30-ONR ..... p 743 N95-16783 #
TR-31-ONR ..... p 902 N95-17711 #
TR-32 ..... p 904 N95-17712
TR-33-ONR ..... p 874 N95-16799 #
TR-35 ..... p 874 N95-16629 #
TR-36 ..... p 743 N95-16630 #
TR-4-ONR ..... p 873 N95-16482 #
TR-40-ONR ..... p 747 N95-17685 #
TR-477 ..... p 833 N95-16040 #
TR-479 ..... p 845 N95-16082
TR-486 ..... p 845 N95-16083
TR-495 ..... p 859 N95-16022 #
TR-499 ..... p 859 N95-15951 #
TR-4 ..... p 818 N95-16112 #
TR-4 ..... p 730 N95-16973
TR-501 ..... p 859 N95-15950 #
TR-503 ..... p 859 N95-15949 #
TR-505 ..... p 859 N95-15948 #
TR-506 ..... p 864 N95-16039 #
TR-513 ..... p 845 N95-16113 #
TR-519 ..... p 839 N95-17261 #
TR-521 ..... p 839 N95-16883 #
TR-59 ..... p 868 N95-16162 #
TR-5 ..... p 723 N95-16016 #
TR-5 ..... p 897 N95-16445 #
TR-62 ..... p 728 N95-16406 #
TR-74 ..... p 746 N95-17485
TR-7 ..... p 741 N95-16409
TR-8 ..... p 742 N95-16449 #
TR-9-ONR ..... p 733 N95-16104 #
TR-93(3507)-1 ..... p 713 N95-16302
TR-93-14 ..... p 860 N95-16169
TR-93-20 ..... p 865 N95-17426
TR-94(4925)-4 ..... p 752 N95-16143 #
TR-94(4935)-7 ..... p 901 N95-17620
TR-94-01 ..... p 745 N95-17434
TR-94-08 ..... p 861 N95-16395
TR-94-12 ..... p 742 N95-16427
TR-996 ..... p 885 N95-16494 #
TR-9 ..... p 744 N95-16865 #

TRS-465 ..... p 842 N95-17732

UC-904 ..... p 899 N95-16913

UCB/CSD-94-823 ..... p 844 N95-15940

UCLA ENG-93-43 ..... p 675 N95-17493 * #

UCRL-CR-117234 ..... p 745 N95-16935
UCRL-CR-118201 ..... p 732 N95-17642

UCRL-ID-116573-PHASE-1-2 ..... p 797 N95-17920 #
UCRL-ID-117079 ..... p 765 N95-16925
UCRL-ID-117229 ..... p 749 N95-16542 #
UCRL-ID-117435 ..... p 722 N95-17745 #
UCRL-ID-117530 ..... p 782 N95-17717 #
UCRL-ID-117543 ..... p 797 N95-17718 #
UCRL-ID-117603 ..... p 732 N95-17639

UCRL-JC-114014-REV-1 ..... p 751 N95-17738 #
UCRL-JC-114062 ..... p 777 N95-16929
UCRL-JC-114732 ..... p 736 N95-17378 #
UCRL-JC-114823 ..... p 775 N95-17380 #
UCRL-JC-114954 ..... p 779 N95-17688 #
UCRL-JC-114987 ..... p 777 N95-17168 #
UCRL-JC-115121 ..... p 902 N95-17742 #
UCRL-JC-115149 ..... p 899 N95-16867 #
UCRL-JC-115511 ..... p 779 N95-17689 #
UCRL-JC-115599 ..... p 779 N95-17635
UCRL-JC-115712-REV-1 ..... p 765 N95-16915
UCRL-JC-115839 ..... p 836 N95-16536 #
UCRL-JC-115911 ..... p 884 N95-16366 #
UCRL-JC-116229 ..... p 834 N95-16220 #
UCRL-JC-116231 ..... p 860 N95-16221 #
UCRL-JC-116246 ..... p 770 N95-16211 #
UCRL-JC-116505-REV-1 ..... p 916 N95-17525 #
UCRL-JC-116618 ..... p 861 N95-16535 #
UCRL-JC-116952 ..... p 745 N95-17379 #
UCRL-JC-117170 ..... p 776 N95-17522 #
UCRL-JC-117488 ..... p 778 N95-17627

UCRL-MA-116567 ..... p 797 N95-17922 #
UCRL-MA-117541 ..... p 749 N95-17919 #

UCRL-52000-94-7 ..... p 710 N95-17359 #

UILU-ENG-94-2216 ..... p 762 N95-16089 #
UILU-ENG-94-2225 ..... p 833 N95-16088 * #
UILU-ENG-94-4010 ..... p 730 N95-16955 #
UILU-ENG-94-4011 ..... p 889 N95-16243 #

UMR-FDB-39 ..... p 740 N95-16092 #

US-PATENT-APPL-SN-012140 ..... p 775 N95-17428
US-PATENT-APPL-SN-019414 ..... p 767 N95-17478
US-PATENT-APPL-SN-034802 ..... p 732 N95-17479
US-PATENT-APPL-SN-067504 ..... p 777 N95-17302
US-PATENT-APPL-SN-082640 ..... p 738 N95-17699
US-PATENT-APPL-SN-083776 ..... p 761 N95-17696
US-PATENT-APPL-SN-099510 ..... p 747 N95-17693
US-PATENT-APPL-SN-106746 ..... p 754 N95-16549 #
US-PATENT-APPL-SN-107431 ..... p 766 N95-16950
US-PATENT-APPL-SN-140388 ..... p 747 N95-17694 #
US-PATENT-APPL-SN-168787 ..... p 766 N95-16948 #
US-PATENT-APPL-SN-168788 ..... p 766 N95-16947 #
US-PATENT-APPL-SN-168789 ..... p 766 N95-16949 #
US-PATENT-APPL-SN-186075 ..... p 915 N95-16854
US-PATENT-APPL-SN-196074 ..... p 887 N95-17695 #
US-PATENT-APPL-SN-223350 ..... p 764 N95-16539 #
US-PATENT-APPL-SN-226586 ..... p 896 N95-16399 #
US-PATENT-APPL-SN-230459 ..... p 760 N95-17480 #
US-PATENT-APPL-SN-245284 ..... p 760 N95-17482
US-PATENT-APPL-SN-246206 ..... p 767 N95-17481
US-PATENT-APPL-SN-268341 ..... p 780 N95-16543 #
US-PATENT-APPL-SN-712796 ..... p 832 N95-17400 *
US-PATENT-APPL-SN-752249 ..... p 746 N95-17462
US-PATENT-APPL-SN-796553 ..... p 767 N95-17463
US-PATENT-APPL-SN-800341 ..... p 858 N95-17465
US-PATENT-APPL-SN-834916 ..... p 761 N95-17697
US-PATENT-APPL-SN-842300 ..... p 883 N95-15960 *
US-PATENT-APPL-SN-861409 ..... p 778 N95-17464
US-PATENT-APPL-SN-936369 ..... p 857 N95-16823 #
US-PATENT-APPL-SN-947593 ..... p 782 N95-17461
US-PATENT-APPL-SN-965329 ..... p 775 N95-17376
US-PATENT-APPL-SN-968890 ..... p 779 N95-17698

US-PATENT-CLASS-250-207 ..... p 767 N95-17478
US-PATENT-CLASS-257-593 ..... p 767 N95-17463
US-PATENT-CLASS-333-109 ..... p 761 N95-17696
US-PATENT-CLASS-340-466 ..... p 858 N95-17465
US-PATENT-CLASS-356-345 ..... p 775 N95-17428
US-PATENT-CLASS-359-183 ..... p 883 N95-15960 *
US-PATENT-CLASS-359-279 ..... p 883 N95-15960 *
US-PATENT-CLASS-364-DIG.1 .... p 832 N95-17400 *
US-PATENT-CLASS-364-231.9 .... p 832 N95-17400 *
US-PATENT-CLASS-364-525 ..... p 761 N95-17697
US-PATENT-CLASS-372-18 ..... p 883 N95-15960 *
US-PATENT-CLASS-372-20 ..... p 777 N95-17302
US-PATENT-CLASS-372-6 ..... p 779 N95-17698
US-PATENT-CLASS-372-95 ..... p 883 N95-15960 *
US-PATENT-CLASS-395-375 ..... p 832 N95-17400 *
US-PATENT-CLASS-395-800 ..... p 832 N95-17400 *
US-PATENT-CLASS-415-104 ..... p 782 N95-17461
US-PATENT-CLASS-422-7 ..... p 738 N95-17699
US-PATENT-CLASS-556-112 ..... p 732 N95-17479
US-PATENT-CLASS-73-862.333 .. p 775 N95-17376

US-PATENT-5,301,127 ..... p 761 N95-17697
US-PATENT-5,305,075 ..... p 775 N95-17428
US-PATENT-5,306,836 ..... p 732 N95-17479
US-PATENT-5,306,904 ..... p 767 N95-17478
US-PATENT-5,307,358 ..... p 777 N95-17302
US-PATENT-5,309,140 ..... p 858 N95-17465
US-PATENT-5,311,055 ..... p 767 N95-17463
US-PATENT-5,312,585 ..... p 738 N95-17699
US-PATENT-5,313,477 ..... p 779 N95-17698
US-PATENT-5,315,881 ..... p 775 N95-17376
US-PATENT-5,320,482 ..... p 782 N95-17461
US-PATENT-5,320,870 ..... p 746 N95-17462
US-PATENT-5,320,978 ..... p 747 N95-17693
US-PATENT-5,323,013 ..... p 778 N95-17464
US-PATENT-5,323,126 ..... p 761 N95-17696
US-PATENT-5,347,392 ..... p 883 N95-15960 *
US-PATENT-5,361,367 ..... p 832 N95-17400 *

USAARL-94-29 ..... p 886 N95-17334 #
USAARL-94-32 ..... p 831 N95-17484 #
USAARL-94-33 ..... p 829 N95-16145 #
USAARL-94-35 ..... p 818 N95-16132 #
USAARL-94-37 ..... p 869 N95-16226 #
USAARL-94-38 ..... p 870 N95-16811 #
USAARL-94-40 ..... p 827 N95-16520 #
USAARL-94-41-VOL-1 ..... p 829 N95-16147 #
USAARL-94-42 ..... p 664 N95-16404 #

USACERL-FF-TR-94/31 ..... p 839 N95-17176 #

USAMRICD-TR-93-04 ..... p 818 N95-17666
USAMRICD-TR-94-02 ..... p 821 N95-16491 #

USARIEM-TR-94-18 ..... p 819 N95-16228 #

USARIEM-T94-16 ..... p 821 N95-16809 #

USATEC-R-229 ..... p 666 N95-17508

USCG-D-10-94 ..... p 805 N95-16414

UTD-23253-961 ..... p 798 N95-16432 * #

UTHSCSA-OPH-94-01 ..... p 822 N95-16871 #

UTK-PSL-94-3 ..... p 755 N95-16968 #

UVA/525771/MSE94/101 ..... p 738 N95-17664 #

WES/TR/EL-94-4-VOL-1 ..... p 804 N95-16118 #

WES/TR/GL-94-29 ..... p 799 N95-16872 #

WES/TR/SL-94-15 ..... p 781 N95-17335

WHC-EP-0772 ..... p 737 N95-17637

WL-TR-93-3048 ..... p 655 N95-16808 #
WL-TR-93-3112 ..... p 708 N95-16304
WL-TR-94-1049 ..... p 834 N95-16107
WL-TR-94-1093 ..... p 909 N95-16879 #
WL-TR-94-2055 ..... p 780 N95-16139 #
WL-TR-94-3127 ..... p 784 N95-15953 #
WL-TR-94-4006 ..... p 784 N95-17507
WL-TR-94-4027 ..... p 737 N95-17398
WL-TR-94-4096 ..... p 764 N95-16814 #
WL-TR-94-5028 ..... p 881 N95-17619
WL-TR-94-7033 ..... p 671 N95-16381

WORLD-BANK-TP-244 ..... p 794 N95-17298

WSRC-IM-90-83-14 ..... p 841 N95-17515 #

WSRC-TR-93-0106 ..... p 795 N95-16557 #

APPENDIX

NASA SCIENTIFIC AND TECHNICAL INFORMATION OFFICE PRODUCTS AND SERVICES

The NASA Scientific and Technical Information (STI) Office provides for the collection and announcement of aerospace-related reports and literature obtained worldwide through agreements and exchanges. The result of the collection is the comprehensive NASA STI Database that covers aeronautics, space, and supporting disciplines.

The STI Database, documents generated or obtained by NASA, and products and services derived from or supporting the database are made available to the NASA research community and to the public. Descriptions and sources of these items are presented in the following pages.

Scientific and Technical Aerospace Reports (STAR) is an abstract journal, listing citations with abstracts for aerospace-related reports obtained from worldwide sources. *STAR* is issued on the first of each month, and announces current documents that have been entered into the NASA STI Database during the previous month. The reports are of the following types:

- NASA, NASA contractor, and NASA grantee reports;
- Reports issued by other U.S. Government agencies, domestic and foreign institutions, universities, and private firms;
- Translations in report form;
- NASA-owned patents and patent applications
- Other U.S. Government agency and foreign patents and patent applications
- Domestic and foreign dissertations and theses.

Journal, book, and conference literature, journal translations, and certain foreign dissertations having the same subject scope as *STAR* are announced in a companion journal, *NASA Open Volumes on Aerospace (NOVA). NOVA* is issued on the 15th of each month and is available from the NASA Center for AeroSpace Information, at the address below.

ELIGIBILITY AND REGISTRATION FOR NASA STI PRODUCTS AND SERVICES

Organizations of the type listed below that have registered with NASA can receive products and services.

- NASA offices and installations, contractors, subcontractors, grantees, and consultants;
- Other U.S. Government agencies and their contractors;
- Libraries in the United States that have arrangements with NASA to maintain collections of NASA documents for public reference;
- Other organizations in the United States having a need for NASA documents in work related to aeronautics and space research;
- Organizations abroad that have established reciprocal documents exchange arrangements with NASA.

The central service points—central points of document acquisition and control within qualified organizations—or individuals are eligible to register for NASA STI products and services. Domestic organizations or individuals may be eligible to receive various classes of NASA publications and services and should address their requests for registration or further information to:

ATTN: Registration Services
NASA Center for AeroSpace Information
800 Elkridge Landing Road
Linthicum Heights, MD 21090-2934
301-621-0390

Organizations abroad should direct requests to:

National Aeronautics and Space Administration
Scientific and Technical Information Office (JTT)
International STI Office
Washington, DC 20546-0001
USA
703-271-5640

SUBJECT SCOPE

The subject scope of *STAR* and *NOVA* includes all aspects of aeronautics and space research and development, supporting basic and applied research, and applications. Aerospace aspects of Earth resources, energy development, conservation, oceanography, environmental protection, urban transportation, and other topics of high national priority are also covered.

HOW TO USE *STAR* SUBJECT CATEGORIES

Abstracts in *STAR* are categorized by 10 major subject divisions that are divided further into 76 specific subject categories. The subject divisions and categories are listed in the Table of Contents together with a note for each that defines its scope and provides any cross-references. For example:

16 SPACE TRANSPORTATION

Includes passenger and cargo space transportation, e.g., shuttle operations; and space rescue techniques. For related information see also *03 Air Transportation and Safety* and *18 Spacecraft Design, Testing and Performance*. For space suits see *54 Man/System Technology and Life Support*.

CROSS-REFERENCES

Individual *STAR* abstracts are not ordinarily cross-referenced, except for certain conference reports or book translations that have had separate abstracts written for their component papers or chapters. Citations and abstracts of the components follow immediately after those of the parent document. When the subject content of a component differs sufficiently from the general content of the parent, a cross-reference citation also is printed at the end of the category to which it normally would have been assigned if it were independent.

DOCUMENTS ON MICROFICHE

Documents available on microfiche are designated by a pound sign (#) following the accession number.

LIMITED REPRODUCIBILITY

A note of limited reproducibility appears in the citation, if there are factors affecting the reproducibility of more than 20% of the document. These factors include faint or broken type, color photographs, black and white photographs, foldouts, dot matrix print, or some other factor that limits the reproducibility of the document. This notation also appears on the microfiche header.

NASA PATENTS AND PATENT APPLICATIONS

Patents and patent applications owned by NASA are announced in *STAR* under appropriate subject categories and are referenced in the *STAR* indexes. In the Report Number Index, patents are indexed by the NASA Case Number, and the U.S. Patent Class. Patent applications are indexed by the NASA Case Number and the U.S. Patent Application Serial Number.

Printed copies of patents (which are not microfiched) are available for purchase from the U.S. Patent and Trademark Office.

When ordering patents, the U.S. Patent Number should be used, and payment must be remitted in advance, by money order or check payable to the Commissioner of Patents and Trademarks. Prepaid purchase coupons for ordering are also available from the U.S. Patent and Trademark Office.

NASA patent application specifications are sold in both paper copy and microfiche by the NASA Center for AeroSpace Information (CASI). The N accession number should be used in ordering either paper copy or microfiche from CASI.

The patents and patent applications announced in *STAR* are owned by NASA and are available for royalty-free licensing. Requests for licensing terms and further information should be addressed to:

National Aeronautics and Space Administration
Associate General Counsel for Intellectual Property
Code GP
Washington, DC 20546-0001

SOURCES FOR DOCUMENTS

One or more sources from which a document announced in *STAR* is available to the public is ordinarily given on the last line of the citation. The most commonly indicated sources and their acronyms or abbreviations are listed below, and their addresses are listed on page A-6. If the publication is available from a source other than those listed, the publisher and his address will be displayed on the availability line or in combination with the corporate source line.

Avail: CASI. Sold by the NASA Center for AeroSpace Information. Prices for hard copy (HC) and microfiche (MF) are indicated by a price code following the letters HC or MF in the *STAR* citation. Current values for the price codes are given in the tables on page A-7.

NOTE ON ORDERING DOCUMENTS: When ordering publications from NASA CASI, use the N accession number or other report number. It is also advisable to cite the title and other bibliographic identification.

Avail: SOD (or GPO). Sold by the Superintendent of Documents, U.S. Government Printing Office, in hard copy.

Avail: BLL (formerly NLL): British Library Lending Division, Boston Spa, Wetherby, Yorkshire, England. Photocopies available from this organization at the price shown. (If none is given, inquiry should be addressed to the BLL.)

Avail: DOE Depository Libraries. Organizations in U.S. cities and abroad that maintain collections of Department of Energy reports, usually in microfiche form, are listed in *Energy Research Abstracts*. Services available from the DOE and its depositories are described in a booklet, *DOE Technical Information Center - Its Functions and Services* (TID-4660), which may be obtained without charge from the DOE Technical Information Center.

Avail: ESDU. Pricing information on specific data, computer programs, and details on Engineering Sciences Data Unit (ESDU) topic categories can be obtained from ESDU International Ltd. Requesters in North America should use the Virginia address while all other requesters should use the London address, both of which are on page A-6.

Avail: Fachinformationszentrum Karlsruhe. Gesellschaft für wissenschaftlich-technische Information mbH 76344 Eggenstein-Leopoldshafen, Germany.

Avail: HMSO. Publications of Her Majesty's Stationery Office are sold in the U.S. by Pendragon House, Inc. (PHI), Redwood City, CA. The U.S. price (including a service and mailing charge) is given, or a conversion table may be obtained from PHI.

Avail: Issuing Activity, or Corporate Author, or no indication of availability. Inquiries as to the availability of these documents should be addressed to the organization shown in the citation as the corporate author of the document.

Avail: NASA Public Document Rooms. Documents so indicated may be examined at or purchased from the National Aeronautics and Space Administration (JBD-4), Public Documents Room (Room 1H23), Washington, DC 20546-0001, or public document rooms located at NASA installations, and the NASA Pasadena Office at the Jet Propulsion Laboratory.

Avail: NTIS. Sold by the National Technical Information Service. Initially distributed microfiche under the NTIS SRIM (Selected Research in Microfiche) are available. For information concerning this service, consult the NTIS Subscription Section, Springfield, VA 22161.

Avail: Univ. Microfilms. Documents so indicated are dissertations selected from *Dissertation Abstracts* and are sold by University Microfilms as xerographic copy (HC) and microfilm. All requests should cite the author and the Order Number as they appear in the citation.

Avail: US Patent and Trademark Office. Sold by Commissioner of Patents and Trademarks, U.S. Patent and Trademark Office, at the standard price of $1.50 each, postage free. (See discussion of NASA patents and patent applications on page A-3.)

Avail: (US Sales Only). These foreign documents are available to users within the United States from the National Technical Information Service (NTIS). They are available to users outside the United States through the International Nuclear Information Service (INIS) representative in their country, or by applying directly to the issuing organization.

Avail: USGS. Originals of many reports from the U.S. Geological Survey, which may contain color illustrations, or otherwise may not have the quality of illustrations preserved in the microfiche or facsimile reproduction, may be examined by the public at the libraries of the USGS field offices whose addresses are listed on page A-6. The libraries may be queried concerning the availability of specific documents and the possible utilization of local copying services, such as color reproduction.

FEDERAL DEPOSITORY LIBRARY PROGRAM

In order to provide the general public with greater access to U.S. Government publications, Congress established the Federal Depository Library Program under the Government Printing Office (GPO), with 53 regional depositories responsible for permanent retention of material, inter-library loan, and reference services. At least one copy of nearly every NASA and NASA-sponsored publication, either in printed or microfiche format, is received and retained by the 53 regional depositories. A list of the regional GPO libraries, arranged alphabetically by state, appears on page A-8. These libraries are *not* sales outlets. A local library can contact a regional depository to help locate specific reports, or direct contact may be made by an individual.

PUBLIC COLLECTION OF NASA DOCUMENTS

An extensive collection of NASA and NASA-sponsored publications is maintained by the British Library Lending Division, Boston Spa, Wetherby, Yorkshire, England for public access. The British Library Lending Division also has available many of the non-NASA publications cited in *STAR*. European requesters may purchase facsimile copy or microfiche of NASA and NASA-sponsored documents, those identified by both the symbols # and * from ESA — Information Retrieval Service European Space Agency, 8-10 rue Mario-Nikis, 75738 CEDEX 15, France.

SUBMITTING DOCUMENTS

All users of this abstract service are urged to forward reports to be considered for announcement in *STAR*. This will aid NASA in its efforts to provide the fullest possible coverage of all scientific and technical publications that might support aeronautics and space research and development. If you have prepared relevant reports (other than those you will transmit to NASA, DOD, or DOE through the

usual contract- or grant-reporting channels), please send them for consideration to the NASA Center for AeroSpace Information, 800 Elkridge Landing Road, Linthicum Heights, MD 21090-2934.

Reprints of journal articles, book chapters, and conference papers are also welcome. These will be considered for announcement in *STAR's* companion journal, *NOVA*.

You may specify a particular source to be included in a report announcement if you wish; otherwise the report will be placed on a public sale at the NASA Center for AeroSpace Information. Copyrighted publications will be announced but not distributed or sold.

PURCHASE OF *STAR*

STAR is publicly available on annual subscription from the NASA Center for AeroSpace Information (CASI). 1995 *STAR* subscription prices are $100.00/domestic and $125.00/foreign. Single copy prices: $33.00/domestic, $41.00/foreign.

An annual, cumulative *STAR Index* is also available at $70.00/domestic and foreign.

STAR is available to registered users on annual subscription from the NASA Center for AeroSpace Information, ATTN: Registration Services, 800 Elkridge Landing Road, Linthicum Heights, MD 21090-2934.

ADDRESSES OF ORGANIZATIONS

British Library Lending Division
Boston Spa, Wetherby, Yorkshire
England

Commissioner of Patents and Trademarks
U.S. Patent and Trademark Office
Washington, DC 20231

Department of Energy
Technical Information Center
P.O. Box 62
Oak Ridge, TN 37830

European Space Agency-
Information Retrieval Service ESRIN
Via Galileo Galilei
00044 Frascati (Rome) Italy

Engineering Sciences Data Unit International
P.O. Box 1633
Manassas, VA 22110

Engineering Sciences Data Unit
International, Ltd.
251-259 Regent Street
London, W1R 7AD, England

Fachinformationszentrum Karlsruhe
Gesellschaft für wissenschaftlich-technische
Information mbH
76344 Eggenstein-Leopoldshafen, Germany

Her Majesty's Stationery Office
P.O. Box 569, S.E. 1
London, England

NASA Center for AeroSpace Information
800 Elkridge Landing Road
Linthicum Heights, MD 21090-2934

National Aeronautics and Space Administration
Scientific and Technical Information Office
(JTT)
Washington, DC 20546-0001

National Technical Information Service
5285 Port Royal Road
Springfield, VA 22161

Pendragon House, Inc.
899 Broadway Avenue
Redwood City, CA 94063

Superintendent of Documents
U.S. Government Printing Office
Washington, DC 20402

University Microfilms
A Xerox Company
300 North Zeeb Road
Ann Arbor, MI 48106

University Microfilms, Ltd.
Tylers Green
London, England

U.S. Geological Survey Library National Center
MS 950
12201 Sunrise Valley Drive
Reston, VA 22092

U.S. Geological Survey Library
2255 North Gemini Drive
Flagstaff, AZ 86001

U.S. Geological Survey
345 Middlefield Road
Menlo Park, CA 94025

U.S. Geological Survey Library
Box 25046
Denver Federal Center, MS914
Denver, CO 80225

NASA CASI PRICE CODE TABLE

(Effective January 1, 1995)

CASI PRICE CODE	NORTH AMERICAN PRICE	FOREIGN PRICE
A01	$ 6.00	$ 12.00
A02	9.00	18.00
A03	17.50	35.00
A04-A05	19.50	39.00
A06-A09	27.00	54.00
A10-A13	36.50	73.00
A14-A17	44.50	89.00
A18-A21	52.00	104.00
A22-A25	61.00	122.00
A99	Call For Price	Call For Price

IMPORTANT NOTICE

For users not registered at the NASA CASI, prepayment is required. Additionally, a shipping and handling fee of $1.00 per document for delivery within the United States and $9.00 per document for delivery outside the United States is charged.

For users registered at the NASA CASI, document orders may be invoiced at the end of the month, charged against a deposit account, or paid by check or credit card. NASA CASI accepts American Express, Diners' Club, MasterCard, and VISA credit cards. There are no shipping and handling charges. To register at the NASA CASI, please request a registration form through the NASA Access Help Desk at the address or numbers below.

NASA Center for AeroSpace Information
800 Elkridge Landing Road
Linthicum Heights, MD 21090-2934
Telephone: (301) 621-0390
E-mail: help@sti.nasa.gov
Fax: (301) 621-0134

FEDERAL REGIONAL DEPOSITORY LIBRARIES

ALABAMA

AUBURN UNIV. AT MONTGOMERY LIBRARY
Documents Dept.
7300 University Dr.
Montgomery, AL 36117-3596
(205) 244-3650 Fax: (205) 244-0678

UNIV. OF ALABAMA
Amelia Gayle Gorgas Library
Govt. Documents
P.O. Box 870266
Tuscaloosa, AL 35487-0266
(205) 348-6046 Fax: (205) 348-0760

ARIZONA

DEPT. OF LIBRARY, ARCHIVES, AND PUBLIC RECORDS
Research Division
Third Floor, State Capitol
1700 West Washington
Phoenix, AZ 85007
(602) 542-3701 Fax: (602) 542-4400

ARKANSAS

ARKANSAS STATE LIBRARY
State Library Service Section
Documents Service Section
One Capitol Mall
Little Rock, AR 72201-1014
(501) 682-2053 Fax: (501) 682-1529

CALIFORNIA

CALIFORNIA STATE LIBRARY
Govt. Publications Section
P.O. Box 942837 - 914 Capitol Mall
Sacramento, CA 94337-0091
(916) 654-0069 Fax: (916) 654-0241

COLORADO

UNIV. OF COLORADO - BOULDER
Libraries - Govt. Publications
Campus Box 184
Boulder, CO 80309-0184
(303) 492-8834 Fax: (303) 492-1881

DENVER PUBLIC LIBRARY
Govt. Publications Dept. BSG
1357 Broadway
Denver, CO 80203-2165
(303) 640-8846 Fax: (303) 640-8817

CONNECTICUT

CONNECTICUT STATE LIBRARY
231 Capitol Avenue
Hartford, CT 06106
(203) 566-4971 Fax: (203) 566-3322

FLORIDA

UNIV. OF FLORIDA LIBRARIES
Documents Dept.
240 Library West
Gainesville, FL 32611-2048
(904) 392-0366 Fax: (904) 392-7251

GEORGIA

UNIV. OF GEORGIA LIBRARIES
Govt. Documents Dept.
Jackson Street
Athens, GA 30602-1645
(706) 542-8949 Fax: (706) 542-4144

HAWAII

UNIV. OF HAWAII
Hamilton Library
Govt. Documents Collection
2550 The Mall
Honolulu, HI 96822
(808) 948-8230 Fax: (808) 956-5968

IDAHO

UNIV. OF IDAHO LIBRARY
Documents Section
Rayburn Street
Moscow, ID 83844-2353
(208) 885-6344 Fax: (208) 885-6817

ILLINOIS

ILLINOIS STATE LIBRARY
Federal Documents Dept.
300 South Second Street
Springfield, IL 62701-1796
(217) 782-7596 Fax: (217) 782-6437

INDIANA

INDIANA STATE LIBRARY
Serials/Documents Section
140 North Senate Avenue
Indianapolis, IN 46204-2296
(317) 232-3679 Fax: (317) 232-3728

IOWA

UNIV. OF IOWA LIBRARIES
Govt. Publications
Washington & Madison Streets
Iowa City, IA 52242-1166
(319) 335-5926 Fax: (319) 335-5900

KANSAS

UNIV. OF KANSAS
Govt. Documents & Maps Library
6001 Malott Hall
Lawrence, KS 66045-2800
(913) 864-4660 Fax: (913) 864-3855

KENTUCKY

UNIV. OF KENTUCKY
King Library South
Govt. Publications/Maps Dept.
Patterson Drive
Lexington, KY 40506-0039
(606) 257-3139 Fax: (606) 257-3139

LOUISIANA

LOUISIANA STATE UNIV.
Middleton Library
Govt. Documents Dept.
Baton Rouge, LA 70803-3312
(504) 388-2570 Fax: (504) 388-6992

LOUISIANA TECHNICAL UNIV.
Prescott Memorial Library
Govt. Documents Dept.
Ruston, LA 71272-0046
(318) 257-4962 Fax: (318) 257-2447

MAINE

UNIV. OF MAINE
Raymond H. Fogler Library
Govt. Documents Dept.
Orono, ME 04469-5729
(207) 581-1673 Fax: (207) 581-1653

MARYLAND

UNIV. OF MARYLAND - COLLEGE PARK
McKeldin Library
Govt. Documents/Maps Unit
College Park, MD 20742
(301) 405-9165 Fax: (301) 314-9416

MASSACHUSETTS

BOSTON PUBLIC LIBRARY
Govt. Documents
666 Boylston Street
Boston, MA 02117-0286
(617) 536-5400, ext. 226
Fax: (617) 536-7758

MICHIGAN

DETROIT PUBLIC LIBRARY
5201 Woodward Avenue
Detroit, MI 48202-4093
(313) 833-1025 Fax: (313) 833-0156

LIBRARY OF MICHIGAN
Govt. Documents Unit
P.O. Box 30007
717 West Allegan Street
Lansing, MI 48909
(517) 373-1300 Fax: (517) 373-3381

MINNESOTA

UNIV. OF MINNESOTA
Govt. Publications
409 Wilson Library
309 19th Avenue South
Minneapolis, MN 55455
(612) 624-5073 Fax: (612) 626-9353

MISSISSIPPI

UNIV. OF MISSISSIPPI
J.D. Williams Library
106 Old Gym Bldg.
University, MS 38677
(601) 232-5857 Fax: (601) 232-7465

MISSOURI

UNIV. OF MISSOURI - COLUMBIA
106B Ellis Library
Govt. Documents Sect.
Columbia, MO 65201-5149
(314) 882-6733 Fax: (314) 882-8044

MONTANA

UNIV. OF MONTANA
Mansfield Library
Documents Division
Missoula, MT 59812-1195
(406) 243-6700 Fax: (406) 243-2060

NEBRASKA

UNIV. OF NEBRASKA - LINCOLN
D.L. Love Memorial Library
Lincoln, NE 68588-0410
(402) 472-2562 Fax: (402) 472-5131

NEVADA

THE UNIV. OF NEVADA LIBRARIES
Business and Govt. Information Center
Reno, NV 89557-0044
(702) 784-6579 Fax: (702) 784-1751

NEW JERSEY

NEWARK PUBLIC LIBRARY
Science Div. - Public Access
P.O. Box 630
Five Washington Street
Newark, NJ 07101-7812
(201) 733-7782 Fax: (201) 733-5648

NEW MEXICO

UNIV. OF NEW MEXICO
General Library
Govt. Information Dept.
Albuquerque, NM 87131-1466
(505) 277-5441 Fax: (505) 277-6019

NEW MEXICO STATE LIBRARY
325 Don Gaspar Avenue
Santa Fe, NM 87503
(505) 827-3824 Fax: (505) 827-3888

NEW YORK

NEW YORK STATE LIBRARY
Cultural Education Center
Documents/Gift & Exchange Section
Empire State Plaza
Albany, NY 12230-0001
(518) 474-5355 Fax: (518) 474-5786

NORTH CAROLINA

UNIV. OF NORTH CAROLINA - CHAPEL HILL
Walter Royal Davis Library
CB 3912, Reference Dept.
Chapel Hill, NC 27514-8890
(919) 962-1151 Fax: (919) 962-4451

NORTH DAKOTA

NORTH DAKOTA STATE UNIV. LIB.
Documents
P.O. Box 5599
Fargo, ND 58105-5599
(701) 237-8886 Fax: (701) 237-7138

UNIV. OF NORTH DAKOTA
Chester Fritz Library
University Station
P.O. Box 9000 - Centennial and University Avenue
Grand Forks, ND 58202-9000
(701) 777-4632 Fax: (701) 777-3319

OHIO

STATE LIBRARY OF OHIO
Documents Dept.
65 South Front Street
Columbus, OH 43215-4163
(614) 644-7051 Fax: (614) 752-9178

OKLAHOMA

OKLAHOMA DEPT. OF LIBRARIES
U.S. Govt. Information Division
200 Northeast 18th Street
Oklahoma City, OK 73105-3298
(405) 521-2502, ext. 253
Fax: (405) 525-7804

OKLAHOMA STATE UNIV.
Edmon Low Library
Stillwater, OK 74078-0375
(405) 744-6546 Fax: (405) 744-5183

OREGON

PORTLAND STATE UNIV.
Branford P. Millar Library
934 Southwest Harrison
Portland, OR 97207-1151
(503) 725-4123 Fax: (503) 725-4524

PENNSYLVANIA

STATE LIBRARY OF PENN.
Govt. Publications Section
116 Walnut & Commonwealth Ave.
Harrisburg, PA 17105-1601
(717) 787-3752 Fax: (717) 783-2070

SOUTH CAROLINA

CLEMSON UNIV.
Robert Muldrow Cooper Library
Public Documents Unit
P.O. Box 343001
Clemson, SC 29634-3001
(803) 656-5174 Fax: (803) 656-3025

UNIV. OF SOUTH CAROLINA
Thomas Cooper Library
Green and Sumter Streets
Columbia, SC 29208
(803) 777-4841 Fax: (803) 777-9503

TENNESSEE

UNIV. OF MEMPHIS LIBRARIES
Govt. Publications Dept.
Memphis, TN 38152-0001
(901) 678-2206 Fax: (901) 678-2511

TEXAS

TEXAS STATE LIBRARY
United States Documents
P.O. Box 12927 - 1201 Brazos
Austin, TX 78701-0001
(512) 463-5455 Fax: (512) 463-5436

TEXAS TECH. UNIV. LIBRARIES
Documents Dept.
Lubbock, TX 79409-0002
(806) 742-2282 Fax: (806) 742-1920

UTAH

UTAH STATE UNIV.
Merrill Library Documents Dept.
Logan, UT 84322-3000
(801) 797-2678 Fax: (801) 797-2677

VIRGINIA

UNIV. OF VIRGINIA
Alderman Library
Govt. Documents
University Ave. & McCormick Rd.
Charlottesville, VA 22903-2498
(804) 824-3133 Fax: (804) 924-4337

WASHINGTON

WASHINGTON STATE LIBRARY
Govt. Publications
P.O. Box 42478
16th and Water Streets
Olympia, WA 98504-2478
(206) 753-4027 Fax: (206) 586-7575

WEST VIRGINIA

WEST VIRGINIA UNIV. LIBRARY
Govt. Documents Section
P.O. Box 6069 - 1549 University Ave.
Morgantown, WV 26506-6069
(304) 293-3051 Fax: (304) 293-6638

WISCONSIN

ST. HIST. SOC. OF WISCONSIN LIBRARY
Govt. Publication Section
816 State Street
Madison, WI 53706
(608) 264-6525 Fax: (608) 264-6520

MILWAUKEE PUBLIC LIBRARY
Documents Division
814 West Wisconsin Avenue
Milwaukee, WI 53233
(414) 286-3073 Fax: (414) 286-8074

•U.S. GOVERNMENT PRINTING OFFICE: 1995-387-253/20003

National Aeronautics and
Space Administration
Code JTT
Washington, DC 20546-0001